



INTERNATIONAL YEAR OF LIGHT 2015



2015 OPTICS + PHOTONICS TECHNICAL SUMMARIES.

NANOSCIENCE + ENGINEERING OPTICS + PHOTONICS FOR SUSTAINABLE ENERGY ORGANIC

PHOTONICS + ELECTRONICS OPTICAL ENGINEERING + APPLICATIONS

WWW.SPIE.ORG/OP

San Diego Convention Center San Diego, California, USA

Conferences & Courses: 9-13 August 2015

Exhibition: 11–13 August 2015

CONTENTS

NanoScience + Engineering



```
Symposium Chair
Satoshi Kawata.
Osaka Univ. (Japan)
```

Symposium Chair Manijeh Razeghi, Northwestern Univ. (USA)



Symposium Co-chair David L. Andrews, Univ. of East Anglia Norwich (United Kingdom)



Symposium Co-chair James G. Grote, Air Force Research Lab. (USA)

Optics + Photonics for Sustainable Energy



Symposium Chair		
Oleg V. Sulima,		
GE Global Research (USA)		

Organic Photonics + Electronics



Symposium Chair Zakya H. Kafafi, National Science Foundation, ret (USA)

Nano	Science + Engineering
9544:	Metamaterials, Metadevices, and Metasystems 2015
9545:	Nanophotonic Materials XII
9546:	Active Photonic Materials VII
9547:	Plasmonics: Metallic Nanostructures and Their Optical Properties XIII
9548:	Optical Trapping and Optical Micromanipulation XII
9549:	Physical Chemistry of Interfaces and Nanomaterials XIV
9550:	Biosensing and Nanomedicine VIII 115
9551:	Spintronics VIII 124
9552:	Carbon Nanotubes, Graphene, and Emerging 2D Materials for Electronic and Photonic Devices VIII
9553:	Low-Dimensional Materials and Devices 162
9554:	Nanoimaging and Nanospectroscopy III 172
9555:	Optical Sensing, Imaging, and Photon Counting: Nanostructured Devices and
0550	Applications 183
9556:	Nanoengineering: Fabrication, Properties, Optics, and Devices XII
Optic	al Engineering + Applications
0570.	The Netwood Light What are Distance 21/1 244

. .

9570: The Nature of Light: What are Photons? VI . . 344 9571: Fourteenth International on Solid State Lighting and LED-based Illumination Systems. 356 9572: Nonimaging Optics: Efficient Design for Illumination and Solar Concentration XII 364 9573: Optomechanical Engineering 2015. 370 9574: Material Technologies and Applications to Optics, Structures, Components, 9575: Optical Manufacturing and Testing XI..... 383 Applied Advanced Optical Metrology 9576: 9577: Optical Modeling and Performance Predictions VII 402 9578: Current Developments in Lens Design and Optical Engineering XVI..... 407 9579: Novel Optical Systems Design and Optimization XVIII 415 9580: Zoom Lenses V 423 Optical System Alignment, Tolerancing, 9582: and Verification IX 434 9583: An Optical Believe It or Not: Key Lessons Learned IV 438 9584: Ultrafast Nonlinear Imaging and 9585: Terahertz Emitters, Receivers, and Applications VI..... 451 9586: Photonic Fiber and Crystal Devices: Advances in Materials and Innovations in Device Applications IX..... 460 9587: Optical Data Storage 2015 472 9588: Advances in X-Ray/EUV Optics and Components X..... 477 9589: X-Ray Lasers and Coherent X-Ray Sources: Development and Applications XI...... 482 9590: Advances in Laboratory-based X-Ray Sources, Optics, and Applications IV 492 9591: Target Diagnostics Physics and Engineering f or Inertial Confinement Fusion IV 496 9592: X-Ray Nanoimaging: Instruments and Methods II 502 9593: Hard X-Ray, Gamma-Ray, and Neutron Detector Physics XVII 510 9594: Medical Applications of Radiation

	Technology VII
9562:	Next Generation Technologies for
	Solar Energy Conversion VI
9563:	Reliability of Photovoltaic Cells, Modules,
	Components, and Systems VIII 252
Orga	nic Photonics + Electronics
9564:	Light Manipulating Organic Materials
	and Devices II
9565:	Liquid Crystals XIX
9566:	Organic Light Emitting Materials and
	Devices XIX
9567:	Organic Photovoltaics XVI 303
9568:	Organic Field-Effect Transistors XIV 326
9569:	Printed Memory and Circuits
9595:	Radiation Detectors: Systems and
	Applications XVI
9596:	Signal and Data Processing of Small
	Targets 2015 533
9597:	Wavelets and Sparsity XVI 538
9598:	Optics and Photonics for Information
	Processing IX 545
9599:	Applications of Digital Image
0000	Processing XXXVIII
9600:	Image Reconstruction from Incomplete Data VIII
9601:	UV, X-Ray, and Gamma-Ray Space
	Instrumentation for Astronomy XIX 587
9602:	UV/Optical/IR SpaceTelescopes and
	Instruments: Innovative Technologies
	and Concepts VII
9603:	Optics for EUV, X-Ray, and Gamma-Ray Astronomy VII
9604:	Solar Physics and Space Weather
	Instrumentation VI
9605:	Techniques and Instrumentation for
	Detection of Exoplanets VII
9606:	Instruments, Methods, and Missions for
	Astrobiology XVII 649
9607:	Earth Observing Systems XX 658
9608:	Infrared Remote Sensing and
	Instrumentation XXIII
9609:	Infrared Sensors, Devices, and Applications V
9610:	Remote Sensing and Modeling of
3010.	Ecosystems for Sustainability XII
9611:	Imaging Spectrometry XX
9612:	Lidar Remote Sensing for Environmental
	Monitoring XV
9613:	Polarization Science and Remote
	Sensing VII
9614:	Laser Communication and Propagation
00/5	through the Atmosphere and Oceans IV 736
9615:	Quantum Communications and Quantum
9616:	Imaging XIII
3010:	Space Environments IX
9617:	Unconventional Imaging and Wavefront
	Sensing XI

9557: Nanobiosystems: Processing,

9561: Thin Films for Solar and Energy

Characterization, and Applications VIII..... 207 9558: Nanostructured Thin Films VIII 212

Solar Energy Applications X 223 9560: Solar Hydrogen and Nanotechnology X..... 227

Optics + Photonics for Sustainable Energy

9559: High and Low Concentrator Systems for

Sunday - Thursday 9 -13 August 2015 Part of Proceedings of SPIE Vol. 9544 Metamaterials, Metadevices, and Metasystems 2015

9544-1, Session 1

Propagating and localized toroidal excitations in free space and metamaterials (Invited Paper)

Nikolay I. Zheludev, Optoelectronics Research Ctr. (United Kingdom) and Nanyang Technological Univ. (Singapore); Vassili A. Fedotov, Nikitas Papasimakis, Vassili Savinov, Univ. of Southampton (United Kingdom); Tim A. Raybould, Optoelectronics Research Ctr. (United Kingdom)

Invited: The emerging field of toroidal electrodynamics involves the study and exploitation of peculiar localized and propagating electromagnetic excitations that topologically resemble a torus. Here we present an overview of our recent advances in the field enabled by a metamaterial approach, which includes the engineering of non-trivial non-radiating electromagnetic sources and an exotic type of optical activity. We also present an analytical technique for evaluating the role of the toroidal excitations in material systems. Finally, we examine the propagation of toroidal electromagnetic perturbations in free space (so-called 'focused doughnuts'), which present a platform for observing and studying unique light-matter interactions.

9544-2, Session 1

Observation of an anapole with dielectric nanoparticles (Invited Paper)

Andrey E. Miroshnichenko, The Australian National Univ. (Australia)

A possible existence of nonradiating sources has puzzled physicists since the early days of electromagnetic theory, particularly in connection with models of stable atoms and electrons configurations. . One intriguing example of such a nonradiating source is known as "anapole". The term "anapole" (which means "without poles" in Greek) was introduced in the physics of elementary particles by Yakov Zel'dovich. An anapole mode can be considered as a superposition of electric and toroidal dipole moments, resulting in destructive interference of the radiation fields due to similarity of their far- field scattering patterns. We demonstrate experimentally that dielectric nanoparticles can realize a radiationless anapole mode in visible. We achieve a spectral overlap of the toroidal and electric dipole modes through a geometry tuning in silicon nano-discs and observe a highly pronounced dip in the far-field scattering accompanied by the specific near-field distribution associated with the anapole mode. This radiationless excitation makes the nanodisk invisible in the far-field at the anapole mode wavelength. The anapole mode offers a new way to achieve an invisibility condition for lossless dielectric nanostructures based on the cancelation of radiation scattering. The anapole mode is not only limited to the disk geometries but it can also be observed for spheres or other dielectric nanostructures where the electric dipole contribution vanishes due to a switch to a "higher-order dipole" mode. The anapole physics provides a unique playground for the study of electromagnetic properties of nontrivial excitations of complex fields, reciprocity violation, Aharonov-Bohm like phenomena at optical frequencies, and other related phenomena.

9544-3, Session 1

Probing metamaterials with structured light

Yun Xu, Jingbo Sun, Jinwei Zeng, Zhaxylyk Kudyshev, Univ. at Buffalo (United States); Apra Pandey, CST of America,

Inc. (United States); Ying Liu, Natalia M. Litchinitser, Univ. at Buffalo (United States)

OPTICS+

PHOTONICS NANOSCIENCE+

ENGINEERING

We propose and demonstrate a reliable and inexpensive tool for optical characterization of photonics metamaterials and metasurfaces. Existing characterization methods of metamaterials (or more precisely negative index metamaterials), including conventional interferometry and ellipsometry, are rather complex and expensive.

The "measurable" difference between, for example, positive index materials and negative index materials is that the former introduces a phase delay to transmitted light beam and the latter one introduces a phase advance. Here, we propose to use optical vortex interferometry to directly "visualize" phase delay or phase advance.

In the proposed setup a laser beams at the wavelength of 633 nm is separated in two by a beam splitter. One beam is transmitted through a spiral phase plate in order to generate a beam with an orbital angular momentum, and the second beam is transmitted through a nanostructured sample. Two beams are subsequently recombined by a beam splitter to form spiral interferogram. Spiral patterns are then analyzed to determine phase shifts introduced by the sample. In order to demonstrate the efficiency of the proposed technique, we fabricated four metasurface samples consisting of metal nano-antennas introducing different phase shifts and experimentally measured phase shifts of the transmitted light using the proposed technique. The experimental results are in good agreement with numerical simulations.

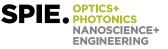
In summary, we report a novel method to characterize metasurfaces and metamaterials using optical vortex interferometry. The proposed characterization approach is simple, reliable and particularly useful for fast and inexpensive characterization of phase properties introduced by metamaterials and metasurfaces.

9544-4, Session 1

Large magnetic to electric field contrast in azimuthally polarized vortex beams generated by a metasurface

Mehdi Veysi, Caner Guclu, Filippo Capolino, Univ. of California, Irvine (United States)

We investigate azimuthally E-polarized vortex beams with enhanced longitudinal magnetic field. Ideally, such beams possess strong longitudinal magnetic field on the beam axis where there is no electric field. First we formulate the electric field vector and the longitudinal magnetic field of an azimuthally E-polarized beam as an interference of right- and lefthand circularly polarized Laguerre Gaussian (LG) beams carrying the orbital angular momentum (OAM) states of -1 and +1, respectively. Then we propose a metasurface design that is capable of converting a linearly polarized Gaussian beam into an azimuthally E-polarized vortex beam with longitudinal magnetic field. The metasurface is composed of a rectangular array of double-layer double split-ring slot elements, though other geometries could be adopted as well. The element is specifically designed to have nearly a 180° transmission phase difference between the two polarization components along two orthogonal axes, similar to the optical axes of a half-wave plate. By locally rotating the optical axes of each metasurface element, the transmission phase profile of the circularly polarized waves over the metasurface can be tailored. Upon focusing of the generated vortex beam through a lens with a numerical aperture of 0.7, a 41-fold enhancement of the magnetic to electric field ratio is achieved on the beam axis with respect to that of a plane wave. Generation of beams with large magnetic field to electric field contrast can find applications in future spectroscopy systems based on magnetic dipole transitions, which are usually much weaker than electric dipole transitions.



9544-5, Session 1

Plasmonic magnetization during circularly polarized excitation

Matthew T. Sheldon, Texas A&M Univ. (United States)

In contrast with linearly polarized excitation, which necessarily has zero magnitude electrical field twice during an optical cycle, the electrical field vector of circularly polarized light has constant magnitude. During an optical cycle the electric field vector rotates in the plane normal to the wave propagation. Consequently, if plasmonic structures are resonant with circularly polarized excitation, it is possible for them to exhibit regions of strongly modified carrier density for the duration of the optical cycle.

Here, we study a class of achiral toroid and 'sun burst' nano-patterned plasmonic surfaces that show persistent, circulating charge density waves during circularly polarized illumination. The direction of the continuously circulating wave (clockwise or counterclockwise) depends on the handedness of the incident beam. Our interest stems from whether these charge density waves can support circular electric currents (DC) manifest experimentally as static magnetic fields during illumination. Using fullwave optical modeling (FDTD method), and mechanistic calculations of the circulating potential acting on electrons in the toroid resonators, we outline the conditions that maximize optical excitation of both circulating displacement currents and electron transport currents. We show that in the limit of very weak coupling to the solenoid-like electron transport, or when < 1 x 10⁻⁶% of the plasmonically active electron population enters the circular transport modes, relatively strong magnetic fields, > 1 G, can be expected. We discuss scanning probe measurements for monitoring the induced magnetic field, as well as the relationship between this phenomenon and the inverse Faraday effect observed in continuous media.

9544-6, Session 2

Enhanced light-matter coupling in Sibased metamaterials (Invited Paper)

Luca Dal Negro, Boston Univ. (United States)

I will present our results on the design, nanofabrication and optical characterization of silicon-compatible metamaterials for applications to light sources and highly nonlinear optical components. In particular, I will discuss recent work on loss-reduction in metamaterials with tunable negative permittivity in the near-infrared spectral range. Rare earth doping of conductive oxides and nitrides with different compositions will also be discussed as an alternative approach to active plasmon alloys and epsilon-near-zero (ENZ) media with tunable polaritonic responses across the 1-2 micrometer spectral range. Experiments will be presented addressing change modulation, enhanced light scattering, emission, second and third harmonic generation on a chip.

9544-7, Session 2

Recent advances in metamaterial multiphysics (Invited Paper)

Mikhail Lapine, Univ. of Technology Sydney (Australia)

In this contribution, I will present an overview of our recent achievements in exploiting novel degrees of freedom in metamaterial design, which enable sophisticated nonlinear coupling mechanisms and bring enhancement to nonlinear behaviour. One of the paradigms makes use of various types of mechanical feedback, achieved by embedding electromagnetic resonators within elastic medium or engineering explicit elastic links between them — such arrangements lead to broad-band self-adjustable resonances, self-oscillations, chaotic regimes and spontaneous symmetry breaking. With this respect, we have analysed a range of implementations from microwaves to optics. Another concept benefits from multi-frequency operation, where the properties in completely distinct frequency ranges become entangled through specific metamaterial design — for example,

direct optical coupling can be introduced between microwave resonators, providing an independent interaction channel which can be exploited for nonlinear "traffic lights" between otherwise independent waveguides so that one signal is suppressed or enhanced depending on the power of a competing signal. Alternatively, such an optical path may be used to achieve nonlinear mutual interaction. Finally, we explore the benefits which hyperbolic metamaterials can bring to classical nonlinear processes. The use of hyperbolic dispersion, which supports arbitrary k-vectors, eventually allows for unusual phase matching solutions, with a rich choice of matching combinations. This design overcomes the limitations of both the conventional birefringent and quasi phase matching, making harmonics generation easily possible with nonlinear materials where the classical approaches fail.

9544-8, Session 2

Coherent effects in nonlinear metamaterial-based devices (Invited Paper)

Alessandro Salandrino, The Univ. of Kansas (United States)

Nonlinear optical interactions are at the foundation of ultrafast control of photons with other photons, and are essential for the realization of integrated all-optical processors. The problem posed by the weak nature of nonlinear effects is typically circumvented by designing devices relying on long propagation lengths and operating under high intensity excitation fields. However such an approach precludes dense integration and hardly complies with the low power, low weight, and small size requirements of modern telecommunication systems. Metamaterials can provide novel strategies to address the shortcomings of conventional nonlinear optics.

Nanostructured media and metamaterials have revolutionized the technological landscape, and for this reason a variety of concepts from classical nonlinear optics such as phase-matching should be revisited in order to account for the new properties offered by these artificial media. One unique characteristic of metamaterials and nanostructured media is the possibility of controlling electromagnetic fields over length-scales comparable to, or smaller than the operating wavelength. In addition to field enhancement effects, metamaterials offer an unprecedented control over the phase of electromagnetic fields, which is of paramount importance in coherent optical processes.

Here we explore frequency conversion effects in nanostructured media under structured illumination. The coherent interactions arising in such ensembles of nanostructures lead to a very rich phenomenology and a unique set of degrees of freedom with which to engineer the overall nonlinear response. Here we discuss the control of nonlinear emission direction, the control of nonlinear emission polarization and novel phasematching schemes.

9544-9, Session 2

Active control of light beam in transformation optics

Hui Liu, Nanjing Univ. (China)

The control of electromagnetic radiation in transformation optical metamaterials brings the development of vast variety of optical devices. Of a particular importance is the possibility to control the propagation of light with light. In this work, we use a structured planar cavity to enhance the thermo-optic effect in a transformation optical waveguide. In the process, a control laser produces apparent inhomogeneous refractive index change inside the waveguides. The trajectory of a second probe laser beam is then continuously tuned in the experiment. The experimental results agree well with the developed theory. The reported method can provide a new approach toward development of transformation optical devices where active all-optical control of the impinging light can be achieved.

9544-91, Session 2

Transparency and coherence in rf SQUID metamaterials (Invited Paper)

Steven M Anlage, Univ. of Maryland, College Park (United States)

We have developed active metamaterials based on macroscopic quantum effects capable of quickly tuning their electrical and magnetic responses over a wide frequency range. These metamaterials are based on superconducting elements to form low insertion loss, physically and electrically small, highly tunable structures for the next generation rf electronics. The meta-atoms are rf superconducting quantum interference devices (SQUIDs) that incorporate the Josephson effect. RF SQUIDs have an inductance which includes a contribution from the Josephson inductance of the junction. This inductance is strongly tunable with dc and rf magnetic fields and currents. The rf SQUID metamaterial is a richly nonlinear effective medium introducing qualitatively new macroscopic guantum phenomena into the metamaterials community, namely magnetic flux quantization and the Josephson effect. The coherence of the metamaterials is strongly sensitive to the environment and measurement conditions. The metamaterials also display a unique form of transparency whose development can be manipulated through multiple parametric dependences. Further features such as breathers, superradiance, and selfinduced transparency, along with entry into the fully quantum limit, will yield qualitatively new metamaterial phenomena.

This work is supported by the NSF-GOALI and OISE Programs through Grant No. ECCS-1158644 and the Center for Nanophysics and Advanced Materials (CNAM).

9544-10, Session 3

Nanostructured photonic metamaterials reconfigurable with light, nanomechanical, and electromagnetic forces (Invited Paper)

Jun-Yu Ou, Univ. of Southampton (United Kingdom); João Valente, Optoelectronics Research Ctr. (United Kingdom); Artemios Karvounis, Univ. of Southampton (United Kingdom); Weiping Wu, Eric Plum, Optoelectronics Research Ctr. (United Kingdom); Kevin F. MacDonald, Univ. of Southampton (United Kingdom); Nikolay I. Zheludev, Univ. of Southampton (United Kingdom) and Nanyang Technological Univ. (Singapore)

Invited: Active and dynamic manipulation of metamaterial optical properties is the foundation for metamaterial devices. Such metadevices will translate metamaterials from fundamental scientific research to practical applications including optical switches, optical modulators, tunable spectral filters, and programmable transformation optics devices. Here we develop reconfigurable photonic metamaterials that offer a flexible platform for fast dynamic control of metamaterial optical properties.

The properties of any metamaterial structure strongly depend on the spatial arrangement of its building blocks. By constructing metamaterials on elastically deformable scaffolds we can dynamically control the nanoscale spacing among constituent elements across the entire metamaterial array. Based on this approach, we use electrostatic, Lorentz and near field optical forces to drive high-contrast, high-speed active tuning, modulation and switching of photonic metamaterial properties and to deliver exceptionally large opto-mechanical nonlinearities.

9544-11, Session 3

Latest progress in spasers (Invited Paper)

Mark I. Stockman, Georgia State Univ. (United States)

Nanoplasmonics deals with collective electron excitations at the surfaces

of metal nanostructures, called surface plasmons. The surface plasmons localize and nano-concentrate optical energy creating highly enhanced local fields. Nanoplasmonics has numerous applications in science, technology, biomedicine, environmental monitoring, and defense.

SPIE

OPTICS+

PHOTONICS

NANOSCIENCE+ ENGINEERING

There is an all-important need in active devices capable of generating and amplifying coherent optical fields on the nanoscale analogous to lasers and amplifiers of the conventional optics or transistors of microelectronics. Such an active device is the spaser (surface plasmon amplification by stimulated emission of radiation), also called plasmonic nanolaser. We will focus on the newest ideas and achievements in spasers.

We will present two new theoretical ideas in the field of spasers: spaser with electric pumping via quantum wire [D. Li and M. I. Stockman, Electric Spaser in the Extreme Quantum Limit, Phys. Rev. Lett. 110, 106803-1-5 (2013)] and quantum-cascade graphene spaser [V. Apalkov, M. I. Stockman, Proposed graphene nanospaser. Light Sci. Appl. 3, e191-191-196 (2014)]. We will consider the latest progress in applications of spasers. Among them is a recent breakthrough in ultrasensitive detection of explosives using the spaser [R.-M. Ma, S. Ota, Y. Li, S. Yang, X. Zhang, Explosives Detection in a Lasing Plasmon Nanocavity, Nat. Nano 9, 600-604 (2014)]. Another recent breakthrough to be presented is an application of the spaser as an ultrabright nanolabel and an efficient theranostic agent in biomedicine (cancer diagnostics and treatment) [E. I. Galanzha, R. Weingold, D. A. Nedosekin, M. Sarimollaoglu, A. S. Kuchyanov, R. G. Parkhomenko, A. I. Plekhanov, M. I. Stockman, and V. P. Zharov, Spaser as Novel Versatile Biomedical Tool, arXiv:1501.00342, 1-33 (2015)].

9544-12, Session 3

Active hyperbolic metamaterials (Invited Paper)

Vinod M. Menon, The City College of New York (United States)

Hyperbolic metamaterials (HMMs) have become one of the most attractive classes of metamaterials due to their wide array of applications in combination with ease of realization. Here we will discuss our recent work on "active hyperbolic metamaterials" where demonstrate enhanced light emission and extraction from metamaterials embedded with quantum dots. We will also discuss our recent efforts on realizing tunable HMMs as well as sub-wavelength cavities.

9544-13, Session 3

Gain-enhanced hyperbolic metamaterials at telecommunication frequencies

Joseph S. T. Smalley, Univ. of California, San Diego (United States); Felipe Vallini, Univ. of California San Diego (United States); Boubacar Kante, Shiva Shahin, Conor Riley, Yeshaiahu Fainman, Univ. of California, San Diego (United States)

Using effective medium theory (EMT), Bloch's theorem (BT), and the transfer matrix method (TMM), we analyze the possibility of gainenhanced transmission in metamaterials with hyperbolic dispersion at telecommunication frequencies. We compare different combinations of dissipative metals and active dielectrics, including noble metals, transparent conducting oxides (TCO), III-V compounds, and solid-state dopants. We find that both indium gallium arsenide phosphide (InGaAsP) and erbium-doped silica (Er:SiO2), when combined with silver, show promise as a platform for demonstration of pump-dependent transmission. On the other hand, when these active dielectrics are combined with aluminum-doped zinc oxide (AZO), a low-loss TCO, gain-enhanced transmission is negligible. Results based on EMT are compared to the more accurate BT and TMM. When losses are ignored, quantitative agreement between these analytical techniques is observed near the center of the first Brillouin zone of a one-dimensional periodic structure. Including realistic levels of loss and gain, however, EMT predictions become overly optimistic compared to BT and TMM. We also



discuss the limitations to assumptions inherent to EMT, BT, and TMM, and suggest avenues for future analysis.

9544-14, Session 3

Giant gain enhancement in slow-wave photonic crystals with a degenerate band edge

Mohamed A. K. Othman, Filippo Capolino, Alexander Figotin, Univ. of California, Irvine (United States); Farshad Yazdi, Univ. of California Irvine (United States)

Recent photonic crystal technologies have enabled a new class of lowthreshold laser sources that showed a substantial enhancement in the performance utilizing a Fabry-Perot configuration. In the pursuit of higher gain and more efficient sources, we here propose a novel slow-wave Fabry-Perot cavity (FPC) made of a photonic crystal for laser applications that utilizes a degeneracy condition of the structural eigenmodes, namely, the degenerate band edge (DBE) condition. We show here that FPCs operating very close to the DBE can be used to enhance gain in laser devices to unprecedented levels. Light confinement in this configuration allows a huge increase in the photon lifetime in the cavity. Consequently, when active materials are integrated into an FPC with a DBE, round trip gain experienced by photons is significantly increased for photons travel with extremely low group velocities yielding a gigantic transmission gain. We show in particular giant enhancement of the gain in an FPC with a DBE compared to an FPC with a photonic crystal with a regular band edge, up to a few orders of magnitude. We also investigate the role of the local density of states (LDOS) which provides an explanation of the origin of gain enhancement mechanism in the PFC with a DBE. The proposed gain mechanism has a promising potential for many applications, including, but not limited to, high efficiency, low threshold laser devices as well as high power microwave amplifiers.

9544-15, Session 4

Collective Förster energy transfer modified by planar plasmonic mirror (*Invited Paper*)

Alexander N. Poddubny, Ioffe Physical-Technical Institute (Russian Federation)

This is an invited presentation devoted to the Förster energy transfer in plasmonic systems.

Förster energy transfer processes are now actively studied in various fields that bridge physics, biology and medicine. One can try to control the efficiency of the transfer by embedding the donors and acceptors into the structured electromagnetic environment. Available experimental studies yields contradictory reports on suppressed [1], enhanced [2] or unaffected [3] transfer.

We present a rigorous Green function theory of the collective Förster energy transfer between the arrays of donor and acceptor molecules lying on the planar metallic mirror that has been previously available only for spherical nanoparticles [4]. We reveal strong modification of the effective transfer rate by the mirror. The rate can be either suppressed or enhanced depending on the relative positions between acceptor and donor arrays. This is a collective effect, completely absent for a single donor-acceptor pair put above the mirror. Our results may explain the slowdown of the transfer rate recently observed in experiment for dye molecules put on top of plasmonic mirrors and layered hyperbolic metamaterials [1].

[1] T. Tumkur, J. Kitur, C. Bonner, A. Poddubny, E. Narimanov and M. Noginov, Faraday Discuss., 2014 , DOI: 10.1039/C4FD00184B

[2] C. Blum, N. Zijlstra, A. Lagendijk, M. Wubs, A. P. Mosk, V. Subramaniam, and W. L. Vos, Phys. Rev. Lett. 109, 203601 (2012).

[3] P. Andrew and W. L. Barnes, Science 290, 785 (2000).

[4] V.N. Pustovit, A.M. Urbas, and T.V. Shahbazyan, Phys. Rev. B 88, 245427(2013)

9544-16, Session 4

Nitrogen-vacancy single-photon emission enhanced with nanophotonic structures (Invited Paper)

Vladimir M. Shalaev, Mikhail Y. Shalaginov, Purdue Univ. (United States); Vadim V. Vorobyov, Photonic Nano-Meta Technologies (Russian Federation); Simeon Bogdanov, Purdue Univ. (United States); Alexey V. Akimov, Russian Quantum Ctr. (Russian Federation); Alexei Lagutchev, Alexander V. Kildishev, Alexandra Boltasseva, Purdue Univ. (United States)

Efficient generation of single photons is essential for the development of photonic quantum technologies. We have demonstrated that coupling a nanodiamond nitrogen-vacancy (NV) center to CMOS-compatible nanophotonic structures results in significant reduction of the excited state lifetime, increase in the collected single-photon emission, and modification of radiation pattern. In addition, we studied the effect of increased photonic density of states on spin dependent fluorescence contrast.

9544-17, Session 4

Super-coulombic Van der Waals interactions in metamaterials (Invited Paper)

Cristian L. Cortes, Ward D. Newman, Zubin Jacob, Univ. of Alberta (Canada)

We use Rytov's fluctuational electrodynamics to show that Van Der Waals interactions are fundamentally modified by metamaterials. We verify the conditions under which the effect is strongest and also show initial experimental results to prove the same. En route to developing the van der waals theory in metamaterials we have also adopted a unique approach to quantization in lossy dispersive media.

9544-18, Session 4

Effect of nonlocal dielectric environments on chemical reactions

Vanessa N. Peters, Norfolk State Univ. (United States); Thejaswi U Tumkur, Guohua Zhu, Mikhail A Noginov, Norfolk State Univ (United States)

Proximity to metallic surfaces, plasmonic structures, cavities and other inhomogeneous dielectric environments is known to control spontaneous emission, energy transfer, scattering, and many other phenomena of practical importance. The aim of the present study was to demonstrate that, in spirit of the Marcus theory, the rates of chemical reactions can, too, be influenced by nonlocal dielectric environments, such as metallic films and metal/dielectric bilayer or multilayer structures. We have experimentally shown that metallic and composite metal/dielectric substrates can, indeed, control ordering as well as photodegradation of thin poly-3-hexylthiophene (p3ht) films. In many particular experiments, p3ht films were separated from metal by a dielectric spacer, excluding conventional catalysis facilitated by metals and making modification of the nonlocal dielectric environment a plausible explanation for the observed phenomena. This first step toward understanding of a complex relationship between chemical reactions and nonlocal dielectric environments is to be followed by the theory development and a broader scope of thorough experimental studies.

9544-19, Session 4

Effect of photonic density of states on spin-flip induced fluorescence contrast in diamond nitrogen-vacancy center ensembles

Mikhail Shalaginov, Simeon Bogdanov, Jing Liu, Alexei Lagutchev, Alexander V. Kildishev, Dimitrios Peroulis, Joseph M. Irudayaraj, Alexandra Boltasseva, Vladimir M. Shalaev, Purdue Univ. (United States)

Diamond based nitrogen-vacancy (NV) centers are promising solid state defects for applications in quantum information technologies. On the one hand, there is a growing interest in enhancing their single-photon emission by coupling them to plasmonic structures. On the other hand, the dependence of emission intensity on the electron spin state enables room temperature quantum information readout. We study the fluorescence contrast resulting from the spin resonance in the conditions of an increased photonic density of states. Fluorescence observations from NV center ensembles in diamond nanocrystals coupled to structures supporting plasmonic modes experimentally confirm the analytical results.

9544-500, Session Plen

Extreme Imaging and Beyond

Keisuke Goda, The Univ. of Tokyo (Japan)

Imaging is an effective tool in scientific research, manufacturing, and medical practice. However, despite its importance, it is not easy to observe dynamical events that occur much faster or slower than the human time scale (found in photochemistry, phononics, fluidics, MEMS, and tribology). Unfortunately, traditional methods for imaging fall short in visualizing them due to their technical limitations. In this talk, I will introduce radically different approaches to imaging. I will first discuss ultrafast imaging and then talk about ultraslow imaging. I will show how these imaging tools help us better understand dynamical processes.

9544-501, Session Plen

Nano-bio-optomechanics: nanoaperture tweezers probe single nanoparticles, proteins, and their interactions

Reuven Gordon, Univ. of Victoria (Canada)

Nanoparticles in the single digit nanometer range can be easily isolated and studied with low optical powers using nanoaperture tweezers. We have studied individual proteins and their interactions with small molecules, DNA and antibodies. Recently, using the fluctuations of the trapped object, we have pioneered a new way to "listen" to the vibrations of nanoparticles in the 100 GHz - 1 THz range; the approach is called extraordinary acoustic Raman (EAR). EAR gives unprecedented low frequency spectra of individual proteins in solution, allowing for identification and analysis, as well as probing their role in biological functions. We have also used EAR to study the elastic properties, shape and size of various individual nanoparticles.

9544-502, Session Plen

Device Applications of Semiconductor Nanoantennas and Metafilms

Mark L. Brongersma, Geballe Lab. for Advanced Materials (GLAM) (United States)

Semiconductor nanostructures are at the heart of modern-day electronic devices and systems. Due to their high refractive index, they also provide

a myriad of opportunities to manipulate light. When properly sized and shaped, they can support strong optical resonances that boost light-matter interaction over bulk materials and enable their use in controlling the flow of light at the nanoscale. In this presentation, I will discuss the use of individual, resonant nanostructures and dense arrays thereof (metafilms) in a variety of optoelectronic devices and illustrate how the performance of these devices can be improved by engineering the constituent nanostructure, size, shape, and/or spacing.

OPTICS+
 PHOTONICS

NANOSCIENCE+ ENGINEERING

9544-20, Session 5

Photonic hypercrystals (Invited Paper)

Evgenii E. Narimanov, Purdue Univ. (United States)

We introduce a new "universality class" of artificial optical media - photonic hyper-crystals. These hyperbolic metamaterials with periodic spatial variation of dielectric permittivity on subwavelength scale, combine the features of optical metamaterials and photonic crystals.

9544-21, Session 5

Non-resonant hyperlens in the visible range (Invited Paper)

Natalia M. Litchinitser, Jingbo Sun, Mikhail I. Shalaev, Univ. at Buffalo (United States)

A metamaterial hyperlens offers a unique solution to overcome the diffraction limit by transforming evanescent waves responsible for imaging subwavelength features of an object into propagating waves. However, the first realizations of optical hyperlenses were limited by a narrow working bandwidth and significant resonance-induced loss. Here, we report the first experimental demonstration of a non-resonant waveguide-coupled hyperlens operating in the visible wavelength range that was fabricated using a combination of top-down and bottom-up fabrication approaches. A detailed investigation of various materials systems proves that a radial fan-shaped configuration is superior to the concentric layer-based configuration in that it relies on non-resonant negative dielectric response, and, as a result, enables broadband and low-loss performance in the visible range. While the majority of applications of a hyperlens is expected to be in optical frequency range, the challenge of fabricating non-resonant radial structures at optical frequencies has not been overcome until now.

9544-22, Session 5

Sub-diffractional, volume-confined polaritons in a natural hyperbolic material: hexagonal boron nitride

Joshua D. Caldwell, U.S. Naval Research Lab. (United States); Andrey V. Kretinin, The Univ. of Manchester (United Kingdom); Yiguo Chen, Vincenzo Giannini, Imperial College London (United Kingdom); Michael M. Fogler, Univ. of California, San Diego (United States); Yan Francescato, Imperial College London (United Kingdom); Chase T. Ellis, Joseph G. Tischler, U.S. Naval Research Lab. (United States); Colin R. Woods, The Univ. of Manchester (United States); Alexander J. Giles, U.S. Naval Research Lab. (United States); Kenji Watanabe, Takashi Taniguchi, National Institute for Materials Science (Japan); Stefan A. Maier, Imperial College London (United Kingdom); Kostya S. Novoselov, The Univ. of Manchester (United Kingdom)

Strongly anisotropic media where principal components of the dielectric tensor have opposite signs are called hyperbolic. These materials permit highly directional, volume-confined propagation of slow-light modes



at deeply sub-diffractional size scales, leading to unique nanophotonic phenomena. The realization of hyperbolic materials within the optical spectral range has been achieved primarily through the use of artificial structures typically composed of plasmonic metals and dielectric constituents. However, while proof-of-principle experiments have been performed, the high plasmonic losses and inhomogeneity of the structures limit most advances to the laboratory. Recently, hexagonal boron nitride (hBN) was identified as a natural hyperbolic material (NHM), offering a low-loss, homogeneous medium that can operate in the mid-infrared. We have exploited the NHM response of hBN within periodic arrays of conical nanoresonators to demonstrate 'hyperbolic polaritons,' deeply sub-diffractional guided waves that propagate through the volume rather than on the surface of a hyperbolic material. We have identified that the polaritons are manifested as a four series of resonances in two distinct spectral bands that have mutually exclusive dependencies upon incident light polarization, modal order, and aspect ratio. These observations represent the first foray into creating NHM building blocks for midinfrared to terahertz nanophotonic and metamaterial devices. This talk will also discuss potential near-term applications stemming from these developments.

9544-23, Session 5

Practical realization of deeply subwavelength multilayer metal-dielectric nanostructures based on InGaAsP

Joseph S. T. Smalley, Univ. of California, San Diego (United States); Felipe Vallini, Univ. of California San Diego (United States); Sergio Montoya, Eric E. Fullerton, Yeshaiahu Fainman, Univ. of California, San Diego (United States)

Using established nanofabrication techniques, we realize deeply subwavelength multilayer metal-dielectric nanostructures composed of silver and indium gallium arsenide phosphide (InGaAsP). In contrast to most, if not all, subwavelength multilayer metal-dielectric systems to date, the Bloch vector of the fabricated structure is parallel to the plane of the substrate, making it suitable for waveguide integration. InGaAsP multiple quantum wells (MQWs) are epitaxially grown on InP normal to the Bloch vector of the resulting multilayer. The associated carrier population of the MQWs allows for active control of the behavior of the nanostructure via external optical pumping. Individual layer thicknesses of 30nm are repeatedly achieved via electron-beam lithography, reactive ion etching of InGaAsP, and sputter deposition of silver. Resulting 60nm periods of the one-dimensional periodic structure are 25 times smaller than telecommunication wavelengths in vacuum. The realized multilayer nanostructures hold promise as a platform for active and tunable hyperbolic metamaterials at telecommunication frequencies.

9544-24, Session 5

Semiconductor-dielectric Multilayer surface magnetoplasmon planar hyperlens

Bo Han Cheng, Academia Sinica (Taiwan); Hong Wen Chen, Yung-Chiang Lan, National Cheng Kung Univ. (Taiwan); Din Ping Tsai, Academia Sinica (Taiwan)

The magnetically controlled planar hyperlens which consists of an InSb-PMMA multilayered structure is proposed and analyzed. The ability of the proposed hyperlens to resolve subwavelength structures at THz region is demonstrated by electromagnetic numerical simulation. The asymmetric field pattern in the hyperlens is caused by the surface magnetoplasmon (SMP) propagating in the InSb-PMMA waveguide. By using transfer matrix method and the effective medium approach of the investigated components, the role of SMP played in the super-resolution is elucidated. Furthermore, the super-resolution of the proposed device under various frequencies is accomplished by merely changing the value of external magnetic field. The proposed device would provide a practical route for multi-functional material, real-time super-resolution imaging, photolithography, and THz imaging.

9544-25, Session 5

Probing the ultrathin limit of hyperbolic metamaterial: nonlocality induced topological transitions

Long Chen, Cheng Zhang, Jing Zhou, L. Jay Guo, Univ. of Michigan (United States)

An ideal hyperbolic metamaterial (HMM), which has a perfect hyperbolic dispersion curve, theoretically can support modes with indefinite wavenumbers, leading to large photon local density of states (LDOS) and many applications such as enhancing light-matter interactions, spontaneous emission and thermal radiation. Here in this presentation, HMMs based on ultrathin metal-dielectric multilayers have been studied by considering the nonlocal response of electrons in metal. Based on the hydrodynamic model of the nonlocal response, we investigate the effect of nonlocality on the performance (dispersion relation, ray refraction, LDOS and spontaneous emission) of HMMs when gradually approaching the ultrathin limit of the unit cell. We show that nonlocality will induce topological transitions of the iso-frequency surfaces and limit the wavenumber as well as LDOS for both type I and type II HMMs. Under nonlocal treatment, the iso-frequency surface of type II HMM transforms from a hyperbola to a bullet shape, while for type I HMM, the surface splits into two branches: a cylindrical-like branch at high k region and an elliptical branch at the low k region. In the high k region, the nonlocality set a cut-off k for the allowed wavenumbers in both type I and type II HMMs. This cut-off k which is defined by the electron Fermi velocity of the metal intrinsically limits the LDOS and lightmatter interactions. These results indicate that in the aim of achieving high performance HMMs, merely thinning the constituent films according to the local theories is no longer valid.

9544-26, Session 5

Tunable VO2/Au hyperbolic metamaterial

Srujana Prayakarao, Norfolk State Univ. (United States); Brock Mendoza, Andrew Devine, Cornell Univ. (United States) and Norfolk State Univ. (United States); Chan Kyaw, Morehouse College (United States) and Norfolk State Univ. (United States); Robert B. Van Dover, Cornell Univ. (United States); Mikhail A. Noginov, Norfolk State Univ. (United States)

Vanadium oxide (VO2) is known to undergo a semiconductor-to-metal transition at 68°C. Therefore, it can be used as a tunable component of an active metamaterial. The lamellar metamaterial designed and studied in this work is composed of subwavelength VO2 and Au layers and is predicted to have the temperature controlled transition from the hyperbolic phase to the metallic phase. The VO2 films and VO2/Au lamellar metamaterial stacks have been fabricated and studied in the electrical conductivity as well as optical (transmission, reflection) experiments. The temperature depended changes in the absorption and transmission spectra of metamaterials and films have been observed experimentally and compared with the theory predictions.

9544-27, Session 6

Infrared spectroscopy with tunable graphene plasmons (Invited Paper)

Andrea Marini, Iván Silveiro, Javier Garcia de Abajo, ICFO -Institut de Ciències Fotòniques (Spain)

We propose the exploitation of plasmons in graphene nanoislands as



a promising platform for sensing through surface-enhanced infrared absorption and Raman scattering. Our calculations indicate that the large electrical tunability of graphene enables the identification of molecular resonances by recording broadband absorption or inelastic scattering, replacing wavelength-resolved light collection by a signal integrated over photon energy as a function of the graphene doping level. Our results pave the way for the development of novel cost-effective sensors capable of identifying spectral signatures of molecules without using spectrometers and laser sources.

9544-28, Session 6

Nano-photonic phenomena in van der Waals heterostructures (Invited Paper)

Dmitri N. Basov, Univ. of California, San Diego (United States)

van der Waals (vdW) crystals consist of individual atomic planes coupled by vdW interaction, similar to graphene monolayers in bulk graphite. We investigated van der Waals heterostructures assembled from atomically thin layers of graphene and hexagonal boron nitride (hBN). We launched, detected and imaged plasmonic, phonon polaritonic and hybrid plasmonphonon polariton waves in a setting of an antenna based nano-infrared apparatus. Hyperbolic phonon polaritons in hBN enabled sub-diffractional focusing in infrared frequencies. Because electronic, plasmonic and phonon polaritonic properties in van der Waals heterstructures are intertwined, gate voltage and/or details of layer assembly enable efficient control of nanophotonic effects.

9544-29, Session 6

Second-harmonic generation from atomic-scale ABC-type laminate optical metamaterials (Invited Paper)

Luca Alloatti, Massachusetts Institute of Technology (United States) and Institute of Photonics and Quantum Electronics Karlsruhe Institute of Technology (Germany); Clemens M. Kieninger, Andreas M. Frölich, Matthias Lauermann, Tobias Frenzel, Kira Köhnle, Wolfgang Freude, Karlsruher Institut für Technologie (Germany); Juerg Leuthold, ETH Zürich (Switzerland); Christian Koos, Martin Wegener, Karlsruher Institut für Technologie (Germany)

We introduce ABC laminate metamaterials composed of layers of three different dielectrics. Each layer has zero bulk second-order optical nonlinearity, yet centro-symmetry is broken locally at each inner interface. To achieve appreciable effective bulk metamaterial second-order nonlinear optical susceptibilities, we densely pack many inner surfaces to a stack of atomically thin layers grown by conformal atomic-layer deposition. For the ABC stack, centro-symmetry is also broken macroscopically. Our experimental results for excitation at around 800 nm wavelength indicate interesting application perspectives for frequency conversion or electrooptic modulation in silicon photonics.

9544-111, Session 6

Metamaterials with magnetic hyperbolic dispersion

Sergey S. Kruk, The Australian National Univ. (Australia); Zi Jing Wong, Univ. of California, Berkeley (United States); Ekaterina Pshenay-Severin, Friedrich-Schiller-Univ. Jena (Germany) and The Australian National Univ. (Australia); Kevin O'Brien, Univ. of California, Berkeley (United States); Dragomir N. Neshev, Yuri S. Kivshar, The Australian National Univ. (Australia); Xiang Zhang, Univ. of California, Berkeley (United States)

Strongly anisotropic media, where the principal components of the dielectric permittivity and/or permeability tensor have opposite signs, are called hyperbolic media. The study of hyperbolic media and hyperbolic metamaterials have attracted significant attention in recent years for their interesting properties such as high density of states, all-angle negative refraction, and hyperlens imaging beyond the resolution of conventional systems. In previous studies hyperbolic media were realized as uniaxial materials whose axial and tangential dielectric permittivities have opposite signs. Such media are typically realized using the metamaterial concept in the form of metal-dielectric multilayered structures, or arrays of conducting nanowires, while several examples of natural hyperbolic media have been demonstrated as well. However, the hyperbolic dispersion in all artificial and natural optical media demonstrated to date has its origin in the electric response. This restricts fundamentally the functionality of these materials for only one polarization of light and places severe limitation for the impedance matching with a free space. Importantly, the concept of generalized hyperbolic media with both electric and magnetic response does not have these restrictions. Here we present the first demonstration of a magnetic hyperbolic dispersion in a three-dimensional metal-dielectric multilayer metamaterial with principal components of the effective magnetic permeability tensor having opposite signs. We provide a systematic direct measurement of a topology-driven transition between elliptic and hyperbolic metamaterials observed through a structural modification of their dispersion, reported for the time for any type of metamaterial. Our findings show the possibility for realization of efficient hyperbolic media for unpolarised light.

9544-30, Session 7

Transparent conducting oxides as plasmonic component in near infrared (Invited Paper)

Jongbum Kim, Nathaniel Kinsey, Aveek Dutta, Purdue Univ. (United States); Marcello Ferrera, Purdue Univ. (United States) and Heriot-Watt Univ. (United Kingdom); Clayton Devault, Alexander V Kildishev, Vladimir M. Shalaev, Alexandra Boltasseva, Purdue Univ. (United States)

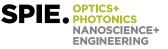
The development of new plasmonic materials enables novel optical devices, and they in turn assist in the progress of optical communications. As a result of the significant attention in searching for alternative materials, transparent conducting oxides (TCOs) have been proposed as promising plasmonic compounds at telecommunication wavelengths [1]. They are eminently practical materials because they are CMOS-compatible, can be grown on many different types of substrates, patterned by standard fabrication procedures, and integrated with many other standard technologies.

Due to the ability of TCO nanostructures to support strong plasmonic resonance in the NIR, metasurface devices, such as a quarter wave plate, have been demonstrated whose properties can be easily adjustable with post processing such as thermal annealing [2,3]. Additionally, TCOs can be used as epsilon near zero (ENZ) materials in the NIR. From our recent study of the behavior of nanoantennae sitting upon a TCO substrate, we found that TCOs serve as an optical insulating media due to the high impedance of TCOs at the ENZ frequency, enabling emission shaping.

Finally, the optical properties of TCOs can be varied by optical or electrical means. Current research is focused on studying the ultrafast carrier dynamics in doped zinc oxide films using pump-probe spectroscopy. We have shown that aluminum doped zinc oxide films can achieve a 40% change in reflection with ultrafast dynamics (<1ps) under a small fluence of 3mJ/cm2. Consequently, TCOs are shown to be extremely flexible materials, enabling fascinating physics and unique devices for applications in the NIR regime.

References

[1] A. Boltasseva and H. Atwater, Science 331(6015), 290-291, 2011.



[2] J. Kim et al, Selected Topics in Quantum Electronics, IEEE Journal of, 19, 4601907-4601907, 2013.

[3] J. Kim et al, CLEO: QELS_Fundamental Science. Optical Society of America, 2014.

This work was supported by ONR MURI N00014-10-1-0942

9544-31, Session 7

Towards low-loss, infrared and THz nanophotonics and metamaterials: surface phonon polariton modes in polar dielectric crystals (Invited Paper)

Joshua D. Caldwell, U.S. Naval Research Lab. (United States); Lucas Lindsey, Oak Ridge National Lab. (United States); Vincenzo Giannini, Imperial College London (United Kingdom); Igor Vurgaftman, Thomas L. Reinecke, U.S. Naval Research Lab. (United States); Stefan A. Maier, Imperial College London (United Kingdom); Orest J. Glembocki, Oak Ridge National Lab. (United States) and U.S. Naval Research Lab. (United States)

The field of nanophotonics is based on the ability to confine light to subdiffractional dimensions. Up until recently, research in this field has been primarily focused on the use of plasmonic metals. However, the high optical losses inherent in such metal-based surface plasmon materials has led to an ever-expanding effort to identify, low-loss alternative materials capable of supporting sub-diffractional confinement. One highly promising alternative are polar dielectric crystals whereby sub-diffraction confinement of light can be achieved through the stimulation of surface phonon polaritons within an all-dielectric, and thus low loss material system. Both SiC and hexagonal BN are two exemplary SPhP systems, which along with a whole host of alternative materials promise to transform nanophotonics and metamaterials in the mid-IR to THz spectral range. In addition to the lower losses, these materials offer novel opportunities not available with traditional plasmonics, for instance hyperbolic optical behavior in natural materials such as hBN, enabling super-resolution imaging without the need for complex fabrication. This talk will provide an overview of the SPhP phenomenon, a discussion of what makes a 'good' SPhP material and recent results from SiC and the naturally hyperbolic material, hBN from our research group.

9544-32, Session 7

Spectroscopy of semiconductor metadevice building blocks

Nikita A. Butakov, Jon A. Schuller, Univ. of California, Santa Barbara (United States)

Inspired by the potential of designing highly efficient nanophotonic optical elements, numerous researchers are currently exploring the use of dielectric resonators in constructing meta-devices. A wide range of optical components have been demonstrated, including metasurfaces that act as two-dimensional lenses, gratings, and axicons. At the core of these devices is a dielectric building block, typically a Silicon nanodisk or nano-rod, that supports Mie-like leaky mode excitations with a geometrically tunable amplitude and phase response. Here we present a comprehensive experimental characterization of these building blocks. We elucidate their multipolar mode structure, and explain the dependence on the underlying substrate. We find that fundamentally new buried magnetic modes emerge in high-index substrates, and that Fabry-Perot effects in silicon-on-insulator platforms can be utilized to enhance or suppress specific modes. When individual resonators are arranged into arrays with sub-wavelength periodicities, inter-particle coupling leads to a shift in the resonant response. When the periodicities are on the same order as the operating wavelength, the localized resonances may couple with the global diffraction modes, leading to the possible formation of distinct high-qualityfactor surface-lattice-resonant modes, similar to those encountered in

plasmonic gratings. We conclude by exploring the behavior of resonators constructed out of active materials, such as polar materials that support phonon-polariton excitations, and phase-change materials with tunable dielectric constants.

9544-33, Session 7

Properties of infrared doped semiconductor Mie resonators

Tomer Lewi, Univ. of California Santa Barbara (United States); Prasad P. Iyer, Nikita A. Butakov, Jon A. Schuller, Univ. of California, Santa Barbara (United States)

Dielectric optical antenna resonators have recently emerged as a viable alternative to plasmonic resonators for metamaterials and nanophotonic devices, due to their ability to support multipolar Mie resonances with low losses. In this work, we experimentally investigate the mid-infrared Mie resonances in Si and Ge subwavelength spherical particles. In particular, we leverage the electronic and optical properties of these semiconductors in the mid-infrared range to design and tune Mie resonators through free-carrier refraction.

Si and Ge semiconductor spheres of varying sizes of 0.5-4 ?m were fabricated using femtosecond laser ablation. Using single particle infrared spectroscopy, we first demonstrate size-dependent Si and Ge Mie resonances spanning the entire mid-infrared (2-16 ?m) spectral range. Subsequently we show that the Mie resonances can be tuned by varying material properties rather than size or geometry. We experimentally demonstrate doping-dependent resonance frequency shifts that follow simple Drude models of free-carrier refraction. We show that Ge particles exhibit a stronger doping dependence than Si due to the smaller effective mass of the free carriers. Using the unique size and doping dispersion of the electric and magnetic dipole modes, we identify and demonstrate a size regime where these modes are spectrally overlapping. We also demonstrate the emergence of plasmonic resonances for high doping levels and long wavelengths. These findings demonstrate the potential for tuning infrared semiconductor Mie resonances by optically or electrically modulating charge carrier densities, thus providing an excellent platform for tunable electromagnetic metamaterials.

9544-34, Session 7

All dielectric near-field transducers for optical field concentration at the nanometer scale and heat assisted magnetic recording (Invited Paper)

Andrey K. Sarychev, Institute for Theoretical and Applied Electrodynamics (Russian Federation); Sergey Vergeles, L.D. Landau Institute for Theoretical Physics (Russian Federation) and Moscow Institute of Physics and Technology (Russian Federation); Alexei L. Bogdanov, Stanley Burgos, HGST (United States)

Concentration of light into nanospots is greatly beneficial for applications such as heat assisted magnetic recording (HAMR), biomedical imaging and sensing, optical microscopy with single-molecule resolution, quantum plasmonics, nanolasing, etc. We propose novel, all-dielectric near field transducers (NFT), which allow focusing light into a hot spot, much smaller than the wavelength. In existing HAMR heads with metal plasmonic NFT, light is typically concentrated at a metallic tip, which appears to be one of the hottest spots of the whole head and, thus, is most severely affected by thermal stress, dramatically shortening usable lifetime of the head. However, if the NFT optical components are fully dielectric and optically lossless, the hottest temperature spot is at the surface of the targeted media in the vicinity of the tip, but not within the NFT itself. Thus, the aforementioned detrimental thermal effects can be significantly reduced and head life time is greatly increased opening new venue in the magnetic recording.



We propose the dielectric NFT in the form of the pumped dielectric resonator.

The electric field concentrates at the tip of the prolate dielectric beak attached to the resonator. For a sufficiently elongated beak, the intensity of the field just outside the tip of the beak is Eps times larger than the resonator field, where Eps is the permittivity of the resonator+beak. A cascade enhancement of the electric field is being achieved: first, there is a resonance in the dielectric resonator, and then the resonant field is further amplified due to the dipole polarization of the beak.

9544-110, Session 7

Nonlinear optical metamaterials (Invited Paper)

Xiang Zhang, Univ. of California, Berkeley (United States)

Nonlinear metamaterials, manmade structures in which the electromagnetic fields can change material properties, have potential for frequency conversion, amplification, and switching. Phase-matching is critical for coherent nonlinear optical processes, allowing nonlinear sources to combine constructively, resulting in more efficient emission. We discuss phase matching in zero index optical metamaterials, single plasmonic nanostructures, and others.

9544-35, Session 8

Nonlinearities in hyperbolic plasmonic metamaterials (Invited Paper)

Andres D. Barbosa Neira, Silvia Peruh, Giuseppe Marini, Mazhar Nasir, Alexey V. Krasavin, Nicolas Olivier, Wayne Dickson, Gregory A. Wurtz, Anatoly V. Zayats, King's College London (United Kingdom)

We will present experimental studies and numerical modeling of nonlinear optical processes in plasmonic metamaterials based on assemblies of metallic nanorods and other complex geometries. Second- and third-order nonlinear optical response originating from a plasmonic component of the metamaterial will be discussed. Such plasmonic metamaterials can be used for engineering enhanced nonlinear optical properties with the required spectral and temporal response. We will also discuss a novel concept of an on-chip ultrafast all-optical modulator based on a hyperbolic metamaterial integrated in a silicon waveguide.

9544-36, Session 8

Mid-infrared hyperbolic metamaterial based on graphene-dielectric multilayers (Invited Paper)

Theodore B. Norris, You-Chia Chang, Che-Hung Liu, Chang-Hua Liu, Univ. of Michigan (United States); Siyuan Zhang, Seth R. Marder, Georgia Institute of Technology (United States); Zhaohui Zhong, Univ. of Michigan (United States)

Graphene is an interesting building block for metamaterials due to its atomic thickness and the ability to modify the optical properties by chemical doping or electrical gating. We have designed and fabricated a hyperbolic metamaterial composed of alternating Al2O3 and chemical-vapor-deposited (CVD) graphene. This hyperbolic metamaterial operates in the mid-infrared range, where CVD graphene has minimal loss. The effective medium approximation can accurately describe the metamaterial due to large wavelength-to-periodicity ratio. Fabrication is done by repeated graphene transfer and atomic layer deposition. Using an infrared ellipsometer, the anisotropic effective permittivities is measured, showing a transition from

elliptical to hyperbolic dispersion.

9544-37, Session 8

LCR model for the design of hyberbolic metamaterials

Christopher Rosenbury, Daniel B. Fullager, Michael A. Fiddy, The Univ. of North Carolina at Charlotte (United States)

In an HMM, we assumed laver thicknesses are small on the scale of the wavelength and alternate layers can have positive and negative permittivity. Surface plasma waves are generated on the boundaries. These plasma waves create image charge distributions in neighboring conducting layers due to the small separation between sheets. These image charge distributions have a phase lag due to the interaction of the inductance and the capacitance. As the image charge distributions propagate through the layers, the lag increases. This effect gives a volume distribution of modes for any single frequency of generated plasma waves. One can physically interpret this as what gives rise to the hyperbolic density of states in a HMM. By treating the HMM as an LCR circuit, the density of states and the dispersion relation can be engineered to fit any desired parameters since such changes can be directly tied to alterations in the physical parameters of the structure. As the number of layers increases and hence the number of occupied modes increases, the transfer of energy into increasing high k-modes occurs and this can also be understood using the LCR model. Finite feature sizes in the HMM will limit the maximum k vector by diffraction. This makes the LCR model a valuable tool in the design of HMM's.

9544-39, Session 8

Optical mode confinement in threedimensional Al/SiO2 nano-cavities with hyperbolic dispersion

Carla M. Bacco, Priscilla N. Kelly, Lyuba Kuznetsova, San Diego State Univ. (United States)

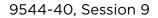
Today's technological needs are demanding for faster and smaller optical components. Optical microcavities offer a high confinement of electromagnetic field in a small volume, with dimensions comparable to the wavelength of light, which provides a unique system for the enhancement of light-matter interactions on the nanoscale. However, further reducing the size of the optical cavity (from microcavity to nanocavity) is limited to the fundamental diffraction limit. In hyperbolic metamaterials, large wavevectors can be achieved [1]. Therefore, optical cavities, created from hyperbolic metamaterials, allow the confinement of the electromagnetic field to an extremely small volume with dimensions significantly smaller than the wavelength of light.

This paper presents the results of numerical study of the optical mode confinement in nanocavities with hyperbolic dispersion using nanolayered AI/SiO2 hyperbolic metamaterial [2] with different AI fill fractions. The fundamental properties of the optical modes and resonance frequencies for the nanocavities are studied using the finite-difference time-domain numerical technique. Numerical simulations show that the light can be adequately confined to a space 22 times smaller than a silicon oxide disk. Reducing the cavity size further doubled the Purcell factor for the disk with aluminum doping.

Beyond this point, the cavities exhibited antenna-like properties. This paper will also focus on other variables of mode confinement such as quality factor, loss, and fill fraction. Potential future applications for three-dimensional nanocavities with hyperbolic dispersion include: silicon photonics optical communications networks, ultrafast LEDs and biological nanoparticles sensing.

[1] Science 336, 205 (2012)

[2] Frontiers in Optics 2014, paper FTh1D.3



Thermal radiation of metallic surfaces and hyperbolic metamaterials

Mikhail A. Noginov, A. Mozafari, Thejaswi U. Tumkur, John K. Kitur, Norfolk State Univ. (United States); Evgenii E. Narimanov, Purdue Univ. (United States)

We studied angular distributions and spectra of thermal radiation of lamellar metal/dielectric metamaterials with hyperbolic dispersion and compared them with the corresponding characteristics of simple metallic films and pairs of metallic and dielectric layers. The spectra of thermal radiation, in the mid-infrared part of the spectrum, were nearly flat and featureless, in a good agreement with the model predictions. The angular distributions of thermal emission closely followed the Lambert's law, ?cos?. The thermal radiation properties of hyperbolic metamaterials were not much different from those of simpler metallic structures.

9544-41, Session 9

Rare-Earth frequency converters for thermophotovoltaics-revisiting century old claims

Ekembu K. Tanyi, Brandi T. Burton, Norfolk State Univ. (United States); Evgenii E. Narimanov, Purdue Univ. (United States); Mikhail A. Noginov, Norfolk State Univ. (United States)

Harnessing more energy from the sun has led to the development of materials which can efficiently trap the sun radiation in the whole spectrum and re-emit it into a narrow spectral band corresponding to the band gap of a photovoltaic device. The field of metamaterials is largely aimed at designing nanostructured surfaces with tailored absorption (emission) spectra. Many rare-earth doped crystals and glasses can efficiently absorb light throughout the whole visible and near-infrared range of the spectrum and emit radiation at longer wavelengths (1.5 to 3 microns). We report studies of absorption and thermal emission of several rare-earth doped crystals.

9544-42, Session 9

Energy conversion and photo-thermal effect within plasmonic absorption metamaterials in infrared region

Yongqian Li, Chenglin Zhang, Lei Su, Xiaoying Li, Northwestern Polytechnical Univ. (China); Zili Zhou, Science and Technology on Metrology and Calibration Lab. (China)

The energy-conversion process and photo-thermal effect within a plasmonic absorber metamaterials (PAM) were investigated theoretically using the Poynting theorem. The Ohmic loss and dielectric loss were calculated to estimate the amount of heat energy produced. The heat-generation within the PAM was studied numerically. From the microscopic details, the heat-generation owing to the electric current accounts for the majority of the energy conversion, while the magnetic resonance plays a negligible role. The distinct resonant peaks of the PAMs are attributed to the polarization sensitive excitation of plasmonic resonance. The strong field confinement and redistribution inside the structure of the PAM were investigated for use in a subsequent thermal-detection design. Field redistribution and enhancement associated with multiplex resonant electromagnetic wave passing through the PAM medium provided insight into the energy conversion processes inside the nanostructure.

9544-43, Session 9

Design and analysis of chevrons shaped split ring resonator in the mid-infrared region

Neerad Nandan, Than Singh Saini, Ajeet Kumar, Ravindra K. Sinha, Delhi Technological Univ. (India)

The terahertz region of the electromagnetic spectrum is relatively new area of interest and incorporates a wide range of applications from image sensing to spectroscopy and many more yet to be discovered. In the area of metamaterials many new designs have been discovered, but "chevrons" shaped split ring resonators (ch-SRRs) in the mid-infrared region has not been studied to the best of our knowledge. This paper presents the analysis and simulation of ch-SRRs in the mid infrared region. Tunability of SRRs is important for various industrial and scientific applications and hence this paper analyzes the tunability of the ch-SRRs by variation of angle. The device is simulated in two configurations i.e., one with two chevrons shaped SRRs on the same plane of the dielectric substrate and the other with each of the two chevron shaped SRRs on the opposite plane of the substrate. Standard polarization method for SRR has been used. Gold SRRs is used, since we are working in the terahertz region Lorentz-Drude model is employed. The ch-SRRs have been embedded upon the silicon substrate. The numerical simulation software uses finite element method (FEM) method to simulate the results. The results obtained for reflectance and transmittance are of particular interest. The effective medium parameters viz. Impendence, permittivity, permeability and refractive index obtained for the split ring resonator are also evaluated. This design is improvement over single chevron design with respect to the sharpness of reflectance as well as transmittance curves which may be of specific interest.

9544-44, Session 9

Colossal optical transmission through buried metal gratings

Christopher M. Roberts, Univ. of Massachusetts Lowell (United States); Runyu Liu, Xiang Zhao, Lan Yu, Xiuling Li, Daniel M. Wasserman, Univ. of Illinois at Urbana-Champaign (United States); Viktor A. Podolskiy, Univ. of Massachusetts Lowell (United States)

In Extraordinary Optical Transmission (EOT), a metallic film perforated with an array of [periodic] apertures exhibits transmission over 100% normalized to the total aperture area, at selected frequencies. EOT devices have potential applications as optical filters and as couplers in hybrid electro-optic contacts/devices. Traditional passive extraordinary optical transmission structures, typically demonstrate un-normalized transmission well below 50%, and are typically outperformed by simpler thin-film techniques. To overcome these limitations, we demonstrate a new breed of extraordinary optical transmission devices, by "burying" an extraordinary optical transmission grating in a dielectric matrix via a metal-assistedchemical etching process. The resulting structure is an extraordinary optical transmission grating on top of a dielectric substrate with dielectric nano-pillars extruded through the grating apertures. These structures not only show significantly enhanced peak transmission when normalized to the open area of the metal film, but more importantly, peak transmission greater than that observed from the bare semiconductor surface. The structures were modeled using three-dimensional rigorous coupled wave analysis and characterized experimentally by Fourier transform infrared reflection and transmission spectroscopy, and the good agreement between the two has been demonstrated. The drastic enhancement of light transmission in our structures originates from structuring of high-index dielectric substrate, with pillars effectively guiding light through metal apertures.





9544-45, Session 9

Experimental verification of classical electromagnetically induced transparency in conductors

Adil-Gerai Kussow, Yassine Ait-Ei Aoud, Alkim Akyurtlu, Univ. of Massachusetts Lowell (United States)

The effect of electromagnetically induced transparency in non-Ohmic conductors, being based on the concepts of classical nonlinear optics was discussed recently. We report an experimental demonstration of this effect within the mid-IR wavelength range. A low-dispersion semiconductor, i.e. ZnTe, and a highly dispersive Au were subjected to bichromatic parametric irradiation with a certain frequencies, amplitudes, phases, and polarizations of a constituent waves. When a specific phase matching conditions are satisfied, experimental evidence for strong signature of EIT was found. The optical losses were considerably reduced in both materials. This effect can be utilized to improve the optical quality of metamaterials.

9544-46, Session 10

Guiding electromagnetic waves around sharp corners: topologically protected photonic transport in meta-waveguides (Invited Paper)

Gennady B. Shvets, The Univ. of Texas at Austin (United States); Alexander B. Khanikaev, Queens College (United States); Tzuhsuan Ma, Kueifu Lai, The Univ. of Texas at Austin (United States)

Science thrives on analogies, and a considerable number of inventions and discoveries have been made by pursuing an unexpected connection to a very different field of inquiry. For example, photonic crystals have been referred to as "semiconductors of light" because of the far-reaching analogies between electron propagation in a crystal lattice and light propagation in a periodically modulated photonic environment. However, two aspects of electron behavior, its spin and helicity, escaped emulation by photonic systems until recent invention of photonic topological insulators (PTIs). The impetus for these developments in photonics came from the discovery of topologically nontrivial phases in condensed matter physics enabling edge states immune to scattering. The realization of topologically protected transport in photonics would circumvent a fundamental limitation imposed by the wave equation: inability of reflections-free light propagation along sharply bent pathway. Topologically protected electromagnetic states could be used for transporting photons without any scattering, potentially underpinning new revolutionary concepts in applied science and engineering.

I will demonstrate that a PTI can be constructed by applying three types of perturbations: (a) finite bianisotropy, (b) gyromagnetic inclusion breaking the time-reversal (T) symmetry, and (c) asymmetric rods breaking the parity (P) symmetry. We will experimentally demonstrate (i) the existence of the full topological bandgap in a bianisotropic, and (ii) the reflectionless nature of wave propagation along the interface between two PTIs with opposite signs of the bianisotropy.

9544-47, Session 10

Light emission in nonlocal plasmonic metamaterials (Invited Paper)

Viktor A. Podolskiy, Brian Wells, Univ. of Massachusetts Lowell (United States); Pavel Ginzburg, Anatoly V. Zayats, King's College London (United Kingdom)

Plasmonic metamaterial composites are often considered to be promising building blocks for a number of applications that include subwavelength

light manipulation, imaging, and quantum optics engineering. These applications often rely on effective medium response of metamaterial composites and require metamaterial to operate in exotic (hyperbolic, or epsilon-near-zero) regimes. However, the behaviour of metamaterials is often different from the predictions of effective medium. In this work we aim to understand the implications of composite nature of metamaterials on their optical properties. Plasmonic nanowire metamaterials are a convenient metamaterial platform that is capable of realization of ENZ, hyperbolic, and elliptic responses depending on light frequency and metamaterial geometry. In this work we show that the response of metamaterial in elliptical regime may be strongly affected by the additional electromagnetic wave that represents collective excitation of cylindrical surface plasmons in nanowire arrays. We present an analytical description of optical properties of additional wave and analyse the effect of this mode on quantum emitters inside nanorod metamaterials.

9544-48, Session 10

Metamaterials for group-velocity dispersion compensation

Philippe Tassin, Chalmers Univ. of Technology (Sweden); Babak Dastmalchi, Thomas Koschny, Costas M. Soukoulis, Ames Lab. (United States) and U.S. Dept. of Energy (United States) and Iowa State Univ. of Science and Technology (United States)

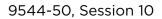
In this contribution, we present our results concerning metamaterials for group-velocity dispersion compensation. Resonant metamaterials usually exhibit substantial dispersion, which is considered a shortcoming for many applications. But we can also take advantage of the ability to tailor the dispersive response of a metamaterial, introducing a new method of group-velocity dispersion compensation. The method consists of stacking a number of highly dispersive sheet metamaterials and is capable of compensating the dispersion of optical fibers with either negative or positive group-velocity dispersion coefficients. We demonstrate that the phase-engineered metamaterial, essentially consisting of a metasurface exhibiting the classical analogue of electromagnetically induced transparency, can provide strong group-velocity dispersion management without being adversely affected by large transmission loss, while at the same time offering high customizability and a small footprint.

9544-49, Session 10

Multi-foci metalens for spin and orbital angular momentum interaction

Shengtao Mei, Cheng-Wei Qiu, Muhammad Qasim Mehmood, Kun Huang, National Univ. of Singapore (Singapore)

The emergence of two-dimensional version of Metamaterial, named metasurface, provides an intriguing methodology for designing miniaturized and integrated optical devices owing to their ultrathin merit. Here we theoretically propose and experimentally demonstrate a multi-foci metalens for spin-orbital angular momentum interaction (SOI). The designed metasurface consists of a monolayer of metallic nano-void antenna with spatially varying orientation. Compared with traditional lens, such flat lens takes advantage of its ultrathin trait to multi orbital angular momentum (OAM) focal points, namely, OAM with different topological charge are focused onto different focal planes. Meanwhile, due to the dual-polarity feature brought by the Pancharatnam-Berry phase based metasurface, we observe several pairs of OAM focal points with opposite topological charges on both sides of the metalens. These pairs correspond to different parts of the multiple ring-shape lens, in which real and virtual OAM foci are achieved by opposite helical incident light. It is also observed that only linearly polarized lights can produce both real and virtual OAM foci simultaneously. The designed metalens may find potential applications in multi-particle manipulation, angular-momentum-based quantum information processing and integrated nano-optoelectronics.



Birefringence modulation of thermallydriven metal nanograting

Takashi Shimura, Miho Ishii, Kentaro Iwami, Hideaki Nagasaki, Norihiro Umeda, Tokyo Univ. of Agriculture and Technology (Japan)

Subwavelength metallic grating has been known to have giant birefringence for visible light. The authors have been produced Au nanograting half wave plate for visible light. Recently, reconfigurable photonic metamaterial fabricated on Au/Si3N4 bimorph beams have been reported that modulate transmittance of near-infrared light by thermal deflection of beams. In this paper, nanograting of thermally-driven bimorph beams was developed that modulate birefringence for at the wavelength of 650 nm. The nanoslits are consisted of Au/SiO2 bimorph beams, and actuated by Joule heating. The width and length of the beam is 300 nm and 20 ?m, respectively. The thickness of Au and SiO2 is 200 nm, respectively. From FDTD simulation, the phase difference at 650 nm is calculated to be modulated from 0 to 45 degree by actuating bimorph beams. The phase modulator is fabricated on the glass substrate using EB lithography, lift-off process and sacrificial layer etching. The phase difference of fabricated modulator was measured at the wavelength range of from 500 to 800 nm with a driving voltage of 10 V. Phase modulation is obtained on the broad wavelength range, and the maximum variation is -3.3 degree at 646 nm. The drive current is 100 mA. Measured modulation was relatively small to simulation. As it is considered to be due to small displacement of beams and it can be improved by refining fabrication process. Because of the modulating characteristics and ultra-small scale, this modulator is expected to be applied as a new display module.

9544-51. Session 10

Building novel nanophotonics devices using symmetry considerations

Boubacar Kante, Univ. of California, San Diego (United States)

Symmetries play a fundamental role in engineering. In this talk, I will show how symmetry considerations can enable novel nanophotonics devices with advanced functionalities. Novel electromagnetic cavities that can hold light for an infinite amount of time will be introduced as well as the design of novel metamaterials built solely from symmetry considerations. I will present a realized closed ring negative index metamaterial and a self-assembled symmetry breaking metamaterials with controllable optical response.

9544-52, Session 11

Laser processing of metamaterial structures (Invited Paper)

Alberto Piqué, Nicholas A. Charipar, Heungsoo Kim, Eric Breckenfeld, Scott A. Mathews, U.S. Naval Research Lab. (United States)

The use of metamaterials structures has been the subject of extensive discussions given their wide range of applications. However, a large fraction of the work available to date has been limited to simulations and proofof-principle demonstrations. One reason for the limited success inserting these structures into functioning systems and real-world applications is the high level of complexity involved in their fabrication. Direct-write processes are ideally suited for the fabrication of arbitrary periodic and aperiodic structures found in most metamaterial and plasmonic designs. For these applications, laser-based processes offer numerous advantages since they can be applied to virtually any surface over a wide range of scales. Furthermore, laser direct-write or LDW allows the precise deposition and/ or removal of material thus enabling the fabrication of novel metamaterial designs. This presentation will show examples of metamaterial and

plasmonic structures developed at the Naval Research Lab using LDW, and discuss the benefits of laser processing for these applications. This work was sponsored by The Office of Naval Research.

OPTICS+

NANOSCIENCE+ ENGINEERING

SPIE. PHOTONICS

9544-53, Session 11

Large-area, low-cost plasmonic perfect absorber sensor fabricated by laser **interference lithography** (Invited Paper)

Shahin Bagheri, Nikolai Strohfeldt, Andreas Tittl, Harald Giessen, Univ. Stuttgart (Germany)

We employ laser interference lithography as a reliable method to create nanowire and nanorod arrays in photopolymers for manufacturing plasmonic perfect absorber sensors over a homogeneous area as large as 2 cm2. Subsequently we transfer the fabricated pattern into a metal layer by using argon ion beam etching techniques. Geometry and periodicity of our large-area metallic nanostructures are precisely controlled by adjusting the interference conditions during single- and double-exposure processes, resulting in structures with spectrally selective perfect absorption of light from the visible to the mid-infrared wavelength range. We also demonstrate the applicability of our large-area structures for hydrogen detection schemes by measuring the hydrogen sensing performance of a palladiumbased perfect absorber operating in the visible wavelength range. Since palladium changes its optical properties upon hydrogenation, exposure of the sample to hydrogen gas causes fast and reversible changes in the absorption of light which is easily measured by an FTIR microscope. Our large-area perfect absorber sensor provides nearly perfect absorption of light at 730 nm, and the reflectance changes from 1 % to 5 % in the presence of hydrogen. The large-area and fast fabrication process makes our approach highly attractive for simple and low-cost sensor fabrication, which is suitable for industrial production of plasmonic devices in the near future.

9544-54, Session 11

Design and analysis of near-perfect metamaterial reflector in visible range

Ravindra K. Sinha, Nishant Shankhwar, Delhi Technological Univ. (India)

A unit cell was simulated in frequency domain using COMSOL Multiphysics and s parameters were obtained. Reflection and transmission coefficients were analysed to optimize the Aspect ratio (height/base diameter) of cone in order to achieve highest reflectivity. Using s-parameters, material properties-effective refractive index (neff), permittivity (?), permeability (μ) and impedance (?) were calculated. The underlying principle for this property is Mie Resonance in dielectric. Reflectivity is high when either electric or magnetic (but not both) resonance exists and real part of impedance is close to zero. These conditioned are satisfied and the structure shows high reflectivity in the range 650nm-730nm leading to ~99.99% reflectivity at wavelengths 660nm and 720nm.

9544-55, Session 11

The Silicon photomultiplier as a metasystem with designed electronics as metadevice for a new receiver-emitter in visible light communications

Rafael M. Gutierrez, Luis Castañeda, Javier Castaño, Univ. Antonio Nariño (Colombia)

A Silicon Photomultiplier, SiPM, can be considered a metasystem of microscopic Avalanche Photodiodes, APDs, which embedded in a specific purpose electronic, becomes a metadevice with unique and useful advanced



functionalities by transforming microscopic quantum processes of the radiation-matter interaction into macroscopic detectable classical electronic signals. This metadevice provides new capacities to capture, transmit and analyze information with increased efficiency and security. The SiPM is a very small state of the art photo-detector made of a matrix arrangement of many APDs (thousands by mm2), with very high efficiency and sensitivity, it has a well define frequency response, is unaffected by magnetic fields and has very high photo-electric gain. New results of R&D, some of them performed at the "Laboratorio de Detectores" of the Universidad Antonio Nariño, demonstrate that the metadevice constituted by the SiPM and an appropriated designed electronics, has a very good response to controlled light pulses in the presence of background light without presenting saturation. In this work we present some results of this metadevice to understand and profit its advanced functionalities in transforming photodetection into electronic signals to propose a new receiver-emitter device for Visible Light Communication, VLC. This metadevice is highly sensitive to fast and low intensity pulses and does not show saturation, therefore, it does not need filters; both are challenges of the receiver-emitter devices presently used in VLC. This new VLC receiver-emitter metadevise, could facilitate new and diverse applications by introducing and developing state of the art high energy physics photo-detectors into VLC.

9544-58, Session 11

Metamaterial-based single pixel imaging system (Invited Paper)

Willie Padilla, Duke Univ. (United States); Claire M. Watts, Boston College (United States); Christian Nadell, Duke Univ. (United States); John A. Montoya, Sanjay Krishna, The Univ. of New Mexico (United States)

Single pixel cameras are useful imaging devices where it is difficult or infeasible to fashion focal plan arrays. For example in the Far Infrared (FIR) it is difficult to perform imaging by conventional detector arrays, owing to the cost and size of such an array. The typical single pixel camera uses a spatial light modulator (SLM) - placed in the conjugate image plane – and is used to sample various portions of the image. The spatially modulated light emerging from the SLM is then sent to a single detector where the light is condensed with suitable optics for detection. Conventional SLMs are either based on liquid crystals or digital mirror devices. As such these devices are limited in modulation speeds of order 30 kHz. Further there is little control over the type of light that is modulated.

We present metamaterial based spatial light modulators which provide the ability to digitally encode images – with various measurement matrix coefficients – thus permitting high speed and fidelity imaging capability. In particular we use the Hadamard matrix and related S-matrix to encode images for single pixel imaging. Metamaterials thus permit imaging in regimes of the electromagnetic spectrum where conventional SLMs are not available. Additionally, metamaterials offer several salient features that are not available with commercial SLMs. For example, metamaterials may be used to enable hyperspectral, polarimetric, and phase sensitive imaging. We present the theory and experimental results of single pixel imaging with digital metamaterials in the far infrared and highlight the future of this exciting field.

9544-56, Session 12

Device applications of metafilms and metasurfaces (*Invited Paper*)

Mark L. Brongersma, Geballe Lab. for Advanced Materials (GLAM) (United States)

Many conventional optoelectronic devices consist of thin, stacked films of metals and semiconductors. In this presentation, I will demonstrate how one can improve the performance of such devices by nano-patterning the constituent layers at length scales below the wavelength of light. The resulting metafilms and metasurfaces offer opportunities to dramatically modify the optical transmission, absorption, reflection, and refraction

properties of devices. This is accomplished by encoding the optical response of nanoscale resonant building blocks into the effective properties of the films and surfaces. To illustrate these points, I will show how nanopatterned metal and semiconductor layers can be used to enhance the performance of solar cells, photodetectors, and enable new imaging technologies. I will also demonstrate how the use of active building blocks can facilitate the creation of active metafilm devices.

9544-57, Session 12

Mechanics meets plasmonics: new devices and sensors (Invited Paper)

Ertugrul Cubukcu, Univ. of Pennsylvania (United States)

In this talk, we will discuss our recent result on new types of devices and sensors enabled by on chip integration of plasmonic resonators and mechanical microresonators. In the first part, we will talk about low noise infrared thermal optomechanical detectors based on nanoantenna light absorbers. In the second part, we will present our work on hybrid multimode optomechanical biosensors with an ultra large dynamic sensing range. In the last part, voltage tunable Fano resonances arising from the coupling of Fabry-Perot and nanoantenna resonances in a metamaterial perfect absorber that supports strong optomechanical coupling will be introduced.

9544-59, Session 12

Design theory of thin film hyperbolic metamaterial collimators

Daniel B. Fullager, Michael A. Fiddy, The Univ. of North Carolina at Charlotte (United States)

Hyperbolic metamaterial (HMM) research has led to the fabrication of devices which have unbounded k-space ellipsoids. Alternating layers of films with alternating signs of relative permittivity or permeability in a given direction enable multi-layer surfaces that are, in theory, either perfectly reflective or transmissive at an angle dependent upon the free space wave vector and ratios of the permittivity or permeability in the normal and transverse directions. By having knowledge of the electromagnetic properties of the constituent materials of a multi-layer HMM over a given bandwidth, the functionality of these structures can be altered by changing the fill fraction of the constituents. One potential device design that results is that of a flat electromagnetic wave collimator. The degree to which a multi-layer HMM collimates comes from the contrast in the magnitudes of the relative permeability or permittivity in the normal and transverse directions. With large material parameter contrast at a given frequency, the transverse wave vectors that allow for successful EM wave propagation at the HMM/atmosphere interface approach zero. This leads to propagation of a narrow angular cone of waves relative to the surface normal of the HMM. Herein we show that the transfer matrix method is in relatively good agreement with finite element method electromagnetic simulations performed in COMSOL's RF module and compare dispersion relations of known materials to the resulting collimation generated in a corresponding HMM. We thereby use existing material data and predictive theories show how to tailor the frequency response of HMMs.

9544-60, Session 12

Engineering optical systems using transformation optics

Saul Wiggin, Queen Mary, Univ. of London (United Kingdom)

This paper presents a method for calculating theZernike aberrations in a lens design using transformation optics FDTD. Currently there is no literature on calculating imageaberrations in FDTD. In this paper I divulge the methods tocalculate the Zernike aberration using a polynomial fitting for a wavefront.



The results are shown to match very well with the Zernike aberrations in an equivalent lens in $\ensuremath{\mathsf{ZEMAX}}$

9544-61, Session 12

Plasmonic photocathodes

Rosa A. Lukaszew, Zhaozhu Li, Kaida Yang, Jose Riso, The College of William & Mary (United States)

Surface Plasmon polaritons (SPPs) on patterned surfaces have drawn attention since this approach enables enhancement of the electric field intensity near the patterned surface, which may be important for specific applications, such as photoemission. Due to interaction of the incident light with the nanopatterm, SPPs can exhibit a different response as consequence of the choice of the pattern parameters. This may offer improved performance in certain applications, for example increased quantum efficiency in metallic photocathodes exploiting this phenomenon. In the present case we utilized conformal growth of metallic layers onto optical gratings but applying oblique shadow thin film deposition to modify the conformal growth compared to normal incidence, leading to an increase of the grating amplitude while also reducing emittance compared to other designs. We have carried out measurements and simulations of the surface plasmon resonance (SPR) response of such sample and compared it with that of a film grown at normal incidence. The comparison of the SPR dip in reflectivity for each type of sample shows a significant change, with a narrower and deeper response for the obliquely deposited one compared to the normal deposition. The observed results are attributed to lower radiative damping of the SPP in the latter. Previous reports associate lower damping with enhanced electric fields in SPR excitations, thus, the observed narrower SPR feature in the obliquely deposited sample measurements and simulations reported is also correlated with enhancement of the SPPs localized electric field. Measurements of the photocurrent in the two types of samples will also be presented and discussed in this context.

This project is funded under Department of Energy (DOE) and the award # is DE-SC0008546

9544-62, Session 12

Stripe-teeth metamaterial AI- and Nbbased rectennas

Richard M. Osgood III, Stephen A. Giardini, Joel B. Carlson, U.S. Army Natick Soldier Research, Development and Engineering Ctr. (United States); Prabhuram Joghee, Ryan P. O'Hayre, Colorado School of Mines (United States); Kenneth Diest, Mordechai Rothschild, MIT Lincoln Lab. (United States)

Unlike a semiconductor, where the absorption is limited by the band gap, a "microrectenna array" could theoretically very efficiently rectify any desired portion of the infrared frequency spectrum (25 - 400 THz). We investigated vertical metal-insulator-metal (MIM) diodes that rectify vertical high-frequency fields produced by a metamaterial planar stripe-teeth Al or Au array (above the diodes), similar to stripe arrays that have demonstrated near-perfect absorption in the infrared due to critical coupling [1]. Using our design rules that maximize asymmetry (and therefore the component of the electric field pointed into the substrate, analogous to Second Harmonic Generation), we designed, fabricated, and analyzed these metamaterial-based microrectenna arrays. NbOx and Al2O3 were produced by anodization and ALD, respectively. Smaller visible-light Pt-NbOx-Nb rectennas have produced output power when illuminated by visible (514 nm) light [2].

The resonances of these new Au/NbOx/Nb and Al/Al2O3/Al microrectenna arrays, with larger dimensions and more complex nanostructures than in Ref. 1, were characterized by microscopic FTIR microscopy and agreed well with FDTD models, once the experimental refractive index values were entered into the model. Current-voltage measurements were carried out, showed that the Al/Al2O3/Al diodes have very large barrier heights and breakdown voltages, and were compared to our model of the MIM diode. We calculate

expected THz-rectification using classical [3] and quantum [4] rectification models, and compare to measurements of direct current output, under infrared illumination.

[1] C. Wu, et. al., Phys. Rev. B 84 (2011) 075102.

[2] R. M. Osgood III, et. al., Proc. SPIE 8096, 809610 (2011).

[3] A. Sanchez, et. al., J. Appl. Phys. 49 (1978) 5270.

[4] J. R. Tucker and M. J. Feldman, Rev. of Mod. Phys. 57, (1985)1055.

9544-63, Session 13

Understanding of increased diffuse scattering in regular arrays of fluctuating resonant particles (Invited Paper)

Andrei Andryieuski, DTU Fotonik (Denmark); Mihail Petrov, National Research Univ. of Information Technologies, Mechanics and Optics (Russian Federation); Andrei Lavrinenko, DTU Fotonik (Denmark); Sergei Tretyakov, Aalto Univ. School of Science and Technology (Finland)

In this presentation we will discuss the analytical and numerical approaches to modeling electromagnetic properties of geometrically regular subwavelength 2D arrays of random resonant plasmonic particles.

Amorphous metamaterials and metasurfaces attract interest of the scientific community due to promising technological implementations with costefficient methods of large-scale chemical nanoparticles synthesis as well as their self-organization. Random fluctuations of the particles size, shape, and/or composition are inevitable not only in the bottom-up synthesis, but also in conventional electron beam and photolithography fabrication. Despite the significant progress in large-scale fabrication, modeling and effective properties prediction of random/amorphous metamaterials and metasurfaces is still a challenge, which we address here. We present our results on analytical modelling of metasurfaces with regular periodic arrangements of resonant nanoparticles of random polarizability/size/ material at normal plane-wave incidence. We show that randomness of the polarizability is related to increase in diffused scattering and we relate this phenomenon to a modification of the dipoles' interaction constant. As a result, we obtain a simple analytical formula which describes diffuse scattering in such amorphous metasurfaces. Employing the supercell approach we numerically confirm the analytical results.

The proposed approach can be easily extended from electrical dipole arrays and normal wave incidence to more general cases of electric and magnetic resonant particles and oblique incidence.

9544-64, Session 13

Giant field fluctuations in dielectric metamaterials and SERS sensors

Andrey K. Sarychev, Konstantin N. Afanasiev, Irina A. Boginskaya, Institute for Theoretical and Applied Electrodynamics (Russian Federation); Igor A. Budashov, N.M. Emanuel Institute of Biochemical Physics (Russian Federation); Igor V. Bykov, Institute for Theoretical and Applied Electrodynamics (Russian Federation); Ilya N. Kurochkin, N.M. Emanuel Institute of Biochemical Physics (Russian Federation); Andrey N. Lagarkov, Institute for Theoretical and Applied Electromagnetics (Russian Federation); Ilya A. Ryzhikov, Andrey V. Ivanov, Alexander V. Vaskin, Institute for Theoretical and Applied Electrodynamics (Russian Federation)

Sensor for the detecting and analyzing bio and chemical substances is the important practical application for the modern metamaterials. We suggest the new dielectric metamaterials with special structure, where the local



electromagnetic field is much enhanced in comparison with the amplitude of the incident light. The metamaterial has facet structure, where each elementary cell separate by the gaps from the rest of the material. Each facet operates as a micro resonator of Fabry-Perot type. The incident light excites these micro resonators that have various resonance frequencies. The em field oscillations in the facets interact and form the collective modes. In spite of the collective nature, the modes are spatially localized in so called hot spots, where local field has maxima. The incident light pumps energy in the localized mode increasing the local em field. The local field enhancement is mainly restricted by the radiation loss. The scale of the local field localization is about few microns in the proposed metamaterials. The metal nanoparticles, being placed at the surface of the dielectric metamaterial, are excited by the giant local field. The strong local electric field in the metamaterial excites surface plasmon in the metal nanoparticle, placed at the surface of the metamaterial. The enhancement factor of the local field is multiplied by the enhancement factor of the plasmon resonance. The cascade enhancement results in the strong SERS in the analyte molecules adsorbed at the surface of the metal nanoparticles.

9544-65, Session 13

Opto-mechanical interactions in split ball resonators

Yue Sun, Sergey V. Suchkov, Andrey E. Miroshnichenko, Andrey A. Sukhorukov, The Australian National Univ. (Australia)

We demonstrate that a gold split-ball resonator (SBR) in the form of a spherical nanoparticle with a cut supports both optical magnetic and acoustic modes, which have strong field confinement around the cut. Such localization away from the bottom is expected to lead to an immunity to anchor loss and thus potentially high quality factors of acoustic oscillations when positioned on a substrate. As a result, when a planewave pulse excites the optical resonance, it can then efficiently drive the acoustic vibration through laser heating and/or optical forces. We estimate the overall heat variation by modelling the optical energy dissipation inside the SBR due to the dispersive and absorbing nature of gold at optical wavelengths. The optically induced force is given by the time averaged Lorentz force density. We simulate the mechanical vibrations under the optical excitation through time-dependent simulations using solid mechanics module of COMSOL software. Assuming a moderate quality factor of 10, under a plane wave pulsed laser pump which gives 100K temperature change to the SBR, both the laser heating and optical forces lead to the excitation of the acoustic mode at the same frequency with different magnitudes of 200pm and 10pm, resulting 10% and 0.5% modification of the total optical scattering, respectively. These results show that the SBRs support strong opto-mechanical coupling and are promising in applications such as surfaceenhanced Raman spectroscopy and detection of localised strain.

9544-66, Session 13

Ultrahigh-capacity non-periodic photon sieves operating in visible light

Cheng-Wei Qiu, Shengtao Mei, National Univ. of Singapore (Singapore); Hong Liu, A*STAR Institute of Materials Research and Engineering (Singapore); Kun Huang, National Univ. of Singapore (Singapore); Jinghua Teng, A*STAR Institute of Materials Research and Engineering (Singapore)

Miniaturization of optical structures makes it possible to control light at the nanoscale, but on the other hand imposes a challenge of accurately handling numerous unit elements in the miniaturized devices. Up to date, photonic structures of periodic or quasi-periodic arrangement have been predominantly developed and investigated. Breaking such a convention by engineering aperiodic and random nanophotonics to govern complex optical responses, we can go for technological innovations in light manipulation, optical microscopy, and nanolithography. Here, we report both the new analytical model and experimental demonstration of the photon sieves made of ultrahigh capacity of subwavelength holes (over 34 thousands) arranged in two different structural orders of randomness and aperiodicity. The random photon sieve produces uniform optical hologram with high diffraction efficiency and free from twin-images usually seen in conventional holography while the aperiodic photon sieve manifests far-field sub-diffraction limit focusing in air. A hybrid approach resulting in an analytical solution is developed to make the design of random and aperiodic photon sieve viable for high-accuracy control of the amplitude, phase and polarization of visible light beyond the evanescent range. The polarization independence of the photon sieve will also greatly benefit its applications in optical imaging and spectroscopy.

9544-67, Session 13

A non-Monte Carlo approach to analyzing 1D Anderson localization in dispersive metamaterials

Glen J. Kissel, Univ. of Southern Indiana (United States)

Monte Carlo simulations have been used to study Anderson localization in models of one-dimensional random stacks. Because such simulations can use substantial computational resources and because the randomness of random number generators used in such simulations has been called into question, a non-Monte Carlo approach is of interest. This paper makes use of a non-Monte Carlo methodology, limited to discrete random variables, to determine the Lyapunov exponent, or its reciprocal, frequently known as the localization length, for a one-dimensional random stack model. proposed by Asatryan, et al., consisting of alternating and non-alternating layers of positive and negative index materials that include the effects of dispersion and absorption, as well as previously studied off-axis incidence and polarization effects. In the paper, Furstenberg's integral formula is used to calculate the Lyapunov exponent of an infinite product of random matrices modeling the one-dimensional stack. The integral formula requires integration with respect to the probability distribution of the randomized layer parameters, as well integration with respect to the so-called invariant probability measure of the direction of the vector propagated by the long chain of random matrices. The non-Monte Carlo approach is made possible by a numerical procedure of Froyland and Aihara which calculates the invariant measure as the left eigenvector of a certain sparse row-stochastic matrix, thus avoiding the use of any random number generator. The results show excellent agreement with the Monte Carlo generated simulations which made use of continuous random variables, while also frequently providing dramatic reductions in computation time.

9544-68, Session 14

Tunable metasurfaces (Invited Paper)

Harry A. Atwater Jr., California Institute of Technology (United States)

Metasurfaces composed of sub-wavelength artificial structures show promise for extraordinary light-manipulation and development of ultrathin optical components such as lenses, wave plates, orbital angular detection, and holograms over a broad range of the electromagnetic spectrum. However structures developed to date do not allow for post-fabrication control of antenna properties. We have investigated the integration of the transparent conductor indium tin oxide (ITO) active elements to realize gate-tunable phased arrays of subwavelength patch antenna in a metasurface configuration to enable gate tunable permittivity. The magnetic dipole resonance of each patch antenna interacts with the carrier densitydependent permittivity resonance of the ITO to enable phase and amplitude tunability. Operation of patch antennas and beam steering phased arrays will be discussed.



9544-69, Session 14

Vertical split-ring resonators for plasmon coupling, sensing, and metasurface (Invited Paper)

Din Ping Tsai, Academia Sinica (Taiwan) and National Taiwan Univ. (Taiwan); Pin Chieh Wu, Wei-Lun Hsu, Wei Ting Chen, Yao-Wei Huang, Chun Yen Liao, Wei-Yi Tsai, National Taiwan Univ. (Taiwan); Ai Qun Liu, Nanyang Technological Univ. (Singapore); Nikolay I. Zheludev, Optoelectronics Research Ctr. (United Kingdom); Greg Sun, Univ. of Massachusetts Boston (United States)

Plasmonic metamaterials composed of artificial structures in subwavelength scale exhibit many unconventional properties for light manipulation, and it is also very promising for photonic devices, high-sensitivity optical sensor, etc. Split-ring resonator (SRR), one kind of building block of metamaterials, has attracted wide attentions due to the resonance excitation of electric and magnetic dipolar response. Here, the fundamental plasmon properties and potential applications in novel three dimensional vertical split-ring resonators (VSRRs) are designed and discussed.

The resonant properties arose from the electric and magnetic interactions between the VSRR and light are theoretically and experimentally studied. Tuning the configuration of VSRR unit cells is able to generate various novel coupling phenomena in VSRRs, such as plasmon hybridization and Fano resonance. The magnetic resonance plays a key role in plasmon coupling in VSRRs. The VSRR-based refractive-index sensor will be demonstrated. Due to the unique structural configuration, the enhanced plasmon fields localized in VSRR gaps can be lifted off from the dielectric substrate, allowing for the increase of sensing volume and enhancing the sensitivity. We perform a VSRR based metasurface for light manipulation in optical communication frequency. By varying the prong heights, the 2ϖ phase modulation can be achieved in VSRR for the design of metasurface. Because the phase shift is changed via the upright configuration rather than the one parallel to the substrate, it can be used for high area density integration of metal nanostructures and opto-electronic devices.

9544-70, Session 14

Cascaded meta-surfaces for broadband antenna isolation

Joseph A. Miragliotta, David Shrekenhamer, Robert Scott, Allan Jablon, Jerry Friedman, Derek Harshbarger, Johns Hopkins Univ. Applied Physics Lab., LLC (United States); Daniel F. Sievenpiper, Univ. of California, San Diego (United States)

We report a computational and experimental study using meta-surfaces to enhance isolation between antennas that share a common ground plane. Our current emphasis is on the development of a high-impedance surface (HIS) that enables broadband isolation between transmit and receive antennas. The unit cell geometry in each of the arrays is the Sievenpiper mushroom, which contains a band gap that inhibits the propagation of surface waves within a very specific frequency region. In addition to its ease of fabrication, this simple unit cell structure is quite amenable to tailoring the frequency of the band gap through subtle changes to the geometric parameters such as via radius. For our specific HIS, we have formed a cascade of HIS unit cells and have thus expanded the isolation bandwidth to provide greater than 1 octave isolation relative to the bare ground plane. In addition to bandwidth, the HIS was designed to exhibit a 10 dB enhancement to isolation relative to an uncoated ground plane for operation between the X- through Ku-band (~ 8 to 18 GHz). Computational optimization was performed on the cascaded structure when selecting the unit cell and array parameters to assure maximum isolation amplitude and bandwidth.

9544-71, Session 14

Anisotropic meta-surfaces for enhanced antenna isolation

Joseph A. Miragliotta, David Shrekenhamer, Johns Hopkins Univ. Applied Physics Lab., LLC (United States); Daniel F. Sievenpiper, Univ. of California, San Diego (United States)

Electromagnetic band gap structures, also referred to as high impedance surfaces (HIS), inhibit the propagation of surface electromagnetic waves within a given frequency range and are an effective means to enhance the isolation between antenna that share a common ground plane. To date, the majority of HIS structures that have been designed, fabricated and tested for antenna isolation applications have relied on an isotropic distribution of unit cells within the overall surface structure, which results in a corresponding isotropic impedance profile. Although this type of impedance profile is sufficient for antenna systems on flat ground plane surfaces, they have limited performance when incorporated onto surfaces that have significant curvature. In this report, we discuss results from our computational and experimental investigation associated with enhanced antenna isolation on a non-planar ground plane via an anisotropic HIS. Unit cell anisotropy within the array was created by a number of approaches, including a variation in the aspect ratios of both rectangular and diamond shape profiles. Data associated with the isolation performance of the anisotropic impedance surface is compared to the corresponding results from an isotropic HIS in the 8 to 18 GHz microwave region.

9544-72, Session 14

Plasmon drag effect in plasmonic metasurfaces

Vincent Rono, Norfolk State Univ. (United States); Matthew LePain, Georgia Southern Univ. (United States); Rabia Hussain, Norfolk State Univ. (United States); David Keene, Maxim Durach, Georgia Southern Univ. (United States); Natalia Noginova, Norfolk State Univ. (United States)

Plasmon drag effect (PLDE) is the generation of dc electric currents associated with the excitation and propagation of surface plasmon polaritons in metal nanostructured systems. In order to better understand the mechanism of the effect and explore its properties, we experimentally study PLDE in the dependence on light intensity, wavelength and angle of incidence in hyperbolic metasurfaces of different periodicity and surfaces with random roughness. The results are discussed theoretically in a frame of the hydrodynamic loss approach.

9544-73, Session 14

Cramér-Rao bounds for metasurfaces susceptibilities

Thomas Lepetit, Boubacar Kante, Univ. of California, San Diego (United States)

Over the past fifteen years, a lot of efforts have been focused on understanding the effective properties of metamaterials [1]. In the last few years, metasurfaces in particular have been widely investigated [2]. Several homogenization methods dedicated to them have been proposed but, due to the topic's complexity, none have yet to be widely accepted.

We considered a specific homogenization method dedicated to metasurfaces, namely Generalized Sheet Transition Conditions (GSTC, [3]). This method was chosen because it is compatible with retrieval from reflection and transmission coefficients. In this method, method, method characterized by electric and magnetic susceptibilities. In the literature, retrieved effective parameters have been shown to violate causality around resonances and this has been attributed to spatial dispersion [4]. In order to determine if spatial dispersion is the only source of this phenomenon,

we have investigated the statistical properties of estimators that have been put forward for these susceptibilities. We have thus computed the Cramér-Rao lower bounds on the variance of these estimators. We have shown that this bound increases substantially around resonances making retrieval possible only for very high Signal-to-Noise Ratio (SNR, [5]). Therefore, in experiments, issues arising from spatial dispersion and noise compound and result in non-physical effective parameters. To mitigate this, we have proposed a least-squares estimator for susceptibilities that has a better performance with respect to noise.

Sensitivity to noise is particularly acute for low-loss metasurfaces. It often results in required SNRs that are unachievable in practice. The present work is thus relevant to the development of loss-compensated metasurfaces for which the issues posed by retrieval will have to be closely considered for accurate and robust device characterization.

References

 D. R. Smith et al., "Determination of effective permittivity and permeability of metamaterials from reflection and transmission coefficients", Phys. Rev. B 65, 195104 (2002).

2. N. Yu et al., "Light propagation with phase discontinuities: Generalized laws of reflection and refraction", Science 334, 333 (2011).

3. C. L. Holloway et al., "An overview of the theory and applications of metasurfaces: The two-dimensional equivalents of metamaterials", IEEE Antennas Propag. Mag. 54, 10 (2012).

4. C. R. Simovski, "On electromagnetic characterization and homogenization of nanostructured metamaterials", J. Opt. 13, 1 (2011).

5. T. Lepetit and B. Kanté, "Cramér-Rao bounds for determination of electric and magnetic susceptibilities in metasurfaces", accepted for publication in Optics Express.

9544-95, Session PWed

Hybrid plasmonic nanosandwich structures

Soad Alsheheri, Marjan Saboktakin, Mohammed Matin, Univ. of Denver (United States)

Plasmonic properties of gold and silver nanoparticles has several applications in the last decade. Of the several shapes of nanoparticles, triangular nanoprisms are of significant interest to us. In this study, Ag and Au nanoprisms with different edge length and thicknesses were simulated by using Finite- difference time-domain (FDTD) simulation technique. The edge length are varied between 90 to 150 nm and thicknesses are between 10 to 50 nm of Ag and Au nanoprisms. The increase in edge length and thicknesses were found red shift to the plasmonic peak of the nanostructures. The dipole resonance peak occurs at ~700 nm for an Au nanoprism with an edge length of 90 nm and a thickness of 10 nm while it occurs at ~800 nm for an Ag nanoprism of the same size and shape. The plasmonic dipole resonance of these Ag nanoparticles varied between 725 nm and 913 nm with varying nanoprism thickness from 10 nm to 50 nm. Similarly, the dipole resonance peak for Au nanoparticles have experienced a blue shift from 721 nm corresponding to the thickness of 10 nm to 636 nm corresponding to the thickness of 50 nm. After studying the plasmonic resonance of individual Au and Ag nanoprisms, we constructed hybrid plasmonic nanoprisms in the form of gold (Au)-dielectric- silver (Ag) sandwich structures. Moreover, by creating the sandwich structure (Au/ dielectric/ Ag), the ability to tune the plasmonic resonance will be by having two peaks that can control the strength of each of them depending on the application.

9544-96, Session PWed

Adjustment characteristics in terahertz transmission through a split ring resonator-based metamaterial

Jun Luo, Yehua Bie, Xinyu Zhang, Hongshi Sang, Changsheng Xie, Huazhong Univ. of Science and Technology (China) The artificially structured metamaterials has led to many potential applications in terahertz regime, but the role in adjusting the terahertz transmission still needs to be carefully investigated. Currently, designs with split ring resonator (SRR) based metamaterials can provide a promising approach for understanding the terahertz transmission characteristics. In the experiments, a SRR-based metamaterial is proposed for presenting terahertz transmission characteristics. The substrate of the metamaterial is an n-type gallium arsenide (n-GaAs) film grown over a semi-insulating GaAs wafer. Then, the metallic film, fabricated on n-GaAs, is patterned into an arrayed four-gap microstructure according to traditional ultraviolet photolithography methods. The metal film and n-GaAs film form a Schottky contact. In the experiments, the transmission frequency spectrum of the metamaterial has an obvious fluctuation with a frequency interval of f = 0.15 THz in the 0.6-1.23 THz and 1.52-2.4 THz range, and the experimental results show that the frequency region of the intensive oscillatory signal essentially agrees with that of the metamaterial characteristic transmission spectrum in the 0.5–2.5 THz range. The terahertz characteristic transmission spectrum of the fabricated metamaterial are measured at the central frequency of ~1.0 THz and ~1.5 THz, this oscillation characteristics can be explained by dipole resonance. The measured time-domain transmission signals and corresponding frequency responses based on the metamaterial agree well with simulation results, including resonance frequency, surface current and electric field. Therefore, our research shows a potential application of the transmission adjusting roles in terahertz regime.

SPIE. PHOTONICS

NANOSCIENCE+ ENGINEERING

9544-97, Session PWed

Plasmon coupling in vertical split-ring resonator magnetic metamolecules

Mu Ku Chen, Pin Chieh Wu, Wei-Lun Hsu, Wei Ting Chen, National Taiwan Univ. (Taiwan); Din Ping Tsai, Academia Sinica (Taiwan); Yi-Teng Huang, Yao-Wei Huang, Chun Yen Liao, National Taiwan Univ. (Taiwan)

Vertical split-ring resonators (VSRRs) were fabricated which behave as magnetic metamolecules sensitive to both incident electric and magnetic fields with the stronger induced magnetic dipole moments upon excitation in comparison to planar SRRs. Using these metamolecules with different spacing in VSRR dimers, we investigate the hybridization of the magnetic plasmon modes associated with each constituent VSRRs. We found that plasmon coupling can be precisely controlled by varying the gap separation between VSRRs. The resulting wide tuning range of these hybrid modes offers the possibility of developing frequency selective functional devices such as sensors and filters based on plasmon coupling with high sensitivity.

9544-98, Session PWed

Active metasurface grating for broadband electronic modulation of free space terahertz waves

Muhammad Tayyab Nouman, Jae Hyung Jang, Sungbae J. Lee, Gwangju Institute of Science and Technology (Korea, Republic of)

Terahertz frequency band promises applications in vast number of areas. To actively control and manipulate terahertz waves, various devices based on active metasurfaces have been demonstrated. However, they all exhibit narrowband nature. In this paper, design of a broadband electronic terahertz modulator, using an active metasurface, is proposed and numerically evaluated. The proposed design exploits the small slits in a metallic plate that modify its Drude like response to a Lorentzian response. The design consists of a metallic grating on a doped gallium arsenide substrate, where the grating bars form a Schottky contact with the substrate. Application of voltage bias across Schottky contact permits control of the carrier concentration in the slits. Under zero bias the carrier concentration in the slits is large so that whole surface acts as a metal plate exhibiting a Drude like response. Upon application of a large negative voltage to the Schottky contact, the charge carriers in the slits are depleted and the metasurface



exhibits a Lorentzian response, thus achieving the modulation. Grating dimensions are optimized for maximum modulation depth and bandwidth using an electromagnetic simulation tool. Simulation results promise superior performance in terms of modulation depth and insertion loss, compared to the previously demonstrated broadband electronic modulators. This work is supported by National Research Foundation of Korea through a grant (No. 20110017603).

9544-99, Session PWed

Shaping the light distribution of strongly focused systems for efficient excitation of optical nano-circuits

Boris Okorn, Jordi Sancho-Parramon, Institut Ruder Bo?kovic (Croatia); Silvio Hrabar, Univ. of Zagreb (Croatia)

Optical nano-circuits and metatronics have emerged as a promising alternative to classical electronic circuits that could enable operations at higher frequencies. Large efforts have been devoted to investigation of optical nano-circuits but so far all studies either bypass the problem of excitation of the metatronic system. In the present study we theoretically investigate how shaping the light distribution that illuminates a high numerical aperture lens can be used to efficiently couple light to given elements of optical nano-circuits located at the focal plane of the lens. In addition to standard plane waves, we consider illumination schemes that provide peculiar light distributions at focus, such as cylindrical vector beams. These results show that light excitation may be included as an additional degree of freedom in the optimization of optical nano-circuits and metatronics designs.

9544-100, Session PWed

Quantum toroidal moments of nanohelix eigenstates

Johnny Williamson, Mario R. Encinosa, Florida Agricultural and Mechanical Univ. (United States)

Developments in the area of metamaterial research have generated interest in toroidal moments and their treatment in the guantum regime. A quantum mechanical method of determining toroidal moments due to current circulating on a toroidal helix is presented. The Laplacian of the toroidal helix manifold is determined and used to develop the Hamiltonian of a negatively charged spinless particle constrained to motion in the vicinity of a toroidal helix having loops of arbitrary eccentricity. In the limit that the particle is constrained to the toroidal helix, the particle's wave function is assumed to decouple into components tangential and normal to the toroidal helix. Once confined to the toroidal helix, only the motion along the manifold is nontrivial. An additional term arises in the Hamiltonian that depends on the curvature of the toroidal helix. Using this resulting Hamiltonian, the three dimensional Schrodinger equation is effectively reduced to a one dimensional form inclusive of curvature effects. The curvature term that arises from the dimensional reduction procedure is periodic over the azimuthal angle of the system. Thus a Blochtype formalism is utilized to define a basis set which is used to find the Hamiltonian matrix. This Hamiltonian matrix is diagonalized and the energies and low-lying eigenfunctions of the toroidal helix system are calculated. The eigenfunctions are used to calculate probability currents which in turn are used to calculate corresponding toroidal moments. A disagreement, not predicted by a classical treatment, arises between toroidal moments of elliptic toroidal helix systems when vertical and horizontal eccentricity are transposed.

9544-101, Session PWed

Mie resonance in the arrays of dielectric rods in air

Ravindra K. Sinha, Reena Dalal, Yogita Kalra, Delhi Technological Univ. (India)

Mie resonance in square arrays of dielectric rods has been reported. Arrays in square lattice of dielectric rods with very high permittivity in air have been considered. Light of transverse electric mode has been launched on the square arrays of cylindrical dielectric rods. Mie resonance of first two orders has been observed in the dielectric rods, due to which electric and magnetic dipoles are generated in the rods. At optimized parameters the electric field is confined in the dielectric rods and magnetic field is rotating around the dielectric rods. Simulations are done for different values of permittivity from 40 to 100. Materials like titanium dioxide and strontium titanate have very high permittivity. We observe better results at the permittivity ?r = 60 in our design. Negative value of effective permittivity and effective permeability at different frequencies in the range of 0.1 THz to 2.5 THz has been obtained. Thus, electric resonance and magnetic resonance at different frequencies has been observed.

9544-102, Session PWed

Taming microwave propagation with hyperbolic and chiral metal-dielectric metamaterials

Brittany Bates, Brandon Allison, Nicole Greene, Vincent Rono, Natalia Noginova, Norfolk State Univ. (United States)

Bulk lamellar metal-dielectric structures as well as layers of wires arranged in aligned or chiral manner have been fabricated and studied in microwave free space propagation experiments. We have shown that a ~ 10 cm x 10 cm x 10 cm x 10 cm x 10 cm cm a polarizer. Rotation of polarization (optical activity) has been demonstrated in chiral structures. We have further explored use of natural magnetic materials as constituent ingredients of metamaterials as well as the possibility to tune material parameters at microwave range with external magnetic fields.

9544-103, Session PWed

Simulation of space-time cloaking using FDTD for terahertz frequency range

Egor A Gurvitz, Mikhail V Sharaevsky, ITMO University (Russian Federation); Mikhail K. Khodzitky, National Research Univ. of Information Technologies, Mechanics and Optics (Russian Federation)

Recently, investigation of metamaterials gave new turn of scientific development. Their unique properties design devices which can control wave in space and time. Metamaterials already have been applied in the field of antennas, cloaking, high resolution imaging, etc [1]. Generally these applications require spatial distribution of constitutive parameters. This work is based on the theory of transformation optics [2] and field theory [3] and these theories extend the mathematical apparatus of object concealment for time applications [4]. Using FDTD numerical simulation of the electromagnetic fields distribution in the cloaking medium with non ordinary constitutive parameters for two space dimensions and time was shown. The work is focused on magneto-electric interactions of incident wave and the medium, which possesses constitutive parameters tensors with non diagonal components.

Filippo Capolino, Metamaterials Handbook, CRC Press, 2007
 Ulf Leonhardt, Thomas Philbin, Geometry and Light: The Science of



Invisibility, Dover Books on Physics, 2010

 L D Landau, E.M. Lifshitz, Theory of Fields, Nauka, 1973
 Moti Fridman, Alessandro Farsi, Yoshitomo Okawachi & Alexander L. Gaeta, Demonstration of temporal cloaking, Nature 481, 62–65, 2012

9544-104, Session PWed

Temperature-controlled infrared broadband cloaking with the bilayer of semiconductor and superconductor

Xiaohua Wang, Nanjing Univ of Aeronautics and Astronautics (China); Youwen Liu, Nanjing Univ. of Aeronautics and Astronautics (China)

From the beginning of this century, metamaterial has attracted more and more attention owing to its unique properties and many potential applications. Among these applications, electromagnetic cloaking is undoubtedly paid more attention. Up to now, many research groups have investigated electromagnetic cloaking using the following approaches: transformation optics and scattering cancellation. Usually, the latter is relatively easy to realize, because the cloaking is obtained by using isotropic and homogeneous plasmonic materials, whilst the former may achieve perfect cloaking with the use of the anisotropic and inhomogeneous metamaterials.

Superconductor is a good plasmonic material because of low loss and temperature-tunability in THz and infrared band. In this contribution, we design the invisibility cloak made of the two materials of semiconductor (n-type germanium) and high-temperature superconductor (YBa2Cu3O7). Based on the Mie theory, we derive the formula of total scattering cross-section and the cloaking condition of the composite structure under the long-wavelength approximation. This invisibility cloak may reduce the total scattering cross-section of the composite structure of 90% over a broadband frequency of near 20 THz and the cloaking frequency may be tuned by the applied temperature. Further, we discuss numerically the effect of the structure parameters on the cloaking performance of the composite structure. The results show that the cloaking frequency may be tuned by changing the thickness of the outer semiconductor layer, and the tuning range of this bilayer structure is wider than that of single superconductor layer. It can provide a feasible way to design a broadband tunable cloak.

9544-105, Session PWed

A new type of metamaterial panel for invisible using

Hongwei Sun, Fei Yan, Jari Tooling Technology Co. (China)

This paper presents modeling, analysis techniques and experiment of metamaterial panel for Broadband Vibration Absorption. For a unit cell of an infinite fmetamaterial panel, governing equations are derived using the extended Hamilton principle. The concepts of negative effective mass and stiffness and how the spring-mass-damper subsystems create a stopband are explained in detail. Numerical simulations reveal that the actual working mechanism of the proposed metamaterial panel is based on the concept of conventional mechanical vibration absorbers. It uses the incoming elastic wave in the panel to resonate the integrated membrane-mass-damper absorbers to vibrate in their optical mode at frequencies close to but above their local resonance frequencies to create shear forces and bending moments to straighten the panel and stop the wave propagation. Moreover, a two-dimension acoustic metamaterial panel consisting of lumped mass and elastic membrane is proposed in the lab. We do experiments on the model and The results validate the concept and show that, for two-dimension acoustic foam metal metamaterial panel do exist two vibration modes. For the wave absorption, the mass of each cell should be considered in the design. With appropriate design calculations, the proposed two-dimension acoustic foam metal metamaterial panel can be used for absorption of low-frequency waves and hence expensive micromanufacturing techniques are not needed for design and manufacturing of

such foam metal metamaterial panel for low-frequency waves absorption/ isolation.

9544-106, Session PWed

Controlling the bandwidth of metamaterial properties

Morteza Karami, Michael A. Fiddy, The Univ. of North Carolina at Charlotte (United States)

We have studied meandering wire or S-shaped resonators which are well known for exhibiting overlapping negative permittivity and permeability to achieve negative and zero index bulk metamaterials. The resonators are continuously connected in one direction and their dimensions are readily chosen so that resonant frequencies lie in the frequency range of choice, e.g. 5-10 GHz. Two sets of S-elements are placed on either side of a substrate (FR4). The bulk properties of this metamaterial are determined from scattering parameters and the retrieval method assumes an infinite array of meta-atoms in the plane perpendicular to the plane of incidence and periodic boundary conditions in the other two dimensions. The retrieved refractive index values are consistent with expectations, do not arise from diffraction phenomena, and their dependence on the collective resonant properties of the metamaterial is clear. Moreover, predictable properties are found when the S elements, originally made from copper, are made from a high permittivity dielectric such as barium strontium titanate. Inserting rod-like structures in the FR4 substrate has the effect of shifting and broadening/smearing the electrical resonance, with little change to the magnetic resonance. Addition of more rods can eventually shift and suppress the magnetic resonance while shift the bulk plasma frequency to higher frequencies. This combination of effects, now understood, allows one to design an index value with a prescribed bandwidth, to some extent. By replacing the metal with a high permittivity dielectric, the associated losses are reduces as we will show.

9544-107, Session PWed

Full control of light using plasmonic metasurfaces

jianxiong li, Nankai university (China); Shuqi Chen, Nankai Univ. (China); Jianguo Tian, Nankai university (China)

Harnessing light for modern photonic applications often involves the control and manipulation of light polarization and phase. The polarization and phase are among the basic properties of light, and their manipulation enables many optical applications and plays an increasingly important role in investigating light-matter interactions. However, so far it is still challenging to simultaneously manipulate the polarization state into an arbitrary direction and a phase variation spanning over the entire 2ϖ range.

Here, we propose and validate dual-layer plasmonic metasurfaces that can provide simultaneous manipulation of the phase and polarization of the transmitted light. An arbitrary spatial field distribution of the optical phase is obtained by using plasmonic metasurfaces consisting of six sub-units, where the orientation of these sub-units can be tuned to further control the polarization. We have proposed and experimentally validated plasmonic metasurfaces achieving simultaneous control of the phase and polarization direction of light. For linearly polarized incident light, the metasurface enables near-perfect anomalous refraction without converting the polarization to its cross-direction; while for circularly polarized incident light, the out-coupling polarization can be further controlled by the orientation of the nano-apertures. This capability also allowed us to create arbitrary vector optical fields, and as an example we generated a radially polarized beam from the circularly polarized incident light. The demonstration is in the nearinfrared wavelength range, which indicates that the approach can be easily translated to mid-infrared, terahertz, and microwave frequency regimes. The new degrees of freedom of metasurfaces facilitate arbitrary manipulation of light and will profoundly affect a wide range of photonic applications.



9544-108, Session PWed

Acoustic metamaterial panel for potential invisible using based on multi-cells

Fei Yan, Hongwei Sun, Jari Tooling Technology Co., Ltd. (China); Guochang Lin, Ge He, Harbin Institute of Technology (China)

This paper presents modeling, and analysis techniques of acoustic metamaterial panel for Invisible Using. For a unit cell of an infinite metamaterial panel, governing equations are derived using the extended Hamilton principle. Numerical simulations reveal that the actual working mechanism of the proposed metamaterial panel is based on the concept of conventional mechanical vibration absorbers. It uses the incoming elastic wave in the panel to resonate the integrated membrane-mass-damper absorbers to vibrate in their optical mode at frequencies close to but above their local resonance frequencies to create shear forces and bending moments to straighten the panel and stop the wave propagation. Moreover, we explain the negative effective mass and negative effective stiffness in acoustic metamaterials.

9544-109, Session PWed

Paraxial cloaking: ray optics and full-field

Joseph S. Choi, John C. Howell, Univ. of Rochester (United States)

We complete a paraxial cloaking formalism to include full-field (phase + amplitude) matching of light fields. Omnidirectionality is the only remaining property of what may be considered an "ideal" invisibility cloak that is broadband for the visible spectrum. Interestingly, our design remains isotropic, though some instances require metamaterials or anomalous dispersion. This suggests that anisotropy may be a characteristic of cloaking for all directions in three-dimensions. Our work also confirms the growing literature on the exclusiveness between broadband versus zero scattering cross-section.

9544-74, Session 15

Visible-frequency metasurfaces for broadband anomalous reflection and highefficiency spectrum splitting

Zhongyang Li, Edgar Palacios, Serkan Bütün, Koray Aydin, Northwestern Univ. (United States)

Metasurfaces offer new degrees of freedom in moulding the optical wavefronts by introducing abrupt and drastic changes in the amplitude, phase and/or polarization of electromagnetic radiation at the wavelength scale. By carefully arranging multiple subwavelength anisotropic or gradient optical resonators, metasurfaces have been shown to enable anomalous transmission, anomalous reflection, optical holograms and spin-orbit interaction. However, experimental realization of highperformance metasurfaces that can operate at visible frequency range has been a significant challenge due to high optical losses of plasmonic materials and difficulties in fabricating several subwavelength plasmonic resonators with high uniformity. Here, we propose a highly-efficient yet a simple metasurface design comprising of a single, anisotropic trapezoidshape antenna in its unit cell. We demonstrate broadband (450 - 850 nm) anomalous reflection and spectrum splitting at visible and near-IR frequencies with 85% conversion efficiency. Average power ratio of anomalous reflection to the strongest diffraction mode was calculated to be on the order of 1000 and measured to be on the order of 10. The anomalous reflected photons have been visualized using a CCD camera, and broadband spectrum splitting performance has been confirmed experimentally using a free space, angle-resolved reflection measurement setup. Metasurface design proposed in this study is a clear departure from conventional metasurfaces utilizing multiple, anisotropic and/or gradient optical

resonators, and could enable high-efficiency, broadband metasurfaces for achieving flat high SNR optical spectrometers, polarization beam splitters, directional emitters and spectrum splitting surfaces for photovoltaics.

9544-75, Session 15

Metasurfaces for amplitude, phase, and polarization control (*Invited Paper*)

Uriel Levy, Boris Desiatov, Meir Grajower, Jonathan Bar David, The Hebrew Univ. of Jerusalem (Israel)

In this talk we present our recent work on dielectric metasurfaces for phase, amplitude and polarization control. We show new results in the near IR and the mid IR regime, in which the control over the properties of light can be achieve by controlling the retardation of a subwavelength periodic structure or by controlling the resonances of nano beams in semiconductors. We discuss approaches for achieving broadband retardation of light by tailoring the dispersion properties of the metasurface. Both guided mode and free space configurations are considered. The effect of introducing metals is also analyzed and demonstrated. Finally, we also discuss and demonstrate tunable metasurfaces.

9544-76, Session 15

Light manipulation by resonant dielectric nanostructures and metasurfaces (Invited Paper)

Arseniy I. Kuznetsov, A*STAR - Data Storage Institute (Singapore)

Resonant nanostructures made of high-refractive index dielectric materials offer a new way for manipulation of light at nanoscale. Due to their inherently high magnetic and electric resonant response and low losses at optical frequencies these nanostructures offers unique functionalities, which are not achievable with conventional nanoscale plasmonics. Simple examples are strong magnetic near-field enhancement and directional scattering by nanoparticles of spherical shape, also known as a Kerker's effect. In this talk, I will review this new rapidly developing research direction and present several new results of our team, which demonstrate a huge potential of dielectric nanoantennas for various applications. Fist will be experimental demonstration of highly localized magnetic and electric fields in silicon nanodimer antennas, which can be excited at any polarization of incoming light. Second will show low-loss light propagation in silicon nanoparticle waveguides, which can be much longer than in plasmonic waveguide of similar dimensions. Finally I will present how the light can be manipulated with almost fully transparent resonant dielectric metasurfaces having a full 2ϖ control over the phase of incoming light at visible and near-IR wavelengths.

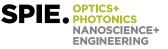
9544-77, Session 15

Metasurface-enabled quantum vacuum effects over macroscopic distances

Pankaj K. Jha, Xingjie Ni, Chihhui Wu, Yuan Wang, Xiang Zhang, Univ. of California, Berkeley (United States)

Quantum vacuum engineering is an active field of research. Here we use recent advances in the field of metasurface (2D-array of sub-wavelength scale nano-antennas) to construct an anisotropic quantum vacuum (AQV) in the vicinity of a quantum emitter located at some macroscopic distance from the metasurface. Such AQV can induce quantum interference among several atomic transitions, even when the transition dipole moment corresponding to the decay channels are orthogonal.

Recently, there have been few theoretical proposal to use metamaterials to engineer the back-action. All these approaches, which works in the near



field (few tens of nanometers from the surface), suffers from trapping an atom at these distance, surface interactions like quenching, Casimir force etc. Hence it's pivotal to construct the back-action over macroscopic distance. We harness the polarization dependent response of a metasurface to engineer the back-action of the spontaneous emission from the atom to itself. We show strong anisotropy in the decay rate of a quantum emitter which is a manifestation of AQV.

Engineering light-matter interaction over macroscopic distances opens new possibilities for long-range interaction between quantum emitters for quantum information processing, spin-optics/spintronics etc.

9544-78, Session 15

All-dielectric metasurfaces for structured light generation

Mikhail Shalaev, Jingbo Sun, Univ. at Buffalo (United States); Apra Pandey, CST of America, Inc. (United States); Kirill Nikolsky, M.V. Lomonosov Moscow State Univ. (Russian Federation); Natalia M. Litchinitser, Univ. at Buffalo (United States)

Recent progress in nanostructured optical materials has enabled new ways of manipulating intensity, polarization and phase distribution of light beams. Metamaterials and metasurfaces facilitate a new class of ultra-compact optical elements. In particular, optical metasurfaces allow precise control of phase and wave-front properties of light beams. To date, most work has been focused on metal-dielectric structures relying on resonant response of metallic nanoantennas. There are several challenges associated with this approach, including anisotropic and polarization-dependent properties of the structures and ohmic losses introduced by metals. These problems can be addressed using all-dielectric metasurfaces instead of more conventional metal-dielectric counterparts. Here, we demonstrate subwavelength-thick efficient all-dielectric matasurfaces enabling generation/conversion of light beams with orbital angular momentum (OAM) operating in transmission mode. We utilize the strong resonant response of high-permittivity dielectric meta-atoms in the near-IR spectral range. Such nanostructures support both electric and magnetic dipolar Mie-type resonances and possess very low intrinsic losses. Such all-dielectric metasurfaces having both electric and magnetic responses can be designed to be polarization independent, enable high transmission and are compatible with existing complementary metaloxide-semiconductor (CMOS) processes, which makes them attractive for practical applications in optoelectronics and communication industries.

9544-79, Session 15

Dynamically reconfigurable metasurfaces

Prasad P. Iyer, Nikita A. Butakov, Jon A. Schuller, Univ. of California, Santa Barbara (United States)

Recently, the use of phased array metasurfaces to control the phase and amplitude of electromagnetic waves at subwavelength dimensions have led to large number of devices ranging from flat optical elements to holographic projections. Here we analytically (& numerically using FDTD techniques) develop a design principle to form reconfigurable metasurfaces that control the phase of transmitted beam between 0 and 2ω in a lossless manner. For a linearly polarized plane wave incident on a sub-wavelength array of dielectric resonators, we engineer the size of the individual resonators and the array periodicity such that the fundamental Electric and Magnetic dipole resonances of the device cross each other. This mode crossing caused by coupling of individual resonator modes with the surface lattice resonances, constructively interferes with the incident plane wave enabling us to form lossless metasurfaces. By optically pumping charge carriers into the resonators, we can tune the refractive index of the individual resonators leading to arbitrary control over the phase of the transmitted beam between O and 2ω with less than 3dB loss in intensity. Further, we extend these strategies by redesigning the resonator elements by forming core-shell (metal-dielectric) resonators to cause the resonance matching within each resonator. This enables the mode crossing to be independent of the

periodicity of the resonator elements while preserving the arbitrary control over the phase through charge carrier modulation. Such metasurfaces with spectrally overlapping electric and magnetic dipole modes may form the basis for a range of metadevices with unprecedented control over the Electromagnetic wave front.

9544-80, Session 16

Metagratings for tunable unidirectional steering and focusing of surface plasmons (Invited Paper)

Federico Capasso, Daniel Wintz, Harvard School of Engineering and Applied Sciences (United States); Patrice Genevet, Singapore Institute of Manufacturing Technology (Singapore) and Harvard School of Engineering and Applied Sciences (United States); Antonio Ambrosio, Harvard School of Engineering and Applied Sciences (United States) and Univ. degli Studi di Napoli Federico II (Italy); Alex Woolf, Harvard School of Engineering and Applied Sciences (United States)

In this paper, we present new results on the controlled directional steering and focusing of surface plasmon polaritons (SPPs) via 1D and 2 D metagratings by changing the angle of incidence, the incident wavelength and polarization. These findings build on previous work of our group on polarization controlled steering of SPPS using fishbone meta gratings and greatly expand on the functionality of the latter using novel designs.

First we show that by creating a running wave of polarization along a one dimensional metallic metagrating consisting of subwavelength spaced rotated apertures that propagates faster than the SPP phase velocity, we can generate surface plasmon wakes, which are the two-dimensional analogue of Cherenkov radiation. The running wave of polarization travels with a speed determined by the angle of incidence and the photon spin angular momentum. We utilize this running wave of polarization to demonstrate controlled steering of the wakes by changing both the angle of incidence and the polarization of light, which we measure through near-field scanning optical microscopy.

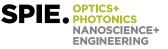
Next we report a simple 2D metagrating design strategy that can be used for focusing, polarization beam splitting, waveguide coupling, and even phase control at the focus of an SPP beam. We experimentally verify our 2D metasurface by creating a four wavelength plasmonic demultiplexer, which also has polarization selectivity (on/off). The wavelength demultiplexer is designed such that each of the four wavelengths is focused to a different spot outside of the structure. Coupling of free space light to SPPs is achieved by milling subwavelength apertures into a thin gold film. This methodology can be easily extended to any wavelength where SPPs exist, for an arbitrary number of wavelengths, and with polarization selectivity and phase control at the focus as well.

9544-81, Session 16

Metasurfaces and epsilon-near-zero modes in semiconductors (Invited Paper)

Igal Brener, Salvatore Campione, Sandia National Labs. (United States); Francois Marquier, Institut d'Optique (France)

Thin layers of semiconductors where the permittivity crosses zero, support a particular polariton mode called epsilon-near-zero (ENZ) mode. This zero crossing can be obtained near optical phonon resonances in dielectrics or the plasma frequency in doped semiconductors. The coupling of metamaterial resonators to these ENZ modes leads to particularly large Rabi splittings. ENZ layers can be added to metamaterial-based strongly coupled systems to increase this coupling even further. I will discuss several examples of these coupled systems that include metasurfaces, phonons, intersubband transitions and ENZ modes.



9544-82, Session 16

Carpet cloak with graded dielectric metasurface

LiYi Hsu, Thomas Lepetit, Boubacar Kante, Univ. of California, San Diego (United States)

We demonstrate a method to hide a Gaussian-shaped bump on a ground plane from an incoming plane wave. In essence, we use a graded metasurface to shape the wavefronts like those of a flat ground plane[1,2]. The metasurface provides additional phase to the electromagnetic field to control the reflection angle. To mimic a flat ground plane, the reflection angle is chosen to be equal to the incident angle. The desired phase distribution is calculated based on generalized Snell's laws[3]. We design our metasurface in the microwave range using sub-wavelength dielectric resonators. We verify the design by full-wave time-domain simulations and show that the result matches our theory well. This approach can be applied to hide any object on a ground plane not only at microwave frequencies but also at higher frequencies up to the infrared.

1. Jensen Li and J. B. Pendry, Hiding under the Carpet: A New Strategy for Cloaking. Phys. Rev. Lett. 101, 203901 (2008)

2. Andrea Alù, Mantle cloak: Invisibility induced by a surface. Phys. Rev. B 80, 245115 (2009)

3. Yu N, et al. Light propagation with phase discontinuities: Generalized laws of reflection and refraction. Science 334(6054):333-337 (2011)

9544-83, Session 16

Ultra-thin metasurface carpet cloak

Xingjie Ni, Zi Jing Wong, Michael Mrejen, Yuan Wang, Univ. of California, Berkeley (United States); Xiang Zhang, Univ. of California, Berkeley (United States) and Lawrence Berkeley National Lab. (United States)

We experimentally demonstrate a three-dimensional ultra-thin metasurface carpet cloak can cover on an arbitrary-shaped object and make it undetectable by the visible light. Our metasurface cloak consists of subwavelength-scale nanoantennas which provide a distinct phase shift to the reflected electromagnetic waves. Based on this phase control capability, we design a metasurface so that at each local point on the interface of the cloaked region the phase of the light scattered by the interface is the same as that reflected from a flat mirror. One of the most significant problem of the plasmonic metasurface designs resides in their poor overall efficiency. In our carpet cloak case, we adapt an ultrathin dielectric space layer to create a gap plasmon resonance. The overall reflectivity can be close to 90% with proper optimization.

9544-84, Session 16

Flat optical beam shapers based on alldielectric Huygens' metasurfaces

Katie E. Chong, Isabelle Staude, The Australian National Univ. (Australia); Anthony James, Jason Dominguez, Sheng Liu, Salvatore Campione, Ganapathi S. Subramania, Ting S. Luk, Sandia National Labs. (United States); Manuel Decker, Dragomir N. Neshev, The Australian National Univ. (Australia); Igal Brener, Sandia National Labs. (United States); Yuri S. Kivshar, The Australian National Univ. (Australia)

Functional optical metasurfaces have gained a lot of attention in the last couple of years for their potential in ultra-thin flat optics; however their practicality has been restricted by their low efficiencies caused by reflection losses, undesired polarization conversion or the intrinsic loss of metals at optical frequencies, for example. Here, we study highly efficient

polarization-independent beam shapers based on all-dielectric Huygens' metasurfaces [1]. Our beam shapers consist of subwavelength arrays of silicon nanodisks fabricated using electron-beam lithography and reactiveion etching on silicon-on-insulator wafers. Each nanodisk radiates as a pair of crossed electric and magnetic dipoles in the forward direction into the farfield [2], thereby emulating the behavior of a Huygens' source. As a result, they can impose local phase shifts on the arbitrarily polarized incident light field and allows for wavefront control of the incident wave. By systematically varying the geometry of the nanodisks in the arrays and arranging them in four quadrants, a phase shift of 0, $\frac{\pi}{2}$, $\frac{\pi}{2}$ or $\frac{3\pi}{2}$ radians is imposed onto the incident light in each quadrant. Therefore a spatial phase gradient in the azimuthal direction is produced, covering the full 2ϖ range and leading to the generation of a vortex beam. Our beam shapers can achieve transmittance efficiencies close to the theoretical limit of 100%, thereby paving a way to practical lossless flat optics that are compatible with standard and well-established nanofabrication procedures, making mass production of such meta-devices achievable.

M. Decker, I. Staude, et al. Adv. Opt. Mat. Accepted.
 I. Staude, et al. ACS Nano, 7, 7824 (2013)

9544-85, Session 17

An atom/metamaterial hybrid system (Invited Paper)

David Wilkowski, Nanyang Technological Univ. (Singapore); Eng Aik Chan, Syed Abdullah Aljunid, Giorgio Adamo, Centre for Disruptive Photonic Technologies (Singapore); Martial Ducloy, Centre for Disruptive Photonic Technologies (Singapore) and Laboratoire de physiques des Lasers (France); Nikolay Zheludev, Centre for Disruptive Photonic Technologies (Singapore) and Optoelectronics Research Centre & Centre for Photonic Metamaterials (United Kingdom)

We report recent studies on an atom/surface Metamaterial Hybrid device. The plasmonic resonance of the Metamaterial is designed to cover a transition of Caesium atom. We use the selective reflection spectroscopy to probe the system. This technic reveals the sub-Doppler structure of the atomic line. Thus we succeed to couple two systems, where those resonance linewidths differ by more than 6 orders of magnitude. As a consequence we observe Fano-like resonance shapes which we interpret as a mixing of the reactive and the dissipative response of the atomic dipole operator. On top of it, the selective reflection spectroscopy probes atoms which are located at the vicinity of metamaterial. Hence Casimir-Polder interaction can observe and tune through the surface plasmonic resonance of the metamaterial.

Several interesting applications of this new type of hybrid system are envisioned. First, taking advantage of the strong nonlinearity of the atom response, efficient nanophotonic devices like optical switch at few photons level could be in principle implemented. Second, surface metamaterials may provide a new platform to cool and manipulate atoms for nano sensing devices.

9544-86, Session 17

Metamaterial models of curved spacetime

Tom G. Mackay, The Univ. of Edinburgh (United Kingdom); Akhlesh Lakhtakia, The Pennsylvania State Univ. (United States)

In the early 20th century, Igor Tamm established a formal equivalence between the electromagnetic properties of vacuous curved spacetime and a certain fictitious material in flat spacetime. This fictitious medium - known as the Tamm medium - is generally bianisotropic and nonhomogeneous. The Tamm medium offers the possibility of exploring the electromagnetic properties of certain curved spacetime scenarios that may be impractical



to explore by direct methods. The realization of various Tamm mediums as metamaterials is considered here. The approach taken is based on the homogenization of relatively simple component materials, with the inverse Bruggeman formalism exploited to determine appropriate constitutive parameters. The bianisotropic nature of Tamm mediums can be accommodated via the homogenization of chiral (or otherwise magnetoelectric) component materials. Typically, Tamm mediums are highly anisotropic in regions corresponding to relatively large spacetime curvature (e.g., in the vicinity of spacetime singularities). In principle at least, such high degrees of anisotropy may be achieved by homogenizing component particles that are highly elongated. The nonhomogeneous nature of Tamm mediums can be accommodated by adopting a piecewise homogeneous approach, which is valid for sufficiently-long wavelength regimes. The spacetime scenarios considered include those of gravitational plane waves, Schwarzschild-(anti-)de Sitter, and cosmic strings.

9544-87, Session 17

Electron beam excitation of CSRR loaded waveguide for Cherenkov radiation

Emmy Sharples, The Cockcroft Institute (United Kingdom) and Lancaster Univ. (United Kingdom); Rosa Letizia, Lancaster Univ. (United Kingdom) and The Cockcroft Institute (United Kingdom)

An electron beam is used to excite a unique electromagnetic response from a complementary split ring resonator (CSRR) metasurface loaded waveguide and investigate it as a backward propagating Cherenkov radiation source. This novel structure comprises of a metallic WR-284 waveguide loaded with four layers of CSRR-metasurface 1 mm thick, with sufficient spacing between the metasurface layers for electron beam propagation. The loaded waveguide exhibits left handed behaviour around 5.86 GHz where a TM-like mode exists. The transverse confinement of this mode between the CSRRs leads permeability and permittivity to be simultaneously negative. The structure has been optimised to reduce the surface current on the metasurface, improve the fabrication suitability and minimise the effect of hybrid modes.

The structure is suitable for beam-based applications as it exhibits strong beam coupling parameters and excitation of longitudinal wake impedance at the frequency of the TM-like mode. The beam coupling parameters exhibited are high with R/Q of 36 ? and shunt impedance of 177 k?. Strong excitation of the longitudinal wake impedance of 10 k?, with minimal transverse wake impedance and minimal beam disruption, has been observed for this mode. Results from particle-in-cell simulations will be shown to verify that backward propagating Cherenkov is radiated when a suitable electron beam propagates between the central layers of the waveguide. This investigation can lead to new solutions for non-destructive beam detection and wakefield acceleration which can potentially be scaled to higher frequency ranges.

9544-88, Session 17

Synchrotron infra-red spectral microscopy of metal-dielectric-metal cavity metamaterial absorbers

Janardan Nath, Deep Panjwani, Mehmet Yesiltas, Univ. of Central Florida (United States); Carol J. Hirschmugl, Univ. of Wisconsin-Milwaukee (United States); Farnood K. Rezaie, Robert E. Peale, Univ. of Central Florida (United States)

Metamaterial absorbers typically comprise a periodically-structured metal surface, a dielectric spacer, and a metal ground plane, which together give rise to strong absorption resonances. Using diffraction-limited synchrotronbased infrared spectral microscopy in the 2-8 micron wavelength range, we succeeded in measuring the spatial distribution of absorption for a single unit cell of such an absorber, for which the surface structure comprised a single isolated 2 micron x 2 micron square of 100 nm thick gold on a 100 nm thick electron-beam evaporated layer of SiO2. The ground-plane was an optically thick Au film on a Si substrate. The reflectance spectrum revealed a fundamental absorption band at 6.4 micron wavelength and a higher-order resonance at 2.5 microns. For comparison, a reflectance spectrum for a device comprising a 2D 3-micron-period array of such squares on similar layers revealed similar resonances, which differed only by being about twice stronger and red shifted by less than 2%. These experiments confirm a waveguide standing wave resonance model, which is independent of the periodicity of the 2D array, where resonances and their harmonics depend on the lateral dimension of the squares and the thickness of the dielectric and on no other geometrical parameters. Specifically, interaction among the neighboring cavities is unimportant. Devices of the type considered have application to infrared bolometers and potentially for localization of heat in medical therapy.

9544-89, Session 17

Double Fano resonances in a composite metamaterial possessing tripod plasmonic resonances

Jeong-Weon Wu, Y. U. Lee, E. Y. Choi, E. S. Kim, J. H. Woo, B. Kang, J. Kim, Ewha Womans Univ. (Korea, Republic of); Byung Cheol Park, T. Y. Hong, Jae Hoon Kim, Yonsei Univ. (Korea, Republic of)

We experimentally demonstrate a classical analogue of double Fano resonances in a planar composite metamaterial possessing tripod plasmonic resonances, where a common subradiant dipole corresponding to the dark mode is coupled with two superradient dipoles corresponding to two bright modes. The composite metamaterial is structured such that four-rod resonators (FRR) are embedded inside double-split ring resonators (DSRR) superlattice. Two dipole resonances of DSRR are superradiant modes and one dipole resonance of FRR is subradiant mode. Proximity of the inner diameter of DSRR and the rod-length of FRR permits near field coherent couplings, and the composite metamaterial is a tripod metamaterial system possessing two superradiant dipole resonances of DSRR coupled coherently with one common subradiant dipole resonance of FRR in near field, similar to a tripod atomic system with four atomic levels coupled coherently by coherent optical fields. Important finding is that double Fano resonances in the composite metamaterial are correlated, showing up as a transfer of the absorbed power from one superradiant dipole to the other superradient dipole in DSRR. The general feature of plasmonic Fano resonance is examined where both superradiant and subradiant oscillators are externally driven. Analysis based on two coupled oscillators model leads to the fact that the characteristic asymmetric Fano resonance formula of plasmonic structure is kept the same with a modication in the asymmetry parameter q.

9544-92, Session 18

Polarization and angle dependent electromagnetic response of microwave metamaterials

David A. Lee, The MITRE Corp. (United States); James L. Vedral, Univ. of Colorado at Colorado Springs (United States); Randall Musselman, U.S. Air Force Academy (United States); Anatoliy O. Pinchuk, Univ. of Colorado at Colorado Springs (United States)

Microwave metamaterials are of interest for antenna applications, such as Radome shielding. In this work we present experimental and theoretical results on angle dependent transmission through a slab of microwave negative index metamaterials. We used S-shaped Split Ring Resonator (SSRR) as a unit cell to design, fabricate, and test a negative index metamaterial slabs in the X-Ku and K microwave bands. We tested the negative index of refraction by cutting the slabs into prisms and measuring the refraction of a plane electromagnetic wave in an anechoic chamber.



Angle dependent transmission through a uniform slab of microwave metamaterial was measured for a linear polarized incident electromagnetic wave. Theoretical simulations by using the HFSS package showed a good agreement between the theory and experiments. We then fabricated a set of single axis boards (1 D metamaterial) and a set of two-dimensional interlocked metamaterial slabs (2D metamaterial), and tested them in the anechoic chamber. The transmission spectra S21 were measured as a function of the orientation of the metamaterial slabs within the incoming linearly polarized electromagnetic waves. The single axis board (1 D metamaterial) exhibited a strong anisotropic response with respect to the incoming linearly polarized electromagnetic wave. The dual interlocked metamaterial slab, however, did not exhibit this response. We conclude that the dual axis 2D metamaterial slab is isotropic with respect to the linearly polarized incoming electromagnetic wave.

9544-93, Session 18

Extraordinary terahertz transmission through electrically small particles

Mohammed R. AlShareef, King Abdulaziz City for Science and Technology (Saudi Arabia); Omar M. Ramahi, Univ. of Waterloo (Canada)

An array composed of six electrically small resonators and a transmission line is proposed to enhance terahertz (THz) waves' transmittance. Silver is the metal of choice for the proposed array. 3000 of the proposed array are fabrication on an intrinsic double-side polished silicon wafer using nanotechnology tools, followed by a THz time-domain spectroscopy (THZ-TDS) measurement, to validate the numerical findings experimentally.

In detail, Transmission mode THz-TDS experimental setup was applied. This setup mainly consisted of Ti:sapphire femtosecond laser, transmitter and receiver photoconductive antennas and four off-axis mirrors. First, the femtosecond laser pulses excite the THz emitter (transmitter antenna) which in turns generates THz pulses. The THz pulses are then collimated by the first off-axis mirror followed by focusing the beam on the sample with aid of the second off-axis mirror. The transmitted THz beam that passes through the sample is collimated again by the third off-axis mirror and then focused by the fourth off-axis mirror on the THz detector.

The silicon wafer with and without the metallic structure were at the focus of THz beam. The measured THz temporal pulses, in transient mode, of the sample and the reference (pure silicon) were Fourier transformed to THz spectrums. Next, the transmission was obtained from the ratio between the sample and reference spectrums.

At the resonance frequency of the structures (around 0.4 THz), an extraordinary transmission was observed. This phenomenon is attributed mainly to the periodic structure composed of the sub-wavelength unit cells.

9544-94, Session 18

Two layer metamaterials for selective frequency transmission in the terahertz region

Mayer A. Landau, Air Force Research Lab. (United States)

We have fabricated a metamaterial tunable filter for dynamic frequency selection in the terahertz region. The metamaterial consists of a sandwich of two meta-surfaces grown on high resistivity silicon wafers. The first meta-surface consists of a two-dimensional array of gold double split ring resonators and the second meta-surface consisits of an array of gold cut rods. Both meta-surfaces are fabricated for a response in the terahertz region. Our terahertz pulses are produced using the standard Austin switch technique. The terahertz pulse is focused onto the two meta-surfaces which are sandwiched together to produce a transmission window. Together, with the right orientation, translation, and parallelism of the two meta-surfaces, we achieve filtering of terahertz pulses. Since the unit cells for the inclusions are on the order of 100 microns, control of the translation, orientation, and parallelism of the two meta-surfaces with respect to each other and with respect to the orientation and direction of the impinging terahertz field is a challenge. We describe our technique for doing this and present data on our frequency filtering in the terahertz.

Conference 9545: Nanophotonic Materials XII

Wednesday - Thursday 12-13 August 2015

Part of Proceedings of SPIE Vol. 9545 Nanophotonic Materials XII



9545-2, Session 1

Surface functionalized spherical nanoparticles: an optical assessment of local chirality

Jamie M. Leeder, David L. Andrews, Henryk T. Haniewicz, Univ. of East Anglia (United Kingdom)

Electromagnetic radiation propagating through any molecular system typically experiences a characteristic change in its polarization state as a result of light-matter interaction. Circularly polarized light is commonly absorbed or scattered to an extent that is sensitive to the incident circularity, when it traverses a medium whose constituents are chiral. This research assesses specific modifications to the properties of circularly polarized light that arise on passage through a system of surfacefunctionalized spherical nanoparticles, through the influence of chiral molecules on their surfaces. Non-functionalized nanospheres of atomic constitution are usually inherently achiral, but can exhibit local chirality associated with such surface-bound chromophores. The principal result of this investigation is the quantification of functionally conferred nanoparticle chirality, manifest through optical measurements such as circularly polarized scattering and emission.

The relative position of chiral chromophores fixed to a nanoparticle sphere are first determined by means of spherical coverage co-ordinate analysis. For both emission and scattering, the total electromagnetic field received by a spatially fixed, remote detector is determined. It is shown that bound chromophores will accommodate both electric and magnetic dipole transition moments, whose scalar product represents the physical and mathematical origin of chiral properties identified in the detected signal. Results are reported for both oriented and isotropically averaged systems, the latter accounting for solutions (or randomly oriented) cases where the associated transition moments are uncorrelated with the detector. The analysis concludes with discussion of the magnitude of circular differential optical effects, and their potential significance for the characterization of surface-functionalized nanoparticles.

9545-3, Session 1

Semiconductor nanoplatelets: a new colloidal system for low-threshold, high-gain stimulated emission

Matthew A. Pelton, Univ. of Maryland, Baltimore County (United States) and Argonne National Lab. (United States); Chunxing She, Univ. of Chicago (United States); Igor Fedin, Dmitriy Dolzhnikov, Sandrine Ithurria, The Univ. of Chicago (United States); Erfan Baghani, Stephen K. O'Leary, The Univ. of British Columbia (Canada); Arnaud Demortiere, Illinois Institute of Technology (United States); Richard D. Schaller, Argonne National Lab. (United States); Dmitri V. Talapin, The Univ. of Chicago (United States) and Argonne National Lab. (United States)

Quantum wells (QWs) are thin semiconductor layers than confine electrons and holes in one dimension. They are widely used for optoelectronic devices, particularly semiconductor lasers, but have so far been produced using expensive epitaxial crystal-growth techniques. This has motivated research into the use of colloidal semiconductor nanocrystals, which can be synthesized chemically at low cost, and can be processed in the solution phase. However, initial demonstrations of optical gain from colloidal nanocrystals involved high thresholds.

Recently, colloidal synthesis methods have been developed for the production of thin, atomically flat semiconductor nanocrystals, known as nanoplatelets (NPLs). We investigated relaxation of high-energy carriers in colloidal CdSe NPLs, and found that the relaxation is characteristic of a

QW system. Carrier cooling and relaxation on time scales from picoseconds to hundreds of picoseconds are dominated by Auger-type exciton-exciton interactions. The picosecond-scale cooling of hot carriers is much faster than the exciton recombination rate, as required for use of these NPLs as optical gain and lasing materials.

We therefore investigated amplified spontaneous emission using closepacked films of NPLs. We observed thresholds that were more than 4 times lower than the best reported value for colloidal nanocrystals. Moreover, gain in these films is 4 times higher than gain reported for other colloidal nanocrystals, and saturates at pump fluences more than two orders of magnitude above the ASE threshold. We attribute this exceptional performance to large optical cross-sections, relatively slow Auger recombination rates, and narrow ensemble emission linewidths.

9545-5, Session 1

Manipulating the spatial extent of the exciton diffusion through QDs assembly by controlling dimensionality, energy landscape, and exciton density (Invited Paper)

Keiko Munechika, Jiye Lee, Dimitrios Simatos, Mauro Melli, Steve Whitelam, Alexander Weber-Bargioni, The Molecular Foundry (United States)

Semiconductor quantum dots are considered a promising material class with the potential of highly tunable and novel optoelectronic properties. Recent research efforts have shown that quantum dots, assembled in well-ordered 1D, 2D and 3D geometries have the potential to funnel excitons via Förster Resonance Energy Transfer (FRET) through the nanocrystal composite. Understanding the inter quantum dot coupling and the spatial extend of exciton diffusion is key to design material for the deliberate control of energy transport through them. In this regard, we study Förster Resonance Energy Transfer (FRET) between CdSe quantum dots in a well-defined 2D assembly with different interparticle distances. We then examine the spatial extent of FRET coupling between quantum dots using confocal fluorescence hyperspectral imaging. We spatially map out the degree of the coupling between the neighboring quantum dots by exciting the quantum dots at a known location and collect fluorescence signals at various distances relative to the excitation. We show that by varying the dimensionality, energy landscape, and exciton density, we are able to manipulate the spatial extent of exciton diffusion through the QDs assembly. Modeling was done in conjunction the experiments and well described our observations in each case. The results provide in-depth understanding into the spatial extent of exciton diffusion via FRET through ordered quantum dot assemblies and provide useful insights in engineering nano-building structures to direct and enhance the direction of the exciton transport to a preferred sites.

9545-6, Session 2

Nitride semiconductor nanostructures for classical and quantum light generation (Invited Paper)

Yong-Hoon Cho, KAIST (Korea, Republic of)

No abstract available



9545-7, Session 2

Carrier localization in In-rich InGaN/GaN multiple quantum wells for green lightemitting

Hyun Jeong, Univ. de Technologie Troyes (France); Mun Seok Jeong, Sungkyunkwan Univ. (Korea, Republic of); Gilles Lerondel, Univ. de Technologie Troyes (France)

Carrier localization of In-rich InGaN/GaN MQWs was investigated via spatially resolved optical characterization using NSOM and confocal TRPL. To assess the correlation between carrier localization and crystal quality, sapphire and GaN have been used as substrates for the growth of InGaN/GaN MQWs. We found a strong correlation between the carrier localization and the crystal quality based on temperature dependent PL results. The distribution of luminescent clusters on both samples was shown to be quite different as revealed by the NSOM analysis. The clear relation between the luminescent clusters and the longer PL decay time regions strongly support the claim that carrier localization is strongly affected by the crystal quality. Accurate understanding of the optical characteristics of In-rich InGaN/GaN MQWs is the way to overcome the "green gap" issue, which would ultimately lead to pure white LEDs.

9545-8, Session 2

CdTe quantum dots fluorescent probes for determination of 2,4-dichlorophenol compounds based on the Fe(III)PcTs-BuOOH catalysis system

Tong Yilin, Hongqi Li, Haiqing Chen, Hankou Univ. (China)

A new fluorescent probe based on the fluorescence of CdTe quantum dot was established and studied for the determination of contaminant 2,4-dichlorophenol(DCP) compounds. In the presence of 4-AAP, DCP was catalyzed by iron(II) phthalocyanine (Fe(II)Pc), the reaction product dye was generated, which quenched the fluorescence of CdTe quantum dots. t-BuOOH was added in the system to be as oxidizing agent, greatly accelerated the oxidation effect of DCP. The water soluble CdTe quantum dot was prepared. The effects of reaction conditions on the fluorescence and catalysis oxidation of DCP were studied and the optimal reaction conditions were obtained. In the concentration range of 1.0?10-6mol/L L-9.0?10-6mol/L and 1.0?10-5mol/L ~1.3?10-4mol/L, there is a good linear relationship between the change value of CdTe quantum dot Fluorescence intensity PO/P and DCP concentration. This method has good repeatability and ability of resisting disturbance.

9545-9, Session 2

Nanostructured organosilicon luminophores as a new concept of nanomaterials for highly efficient downconversion of light

Sergey A. Ponomarenko, Institute of Synthetic Polymeric Materials (Russian Federation) and Moscow State Univ. (Russian Federation) and LumInnoTech LLC (Russian Federation); Nikolay M. Surin, Oleg V. Borshchev, Maxim S. Skoroteckiy, Institute of Synthetic Polymeric Materials (Russian Federation) and LumInnoTech LLC (Russian Federation); Aziz M. Muzafarov, Institute of Synthetic Polymeric Materials (Russian Federation) and A.N. Nesmeyanov Institute of Organoelement Compounds (Russian Federation) Organic luminophores are widely used in various optoelectronic devices, which serve for photonics, nuclear and particle physics, quantum electronics, medical diagnostics and many other fields of science and technology. Improving their spectral-luminescent characteristics for particular technical requirements of the devices is a challenging task. In this work we report on a new concept to universal solution of this problem by creation of nanostructured organosilicon luminophores (NOLs), which are a particular type of dendritic molecular antennas. A NOL consists of two types of covalently bonded via silicon atoms organic luminophores with efficient Förster energy transfer between them (Sci. Rep. 2014, 4, 6549). They combine the best properties of organic luminophores and inorganic quantum dots: high absorption cross-section, excellent photoluminescence quantum yield, fast luminescence decay time, good processability and low toxicity. A smart choice of organic luminophores allowed us to design and synthesize a library of NOLs, absorbing from VUV to visible region and emitting at the desired wavelengths having maxima varying from 390 to 650 nm. Using NOLs in plastic scintillators, widely utilized for radiation detection and in elementary particles discoveries, led to a breakthrough in their efficiency, which combines both high light output and fast decay time. Moreover, for the first time plastic scintillators, which emit light in the desired wavelength region ranging from 370 to 700 nm, have been created. Thin films of NOLs themselves or their composites with optical plastics are transparent, which leads to efficient down-conversion of light useful for different types of optical detectors.

9545-10, Session 3

Terahertz devices based on carbon nanomaterials (Invited Paper)

Junichiro Kono, Rice Univ. (United States)

Carbon nanomaterials attract much attention due to novel electronic, photonic, and mechanical properties that can find application in a variety of devices. In particular, they have promising properties for developing optoelec-tronic devices at long wavelengths, i.e., in the mid-infrared (MIR) and terahertz (THz) ranges, including polarizers, modulators, detectors, and sources. It has been predicted that they have superior performance over existing devices in these ranges. In this talk, after reviewing the past, current, and future of the THz science and technology of gra-phene and carbon nanotubes, we will present some of our latest results on THz dynamic conductivity and ultrafast carrier dynamic as well as THz devices including polarizers, modulators, and detectors.

9545-11, Session 3

Theoretical design of nano-layered AI/ SiO2 metamaterial with hyperbolic dispersion with minimum losses

Priscilla N. Kelly, Daniel White, Lyuba Kuznetsova, San Diego State Univ. (United States)

Motivated by a greater need for increased performance in modern-day technology, this paper will show the results of theoretical calculations for the optical properties of AI/SiO2 nanolayered metamaterial with hyperbolic dispersion. Our main focus is on finding the conditions for low losses since losses might outweigh any increase in speed for use of metamaterial devices today. Using the Effective Medium approximation (EMA) with non-local corrections, we have investigated effect of three major variables (number and thickness of the Al layers and Al fill fraction) on inherent losses and hyperbolic dispersion. Our model predicts a variation of the dielectric permittivity only in the perpendicular direction as the number of Al layers changes. This is an important factor to consider when reducing losses. The first of the trends is to find the saturation limit of non-local corrections in Al/SiO2 layers. This will tell us when the number of layers reaches the EMA, therefore the full range of optical effects AI/SiO2 layers is capable of. The second and third effects, AI fill fraction with a fixed layer height and thickness of a single layer in a sample of 20 layers, will be investigated to minimize losses. Both of these effects determine the transition wavelength



to hyperbolic dispersion which allows for fine tuning of this dispersion for future applications. The paper will also discuss the repercussions these properties will have on the manufacturing techniques and future applications of AI/SiO2 devices.

9545-12, Session 3

Spectral tunability of the spacer layer in metasurface absorbers

Kai Liu, Nan Zhang, Dengxin Ji, Haomin Song, Xie Zeng, Qiaoqiang Gan, Univ. at Buffalo (United States)

Potential solar energy applications of metamaterial absorbers require spectrally tunable resonance to ensure the overlap with intrinsic absorption profiles of active materials. Although those resonance peaks of metamaterial absorbers can be tuned precisely by lithography-fabricated nanopatterns with different lateral dimensions, they are too expensive for practical large-area applications. In this work, we will report another freedom to tune the spectral position of the super absorbing resonance, i.e. the spacer thickness. The structure was fabricated by evaporating an optically opaque metallic ground plate, a dielectric spacer layer, and a top metallic thin film followed by thermal annealing processes to form discrete nanoparticles. As the spacer thickness increases from 10-90 nm, two distinct shifts of the absorption peak can be observed [i.e. a blue-shift for thinner (10-30 nm) and a red-shift for thicker spacer layers (30-90 nm)]. To understand the physical mechanism, we characterized effective optical constants of top nanopattern layer and loaded them into numerical simulation models. A good agreement with experimental data was only observed in the thick spacer region (i.e. 30-90 nm). The optical behavior for thinner spacers cannot be explained by effective medium theory and interference mechanism. Therefore, a microscopic study has to be performed to reveal strongly coupled modes under metallic nanopatterns, which can be interpreted as separate antennas strongly coupled with the ground plate. Since the resonant position is sensitive to the spacer thickness, a tunable super absorbing metasurface is realizable by introducing spatial tunable materials like stretchable chemical/biomolecules.

9545-13, Session 3

Highly efficient excitonic emission of CBD grown ZnO micropods

Roy Aad, Anisha Gokarna, Komla Nomenyo, Univ. de Technologie Troyes (France); Patrice Miska, Univ. de Lorraine (France); Wei Geng, Christophe Couteau, Gilles Lérondel, Univ. de Technologie Troyes (France)

Due to its wide direct band gap and large exciton binding energy allowing for efficient excitonic emission at room temperature, ZnO has attracted attention as a luminescent material in various applications such as UV-light emitting diodes, chemical sensors and solar cells. While low-cost growth techniques, such as chemical bath deposition (CBD), of ZnO thin films and nanostructures have been already reported; nevertheless, ZnO thin films and nanostructures grown by costly techniques, such as metalorganic vapour phase epitaxy, still present the most interesting properties in terms of crystallinity and internal quantum efficiency.

In this work, we report on highly efficient and highly crystalline ZnO micropods grown by CBD at a low temperature (< 90°C). XRD and low-temperature photoluminescence (PL) investigations on as-grown ZnO micropods revealed a highly crystalline ZnO structure and a strong UV excitonic emission with internal quantum efficiency (IQE) of 10% at room temperature. Thermal annealing at 900°C of the as-grown ZnO micropods leads to further enhancement in their structural and optical properties. Low-temperature PL measurements on annealed ZnO micropods showed the presence of phonon replicas, which was not the case for as-grown samples. The appearance of phonon replicas provides a strong proof of the improved crystal quality of annealed ZnO micropods. Most importantly, low-temperature PL reveals an improved IQE of 15% in the excitonic emission of ZnO micropods. The ZnO micropods IQE reported here are comparable

to IQEs reported on ZnO structures obtained by costly and more complex growth techniques. These results are of great interest demonstrating that high quality ZnO microstructures can be obtained at low temperatures using a low-cost CBD growth technique.

9545-14, Session 3

High-speed tip-enhanced Raman imaging (*Invited Paper*)

Marc Chaigneau, HORIBA Jobin Yvon S.A.S. (France); Andrey V. Krayez, AIST-NT Inc. (United States); Ophélie Lancry, HORIBA Jobin Yvon S.A.S. (France); Sergey A. Saunin, AIST-NT Inc. (United States)

Tip Enhanced Raman Scattering (TERS), a technique that provides molecular information on the nanometer scale, has been a subject of great scientific interest for 15 years. But regardless of the recent achievements and applications of TERS, ranging from material science and nanotechnology, strain measurement in semiconductors, to cell biological applications, the TERS technique has been hampered by extremely long acquisition times, measured in hours, required for collection of reasonably high pixel density TERS maps.

In this talk, specifics of the TERS setup that enable fast, high pixel density nano-Raman imaging will be discussed: The innovative integration of technologies brings high-throughput optics and high-resolution scanning for high-speed imaging without interferences between the techniques. The latest developments in near-field optical probes also provide reliable solutions for academic and industrial researchers alike to easily get started with nanoscale Raman spectroscopy. Thanks to those latest instrumental developments, we will present the nanoscale imaging of chemical and physical properties of graphene, carbone nanotubes and self-assembled monolayers of organic molecules, with a spatial resolution routinely obtained in TERS maps in the 15 - 20 nm range and a best resolution achieved being of 7 nm

9545-15, Session 4

Design of metal/dielectric/nanocrystals core/shell/shell nano-structures for the fluorescence enhancement of cadmiumfree semiconductor nanocrystals (Invited Paper)

Théo Chevallier, Gilles Le Blevennec, Frederic Chandezon, Commissariat à l'Énergie Atomique (France)

AgInS2-ZnS (ZAIS) quaternary semiconductors nanocrystals are versatile cadmium-free luminescent nanomaterials that are ideal for the development of innovative white-LED devices. By grafting ZAIS nanocrystals to carefully chosen metal@dielectric core@shell nanoparticles, both the absorption and emission processes can be tuned and enhanced. A simulation was used to predict the nano-optical behavior of a silver@oxide@nanocrystals structures and find the most efficient structures before synthesizing and testing them.

This study shows the potential of silver@oxide@ZAIS nanocrystals nanostructures and highlights the use of simulation as a guiding tool for the design of efficient photonic nanostructures targeting specific applications.

9545-16, Session 4

Adiabatic mode coupler on ion-exchanged waveguides for the efficient excitation of surface plasmon modes

Josslyn Beltran Madrigal, Univ. de Technologie Troyes (France); Martin Berthel, Institut NÉEL (France); Florent



Gardillou, Teem Photonics S.A. (France); Ricardo Tellez Limon, Christophe Couteau, Univ. de Technologie Troyes (France); Denis Barbier, Teem Photonics S.A. (France); Aurelien Drezet, Institut NÉEL (France); Rafael Salas-Montiel, Univ. de Technologie Troyes (France); Serge Huant, Institut NÉEL (France); Sylvain Blaize, Wei Geng, Univ. de Technologie Troyes (France)

Several works have already shown that the excitation of plasmonic structures through waveguides enables a strong light confinement and low propagation losses [1]. This kind of excitation is currently exploited in areas such as biosensing [2], nanocircuits[3] and spectroscopy[4].

The efficient excitation of surface plasmon modes (SPP) with guided modes supported by high-index-contrast waveguides, such as silicon-oninsulator waveguides, had already been shown [1,5]. However, the use of weak-confined guided modes of a glass ion exchanged waveguide as a SPP excitation source represents a technological challenge, because the mismatch between the size of their respective electromagnetic modes is so high that the resultant coupling loss is unacceptable for practical applications.

In this work, we describe how an adiabatic taper structure formed by an intermediate high-index-contrast layer placed between a plasmonic structure and an ion-exchanged waveguide decreases the mismatch between effective indices, size, and shape of the guided modes. This hybrid structure concentrates the electromagnetic energy from the micrometer to the nanometer scale with low coupling losses to radiative modes. The electromagnetic mode confined to the high-index-contrast waveguide then works as an efficient source of SPP supported by metallic nanostructures placed on its surface.

We theoretically studied the modal properties and field distribution along the adiabatic coupler structure. In addition, we fabricated a highindex-contrast waveguide by electron beam lithography and thermal evaporation on top of an ion-exchanged waveguide on glass. This structure was characterized with the use of near field scanning optical microscopy (NSOM). Numerical simulations were compared with the experimental results.

[1] N. Djaker, R. Hostein, E. Devaux, T. W. Ebbesen, and H. Rigneault, and J. Wenger, J. Phys. Chem. C 114, 16250 (2010).

[2] P. Debackere, S. Scheerlinck, P. Bienstman, R. Baets, Opt. Express 14, 7063 (2006).]

[3] A. A. Reiserer, J.-S. Huang, B. Hecht, and T. Brixner. Opt. Express 18(11), 11810–11820 (2010).

[4] R. Salas-Montiel, A. Apuzzo, C. Delacour, Z. Sedaghat, A. Bruyant et al. Appl. Phys Lett 100, 231109 (2012)

[5] A. Apuzzo M. Févier, M. Salas-Montiel et al. Nano letters, 13, 1000-1006

9545-17, Session 4

Multiscale modeling of the plasmonic and light trapping response of random nanostructured TiO2-photoelectrodes

Ivonne Carvajal, George P. Demopoulos, Raynald Gauvin, McGill Univ. (Canada)

Random nanostructured materials possess electromagnetic properties that greatly differ from those of ordinary bulk materials. The capacity to control the optical response of the material by tuning its internal structure has rendered these architectures into a promising light trapping technology for solar energy conversion and photocatalytic applications. However, a rigorous electromagnetic computation of these structures in large-scale systems is computationally demanding and impractical. Here, we present a multiscale optical model approach to study random nanostructured TiO2-photoelectrodes for solar cell applications. In this approach, Maxwell's electromagnetic equations are solved with the generalized-multiparticle-Mie theory for a system of aggregated TiO2 nanoparticles in a subwavelength volume. The results are then implemented in a Monte Carlo algorithm to simulate the propagation of light within the photoelectrode. We investigate

the influence of the TiO2 crystal phase, porosity, and pore and particle size distributions on the photoelectrode transmitted, reflected and absorbed spectra. Results of the simulations agree with the observed experimental data. We show that careful engineering of the internal structure and of the photoelectrode gives accurate control on the coupling of incident light with the nanostructured film over the UV to near-IR spectrum range that can lead to enhanced solar energy conversion efficiency. Our approach provides for the first time insight into the spatial distribution of electron generation within the photoelectrode that is of great importance for the design and optimization of the photoelectrode. Finally, we show the potential of this model to investigate randomly structured materials composed of nanowires.

9545-18, Session 4

New design of photonic band gap filter: the random dimer effect

Brezini Abderrahmane, Univ. d'Oran (Algeria); Fares Kanouni, Ctr. de Recherche (Algeria); Qin Zou, Institut Telecom Sud Paris (France)

A new type of optical filter using photonic band gap materials is suggested. We consider photonic superlattices composed of two alternating photonic crystals. The structure is denoted as A/B/A/B.....A/B, where photonic crystals A and B act as photonic wells and barriers, respectively. The propagation of electromagnetic waves in such one dimensional disordered photonic crystal is investigated by means the transfer matrix formalism. In particular the presence of short range correlation in disorder into the sample induces the suppression of localization. By introducing a short range intentionally binary disorder provides predicted resonance breaking down the Anderson localization. By properly adjusting the intrinsic dimer unit cell parameter i.e. dimer dielectric constants ?d, light can be transmitted over the whole sample with a very large localization length ? through a ballistic canal. Such findings open up possibilities in performing new design optical filter. Moreover with increasing the degree of disorder, by means the dimer concentration cd and the period number N, the quality in transmitting light around the resonance is significantly improved with the smoother corresponding allowed mini band.

9545-19, Session 4

Optical properties of polyaniline-coated silica spheres: aging effect in acetone

Byeong-Wu Kim, Sang-Jo Kim, So-Yeon Kang, Sang-Hyeon Moon, Eun-Hye Park, Kwang-Sun Kang, Kyungil Univ. (Korea, Republic of)

Polyaniline (PAn)-coated silica spheres have been synthesized by attaching various amounts of N-[3-(trimethoxysilyl)propyl]aniline (TMSPA) and polymerizing with ammonium persulfate. The ratios of tetraethoxy orthosilicate and TMSPA were 10:1 (PAn-A), 5:1 (PAn-B), and 3:1 (PAn-C). After polymerization of the aniline moieties the -OH absorption peak drastically reduced and the new sharp peaks appeared at 1398 cm-1 and 617 cm-1 representing C-N and C-S stretching vibrations, respectively. The polymerized spheres were soaked into the acetone for three months. New absorption peak at 1712 cm-1 representing C=O stretching vibration of an ester appears after three months storage in acetone and becomes stronger with the smaller amount of PAn. Although the sphere film color is gray when it is dried, the color turned to dark when it was wetted with methanol. Complicated solvatochromic behavior was observed for whole UV-visible range depending on the solvent. The solution color changed from clear to dark brown, brown, and yellow for the PAnA, PAnB and PAnC, respectively. The absorption peaks of the dried solution for PAn-A and PAn-B at 3230, 2972, 2926, 1712, 1434/1377, and 1051 cm-1 represent C-OH, R-CH3, R2-CH2, -C=O, C-H, and Si-O-Si absorption, respectively. Photoluminescence peak of the solution shifted toward longer wavelength with the decrease the amount of PAn. The sequence of the amount of new material formation is PAn-A > PAn-B > PAn-C.



9545-30, Session PWed

Investigation of Ta nanoparticles characteristics produced by laser ablation method

Fariba Azadi Kenari, Mohammad Reza Hantehzadeh, Islamic Azad Univ. (Iran, Islamic Republic of)

In this paper the characteristics of Tantalum nano particles produced by laser ablation method is investigated experimentally with a first harmonic of a Q-switched Nd:YAG laser of 1064 nm wavelengths at 6 ns pulse. Spherical nano particles of Ta have been produced successfully by using a 1?cm?^2 Ta bulk plate in Ethanol.The fluency of laser is 105 j/?cm?^(-2) .By using some molecular-scale devices such as transmission Electron Microscopy (TEM),photo luminescence (PL), X-ray diffraction (XRD) and absorption spectroscopy we determined the optical characteristic, size, band gap energy,crystlline characteristics and size of nano particles.And at the end, some applications of Ta have been noticed.

9545-31, Session PWed

Resonant tunneling in 2D-photonic superlattices

Fares Kanouni, Ctr. de Développement des Téchnologies Avancées (Algeria); abderrahmane Brezini, Thin films and nanostructures Laboratory LaMiN, Polytechnic School, Oran, 31000, Algeria (Algeria); fahima arab, radouane graine, Ctr. de Développement des Téchnologies Avancées/ research unit in optics and photonics (Algeria)

Transmissions and resonant tunneling of two-dimensional (2D) photonic superlattices (PhSLs) are discussed. We consider PhSL composed of two alternating 2D-photonic crystals. The structure is denoted as A/B/A/B..... A/B, where photonic crystals A and B act as photonic wells and barriers, respectively. The transmission coefficient is calculated using the Transfer Matrix Method (TMM) in combination with Bloch theorem. The transmission spectra of the PhSLs indicate that the formation of photonic minibands and minigaps inside the wells. The positions and number of the minibands can be artificially tuned by varying the well width. By appropriately choosing the structure parameters, these interesting results can be used to develop new photonic devices.

9545-32, Session PWed

Broadband ENZ metamaterials based on metal-polymer composite films

Pavlo Pinchuk, Ke Jiang, Univ. of Colorado at Colorado Springs (United States)

Epsilon-near-zero metamaterials are of interest for a broad range of potential applications in photonics, photovoltaics, and communications. In this work we present the experimental and theoretical results on a broadband ENZ metamaterial composite film based on gold metal nanoparticles of different sizes embedded in a polymer thin film. Gold metal nanoparticles of the sizes ranges 10 - 50 nm were synthesized using chemical reduction of gold chloride with borohydride. The solutions of the nanoparticles were characterized by using the UV-VIS spectroscopy, DLS, and SEM microscopy. The nanoparticles were then mixed and embedded into composite thin polymer films. The thin films were characterized by UV-VIS spectroscopy. The optical absorption spectra were then used to retrieve the complex dielectric permittivity of the solutions of the nanoparticles and the composite thin films by using Kramers-Kronig integrals. The Maxwell-Garnett effective medium theory was then used to calculate the effective complex dielectric permittivity of the composite polymer films.

9545-33, Session PWed

Using of radiation intensity dependence on excitation level for the analysis of surface plasmon resonance effect on ZnO luminescence

Stepan I. Rumyantsev, Mikhail V. Ryzhkov, Charus M. Briskina, Valery M. Markushev, Institute of Radio Engineering and Electronics (Russian Federation); Andrey P. Tarasov, Moscow Institute of Physics and Technology (Russian Federation) and Institute of Radio Engineering and Electronics (Russian Federation); Andrey A. Lotin, Institute on Laser and Information Technologies (Russian Federation)

For the analysis of surface plasmon (SP) resonance effect on ZnO luminescence the system of rate equations (SRE) is proposed. It contains a set of parameters that characterizes processes participating in luminescence: zone-zone excitation, excitons formation and recombination, formation and disappearance of photons and SP. It is shown that utilizing SRE experimental ZnO microstructure radiation intensity dependence on photoexcitation level can be approximated. Thus the values of these parameters can be estimated and used for luminescence analysis.

This approach was tested on ZnO microfilms with different thickness of Ag island film covering. It was revealed that the increase of cover thickness leads to the increase of losses and probability of photons to SP conversion decrease.

Based on SRE parameters dependence of luminescence intensity of ZnO microstructures covered by Ag with MgO spacer on its thickness was simulated. It turns out that it is possible to obtain the result near to the experimental one if we assume exponential decrease of probability of photons hit in Ag-cover with the increase of spacer thickness.

In order to take into account visible emission rate equations for levels populations in energy gap and for corresponding photons and SP were added to SRE. Using such SRE it is shown that the form of visible luminescence intensity dependence on excitation level (P) like (P) raised to the power of 1/3 as obtained elsewhere (Studenikin et al., J.Appl.Phys.91, 5060, 2002) is possible only for emission of donor-acceptor pairs.

9545-34, Session PWed

Visible-light response of TiO2 photocatalysts introduced by annealing

Fangzhou Liu, The Univ. of Hong Kong (Hong Kong, China); Mu Yao Guo, Alan Man Ching Ng, South Univ. of Science and Technology of China (China) and The Univ. of Hong Kong (Hong Kong, China); Aleksandra B. Djuri?i?, Wai Kin Chan, The Univ. of Hong Kong (Hong Kong, China)

TiO2 has been one of the most investigated photocatalysts for its high effectiveness and efficiency for degradation of various organic compounds. Several major crystal phases of TiO2, such as anatase and rutile, as well as the commercially available form with mixed phases, all exhibit considerable photocatalytic activities. However, due to their large band-gaps, these TiO2 forms are primarily active under UV illumination which only accounts for a very small portion of solar energy. To overcome this restriction, efforts have been made by doping TiO2 with metal or non-metal atoms, coupling with narrow band-gap materials, oxygen deficiency, as well as the investigation of carbon-titania composites. Oxygen deficient TiO2 has been reported as a visible-light-active photocatalyst due to the midgap states below the conduction band introduced by oxygen vacancies. Based on this understanding, various techniques can be utilized to enable visible-light photoactivity of TiO2 materials.

In this work, we proposed a simple approach to obtain visible-lightresponsive TiO2 photocatalysts. TiO2 nanoparticles with different crystal



phases (anatase, rutile, and anatase-rutile mixture) were annealed together with Cu foil in vacuum at specified temperatures. The as-fabricated samples exhibited enhanced photocatalytic activities under solar illumination with UV block filter compared to initial materials. Other characterizations were performed to detect the changes of the materials corresponding to visiblelight activation. Possible mechanisms were explained in detail.

References

Fujishima, A., Zhang, X., Tryk, D. A., Surf. Sci. Rep. 63, 515-582 (2008).
 Lin, Z., Orlov, A., Lambert, R. M., Payne, M. C., J. Phys. Chem. B 109, 20948-20952 (2005).

9545-35, Session PWed

Photovoltaic study of dye sensitized solar cells based on TiO2, ZnO:Al3+ nanoparticles

Ruben A. Rodríguez-Rojas, Humberto E. Sanchez, Jesus Castañeda-Contreras, Virginia F. Marañon-Ruiz, Héctor Pérez Ladrón de Guevara, Univ. de Guadalajara (Mexico); Tzarara López-Luke, Elder De la Rosa-Cruz, Ctr. de Investigaciones en Óptica, A.C. (Mexico)

A technique to fabricate dye (rhodamine B) sensitized solar cells based on titania oxide and zinc oxide nanoparticles is reported. The TiO2 was synthesized using the sol-gel method and the ZnO was synthesized by hydrolysis method to obtain nanoparticles of ~ 5 nm and 150 nm respectively. ZnO was doped with Al3+ in order to enhance the photovoltaic efficiency in order to promote the electrons mobility. The photovoltaic conversion characterization of films of TiO2, ZnO and ZnO:AI3+ nanoparticles is also reported. The generated photocurrent was measured by two methods; one of those uses a three electrode electrochemical cell and the other use an electronic array where the cells were exposed to UV lamp and the sun light. The role of the TiO2, ZnO and Al3+ doped ZnO nanoparticles is discussed to obtain a better efficiency in the generation of photocurrent (PC). The results exhibited by the electrochemical cell method, efficiencies of 0.55 (PC=187 µA/cm2) and 0.22 (PC=149 µA/cm2) for TiO2 and undoped ZnO respectively. However, when ZnO is doped with Al3+ at the higher concentration the efficiency was 0.44. While using the electronic array the results exhibited efficiencies of 0.31 (PC=45 µA/cm2) and 0.09 (PC=16 μ A/cm2) for TiO2 and undoped ZnO respectively. However, when ZnO is doped with Al3+ at the higher concentration the efficiency was 0.44 and 0.48 for electrochemical cell and electronic array respectively. This shows that AI3+ enhances the photogenerated charge carriers increasing the mobility of electrons.

9545-36, Session PWed

Photodisaggregation of silver nanoparticles suspended in ethanol

Gabriel J. Ortega, Alfonso Padilla-Vivanco, Carina Toxqui-Quitl, Univ. Politécnica de Tulancingo (Mexico); Placido Zaca, Fernando Chávez, Benemérita Univ. Autónoma de Puebla (Mexico); O. Goiz, Instituto Politécnico Nacional (Mexico)

An experimental study about of aggregation and disaggregation of silver nanoparticles suspended in ethanol is presented. Disaggregate process is implemented when a non-colloidal solution of silver nanoparticles whose size are less than 100 nm is irradiated with a pulsed laser via an optical fiber. Results show that, it is possible to disaggregate and aggregate nanoparticles with certain sizes only by controlling the laser energy. A colloidal solution with a spectrum extinction characteristic and particular color is obtained when a non-colloidal solution is irradiated with a laser energy greater than 100 nJ. Furthermore, we also show that, the laser light also provokes aggregation of silver nanoparticles with certain sizes when a colloidal solution is irradiated with an energy laser greater than 100 nJ. Experimental results are presented.

9545-37, Session PWed

Suppressing spontaneous polarization of p-GaN by graphene oxide passivation: augmented light output of GaN UV-LED

Hyun Jeong, Univ. de Technologie Troyes (France); Mun Seok Jeong, Sungkyunkwan Univ. (Korea, Republic of)

GaN-based ultraviolet (UV) LEDs are widely used in numerous applications, including white light pump sources and high-density optical data storage. However, one notorious issue is low hole injection rate in p-type transport layer due to poorly activated holes and spontaneous polarization, giving rise to insufficient light emission efficiency. Therefore, improving hole injection rate is a key step towards high performance UV-LEDs. Here, we report a new method of suppressing spontaneous polarization in p-type region to augment light output of UV-LEDs. This was achieved by simply passivating graphene oxide (GO) on top of the fully fabricated LED. The dipole layer formed by the passivated GO enhanced hole injection rate by suppressing spontaneous polarization in p-type region. The homogeneity of electroluminescence intensity in active layers was improved due to band filling effect. As a consequence, the light output was enhanced by 60% in linear current region. Our simple approach of suppressing spontaneous polarization of p-GaN using GO passivation disrupts the current state of the art technology and will be useful for high-efficiency UV-LED technology.

9545-38, Session PWed

A simple method for p-type doping of monolayer MoS2 using graphene oxide

Hye Min Oh, Young Hee Lee, Mun Seok Jeong, Sungkyunkwan Univ. (Korea, Republic of)

We propose a novel and simple method for p-type doping of monolayer MoS2 by spin-casting of graphene oxide sheet (GO). The GO sheets act as a p-type dopant because of their large number of functional groups, which exhibit electron-withdrawing characteristics. Increased PL intensity and shifted peak positions in the PL and Raman spectra, which served as evidence of the p-type doping of the MoS2, were clearly observed. Moreover, the current versus voltage curves recorded for backward and forward bias also confirmed the rectifying behavior of a MoS2 p-n junction diode. The observed p-type doping effect can be explained by the numerous electron-withdrawing groups present on GO sheets. Moreover, using confocal PL/Raman spectroscopic analysis, we observed that the p-type doping of MoS2 is extremely sensitive to the thickness of the coated GO sheets. Our technique for the p-type doping of MoS2 through contact with GO sheets offers remarkable advantages for optoelectronic applications; the process is simple and low in cost, and it allows the largescale fabrication and the modulation of doping concentration by controlling the thickness of the coated GO sheets.

9545-39, Session PWed

Determination of refractive index and absorbance modulation amplitudes from angular selectivity of holograms in polymer material with phenanthrenequinone

Vladimir N Borisov, Andrey N Veniaminov, ITMO University (Russian Federation)

Amplitude and phase contributions to mixed volume holographic gratings were extracted from measured contours of angular selectivity. Holograms for the investigation were recorded in the glassy polymer material with phenanthrenequinone (PQ) using the DPSS CW laser (532 nm) and then self-developed due to molecular diffusion of PQ, reaching diffraction



efficiency about 40%. Refractive index and absorbance modulation amplitudes of those holograms were obtained as adjustable parameters from theoretical equations by fitting angular dependences of zeros and 1st orders diffraction efficiency measured at 450, 473, 532, and 633 nm at the different stages of hologram development. Mixed gratings manifest themselves in asymmetrical transmittance selectivity contours with one minimum and one maximum shifted with respect to the Bragg angle, while symmetrical contours with a minimum or a maximum are characteristic of pure phase and amplitude gratings, respectively. In the course of hologram development, it converts from a predominantly amplitude-mixed to almost purely phase one in the case of readout using a light within the absorption band of PQ and maintains the phase nature besides it. The value of refractive index amplitude is ranging from 5?10-6 to 10-4 and the value of absorbance amplitude is up to 140 m-1.

9545-40, Session PWed

Synthesis, characterization, and electrical properties of Pd doped ZnO nanoparticles with enhanced visible light phtocaralytic activity

Omar Abdullah Al-Hartomy, Mohammad Mujahid, Univ. of Tabuk (Saudi Arabia)

Synthesis of pure and Pd doped ZnO has been carried out using easy hydrothermal method which is less time-consuming, inexpensive and give high yields. The synthesized materials are characterized by standard analytical techniques, such as X- ray Diffraction analysis (XRD), Scanning Electron Microscopy (SEM), Transmission Electron Microscopy (TEM) and UV-Visible Spectroscopy. The XRD analysis shows no change in crystal structure of ZnO after doping with different concentration of Pd indicating single phase polycrystalline material. The SEM images confirm that Pd are well incorporated on the surface of ZnO. The UV-Visible absorption analysis technique indicate that the doping of Pd into the ZnO lattice shift the absorption band towards the visible region. The electrical properties of the synthesized particle have been performed by monitoring the dielectric constant (?), dielectric loss (tan ?) and ac conductivity with respect to frequency. The dielectric constant and dielectric loss decreases with the increase in frequency upto certain limit, after then on further increase in frequency, they became independent. The a.c. conductivity increases with the increase of frequency. The dielectric property also decreases by increase of the dopant concentration.

9545-20, Session 5

Rh6G released from solid and nanoporous SiO2 spheres prepared by sol-gel route

Jorge A. Garcia-Macedo, Pedro Francisco-Santiago, Alfredo Franco, Univ. Nacional Autónoma de México (Mexico)

Porous silica nanoparticles are considering good systems for drug cargo and liquid separation. In this work we studied the release of rhodamine 6G from solid and porous silica nanoparticles. Solid SiO2 spheres were prepared by sol-gel method. Nanoporous channels were produced by using a surfactant that was removed by chemical procedure. Rh6G was incorporated into the channels by impregnation. The hexagonal structure of the pores was detected by XRD and confirmed by HRTEM micrographs. N2 adsorption-desorption isotherm Type V, was obtained by BET in the nanoporous particles. Surface area was bigger in the nanoporous spheres than in the solid ones. Rh6G released from the particles by stirring them in water at controlled speed was studied as function of time by photoluminescence. Released ratio was faster in the solid nanoparticles than in the porous ones. In the last case, a second release mechanism was observed. It was related with rhodamine coming out from the porous.

9545-21, Session 5

Fabrication and characterization of p-ZnO:(P,N)/n-ZnO:Al homojunction ultraviolet (UV) light emitting diodes

Amiruddin Rafiudeen, T. Srinivasa Reddy, Shaheer Cheemadan, M.C. Santhosh Kumar, National Institute of Technology, Tiruchirappalli (India)

ZnO possess distinctive characteristics such as low cost, wide band gap (3.36 eV) and large exciton binding energy (60meV). As the band gap lies in ultra violet (UV) region, ZnO is considered as a novel material for the fabrication of ultra violet light emitting diodes (UV-LEDs). However, ZnO being intrinsic n-type semiconductor the key challenge lies in realization of stable and reproducible p-type ZnO. In the present research dual acceptor group-V elements such as P and N are simultaneously doped in ZnO films to obtain the p-type characteristics. The deposition is made by programmable spray pyrolysis technique upon glass substrates at 697K. The optimum doping concentration of P and N were found to be 0.75 at% which exhibits hole concentration of 4.48 x 10¹⁸ cm⁻³ and resistivity value of 9.6 Ω .cm. The deposited p-ZnO were found to be stable for a period over six months. Highly conducting n-type ZnO films is made by doping aluminum (3 at%) which exhibits higher electron concentration of 1.52 x 10¹⁹ cm-3 with lower electrical resistivity of $3.51 \times 10-2 \Omega$.cm. The structural, morphological, optical and electrical properties of the deposited n-ZnO and p-ZnO thin films are investigated. An efficient p-n homojunction has been fabricated using the optimum p-ZnO:(P,N) and n-ZnO:Al layers. The current-voltage (I-V) characteristics show typical rectifying characteristics of p-n junction with a low turn on voltage. Electroluminescence (EL) studies reveals the fabricated p-n homojunction diodes exhibits strong emission features in ultra-violet (UV) region around 378 nm.

9545-22, Session 5

Control of photoinduced fluorescence enhancement of colloidal quantum dots using metal oxides

Seyed M. Sadeghi, Waylin J. Wing, Kira Patty, The Univ. of Alabama in Huntsville (United States)

It is well known that irradiation of colloidal quantum dots can dramatically enhance their emission efficiencies, leading to so-called photoinduced fluorescence enhancement (PFE). This process is the result of the photochemical and photophysical properties of quantum dots and the way they interact with the environment in the presence of light. In this contribution we will discuss the results of our recent investigations regarding the impact of metal oxides on PFE of guantum dots. For this, using spectroscopic techniques, we investigated emission of different types of quantum dots (with and without shell) in the presence of various types of metal oxides while being irradiated with a laser field. We observed significant increase of PFE when quantum dots are deposited on about one nanometer of aluminum oxides, suggesting such oxide can profoundly increase quantum yield of such quantum dots. On the other hand, copper oxide can lead to significant suppression of emission of quantum dots, making them nearly completely dark. We discovered for certain types of quantum dots, aluminum oxide can be used to reduce the adverse impact of photo-oxidation, allowing reduction of guantum dot core sizes without significant increase of their non-radiative decay rates. We discuss these results in terms of impact of aluminum oxide on coulomb blockade caused by photo-ionization in quantum dots and the way laser intensity influence this process. The results of this study show how metal oxides can be used to induce or accelerate certain types of photo-induced processes in quantum dots, providing us unique tools to explore and utilize their photophysics and photochemistry.



9545-23, Session 5

Optical thin film materials and devices for harsh environment, high temperature sensing applications

Paul R. Ohodnicki Jr., Zsolt Poole, Thomas Brown, John Baltrus, National Energy Technology Lab. (United States); Kevin Chen, Aidong Yan, Univ. of Pittsburgh (United States)

Optical sensors display a number of advantages for extreme temperature, harsh environment sensing applications. A research program has therefore been established at the National Energy Technology Laboratory in the area of functional optical sensor materials for harsh environment sensing applications. The presentation will provide an overview of research technical developments in the specific area of optical nanocomposite based sensing layers consisting of metal oxides integrated with noble metal nanoparticles for optical H2 sensing applications at ambient and elevated temperatures.

Two different types of functional sensor layers will be investigated, namely (1) Pd and AuPd-alloy nanoparticle incorporated silica based sensing layers as well as (2) Pd / nanostructured TiO2 based sensing layers. Film characterization results will be presented for films deposited on planar substrates and characteristic elevated temperature sensing responses for fabricated prototype sensors will be presented at temperatures that are relevant for typical fuel gas streams in solid oxide fuel cell applications, for example. The results demonstrate that in the presence of oxidizing gas species at elevated temperatures, oxidation and reduction reactions of Pd-based nanoparticles can play a significant or even dominant role in the measured sensing response. In the absence of oxidizing gas species, responses are likely to be dictated by a combination of characteristic absorption of the oxide matrix and/or the direct interaction H2 with the Pd-based nanoparticles. Theoretical modeling results that help to explain the reported observations will also be discussed.

9545-24, Session 5

Enhanced luminescence excitation via efficient optical energy transfer (Invited Paper)

Roy Aad, Komla D. Nomenyo, Univ. de Technologie Troyes (France); Bogdan Bercu, Univ. de Reims Champagne-Ardenne (France); Christophe Couteau, Univ. de Technologie Troyes (France); Vincent Sallet, Univ. de Versailles Saint-Quentin-en Yvelines (France); David J. Rogers, Nanovation (France); Michael Molinari, Univ. de Reims Champagne-Ardenne (France); Gilles Lérondel, Univ. de Technologie Troyes (France)

Luminescent nanoscale materials (LNMs) have received widespread interest in sensing and lighting applications due to their enhanced emissive properties. For sensing applications, LNMs offer improved sensitivity and fast response time which allow for lower limits of detection. Meanwhile, for lighting applications, LNMs, such as quantum dots, offer an improved internal quantum efficiency and controlled color rendering which allow for better lighting performances. Nevertheless, due to their nanometric dimensions, nanoscale materials suffer from extremely weak luminescence excitation (i.e. optical absorption) limiting their luminescence intensity, which in turn results in a downgrade in the limits of detection and external quantum efficiencies. Therefore, enhancing the luminescence excitation is a major issue for sensing and lighting applications.

In this work, we report on a novel photonic approach to increase the luminescence excitation of nanoscale materials. Efficient luminescence excitation increase is achieved via a gain-assisted waveguided energy transfer (G-WET). The G-WET concept consists on placing nanoscale materials atop of a waveguiding active (i.e. luminescent) layer with optical gain. Efficient energy transfer is thus achieved by exciting the nanoscale

material via the tail of the waveguided mode of the active layer emission. The G-WET concept is demonstrated on both a nanothin layer of fluorescent sensitive polymer and on CdSe/ZnS quantum dots coated on ZnO thin film, experimentally proving up to an 8-fold increase in the fluorescence of the polymer and a 3-fold increase in the luminescence of the CdSe/ZnS depending of the active layer emission regime (stimulated vs spontaneous emission). Furthermore, we will discuss on the extended G-WET concept which consists on coating nanoscale materials on a nanostructured active layer. The nanostructured active layer offers the necessary photonic modulation and a high specific surface which can presumably lead to a more efficient G-WET concept. Finally, the efficiency as well as the observation conditions of the GWET will be discussed and compared with more conventional charge transfer or dipole-dipole energy transfer.

9545-25, Session 6

Optical property tuning of bismuth chalcogenides using chemical intercalation (Invited Paper)

Jie Yao, Univ. of California, Berkeley (United States)

Two-dimensional (2D) materials with natural layer structures have been proven to provide extraordinary physical and chemical properties. Bismuth chalcogenides are examples of such two-dimensional materials. They are strongly bonded within layers and weak van der Waals interaction ties those layers together. Such naturally layered structure allows chemical intercalation of foreign atoms into the van der Waals gaps. Here, we show that by adding large number of copper atoms into van der Waals gaps of bismuth chalcogenides, we observed counter-intuitive enhancement of optical transparency together with improved electrical conductivity, which is on the contrary to most bulk materials in which doping reduces the light transmission. This surprising behavior is caused by substantial tuning of material optical property and nanophotonic anti-reflection effect unique to ultra-thin nanoplates. With the intercalation of copper atoms, large number of electrons have been added into the semiconducting material system and effectively lift the Fermi level of the resulting material to its conduction band, as proved by our density-functional-theory computations. Occupied lower states in the conduction band do not allow the optical excitation of electrons in the valence band to the bottom of the conduction band, leading to an effective widening of optical band gap. Optical transmission is further enhanced by constructive interference of reflected beams as bismuth chalcogenides have large permittivity than the environment. The synergy of these two effects in two-dimensional nanostructures can be exploited for various optoelectronic applications including transparent electrode. The reversible intercalation process allows potential dynamic tuning capability.

9545-26, Session 6

Utilizing homogenous FRET to extend molecular photonic wires beyond 30 nm

Sebastian A. Diaz, Susan Buckhout-White, Mario G. Ancona, Joseph S. Melinger, Igor L. Medintz, U.S. Naval Research Lab. (United States)

Molecular photonic wires (MPWs) present interesting applications in energy harvesting, artificial photosynthesis, and nano-circuitry. MPWs allow the directed movement of energy at the nanoscopic level. Extending the length of the energy transfer with a minimal loss in efficiency would overcome an important hurdle in allowing MPWs to reach their potential. We investigated Homogenous Förster Resonance Energy Transfer (HomoFRET) as a means to achieve this goal. We designed a simple, self-assembled DNA nanostructure with specifically placed dyes (Alexa488-Cy3-Cy3.5-Alexa647-Cy5.5) at a distance of 3.4 nm, a separation at which energy transfer should theoretically be very high. The input of the wire was at 466 nm with an output up to 697 nm. Different structures were studied where the Cy3.5 section of the MPW was extended from one to six repeats. We found that though the efficiency cost is not null, HomoFRET can be extended up to six repeat dyes with only a 22% efficiency loss when compared to a



single step system. The advantage is that these six repeats created a MPW which was 17 nm longer, almost 2.5 times the initial length. To confirm the existence of HomoFRET between the Cy3.5 repeats fluorescence lifetime and fluorescence lifetime anisotropy was measured. Under these conditions we are able to demonstrate the energy transfer over a distance of 30.4 nm, with an end-to-end efficiency of 2.0%, by utilizing a system with only five unique dyes.

9545-27, Session 6

TiO2 membranes for concurrent photocatalytic organic degradation and corrosion protection

Robert Liang, Melisa Hatat, Horatio He, Y. Norman Zhou, Univ. of Waterloo (Canada)

Organic contaminants and corrosion products in water treatment effluents are a current and emerging global problem and the development of effective methods to facilitate the removal of organic contaminants and create effective corrosion control strategies are required to mitigate this problem. TiO2 nanomaterials that are exposed to UV light can generate electron-hole pairs, which undergo redox reactions to produce hydroxyl radicals from adsorbed molecular oxygen. They hydroxyl radicals are able to oxidize organic contaminants in water. This same process can be used in conjunction to protect metals from corrosion via cathodic polarization. In this work, TiO2 nanomaterials were synthesized and deposited as films on conductive substrates via electrophoretic deposition. These films were characterized for their material and structural properties using XRD, XPS, and SEM. An illuminated TiO2 film on a conductive surface served as the photoanode and assisted in the cathodic protection of steel and the degradation of organic pollutants, in this case glucose. This proof-ofconcept relied on photoelectrochemical experiments conducted using a potentiostat and a xenon lamp illumination source to mimic solar radiation. The open-circuit potential changes along with weight loss measurements was measured and determined whether a metal was protected from corrosion under illumination. The electrical characteristics of the TiO2 film or membrane under dark and arc lamp illumination conditions were analyzed using electrochemical impedance spectroscopy. Furthermore, the effect of organic contaminants on the photocathodic protection mechanism and the oxidation of glucose during this process were explored.

9545-28, Session 6

Optically active quantum dots

Yurii K. Gun'ko, Trinity College Dublin (Ireland)

The main goal of our research is to develop new types of technologically important optically active quantum dot (QD) materials, study their properties and explore their applications. For the first time chiral II-VI QDs (penicillamine stabilised) have been prepared by us using microwave induced heating with the racemic (Rac), D- and L-enantiomeric forms of penicillamine as stabilisers. Circular dichroism (CD) studies of these QDs have shown that D- and L-penicillamine stabilised particles produced mirror image CD spectra, while the particles prepared with a Rac mixture showed only a weak signal. It was also demonstrated that these QDs show very broad emission bands between 400 and 700 nm due to defects or trap states on the surfaces of the nanocrystals. These QDs have demonstrated highly specific chiral recognition of various biological species including aminoacids and DNA. The utilisation of chiral stabilisers also allowed the preparation of new water soluble white emitting CdS nano-tetrapods, which demonstrated circular dichroism in the band-edge region of the spectrum. Biological testing of chiral CdS nanotetrapods displayed a chiral bias for an uptake of the D- penicillamine stabilised nano-tetrapods by cancer cells. Then we have developed a range of ZnS and ZnSe based chiral nanostructures have doped them by various metal ions. These nanostructures have been used for in vitro photodynamic therapy studies. It is expected that this research will open new horizons in the chemistry of chiral nanomaterials and their application in nanobiotechnology, photonics, medicine and optical chemo- and bio-sensing.

Conference 9546: Active Photonic Materials VII

Sunday - Thursday 9-13 August 2015

Part of Proceedings of SPIE Vol. 9546 Active Photonic Materials VII



9546-1, Session 1

Meta-infrared detectors for 4th generation infrared imagers (Invited Paper)

Sanjay Krishna, The Univ. of New Mexico (United States)

There is an increased emphasis on obtaining detectors with spectropolarimetric functionality at the pixel level. Meta-infrared detectors in which infrared detectors are combined with metamaterials are a promising way to realize this. The infrared region is appealing due to the low metallic loss, large penetration depth of the localized field and the larger feature sizes compared to the visible region. We will discuss approaches to realize multicolor detectors using these approaches.

9546-2, Session 1

Wideband and wide angle thermal emitters for use as lightbulb filaments

Christopher H. Granier, Simon G. Lorenzo, Jonathan P. Dowling, Georgios Veronis, Louisiana State Univ. (United States)

Lighting is a field that has been widely researched. Recently this research has been focused on creating energy-efficient visible light sources. One of the most recently commercially introduced products is the light emitting diode (LED) bulb, which is highly energy efficient; however, these bulbs are extremely expensive. Compact fluorescent bulbs (CFL) are energy-efficient and less expensive. While CFL bulbs are cheaper than LED bulbs, they contain toxic mercury and are more expensive than traditional tungstenfilament based bulbs. Tungsten bulbs are extremely cheap to mass produce and contain no poisonous elements; however, they are the most energy inefficient of any bulb used today. Here, we present optimized aperiodic structures for use as broadband, broad-angle thermal emitters which are capable of drastically increasing the efficiency of tungsten lightbulbs. Onedimensional layered structures without texturing are preferable to more complex two- and three-dimensional structures because of the relative ease and low cost of fabrication. These aperiodic multilayer structures designed with alternating layers of tungsten and air or tungsten and silicon carbide on top of a tungsten substrate exhibit broadband emittance peaked around the center of the visible wavelength range. We design structures using a genetic optimization algorithm coupled to a transfer matrix code which computes thermal emittance. We investigate the properties of these genetic-algorithm-optimized aperiodic structures for use as filaments in lightbulbs, and compare their performance with conventional lightbulbs. We find that the genetic-algorithm-optimized structures greatly enhance the emittance over the visible wavelength range, while also increasing the overall efficiency of the bulb.

9546-3, Session 1

Intensity tunable mid-wavelength infrared broadband absorbers based on planar nanometric film coatings employing thermochromic phase change material

Hasan Kocer, Turkish Military Academy (Turkey); Serkan Bütün, Edgar Palacios, Zizhuo Liu, Koray Aydin, Northwestern Univ. (United States)

Spectrally selective resonant absorption can be achieved using plasmonic and metamaterial based nano/micro-structured materials, where the resonant bandwidth and absorption intensity can be engineered by controlling the size and geometry of nanostructures. Here, a simple, lithography-free approach was demonstrated for obtaining a resonant and dynamically tunable broadband absorber based on vanadium dioxide (VO2) thermochromic phase transition. Using metal-insulator-metal planar nanometric film coatings, where top layer is chosen to be an ultrathin (20 nm) VO2 film, broadband, angular and polarization-independent IR light absorption tuning (from ~90 % to ~30 % in measured absorption intensity) was demonstrated over the entire mid wavelength infrared spectrum. VO2 undergoes a structural transition from an insulating phase to a metallic phase at 68 °C. This reversible phase change occurs on a sub-picosecond timescale. In order to better understand the absorption mechanism in VO2 based absorbers for two different phases, local electric field intensities and absorbed powers were calculated for insulator VO2 and metal VO2 based absorbers at 4 μ m wavelength using finite difference time domain simulations. The numerical and experimental results indicate that the bandwidth of the absorption bands can be controlled by changing the dielectric spacer layer thickness. Broadband tunable absorbers can find applications in absorption filters, thermal emitters, thermophotovoltaics and sensina.

9546-4, Session 1

Optimization of Er and Yb dopant concentrations and ratios for efficient high-brightness mid-infrared light sources

Behsan Behzadi, Mani Hossein-Zadeh, Ravi Jain, The Univ. of New Mexico (United States)

We will describe our experimental and theoretical studies on the optimization of the Er and Yb concentrations for high-brightness midinfrared light sources. Although many aspects of these studies apply to numerous host crystals and glasses, our initial studies have focused on ZBLAN glasses as hosts, and the impact of this data on the design of next-generation mid-infrared fiber and microresonator lasers and luminescent sources in the 3 um spectral region. High doping densities (> 5 mol%) of Er and Yb are preferred for high pump absorption, particularly for the small dimensions of the doped 3 um microresonator lasers, but the density and ratio of these dopants have to selected carefully for optimization of the Pb-Er forward energy transfer, and appropriate optimization of the energy transfer upconversion processes and the upper and lower laser lifetimes and their ratios.

9546-5, Session 1

Phased arrays based on second harmonic generation from metamaterials coupled to semiconductor heterostrustures (Invited Paper)

Omri Wolf, Salvatore Campione, Alexander Benz, Sandia National Labs. (United States); Arvind P. Ravikumar, Princeton Univ. (United States); Sheng Liu, Ting S. Luk, Emil A. Kadlec, Eric A. Shaner, John F. Klem, Michael B. Sinclair, Igal Brener, Sandia National Labs. (United States)

No Abstract Available

9546-6, Session 2

Hybrid optical-thermal nanoantennas for enhanced light focusing and radiative cooling (Invited Paper)

Svetlana V. Boriskina, Gang Chen, Massachusetts Institute of Technology (United States)



Metallic nanoparticles supporting localized surface plasmon resonances have become an indispensable tool in sensing and nanoscale imaging applications. However, the high plasmon-enhanced electric field intensity in the visible and near-IR range that enables the above applications also causes excessive heating of metal nanoparticles, which is a major drawback in plasmonics. In my talk I will discuss the design of hybrid optical-thermal nano-antennas that simultaneously enable intensity enhancement at the operating wavelength in the visible and reduction of the operating temperature via a combination of reduced absorption and radiative cooling.

9546-7, Session 2

Broadband nonresonant funneling of light via ultrasubwavelength channels

Ganapathi S. Subramania, Sandia National Labs. (United States); Stavroula Foteinopoulou, The Univ. of New Mexico (United States); Igal Brener, Sandia National Labs. (United States)

Efficient control of light-matter interaction at deeply subwavelength scales is key to many photonics applications such as detectors, sensors and novel light sources. Enhancing and funneling light efficiently through nanoscale channels can dramatically improve the performance of such devices by making them compact and more efficient. Currently, this is accomplished by utilizing the extraordinary optical transmission phenomenon wherein structural surface plasmon resonances are excited in perforated nanostructured metal films. As a result the phenomenon is inherently narrowband with low transmission. Here, we introduce a new paradigm structure consisting of a double-grooved metallic nanostructure platform that can outperform extraordinary optical transmission structures while operating nonresonantly across broadband (Phys. Rev. Lett. 107, 163902(2011)). Our platform consists of a continuous periodic metallic nanostructure composed of an array of connected large (~100-200nm) and small (~ 15-20nm) rectangular slits. The key feature of our platform is that the optical power can be channeled through an area as small as ~ (?/500)2 associated with optical field enhancement and high transmission while operating across a broad wavelength band in the mid-infrared (~ 2- 20 ?m). We will discuss the nonresonant mechanism underlying this phenomenon based on a simple quasistatic picture that shows excellent agreement with our numerical simulations.

We will also show experimental implementations of this platform and discuss pertinent results.

Sandia National Laboratories is a multi-program laboratory managed and operated by Sandia Corporation, a wholly owned subsidiary of Lockheed Martin Corporation, for the U.S. Department of Energy's National Nuclear Security Administration under contract DE-AC04-94AL85000.

9546-8, Session 2

Mid-IR phonon-polaritonics: superabsorpion and super-steering (Invited Paper)

Ganga C. R. Devarapu, Univ. of St Andrews (United Kingdom); Stavroula Foteinopoulou, The Univ. of New Mexico (United States)

Plasmonics has been a growing field in the last decade, exploring strong light control by resonant coupling between light and free electron oscillations at nanostructured metal surfaces. However, metals respond only poorly to mid-IR light, as the light penetration depth, known as skin-depth, is very small at such frequencies. The exciting physics and capabilities of plasmonics is transferrable to the mid-IR regime with materials of strong phonon-resonant response to EM radiation. We discuss here judicious designs of such phonon-polaritonic microstructures that can demonstrate near-perfect absorption within a thin material layer as thick as one-thousandth the impinging lights wavelength, highly asymmetric absorption as well as super-steering of a light beam beyond 90 deg.

9546-9, Session 3

Recent progress in photonic crystals and their device applications (*Invited Paper*)

Susumu Noda, Kyoto Univ. (Japan)

No Abstract Available

9546-10, Session 3

Photonic crystal enhanced light emission from silicon (Invited Paper)

Liam O'Faolain, Univ. of St. Andrews (United Kingdom)

Realising efficient light emission from silicon is a major challenge for silicon photonics due to the material's indirect band gap. Overcoming this barrier would enable a host of important applications ranging from low power optical interconnects to biosensing. In this work, we take both a material and device engineering route. We deposit the optically active ytterbium disilicate on top of a silicon photonic crystal nanocavity. We demonstrate an enhancement of the Erbium emission due to the coupling with the cavity fundamental modes and show that the concentration in the excited state is about 30%

9546-11, Session 3

Exploiting lossy resonances for arbitrary nonlinear power response (Invited Paper)

Michelle L. Povinelli, Roshni Biswas, The Univ. of Southern California (United States)

No Abstract Available

9546-12, Session 3

Near thresholdless laser operation at room temperature (Invited Paper)

Pablo A. Postigo, Instituto de Microelectrónica de Madrid (Spain)

We report a near-thresholdless laser operating at room temperature under continuous wave excitation [1]. Our laser is based on a two-dimensional photonic crystal cavity on GaAs material [2] coupled to a single embedded layer of self-assembled InAsSb quantum dots (QDs), which provides efficient luminescence at room temperature [3]. Laser emission centered at the 1.3 ?m telecommunications window is obtained with a spontaneous coupling factor ?=0.85 and a threshold of 861 nW in net absorbed power. Our results demonstrate the feasibility to produce near thresholdless laser operation at room temperature for on-chip applications.

[1] I. Prieto et al., "Near thresholdless laser operation at room temperature" Optica, Vol. 2 Issue 1, pp.66-69 (2015)

[2] I. Prieto et al., "Fabrication of high quality factor GaAs/InAsSb photonic crystal microcavities by inductively coupled plasma etching and fast wet etching," J. Vac. Sci. Technol. B 32, 011204 (2014).

[3] A. G. Taboada et al., "Effect of Sb incorporation on the electronic structure of InAs quantum dots," Phys. Rev. B 88, 085308 (2013).



9546-13, Session 4

Transverse Anderson localization and image transport through disordered fibers (Invited Paper)

Arash Mafi, The Univ. of New Mexico (United States); Salman Karbasi, Univ. of California, San Diego (United States); John Ballato, Clemson Univ. (United States); Karl Koch, Corning Incorporated (United States)

Disordered optical fibers show novel waveguiding properties that can be used for various device applications, such as beam-multiplexed optical communications and endoscopic image transport. The quality of the transported image is shown to be comparable with or better than some of the best commercially available multicore image fibers with less pixelation and higher contrast. Design, fabrication, characterization, and on-going efforts on the best practices for image transport in disordered optical fibers will be discussed. Novel nonlinear behavior of these fibers will also be covered.

9546-14, Session 4

Hyperuniform photonic slabs for high-Q cavities and low-loss waveguides

Timothy Amoah, Marian Florescu, Univ. of Surrey (United Kingdom)

Hyperuniform disordered photonic structures are a new class of photonic solids, which display large, isotropic photonic band gaps (PBG) comparable in size to the ones found in photonic crystals. The existence of large band gaps in HUD structures contradicts the long-standing intuition that Bragg scattering and long-range translational order is required in PBG formation, and demonstrates that interactions between "Mie-like" local resonances and multiple scattering can induce on their own PBGs.

The HUD structures combine advantages of both statistical isotropy due to disorder character and controlled scattering properties due to hyperuniformity (due to constraints imposed on the disorder) and uniform local topology.

Using FDTD and band structure simulations, we demonstrate efficient confinement of TE radiation and high-Q optical cavities and low-loss waveguides, in a trihedrally coordinated "relaxed" network lattice obtained from a centroidal tessellation protocol. For two-dimensional structures, quality factors exceeding Q > 10⁻⁹ are achieved. We further show that for 3D finite-height photonic slab high quality factors exceeding Q > 20, 000 can be maintained. Moreover, a multitude of cavity modes can be obtained, which can be classified according to their symmetry (monopole, dipole, quadrupole, etc.) of the confined electromagnetic wave pattern.

Our results put to rest the presumption that disorder would induce significant out of plane scattering in disordered structures as compared to their periodic counterparts and demonstrate the ability of disordered HUD PBG materials to serve as a general-purpose design platform for integrated optical micro-circuitry, including active devices such as optical microcavity lasers and modulators.

9546-15, Session 4

Periodic, quasiperiodic, aperiodic, and random plasmon particle array lasers (Invited Paper)

A. Femius Koenderink, Hinke Schokker, FOM Institute for Atomic and Molecular Physics (Netherlands)

No Abstract Available

9546-16, Session 4

Engineering active aperiodic nanostructures (Invited Paper)

Luca Dal Negro, Boston Univ. (United States)

Efficient approaches to electromagnetic field localization and enhancement are essential for optoelectronic components that leverage broadband enhancement of optical cross sections, such as optical biosensors, photodetectors, light sources and on-chip nonlinear elements. In this context, the ability to tailor light-matter interactions by aperiodic order in metal-dielectric nanostructures can provide exciting opportunities. In this talk, I will discuss recent work on the development of aperiodic structures with enhanced radiation rates over broad frequency spectra. Tuning light propagation and diffusion in aperiodic metamaterials will be discussed, and applications to solar harvesting and broadband lasers with structured emission will be presented.

9546-17, Session 5

Understanding disordered materials for new unconventional light sources (Invited Paper)

Cefe López, Consejo Superior de Investigaciones Científicas (Spain)

No Abstract Available

9546-18, Session 5

High Q photonic crystal cavities realized using deep ultraviolet lithography

Liam O'Faolain, Univ. of St. Andrews (United Kingdom)

As extremely precise fabrication processes are required for the realisation of high performance PhCs, Ultra-high Q PhC cavities demonstrated to date have been patterned using electron beam lithography because not only must the etched sidewalls be vertical and smooth but positioning accuracies at the nanometre level are also. To date, tThihis combination has prevented the realisation of high Q-factor devices using Deep-UV Photolithography (DUV), a key prerequisite for the mass manufacturing of silicon based optical devices. For example, DUV photomasks typically have a 5-10nm design grid (minimum increment in feature position), which prevents the nanometer scale positioning required for most ultra-high Q cavity designs. In this work, we use a recently developed 2D PhC resonator design that shows increased tolerance to fabrication imperfections and improved compatibility with DUV patterning to realise high optical Q-factors of ~200,000.

9546-19, Session 5

3D optical metamaterials formed by holographic assembly and directed solidification of eutectics (*Invited Paper*)

Paul V. Braun, Univ. of Illinois at Urbana-Champaign (United States)

Nanoscale integration of materials in three dimensions is critical for the realization of a number of highly functional optical metamaterials. Starting with structures enabled via eutectic solidification and holographic lithography, our team is applying unique template-based and post-synthetic materials transformations in conjunction with powerful computational design tools to develop the scientific underpinnings of, and to produce, 3D metamaterials derived from directionally solidified eutectics. Our approach



involves close interactions among computational design, photonic theory, eutectic materials development, template fabrication, materials chemistry, and optical characterization.

9546-20, Session 6

Highly-nonlinear quantum-engineered polaritonic metasurfaces (Invited Paper)

Mikhail A. Belkin, The Univ. of Texas at Austin (United States)

Intersubband transitions in n-doped semiconductor heterostructures provide the possibility to guantum engineer one of the largest known nonlinear optical responses in condensed matter systems, limited however to electric field polarized normal to the semiconductor layers. We have recently integrated these nonlinearities into laser waveguides to produce room-temperature terahertz quantum cascade laser sources based on efficient intra-cavity difference-frequency mixing [1,2]. Here we show that by coupling of electromagnetic modes in plasmonic metasurfaces with guantum-engineered intersubband transitions in semiconductor heterostructures one can create ultra-thin highly-nonlinear polaritonic metasurfaces for normal light incidence. Experimentally, we realized midinfrared metasurfaces with giant electro-optic effect that display ultrafast electrical tuning of reflectivity [3] and giant nonlinearity for second harmonic generation [4]. Structures discussed here represent a novel kind of hybrid metal-semiconductor metamaterials in which exotic optical properties are produced by coupling electromagnetically-engineered modes in dielectric and plasmonic nanostructures with quantum-engineered intersubband transitions in semiconductor heterostructures.

[1] K. Vijayraghavan, Y. Jiang, M. Jang, A. Jiang, K. Choutagunta, A. Vizbaras, F. Demmerle, G. Boehm, M. C. Amann, and M. A. Belkin, "Broadly tunable terahertz generation in mid-infrared quantum cascade lasers," Nature Commun. 4, 2021 (2013).

[2] S. Jung, A. Jiang, Y. Jiang, K. Vijayraghavan, X. Wang, M. Troccoli, and M.A. Belkin "Broadly tunable monolithic room-temperature terahertz quantum cascade laser sources," Nature Comm., 5, 4267 (2014).

[3] J. Lee, S. Jung, P. Y. Chen, F. Lu, F. Demmerle, G. Boehm, M. C. Amann, A. Alu, and M.A. Belkin, "Ultrafast electrically tunable polaritonic metasurfaces," Adv. Opt. Matt., 2, 1057-1063 (2014).

[4] J. Lee, M. Tymchenko, C. Argyropoulos, P. Y. Chen, F. Lu, F. Demmerle, G. Boehm, M. C. Amann, A. Alu, and M.A. Belkin, "Giant nonlinear response from plasmonic metasurfaces coupled to intersubband transitions," Nature, 511, 65 (2014).

9546-21, Session 6

Alternative materials lead to practical nanophotonic components (Invited Paper)

Nathaniel Kinsey, Purdue Univ. (United States); Marcello Ferrera, Purdue Univ. (United States) and Heriot-Watt Univ. (United Kingdom); Clayton DeVault, Jongbum Kim, Alexander V. Kildishev, Vladimir M. Shalaev, Alexandra Boltasseva, Purdue Univ. (United States)

Recently, there has been a flurry of research in the field of alternative plasmonic materials, but for telecommunication applications, CMOS compatible materials titanium nitride and doped zinc oxides are among the most promising materials currently available. TiN is a gold-like ceramic with a permittivity cross-over near 500nm. In addition, TiN can attain ultra-thin, ultra-smooth epitaxial films on substrates such as c-sapphire, MgO, and silicon. Partnering TiN with CMOS compatible silicon nitride enables a fully solid state waveguide which is able to achieve a propagation length greater than 1cm for a ~8?m mode size at 1.55?m.

Utilizing doped zinc oxide films as a dynamic material, high performance modulators can also be realized due to the low-loss achieved by the TiN/Si3N4 waveguide. Simply by placing a thin layer of aluminum doped zinc

oxide (AZO) on top of the waveguide structure, a modulator with very low insertion loss is achieved. Our recent work has investigated optical tuning of AZO films by the pump-probe method, demonstrating a change in the refractive index of -0.17+0.25i at 1.3?m with an ultrafast response of 1ps. Assuming this change in the refractive index for the AZO film, a modulation of ~0.7dB/?m is possible in the structure with ~0.5dB insertion loss and an operational speed of 1THz. Further optimization of the design is expected to lead to an increased modulation depth without sacrificing insertion loss or speed.

Consequently, nanophotonic technologies are reaching a critical point where many applications including telecom, medicine, and quantum science can see practical systems which provide new functionalities.

9546-22, Session 6

Understanding carrier injection effects upon the Reststrahlen band of SiC using transient infrared spectroscopy

Bryan T. Spann, Ryan Compton, Adam D. Dunkelberger, James P. Long, U.S. Naval Research Lab. (United States); Paul Klein, Sotera Defense Solutions, Inc. (United States); Daniel Ratchford, Josh D. Caldwell, Jeff C. Owrutsky, U.S. Naval Research Lab. (United States)

Sub-diffractional confinement of light has led to advancements in imaging, metamaterials, nano-manufacturing, plasmonics, and other fields. One potential route to sub-diffractional confinement is via stimulated surface phonon polaritons (SPhPs). SPhPs couple infrared photons with optical phonons and consequently their lifetimes can be longer than surface plasmon polaritons (SPPs), whose lifetimes are dominated by electron scattering events. Thus, materials capable of generating SPhPs are of general interest to study. SPhPs are activated by photons with energies near the Reststrahlen band of semiconductors such as SiC. In this work we examine aspects of carrier dynamics by photo-injecting electrons into the SiC conduction band using a pulsed 355 nm laser and probe the resulting dynamics near the Reststrahlen band using a tunable CO2 laser. The fluence of the pump laser was varied to provide photo-injection levels ranging from ~1x10^17 to 1x10^19 free carriers. Probing the excited-state dynamics near the blue-edge of the Reststrahlen band resulted in complex transient behavior, showing both positive and negative changes in transient reflectance depending on the level of photo-injected carriers and probe energy. Numerical calculations of the SiC reflectance spectra with different doping levels were done to simulate the initial photo-injection level provided by the transient experiment. The computed spectra and the experimentally measured excited spectra for different photo-injection levels were compared and resulted in qualitative agreement.

9546-23, Session 6

Ultrafast dynamics of Al-doped zinc oxide under optical excitation

Nathaniel Kinsey, Clayton T. DeVault, Jongbum Kim, Purdue Univ. (United States); Marcello Ferrera, Purdue Univ, (United States) and Heriot-Watt Univ. (United Kingdom); Alexander V. Kildishev, Vladimir M. Shalaev, Alexandra Boltasseva, Purdue Univ. (United States)

There is a continual need to explore new and promising dynamic materials to power next-generation switchable devices. In recent years, transparent conducting oxides have been shown to be vital materials for such systems, allowing for both optical and electrical tunability. Using a pump-probe technique, we investigate the optical tunability of CMOS-compatible, highly aluminum doped zinc oxide (AZO) thin films. The sample was pumped at 325 nm and probed with a weak beam at 1.3 ?m to determine the timescale and magnitude of the changes by altering the temporal delay between the pulses with a delay line.



For an incident fluence of 3.9 mJ/cm2 a change of 40% in reflection and 30% (max 6.3dB/?m modulation depth) in transmission is observed which is fully recovered within 1ps. Using a computational model, the experimental results were fitted for the given fluence allowing the recombination time and induced carrier density to be extracted. For a fluence of 3.9 mJ/cm2 the average excess carrier density within the material is $0.7?10^{-}20\text{cm}{-}3$ and the recombination time is 88fs. The ultrafast temporal response is the result of Auger recombination due to the extremely high carrier concentration present in our films, $-10^{-}21 \text{ cm}{-}3$. By measuring and fitting the results at several incident fluence levels, the recombination time versus carrier density was determined and fitted with an Auger model resulting in an Auger coefficient of C = $1.03?10^{-}20\text{cm}{-}6\text{sec}$. Consequently, AZO is shown to be a unique, promising, and CMOS-compatible material for high performance dynamic devices in the near future.

9546-24, Session 6

Advanced electrodynamic mechanisms for the nanoscale control of light by light (Invited Paper)

David L. Andrews, Univ. of East Anglia (United Kingdom)

A wide range of mechanisms is available for achieving rapid optical responsivity in material components. Amongst them, some of the most promising for potential device applications are those associated with an ultrafast response and a short cycle time. These twin criteria for photoresponsive action substantially favor optical, over most other, forms of response such as those fundamentally associated with photothermal, photochemical or optomechanical processes.

The engagement of nonlinear mechanisms to actively control the characteristics of optical materials is not new. Indeed, it has been known for over fifty years that polarization effects of this nature occur in the optical Kerr effect – although in fluid media the involvement of a molecular reorientation mechanism leads to a significant response time. It has more recently emerged that there are other, less familiar forms of optical nonlinearity that can provide a means for one beam of light to instantly influence another. In particular, major material properties such as absorptivity or emissivity can be subjected to instant and highly localized control by the transmission of light with an off-resonant wavelength.

This presentation introduces and compares the key electrodynamic mechanisms, discussing the features that suggest the most attractive possibilities for exploitation. The most significant of such mechanistic features include the off-resonant activation of optical emission, the control of excited-state lifetimes, the access of dark states, the inhibition or redirection of exciton migration, and a coupling of stimulated emission with coherent scattering. It is shown that these offer a variety of new possibilities for ultrafast optical switching and transistor action, ultimately providing all-optical control with nanoscale precision.

9546-25, Session 7

Photonic quantum technologies (Invited Paper)

Jeremy L. O'Brien, Univ. of Bristol (United Kingdom)

The impact of quantum technology will be profound and far-reaching: secure communication networks for consumers, corporations and government; precision sensors for biomedical technology and environmental monitoring; quantum simulators for the design of new materials, pharmaceuticals and clean energy devices; and ultra-powerful quantum computers for addressing otherwise impossibly large datasets for machine learning and artificial intelligence applications. However, engineering quantum systems and controlling them is an immense technological challenge: they are inherently fragile; and information extracted from a quantum system necessarily disturbs the system itself. Of the various approaches to quantum technologies, photons are particularly appealing for their low-noise properties and ease of manipulation at the single qubit level. We have developed an integrated waveguide approach to photonic quantum circuits for high performance, miniaturization and scalability. We will described our latest progress in generating, manipulating and interacting single photons in waveguide circuits on silicon chips.

9546-26, Session 7

Deterministic placement of fabricated InGaN quantum dots in photonic structures (Invited Paper)

Arthur J. Fischer, Xiaoyin Xiao, Ping Lu, Ganapathi S. Subramania, Jeffrey Y. Tsao, Daniel D. Koleske, Sandia National Labs. (United States)

InGaN quantum dots (QDs) are desired for a wide variety of applications including emitters for full-color compact projectors, solid state lighting, and single photon sources. InGaN QDs can be fabricated using a process called quantum-size-controlled photoelectrochemical (PEC) etching where quantum size effects enable a self-terminated etch process. The process starts with InGaN quantum wells (QWs) which are PEC-etched to form layers of QDs. QW emission at ~500 nm can be blue-shifted by almost 100 nm via PEC etching showing a dramatic increase in confinement when going from QWs to QDs. Photoluminescence linewidths as narrow as 6 nm FWHM have been observed at low temperature for ensembles of PEC-etched QDs showing an improved size distribution compared to Stranski-Krastanov QDs. This process can potentially produce extremely uniform QD size distributions which would be very beneficial for QD laser diodes. At the same time, this process also has the potential to allow for deterministic placement of QDs at specific locations, for example at a field maximum in a photonic structure. Through careful device design, it is possible to perform PEC etching and to leave a single InGaN QD inside a photonic crystal cavity at the optimum position for efficient emitter-cavity coupling. This has clear implications for use in single photon sources for quantum information processing applications. Sandia National Laboratories is a multiprogram laboratory managed and operated by Sandia Corporation, a wholly owned subsidiary of Lockheed Martin Corporation, for the U.S. Department of Energy's National Nuclear Security Administration under contract DE-AC04-94AL85000.

9546-27, Session 7

Towards scalable networks of solid state quantum memories in a photonic integrated circuit (Invited Paper)

Dirk R. Englund, Massachusetts Institute of Technology (United States)

A central goal of quantum information science is the entanglement of multiple quantum memories that can be individually controlled. Here, we discuss progress towards photonic integrated circuits designed to enable efficient optical interactions between multiple spin qubits in nitrogen vacancy (NV) centers in diamond. We describe NV-nanocavity systems in the strong Purcell regime with optical quality factors approaching 10,000 and electron spin coherence times exceeding 200 ?s; implantation of NVs with nanometer-scale apertures, including into cavity field maxima; hybrid on-chip networks for integration of multiple functional NV-cavity systems; and scalable integration of superconducting nanowire single photon detectors on-chip.

9546-28, Session 7

Quantum optics in directional onedimensional photonic reservoirs (Invited Paper)

Immo Söllner, Peter Lodahl, Niels Bohr Institute (Denmark)



We present a novel photonic crystal waveguide, engineered to support broadband modes with circular in-plane polarization. We show experimental evidence that for single-photon emitters with circular dipoles these waveguides act as near-lossless unidirectional photonic reservoirs, where the emission direction is given by the helicity of the dipole. This directional coupling has a strong effect on the scattering of single photons transmitted through the system and we discuss how counter-propagating photons acquire a relative phase of ϖ . Combining this effect with photonic structures that can map a phase to a propagation path, we show how one can create nonreciprocal photonic elements.

9546-29, Session 7

Integrated single photon detectors for chip scale quantum key distribution

(Invited Paper)

Paul S. Davids, Chris DeRose, Nick Martinez, Douglas Trotter, Andrew Starbuck, Andrew Pomerene, Ryan Camacho, Anthony Lentine, Sandia National Labs. (United States)

In this talk, we will present our recent progress in the development of quantum key distribution (QKD) on a chip based on our integrated Si photonics platform. An essential integrated building block in discrete variable chip-scale QKD is a waveguide coupled single photon detector. Our single photon detector is based on a compact separate absorption and multiplication avalanche photodiode device design with integrated waveguide coupling. Various device designs and experimental Geiger mode device characteristics will be presented.

9546-30, Session 7

Integrated laser-written quantum photonics (Invited Paper)

Markus Gräfe, René Heilmann, Armando Perez-Leija, Maxime Lebugle, Diego Guzman-Silva, Matthias Heinrich, Alexander Szameit, Friedrich-Schiller-Univ. Jena (Germany)

No Abstract Available

9546-31, Session 8

Whispering-gallery-mode optical resonators around an exceptional point (Invited Paper)

Bo Peng, Sahin K. Ozdemir, Huzeyfe Yilmaz, Washington Univ. in St. Louis (United States); M. Liertzer, Technische Univ. Wien (Austria); Faraz Monifi, C. M. Bender, Washington Univ. in St. Louis (United States); Franco Nori, RIKEN (Japan) and Univ. of Michigan (United States); Lan Yang, Washington Univ. in St. Louis (United States)

I will report our experiments on unconventional control of light flow in highquality whispering-gallery-mode (WGM) resonators around an exceptional point (EP), which is characterized by the coalescence of the eigenvalues and eigenstates of a system. The presence of an EP affects the system significantly, leading to nontrivial physics with interesting counterintuitive features. In the experiment, we show that when the resonator system is operated in the vicinity of an EP, the effect of loss could be reversed. Specifically, we demonstrate that the lasing power increases with increasing the loss introduced to the system.

9546-32, Session 8

Ultrafast plasmonic nanowire lasers near the surface plasmon frequency (Invited Paper)

Themistoklis P. H. Sidiropoulos, Imperial College London (United Kingdom); Robert Roder, Sebastian Geburt, Friedrich-Schiller-Univ. Jena (Germany); Ortwin Hess, Stefan A. Maier, Imperial College London (United Kingdom); Carsten Ronning, Friedrich-Schiller-Univ. Jena (Germany); Rupert F. Oulton, Imperial College London (United Kingdom)

No Abstract Available

9546-33, Session 8

III-V GaAs based plasmonic lasers

Lucas Lafone, Ngoc Nguyen, Imperial College London (United Kingdom); Ed Clarke, Univ. of Sheffield (United Kingdom); Paul Fry, The Univ. of Sheffield (United Kingdom); Rupert F. Oulton, Imperial College London (United Kingdom)

Plasmonics is a potential route to new and improved optical devices. Many predict that sub wavelength optical systems will be essential in the development of future integrated circuits, offering the only viable way of simultaneously increasing speed and reducing power consumption. Realising this potential will be contingent on the ability to exploit plasmonic effects within the framework of the established semiconductor industry and to this end we present III-V (GaAs) based surface plasmon laser platform capable of effective laser light generation in highly focussed regions of space. Our design utilises a suspended slab of GaAs with a metallic slot printed on top. Here, hybridisation between the plasmonic mode of the slot and the photonic mode of the slab leads to the formation of a mode with confinement and loss that can be adjusted through variation of the slot width alone. As in previous designs the use of a hybrid mode provides strong confinement with relatively low losses, however the ability to print the metal slot removes the randomness associated with device fabrication and the requirement for etching that can deteriorate the semiconductor's properties. The deterministic fabrication process and the use of bulk GaAs for gain make the device prime for practical implementation.

9546-34, Session 8

Time-resolved lasing dynamics for plasmonic system with gain

Jieran Fang, Jingjing Liu, Zhuoxian Wang, Xiangeng Meng, Ludmila J. Prokopeva, Vladimir M. Shalaev, Alexander V. Kildishev, Purdue Univ. (United States)

To study the light-matter interaction between plasmonic systems and gain media, numerous theoretical and numerical methods have been proposed. Among them, because of its accurate treatment of the quantum property of gain media, the time domain (TD) multi-physics approach is viewed as the most powerful method, especially for analysis of transient dynamics. Even though the finite difference, finite-volume and finite element TD methods can be readily coupled to a multi-level atomic system through auxiliary differential equations, for each of them however there is limited information on accurate TD kinetic parameters fitted with experimental measurements. In this work, we develop a multi-physics time domain model to inspect our most recent lasing experiment with a silver nanohole array. We use a classical finite difference time-domain (FDTD) model coupled to the rate equations of a 4-level gain system. To retrieve kinetic energy parameters for accurate modeling, we first fit 1-D simulations with pump-probe experiments



studying Rhodamine-101 (R-101) dye embedded in epoxy on an indium tin oxide silica substrate. The retrieved parameters are then fed into a 3-D model to study the lasing behavior of the R-101-coated nanohole array. The simulated emission intensity shows a clear lasing effect, which is in good agreement with the experimental measurements. By tracing the population inversion and polarization dynamics, the amplification and lasing regimes inside the nanohole cavity can be clearly distinguished. With the help of our systematic approach, we can further improve understanding of the timeresolved physics of active plasmonic nanostructures with gain.

9546-35, Session 8

Single mode parity-time laser

Zi Jing Wong, Liang Feng, Renmin Ma, Yuan Wang, Xiang Zhang, Univ. of California, Berkeley (United States)

In optoelectronics, optical loss is usually undesired, as it is responsible for power dissipation and light attenuation. The concept of parity-time (PT) symmetry, however, exploits the interplay between the material loss and gain to attain novel optical phenomena such as exceptional point and unidirectional light propagation. Here we experimentally demonstrate a PT symmetry laser that allows unique control of the resonant modes. In contrast to conventional ring cavity lasers with multiple competing modes, our on-chip InGaAsP/InP based PT microring laser exhibits intrinsic singlemode lasing regardless of the gain spectral bandwidth. Thresholdless parity-time symmetry breaking due to the rotationally symmetric structure leads to stable single-mode operation with the selective whispering gallery mode order. Our chip-scale semiconductor platform provides a unique route towards fundamental exploration of PT physics and next-generation active optoelectronic devices for optical communication and computing.

9546-36, Session 8

Simultaneous unidirectional lasing and reflectionless modes in PT-symmetric cavities (Invited Paper)

Hamidreza Ramezani, Hao-kun Li, Yuan Wang, Univ. of California, Berkeley (United States); Xiang Zhang, Univ. of California, Berkeley (United States) and Lawrence Berkeley National Lab. (United States)

We introduce a new family of spectral singularities with highly directional response in parity-time (PT) symmetric cavities. These spectral singularities support modes with infinite reflection from one side and zero reflection from the other side of the cavity, results in simultaneous unidirectional laser and unidirectional reflectionless parity-time symmetric cavity. Such unidirectional spectral singularities emerge from resonance trapping induced by the interplay between parity-time symmetry and Fano resonances.

9546-37, Session 8

Cavity-free stopped-light nanolasing in nanoplasmonic heterostructures (Invited Paper)

Ortwin Hess, Imperial College London (United Kingdom)

Going beyond traditional cavity-concepts, recently conceived nanolasers employ plasmonic resonances for feedback, allowing them to concentrate light into mode volumes that are no longer limited by diffraction [1]. The use of localized surface plasmon resonances as cold-cavity modes, however, is only one route to lasing on subwavelength scales. Lasing, in fact, does not require modes predefined by geometry but merely a feedback mechanism [2].

Here we demonstrate that the concept of dispersion-less stopped-light [3]

allows by combination of nanoplasmonics with quantum gain materials [4] stopped-light lasing in hybrid nanoplasmonic heterostructures. Thereby, photons are trapped and amplified in space just at the point of their emission. It will be discussed that, at the stopped-light point, a stable lasing mode can form over a finite region of gain material due to the arising local (cavity-free) feedback in the form of a sub-wavelength optical vortex. We discuss the remarkable spatio-temporal dynamics of nanoplasmonic stopped-light lasing is studied on the basis of a Maxwell-Bloch Langevin approach [4]. Moreover, a new rate-equation framework is shown to grasp the particular physics of stopped-light lasing involving [4]. The observed high-? characteristics and picosecond relaxation oscillations of cavity-free stopped-light lasing can potentially allow for the design of thresholdless plasmonic laser diodes that can be modulated with THz speeds.

[1] O Hess and KL Tsakmakidis, Science 339, 654 (2013).

[2] J M Hamm and O Hess, Science 340, 1298 (2013).

[3] KL Tsakmakidis, TW Pickering, JM Hamm, AF Page and O Hess, Phys Rev Lett 112, 167401 (2014).

[4] T Pickering, J M Hamm, A F Page, S Wuestner and O Hess, Nature Communications 5, 4971 (2014).

9546-38, Session 9

Auger-decay engineering in quantum dots in relation to applications in LEDs and lasers (Invited Paper)

Victor I. Klimov, Los Alamos National Lab. (United States)

Multicarrier dynamics in colloidal quantum dots (QDs) are normally controlled by nonradiative Auger recombination wherein the energy of an electron-hole pair is converted not into a photon but instead transferred to a third carrier (an electron or a hole). Auger decay is extremely fast in QDs (time scales of tens-to-hundreds of picoseconds) due to both close proximity between interacting charges and elimination of restrictions imposed by translational momentum conservation. Photoluminescence (PL) quenching by nonradiative Auger processes complicates realization of applications that require high emissivity of multicarrier states such as lightemitting diodes (LEDs) and lasers. Therefore, the development of "Augerrecombination-free" QDs is an important current challenge in the field of colloidal nanostructures.

Previous single-dot spectroscopic studies have indicated a significant spread in Auger lifetimes across an ensemble of nominally identical QDs. It has been speculated that in addition to dot-to-dot variation in physical dimensions, this spread is contributed to by variations in the structure of the QD interface, which controls the shape of the confinement potential. Here we directly evaluate the effect of the composition of the core-shell interface on single- and multi-exciton dynamics via side-by-side measurements of individual core-shell CdSe/CdS nanocrystals with a sharp vs. smooth (graded) interface. We observe that while having essentially no effect on single-exciton decay, the interfacial alloy layer leads to a systematic increase in the biexciton lifetime indicating suppression of Auger recombination. We demonstrate that using QDs with "engineered interfaces" we can considerably improve the performance of QD LEDs and lasers.

9546-39, Session 9

Nanowire quantum dots for quantum optics (Invited Paper)

Valery Zwiller, Michael Reimer, Klaus Joens, Lucas Schweickert, Technische Univ. Delft (Netherlands)

We demonstrate the generation of single photons as well as pairs of entangled photons with quantum dots in semiconducting nanowires, we show applications to quantum optics including generation, manipulation and detection of light at the nanoscale.



9546-40, Session 9

Redefining giant quantum dot functionality through synthesis and integration: from multifunctionality to directed photoluminescence (Invited Paper)

Jennifer A. Hollingsworth, Los Alamos National Lab. (United States)

Thick-shell or "giant" core/shell nanocrystal quantum dots (gQDs) are efficient and stable emitters. Their characteristic properties of nonblinking and non-photobleaching emission, as well as suppressed nonradiative Auger recombination and minimal self-reabsorption (due to a large effective Stokes shift) make them relevant to both single-emitter and many-emitter applications, e.g., live-cell single-molecule tracking in the biosciences and down-conversion phosphors for solid-state lighting. Here, I will discuss how gQDs are also ideal "building blocks" for achieving additive functionalities through synthesis and modified emission properties through integration with fabricated photonic structures. gQDs have been synthetically incorporated into the interior of a gold shell, resulting in "plasmonic gQDs" that exhibit efficient photoluminescence combined with efficient photothermal transduction and thermometry. Furthermore, through direct patterning of gQDs into all-dielectric antennas, we show an approach for realizing emitter-antenna couples (toward controlling the motion of photons) that is both deterministic and reproducible.

9546-41, Session 9

Controlled growth of CdSe quantum dots on silica spheres

Byoung-Ju Kim, Donghyun Jo, Se-Han Lim, Do-Kyoon Kim, Jin-Young Park, Jong-Hwa Jeon, Kwang-Sun Kang, Kyungil Univ. (Korea, Republic of)

Various sizes of CdSe quantum dots have been fabricated on the surface of the monodisperse silica spheres and five different photoluminescence (PL) peaks are observed from the CdSe quantum dots. The monodisperse silica spheres were synthesized with Stöber synthetic method. The surface of the spheres was modified with 100:1 ratio of phenylpropyltrimethoxysilane (PTMS) and mercaptopropyltrimethoxysilane (MPTMS). The MPTMS works as a covalent bond formation with CdSe quantum dots, and the PTMS acts as a separating quantum dots to prevent PL quenching by neighboring quantum dots. The Fourier transform infrared (FTIR) spectrum of the surface modified spheres (SMSiO2) shows strong absorption peak at 2852 and 2953 cm-1 representing the characteristic absorption of -CH or -CH2. The FTIR absorption peak at 1741 cm-1 represents the characteristic absorption of CdSe quantum dots. The field emission scanning electron microscope image shows the average diameter of the spheres ranging approximately 418 nm. The ultraviolet-visible transmittance spectrum shows stop band at 880 nm. The PL spectrum shows five different emission bands at 434, 451, 468, 492 and 545 nm, which indicates the formation of several different sizes of CdSe quantum dots.

9546-42, Session 10

Collective properties and strong coupling in the near-field of a meta-surface (Invited Paper)

Didier Felbacq, Emmanuel Rousseau, Univ. Montpellier 2 (France)

Meta-surfaces are the 2D analogues of metamaterials. Meta- surfaces are generally seen as devices able to control the far-field behavior of light. However, because of their resonant properties, meta-surfaces also have

interesting properties in the near-field. In the present work, we aim at initiating the study of the guantum electrodynamics of meta- surfaces. In standard cavity quantum electrodynamics, one studies the coupling between an emitter, such as an atom, or quantum dot or a superconducting qubit, and the electromagnetic modes. Depending on the ratio between the light-matter coupling and that to the irreversible mechanisms, two regimes can occur: the weak coupling and the strong coupling. In the strong coupling regime, the coupling dominates the losses, the emitter and the meta-surface can exchange photons periodically in time, which leads to hybrid excited states. From an experimental point of view, this regime leads to the onset of a double peak in the emitted spectrum, due to the anti-crossing of the dispersion curves of the light and matter modes. In the present work, the coupling of a quantum emitter with the photonic surface modes supported by a meta-surface is investigated. The meta-surface is made of a periodic set of parallel nano wires. From a theoretical point of view, the meta-surface can be described by an effective impedance model, which allows to derive the density of electromagnetic modes due to the meta- surface. Further, it allows to obtain the dressed susceptibility of the quantum emitter and to exhibit the strong coupling regime.

9546-43, Session 10

Coherent coupling between a molecular vibration and Fabry-Perot optical cavity to give hybridized states in the strong coupling limit

James P. Long, Jeff C. Owrutsky, Kenan P. Fears, Walter J. Dressick, Adam D. Dunkelberger, Ryan Compton, Bryan T. Spann, Blake S. Simpkins, U.S. Naval Research Lab. (United States)

Coherent coupling between an optical-transition and confined optical mode, when sufficiently strong, gives rise to new modes separated by the vacuum Rabi splitting. Such systems have been investigated for electronic-state transitions, however, only very recently have vibrational transitions been considered. Here, we bring strong polaritonic-coupling in cavities from the visible into the infrared where a new range of static and dynamic vibrational processes await investigation.

First, we experimentally and numerically describe coupling between a Fabry-Perot cavity and carbonyl stretch (~1730 cm 1) in polymethylmethacrylate. As is requisite for "strong coupling", the measured vacuum Rabi splitting of 132 cm 1 is much larger than the full width of the cavity (34 cm-1) and the inhomogeneously broadened carbonyl-stretch (24 cm-1). Agreement with classical theories providea evidence that the mixed-states are relatively immune to inhomogeneous broadening. Next, we investigate strong and weak coupling regimes through examination of cavities loaded with varying concentrations of urethane. Rabi splittings increases from 0 to ~104 cm-1 with concentrations from 0-20 vol% and are in excellent agreement to an analytical description using no fitting parameters. Ultra-fast pump-probe measurements reveal transient absorption signals over a frequency range well-separated from the vibrational band as well as modifications of energy relaxation times. Finally, we demonstrate coupling to liquids using the C-O stretching band (~1985 cm-1) of Mo(CO)6 in an aqueous solution.

Opening the field of polaritonic coupling to vibrational species promises to be a rich arena amenable to a wide variety of infrared-active bonds that can be studied statically and dynamically.

9546-44, Session 10

Applications of Fano resonances to active photonic devices (Invited Paper)

Andrey E. Miroshnichenko, The Australian National Univ. (Australia)

The current surging interest in various applications of nanoscale lightmatter interactions, including biosensing, nanoantennas, photovoltaic



devices and many others, has triggered enormous effort into the old and fundamental problem of manipulation of a particle's scattering and absorption characteristics. In the recently emerging fields of nanophotonics, various novel phenomena have been demonstrated involving interaction of nanoparticles with light, such as super-scattering, control of the direction of the scattered light by metasurface, coherent perfect absorption of light by surface plasmons, Fano resonances in plasmonic and all-dielectric oligomers . At the same time, the interest in artificial magnetic responses that was fostered by the field of metamaterials has lead to the observation of artificial magnetic modes in nanoparticles and, since then, many related novel scattering features based on the interplay of both electric and magnetic responses have been demonstrated. To make further breakthroughs in different applications based on the particles scattering, there is a fundamental challenge to overcome: polarization dependence. The polarization-independent absorption is, then, quite counter-intuitive because the near field profile of the electromagnetic field does depend on the incident polarization yet the overall absorption cross-section does not. It implies that the variation of the near field with the incident polarization does not affect the overall integral absorption cross-section. It has the main implication to the origin of the Fano resonance in oligomer-like structures. By studying the near-field and discrete dipole modes distribution we reveal the necessary conditions for the Fano resonance to occur in such structures.

9546-45, Session 10

Strong light matter coupling in twodimensional semiconductors (Invited Paper)

Vinod M. Menon, The City College of New York (United States)

Transition metal dichalcogenides (TMDs) have emerged as an attractive class of two-dimensional (2D) semiconductors that show unprecedented strength in its interaction with light. Here we will discuss our recent work on embedding such a 2D TMD layer of molybdenum disulphide in a dielectric microcavity showing the forming of strongly coupled half-light half-matter quasiparticles called microcavity polaritons. Realizing strong coupling at room temperature in a disorder free landscape such as 2D materials offers a practical and attractive route to realizing devices such as switches and logic gates that exploit the benefits of the half-light half-matter composition of the polaritons.

9546-46, Session 11

Phonon-modified spontaneous emission from quantum dots in structured photonic reservoirs: breakdown of Fermi's golden rule (Invited Paper)

Stephen Hughes, Queen's Univ. (Canada)

The spontaneous emission rate of a two-level atom coupled to a structured photonic reservoir is determined by the local density of photonic states (LDOS) at the emitter frequency, according to Fermi's golden rule. Such a relation is also supposed to hold true for semiconductor quantum dots (QDs), which behave as artificial atoms in a solid state medium [1]. A sharp atom-like transition along with an ability to couple to microcavity structures such as photonic crystal reservoirs makes QDs promising as scalable qubits at optical frequencies. However, coupling with phonons renders a QD different compared to a simple two-level atom, as has been demonstrated in a number of recent experiments [1].

In this talk, we will describe how the spontaneous emission rate of a QD coupled to structured photonic reservoir is actually determined by the broadband frequency dependence of the LDOS, in clear violation of Fermi's golden rule [2]. A self-consistent polaron master equation approach including both a photon and a phonon reservoir is utilized in determining the phonon-modified spontaneous emission rate. The theory makes no specific assumption about the structure of the reservoirs and we will

exemplify the cases of a microcavity and a coupled-cavity waveguide. In particular, we find a significant breakdown of the Fermi's golden rule when the damping rates of the phonon bath and photon bath compare [2]. We will also make a direct connection to recent experiments and show how the broadband frequency dependence of the LDOS influences the PL spectra from coherently excited QDs [3].

[1] e.g., see A. Ulhaq, S. M. Ulrich, D. Richter, M. Jetteri, P. Michler, C. Roy, and S. Hughes, Phys. Rev. B 86, 241304(R) (2012); A. Ulhaq, S. Weiler, C. Roy, S. M. Ulrich, M. Jetter, S. Hughes, and P. Michler, Opt. Express 21, 4382 (2013).

[2] K. Roy-Choudhury and S. Hughes, e-print: arXiv:1406.3649 (2014).
 [3] ibid., e-print: arXiv:1411.6050 (2014).

9546-47, Session 11

Improving emission in nanorod arrays using quasi-aperiodic inverse design

P. Duke Anderson, Michelle L. Povinelli, The Univ. of Southern California (United States)

Photonic structure plays a significant role in determining the brightness and efficiency of nanoemitter systems. Using photonic crystal slabs it is possible to affect these quantities in various ways. First, positioning a leaky mode near the emission frequency allows more light to be extracted from within the slab. Second, concentrating high electric field intensity near emitter locations significantly enhances the spontaneous emission rate. However, a large body of work has suggested these two contributing factors are in competition, making it difficult to simultaneously achieve high electric field intensity and light extraction. In previous work, we identified one mode in an array of GaN nanorods which exhibited a 25X enhancement in extracted power, relative to a uniform slab. However, the mode was uncoupled to normal radiation and, consequently, produced a sharp dip in extraction efficiency. Here, we improve upon the previous design by investigating a new class of quasi-aperiodic nanorod array structures. Using an inverse design algorithm, we identify one optimized structure which achieves maximum theoretical light extraction while maintaining a high spontaneous emission rate. Overall, the optimized structure achieves a 48% increase in extracted power and a 20-48% increase in external quantum efficiency relative to the previous periodic design.

9546-48, Session 11

Photonic and plasmonic nanoresonators: a modal approach (Invited Paper)

Christophe Sauvan, Jean-Paul Hugonin, Lab. Charles Fabry (France); Philippe Lalanne, Lab. Photonique Numérique et Nanosciences (France)

Photonic and plasmonic resonators are dielectric or metallic optical devices that confine light at a scale smaller than the wavelength. The eigenmodes of the system are obviously powerful and intuitive tools to describe light scattering and light-matter interactions mediated by the resonant structure. However, owing to the presence of energy dissipation (by radiation or absorption), using the eigenmodes of nanoresonators is an open issue that has been solved only recently. We have developed a modal formalism that relies on the concept of guasinormal modes with complex eigenfrequencies. The theory is capable of handling any photonic or plasmonic resonator with strong radiation leakage, absorption and material dispersion. The normalization of the quasinormal modes constitutes one of the key points of the theory that we will discuss in this presentation. We will then show that the modal formalism provides a powerful tool to calculate and understand light-matter interactions in complex photonic or plasmonic systems. In particular, it allows understanding the physical mechanisms at play in the extremely large Purcell factors observed recently for emitters coupled to plasmonic nanoantennas.



9546-49, Session 12

Novel topological states in photonics (Invited Paper)

Marin Soljacic, Massachusetts Institute of Technology (United States)

Topologically non-trivial states have been raising a substantial interest in the electronics community because of their novel and unique properties. Similarly, topological states in photonics display an equally diverse range of novel and surprising phenomena.

Some of our recent results in this area will be presented.

9546-50, Session 12

Gyromagnetically induced transparency of metasurfaces (Invited Paper)

Gennady B. Shvets, Hossein Mousavi, The Univ. of Texas at Austin (United States); Alexander Khanikaev, Queens College (United States); Jeffery W. Allen, Monica Allen, Air Force Research Lab. (United States)

The concept of symmetry pervades modern physics. Through the conservation laws derived from various symmetries, high-level restrictions and selection rules can be derived for a variety of physical systems without any need for detailed investigations of their specific properties. The spatial symmetries of electric charge distribution on the metamaterial's surface determine whether the EM resonance is "bright" (radiatively coupled to) or "dark" (radiatively de-coupled from) the EM continuum. As we demonstrate in this talk, other (non-spatial) symmetries and their breaking can also be crucial to determine the properties of EM resonances and enable their mutual coupling, which in turn can give rise to EM Fano interferences.

I will consider a meta-surface formed by a two-dimensional array of double-antenna meta-molecules resting on a gyromagnetic ferrite substrate. In conclusion, I will use simple symmetry considerations to predict and numerically demonstrate two phenomena that occur in metasurfaces when symmetry of the system is reduced by a gyromagnetic substrate: gyromagnetically induced transparency and nonreciprocal Fano interference. These phenomena hold significant promise for practical applications such as the dynamic control of resonant EM interactions using magnetic fields produced by the external currents, mitigation of co-site interference and improving isolation. Spectral positions, radiative lifetimes and quality factors of Fano resonances can be controlled by the magnitude of the external magnetic field. This class of effects may lead to a new generation of tunable and nonreciprocal Fano resonant systems for various applications where strong field enhancement, tunability and nonreciprocity are simultaneously required.

9546-51, Session 12

Using time-dependent effective gauge field for photons to achieve dynamic localization of light

Luqi Yuan, Shanhui Fan, Stanford Univ. (United States)

We study a problem of achieving three-dimensional dynamic localization of light in a dynamically-modulated resonator lattice. An effective gauge potential for photons has been previously shown to exhibit in such lattice. Dynamic localization of light can be achieved by varying the effective gauge potential sinusoidally in time. Furthermore, the rotating wave approximation was used in previous works on such effective gauge potential for photons. Here, we find that the effect of dynamic localization persists even in the regime where the counter-rotating term has to be taken into count.

9546-53, Session 12

Transport properties of pseudospin-1 photons (Invited Paper)

Che Ting Chan, Anan Fang, Zhao-Qing Zhang, Hong Kong Univ. of Science and Technology (Hong Kong, China); Steven G. Louie, Hong Kong Univ. of Science and Technology (Hong Kong, China) and Univ. of California, Berkeley (United States) and Lawrence Berkeley National Lab. (United States)

Pseudospin is of central importance in governing many unusual transport properties of graphene and other artificial systems which have pseudospins of ?. These unconventional transport properties are manifested in phenomena such as Klein tunneling, and collimation of electron beams in one-dimensional external potentials. Here we show that in certain photonic crystals (PCs) exhibiting conical dispersions at the center of Brillouin zone, the eigenstates near the "Dirac-like point" can be described by an effective spin-orbit Hamiltonian with a pseudospin of 1. This effective Hamiltonian describes within a unified framework the wave propagations in both positive and negative refractive index media which correspond to the upper and lower conical bands respectively. Different from a Berry phase of $\boldsymbol{\varpi}$ for the Dirac cone of pseudospin-? systems, the Berry phase for the Dirac-like cone turns out to be zero from this pseudospin-1 Hamiltonian. In addition, we found that a change of length scale of the PC can shift the Dirac-like cone rigidly up or down in frequency with its group velocity unchanged, hence mimicking a gate voltage in graphene and allowing for a simple mechanism to control the flow of pseudospin-1 photons. As a photonic analogue of electron potential, the length-scale induced Dirac-like point shift is effectively a photonic potential within the effective pseudospin-1 Hamiltonian description. At the interface of two different potentials, the 3-component spinor gives rise to distinct boundary conditions which do not require each component of the wave function to be continuous, leading to new wave transport behaviors as shown in Klein tunneling and supercollimation. For examples, the Klein tunneling of pseudospin-1 photons is much less anisotropic with reference to the incident angle than that of pseudospin-? electrons, and collimation can be more robust with pseudospin-1 than pseudospin-?. The special wave transport properties of pseudospin-1 photons, coupled with the discovery that the effective photonic "potential" can be varied by a simple length-scale change, may offer new ways to control photon transport. We will also explore the difference between pseudospin-1 photons and pseudospin-? particles when they encounter disorder.

9546-54, Session 13

Light scattering in pseudo-passive media with uniformly balanced gain and loss (Invited Paper)

Tsampikos Kottos, Ali Basiri, Wesleyan Univ. (United States); Ilya Vitebskiy, Air Force Research Lab. (United States)

We introduce a class of metamaterials with uniformly balanced gain and loss associated with complex permittivity and permeability constants. The refractive index of such a balanced pseudo-passive metamaterial is real. An unbounded uniform pseudo-passive medium has transport characteristics similar to those of its truly passive and lossless counterpart with the same real refractive index. However, bounded pseudo-passive samples show some unexpected scattering features which can be further emphasized by including such elements in a photonic structure.



9546-55, Session 13

Giant amplification of light in nonhermitian photonic materials (Invited Paper)

Hakan E. Tureci, Konstantinos G. Makris, Princeton Univ. (United States); Li Ge, College of Staten Island (United States)

In photonics and quantum optics, a key challenge facing any technological application has traditionally been the mitigation of optical losses. Recent work has shown that a new class of optical materials, called Parity-Time symmetric materials, that consist of a precisely balanced distribution of loss and gain can be exploited to engineer novel functionalities for propagating and filtering electromagnetic radiation. Here we show a generic property of optical systems that feature an arbitrary distribution of loss and gain, described by non-Hermitian operators, namely that overall lossy optical systems can transiently amplify certain input signals by several orders of magnitude. We present a mathematical framework to analyze the dynamics of wave propagation in media with an arbitrary distribution of loss and gain and construct the initial conditions to engineer such non-Hermitian power amplifiers.

9546-56, Session 13

Parity-time anti-symmetric parametric amplifier (Invited Paper)

Diana A. Antonosyan, Alexander S. Solntsev, Andrey A. Sukhorukov, The Australian National Univ. (Australia)

We consider a directional coupler composed of two waveguides in quadratically nonlinear medium, where one waveguide is lossy. The loss can be introduced, for example, by depositing a thin layer of metal. In the linear regime, at low light intensities, such coupler realizes PT-symmetric optical system. We analyze the process of optical parametric amplification based on nonlinear mixing between a strong pump, and signal and idler waves. We model the wave propagation in the undepleted pump regime using coupled-mode equations. We reveal that the Hamiltonian possesses an anti-PT symmetry (with a negative sign). We find that if the eigenmode profile is PT-symmetric, then generally the gain coefficients of modes are different. On the other hand, if the mode profile has a broken PT-symmetry, then there appear mode pairs with the same gain coefficients. We emphasize that the modal PT-symmetry has opposite relation to gain in contrast to the previously studied PT-symmetric systems.

We demonstrate that the modal PT-breaking can be controlled by the pump beam. Due to the electronic nature of quadratic nonlinearity, such tuning can be ultrafast, directly following the pump profile in real time. For a pump amplitude over the threshold, there appears one mode exhibiting strong gain, whereas at lower pump powers, signal periodically switches between the waveguides due to a beating between two modes exhibiting the same negative gain.

9546-57, Session 13

PT-symmetric scatterers (Invited Paper)

Mohammad-Ali Miri, Nicholas Nye, Mercedeh Khajavikhan, Demetrios N. Christodoulides, CREOL, The College of Optics and Photonics, Univ. of Central Florida (United States)

No Abstract Available

9546-73, Session PWed

Intense terahertz-pulse generation by four-wave mixing process in induced gas plasma

Surawut Wicharn, Srinakharinwirot Univ. (Thailand); Prathan Buranasiri, King Mongkut's Institute of Technology Ladkrabang (Thailand)

In this article, we have numerically investigated an intense terahertz (THz) pulses generation in gaseous plasma based on the third-order nonlinear effect, four-wave mixing (FWM) process. We have proposed that the fundamental fields and second-harmonic field of ultra-short pulse lasers are combined and focused into a very small gas chamber to induce a gaseous plasma, which intense THz pulse is produced. To understand the THz generation process, the first-order multiple-scale perturbation method has been utilized to derive a set of nonlinear coupled-wave equations for interacting fields such as two fundamental fields, a second-harmonic field, and a THz field. Then, we have seek for the optimal conditions of intense THz-pulse generation, simulated output THz field using numerical method, and calculated output energy and conversion efficiency of this process.

9546-74, Session PWed

Direct measure of the photo-induced nanoscale surface displacement in solids using atomic force microscopy

Samuel T. Souza, Eduardo J. Fonseca, Carlos Jacinto, Univ. Federal de Alagoas (Brazil); Nelson G. C. Astrath, Thiago P. Rodrigues, Luis C. Malacarne, Univ. Estadual de Maringá (Brazil)

The light-matter interaction induces a large number of effects that are of fundamental interest in the development and characterization of new materials. In this direction, phothothermal methods are largely employed in the determination of thermal, optical, and mechanical properties, in addition to the study of amplitude and dynamic of the material response. In this work, we investigate the photo-induced nano-expansion in solids by a direct measure using atomic force microscopy. The results were comparable with those ones obtained from the thermal mirror technique, presenting good agreement between the techniques. The results presented here open possibilities to optically induce nanoscale-controlled positioning in a bidimensional system

9546-75, Session PWed

Using dilute-P GaNP alloy as improved visible active region

Chee-Keong Tan, Zhangji Zhao, Nelson Tansu, Lehigh Univ. (United States)

Group III-Nitride semiconductor alloy especially InGaN alloy has been extensively studied as the active region for the solid state lighting applications. Recent studies suggested dilute-As GaNAs alloy as an alternative candidate to improve the nitride-based active region due to the suppression of the interband Auger recombination. In conjunction with dilute-As GaNAs alloy, previous works indicated the potential of dilute-P GaNP alloy as a novel source for light emitters. Nonetheless the details of the electronic properties of dilute-P GaNP alloy are severely lacking, prohibiting further development of the alloys into effective photonic devices. Understanding the electronic properties of dilute-P GaNP alloy is thus a critical first step towards device implementation for realizing practical devices.

In this work we provide the analysis of the electronic properties of dilute-P GaNP alloys by utilizing First-Principle Density Functional Theory



(DFT) calculation. Our DFT analysis indicates significant band structure modifications of the GaN alloy when the N atoms are replaced with Phosphorus (P) atoms in the GaN alloy. The electronic properties of the dilute-P GaNP alloys are analyzed as follow: (a) band gap energy, (b) carrier effective masses and (c) split-off energy. Additionally, further analysis shows minimal interband Auger recombination in the dilute-P GaNP alloys as compared to InGaN alloy, implying the advantage of GaNP alloys as a visible light emitting material. The electronic properties of the dilute-P GaNP alloy will be discussed in details. The interband Auger recombination rates for the dilute-P GaNP alloy in comparison to InGaN alloy will also be provided.

9546-76, Session PWed

Selectively reflective transparent sheets

Remi Wache, Steven K. Clowes, Marian Florescu, Stephen J. Sweeney, Univ. of Surrey (United Kingdom)

The aim of the present work is to investigate the possibility to selectively reflect certain wavelengths while maintaining the optical properties at other wavelengths. This is of particular interest for transparent materials which for specific applications may require reflection at a specific band gap. Although there exist currently techniques such as coatings to produce this selective reflection, this work focus on new approaches for a mass production of polyethylene sheet which incorporates either additives or surface patterning for selective reflection between 8 to 13 μ m.

Typical additives used to produce a greenhouse effect in plastics include particles such as clays, silica or hydroxide materials. However, the absorption of thermal radiation is less efficient that the decrease of emissivity as it can be compared with the inclusion of lambertian materials.

Band gap engineering by the periodic structuring of metamaterials is known in nature for producing the vivid bright colours in certain insects via strong wavelength selective reflection. Research to artificially engineer such structures has mainly focused on wavelengths in the visible and near infrared. However few studies to date have been carried out to investigate the properties of metastructures in the mid infrared range even though the patterning of microstructure should be easier than the fabrication of nanostructures in photonic crystals. Preliminary results on the diffuse reflectivity given by simulation tools will be presented and the technical feasibility of these two approaches will be discussed.

9546-77, Session PWed

Omnidirectional mirror in two-dimensional photonic crystal with a periodic gain-loss modulation

Carlos Ivan Ham-Rodriguez, Jesus Manzanares-Martinez, Univ. de Sonora (Mexico); Paola Castro-Garay, Universidad de Sonora (Mexico); Betsabe Manzanares-Martinez, Yohan Jasdid Rodriguez-Viveros, Univ. de Sonora (Mexico); Damian Moctezuma-Enriquez, Ctr. de Investigación en Materiales Avanzados, S.C. (Mexico)

Recently has been demonstrated that the light propagation can be forbidden in gain-loss composite media as result of simultaneous absorption and enhancement of electromagnetic waves. The gain-loss media have a great potential in the design of electro-optical devices because the complex difractions of propagating and evanescent waves allow exotic possibilities for the modification of the spontaneous emission of atoms and molecules.

Gain-loss media has been for a long time an essential component in the design of Distributed Feedback Lasers. More recently gain-loss media has been intensively studied because in principle, it is possible to compensate the losses of evanescent fields such as the surface plasmons allowing new posibilities for the plasmonic-based technology.

In this work we study the Photonic Band Gaps (PBG) that are result of the destructive interference of electromagnetic waves interacting with a twodimensional gain loss media. The composite system is made of cylinders with gain embedded in a lossy background. We have chose a combination of the constitutive parameters which give an zero average of gain or loss in the unit cell. We have found the parameters to obtain a robust band gap for the normal direction to the TX direction of a square lattice. We have also found the ambient conditions to design an Omnidirectional Mirror which have a stop band for all the imping propagating waves, irrespectively of their polarization or angle of incidence.

9546-78, Session PWed

Moving femtosecond soliton in layered structure with cubic nonlinearity

Vyacheslav A. Trofimov, Tatyana M. Lysak, Lomonosov Moscow State Univ. (Russian Federation)

We discuss soliton mode of laser femtosecond pulse propagation in layered structure with cubic nonlinear response in certain layers. Soliton under consideration occupies a few layeres. It moves across the layers without its shape destroying. Using computer simulation we investigate the features of soliton reflection from ambient linear medium. Soliton reflection depens in strong way on optical properties for boundary layers. However, in any situation a part of soliton leaves the photonic crystal during some time interval.

9546-58, Session 14

Engineering light absorption in semiconductor metafilms (Invited Paper)

Mark L. Brongersma, Geballe Lab. for Advanced Materials (GLAM) (United States)

The optical properties of semiconductors are typically considered intrinsic and fixed. I will discuss how the rapid developments in the understanding of high-index semiconductor nano-antennas can be leveraged to create ultrathin semiconductor metafilms with designer absorption spectra. Such metafilms are constructed by placing one or more types of semiconductor antennas into a dense array with subwavelength spacings. As semiconductor antennas are only weakly-interacting and feature absorption cross sections that can exceed their geometrical cross section, very strongly absorbing metafilms can be created whose spectral absorption properties can directly be linked to the resonant properties of the constituent building blocks. The ability to create semiconductor metafilms with custom absorption spectra opens up new design strategies for planar optoelectronic devices and solar cells.

9546-59, Session 14

Exchanging Ohmic losses in metamaterial absorbers with useful optical absorption for photovoltaics (Invited Paper)

Durdu O. Guney, Michigan Technological Univ. (United States)

Using metamaterial absorbers, we have shown that metallic layers in the absorbers do not necessarily constitute undesired resistive heating problem for photovoltaics. Tailoring the geometric skin depth of metals and employing the natural bulk absorbance characteristics of the semiconductors in those absorbers can enable the exchange of undesired resistive losses with the useful optical absorbance in the active semiconductors. Thus, Ohmic loss dominated metamaterial absorbers can be converted into photovoltaic near-perfect absorbers with the advantage of harvesting the full potential of light management offered by the metamaterial absorbers. Based on experimental permittivity data for indium gallium nitride, we have shown that between 75%–95% absorbance can be achieved in the semiconductor layers of the converted metamaterial absorbers. Besides other metamaterial and plasmonic devices, our results



may also apply to photodectors and other metal or semiconductor based optical devices where resistive losses and power consumption are important pertaining to the device performance.

9546-60, Session 14

Optimized super-absorption in nanostructured thin films via a genetic algorithm (Invited Paper)

Alexandre Mayer, Jérôme Muller, Aline Herman, Olivier Deparis, Univ. of Namur (Belgium)

Genetic algorithms mimic natural selection in order to determine globally optimal solutions for complex problems in physics. The idea consists in working with a population of individuals, each of them representing a possible solution of the problem. The initial population consists of random individuals. We then select the best individuals. We breed them to determine new individuals for the next generation. We finally introduce random mutations in the coding of parameters. When repeated from generation to generation, this strategy leads to globally optimal solutions in a time that grows only linearly with the number of parameters to determine.

We used this approach to achieve super-absorption in nano-structured thin films (40 microns) of crystalline silicon. The device considered includes a periodic array of inverted pyramids on the front side with a conformal anti-reflection coating (SiNx and a-Si layers) and a reflector on the back side (a-Si and ITO layers). The geometrical parameters of these pyramids and the different layer thicknesses must be adjusted in order to maximize the absorption of solar radiation in the c-Si. The genetic algorithm provides solutions that lead to short-circuit currents of the order of 35-40 mA/ cm?, which compare very well with the maximum of 43.5 mA/cm? one can achieve with c-Si.

[1] A. Mayer et al., Genetic algorithms used for the optimization of lightemitting diodes and solar thermal collectors, Proc. of SPIE 3987, 918705 (2014).

[2] V. Depauw et al., Nanophotonics for ultra-thin crystalline silicon photovoltaics: when photons (actually) meet electrons, EU PVSEC Proceedings, 1461 (2014).

9546-61, Session 14

A new avenue for high efficiency solar cells: interaction of hot electrons with plasmons (*Invited Paper*)

Krzysztof Kempa, Michael J. Naughton, Boston College (United States)

Hot electrons rapidly dissipate their extra free energy, typically into heat. This is the origin of the Shockley-Queisser efficiency limit of the single junction solar cells. An even faster mechanism of electron-plasmon scattering is available in metals. We demonstrate by detailed simulations, that an ultra-thin solar cell with a composite metamaterial/plasmonic collector could yield efficiency exceeding the Shockley-Quasar limit. The composite collector has a double function: firstly, it is designed to participate in efficiently trapping light, and secondly, it is a plasmonic resonator tuned to absorb the energy of hot electrons, thus protecting them from phonon losses.

9546-62, Session 14

Large-area, lithography-free perfect absorbers, color filters, and photodectors at visible frequencies using ultra-thin silver or amorphous silicon films

Zhongyang Li, Serkan Bütün, Koray Aydin, Northwestern Univ. (United States)

Plasmonic materials and metamaterials have been widely utilized to achieve spectral transmission, reflection and absorption filters based on localized or delocalized resonances arising from the interaction of photons with nanoscale patterns. However, the realization of visible-frequency, highperformance, large-area, optical filters based on nanoplasmonic materials is rather challenging due to nanofabrication related problems (cost, fabrication imperfection, surface roughness) and optical losses of metals. Here, we propose and demonstrate large-area perfect absorbers and transmission color filters and photodectors that could overcome the difficulties associated with nanofabrication using a lithography-free approach. Our resonant flat optical design is based on a modified, asymmetric metal-insulator/semiconductor-metal (MI/SM) based Fabry-Perot cavity incorporated with plasmonic, lossy ultra-thin (~ 30 nm) Ag or (~ 5-15 nm) amorphous Si films. We demonstrated a narrow bandwidth (~17 nm) super absorber with 97% maximum absorption with a performance comparable to nanostructure/nanoparticle-based super absorbers. We also investigated transmission filters in which different colors can be obtained by controlling the spacer thickness of silicon dioxide or amorphous silicon. With measured performance of transmission peak intensity reaching 60% and a narrowband of ~ 40 nm, our color filters exceed the performance of widely studied plasmonic nanohole array based color filters and make a good candidate for large-area narrow-band photodetection devices. Such plasmonic loss incorporated Fabry-Perot cavities using ultra-thin metallic or semiconductor films could suggest active and practical applications in spectrally selective optical (color and absorber) filters, optoelectronic devices with controlled bandwidth such as narrow-band photodetectors, and light-emitting devices.

9546-63, Session 15

Transforming Cherenkov radiation in metamaterials (Invited Paper)

Vincent Ginis, Jan Danckaert, Irina Veretennicoff, Vrije Univ. Brussel (Belgium); Philippe Tassin, Chalmers Univ. of Technology (Sweden)

In this contribution, we explore the generation of light in transformationoptical media. When charged particles move through a transformationoptical material with a speed larger than the phase velocity of light in the medium, Cherenkov light is emitted. We show that the emitted Cherenkov cone can be modified with longitudinal and transverse stretching of the coordinates. Transverse coordinates stretching alters only the dimensions of the cone, whereas longitudinal stretching also changes the apparent velocity of the charged particle. These results demonstrate that the geometric formalism of transformation optics can be used not only for the manipulation of light beam trajectories, but also for controlling the emission of light, here for describing the Cherenkov cone in an arbitrary anisotropic medium. Subsequently, we illustrate this point by designing a radiator for a ring imaging Cherenkov radiator. Cherenkov radiators are used to identify unknown elementary particles by determining their mass from the Cherenkov radiation cone that is emitted as they pass through the detector apparatus. However, at higher particle momentum, the angle of the Cherenkov cone saturates to a value independent of the mass of the generating particle, making it difficult to effectively distinguish between different particles. Using our transformation optics description, we show how the Cherenkov cone and the cut-off can be controlled to yield a radiator medium with enhanced sensitivity for particle identification at higher momentum.



9546-64, Session 15

Guiding light by plasmonic resonant solitons in metallic nanosuspensions

Trevor S. Kelly, Akbar Samadi, Anna Bezryadina, San Francisco State Univ. (United States); Zhigang Chen, San Francisco State Univ. (United States) and Nankai Univ. (China)

In typical colloidal suspensions, the corresponding optical polarizability is positive, and thus enhanced scattering takes place as optical beams tend to catastrophically collapse during propagation. Recently, light penetration deep inside scattering suspensions has been realized by engineering dielectric or plasmonic nanoparticle polarizibilities. In particular, we have previously demonstrated two types of soft-matter systems with tunable optical nonlinearities - the dielectric and metallic colloidal suspensions, in which the effects of diffraction and scattering were overcome, hence achieving deep penetration of a light needle through the suspension.

In this work, we show that waveguides can be established in soft matter systems such as metallic nanosuspensions through the formation of plasmonic resonant solitons. First, we show that, due to plasmonic resonance, a 1064nm laser beam (probe) would not experience appreciable nonlinear self-action while propagating through 4cm cuvette containing the metallic nanosuspension of gold spheres (40nm), whereas a 532nm laser beam (pump) can readily form a spatial soliton due to nonlinear selftrapping. Second, we demonstrate effective guidance of the probe beam, which would otherwise diffract significantly through the nanosuspensions, due to the soliton-induced waveguide from the pump beam. Such guidance was observed when the power of the probe beam was varied from 20mW to 500mW at constant pump beam power, with more pronounced guidance realized from lower to higher probe beam power. Interestingly, due to the presence of the probe beam, the pump beam undergoes self-trapping at an even lower power. These results may bring about the possibility of engineering plasmonic soliton-based waveguides for many applications.

9546-65, Session 15

Magneto-optical switches in metaldielectric-metal plasmonic waveguides

Ali Haddadpour, Vahid Foroughi Nezhad, Louisiana State Univ. (United States); Zongfu Yu, Univ. of Wisconsin-Madison (United States); Georgios Veronis, Louisiana State Univ. (United States)

The magneto-optical effect has been used to control the propagation of surface plasmon polaritons in plasmonic waveguides. Here we investigate single-interface metal-dielectric and metal-dielectric-metal plasmonic waveguides in which either the dielectric or the metal is a magneto-optical material. We derive the dispersion relation of these waveguides, and investigate the effect of an externally applied static magnetic field. We find that in metal-dielectric-metal waveguide structures in which the dielectric is a magneto-optical material, the symmetry of the structure prohibits any non-reciprocal propagation in the system. Moreover, the induced change in the propagation constant of the supported modes in the presence of an externally applied static magnetic field is relatively small. In addition, we find that using a magneto-optical metal in a single-interface metal-dielectric plasmonic waveguide results in non-reciprocal propagation of the plasmonic modes along the interface. We also find that in metal-dielectric-metal plasmonic waveguides in which the metal is a magneto-optical material, the propagation constant of the supported modes is dependent on the relative direction of the applied magnetic fields to the upper and lower metal regions. If the applied magnetic fields to the two metal regions are equal and in the same direction, the induced changes in the propagation constants of the modes propagating in the positive and negative directions are the same. On the other hand, if the directions of the applied external magnetic fields are opposite, the propagation constants of the modes propagating in the positive and negative directions are different. We finally investigate Fabry-Perot cavity magneto-optical switches.

9546-66, Session 15

Second order nonlinearity in Si by inhomogeneous strain and electric fields (Invited Paper)

Jörg Schilling, Clemens Schriever, Martin-Luther-Univ. Halle-Wittenberg (Germany); Federica Bianco, Scuola Normale Superiore (Italy); Massimo Cazzanelli, Lorenzo Pavesi, Univ. degli Studi di Trento (Italy)

Inhomogeneous strain was recently used to artificially generate a dipolar second order nonlinear susceptibility in silicon. However this is not the only way to break silicon's centrosymmetry. Second harmonic generation (SHG) was measured on several Si strip waveguides, which were strained by the deposition of stressed SiNx and SiO2 layers. A substantial offset of the SHG signal for all SiNx-covered waveguides was detected. This could be attributed to a local electric field near the Si/SiNx-interface generated by fixed charges in the cladding. This electric field induced SHG (EFISH) contributes constructively to the strain caused SHG and opens ways to electrically create and control a second order nonlinearity in Si waveguides.

9546-67, Session 16

Nano-optoelectronics with atomically thin material (*Invited Paper*)

Nick Vamivakas, Univ. of Rochester (United States)

No Abstract Available

9546-68, Session 16

In-the-cloud optimization tool for retrieving experimentally fitted conductivity of graphene

Ludmila J. Prokopeva, Purdue Univ. (United States) and Novosibirsk State Univ. (Russian Federation) and Institute of Computational Technologies (Russian Federation); You-Chia Chang, Univ. of Michigan (United States); Naresh K. Emani, Purdue Univ. (United States) and Data Storage Institute (Singapore); Ted Norris, Univ. of Michigan (United States); Alexander V. Kildishev, Purdue Univ. (United States)

Graphene is one of the emerging active nanophotonics materials with optical properties that can be controlled in real time by an applied bias voltage. Different applications from sensing to active nanophotonics have been discussed in the literature recently and the field is still developing especially with an eye on structured and multi-layer graphene. To design new devices there is a need for precise modeling of multivariate and dynamic optical responses of graphene elements in frequency and time domains. Taking into account the complexity that comes along with multiple unknown parameters, including edge effects in nanostructured graphene elements, graphene impurities, imperfections of characterization optics etc., it is hard to build an adequate multivariate model to reach good quantitative agreement with experiment.

Here, we present an approach that uses optimization methods to retrieve the optical properties of a given graphene sample from experiment. We show that with these techniques good quantitative agreement with experiments can be achieved; additionally we encapsulate our techniques in an online data-fitting tool. The tool includes several options to precisely fit the conductivity function to a given experiment - general spline approximations and physically meaningful random phase approximation models for frequency domain solvers, along with the relaxed Lorentz oscillator models for confident time domain simulations. A pilot version of



our free online tool entitled Photonics2D-Fit (to be staged at nanoHUB.org) is presented.

9546-69, Session 16

Enhanced infrared transmission from gold wire-grid arrays via surface plasmons in continuous graphene

Zizhuo Liu, Serkan Bütün, Edgar Palacios, Koray Aydin, Northwestern Univ. (United States)

Enhanced transmission of light through nanostructures has always been of great interest in the field of plasmonics and nanophotonics. With the aid of near-field effects, the transmission of the electromagnetic waves can be enhanced or suppressed. Much of the work on enhanced transmission has been shown to be frequency-selective. However it is possible to increase the transmission over a large frequency range by using graphene, which has shown broadband properties in many applications.

Here, we propose enhanced transmission in wire grid gold structure making use of continuous graphene sheets. We use finite-difference time-domain simulations to study the optical properties of this graphene-metal hybrid structure at mid infrared (mid-IR) wavelengths. The grating structure in wire grid gold provides an ideal platform to match the momentum and excite the surface plasmon polaritons (SPPs) in monolayer graphene. Our numerical calculations show that the local electromagnetic field around the graphene is largely enhanced due to surface plasmons. Moreover, with the highly confined SPPs coupling with the incident light, the transmission through the whole structure can be broadly enhanced in the mid infrared region. We also analyze the effect of the spectrum with different periods and gold nanowire widths to evaluate the size effects of the plasmons in graphene. In addition, by tuning the Fermi level, one can control the wavelength range at which the transmission is enhanced. The mechanism of the enhancement will be explained in the calculated electric field distribution. And we will also highlight the opportunities of graphene for applications such as tunable transmission and active photonic modulator.

9546-70, Session 17

Enhancing and inhibiting stimulated Brillouin scattering in photonic integrated circuits (Invited Paper)

Benjamin J. Eggleton, Moritz Merklein, Thomas F. S. Buettner, Irina V. Kabakova, The Univ. of Sydney (Australia)

On-chip nonlinear optics is a thriving research field, which creates transformative opportunities for manipulating classical or quantum signals in small-footprint integrated devices. Since the length scales are short, nonlinear interactions need to be enhanced by exploiting materials with large nonlinearity in combination with high-Q resonators or slowlight structures. This, however, often results in simultaneous enhancement of competing Q2 nonlinear processes, which limit the efficiency and can cause signal distortion. Here, we exploit the frequency dependence of the optical density-of-states near the edge of a photonic bandgap to selectively enhance or inhibit nonlinear interactions on a chip. We demonstrate this concept for one of the strongest nonlinear effects, stimulated Brillouin scattering using a narrow-band one-dimensional photonic bandgap structure: a Bragg grating. The stimluated Brillouin scattering enhancement enables the generation of a 15-line Brillouin frequency comb.

In the inhibition case, we achieve stimulated Brillouin scattering free operation at a power level twice the threshold

9546-71, Session 17

Optical pulse engineering and processing using nonlinearities of tapered and photonic crystal waveguides made of silicon (Invited Paper)

Nicolae-Coriolan Panoiu, Spyros Lavdas, Jie You, Univ. College London (United Kingdom); Richard M. Osgood Jr., Columbia Univ. (United States)

We present recent results pertaining to pulse reshaping and optical signal processing using optical nonlinearities of silicon-based tapered photonic wires and photonic crystal waveguides. In particular, we show how nonlinearity and dispersion engineering of tapered photonic wires can be employed to generate optical similaritons and achieve more than 10? pulse compression. We also discuss the properties of four-wave mixing pulse amplification and frequency conversion efficiency in long-period Bragg waveguides and photonic crystal waveguides. Finally, the influence of linear and nonlinear optical effects on the transmission bit-error rate in uniform photonic wires and photonic crystal waveguides made of silicon is discussed.

9546-72, Session 17

Nonlocal and quantum tunneling contributions to harmonic generation in nanostructures: electron cloud screening effects (Invited Paper)

Michael Scalora, U.S. Army Aviation and Missile Command (United States)

We investigate theoretically second and third harmonic generation from metal-based nanostructures and predict that nonlocal and quantum tunneling phenomena can significantly exceed expectations based solely on local, classical electromagnetism. Mindful that the diameter of typical transition metal atoms is approximately 3Å, we adopt a theoretical model that treats nanometer-size features and/or sub-nanometer size gaps or spacers by taking into account: (i) the limits imposed by atomic size to fulfill the requirements of continuum electrodynamics; (ii) spillage of the nearly-free electron cloud into the surrounding vacuum; and (iii) the increased probability of quantum tunneling as objects are placed in close proximity. Our treatment also includes the dynamics of bound charges in wavelength ranges where their contribution to the linear dielectric constant becomes pivotal. The model is an attempt to simplify a classical electrodynamic picture by incorporating a thin layer of free-electrons at the metal surface that screens an internal, polarizable medium.

Conference 9547: Plasmonics: Metallic Nanostructures and Their Optical Properties XIII



Sunday - Thursday 9 -13 August 2015

Part of Proceedings of SPIE Vol. 9547 Plasmonics: Metallic Nanostructures and Their Optical Properties XIII

9547-1, Session 1

Transverse spin of surface plasmon polaritons and spin-orbit coupling effects in light scattering by plasmonic nanostructures (Invited Paper)

Francisco J. Rodríguez-Fortuño, Daniel O'Connor, Pavel Ginzburg, Gregory A. Wurtz, Anatoly V. Zayats, King's College London (United Kingdom)

We will present the experimental and theoretical studies of the photonic spin-orbit coupling effects facilitated by a nanoparticle near a planar surface. Due to spin-orbit coupling, circularly polarized light of opposite handedness may take different trajectories when interacting with such a system, e.g. impinging on a polarizable particle placed above a metallic surface supporting surface plasmon polaritons or other guided modes. The transverse spin carried by surface plasmons is intimately linked to the polarization of light after their scattering on nanostructures. Circular polarizations of opposite handedness are radiated into mirror-symmetric directions, dependent on the surface plasmon propagation direction. This spin-orbit coupling effect is an optical analogue of the inverse spin Hall effect and has important implications for optical forces, optical information processing, quantum optical technology and topological surface metrology.

9547-2, Session 1

Generation of quantum entangled states in nonlinear plasmonic structures and metamaterials

Alexander N. Poddubny, loffe Physical-Technical Institute (Russian Federation) and National Research Univ. of ITMO (Russian Federation); Andrey A. Sukhorukov, The Australian National Univ. (Australia)

The practical development of quantum plasmonic circuits incorporating non-classical interference [1] and sources of entangled states calls for a versatile quantum theoretical framework which can fully describe the generation and detection of entangled photons and plasmons. However, majority of the presently used theoretical approaches are typically limited to the toy models assuming loss-less and nondispersive elements or including just a few resonant modes. Here, we present a rigorous Green function approach describing entangled photon-plasmon state generation through spontaneous wave mixing in realistic metal-dielectric nanostructures.

Our approach is based on the local Huttner-Barnett quantization scheme [2], which enables problem formulation in terms of a Hermitian Hamiltonian where the losses and dispersion are fully encoded in the electromagnetic Green functions. Hence, the problem can be addressed by the standard quantum mechanical perturbation theory, overcoming mathematical difficulties associated with other quantization schemes. We derive explicit expressions with clear physical meaning for the spatially dependent two-photon detection probability, single-photon detection probability and single-photon density matrix. In the limiting case of low-loss nondispersive waveguides our approach reproduces the previous results [3,4]. Importantly, our technique is far more general and can quantitatively describe generation and detection of spatially-entangled photons in arbitrary metal-dielectric structures taking into account actual losses and dispersion. This is essential to perform the design and optimization of plasmonic structures for generation and control of quantum entangled states.

[1] J.S. Fakonas, H. Lee, Y.A. Kelaita and H.A. Atwater, Nature Photonics 8, 317(2014)

[2] W. Vogel and D.-G. Welsch, Quantum Optics, Wiley (2006).

[3] D.A. Antonosyan, A.S. Solntsev and A.A. Sukhorukov, Phys. Rev. A 90

043845 (2014) [4] L-G Helt LE Sine and M L Steel

[4] L.-G. Helt, J.E. Sipe and M.J. Steel, arXiv: 1407.4219

9547-3, Session 1

Efficient far field transmission of orbital angular momentum light states

Denis Garoli, Pierfrancesco Zilio, Istituto Italiano di Tecnologia (Italy); Giuseppe Parisi, twistoff s.r.l. (Italy); Francesco Tantussi, Istituto Italiano di Tecnologia (Italy); Felix Ritort, Univ. de Barcelona (Spain); Tommaso Ongarello, Institut d'Électronique Fondamentale (France); Francesco De Angelis, Istituto Italiano di Tecnologia (Italy); Yuri Gorodetski, Ariel Univ. (Israel)

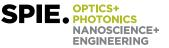
Nowadays light carrying orbital angular momentum (OAM) constitutes the focus of multiple and variegate research interests, ranging from astronomy to microscopy and plasmonics. Surface plasmon polaritons carrying OAM, from now on called Plasmonic vortices (PVs), can be generated by exploiting particular chiral grating couplers, which have been called plasmonic vortex lenses (PVLs). Once generated, PVs can interact with nanostructures placed at the center of the PVL, creating a number of interesting optical effects. We introduce new simulative and experimental results on generation of OAM light states both in near and far-field optical regime. PVLs coupled with nanostructures placed at the center will be used in order to investigate interesting optical behaviors. We propose an innovative holey PVL architecture which is able to convert impinging light to an almost pure and well defined OAM state, both in its evanescent and propagating parts. We then extend the investigation by introducing a vertical nanotip at the center of our structure. Although this kind of structures has been investigated for its plasmonic nanofocusing effects, here we use it as a perfect plasmonto-far-field OAM decoupler. Indeed, by increasing the curvature radius at the cone base, a perfect decoupling of plasmonic vortex into free space propagating structured light can be obtained, without any plasmonic back reflection at the tip base. This structure has interesting applications to nanoparticle trapping and manipulation. We show that the vertical nanotip can be actually used as "nano-launcher" of particles, inducing at the same time an non-zero angular momentum on their motion.

9547-4, Session 1

Magneto-optical response of a periodic metallic nano-structure (Invited Paper)

Yakov M. Strelniker, Bar-Ilan Univ. (Israel); David J. Bergman, Tel Aviv Univ. (Israel)

When an applied magnetic field has an arbitrary direction with respect to the lattice axes of a periodically nano-structured metal-dielectric metamaterial, the macroscopic or bulk effective permittivity tensor becomes anisotropic and all its components can be nonzero. This effect can be especially strong and significant in the vicinity of surface plasmon and cyclotron resonances (the frequencies of which are also sensitive to the value and direction of the applied external magnetic field). A similar effect for the case of dc effective conductivity is already verified experimentally (since magneto-conductivity tensor can be measured directly). However, this prediction for the permittivity has not yet been tested experimentally (since the permittivity tensor cannot be measured directly). What can be measured directly is the Voigt rotation, for which general exact analytical expressions were not published previously. In this work we have studied analytically and numerically the rotation and ellipticity of polarization of the light propagating through a metamaterial film with periodic nanostructure for arbitrary direction of the applied static magnetic field, including both Voigt and Faraday configurations. In the Voigt configuration we found a



strong dependence of the above mentioned effects on the direction of the applied magnetic field.

9547-5, Session 2

Perfect optical imaging of a Veselago Lens: Eigenstate based analysis (Invited Paper)

David J. Bergman, Asaf Farhi, Tel Aviv Univ. (Israel)

The Veselago Lens is analyzed by expanding the electric field of a time dependent point charge in a complete set of eigenstates of Maxwell's equations for a two-constituent composite medium with electric permittivities ?1, ?2 and a magnetic permeability equal to 1 everywhere which has the appropriate microstructure. An exact expression for the local electric field in the form of a one dimensional integral is obtained from which we are able to calculate that field numerically very rapidly and with great precision. In the quasistatic regime it was found earlier that this field diverges in some parts of the system when $2^{1/2} = -1$ and 2^{1} , 2^{2} are both real. That is precisely where the Veselago Lens has been predicted to provide imaging the resolution of which is not limited by the wavelength. Moreover, the dissipation rate then also diverges sometimes. That analysis will now be extended to the non-quasistatic regime. Among the surprising results is the fact that the best sub-wavelength resolution is obtained not at the geometric optics foci of the Veselago Lens but at points on the ?1, ?2 interface.

9547-6, Session 2

Beam engineering for selective and enhanced coupling to multipolar resonances

Tanya Das, Jon A. Schuller, Univ. of California, Santa Barbara (United States)

Multipolar light-matter interactions in sub-wavelength nanostructures depend on both nanostructure properties and properties of the illuminating beam. Conventionally, researchers manipulate the former and engineer the resonant properties of nanostructures. Instead, we concentrate on the latter and demonstrate via electromagnetics calculations that unconventional light sources can be used to selectively excite and enhance coupling to specific multipolar resonances. Building on Mie theory, we describe an analytical method for determining the optical response of nanoparticles (NPs) illuminated by any focused beam of interest. The illuminating source is decomposed into an angular spectrum of plane waves, and the NP response is determined by superimposing the response of the plane waves. We show that the multipolar light-matter interaction can alternately be expressed as a product of illumination-independent multipole moments and particleindependent field quantities: a vastly simplified approach for calculating light scattering and absorption in complex illumination conditions. Using these methods, we study the scattering spectra of a spherical NP under several types of illumination. We show that the spectra vary significantly with different illumination conditions, and show how to achieve selective excitation of desired multipolar modes. Additionally, we demonstrate the existence of longitudinal quadrupole excitations that cannot be accessed with conventional linearly polarized illumination. This work enables a new understanding of light-matter interactions in metamaterials, and lays the foundation for researchers to identify, quantify, and manipulate multipolar light-matter interactions through optical beam engineering.

9547-7, Session 2

Ultrafast coherent dynamics of Rydberg electrons bound in the image potential near a single metallic nanoobject (Invited Paper)

Jörg Robin, Jan Vogelsang, Carl von Ossietzky Univ. Oldenburg (Germany); Benedek J. Nagy, Wigner Research Ctr. for Physics of the H.A.S. (Hungary); Petra Gross, Christoph Lienau, Carl von Ossietzky Univ. Oldenburg (Germany)

Image potential states are well established surface states of metallic films [1]. For a single metallic nanostructure these surface states can be localized in the near-field arising from illumination by a strong laser field. Thus single metallic nanostructures offer the unique possibility to study quantum systems with both high spatial and ultrafast temporal resolution. Here, we investigate the dynamics of Rydberg states localized to a sharp metallic nanotaper.

For this purpose we realized a laser system delivering few-cycle pulses tunable over a wide wavelength range [2]. Pulses from a regenerative titanium:sapphire amplifier generate a white light continuum, from which both a proportion in the visible and in the infrared are amplified in two non-collinear optical parametric amplification (NOPA) stages. Difference frequency generation (DFG) of both stages provides pulses in the near-infrared.

With a precisely delayed sequence of few-cycle pulses centered around 600 nm (NOPA#1 output) and 1600 nm (DFG output) we illuminate the apex of a sharply etched gold tip. Varying the delay we observe an exponential decay of photoemitted electrons with a distinctly asymmetric decay length on both sides, indicating the population of different states. Superimposed on the decay is a clearly discernible quantum beat pattern with a period of <50 fs, which arises from the motion of Rydberg photoelectrons bound within their own image potential. These results therefore constitute a step towards controlling single electron wavepackets released from a gold tip opening up fascinating perspectives for applications in ultrafast electron microscopy [3].

[1] Höfer, U. et al. Science 277, 1480 (1997)

[2] Vogelsang, J., Robin J. et al. Opt. Express 22, 25295 (2014)[3] Petek, H. et al. ACS Nano 8, 5 (2014)

9547-8, Session 2

Heat generation, hot electrons, and transparency windows in plasmonic nanostructures (Invited Paper)

Alexander Govorov, Ohio Univ. (United States)

We investigate the effects of generation of heat and hot plasmonic carriers in metal nanostructures. The problem of heat release from optically-excited plasmonic nanocrystals is treated classically [1,2] whereas the hot electron problem is calculated using the quantum mechanical approach based on the equation of motion for the density matrix [3-5]. The energy distribution of optically-excited plasmonic carriers is very different in metal nanocrystals with large and small sizes. In large nanocrystals, most excited carriers have very small energies and the electron distribution resembles the case of a plasmon wave in bulk. For gold nanocrystal with smaller sizes (less than 20nm), the energy distribution of hot carriers becomes flat and has a large number of carriers with high energy [3-5]. Therefore, smaller nanocrystals are preferable for injection of plasmonic carriers into semiconductors or into molecules on the surface. The physical reason for the above behavior is non-conservation of momentum in a nanocrystal. The geometry, type of metal, and orientation of the external electric field are important to obtain high quantum efficiencies of generation and injection of plasmonic electrons [3-5]. Other important properties and limitations: (1) Intraband transitions are preferable for generation of energetic electrons and dominate the absorption for relatively long wavelengths (approximately



>600 nm), (2) inter-band transitions efficiently generate energetic holes in the d-band of gold and (3) the carrier-generation and absorption spectra can be significantly different [3-5]. The d-band hole generation can be used for efficient plasmonic photochemistry [6]. Along with the optical-energy conversion processes, we are looking at plasmonic and hybrid metastructures with unusual properties such as strong chirality and transparency windows [7,8,9]. The results obtained in this study can be used to design a variety of plasmonic nanodevices based on hot electron injection for photo-catalysis, light-harvesting, and solar cells.

[1] A. Govorov and H.H. Richardson, NanoToday 2, 20 (2007).

[2] S. Baral, A. Green, M. Livshits, A. Govorov and H.H. Richardson, ACS Nano 8, 1439-1448 (2014).

[3] A. O. Govorov, H. Zhang and Y. K. Gun'ko, J. Phys. Chem. C 117, 16616 (2013).

[4] H. Zhang and A. O. Govorov, J. Phys. Chem. C 118, 7606 (2014).

[5] A.O. Govorov, H. Zhang, V. Demi, and Y. K. Gun'ko, NanoToday, 9, 85 (2014) [Editors' Highlights].

[6] L. Weng, H. Zhang, A. O. Govorov, and M. Ouyang, Nature Communications 5, 4792 (2014).

[7] A. Kuzyk, R. Schreiber, Z. Fan, G. Pardatscher, E.-M. Roller, A. Högele, F.C. Simmel, A. O. Govorov, T. Liedl, Nature, 483, 311 (2012).

[8] M. L. Kerfoot, A.O. Govorov, D. Lu, R. J. O. Babaoye, Y. N. Gad, C. Czarnocki, M. Tsukamoto, A. S. Bracker, D. Gammon, M. Scheibner, Nature Communications (2014).

[8] H. Zhang, H. V. Demir, A.O. Govorov, ACS Photonics 1, 822 (2014).

9547-9, Session 3

Thermal phenomena in quantum plasmonics (Invited Paper)

Andrey K. Sarychev, Institute for Theoretical and Applied Electrodynamics (Russian Federation); Gennady Tartakovsky, Advanced Systems and Technologies (United States); Sergey Vergeles, L.D. Landau Institute for Theoretical Physics (Russian Federation); Vladimir Parfenyev, Moscow Institute of Physics and Technology (Russian Federation)

Plasmon nanolasers, also known as SPASERs, were suggested by Bergman and Stockman in 2003. Quantum plasmonics attract much attention in recent years due to the numerous potential applications in the plasmonics. We consider thermal effects in the metal nanoresonator immersed in the active, laser medium. The size of the resonator is much less than the wavelength. The plasmon field inside the nanoresonator operates as a quantum object. Due to the nanosize of the resonator, the internal plasmon electric field is about the atomic field even for few plasmon quants. The coupling between the plasmon field and plasmon resonator is anomalous strong. We develop the quantum dynamics of the plasmon field and show that the SPASER may be the subject of thermal instability. The loss in SPASER increases with increasing the temperature when the average number of the plasmons is maintained at the stationary level. Therefore, the heat generation increases with increasing the temperature. This positive feedback results in the thermal instability. When the energy, accumulated in the plasmon nanoresonator, exceeds the instability threshold the temperature increases exponentially. We find the increment of the temperature growth and lifetime as function of the loss in metal and the structure of the plasmon resonator. We consider how the thermal instability influences the luminescence and find how the lasing threshold is changed. The coherence of the light emitted by the plasmon laser is also considered. The thermal stability of the nanolaser is crucial for any practical application.

9547-10, Session 3

Plasmonic laser sensors

Renmin Ma, Sadao Ota, Yimin Li, Sui Yang, Xiang Zhang,

Univ. of California, Berkeley (United States)

Perhaps the most successful application of plasmonics to date has been in sensing, where the interaction of a nanoscale localized field with analytes leads to high-sensitivity detection in real time and in a label-free fashion. However, all previous designs have been based on passively excited surface plasmons, in which sensitivity is intrinsically limited by the low quality factors induced by metal losses. It has recently been proposed theoretically that surface plasmon sensors with active excitation (gain-enhanced) can achieve much higher sensitivities due to the amplification of the surface plasmons. Here, we experimentally demonstrate an active plasmon sensor that is free of metal losses and operating deep below the diffraction limit for visible light. Loss compensation leads to an intense and sharp lasing emission that is ultrasensitive to adsorbed molecules. We validated the efficacy of our sensor to detect explosives in air under normal conditions and have achieved a sub-part-per-billion detection limit, the lowest reported to date for plasmonic sensors with 2,4-dinitrotoluene and ammonium nitrate. The selectivity between 2,4-dinitrotoluene, ammoniumnitrate and nitrobenzene is on a par with other state-of-the-art explosives detectors. Our results show that monitoring the change of the lasing intensity is a superior method than monitoring the wavelength shift, as is widely used in passive surface plasmon sensors. We therefore envisage that nanoscopic sensors that make use of plasmonic lasing could become an important tool in security screening and biomolecular diagnostics.

9547-11, Session 3

Near-field imaging and spectroscopy of hybridized plasmons (Invited Paper)

Martin Aeschlimann, Technische Univ Kaiserslautern (Germany)

Understanding light-matter interactions such as the dynamic response of a metal to incident light is essential for advancing fundamental research and technological applications e.g. designing plasmonic devices such as nanoantenna directional emitters. The near-field response is determined on a length scale that is intrinsically smaller than the optical diffraction limit and so we use electrons to image the near-field distribution.

We combine photoemission electron microscopy (PEEM) with a variable wavelength laser light source, an optical parametric oscillator (OPO), to perform near-field imaging & spectroscopy of whispering gallery resonator (WGR)1 arrays. These ultrahigh spatially and spectrally resolved measurements show characteristic spectral peaks and near-field mode distributions due to the excitation of different plasmon resonances. Controlling the interference between dipole and quadrupole modes allows us to direct the emission from the nanoantenna.

Additionally we perform femtosecond 2-dimensional coherence spectroscopy2 on a microcavity system containing two well separated WGR nanoantennas. Hybridization of a propagating surface plasmon polariton and the localized surface plasmon in a cavity enables energy transfer between the two coupled nanoantennas.

[1] E. J. R. Vessseur, F. J. García de Abajo and A. Polman Nano Letters 9 3147 (2009)

[2] M. Aeschlimann et al, Science 333, 1723 (2011)

9547-12, Session 4

Ultrafast nanoelectronics: steering electrons in infrared near-fields (Invited Paper)

Georg Herink, Claus Ropers, Georg-August-Univ. Göttingen (Germany)

Plasmonic nanostructures can break the diffraction limit and confine optical fields on the nanoscale. The coupling of intense femtosecond transients to the apex of metallic nanotips enables ultrafast electron point sources which find applications in ultrafast electron microscopy and time-resolved



diffraction instruments. In this contribution, we demonstrate the impact of near-field localization onto strong-field photoemission and present the control of electron trajectories via the momentary electric near-field. The photoemission dynamics at single gold and tungsten nanotips are experimentally studied over a broad range of excitation frequencies, spanning from 1 - 400 Terahertz (THz). The transition from oscillatory electron acceleration to a field-driven interaction is presented as a result of intense, long-wavelength and localized excitation.

The high field enhancement at lower frequencies is demonstrated to induce localized field emission from a nanotip with moderate incident fields as provided by table-top THz sources. Such THz-induced cold field emission can be used, e.g., for the temporal tracking of optically excited hot-electron dynamics in nanostructures. Moreover, the field-driven electron acceleration in the enhanced THz near-field is employed in a pump-probe scheme to temporally map the local THz-response of the nanostructure by projecting the momentary apex near-field onto the kinetic energy of femtosecond electron pulses. Besides the electrical characterization of nanostructures at THz-frequencies, the temporally and spatially confined interaction of free electrons with ultrashort near-fields is expected to enable a novel class of ultrafast vacuum micro- and nanoelectronic devices, and first applications are presented in this talk.

9547-13, Session 4

Mapping near-field plasmonic interactions of silver particles with scanning near-field optical microscopy measurements

Patrick Andrae, Helmholtz-Zentrum Berlin für Materialien und Energie GmbH (Germany) and Freie Universtität Berlin (Germany); Min Song, Helmholtz Zentrum Berlin (Germany); Mohamed Haggui, Paul Fumagalli, Freie Univ. Berlin (Germany); Martina Schmid, Helmholtz-Zentrum Berlin für Materialien und Energie GmbH (Germany) and Freie Univ. Berlin (Germany)

A scanning near-field optical microscope (SNOM) is a powerful tool to investigate optical effects that are smaller than Abbe's limit. Its greatest strength is the simultaneous measurement of high-resolution topography and optical near-field data that can be correlated to each other. However, the resolution of an aperture SNOM is always limited by the probe. It is a technical challenge to fabricate small illumination tips with a welldefined aperture and high transmission. The aperture size and the coating homogeneity will define the optical resolution and the optical image whereas the tip size and shape influence the topographic accuracy. Although the technique has been developing for many years, the correlation between simulated near-field data and measurement is still not convincing.

To overcome this challenge, the mapping of near-field plasmonic interactions of silver nanoparticles is investigated. Different nanocluster samples with diverse distributions of silver particles are characterized via SNOM in illumination and collection mode. This will lead to topographical and optical images that can be used as an input for SNOM simulations with the aim of estimating optical artifacts. Including tip, particles, and substrate, the COMSOL simulations are based on the real set-up and settings. Correlating the high-precision SNOM measurement and the detailed simulation of a full image scan will enable us to draw conclusions regarding near-field enhancements caused by interacting particles.

We will discuss how different tip shapes, particle distributions, and roughness can affect the optical image. Providing the influence of critical measurement parameters (tip-sample distance, step size, integration time), we will improve the SNOM set-up and the resolution of the resulting images.

9547-14, Session 4

Probing plasmonic hot spots on single gold nanowires using combined near field techniques

Patrick Hsia, Sylvie Marguet, CEA-Ctr. de SACLAY (France); Sergei Kostcheev, Renaud J. B. Bachelot, Institut Charles Delaunay (France) and Lab. de Nanotechnologie et Instrumentation Optique (France); Ludovic Douillard, Fabrice Charra, Céline Fiorini-Debuisschert, CEA-Ctr. de SACLAY (France)

Gold nanowires are known to sustain surface plasmons (SP) when they are excited by visible or near-infrared light. SPs correspond to the collective oscillation of conduction electrons which leads to high localized field enhancements called "hot spots". They find various applications such as the optimization of the efficiency of solar cells or the generation of nanosource of light. Comparative characterizations between wires made by colloidal chemistry and by e-beam lithography have been undertaken using complementary near field characterization techniques. Considering comparable excitation conditions, we show that wires made by colloidal synthesis exhibits rather stronger field enhancement effects, their twophoton luminescence (2PL) emission spectrum clearly revealing their crystalline properties.

Simultaneous characterization of the topography and the optical properties of single nanowires was performed both by correlated atomic force microscopy (AFM) coupled with 2PL and by combined low-energy and photoemission electron microscopy (LEEM/PEEM), respectively to get an insight in both the radiative and non-radiative channels of relaxation of the SP. Finally, we present a new near-field technique where the second harmonic signal generated by locally oriented molecules under a tip plays the role of an active probe, enabling to reveal the optical properties of nanoobjects (hot spots). The optical resolution obtainable with this technique is directly linked to the tip apex while the resolution in 2PL depends on the size of the spot. This technique will be further compared to the ones mentioned above and its possibilities will be presented.

9547-15, Session 4

Ultrafast dynamics via coherent excitonplasmon coupling in quantum dot-metallic nanoparticle systems

Seyed M. Sadeghi, The Univ. of Alabama in Huntsville (United States)

When a guantum dot is in the vicinity of a metallic nanoparticle and is driven by a laser field, quantum coherence can renormalize the plasmon field of the metallic nanoparticle, forming a coherent-plasmonic field (CP field). In this contribution we demonstrate that for a given form of variation of this laser field with time, the CP field around the metallic nanoparticle can have offer different forms of field ultrafast dynamics, depending on location. In other words, the coherent exciton-plasmon coupling in such a system can generate distinctive position-dependent coherent-plasmonic dynamics, designating each location around the metallic nanoparticle with a characteristic time-position coordinate. We discuss the way such a process depends on the applied laser field frequency and polarization, quantum dot transition energies, and spacing between the quantum dot and metallic nanoparticle. We also discuss how such a process allows quantum dot-metallic nanoparticle acts as coherent antenna, offering novel ways for adsorption-free detection of certain nanoscale materials. These investigations are carried out by demonstrating that the coherent dynamics responsible for these effects can persist even in the presence of the ultrafast polarization dephasing of the quantum dots. This part of our investigation highlights the prospect of generation and preservation of quantum coherence effects in hybrid quantum dot-metallic nanoparticle systems at elevated temperatures. Therefore, even when the decoherence times of the quantum dots are of the order of several hundreds of femtoseconds, as observed at room temperature, such coherent dynamics can remain guite distinct and observable.

9547-16, Session 4

Efficient coupling and transport of a surface plasmon at 780 nm in a gold nanostructure (Invited Paper)

Yu Gong, Alan G. Joly, Patrick El Khoury, Wayne P. Hess, Pacific Northwest National Lab. (United States)

Nonlinear photoemission electron microscopy (PEEM) is used to map propagating surface plasmons launched from lithographically patterned nanostructures, such as individual nanoholes nanohole arrays and trenches, in noble metal films. The propagation of a coherent surface plasmon is followed, in real time, using a pump-probe technique and locked femtosecond pulse pairs. In effect we produce a movie of plasmon propagation. The plasmon velocity is determined and dispersion properties characterized. Strong near field photoemission patterns are observed in the PEEM images. A damped elongated ring-like photoemission beat pattern is observed from individual nanoholes following low angle of incidence irradiation. In studies of plasmonic nanohole arrays, with sub-15 fs laser pulses centered at 780 nm, focusing of propagating plasmons is optimized as a function of the number of rows and columns constituting the array. The recorded photoemission patterns are attributed to constructive and destructive interference between propagating surface plasmons launched from the individual nanoholes which comprise the array. By exploiting the wave nature of propagating surface plasmons, we demonstrate how varying the array geometry (hole diameter, pitch, and number of rows/ columns) ultimately yields intense localized photoemission patterns. Through a combination of PEEM experiments and finite-difference timedomain simulations, we identify the parameters for optimal array geometry for efficient light coupling and interferometric plasmonic lensing. We also describe an exemplary practical application of the nanohole array-based plasmonic lenses, namely, enhanced photoemission from a vertex of a strategically positioned gold triangle.

9547-18, Session 5

Multicolor fluorescence microscopic imaging of cancer cells on the plasmonic chip

Keiko Tawa, National Institute of Advanced Industrial Science and Technology (Japan) and Kwansei Gakuin Univ. (Japan); Chisato Sasakawa, Shohei Yamamura, Izumi Shibata, Masatoshi Kataoka, National Institute of Advanced Industrial Science and Technology (Japan)

A plasmonic chip which is a metal coated substrate with grating structure can provide the enhanced fluorescence by the grating-coupled surface plasmon field. In our previous studies, bright epi-fluorescence microscopic imaging of neuron cells and sensitive immunosesnsing have been reported. In this study, two kinds of breast cancer cells, MCF-7 and MDA-MB231, were observed with epi-fluorescence microscope on the plasmonic chip with 2D hole-arrays. They were multicolor stained with 4', 6-diamidino-2-phenylindole (DAPI) and allophycocyanin (APC)-labeled anti-epithelial cell adhesion molecule (EpCAM) antibody. Our plasmonic chip provided the brighter fluorescence images of these cells compared with the glass slide. Even in the cells including few EpCAM, the distribution of EpCAM was clearly observed in the cell membrane. It was found that the plasmonic chip can be one of the powerful tools to detect the marker protein existing around the chip surface even at low concentration.

9547-19, Session 5

NIR and MIR charge transfer plasmons in wire-bridged antennas

Yue Zhang, Fangfang Wen, Samuel Gottheim, Nicholas S.

King, Yu Zhang, Peter Nordlander, Naomi J. Halas, Rice Univ. (United States)

SPIE. PHOTONICS

NANOSCIENCE+ ENGINEERING

We investigate optical properties of wire-bridged plasmonic nanoantennas. Here we found two spectral features: a dipolar plasmon in the visible and a Charge Transfer Plasmon (CTP) in the infrared. The CTP depends sensitively on the conductance of the junction wire, offering a controllable way for tuning the plasmon resonance to the desired wavelength regime via junction geometries. Here we use single-particle dark field spectroscopy from UV, visible to IR to identify plasmonic modes in different spectrum regimes. The simulations using Finite-difference time-domain (FDTD) method are in good agreement with experiment: Increasing the junction wire width and concurrently the junction conductance blue shifts resonance positions, and simultaneously modifies scattering strengths, the linewidth of CTP and dipolar plasmon. We notice that CTP in a much longer wavelength regime and preserving a narrow line width, an important implication for designing IR plasmons with a high quality factor for enhanced spectroscopy and sensing applications. We also extend the CTP to the IR regime by increasing the wire length to create IR plasmon while keeping the line width of the resonance. Our work offers a way for studying the charge transfer properties in plasmonic nanostructures. Not only it adds another degree in understanding the charge transfer properties in plasmonic nanostructures but also offers an optical platform for studying molecules transport at optical frequencies and related applications.

9547-20, Session 5

Nanoporous antennae for high quality factor infrared sensing

Denis Garoli, Eugenio Calandrini, Istituto Italiano di Tecnologia (Italy); Sandro Cattarin, CNR-IENI (Italy); Pierfrancesco Zilio, Alessandro Alabastri, Andrea Toma, Ermanno Miele, Francesco De Angelis, Istituto Italiano di Tecnologia (Italy)

In the last decade, the research efforts was focused on the quest of novel plasmonic materials. In particular, the mid-infrared and THz spectral ranges present the advantage of direct probing of the vibrational spectra of the sample but suffers the limit imposed by diffraction. The capability of plasmonics to squeeze and enhance the light in the so-called hot-spots offers a new path for the development of highly-selective optical sensors for biomedical applications.

We introduce a novel material platform for mid-infrared plasmonics and sensing based on nanoporous gold grown by means of Au and Ag cosputtering. Nanoporous gold can be formed by dealloying Au-Ag alloys and its nanostructural features depends on the initial alloy composition. To this goal, co-sputtering technique offers the advantages of complete tuning of the growth parameters and high-scalability. The optical response is completely determined by the nanostructural film features.

Plasma frequency around 3000 cm-1 has been obtained and nanoantenna arrays have been fabricated by means of electron beam lithography and reactive ion etching. Antennas are engineered to support localized plasmon resonances in the 1500-1700 cm-1 range. This device is exploited for the detection of protein conformational states, in their native environment, at extremely low concentration, in the amide-I and -II band range. The employment of nanoporous gold offers the unique advantages of augmented analyte delivery by infiltration inside the sensor, high-effective surface area and versatile functionalization, without affecting the device fabrication by porousity.

9547-21, Session 5

Plasmonic holography: obtaining wide angle, broadband, and high efficiency (Invited Paper)

Jacob Scheuer, Yuval Yifat, Michal Eitan-Wiener, Zeev Iluz, Yael Hanein, Amir Boag, Tel Aviv Univ. (Israel)



We demonstrate wide-angle, broadband and efficient reflection holography by utilizing coupled dipole-patch nano-antenna cells to impose an arbitrary phase profile on of the reflected light. High fidelity images were projected at angles of up to 450 with respect to the impinging light with efficiencies exceeding 50% over an optical bandwidth of 200nm. The demonstration of such reflectarrays opens new avenues towards expanding the limits of large angle holography and rendering it a practical technology.

9547-87, Session 5

Tuning plasmonic cavity modes by the symmetry breaking of metasurface (Invited Paper)

Hui Liu, Nanjing Univ. (China)

A plasmonic cavity composed from metasurface is designed and experimentally demonstrated. Due to the symmetry breaking of the metasurface, the degeneracy of the different polarized cavity states is lifted. It shifts the resonating frequencies of two polarized cavity modes, in which one is blue-shifted and another is red-shifted. Combining with a photothermal effect, we demonstrate that the polarized cavity states can be experimentally tuned by varying the reflection phase of the metasurface through the incident laser intensity. This reported metacavity can be applied in cavity quantum optics, lasers and other light-matter interaction processes.

9547-22, Session 6

Strongly coupled plasmon-nanocavity modes for broadband, near-field induced absorption in ultrathin semiconductor coatings (Invited Paper)

Carl Hagglund, Uppsala Univ. (Sweden)

Ultrathin nanocomposite layers comprising noble metal nanoparticles and semiconductor coatings can support localized surface plasmon resonances (LSPRs) with very large cross sections for absorption and scattering of light. These plasmon resonances are highly sensitive to details of the geometry as well as to the permittivity of the metal and semiconductor components, allowing their effective optical properties to be adapted to a range of important applications including solar energy conversion.

By employing such a nanocomposite system as an essentially two dimensional absorber layer in an absorber/spacer/reflector stack, extreme levels of absorption per unit volume can be accomplished through optical impedance matching.1 This is of high interest for solar cells, where it may enable a two orders of magnitude reduction of the absorber layer thickness, implying potentially large gains in terms of cost reductions and conversion efficiency. However, in order to exploit such ultrathin nanocomposite layers for efficient solar energy conversion, the absorption must cover a broad spectral range and losses in the form of Joule heating of the metal components must be minimized.

These challenges may be approached by exploiting plasmon near-field induced absorption in heavily damping semiconductor coatings.2 The damping broadens the LSPR and channels a high fraction of the absorption into the semiconductor layer while it suppresses Joule heating. Additional benefits can be gained through strong coupling of the damped LSPR and a Fabry-Perot nanocavity mode supported by the absorber/spacer/reflector system. This results in additional peak width and even anticrossing behavior when the coupling is strong enough compared to the overall damping. Based on a 10 nm thick semiconductor coating grown on a gold nanoparticle array by atomic layer deposition, these effects are experimentally verified and used to demonstrate a very high average semiconductor absorption across the spectral range targeted for solar energy applications.

1 Hägglund, C. et al. Self-assembly based plasmonic arrays tuned by atomic layer deposition for extreme visible light absorption. Nano Lett. 13, 3352-3357, (2013).

2 Hägglund, C. & Apell, S. P. Plasmonic near-field absorbers for ultrathin solar cells. The Journal of Physical Chemistry Letters 3, 1275-1285, (2012).

9547-23, Session 6

Cooperative energy transfer in plasmonic systems

Tigran V. Shahbazyan, Jackson State Univ. (United States); Vitaliy N. Pustovit, Augustine M. Urbas, Air Force Research Lab. (United States)

Forster's energy transfer between donor and acceptor fluorophores, e.g., dye molecules or semiconductor quantum dots, underpins diverse phenomena in biology, chemistry and physics. While Forster's transfer between isolated fluorophores is efficient only for relatively short donoracceptor separations below 10 nm, plasmon-mediated transfer channels that arise when fluorophores are placed near metal nanostructures lead to significant increase of energy transfer rate for larger donor-acceptor distances. The fraction of the donor energy absorbed by the acceptor is determined by ta subtle interplay between transfer, radiation and dissipation channels. We describe a cooperative amplification mechanism for plasmonmediated energy transfer from a large ensemble of donors to fewer acceptors. The plasmonic coupling between donors' gives rise to robust superradiant and subradiant states and the energy transfer takes place from these collective states rather than from many individual donors. We show that the transfer efficiency from superradiant states is significantly amplified relative to that from the same number of individual donors due to the large matrix element of superradiant states with acceptor's electric field. At the same time, energy transfer from subradiant states is amplified as well due to their reduced Ohmic and radiative losses.

9547-24, Session 6

Surface plasmon strengthened nonlinearity in indium-tin-oxide coated Cu-doped potassium sodium barium strontium niobate crystals

Hua Zhao, Liang Li, Jingwen Zhang, Harbin Institute of Technology (China)

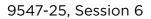
Since the electromagnetic fields associated with the surface plasmon polaritons (SPPs) are localized at interfaces and often intensified greatly [1], the nonlinearity of optical materials were strengthened greatly [2]. In the past years, researchers tuned the plasma frequency of semiconductor indium tin oxide (ITO) thin films towards shorter wave by applying external electric field [3]. We used internal photovoltaic field to tune ITO plasma frequency from IR to visible band in lithium niobate [4]. In this work, we employed fast response, pyroelectric Cu-doped (K0.5Na0.5)0.2(Sr0.75 Ba0.25)0.9Nb2O6 (KNSBN) crystals in modifying ITO coating to support visible SPP to strengthen its nonlinearity in KNSBN. As the result, (1) a 2 dimensional diffraction pattern was observed with only two writing beams; (2) The reflectivity on the very first surface was changed 2.3%, equivalent to 0.023 refractive index change; (3) as high as 3.0% energy transferring to the reflection on the first surface was measured, resulting unambiguously from energy transferring in subwavelength scale. All these results, beyond reach of conventional photorefractive theory, consist with our theoretical consideration based on SPP excitation. The phase grating mediated SPP excitation is promising in designing photonic devices.

[1] S. Hayashi, and T. Okamoto, J. Phys. D: Appl. Phys. 45, 433001 (2012).

[2] P. Gadenne and J. C. Rivoal, Topics Appl. Phys. 82, 185-215 (2002).

[3] E. Feigenbaum, K. Diest, and H. A. Atwater, Nano Lett. 10, 2111 (2010).

[4] H. Wang, H. Zhao, C. Xu, L. Li, G. Hu, and J. Zhang, Appl. Phys. Express, 7, 102001 (2014).



Enhancing second-order nonlinearity on Au-nanorods at localized surface plasmon resonance with nonlinear optical polymers

Atsushi Sugita, Takuma Hirabayashi, Shunsuke Nihashi, Atsushi Ono, Yoshimasa Kawata, Univ. of Shizuoka (Japan)

We will present second harmonic generations (SHG) from Au nanorods coated with nonlinear optical (NLO) polymers. Nonlinear Plasmonics, the technologies of mixing multiple Surface Plasmon (SP)-enhanced optical fields, have attracted great attentions as one of the most important basic technologies for next-generation high-speed, high-density and ultracompact integrated photonic devices. Most of the previous studies have exploited the nonlinearities of metal surfaces, where the SP waves were generated. In the present study, we challenged enhancing the nonlinearities of the metal surfaces with the NLO polymers. The three kinds of the NLO polymers with different transition frequencies were prepared. The localized Surface Plasmon (LSP) waves were excited with Au-nanorods. The LSP resonant frequencies were tuned by changing the aspect ratio of the nanorods. The NLO polymer thin film with 50 nm-thickness was coated on the nanorods. When the excitation light wavelength agreed with the LSP resonant wavelength, the nanorods emitted the intense SHG waves, whether or not the NLO polymers were coated. However, the SHG conversion efficiency of the NLO polymer coated nanorods was higher than that of the pristine nanorods. Furthermore, the conversion efficiencies were higher, as the transition wavelengths of the NLO polymers were closer to the excitation light wavelength. The 3.5-fold enhancement in the conversion efficiency was recorded from the nanorods whose absorption peak was the closest to the LSP excitation wavelength, comparing with that from the pristine nanorods. The results proved that the enhancements of the nonlinearities due to the near-resonant excitations were available for the nonlinear plasmonics.

9547-26, Session 6

A comparative study of second-harmonic generation in plasmonic and dielectric gratings made of centrosymmetric materials

Martin Weismann, Univ. College London (United Kingdom) and Photon Design Ltd. (United Kingdom); Dominic F. G. Gallagher, Photon Design (United Kingdom); Nicolae-Coriolan Panoiu, Univ. College London (United Kingdom)

We present a new numerical method for the analysis of second-harmonic generation (SHG) in one- and two-dimensional (1D, 2D) diffraction gratings containing centrosymmetric quadratically nonlinear materials. Thus, the nonlinear optical properties of a material are determined by its symmetry properties: non-centrosymmetric materials lack inversion symmetry and therefore allow local even-order SHG in the bulk of the material, whereas this process is forbidden in centrosymmetric materials. The inversion symmetry of centrosymmetric materials is broken at their surface whence they allow local surface SHG. Additionally, centrosymmetric materials give rise to nonlocal (bulk) SHG.

Our numerical method extends the linear generalized source method (GSM), which is an efficient numerical method for solving the problem of linear diffraction in periodic structures of arbitrary geometry. The nonlinear GSM is a three-step algorithm: for a given excitation at the fundamental frequency the linear field is computed using the linear GSM. This field gives rise to a nonlinear source polarization at the second harmonic (SH) frequency. This nonlinear polarization comprises surface and bulk polarizations as additional source terms and is subsequently used to compute the nonlinear near- and far-field optical response at the SH.

We study the convergence characteristics of the nonlinear GSM for 1D and 2D periodic structures and emphasize the numerical intricacies caused by the surface SH polarization term specific to centrosymmetric materials. In

order to illustrate the practical significance of our numerical method, we apply it to metallic gratings made of Au and Ag as well as dielectric grating structures made of silicon and investigate the relative contribution of the bulk and surface nonlinearity to the nonlinear optical response at the SH. Particular attention is paid to optical effects that have a competing influence to the nonlinear optical response of the grating structures, namely the resonant local field enhancement and optical losses.

OPTICS+

NANOSCIENCE+ ENGINEERING

SPIE. PHOTONICS

9547-27, Session 7

Surface-enhanced Raman spectroscopy on engineered plasmonic metamaterials for "label free" biosensing (Invited Paper)

Massimo Rippa, Rossella Capasso, Marianna Pannico, Pietro La Manna, Pellegrino Musto, Consiglio Nazionale delle Ricerche (Italy); Jun Zhou, Ningbo Univ. (China); Lucia L. Petti, Consiglio Nazionale delle Ricerche (Italy)

The last decade has been characterized by artificial electromagnetic (EM) materials, including photonic crystals (PCs) and photonic quasi-crystals (PQCs), making these very attractive given that there are new possibilities to control the EM field in innovative way. Quasiperiodic crystals (QCs) are a new class of materials that have fascinating optical properties lying somewhere between those of disordered and period structures. With the use of PCs and PQCs, it is possible to synthesize novel artificial structures characterized by selective EM responses, which, in turn, undergo significant frequency shifts, in presence of biological material.

In the present work we studied artificial EM nanomaterials to develop innovative plasmonic nanobiosensors based on Surface Enhanced Raman Scattering (SERS) substrates and working in the visible and NIR frequency bands. Fabricated gold PQCs in a Thue Morse arrangement are proposed for the engineering of reproducible SERS substrates. Scanning electron microscopy, UV/Vis absorption spectroscopy, dark field microscopy and atomic force microscopy (AFM) are used to characterize the experimental structure. Using a molecular monolayer of pMA (p-mercaptoaniline) as a Raman reporter, we show that high values of SERS enhancement factors can be achieved in photonic structures.

9547-28, Session 7

Nonradiative Energy Transfer in Layered **Metal-Dielectric Nanostructure Mediated** by Surface Plasmon

Sepideh Golmakaniyoon, Nanyang Technological Univ. (Singapore) and LUMINOUS! Ctr. of Excellence for Semiconductor Lighting and Displays (Singapore); Xiaowei Sun, Hilmi V. Demir, Nanyang Technological Univ. (Singapore)

Plasmon resonance energy transfer has received great attention in semiconductor nanoparticles structures. The conventional sandwich configuration consists of donor-metal nanostructure-acceptor has been successfully applied to improve the nonradiative energy transfer efficiency from the excited donor dipole to the acceptor molecule via surface plasmon coupling at the interfaces. Here we demonstrate that the cascaded plasmon coupling gives rise to more efficient energy transfer mechanism compared to single plasmon coupling. The approach has been illustrated through the analytical simulation of an oscillating dipole near the stratified nanostructure of silver-dielectric-silver-acceptor. The overlaps of the surface plasmon modes at the silver-dielectric and dielectric-silver interfaces lead to the stronger cross coupling in comparison with the single silver layer configuration. Moreover, the experimental results are in good agreement with the analytical simulation. The consistency confirms more than 100% plasmon resonance energy transfer enhancement in the donor-silver-dielectric-silver-acceptor configuration compared to the donor-silver-acceptor structure. The current approach uniquely allows



designing the optoelectronic devices with less photoluminous quenching and more efficient energy transfer process due to the reduction in total metal thickness and stronger surface plasmon coupling at the boundaries, respectively.

9547-29, Session 7

Integrated ring grating-nanoantenna structure for plasmon/emitter coupling

Nancy Rahbany, Wei Geng, Rafael Salas-Montiel, Sylvain Blaize, Renaud J. B. Bachelot, Univ. de Technologie Troyes (France); Christophe Couteau, Univ. de Technologie Troyes (France) and Nanyang Technological Univ. (Singapore)

There is a growing interest nowadays in the study of strong light-matter interaction at the nanoscale [1], specifically between surface plasmon polaritons and emitters [2]. Researchers in the fields of plasmonics, nanooptics and nanophotonics are constantly exploring new ways to control and enhance surface plasmon launching, propagation, and localization [3]. Moreover, emitters placed in the vicinity of metallic nanoantennas exhibit fluorescence rate and guantum yield enhancement [4] due to the increase in the electromagnetic confinement in the region [5]. However, numerous applications such as optical electronics, nanofabrication and sensing devices require a very high optical resolution which is usually limited by the diffraction limit. Targeting this problem, we introduce a novel plasmonic structure consisting of metallic nanoantennas integrated in the center of ring diffraction gratings [6, 7]. Propagating surface plasmon polaritons (SPPs) are generated by the ring grating and couple with localized surface plasmons (LSPs) at the nanoantennas, which excites dye molecules placed in the gap. Numerical FDTD simulations as well as experimental optical characterization results are presented. Ring gratings containing nanoprisms, single bowtie nanoantennas and double bowtie nanoantennas were fabricated using Electron Beam Lithography (EBL). Plasmon-emitter coupling was studied upon measuring the photoluminescence spectrum of dye molecules placed in the nanoantenna gap, where a comparison between the different nanoantennas is provided. The combination of the sub-wavelength confinement of LSPs and the high energy of propagating SPPs in our structure leads to precise nanofocusing at the nanoscale, which can be implemented to reach the strong coupling regime between emitters and surface plasmons.

[1] Tame, M. S., et al. "Quantum plasmonics," Nat. Phys. 9.6 (2013): 329-340.

[2] Törmä, P., & Barnes, W. L., "Strong coupling between surface plasmon polaritons and emitters," ArXiv Preprint. (2014): ArXiv14051661.

[3] Barnes, W. L., et al. "Surface plasmon subwavelength optics," Nature 424.6950 (2003): 824–830.

[4] Kinkhabwala, A., et al. "Large single-molecule fluorescence enhancements produced by a bowtie nanoantenna," Nature Photonics 3 (2009): 654–657.

[5] Maier, S. A., et al. "Local detection of electromagnetic energy transport below the diffraction limit in metal nanoparticle plasmon waveguides," Nature Materials 2.4 (2003): 229–232.

[6] Rahbany, N., et al. "A concentric plasmonic platform for the efficient excitation of surface plasmon-polaritons," Submitted to Optics Express (2015).

[7] Rahbany, N., et al. "Integrated plasmonic double bowtie / ring grating structure for enhanced electric field confinement," Submitted to Nanospectroscopy (2015).

9547-30, Session 7

Fluorescence enhancement using Fanoresonant a plasmonic nanostructure with selective functionalization of molecules at the electromagnetic hot spot

Xiaolong Wang, Olivier J. F. Martin, Ecole Polytechnique

Fédérale de Lausanne (Switzerland)

In recent years, one has paid significant attention to plasmonic nanostructures due to their potential for practical applications. Especially, in most plasmonic nanostructures, the local density of optical states is strongly enhanced and confined in the nanogap region - like for example in plasmonic antennas – which results in the so-called electromagnetic hot spots. In this work, we use 4-nanorod structures made with silver to generate and tune Fano resonances exhibiting an asymmetric and narrow lineshape. In such a system, a strongly enhanced electromagnetic field is created in the nanogap when the two antenna modes undergo destructive interference, i.e. at the Fano resonance. The local near field is thus strongly enhanced since most of the energy is not radiated into the far field at that wavelength. We will show that using a 4-nanorod structure in silver, we can easily tune the Fano resonance through the fluorescence spectrum of the molecule under study, thus exploring the different resonance conditions between the molecule absorption/emission bands and the plasmonic nanostructure; both the excitation and emission rates of the molecule can be enhanced when it is placed within the hot spot. To this end, we have developed a double electron beam lithography process to fabricate the plasmonic nanostructures and then selectively immobilize the molecule in the hot spot, in order to investigate the fluorescence enhancement under well-controlled conditions. The fluorescence enhancement is demonstrated by measuring the fluorescence lifetime and the fluorescence count rate. The experimental results are supported by theoretical modelling and numerical calculations with the Green's tensor method.

9547-31, Session 7

Plasmon enhanced linear and nonlinear photoluminescence in planar nanoparticle arrays

Gary F. Walsh, U.S. Army Natick Soldier Research, Development and Engineering Ctr. (United States) and Boston Univ. (United States); Luca Dal Negro, Boston Univ. (United States)

Light emission from metal nanoparticles has potential appications as a highly sensitive refractive index detector. In order for this protential to be realized the mechanics of plasmon enhanced photoluminescence (PL) in planar nanoparticle arrays must be understude. We present an experimental exploreation of emission spectra and realitive efficiency of gold PL in nanoplasmonic arrays. We demonstrate tunability of metal PL by nanoparticle size and discover the critical role of near-field interparticle coupling on emission efficiency. We show that direct excition of plasmon resonances by photoexcited electron-hole pairs is the primary contributer to the metalic nanoparticle emission spectrum. We additionally show that emission is quenched by near-field interactions between nanoparticles leading to spectral broading by increased non-radiative plasmon decay. Finally, we show a correlation between plasmon life-time and PL efficiency. We explore this phenominan for both linear and nonlinear PL. Experimental results are supported by numerical simulations of plasmon life-time.

9547-32, Session 7

Probing and controlling large Purcell enhancement in plasmonic nanoantennas

Maiken H. Mikkelsen, Duke Univ. (United States)

Plasmonic cavities and nanoantennas can strongly modify the excitation and decay rates of nearby emitters by altering the local density of states. Here, we demonstrate large enhancements of fluorescence and spontaneous emission rates of molecules embedded in plasmonic nanoantennas with sub-10-nm gap sizes. The nanoantennas consist of colloidally synthesized silver nanocubes coupled to a metallic film which is separated by a 5-15 nm self-assembled polyelectrolyte spacer layer with embedded molecules. Each nanocube resembles a nanoscale patch antenna whose plasmon resonance can be changed independent of its local field enhancement.



By varying the size of the nanopatch, we tune the plasmon resonance by ~200 nm throughout the excitation, absorption, and emission spectra of the embedded molecules demonstrating giant fluorescence enhancement for antennas resonant with the excitation wavelength [A. Rose, T.B. Hoang, F. McGuire, J.J. Mock, C. Ciraci, D.R. Smith & M.H. Mikkelsen, Nano Letters 14, 4797 (2014)]. Next, we directly probe and control the nanoscale photonic environment of the embedded emitters including the local field enhancement, dipole orientation and spatial distribution of emitters. This enables the design and experimental demonstration of Purcell factors exceeding 1,000, while maintaining high quantum efficiency and directional emission [G.M. Akselrod, C. Argyropoulos, T.B. Hoang, C. Ciracì, C. Fang, J. Huang, D.R. Smith & M.H. Mikkelsen, Nature Photonics 8, 835 (2014)]. Full-wave simulations incorporating the nanoscale environment accurately predict the experimentally observed emission dynamics and reveal design rules for future devices. Finally, progress on coupling colloidal quantum dots to the plasmonic nanopatch antennas will be discussed.

9547-33, Session 8

Second harmonic excitation spectroscopy in studies of Fano-type coupling in plasmonic arrays

Gary F. Walsh, U.S. Army Natick Soldier Research, Development and Engineering Ctr. (United States) and Boston Univ. (United States); Jacob T. Trevino, The City Univ. of New York Advanced Science Research Ctr. (United States) and Boston Univ. (United States); Emanuele Francesco Pecora, Stanford Univ. (United States) and Boston Univ. (United States); Luca Dal Negro, Boston Univ. (United States)

Scattering by plasmon resonances of metallic nanoparticles can be tailored by particle material, size, shape, and local as well as long-range order. In this presentation we discuss a series of experiments in which long-range Fanotype coupling between grating resonances and localized surface palsmon (LSP) resonances were studied using second harmonic excitation (SH-E) spectroscopy. By tuning the excitation wavelength of a femtosecond laser and measuring the relative second harmonic (SH) signal we demonstrated that when long-range grating resonances spectrally overlap with those of the LSPs, electromagnetic field enhancement occurs on the surface of the nanoparticles leading to an increase in nonlinear scattering. This effect has been demonstrated for periodic arrays of monomers and dimers, bi-periodic antenna arrays for multi-spectral focusing to a single point, and chirped nanoparticle structures for broadband field enhancement. Results are supported by finite difference time domain simulations showing that electromagnetic fields are enhanced close on the surface of the nanoparticles when long-range structural resonances are excited. These studies have revealed design principles for engineering the interplay of photonic and plasmonic coupling for future linear and nonlinear plasmonic devices.

9547-34, Session 8

Predicting nonlinear properties of metamaterials from the linear response

Kevin O'Brien, Haim Suchowski, Junsuk Rho, Alessandro Salandrino, Boubacar Kante, Xiaobo Yin, Xiang Zhang, Univ. of California, Berkeley (United States)

Nanostructures and metamaterials have attracted interest in the nonlinear optics community due to the possibility of engineering their nonlinear responses. Much debate surrounds whether the nonlinear susceptibility can be represented by an anharmonic oscillator model (Miller's rule) which implies a direct relation between the nonlinearity and a product of its linear susceptibilities. In this work we show experimentally that Miller's rule does not apply in general and that nonlinear scattering theory accurately predicts the optimal geometry for nonlinear emission.

We study the geometry dependence of the second harmonic and third harmonic emission from gold nanostructures by designing arrays of nanostructures whose geometry varies from bars to split ring resonators. We change the length (and volume) of the nanostructure on one axis, and change the morphology on the other axis. We observed that the maximum second harmonic generation does not occur at the morphology indicated by a nonlinear oscillator model with parameters derived from the far field transmission; however, we find a near field overlap integral accurately predicts the optimal geometry. We show that the optimum geometry for nonlinear generation can be predicted from an overlap integral between the local nonlinear susceptibility and the mode of the nanostructure at the emission wavelength. This conclusion is independent of the specific structure studied and may be applied in order to predict the nonlinear generation from any plasmonic nanostructure or metamaterial.

9547-35, Session 8

Multi-coupled resonant splitting with a nano-slot metasurface and PMMA phonons

Michael F. Finch, Brian A. Lail, Florida Institute of Technology (United States)

Coupled-resonances can be used in applications that include, but are not limited to, surface-enhanced infrared spectroscopy (SEIRS), surfaceenhanced Raman spectroscopy (SERS), biosensing, and index sensing. Fano resonance in analogue plasmonic systems has been described as the coupling of a bright (superradiant) mode and a dark (subradiant) mode via the near field. Dark and bright mode interactions are investigated with the use of a Fano resonant metamaterial (FRMM) where the metamaterial is a dual nano-slot metasurface on a silicon cavity. The FRMM is numerically simulated using Ansys high frequency structural simulator (HFSS). The FRMM is coupled to the carbon double bond in polymethyl methacrylate (PMMA) to demonstrate mode splitting and signal enhancement. Then the dual nano-slot is compared to the complementary dual nano-rod configuration.

9547-36, Session 8

Local field enhanced second-harmonic response of organic nanofibers

Oksana Kostiu?enko, Till Leißner, Jacek Fiutowski, Jonathan R. Brewer, Horst-Günter Rubahn, Univ. of Southern Denmark (Denmark)

Organic CNHP4 nanofibers showing a strong second-harmonic (SH) response have been successfully implemented as active components in a metal-organic hybrid system. Using nondestructive roll-on transfer technique nanofibers were transferred from the growing mica substrates onto electron-beam lithography-defined regular arrays of gold, titanium and silicon oxide. As shown in a femtosecond laser scanning microscopy study the fiber-substrate interplay leads (only) on gold to a significantly enhanced SH signal. We suggest that this effect is driven by the local field enhancement i.e. the excitation of surface plasmon polaritons (SPP) and lightning rod effects, since in case of Ti and SiO2 no SPPs are excited at a laser wavelength of 790 nm and the used array dimensions. Furthermore, we observe a considerably reduced fluorescence lifetime for the fibers deposited on gold arrays supporting the assumption of strong interaction between gold substrate and fibers. In summary we show that by adjusting substrate and fiber properties the SH response can be locally controlled.

9547-37, Session 8

Plasmonic coupling of gold curvilinear nanorods with nanogap

Yukie Yokota, Takuo Tanaka, RIKEN (Japan)

Conference 9547: Plasmonics: Metallic Nanostructures and Their Optical Properties XIII



The local-mode surface plasmon resonances of a closely-spaced dimer of two identical metal nanostructures, such as straight nanorods, nanoparticles, strongly interact due to dipole-dipole coupling. These strong interactions have been exploited in various applications, such as surface-enhanced Raman scattering, biosensing, and near-field optical spectroscopy. Nevertheless, there are few reports about the spectral properties of LSP on a pair of two intricately-shaped nanostructures. We fabricated gold curvilinear nanorods dimers with various gap widths and structural configurations using electron beam lithography and lift-off technique. In this work we present detailed studies of plasmonic coupling of gold curvilinear nanorod dimer with controlling gap distance. When the linearly polarized light that oscillates parallel to the long axis of curvilinear nanorod is irradiated on the sample structures, transmission spectrum of gold curvilinear nanorod monomers has one resonant peak in near-infrared region and the peak position is the same as that of the structures of the arc length of curvilinear nanorod. Compared to transmission spectrum of curvilinear nanorod monomers, the plasmon resonance peak of curvilinear nanorod dimers that has 10nm nanogap with outside center of curved portion in the y-axis symmetry was blue shift.

9547-38, Session 9

Graphene plasmonics: multiple sharp Fano resonances in silver split concentric nanoring resonator dimers on a metasurface

Arash Ahmadivand, Nezih Pala, Florida International Univ. (United States)

Graphene plasmonics has been introduced as an alternative strategy in designing and fabricating plasmonic structures and devices in nanoscale regime. Tighter confinement and significant decay length are the major features which persuaded researchers to employ graphene plasmonics instead of regular noble metals in various applications. Herein, we propose to use graphene plasmons as a platform for inducing strong dark modes in silver split concentric nanoring resonator dimers on a multilayer metasurface composed of graphene sheet and silicon substrate. Using numerical methods, we examined the possibility of appearing pronounced double Fano resonant modes as strong hot spots and also, the influence of carbon atoms sheet in intensifying the intensity of Fano dips is reported. Employing the geometrical versatility of concentric rings in designing a colloidal dimer structure, we enhanced the tunability and performance of the appeared Fano resonant mode in the visible to the near infrared region. It is shown that a thin layer of graphene with a few nanometers thickness under the dimer structure helps to localized huge amount of optical energy to produce hot spots. Our theoretical results paves a method toward inducing pronounced Fano resonances via tremendous electromagnetic field confinement and ultrastrong near-field coupling. This understating opens new avenues to utilize simple dimers in designing metamaterial structures to use in fabricating biochemical and DNA sensors, and photodetectors.

9547-39, Session 9

Graphene spports the manipulating mode propagation in the hybird plasmonic nanowaveguides

Xiaosai Wang, Jiangnan Univ. (China); Jicheng Wang, Jiangnan Univ. (China) and Purdue Univ. (United States); Ci Song, Sinian Qu, Lin Sun, Jiangnan Univ. (China)

We propose a new type of plasmonic waveguide in a graphene-coated V-groove. A graphene layer treated as an ultra-thin "metal" layer could support transverse magnetic (TM) polarized surface plasmon polaritons (SPPs) when the imaginary of the graphene's conductivity is larger than zero. The graphene permittivity can be controlled by varying the chemical potential in the terahertz frequencies. The subwavelength confinements and the propagation of the SPPs modes of the graphene waveguide

structure are reached. The mode field energies can be well confined in the V-groove and be adjusted by changing the depth of the groove, the opening angle of the channel and the chemical potential of graphene. The mode confinements become weaker as increasing the depth of the groove, the angle of V-groove and the chemical potential of grapheme, respectively. The field energies of SPPs could be mainly focused at the bottom of graphene-coated V-groove if the groove is deep enough. In addition, the mode distributions of the graphene-coated nanowire are also discussed. By changing the nanowire radius and the chemical potential of graphene, we can reach different characteristic of SPP modes. And the m=5 mode can be achieved when the radius R=100nm at 30THz. The relationship between effective index and propagation length with the radius are discussed, respectively. Based on those two structures, we propose a hybrid plasmonic waveguide with a graphene-coated nanowire placing in a graphene-coated V-groove. The mode field energies are strongly confined between the graphene-coated nanowire and the V-groove.

9547-40, Session 9

Observation of Fano resonances in highly doped semiconductors plasmonic resonators

Thierry Taliercio, Vilianne Ntsame Guilengui, Univ. Montpellier 2 (France); Jean-Baptiste Rodriguez, Univ. of Montpellier (France); Laurent Cerutti, Eric Tournié, Univ. Montpellier 2 (France)

All-semiconductor plasmonics gives the opportunity to build new plasmonic structures with embedded resonators of highly doped semiconductor (HDSC) in a matrix of un-doped semiconductor for mid-IR applications. In this work, we report on the excitation of Fano resonances in the midinfrared range using plasmonic resonators based on HDSC. Using adequate semiconductors, InAsSb and GaSb grown by molecular beam epitaxy (MBE), we have designed the right structure to obtain the expected optical properties. The samples are lattice matched to the GaSb substrate which offers the possibility to integrate the plasmonic resonators at the heart of photonic devices. The embedded nanostructures have been studied by highresolution transmission electron-microscopy (HR-TEM) to accurately retrieve the geometrical parameters of the resonator. These actual geometrical parameters have then been used to model the optical properties of the HDSC resonators by the FDTD technique and a model based on Fano resonances. Excellent agreement has been achieved between simulation and experiments. We show that it is possible to control the optical properties of the plasmonic resonators by adjusting their geometrical parameters or the doping level of the HDSC. This work demonstrates the possibility to develop all-semiconductor plasmonics for photonic applications in the mid-IR range.

9547-41, Session 9

Alloyed thin-films and nanostructures with dielectric function on demand

Chen Gong, Allen Chang, Ellen Cesewski , Marina S. Leite, Univ. of Maryland, College Park (United States)

If one could arbitrarily modulate the dielectric function of metals, this would permit an exceptional control of the plasmon resonances in nanostructures and thin-films, leading to the development of a new class of materials with tunable optical responses for the fabrication of optoelectronic devices with unique characteristics. Here we present plasmonic thin-films and nanoparticles based on alloyed metals, formed by the combination of Ag, Al, Au and Cu. We modulate the dielectric function of the alloys by modifying its chemical composition. We measure the surface plasmon propagation for the different alloys, and control the angle of propagation as a function of the thin-film composition. Further, we fabricate nanoparticles also with tunable chemical composition and optical response. We spatially and spectrally resolve the scattering and transmission characteristics by NSOM measurements of the alloyed nanostrustures. Mie calculations are used to corroborate our results, showing that the scattering efficiency of the alloys



nanostructures strongly depend on its composition. These new materials can be used for the design of metamaterials with dielectric function on demand.

9547-42, Session 10

Plasmonics for the industry (Invited Paper)

Benjamin Gallinet, Ctr. Suisse d'Electronique et de Microtechnique SA (Switzerland)

Metallic nanostructures interact strongly with light through surface plasmon modes and many application fields have been proposed during the past decade, including light harvesting to sensing and structural colors. However, their implementation for the industry requires the development of up scalable and cost effective manufacturing processes. The fabrication at wafer scale of plasmonic nanostructures and metamaterials using nano imprint lithography is reported. After structuring, one or several evaporations of various plasmonic materials are performed with a tilt angle with respect to the substrate, which increases the light interactions with the different metallic layers as well as enlarges the design possibilities. A step and repeat process is used to increase further the area of nanostructured surface. The measured optical properties of the fabricated structures show a very good agreement compared to numerical calculations using the rigorous coupled wave analysis and the surface integral method. These numerical calculations together which structural characterization, increase the process control and enable the design of the nanostructures for specific applications. In particular, nanostructures with a shape similar to split ring resonators and which support high order plasmonic modes showing Fano resonances are shown to be promising for sensing applications. Another kind of plasmonic substrates is reported, which shows unique color effects with a large palette of colorations. With a specific design, the structural colors are associated with a strong interaction between the polarizations which increases the complexity of the color effect rendered to the user. Finally, the potential of plasmonic nanostructures for the management of solar light is discussed.

9547-43, Session 10

Optical dark field and electron energy loss imaging and spectroscopy of symmetryforbidden modes in loaded nanogap antennas

Todd Brintlinger, U.S. Naval Research Lab. (United States); Andrew Herzing, National Institute of Standards and Technology (United States); James P. Long, Igor Vurgaftman, Rhonda Stroud, Blake S. Simpkins, U.S. Naval Research Lab. (United States)

Theoretical work has identified a new type of hybrid nanoresonator akin to a loaded-gap antenna, wherein the gap between two collinearly aligned metal nanorods is filled with active dielectric material. The gap optical load has a profound impact on resonances supported by such a "nanogap" antenna, and thus provides opportunity for (i) active modulation of the antenna resonance and (ii) delivery of substantial energy to the gap material. To this end, we have (i) used a bottom-up technique to fabricate nanogap antennas (Au/CdS/Au); (ii) characterized the optical modes of individual antennas with polarization- and wavevector-controlled dark-field microscopy; (iii) mapped the spatial profiles of the dominant modes with electron energy loss spectroscopy and imaging; and (iv) utilized full-wave finite-difference time-domain simulations to reveal the nanoscopic origin of the radiating modes supported on such nanogap antennas.

In addition to conventional transverse and longitudinal resonances, these loaded nanogap antennas support a unique symmetry-forbidden gap-localized transverse mode arising from the splitting of degenerate transverse modes located on the two gap faces. This previously unobserved mode is strong (E2 enhanced ~20), tightly localized in the nanoscopic (~30 nm separation) gap region, and is shown to red-shift with decreased gap size and increased gap dielectric constant. In fact, the mode is highly suppressed in air-gapped structures which may explain its absence from the literature to date. Understanding the complex modal structure supported on hybrid nanosystems is necessary to enable the multi-functional components many seek.

9547-44, Session 10

Epitaxial silver as a plsamonic materials platform: from plasmonic nanolasers to long range plasmonic wave propagations (Invited Paper)

Chih-Kang Shih, The Univ. of Texas at Austin (United States)

Plasmonics is an emerging field which harnesses surface plasmon polaritons (SPPs)-hybrid modes of photons and surface plasmons-to achieve confinement of electromagnetic fields at a deeply subwavelength scale. It has the potential of providing a true alternative to electronic circuits and operations, with orders of magnitude gains in terms of speed, frequency of operation and available bandwidths. Despite impressive conceptual demonstrations, the field of plasmonics faces a severe material limitation: SPPs are highly damped in current plasmonics materials and cannot travel beyond a few wavelengths if confined to sub-wavelength scales. Thus far, most plasmonics applications utilize thermally deposited noble metal (e.g. Ag and Au) films which are granular and are therefore subjected to high scattering loss. We show that this adverse effect can be eliminated by developing epitaxial silver films on semiconductor (EpSoS) a plasmonic platform. By using the EpSoS platform, we demonstrate two key applications: CW operation of plasmonic nanolaser with ultra-low thresholds and extra-ordinary long propagation length for SPP in the visible wavelength range. These demonstrations lay foundation for potential integration of nanophotonics.

*The research work on plasmonic nanolaser was carried out in collaboration with Professor S. Gwo of National Tsing-Hua University. The work on long range plasmonic wave propagations was carried in collaboration with Professor X.Q. Li of the University of Texas at Austin.

9547-45, Session 10

Femtosecond control of magneto-optical effects in magnetoplasmonic crystals (Invited Paper)

Andrey A Fedyanin, Maksim R Shcherbakov, Polina P Vabishchevich, Lomonosov Moscow State Univ (Russian Federation); Aleksandr Yu. Frolov, Lomonosov Moscow State Univ. (Russian Federation); Artem V Chetvertukhin, Tatiana V Dolgova, Lomonosov Moscow State Univ (Russian Federation)

In magnetoplasmonics, it is possible to tailor the magneto-optical properties of nanostructures by exciting surface plasmon-polaritons. Thus far, magnetoplasmonic effects have been considered to be static. Here, manifestations of a time-dependent transversal magneto-optical Kerr effect were experimentally demonstrated in femtosecond laser pulses reflected from a one-dimensional iron-based magnetoplasmonic crystal. The effect is attributed to exciting surface plasmons with magnetization-dependent dispersion. Measurements of temporal dependence of transversal magneto-optical Kerr effect were performed for a one-dimensional magnetoplasmonic crystal based on a commercially available digital versatile disk polycarbonate template that had periodic corrugations with a depth of approximately 50 nm and a period of 750 nm. The dielectric template was covered by a 100-nm layer of polycrystalline iron deposited by magnetron sputtering and protected by a 20-nm-thick silica layer from the top. The Kerr effect evolution was demonstrated to have either a positive or negative time derivative, depending on the position of the incident pulse's carrier wavelength with respect to the plasmonic resonance. Proper



justification was given for this effect using the Lorentzian spectral line shape approach. Iron-based plasmonic crystal studied is a promising tool for manipulating femtosecond laser pulses with an external magnetic field that may have applications in active, plasmon-based telecom devices.

9547-46, Session 10

A plasmonic walker (Invited Paper)

Na Liu, Max-Planck Institut für Intelligente Systeme (Germany)

Construction of 3D reconfigurable plasmonic nanostructures witnesses major technological limitations, arising from the required subwavelength dimensions and controlled 3D motion. There have been considerable efforts on integration of plasmonic nanostructures with active platforms using top-down techniques. Here we lay out and implement a multi-disciplinary strategy to create active 3D plasmonic nanostructures by merging plasmonics and DNA nanotechnology on the nanoscale.

We demonstrate the first plasmonic walker, which can carry out directional, progressive, and reverse nanoscale walking on a DNA origami track. The plasmonic walker comprises an anisotropic gold nanorod as its 'body' and discrete DNA strands as its 'feet'. Specifically, our plasmonic walker carries optical information and can in situ optically report its own walking directions and consecutive steps at nanometer accuracy, through dynamic coupling to a plasmonic stator immobilized along its walking track. The dynamic process in real time.

Our concept may enable a variety of smart nanophotonic platforms for studying dynamic light-matter interaction, which requires controlled motion at the nanoscale well below the optical diffraction limit.

9547-47, Session 10

From light modulation to far-field excitation of graphene plasmons: science and applications of graphene-integrated metasurfaces (Invited Paper)

Gennady B. Shvets, The Univ. of Texas at Austin (United States)

Graphene has emerged as a promising optoelectronic material because its optical properties can be rapidly and dramatically changed using electric gating. Graphene's weak optical response, especially in the infrared part of the spectrum, remains the key challenge to developing practical graphene-based optical devices such as modulators, infrared detectors, and tunable reflect-arrays. We demonstrate experimentally and theoretically demonstrated that a plasmonic metasurface with two Fano resonances can dramatically enhance the interaction of infrared light with single layer graphene.

An order of magnitude modulation of the reflected light was accomplished by designing a novel type of a metasurface supporting double Fano resonances and integrating it with an under-layer of graphene. The unique aspect of such modulator is its high baseline reflectivity and large reflectivity extinction coefficient (modulation depth). Using laser interferometry, we demonstrate that the phase of the reflected infrared light can also be modulated by back-gating graphene. This work paves the way to future development of ultrafast opto-electronic devices such as dynamically reconfigurable holograms, single-detector imagers, dynamical beam-steering devices, and reconfigurable biosensors. Moreover, we will show that strong non-local response of graphene can be induced by exciting graphene plasmons which are confined inside the narrow gaps in the plasmonic metasurface. Such graphene plasmons excitation dramatically boosts the intensity of the infrared light confined by the metasurface.

9547-17, Session 11

Surface plasmon resonance gas sensing by electrons injection

Enrico Gazzola, Michela Cittadini, Laura Brigo, Giovanna Brusatin, Massimo Guglielmi, Filippo Romanato, Alessandro Martucci, Univ. degli Studi di Padova (Italy)

Surface Plasmon Resonance (SPR) sensing is based on the principle that the conditions for the resonant excitation of a plasmonic mode by an incident light beam are highly sensitive to variations of the refractive index (RI) of the environment. We report a case in which this variation can be attributed to electrons injection by the analyte into the structure.

We fabricated two kinds of high-performance plasmonic structures for hydrogen sensing, based on nanoporous TiO2 anatase sensitive layers. In the first, a TiO2 film was deposited above a metallic plasmonic grating, which can support propagating surface plasmon polaritons. The second consisted of TiO2 film with embedded gold nanoparticles, supporting localized surface plasmon modes, deposited on a flat surface.

In both cases, reversible shifts of the resonance wavelength are observed when the sensors are exposed to 5% H2 in N2 carrier at 300°C, with respect to N2 alone at the same temperature. The shifts range from 2 to 7 nm and their direction is consistent with a decrease of the RI of the environment.

Since the presence of the analyte modifies in a negligible way the RI of the atmosphere, the observed shifts cannot be explained only by the RI change induced by the gas filling the pores in the sensitive layers.

For this reason we propose a different interaction mechanism. At 300°C, H2 can dissociate by reacting with oxygen into the TiO2 matrix and donate electrons; the high temperature also promotes the formation of intragap states in the TiO2 band structure that allows the injected electrons to reach the conduction band. According to the Drude-Lorentz model, the injection of electrons decreases the RI, causing the shift of the plasmonic resonance.

This interpretation is consistent with the observed effects in both kinds of structure.

9547-48, Session 11

Comparison between plasmonic and dielectric nanoantennas for surfaceenhanced spectroscopies (Invited Paper)

Stefan A. Maier, Imperial College London (United Kingdom)

We evaluate the performance of dielectric nanoantennas composed out of silicon disks separated by a nanoscale gap for surface-enhanced spectroscopies. Contrary to plasmonic nanonantennas, the new system does not exhibit quenching of fluorescence, and can also sustain electromagnetic hot spots comparable in size to those of their plasmonic counterparts. Dielectric and metallic systems will be experimentally compared in terms of performance in surface-enhanced fluorescence and Raman, as well as in terms of local heat generation upon external illumination. Conclusions for applications in optical biosensing will be drawn.

9547-50, Session 11

Wafer-scale plasmonic and photonic crystal sensors

Matthew C. George, MOXTEK, Inc. (United States); Jui-Nung Liu, Univ. of Illinois at Urbana-Champaign (United States); Arash Farhang, Brent Williamson, Mike Black, Ted Wangensteen, James Fraser, Rumyana Petrova, MOXTEK, Inc. (United States); Brian T. Cunningham, Univ. of Illinois at Urbana-Champaign (United States)



200 mm diameter wafer-scale fabrication, metrology, and optical modeling results will be reviewed for surface plasmon resonance (SPR) sensors based on 2D metallic nano-dome and nano-hole arrays (NHA) as well as 1D photonic crystal sensors based on leaky-waveguide mode resonance, with potential applications in label free sensing, surface enhanced Raman spectroscopy (SERS), and surface-enhanced fluorescence spectroscopy (SEFS). Potential markets include micro-arrays for medical diagnostics, forensic testing, environmental monitoring, and food safety.

1-D and 2-D nanostructures were fabricated on glass, fused silica, and silicon wafers using optical lithography and semiconductor processing techniques. Wafer-scale optical metrology results are compared to FDTD modeling and presented along with application-based performance results, including label-free plasmonic and photonic crystal sensing of both surface binding kinetics and bulk refractive index changes. In addition, SERS and SEFS results from a line scan microscope will be presented for several 1D photonic crystal and 2D metallic array structures. Normal incidence extraordinary optical transmission (EOT) results for a 550 nm pitch NHA showed good bulk refractive index sensitivity, however an intensity-based design with 665 nm pitch was chosen for use as a compact, label-free sensor at both 650 and 632.8 nm wavelengths. The optimized NHA sensor gives an SPR shift of about 480 nm per refractive index unit when detecting a series of 0-40% glucose solutions, but shows about 10 times greater surface sensitivity when operating at 532 nm. Narrow-band photonic crystal resonance sensors showed quality factors over 200, with reasonable wafer-uniformity in terms of both resonance position and peak height.

9547-52, Session 11

Hot electron pump: a plasmonic rectifying antenna

Ahmet A. Yanik, Golam I. Hossain, Univ. of California, Santa Cruz (United States)

Plasmonic nanostructures have been widely explored to improve absorption efficiency of conventional solar cells, either by employing them as a light scatterer, or as a source of local field enhancement. Unavoidable ohmic loss associated with the plasmonic metal nanostructures in visible spectrum. limits the efficiency improvement of photovoltaic devices by employing this local photon density of states (LDOS) engineering approach. Instead of using plasmonic structures as efficiency improving layer, recently, there has been a growing interest in exploring plasmoinc nanoparticle as the active medium for photovoltaic device. By extracting hot electrons that are created in metallic nanoparticles in a non-radiative Landau decay of surface plasmons, many novel plasmonic photovoltaic devices have been proposed. Moreover, these hot electrons in metal nanoparticles promises high efficiency with a spectral response that is not limited by the band gap of the semiconductors (active material of conventional solar cell). In this work, we will show a novel photovoltaic configuration of plasmonic nanoparticle that acts as an antenna by capturing free space ultrahigh frequency electromagnetic wave and rectify them through an ultrafast hot electron pump and eventually inject DC current in the contact of the device. We will introduce a bottom-up quantum mechanical approach model to explain fundamental physical processes involved in this hot electron pump rectifying antenna and it's ultrafast dynamics. Our model is based on nonequilibrium Green's function formalism, a robust theoretical framework to investigate transport and design nanoscale electronic devices. We will demonstrate some fundamental limitations that go the very foundations of quantum mechanics.

9547-53, Session 11

Tunable optical extinction of nanoantennas for solar energy conversion from near-infrared to visible

Raymond A Wambold, The Pennsylvania State University (United States); James M Chen, Kansas State University (United States); Paul H Cutler, Nicholas M Miskovsky, Scitech Associates, LLC (United States); Jie Qi, The University of Connecticut (United States); Gary J Weisel, The Pennsylvania State University, Altoona (United States); Brian G Willis, The University of Connecticut (United States); Darin T. Zimmerman, Penn State Altoona (United States)

We demonstrate tunable optical extinction of nano-antennas, designed to collect and rectify solar radiation from near-infrared to visible. By employing a confocal, transmission arrangement with a broadband light source and detection from 400 - 1700 nm, we determine the spectrum of the (absorbed + scattered) light from a beam incident on thin-film metallic nano-antennas. The two-terminal rectifying antennas (rectennas) employ geometric asymmetry intended to produce a self-biased junction and a photo-assisted DC tunneling current. To fabricate the antenna arrays with junction gaps in the tunneling regime, we use standard electron-beam lithography of palladium, followed by selective atomic-layer deposition (ALD) of copper. We examine the variation in extinction spectra with device morphology and show that the resonance peak is progressively red-shifted with increasing cycles of ALD. Using actual device dimensions as determined from Scanning Electron Microscopy, we also demonstrate that our experimental results are in good agreement with three-dimensional Finite Difference-Time Domain simulation results.

9547-54, Session 12

3D chiral nanoplasmonics: fabrication, chiroptic engineering, mechanism, and application in enantioselection

Zhifeng Huang, Hong Kong Baptist Univ. (Hong Kong, China)

Chirality does naturally exist, and the building blocks of life (e.g. DNA, proteins, peptides and sugars) are usually chiral. Chirality inherently imposes chemical/biological selectivity on functional molecules; hence the discrimination in molecular chirality from an enantiomer to the other mirror image (i.e. enantioselection) has fundamental and application significance. Enantiomers interact with left and right handed circularly polarized light in a different manner with respect to optical extinction; hence, electronic circular dichroism (ECD) has been widely used for enantioselection. However, enantiomers usually have remarkably low ECD intensity, mainly owing to the small electric transition dipole moment induced by molecular sizes compared to the ECD-active wavelength in the UV-visible-near IR region. To enhance ECD magnitude, recently it has being developed 3D chiral nanoplasmonic structures having a helical path, and the dimensions are comparable to the ECD wavelength. However, it is still ambiguous the origin of 3D chiroplasmonics, and there is a lack of studying the interaction of 3D chiroplasmoncs with enantiomers for the application of enantioselection.

Herein, we will present a one-step fabrication of 3D silver nanospirals (AgNSs) via low-substrate-temperature glancing angle deposition. AgNSs can be deposited on a wide range of substrates (including transparent and flexible substrates), in an area on the order of cm2. A set of spiral dimensions (such as spiral pitches, number of turns and handedness) have been easily engineered to tune the chiroptic properties, leading to studying the chiroplasmonic principles together with finite element simulation and the LC model. At the end, it will be demonstrated that 3D chiroplasmonics can differentiate molecular chirality of enantiomers with dramatic enhancement in the anisotropy g factor. This study opens a door to sensitively discriminate enantiomer chirality.

9547-55, Session 12

Modeling and engineering of threedimensional chiroplasmonic silver nano structures

Junhong Deng, Fan Bai, Jack Ng, Zhifeng Huang, Hong

Conference 9547: Plasmonics: Metallic Nanostructures and Their Optical Properties XIII



Kong Baptist Univ. (Hong Kong, China)

Fabrication of 3D chiral nanoplasmonic structures is always challenging, while the principles for their chiroptical properties are still ambiguous.

We will present a combined experimental and theoretical study on 3D chiroplasmonic activity of silver nanospirals (AgNSs), fabricated on sapphire by low temperature glancing angle deposition. AgNSs exhibit bisignated CD spectra in the UV-visible range, in the form of not only individual AgNSs or an array. Compared to individual AgNSs, the array of AgNSs show CD with an intensity 3 order of magnitude higher. It is demonstrated the engineering of chiroplasmonic CD via adjusting spiral parameters, including spiral pitches, number of turns and handedness.

Finite element simulations were performed and are in good agreement with the experiments. A LC theory is also employed to explain the difference of chiroplasmonic CD in the UV and visible region.

9547-56, Session 12

Twisted nanosphere lithography: use colloidal Moiré patterns as masks

Kai Chen, National Institute for Materials Science (Japan); Bharath B. Rajeeva, Michael Rukavina, The Univ. of Texas at Austin (United States); Thang Duy Dao, Satoshi Ishii, Masakazu Aono, Tadaaki Nagao, National Institute for Materials Science (Japan); Yuebing Zheng, The Univ. of Texas at Austin (United States)

Nanosphere lithography (NSL) uses self-assembled layers of monodisperse micro-/nano-spheres as masks to fabricate plasmonic metal nanoparticles. Different variants of NSL have been proposed with the combination with dry etching and/or angled-deposition. These techniques have employed to fabricate a wide variety of plasmonic nanoparticles or nanostructures. Here we report another promising extension - twisted nanosphere lithography (T-NSL), which incorporates in-plane twisting between neighboring monolayers, to extend the patterning capability of conventional NSL. In conventional NSL, the masks, either a monolayer or bilayer, are formed by spontaneous self-assembly. Therefore, the resulted colloidal crystal configurations are limited. In this work we used sequential stacking of polystyrene nanosphere monolayers to form a bilayer crystal at the air/water interfaces. During this layer-by-layer stacking process, a crystal domain in the top layer gains the freedom to positon itself in a relative angle to that in the bottom layer allowing for the formation of Moiré patterns. Subsequent O2 plasma etching results in a variety of complex nanostructures that have not been reported before. Using etched Moiré patterns as masks, we further fabricated the corresponding gold nanostructures and characterized their scattering optical properties. We believe this facile technique provides a new strategy to fabricate novel and complex plasmonic nanostructures or metasurfaces.

9547-57, Session 12

Angled nanospherical-lens lithography as a high-throughput method to fabricate various nanodisk cluster arrays

Yi-Hsin Chien, Chang-Han Wang, Chi-Ching Liu, Yun-Chorng Chang, Academia Sinica (Taiwan)

Nanospherical-Lens Lithography (NLL) is a low-cost nano-fabrication technique that has the ability to fabricate nanodisk arrays that cover a very large area. Polystyrene nanospheres are functioning as nanoscale focusing lenses to focus the incoming ultraviolet light and exposure the underlying photoresist (PR) layer. PR hole arrays form after developing. Metal nanodisk arrays can be fabricated following metal evaporation and lifting-off processes. Nanodisk or nano-ellipse arrays with various sizes and aspect ratios are routinely fabricated in our research group.

In this study, we have expended the capabilities of NLL by performing the

UV exposures with a designated tilted angle. The exposure will result in a PR hole at an off-center location. The distance between the PR hole and the center depends on the exposure angle. With this angled-exposure technique, we can successfully fabricate nanodisk oligomers by performing multiple angled-exposures. We can also control the size of each nanodisk by preciously controlling the exposure angle and duration. Array of self-similar nanodisk chain can also be obtained. Both nanodisk oligomers and self-similar chain have been demonstrated to exhibit huge field enhancement, which is especially important for sensitive Raman platforms. Technique proposed in this study will help to find suitable industrial applications since it is both high-throughput and low-cost. We also believe the proposed method is versatile enough to fabricate more complex nanodisk systems that will demonstrate novel function in the near future.

9547-58, Session 12

From nanoparticles to nanostructures for plasmonic-related applications (Invited Paper)

Bin Ren, Bowen Liu, Xu Yao, Shu Chen, Liang Zhang, Lei Wang, Zhilin Yang, Xiamen Univ. (China)

Compared with some precise nanofabrication methods, such as EBL and FIB, holographic lithography (HL) is a convenient way to fabricate periodic structures in a large area and with superb uniformity. In this work, we developed the deep UV HL with 266 nm laser to obtain structure with a periodicity between 100 nm to 1?m, which cannot be achieved by traditional photolithography. We further developed a strategy to fabricate hybrid periodical dimmer arrays by deep UV HL and lift-off process, followed by selectively surface functionalization. Thermal treatment was employed to as an effective approach to tune the gap size, which provides an additionally adjustable factor. By coating the substrate with gold and the obtained nanostructures with gold or silver, we have obtained periodical dimmer arrays can be used as an effective plasmonics structure, and have potential application as a platform for high-efficiency surface- and bio- analysis.

9547-59, Session 13

Perfect light trapping in mid-IR using patterned ZnO structures (Invited Paper)

Shivashankar R. Vangala, Nima Nader, Justin W. Cleary, Air Force Research Lab. (United States); Junpeng Guo, The Univ. of Alabama in Huntsville (United States); Kevin D. Leedy, Joshua R. Hendrickson, Air Force Research Lab. (United States)

Plasmonic assisted mid-IR light trapping using 1D grating structures patterned in Ga-ZnO is demonstrated. FDTD simulations of these structures with proper grating period and depth show the light trapping into a resonant mode resulting in a close to 100% reflection dip in the 4-8 μm wavelength regime. The 1D grating structures of different periods are fabricated using standard photolithography followed by etching. The resonant reflection dips in the experimentally measured spectra well agree with the FDTD simulation, exhibiting light trapping in the mid-IR as predicted.

9547-60, Session 13

Terahertz metal grid polarizer with bridges on quartz substrate

John S. Cetnar, Air Force Research Lab. (United States); Junpeng Guo, The Univ. of Alabama in Huntsville (United States); Elliott R. Brown, Wright State Univ. (United States)

Conference 9547: Plasmonics: Metallic Nanostructures and Their Optical Properties XIII



The metal wire-grid polarizer is a venerable device that is used on radiation throughout the electromagnetic spectrum. It usually consists of a 1D-periodic array of subwavelength metallic wires in free space or mounted on a low-loss dielectric substrate, the plane of the grid being oriented perpendicular to the propagation direction. Herein is presented a new structure, a subwavelength wire-grid polarizer for the terahertz region that acts not only as a wideband polarizer but also as a transparent electrode. This function is achieved by the addition of periodically placed metallic bridges that connect the parallel metal wires of the polarizer. The bridges allow for the uniform distribution of an electrostatic potential over all wires while maintaining the polarizing functionality of the metal wire grid polarizer.

Full-wave electromagnetic simulations were performed on the device. The transmittance was computed in both perpendicular polarization and parallel polarization from 100 to 4000 GHz, and the extinction ratio was calculated across the same range. Furthermore, fill-factor studies were performed to understand how device performance is affected by varying slot width and bridge length, as well as bridge offset. The simulation results showed extraordinary optical transmission through the device for perpendicular polarization, creating excellent transmittance and extinction ratios over the frequency range. The perpendicular polarization transmittance and extinction ratio at 1 THz was calculated to be -1 dB and -36 dB respectively. Meanwhile, the bridges allow the device to behave like a DC electrode.

9547-61, Session 13

Optical force acting on metallic nanostructure (Invited Paper)

Che Ting Chan, Shubo Wang, Kun Ding, Hong Kong Univ. of Science and Technology (Hong Kong, China); Xulin Zhang, Jilin Univ. (China)

Light can exert radiation pressure on any object it encounters and the resulting optical force can be used to manipulate particles. Conventional studies of optical force in typical systems are mainly concerned with the scattering force and gradient force. We show that rich physics can be explored when chiral nanostructures are considered. We present analytical formula and full-wave simulation results for optical forces acting on metallic helix nanostructures. We found that the structural chirality can be coupled with light's chirality (spin) and results in optical spin force terms which can be used to realize optical pulling force and sideway force acting on chiral particles. The sideway force can laterally push particles with opposite chirality to the different side of an interface and hence may serves as a possible approach to separate chiral particles or molecules. We also show that such chiral metallic nanostructures, when properly arranged, can induce scattering force through a dominating toroidal-moment mode which plays a clear and indispensable role in the view point of source (charge and current) distribution. We show that such a scattering force can also be explained by an electric dipole mode in the radiation far-field. Our results build the connection between the source picture and the field picture and help understanding the role played by complex electromagnetic multipoles in optical force system.

9547-62, Session 13

Electrothermoplasmonic flow for plasmonassisted optical trapping (Invited Paper)

Justus Ndukaife, Alexander V. Kildishev, Agbai Agwu Nnanna, Steven T. Wereley, Vladimir M. Shalaev, Alexandra Boltasseva, Purdue Univ. (United States)

Plasmonic nanostructures, which support highly localized and enhanced electromagnetic field are now actively researched as a means for efficient trapping of nanoscale objects, not addressable by conventional diffractionlimited optical tweezers. An issue of critical concern is how to efficiently transport and deliver the suspended particles to the illuminated plasmonic nanostructure. There are primarily two main approaches that researchers employ for trapping of particles with plasmonic nanostructure(s) on a substrate. The first approach involves illuminating arrays of closelyspaced plasmonic nanostructures. However resonant illumination of the nanostructures results in collective heating and this produces strong fluid convection that exerts drag forces on the particles. Elucidating the roles of these heating-induced forces and optical gradient forces arising from plasmonic field enhancement have so far remained elusive. The other scheme involves illuminating a single plasmonic nanostructure. However, due to the absence of thermoplasmonic convection in this case, the dynamics of the suspended particle to be trapped becomes dictated by Brownian motion- an inherently slow process. We will discuss a new fluid flow mechanism, which we have termed electrothermoplasmonic (ETP) flow to resolve this dilemma. ETP flow harnesses intrinsic plasmonic heating combined with AC electric field to generate on-demand fluid and particle transport, which means that particles could be rapidly transported for trapping in sub-wavelength plasmonic hotspots only when desired, and without any competition between heating-induced forces and optical gradient forces. These new capabilities certainly provide new directions for research in the field of plasmon-assisted optical trapping, which will be discussed.

9547-63, Session 14

Non-quasi-static eigenstates of Maxwell's equations in a two-constituent composite medium and their application to a calculation of the local electric field of an oscillating electric dipole

Asaf Farhi, David J. Bergman, Tel Aviv Univ. (Israel)

In conventional optics the image is formed only by the propagating waves and the information encoded in the evanescent waves is lost. This limits the resolution which is inversely proportional to the wavelength of the light. A flat slab with a negative refractive index metamaterial can focus at a point the radiation from a point source. Such a slab can also amplify evanescent waves and thus enable the generation of an image by both propagating and non propagating waves, theoretically leading to unlimited resolution.

The imaging of an electric point charge in a composite structure composed of a \$epsilon_1\$ slab surrounded by a \$epsilon_2\$ medium, was recently analyzed by expanding the local electric potential in a series of the quasistatic eigenfunctions of the composite structure. Numerical evaluations of the electric potential, using realistic values for the electric permittivities and the slab thickness, revealed that the maximum concentration of the electric field occurs not at the geometric optics foci but at the interfaces between the negative permittivity slab and the surrounding medium.

Here we describe an exact calculation of the local electric field $f E_{(bf r)} f r$ by for the full Maxwell's equations

where mu=1 everywhere in the system. For this purpose we first calculate all the eigenstates of Maxwell's equations for the composite structure. These eigenstates are then used to develop an exact expansion for the physical values of $fb E{(b r)}$ in the system for the case of a time dependent point charge $q e^{-imega t}$ in the puilties medium.

9547-64, Session 14

Retrieving the polarizability tensor of wire media

Jacob Ben-Yakar, Tel Aviv Univ. (Israel); Yonatan Sivan, Ben-Gurion Univ. of the Negev (Israel); David J. Bergman, Tel Aviv Univ. (Israel)

Metamaterials consisting of long, circular, cylinders are very popular. It is a fundamental challenge to characterize the effective electromagnetic response of such composites. In this framework, the radius of cylinder is assumed to be considerably smaller than the external wave length, thus the dominant scattered EM fields can be approximately replaced by dipole fields. Previous works dealt mainly with two dimensional (2D) scenarios, i.e.,



characterizing the effective electromagnetic response for light propagation perpendicular to the cylinder axis.

In this work, we generalize this treatment to three dimensions (3D), i.e., we characterize the effective electromagnetic response for light propagation at any angle, and find that the resulting electromagnetic response is non-local, i.e., it depends on the wavevector component parallel to the cylinder axis.

We retrieve analytically, the full polarizability tensor and show that it has different contributions for different polarized incoming EM waves (transverse electric and transverse magnetic with respect to the cylindrical axis).

It is also diagonal, i.e., it contains no magneto-electric coupling, showing that claims in previous studies were incorrect. Having closed form expressions for polarizability allows us to use effective medium approximation methods, and tailor the spectral response for both electric and magnetic dipolar contributions. It is important to emphasize that for the first time, this gives a fully systematic way to characterize the magnetism.

Our analysis holds for additional structures based on cylindrical geometry, such as hole arrays, all-dielectric metamaterials, and multi-layer cylinders. It can be used to explain the electromagnetic response of wire media attributed with a negative refractive index, effective magnetism and hyperbolic dispersion relations. In addition, this approach can be applied to more complex unit cells e.g., consisting of clusters of parallel cylinders.

9547-65, Session 14

Distinguishing between plasmon-induced and photoexcited carriers in a device geometry

Hangqi Zhao, Bob Y. Zheng, Alejandro Manjavacas, Michael J. McClain, Peter Nordlander, Naomi J. Halas, Rice Univ. (United States)

The use of surface plasmons, charge density oscillations of conduction electrons of metallic nanostructures, could drastically alter how sunlight is converted into electricity or fuels by increasing the efficiency of lightharvesting devices through enhanced light-matter interactions. Surface plasmons can decay directly into energetic electron-hole pairs, or "hot" carriers, which can be used for photocurrent generation or photocatalysis. However, little has been understood about the fundamental mechanisms behind plasmonic carrier generation. Here we use metallic nano-wire based hot carrier devices on a wide-bandgap semiconductor substrate to show that plasmonic hot carrier generation is proportional to field intensity enhancement instead of bulk material absorption. We also show that interband carrier generation results in less energetic carriers than plasmoninduced generation, and a plasmon is required to inject electrons over a large energy barrier. Finite Difference Time Domain (FDTD) method is used for theoretical calculations, which match well with experimental results. This work points to a clear route to increasing the efficiency of plasmonic hot carrier devices and drastically simplifies the theoretical framework for understanding the mechanisms of hot carrier generation.

9547-66, Session 14

Taming surface plasmons with adjacent molecules (Invited Paper)

Mikhail A. Noginov, Norfolk State Univ. (United States)

In this presentation, we will review the plethora of physical phenomena related to interaction of surface plasmons (and, more generally, metallic nanostructures and environments) with adjacent molecules. We will start the discussion with a more familiar subject of compensation of loss by gain and stimulated emission. After that we will review our recent experiments demonstrating strong coupling of surface plasmons and dye molecules as well as the effect of metallic surfaces on Förster energy transfer, van der Waals interactions, and chemical reactions.

9547-97, Session PWed

Photoconductively excited plasmonic modulator-switch

John S. Cetnar, David E. Zelmon, David H. Tomich, Air Force Research Lab. (United States)

A novel plasmonic modulator-switch for the long-wave infrared (LWIR) region is presented. The device consists of a thin metal film, an underlying photoconductive substrate, input and output reflection gratings located on top of the film on opposite ends of the device, and a limited aperture detector located over the out-couple grating. LWIR incident at a given angle is in-coupled, generating surface plasmons (SPs). Since the underlying metal film is thinner than the SP penetration depth, the SPs are couple on both the top and the bottom of the thin film and propagate on both sides of the metal film toward the out-coupling grating. When free carriers in the photoconductive substrate are excited by laser illumination, the electrical properties of the substrate are changed. This change in substrate electrical properties is sensed by the propagating SPs and thus changes the wavevector of the SPs. The SP wavevector change will cause the out-coupled radiation magnitude and angle to change. Thus, the radiation incident on the detector is modulated implementing a plasmonic modulatorswitch.

Full-wave electromagnetic simulations were performed on the device. The reflected power at various angles was calculated for a fixed incident angle at ? = 10 ?m using various geometries and substrate materials. The substrate materials modelled include III-V compound semiconductors and Si. The dielectric functions for these materials were computed as functions their free carrier concentration to simulate excited and unexcited states. This paper reports on how device performance was affected by variation of these geometric and material parameters.

9547-99, Session PWed

Study of the plasmonic properties of ordered arrays of Ag and Au nanoparticles fabricated by a combination of nanosphere lithography with ion implantation

Octavio Graniel, Cecilia Salinas, Erick Flores-Romero, Univ. Nacional Autónoma de México (Mexico); Ulises Morales, Univ. de Guanajuato (Mexico); Juan-Carlos Cheang-Wong, Univ. Nacional Autónoma de México (Mexico)

Colloidal silica particles are being intensively studied due to their potential applications in catalysis, intelligent materials, optoelectronic devices, photonic bandgap crystals, masks for lithographic nanopatterning. In nanoscale electronic, photonic and plasmonic devices, feature dimensions shrink towards a critical limit, and new experimental approaches have to be explored in lithographic patterning to create ordered arrays of metallic nanostructures with useful optical properties. Nanosphere lithography uses self-assembled monolayers of spherical submicrometer-sized silica particles prepared by sol-gel and deposited onto silica glass plates. This silica monolayer is then used as a mask to create regular arrays of nanoscale features in the sample by 1-2 MeV Ag and Au ion implantation. By this way, after removal of the silica particles and an adequate thermal annealing of the as-implanted samples, the formation of Ag or Au nano-objects embedded in silica plates was confirmed by the presence of the surface plasmon resonance in the optical absorption spectra. The size and shape of the array of metallic nanostructures were studied by electron microscopy. The amount of implanted ions was measured by Rutherford Backscattering Spectrometry. The long range order of the metallic nanoparticle assembly and its plasmonic properties were characterized by a Fast Fourier Transform study and optical absorption measurements, respectively.



9547-100, Session PWed

Plasmonic analog of electromagneticinduced transparency of asymmetrical slots waveguide

Lin Sun, Jiangnan Univ. (China); Jicheng Wang, Jiangnan Univ. (China) and Purdue Univ. (United States); Baojie Tang, Xiaosai Wang, Jiangnan Univ. (China)

The optical phenomenon analogous to electromagnetically induced transparency (EIT) has been proposed numerically in the plasmonic system composed of unsymmetrical grooves shaped metal-insulator-metal (MIM) waveguide. Based on the coupled mode theory (CMT) and Fabry-Perot model, the formation and evolution mechanisms of plasmoninduced transparency by direct and indirect couplings are exactly analyzed. The analysis shows that the EIT-like spectral response and Fano resonances can be tuned easily by adjusting the geometrical parameters of the groove structures, including the coupling distances and groove lengths. We observe that both the wavelengths of resonance modes present red shift and the transparency window progressively widens with the increase of the difference of the two groove lengths. In addition, the plasmonic system with unsymmetrical third-groove structure is also proposed. The numerical results are simulated by finite element method (FEM) to validate the correctness of the uniform theoretical description. The results may open up avenues for designing nanoscale optical switch, ultrasensitive sensors, and slow light devices in highly integrated optical circuits.

9547-101, Session PWed

Spectral magnetooptical tunability using Bragg plasmons

Emil Melander, Sebastian M. George, Uppsala Univ. (Sweden); Evangelos Th. Papaioannou, Technische Univ. Kaiserslautern (Germany); Marc A. Verschuuren, Philips Research (Netherlands); Björgvin Hjörvarsson, Vassilios Kapaklis, Uppsala Univ. (Sweden)

Magnetoplasmonics is a field where external magnetic fields are utilized to control the optical properties that come from plasmons. Active control of plasmonics has many applications in energy harvesting and nanosensing. [1]

We demonstrate experimentally the optical and magnetooptical response from Bragg plasmons [2] using diffraction from magnetoplasmonic nanodisks arranged in a periodic 2D square pattern from the coupled islands. The circular islands are 450 nm in diameter and have a lateral periodicity of 512 nm. This enables diffraction parallel to the surface which in turn yields Bragg plasmon excitation due to the electric field enhancement. The alloy is a combination of Fe and Pd, Fe20Pd80, in order to have a simple material that has both the magnetic functionality as well as the plasmonic.

Specular reflectivity and transverse magnetooptical Kerr effect (TMOKE) spectra [3] are compared to show how the optical measurements relate to the magnetooptical enhancement. The experimental data is compared to a simple diffraction model that accounts for the lateral dimensions of the nanostructure and the diffraction which gives the Bragg plasmon onset. In this way we show the link between the Bragg plasmon excitation and the changes in TMOKE asymmetry.

[1] Gaspar Armelles and Alexandre Dmitriev, "Focus on magnetoplasmonics", New J. Phys. 16 045012, 2014

 $\ensuremath{\left[2\right]}$ Melander et al., "Spectral magnetooptical tunability from Bragg plasmons", to be submitted

[3] Melander et al., "Influence of the magnetic field on the plasmonic properties of transparent Ni anti-dot arrays", Appl. Phys. Lett. 101, 063107 (2012)

9547-102, Session PWed

The effect of truncation in plasmon resonance of metal nanoprisms

Soad Alsheheri, Marjan Saboktakin, Mohammad Matin, Univ. of Denver (United States)

Plasmonic properties of gold and silver nanoparticles has several applications in the recent years. Of the several shapes of nanoparticles, triangular nanoprisms are of significant interest to us. The interest mostly arises from the multiple absorption bands in these particles associated with the multiple axes of their triangular shape as each of these axes can support propagating and localized surface plasmons. As a result, nanoprisms, are among the anisotropic plasmonic particles which exhibit LSPR in different orientations depending on the polarization of the incident light. Further, triangular nanoprisms provide us the opportunity of tuning their LSPR properties by suitably modifying their structural parameters such as particle thickness, particle edge length and height. Despite the several advantages of triangular nanoprisms, it has been a challenge to synthesize these nanomaterials with absolute precision in edge lengths. Often times, the triangular nanoprisms we synthesize through various methods will not have sharp edge lengths, instead they are seen as truncated. In this project, we have studied the effect of truncation in plasmon resonance. Truncation (TR = a/l). The TR values we studied are 0.006, 0.03, 0.06, 0.1, 0.13 and 0. The edge lengths we studied is 150 nm and thickness of prism is 15nm, 25nm, and 35 nm. Further, we measured the plasmon resonance for 1 snip, 2 snip and 3 snips. For 15 nm thickness of nanoprism, with edge length of 150 nm, with increase in TR value, plasmon resonance saw a blue shift for one snip. However, when the snips increased to 2 and 3 no shift in values of plasmon resonance were found. However, when the thickness of nanoprism changed from 15nm to 35 nm, plasmon resonance found a blue shift.

9547-103, Session PWed

Plasmonic devices based on the dual coupled grapheme-integrated ring resonators

Jicheng Wang, Jiangnan Univ. (China) and Purdue Univ. (United States); Xiushan Xia, Jiangnan Univ. (China); Xiuye Liang, Jiangnan Univ (China); Jing Chen, Jiangnan Univ. (China); Dongdong Liu, Nanjing Univ. of Science & Technology (China)

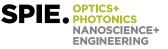
We have proposed a couple of plasmonic devices based on graphene sheets and ring resonators. The highly frequency-tunable multi-mode plasmonically induced transparency (PIT) device based on monolayer graphene and rings for the mid-IR region is presented in theory firstly. The multi-mode transparency windows in the spectral responses and slow light effects can be achieved in plasmonic configuration composed of two graphene resonators coupled with single-layer graphene waveguide. By varying the Fermi energy of the graphene, the multi-mode PIT resonance can be dynamic controlled without reoptimizing the geometric parameters of the structures. Based on the coupled mode theory (CMT) and Fabry-Perot (FP), we numerically investigated direct coupling and indirect coupling in the graphene-integrated PIT systems. In addition, the theoretical plasmonic devices based on graphene sheets and ring resonators are also proposed to perform as 1?2 optical spatial switch or ultra -compact Mach-Zehnder interferometer. The finite element method (FEM) is carried on to verify our designs. Those designs may pave the ways for the further development of the compact high-performance plasmonic communication devices.

9547-104, Session PWed

Fano resonances in nanoscale plasmonic structure

Yundong Zhang, Hui Li, Xuenan Zhang, Yongfeng Wu,

Conference 9547: Plasmonics: Metallic Nanostructures and Their Optical Properties XIII



Harbin Institute of Technology (China)

We investigate a plasmonic waveguide system using the finite-difference time-domain method, which consists of a metal-insulator-metal waveguide coupled with a circle and a disk cavity. Numerical simulations results show that the sharp and asymmetric Fano-line shapes can be created in the waveguide. Fano resonance strongly depends on the structural parameters. This has important applications in highly sensitive and multiparameter sensing in the complicated environments.

9547-105, Session PWed

Investigation of the reflection and transmission of nano-scale gold films

Haoliang Qian, Yuzhe Xiao, Dominic Lepage, Zhaowei Liu, Univ. of California, San Diego (United States)

With the shrunk of the plasmonic device dimensions into the nano region, the field of quantum plasmonics has emerged and drawn much attention recently. Ultra-thin metal film is an ideal platform to study the quantum behavior of electrons, and is the focus of this paper. This paper demonstrates a combined experimental and theoretical investigation of the optical properties of gold nano films with thickness varying from 30 nm to 2.5 nm. More specifically, accurate reflection and transmission measurements are performed for the gold films with thickness down to 2.5 nm. The optical constants (n and k) are extracted using Newton's method with a multilayer transmission code. A new theoretical model based on the self-consistent solution of the coupled Schrodinger and Poisson equations is applied to gold quantum wells for the first time and its predictions agree excellently experiment over a very broadband spectral range (1 to 2 um). This guantum model not only can explain the experimental results, it also predicts the values of the electron parameters in gold quantum well, such as the effective mass and relaxation time. Such a theory can be easily generalized to other quantum structures, such as quantum dots and quantum wires, and should be very useful in the field of quantum plasmonics.

9547-106, Session PWed

High order gap modes in film-coupled ?/10 nanoantennas

Chua-Zu Huang, Ming-Jing Wu, National Cheng Kung Univ. (Taiwan); Shiuan-Yeh Chen, National Cheng Kung Univ (Taiwan)

The high order gap modes in the film-coupled nanoantenna are identified experimentally and theoretically. Recently, several reports show that a particle-film structure with a gap on the few-nanometer scale provides a stable platform for investigating the induced enhanced field and its interaction with molecules nearby. The concentrated enhanced field within the gap is usually dominated by the well-known gap dipole mode. However, when the gap size decreases, the increasing high enhanced field is accompanied by the induced high order modes. These high order modes are usually thought to be "dark" (not radiate efficiently) and only affect the distribution of the near-field. However, in our far-field scattering measurements, it is found that these high order modes also have substantial influence on the far-field scattering profile. In addition, it is also shown that several high order modes could exist even in this small structure (~?/10) within the relatively narrow spectral range. Therefore, the evaluation of nanoantenna bandwidth needs to take this factor into account. The relation between far-field scattering profiles, spectra, and near-field distribution were elucidated through the optical measurements and simulations. Our findings provide a guideline for probing the interaction between the gap field and the molecules nearby and can be extended for designing extremely compact nanophotonic devices.

9547-107, Session PWed

The influence of annealing on Au films deposited on Ge seed layers

Vesna Janicki, Jordi Sancho-Parramon, Boris Okorn, Institut Ruder Bo?kovic (Croatia); Eva Kova?evi?, CNRS/ Université d'Orléans (France); Hrvoje Zorc, Institut Ruder Bo?kovic (Croatia)

Ultrathin compact metal films are important for plasmonic and metamaterial devices. This kind of films can be obtained by electron beam evaporation technique on a pre-deposited Ge seed layer. The role of the seed layer is to reduce the percolation threshold of metal islands. In this way thinner compact metal layers having lower losses are formed. Similarly as the growth of metal island films is promoted if the substrate is heated, annealing of a compact metal film can result in breaking the surface continuity of the layer and formation of metal islands.

The influence of annealing on metal islands and compact Au films formed on the substrates with and without Ge seed layer is studied in this work. A serial of samples with different thicknesses of Au was annealed at different temperatures. Optical and structural measurements, ellipsometry and scanning electron microscopy at the first place, were performed and used for characterization of the samples. As expected, the obtained results present formation of discontinuous layers with the increase of the temperature. However, even in the conditions of elevated temperature, Ge seed layer is shown to promote percolation, postponing or even preventing the breakdown of the continuity of the film.

9547-108, Session PWed

Influence of plasmonic nanoantennas on the optical properties of ultra-thin conjugated polymer films

Binxing Yu, Joseph Woo, Rutgers, The State Univ. of New Jersey (United States); Sarah Goodman, Massachusetts Institute of Technology (United States); Deirdre M. O'Carroll, Rutgers, The State Univ. of New Jersey (United States)

Conjugated polymers have been intensively studied in the recent years due to their remarkable electronic and optical properties which include high conductivities, excitonic absorption, photoluminescence and electroluminescence. However, their limited spectral absorption bandwidths have limited their applications in photodetection and photovoltaic devices, which makes improving light-harvesting in ultra-thin conjugated polymer active layers an ongoing topic of interest in the optoelectronic community.

Here, we present how a a metal nanoantenna/poly(3-hexylthiophene) (P3HT)/metal film system can be designed to affect the enhancement and localization of electric fields in polymer thin films. We theoretically and experimentally investigate the tunability of the subwavelength resonant modes supported by the system and their impact on the spectral response of sub-50 nm thick conjugated polymer layers. Significant absorption enhancement up to 6 times in polythiophene is obtained using this system which is also validated by agreement with full-field electromagnetic simulation data. Single nanoparticle dark-field scattered-light spectroscopy and simulations also revealed evidence for the excitation of both localized surface plasmons (LSPs) of the nanoparticle and propagating surface plasmon polaritons (SPPs) of the metallic film. Distinct resonance features observed in the scattering spectra were assigned to specific modes based on an image-dipole interaction model as well as the coupling and interplay between LSPs and SPPs.Upon modifying factors such as: polymer spacer thickness, nanoparticle height and material type, we could alter bandwidth, intensity of the individual modes and optimize degree of electromagnetic field localization in the polymer. The analysis in this study would be useful for proposing new concepts for manipulation and control of light-matter interactions in nanoscale material volumes, which is of utmost importance for the optimization of ultra-thin film devices exploiting near-field



phenomena, such as surface plasmon-enhanced thin-film solar cells and light-emitting devices.

9547-109, Session PWed

Surface plasmon resonance in diabolo metal bar optical antenna arrays

Junpeng Guo, Hong Guo, The Univ. of Alabama in Huntsville (United States)

Surface Plasmon Resonance in Diabolo Metal Bar Optical Antenna Arrays

Hong Guo, Blake Simpkins, Joshua Caldwell, Junpeng Guo

Abstract: We investigated a new configuration of optical antennas: metal bar antennas with reduced waist width with respect to rectangular bars. Previously investigated bowtie optical antennas consist of two triangle shape metal patches with a small gap between the two metal patches. The excitation polarization is along the small gap of the triangle metal patches and the electromagnetic field enhancement occurs inside the gap between the two metal patches. For the narrow waist metal bar antennas investigated here, there are no gaps in the structure. The excitation polarization is along the longitudinal dimension of the metal antennas. It was found that the resonance wavelength and near field enhancement of diabolo metal bar antennas can be tuned by varying the waist width of the Diabolo Metal Bar Optical Antennas.

9547-110, Session PWed

A two-electrode electrochemical surface plasmon resonance sensor for investigating the electropolymerization of polyaniline

Bing Zhang, Zhejiang Univ. (China); Yazhuo Li, Jianghan Univ. (China); Yizhang Wen, Peijun Cai, Xiaoping Wang, Zhejiang Univ. (China)

A novel electrochemical surface plasmon resonance (EC-SPR) sensor has been developed based on the surface plasmon resonance (SPR) combined with a two-electrode electrochemical configuration. The theory of potential-modulated for EC-SPR was described, and several factors which can induce the change of the SPR resonance angle were revealed. Comparing with the conventional three-electrode electrochemical system, the reference electrode has been eliminated in this design, and the active carbon (AC) electrode employed as the counter electrode. Due to the large specific surface area, AC presents considerable double layer capacitance at the interface of electrode and electrolyte, which can provide a constant potential during the electrochemical reactions. Using an angle modulation SPR sensor and the resolution of that is 5?10-6 RIU (refractive index units), a real-time data-smoothing algorithm is adopted to reduce the noise of the data, which can guarantee an accurate result of the resonance angle of SPR. The EC-SPR setup was used for investigating the electropolymerization of polyaniline by applying a potential of cyclic voltammetry, both of the electrochemical current and the resonance angle shift of SPR are recorded to monitor the growth process of the polymer. Comparing with the threeelectrode configuration, the novel AC two-electrode system can also obtain detailed information about the polymerization process from the resonance angle shift curves, including the change of thickness and dielectric constant, deposition and transitions between different redox states of the polymer film. Experimental results demonstrated that this two-electrode EC-SPR configuration is suitable for analyzing the electropolymerization process of a conducting polymer.

9547-111, Session PWed

Surface plasmons leaky radiation of the flat metal

Ping Wang, Sichuan University (China)

We derive the Fano equation to present the reflection spectrum derived from the three-layer Fresnel reflection equation, which are asymmetric curves resulted from interference between direct reflectance and surface plasmons leaky radiation. When surface plasmons propagate on the metal surface, part of the excited surface plasmons leaks out as a radiation wave into prism. Therefore the reflection consists of two parts: direct reflectance and the leaky radiation. The whole incident light energy can be divided into three parts: direct reflectance, the surface plasmons leaky radiation and propagating surface plasmons which is confined in metal and ultimately converts into heat because of the metal absorption. By fitting the rigorous electromagnetic calculation with the Fano equation, we obtain each contribution to reflection of the three parts. The surface plasmons leaky radiation decreases with the increase of metal thickness. It approximates to zero with metal thickness thicker than 35nm and the leaky radiation is quite strong at ultra-thin metal film due to the optical tunneling effect. When the sum of direct reflectance and leaky radiation reach the value close to zero the propagating surface plasmons reach the value close to unity at about 45nm metal thickness.Compares to our investigation of grating coupler, we learn the surface plasmons leaky radiation of flat metal is quite weak than resonance radiation coupled out by grating, especially at thick metal, because they are in different radiation mechanism.

9547-112, Session PWed

Polarization conversion with crossed plasmonic polarizers

Xiaobin Cui, Chengping Huang, Nanjing Tech Univ. (China)

Conventionally, a pair of linear polarizers can be used to generate and rotate the linear polarization. However, according to the Malus law, the transmission or conversion efficiency decreases with the rotating angle. It is well known that, when the two linear polarizers are orthogonal to each other, the transmission of light will be blocked. This effect also prohibits the 90-degree polarization conversion with two crossed polarizers. We propose that a pair of specially-designed orthogonal plasmonic polarizers may break through the above limitation to induce both high transmission and 90-degree polarization conversion. We present the experimental demonstration of such effect in both optical frequency and microwave regime. Moreover, based on this effect, a super polarization converter that switches the incident polarization to arbitrary direction has also been designed and realized in the microwave band. The results may be used to construct new types of plasmonic devices, e.g., the polarization converters, one-way transmitters, subwavelength switches and modulators, etc.

9547-113, Session PWed

Hybrid spherical cap plasmonic waveguide for tight mode confinement and long propagation length

Kai Li, Maojin Yun, Xiaohui Ge, Weijin Kong, Qingdao Univ. (China)

The special abilities of plasmonic waveguide including tight field confinement and beyond diffraction limit within nano-scale structure have been exploited in many different fields. In order to overcome the trade-off between tight mode confinement and long propagation length, many kinds of nano-scale structures have been proposed in recent years. In this paper, a novel hybrid plasmonic waveguide consisting of the layer of metal Ag, a spherical cap with low-index dielectric layer placed above the metal Ag and a high-index dielectric layer placed above the spherical cap is proposed and analyzed theoretically. The relations between the characteristics of

Conference 9547: Plasmonics: Metallic Nanostructures and Their Optical Properties XIII



the bound modes, such as mode confinement, propagation lengths, and parameters of the spherical cap, the curvature and width, are numerically investigated in detail. The simulation results show that the nano-scale confinement can be realized. The simulation results show that the performance of the proposed spherical cap hybrid plasmonic waveguide is better than the rectangle or cylindrical hybrid plasmonic waveguide. Such hybrid plasmonic waveguide has a tight mode confiment and long propagation length. This novel stucture provides promising applications for high-integration density photonic components.

9547-114, Session PWed

Cylindrical hybrid plasmonic waveguide for a nano-scale light confinement

Chao Liu, Mei Wang, Maojin Yun, Weijin Kong, Qingdao Univ. (China)

In order to improve integration density, it is essential to develop a nanoscale optical waveguide which is the key element to build varies of optical components. In this paper, a novel cylindrical hybrid plasmonic waveguide, which has a air core surrounded by a metal-layer and a silicon layer, is proposed to achieve nano-scale confinement of light at the operating wavelength of 1550nm. And there is a low-index material nano-layer between the metal layer and the silicon layer, in which the field enhancement provides a nano-scale confinement of the optical field. The relations between the characteristics of the bound modes, including the effective mode indices, propagation lengths, mode sizes, mode shapes and parameters of the plasmonic waveguide are numerically investigated in detail. The simulation results show that the nano-scale confinement can be realized and the proposed hybrid plasmonic waveguide has a potential application in high density photonic integration.

9547-115, Session PWed

Coupled plasmon hybrid modes in aggregates of metal nanowires

Nadiia P. Stognii, Kharkiv National Univ. of Radio Electronics (Ukraine) and Institute of Radiophysics and Electronics (Ukraine); Nataliya K. Sakhnenko, Kharkiv National Univ. of Radio Electronics (Ukraine)

Investigation of the plasmonic resonances in aggregates of metal nanowires is presented. Mechanism of plasmonic mode coupling in a system of metal wires that can be considered as hybridization combinations of isolated wire plasmons is investigated

9547-116, Session PWed

Plasmon enhanced luminescence upconversion in Au and NaYF4:Yb3+,Er3+ nanoparticle clusters

Chenchen Mao, Univ. of Colorado at Boulder (United States); Liangcan He, Jennifer N. Cha, Univ. of Colorado Boulder (United States); Wounjhang Park, Univ. of Colorado at Boulder (United States)

Rare-earth activated upconversion materials present exciting new possibilities in solar energy conversion, bioimaging and medicine. For viable applications, however, the efficiency must be enhanced which may be accomplished by surface plasmon. Also, solution-processed nanocomposites are desired for most bio-applications and organic devices.

In this study, SiO2 coated NaYF4: Yb3+, Er3+ upconversion nanoparticles (UCNPs) by the co-precipitation method. Then, Au nanostars or nanospheres were synthesized, thiol-streptavidin stabilized, and attached

to the biotinylated UCNPs through the strong interaction between biotin and streptavidin. The Au-UCNP clusters showed various extinction spectra depending on the shape of the Au nanomaterial. Au nanospheres presented resonance at 520 nm while two types of Au nanostars exhibited resonances at 700 nm and 980 nm, respectively. The plasmon resonance can lead to enhanced upconversion through a complex mechanism involving absorption, emission and energy transfer. Also, metal surface introduces quenching which has to be minimized mainly by adjusting the SiO2 coating thickness.

Due to the interplay of many different processes, the upconversion luminescence was highly sensitive to the exact geometry of the nanocluster. Among the set of Au-UCNP clusters we studied, the highest enhancement was observed from the UCNP coupled to Au nanostar with 700 nm resonance. Enhancement factors for green and red emission were 3.4 and 2.7, respectively. The SiO2 coating thickness was 10 nm. A complete analysis of the experimental data together with quantum electrodynamics based theoretical models will be presented at the conference.

9547-117, Session PWed

Plasmonic local heating beyond diffraction limit by the excitation of magnetic polariton

Liping Wang, Hassan Alshehri, Arizona State Univ. (United States)

In recent years, optical local heating in the nanoscale has attracted great attention due to its unique features of small hot spot size and high energy density. Plasmonic local heating can provide solutions to several issues such as data storage and cancer treatment. Research conducted in this field to achieve plasmonic local heating has mainly utilized the excitation of localized surface plasmon (LSP) or surface plasmon resonance (SPR). However, achieving plasmonic local heating by the excitation of magnetic polariton (MP) has not been researched extensively yet.

In this work, we numerically investigate the radiative properties of a metamaterial nanostructure composed of a gold nanowire suspended on a gold thin film. HFSS (High Frequency Structural Simulator) simulation shows that the proposed structure exhibits a selective absorption peak at 655 nm due to the excitation of MP at the resonance wavelength. The electromagnetic field of the structure at resonance is plotted to explain the mechanism of MP. Geometric and incidence angle effects on the resonance wavelength and the absorptance spectra are also studied, and the physical mechanisms are elucidated. Furthermore, an inductor-capacitor circuit model is employed to predict the resonance wavelength for MP and compare with the HFSS results. Temperature distributions of the respective simulations are then obtained employing ANSYS steady state thermal software. Temperature distributions show relatively high temperature where electromagnetic energy is confined; hence localized heating is achieved. The findings of this work may facilitate applications in the fields of data storage, optical local heating, and optical sensing.

9547-118, Session PWed

Enhancing resonance dynamics in plasmonics

Ashok Kodigala, University of California, San Diego (United States); Thomas Lepetit, Boubacar Kante, Univ. of California, San Diego (United States)

A budding topic of interest is that of applications in the field of plasmonics which currently range from chemical and biological sensing to enhanced photovoltaics. At the core of these plasmonic devices are resonances that govern their unique function and the ability to manipulate said resonances is crucial to their design. In order to manipulate resonances, we must be able to observe them quantitatively. Conventionally, the approach to examining plasmonic resonances is to identify the peaks and troughs of reflection and transmission spectra. This methodology is qualitative in nature and is



insufficient for non-symmetric or Fano resonances. This approach is even worse for cases with multiple overlapping resonances. Here, we describe an effective Hamiltonian formalism to study and tailor plasmonic resonances at optical frequencies. Using this approach, we compute the complex poles of the scattering matrix which quantitatively relate to both the resonance frequencies and linewidths. As such, we are able to track the dynamics of resonances and study in detail the coupling behavior between multiple plasmonic particles. As a further consequence, we can design novel plasmonic systems that offer a very large degree of resonance tunability.

9547-119, Session PWed

Optica fiber tip with point light source of SPPs driven by three-dimensional nanostructured asymmetric metalinsulator-metal layer cap

Yasushi Oshikane, Motohiro Nakano, Osaka Univ. (Japan); Kensuke Murai, National Institute of Advanced Industrial Science and Technology (Japan)

Numerical analysis of three dimensional optical electro-magnetic field in a circular-truncated conical optical fiber covered by asymmetric MIM structure has been performed by a commercial finite element method package, COMSOL Multiphysics coupled with Wave Optics Module. The outermost thick metallic layer has twin nano-hole, and the waveguiding twin-hole could draw surface plasmon polaritions (SPPs) excited in the MIM structure to the surface. Finally the guided two SPPs could unite each other and may create a single bright spot. The systematic simulation is continuing, and the results will give us valuable counsel for control of surface plasmon polaritons (SPPs) appearing around the MIM structure and twin nano-hole. (1) Optimal design of the 3D FEM model for 8-core Xeon server and rational approach for the FEM analysis, (2) behavior of SPPs affected by wavelength and polarization of light travel through fiber, (3) change in excitation condition of SPPs caused by shape of the MIM structure and twin-hole, (4) effectiveness of additional nanostructures that are aimed at focusing control of two SPPs come out from the corners of twin-hole, (5) scanning ability of the MIM/twin-hole probe at nanostructured sample saurface (i.e. amount of forward and backward scattering of SPPs) will be presented and discussed. Several FIBed prototypes and their characteristic of light emission will also reported.

9547-120, Session PWed

Revealing the dispersive phase change in a slit-groove plasmonic interferometer structure

Xie Zeng, Univ. at Buffalo (United States); Haifeng Hu, Northeastern Univ. (China); Yongkang Gao, Alcatel-Lucent Bell Labs. (United States); Dengxin Ji, Nan Zhang, Haomin Song, Kai Liu, Qiaoqiang Gan, Univ. at Buffalo (United States)

The investigation on light interaction with individual slits has a long history in physical optics, resulting in many fundamental progresses. In recent years, there has been considerable growth in plasmonics research due to their subwavelength confinement of electromagnetic (EM) waves. To better understand surface plasmon polariton (SPP) mediated interactions between optical nano-objects at metallodielectric interfaces, researchers have performed numerous theoretical and experimental studies of the physics of nanostructures. However, there are still many open questions regarding fundamental understanding on surface plasmon waves. For instance, phase is an inherent and important feature for coherent processes, particularly for EM waves. In previously reported literature, the phase change during the SPP coupling was considered as a constant for different wavelengths, resulting in a mismatch between experiment and theoretical modeling. In this work, we propose an approach to extract the phase change dispersion during the interaction between free-space light, SPPs and nanogrooves. Using the far-field transmission and scattering image from a tilted slitgroove plasmonic interferometer structure, the intrinsic phase dispersion ?0(?) as the function of wavelength was successfully extracted, revealing more fundamental physics of SPP-nano-object interactions. This approach can also be applied to extract intrinsic phase dispersion of other plasmonic nano-objects with different shapes, which is essential for plasmonic subwavelength optics on a chip.

9547-121, Session PWed

Enhanced light emission and absorption from monolayer MoS2 using single plasmonic optical antenna

Edgar Palacios, Serkan Bütün, Spencer Park, Lincoln J. Lauhon, Koray Aydin, Northwestern Univ. (United States)

In the last few years 2D transition metal dichalcogenides exhibiting direct bandgap behavior have received much attention because of their performance advantages in field-effect transistors, detector applications and flexible electronic devices operating in the visible spectrum. Among these materials, MoS2 has shown impressive results but the advantages stemming from its monolayer thickness also present a disadvantage- reduced lightmatter interaction. By utilizing the light confining effects of plasmonic nano-structures it is possible to strongly couple plasmonic resonances with single layer MoS2 and increase light matter interactions. Recently, we have modeled and experimentally verified the strong optical interactions of localized surface plasmons from Ag nanodiscs with monolayer MoS2 resulting in a twelve-fold photoluminescence enhancement. Herein, we will present our latest results on the detection of single Au nanoantennas through enhanced photoemission from monolayer MoS2. By engineering the length of Au dipole and bowtie nanoantennas we tune the resonant frequency to support the excitation or emission fields resulting in improved light emission and absorption for the next generation of 2D based photonics, detectors and solid state lighting.

9547-122, Session PWed

Plasmonic dark modes excited by strongly focused illumination

Jordi Sancho-Parramon, Institut Ruder Bo?kovic (Croatia) and Univ. of Barcelona (Spain); Salvador Bosch Puig, David Maluenda, Univ. de Barcelona (Spain); Hrvoje Zorc, Institut Ruder Bo?kovic (Croatia)

Surface plasmons with a charge distribution having a net dipole moment are known as bright modes, as they can easily couple to light. On the other hand, resonances with a zero dipole moment are termed dark as they cannot be excited by homogeneous illumination. Over the last years, dark modes have attracted significant interest due to their potential for sensing applications. Compared to bright modes, they show strong electromagnetic near-field enhancement and high quality factors. In addition, the interference of dark and bright modes can lead to Fano-like resonances.

In symmetric structures, dark plasmon modes can be excited by nonoptical means such as an electron beam. Generation of dark modes by light requires breaking the excitation symmetry that can be achieved using inhomogeneous illumination, evanescent waves, retardation effects, localized emitters or spatial phase shaping. In the present work, we show that strongly focused illumination can lead to excitation of dark modes. We first use rigorous vectorial diffraction theory to compute the distribution of light at the focus and then numerically calculate the response of particle clusters and core-shell particles. Controlling the distribution of light arriving at the focusing lens by, for instance, pupil filters enables enhancing the excitation of dark modes. Overall, these results present guidelines for the excitation of dark plasmon modes using standard optical instrumentation.



9547-123, Session PWed

Fabrication of alternative plasmonic materials with room temperature highpower impulse magnetron sputtering

Zih-Ying Yang, Yi-Hsun Chen, National Chiao Tung Univ. (Taiwan); Bo-Huei Liao, Instrument Technology Research Ctr. (Taiwan); Kuo-Ping Chen, National Chiao Tung Univ. (Taiwan)

Low loss alternatives plasmonic materials like titanium nitride (TiN), have received significant interests in recent years. TiN has low loss in the visible and NIR wavelengths and the optical properties can be adjusted. In addition, the high melting temperature and bio-compactable properties make TiN with strong potentials in many applications. However, there is less discussion on the relevance of electrical and optical characteristics of TiN thin films. In this work, the room temperature fabrication process of TiN thin film is proposed, which is suitable for flexible substrate. Compared to the conventional magnetron sputtering, reactive high power impulse magnetron sputtering (HiPIMS) could provide higher degree of ionization of the sputtered metal and higher rate of molecular gas dissociation. Thus, the improvement in density, roughness, and electrical conductivity at lower temperature process could be achieved. Since TiN are non-stoichiometric materials, their composition could be changed by preparation method. In this study, 40 nm TiN thin films were deposited on B270 glass by HiPIMS at room temperature. First, the effects of DC power parameter on the conductivity, crystallinity, optical resonant properties of the TiN thin film will be investigated. Then, the relationship between electrical and optical properties will be shown. When the DC power is increasing, the ellipsometry results show that the dielectric function will change from dielectric to conductor. From four-point probe measurements, the resistivity decreases to 1/16 times as the power increases. In addition, increasing power would result in plasmon resonance blue-shifted from 515 nm to 460 nm.

9547-124, Session PWed

Plasmonic hydrogels for ultrasensitive and in situ detection of a quorum-sensing signaling molecule by surface-enhanced Raman scattering spectroscopy

Verónica Montes García, Gustavo Bodelon-Gonzalez, Sergio Rodal-Cedeira, Vanesa López Puente, Celina Costas, Univ. de Vigo (Spain); Luis M. Liz-Marzán, CIC BiomaGUNE (Spain); Isabel Pastoriza-Santos, Jorge Perez-Juste, Univ. de Vigo (Spain)

In nature most bacteria exist in biofilms regulated by a cell-to-cell communication process termed quorum sensing (QS). The understanding of how microbial populations communicate and behave is important for developing new therapeutic compounds. Herein we report the use of Surface-enhanced Raman scattering (SERS) spectroscopy as an ultrasensitive tool for direct, in vivo plasmonic detection of a Pseudomonas aeruginosa QS-regulated molecule termed pyocyanin. With this aim, we report the design and characterization of a novel nanostructured plasmonic substrate to be used as SERS active sensing platform.

The nanostructure is based on poly(N-isopropylacrylamide) (pNIPAM) hydrogels doped with gold nanorods with high scattering contribution. The plasmonic substrates allowed simple, fast and ultrasensitive detection (up to 10-10 M) and quantification of pyocyanin produced from bacteria grown in liquid culture. Importantly, the inherent properties of the plasmonic hydrogels enabled bacterial growth as biofilm and simultaneous SERS detection of pyocyanin. This study shows for the first time in situ plasmonic imaging and monitoring of QS, demonstrating the suitability of this plasmonic platform for spectroscopic analysis of microbial communication and behavior.

9547-125, Session PWed

Mapping of transmission spectrum between plasmonic and nonplasmonic single slits

Shih-Hui Chang, Yulun Su, National Cheng Kung Univ. (Taiwan)

In contrast to conventional emphases on plasmonic effects, mapping of the transmission spectrum between a plasmonic and non-plasmonic 2D single slit are demonstrated. At resonant transmission, plasmonic and nonplasmonic single slits exhibit similar near-field mode at their corresponding resonant wavelengths. Their resonant transmission wavelengths can be transformed via a simple mapping with surface plasmon dispersion relation. To further extend the mapping for non-resonant condition, complex reflection and transmission coefficients at the end faces of a semi-infinite slit are analyzed to reconstruct the whole transmission spectra. The complex reflection coefficients are found similar at the same effective wavelength for both plasmonic and non-plasmonic cases. The reconstructed spectrum by a Fabry-Perot model matches the transmission spectrum of a non-plasmonic slit and can be transformed into that of a plasmonic case by wavelength stretching with plasmonic waveguide dispersion. The transmission cross section is bounded by $?/(\varpi d)$. Width-dependent red shifts of the transmission spectrum are associated with effective capacitances at the slit end faces. Same mapping method applies for a single slit with substrate or periodic structure. Furthermore, the optical property of a plasmonic slit can be achieved by a non-plasmonic slit via dimension scaling. The focusing lens effect of a plasmonic slit array can be mimicked by a non-plasmonic slit array with dimension scaling. The unified transmission properties of plasmonic and non-plasmonic 2D single slits can simplify the design of slit structures for plasmonic applications.

9547-126, Session PWed

Detectivity comparison of bolometric optical antennas

Alexander Cuadrado, José Manuel López-Alonso, Juan Carlos Martínez-Antón, Jose-Miguel Ezquerro, Univ. Complutense de Madrid (Spain); Francisco Javier González, Univ. Autónoma de San Luis Potosí (Mexico); Javier Alda, Univ. Complutense de Madrid (Spain)

The actual application of optical antennas in detection devices strongly depends on its ability to produce an acceptable signal-to-noise ratio for the given task. It is known that, due to the intrinsic problems arising from its sub-wavelength dimensions, optical antennas produce very small signals. The guality of these signals depends on the involved transduction mechanism. The contribution of different types of noise should be adapted to the transducer and to the signal extraction regime. Once noise is evaluated and measured, the specific detectivity, D*, becomes the parameter of interest when comparing the performance of antenna coupled devices with other detectors. In this contribution we are interested in the evaluation and comparison of D* values for several arrangements of bolometric optical antennas working in the infrared. The values obtained for D* will be related with those characterizing conventional optical detectors. At the same time, some strategies, related with the adequate choice of materials and geometries will be discussed in order to improve this parameter.

9547-127, Session PWed

Analysis of the spectral response of fractal antennas related with its geometry and current paths

Alexander Cuadrado, José Manuel López-Alonso, Juan



Carlos Martínez-Antón, Jose-Miguel Ezquerro, Univ. Complutense de Madrid (Spain); Francisco J. Gonzalez, Univ. Autónoma de San Luis Potosí (Mexico); Javier Alda, Univ. Complutense de Madrid (Spain)

Fractal antennas have been proposed to improve the bandwidth of resonant structures and optical antennas. Their multiband characteristics are of interest in radiofrequency and microwave technologies. In this contribution we link the geometry of the current paths built-in the fractal antenna with the spectral response. We have seen that the actual currents flowing through the structure are not limited to the portion of the fractal that should be geometrically linked with the signal. This fact strongly depends on the design of the fractal and how the different scales are arranged within the incoming radiation could be of help to spectrally select the response of the multiband design.

9547-128, Session PWed

Nanoporous gold leaves: preparation, optical characterization, and biosensing capabilities

Gianluca Ruffato, Univ. degli Studi di Padova (Italy); Denis Garoli, Eugenio Calandrini, Pierfrancesco Zilio, Francesco De Angelis, Istituto Italiano di Tecnologia (Italy); Filippo Romanato, Univ. degli Studi di Padova (Italy); Sandro Cattarin, CNR-IENI (Italy)

Porous gold films have recently attracted increasing interest due to the unique properties related to their very high specific surface area. This particular material finds applications in many fields from electrochemistry to nanofluidic, solar cell and enhanced spectroscopy. Among the different fields of application, nanoporous gold (NPG) demonstrates also intriguing properties as plasmonic material. There is still a great desire to develop materials with optimized photonic properties taking advantage of electromagnetic resonances and concomitant enhancement of the electromagnetic near-field owing to surface plasmons. NPG has been extensively studied also as plasmonic platform for biosensing applications. In almost the cases it was prepared as thin film on a bulk substrate. A possible alternative approach is to prepare the NPG as self-standing film. This leads to a perfect symmetric configuration where the metal is immersed in an homogeneous medium. In order to exploit symmetric plasmonic modes this configuration can be extremely interesting. Here we present a reproducible NPG self-standing leaves preparation. We then investigate the material's optical response from the visible up to the medium infrared (MID-IR). The material has been nanostructured in order to support propagating symmetric plasmonics modes. Biosensing performances have been tested both in the optical and in the MID-IR spectral range. This platform was exploited for the detection of both self-assembly monolayer of very small molecules (alcane-thiol) and of protein conformational states. The employment of nanoporous gold offers the unique advantages of augmented analyte delivery by infiltration inside the sensor and versatile functionalization.

9547-129, Session PWed

Optical monitoring of the doping level of semiconductor by Brewster "mode"

Thierry Taliercio, Eric Tournié, Laurent Cerutti, Univ. Montpellier 2 (France); Jean-Jacques Greffet, Lab. Charles Fabry (France)

Develop plasmonic materials compatible with complementary metal oxide semiconductor (CMOS) technology is one of the fundamental challenges for plasmonics to imagine a possible industrialization of plasmonic applications other than bio-detection. Several approaches have been proposed to reach this goal notably using highly doped semiconductor (HDSC). However, it is indispensable to control accurately the plasma frequency, wp, of the HDSC to adjust the plasmonic resonances of the metallic nanostructures. We have developed a new non-destructive optical technique to measure wp by the intermediate of the Brewster "mode". When we investigate highly-doped InAsSb layers lattice matched onto GaSb substrates by angular-dependent reflectance, we evidenced a resonant dip near the plasma frequency of thin layers. Based on Fresnel coefficient in the case of transverse electromagnetic wave, we propose that this resonance is due to the excitation of a leaky electromagnetic mode, the Brewster "mode", propagating in the metallic layer deposited on a dielectric material. Investigating series of samples allowed us to realize abacus linking plasma frequency to carrier density. Potential interest of this mode for in-situ monitoring during device fabrication is also discussed.

9547-130, Session PWed

Fabrication of plasmonic thin films and its characterization by optical method and FDTD simulation technique

Anton Kuzma, Frantisek Uherek, Slovenska Technicka Univ. (Slovakia) and International Laser Ctr. (Slovakia); Jaroslava ?kriniarová, Slovenska Technicka Univ. (Slovakia); Du?an Pudi?, Univ. of ?ilina (Slovakia); Martin Weis, Martin Donoval, Slovenska Technicka Univ. (Slovakia)

In this paper we present optical properties of thin metal films deposited on the glass substrate by the physical vapor deposition system. Localized surface plasmon polaritons of different film thicknesses have been spectrally characterized by optical methods. Evidence of the Au and Ag nanoparticles in deposited thin films have been demonstrated by Scanning Electron Microscope (SEM) and Atomic Force Microscope (AFM) and their dimensions as well as separations have been evaluated. As a first approximation, the simulation model of deposited nanoparticles without assuming their dimension and separation distributions has been created. Simulation model defines relation between the nanoparticle dimensions and their separations. Model of deposited nanoparticles has been simulated by the Finite-Difference Time-Domain (FDTD) simulation method. The pulsed excitation has been used and transmission of optical radiation has been calculated from the spectral response by Fast Fourier Transform (FFT) analyses. Plasmonic extinctions have been calculated from measured spectral characteristics as well as simulated characteristics and compared with each other. The nanoparticle dimensions and separations have been evaluated from the agreement between the simulation and experimental spectral characteristics. Surface morphology of thin metal film has been used as an input for the detail simulation study based on the experimental observation of metal nanoparticle distribution. Hence, this simulation method includes appropriate coupling effects between nanoparticles and provides more reliable results. Obtained results are helpful for further deep understanding of thin metal films plasmonic properties and simulation method is demonstrated as a powerful tool for the deposition technology optimizations.

9547-131, Session PWed

Bianisotropic metamaterials for enhanced chiral fields and forces

Hossein Alizadeh, Björn M. Reinhard, Boston Univ. (United States)

The two enantiomers (mirror-images) of a biomolecule can show drastically different behaviors, requiring the development of sensitive approaches for their identification and separation. Plasmonic nanostructures have shown promise for enhancing the sensitivities of chiral spectroscopies, but the generation of chiral near fields with a specific handedness in the spatial domain surrounding the plasmonic structures remains a challenge. Here we demonstrate that achiral bianisotropic structures, which couple the electric and magnetic fields, can achieve high enhancements of optical chirality in an extended spatial region. Magneto-electric coupling in such structures



facilitates electrically excited magnetic resonances in the near IR and optical regimes, which in turn can result in highly enhanced optical chirality in an extended region of space. We apply this concept to achiral double split ring resonators (DSRRs) and demonstrate their potential in generating enhanced chiral fields and forces. Also, the behavior of optical chirality density gradient and chirality flux in such structures is examined, and it is shown that plasmonically generated chiral forces may pave the way to a new class of chiral biosensors.

9547-132, Session PWed

Engineering metal-nanoantennae/dye complexes for maximum fluorescence enhancement

Xiang Meng, Richard R. Grote, Jerry I. Dadap Jr., Columbia Univ. (United States); Nicolae-Coriolan Panoiu, Univ. College London (United Kingdom); Richard M. Osgood Jr., Columbia Univ. (United States)

We theoretically investigate the fluorescence enhancement of a molecule placed in a variable (4 - 20 nm) gap of a plasmonic dimer, with different dye molecules as well as different nanoparticle geometries, using a fully vectorial three-dimensional finite-difference time-domain (3D FDTD) method. This work extends previous studies on molecular fluorescence in the vicinity of metal interfaces and single nanoparticles and shows how the radiative emission of a molecule can be further enhanced by engineering the geometry of a plasmonic structure. Through the use of rigorous 3D FDTD calculations, in conjunction with analytic guidance based on temporal coupled-mode (TCM) theory, we achieve accurate fluorescence enhancement calculations for arbitrary-shaped metal nanoparticle antennae. We have obtained the antennae configurations for the optimimized fluorescence enhancement of each of a selected set of dye molecules, which are matched to three different antennae geometries. Our results provide guidance for the rational design of optimized metallic nanoparticle complexes for maximum fluorescence enhancement. Finally, we note that this approach provides a design procedure for antennae assemblies that is useful both for general understanding of molecule-metal structure interaction and experimental efforts in plasmon-enhanced molecular spectroscopy.

9547-133, Session PWed

Plasmon resonance in ellipsoids and ellipsoidal dimers

Catalina B. Lopez-Bastidas, Univ. Nacional Autónoma de México (Mexico); Leonardo Baez, Ctr. de Investigación Científica y de Educación Superior de Ensenada B.C. (Mexico); Jesus Manzanares-Martinez, Univ. de Sonora (Mexico)

Ellipsoidal nanoparticles represent an interesting system to study beyond spherical nanoparticles since the loss of symmetry is easily controled by a single parameter.

The resulting split in plasmon resonance frequency can be tuned modifying the same parameter. Furthermore the presence of more than one mode can be controled by the polarization of the exciting field. When two or more such structures are present the enhancement of the local fields can have strong effects on the optical spectra of system.

We calculate the optical properties of ellipsoidal nanoparticles and ellipsoidal dimers and compare quasi-static approximations with numerical solution of electrodynamic equations.

9547-134, Session PWed

Prospect of detection and recognition of single biological molecules using ultrafast coherent dynamics in quantum dotmetallic nanoparticle systems

Seyed M. Sadeghi, The Univ. of Alabama in Huntsville (United States)

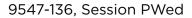
Conventional plasmonic sensors are based on intrinsic resonances of metallic nanoparticles (localized surface plasmons). In such sensors detection is done by investigating wavelength shifts of such resonances. In this contribution we propose ultra-sensitive time-domain nanosensors based on the impact of ultra-small changes in environmental conditions on the coherent dynamics of hybrid systems consisting of one metallic nanoparticle and one quantum dot. Interaction of these systems with a laser field generates quantum coherence, allowing us to convert minuscule changes in the environment into dramatic optical events detectable by conventional and simple electronic and optical means. These sensors are not based on excitons or plasmons as in conventional sensors, but rather they utilize the way ultra-small changes in the refractive index of environment modify dynamics of coherent exciton-plasmon coupling and the collective molecular resonances (plasmonic meta-resonances) of the hybrid quantum dot-metallic nanoparticle systems. We show when the laser field and the structural conditions of these systems are properly adjusted such that these systems are close to their collective resonances, adsorption of a single molecule to can make the dark (non-emissive), offering large extinction ratio of detection. We show one can adjust the laser field, in terms of its temporal width and intensity, such that these processes can be sensitive for a certain size of molecule, suggesting the possibility of recognition of molecules. A prime feature of our investigation is that it includes the ultrafast quantum dephasing of quantum dots which can happen at elevated temperatures.

9547-135, Session PWed

Field enhancement with plasmonic nano antennas on silicon-based waveguides

Mahsa Darvishzadeh Varcheie, Caner Guclu, Regina Ragan, Ozdal Boyraz, Filippo Capolino, Univ. of California, Irvine (United States)

Plasmonic nanoantennas have been investigated due to the capability to provide strong near-field enhancements when illuminated by an external electromagnetic field. Surfaces made of plasmonic nanoantennas have been demonstrated to increase signal intensity in surface enhanced Raman scattering by several orders of magnitude. Measurement techniques, however, are expensive and bulky using standard methods for illumination and detection of Raman scattering signals. Our goal is to investigate novel optical structures to develop spectroscopy systems that are inexpensive and mobile by utilizing nanoantennas that are integrated with dielectric waveguides. Particularly, dimers made of gold nanospheres assembled from colloidal solution on top of silicon nitride waveguide are used in this work. This optical structure eliminates the complexity of illumination and detection in traditional schemes, reducing both cost and volume. Resonant dimer nanoantennas are excited by the guided field that exhibits evanescent decay outside of the waveguide. Simulations show that a very strong electric field builds up in the dimer gap with a 25-100 fold field enhancement as compared to the waveguide's modal field at the same location. We further investigate how the field enhancement varies with the dimer location and orientation and how it depends on the waveguide geometry and modes. This is important information to guide level of control of placement on waveguide surfaces using colloidal assembly. Full-wave simulations demonstrate the effectiveness of the investigated optical structures to achieve similar signal enhancement obtained with standard instrumentation measuring signals from dimers scattered light on a planar substrate illuminated by a plane wave.



Angle-resolved far-field scattering spectra of single Ag nanowire over the entire semimeridian

Jinhyung Kim, Ho-Seck Ee, KAIST (Korea, Republic of); Min-Soo Hwang, Kwang-Yong Jeong, Korea Univ. (Korea, Republic of); Ju-Hyung Kang, Korea Univ. (Korea, Republic of) and KAIST (Korea, Republic of); Hong-Gyu Park, Korea Univ. (Korea, Republic of); Min-Kyo Seo, KAIST (Korea, Republic of)

Scattering properties of a plasmonic nanowire have been investigated through dark-field microscopy, back-focal plane imaging and so on. Surface plasmon polaritons (SPPs) supported by the metallic nanowire have a large wavevector and cause strong scattering radiations to the direction of a large angle even beyond the numerical aperture (N.A.) of the microscope objective employed in the conventional methods. To overcome this limitation and obtain the full information of scattering characteristics, we directly measured far-field scattering spectra of a single Ag nanowire over the entire semi-meridian with varying detection angle. SPPs of the nanowire on a coverslip are excited by white-light illumination focused on one end of the nanowire by an objective. The detection part, 0.23 m distant from the nanowire, scans the entire northern semi-meridian with an angular resolution of 2 degrees and collects scattering radiations into an optical fiber attached to a spectrometer. Beyond the N.A. of the focusing objective, purely scattered signal is detected, while, within the N.A., the extinction by the nanowire is observed. The angle-resolved scattering spectra reveal that the far-field scattering pattern of the nanowire carries two features of the near-field: Fabry-Perot resonances of SPPs propagating along the nanowire and phase-matching conditions between SPPs and free-propagating radiation depending on the emission angle and wavelength. The dispersion relation of SPPs can also be precisely retrieved, since the resolved angle corresponds to the wavevector. We believe that the study on the angleresolved far-field scattering spectra will be useful to understand scattering characteristics of a desired optical nanostructure.

9547-137, Session PWed

A low-cost, high-sensitivity surface enhanced raman scattering substrate by Si nanowire arrays decorated with Au nanoparticles and backplane

Bi-Shen Lee, National Tsing Hua Univ. (Taiwan); Ding-Zheng Lin, Industrial Technology Research Institute (Taiwan); Ta-Jen Yen, National Tsing Hua Univ. (Taiwan)

Raman spectra provide rich vibrational signals that represent the fingerprint of molecules, and more importantly, such signals are insensitive to water so that recently the technique of Raman scattering emerges a promising method for environmental and biological trace analysis. Nevertheless, the scattering cross section of Raman signals is usually small, and therefore it is crucial to further enhance the signals of Raman scattering. In this work, we demonstrate a low-cost and highly sensitive surface enhanced Raman scattering (SERS) substrate, which is comprised of the silicon nanowire (SiNW) array decorated with Au nanoparticles (AuNPs) on the surface and incorporated with a layer of Au backplane at the bottom. Firstly, the SiNW array was prepared by a metal-assisted chemical etching (MaCE) method as a template of the SERS substrate. Then, the gold nanoparticles (AuNPs), which were decorated on the surface of SiNWs array by an electron-beam evaporator under oblique angle deposition (OAD), enable localized surface plasmon resonance (LSPR) to substantially intensify the signal of Raman scattering from the analyte. Besides, we deposited an additional Au layer at the bottom of the SiNW array by electron-beam deposition under normal incidence. This additional Au layer, termed as a metal backplane (MBP), facilitates to reflect the back-scattered field rather than being absorbed by the silicon substrate, leading to the further enhancement of the SERS

signals. Finally, the performance of this SERS substrate was optimized by a statistical Taguchi method. Our experimental verification indicates that for the analyte of 10-2 M self-assembled monolayer (S.A.M.) of thiophenol molecules, our tailored SERS substrate presents the average Raman signal up to1740 counts per second under a near infrared laser excitation (785 nm), which is 1.78 times stronger than a commercialized SERS substrate (Klarite*). Furthermore, our low-cost and high-sensitivity SERS substrate preforms reliably, showing a small coefficient of variation (C.V.) about 4.2%

SPIE. PHOTONICS

NANOSCIENCE+ ENGINEERING

9547-138, Session PWed

Third-harmonic generation from core/shell structure nanoparticle

Liwei Liu, Yue Wang, Yu Ren, Yueshu Feng, Siyi Hu, Changchun Univ. of Science and Technology (China)

In this paper, we report the third harmonic generation (THG) from Au-Cu2S nanoparticles, We characterized the THG efficiency of Au-Cu2S nanoparticles experimentally and theoretically, comparing to Cu2S quantum Dots (QDs), Au-Cu2S nanoparticles exhibited stronger THG signal and intensity, we performed experiments pumped by femtosecond laser pulses. Our studies suggest that these Au-Cu2S nanoparticles can be used for nonlinear optics detection, optics Harmonic imaging, and electric detection.

9547-139, Session PWed

Nanoscale dimples for field enhancement of organic thin films

Arkardiusz J. Goszczak, Jost Adam, Pawel P. Cielecki, Jacek Fiutowski, Horst-Günter Rubahn, Univ. of Southern Denmark (Denmark)

A promising method for improving the power conversion efficiencies of organic solar cells (OSCs) is by incorporating structured electrodes in their thin film architecture, improving the light absorption in the device's active layers. A cheap and large-scale production compatible method for structuring the electrodes in OSCs is by the use of Anodic Alumina Oxide (AAO) membranes. Here, nano-scale pores of controlled dimensions are formed through anodic oxidation of sputter deposited high purity aluminum (AI) films. The AI deposition conditions are controlled in order to modify the roughness and the grain size of the Al layers, as those parameters critically affect the subsequent pore formation during the anodization process. The anodization of the AI layers occurs in an electrochemical cell in H2SO4, H2C2O4 and H3PO4 solutions, in order to tune the AAO pore diameter and interpore distance. Following anodization, the fabricated AAO is selectively etched away in H2CrO4/H3PO4 mixtures, in order to reveal the underlying Al nanoscale dimples, which are present at the bottom of the pores. We investigate the light-trapping properties of these dimples as a function of their dimensions and ordering. The dimples' optical properties are characterized via reflection measurements, supported by non-destructive laser ablation of polymer coatings. The resulting polarization-dependent field enhancement measurements are compared to FDTD calculations to further explain the mechanisms of light-trapping in dimple-structured organic thin film devices.

9547-140, Session PWed

Structure, configuration, and sizing of Ni nanoparticles generated by ultrafast laser ablation in different media

David Muñetón Arboleda, Ctr. de Investigaciones Ópticas (Argentina); Jesica M. Santillán, Ctr. de Investigaciones Ópticas (Argentina) and Univ. Nacional de Catamarca (Argentina); Luis J. Mendoza Herrera, Ctr. de Investigaciones Ópticas (Argentina); Marcela B. Fernández

Conference 9547: Plasmonics: Metallic Nanostructures and Their Optical Properties XIII



van Raap, Univ. Nacional de la Plata (Argentina) and Facultad de Ciencias Exactas (Argentina); Diego Muraca, Univ. Estadual de Campinas (Brazil); Daniel C. Schinca, Lucia B. Scaffardi, Ctr. de Investigaciones Ópticas (Argentina) and Univ. Nacional de la Plata (Argentina)

In recent years, nickel nanoparticles (Nps) have increased scientific interest because of their extensive prospects in catalysts, conducting pastes, information storage, large-scale batteries and biomedicine.

Several works on Ni Nps generation by laser ablation have appeared in the literature in the last years, using different pulsed laser regimes and different media have been published recently.

However, there are no works reporting on the use of fs-regime laser ablation of Ni in liquids and the corresponding characterization of the obtained colloids. In this work we analyze the characteristics of species, structure (bare core or core-shell), configuration and size distribution of Nps generated by fs pulse laser ablation over a Ni solid target in n-heptane and water. We report the presence of NiO-Ni core-shell and hollow Ni Nps in these colloids obtained, discussing a mechanism for the formation of different species present in the colloidal suspensions. These were experimentally characterized using AFM and TEM microscopy, as well as Optical Extinction Spectroscopy (OES). Extinction spectra were modeled using Mie theory through an appropriate modification of the complex experimental dielectric function, taking into account a size-dependent corrective term for each free and bound electron contribution. Experimental UV-visible-NIR spectra were reproduced considering a size distribution of bare core, hollow and core-shell structures Nps.

In both media, Ni Nps shape and size distribution agrees with that derived from TEM and AFM analysis.

9547-141, Session PWed

Surface plasmon polariton interface of left-handed metamaterial with cylindrical anisotropy and dielectric medium

Semen Andronaki, Egor Gurvitz, Mikhail Khodzitsky, Anna Vozianova, ITMO Univ (Russian Federation)

In recent years the role of surface plasmons polaritons (SPP) in nano-optics [1] gaining popularity because of the wide applications in areas such as the development of waveguides, biosensors, near-field microscopy and cloaking devices [2]. Therefore it needs to search new ways to generate the SPP due to high actuality of plasmonic applications in terahertz frequency range. In this paper the mechanism of excitation of SPP at the interface of left-handed metamaterial with cylindrical anisotropy and dielectric medium at THz frequency range [3]. Numerical simulation of this structure was performed using COMSOL Multiphysics, Frequency Domain solver.

1. Azad, Abul K., et al. Selected Topics in Quantum Electronics, IEEE Journal of 19.1 (2013): 8400416-8400416.

2. Liu, Yongmin, et al. Nano letters 10.6 (2010): 1991-1997.

3. Carbonell, Jorge, et al. New Journal of Physics 13.10 (2011): 103034.

9547-142, Session PWed

Fabrication and optical properties of gold nano aperture array using plating technique for plasmonic infrared filter

Hong-Kun Lyu, Hui-Sup Cho, Young-Jin Park, DGIST (Korea, Republic of); Sung-Hyun Jo, Jang-Kyoo Shin, Kyungpook National University (Korea, Republic of)

We report on plating technique to fabricate the gold nano aperture array and the optical properties. Firstly, we designed a structural model of the gold nano aperture array and simulated the spectral variation in the wavelength transmission. For the simulation, we used a commercial computer simulation tool utilizing the FDTD method. SiO2 was used as the substrate insulator, top-side insulator, and the fill material in the cylindrical aperture. We applied gold as the metal layer; dispersion information for gold was derived from the Lorentz–Drude model. Next, we fabricated the nano aperture array on the glass substrate. To apply a plating technique, the seed layer was formed on the substrate, and the PR pattern of the nono aperture array was built up using electron-beam lithograph machine. And then, we formed the gold plating layer in an optimized bath. Finally, the PR pattern was removed in the PR stripper. Furthermore, we measured the optical characteristics of gold nono aperture array using UV-VIS-IR spectrophotometer.

9547-143, Session PWed

Solid state oxidation of copper nanoparticles: a plasmonic perspective

Mariano D. Susman, Yishai Feldman, Tatyana Bendikov, Hagai Cohen, Alexander Vaskevich, Israel Rubinstein, Weizmann Institute of Science (Israel)

No Abstract Available

9547-145, Session PWed

Separation of surface plasmon polariton modes generated in a multilayer structure

Boram Kim, Hong-Gyu Ahn, Kyongseok Kim, Sung-Ho Lee, Daeyeon Kim, Yu-mee Jeoug, Seung-Han Park, Yonsei Univ. (Korea, Republic of)

In a thin metallic film surrounded by the dielectric media with different refractive indices, two different modes of surface plasmon polariton (SPP) are generated. These two modes are called long-range SPP and short-range SPP, respectively. By varying the thickness of the metallic film, amplitude ratio of the two modes can be controlled. In addition, these modes can be mixed as long as the film thickness is thin enough (closed to the skin depth). In this talk, the field distributions generated by the SPPs are presented.

9547-77, Session 15

Imaging metallic nanostructures with second and third order nonlinear optical response (Invited Paper)

Emeric Bergmann, Christian Jonin, Emmanuel Benichou, Pierre-François Brevet, Institut Lumière Matière (France)

Imaging metallic structures to determine their nanoscale optical properties is of utmost importance not only to reveal their morphology but also their ability to be incorporated into devices. Combining linear and nonlinear optical imaging may then turn to be highly fruitful because the corresponding optical responses stem from different origins. For instance, odd order responses like the first linear and the third order responses essentially probe volume effects whereas even orders like the second order response probe surface effects in centrosymmetric media, like gold and silver. These effects may arise from the fabrication methods employed to produce the structures like manufacturing defects appearing as shape distortions. This striking difference between the different contributions to the nonlinear optical response of these metallic structures can therefore be used to reveal a highly refined picture of the nanostructures.

We report in this study the combined first, second and third order responses from single gold metallic nanoparticles as well as their assemblies. The different features observed will be discussed in light of the origin of the different orders observed.



9547-78, Session 15

Interfacing ion-exchanged waveguide for the efficient excitation of surface plasmons

Josslyn Beltran Madrigal, Univ. de Technologie Troyes (France); Martin Berthel, Institut NÉEL (France); Florent Gardillou, Teem Photonics S.A. (France); Ricardo Tellez Limon, Christophe Couteau, Univ. de Technologie Troyes (France); Denis Barbier, Teem Photonics S.A. (France); Aurelien Drezet, Institut NÉEL (France); Rafael Salas-Montiel, Univ. de Technologie Troyes (France); Serge Huant, Institut NÉEL (France); Sylvain Blaize, Univ. de Technologie Troyes (France)

Several works have already shown that the excitation of plasmonic structures through waveguides enables a strong light confinement and low propagation losses [1]. This kind of excitation is currently exploited in areas such as biosensing [2], nanocircuits[3] and spectroscopy[4].

Efficient excitation of surface plasmon modes (SPP) with guided modes supported by high-index-contrast waveguides, such as silicon-on-insulator waveguides, had already been shown [1,5], however, the use of weak-confined guided modes of an ion exchanged waveguide on glass as a source of excitation of SPP represents a scientific and technological breakthrough. This is because the integration of plasmonic structures into low-index-contrast waveguide increases the bandwidth of operation and compatibility with conventional optical fibers.

In this work, we describe how an adiabatic tapered coupler formed by an intermediate high-index-contrast layer placed between a plasmonic structure and an ion-exchanged waveguide decreases the mismatch between effective indices, size, and shape of the guided modes. This hybrid structure concentrates the electromagnetic energy from the micrometer to the nanometer scale with low coupling losses to radiative modes. The electromagnetic mode confined to the high-index-contrast waveguide then works as an efficient source of SPP supported by metallic nanostructures placed on its surface.

We theoretically studied the modal properties and field distribution along the adiabatic coupler structure. In addition, we fabricated a highindex-contrast waveguide by electron beam lithography and thermal evaporation on top of an ion-exchanged waveguide on glass. This structure was characterized with the use of near field scanning optical microscopy (NSOM). Numerical simulations were compared with the experimental results.

[1] N. Djaker, R. Hostein, E. Devaux, T. W. Ebbesen, and H. Rigneault, and J. Wenger, J. Phys. Chem. C 114, 16250 (2010).

[2] P. Debackere, S. Scheerlinck, P. Bienstman, R. Baets, Opt. Express 14, 7063 (2006).]

[3] A. A. Reiserer, J.-S. Huang, B. Hecht, and T. Brixner. Opt. Express 18(11), 11810–11820 (2010).

[4] R. Salas-Montiel, A. Apuzzo, C. Delacour, Z. Sedaghat, A. Bruyant et al. Appl. Phys Lett 100, 231109 (2012)

[5] A. Apuzzo M. Févier, M. Salas-Montiel et al. Nano letters, 13, 1000-1006

9547-79, Session 15

Controlling light scattering and emission at subwavelength scale with plasmonic nanopatch antennas

Zilong Wu, Yuebing Zheng, The Univ. of Texas at Austin (United States)

Controlling light scattering and emission at subwavelength scale has significant implications for solar energy conversion, sensing, and nanophotonic devices. Plasmonic nanopatch antennas (PNAs), which consist of plasmonic nanoparticle coupled with metallic films, have shown directionality of radiation and large emission rate enhancement due to the strong plasmonic waveguide modes within the spacer layer. Herein, we comparatively study the light scattering and emission behaviors of a series of plasmonic nanopatch antennas (PNAs) with different plasmonic nanoparticles (i.e., nanosquare, nanotriangle, nanorod, and nanodisk) to develop the design rules of the PNAs. Using finite-difference timedomain (FDTD) simulations, we show that the shape and size of plasmonic nanoparticles can be tuned to control the resonance peak, intensity, directionality, and spatial distribution of the scattering light as well as the directionality, spatial distribution, spontaneous emission rate, quantum efficiency, and radiation enhancement factor of light emission. For example, high radiative quantum efficiency (0.74) and radiation enhancement factor (>20) can be achieved by disk PNA, while triangle PNA shows remarkable spontaneous emission rate enhancement of over 2,500. The effects of locations of emitters relative to the PNAs on the emission properties are also examined. Our results pave the way towards the rational design of PNAs for the optimal light scattering and emission as required by targeted applications.

9547-80, Session 15

Controlling the ultrafast hot electron dynamics in hybrid plasmonic nanostructures

Hayk Harutyunyan, Emory Univ. (United States)

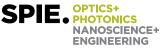
Plasmons hold promise for applications in photonic circuitry because of their ability to squeeze light into sub-wavelength dimensions and also for their ultrafast response times. To this end, it is important to fabricate plasmonic systems that can generate large optical signals at ultrafast timescales. Plasmonic devices based on Kerr-type nonlinear optical effects, typically demonstrate picosecond timescales attributed to electron -- phonon scattering. By designing and fabricating metal-oxide hybrid nanosystems with ultra-high field enhancements we were able to demonstrate much faster, femtosecond dynamics of the optical response based on hot electron generation. Moreover, our experiments show that the nonlinear optical response can be further tuned in both time and spectral domains by tuning the material composition of our hybrid nanomaterials.

9547-81, Session 15

Resonant elements contactless coupled to bolometric micro-stripes

Alexander Cuadrado, José Manuel López-Alonso, Juan Carlos Martínez-Antón, Jose-Miguel Ezquerro, Univ. Complutense de Madrid (Spain); Francisco J. Gonzalez, Univ. Autónoma de San Luis Potosí (Mexico); Javier Alda, Univ. Complutense de Madrid (Spain)

One of the main technical difficulties in the fabrication of optical antennas working as light detectors is the proper design and manufacture of auxiliary elements as lead lines and signal extraction structures. These elements need to be quite small to reach the location of the antennas and should have a minimal effect on the response of the device. Unfortunately this is not an easy task and signal extraction lines resonate along with the antenna producing a complex signal that usually masks the one given by the antenna. In order to decouple the resonance from the transduction we present in this contribution a parametric analysis of the response of a bolometric stripe that is surrounded by resonant dipoles with different geometries and orientations. We have checked that these elements should provide a signal proportional to the polarization state of the incoming light.



9547-82, Session 15

Hybridization models of gold nanoantennas arrays in polarization dependent evanescent waves

Kuo-Ping Chen, Yi-Hsun Chen, Che-Yuan Chang, Yu-Lun Kuo, Zhen-hong Yang, National Chiao Tung Univ. (Taiwan)

The plasmonic coupling of nanoantennas could be explained by the plasmon hybridization model introduced. For symmetric nanoparticles pairs, the coupled mode can be shifted to higher or lower frequencies, depending on the phase of the fields from each nanoparticle. In p-polarization, the inphase response is called bonding mode and out of phase response is called antibonding mode, which are analogous to the molecular orbital theory. The bonding mode, located at a lower energy level, could be strongly excited by normal incidence, but antibonding mode, located at a higher energy level, could hardly excited by normal incident plane wave and which is not easy to be observed. In literatures, the antibonding mode could only be excited by highly focused laser beams, the radiation from a local emitter, and the evanescent field produced by total internal reflection9. Although the observation is not easy, the antibonding mode has brought a lot of attention because of the slower radiative decay and narrower linewidths. However, there are not many researches discussing the sensor application of the plasmonic antibonding mode of nanoantenans arrays.

In this work, gold nanoantennas antibonding mode in TM and TE polarized evanescent field is investigated and the sensitivity to the refractive index change of surrounding medium is compared to bonding mode in normal incidence. Furthermore, in normal incidence, due to the impedance mismatch between the dielectric and substrate, strong reflectance happens at the resonance in bonding mode which could reduce the coupling efficiency. In order to achieve higher energy coupling efficiency, total internal reflection could be used to minimize the impedance mismatch and transfer the input energy into antibonding mode plasmonic resonance.

9547-83, Session 16

Detecting single DNA molecule interactions with optical microcavities (*Invited Paper*)

Frank Vollmer, Max-Planck-Institut für die Physik des Lichts (Germany)

Detecting molecules and their interactions lies at the heart of all biosensor devices, which have important applications in health, environmental monitoring and biomedicine. Achieving biosensing capability at the single molecule level is, moreover, a particularly important goal since single molecule biosensors would not only operate at the ultimate detection limit by resolving individual molecular interactions, but they could also monitor biomolecular properties which are otherwise obscured in ensemble measurements. For example, a single molecule biosensor could resolve the fleeting interaction kinetics between a molecule and its receptor, with immediate applications in clinical diagnostics.

We have now developed a label-free biosensing platform that is capable of monitoring single DNA molecules and their interaction kinetics[1], hence achieving an unprecedented sensitivity in the optical domain, Figure 1. We resolve the specific contacts between complementary oligonucleotides, thereby detecting DNA strands with less than 2.4 kDa molecular weight. Furthermore we can discern strands with single nucleotide mismatches by monitoring their interaction kinetics.

Our device utilizes small glass microspheres as optical transducers[1,2, 3], which are capable of increasing the number of interactions between a light beam and analyte molecules. A prism is used to couple the light beam into the microsphere.

Ourr biosensing approach resolves the specific interaction kinetics between single DNA fragments. The optical transducer is assembled in a simple three-step protocol, and consists of a gold nanorod attached to a glass microsphere, where the surface of the nanorod is further modified with oligonucleotide receptors. The interaction kinetics of an oligonucleotide receptor with DNA fragments in the surrounding aqueous solution is monitored at the single molecule level[1].

The light remains confined inside the sphere where it is guided by total internal reflections along a circular optical path, similar to an acoustic wave guided along the wall of St. Paul's Cathedral. These so called whispering gallery modes (WGM) propagate with little loss, so that even a whisper can be heard on the other side of the gallery. In the optical case, the light beam can travel many thousand times around the inside of the microsphere before being scattered or absorbed, thereby making numerous interactions with an analyte molecule, bound to microsphere from surrounding sample solution. The most part of the light intensity, however, remains inside the microsphere, just below the reflecting glass surface, resulting in a relatively weak interaction between the light and the bound molecule.

To enhance this interaction further, we attach tiny 42 nm x 12 nm gold nanorods to the glass surface. When passing a nanorod, the lightwave induces oscillations of conduction electrons, resulting in so called plasmon resonance. These nanorod plasmons greatly enhance the light intensity on the nanorod, so that the interaction of the light with a molecule attached to the nanorod is also enhanced[4-6]. This enhanced interaction results in an increase in sensitivity by more than a factor of one thousand, putting our experiments of single DNA molecule detection within reach.

For the specific detection of nucleic acids, we attach single-stranded DNA to the nanorod and immerse our device in a liquid solution. When a matching, i.e. complementary DNA fragment binds from solution to the "bait" on the nanorod, the enhanced interaction with the light results in an observable shift of the WGM wavelength. Since light propagates in a WGM only for a very precise resonance wavelength or frequency, this shift can be detected with great accuracy[3]. On our current biosensor platform, we detect wavelength shifts with an accuracy of less than one femtometer, resulting in an extremely high sensitivity for biosensing, which we leverage for the specific detection of single 8 mer oligonucleotides as well as the detection of less than 1 kDa intercalating small molecules[1].

[1] M. D. Baaske, M. R. Foreman, and F. Vollmer, "Single molecule nucleic acid interactions monitored on a label-free microcavity biosensing platform," Nature Nanotechnology, vol. 9, pp. 933-939, 2014.

[2] Y. Wu, D. Y. Zhang, P. Yin, and F. Vollmer, "Ultraspecific and Highly Sensitive Nucleic Acid Detection by Integrating a DNA Catalytic Network with a Label-Free Microcavity," Small, vol. 10, pp. 2067-2076, 2014.

[3] M. R. Foreman, W.-L. Jin, and F. Vollmer, "Optimizing Detection Limits in Whispering Gallery Mode Biosensing," Optics Express, vol. 22, pp. 5491-5511, 2014.

[4] M. A. Santiago-Cordoba, S. V. Boriskina, F. Vollmer, and M. C. Demirel, "Nanoparticle-based protein detection by optical shift of a resonant microcavity," Applied Physics Letters, vol. 99, Aug 2011.

[5] M. R. Foreman and F. Vollmer, "Theory of resonance shifts of whispering gallery modes by arbitrary plasmonic nanoparticles," New Journal of Physics, vol. 15, p. 083006, Aug 2013.

[6] M. R. Foreman and F. Vollmer "Level repulsion in hybrid photonicplasmonic microresonators for enhanced biodetection" Phys. Rev. A 88, 023831 (2013).

9547-84, Session 16

Impedance-matching analysis in IR leakywave antennas

Navaneeth Premkumar, Yuancheng Xu, Brian A. Lail, Florida Institute of Technology (United States)

Planar leaky-wave antennas (LWA) that are capable of full-space scanning have long since been the pursuit for applications including integration onto vehicles and into cameras for wide-angle of view beam-steering scenarios. Recently such a leaky-wave surface (LWS) was designed for long-wave infrared frequencies with frequency scanning capability. The LWS is based on a microstrip patch array design of a leaky-wave impedance surface and is made up of gold microstrip patches on a grounded zinc sulphide substrate. A 1D composite right/left-handed (CRLH) metasurface made by periodically stacking a unit cell of the LWS in the longitudinal direction to

Conference 9547: Plasmonics: Metallic Nanostructures and Their Optical Properties XIII



form a LWA was designed. This paper deals with loading the LWA with a nickel bolometer to collect leaky-wave signals. The LWA radiates a backward leaking wave at 30 degrees at 28.2THz and scans through broadside for frequencies 20THz through 40THz. The paper deals with effectively placing the bolometer in order for the collected signal to exhibit the designed frequency regime. An effective way to impedance match the load to the antenna is also explored. The benefit of such a metasurface/holographic antenna-coupled detector is its ability to provide appreciable capture crosssections while delivering smart signals to sub-wavelength sized detectors. Due to their high-gain, low-profile, and ease of fabrication, this IR LWA harbors great potential in the areas of high resolution infrared imaging and uncooled multiband focal plane arrays.

9547-85, Session 16

Infrared surface phonon polariton waveguides on SiC substrate

Yuchen Yang, Franklin Manene, Brian A. Lail, Florida Institute of Technology (United States)

Surface plasmon polariton (SPP) waveguides harbor many potential applications at visible and near-infrared (NIR) wavelengths. However, the highly lossy metal in the waveguide yields very weak or nonexistent response in the mid and long wave infrared range. This is one of the major reasons for the rise in popularity of surface phonon polariton (SPhP) waveguides in recent research and micro-fabrication pursuit. Silicon carbide (SiC) is a good candidate in SPhP waveguides since it has negative dielectric permittivity in the LWIR spectral region, indicative that coupling to surface phonon polaritons is realizable. Introducing surface phonon polaritons for waveguiding provides good modal confinement and enhanced propagation length. A hybrid waveguide structure at long-wave infrared (LWIR) is demonstrated in which an eigenmode solver approach in Ansys HFSS was applied. The effect of a three layer configuration i.e., silicon wire on a benzocyclobutene (BCB) dielectric slab on SiC, and the effects of varying their dimensions on the modal field distribution and on the propagation length, is studied.

9547-86, Session 17

Broadband toroidal response in threedimensional plasmonic metamaterial (Invited Paper)

Din Ping Tsai, Academia Sinica (Taiwan) and National Taiwan Univ. (Taiwan); Chun Yen Liao, Wei Ting Chen, Pin Chieh Wu, Yao-Wei Huang, Wei-Yi Tsai, Mu Ku Chen, Hao Tsun Lin, Yi-Teng Huang, Ting-Yu Chen, Jia Wern Chen, National Taiwan Univ. (Taiwan); Vassili Savinov, Nikolay I. Zheludev, Univ. of Southampton (United Kingdom)

The unusual property of toroidal dipole response [1] is a non-radiating configuration which results from destructive interference between electromagnetic fields [2]. The toroidal dipole moment is usually neglected because of the intensity is much weaker than electric or magnetic dipole moment. Recently, the toroidal moments signal has been amplified significantly by using metamaterials [3, 4].

In this paper, we design a new toroidal metamaterials by using mutual coupling between a dumbbell-shaped gold plate and a vertical split-ring resonator (VSRR). Using double alignment e-beam lithography technology, we fabricate sample that shows the resonant toroidal responses at optical region. The numerical calculation of radiated power for various multipole moments is also performed for the verification of toroidal response.

The authors acknowledge financial support from Ministry of Science and Technology, Taiwan (Grant Nos. 103-2745-M-002-004-ASP, 102-2745-M-002-005-ASP, 102-2911-I-002-505, 100-2112-M-019-003-MY3, and 100- 2923-M-002-007-MY3) and Academia Sinica (Grant No. AS-103-TP-A06). They are also grateful to National Center for Theoretical Sciences, Taipei Office, Molecular Imaging Center of National Taiwan University, National Center for High-Performance Computing, Taiwan, and Research Center for Applied Sciences, Academia Sinica, Taiwan for their support References:

1. Ia. B. Zel'dovich, "The relation between decay asymmetry and dipole moment of elementary particles," Sov. Phys. JETP 6, 1184 (1958).

2. A. D. Boardman, K. Marinov, N. Zheludev, and V. A. Fedotov, "Dispersion properties of nonradiating configurations: finite-difference time-domain modeling," Phys. Rev. E Stat. Nonlin. Soft Matter Phys. 72, 036603 (2005).

3. T. Kaelberer, V. A. Fedotov, N. Papasimakis, D. P. Tsai, and N. I. Zheludev, "Toroidal dipolar response in a metamaterial," Science 330, 1510 (2010)

4. W. T. Chen, C.-J. Chen, P. C. Wu, S. Sun, L. Zhou, G.-Y. Guo, C. T. Hsiao, K.-Y. Yang, N. I. Zheludev, and D. P. Tsai, "Optical magnetic response in three-dimensional metamaterial of upright plasmonic metamolecules," Opt. Express 19, 12837 (2011)

9547-88, Session 17

Low-cost and high-throughput realization of metasurface-based absorber/emitter for thermal-photovoltaic cells

Alireza Bonakdar, Sung Jun Jang, Hooman Mohseni, Northwestern Univ. (United States)

A thermal photovoltaic cell (TPV) is an optical heat engine that can extract energy from an emitter with elevated temperature. In theory, the efficiency of a TPV can reach to 80% by wavelength conversion, yet in practice, only 3.2% efficiency has been achieved. The main physical drawback is to maintain the device operation at very high temperature while managing total solar spectrum absorption and efficient coupling of the narrowband thermal radiation into the photovoltaic cell. In this vein, utilizing of a nanophotonic structure to undergo the wavelength conversion of solar energy is inevitable. Furthermore, low cost, large area and high throughput realization of such a structure brings TPV beyond the research lab.

Simultaneous tailoring of UV/visible and mid-infrared spectrums requires sub-100-nm feature size, which is challenging with conventional photolithography if it is not impossible. We have developed a microsphere deep-UV lithography that can produce minimum feature size of ~ 50 nm at extremely low cost and high throughput. In this work, we demonstrate a metasurface platform fabricated with this lithography technique which has omni-polarization and -angle absorption in visible spectrum and efficient emission at mid-infrared as confirmed both by FDTD simulation and Fourier transform infrared spectroscopy (FTIR) measurement. The developed technique is promising technology to expedite TPV in real-life energy harvesting applications.

9547-89, Session 17

Determination of effective permittivity and permeability for plasmonic absorber metamaterials in infrared

Yongqian Li, Xiaoying Li, Northwestern Polytechnical Univ. (China)

The estimation of effective optical properties of the nanostructures absorber materials will help to understand its absorption, reflection and radiation characteristics. The effective optical parameters of the metamaterials are estimated by the S-parameters proposed by Smith D.R in 2002, which assumes the inhomogeneous metamaterials to be homogeneous bulk material. Here we present an analytical theory in which the Drude-Lorentz model is adopted to describe the dispersion relations of plasmonic absorber metamaterials in infrared. Based on the effective electron density and the equivalent circuit analysis, a functional description between the geometrical parameters and its optical parameters has been built. The model establishes the quantitative relationship between structure parameters, material parameters and its optical constants. The present simulations and experiments result illustrated the proposed algorithm and the impact on

the retrieved optical parameters of the perfect absorption metamaterials. An accurate prediction for their dispersive behavior can be obtained at IR wavelengths.

9547-90, Session 17

Structured light-matter interactions in optical nanostructures (Invited Paper)

Natalia M. Litchinitser, Jingbo Sun, Mikhail I. Shalaev, Tianboyu Xu, Yun Xu, Univ. at Buffalo (United States); Apra Pandey, CST of America, Inc. (United States)

We show that unique optical properties of metamaterials open unlimited prospects to "engineer" light itself. For example, we demonstrate a novel way of complex light manipulation in few-mode optical fibers using metamaterials highlighting how unique properties of metamaterials, namely the ability to manipulate both electric and magnetic field components, open new degrees of freedom in engineering complex polarization states of light. We discuss several approaches to ultra-compact structured light generation, including a nanoscale beam converter based on an ultra-compact array of nano-waveguides with a circular graded distribution of channel diameters that coverts a conventional laser beam into a vortex with configurable orbital angular momentum and a novel, miniaturized astigmatic optical element based on a single biaxial hyperbolic metamaterial that enables the conversion of Hermite-Gaussian beams into vortex beams carrying an orbital angular momentum and vice versa. Such beam converters is likely to enable a new generation of on-chip or all-fiber structured light applications. We also present our initial theoretical studies predicting that vortexbased nonlinear optical processes, such as second harmonic generation or parametric amplification that rely on phase matching, will also be strongly modified in negative index materials. These studies may find applications for multidimensional information encoding, secure communications, and quantum cryptography as both spin and orbital angular momentum could be used to encode information; dispersion engineering for spontaneous parametric down-conversion; and on-chip optoelectronic signal processing.

9547-91, Session 18

On chip integration and light-matter interactions in active plasmonic devices (Invited Paper)

Uriel Levy, Liron Stern, Boris Desiatov, Meir Grajower, The Hebrew Univ. of Jerusalem (Israel)

In this talk we demonstrate light matter interactions in active plasmonic devices. We begin by describing our recent results on plasmonic enhanced silicon Schottky detectors for the near IR and the role of structural optimization in enhancing the functionality of these detectors. Next, we deal with the important task of measuring the temperature of plasmonic devices at the nanoscale. Finally, we describe our recent results related to a coupled plasmonic-atomic system which provides the capability of controlling the resonant lineshape at will.

9547-92, Session 18

Optical switching of nematic liquid crystal film arising from induced electric field of localized surface plasmon resonance

Makiko T. Quint, Silverio Delgado, Zachary S. Nuno, Linda S. Hirst, Sayantani Ghosh, Univ. of California, Merced (United States)

We demonstrate a method to control nematic liquid crystal (LC) molecular orientation in a few micron thick films by utilizing the localized surface plasmon (LSP) effect of gold nano-particles (AuNPs). This re-orientation

is reversible and repeatable, and does not require any specific alignment coatings and additional applied electric field, instead responding to excitation resonant with the LSP absorption band. Our samples have AuNPs with peak absorption in the spectral range of 500 - 550 nm and these AuNPs are deposited on a glass slide with a coating of LC molecules on top. We use optical techniques for quantitative analysis, such as measuring the LC switching time-scales and threshold power requirements in our samples, and we analyze these characteristics by plotting the optical transmission through the samples as a function of time to extract the time-scale over which the LC re-orientation takes place. Our results show that while the total transmission intensity increases strongly with incident power, it shows weak dependence on temperature. Further, we are able to control and vary the in-plane directionality of the LC molecules by altering the linear polarization of the incident excitation. Based on our results, these devices have the potential to act as optically activated LC switches and enhance the performance of current LC devices. It may lead to the design of completely new devices such as electronic skins, ultra-thin low power displays, and autonomous filters.

OPTICS+PHOTONICS

NANOSCIENCE+ ENGINEERING

9547-93, Session 18

TCO/metal hybrid structures for surface plasmon enhanced light emitting in the near infrared range

Xu Fang, Shiyu Zhang, Liang Xia, Hui Ye, Zhejiang Univ. (China)

Transparent conductive oxides (TCOs, such as Sn:In2O3, AI:ZnO, Ga: ZnO et al) have re-drawn people's attention as alternative candidates of noble metals (particularly Ag or Au) in the field of plasmonic for the reasons of property tunable and low losses et al. However even for Sn:In2O3 (ITO, reported highest conductivity), the metallic property lies in the near infrared (NIR) range exhibiting the real part permittivity ?' was around -3 at communication wavelength of 1.55?m. Under this circumstance, surface plasma polaritons (SPPs) was hard to be exited on the interface between ITO and surrounded dielectric materials with large permittivity. Hence, in order to explore the potential use of TCOs in the applications of silicon photonics (for permittivity of silicon and germanium are 11.6 and 16 at 300K, respectively), we design a hybrid structure of ITO/metal or ITO/metal/ITO as surface plasmonic materials in NIR. The electrical and optical property of hybrid structure was manipulated accordingly by changing the portion of the introduced metal while maintaining a lower loss than bare metals. The highest carrier concentration of the hybrid structure reached 3?10^22cm^-3, definitely the same magnitude of noble metals. Magnetron sputtering and atomic layer deposition (ALD) can be used to deposit the hybrid ITO/ metal structure, in which metal represents gold (Au), and iridium (Ir). The normalized radiative decay rate of light emitted by germanium quantum dots reaches a maximum enhancement of ~8-fold with the assistance of ITO/metal hybrid structure according to the finite difference time domain (FDTD) simulation.

9547-94, Session 18

Optics and nonlinear buckling mechanics in large-area, highly stretchable arrays of plasmonic nanostructures

Hui Zhang, Rice Univ. (United States); Li Gao, Univ. of Illinois at Urbana-Champaign (United States); Yihui Zhang, Northwestern Univ. (United States); Xu Xie, Univ. of Illinois at Urbana-Champaign (United States); Sage Doshay, Stanford Univ. (United States); Hui Fang, Univ. of Illinois at Urbana-Champaign (United States); Jonathan A. Fan, Stanford Univ. (United States); Peter Nordlander, Rice Univ. (United States); Yonggang Huang, Northwestern Univ. (United States); John A. Rogers, Shad Deesha, Siyi Xu, Univ. of Illinois at Urbana-Champaign (United States)



Large scale, dense arrays of plasmonic nanodisks (Au) on low modulus, high elongation elastomeric substrates (PDMS) represent a class of tunable optical system, with reversible ability to shift plasmon resonances, originating from array deformation, over a range of nearly 600nm in the visible region. At the most extreme levels of mechanical deformation (strains >100%), non-linear buckling processes transform initially planar arrays into three dimensional configurations, in which the nanodisks rotate out of the plane, giving rise to an increase of transition rate, to form linear arrays with 'wavy' geometries. Analytical and finite element models capture not only the physics of these buckling processes, including all of distinct modes that occur, but also the quantitative effects of these deformations on the plasmonic responses. The results have relevance to mechanically tunable optical systems, with potential relevance to soft optical sensors that integrate on or in the human body.

9547-95, Session 18

Exploiting local light helicity to direct emission (*Invited Paper*)

Laurens K. Kuipers, FOM Institute for Atomic and Molecular Physics (Netherlands)

Beams propagating in free space can carry angular orbital momentum [1]. The heart of such a beam is typically formed by a vortex or optical singularity. Optical singularities occur in many far-field optical phenomena, e.g., diffraction patterns or caustics [2]. It turns out that such singularities also readily occur in light fields surrounding photonic nanostructures. This is of particular interest as those near fields often contain all 6 vector components of the electro-magnetic field, i.e., the waves cannot be considered as purely transverse.

Here, we will show how ubiquitous optical singularities at the nanoscale seem to be. We illustrate this by visualizing the fields around two prototypical photonic nanostructures: a subwavelength hole in a metal film and a photonic crystal waveguide. Vector-field-selective near-field microscopy is used to locate the singularities and investigate their topology. We show that by controlling the incident beam, in the case of the hole, we can control the spatial positions of the singularities [3]. For the photonic crystal waveguide we identify both phase- and polarization singularities. By separating the contributions for the electric and magnetic field [4,5] we show that singularities indeed occur in both fields. We trace the positions of the singularities at different heights, i.e., orthogonal to the propagation direction of the light. The lateral positions are not fixed with respect to the geometry and, perhaps more interestingly, that the trajectory of the electric fields singularities are different from their magnetic cousins [6].

The existence of the singularities at the nanoscale results in a local helicity in the field. We show that this helicity can be used to control the emission of circular dipoles, i.e., dipoles that are associated with orbital angular momentum-changing transitions which are prevalent in solid-state qubits. We experimentally map the coupling of classical, circular dipoles to photonic modes in a photonic crystal waveguide. We show that, depending on the combination of the local helicity of the mode and the dipole helicity, circular dipoles can couple to left- or rightwards propagating modes with a near-unity directionality. The maps are in excellent agreement with calculations [7]. Our measurements, therefore, demonstrate the possibility of coupling spin to photonic pathway opening avenues for new ways to process quantum information.

[1] L. Allen, L., et al., Phys.Rev. A 45, 8185, (1992).

[2] J.F. Nye, Natural Focusing and fine structure of light, Institute of Physics Publishing, Bristol, 1999.

[3] de Hoogh, A., Rotenberg, N., and Kuipers, L., J. Opt. 16, 114004 1/8, (2014).

[4] le Feber, B., Rotenberg, N., Beggs, D.M., and Kuipers, L., Nature Photonics 8, 43-46, (2014). [5] Rotenberg, N., and Kuipers, L., Nature Photonics 8, 919-926, (2014).

[6] Rotenberg, N., le Feber, B., Visser, T.D., and Kuipers, L., submitted.

[7] le Feber, B., Rotenberg, N., and Kuipers, L., Nature Comm. 6, 6695 (2015).

Sunday - Wednesday 9 -12 August 2015

Part of Proceedings of SPIE Vol. 9548 Optical Trapping and Optical Micromanipulation XII

9548-1, Session 1

Interaction between spin and orbital angular momentum of light in optical tweezers (Invited Paper)

Halina Rubinsztein-Dunlop, David Carberry, Timo A. Nieminen, The Univ. of Queensland (Australia); Daryl C. Preece, Univ. of California, San Diego (United States); Alexander B. Stilgoe, The Univ. of Queensland (Australia)

Since 1995 the transport of optical angular momentum by optical vortex beams or/and Gaussian beams carrying spin angular momentum has been applied to the rotation and twisting of microscopic objects in optical traps. Even earlier, optical vortex traps had been proposed as a method to reduce the scattering forces that oppose optical trapping; in the ray optics picture, only high-angle rays contribute to the gradient force, and the use of a hollow beam eliminates the low-angle rays that would still contribute to the scattering force.

A large variety of methods have been used to sculpt beams carrying orbital angular momentum and spin angular momentum and to determine the optimum geometries that yield maximum efficiency of transfer of these light momenta to microscopic objects. The transfer of spin can be quantitatively measured by simply analysing the state of polarisation of the light transmitted through a spinning object if only all of the transmitted light can be collected for analysis. However a direct measurement of orbital angular momentum for highly focused beams is more difficult. We present overview of these methods and describe a direct quantitative measurement of the orbital angular momentum, in non-paraxial geometry. We study the coupling between the spin and orbital angular momentum. We also investigate, both theoretically and experimentally optimal geometries of these beams to couple to optimally designed microstructures and their applications in studies of biological and bioanalog systems.

9548-2, Session 1

Transverse spin and momentum of structured light (Invited Paper)

Konstantin Y. Bliokh, RIKEN (Japan)

No Abstract Available

9548-3, Session 1

Angular momentum transfer to trapped particles in vacuum

Kishan Dholakia, Yoshihiko Arita, Tom Vettenburg, Juan Aunon, Univ. of St. Andrews (United Kingdom); Ewan Wright, College of Optical Sciences, The Univ. of Arizona (United States); Susan E. Skelton, Michael Mazilu, Univ. of St. Andrews (United Kingdom)

Optical manipulation of mesoscopic particles remains a very powerful method for both fundamental and applied science. The field has seen great advances for the biosciences including new studies of single molecules and force studies on cells. In the physical sciences, studies have also seen groundbreaking work in many areas. In this paper we describe some of the recent work at St Andrews looking particularly at the trapping of particles in liquid, air and vacuum with an emphasis on optical angular momentum transfer.

An optically trapped nano- or micro- particle in vacuum is an ideal system for investigating quantum effects as the particle is well isolated from

the thermal environment. Recently, we have worked on the rotation of birefringent particles (vaterite) in vacuum and also studied these particles and silica particles in beams with orbital angular momentum.

SPIE. PHOTONICS

NANOSCIENCE+

ENGINEERING

9548-4, Session 1

Optical trapping using focused optical vortices with broadband flat spiral zone plates

Mark Jayson M. Villangca, DTU Fotonik (Denmark); Shengtao Mei, Muhammad Qasim Mehmood, Cheng-Wei Qui, National Univ. of Singapore (Singapore); Jesper Glückstad, DTU Fotonik (Denmark)

Light has been used to exert microscopic force on dielectric particle through conservation of linear momentum as light refracts through the particle. In the past years, it has been realized that light can also impart orbital angular momentum (OAM) by incorporating a helical phase profile. This is normally done using a spatial light modulator (SLM) and the generated beam is commonly called as optical vortex or Laguerre-Gaussian (LG) beam. It has been used in trapping of low-index particles [1] and has been extended to optical communications [2]. However, increasing the topological charge of LG beam results in large dark spot in the center due to phase singularity and thus not suitable for applications requiring high photon density. One approach is to use helico-conical beam or optical twister where the phase profile is dependent on the radial and angular coordinates [3]. Experimental results show that optical twister is capable of trapping particle and imparting OAM [4]. In this work, we demonstrate nanostructured logarithmic-spiral flat spiral zone plates (LSZP); etched through 100 nm chromium film followed by the electron beam lithography (EBL). Numerical calculations and optical characterizations of the LSZP, on the transmission side, reveal the phenomenon of spatial focusing of optical vortex. Further investigations unveil that our device maintains its intriguing ability of OAM focusing under entire visible spectrum and different polarization states [5]. Owing to compactness of the LSZP, it may be integrated in microfluidics systems to perform localized trapping and stirring, while putting an array of LSZPs may be useful for applications such as particle sorting.

References

1. V. Garcés-Chávez, K. Volke-Sepulveda, S. Chávez-Cerda, W. Sibbett, and K. Dholakia, "Transfer of orbital angular momentum to an optically trapped low-index particle," Phys. Rev. A 66, 1–8 (2002).

2. J. Wang, J.-Y. Yang, I. M. Fazal, N. Ahmed, Y. Yan, H. Huang, Y. Ren, Y. Yue, S. Dolinar, M. Tur, and A. E. Willner, "Terabit free-space data transmission employing orbital angular momentum multiplexing," Nat. Photonics 6, 488–496 (2012).

3. C. A. Alonzo, P. J. Rodrigo, and J. Glückstad, "Helico-conical optical beams?: a product of helical and conical phase fronts," 13, 599–602 (2005).

4. V. R. Daria, D. Z. Palima, and J. Glückstad, "Optical twists in phase and amplitude.," Opt. Express 19, 476–81 (2011).

5. H. Liu, M. Mehmood, and K. Huang, "Twisted Focusing of Optical Vortices with Broadband Flat Spiral Zone Plates," Adv. Opt. Mater. 2, 1193–1198 (2014).

9548-5, Session 1

Resonance near field coupling induced optical counter torque for plasmonic particle cluster

Jun Chen, Shanxi Univ. (China) and Hong Kong Baptist Univ. (Hong Kong, China); Neng Wang, Fudan Univ. (China) and Hong Kong Baptist Univ. (Hong Kong, China);



Liyong Cui, Xiao Li, Hong Kong Baptist Univ. (Hong Kong, China); Zhifang Lin, Fudan Univ. (China); Jack Ng, Hong Kong Baptist Univ. (Hong Kong, China)

Light induced torques are common tools for micro-particle manipulation. While novel and interesting ways were invented, applying strong optical torque over a large area is still a challenging task. One major reason is that angular momentum conservation must be fully fulfilled.

A simple argument shows the tendency for two strongly scattering objects to develop counter torques that are much stronger than the total torque. The effect is quite significant for metal particle cluster at resonance, but can also be observed in other structures. Advantages include, but not limited to, strong torque that is significantly stronger than that of a single isolated object, and large torque to extinction cross section ratio allowing multiple rotors to work in tandem. Our work contributes to the understanding of optical rotation and introducing novel ways to manipulate the internal degree of freedom of a structured particle.

9548-6, Session 2

Trapping of highly birefringent rutile nanocylinders in the optical torque wrench

Yera Y. Ussembayev, Seungkyu Ha, Richard Janissen, Maarten M. van Oene, Nynke H. Dekker, Technische Univ. Delft (Netherlands)

The optical torgue wrench (OTW) is a powerful technique to measure the torsional properties of different biomolecules, including DNA, DNAprocessing protein complexes and rotary motors, such as the bacterial flagellar motor. To date, quartz (SiO2) has proven to be a convenient birefringent material out of which to synthesize the micron-sized particles essential for this technique. However, the relatively low birefringence of quartz, which limits the maximal torque that can be applied in OTW, hampers the study of certain biological systems. A more attractive material is rutile (TiO2), which has a thirty-fold higher birefringence. To date, however, the application of rutile in the trapping has been restricted due to its high refractive index, which results in low trapping efficiency. Here, we have employed finite element method calculations to determine the optimal dimensions of submicron-sized rutile cylinders for tight stable optical trapping. Using these calculations as a guideline, we have designed and developed a nanofabrication protocol that allows us to produce rutile cylinders with the desired sizes at high yield. We have characterized the fabricated cylinders in the OTW setup and quantified both their linear and angular trapping properties. In addition, we demonstrate full translational and rotational control of these functionalized cylinders tethered to individual DNA molecules for use in single-molecule applications.

9548-7, Session 2

Initiating optics immersions

Gabriel C. Spalding, Illinois Wesleyan Univ. (United States)

To ensure an increased supply of well-prepared graduate students, and to spread awareness of the research opportunities we offer, it is proposed that your institution serve as a site for a 2.5-day training workshop for those advanced lab instructors who mentor undergraduates at the stage when they are considering their graduate school options. Data clearly suggests that enormous impact can be achieved by reaching out to an identifiable and relatively small cohort of individuals who collectively play a crucial role in the experimental instruction of nearly all students with a major or minor in physics at US institutions. Mentor stipends are available, and logistics, advertising, registration, and follow-up for these Optics Immersions will be coordinated by ALPhA, the "Advanced Laboratory Physics Association."

9548-8, Session 2

A simple explanation of opto-mechanical cooling by the back action of cavity photons

Masud Mansuripur, College of Optical Sciences, The Univ. of Arizona (United States)

We present a simple classical analysis of the light reflected from a Fabry-Perot cavity consisting of a fixed (dielectric) front mirror and a vibrating rear mirror. In the adiabatic approximation, the returning light exhibits sideband symmetry, which will go away as the photon lifetime becomes comparable to or longer than the oscillation period of the rear mirror. When the oscillation period is short compared to the cavity photon lifetime, one must approach the problem differently, treating the vibrating mirror as a scatterer which sends a fraction of the incident light into the sideband frequencies. With proper detuning, the internal radiation pressure can be shown to slow down the oscillating mirror. This is the principle of cooling a vibrating mirror by the back action of the cavity photons.

9548-9, Session 3

Nano-optomechanics with optically levitated dielectric nanoparticles (Invited Paper)

Levi Neukirch, Brandon Rodenburg, Mishkatul Bhattacharya, Nick Vamivakas, Univ. of Rochester (United States)

The inability to leverage resonant scattering processes involving internal degrees of freedom differentiates optical cooling experiments performed with levitated dielectric nanoparticles, from similar atomic and molecular traps. Trapping in optical cavities or the application of active feedback techniques has proven to be effective ways to circumvent this limitation. We present our nanoparticle optical cooling apparatus, which is based on parametric feedback modulation of a single-beam gradient force optical trap. This scheme allows us to achieve effective center-of-mass temperatures well below 1 kelvin for our ? 1 ? 10?18 kg particles, at modest vacuum pressures. We will also discuss experiments in which the levitated nanoparticle contains a single optically active quantum emitter. The method provides a versatile platform, with parameter tunability not found in conventional tethered nanomechanical systems. Potential applications include investigations of nonequilibrium nanoscale thermodynamics, ultrasensitive force metrology, and mesoscale quantum mechanics and hybrid systems.

9548-10, Session 3

Experimental opto-mechanics with levitated nanoparticles: towards quantum control and thermodynamic cycles (Invited Paper)

Nikolai Kiesel, Florian Blaser, Uros Delic, David Grass, Univ. Wien (Austria); Andreas Dechant, Eric Lutz, Friedrich-Alexander-Univ. Erlangen-Nürnberg (Germany); Marzieh Bathaee, Sharif Univ. of Technology (Iran, Islamic Republic of); Markus Aspelmeyer, Univ. Wien (Austria)

Combining optical levitation and cavity optomechanics constitutes a promising approach to prepare and control the motional quantum state of massive objects (>10^9 amu). This, in turn, would represent a completely new type of light-matter interface and has, for example, been predicted to enable experimental tests of macrorealistic models or of non-Newtonian gravity at small length scales. Such ideas have triggered significant



experimental efforts to realizing such novel systems.

To this end, we have recently successfully demonstrated cavity-cooling of a levitated sub-micron silica particle in a classical regime at a pressure of approximately 1mbar. Access to higher vacuum of approx. 10⁻⁶ mbar has been demonstrated using 3D-feedback cooling in optical tweezers without cavity-coupling.

Here we will illustrate our strategy towards trapping, 3D-cooling and quantum control of nanoparticles in ultra-high vacuum using cavity-based feedback cooling methods and clean particle loading with hollow-core photonic crystal fibers. We will also discuss the current experimental progress both in 3D-cavity cooling and HCPCF-based transport of nanoparticles.

As yet another application of cavity-controlled levitated nanoparticles we will show how to implement a thermodynamic Sterling cycle operating in the underdamped regime. We present optimized protocols with respect to efficiency at maximum power in this little explored regime. We also show that the excellent level of control in our system will allow reproducing all relevant features of such optimized protocols. In a next step, this will enable studies of thermodynamics cycles in a regime where the quantization of the mechanical motion becomes relevant.

9548-11, Session 3

Dispersive light-matter interaction in programmable optical tweezers

Bianca J. Sawyer, Milena S. J. Horvath, Amita B. Deb, Niels Kj?rgaard, Univ. of Otago (New Zealand)

Off-resonant probing via the dispersive light-matter interaction is a powerful metrological tool in the manipulation and control of trapped ultracold gases. We have developed a robust interrogation system that uses frequency modulation spectroscopy to measure the quantum state-dependent phase shift incurred on an off-resonant optical probe when transmitted by an atomic medium. This is routinely used to track a number of dynamic atomic processes in real time. An important design consideration for such a scheme is the three-dimensional mode-matching at the interface between light and matter when coupled by this dispersive interaction. The geometry of the ellipsoidal ensemble of trapped atoms should be adjusted such that scattering of the axially propagating probe field is optimized in the forward direction. This allows the maximum signal to be collected by the photodetection optics.

The trapping potential for our ultracold gas is generated by programmable optical tweezers, which preform precise spatial micro-manipulation of the ensemble. The unit consists of a versatile vertical tweezer beam and intersecting static horizontal waveguide. The vertical beam can be split into multiple time-averaged potentials, producing a one-dimensional array of cold clouds.

As an application, we use the tweezers as a pair of laser "test tubes" to independently prepare two clouds of ultracold 87Rb in different internal quantum states. The samples are then brought together and an external magnetic field is swept across a Feshbach resonance. Dispersive probing is used to track the resulting dynamics and identify the resonant magnetic field value.

9548-13, Session 4

Extinction cross section measurements for a single optically trapped particle (Invited Paper)

Michael I. Cotterell, Univ. of Bristol (United Kingdom); Thomas C. Preston, McGill Univ. (Canada); Bernard J. Mason, Univ. of Bristol (United Kingdom); Andrew J Orr-Ewing, Jonathan P Reid, University of Bristol (United Kingdom)

Bessel beam (BB) optical traps have become widely used to confine single

and multiple aerosol particles across a broad range of sizes, from a few microns to < 200 nm in radius. The radiation pressure force exerted by the core of a single, zeroth-order BB incident on a particle can be balanced by a counter-propagating gas flow, allowing a single particle to be trapped over many hours. The pseudo non-diffracting nature of BBs enables particles to be confined over macroscopic distances along the BB core propagation length; the particle's position along this length can be finely controlled by modulating the BB laser power. We exploit this property to optimise the particle's position at the centre of the TEMOO mode of a high finesse optical cavity, allowing cavity ring-down spectroscopy (CRDS) to be performed on single aerosol particles and their optical cross section, ?ext, measured. Further, the variation in the light from the illuminating BB elastically scattered by the particle is recorded as a function of scattering angle. Such intensity distributions are fitted to Mie theory to determine the particle's radius. The trends in ?ext with particle radius are modelled using cavity standing wave Mie simulations and a particle's varying refractive index with changing relative humidity is determined. We demonstrate ?ext measurements on sub-micrometre aerosol and determine the lowest limit in particle size that can be probed by this technique. The BB-CRDS method will play a key role in reducing the uncertainties associated with atmospheric aerosol radiative forcing, among the largest uncertainties in climate modelling.

9548-14, Session 4

Quadruple Bessel beam trap for single droplet studies

Grégory David, Ruth Signorell, ETH Zürich (Switzerland)

Metastable submicron droplets play an important role in atmospheric processes. In this context, we use Bessel beam optical traps, which enable us to isolate a single submicron droplet for a long time (several hours or days) in air. However, the stability of a single counter-propagating Bessel beam (CPBB) trap is very sensitive to the alignment [1]. Its trapping position may change with the particle size and the particle may wobble by several tens of micrometers. This can be a major problem for single droplet studies, such as broadband light scattering and photo-acoustic measurements. We suggest a new type of trap, which is much less sensitive to small optical misalignment [1]: the quadruple Bessel beam trap (QBB) consisting of two sets of CPBBs perpendicularly arranged. This presentation shows the first experimental realization and characterization of the stability and confinement of single droplets in a QBB trap and compares it with numerical simulations of the three-dimensional droplet dynamics [2].

The QBB trap is shown to be more predictable and several times more stable than the CPBB trap, while it confines the particle much more tightly by several orders of magnitude. QBB traps are thus better suited for single droplet studies. In addition we will present results for the water uptake/ release and for the aging of metastable submicron droplets.

References

[1] Thanopulos I., D. Luckhaus, T. C. Preston and R. Signorell. J. Appl. Phys., 115, 154304, 2014.

[2] David G., et al., manuscript in preparation.

9548-15, Session 4

Measuring forces and dynamics for optically levitated 20um PS particles in air using electrostatic modulation

Haesung Park, Thomas W LeBrun, National Institute of Standards and Technology (United States)

Optical trapping in air and vacuum has become the subject of increased attention due its applications to precision measurement and fundamental physics. Unlike traditional studies of trapping in fluids (in support of biological measurement, colloid science, cell sorting, and nanotechnology), trapping in air or vacuum can present an underdamped system where inertia rather than damping dominates dynamics. Under these conditions, the full

nonlinear, three-dimensional nature of the trapping force can give rise to much more complex behavior. We use electrostatic modulation to study the forces on a $20\mu m$ polystyrene bead trapped in air, and measure the dynamics of the particle's motion under impulse excitation.

A ring-type piezoelectric launcher allows us to introduce a selected target particle into the optical trap, where it remains stably trapped indefinitely (> 6 hrs). We combine quadrant photodiode measurement with video microscopy to measure the particle motion after electrostatic impulse both accurately and at high speed. An advantage of electrostatic modulation is the ability to excite particle motion rapidly and without changing the trapping beam or surrounding medium. We use this to determine the stiffness and damping directly and independently of each other without assumptions about temperature. In addition, we show that the full force curve can be measured with no assumptions beyond Newton's equations.

9548-16, Session 4

Optical trapping of individual gold nanoparticles in air

Liselotte Jauffred, Lund Univ. (Sweden); Seyed Mohammad-Reza Taheri, Univ. of Zanjan (Iran, Islamic Republic of); Regina K. Schmitt, Heiner Linke, Lund Univ. (Sweden); Lene B. Oddershede, Niels Bohr Institute (Denmark)

Since the ground breaking particle levitation experiments by Ashkin in 1975, huge efforts have been put into controlling micro- and nanometer sized particles in both air and liquids. Till date, most progress has been done in liquids with aerosol trapping proving more challenging. By utilizing an air chamber designed to have a minimum of turbulence [1] and a laser beam with a minimum of aberration, we succeeded to trap individual gold nanoparticles with diameters between 80 nm and 200 nm in air using a 1064 nm laser. The positions visited by the trapped gold nanoparticle were quantified using a quadrant photodiode placed in the back focal plane. The time traces were analyzed and the trapping stiffness characterizing gold aerosol trapping determined and compared to aerosol trapping of nanometer sized silica and polystyrene particles. Calibration, however, is not trivial as the 'normal' assumption of an underdamped system, underlying the Langevin approach, is not a priori valid in the case of trapping metallic nanoparticles in air. Based on our analysis, we conclude that gold nanoparticles trap more strongly in air than similarly sized polystyrene and silica particles, and that the spring constants characterizing aerosol trapping of gold nanoparticles are approximately half of those characterizing trapping of gold nanoparticles in water [2]. The gold nanoparticles absorb part of the irradiating laser light and we also discuss the associated nanoparticle heating, which is even more pronounced in air than in water [3] due to a lower thermal conductance.

[1] S.M.R. Taheri, M. Sadeghi, E. Madadi, S.N.R. Reihani, Opt. Commun. 2014, vol. 329 p. 196–199 (2014).

[2] P.M. Hansen, V.K. Bhatia, N. Harrit, and L. Oddershede, Nano Letters, vol. 5 p.1937-1942 (2005).

[3] P.M. Bendix, S.N.S. Reihani and L.B. Oddershede, ACS Nano, vol. 4 p.2256-2262 (2010)

9548-17, Session 5

Optical trapping of microdroplet containing a single nanomaterial in helium gas (Invited Paper)

Yosuke Minowa, Masaaki Ashida, Ryoichi Kawai, Osaka Univ. (Japan)

Quantum dots or nanometer-sized semiconductor nanocrystals are fascinating quantum emitters having a discrete energy level structure which is tunable through the quantum confinement effect. In particular, chemically synthesized colloidal quantum dots are promising as they can be mass produced and their size can be precisely controlled. Colloidal quantum dots can be treated as an isolated single particle. Therefore, manipulation and alignment of colloidal quantum dots would enable the realization of the ideal platform to investigate the mutual interaction among quantum emitters and the ultra strong coupling between light and matter. Optical manipulation is one of the universal techniques to control the motion/position of microparticles and atoms. However, researches on optical manipulation of quantum dots are scarce. The difficulties arise from the relatively small polarizability, which normally tends to decrease with decreasing the particle's size in the Rayleigh regime. Here, we report on the optical trapping of a single quantum dot within the microdroplet in helium gas. The liquid droplet behaves as an optically-transparent container with a larger volume enabling the stable optical trapping. We detected bright single photon emission from the trapped quantum dot through the two photon excitation process. We also observed intensity and spectral fluctuation, which are well known features of a solid state quantum emitter. Our results can lead to the isolation of nanomaterials from their environment or substrates and provide unprecedented information on their intrinsic material properties which are obscured by the environmental fluctuation.

SPIE. PHOTONICS

NANOSCIENCE+ ENGINEERING

9548-18, Session 5

Steering a jet of particles into an x-ray beam with optically induced forces

Richard A. Kirian, Arizona State Univ. (United States); Niko Eckerskorn, The Australian National Univ. (Australia); Salah Awel, Max Wiedorn, Jochen Küpper, Henry N. Chapman, Ctr. for Free-Electron Laser Science (Germany); Andrei V. Rode, The Australian National Univ. (Australia)

Optical trapping of light-absorbing particles in a gas environment has shown to be governed by laser-induced thermal or photophoretic forces, which can be orders of magnitude higher than the force of the light-induced radiation pressure. Guiding of particles with photophoretic forces over large distances in open air was recently realised by an optical pipeline, formed by a vortex laser beam of doughnut-like intensity profile, with a high-intensity ring of light that surrounds a dark core. The exact formation mechanism of photophoretic force and the influence on the particle movement are still unclear. Here we report on our efforts to utilize the optical pipeline concept to guide particles into the focus of an x-ray free-electron laser (XFEL). XFELs produce coherent femtosecond-duration pulses of highenergy x-rays with immense brightness. In the "diffract-and-destroy" mode, such pulses destroy any illuminated target, but terminate prior to the onset of atomic motion and hence overcome fundamental problems associated with radiation damage. Through coherent diffractive imaging methods, one can form single-shot nanometer-resolution projection images of thick irreproducible targets such as cells, or Angstrom-resolution 3D electron density maps from reproducible macromolecules exposed in many orientations. The combination of a touch-free optical system for pin-point delivery of bioparticles to the focal spot of an XFEL would significantly enhance the efficiency of XFEL-based serial diffractive imaging experiments.

9548-20, Session 5

Bistable dynamics of a levitated nanoparticle

Francesco Ricci, ICFO - Institut de Ciències Fotòniques (Spain); M. Spasenovic, Univ. of Belgrade (Serbia) and ICFO - Institut de Ciències Fotòniques (Italy); Raúl A. Rica, ICFO - Institut de Ciències Fotòniques (Spain); Lukas Novotny, ETH Zürich (Switzerland); Romain Quidant, ICFO - Institut de Ciències Fotòniques (Spain)

Bistable systems are ubiquitous in nature. Classical examples in chemistry and biology include relaxation kinetics in chemical reactions [1] and stochastic resonance processes such as neuron firing [2,3]. Likewise, bistable systems play a key role in signal processing and information handling at the



nanoscale, giving rise to intriguing applications such as optical switches [4], coherent signal amplification [5,6] and weak forces detection [5].

The interest and applicability of bistable systems are intimately connected with the complexity of their dynamics, typically due to the presence of a large number of parameters and nonlinearities. Appropriate modeling is therefore challenging. Alternatively, the possibility to experimentally recreate bistable systems in a clean and controlled way has recently become very appealing, but elusive and complicated. With this aim, we combined optical tweezers with a novel active feedback-cooling scheme to develop a well-defined opto-mechanical platform reaching unprecedented performances in terms of Q-factor, frequency stability and force sensitivity [7,8]. Our experimental system consists of a single nanoparticle levitated in high vacuum with optical tweezers, which behaves as a non-linear (Duffing) oscillator under appropriate conditions. Here, we prove it to be an ideal tool for a deep study of bistability.

We demonstrate bistability of the nanoparticle by noise activated switching between two oscillation states, discussing our results in terms of a doublewell potential model. We also show the flexibility of our system in shaping the potential at will, in order to meet the conditions prescribed by any bistable system that could therefore then be simulated with our setup. References

[1] T. Amemiya, T. Ohmori, M. Nakaiwa, T. Yamamoto, and T. Yamaguchi, "Modeling of Nonlinear Chemical Reaction Systems and Two-Parameter Stochastic Resonance," J. Biol. Phys. 25 (1999) 73

[2] F. Moss, L. M. Ward, and W. G. Sannita, "Stochastic resonance and sensory information processing: a tutorial and review of application" Clinical neurophysiology 115 (2004) 267

[3] M. Platkov, and M. Gruebele, "Periodic and stochastic thermal modulation of protein folding kinetics" J. Chem. Phys. 141 (2014) 035103

[4] T. Tanabe, M. Notomi, S. Mitsugi, A. Shinya and E. Kuramochi. "Fast bistable all-optical switch and memory on a silicon photonic crystal onchip". Opt. Lett., 30 (2005) 2575

[5] R. L. Badzey and P. Mohanty. "Coherent signal amplification in bistable nanomechanical oscillators by stochastic resonance" Nature, 437 (2005) 995

[6] W. J. Venstra, H. J. R. Westra, and H. S. J. van der Zant. "Stochastic switching of cantilever motion," Nature Communications, 4 (2013) 3624

[7] J. Gieseler, B. Deutsch, R. Quidant, and L. Novotny "Subkelvin parametric feedback cooling of a Laser-Trapped nanoparticle" Phys. Rev. Lett. 109 (2012) 103603

[8] J. Gieseler, M. Spasenovi?, L. Novotny, and R. Quidant, "Nonlinear Mode Coupling and Synchronization of a Vacuum-Trapped Nanoparticle," Phys. Rev. Lett. 112 (2014) 103603

9548-21, Session 6

Continuum electrodynamics and the Abraham-Minkowski controversy

Michael E. Crenshaw, U.S. Army Aviation & Missile Research, Development & Engineering Ctr. (United States)

The Abraham--Minkowski controversy refers to a long-standing inability to deal with issues involving the momentum of an electromagnetic field in a linear dielectric medium. In 1908, Minkowski derived a tensor energy-momentum continuity equation. Abraham subsequently argued that the Minkowski tensor violates conservation of angular momentum because the tensor is not symmetric. Based on the continuing work in the field, the resolutions that have been proposed over the last century have not been persuasive.

We treat continuum electrodynamics as an axiomatic formal theory based on the macroscopic Maxwell equations applied to a thermodynamically closed system consisting of an antireflection coated block of a linear dielectric situated in free-space that is illuminated by a quasimonochromatic field. We demonstrate that the Abraham and Minkowski formulations of the continuity of energy and momentum are valid theorems of the formal theory of continuum electrodynamics that are proven false by conservation laws. Furthermore, we show that another valid theorem of continuum electrodynamics is contradicted by special relativity. Our options are: 1) that the axioms of the formal theory, the macroscopic Maxwell equations, are proven false by conservation laws and relativity, 2) that conservation and relativity are proven false by continuum electrodynamics, or 3) all of the above. Electrodynamics, conservation, and relativity are fundamental principles of physics that are intrinsic to the vacuum in which the speed of light is c. The contradictions are resolved by a reformulation of physics for a region of space in which the speed of light is c/n.

9548-22, Session 6

Electromagnetic angular momentum

Masud Mansuripur, College of Optical Sciences, The Univ. of Arizona (United States)

In addition to energy and linear momentum, electromagnetic (EM) fields possess the capacity to carry spin and orbital angular momentum. With a view to Maxwell's macroscopic equations and the laws governing EM force and torque, we discuss the fundamental properties of EM angular momentum and point out several facts concerning the angular momentum content and behavior of static as well as dynamic fields. Certain paradoxes arise from the exchange of angular momentum between fields and material media, all involving the conservation of angular momentum, especially when the media are endowed with magnetic properties. We examine the origin of these paradoxes, discuss their connection to the Abraham-Minkowski controversy, and explain how the paradoxes can be resolved.

9548-23, Session 6

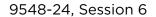
Physics of electromagnetic and material stresses in optical manipulation

Brandon A. Kemp, Cheyenne J. Sheppard, Arkansas State Univ. (United States)

Modeling the dynamics optical manipulation experiments relies upon a precise mathematical representation of electromagnetic fields and the interpretation of optical momentum and stresses in materials. However, the momentum of light within media has been an issue of debate over the past century. Multiple mathematically energy-momentum models have been advanced, each, under certain conditions, agreeing with experimental observation and mathematically consistent with classical electromagnetism.

The modern view is that the various formulations of electrodynamics represent different divisions of the total energy-momentum tensor, with the separation of field and matter being ambiguous. Recently, a proposed view of photon momentum identified two leading forms as the kinetic and canonical momenta. The Abraham momentum is responsible for the overall center-of-mass translation of a material, while the Minkowski momentum is responsible for translations with respect to the surrounding medium. However, the Abraham momentum corresponds to multiple, unique electromagnetic energy-momentum tensors that attempt to separate field from material responses (e.g. Abraham, Chu, and Einstein-Laub). However, only the form of the kinetic momentum density has been revealed, while the formulation that uniquely separates the kinetic stress tensor has remained ambiguous.

In this correspondence, multiple formulations are considered within the framework of relativistic electrodynamics. We apply various mathematical techniques to identify the kinetic subsystem of electrodynamics. While optical manipulation is usually modeled using a stationary medium approximation, the lessons from relativistic electrodynamics reveal a specific distribution of electromagnetic stress in media. The physics of optical and static manipulation of dielectric particles are described within this framework.



Discriminatory effects in the optical binding of chiral nanoparticles

Kayn A. Forbes, Univ. of East Anglia (United Kingdom); David S Bradshaw, David L Andrews, Univ of East Anglia (United Kingdom)

The laser-induced intermolecular force that exists between two or more particles subjected to a moderately intense laser beam is termed 'optical binding'. Completely distinct from the single-particle forces that give rise to optical trapping, the phenomenon of optical binding is a manifestation of the coupling between optically induced dipole moments in neutral particles. In conjunction with optical trapping, the optomechanical forces in optical binding afford means for the manipulation and fabrication of optically bound matter. The Casimir-Polder potential that is intrinsic to all matter can be overridden by the optical binding force in cases where the laser beam is of sufficient intensity. Chiral discrimination can arise when the laser input has a circular polarization, if the particles are themselves chiral. Then, it emerges that the interaction between particles with a particular handedness is responsive to the left- or right-handedness of the light. The present analysis, which expands upon previous studies of chiral discrimination in optical binding, identifies a novel mechanism that others have previously overlooked, signifying that the discriminatory effect is much more prominent than originally thought. The new theory leads to results for freely-tumbling chiral particles subjected to circularly polarized light. Rigorous conditions are established for the energy shifts to be non-zero and display discriminatory effects with respect to the handedness of the incident beam. Detailed calculations indicate that the energy shift is larger than those previously reported by three orders of magnitude.

9548-25, Session 6

1D problems of radiation pressure on elastic solids

Tomaz Pozar, Janez Mo?ina, Univ. of Ljubljana (Slovenia)

When light exerts pressure on elastic solids, the properties of both, light and matter change. In the simplest cases, the energy and momentum transferred between the light and matter can be solved in one dimension.

We treat the light-matter interaction solely due to radiation pressure using the fundamental nonrelativistic conservation principles of energy and momentum with the assumption that solids are considered as elastic objects. This optodynamic approach only assumes that the momentum of a light pulse propagating in vacuum equals its energy divided by the speed of light and that the speed of light is constant in any reference frame. The methodology intentionally avoids other known properties of light, such as the fact that light is an electromagnetic wave and that its energy is quantized. Since we handle solids as elastic objects, the results are consistent with the principles of causality and agree with recent experimental observations.

Employing the above mentioned assumptions, we shall tackle the problem of reflection of a laser pulse from a fully reflective mirror and show that its reflection gives rise to an elastic wave with measurable amplitude that propagates within the mirror and that our results predict a larger Doppler shift in the reflected pulse for the most common setting, when the mirror is initially at rest, compared to the results obtained when the mirror is treated as rigid.

Similarly, we will revisit the Balazs thought experiment. The final example will explain the infinite expansion of a fully reflective 1D resonator filled with light.

9548-26, Session 6

Optodynamic description of optical manipulation

Tomaz Pozar, Janez Mo?ina, Univ. of Ljubljana (Slovenia)

SPIE. PHOTONICS

NANOSCIENCE+ ENGINEERING

We treat optical manipulation of solid objects from the perspective of optodynamics, a research field which investigates light-induced motion of macroscopic matter. Contrary to general notion of optical manipulation which investigates the means to move an object as a whole, optodynamics also focuses on the redistribution of the acquired momentum from the initial, time-developing, extremely low-amplitude propagating mechanical waves to the final net motion of the object.

When a solid object is manipulated/propelled by a pulse of light, various types of mechanical waves are generated whenever and wherever light exchanges momentum with matter. In the case of opaque objects, the following elastic waves are launched from the illuminated surface towards the bulk of the solid: ablation-induced waves (AIWs) resulting from material recoil, thermoelastic waves (TEWs) caused by light absorption and the subsequent thermal expansion, and the light-pressure-induced waves (LIWs) emanating exclusively from the photon linear momentum transfer (radiation pressure). Even though the macroscopic motion of the object is the superposition of all these waves, only AIWs and the much weaker LIWs are involved in the translation of the object's center of mass.

In this contribution, we will present two unique measurements revealing AIWs and LIWs, and discuss the time-development of the transferred momentum. We shall report on the measurements that show how TEWs can be sufficiently suppressed in order to discern the presence of LIWs. The required experimental techniques will be reviewed. The Abraham-Minkowski debate and Balazs thought experiment shall also be theoretically expanded to include elastic wave motion.

9548-27, Session 7

A model for traumatic brain injury using laser induced shockwaves

Aaron R. Selfridge, Daryl C. Preece, Veronica Gomez, Linda Z. Shi, Univ. of California, San Diego (United States); Michael W. Berns, Univ. of California, Irvine (United States)

Traumatic brain injury (TBI) represents a major treatment challenge in both civilian and military medicine; on the cellular level, its mechanisms are poorly understood. As a method to study the dysfunctional repair mechanisms following injury, laser induced shockwaves (LIS) are a useful way to create highly precise, well characterized mechanical forces.

We present a simple model for TBI using laser induced shockwaves as a model for damage. Our objective is to develop an understanding of the processes responsible for neuronal death, the ways in which we can manipulate these processes to improve cell survival and repair, and the importance of these processes at different levels of organization.

The physics of shockwave creation has been modeled and can be used to calculate forces acting on individual neurons. By ensuring that the impulse is in the same regime as that occurring in practical TBI, the LIS model can ensure that in vitro conditions and damage are similar to those experienced in TBI. This model will allow for the study of the biochemical response of neurons to mechanical stresses, and can be combined with microfluidic systems for cell growth in order to better isolate areas of damage.

9548-28, Session 7

Periodic cavitation in an optical tweezer

Viridiana Carmona-Sosa, José E. Alba-Arroyo, Pedro A. Quinto-Su, Univ. Nacional Autónoma de México (Mexico)

We show that microscopic explosions (cavitation) can be generated periodically in an optical tweezer. An absorbing microparticle is attracted



to the trapping beam waist where it is superheated resulting in a cavitation bubble that impulsively pushes the particle close to the starting position where the cycle restarts.

We find that multiple microparticles can briefly coexist oscillating in asingle optical trap, increasing the frequency of microscopic explosions.

9548-29, Session 7

Interesting physics and applications using microbubbles in thermo-optic tweezers

Basudev Roy, Subhrokoli Ghosh, Soumyajit Roy, Ayan Banerjee, Indian Institute of Science Education and Research Kolkata (India)

We have developed a technique of generating a micro-bubble inside an optical trap by using a material (Mo-based Soft Oxometalate (SOM) compound) that absorbs at the trapping laser wavelength. A high concentration aqueous dispersion of the SOMs is taken in a sample chamber, and the trapping laser is focused on SOMs adsorbed on one of the surfaces of the chamber, so as to create a 'hot spot' due to which a microbubble is nucleated. Due to the temperature gradient on the bubble, a surface tension gradient results, which leads to Marangoni type flows around the bubble. The resultant Marangoni flow around the bubble causes self-assembly of material at its base, which undergoes a phase transition into a crystalline state when the laser spot is translated causing the bubble to follow due to convective effects [1]. We have used this technique to pattern materials ranging from dyes to carbon nano-tubes to conducting polymers which co-assemble in a mixture with the SOMs. The method is rather universal and has been used to develop catalytic chips [2] and solution processed printable electronics. The flow generated by the bubbles can be studied by mapping the trajectories of probe particles in the vicinity of the bubble. We show interesting self-assembly of the particles on the bubble surface, as well as manipulation of trajectories of the particles by multiple bubbles. The bubble can also be used to capture, transport, and release particles in a perfectly controlled manner.

9548-30, Session 8

Reactive oxygen species production in single cells following laser irradiation

Michelle L. Duquette, Justine Kim, Linda Z. Shi, Michael W. Berns, Univ. of California, San Diego (United States)

Region specific DNA breaks can be created in single cells using laser light that damages DNA but does not directly generate reactive oxygen species (ROS). We have examined the cellular response to directly generated DNA breaks in single cells. Using a combination of ROS specific dyes and oxidase inhibitors we have found that the oxidase and chromatin remodeling protein Lysine demethylase I (LSD1) generates detectable ROS as a byproduct of its chromatin remodeling activity during the initial DNA damage response. ROS is produced at detectable amounts primarily within the first 3 minutes post irradiation. LSD1 activity has been previously associated with transcriptional regulation therefore these findings have implications for regulation of gene expression following DNA damage particularly in cells with altered redox states.

9548-31, Session 8

Integrated 3D macro-trapping and lightsheet imaging system

Zhengyi Yang, Peeter Piksarv, David E. K. Ferrier, Frank J. Gunn-Moore, Kishan Dholakia, Univ. of St. Andrews (United Kingdom)

Light-sheet imaging technique is particular suitable for forming three-

dimensional (3D) image of large samples. Construction of 3D image needs scanning sample along the detection axis, which is currently accomplished by moving the fixed sample in agent such as agarose. However, this fixing agent limits the development of the living sample, moreover the refractive-index mismatch between this agent and water introduces optical aberration which degrade the quality of image. Here we demonstrate a light-sheet imaging system integrated with dual-beam trap. The specimen was trapped by two counter-propagating beams and moved optically by a scanning mirror. Trapping and imaging of BY-2 cells and Pomatoceros lamarckii larva were successfully demonstrated.

9548-32, Session 8

Single-cell diffraction tomography with optofluidic rotation about a tilted axis

Paul Müller, Mirjam Schürmann, Jochen Guck, Technische Univ. Dresden (Germany)

The refractive index is an inherent property of every biological cell and its measurement does not require any markers. The knowledge of the three-dimensional refractive index distribution inside a cell helps to better characterize cell shape, dry mass, or volume. Its measurement thus complements techniques that investigate the inner structure of cells.

Optical diffraction tomography is a technique that produces refractive index maps with sub-cellular resolution. The refractive index can be inferred from quantitative phase maps which are recorded with imaging techniques such as digital holographic microscopy (DHM). We combine DHM with optical micromanipulation techniques to obtain tomographic projections of single biological cells in the visible spectrum of light. We employ optical diffraction tomography with the Rytov approximation to reconstruct the three-dimensional refractive index distribution of single cells from these projections. Optical diffraction tomography opens the possibility to monitor structural changes in cells, but also enables us to derive their optical properties which are of high interest for applications that involve optical forces.

9548-33, Session 9

Acoustic force spectroscopy (Invited Paper)

Iddo Heller, Vrije Univ. Amsterdam (Netherlands)

No Abstract Available

9548-34, Session 9

Structured interference force for enhanced optical trapping (Invited Paper)

Michael A. Taylor, The Univ. of Queensland (Australia) and Research Institute of Molecular Pathology (Austria); Muhammad Waleed, Alexander B. Stilgoe, Halina Rubinsztein-Dunlop, Warwick P. Bowen, The Univ. of Queensland (Australia)

Interferometry can completely redirect light, providing the potential for exceptionally strong and controllable optical forces. When a beamsplitter combines two fields, the output power is directed via the relative phase between the incident fields. Since the phase changes with beamsplitter displacement, the interference force can be used to stably trap; with displacements as small as (?/4n) able to completely redirect the light. The resulting change in optical momentum causes an opposing optical force. However, optical forces are most useful for trapping and manipulating small scattering particles. Optical scattering is not generally thought to allow efficient interference; essentially, it appears that small particles cannot act as beamsplitters. As such, optical traps have relied upon much weaker



deflection-based forces.

Here we show that efficient interference can be achieved by appropriately structuring the incident light. This relies on Mie scattering fringes to combine light which is incident from different incident angles. This results in a force, which we call the structured interference force, which offers order-of-magnitude higher trap stiffness over the usual Gaussian trap. We demonstrate structured interference force trapping (SIFT) of 10?m diameter silica spheres with a stiffness 20.1 times higher than is possible using Gaussian traps, while also increasing the measurement signal-to-noise ratio by two orders of magnitude. This is demonstrated using only phase control of the incident light, making the technique directly compatible with most existing holographic optical traps. These results are highly relevant to many applications, including cellular manipulation, fluid dynamics, micro-robotics, and tests of fundamental physics.

9548-35, Session 9

Mapping of independent force and position measurements for calibration of non-Hookean optical traps

Ann A. Bui, Alexander B. Stilgoe, Timo A. Nieminen, Halina Rubinsztein-Dunlop, The Univ. of Queensland (Australia)

Optical tweezers use highly focussed beams to trap microscopic particles in three dimensions. It is possible to carry out quantitative force measurements, on the order of piconewtons, if calibration of the system is done first. This requires finding the optical force for a given trapping power and position in the trap. Two tools commonly used for calibration are the camera and position-sensitive detector (PSD). Both are commonly used to track trapped particles, but they give complementary information. The camera gives the position of the particle. The PSD measures the defection of the beam, which is the force exerted on the particle. Since these data are obtained on different instruments, usually at vastly different rates, there is difficulty in synchronising the force and position data. Here we look at a force calibration method, without synchronising the data, by mapping force and position measurements. If the force-position relation is monotonic, then the median of the force distribution corresponds to the median of the position distribution; in general, the nth percentile of one corresponds to the (100-n)th percentile of the other. This intuitively works for traps whose force-position relations are monotonic, which includes Hookean traps like a single round symmetric trap. We discuss the limits at which this method can be applied to non-Hookean trapping arrangements, such as independent or coherent double-well traps.

9548-36, Session 9

A new method for calibrating the nonlinear range of a single-beam optical trap

Jamianne C. Wilcox, Benjamin J. Lopez, Otger Campas, Megan T. Valentine, Univ. of California, Santa Barbara (United States)

Optical traps allow for the precise application and measurement of pico-Newton forces in a wide variety of situations, and are particularly well suited for biophysical measurements of motor proteins and cells. Nearly all experiments exploit the linear regime of the optical trap, where force and displacement are related by a simple spring constant that does not depend on the trapped object's position. This typically limits the useful force range to < 100 pN for high-NA objective lenses and reasonable laser powers. Several biological studies require larger forces, which are not accessible in the linear regime of the trap. The best means to extend the maximum force is to make use of the entire nonlinear range; however, current techniques for calibrating the full nonlinear regime are limited. Here we report a new method for calibrating the nonlinear trap region that uses the fluctuations in the position of a trapped object when it is displaced from the center of a single gradient optical trap by controlled flow. From the position fluctuations, we measure the local trap stiffness, in both the linear and non-linear regimes. This approach requires only knowledge of the system

temperature, and is especially useful for measurements involving trapped objects of unknown size, or objects in a fluid of unknown viscosity.

9548-37, Session 9

Measurement of radiation pressure in an ambient environment

Dakang Ma, Joseph L. Garrett, Jeremy N. Munday, Univ. of Maryland, College Park (United States)

Light reflected off a material or absorbed within it exerts radiation pressure through the transfer of momentum. Although this effect is small, microscale mechanical transducers have progressed to the point that radiation pressure can play an important role in these systems. Understanding these effects and distinguishing radiation pressure from photothermal effects is thus of great importance for future optomechanical devices. Here we discuss our recent measurements of radiation pressure on a silicon nitride microcantilever under ambient conditions. Using our technique, we are able to separately identify the radiation pressure and photothermal forces through an analysis of the cantilever's frequency response. Additionally, the radiation pressure is found to be much stronger than the effective photothermal forces when excitation occurs near the free end of the cantilever. In such a regime (where the photothermal forces make up less than 1% of the total cantilever amplitude at resonance), we measure the force resulting from the radiation pressure. Measured forces range from 1-10 pN for illumination powers of 1-9 mW at 660 nm. A model is used to calculate the radiation pressure, which is found to agree with experimental results within the measured and calculated uncertainties. We envision this method as a practical way to determine the response of optomechanical devices and as an alternative method for cantilever spring constant calibration. Further, we expect this technique to be an effective method for the study of optical forces on exotic metamaterials, which might be hindered by photothermal forces.

9548-38, Session 10

Photonic force microscopy of surface electromagnetic waves in a onedimensional photonic crystal

Daniil Shilkin, Evgeny V. Lyubin, Lomonosov Moscow State Univ. (Russian Federation); Irina V. Soboleva, Lomonosov Moscow State Univ. (Russian Federation) and A.N. Frumkin Institute of Physical Chemistry and Electrochemistry (Russian Federation); Andrey A. Fedyanin, Lomonosov Moscow State Univ. (Russian Federation)

The Bloch Surface Electromagnetic Waves (SEWs) providing large field enhancement in all-dielectric structures are shown to be promising tool for optical manipulation of dielectric microparticles. In our work, momentum of the SEW at a one-dimensional photonic crystal/water interface is experimentally demonstrated to be transferred to a 1-?m polystyrene microsphere trapped by optical tweezers in the vicinity of the photonic crystal surface. By means of optical microscopy, the interaction force generated by the SEW evanescent field is shown to be large enough for particles localization near the surface and propulsion along the SEW propagating direction. Using photonic force microscopy, the force is measured quantitatively as a function of the exciting beam angle of incidence and the distance from the photonic crystal surface. The force is shown to decay exponentially with moving off the surface at large distances, but there is a surprising diminution of the force at surface/particle gaps less than 150 nm. The maximum force of 0.25 fN at the exciting radiation intensity of 1.6 kW/cm? is observed at the SEW excitation resonance. The SEW-induced gradient force was estimated in the dipole approximation. Because of the small width of the resonance (0.1° in our experiment), the angular divergence of the exciting radiation should be taken into account. The results are in a good agreement with the experimental data.



9548-39, Session 10

Optical epitaxial growth of gold nanoparticle arrays

Ningfeng Huang, The Univ. of Southern California (United States); Luis J. Martinez, The Univ. of Southern California (United States) and Ecole Normale Supérieure de Cachan (France); Eric Jaquay, Michelle L. Povinelli, The Univ. of Southern California (United States)

We demonstrate optical trapping of a periodic array of closely spaced gold nanoparticles. To achieve the experimental result, we considered competition between optical gradient forces and strong interparticle interactions. We achieve control of the gradient forces using a photoniccrystal template designed to create a periodic optical trapping potential. We modeled the interparticle interactions using a kinetic Monte Carlo approach. The results predict the formation of different particle superstructures (such as chains or filled-in arrays) depending on lattice constant and symmetry. Using the model prediction, we designed and demonstrated a template that allows trapping of a regular periodic array.

9548-40, Session 10

Submicron particle manipulation using slotted tapered optical fibers

Mark J. Daly, Viet Giang Truong, Síle Nic Chormaic, Okinawa Institute of Science and Technology Graduate Univ. (Japan)

Optical micro- and nanofibers (MNFs) have, in recent years, been used for trapping and manipulating micron, and even submicron scale particles with varying degrees of success. Despite their versatility, their applications to the trapping of submicron particles without a high refractive index have remained somewhat limited. To increase their performance in this regime, we demonstrate the use of a slotted tapered optical fiber (STOF), which was previously proposed in the context of cold atom trapping. This fiber has an increased evanescent field via nanostructuring, hence increasing the trapping strength for submicron particles. The structuring process consists of the removal of a rectangular section of the fiber with a focused ion beam, thus producing a region of increased electric field, when compared to that of an unstructured fiber. The STOF, with typical slot dimensions of 20 μ m by 300 nm, can be used to propel and trap submicron particles. Using 1064 nm trapping beams, which are propagated through a STOF, particles can be localized to the slot region. We present the trapping and manipulation of submicron fluorescent particles, with diameters in the range of 100 -300 nm, using this novel fiber design, alongside a brief presentation of the operational abilities and fabrication process of a STOF. The STOF's increased ability to trap submicron particles reliably within its evanescent field may lead to future applications in particle sorting, particle counting, and even opening up the possibility of performing in situ spectroscopic measurements on STOF trapped particles.

9548-41, Session 11

Optical manipulation of single microparticle for microfluidic flow rate sensing

Yuan Gong, Univ. of Electronic Science and Technology of China (China)

Sensitive flowmeter with large dynamic range is highly desirable for microfluidic applications. We developed an optofluidic flow rate sensor, with a dynamic range of 3 orders of magnitude and a minimum detectable flow rate change (MDFRC) as low as 5 nL/min, based on optical manipulation of a microparticle by a single mode fiber (SMF). A single polystyrene microsphere was trapped on the optical axis by the 980nm laser emitting

from SMF and the force balance between optical force and flow force was used for sensing. The manipulation distance was detected as a function of the flow rate. The measurement range of the flow rate is 20 - 22000 nL/ min with laser power of 11.43 mW to 146.31 mW. The maximum manipulation distance is about 715 ?m. The MDFRC can achieve 5nL/min at low rate range between 20 nL/min and 100nL/min which is 2 orders of magnitude better than the state-of-the-art microfluidic flowmeters. At other ranges, the MDFRC is around 5% of the measurand. The experimental results indicates that the sensor has a good repeatability for flow rate measurement. Theoretical analysis and numerical simulations were also provided and used for experimental discussion.

9548-42, Session 11

Optically-induced circulation of dielectric particles with fiber optic Bessel beam

Boram Joo, Sungrae Lee, Kyunghwan K. Oh, Yonsei Univ. (Korea, Republic of)

Bessel beams are important for applications in optical trapping because they have non-diffracting and self-reconstructing properties. Bessel beams are usually generated by bulk optic systems using ring apertures or axicons. We fabricated a fiber device to generate a Bessel-like beam that is significantly more compact than a conventional bulk-optic Bessel beam generation system. This Bessel beam generation(BBG) device is composed of two fiber segments: a single mode fiber section and a coreless silica fiber(CSF), both with diameter 125?m. The fundamental LPO1 mode from the input SMF excites LPOm higher order modes in the CSF to form an interferometric concentric intensity distribution similar to a Bessel function. This alignment-free and micro-scale BBG device is well-suited for "Lab on a Chip" systems.

In this experiment, the BBG devices are connected to 980 nm He-Ne laser diodes. Three BBG devices are located inside a solution of polystyrene beads (n=1.55, D=15?m) and water to form a 3-beam array. The polystyrene beads are trapped by the beams and transported along the beam propagation direction. At the points where the Bessel-like beams are crossed, the bead changes its path from the initial trapping beam to the next beam. We were able to change the bead's path at a crossing of 120 degrees by utilizing the optical power difference between the beams. We set up a triangular beam route with three BBG devices. By controlling the speed and angular motion of the particles, we have demonstrated optically induced circulation of particles along triangular routes. This technique is applicable to the control of motion of living cells in a microscopic environment.

9548-43, Session 11

Ultrathin optical fibers for particle trapping and manipulation

Síle G. Nic Chormaic, Okinawa Institute of Science and Technology Graduate Univ. (Japan); Aili Maimaiti, Okinawa Institute of Science and Technology Graduate Univ. (Japan) and Univ. College Cork (Ireland); Marios Sergides, Ivan Gusachenko, Viet Giang Truong, Okinawa Institute of Science and Technology Graduate Univ. (Japan)

In recent years, optical micro- and nanofibres (MNF) have shown their potential as trapping devices across a range of particle size regimes, from atoms to microparticles. The fibers, with waist diameters close to or less than the wavelength of the guided light, have unique properties due to the strong evanescent field that extends from the waist region into the surrounding environment. This field can have very high intensities for very low guided light powers over the full length of the nanofiber, which is typically a few millimeters. This provides experimentalists with a relatively easy method of extending the interaction length between a tightly focused light beam and the surrounding environment. To date, most work on micron sized particles around optical MNFs has dealt with multiparticle trapping



and propulsion, and has been limited to fundamental mode propagation within the optical fiber. Research on higher order mode (HOM) particle trapping and manipulation was avoided due to the difficulties in fabricating MNFs that permit HOM propagation. Here, we report on HOM propagation in MNFs and the speed enhancement that can be achieved for dielectric particles moving under the influence of this mode. Optical binding using HOMs in MNFs has also been investigated. Detailed simulations support the experimental results and provide insight into the inter-dynamics of particle assembly within the multiparticle chains.

9548-44, Session 12

Stochastic thermodynamics with a Brownian particle in an optical trap (Invited Paper)

Ignacio A. Martinez, ICFO - Institut de Ciències Fotòniques (Spain) and Ecole Normale Supérieure de Lyon (France); Édgar Roldán, ICFO - Institut de Ciències Fotòniques (Spain) and Max-Planck-Institut für Physik komplexer Systeme (Germany) and Grupo Interdisciplinar de Sistemas Complejos (Spain); Luis Dinis, Grupo Interdisciplinar de Sistemas Complejos (Spain) and Univ. Complutense de Madrid (Spain); Pau Mestres, ICFO - Institut de Ciències Fotòniques (Spain); Juan M. R. Parrondo, Grupo Interdisciplinar de Sistemas Complejos (Spain) and Univ. Complutense de Madrid (Spain); Raúl A. Rica, ICFO - Institut de Ciències Fotòniques (Spain)

Stochastic thermodynamics [1,2] is a recently developed framework to deal with the thermodynamics at the microscope, where thermal fluctuations strongly influence their behaviour. Typical such systems are colloids and biomolecules or cells. These thermal fluctuations do not only lead to Brownian motion, but to a continuous and unavoidable heat exchange between the suspending medium and the particles, leading to a very interesting phenomenology. In order to explore such phenomenology and to test theoretical results obtained from stochastic thermodynamics, we developed an "experimental simulator" of thermodynamic devices in the microscale with an optically trapped bead that is subject to an external noise that mimics a controllable thermal bath. The noise is applied by means of electric fields acting on the charge of the trapped particle.

In this talk, I will present some of the results we obtained with this simulator, demonstrating excellent control over the effective temperature of the system and a control parameter. This allows us to perform a variety of equilibrium and non-equilibrium thermodynamic processes [3-5]. In particular, we were able to realize microadiabatic processes, where no heat is exchanged on average between the particle and the medium [6]. This achievement allowed us to implement a Carnot microengine as a concatenation of isothermal and adiabatic processes [7], whose theoretical study is playing a key role in the foundations of stochastic thermodynamics. References

K Sekimoto; Lecture Notes in Physics (Springer, Berlin, 2010), Vol. 799.
 U Seifert; Rep. Prog. Phys. 75 (2012) 126001

[3] IA Martínez, É Roldán, JMR Parrondo, D Petrov; Phys. Rev. E 87 (2013) 032159

[4] É Roldán, IA Martínez, L Dinis, RA Rica; Appl. Phys. Lett. 104 (2014) 234103

[5] P Mestres, IA Martinez, A Ortiz-Ambriz, RA Rica, E Roldan ;Phys. Rev. E 90 (2014) 032116

[6] IA Martínez, É Roldán, L Dinis, D Petrov, RA Rica; Phys. Rev. Lett. (2015) In press

[7] IA Martinez, E Roldan, L Dinis, D Petrov, JMR Parrondo, RA Rica; (2015) arXiv preprint: 1412.1282

9548-45, Session 12

Auto correlation and relaxation time measurements on metal oxide core: dielectric shell beads in an optical trap

Shruthi S. Iyengar, Praveen Parthasarathi, Rekha Selvan, Sarbari Bhattacharya, Sharath Ananthamurthy, Bangalore Univ. (India)

Optical Tweezers are capable of trapping individual particles of sizes that range from sub micrometers to micrometers. By measuring the fluctuations in the position of the trapped particle with time, one can compute the trap strength experienced by the particle. It is reported that the trap strength of a dielectric bead, increases linearly with increase in the power of the trapping laser. The situation with metallic particles, however, is strongly dependent on the particle size. Available literature shows that metallic Rayleigh particles, despite having scattering no different from dielectric particles of similar sizes, experience enhanced trap strengths due to larger polarizability. On the contrary, micrometer sized metallic particles are poor candidates for trapping due to high reflectivity. We report here that core-shell (metal oxide-dielectric) micrometer sized beads are trapped like dielectric beads, but with reduced corner frequency compared to ordinary dielectric beads at the same laser power. We attribute this anomaly to an increase in the temperature of the surrounding of the bead due to an enhanced dissipation of the laser power as heat. The variation in the auto correlation coefficients and thereby relaxation times of such beads with laser power contrasted with that of ordinary dielectric beads supports our claim. We propose to extend this work towards extracting hydrodynamic correlations between beads where one is a heat source and study its variation as a function of the inter bead separation.

9548-46, Session 12

Tailoring defects in colloidal crystals using an external "non-affine" field

Saswati Ganguly, Indian Association for the Cultivation of Science (India); Surajit Sengupta, TIFR Ctr. for Interdisciplinary Sciences (India); Peter Sollich, King's College London (United Kingdom)

Thermal fluctuations of displacements of particles within a small subvolume in a two-dimensional colloidal crystal may be either affine or non-affine. Displacements are fully affine only if the instantaneous positions of all the particles in the sub-volume can be represented as an uniform deformation of the ideal reference configuration. Mostly however, these displacements are non-affine with the overall deviation from affine-ness being measured by a well defined non-affine parameter X. We show that X has all the characteristics of a thermodynamic variable and may be tuned using the conjugate non-affine field h_X. We show further that the largest contribution to X comes from displacements which are precursors to the creation of elementary dislocation dipoles. Hence, tuning X also automatically changes dislocation concentrations. Finally, we present a proposal for an experiment aiming to construct h_X using laser tweezer techniques. With presently available particle manipulation techniques one can only increase the defect concentration by introducing dislocation dipoles in colloidal crystals. Manipulating h_X , on the other hand, would allow one to both increase or decrease X and, therefore, the defect concentrations. Our method may find application in the study of the stability of crystals or in the manipulation of mechanical properties of colloidal crystals by external fields. A preprint presenting preliminary results from this work is available at http://arxiv.org/abs/1502.00042.



9548-47, Session 12

Plasticity avalanches for colloidal crystals in dynamical optical traps

Cynthia J. Reichhardt, Los Alamos National Lab. (United States); Danielle McDermott, Wabash College (United States); Charles M. Reichhardt, Los Alamos National Lab. (United States)

Colloidal assemblies are an ideal system in which to study general features of equilibrium and nonequilibrium phenomena since, due to their size scale, microscopic information about the particle configurations and dynamics can be accessed directly. Additionally, recent advances in optical trapping techniques permit the manipulation of colloidal particles at individual and collective levels. Here we numerically examine a collection of chargestabilized colloids forming a triangular crystal that is placed in a quasione-dimensional confining potential which could be created using optical means. The potential depth is slowly increased to uniaxially compress the colloidal assembly. During the compression process, colloid motion occurs via both slow elastic distortions as well as short bursts or avalanches in which plastic rearrangements of the colloids occur. These rearrangements are associated with structural changes in the colloid lattice that make the configuration more isotropic and permit new triangular arrangements to fit in the trap. At high compression the avalanches are associated with row reduction events for the number of colloids that fit across the width of the confining potential. We also find that the colloid velocity distributions during the avalanches have power law tails with exponents close to those found for gliding dislocations. We also examine cases in which the colloidal interactions are more complex and consist of both attractive and repulsive components. Here we observe sharp transitions in which the entire structure of the lattice can change, producing sudden volume-collapse type events that result in the formation of a more compact colloidal lattice structure.

9548-48, Session 12

Combined magneto- and optofluidic assembly of colloidal chains of controllable length

Tao Yang, Ning Wu, David WM Marr, Colorado School of Mines (United States)

Because of their unique characteristics, colloids have been used to investigate the fundamental physics of soft materials including both equilibrium phase behavior and kinetic processes. Unlike atoms, colloidal sizes can be conveniently tailored and are typically large enough to be probed individually with interaction strengths and effective ranges that can be modulated over several orders of magnitude. Despite these significant advantages, only relatively simple colloidal models such as spheres have been created: such systems in turn assemble into crystals of fairly limited symmetry, precluding the study of problems associated with complex structure. To push towards the synthesis of more complicated colloidal molecules, we use combined applied magnetic and anisotropic optical fields to fabricate colloidal chains. By integrating these induced forces within microfluidic channels and in flow, we grow colloidal chains one particle at one time, mimicking step-growth polymerization. The key advantage of this method is the ability to precisely control chain length and sequence, both essential for studies of self-assembly. In this, chain length is determined by a balance between the hydrodynamic shear stress, applied magnetic field, and the optical forces applied. Once a desired chain length is achieved, we fix the assembly in situ via the use of thiol-functionalized magnetic beads and a functionalized polyethylene glycol crosslinker. With the ability to perform directed assembly and irreversible fixation in flow, a route to the highthroughput synthesis of colloidal molecules can be achieved.

9548-49, Session 13

Controlling hydrodynamic interactions in driven systems (*Invited Paper*)

David B. Phillips, Rebecca F. Hay, Graham Gibson, Univ. of Glasgow (United Kingdom); Stephen H. Simpson, Institute of Scientific Instruments of the ASCR, v.v.i. (Czech Republic); Miles J. Padgett, Univ. of Glasgow (United Kingdom)

Hydrodynamic interactions in low Reynolds number environments, where inertial forces are dominated by viscous ones, can give rise to some unusual effects.

At the micro-scale, particles continually undergo random walks due to the stochastic forces of Brownian motion. Nearby particles feel correlated Brownian forces, and so their motion is coupled.

The addition of external forces on such particles induces more coupling, as the flow-field generated around a moving particle in turn exerts hydrodynamic forces on surrounding objects. Although the underlying rules at play are well known, they can result in counter-intuitive behaviour, even in simple systems.

In this work we study two such systems. Firstly we show that an optically trapped microsphere in a time-reversible oscillating flow-field (created by a nearby optically trapped microsphere driven in an oscillatory manner) can exhibit a trajectory that breaks time-reversal symmetry. This is a consequence of the competition between the time-dependent hydrodynamic flow and the positiondependent optical force as the microsphere moves in the harmonic potential of the optical trap. We investigate the transfer of energy between the two hydrodynamically coupled particles, and describe how the topology of the resulting trajectories varies as the driven beads motion is altered.

Secondly, we study how such systems can exhibit yet more elaborate effects by moving the driving optical traps according to feedback on the positions of hydrodynamically interacting microspheres.

9548-50, Session 13

Hydrodynamic synchronisation in arrays of hollow beams

Luke J. Debono, Univ. of Bristol (United Kingdom); Stephen Simpson, Institute of Scientific Instruments of the ASCR, v.v.i. (Czech Republic); Simon Hanna, Univ. of Bristol (United Kingdom)

Hydrodynamic synchronisation has previously been observed in pairs of simple rotors controlled by optical tweezers. In one scenario, pairs of beads were driven on circular trajectories by moving Gaussian traps [Kotar et al, PRL 11,228103 (2013)]; in another, rigid spheroids were rotated by the angular momentum in vortex beams [Arzola et al, Opt. Exp. 22, 16207 (2014)]. In both cases, synchronised motion resulted from hydrodynamic interactions (HI). In the present computational study, we examine the stochastic behaviour of ensembles of microspheres trapped in the bright annuli of arrays of LG beams. In this model, the angular momentum of the beams provides the azimuthal driving force, while HI lead to synchronicity. The conditions for synchronisation are explored. Intriguingly, synchronisation is more difficult to achieve as the number of LG beams increases. This results from the long-range nature of HI in the low Reynolds number regime. In square arrays of rotors, the corner rotors are in substantially different environments from those on the edges and on the inside of the array, and experience correspondingly lower synchronisation forces and lower velocities. On the other hand, patches of rotors moving in concert tend to speed up, owing to the additive effects of the hydrodynamic forces. The net result, for large arrays of rotors, is a fragile synchrony; patches of synchronisation forming due to HI, are constantly moving, breaking up and re-forming due to stochastic forces. Learning to control the synchronised motion of large arrays of rotors is viewed as an important step in the development of micro-machines to deliver motion on the macroscopic scale.



9548-51, Session 13

Hydrodynamics of micro-objects near curved surfaces

Shu Zhang, David Carberry, Timo A. Nieminen, Halina Rubinsztein-Dunlop, The Univ. of Queensland (Australia)

Boundary walls have a strong influence on the drag force on optically trapped object near surface. Faxen's correction has shown how a flat surface modifies the hydrodynamic drag. However, to date, the effect of curved walls at microscopic scale on both translational and rotational movement of micro-objects has not been studied. Here we describe our experiments which aim to study the drag force on optically trapped particles moving near walls with different curvatures.

The curved walls were made using 3D laser nano-printing (Nanoscribe), and optical tweezers were used to trap micro-objects near the walls. The translational and rotational motion of the optically trapped particle is related to the drag coefficients. By monitoring the change in the motion of particle, we determined the increase in drag force for particles translating or rotating at different distances from surfaces with different curvatures.

These results are essential for calibrating the drag force on particles, and thus enable accurate rheology at the micron-scale. This opens the potential for microrheology under different conditions, such as within microdevices, biological cells and studies of biological processes

9548-52, Session 13

Boundary element method for optical force calibration in microfluidic dual-beam optical trap

Mehmet E. Solmaz, Izmir Katip Celebi Univ. (Turkey); Barbaros Cetin, Bilkent Univ. (Turkey); Besim Baranoglu, Atilim Üniv. (Turkey); Murat Serhatlioglu, Necmi Biyikli, Bilkent Univ. (Turkey)

The potential use of optical forces in microfluidics environment enables highly selective bioparticle manipulation [1, 2]. Manipulation could be accomplished via trapping or pushing a particle due to optical field. Empirical determination of optical force is often needed to ensure efficient operation of manipulation. The external force applied to a trapped particle in a microfluidic channel is a combination of optical and drag forces. The optical force can be found by measuring the particle velocity for a certain laser power level and the Faxen's law [3] is applied as the multiplicative correction factor for the proximity of the particle to the channel surface. This method is not accurate especially for small microfluidic geometries where the particle size is in Mie regime and is comparable to channel cross section. In this work, we propose to use Boundary Element Method (BEM) to simulate fluid flow within the microchannel with the presence of the particle to predict drag force on the particle. This way, the drag force on the particle will be determined accurately and the optical power will be calibrated. We will perform pushing experiments in a dual-beam optical trap and extracted the particle's position information. We will then obtain the drag force acting on the particle using BEM. We will also compare our results with the traditional drag force correction factor.

9548-53, Session 13

Rotational behavior of oblate spheroids in circularly polarized dual beam optical trap

Martin ?iler, Oto Brzobohat?, Institute of Scientific Instruments of the ASCR, v.v.i. (Czech Republic); Alejandro V. Arzola, Univ. Nacional Autónoma de México (Mexico); Luká? Chvátal, Petr Jákl, Stephen H. Simpson, Pavel Zemánek, Institute of Scientific Instruments of the ASCR, v.v.i. (Czech Republic) We study the rotational dynamics of oblate spheroids in an optical trap which is based on interference of two counter-propagating Gaussian beams that are circularly polarized. Single spheroid may either rotate with a frequency determined by its size and aspect ratio or it may be oriented in a symmetric state where it is not rotating. The experimental results are supported by numerical calculations based on Finite elements method and T-matrix. Furthermore, a pair of spheroids display phase locking behavior and the introduction of additional particles leads to yet more complex behavior.

9548-54, Session 13

Spatial optical solitons in bidisperse fluorescent nanocolloids

M. Yadira Y. Salazar Romero, Instituto de Investigaciones en Materiales (Mexico); Juan Hernández-Cordero, Karen P. Volke-Sepúlveda, Alejandro V. Arzola, Univ. Nacional Autónoma de México (Mexico); Yareni Ayala, Univ Nacional Autónoma de México (Mexico)

We report on the nonlinear effects of light propagation through a fluorescent nanocolloid. The medium was formed by a bidisperse suspension of fluorescent and nonfluorescent nanospheres of similar diameters (60nm and 57nm, respectively) in distilled water. A CW laser beam (532 nm wavelength) was focused into the nano-suspension, generating a spatial optical soliton of a few millimeters in length as a result of the compensation between beam diffraction and the self-focusing nonlinearity. The threshold power and focusing conditions to create the soliton were analyzed as a function of the pump power and hysteresis effects were observed. We also varied the concentration of both types of particles and the size of the nonfluorescent nanospheres and studied their effect in the soliton formation. Thermal effects caused by the absorption of the fluorescent particles are discussed.

9548-55, Session 13

Spatio-temporal formation of amyloid aggregates by laser trapping of domainswapped dimeric cytochrome c

Ken-ichi Yuyama, National Chiao Tung Univ. (Taiwan); Mariko Ueda, Satoshi Nagao, Shun Hirota, Nara Institute of Science and Technology (Japan); Teruki Sugiyama, National Applied Research Labs. (Taiwan); Hiroshi Masuhara, National Chiao Tung Univ. (Taiwan)

Laser trapping of a focused laser beam has been employed to gather molecules in solution spatio-temporally and realized the formation of a small molecular assembly in the focal volume. When the small molecular assembly evolves to a nucleus, it is grown outward from the focal spot, and eventually a crystal or a dense liquid droplet is generated under certain trapping conditions. In this paper, we present the spatio-temporal formation of protein amyloid aggregate by laser trapping in solution. Protein amyloids have recently attracted considerable interest because their accumulation in vivo is related to serious diseases and they have unique morphology of nanometer-scale fibrils. When a continuous-wave laser beam of 1064 nm was focused into a D2O solution of domain-swapped dimeric cytochrome c through an objective lens (100 magnification, NA = 1.4), the proteins were gathered at the focal spot, and a particle-like small assembly was formed in the focal volume. The small assembly greatly extended toward the outside of the focal spot after a certain lag time and eventually reached a diameter of over 10 ?m. Through a few kinds of analyses of the assembly, we confirmed that the large assembly resultant from dimeric cytochrome c consists of amyloid fibrils measuring several hundred nanometers in length and 5-10 nm in diameter. This spatio-temporal formation of amyloids by laser trapping is useful for fabricating and patterning amyloids as well as for elucidating the dynamics and mechanism of amyloid formation.

9548-56, Session 14

Behavior and applications of active Brownian particles in complex and crowded environments (Invited Paper)

Giovanni S. Volpe, Bilkent Univ. (Turkey)

Active Brownian particles, also know as microswimmers and nanoswimmers, have recently come under the spotlight, becoming the focus of the research of many groups around the world from the physical and biophysical communities alike. These swimmers are biological or manmade microscopic and nanoscopic particles that can propel themselves. Their behavior can therefore only be explained and understood within the framework of farfrom-equilibrium physics. Several microscopic biological entities perform active Brownian motion, for example, when moving away from a poison or towards a source of food; a paradigmatic example is the swimming behavior of bacteria such as Escherichia coli. Inspired by these microorganisms, researchers around the world have been developing artificial active particles that can reproduce the swimming behavior of motile biological cells based on very different and varied physical mechanisms; the reason for this interest lies in the potential these manmade micro- and nanomachines hold as autonomous agents for healthcare, sustainability and security applications: for example, by enabling the targeted localization, pick-up and delivery of nanoscopic objects with applications including bioremediation, catalysis, chemical sensing and drug-delivery. In this talk I will review this field of research and present some of my latest results.

9548-57, Session 14

Pattern formation for active particles on optically created ordered and disordered substrates

Charles M. Reichhardt, Dipanjan Ray, Cynthia J. Reichhardt, Los Alamos National Lab. (United States)

There has been tremendous growth in the field of active matter, where the individual particles that comprise the system are self-driven. Examples of this class of system include biological systems such as swimming bacteria and crawling cells. More recently, non-biological swimmers have been created using colloidal Janus particles that undergo chemical reactions on one side to produce self-propulsion. These active matter systems exhibit a wide variety of behaviors that are absent in systems undergoing purely thermal fluctuations, such as transitions from uniform liquids to clusters or living crystals, pushing objects around, ratchet effects, and phase separation in mixtures of active and passive particles. Here we examine the collective effects of active matter disks in the presence of static or dynamic substrates. For colloids, such substrates could be created optically in the form of periodic, random, or guasiperiodic patterns. For thermal particles, increasing the temperature generally increases the diffusion or mobility of the particles when they move over a random or periodic substrates. We find that when the particles are active, increasing the activity can increase the mobility for smaller run lengths but decrease the mobility at large run lengths. Additionally we find that at large run lengths on a structured substrate, a variety of novel active crystalline states can form such as stripes, squares and triangular patterns.

9548-58, Session 14

Study of microparticles' anomalous diffusion in active bath using speckle light fields

Ercag Pince, Sabareesh K. P. Sabareesh, Bilkent Univ. (Turkey); Giorgio Volpe, Univ. College London (United Kingdom); Sylvain Gigan, Univ. Pierre et Marie Curie (France); Giovanni S. Volpe, Bilkent Univ. (Turkey)

Particles undergoing a stochastic motion within a disordered medium is a ubiguitous physical and biological phenomenon. Examples can be given from organelles as molecular machines of cells performing physical tasks in a populated cytoplasm to human mobility in patchy environment at larger scales. Our recent results showed that it is possible to use the disordered landscape generated by speckle light fields to perform advanced manipulation tasks at the microscale. Here, we use speckle light fields to study the anomalous diffusion of micron size silica particles (5 ?m) in the presence of active microswimmers. The microswimmers we used in the experiments are motile bacteria, Escherichia coli (E.coli). They constitute an active background constantly agitating passive silica particles within complex optical potentials. The speckle fields are generated by mode mixing inside a multimode optical fiber where a small amount of incident laser power (maximum power = 12 ?W/?m2) is needed to obtain an effective random landscape pattern for the purpose of optical manipulation. We experimentally show how complex potentials contribute to the anomalous diffusion of silica particles undergoing collisions with swimming bacteria. We observed an enhanced diffusion of particles interacting with the active bath of E.coli inside speckle light fields: this effect can be tuned and controlled by varying the intensity and the statistical properties of the speckle pattern. Potentially, these results could be of interest for many technological applications, such as the manipulation of microparticles inside optically disordered media of biological interests.

OPTICS+

NANOSCIENCE+ ENGINEERING

SPIE. PHOTONICS

9548-59, Session 14

Noise, fluctuations, and nonlinear mechanical properties of living cells

H. Daniel Ou-Yang, Ming Tzo Wei, Dimitrios Vavylonis, Sabrina Jedlicka, Lehigh Univ. (United States)

Living cells are a non-equilibrium mechanical system, largely because intracellular molecular motors consume chemical energy to generate forces that reorganize and maintain cytoskeletal functions. Persistently under tension, the network of cytoskeletal proteins exhibits a nonlinear mechanical behavior where the network stiffness increases with intracellular tension. We examined the nonlinear mechanical properties of living cells by characterizing the differential stiffness of the cytoskeletal network for HeLa cells under different intracellular tensions. Combining optical tweezer-based active and passive microrheology methods, we measured non-thermal fluctuating forces and found them to be much larger than the thermal fluctuating force. From the variations of differential stiffness caused by the fluctuating non-thermal force for cells under different tension, we obtained a master curve describing the differential stiffness as a function of the intracellular tension. Varying the intracellular tension by treating cells with drugs that alter motor protein activities we found the differential stiffness follows the same master curve that describes intracellular stiffness as a function of intracellular tension. This observation suggests that cells can regulate their mechanical properties by adjusting intracellular tension.

9548-60, Session 15

Using optical tweezers to assess the role of inter-protein interactions in collagen self-assembly (Invited Paper)

Tuba Altindal, Marjan Shayegan, Evan Kiefl, Nancy R. Forde, Simon Fraser Univ. (Canada)

Collagen is a structural protein which is capable of self-assembling into hierarchical fibrillar structures. These structures form the basis of the extracellular scaffolding in the connective tissues of vertebrates. Further, collagen-based structures continuously remodel in a dynamic fashion. Collagen self-assembly into fibrils relies on specific interactions between these constituent proteins. Identification and characterization of these interactions is crucial for our understanding of the extracellular environment and cellular decisions prompted by this environment.

Here, we describe the results of the experiments where we probed the frequency-dependent viscoelasticity of collagen solutions with intact and

removed telopeptides using optical-tweezers-based passive microrheology. Telopeptides are short non-helical regions at the ends of triple helical collagen molecules, and their proteolytic removal results in a delay in the onset of fibril formation. We find that the removal of telopeptides significantly reduces elasticity of collagen solutions at timescales from ~10 msec to ~1 sec. By examining the loss modulus, we also find that increasing the concentration of telopeptide-intact collagen results in a growing non-Maxwellian behavior at low frequencies. Telopeptides have previously been postulated to bind transiently to specific sites on adjacent collagen triple helices in solution, and thus may facilitate the otherwise less probable alignment of two collagen molecules in proper register. Our microrheology experiments provide evidence of increased strength and duration of interprotein contact arising from the presence of telopeptides, critical in catalyzing self-assembly of fibrillar collagen systems.

9548-61, Session 15

Viscoelastic properties of subcellular structures measured by fluorescence correlation spectroscopy

Jens-Christian D. Meiners, Rudra P. Kafle, Molly R. Liebeskind, Univ. of Michigan (United States)

Mechanical quantities like the elasticity of cells are conventionally measured by directly probing them mechanically. This, however, is often impractical, and even impossible when subcellular structures inside living cells are concerned. We use a purely optical method instead; an adaptation of fluorescence correlation spectroscopy (FCS) to measure such mechanical quantities in chromosomal DNA in live E. Coli cells.

FCS is a fluorescence technique conventionally used to study the kinetics of fluorescent molecules in a dilute solution. Being a non-invasive technique, it is now drawing increasing interest for the study of more complex systems like the dynamics of DNA or proteins in living cells and cell membranes. Unlike an ordinary dye solution, the dynamics of macromolecules like proteins or entangled DNA in crowded environments is often slow and subdiffusive in nature. This in turn leads to longer residence times of the attached fluorophores in the excitation volume of the microscope and artifacts from photobleaching abound that can easily obscure the signature of the molecular dynamics of interest.

We present a method of calculating the intensity autocorrelation function from the arrival times of the photons on the detector that maximizes the information content while correcting for the effect of photobleaching to yield an autocorrelation function that reflects only the underlying dynamics of the sample. This autocorrelation function in turn is used to calculate the mean square displacement of the fluorophores attached to DNA. By using a suitable integral transform of the mean square displacement, we determine the viscoelastic moduli for lambda-DNA solution and the DNA in E. coli. We note that these mechanical quantities evaluated by an optical technique are in good agreement with similar quantities measured by completely different techniques.

9548-62, Session 15

Calibration of femtosecond optical tweezer as a sensitive thermometer

Dipankar Mondal, Debabrata Goswami, Indian Institute of Technology Kanpur (India)

We present the effects of a femtosecond perturbing heating source on an optical tweezer. Our experiments involve a unique combination of a nonheating femtosecond trapping laser at 780 nm with a femtosecond Infrared (1560 nm) laser at low power (100-800 μW) to cause heating in the trapped volume. We can control the temperature precisely around the optical trap center with such an experimental system. The 1560 nm high repetition rate laser acts as a resonant excitation source for the vibrational combination band of the hydroxyl group (OH) of water, which helps to create the local heating effortlessly within the trapping volume. We have observed for the first time direct effect of temperature on the corner frequency deduced

from power spectrum. This observation leads us to calculate the viscosity as well as the temperature within the vicinity of the trapping zone. These experimental results also support the well-known fact that the behavior of Brownian motion is a response from optically trapped bead due to temperature change of surroundings. Temperature rise near the trapping zone can significantly change the viscosity of the medium. However, we notice that though the temperature and viscosity are changing as per our corner frequency calculations, the trap stiffness remains same throughout our experiments conducted within the temperature range of about 20 K.

SPIE. PHOTONICS

NANOSCIENCE+ ENGINEERING

9548-63, Session 16

Three dimensional living neural networks

Anna M. Linnenberger, Meadowlark Optics, Inc. (United States)

We investigate holographic optical tweezing combined with step-andrepeat maskless projection stereolithography for fine control of 3D position of living cells within a 3D microstructured hydrogel grid. PC12 cells were chosen as a demonstration platform because they can easily differentiate into neuron-like cells, exhibiting properties similar to neurons. PC12 cells are positioned in the monomer solution with optical tweezers at 1064 nm and then are encapsulated by photopolymerization of polyethylene glycol (PEG) hydrogels formed by thiol-ene photo-click chemistry via projection of a 512x512 spatial light modulator (SLM) illuminated at 405 nm. Fabricated samples are incubated in differentiation media containing nerve growth factor such that the PC12 cells cease to replicate and begin to form axon-like structures. By controlling the position and direction of channels between cells within the encapsulating hydrogel structure the formation of the neuron-like circuits is controlled. The samples fabricated with this system are a useful model for future studies of neural circuit formation, neurological disease, cellular communication, plasticity, and repair mechanisms.

9548-64, Session 16

Multi-point optical manipulation and simultaneous imaging of neural circuits through wavefront phase modulation

Samira Aghayee, Dan Winkowski, Patrick Kanold, Wolfgang Losert, Univ. of Maryland, College Park (United States)

The spatial connectivity of neural circuits and the various activity patterns they exert is what forms the brain function. How these patterns link to a certain perception or a behavior is a key question in neuroscience. Recording the activity of neural circuits while manipulating arbitrary neurons leads to answering this question. That is why acquiring a fast and reliable method of stimulation and imaging a population of neurons at a single cell resolution is of great importance. Owing to the recent advancements in calcium imaging and optogenetics, tens to hundreds of neurons in a living system can be imaged and manipulated optically. We describe the adaptation of a multi-point optical method that can be used to address the specific challenges faced in the in-vivo study of neuronal networks in the cerebral cortex. One specific challenge in the cerebral cortex is that the information flows perpendicular to the surface. Therefore, addressing multiple points in a three dimensional space simultaneously is of great interest. Using a liquid crystal spatial light modulator, the wavefront of the input laser beam is modified to produce multiple focal points at different depths of the sample for true multipoint two-photon excitation.

9548-65, Session 16

Trapping and manipulation of bacteria with circular Airy beams

Drew Bischel, Anna S. Bezryadina, Joseph C. Chen, Zhigang Chen, San Francisco State Univ. (United States)



In micromanipulation and optical trapping, rod-shaped objects have a tendency to align along the propagation direction of the beam, which limits simultaneous trapping and observation of the entire cellular structure. We utilize a circular Airy beam (CAB) to optically trap rod-shaped and multi-pronged bacteria in the observation plane and controllably stretch in transverse direction. This is achieved by exploiting the outward transverse acceleration of the autofocusing Airy beam, which acts as a radially outward force along the poles of a bacterium in the sample plane. This beam can be used to trap a multi-pronged bacterium by applying an evenly distributed tunable lateral force to the parts of the cell caught within the adjustable optical ring. We demonstrate that the CAB can be used as a tool to stretch symmetric and asymmetrically mutated S. meliloti cells, as well as bacterial clusters via its radial profile. This approach explores the use of the CAB as a tool for micromanipulation and for studying cellular clustering and aggregation, intercellular interactions, and viscoelasticity of cells with nontrivial morphologies.

9548-66, Session 16

Label-free dynamic optical chromatography for laser analysis of biological samples

Alex V. Terray, U.S. Naval Research Lab. (United States)

Label-free Optical Chromatography is a transformative NRL grown technology that is transitioning to industry. Over the last 12 years, this NRL basic research program has matured from a simple experiment to push a plastic particle with a laser against flow to a fully capable analytical measurement and sorting instrument that measures the subtle optical forces on micron sized particles and cells. This technology has been used to distinguish the optical forces of Bacillus anthracis Sterne spores for biological warfare agent detection and the optical forces of blood components in the body. Recently, we have used this sensitive analysis techniques to identify the host response in macrophage cells exposed to Bacillus anthracis Sterne spores. Through a collaboration with our industry partner LumaCyte, an NRL built prototype sits in UVA's Flow Cytometry Core Facility. Researchers are using it to study cancer, infectious diseases, drug development and more. Because the technology is based on a completely label-free method, the information revealed has the potential to identify previously unknown changes in cells during infection or injury.

9548-67, Session 17

Listening to proteins and viruses with nanoaperture optical tweezers (Invited Paper)

Reuven Gordon, Univ. of Victoria (Canada)

This talk will present a nanoaperture tweezer approach to measure the acoustic spectra of viruses and single proteins. The approach, termed extraordinary optical Raman (EAR), shows promise for uncovering the structure and mechanical properties of nanoparticles as well as the effects of their interactions.

9548-69, Session 17

Characterization of periodic plasmonic nanoring devices for nanomanipulation

Marios Sergides, Viet Giang Truong, James R. Schloss, Bishwajeet S. Bhardwaj, Síle G. Nic Chormaic, Okinawa Institute of Science and Technology Graduate Univ. (Japan)

We study the optical properties of hybrid gold nanodisk and nanohole arrays and present experimental evidence of nanoparticle trapping using

these devices. The fabrication procedure using electron beam lithography (EBL) is also discussed. This hybrid design exhibits a splitting of the resonance modes (low and high energy modes) due to the coupling of the electromagnetic interaction between nanohole and nanodisk plasmons. The devices demonstrate high plasmon resonance tunabilities from the visible to the near-infrared region (NIR) by varying the periodicity, dimension of the disks, and holes of the arrays. This enhancement in the NIR is highly desirable for the purposes of biological sample manipulation where photo damage is low. The characterization of the devices is achieved by excitation using evanescent fields via the Kretschmann configuration. The spectrometric measurements are conducted by monitoring the reflected light at the prism-water interface and the dependency of the plasmon resonance frequency on the incident angle and polarization is investigated. Additionally, these devices consist of grooves connecting the hybrid structures to each other. These regions provide further enhancement of the local electric fields and play the role of the trapping sites. We demonstrate multiple fluorescent dielectric nanoparticle trapping in these grooves. The incident angle and polarization dependency is also considered in the trapping experiments. The results provide good evidence of the potential of this design to be used for the manipulation of biological samples with subdiffraction limit sizes.

9548-70, Session 17

Optical trapping of nanoparticles with significantly reduced laser powers by using counter-propagating beams

Chenglong Zhao, Thomas W. LeBrun, National Institute of Standards and Technology (United States)

Gold nanoparticles (GNP) have wide applications ranging from nanoscale heating to cancer therapy and biological sensing. Optical trapping of GNPs as small as 18 nm has been successfully achieved with laser power as high as 855 mW, but such high powers can damage trapped particles (particularly biological systems) as well heat the fluid, thereby destabilizing the trap.

In this article, we show that counter propagating beams (CPB) can successfully trap GNP with laser powers reduced by a factor of 50 compared to that with a single beam. The trapping position of a GNP inside a counterpropagating trap can be easily modulated by either changing the relative power or position of the two beams. Furthermore, we find that under our conditions while a single-beam most stably traps a single particle, the counter-propagating beam can more easily trap multiple particles. This (CPB) trap is compatible with the feedback control system we recently demonstrated to increase the trapping lifetimes of nanoparticles by more than an order of magnitude. Thus, we believe that the future development of advanced trapping techniques combining counter-propagating traps together with control systems should significantly extend the capabilities of optical manipulation of nanoparticles for prototyping and testing 3D nanodevices and bio-sensing.

9548-71, Session 17

Plasmonic hybridization induced trapping and manipulation of metallic nano-objects

Changjun Min, Shenzhen Univ. (China); Yuquan Zhang, Nankai Univ. (China); Lichao Zhang, Xiaocong Yuan, Shenzhen Univ. (China)

Hybridization in the narrow gaps between the surface plasmon polaritons (SPP) along a metal surface and the localized surface plasmons (LSP) on metallic nano-objects strongly enhance the electromagnetic field. Here, we employ plasmonic hybridization to achieve dynamic trapping and manipulation of metallic nano-objects (particle, nanowire, nanorod, etc.) on a flat metal surface. We first reveal that metallic particles of nanometer to micrometer sizes can be attracted and steadily trapped due to the plasmonic hybridization in a plasmonic tweezers excited by a highly focused radially polarized beam, instead of being repulsed by a conventional optical tweezers due to high scattering force. Next we



demonstrate that trapping and manipulating various metallic nano-objects can be achieved by modifying the property of incident beam. We show that plasmonic hybridization achieved by exciting plasmonic tweezers with a linearly polarized laser beam could induce strong trapping forces and large rotational torques on a single metallic nanowire. The position and orientation of the nanowire could dynamically be controlled by the hybridization-enhanced nonisotropic electric field in the gap. Based on this technique, a plasmonic swallow tail structure is built to demonstrate its potential in the fabrication of lab-on-a-chip plasmonic devices. This work could provide a profound influence on manipulating various metallic nano-objects and have an important contribution to plasmonic lab-on-achip devices for quantum optics, optical characterization, spectroscopy, and sensing applications.

9548-72, Session 17

Aggregation of gold nanorods by optical forces for SERS biosensing in liquid environment

Barbara Fazio, Antonino Foti, Cristiano D'Andrea, Elena Messina, Valentina Villari, Onofrio M. Maragó, Norberto Micali, Istituto per i Processi Chimico-Fisici (Italy); Pietro G. Gucciardi, Consiglio Nazionale delle Ricerche (Italy)

Here we report on a novel concept of label-free, all-optical SERS biosensor for proteins detection in liquid, based on the laser-induced aggregation of gold nanorods (NRs) in proteins buffered solution. Commercial gold NRs dispersed in deionized water and capped with CTAB molecules are mixed with the target proteins dissolved in PBS in a glass microcell. A laser beam is then focused on a micron scale spot inside the liquid solution. Due to radiation pressure, NRs-protein complexes thermally drifting through the laser spot are pushed towards the bottom of the glass microcell. Here they stick and accumulate, forming SERS-active aggregates. BSA has been used as a model protein to test the sensor performances. We reach sensitivities down to 10-7 M, whereas solution phase Raman spectroscopy of BSA is already impossible at concentrations of 10-4 M. This methodology paves the way to a new generation lab-on-chip sensors that implies user-friendly experimental set up allowing for highly sensitive vibrational spectroscopy of biomolecules in their natural habitat.

9548-73, Session 18

Tilted optical trapping of anisotropic single crystal nanorod

Paul Brule-Bareil, Yunlong Sheng, Univ. Laval (Canada)

When a nanorod of typically d=100's nm diameter and h=1-3 micrometers length trapped in the optical tweezers, its orientation is along the trapping beam axis for h/d > 2 and is normal to beam axis for h/d < 2. We report the preliminary experimental observation that some anisotropic single crystal nanorod was stably trapped at a tiled angle to the beam axis. We explain the observation with the T-matrix calculation. In the anisotropic media, as the divergence of is non zero, the conventional vector spherical wave functions (VSWFs) do not individually satisfy the anisotropic vector wave equation. Some new bases, such as the modified VSWFS and qVSWF, have been proposed. Notice that the anisotropic nanorod is floating in the aquatic isotropic medium, we make the VSWF expansions of the incident and scattered fields in terms of , and the VSWF expansion of internal field in the anisotropic nanorod in terms of . Both expansions are therefore legitimate. The boundary condition was chosen as for the normal components of . The internal field is represented as a sum of a set of compoment VSWF expansions to gave better description with more expansion coefficients and to help the convergence of the T-matrix solver. Our calculation showed that when the optical axes of an anisotropic nanorod are not aligned to the nanorod axis, the nanorod may be trapped at a tilted angle position where the lateral torque is zero and its derivative is negative.

9548-74, Session 18

Studies on shape anisotropy in red blood cells

Argha Mondal, Basudev Roy, Sudipta Bera, Ayan Banerjee, Indian Institute of Science Education and Research Kolkata (India)

Red blood cells often demonstrate rotational motion (spin) inside optical tweezers - a phenomenon that has been attributed to both shape anisotropy and form birefringence induced due to the asymmetric shape, resulting in a degree of ambiguity about the cause of such rotation. We show by numerical simulations for a structure similar to RBCs' having large shape anisotropy, that the torque resulting from an imbalance in scattering forces due to shape anisotropy is almost an order of magnitude higher than that due to form birefringence. We also measure the entire Mueller Matrix for a trapped RBC and observe that the measured retardance due to form birefringence is similar to that numerically obtained in our model. In addition, we probe an important signature of shape anisotropy - that of a coupling between translational and rotational motion under the action of the trapping force. We introduce a coupling term as a measure of the shape anisotropy in the coupled Langevin equations, and numerically demonstrate that the cross correlation would indeed depend significantly on the value of the coupling term. We verify this experimentally by measuring the translational and rotational Brownian motion simultaneously using a quadrant photodiode. By trapping single RBCs' of different degrees of shape anisotropy, we demonstrate that the cross-correlation is indeed dependent on the shape anisotropy and fits very well to the solution obtained for the coupled Langevin equation numerically. Indeed, this could be a general technique to determine the presence of any anisotropy in trapped objects.

9548-76, Session PWed

Low frequency dynamical stabilisation in optical tweezers

Christopher J. Richards, Thomas J. Smart, Univ. College London (United Kingdom); David Cubero, Univ. de Sevilla (Spain); Philip H. Jones, Univ. College London (United Kingdom)

It is well known that a rigid pendulum with minimal friction will occupy a stable equilibrium position vertically upwards when its suspension point is oscillated at high frequency. The phenomenon of the inverted pendulum was explained by Kapitza by invoking a separation of timescales between the high frequency modulation and the much lower frequency pendulum motion, resulting in an effective potential with a minimum in the inverted position.

We present here a study of an optical analogue of Kapitza's pendulum that operates in different regimes of both friction and driving frequency. The pendulum is realised using a microscopic particle held in a scanning optical tweezers and subject to a viscous drag force. The motion of the optical pendulum is recorded and analysed by digital video microscopy and particle tracking to extract the trajectory and stable orientation of the particle. In these experiments we enter the regime of low driving frequency, where the period of driving is comparable to, or greater than the characteristic relaxation time of the radial motion of the pendulum with finite stiffness.

In this regime we find stabilisation of the pendulum at angles other than the vertical (downwards) is possible for modulation amplitudes exceeding a threshold value where, unlike the truly high frequency case studied previously, both the threshold amplitude and equilibrium position are found to be functions of friction. Experimental results are complemented by analytical theory and Brownian motion simulations.



9548-77, Session PWed

Laser trapping and assembling of nanoparticles at solution surface studied by reflection micro-spectroscopy

Shun-Fa Wang, Ken-ichi Yuyama, National Chiao Tung Univ. (Taiwan); Teruki Sugiyama, National Applied Research Labs. (Taiwan); Hiroshi Masuhara, National Chiao Tung Univ. (Taiwan)

Nanometer-sized objects like nanoparticles, polymers, and amino acids can be confined in the focal volume by conventional laser trapping in solution. Interestingly, the trapping behavior at a solution surface is different from that inside the solution, namely we have demonstrated laser trappinginduced crystallization of amino acids at a solution surface. In this paper, we present laser trapping dynamics of 200 nm polystyrene nanoparticles at a solution surface studied by reflection micro-spectroscopy. When a CW laser beam of 1064 nm was focused into a surface layer of the colloidal D2O solution through an objective lens (60 magnification, NA = 0.9), nanoparticle were gathered at and around the focal spot, and eventually a nanoparticle assembly with a size much larger than the focal volume was formed. The resultant assembly showed structural color in transmission and backscattering images, meaning that constituent nanoparticles are periodically packed in the assembly. The reflection micro-spectroscopy revealed that the nanoparticle assembly has a reflection band in visible region and the peak position is shifted to shorter wavelength with the narrowing of band width during the assembly growth. This result indicates that the nanoparticle packing structure in the assembly becomes homogeneous with the decrease in inter-particle distance under the laser irradiation. Turing off the laser led to the diffusion of constituent nanoparticles, meaning that the assembly is temporarily formed under dynamic force balance between optical trapping and inter-particle force. Reflection spectra of the nanoparticle assembly were measured under various laser trapping conditions, and we discuss the trapping and assembly dynamics of nanoparticles based on the spectral change.

9548-79, Session PWed

Magnon-like properties of spin-3/2 chains

Jhon James J. Hernández Sarria Sr., Univ. del Valle (Colombia) and Ctr. for Bioinformatics and Photonics (Colombia); Karem Cecilia C. Rodríguez Ramírez, Univ. del Valle (Colombia)

Ultracold gases is optical lattices constitute an extraordinary tool for the analysis of strongly-correlated gases under extremely well-controlled condition. In this work, we study the magnon-like properties of repulsively interacting spin-3/2 fermions in one-dimensional optical lattices. For large-enough interactions, the system enters into the Mott-insulator regime with maximally one fermion per site.

We perform the Holstein-Primakoff transformation to the fermionic system. This is a useful technique based on the expansion of the spin operators in terms of the creation and annihilation operators of the harmonic oscillator, i.e. magnon-like position-operators. In this way, we obtain a spinless bosons system described by an extended Bose-Hubbard model with a hole-like lowest band. The magnon-like model involves single, pair and correlated nearest neighbors hopping terms beside the on-site and nearest neighbor interactions.

The magnetic phases present in the Mott-insulator of the spin-3/2 lattice fermions namely the gapless spin liquid and the gapped spin Peierls quantum phases, previously studied, are analyzed in the mirror frame of their bosonic counterpart. Since the transformation is not linear and the coupling between the oscillators has important consequences for many properties of ordered systems, we perform the ground-state characterization as a function of the spin-changing collision strength including the calculation of several observables such as the magnetization and spin-spin and dimer-dimer correlations in the magnon-like frame-work.

This kind of work pave the path of revealing magnetic phases signatures in

the state-of-the-art spinless boson experiments. The many-body numerical calculations are performed using the Matrix Product State formalism.

9548-80, Session PWed

Correlated fluctuations of optically trapped particles

Thomas J. Smart, Christopher J. Richards, Univ. College London (United Kingdom); Xian Han, National Univ. of Defense Technology (China); Stefan Siwiak-Jaszek, Philip H. Jones, Univ. College London (United Kingdom)

We present a study of correlated Brownian fluctuations between optically confined particles in a number of different configurations. First we study colloidal particles held in separate optical tweezers. In this configuration the particles are known to interact through their hydrodynamic coupling, leading to a pronounced anti-correlation in their position fluctuations at short times. We study this system and the behaviour of the correlated motion when the trapped particles are subject to an external force such as viscous drag. The experiments are complemented by Brownian motion simulations.

The second system considered is a chain of optically bound particles in an evanescent wave surface trap. In this configuration the particles interact both through hydrodynamic and optical coupling. Using digital video microscopy and subsequent particle tracking analysis we study the thermal motion of the chain and map the variation in fluctuation correlation amplitude between pairs of particles. We further analyse the dynamics by constructing the normal modes of the particle chain, extracting the mode amplitudes and autocorrelation decay times.

Finally we examine the potential of these systems for probing fluctuation theorems of thermodynamics when applied to systems of coupled or interacting particles. In these systems with well-controlled coupling of a well-defined number of particles we calculate the distribution of the dissipation function (entropy production) in the system when one particle is subject to an external driving force.

9548-81, Session PWed

Three-dimensional thermal noise imaging of collagen networks

Tobias F. Bartsch, The Rockefeller Univ. (United States); Martin D. Kochanczyk, Emanuel N. Lissek, The Univ. of Texas at Austin (United States); Janina Lange, Friedrich-Alexander-Univ. Erlangen-Nürnberg (Germany); Ernst-Ludwig Florin, The Univ. of Texas at Austin (United States)

Extracellular biopolymer networks show interesting mechanical properties that are essential for living organisms. In particular, a highly nonlinear elastic response to strain is seen, which gives biopolymer networks the ability to comply with small stresses but resist to large ones. The macroscopic mechanical properties have their origin in the properties of the individual filaments and the properties of the network that they form, like cross-linking geometry and pore size distribution. While the macroscopic properties of biopolymer networks have been extensively studied, there has been a lack of experimental techniques that can simultaneously determine mechanical and architectural properties of the network in situ with single filament resolution. Thermal Noise Imaging (TNI) is a novel scanning probe technique that utilizes the confined thermal motion of an optically trapped particle as a three-dimensional, noninvasive scanner for soft, biological material. It achieves nanometer precision in probe position detection with MHz bandwidth. Using feedback control we have recorded thermal noise images on the micrometer scale inside a collagen I network for the first time, extracting quantitative information about cross-linking geometry and network architecture from the data. We are also able to quantify filament fluctuations by monitoring the forward scattered light from the collagen network structure. We find that the transverse fibril fluctuations are negligible compared to their diameter, and cannot account for strain



stiffening behavior. This is in agreement with recent models of stiff filament networks and points towards elastic deformations and structural changes as the origin of the nonlinear response to force. Thermal Noise imaging will allow us to study network deformations and force distribution on the single filament level under local and global stresses.

9548-82, Session PWed

A study of red blood cell deformability in diabetic retinopathy using optical tweezers

Thomas J. Smart, Christopher J. Richards, Rhythm Bhatnagar, Univ. College London (United Kingdom); Carlos Pavesio, Moorfields Eye Hospital NHS Foundation Trust (United Kingdom) and Univ. College London (United Kingdom); Philip H. Jones, Univ. College London (United Kingdom); Rupesh Agrawal, Moorfields Eye Hospital NHS Foundation Trust (United Kingdom) and Univ. College London (United Kingdom) and Tan Tock Seng Hospital (Singapore)

Red blood cells (RBCs) possess an ability to undergo significant cellular deformation, allowing them to pass through capillaries in the human microcirculation system whose diameters are smaller than their own. There is evidence that diabetes mellitus impairs RBC deformability and it has been suggested that this may be part of the cause of microangiopathy. A common complication of diabetes mellitus, microangiopathy is a disease that can cause capillaries to bleed, leak protein and slow the flow of blood. In the eye, this may lead to diabetic retinopathy - microangiopathy in the retina caused by high blood sugar levels, which can cause blindness.

Here we present an investigation into the deformability of RBCs in patients with diabetic retinopathy using optical tweezers. We compare the deformability with those of RBCs in healthy patients as well as to those with other retinal vascular disorders: Behcet's disease and birdshot chorioretinopathy.

To extract a value for the deformability of RBCs we use a dual-trap optical tweezers set-up to stretch individual RBCs. RBCs are trapped directly (i.e. without micro-bead handles), so rotate to assume a 'side-on' orientation. Video microscopy is used to record the deformation events and shape analysis software is used to determine parameters such as maximum RBC length. 3D imaging of individual RBCs is also performed using defocusing microscopy to ascertain the radius, volume, surface area and sphericity index to test the hypothesis that it is increased volume and sphericity index of RBCs that leads to the decreased deformability of the pathological cells.

9548-83, Session PWed

Absortion model of different fluids in an optical fiber trap using CFD

Jenny Emmanuelle Hernández Zavala, Univ. Veracruzana (Mexico); Hector H. Cerecedo, Univ. Autonoma Veracruzana (Mexico)

It is important to determine the heat absorption of a fluid where a microparticle is merge in an optical fiber trap and to be capable to predict the impact in the particle movement. In this sense, this document presents a first approach to study the thermal behavior of an initially static fluid radiated by infrared light (980nm, 100mW) transmitted by a single-mode optical fiber, for this simulation temperature and radiation pressure are calculated based on the intensity delivered by a laser diode.

With the help of Computing Fluid Dynamics (CFD) it is possible to study the absorption of heat of a specific fluid due to thermal radiation. Experiments show that as the particle moves along the axis, temperature decreases, having the points of mayor temperature around the axis, with a different thermal spectrum depending on the substance and heat model used.

9548-84, Session PWed

Noticeable nonlinear optical effect in plasmon-assisted radiation force

Masayuki Hoshina, Osaka Prefecture Univ. (Jordan); Nobuhiko Yokoshi, Hajime Ishihara, Osaka Prefecture Univ. (Japan)

For the optical manipulation of nanoparticles, the light of extremely high intensity is required in order to gain the radiation force overwhelming the effects of fluctuating environment. One of the ways to produce such a high intensity field is to utilize localized surface plasmons (LSP) induced on the metallic nanostructures [1]. Although there exist many works to investigate and demonstrate the LSP-assisted optical manipulation [2], theoretical analyses have been limited within the linear response theory. However, the recent works of our group have revealed essential roles of optical nonlinearity in resonant molecular trapping by the conventional method [3]. Thus, considering the great enhancement of the field intensity by LSP, a theoretical method incorporating the optical nonlinearity is also desired for the system including arbitrary-shaped metallic structures.

In this work, we develop a new calculation method for the LSP-assisted optical manipulation based on the quantum master equation combined with the discrete dipole approximation method. This method enables us to investigate the radiation force including the strong nonlinear optical effect such as absorption saturation of the excited states. Our demonstration reveals that the consideration of optical nonlinearity leads to significantly different behavior of molecules near the resonant region even for the incident intensity around a few kW/cm2.

S. Zhang, K. Bao, et al, Nano Lett. 11, 1657 (2011). [2] M. L. Juan, M. Righini, and R. Quidant: Nature. Photon. 5 349 (2011). [3] T. Kudo and H. Ishihara, Phys. Rev. Lett. 109, 087402 (2012), Phys. Chem. Chem. Phys. 15, 14595 (2013).

9548-85, Session PWed

Three-dimensional trapping with a focused Bessel beam

Yareni Ayala, Karen P. Volke-Sepúlveda, Alejandro V. Arzola, Univ. Nacional Autónoma de México (Mexico)

A Bessel beam generated with an axicon lens is focused by a low numerical aperture objective lens to create an optical levitation trap. This configuration allows a full three dimensional trapping of solid glass spheres of few microns in diameter immerse in water. We establish a comparison with an optical levitation trap generated with a Gaussian beam under the same focusing conditions. In both cases the particles are lifted up in an axial position above the focal region that depends on the incident power. The spatial stability is investigated in both cases as a function of axial position, which in turn depends on the input optical power.

9548-86, Session PWed

Non-radially symmetric dark-hollow optical beams for manipulation elongated microobjects

Aleksey P. Porfirev, Samara State Aerospace Univ. (Russian Federation); Roman V. Skidanov, Image Processing Systems Institute (Russian Federation)

We theoretically and experimentally investigate shaping of non-radially symmetric dark-hollow optical beams (DHOBs) generated by superimposed non-coaxial Bessel beams. Transverse dimensions of the traps can be changed by varying a number of Bessel beams. Thus it is possible to adjust the size of the trap to the size of the captured objects. We used scalar theory diffraction to theoretically investigate shaping of DHOBs. Also the generation of non-radially symmetric DHOBs, especially by using the



laser radiation with different wavelengths (from 400 to 1000 microns), is experimentally investigated. In this experiments, we used EKSPLA NT200 series tunable laser systems (output wavelength range from 335 nm to 12 000 nm, Lithuania). We used diffractive optical elements and a spatial light modulator PLUTO VIS (Holoeye Pluto-Vis, Germany) to demonstrate experimentally the generation of DHOBs. Dynamically forming by a spatial light modulator non-radially symmetric DHOBs can create a device to manipulate elongated microobjects. Trapping of non-spherical particles is essential for microassembling and driving microstructures in optofluidic systems and for manipulating of biological microobjects, that are mostly non-spherical.

9548-87, Session PWed

Creation of three-dimensional volume chain under high numerical aperture illumination

Jiming Wang, Nanjing Univ. of Aeronautics and Astronautics (China)

Recently, the beams with unconventional polarization states have attracted increasing interests in their generation, manipulation, and focusing. The polarizations of this vector beams are spatially inhomogeneous in the transverse cross-section. Generalized vector beams can be obtained through engineering the phase, polarization and amplitude of the incoming beams. For their unique properties, the beams meet potential applications in many fields. As a new way to explore phenomenon and physics on nano-scale, the focused field with desired intensity shaping and polarization structuring in the focal volume has been investigated in a high-numerical-aperture (NA) imaging system. In this paper, we attempt to construct a focused field with a shape of complex chain. Here the three-dimensional uniform optical chain consists of arrayed bubbles with high radial barrier and quasi-periodic location. Except for this bubbles array along the optical axis, the dark fields exist in the focused field. In the rz plane, the focused field presents a volume feature of chain, so-called volume chain. Ten holes appear and six of them exist beside the z-axis at r=0.42?. The six formed holes is located at the cross section of the dark fields at r=0.42? and the other four arrange along z-axis at r=0. This focused field as a tool can provide effective optical manipulation. Optical bubbles generated by the vectorial beam have the trapping capability of the low-refractive-index particles. The constructed optical chain may be used as an effective tool for multiple particles trapping, delivering and self-assembling.

9548-88, Session PWed

Single-shot multiphoton fabrication of polygonized structures by a novel fresnel zone lens via spatial light modulator

Chenchu Zhang, Dong Wu, Yanlei Hu, Jiawen Li, Zhaoxin Lao, Bin Xu, Jiaru Chu, Wenhao Huang, Univ. of Science and Technology of China (China)

Recently, annular beams has been developed to rapidly fabricate microscope tubular structures via two-photon polymerization, but the distribution of light field is limited to ring pattern. Here a novel Fresnel lens is designed and applied to modulate the light field into a uniform quadrangle or hexagon shape with controllable diameters. By applying spatial light modulator to load the phase information of Fresnel lens, quadrangle and hexagon structures are achieved through single exposure of a femtosecond laser. A 3?6 array of structures is made within 9 seconds. Comparing with the conventional holographic processing, this method shows higher uniformity, high efficiency, better flexibility, and easy-operation. The novel approach exhibited the promising prospect in rapidly fabricating structures such as tissue engineering scaffolds and various shape tubular arrays.

9548-89, Session PWed

Analysis of the phage lambda DNA packaging motor by optical tweezers measurements and site-directed mutagenesis of residues involved in ATP binding

Mariam Ordyan, Damian J. Deltoro, Douglas E. Smith, Univ. of California, San Diego (United States)

We use optical tweezers to measure molecular-motor driven packaging of single DNA molecules into single viral proheads. Analysis of the sequence of the lambda gpA motor protein suggests it contains a "Walker A"-like ATP binding region spanning amino acids K76 to S83 that is essential for motor function. Systematic alteration of the amino acids in this region by genetic mutations causes moderate to nearly complete impairment of viral replicationOptical tweezers measurements of mutants exhibiting moderate impairment in viral productionreveal clear impairments in DNA translocation in every case. We characterize the impairments by determining motor velocity distributions from ensembles of single-molecule packaging events. Our findings support the hypothesis that this region corresponds to a Walker A motif and shed light on the relative importance of different amino acids within this region for DNA translocation. Relationships between the functional roles and positions of specific amino acids in the protein structure are explored via the use of a structural model based on homology with other ATP binding proteins.

9548-90, Session PWed

Single-molecule mechanics of the molecular spring that underlies hearing

Tobias F. Bartsch, Albert J. Hudpeth, The Rockefeller Univ. (United States)

The astounding sensitivity, frequency selectivity, and dynamic range of mammalian hearing result from the ear's sensory receptors, the hair cells of the inner ear. Atop each hair cell stands a hair bundle, a cluster of stiff stereocilia, whose deflection causes mechanically gated ion channels to open. One candidate for the mechanical element that converts bundle deflection to a force capable of opening the channels is the tip link, a biopolymer of cadherin molecules that connects pairs of adjacent stereocilia. The link's elasticity results both from the extensibility of individual cadherin domains, which was recently explored by molecular-dynamics simulations, and from the rearrangement of the domains relative to each other, which is stabilized by Ca2+ binding and remains unexplored.

We show that the elasticity of the tip link's constituents can be measured in the physiologically relevant low-force regime by a single-molecule experiment with a custom-built photonic force microscope. In our assay thermal forces are exploited to sample the proteins' energy landscapes. A single protein molecule is positioned between a fixed glass substrate and a probe nanoparticle held in a weak optical trap. The three-dimensional spatial probability distribution of the probe's thermal motion is measured with nanometer precision and megahertz bandwidth by interfering on a quadrant-photodiode the unscattered trapping beam with light scattered forward by the probe. The protein's energy landscape can be computed directly from the measured spatial probability distribution.

We next intend to investigate the effects on the proteins' energy landscapes, and thus on their mechanical properties, of varying the Ca2+ concentration and of pathologically relevant mutations.

Conference 9549: Physical Chemistry of Interfaces and Nanomaterials XIV



Part of Proceedings of SPIE Vol. 9549 Physical Chemistry of Interfaces and Nanomaterials XIV

9549-1, Session 1

Interface design principles for high efficiency organic semiconductor devices (Invited Paper)

Adiitya D. Mohite, Los Alamos National Lab. (United States)

Present day electronic devices are enabled by design and implementation of precise interfaces that control the flow of charge carriers. However, unlike the well-controlled interfaces in conventional electronics based on silicon and other inorganic materials, organic semiconductor interfaces are relatively poorly characterized and understood. Here, we describe how precise manipulation and control of organic-organic interfaces using interface modification strategies can overcome a long-standing bottleneck of interface recombination at the donor-acceptor interface in an organic photovoltaic device. These strategies lead to a dramatic increase in the average power conversion efficiency by 2-5 times in a model bilayer system and when applied to practical architectures like the bulk heterojunction result in a dramatic increase in the overall efficiency from 4.1% to ~8.0 %. Moreover, these interface strategies are applicable to a wide variety of donor-acceptor systems,, making them both fundamentally interesting and technologically relevant for achieving high efficiency organic electronic devices

In addition, I will also briefly describe our most recent work on organicinorganic perovskite solar cells. We have developed a new solutionbased hot-casting technique to grow continuous, pin-hole free thin-films of organometallic perovskites with millimeter-scale crystalline grains. Photovoltaic devices show hysteresis-free response, which had been a fundamental bottleneck for stable operation of perovskite devices. Characterization and modeling attribute the improved performance to reduced bulk defects and improved charge-carrier mobility in large-grain devices.

9549-3, Session 1

In situ transient optical studies of bulk and interfacial recombination processes in nanostructured photocatalytic materials

(Invited Paper)

Matthew Y. Sfeir, Kannatassen Appavoo, Mingzhao Liu, Brookhaven National Lab. (United States)

Generating hydrogen-fuel by photoelectrochemical (PEC) water splitting is a promising renewable energy technology and also a complex and fascinating mesoscale science problem. Efficient photocatalytic water splitting requires both a high quantum yield for transport of charge carriers to the reactive interface (occurring on ps timescales) and for charge transfer (occurring on ns and longer time scales). Using in situ ultrafast optical methods, we have developed an experimental framework to separately measure recombination losses during charge separation and interfacial charge transfer in nanostructured semiconductor photocatalysts. This approach allows us to quantify and understand the origins of differences in performance between different materials through concurrent electrical characterization and in situ optical studies carried out in a customized PEC cell. Using a transient emission technique with sub-ps resolution, we preferentially probes the photogenerated excitons and directly monitor parasitic recombination processes that occur on timescales shorter than interfacial charge transfer. Performing these measurements at various applied potential, we tune the depletion region to direct the flow of photogenerated minority carriers and to correlate the measured carrier dynamics to the electrical properties of the photoelectrochemical device. Losses occurring on picosecond timescales are found to represent a major loss channel in heavily doped nanostructured photocatalytic materials, even when the size of the nanostructure is below

its carrier diffusion length. Furthermore, this approach allows us to evaluate the role of ultrathin (~ 1 nm) surface layers, which, in our model system, provides enhanced chemical activity in addition to reducing corrosion.

OPTICS+ PHOTONICS NANOSCIENCE+

ENGINEERING

9549-4, Session 1

Avoding the kinetics of the bulk heterojunction: self-assembled materials and sequential processing for organic photovoltaics (Invited Paper)

Benjamin Schwartz, Univ. of California, Los Angeles (United States)

One of the key issues with improving the efficiency of conjugated polymerbased phovoltaics is controlling the nm-scale morphology of the two active components. Typically, efficiency is optimized by trial-and-error: component weight ratios, solvent additives, post-processing thermal annealing, etc. are all used to attempt to obtain the desired bulk heterojunction (BHJ) interpenetrating network. In this talk, we discuss some of our recent work aimed at using alternate, more reproducible methods for controlling BHJ morphology. We present results showing new amphiphilic semiconducting polymers and fullerenes that spontaneously selfassembly into co-axial cylindrical micelles in solution, and thus provide a built-in connected network when cast into gels that form thin films. Photoexcitation of the polymer in these systems produces separated charges on sub-ps time scales, and the separated charges are stable for weeks to months in air-free environments. The stability of the charge-separated pair can be controlled by changing the gel morphology. We also show that sequential processing of the polymer and fullerene components can provide an exquisite degree of control of the nm-scale morphology of a BHJ, and that the degree of crystallinity of the polymer controls both the amount of intercalated fullerene and the geometry of the interpenetrating network.

9549-5, Session 2

Interfacial considerations in organo-halide perovskite optoelectronics (Invited Paper)

Paul Meredith, Qianqian Lin, Ardalan Armin, Dani Lyons, Ravi Nagiri, Paul L. Burn, The Univ. of Queensland (Australia)

The organo-halides perovskites have recently emerged as one of the leading candidates for low cost, next generation thin film photovoltaics [1]. The working principles of CH3NH3Pbl3-based homojunction solar cells were recently disclosed by Lin et al. [2] who proposed the material to be non-excitonic with high static dielectric constant. Lin et al. also discussed the origin of the cell Voc, suggesting that it arises directly from the difference in work functions between the anode and cathode consistent with minimal chemical potential loss across the perovskite homojunction. In this regard the interface between the active layer and both electrodes is critical, and this was demonstrated using a range of semiconducting polymers to modify the anode electronics.

In our paper we will discuss these interfacial considerations, and also highlight the differences between solution processed and evaporated perovskites on various work function modified anodes. In principle, the cell Voc could be optimised by increasing the electrode work function difference, but in practise this is very difficult due to surface energy considerations which control the morphology and quality of the subsequent perovskite active layer. These principles are not only relevant to solar cells but organo-halide perovskite optoelectronics in general.

[1] Liu et al., Nature 501, 395-398 (2013).

[2] Lin, et al., Nature Photonics, DOI:10.1038/NPHOTON.2014.284 (2014).



9549-6, Session 2

Investigation on the initial photophysics in hybrid perovskite-polymer solar cells

Jan C. Brauer, Univ. de Fribourg (Switzerland); Arianna Marchioro, Univ. of Washington (United States); Yong Hui Lee, Mohammad K. Nazeeruddin, Jacques-Edouard Moser, Ecole Polytechnique Fédérale de Lausanne (Switzerland); Natalie Banerji, Univ. de Fribourg (Switzerland)

Perovskite solar cells based on alkali-metal halides represent an emerging photovoltaic technology that has attracted a lot of attention in the scientific community due to an incredible increase in efficiency over the last years starting from 3-4 % in 2009 to a certified efficiency over 20% in 2015. These performances rivaling the best thin-film photovoltaic devices in combination with their ease of fabrication present a major breakthrough in the quest for renewable energy devices. A variety of cell architecture including the use of a mesopourous TiO2 or Al2O3 scaffolds, planar TiO2/ perovskite heterojunctions as well as architectures using purely organic charge transport layers sandwiching the central perovskite layer have been investigated in literature. While a lot of effort has been invested in order to improve device performance, the fundamental understanding of the involved mechanisms and material-properties is lagging behind.

In this work we investigate the early photophysics of hybrid perovskitepolymer solar cells by means of ultrafast transient absorption spectroscopy and THz spectroscopy. We were particularly interested in the charge transfer reactions at the perovskite-TiO2 and perovskite-polymer interfaces since theses reactions are crucial for the proper functioning of the cell. In this regards we investigated the influence of the choice of the organic holeconductor with respect to the early time dynamics of the charge transfer reaction as well as the quenching efficiency in comparison to the standard organic hole-conductor spiro-MeOTAD.

9549-7, Session 2

Mapping the electrical properties of methylammonium lead triodide perovskite films using conductive tip atomic force microscopy for photovoltaic applications

James G. Stanfill, R. Clayton Shallcross, Neal R. Armstrong, The Univ. of Arizona (United States)

This paper focuses on our recent studies of the mapping of the electrical properties of ultrathin methylammonium lead triodide (MAPbI3) perovskite (PVSK) films on bare and chemically modified metal oxide surfaces through conductive tip atom force microscopy (cAFM). Despite the impressive growth in PV efficiencies using PVSK active layers, we hypothesize that the charge harvesting efficiencies in fully optimized PV platforms using these active layers, especially those obtained by massively scalable processing approaches, will be dependent upon PVSK crystal morphologies, orientations, and energetic heterogeneity in ways that can be uniquely probed by cAFM. Our approach has been to control nucleation free energy of either the stoichiometric PVSK film (direct deposition), or the PbI2 precursor (two-step deposition) using surface modifiers which vary in polarity and functional groups that might incorporate into the PbI2 or PVSK during the initial 1-2 nm of film growth. Correlations will be shown between differences in crystalline morphology, which low-index faces are exposed, and the long range order in the PVSK lattice, with dark J/V behavior, on substrates and with cAFM tips designed to produce either rectifying behavior or a purely ohmic contact. These dark electrical properties are correlated with band edge energetics and density-of-states observed above the valence band edge, out to the Fermi energy, obtained with high sensitivity UV-photoemission spectroscopies and finally to differences in PV device performance.

9549-8, Session 2

Induction of photocurrent by the hole transporting layer to adjacent photoactive perovskite sensitized TiO2 thin film for the solar cell application

Sadia Ameen, Mohammed Nazim, Hyung-Kee Seo, Hyung-Shik Shin, Chonbuk National Univ. (Korea, Republic of)

The high performance perovskite solar cell is fabricated using unique and well-defined morphology of polyaniline nanoparticles (PANI-NPs) as efficient hole transporting layer (HTL) with methyl ammonium lead iodide perovskite (CH3NH3PbI3) as sensitizer to fabricate the high performance perovskite solar cell. PANI NPs are simply synthesized by the oxidative chemical polymerization of aniline monomer at 0-5 oC. The reasonable solar-to-electricity conversion efficiency of ~6.29 % with high short circuit current (JSC) of ~17.97 mA/cm2 and open circuit voltage (VOC) of ~0.877 V are accomplished by Ag/PANI-NPs/CH3NH3PbI3/mp-TiO2/bl-TiO2/FTO perovskite solar cell. The IPCE measurement reveals that the fabricated Ag/ PANI-NPs/CH3NH3PbI3/mp-TiO2/bl-TiO2/FTO perovskite solar cell presents the maximum value of ~51% in the wavelength range of ~450-700 nm and drops at longer wavelengths. The transient photocurrent and photovoltage studies reveal that the fabricated solar cell shows better charge transport time, diffusion coefficient, diffusion length and the charge collection efficiency. Herein, the use of PANI NPs as HTL improves the charge carrier generation and the charge collection efficiency of the fabricated solar cell.

9549-9, Session 3

Linking molecular features of conjugated polymers, acceptors, and additives to the blend morphology for organic electronics applications (*Invited Paper*)

Arthi Jayaraman, Univ. of Delaware (United States)

Organic solar cells consist of an active layer made of an electron donating species (e.g. conjugated polymer) and an electron accepting species (e.g. fullerene derivative). The efficiency of a solar cell is dependent on the spatial organization or morphology of the donor and acceptor materials. The donor-acceptor blend morphology is dependent on the chemistry and architecture of the conjugated polymer and its interactions with the acceptor material (fullerene derivatives), and other additive material. This talk will present our recent work using theory and simulation techniques to connect molecular features of polymers and nanoscale additives to the blend/composite morphology, thereby guiding synthesis of new materials for organic photovoltaic applications.

9549-10, Session 3

Describing and quantifying tightly packed molecular aggregate properties using innovative electronic structure methods (Invited Paper)

Clémence Corminboeuf, Ecole Polytechnique Fédérale de Lausanne (Switzerland)

Improving the performance of organic materials (e.g., charge-carrier mobility in field-effect transistors) relies upon the adjustment of the ϖ -conjugated molecules or chains at the molecular level. A relevant and efficient strategy consists in fine-tuning specific non-covalent interactions, which dictate the lateral displacements, intermolecular distances and relative orientation of the ϖ -conjugated moleties. The use of efficient computational schemes can be very useful to identify promising structural patterns and analyze their electronic structure properties. This talk will discuss novel electronic structure approaches capable of modeling and

Conference 9549: Physical Chemistry of Interfaces and Nanomaterials XIV



analyzing the structures, energies and properties of molecular assemblies relevant to the field of organic electronics. Special emphasis will be placed on molecular architectures designed to feature unusually close ϖ -stacking interactions. The proposed electronic structure approaches will range from the DORI (i.e., density overlap region indicator) molecular descriptor capable of visualizing and comparing the "electronic compactness" of quatertiophene-based crystals and up to recently introduced density functional-based schemes aiming at improving the electronic structure description of large-sale systems and overcoming the obvious failures of standard DFT methods. In this context, we will also address lingering difficulties associated with the accurate description of ground and excited state properties of molecular aggregates using standard density functionals and post-Hartree-Fock approaches.

9549-11, Session 3

Diffusion, recombination, and photon emission properties of interacting excitons in semiconductor carbon nanotubes

(Invited Paper)

Andrei Piryatinski, Los Alamos National Lab. (United States); David H. Dunlap, The Univ. of New Mexico (United States); Oleksiy Roslyak, Fordham Univ. (United States); Han Htoon, Los Alamos National Lab. (United States)

Semiconductor single-walled carbon nanotubes (SWCNTs) are near-perfect 1D materials with great potential for applications in opto-electronic and photonic devices. Their unique optical properties are determined by highly mobile interacting excitons. Motivated by recent experimental studies, we examine competition between exciton diffusion dynamics and their local interactions resulting in the exciton-exciton annihilation (EEA). Treating the EEA as the exciton coalescence reaction, we propose a mean field model based on non-linear diffusion equation for exciton density with generalized time-dependent EEA coefficient. This model interpolates between shorttime Auger recombination and long-time diffusion-limited recombination dynamics. While exciton key model parameters such as diffusion and Auger recombination constants are physically independent quantity, we demonstrate that environment disorder perturbing the exciton energy landscape gives rise to their correlation. Our model based simulations reveal important dependence of the exciton emission profile on exciton population prepared by optical pule. These results are rationalized by partitioning exciton density into spatial diffusion length segments that are identify as independent guantum emitters. This coarse-grained model is further applied to interpret the photon counting statistics available from 2nd order photon correlation measurements. Provided exciton density is prepared on the scale larger than exciton diffusion length (i.e., case of multiple independent emitters), our calculations show strong photon bunching. Reduction of the exciton density spread to the diffusion lengthscale causes photon antibunching whose degree is limited by the strength of the EEA processes. These findings have strong implications toward development of SWCNTbased room-temperature single photon sources.

9549-12, Session 3

Impact of mesoscale order on open-circuit voltage in organic solar cells

Carl Poelking, Max-Planck-Institut für Polymerforschung (Germany); Max L. Tietze, Chris Elschner, Technische Univ. Dresden (Germany); Selina Olthof, Dirk Hertel, Univ. zu Köln (Germany); Björn Baumeier, Max-Planck-Institut für Polymerforschung (Germany); Frank Würthner, Julius-Maximilians-Univ. Würzburg (Germany); Klaus Meerholz, Univ. zu Köln (Germany); Karl Leo, Technische Univ. Dresden (Germany); Denis Andrienko, Max-Planck-Institut für Polymerforschung (Germany) Structural order in organic solar cells is paramount: it reduces energetic disorder, boosts charge and exciton mobilities, and assists exciton splitting. Owing to spatial localization of electronic states, microscopic descriptions of photovoltaic processes tend to overlook the influence of structural features at the mesoscale. Long-range electrostatic interactions nevertheless probe this ordering, making local properties depend on the mesoscopic order. Using a technique developed to address spatially aperiodic excitations in thin films and in bulk, we show how inclusion of mesoscale order resolves the controversy between experimental and theoretical results for the energy-level profile and alignment in a variety of photovoltaic systems, with direct experimental validation. Optimal use of long-range ordering also rationalizes the acceptor-doner-acceptor paradigm for molecular design of donor dyes. We predict open-circuit voltages of planar heterojunction solar cells in excellent agreement with experimental data, based only on crystal structures and interfacial orientation.

Reference: Nature Materials, (2014) doi:10.1038/nmat4167

9549-13, Session 3

Modeling electric field-induced quenching in conjugated polymers and oligomers

Christian M. Legaspi, Linda A. Peteanu, David J. Yaron, Carnegie Mellon Univ. (United States)

The phenomenon of electric field-induced emission guenching is important in organic light-emitting diodes which require the application of large electric fields for their function. Past experimental work on light-emitting polymers and oligomers showed that field-induced quenching (FIQ) efficiencies are higher in non-rigid molecules such as poly(p-phenylene vinylene) or PPV, than in similar, more planar molecules.(ref 1) Based on this relationship, we proposed that the applied field enhances internal conversion decay channels.(refs 2,3) The current study builds on this idea by examining FIQ in PPV oligomers of varying length using computational methods. Calculations performed at the INDO/S-CI level show the presence of free electron-hole pair (FEHP) states which are stabilized by the uniform external electric field. These FEHP states undergo an avoided crossing with the fluorescent 1Bu bound exciton state at sufficiently high field magnitudes. The magnitude of the electronic coupling between the FEHP and 1Bu state, determined from these avoided crossings, is found to be a function of the field at which these states cross. This function is universal in that it applies across different length oligomers and across different FEHP states on the same oligomer. A model for FIQ is developed by combining this electronic-coupling function with Marcus theory and a simple model for the surrounding dielectric medium. To better reproduce the gradual increase of quenching with field seen in experiment (ref 3), inhomogeneous broadening of state energies is also included. The resulting model yields reasonable quantitative agreement with FIQ magnitudes, dependence on oligomer length, and threshold field strengths at which guenching is observed.

(1) Moscatelli, A.; Livingston, K.; So, W. Y.; Lee, S. J.; Scherf, U.; Wildeman, J.; Peteanu, L. A. Electric-Field-Induced Fluorescence Quenching in Polyfluorene, Ladder-Type Polymers, and MEH-PPV: Evidence for Field Effects on Internal Conversion Rates in the Low Concentration Limit. J. Phys. Chem. B 2010, 114, 14430–14439.

(2) Smith, T. M.; Hazelton, N.; Peteanu, L. A.; Wildeman, J. Electrofluorescence of MEHPPV and Its Oligomers: Evidence for Field-Induced Fluorescence Quenching of Single Chains. J. Phys. Chem. B 2006, 110, 7732–42.

(3) Smith, T.; Kim, J.; Peteanu, L.; Wildeman, J. Electric Field Effects on Internal Conversion: An Alternative Mechanism for Field-Induced Fluorescence Quenching of MEHPPV and Its Oligomers in the Low Concentration Limit. J. Phys. Chem. C 2007, 111, 10119–10129.

9549-15, Session 4

Singlet, triplet, electron and hole transport along single polymer chains (Invited Paper)

Matthew Bird, Brookhaven National Lab. (United States);

Conference 9549: Physical Chemistry of Interfaces and Nanomaterials XIV



Gina Mauro, Brookhaven National Lab. (United States) and Dowling College (United States); Xiang Li, Brookhaven National Lab. (United States); Lori Zaikowski, Brianne Karten, Dowling College (United States); Sada Asauoka, Kyoto Institute of Technology (Japan); Qin Wu, Hung-Cheng Chen, Andrew Cook, John Miller, Brookhaven National Lab. (United States)

The diffusion of singlet and triplet excitons along single polyfluorene chains in solution has been studied by monitoring their transport to end traps. Time-resolved transient absorption and steady state fluorescence were used to determine fractions of excitons that reach the end caps. In order to accurately determine the singlet diffusion coefficient, the fraction of polymer ends that have end traps was determined through a combination of NMR and triplet quenching experiments. The distributions of polymer lengths were also taken into account and the resulting analysis points to a surprisingly long singlet diffusion length of 34nm. Experiments on triplet transport also suggest that the entire 100nm+ chain is accessible to the triplet during its lifetime suggesting a lack of hindrance by defects or traps on this timescale.

Pulse radiolysis microwave conductivity measurements were performed on single chains of homo polymers and alternating donor-acceptor copolymers. Through the careful addition of electron or hole scavengers, the electron and hole mobilities could be independently extracted for a series of common OPV polymers. A surprising result has been the similarity of electron and hole mobility in polymers where quantum chemical calculations would suggest large asymmetries in the localization of their respective wavefunctions.

9549-16, Session 4

Cross-linking high-k fluoropolymer gate dielectrics enhances the charge mobility in rubrene field effect transistors

Jwala M. Adhikari, Enrique D. Gomez, Matthew R. Gadinski, Qing Wang, The Pennsylvania State Univ. (United States)

Polymer dielectrics have the potential to incorporate the chemical and mechanical flexibility of polymers into gate insulators. For example, polymers can be functionalized with polar groups to enhance the dielectric constant. Nevertheless, fluctuations in chain conformations at the semiconductor-dielectric interface can introduce energetic disorder and limit charge mobilities in organic thin-film transistors. Here we demonstrate a photopatternable high-K fluoropolymer, poly(vinylidene fluoridebromotrifluoroethylene) P(VDF-BTFE), with a dielectric constant between 8 and 11. The bromotrifluoroethylene moiety enables photo-crosslinking and stabilization of gate insulator films while also significantly enhancing the population of trans torsional conformations in the chain backbones. Using rubrene single crystals as the active layer, charge mobilities exceeding 10 cm2/Vs are achieved in thin film transistors with cross-linked P(VDF-BTFE) gate dielectrics, in contrast to 4 cm2/Vs without crosslinking. We hypothesize that crosslinking reduces energetic disorder at the dielectricsemiconductor interface by suppressing segmental motion and controlling chain conformations of P(VDF-BTFE), thereby leading to approximately a three-fold enhancement in the charge mobility of rubrene thin-film transistors over devices incorporating uncross-linked dielectrics or silicon oxide.

9549-17, Session 4

The deactivation of a conducting polymer

Ricardo I. Tucceri, Univ. Nacional de la Plata (Argentina)

The aim of this work was to study the effect of prolonged potentiodynamic cycling (PPC) on the conducting properties of poly(o-aminophenol) (POAP) film electrodes. PPC reduces strongly the electron transport rate at POAP films. This effect is called here deactivation. Cyclic Voltammetry (CV) and

Rotating Disc Electrode Voltammetry (RDEV) were employed in this study. The attenuation of the voltammetric response of the polymer with the increase in the number of oxidation-reduction cycles allowed one to define a degree of deactivation. RDEV was employed to obtain the dependence of the electron-transport rate on the degree of deactivation of the polymer. RDEV data were interpreted in terms of the electron hopping model. POAP films maintain their conducting properties almost unaltered for about 500 potential cycles at a scan rate of 0.010 V s-1. However, a loss of conductivity was observed as the number of potential cycles was extended beyond 500. The slower electron transport with the increase in the degree of deactivation was attributed to the increase of the electron hopping distance between redox sites.

9549-18, Session 5

Excited state dynamics in next-generation photovoltaic materials (Invited Paper)

Cody W. Schlenker, Univ. of Washington (United States)

Interface states and defect states are often responsible for some of the most interesting processes observed in next-generation solid-state optical devices such as organic and hybrid photovoltaics. We explore these states in a range of organic and hybrid materials by using transient optical absorption spectroscopy and field-dependent excited state spectroscopy. In all-organic systems, we find evidence for a connection between nanostructure and charge recombination mechanisms that appears to be correlated with the susceptibility of different interfacial spin states to be influenced by an electric field. We will also discuss our recent work focused on using transient optical spectroscopy to understand the role of photon energy and flux in determining excited state population kinetics in hybrid systems.

9549-19, Session 5

Photo-induced electron transfer processes in doped conjugated polymer films (Invited Paper)

Garry Rumbles, National Renewable Energy Lab. (United States) and Univ. of Colorado (United States); Obadiah G. Reid, Univ. of Colorado at Boulder (United States) and National Renewable Energy Lab. (United States); Jaehong Park, National Renewable Energy Lab. (United States); Jessica Ramirez, Hilary Marsh, Univ. of Colorado at Boulder (United States); Tyler T. Clikeman, Colorado State Univ. (United States)

With increasing knowledge of the role of the different phases in the bulk heterojunction organic solar cell, the primary site for charge generation is now considered to be the mixed phase, and not the clean interface between neat polymer and neat fullerene. To gain a better understanding of the primary charge generating and recombination steps in this region of the system, we focus our studies on the role of the solid-state microstructure of neat polymers and light-doping of these polymers with a variety of electron-accepting dopants at low concentration.

This presentation will describe some recent work on the doping of polythiophene and polyfluorene derivatives with fullerenes, phthalocyanines and perylenes, which provide a range of reduction potentials that serve to control the driving force for electron transfer processes. Results from flash photolysis, time-resolved microwave conductivity (fp-TRMC), femtosecond transient absorption spectroscopy (fTA) and photoluminescence spectroscopy will be presented.



9549-20, Session 5

Using the Stark effect to understand charge generation in organic solar cells

Natalie Banerji, Univ. de Fribourg (Switzerland)

The photoactive material of organic solar cells commonly consists of a conjugated polymer blended with a fullerene derivative, yielding a complex network of intermixed and phase-pure domains. The charges that are photo-generated in the blend create an electric field in their vicinity, which can affect neighboring molecules and shift their absorption spectrum (Stark effect). The corresponding electro-absorption signature is a powerful tool to understand charge generation in the organic materials. We have investigated pBTTT:PCBM samples with a variety of well-defined microstructures, exploiting the Stark effect in two complementary ways. First, we have studied the evolution of the electro-absorption signal present in ultrafast transient absorption data (no external bias). This has allowed for the first time to directly visualize the migration of charges from intermixed to phase-pure regions, leading to significant insight to the still poorly understood mechanism by which the neat domains favour spatial separation of charges. Second, we have looked at the field-dependent generation and transport of charges in full solar cell devices with externally applied reverse bias, where the photo-generated charged cause a time-resolved reduction of the electro-absorption induced by the external field.

9549-21, Session 5

Exciton dissociation at organic small molecule donor-acceptor interfaces

Steven W. Robey, National Institute of Standards and Technology (United States)

Exciton dissociation at organic semiconductor donor-acceptor (D-A) heterojunctions is critical for the performance of organic photovoltaic (OPV) structures. Interfacial charge separation and recombination processes control device efficiency. We have investigated these fundamental interfacial issues using time-resolved two-photon photoemission (TR-2PPE), coupled with the formation of well-controlled D-A structures by organic molecular beam epitaxy. The interfacial electronic and molecular structure of these model interfaces was well-characterized using scanning tunneling microscopy and ultraviolet photoemission. Exciton dissociation dynamics were investigated by using a sub-picosecond pump pulse to create Pc ϖ ? ϖ * transitions, producing a population of singlet (S1) Pc excitons. The subsequent decay dynamics of this population was monitored via photoemission with a time-delayed UV pulse. For CuPcC60 interfaces, S1 exciton population decay in the interfacial CuPc layer was much faster than decay in the bulk due to interfacial charge separation. The rate constant for exciton dissociation was found to be \approx 7 x 10 12 sec-1 (\approx 140 fs). Excitons that lose energy via intersystem crossing (ISC) to triplet levels dissociate approximately 500 to 1000 times slower. The dependence of exciton dissociation on separation was also studied. Exciton dissociation falls of rapidly with distance from the interface. Dissociation from the 2nd, and subsequent, layers of H2Pc is reduced by at least a factor of 10 from that in the interfacial layer. Finally, investigations of the relative efficiency for interfacial exciton dissociation by alternative acceptors based on perylene cores, (perylene tetracarboxylic dianhydride, or PTCDA) compared to fullerene-based acceptors such as C60 will also be discussed.

9549-22, Session 5

Fluorescence and UV/VIS absorption spectroscopy studies on polymer blend films for photovoltaics

Jan van Stam, Camilla Lindqvist, Rickard Hansson, Leif K. E. Ericsson, Ellen Moons, Karlstad Univ. (Sweden)

The quinoxaline-based polymer TQ1 (poly[2,3-bis-(3-octyloxyphenyl)

quinoxaline-5,8-diyl-alt-thiophene-2,5- diyl]) [1] is a promising candidate as electron donor in organic solar cells. In combination with the electron acceptor [6,6]- phenyl-C71-butyric acid methyl ester (PC70BM), TQ1 has resulted in solar cells with power conversion efficiencies of 7 % [2].

We have studied TQ1 films, with and without PC70BM, spin-casted from different solvents, by fluorescence spectroscopy and UV/VIS absorption spectroscopy. We used chloroform (CF), chlorobenzene (CB), and o-dichlorobenzene (o-DCB) as solvents for the coating solutions and 1-chloronaphthalene (1-CN) as solvent additive. 1-CN addition has been shown to enhance photo-conversion efficiency of these solar cells [2,3]. Phase-separation causes lateral domain formation in the films and the domain size depends on the solvent [2,3]. These morphological differences coincide with changes in the spectroscopic patterns of the films.

From a spectroscopic point of view, TQ1 acts as fluorescent probe and PC70BM as quencher. The degree of fluorescence quenching is coupled to the morphology through the distance between TQ1 and PC70BM. Furthermore, if using a bad solvent for PC70BM, morphological regions rich in the fullerene yield emission characteristic for aggregated PC70BM [4]. Clear differences were found, comparing the TQ1:PC70BM blend films casted from different solvents and at different ratios between the donor and acceptor. The morphology also influences the UV/VIS absorption spectra, yielding further information on the composition.

The results show that fluorescence and UV/VIS absorption spectroscopy can be used to detect aggregation in blended films and that these methods extend the morphological information beyond the scale accessible with microscopy.

References:

- [1] E.Wang et al., Adv. Mater. 2010, 22, 5240-5244.
- [2] Y. Kim et al., Energy Environ. Sci. 2013, 6, 1909-1916

[3] R. Hansson et al., submitted.

[4] S. Cook et al., Chem. Phys. Lett. 2007, 445, 276-280.

9549-2, Session 6

Electronic coupling at hybrid organic/ inorganic interfaces (Invited Paper)

Oliver L. A. Monti, The Univ. of Arizona (United States)

Hybrid organic / inorganic interfaces play a central role in organic optoelectronics as charge harvesting layers or charge-recombination layers. The properties that determine electronic structure, dynamics and charge collection efficiencies are however at present poorly understood. I will discuss recent results for the paradigmatic interface of organic semiconductors with highly conductive ZnO films. Using a wide range of steady-state and time-resolved spectroscopic approaches, I will show how defect-driven strong electronic interactions determine interfacial energylevel alignment, carrier dynamics on the sub-fs time-scale and device function. These interactions can be controlled by judicious preparation of the interface, with immediate consequences for carrier-harvesting efficiencies.

9549-23, Session 6

Ultrafast excited-state dynamics at interfaces: fluorescent DNA probes at the dodecane/water interface (Invited Paper)

Giuseppe Licari, Eric Vauthey, Univ. de Genève (Switzerland)

Although liquid/liquid interfaces play a key role in many area of science and technology, their properties are only partially understood. Our strategy to obtain an insight into these properties is to investigate the ultrafast excited-state dynamics of environment-sensitive molecular probes at liquid interfaces using time-resolved surface second harmonic generation (SSHG), and to compare it with the dynamics of the same molecules in bulk solutions. This approach gives additionally rich information on how the

Conference 9549: Physical Chemistry of Interfaces and Nanomaterials XIV



chemical reactivity may change when going from the bulk liquid phase to the interface.

This will be illustrated by several examples, concentrating on results obtained with several fluorescent DNA probes, such as YO (oxazol yellow) and the homodimeric probe YOYO, as well as with chiral helicenium dyes. Stationary and time-resolved SSHG measurements reveal substantial differences in the structure and the excited-state lifetime of these DNA probes at the interface compared to bulk water. For example, whereas some of these dyes form H aggregates in aqueous solution, J aggregation is observed at the alkane/water interface. Similarly, the excited-state lifetime of these flexible molecules increase substantially when going from the bulk phase to the interface, pointing to higher friction.

The sensitivity of SSHG to the chirality of the interface has been used to observe the intercalation of these dyes in B-DNA. Our effort to exploit this sensitivity to measure temporal photoinduced changes of optical activity and hence to monitor structural dynamics will be illustrated with results obtained with helicenium dyes.

9549-24, Session 6

Absolute polaron yield generated in donor-acceptor P3HT:fullerene bulk heterojunction composites (Invited Paper)

Saptaparna Das, Alia A. Latif, William Thornbury, Barry C. Thompson, Stephen E. Bradforth, The Univ. of Southern California (United States)

Broadband pump-probe spectroscopy over the entire time range (200 fs to 500 ns) relevant to monitor the polaron generation and recombination dynamics were performed on the bulk heterojunction composites of poly (3-hexylthiophene) (P3HT) and poly(3-hexylthiophene-thiophene-diketopyrrolopyrrole) (P3HTT-DPP-10%) with [6,6]-phenyl-C61-butyric acid methyl ester (PCBM) as the acceptor. The modeling of the polaron dynamics with the Debye-Smoluchowski diffusion model provides the charge separation length at the polymer:fullerene interface. Using the polaron cross-section obtained from the chemical doping measurements, the computed polaron yield over the entire time range reveals how many photo-generated charges are created and survive in P3HT:PCBM and P3HTT-DPP-10%:PCBM bulk-heterojunction thin films.

9549-25, Session 6

Photoinduced carrier generation and recombination dynamics of a trilayer cascade heterojunction composed of poly(3-hexylthiophene), titanyl phthalocyanine, and C60

Jaehong Park, Obadiah G. Reid, Garry Rumbles, National Renewable Energy Lab. (United States)

We demonstrated that the combination of flash-photolysis time-resolved microwave conductivity experiments (fp-TRMC) and classic fs-ns pumpprobe transient absorption spectroscopy can serve to complement each other and can be utilized to elaborate photoinduced carrier generation and recombination dynamics for more complicated trilayer cascade heterojunction system (P3HT/TiOPc/C60) composed of poly(3hexylthiophene) (P3HT), titanyl phthalocyanine (TiOPc), and C60. Carrier generation following selective photoexcitation of TiOPc is independently observed at both the P3HT/TiOPc and TiOPc/C60 interfaces. Moreover, fp-TRMC results show that the yield-mobility product (???) of the trilayer (P3HT/TiOPc/C60) exceeds the sum of ??? each bilayer (P3HT/TiOPc and TiOPc/C60), suggesting that carriers generated at one interface undergo a second charge transfer step at the other interface. Pump-probe transient absorption spectroscopic studies probe carrier generation through hole and electron transfer processes at the interfaces of P3HT/TiOPc and TiOPc/C60, respectively. Each bilayer (P3HT/TiOPc) and (TiOPc/C60) exhibited ultrafast electron/hole transfer as well as exciton-diffusion limited processes. These transient absorption results indicates that following initial charge generation processes to produce $P3HT \cdot +/TiOPc - \cdot$ and $TiOPc \cdot +/C60 - \cdot$ at each interface from ($P3HT/TiOPc^*/C60$) via electron transfer and hole transfer processes, the final charge separated product of ($P3HT \cdot +/TiOPc/C60 - \cdot$) is responsible for the long-lived photoconductance signals in fp-TRMC.

9549-26, Session 6

Cause of absorption band shift of disperse red-13 attached on silica spheres

Byoung-Ju Kim, Hyung-Deok Kim, Na-Rae Kim, Byeong-Gyu Bang, Eun-Hye Park, Tea Wuk Kang, Kwang-Sun Kang, Kyungil Univ. (Korea, Republic of)

A reversible color change and large absorption band shift have been observed for the disperse red-13 (DR-13) attached on the surface of the monodisperse silica spheres. Two step synthetic processes including urethane bond formation and hydrolysis-condensation reactions were used to attach the DR-13 on the surface of the silica spheres. After the reaction, the characteristic absorption peak at 2270 cm-1 representing the -N=C=O asymmetric stretching vibration disappeared, and the a new absorption peak at 1700 cm-1 corresponding the C=O stretching vibration appeared. A visual and reversible color change was observed before and after wetting in alcohol. Although the absorption peak of DR-13 in alcohol is at 510 nm, the absorption peak shifts to 788 nm when it is dried. The absorption peak shifts to 718 nm when it is wetted in alcohol. This result can be explained by the formation of intramolecular charge transfer band.

9549-27, Session 7

Nano-optical spectroscopic imaging of MoS2: probing 2D materials at the length scales that matter (Invited Paper)

James P. Schuck, The Molecular Foundry (United States)

No Abstract Available

9549-28, Session 7

Surface-enhanced, multi-dimensional attenuated total reflectance spectroscopy (Invited Paper)

Jan Philip Kraack, Univ. of Zürich (Switzerland); Davide Lotti, Univ. of Zurich (Switzerland); Peter Hamm, Univ. of Zürich (Switzerland)

Vibrational dynamics of molecules at solid-liquid interfaces attract attention due to their involvement in heterogeneous catalysis.1 This includes simple samples like small molecules (e.g., CO) and large organic molecules (e.g., self-assembled monolayers) on metallic substrates. It is therefore desirable to develop spectroscopic techniques for obtaining surface-sensitive molecular information.

We present a new method for delivering coherent, time-resolved twodimensional (2D) infrared (IR) spectra from adsorbates on metallic thin films.2,3 The technique is based on reflection absorption spectra obtained under total reflection conditions at interfaces of different refractive index materials. Details of femtosecond 2D ATR IR spectroscopy are presented along with benefits and challenges. 2D ATR IR spectroscopy is used to resolve ultrafast interfacial dynamics of molecules on metallic thin films. We characterize surface-enhancement effects due to the presence of the metal. The experiments focus on the impact of different chemical environments on samples vibrational dynamics. The technique is capable for a surfacesensitive characterization of vibrational lifetimes, dephasing, spectral diffusion and sample inhomogeneity. Finally, we discuss the future scope



of 2D ATR IR spectroscopy regarding its applicability on more complex samples such as heterogeneous photocatalysts or transient intermediates in spectro-electrochemistry.

1 H. Arnolds and M. Bonn, Surf. Sci. Rep. 65, 45 (2010).

2 J.P. Kraack, D. Lotti, and P. Hamm, J. Phys. Chem. Lett. 18, 2325 (2014). 3 J.P. Kraack, D. Lotti, and P. Hamm, J. Chem. Phys. submitted (2015).

9549-29, Session 7

Ultrafast carrier photogeneration dynamics in polymer: fullerene solar cells probed by photocurrent-detected two-dimensional coherence spectroscopy (Invited Paper)

Carlos Silva, Univ. de Montréal (Canada)

In solar cells that incorporate semiconductor polymers as electron donors and fullerene derivatives as acceptors, a number of reports based on ultrafast optical probes reveal that charges can be generated on timescales significantly faster than ~100 fs in certain solid-state microstructures. Techniques that have been applied in these studies include variants of visible transient absorption and photoluminescence spectroscopy, terahertz spectroscopy, time-resolved infrared spectroscopy, and femtosecond stimulated Raman spectroscopy. These probes allow measurement of population dynamics of relevant photoexcitations (excitons, polarons) but do not reveal directly how these interact to produce photocarriers. Here, we present a non-linear coherent spectroscopy, photocurrent-detected twodimensional spectroscopy (2DPC), which is an ultrafast optical thechnique belonging to a family of 2D Fourier- domain spectroscopies that allows measurement of correlations between optical transitions induced by short optical pulses. In our implementation, spectral correlations are detected via the time-integrated photocurrent produced in a photovoltaic diode. Four collinear ultrashort laser pulses (10 fs, centered at 600 nm in our experimental setup) excite the semiconductor polymer in the solar cell, with a variable delay that is independently controlled between each pulse in the sequence. Each pulse separately excites a quantum wavepacket with spectral phase and amplitude imparted by that pulse, while the effect of the pulse sequence is to collectively excite multiple quantum coherences. Interferences between the various combinations of the wavepackets determine linear and non-linear contributions to the material optical response. The fourth-order signal terms of the detected photocurrent are read using phase-sensitive detection schemes with reference waveforms corresponding to a modulation of specific phase combinations of the four femtosecond excitation pulses. By scanning the time delay between the pulses 1 and 2, as well as that between pulses 3 and 4 (coherence times), at a fixed delay between pulses 2 and 3 (population waiting time), one measures a two-dimensional coherence decay function that is Fourier transformed to produce a 2D photocurrent correlation excitation spectrum. Measurement of such spectra at different population waiting times provides insight into the role of spectral correlations and state coherence in photocurrent generation in such complex functional materials. We focus on solar cells produced by blends of a common carbazole-thiophenebenzothiadiazole polymer, PCDTBT (the donor polymer), and PCBM (the fullerene acceptor), in which we analyse the dynamics of total photocurrent generation via the time evolution of diagonal and off-diagonal spectral correlations. We address the role of vibronic coherence as well as resonant tunneling in charge separation pathways on ultrashort timescales.

9549-30, Session 7

Controlling electron transfer in condensed phase with bond specific Infrared excitation (Invited Paper)

Milan Delor, Paul A. Scattergood, The Univ. of Sheffield (United Kingdom); Igor V. Sazanovich, Gregory M. Greetham, STFC Rutherford Appleton Lab. (United Kingdom); Anthony J. H. M. Meijer, The Univ. of Sheffield (United Kingdom); Anthony W. Parker, Michael Towrie, STFC Rutherford Appleton Lab. (United Kingdom); Julia A. Weinstein, The Univ. of Sheffield (United Kingdom)

The ability to direct chemical change by targeted external perturbation is a long sought after gateway to controllable reactivity. Photochemically driven electron transfer (ET), one of the few elementary processes, is a particularly attractive target for such optical control. A key but elusive factor that often determines the mechanism of ET is nuclear-electronic (vibronic) coupling, known to considerably affect ultrafast photoinduced ET in a vast range of biochemical systems. Vibronic effects are particularly difficult to probe in condensed phase due to the convolution of multiple electronic and structural processes occurring on ultrafast timescales. We use the frequency-domain Transient 2-Dimensional Infrared (T-2DIR) pulse sequence (UV pump, narrowband IR pump, broadband IR probe) to elucidate the interplay between vibrational and electronic processes in charge transfer complexes. We demonstrate the application of this technique to covalent Donor-Bridge-Acceptor systems, where the Donor and Acceptor are tethered together by a strongly IR-active Pt-acetylide bridge which is the target for the IR pulse.

Using 400 - 470 nm excitation, we optically populate a gateway state [D-B-A]*, which branches over separate pathways, and then introduce a ~2-ps, ~15 cm(-1) IR-pulse to selectively perturb IR-vibrations coupled to a charge-separation pathway. e show that vibrationally exciting intramolecular bridge vibrations during visible-light induced ET between donor and acceptor can result in substantial modulation of ET rates and photoproduct yields, and in some cases, completely switches off charge-separation.

9549-31, Session 8

Exciton and polaron interactions in self-assembled conjugated polymer aggregates (Invited Paper)

John K. Grey, The Univ. of New Mexico (United States); Jian Gao, Lawrence Berkeley National Lab. (United States); Alan Thomas, The Univ. of New Mexico (United States)

We study exciton coupling and interconversion between neutral and charged states of different spin in pi-stacked conjugated polymer aggregates. Rigorous self-assembly approaches are used to prepare aggregate nanofibers that permit reliable control of polymer chain conformational and packing (intra- and interchain) order within these structures. Exciton coupling can be tuned between the H- and J-aggregate limits which has important implications for determining the fates of excitons and polarons. Single molecule intensity modulation spectroscopy was performed on individual nanofibers and large quenching depths of emissive singlet excitons by triplets are found in J-aggregate type structures. We propose that high intrachain order leads to exciton delocalization that effectively lowers singlet-triplet energy splittings thus increasing triplet yields. Exciton-polaron and polaron-polaron interactions are next investigated in both H- and J-type nanofibers where polarons are injected by charge transfer doping. We find that the enhanced intrachain order of J-aggregates enables efficient intrachain polaron transport and leads to significantly larger doping efficiencies than less ordered H-aggregates. As polaron densities increase, signatures of spin-spin interactions between polarons on adjacent chains become appreciable leading to the formation of a spinless bipolaron. Overall, these studies demonstrate the potential for controlling and directing exciton and polaron interactions via tuning of subtle intra- and interchain ordering characteristics of aggregates, which could benefit various polymeric optoelectronic applications.

9549-32, Session 8

Controllable supramolecular architectures for modulating the optical properties

Yongjun Li, Runsheng Jiang, Institute of Chemistry (China)

There is growing interest in the design of pi-conjugated systems that

Conference 9549: Physical Chemistry of Interfaces and Nanomaterials XIV



can self-assemble into uniform aggregates with specific shape and novel functionalities. Indeed, an effective way to shape supramolecular architectures is through molecular self-assembly technology based on intramolecular, intermolecular, and molecule-substrate interactions. The optical properties of the conjugated molecules can also be influenced by different conformations and spatial arrangements, such as observed in conformation-dependent fluorescent enhancement induced by laser irradiation.

A thiophene-substituted perylene bisimide has been synthesized and used to demonstrate a relatively simple associated approach to the construction of nano- and microstructures with zero and two dimensions. The thiophene substituted perylene bisimide showed conformationdependent hypochromatic shift and fluorescent enhancement behavior in the solid state, which is induced by tuning the intramolecular charge transfer from the trithiophene unit to the perylene bisimide through light-induced conformation changes of the trithiophenes. The mechanism differs from the fluorescent bleaching of normal solid-state fluorescent materials, and suggests potentially important applications in optical devices. This work demonstrates the importance of controlling molecular conformation in molecular aggregation systems to modulate optical properties.

1. Y. J. Li, T. F. Liu, H. B. Liu, M. Z. Tian, Y. L. Li, Acc. Chem. Res., 2014, 47(4),1186–1198.

2. R. S. Jiang, Z. Xue, Y. J. Li, Z. H. Qin, Y. L. Li, D. B. Zhu, Eur. J. Org. Chem. 2014, 5004–5009.

3. Y. W. Yu, Q. Shi, Y. J. Li, T. F. Liu, L. Zhang, Z. G. Shuai, Y. L. Li, Chem. Asian J. 2012, 7, 2904–2911.

9549-33, Session 8

Characterization of nano-sized iron particle layers spin coated on glass substrate

Sunil Dehipawala, Queensborough Community College (United States); Pubudu Samarasekara, Rasika Dahanayake, Univ. of Peradeniya (Sri Lanka); George Tremberger Jr., Tak D. Cheung, Queensborough Community College (United States); Harry D. Gafney, Queens College (United States)

Nanometer scale iron particles have a variety of technological applications. They are vastly utilized in optical and microwave devices. Thin films with various compositions of iron (III) nitrate and ethylene glycol were deposited on glass substrate using the spin coating technique. The micro structures of iron particles in films prepared under different conditions were investigated using X-ray Absorption spectroscopy and Mossbauer spectroscopy.

9549-34, Session 8

Influence of the molecular orientation on the optical properties and photomodification of cyanine thin film

Anton A Starovoytov, ITMO University (Russian Federation); Elena N. Kaliteevskaya, Valentina P. Krutyakova, Tatiana K. Razumova, National Research Univ. of Information Technologies, Mechanics and Optics (Russian Federation)

Cyanine dyes have a good ability to form layers from solutions of organic solvents. Due to the high polarizability of the electron cloud in the conjugation chain, the cyanines are optical materials with large nonlinear susceptibility. The photorecording cyanine layers are widely used in optical discs. Photochemical switches with subpicosecond response time are developed based on cyanine films. Ionic cyanines are used in light-emitting electrochemical cells.

The structural photomodification of the multicomponent cyanine thin

films was studied. Samples were prepared by spin-coating of the ethanol solution of cyanine dye on the glass substrate. The spectrum of the film shows different bands of components, formed by dye molecules. Optical properties of the films were determined by the relative concentrations of the components and their orientation angles, which depend on the temperature of the substrate during coating of the layer.

Photoinduced modification of the film structure was provided by laser pulses (duration of 10 ns). Laser irradiation carried out in the absorption range of different monomer and aggregate components of the films. Photoinduced changes in the absorption spectra of film associated with the variation of the relative concentrations of the components and their orientation angles. The dependences of angle on the total photoexcitation energy, which was determined by the number of laser pulses, had the form of saturating functions. With increasing pulse energy, the limiting angles grow. The limiting angle vs. pulse energy dependences are the saturating functions. Maximum limiting angles depend on the initial orientation angles of the component.

9549-60, Session 8

SHG techniques to investigate the surface and the bulk of aqueous solutions

Anthony Maurice, Institut Lumière Matière (France); Q. Ma, Institut Lumière Matière (France) and Commissariat à l'Énergie Atomique (France); Fabrice Canto, Laurent Couston, Commissariat à l'Énergie Atomique (France); Olivier Diat, Institut de Chimie Séparative de Marcoule (France); Emmanuel Benichou, Pierre-François Brevet, Institut Lumière Matière (France)

During the last years, ion extraction processes were widely used in industry to separate and concentrate ionic species in solutions. These processes are of considerable interest both from the fundamental and the industrial point of view, particularly in the fields of ore extraction or nuclear waste treatment. In all cases, the region of interest is the interface between the two media, where the structure and the dynamics remain elusive. In order to access the interface and the bulk solution at the same time with a high contrast, we have developed a method based on second harmonic generation, namely the conversion of two photons into a single one at the sum energy

We will present our recent results obtained for simple multivalent cations and different counter-anions, standard organic dye molecules and metallic nanoparticles. SHG profiles of these species at air-liquid and liquid-liquid interfaces exhibit two distinct regions. The first one corresponds to the interface where the bulk centrosymmetry is broken whereas the second one corresponds to the bulk volume of the phases where incoherent second harmonic is generated. A general framework to describe these data sets will be provided and the structure of the interface discussed in light of these results.

9549-35, Session 9

Mapping optoelectronic processes at their native length scale in perovskite PV materials (Invited Paper)

Alexander Weber-Bargioni, The Molecular Foundry (United States)

No Abstract Available



9549-36, Session 9

Interfacial energy landscapes of organic semiconductors probed on the submolecular scale by STM (Invited Paper)

Sarah A. Burke, Agustin E. Schiffrin, Katherine Cochrane, Martina Capsoni, Tanya Roussy, The Univ. of British Columbia (Canada)

The inter- and intra- molecular energy transfer underlying applications in electronics, optoelectronics and catalysis relies on both the spatial distribution of electronic states and their energy level alignment across interfaces. As models for organic photovoltaic and catalytic materials, we are investigating well-controlled nanostructures of the organic semiconductor PTCDA, and an iron-terpyridine coordination polymer. Scanning tunneling microscopy and spectroscopy, operated in a spectroscopic mapping mode, allows us to visualize position and orientation of molecules alongside the spatial distribution of states and shifts in the energy level alignments across these organic nanostructures. In small clusters of PTCDA, we have found a pronounced shift in the energy level alignment and change in the semiconducting gap of up to 0.5eV, likely due to the abrupt change in the local polarization environment. This interfacial energy level shift has potential consequences for electronic devices and organic heterostructures for photovoltaics where the distinct local environment of the interface would need to be considered. On-surface coordination of iron-terpyridine chains was used to generate well-controlled and clean metal-ligand complexes as a model for dyes and catalytic systems. Taking inspiration for existing molecular complexes, this surfacebound macromolecular system exhibits spatial and energetic characteristics that mimic the molecular complexes, most notably showing a metalcentered HOMO and ligand-centered LUMO that indicates a low-lying MLCT optical excitation exploited in related photoactive dyes. In each of these examples, the sub-molecular resolution spectroscopy yields high resolution energetic and spatial information that can be used to understand the local electronic landscape.

9549-37, Session 9

Super-resolution imaging with mid-IR photothermal microscopy on the single particle level

Zhongming Li, Gregory V. Hartland, Univ. of Notre Dame (United States)

Photothermal microscopy, as a label-free imaging technique, has achieved single molecule sensitivity. However, the analytes are usually restricted to be natural absorbers in the visible light region. Mid-IR imaging, on the other hand, encounters difficulties of diffraction-limited spatial resolution and scarcity of ideal detectors. Here we present Mid-IR photothermal heterodyne imaging (MIR-PHI) microscopy, which overcomes the diffraction limit and is universally applicable to any analyte. It can also provide spectroscopic information for further identification. In MIR-PHI, a tunable Mid-IR pulsed laser at 150 kHz is used as a heating beam to transmit thermal energy to an analyte particle. Energy relaxation creates a temperature gradient, changing the refractive index of the surrounding solvent and creating a thermal lens around this particle. A collinear counter propagating probe beam (a 532 nm CW laser) is modified by the thermal lens and generates a super-resolution photothermal image. We studied 1.1 µm polystyrene beads on the single particle level using this technique. Images were recorded at 3030 cm-1, which corresponds to the strong absorption from aromatic C-H stretches. Various solvents with different heat capacities and refractive indices are tested for the best image contrast. Spectra were recorded in the 2.5 to 3.7 μ m and 5.4 to 9.6 μ m regions, which cover the majority of both of the functional group frequency region and the fingerprint region. The spectra obtained can be used to distinguish different materials. The wide applicability and high sensitivity of this technique make it promising for biological imaging and identification.

9549-38, Session 10

Emergence of collective luminescence in mesoscopic conjugated polymer aggregates by coherent and incoherent processes (Invited Paper)

Jan Vogelsang, Thomas Stangl, Philipp Wilhelm, Univ. Regensburg (Germany); Klaas Remmerssen, Sigurd Höger, Univ. Bonn (Germany); John Lupton, Univ. Regensburg (Germany)

Many applications of conjugated polymers depend critically on the nature of excitation energy transport in these materials. Bulk measurements regarding these processes have the inherent disadvantage that an average physical or chemical mechanism is probed, which can mask important microscopic mechanisms, taking place on smaller subunits. An example of this problem is coherent coupling between multiple chromophores, which leads to efficient energy transport and is therefore masked by photoluminescence quenching in the bulk.

By employing single molecule and aggregate spectroscopy on well-defined conjugated polymer chains and differently sized aggregates composed of multiple chains, we unravel the following non-intuitive behaviour in the material poly(phenylene-ethynylene): (i) aggregation by solvent vapour annealing [1] of multiple chains leads to coherent coupling between chromophores, best described in the context of H-aggregation [2] or excimer-like states [3] and resulting in a ~10-fold increase in the excited state lifetime. (ii) This coupling between chromophores in aggregates is so efficient that photon anti-bunching occurs in aggregates consisting of up to ~20 chains, even though single chains do not show such an effect. (iii) Quenching, due to photochemical guenchers, becomes increasingly dominant with increasing aggregate size, resulting in a strong blinking behaviour of the photoluminescence. These incoherent guenching processes, mediated by FRET, lead to a decrease of the excited state lifetime in the aggregate and also to a decrease in the fidelity of photon antibunching. Our results demonstrate that important intermolecular processes take place in the mesoscopic size regime, which do not exist on the single chain and are masked in the bulk, but influence the bulk properties.

[1] J. Vogelsang, T. Adachi, J. Brazard, D. A. V. Bout, and P. F. Barbara, (2011) Nature Mater. 10, 942.

[2] M. Kasha, (1963) Radiation Res. 20, 55.

[3] S. A. Jenekhe and J. A. Osaheni, (1994) Science 265, 765.

9549-39, Session 10

Transient absorption microscopy studies of single metal and semiconductor nanostructures (Invited Paper)

Paul Johns, Mary Sajini-Devadas, Gregory V. Hartland, Univ. of Notre Dame (United States)

Single particle spectroscopy is capable of providing detailed information about how differences in size, shape and environment affect the properties of nanomaterials. In this talk results from transient absorption experiments performed with diffraction limited spatial resolution will be presented. This technique allows us to perform ultrafast measurements on single nanostructures, and provides information about their dynamics that is washed out in ensemble experiments. The systems that have been examined to date include metal nanoparticles and nanowires, carbon nanotubes, and semiconductor nanowires. The time scales of interest range from a few hundred fs to several ns, and the results provide detailed information about how nanomaterials interact with their environment. In particular, recent results on the damping of the breathing modes of Au nanowires will be described. These modes are impulsively excited by rapid heating from the pump laser. Their damping strongly depends on the viscosity of the surrounding medium. Analysis of the results for viscous to moderately viscous solvents shows that viscoelastic effects have to be included to properly describe the experiments. Viscoelasticity is normally only

Conference 9549: Physical Chemistry of Interfaces and Nanomaterials XIV



important in complex fluids, such as concentrated colloidal dispersions. It appears here because of the high frequencies inherent to the vibrational modes of nanomaterials. Imaging experiments that provide information about the propagation of surface plasmon polaritons (SPPs) in metal nanowires will also be described. These measurements have been used to determine how the SPPs couple between nanostructures. This was achieved by investigating Au nanowires with gaps that were created by focused ionbeam milling.

9549-40, Session 10

Single-molecule methods to quantify adsorptive separations (Invited Paper)

Christy Landes, Rice Univ. (United States)

Interfacial adsorption and transport are the chemical and physical processes that underlie separations. Although separations technology accounts for hundreds of billions of dollars in the global economy, the process is not wellunderstood at the mechanistic level and instead is almost always optimized empirically. One of the reasons is that access to the underlying molecular phenomena has only been available recently via single-molecule methods. There are still interesting challenges because adsorption, desorption, and transport are all dynamic processes, whereas much of the advances in super-resolution imaging have focused on imaging static materials. Our lab has focused in recent years on developing and optimizing data analysis methods for quantifying the dynamics of adsorption and transport in porous materials at nanometer-resolution spatial scales. Our methods include maximizing information content in dynamic single-molecule data and developing methods to detect change-points in binned data. My talk will outline these methods, and will address how and when they can be applied to extract dynamic details in heterogeneous materials such as porous membranes.

9549-42, Session 10

Stability studies on promethazine unexposed and exposed to UV laser radiation

Agota Simon, Adriana Loredana Smarandache, Tatiana Tozar, Viorel V. Nastasa, National Institute for Laser, Plasma and Radiation Physics (Romania) and Univ. of Bucharest (Romania); Ruxandra Pirvulescu, Univ. of Medicine and Pharmacy Carol Davila (Romania); Mihail Lucian Pascu, National Institute for Laser, Plasma and Radiation Physics (Romania) and Univ. of Bucharest (Romania)

Since multiple drug resistance evolved, it became crucial to develop new medicines and to improve the action of the existing ones. A method to cope with these requirements consists in the generation of new photoproducts with possible bactericide, fungicidal effects, by modifying the parental compound at the molecular level by exposure to UV laser beam. This is particularly applied on phenothiazines which are photosensitive non-antibiotics.

The phenothiazine derivative Promethazine (PMZ), was investigated from the point of view of its stability before and after exposure to UV laser radiation. PMZ is a neuroleptic drug with antihistaminic, antiemetic and anticholinergic properties.

Stability studies of samples are imperative prior to be used in preclinical applications. PMZ solutions have been studied by pH measurements, absoption spectroscopy, laser induced fluorescence and FTIR before and after irradiation. Samples (exposed and unexposed to UV laser beam) of different concentrations have been prepared, to examine their time stability while kept in different conditions: laboratory temperature and exposed to white light, laboratory temperature in the dark, fridge in the dark. This study involved the exposure of solutions utilizing the 4th harmonic (266nm) of a Nd:YAG pulsed laser beam. Stability measurements have been performed monitoring samples evolution for long time intervals after exposure. First

results about applications of irradiated phenothiazines samples on infected rabbit eyes are reported.

Acknowledgements: The NILPRP authors acknowledge research financing by CNCS – UEFISCDI by project number PN-II-ID-PCE-2011-3-0922 and by the Ministry of Education via NUCLEU project PN 0939/2009. Smarandache, Tozar and Nastasa were supported by POSDRU/159/1.5/S/137750.

9549-43, Session 11

Effect of surface stoichiometry and interfacial interactions on ultrafast carrier dynamics of crystalline CdTe (Invited Paper)

Xing He, Napat Punpongjareorn, Chengyi Wu, Karjini Rajagopal, Ding-Shyue Yang, Univ. of Houston (United States)

To improve the efficiency of optoelectronic devices, it is critical to understand the carrier dynamics of photoactive materials and the mechanisms involved, including those effects caused by different surface stoichiometry and/or interfacial interactions. A good example is CdTe, which exhibits cost-effective high performance in thin-film photovoltaic cells; it is also known to show surface oxidation, which may affect device efficiency and hence limit the production methods used. In this contribution, we present ultrafast carrier dynamics of crystalline CdTe specimens with different surface conditions using transient reflectivity measurements, following a femtosecond above-gap excitation. The distinct differences observed in the dynamics and the time constants for oxidized and stoichiometrically restored specimens indicate the major role of surface tellurium oxide on the relaxation of photoinduced carriers. The much slower recovery observed on oxidized surfaces is attributed to a transfer (and trapping) of electrons to the tellurium atoms with a high oxidation state, which signifies a charge separation near the surface. To distinguish the effect caused by oxygen adsorption, we also examined the carrier dynamics of CdTe surfaces covered by a thin layer of water molecules for comparison. These results, which show clear interfacial effects, may have broader implications for the understanding of carrier dynamics in nanostructured and polycrystalline specimens under different chemical environments, as such materials exhibit a high surface-to-volume ratio.

9549-44, Session 11

Quadratic nonlinear optics of liquids: from bulk to surfaces and interfaces (Invited Paper)

Anthony Maurice, Isabelle Russier-Antoine, Christian Jonin, Emmanuel Benichou, Pierre-François Brevet, Institut Lumière Matière (France)

Quadratic nonlinear optical processes entailing the conversion of two photons at a fundamental energy into one photon with the sum energy are gaining a wider interest over the years, fueled by the development of highly spatially resolved microscopy techniques. These processes obey strict parity rules in order to occur. They are for instance forbidden in media possessing inversion symmetry like liquids. However this constraint may be turned into a benefit when used in special cases where it is broken by a small amount. One of these processes, second harmonic generation, namely the degenerate process of photon addition, can thus be used to investigate liquids on short scales, within the bulk or at the interface. This property will be illustrated through several examples of nanoscale molecular organization.



9549-45, Session 11

High resolution patterning electronic polymers using dopant induced solubility control (Invited Paper)

Adam J. Moule, Ian E. Jacobs, Jun Li, Stephanie L. Burg, David J. Bilsky, Brandon T. Rotondo, Pieter Stroeve, Univ. of California, Davis (United States)

Organic electronics promise to provide flexible, large-area circuitry such as photovoltaics, displays, and light emitting diodes that can be fabricated inexpensively from solutions. A major obstacle to this vision is that most conjugated organic materials are miscible, making solution-based fabrication of multilayer or micro- to nanoscale patterned films problematic. Here we demonstrate that the solubility of prototypical conductive polymer poly(3-hexylthiophene) (P3HT) can be reversibly "switched off" using high electron affinity molecular dopants, then later recovered with light or a suitable dedoping solution. Using this technique, we are able to stack mutually soluble materials and laterally pattern polymer films using evaporation of dopants through a shadow mask or with light, achieving sub-micrometer, optically limited feature sizes. After forming these structures, the films can be dedoped without disrupting the patterned features; dedoped films have identical optical characteristics, charge carrier mobilities, and NMR spectra as as-cast P3HT films. This method greatly simplifies solution-based device fabrication, is easily adaptable to current manufacturing workflows, and is potentially generalizable to other classes of materials.

9549-46, Session 11

Effect of substrate on Scanning Kelvin Probe Microscopy (SKPM) of interface polarity at carbon nanotube/fullerene junctions

Olivia Alley, Johns Hopkins Univ. (United States); Meng-Yin Wu, Univ. of Wisconsin-Madison (United States); Josue F. Martinez Hardigree, Johns Hopkins Univ. (United States); Michael S. Arnold, Univ. of Wisconsin-Madison (United States); Howard E. Katz, Johns Hopkins Univ. (United States)

Using our method of SKPM of lateral junctions, we have observed the interfacial potential between semiconducting carbon nanotubes and phenyl-C61 butyric acid methyl ester (PCBM). The lateral junctions are made using a fluoro-polymer based lithography and dry etching technique. We determined that the polarity of this potential is reversed when the lateral junction is made on Al2O3 compared to when it is made on SiO2. We did not observe this reversal for a polyemer/PCBM junctions made on these two substrates. There are several possible reasons behind this difference. First, the carbon nanotube layer is thinner and more conductive than the polymer layer, so the substrate will have more of an effect on the potential at the surface. Additionally, others have found that insulators with larger dielectric constants, such as Al2O3, alter the electronic states of adjacent organic semiconductors (OSCs). This is both from greater dipolar disorder in the insulator, and a greater degree of polaron formation in the OSC. We think these effects extend to this situation, and lead to greater charge trapping near the dielectric interface. It is only evident in the nanotube/PCBM system because the effects only extend a few nm beyond the interface with the insulator. The surface of the thicker polymer film therefore is not affected.

9549-47, Session 12

Interface engineering to eliminate biasstress effect in quantum dot transistors (Invited Paper)

Matt Law, Univ. of California, Irvine (United States)

Colloidal quantum dot (QD) solids are the subject of active research with applications emerging in light-emitting diodes, field-effect transistors, and solar cells. In this talk, I describe the use of atomic layer deposition (ALD) infilling to engineer the surfaces and interfaces of PbSe QD films in order to produce high-performance QD field-effect transistors (FETs) that completely lack bias-stress effect (i.e., drain current transients caused by charge trapping near the dielectric/channel interface). This ALD "matrix engineering" approach includes steps designed to manage ligand concentrations, passivate surface states, and arrest ionic motion within the films, resulting in the first high-mobility (-14 cm V-1 s-1), environmentally stable, and transient-free PbX QD transistors. Two bias-stress mechanisms in QD FETs are identified and discussed. The implications of these mechanisms for the operation of QD solar cells is highlighted.

9549-48, Session 12

Exciton formation dynamics in Si quantum dots and functionalized CdSe nanorods studied with time-resolved THz spectroscopy

Matthew C. Beard, National Renewable Energy Lab. (United States)

Time-resolved THz spectroscopy is typically used to probe the complex photoconductivity in a non-contact fashion with sub-picosecond temporal resolution. As such the THz spectra is sensitive to the nature of carriers within nanostructures. We show that the THz probe can distinguish between free-carriers and excitons. The THz probe therefore distinguishes the initially produced hot-carriers from excitons that are formed on a longer timescale. We report size-dependent exciton formation dynamics within colloidal silicon quantum dots. We find that the exciton formation time increases from -600 fs - 1 ps, as the size of the QD is reduced. At longer delay times we extract the exciton-polarizability, which follows an -r^4 dependence, consistent with previous reports for quantum-confined excitons. The ability to differentiate between excitons and free carriers makes time-resolved terahertz spectroscopy a powerful technique for understanding the complex carrier relaxation processes that can occur in semiconductor nanocrystals.

We studied the exciton formation dynamics within methylene blue (MB) sensitized CdSe nanorods (NRs). In the absence of MB, free charge-carriers are initially produced that then form excitons within the CdSe NRs within ~ 2 ps. In the presence of MB, photoexcited electrons reduce the MB within ~ 3 ps and the hole remains delocalized. In the subsequent 17 ps the hole becomes localized on the reduced MB as it is trapped by the Coulomb potential that arises from the reduced MB. Our results explain why dot-inrod systems work better than NRs in photocatalytic systems and should allow for designing a better photocatalytic system based on CdSe NRs.

9549-49, Session 12

Tunable emission properties of Au nanoclusters

Woong Young So, Anindita Das, Hee Young Byun, Carnegie Mellon Univ. (United States); Santosh Kumar, Henkel Corp. (United States); Rongchao Jin, Linda A. Peteanu, Carnegie Mellon Univ. (United States)

Despite the significant interest in the fluorescence properties of gold nanoclusters, the emission mechanism remains unclear. This study reports

Conference 9549: Physical Chemistry of Interfaces and Nanomaterials XIV

the fluorescence properties of two structural forms of Au25, a nano-sphere (Au25PET18) and a nano-rod ([Au25(PPh3)10(PET)5Cl2]2+) in several different solvent environments. For both materials, the strongest emission is observed for excitation at energies higher than the HOMO-LUMO gap of the material with the nano-rod form being significantly more emissive than the nano-sphere. Increasing the polarity of the solvent results in a substantial enhancement of the emission intensity of the nano-rod which is evident in both bulk studies and at the single-molecule level. This enhancement effect requires the presence of the solvent and does not persist in the solid state. In addition, the fluorescence maximum is strongly red shifted in more polar solvents which suggest that the emitting state has a highly dipolar character. Similar to what has been previously reported for CdSe guantum dots and silver nanoparticles[1,2], the emission intensity of the nano-rod in solution increased by up to 250% after illumination for several minutes at relatively low laser powers. Implications of these observations for the emission mechanism of gold nanoclusters will be discussed.

 Noseung, M.; Yoon, J.B.; Allen, J.B. Nano Lett. 2003, 3, 747-749
 Geddes, C.D.; Parfenov, A.; Gryczynski, L.; Lakowicz, J. R. J. Phys. Chem. B 2003, 107, 9989-9993

9549-50, Session 12

Electronic logic gates from threesegment nanowires featuring two P-N heterojunctions

Huibiao Liu, Yuliang Li, Chinese Academy of Sciences (China)

We have fabricated a novel heterojunction structure combining one inorganic and two organic semiconductors. The different segments exhibited distinct self-assembly behavior, allowing us to control the production of 1D three-segment nanowires featuring two diodes in series on two interfaces; the isolated organic/inorganic semiconductor wires displayed the novel properties of a two-input OR logic gate. We suspect that these devices might have applicability for fundamental research in the field of nanoscience and to applications in the field of nanotechnology, with great potential to produce new molecular electronic devices.

9549-51, Session 13

Photophysical versus structural properties in hybrid lead-halide perovskites (Invited Paper)

Annamaria Petrozza, Istituto Italiano di Tecnologia (Italy)

Hybrid perovskites represent a new, disruptive, technology in the field of optoelectronics. They have the potential to overcome the performance limits of current technologies and achieving low cost and high integrability. Hybrid halide perovskite, e.g. CH3NH3PbX3 [X = Cl, Br, or I], are usually deposited as polycrystalline thin-films with variable mesoscale morphology depending on the growth conditions. The obtained grain size ranges from tens to thousands of nm. Over the last two years the impressive improvement of photovoltaic performance has been driven by radical evolution of the device architecture and processing methodologies. However, there is a considerable lack of understanding of material properties, both as pristine films and their embodiment in a device.

Here we demonstrate that the electron-hole interaction is sensitive to the microstructure of the material. We find that by control of the material processing during fabrication both free carrier and Wannier excitonic regimes are accessible, with strong implications for optoelectronic devices. The long-range order of the organic cation dipole field is disrupted by polycrystalline disorder introducing domain walls where dipole twinning breaks down. The variations in electrostatic potential found for smaller crystallites suppress exciton formation, while larger crystals of the same composition demonstrate an unambiguous excitonic statel,2. In addition, we demonstrate that it is also possible to design the emissive properties for a single material composition by designing the processing routs3. By



simply tuning the average crystallite dimension in the film from tens of nanometers to a few micrometers, it is possible to tune the optical band gap of the material along with its photoluminescence lifetime. We demonstrate that larger crystallites present smaller bandgap and longer lifetime which correlates to a smaller rediative bimolecular recombination coefficient. We also show that they present a higher optical gain, becoming preferred candidates for the realization of lasing devices.

 [1] G. Grancini et al, The Journal of Physical Chemistry Letters, 5, 3836, 2014
 [2] G. Grancini et al, Exciton Stabilization in Hybrid Lead-Halide Perovskites, manuscript submitted.

[3] V. D'Innocenzo et al, Tuning the light emission properties by band gap engineering in hybrid lead-halide perovskite Journal of the American Chemical Society, 136, 17730, 2014

9549-52, Session 13

Effect of substrate surface free energy on the optoelectronic and morphological properties of organolead halide perovskite solar cell materials

R. Clayton Shallcross, James G. Stanfill, Neal R. Armstrong, The Univ. of Arizona (United States)

Here, we show how the surface free energy of the electron-collecting oxide contact has a very pronounced effect on the nucleation free energy of solution-processed organolead halide perovskite thin films, which influences the crystal size/orientation, band-edge energies, conductivity and, ultimately, the performance of solar cell devices. While a great deal of the research community's attention has been focused on the perovskite deposition methodology (e.g., starting precursors, annealing conditions, etc.), we demonstrate how the surface free energy of the oxide contact itself can be modified to control morphology and optoelectronic properties of the resulting hybrid perovskite thin films. The surface free energy of high-quality oxide contacts deposited by chemical vapor deposition (CVD) and atomic layer deposition (ALD) is modified by functionalization with a variety of selfassembled monolayers. We explore a number of deposition methodologies (e.g., a variety of single step and sequential step approaches) and their effect on the morphological and electronic properties of the resulting perovskite thin films deposited on these modified oxide contacts. Standard atomic force microscopy (AFM) and its conductive analog (cAFM) show how the oxide surface free energy ultimately affects the nanoscale morphology and charge transport characteristics of these semiconductor films. Photoelectron spectroscopy is used to elucidate the chemical composition (e.g., X-ray photoelectron spectroscopy ? XPS), band edge energies (e.g., ultraviolet photoelectron spectroscopy ? UPS), and the presence of gap states above the valence band (high sensitivity UPS measurements near the Fermi energy) of the hybrid perovskite materials as a function of the oxide surface free energy.

9549-53, Session 14

Optical processes in molecular junctions *(Invited Paper)*

Abraham Nitzan, Tel Aviv Univ. (Israel); Michael Galperin, Univ. of California, San Diego (United States); Maxim Sukharev, Arizona State Univ. (United States)

The interaction of light with molecular conduction junction is attracting growing interest as a challenging experimental and theoretical problem on one hand, and because of its potential application as a characterization and control tool on the other. From both its scientific aspect and technological potential it stands at the interface of two important fields: molecular electronics and molecular plasmonics. I shall review the present state of the art of this field and our work on optical response, Raman scattering, temperature measurements, light generation and photovoltaics in such systems.



9549-54, Session 14

Site models for including effects of torsions and disorder on charge and energy transport in organic semiconductors (Invited Paper)

David J. Yaron, Nicolae M. Albu, Christopher R. Collins, Christian M. Legaspi, Carnegie Mellon Univ. (United States)

In organic molecules with extensive pi conjugation, the motion of charge and energy is strongly influenced by disorder and motion in the torsional degrees of freedom. Site models provide a computationally efficient description and make it possible to carry out the ensemble and time averaging needed to gain insight into the phenomena. The development of site models from quantum chemical calculations on a large set of representative oligomers will be discussed. An important feature of conjugated polymers, that is well described by site models, is an increase in the torsional barrier in the vicinity of an exciton or charge. This leads, for instance, to rapid planarization of the excited state following photoexcitation. A Brownian dynamics model of this excited-state relaxation reveals universal behaviors that apply across a wide range of polymer systems. Among these universal features is the prediction of two timescales for the relaxation such that short-time and longer-time dynamics differ substantially. Similar to the planarization associated with photoexcitation, oxidation or reduction to form a charge on the polymer increases the torsional potential and so leads to self-trapping of the charge on a planarized region of the polymer. Our models suggest that the solutionphase charge mobility, as measured by microwave reflectivity, is established by the stochastic motion of this planarized, charged region along the polymer chain.

9549-55, Session 14

Size-dependent Hamaker constants for silver and gold nanoparticles

Pavlo Pinchuk, Ke Jiang, Univ. of Colorado at Colorado Springs (United States)

Hamaker-Lifshitz constants are material specific constants that are used to calculate van der Waals forces between colloidal particles. Typically, these constants do not depend on the size of the interacting particles in the colloids. According to the Lifshitz theory, the Hamaker-Lifshitz constants can be calculated by taking integrals that include dielectric permittivity of the interacting particles as a function of the frequency. The complex dielectric permittivity of the interacting metal nanoparticles can be calculated by using the Drude model that describes the response of free conducting electrons to the external excitations. Usually, the complex dielectric permittivity of bulk metals does not depend on the size of the interacting objects. However, metal nanoparticles with sizes smaller than the mean free path of the electrons in the bulk metals exhibit size-dependent dielectric complex permittivity. The size dependence of the complex dielectric permittivity is the result of the scattering of the free conduction electrons from the surface of the nanoparticles. This leads to the size dependence of the Hamaker-Lifshitz constants for metal nanoparticles. In this work we show theoretically that scattering of the free conducting electrons inside silver and gold nanoparticles with the size of 1 - 50 nm leads to their size-dependent Hamaker-Lifshitz constants. We calculate numerically the Hamaker-Lifshitz constants for silver nanoparticles with different diameters. The results of the study might be of interests for understanding colloidal stability of metal nanoparticles.

9549-56, Session 14

Effect of excess charge on metallic nanoclusters

Shideh Ahmadi, Nanyang Technological Univ. (Singapore);

Xi Zhang, Shenzhen Univ. (China); Yinyan Gong, China Jiliang Univ. (China); Changqing Sun, Nanyang Technological Univ. (Singapore)

Charged Ag, Cu, Pt, and Rh nanostructures have attracted enormous research interest recently due to their unique properties comparison with their bulk counterparts. The effect of excess charge on metallic nanoclusters with Cuboctahedral and Marks decahedral structures has been studied using density functional theory (DFT) calculations, bond order-length-strength correlation (BOLS) [1] and nonbonding electron polarization (NEP) [2] theories. Our calculations are consistent, in trend, with experimental observations such as X-ray-absorption fine structure, scanning tunneling microscope/spectroscopy, and ultraviolet photoelectron spectra. The agreement confirmed the predications based on BOLS-NEP notation, suggesting that the bonds between under-coordinated atoms in the surface skin of nanostructures become shorter and stronger, inducing entrapment and polarization, which give rise to observed unique catalytic and magnetic behaviors.

1. C. Q. Sun, Relaxation of the Chemical Bond. (Springer Series in Chemical Physics, 2014).

2. Sun CQ. Nanoscale 10, 1930 (2010).

9549-57, Session 14

Multiscale molecular modeling of tertiary supported lipid bilayers (Invited Paper)

Holden T. Ranz, Roland Faller, Univ. of California, Davis (United States)

Lipid bilayer structures supported on solid substrates are highly important experimental analogs for understanding cell membranes. We use and adapt different variations of the Martini model to study the differences in phase behavior between supported and free bilayers and to explain observed experimental discrepancies. The same phases are found in both cases but the phase boundaries are different both in temperature and concentration. We study the impact of the surface and the effect of the water layer between surface and membrane. We also find differences in the structure of the membranes. We particularly study for the first time computationally the effect of cholesterol in supported bilayers.

9549-58, Session PWed

Electronic and optical properties of novel carbazole-based donor-acceptor compounds for applications in blueemitting organic light-emitting devices

Christian M. Legaspi, Regan E. Stubbs, Linda A. Peteanu, David J. Yaron, Carnegie Mellon Univ. (United States); Abraham Kemboi, Jesse Picker, Eric Fossum, Wright State Univ. (United States)

The optical and electronic properties of polythiophenes and other poly(heterocycles) have received extensive study due to their applications in photovoltaic devices and organic transistors. Several short oligometric thiophenes are highly emissive making them promising materials for organic lighting and displays. This study focuses on the effect of steric hindrance on the electronic spectroscopy of a series of bithiophenes with emphasis on identifying those structural properties that give rise to high emission yields. The simplest member of this series is 2,2'-bithiophene (2T), which computations have shown to have a highly twisted ground state.1-4 Substitution in the inner ring positions (3 and 3') with bromo (33'Br2T) and methyl (33'Me2T) substituents show distinctly different optical properties from 2T or 55'Br2T, a derivative brominated in the outer ring positions (5 and 5'). 33'Br2T and 33'Me2T exhibit very large Stokes shifts compared to 2T and 55'Br2T. Perhaps most interestingly, the excitation spectra of 33'Br2T

Conference 9549: Physical Chemistry of Interfaces and Nanomaterials XIV



and 33'Me2T do not overlap their respective absorption spectra except in a low-absorbing red tail not present in 2T or 55'Br2T. Excitation in the red tail shows a greater than ten-fold increase in the quantum yield as compared to excitation at the absorption maxima. This study explores this unusual behavior by use of ultrafast spectroscopy to probe excited state dynamics and theoretical calculations of the torsional energy surfaces and excitedstate structure. We theorize the mechanism is related to the presence of small populations of highly-emissive conformers and that torsion about inter-ring angle greatly influences the electronic properties of these thiophene oligomers.

(1) Di Césare, N.; Belletête, M.; Raymond, F.; Leclerc, M.; Durocher, G. Conformational and Spectroscopic Analysis of Selected 2,2'-Bithiophene Derivatives. J. Phys. Chem. A 1997, 101, 776–782.

(2) Alemán, C.; Domingo, V. M.; Fajarí, L.; Juliá, L.; Karpfen, A. Molecular and Electronic Structures of Heteroaromatic Oligomers: Model Compounds of Polymers with Quantum-Well Structures. J. Org. Chem. 1998, 63, 1041–1048.

(3) Millefiori, S.; Alparone, A.; Millefiori, A. Conformational Properties of Thiophene Oligomers. J. Heterocycl. Chem. 2000, 37, 847-853.

(4) Wakamiya, A.; Yamazaki, D.; Nishinaga, T.; Kitagawa, T.; Komatsu, K. Synthesis and Properties of Novel Oligothiophenes Surrounded by Bicyclo[2.2.2]octene Frameworks. J. Org. Chem. 2003, 68, 8305–8314.

9549-59, Session PWed

Growth of axial nested P-N heterojunction nanowires for high performance diode

Huibiao Liu, Chinese Academy of Sciences (China)

Heterojunction nanomaterials have attracted the interests of a broad range of scientists and engineers to explore fundamental scientific understanding the formation of heterojunction nanostructure, special properties with enhanced electrical and optical performance and the relationship between functionality and molecule structures. In this work, we synthesized a novel axial nested P-N heterojunction nanowire combined inorganic semiconductor PbS and organic conjugated polymers polypyrrole (PPy). The nested P-N heterojunction nanowires (NWs) show higher rectification ratio (exceeded 100), long-term stability and high unilateral conductivity due to the producing bigger area of junction.



Sunday - Wednesday 9 -12 August 2015 Part of Proceedings of SPIE Vol. 9550 Biosensing and Nanomedicine VIII

9550-1, Session 1

Semiconductor quantum dots as delivery and imaging platforms for intracellular assembly

Lauren D. Field, James B. Delehanty, Igor L. Medintz, U.S. Naval Research Lab. (United States)

The efficient and specific intracellular delivery of nanoparticle-based drug formulations is a critical area of research which can allow for further understanding of cellular processes and increased efficacy of therapeutic treatments. The visualization of these delivery mechanisms is often achieved using florescent molecules, some of which are bulky and can interfere with the processes being studied. Alternatively, semiconductor nanocrystals or quantum dots (QDs) are nanoscale particles that provide a scaffold for both drugs and targeting moieties while providing superior optical properties that include size-tunable photoluminescence and resistance to photobleaching. Utilizing this nanoparticle platform, delivery methods and intracellular assembly can be studied. Potential delivery mechanisms include either specific delivery using targeting ligands or direct cytosolic administration through microinjection or electroporation. Once within the cytosol, the QDs can assemble to targeted proteins, a process that can be visualized through the use of Förster resonance energy transfer (FRET). Here, we characterize the effectiveness of various delivery methods and the role of QD surface chemistry in mediating intracellular QD delivery and assembly to targeted proteins.

9550-2, Session 1

Using a narrow linewidth spectral filter for calibration of the spectrometer in spectral domain optical coherence tomography

Tong Wu, Nanjing Univ. of Aeronautics and Astronautics (China)

Calibration of the pixel-wavelength relationship is necessary for a custombuilt spectrometer in a spectral domain optical coherence tomography (SDOCT) system. A calibration method based on a narrow linewidth spectral filter (NLSF) is proposed and presented in this paper. Through detecting the narrow linewidth spectral light generated by the NLSF with the spectrometer and a commercial optical spectrum analyzer (OSA) simultaneously, the absolute wavelength corresponding to each pixel can be measured accurately. The wavelength filtering performance and the spectral resolution of the NLSF is theoretically modeled, and the generated narrow linewidth spectral signal can be covering the whole bandwidth of the light source with a measured linewidth of 0.2 nm. The proposed method may be applied to the general calibration process for the various type of spectrometer.

9550-3, Session 1

Biodegradable bisphosphonate nanoparticles for imaging and therapeutic applications in osteosarcoma

Safra Rudnick-Glick, Enav Corem-Salkmon, Igor Grinberg, Eran Gluz, Shlomo Margel, Bar-Ilan Univ. (Israel)

Osteosarcoma (OS) is amongst the most commonly diagnosed bone tumors occurring in adolescence, young adults and adults over the age of 65. Current treatment is based on a combination of surgery and chemotherapy. Chemotherapy has improved the survival rate, however it is associated with severe side effects due to the use of high dosages, nonspecific uptake and poor bone blood supply. At present bisphosphonates (BP) are widely used in the treatment of bone disorders including OS. We have engineered a unique biodegradable BP nanoparticle that possesses a dual functionality: 1) covalent attachment of a dye (e.g., NIR dye) or drug to the nanoparticles through the primary amine groups on the surface of the nanoparticle; 2) chelation to the bone mineral hydroxyapatite through the BP on the surface of the nanoparticle. Due to a high concentration of PEG in the BP nanoparticles they possess a relatively long plasma half-life time. Therefore, the nanoparticle has potential for use both in diagnosis and therapy of OS. Doxorubicin was conjugated to the free amine on the surface of the BP nanoparticles, in vitro experiments on osteosarcoma cells demonstrated that the doxorubicin-conjugated BP nanoparticles possess a higher efficacy than the free doxorubicin. Further investigation in vivo confirmed that both in chicken embryo and mouse models the doxorubicin-conjugated nanoparticle was significantly more effective in inhibiting tumor growth compared to free doxorubicin at a similar concentration. Additionally, we have shown that these BP nanoparticles preferentially target OS tumor tissue, thus increasing anti-cancer drug bioavailability at targeted site.

9550-4, Session 1

Enhanced in-vivo optical coherence tomography of live mouse brain by the use of implanted micro-lens (Invited Paper)

Iman Hassani Nia, Daniel Dombeck, Hooman Mohseni, Northwestern Univ. (United States)

Near-infrared optical coherence tomography (OCT) has gained a lot of attention due to the fact that it is relatively cheap, non-invasive and provides high resolution and fast method of imaging. However the main challenge of this technique is the poor signal to noise ratio of the images of the tissue at large depths due to optical scattering. The signal to noise ratio can be improved by increasing the source power, however the laser safety standards (ANSI Z136.1) restricts the maximum amount of power that can be used safely to characterize the biological tissue. In this talk, we discuss the advantage of implanting a micro-lens inside the tissue to have a higher signal to noise ratio for confocal and OCT measurements. We explain the theoretical background, experimental setup and the method of implanting the micro lens at arbitrary depths within a live mouse brain. The in-vivo 3D OCT and two-photon microscopy images of live mouse with implanted micro-lens are presented and significant enhancement of signal to noise ratio is observed. The confocal and OCT measurements have been performed with super-luminescent LEDs emitting at 1300 nm. We believe that the high resolution and high sensitivity of this technique is of fundamental importance for characterization of neural activity, monitoring the hemodynamic responses, tumors and for performing image guided surgeries.

9550-5, Session 1

Probing cellular forces with an elastic optical micro-cavity

Nils M. Kronenberg, Philipp Liehm, Anja Steude, Malte C. Gather, Univ. of St. Andrews (United Kingdom)

Mechanical forces at the cellular level are increasingly recognized as an important factor in numerous biological processes. Here, we present a completely new approach to measure cellular forces which overcomes limitations of existing methods such as traction force microscopy (TFM). The centerpiece of our innovation is a novel optical micro-cavity sensor that enables fast force mapping across a large field of view by analyzing changes in resonance wavelength. Our approach avoids phototoxic effects and therefore allows the measurement of cellular forces at high frame rates over hours or days. Being based on wide-field imaging, the method measures



deformation at each point of the image simultaneously and with diffraction limited lateral resolution. Vertical displacements are detected with accuracy far beyond conventional confocal microscopy (5 nm or better). Force maps can be recorded without the need for zero-force images, increasing throughput, eliminating the need to detach non-migrating cells after force mapping and allowing measurements of multiple cells on one substrate. Additionally, the optics needed for the readout of the new biosensor can be readily integrated with a conventional inverted microscope. In this presentation, we will discuss the fabrication of our micro-cavity sensors and provide detailed investigations of force and spatial resolution of the device by means of AFM indentation analysis. Cell mechanical measurements of different cell lines will be presented and links between recorded force patterns and subcellular structures labelled by fluorescence staining will be discussed.

9550-6, Session 1

Beta-cyclodextrin functionalized gold nanoparticles for trace cancer biomarker quantification

Jian Wu, Fraser Hof, Reuven Gordon, Univ. of Victoria (Canada)

We demonstrate the application of beta-cyclodextrin (?-CD) functionalized gold nanoparticles (AuNPs) as a platform for surface enhanced Raman scattering (SERS) quantification of the exogenous cancer biomarker Acetyl Amantadine (AcAm). We utilize the ?-CD encapsulation to capture the hydrophobic AcAm from solution, followed by drying and detection using SERS. We achieve a detection limit of 0.6 ng/mL using this platform. Compared with our previous ?-CD functionalized Klarite [1] and polystyrene functionalized gold nanorods [2], this platform shows better sensitivity and lower cost, which is promising for clinical adoption for early cancer detection.

[1] G. Cao, G. Hajisalem, W. Li, F. Hof, R. Gordon, "Quantification of an exogeneous cancer biomarker in urinalysis by Raman spectroscopy," Analyst 139, 5375-5378 (2014).

[2] J. Wu, W. Li, G. Hajisalem, A. Lukach, E. Kumacheva, F. Hof, and R. Gordon, "Trace cancer biomarker quantification using polystyrene-functionalized gold nanorods," Biomedical Optics Express, 5(12), 4101-4107 (2014)

9550-7, Session 1

A three-camera imaging microscope for high-speed single-molecule tracking and super-resolution imaging in living cells (Invited Paper)

Brian P. English, Timothée Lionnet, Robert H. Singer, Howard Hughes Medical Institute (United States)

Most cellular processes are the result of multiple factors coming together at precise subcellular locations to form complexes. Our aim is to develop quantitative single-molecule assays to study when and where molecules are interacting inside living cells and where enzymes are active. To this end we present a three-camera imaging microscope for fast tracking of multiple interacting molecules simultaneously, with high spatiotemporal resolution. The system was designed around an ASI RAMM frame using three separate tube lenses and custom multi-band dichroics to allow for enhanced detection efficiency. The frame times of the three Andor iXon Ultra EMCCD cameras were hardware synchronized to the laser excitation pulses of the three excitation lasers, such that the fluorophores are effectively immobile during imaging and do not yield blurred-out views of the diffraction-limited spots. Stroboscopic illumination allows robust detection from even rapidly moving objects, and since snapshots can be spaced out with varying time intervals, stroboscopic illumination enables a direct comparison to be made between fast and slow molecules under identical light dosage. We developed algorithms that accurately track and co-localize multiple

interacting biomolecules. The three-color microscope combined with our co-movement algorithms have made it possible to simultaneously image and track when mRNA may be translated by ribosomes, how the chromosome environment affects diffusion kinetics as well as other systems. Such multiplexed single-molecule measurements at a high spatiotemporal resolution inside living cells will provide a major tool for testing models relating molecular architecture and biological dynamics.

9550-8, Session 1

Nanostructured silicon biosensors (Invited Paper)

Sharon M. Weiss, Vanderbilt Univ. (United States)

Optical biosensors based on nanostructured silicon hold great promise as low-cost, lab-on-chip sensor array elements due to their compatibility with both standard microelectronics processing and standard surface functionalization techniques. The sensitivity of these optical biosensors is fundamentally derived from the level of interaction between light and the target molecules to be detected. This light-matter interaction can be strengthened by either designing the sensor structure in such a way as to promote strongly confined fields in selected regions where molecules can attach or by increasing the number of target molecules that are captured in regions where light is localized. The former approach can be achieved through modifications to the nanostructured silicon photonic sensor geometry while the latter approach is achieved through modifications to the surface chemistry of the sensor. This talk will discuss both approaches to increasing light-matter interaction, and hence sensitivity, of nanostructured silicon photonic biosensors. In particular, several biosensor designs, including photonic crystals with multiple defect holes, suspended ring resonators, and Bloch surface wave structures will be described in the silicon-on-insulator and porous silicon materials systems. A method of insitu bioreceptor synthesis will also be discussed as a means of increasing bioreceptor density. Several illustrative examples of specific molecular detection using nanostructured silicon optical biosensors will be presented.

9550-9, Session 2

Detection of cancerous biological tissue areas by means of infrared absorption and SERS spectroscopy of intercellular fluid

Martynas Velicka, Vidita Urboniene, Justinas Ceponkus, Milda Pucetaite, Feliksas Jankevicius M.D., Valdas Sablinskas, Vilnius Univ. (Lithuania)

Precise identification of cancerous biological tissue areas during the surgical segmental resection has high importance since information about location of borders between normal and cancerous tissues is needed. Most of the identification methods used nowadays are based on histopathology, which is time consuming procedure and cannot be performed directly in the operating room during the surgery.

We present a novel approach for the detection of cancerous kidney tissue areas by measuring surface-enhanced Raman (SERS) spectrum of its intercellular fluid taken from the tissue. Thickness of the dried film of the fluid on optical substrate is in nanometric scale and conventional Raman spectroscopy cannot be used unless some enhancement of the Raman signal is applied. Determination of cancerous and normal kidney tissue areas was performed by using differences in the SERS spectra of the fluid taken from the corresponding tissue areas.

The samples were prepared by sliding the kidney tissue over the calcium fluoride optical substrate and covering the dried fluid film by silver nanoparticle colloidal solution. In order to suppress fluorescence background the measurements were performed in NIR region with the excitation wavelength of 1064 nm and 785 nm. The most significant spectral differences were found in the region between 400-1300 cm-1, where spectral bands related to various vibrations of fatty acids, glycolipids and carbohydrates are located. We found for the first time that SERS spectra of



intercellular fluid can be used for detection of cancerous areas of biological tissue and the method has potential to be used directly during the surgery.

9550-10, Session 2

Colloidal assembly of surface enhanced Raman scattering sensors for monitoring airway infections (Invited Paper)

Regina Ragan, Nicholas Sharac, Univ. of California, Irvine (United States); Salvatore Campione, Sandia National Labs. (United States); Katrine Whiteson, Filippo Capolino, Univ. of California, Irvine (United States)

Since doctors first used flies to detect glucose in the urine of diabetic patients, the biomarkers primarily used in medical diagnostics and disease monitoring have been small molecule metabolites. Current tools such as clinical culturing take days to obtain results, leaving physicians to choose antibiotic treatment based on trial and error. Pilot breath and sputum metabolite profile studies using Gas chromatography-Mass spectroscopy (GC-MS) paired with microbial DNA sequencing, establishing that fermentation products such as 2,3-butanedione are present in the ppb range in cystic fibrosis patients. Though single molecule detection limits have been demonstrated using nanostructured surfaces previously, issues of cost, shelf life, reproducibility in detection response, and integration have limited technological impact. We have created and developed a low-cost colloidal assembly process using covalent nanoparticle-substrate interactions to produce arrays of ad hoc clusters of nanoparticles. Full-wave simulations show the dependence of electric field enhancements on geometric arrangement of and gap spacing between nanoparticles in clusters. Transmission electron microscopy data shows that by varying driving forces for assembly, diffusion versus electrophoresis, nanoparticle clusters with gaps between nanoparticles of 4 nm down to 1 nm, respectively, are obtained. SERS characterization measurements demonstrate robust SERS sensors reaching ppb detection limits for small volatile molecules reproducibly over large areas. Samples have a tested shelf life of two years indicating that materials, chosen for integration in micro-optofluidic chips, do not degrade over time. Our platform aims to achieve the elusive goal of providing easy to use technology alongside ppb detection for patient diagnosis and treatment.

9550-11, Session 2

Detection of p17-1 peptide (HIV) based in surface enhanced Raman scattering (SERS)

Leandro de B. Carneiro, Chemistry Institute (Brazil) and Univ. of Victoria (Canada); Alexandre Brolo, Univ. of Victoria (Canada); Sidney Ribeiro, Univ. Estadual Paulista "Júlio de Mesquita Filho" (Brazil)

SERS offers great promises for simplified and sensitive detection of biomolecular interactions that are relevant for early disease diagnostics.

Human immunodeficiency virus (HIV) has been a problem for decades. There are several methods of diagnostics based on antibodies specific reactions, such as Western blotting and enzyme-linked immunosorbent assays (ELISAs). However, new strategies have been developed for rapid HIV diagnostics and, as a proof-of-concept, peptide p17-1 was considered here.

The matrix protein p17 is a structural protein that is essential in the life cycle of the retrovirus . The early stages of the virus replication involve the pre integration of the DNA complex into the nucleus. P17 plays a role in RNA viral binding and transport to the membrane

The fabrication and characterization of a new SERS platform for HIV detection based on peptide p17-1 is described. Self-Assembled monolayers (SAM) were obtained by immersion of the gold surface into ethanolic solution of 11-Mercaptoundecanoic acid (MUA). To activate the COOH functional group at the gold surface EDC/NHS (1-ethyl-3-(-3dimethylaminopropyl) carbodiimid/ N-hydroxysuccinimide) was used. The prepared substrates were immersed in a solution containing of the anti-p17 (100µg/ml). Gold substrates were immobilization with the peptide p17-1 (0.1µM sequence LSGGELDRWEKIRLPGG). SERS probes were prepared with gold nanoparticles and are coated with a Raman reporter molecule (Nile Blue A) and, functionalized with an anti-p17. These structures (SERS probe and Au substrate) allow for a sandwich assay, a strategy regularly used for high-sensitivity detection . Spectral variations were analysed through a statistical approach and also considering false positive possibility. Statistical distribution shows high intensity for surface exposed to solution containing the peptide p17-1 when compared with negative controls. The suggest approach to detect peptide p17 is promising and could be further tested using real blood.

References

Becker, P. D.; Fiorentini, S.; Link, C.; Tosti, G.; Ebensen, T.; Caruso, A.; Guzman, C. A., Vacine, 2006,24, 5269–5276, Bukrinskaya A G, Vorkunova G K, Tentsov Y. AIDS, Res Hum Retroviruses 1992; (10):1795–801

Vorkunova G K, Tentsov L., Mol. Biol, 1993, 1, 49-57. Fan, M.; Brolo, A. G.; Phys. Chem. Chem. Phys., 2009, 11, 7381-738

9550-12, Session 2

Using Raman spectroscopy and SERS for in-situ studies of rhizosphere bacteria

Sneha Polisetti, Nameera Baig, Univ. of Notre Dame (United States); Amber Bible, Jennifer Morrell-Falvey, Mitchel Doktycz, Oak Ridge National Lab. (United States); Paul W. Bohn, Univ. of Notre Dame (United States)

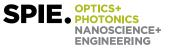
Bacteria colonize plant roots to form a symbiotic relationship with the plant and can play an important role in promoting plant growth. Raman spectroscopy is a useful technique to study these bacterial systems and the chemical signals they utilize to interact with the plant. We present a Raman study of Pantoea sp. YR343 that was isolated from the rhizosphere of Populus deltoides (Eastern Cottonwood). Pantoea sp. YR343 produces yellowish carotenoid pigments that play a role in protection against UV radiation, in the anti-oxidative pathways and in membrane fluidity. Raman spectroscopy is used to non-invasively characterize the membrane bound carotenoids. The spectra collected from a mutant strain created by knocking out the crtB gene that encodes a phytoene synthase responsible for early stage of carotenoid biosynthesis, lack the carotenoid peaks. Surface Enhanced Raman Spectroscopy is being employed to detect the plant phytoharmone indoleacetic acid that is synthesized by the bacteria. This work describes how Raman spectroscopy is utilized as a label free, non-destructive method of studying plant-bacteria interactions in the rhizosphere.

9550-13, Session 3

Advances in macromolecular data storage (Keynote Presentation)

Masud Mansuripur, College of Optical Sciences, The Univ. of Arizona (United States)

Many of the traditional problems in disk and tape data storage can be overcome if data-blocks were to be released from the confines of a disk (or tape) and allowed to float freely between read/write stations (i.e., heads) and permanent "parking spots." The heads and parking spots thus become fixed structures within an integrated chip, while the macromolecular data blocks themselves become the (mobile) storage media. In this scheme, a large number of read/write heads could operate in parallel, the heads and parking spots would be constructed (layer upon layer) in a truly 3-dimensional fashion, and individual nanometer sized molecules—strung together in a flexible macromolecular chain—would be used to represent the zeros (Os) and ones (1s) of binary information. We discuss the potential advantages of this alternative scheme for secondary data storage and, to demonstrate the feasibility of the concept, present results of experiments



based on DNA molecules that travel within micro-fluidic chambers. Since our first proposals to develop macromolecular data storage systems, other groups have contributed to developments in DNA-based techniques for information storage and processing. In this presentation we will discuss the latest developments reported by other groups as well.

9550-14, Session 3

Mid-Infrared (~2.8 μm to ~7.1 μm) interband cascade lasers (Keynote Presentation)

Sven Höfling, Univ. of St. Andrews (United Kingdom); Robert Weih, Matthias Dallner, Julius-Maximilians-Univ. Würzburg (Germany); Julian Scheuermann, Lars Nähle, Marc Fischer, Johannes Koeth, nanoplus GmbH (Germany); Martin Kamp, Julius-Maximilians-Univ. Würzburg (Germany)

20 years after their first reference [1] interband cascade lasers (ICLs) have become a mature and competitive semiconductor laser source in the mid-infrared region. The carrier rebalancing concept that was introduced in 2011 [2] drastically improved the performance. As a consequence the wavelength window that is accessible for ICLs operating at ambient temperatures could be extended. For GaSb based ICLs cw-emission at room temperature could be achieved up to a wavelength of 5.6 μ m [3]. As the need for thicker claddings at longer wavelengths makes the growth of the superlattice claddings increasingly difficult and limits the heat dissipation, a plasmon waveguide structure with highly doped InAs-layers grown on InAs-substrates is typically used for ICLs emitting up to ~7 μm in pulsed mode at room temperature [4]. With regard to the short wavelength limit of ICLs, we present cw emission of a GaSb based ICL emitting at 2.8 μ m and with regard to the long wavelength limit we present room temperature pulsed operation of an InAs based plasmonic waveguide ICL up to 7.1 μ m. Furthermore, we show single mode emitting ICLs with distributed feedback gratings emitting between 2.8 and 5.2 μ m.

[1] R. Q. Yang, Superlatt. Microstruct. 17 77 (1995)

[2] I. Vurgaftman, W. W. Bewley, C. L. Canedy, C. S. Kim, M. Kim, C. D. Merritt, J. Abell, J. R. Lindle and J. R. Meyer, Nature Commun. 2 585 (2011)

[3] W. W. Bewley, C. L. Canedy, C. S. Kim, M. Kim, C. D. Merritt, J. Abell, I. Vurgaftman and J. R. Meyer, Opt. Expr. 20 3235-3240 (2012)

[4] M. Dallner, S. Höfling and M. Kamp,, Electron. Lett., 49, 4, (2013)

[5] Z. Tian, L. Li, H. Ye, R.Q. Yang, T.D. Mishima, M.B. Santos, and M.B. Johnson, Electron. Lett., 48, 2, (2012)

9550-15, Session 3

Towards novel compact laser sources for non-invasive diagnostics and treatment *(Keynote Presentation)*

Edik U. Rafailov, Aston Univ. (United Kingdom)

In the past decades, progress in compact semiconductor based laser technologies has brought to science and industry an enormous number of new applications. Such laser systems which were mostly utilised in the communication and other industries are now becoming adopted in biology and medicine. In this talk we would like to discuss and review some of the most promising biomedical applications where novel compact lasers are being used. Particularly we are focussing on the development of compact non-invasive diagnostics system for monitoring main body parameters in parallel, like blood perfusion, blood and tissue oxygen saturation based on Doppler Flowmetry, tissue oximetry and fluorescent spectroscopy techniques.

9550-16, Session 4

Switchable bioelectronics on graphene interface (Invited Paper)

Onur Parlak, Linköping Univ. (Sweden); Ashutosh Tiwari, Linköping Univ (Sweden); Anthony P. F. Turner, Linköping Univ. (Sweden)

Smart and flexible bioelectronics on graphene have emerged as a new frontier in the field of biosensors and bioelectronics. Graphene has begun to be seen as an ideal signal transducer and a promising alternative for the production of low-cost bioelectronic devices.1-2 However, biological systems used in these devices suffer from a lack of control and regulation. There is an obvious need to develop "switchable" and "smart" interfaces for both fundamental and applied studies. Here, we report the fabrication of a stimuli-responsive graphene interface, which is used to regulate biomolecular reactions.

The present study aims to address the design and development of a novel auto-switchable graphene bio-interface that is capable of positively responding, by creating smart nanoarchitectures. By changing the external conditions such as temperature, light and pH of the medium, we acheived control of the biochemical interactions. In the negative mode, access of an associated enzyme to its substrate is largely restricted, resulting in a decrease in the diffusion of reactants and the consequent activity of the system. In contrast, the biosubstrate could freely access the enzyme facilitating bioelectrocatalysis in a positive response.

Using electrochemical techniques, we demonstrated that interfacial bioelectrochemical properties can be tuned by modest changes in conditions. Such an ability to independently regulate the behaviour of the interface has important implications for the design of novel bioreactors, biofuel cells and biosensors with inbuilt self-control features.

9550-17, Session 4

Evaluating cells and protocells as therapeutic vehicles (Invited Paper)

Natalie Adolphi, The Univ. of New Mexico (United States); Jaclyn Murton, Sandia National Labs. (United States); Helen Hathaway, The Univ. of New Mexico (United States); Yu-Shen Lin, Jason Townson, Oncothyreon (United States); Jeff Norenberg, The Univ. of New Mexico (United States); Eric Carnes, Carlee Ashley, Jeff Brinker, Sandia National Labs. (United States)

Mesoporous silica nanoparticle-supported lipid bilayers (protocells) can be loaded with a variety of drugs and/or imaging probes and modified using various surface chemistries. To enhance delivery of protocells to solid tumors, we investigated a novel delivery method, in which circulating mononuclear cells (MCs), which naturally infiltrate tumors, are used to actively deliver protocells to tumor tissue. MCs were extracted by density gradient separation from the spleens of immune-competent polyomavirus middle T (PyMT) transgenic mice, which spontaneously develop epithelial mammary tumors that mimic human breast cancer. MCs were loaded with DOPC (1,2-dioleoyl-sn-glycero-3-phosphocholine)-coated polydisperse protocells (diameter <200 nm), further modified with PEG (polyethylene glycol), DOPS (1,2-dioleoyl-sn-glycero-3-phosphoserine), or DOTAP (1,2-dioleoyl-3-trimethylammonium-propane) and injected into tumor-bearing PyMT-FVB mice or FVB mice lacking the transgene, which have normal mammary glands. We observed the biodistribution of protocell-loaded MCs and directly-injected protocells in vivo by SPECT-CT imaging, and post-mortem via fluorescence microscopy and flow cytometry, demonstrating that MC-mediated delivery enhances localization of protocells to mammary tumors compared to direct injection. Further, both direct injection and MC-mediated delivery resulted in higher protocell concentrations in mammary tumors, relative to normal mammary tissue. In normal mice, we also demonstrated that fully-differentiated macrophages can be used to direct protocells to the lung. Additionally, we performed in vivo SPECT-CT to quantify the biodistribution of monosized mesoporous



silica particles as a function of diameter (25, 50, 90, 150 nm) in normal rats, demonstrating that smaller particle size correlates with increased circulation time and decreased uptake by the liver and spleen.

9550-18, Session 4

Effect of PKC? expression to cell death after photoactivation of Hypericin delivered to cell through different drug delivery systems

Matú? Mi?uth, Jaroslava Joniova, Pavol Jozef ?afárik Univ. in Kol?ice (Slovakia); Pavol Mi?kovsk?, Zuzana Nadova, Pavol Jozef ?afárik Univ. in Kol?ice (Slovakia) and Ctr. for Interdisciplinary Sciences (Slovakia)

Low-density lipoprotein (LDL), a natural in vivo carrier of cholesterol in the vascular system, plays a key role in the delivery of hydrophobic photosensitizer (pts) to tumor cells in PDT, including hypericin (Hyp), a potent natural pts. Hyp under light illumination causes antiproliferative and cytotoxic effects (necrosis as well as apoptosis) in many tumor cell lines.

These properties together with minimal dark toxicity, tumor selectivity and high clearance rate from the host body, make Hyp a promising agent for PDT of cancer as well as for tumor photo-diagnosis.

In the present study we aim to investigate the consequences on cell survival and cell death induced by photo-activated Hyp delivered to the cells through different drug delivery systems including LDL.

Hyp incorporation and redistribution, cell survival and type of the cell death were assessed by confocal fluorescence imaging and flow cytometry.

We have evaluated the influence of photo-activated Hyp delivered to the cells thhrough different drug delivery systems on cell death in nontransfected and transfected (PKCa-) human glioma cells (U-87 MG).

No significant differences were detected in cell survival between nontransfected and transfected PKCa- cells when Hyp was delivered without any carrier. However, the type of cell death was notably affected by silencing the pkca gene. Photo-activation of Hyp strongly induced apoptosis in nontransfected cells, but the level of necrotic cells in transfected PKCa- cells increased significantly. We suggest that PKCa, as Bcl-2 kinase, indirectly protects U-87 MG cells against oxidative stress and subsequent cell death.

9550-19, Session 4

Enhanced kinetics of quantum dot bound enzymatic nanosensors

Joyce Breger, Scott Walper, Mario G. Ancona, Michael Stewart, Kimihiro Susumu, Sebastian A. Diaz, Igor L. Medintz, U.S. Naval Research Lab. (United States)

Nanosensors employing quantum dots (QDs) and functional moieties such as enzymes offer tremendous promise for disease surveillance/diagnostics and chemical/biological threat activity. Advantages of QDs over other nanoscaffolds include their small size and inherent photochemical properties such as size tunable fluorescence, ease in attaching functional moieties, and resistance to photobleaching. Making QDs well-suited for rapid, optical measurement applications.

The mechanisms for increased catalytic activity of enzymes attached to nanoparticles was investigated by attaching various ratios of phosphotriesterase (PTE) enzymes to two distinctly sized QDs, with emission maxima centered at 525 or 625 nm. PTE catalyzes the detoxification of organophosphate pesticides to p-nitrophenol. To confirm assembly and characterize QD-PTE bioconjugates dynamic light scattering and gel electrophoresis were employed.

PTE activity was assayed using paraoxon, an analog of sarin, as a substrate. The conversion of paraoxon to p-nitrophenol was monitored over time by measuring the absorbance. Absorbance values were converted to concentration by employing a p-nitrophenol standard curve. Enzymatic activity and characteristic parameters were determined by fitting the initial rates of the progress curves to a Michaelis-Menten single substrate model.

We attempt to elucidate the mechanisms for enhanced catalytic activity when attached to nanoparticle surfaces as compared to free enzyme in solution. PTE hydrolytic activity was studied when attached to two differently sized QDs and significant enhancement in activity was observed when attached to QDs as compared to free enzyme with more dramatic increases when PTE was attached at lower ratios to the smaller sized QDs.

9550-20, Session 4

Nanoplasmonic lenses for bacteria sorting (Invited Paper)

Xiangchao Zhu, Ahmet A. Yanik, Univ. of California, Santa Cruz (United States)

We demonstrate that patches of two dimensional arrays of circular plasmonic nanoholes patterned on gold-titanium thin film enables subwavelength focusing of visible light in far field region. Efficient coupling of the light with the excited surface plasmon at metal dielectric interface results in strong light transmission. As a result, surface plasmon plays an important role in the far field focusing behavior of the nanohole-aperture patches device. Furthermore, the focal length of the focused beam was found to be predominantly dependent on the overall size of the patch, which is in good agreement with that calculated by Rayleigh-Sommerfield integral formula. The focused light beam can be utilized to separate bio-particles in the dynamic range from 0.1 ?m to 1 ?m through mainly overcoming the drag force induced by fluid flow. In our proposed model, focused light generated by our plasmonic lenses will push the larger bio-particles in size back to the source of fluid flow and allow the smaller particles to move towards the central aperture of the patch. Such a new kind of plasmonic lenses open up possibility of sorting bacterium-like particles with plasmonic nanolenses, and also represent a promising tool in the field of virology.

9550-21, Session 4

Nano scaffolds and stem cell therapy in liver tissue engineering

Laila M. Montaser, Menoufia Univ. (Egypt)

Tissue engineering and regenerative medicine have been constantly developing of late due to the major progress in cell and organ transplantation, as well as advances in materials science and engineering. Although stem cells hold great potential for the treatment of many injuries and degenerative diseases, several obstacles must be overcome before their therapeutic application can be realized. These include the development of advanced techniques to understand and control functions of micro environmental signals and novel methods to track and guide transplanted stem cells. A major complication encountered with stem cell therapies has been the failure of injected cells to engraft to target tissues. The application of nanotechnology to stem cell biology would be able to address those challenges. Combinations of stem cell therapy and nanotechnology in tissue engineering and regenerative medicine have achieved significant advances. These combinations allow nanotechnology to engineer scaffolds with various features to control stem cell fate decisions. Fabrication of Nano fiber cell scaffolds onto which stem cells can adhere and spread, forming a niche-like microenvironment which can guide stem cells to proceed to heal damaged tissues. In this paper, current and emergent approach based on human stem cells in the field of liver tissue engineering is presented for specific application in an animal model. The combination of stem cells and tissue engineering opens new perspectives in tissue regeneration for stem cell therapy because of the potential to control stem cell behavior with the physical and chemical characteristics of the engineered scaffold environment.



9550-22, Session 4

A creatinine biosensor based on admittance measurement

Congo Tak-Shing Ching, Tai-Ping Sun, Deng-Yun Jheng, Hou-Wei Tsai, Hsiu-Li Shieh, National Chi Nan Univ. (Taiwan)

Kidney disease is reportedly increasing in developed countries, including the US, Canada, Australia, and Europe. It imposes a substantial economic burden. Measurement of blood creatinine level is clinically important for the evaluation of renal dysfunction. Clinically, the normal physiological blood creatinine level is between 44 uM and 106 uM. Regular check of blood creatinine level can reduce the incidence rate for the people who are at the high risk of renal dysfunction. Biosensor provides point-of-care testing so as to achieve regular check of blood creatinine level at home. No paper has been found in the literatures on developing creatinine biosensor based on admittance measurement. Therefore, this study aims to develop a simple and reliable creatinine biosensor based on admittance measurement.

The creatinine biosensor was fabricated with the enzyme "creatinine deiminase" immobilized on screen-printed graphite electrodes by simple drop coating method.

Admittance measurement at specific frequency ranges (22.80 – 84.71 Hz) showed biosensor having an excellent linear (r2 > 0.95) response range (50 – 250 uM), with the maximum sensitivity of -3x10-6 Siemens/uM. Intraclass correlation coefficient (ICC) showed that the biosensor has excellent reliability and validity (ICC = 0.98). And the biosensor was reliable enough to determine the concentrations of creatinine (50 – 250 uM) with the coefficient of variation of about 5.5%.

In conclusion, a simple and reliable creatinine biosensor was developed and it is capable of precisely determining blood creatinine levels in both the normal physiological and pathological ranges.

9550-23, Session 4

Quantitative fluorescence nanoscopy for cancer biomedicine

Li-Jung Lin, Oregon Health & Science Univ. (United States); Tao Huang, Oregon Health and Science Univ (United States); Alec Peters, Xiaolin Nan, Oregon Health & Science Univ. (United States)

Cancer is a major health threat worldwide. Options for targeted cancer therapy, however, are often limited, in a large part due to our incomplete understanding of how key processes including oncogenesis and drug response are mediated at the molecular level. New imaging techniques for visualizing biomolecules and their interactions at the nanometer and single molecule scales, collectively named fluorescence nanoscopy, hold the promise to transform biomedical research by providing direct mechanistic insight into cellular processes. We discuss the principles of quantitative single-molecule localization microscopy (SMLM), a subset of fluorescence nanoscopy, and their applications to cancer biomedicine. In particular, we will examine oncogenesis and drug resistance mediated by mutant Ras, which is associated with ~1/3 of all human cancers but has remained an intractable drug target. At ~20 nm spatial and single-molecule stoichiometric resolutions, SMLM clearly showed that mutant Ras must form dimers to activate its effector pathways and drive oncogenesis. SMLM further showed that the Raf kinase, one of the most important effectors of Ras, also forms dimers upon activation by Ras. Moreover, treatment of cells expressing wild type Raf with Raf inhibitors induces Raf dimer formation in a manner dependent on Ras dimerization. Together, these data suggest that Ras dimers mediate oncogenesis and drug resistance in tumors with hyperactive Ras and can potentially be targeted for cancer therapy. We also discuss recent advances in SMLM that enable simultaneous imaging of multiple biomolecules and their interactions at the nanoscale. Our work demonstrates the power of quantitative SMLM in cancer biomedicine.

9550-24, Session 5

Resonant waveguide grating imagers for single cell analysis and high throughput screening (Invited Paper)

Ye Fang, Corning Incorporated (United States)

Resonant waveguide grating (RWG) biosensor systems use a microtiter plate array of diffractive nanograting waveguide structures to establish evanescent waves under illumination for measuring tiny changes in local refractive index arising from the dynamic mass redistribution (DMR) of living cells upon stimulation. Whole-plate RWG imager enables highthroughput profiling and screening of drugs in the context of distinct cellular phenotypes including cell adhesion, proliferation, signaling, and infection. RWG imager under microfluidics not only manifests distinct receptor signaling waves, but also differentiates long-acting agonism and antagonism. Spatially resolved RWG imager allows for single cell analysis including cell-to-cell variability of receptor signaling and the invasion of cancer cells in a spheroidal structure through 3-dimensional extracellular matrix. High frequency RWG imager permits real-time detection of druginduced cardiotoxicity. The wide coverage in target, pathway, assay, and cell phenotype has made RWG biosensor systems widely accepted in both basic research and early drug discovery processes.

9550-25, Session 5

Motion behaviour of mammalian AT-SC under evanescent field illumination

Mukhzeer Mohamad Shahimin, Univ. Malaysia Perlis (Malaysia); Fhataheya Buang, Univ. Kebangsaan Malaysia (Malaysia); Nor Azura Malini B. Ahmad Hambali, Vithyacharan Retnasamy, Mohamad Halim Abdul Wahid, Univ. Malaysia Perlis (Malaysia); Ali Hussain Reshak, Univ. of West Bohemia (Czech Republic)

The motion behaviour of mammalian adipose tissue derived stem cells (AT-SC) on an integrated channel waveguide under the evanescent field illumination is demonstrated and analysed. An approximately 20µm diameter pseudospherical cells in aqueous medium are deposited in a reservoir over a copper ion-exchanged channel waveguide. Light from a tuneable laser operating at ~1064nm was coupled into the waveguide, causing the cells under the illumination of evanescent field and moved in a skewed stochastic motion in accordance to the laser power. The trajectory angle of the motion of the cells towards the illuminated channel waveguide was investigated and analysed to distinguish the factors that affect such behaviour. The cells reach a position relative to the illuminated channel that is dictated by the compounded effect of convectional current and evanescent field. The observations deduced that motion due to the optical field exists and were more pronounced when considering the trajectory angle towards the output facet. However, the optical forces are not significantly large enough to counter the motion due to the convection current. The results are discussed in light of the potential application of optical channel waveguides for bioanalytical applications, namely in the identification, sorting and analysis of differently sized mammalian cells without recourse to fluorescence or antibody staining.

9550-26, Session 5

Rational design of on-chip refractive index sensors based on lattice plasmon resonances

Linhan Lin, Yuebing Zheng, The Univ. of Texas at Austin (United States)

Lattice plasmon resonances (LPRs), which originate from the plasmonicphotonic coupling in gold or silver nanoparticle arrays, possess ultra-



narrow linewidth by suppressing the radiative damping and provide the possibility to develop the plasmonic sensors with high figure of merit (FOM). However, the plasmonic-photonic coupling is greatly suppressed when the nanoparticles are immobilized on substrates because the diffraction orders are cut off at the nanoparticle-substrate interfaces. Here, we develop the rational design of LPR structures for the high-performance, on-chip plasmonic sensors based on both orthogonal and parallel coupling. Our finite-difference time-domain simulations in the core/shell SiO2/Au nanocylinder arrays (NCAs) reveal that new modes of localized surface plasmon resonances (LSPRs) show up when the aspect ratio of the NCAs is increased. The height-induced LSPRs couple with the superstrate diffraction orders to generate the robust LPRs in asymmetric environment. The high wavelength sensitivity and narrow linewidth in these LPRs lead to the plasmonic sensors with high FOM and high signal-to-noise ratio (SNR). Wide working wavelengths from visible to near-infrared are also achieved by tuning the parameters of the NCAs. Moreover, the wide detection range of refractive index is obtained in the parallel LPR structure. The electromagnetic field distributions in the NCAs demonstrate the heightenabled tunability of the plasmonic "hot spots" at the sub-nanoparticles resolution and the coupling between these "hot spots" with the superstrate diffraction waves, which are responsible for the high performance LPRsbased on-chip refractive index sensors.

9550-28, Session 5

Ultra-broadband plasmonic super absorbers for universal surface enhanced Raman spectroscopy substrate

Nan Zhang, Kai Liu, Haomin Song, Xie Zeng, Dengxin Ji, Qiaoqiang Gan, Univ. at Buffalo (United States)

Although Raman spectroscopy has been commercialized, low-cost and large-area surface enhanced Raman spectroscopy (SERS) substrates with localized enhanced field are heavily required. However, currently dominant manufacturing techniques are expensive and complicated for large-area fabrication. Furthermore, most SERS substrates can only be used for individual excitation wavelengths. In this work, we will report an ultra-broadband super absorbing metasurface to enhance SERS signals in a broadband region (i.e. from 450 nm to 1000 nm). The design consisting of an Ag ground plate, a SiO2 spacer, and a layer of Ag nanoparticles was fabricated using simple film deposition and thermal annealing techniques. A broadband absorption over 80% from 414 nm to 956 nm was obtained, resulting in localized field enhancement between adjacent nanoparticles. We employed this metasurface to test its broadband SERS signal by adsorbing 1,2-Bis(4-pyridyl)-ethylene (BPE) molecules on top of it. We employed 5 laser lines (i.e., 514, 532, 633, 671 and 785 nm) to excite the sample and observed fingerprint signature of BPE molecules under all 5 excitation wavelengths with the average enhancement factor up to 5.3?107. Therefore, the designed SERS substrate can work for almost "all" available excitation wavelengths over a broadband, which is particularly useful for sensing a broad spectrum of chemicals on the same chip.

9550-29, Session 5

Plasmonic nanoparticles sensors utilizing hybrid modes, electrical excitation, and anisotropic particles

Wolfgang Fritzsche, Andre Dathe, Pavel Kliuiev, Jacqueline Jatschka, Uwe Hübner, Mario Ziegler, Matthias Thiele, Steffen Trautmann, Janina Wirth, Frank Garwe, Andrea Csaki, Ondrej Stranik, Leibniz-Institut für Photonische Technologien e.V. (Germany)

Surface Plasmon Resonance (SPR) in metallic nanostructures is an optical effect that can be exploited for the detection of small molecules. There is a broad range of metallic nanostructures supporting different SPR modes, and nanostructures can be even geometrically combined leading to the creation

of new hybridised SPR modes.

In our study, we investigated the properties of a hybridised SPR mode (gap modes GM) created by the placement of metallic nanoparticles onto metallic layers and its use as a sensitive sensor.

A tunneling current passing through a metal-insulator-semiconductor structure can generate supported SPR modes, that can be scattered through GM, which was experimentally confirmed.

Moreover, we were able to experimentally follow the degradation of anisotropic (silver nanoprism) nanoparticles under ambient conditions in real time. Using atomic force microscopy and optical spectroscopy we observed an anisotropic corrosion that is starting from the tips of the nanoparticles.

9550-30, Session 5

Wafer-scale aluminum plasmonics for biosensing applications

Arash Farhang, Matthew C. George, Brent Williamson, Mike Black, Ted Wangensteen, James Fraser, Rumyana Petrova, MOXTEK, Inc. (United States)

Moxtek has leveraged existing capabilities in wafer-scale patterning of sub-wavelength wire grid polarizers into the fabrication of 1D and 2D periodic aluminum plasmonic structures. This work will discuss progress in 200 mm diameter wafer-scale fabrication of post and grating based aluminum nanostructures for SPR sensing as well as optical modeling results and device performance. More specifically, hybrid systems combining such periodic nanostructure arrays with a thin underlying metallic film on a glass substrate are investigated. These structures are of great interest as they combine the capabilities of both SPR and LSPR based sensors. The enhanced sensing advantage they offer is based on a nanofocusing mechanism. Specifically, the propagating surface plasmon launched on the metallic film couples to the nanostructure array and is thereby focused into a smaller volume than simply the evanescent plasmon field. This in turn results in a more enhanced surface sensitivity. This advantage, combined with the fact that the structures are operable in the same prism based configuration of standard SPR, i.e. existing commercial sensing platforms, makes them an obvious choice for future use. Potential markets include medical diagnostics, forensic testing, environmental monitoring, and food safetv.

9550-31, Session 5

Real-time protein aggregation monitoring based on a simultaneous light scattering investigation and a bloch surface wavebased approach

Sara Santi, Elsie Barakat, Ecole Polytechnique Fédérale de Lausanne (Switzerland); Reinhard Neier, Univ. of Neuchâtel (Switzerland); Hans Peter Herzig, Ecole Polytechnique Fédérale de Lausanne (Switzerland)

The misfolding and aggregation of amyloid proteins has been associated with incurable diseases such as Alzheimer's or Parkinson's disease. In the specific case of Alzheimer's disease, recent studies have shown that cell toxicity is caused by soluble oligomeric forms of Amyloid-beta (A?) peptide aggregates appearing in the early stages of aggregation, rather than by insoluble fibrils. Research on new strategies of diagnosis is imperative to detect the disease prior to the onset of clinical symptoms.

Here, we propose the use of an optical method for protein aggregation dynamic studies using a Bloch surface wave (BSW) based approach. A onedimension photonic crystal made of a periodic stack of silicon oxide and silicon nitride layers is used to excite a Bloch surface wave, which is sensitive to variation of the refractive index of an aqueous solution. The aim is to detect the early dynamic events of protein aggregation and fibrillogenesis of the amyloid-beta peptide A?42, which plays a central role in the onset



of the Alzheimer's disease. The detection principle relies on the refractive index changes caused by the depletion of the A?42 monomer concentration during oligomerization and fibrillization.

We demonstrate the efficacy of the BSW approach by monitoring in realtime the first crucial steps of A?42 oligomerization and in the presence of small molecular probes able to interfere with the dynamics of amyloid formation. Moreover, we improved the setup to perform a simultaneous light scattering measurement, with the purpose of real-time monitoring the size change of the A? aggregates, throughout fibrillization.

9550-32, Session PWed

Fluorescent cy5 silica nanoparticles for cancer cell imaging

Claire L. O'Connell, Robert I. Nooney, Macdara Glynn, Jens Ducrée, Colette McDonagh, Dublin City Univ. (Ireland)

Cancer is a leading cause of death worldwide, with metastasis responsible for the majority of cancer-related deaths. Circulating tumour cells (CTCs) play a central role in metastasis. Fluorescent silica particles (NPs), of diameter -50 nm which contain a large concentration of Cy5 dye molecules and are extremely bright, have been developed to detect these rare CTCs. Due to this brightness, the particles have superior performance compared to single Cy5 dye molecule labels, for detecting cancer cells.

Fluorescence measurements show that the NPs are almost 100 times brighter than the free dye. They do not photobleach as readily and, due to the biocompatible silica surface, they can be chemically modified, layer by layer, in order to bind to cells.

The choice of these chemical layers, in particular the NP to antibody linker, along with the incubation period and type of media used in the incubation, has a strong influence on the specific binding abilities of the NPs.

In this work, NPs have been shown to selectively bind to the MCF-7 cell line by targeting epithelial cellular adhesion molecule (EpCAM) present on the MCF-7 cell membrane by conjugating anti-EpCAM antibody to the NP surface. Results have shown a high signal to noise ratio for this cell line in comparison to a HeLa control line.

NP attachment to cells was verified qualitatively with the use of fluorescence microscopy and quantitatively using image analysis methods. Once the system has been optimised, other dyes will be doped in the silica and their use in multiplexing will be investigated.

9550-33, Session PWed

Probing the interaction between Congo Red and ?-amyloid for diagnosis and inhibition of brain plaque formation in Alzheimer's disease

Kristine A. Zhang, Yat Li, Univ. of California, Santa Cruz (United States)

Alzheimer's disease (AD), the most common form of dementia, is an age-related neurodegenerative disorder and the seventh leading cause of death in the United States. One strong pathological indicator of AD is senile plaques, which are aggregates of fibrils formed from assemblies of 40- or 42- residue peptides, known as amyloid ?-peptides (A?). Thus, detection and inhibition of A? aggregation are actively investigated with the objective to prevent and treat AD. Congo red (CR) is one of the most widely used dye molecules for probing as well as inhibiting A? aggregation. However, the nature of interaction between CR and A? is not well understood at the molecular level, which hinders progress in this area. In this research, we have systematically studied the fundamental interaction between CR and A? using a combination of spectroscopic techniques. Compared to CR alone, interaction with A? results in a red-shifted or new absorption peak near 520 nm and significantly enhanced photoluminescence as well as surfaceenhanced Raman scattering (SERS) signal. The results led us to propose a new model to explain the interaction between CR and A?, which suggests

that CR exists primarily in a micellar or aggregated form in water down to about 0.5 ?M and, upon interacting with A? or similar proteins or peptides, dissociates into monomers. The results and new model have significant implications for developing new molecules and strategies to detect and inhibit brain plaque formation and thereby prevent and treat neurological diseases like AD in the long term.

9550-35, Session PWed

Evaluation of performance of portable respiratory monitoring system based on micro-electro-mechanical-system for respiratory gated radiotherapy

Jiwon Sung, Korea Univ. (Korea, Republic of) and Kyung Hee Univ. Hospital at Gangdong (Korea, Republic of); Dong Wook Kim, Weon Kuu Chung, Kyung Hee Univ. Hospital at Gangdong (Korea, Republic of)

Purpose:

This study evaluated the accuracy of the hand-made portable respiratory monitoring system (PRMS) based on Micro-electro-mechanical-system (MEMS) sensor.

Methods and materials:

The performance of the PRMS was estimated by comparing the actual and measured movements of linear motion by using a one-dimensional motion phantom which moved with periods of 3.50s ~ 7.50s and amplitude of 2.5cm. The PRMS was also tested for radiation hardness by irradiating accumulated radiation to MEMS sensor.

Results:

The difference between signal of the PRMS and real motion were measured up to 1% for periods and 3% for amplitude. The signal from PRMS was well matched with the motion of 1D motion phantom for direction, timing and amplitude. And maximum permissible exposure dose to PRMS was up to 900Gy approximately.

Conclusion:

In term of simplicity and convenience, we found the possibility of the PRMS as the patient training for respiratory gated radiotherapy. We have plan to apply the PRMS to the person or patients and evaluate it help them to make regular breathing by training. So we expect more detail of study for more realistic situation and it can be established in near future.

9550-36, Session PWed

Decoding the LasR quorum sensing communication system of Pseudomonas aeruginosa by SERS

Vanesa Lopez-Puente, Celina Costas, Cristina Fernandez-Lopez, Gustavo Bodelon-Gonzalez, Jorge Perez-Juste, Isabel Pastoriza-Santos, Univ. de Vigo (Spain); Luis M. Liz-Marzan, CIC biomaGUNE (Spain) and IKERBASQUE. Basque Foundation for Science (Spain)

Quorum sensing (QS) is a bacterial cell-to-cell communication system that relies in the activation of receptor proteins by small diffusible signals, which results in the regulation of important cellular processes including virulence, antibiotic resistance and biofilm formation. The study of such protein-ligand interactions provides a molecular framework for the development of QS modulators. Herein, we have applied Surface-enhanced Raman scattering (SERS) spectroscopy for investigating the conformational changes in the structure of LasR from Pseudomonas aeruginosa upon interaction with different QS modulators. With this aim, we generated plasmonic SERS substrates consisting in gold nanoparticles thin films. Then, we genetically modified the ligand-binding domain of LasR to incorporate a C-terminal cysteine that enabled precise control over the protein orientation onto



the gold surface. Based on SERS analyses we demonstrate structural rearrangements in the LasR polypeptide as a result of ligand binding. This study shows for first time SERS detection of conformational changes in a QS receptor, demonstrating its capacity as a powerful tool for the analysis of protein-ligand interactions. Therefore this spectroscopic technique could be successfully used as complementary tool for accelerating drug discovery.

9550-37, Session PWed

Low-temperature UV-resonance Raman spectroscopy: toward less damaging biomolecular imaging

Yuika Saito, Hikaru Yoshino, Yasuaki Kumamoto, Atsushi Taguchi, Satoshi Kawata, Osaka Univ. (Japan)

There has been a considerable interest on applying UV resonant Raman spectroscopy to biological materials, because of a high sensitivity and molecular selectivity caused by the resonant effect. The main drawback of UV resonance Raman spectroscopy is photodegradation during a laser exposure that cause a serious problem for observation of an actual biological processes especially in a microscopic imaging where the observation volume cannot be refreshed. Therefore, it is essential to figure out the origin of a photodegradation and choosing appropriate experimental parameter including environmental conditions .

In this work, the temperature-dependent photodegradation during UVresonance Raman spectroscopy was investigated. Photodegradation was quantitatively probed by monitoring the temporal evolution of UVresonance Raman spectra obtained from bacteriochlorophyll (BChl) showing resonance effect at a 355-nm excitation wavelength. At 80 K, the molecular photodecomposition rate was 5-times lower than at room temperature. The decomposition rates of BChl followed the Arrhenius formula, indicating that the mechanism of photodegradation can be explained by a thermal activation process.

Conference 9551: Spintronics VIII

Sunday - Thursday 9 -13 August 2015 Part of Proceedings of SPIE Vol. 9551 Spintronics VIII

9551-1, Session 1

Electrical control of the perpendicular magnetization in Pt/[Co/Ni]3/Al multilayers (Invited Paper)

Juan-Carlos Rojas-Sánchez, Unité Mixte de Physique CNRS/Thales (France) and Univ. Paris-Sud 11 (France); Joao Sampaio, Univ. Paris-Sud 11 (France); Piotr Laczkowski, Nicolas Reyren, Cyrile Deranlot, Sophie Collin, Henri Jaffrès, Unité Mixte de Physique CNRS/ Thales (France) and Univ. Paris-Sud 11 (France); Alexandra Mougin, Univ. Paris-Sud 11 (France); Albert Fert, Jean-Marie George, Unité Mixte de Physique CNRS/Thales (France) and Univ. Paris-Sud 11 (France)

The spin to charge current conversion (SCCC) due to spin-orbit coupling (SOC) opens the way to manipulate the magnetization by electrical means. SCCC results either from bulk effects, in particular through Spin Hall Effect (SHE) [1-3], or from interfacial effects, for example in our recent experimental discovery of Rashba-Edelstein Effect (REE) [4]. We have investigated the SCCC by SHE in metals such as Pt [1,2], Au and AuW [3]. In the case of 2D systems, we recently demonstrated a large SCCC efficiency in Rashba type Ag/Bi interface [4]. An even larger effect can be even anticipated if topological insulators are used.

We will present a practical application of this SCCC to control the magnetization due to the spin-orbit torque induced by SHE [5-8], and focus on the case of Pt/(Co/Ni)3/AI multilayers with perpendicular magnetization. Using both the anomalous Hall Effect and Kerr experiments in patterned Hall bars, we are able to establish a scenario for the reversal mechanism involving domain wall motions and spin-orbit torques induced by SHE in Pt.

[1] J-C. Rojas-Sánchez et al. PRL 112, 106602 (2014). [2] J.-C. Rojas-Sánchez et al. SPIE 9167, Spintronics VII, 916729 (2014). [3] P. Laczkowski et al. APL 104, 142403 (2014). [4] J C Rojas Sánchez et al. Nat. Comm. 4:2944 (2013). [5] A. V. Khvalkovskiy et al. PRB 87, 020402 (2013). [6] I. M. Miron et al. Nature 476, 189 (2011). [7] L. Liu et al. PRL 109, 096602 (2012). [8] N. Perez et al. APL 104, 092403 (2014).

9551-2, Session 1

Ultra-fast three terminal perpendicular spin-orbit torque MRAM (Invited Paper)

Olivier Boulle, Murat Cubukcu, Claire Hamelin, SPINTEC (France); Nathalie Lamard, CEA-LETI (France); Liliana Buda-Prejbeanu, SPINTEC (France); Nikolai Mikuszeit, CEA-LETI (France); Kevin Garello, Pietro Gambardella, ETH Zürich (Switzerland); Juergen Langer, Berthold Ocker, SINGULUS TECHNOLOGIES AG (Germany); Mihai Miron, Gilles Gaudin, SPINTEC (France)

The discovery that a current flowing in a heavy metal can exert a torque on a neighboring ferromagnet has opened a new way to manipulate the magnetization at the nanoscale. This "spin orbit torque" (SOT) has been demonstrated in ultrathin magnetic multilayers with structural inversion asymmetry (SIA) and high spin orbit coupling, such as Pt/Co/AlOx multilayers. We have shown that this torque can lead to the magnetization switching of a perpendicularly magnetized nanomagnet by an in-plane current injection. The manipulation of magnetization by SOT has led to a novel concept of magnetic RAM memory, the SOT-MRAM, which combines non volatility, high speed, reliability and large endurance. These features make the SOT-MRAM a good candidate to replace SRAM for non-volatile cache memory application.

We will present the proof of concept of a perpendicular SOT-MRAM cell composed of a Ta/FeCoB/MgO/FeCoB magnetic tunnel junction

and demonstrate ultra-fast (down to 300 ps) deterministic bipolar magnetization switching. Macrospin and micromagnetic simulations including SOT cannot reproduce the experimental results, which suggests that additional physical mechanisms are at stacks. Our results show that SOT-MRAM is fast, reliable and low power, which is promising for nonvolatile cache memory application. We will also discuss recent experiments of magnetization reversal in ultrathin multilayers Pt/Co/AIOx by very short (<200 ps) current pulses. We will show that in this material, the Dzyaloshinskii-Moryia interaction plays a key role in the reversal process.

OPTICS+

 PHOTONICS NANOSCIENCE+

ENGINEERING

9551-3, Session 1

Spin-transfer torques from spinorbit interactions in heavy metals and topological insulators (Invited Paper)

Daniel C. Ralph, Cornell Univ. (United States)

The manipulation of magnetic devices using spin transfer torque in conventional magnetic tunnel junctions faces a fundamental limit in efficiency. This conventional torgue can be no stronger than the equivalent of one unit of hbar angular momentum transferred per unit charge in the applied current. I will discuss recent experiments which investigate the use of spin-orbit interactions in two different classes of materials to achieve magnetic manipulation with much better efficiency. First I will discuss the use of the spin Hall effect in certain heavy metals, which can provide spin-transfer torques that are more than a factor of 10 stronger per unit current than conventional spin torque in magnetic tunnel junctions. These torques can switch magnetic devices with either in-plane or perpendicular anisotropy, and can also drive very rapid domain wall motion in perpendicularly-magnetized samples. I will describe our efforts to identify the materials and device geometries that can provide the strongest spin Hall effects for applications, and to understand the physical mechanisms at work. Second, I will describe initial experiments on topological insulator/ ferromagnet bilayers, which suggest that spin-momentum locking in the surface state of the topological insulator may generate spin-transfer torques at least another order of magnitude more efficient even than in the heavy metals.

9551-4, Session 1

Spin-transfer torque excited by spin-orbit effects in ferromagnetic bilayers (*Invited Paper*)

Tomohiro Taniguchi, National Institute of Advanced Industrial Science and Technology (Japan); Julie Grollier, Unité Mixte de Physique CNRS/Thales (France); Mark D. Stiles, National Institute of Standards and Technology (United States)

Spin-orbit effects in nonmagnetic heavy metals have attracted much attention because of their potential application to nanostructured magnetic devices. In a ferromagnetic/nonmagnetic bilayer system, an in-plane electric field applied to the nonmagnet produces spin current flowing in the direction perpendicular to the electric field by the spin-Hall effect. The spin current injected into the attached ferromagnet excites magnetization dynamics by the spin-transfer effect. Recent experiments have demonstrated switching of a perpendicular ferromagnet by this spintransfer torque.

Spin-orbit effects are also observed in ferromagnets in the anomalous Hall effect and the anisotropic magnetoresistance. These effects also produce the spin-transfer torques in ferromagnetic bilayers. Based on spin transport theory and spin-dependent Landauer formula, we developed a theory of interlayer spin-transfer torque excited by the anomalous Hall effect and the anisotropic magnetoresistance in a ferromagnetic bilayer [1]. We derive an analytical formula of the spin-transfer torque, and show that

Conference 9551: Spintronics VIII



the spin-transfer torque can point to an arbitrary direction by changing the magnetization direction, in contrast to spin-Hall systems in which the direction of the spin-transfer torque is geometrically determined. It enables us to control the magnetization direction more efficiently than with spin-Hall systems. For example, by choosing an appropriate magnetization direction of one ferromagnet, the spin-transfer torque enables us to switch another perpendicular ferromagnet with low current and high accuracy. Coupled domain wall motion can also be excited.

[1] T. Taniguchi. J. Grollier, and M. D. Stiles, arXiv:1411.4863.

9551-5, Session 2

Resonant optical control of the currentinduced spin polarization in a twodimensional electron system (Invited Paper)

Felix G. G. Hernandez, Gennady Gusev, Univ. de São Paulo (Brazil); Askhat Bakarov, A.V. Rzhanov Institute of Semiconductor Physics (Russian Federation)

Semiconductor quantum wells are largely explored systems for the future development of spintronic devices using optical or electrical techniques. For the successful implementation in practical technological platforms, the combination of such methods will be a desirable target for the steps of generation, control with amplification, and detection. Nowadays, the reported studies using optical detection, for example, Kerr rotation, are mainly divided in two branches depending on the spin polarization trigger used: light or electrical current. Among the optical techniques for the generation of spin polarization, those using periodical excitation are very attractive because they lead to remarkable phenomena such as the resonant spin amplification (RSA). On the other side, electrical generation of spin polarization (CISP) opens a possibility to develop spin current sources added to the tuning capability of the spin-orbit interaction. In a combination of optical and electrical techniques, the situation where a CISP signal is controlled by an optical pulse has not been reported. Here, we address the amplification and reorientation of the CISP by periodic optical excitation in resonance with a variable external magnetic field. We explored the manipulation of the spin polarization in a 2DEG by the applied electrical voltage, optical pulse power, and the signal amplitude dependence on the temperature and device geometry. The experimental data displays a RSA pattern with long-lived spin coherence oscillations where the polarization amplitude is enhanced by the electric field, the spin lifetime is independent of the current level but strongly damped by high optical power and temperature.

9551-6, Session 2

Dynamics of coupled carriers and Mn spins in a positively charged Mn-doped quantum dot (Invited Paper)

Lucien Besombes, Institut NÉEL (France)

Semiconductor quantum dots (QDs) allow for the manipulation of single charge and spins in a solid-state system. It has been shown that the optical properties of a QD can also be used to access the spin of individual or pairs of magnetic atoms. A magnetic atom spin can be prepared by the injection of spin polarized carriers and its spin state can be read through the energy and polarization of the photons emitted by the QD. Information processing using individual magnetic atom spins will require fast coherent control of a single spin and tuning the coherent coupling between two or more spins. The controlled exchange coupling of a carrier spin with the spin of individual magnetic atoms could be used to transfer information between localized spins.

Using the resonant photoluminescence (PL) of the positively charged exciton as a probe we analyze here the dynamics of coupled carriers and individual Mn spins in a p-doped CdTe/ZnTe QD. The electron-Mn spin relaxation channels are identified in the energy and polarization of the

resonant PL. The auto-correlation of the resonant PL reveals a large photon bunching resulting from the spin fluctuations of the electron-Mn and hole-Mn complexes. The dynamics of the coupled hole-Mn spins is directly measured in time resolved resonant optical pumping experiments and the coherent dynamics of coupled electron and Mn spins is observed in the time resolved resonant PL. We show that a p-doped magnetic QD forms an ensemble of ten independent optical ? systems that could be used for a coherent manipulation of the coupled hole-Mn spins.

9551-7, Session 2

Semiconductor-based interface between photons and quantum registers using spins in self-assembled quantum dots (Invited Paper)

Danny Kim, Thaddeus D. Ladd, Matthew Rakher, Nathan C. Jones, Andrey A. Kiselev, Richard S. Ross, HRL Labs., LLC (United States)

Self-assembled semiconductor quantum dots are prime candidates as coherent spin-to-photon interfaces in proposed quantum repeaters or quantum networks. The spin of a trapped electron acts as the stationary or storage qubit while recombination from atom-like energy levels produces single photons. A strong optical transition dipole in the semiconductor medium provides salient advantages, such as quantum gates completed in picoseconds using ultrafast lasers, near unity photon extraction efficiency when embedded in engineered nanostructures, and the ability to provide a deterministic single photon turnstile operating at 100 MHz. These properties have enabled experiments demonstrating ultrafast one- and two-qubit gates, spin echo, and spin-photon entanglement.

This talk will present preliminary experiments and simulations towards realizing a semiconductor-based architecture for spin/photon interconversion based on self-assembled quantum dots. One key limitation of these dots for quantum memory is the short decoherence time due to nuclear field fluctuations. Although the demonstrated ratio of T2 to the single-qubit optical gate time (105) exceeds many systems, high-fidelity multi-qubit logic is still required for most quantum network architectures. A logic-enabled memory register larger than a few self-assembled dots is challenging to build with self-assembly, motivating architectures which transfer the spin information from these dots to microfabricated arrays of electrically gated dots. Critical performance parameters for this transfer are the coherence time and control fidelity of the self-assembled dots; we therefore investigate optical dynamical decoupling and composite pulse sequences and compare the performance to the requirements of future integrated devices.

9551-8, Session 3

Spin-orbit torques in magnetic bilayers *(Invited Paper)*

Paul M. Haney, Mark D. Stiles, National Institute of Standards and Technology (United States); Hyun-Woo Lee, Pohang Univ. of Science and Technology (Korea, Republic of); Aurélien Manchon, King Abdullah Univ. of Science and Technology (Saudi Arabia); Kyung-Jin Lee, Korea Univ. (Korea, Republic of)

Spintronics aims to utilize the coupling between charge transport and magnetic dynamics to develop improved and novel memory and logic devices. Future progress in spintronics may be enabled by exploiting the spin-orbit coupling present at the interface between thin film ferromagnets and heavy metals. In these systems, applying an in-plane electrical current can induce magnetic dynamics in single domain ferromagnets, or can induce rapid motion of domain wall magnetic textures. There are multiple effects responsible for these dynamics. They include spin-orbit torques and a chiral exchange interaction (the Dzyaloshinskii-Moriya interaction) in the



ferromagnet. Both effects arise from the combination of ferromagnetism and spin-orbit coupling present at the interface. There is additionally a torque from the spin current flux impinging on the ferromagnet, arising from the spin hall effect in the heavy metal. Using first principles calculations, we identify spin-orbit hybridization at the ferromagnet-heavy metal interface as central to the spin-orbit torques present in Co-Pt bilayers. We additionally propose that the transverse spin current (from the spin hall effect) is locally enhanced over its bulk value due to scattering at an interface which is oriented normal to the charge current direction.

9551-9, Session 3

Spin orbit torques and chiral spin textures in ultrathin magnetic films (Invited Paper)

Geoffrey S. Beach, Massachusetts Institute of Technology (United States)

Spin orbit coupling at interfaces can give rise to chiral magnetic textures such as homochiral domain walls and skyrmions, as well as current-induced torques that can effectively manipulate them [1-3]. This talk will describe interface-driven spin-orbit torques and Dzyaloshinskii-Moriya interactions (DMIs) in ultrathin metallic ferromagnets adjacent to nonmagnetic heavy metals. We show that the DMI depends strongly on the heavy metal, differing by a factor of -20 between Pt and Ta [4], and describe the influence of strong DMI on domain wall dynamics and spin Hall effect switching [5]. We present high-resolution magnetic force microscopy imaging of static magnetic textures that directly reveal the role of DMI and allow its strength to be quantified. Finally, we will describe how SOTs can be enhanced through interface engineering [6] and tuned by a gate voltage [7] by directly controlling the interfacial oxygen coordination at a ferromagnet/ oxide interface [8].

[1] A. Thiaville, et al., Europhys. Lett. 100, 57002 (2012).

[2] S. Emori, et al., Nature Mater. 12, 611 (2013).

[3] J. Sampaio, V. Cros, S. Rohart, A. Thiaville, and A. Fert, Nature Nano. 8, 839 (2013).

[4] S. Emori, et al., Phys. Rev. B 90, 184427 (2014).

[5] N. Perez, et al., Appl. Phys. Lett. 104, 092403 (2014).

[6] S. Woo, et al., Appl. Phys. Lett. 105, 212404 (2014).

[7] S. Emori, et al., Appl. Phys. Lett. 105, 222401 (2014).

[8] U. Bauer, et al., Nature Mater. 14, 174 (2015).

9551-10, Session 3

Anatomy of spin-orbit phenomena at ferromagnetic/nonmagnetic material interfaces (Invited Paper)

Hongxin Yang, Ali Hallal, Bernard Dieny, SPINTEC (France) and Univ. Grenoble Alps (France) and Ctr. National de la Recherche Scientifique (France); Andre Thiaville, Stanislas Rohart, Univ. Paris-Sud 11 (France) and Ctr. National de la Recherche Scientifique (France); Albert Fert, Unité Mixte de Physique CNRS/Thales (France) and Univ. Paris-Sud 11 (France); Mairbek Chshiev, SPINTEC (France) and Univ. Grenoble Alps (France) and CEA-INAC (France)

Spin-orbit coupling based phenomena such as perpendicular magnetic anisotropy (PMA) and Dzyaloshinskii-Moriya interaction (DMI) at interfaces between ferromagnetic (FM) metal and nonmagnetic (NM) insulator or metal have been an object of increased interest for spintronics including spin orbitronics in a view of ultra-dense information storage and spintronic devices such as MRAM. In this talk we elucidate mechanisms responsible for the PMA and DMI from first-principles for Co(Fe)|MgO and Co|Pt interfaces, respectively. First, we unveil the nature of PMA at Fe|MgO interfaces by evaluating the orbital and layer resolved contributions to magnetic anisotropy in Fe/MgO interfaces and MTJs with di?erent interfacial conditions [1,2]. It is demonstrated that the origin of the large PMA values is far beyond simply considering the hybridization between Fe-3d and O-2p orbitals at the interface between the metal and the insulator. Our on-site projected analysis show that the anisotropy energy is not localized at the interface but it rather propagates into the bulk showing an attenuating oscillatory behavior which depends on orbital character of contributing states and interfacial conditions [2]. Next, we calculate and clarify the main features and microscopic mechanisms of DMI in Co/Pt bilayers [3]. Here we found that DMI is predominantly located at the interfacial Co layer, originating from spin-orbit energy provided by the adjacent NM layer. Furthermore, no direct correlation is found between DMI and proximity induced magnetism in Pt. The thickness dependencies as well as the impact of interfacial mixing on DMI values in Co/Pt inetrfaces will be also discussed. These results clarify underlying mechanisms of DMI at FM/NM bilayers and should help optimizing material combinations for skyrmion- and DW-based storage and memory devices. [1] H.-X. Yang et al, Phys. Rev. B 84, 054401 (2011):

[2] A. Hallal et al, Phys. Rev. B 88, 184423 (2013); [3] H.-X. Yang et al, arXiv:1501.05511.

9551-11, Session 4

Long-range transfer of spin information using a single electron (Invited Paper)

Tristan Meunier, Ctr. National de la Recherche Scientifique (France)

The recently demonstrated on-demand transfer of a single electron using surface acoustic waves in AlGaAs heterostructures [1,2] opens the route towards electronics at the single electron level and is a promising strategy to scale up the system of electron spin qubits.

We will discuss the result of an experiment where the spin of an electron, initially prepared in a specific spin states in a first dot, is measured in a second dot four microns away after transfer. We demonstrate that spin information is preserved during the transfer with a fidelity close to 30%. We will discuss possible source of depolarization during the transfer and prior to the transfer.

9551-12, Session 4

Spin dynamics of isolated carrier spins in semiconductors (Invited Paper)

Michael Oestreich, Fabian Berski, Ramin Dahbashi, Julia Wiegand, Leibniz Univ. Hannover (Germany); Klaus Pierz, Physikalisch-Technische Bundesanstalt (Germany); Andreas D. Wieck, Ruhr-Univ. Bochum (Germany); Jens Hübner, Leibniz Univ. Hannover (Germany)

The spin of localized carriers is a prospective candidate for future quantum information systems like for example quantum repeaters or quantum information processing. In this talk we will present new results on the intriguing interaction of single and ensembles of localized spins with the surrounding nuclear spin bath and the subtle influence of electrically active defects in close vicinity of the corresponding spins. In the field of the central spin problem, we will discuss higher order spin correlations as an appropriate tool to shed more light on the complex type of spin interaction. We will furthermore elaborate on the coupling of light and spins in direct and indirect semiconductors at very low temperatures. We will experimentally verify the predicted multifaceted longitudinal and transverse spin relaxation times of localized carriers and explain the appearance of unexpected features in the spin noise spectrum which emerge as extremely sharp spin noise peaks indicating spin coherence times in the millisecond regime. Finally, we will show recent advances in the technique spin noise spectroscopy in view of an enhanced sensitivity and surprising observations concerning the magnetic field dependence of the longitudinal spin relaxation time of single electrons and holes in individually addressed



quantum dots and strong signatures of anisotropic spin interaction in nominally symmetric quantum systems.

9551-13, Session 4

Ultrafast phase-sensitive probes of the exchange interaction at ferromagnet/ semiconductor interfaces (Invited Paper)

Ezekiel Johnston-Halperin, The Ohio State Univ. (United States)

We investigate the ultrafast exchange mechanism between the magnetization of a metallic ferromagnet and the free carriers of an adjacent non-magnetic semiconductor using ultrafast optical pump probe techniques. Using Fe/MgO/GaAs heterostructures we explore the exchangedriven ferromagnetic proximity polarization (FPP) mechanism, which has previously been reported to lead to a non-equilibrium polarization of the free carriers in the GaAs layer that develops on timescales of less than 50 ps. This non-equilibrium electron polarization leads to a hyperpolarization of the nuclear spin system via the contact hyperfine interaction, which in turn dramatically modifies the ensemble spin dynamics of the free carriers. Here, we use the time and phase sensitivity of time-resolved Kerr rotation measurements to explore the role of inhomogeneity in both the exchange and hyperfine fields in determining the ensemble dephasing time, T2*, of spins in the GaAs. We find an unexpected and dramatic dependence of T2* on the effective nuclear field that suggests significant inhomogeneity in the local hyperfine interaction at low temperatures due to carrier freeze-out (i.e. localization at Si donor sites). These results provide a powerful new tool to explore the time dependent exchange interaction at ferromagnetic/ non-magnetic interfaces, with the potential to dramatically improve our understanding of dynamic spin phenomena ranging from spin-thermal interactions in heterostructures to ferromagnetic resonance driven spin pumping.

9551-14, Session 5

Spin-pumping-induced spin transport in semiconductors and related phenomena (*Invited Paper*)

Masashi Shiraishi, Yuichiro Ando, Kyoto Univ. (Japan)

Spin pumping is currently recognized as a quite potential tool for injecting spins and generating pure spin current into condensed matters, such as nonmagnetic metals [1], inorganic semiconductors [2], organic semiconductors [3], magnetic insulator [4], and so on. For detection of the generated spin current, the inverse spin Hall (ISHE) effect [5] is now widely used. We have been investigating spin transport properties and spin polarization in semiconductors and topological insulators by using spin injection (Si [2], Graphene [6], GaAs [7] and Ge [8]) and electrical spin injection (Si [9], Graphene [10]) and BiSbTeSe [11]), and will present these recent results. In the course of these studies, we found that non-negligible electromotive forces can be generated from ferromagnetic metals, NiFe and Co [12], due to the self-induced ISHE. The detail of this interesting feature will be also presented.

References:

[1] S. Mizukami et al., PRB 2001. [2] E. Shikoh, M. Shiraishi et al., PRL 2013. [3] K. Ando et al., Nature Mater. 2013. [4] Y. Kajiwara et al., Nature 2010. [5] E. Saitoh et al., APL 2006. [6] Z. Tang, M. Shiraishi et al., PRB(R) 2013. [7] A. Yamamoto, Y. Ando et al., submitted. [8] S. Dushenko, Y. Ando, M. Shiraishi et al., submitted. [9] T. Sasaki, Y. Ando, M. Shiraishi et al., Phys. Rev. Applied, 2014. [10] M. Shiraishi et al., Adv. Func. Mat. 2009. [11] Y. Ando, M. Shiraishi et al., Nano Lett. 2014. [12] A. Tsukahara, Y. Ando, M. Shiraishi et al., PRB 2014.

9551-15, Session 5

Hot electrons transport in devices combining tunnel and Schottky barriers (Invited Paper)

Christopher Vautrin, Yuan Lu, Sylvain Le Gall, Guillaume Salla, Sylvie Robert, Olivier Lenoble, François Montaigne, Institut Jean Lamour (France); Ming-Wei Wu, Univ. of Science and Technology of China (China); Daniel Lacour, Michel Hehn, Institut Jean Lamour (France)

We have recently unveiled experimentally a new interfacial trapping phenomenon for hot electron injection in silicon [1]. The transport measurements indicate that an interfacial charge trapping and a backscattering-induced collector current limitation take place when the temperature is lower than 25?K. This results in a rapid decrease of the magneto-current ratio. In this presentation we will demonstrate an electrical control of this trapping effect thanks to a magnetic tunnel transistor made on wafer bonded substrate [2]. A model taking into account the effects of both electric field and temperature will be presented. It closely reproduces the experimental results and allows extraction of the trapping binding energy (1.6 meV). Finally we will also discussed the difficulties encountered during realization of equivalent devices having out of plane magnetizations. Links between Schottky barriers preparation techniques and the existence of perpendicular magnetic anisotropy in a CoNi multilayer are established made. A solution to join in the same devices a Schotkky barrier and perpendicular anisotropy will be revealed [3].

[1]Y. Lu, D. Lacour et al, Appl. Phys. Lett. 103, 022407 (2013)
[2]Y. Lu, D. Lacour et al, Appl. Phys. Lett. 104, 042408 (2014)
[3]C. Vautrin, D. Lacour et al, to be published (2015)

9551-16, Session 5

The role of interface states in the electrical and dynamical spin injection in silicon and germanium (Invited Paper)

Matthieu Jamet, Commissariat à l'Energie Atomique (France) and Univ. Grenoble Alps (France); Fabien Rortais, Simon Oyarzun, Commissariat à l'Énergie Atomique (France) and Univ. Grenoble Alps (France); Juan-Carlos Rojas-Sánchez, Piotr Laczkowski, Unité Mixte de Physique CNRS/Thales (France) and Univ. Paris-Sud 11 (France); Céline Vergnaud, Commissariat à l'Energie Atomique (France) and Univ. Grenoble Alps (France); Clarisse Ducruet, Crocus Technology (France); Cyrille Beigné, Commissariat à l'Énergie Atomique (France) and Univ. Grenoble Alps (France); Nicolas Reyren, Unité Mixte de Physique CNRS/Thales (France) and Univ. Paris-Sud 11 (France); Jean-Philippe Attané, Commissariat à l'Énergie Atomique (France) and Univ. Grenoble Alps (France); Laurent Vila, Commissariat à l'Energie Atomique (France) and Univ. Grenoble Alps (France); Gérard Desfonds, Serge Gambarelli, Commissariat à l'Énergie Atomique (France) and Univ. Grenoble Alps (France); Julie Widiez, Commissariat à l'Energie Atomique (France); Henri Jaffrès, Jean-Marie George, Unité Mixte de Physique CNRS/Thales (France) and Univ. Paris-Sud 11 (France)

Electrical spin injection from ferromagnetic metals to silicon (Si) and germanium (Ge) is the first and basic requirement for the development of spintronic devices and their integration with mainstream semiconductor (SC) technology. The main obstacle to efficient spin injection is the conductivity mismatch between the ferromagnetic metal and Si, Ge and



requires tunneling spin injection through an oxide barrier (Ox). However, tunneling spin injection raises other important issues in the interpretation of electrical spin signals. In particular, the possible presence of localized states within the Ox or at the Ox/SC interface may lead to wrong conclusions. To study the exact origin of the spin signals measured in three and fourterminal geometries, we have grown Ta/CoFeB/MgO/SOI and GeOI samples with n and p type doping using variable MgO thicknesses. The use of SOI and GeOI substrates allows us to apply back gate voltages to the SC channel to vary its resistivity. Moreover we have used three different techniques to grow the MgO tunnel barrier: by sputtering of MgO or Mg followed by a plasma oxidation and e-beam evaporation of MgO. Using the Mg and plasma oxidation growth of the tunnel barrier, though less flexible than the other techniques, allowed us to show the temperature transition from the spin accumulation into interface states to the spin accumulation into the conduction band of n-Ge and n-Si. For this purpose, both electrical and dynamical spin injection measurements were carried out as a function of temperature and bias voltage for different MgO tunnel barriers.

9551-17, Session 6

Understanding bilayers of metals and magnetic insulators (Invited Paper)

Gerrit E. W. Bauer, Tohoku Univ. (Japan) and Delft Univ. of Technology (Netherlands)

The spintronics based on magnetic and non-magnetic elemental metals and their alloys has been very successful in the last decade. Discoveries such as the giant magnetoresistance, tunnel magnetoresistance, spintransfer torque, (inverse) spin Hall effect, spin-orbit torques etc. not only lead to fundamental new physical insights, but also to functionalities that are employed in new nanoscale devices such as switches, memories, and sensors.

Magnetic insulators form another class of versatile materials with great technological importance. They have been central to the research in magnetism up to the 80's of the last century, but were later largely forgotten. The most important magnetic insulators are arguably the manmade yttrium iron garnets, ferrimagnets with Curie transitions far above room temperature and record magnetic quality [1-3]. In recent years, magnetic insulators have attracted much interest from the spintronics community, because K. Uchida, E. Saitoh c.s., demonstrated that they can be actuated thermally [4] and electrically [5] and thereby integrated into conventional electronics and thermoelectric devices. The discovery of entirely new phenomena, such as the spin Seebeck effect, raises the hope for a new and green spintronics [6].

This contribution reviews recent (published in 2014 [7-15] and yet unpublished) progress in the theoretical spin(calori)tronics of YIG and its heterostructures with normal metals,. After an elementary introduction into the basic physical concepts, a number of recent key theoretical insights and, where possible experimental evidence, will be reviewed. Topics such as spin Peltier effect, the figure or merit of spin Seebeck generators, exchange magnon-polaritons, acoustically induced spin pumping, current-induced spin torque resonance facilitated by the spin Hall magnetoresistance, and others will be presented.

I gratefully acknowledge collaboration with many researchers (see Refs. [5-16]). This work was supported by the FOM Foundation, Reimei program of the Japan Atomic Energy Agency, EU-FET "InSpin", the ICC-IMR, DFG Priority Program 1538 "Spin-Caloric Transport", and JSPS Grants-in-Aid for Scientific Research (Grant Nos. 25247056, 25220910, 26103006).

[1] V. Cherepanov, I. Kolokolov, V. L'vov, The Saga of YIG: Spectra, Thermodynamics, Interaction and Relaxation of Magnons in a Complex Magnet, Phys. Rep. 229, 81 (1993).

[2] Recent Advances in Magnetic Insulators -- From Spintronics to Microwave Applications, M. Wu and A. Hoffmann (eds.), Solid State Physics 64, 1 (2013).

[3] R. L. Stamps, S. Breitkreutz, J. Åkerman, A. Chumak., Y. Otani, G. E. W. Bauer, J.-U. Thiele., M. Bowen., S.A. Majetich, M. Kläui, I. L. Prejbeanu, B. Dieny, N. M. Dempsey, and B. Hillebrands, The 2014 Magnetism Roadmap, J. Phys. D 47, 333001 (2014).

[4] K. Uchida, J. Xiao, H. Adachi, J. Ohe, S. Takahashi, J. Ieda, T. Ota, Y.

Kajiwara, H. Umezawa, H. Kawai, G. E.W. Bauer, S. Maekawa, and E. Saitoh, Nature Mater. 9, 894 (2010).

[5] Y. Kajiwara, K. Harii, S. Takahashi, J. Ohe, K. Uchida, M. Mizuguchi, H. Umezawa, H. Kawai, K. Ando, K. Takanashi, S. Maekawa, and E. Saitoh, Nature 464, 262 (2010).

[6] A. Kirihara, K. Uchida, Y. Kajiwara, M. Ishida, Y. Nakamura, T. Manako, E. Saitoh, and S. Yorozu, Spin-current-driven thermoelectric coating, Nature Mat. 11, 686 (2012).

[7] A. B. Cahaya, O. A. Tretiakov, G. E. W. Bauer, Spin Seebeck Power Generators, Appl. Phys. Lett. 104, 042402 (2014).

[8] A. Kamra and G. E. W. Bauer, Actuation, propagation, and detection of transverse magnetoelastic waves in ferromagnets, Solid State Commun. 198, 35–39 (2014); A. Kamra, H. Keshtgar, P. Yan, G. E. W. Bauer, Coherent elastic excitation of spin waves, arXiv:1412.5820.

[9] J. Flipse, F. K. Dejene, D. Wagenaar, G. E. W. Bauer, J. Ben Youssef, B. J. van Wees, Observation of the spin Peltier effect, Phys. Rev. Lett. 113, 027601 (2014).

[10] M. Schreier, G. E. W. Bauer, V. Vasyuchka, J. Flipse, K. Uchida, J. Lotze, V. Lauer, A. Chumak, A. Serga, S. Daimon, T. Kikkawa, E. Saitoh, B. J. van Wees, B. Hillebrands, R. Gross, S. T. B. Gönnenwein, Sign of inverse spin Hall voltages generated by ferromagnetic resonance and temperature gradients in yttrium iron garnet|platinum bilayers, arXiv:1404.3490

[11] T. Chiba, G. E. W. Bauer, S. Takahashi, Current-induced spin torque resonance for magnetic insulators, Phys. Rev. Applied 2, 034003 (2014);
M. Schreier, T. Chiba, A. Niedermayr, J. Lotze, H. Huebl, St. Geprägs, S. Takahashi, G. E. W. Bauer, R. Gross, S. T. B. Goennenwein, Current-induced spin torque resonance of a magnetic insulator, arXiv:1412.7460.

[12] H. Skarsvåg, G. E. W. Bauer, and A. Brataas. Current-induced magnetization dynamics in two magnetic insulators separated by a normal metal, Phys. Rev. B 90, 054401 (2014).

[13] V. L. Grigoryan, W. Guo, G. E. W. Bauer, J. Xiao, Intrinsic magnetoresistance in metal films on ferromagnetic insulators, Phys. Rev. B 90, 161412(R) (2014)

[14] A. Kamra, F. P. Witek, S. Meyer, H. Huebl, S. Geprägs, R. Gross, G. E. W. Bauer, and S. T. B. Goennenwein, Spin Hall noise, Phys. Rev. B 90, 214419 (2014).

[15] Y. Cao, P. Yan, H. Huebl, S. T.B. Goennenwein, G.E.W. Bauer, Magnon-polaritons in Microwave Cavities, arXiv:1412.5809

9551-18, Session 6

Spintronics in complex oxide hybrid and heterostructures (Invited Paper)

Georg Schmidt, Martin-Luther-Univ. Halle-Wittenberg (Germany)

Complex oxides are an interesting class of materials for spintronics research and applications. Among others they have been used in tunnelling magnetoresistance elements because of high spin polarization or in hybrid structures for spin pumping [1] where ferromagnetic insulators like yttrium iron garnet (YIG) greatly facilitate the interpretation of experimental results.

In this presentation further progress in the utilization of ferromagnetic oxides for spintronics will be shown. On the one hand spin pumping and inverse spin-Hall effect in all-oxide heterostructures are presented. In these structures complex oxides are not only the source of spin pumping but they also act as the detecting spin sink which exhibits the inverse spin-Hall effect.

In addition new experiments on tunnelling anisotropic magnetoresistance (TAMR) in oxides will be shown. While TAMR in inorganic systems was limited to a few % until recently [2], we demonstrate that in a fully epitaxial stack of a ferromagnetic oxide and a complex oxide tunnel barrier TAMR can be as large as 65 %.

References

[1] K. Uchida et al. Nature Materials 9, 894 (2010)

[2] C. Gould et al., Phys. Rev. Lett. 93, 117203 (2004)



9551-19, Session 6

Spin wave propagation in magnetic insulator thin film of nanometer thickness (Invited Paper)

Haiming Yu, BeiHang Univ. (China) and Technische Univ. München (Germany); Olivier d'Allivy Kelly, Unité Mixte de Physique CNRS/Thales (France) and Univ Paris-Sud 11 (France); Vincent Cros, Rozenn Bernard, Paolo Bortolotti, Abdelmadjid Anane, Unité Mixte de Physique CNRS/ Thales (France) and Univ. Paris-Sud 11 (France); Florian Brandl, Rupert Huber, Ioannis Stasinopoulos, Dirk Grundler, Technische Univ. München (Germany)

Wave control in the solid state has opened new avenues in modern information technology. Surface-acoustic-wave-based devices are found as mass market products in 100 millions of cellular phones. Spin waves (magnons) would offer a boost in today's data handling and security implementations, i.e., image processing and speech recognition. However, nanomagnonic devices realized so far suffer from the relatively short damping length in the metallic ferromagnets amounting to a few 10 micrometers typically. Here we demonstrate that nm-thick YIG films overcome the damping chasm. Using a conventional coplanar waveguide we excite a large series of short-wavelength spin waves (SWs). From the data we estimate a macroscopic of damping length of about 600 micrometers. The intrinsic damping parameter suggests even a record value about 1 mm allowing for magnonics-based nanotechnology with ultra-low damping. In addition, SWs at large wave vector are found to exhibit the non-reciprocal properties relevant for new concepts in nanoscale SW-based logics. We expect our results to provide the basis for coherent data processing with SWs at GHz rates and in large arrays of cellular magnetic arrays, thereby boosting the envisioned image processing and speech recognition.

9551-20, Session 6

Role of transparency of platinumferromagnet interface in determining intrinsic magnitude of spin Hall effect (Invited Paper)

Wei Han, Peking Univ. (China)

The spin Hall effect is a phenomenon in which electrical current generates pure spin currents in thin layers formed from materials with large spin orbit coupling. What determines the magnitude of the effect is of considerable debate. Whilst the spin Hall effect has been observed in a number of conducting materials one of the most interesting materials is platinum due, not only to the substantial large spin Hall effect that it exhibits, but also because Pt exhibits several other important properties related to its large spin orbit coupling including perpendicular magnetic anisotropy, a Dzyaloshinsky-Moriya exchange interaction, and a proximity induced magnetic moment when coupled to a magnetic layer.

The magnitude of the SHE is not easy to measure and most often is inferred from the effect of the spin current on neighboring magnetic moments. The spins diffuse from the non -magnetic layer in which they are formed across the interface into the magnetic material. What we show in our paper is that the "transparency" of this interface to the spin current strongly affects the magnitude of the spin Hall effect. The transparency has been ignored in all measurements of the SHE to date. In our manuscript we use a spin torque ferromagnetic resonance (ST-FMR) technique to measure the SHE. When the transparency is neglected we show that the magnitude of the SHE in platinum measured using ST-FMR can vary by more than a factor of 2 with different magnetic metals! The SHE should, however, not depend on the ferromagnet since it is an intrinsic property of the material itself. We show that we can readily account for our observations by taking account of the transparency of the platinum / magnet interface that we measure in independent measurements using the phenomenon of spin pumping. This is an enormous effect! For example, we find for the platinum/ permalloy

interface only 1 in 4 spins cross the interface! This means that the spin current generated in the platinum layer from the SHE is 4 times larger than is inferred from the perturbation of the magnetic layer from the spin torque created by the spins that cross the interface. Correspondingly, this means that the magnitude of the SHE is also 4 times larger than was inferred from ST-FMR or related experiments which ignores the interface transparency.

Our work points to the importance of the interface transparency in understanding the origin of the SHE and how it can be used technologically. In hindsight the role of the interface transparency seems so important that it is surprising that it has been overlooked. Thus, we believe our paper will be of considerable interest and will play an important role in developing a detailed understanding of the physics underlying the spin Hall effect.

9551-21, Session 6

Quantum Well state oscillations of pure spin currents in Fe/Au/Pd(001) structures (*Invited Paper*)

Bret V. Heinrich, Eric Montoya, Simon Fraser Univ. (Canada)

Interlayer exchange coupling and spin pumping are caused by instantaneous and time delayed spin dependent potential at FM (ferromagnet) /NM (normal metal) interface, respectively. Therefore one can expect that in some structures the spin pumping contribution to the interface damping can result also in an oscillatory behavior with the NM layer thickness as it is observed readily for the interlayer coupling. Since no oscillatory behavior of spin pumping was found in FM/simple NM systems, we investigated spin pumping in Fe/Au/Pd(001); the Pd layer exhibits thermally excited spin fluctuations resulting in a large spin current decoherence in Pd on the length scale of 10 nm which is significantly smaller than the spin diffusion length in normal Au. Spin pumping contribution to the Gilbert damping in Fe/Au/Pd reached an asymptotic value corresponding to a thick Au layer on much shorter length scale than that expected for the spin diffusion length in Au. This behavior was possible to explain using a partial reflection of spin current at the Au/Pd interface which is caused by different Fermi velocities in Au and Pd. Surprisingly, for the Au layer thickness less than the momentum mean free path, the interface damping oscillated with a periodicities corresponding to long (belly of the Fermi surface) and short (necks) spanning k-vectors in Au(001) of the static interlayer exchange coupling. This means that even in the time irreversible process of spin pumping collective quantum well states play a significant role when the Au spacer is thinner that the electron momentum mean free path.

9551-22, Session 7

Origin of the spin-orbit interaction (Invited Paper)

Gianfranco Spavieri, Univ. de los Andes (Venezuela); Masud Mansuripur, College of Optical Sciences, The Univ. of Arizona (United States)

We consider a semi-classical model to describe the origin of the spin-orbit interaction in a simple system such as the hydrogen atom. The interaction energy U is calculated in the rest-frame of the nucleus, around which an electron, having linear velocity v and magnetic dipole-moment ?, travels in a circular orbit. The interaction energy U is due to the coupling of the induced electric dipole p=(v/c)?? with the electric field En of the nucleus. According to quantum mechanics, the radius of the electron's orbit remains constant during a spin-flip transition. Under such circumstances, our model predicts that the energy of the system changes by Δ E=?U, the factor ? emerging naturally as a consequence of equilibrium and the change of the kinetic energy of the electron. The correct ? factor for the spin-orbit coupling energy is thus derived without the need to introduce the well-known Thomas precession in the rest-frame of the electron.



9551-23, Session 7

Rashba spin-orbit effect and its electric field control at the surfaces and interfaces for spintronics applications (*Invited Paper*)

Sashi Satpathy, Univ. of Missouri (United States); Kavungal Veedu Shanavas, Oak Ridge National Lab. (United States)

The Rashba effect [1] describes the momentum-dependent spin splitting of the electron states at a surface or interface. It is the combined result of the relativistic spin-orbit interaction (SOI) and the inversion-symmetry breaking. The control of the Rashba effect by an applied electric field is at the heart of the proposed Rashba-effect-based spintronics devices for manipulating the electron spinfor manipulating the electron spin in the semiconductors. The effect is expected to be much stronger in the perovskite oxides owing to the presence of high-Z elements.

In this talk, I will introduce the Rashba effect and discuss how the Rashba SOI at the surfaces and interfaces can be tuned by manipulating the two dimensional electron gas (2DEG) by an applied electric field. The effect can be understood in terms of a tight-binding model Hamiltonian for the d orbitals incorporating the effect of electric field in terms of effective orbital overlap parameters [3]. From first principles calculations we see that the Rashba SOI originates from the first few layers near the surface and it therefore can be altered by drawing the 2DEG to the surface or by pushing the 2DEG deeper into the bulk with an applied electric field. These ideas will be illustrated by a comprehensive density-functional study of polar perovskite systems [4].

References

[1] E. I. Rashba, Sov. Phys. Solid State 2, 1109 (1960)

[2] A. Ohtomo and H. Hwang, Nature 427, 423 (2004); Z. Popovic, S. Satpathy, and R. Martin, Phys. Rev. Letts. 101, 256801 (2008)

[3] K. V. Shanavas and S. Satpathy, Phys. Rev. Lett. 112, 086802 (2014); K. V. Shanavas, Z. S. Popovic, and S. Satpathy, Phys. Rev. B 90, 165108 (2014)
 [4] K. V. Shanavas, J. Electron Spectrosc., In press (2015)

9551-24, Session 7

Microscopic theory of the inverse Edelstein effect (Invited Paper)

Roberto Raimondi, Univ. degli Studi di Roma Tre (Italy); Ka Shen, Giovanni Vignale, Univ. of Missouri (United States)

The spin Hall effect (SHE) and the inverse spin Hall effect (ISHE) are well established phenomena in current spintronics research. A third important effect is the current-induced spin polarization, which, within the Rashba model for a spin-orbit coupled two-dimensional disordered electron gas, has been predicted by Edelstein in 1990 and it is referred to as the Edelstein effect (EE). This effect is deeply connected to the above two effects thanks to a constraint dictated by the equation of motion. Less known is the inverse Edelstein effect (IEE), which is the Onsager reciprocal of the EE and according to which a charge current is generated by a non-equilibrium spin polarization. The IEE has been recently observed (Nature Commun. 4, 2944 (2013)) in a hybrid ferromagnetic-metal system. In this talk I provide a precise microscopic definition of the IEE and its description within the Rashba model. It turns out that the effect has a surprisingly simple interpretation when the spin-charge coupled drift-diffusion equations governing it are cast in the language of a SU(2) gauge theory, with the Rashba spin-orbit coupling playing the role of a generalized spin-dependent vector potential. After sketching briefly the derivation of the drift-diffusion equations, the latter are applied to the interpretation of the experiments. The role of spin-orbit coupling due to impurities is also considered, by showing that the strenght of the IEE can be controlled by the ratio of the spin relaxation rates associated to the two type of spin-orbit coupling.

9551-25, Session 7

Spin-orbit torques and the Dzyaloshinskii-Moriya interaction in Ta/CoFeB/MgO nanowires (Invited Paper)

Thomas A. Moore, Univ. of Leeds (United Kingdom)

The interaction between current and magnetization in Ta/CoFeB/MgO is of interest because this materials stack is already used for the fabrication of spintronic devices whose functionality is based on spin torque. With the advent of spin-orbit torques, the challenge is to understand what governs the torques and the strength and sign of the Dzyaloshinskii-Moriya interaction (DMI).

Firstly, we demonstrate spin-orbit torque switching of the magnetization in Ta/Co20Fe60B20/MgO nanowires by current pulse injection along the nanowires, both with and without a magnetic field collinear to the current. A component of magnetization along the current direction is required for the switching to occur, and we find that this may be present, even in zero field, due to thermally generated fluctuations. Our data are analysed using a generalized Neel-Brown model which enables the attempt frequency and effective energy barrier to be extracted.

Secondly, we observe current-induced domain wall motion in Ta/ Co20Fe60B20/MgO nanowires against the electron flow when no magnetic field is applied. A field along the nanowires strongly affects the domain wall velocity, the magnitude and direction of which is in agreement with the spin-orbit torque model. A DMI effective field of 7.8+/-1.2 mT is measured, resulting in a DMI constant +0.06+/-0.01 mJ/m2, corresponding to right-handed domain walls. The positive DMI constant is attributed to the diffusion of B in the Ta layer and its segregation at the Ta/CoFeB interface. Using 1D model simulations that include pinning we reproduce the experimental data and extract a spin Hall angle of -0.11 for Ta.

9551-26, Session 7

Transport at spin-orbit and exchange-split interfaces and universal giant asymmetry

Huong Thi Dang, Ecole Polytechnique (France); Henri Jaffrès, Unité Mixte de Physique CNRS/Thales (France); T. L. Hoai Nguyen, Vietnam Academy of Science and Technology (Viet Nam); Henri-Jean Drouhin, Ecole Polytechnique (France)

We report on theoretical investigations and k.p calculations of carrier tunneling, both electrons and holes, in model systems and heterostructures composed of exchange-split III-V semiconductors, involving spin-orbit interactions. The two media are separated-or not-by a thin tunnel barrier made out of a (III-V) semiconductor. In a 2x2 exchange-split band model, we show that, when Dresselhaus interactions are included in the conduction band of two exchange-split semiconductors in contact in the antiparallel states of magnetization, the electrons are differently transmitted with respect to an axis orthogonal to both normal axis of the interface and of the magnetization. The transmission asymmetry (A) between +k// and -k// incidence is shown to be maximal (A=100%) at some points of the Brillouin zone corresponding to a totally quenched transmission at some given incidence angles. More generally, we derive a universal character of the transmission asymmetry A vs. the in-plane incidence wavevector, the reduced kinetic energy and exchange parameter, A being universally scaled by a unique function, independent of the spin-orbit strength and of material parameters. This particular asymmetry feature is reproduced by a more complete 14x14 band model involving coupling with the conduction band. On the other hand, calculations performed in the valence-band of equivalent model heterostructures and including tunnel barriers in both 6x6 (without inversion) and 14x14 k.p band model more astonishingly highlight. the same trends in the transmission asymmetry (A) which is related to the difference of orbital chirality and to the related branching (overlap) of the corresponding evanescent wavefunctions responsible for tunneling current. In both cases of electrons and holes, the asymmetry appears to be robust and persists only when a single electrode is magnetic.



9551-27, Session 8

Spin and phase relaxation dynamics in GaN and GaN/AlGaN quantum wells (Invited Paper)

Mathieu Gallart, Marc Ziegler, Bernd H. Hönerlage, Pierre Gilliot, Institut de Physique et Chimie des Matériaux de Strasbourg (France); Eric Feltin, Jean-François Carlin, Raphaël Butté, Nicolas Grandjean, Ecole Polytechnique Fédérale de Lausanne (Switzerland)

By performing time-resolved optical non-degenerate pump-probe experiments, we study the relaxation dynamics of spin-polarized excitons in wurtzite epitaxial GaN and in nitride nanostructures. Those materials are indeed promising candidates for spintronic applications because of their weak spin-orbit coupling and large exciton binding energy (~ 17?meV and ~ 26meV in bulk GaN, respectively).

In epilayers, we show that the high density of dislocations increases dramatically the spin relaxation of electrons and holes through the defect assisted Elliott-Yafet mechanism. That makes the exciton dephasing time very short.

In high quality GaN/AlGaN quantum wells, both the exciton-spin lifetime ?S and the exciton dephasing-time T2 were determined via pump-probe spectroscopy using polarized laser pulses and time-resolved four wavemixing experiments. The evolution of both quantities with temperature shows that spin relaxation occurs in the motional narrowing regime up to 80 K. Above this threshold, the thermal energy becomes large enough for excitons to escape from the QW. Such measurements demonstrate that GaN-based heterostructures can reach a very high degree of control that was previously mostly restricted to conventional III-V semiconductors and more specifically to the arsenide family.

9551-28, Session 8

Ultrafast magneto-optical spectroscopy of BiFeO3-BaTiO3 based structures (Invited Paper)

Giti A. Khodaparast, Brenden A. Magill, Michael A. Meeker, Anuj Chopra, Yuon Zhou, Hyun-Cheol Song, Virginia Polytechnic Institute and State Univ. (United States); Michael Bishop, Stephen A. McGill, National High Magnetic Field Lab. (United States); Christopher J. Stanton, Univ. of Florida (United States); Shashank Priya, Virginia Polytechnic Institute and State Univ. (United States)

Ultrafast optical spectroscopy can provide insight into fundamental microscopic interactions, dynamics and the coupling of several degrees of freedom. Pump/ probe studies can reveal the answer to questions like "What are the achievable switching speeds in multiferroics?", "What is the influence of the crystallographic orientation and domain states on the available switching states?", and "What is the effect of the hetrostructure on promoting the coupling between the varying field excitations?". In this presentation, we report on two color (400/800nm) ultrafast pumpprobe differential reflectance spectroscopy of BiFeO3-BaTiO3 structures to probe the coupling between optical and acoustic phonons to spin waves. The data presented here is a combination of different transient reflectivity measurements to probe both the carrier and spin dynamics. The (001)-BiFeO3-BaTiO3 thin films were prepared using pulsed laser deposition on vicinal SrTiO3 substrates using La0.70 Sr0.30MnO3 bottom electrodes. Crystal orientation and topography were analyzed by x-ray diffraction and atomic force microscopy. . Our results are important to developing devices on the basis of this material system.

This work was supported by the AFOSR through grant FA9550-14-1-0376,NSF-Career Award DMR-0846834, and the Virginia Tech Institute for Critical Technology and Applied Science.

9551-29, Session 8

Ultrafast spectroscopy in high magnetic fields using the 25 Tesla Split Florida Helix (Invited Paper)

David J. Hilton, The Univ. of Alabama at Birmingham (United States)

Two-dimensional systems offer a rich array of physical phenomena that include the integer and fractional quantum Hall effects, both of which have been observed in multiple materials systems to date. The mitigation and control of coherence in quantum states in 2D systems is an area of great current interest that is critical for the development of the next generation of solid state electronics based on guantum phenomena. In the first experiments that I will discuss, we investigate the terahertz frequency properties of a high mobility (? \geq 106 cm2 V-1 s-1) gallium arsenide twodimensional electron gas (2DEG) at cyclotron resonance in a perpendicular magnetic field, which results in the formation of a spectrum of Landau levels. Our experiments reveal a strong increase in the decoherence at low temperatures and a power law dependence to the decoherence time from T = 0.4 - 100 K. In the second part of the talk, I will discuss our high fluence, nondegenerate pump-probe spectroscopic experiments of GaAs in the Florida Split Helix magnet at 15 K and 25 T. We model the electronic component of our data with an approximate four level system, from which we have extracted scattering and recombination rates in high magnetic field. We also observe coherent phonons, which were isolated and fitted to a sinusoid with an oscillation frequency of 43.5 GHz at 25 T, which is 3.0% larger than the previously measured zero field frequency.

9551-30, Session 9

Time-resolved spectroscopy of coupled spin-valley-dynamics in monolayer transition metal dichalcogenides at low temperatures (Invited Paper)

Gerd Plechinger, Philipp Nagler, Christian Schüller, Tobias Korn, Univ. Regensburg (Germany)

The recent interest in semiconducting transition metal dichalcogenides (TMDs) such as MoS2, and WS2 has been kindled by their fascinating optical properties and peculiar band structure, which suggest potential applications for spintronics. In contrast to the bulk crystals, single-layer TMDs have a direct bandgap located at the K points in the Brillouin zone. They show strong excitonic effects due to the two-dimensional carrier confinement, and a coupling of valley and spin degrees of freedom. In these materials, optical selection rules allow valley-selective excitation of spin-polarized electron-hole pairs using resonant, circularly-polarized excitation, and the valley polarization can directly be determined by helicity-resolved photoluminescence.

Here, we demonstrate the exfoliation of large-area monolayer flakes prepared from bulk TMD crystals. The flakes are first characterized using Raman and photoluminescence measurements. We then utilize timeresolved Kerr rotation (TRKR) measurements to probe the valley dynamics in the monolayer flakes at low temperatures. This technique allows resonant excitation of the excitonic transitions and yields sub-picosecond resolution.

We find valley lifetimes of about 60 ps at a temperature of 4 K in monolayer MoS2 for resonant excitation. With increasing temperatures, we observe a dramatic decrease of the valley lifetimes, indicating that valley dephasing is mediated by phonon-related scattering processes. The MoS2 valley lifetime can be significantly enhanced by mildly annealing the samples in vacuum to remove surface adsorbates, indicating that these adsorbates, acting as scattering centers, also play an important role in valley depolarization.

Financial support by the DFG via SFB 689, GRK1570 and KO3612-1/1 is gratefully acknowledged.



9551-31, Session 9

Disentangling intra and intervalley dynamics in monolayer MoS2 by ultrafast optical techniques (Invited Paper)

Stefano Dal Conte, CNR-Istituto di Fotonica e Nanotecnologie (Italy) and Politecnico di Milano (Italy)

The field of spintronics has recently experienced a strong boost after the advent of atomically thin Transition Metal Dichalcogenides (TMDs). In this work we measure separately the spin and valley relaxation dynamics of both electrons and holes in the prototypical TMD monolayer MoS2. We combine together two ultrafast optical spectroscopy techniques i.e. Time Resolved Circular Dichroism (TRCD) and Time Resolved Faraday Rotation (TRFR) in order to disentangle intra and intervalley relaxation processes. TRCD experiments are performed by exciting the sample with an ultrashort circularly polarized pulse, resonant with the optical gap, and measuring the difference between the transient absorption response probed by co- and counter- circularly polarized pulses. These measurements reveal an extremely fast intravalley relaxation of the spin of the photoexcited electrons and demonstrate that the valley polarization is strongly quenched after few ps. TRFR experiments are performed in a two-color configuration, i.e. the energy of the probe pulse is tuned well below the absorption gap. In these conditions, the Faraday rotation transient signal is related to an unbalanced distribution of the photoexcited carrier orbital degrees of freedom. Since the orbital momentum in MoS2 single layer is locked with the valley index, TRFR measurements probe exclusively the intervalley dynamics of electrons and holes. The combination of TRFR and TRCD allows us to disentangle intervalley and intravalley dynamics. Both TRCD and TRFR experiments are quantitatively explained by a set of rate equations which take into account intervalley and intravalley relaxation channels.

9551-32, Session 9

Exciton fine structure and spin/valley dynamics in nanosystems (Invited Paper)

Mikhail M. Glazov, loffe Physical-Technical Institute (Russian Federation)

In my invited talk the fine structure of neutral and charged excitons for GaAs/AlGaAs quantum dots (QDs) grown on (111) plane as well for transition metal dichalcogenides (TMDCs) monolayers will be discussed. These, at first glance, different systems posses similar trigonal symmetry, which makes exciton fine structure and spin dynamics unusual compared with standard low-dimensional semiconductors. The effects of long-range exchange interaction induced mixing of excitons in two valleys of TMDCs and of magneto-induced mixing of bright and dark excitonic states in trigonal QDs are predicted and confirmed experimentally. Manifestations of excitonic spin/valley dynamics in photoluminescence, pump-probe Kerr rotation and spin noise are discussed.

The presentation will be based on the following references:

[1] G. Sallen, B. Urbaszek, M. M. Glazov, et al., Dark-Bright Mixing of Interband Transitions in Symmetric Semiconductor Quantum Dots, Phys. Rev. Lett. 107, 166604 (2011).

[2] L. Bouet, M. Vidal, T. Mano, N. Ha, T. Kuroda, M. V. Durnev, M. M. Glazov, et al., Charge tuning in [111] grown GaAs droplet quantum dots, Appl. Phys. Lett. 105, 082111 (2014).

[3] M. M. Glazov, et al., Exciton fine structure and spin decoherence in monolayers of transition metal dichalcogenides Phys. Rev. B 89, 201302(R) (2014).

[4] C. R. Zhu, K. Zhang, M. Glazov, et al., Exciton valley dynamics probed by Kerr rotation in WSe2 monolayers, Phys. Rev. B 90, 161302(R) (2014).

9551-33, Session 9

Generation of valley-spin currents in 2D transition metal dichalcogenides (Invited Paper)

Wang Yao, The Univ. of Hong Kong (Hong Kong, China)

The recent emergence of two-dimensional transition metal dichalcogenides (TMDs) provides a new laboratory for exploring the internal quantum degrees of freedom of electrons for new electronics [1]. These include the real electron spin and the valley pseudospin that labels the degenerate band extrema in momentum space. The generation and control of spin and valley pseudospin currents are at the heart of spin and valley based electronics. We will discuss two mechanisms for generating spin and valley currents of electrons in 2D transition metal dichalcogenides: (I) the valley and spin Hall current arising from the Berry curvatures [2,3]; and (II) the nonlinear valley and spin currents arising from Fermi pocket anisotropy [4]. We discuss the possibility to observe and distinguish the two effects as distinct patterns of polarized electroluminescence at pn junction in monolayer TMDs. We show that the nonlinear current response allow two unprecedented possibilities to generate pure spin and valley flows without net charge current, either by an AC bias or by an inhomogeneous temperature distribution. We will also discuss the valley Hall effect of charged excitons in monolayer TMDs, which arises from the exchange interaction between the electron and hole constituents [5].

Ref:

[1] X. Xu, W. Yao, D. Xiao and T. F. Heinz, Spins and pseudospins in layered transition metal dichalcogenides, Nature Physics 10, 343 (2014).

[2] D. Xiao, W. Yao and Q. Niu, Valley Contrasting Physics in Graphene: Magnetic Moment and Topological Transport, Phys. Rev. Lett. 99, 236809 (2007).

[3] D. Xiao, G. Liu, W. Feng, X. Xu and W. Yao, Coupled spin and valley physics in monolayers of MoS2 and other group VI dichalcogenides, Phys. Rev. Lett. 108, 196802 (2012).

[4] H. Yu, Y. Wu, G. Liu, X. Xu and W. Yao, Nonlinear valley and spin currents from Fermi pocket anisotropy in 2D crystals, Phys. Rev. Lett. 113, 156603 (2014).

[5] H. Yu, G. Liu, P. Gong, X. Xu and W. Yao, Dirac cones and Dirac saddle points of bright excitons in monolayer transition metal dichalcogenides, Nature Communications 5, 3876 (2014).

9551-34, Session 9

Spin relaxation and intervalley scattering in 2D semiconductors (Invited Paper)

Aubrey Hanbicki, Marc Currie, U.S. Naval Research Lab. (United States); George Kioseoglou, Univ. of Crete (Greece); C. Stephen Hellberg, Kathleen M. McCreary, Adam L. Friedman, Berend T. Jonker, U.S. Naval Research Lab. (United States)

Monolayer transition metal dichalcogenides, MX2 (M = Mo, W and X = S, Se), are direct-gap semiconductors with some interesting properties. First, the low-dimensional hexagonal structure leads to two inequivalent K-points, K and K', in the brillioun zone. Second, this valley index and spin are intrinsically coupled, and spin-dependent selection rules enable one to independently populate and interrogate a unique K valley with circularly polarized light. Here we probe the degree of circular polarization of the emitted photoluminescence as function of the photo-excitation energy and temperature to elucidate spin-dependent inter- and intravalley relaxation mechanisms. Monolayer flakes of MoS2 and MoSe2 show a strong depolarization as the excitation energy is increased. However, WS2 maintains significant polarization for high excitation energies, even at room temperature when properly prepared. We discuss the behavior of the polarization in terms of various phonon assisted intervalley scattering processes. This work was supported by NRL and the NRL Nanoscience Institute



9551-35, Session 10

Valley dynamics and excitonic effects in transition metal dichalcogenide monolayers (Invited Paper)

Gang Wang, Xavier Marie, Iann Gerber, Thierry Amand, Delphine Lagarde, Louis Bouet, Maël Vidal, Andréa Balocchi, Bernhard Urbaszek, Lab. de Physique et Chimie des Nano-objets (France) and Ctr. National de la Recherche Scientifique (France) and Univ. de Toulouse (France)

The closely related transition metal dichalcogenides (TMDC) MoS2, MoSe2, WSe2 and WS2 have a direct optical bandgap in the visible region around 1.8 eV when thinned down to one monolayer (ML) and show strong optical absorption (>10% / ML). ML TMDCs provide unique and convenient access to controlling the electron valley degree of freedom in k-space in the emerging field of 'valleytronics'. We show how the electron valley index can be initialized and read out optically in time and polarization resolved photoluminescence measurements [1]. The polarization properties of bilayers will be discussed for comparison [2].

When electrons and holes are simultaneously present in a ML, they will form excitons as the Coulomb interaction is enhanced by the strong quantum confinement, the large effective masses and the reduced dielectric screening in these ideal 2D systems. We determine large exciton binding energies of typically 0.5eV. We will demonstrate a variation over several orders of magnitude of the non-linear and linear optical response of ML WSe2 and MoSe2. This is achieved by tuning the optical excitation 'ON' and 'OFF' resonance with respect to the ground (1s) and excited (2s, 2p, ...) exciton states. We show that at these particular energies, identified in 1 and 2-photon excitation spectroscopy, the light-matter interaction is strongly enhanced [3].

[1] D. Lagarde et al, PRL 112, 047401 (2014)& G. Wang et al,PRB 90, 075413 (2014)

[2] G. Wang et al APL105, 182105 (2014)[3] G. Wang et al arxiv 1404.0056

9551-36, Session 10

Homoepitaxial graphene tunnel barriers for spin transport (Invited Paper)

Adam L. Friedman, U.S. Naval Research Lab. (United States)

Tunnel barriers are key elements for both charge-and spin-based electronics, offering devices with reduced power consumption and new paradigms for information processing. Such devices require mating dissimilar materials, raising issues of heteroepitaxy, interface stability, and electronic states that severely complicate fabrication and compromise performance. Graphene is the perfect tunnel barrier. It is an insulator out-of-plane, possesses a defect-free, linear habit, and is impervious to interdiffusion. Nonetheless, true tunneling between two stacked graphene layers is not possible in environmental conditions (magnetic field, temperature, etc.) usable for electronics applications. However, two stacked graphene layers can be decoupled using chemical functionalization. Here, we demonstrate homoepitaxial tunnel barrier devices in which graphene serves as both the tunnel barrier and the high mobility transport channel. Beginning with multilayer graphene, we fluorinate or hydrogenate the top layer to decouple it from the bottom layer, so that it serves as a single monolayer tunnel barrier for both charge and spin injection into the lower graphene transport channel. We demonstrate successful tunneling by measuring non-linear IV curves, and a weakly temperature dependent zero bias resistance. We perform lateral transport of spin currents in non-local spin-valve structures and determine spin lifetimes with the non-local Hanle effect to be commensurate with previous studies (~200 ps). However, we also demonstrate the highest spin polarization efficiencies (~45%) yet measured in graphene-based spin devices [1].

[1] A.L. Friedman, et al., Homoepitaxial tunnel barriers with functionalized graphene-on-graphene for charge and spin transport, Nat. Comm. 5, 3161 (2014).

9551-37, Session 10

Long distance spin transport in CVD graphene and spin filtering with h-BN barrier (Invited Paper)

Saroj P. Dash, Chalmers Univ. of Technology (Sweden)

Spintronics research in two dimensional (2D) atomic crystals is considered to be very promising. It provides a large class of materials proposed to be important for long distance spin transport and insulators for spin polarized tunneling. Here we will present two important advancements in graphene spintronics: (i) Long distance spin communication in CVD graphene on SiO2/Si substrate at room temperature, and (ii) Spin filtering in ferromagnet/hBN-graphene van der Waals heterostructures. Graphene is proposed to be an ideal material for spin transport channels due to the high mobility and long spin lifetime of the carriers. We demonstrated the effect of ferromagnetic tunnel contacts [1] and channel length dependence on the spin signal, achieving spin transports over distances of 16 µm and spin lifetimes up to 1.2 ns in CVD graphene [2]. These spin parameters are up to five times higher than previous reports on CVD graphene and highest at room temperature for any form of pristine graphene on industrial standard SiO2¬¬¬/Si substrates. Our detailed investigations reinforce the observed performance over a wafer scale demonstrating CVD graphene as an excellent material for long distance spin transport in lateral spin based devices. Furthermore, using the h-BN as a tunnel barrier on graphene, we observe an enhancement in spin polarization [3], and negative spin polarization for thicker h-BN layers [4]. The large magnitude of spin polarization together with its negative sign provides experimental evidence of the spin filtering across the ferromagnet/hBN-graphene van der Waals heterostructures. These results highlight the potential role of 2D atomic crystals in future spintronic devices.

References

[1] A. Dankert et al., Spin Transport and Precession in Graphene measured by Nonlocal and Three-Terminal Methods; Applied Physics Letters 104, 192403 (2014).

[2] M. V. Kamalakar et al., Long Distance Spin Communication in CVD Graphene, Submitted.

[3] M. V. Kamalakar et al., Enhanced Tunnel Spin Injection into Graphene using Chemical Vapor Deposited Hexagonal Boron Nitride; Scientific Reports 4, 61446 (2014); Appl. Phys. Lett. 105, 212405 (2014).

[4] M. V. Kamalakar et al., Spin Filtering in Ferromagnet/ hBN – Graphene van der Waals Heterostructures, Submitted.

9551-38, Session 10

Spintronic and optical properties of 2D materials (Invited Paper)

Roland K. Kawakami, Univ. of California, Riverside (United States)

As atomically-thin conductors, two dimensional (2D) materials enable new behaviors for spintronics and optoelectronics. The ability to stack 2D materials with differing properties allows one to combine and manipulate their electronic, spintronic, and optical properties at the atomic scale. The majority of our work has focused on graphene, which has been demonstrated to be an excellent spin channel material with extremely long spin diffusion lengths at room temperature (several microns). We have demonstrated efficient spin injection and spin transport in graphene, investigated the effects of adatom doping. Most strikingly, spin transport has been utilized as a very sensitive magnetometer to detect the formation of magnetic moments due to point defects including hydrogen adatoms and lattice vacancies. Beyond graphene, we have investigated new 2D semiconductors including transition metal dichalcogenides and germanane.



Both have direct bandgap transitions with optical selection rules that permit the optical excitation of spin polarization and/or valley polarization. Our efforts include the combined optical and electrical study of 2D semiconductors and their junctions with graphene and metals via transport, photoluminescence, photoconductivity, and ultrafast optics.

9551-39, Session 10

Graphene: new venues for spintronics (*Invited Paper*)

Pierre Seneor, Unité Mixte de Physique CNRS/Thales (France)

The recent discovery of graphene has opened novel exciting opportunities in terms of functionalities and performances for spintronics devices. We will present experimental results on the impact and potential of graphene for spintronics. We will show that unprecedented highly e?cient spin information transport can occur in graphene [1] leading to large spin signals and macroscopic spin di?usion lengths (?100 microns), potentially a key enabler for the advent of envisioned beyond-CMOS spinbased logic architectures. Furthermore, we will show that a thin graphene passivation layer can prevent the oxidation of a ferromagnet [2], enabling its use in novel humide/ambient low-cost processes for spintronics devices (such as Atomic Layer Deposition (ALD) already used intensively in micro-electronics industry but absent from spintronics), while keeping its highly surface sensitive spin current polarizer/analyzer behavior and adding new enhanced spin filtering property with almost full spin polarization reversal [3]. This could be of strong interests for MTJs or molecular spintronics [4]. These different experiments unveil promising uses of graphene for spintronics.

[1] B. Dlubak et al. Nature Physics 8, 557 (2012); P. Seneor et al. MRS Bulletin 37, 1245 (2012).

[2] B. Dlubak et al. ACS Nano 6, 10930 (2012); R. Weatherup et al. ACS Nano 6, 9996 (2012).

[3] M.-B. Martin et al. ACS Nano 8, 7890 (2014).[4] M. Galbiati et al. MRS Bulletin 39, 602 (2014)

9551-40, Session 11

Properties of light emission from multilayer InGaAs/GaAsP solid-state spinlasers and VECSELs

Tibor Fördös, Ecole Polytechnique (France) and V?B-Technical Univ. of Ostrava (Czech Republic); Henri Jaffrès, Unité Mixte de Physique CNRS/Thales (France); Kamil Postava, V?B-Technical Univ. of Ostrava (Czech Republic); Jean-Marie George, Unité Mixte de Physique CNRS/ Thales (France); Jaromír Pi?tora, V?B-Technical Univ. of Ostrava (Czech Republic); Henri-Jean Drouhin, Ecole Polytechnique (France)

Spin-polarized light sources such as spin-polarized light-emitting diodes (spin-LEDs) and spin-polarized lasers (spin-lasers and VECSELS) are prospective devices in which the spin information carried-out by the injected electrons is encoded into the circular polarization of emitted photons [1]. We will first report on a new approach for modeling of polarized light emission from spin-polarized vertical-cavity surface-emitting lasers and diodes with multiple quantum well dipole sources. The proposed method [2] is based on a 4x4 matrix formalism describing propagation of electromagnetic field in multilayer system and including boundary conditions of Maxwell equations on interfaces as well as dipolar sources in active regions or quantum wells to describe spontaneous (spin-LEDs) and stimulated (spin-VECSELs) emission. Impact of the particular linear birefrigence of the overall heterostructure [3] caused by in-plane symmetry breaking due to lattice strain, residual stress, on the emitted polarization state is demonstrated on InGaAs/GaAsP MQW laser structure characterized by a series of experiments using Mueller matrix spectroscopic ellipsometry.

In particular, we will give, by numerical methods, the properties of the output laser modes under spin-polarized carrier pump (optical and electrical) vs. the degree of linear birefringence within the heterostructure competing with the circular gain imposed by optical recombination.

[1] N. C. Gerhardt and M. R. Hoffmann, 'Spin-Controlled Vertical-Cavity Surface-Emitting Lasers', Advances in Optical Technologies, volume 2012, 268949, (2012)

[2] Tibor Fördös, Kamil Postava, Henri Jaffrès and Jaromír Pi?tora, 2014 J. Opt. 16 065008 (2014)

[3] J. Frougier et al. Appl. Phys. Lett. 103, 252402 (2013)

9551-41, Session 11

Electron spin injection and transport in (110) quantum wells for room temperature operation of spin-controlled vertical-cavity surface-emitting lasers (Invited Paper)

Nobuhide Yokota, Kazuhiro Ikeda, Nara Institute of Science and Technology (Japan); Nozomi Nishizawa, Hiro Munekata, Tokyo Institute of Technology (Japan); Hitoshi Kawaguchi, Nara Institute of Science and Technology (Japan)

Spin-controlled vertical-cavity surface-emitting lasers (sc-VCSELs) have been attracting researchers' interest because they can achieve oscillation with a single circular polarization mode controlled by electron spin polarization in the active region. A long electron spin relaxation time ts is crucial for sc-VCSELs to exhibit a high degree of circular polarization PC. (110)-oriented quantum wells (QWs) are thus attractive owing to their ts much longer than (100)-oriented QWs even at room temperature (RT). In this presentation, we report our recent studies toward realization of sc-VCSEL operating at RT.

We investigated electrical spin injection into (110) GaAs QWs in lightemitting diodes having Fe/crystalline-AlOx (Fe/x-AlOx) tunnel barrier contacts. A Pc of 2.6% was obtained at RT even with a current density of 1.5 kA/cm2 required for VCSELs to oscillate. The degree of initial electron spin polarization in the QWs estimated from the measured value of Pc was 9.3% at RT, which suggests that lasing with a high Pc value can be achieved under electrical spin injection in VCSELs with the Fe/x-AlOx contacts.

Observation of a 37-um electron spin transport at RT in (110) GaAs QWs with an in-plane electric field of 1.75?kV/cm suggests that (110) QWs are useful as a spin transport layer for sc-VCSELs.

The electron spin relaxation originating from the D'yakonov-Perel' and Bir-Aronov-Pikus mechanisms was found to be small in both (110) and (100) InGaAs/InAIAs QWs. This result implies that the sc-VCSEL operating at RT and a telecom wavelength of 1.55 um will be obtained by using conventional (100) InGaAs/InAIAs QWs.

9551-42, Session 11

Growth condition dependence of carrier and spin lifetimes in GaAs-based quantum wells (Invited Paper)

Satoshi Iba, Hidekazu Saito, National Institute of Advanced Industrial Science and Technology (Japan); Ken Watanabe, Yuzo Ohno, Univ. of Tsukuba (Japan); Shinji Yuasa, National Institute of Advanced Industrial Science and Technology (Japan)

Spin-polarized light-emitting diode (spin-LED), which consists of a ferromagnetic (FM) contact and semiconductor quantum well (QW), is an essential element for future spin-optical devices such as spin laser [1,2]. So far, the FM contact has attracted much attention to achieve a highly circularly polarized electroluminescence (EL). However, it is also important



to study carrier and spin dynamics in the QW part because the polarizability strongly depends on those properties [1]. In this study, we systematically investigated the effect of growth conditions on the carrier and spin lifetimes in the (001) GaAs/AlGaAs QWs at room temperature.

All the undoped samples were grown using MBE under the different As4/ Ga flux ratios and growth temperature conditions. The carrier lifetimes (t_c) strongly depend on both the As4/Ga ratio and the growth temperature (0.4-9 ns), whereas the spin relaxation times (t_s) are almost constant at about 0.2 ns. These results suggest that the circular polarization of the PL (P_PL) is largely affected by the growth conditions because the P_PL is given by t_s/(t_c+t_s)P_s, where the P_s is the electron spin polarization (constant in our measurements). Actually, we confirmed that the P_PL values depend considerably on growth conditions as expected from the t_c and t_s values. Hence, choosing the appropriate growth condition of the QW is indispensable for obtaining a high EL polarization from the spin-LED. Reference

M. Holub and P. Bhattacharya, J. Phys. D: Appl. Phys. 40 R179 (2007).
 J. Sinova and I. ?uti?, Nature Mater. 11, 368 (2012).

9551-43, Session 11

Continuous visible-light emission at room temperature in Mn-doped GaAs and Si light-emitting diodes (Invited Paper)

Masaaki Tanaka, Pham Nam Hai, Le Duc Anh, The Univ. of Tokyo (Japan)

We demonstrate visible-light electroluminescence due to d-d transitions in GaAs:Mn based light emitting diodes (LEDs) [1][2]. We prepared p+n junctions with a p+GaAs:Mn layer. At a reverse bias voltage (-3 to -6V), holes are injected from the n-type layer to the depletion layer and accelerated by the intense electric field, and excite the d electrons of Mn in the p+GaAs:Mn layer by impact excitations. We observe visible-light emission E1 = 1.89eV and E2 = 2.16eV, which are exactly the same as the 4T1 -> 6A1 and 4A2 -> 4 T1 transition energy of Mn.

Furthermore, by utilizing optical transitions between the p-d hybridized orbitals of Mn atoms doped in Si, we demonstrate Si-based LEDs that continuously emit reddish-yellow visible light at room temperature. The Mn p-d hybrid states are excited by hot holes that are accelerated in the depletion layers of reverse biased Si pn junctions. Above a threshold reverse bias voltage of about -4V, our LEDs show strong visible light emission with two peaks at EI = 1.75eV and E2 = 2.30eV, corresponding to optical transitions from the t-a (spin-down anti-bonding) states to the e- (spin-down non-bonding) states, and from the e- to the t+a (spin-up anti-bonding) states. The internal quantum efficiency of the EI and E2 transitions is 3-4 orders of magnitude higher than that of the indirect band-gap transition [3].

P. N. Hai, et al., APL 104, 122409 (2014).
 P. N. Hai, et al., JAP 116, 113905 (2014).

[3] P. N. Hai, et al., submitted.

9551-44, Session 12

Time-evolution of wave-packets in topological insulators (Invited Paper)

Gerson J. Ferreira, Univ. Federal de Uberlândia (Brazil); Poliana H. Penteado, José Carlos Egues, Univ. de São Paulo (Brazil)

The electronic structure of topological insulators (TIs) are well described Dirac-like equations, e.g. the BHZ model, with a mass term that changes sign at some interface. This simplistic description includes a pseudo-spinorbit coupling that is intrinsic to the Dirac Hamiltonian. Consequently, the TIs share common properties with the Dirac equation. Among them, the interference between positive and negative energy bands leads to the relativistic oscillatory motion known as the Zitterbewegung. Here we discuss the ballistic time-evolution (pico and nanoseconds) of wave-packets in TIs in the presence of an external electric field. We show that the guiding center of large wave-packets have a finite motion transversal to the electric field equivalent to side-jump in Rashba GaAs. However, for narrow wave-packets the dynamics change and the guiding center description is not complete. We also discuss the reflection of a wave-packet colliding with the edge of the system and the effects of the edge states.

Acknowledgement: We acknowledge support from CAPES, CPNq, FAPEMIG, FAPESP, and NAP Q-NANO from PRP/USP.

9551-45, Session 12

Skyrmions in quasi-2D chiral magnets with broken bulk and surface inversion symmetry (Invited Paper)

Mohit Randeria, The Ohio State Univ. (United States); Sumilan Banerjee, Weizmann Institute of Science (Israel); James Rowland, The Ohio State Univ. (United States)

Most theoretical studies of chiral magnetism, and the resulting spin textures, have focused on 3D systems with broken bulk inversion symmetry, where skyrmions are stabilized by easy-axis anisotropy. In this talk I will describe our results on 2D and quasi-2D systems with broken surface inversion, where we find [1] that skyrmion crystals are much more stable than in 3D, especially for the case of easy-plane anisotropy. These results are of particular interest for thin films, surfaces, and oxide interfaces [2], where broken surface-inversion symmetry and Rashba spin-orbit coupling naturally lead to both the chiral Dzyaloshinskii-Moriya (DM) interaction and to easy-plane compass anisotropy. I will then turn to systems that break both bulk and surface inversion, resulting in two distinct DM terms arising from Dresselhaus and Rashba spin-orbit coupling. I will describe [3] the evolution of the skyrmion structure and of the phase diagram as a function of the ratio of Dresselhaus and Rashba terms, which can be tuned by varying film thickness and strain.

S. Banerjee, J. Rowland, O. Erten, and M. Randeria, PRX 4, 031045 (2014).
 S. Banerjee, O. Erten, and M. Randeria, Nature Phys. 9, 626 (2013).

[3] J. Rowland, S. Banerjee and M. Randeria, (unpublished).

9551-46, Session 12

Spirals and skyrmions in two dimensional oxide heterostructures (Invited Paper)

Xiaopeng Li, Univ. of Maryland, College Park (United States); W. Vincent Liu, Univ. of Pittsburgh (United States); Leon Balents, Univ. of California, Santa Barbara (United States)

Metallic interfaces between insulating oxides such as STO-LAO or STO-GTO provide a versatile platform to study two dimensional electron liquids. Numerous experiments have observed magnetism and significant spin-orbit effects in such structures. We construct the general free energy governing long-wavelength magnetism in two-dimensional oxide heterostructures, which applies irrespective of the microscopic mechanism for magnetism. This leads, in the relevant regime of weak but non-negligible spin-orbit coupling, to a rich phase diagram containing in-plane ferromagnetic, spiral, cone, and skyrmion lattice phases, as well as a nematic state stabilized by thermal fluctuations.



9551-47, Session 12

Electrical injection and detection of spinpolarized currents in 3D topological insulators (Invited Paper)

Jifa Tian, Purdue Univ. (United States)

Topological insulators (TIs) are an unusual phase of quantum matter with nontrivial spin-momentum locked topological surface states (TSS). The electrical detection of spin-momentum locking of the TSS in 3D TIs has been lacking till very recently. In this talk, we will present the spin potentiometric measurements in thin flakes exfoliated from 3D TI Bi2Te2Se (BTS221) and Bi2Se3 bulk crystals, using two outside nonmagnetic (Au) contacts for driving a DC spin helical current and a middle ferromagnetic (FM)-Al2O3 tunneling contact for detecting spin polarization. The voltage measured by the FM electrode exhibits a hysteretic step-like change when sweeping an in-plane magnetic field between opposite directions along the easy axis of the FM contact to switch its magnetization. Importantly, the direction of the voltage change can be reversed by reversing the direction of the DC current, and the amplitude of the change as measured by the difference in the detector voltage between opposite magnetization increases linearly with increasing bias current, consistent with the current-induced spin polarization of spin-momentum-locked TSS. Our work directly demonstrates the electrical injection and detection of spin polarization in TI and may enable utilization of spin-helical TSS for future applications in nanoelectronics and spintronics.

9551-48, Session 13

Magnon Hall effect (Invited Paper)

Yoshinori Onose, The Univ. of Tokyo (Japan)

In itinerant ferromagnets, the Hall effect proportional to the magnetization, which is termed anomalous Hall effect, is driven by the relativistic spin-orbit interaction, and does not require the Lorentz force. Therefore, an important question is whether charge neutral magnons can show the anomalous Hall effect.

Recently, we have succeeded in observing the magnon Hall effect for the first time in terms of thermal transport. We also observe the distinct effect of lattice geometry on the magnon Hall effect, which can be well explained by the picture of the Dzyaloshinskii-Moriya interaction-induced magnon Hall effect.

9551-49, Session 13

Magnonic Hall effect and topological magnonic crystals (Invited Paper)

Shuichi Murakami, Tokyo Institute of Technology (Japan)

In electronic systems it is well established that when there is a magnetic field or spontaneous magnetization, the Hall effect, and in some cases the quantum Hall effect appears. We theoretically pursue analogs of these phenomena in magnons (spin waves) and plasmons. In the case of magnons in ferromagnets, the Hall effect or quantum Hall effect requires some kind of a spin-orbit coupling (similar to electronic systems), and we show that the dipolar interaction, as well as the Dyaloshinskii-Moriya interaction, plays the role. By calculating the Berry curvature from the wavefunction, we can calculate thermal Hall effect for magnons in ferromagnets with dipolar interaction. We found that only the magnetostatic forward volume-wave mode exhibits the thermal Hall effect while the backward mode and the surface mode do not. In addition, by introducing some artificial spatial periodicity into the magnet, for example by fabricating nanostructures with two different magnets in a periodic structure or by making a periodic array of nanomagnets, we theoretically find appearance of quantum Hall effect in a certain range of the magnetic field. There appear chiral edge states which propagate along the edge of the magnet in one way. We call this a topological magnonic crystal. In the plasmon case, we should begin

with constructing a fundamental band theory, and we theoretically show that on a metal surface with corrugations forming a triangular lattice under the magnetic field, the quantum Hall effect appears. It can be called a topological plasmonic crystal.

9551-50, Session 13

Magnon Hall effect and planar Righi-Leduc effect measured in NiFe and YIG ferromagnets

Benjamin Madon, Do Chung Pham, Ecole Polytechnique (France); Daniel Lacour, Institut Jean Lamour (France); Abdelmadjid Anane, Unité Mixte de Physique CNRS/Thales (France) and Univ. Paris-Sud 11 (France); Rozenn Bernard, Vincent Cros, Unité Mixte de Physique CNRS/Thales (France) and Univ. Paris Sud 11 (France); Michel Hehn, Institut Jean Lamour (France); Jean-Eric Wegrowe, Ecole Polytechnique (France)

A pure magneto-thermal signal (described by the anisotropic Fourier law) was measured in ferromagnets that possess a chiral structure (Lu2V2O7): this is the magnon hall effect (or equivalently "anomalous Righi-Leduc effect") [1], that is the thermal analogue of the electric anomalous Hall effect. It has then been proposed [2] that the effect could be universal, in the sense that it can also be measured in ferromagnetic materials without specific crystalline structures, like NiFe (metallic) or Yttrium Iron Garnets (YIG, electric insulator). Furthermore, it has been predicted that the Magnon-Hall effect should be associated with the "Planar Righi-Leduc effect" (which is the thermal analogue of the electric planar-Hall effect).

We report here about a comparative study of the Magnon-Hall and planar Righi-Leduc effect performed on both NiFe and YIG ferromagnets. For the first time, the magneto-thermal effect is measured with a thin electrode deposited on the top of a ferromagnetic layer. This electrode plays the role of the thermocouple. The corresponding magneto-thermo-voltage is measured as a function of the quasi-static magnetization states. It is shown that, for a heat current confined in the plane of the ferromagnetic layer and oriented perpendicular to the electrode, the Magnon-Hall signal follows a 360° periodicity as a function of the out-of-plane angle of the magnetization, while the Planar Righi-Leduc signal follows a 180° periodicity as a function of the in-plane angle.

The relation between these observations and the occurrence of the inverse spin-Hall effect (which is responsible for the spin-Seebecl effect[3]) is discussed.

[1] Y. Onose et al, Science 329, 297 (2010).

[2] J.-E. Wegrowe et al. Phys. Rev. B 89, 094409 (2014)

[3] K. Uchida et al., Nature 455, 778-781 (2008).

9551-51, Session 14

Helimagnetism in nanometer small bilayer iron islands (Invited Paper)

Dirk Sander, Max-Planck-Institut für Mikrostrukturphysik (Germany)

We report a novel noncollinear magnetic order in individual nanostructures of a prototypical magnetic material, bilayer iron islands on Cu (111) [1]. Spin-polarized scanning tunnelling microscopy reveals a magnetic stripe phase with a period of 1.28 nm, which is identified as a one-dimensional helical spin order. Ab initio calculations reveal reduced-dimensionalityenhanced long-range antiferromagnetic interactions as the driving force of this spin order. Our findings point at the potential of nanostructured magnets to establish noncollinear magnetic order in a nanostructure, which is magnetically decoupled from the substrate.

[1] S.H. Phark, J.A. Fischer, M. Corbetta, D. Sander, K. Nakamura, J. Kirschner, Nature Comm. 5, 5183 (2014).



9551-52, Session 14

Toward the realization of a single atom magnet (Invited Paper)

Fabio Donati, Ecole Polytechnique Fédérale de Lausanne (Switzerland)

Single atoms adsorbed on a solid surface represent a paradigm for investigating the ultimate size limit of a magnet. The main request for their use in information storage and computation is the magnetic bistability, which requires protecting the magnetization of an atom against thermal fluctuations and quantum tunneling. Different strategies have been attempted in this direction, aiming to increase the magnetic anisotropy energy of the adsorbed atom, decouple its spin from the conduction electron of the substrate, and tailor the angular symmetry of the crystal field of the surface. However, the complexity of the interactions between magnetic atoms and surface electrons makes the experimental realization of a single atom magnet a challenging task.

In this talk, I will present the recent advancements in the field, discussing the results achieved in the engineering of the magnetic properties of transition metal and rare earth atoms. First, I will describe how graphene can be successfully used to induce a large magnetic anisotropy in adsorbed Co atoms [Phys. Rev. Lett. 111, 236801 (2013); 113, 177201 (2014)]. For the same atoms, I will show how the magnetic anisotropy can be enhanced to the maximum limit of 58 meV imposed by the spin-orbit coupling by exploiting the almost cylindrical crystal field environment offered by the MgO/Ag(100) surface [Science 344, 988 (2014)]. Finally, I will illustrate how the magnetism of Ho and Er atoms can be tailored via the interaction with closed packed metal surfaces [Phys. Rev. Lett. 113, 237201 (2014)].

9551-53, Session 14

Geometrical phase and inertial regime of the magnetization: Hannay angle and magnetic monopole (Invited Paper)

Jean-Eric Wegrowe, Ecole Polytechnique (France)

It is well known that the Landau-Lifshitz-Gilbert (LLG) equation for a macroscopic magnetic moment find its theoretical limit of validity at very short time scales or equivalently at very high frequencies. The reason for this limit of validity is well understood in terms of separation of the characteristic times between slow (the magnetization) and fast (the environment) degrees of freedom, as pointed-out in the stochastic derivation of the LLG equation first proposed by W. F. Brown in 1963 [1]. Indeed, the ferromagnetic moment is a slow collective variable, but fast degrees of freedom are also playing a role in the dynamics, and especially the angular momentum responsible for inertia. In the last couple of years. the generalization of the LLG equation with inertia (ILLG) has been derived by different means [2,3,4]. The signature of the inertial regime of the magnetization is the nutation oscillation - added to the usual precession - that can be measured by resonance experiments (but it has not been observed up to know). However, we show that even for the pure precession movement, the fast degrees of freedom can also play an important role.

We developed an approach in terms of geometrical phase (defining the corresponding Hannay angle [5], which is the classical analog to the quantum Berry phase), that has recently been used with success to analogous problems [6]. We calculated the Hannay angle for the precession of the magnetization in the case of the inertial effect. This analysis allows the slow vs. fast variable expansion to be calculated in the specific case of pure precession. The result is interpreted in terms of classical magnetic monopole.

[1] W. F. Brown, "Thermal Fluctuation of a Single_Domain Particle" Phys. Rev. 130 (1963), 1677 (1963)

[2] M. Faehnle, D. Steiauf, and Ch. Illg, "erratum: Generalized Gilbert equation including inertial damping: Derivation from an extended breathing Fermi surface model" Phys. Rev. B 88 (2013), 219905.

[3] J.-E. Wegrowe, C. Ciornei "Magnetization dynamics, Gyromagnetic Relation, and Inertial Effects", Am J. Phys. 80, 607 (2012).

 $\ensuremath{\left[4\right]}$ M.-C. Ciornei, J. M. Rubi, and J.-E. We growe, "Magnetization dynamics in the inertial regime: Nutation predicted at

short time scales", Phys. Rev. B 83, 020410(R) (2011).

[5] J. H. Hannay "Angle variable holonomy in adiabatic excursion of an integrable Hamiltonian", J. Phys. A 18, 221 (1985)

[6] M. V. Berry a,d P. Shukla "Slow Maniforld and Hannay angle in the spinning top", Eur. J. Phys. 32, 115 (2011)

9551-54, Session 14

Laser-induced spin precession for magnetic alloy films in THz wave range (Invited Paper)

Shigemi Mizukami, Tohoku Univ. (Japan)

No Abstract Available

9551-55, Session 14

Magnetism in thin films: a spin-resolved investigation of single and multi-layer systems (Invited Paper)

Alberto Calloni, Politecnico di Milano (Italy)

An overview of our past and present activity in the study of the magnetic properties of ultrathin films of transition metal elements is presented, with emphasis on spin resolved electron spectroscopy results. The development of perpendicular anisotropies, the observation of oscillatory magnetic coupling and giant magnetoresistence in such multilayer systems are widely exploited by the microelectronic industry for data manipulation and storage. The practical realization and characterization of selected model systems is devised to investigate some of these peculiar magnetic phenomena. In this respect, specific topics will be discussed, such as: (i) the epitaxial growth of monolayer range thin films of Fe and Ni on non-magnetic substrates [such as W(110)], focusing on the occurrence of a spontaneous magnetization as a function of the film thickness and the crystal structure evolution. (ii) The characterization of the magnetic phenomena occurring at the interface/ surface of magnetic films. In particular, recent results on the coupling of a thin Cr layer to a Fe(100) substrate, where a layered antiferromagnetic order is induced, will be illustrated, together with some strategies devised to tune the anisotropy energy in thin films made of stacked Fe/Ni(111) and Co/ Ni(111) layers, eventually leading to perpendicular magnetization. The role of structural (i.e. the effect of film strain) chemical (i.e. the stability of the interface against atomic diffusion) and procedural issues (i.e. the different strategies devised to promote the layer-by-layer growth of atomically flat interfaces), often the key ingredients for the determination of the magnetic behavior of such systems, will be highlighted.

9551-56, Session 15

Voltage control of nanoscale magnetoelastic elements: theory and experiments (Invited Paper)

Gregory P. Carman, Univ. of California, Los Angeles (United States)

Electromagnetic devices rely on electrical currents to generate magnetic fields. While extremely useful this approach has limitations in the small-scale. To overcome the scaling problem, researchers have tried to use electric fields to manipulate a magnetic material's intrinsic magnetization (i.e. multiferroic). The strain mediated class of multiferroics offers up to 70% of energy transduction using available piezoelectric and magnetoelastic materials. While strain mediated multiferroic is promising, few studies exist on modeling/testing of nanoscale magnetic structures.



This talk presents motivation, analytical models, and experimental data on electrical control of nanoscale single magnetic domain structures. This research is conducted in a NSF Engineering Research Center entitled Translational Applications for Nanoscale Multiferroics TANMS. The models combine micromagnetics (Landau-Lifshitz-Gilbert) with elastodynamics using the electrostatic approximation producing eight fully coupled nonlinear partial differential equations. Qualitative and guantitative verification is achieved with direct comparison to experimental data. The modeling effort guides fabrication and testing on three elements, i.e. nanoscale rings (onion states), ellipses (single domain reorientation), and superparamagnetic elements. Experimental results demonstrate electrical and deterministic control of the magnetic states in the 5-500 nm structures as measured with Photoemission Electron Microscopy PEEM, Magnetic Force Microscopy MFM, or Lorentz Transmission Electron Microscopy TEM. These data strongly suggests efficient control of nanoscale magnetic spin states is possible with voltage.

9551-57, Session 15

Reversible electric field driven magnetic domain wall motion (*Invited Paper*)

Kevin J. A. Franke, Aalto Univ. School of Science and Technology (Finland); Ben Van de Wiele, Univ. Gent (Belgium); Yasuhiro Shirahata, Tokyo Institute of Technology (Japan); Sampo J. Hämäläinen, Aalto Univ. School of Science and Technology (Finland); Tomoyasu Taniyama, Tokyo Institute of Technology (Japan); Sebastiaan van Dijken, Aalto Univ. School of Science and Technology (Finland)

Control of magnetic domain wall motion by electric fields has recently attracted scientific attention because of its potential for magnetic logic and memory devices. Here, we report on a new mechanism for reversible and deterministic motion of magnetic domain walls using an electric field only. Full electric-field control over the magnetic domain-wall velocity in the absence of a magnetic field or spin-polarized electric current is demonstrated using epitaxial Fe films on single-crystal BaTiO3 substrates with alternating in-plane (a domains) and out-of-plane (c domains) ferroelectric polarization [1]. The magnetic domain walls of the Fe film are strongly pinned onto the a-c boundaries of the BaTiO3 substrate by abrupt changes in the symmetry and strength of magnetic anisotropy as a result of strain transfer and inverse magnetostriction [2]. Repeatable back-and-forth motion of a ferroelectric a-c boundary and a pinned magnetic domain wall is realized by the application of positive and negative out-of-plane voltage pulses. The domain-wall velocity is varied over 5 orders of magnitude by adjusting the electric-field strength. Patterning of the magnetic film reveals that near-180° transverse magnetic domain walls can be stabilized in magnetic nanowires on top of BaTiO3 due to competing shape anisotropy. Moreover, the driving mechanism is not affected by pinning centers such as grain boundaries or notches that usually influence the motion of magneticfield or electric-current driven magnetic domain walls.

I. K. J. A. Franke, B. Van de Wiele, Y. Shirahata et al., Phys. Rev. X 5, 011010 (2015)

2. T. H. E. Lahtinen, Y. Shirahata, L. Yao et al., Appl. Phys. Lett. 101, 262405 (2012)

9551-58, Session 15

Magnetoelectric imaging of multiferroic heterostructures (Invited Paper)

Massimo Ghidini, Arnaud Lesaine, Bonan Zhu, Xavier Moya, Wenjing Yan, Sam Crossley, Bhasi Nair, Rhodri Mansell, Russell P. Cowburn, Crispin H. W. Barnes, Univ. of Cambridge (United Kingdom); Florian Kronast, Sergio Valencia, Helmholtz-Zentrum Berlin für Materialien und Energie GmbH (Germany); Francesco Maccherozzi, Sarnjeet S. Dhesi, Diamond Light Source Ltd. (United Kingdom); Neil Mathur, Univ. of Cambridge (United Kingdom)

Electrical control of magnetism has been demonstrated in multiferroic compounds and ferromagnetic semiconductors, but electrical switching of a substantial net magnetization at room temperature has not been demonstrated in these materials. This goal has instead been achieved in heterostructures comprising ferromagnetic films in which electrically driven magnetic changes arise due to strain or exchange bias from ferroic substrates, or due to charge effects induced by a gate. However, previous work focused on electrical switching of an in-plane magnetization or involved the assistance of applied magnetic fields.

In heterostructures made of juxtaposed ferroelectric and ferromagnetic layers, we have shown electrical control with no applied magnetic field of the perpendicular magnetization of small features [1] and of magnetic stripe domains patterns [2].

Here we investigate Ni81Fe19 films on ferroelectric substrates with and without buffer layers of Cu, whose presence precludes charge-mediated coupling. Ni81Fe19 has virtually zero magnetostriction, but sufficiently thin films show large magnetostriction, and thus, on increasing film thickness through the threshold for zero magnetostriction, we have seeked the crossover from charge- to strain-mediated coupling.

We will then show that strain associated with the motion of 90°ferroelectric domain walls in a BaTiO3 substrate, can switch the magnetization of an array of overlying single-domain Ni dots.

[1] M. Ghidini, R. Pellicelli, J. L. Prieto, X. Moya, J. Soussi, J. Briscoe, S. Dunn and N. D. Mathur, Nature Communications 4 (2013) 1453.

[2] M. Ghidini, F.Maccherozzi, X. Moya, L. C. Phillips, W.Yan, J. Soussi, N. Métallier, M.Vickers, , N. -J.Steinke, R. Mansell, C. H. W. Barnes, S. S. Dhesi, and N. D. Mathur, Adv. Mater.doi: 10.1002/adma.201404799 (2015).

9551-59, Session 15

Non-collinear magnetic structure in La2/3Sr1/3MnO3/LaNiO3 superlattices (Invited Paper)

Anand Bhattacharya, Argonne National Lab. (United States)

Non-collinear magnetic textures give rise to interesting charge and spin transport properties, and allow for control of of magnetism using small electric currents. While these textures have been observed in a number of bulk materials and in thin films, realizing non-collinear magnetism in heterostructures may lead to new avenues to control their properties using tailored interfaces and gate electric fields. We have discovered a non-collinear magnetic coupling in superlattices comprised of two metallic perovskites,

La2/3Sr1/3MnO3 (LSMO) and LaNiO3 (LNO). The angle between the magnetization of the LSMO layers varies in an oscillatory manner with the thickness of the intervening LNO. The magnetic field and temperature dependence of this angle cannot be explained using models that incoporate bilinear and biquadratic coupling, commonly used to describe non-collinear magnetism in conventional metallic heterostructures. Furthermore, we observe substantial electron transfer from the LSMO into the LNO layer, causing the Ni sites in the vicinity of interfaces to be in approximately a 2+ oxidation state. We propose a model where these localized Ni2+ spins in the LNO couple to a momentum dependent spin susceptibility, giving rise to a spiral magnetic structure within the LNO. All our superlattices are synthesized using oxide-MBE, and characterized with a variety of means, including neutron scattering.



9551-60, Session 15

Efficient spin-to-charge conversion at LaAIO3/SrTiO3 interfaces (Invited Paper)

Edouard Lesne, Juan-Carlos Rojas-Sánchez, Unité Mixte de Physique CNRS/Thales (France); Simon Oyarzun, Yu Fu, CEA-INAC (France); Nicolas Reyren, Eric Jacquet, Vincent Cros, Unité Mixte de Physique CNRS/Thales (France); Gérard Desfonds, Serge Gambarelli, Matthieu Jamet, Jean-Philippe Attané, CEA-INAC (France); Jean-Marie George, Albert Fert, Agnès Barthélémy, Unité Mixte de Physique CNRS/Thales (France); Laurent Vila, CEA-INAC (France); Henri Jaffrès, Unité Mixte de Physique CNRS/ Thales (France) and Peter Grünberg Institute (Germany) and Institute for Advanced Simulation (Germany); Manuel Bibes, Unité Mixte de Physique CNRS/Thales (France)

The Rashba effect is a manifestation of spin-orbit interaction (SOI) in solids, where the spin degeneracy associated with the spatial inversion symmetry is lifted due to a symmetry-breaking electric field normal to the heterointerface [1] and giving rise to an electric field modulation effect at e.g. the canonical LaAIO3/SrTiO3 interface, as demonstrated very recently [2]. On the other hand, Eldelstein was the first to realize that in a Rashba two-dimensional electron system, the flow of a charge current is accompanied by a non-zero spin accumulation coming from uncompensated spin-textured Fermi surfaces [3]. Recently, the converse effect, corresponding to a spin-to-charge conversion through SOI (inverse Edelstein effect or IEE), was demonstrated at Ag/Bi(111) interfaces [3].

Here we report on spin-pumping experiments performed on a series of NiFe/LaAIO3/SrTiO3 heterostructures, with possible evidence of efficient spin-to-charge conversion from perpendicular spin injection by spin-pumping method to lateral current measured in voltage detection method. We tentatively interpret these results in terms of the large SOI at the LaAIO3/SrTiO3 interface [5], discuss the corresponding electrostatic modulation of the IEE by a back-gate voltage and give perspectives for oxide-based spintronics free of ferromagnetism.

[1] Y. A. Bychkov & E. I. Rashba, J. Phys. C 17, 6039 (1984).

[2] G. Herranz et al., Nat. Commun. 6, 6028 (2015).

[3] V. M. Edelstein, Solid State Commun. 73, 233 (1990).

[4] J. C. Rojas-Sánchez et al., Nat. Commun. 4, 2944 (2013).

[5] A. D. Caviglia et al., Phys. Rev. Lett. 104, 126803 (2010).

9551-61, Session 16

Periodic and quasiperiodic artificial spin ices: magnetic structure and dynamics (Invited Paper)

Christopher H. Marrows, Univ. of Leeds (United Kingdom)

Artificial spin ices are frustrated systems constructed using nanotechnology, where single-domain magnetic nanoislands are arranged in such a manner that their magnetostatic interactions cannot all be simultaneously satisfied. They are often described as designer metamaterials, since all the system parameters can be tuned during the design of the lithography pattern. They are often touted to be model statistical mechanical systems, yet most instances to date are athermal systems described by an effective thermodynamics. Here we report on square ice systems where the island size has been shrunk to the point where the energy barrier to reversal is of the order of kT, and the moment of the islands therefore fluctuates as time passes. These islands are too small to be imaged by conventional magnetic microscopy techniques. Real space X-ray transmission microscopy and reciprocal space X-ray photon correlation spectroscopy studies, both using soft X-rays with XMCD contrast, show the thermally activated dynamics of the system as it explores its phase space.

We have also prepared systems based on Penrose tilings. These have a

multiplicity of different structural vertex types, each with its own energy spectrum. MFM shows that high-magnetic charge configurations are avoided, but long-range magnetic order is difficult to observe. Analysis of the vertex energies suggests that the structure can be divided into two parts: a percolating 'skeleton' that possesses a rigid twofold ground state, containing spins that are 'flippable' and do not affect the overall system energy, a signature of true frustration.

9551-62, Session 16

Unconventional spin textures in magnetically frustrated topologies (Invited Paper)

Nicolas Rougemaille, Ioan Chioar, Institut NÉEL (France); Michel Hehn, Daniel Lacour, François Montaigne, Institut Jean Lamour (France); Benjamin Canals, Institut NÉEL (France)

Frustration is a general concept in physics and can be found in many condensed matter systems. Frustration arises when all pairwise interactions can not be satisfied simultaneously, for example due to the system geometry. In some cases, frustration effects lead to an extensively degenerate ground state, i.e a low-temperature manifold built with a infinite number of configurations with identical energy. Frustrated systems may then have a finite entropy, even at zero temperature.

Progress in fabrication and characterization techniques allowed researchers to produce, artificially, two-dimensional frustrated arrays of nanostructures and to investigate their collective magnetic behavior. These studies have stimulated new research activities motivated by the quest for exotic magnetic phases in condensed matter physics, bringing together the communities of magnetic frustration, statistical physics, and nanomagnetism.

In this contribution, we'll show, experimentally (magnetic imaging techniques) and theoretically (mainly Monte Carlo simulations), that simple magnetic topologies can lead to unconventional, non-collinear spin textures. For example, kagome arrays of ferromagnetic nano-islands with ferromagnetic nearest neighbor interactions do not show magnetic order. Instead, these systems are characterized by spin textures with intriguing properties, such as chirality, coexistence of magnetic order and disorder, and charge crystallization. However, in kagome arrays of ferromagnetic nanodisks with antiferromagnetic interactions between neighboring elements, the system is also characterized by a new magnetic phase, but with a still unknown spin texture.

9551-63, Session 16

Direct visualization of the thermodynamics of artificial spin ice systems (Invited Paper)

Alan Farhan, Paul Scherrer Institut (Switzerland)

Recent years have shown a significant amount of research being directed towards investigations on artificial spin ice systems [1, 2], which mimic the behavior of geometrically frustrated pyrochlore spin ice [3]. Here, we present first direct observations of thermally induced magnetic relaxation in extended arrays of artificial square ice [4] and building block structures of artificial kagome spin ice [5, 6]. While thermal relaxation leads to a clear route towards the ground state in artificial square ice [4], we observe an increasing difficulty in accessing the predicted ground state configuration in artificial kagome spin ice an ideal system to visualize an optimization of applied annealing procedures. From a general point of view, our methods offer the possibility to observe and investigate the thermodynamics of two-dimensional frustrated systems in real space and time, and provide a way to directly investigate the nature of complex stochastic processes.

[1] C. Nisoli and P. Schiffer, Review of Modern Physics 85, 1473 (2013).

[2] L. J. Heyderman and R. L. Stamps, Journal of Physics-Condensed Matter 25, 363201 (2013).



[3] M. J. Harris et al., Physical Review Letters 79, 2554 (1997).
[4] A. Farhan et al., Physical Review Letters 111, 057204 (2013).
[5] A. Farhan et al., Nature Physics 9, 375 (2013).

[6] A. Farhan et al., Physical Review B 89, 214405 (2014).

9551-64, Session 17

Artificial spin ice: from scientific toy to material by design (Invited Paper)

Cristiano Nisoli, Los Alamos National Lab. (United States); Peter Schiffer, Ian Gilbert, Univ. of Illinois at Urbana-Champaign (United States)

Frustration, the presence of constraints/interactions that cannot be completely satisfied, is ubiquitous in the physical sciences as well as in life and a source of degeneracy and disorder which gives rise to new and interesting physical phenomena. In the past years a new perspective has opened in the study of frustration through the creation of artificial frustrated magnetic systems, consisting of arrays of lithographically fabricated singledomain ferromagnetic nanostructures that behave like giant lsing spins. The interactions can be controlled through their geometric properties and arrangement: The degrees of freedom of the material can be directly tuned, but also individually observed. Experimental studies have unearthed intriguing connections to the out-of-equilibrium physics of disordered systems and non-thermal "granular" materials, while revealing strong analogies to spin ice materials and their fractionalized magnetic monopole excitations, lending the enterprise a distinctly interdisciplinary flavor.

In this talk we outline the more recent developments and future vistas for progress in this rapidly expanding field. We show how recent results have opened paths to new territories. Higher control, inclusive of genuine thermal ensembles have replaced the earlier and coarser methods based on magnetic agitation. Dynamical versions are now being realized, characterized in real time via PEEM, revealing statistical mechanics in action. This has lead us to afford implementation of new geometries, not found in nature, for dedicated bottom up design of desired emergent properties. Born as a scientific toy to investigate frustration-by-design, artificial spin ice might now be used to open "a path into an uncharted territory, a landscape of advanced functional materials in which topological effects on physical properties can be explored and harnessed."

9551-65, Session 17

Controlling electric and magnetic currents in artificial spin ice (Invited Paper)

Will R. Branford, Imperial College London (United Kingdom)

I will discuss the collective properties of arrays of single domain nanomagnets called Artificial Spin Ice.1 The shape of each nanomagnet controls the magnetic anisotropy and the elements are closely spaced so dipolar interactions are important. The honeycomb lattice geometry prevents the satisfaction of all dipole interactions. Here I will show direct magnetic imaging studies of magnetic charge flow.2 The magnetic charge is carried by transverse domain walls and the chirality of the domain wall is found to control the direction of propagation.3,4 Injection of domain walls within the arrays with local fields is also explored.5

References

1 Branford, W. R., Ladak, S., Read, D. E., Zeissler, K. & Cohen, L. F. Emerging Chirality in Artificial Spin Ice. Science 335, 1597-1600, (2012).

2 Ladak, S., Read, D. E., Perkins, G. K., Cohen, L. F. & Branford, W. R. Direct observation of magnetic monopole defects in an artificial spin-ice system. Nature Physics 6, 359-363, (2010).

3 Burn, D. M., Chadha, M., Walton, S. K. & Branford, W. R. Dynamic interaction between domain walls and nanowire vertices. Phys. Rev. B 90, 144414, (2014).

4 Zeissler, K., Walton, S. K., Ladak, S., Read, D. E., Tyliszczak, T., Cohen, L. F. & Branford, W. R. The non-random walk of chiral magnetic charge carriers in artificial spin ice. Sci Rep-Uk 3, 1252, (2013).

5 Pushp, A., Phung, T., Rettner, C., Hughes, B. P., Yang, S. H., Thomas, L. & Parkin, S. S. P. Domain wall trajectory determined by its fractional topological edge defects. Nature Physics 9, 505-511, (2013).

9551-66, Session 17

Ordering and thermal excitations in dipolar coupled single domain magnet arrays (Invited Paper)

Erik Östman, Uppsala Univ. (Sweden); Unnar Arnalds, Univ. of Iceland (Iceland); Vassilios Kapaklis, Björgvin Hjörvarsson, Uppsala Univ. (Sweden)

For a small island of a magnetic material the magnetic state of the island is mainly determined by the exchange interaction and the shape anisotropy. Two or more islands placed in close proximity will interact through dipolar interactions. The state of a large system will thus be dictated by interactions at both these length scales. Enabling internal thermal fluctuations, e.g. by the choice of material, of the individual islands allows for the study of thermal ordering in extended nano-patterned magnetic arrays [1,2]. As a result nano-magnetic arrays represent an ideal playground for the study of physical model systems.

Here we present three different studies all having used magneto-optical imaging techniques to observe, in real space, the order of the systems. The first study is done on a square lattice of circular islands. The remanent magnetic state of each island is a magnetic vortex structure and we can study the temperature dependence of the vortex nucleation and annihilation fields [3]. The second are long chains of dipolar coupled elongated islands where the magnetization direction in each island only can point in one of two possible directions. This creates a system which in many ways mimics the Ising model [4] and we can relate the correlation length to the temperature. The third one is a spin ice system where elongated islands are placed in a square lattice. Thermal excitations in such systems resemble magnetic monopoles [2] and we can investigate their properties as a function of temperature and lattice parameters.

[1] V. Kapaklis et al., New J. Phys. 14, 035009 (2012)

[2] V. Kapaklis et al., Nature Nanotech 9, 514(2014)

[3] E. Östman et al., New J. Phys. 16, 053002 (2014)

[4] E. Östman et al.,Thermal ordering in mesoscopic Ising chains, In manuscript.

9551-67, Session 18

Majorana modes and Kondo effect in a quantum dot attached to a topological superconducting wire (*Invited Paper*)

Edson Vernek, Univ. Federal de Uberlândia (Brazil); David Ruiz-Tijerina, Luis G. Dias da Silva, José Carlos Egues, Univ. de São Paulo (Brazil)

Quantum dot attached to topological wires has become an interesting setup to study Majorana bound state in condensed matter[1]. One of the major advantage of using a quantum dot for this purpose is that it provides a suitable manner to study the interplay between Majorana bound states and the Kondo effect.

Recently we have shown that a non-interacting quantum dot side-connected to a 1D topological superconductor and to metallic normal leads can sustain a Majorana mode even when the dot is empty. This is due to the Majorana bound state of the wire leaking into the quantum dot. Now we investigate the system for the case in which the quantum dot is interacting[3]. We explore the signatures of a Majorana zero--mode leaking into the quantum dot, using a recursive Green's function approach. We then study the Kondo

Conference 9551: Spintronics VIII



regime using numerical renormalization group calculations. In this regime, we show that a "0.5" contribution to the conductance appears in system due to the presence of the Majorana mode, and that it persists for a wide range of the dot parameters. In the particle-hole symmetric point, in which the Kondo effect is more robust, the total conductance reaches \$3e^2/2h\$, clearly indicating the coexistence of a Majorana mode and the Kondo resonance in the dot.

However, the Kondo effect is suppressed by a gate voltage that detunes the dot from its particle-hole symmetric point as well as by a Zeeman field. The Majorana mode, on the other hand, is almost insensitive to both of them. We show that the zero--bias conductance as a function of the magnetic field follows a well--known universal curve. This can be observed experimentally, and we propose that this universality followed by a persistent conductance of \$0.5,e^2/h\$ are evidence for the presence of Majorana--Kondo physics.

This work is supported by the Brazilians agencies FAPESP, CNPq and FAPEMIG.

[1] A. Y. Kitaev, Ann.Phys. {bf 303}, 2 (2003).

[2] E. Vernek, P.H. Penteado, A. C. Seridonio, J. C. Egues, Phys. Rev. B {bf 89}, 165314 (2014).

[3] David A. Ruiz-Tijerina, E. Vernek, Luis G. G. V. Dias da Silva, J. C. Egues, arXiv:1412.1851 [cond-mat.mes-hall].

9551-68, Session 18

Universal parity-crossing statistics in spinpolarized hybrid normal-superconductor nanostructures (Invited Paper)

Inanc Adagideli, Sabanci Univ. (Turkey)

We focus on topologically protected crossings of Andreev bound states in spin-polarized normal-superconductor hybrid structures [1]. Such crossings, signaling a change in the ground state fermion parity, became the focus of recent attention as they are regarded to be precursors to Majorana fermions that appear in the long-wire limit. In recent work, we showed how a topological state can be induced from regular or irregular scattering in (i) p-wave superconducting wires and (ii) Rashba wires in proximity to an s-wave superconductor. We also related the topological properties of such nanowires to their normal state properties such as conductance [2]. In the present work, we build on these results and study the correlation between parity-crossings in the superconducting state and the normal state properties of a hybrid nanostructure. Surprisingly, we find that the crossing points as well as their statistics are universal and are described solely by their normal-state properties. We obtain formulae for mean spacing between parity crossings as well as crossing statistics in disordered wires/ cavities. We finally discuss under what conditions these crossings signal Majorana fermions. [1] I. Adagideli et al . [2] I. Adagideli, M. Wimmer, A. Teker, Phys Rev B 89, 144506 (2014)

9551-69, Session 18

Magnetic noise from Kondo charge traps (Invited Paper)

Luis G. Dias da Silva, Univ. de São Paulo (Brazil); Rogério de Sousa, Univ. of Victoria (Canada)

Magnetic noise impacts a wide variety of solid-state devices, from quantum bits in superconductor and semiconductor-based quantum computer architectures to spintronic devices made of metals and semiconductors. Developing a theory of magnetic noise will have great impact in minimizing fluctuations in these devices. Magnetic noise is commonly detected as flux noise in superconducting quantum interference devices (SQUIDs). At low frequencies, SQUID flux noise spectral density decreases with frequency as \$1/f^{alpha}\$ with \$alpha=0.5-0.8\$ in a wide variety of devices. However, at higher frequencies (above ~1-GHZ) flux noise was found to be Ohmic, i.e. increasing linearly with frequency. This puzzling behavior is not explained by any model of magnetic fluctuations.

Here we present a theory for the magnetic noise produced by local charge traps, elucidating the kind of noise that the majority of defects produce in a typical solid-state device. Our numerical renormalization group calculations reveal a deviation from 1/f behavior in the magnetic noise of charge traps in the Kondo regime over a wide range of frequencies. Remarkably, such behavior is not present in the charge noise, which is dominated by single-particle processes, consistent with a mean-field picture. The results show that, when Kondo correlations are present, magnetic noise originating from charge traps has a many-particle character, while charge noise does not. Since Kondo temperatures can be relatively high in charge traps, these findings indicate that electron-electron interactions can lead to a strong contribution to the magnetic noise that has not been captured by current models.

9551-99, Session PWed

Intrinsic spin Hall effect of vector beam with rotational symmetry-breaking

Xiaohui Ling, Shenzhen Univ. (China); Zhiping Dai, Hengyang Normal Univ. (China); Xunong Yi, Shenzhen Univ. (China); Liezun Chen, Youwen Wang, Hengyang Normal Univ. (China); Shuangchun Wen, Shenzhen Univ. (China)

We report the observation of intrinsic photonic spin Hall effect (SHE) of cylindrical vector beam by breaking its rotational symmetry using a fanshaped aperture to block part of the vector beam. The spin accumulation occurs at the edge of the beam, and the spin-dependent splitting increases with the topological charge of the vector beam and restricts by the aperture angle. The underlying mechanism is attributed to the discontinuous local energy flow that results from the broken, opposite vortex phases. It is large enough to be directly observed without using a weak measurement technology. Because of the inherent nature of the phase and independency of light-matter interaction, the observed photonic SHE is intrinsic. This enables us to observe a direct and giant photonic SHE. Our findings reveal that the photonic SHE may be manipulated (enhanced or inverted) by directly tailoring the polarization geometry of light, which may provide a possible route for generation and manipulation of spin-polarized photons, and enables spin-controlled photonics applications.

9551-100, Session PWed

Fabrication of Fe/MgO/Fe low-resistance nano-contact on pn-GaAs photodetector as a memory element for a high-speed non-volatile optical memory

Vadym Zayets, Hidekazu Saito, Koji Ando, Shinji Yuasa, National Institute of Advanced Industrial Science and Technology (Japan)

The high-speed non-volatile optical memory has been proposed [1], which is utilized a high-speed spin injection of a spin-polarized photo current from a semiconductor-made pn-junction into a metal nanomagnet. The demultiplexing of a train of optical pulses at the speed of 2200 GBit/s was experimentally demonstrated for this memory [1].

For the successful operation of the memory it is essential to inject photoexcited electrons form the semiconductor detector into the nanomagnet within a time interval shorter than the spin life time in the semiconductor. The spin life time in the GaAs is short and it does not exceed 100 picoseconds at room temperature. In the case of the injection time longer than the spin life time, the spin information is lost inside the semiconductor before it is injected into the nanomagnet.

The injection time significantly depends on the nanocontact resistance. The lowest contact resistance is important to shorten photocurrent injection time from the pn-photodetector to the nanomagnet. The photocurrent was excited by 170-fs 10-pJ optical pulses at wavelength of 860 nm. The area



of the MTJ nanocontact was 0.01 um2. The tunnel magneto resistance was 100%. The injection time was measured to be 3 ns, 350 ps and 75 ps for the MTJ nanocontacts with contact resistance of 7000, 250 and 30 Ohm um2. The injection time shorter than the spin life time in the GaAs is achieved. The dependence of the tunnel magneto-resistance on the light intensity was observed.

[1] V. Zayets, APL 94 (2009) pp. 121104

9551-101, Session PWed

Band structure of thin films materials

Amine Elhaimeur, Zouhair Sofiani, Univ. Ibn Tofail (Morocco)

Calculations of ferromagnetic properties using local density approximation (LDA) based on the parameterization given by Moruzzi, Janak, and Williams (MJW), were investigated in datail. We found that Nickel concentration in ZnO could induce magnetism effects. These effects from Ni impurties incorporation in ZnO matrice are explored using the Korringa-Rostocker potential approximation (KKR-CPA). The magnetic effect is due to the hybredization between 3d and 2p oxygen of Zn, O, and nickel atoms.

9551-102, Session PWed

The titanium-antisite (TiO) magnetism effect on TiO.98CrO.02O2(0.98)(TiO)0.02 system within ab-initio calculation

Zakaryaa Zarhri, Univ. Mohammed V (Morocco)

The ab-initio calculations, based on the Korringa Kohn Rostoker approximation approach combined with Coherent Potential Approximation (KKR-CPA) were used to study the magnetic properties of the Titanium antisite (TiO) and Chromium (Cr) doped TiO2. In the considered systems, we used different concentrations for TiO defect and Cr doping. In TiO2(0.98) (TiO)0.02, the obtained results indicate that TiO is an acceptor having the half-metal behavior. TiO[3d] band is located at the Fermi level, although isn't 100% polarized, the ferromagnetic (FM) state is verified as being more stable than Disordred Local Moment (DLM) one. For Ti0.98Cr0.02O2 the Cr introduced new states which give the material half-metallic feature. The majority spin of Cr impurity are located at the Fermi level and the conduction electrons around the Fermi level are 100% spin polarized. This indicates the stability of (FM) state. Moreover, in Ti0.98Cr0.02O2(0.98) (TiO)0.02, the top of the conduction band (TCB) related to TiO2 shifted to lower energy and the n-type of TiO2 is verified. the majority spin of Cr[3d] are located at 0.025 Ry close Fermi level. The predicted Curie temperatures (Tc) were calculated using the Mean Field Approximation (MFA) and we predicted that TiO defect in Cr doped TiO2 makes Tc higher. This kind of defect makes the material useful for spinotronics's applications and devices.

9551-103, Session PWed

Description of the spin proximity effect from a solution of the modified Boltzmann transport equations

Vadym Zayets, National Institute of Advanced Industrial Science and Technology (Japan)

The spin proximity effect was measured experimentally [1,2]. The Spin Proximity effect describes the fact that at a contact between two conductors, the spin accumulation diffuses from the conductor of a higher spin polarization to the conductor of a smaller spin polarization. For example, in the vicinity of a contact between a ferromagnetic and non-magnetic metals, in the ferromagnetic metal the equilibrium spin accumulation becomes smaller than in the bulk and the electron gas in the non-magnetic metal becomes spin-polarized. When a drift current flows through the contact, the spin accumulation is drifted from one metal to the other metal, because of the spin injection. The spin injection only modifies the distribution of the spin accumulation across the contact, which was initially established due to the Spin Proximity effect.

From a solution of the modified Boltzmann transport equations [3,4] it was found that the contributions of the electrons and holes to the spin injection are of opposite signs. In contrast, the contributions of the electrons and holes to the Spin Proximity effect are of the same sign. For this reason, in a metal a significant drift current is required in order to modify the distribution of the spin accumulation across a contact enough so that the modification can be detected.

The features of the spin Proximity effect will be discussed.

[1] S. A. Crooker et al., Science 309, 2191 (2005).

[2] M. Furis, et al. New Journal of Physics 9, 347 (2007).

[3] V. Zayets J. Mag. and Mag. Mat. 356 52-67 (2014) 52-67

[4] V. Zayets, ArXiv 1410.7511; https://staff.aist.go.jp/v.zayets/spin3_intro_41. html

9551-104, Session PWed

Ultrafast affection of electron spin dynamics in GaAs by a ferromagnetic film

Dagmar Butkovi?ová, Petr N?mec, Charles Univ. in Prague (Czech Republic); Kamil Olejník, Vít Novák, Institute of Physics of the ASCR, v.v.i. (Czech Republic); Tomá? Janda, Franti?ek Trojánek, Charles Univ. in Prague (Czech Republic); Tomá? Jungwirth, Institute of Physics of the ASCR, v.v.i. (Czech Republic)

Spin-polarized electrons can be optically injected in semiconductor by absorption of circularly-polarized light. If an external magnetic field Hext perpendicular to the light propagation direction is applied, the electron spins presses around this field. Consequently, an oscillatory signal reflecting the electron spin dynamics in the material can be measured using the timeresolved pump-probe magneto-optical technique.

We studied the electron spin dynamics in GaAs substrate overgrown by a thin (~ 20 nm) epilayer of ferromagnetic semiconductor (Ga,Mn)As with different Mn doping [1] at temperature of 15 K using the light tuned to ~ 25 meV above the band gap of GaAs. Since the light penetration depth is much bigger than the thickness of the (Ga,Mn)As epilayer, the spin-polarized electrons are injected in both (Ga,Mn)As and GaAs. We observed that the presence of a thin ferromagnetic layer induced a very pronounced initial phase shift of the measured oscillations relative to the initial phase present in a bare GaAs. This phase shift of the electron spin precession arises within ~ 50 ps after the impact of a laser pulse on the sample, is dependent on the sample temperature and it disappears if an insulating barrier is inserted between GaAs and (Ga,Mn)As. Overall, our experimental data suggest that there is an ultrafast mechanism by which the ferromagnetic layer can modify the electron spin dynamics in the adjacent paramagnetic semiconductor. [1] N?mec et al, Nature Communications 4, 1422 (2013).

9551-105, Session PWed

Giant stress field in a single Ni nanowire generated by an external mechanical strain

Giuseppe Melilli, CEA-Ctr. de SACLAY (France); Marie-Claude Clochard, Commissariat à l'Énergie Atomique (France); Mohamed tabellout, Univ. du Maine (France); Daniel Lacour, Laurent Bouvot, Univ. de Lorraine (France); Nicolas Biziere, Ctr. d'Elaboration de Matériaux et d'Etudes Structurales (France); Jean-Eric Wegrowe, Ecole Polytechnique (France)

The effects of thermoelastic and piezoelectric strain of an active track-



etched ?-PVDF polymer matrix on an electrodeposited single-contacted Ni nanowire (NW) are investigated at the nanoscale by measuring the change of magnetization (i.e. using the inverse magnetostriction effect). The magnetization state is measured locally by anisotropic magnetoresitance (AMR). The ferromagnetic NW plays thus the role of a mechanical probe that allows the effects of mechanical strain to be characterized and described qualitatively and quantitatively.

The inverse magnetostriction was found to be responsible for a quasidisappearance of the AMR signal for a variation of the order of $?T \approx 10$ K. In other terms, the variation of the magnetization due to the stress compensates the effect of external magnetic field applied on the NW resistance.

The induced stress field in a single Ni NW was found 1000 time higher than the bulk stress field (due to thermal expansion measured on the PVDF). This amplification could be attributed to three nanoscopic effects: (1) a stress mismatch between the Ni NW and the membrane, (2) a non-negligible role of the surface tension on Ni NW Young modulus, and (3) the possibility of non-linear stress-strain law.

We investigate here the role of these different contributions using various types of track-etched polymer membranes leading, after electrodeposition, to embedded Ni NWs of different diameters and orientations.

9551-107, Session PWed

Controlled switching and frequency tuning of polarization oscillations in verticalcavity surface-emitting lasers

Markus Lindemann, Henning Höpfner, Nils C. Gerhardt, Martin R. Hofmann, Ruhr-Univ. Bochum (Germany); Tobias Pusch, Rainer Michalzik, Univ. Ulm (Germany)

Spintronic lasers offer promising perspectives for novel concepts and characteristics superior to conventional purely charge-based devices. This applies in particular to spin-polarized vertical-cavity surface-emitting lasers (spin- VCSELs), which exhibit ultrafast spin and polarization dynamics. Using pulsed spin-injection, oscillations in the circular polarization degree can be generated, which have the potential to be much faster than conventional relaxation oscillations and may exceed frequencies of 100 GHz. The oscillations originate from the coupled carrier-spin-photon system in birefringent VCSEL cavities. The polarization oscillations are independent from conventional relaxation oscillations and thus can be the cornerstone for ultrafast directly modulated spin-VCSELs in the near future. It is possible to switch the oscillations on and off, depending on phase and amplitude conditions of two consecutive excitation pulses. Even half-cycles can be generated, which is the basis for short polarization pulses, only limited by the polarization oscillation resonance frequency. Experimental results of oscillation switching are given using an 850 nm oxide-confined singlemode VCSEL. In order to increase the polarization oscillation frequency, birefringence has to be tuned to higher values. We demonstrate a method to manipulate the birefringence by adding mechanical strain to the substrate in vicinity of the VCSEL. With this method the polarization oscillation frequency can be tuned over a wide range of several tens of GHz. The results are compared to the theory with simulations using the spin-flip-model.

9551-108, Session PWed

Spin relaxation dynamics of an individual Co2+ ion in a CdTe/ZnTe quantum dot

Aleksander M. Bogucki, Mateusz Goryca, Kacper Oreszczuk, Tomasz Smolenski, Jakub Kobak, Wojciech Pacuski, Piotr Kossacki, Univ. of Warsaw (Poland)

Studies of single dopants in semiconductors constitute one of the research areas of the dynamically developing field of solotronics.

In this work we present studies of spin dynamics of a single Co2+ ion embedded in a CdTe/ZnTe quantum dot (QD) – a new system of single

magnetic ion in semiconductor QD. In order to determine spin-relaxation time of the single Co2+ ion we performed time-resolved measurements of the QD photoluminescence under quasi-resonant, modulated excitation for various magnetic fields. It is experimentally simpler than the method previously used for the Mn2+ ion. The obtained relaxation times stay in an agreement with the values determined previously under non-resonant excitation and are much shorter than those reported for the Mn2+ ion.

We discuss the impact of the local strain on the spin relaxation. The Co2+ ion has non-zero orbital momentum, thus it is more sensitive to the local anisotropy of surrounding lattice than the Mn2+ ion. Analyzing different dots, we show that local distortion has minor influence on the cobalt relaxation time. This new observation can help to determine the spin-lattice relaxation mechanism of a single magnetic ion in a QD.

We also show that similarly to the case of the QDs with Mn2+ ions, qusiresonant injection of spin polarized excitons leads to the orientation of the Co2+ spin. The time resolved measurements of this effect reveals that the spin orientation efficiency per one exciton for a Co2+ ion in a CdTe dot is much larger than for Mn2+ ion in a similar dot.

9551-109, Session PWed

Spin-lasers: from threshold reduction to large-signal analysis

Sean Bearden, Evan Wasner, Univ. at Buffalo (United States); Jeongsu Lee, Univ. at Buffalo (United States) and Univ. of Regensburg (Germany); Igor Zutic, Univ. at Buffalo (United States)

Lasers in which spin-polarized carriers are injected provide paths to different practical room temperature spintronic devices, not limited to magnetoresistive effects. Considering spin-lasers, it is necessary to revisit simple concepts in spintronics. Is longer spin relaxation always better? How does a simultaneous spin relaxation of electrons and holes affect the device operation? Unfortunately, the proper framework to investigate such questions is usually overlooked. Theoretical studies mostly focus only on spin-polarized electrons, the holes are merely spectators with vanishingly short spin relaxation time, losing their spin polarization instantaneously. Unlike the conventional understanding of spintronic devices, an optimal performance of such spin-lasers can arise for finite, not infinite, spin relaxation time. By considering spin-relaxation times of both electrons and holes, we elucidate advantages of spin-lasers over their conventional (spin-unpolarized) counterparts. In addition to the steady-state threshold reduction, spin-lasers can improve transient operation leading to shorter turn-on delay times, reduced ringing of emitted light, and an enhanced bandwidth [1,2].

[1] J. Lee, S. Bearden, E. Wasner, and I. Zutic, Appl. Phys. Lett. 105, 042411 (2014).

[2] E. Wasner, S. Bearden, J. Lee, and I. Zutic, preprint.

9551-71, Session 19

Spin photonics and spin-photonic devices with dielectric metasurfaces (Invited Paper)

Hailu Luo, Yachao Liu, Shizhen Chen, Yougang Ke, Xinxing Zhou, Hunan Univ. (China)

Dielectric metasurfaces with spatially varying birefringence fabricated by transparent materials can exhibit exceptional abilities for controlling the photonic spin states. We present here some of our works on spin photonics and spin-photonic devices with dielectric metasurfaces. We develop a hybrid-order Poincare sphere to describe the evolution of spin states of wave propagation in the metasurface. We extend the orbital Poincare sphere and high-order Poincare sphere to a more general form. The spin evolution in the metasurface with special geometry can be conveniently described by state evolution along the longitude and the latitude lines on

Conference 9551: Spintronics VIII



the hybrid-order Poincare sphere. Similar to that in previously proposed Poincare spheres, the Berry curvature can be regarded as an effective magnetic field with monopole centered at the origin of sphere and Berry connection can be interpreted as the vector potential. Both the Berry curvature and the Pancharatnam-Berry phase on the hybrid-order Poincare sphere are demonstrated to be proportional to the variation of total angular momentum. Moreover, we show that the dielectric metasurfaces can provide great flexibility in the design of novel spin-photonic devices such as spin filter and spin-dependent beam splitter. The high transmission efficiency of dielectric metasurfaces makes it possible to utilizing the spin-dependent effect based on Pancharatnam-Berry phase in optical far field, which would substantially facilitate the development of spin-dependent devices in photonics.

9551-72, Session 19

Spin-photonic devices based on crystalline-AIOx / GaAs for emission and detection of circular polarized light (Invited Paper)

Hiro Munekata, Masaki Aoyama, Ronel Roca, Nozomi Nishizawa, Tokyo Institute of Technology (Japan)

In the papers published in APL 2014 [1] and JMSJ 2014 [2], we reported electrical helicity switching of circularly polarized light (CPL) at 1 KHz with spin-LEDs having dual spin injection electrodes [3] of Fe and detection of CPL up to RT by operating reversely the spin-LEDs. Those LEDs consisted of a n-AlGaAs/InGaAs/p-AlGaAs double heterojunction and a newly developed crystalline x-AlOx tunnel barrier [4]. Presented here are helicity switching of CPL at 1 MHz and a phenomenological model of spin photodiode (PD), the recent progresses towards the realization of spin-photonics based devices. The same type of a dual-electrodes spin-LED is used for experiments. Only a quarter waveplate and a linear polarizer are used to distinguish helicity of electroluminescence (EL). The degree of EL-CPL is 10 to 15 % at around peak wavelength of 840 nm. Alternating a current between the two electrodes with the frequency of 1 MHz has yielded dynamic change in the intensity output, indicating helicity switching at same frequency. A model of spin-PD is based on a picture that a spin polarized photo-current yielded in a pn junction is split into two independent spin channels R(up) and R(down) including those due to spin-dependent tunneling. The advantage of our model is the direct estimation of relaxation of carrier spin polarization gmma from experimental data; e.g., gamma = 0.4 % at low temperatures referring the data shown in ref. 2.

[1] APL 104(2014)111102, [2] JMSJ 38(2014)147, [3] SST 17(2002)285, [4] JAP 114(2013)0333507.

9551-73, Session 19

Development of plasmonic isolator for integration into photonic integrated circuits (Invited Paper)

Vadym Zayets, Hidekazu Saito, Koji Ando, Shinji Yuasa, National Institute of Advanced Industrial Science and Technology (Japan)

An optical isolator is an important component of an optical network. At present, there is a significant commercial demand for an optical isolator, which can be integrated into the Photonic Integrated Circuits (PIC). A new design of an integrated optical isolator, which utilizes unique non-reciprocal properties of surface plasmons, has been proposed [1]. The main obstacle for a practical realization of the proposed design is a substantial propagation loss of the surface plasmons in structures containing a ferromagnetic metal. The reduction of the propagation loss of a surface plasmon is the key to make the plasmonic isolator competitive with other designs of the integrated isolator.

We studied experimentally optical and magneto-optical properties of a

Fe plasmonic waveguide integrated with an AlGaAs rib waveguides and a Co plasmonic waveguide integrated with Si nanowire waveguides. It was demonstrated experimentally that by utilizing a double-dielectric plasmonic waveguide it is possible to reduce significantly the optical loss in a plasmonic waveguide. For Fe/SiO2/AlGaAs double-dielectric plasmonic waveguide the low optical loss of 0.03 dB/um is obtained. As far as we know at present it is a lowest optical loss demonstrated for a plasmon propagating at a surface of a ferromagnetic metal. For Co/ Ti2O3/SiO2 double-dielectric plasmonic waveguide integrated with a Si nanowire waveguide on a Si substrate the optical loss of 0.7 dB/um was demonstrated. The designs of the plasmonic isolator utilizing a ring resonator or a non-reciprocal coupler were studied.

[1] V. Zayets, H. Saito, S. Yuasa, and K. Ando,, Materials 5, 857 (2012).

9551-74, Session 19

Integrated optical isolators using magnetic surface plasmon (Invited Paper)

Hiromasa Shimizu, Terunori Kaihara, Saori Umetsu, Masashi Hosoda, Tokyo Univ. of Agriculture and Technology (Japan)

Optical isolators are one of the essential components to protect semiconductor laser diodes (LDs) from backward reflected light in integrated optics. In order to realize optical isolators, nonreciprocal propagation of light is necessary, which can be realized by magnetic materials. Semiconductor optical isolators have been strongly desired on Si and III/V waveguides. We have developed semiconductor optical isolators based on nonreciprocal loss owing to transverse magneto-optic Kerr effect, where the ferromagnetic metals are deposited on semiconductor optical waveguides1). Use of surface plasmon polariton at the interface of ferromagnetic metal and insulator leads to stronger optical confinement and magneto-optic effect. It is possible to modulate the optical confinement by changing the magnetic field direction, thus optical isolator operation is proposed2, 3). We have investigated surface plasmons at the interfaces between ferrimagnetic garnet/gold film, and applications to waveguide optical isolators. We assumed waveguides composed of Au/Si(38.63nm)/ Ce:YIG(1700nm)/Si(220nm)/Si , and calculated the coupling lengths between Au/Si(38.63nm)/Ce:YIG plasmonic waveguide and Ce:YIG/ Si(220nm)/Si waveguide for transversely magnetized Ce:YIG with forward and backward directions. The coupling length was calculated to 232.1um for backward propagating light. On the other hand, the coupling was not complete, and the length was calculated to 175.5um. The optical isolation by using the nonreciprocal coupling and propagation loss was calculated to be 43.7dB when the length of plasmonic waveguide is 700um.

1) H. Shimizu et al., J. Lightwave Technol. 24, 38 (2006). 2) V. Zayets et al., Materials, 5, 857-871 (2012). 3) J. Montoya, et al, J. Appl. Phys. 106, 023108, (2009).

9551-75, Session 20

Electrical generation and manipulation of spin polarization in semiconductors (Invited Paper)

Vanessa Sih, Univ. of Michigan (United States)

Utilizing spins for information processing requires developing methods to generate and manipulate spin polarization. Current-induced spin polarization is a phenomenon in which carrier spins in a semiconductor are oriented when subjected to current flow. However, the mechanism that produces this spin polarization remains an open question. Existing theory predicts that the spin polarization should be proportional to the spin-orbit splitting, yet no clear trend has been observed experimentally. We perform experiments on semiconductor samples designed so that the magnitude and direction of the in-plane current and applied magnetic field can be varied and measure the electrical spin generation efficiency and spin-orbit splitting using optical techniques. These techniques can sensitively measure the electron g-factor and effective magnetic fields produced by spin-



orbit splitting and nuclear spin polarization. Contrary to expectation, the magnitude of the current-induced spin polarization is shown to be larger for momentum directions corresponding to smaller spin-orbit splitting [1]. In addition, angle-dependent measurements demonstrate that the steady-state spin polarization is not along the direction of the spin-orbit field, which we attribute to anisotropic spin relaxation. Furthermore, we show that this electrically-generated electron spin polarization can produce a nuclear spin hyperpolarization through dynamic nuclear polarization [2].

This work is supported by AFOSR, DTRA, NSF, and ONR.

[1] B. M. Norman et al., Phys. Rev. Lett. 112, 056601 (2014).

[2] C. J. Trowbridge et al., Phys. Rev. B 90, 085122 (2014).

9551-76, Session 20

Spinor effects in the pattern formation of polaritons in semiconductor microcavities (*Invited Paper*)

Rudolf Binder, Ming Ho Luk, The Univ. of Arizona (United States); K. P. Chan, The Chinese Univ. of Hong Kong (Hong Kong, China); Przemyslaw Lewandowski, Univ. Paderborn (Germany); Ombline Lafont, Ctr. National de la Recherche Scientifique (France); Vincenzo Ardizzone, Emmanuel Baudin, Lab. Pierre Aigrain (France); Nai-Hang Kwong, College of Optical Sciences, The Univ. of Arizona (United States); Yuen Chi Tse, The Chinese Univ. of Hong Kong (Hong Kong, China); Andreas Luecke, Univ. Paderborn (Germany); C.Y. Tsang, The Chinese Univ. of Hong Kong (Hong Kong, China); Marco Abbarchi, Lab. Pierre Aigrain (France); Jacqueline I. Bloch, Elisabeth Galopin, Aristide Lemaitre, Lab. de Photonique et de Nanostructures (France); Philippe Roussignol, Lab. Pierre Aigrain (France); Pui Tang Leung, The Chinese Univ. of Hong Kong (Hong Kong, China); Jérôme Tignon, Lab. Pierre Aigrain (France); Stefan Schumacher, Univ. Paderborn (Germany)

Semiconductor microcavities form an important class of semiconductor systems in which light is strongly coupled to excitons. The resulting polaritons have advantageous dispersion relations that, in the past, have allowed for the observations of many prominent effects, ranging from Bose condensation to the optical spin Hall effect. Our group has recently predicted and observed formation of patterns in the spatial polariton density and far-field emission signals. These patterns are created by a coherent optical pump field that enters the microcavity in normal incidence and that is tuned above the minimum of the lowest polariton branch. Fourwave mixing instabilities involving pump photons and polaritons on the elastic circle (off-axis polaritons) are the main process for pattern formation. An important aspect of patterns involving linearly polarized pump fields is the TE/TM splitting, which in the past has been associated with important characteristics of semiconductor microcavities, including the optical spin Hall effect.

In our previous research, we have investigated spin-dependent excitonexciton interaction in semiconductor quantum wells and microcavities, and recently we found that the TE/TM splitting, together with the spindependent exciton-exciton interaction, leads to specific characteristics in the polariton pattern formation. For example, the spin-dependent excitonexciton interaction favors a linearly x-polarized pump beam to produce y-polarized off-axis polaritons. Depending on the pump conditions, this can create patterns involving TE or TM polarized polaritons. The patterns offer the possibility of external control as they can be rotated simply through rotation of the pump polarization. We review the theoretical framework as well as experimental results.

9551-77, Session 20

Effect of the Pauli principle on photoelectron spin transport in p+ GaAs (Invited Paper)

Daniel Paget, Ecole Polytechnique (France)

In p+ GaAs thin films, the effect of photoelectron degeneracy on spin transport is investigated theoretically and experimentally by imaging the spin polarization profile as a function of distance to the light excitation spot. Under degeneracy of the electron gas (high concentration, low temperature), a dip at the center of the polarization profile appears, with a polarization maximum at a distance of about 2μ m from the center. This counterintuitive result reveals that photoelectron diffusion depends on spin, as a direct consequence of the Pauli principle which causes a concentration dependence of the spin stiffness while the spin dependence of the mobility is found weak in doped material.

The various effects which can modify spin transport in a degenerate electron gas under local, circularly-polarized, laser excitation are considered. A comparison of the data with a numerical solution of the coupled diffusion equations reveals that ambipolar coupling with holes increases the steadystate photo-electron density at the place of excitation and therefore the amplitude of the degeneracy-induced dip. Thermoelectric currents are predicted to depend on spin under degeneracy (spin Soret currents), but these currents are negligible except at very high excitation power where they play a relatively small role. Coulomb spin drag and bandgap renormalization are negligible due to electrostatic screening by the hole gas.

9551-78, Session 20

Efficient conversion of light to charge and spin in Hall-bar microdevices

Lukas Nadvornik, Institute of Physics of the ASCR, v.v.i. (Czech Republic); James A. Haigh, Hitachi Cambridge Lab. (United Kingdom); Kamil Olejnik, Institute of Physics of the ASCR, v.v.i. (Czech Republic); Andrew C. Irvine, Univ. of Cambridge (United Kingdom); Vit Novak, Tomá? Jungwirth, Institute of Physics of the ASCR, v.v.i. (Czech Republic); Joerg Wunderlich, Hitachi Cambridge Lab. (United Kingdom)

During the last decade, the spin related Hall effects have developed from subtle academic phenomena to practical tools for exploring a variety of fields in the fundamental and applied spintronics research. One of the recently proposed concepts, where these effects can find utility, is the spin Hall based polarimeter.

In this contribution, we report an experimental study of the direct conversion of light into electrical signals in GaAs/AlGaAs Hallbar microdevices. Our approach based on different modulation frequencies of the intensity and polarization of the laser beam allows us to disentangle the charge and spin dependent parts of the induced electrical signal, and to link them to the incident light intensity and polarization, respectively.

In our electrical polarimeter, the degree of circular polarization of incident light is directly converted into transverse electrical voltage via spin-orbit interaction acting on optically generated spin-polarized photocarriers. We demonstrate that the efficiency of the light to spin conversion is strongly enhanced by adding a drift component to the transport of the spinpolarized photocarriers, as compared to a purely diffusive transport regime of the device. We show that this is in agreement with the theory of spinrelated Hall effects.

For a micron-size focused laser beam, the experiments also demonstrate that the light to charge and spin conversion efficiency depends on the precise position of the light spot, reflecting the spatially dependent response function of the Hall cross.

All these observations may find utility in designing spin Hall based convertors, modulators, polarimeters or other related opto-spintronic microdevices.



9551-79, Session 21

Current-induced magnetization dynamics and thermal stability of perpendicular STT-MRAM devices (Invited Paper)

Huanlong Liu, Luc Thomas, Guenole Jan, Son Le, Yuan-Jen Lee, Jian Zhu, Ru-Ying Tong, Keyu Pi, Yu-Jen Wang, Tom X. Zhong, Terry Torng, Po-Kang Wang, Headway Technologies, Inc. (United States)

Spin-transfer torque-magnetic random access memory (STT-MRAM) devices, combining non-volatility and fast read/write operations, have the potential of becoming next generation "universal memory". In this presentation, we will discuss some of the interesting challenges we face in developing the STT-MRAM technology. Firstly, we will show that millions of devices can be switched reliably by electrical pulses as short as sub-nanoseconds. However, complex magnetization dynamics is occasionally observed, especially for large devices in the deep statistics regime. We will discuss the origin of these phenomena and how they can be avoided by improving the design of the MTJ stacks. Secondly, we will address the thermal stability of the devices. In particular, we will discuss methods of evaluating the energy barrier Eb at different temperatures in order to assess data retention of different MTJ designs.

9551-80, Session 21

Spintronic devices for space applications *(Invited Paper)*

Malik Mansour, Lab. de Physique des Plasmas (France)

In this presentation we aim to review some implementations of spintronic devices in the frame of space applications. Because they are compact and can easily be adapted to a space environment, we will show that magnetoresistive effects based sensors (MR) (as AMR, GMR or TMR sensors) can not only be used as positioning sensing devices but are also new assets to develop highly integrated space magnetometers dedicated to space science. Their sensitivity as well as their ability to cover a large frequency range allows using them for magnetometry applications ranging from the Martian soil mapping up to the measurement of interplanetary magnetic waves fluctuations. Whether used alone or as part of new instrumental concepts we will endeavor to show that MR sensors have the potential to be a must in the field of magnetic measurement in a space environment.

9551-81, Session 21

Monolithic integration of focused 2D GMR spin valve magnetic field sensor for highsensitivity (compass) applications (Invited Paper)

Olaf Ueberschär, Fraunhofer-Institut für Elektronische Nanosysteme (Germany); Maria J. Almeida, Fraunhofer-Institut für Elektronische Nanosysteme (Germany) and Technische Univ. Chemnitz (Germany); Patrick Matthes, Technische Univ. Chemnitz (Germany); Mathias Müller, Hochschule Mittweida (Germany); Ramona Ecke, Fraunhofer-Institut für Elektronische Nanosysteme (Germany); Horst Exner, Hochschule Mittweida (Germany); Stefan E. Schulz, Fraunhofer-Institut für Elektronische Nanosysteme (Germany) and Technische Univ. Chemnitz (Germany)

We have designed and fabricated 2D GMR spin valve sensors on the basis of IrMn/CoFe/Cu/CoFe/NiFe nanolayers in monolithic integration for high sensitivity applications. For a maximum signal-to-noise ratio, we realize a

focused double full bridge layout featuring an antiparallel exchange bias pinning for neighbouring meanders and an orthogonal pinning for different bridges. This precise alignment is achieved with microscopic precision by laser heating and subsequent in-field cooling.

Striving for maximum signal sensitivity and minimum hysteresis, we study in detail the impact of single meander geometry on the total magnetic structure and electronic transport properties. The investigated geometrical parameters include stripe width, stripe length, cross bar material and total meander length. In addition, the influence of the relative alignment between reference magnetization (pinned layer) and shape anisotropy (free layer) is studied. The experimentally obtained data are moreover compared to the predictions of tailored micromagnetic simulations.

Using a set of optimum parameters, we demonstrate that our sensor may readily be employed to measure small magnetic fields, such as the ambient (geomagnetic) field, in terms of a 2D vector with high spatial (-200 μm) and temporal (-1 ms) resolution.

9551-82, Session 21

State of the art of the equivalent magnetic sensor noise: from intrinsic sensor performances to application, the challenges (Invited Paper)

Christophe Dolabdjian, Univ. de Caen Basse-Normandie (France)

This talk deals with on the problematic of the development on highly sensitive magnetic sensors to applications. The sensor performances were described and analysed, mainly, in term of intrinsic or equivalent input magnetic noise in the Tesla per square root Hertz. Based on our laboratory researches, three sensor technologies were outlined: Giant MagnetoResistance, Magneto(Elasto)Electric and Magneto-Impedance devices. These sensors are based on different physical principles. In each case, a soft magnetic material is used and can be seen as an intrinsic or as an extrinsic sensing element, which is coupled to the active part of the sensor. The material properties and conditioning electronic parameters were detailed versus sensor working principles. Both have to be well considered in highly sensitive magnetic magnetometer development. To improve this analysis, the relation between the sensitivity and the equivalent input magnetic noise of the sensors and the sensor material properties have to be study, carefully! We notice that sensor noise improvements can be done, only, by considering a system theory or systems engineering approach, which includes the material properties, the working principle, the conditioning electronics and often, the fluctuation dissipation theorem! The general trends, predicted by the (and our) theoretical models, which are associated to these different sensor technologies, are very well supported by experiments. These analyses provide a view of the technological limits and insights for material, design, working principle, optimization and used. To conclude this presentation, some applications (NDT, magnetic detection, magnetorelaxometry, imagery of NMPs, biomagnetism...) as example, will be given. The link between the intrinsic sensor noise and performances and measurement problematics will be pointed out.

9551-83, Session 22

Tailoring and manipulating spin in semiconductor nanostructures (Invited Paper)

Christopher J. Stanton, Gary D. Sanders, Univ. of Florida (United States)

There has been much interest in III-V and II-VI dilute magnetic semiconductors in which incorporation of magnetic impurities, such as manganese, is used to tailor the electronic, magnetic, and magneto-optical properties. In particular, carrier-induced ferromagnetism in dilute magnetic semiconductors has opened up opportunities for device applications. We present a theory for the electronic and magneto-optical properties of



magnetically doped semiconductor nanostructures and investigate how the effects of i) guantum confinement, ii) interfacial strain and iii) precise control of the magnetic impurity position can be used to change and tune these properties. We study two systems: 1) quantum wells and 2) core shell quantum dots. Calculations in the quantum wells are based on an 8 band calculation and allows for valence/conduction band mixing in narrow gap materials. The spherical guantum dots consist of an inner core surrounded by an outer shell. This core-shell quantum dot is doped by magnetic Mn impurities all of which are implanted at a preselected and controllable radius on a spherical surface within the dot. The electronic states in the presence of a magnetic field are treated in an effective mass model which includes the s-d and p-d exchange interaction with the Mn electrons. Strain in both systems due to the lattice is assumed to be pseudomorphic and the effect of this strain field on the electronic and spin states is included. The optical properties are computed using electronic states from our calculations using Fermi's golden rule.

This work was supported by the NSF through grant DMR-1105437.

9551-84, Session 22

100% spin polarized surface resonance in the half metallic Heusler compound Co2MnSi (Invited Paper)

Martin Jourdan, Johannes Gutenberg Univ. Mainz (Germany); Jan Minar, Juergen Braun, Ludwig-Maximilians-Univ. München (Germany); Alexander Kronenberg, Johannes Gutenberg Univ. Mainz (Germany); Stanislav Chadov, Max-Planck-Institut für Chemische Physik Fester Stoffe (Germany); Benjamin Balke, Johannes Gutenberg Univ. Mainz (Germany); Andrey Gloskovskii, Deutsches Elektronen-Synchrotron (Germany); Michaela Kolbe, Hans-Joachim Elmers, Gerd Schoenhense, Johannes Gutenberg Univ. Mainz (Germany); Hubert Ebert, Ludwig-Maximilians-Univ. München (Germany); Claudia Felser, Max-Planck-Institut für Chemische Physik Fester Stoffe (Germany); Mathias Klaeui, Johannes Gutenberg Univ. Mainz (Germany)

The magnitude of the room temperature spin polarization of ferromagnetic materials is a key property for their application in spin transport-based electronics. Thus Heusler compounds, due to their predicted bulk half-metallic properties, i.e. 100% spin polarization at the Fermi energy, are in the focus of interest. However, for most applications it is not the bulk but the surface or interface of the material, which is relevant.

Investigating optimized thin films of the compound Co2MnSi by in situ spinresolved UPS, we were able to demonstrate for the first time half-metallicity in combination with directly measured 93(+7/-11) % spin polarization at room temperature in the surface region of a Heusler thin film [Jou14]. Our novel band structure and photoemission calculations including all surfacerelated effects [Bra14] show that the observation of a high spin polarization in a wide energy range below the Fermi energy is related to a stable surface resonance in the majority band of Co2MnSi extending deep into the bulk of the material. Spin-integrated ex situ HAXPES with a photon energy of 6 keV on Co2MnSi thin films and spin-integrated in situ UPS was carried out. The UPS and the HAXPES results fundamentally agree although the information depth of both experiments varies from less than 1 nm to 20 nm. Nearly quantitative agreement of the calculations with the experiments for both, UV and hard X-ray photon energies, was obtained.

[Jou14] M. Jourdan et al. Nat. Commun. 5, 3974 (2014).

[Bra14] J. Braun et al., New J. Phys. 16, 015005 (2014).

9551-85, Session 22

Valence control of Eu ions in Eu-doped GaN grown by organometallic vapor phase epitaxy (Invited Paper)

Yasufumi Fujiwara, Masaaki Matsuda, Wanxin Zhu, Takanori Koijma, Atsushi Koizumi, Osaka Univ. (Japan)

We have intensively investigated rare-earth (RE)-doped III-V semiconductors grown by atomically controlled organometallic vapor phase epitaxy and fabricated new types of functional devices using the materials. Eu-doped GaN has been identified as a promising red emitter because it has excellent luminescence properties in the red spectral region, resulting from the specific optical properties of RE materials, such as a sharp, intense, and temperature-independent emission peak due to the intra-4f shell transitions. We have succeeded in growing Eu-doped GaN layers with high crystalline quality, and have demonstrated for the first time a low-voltage currentinjected red emission from p-type GaN /Eu-doped GaN/n-type GaN LEDs with an applied voltage of as low as 3 V [1]. A main emission line with a half width of less than 1 nm was observed at 621 nm, which can be assigned to the 5D0-7F2 transition of Eu3+ ions. By optimizing growth conditions and device structures, the light output power has been increasing steadily to sub-mW at an injected current of 20 mA [2]. The valence of Eu ions can be controlled by codoping with other elements. In AlxGa1-xN with high Al contents, Eu2+ state with a magnetic moment was obviously revealed by XANES, while the volume increased with the Al content [3]. These results suggest strongly a possibility to create novel devices for combined applications of optronics and spintronics.

A. Nishikawa, Y. Fujiwara et al., Appl. Phys. Express 2, 071004 (2009).
 Y. Fujiwara et al., Jpn. J. Appl. Phys. 53, 05FA13 (2014).
 A. Koizumi, Y. Fujiwara et al., Opt. Mater., in press (2015).

9551-86, Session 22

Novel 2D electron gases at the surface of transition-metal oxides: fundamentals and perspectives for spintronics (*Invited Paper*)

Andrés F. Santander-Syro, Univ Paris-Sud 11 (France)

Transition-metal oxides (TMOs) show remarkable properties, such as hightemperature superconductivity or large magnetoresistance. The realization of two-dimensional electron gases (2DEGs) at surfaces or interfaces of TMOs, a field of current intense research, is crucial for harnessing the functionalities of these materials for future applications. Additionally, these 2DEGs offer the possibility to explore new physics emerging from the combined effects of electron correlations and low-dimensional confinement.

Recently, we discovered that 2DEGs can be simply realized at the surface of various insulating transparent TMOs, such as the quantum paraelectric SrTiO3 [1] or the strong spin-orbit coupled KTaO3 [2]. In this talk, I will show that by choosing various surface terminations one can additionally tailor the electronic structure and symmetries of these 2DEGs [3-4], paving the way for the quest of topological states in correlated oxides. Furthermore, I will discuss our latest observation of a giant spin splitting, of 100 meV, of bands with opposite spin chiralities in the 2DEG at the surface of SrTiO3 [5]. These results show that confined electronic states at oxide surfaces can be endowed with novel properties, not present in the bulk, which are promising for technological applications.

[1] A. F. Santander-Syro et al., Nature 469, 189 (2011).

- [2] A. F. Santander-Syro et al., Phys. Rev. B 86, 121107(R) (2012).
- [3] C. Bareille et al., Sci. Rep. 4, 3586 (2014).
- [4] T. C. Rödel et al., Phys. Rev. Applied 1, 051002 (2014).
- [5] A. F. Santander-Syro et al, Nature Mater. 13, 1085 (2014).



9551-87, Session 23

Spin electronic magnetic sensor based on functional oxides for medical imaging (Invited Paper)

Aurelie Solignac, Commissariat à l'Énergie Atomique (France); Georg Kurij, Ruben Guerrero, Guillaume Agnus, Thomas Maroutian, Institut d'Électronique Fondamentale (France); Claude Fermon, Myriam Pannetier-Lecoeur, Commissariat à l'Énergie Atomique (France); PHILIPPE LECOEUR, Institut d'Électronique Fondamentale (France)

There is a strong interest in developing ultrasensitive sensors able to detect magnetic signals coming from the body, in particular those produced by the electrical activity of the heart or of the brain. Magnetoresistive sensors, stemming from spin electronics, are very promising devices. For example, tunnel magnetoresistance (TMR) junctions based on MgO tunnel barrier have a high sensitivity. Nevertheless, TMR also often have high level of noise. Full spin polarized materials like manganite La0.67Sr0.33MnO3 (LSMO) are attractive alternative candidates to develop such sensors because LSMO exhibits a very low 1/f noise when grown on single crystals [1], and a TMR response has been observed with values up to 2000% [2]. This kind of tunnel junctions, when combined with a high Tc superconductor loop, opens up possibilities to develop full oxide structures working at liquid nitrogen temperature and suitable for medical imaging. In this work, we investigated on LSMO based tunnel junctions the parameters controlling the overall system performances, including not only the TMR ratio, but also the pinning of the reference layer and the noise floor [3]. We especially focused on studying the effect of the quality of the barrier, the interface and the electrode, by playing with materials and growth conditions.

[1] A. Solignac et al., Journal of Physics: Conference Series 303, 012059 (2010)

[2] R. Werner et al., Appl. Phys. Letters, 98, 162505 (2011)

[3] R. Guerrero, A. Solignac et al., Appl. Phys. Lett. 100, 142402 (2012)

9551-88, Session 23

Development of micronic GMRmagnetoresistive sensors for nondestructive sensing applications (Invited Paper)

Henri Jaffrès, Yves LeMaitre, Sophie Collin, Frédéric Nguyen Vandau, Unité Mixte de Physique CNRS/Thales (France); Natalia Sergeeva-Chollet, CEA-Ctr. de SACLAY (France); Jean-Marc Decitre, CEA-Ctr. de SACLAY (France)

We will present our last development of GMR-based magnetic sensors devoted to sensing application for non-destructive control application. In these first realizations, we have chosen a so-called shape anisotropy exchange biased strategy to fulfill the field-sensing criteria in the uT range in devices made of micronic single elements. Our devices realized by optical lithography, and whose typical sizes range from 150 μ m x 150 μ m to 500 μm x 500 μm elements, are made of trilayers GMR-based technology and consist of several circuitries of GMR elements of different lengths, widths and gaps. To obtain a full sensing linearity and reversibility requiring a perpendicular magnetic arrangement between both sensitive and hard layer, the magnetization of the latter have been hardened by pinning it with an antiferromagnetic material. The specific geometry of the design have been engineered in order to optimize the magnetic response of the soft layer via the different magnetic torques exerted on it essentially played by the dipolar fields or shape anisotropy, and the external magnetic field to detect. The smaller dimensions in width and in gap are then respectively of 2 μ m and 3 μm to benefit of the full shape anisotropy formatting the magnetic response.

9551-89, Session 23

3D magnetic surfaces (Invited Paper)

Denys Makarov, Leibniz-Institut für Festkörper- und Werkstoffforschung Dresden (Germany)

Conventionally magnetic films and structures are fabricated on flat surfaces. The topology of curved surfaces has only recently started to be explored and leads to new fundamental physics and applied device ideas. Advancing in this field calls for the understanding of the magnetic responses of thin films on curved surfaces. Here, two basic geometries, i.e. hemi-spherical [1,2] and tubular [3,4], will be addressed. To enable the microscopic characterization of 3D architectures, we put forth the concept of magnetic soft x-ray tomography. I will introduce this concept and present the angle-and layer-resolved imaging of rolled-up tubes [4,5].

Based on this knowledge, we fabricated flexible [6,7], printable [8] and stretchable [9] magnetic sensorics. The unique mechanical properties open up new application potential of magnetic field sensors for printable electronics and smart skins, allowing to sense and manipulate objects of the surrounding us physical as well as digital world.

[1] T. Ulbrich et al., Phys. Rev. Lett. 96, 077202 (2006).

[2] D. Makarov et al., Appl. Phys. Lett. 93, 153112 (2008).

[3] E. Smith et al., Phys. Rev. Lett. 107, 097204 (2011).

[4] R. Streubel et al., Nano Lett. 14, 3981 (2014).

[5] R. Streubel et al., Adv. Mater. 26, 316 (2014).

[6] G. Lin et al., Lab Chip 14, 4050 (2014).

[7] M. Melzer et al., Adv. Mater. DOI: 10.1002/adma.201405027

[8] D. Karnaushenko et al., Adv. Mater. 24, 4518 (2012) & Adv. Mater. DOI: 10.1002/adma.201403907

[9] M. Melzer et al., Nano Lett. 11, 2522 (2011) & Adv. Mater. DOI: 10.1002/ adma.201403998

9551-90, Session 24

Organic analogues of diluted magnetic semiconductors: bridging quantum chemistry to condensed matter physics (Invited Paper)

Madalina I. Furis, Naveen Rawat, Kim Ngan Hua, The Univ. of Vermont (United States); Stephen A. McGill, National High Magnetic Field Lab. (United States)

The selective coupling between polarized photons and electronic states in materials enables polarization-resolved spectroscopy studies of exchange interactions, spin dynamics, and collective magnetic behavior of conduction electrons in semiconductors. At the University of Vermont we employ Magnetic Circular Dichroism (MCD) and polarization-resolved photoluminescence (PL) spectroscopy techniques to investigate the excitonic and magnetic properties of electrons in crystalline thin films of small molecule organic semiconductors.

We focus on the collective magnetic properties of d-shell ions (Cu2+, Co2+ and Mn2+) metal phthalocyanine (Pc) thin films that one may think of as organic analogues of diluted magnetic semiconductors (DMS). These films were deposited in-house using a recently developed pen-writing method that results in crystalline films with macroscopic long range ordering and improved electronic properties, ideally suited for spectroscopy techniques.

Our experiments reveal that, in analogy to DMS, the extended ϖ -orbitals of the Pc molecule mediate the spin exchange between highly localized d-like unpaired spins. We established that exchange mechanisms involve different electronic states in each species and/or hybridization between d-like orbitals and certain delocalized ϖ -orbitals. More recently, we focused our studies on "alloys" made of a mixture of Mn2+, Co2+ and metal-free (H2) soluble derivatives of the Pc molecule that offer insight into the possibility of tuning the magnetic interactions in these organic systems. Unprecedented 25T MCD and PL experiments conducted in the unique Florida State Split HELIX



magnet at the National High Magnetic Field Laboratory (NHMFL) reveal that we may be able to induce an exchange mechanism that involve different band edge states by varying the mixing ratio.

9551-91, Session 24

Photocontrol of magnetism above 77 K in nanoscaled heterostructures of cyanometallate coordination networks (Invited Paper)

Mark W. Meisel, Daniel R. Talham, Univ. of Florida (United States)

Using nanometer-sized heterostructures of cyanometallate coordination networks, specifially core@shell nanoparticles of CoFe@CrCr-PBA (PBA = Prussian blue analogues), irradiation by white light at 80 K modifies the magnetic response, and these changes remain intact and persist without continued irradiation to nominally 125 K [1]. Preliminary pressure studies indicate the photoinduced changes can be maintained up to 200 K, the transition temperature of the ferromagnetic CrCr-PBA component. The effect, which we first reported up to 70 K [2,3], arises from thermally induced interface strain, which is relaxed by irradiation of the photactive consituent, CoFe-PBA. The ferromagnetic domains in the strained interface region are affected and generate the persistent changes of the magnetism. Our understanding of this photo-magnetostructural mechanism enabled us to extend the phenomenon to include photoactive spin-crossover systems [4] and other ferromagnetic PBAs [5]. The potential path to higher temperatures will be sketched. This presentation is coauthored with Daniel R. Talham, UF Chemistry, and supported by the NSF via DMR-1405439 (DRT), DMR-1202033 (MWM), and DMR-1157490 (NHMFL), and by the UF Division of Sponsored Research.

[1] O.N. Risset, T.V. Brinzari, M.W. Meisel, D.R. Talham, submitted.

[2] D.M.Pajerowski, M.J. Andrus, J.E. Gardner, E.S. Knowles, M.W. Meisel, D.R. Talham, J. Am. Chem. Soc. 132 (2010) 4058.

[3] M.F. Dumont, E.S. Knowles, A. Guiet, D.M. Pajerowski, A.Gomez, S.W. Kycia, M.W. Meisel, D.R. Talham, Inorg. Chem. 50 (2011) 4295.

[4] C.R. Gros, M.K. Peprah, B.D. Hosterman, T.V. Brinzari, P.A. Quintero, M. Sendova, M.W. Meisel, D.R. Talham, J. Am. Chem. Soc. 136 (2014) 9846.
[5] O.N. Risset, P.A. Quintero, T.V. Brinzari, M.J. Andrus, M.W. Lufaso, M.W. Meisel, D.R. Talham, J. Am. Chem. Soc. 136 (2014) 15660.

9551-92, Session 24

Tailoring spintronics interfaces with organic molecules (Invited Paper)

Mirko Cinchetti, Technische Univ. Kaiserslautern (Germany)

Control of spin on the shortest and fastest scale is the holy grail of modern research in magnetism, as it holds the key to the ultimate miniaturization of energy-efficient and non-volatile spintronics devices. A very promising approach to this end is the deposition of isolated organic molecules, as small atomic-scale units, on a magnetic surface. The hybridization between the electronic bands at the surface of the magnet and the orbitals of the molecule can lead to a drastic change of the magnetic properties of the atoms coupled to the molecule. As hybridization can be controlled through the electronic properties of the organic components, the intrinsic multifunctionality of organic molecules could make hybrid interfaces the long-sought ultrafast handle for spin down to the atomic scale. Recent progress in organic spintronics and molecular spintronics has thus focused on the remarkably promising functionality of hybrid interfaces formed between magnetic surfaces and organic molecules — 'spinterfaces'.

In this talk I will show that the versatility of organic molecules for spin applications is not only limited to interfaces formed with magnetic materials, but extends to the much broader class of non-magnetic spintextured materials, like Rashba systems and topological insulators. In this context, the unique combination of chemical synthesis and state-of-the-art theoretical and experimental methods allows one to define the fundamental and general design rules of spinterfaces with stable and tunable spintronics properties, opening new and still unexplored avenues where the spin functionality of spin-textured surfaces is tailored both locally (on the molecular scale) and temporally (on the femtosecond time-scale).

9551-93, Session 25

Fundamental electric circuit elements based on the linear and nonlinear magnetoelectric effects (Invited Paper)

Young Sun, Dashan Shang, Yisheng Chai, Zexian Cao, Jun Lu, Institute of Physics (China)

From the viewpoint of electric circuit theory, the three fundamental twoterminal passive circuit elements, resistor R, capacitor C, and inductor L, are defined in terms of a relationship between two of the four basic circuit variables, charge q, current i, voltage v, and magnetic flux ?. From a symmetry concern, there should be a fourth fundamental element defined from the relationship between charge q and magnetic flux ?. Here we present both theoretical analysis and experimental evidences to demonstrate that a two-terminal passive device employing the magnetoelectric (ME) effects can exhibit a direct relationship between charge q and magnetic flux ?, and thus is able to act as the fourth fundamental circuit element. The ME effects refer to the induction of electric polarization by a magnetic field or magnetization by an electric field, and have attracted enormous interests due to their promise in many applications. However, no one has linked the ME effects with fundamental circuit theory. Both the linear and nonlinear-memory devices, termed transtor and memtranstor, respectively, have been experimentally realized using multiferroic materials showing strong ME effects. Based on our work, a full map of fundamental two-terminal circuit elements is constructed, which consists of four linear and four nonlinear-memory elements. This full map provides an invaluable guide to developing novel circuit functionalities in the future.

9551-94, Session 25

Emerging functionalities in devices with complex oxides (Invited Paper)

Tamalika Banerjee, Univ. of Groningen (Netherlands)

Interfaces of complex oxides host new physical phenomena and novel functionalities due to the interplay between strain, charge-transfer, orbitalreconstruction etc. Electronic devices on oxide semiconductors such as Nb doped SrTiO_3, bring in additional functionalities derived from temperature and electric field dependence of their dielectric permittivity, allowing manipulation by electric and magnetic field and tuning by spin-orbit relativistic effects. In this talk, I will discuss emerging functionalities that have been observed at oxide interfaces a) between Nb doped SrTiO 3 and SrRuO 3- a pervoskite metal, where ferromagnetism and metallicity evolve with decreasing temperature and increasing thickness, influencing electronic transport at the interface b) between carefully tuned spin injection contacts and Nb doped SrTiO 3, exhibiting an unusal bias dependence of the spin lifetime and features that demonstrate a strong influence of the interface electric field on spin accumulation and charge transport, unlike that found in conventional semiconductors and c) influence of dielectric screening on charge and spin transport when complex oxides are integrated with graphene. Our findings open up new directions in the field of oxide electronics and spintronics.



9551-95, Session 25

Tuning magnetic nanostructures and flux concentrators for magnetoresistive sensors (Invited Paper)

Xiaolu Yin, Univ. of Nebraska-Lincoln (United States); Yen-Fu Liu, Sy-Hwang Liou, Univ. of Nebraska-Lincoln (United States)

The methods for the optimization of the magnetoresistive (MR) sensors are to reduce sources of noises, to increase the signal, and to understand the involved fundamental limitations. The high-performance MR sensors are resulting from the important MTJ properties, such as tunneling magnetoresistance ratio (TMR), coercivity (Hc), exchange coupling field (He), domain structures, and noise property as well as the external magnetic flux concentrators. All these parameters are sensitively controlled by the magnetic nanostructures, which can be tuned by varying junction geometry, magnetic annealing process and so on. With all the efforts, we had achieved optimized magnetic sensor with a sensitivity as high as 5,146 %/mT. This sensitivity is currently the highest among all MR-type sensors that has been reported. The estimated noise of our magnetoresistive sensor is 47 pT/Hz1/2 at 1 Hz and 1.4 pT/Hz1/2 at 1 kHz, respectively. This magnetoresistance sensor dissipates only 100 μ W of power while operating under an applied voltage of 1 V at room temperature.

9551-106, Session 25

Towards high-frequency operation of polarization oscillations in spin verticalcavity surface-emitting lasers (Invited Paper)

Markus Lindemann, Nils C. Gerhardt, Martin R. Hofmann, Ruhr-Univ. Bochum (Germany); Tobias Pusch, Rainer Michalzik, Univ. Ulm (Germany)

Compared to purely charge based devices, spintronic lasers offer promising perspectives for new superior device concepts. Especially vertical-cavity surface-emitting lasers with spin-polarization (spin- VCSELs) feature ultrafast spin and polarization dynamics. Oscillations in the circular polarization degree can be generated using pulsed spin-injection. The oscillations evolve due to the carrier-spin-photon system, which is coupled for the linear modes in the VCSEL's cavity via birefringence. The polarization oscillations are independent of the conventional relaxation oscillations and have the potential to exceed frequencies of 100 GHz. The oscillations are switchable and can be the basis for ultrafast directly modulated spin-VCSELs for e.g. communication purposes. The polarization oscillation frequency is mainly determined by the birefringence. We show a method to tune the birefringence and thus the polarization oscillation frequency by adding mechanical strain to the substrate in vicinity of the laser. We demonstrate first experimental results for high frequency operation using 850 nm oxide-confined single-mode VCSELs. The results are compared with simulations using the spin-flip-model for high birefringence values. By means of this model, theoretical limitations of high frequency operation beyond 100 GHz are discussed.

9551-96, Session 26

An efficient biological source for light induced spin injection: photosystem I (Invited Paper)

Chanoch Carmeli, Tel Aviv Univ. (Israel); Ron Naaman, Weizmann Institute of Science (Israel); Itai Carmeli, Omri Heifler, Tel Aviv Univ. (Israel); Karuppannan S. Kumar, National Univ. of Singapore (Singapore) Recent research in spintronics is aimed at introducing spin-based devices in medical and biological applications. An essential component in these devices is the spin injector. We observed very high spin selectivity in electron transfer the chlorophyll protein complex photosystem I (PSI). Light-induced spin injection was observed by adsorbing the PSI complex on a silver substrate, exciting it with red light and using a spin analyzer device developed recently for detecting spin polarization. It was found that the photoexcitation-induced charge separation across PSI is spin selective and that the system has an efficiency of almost 100% in spin-specific injection. Temperature dependence studies revealed that the injection is especially efficient at room temperature. The observation that the nanosize protein operates at room temperature and in a dry environment renders PSI as a possible spintronic component for applications in nano optoelectronic devices. At physiological relevant temperatures the spin selectivity is extremely high and is superior to the spin polarization obtained by most inorganic spin injectors at room temperature. This finding opens the possibility of combining spintronics with bio-applications having a bio-system-based spin injector. Since the system properties are not related to the exchange interaction, that controls magnetism, this system can be miniaturized to a scale of a few nm. This size is difficult to obtain with ferromagnetic-based devices which become superparamagnetic and their spin orientation is not stable at temperatures relevant to many applications.

9551-97, Session 26

Spin injection and relaxation in a highly doped organic polymer film (*Invited Paper*)

Motoi Kimata, Daisuke Nozaki, Yasuhiro Niimi, The Univ. of Tokyo (Japan); Hiroyuki Tajima, Univ. of Hyogo (Japan); YoshiChika Otani, The Univ. of Tokyo (Japan)

The organic semiconductors (OSCs) are promising candidates for longdistance spin current transport. However, most of the OSCs have a strongly disordered structure, so that the transport and relaxation properties of spin currents in OSCs have not been fully understood unlike the usual metallic materials. To resolve this problem, we have performed the systematic studies on the spin current transport and relaxation mechanism in a highly doped OSC, PEDOT: PSS. In this study, we have respectively carried out spin pumping, electron paramagnetic resonance, and charge transport experiments to determine the spin diffusion length (SDL), the spin lifetime and spin diffusion constant. The obtained SDL of the order of one hundred nanometers is comparable to the calculated SDL using the experimentally obtained spin lifetime and the spin diffusion constant. However, the spin lifetime is much shorter than the reported value, meaning that the spin relaxation mechanism in doped OSCs is guite different from the previous discussions. In the present work, we propose the overall spin transport and relaxation mechanism in the hopping conduction regime of doped OSCs: the spin angular momentum is almost preserved in the hopping event, on the other hand, the spin relaxation mainly occurs within the nano-scale OSC crystal grains.

9551-98, Session 26

Tuning exchange interactions in organometallic semiconductors

Naveen Rawat, Madalina I. Furis, The Univ. of Vermont (United States)

Development of organic semiconductors has emerged as a leading area of research as they are expected to overcome limitations of inorganic semiconductor devices for certain applications where low cost manufacturing, device transparency in the visible range of white light spectrum or mechanical flexibility are more important than fast switching times. Solution processing methods produce thin films with millimeter -sized crystalline grains at very low cost manufacturing prices, ideally suited for optical spectroscopy investigations of long range many-body effects in organic systems. Our research is focused on a quest for magnetic organic semiconductor systems where magnetic ordering is achieved through a



tunable carrier-mediated spin exchange interaction, an organic analogue of an RKKY mechanism.

To this end we synthesized an entire family of organo-soluble 3-d transition metal Pc's and we successfully employed a novel solution-based pen-writing deposition technique to fabricate long range ordered thin films of mixtures of metal-free (H2Pc) molecule and Organo-metallic Phthalocyanines (MPc's) without any loss of long range order.

Our previous studies on the parent MPc crystalline thin films identified different electronic states mediating exchange interactions in these materials. This understanding of spin-dependent exchange interaction between delocalized ϖ -electrons with unpaired d-spins has driven us to further tune these interactions by mixing Co or MnPc and H2Pc in different ratios ranging from 1:1 to 1000:1 H2Pc:MPc. Variable temperature Magnetic Circular Dichroism (VTVH-MCD) reveal that magnetic exchange switches sign from AFM to FM as a function of ratio in the 1:1 through 10:1 range. The magnitude of the exchange is also tunable as a function of the average distance between unpaired spins in these materials. Furthermore, high magnetic field (B < 25T) MCD and Magneto-PL show evidence of spin-polarized band-edge excitons in the same materials.

Conference 9552: Carbon Nanotubes, Graphene, and Emerging 2D Materials for Electronic and Photonic Devices VIII



Sunday - Wednesday 9 -12 August 2015

Part of Proceedings of SPIE Vol. 9552 Carbon Nanotubes, Graphene, and Emerging 2D Materials for Electronic and Photonic Devices VIII

9552-1, Session 1

Using wafer-scale epitaxial graphene for producing twisted bilayers with controlled twist angle for electronics applications (Invited Paper)

Christos D. Dimitrakopoulos, Univ. of Massachusetts Amherst (United States)

Graphene's exceptional properties make it attractive for technological applications in many areas, including high-speed electronics. The establishment of processes for producing high quality, large-scale graphene is necessary for such applications. Large area growth of epitaxial graphene on the Si-face of hexagonal SiC (0001) wafers exhibits manageable growth kinetics, and most importantly, its azimuthal orientation is fixed, as it is determined by the structure of the single crystal substrate. Therefore, this is a viable method for producing graphene with uniform coverage and structural coherence at wafer-scale.[1],[2]

Semi-insulating SiC is a good substrate for graphene RF transistors, however, its cost is so high that potentially only niche applications of graphene on SiC (e.g. defense or space related) can be viable.

Furthermore, to enable hybrid electronics, where standard circuits built on Si perform digital logic functions while graphene that does not exhibit a band gap is used for ultrafast analog devices, we would need to transfer epitaxial graphene onto Si wafers. To address these issues, we have developed a method in which a graphene film grown on a 4" SiC wafer is exfoliated via the stress induced by an overgrown Ni film and transferred to other substrates, resulting in a wafer-scale monolayer of graphene that is continuous and has a single azimuthal orientation.[3] This growth and transfer process can be repeated on the same SiC wafer hundreds to thousands of times, dramatically reducing the cost per wafer-sized graphene layer. The characterization of the transferred films shows that they are of quality similar to the pristine films on SiC.

Capitalizing on this new method for single crystal epitaxial graphene transfer, we have initiated a project to produce bilayers of graphene with deterministically controlled twist angles. The inspiration for this experimental work is recent theoretical work by Maroudas and coworkers4 that predicts the opening of substantial band gaps at specific twist angles in bilayer graphene. We will report our methods for producing twisted bilayers with controlled twist angle, their characterization and device results.

[1] C. Dimitrakopoulos, Y.-M. Lin, A. Grill, D. B. Farmer, M. Freitag, Y. Sun, S.-J. Han, Z. Chen, K. A. Jenkins, Y. Zhu, Z. Liu, T. J. McArdle, J. A. Ott, R. Wisnieff, Ph. Avouris J. Vac. Sci. Technol. B 28, 985-992, (2010).

[2] Y.-M. Lin, C. Dimitrakopoulos, K. A. Jenkins, D. B. Farmer, H.-Y. Chiu, Ph. Avouris Science 327, 662 (2010).

[3] J. Kim, H. Park, J. B. Hannon, S. W. Bedell, K. Fogel, D. K. Sadana, C. Dimitrakopoulos Science 342, 833-836 (2013).

[4] A. R. Muniz, D. Maroudas Phys. Rev. B 86, 075404 (2012)

9552-2, Session 1

Lithographically defined 3-dimensional graphene scaffolds (Invited Paper)

D. Bruce Burckel, Sandia National Labs. (United States)

Graphene, single atomic layer 2-dimensional sheets of sp2-bonded carbon atoms, has attracted significant attention since the "Scotch tape" exfoliation method was demonstrated as a method to prepare useable areas of material. The excitement over potential applications for graphene has placed renewed interest in development of alternative, scalable methods to prepare graphene. Transition metals (e.g. nickel and copper) are known to catalyze the formation of sp2 bonds when carbon is deposited on them, forming a route to production of graphene. Recently we have demonstrated fabrication of 3D graphene following a variation of this process. Starting from lithographically defined photoresist structures which are converted to sp3 bonded carbon by heating to ~1000 degrees C in a reducing atmosphere, nickel is deposited conformally on the exterior of the carbon scaffold and subsequently annealed. During the anneal process, the carbon diffuses through the nickel and emerges on the exterior of the nickel as sp2 bonded carbon. The 3D topology of the scaffold results in buckling of the graphene to accommodate the non-2D nature of the structure, but otherwise, high quality graphene is formed, suitable for a variety of electrochemical applications. This paper will detail the fabrication, characterization and electrochemical application of these 3D graphene scaffolds

Supported by the Laboratory Directed Research and Development program at Sandia National Laboratories. Sandia National Laboratories is a multiprogram laboratory managed and operated by Sandia Corporation, a wholly owned subsidiary of Lockheed Martin Corporation, for the U.S. Department of Energy's National Nuclear Security Administration under contract DE-AC04-94AL85000.

9552-3, Session 1

III-V nanowires and 2D van der Waals sheets: interfaces and devices (Invited Paper)

Xiuling Li, Univ. of Illinois at Urbana-Champaign (United States)

Vertical and planar III-V nanowire growth on 2D van der Waals sheets by MOCVD will be presented, along with axial and radial p-n junction based solar cells.

9552-4, Session 1

Engineering catalytic activity via ion beam bombardment of catalyst supports for vertically aligned carbon nanotube growth (Invited Paper)

Ahmad E. Islam, Air Force Research Lab. (United States) and National Research Council (United States) and National Academy of Sciences (United States); Pasha Nikolaev, Air Force Research Lab. (United States); Placidus B. Amama, Kansas State Univ. (United States); Sammy Saber, Air Force Research Lab. (United States); Dmitri Zakharov, Brookhaven National Lab. (United States); Daniel Huffman, Gordon Sargent, Michelle Erford, Sheldon Semiatin, Air Force Research Lab. (United States); Eric A. Stach, Brookhaven National Lab. (United States); Benji Maruyama, Air Force Research Lab. (United States)

We have developed a method to control catalyst activity for super-growth of vertically aligned carbon nanotubes (VA-CNT) by defect engineering the catalyst support. In earlier work, we showed the importance of the structure and surface state of different alumina catalyst supports as a

Conference 9552: Carbon Nanotubes, Graphene, and Emerging 2D Materials for Electronic and Photonic Devices VIII



distinguishing characteristic driving catalyst lifetime and carbon nanotube yield. Our comparison of different types of alumina deposited using e-beam evaporation, magnetron sputtering, and atomic layer deposition gave insight into the mechanisms of catalyst deactivation, but did not give us direct control over the catalyst activity. Here we used ion beam bombardment to control activity transforming sapphire, a substrate that normally does not support VA-CNT growth, into a substrate that supports super-growth of VA-CNT as good as the best deposited alumina's. A wide range of surface characterization techniques were used to characterize the material transformation induced by ion beam bombardment and hence to study the catalyst activity during VA-CNT growth. By tuning the degree of ion beam bombardment, we purposely control the structure and chemistry of the support, the resultant catalyst diameter and areal density, and ultimately the activity of the catalyst. This ability to control the catalyst activity enables us to grow VA-CNTs with tunable height and also offers a versatile way to pattern VA-CNT growth by masked ion bombardment. The capability to grow carbon nanotubes on substrates that otherwise do not support growth offers promising applications in many electronic, thermal, energy storage uses of carbon nanotubes.

9552-5, Session 1

Noncontact carrier dynamic characterization of hybrid graphene-based thin films by terahertz pulsed and CW techniques

Ehsan Dadrasnia, Sujitha Puthukodan, Univ. Carlos III de Madrid (Spain); Guillaume Ducournau, Jean-François Lampin', Univ. des Sciences et Technologies de Lille (France); Frédéric Garet, Jean-Louis Coutaz, IMEP-LAHC (France); Horacio R. Lamela Rivera, Univ. Carlos III de Madrid (Spain)

The graphene-based thin films are usually stacked on substrate for different optoelectronic devices. A profoundly study of the graphenes' electrical and optical characterization is necessary in order to be applied them in novel optic and electronic applications. Four-point probe (Klarskov et al.,Nanotechnol., 2011) or van der Pauw (Li et al.,Nano Letters, 2009) method, and Hall effect measurements (Zhang et al.,Nature, 2005) applied to measure the characteristics of the graphene-like materials as contact techniques. Four-point probe and van der Pauw measure only the conductivity or resistivity, while Hall effect method measures the carrier density and the carrier mobility. The contacting issue may damage such fragile device and thus may prevent a multiple measurement procedure and/ or a subsequent use of the tested devices.

We have recently reported the noncontact and nondestructive pulsed terahertz time-domain spectroscopy (THz-TDS) (Dadrasnia et al.,Appl. Phys. Lett., 2014, Dadrasnia et al.,Adv. Condens. Matter Phys,2014) and continuous wave (CW) techniques (Puthukodan et al.,Electron. Lett., 2014, Dadrasnia et al.,J. SPECTROSC.,2014) to measure the electrical conductivity of such high conductance graphene and carbon-based materials at AC and DC levels.

The novelty of this new work is to apply non-Drude responses to demonstrate the potential features of both THz CW and TDS transmission/ reflection measurements not only to derive the electrical conductivity, but also to study the optical and ultrafast mobility carrier transport parameters without the need for application of gating potentials. In this study, we test this approach for nanometric hybrid silver nanowires-graphene films grown using common chemical vapor deposition on the top of a quartz substrate.

9552-40, Session 1

Design of nanomaterials for energy storage (Invited Paper)

Cengiz Sinan Ozkan, Univ. of California, Riverside (United States)

I will describe innovative approaches for the design and synthesis of hierarchical three dimensional graphene hybrid materials which possess characteristics including ultra large surface area, tunability, and high conductivity which are appealing to diverse energy storage systems. Next, I will talk about three-dimensional cone-shape carbon nanotube clusters decorated with amorphous silicon for lithium ion battery anodes. An innovative silicon decorated cone-shape CNT clusters (SCCC) is prepared by depositing amorphous silicon onto CCC. The seamless connection between silicon decorated CNT cones and graphene facilitates the charge transfer in the system and provides a binder-free technique for fabricating lithium ion batteries.

9552-7, Session 2

Genomics with graphene nanotechnology (*Invited Paper*)

Jean-Pierre Leburton, Univ. of Illinois at Urbana-Champaign (United States)

The single-atom thickness of monolayer graphene makes it an ideal candidate for DNA sequencing as it can scan molecules passing through a nanopore at high resolution. Additionally, unlike most insulating membranes, graphene is electrically active, and this property can be exploited to control and electronically sense biomolecules. We show that the shape of the edge as well as the shape and position of the nanopore can strongly affect the electronic conductance through a lateral constriction in a graphene nanoribbon as well as its sensitivity to external charges. In this context the geometry of the graphene membrane can be tuned to detect the rotational and positional conformation of a charge distribution inside the nanopore. We show that a quantum point contact (QPC) geometry is suitable for the electrically-active graphene layer and propose a viable design for a graphene-based DNA sequencing device.

9552-8, Session 2

Optoelectronic properties of CZTS(e) as revealed by low-temperature photoluminescence studies (Invited Paper)

Talia Gershon, IBM Thomas J. Watson Research Ctr. (United States); Byungha Shin, KAIST (Korea, Republic of); Tayfun Gokmen, Yun S. Lee, Supratik Guha, IBM Thomas J. Watson Research Ctr. (United States)

CZTSSe photovoltaic devices have long held promise as earth-abundant substitutes for the commercial thin film absorber material CIGS. Efficiencies up to 12.6% have been demonstrated with the mixed sulfo-selenide CZTSSe, however this performance is well below the levels achieved with CIGS (>20%). A leading explanation of the lower performance relates to the highly defective nature of the CZTSSe bulk, which causes electrical distortions of the valence and conduction bands and hence a reduction in quasi Fermi level splitting in the material under illumination, and ultimately a low Voc. This talk will describe a method for examining the bulk defects in CZTS and CZTSe materials using low-temperature photoluminescence measurements (4K). It will be shown that a larger concentration of defects as measured using this technique is correlated with a reduction in device Voc. The talk will also discuss some of the optoelectronic consequences of sodium incorporation into CZTS(e), including a change in the energetic depth of the optically-active defects with respect to the band gap and a change in the radiative luminescence efficiency. The results presented will help explain the empirical observation that the presence of sodium in the absorber is correlated with high performance CZTSSe photovoltaic devices.

9552-9, Session 2

Bromination of graphene: a new route to making high performance transparent conducting electrodes with low optical losses

Ahmed E. Mansour, Aram Amassian, King Abdullah Univ. of Science and Technology (Saudi Arabia); Minas H. Tanielian, Boeing Research and Technology (United States)

The high optical transmittance, electrical conductivity, flexibility and chemical stability of graphene have triggered great interest in its application as a transparent conducting electrode material and as a potential replacement for indium doped tin oxide. However, currently available large scale production methods such as chemical vapor deposition produce polycrystalline graphene, and require additional transfer process which further introduces defects and impurities resulting in a significant increase in its sheet resistance. Doping of graphene with foreign atoms has been a popular route for reducing its sheet resistance which typically comes at a significant loss in optical transmission.

Herein, we report the successful bromine doping of graphene resulting in air-stable transparent conducting electrodes with up to 80% reduction of sheet resistance reaching -180 ?/? at the cost of 2-3% loss of optical transmission in case of few layer graphene and 0.8% in case of single layer graphene. The remarkably low tradeoff in optical transparency leads to the highest enhancements in figure of merit reported thus far. Furthermore, our results show a controlled increase in the workfunction up to 0.3 eV with the bromine content. These results should help pave the way for further development of graphene as potentially a highly transparent substitute to other transparent conducting electrodes in optoelectronic devices.

9552-10, Session 2

Thermal instability of field emission from carbon nanotubes studied using multiphysics simulation by considering space charge effect

Ahmad E Islam, Air Force Research Laboratory (United States) and National Research Council (United States) and National Academy of Sciences (United States); Steven B. Fairchild, Benji Maruyama, Air Force Research Lab. (United States)

Thermal stability is an important concern for practical use of high-current field emitters in display, X-ray generation, Hall thruster, and microplasma generation. Carbon nanotubes (CNTs) and their bundles have high thermal conductivity and offers great promise in this aspect, as evident from the wide-scale availability of experiments with CNT-based emitters. Analysis of these experiments is often carried out using – classical Fowler-Nordheim (FN) equation and heat equation with no self-consistency, infinite conductivity for CNT, and a linear potential profile near the emission points. Ideal work-function of CNT is typically assumed during extraction of critical parameters like field enhancement factor, area of emission – making these extractions physically irrelevant. Additionally, the space-charge effect – one of the most important aspect of high-current field emission – is never considered during data analysis.

In this work, we use a self-consistent numerical framework for the first time to study thermal stability of field emission in CNT-based emitters by considering proper electrostatics, quantum-mechanical tunneling (with FN equation as the limiting case), heat flow, and space charge effect. Our self-consistent numerical simulation compares well with the available experimental results. This comparison suggests consideration of finite CNT conductivity and proper workfunction as key for accurate extraction field enhancement factor. Developed framework also offers a unique opportunity to study temperature rise in the emission areas and suggests options for improving thermal stability and hence mitigating thermal runaway. The analysis also identifies the role of impurity in reducing the space charge effect.

OPTICS+ PHOTONICS

NANOSCIENCE+ ENGINEERING

9552-11, Session 2

Study of 2D triangular lattice of multiwall carbon nanotube arrays

Xingxing Wu, Mei Wang, Maojin Yun, Weijin Kong, Qingdao Univ. (China)

A triangular lattice photonic crystal is formed with the periodic arrays of multiwall carbon nanotube. With the Drude-Lorentz model, the photonic properties of the designed multiwall carbon nanotube photonic crystal are investigated by means of optical transmission measurements. In order to find the relations between optical properties and different parameters of the photonic crystals, such as radius and intermediate spacing of the nanotube, the transverse electric (TE) and transverse magnetic (TM) waves propagation should be considered respectively. The transmission spectrum and simulation results show that a strong metamaterial cut-off filtering effect at the plasma frequency is obtained with the designed multiwall carbon nanotube photonic crystal. It can be used in high pass filters, waveguides, switches and diffraction gratings which based on the computational analysis.

9552-12, Session 2

Mitigation of charged impurity effects in graphene field-effect transistors with polar organic molecules

Barrett C. Worley, Seohee Kim, Deji Akinwande, The Univ. of Texas at Austin (United States); Peter J. Rossky, Rice Univ. (United States); Ananth Dodabalapur, The Univ. of Texas at Austin (United States)

Recent developments in monolayer graphene production allow its use as the active layer in field-effect transistor technology. Favorable electrical characteristics of monolayer graphene include high mobility, operating frequency, and good stability. These characteristics are governed by such key transport physical phenomena as electron-hole transport symmetry, Dirac point voltage, and charged impurity effects. Doping of graphene occurs during device fabrication, and is largely due to charged impurities located at or near the graphene/substrate interface. These impurities cause scattering of charge carriers, which lowers mobility. Such scattering is detrimental to graphene transistor performance, but our group has shown that coating with fluoropolymer thin films or exposure to polar organic vapors can restore favorable electrical characteristics to monolayer graphene. By partially neutralizing charged impurities and defects, we can improve the mobility by approximately a factor of 2, change the Dirac voltage by fairly large amounts, and reduce the residual carrier density significantly. We hypothesize that this phenomena results from screening of charged impurities by the polar molecules. To better understand such screening interactions, we performed computational chemistry experiments to observe interactions between polar organic molecules and monolayer graphene. The molecules interacted more strongly with defective graphene than with pristine graphene, and the electronic environment of graphene was altered. These computational observations correlate well with our experimental results to support our hypothesis that polar molecules can act to screen charged impurities on or near monolayer graphene. Such screening favorably mitigates charge scattering, improving graphene transistor performance.



9552-13, Session 2

On-chip high power porous silicon lithium ion batteries with stable capacity over 10000 cycles (Invited Paper)

Andrew S. Westover, Daniel Freudiger, Zarif Gani, Keith Share, Landon Oakes, Rachel E. Carter, Cary L. Pint, Vanderbilt Univ. (United States)

We demonstrate the operation of a graphene-passivated on-chip porous silicon material as a high rate lithium ion battery anode with over 50x power density and 100x energy density improvement compared to identically prepared on-chip porous silicon supercapacitors. We demonstrate this Faradaic storage behavior to occur at fast charging rates (1-10 mA/cm2) where lithium locally intercalates into the nanoporous silicon, but not underlying bulk silicon material. This prevents the degradation and poor cycling performance that is commonly observed from deep storage in bulk silicon materials. As a result, this device exhibits cycling performance that exceeds 10,000 cycles with capacity above 0.1 mAh/cm2, without notable capacity fade. This work demonstrates a practical route toward high power, high energy, and long lifetime all-silicon on-chip storage systems relevant toward integration of energy storage into electronics, photovoltaics, and other silicon-based technology.

9552-14, Session 3

Two-dimensional material electronics and photonics (*Invited Paper*)

Wenjuan Zhu, Univ. of Illinois at Urbana-Champaign (United States)

Two-dimensional (2D) materials has attracted intense interest in research in recent years. As compared to their bulk counterparts, these 2D materials have many unique properties due to their reduced dimensionality and symmetry. A key difference is the band structures, which lead to distinct electronic and photonic properties. The 2D nature of the materials also plays an important role in defining their exceptional properties of mechanical strength, surface sensitivity, thermal conductivity, tunable band-gap and interaction with light. These unique properties of 2D materials open up broad territories of applications in computing, communication, energy, and medicine. In this talk, I will present our work on understanding the electrical properties of graphene and MoS2, in particular current transport and band-gap engineering in graphene, interface between gate dielectrics and graphene, and gap states in MoS2. I will also present our work on the nano-scale electronic devices (RF and logic devices) and photonic devices (plasmonic devices and photo-detectors) based on graphene and transition metal dichalcogenides.

9552-15, Session 3

Optical selection rule based on valleyexciton locking in monolayer TMDC

Jun Xiao, Ziliang Ye, Ying Wang, Hanyu Zhu, Yuan Wang, Xiang Zhang, Univ. of California, Berkeley (United States)

Layered transition metal dichalcogenide (TMDC) with hexagonal lattice structure has six valleys at corners of the Brillouin zone. The nontrivial Berry curvature distribution renders the adjacent valleys with distinguishable valley angular momentum, which enables itself as an ideal 2D valleytronic platform. Recent studies reported strong excitonic effect in monolayer WS2 and each excitonic state is identified with a well-defined orbital angular momentum, however the anticipated selection rules involve nonlinear optical processes are not clear. Here we show valley angular momentum (VAM) together with exciton angular momentum (EAM) impose different valley-exciton locked selection rules for second harmonic generation (SHG) and two photon luminescence (TPL) in monolayer WS2. Moreover, the two-photon induced valley populations yield net circular polarized photoluminescence after a sub-ps interexciton relaxation. The work demonstrates a new approach to control valley population at different excitonic states for next generation of optical circuits and quantum information computing.

9552-16, Session 3

Second-harmonic generation in an atomic phase-matched nonlinear 2D crystal

Mervin Zhao, Ziliang Ye, Yu Ye, Hanyu Zhu, Yuan Wang, Univ. of California, Berkeley (United States); Yoshihiro Iwasa, The Univ. of Tokyo (Japan); Xiang Zhang, Univ. of California, Berkeley (United States)

The second harmonic generation (SHG) produced from two-dimensional atomic crystals have been utilized recently in studying the grain boundaries and electronic structure of such ultra-thin materials. However, the SHG in many of these crystals, such as transition metal dichalcogenides (TMDCs), only occur in odd numbered layers with limited intensity due to their noncentrosymmetric nature. Here, we probe the SHG from the bulk noncentrosymmetric molybdenum disulfide (MoS2). Whereas the commonly studied 2H crystal phase's anti-parallel nonlinear dipoles in adjacent layers give an oscillatory SH response, the parallel nonlinear dipoles of each atomic layer in the 3R phase constructively interfere to amplify the nonlinear light. Due to this interference, we observed the atomically phase-matched condition yielding a quadratic dependence between the intensity and layer number. Additionally, we probed the layer evolution of the A and B excitonic transitions in 3R-MoS2 using SHG spectroscopy and found distinct electronic structure differences arising from the crystal geometry. These findings demonstrate the dramatic effect of the symmetry and layer stacking of these atomic crystals.

9552-17, Session 3

Monolayer tungsten disulfide laser

Yu Ye, Zi Jing Wong, Univ. of California, Berkeley (United States); Xiufang Lu, Univ. of Science and Technology of China (China); Hanyu Zhu, Yuan Wang, Univ. of California, Berkeley (United States); Xianhui Chen, Univ. of Science and Technology of China (China); Xiang Zhang, Univ. of California, Berkeley (United States)

When transition metal dichalcogenide (TMDC) crystals are thinned to monolayers, they undergo an indirect to direct bandgap transition, enabling rich electroluminescent and photoluminescent behaviors. Coupling and integration of TMDC monolayers with photonic crystal and distributed Bragg reflector microcavities have recently been reported with Purcell enhancement of spontaneous emission and strong lightmatter interaction. However, realization of laser - a fundamental building block of optoelectronic system - remains a bottleneck, mainly due to the limited overall materials gain volume and difficulty to design efficient optical confinement structure. In fact, the quantum confinement on these layered d-electron materials leads to layer-dependent evolution of electronic structure with step like density of states for monolayers comparing to their bulk counterparts, Making TMDC monolayers a unique optical gain medium for superior lasing characteristics. Here, we report the first realization of monolayer tungsten disulfide (WS2) laser embedded in a microdisk resonator. To reduce the 2D material lasing threshold, we utilized a whispering gallery mode resonator with a high quality factor. The Si3N4/WS2/HSQ sandwich configuration provides a strong feedback and mode overlap. An excitonic laser emission has bee observed in the visible wavelength. Our work marks a major step towards monolayer-based on-chip active optoelectronics and integrated 2D photonic platforms for new optical communication and computing applications.



9552-18, Session 3

Plasmonic gold nanorods enhance the photoluminescence of a two-dimensional molybdenum disulfide (MoS2) monolayer

Min-Hsiung Shih, Kevin Lee, Yi-Huan Chen, Academia Sinica (Taiwan)

Enhancing the Photoluminescence (PL) of a weak emitter, such as the 2-D atomic layers of molybdenum disulfide (MoS2), is critical for developing the next generation optoelectronic devices such as flexible mobiles, ultrathin light-emitting diodes, and atomically thin phototransistors. MoS2, which is one of the transition metal dichalcogenide (TMD) semiconductors, has received great attention due to its excellent optical and electronic properties and potential applications in field-effect transistors, light emitting and sensing devices. This study presents the enhanced photoluminescence (PL) of a MoS2 monolayer incorporating a MoS2 monolayer in the presence of gold (Au) nanorods. A localized surface plasmon wave of Au nanorods that generated around the MoS2 monolayer can provide resonance wavelength overlapping with that of the MoS2 gain spectrum. These spatial and spectral matches between the localized surface plasmon polariton waves and that from MoS2 emission drastically enhanced the light emission from the MoS2 monolayer. Upon optimizing the Au nanorod density in the system, we obtained more than six-fold intensity enhancement of the PL that was generated from the MoS2 monolayer incorporating Au nanorods, as compared to the intensity of the PL from the pristine MoS2 monolayer. The plasmonic Au nanostructures approach provides a valuable avenue to enhancing the emitting efficiency of the 2-D nano-materials and their devices for the future optoelectronic devices and systems.

9552-20, Session 3

Pulsed laser annealing for advanced performance of mechanically flexible and optically transparent multilayer MoS2 transistors (Invited Paper)

Hyuk-Jun Kwon, Univ of California Berkeley (United States); Woong Choi, Kookmin Univ. (Korea, Republic of); Min Suk Oh, Display Convergence Research Center, Korea Electronics Technology Institute (Korea, Republic of); Sunkook Kim, Kyung Hee Univ. (Korea, Republic of); Costas P Grigoropoulos, Univ of California Berkeley (United States)

Laser enables the achievement of superb interfacial characteristics between electrode and semiconducting material contact surface and is also useful for a reduction in contact resistance. The irradiation of a pulsed laser with high energy density and short wavelength onto the electrodes leads to thermal annealing at the locally confined small area that needs high temperature without inflicting thermal damage. This contrasts conventional thermal annealing that affects the entire panel, including unwanted areas in which the annealing process should be excluded.

We demonstrate that mechanically flexible and optically transparent (more than 81% transmittance in visible wavelength) multilayered molybdenum disulfide (MoS2) thin-film transistors (TFTs) in which the source/drain electrodes are selectively annealed using picosecond laser achieve the enhancement of device performance without plastic deformation, such as higher mobility, increased output resistance, and decreased subthreshold swing. Numerical thermal simulation for the temperature distribution, transmission electron microscopy (TEM) analysis, current-voltage measurements, and contact-free mobility extracted from the Y-function method (YFM) enable understanding of the compatibility and the effects of pulsed laser annealing process; the enhanced performance originated not only from a decrease in the Schottky barrier effect at the contact, but also an improvement of the channel interface. Furthermore, these results show that the laser annealing can be a promising technology to build up a high performance transparent and flexible electronics.

9552-21, Session 3

Cavity coupled MoS2 light sources (Invited Paper)

Ertugrul Cubukcu, Jason C. Reed, Fei Yi, Hai Zhu, Univ. of Pennsylvania (United States)

Emerging transition metal dichalcogenide (TMDC) materials such as MoS2 exhibit a direct electronic bandgap at the monolayer limit. Besides. this material exhibits giant resonant second order optical nonlinear susceptibility. Here, we utilize these unique properties coupled to optical microcavities. In the first part of this talk, we will show our recent results on a wavelength tunable integrated narrowband light source with a chemically enhanced MoS2 layer integrated into a microdisk cavity with a sub-wavelength notch coupler for easy excitation and light extraction. Here, we fabricate SiO2 micro disk resonators that support high-quality factor whispering gallery modes. These microdisk cavities contain a monolayer of the MoS2 crystal directly embedded as part of the fabrication process. In the second part, we will present our recent results on the optomechanical control of second harmonic generation from monolayer MoS2. This work relies on a one-dimensional Fabry-Perot type microcavity, which is doubly resonant with fundamental and second harmonic beams. We envision that this work will pave the way for nanophotonic light sources with atomically thin active media for next generation optoelectronic sensors and systems.

9552-22, Session 3

Towards graphene electronics (Invited Paper)

Eric Borguet, Temple Univ. (United States)

Thirty years ago there were two classic forms of carbon (diamond and graphite). Since then, three new carbon allotropes (buckyballs, carbon nanotubes and graphene), all involving only sp2 carbons, have been discovered. While there is much excitement about graphene, another interesting carbon-based material, graphyne (a two dimensional network of sp and sp2 carbon centers.) has been suggested.

Even though bulk graphyne is not known in nature, it has been the subject of theoretical calculations which suggest exciting properties for graphynes beyond those of graphene. While macroscopic samples of graphyne are not currently available, molecular units of graphyne, called carbo-benzenes, have been synthesized by our collaborators in Toulouse.

We report the single molecule electrical measurements on molecular carbo-benzenes, connected to gold electrodes via amine anchoring groups, determined using scanning tunneling microscope break junction (STM-BJ) methods. Our results show that these highly conjugated macroaromatics with NH2 metal-anchoring functions are superior in conductivity (-100 nS) compared with molecules of similar length (1.94 nm). These experimental results are rationalized by high level calculations performed by our colleagues at Northwestern. Cutting one side of the macro-aromatic circuit results in a two orders of magnitude smaller junction conductance. Furthermore, single carbo-benzene-mediated junctions exhibit field-effect transistor behavior when an electrochemical gate potential is applied, opening the way for device applications.

9552-23, Session 3

Tin disulfide: large-area growth and characterization

Zafer Mutlu, Mihrimah Ozkan, Cengiz S. Ozkan, Univ. of California, Riverside (United States)

Tin disulfide (SnS2), an emerging two-dimensional (2D) layered metal dichalcogenide semiconductor, has promising potential applications in electronic and optoelectronic devices. Here we demonstrate the large-area growth of atomically thin SnS2 films directly on device-compatible SiO2, MgO and sapphire substrates by a scalable chemical vapor deposition

Conference 9552: Carbon Nanotubes, Graphene, and Emerging 2D Materials for Electronic and Photonic Devices VIII



(CVD) method using pre-deposited Sn films and S powders as the reactants. Growth temperature, pressure and pre-deposited film thickness are found to critically impact the quality of the as grown films. The films grown under optimal conditions are found to be of high structural quality. The compositional analysis of the layers is done by X-ray photo?emission spectroscopy. The thickness and surface roughness of the films are determined by atomic force microscopy. High resolution transmission electron microscopy and Raman spectroscopy indicate that the number of layers range from single layer to a few layers. The charge-carrier mobility is measured through the back-gate field-effect transistor configuration. The growth approach developed here can be now used to build broken-gap hetero-structures of 2D materials stacked in the vertical direction such as SnS2/MoTe2 with ultimate control over their morphology, composition, and dimensionality.

9552-24, Session 3

Control of light-matter interaction in 2D atomic crystals (Invited Paper)

Vinod M. Menon, The City College of New York (United States)

In this talk I will review recent efforts at enhancing the interaction of light with excitons in 2D atomic crystals of transition metal dichalcogendeis (TMD) using optical microcavities. Approaches to enhance spontaneous emission using one dimensional dielectric microcavities, two-dimensional photonic crystals and metamaterials will be discussed. Following this, I will discuss the regime of strong coupling between excitons and photons resulting in the formation of microcavity polaritons in these systems. The possibility to exploit the unique properties of 2D atomic crystals such as valley polarization in photonic applications will be briefly addressed. Finally I will discuss some potential applications of such microcavity enhanced 2D atomic crystal based devices.

9552-41, Session 3

Tunable WS2 microfiber saturable absorber as mode-locker and Q-switcher in an all-fiber laser

Reza Khazaeinezhad, Yonsei Univ. (Korea, Republic of); Sahar Hosseinzadeh Kassani, Harvard Medical School (United States); Hwanseong Jeong, Ajou Univ. (Korea, Republic of); Kyung Jun Park, Byoung Yoon Kim, KAIST (Korea, Republic of); Dong-II Yeom, Ajou Univ. (Korea, Republic of); Kyunghwan Ken Oh, Yonsei Univ. (Korea, Republic of)

Ultrafast lasers are used in a variety of applications, ranging from optical communications to medical diagnostics, biomedical imaging and industrial materials processing. Developments of new gain media and mode-locking technologies have changed the outlook of ultrafast lasers over the past two decades. Saturable Absorber (SA) is a key component in passive modelocked and Q-switched fiber lasers. Over the past couple of decades, a large range of SA materials have been demonstrated, including toxic dyes, semiconductors with costly fabrication process and narrow spectral band, and carbon materials such as Carbon nano tubes (CNTs) and graphene with diameter and chirality absorption dependent and uses hazardous organic solvents such as dichlorobenzene as well as polymer composites for homogeneous dispersion. Nevertheless, all these SAs have their own drawbacks, and are thus unable to fully satisfy the key SA requirements for ultrafast lasers. These limitations motivate research on new materials for alternative SA materials and novel designs. Recently, Transition Metal Dichalcogenides such as MoS2 and WS2 have been attracted intensive attentions due to their unique characteristics in the field of nonlinear optical materials [1-5]. The reported nonlinear optical absorption of MoS2 through Z-scan measurements confirmed that MoS2 not only has significant saturable absorber performance in broadband wavelengths but also

demonstrates a higher saturable absorption response than graphene [6]. In this study, we experimentally demonstrated application of WS2 as a SA in a passively Er-doped fiber laser, successfully achieving tunable ultrafast pulses as well as Q-switching operation. We propose a novel tunable saturable absorber based on the WS2-deposited tapered fiber without using any kind of polymer. The use of polymers has many disadvantages, such as decreasing the damage threshold, increasing the non-saturable loss due to absorption. Tapered fibers were fabricated via the standard flame brushing method and WS2 nano-sheets were optically deposited along the interaction length of the tapered fibers by evanescent field interactions. Subsequently, we built a ring laser including the fabricated SAs and tunable ultrafast pulses based on waist diameter of tapered fiber and Qswitched pulses were obtained.

References

[1] R. Khazaeinezhad, S. H. Kassani, T. Nazari, H. Jeong, J. Kim, K. Choi, J. U. Lee, J. H. Kim, H. Cheong, D. Yeom, and K. Oh, "Saturable optical absorption in MoS2 nano-sheet optically deposited on the optical fiber facet," Opt. Commun.335, 224–230 (2015).

[2] Wang, S., Yu, H., Zhang, H., Wang, A., Zhao, M., Chen, Y., Mei, L. & Wang, J., Broadband Few-Layer MoS2 Saturable Absorbers. Adv. Mater. 26, 3538–3544 (2014).

[3] R. Khazaeizhad, S. H. Kassani, H. Jeong, D.-I. Yeom, and K. Oh, "Modelocking of Er-doped fiber laser using a multilayer MoS2 thin film as a saturable absorber in both anomalous and normal dispersion regimes," Opt. Express 22, 23732-23742 (2014).

[4] D. Mao, Y. Wang, C. Ma, L. Han, B. Jiang, X. Gan, S. Hua, and J. Zhao, , "WS2 mode-locked ultrafast fiber laser." Sci. Rep. 5, 7965 (2015).

[5] S. H. Kassani, R. Khazaeinezhad, H. Jeong, T. Nazari, D.-I. Yeom, and K. Oh, "All-fiber Er-doped Q-Switched laser based on Tungsten Disulfide saturable absorber," Opt. Mater. Express 5, 373-379 (2015)

[6] K. Wang, J. Wang, J. Fan, M. Lotya, A. O'Neill, D. Fox, Y. Feng, X. Zhang, B. Jiang, Q. Zhao, H. Zhang, J. N. Coleman, L. Zhang, and W. J. Blau, "Ultrafast saturable absorption of two-dimensional MoS2 nanosheets," ACS Nano 7(10), 9260–9267 (2013).

9552-25, Session Key

Plastic events in soft glass materials (Keynote Presentation)

Roberto Benzi, Univ. degli Studi di Roma "Tor Vergata" (Italy)

Many materials around us respond elastically to small applied stresses, but flow once a threshold stress (the yield stress) is exceeded. This is the case for food products, powders, cosmetics, foams, etc... It turns out that understanding the yield stress transition in these materials, often called soft glasses, is a challenging question. Similar to structural glasses, soft glasses exhibit aging and complex dynamics. Also, the size of the elementary building block of a soft glass is usually ranging from 1 micron to 1mm, ruling out the possibility to investigate the problem by molecular dynamics.

Recently, a new approach has been proposed: using a mesoscopic formulation of the system, the dynamics of relative simple soft glasses, like foams or micro emulsions, has been investigated. Numerical simulations allow the computation of several important properties of the systems, such as the yield stress transition. In this talk, I will review the new approach and explain how the complexity of soft glass dynamics may be disentangled in a systematic way.

9552-26, Session 4

A graphene-based non-volatile memory

Loic Loisel, Ecole Polytechnique (France) and Nanyang Technological Univ. (Singapore); Ange Maurice, Nanyang Technological Univ. (Singapore); Bérengère Lebental, Ecole Polytechnique (France) and Institut Francais



des Sciences et Technologies des Transports de l'amenagement et des Reseaux (France); Stefano Vezzoli, Nanyang Technological Univ. (Singapore); Costel-Sorin Cojocaru, Ecole Polytechnique (France); Beng Kang Tay, Nanyang Technological Univ. (Singapore)

We report on the demonstration and characterization of a non-volatile graphene-based memory, where the resistance level can be reversibly modulated with a contrast exceeding 400. We study two-terminal devices consisting of highly crystalline (Raman I(D)/I(G) \approx 0.2) monolayer CVD-graphene micro-ribbons transferred on SiO2 after growth on Cu. Electrical characterizations right after fabrication show the expected Ohmic behavior with k? resistance level and no memory effect.

A breakdown technique turns the resistive devices into memories: we apply a voltage sweep up to 30V (a few mA). During the sweep, several moderate jumps in resistance are observed, followed by a final rise to a high resistance state (several M?). As evidenced by Raman mapping, the resulting material is highly disordered graphene (I(D)/I(G) \approx 1.3) covering the whole device width. After breakdown, the resistance can be reversibly set at two wellseparated levels (e.g. 0.1 M? and 10 M?) by applying low voltage pulses (10V; 1-100 ?A) in vacuum. Both conductance states feature the Poole-Frenkel conduction mode, as is typical in disordered carbon. No loss of matter or physical gap is observed with either SEM or AFM.

Overall, our results suggest that the reversible switching is mostly due to thermally-induced increase or decrease in sp2 grain size in disordered graphene. This is significantly different from the commonly reported switching mechanism based on conducting filaments bridging a physical gap.

9552-27, Session 4

Plasmonic sensing structure of carbon nanotubes and gold nanoparticles for hydrogen detection

Marco Angiola, Univ. degli Studi di Padova (Italy); Chris Rutherglen, Carbonics, Inc. (United States); Kosmas Galatsis, Univ. of California, Los Angeles (United States); Alessandro Martucci, Univ. degli Studi di Padova (Italy)

Large attention has been directed toward carbon nanotubes as material for chemical sensors. However, little attention was paid toward the different behavior of the metallic and semiconductive carbon nanotubes as optical sensing materials.

Semiconductive or metallic Single Wall Carbon Nanotubes (SWCNTs) have been deposited on gold nanoparticles (NPs) monolayer and used as plasmonic based gas sensor.

The coupling between SWCNTs and Au NPs has the aim of combining the reactivity of the nanotubes towards hazardous gases, such as H2, CO, NO2, with the Localized Surface Plasmon Resonance (LSPR) of gold NPs. The LSPR is known to be extremely sensitive to the changes in the dielectric properties of the surrounding medium, a characteristic that has been widely exploited for the preparation of sensing devices. While the use of SWCNTs for gas sensing has been covered in multiple reports, to the best of our knowledge this is the first time that SWCNTs are used as sensing material in an optical sensor for the detection of reducing and oxidizing gases.

Two different techniques, ink-jet printer and dropcasting, were used for depositing the transparent CNTs film on the plasmonic layer. Both the deposition techniques proved to be effective for the development of transparent optical sensing films.

Metallic SWCNTs showed high sensitivity toward H2 at low temperature and an enhancement of performance at 300°C with the detection of low concentration of H2 and NO2. On the contrary, the semiconductive SWCNTs displayed very poor gas sensing properties, especially for the thinner film.

9552-28, Session 4

Perfect extinction of terahertz waves in monolayer graphene over 2-nm-wide metallic apertures (Invited Paper)

Hyeong-Ryeol Park, Univ of Minnesota Twin Cities (United States); Seon Namgung, Univ. of Minnesota, Twin Cities (United States); Xiaoshu Chen, Univ of Minnesota Twin Cities (United States); Nathan C Lindquist, Bethel University (United States); Yan Francescato, Vincenzo Giannini, Stefan A Maier, Imperial College London (United Kingdom); Sang-Hyun Oh, Univ of Minnesota Twin Cities (United States)

2D materials such as graphene possess unique electrical and optical properties that are not present in bulk materials. Due to their atomicscale thickness, however, 2D materials usually interact only weakly with electromagnetic waves, presenting challenges for realizing highperformance optoelectronic devices. This work demonstrates that by confining light into ultra-small metallic gaps, it is possible to dramatically boost this interaction with graphene. As an extreme case, terahertz waves are squeezed into 2-nm-wide gaps, which are ~100000 times smaller than the wavelength, allowing them to interact with 99% efficiency with monolayer graphene. This experiment is made possible by a new technique called atomic layer lithography to define sub-10-nm-wide and millimeterlong gaps in a metal film. Interestingly, while the gaps cover only 0.002% of the surface, 25% of incident THz energy passes through the metal film. The mechanism behind this dramatically enhanced transmission is partly in the shape of the gaps themselves: these annular gaps are able to efficiently funnel the THz waves along the loop. Furthermore, since the annular gaps are so narrow, the energy density becomes very high inside the gap and near the surface. Therefore, by placing graphene at the exit side of these gaps, 99% of the transmission is blocked since the graphene can now efficiently absorb the strongly confined waves. As an application of this strong absorption, we also demonstrate the construction of a highquality THz modulator. Nanogaps are integrated with an ionic gel gate and the enhanced intraband absorption in the graphene leads to a very large modulation depth of 80% with an operational voltage as low as 1.5 V. Besides graphene, such ultra-strong light-matter interactions mediated by nanogap structures could also benefit many applications involving other 2D materials.

9552-30, Session 4

Materials and other needs for advanced phase change memory (Invited Paper)

Norma E. Sosa, IBM Thomas J. Watson Research Ctr. (United States)

Phase change memory (PCM), with its long history, may now hold its brightest promise to date. This bright future is being fueled by the "push" from big data. PCM is a non-volatile memory technology used to create solid-state random access memory devices that operate based the resistance properties of materials. Employing the electrical resistance differences—as opposed to differences in charge stored—between the amorphous and crystalline phases of the material, PCM can store bits, namely one's and zero's. Indeed, owing to the method of storage, PCM can in fact be designed to hold multiple bits thus leading to a high-density technology twice the storage density and less than half the cost of DRAM, the main kind found in typical personal computers. It has been long known that PCM can fill a need gap that spans 3 decades in performance from DRAM to solid state drive (NAND Flash). Furthermore, PCM devices can lead to performance and reliability improvements essential to enabling significant steps forward to supporting big data centric computing. This talk will focus on the science and challenges of aggressive scaling to realize the density needed, how this scaling challenge is intertwined with materials needs for endurance into the giga-cycles, and the associated forefront research aiming to realizing multi-level functionality into these nanoscale programmable resistor devices.



9552-31, Session 4

Photodetector based on carbon nonotubes

Valeri Timoshenkov, National Research Univ. of Electronic Technology (Russian Federation); Alexandr Pavlov, Evgeni Kitsyuk, Roman Ryazanov, Institute of Nanotechnologies of Microelectronics Russian Academy of Sciences (Russian Federation); Yuri Adamov, National Research Univ. of Electronic Technology (Russian Federation)

Photodetector based on carbon nanotubes (CNT) was investigated. Optical sensor (size 2x8mm) was done on quartz susbtrate (size 5x10.5mm). Samples of photodetectors sensors were produced by planar technology. This technology included deposition of first metal layer (AL), lithography for formation of pads, etching, and formation of local catalyst area by inverse lithography. Catalyst layer for selective synthesize was deposited by standard procedure of magnetron sputtering and consist of Ti/Ni (thickness is 10/2 nm). The catalyst photoresist was removed after sputtering. This procedure forms local synthesis area. After cutting a substrate to chips 5x10.5 mm samples were ready to synthesis. Vertically-aligned multi-wall carbon nanotubes were directly synthesized on quartz chips by PECVD method.

The growing of carbon nanotubes started from catalyst nanoclusters. It was performed by oxidizing annealing at 280°C in O2 environment and reducing annealing at 450 ?C in H2 environment. Synthesis of multiwall carbon nanotubes was carried out in gas mixture composition - C2H2, H2 and NH3. Temperature of substrate holder (550 ?C) was controlled by thermo sensor. Plasma energy generator creates of radio frequency (RF) with energies of 20 W and low frequency (LF) with energy 30 W. The operating pressure was 2 Torr.

The morphology of the nanotubes was observed by scanning electron microscopy. Height of CNT array is approximately 2 μm and average diameter is about 40 nm.

Spectrum sensitivity of photodetector was investigated for 0.4u - 0.8u wavelength. Resistivity of CNT layers over temperature was detected in the range of -40 ?C to 150 ?C.

9552-32, Session 5

Wafer-scale single-crystalline graphene and its application for semiconductor layer transfers (Invited Paper)

Jeehwan Kim, IBM Thomas J. Watson Research Ctr. (United States); Hongsik Park, Kyungpook National Univ. (Korea, Republic of); Can Bayram, Univ. of Illinois at Urbana-Champaign (United States); Christos D. Dimitrakopoulos, Univ. of Massachusetts Amherst (United States); James Hannon, IBM Thomas J. Watson Research Ctr. (United States)

The performance of optimized graphene devices is ultimately determined by the quality of the graphene itself. Graphene grown on SiC has a single orientation, but its thickness cannot be limited to one layer. We have developed a method for manipulating these graphene layers with a singleatom-thickness precision. A graphene film of one or two monolayers grown on SiC is exfoliated via the stress induced with a nickel film. The excess graphene is selectively removed with a second exfoliation process with a gold film, resulting in a flat, single-oriented, monolayer graphene film.

This single-oriented graphene can be a template for the growth and transfer of single-crystalline films if films can be epitaxially grown on graphene. We, for the first time, demonstrated direct van der Waals growth of high-quality single-crystalline GaN films on this graphene. The GaN film was released and transferred onto Si substrates. The post-released graphene/SiC substrate was reused for multiple growth and transfer cycles of GaN films. This technique will be generally applied for growing other single-crystalline 3D and 2D materials on graphene and transfer.

References

1. Jeehwan Kim, Hongsik Park, James B. Hannon, Stephen W. Bedell, Keith Fogel, Devendra K. Sadana, Christos Dimitrakopoulos, "Layer?resolved graphene transfer via engineered strain layers", Science, Vol. 342, 833 (2013)

2. Jeehwan Kim, Can Bayram, Hongsik Park, Cheng?Wei Cheng, Christos Dimitrakopoulos, John A. Ott, Kathleen B. Reuter, Stephen W. Bedell, and Devendra K. Sadana, "Principle of direct van der Waals epitaxy of single?crystalline films on epitaxial graphene", Nature Communications, Vol. 5, 4836 (2014)

9552-33, Session 5

Metal-assisted exfoliation (MAE): green process for transferring graphene to flexible substrates and templating of subnanometer plasmonic gaps (Invited Paper)

Aliaksandr V. Zaretski, Brandon C. Marin, Herad Moetazedi, Tyler J Dill, Liban Jibril, Casey Kong, Andrea R. Tao, Darren J. Lipomi, Univ. of California, San Diego (United States)

This paper describes a new technique, termed "metal-assisted exfoliation," for the scalable transfer of graphene from catalytic copper foils to flexible polymeric supports. The process is amenable to roll-to-roll manufacturing, and the copper substrate can be recycled. We then demonstrate the use of single-layer graphene as a template for the formation of subnanometer plasmonic gaps using a scalable fabrication process called "nanoskiving." These gaps are formed between parallel gold nanowires in a process that first produces three-layer thin films with the architecture gold/single-layer graphene/gold, and then sections the composite films with an ultramicrotome. The structures produced can be treated as two gold nanowires separated along their entire lengths by an atomically thin graphene nanoribbon. Oxygen plasma etches the sandwiched graphene to a finite depth; this action produces a sub-nanometer gap near the top surface of the junction between the wires that is capable of supporting highly confined optical fields. The confinement of light is confirmed by surface-enhanced Raman spectroscopy measurements, which indicate that the enhancement of the electric field arises from the junction between the gold nanowires. These experiments demonstrate nanoskiving as a unique and easy-to-implement fabrication technique that is capable of forming sub-nanometer plasmonic gaps between parallel metallic nanostructures over long, macroscopic distances. These structures could be valuable for fundamental investigations as well as applications in plasmonics and molecular electronics.

9552-34, Session 5

Graphene growth on SiC(0001) and SiC(000-1): effect of substrate termination, hydrogen etching, and growth ambient (Invited Paper)

Zachary R. Robinson, Gell Jernigan, Marc Currie, Jennifer Hite, Konrad Bussmann, U.S. Naval Research Lab. (United States); Luke Nyakiti, Texas A&M Univ. (United States); Nelson Garces, Anindya Nath, Virginia Wheeler, Rachael Myers-Ward, James Wollmershauser, Boris Feygelson, U.S. Naval Research Lab. (United States); James Hannon, IBM T.J. Watson Research Laboraotry (United States); D. Kurt Gaskill, Charles Eddy Jr., U.S. Naval Research Lab. (United States)

Graphene of high crystal quality and single-layer thickness can be grown epitaxially by low pressure sublimation (LPS) on SiC(0001). On SiC(000-1), which is the C-terminated polar surface, there has been much less success growing uniform, single-layer films. In this work, a systematic study of



surface preparation by in situ hydrogen etching follow by LPS in an argon ambient was performed. Hydrogen etching is an important first step in the graphene growth process because it removes damage caused by polishing the surface. However, etching at too high of a temperature or for too long can result in pit formation due to the preferential etching of screw dislocations that intersect the surface. It was found that temperatures above 1450 °C in 200mbar of hydrogen result in pitting of the surface, whereas etch temperatures at and below 1450 °C can result in atomically flat terraces of ~1 ?m. Following the hydrogen etch optimization, a systematic study of argon-mediated graphene growth was carried out by varying temperature and pressure. By performing simultaneous growth on the 4H and 6H substrates, it was found that subtle differences in substrate properties can lead to drastic differences in graphene growth morphology and thickness. However, for all of the films the graphene was found to have non-uniform thickness. Further, x-ray photoelectron spectroscopy and low energy electron microscopy measurements reveal that trace amounts of oxygen that may be present during growth significantly affect the graphene growth process. Recent results will be discussed.

9552-35, Session 5

Theoretical insights into multibandgap hybrid perovskites for photovoltaic applications (Invited Paper)

Jacky EVEN, Daniel SAPORI, Laurent PEDESSEAU, Alain ROLLAND, Institut National des Sciences Appliquées de Rennes (France); Mikaël KEPENEKIAN, CNRS, Institut des Sciences Chimiques de Rennes (France); Roberto Robles, ICN2 - Institut Catala de Nanociencia i Nanotecnologia (Spain); Shijian Wang, Yong Huang, Alexandre Beck, Olivier Durand, Institut National des Sciences Appliquées de Rennes (France); Claudine KATAN, CNRS, Institut des Sciences Chimiques de Rennes (France)

In this review, we examine recent theoretical investigations on 3D [1] and layered hybrid perovskites (HOP) [2] that combine classical solid-state physics concepts and density functional theory (DFT) simulations as a tool for studying their exceptional photovoltaic and optoelectronic properties. Such an approach allows one to define a new class of semiconductors, where the pseudocubic high temperature perovskite structure plays a central role. A general symmetry analysis of electronic Bloch states, lattice strain, molecular rotations and optical phonons yield new insight into the influence of lattice distortions, including loss of inversion symmetry, as well as spin-orbit coupling. Electronic band folding and degeneracy, phase transitions, effective masses, carrier transport and optical absorption are analyzed. Screening mechanisms related to thermally activated molecular rotations are important for room temperature optical and transport properties of 3D HOP. Concepts of Bloch and envelope functions, as well as confinement potential are discussed. Dielectric confinement in layered HOP is determined and compared to the one in colloidal nanoplatelets [3]. A new method for the numerical computation of dielectric constant and selfenergy profiles is proposed. Non-radiative Auger effects are analyzed for the first time close to the electronic band gap of 3D hybrid perovskites. The new theoretical concepts will be compared to recent experimental investigations on the excitonic properties of both 3D and layered HOP [4].

[1] J. Even, et al, J. Phys. Chem. Lett. 4, 2999 2013 Phys. Status Solidi Rap. Res. Lett. 8, 31 2014 J. Phys. Chem. C, 118, 11566 2014 C Katan et al J. of Mat. Chem. A, DOI: 10.1039/C4TA06418F

[2] J. Even, et al, Phys. Rev., B 86, 205301 2012 Chem. Phys. Chem. 15, 3673 2014

[3] R. Benchamekh, et al Phys. Rev. B, 89, 035307 2014 J. Even et al Phys. Chem. Chem. Phys., 16, 25182 2014

[4] H.-H. Fang, el al. Adv. Func. Mat., DOI: 10.1002/adfm.20140442 G. Lanty, et al. J. Phys. Chem. Lett. 5, 3958 2014

9552-36, Session 5

High aspect ratio CNT structures produced by energetic ion bombardment

Gregory A. Konesky, National Nanotech, Inc. (United States)

Earlier research has sought to utilize the exceptional thermal conductivity of CNTs to produce a heat spreader by bulk cross-linking the CNTs into an interpenetrating network. An isotropic thermal conductivity of 2150 W/m-K was measured in a 5 ?m thick MWCNT film which had been subject to argon ion bombardment with an ion energy of 4 keV and a fluence on the order of 10^17 ions/cm2. While energetic ions will randomly bombard the entire CNT network, on occasion, one will strike a junction where two or more CNTs are touching, momentarily disrupting them. CNTs have the remarkable ability to self-heal, and in doing so, the disrupted junction self-heals into a new interpenetrating junction. However, practical heat spreader applications require films at least 100 times thicker than this initial demonstration. In an attempt to achieve this, substantially higher ion energies and fluence were applied. But rather than forming interpenetrating junctions deeper into the bulk of a CNT thick film, an interesting new form of high aspect ratio structure results, where groups of CNTs are now vertically aligned, even though the original CNT thick film was randomly oriented. There is also a sharp transition at the base of these structures from the new aligned form to the original randomly oriented form. We consider various aspects of ion-induced sputter dynamics coupled to the growth processes of CNTs to account for these new aligned high aspect ratio structures. The role of ion channeling within and between CNTs is also considered.

9552-37, Session 5

Synthesis of large-size graphene by chemical vapor deposition

Ruizhe Wu, Yao Ding, Lin Gan, Zhengtang Luo Luo, Hong Kong Univ. of Science and Technology (Hong Kong, China)

The major obstacle for graphene application is the difficulty to obtain graphene of large size while retain the long range structural order. To synthesis single crystal graphene with large dimension, we developed multiple strategies to enlarge the graphene size by controlling the nucleation density during the initiation stage of chemical vapor deposition processes, or through continued growth. Electron diffraction and Raman mapping measurement show that the graphene flakes are single crystal in nature. Electron transport measurement in Hall bar configuration demonstrate that the graphene exhibit high carrier mobility and exceptional electronic properties. Our method allows the production of high quality graphene film of long range electronic connectivity and structure coherence.

9552-38, Session 5

Nanoscale thermocapillarity enabled purification for horizontally aligned arrays of single-walled carbon nanotubes (Invited Paper)

Sung Hun Jin, Incheon National Univ. (Korea, Republic of)

Among the remarkable variety of semiconducting nanomaterials that have been discovered over the past two decades, single-walled carbon nanotubes remain uniquely well suited for applications in high-performance electronics, sensors and other technologies. The most advanced opportunities demand the ability to form perfectly aligned, horizontal arrays of purely semiconducting, chemically pristine carbon nanotubes. Here, we present strategies that offer this capability. Nanoscale thermos-capillary flows in thin-film organic coatings followed by reactive ion etching serve as highly efficient means for selectively removing metallic carbon nanotubes from electronically heterogeneous aligned arrays grown on quartz substrates. The



low temperatures and unusual physics associated with this process enable robust, scalable operation, with clear potential for practical use.

Especially for the purpose of selective joule heating over only metallic nanotubes, two representative platforms are proposed and confirmed. One is achieved by selective joule heating associated with thin film transistors with partial gate structure. The other is based on a simple, scalable, large-area scheme through microwave irradiation by using micro-strip dipole antennas of low work-function metals. In this study, based on purified semiconducting SWNTs, we demonstrated field effect transistors with mobility (> 1,000 cm^2/Vsec) and on/off switching ratio (~10,000) with current outputs in the milliamp range. Furthermore, as one demonstration of the effectiveness over large area-scalability and simplicity, implementing the micro-wave based purification, on large arrays consisting of ~20,000 SWNTs completely removes all of the m-SWNTs (~7,000) to yield a purity of s-SWNTs that corresponds, quantitatively, to at least to 99.9925% and likely significantly higher.

9552-6, Session PWed

Study of SWCNT functionalization by means of SERS

Justinas Ceponkus, Martynas Velicka, Milda Pucetaite, Jorinta Jakubauskaite, Valdas Sablinskas, Vilnius Univ. (Lithuania)

Raman spectroscopy is known to provide information about the quality of the SWCNT's. The information is based on the intensity ratio of D and G spectral modes and the frequency of RBM modes. However due to resonance nature of Raman spectrum of the nanotubes this method is not suitable to detect functionalization of the nanotubes.

Surface enhanced Raman spectroscopy (SERS) is known to enhance the Raman bands up to fourteen orders of magnitude. The use of this technique provides possibility to detect even small amounts of chemical groups attached to the SWCNT. Enhancement effect of particular spectral band in the SERS spectra strongly depends on the strength of adsorption of molecule under studies on the metal particle as well as on the distance of particular chemical group from the metal surface. Since preferable adsorption sites of the functionalized nanotube are the functional groups, SERS technique allows detecting small amounts of functional groups despite strong resonance Raman from backbone of SWCNT.

In this study COOH functionalized nanotubes were dispersed in silver colloid and dried on the standard silver plate for Raman measurements.

Spectra of SWCNT without colloid in the spectral range between 50 and 1800 cm-1 exhibit only three main spectral features: G band at 1590 cm-1, D band at 1350 cm-1, and RBM modes between 200 and 400 cm-1. Spectra of SWCNT with the colloid exhibit several additional spectral bands which do not belong to the colloid. These bands attributed to vibrations of C-C-O, C-C and C-O from the functional groups and the carbon atom of the SWCNT attached to the corresponding group. The bands associated with the vibrations involving O atom is an indication that silver nanoparticles interact with the functional group attached to SWCNT.

9552-39, Session PWed

Use of carbon nanotubes as an anti-icing and de-icing material for aircrafts

Ashwin Kumar Kuchibhotla, Kumar Ravi, Badrinath Vadakkapattu Canthadai, B. V. Reddi, Esakkimuthuraju Murugan, Vidya Jyothi Institute of Technology (India)

Anti-icing and De-icing of aircrafts efficiently is essential and also a major concern for safe operation of a flight.

Traditional methods of anti-icing and de-icing of aircrafts such as heating, deicer boot and deicing fluids make use of salts, waxes and fluids which are toxic to the soil and harm aquatic life. These need to be done every time before take-off. The use of carbon nanotubes delivers significant performance improvements. However, the applicability of this technique has

not yet been evaluated.

We propose a novel idea which incorporates the use of carbon nanotubes as an anti-icing and de-icing material.

This paper describes the synthesis of carbon nanotubes by carbon vapor deposition process which is used to create a super hydrophobic coating to be coated on the surface of different aircraft parts. It repels the water by reduction of surface energy and prevents formation of ice on the aircraft.

The results of this study introduce the concept of super hydrophobic coatings of carbon nanotubes which may provide an improvised method of anti-icing and de-icing.

9552-42, Session PWed

Synthesis and characterization of covalently bound benzocaine graphite oxide derivative

Ahmad Kabbani, Lebanese American Univ. (Lebanon); Mohamad Kabbani, Rice Univ. (United States); Khadija Safadi, Beirut Arab Univ. (Lebanon)

(Graphite oxide (GO) derived materials include chemically functionalize or reduced graphene oxide (exfoliated from GO) sheets, assembled paperlike forms, and graphene-based composites Due to the attached oxygen functional groups, GO was used to prepare different derivatives which result in some physical and chemical properties that are dramatically different from their bulk counterparts. The present work discusses the covalent cross linking of graphite oxide to benzocaine or ethyl ester of para-aminobenzoic acid, structure I, used in many over-the-counter ointment drug. Synthesis is done via diazotization of the amino group. The product is characterized via IR, Raman, X-ray photoelectron spectroscopy as well as electron microscopy.

Conference 9553: Low-Dimensional Materials and Devices



Wednesday - Thursday 12-13 August 2015 Part of Proceedings of SPIE Vol. 9553 Low-Dimensional Materials and Devices

9553-1, Session 1

Using electric field manipulation to fabricate nanoscale fibers on large areas: a path to electronic and photonic devices (Invited Paper)

Jack L Skinner, Montana Tech (United States)

Traditional fabrication methods used for the integrated circuit (IC) and the microelectromechanical systems (MEMS) industry have been developed specifically for two-dimensional fabrication on planar surfaces. While electrospinning (ES) has been in existence for over 100 years, its full potential as a fabrication technology has not been reached. ES is not currently being used for commercial fabrication of electronic or photonics devices. The focus of this presentation is on computational and experimental methods focused on spatial fiber control with the aim of expediting the adoption of ES as a common-place fabrication method.

Both analytical and numerical methods are used for modeling fiber deposition. Forces leading to fiber formation and deposition are modeled by integrating the electrostatic force acting on the fiber within a circular area at an elevation 1 mm above the collection plate. A shape function is used to estimate the electrostatic field distribution for the surface integral. Experimental depositions of fibers with nominal sizes of 100 nm were compared with analytical results with reasonable agreement. COMSOL Multiphysics was used to estimate the field strength for given configurations of the ES spinneret and collection plate. We also use active field control to align fibers across electrodes and passive electrostatic lenses to confine the electrostatic field to achieve control over fiber deposition. Applications of our fibers range from being directly used as sensors or in subsequent pattern transfer. The strength of ES as a fabrication technology is in rapid patterning of nanoscale features over large areas with inexpensive materials.

9553-2, Session 1

Structural modulation of nanowire interfaces grown over selectively disrupted single crystal surfaces

Elias J Garratt, Babak Nikoobakht, National Institute of Standards and Technology (United States)

Recent breakthroughs in deterministic approaches to the fabrication of nanowire arrays have demonstrated the possibility of fabricating such networks using low-cost scalable methods. In this regard, we have developed a scalable growth platform for lateral fabrication of nanocrystals with high precision utilizing lattice match and symmetry. Using this planar architecture, a number of homo- and heterostructures have been demonstrated including ZnO nanowires grown over GaN. The latter combination produces horizontal, epitaxially formed crystals aligned in the plane of the substrate containing a very low number of intrinsic defects. We use such ordered structures as model systems in the interests of gauging the interfacial structural dynamics in relation to external stimuli. Using nanosecond pulses of focused ion beams to slightly modify the substrate surface and selectively form lattice disorders in the path of nanowire growth, we examine the nanocrystal, namely: its directionality and lattice defects. High resolution electron and cathodoluminescence microscopies are used to reveal some interesting optical and structural effects; for instance, a minimum threshold of surface defects that can divert nanowires. We also discuss data indicating formation of surface strains and show their mitigation during the growth process as well as high tolerance of such epitaxial systems to the imposed artificial defects.

9553-3, Session 1

Integrated vapor-liquid-solid silicon mass sensors (Invited Paper)

Brian A Bryce, NIST (United States); Jason J. Gorman, National Institute of Standards and Technology (United States); Sergiy Keylyuk, National Institute of Science and Technology (United States); Albert Davydov, NIST (United States)

No Abstract Available

9553-4, Session 1

Silicon-Germanium epitaxy for radial nanowire heterostructures (Invited Paper)

Yung-Chen Lin, Jinkyoung Yoo, Los Alamos National Lab. (United States)

Radial epitaxy enables researchers to modulate composition in nanostructures along radial direction precisely. Radial nanowire heterostructures have been considered as suitable building blocks for electronic and photonic devices with three-dimensional architectures for transistors, photovoltaic devices, and energy storages. From the perspective of fundamental understanding o materials behavior radial heterostructure is very interesting platform to study strain relaxation since defect formation in nanowire heterostructure can be occurred in both core and shell regions. Here we report the observation of cross-over of defect formation region from shell to core in silicon (Si)/germanium (Ge) core/shell NW heterostructures, which are technologically important nanomaterials. We observed that stacking faults primarily nucleated around Si/Ge interface and extended to the Ge shell. As the Ge shell thickness increases, stacking faults can be found in the Si core. Furthermore we will discuss the carrier transport characteristics of Si/Ge radial heterostructures with various growth sequences.

9553-5, Session 1

On the MOVPE growth and properties of device-quality GaAs-AlGaAs core-(multi) shell nanowire structures (Invited Paper)

Paola Prete, Istituto per la Microelettronica e Microsistemi (Italy); Nico Lovergine, Univ. del Salento (Italy)

No Abstract Available

9553-6, Session 1

Absorption enhancement and carrier diffusion in single lead sulfide nanowire Schottky solar cells (Invited Paper)

Yiming Yang, Xingyue Peng, Steven Hyatt, Dong Yu, Univ. of California, Davis (United States)

Light trapping in sub-wavelength semiconductor nanowires (NWs) offers a promising approach to simultaneously reducing material consumption and enhancing photovoltaic performance. Nevertheless, the absorption efficiency of a NW, defined by the ratio of optical absorption cross section

Conference 9553: Low-Dimensional Materials and Devices



to the NW diameter, lingers around 1 in existing NW photonic devices, and the absorption enhancement has suffers from a narrow spectral width. The degree of absorption enhancement is expected to substantially scale up with material refractive indices. Here, we show that the absorption efficiency can be significantly improved in NWs with higher refractive indices, by an direct experimental observation of up to 350% external quantum efficiency (EQE) in lead sulfide (PbS) NW resonators, a 3-fold increase compared to Si NWs. Furthermore, broadband absorption enhancement is achieved in single tapered NWs, where light of various wavelengths is absorbed at segments with different diameters analogous to a tandem solar cell. Overall, the single NW Schottky junction solar cells benefit from optical resonance, near bandgap open circuit voltage, and long minority carrier diffusion length, demonstrating power conversion efficiency (PCE) comparable to single Si NW coaxial p-n junction cells, but with much simpler fabrication processes.

9553-7, Session 2

Ordered arrays of bottom-up III-nitride core-shell nanostructures (Invited Paper)

Daniel F. Feezell, Ashwin K. Rishinaramangalam, Rhett Eller, Saadat Mishkat Ul Masabih, Michael Fairchild, Darryl M. Shima, Ganesh Balakrishnan, Steven R. J. Brueck, The Univ. of New Mexico (United States)

III-nitrides are the preferred materials for high-brightness light-emitting diodes (LEDs) for solid-state lighting and diode lasers for high-density optical data storage. However, III-nitrides grown on the conventional polar c-plane using sapphire substrates suffer from polarization-related electric fields and high dislocation densities. Growth on nonpolar/semipolar freestanding GaN substrates is one option to address these issues, although the high costs associated with this approach are a concern. Another option is to realize nonpolar/semipolar active regions using nanoscale bottom-up selective-area epitaxy (SAE) on sapphire substrates. The SAE technique results in three-dimensional GaN nanostructure cores with large nonpolar/ semipolar surface areas and low dislocation densities on inexpensive substrates. Subsequent growth of InGaN shells on the core templates can be used to fabricate nonpolar/semipolar quantum-well active regions. In this work, we use bottom-up SAE and catalyst-free metal organic chemical vapor deposition (MOCVD) to fabricate ordered arrays of various core-shell nanostructures, including GaN-InGaN nanowalls, pyramidal nanostripes, and nanowires. Scanning electron microscopy, cross-sectional transmission electron microscopy, and micro-photoluminescence are utilized to examine the dependence of geometry, surface morphology, and guantum-well emission on epitaxial growth conditions. Progress toward applying these nanostructures to electrically injected LEDs for solid-state lighting and nanophotonics will also be discussed.

9553-8, Session 2

Interfacial reactions of gold and tolerance of nanoscale heterojunctions to crystal disorder in surface-directed vapor-liquidsolid growth of nanocrystals (Invited Paper)

Babak Nikoobakht, National Institutes of Standards and Technology (United States)

No Abstract Available

9553-9, Session 2

Consequences of quantum size effects in 2D and 1D nano-epitaxy (*Invited Paper*)

Bene Poelsema, University of Twente (Netherlands)

No Abstract Available

9553-10, Session 2

Understanding and controlling III-V nanowire growth at the atomic scale (Invited Paper)

Jerry Tersoff, IBM Watson Research Center (United States)

No Abstract Available

9553-11, Session 3

Template-assisted synthesis of III-nitride and metal-oxide nano-heterostructures using low-temperature atomic layer deposition for energy, sensing, and catalysis applications (Invited Paper)

Necmi Biyikli, Cagla Ozgit-Akgun, Hamit Eren, Ali Haider, Tamer Uyar, Fatma Kayaci, Mustafa Ozgur Guler, Ruslan Garifullin, Ali K. Okyay, Gamze M. Ulusoy, Eda Goldenberg, Bilkent Univ. (Turkey)

Recent experimental research efforts on developing functional nanostructured III-nitride and metal-oxide materials via low-temperature atomic layer deposition (ALD) will be reviewed. Ultimate conformality, a unique propoerty of ALD process, is utilized to fabricate core-shell and hollow tubular nanostructures on various nano-templates including electrospun nanofibrous polymers, self-assembled peptide nanofibers, metallic nanowires, and multi-wall carbon nanotubes (MWCNTs). III-nitride and metal-oxide coatings were deposited on these nano-templates via thermal and plasma-enhanced ALD processes with thickness values ranging from a few mono-layers to 40 nm.

Metal-oxide materials studied include ZnO, TiO2, HfO2, ZrO2, and Al2O3. Standard ALD growth recipes were modified so that precursor molecules have enough time to diffuse and penetrate within the layers/pores of the nano-template material. As a result, uniform and conformal coatings on high-surface area nano-templates were demonstrated. Substrate temperatures were kept below 200C and within the self-limiting ALD window, so that temperature-sensitive template materials preserved their integrity III-nitride coatings were applied to similar nano-templates via plasma-enhanced ALD (PEALD) technique. AIN, GaN, and INN thinfilm coating recipes were optimized to achieve self-limiting growth with deposition temperatures as low as 100C. BN growth took place only for >350C, in which precursor decomposition occured and therefore growth proceeded in CVD regime. III-nitride core-shell and hollow tubular single and multi-layered nanostructures were fabricated.

The resulting metal-oxide and III-nitride core-shell and hollow nano-tubular structures were used for photocatalysis, dye sensitized solar cell (DSSC), energy storage and chemical sensing applications. Significantly enhanced catalysis, solar efficiency, charge capacity and sensitivity performance are reported. Moreover, core-shell metal-oxide and III-nitride materials showed promise to be used in applications where flexibility is critical like functional membranes, textile and flexible electronic applications.

9553-12, Session 3

Simultaneous optical and structural investigation of nanomaterials and nanostructures for LEDs (Invited Paper)

Marcus Mueller, Otto-von-Guericke Univ. Magdeburg (Germany); Frank Bertram, Gordson Schmidt, Jürgen Christen, Otto-von-Guericke-Univ. Magdeburg (Germany)

In the past few years, tremendous progress has been achieved on epitaxial growth and processing of group III nitride nano- and microrods. Furthermore, these growth improvements have allowed the fabrication of optoelectronic devices based nanorods as active elements, i.e. light emitting diodes (LEDs). However, their efficiency is still far behind the performance of conventional GaN-based light emitting diodes.

The controlled growth of GaN nanorods offers a potential benefit for achieving higher efficiencies of III-Nitride based optoelectronic devices due to a high surface to volume ratio. Nanorods have a very large active area compared to their footprint. Since the active region is wrapped around the three-dimensional core (for core shell structures), the active layer scales with the rod's aspect ratio (i.e. the ratio of height and diameter). Therefore, by controlling their density, diameter and height, a tremendous increase of active surface can be achieved. Additionally, the low defect density in nanorods allows the characterization of single extended defects which is of high interest for a clear understanding of the formation of these defects.

In this study we present a direct nano-scale correlation of the optical properties with the actual real crystalline structure of single GaN nanorods using low temperature CL spectroscopy in a scanning transmission electron microscope (STEM). We concentrate on the crystalline quality, local In incorporation, n- and p-layer quality and defects of the complete structures.

9553-13, Session 3

Sonochemically grown 1D ZnO nanostructures and their applications (Invited Paper)

Yavuz Bayam, Gediz Univ. (Turkey); Debora Rodrigues, Univ. of Houston (United States); Rukayya K. Bala, Gediz Üniv. (Turkey); Tugba O. Okyay, Univ. of Houston (United States); Enis E. Tural, Sinem Duyar, Gediz Üniv. (Turkey)

Upon irradiation of liquid with high intensity of sound, the alternate expansion and compression of the acoustic wave create bubbles. These bubbles oscillate and accumulate ultrasonic energy and grow until they reach an unstable size. They eventually collapse and release the concentrated energy stored. The implosive collapse of bubbles generate a hot spot with very high temperature of 5000 K and pressure of 1000 atm, with high heating and cooling rate above 1010 K/s. This phenomenon causes high energy chemical reactions within a short time.

ZnO nanorods of different size were synthesized by sonochemical method. The long sonication period at the maximum amplitude produced the best result, with ZnO nanorods densly grown on the substrate.

The surface morphology, crystal structure and elemental analysis of the grown nanorods sample were observed by optical microscope, SEM, EDS and Raman Spectroscopy.

The antibacterial properties of the sonochemically synthesized ZnO nanorods toward E.coli and B.subtilis was investigated. It was found that the sample sonicated for long period at the maximum amplitude exhibited the highest antibacterial properties.

Gas sensing measurements of sonochemically grown ZnO nanorod network in between Au interdigitated electrodes were carried out for the gas sensing characterization. The gas sensing measurements were carried out for two oxidizing gases (O2 and CO2) and five reducing gases (CO, C2H5OH, C3H7OH, CHCI3, CH2CI2). Same device has also been utilized and tested as humidity sensor. The results suggest that sonochemical method is a very good candidate for production of high performing, low cost gas and humidity sensors.

9553-14, Session 4

Imaging local electrical and optical responses in nanostructured devices (Invited Paper)

Marina S. Leite, Univ. of Maryland, College Park (United States)

SPIE. PHOTONICS

NANOSCIENCE+ ENGINEERING

If one had the option to resolve the local electrical and optical responses of nanostructured devices at the nanometer scale, this would enable unprecedented correlation between the structural properties of materials and carriers' recombination and collection, allowing for the design of next generation devices with improved performance. Currently, macroscopic electrical and optical characteristics of low-dimensional systems is very well understood, however, a direct correlation between the local electrical and optical responses is still missing. Here we combine scanning probe microscopy techniques to map the voltage and the current generated by optoelectronic devices. By implementing a variant of Kelvin probe force microscopy (KPFM) we map the open-circuit voltage (Voc) of working devices with spatial resolution < 100 nm by measuring the difference between the contact potential difference under illumination and in the dark, which is equal to the photo-generated voltage of the device (and is proportional to the Fermi level splitting). By applying scanning photocurrent microscopy we image local variations in photocurrent, also with nanoscale resolution. We combine these methods to resolve recombination and collection within polycrystalline devices with high spatial resolution. Moreover, we quantify the contribution of (i) increased scattering, (ii) field enhancement, and (iii) waveguiding to solar cells' performance improvement caused by metallic nanostructures. We decorate the solar cells with noble metal and alloved nanoparticles, and spectrally resolve the effect of scattering enhancement, and the waveguiding contribution by varying the periodicity of the NPs array, and measuring the local changes in Voc as a function of wavelength.

9553-15, Session 4

Latest advances in low-cost solar water splitting nanodevices (Invited Paper)

Lionel Vayssieres, Xi'an Jiaotong Univ. (China)

The demand of low cost materials has become one of the major challenges scientists face to address critical contemporary issues such as sustainable energy sources. For instance, one of the promising alternatives for the transition of fossil fuel-based energy to a clean and renewable technology relies on the widespread implementation of solar-related energy systems, however, the high cost of energy production poses an intrinsic limitation. In this context, low cost materials development is required to balance the necessary increase in power generation and conversion efficiency and the costs of implementation and operation. Furthermore, a better comprehensive understanding of materials growth and properties relationships using quantum confinement and nanoscale strategies to raise the theoretical limits by changing the fundamental physics and chemistry is the key to success. Such ideas will be demonstrated by the thermodynamic modeling and low-cost design of crystalline arrays of quantum rods- and dots-based oxides with controlled orientation, size, and shape onto various substrates at nano-, meso-, and micro-scale by aqueous chemical growth at low-temperature. Tailored dimensionality effects on their surface chemistry, electronic structure, and energetics for a low cost and sustainable generation of hydrogen from the two most abundant and geographicallybalanced free resources available on this planet, that is the sun and seawater will also be presented.

9553-16, Session 4

Thermoelectric pellets made of Si nanowires

Kate J Norris, Univ of California Santa Cruz (United



States); Gary S Tompa, Nick M Sbrockey, Structured Materials Industries, Inc. (United States); Nobuhiko P Kobayashi, Univ of California Santa Cruz (United States)

No Abstract Available

9553-17, Session 5

Resonant spectroscopy of individual CdSe quantum dots containing single Mn2+ ions in (Zn,Cd)Se barrier

Justyna Piwowar, Wojciech Pacuski, Tomasz Smolenski, Mateusz Goryca, Aleksander M. Bogucki, Andrzej Golnik, Piotr Kossacki, Jan Suffczynski, Univ. of Warsaw (Poland)

We present design, a Molecular Beam Epitaxy growth, and results of polarization resolved, resonant spectroscopy of CdSe Quantum Dots (QDs) embedded in Zn1-xCdxSe (x up to 30%) barrier, innovative with respect to, e.g, our previous studies[1-2].

Micro-Photoluminescence at 1.7 K-300 K temperatures range reveals the QDs energy emission shifted to 1.9 - 2.3 eV from 2.3 - 2.5 eV, proper for CdSe QDs in ZnSe barrier. A typical pattern of excitonic emission spectrum of a single CdSe/(Zn,Cd)Se QD is determined.

Photoluminescence Excitation (PLE) measurements on individual QDs are performed using a tunable Rhodamine 590 dye laser operating at 2.05-2.20 eV as the excitation source. Sharp (FWHM down to 200 ueV) maxima are found in PLE spectra, reflecting the resonant transfer of photoexcitation to the emitting QD state. Effects of optical control of confined exciton spin[2] are studied through polarization resolved PLE. In particular, transfer of optical polarization between absorbing and emitting states with 18% efficiency is found.

The CdSe/(Zn,Cd)Se QDs are suitable for implementation as temperature robust non-classical light sources or as building blocks for lasers operating at the short wavelength transmission window of plastic optical fibers. Incorporation of single Mn2+ ions makes them promising for efficient optical single ion spin orientation. The QD transitions energy below energy of Mn2+ ion internal transition (2.1 eV) is beneficial for high quantum yield of magnetooptical devices involving CdSe/(Zn,Cd)Se QDs doped with many Mn2+ ions.

[1] J. Kobak et al., Nature Communications 5, 3191 (2014).

[2] T. Smole?ski et al., accepted to Physical Review B

9553-18, Session 5

Photoluminescence study of the increased hole confinement in CdTe quantum dots

Malgorzata M. Pilat, Univ. of Warsaw (Poland); Lukasz Klopotowski, Piotr Wojnar, Krzysztof Fronc, Grzegorz Karczewski, Tomasz Wojtowicz, Jacek Kossut, Institute of Physics (Poland)

At low temperature single CdTe quantum dot (QD) photoluminescence (PL) spectra contains four transitions resulting from the ground state, s-shell carriers recombination: the neutral exciton (XO), positively and negatively charged excitons (X+ and X-, respectively), and the biexciton (2X). With increasing temperature these PL peaks redshift, broaden, and decrease the intensity. The redshift is related to the bandgap shrinkage, while increased exciton-acoustic phonon coupling results in peaks broadening. The quenching of the PL intensity comes from thermal activation of carriers to other QDs or to excited states within the same dot.

To define the confinement conditions in the conduction and valence band separately we investigated the influence of temperature on particular charge state (X+ and X-). For CdTe QDs in ZnTe barriers, we find that the PL vanishes at about 65 K. Importantly, we observe decreasing of the normalized X+ intensity, while the X- intensity remains approximately constant. On the contrary, for CdTe QDs in ZnMgTe barriers, the PL is visible up to 115 K and the decrease of the normalized X+ intensity is substantially slower. These results point out that Mg incorporation in the barrier increases the hole confinement along the growth axis. As a consequence, the hole states are moved further apart in energy compared to those in CdTe dots in ZnTe barriers, inhibiting the thermal activation of s-shell carriers to excited states. Our result demonstrate that a proper design of the valence band structure should lead to room temperature emission from CdTe QDs.

9553-19, Session 5

HgTe colloidal quantum dot LWIR infrared photodetectors

Richard E. Pimpinella, Anthony Ciani, Sivananthan Labs., Inc. (United States); Philippe Guyot-Sionnest, The Univ. of Chicago (United States); Christoph H. Grein, Univ. of Illinois at Chicago (United States)

The majority of modern infrared imaging devices are based on epitaxially grown bulk semiconductor materials. Colloidal quantum dot (CQD) based infrared devices provide great promise for significantly reducing cost as well as significantly increased operating temperatures of infrared imaging systems. In addition, CQD based infrared devices greatly benefit from band gap tuning by controlling the CQD size rather than the composition. LWIR Photoresponsive thin films were fabricated by synthesizing HgTe quantum dots through colloidal synthesis similar to the fabrication process for MWIR HgTe CQDs [1,2]. We will describe the optical response of the HgTe CQD in the 8-12 μ m cutoff range as a function of temperature.

[1] Lhuillier, E., Keuleyan, S., Zolotavin, P. and Guyot-Sionnest, P. Adv. Mater., 25: 137–141 (2013)

[2] Sean Keuleyan, Emmanuel Lhuillier, Vuk Brajuskovic, Philippe Guyot-Sionnest. Nature Photonics 5, 489–493 (2011)

9553-20, Session 5

Novel quantum dot cascade laser

Ning Zhuo, Feng-Qi Liu, Institute of Semiconductors (China)

Quantum cascade lasers are semiconductor laser sources based on intersubband transitions in multiple quantum well systems. Their unique operation principle and good performance have established themselves as the leading tunable coherent semiconductor source in the infrared and terahertz ranges of the electromagnetic spectrum. In principle, such lasers are restricted in broad tunability, surface emission, and high wallplug efficiency. Theoretical works have predicted that these issues can be raveled out in a quantum dot cascade laser, in which quantum well active region is replaced by quantum-dot active region. By making use of self-assembled quantum dots in the Stranski–Krastanow growth mode and two-step straincompensation active region design, an unambiguous quantum dot cascade laser based on InAs/InGaAs/InAIAs heterostructure is directly proven.

9553-43, Session PWed

Fatigue analysis of optimized chevron with Z shape arms

Margarita Tecpoyotl-Torres, Ramón Cabello-Ruiz, Jose Gerardo Vera-Dimas, Jose Alfredo Rodriguez-Ramirez, J. Jesús Escobedo-Alatorre, Alejandra Ocampo Díaz, Univ. Autónoma del Estado de Morelos (Mexico)

Micro-Electromechanical Systems have been widely used in military applications, radio frequency systems, pressure sensors, automotive industry, among several others. Due to the diversity and multiple energy domains involved, MEMS devices are vulnerable to several mechanical

Conference 9553: Low-Dimensional Materials and Devices



failures such as fatigue. Most MEMS devices contain moving parts that are subjected to cyclic loading, which degrade device's efficiency. Due to the high importance of MEMS in various applications, it is necessary to know the lifetime of them to prevent any damage or process discontinuity to which the system is subject. There have been several investigations in particular on the fatigue analysis in presence of cracks, however in terms of lifetime under cycling load, information is not abundant. The fatigue analysis can be performed for characterizing the ability of a material to support many cycles that a device component experiences during its usable lifetime. In this paper, a theoretical fatigue analysis of an optimized chevron with Z shape arms is shown. Simulations are made to validate calculations, using Ansys 15.0, to obtain the arms lifetime of the component. Especial attention is given on arms because they are subjected to greater efforts in the presence of cyclic loading.

9553-44, Session PWed

Structural and electrical properties of zinc oxide doped with aluminium oxide thin films prepared via atomic layer deposition

Baojun Yan, Shulin Liu, Institute of High Energy Physics (China)

Zinc oxide (ZnO) doped with aluminum oxide (Al2O3) and pure Al2O3 thin films were grown on Si (100), quartz and porous substrates by atomic layer deposition at 200°C using diethylzinc, trimethylaluminium, and deionized water as precursors. All prepared samples thicknesses are varied nominally from 80 nm to 250 nm with a varying number of alternating ZnO and Al2O3 layers. Samples thickness and ellipsometric spectra were measured using a spectroscopic ellipsometer (SE), and the parameters determined by computer simulation matched with the experimental results well. The morphologies of all samples were clearly shown by scanning electron microscopy (SEM). The element distribution measured by energy dispersive x-ray (EDX) was evenly distributed implied the film composition is uniform. The data from x-ray diffraction (XRD) suggest that layer growth appears to be substrate sensitive and film thickness and deposition temperature also have influences on the crystallization of films. The surface chemical states of deposited samples were investigated by x-ray photoemission spectrum (XPS) and the results show the carbon atom contamination is apparent in the films growth which has probably severe influence on the electrical properties. The effects of nano oxide thin film thicknesses on the electrical properties of samples prepared on porous substrate were studied. Before electrical measurement, electrodes were fabricated by electron beam evaporation method firstly. By applied high direct voltages (DC 800 V) on the two ends of the samples measured at vacuum condition, the I-V curves and resistances can be obtained precisely. The resistance jitter phenomenon of samples was observed and we proposed a current transport model within the oxide layers to elucidate the experimental phenomenon.

9553-45, Session PWed

Charge trapping and recombination in Ge nanoislands grown on Si (001)

Anastasiia A. Mykytiuk, Sergey V. Kondratenko, National Taras Shevchenko Univ. of Kyiv (Ukraine); Yu. N. Kozyrev, Chuiko Institute of Surface Chemistry (Ukraine); Volodymyr S. Lysenko, V.E. Lashkaryov Institute of Semiconductor Physics (Ukraine)

In nanosize semiconductor heterostructures quantum size effects can result in changes of the electron spectrum.

In our sample Ge was deposited on boron doped p-Si(100) substrate with temperature of 600 degrees centigrade. For in-plane photoconductivity studies ohmic contacts were formed by annealing of Au at 370 degrees centigrade into the planar surface normal to the epitaxial layers.

Transient in-plane photocurrent of the Ge-Si heterostructure with Ge nanoislands on p-Si (001) upon exposing with different photon energies

at 120 K were studied. When only nanoislands were excited we observed a comparably fast relaxation. When the temperature drops to 120 K the long-term relaxation of the photocurrent is observed.

Using the Kelvin probe method we recorded the fluctuations of the electrostatic potential in the Si-Ge heterostructures with Ge nanoclusters.

It was shown that Ge nanoislands can accumulate positive charge, which affects the contact-potential difference (CPD) within the nanoisland by varying it by 5 to 10 mV depending on the size of the nanoisland. The CPD increases with the increasing of the nanoisland diameter.

The recombination efficiency of the electron-hole pairs involving quantum confinement states in nanoislands is higher in comparison with the rate of recombination of the carriers photogenerated in Si substrate. It was found that when we have selective photoexcitation, recombination of electron-hole pairs in SiGe nanoislands is defined by spatial separation of nonequilibrium charge carriers, when the holes are captured in the valence band states of SiGe nanoislands and electrons are in silicon environment.

9553-46, Session PWed

Logic gates based on nonlinear light interaction in subwavelength discrete systems

Gregorio Mendoza González, Erwin A. Martí Panameño, Benemérita Univ. Autónoma de Puebla (Mexico)

We study the dynamics of nonlinear propagation and interaction of two optical fields in arrays of dielectric subwavelength waveguides of circular and square cross section. Applying the finite difference time-domain method, we numerically solve the Maxwell's equations considering real values for the constitutive relations. The arrays under study are formed by a finite number of parallel waveguides with identical parameters: a subwavelength dimension in cross section, Kerr nonlinearity, length of tens of micrometers and the separation between the waveguides is constant. In our study, we focus on the determination of specific values of the physical parameters before mentioned, to obtain light self-trapping. For this, we also determine the properties of the incident optical fields: complex amplitude, wavelength, angle of incidence and phase difference. As a result we observe the dependence of the total energy output to the parameters of phase difference and angle of incidence. This allows us to conclude about the possibility to control the nonlinear interaction properties of two optical fields, generating a single output beam, whose position can be controlled by the selection of the system parameters. These results allow us to reproduce the behavior of an AND gate.

9553-47, Session PWed

Raman spectroscopy studying of guanajuatite (Bi2Se3): natural topological insulator

Malgorzata M. Pilat, Katarzyna Golasa, Magdalena Grzeszczyk, Adam Babinski, Univ. of Warsaw (Poland)

Topological insulators are a new class of materials which are semiconducting in bulk but conducting on their surface. One of its representatives is bismuth selenide (Bi2Se3), which occurs naturally as a mineral called guanajuatite. Bi2Se3 has a layered structure consisting of quintuples – alternating monoatomic layers of bismuth and selenium in the stoichiometric ratio. While atoms inside the quintuple are strongly bounded, individual quintuples interact with each other only via relatively weak van der Waals effect. We present micro-Raman spectroscopy studies of the natural Bi2Se3. Four Raman active phonon modes (two each Alg and Eg corresponding to vibrations crosswise and along quintuple respectively) are studied in a wide range of temperature (4-300 K) and the results are compared with spectra obtained on a synthesized material. A linear temperature dependence of active Raman modes energy enables us to determine the first order temperature coefficient of the phonons. Results span the range from 1.01 to 1.71 cm-1/K depending on the mode, which is in accord with previous



works on Bi2Se3. It is shown that the widths of the observed Raman peaks in guanajuatite are similar to the corresponding values in the synthesized Bi2Se3 confirming the quality of natural crystals.

9553-21, Session 6

Physics of artificially-engineered AlGaN and InGaN based digital alloys

Wei Sun, Chee-Keong Tan, Nelson Tansu, Lehigh Univ. (United States)

The pursuit of III-Nitride based semiconductor in optoelectronic application has been primarily driven by the attribute of broadband coverage through the use of AIN and INN materials. However, the phase separation in growing high Al/In-content ternary alloy has been one of the largest barriers in applying the application of nitride-based ternary semiconductor. Meanwhile, the large built-in polarization induced by the strain effect within the active region also causes significant charge separation issue. Thus, a new approach in extending the bandgap coverage and suppressing charge-separation in nitride-based alloy needs to be pursued.

In this work, we propose novel artificially-engineered AlGaN and InGaN based digital alloys to overcome the limitations presented by the epitaxy of phase-separated III-Nitride ternary material and the carrier separation issue in the polarized material system. The proposed digital alloy structure is a short period superlattice that is formed by desired thin film alloy layers alternately, in which the thickness of each layer is represented by a number of monolayer (ML). By adjusting the thickness of GaN layer (m ML) and AlN or InN layer (n ML), the Al/In-content and the band structure of AlGaN or InGaN digital alloy can be engineered correspondingly. Due to the usage of thin film GaN and InN/AlN layers, the large quantum coupling and suppressed charge separation could increase the wavefunction overlap of carriers significantly. The use of this digital alloy demonstrated the suitability of this method in extending the bandgap coverage and suppressing charge separation in nitride-based semiconductors.

9553-22, Session 6

Electrical generation and control of valley carrier in monolayer TMDC

Yu Ye, Xiaobo Yin, Univ. of California, Berkeley (United States); Hailong Wang, Institute of Semiconductors (China); Ziliang Ye, Hanyu Zhu, Yuan Wang, Univ. of California, Berkeley (United States); Jianhua Zhao, Institute of Semiconductors (China); Xiang Zhang, Univ. of California, Berkeley (United States)

Electrical control of the flow of charges is at the heart of modern electronics. The spintronics exploits the spin degree of freedom (DOF) of electrons for information processes such as magnetoresistive random-access memory. Recently, the atomic membrane of transition metal dichalcogenides (TMDCs) was found possesses a nonequivalent carrier distribution in crystal momentum valley space, which makes the valley index of electrons a new DOF for information processing. A variety of valleytronic devices such as valley filters and valves have been proposed, and optical valley excitation has been observed. However, to realize its potential in electronics, one has to electrically control of valley DOF, which remains the critical challenge to date. Here, we experimentally demonstrate electrically valley generation and control. Valley polarization is achieved through spin injection via a diluted ferromagnetic semiconductor and measured by the helicity of electroluminescence using the unique spin-valley locking. We also report a new scheme of electronic devices combining both the spin and valley DOFs. Such a direct electrical generation and control of valley carriers opens the new dimension in utilizing both spin and valley for next-generation electronics and computing.

9553-23, Session 6

Optical study of interlayer coupling and stacking-dependent electronic structure in MoS2

Ze-Xiang Shen, Jiaxu Yan, Juan Xia, Zheng Liu, Nanyang Technological Univ. (Singapore)

The optical and electronic structures of two dimensional transition metal dichalcogenide (2DTMD) materials often show very strong layer-dependent properties. Detailed understanding of the inter-layer interaction will help greatly in tailoring the properties of 2D TMD materials for applications. Raman/Photoluminescence (PL) spectroscopy and imaging have been extensively used in the study of nano-materials and nano-devices. They provide critical information for the characterization of the materials such as electronic structure, optical property, phonon structure, defects, doping and stacking sequence.

In this talk, we use Raman and PL techniques to study few-layer MoS2 samples. The Raman and PL spectra show clear correlation with layer-thickness and stacking sequence. Our ab initio calculations reveal that difference in the electronic structures mainly arises from competition between spin-orbit coupling and interlayer coupling in different structural configurations.

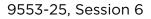
9553-24, Session 6

The role of ultra-thin SiO2 layers in metal-insulator-semiconductor (MIS) photoelectrochemical devices (Invited Paper)

Daniel V. Esposito, Columbia Univ. (United States)

Solid-state junctions based on a metal-insulator-semiconductor (MIS) architecture are of great interest for a number of optoelectronic applications such as photovoltaics, photoelectrochemical cells, and photodetection. One major advantage of the MIS junction compared to the closely related metal-semiconductor junction, or Schottky junction, is that the thin insulating layer (I-3 nm thick) that separates the metal and semiconductor can significantly reduce the density of undesirable interfacial mid-gap states. The reduction in mid-gap states helps "un-pin" the junction, allowing for significantly higher built-in-voltages to be achieved. A second major advantage of the MIS junction is that the thin insulating layer can also protect the underlying semiconductor from corrosion in an electrochemical environment, making the MIS architecture well-suited for application in (photo)electrochemical applications.

In this presentation, discontinuous Si-based MIS junctions immersed in electrolyte are explored for use as i.) photoelectrodes for solar-water splitting in photoelectrochemical cells (PECs) and ii.) position-sensitive photodetectors. The development and optimization of MIS photoelectrodes for both of these applications relies heavily on understanding how processing of the thin SiO2 layer impacts the properties of nano- and micro-scale MIS junctions, as well as the interactions of the insulating layer with the electrolyte. In this work, we systematically explore the effects of insulator thickness, synthesis method, and chemical treatment on the photoelectrochemical and electrochemical properties of these MIS devices. It is shown that electrolyte-induced inversion plays a critical role in determining the charge carrier dynamics within the MIS photoelectrodes for both applications.



Challenges and future perspectives in HVPE-GaN growth (Invited Paper)

Michal Bockowski, Institute of High Pressure Physics (Poland) and TopGaN Ltd. (Poland)

No Abstract Available

9553-26, Session 6

Functional 2-dimensional nanomaterial inks for photonics and (opto)electronics (Invited Paper)

Tawfique Hasan, Univ. of Cambridge (United Kingdom)

Layered nanomaterial crystals with interesting electronic and optical properties are an attractive proposition for flexible photonic and optoelectronic devices. The most widely investigated layered material is graphene, which heralds the possibility of truly flexible and perhaps, transparent electronics. Other graphene-like layered nanomaterials, for example, semiconducting metal dichalcogenides complementary (opto) electronic properties, strengthening the offering from layered materials. Together, graphene and related layered materials thus represent a family of materials attractive for next generation flexible electronic components, devices and systems.

For large area applications, growth of layered materials typically requires high temperature (-1000 C). This is further complicated during their transfer deposition on to the target substrates. An alternative and economic approach is to use inks of exfoliated layers from their chemically untreated bulk crystals. This process can be carried out at room temperature and does not involve harsh chemicals. More importantly, the inks offer device fabrication and integration strategy through different processes, such as polymer composites, digital and lithographic printing as well as roll-to-roll (R2R) and spray coating over large area.

I will discuss several photonic and (opto)electronic applications using graphene, the most established ink platform to date. This will include ultrafast lasers, transistors, hybrid nanomaterial transparent and nontransparent conductors and electrodes on silicon/glass, plastic and paper substrates. I will briefly address other layered material inks and their printability. I will conclude with a short perspective in terms of materials, printing technologies and devices that may evolve from this materials technology platform.

9553-27, Session 7

Synthesis of one-dimentional nanostructures for gas sensing and photovoltaic applications (Invited Paper)

Hakan Karaagac, Elif Peksu, M. Saif Islam, Istanbul Technical Univ. (Turkey)

In recent years, ZnO,(TiO2 and Silicon (Si) nanowires (NWs) have attracted a significant attention due to their unique properties which can be employed for many applications including field ionization gas sensors, photodetectors, and solar cells. In this work, three-dimentional p-n heterojunctions were used for the fabrication of field ionization gas sensors and solar cells. P-Si micro-pillars/ZnO NWs, n-TiO2-nanorod/p-CdTe and n-Si-NW/p-Ag(Ga,In) Se2(AGIS) material combinations were preferred for the construction field-ionization gas sensor, a core-shell and a thin-film embedded type of solar cells, respectively. Well-aligned Si NWs were derived from a silicon (100) wafer by using Ag-assisted electroless etching technique. The synthesized Si-NWs embedded into a sputter deposited chalcopyrite thin film (AGIS) to fabricate a thin film embedded solar cell. High aspect ratio well oriented silicon micropillars (MPs) were synthesized using the deep reactive ion Etching process with the BOSCH recipe. Field ionization gas sensor based

on p-Si-MPs/n-ZnO-NWs was fabricated from growing hydrothermally dense arrays of ZnO nanowires onto the high aspect ratio vertically oriented silicon MPs. The constructed structure was tested for many target gases including He, N2, NH3 and O2, which showed very promising results. It was observed that nanowires with controlled doping of metal offer unique advantage for FI applications due to high density of surface states associated with the impurities. Especially, unoccupied local states formed by doping Si-NWs with gold resulted in a nearly 5 order of magnitude enhancement in field ionization current. In this talk, the performance of all the fabricated devices will be presented in detail.

OPTICS+PHOTONICS

NANOSCIENCE+ ENGINEERING

9553-28, Session 7

Flexible and stackable non-volatile resistive memory for high integration (*Invited Paper*)

Shawkat Ali, Jinho Bae, Chong Hyun Lee, Jeju National Univ. (Korea, Republic of)

"N/A": However, I filled in the box to help understand our idea.

Organic and printed electronics have been initiated and developed since various electronic applications have been substantially demanded for flexible electronic technology, good prototyping, mass production with low cost, and eco-friendly fabrication process. In these flexible electronic systems, a research of the flexible memory for high integration becomes an important topic. In order to produce a memory of high data storage capacity, it introduces constraints of low power consumption, high read/ write speed, and decreasing device size in higher memory density. For the last decade, resistive crossbar array architectures suitable for easy fabrication and low power consumption are being considered to solve these constraints. However, it reveals several problems such as sneak path, crosstalk, and power requirement, which limits the memory size and performance as the memory integration increases. In this paper, we propose a novel flexible and stackable resistive random access memory (ReRAM) array with multi-layered crossbar structures, which comprises of small size printed resistive switching elements and printed pull-up resistors. With the architecture of the proposed memory, the basic memory block of ReRAM is based on one resistor and multi-layered column memristor (1R-MCM) structure, which can be easily extended to 3 dimensional columns. Especially, it can be applied for higher memory density because it has 3 dimensional structure with multiple memory layers on a same area. For a high integration, the proposed memory device is also fabricated on polyethyleneterephthalate (PET) flexible substrate by using direct-printed technology, electrohydrodynamic (EHD) system printable to micrometer scale patterns at room temperature and normal air pressure. To fabricate the proposed memory device, the materials, silver (Ag) for top and bottom electrodes, PVP for memristor, and (MEH:PPV and PMMA in acetonitrile) for pull-up resistors are used. In random access of the proposed memory device, zero detection error was obtained in reading a logic data, and cell to cell interference was not occurred. Lower power consumption realized by the low current memristive elements with high OFF/ON ratio and higher retention time by flexible encapsulation were achieved. The proposed ReRAM based on 1R-MCM also demonstrated as high read/write speed as the data writing with a short delay time and data reading without delay. To overcome several limitations of flexible memory devices including, high speed, low power easy fabrication, the proposed memory device can create a new approach to be used in electronic applications.

9553-29, Session 7

Nanoscale characterization and modeling of the variability in metal oxide resistive switching memory (Invited Paper)

Matthew J. Marinella, David R. Hughart, Patrick R. Mickel, Stephen W. Howell, Ed Bielejec, George Vizkelethy, Jose L. Pacheco, Rudeger H.T. Wilke, Sapan Agarwal, Conrad D. James, Sandia National Labs. (United States)

Conference 9553: Low-Dimensional Materials and Devices



Metal oxide based resistive switching memory is a promising device technology for advanced memory and neuromorphic computing. However, the key hurdle in moving this technology forward as a memory and analog circuit element is the significant variability in electrical characteristics. This electrical variability can be categorized by (1) device to device variation, (2) cycle to cycle, or temporal write variation, and (3) read noise. The goal of this work is to correlate nanoscale physical properties of the switching film and electrodes with electrical variability. First, we will present methodologies used to electrically assess the temporal variability and the read noise. These results are then correlated with the results of nanoscale characterization of morphological, and electrical properties of the switching films using conducting atomic force microscopy (CAFM). In addition, we will present spatial maps of switching regions in the oxide produced by probing the switching film with a nanoscale ion beam while correlating the beam position with in situ electrical response (indicating the filament region). We will then present density functional theory (DFT) modeling, which provides further evidence of the origins of variability. Finally, we will discuss how methods to improve the electrical variability of devices, and the feasibility of using transition metal oxide memories for analog computation.

Sandia National Laboratories is a multi-program laboratory managed and operated by Sandia Corporation, a wholly owned subsidiary of Lockheed Martin Corporation, for the U.S. Department of Energy's National Nuclear Security Administration under contract DE-AC04-94AL85000.

9553-30, Session 7

Tantalum oxide nanoscale resistive switching devices: TEM/EELS study

Kate J Norris, Univ of California Santa Cruz (United States); Jiaming Zhang, Emmanuelle Merced-Grafals, Srinitya Musunuru, Max Zhang, Katy Samuels, Hewlett-Packard Labs. (United States); Jianhua J Yang, Hewlett-Packard Laboratories (United States); Nobuhiko P Kobayashi, Univ of California Santa Cruz (United States)

No Abstract Available

9553-31, Session 8

Extended defect structures observed in (AlxGa1-x)0.5In0.5P light emitting diodes grown by MOVPE (Invited Paper)

Andreas Rudolph, OSRAM Opto Semiconductors GmbH (Germany)

Scanning transmission electron microscopy (STEM) annular dark field (ADF), high angle annular dark field (HAADF), cathodoluminescence (CL) and energy-dispersive X-ray spectroscopy (EDX) analysis were carried out to investigate the structural and optical properties of (AlxGa1-x)0.5ln0.5P light emitting diodes (LEDs). Extended defect structures were observed in the LED active region, which exhibit defect emission that is shifted by 0.25 eV relative to the multi quantum well (MQW) emission. The morphology and composition of the defect structures was elucidated and the results confirmed by growth experiments and photoluminescence (PL) measurements.

9553-32, Session 8

Electrically injected AlGaN nanowire deep ultraviolet lasers (*Invited Paper*)

Zetian Mi, McGill Univ. (Canada)

No Abstract Available

9553-33, Session 8

Selective area metal-organic vapor-phase epitaxy growth of InP nanowires for optoelectronic device applications (Invited Paper)

Lan Fu, Australian National Univ (Australia); Q. Gao, The Australian National Univ. (Australia); F. Wang, Y. Guo, Australian National Univ (Australia); Z. Y. Li, K. Peng, L. Li, K. Vora, The Australian National Univ. (Australia); H. H. Tan, Australian National Univ (Australia); C. Jagadish, The Australian National Univ. (Australia)

No Abstract Available

9553-34, Session 8

Engineering heterojunctions with carbon nanostructures: towards high-performance optoelectronics (Invited Paper)

Judy Z Wu, Univ of Kansas (United States)

No Abstract Available

9553-35, Session 8

Optoelectronics in two-dimensional semiconductor alloys (*Invited Paper*)

François Léonard, Sandia National Labs. (United States)

Two -dimensional transition-metal dichalcogenides (2D-TMDs) have attracted attention for applications in electronics and photonics, as well as for the wealth of new scientific phenomena that arise at low dimensionality. Recently, the ability to grow 2D-TMDs by chemical vapor deposition has opened the path to large area devices, but also to the synthesis of semiconductor alloys with tunable bandgaps. In this presentation, I will discuss our recent experimental work in exploring the optoelectronic properties of 2D MoS_2(1-x)Se_2x alloys spanning the compositional range. In particular, we report the observation of a new regime of operation where the photocurrent depends superlinearly on light intensity. We use spatiallyresolved photocurrent measurements on devices consisting of CVD-grown monolayers to show the photoconductive nature of the photoresponse, with the photocurrent dominated by recombination and field-induced carrier separation in the channel. Time-dependent photoconductivity measurements show the presence of persistent photoconductivity for the S-rich alloys, while photocurrent measurements at fixed wavelength for devices of different alloy compositions show a systematic decrease of the responsivity with increasing Se content associated with increased linearity of the current-voltage characteristics. A model based on the presence of different types of recombination centers is presented to explain the origin of the superlinear dependence on light intensity, which emerges when the non-equilibrium occupancy of initially empty fast recombination centers becomes comparable to that of slow recombination centers.

9553-36, Session 9

Formation and properties of 3D metamaterial composites fabricated using nanometer scale laser lithography (Invited Paper)

Sharka M. Prokes, Frank K. Perkins, Orest J. Glembocki, U.S. Naval Research Lab. (United States)

No Abstract Available

9553-37. Session 9

Observation of direct electron-electron interaction in suspended MQW structures

Iman Hassani Nia, Sung Jun Jang, Hooman Mohseni, Northwestern Univ. (United States)

Suspended structures have been used not only for a wide range of Micro Electro Mechanical systems (MEMs) but also particularly for highly sensitive bolometers. The advantage of using such devices is that they provide a very high thermal isolation to the environment which makes it possible to detect any physical phenomenon by its temperature signature. On the other hand, by carefully designing Multiple Quantum Well (MQW) structures, scientists have been able to tailor the electronic energy levels in such a way to obtain the desired performance for lasers and detectors in particular. Inspired by the virtue of the suspended structures and MQWs, we have fabricated pristine suspended MQW structures with minimal damage to the active region using a novel method. We furthermore measured the temperature of these devices using ultra-accurate micro-thermometers. By using two separate lasers and performing heterodyne detection of the resulting change in the temperature, we observed direct signature of electron and electron interaction in our devices. We attribute these effects to various recombination mechanisms in the III-V MQW structure. To have a better understanding of these phenomena, we have performed our experiments from 78 K up to room temperature. The results have been interpreted by rigorous self-consistent solution of Poisson and Schrodinger equations and also solving the carrier rate equations. We believe that our findings will open up new aspects of III-V semiconductors physics and particularly its applications for sensing.

9553-38, Session 9

Chemical modification approaches for improved performance of Na-ion battery electrodes

Bryan Byles, Mallory Clites, Ekaterina Pomerantseva, Drexel Univ. (United States)

Recent concerns in regards to the long-term sustainability of lithium has shifted the focus of energy storage research towards utilizing other charge carrying ions in intercalation based metal-ion batteries. Sodium has received much attention as an alternative to lithium due the fact that it is more abundant and less expensive. However, there are limited numbers of electrochemically active Na-ion battery electrode materials. We present chemical approaches that results in the improved performance of materials known to reversibly intercalate sodium ions through the modification of materials composition. In this work, we study two different chemical modification processes. The first approach is based on the chemical preintercalation of sodium ions. Vanadium pentoxide was used as a model "host" material to investigate this process. By varying the Na:V ratio in the precursors, more than one sodium ion per vanadium oxide unit cell was inserted and reversibly cycled in electrochemical tests. The second chemical modification approach we investigated involved post-synthesis treatments, including hydrothermal treatment and annealing of sodium pre-intercalated vanadium oxides. These methods have proven to improve performance

through enhancing capacity and capacity retention, respectively. An alternative post-synthesis treatment involves the reaction of electrode materials with acids. To study this method we used nanostructured manganese oxides. Formation of defects during acid leaching resulted in facilitated diffusion of Na ions into the crystal structure of the material and improved its electrochemical performance. Overall, these pre- and post-synthesis approaches prove to be an efficient means of improving performance of Na-ion batteries.

OPTICS+

NANOSCIENCE+ ENGINEERING

SPIE. PHOTONICS

9553-39, Session 9

Deposition and characterizations of ultrasmooth silver thin films assisted with a germanium wetting layer

Junce Zhang, David M. Fryauf, Matthew P. Garrett, Univ. of California, Santa Cruz (United States); Logeeswaran Veerayah Jayaraman, Univ. of California, Davis (United States); Atsuhito Sawabe, Aoyama Gakuin Univ. (Japan); M. Saif Islam, Univ. of California, Davis (United States); Nobuhiko P. Kobayashi, Univ. of California, Santa Cruz (United States)

The structural properties of thin (15nm) silver (Ag) films deposited on SiO2/ Si(100) substrates with a germanium (Ge) wetting layer were studied. The Ag thin films with different Ge wetting layer thicknesses were characterized by cross-sectional transmission electron microscopy (XTEM), reflection high energy electron diffraction (RHEED), X-ray diffractometry (XRD), grazing incidence X-ray diffractometry (GIXRD), X-ray reflection (XRR) and Fourier transform infrared spectroscopy (FTIR). The surface of Ag thin films was found to be significantly smoothened by introducing a Ge wetting layer with a thickness in the range of 1-2nm. However, as the Ge wetting layer thickness increased beyond 2nm, the surface roughness increased concomitantly. The role of 1-2nm Ge wetting layer in the Ag film deposition is discussed by the surface energy of Ge, the bond dissociation energy of Ag-Ge, and the deposition mechanisms of Ag thin films on a given characteristic Ge wetting layer. Additionally, Ge island formation, precipitation of Ge from Ag-Ge alloys and penetration of Ge into SiO2 are suggested for the Ge beyond 2nm. This demonstration of ultrasmooth Ag thin films would offer an advantageous material platform with scalability for applications such as molecular anchors, optical metamaterials, plasmonic devices, and several areas of nanophotonics.

9553-40. Session 9

Thin film thermoelectric metal-organic framework with high Seebeck coefficient and low thermal conductivity

Kristopher J. Erickson, Francois Leonard, Vitalie N. Stavila, Michael E. Foster, Catalin D. Spataru, Reese Jones, Sandia National Labs. (United States); Brian Foley, Patrick Hopkins, Univ. of Virginia (United States); Mark D. Allendorf, A. Alec Talin, Sandia National Labs. (United States)

Inorganic, low bandgap semiconductors such as Bi2Te3 have adequate efficiency for some thermoelectric energy conversion applications, but have not been more widely adopted because they are difficult to deposit over complex and/or high surface area structures, are not eco-friendly, and are too expensive. As an alternative, conducting polymers have recently attracted much attention for thermoelectric applications motivated by their low material cost, ease of processability, non-toxicity, and low thermal conductivity. Metal-organic frameworks (MOFs), which are extended, crystalline compounds consisting of metal ions interconnected by organic ligands, share many of the advantages of all-organic polymers including solution processability and low thermal conductivity. Additionally, MOFs and Guest@MOF materials offer higher thermal stability (up to ~300

Conference 9553: Low-Dimensional Materials and Devices



oC in some cases) and have long-range crystalline order which should improve charge mobility. A potential advantage of MOFs and Guest@ MOF materials over all-organic polymers is the opportunity for tuning the electronic structure through appropriate choice of metal and ligand, which could solve the long-standing challenge of finding stable, high ZT n-type organic semiconductors. In our presentation, we report on thermoelectric measurements of electrically conducting TCNQ@Cu3(BTC)2 thin films deposited using a room-temperature, solution-based method, which reveal a large, positive Seebeck coefficient. Furthermore, we use time-dependent thermoreflectance (TDTR) to measure the thermal conductivity of the films, which is found to have a low value due to the presence of disorder, as suggested by molecular dynamics simulations. In addition to establishing the thermoelectric figure of merit, the thermoelectric measurements reveal for the first time that holes are the majority carriers in TCNQ@Cu3(BTC)2.

9553-41, Session 9

High-throughput screening of substrates for synthesis and functionalization of 2D materials

Arunima Singh, Albert V Davydov, Francesca Tavazza, National Institute of Standards and Technology (United States); Kiran Mathew, Cornell Univ. (United States); Richard Hennig, Univ. of Florida (United States)

No Abstract Available

9553-42, Session 9

Titanium hafnium oxide alloys: study of the dependence of microstructures and optical properties on RF substrate bias during deposition

Juan Jose Diaz Leon, Matthew P Garrett, David M Fryauf, Junce Zhang, Kate J Norris, Univ of California Santa Cruz (United States); Sharka M. Prokes, U.S. Naval Research Lab. (United States); Nobuhiko P Kobayashi, Univ of California Santa Cruz (United States)

No Abstract Available

Conference 9554: Nanoimaging and Nanospectroscopy III



Sunday - Wednesday 9 -12 August 2015 Part of Proceedings of SPIE Vol. 9554 Nanoimaging and Nanospectroscopy III

9554-2, Session 1

Super-resolution imaging of plasmonic nanostructures (Invited Paper)

Katherine A. Willets, Temple Univ. (United States)

Noble metal nanoparticles have attracted significant attention due to their ability to support localized surface plasmons, which generate local electromagnetic field enhancements, produce strong environmentallysensitive nanoparticle color, lead to localized heating, and even produce energetically excited (or hot) electrons. In order to impart additional function to these materials, hybrid nanostructures, in which organic or inorganic materials are covalently attached to the nanoparticle surface, have been synthesized, allowing plasmonic nanoparticles to be used in biosensing, drug delivery, and photonic applications. One challenge is knowing the nature of the assembly of these molecules onto the surface of the nanoparticles, which is complicated by their small size and lack of contrast in traditional surface characterization techniques, such as electron microscopy. This talk will describe super-resolution optical imaging of fluorescently-labeled molecules covalently attached to the surface of gold nanorods, highlighting some of the unique challenges of performing superresolution imaging on plasmonic nanostructures, as well as providing insight into local binding heterogeneity.

9554-3, Session 1

Transient absorption microscopy for labelfree super-resolution imaging (*Invited Paper*)

Christophe Silien, Ning Liu, University of Limerick (Ireland); Aladin Mani, LaserSpec (Belgium); Susan Daly, Mahendar Kumbham, Kevin O'Dwyer, University of Limerick (Ireland); Paolo Bianchini, Alberto Diaspro, Istituto Italiano di Tecnologia (IIT) (Italy); Yurij Fedutik, Alexei Antipov, PlasmaChem GmbH (Germany); Syed A.M. Tofail, University of Limerick (Ireland); André Peremans, Laserspec (Belgium)

No Abstract Available

9554-4, Session 1

Developments in fluorescence nanoscopy

Alexander Egner, Claudia Geisler, Laser-Laboratory Göttingen e.V. (Germany); Haugen Grefe, Jennifer Schubert, Laser-Lab. Göttingen e.V. (Germany)

No Abstract Available

9554-5, Session 1

isoSTED microscopy in living cells

Rene Siegmund, Claudia Geisler, Alexander Egner, Laser-Laboratory Göttingen e.V. (Germany)

No Abstract Available

9554-53, Session 1

New results on the single molecule localization problem in two and three dimensions (Invited Paper)

Raimund J. Ober, Texas A&M Univ (United States)

New results on the single molecule localization problem in two and three dimensions

9554-6, Session 2

Expanding the horizon of plasmonenhanced Raman spectroscopy: from SERS to SHINERS, TERS, and EERS (Invited Paper)

Jian-Feng Li, Yi-Fan Huang, Song-Yuan Ding, Zhi-Lin Yang, De-Yin Wu, Bin Ren, Zhong-Qun Tian, Xiamen Univ. (China)

In the about four decades, surface-enhanced Raman scattering (SERS) has gone through a tortuous pathway to develop into a family of plasmonenhanced Raman spectroscopy (PERS). Surface plasmons (SPs) or surface plasmon resonance (SPR), either localized surface plasmons or propagating surface plasmons, can significantly increase the intensity of Raman scattering from a molecule adsorbed at or close to the nanostructures. Although SERS is comparable to the sensitivity of fluorescence, there are two significant drawbacks to the commonplace application of SERS: a lack of substrate/molecule generality and a lack of morphology generality. To bypass these obstacles, many groups including ours have utilized different nanostructures to invent Tip-enhanced Raman spectroscopy (TERS) and shell-isolated nanoparticle-enhanced Raman spectroscopy (SHINERS). High-quality Raman spectra were obtained on various molecules adsorbed at Pt, Au and Rh single-crystal surfaces and from Si surfaces with hydrogen monolayers. Very recently we employed electron-enhanced Raman spectroscopy (EERS) to expend the study from surface reaction active sites to the electronic jellium at electrode-electrolyte interfaces. PERS have significantly expanded the versatility of Raman spectroscopy in surface science and trace analysis on complex systems, for wide applications in surface, materials and life sciences, as well as for molecular electronics, inspection of food safety and drug. In the PERS family each member with its own operation mode has its strength and limitations, their features will be summarized and correlated. Finally, an outlook on further developments of PERS will be given with emphasis on the emerging methodology.

J. F. Li et al., Nature, 2010, 464, 392-395.

9554-7, Session 2

Photo induced force microscopy: nanoscale imaging of optical polarizability (Invited Paper)

Hemantha K. Wickramasinghe, Univ. of California, Irvine (United States)

We review the application of Atomic Force Microscopy (AFM) for mapping optical near-fields with nanometer resolution. By detecting the optical force between a gold coated AFM probe and its image dipole on a glass substrate, we profile the electric field distributions of tightly focused laser beams with different polarizations. The experimentally recorded focal force maps agree well with theoretical predictions . We experimentally estimate the aspect ratio of the apex of gold coated AFM probe using only optical forces. We show that the optical force between a sharp gold coated

Conference 9554: Nanoimaging and Nanospectroscopy III



AFM probe and a sample can be used to map the spatial distribution of polarizability. Recent results using this method will be presented. Photo Induced Force Microscopy (PIFM) allows for background free, thermal noise limited mechanical imaging of optical phenomenon over wide range of wavelengths from Visible to RF with detection sensitivity limited only by AFM performance.

9554-8, Session 2

Experimental correlation of electric fields and Raman signals in SERS and TERS (Invited Paper)

Zachary D. Schultz, Hao Wang, Daniel T. Kwasnieski, James M. Marr, Univ. of Notre Dame (United States)

Enhanced Raman scattering from plasmonic nanostructures associated with surface enhanced (SERS) and tip enhanced (TERS) is seeing a dramatic increase in applications from bioimaging to chemical catalysis. The importance of gap-modes for high sensitivity indicates plasmon coupling between nanostructures plays an important role. However, the observed Raman scattering can change with different geometric arrangements of nanoparticles, excitation wavelengths, and chemical environments; suggesting differences in the local electric field.(1, 2) Our results indicate that molecules adsorbed to the nanostructures are selectively enhanced in the presence of competing molecules. This selective enhancement arises from controlled interactions between nanostructures, such as an isolated nanoparticle and a TERS tip.(3, 4) Complementary experiments suggest that shifts in the vibrational frequency of reporter molecules can be correlated to the electric field experienced by the molecule.(5) Here we present a strategy that utilizes the controlled formation of coupled plasmonic structures to experimentally measure both the magnitude of the electric fields and the observed Raman scattering.

References:

1. Halas, N. J.; Lal, S.; Chang, W. S.; Link, S.; Nordlander, P. Chem. Rev. 2011, 111, (6), 3913-3961.

2. Schultz, Z. D.; Marr, J. M.; Wang, H. Nanophotonics 2014, 3, (1-2), 91-104.

3. Wang, H.; Carrier, S.; Park, S.; Schultz, Z. D. Faraday Discuss. 2015, In Press.

4. Wang, H.; Schultz, Z. D. ChemPhysChem 2014, 15, (18), 3944-9.

5. Marr, J. M.; Schultz, Z. D. The Journal of Physical Chemistry Letters 2013, 4, (19), 3268-3272.

9554-9, Session 2

Nano-antenna-controlled tunable enhancement in tip-enhanced Raman spectroscopy

Prabhat Verma, Osaka Univ. (Japan)

Tip-enhanced Raman spectroscopy (TERS) utilizes a nano-tip as plasmonic nano-antenna for enhancement and confinement of light for nanospectroscopy and nano-imaging. Usually, the tips for TERS are prepared by evaporating metal on an AFM cantilever tip to form a thin layer of metallic nanoparticles on the surface. By controlling the shape and size of these metallic nanoparticles, one can tunably control the surface plasmon resonance, and hence the enhancement in TERS. I will show some results of numerical simulations and will demonstrate how we can tune the enhancement in TERS by precisely truncating the length of silver on the tip.

9554-10, Session 3

Nanospectroscopy for nano-chemistry and nanostructures (Invited Paper)

Debdulal Roy, National Physical Lab. (United Kingdom)

The first part of the talk will focus on measuring nanochemistry in catalysis. Chemical mapping of a photocatalytic reaction with nanoscale spatial resolution is demonstrated for the first time using tip-enhanced Raman spectroscopy (TERS). An ultrathin alumina film applied to the Ag-coated TERS tip blocks catalytic interference whilst maintaining near-field electromagnetic enhancement, thus enabling spectroscopic imaging of catalytic activity on nanostructured Ag surfaces.

The second part focuses on detects in graphene. Defects in a 2D material, like graphene, directly impact its key performances including high electrical conductivity, high tensile strength and chemical inertness. Measuring single defect in few nanometres length scale has not been realised without the help of high resolution transmission electron microscopy. Here we present a simple and elegant way of measuring single defects, OD point defects and ID line defects in the 2D plane of single layer of atoms in graphene using tip-enhanced Raman spectroscopy. Spectroscopic measurements provide great deal of information ranging from fundamental light scattering from defects to measuring the extent that a defect influences the properties of a 2D material.

9554-11, Session 3

Seeing molecular vibrations: chemical imaging for biomedicine (Invited Paper)

Wei Min, Columbia Univ. (United States)

Here we discuss an emerging chemical imaging platform, stimulated Raman scattering (SRS) microscopy, which can enhance the otherwise feeble spontaneous Raman eight orders of magnitude by virtue of stimulated emission. When coupled with stable isotopes (e.g., deuterium and 13C) or bioorthogonal chemical moieties (e.g., alkynes), SRS microscopy is well suited for probing in vivo metabolic dynamics of small bio-molecules which cannot be labeled by bulky fluorophores. Physical principle of the underlying optical spectroscopy and exciting biomedical applications such as imaging lipid metabolism, protein synthesis, DNA replication, protein degradation, RNA synthesis, glucose uptake, drug trafficking and tumor metabolism will be presented.

9554-12, Session 3

Infrared near-field nanospectroscopy: chemical identification, nanoellipsometry, and nanotomography (Invited Paper)

Alexander A. Govyadinov, CIC nanoGUNE Consolider (Spain)

Scattering-type scanning near-field optical microscopy (s-SNOM) brings the power of infrared imaging and spectroscopy to the nanometer scale. The spatial resolution of about 10 - 20 nm opens a new era for modern applications in analytical chemistry, materials and bio sciences. After a brief overview of fundamentals and applications of s-SNOM, this talk will present recent achievements in broadband infrared nanospectroscopy (nano-FTIR) of polymers and proteins. Particularly, it will show how nanoscale chemical identification and quantitative recovery of local dielectric properties can be achieved. Finally, our progress towards near-field nanotomography will be discussed.

9554-13, Session 3

Investigation of surface plasmons in nano-squares using electron energy loss spectroscopy

Yue Zhang, Rice Univ. (United States); Edson Bellido Sosa, McMaster Univ. (Canada); Alejandro Manjavacas, Yang Cao, Rice Univ. (United States); Gianluigi A. Botton, McMaster



Univ. (Canada); Peter Nordlander, Rice Univ. (United States)

Electron energy-loss spectroscopy (EELS) has great advantages to study surface plasmon. This method allows us to image surface plasmon with nanometer spatial resolution. Furthermore, EELS perfectly identifies dark modes in addition to bright modes. Here, we present an experimental and theoretical study of silver nano-squares. EELS performed in a scanning transmission electron microscope (STEM-EELS) is used to acquire spectra and maps of plasmon resonances of lithographically patterned silver nano-squares. The simulations give EELS spectra and photonic local density of states (LDOS) maps at plasmon resonances, using Finite-Difference Time-Domain (FDTD). The simulation and experiment are in good agreement, and observed modes that are not captured by optical measurements: besides multipolar bright and dark modes, plasmonic modes confined to the center of the structures are also successfully found. Our study fully explains the optical properties of nano-squares.

9554-14, Session 4

Accelerating beams for advanced imaging in biomedicine (Invited Paper)

Kishan Dholakia, Univ. of St. Andrews (United Kingdom)

I will describe the use of shaped light fields namely propagation invariant ('non-diffracting') light fields and complex beam shaping for advanced studies in imaging. Propagation invariant light fields, as the name suggests retain their transverse intensity profile upon propagation. Bessel light fields and Airy light fields are prime examples of such beams. In terms of imaging, single plane illumination (light sheet) microscopy (SPIM) offers a myriad of unique advantages. Detection orthogonal to the illumination allows rapid imaging of large, three-dimensional, samples of living tissue. Illumination with a thin sheet of light ensures high contrast by minimizing the fluorescent background. Moreover, by restricting the sample exposure to a single plane, photo-bleaching and damage are minimized. This is crucial when imaging photo-sensitive samples over a larger period of time. Recent enhancements to the original technique attempt to overcome the inherent trade off between axial resolution and field-of-view of conventional light sheet microscopy. Until recently, this was only achieved by compromising on one or more of its key advantages: high contrast, time-resolution, or minimal sample exposure. I will discuss the use of propagation invariant light fields for the enhancement within this imaging modality particularly Airy modes. The extension to combining this approach with super-resolution will be described

9554-15, Session 4

Nanophotonic measurement of the dark fraction in red fluorescent proteins (Invited Paper)

Jord C. Prangsma, Robert Molenaar, Christian Blum, Univ. Twente (Netherlands); Vinod Subramaniam, FOM Institute for Atomic and Molecular Physics (Netherlands)

All complex fluorophores such as fluorescent proteins display a fraction of the population that absorb light but do not emit fluorescence. Accurate measurement of this 'dark' fraction is of critical importance for quantitative microscopy in cell biology. We used a nanophotonic method to measure the dark fraction of several frequently used red fluorescent proteins. The results we obtain show that most RFPs have a considerable 30% fraction of absorbing but not emitting fluorophores. Our findings have direct implications in quantitative microscopy such as in the interpretation of intensity-based FRET measurements, and prove an important bottleneck in the development of enhanced fluorescent proteins.

9554-16, Session 4

Supercritical angle fluorescence for absolute super-localization nanoscopy (Invited Paper)

Nicolas Bourg, Institut des Sciences Moléculaires d'Orsay (France); Guillaume Dupuis, Sandrine Lécart, Univ. Paris-Sud 11 (France); Emmanuel Fort, Institut Langevin (France); Sandrine Lévêque-Fort, Institut des Sciences Moléculaires d'Orsay (France)

We propose to take advantage of Supercritical Angle Fluorescence (SAF) emission, also called forbidden light, to obtain an isotropic and absolute 3D localization precision in superlocalization microscopy. When a fluorophore is located in the vicinity of the coverslip interface, its near-field component can become propagative and emitted above the critical angle. As this SAF emission decreases exponentially with the dye/interface distance, absolute nanometric axial position of each fluorescent dye can be extracted. An isotropic 3D localization precision of 20nm within an axial range of -150 nm above the coverslip can be achieved, allowing to observe the 3D hollowness of microtubules.

9554-17, Session 4

Optical coherence tomography for nanoparticles quantitative characterization

Michal Trojanowski, Maciej Kraszewski, Marcin R. Str?kowski, Jerzy Pluci?ski, Gdansk Univ. of Technology (Poland)

The unique features of nanocomposite materials depend on the type and size of nanoparticles, as well as their placement in the composite matrices. Therefore the nanocomposites manufacturing process requires inline control over certain parameters of nanoparticles such as dispersion and concentartion. Keeping track of nanoparticles parameters inside a matrix is currently a difficult task due to lack of a fast, reliable and cost effective way of measurement that can be used for large volume samples. Currently used methods like scanning electron microscopy and transmission electron microscopy (SEM, TEM) are costly, time consuming and invasive. To overcome those difficulties we propose the usage of Low Coherence Interferometry (LCI) based methods such as Optical Coherence Tomography (OCT). OCT is an optical measurement method which is a non-destructive and non-invasive technique. It is capable of creating tomographic images of inner structure by gathering depth related backscattered signal from scattering particles. OCT can analyse, in a single shot, area of the micrometre range. To increase OCTs measurement capabilities we are using additional system extensions such as Spectroscopic OCT (SOCT) and Polarization Sensitive (PS-OCT). With such additions we are able to measure several parameters such as extinction coefficient, absorption coefficient, scattering spectra and polarization. Those parameters allow us to quantitatively estimate nanoparticles, size, orientation and dispersion. Gaining those information allows to calculate volume concentration of nanoparticles. In addition we analyse different types of particles, metallic and oxides. To fully characterize nanoparticles it is necessary to find and differentiate those that are single particles from agglomerated ones. In this contribution we present our research results on using the LCI based measurement techniques for evaluation of materials with nanoparticles. The laboratory system and signal processing algorithms are going to be shown in order to express the usefulness of this method for inline constant monitoring of the nanocomposite material fabrication.

9554-18, Session 4

Microscopic ellipsometry image of microspheres on a substrate

Fu-Chen Hsiao, Yu-Da Chen, Buu Trong H. Ngo, Huai-Yi Xie,

Conference 9554: Nanoimaging and Nanospectroscopy III



Yia-Chung Chang, Academia Sinica (Taiwan)

We performed experimental measurements and theoretical simulation based on an efficient half-space Green's function method[1.2] to investigate the diffraction patterns of light scattering from silicon and ZnO microspheres on a substrate. The microscopic ellipsometry image for s- and p-polarized reflectance and their phase difference (Rs, Rp, and ?) was taken by a modified Optrel MULTISKOP system with rotating compensator configuration for various angles of incidence and wavelengths ranging from 450nm to 750nm. An 80X objective was used and the pixel size for our image is around 200nm. The images obtained display clear diffraction patterns, which is analyzed by an efficient full-wave simulation. By expanding the electromagnetic fields within the microsphere in terms of spherical harmonics[2,3] and use the half-space Green's function method to solve the scattered field, we obtain accurate near-filed distributions on the focal plane. The near-field distributions are then converted to images observed by the CCD camera via a near-field to far-field transformation. The simulated images are then compared with experimental results to gain deep understanding of these diffraction patterns. Mode profiles of the resonant cavity modes are observed and identified theoretically.

[1] S.-H. Hsu, Y.-C. Chang, Y.-C. Chen, P.-K. Wei, Y. D. Kim, Optics Exp. 18, 1310 (2010).

[2] H-Y Xie, Y-C Chang, G. Li, S-H Hsu, Optics Exp., 21, 3091 (2013)
 [3] H.-Y. Xie and Y.-C. Chang, J. Opt. Soc. Am. B 30, 2215 (2013)

9554-1, Session 5

Nanoscopy of thick specimens using adaptive optics (Invited Paper)

Martin J. Booth, Univ. of Oxford (United Kingdom)

Optical nanoscopes provide nanometric resolution of specimens through combinations of optical and photophysical effects. Their performance is however often compromised by aberrations, especially when imaging deep into cells or tissues. We present advances in adaptive optics for compensation of aberrations in STED and single molecule switching (STORM/PALM) microscopy. Aberration correction permits 3D STED microscopy tens of micrometres inside inhomogeneous tissue. Adaptive STORM microscopy leads to significant increases in the number of detected emitters and localization precision. We also show that aberration correction is necessary to avoid localization errors in 3D STORM microscopes.

9554-19, Session 5

Optimizing STED and single-molecule switching nanoscopy for biological applications (Invited Paper)

Edward Allgeyer, Xiang Hao, Fang Huang, Emil Kromann, Yu Lin, Mary Grace Velasco, Yongdeng Zhang, Joerg Bewersdorf, Yale Univ. (United States)

This presentation will provide an overview over our current method developments in STED and single-molecule switching nanoscopy (FPALM, PALM, STORM, GSDIM, dSTORM, ...) towards routine application in cell biology, in particular in living cells. We will discuss, in particular, recent advances in speeding up SMS nanoscopy with sCMOS camera detection and novel algorithms, and the use of recently developed live-cell compatible fluorophores for multicolor STED as well as SMS nanoscopy.

9554-20, Session 5

Quantitative high spatiotemporal resolution imaging of biological processes (Invited Paper)

Joseph S. Borbely, Jason Otterstrom, Nitin Mohan, Carlo Manzo, Melike Lakadamyali, ICFO - Institut de Ciències Fotòniques (Spain)

In the recent years, super-resolution microscopy has emerged as a powerful tool to image cells at the nanoscale, giving important insights into biological processes at the molecular level. These methods have been so revolutionary that their impact has recently been recognized by the Nobel Prize in Chemistry. While exciting developments over the last decade have significantly advanced the capabilities of super-resolution microscopy, important challenges remain in pushing its applications in biology. One limitation is the compromise between spatial and temporal resolution that make these methods poorly suited to study dynamic processes. Another challenge is our limited capability to extract quantitative information from the super-resolution images, which is confounded by the photophysics of the fluorophores. I will show how we are developing new approaches to overcome these challenges and demonstrate two novel biological applications of super-resolution microscopy. In the first part of my talk, I will summarize our ongoing efforts to use a combination of single particle tracking and super-resolution microscopy to study how molecular motors such as dynein and kinesin overcome road blocks to transport their cargo. In the second part of my talk, I will show how we are using highly quantitative approaches to decipher the nanoscale organization of chromatin inside intact nuclei at the single cell level. Overall, I will demonstrate that quantitative, high spatio-temporal resolution imaging holds great promise for solving important mysteries in biology.

9554-21, Session 5

Optical nanoscopy to reveal structural and functional properties of liver cells (Invited Paper)

Peter McCourt, UiT The Arctic Univ. of Norway (Norway); Thomas R. Huser, Univ. Bielefeld (Germany); Karen K. Sørensen, Cristina I. Øie, UiT The Arctic Univ. of Norway (Norway); Viola Mönkemöller, Univ. of Bielefeld (Germany); Balpreet S. Ahluwalia, UiT The Arctic Univ. of Norway (Norway)

The advent of optical nanoscopy has provided an opportunity to study fundamental properties of nanoscale biological functions, such as liver sinusoidal endothelial cells (LSEC) and their fenestrations. The fenestrations are nano-pores (50-200 nm) on the LSEC plasma membrane that allow free passage of molecules through cells. The fenestrated LSEC also hase a voracious appetite for waste molecules, viruses and nanoparticles. LSEC daily remove huge amounts of waste, nanoparticles and virus from the blood. Pharmaceuticals also need to pass through these fenestrations to be activated (e.g. cholesterol reducing statins) or detoxified by hepatocytes. And, when we age, our LSEC fenestrations become smaller and fewer. Today, we study these cells and structures using either conventional light microscopy on living cells, or high-resolution (but static) methods such as transmission and scanning electron microscopy on fixed (i.e. dead) tissue. Such methods, while very powerful, yield no real time information about the uptake of virus or nanoparticles, nor any information about fenestration dynamics. Therefore, to study LS-SEC, we are now using optical nanoscopy methods, and developing our own, to map their functions in 4 dimensions. Attaining this goal will shed new light on the cell biology of the liver and how it keeps us alive. This paper describes the challenges of studying LS-SEC with light microscopy, as well as current and potential solutions to this challenge using optical nanoscopy.



9554-22, Session 5

Chip-based optical microscopy for imaging membrane sieve plates of liver scavenger cells

Øystein I. Helle, Cristina I. Øie, Peter McCourt, Balpreet S. Ahluwalia, UiT The Arctic Univ. of Norway (Norway)

Liver sinusoidal scavenger endothelial cells (LSECs) are engaged in blood clearance activity. LSECs are uniquely characterized structurally with fenestration (nano-holes of ~50-200 nm diameter) grouped in sieve plates, which allows small soluble material, but not larger particles to pass through the sinusoidal wall. As fenestrations and sieve plates are present only on the cell membrane, TIRF (total internal reflection microscopy) configuration is preferred over epi- fluorescence. In TIRF microscopy surface evanescent field is used to excite the sample. Here, we use the evanescent field on top of optical waveguides to image cell membrane network and sieveplates (holes in the membrane) of liver cells. In waveguide excitation, the evanescent field is dominant only near the surface (~100-150 nm) providing default optical sectioning and illuminating fluorophores that are in close proximity to the surface and thus benefiting higher signal-to-noise ratio. This method represents an integrated, on-chip optical microscopy approach, with a possible extension towards super-resolution imaging methods. Waveguide platform is compatible with fast optical fiber components (couplers, adapters, switches) allowing easy multiplexing to different wavelengths. In this paper, we will discuss the challenges and opportunities provided by integrated optical microscopy for imaging cell membranes.

9554-23, Session 5

Nanoscopic lithography and applications

Jaroslaw Jacak, Richard Wollhofen, Thomas A. Klar, Johannes Kepler Univ. Linz (Austria)

STED-lithography is a powerful tool for maskless two and three dimensional structuring far below the diffraction limit of any desired geometry [1]. Similar to STED-microscopy [2, 3], optically excited starters of polymerization are depleted by a second laser beam which confines the excitation volume. An appropriate beam shaping reduces the volume, where initiators of polymerization are in the excited state, which initiates the polymerization in the adjacent region of the focal spot.

Using a 110 fs pulsed laser (780 nm) for multy-photon polymerization (MPP) and a 532 nm CW laser for STED, we are able to obtain structure sizes of 55 nm in all three dimensions (?/14 for 780 nm excitation) and manufacture two separated lines with 120 nm lateral distance, which marks the best resolution in STED lithography reported so far [5, 6].

Various two-and three-dimensional acrylate nanostructures are fabricated on glass supports with precisely controlled size, geometry and chemical properties. Tuning the polymer properties, we are able to create structures allowing an easy biofunctionalization with proteins approaching the single protein level [7]. In contrast, we can also inhibit adhesion of proteins or cells to the structures by using another composition of the polymer. We use direct stochastic optical reconstruction microscopy (dSTORM) and statistical fluorescence analysis methods to determine the protein density on nanoscopic structures fabricated via STED-lithography.

References

1. Fischer J, von Freymann G, Wegener M: The Materials Challenge in Diffraction-Unlimited Direct-Laser-Writing Optical Lithography. Advanced Materials 2010, 22:3578-+.

2. Klar TA, Hell SW: Subdiffraction resolution in far-field fluorescence microscopy. Opt Lett 1999, 24:954-956.

3. Klar TA, Jakobs S, Dyba M, Egner A, Hell SW: Fluorescence microscopy with diffraction resolution barrier broken by stimulated emission. Proc Natl Acad Sci U S A 2000, 97:8206-8210.

 Maruo S, Nakamura O, Kawata S: Three-dimensional microfabrication with two-photon-absorbed photopolymerization. Opt Lett 1997, 22:132-134.
 Wollhofen R, Katzmann J, Hrelescu C, Jacak J, Klar TA: 120 nm resolution and 55 nm structure size in STED-lithography. Opt Express 2013, 21:10831-10840.

6. Klar TA, Wollhofen R, Jacak J: Sub-Abbe resolution: from STED microscopy to STED lithography. Physica Scripta 2014, 014049.

7. Wiesbauer M, Wollhofen R, Vasic B, Schilcher K, Jacak J, Klar TA: Nano-Anchors with Single Protein Capacity Produced with STED Lithography. Nano Lett 2013, 13:5672-5678.

9554-24, Session 6

Visualisation of plasmonic fields at the nanoscale with single molecule localisation microscopy (Invited Paper)

Christian Steuwe, KU Leuven (Belgium) and Univ. of Cambridge (United Kingdom); Miklos Erdelyi, Univ. of Cambridge (United Kingdom); Gabor Szekeres, Mária Csete, Univ. of Szeged (Hungary); Jeremy J. Baumberg, Univ. of Cambridge (United Kingdom); Sumeet Mahajan, Univ. of Southampton (United Kingdom); Clemens F. Kaminski, Univ. of Cambridge (United Kingdom)

In this paper we demonstrate a novel method for combining surface enhancement on nanostructures with high resolution localisation microscopy [1] for in situ imaging of plasmonic hotspots in three dimensions [2]. We show that this technique allows for the characterisation of surfaces on the nanoscale enabling visualization of plasmon active areas, hence offering complementary information to results obtained by optical scattering or other far-field optical methods. The data is amenable for comparison with simulations obtained by boundary element and finite difference timedomain methods. For performing surface enhanced localisation microscopy (SELM) on metal surfaces we place fluorophores at precisely defined distances away from the surface to obtain the best field enhancement and overcome quenching. Using this technique we characterise plasmonic 'hotspots' on two types of substrates previously used in surface enhanced Raman spectroscopy such as Klarite®, a pyramidally pitted material [3] and sphere segment void (SSV) nanostructured substrates which can offer tunable plasmonic properties [4][5].

Furthermore, we investigate the photo-switching behaviour of fluorophores in the vicinity of the enhanced optical field of the metal and demonstrate the possibility of switching fluorophores between a dark and bright state thus obviating the need of any oxidising or reducing agents usually required for photoswitching superresolution methods [1].

[1] van de Linde et al., Nat. Protocols, 6, 991 (2011)

- [2] Steuwe et al, Nanoletters, In revision
- [3] Perney et al., Phys. Rev. B, 76,1 (2007)
- [4] Mahajan et al., J. Phys. Chem. C, 21, 9284 (2009)
- [5] Steuwe et al., Nanoletters 11, 5339 (2011)

9554-25, Session 6

Visible-wavelength two-photon excitation microscopy (Invited Paper)

Katsumasa Fujita, Masahito Yamanaka, Kumiko Uegaki, Yoshiyuki Arai, Kenta Saito, Nicholas I. Smith, Yasuo Yonemaru, Kentaro Mochizuki, Satoshi Kawata, Takeharu Nagai, Osaka Univ. (Japan)

We proposed and investigate the use of visible light for two-photon excitation of fluorescent proteins. We found that various kinds of fluorescent proteins can be excited by absorbing two photons at the wavelength of 525 nm to emit fluorescence. We used an OPO system pumped by 200-fs pulsed laser oscillating at 400 nm to produce 525 nm pulsed laser light for the visible-wavelength two-photon excitation and successfully demonstrated the simultaneous observation of four fluorescent protein, Sirius, mseCFP,

Conference 9554: Nanoimaging and Nanospectroscopy III

mTFP1, and EGFP expressed in HeLa cells. The fluorescence signal we have obtained from the fluorescent proteins was more than 100 times stronger than that of autofluorescence from endogenous molecules. We have confirmed that Sirius, mseCFP, mTFP1, and EGFP shows fluorescence response quadratic to the excitation intensity of pulsed laser light at 525 nm. We also measured the excitation spectra, and the results indicate the contribution of resonant two-photon excitation to the result of imaging with low autofluorescence background. With using 100-nm diameter fluorescence beads with fluorescence emission at 440 nm, we have confirmed that the spatial resolutions of 120 nm and 280 nm can be obtained for the lateral and axial directions, respectively, with two-photon excitation in multifocus confocal microscopy and successfully demonstrated the video-rate two-color fluorescence imaging with high spatial resolution.

9554-26, Session 6

Resolution enhancement in a double-helix phase engineered scanning microscope (RESCH microscope) (Invited Paper)

Alexander Jesacher, Monika Ritsch-Marte, Medizinische Univ. Innsbruck (Austria); Rafael Piestun, Univ. of Colorado at Boulder (United States)

Recently we introduced RESCH microscopy [1] – a scanning microscope that allows slightly refocusing the sample after the acquisition has been performed, solely by performing appropriate data post-processing. The microscope features a double-helix phase-engineered emission point spread function in combination with camera-based detection. Based on the principle of transverse resolution enhancement in Image Scanning Microscopy [2,3], we demonstrate similar resolution improvement in RESCH. Furthermore, we outline a pathway for how the collected 3D sample information can be used to construct sharper optical sections.

 A. Jesacher, M. Ritsch-Marte and R. Piestun, accepted for Optica.
 C.J.R. Sheppard, "Super-resolution in Confocal imaging," Optik, 80, 53-54 (1988).

[3] C.B. Müller and J. Enderlein "Image Scanning Microscopy," Phys. Rev. Lett. 104, 198101 (2010).

9554-27, Session 6

Nonlinear fluorescence probe using photoinduced charge separation

Kentaro Mochizuki, Lanting Shi, Shin Mizukami, Masahito Yamanaka, Osaka Univ. (Japan); Mamoru Tanabe, FUJIFILM Corp. (Japan); Wei-Tao Gong, Almar F. Palonpon, Shogo Kawano, Satoshi Kawata, Kazuya Kikuchi, Katsumasa Fujita, Osaka Univ. (Japan)

Two-photon excitation microscopy (TPEM) provides spatial resolution beyond the optical diffraction limit using the nonlinear response of fluorescent molecules. One of the strong advantages of TPEM is that it can be performed using a laser-scanning microscope without a complicated excitation method or computational post-processing. However, TPEM has not been recognized as a super-resolution microscopy due to the use of near-infrared light as excitation source, which provides lower resolution than visible light. In our research, we aimed for the realization of nonlinear fluorescence response with visible light excitation to perform super-resolution imaging using a laser-scanning microscope. The nonlinear fluorescence response with visible light excitation is achieved by developing a probe which provides stepwise two-photon excitation through photoinduced charge separation. The probe named nitro-bisBODIPY consists of two fluorescent molecules (electron donor: D) and one electron acceptor (A), resulting to the structure of D-A-D. Excited by an incident photon, nitro-bisBODIPY generates a charge-separated pair between one of the fluorescent molecules and the acceptor. Fluorescence emission is

obtained only when one more incident photon is used to excite the other fluorescent molecule of the probe in the charge-separated state. This stepwise two-photon excitation by nitro-bisBODIPY was confirmed by detection of the 2nd order nonlinear fluorescence response using a confocal microscope with 488 nm CW excitation. The physical model of the stepwise two-photon excitation was investigated by building the energy diagram of nitro-bisBODIPY. Finally, we obtained the improvement of spatial resolution in fluorescence imaging of HeLa cells using nitro-bisBODIPY.

SPIE. PHOTONICS

NANOSCIENCE+ ENGINEERING

9554-28, Session 6

A new method of single-particle spectroscopy with optical microresonators

Kevin Heylman, Randall H. Goldsmith, Kassandra A. Knapper, Erik Horak, Univ. of Wisconsin-Madison (United States)

Single-particle spectroscopy is a powerful technique for characterizing disordered materials, individual nanoparticles, and plasmonic nanostructures. This type of spectroscopy is typically performed via luminescence; however, important target systems such as plasmonic nanoparticles and conducting polymers typically cannot be made to luminesce. Absorption spectroscopy not only lacks this drawback, it offers additional information; in particular, the electronic structure and orientation of single nanoparticles can be determined. Previous efforts have typically employed photothermal microscopy, where the absorbing particle dissipates nanowatts of heat to its local environment through non-radiative relaxation after optical excitation. The extension of this technique to objects with small absorption cross-sections has been hampered by the intrinsically low sensitivity of existing methods for reading out this small heat flux.

In this work we employ ultrahigh-quality-factor optical microresonators to detect this dissipated heat, substantially augmenting the sensitivity and versatility of photothermal absorption spectroscopy. Tuning the excitation wavelength and measuring the resulting variation in dissipated heat leads to an absorption spectrum of a single nano-object. Finite-element simulations in COMSOL Multiphysics are used to correlate the observed resonance shift to an absolute absorption cross-section at each wavelength. Rotating the linear polarization angle of the excitation light, by contrast, gives information about the transition dipole of the absorber. This single-particle linear dichroism can be used to determine the orientation of anisotropic plasmonic nanoparticles, or the degree of crystallinity of organic nanoparticles. Combining the information content of optical absorption spectroscopy with the specificity of single-particle imaging provides a valuable new tool for nanospectroscopy.

9554-29, Session 7

Electrochemical tip-enhanced Raman spectroscopy (Invited Paper)

Zhicong Zeng, Shengchao Huang, Tengxiang Huang, Maohua Li, Bin Ren, Xiamen Univ. (China)

Tip-enhanced Raman spectroscopy (TERS) can not only provide very high sensitivity but also high spatial resolution, and has found applications in various fields, including surface science, materials, and biology. Most of previous TERS studies were performed in air or in the ultrahigh vacuum. If TERS study can be performed in the electrochemical environment, the electronic properties of the surface can be well controlled so that the interaction of the molecules with the substrate and the configuration of the molecules on the surface can also be well controlled.

However, the EC-TERS is not just a simple combination of electrochemistry with TERS, or the combination of EC-STM with Raman. It is a merge of STM, electrochemistry and Raman spectroscopy, and the mutual interference among these techniques makes the EC-TERS particularly challenge: the light distortion in EC system, the sensitivity, the tip coating to work under EC-STM and retain the TERS activity and cleanliness.

We designed a special spectroelectrochemical cell to eliminate the

Conference 9554: Nanoimaging and Nanospectroscopy III



distortion of the liquid layer to the optical path and obtain TER spectra of reasonably good signal to noise ratio for surface adsorbed molecules under electrochemical potential control. For example, potential dependent TERS signal have been obtained for adsorbed aromatic thiol molecule, and much obvious signal change compared with SERS has been found, manifesting the importance of EC-TERS to reveal the interfacial structure of an electrochemical system.

We further extended EC-TERS to electrochemical redox system, and clear dependence of the species during redox reaction can be identified.

9554-30, Session 7

Nanoscale chemical identification of different molecular species by plasmon enhanced Raman spectroscopy (Invited Paper)

Zhenchao Dong, Univ. of Science and Technology of China (China)

No Abstract Available

9554-31, Session 7

Tip-enhanced Raman spectroscopy in graphene and GaN nanostructures (Invited Paper)

Janina Maultzsch, Technische Univ. Berlin (Germany)

Application of tip-enhanced Raman spectroscopy (TERS) to nanostructured materials can give valuable information about local deformations, disorder, as well as nm-scale variations in composition, strain, and doping. Here we present examples for carbon and semiconductor nanomaterials. TERS measurements on approximately 10nm wide graphene folds show the differences in strain and substrate-induced doping levels between the fold and the unfolded graphene. In GaN layers we investigate the different enhancement in TERS for different Raman modes, as well as polarization-dependent selection rules.

9554-32, Session 7

Polarization analysis in near-field Raman spectroscopy (*Invited Paper*)

Yuika Saito, Toshihiro Mino, Prabhat Verma, Osaka Univ. (Japan)

TERS has emerged over the past decade as a powerful tool for Raman spectroscopy that shows high sensitivity and capability of nano-scale imaging with high spatial resolution. TERS utilizes a metallic nano-tip, which confines and enhances the propagating light into near-field in the close vicinity of the apex. Besides the nano-scale spatial resolution, polarization analysis in TERS is of tremendous advantage, as it allows one to study highly directional intrinsic properties of a sample at the nanoscale. In this study, we have developed a method to analyze the polarization of near-field light in TERS from the scattering pattern produced by the induced dipole in the metallic tip. Under dipole approximation, we measured the image of the dipole at a plane away from the focal plane, where the information about the direction of the dipole oscillation was intact. The direction of the dipole oscillation was determined from the defocused pattern, and then the polarization of near-field light was evaluated from the oscillation direction by calculating the intensity distribution of near-field light We used those evaluated tips to measure nano-images from single-walled carbon nanotubes and confirmed that the contrast of the TERS image depended on the oscillation direction of the dipole, which were also found in excellent agreement with the calculated TERS images, verifying that the polarization of the near-field was quantitatively estimated by our technique.

9554-33, Session 7

Fast reproducible TERS imaging for real world applications

Dmitry Evplov, Vasily Gavrilyuk, Andrey Krayev, Sergey Saunin, AIST-NT Inc. (United States)

Since the discovery in 2000 Tip Enhanced Raman Scattering (TERS) has been a subject of great scientific interest due to the huge potential of the nanoscale chemical imaging. For number of reasons, both fundamental and engineering, successful TERS measurements were achieved in very limited number of the laboratories around the world. The real-life application of TERS as an analytical method has been hampered by the complexity of the experimental setups, poor reproducibility and extremely long acquisition times, measured in hours, required for collection of reasonably high pixel density TERS maps.

We report successful chemically specific high pixel density, high speed (less than 10 minutes per map) TERS imaging of complex samples comprised of Graphene oxide, Carbon nanotubes of different chirality, fullerene and self-assembled layers of organic molecules. The spatial resolution routinely obtained in such chemically specific TERS maps is in the 15 - 20 nm range, with the best resolution achieved being 7 nm.

The ease of use of the TERS imaging system and high speed TERS imaging capability enabled by advanced hardware and software move TERS closer to become a real life analytical method for chemically specific imaging at the nano scale.

9554-34, Session 8

Molecule-to-nanoantenna coupling investigated by polarization-sensitive SERS (Invited Paper)

Pietro G. Gucciardi, Consiglio Nazionale delle Ricerche (Italy)

When molecules are near-field coupled with optical nanoantennas their scattering properties are strongly affected by the radiation properties of the nanoantenna itself. In Surface Enhanced Raman Scattering (SERS) the Raman scattering cross section is greatly enhanced, the field orientation and polarization are modified by the nanoantenna radiation modes. Here we discuss how the polarization of the Raman field, inelastically scattered by molecules in SERS, is modified by the interaction with optical nanoantennas in a model beyond the E⁴ approximation. The polarized SERS intensity is discussed for different nanoantenna geometries. Insights on how to recover information on the Raman polarizability tensor based on the SERS measurements are given.

9554-35, Session 8

Multi-targeting SERS bio-imaging (Invited Paper)

Aiguo Shen, Jiming Hu, Wuhan Univ. (China)

Surface-enhanced Raman scatter (SERS) technique has been fully demonstrated to be highly suitable for multi-targeting assay and bioimaging since due to its high sensitivity and multiolex etection capability. Herein, we describe recent advances in this domain including the design and synthesis of SERS substrates and tags, label-free/separation-free SERS assay and in vitro/in vivo SERS bio-imaging in our group. Especially, a focusing introduction is given on novel SERS active micropipettes for micro-area sampling and quantitative, separation-free detection of multiple organic residues, and the multi-targeting SERS imaging of a live cell which allow simutaneous label-free imaging of nuclear and label imaging of membrane in the process of drug induced cellular apoptosis.



9554-36, Session 8

Fan-shaped gold nanoantennas above reflective substrates for surface-enhanced infrared absorption (SEIRA)

Xiao Yang, Lisa V. Brown, Ke Zhao, Bob Y. Zheng, Peter Nordlander, Naomi J. Halas, Rice Univ. (United States)

Surface-enhanced infrared absorption (SEIRA) has been gaining substantial attention by using plasmonic nanoantennas to amplify near-field intensities so that it can extend IR spectroscopy to zeptomolar quantities and ultimately to the sigle-molecule level. Here we report a new nanoantenna for SEIRA detection, consisting of a fan-shaped Au structure positioned at a well-specified distance above a reflective plane with an intervening silica spacer layer. This antenna can be easily tuned to overlap vibrational modes within a broad spectral range from the near-IR into terahertz regimes. Our finite difference time domain (FDTD) simulations reveal a maximum SEIRA enhancement factor of 105 in the antenna junction area, which is corresponding to the experimental detection of 20-200 zeptomoles of octadecanethiol, using a standard commercial FTIR spectrometer. Our optimized antenna exhibits an order of magnitude greater SEIRA sensitivity than previous record-setting designs, which opens new opportunities for using infrared spectroscopy to analyze exceptionally small quantities of molecules.

9554-37, Session 8

Shell-isolated nanoparticle-enhanced Raman spectroscopy: principle and applications

Jian-Feng Li, Zhong-Qun Tian, Xiamen Univ. (China)

Surface-enhanced Raman spectroscopy (SERS) is a powerful technique that yields fingerprint vibrational information with ultra-high sensitivity. However, only roughened Ag, Au and Cu surfaces can generate strong SERS effect. The lack of materials and morphology generality has severely limited the breadth of SERS practical applications on surface science, electrochemistry and catalysis.

Shell-isolated nanoparticle-enhanced Raman spectroscopy (SHINERS) was therefore invented to break the long-standing limitation of SERS. In SHINERS, Au@SiO2 core-shell nanoparticles were rationally designed. The gold core acts as plasmonic antenna and encapsulated by an ultra-thin, uniform and pinhole-free silica shell, can provide high electromagnetic field to enhance the Raman signals of probed molecules. The inert silica shell acts as tunneling barrier prevents the core from interacting with the environment.

SHINERS has already been applied to a number of challenging systems, such as hydrogen and CO on Pt(hkl) and Rh(hkl), which can't be realized by traditional SERS. Combining with electrochemical methods, we has investigated the adsorption processes of pyridine at the Au(hkl) single crystal/solution interface, and in-situ monitored the surface electro-oxidation at Au(hkl) electrodes. These pioneering studies demonstrate convincingly the ability of SHINERS in exploring correlations between structure and reactivity as well as in monitoring intermediates at the interfaces. SHINERS was also explored from semiconductor surface for industry, to living bacteria for life science, and to pesticide residue detection for food safety. The concept of shell-isolated nanoparticle-enhancement is being applied to other spectroscopies such as infrared absorption, sum frequency generation and fluorescence.

Jian-Feng Li et al., Nature, 2010, 464, 392-395.

9554-38, Session 8

Dynamic placement of plasmonic hotspots for super-resolution chemical imaging

Nathan C. Lindquist, Christopher T. Ertsgaard, Rachel M. McKoskey, Isabel S. Rich, Bethel Univ. (United States)

We demonstrate dynamic placement of plasmonic "hotspots" for superresolution chemical imaging via Surface Enhanced Raman Spectroscopy (SERS). A silver nanohole array surface was first coated with various biological samples and illuminated with a laser. After optical filtering, the SERS hotspots could be imaged over a wide field of view on a CCD camera. Due to the large plasmonic field enhancements, blinking behavior of the SERS hotspots was observed and processed using a Stochastic Optical Reconstruction Microscopy (STORM) algorithm enabling localization of the hotspots to within 10 nm. However, illumination of the sample with a single static laser beam (i.e., a slightly de-focused Gaussian beam) only produced SERS hotspots in fixed locations on the surface, leaving noticeable gaps in any final super-resolution STORM image. But, by using a spatial light modulator (SLM), the illumination profile of the beam could be altered, shifting any hotspots across the nanohole array surface in sub-wavelength steps (i.e., shift a hotspot's position by <100 nm with an illumination wavelength of 660 nm). Therefore, by properly structuring an illuminating light field with the SLM, we show the possibility of positioning plasmonic hotspots over a metallic nanohole surface on-the-fly. Using this and our SERS-STORM imaging technique, we show potential for high-resolution chemical imaging without the noticeable gaps that were present with static laser illumination. Interestingly, even illuminating the surface with randomly shifting SLM phase profiles was sufficient to completely fill in a wide field of view for super-resolution SERS imaging of a single strand of collagen protein fibrils.

9554-39, Session 9

Nanospectroscopy of hybrid metallicinorganic and metallic-organic systems (Invited Paper)

Monika Fleischer, Eberhard Karls Univ. Tübingen (Germany)

Plasmonic nanostructures acting as optical antennas are employed to locally create electrical near-fields and concentrate energy. Through the nanostructures' plasmon resonances the enhancement effects are spectrally dependent. The nanostructure material and geometry can be tailored to match either an exciting wavelength, or particular transitions of a nanosystem that is coupled to the nanoantenna. Such hybrid structures present interesting systems for near-field enhancement studies, single nanoemitter spectroscopy, for the modification of polarization and radiation characteristics, or for sensors and device applications.

In this presentation different hybrid nanostructures are introduced. Plasmonic nanostructures are fabricated by electron beam lithography, either in a lift-off process or by etch-mask transfer techniques. The geometry and plasmonic modes of the metallic nanostructures are thoroughly characterized by scanning electron microscopy, atomic force microscopy, numerical simulations, and nanospectroscopy [1-4]. To prepare hybrid systems based on these structures, nanoscale control over the positioning of nanoemitters within the high near-field regions of the plasmonic nanoantennas, or nanoscale thickness control over organic layer deposition are required. Firstly, strategies for the self-aligned fabrication of nanocone-nanoemitter structures by back-etching, dry ablation, and dielectrophoresis are demonstrated [4]. Secondly, nanogratings coupled to organic thin-films are discussed [3]. The respective hybrid systems are investigated by microscopy, dark-field scattering, extinction and Raman spectroscopy.

[1] C. Schäfer et al., Nanoscale 5, 7861 (2013)

- [2] A. Horrer et al., Small 9, 3987 (2013)
- [3] D.A. Gollmer et al., Microelectron. Eng. 119, 122 (2014)
- [4] C. Schäfer et al., Lab Chip 15, 1066 (2015)



9554-40, Session 9

Live cell imaging using Au-NNP (Nanobridged Nanogap Particles) (Invited Paper)

Yung Doug Suh, Korea Research Institute of Chemical Technology (Korea, Republic of)

Single-particle tracking Live-Cell imaging using Au-NNP(Nanobridged Nanogap Particles) will be presented. Due to a stable plasmonic amplification of Raman signal from the intra-nanogap of Au-NNP, we have a stable and strong Raman signal enough for single particle imaging of Au-NNP in live cell. Multiplex imaging by encoding different Raman dyes into this nanogap and its application will be also discussed.

9554-41, Session 9

Morphologically controlled devices for SERS/TERS-like applications at the nanoscale (Invited Paper)

Remo Proietti Zaccaria, Istituto Italiano di Tecnologia (Italy)

Top-down fabrication allows for the realization of morphologically controlled micro/nano devices down to few nanometers scale. We investigate a number of applications based on this fabrication technique, with special emphasis towards nanoplasmonics. In particular, we shall focus on quasi-2D and 3D SERS devices, to move on with TERS structures especially designed to provide superfocusing characteristic. This feature, besides having tremendous impact in improving the TERS spatial resolution, is at the core of a new kind of nanoscopy technique based on hot-electrons transfer.

Finally, we shall provide a flavor of a new paradigm, namely the magnetic field enhancement and concentration from 2D SERS-like nanodevices.

9554-42, Session 9

Magnetic plasmonic Fano resonance at optical frequency (Invited Paper)

Zheyu Fang, Yanjun Bao, Peking Univ. (China)

We demonstrate a purely magnetic plasmon Fano resonance at optical frequency with Au split ring hexamer nanostructure excited by an azimuthally polarized incident light. Collective magnetic plasmon modes induced by the circular electric field within the hexamer and each of the split ring can be controlled and effectively hybridized by designing the size and orientation of each ring unit. With control of the magnetic Fano resonance, the split ring hexamer configuration can be further extended to obtain a double Fano resonance, which shows potential in the narrow line-shape engineering and low-loss magnetic plasmon resonance applications.

9554-43, Session 9

Metallic nanorods array for magnified subwavelength imaging

Yoshiro Ohashi, Bikas Ranjan, Yuika Saito, Prabhat Verma, Osaka Univ. (Japan)

Earlier, our group proposed a lens made of metallic nanorods, stacked in 3D arrays tapered in a conical shape. This nanolens could theoretically realize super-resolution color imaging in the visible range. The image could be magnified and transferred through metallic nanorods array. Lithography or self-assembly are common ways to fabricate such nanostructured devices. However, to precisely arrange nanorods is challenging due to the limitations to scale down components, and to increase accuracy of assembling particles

in large area.

Here we experimentally demonstrated 2D nanolens with long chains of metallic nanorods placed at tapered angles in a fan-like shape to magnify images. In the fabrication, we chemically synthesized gold nanorods coated with CTAB surfactant to ensure a 10 nm gap between the rods for the resonance control of nanolens. And we prepared trenches patterned by FIB lithography on a PMMA coated glass substrate. The different hydrophobicity of PMMA and CTAB coats enabled to optimize capillary force in gold nanorod solution and selectively assemble nanorods into hydrophilic trenches. Finally, we obtained 2D nanolens after lift-off of the PMMA layer.

We numerically estimated the resonance property of nanorods chain and found a broad peak in the visible range located at a wavelength of 727 nm. The broadness of this peak (~178 nm) confirms that a broad range of wavelength can be resonant with this structure. This phenomenon was also confirmed experimentally by optical measurements. These results show that the combination of lithography and self-assembly has the potential to realize plasmonic nanolens.

9554-44, Session 10

Raman identification of edge misalignment of bilayer graphene down to the nanometer scale (Invited Paper)

Ping-Heng Tan, Institute of Semiconductors (China)

No Abstract Available

9554-45, Session 10

Space and time localization of the Raman scattering in graphene systems (Invited Paper)

Ado Jorio, Univ. Federal de Minas Gerais (Brazil)

This work focuses on the localization aspects of Raman spectroscopy. The materials under study are graphene related systems. Spatial localization is considered in tip-enhanced Raman spectroscopy (TERS), with focus on the specific aspects of TERS in two-dimensional systems. Time localization is considered in the correlation between the Stokes (S) and anti-Stokes (aS) scattering events, which leads to corrections in the broadly used relation between the S/aS ratio and the boson statistics. This phenomenon is shown to be special for low-dimensional systems under specific resonance conditions.

9554-46, Session 10

Nonlinear photo-oxidation of graphene and carbon nanotubes probed by four wave mixing imaging and spectroscopy (Invited Paper)

Mika Pettersson, Jukka Aumanen, Andreas Johansson, Juha Koivistoinen, Pasi Myllyperkiö, Univ. of Jyväskylä (Finland)

Graphene has high potential for becoming the next generation material for electronics, photonics and optoelectronics. However, spatially controlled modification of graphene is required for applications. Here, we report patterning and controlled tuning of electrical and optical properties of graphene by laser induced non-linear oxidation. We use four wave mixing (FWM) as a key method for imaging graphene and graphene oxide patterns with high sensitivity. FWM produces strong signal in monolayer graphene and the signal is highly sensitive to oxidation providing good contrast between patterned and non-patterned areas. We have also performed photo-oxidation and FWM imaging for air suspended carbon nanotubes.

SPIE. PHOTONICS NANOSCIENCE+ ENGINEERING

9554-48, Session PWed

Multiplexed label-free detection of single proteins

Aleksandar Sebesta, Alexander Weigel, Philipp Kukura, Univ. of Oxford (United Kingdom)

Optical detection of single molecules usually relies on the fluorescent properties of the molecule or a label. Samples like proteins are purely refractive in the visible and near infrared, and thus not detectable by fluorescence without additional labelling. Recent alternative approaches used the local refractive index sensitivity of surface plasmon resonances to sense proteins as small as 53 kD even without any labels. 1,2

So far, all of these methods relied on the subsequent readout of one gold nanoparticle at a time. We present a novel wide-field detection scheme, which allows us to simultaneously monitor the surface plasmon resonance of multiple gold nanorods. The setup is based on a home-built ultrasensitive darkfield microspectroscope, which was shown to be 2 orders of magnitude more sensitive than the current state of the art, and capable of detecting and characterising 10 nm diameter gold nanospheres.3 Here, we directly recorded 2-dimensional, spectrally dispersed images of a gold nanorod array. The spectral positions were referenced with additional monochromatic illumination, allowing us to use the full 2D space of the sensor without any slit in the detection path. We present simultaneous readout traces of multiple gold nanorods with single-protein sensitivity. The technique not only increases the number of detected events for a given bulk concentration, but also allows us to distinguish general fluctuations and correlated noise from particle-specific protein binding steps. Together with the simple experimental implementation, our approach paves the way towards routine and efficient label-free detection down to the single molecule level.

Zijlstra P., Paulo P.M.R and Orrit M., Nat. Nanotechnol., 2012, 7, 379-382
 Ament I., Prasad J, Henkel A., Schmachtel S. and So?nnichsen C., Nano

Lett. 2012, 12, 1092?1095 [3] Weigel A., Sebesta A., Kukura P., ACS Photonics, 2014, 1, 848-856

9554-49, Session PWed

Spectral analysis of photonic nanojet and exploring different microstructures with jet-like photonic beam for imaging applications

Mohsen Rezaei, Alireza Bonakdar, Hooman Mohseni, Northwestern Univ. (United States)

Resolution in all imaging devices using conventional photonics is limited on Abbe diffraction limit. Overcoming this limit has frequently been the goal to achieve high resolution -beyond diffraction limit- imaging or lithography. In this work we evaluate the photonic jet (PJ) which is essentially light confinement beyond diffraction limit using dielectric microspherers. In PJ evanescent and propagative field are contributing, and resulting in confined optical mode beyond the diffraction limit. PJ has received a tremendous attention within the last decade, with numerous applications in imaging, lithography and enhancing light matter interaction. The main problem in using PJ for lithography and imaging is its severe aberration due to curvature of the microspheres. We proposed a new "hourglass" structure, which can produce a jet like focusing, but with a planar focal plane. We will evaluate the spectral and spatial quality of the jet of light produced in this structure, and compare it with those produced by microspheres.

9554-50, Session PWed

Photo-induced magnetic force using nano probes

Caner Guclu, Univ of California Irvine (United States); Venkata A. Tamma, H. Kumar Wickramasinghe, Filippo

Capolino, Univ. of California, Irvine (United States)

A theoretical investigation of the photo-induced magnetic force between nanostructures is presented as an initial assessment of the strength of magnetic field - matter interactions at optical frequencies. Atomic Force Microscopy (AFM) using static magnetism is an established method; whereas optical magnetic effects have not been of use in AFM due to vanishing natural magnetism in molecules and nanostructures at optical frequencies. Nevertheless, recently it has been shown that artificial magnetism can be established in engineered nanostructures and here we report that it can lead to detectable magnetic force levels. In particular we consider two examples of nanoprobes, namely a Si nanosphere and a circular cluster of plasmonic nanospheres. Both structures, either via a Mie magnetic resonance or by a collective plasmonic resonance, respectively, exhibit strong magnetic polarizability. These structures can be used as nanoprobes to detect magnetic fields and forces at optical frequencies. In particular we investigate the case of two nanoprobes interacting with each other, as an exemplary interacting structure, and the dependence of force magnitude and direction on the inter-probe disposition. We report forces in piconewton range when the nanoprobes are illuminated with a LASER beam intensity of 133 W/cm^2. Results show that Scanning Probe Microscopy (SPM) can be based on photo-induced magnetic nanoprobe for the investigation of artificial magnetism and weak magnetic-dipole transitions at optical frequencies. Such nanoprobes can enhance magnetic transitions and even lead to detection by force microscopy with nanoscale precision.

9554-51, Session PWed

Shell-isolated silver nanoparticles for plasmon-enhanced spectroscopies

Chaoyu Li, Meng Meng, Shaorong Huang, Jianfeng Li, Zhongqun Tian, Xiamen Univ. (China)

In 2010, our group has invented a novel strategy called Shell-Isolated Nanoparticle-Enhanced Raman Spectroscopy (SHINERS) to overcome the substrate and surface generalities of surface-enhanced Raman scattering (SERS). The SERS-active Au nanospheres are coated with the ultrathin silica shell to prevent the interference from the environment, while the Au cores can provide strong electromagnetic (EM) field to enhance the probe molecules nearby. In-situ SHINERS technology has already been applied to a number of challenging systems.

In plasmonics, silver nanostructures have plenty of advantages over other noble metals due to its special dielectric property in visible and nearinfrared regions. Herein, we use silver nanoparticles as cores instead of gold ones in the synthesis of SHINERS particles so that we can obtain a much stronger localized optical field in the applications of plasmon-enhanced spectroscopies, such as Raman, fluorescence, and etc.

The Ag nanospheres are synthesized by the seed-mediated growth method in which citrate ions acts as surface protection ligands. The as-prepared Ag@SiO2 nanoparticles could be introduced as signal amplifier to probe the surface adsorbates on the well-defined substrate, monitor the surface catalytic reactions and bear great potentials on plasmon mediated photocatalysis.

References

J. F. Li, Y. F. Huang, Y. Ding et al., Nature 464, 392 (2010).
 J. F. Li, X. D. Tian, S. B. Li et al., Nat. Protocols 8, 52 (2013).

9554-52, Session PWed

Nanodiamonds as cellular marker for super-resolution STED-TEM correlative microscopy

Neeraj Prabhakar, Åbo Akademi Univ. (Finland)

We describe a correlative STED-TEM method and application of nanodiamonds (ND) as a unique dual purpose label for TEM and STED. NDs have excellent photostability, no-blinking, far red emission and fluorescence

Conference 9554: Nanoimaging and Nanospectroscopy III



originating from NDs has been shown to be depleted by STED laser allowing it to be resolved up to 6 nm, thus making an ideal super-resolution optical probe. Moreover, the electron dense nature of nanodiamonds allows it to be detected by TEM. First, we used nanogold (Au NP) ink pattern printed coverslips to grow MDA-MB-231 cells. Cells were then labeled with NDs and detected by live cell imaging. Au NP printed coverslips served as a landmark to mark and locate the position of cells with respect to intracellular fluorescent NDs. Therefore, this technique acted as a sophisticated method to precisely localize any cell of interest. Second, once the cell of interest was identified and fixed, nano-gold patterns allowed the re-identification in the block face, thus led to embedding and sectioning of the same cell. 70 nm thin sections of ND containing cells were prepared and imaged with TEM. ND allowed cells to be detected in TEM along with sub-cellular features. Finally, the TEM section was imaged with STED microscope exploiting NDs. as dual. The images obtained from both modalities were correlated with nanometer precision using our open source software. The current work demonstrates the potential of achieving correlative optical resolution with respect to TEM resolution.

Conference 9555: Optical Sensing, Imaging, and Photon Counting: Nanostructured Devices and Applications

Tuesday - Thursday 11-13 August 2015

Part of Proceedings of SPIE Vol. 9555 Optical Sensing, Imaging, and Photon Counting: Nanostructured Devices and Applications

9555-1, Session 1

Solar-blind photodetectors and focal plane arrays based on AlGaN

Ryan McClintock, Northwestern Univ. (United States)

III-Nitride material system (AlGaInN) possesses unique optical, electrical and structural properties such as a wide tunable direct bandgap, inherent fast carrier dynamics; good carrier transport properties, high breakdown fields; and high robustness and chemical stability. Recent technological advances in the wide bandgap AIGaN portion of this material system have led to a renewed interest in ultraviolet (UV) photodetectors. These detectors find use in numerous applications in the defense, commercial and scientific arenas such as covert space-to-space communications, early missile threat detection, chemical and biological threat detection and spectroscopy, flame detection and monitoring, UV environmental monitoring, and UV astronomy. Back illuminated detectors operating in the solar blind region are of special interest. Back illumination allows the detector to be hybridized to a silicon read-out integrated circuit, epi-side down, and still collect light through the back of the transparent sapphire substrate. This allows the realization of solar blind focal plane arrays (FPAs) for imaging applications. Solar-blind FPAs are especially important because of the near total absence of any background radiation in this region.

In this talk, we will present our recent back-illuminated solar-blind photodetector, mini-array, and FPA results. By systematically optimizing the design of the structure we have realized external quantum efficiencies (EQE) of in excess of 89% for pixel-sized detectors. Based on the absence of any anti-reflection coating, this corresponds to nearly 100% internal quantum efficiency. At the same time, the dark current remains below -2 ? 10-9 A/ cm2 even at 10 volts of reverse bias. The detector has a very sharp falloff starting at 275 with the UV-solar rejection of better than three orders of magnitude, and a visible rejection ratio is more than 6 orders of magnitude. This high performance photodetector design was then used as the basis of the realization of solar-blind FPA. We demonstrated a 320x256 FPA with a peak detection wavelength of 278nm. The operability of the FPA was better than 92%, and excellent corrected imaging was obtained.

9555-3, Session 1

Growth of AlGaN on silicon substrates: a novel way to make back-illuminated ultraviolet photodetectors (Invited Paper)

Ryan McClintock, Manijeh Razeghi, Northwestern Univ. (United States)

AlGaN, with its tunable wide-bandgap is a good choice for the realization of ultraviolet photodetectors. AlGaN films tend to be grown on foreign substrates such as sapphire, which is the most common choice for backilluminated devices. However, even ultraviolet opaque substrates like silicon holds promise because, silicon can be removed by chemical treatment to allow back-illumination, and it is a very low-cost substrate which is available in large diameters up to 300 mm. However, Implementation of silicon as the solar-blind PD substrates requires overcoming the lattice-mismatch (17%) with the AlxGa1-xN that leads to high density of dislocation and crackinitiating stress.

In this talk, we report the growth of thick crack-free AlGaN films on (111) silicon substrates through the use of a substrate patterning and mask-less selective area regrowth. This technique is critical as it decouples the epilayers and the substrate and allows for crack-free growth; however, the masking also helps to reduce the dislocation density by inclining the growth direction and encouraging dislocations to annihilate. A back-illuminated

p-i-n PD structure is subsequently grown on this high quality template layer. After processing and hybridizing the device we use a chemical process to selectively remove the silicon substrate. This removal has minimal effect on the device, but it removes the UV-opaque silicon and allows backillumination of the photodetector. We report our latest results of backilluminated solar-blind photodetectors growth on silicon.

9555-4, Session 1

Ultraviolet avalanche photodiodes

Ryan McClintock, Manijeh Razeghi, Northwestern Univ. (United States)

The III-Nitride material system is rapidly maturing; having proved itself as a material for LEDs and laser, and now finding use in the area of UV photodetectors. However, many UV applications are still dominated by the use of photomultiplier tubes (PMT). PMTs are capable of obtaining very high sensitivity using internal electron multiplication gain (typically ~106). It is highly desirable to develop a compact semiconductor-based photodetector capable of realizing this level of sensitivity. In principle, this can be obtained in III-Nitrides by taking advantage of avalanche multiplication under high electric fields – typically 2.7 MV/cm, which with proper design can correspond to an external reverse bias of less than 100 volts.

In this talk, we review the current state-of-the-art in III-Nitride solar- and visible-blind APDs, and present our latest results on GaN APDs grown on both conventional sapphire and low dislocation density free-standing c- and m-plane GaN substrates. Leakage current, gain, and single photon detection efficiency (SPDE) of these APDs were compared. The spectral response and Geiger-mode photon counting performance of UV APDs are studied under low photon fluxes, with single photon detection capabilities as much as 30% being demonstrated in smaller devices. Geiger-mode operation conditions are optimized for enhanced SPDE

9555-5, Session 2

+1 360 676 3290 · help@spie.org

Colloidal quantum dots for mid-infrared detection (*Invited Paper*)

Philippe Guyot-Sionnest, The Univ. of Chicago (United States)

Colloidal quantum dots present an opportunity as infrared and liquid processed materials. Initial results in 2011 showed mid-infrared detection with HgTe colloidal quantum dots in the mi-IR range, 3-5 microns. This has been now extended to the long-wave IR, 8-12 microns. The infrared response from the HgTe colloidal quantum dots arises from the absorption of light across the gap created by the confinement. The large dots absorbing the LWIR are about 20 nm in size and the size dispersion will need improvements. While Interband absorption requires the material to be zero or small-gap semiconductors, intraband transitions have no such limitations. However, this requires doped colloidal quantum dots. Two colloidal quantum dot materials, the small gap (0.6 eV) b-HgS and the zero-gap HgSe turn out to be stably doped with electrons. This has led to the observation of Mid-IR intraband photoconduction in both systems and alternative materials for IR detection.

There are several basic challenges, besides fabrication and reliability. The proximity of the surface from the excitation leads to very short excited lifetimes due to nonradiative processes. Controlling the surface will be the avenue to lengthen the lifetime, while plasmonic coupling may lead to shorter radiative lifetime. Since the surface is easily chemically modified, it also leads to strong changes in the Fermi level and this will need to be controlled.



In this talk, I will describe my understanding of the potential and limitations of this material approach to infrared detection, while discussing aspects of transport, photoluminescence, doping and photovoltaic responses.

9555-6, Session 2

Colloidal quantum dot Vis-SWIR imaging: demonstration of a focal plane array and camera prototype (Invited Paper)

Ethan J. D. Klem, Christopher W. Gregory, Dorota S. Temple, Jay S. Lewis, RTI International (United States)

RTI has developed a photodiode technology based on solution-processed PbS colloidal quantum dots (CQD). These devices are capable of providing low-cost, high performance detection across the Vis-SWIR spectral range. At the core of this technology is a heterojunction diode structure fabricated using techniques well suited to wafer-scale fabrication, such as spin coating and thermal evaporation. This enables RTI's CQD diodes to be processed at room temperature directly on top of read-out integrated circuits (ROIC), without the need for the hybridization step required by traditional SWIR detectors. Additionally, the CQD diodes can be fabricated on ROICs designed for other detector material systems, effectively allowing rapid prototype demonstrations of CQD focal plane arrays at low cost and on a wide range of pixel pitches and array sizes.

We will show the results of fabricating CQD arrays directly on top of commercially available ROICs. Specifically, the ROICs are a 640 x 512 pixel format with 15 μm pitch, originally developed for InGaAs detectors. We will show that minor modifications to the surface of these ROICs make them suitable for use with our CQD detectors. Once completed, these FPAs are then assembled into a demonstration camera and their imaging performance is evaluated. In addition, we will discuss recent advances in device architecture and processing resulting in devices with room temperature dark currents of 2-5 nA/cm^2 and sensitivity from 350 nm to 1.7 μm .

This combination of high performance, dramatic cost reduction, and multi-band sensitivity is ideally suited to expand the use of SWIR imaging in current applications, as well as to address applications which require a multispectral sensitivity not met by existing technologies.

9555-7, Session 2

Colloidal quantum dot photodetectors *(Invited Paper)*

Valerio Adinolfi, Edward H. Sargent, Univ. of Toronto (Canada)

Colloidal quantum dots (CQDs) are emerging solution processed materials combining low cost, easy deposition on large and flexible substrates, and bandgap tunability. The latter feature, which allows spectral tuning of the absorption profile of the semiconductor, makes these materials particularly attractive for light detection applications. Lead sulfide (PbS) CQDs, in particular, have shown astonishing performance as a light sensitive material operating at visible and infrared (IR) wavelengths. Early studies of PbS CQDs used as a photosensitive resistor (photoconductor) showed an impressive responsivity - exceeding 1000 A/W - and a detectivity (D*) higher then 10^13 Jones. This impressive D* was preserved in the successive development of the first PbS CQD photodiode, showing the possibility to realize fast - f_3db > 1Mhz - and sensitive IR detectors. Currently, the field is moving toward the development of hybrid devices and phototransitors. PbS CQDs have been combined in field effect transistors (FETs) with graphene and MoS2 channels, showing ultra-high gain (exceeding 10^8 electrons/ photons) and high D*. Recently a photo-junction FET (photo-JFET) has been reported that breaks the inherent dark current/gain/bandwidth compromise affecting photoconductive light detectors. With this presentation we offer a broad overview on CQD photodetection highlighting the past achievements, the benefits, the challenges and the prospects for the future research on this field.

9555-8, Session 2

Superlattice infrared photodetector research at the jet propulsion laboratory (Invited Paper)

NANOSCIENCE+ ENGINEERING

Sarath D. Gunapala, David Z. Y. Ting, Alexander Soibel, Sir B. Rafol, Arezou Khoshakhlagh, Linda Höglund, Cory J. Hill, Sam A. Keo, John K. Liu, Jason M. Mumolo, Edward M. Luong, Jet Propulsion Lab. (United States)

Recently, 320x256 pixel focal plane arrays (FPAs) with 30?m pixel pitch were fabricated with LWIR CBIRD material by dry etching through the top contact, hole-barrier superlattice (SL), photosensitive absorber SL, electron-barrier SL into the 0.5µm thick doped GaSb detector common layer. Some imagery was performed at a temperature of 78 K. The measured mean NE?T was 18.6 mK at a flat plate blackbody temperature of 300K with f/2 cold stop. The experimentally measured FPA quantum efficiency is 45%. The horizontal and vertical modulation transfer functions (MTFs) at Nyquist frequency based on pixel pitch, a, (= 1/2a, a = 30?m) ~16.67cycles/ mm are about ~0.49 and ~0.52, respectively. The image quality of the natural scene attests to the very good MTF behavior at low and high frequencies. The FPA MTF can be separated into the product of two components. The geometric aperture MTF is related to the pixel size and the diffusion MTF related to electro-optical properties. The diffusion MTF depends on the diffusion length and geometry. The CBIRD pixels are delineated down to the bottom contact and it is expected that no lateral carrier diffusion into the next neighbor can occur. The disadvantage is that the fill factor is less than 100%. Shorter wavelengths on the other hand can be absorbed near the top surface and can diffuse to the next neighbor. In CBIRD FPA, the only channel left for the charge carriers to diffuse to an adjacent pixel is through the thin detector common layer of the FPA.

9555-9, Session 2

Identification of point defect candidates in strained-layer type-II superlattices for infrared detectors: ab initio electronic structure studies (Invited Paper)

Nicholas Kioussis, California State Univ., Northridge (United States)

The InAs/GaSb and InAs/InAsSb type-II strain-layer superlattices (T2SLS) are of great importance and show great promise for mid-wave and longwave infrared (IR) detectors for a variety of civil and military applications. The T2SLS offer several advantages over present day detection technologies including suppressed Auger recombination relative to the bulk MCT material, high quantum efficiencies, and commercial availability of low defect density substrates. While the T2SLS detectors are approaching the empirical Rule-07 benchmark of MCT's performance level, the dark-current density is still significantly higher than that of bulk MCT detectors. One of the major origins of dark current is associated with the Shockley-Read- Hall (SRH) process in the depletion region of the detector.

I will present results of ab initio electronic structure calculations of the stability of a wide range of point defects [As and In vacancies, In, As and Sb antisites, In interstitials, As interstitials, and Sb interstitials] in various charged states in bulk InAs, InSb, and InAsSb systems and T2SLS. I will also present results of the transition energy levels. The calculations reveal that compared to defects in bulk materials, the formation and defect properties in InAs/InAsSb T2SLS can be affected by various structural features, such as strain, interface, and local chemical environment. I will present examples which demonstrate that the effect of strain or local chemical environment shifts the transition energy levels of certain point defects either above or below the conduction band minimum, thus suppressing their contribution to the SRH recombination.

9555-10, Session 3

III-V strain layer superlattice based band engineered avalanche photodiodes

(Invited Paper)

Sid Ghosh, Raytheon Space and Airborne Systems (United States)

Laser detection and ranging (LADAR)-based systems operating in the Near Infrared (NIR) and Short Wave Infrared (SWIR) have become popular optical sensors for remote sensing, medical, and environmental applications. Sophisticated laser-based radar and weapon systems used for long-range military and astronomical applications need to detect, recognize, and track a variety of targets under a wide spectrum of atmospheric conditions. Infrared APDs play an important role in LADAR systems by integrating the detection and gain stages in a single device. Robust silicon-APDs are limited to visible and very near infrared region (< 1 um), while InGaAs works well up to wavelengths of about 1.5um. Si APDs have low multiplication or excess noise but are limited to below 1um due very poor quantum efficiency above 0.8um. InGaAs and Ge APDs operate up to wavelengths of 1.5um but have poor multiplication or excess noise due to a low impact ionization coefficient ratio between electrons and holes. For the past several decades HgCdTe has been traditionally used in longer wavelength (> 3um) infrared photon detection applications. Recently, various research groups (including Ghosh et. al.) have reported SWIR and MWIR HgCdTe APDs on CdZnTe and Si substrates. However, HgCdTe APDs suffer from low breakdown fields due to material defects, and excess noise increases significantly at high electric fields

During the past decade, InAs/GaSb Strain Layer Superlattice (SLS) material system has emerged as a potential material for the entire infrared spectrum because of relatively easier growth, comparable absorption coefficients, lower tunneling currents and longer Auger lifetimes resulting in enhanced detectivities (D*). Band engineering in type II SLS allows us to engineer avalanche properties of electrons and holes. This is a great advantage over bulk InGaAs and HgCdTe APDs where engineering avalanche properties is not possible.

The talk will discuss the evolution of superlattice based avalanche photodiodes and some of the recent results on the work being done at Raytheon on SWIR avalanche photodiodes.

9555-12, Session 3

Recent progress in high gain InAs avalanche photodiodes (Invited Paper)

Seth Bank, Scott J. Maddox, The Univ. of Texas at Austin (United States); Wenlu Sun, Univ. of Virginia (United States); Hari P. Nair, The Univ. of Texas at Austin (United States); Joe C. Campbell, Univ. of Virginia (United States)

InAs possesses nearly ideal material properties for the fabrication of nearand mid-infrared avalanche photodiodes (APDs), which result in strong electron-initiated impact ionization and negligible hole-initiated impact ionization [1]. Consequently, InAs multiplication regions exhibit several appealing characteristics, including extremely low excess noise factors and bandwidth independent of gain [2], [3]. These properties make InAs APDs attractive for a number of near- and mid-infrared sensing applications including remote gas sensing, light detection and ranging (LIDAR), and both active and passive imaging. Here, we discuss our recent advances in the growth and fabrication of high gain, low noise InAs APDs. Devices yielded room temperature multiplication gains >300, with much reduced ($\sim 10x$) lower dark current densities. We will also discuss a likely key contributor to our current performance limitations: silicon diffusion into the intrinsic (multiplication) region from the underlying n-type layer during growth. Future work will focus on increasing the intrinsic region thickness, targeting gains >1000. This work was supported by the Army Research Office (W911NF-10-1-0391).

[1] A. R. J. Marshall, C. H. Tan, M. J. Steer, and J. P. R. David, "Electron dominated impact ionization and avalanche gain characteristics in InAs

photodiodes," Applied Physics Letters, vol. 93, p. 111107, 2008.

[2] A. R. J. Marshall, A. Krysa, S. Zhang, A. S. Idris, S. Xie, J. P. R. David, and C. H. Tan, "High gain InAs avalanche photodiodes," in 6th EMRS DTC Technical Conference, Edinburgh, Scotland, UK, 2009.

ENGINEERING

[3] S. J. Maddox, W. Sun, Z. Lu, H. P. Nair, J. C. Campbell, and S. R. Bank, "Enhanced low-noise gain from InAs avalanche photodiodes with reduced dark current and background doping," Applied Physics Letters, vol. 101, no. 15, pp. 151124–151124–3, Oct. 2012.

9555-13, Session 3

Evaluation of different processing steps on the dark current of electron-injection detectors

Mohsen Rezaei, Sung Jun Jang, Hooman Mohseni, Northwestern Univ. (United States)

Our recently published results show a much reduced dark current and enhanced speed from our second-generation electron-Injection detectors, due to the introduction of an isolation method. However, these results have been limited to single-element detectors. A natural next step is to incorporate these new devices into a focal plane array (FPA), since we have already achieved very attractive results from an FPA based on the first-generation devices, isolation introduces new processing steps and a robust procedure is required for realization of focal plane arrays (FPA) with good uniformity and yield. Here we report our systematic evaluation of the processing steps, and in particular the effect of the processing temperature, on the device dark current and uniformity. Our goal is to produce ultra-low dark current FPA based on isolated electron-injection detectors, and to approach single-photon sensitivity.

9555-14, Session 3

Effect of temperature on superconducting nanowire single-photon detector noise

Andrea Bahgat Shehata, Alessandro Ruggeri, Franco Stellari, Alan J. Weger, Peilin Song, IBM Thomas J. Watson Research Ctr. (United States); Kristen Sunter, Karl K. Berggren, Massachusetts Institute of Technology (United States); Vikas Anant, Photon Spot, Inc. (United States)

Today Superconducting Nanowire Single-Photon Detectors (SNSPDs) are commonly used in different photon-starved applications, including testing and diagnostics of VLSI circuits. Detecting very faint signals in the nearinfrared wavelength range requires not only good detection efficiency, but also very low Dark Count Rate (DCR) and jitter. For example, low noise is crucial to lower the Bit Error Rate (BER) in Quantum Key Distribution (QKD), or to enable ultra-low voltage optical testing of integrated circuits. In this paper we study the effect of temperature on the noise of superconducting single-photon detectors made of NbN meanders. We show that two different regimes can be identified in the DCR vs. bias current characteristics. At high bias the dark count rate is dominated by the intrinsic noise of the detector that depends on its switching current, while at low bias current it is dominated by the detection of stray photons that get onto the SNSPD. Changing the detector temperature changes its switching current and only affects the high bias branch of the characteristics: a reduction of the DCR can be achieved by lowering the SNSPD base temperature. On the other hand, changing the temperature of the single-photon light source (in our case VLSI circuits) only affects the low bias regime: a lower target temperature leads to a smaller DCR.

9555-15, Session 4

IR CMOS: near infrared enhanced digital imaging (Invited Paper)

Martin U. Pralle, James E. Carey, Thomas Joy, Chris J. Vineis, Chintamani Palsule, SiOnyx Inc. (United States)

SiOnyx has demonstrated imaging at light levels below 1 mLux (moonless starlight) at video frame rates with a 720P CMOS image sensor in a compact, low latency camera. Low light imaging is enabled by the combination of enhanced quantum efficiency in the near infrared together with state of the art low noise image sensor design. The quantum efficiency enhancements are achieved by applying Black Silicon, SiOnyx's proprietary ultrafast laser semiconductor processing technology. In the near infrared, silicon's native indirect bandgap results in low absorption coefficients and long absorption lengths. The Black Silicon nanostructured layer fundamentally disrupts this paradigm by enhancing the absorption of light within a thin pixel layer making 5 microns of silicon equivalent to over 300 microns of standard silicon. This results in a demonstrate 10 fold improvements in near infrared sensitivity over incumbent imaging technology while maintaining complete compatibility with standard CMOS image sensor process flows. Applications include surveillance, nightvision, and 1064nm laser see spot. Imaging performance metrics will be discussed.

Demonstrated performance characteristics:

Pixel size : 5.6 & 10 um Array size: 720P/1.3Mpix Frame rate: 60 Hz Read noise: 2 ele/pixel Spectral sensitivity: 400 to 1200 nm (with 10x QE at 1064nm) Daytime imaging: color (Bayer pattern) Nighttime imaging: moonless starlight conditions 1064nm laser imaging: daytime imaging out to 2Km

9555-16, Session 4

Si based mid-infrared GeSn photo detectors and light emitters on silicon substrates (Invited Paper)

Shui-Qing Yu, Wei Du, Benjamin R. Conley, Seyed A. Ghetmiri, Aboozar Mosleh, Thach Pham, Perry Grant, Yiyin Zhou, Huong Tran, Sattar Al Kabi, Univ. of Arkansas (United States); Amjad Nazzal, Wilkes Univ. (United States); Greg Sun, Richard A. Soref, Univ. of Massachusetts Boston (United States); Joe Margetis, John Tolle, ASM America Inc. (United States); Baohua Li, Arktonics, LLC (United States); Hameed A. Naseem, Univ. of Arkansas (United States)

The Ge1-xSnx alloy is a promising material for active and passive photonics on Si due to its identified direct bandgap, industry scalable growth, compatibility with complementary metal-oxide-semiconductor (CMOS) process, capability of monolithic integration on Si and broad wavelength coverage in infrared. The GeSn-based optoelectronic devices can be widely used in Si photonic applications such as active imaging, sensing, Ladar signal processing and high speed optical interconnects, et al.

In this work, high performance GeSn photoconductor and light emitting diodes (LED) have been demonstrated. For the photoconductor, the high responsivity was achieved due to high photoconductive gain, which is attributed to the novel optical and electrical design. A side by side comparison of spectral detectivity with other mature photo detectors indicates that the GeSn photoconductor is comparable with commercially available detectors such as InGaAs, InAs and Ge. The longwave cutoff at 2.4 ?m was also observed at room temperature. For LED, temperature-dependent study was conducted. The electroluminescence (EL) spectra

at different temperatures were obtained and EL peak shift was observed. Moreover, the emission power at different temperatures was measured. High power emission at 2.1 ?m was achieved.

PHOTONICS

NANOSCIENCE+ ENGINEERING

9555-17, Session 4

Optical absorption in 3D topological insulator Bi2Te3 with applications to THz detectors

Parijat Sengupta, Enrico Bellotti, Boston Univ. (United States)

Topological insulators (TI) are a new class of materials that have an energy gap in bulk but possess gapless states bound to the sample surface or edge that have been theoretically predicted and experimentally observed [1]. The topological state in Bi2Te3 is characterized by a linear dispersion and a Dirac cone at the ?point. The optical absorption on the surface of a TI is given by the standard graphene-like $2\pi/2$ when a linear dispersion is assumed. Realistically, at k-points away from ?, higher order cubic terms in k that represent the underlying hexagonal symmetry [2] of the crystal dominate and give rise to warping of bands. The optical absorption of a ferromagnetic coated gapped 3D TI film with warping terms considered is longer $2\pi/2$ but significantly modified. We demonstrate, by using wave functions from a continuum-Hamiltonian and Fermi-golden rule, the absorption spectrum on the surface of a TI as a function of the chemical potential, film-thickness and incident photon energy. A linear response theory based calculation is also performed using the Kubo formula to determine the longitudinal optical conductivity whose real part gives absorption as a function of photon frequency. The absorption in materials with Dirac fermions which is significantly higher than in normal THz detectors [3] can be further modulated in a TI by explicitly including the warping term making them highly efficient and tunable photodetectors.

M.Hasan and C.Kane, Rev.Mod.Phys. 82, 3045(2010)
 L.Fu, Phys.Rev.Lett.103, 266801(2009)
 X.Zhang et al., Phys. Rev B, 82, 245107(2010)

9555-18, Session 4

Design tradeoffs of II-VI and III-V superlattices for VLWIR sensing (Invited Paper)

Gail J. Brown, Frank Szmulowicz, Air Force Research Lab. (United States)

There are three leading options for creating superlattice materials to cover the very long wavelength infrared (VLWIR) sensing range: InAs/InGaSb, InAs/InAsSb and HgTe/CdTe. Each of these material systems has some advantages and disadvantages in the very narrow band gap regime, i.e. 100 to 50 meV. The results of an analysis of the design tradeoffs for these three superlattice materials will be presented. Areas to be discussed are: sensitivity to variations in layer widths and composition, absorption coefficient, carrier mobilities and lifetimes. Comparisons to experimental results, where available, will also be performed to support the design analysis. A review of the state-of-the-art for these three superlattice materials for VLWIR sensing will also be covered.

9555-19, Session 5

Full-band structure modeling of the radiative and non-radiative properties of semiconductor materials and devices (*Invited Paper*)

Enrico Bellotti, Hanqing Wen, Benjamin Pinkie, Masahiko



Matsubara, Boston Univ. (United States); Francesco Bertazzi, Politecnico di Torino (Italy)

Understanding the radiative and non-radiative properties of semiconductor materials is a prerequisite for optimizing the performance of existing light emitters and detectors and for developing new device architectures based on novel materials. Due to the ever increasing complexity of novel semiconductor systems and their relative technological immaturity, it is essential to have design tools and simulation strategies that include the details of the microscopic physics and their dependence on the macroscopic (continuum) variables in the macroscopic device models. Towards this end, we have developed a robust full-band structure based approach that can be used to study the intrinsic material radiative and non-radiative properties and evaluate the same characteristics of low-dimensional device structures. A parallel effort is being carried out to model the effect of substrate driven stress/strain and material guality (dislocations and defects) on microscopic quantities such as non-radiative recombination rate. Using this modeling approach, we have extensively studied the radiative and non-radiative properties of both elemental (Si and Ge) and compound semiconductors (HgCdTe, InGaAs, InAsSb and InGaN). In this work we outline the details of the modelling approach, specifically the challenges and advantages related to the use of the full-band description of the material electronic structure. We will present a detailed comparison of the radiative and Auger recombination rates as a function of temperature and doping for HgCdTe and InAsSb that are two important materials for infrared detectors and emitters. Furthermore we will discuss the role of non-radiatiave Auger recombination processes in explaining the performance of light emitter diodes. Finally we will present the extension of the model to low dimensional structures employed in a number of light emitter and detector structures.

9555-20, Session 5

Three-dimensional numerical modeling for ultra-sensitive noninvasive size-dependent nanoparticle detection technique using subwavelength silicon microcavities

Jeffrey P. Dionne, Lyuba Kuznetsova, San Diego State Univ. (United States)

Resonant microcavities that use whispering gallery modes (WGMs) allow sensitivity to a single bonding event [1] that makes silicon microcavity a promising candidate for a compact, label-free biosensor. The fact that the microdisk's size is comparable with a wavelength is extremely important because the fraction of the light that is absorbed per pass when interacting with a biological molecule is inversely proportional to the cross-sectional area of the optical mode. In addition, it has been recently proposed [2] that silicon is a promising material for mid-IR because of its low loss that opens up an opportunity for the detection of many biological nanoparticles.

In this work we use the three-dimensional finite-difference time-domain numerical simulations (COMSOL Multiphysics) to investigate a system, consisting of a silicon microdisk cavity (1?m radius, 250nm thickness), for the detection of different viruses of the same type by observing the effects that a spherical nanoparticle has on the frequency resonances of the silicon microdisk's WGMs. Numerical simulations show that the observed spectral shift for a nanoparticle with radius R=200 nm is significantly higher for the lower order modes (TM15 mode at ~1960nm) compare to the higher order modes at ~1130 nm. The observed spectral shift varies between 1.4-1.9 nm for the TM15 mode with an attached nanoparticle with radiuses between 100-300 nm. This frequency shift size-dependence makes it possible for the mature and immature HIV-1 viruses to be identified by the resonant frequency change in the transmission spectrum.

References

[1]Nature Methods 5, 591(2008) [2]Nature Photonics 4, 495(2010)

9555-21, Session 5

Electro-optical characteristics of p+n In0.53Ga0.47As photodiodes in large format dense focal plane arrays (Invited Paper)

Roger E. DeWames, FulcrumIT (United States): Kyle Witte, Patrick G. Maloney, U.S. Army Night Vision & Electronic Sensors Directorate (United States); Adam R. Wichman, Enrico Bellotti, Boston Univ. (United States); Manijeh Razeghi, Northwestern Univ. (United States)

This paper is concerned with focal plane array (FPA) data and applying analytical and three dimensional (3D) numerical simulation methods to capture the right physical effects and processes limiting performance. For shallow homojunction p+n designs, T <300K, in the analytical model the variations from bulk G-R dark current behavior are modeled with a perimeter dependent shunt current conjectured to be of origin at the InP/ InGaAs interface. A major result of the device's 3D numerical simulation is the prediction of a perimeter G-R current not associated with the properties of the metallurgical interface. For junctions positioned in the larger band gap InP cap layer, the QE is bias dependent and relatively large reverse bias \geq 0.9 volts are needed for the QE to saturate to the shallow homojunction value; at this bias voltage the dark current is larger than the shallow homojunction value. The 3D numerical and analytical models agree in predicting and explaining the measured radiatively limited diffusion current of origin in the n-side of the junction; the calculation of the area dependent G-R current is also in agreement. Substrate removal extends the quantum efficiency (QE) spectral band into the visible; dead layer effects limit the QE to 10% at a wavelength of 0.5 ?m.

9555-22. Session 5

Real-time baseline correction technique for MWIR and LWIR time-resolved photoluminescence spectroscopy

Zhi-Yuan Lin, Yong-Hang Zhang, Arizona State Univ. (United States)

The time-resolved photoluminescence (TRPL) measurement provides rich information about carrier dynamics and recombination mechanisms. However, TRPL measurements are guite challenging in mid-wave infrared (MWIR) and long-wave infrared (LWIR) regimes due to noise in photodetectors and data acquisition systems. Our analysis and experimental results show that the noise in a conventional TRPL system using a traditional averaging method is dominated by 1/f noise from 10 Hz to 3 kHz. The signal is also mixed with sub-Hertz noise associated with the boxcar baseline oscillation, commonly known as the "baseline drift" issue which results from numerous fluctuations in the system. A real-time baseline correction method is proposed and demonstrated to suppress these low frequency noise sources. The real-time baseline correction method is realized by modulating the signal. The modulation can be achieved by either electrical, mechanical, or optical approaches. Analysis indicates that the noise of this method is proportional to the noise spectral density at the modulation frequency, this argument is confirmed by the simulation results. The simulated noise achieved by the real-time baseline correction method is much lower than the traditional method. Experimental results show that the low frequency baseline oscillations associated with the traditional TRPL experiments are absent using the real-time baseline correction technique, and the noise of the measurement is significantly reduced. This work establishes a more efficient experimental method for TRPL measurements on weak MWIR and LWIR PL signals, such as the InAs/InAsSb type-II superlattice samples which are used here to demonstrate the proposed method.

9555-23, Session 6

Benefits of small pixel focal plane array technology (Invited Paper)

John T. Caulfield, Jon Paul Curzan, Cyan Systems (United States)

There are known limits in undersampled and critically sampled sensors regarding resolution and aliasing. Improved imaging systems using smaller sub diffraction sized pixels have shown good initial imaging results. Oversampling the image using sub-diffraction size pixels offers much more than improved resolution, smaller FPAs, optics, and dewar systems. Oversampled pixels results in processing techniques for smaller pixels that enable a number of related systems benefits such as improved Instantaneous Field of View (IFOV), Noise Equivalent Power (NEP), False Alarm Rate, and detection range, as well as other system level benefits.

Cyan Systems has developed and recently demonstrated a small pixel ROIC/ FPA that demonstrates these advanced resolutions features.

We will show data from the first 2.4 Megapixel 5 micron pitch ROIC and demonstrate that spatial oversampling can improve aliasing, sensitivity, and drive reductions in False Alarms through oversampled correlated processing. Oversampled pixels allow larger format FPAs and smaller optics, resulting in reductions in size, power, and weight. Oversampled IR sensors will also improve detection and acuity in turbulent and hazy conditions over larger pixel IR focal plane array sensors.

We will review the phenomena of smaller pixels having improved SNR, and how using temporal and spatial oversampling can compensate and effectively increase SNR lost with smaller pixels. We will quantify the limits of performance of Oversampling based on theory, and also with Monte Carlo type analysis using realistic parameters such as shot noise and thermal noise. We will show quantitative data to illustrate the improvements in resolution, NEP, detection range, and false alarm suppression of the oversampled IR sensor as the temporal and spatial oversampling are increased.

9555-24, Session 6

Design methodology: ASICs with complex in-pixel processing for pixel detectors

Farah Fahim, Hooman Mohseni, Northwestern Univ. (United States); Grzegorz Deptuch, James R. Hoff, Alpana Shenai, Fermi National Accelerator Lab. (United States); Bruce Cauble, Cadence Design Systems, Inc. (United States)

The development of Application Specific Integrated Circuits (ASIC) for pixel detectors with complex in-pixel processing using Computer Aided Design (CAD) tools that are, themselves, mainly developed for the design of conventional digital circuits requires a specialized approach. Mixed signal pixels often require parasitically aware detailed analog front-ends and extremely compact digital back-ends with more than 1000 transistors in small areas below 100µm x 100µm. These pixels are tiled to create large arrays, which have the same clock distribution and data readout speed constraints as in, for example, micro-processors. The methodology uses a modified mixed-mode on-top digital implementation flow to not only harness the tool efficiency for timing and floor-planning but also to maintain designer control over compact parasitically aware layout.

The design methodology of two pixel detector ASICs for two diverse applications is discussed. It proposes the modification of the standard approach and uses an iterative design flow, which needs to be adapted based on the area constraints of the digital pixel and the peripheral functionality for the ASIC. Custom digital layouts require parasitic information to be extracted using Assura QRC and subsequently using Encounter in timing mode to extract the timing and delay files. Adapting the design flow of EDI primarily developed for high-speed microprocessor layouts, allows the designer of pixel detector ASICs to distribute high-speed clocks with low jitter across a large array.

9555-25, Session 6

Fusion: ultra-high-speed and ir image sensors (Invited Paper)

NANOSCIENCE+ ENGINEERING

Takeharu Goji Etoh, Ritsumeikan Univ. (Japan)

It has been thought that there is no need to develop IR ultra-high-speed video cameras, since movement of heat is slower than motions. However, most of targets of ultra-high-speed video cameras operating at more than 1 Mfps, such as combustion, crack propagation, collision, laser plasma, discharge, a tire under a sudden brake and an air bag, generate sudden heat. Researchers in these fields require tools to measure the motion and the heat simultaneously.

Ultra-high frame rate imaging is achieved by an in-situ storage image sensor. Each pixel of the sensor is equipped with multiple memory elements to record a series of image signals simultaneously at all pixels. Image signals stored in each pixel are read out after an image capturing operation. In 2002, we developed an in-situ storage image sensor operating at 1 Mfps. However, the fill factor of the sensor was only 15% due to a light shield covering the wide in-situ storage area. Therefore, in 2011, we developed a backside illuminated in-situ storage image sensor to increase the sensitivity with 100% fill factor and a very high quantum efficiency. The sensor also achieved a much higher frame rate,16.7 Mfps, thanks to the wiring on the front side with more freedom.

This paper proposes development of an ultra-fast IR image sensor in combination of advanced nano-technology for IR imaging and the BSI insitu storage image sensor technology, and discuss the relating fundamental issues

9555-26, Session 6

Infrared detectors based on InAs/GaSb superlattice materials (Invited Paper)

Sanjay Krishna, The Univ. of New Mexico (United States)

Heteroengineered structures with unipolar barriers such as nBn, CBIRD, M-structure, N-structure, pBiBn and cascade structures have taken advantage of the unique bandstructure engineering properties of the 6.1A InAs/GaSb/AISb family. In this talk, I will review some of the approaches that we have developed in our group nBn, pBiBn and interband cascade detectors. The performance characteristics of these detectors will be discussed in detail in the presentation.

9555-42, Session PWed

Tunable sensitivity phase detection of multichannel transmitted-type guided-mode resonance (GMR) sensor

Wen-Kai Kuo, National Formosa Univ. (Taiwan)

We report a multichannel transmitted-type guided-mode resonance (GMR) sensor by utilizing a phase-shift interferometer (PSI) for phase detection with tuning sensitivity. The GMR sensor grating structure was fabricated by nano-imprinting technique and a thin titanium dioxide (TiO2) film was coated onto the grating surface by sputtering process. In our system, a cylindrical lens with focal length of 60 mm to form a V-shaped convergent beam with incident angles ranging from 12 degree to 16 degree. Two liquidcrystal modulators (LCM) able to produce over one wavelength retardation were used to produce five-step phase shift in the PSI system. A low-cost web-camera with 130 Mega pixels was used to capture these phase shift images of the multichannel GMR sensor and then the five-step phaseshift reconstruction algorithm can obtain spatial phase-shift information. Because intensity and phase curves of the transmitted light, the phase detection sensitivity can be tuned by rotating a polarizer in front of the web-camera. Experimental result shows that the detection sensitivity tuning approximately from 10E-5 to 10E-7 RIU can be obtained in our system. In conclusion, this tunable sensitivity phase detection functions can provide

a more flexible GMR sensor detection method. Moreover, the multichannel scheme can provide low-cost and high throughput detection.

9555-43, Session PWed

Ellipsoid type microchannel plate photomultiplier tube for neutrino center detector

Shulin Liu, Baojun Yan, Institute of High Energy Physics (China)

In order to determine neutrino mass hierarchy and precisely measure oscillation parameters, Chinese scientists will establish super large neutrino experimental station in Jiangmen city, Guangdong province. The central detector in the experimental station needs 18000 surround 20" photomultiplier tubes (PMTs) with high detection efficiency. In order to develop and implement mass production of the large size PMTs, project group use the ellipsoid type high borosilicate glass as vacuum bulbs which were smelted and blown with low background materials and adopt gradual transition of glass section to achieve Kovar metal sealing. Choose the bialkali photocathode which is easy to make and its spectral range is the best matching with emission spectra of liquid scintillator. By optimizing the process, a kind of new photocathode is fabricated which has high quantum efficiency, low noise and good uniformity. Microchannel plate (MCP) electron multiplier is made of two MCPs which have high open area ratio and high gain. By adjusting the two pieces of MCP position and the corresponding gap voltage, the overall gain of MCPs is about 107 with good single photoelectron peak to valley ratio. The measured signal quality is good by excellent designing of the anode and the signal lead wire. At current process, the performance of ellipsoid type 20" MCP-PMT are quantum efficiency ~30%, collection efficiency more than 80%, photoelectron transit time spread less than 20 ns and the single photoelectron peak to valley ratio greater than 3. Further optimization of MCP-PMTs can meet the needs of Jiangmen Underground Neutrino Observatory (JUNO).

9555-44, Session PWed

Whispering-gallery microresonators and microlasers for nanoscale sensing and beyond

Sahin Kaya Ozdemir, Lan Yang, Washington Univ. in St. Louis (United States)

Optical sensors based on Whispering-Gallery-Mode (WGM) resonators have emerged as front-runners for label-free. ultra-sensitive detection of nanoscale materials and structures due to their superior capability to significantly enhance the interactions of light with the sensing targets. A WGM resonator traps light in circular orbits in a way similar to a whisper, i.e., a sound wave, traveling along a circular wall, an effect found in the whispering gallery of a cathedral dome. The basis for resonator sensors is that the physical associations and interactions of nanomaterials on the surface of a high-Q optical WGM resonator alter the trajectory and lifetime of photons in a way that can be measured and quantified. I will first present the discovery of using ultra-high-Q microresonators for ultrasensitive self-referencing detection and sizing of single virion, dielectric and metallic nanoparticles. I will introduce sol-gel process as a convenient and efficient method to incorporate optical gain dopants into silica resonators, providing a route to achieve arrays of microlasers on silicon wafer with emission spectral windows from visible to infrared. Then I will discuss using optical gains in a microlaser to improve the detection limit beyond the reach of a passive microresonator. These recent advancements in WGM microresonators will enable a new class of ultra-sensitive and low-power sensors for investigating the properties and kinetic behaviors of nanomaterials, nanostructures, and nanoscale phenomena. In the end, I will discuss exploration of nanoparticles as nanocouplers introducing a new channel to harvest light from free space into high-Q WGM resonators.

9555-45, Session PWed

Modeling and analysis of hybrid pixel detector deficiencies for scientific applications

NANOSCIENCE+ ENGINEERING

Farah Fahim, Hooman Mohseni, Northwestern Univ. (United States); Grzegorz Deptuch, Fermi National Accelerator Lab. (United States); James R. Hoff, Fermi National Accelerator Lab. (United States)

Semiconductor hybrid pixel detectors often consist of a pixellated sensor layer bump bonded to a matching pixelated readout integrated circuit (ROIC). The sensor can range from high resistivity Si to III-V materials, whereas a Si CMOS process is typically used to manufacture the ROIC. Independent, device physics and electronic design automation (EDA) tools are used to determine sensor characteristics and verify functional performance of ROICs respectively with significantly different solvers. Some physics solvers provide the capability of transferring data to the EDA tool. However, single pixel transient simulations are either not feasible due to convergence difficulties or are prohibitively long. A simplified sensor model, which includes a current pulse in parallel with detector equivalent capacitor, is often used; even then, spice type top-level (entire array) simulations range from days to weeks.

In order to analyze detector deficiencies for a particular scientific application, accurately defined transient behavioral models of all the functional blocks is required. Furthermore, various simulations, such as transient, noise, Monte Carlo, inter-pixel effects, etc. of the entire array need to be performed, within a reasonable time frame without trading off accuracy. This work uses, Cadence Wreal, a mathematical real number modeling language, to model the sensor and the analog front-end of the pixel as complex mathematical functions. Parasitically aware digital timing is extracted in a standard delay format (sdf) from the pixel digital back-end layout as well as the periphery of the ROIC. For any given input, detector level worst-case and best-case simulations are performed using the Cadence Incisive environment to determine the output. Each top-level transient simulation takes no more than 10-15 minutes. The impact of changing key parameters such as sensor poissonian shot noise, analog front-end bandwidth, jitter due to clock distribution etc. can be accurately analyzed to determine ROIC architectural viability and bottlenecks. Hence the impact of the detector parameters on the scientific application can be studied.

9555-27, Session 7

High grain, low noise organic and nanoelectronic photodetectors (Invited Paper)

Jinsong Huang, Univ. of Nebraska-Lincoln (United States)

The dramatically reduction of cost of photodetectors without comprising their performance will enable new applications in many fields. In this talk, I will brief our progress in the development of sensitive photodetectors/ photon counters using low-cost solution processable organic and nanoelectronic materials. Four types of device structures will be compared in terms of device gain, noise, sensitivity, response speed and linear dynamic range: 1) traditional diode structure, 2) a structure combine the photodiode and photoconductor through the interface trap triggered secondary charge injection, 3) an organic phototransistor that has combined photoconductive gain and photovoltaic gain, and 4) quantum dots modulated transistor channel conductance. Broad response spectrum from UV to NIR will be demonstrated, and active material limited performance will be discussed.

Solution-Processed Nanoparticle Super-Float-Gated Organic Field-Effect Transistor as Un-cooled Ultraviolet and Infrared Photon Counter

Yongbo Yuan, Qingfeng Dong, Bin Yang, Fawen Guo, Qi Zhang, Ming Han, and Jinsong Huang^{*}, Scientific Reports, 3, 2707 (2013)

A nanocomposite ultraviolet photodetector enabled by interfacial trapcontrolled charge injection

Fawen Guo, Bin Yang, Yongbo Yuan, Zhengguo Xiao, Qingfeng Dong, Yu Bi,



and Jinsong Huang*, Nature Nanotechnology, 7, 798-802, (2012)

Large Gain, Low Noise Nanocomposite Ultraviolet Photodetectors with a Linear Dynamic Range of 120 $\rm dB$

Yanjun Fang, Fawen Guo,Zhengguo Xiao, Jinsong Huang*, Advanced Optical Materials, 348-353 (2014)

High Gain and Low-Driving-Voltage Photodetectors Based on Organolead Triiodide Perovskites

Rui Dong, Yanjun Fang, Jungseok Chae, Jun Dai, Zhengguo Xiao, Qingfeng Dong,Yongbo Yuan, Andrea Centrone,Xiao Cheng Zeng , Jinsong Huang*. ,Advanced Materials, 2015

9555-28, Session 7

Dielectrophoresis based integration of nanostructures and their sensorial application

Christian Leiterer, Macquarie Univ. (Australia); Gerald Brönstrup, Helmholtz-Zentrum Berlin für Materialien und Energie GmbH (Germany); Steffen Berg, Norbert Jahr, Institut für Photonische Technologien eV (Germany); Wolfgang Fritzsche, Leibniz-Institut für Photonische Technologien e.V. (Germany)

This presented work deals with utilization of bottom-up nanostructures in the field of optical basic research, optoelectronic and chemoresistive sensing and their microintegration using AC electrical fields. It focuses on three types of nanostructured materials in particular: DNA/DNAsuperstructures, gold nanoparticle and semiconducting nanowire e.g. silicon, gallium arsenide, zinc oxide.

The focus of DNA micro integration lies hereby in determining conditions allowing the handling of single DNA molecules on a microelectrode substrate in a stretched conformation, which enables subsequent investigation and experimenting on single DNA molecules in an organized and ordered fashion. The micro integration based on dielectrophoresis of gold nanoparticles and silicon nanowires focuses on applying contact to these nanostructures in order to use them as optoelectronic or chemo resistive sensors. In order to achieve this, a micro integration process was developed to apply contact to silicon nanowires and gold nanoparticles as basis for their sensorial application. The contacted nanostructures were characterized electrically to optimize the integration procedure to acquire best possible sensing capabilities. Silicon nanowires were demonstrated to work as wavelength sensitive optical sensors and gold nanoparticle as chemo resistive sensor.

9555-29, Session 7

Spectrometer with nanophotonic structure based on compressive sensing

Zhu Wang, Zongfu Yu, Univ. of Wisconsin-Madison (United States)

This talk will introduce a new method of spectral analysis based on compressive sensing, which is based on nanophotonic structures and thus has the potential to achieve high resolution in a compact device size. This method will solve the common problems that exist in traditional spectrometers--bulky and expensive. Also the complex interferences in nanostructures will offer diverse spectral features suitable for compressive sensing.

9555-30, Session 7

Localised surface plasmon fiber device coated with carbon nanotubes for the specific detection of CO2

Thomas Allsop, Raz Arif, Aston Univ. (United Kingdom); Ron Neal, Plymouth Univ. (United Kingdom); Kyriacos Kalli, Cyprus Univ. of Technology (Cyprus); Vojta Kundrat, Aleksey G. Rozhin, Aston Univ. (United Kingdom); Philip F. Culverhouse, Plymouth Univ. (United Kingdom); David J. Webb, Aston Univ. (United Kingdom)

We explored the potential of a carbon nanotube (CNTs) coating working in conjunction with a recently developed localised surface plasmon (LSP) device (based upon a nanostructured thin film/array of nano-wires of platinum) with ultra-high sensitivity to changes in the surrounding indices. The uncoated LSP sensor's transmission resonances exhibited a refractive index sensitivity of dl/dn ~ -6200nm/RIU and dl/dn ~5900dB/RIU, which is the highest reported spectral sensitivity of a fiber optic sensor to bulk index changes within the gas regime. The complete device provides the first demonstration of chemically specific gas sensing capabilities of CNTs utilising their optical characteristics. This is proven by investigating the spectral response of the sensor before and after the adhesion of CNTs to alkane gases along with carbon dioxide. The device shows a distinctive spectral response in the presence of gaseous CO2 over and above what is expected from general changes in the bulk refractive index. This fiber device yielded a limit of detection of 150ppm for CO2 at a pressure of one atmosphere. Additionally the adhered CNTs actually reduce sensitivity of the device to changes in bulk refractive index of the surrounding medium. The polarisation properties of the LSP sensor resonances are also investigated and it is shown that there is a reduction in the overall azimuthal polarisation after the CNTs are applied. These optical devices offer a way of exploiting optically the chemical selectivity of carbon nanotubes, thus providing the potential for real-world applications in gas sensing in many inflammable and explosive environments.

9555-31, Session 7

A novel sensing and tracing technology based on the hollow-core plastic optical fiber and cone-shape optical coupler in a sun-lighting system

Lingyu Zhang, Deming Liu, Xiaolei Li, Huazhong Univ. of Science and Technology (China)

A novel sensing and tracing technology used for the sun-lighting system is reported in this paper. The system is composed of an azimuth angle sensor, an optical fiber, a sunlight coupling unit, and a sunlight tracing control unit. A hollow-core plastic fiber is designed and fabricated and used to receive and transmit the sunlight. A cone-shape optical coupler is designed and used to trap in more sunlight. Compare with the traditional the traditional sensing and tracing technology, both of the receive angle of the optical fiber and the coupling efficiency of the sunlight to the optical fiber are substantially increased, and therefore the requirement for the sensing and tracing technology. But herefore the cost of the optical fiber sunlighting system is also reduce. This new sensing and tracing technology has been used in an optical fiber sun-lighting system, the sunlight could be transmitted a length of 50m to 100m. The application of this optical fiber sun-lighting in an underground garage would be introduced.

9555-32, Session 8

Colloidal semiconductor nanocrystals for biosensing and optoelectronic applications (Invited Paper)

Richard D. Schaller, Argonne National Lab. (United States) and Northwestern Univ. (United States)

Colloidally synthesized, quantum-confined semiconductor nanocrystals offer size-tunable energy gaps, large photoluminescence quantum efficiencies at room temperature, scalable synthesis, and low cost solution processing. Owing to these characteristics, significant interest exists in the development of these materials for use in optoelectronic and sensing applications. Despite high room temperature photoluminescence quantum yields of nanocrystals that in some cases can approach unity, many devices such as displays, lighting, and optical amplifiers experience elevated temperatures during operation. For three semiconductor compositions (cadmium selenide, indium phosphide, and silicon), we utilize static and time-resolved optical characterizations to improve understanding of carrier dynamics under operational conditions. Specifically, we measure quantum yield vs elevated temperature, reveal reversible as well as irreversible exciton guenching pathways, and investigate the role of surface termination on exciton integrity with temperature. This work points to strategies to improve upon the performance of these materials in high temperature applications. We have also made use of these materials in biological sensing applications where we exploit the large absorption cross-sections and high optical stability of some nanocrystals compositions. Using these materials, we report a selective, stable, fast and sensitive all-optical pathogen detection assay.

9555-33, Session 8

Development of optical nanosensor for intracellular pH measurement and imaging

Aleksandar Secenji, Barbara Horváth, Univ. of Pécs (Hungary)

The living cells are dynamic continuously changing systems. To fully understand their working mechanisms, there is a need for real time monitoring of most important parameters. Real time measurement of pH can provide detailed information of H+ transport, H+ consuming and producing reactions, and buffering. There are several techniques for intracellular pH monitoring like NMR imaging or confocal scanning microscopy. These techniques are related to expensive equipment, and in some cases to time-consuming procedures.

A simple fluorescent microscope equipped with RGB camera and use of pH sensitive fluorescent dye is an alternative for real time pH imaging. Unfortunately the free dyes interact with cell components and they are toxic in most of the cases. In the recent times nanoparticle based optical nanosensors are used due to their many advantages instead of dyes.

The main aim of our work is to develop an optical nanosensor, which is suitable for intracellular pH imaging with RGB camera. For this reason a core-shell type of nanosensor have been synthesized. The core of the nanoparticle contains a reference dye, octaethylporphyrin (OEP) (?exc= 400 nm, ?em=620 nm) entrapped in modified Stöber silica, made of phenyltriethoxysilane. The shell synthesis was made with pH sensitive N-allyl-4-isopropylpiperazine-1,8-naphtalamide (AiPPN) (?exc= 400 nm, ?em=527 nm). OEP emission is detected with the red channel of RGB camera and the AiPPN with green channel. The surface modification was performed with aminopropyltriethoxysilane and aminobuthyl[3-(triethoxysilyl)propyl]urea to provide a positively charged particles. The particles had a narrow size distribution, main diameter was 140 nm.

In the future we will test our optical pH sensor in live cells.

9555-34, Session 8

Fresnel-zones-patterned nanoparticles as fluorophore in biological sensing and imaging

OPTICS+ PHOTONICS

NANOSCIENCE+ ENGINEERING

Lujiang Qian, Yu Zhou, Qingfeng Zhang, Rui Wang, Yifan Chen, South Univ. of Science and Technology of China (China)

This paper proposes a new approach of implementing Fresnel-zonespatterned nanoparticles (FZPN) as the fluorophore to enhance the fluorescence intensity in biological sensing and imaging applications. The FZPN used to label a biological object-of-interest (e.g., tissue, cell) can reemit light upon light excitation. Biocompatible nanoparticles bonded to the object-of-interest are arranged according to the amplitude transmittance function of a Fresnel zone plate (ZP). Such structures are expected to increase significantly the penetration depth of fluorescence microscopy.

Firstly, given the wavelength of fluorescence and the desired focal length of a virtual ZP where the nanoparticles are to be placed, the circular diffraction grating with radially varying line period on the ZP can be calculated.

Subsequently, a number of nanoparticles are positioned at locations where the amplitude transmittance of the virtual ZP is equal to 1 (i.e., transparent). On the other hand, the locations where the amplitude transmittance is equal to 0 (i.e., opaque) remain empty. Each nanoparticle can be treated as a point source as its size is much smaller than the wavelength of the impinging light. As a result, the backscatter radiation pattern of a nanoparticle in the far field is similar to the pattern of a dipole. Furthermore, the mean free path of photon in biological tissues is around 100 um, which is comparable to the size of the virtual ZP. Thus, it can be assumed that the backscatter lighwaves of all nanoparticles are correlated. When a coherent light impinges on the FZPN, the re-emitted lightwaves will interfere constructively and form a bright spot at the desired focus of the virtual ZP. This phenomenon is due to the useful analogy between the FZPN and the classical ZP using diffraction to focus light, both of which follow the Huygens-Fresnel principle. By focusing microscope objective lens on the bright spot, one could sense and image the object-of-interest with a high sensitivity. In the full-length paper, the influence of the ZP size on the scattering field will be analyzed. Furthermore, the effect of the variation of the opacity (e.g., binary or sinusoidal ZP) will be discussed.

9555-35, Session 9

With electroluminescence microcopy towards more reliable AlGaN/GaN transistors (Invited Paper)

Martina Baeumler, Michael Dammann, Matthias Wespel, Helmer Konstanzer, Vladimir M. Polyakov, Stefan Müller, Stephan Maroldt, Wolfgang Bronner, Peter Brückner, Fouad Benkhelifa, Patrick Waltereit, Rüdiger Quay, Michael Mikulla, Joachim Wagner, Oliver Ambacher, Fraunhofer-Institut für Angewandte Festkörperphysik (Germany)

Long-term stability and reliability of AlGaN/GaN high electron mobility transistors (HEMT) devices can be validated by various stress tests which allow studying the physical mechanisms responsible for degradation. Electroluminescence microscopy (ELM) allows to monitor microscopic changes in the device related to the degradation process. As the electroluminescence (EL) intensity is related to the kinetic energy and density of the channel electrons accelerated in the electric field, both local current and electric field changes can result in an increase or decrease of the EL intensity. Although the spatial resolution is limited to a few microns, ELM benefits from the fact that submicron imperfections at the Schottky interface of the gate electrode result in strong local current variations. To distinguish between current and field effects, additional techniques as infrared thermography have been applied. The electric field distribution in source drain direction Fx peaks at the drain side edge of the gate foot and the field plates. Fx is strongly dependent on the gate design and

Conference 9555: Optical Sensing, Imaging, and Photon Counting: **SPIE**, OPTICS+ Nanostructured Devices and Applications

the passivation /semiconductor interface trap density. The latter can be extracted by comparing the EL intensity profiles in source drain direction, recorded at different drain source voltages, to simulated electric field profiles. The results will be compared to CV measurements. ELM has been used to selectively identify suitable positions for further failure analysis of focused ion beam prepared cross sections by scanning and transmission electron microscopy. Process induced imperfections as well as damage at the Schottky interface after stress have been localized.

9555-36, Session 9

Micro-nanofluidic biochip and detector for fast clinical diagnostic at aM nucleic acid concentration

Guoliang Huang, Tsinghua Univ. (China); Qin Huang, National Engineering Research Ctr. for Beijing Biochip Technology (China)

Molecular diagnostics is one of the most important tools currently in use for clinical pathogen detection due to its high sensitivity and specificity. In this paper, a sensitive DNA isothermal amplification method for the detection of DNA at aM (10-18 M) concentrations for fast clinical diagnostic was developed using a PC micro-nanofluidic chip. One important aspect of the microfluidic chip with a surface inert to bio-molecules was the surface contact angle increasing from 71.3° on original surface to 103° on the inert processed surface. A portable confocal optical fluorescence detector was specifically developed for the micro-nanofluidic chip that was capable of highly sensitive real-time detection of amplified products for sequence-specific molecular identification near the optical diffraction limit with low background. The isothermal nucleic acid amplification in the micro-nanofluidic chip could be performed at a minimum DNA template concentration of 1.3 aM, and a detection limit of less than 5 copies of genomic DNA was obtained. We used the whole system and method for the molecular diagnostics of four clinical pathogens with nucleic acid extracted from stool samples, and the result showed that the response time was clearly reduced to 45 minutes for multi-target parallel detection. This novel micro-nanoliter fluidic detection system and method could be used to develop a Micro Total Analysis System as a clinically relevant pathogen molecular diagnostic method via the amplification of targets, and with potential applications in nanobiotechnology, nanomedicine, and clinical molecular diagnostics.

9555-37, Session 9

Polarization-based optical fiber sensor of steel corrosion

Wenbin Hu, Cheng Zhu, Xing Zheng, Min Gao, Donglai Guo, Wuhan Univ. of Technology (China); Wei Chen, School of Materials Science and Engineering, Wuhan Univ. of Technology (China)

A polarizer formed by a metal-coated D-shape optical fiber, has been demonstrated since 1980. By employing this micro-structure, a high extinction ratio of odd and even fundamental mode can be achieved. A novel sensor form by an iron-coated optical fiber polarizer is presented for corrosion real-time monitoring.

The sensor is fabricated by sputtering an iron film with a thickness of 10 - 50 nm on a side-polished single mode fiber. The birefringence characteristic of the newly-formed metal film is varying during the corrosion of the Fe(C) film, and is eliminated as the occurrence of the film spalling at a severe corrosion stage. Two corrosion-dependent optical characteristics (the extinction ratio and optical power loss) contribute to probe the corrosion status. If installed in steel structures, the status of iron-film corrosion indicates the status of steel corrosion.

An experiment is conducted by immersing the sensors in an accelerated corrosive environment with a NaCl solution (3.5 wt%). The experimental results show that the sensors can perform as corrosion indicators of the

initial corrosion occurred on the coated film. The extinction ratio varies significantly while the well-crystallize iron is corroded. The optical power loss depends on the spalling of the coated film. By establishing the relation between the corrosion-dependent optical characteristics and the corrosive status, the initial corrosion can be traced and evaluated.

NANOSCIENCE+ ENGINEERING

9555-38, Session 9

An optical fiber lateral stress sensor based on a Sagnac interferometer structure

Shun Wang, Ping Lu, Li Liu, Hao Liao, Jiangshan Zhang, Deming Liu, Xinyue Jiang, Huazhong Univ. of Science and Technology (China)

In this article, we propose and demonstrate an optical fiber lateral stress sensor based on a Sagnac interferometer (SI). The SI structure consists of an optical fiber coupler with splitting ratio about 50:50. By inserting a section of polarization-maintaining photonic crystal fiber (PM-PCF) in the sensing loop of the SI structure, a inline interference between the two orthogonal polarization modes (Mx and My) of the PM-PCF is realized. Theoretical study shows that the reflection spectrum of the SI is depended on not only the refractive index difference of the two orthogonal polarization modes (Mx and My) but also the length of the PM-PCF (L). The chosen PM-PCF, whose cross section contains two big air holes side by side which are surrounded by many small air holes. Due to the large asymmetry of the two perpendicular axes x and y, the refractive index difference of the two orthogonal polarization modes, Mx and My, will be very large. Thus resulting in great changes in the wavelength drift induced by the lateral stress applied on the fiber side which changes the refractive index difference of the two orthogonal polarization modes, Mx and My. By suitably selecting the length of PM-PCF and keeping a good state of polarization in the SI loop, a highly sensitive optical fiber lateral stress sensor can be achieved. Experimental results show that the sensor achieves the highest sensitivity of lateral stress strain 1.28 nm/kPa, which demonstrating the ability for lateral stress measurement with high accuracy.

9555-39, Session 9

Spectropolarimetry screening of cytological smears from cervical on the presence of HPV

Sergey B. Yermolenko, Yuriy Fedkovych Chernivtsi National Univ. (Ukraine); Alexander P. Peresunko, Julia G. Karpenko, Bukovinian State Medical Univ. (Ukraine)

Diagnosis of cervical cancer is an actual issue in oncology and gynecology that needs new, innovative approaches. The main concept of the etipathogenesis of cervical cancer is recognized as viral hypothesis. The human papilloma virus (HPV) occupies a central place in it which has the greatest potential for oncology and is a major factor exogenous factor in cervical carcinogenesis.

Pathogenetic cytological feature of the infection of cervical epithelium with human papilloma virus is the presence of koylotsity or "air" cells (balloon-cells) with a halo around the nucleus. These cells are intermediate or surface layer of keratinized squamous epithelium with characteristic large transparent, clearly delineated perinuclear area. So, koylotsitoz can be considered as a marker of human papilloma virus infection.

Assistance in objectification and improving of the accuracy of diagnosis of cervical pathology can provide non-contact optical methods, including a spectro- polarimetry one.

In the method of spectropolarimetry screening of cytological smears of the cervix for the presence of human papillomavirus (HPV) is offered the following. Native cytological smears of the cervix are irradiated in a wide spectral range and examined changes in polarization parameters and modeling anisotropic structure of cervix values of linear dichroism and its spectral dependence in the spectral range of ? = 330 - 750 nm, with a



maximum value at koylotsity reaction in cytological smears in area of $\ref{eq:stars}$ = 395-415 nm.

9555-46, Session 9

Interaction of two nano particle plasmons for sensor application

Naresh C. Das, U.S. Army Research Lab. (United States)

By combining plasmon wave of two different nano particles, from aluminum (Al) and gold (Au) nano-particles, we observed plasmon resonance peak at two different wavelengths. We used electron beam lithography along with angle metal evaporation techniques to deposit metal particle plasmon layer with nanometer-scale separation. The coupled plasmon layer has two peaks at 525 and 650 nm, which are different from the constituent metal plasmon layers (Al and Au, respectively).

The area of creating artificial molecules by combining more than one nanoparticle (NP) has received significant interest recently. Similar to the way atoms join together in different combination to form all the substances in the universe, we too can make groups of new materials by combining artificial atoms or NPs1. The strong interaction of plasmon waves from different NPs can render many applications possible, including sensors2, and enhanced electro catalytic reactions3. We used an electron beam lithography process along with angle evaporation techniques to achieve nanometer-scale metallic particles with very close proximity. Gold (Au) and aluminum (AI) metal particles were chosen for the plasmonic coupling experiment because of their distinguished plasmonic behavior with peak wavelengths separated by few 100 nm. We used a variable angle ellipsometer model M-200 from J. Wolman and Company to measure change in phase difference, ?, due to plasmonic NPs. The peak resonance wavelength for different plasmonic material was determined.

Two metallic NPs were deposited using different angles of evaporation of substrate with respect to metal crucible. We observed two peaks: one narrow plasmon peak at 525 nm showing a contribution from the AI NPs and another broad plasmon peak at 650 nm due to the Au NPs.

We have shown two-color plasmon absorption peaks due to Al and Au NPs with a nanometer-scale separation between them. The position and peak height of the coupled plasmon curves are different from the individual peaks of Al and Au NPs, respectively.

References:

1H. Haken, H. C. Wolf, In Molecular physics and elements of quantum chemistry; Springer: Berlin, (2003).

2 M. Kauranen and A. V. Zayats, Nature Photonics, 6, 737, (2012).

3N.C. Das, Journal of Applied Physics, 110, 046101 (2011).

Bio: Dr. Naresh Das is working at Army research laboratory since 2000. He has published more than 100 papers in international journals and conferences. His areas of interest include IR/UV LEDs, detectors and solar cells. He has worked at NASA Goddard space flight center, AF research lab in Albuquerque, IIT Mumbai and BHEL Bangalore, India.

Tuesday - Wednesday 11-12 August 2015

Part of Proceedings of SPIE Vol. 9556 Nanoengineering: Fabrication, Properties, Optics, and Devices XII

9556-2, Session 1

Technical requirements, manufacturing processes, and cost efficiency for transparent electrodes based on silver nanowires and carbon nanotubes

Thomas Ackermann, Univ. Stuttgart (Germany) and Fraunhofer-Institut für Produktionstechnik und Automatisierung (Germany); Serhat Sahakalkan, Ivica Kolaric, Fraunhofer-Institut für Produktionstechnik und Automatisierung (Germany); Engelbert Westkaemper, Univ. Stuttgart (Germany); Siegmar Roth, Sineurop Nanotech GmbH (Germany)

As product life cycles of displays become shorter the electronic industry is seeking for the usage of alternative materials to conventional indium tin oxide (ITO) as a material for transparent electrodes. Several materials such as nano carbon or silver nanowires have been discussed in literature. However a commercial replacement of ITO has not set on yet since each of the alternative materials perform well in a certain property but underperforms in another compared to ITO. We will present our recent results on transparent conductive films made of co-percolating silver nanowires and carbon nanotubes. This combination leads to superior optoelectrical performance of the ultra-transparent electrodes. We will outline the huge potential of electrical co-percolation of rodlike conductors based on theoretical and experimental data.

Furthermore we will report on scalable manufacturing processes of these films on commercial smart phone cover glasses and flexible foils for roll-to-roll manufacturing. The liquid film coating technique is analyzed with regard to technical suitability and cost efficiency. We were able to produce transparent conductive films with material costs less than three US Dollars per square meter. The ultra-transparent electrodes exhibit optical transmission of 98 % with sheet resistance of 60 Ohm/sq. The optical haze, which is usually a crucial drawback of silver nanowire films, is within the industrial tolerance of today's quality standards.

Transparent conductive films are an important research topic. Our contribution will discuss fundamental principles such as electrical percolation theory as well the industrial feasibility of ITO replacement.

9556-3, Session 1

Fast water vapor transmission rate measurement system by graphene-based device

Yung-Hsiang Hsieh, Cheng-Chung Lee, Chien-Cheng Kuo, National Central Univ. (Taiwan)

Flexible organic light emitting diode display is candidate for next generation display device but the water vapor and oxygen is easy to damage the organic element. Therefore, the organic element need barrier film to protect it. Water vapor transmission rate (WVTR, unit: g/m2/day)is used to evaluate the quality for encapsulation of organic element, which is estimated for encapsulating organic element is 10-6 g/m2/day at least in the flexible organic light emitting diode. There are two main ways to measure the WVTR for encapsulation of organic element but they had some disadvantage like that measure for long time or non-reusable. In recent years, graphene is found to be a good gas sensor. Graphene has fast response time and sensitive characteristics. The charge transfer between the molecules and the graphene surface when the molecules absorb on graphene in seconds. In this study, we made a fast WVTR measurement system by graphene-based device. The graphene-based device is prepared by transferred the graphene which is grown by chemical vapor deposition

(CVD) on glass subtrate first and then deposited the metal electrode with mask. The source voltage of graphene-based device kept 1V. Calculating the change of device resistance due to charge transfer between the molecules and the graphene surface that could be conversion to how many water molecules absorb on graphene. Using physically plausible model to calculate the adsorption/desorption of the molecules on the graphene surface.

9556-4, Session 1

Invoking the frequency dependence in square modulated light intensity techniques for the measurement of electron time constants in dye-sensitized solar cells

Hamid M. Ghaithan, Saif M. Qaid, King Saud Univ. (Saudi Arabia); Mahmoud Hezam, King Saud Univ. (Saudi Arabia) and Ecole Polytechnique Fédérale de Lausanne (Switzerland); Muhemmad B. Siddique, Univ. of Management and Technology (Pakistan) and Univ. of Management and Technology (Pakistan); Idriss M. Bedja, Abdullah S. Aldwayyana, King Saud Univ. (Saudi Arabia)

Dye-sensitized solar cells (DSSCs) have been considered as one of the most promising new generation solar cells. Enormous research efforts have been invested to improve the efficiency of solar energy conversion which is determined by the light harvesting efficiency, electron injection efficiency and undesirable electron lifetime. A simple, cheap and trustable laser-induced photovoltage and photocurrent decay (LIPVCD) technique is adopted in this work in order to determine the electron lifetime (?e) and electron transport (?tr) in DSSCs. In LIPVCD technique, DSSC is illuminated by a small squared intensity-modulated laser beam. Time-based response of the DSSC is recorded using a transient digitized oscilloscope for further analysis. Sensitization dye used studied DSSCs has an absorption wavelength peak at 532 nm which is obtainable using a proper laser diode. Present LIPVCD technique, using single wavelength, is tested with standard solar cells to give comparable results with other standard techniques (i.e. IMVS, IMPS and OCVD).

Measurements are performed at open-circuit and short-circuit for a variety of DSSCs, so that the photovoltage and photocurrent decay data are acquired and interpreted in the time domain. Studied DSSCs are fabricated with various electrodes include TiO2 nanoparticles and ZnO nanowire based DSSC. It has found that ?tr is much faster than ?e for all tested cells.

9556-5, Session 1

Optical and structural properties of cosputtered Cu-Si-O and Cu-Ge-O thin films

Lirong Sun, Air Force Research Lab. (United States) and General Dynamics Information Technology (United States); Neil R. Murphy, John G. Jones, Air Force Research Lab. (United States); John T. Grant, Air Force Research Lab. (United States) and Univ. of Dayton Research Institute (United States)

The co-sputtered Cu-Si-O and Cu-Ge-O thin films were prepared using reactive DC, pulse DC and modulated pulse power magnetron sputtering (MPPMS) on two separate Cu and Si or Cu and Ge targets simultaneously. The powers on each target and Oxygen/Argon flow ratio f(O2) were varied to have different stoichiometies determined by XPS. The film thickness, refractive index n and extinction coefficient k were extracted from in situ ellipsometry and the reactive plasma discharge was monitored by optical





emission spectroscopy in real time during film growth. The grazing incident x-ray diffraction measurements reveal that the films deposited at low f(O2) have the nanocrystalline structure of cuprous Cu2O with diffraction peaks of (11) and (200). The films deposited at high f(O2) (\geq 1) have cupric oxide CuO phase. The optical constant n and k, film density and band gap of the co-sputtered film were investigated and determined by in situ ellipsometry, X-ray reflectivity and UV-Vis-NIR spectroscopy. Their structural, chemical and optical properties are able to be tuned by incorporating Cu2O, CuO and the mixtures of them into Silicon oxide or Germanium oxide matrix with varying target powers and oxygen/Argon ratio for applications in optical coatings and optical filters.

9556-6, Session 2

Ultra-slim coherent backlight unit for mobile holographic display (Invited Paper)

Chil-Sung Choi, SAMSUNG Electronics Co., Ltd. (Korea, Republic of); Alexander V. Morozov, Alexander Koshelev, Sergey Dubynin, German Dubinin, SAMSUNG Advanced Institute of Technology (Russian Federation); Sung-Hoon Lee, Jae-Seung Chung, Geeyoung Sung, Jungkwuen An, Hoon Song, Juwon Seo, Hojung Kim, Wontaek Seo, Samsung Advanced Institute of Technology (Korea, Republic of); Andrey Putilin, P.N. Lebedev Physical Institute (Russian Federation); Sergey Kopenkin, Yuriy Borodin, P.N. Lebedev Physical Institute (Russian Federation); Sun II Kim, Hong-Seok Lee, U-in Chung, Sungwoo Hwang, Samsung Advanced Institute of Technology (Korea, Republic of)

The proposed paper relates to illumination devices for holographic display using coherent radiation from laser source. These backlighting systems are known for providing uniform and effective illumination in visualization devices. Backlight units using lens optics, which is bulky, have been implemented to a holographic display, but very few attempts have been made in minimizing the size of backlight units that can be used in the flat panel holographic display. Thickness is one of the key parameters in modern backlighting systems that need to be minimized to reduce the overall size of the display devices.

We propose slim coherent backlight unit for a mobile holographic display. This backlight unit consists of glass substrate for waveguide and two surface gratings produced by two-beam interference. Two surface gratings are used to solve chromatism, whereas the input grating has chromatic aberrations. Red, green, and blue components propagate in waveguide separately with different angles, which can be compensated by only one output grating for each channel.

The area of backlight illumination is 150 by 85mm (5.5 inch), and the thickness is 0.7mm which is thin compared to other conventional coherent backlight units. This backlight unit exhibits a total efficiency of 0.1%, preserving the collimation and a uniformity of 80% over the whole area. Although the efficiency of backlight unit is very low, brightness of backlight is sufficient when viewing window concept is applied.

9556-7, Session 2

Scalable nanostructuring on polymer by a SiC stamp: optical and wetting effects

Aikaterini Argyraki, Weifang Lu, Paul M. Petersen, Haiyan Ou, DTU Fotonik (Denmark)

A method for fabricating scalable antireflective nanostructures on polymer surfaces (polycarbonate) is demonstrated. The transition from small scale fabrication of nanostructures to a scalable replication technique can be quite challenging. Here, an area per print corresponding to a 2-inch-wafer, is presented. The initial nanopatterning is performed on SiC in a 2-step process. Depending on the nanostructures the transmission of the SiC surface can be increased or suppressed (average height of nanostructures ~300nm and ~600nm, respectively) while the reflectance is decreased, when compared to a bare surface. The reflectance of SiC can be suppressed down to 0.5% when the ~600nm nanostructures are applied on the surface (bare surface reflectance 25%). It is observed that the texture of the green SiC colour is changed when the different nanostructures are apparent.

The ~600nm SiC nanostructures are replicated on polymer through a process flow that involves hot embossing and galvanization. The resulted polymer structures have similar average height and exhibit more rounded edges than the initial SiC nanostructures. The polymer surface becomes antireflective and hydrophobic after nanostructuring. The contact angle changes from 68 (bare) to 123 (nanostructured) degrees. The optical effect on the polymer surface can be maximized by applying a thin Al layer coating on the nanostructures (bare polymer reflectance 11%, nanostructured polymer reflectance 5%, Al coated nanostructured polymer reflectance 3%).

The optical measurements were performed with an integrating sphere (8/8deg incident angle) and a spectrometer (QE 65000, Ocean Optics). The nanostructures applied were characterized with scanning electron microscopy (SEM, Zeiss Supra VP40).

9556-8, Session 2

Re-usable metal-metal stamping for three-dimensional active metamaterial fabrication

Robert L. Brown, Alan Selewa, Sung Jun Jang, Alireza Bonakdar, Mohsen Rezaei, Hooman Mohseni, Northwestern Univ. (United States)

Metamaterials are man-made materials composed of sub-wavelength components that display properties not found in nature such as negative refraction, superlensing, cloaking, polarization control, and wavelength filtering. There is much interest in 3D-metamaterials, including stacks of 2D metamaterials like metasurfaces and Frequency Selective Surfaces, which can increase the optical path and interaction of light and metamaterial significantly. Recent progress in metamaterial stacks involves methods that either rely on time-consuming and expensive techniques or fabrication that has little process flexibility. Furthermore, the benefits of having multiple stacks can be negated by the increase in interaction length with lossy metal components. We propose a method of additive metal-metal welding using a conformal stamp that will allow the transfer of multiple stacks of metal, semiconductors, and dielectrics to fabricate stacks of 3D optically active metamaterials. This method offers three advantages over standard methods and materials: 1) The ability to re-use stamps eliminates the need for optical or electron-beam patterning of each layer. 2) Because the stamp is conformal, layers do not need to be perfectly flat. 3) This process relies on metal-metal fusion and can transfer materials already connected to the metal along with the metal. With the ability to transfer semiconductors comes the opportunity to interact with these materials optically or electrically. This opens the door for loss compensation by the use of gain media, tunability of a semiconductor load, or the taking advantage of nonlinear optical processes.

9556-9, Session 2

Nanofabrication of ultra-low reflectivity black silicon surfaces and devices

Victor E. White, Karl Y. Yee, Kunjithapatham Balasubramanian, Pierre M. Echternach, Richard E. Muller, Matthew R. Dickie, Eric Cady, Daniel J. Ryan, Michael Eastwood, Byron E. Van Gorp, Jet Propulsion Lab. (United States); A. J. Eldorado Riggs, Niel Zimmerman, N. Jeremy Kasdin, Princeton Univ. (United States)

Optical devices with features exhibiting ultra low reflectivity on the



order of 10-7 specular reflectance in the visible spectrum are required for coronagraph instruments and some spectrometers employed in space research. Nanofabrication technologies have been developed to produce such devices with various shapes and feature dimensions to meet these requirements. Infrared reflection is also suppressed significantly with chosen wafers and processes. Particularly, devices with very high (>0.9) and very low reflectivity (<10-7) on adjacent areas have been fabricated and characterized. Significantly increased surface area due to the long needle like nano structures also provides some unique applications in other technology areas. We present some of the approaches, challenges and achieved results in producing and characterizing such devices currently employed in laboratory testbeds and instruments.

9556-10, Session 3

Development of 3D photonic crystals using sol-gel process for high power laser applications

Florence Benoit, Bertrand Bertussi, Eva Dieudonné, Nicolas Mallejac, Karine Vallé, Philippe Belleville, Commissariat à l'Énergie Atomique (France); Clément Sanchez, Collège de France (France); Stefan Enoch, Institut Fresnel (France)

Three-dimensional photonic crystals (PCs) are periodic materials with a modulated refractive index on a length scale close to the light wavelength of interest. This optical property allows the preparation of precise optical components like highly reflective mirrors [1].

Moreover, these structured materials are known to have a high laser-induced damage threshold (LIDT) in the sub-nanosecond range [2] compared to multi-layered dielectric mirrors. This property is obtained because only one high LIDT material (silica) is used. The second material used in the layer stack is replaced by air.

In this work, we propose to develop a bottom-up approach based on sol-gel chemistry to prepare 3D PCs. PCs are obtained using the self-assembly of narrow-sized distribution colloidal silica particles.

We will firstly describe the synthesis of narrow-sized distribution colloidal silica particles prepared with a polydispersity index below 1.05 and the Langmuir-Blodgett technique used to deposit the organized single layer of particles onto hydrophilic substrates exhibiting good uniformity at large scale.

Then we will illustrate first results through various characterisations of PC samples made in different conditions (optical measurements, SEM (Scanning Electron Microscopy)).

In order to understand experimental results, we have used a numerical modelling based on an ideal opal network with and without on purpose defect embedding. Thanks to this study, we present the new routes we have investigated in order to realize PC samples with optimized optical properties.

[1]- N. Bonod & J. Neauport, "Design of a full silica pulse compression grating," Optics letters 33 (5), 458-460 (2008).

[2]- M. Mero, J. Liu, W. Rudlph, D. Ristau, K. Starke, "Scaling laws of femtosecond laser pulse induced breakdown in oxide films," Phys. Rev. B 71, 115109 (2005)

9556-11, Session 3

Enhancement in light emission efficiency of silicon-rich oxide/SiO2 multilayer structures deposited by hydrogen ionbeam assisted sputtering

Sheng Wen Fu, National Cheng Kung Univ. (Taiwan)

Recently, the silicon-rich oxide (SRO)/SiO2 multilayer (ML) structures have drawn a great attention owing to their potential optoelectronic applications, especially for the visible light emitting devices (LED). In this

study, we prepared SRO/SiO2 multilayers by hydrogen ion-beam assisted sputtering (HIBAS) with different hydrogen anode voltage for the LED application. The property of the prepared samples was determined by Fourier transform infra-red (FTIR), X-ray photoelectron spectroscopy (XPS), photoluminescence (PL) and electroluminescence (EL) analysis.

Figure 1 shows the PL spectrum measurement of SRO/SiO2 films corresponding to different HIBAS energy by 325 nm and 532 nm excitation wavelength. In the range from 450 nm to 650 nm, it is a blue shift from 535 to 550 nm and the PL peaks intensity decrease corresponding to the HIBAS energy from 0 V to 116 V. In contrast, in the range from 650 nm to 1000 nm, the PL intensity increase significantly when HIBAS energy 70V and 116V treated SRO/SiO2 films compared that by 0 V.

The references showed that the PL band at the range from 450 nm to 650 nm and from 650 nm to 1000 nm have been associated with defect-related effects at the Si nanoclusters/SiO2 matrix interface and quantum confinement effects, respectively [1,2,3]. The 520-550 nm PL band has been commonly attributed to the E' center [O3?Si?] (510-550 nm) as a result of point defect [4]. Therefore, HIBAS could enhance the PL intensity owing to improvement of the Si nanocluster appearence. Furthermore, a red shift of PL in the 780-880 nm with samples treated by 70 V and 116 V is observed, which demonstrate the HIBAS gives more energy to synthesize and increase the nucleation of Si nanocluster size.

As shown in Figure 2(a), the EL spectra of the devices with three HIBAS energy were measured at the same injection current of 1 A. The peak EL intensity of the device treated with HIBAS 70 V and 116 V is about 3 and 5 times larger than the that by HIBAS 0 V, respectively. It is obvious that the improvement in the EL can be acquired by HIBAS. In addition, the blue shift of the EL peak from 552 nm to 512 nm is apparent with increasing HIBAS energy, which is in good agreement with the PL result. Figure 2(b) shows the integrated EL intensity as function of the injection current by HIBAS devices. Firstly, before the maximum of the EL in all samples, there is a linear relation between the integrated EL intensity and the injection current, which indicated that the light emission is resulted from the recombination of electrons and holes in the SRO/SiO2 films.

One can see that there is a linear relationship between the integrated EL intensity and the electrical input current, implying that the EL is originated from the recombination of the holes and electrons injected from the ITO gate and the Al electrode, respectively. Secondly, the external quantum efficiency (EQE) means the number of photons emitted externally divided number of carriers passing junction, therefore, the slope in figure 2(b) is directly proportional to EQE. The slope of HIBAS of 0 V : 70 V : 116 V is 1 : 3.6 : 7.1, which mean that HIBAS 116 V treatment drastically improve the EQE over 7 times than HIBAS 0 V. Furthermore, there are the maximum of EL intensity on all over the devices and the injection current could be adjust over 2.4 A without EL intensity decay for HIBAS 116 V device.

In conclusion, we approve the HIBAS effectively improve the SRO/ SiO2 based LED, where the intensity of EL was 15 times higher than the conventional devices at the same operated power.

9556-12, Session 3

Auger recombination in nanoscale III-Nitride material system

Chee-Keong Tan, Nelson Tansu, Lehigh Univ. (United States)

The development in III-Nitride light emitting devices have been impeded by the efficiency droop issue in which the internal quantum efficiency of the devices reduces when operating at high current density. Recent research on the efficiency droop increasingly identified current injection efficiency quenching and Auger recombination as the important mechanisms in leading to the efficiency droop issue. Recent studies affirmed the important role of Auger recombination process in the InGaN material system, even though the reported theoretical and experimental Auger coefficient values remain in disparity. Most studies in investigating the Auger recombination processes have been focused in the bulk nitride system and the literature of the Auger recombination processes in low-dimensional III-Nitride material system such as InGaN quantum well (QW) is still highly limited. Describing the Auger recombination processes in the nitride-based QW system is thus critical in exploring the underlying fundamental issues in the material



system for future prospective device engineering.

In this work we employed a numerical method to analyze the Auger recombination process in the III-Nitride QW system. The Auger recombination coefficient values for the low-dimensional III-Nitride material systems are investigated for InGaN QW. Specifically, the Auger recombination rates are analyzed as a function of InGaN active layer thickness by incorporating various parameters extracted from experiments. Our finding implies more dominant Auger recombination processes in the InGaN QW system when the active layer thickness reduces. The comparison of Auger recombination rates for InGaN QW material systems with various QW thicknesses will be discussed in details.

9556-13, Session 3

Development, electrical, and optical characterization of nanoscale FDSOI MOSFET devices based on quantum well structure for optical communication between chips and internal blocks

Avi Karsenty, Jerusalem College of Technology (Israel); Avraham Chelly, Bar-Ilan Univ. (Israel); Roi Zolberg, Roi Sabo, Jerusalem College of Technology (Israel)

Highlights

? Scientific background: The long term ongoing scaling of CMOS technology is moving the clock speed of future generations ULSI to the ten GHz frequencies and above. In such frequencies, the signal propagation delay on chip and on the circuit board, as well as signal cross talk, impose severe limitations on system design and performance. The direct solution to this problem is to move to optical signal transmission in the critical paths. Unfortunately the indirect energy band structure of silicon prevents the construction of simple and efficient light emitting devices as in the III-V materials such as GaAs. In recent years there is an ongoing wide research effort to find processes and mechanisms of light emission in silicon in spite of the basic physical limitations. The most promising directions are based on quantum effects in nanoscale silicon structures.

? The need/market (if applicable): The merging of the microelectronics with the communication in general and with optical communication in particular, pushes vigorously the efforts to realize on the same silicon chips both electronic and electro-optic functions. This is further motivated by the limitations of the metal wiring on chip and on the PC board, to transfer the electronic signals in the 10GHz range and above. The indirect band structure of silicon is a basic obstacle to the realization of light emitting devices in this material.

? Existing methods/techniques: The efforts for the development of light emitting devices in silicon concentrated in the last decades on quantum structures which indeed exhibit some photoluminescence in the visible range with efficiencies approaching that of Gallium Arsenide. However there is currently no practical light emitting silicon device either because of lack of efficiency, reproducibility and reliability. In particular most of these devices are not compatible with CMOS technology.

? Problems with existing solutions: As the QW MOSFET processing is compatible with standard CMOS technology, and SOI CMOS on SOI wafers is a commercial process, the expected light emission at preferred wavelengths in correlation with the silicon thickness in the transistor, may lead to the development of modified SOI CMOS technology that will include both standard CMOS transistors for the performance of the electronic functions, and Quantum Well Transistor devices for optical communication.

9556-14, Session 3

PbSe/PbSrSe MQW characteristic temperature relationship with laser cavity length

Majed Khodr, American Univ. of Ras Al Khaimah (United Arab Emirates)

A potential materials system that may play a key role in IR spectroscopy applications is PbSe/Pb 0.934 Sr0.066 Se quantum well structure. In this work, the characteristic temperature (TO) relationship with laser cavity length was studied for this material system at three temperature ranges 77< T<150 K, 150< T<300 K, and 77< T<300 K. It was noticed that TO is high for short cavity lengths then decreases to an almost constant value after some critical length. The data were best fitted to a second degree polynomials which can be used to determine these critical values. Also, we analyzed the effects of quantum efficiency on the characteristic temperature values. Inclusion of theoretical values for the quantum efficiency due to Auger recombination and leakage current reduces the characteristic temperature TO in these ranges. It was found that inclusion of the quantum efficiency decreases the characteristic temperature by 60% for a wide range of cavity lengths.

9556-16, Session 4

All-polymer based fabrication process for an all-polymer flexible and parallel optical interconnect

Jilin Yang, Tao Ge, Chris Summitt, Sunglin Wang, Yuzuru Takashima, Thomas D. Milster, College of Optical Sciences, The Univ. of Arizona (United States)

We demonstrate a new all-polymer based fabrication process for an all-polymer flexible and parallel optical interconnect cable having a vertical light coupler, which can not only cut down the cost by eliminating metallization process for alignment but also facilitate both in production and application. Throughout the process we used polyimide as the substrate, coated Epocladd as claddings, then Poly-10 and WPR 5100 were used to fabricate waveguides and 45 degree mirror coupler, respectively. As a key process tool, instead of conventional mask aligner lithography, we applied maskless lithography technology to print both of the waveguides and mirror coupler thereby eliminating the time and cost spent on the production of masks. In addition, precisely aligned mirror coupler to waveguides are achieved by using polymer-based, non-metallic, and transparent alignment marks. Such alignment marks are easy to be detected by camera, when a layer of high reflective material, generally Cr metal, is patterned. However transparent polymer material is used in our process, as alignment marks made of it which are actually buried phase structures would be hardly to be observed by conventional camera. Hence to increase the contrast of the alignment marks, we proposed a feature specific alignment system for which the shape and depth of the alignment marks are optimized for phasebased imaging, such as phase contrast and Schlieren imaging. Our results showed a contrast enhancement of alignment marks image compared to that of a conventional imaging system. At last, through this proposal we fabricated a flexible optical interconnect for testing.

9556-17, Session 4

Tolerance analysis of the pulse signal of a noval lateral deformable optical NEMS grating transducer

Chen Wang, Jian Bai, Zhejiang Univ. (China)

In this paper we discuss a tolerance analysis of the pulse signal of a novel opto-mechanical zeroth-order grating transducer in terms of fabrication, illumination as well as alignment. This device gives out rapid variation of



reflective intensity with the displacement of the nanostructured grating elements and the original sinusoidal signal of the device develops into a new signal form, i.e. pulse signal with the decrease of the air gap between two layers of gratings. As the slop of the pulse signal, namely 2.481%/ nm is 8 times higher than that of the original signal form, namely 0.3%/ nm, the sensitivity of the structure is improved 8 times higher. Since the special function of the device is originated from its extreme sensitivity to variation of its parameters and the size of the structure is in sub-wavelength dimension, the parameter setting of the device is crucial to its performance and also imposes a high demand on the state-of-art processing technology. Thus, in this paper a tolerance analysis of the device in terms of fabrication, illumination, alignment is discussed in detail to get a better understanding of the tolerance of the pulse signal and a guidance of successful realization of an actual device.

9556-18, Session 4

Design of SiOx slab optical waveguides

Eder Lizarraga, Ctr. de Investigación Científica y de Educación Superior de Ensenada B.C. (Mexico); Alicia Oliver, Univ. Nacional Autónoma de México (Mexico); Rafael Salas, Univ. de Technologie Troyes (France); Heriberto Márquez, Ctr. de Investigación Científica y de Educación Superior de Ensenada B.C. (Mexico); Veronica Vazquez, CIO (Mexico)

Integrated optics is a growing field looking for materials for building passive and active components preferably based in silicon to be compatible with microelectronic industry. SiOx is a suitable candidate for the development of both kind of components due to the potential of precipitation of silicon nanoparticles, which can lead to active components and being a platform of hybrid photonic-plasmonic devices. High refractive contrast between the substrate (SiO2) and the core (SiOx) may be achieved, leading to strong confinement in the core, allowing submicron sized optical waveguides. The advantages of this submicron waveguides is the enhancement of nonlinear effects waveguide and the possibility of making a denser integrated circuit. A modal analysis of the light in the slab waveguide will allow us to select the appropriated guide physical structure. In this work, an analysis of dispersion relation curves b-V of SiOx slab optical waveguides is presented. Here is considered that SiOx refractive index can range between 1.457-1.9, and core thickness between 100 nm- 1000 nm. Starting from the normalized dispersion relation and the distribution of the electric field in the waveguide, the cutoff wavelength or thickness, effective refractive index, effective guide thickness and confinement factor of a selected mode are calculated.

9556-19, Session 4

Design and fabrication of sinusoidal spectral filters for multispectral imaging

Chuan Ni, Jie Jia, Keigo Hirakawa, Andrew M. Sarangan, Univ. of Dayton (United States)

Multispectral imaging beyond the minimal metametric RGB colors still remains a challenge, especially in portable inexpensive systems. We report a novel discrimination technique which utilizes an array of multichroic filters that have a sinusoidal transmission spectra in the frequency domain, known as the Spectra Filter Array (SFA). These spectrally periodic filters are not only convenient for Fourier analysis, but are also highly desirable for preserving the signal integrity. Since the SFA is posed as an optimal sampling of hyperspectral images, it allows for the reconstruction of the full spectrum from subsequent demosaicking algorithms.

Unlike conventional Color Filter Arrays (CFA) which utilizes absorption dyes embedded in a polymeric material, the sinusoidal multichroic filters require an all-dielectric interference filter design. However, the goal of most dielectric filter designs is to achieve sharp transitions with high-contrast. A smoothly varying sinusoidal transition is more difficult with conventional approaches. However, this can be achieved by trading off the contrast. Following the principles of a simple Fabry-Perot cavity, we have designed and built interference filters from 0.5 sinusoidal periods to 2.5 sinusoidal periods from 450nm to 900nm spectral range. Also, in order to maintain a uniform period across the entire spectrum, the material must have a very low dispersion. In this design, we have used ZnS as the cavity material. The six filters have been used in a multispectral imaging test bed.

9556-20, Session 4

Detection of coating fluorophores' densities in improved Q-factor cavities

Nader Shehata, Ishac L. N. Kandas, Virginia Polytechnic Institute and State Univ. (United States) and Alexandria Univ. (Egypt); Chalongrat Daengngam, Prince of Songkla Univ. (Thailand)

This work investigates the relationship between spherical silica cavity Q-factors and the density of coated second order nonlinearities optical structures such as prosion brown (PB) and PCBS. In particular, we fabricate multiple functional cavity with different ionic self-assembled multilayer (ISAM) film thickness in nanometers range (about 1 nm for each one bilayer) and PB/ PCBM densities. The Q factors of these cavities are mainly limited by optical absorption in the case of the ISAM film, and a combination of optical absorption and scattering of the coated fluorophores. The nonlinear optical materials reduce Q-factor to the range of 106-107, which is in the range of producing second harmonic signal. That could help in evaluating the effective density of fluorophores of both coating materials. This work is helpful in different applications including optical communication infrastructure.

9556-21, Session 4

Applications of silicon microspheres as microphotonic filters

Muhammad Zakwan, Ulas S. Gökay, Ali Serpengüzel, Koç Univ. (Turkey)

Elastic light scattering is performed in silicon microspheres at near-infrared telecommunication wavelengths. Lorentzian and Fano lineshape whispering gallery mode resonances are experimentally observed and numerically simulated. The quality factors of the resonances are on the order of 100,000. Possible applications of silicon microspheres include Lorentzian and Fano filters for optical channel dropping and modulation for wavelength division multiplexing.

9556-22, Session 5

Nanofabrication at 1nm resolution by quantum optical lithography

Eugen Pavel, Storex Technologies Inc. (Romania)

A major problem in the optical lithography was the diffraction limit. Here, we report and demonstrate a lithography method, Quantum Optical Lithography [1,2], able to attain 1 nm resolution by optical means using new materials (fluorescent photosensitive glass-ceramics and QMC-5 resist). The performance is several times better than that described for any optical or Electron Beam Lithography (EBL) methods. In Fig. 1 we present TEM images of 1 nm lines recorded at 9.6 m/s.

References

[1] E. Pavel, S. Jinga, B.S. Vasile, A. Dinescu, V. Marinescu, R. Trusca and N. Tosa, "Quantum Optical Lithography from 1 nm resolution to pattern transfer on silicon wafer", Optics and Laser Technology, 60 (2014) 80–84.

[2] E. Pavel, S. Jinga, E. Andronescu, B.S. Vasile, G. Kada, A. Sasahara, N. Tosa, A. Matei, M. Dinescu, A. Dinescu, and O.R. Vasile, "2 nm Quantum Optical Lithography", Optics Communications, 291 (2013) 259–263



9556-24, Session 5

Plasmonic structures fabricated via nanomasking sub-10 nm lithography technique

Stephen J. Bauman, Desalegn Debu, Joseph B. Herzog, Univ. of Arkansas (United States)

Fabrication of nanostructures below the resolution limit of typical lithography techniques helps push the boundaries of plasmonics and nano-optics research. Smaller nanoscale (<10 nm) metallic structures and gaps allow for plasmonic enhancement of incident light which is beneficial in various applications such as biosensing, photovoltaic absorption enhancement, surface enhanced spectroscopies, and photocatalysis. However, this high structural resolution can be difficult to obtain with typical techniques. A new nanomasking technique has been developed which allows for fabrication of nanostructures and nanogaps down to sizes less than 10 nm by using a two-step electron beam lithography (EBL) and deposition method with the potential for mass production scalability. This technique improves upon existing alternatives for creation of truly nanoscale features. It provides control over geometrical variation, two-dimensional fabrication, and the ability to simultaneously create many plasmonic hotspots over a large area. This work has fabricated such structures with sub-20 nm metal features and sub-10 nm gaps. Structures can potentially be tuned to specific wavelengths by controlling structure and gap widths. Further work will involve determination of line edge and line width roughness, comparisons of different metals, varying structure heights, and continued scaling up of the technique to determine its feasibility for mass producible plasmonic enhancement and nano-optics applications. Additional future work includes theoretical models in conjunction with experimental optical characterization results.

9556-25, Session 5

Optomechanical nanoantenna

Alireza Bonakdar, Sung Jun Jang, Robert L. Brown, Iman Hassani Nia, Mohsen Rezaei, Hooman Mohseni, Northwestern Univ. (United States)

Optical nonlinearity is a necessary condition for optoelectronic signal processing devices such as modulators, wavelength mixers, and non-magnetic isolators. Unfortunately, nature does not provide us with materials that have large optical nonlinearity, setting limitations on the device performance and power consumption. In addition, implantation of nonlinear materials is a difficult task, since they are not necessarily compatible with the standard III-V semiconductor technology. Previously, we introduced the concept of optomechanical nanoantenna as a promising nanophotonic building blocks to exhibit giant nonlinear response. Here, we designed, fabricated and characterized an optomechanical nanoantenna (OMNA), which shows dramatic change in scattering properties by minuscule changes in geometry. The OMNA is highly compact compared with other types of the developed optomechanical devices due to the plasmonic effect that squeezes optical field many orders of magnitude bellow the diffraction limit setting a sub-wavelength resonance length of the antenna.

We fabricated the OMNA using electron beam lithography and suspended its reconfigurable parts via isotropic RIE etching of a sacrificial layer. In order to explore the nonlinearity response of OMNA, we used pump-probe scheme. Pump laser is responsible to generate optical force at the gap of the antenna and subsequently induces deformation on the antenna. The modification on the antenna's response to the probe due to mechanical deformation can be detected as the amount of the change in the captured reflection and transmission signals. This work brings new opportunities toward material-less nonlinear optics.

9556-26, Session 5

Optimizing a subwavelength grating lens for large incidence angles

Lukas Elsinger, Technische Univ. Graz (Austria) and ams AG (Austria); Peter Hadley, Technische Univ. Graz (Austria); Rainer Minixhofer, Anderson P. Singulani, ams AG (Austria)

Flat transmissive lens designs for infrared sensor applications based on subwavelength gratings were analyzed using a finite difference time domain program (Lumerical). The lens structure consisted of periodically arranged silicon pillars placed on a sapphire substrate. Broadband transmission in a >1.5 μ m wavelength band around the design wavelength of ? = 4 μ m was observed. For the initial design the pillar height was 2.5 µm, the pitch was 1.8 μ m and the filling factor varied between 30% and 70%, resulting in a change of the transmitted phase over 2ϖ , while the transmitted power remained >90%. The Huygens-Fresnel principle was then used to find the correct filling factor at each position for a focusing lens. Other authors have reported severe corruption of the focal spot quality for incidence angles >10° with similar lens designs. While for other usage this might be satisfactory, for sensor applications the lens also has to work at large incidence angles. A parametric sweep of the initial design with varying incidence angle showed a drop in the transmittance appearing at a filling factor of 55-60%, which caused defocusing. The effect of the transmission drop was accompanied by a phase discontinuity. This was investigated numerically and a phenomenological explanation is presented. The subwavelength structure was then optimized to work for a lens design with large incidence angles. A finite element method package (Comsol) was used to characterize the quality of the focal spot at different incidence angles.

9556-27, Session 5

Research on input shaping algorithm for rapid positioning of ultra-precision dual-stage

Fazhi Song, Yan Wang, Xinglin Chen, Ping He, Harbin Institute of Technology (China)

As a high-precision servo motion platform, the dual-stage lithographic system uses lots of long-stroke air-bearing linear motors to achieve rapid positioning. Residual vibration, resulting from direct drive, almost zero damping, parallel decoupling structure and high velocity, leads to too long settling time and is one of the key factors in slowing the speed of positioning. To suppress the residual vibration and realize the high positioning precision in shorter settling time, this paper designs proportional integral derivative (PID) controller with input shaping algorithm for the air-bearing linear motor. The simulation of the system is performed by MATLAB/Simulation. The experimental results indicate that the input shaping algorithm proposed in this paper brings about significant reduction in the positioning time of the linear motor.

9556-28, Session 6

Nanomanufacturing concerns about measurements made in the SEM: Part IV: charging and its mitigation (Invited Paper)

Michael T. Postek, András E. Vladár, National Institute of Standards and Technology (United States)

This is the fourth of a series of tutorial papers discussing various causes of measurement uncertainty in scanned particle beam instruments, and some of the solutions researched and developed at NIST and other research institutions. Scanned particle beam instruments especially the scanning electron microscope (SEM) have gone through tremendous evolution to become indispensable tools for many and diverse scientific



and industrial applications. These improvements have significantly enhanced their performance and made them far easier to operate. But, ease of operation has also fostered operator complacency. In addition, the perceived user-friendliness has reduced the need for extensive operator training. Unfortunately, this has led to the concept that the SEM is just another expensive digital camera or another peripheral device connected to a computer and that all of the issues related to obtaining guality data have been solved. Hence, a person using these instruments may be lulled into thinking that all of the potential pitfalls have been fully eliminated and they believe everything they see on the micrograph is always correct. But, as described in this and the earlier presentations, this may not be the case. Care must always be taken when guantitative data are being recorded. The first paper in this series discussed some of the issues related to signal generation in the SEM, including instrument calibration, electron beam-sample interactions and the need for physics-based modeling to understand the actual image formation mechanisms to properly interpret SEM images. The second paper, discussed another major issue confronting the microscopist: specimen contamination and methods of contamination elimination. The third paper discussed mechanical vibration and stage drift and some useful solutions and this fourth contribution discusses some of the issues related to specimen "charging" and some possible solutions for its mitigation.

9556-29, Session 6

Helium ion microscopy of electrospun nano-composites (Invited Paper)

Eva M. Campo, Bangor Univ. (United Kingdom); Chuong T. Huynh, Carl Zeiss Microscopy, LLC (United States); Eduardo Larios, Univ. of Texas at San Antonio (United States); Mohan Ananth, Carl Zeiss Microscopy, LLC (United States)

Carbon Nanotubes and polymer nanocomposites have attracted much attention in the last couple of decades. Convenient processing of polymers in microtechnology environments, combined with exceptional properties of CNTs are expected to produce a variety of structural and functional applications. Some examples include high-strength composites, artificial muscles, energy storage and conversion devices, sensors, field emission displays, radiation sources, nanometer sized semiconductor devices, as well as probes and interconnects. However, despite a promising application space, effective processing and manufacturing remains elusive due to the poor understanding of processing effects on interfaces. As a result, understanding of dynamics at the CNT-polymer interface sits at the core of this promising material system. In fact, interfacial dynamics between polymers and nanofillers upon electrospinning is a largely unexplored field of research, and in this work we propose an exploration through innovative microscopy techniques.

Indeed, the advent of Helium Ion Microscopy (He-IM) could impose an inflexion point towards the understanding of the extremely dynamical character of electrospinning. Absence of surface treatments prior to irradiation unveils previously unreported conformation arrangements between CNTs and hosting polymer blend, possibly pointing at complex dynamical processes upon fiber collection during electrospinning. These results further highlight the value of He-IM in the study of soft matter and nanocomposites.

9556-30, Session 6

Controlling orientation of carbon nanotubes by using direct laser writing

Shota Ushiba, Osaka Univ. (Japan); Satoru Shoji, The Univ. of Electro-Communications (Japan); Kyoko Masui, Osaka Univ. (Japan); Junichiro Kono, Rice Univ. (United States); Satoshi Kawata, Osaka Univ. (Japan)

Single wall carbon nanotubes (SWNTs), which consist of a rolled-up

single layer graphene with a 1 nm diameter cylindrical shape, exhibit remarkable mechanical, electrical, thermal, and optical properties. The intrinsic characteristics make them ideal candidates as advanced filler materials in composites, leading to a wide range of applications such as MEMS and photomechanical actuators. In our previous research, we demonstrated 3D micro fabrication of SWCNT/polymer composite by using direct laser writing based on two photon polymerization (TPP). Our method allows one to fabricate arbitrary 3D micro structures, and SWCNTs are uniformly distributed throughout the whole structures. Here, we present a technique to orient SWCNTs in a desired direction. Polarized micro Raman spectroscopy is used to elucidate the orientation direction of SWCNTs in structures with high spatial resolution. The G-band peak intensity significantly varies in intensity as a function of angles between the polarization of incident light and nanowire axis. The G-band intensity becomes largest when the polarization of the laser beam is parallel to the nanowire axis, while it becomes smallest when the polarization is perpendicular. This result clearly indicates that the SWCNTs are uniaxially aligned inside the wire. We also demonstrate controlling orientation of CNTs in 3D structures by changing laser scanning direction. The alignment would further improve properties of the composite such as mechanical and electrical properties.

9556-31, Session 6

Self-assembly based nanometre scale patterning for nanowire growth

Abhishek Chandramohan, Durham Univ. (United Kingdom); Rong Sun, Lund Univ. (Sweden); Natalia Kaliteevskaya, Durham Univ. (United Kingdom); Jonas Johansson, Kimberly A. Dick, Lund Univ. (Sweden); Budhika Mendis, Michael C. Petty, Andrew J. Gallant, Dagou A. Zeze, Durham Univ. (United Kingdom)

Periodic nanostructure arrays have been ubiquitously exploited lately due to their properties and prospective applications in production of templates for self-induced and gold (Au)-catalysed nanowires (NWs) as this approach is relatively cheap, time-efficient and do not require electron beam lithography. The technique consists creating nanoholes in SiO2 to expose the silicon Si (111) beneath where self-induced NWs can nucleate, while nanodots deposited onto the Si (111) surface serve as catalyst seeds.

For Au-catalysed NWs, a monolayer of self-assembled polystyrene nanospheres (PNS 300nm) was created on a 2 inch Si wafer by spin coating and later etched for a short time before a very thin Au-catalyst layer was deposited. In turn, for self-induced, PNS monolayer was created onto a SiO2-Si substrate. A longer etch was required to reduce PNS diameter significantly to leave relatively larger spacing where chromium is blanket deposited. PNS were lifted off by sonicating the samples in toluene produce the periodic arrays of nanodots and nanoholes, respectively. The underlying SiO2 was etched further through the nanoholes to uncover the Si below. 200 nm holes and 30-70 nm dots were demonstrated through the bespoke methods. The patterned substrates served as master templates, subsequently copied using polydimethylsiloxane (PDMS) to produce a flexible stamp for nanoimprint lithography. A bi-layer resist lift off process was developed to print the replicated nanodots or nanoholes on large-area substrates onto which III-V NWs were subsequently grown.

9556-32, Session 7

Janus tectons: a versatile platform for selfassembling chromophores on sp2-carbon based substrates (Invited Paper)

Ping Du, David Kreher, Fabrice Mathevet, Univ. Pierre et Marie Curie (France); Fabrice Charra, Commissariat à l'Énergie Atomique (France); André-Jean Attias, Univ. Pierre et Marie Curie (France)

In view of the demanding forthcoming applications in nanotechnology, it is



of prime interest to create functions out-off the plane and fully exploit the room above the substrate. Accessing the third dimension is so a mandatory step for nanooptics/electronics. Previously we introduced the Janus-like 3D tecton concept. It consists of a dual-functionalized unit presenting two faces linked by a rigid spacer: one face (A) is designed for steering 2D selfassembly, the other one (B) is a functional molecule. The objective is to take advantage of the in-plane self assembling of building blocks lying on face A to control the positioning of out-off plane active unit B, linked to the base by a rigid pillar. Here we present a series of Janus tectons incorporating chromophores ranging from fluorescent dyes to photoswitchable molecules. We will present the optical properties in solution as well as the properties of the self-assembled functional monolayers on flat sp2-carbon based substrates like HOPG and graphene.

9556-33, Session 7

Linear and nonlinear optical processing of polymer matrix nanocomposites

Travis J. DeJournett, Karen Han, Lauren R. Olasov, Fan W. Zeng, Brennan Lee, James B. Spicer, Johns Hopkins Univ. (United States)

This work focuses on the scalable synthesis and processing of nanostructures in polymer matrix nanocomposites (PMNCs) for applications that require photochemical functionality of these nanostructures. An in situ vapor deposition process using various metal and metal oxide precursors has been used to create a range of nanocomposites that display photochromic and photocatalytic behaviors. Under specific processing conditions, these composites consist of discrete nanoparticles distributed uniformly throughout the bulk of an optically transparent polymer matrix. Incorporating other chemical species as supplementary deposition agents in the synthesis process can modify these particles and produce complicated nanostructures with enhanced properties. In particular, work has been carried out to structure nanoparticles using laser irradiation. Starting with metallic or metal oxide nanoparticles in the polymer matrix, localized chemical vapor deposition in the near-particle environment has been carried out using laser irradiation to decompose chemical precursors leading to the formation of secondary structures surrounding the seed nanoparticles. Control of the spatial and temporal characteristics of the excitation source allows for synthesis of nanocomposites with a high degree of control over the location, composition and size of nanoparticles in the matrix and presents the opportunity to produce patterned materials with spatially varying properties.

9556-34, Session 7

High contact angle hysteresis of nanopillared quartz surfaces

Ming-Tsung Hung, Shing-Lung Chen, Shang Yang, National Central Univ. (Taiwan)

Introducing micro/nanostructure on the surfaces is an effective way to achieve superhydrophobicity. However, it usually exhibits very low contact angle hysteresis. In this study, we present a nanopillared quartz surface with large contact angle and high hysteresis. Quartz is a very unique material with great optical, electrical, thermal, and mechanical properties, but with very low manufacturability. The nanopillar structures are fabricated by a cost-effective wet etching of ammonium bifluoride solution. A nanometerthick platinum layer is deposited on the substrate and annealed to form nanoparticles prior the etching as an etching mask. Different pillar lengths and densities are fabricated by controlling the etching conditions with different etching masks. In the contact angle measurements, the surfaces turn into hydrophobic on the nanostructured samples and with high hysteresis. Compared with the theoretical models, it suggests that the droplet penetrates into the structures and partially contacts the bottoms surface. The ratio of the bottom contacting area decreases with the increase of the structure density and the increase of the structure height. The hysteresis is roughly proportion to the penetrating contact area, where the

movement of the droplet is impeded. The situation becomes severe when the droplets have larger portion touching the bottom surface.

9556-35, Session 7

Nanoscale patterning of poly (L-lactic acid) (PLLA) films with nano-imprinting methods

Akshit Peer, Iowa State Univ. (United States) and Ames Lab. (United States); Rabin Dhakal, Iowa State Univ. (United States); Rana Biswas, Iowa State Univ. (United States) and Ames Lab. (United States); Jaeyoun Kim, Iowa State Univ. (United States)

Many diverse biological applications can benefit from nanoscale texturing of materials for bio-medical functions. Texturing of bio-materials can increase the available surface area so that they can be coated with larger doses of therapeutic agents. We demonstrate nanotexturing of poly (L-lactic acid) (PLLA) – a material used for drug-eluting coronary stents and cell growth template.

We develop a rapid technique for texturing PLLA films based on nanoimprinting. A master pattern consisting of a periodic array of holes or nanocones with sub-micron pitch was developed on a master substrate by lithography. The inverse of this pattern was transferred to a polydimethylsiloxane (PDMS) mold by nanoimprinting.

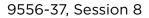
We investigated the transfer of the PDMS pattern onto PLLA films by dropcasting the PLLA solution on the mold, and imprinting PLLA films with the PDMS mold, under elevated pressure and temperature. PLLA was dissolved in chloroform and the solution was either drop casted directly on the PDMS mold or was spin coated on the glass substrate to be stamped later by the PDMS mold. We successfully achieved nanoarrays of holes with pitch ~700 nm, and hole diameter ~500 nm, with triangular lattice periodicity and varying depths on PLLA films. SEM images demonstrate that drop-casting achieves the most reliable transfer of patterns onto the PLLA, whereas nanoimprinting the PLLA films results in shallower and less resolved features. We compare the nanopatterns on PLLA to those on a polystyrene film. We will describe the optical reflectance from these films and compare the results with simulations.

9556-36, Session 8

Nanomanufacturing-related programs at NSF (Invited Paper)

Khershed P. Cooper, National Science Foundation (United States)

The National Science Foundation is meeting the challenge of nanoscience and technology implementation through several nanomanufacturingrelated research programs. The goal of the core Nanomanufacturing (NM) and the inter-disciplinary Scalable Nanomanufacturing (SNM) programs is to meet the barriers to manufacturability at the nano-scale by developing the fundamental principles for the manufacture of nano-scale materials, structures, devices, and engineered systems. These programs address issues such as scalability, reliability, quality, performance, yield, metrics, and cost among others. The programs seek nano-scale manufacturing ideas that are transformative, that will be widely applicable and that will have far-reaching technological and societal impacts. It is envisioned that these basic research programs will provide the knowledge base for larger programs such as the manufacturing Nano Science and Engineering Centers (NSECs), the Nanosystems Engineering Research Centers (ERCs), the STTR/SBIR program and the current and future nano-related National Network for Manufacturing Innovation (NNMI) Institutes. In this talk these different programs will be briefly described. The presentation will include discussions on novel approaches to nanomanufacturing and process integration and their implications for measurement and control protocols. Nanomanufacturing concepts and ideas will be illustrated by examples of projects from the NM and SNM programs.



Challenges and needs for automating nano image processing for material characterization (Invited Paper)

Yu Ding, Satish T. S. Bukkapatnam, Texas A&M Univ. (United States)

Working with various nanomanufacturing processes, the authors realize that measurements revealing the structure and function of nano subjects are most likely in an image format. Consequently, image processing techniques are inevitably needed to extract critical information pertinent to a subject's formation as well as interaction with the host materials. These nano images are of large data size and contain complicated features. The current nano image processing methods are slow, expensive and labor intensive. There is a strong need to develop fast and reliable methods and procedures, enabling process control compatible automated processing of nano images.

The international standard on nanotechnology leaves it for the users to identify an appropriate data analysis algorithm or to seek a third party software solution. When an incapable image processing tool is used, this approach leaves a gap in the whole loop of nano metrology on imaging data. The high resolution enabled by the physical instruments may not be preserved.

The authors believe that nano images have their uniqueness. Features valid, and techniques favored, in the general image processing or bio-imaging field may no longer be effective in nano imaging. Specialized image processing techniques are needed to address the challenges. Towards that goal, the authors will discuss the recent developments of image processing methods, specifically tailored for nano image data, as well as the nearand medium-term needs in the area of nano metrology and imaging. The authors will also share their perspectives on how some of the research challenges may be addressed.

9556-38, Session 8

Scatterometry reference standards to improve tool matching and traceability in lithographical nanomanufacturing

Emil Agocs, Bernd Bodermann, Physikalisch-Technische Bundesanstalt (Germany); Sven Burger, JCMwave GmbH (Germany); Gaoliang Dai, Johannes Endres, Hermann Gross, Physikalisch-Technische Bundesanstalt (Germany); Poul-Erik Hansen, Danish Fundamental Metrology Institut (Denmark); Sebastian Heidenreich, Michael Krumrey, Physikalisch-Technische Bundesanstalt (Germany); Bernd Loechel, Juergen Probst, Helmholtz-Zentrum Berlin für Materialien und Energie GmbH (Germany); Frank Scholze, Victor Soltwisch, Matthias Wurm, Physikalisch-Technische Bundesanstalt (Germany)

Scatterometry is an important and high sensitivity metrology technique to support the lithographic nanomanufacturing process in semiconductor industry. However, today it is usually not applied for absolute measurements of critical dimensions (CD) and quality control due to the lack of traceability. The reasons for this have been some possible sources of systematic measurement deviations caused by a number of approximations and assumptions commonly applied in measurements and data analysis as well as the lack of reliable standard samples. To establish scatterometry as traceable and absolute method for dimensional measurements we have investigated the influences of some of these approximations and we have developed, characterised and calibrated scatterometry standard samples suitable for tool validation [1].

We investigated both experimentally and by numerical simulations the influences of different tool or sample specific approximations and discuss and quantify their influences on the measurement uncertainty budget.

Two different standard samples, based either on Si or on Si3N4, have been developed. The etched gratings have periods down to 50 nm and contain areas for AFM measurements for comparison. We have characterised these samples using AFM, optical, EUV as well as X-Ray scatterometry and spectroscopic ellipsometry. For the calibration a combined analysis of DUV and EUV scatterometry, spectroscopic ellipsometry and GISAXS measurement data supported by AFM results will be applied using Bayes algorithms.

OPTICS+

NANOSCIENCE+ ENGINEERING

SPIE. PHOTONICS

We report on the status of these developments and discuss the final design and aimed specifications of these standard samples and of possible future extensions.

[1] http://www.ptb.de/emrp/ind17.html, http://www.euramet.org

9556-39, Session 8

Quantitative tool characterization of 193 nm scatterfield microscope

Martin Y. Sohn, Bryan M. Barnes, Hui Zhou, Richard M. Silver, National Institute of Standards and Technology (United States)

Evaluation of uncertainties is a critical element in guantitative nanoscale measurements using optical microscopy techniques. Instrument characterization underlies the quantitative evaluation of measurements of deep sub-wavelength features. The scatterfield microscopy technique, which articulates the illumination at the sample plane, is an efficient method for angle- and polarization-resolved microscope characterization to enable the uncertainty evaluations. The tool characterization results are used for the Fourier space normalization of electromagnetic simulation to permit comparisons with experimental imaging data. For this purpose the NIST 193 nm scatterfield microscope operating with an ArF Excimer laser was characterized. The illumination and collection optics were scanned angularly, utilizing a small aperture at the conjugate back focal plane of the objective lens so that the optics train was characterized with respect to angularly discrete cones of the illumination beam. Each cone beam can be approximated as a plane wave by using Köhler configuration, simplifying the analysis of the scattered light induced by the discrete illumination beam at the sample plane. Under this approximation, the illumination and entire tool function sets were measured at sample and imaging CCD planes, respectively, producing the collection tool function set numerically. We report tool imperfection effects upon these tool functions, specifically, comparing to the optical simulations of the designed optical paths varied with misalignments and aberrations that lead to changes in the tool functions. Through these comparisons, we investigate the relationship between the microscope tool imperfection factors to the deviations in the illumination as well as in the collected scattered light.

9556-40. Session 8

Laser velocimetry for measurement of non-sinusoidal vibration in sub-nanometer scale without lock-in amplifiers

How-Foo Chen, Wei-Lun Chiang, National Yang-Ming Univ. (Taiwan)

Laser velocimetry capable of measuring slow motion or small displacement normal to vibrational surface always find its position in industry and scientific applications, even in life science, such as mechnobiology of cells. However, measurement of small velocity or displacement down to sub-nanometer scale is always a challenge due to the significant amount of low-frequency noise from environment, detectors, and circuits. When such sensitivity is required, utilization of lock-in amplifiers is necessary to filter out the noise and to satisfy the requirement. But the measurement is then also limited to single-point detection. Without lock-in amplifiers, the measurement sensitivity is usually limited to the micron scale at the smallest. Utilizing self-mixing dynamics of a semiconductor laser for velocity measurement usually has the sensitivity limited to about



centimeter per second and also to a single-point measurement because one laser can be used only for one detection point. Different from those technologies, we have developed a laser Doppler velocimetry in a Mach-Zehnder configuration. A heterodyne scheme combined with a downconversion scheme, digital filtering, and Hilbert transform is used to gain the measurement sensitivity down to sub-nanometer scale without the usage of a lock-in amplifier. Environment perturbation in tens of nanometer scale can be removed by empirical mode decomposition (EMD). The setup can detect sub-nanoscale displacement and velocity of a surface with nonsinusoidal vibration frequency down to sub-Hertz. Lack of lock-in amplifiers promises this Doppler velocimetry technology not limited to single-point measurement of a surface vibrating down to sub-nanometer scale.

9556-41, Session PWed

Self-assembly of composite materials based on carbon nanotubes

Dmitrii Zhukalin, Andrei V. Tuchin, Larisa A. Bityutskaya, Voronezh State Univ. (Russian Federation)

One of the urgent problems of condensed matter physics is the study of interrelation between the formation process and the properties of self-organized structures. The main goal of this work is to study nonlinear dynamic processes during the aggregation of short carbon nanotubes in a drying drop. The autowave process is characteristic of dynamically ordered structures and can be seen in physical, chemical, biological and medical systems. Recently, a drying drop has been used as a reactor with distributed active medium, allowing to observe nanoprocesses in a contained environment. Taking into account the dynamic conditions of the drying drop, including the capillary flows, temperature gradient and gradually increasing concentration of the components - "The Droplet reactor" is of great interest in studying the self-assembly and self-organization of nanoparticles.

The colloidal suspension containing short carbon nanotubes in distilled water was used as the active medium. The dynamics of the thermophysical properties of aggregation process, as well as morphology was investigated in situ. The phenomenon of formation of the thermal autowave spatio-temporal structures was observed. According to its distinctive features (disequilibrium, nonlinearity, spontaneity, openness), the autowave process of aggregation of nanotubes can be seen as a dissipative structure with the increasing amplitude of temperature fluctuations. As a result of this aggregation, fractal structures are formed.

It can therefore be concluded that autowave processes represent unique thermodynamic characteristics of self-organization. Thus, autowave processes can be used for diagnostic and identification purposes during the synthesis of various functional materials.

9556-42, Session PWed

Non-circular nanohole array as selective emitter for thermophotovoltaic system

Jin Hwan Kim, Moo Whan Shin, Yonsei Univ. (Korea, Republic of)

We fabricated two-dimensional tantalum (Ta) photonic crystal with noncircular nanohole array as a selective emitter for the thermophotovoltaic system. We optimized geometric parameters (pitch, diameter, and depth) for each of patterns of rectangular, hexagonal, and circular nanohole array by using finite difference time domain (FDTD) techniques. The cutoff wavelength of the selective emitter was designed to coincide with the bandgap energy of a promising low-bandgap (0.55 eV, 2.25 ?m) photovoltaic material, InGaAsSb. The three types of nanohole arrays were thoroughly investigated in the aspect of spectral selectivity, and fabricability (minimum feature size, and aspect ratio). Spectral selectivity was defined as the ratio of summation of emissivity for the useful wavelength range from 1 to 2.25 ?m to that from 1 to 4 ?m, and the optimized spectral selectivity was over 0.9. The non-circular nanohole arrays showed similar spectral selectivity compared to typical circular nanohole array even with relatively large feature size and low aspect ratio. We tried to transfer the optimized non-circular pattern onto polycrystalline Ta substrates via typical photolithography process. The fluorine based deep reactive ion etching was developed for the Ta emitter to exhibit clear vertexes of polygonal shape and relatively high aspect ratio. Emissivity of the emitters was measured by using the UV-Vis-NIR spectrophotometer, and the measurement verified the simulated results.

9556-43, Session PWed

Design and fabrication of multilayer dielectric gratings for spectral beam combining

Hyun-Ju Cho, Daeduk College (Korea, Republic of); Yong-Soo Lee, Hyun-Tae Kim, Doosan DST Co., Ltd. (Korea, Republic of)

Metal gratings are mostly used on low energy optics, buy it has low diffraction efficiency and laser damage threshold. Spectral beam combining is a method to make high power laser beam using diffraction gratings. Multilayer dielectric (MLD) high reflectance mirror is designed for high efficiency gratings using HfO2 and SiO2 for high laser damage threshold. On the top of the mirror, polarization dependent SiO2 grating structure is simulated by finite domain time division (FDTD) method at 1060nm for spectral beam combining. To estimate the far field diffraction characteristics, we first calculate near field electromagnetic wave properties at the substrate region and these are transformed to angular diffraction characteristics at about 1 meter apart from the grating. Multilayer dielectric mirrors is deposited by electron beam evaporation method at the substrate temperature 250? and the reflectance of the deposited mirror was measured by spectrophotometer. Four types of high efficiency MLD gratings are selected and these are fabricated by lithography and reactive ion etching method. To fabricate the designed submicron structure, 4X stepper is used for pattern formation on the photo resistor. We use fused silica as a substrate and additional dummy silicon wafer substrates are used for grating structure confirmation using scanning electron microscope. The diffraction efficiencies are measured by the angle resolved power measurements method and these are compared with simulated results.

9556-44, Session PWed

Advanced length scaling method of optical nanoantennas

Seunguk Kim, Jeonghee Shin, Jae-Eun Jang, Byoungok Jun, Daegu Gyeongbuk Institute of Science & Technology (Korea, Republic of)

Due to the tiny size of optical nanoantennas, some typical radio frequency (RF) antenna theory, especially length scaling regime, are unsuitable for optical region. Various approaches to obtain meaningful scaling method have been recently studied and estimated. However, suggested models so far still have some mismatches from the real values of optical nanoantennas in visible light and near infrared (NIR) regions. Even if simplified dielectric constant of metals is available near the ultraviolet (UV) range, it shows appreciable difference with the real dielectric constant of metals in visible to NIR regions, so that it induces severe deviation for the dimensional factors of optical nanoantennas such like a length and a width. Here, to improve the accuracy of scaling regime, we used waveguide theory and tried to find a well-defined dielectric constant of metals based on Lorentz-Drude model. Also, metallic monopole nanoantennas which have various dimensional conditions were formed on the dielectric (SiO2) layer to confirm whether our simulation is well-matched with real values. As a result, the characteristics of fabricated optical nanoantennas are well matched with simulated values in visible light and NIR regions. The deviation of geometric parameters, especially lengths, between simulated and experimental values is less than 5 nm.



9556-45, Session PWed

Design of optical channel waveguides in SiO2 by ion implantation

Helena De los Reyes, Ctr. de Investigación Científica y de Educación Superior de Ensenada B.C. (Mexico); Gloria V. Vázquez, Ctr. de Investigaciones en Óptica, A.C. (Mexico); David M. Salazar, Ctr. de Investigación Científica y de Educación Superior de Ensenada B.C. (Mexico); Alicia Oliver, Univ. Nacional Autónoma de México (Mexico); Heriberto Márquez, Ctr. de Investigación Científica y de Educación Superior de Ensenada B.C. (Mexico)

Design of optical channel waveguides straight, curved, and S-bends based on silver ion implantation in substrate of SiO2 is presented. Step index profiles have been reached using a sequential multiple ion implantation process with energies of implantation from 4.3 to 9 MeV and fluences of 1014 to 1015 ions/cm2 and are used for three-dimensional (3-D) beam propagation method calculations. (BPM). An analysis of modal optical confinement was done by means of effective index method (EIM) for selecting the right dimensions of channel waveguides. Here is considered core index range between 1.4623-1.4662 which is related with fluence. Depth and width for the waveguides were chosen to provide single mode operation. Bending losses are determined as function of bending radius, refractive index change (Δn), and wavelength. The results are presented taken in consideration bending and transition losses.

9556-46, Session PWed

Influence of wetting states on optical characteristics of Si nanopatterns

Minji Gwon, Sujung Kim, Ewha Womans Univ. (Korea, Republic of); Jiaqi Li, IMEC (Belgium) and KU Leuven (Belgium); Xiumei Xu, IMEC (Belgium); Eunsongyi Lee, Ewha Womans Univ. (Korea, Republic of) and The Univ. of Manchester (United Kingdom); Dong-Wook Kim, Ewha Womans Univ. (Korea, Republic of); Chang Chen, IMEC (Belgium) and KU Leuven (Belgium)

Nowadays, state-of-the-art nanofabrication techniques allow us to produce sub-100 nm-scaled devices in the mass production level. Such development of nanotechnology requires reliable wet cleaning of nano-patterned Si wafers. Establishment of desirable cleaning processes definitely requests characterization methods to examine wettability in nano-patterned Si wafers. Recently, we proposed that simple optical reflectance measurements could quantitatively determine the instantaneous water imbibition depths and define the actual wetting state on Si nanopillars (NPs) (diameter: 40 nm) [Xu et al., ACS Nano 8, 885 (2014)]. In this work, we carried out simulation studies of optical characteristics of Si nanopillar (NP) arrays (diameter: 40~130 nm and height: 420 nm) using finite differential time domain (FDTD) method. Reflectance spectra of wetting and non-wetting NPs showed clear difference. The spectra in the long wavelength range were well explained by the interference at the top and bottom of the NPs. As the diameter of NPs increased, resonant guided modes in individual NPs and coupled guided modes appeared in visible range. Wettability of such large-sized NP arrays also did influence the resonant mode excitation. Our results showed that simple optical reflectance measurements were useful to examine surface wettability of nanopatterns.

9556-47, Session PWed

Nanoindentation for surface modification of nanofilms

Angelika Luchenko, V.E. Lashkaryov Institute of

Semiconductor Physics (Ukraine); Mykola M. Melnichenko, National Taras Shevchenko Univ. of Kyiv (Ukraine)

The miniaturization of the dimensions of functional elements and nanostructuring of materials require solving the issues of preparation and control of physical and chemical properties on the micro- and nanolevels under both static and dynamic conditions. Nanoindentation as a set of approaches, methods and specific hardware is practically the only universal tool for probing the mechanical behavior of submicron materials with nanovolumes, ultra-thin surface layers and films. At the same time physical and chemical properties of nano-objects and nanostructures can differ strongly to the macroscopic properties.

Here we show it is practically to use a scanning tunneling microscope for indentation in the continuous micro- and nano-range. A maximum load of 2.64 cN (and 0.4 cN minimum) was applied on a piezo-scanner to achieve the indentation. The relaxation after the surface is structurally modified by contact was investigated. It is shown that within a few hours of modification there is clear evidence of inevitable loss of information about the morphology initially modified area. These images demonstrate the fundamental possibility of conducting research on the observation of diffusion and relaxation processes at the nanoscale with a scanning tunneling microscope. The possibility of modifying the sample surface for subsequent applications in which it is necessary to reduce the average elevation on the surface. Nano-objects on the surface of the experimental samples were created by using the developed technique.

9556-48, Session PWed

Optical properties of LED with patterned 1D photonic crystal

Pavol Hronec, Jaroslava ?kriniarová, Anton Kuzma, Jaroslav Ková? Jr., Slovenska Technicka Univ. (Slovakia); Anna Bencurova, Stefan Hascik, Pavol Nemec, Slovak Academy of Sciences (Slovakia)

In this paper we focus on the application of the one-dimensional photonic crystal (1D PhC) structures on the top of Al0.295Ga0.705As/GaAs multiquantum well light emitting diode (MQW LED). 1D PhC structures with periods of 500 nm, 600 nm, 700 nm, 800 nm and 900 nm were fabricated by the E-Beam Direct Write (EBDW) Lithography. Effect of 1D PhC period on the light extraction enhancement was studied by experimental method and it was simulated by FDTD simulation method. Simulations were prepared with unpolarized and incoherent light source to simulate appropriate properties of real LEDs and their far fields for different periods of 1D PhC patterned on LEDs.

On the LED heterostructure with patterned 1D PhC, the ohmic contacts were prepared by thermal evaporation of gold based contact metals onto the pattern semiconductor surface: AuBe alloy for p-type upper contact and AuGeNi alloy for n-type bottom contact, respectively. Contacts were shaped by conventional lift-off procedure. Subsequently the samples were alloyed at 450?C for 2 minutes in flowing forming gas. Finally, MESA etching was performed by wet chemical etching for isolation of devices.

LEDs light-current characteristics are measured by using integrating sphere. 1D PhC LED radiation profiles were obtained from Near Surface Light Emission Images (NSLEI). NSLEI measurements were performed by CCD camera and evaluated by image processing. Measurements showed the strongest light extraction enhancement using 600 nm period of PhC. Investigation of PhC LED radiation profiles showed strong light decoupling when light reaches PhC structure.

9556-49, Session PWed

The significance of the number of periods and period size in 2D photonic crystal waveguides

Mirsaeid Sarollahi, Jonathan Mishler, Stephen J. Bauman,



Salvador Barraza-Lopez, Paul Millett, Joseph B. Herzog, Univ. of Arkansas (United States)

This work investigates the significance of the number of periods in twodimensional photonic crystals in addition to other parameters including period length and material properties. Straight and curved 2D photonic crystal waveguide models have been developed to study various photonic crystal properties and parameters. The number of photonic crystal posts (number of periods), wavelength, diameters of photonic crystal pots, period length of photonic crystals and material properties have been investigated to determine their effect on the losses in the waveguide. The models focus on a hexagonal period and have been designed to study transmission properties of the waveguide. Additionally, a simplified study focuses specifically on the transmission of light through photonic crystal layers. This flexible model will reveal a thorough analysis of photonic crystal properties. Future work plans to investigate multiple incident angles, polarization, and create a similar 3D model.

9556-50, Session PWed

Optical enhancement of photoluminescence with colloidal quantum dots

Gabrielle Abraham, David A. French, Pooja Bajwa, Colin D. Heyes, Joseph B. Herzog, Univ. of Arkansas (United States)

Unique plasmonic structures will be investigated with optical spectroscopy measurements. A new fabrication method has been developed which can create plasmonic structures with features that are below the limit of electron beam lithography. With these smaller dimensions, the plasmonic devices could produce interesting optical properties. This work will focus on measuring these structures with dark-field reflection spectroscopy. Dark-field spectroscopy is a valuable method for capturing and examining low signals of spectra. This is particularly useful when studying the scattering and resonant frequencies of the spectra produced by plasmonic nanodevices. Additional investigations include examining potential plasmonic enhancement in micro photoluminesce spectroscopy with these novel nanostructures. Both computational modeling and spectroscopy experimental results will be presented. This study analyzes how the geometry and environment of the structures; including thickness, size, and adhesion layer effects; alters the spectral intensity of the resultant scattered light.

9556-52, Session PWed

Wearable and stretchable substrates fabricate for display by O2-plasma surface treatment

Sang Chul Lim, Myung Chan An, Dong IC Lee, Se Hyuk Yeom, Chang Taek Seo, Gyu Seok Choi, Gumi Electronics & Information Technology Research Institute (Korea, Republic of)

Bi-layer substrates under uniaxial compression exhibit micron-scale features that can impart mechanical flexibility in functional electronic devices including interconnects, transistors and solar cells. Bi-layer substrates are produced by forming thin rigid oxide membranes on pre-strained elastomeric substrates using oxygen plasma treatment. The wrinkle process comprises stretching of a soft elastic polydimethylsiloxane(PDMS) substrate and subsequent oxygen plasma treatment, resulting in a hard SiO2-like (SiOx-) layer on the surface.

These were treated on one side with oxygen plasma for 5, 10, 15 min to create a nanoscale silica skin, thus presenting identical surface chemistry in all experiments. This paper presents a cost-effective and simple method to form wrinkled stiff SiOx thin films on PDMS substrates at room temperature by oxygen plasma on pre-strained PDMS. The orientation of the generated structures was always perpendicular to the pre-stretched direction and

the pitch of the structure could be adjusted ranging from 1.1 ?m to 3 ?m by controlling the strength of the pre-stretched strain and the thickness of the surface metal film. Upon relaxation, highly controlled and regular wrinkling of the silica skin resulted.

Systemic studies have been conducted to understand the dependence of the wavy profile on the PDMS pre-strain, oxygen plasma exposure time, and PDMS modulus. The mechanics analysis has been verified to be quantitatively or qualitatively accurate by experimental comparisons. The wrinkled SiOx/PDMS system is stretchable and provides a wavy mold for stretchable electrodes. The constant electrical resistance during mechanical stretching shows the stretchablity of this system. In this study, the metal thin film/contoured substrate is stretchable and has been demonstrated as stretchable electrical conductors.

9556-53, Session PWed

Keratin/poly (vinyl alcohol) blended nanofibers with high optical transmittance

Hak Yong Kim, Chonbuk National University (Korea, Republic of)

In conclusion, highly optically transparent composite NFs were fabricated by simple process involving immersion of human hair derived keratin/ PVA electrospun composite NFs in water without adding any additive. Thus obtained transparent composite NFs were characterized in detail by applying various techniques. On the basis of experimental results, the composite NFs having enhanced mechanical strength and flexibility could exhibit high optical transparency (about 88%) at a wave length of 600 nm. To the best of our knowledge this type of report has not been published so far and we expect that this type of synthesis technique would be a new paradigm for fabricating different composite NFs reinforced with keratin as a transparent substrate to encourage the use of natural and environmentally friendly materials.

9556-54, Session PWed

Development of EUV scatterometer with high-harmonic-generation EUV source for nano-scale grating

Chia-Liang Yeh, Industrial Technology Research Institute (Taiwan)

We have developed a EUV scatterometer using a focused high-order harmonic generation (HHG) source for nano-scale grating measurement. The coherent light source with multiple discrete wavelengths of 25-35 nm was pumped by a table top Ti:sapphire laser system. A charge-couple-device (CCD) camera directly records the diffraction image of the zero and the first order diffraction information from the grating samples. The grating structure can be reconstructed base on the calculations from the location and the intensity distribution of diffraction pattern.

9556-55, Session PWed

Modeling and adaptive neural network control of the short-stroke wafer stage

Yiguang Wang, Xinglin Chen, Yan Wang, Zhenxian Fu, Sheng Qiang, Harbin Institute of Technology (China)

The short-stroke wafer stage for lithography is a six degrees of freedom (DOF) ultra-precision moving body driven by six voice coil motors (VCM). To improve the exposure quality of wafer scanner, focusing and leveling are required during the exposure. Due to coupling, however, the vertical adjustment of the stage has a great coupling impact on the horizontal motion. To solve this problem, a novel 6-DOF model, based on dynamics and kinetics modeling, is proposed for the short-stroke wafer stage.



Compared with the conventional model, no coupling effect is neglected in this model. Based on this model, a robust adaptive neural network multiple input multiple output (MIMO) controller is proposed for the short-stroke wafer stage. The external disturbances, un-modeled dynamics and model uncertainties involved in the control system are considered as a lumped effect in the proposed method and can be estimated by a radial basis function (RBF) neural network real time online. The stability analysis of the proposed control strategy is conducted based on the lyapunov method. To verify the correctness and effectiveness of the proposed model and control method, a simulation is carried out. The results show that, under considered measurement noise, external disturbances and un-modeled dynamics, the system stability and tracking convergence can be guaranteed and nanoscale tracking accuracy can be achieved.

9556-56, Session PWed

Optical reflectivity as an inspection tool for metallic nanoparticles deposited randomly on a flat substrate

Omar W. Vázquez-Estrada, Ctr. de Ciencias Aplicadas y Desarrollo Tecnológico (Mexico); Gesuri Morales-Luna, Alipio G. Calles, Alejandro Reyes-Coronado, Univ. Nacional Autónoma de México (Mexico); Augusto García-Valenzuela, Ctr. de Ciencias Aplicadas y Desarrollo Tecnológico (Mexico)

Nowadays we have different tools to determine the surface coverage fraction of a monolayer of nanoparticles deposited on the surface of a flat substrate, for example: electron microscope, scanning electron microscope-SEM, atomic force microscope-AFM, among others. These techniques have several limitations such as the analysis of a small area and sometimes the sample can be destroyed or altered by the analysis itself. In this work, we present a multiple scattering model for the reflectance of a monolayer of spherical particles supported onto a flat substrate, which allows us to determine indirectly the surface covered fraction of the monolayer, by measuring the reflection of coherent light scattered by the system. Additionally, this model can be extended to study the reflectance spectra in real time of a forming monolayer, estimating the surface coverage fraction supported in any type of flat substrate (e.g. silica, glass, quartz). The advantages of this technique are that the sample is not damaged during the analysis and it also allows to sense large areas of the sample by simply modifying the width of the laser spot. Currently, we are in the process of determining the best configuration to perform optical reflectivity measurements, in order to estimate the surface coverage fraction of a monolayer of spherical nanoparticles deposited on the surface, either varying the angle of incidence of a laser beam or by using reflectivity spectra at a fixed angle of incidence. Specifically, we are studying the minimum value of the surface coverage that can be guantified using optical reflectivity measurements, assuming different sensitivities and noise scenarios with detectors commonly found in most optical laboratories.

9556-57, Session PWed

Viability of sizing metallic nanoparticles in suspension from effective refractive index measurements

Gesuri Morales-Luna, Univ Nacional Autónoma de México (Mexico); Roberto Márquez-Islas, Univ. Nacional Autónoma de Mexico (Mexico); Omar W. Vázquez-Estrada, Humberto Contreras-Tello, Univ Nacional Autónoma de México (Mexico); Augusto García-Valenzuela, Univ. Nacional Autónoma de México (Mexico)

Many nanofluids of technological interest consist of suspensions of metallic nanoparticles. Optical determination of the particles' size is of interest since it can be done in situ. In cases when a plasmonic resonance in the extinction spectrum is clearly visible (e.g. with Ag and Au nanoparticles) one can use its location in the spectrum to infer the particles size. In the absence of a clean resonance peak, due for instance to a distribution in particles shape and size, or for metals with higher losses (eg. Cu or Fe), such method cannot be used. A general and accurate measurement of particles' size in absorbing nanofluids from optical measurements is therefore not available today and further research is needed. Recently we developed a novel methodology based on measurements of optical properties of a nanofluid to determine the size and refractive index of nanoparticles in suspension [1]. However, the method is limited to cases where the absorption is much smaller than the scattering cross-sections, which is not satisfied by metallic nanoparticles within the VIS-IR spectrum. In this work we explore variations of the original method also relying on measurements of the extinction coefficient and refractive index of nanofluids to size metallic nano-particles. The viability of the new method, achievable accuracy and precision is investigated theoretically and experimentally. Additionally we explore the possibility of exploiting dependent-scattering effects for characterizing nanoparticles in suspension. Such effects in nanofluids are already strong for relatively small volume fractions of about 2%.

[1] Optics Letters 39, pp. 559-562 (2014).

9556-58, Session PWed

Wafer defect inspection using compoment tree of SEM images

SungHyon Kim, Il-suk Oh, Chonbuk National Univ. (Korea, Republic of)

This paper proposes a novel defect detection method using component tree of SEM images. The component tree contains rich information about the topological structure of images such as stiffness of intensity changes, area and volume of lobes. The information is very effective in detecting suspicious spot for the defects. A quasi-linear algorithm for constructing the component tree and computing those features is available.

This paper modifies the original component tree algorithm to be suitable to the defect detection. One is to exclude the pixels near the ground level in the initial stage of constructing the component tree. The experiment showed that the scheme speeded up whole process about 10 times.

The other idea is to detect significant lobes by using both the volume and area attributes. To find out significant lobes, the original algorithm deletes repeatedly the leaf nodes in decreasing order of volume. It produced a merged pattern of nearby defects. The modified algorithm uses both the volume and area attributes. It repeats the operation of deleting the leaf nodes in decreasing order of volume. The algorithm exempts the leaf node from the deletion whose parent's area is less than a, where a is the predefined area threshold. If no leaf node is found any more, the process finishes. The n nodes with the largest volume are output as suspicious defects.

The experiments performed with actual SEM images and printed electronics images showed promising results. For a 1000*1000 image, the proposed algorithm ran whole process in 1.36 seconds.

Conference 9557: Nanobiosystems: Processing, Characterization, and Applications VIII



Monday - Wednesday 10-12 August 2015

Part of Proceedings of SPIE Vol. 9557 Nanobiosystems: Processing, Characterization, and Applications VIII

9557-1, Session 1

Developments of salmon DNA as intelligent materials (Keynote Presentation)

Naoya Ogata, Chitose Institute of Science and Technology (Japan)

No Abstract Available

9557-2, Session 1

DNA-based membranes: development and applications (Invited Paper)

François Kajzar, Mihaela Mindroiu, Gratiela Tihan, Ana-Maria Manea, Univ. Politehnica of Bucharest (Romania); Agnieszka Pawlicka, Univ. de São Paulo (Brazil); Ileana Rau, Univ. Politehnica of Bucharest (Romania)

In this paper we will present the results of our research on developing new deoxyribonucleic acid (DNA)-based conducting membranes for application in electrochromic devices. Improvements of performances of DNA-based solid bioelectrolyte in smart windows were achieved by adding plasticizer like glycerol and different amounts of photosensitive chromophores, such as Nile Blue. The results were obtained and analyzed by a variety of experimental tools and techniques such as FT-IR, UV-VIS spectroscopy, fluorescence, electric conductivity, contact angle, charge density measurements, and cyclic voltammetry. The biomembranes with the highest ionic conductivity values were successfully applied in smart windows with glass/ITO/WO3/DNA-based membranes/CeO2-TiO2/ITO/glass configuration which have shown a good change of transmittance under the applied electric field. The obtained results suggest that the DNA-based electrolytes are promising materials to be applied in electrochromic devices

Acknowledgments

The authors acknowledge the financial support of Romanian Ministry of Education, Research, Youth and Sports, through the UEFISCDI organism, under Contract Number 279/7.10.2011, Code Project PN-II-ID-PCE-2011-3-0505. They would like to acknowledge also the EU support for this work within the FP7 program, grant number FP7 PIRSES-GA-2009-247544, project BIOMOLEC: Functionalized biopolymers for application in molecular electronics and in photonics

9557-3, Session 1

Nucleobase passivation layers for photonic and electronic devices (Invited Paper)

Fahima Ouchen, Adrienne Williams, Donna M. Joyce, Emily M. Heckman, Air Force Research Lab. (United States); Perry P. Yaney, Univ. of Dayton (United States); James G. Grote, Air Force Research Lab. (United States)

No Abstract Available

9557-4, Session 2

3D printing by nonlinear photochemistry for bio-applications (*Invited Paper*)

Patrice L. Baldeck, Univ. Joseph Fourier (France)

No Abstract Available

9557-5, Session 2

Single molecule spectroscopy of conjugated polymers in solution (Invited Paper)

Ifor D. Samuel, Paul A. Dalgarno, Francisco Tenopala Carmona, Univ. of St. Andrews (United Kingdom); Stephanie Fronk, Guillermo C. Bazan, Univ. of California, Santa Barbara (United States); Carlos Penedo, Univ. of St. Andrews (United Kingdom)

Conjugated polymers are an important class of organic semiconductor that can readily be deposited from solution to make thin films for a range of optoelectronic devices including light-emitting diodes, solar cells and transistors. These in turn have been used to make biophotonic devices including a wearable light source for skin cancer treatment and a muscle contraction sensor. As the devices are made from solution, it is important to understand the polymer in solution including the influence of conformational disorder. Single molecule spectroscopy has been a remarkably effective tool in the study of biological molecules in solution, but so far its application to conjugated polymers has been restricted to solid films consisting of dilute blends of conjugated polymers with nonconjugated host polymers. We have developed a process to immobilise poly(3-hexylthiophone) on a surface and will report single-molecule fluorescence measurements of this polymer in solution.

9557-6, Session 2

Novel photonics polymers for 4K/8K real color display system in bio-imaging (Invited Paper)

Yasuhiro Koike, Keio Univ. (Japan)

The real-color and high-resolution display has been strongly required especially in medical- and bio-imaging fields. For example, with such an advanced display, very initial stage of cancer cell will be detected, which cannot be observed with a naked eye through conventional microscope. 4K/8K Liquid Crystal displays (LCDs) for these medical and bio-imaging applications have been intensively studied, however the color degradation deviated from real color has been a serious problem. Such a color degradation is mainly caused by the birefringence of several films used in LCD panel. We have proposed the zero-zero birefringent polymer which exhibit no birefringence even by both orientation of polymer chains and adding stress to polymer matrix. With this, the color degradation, especially color-shift caused by changing viewing angle, has been much improved. For transmitting required data signal for 4K/8K display, tremendously large bit rate such as 100 Gbps is needed, which means the paradigm-shift from electrical wire to optical fiber communication around 4K/8K displays. We have developed the world's fastest graded-index plastic optical fiber (GI POF) covering 40 Gbps, which is one of strong candidates for realizing such advanced imaging systems. Details of our photonics polymers towards 4K/8K systems will be described in my presentation.

9557-7, Session 3

Biological matrices for light amplification (Keynote Presentation)

Jaroslaw Mysliwiec, Konrad Cyprych, Lech Sznitko, Adam Szukalski, Kacper Parafiniuk, Andrzej Miniewicz, Marek Samoc, Piotr Hanczyc, Antoni C. Mitus, Grzegorz Pawlik, Wroclaw Univ. of Technology (Poland); Francois Kajzar,



Ileana Rau, Univ. Politehnica of Bucharest (Romania)

In recent years there has been a growing interest in biopolymers as functional materials for photonic applications. From the rich world of organic materials, biopolymers are of particular interest as they often exhibit unusual properties that are not easily replicated in conventional organic or inorganic materials. Furthermore, natural biomaterials are renewable resources and are inherently biodegradable. Here we show results of studies carried out on selected biological matrices doped with luminescent dyes for light amplification based on periodical gain or refractive index modulation, or on random but coherent light scattering in amplifying medium. The employed biological self-assembling templates were deoxyribonucleic acid (DNA), collagen, lysozyme type fibrils or starch. Laser action was studied in slab planar waveguides doped with dyes like Rhodamine, stilbene, Nile blue or derivatives of pyrazoline. It has been shown that simple incorporation of highly luminescent dye into a biopolymeric matrix can lead to efficient solid laser materials. Additionally, naturally occurring inhomogeneities of biopolymer layers prepared by a drop casting process can scatter emitted light in such a way that feedback is introduced to the system and coherent and incoherent random lasing can be observed. The mechanisms of diffusive transport of light, its amplification and randomization in biopolymeric matrices were studied theoretically in terms of non-standard diffusion approach, including sub/super diffusion.

9557-8, Session 3

Optical amplification in DNA-surfactant complexes incorporating hemicyanine dyes with long and short alkyl chains (Invited Paper)

Yutaka Kawabe, Yuki Suzuki, Chitose Institute of Science and Technology (Japan)

Hemicyanine dyes are promising materials for solid-state tunable dye lasers because of their high activity for light amplification and superior durability under optical pumping when doped in DNA-surfactant complexes [1]. A hemicyanine with a long alkyl chain, 4-[4-(dimethylamino) stylyl]-1-dococylpyridium bromide (DMASDPB or Hemi22) has been usually incorporated in the complex films prepared by various methods, demonstrating amplified spontaneous emission (ASE), laser oscillation and its wavelength tuning. While these achievements seemed to have confirmed the importance of intercalation or groove-binding of the dyes to DNA strand, our recent results for the hemicyanine and other dyes suggested that the influence from surfactant molecules was more essential than that from DNA itself [2].

Considering that dye-DNA interaction mode depended on the size and structure of molecules, another hemicyanine, 4-[4-(dimethylamino)stylyl]-1-methylpyridium iodide (DMASMPI or Hemi1) with methyl substituent instead of C22 of Hemi22, was doped in the complex for comparison. The dye had high solubility in water and gave fluorescence enhancement when dissolved in aqueous solution with DNA, indicating direct interaction between the dye and DNA double strand. DMASMPI also showed ASE under optical pumping with a threshold value nearly identical to that for DMASDPB. Lasing characteristics of the dyes and related topics will be presented.

[1] Y. Kawabe, L. Wang, T. Nakamura and N. Ogata, Appl. Phys. Lett. 81, 1372 (2002).

[2] T. Suzuki and Y. Kawabe, Opt. Mater. Exp. 4, 1411 (2014).

9557-9, Session 3

DNA based electrolyte/separator for lithium battery application

Jitendra Kumar, University of Dayton (United States); Fahima Ouchen, Air Force Research Lab (United States); Guru Subramanyam, University of Dayton (United States); James G. Grote, Air Force Research Lab. (United States)

No Abstract Available

9557-10, Session 3

Disorder and broad-angle iridescence from morpho-inspired structures (*Invited Paper*)

Bokwang Song, Seok Chan Eom, Jung Hoon Shin, KAIST (Korea, Republic of)

The ordered, lamellae-structured ridges on the wing scales of Morpho butterflies give rise to their striking blue iridescence by multilayer interference and grating diffraction. At the same time, the random offsets among the ridges broaden the directional multilayer reflection peaks and the grating diffraction peaks that the color appears the same at various viewing angles, contrary to the very definition of iridescence. While the overall process is well understood, there has been little investigation into confirming the roles of each factor due to the difficulty of controllably reproducing such complex structures. Here, we propose and fabricate Morpho-inspired structures with controlled random offsets. By selective etching of a monolayer of random-sized silica microspheres on a Si wafer, vertical offsets are controlled guantitatively. And directional deposition of 8 pairs SiO2/TiO2 multilayers generates their brilliant blue reflection. We find that while random offsets are necessary, it alone is not sufficient to produce the broad-angle reflection of Morpho butterflies. We identify diffraction as a critical factor for the bright, anisotropic broadening of the reflection peak of Morpho butterflies to a solid angle of 0.23 sr, and suggest random macroscopic surface curvature as a practical alternative, with an isotropic broad reflection peak whose solid angle can reach 0.11 sr at an incident angle of 60o. Furthermore, Morpho-inspired structures applying grating diffraction will be presented to fully reproduce the reflection of Morpho butterflies.

9557-11, Session 4

Nanoparticle-based biomimetic functional materials (Invited Paper)

Kuniharu Ijiro, Hokkaido Univ. (Japan)

Self-assembly originated from molecules, is ubiquitous from nature to unnature systems. The formation of double-stranded structure of DNA, virus, molecular crystals, liposomes etc. are all instances of molecular self-assembly. In the biological system, for example, virus is an impressive feat of molecular engineering by assembly of hundreds of proteins through the weak hydrophobic effect. We propose a robust strategy for the sizecontrollable fabrication of gold nanoparticle vesicles(AuNVs) which are biomimetic nanostructures of virus consisted of gold nanoparticles instead of proteins by using carbohydrate terminated fluorinated surface ligand self-assembly with 5~40nm AuNPs, indicating that carbohydrate can act as stronger molecular glue than oligo(ethylene glycol). Carbohydrate was introduced to tune the hydrophilic effect of the ligand by varying the number of glucose (namely, glucose, maltose, and maltotriose). AuNVs size could be efficiently controlled by varying surface ligands, water content in dioxane, and AuNPs size. We find some similarities between VLPs and AuNVs composed of 30nm gold nanoparticles. Photonic properties of not only AuNVs but also other self-assemblies of nanoparticles were measured. Strong surface-enhanced Raman scattering (SERS) of molecules were detected from the AuNVs and self-assembled gold nanoparticles.

9557-12, Session 4

Gold based hybrid nanosystems as potential agents for diagnostic and therapy (Invited Paper)

Frederic Lerouge, Ecole Normale Supérieure de Lyon (France); Julien R. G. Navarro, KTH Royal Institute of Technology (Sweden); Cristina Cepraga, BASF SE (France); Arnaud Favier, Marie Thérèse Charreyre, Denis Chateau, Frederic Chaput, Cyrille Monnereau, Chantal



Andraud, Patrice L. Baldeck, Ecole Normale Supérieure de Lyon (France)

The tremendous developments in the design of gold based nanomaterials opened the way to a lot of applications in nanomedicine. In this context optical nanosystems for imaging and/or therapy present a great interest. Recent works showed that sharp and edgy nanostructures appear to exhibit interesting features since their surface Plasmon band provide a strong field making them suitable for detection and therapy.

A complete study of bio compatible polymer functionalized gold nanostars and bipyramidal-like nanostructures will be presented. The synthesis of the nanoparticles will be described together with their photophysical properties, in suspension or on single objects. The use of multifunctional polymers enables their anchoring on the particles and their functionalization with organic dyes presenting interesting photophysical properties. Darkfield microscopy shows that the biocompatible gold nanoparticles are internalized after incubation with cancer cells. Finally, the study on these hybrid nanostructures is deepened, showing very interesting chromophoreparticle interactions.

9557-13, Session 4

Solution-processed low dimensional nanomaterials with self-assembled polymers for flexible photo-electronic devices (Invited Paper)

Cheolmin Park, Yonsei Univ. (Korea, Republic of)

Self assembly driven by complicated but systematic hierarchical interactions offers a qualified alternative for fabricating functional micron or nanometer scale pattern structures that have been potentially useful for various organic and nanotechnological devices. Self assembled nanostructures generated from synthetic polymer systems such as controlled polymer blends, semicrystalline polymers and block copolymers have gained a great attention not only because of the variety of nanostructures they can evolve but also because of the controllability of these structures by external stimuli. In this presentation, various novel photo-electronic materials and devices are introduced based on the solution-processed low dimensional nanomaterials such as networked carbon nanotubes (CNTs), reduced graphene oxides (rGOs) and 2 dimensional transition metal dichalcogenides (TMDs) with self assembled polymers including field effect transistor, electroluminescent device, non-volatile memory and photodetector. For instance, a nanocomposite of networked CNTs and a fluorescent polymer turned out an efficient field induced electroluminescent layer under alternating current (AC) as a potential candidate for next generation displays and lightings. Furthermore, scalable and simple strategies employed for fabricating rGO as well as TMD nanohybrid films allowed for high performance and mechanically flexible non-volatile resistive polymer memory devices and broad band photo-detectors, respectively.

9557-14, Session 5

Quick response AC-operated electrochemiluminescent cell with DNA/Ru complex (Invited Paper)

Norihisa Kobayashi, Chiba Univ. (Japan)

No Abstract Available

9557-15, Session 5

Exploring surface plasmon-polariton resonance (SPR) in an interferometer configuration (Invited Paper)

Perry P. Yaney, University of Dayton (United States); Fahima Ouchen, Air Force Research Lab (United States); James G. Grote, University of Dayton (United States)

No Abstract Available

9557-16, Session 5

Towards modeling of random lasing in dye doped bio-organicbased systems: ray-tracing ad cellular automaton analysis (Invited Paper)

Antoni C. Mitus, Krzysztof Lankowski, Pawe? Stopa, Witold Zaklukiewicz, Grzegorz Pawlik, Jaroslaw Mysliwiec, Wroclaw Univ. of Technology (Poland); François Kajzar, Ileana Rau, Univ. Politehnica of Bucharest (Romania)

One of many photonic applications of biopolymers as functional materials is random lasing resulting from an incorporation of highly luminescent dyes into biopolymeric matrix, which leads to a random but coherent light scattering in amplifying medium. In spite of numerous theoretical and experimental studies the origin of the coherence is still not clear and various scenarios are discussed. In particular, inhomogeneity of biopolymeric layers can hypothetically promote the feedback in the scattering of the emitted light resulting in coherent and incoherent random lasing. In this paper we analyze the light scattering in a model system of scattering centers of various shapes and dimensions using ray-tracing techniques. We analyze the trajectories appear. Lasing in model systems is studied using a generalized version of cell-automaton model of Wiersma [1].

[1] S. Lepri, S. Cavalieri, G.-L. Oppo, and D.S. Wiersma, Phys. Rev. A75, 063820 (2007).

9557-17, Session 6

DNA-nucleobases: gate dielectric for flexible GFET-based sensor applications (*Invited Paper*)

Adrienne Williams, Fahima Ouchen, Steve S. N. Kim, Air Force Research Lab. (United States); Said Elhamri, Univ. of Dayton (United States); Eva M. Campo, A. Douglas Winter, Bangor Univ. (United Kingdom); Gregory Kozlowski, Wright State Univ. (United States); Rajesh R. Naik, James G. Grote, Air Force Research Lab. (United States)

In this study, physically vapor deposited (PVD) deoxyribonucleic acid (DNA) nucleobase guanine was physically vapor deposited (PVD) in the fabrication of test platforms in potential application in a bio-based fieldeffect transistor. Another test platform was fabricated by spin coat of polymethylmethacrylate (PMMA) as a gate dielectric onto PVD guanine as a passivation layer. These test platforms were used for comparison of the dielectric properties of the guanine and PMMA to an already-established gate dielectric material for organic thin film transistors. During this time, there were no observed changes in the graphene's transport properties due to guanine and PMMA layers. It appears that guanine does not affect the charge carrier mobility of the graphene, but PMMA decreases the mobility of graphene as a gate dielectric standalone. Other transport properties of the graphene, such as charge carrier concentration, conductivity type,

Conference 9557: Nanobiosystems: Processing, Characterization, and Applications VIII

and resistivity were studied as well. These test platforms can be used as a potential device in biosensors, environmental, computer processing and graphene-based electronics.

9557-18, Session 6

Harvesting of living cell sheets from conjugated polymer surfaces via phothothermal disassembly of a protein layer (Invited Paper)

Eunkyoung Kim, Yonsei Univ. (Korea, Republic of)

Various types of cells, e.g. human mesenchymal stem cells (MSCs) and human dermal fibroblasts, were efficiently and selectively harvested by near-infared (NIR) light using the photothermal effect of a conjugated polymer (CP) nano-thin film. CP-coated substrates were prepared via a simple and fast solution-casting polymerization (SCP) technique. The absorption of CP thin films in NIR region was effectively triggered cell harvesting upon exposure to an NIR source. In the case of MSCs culture system, the proliferation and harvesting of MSCs on the PEDOT surface were controlled quantitatively by controlling the NIR absorption of the CP film through electrochemical doping. This light-induced cell detachment method based on CP films provides the temporal and spatial control of cell harvesting, as well as cell patterning. In the case of fibroblasts culture system, various patterned cell sheets were harvested via the photo-induced local heating of CP films that induced protein disassembly. Such disassembly of proteins allowed a fast detachment of a cell sheet with cell-to-cell interactions. This CP-based substrate can be used for repetitive culture and detachment of cells with no photodegradation and photobreakage in the CP films by NIR exposure.

9557-19, Session 6

Creation of carbon nanotube based biosensors through dielectrophoretic assembly

Nilan S. Mani, Centerville High School (United States); Steve Kim, UES (United States); Kaushik Annam, Danielle Bane, Univ. of Dayton (United States); Guru Subramanyam, University of Dayton (United States)

No Abstract Available

9557-20, Session 6

Metal pattern formation by using DNA brushes (Invited Paper)

Hideyuki Mitomo, Satoshi Nakamura, Shigeaki Suzuki, Yasutaka Matsuo, Kenichi Niikura, Kuniharu Ijiro, Hokkaido Univ. (Japan)

DNA has attracted much attention as templates for the fabrication of nanodevices because of its characteristic double-helix structure and functional molecular recognition. Many kinds of DNA-templated nanomaterials such as nanowires or nanoparticle assembly have been reported. However, in many cases, systematic assembly of nanomaterials up to micrometer scale is required to make usable devices. In this study, we have prepared DNA brushes, those are brush-like structures composed of DNA polymers, through the immobilization of oligonucleotides through the streptavidin-biotin interaction and polymerization of them on glass substrates to develop a fabrication method of large scale metal pattern by using DNA as a template. The length and density of the DNA polymers on the prepared DNA brush were determined by gel electrophoresis and UV absorption measurements. 2D-patterned DNA brush was prepared by patterned denaturation of streptavidin through the UV irradiation. The height and morphology change of the DNA brushes depending on the external environments were observed by atomic force microscopy and fluorescence microscopy. When gold thin film was prepared on 2D-patterned DNA brush through vapor deposition, morphology change of the DNA brush formed 3D metal pattern like a press working of sheet metal. On the other hand, sequence-specific electroless plating on DNA were performed on block-copolymer type DNA brushes to fabricate 3D patterned metal array. These approaches using DNA brushes will work as novel fabrication method for 3D metal pattern.

OPTICS+
 PHOTONICS

NANOSCIENCE+ ENGINEERING

9557-21, Session 6

Ordered auditory neuron growth on mirco-structured nanocrystalline diamond surface (Invited Paper)

Yixiao Cai, Fredrik Edin, Hao Li, Mikael Karlsson, Uppsala Univ. (Sweden)

Recently it has also been shown that nanocrystalline diamond (NCD) can be used for sensitive bio-sensors. Several surface modification methods for NCD has been developed and proteins and DNA has successfully been attached to the NCD surfaces. Previous experiment concerning cell response on NCD surfaces has mainly focused on certain surface chemical modifications, for instance surface termination by using plasma techniques (oxygen, hydrogen, fluorine, ammonia etc). Moreover, these studies have been exploring plain NCD surfaces. In our study we use textured NCD surfaces, consisting of micrometre-sized nail-head-shaped pillars, for neuron growth. The micro structured NCD surface was fabricated by a sequence of micro/nano-fabrication processes including sputtering, photolithography and plasma etching.

The textured NCD surface was created by a sequence of standard micro/ nano-fabrication procedure including sputtering, photolithography and Bosch process of etching. A pattern was fabricated on top by utilizing lithography then followed by inductively coupled plasma (ICP) etching. Pillars of silicon with NCD/AI were thus fabricated and finally AI was etched away in a typical aluminium wet etch. The sample was cleaned again to insure a hydrophilic surface. The CVD system was employed for the following oxygen termination. The surfaces was cultured and incubated with neuron cells continuously for 1 week.

Primary findings reveal axonal growth along the NCD pillar pattern, indicating guided growth of auditory neurons. In this study, the axons were studied by scanning microscopy2 and it showed the potential biocompatibility of such micro-fabricated surface. The obtained morphology revealed a promising neuron guide between each pillar spatial pattern.

9557-22, Session PWed

Picogreen dye as an active medium for plastic lasers

Pradeep Chandran, Cochin Univ. of Science & Technology (India); C P G Vallabhan, Cochin University of Science and Technology (India); P. Radhakrishnan, V. P. N. Nampoori, Cochin Univ. of Science & Technology (India)

With the development of DNA Photonics, the double helical molecular structure has not lost its place being in prime focus among researchers and scientists. From being a biological entity, it has now transformed into a promising nanophotonic material. DNA has found its way to the field of Photonics, and has become a promising material in bio-organic light emitting diodes, bio-organic field effect transistors, light emitting transistors, high energy capacitors, bio-sensors, optical waveguides, optical switches, and as a host material for numerous lumophores/chromophores with enormous fluorescence amplification.

Picogreen is a fluorescent dye used as a probe for quantitation of double stranded DNA. In its pristine form the dye exhibits negligible emission characteristics, but is known to fluorescene with more than a thousand fold

Conference 9557: Nanobiosystems: Processing, Characterization, and Applications VIII



enhancement in the presence of DNA. Such strong enhancement interested us to look out for its potential as lasing medium.

We have therefore fabricated modified DNA lipid complex intercalated with Picogreen dye thin film and observed amplified spontaneous emission at 568 nm and 560 nm while exciting at second and third harmonic frequency respectively from 10 Hz Nd:YAG laser. We estimated an ASE threshold at \sim 0.1 – 0.2 mJ with a spectral narrowing from 70 nm to 5 nm. The film of 3 ?m thick could sustain approximately 200 pulses of 1.5mJ, 532 nm laser radiation before the emission could degrade to 50% of the initial intensity. Here, we see that the DNA not only act as a host material but plays an important role in the luminescence of the dye molecules that could lead to the development of DNA lasers.

9557-23, Session PWed

Enhanced brightness from all solution processable biopolymer LED

Pradeep Chandran, International School of Photonics (India); Manoj A. G. Namboothiry, Indian Institute of Science Education and Research (India); C. P. G. Vallabhan, P. Radhakrishnan, V. P. N. Nampoori, International School of Photonics (India)

Since the discovery of light emission from polymers over two decades ago, especially conjugated polymers paved way for simpler technology viz. solution casting method to make light emitting devices. However in the past few years, biopolymers such as Deoxyribonucliec acid (DNA) has gained tremendous interest among researchers trying to develop BioLED. Marine derived DNA from salmon sperm has been exploited as biodegradeable polymeric material for photonic and electronic applications. Many devices such as optical waveguides, bio-organic light emitting devices, bio field effect transistors and bio sensors are at the research table with promising results. What the DNA could offer in LED application is multifold. Through the emerging field of 'DNA Photonics', it could be exploited as a biodegradable polymeric material for photonics and optoelectronics application. Apart from being biodegradable, abundant, inexpensive and renewable resource, they hold a unique optical and electrical properties. Being optically transparent in the visible region, electrically conductive, tunable resistivity from 1015 to 109 ?-cm by varying its molecular weight, suitable refractive index and dielectric constant, all yielding to be a promising material for optical and optoelectronic devices. Additionally, the HOMO (5.6 eV) and LUMO (0.9 eV) levels support hole transportation and also effectively block electrons enabling it to use as an electron blocking layer in LED which has resulted in increased brightness and luminous efficiency.

Motivated by the potential of DNA as an interesting material in the field of light emitting diodes, much research was directed to designing and developing BioLED. Here, we present the effect of thickness of electron blocking DNA layer in polymer LEDs. In this investigations, a blend of F8BT based green emitting polymer and PFO based blue emitting polymer was used as active layer. We also show an 8 fold increase in brightness of polymer LED by introducing PFN as electron injection and DNA:CTMA as electron blocking layer on either side of the polyfluorene active layer. It has been observed that the variation in thickness of DNA layer even at small values is very crucial.

9557-24, Session PWed

Photoresponsive behavior of azobenzene hybrid materials

Valentin Victor Jerca, "Costin D. Nenitescu" Institute of Organic Chemistry (Romania) and Univ. Politehnica of Bucharest (Romania); Florica Adriana Jerca, "Costin D. Nenitescu" Institute of Organic Chemistry (Romania); Ileana Rau, Ana-Maria Manea, Univ. Politehnica of Bucharest (Romania); François Kajzar, Univ. Politehnica of Bucharest (Romania) and Univ. d'Angers (France); Dan Sorin Vasilescu, Univ. Politehnica of Bucharest (Romania); Dumitru Mircea Vuluga, "Costin D. Nenitescu" Institute of Organic Chemistry (Romania)

Despite of the large number of publications devoted to the study of the E-Z-E isomerization phenomena [1, 2], deciphering the relationship between molecular structure and photo-orientation behavior still remains a problem that needs to be tackled. In accordance, when an azo molecule is substituted with various donor-acceptor groups very different photoresponsive behavior is observed [3]. Embedding azo-derivatives into an organic-inorganic matrix we expect very different behavior as compared to previous studies performed on similar organic polymers [4]. In the case of hybrid matrices, the polymer backbone can undergo different motions when the thermal relaxation of the azo derivative occurs, and can modify the kinetic parameters of the Z-to-E isomerization of the azo chromophore. This information is extremely useful in order to gain control over the overall response time of the material.

Herein, we describe the E-Z-E isomerization of four poly(methacrylateco-methacryloxypropyl trimethoxy-silane) copolymers substituted with different azobenzene moieties in the side-chains (see figure). The E-Z photoisomerization rates and the reaction kinetics of the Z-E thermal relaxation of the copolymers were investigated in solid matrix (thin films) using UV-Vis spectroscopy. In addition, a comparison between the photoresponsive properties of these hybrid materials and similar organic polymers is made.

References:

[1] Zhao, Y.; Ikeda T. Smart Light-Responsive Materials: Azobenzene-Containing Polymers and Liquid Crystals (John Wiley & Sons, Hoboken) 2009.

[2] Sekkat, Z.; Knoll, W. Photoreactive organic thin films (Academic Press, Amsterdam) 2002.

[3] Jerca, F. A.; Jerca, V. V.; Anghel, D. F.; Stinga, G.; Marton, G.; Vasilescu, D. S.; Vuluga, D. M. The Journal of Physical Chemistry: Part C, accepted for publication.

[4] Spiridon, M. C.; Jerca, F. A.; Jerca, V. V.; Vasilescu, D. S.; Vuluga, D. M. European Polymer Journal 2013, 49, (2), 452-463.

Conference 9558: Nanostructured Thin Films VIII



Wednesday - Thursday 12-13 August 2015 Part of Proceedings of SPIE Vol. 9558 Nanostructured Thin Films VIII

9558-1, Session Key

Optical coatings and metamaterials

(Keynote Presentation)

H. Angus Macleod, Thin Film Center, Inc. (United States)

Most optical systems consist largely of a series of surfaces that are shaped and finished so as to manipulate the light in desired ways. Although they succeed in determining the direction of the light, they are less successful in assuring the quality. Modifying the quality of the light, most often in terms of its behavior with respect to wavelength and incident angle, is the task of an optical coating and virtually all optical surfaces in all optical systems carry such treatments. The typical coating consists of a number of thin layers exhibiting interference effects that yield a suitable performance. Unfortunately, coating performance is constrained by the normal properties of interference and this limits its capabilities. Coatings could benefit considerably from the use of metamaterials and those exhibiting a negative index of refraction would be of incredible value. Unfortunately such negative index still appears elusive. Negative refraction has been convincingly demonstrated particularly for p-polarization and this is certainly useful in a number of applications but metamaterials have not so far yielded the complete set of properties representing the true negative index that could transform the field of optical coating.

9558-2, Session 1

Inorganic polarization devices with optical function layers fabricated by glancing angle deposition technique (Invited Paper)

Akio Takada, Nobuyuki Koike, Eiji Takahashi, Dexerials Corp. (Japan)

Polarization devices such as polarizers and waveplates are indispensable for the polarization management in LCDs. Polymer thin films with several polarization functions have been widely used as these polarization devices. Recent trend of LCD projectors, especially in high-end models, towards higher brightness entails that polarization management under strong radiation from the light source is required in the optical unit. Because polymer devices are composed of organic materials, thermal durability would be limited. Therefore, the polarization devices with high thermal durability, namely the absorptive gird polarizer and form birefringent waveplate, were developed. These devices are composed only of inorganic materials and structured with periodic multilaver nanostructures. Glancing angle deposition (GLAD) technique was employed to fabricate their optical functional layers. The structure of the polarizers is featured with a tri-layer consisting of an absorptive layer and a thin SiO2 layer on sub-wavelength pitch gratings made of aluminum. The absorptive layer was deposited only on the top of the SiO2 layer by taking advantage of GLAD and several materials were investigated to optimize the optical properties. On the other hand, the birefringent layer of the waveplate was composed of Ta2O5+TiO2 and formed by the serial bideposition technique in which the azimuth of the substrate is rapidly switched by 180 degrees with each deposition during GLAD. The retardation value can be precisely controlled by the thickness of the birefringent layer. Optical and thermal characterization results showed that these inorganic polarization devices were suitable for the practical application.

9558-3, Session 1

Wideband antireflection coatings combining interference multilayers and a subwavelength structure prepared by reactive ion etching

Stephane Bruynooghe, Carl Zeiss Jena GmbH (Germany); Marcel Schulze, Friedrich-Schiller-Univ. Jena (Germany); Michel Challier, Michael Helgert, Diana A. Tonova, Michael Sundermann, Thomas Koch, Alexandre Gatto, Carl Zeiss Jena GmbH (Germany); Ernst-Bernhard Kley, Friedrich-Schiller-Univ. Jena (Germany)

Transparent multilayer stacks are commonly used to reduce Fresnel reflections in optical systems. It is well established that the refractive index of the outermost layer of an interference layer stack strongly influences the residual reflectance of wideband AR coatings and that the lower the refractive index of the last layer the better the AR properties. Some limitations for the residual reflectance are evident especially for low-index substrates since materials with very low refractive indices are unavailable in nature. In this work, SiO2 thin films were grown by physical vapour deposition and dry etched using a mask-less technology in a plasma containing a fluorine gas compound. During the plasma etching subwavelength stochastic structures which show low refractive index properties are formed using a so-called self-masking effect. The optical and structural properties of the SiO2 nanostructures are examined by spectroscopic ellipsometry, spectralphotometry and scanning electron microscopy. The dependence of the effective refractive index on the structure depth is determined using an optical model based on the effective medium approximation and the index function is discretized in a finite number of homogeneous layers. Owing to their low refractive index properties, the SiO2 nanostructures are combined as outermost layer with a multilayer system prepared by magnetron sputtering in order to realize an antireflective coating with low residual reflectance designed for the 400-900 nm spectral range on a low-index substrate. The AR properties will be presented together with the simulation of the optical properties and the morphology of the nanostructures.

9558-4, Session 2

Biomimetic anti-wetting materials: from molecules to surface properties (Invited Paper)

Frédéric Guittard, T. Darmanin, Univ. de Nice Sophia Antipolis (France)

Superhydrophobicity is characterized by the repellency of water on a surface with an apparent contact angles of water above 150° and various adhesive properties characterized by dynamic contact angle measurements. The potential applications of superhydrophobic materials are extremely wide and include anti-icing coatings, anti-corrosion coatings, anticorrosion coatings, anti-bacteria coatings, textiles, oil/water separation, water purification and desalinization, microfluidic devices, optical devices, batteries, sensors, drug delivery or heterogeneous catalysis. Recent advances in the potential applications of superhydrophobic materials will be carefully described in this presentation and a focus on surfaces built up from electrodeposition of conductive polymers. (see publications and review: www.unice.fr/interface)



9558-5, Session 2

Surface plasmon spectroscopy study of electron exchange between single gold nanorods and metal oxide matrix during hydrogen gas sensing

Michela Cittadini, Univ. degli Studi di Padova (Italy); Sean Collins, Paul Mulvaney, The Univ. of Melbourne (Australia); Alessandro Martucci, Univ. degli Studi di Padova (Italy)

The direct optical monitoring of electron exchange on single plasmonic nanoparticles, involved in chemical reactions with gas molecules, is one of the main challenges in the heterogeneous catalysis and gas sensing fields.

Catalysts are substances that speed up reactions by providing an alternative pathway with lower activation energy than that required for the uncatalysed reaction. A lot of research, both fundamental and applied, has been carried out to investigate how catalysts work and to increase their efficiency.

The present work shows how the use of Dark Field Microscopy (DFM) coupled with surface plasmon spectroscopy, enables the direct observation of the kinetics of H2 gas interaction with single gold nanorods (NR) coupled with Pt nanoparticles (NPs) and/or with metal oxide matrices. The plasmonic particles, gold NRs, act as optical probes, and enable the monitoring of the electron exchange through the measurement of their surface plasmon resonance (SPR) band shift. To improve the redox reaction kinetics, the Au NRs have been coupled with Pt NPs and embedded also into a TiO2 or ZnO low scattering matrix. The Au NRs, the Pt, TiO2 and ZnO NPs have been synthetized by colloid chemistry. Several samples made of bare Au NRs, or Au NRs coupled with only Pt NPs or with Pt and TiO2 NPs or with Pt and TiO2 have been deposited by spin coating on silica substrates.

The longitudinal Au SPR band shift has been monitored by DFM looking at the variation of the scattering spectrum of a single Au NRs in the presence of H2. Time-resolved measurements have been also conducted at fixed wavelength in order to monitor the kinetics of the H2 reaction. With such measurements it was possible to elucidate the importance of the adsorbed oxygen and the TiO2 matrix on the H2 reaction with the Pt NPs.

9558-6, Session 2

Real-time observation of drying kinetics and morphology evolution in organic bulk heterojunctions

Nusret S. Güldal, Tayebeh Ameri, Andres Osvet, Christoph J. Brabec, Friedrich-Alexander-Univ. Erlangen-Nürnberg (Germany)

In organic photovoltaics field, an optimized bulk heterojunction film consists of an electron-donating conjugated polymer and an electron-accepting fullerene derivative, which is organized in a well phase-separated, yet interconnected network. This sensitive morphology, affecting the light absorption, exciton dissociation and subsequent charge generationextraction, is determined by the film formation during solution casting under certain processing conditions. Therefore, a number of previous studies focused on characterizing the thin film formation during solution casting, mainly with in-situ grazing-incidence X-ray scattering methods, accompanied by various optical methods, such as ellipsometry/ reflectometry and UV-VIS absorption. Although these studies provided invaluable information on the matter, the development of nanoscale morphology is yet to be fully understood.

The purpose of this study is to demonstrate a portable in-situ characterization chamber, which can characterize any organic/hybrid thin film during solution casting. The chamber is a miniature doctor blade under controlled atmosphere, equipped with white light reflectometry (WLR), photoluminescence (PL) and laser light scattering (LLS). WLR was used to monitor the thickness reduction of the thin film during the drying, enabling to establish a drying curve. LLS informed the time scale of aggregate/ crystallite formation. PL monitored molecular arrangement and enabled the estimation of microstructure. The combined data is used to understand

the competition between thermodynamics (e.g. solubility, miscibility) and kinetics of morphology formation. In this study, we measured different BHJ systems with binary and ternary solvent mixtures under different processing conditions, from which we built a roadmap for microstructure formation in organic thin films, used in organic photovoltaics.

9558-7, Session 2

Structural and electrical properties of N doped SiC nanostructures obtained by TVA method

Victor Ciupina, Univ. Ovidius Constanta (Romania) and Academy of Romanian Scientists (Romania); Cristian P. Lungu, National Institute for Laser, Plasma and Radiation Physics (Romania); Rodica Vladoiu, Gabriel Prodan, Univ. Ovidius Constanta (Romania); Eugeniu Vasile, Univ. Politehnica of Bucharest (Romania); Corneliu Porosnicu, National Institute for Laser, Plasma and Radiation Physics (Romania); Stefan Antohe, Univ. of Bucharest (Romania); Iuliana M. Stanescu, Marius Belc, Aurelia Mandes, Virginia Dinca, Univ. Ovidius Constanta (Romania); Sorina Iftimie, Univ. of Bucharest (Romania); Valeriu N. Zarovski, National Institute for Laser, Plasma and Radiation Physics (Romania); Virginia Nicolescu, Ceronav (Romania)

Ionized nitrogen doped Si-C thin films at 200°C substrate temperature were obtained by Thermionic Vacuum Arc (TVA) method. To increase the energy of N, C and Si ions, -400V, -600V and -1000V negative bias voltages was applied on the substrate. The 200nm thickness carbon thin films was deposed on Si and glass substrate and then 400nm, 600nm and 1000nm N-SiC coatings on carbon thin films was deposed. To characterize the structure of as-prepared N-SiC coatings, Transmission Electron Microscopy (TEM), High Resolution Transmission Electron Microscopy (HRTEM) and X-Ray and Photoelectron Spectroscopy (XPS) techniques was performed. The crystallinity of N-SiC thin films increase with increasing of acceleration potential drop, i. e. with energy of N, C and Si ions.

Electrical conductivity was measured comparing the potential drop on the structure with the potential drop on a series standard resistance in a constant current mode. To justify the dependence of measured electrical conductivity by the temperature, we assume a thermally activated electrical transport mechanism.

9558-8, Session 3

Constructive and destructive routes to prepare nanostructures on surfaces by low-energy ion beam sputtering (*Invited Paper*)

Bernd Rauschenbach, Leibniz-Institut für Oberflächenmodifizierung e.V. (Germany)

Low energy ion beam induced sputtering is a versatile tool for deposition and also erosion of surface materials. In this contribution results about the evolution of the surface topography during low-energy ion beam erosion with noble gas ions will be given. The destructive route is characterized that under certain conditions, given by the self-organization processes, the ion beam induced erosion process can lead to the formation of well-ordered nanostructures (dots and ripples) on the surface. In contrast, the deposition of sputtered material under glancing angle condition is a sophisticated constructive route to create nanostructures with custom-made structure geometries. The preparation of nanostructures on the base of both routes is demonstrated. At the end, potential applications of nanostructuring in different fields of technology will be discussed.



9558-9, Session 3

Absorption intensity tunability in the near infrared region using phase-change nanostructure

Abdurrahman Ozdemir, Safak Saraydemir, Bilal Barut, Hasan Kocer, Kara Harp Okulu (Turkey)

Nanostructured thin film absorbers embedded with phase-change material (PCM) can provide large level of absorption intensity tunability in the near-infrared region. Germanium Antimonide Tellurite (Ge2Sb1Te4-GST) was employed as the phase-change material in the designed structures. The structure is composed of a periodic grating-type array of 200 nm thick Au buried with 100 nm-thick GST layer from the top of the Au layer. The period of the gratings is 2 μ m and in each period, GST width is 0.5 um. GST was selected as the active PCM because its optical properties undergo a substantial change during a structural transition from the amorphous to the crystalline phase. The optical absorption properties of the designed structures with respect to the geometric and material parameters were systematically investigated using finite-difference time-domain computations. It was shown that absorption intensity in the near-infrared region was tuned from the near-perfect to the near-zero level by switching the PCM from its amorphous to crystalline states. The distributions of the electric field and absorbed power at the resonant wavelengths with respect to different phases of the GST were investigated to further explain the physical origin of the absorption tuning. This study provides a path toward the realization of tunable infrared absorbers for the applications, such as selective infrared emitters, infrared camouflage, sensors, and photovoltaic devices.

9558-10, Session 3

Optical and structural properties of noble metal nanoisLAND

Davide Bacco, Alain J. Corso, Francesca Gerlin, Paola Zuppella, Enrico Tessarolo, Marco Nardello, Maria G. Pelizzo, CNR-IFN UoS Padova (Italy)

Metallic nanostructures are widely studied because of their peculiar optical properties. They possess characteristic absorbance spectra with a peak due to plasmonic resonance. This feature is directly dependent on the nanostructures shape, size, distribution and environment surrounding them. This makes them good candidates for a variety of applications, such as localized surface plasmon resonance sensing (LSPR), surfaceenhanced Raman scattering (SERS) and photovoltaics. A well established technique used to create nanoisland on flat substrates is performing a thermal treatment after the deposition of a thin metal film. While the most widely investigated metal in this context is gold, we have extended our investigation to palladium, which is interesting for sensing applications because it has an excellent hydrogen absorption ability. The morphological properties of the nanoisland depend mainly on the starting thickness of the deposited layer and on the annealing parameters, temperature and duration. The deposition and annealing process has been investigated, and the resulting samples has been tested optically and morphologically in order to optimize the structures in view or their application for sensing purposes.

9558-12, Session 4

Axions, surface states, and the Post constraint in electromagnetics

Akhlesh Lakhtakia, The Pennsylvania State Univ. (United States); Tom G. Mackay, The Univ. of Edinburgh (United Kingdom)

Surface states exist on certain bulk materials confined to bounded regions. We have formulated boundary-value problems to explore the effects of the

surface states on the scattering signatures. Their solutions will be presented with a view to explaining certain aspects of the frequency-domain Maxwell equations and constitutive relations.

9558-13, Session 4

A multiple scattering approach to solving scattering problems by complex objects

Didier Felbacq, Univ. Montpellier 2 (France); Emmanuel Kling, Sagem (France)

There are many numerical approaches to solving the problem of the scattering of a wave by a bounded body. Roughly speaking, these methods can be devided into two families : direct space methods, where space is discretized and the field is calculated at the nodes of a grid and indirect space method, where a, basically, hilbertian basis is used and the field is obtained everywhere in space as a linear combinaison of, basically, Green functions. The Finite Difference, the Finite Element Method belong to the former, whereas the Discrete Dipole Approximation, Bloch wave expansion, possibly under the guise of Rayleigh expansion, or the Boundary Element Method belong to the latter. The list is of course not exhaustive. The direct space methods have the advantage of being able to deal with complex geometry, at the price of a high algorithmic complexity : it requires the use of specific tricks, e.g. Perfectly Matched Layers, in order to deal with the infinite domain. Conversely, indirect space methods handle intrinsically the radiation conditions and are generally simple to code, but are in general not well adapted to complex bodies, whether geometrically or because of their electromagnetic properties. In the present work, we describe a modal methods for solving the problem of the scattering by a bounded body for the Helmholtz operator. The method is very simple to implement and can deal with complex shaped and/or inhomogeneous bodies. It is related to the Discrete Dipole Approximation but is more general and conceptually simpler. The basic idea is that of de-homogenization : the body is decomposed into square cells that are small with respect to the wavelength and such that the permittivity \$epsilon_m\$ of the medium is constant there. Let d be the side of that cell. The cell is then replaced by a a cylinder of radius \$r\$ and permittivity \$epsilon_c\$ such that \$epsilon_m=1+(epsilon_c-1)pi r^2\$. The convergence of the method is ensured by the homogenization result saying that the field diffracted by the collection of cylinders converges towards that diffracted by the original body as \$d\$ tends to 0.

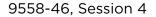
9558-14, Session 4

Nanoengineered composite materials with giant dielectric anisotropy

Tom G. Mackay, Univ. of Edinburgh (United Kingdom)

A nanoengineered composite material was considered in the long wavelength regime. It consisted of a random mixture of two isotropic dielectric component materials. Each component material was composed of oriented spheroidal particles. The Bruggeman formalism was used to estimate the permittivity dyadic of the corresponding homogenized composite material (HCM). The HCM was an orthorhombic biaxial material if the symmetry axes of the two populations of spheroids were mutually orthogonal and a uniaxial material if these two axes were mutually parallel. The degree of anisotropy of the HCM increased as the shape of the component particles became more elongated, with the greatest degrees of anisotropy being attained when the component particles were shaped as needles or discs. Hence, nanoengineered composite materials based on simple oriented component particles may be homogenized to realize extremely large degrees of anisotropy.

Conference 9558: Nanostructured Thin Films VIII



A new fast and accurate spectrophotometric method for the determination of the optical constants of arbitrary absorptance thin films from a single transmittance curve: application to dielectric materials

Jean Desforges, Univ. de Moncton (Canada); Clement Deschamps, Univ. de Poitiers (France); Serge Gauvin, Univ. de Moncton (Canada)

No Abstract Available

9558-31, Session PWed

Nano-heterostructures based on solid solution HgCdTe

obtained using silver ion implantation

Ruslana S. Udovytska, Alexey B. Smirnov, Rada K. Savkina, Fiodor F. Sizov, V.E. Lashkaryov Institute of Semiconductor Physics (Ukraine)

Presented in this work are the results concerning formation of nanoheterostructures Ag2O-Hg1-xCdxTe (x = 0.2) on the surface of solid solution Hg1-xCdxTe (? ~ 0.223). Modification of this ternary chalcogenide semiconductor compound was performed using the method of doping the heterostructure samples with silver ions, which was followed by low-temperature treatment. The energy and dose of implanted ions were 100 keV and 4.8?1013 ?m-2, respectively, while duration of thermal treatment was 5 hours at the temperature 75°? in Ar atmosphere with the excess pressure 4 Pa. These semiconductor nano-heterostructures were characterized using impedance spectroscopy, SEM, AFM-microscopy and X-Ray diffraction. Impedance characteristics of the samples were studied using the impedancemeter Z-3000X within the frequency range 1 Hz...3 MHz with the amplitude of a sinusoidal signal 120 mV. Studied in this work are electro-physical and structural properties of the narrow-band semiconductor compound Hg(Cd)Te with the nano-heteroarchitecture Ag2O-Hg1-xCdxTe (x = 0.2) formed on its surface by using the method of ion implantation in the top-down approach. The state of sample surface was studied using the method of NanoScope Digital Instruments. The data of modelling in the TRIM_2008 determine profile for distribution and depth of localization for the embedded impurity in the sub-surface region of MCT as close to 100 nm. The results GI XRD obtained for irradiated samples confirmed the presence of a disturbed layer with the thickness close to 100 nm as well as formation of metal-oxide nano-heterostructures Ag2O-Hg1-?Cd?Te (? ~ 0.20) on the surface of Hg(Cd)Te solid solution.

9558-32, Session PWed

Atomically thin adhesion promoter for highly stable silver nanowire film

Sungjun Lee, Hyungseok Kang, SungKyunKwan Univ. (Korea, Republic of)

In this manuscript, we demonstrated, for the first time, the atomically-thin conductive adhesion promoter of positively-charged reduced graphene oxide (rGO-NH3+) for transparent highly-stable AgNWs TCEs. The rGO-NH3+ layer was deposited by simple spray-coating onto polymeric substrate. The insertion of the rGO-NH3+ between AgNWs and polymeric substrate dramatically enhanced both chemical and mechanical stabilities of AgNWs. The AgNWs TCEs assisted with the adhesion promoter were extremely stable under harsh conditions including ultrasonication in various solvents, mechanical bending up to 3 % strain, and fatigue over 1000 cycles.

This strong adhesion enhancement was originated from the charge transfer from the negatively-charged hydroxo- and oxo-groups onto AgNWs to the positively-charged protonated amine groups in rGO-NH3+, indicating the formation of ionic bonding. For comparison, positively-charged GO-NH3+ and commercial poly(allylamine hydrochloride) (PAH) were also applied as adhesion promoters. Notably, conductive rGO contributed a uniform current distribution of the mesh-type AgNWs. In addition, the 2D layered structure of atomically-thin rGO-NH3+ adhesion promoter could enhance the water protection properties of the AgNWs films, which is one of the important performance parameters for the water-proof electronic device applications of AgNWs TCEs.

SPIE. PHOTONICS

NANOSCIENCE+ ENGINEERING

9558-33, Session PWed

Growth of Bi2O3 nanocones over large areas by magnetron sputtering

Li-Chia Tien, Ying-Hong Liou, National Dong Hwa Univ. (Taiwan)

Bismuth oxide (Bi2O3) is a multi-functional oxide semiconductor with various properties of interest such as high reflective index, high photoconductive response, luminescence and high oxygen-ion conductivity, potentially useful as optical coatings, electrodes of solid oxide fuel cells (SOFC), supercapacitors, visible-light activated photocatalysts, and gas sensors. Large areas of bismuth oxide (Bi2O3) nanocones were grown onto Si(001) substrates by magnetron sputtering. The samples were characterized by field emission scanning electron microscopy (FE-SEM), X-ray diffraction (XRD), transmission electron microscopy (TEM), and photoluminescence (PL). The obtained tapered nanostructures consist of high-density nanocones with diameters approximately 70–130 nm and lengths of 1-3 ?m. XRD results reveal that the Bi2O3 nanocones can undergo a phase transition from the ? to the ? phase at growth temperatures over 450°C. This phase transition was confirmed by TEM and PL. The growth mechanism of Bi2O3 nanocones was identified as grain boundary-assisted growth, in which a Bi seeding layer is crucial to the formation of the nanostructures. The results herein suggest that introducing a surface seeding layer may provide an effective way to grow various 1D nanostructures over large areas in high yield by magnetron sputtering.

9558-34, Session PWed

Surface treatment of multiferroic thin films using nano-second Nd: YAG laser

Ola G. Allam, National Research Ctr. (Egypt); Yahia Badr, Cairo Univ. (Egypt)

Recent years have seen a huge interest in multiferroic materials for their application as sensors and actuators. However, the scarcity of these materials in single phase and the weak coupling of their ferroic components have directed the research towards multiferroic heterostructures. These systems operate by coupling the magnetic and electric properties of two materials. In this paper, thin films have been grown by chemical solution deposition (CSD) using spin coating technique using rotations peed of 4500 rpm and time of 50 s and dried at 120?C for 20 min The optical, dielectric, magnetic, ferroelectric, ferromagnetic and piezoelectric properties of thin films have been investigated by Uv-Vis spectrophotometer (300-2500) nm, X-Ray Diffraction (XRD), Vibrating Sample Magnometer (VSM), Transmission Electron Microscope (TEM), and Scanning Electron Microscope (SEM) respectively. PZT/CFO thin films sintered at different temperatures from 400°C temperature to 600°C. The as-deposited PZT/CFO show week piezoelectricity and the effective piezoelectric coefficient d33 because, the materials deposited on the films not only PZT layer, but also CFO layer which decrease the piezoelectricity of these films. PZT/CFO Films were then recorded an enhancement in all physical properties (dielectric, optical, structural, surface morphology and magnetic properties) as the sintering temperature increased. The images of thin film before and after treatment with Nd:YAG laser which have Power from 10 mW to 5300 mW, Pulse width: 7 ns, Repetition Rate: 10 Hz and wavelength spectrum in (IR, Vis) laser beam indicate that sample prepared before treated has a lot of porous and



agglomeration which decreases after treatment. *ola_Allam@yahoo.com; phone 002-01008756402; fax 033387697

9558-35, Session PWed

Growth and characterization of La(1-x) Srx MnO3 thin film prepared by pulsed laser deposition

Ali A. A. Abdel Gaied, National Institute of Laser Enhanced Sciences (Egypt)

La(1-x) Srx MnO3 (LSMO) is interesting material for applications as a cathode for solid oxide fuel cell (SOFC), magnetic sensors, electronics, and spintronics. Hydrothermal method was established and successfully scaled up to prepare LSMO (x=0.2, 0.3) nano powder and was characterized to be applied as a target to be deposited on Si (100) substrate by pulsed laser deposition (PLD). In this work, a series of thin films on silicon substrates by PLD are studied at different deposition conditions in high vacuum of ~2 '10-6 Torr. The thin films are prepared by Nd: YAG laser (1064 nm) with 10 Hz repetition rate and 6 ns pulse duration. The substrate temperature and the laser parameters are employed to grow high quality of LSMO thin films on Si(100). Nanostructure of LSMO is an objective to study the possibility of using LSMO as a cathode for the SOFC. The film structure, morphology, and elemental analysis of the films are characterized by X-ray diffraction (XRD), field emission scanning electron microscope (FESEM), high resolution transmission electron microscope (HTEM), thermo gravimetric analysis (TGA), and differential scanning calorimetric (DSC).

*ali_abdelazeem@niles.edu.eg; phone 00201014338414; fax 35708480

9558-36, Session PWed

Simulation and analysis of back scattered light in thin film solar cells with finite difference time domain method

Birhanu Tamene Abebe, Christoph Pflaum, Erlangen Graduate School in Advanced Optical Technologies (Germany)

Recent experiments show that there are localized modes in thin film solar cells as a result of nanostructured interfaces. This will enhance the performance of thin film solar cells by increasing absorption. In this paper we discuss modelling such problem and present the result obtained. A single junction structure with amorphous silicon as an active layer is used for the modelling. The nanostructured interfaces are modelled using data measured by Atomic Scanning Microscopy(AFM). Different stack models and AFM scans are used for comparison. The input wave is Gaussian pulse in time at femtoseconnd scale. Multiple simulations are performed with various pulse width to compare with the experiments. Once the simulation is finished, spatial and temporal Fast Fourier Transform(FFT) is performed on the reflected electric field. This is to analyse the angular and spectral composition of the reflected light. The simulation is done on high performance machines with highly parallel scheme to meet the demand of the big simulation domain.

9558-37, Session PWed

Microwave plasma chemical synthesis of nanocrystalline carbon film structures and study their properties

Valery Timoshenkov, National Research Univ. of Electronic Technology (Russian Federation); Nikolay A. Bushuev, Federal State Unitary Enterprise (Russian Federation); Ravil Yafarov, Institute of Radio Engineering and Electronics (Russian Federation); Sergey Orlov, Dmitri Starykh, Molecular Electronics Research Institute (Russian Federation)

The self-organization effect of diamond nanocrystals in polymer-graphite and carbon films is detected. The carbon materials deposition was carried from ethanol vapors out at low pressure using a highly non-equilibrium microwave plasma. Deposition processes of carbon film structures (diamond, graphite, graphene) is defined. Deposition processes of nanocrystalline structures containing diamond and graphite phases in different volume ratios is identified.

The solid film was obtained under different conditions of microwave plasma chemical synthesis. We investigated the electrical properties of the nanocrystalline carbon films and identified it's from various factors. Influence of diamond-graphite film deposition mode in non-equilibrium microwave plasma at low pressure on emission characteristics was established.

This effect is justified using the cluster model of the structure of amorphous carbon. It was shown that the reduction of bound hydrogen in carbon structures leads to a decrease in the threshold electric field of emission from 20-30 V/m to 5 V/m. Reducing the operating voltage field emission can improve mechanical stability of the synthesized film diamond-graphite emitters. Current density emission at least 100 A/cm2 was obtained.

Nanocrystalline carbon film materials can be used to create a variety of functional elements in micro- and nanoelectronics and photonics such as cold electron source for emission in vacuum devices, photonic devices, cathodoluminescent flat display, highly efficient white light sources. The obtained graphene carbon net structure (with a net size about 6 ?m) may be used for the manufacture of large-area transparent electrode for solar cells and cathodoluminescent light sources.

9558-38, Session PWed

Arrange an asymmetrical metal-dielectric multilayer as a low loss metamaterial

Yi-Jun Jen, Ci-Yao Jheng, Kun-Han Lu, Chien-Ying Chiang, National Taipei Univ. of Technology (Taiwan)

A metal-dielectric (M-D) multilayer has been applied as a subwavelength structure to exhibit negative index of refraction. Periodic MD multilayer or symmetrical five layered MDMDM multilayer has been arranged to exhibit equivalent complex refractive index with negative real part. As the extinction coefficient is much small than the index of refraction, the wave vector and Poynting vector are in opposite directions. How to reduce the extinction coefficient and raise the transmittance becomes an issue. In this work, the metal films within the multilayer are not arranged with the same thickness as well as dielectric films. Under the condition of subwavelength requirement, the thickness of each layer is tuned to increase the transmittance. The previous example of a five layered MDMDM as a negative index metamaterial at a wavelength of 363.8nm is adopted here to do the loss improvement. The previous MDMDM as an Ag and TiO2 multilayer is modified by tuning the thickness of each layer. The figure of merit is increased by a factor of 1.4. As the multilayer is arranged on a BK7 glass as a system of Air/MDMDM/glass, the transmittance could be 70% that is increased by a factor of 1.3. The near field simulation is also adopted here to observe the backward wave propagation a negative refraction phenomenon.

9558-39, Session PWed

Helical structured thin films deposited at a glancing angle

Yi-Jun Jen, Ci-Yao Jheng, San Chan, Chien-Hoa Tseng, National Taipei Univ. of Technology (Taiwan)

Silver nanohelical structured thin films (NHF) were tried to be deposited on a glass substrate using glancing angle deposition technique. At a deposition angle of 89°, silver NHFs were fabricated by introducing liquid



nitrogen to flow under the backside of BK7 glass substrate. The temperature of substrate was reduced to be less than -100°C before deposition. The deposition rate has to be controlled to match the rotation speed of the substrate. Therefore the rotation speed is varied to reach an optimum value. The morphology of each silver NHF was measured and compared with other samples. The screwlike silver NHF is then derived by successful shadowing effect. The circular dichroism (CD) was measured over the visible regime. It is found that the CD values are similar to a previous result which was measured from the one-turn gold NHF grown on a seeded substrate. On the other hand, a linear polarized light is introduced to illuminate the NHA to observe the transmitted polarization state. It is found that the extreme change occurred at a wavelength of 600nm, the linear state of incident light is changed to elliptical polarization state with ellipticity of 0.327. This work is an approach to spiral-like metal nanostructures.

9558-40, Session PWed

Influence of low temperature on the morphology and optical property of a deposited silver nanorod array

Yi-Jun Jen, Ci-Yao Jheng, Jyong-Wei Huang, Yuan-Tai Chang, National Taipei Univ. of Technology (Taiwan)

The substrate cooling technique was introduced in glancing angle deposition to grow slanted silver nanorod array (NRA). The substrate cooling method was applied by introducing liquid nitrogen to flow under the substrate. The morphologies of Ag NRAs deposited with cooling and without cooling are compared in this paper. During deposition, the temperature on the backside of substrate was kept at -140°. The average width of Ag rods is successfully reduced to be 40nm by substrate cooling technique. The effect of substrate cooling on the average tilt angle of silver rods with respect to the surface normal is also measured. For the same deposition angle of 86°, the average tilt angle is 68° that is larger than that of rods grown under room temperature. The tangent rule that represents the relationship between deposition angle and tilt angle of rods is then corrected for low temperature. The associated obvious polarization dependent transmittance and reflectance spectra are also measured in this work. It is found that the difference between s-polarized transmittance and p-polarized transmittance of cooling Ag NRA is larger than that of uncooling Ag NRA. The difference is increased from 8% at a wavelength of 400nm to 3% at a wavelength of 700nm.

9558-41, Session PWed

Nanoengineered hyperbolic materials for optical sensing applications

Tom G. Mackay, The Univ. of Edinburgh (United Kingdom)

Anisotropic dielectric materials characterized indefinite permittivity dyadics (known as hyperbolic materials) are invested for possible optical sensing applications. Such materials present hyperbolic dispersion relations which only allow plane waves to propagate in certain directions. In contrast, anisotropic dielectric materials characterized positive-definite (or negative-definite) permittivity dyadics present elliptical dispersion relations which generally allow plane waves to propagate in all directions. The transition between hyperbolic and elliptical dispersion relations may be exploited for optical sensing. This phenomenon is investigated theoretically by considering the homogenization of a porous hyperbolic material which is infiltrated by an analyte-containing fluid. Factors taken into consideration include the shape, size, and orientation of pores in the hyperbolic material as well as its porosity.

9558-42, Session PWed

Realization of highly transparent conducting thin films by R.F. Magnetron sputtering for photovoltaics

Saheer Cheemadan, Amiruddin Rafiuddin, Srinivasa R. Tippasani, M.C. Santhosh Kumar, National Institute of Technology, Tiruchirappalli (India)

The outstanding electrical and optical properties of transparent conducting oxides (TCOs) have been extensively studied for several decades in the fabrication of optoelectronic devices. Among TCOs, tin-doped indium oxide (ITO) possesses the dominant role in displays (LCDs) and photovoltaic applications. Due to scarcity and toxicity of indium predominant investigation for an alternative TCO is always a keen area of interest in the field of photovoltaics. In this particular research a novel multicomponent TCO has been realized by the mixture of cadmium oxide and zinc oxide with 90:10 and 80:20 ratios respectively. The multicomponent thin film deposition is made by r.f. magnetron sputtering system upon glass substrates. The parameters such as r.f. power and substrate temperature are varied to inspect the optimum multicomponent TCO films. The structural, morphological, electrical and optical properties of the deposited TCO are investigated. Among all examined samples it is observed, CdO:ZnO with ratio of 90:10 deposited at 250 degree and r.f. power at 70W possess an average of 90% transparency in the visible region. Electrical properties reveals the optimum multicomponent TCO possess lower resistivity value in the order of 10-4?.cm. It is perceived the presence of Cd component contributes higher mobility and conductivity to the charge carriers whereas transparency of the films is benefited by the presence of Zn component. The realization of indium-free, low cost multicomponent TCO film is expected to pave path for transparent electrode applications in the area of optoelectronics.

9558-43, Session PWed

Statistical analysis of partial discharges evolved during aging of synthetic nanofilled polypropylene

Prathap Basappa, Charles M. Taylor Jr., Antwarn E. Watson, Rohitha Dhara, Norfolk State Univ. (United States)

Nano-meter sized particles added into the polymer matrix are of growing interest in the insulation industry. Nanofilled polymer show better performance in considerably reducing the space charge and electro luminescene, and increase in electrical breakdown strength and partial discharge resistance and longer life times of electrical insulation. With the addition of natural organo clay nanocomposite particles in isotactic PP matrix, it is reported that aging decreased the remnant breakdown strength of the nanofilled samples whereas, the base polymer is unaffected. It has been reported that under similar aging conditions, the space charge formed in synthetic nanofilled PP samples is more than that in natural nanofilled samples. The aspect ratio of the synthetic nanocomposites is larger compared to the natural nanocomposites which makes their distribution in the polymer matrix more uniform. This uniform distribution of synthetic nanofillers might affect the partial discharge characteristics of synthetic nanofilled samples when compared to the base polymer. This work is intended to study the effect of the inclusion of synthetic nanofillers of different wt % in the polymer matrix on its partial discharge characteristics. The samples will be aged at a constant electric field for a duration of 8 hours. The data regarding the PD characteristics like maximum PD discharge magnitude, mean discharge magnitude, weibull scale and shape parameters will be collected at regular and consistent time intervals. The obtained parameters will be statistically analysed with Time series analyses techniques to forecast and predict the PD behavior.



9558-44, Session PWed

Partial discharge characteristics and residual breakdown strength of natural nanofilled polypropylene films when aged with different voltage profiles

Antwarn Watson, Charles M. Taylor Jr., Rohitha Dhara, Prathap Basappa, Norfolk State Univ. (United States)

It is known from literature that several electrical characteristics such as PD Resistance of Polypropylene (PP) Films can be improved by homogeneous dispersion of Nanofillers into the polymer matrix. Enhancement of PD Characteristics of PP due to the incorporation of Nanofillers indicates an improvement in electrical insulation reliability of PP under high voltage conditions. Partial Discharge measurement is a well-established technique to evaluate the condition, quality and reliability of insulation like PP. In this work, effect of variation in aging voltage on PD characteristics of PP and its remnant breakdown strength will be investigated for unfilled (PP+0%) and natural Nanofilled PP (PP+2% & PP+6%) .Using PD measurement set up several AC voltages (multiple of inception voltage, Vi) will be applied on each sample for a duration of two hours and PD parameters such as average discharge; maximum discharge, Weibull Scale (?) and Shape Factor (?) of PD distribution etc. will be continuously acquired. Variation of applied voltage will influence PD characteristics because of different space charge accumulation threshold voltages for unfilled and Nanofilled PP samples. Above a threshold voltage rate of space charge accumulation is lower in Nanofilled PP than in base PP. Percolation limit of filler concentrations will also play a vital role on the variations in PD characteristics. Above a percolation limit discharges become higher because of the presence of surpassable double layers. After the completion PD measurement experiments, surface erosion of aged PP samples will be measured using Profilometer to investigate effects of change in applied voltage and Nanofillers concentrations on the PD Resistance of PP samples. PD resistance depends on several factors such as bonding between Nanofillers and Polymer Matrix at their interface and number of PD resistive layers in PP polymer matrix. Here, the effect of increasing electrical stress on PP samples on its PD resistance will be investigated. Using microscopic analyses degradation of PP samples will be measured which will provide more accurate information of PD Resistance. At the end, Breakdown Strength Measurement experiment of all unaged and aged PP samples will be conducted to dig into the effect of aging of PP samples on their breakdown strengths .Changes in aging voltage will affect the polymer morphology which will change the breakdown strength in turn .Two parameters (Scale Factor ? and Shape Factor ?) Weibull Distribution will be used to analyze breakdown strength of all samples. Comparison of PD characteristics of all samples (unaged and aged) will be done finally.

9558-45, Session PWed

Effect of type of aging voltage on the residual breakdown strength of polypropylene films with natural and synthetic nanofillers

Charles M. Taylor Jr., Antwarn Watson, Rohitha Dhara, Prathap Basappa, Norfolk State Univ. (United States)

Current literature indicates that the addition of nanometer sized particles into polymers such as Polypropylene (PP) can improve electrical, mechanical, and thermal properties. It is known that the Nanofilled PP performs better than the unfilled PP and there is significant improvement in the electrical characteristics like breakdown strength and PD resistance with the addition of small wt-% addition of nanofiller to the pure polymer matrix. Other workers have investigated into the short term behavior of the unfilled and Nanofilled PP among other polymers and observed that the stress conditions play an important role on the Nanofilled and unfilled PP behavior. When the applied stress is enough to lead to fast breakdown, the nanofilled PP behaves worse than the unfilled PP. However, the Nanofilled PP behaves better than the unfilled PP if the stress is below a particular threshold. In this paper, the investigation into remnant breakdown strength of natural and synthetic Nanofilled and unfilled PP is observed when aged under different types of voltage profiles. Synthetic and natural organoclay samples of 2wt-%, 4wt-%, 6wt-%, and 8wt-% were used in this experiment. The nanocomposites were aged under different aging conditions. They were exposed to constant voltage electric aging (constant voltage), an electric field that increases in a step fashion (step voltage), and an electric field that increases at a constant rate with time (ramp voltage). The various types of voltages were applied to the nanocomposites to observe how they would behave under different aging conditions. The aging conditions play a prominent role on the remnant breakdown strength of the samples as the PD characteristics which affect the sample performance change drastically with the type of aging voltage. During aging, the formation of space charge that causes change in PD characteristics depends on the electric field applied during aging. In the constant electric field aging, space charges formed have more time for their redistribution and the PD characteristics are mainly affected due to the space charges formed during the PD activity. To reduce the effect of space charge redistribution on the PD activity during aging, the samples are aged under an electric field which changes in a step fashion where the applied electric field changes every 10 minutes. To minimize or make the effect of space charge redistribution negligible on the PD characteristics an electric field which constantly increases with time is used. The erosion depth will be used to evaluate the Partial Discharge Resistance. Surface analysis will be conducted using a surface profilometer to measure the erosion depth and a 3D HIROX microscope will also be used to observe and quantify the degradation volume. Breakdown strength analyses will be done on all aged and unaged samples to evaluate the effect of PD on the remnant breakdown strength of samples with and without nanocomposites

9558-15, Session 5

Plasma-etched nanostructures for optical applications (Invited Paper)

Ulrike Schulz, Friedrich Rickelt, Peter Munzert, Norbert Kaiser, Fraunhofer-Institut für Angewandte Optik und Feinmechanik (Germany)

A basic requirement for many optical applications is the reduction of Fresnel-reflections. Besides of interference coatings, nanostructures with sub-wavelength size as known from the eye of the night-flying moth can provide antireflective (AR) properties. The basic principle is to mix a material with air on a sub-wavelength scale to decrease the effective refractive index. To realize AR nanostructures on polymers, the selforganized formation of stochastically arranged antireflective structures using a low-pressure plasma etching process was studied. An advanced procedure involves the use of additional deposition of a thin oxide layer prior etching. A broad range of different structure morphologies exhibiting antireflective properties can be generated on almost all types of polymeric materials. For applications on glass, organic films are used as a transfer medium. Organic layers as thin film materials were evaluated to identify compounds suitable for forming nanostructures by plasma etching. The vapor deposition and etching of organic layers on glass offers a new possibility to achieve antireflective properties in a broad spectral range and for a wide range of light incidence.

9558-16, Session 5

Low temperature near infrared plasmonic gas sensing of gallium and aluminum doped zinc oxide thin films from colloidal inks

Marco Sturaro, Univ. degli Studi di Padova (Italy); Enrico Della Gaspera, Commonwealth Scientific and Industrial Research Organisation (Australia); Alessandro Martucci, Massimo Guglielmi, Univ. degli Studi di Padova (Italy)



We obtained Gallium-doped and Aluminum-doped Zinc Oxide nanocrystals by non aqueous colloidal heat-up synthesis. These nanocrystals are transparent in the visible range but exhibit localized surface plasmon resonances (LSPRs) in the near IR range, tunable and shiftable with dopant concentration (up to 20% mol nominal). GZO and AZO inks can be deposited by spin coating, dip coating or spray coating on glass or silicon, leading to uniform and high optical quality thin films. To enhance absorbtion in the infrared region, samples can be annealed in inert or reductant atmosphere (N2/Argon or H2 in Argon) resulting in plasmon intensity enhancement due to oxygen vacancies and conduction band electrons density increment. Then IR plasmon has been exploited for gas sensing application, according to the plasmon shifting for carrier density variations, due to electrons injection or removal by the target gas/sample chemical interactions. To obtain a functional sensor at low temperature, another treatment was investigated, involving surfanctant removal by dipping deposited films in a solution of organic acid, tipically oxalic acid in acetonitrile; such process could pave the way to obtain similar sensors deposited on plastics. Finally, GZO and AZO thin films proved sensibility to H2 and NOx, and in particular circumstances also to CO, from room temperature to 200°C. Sensibility behavior for different dopant concentration and temperture was investigated both in IR plasmon wavelengths (~2400 nm) and zinc oxide band gap (~370 nm). An enhancement in sensitivity to H2 is obtained by adding Pt nanoparticles, exploiting catalytic properties of Platinum for hydrogen splitting.

9558-17, Session 5

Graphene-metal interfaces for biosensors devices

Paola Zuppella, Francesca Gerlin, Alain J. Corso, Davide Bacco, Enrico Tessarolo, Marco Nardello, Maria G. Pelizzo, CNR-IFN UoS Padova (Italy)

Graphene-metals interfaces are investigated in many subject areas both applicative and speculative. The interest mainly stems from the possibility for CVD synthesis of large area graphene on metals. In this case the metal act as a catalyst for complete dehydrogenetaion of hydrocarbon precursors that leaves carbon behind at the surface. Such bilayer are also very appealing for surface plasmon resonance devices, since graphene acts both as a protective layer and biorecognition element. Several pairs of graphene/ metal interfaces have been studied in terms of SPR performance and physical-chemical properties at the interface. With regard to this last aspect, NEXAFS spectroscopy is a powerful method to study single-, double-, and few- layers graphene and to illustrate any evolution of the electronic states.

9558-18, Session 5

Microfluidic control on nano-plasmonic thin films using Marangoni effect

Kyoko Namura, Kaoru Nakajima, Kenji Kimura, Motofumi Suzuki, Kyoto Univ. (Japan)

Photothermal conversion of gold nanoparticles/dielectric layer/Ag mirror multilayered thin film is highly localized in the surface layer of the gold nanoparticles because of strong interference [1]. Therefore, a focused light on the thin film can be used as a localized and mobile point-heat-source at a micrometer scale. By using this spatio-temporally controlled photothermal conversion, we demonstrated thermally driven microfluidic control around a micro bubble.

The multilayered thin film was fabricated by the dynamic oblique deposition technique. On the film, a shallow cell with 50 ?m height was prepared. The cell was filled with water in which polystyrene spheres with a diameter of 2 ?m were dispersed in order to visualize the flow. Then, we focused a laser (wavelength: 785 nm) onto the sample to manipulate the fluid. The diameter of the laser spot was less than 10 ?m and the laser power at the sample surface was 12 mW.

When the laser was irradiated around a micro bubble with a diameter of ~ 60 ?m, a strong main flow towards the bubble and two symmetric rotation

flow on either side of it develop because of the Marangoni effect. The shape of the rotation flow is controllable by the relative position of the bubble and the laser spot. The flow around the micro bubble can be understood in terms of light refraction and reflection at the bubble surface and actual photothermal conversion positions.

[1] K. Namura, et al., J. Appl. Phys. 114, 074308 (2013).

9558-19, Session 6

The optical and electronic properties of pyrite nanocrystals and solid thin film

Guangmei Zhai, Taiyuan Univ. of Technology (China) and Changzhou Univ. (China) and State Key Lab. of Electronic Thin Films & Integrated Devices (China); Rongwei Xie, Heng Wang, Jitao Zhang, Yongzhen Yang, Hua Wang, Xuemin Li, Xuguang Liu, Bingshe Xu, Taiyuan Univ. of Technology (China)

Pyrite FeS2 has been impeded by the exciting phase purity and defect issues in its application in cost-effective photovoltaic devices since it was first used as thin light absorber for solar energy conversion application in the mid-1980s. However, with the development and progress of nanocrystalbased approach which can use much milder processing condition, and in which surface chemistry and phase impurity issues might take on entirely new character, it is well worthwhile studying the properties of pyrite nanocrystals and solid films. In this work, we report on the optical and electronic properties of phase-purity pyrite nanocrystals (NCs) synthesized via hot-injection method. Also, the effect of surface chemistry of pyrite NCs on their optical and electronic properties was investigated. Our results show that the synthesized pyrite NCs and solid thin films have absorption up to the near infrared region and have an indirect bandgap of around 1.1 eV, exhibiting favorable optical property and bandgap energy for photovoltaic applications. The electron affinity and ionization potential of pyrite NCs passivated with various ligands including organic and atomic ligands were determined by the combination of cyclic voltammetry and optical absorption spectroscopy. It is found that up to 190 mV of energy level shift of pyrite NCs can be obtained between different chemical ligands employed here, indicating a strong dependence of electronic properties of pyrite NCs on their surface chemistry. It is believed that the optical property and energy levels determined here would provide valuable information for the design and fabrication of photovoltaic devices based on pyrite NCs in the future.

9558-20, Session 6

Investigation the stress of the SiOxCyHz thin film deposited by HMDSO/O2 plasma polymerization

Wei-Bo Liao, Ching-Long Cheng, Cheng-Chung Lee, National Central Univ. (Taiwan); Cheng-Chung Jaing, Minghsin Univ. of Science and Technology (Taiwan); Chien-Cheng Kuo, National Central Univ. (Taiwan)

Stress has always had a great impact of thin films. Large stress causes cracking, wrinkling, and peeling of thin films. The total stress of thin films includes intrinsic stress and thermal stress. The intrinsic stress is influenced by the deposition parameters such as the substrate temperature, the deposition rate, the working pressure, and the ion source parameters. The thermal stress is caused by a mismatch in the coefficient of thermal expansion of the thin films and the substrate when the structure is subjected to temperature changes during its fabrication and application. How to reduce the stress of thin films has become a very important issue. There are many ways to eliminate the stress of thin film materials and substrate. In this work, we used an organic thin film to reduce the stress of inorganic thin films. The organic SiOxCyHz thin film was deposited by plasma polymerization process used a mixture source gas by



hexamethyldisiloxane(HMDSO) and oxygen. Growing different properties of SiOxCyHz thin film by four parameters are the flow of oxygen and HMDSO, plasma beam current (Ii) and anode voltage (Vd). The inorganic layers were coated on the SiOxCyHz thin film to reduce the stress of inorganic layers. The transmittance of thin films was measured by Hitachi U4100 spectrometer. The thin film composition and structure has been investigated by X-ray photoelectron spectroscopy (XPS) and Fourier transform infrared (FTIR) spectroscopy. Analyzing the stress of thin films was investigated by phase shift interferometer.

9558-21, Session 6

Investigation of the optoelectronic characteristics of graphene/perovskite/ porous silicon nanowires heterostructure

Wun Wei Lin, National Taipei Univ. of Technology (Taiwan)

This paper focuses on the features of a structure graphene/perovskite/ porous silicon nanowires (PSiNWs). First, the SiNWs on the Si substrate were fabricated by metal-assisted chemical etching (MACE) method in the freshly prepared dilute solution containing HF (48%) and AgNO3 (0.02 mol L-1) (1:1) with different etching time at room temperature. After dipping the wafer in the etching solution, a thick Ag layer is formed on the surface of Si wafer. The wafer is then put into a diluted HNO3 solution (50 wt%) for a short period to remove the Ag layer. It shows that the PSiNWs may have different porosities depending on the etching time and the concentration of AgNO3 in the etching solution . Next, the perovskite is coated on the PSiNWs using a spin coating process at 5000 rpm for 60 s and followed by the rapid thermal annealing (RTA) process in the air at 70oC for 10 mins. Then, the graphene were deposited on the surface of perovskite/SiNWs structure with 2 mins, 5 mins and 10 mins by RF magnetron sputtering. After all, the sample is examined by Scanning Electron Microscope (SEM), Photoluminescence (PL), Hall Measurement. As the I-V curves and PL spectrum is obtained, the optoelectronic characteristics of graphene/ perovskite/PSiNWs and perovskite/PSiNWs two structures and the impact of changes in the thickness of graphene can be discussed.

9558-22, Session 6

Surface morphology of ultrathin graphene oxide films obtained by the SAW atomization

Olga Balachova, Sergey Balashov, Ctr. de Tecnologia da Informacao Renato Archer (Brazil); C. A. S. Costa, Ctr. Nacional de Pesquisa em Energia e Materiais (Brazil); Aristides Pavani Filho, Ctr. de Tecnologia da Informacao Renato Archer (Brazil)

Lately, graphene oxide (GO) thin films have attracted much attention: they can be used as humidity-sensitive coatings in the surface acoustic wave (SAW) sensors; being functionalized, they can be used in optoelectronic or biodevices, etc.

In this research we study surface morphology of thin GO films obtained on Si, LiNbO3 and quartz substrates by successive atomization of submicroliter droplets of aqueous suspension of GO by the SAW atomizer. The advantages of this method are that it allows controlling a process of film deposition, working with microvolumes of liquids and minimizing the "coffee-ring" effect. Deposited films were examined using AFM and electron microscopy. The films may form discrete or continuous coatings at the surface of the substrates with the minimum thickness of 2.5-3 nm which corresponds to few monolayers of GO. The thickness and quality of the deposited films depend on the parameters of the SAW atomization (number of atomized droplets, a volume of the initial droplet, etc.) and on sample surface preparation (activation in oxygen plasma). We study the structure of the obtained films and discuss the uniformity and the degree of the surface coverage as a function of parameters of the film deposition process and sample preparation. Qualitative analysis of adhesion of the films is made by controllable immersion of them into water and subsequent evaluation of morphology of remained films.

9558-23, Session 7

Periodic nanostructures for tunable thin optics (*Invited Paper*)

Francesco Simoni, Univ. Politecnica delle Marche (Italy); Luigino Criante, Istituto Italiano di Tecnologia (Italy) and Univ. Politecnica delle Marche (Italy); Francesco Scotognella, Luca Passoni, Istituto Italiano di Tecnologia (Italy) and Politecnico di Milano (Italy); Francesco Fumagalli, Istituto Italiano di Tecnologia (Italy); Guglielmo Lanzani, Istituto Italiano di Tecnologia (Italy) and Politecnico di Milano (Italy); Fabio Di Fonzo, Istituto Italiano di Tecnologia (Italy)

We report here realization and characterization of porous nanostructures where a periodic refractive index modulation is achieved by stacking layers with different nano-architectures.

One multilayer photonic crystal has been fabricated starting from colloidal dispersion of silicon dioxide and zirconium dioxide using spin coating technique. Improved efficiency of Bragg reflectivity (up to 85% with submicron thickness) has been obtained by an alternative method based on self-assembly from the gas-phase. Due to the high porosity, these systems can be infiltrated with many fluids (liquid/gas). Using nematic liquid crystals, the Bragg reflection band by applying low voltages to the structure can be tuned.

9558-24, Session 7

Effects of silver-nanoparticle layer in chiral sculptured thin films for multiplasmonic sensing

Stephen E. Swiontek, Akhlesh Lakhtakia, The Pennsylvania State Univ. (United States)

Multiple surface-plasmon-polariton (SPP) waves can be guided by the interface of a metal and a chiral sculptured thin film (STF). These multiple SPP waves can be used for more reliable sensing of analytes with high sensitivity, when compared to a single SPP wave in traditional single-SPP-wave scenarios.

An ultra-thin layer of silver nanoparticles can be deposited via physical vapor deposition at different depths of the chiral STF. That layer can eventually act as a site to bind recognition molecules to which analytes of a certain type can attach.

A lanthanum-fluoride chiral STF was deposited on top of a 30-nm-thick aluminum film. An ultra-thin layer of silver nanoparticles was deposited at a certain depth of the chiral STF in order to observe the effects that the nanoparticles have on the multiple SPP waves that were launched. Several samples were then deployed in the Turbadar-Kretschmann-Raether (TKR) configuration. The effects of the depth of the silver-nanoparticle layer in the chiral STF on the angular locations of multiple SPP-wave modes were investigated to determine the optimal depth for multiplasmonic sensing of multiple analytes in aqueous solutions.

9558-26, Session 7

Phoxonic one-dimensional heterostructure with photonic and phononic band gaps at the same frequency

Jesus Manzanares-Martinez, Paola Castro-Garay, Betsabe



Manzanares-Martinez, Univ. de Sonora (Mexico); Damian Moctezuma-Enriquez, Ctr. de Investigación en Materiales Avanzados, S.C. (Mexico); Yohan Jasdid Rodriguez-Viveros, Carlos Ivan Ham-Rodriguez, Univ. de Sonora (Mexico)

The concept of phoXonic Crystals (PxC) has recently been introduced to define a novel class of composite material that allows the simultaneous existence of Photonic and Phononic Band Gaps (PtBG and PnBG, respectively). The periodicity in the dielectric function and in both the elastic constant and densities, allow under certain conditions to obtain ranges of frequency where the electromagnetic and mechanical vibrations can be forbidden.

The PxC can be designed to confine light and sound at a common wavelength. However, the confined waves are of different frequencies and therefore it is required some nonlinear mechanism to couple light and sound.

In this work, we explore for the first time the design of a thin-film based heterostructure where can be obtained a coincidence for the photonic and phononic band gaps.

Our numerical results allow to identify a narrow phoxonic band gap at the GHz regime. We have also explored the behavior of this band gap for the off-axis propagation considering the projected band structure calculation and the oblique incidence for the impinging waves. We consider that the design of an heterostructure with photonic and phononic waves at the same frequency allow to enhance the electromagnetoelastic interaction in piezoelectric materials.

9558-27, Session 8

Self-assembling of molecular nanowires for enhancing the conducting properties of discotic liquid crystals

Ji Hyun Park, Kyungho Kim, Seoul National Univ. (Korea, Republic of); Yoichi Takanishi, Jun Yamamoto, Kyoto Univ. (Japan); Yung Woo Park, Youn Sang Kim, Seoul National Univ. (Korea, Republic of); Giusy Scalia, Seoul National Univ. (Korea, Republic of) and Univ. du Luxembourg (Luxembourg)

The self-organization of discotic liquid crystal molecules in columns has enormous interest for soft nanoelectronic applications. A great advantage of discotic liquid crystal is that defects can be self-annealed in contrast to typical organic materials. Through the overlap of molecular orbitals, the aromatic cores assemble into long range one-dimensional structures. Very thin structured films can be obtained by spin-coating from solution and the resulting morphologies are strongly dependent on the interaction between discotics and solvent molecules. The presence of substrates play an important role in the formation and organization of the nanowires but other factors also contribute. In particular, we have analyzed the effect of solvents, evaporation conditions and the role of interfaces. We have evaluated the arrangement of the molecules in the as-prepared films by Atomic Force Microscopy and by polarizing optical microscopy, when the film features are optically detectable. In addition, x-ray scattering and polarized Raman spectroscopy were performed for understanding the structural organization of the molecular nanowires on substrates. Finally, high control of the overall morphology was confirmed by electrical measurements with one order of magnitude higher conductivity in an aligned sample compared to nonaligned one.

9558-28, Session 8

Room temperature deposition of highly dense TiO2 thin films by filtered cathodic vacuum arc

Elena Guillén, Irene Heras, Gonzalo Rincon Llorente,

Abengoa (Spain); Frank Lungwitz, Helmholtz-Zentrum Dresden-Rossendorf e. V. (Germany); Mercedes Alcon Camas, Ramon Escobar, Abengoa (Spain)

Titanium dioxide is a wide band-gap semiconductor used in many energyconversion and environmental applications. TiO2 properties depend to a great extent on the deposition technique applied for its fabrication. In particular, physical vapor deposition (PVD) techniques are the preferred ones for those applications in which long-term stability and controllable optical properties play an important role. By filtered cathodic vacuum arc (FCVA), it is possible to obtain films with excellent properties deposited at room temperature. This technique produces highly dense films with a good interlayer adhesion due to a high ionization during the plasma deposition. In addition, surface roughness is very low due to the use of magnetic filters. For those reasons, FCVA is a potential alternative to magnetron sputtering as a suitable technique for optical thin film deposition on an industrial scale.

In this work, we carry out a systematic study of TiO2 deposition by FCVA. We have investigated the obtained films for various deposition parameters, analyzing their composition by Rutherford backscattering spectroscopy (RBS), their structure by X-ray diffraction and Raman spectroscopy, their morphology by scanning electron microscopy (SEM) and contact angle, and their optical properties by ellipsometry and reflectance measurements. Optical constants measured by ellipsometry are used as input data for simulation with optical software CODE. RBS measurements showed that resulting films exhibit TiO2 stoichiometry, with porosity below 4%. Contrary to other deposition techniques, no post annealing treatment is needed with FCVA, obtaining transparent, dense TiO2 films in the rutile phase at room temperature.

9558-29, Session 8

Deposition and characterization of Fe-Si based ionic glass thin films

Neil R. Murphy, Air Force Research Lab. (United States); Lirong Sun, General Dynamics Information Technology (United States); John G. Jones, Air Force Research Lab. (United States); John T. Grant, General Dynamics Information Technology (United States)

Ionic glass thin films composed of iron oxides within a dielectric silicon dioxide matrix are deposited by way of reactive co-sputtering. The valence states of the iron oxides are varied through manipulation of the voltage applied to the iron cathode under a constant flow of the reactive oxygen and argon gas mixture. To fabricate these films, a continuous power of 100 watts is applied to the Si cathode, while the Fe cathode power was systematically varied between 20 and 80 watts. Increasing the power applied to the Fe cathode gives rise to an increased flux of metallic atoms, ultimately leading to reduction in the oxygen partial pressure within the chamber via chemisorption. As the oxygen partial pressure decreases, the fraction of Fe within the film increases while the valence state drops from Fe3+ to Fe2+. The transition from Fe3+ to Fe2+ is associated with a large enhancement in NIR absorption and a decreased level of visible absorption. Systematic adjustment of the fraction and valence state of the Fe cations within the dielectric SiO2 matrix allows for a large degree of control over the coloration and NIR absorption behavior of the FexSiyOz films. The ability to control the response of the spectral absorption within visible and NIR wavelengths makes the FexSiyOz thin films a promising candidate for the replacement of lossy metallic materials currently used within induced transmission filters and plasmonic applications.

9558-30, Session 8

Fabrication and characterization of film coatings of silver nanoparticles with different composite agents

Vasyl J. Syrvatka, Yurij I. Slyvchuk, Ivan I. Rozgoni, Institute of Animal Biology NAAS (Ukraine); Nestor O. Piasetskyi,



Ivan Franko National Univ. of L'viv (Ukraine); Oksana V. Shtapenko, Ivan I. Gevkan, Institute of Animal Biology NAAS (Ukraine); Oleksandr I. Bilyy, Roman Y. Serkiz, Ivan Franko National Univ. of L'viv (Ukraine); Iryna O. Matyukha, Svitlana V. Fyodorova, Institute of Animal Biology NAAS (Ukraine)

Unique chemical and optical properties make silver nanoparticles diagnostically relevant as they have the ability to interact with important biomolecules such as DNA and proteins. The main aim of the study was to investigate film coatings of silver nanoparticles with different composite agents for their prospect application as an optical sensors or biomarkers. Silver nanoparticles were prepared by using the chemical reduction of silver nitrate by sodium borohydride. Hyaluronic acid, polyvinylpyrrolidone and polyvinyl alcohol were used as composite agents. Film coatings of silver nanoparticles were done by evaporation at the different temperatures from -60° to +38° C. The structural changes of silver nanoparticles under influence of different chemicals were studied. Ultraviolet-visible spectroscopy was used for examination of surface plasmon resonance band of silver nanoparticles at the all stages of the experiment. Scanning and transmission electron microscopes were used for visualization of structures of film coatings of silver nanoparticles. Energy-dispersive X-ray spectroscopy was used for elemental analysis of the sample surface. The results showed that film coatings of silver nanoparticles have strong optical properties. Furthermore different chemicals lead to structural changes of nanoparticles and modification of their optical properties. Therefore the film coatings of silver nanoparticles have distinctive optical properties and can be applied as optical sensors or biomarkers.

Conference 9559: High and Low Concentrator SPIE. PHOTONICS Systems for Solar Energy Applications X

Monday - Tuesday 10-11 August 2015

Part of Proceedings of SPIE Vol. 9559 High and Low Concentrator Systems for Solar Energy Applications X

9559-17, Session PMon

New trends in solar

Divya Mereddy, Mounica Gampa, Vijay Ram Raju V., Gokaraju Rangaraju Institute of Engineering & Technology (India)

Abstract- Photo voltaic cell (PV cells) is one of the methods of converting solar power to electric power. It consists of semi conductors which exhibit the photovoltaic effect and converts the solar energy to direct current. The output power of the PV cells depends on the angle of incidence of sunlight. These cells are able to produce maximum power only as long as the light rays are perpendicular to the panel's surface. The position of the sun is not stationary so the angle of incidence also changes with time, thereby performance of solar panel also changes with time. By moving the solar panel the panel plane is made always perpendicular to sun rays, so that we can get more efficiency. This is called solar tracking. Depending on the number of axes the panel is moved trackers are differentiated as dual axes and single axes mainly. Single axes tracker can give a good output when the sun's path is stationary, but as it changes with season dual axes tracker gives more efficiency irrespective of the sun's path by following the sun in two axes. In this paper, dual axes solar tracker construction and dual axes method importance over single axes tracking will be explained.

9559-1, Session 1

Fresnel lens characterization for solar concentration efficiency

Christi K. Madsen, Mark Hallam, William Harris, Texas A&M Univ. (United States)

Due to the inexpensive and light weight nature of Fresnel lenses, they are key components in many solar energy concentration systems. The ability to effectively characterize Fresnel lenses over large areas is essential to verifying their system performance and efficiency. Under high concentration, it becomes impractical to perform detailed spatial and spectral measurements under full sun conditions. We have developed a method to characterize large Fresnel lenses for concentrating solar applications. Our Lens Characterization Unit (LCU) analyzes the resultant pattern of an incident laser beam which may be scanned across the lens. Using the LCU, we can evaluate the portion of diffracted light that is concentrated on the receiver area at each incidence point. The wavelength dependence may be quantified using lasers at different wavelengths and the angle of incidence may also be varied.

9559-2, Session 1

Demonstration of an intermediatescale lens-to-channel waveguide solar concentrator

Ran Huang, Yuxiao Liu, Christi K. Madsen, Texas A&M Univ. (United States)

Solar concentrating photovoltaic systems have the potential to reduce total cost and achieve higher efficiency by replacing a large solar cell surface with cheaper optical devices, in which a large area of light can be efficiently collected and concentrated to a small optical device and guided to an array of co-located photovoltaic cells with high optical efficiency. We will present an experimental demonstration for an intermediate-scale lens-to-channel waveguide solar concentrator, in which the sun collected area is much larger than our prior demonstration. In this work, an 8x8 60 mm diameter lens array and a PMMA multimode waveguide are used as the primary

concentrator and the secondary concentrator, respectively. A 45 degree coupler is fabricated to the waveguide to reach the maximum coupling efficiency and to avoid any inherent decoupling loss. In order to achieve higher concentration and a compact structure, a tapered waveguide is integrated to this design, which allows more lenses in a row of the lens array. Simulations indicate that the newly designed lens-to-channel waveguide solar concentrator can have 400x~1000x concentration. The fabrication details of the prototype device will be presented. A critical requirement for this design is maintaining low waveguide propagation losses, which we demonstrate can be less than 0.2 dB/cm.

OPTICS+PHOTONICS

FOR SUSTAINABLE ENERGY

9559-3, Session 1

Direct transmission of concentrated solar radiation via optical fibre bundles to thermal applications

Maryam Rahou, John Andrews, Gary Rosengarten, RMIT Univ. (Australia)

A challenge in high-temperature solar thermal applications is transfer of concentrated solar radiation to the load with minimum energy loss. The use of a solar concentrator in conjunction with bundled optical fibres has advantages in terms of transmission efficiency, and cost-effectiveness compared to a conventional heat transfer system employing heat exchangers and a heat transfer fluid. In this paper, the transmission from a solar concentrator into and through an optical fibre bundle over distances of up to 100 m is estimated using simulation results. A key input to the simulation is the angular distribution of radiation intensity at each point in the aperture plane of the optical fibres. This distribution depends on the optical properties of the solar concentrator. Two different concentrators are investigated to produce the collimated beam incident on the optical fibre bundle: a parabolic dish reflector with a small secondary mirror at a common focal point, producing a collimated beam issuing from a hole at the centre of the dish; and a Fresnel lens with a point focus with a small diameter converging lens located just after this focus. Since solar radiation comprises a broad band of wavelengths, each with very limited spatial coherence, interference effects can be neglected. Hence a ray tracing model is employed covering absorption within the fibres and losses at internal reflections. The intensity of the radiation across the exit plane of the fibre is found by integrating across all directions and wavelengths at each point. For a 15 mm diameter bundle comprising some 27 000 individual low OH fibres, the average transmission per metre length of fibre was found to be 72% with the parabolic reflector, and 65% with the Fresnel lens. Around two thirds of the loss occurred at the entrance plane to the bundle, due to absorption in the packing material between the individual fibres.

9559-4, Session 1

Fabrication and comparison of selective, transparent optics for concentrating solar systems

Robert A. Taylor, Yasitha Hewakuruppu, The Univ. of New South Wales (Australia); Todd Otanicar, The Univ. of Tulsa (United States)

Concentrating optics enable solar thermal energy to be harvested at high temperature (>100oC). As the temperature of the receiver increases, radiative losses can become dominant. In many concentrating systems, the receiver is coated with a selectively absorbing surface (TiNOx, Black Chrome, etc.) to obtain higher efficiency. Commercial absorber coatings are well-developed to be highly absorbing for short (solar) wavelengths, but highly reflective at long (thermal emission) wavelengths. If a solar system requires an analogous transparent, non-absorbing optic - i.e. a

Conference 9559: High and Low Concentrator Systems for Solar Energy Applications X



cover material which is highly transparent at short wavelengths, but highly reflective at long wavelengths – the technology is much less mature.

Low-e glass partially fulfills this need, but only transmits -60% of the full solar spectrum. Optically thin metal films with hole-arrays are another feasible solution, but are often difficult to fabricate. This study investigates combinations of thin film coatings (transparent conductive oxides) and nanoparticle depositions as potential low cost solar covers which can improve upon low-e glass. To our knowledge these materials have not yet been designed and optimized for solar energy applications.

This paper experimentally compares readily available materials deposited on various substrates (quartz, low-e glass, clear glass, and acrylic) and ranks them via an 'efficiency factor for selectivity', which represents the efficiency of radiative exchange in a solar collector. Out of the materials studied, indium tin oxide and thin films of ZnS-Ag-ZnS represent the most feasible solutions for concentrated solar systems. Overall, this study provides an engineering design approach and guide for creating scalable, selective, transparent optics.

9559-5, Session 2

High-temperature selective solar thermal absorber based on Fabry-Perot resonance cavity

Hao Wang, Liping Wang, Arizona State Univ. (United States)

In this work, we will design, fabricate, and characterize a multilayer selective solar absorber made of tungsten and MgF2 thin films. Thin-film optics along with the particle-swam optimization method is used for the optimal design of this novel selective absorber. The selective absorber shows spectral absorptance within solar spectrum as high as 95% and infrared emittance as low as 4%, due to the Fabry-Perot resonance and anti-reflection effect. The designed multilayer solar absorber structure will be fabricated on wafer scale with sputtering and e-beam evaporation. Optical and radiative properties for the fabricated sample will be characterized at both room and high temperatures. An FTIR spectrometer and integrating sphere are available for measuring the specular and hemispherical reflectance at room temperature. A novel FTIR fiber optics setup will be employed to study the normal reflectance at mediate temperatures up to 400°C. More importantly, a home-built high-temperature emissometry facility will be used to directly measure the spectral-directional emittance at high temperature up to 1000°C.

Theoretical calculation estimates a solar-to-thermal efficiency of 90% with x800 concentration at an absorber temperature of 1000°C for the designed multilayer solar absorber. In order to experimentally test the conversion performance and high-temperature stability, a solar simulation with concentrating optics will be used to heat up the sample in a box vacuum chamber, and the stagnation temperature will be measured with different concentration factors. Such a high-performance, high-temperature, low-cost selective solar absorber will greatly increase the performance of various solar thermal systems, especially CSP systems.

9559-6, Session 2

Solar selective coatings based on carbon:transition metal nanocomposites

Irene Heras, Elena Guillén, Abengoa Research (Spain); Matthias Krause, Helmholtz-Zentrum Dresden-Rossendorf e. V. (Germany); Alnhoa Pardo, Fundació CTM Ctr. Tecnològic (Spain); Jose Luis Endrino, Ramon Escobar, Abengoa Research (Spain)

Carbon:Transition Metal nanocomposites were grown by filtered cathodic vacuum arc (FCVA). The metal content was determined by Rutherford backscattering spectroscopy (RBS) and nuclear reaction analysis (NRA). The structure was analysed by X-Ray diffraction (XRD) and Raman spectroscopy measurements. High resolution transmission electron microscopy (HRTEM)

images show the formation of multilayers in the nanocomposite. The optical properties of the deposited coatings were characterized by a combination of ellipsometry, UV-Vis spectrophotometry and FTIR measurements. The reflectance spectra of the films were simulated with the optical software CODE and good agreement between simulated and measured reflectance spectra was found.

9559-7, Session 2

Coupled optical-thermal-fluid and structural analyses of novel light-trapping tubular panels for concentrating solar power receivers

Jesus D. Ortega, Joshua M. Christian, Julius E. Yellowhair, Clifford K. Ho, Sandia National Labs. (United States)

Traditional tubular receivers used in concentrating solar power are formed using tubes connected to manifolds to form panels, which in turn are arranged in cylindrical or rectangular shapes. Previous and current tubular receivers, such as the ones used in Solar One, Solar Two, and most recently the Ivanpah solar plants, have used a black paint coating to increase the solar absorptance of the receiver. However, these coatings degrade over time and must be reapplied, increasing the receiver maintenance cost. This paper presents the thermal efficiency evaluation of novel receiver tubular panels that have a higher effective solar absorptance due to a light-trapping effect created by arranging the tubes in each panel into unique geometric configurations. Similarly, the impact of the incidence angle on the effective solar absorptance and thermal efficiency is evaluated. A goal of this work is to achieve high solar absorptances and thermal efficiencies above 90% without using an external coating on the tubes. Several panel geometries were initially proposed and were down-selected based on structural analyses considering the thermal and pressure loading requirements of molten salt and supercritical carbon-dioxide receivers. The effective solar absorptance of the chosen tube geometries and panel configurations were evaluated using the ray-tracing modeling capabilities of SolTrace. The thermal efficiency was then evaluated by coupling computational fluid dynamics with the ray-tracing results using ANSYS Fluent. Compared to the base case analysis (flat tubular panel), the novel tubular panels have shown an increase in effective solar absorptance and thermal efficiency by several percentage points.

9559-8, Session 2

Testing and optical modeling of novel concentrating solar receiver geometries to increase light trapping and effective solar absorptance

Julius E. Yellowhair, Clifford K. Ho, Jesus D. Ortega, Joshua M. Christian, Charles E. Andraka, Sandia National Labs. (United States)

Concentrating solar power receivers are comprised of panels of tubes arranged in a cylindrical or cubical shape on top of a tower. The tubes contain heat-transfer fluid that absorbs energy from the concentrated sunlight incident on the tubes. To increase the solar absorptance, black paint or a solar selective coating is applied to the surface of the tubes. However, these coatings degrade over time and must be reapplied, which reduces the system performance and increases costs.

This paper presents an evaluation of novel receiver shapes and geometries that create a light-trapping effect, thereby increasing the effective solar absorptance and efficiency of the solar receiver. Several prototype shapes were fabricated from Inconel 718 and tested in Sandia's solar furnace at an irradiance of -30 W/cm2. Photographic methods were used to capture the irradiance distribution on the receiver surfaces. The irradiance profiles were compared to results from ray-tracing models. The effective solar absorptance was also evaluated using the ray-tracing models. Results



showed that relative to a flat plate, the new geometries could increase the effective solar absorptance from 86% to 92% for an intrinsic material absorptance of 86%, and from 60% to 73% for an intrinsic material absorptance of 60%.

Sandia National Laboratories is a multi-program laboratory managed and operated by Sandia Corporation, a wholly owned subsidiary of Lockheed Martin Corporation, for the U.S. Department of Energy's National Nuclear Security Administration under contract DE-AC04-94AL85000.

9559-9, Session 3

Design and analysis of combined photovoltaic-thermal electric systems for reducing intermittency effects of solar illumination

Silvana Ayala Pelaez, Shelby D. Vorndran, Yuechen Wu, Juan Manuel Russo, Raymond K. Kostuk, The Univ. of Arizona (United States)

In this paper we analyze the performance of a combined photovoltaic (PV) and thermal electric generator (TEG) solar energy conversion system to help mitigate the transient effects of solar illumination. The approach takes advantage of the longer time constants of thermal conversion devices to offset the immediate response of PV devices to fluctuations in solar illumination. A thermodynamic analysis of the system is presented and is used to determine the size of a thermal storage block required for different size PV systems. Different materials for the thermal block and efficiencies of the TEG are included in the analysis. A comparison of using a spectrum splitting system to dedicated PV and thermal conversion regions of the collection field is also evaluated. The spectrum splitting system filters shorter wavelengths for use by the PV system and longer wavelengths for thermal conversion. The overall system performance is evaluated using both solar irradiance data available through the SMARTS2 resource and experimental data from a field test site in Tucson Arizona. Preliminary results show that intermittent durations of 2-3 minutes can be achieved with modest size thermal blocks and 2% efficient TEGs. Results from a small scale pilot test are also presented.

9559-10, Session 3

Design and feasibility of high temperature nanoparticle fluid filter in hybrid thermal/ photovoltaic concentrating solar power

Drew DeJarnette, Nick Brekke, Ebrima Tunkara, Hari Parameswar, Kenneth Roberts, Todd Otanicar, The Univ. of Tulsa (United States)

Concentrating solar power utilizes light for both thermal and electrical energy generation through absorbed photons. A parabolic trough concentrator system has been designed for a hybrid concentrating solar thermal collector to reach temperatures up to 300° C. This design incorporates a spectrally tunable nanoparticle fluid filter to absorb subbandgap photons that the photovoltaic cell cannot convert to electrons. Fluid filter housing design will be presented to show how the filter can be incorporated into existing trough concentrator systems. Thermal expansion of the filter is accounted for and optical design of the concentrator is verified using the ray tracing program SolTrace. The SolTrace model shows the feasibility of the filter located between the PV cell and the concentrating mirrors. The nanoparticle fluid filter is modeled to absorb 86% of the subbandgap light in the fluid and transmit 82% of the above-bandgap light to the PV receiver. The current work discusses fabrication and testing of the fluid filter including feasibility of nanoparticle stability at high temperature. Incorporation of temperature variation in the operation of the PV cell which adjusts the working bandgap ensures designed filter is optimized over the entire length of the system. System efficiency is calculated based upon optical, thermal, and photovoltaic models to determine how much solar energy can realistically be converted and what percentages will be usable

directly as electricity and stored as thermal energy. On sun testing will be performed using 14x concentration to verify system level modeling.

9559-11, Session 3

A high temperature hybrid photovoltaicthermal receiver employing spectral beam splitting for linear solar concentrators

Ahmad Mojiri, Cameron C. Stanley, Gary Rosengarten, RMIT Univ. (Australia)

Linear solar concentrators such as parabolic troughs or Fresnel mirrors are used to generate high temperature heat for process applications or power generation. Thermal receivers at their focal point are essentially insensitive to the spectrum of light striking them, and can effectively absorb the whole solar spectrum. Photovoltaic devices can transform a specific range of the solar spectrum into electricity, with high efficiencies. For example, silicon cells optimised for concentrating applications can convert the wavelengths between 700 and 1100nm into electricity with an efficiency of above 30%.

In order to benefit from this, we developed a spectrally splitting hybrid photovoltaic-thermal receiver that can decompose the concentrated light in linear concentrators into different bands. The wavelength between 700 and 1100 nm are sent to silicon cells to be converted directly into electricity. The rest of the solar spectrum is absorbed by a mid-temperature absorber, with above 150°C, for process heat, solar cooling, or thermal power generation.

The proposed spectral beam splitter consists of selective volumetric absorbers including propylene glycol to absorb the wavelengths longer than 1100nm and semiconductor doped glass to absorb wavelengths shorter than 700 nm. The absorbed energy generates heat in the thermal absorber. Separating the spectral beam splitting process into the aforementioned stages helps to reduce the cost of the system and makes it suitable for commercialisation. This receiver was built and tested on a commercial parabolic concentrator generating efficiencies of about 9%for electrical and over 50% for thermal energy at 150°C.

9559-12, Session 3

Concentrating PV module output power using a wireless microcontroller based automatic sun tracker

Ali Abou-Elnour, Ajman Univ. of Science & Technology (United Arab Emirates)

Due to the increasing interest in renewable energies as the main source for future energy, an enormous number of researches are now considering renewable energy generation and applications. In all of these researches, increasing the efficiency (decreasing the costs) of the renewable energy generation is a must to compete with conventional energy resources. Photovoltaic cells are considered as important renewable solar energy elements which convert solar energy into electrical energy in an easily, directly, and environmental friendly way. The amount of the energy generated from a solar energy system depends to a large extend on the relative position of the solar energy module (collector) with respect to the sun position. The sun position with respect to the earth is continuously varying with the time of the day and with the season and consequently the amount of generated energy from a fixed solar module (collector) will be also affected. The initial costs and the output power of fixed solar sun modules are lower than those of movable modules, known as sun trackers, which are designed to follow the movement of the sun to maximize the output power of the module. The cost and the complexity of sun trackers depend on if the tracking is done in one or two dimensions. Although many tracking systems have been designed and implemented in one and two dimensions, the performance of hardware circuits and software programs of these systems can be further enhanced. Moreover, the recent developments in wireless technologies, the intranet and internet topologies, and the rapid developments of computational facilities are opening the ways to design and implement efficient real time wireless monitoring and controlling for

Conference 9559: High and Low Concentrator Systems for Solar Energy Applications X



renewable energy systems.

In the present work, a wireless microcontroller based sun tracker is designed and implemented to concentrate the generated output power resulting from photovoltaic module. Monitoring, controlling, and recording features are fully obtained in the present system using an efficient programming environment. Design equations which are implemented allow the usage of the system anywhere anytime without extra hardware tracking circuits. A carefully design hardware motor deriving circuit is designed and implemented to simplify the controlling program without scarifying the required accuracy. The system generates the motors' controlling signals to allocate the photovoltaic module to receive the maximize amount of the solar energy on its surface from sunrise to sunset. The transmission of all controlling and monitoring signals is wirelessly done to optimize the performance of the system with minimum cost and best quality. The proposed system is successfully implemented for photovoltaic modules under realistic operating conditions

9559-13, Session 4

Simulation of an electrowetting solar concentration cell

K.I. Iftekhar Uddin Khan, Gary Rosengarten, RMIT Univ. (Australia)

Electrowetting control of liquid lenses has emerged as a novel approach for solar tracking and concentration. Recent studies have demonstrated the concept of steering sunlight using thin electrowetting cells without the use of any bulky mechanical equipment. Effective application of this technique may facilitate designing thin and flat solar concentrators. Understanding the behavior of liquid-liquid and liquid-solid interface of the electrowetting cell through trial and error experimental processes is not efficient and time consuming. In this paper, we present a novel simulation model to predict the liquid-liquid and liquid-solid interface behavior of electrowetting cell as a function of various parameters such as applied voltage, dielectric constant, fluidic properties and electrode shape. The simulation model includes measured properties of appropriate liquids. We used Comsol Multiphysics simulations incorporating experimental data of different liquids. We have designed both two dimensional and three dimensional simulation models, which predict the shape of the lenses. The model measures the contact angle using the Young-Lippman equation. The model uses a moving mesh interface with Navier-stokes equation and a Navier slip condition on cell wall. Simulation of the electric field from the electrodes is coupled with Young-Lippman equation. The model can also be applicable for other MEMS electrowetting devices.

9559-14, Session 4

Holographic lens spectrum splitting photovoltaic system for increased diffuse collection and annual energy yield

Shelby D. Vorndran, Yuechen Wu, Silvana Ayala Pelaez, Raymond K. Kostuk, The Univ. of Arizona (United States)

Concentrating and spectrum splitting photovoltaic (PV) modules have a limited acceptance angle and thus suffer from optical loss under off-axis illumination. This loss manifests itself as a substantial reduction in energy yield in locations where a significant portion of insulation is diffuse. In this work, a spectrum splitting PV system is designed to efficiently collect and convert light in a range of illumination conditions. The system uses a holographic lens to concentrate short-wavelength light onto a smaller, more expensive indium gallium phosphide (InGaP) PV cell. The high efficiency PV cell near the axis is surrounded with silicon (Si), a less expensive material that collects a broader portion of the solar spectrum. Under direct illumination, the device achieves increased conversion efficiency from spectrum splitting. Under diffuse illumination, the device collects light with efficiency comparable to a flat-panel Si module. Design of the holographic lens is discussed. Optical efficiency and power output of the module under a range of illumination conditions from direct to diffuse are

simulated with non-sequential raytracing software. Using direct and diffuse Typical Metrological Year (TMY3) irradiance measurements, annual energy yield of the module is calculated for several installation sites. Energy yield of the spectrum splitting module is compared to that of a full flat-panel Si reference module.

9559-15, Session 4

Compound Holographic concentrating system for laterally arranged multiple band gap solar cells

Hiralal L. Yadav, Shivam Nigam, National Institute of Technology, Jamshedpur (India); Asghar Khan, Karim City College (India); N. R. Cakraborty, Kolhan Univ., Chaibasa (India)

To reduce the cost of solar photovoltaic power generation use of concentrators is an attractive proposition. This scheme replaces costly solar cell area with relatively smaller cell area still achieving same out-put power. However, such concentrators concentrate the entire solar spectrum on cells. The portion of solar radiation which does not match the band gap of solar cells degrades the absorber material by overheating. This also leads to fall in efficiency of performance of solar cells. To get rid of absorption of unwanted potion of solar spectrum, spectral splitting and their concentration on laterally arranged multiple band gap solar cells has been proposed and are being extensively investigated both using conventional optical elements and holographic optical elements.

In the present work, use of a compound holographic system consisting of diffraction grating and holographic lens has been proposed to disperse and focus different portion of solar spectrum on laterally arranged solar cells of different band gaps to achieve maximum efficiency operation. Recording, playback geometry and experimental results have been presented in detail. This system is light weight, low cost and can be produced easily.

9559-16, Session 4

Design of a holographic micro-scale spectrum-splitting photovoltaic system

Yuechen Wu, Shelby D. Vorndran, Silvana Ayala Pelaez, Juan Manuel Russo, Raymond K. Kostuk, The Univ. of Arizona (United States)

Micro-scale concentrating PV technology combines the high conversion efficiencies of concentrated photovoltaics (CPV) with the low costs and the simple form of flat panel PV. Some of the benefits of micro-scale PV include: reduced semiconductor material usage; improved heat rejection capacity; and more versatile PV cell interconnect configurations. Spectrum-splitting is also a beneficial technique to increase the efficiency and reduce the cost of photovoltaic systems. It spatially separates the incident solar spectrum into spectral components and directs them to PV cells with matching bandgaps. This approach avoids the current and lattice matching problems that exist in tandem multi-junction systems. In this paper, we apply the ideas of spectrum-splitting in a micro-scale PV system, and demonstrate a holographic micro-scale spectrum-splitting photovoltaic system. This system consists of an off-axis hologram in combination with a micro-lens array. An analysis methodology is developed to determine the optical efficiency of the resulting system, the special characteristics of the dispersed spectrum, and the overall system conversion efficiency when used with different PV cell combinations. Preliminary experimental system performance is also presented.



Sunday - Thursday 9 -13 August 2015 Part of Proceedings of SPIE Vol. 9560 Solar Hydrogen and Nanotechnology X

9560-1, Session 1

Low-cost and high-efficiency solar hydrogen conversion: On materials design and pilot-scale demonstration (Keynote Presentation)

Liejin Guo, Shaohua Shen, Xi'an Jiaotong Univ. (China)

Solar hydrogen conversion via water splitting is an important technology for energy and environment sustainability. Since the pioneering work of Fujisima and Honda in 1972, tremendous research on semiconductor-based photocatalytic and photoelectrochemical water splitting has yielded better understanding of the processes involved in solar hydrogen production, as well as encouraging development of high efficiency photocatalysts/ photoelectrodes for solar hydrogen generation. In the past 15 years, aiming at applicable solar hydrogen conversion in the near future, we have been focusing on the design of low cost and high efficiency semiconductors, which are completely composed of earth-abundant elements, as well as pilot-scale demonstration for large scale solar hydrogen production. In this article, we give a brief overview of recently developed all oxide-based photoanodes and cheap photocatalytic materials without any noble metals for solar water splitting, and also the principles and examples of pilot-scale demonstration for large scale solar hydrogen production.

9560-2, Session 1

Kinetically optimised sensitized TiO2 structures for solar energy conversion (Keynote Presentation)

Yasuhiro Tachibana, RMIT Univ. (Australia)

Sensitisation of nanocrystalline metal oxide has shown great potential as an efficient charge separation system for solar energy conversion devices. Following light absorption by the sensitizer, an electron and a hole can efficiently be separated at the sensitizer/metal oxide interface. A TiO2 nanocrystalline structure was typically employed as an electron acceptor material from the sensitiser. In contrast, a wide variety of sensitisers have been investigated to find a suitable combination with a TiO2 film. After the initial success with a ruthenium complex, typically organic dyes in addition to semiconductor quantum dots and a perovskite film have indicated superior performance as a suitable sensitiser.

To design efficient photovoltaic devices, one could improve photocurrent, however the open circuit photovoltage (Voc) was often decreased. For example, extension of a light absorption wavelength range increased light harvesting efficiency, and thus generated the increased number of photoelectrons (photocurrent). However, the cell often forfeited the Voc by this photocurrent increase. Thus, the design of an interfacial structure is required to increase Voc, while the photocurrent is maintained. In this presentation, we will show some designs to increase Voc without losing the photocurrent. Also, some novel systems to synthesize semiconductor nanocrystals will be demonstrated.

This work was financially supported by JST PRESTO program, Japan. The author also acknowledges Australian Research Council (ARC) LIEF grant (LE140100104) and the Office for University-Industry Collaboration, Osaka University, for the financial supports.

9560-3, Session 1

A theoretical study of photo-induced electron kinetics in composite photocatalytic system (Invited Paper)

Jun Jiang, Univ. of Science and Technology of China (China)

In any optoelectronic applications utilizing photo-excitations of functional materials, one has to efficiently harvest photo-excited electronic states in the materials towards high quantum efficiency. Using first-principle based theoretical tools, we have performed theoretical investigations on the photo-induced electron kinetics behavior in composite structures, including: 1) Develop a quantum mechanics/molecular mechanics simulation protocol for nonlinear spectroscopy of interesting composite-structures under the environmental fluctuations; 2) Develop a rate equation model based on density matrix to capture electronic movements and transitions in the photo-excited material and thereby reflect the inter- and intra-system interactions. Theoretical simulations together with experimental non-linear spectroscopy characterizations, reveal information for photon-electron interactions, electron-hole recombination, and charge migrations, most of which are of key importance for the design of composite photocatalytic systems.

Reference:

[1] Wang, L. L.; Ge, J.; Wang, A. L.; Deng, M. S.; Wang, X. J.; Bai, S.; Li, R.; Jiang, J.*; Zhang, Q.*; Luo, Y.; Xiong, Y. J.* Angew Chem. Int. Ed. 2014, 53, 5107–5111.

[2] Bai, Y.; et. al, Huang, W.X.*; Jiang, J.*, Xiong X. J.*, J. Am. Chem. Soc. 2014, 136, 14650.

[3] Li. R, et. al, Jiang, J.*, Zhang, Q.*, Xiong X. J.*, Adv. Mater. 2014, 26, 4783.
[4] Bai. S., et. al., Jiang, J.*; Zhang Q.*; Luo, Y.; Xie, Y.; Xiong, Y.*, Adv. Mater. 2014, 26, 5689.

[5] Bai, S.; Wang, X. J.; Hu, C.; Xie, M. L.; Jiang, J.*; Xiong, Y. J.* Chem. Commun. 2014, 50, 6094–6097.

9560-4, Session 2

In situ/operando soft x-ray spectroscopy characterization of interfacial phenomena in energy materials and devices (Keynote Presentation)

Yi-Sheng Liu, Per-Anders Glans, Jinghua Guo, Lawrence Berkeley National Lab. (United States)

In many important energy systems such as energy conversion, energy storage and catalysis, advanced materials and functionality in devices are based on the complexity of material architecture, chemistry and interactions among constituents within. To understand and thus ultimately control the energy conversion and energy storage applications calls for the in-situ/ operando characterization tools. Soft X-ray spectroscopy offers some unique features. We will present the instrumentation development of the in-situ/operando soft X-ray spectroscopic in the studies of catalytic and electrochemical reactions in the recent years, and reveal how to overcome the challenge that soft X-rays cannot easily peek into the high-pressure catalytic cells or liquid electrochemical cells. The unique design of in-situ/ operando soft X-ray spectroscopy instrumentation and fabrication principle are presented, and a number of experimental examples are given, including the nanocatalysts and the recent experiment performed for studying the hole generation in a specifically designed photoelectrochemical cell under operando conditions.



9560-5, Session 2

Metal-complex/semiconductor hybrids for carbon dioxide fixation (Invited Paper)

Kazuhiko Maeda, Tokyo Institute of Technology (Japan)

Recently, we reported that carbon nitride (C3N4) functions as a stable photocatalyst for water reduction and oxidation under visible light (> 420 nm). Even though C3N4 is an organic semiconductor, it is capable of oxidizing water into O2 with the aid of a water oxidation cocatalyst like RuO2. The ability of C3N4 to produce O2 from water is very attractive when we construct a CO2 reduction photosystem that is workable using water as an electron source. On the other hand, certain metal complexes based on rhenium or ruthenium are known to catalyze CO2 reduction to CO or HCOOH photocatalytically or electrochemically with high selectivity and quantum yields, although the oxidation ability is relatively low. With these backgrounds, we studied C3N4 as a component of a CO2 photoreduction system that operates under visible light using a metal complex as a cocatalyst. It was found that a hybrid photocatalyst consisting of C3N4 and a small fraction of a ruthenium(II) complex having proper reduction potential and an anchoring group, which respectively work as lightharvesting unit and a catalytic center for CO2 reduction. This simple binary composite, is capable of converting CO2 into HCOOH with a selectivity of >80% and a turnover number of >1000, both of which are the highest among heterogeneous photocatalytic CO2 reduction systems reported to work under visible light.

9560-6, Session 2

The heteropolyacid based photocatalytic intercalated nanomaterials

Jihuai Wu, Jianming Lin, Miaoliang Huang, Huaqiao Univ. (China)

Energy and environment are two issues of the human's top ten problems for the next 50 years. It is indispensable to search new photocatalytic materials in order to solve the issues. The photocatalytic production of hydrogen from water using semiconductor materials is of great interest due to its possible application for converting the sunlight energy into chemical energy. Incorporation of a semiconductor catalyst in the interlayer region of a lamellar compound is a promising method for fabricating an intercalated nanomaterial consisting of host layers with ultrafine particles in the interlayer and enhancing photocatalytic activity of the semiconductor. We have done the researches on the heteropolyacid-based (such as HTaWO6, H2Ca4Ta2Nb4O20, HLaNb2O7, HLaTaxNbyO7, etc) photocatalytic intercalated nanomaterials, including in intercalating type, doping type and loading type nanocomposites. Owing to their layered structure, large specific surface area, small semiconductor size, host-guest coupling effect and quantum size effect, these intercalated nanomaterials show eminent photocatalytic activities. For instances, under irradiation with wavelength less than 290 nm from a 450-W mercury arc, photocatalytic hydrogen yield reach 240, 232, and 220 cm3•h-1?g-1 for photocatalytic materials HLaNb2O7/(Pt,TiO2), H2Ca4Ta2Nb4O2O, and HTaWO6/(Pt, TiO2), respectively, which are higher 70 times than the commercial TiO2 (P25) photocatalyst. Meanwhile, these heteropolyacid-based intercalated nanomaterials have excellent ability for photocatalytic degradation of wastewater, which can be used in environmental improvement. The preparation, composition, structure, properties, formation and photocatalytic mechanism are discussed in this paper.

9560-42, Session 2

Developing plasmonic nanostructures towards enhanced photocatalytic activity (*Invited Paper*)

Dongling Ma, Institut National de la Recherche Scientifique (Canada)

Plasmonic metallic (e.g. Au & Ag) nanostructures have attracted extensive interest in the last decade due to their unique surface plasmon resonance (SPR). SPR arises from collective oscillations of free electrons in plasmonic structures, which can interact with light in a resonant manner and scatter light strongly. It is also characterized by the generation of intense electric fields near the surface. The recent application of plasmonic nanostructures in photocatalysis (including solar water splitting) has led to a new, active research area of plasmon-enhanced photocatalysis. Although exact mechanisms remain elusive in many cases and sometimes can be even controversial for the same materials, the performance enhancement has been confirmed. Herein, I will present some of our recent development in plasmonic nanostructures, their hybridization with semiconductor nanomaterials and the applications of these nanohybrids in photocatalysis. One specific example is about the development of a simple and functionalization-step-free solution process to fabricate nanocomposites made of BiFeO3 nanowires and Au nanoparticles fabricated by pulsed laser ablation in water. The Au nanoparticle-decorated BiFeO3 nanowires exhibit ~30 times higher photocatalytic activity for water oxidation than that exhibited by the Au-free nanowires. Another example is about an integrated nano-architecture, rationally designed to include wide wavelength absorbing nanomaterial, visible-absorbing plasmonic nanocomponent, and high surface-area semiconductor component all in one single structure to maximize photon harvest, beneficial component interactions and thereby photocatalytic efficiency. In addition to introducing new nanohybrids and their photocatalytic activity, the relevant mechanisms (charge transfer and energy transfer) in these specific systems will also be discussed.

9560-204,

Solar hydrogen: harvesting light and heat from sun

Liejin Guo, Xi'an Jiaotong Univ. (China)

My research group in the State Key Laboratory of Multiphase Flow in Power Engineering (SKLMF), Xi'an Jiaotong University has been focusing on renewable energy, especially solar hydrogen, for about 20 years. In this presentation, I will present the most recent progress in our group on solar hydrogen production using light and heat. Firstly, "cheap" photoelectrochemical and photocatalytic water splitting, including both nanostructured materials and pilot-scale demonstration in our group for light-driven solar hydrogen (artificial photosynthesis) will be introduced. Then I will make a deep introduction to the achievements on the thermaldriven solar hydrogen, i.e., biomass/coal gasification in supercritical water for large-scale and low-cost hydrogen production using concentrated solar light.

9560-48, Session PMon

Preparation of N2-plasma assisted visible light active ordered mesoporous nitrogen doped TiO2 thin films for solar energy conversion

Syed Z. Islam, Allen D. Reed, Doo-Young Kim, Stephen E. Rankin, Univ. of Kentucky (United States)

The optical and electronic properties of TiO2 thin films provide tremendous opportunities in several applications including photocatalysts, photovoltaics and photoconductors for energy production and environmental remediation. Despite the attractive features of TiO2 such as low cost and stability under a wide range of conditions, one critical challenge is the innate inability of TiO2 to absorb visible light from the solar spectrum due to its high band gap. In this study, this shortcoming is addressed by doping cubic ordered mesoporous TiO2 thin films (N-TiO2) using nitrogen/argon (N2/Ar) plasma. This represents a rapid, scalable approach to high surface, controlled nanostructure thin films for photocatalytic applications. First, cubic ordered nethod using TiCl4 as precursor and triblock copolymer Pluronic F-127 as the template. Subsequently, the calcined TiO2 films are treated with N2/Ar



plasma under controlled conditions of reaction gas pressures, microwave power, and plasma exposure duration. The primary variable studied here for N-TiO2 films is the duration of plasma exposure (0-210 min). After doping, the films are confirmed to have an accessible, well-ordered cubic mesopore structure by SEM, TEM, STEM and XRD analyses. XPS analysis shows that 2-3% substitutional nitrogen is present in the doped films and that the doping level increases with plasma treatment duration. UV-visible absorbance spectra of N-TiO2 films indicate the enhancement of absorption of visible light and reduction of the bandgap. Finally, the visible-light photocatalytic activity of N-TiO2 films is determined from the photocatalytic degradation of methylene blue under illumination with a visible-light LED. The N-TiO2 films prepared with 150 min plasma treatment show the best photocatalytic activity, with a first-order methylene blue rate coefficient that is 6 times greater than that of undoped TiO2 films. Preliminary experiments also show that the plasma-processed N-TiO2 films on conductive substrates show better visible-light photoelectrochemical activity than undoped TiO2 for hydrogen generation by water splitting.

9560-8, Session 3

A dynamic perspective on charge carriers in quantum-dot sensitized metal oxide nanostructures for photoelectrochemical solar hydrogen generation (Keynote

Presentation)

Jin Zhong Zhang, Univ. of California, Santa Cruz (United States)

Small bandgap semiconductor quantum dots (QDs) are promising sensitizers for metal oxide nanostructures in photoelectrochemical water splitting for hydrogen generation by expanding light absorption into the visible region. Among the several critical steps for charge carriers in this approach, electron transfer (ET) from the QD to MO and charge transport (CT) inside the MO are two of the most important. In one example, we have studied how linker molecules between QD and MO can affect the ET based on ultrafast laser studies. Arene substituted (ortho, meta and para) bifunctional molecular linkers of the HS-[C6H4]-COOH type are designed and employed to link CdSe QDs to TiO2. Interestingly, the CdSe-TiO2 sample with a para substituted linker (representing the longest distance between CdSe and TiO2) shows the best PEC performance as compared to ortho and meta substituted linkers. The ET rate is consistent with PEC measurements in that the CdSe-TiO2 sample with a para substituted linker shows the highest ET rate. Density functional theory (DFT) calculations have been carried to gain insight into the ET mechanism behind. In the meantime, we have explored how to use chemical treatment of the MO to improve CT by introducing bandgap states that serve to mediate electron and hole transport. Furthermore, we have recently started to explore the possibility of using organolead halide peroskite QDs (PQDs) as sensitizers for MO with a focus on understanding the role of bandgap states and their relation to instability of the PQDs, which has important implication for photovoltaic as well as PEC applications.

9560-9, Session 3

Enabling overall water splitting with hematite and Si (Invited Paper)

Dunwei Wang, Boston College (United States)

An important challenge in fulfilling the promises held by photoelectrochemistry water splitting as a solar energy harvesting technology is the mismatch of photocathode and photoanode performance. Often, the photovoltages of the photoanodes are too low, and the turnon potentials are too positive. Similarly, the turn-on potentials of the photocathodes are too negative, making it difficult, sometimes impossible, to achieve complete water splitting without applying external potentials. Here using hematite as a study platform, we examine what limits the turnon potentials in photoelectrochemistry water splitting. Our results show that the poor performance is a combination of unwanted potential drop in the Helmholtz layer that does not contribute to charge separation within the semiconductor photoelectrode and potential loss on the surface the photoelectrode due to structural disorders. We present our strategies to correct these deficiencies. The potential drop in the Helmholtz layer can be harnessed and put back into the semiconductor by depositing catalytic layers such as amorphous NiFeOx. The structural disorders can be readily fixed by a regrowth strategy. Through these simple treatments, we are able to increase the photovoltage of hematite from 0.24 V to 0.80 V, and the turn-on voltage of hematite is lowered to 0.45 V. Complete water splitting at an overall efficiency of 0.91% is achieved by combining hematite with amorphous Si photocathode.

9560-10, Session 3

Insight into materials properties for a photo electrochemical based solar refinery (*Invited Paper*)

Joan Ramón Morante, Institut de Recerca en Energia de Catalunya (Spain) and The Univ. de Barcelona (Spain)

Photo electrochemistry, PEC, processes have attracted great attention as an effective procedure for convert solar photon energy to chemical one. PEC units can produce different solar fuels such as hydrogen, formic acid, methanol, methane or syngas depending on the selected catalyst and the used feed stocks of H2O and CO2. It is always produced with an improved energy balance compared with dark electro catalysis processes. Moreover, it shows a high throughput depending on the used photons absorbed material as well as on the capacity for charge separation and effective role of the used catalyst for cathode and anode electrodes. Different routes for reaching efficiency higher than 10-12% of efficiency have been promoted.

In this contribution, different electrode material option will be reviewed. Example will be presented and charge transfer coefficient discussed from the fine surface characterization. Moreover, the potential use of earth abundant alternative will be discussed considering costs, life time and high yield in the solar fuel production according to the different used catalyst for CO2 reduction. Special attention will be paid on the application of initially photovoltaic absorber materials like silicon, kesterite or CIS combined with protective and photo catalytic active metal oxide layers in order to scale up PEC systems in order to achieve solar refinery yields.

9560-11, Session 4

Surface science insights into surface and interface properties of photoelectrocatalysts for solar fuels (Keynote Presentation)

Bruce E. Koel, Coleman X. Kronawitter, Peng Zhao, Zhu Chen, Princeton Univ. (United States)

A surface science approach can greatly advance understanding of the structure and reactivity of photoelectrocatalysts for solar fuels. Such experiments use well-defined model catalysts under controlled conditions and utilize a range of spectroscopic techniques for characterization of surface and interface properties and the nature and reactivity of surfacebound species. We report on several of our recent studies, which include investigations of the effects of dopant incorporation on the structural and chemical properties of the ?-Fe2O3(0001) surface for water oxidation catalysis, facet-dependent activity and stability of Co3O4 nanocrystals towards OER, and the interaction of water with GaP(110), a semiconductor that is known to enable selective CO2 reduction to methanol in aqueous solutions of CO2 and nitrogen-containing heteroaromatics. For water oxidation on ?-Fe2O3, we found that Ni doping in thin films of model catalysts caused a new termination for the films and induced formation of more stable surface-bound OH groups. For the Co3O4 system, we used the well-defined morphologies of nanocubes and nanooctahedra to demonstrate that the (111) surfaces vastly out-perform the (100) surfaces for OER activity (overpotential and current density). Finally we have



spectroscopically identified in situ the surface-bound species on GaP(110) associated with exposure to water using ambient pressure photoelectron spectroscopy (APPES). These observations on model systems afford further analysis and discussion of the role of surface-bound species in mechanisms for catalyzed water oxidation and CO2 reduction.

9560-12, Session 4

Surface chemistry of molecular catalysts on model photoelectrodes for solar fuels by CO2 reduction (*Invited Paper*)

Coleman X. Kronawitter, Peng Zhao, Bruce E. Koel, Princeton Univ. (United States)

The surface chemistry of catalyst and solvent molecules on photoelectrodes relevant to the production of solar fuels by CO2 reduction is explored by analysis of model systems. At its heart the electroreduction of CO2 is an electrochemical process, but assessing the mechanism of CO2 reduction at semiconductor/catalyst junctions using electrochemistry techniques alone is challenging because of the complex physical chemistry involved in chemical synthesis. Using the presented experimental surface science approach, ultrahigh vacuum conditions are used to facilitate the fabrication of highly characterizable electrode-adsorbate systems, and the use of single crystal surfaces permits analysis of surface chemistry independent of complicating factors such as grain boundaries and morphology. Surface-sensitive corelevel and vibrational spectroscopy measurements on the model systems are used to supplement electrochemistry investigations, and generate unique information describing the role of the electrode surface in CO2 reduction. Specifically the preferential adsorption sites and bonding interactions and reactivities of catalysts and intermediates on III-V semiconductors are considered. Conclusions from experimental results are supported by calculations using density functional theory. This work assists in generating a molecular-level understanding of the heterogeneous processes important to the reaction mechanism of efficient photoelectrocatalytic fuel generation.

9560-13, Session 4

Photocatalytic hydrogen production over CdS: Effects of reaction atmosphere studied by in situ Raman spectroscopy

Lijing Ma, Liejin Guo, Xi'an Jiaotong Univ. (China)

CdS is a well-known efficient photocatalyst for photocatalytic hydrogen production. However, CdS is prone to photocorrosion in the photocatalytic reaction where CdS itself is oxidized by the photogenerated holes. Most of the work reported up to now only focused on the structure of CdS itself. Less attention was, however, paid to the kinetic changes of CdS during photocatalytic reaction, which, in our opinion, is crucial step for its practical utilization. In this report, we developed a facile in situ Raman analysis, aiming to clarify the microstructure changes of CdS during the photocatalytic reaction process. In this study, photocatalytic hydrogen production over CdS in Ar or air atmosphere was studied by various techniques besides of the in-situ Raman. With Raman spectrum, a significant increase in surface lattice strain of CdS is observed only when it is exposed to air, while electron-phonon interactions remain the same regardless of the atmosphere. A direct correlation between interfacial crystal lattice and photo-corrosion of sulfide photocatalyst during its photocatalytic hydrogen production was found based on our in-situ Raman investigation. Finding of photo-corrosion of sulfide photocatalyst at its very early stage with our in-situ Raman technique is expected to provide meaningful guidance for the design of active and stable chalcogenide photocatalysts, which, however, cannot be achieved by traditional characterizing techniques.

9560-14, Session 5

Synchrotron-based spectroscopy for solar energy conversion (Keynote Presentation)

Franz J. Himpsel, Univ. of Wisconsin-Madison (United States)

This overview talk illustrates how synchrotron-based spectroscopy with soft X-rays can contribute to the discovery of new materials for solar cells and solar fuel synthesis. The primary techniques are photoelectron spectroscopy and absorption spectroscopy with soft X-rays, which complement each other in probing occupied and empty electronic states. Both are element-and bond-specific, with absorption spectroscopy also sensitive to the bond orientation [1]. Close coupling with density functional calculations enables discovery and exploitation of systematic trends. Case studies will be presented, such as donor-pi-acceptor complexes for solar cells [2] and hematite nanorod arrays for water splitting [3]. In addition to the energy levels one has to consider the lifetime of the photo-generated carriers. Fourth-generation laser-like synchrotron light sources are on their way which are capable of pump-probe experiments that follow excited charge carriers in real time across a molecular complex or through the charge transport layers in a device.

[1] F. J. Himpsel et al., Design of Solar Cell Materials via Soft X-ray Spectroscopy, J. Electron Spectrosc. Relat. Phenom. 190, 2 (2013).

[2] I. Zegkinoglou et al., Spectroscopy of Donor- ϖ -Acceptor Porphyrins for Dye-Sensitized Solar Cells, J. Phys. Chem. C 117, 13357 (2013).

[3] C. X. Kronawitter et al., Titanium Incorporation into Hematite Photoelectrodes: Theoretical Considerations and Experimental Observations, Energy Environ. Sci. 7, 3100 (2014).

9560-15, Session 5

Interfacial atomic and electronic structure of energy-related material characterized by synchrotron x-ray spectroscopy (Invited Paper)

Chung-Li Dong, National Synchrotron Radiation Research Ctr. (Taiwan)

Owing to the global energy crisis, the scientists are devoted to search new sources of clean energy that meet the human demand for energy. The search for new energy materials that have efficient energy conversion/ generation/storage is one of the most pressing technological challenges. In many promising energy systems such as solar hydrogen, nanostructured catalysts, and smart materials, the interfacial atomic and electronic structure provide the fundamental understanding of the physical and chemical properties of a material. Understanding of these interfacial phenomena is critical and thus can pave a way to better design the material and control the performance. Synchrotron-based x-ray spectroscopy, including x-ray absorption and x-ray emission spectroscopies can be used to investigate the local unoccupied and occupied electronic states. The electronic structure in the conduction band and valence band thus can be obtained. With in situ/in operando technique, it is possible to monitor the change of atomic/electronic structures of an energy material under its working environment. This presentation will report the emerging in situ/in operando characterization based on synchrotron x-ray spectroscopy. A number of recent studies of human-engineered photosynthesis, smart materials, catalytic and electrochemical reactions will be presented.



9560-16, Session 5

Thin film catalyst integration onto silicon: Engineering materials and interfaces for efficient and stable photoanodic water oxidation (Invited Paper)

Ian D. Sharp, Jinhui Yang, Lawrence Berkeley National Lab. (United States)

We provide an overview of different approaches to achieving durable silicon photoanodes and highlight two specific examples of how catalyst integration can be used to improve activity and chemical stability. In the first example, we show that plasma-assisted atomic layer deposition (PE-ALD) of cobalt oxide onto silicon enables efficient and sustained photoelectrochemical water splitting under alkaline conditions. While ALD has recently emerged as a powerful tool for protection of photoelectrodes from corrosion, the composition and structure of deposited materials often differ significantly from those synthesized by other methods. We find that low temperature PE-ALD provides access to structurally disordered, yet conformal, layers that are characterized by higher concentrations of active sites. Engineering the catalyst and the semiconductor/catalyst interface at the nanoscale is essential for simultaneously achieving efficient charge extraction and chemical stability. This work offers insight into the role of structural disorder on catalytic activity and provides a path to higher performance photoelectrodes for solar fuels systems. In the second example, we investigate water oxidation using silicon photoanodes under acidic conditions; at present, the only known catalysts this reaction under acidic conditions are based on iridium or ruthenium. Therefore, it is important to develop integrated semiconductor/catalyst assemblies that minimize the total quantity of catalyst, retain photocatalytic activity, and promote chemical stability. To this end, we have developed multi-layer coatings on silicon that allow photogenerated charge to be efficiently transferred between the light absorber and an ultrathin surface layer of iridium oxide, without adversely affecting the generated photovoltage. In this way, we are able to achieve stable and efficient water oxidation under acidic conditions, while substantially reducing the required quantity of extremely rare iridium in the system. The examples presented here highlight that, although few materials are inherently stable under conditions required for artificial photosynthesis, controlled catalyst integration provides a viable approach to sustained operation in a variety of harsh environments.

9560-17, Session 5

High aspect ratio WO3 nanorod arrays based WO3/BiVO4 Heterojunction for photoelectrochemical water splitting

Jinzhan Su, Xi'an Jiaotong Univ. (China)

Recently, WO3/BiVO4 heterojunction have been investigated and proved to be a good structure for photoelectrochemical water splitting under visiblelight irradiation. In this report, we grew high aspect ratio by annealing ammonium tungsten bronze ((NH4)0.33•WO3) nanorods grown on FTO substrate via a modified solvothermal method and followed with BiVO4 coating by pulse laser deposition. The WO3/BiVO4 heterojunction was characterized by X-ray diffraction (XRD), Raman spectroscopy, and scanning electron microscopy (SEM) and X-ray Photoelectron Spectroscopy (XPS). WO3 nanorod arrays are conformally covered with a BiVO4 layer and a core-shell structure was formed. The WO3/BiVO4 heterojunction promoted the charge carrier separation due to their appropricate band edge positions alignment. The high aspect ratio WO3 nanorod arrays provided larger surface for heterojunction formation which further enhance the performance of nanostructural heterojunction. The photoelectrochemical results showed that the photocurrent was improved compared to bare WO3 nanorod arrays.

9560-18, Session 6

Rational design of titania-based functional nanostructures (Keynote Presentation)

Yadong Yin, Univ. of California, Riverside (United States)

We discuss our recent efforts in the design and architectural control of titania nanostructures and their applications. We first review the synthesis, crystallinity control, and photocatalysis of TiO2 porous nanostructures by discussing several methods for changing the structures from amorphous to crystalline and subsequently ways for enhancing the crystallinity, including those involving the "silica-protected calcination" and "partial etching and re-calcination" strategies. We also discuss the photocatalytic applications of the TiO2 nanoshells and the methods for improving their catalytic activities. In particular, we demonstrate a sandwich-structured photocatalyst that shows an excellent performance in degradation reactions of a number of organic compounds under UV, visible light, and direct sunlight. We will also report a new color switching system based on reversible redox reaction that could be initiated by photocatalytic response of TiO2 nanocrystals. With the assistance of TiO2 nanocrystal-based photocatalysts, UV light irradiation can rapidly reduce the imaging materials and result in obvious color change, while the recoloration can be achieved by re-oxidizing the system with the assistance of visible light irradiation or heating. The excellent performance of the new color switching system promises their potential applications as attractive rewritable media to meet our society's increasing needs for sustainability and environmental conservation.

9560-19, Session 6

From UV/visible to near-infrared light activity: Recent progress in photocatalysis (Invited Paper)

Hong Liu, Shandong Univ. (China)

Photocatalysis is a practical methodology for degradation of organic pollutant for environmental application and hydrogen generation for renewable power source application. Although in most cases the light used for photocatalysis research and application is still artificial light sources at present, the solar light is the real target for for practical photocatalysis. However, up to now, most available photocatalysts are UV and visible or UV-visible light active semiconductor with broad band gap, and there is only a few methods or photocatalyst can realize NIR photocatalystic activity. Therefore, design or find NIR light active photocatalysts and building UV-Vis-NIR full solar light photocatalysis system is great challenge for full utilization of solar energy in environmental and clean energy fields.

Recent years, several methods have been suggested to convers NIR light to visible or UV light and realized NIR light photocatalysis by light conversion nanoparticle-semiconductor hybrid photocatalysts. Most recently, our group proposed to use some semiconductor with impurity energy level, and semiconductor with narrow band gap to achieve NIR light photocatalysis. Based on this mechanism, some oxides, such as Ag2O and Bi2WO6, and some cholcogenides, such as WS2 and In2S3, were discovered to possess high NIR light photocatalytic activity, and some of them possess high photocatalytic properties in UV-Vis-NIR full solar spectrum photocatalytic property.

In this talk, we will summary the principle for design full solar light spectrum photocatalysis systems, or finding new NIR photocatalyst. Several new NIR and full solar spectrum light photocatalysts will be introduced. In addition, the application of full solar light photocatalysts will be reviewed.

9560-20, Session 6

Preparation of Cu2O/TiO2 nanotube arrays and its photoelectrochemical properties as hydrogen-evolving photoanode

Lixia Sang, Jing Zhang, Beijing Univ. of Technology (China)



Cu-based nanomaterials have become a popular sensitizer of TiO2 due to their advantages of low cost, non-toxic, good catalytic activites, narrow band gap, which can replace quantum dots CdS and PbS containing toxic elements Cd and Pb. Cu2O is an environment-friendly p-type semiconductor with narrow band gap (2.0~2.2eV). The present work is focus on the preparation of Cu2O/TiO2 nanotube arrays heterostructures via electrochemical deposition. TiO2 nanotube arrays were prepared by anodic oxidation method and calcined at 450?, then Cu2O were deposited on TiO2 nanotube arrays in a three-electrode system with or without surfactants PVP at different deposition voltages (-0.2V,-0.3V,-0.4V) and different deposition time (5min, 10min, 15min). The results show that the size of Cu2O nanoparticles remarkable decreased with the help of surfactants PVP, and Cu2O deposited on the inner and outer walls of TiO2 nanotube. The resulting Cu2O/TiO2 nanotube arrays have the significant photo response in visible light region. Under irradiation of solar simulator (AM1.5,100mW/cm2), the photocurrent density of the Cu2O/TiO2 nanotube arrays is more than that of pure TiO2 nanotube arrays when Cu2O was deposited at a voltage of -0.3V. In addition, combined with the calculation and analysis of flat band potential, charge carrier density and electron lifetime, the effects of different deposition time and voltage on the photoelectrochemical properties of Cu2O/TiO2 nanotube arrays were further dissicussed.

9560-21, Session 7

Electron dynamics at semiconductormolecule interfaces: Insights from firstprinciples dynamics simulation (Keynote Presentation)

Yosuke Kanai, The Univ. of North Carolina at Chapel Hill (United States)

Dynamics of excited electrons at semiconductor-molecular interfaces is responsible for a number of key interfacial processes of various solar energy conversion and opto-electronic technologies. These processes include interfacial electron transfer and non-radiative recombination. In this talk, I will discuss our recent efforts in my group for addressing several challenges in understanding how atomistic details influence these processes using analytical models with inputs from first-principles calculations and also with first-principles electron dynamics simulations. I will discuss several key aspects of the electron transfer and hot electron relaxation in context of EFRC on Solar Fuels at UNC Chapel Hill. I will also discuss how the results from atomistic theories pose a conceptual challenge when characterizing these interfacial electron processes with a simple kinetic model at these complex interfaces.

9560-22, Session 7

Solution-processed photocathodes for solar water splitting tandem cells (Invited Paper)

Kevin Sivula, Néstor Guijarro, Florian Le Formal, Ecole Polytechnique Fédérale de Lausanne (Switzerland)

A practical solar water splitting device that can produce H2 at a cost less than PV + electrolysis is difficult to envision without it possessing a simple construction that employs widely available materials and inexpensive processing techniques. A tandem cell consisting of 2 solution-processed photoelectrodes (photoanode/photcathode) can reasonably reach this goal. While n-type oxide semiconductors have been established as viable photoanode materials, cheap and stable p-type photocathodes are less developed. In this presentation our groups' progress in the development of solution-processed stable photocathodes is presented and their application toward overall photoelectrochemical water splitting tandem cells is demonstrated. Three classes of promising materials are discussed: copper-based oxides in the delafossite phase, ternary and quaternary chalcogenides, and 2D transition metal chalcogenides. In each case the challenges to maximize photogenerated charge collection in thin films prepared by solution-based deposition approaches are highlighted and the use of bottom-up nanostructuring to gain insight into routes for improvement and overcome these challenges are established. The optimization of these materials for solar water reduction using overlayers and catalysts, and the stability under reasonable operation conditions are addressed. Routes to improve the unassisted and overall solar water splitting performance in tandem cells with commonly used oxide photoanodes are finally outlined.

9560-23, Session 7

Exploring the time-scale of photo-initiated interfacial electron transfer through firstprinciples interpretation of ultrafast X-ray spectroscopy (Invited Paper)

David Prendergast, Lawrence Berkeley National Lab. (United States)

With the advent of X-ray free electron lasers and table-top high-harmonicgeneration X-ray sources, we can now explore changes in electronic structure on ultrafast time scales -- at or less than 1ps. Transient X-ray spectroscopy of this kind provides a direct probe of relevant electronic levels related to photoinitiated processes and associated interfacial electron transfer as the initial step in solar energy conversion. However, the interpretation of such spectra is typically fraught with difficulty, especially since we rarely have access to spectral standards for nonequilibrium states. To this end, direct first-principles simulations of X-ray absorption spectra can provide the necessary connection between measurements and reliable models of the atomic and electronic structure. We present examples of modeling excited states of materials interfaces relevant to solar harvesting and their corresponding X-ray spectra in either photoemission or absorption modalities. In this way, we can establish particular electron transfer mechanisms to reveal detailed working principles of materials systems in solar applications and provide insight for improved efficiency.

9560-24, Session 8

Nanoscale junctions for water splitting photocatalysis (Keynote Presentation)

Frank E. Osterloh, Benjamin A. Nail, Jing Zhao, Jiarui Wang, Kathryn A. Newton, Yuxin Yang, Po Wu, Zongkai Wu, Geetu Sharma, Univ. of California, Davis (United States)

Photochemical charge generation, separation, and transport at nanocrystal interfaces are central to photoelectrochemical water splitting, a pathway to hydrogen from solar energy. Here we use surface photovoltage spectroscopy (SPS) to probe these processes in nanocrystal films of photoanode and photocathode materials, incl. WO3, NiO, C3N4, M:SrTiO3, HCa2Nb3O10, CdSe, p-Si, and BiVO4. Charge injection between nanoparticles can be observed, as well as redox reactions at nanocrystal-liquid interfaces. The ability to monitor these voltage-generating processes with SPS provides new insight into nanoscale charge separation and promotes the development of nanocrystal applications in photoelectrochemical cells, photovoltaics, and as solar fuels photocatalysts.

9560-25, Session 8

Rapid flame processing of metal oxides photoanodes for enhanced solar watersplitting (Invited Paper)

Xiaolin Zheng, Stanford Univ. (United States)

Photoelectrochemical (PEC) water splitting is the simplest and cleanest route that directly converts sun light to hydrogen and potentially it will

232



enable a low cost production of hydrogen. One of the biggest challenges for the realization of the PEC water splitting is to develop an efficient photoanode having a good light absorption, fast charge transport and transfer properties simultaneously. Typically metal oxides are considered to be good candidates because of their excellent photochemical stability and low cost. However, their poor material quality, such as large amount of defects, low surface area, low charge carrier's mobility/conductivity, which largely originated from the preparation method, limits the charge transport and transfer properties.

In this talk, I will present two novel flame processing techniques, i.e., flame reduction and doping, for metal-oxide photoanodes that allows to greatly improve the charge transport and transfer properties, hence improving the PEC water-splitting performance. First, we developed a rapid flame reduction method to generate controllable amount of oxygen vacancies in TiO2 nanowires (NWs) that leads to nearly three times improvement in the PEC water-splitting performance. The flame reduction method has unique advantages of a high temperature (>1000 oC), ultra-fast heating rate, tunable reduction environment, and open-atmosphere operation, so it enables rapid formation of oxygen vacancies (<1min) near the surface region without damaging the nanowire morphology and crystallinity, and even applicable to various metal oxides. Second, we designed an ex-situ novel doping method which combines versatile solution phase chemistry and rapid flame annealing process (i.e., Sol-Flame) to dope TiO2 NWs with cobalt (Co). The sol-flame doping method not only preserves the morphology and crystallinity of the TiO2 NWs, but also allows fine control over the Co dopant profile by varying the concentration of Co precursor solution. Finally, we extended the sol-flame doping method to codope TiO2 NWs with tungsten and carbon (W, C) by sequentially annealing W-precursor coated TiO2 nanowires in flame and CO gas. This is the first experimental demonstration that codoped TiO2:(W, C) nanowires outperform monodoped TiO2:W and TiO2:C and double the saturation photocurrent of undoped TiO2 for PEC water-splitting.

9560-26, Session 8

NH3-treated MoS2 nanosheets for enhanced H2 evolution under visible-light irradiation

Jinwen Shi, Yazhou Zhang, Liejin Guo, Xi'an Jiaotong Univ. (China)

Energy shortage and environmental pollution have become two urgent problems that restrict social development and endanger human survival. In order to resolve the two issues to realize the sustainable development of society, the most effective route is the active development and utilization of clean and renewable energy sources. Exploring and realizing the conversion and storage of solar energy as hydrogen energy is a powerful route to develop and utilize renewable energy. Correspondingly, it is a key task to exploit photocatalysts with high stability, high efficiency, low cost for visiblelight-driven H2 evolution.

Herein, a series of novel photocatalysts (designated as MoS2-N) were explored by treating the MoS2 nanosheets (designated as MoS2), which were prepared by a hydrothermal reaction using Na2MoO4•2H2O as Mo source and CH3CSNH2 as S source, in a tube furnace under flowing NH3 atmosphere at different temperatures. The physiochemical properties of samples were systematically investigated by different instrumental characterizations, and the H2-evolution photocatalytic properties of samples were evaluated, by using HCOOH as the sacrificial reagent and using in-situ photodeposited Pt as the cocatalyst, under visible-light irradiation (? > 420 nm). It was found that, compared with MoS2 that showed no photocatalytic activity due to the lower conduction band position than the redox potential of H+/H2, MoS2-N showed considerable photocatalytic activity due to the high-temperature NH3 treatment that evidently modified the physiochemical properties of pristine MoS2 nanosheets and thus was beneficial for photocatalytic H2 evolution.

9560-27, Session 9

On the surface, confinement, and dimensionality effects of large bandgap oxide semiconductors (Keynote Presentation)

Lionel Vayssieres, Xi'an Jiaotong Univ. (China)

An overview and the latest achievements in surface, dimensionality and confinement effects on large bandgap oxide semiconductors will be presented. The development of low cost visible light-active metal oxide heteronanostructures consisting of earth abundant elements is of crucial importance for the large scale implementation of hydrogen-based energy. Controlled aqueous-based solution chemistry allows the growth of transition metal oxides with tailored orientation, dimensionality and surface chemistry onto various substrates with great purity. For instance, quantum dots grown on the surface of vertically oriented quantum rods can be entirely fabricated from aqueous metal salts without surfactant and at low temperature. These all-oxide heteronanostructures show intermediate bands for efficient visiblelight conversion and highly quantized band structure for band/bandgap engineering. Such unique characteristics, combined with the in-depth investigation of their electronic structure at synchrotron radiation facilities, optical, structural and transport properties provide better fundamental understanding of the energetics and structure-property relationships as well as key trends for efficiency optimization of solar water splitting in neutral aqueous solutions.

9560-28, Session 9

Photocatalytic water splitting: Using a 2-photon approach (Invited Paper)

Brian J. Seger, Bastian Timo Mei, Dowon Bae, Mauro Malizia, Thomas Pedersen, Peter C. Vesborg, Ole Hansen, Ib Chorkendorff, Technical Univ. of Denmark (Denmark)

Modelling has shown that to optimize photoelectrolysis efficiency, a 2 photon tandem device (back to back photocatalysts) should be used. The underlying principle is that one photocatalyst should absorb high energy photons (large band gap) while the other absorbs the low energy photons (small band gap). In theory, either the H2 evolution reaction or the O2 evolution can take place on the large band gap material with the opposite reaction taking place on the small band gap material. I will discuss both possibilities and show how this affects optimal material properties needed for the photocatalysts.

Finding an optimal photocatalyst system can be very difficult, thus we break the water splitting process into 3 parts: 1) Photoabsorption, 2) Photoabsorber/Electrolyte interface and 3) H2 or O2 evolution catalysis. In this talk I will discuss our use of Si, GaP, and Perovskites as photoabsorbers and what we do to maximize photovoltage. To prevent corrosion at the photoabsorber/electrolyte interface we use corrosion protection layers. I will show how TiO2 is a great material for protecting the H2 evolution photocatalyst, whereas NiO is excellent at protecting the O2 evolution catalyst. I will also show our work on improving both the H2 evolution and O2 evolution catalysts.

9560-29, Session 9

Photocatalytic evolution of molecular hydrogen and oxygen over La-doped NaTaO3 particles: Effect of different cocatalysts (Invited Paper)

Irina Ivanova, Leibniz Univ. Hannover (Germany); Tarek Kandiel, Sohag Univ. (Egypt); Amer Hakki, Ralf Dillert, Detlef W. Bahnemann, Leibniz Univ. Hannover (Germany)



To solve the global energy and environmental issues highly efficient systems for solar energy conversion and storage are needed. One of them involves the photocatalytic conversion of solar energy into the storable fuel molecular hydrogen via the water splitting process utilizing metal-oxide semiconductors as catalysts. Since photocatalytic water splitting is still a rather poorly understood reaction, fundamental research in this field is required.

Herein, the photocatalytic activity for water splitting was investigated utilizing La-doped NaTaO3 as a model photocatalyst. The activity of Ladoped NaTaO3 was assessed by the determination of the overall quantum yield of molecular hydrogen and molecular oxygen evolution. In pure water La-doped NaTaO3 exhibits rather poor activity for the photocatalytic H2 evolution whereby no O2 was detected.

To enhance the photocatalytic activity the surface of La-doped NaTaO3 was modified with various cocatalysts including noble metals (Pt, Au and Rh) and metal oxides (NiO, CuO, CoO, AgO and RuO2). The photocatalytic activity was evaluated in pure water, in aqueous methanol solution, and in aqueous silver nitrate solution. The results reveal that cocatalysts such as RuO2 or CuO exhibiting the highest catalytic activity for H2 evolution from pure water, possess, however, the lowest activity for O2 evolution from aqueous silver nitrate solution.

La-doped NaTaO3 modified with Pt shows the highest quantum yield of 33 % with respect to the H2 evolution in the presence of methanol. To clarify the role of methanol in such a photocatalytic system, long-term investigations and isotopic studies were performed. The underlying mechanisms of methanol oxidation were elucidated.

9560-30, Session 9

Effect of potential on the conductivity of electrodeposited Cu2O film

Ying Yang, Juan Han, Xiaohui Ning, Hongsheng Tang, Northwest Univ. (China)

The conductivity (i.e., n-type of p-type) of Cu2O films is controlled by the electrodeposition potential. A slightly acidic solution (pH 4.93) containing cupric acetate and sodium dodecyl sulfate (SDS) is used. Photoelectrochemical measurements at zero bias indicate that the Cu2O films deposited at the potentials of 0.00 V and -0.05 V generate the n-type photocurrents and the films deposited at the potentials negative than -0.10 V generate the p-type photocurrents. The X-ray diffraction (XRD) results show that the n-type films are pure Cu2O, however, the metallic copper appear in the p-type Cu2O films. Mott-Schottky measurements show that the donor concentrations of the n-type Cu2O films decrease and the acceptor concentrations of the p-type Cu2O films increase with the decrease of the deposition potential. The SDS molecules adsorbed on FTO surface and the SDS micelles block the diffusion of Cu2+ ions, resulting in a low diffusion rate of Cu2+ ions. Under this circumstance, the growth of Cu2O films are affected significantly by the overpotential. When the potential is positive than -0.05 V, oxygen vacancies are formed in the films leading to the n-type conductivity; however, when the potential is negative than -0.10 V, the Cu2+ ions are reduced to Cu+ rapidly and part of Cu2+ are reduced to metallic copper, the diffused Cu2+ ions to supply to the growth of Cu2O films are insufficient, hence copper vacancies are formed in the films resulting in the p-type conductivity.

9560-31, Session 10

Materials and devices for efficient solar-to-hydrogen production (Keynote Presentation)

Heli Wang, National Renewable Energy Lab. (United States); Joel W. Ager III, Joint Ctr. for Artificial Photosynthesis (United States) and Lawrence Berkeley National Lab. (United States); Nicolas M. Gaillard, Univ. of Hawai'i (United States) and Hawaii Natural Energy Institute (United States); Eric L. Miller, U.S. Dept. of Energy (United States)

High solar-to-hydrogen (STH) efficiency and high durability has been a significant challenge for hydrogen production via photoelectrochemical (PEC) water splitting. Semiconductor materials' band gap, band edge, optoelectronic efficiency, and stability must be satisfied simultaneously to tackle the challenge.

Metal oxides may be stable, STH efficiencies have been limited by issues related to the wide band gap, absorption, charge mobility, recombination, interfacial kinetics, etc. III-V materials offer an alternative pathway to efficient STH conversion, with stability remains an issue.

Besides the materials requirement, the challenge also requires effective usage of solar spectrum. To address the band-edges mismatch, structures and configurations have been developed for unbiased PEC water splitting. This presentation will discuss different semiconductor materials, STH structures and devices, as well as their STH efficiencies.

9560-32, Session 10

Simultaneous photocharging and photoelectrochemical water splitting over oxide semiconductor thin films (Invited Paper)

Yun Hau Ng, The Univ. of New South Wales (Australia)

Most photoactive semiconductors work under illumination. When the source of light is absent, excited charges recombine instantaneously and photoactivity ceases immediately. Research strategies to extend the applicability of photoactive semiconductors in dark conditions have been formulated by developing multiple-material systems to store the photoexcited charges for later usage. Typically it involves an integrated system to combine a photocatalyst and a battery. In this work, we develop a single oxide material system to achieve the excitation and energy storage. WO3 and MoO3 are the two examples that exhibited the ability to photoexcite thus driving the photoelectrochemical water splitting. At the same time, a portion of the photoexcited charges can be stored within the crystal structure of the oxide, stabilised by the cations in the electrolyte, and subsequently delivered the stored energy in dark condition. A systematic investigation has revealed that a balance between the storage or instant consumption can be achieved by changing the sizes of the cation in the electrolyte, modulating the crystal structure distortion and optimising the crystal facet responsible for each function. This work offers an alternative method in achieving solar energy conversion and storage using a simple single oxide system.

9560-33, Session 10

Efficient and low-cost photoelectrodes for solar water splitting (Invited Paper)

Wenjun Luo, Nanjing Tech Univ. (China)

The consumption of fossil fuels creates energy shortage and serious environment issues, which limits sustainable development of the society. Solar energy is the most abundant renewable energy in the world. However, it needs to be stored as chemical energy due to its low energy density, uneven distribution and discontinuous radiation. Hydrogen is considered as a promising clean energy carrier for the future. Different a conventional PV cell, in a photoelectrochemical water splitting cell, a Schottky-like junction forms at the solid-electrolyte interface and separates photo-generated carriers. Since Fujishima and Honda originally reported that a TiO2 based photoelectrochemical cell could be used to split water into hydrogen and oxygen in 1972 [1], intensive researches have been done to improve the performance of the photoelectrochemical cell in the past forty years [2-3]. However, the solar energy conversion efficiency is still low. Exploring efficient photoelectrodes is a key challenge in solar water splitting for hydrogen production.



In this talk, I will present several kinds of methods to improve a photoelectrode's performance, including heterojunction [4], shallow level doping [5-7], removal of surface recombination centers [8-9], morphology control [10], and suppressing back reaction [11]. After modifying, we have obtained record solar photocurrent on BiVO4 and Ta3N5 photoelectrodes for water splitting.[6], [9] Moreover, we have used the BiVO4 photoelectrode to split natural seawater outdoors, which is more attractive because solar energy and seawater are the most abundant renewable energy source and the most abundant progress in this field and offer guindance to improve photoelectrochemical performance of other materials. References:

[1] Fujishima, A.; Honda, K. Nature 238, 37(1972)

[2] Walter, M. G.; Warren, E. L.; McKone, J. R.; Boettcher, S. W.; Mi, Q.; Santori, E. A.; Lewis, N. S. Chem. Rev. 110, 6446 (2010)

[3] Li,Z.; Luo,W.; Zhang, M.; Feng, J.; Zou, Z. Energy Environ. Sci. 6,347 (2013)

[4]Luo, W.; Tao Yu, T.; Wang, Y.; Li, Z.; Ye, J.; Zou, Z. J. Phys. D: Appl. Phys. 40, 1091 (2007)

[5] Zhao, Z.; Luo, W.; Li, Z.; Zou, Z. Phys. Lett. A 374, 4919 (2010)

[6] Luo, W.; Yang, Z.; Li, Z.; Zhang, J.; Liu, J.; Zhao, Z.; Wang, Z.; Yan, S.; Yu, T.; Zou, Z. Energy Environ. Sci. 4, 4046 (2011)

[7] Luo, W.; Wang, J.; Zhao, X.; Zhao, Z.; Li,Z.; Zou,Z. Phys. Chem. Chem. Phys, 15, 1006 (2013)

[8] Luo, W.; Li, Z.; Yu, T.; Zou, Z. J. Phys. Chem. C. 116, 5076 (2012)

[9] Li, M.; Luo, W.; Cao, D.; Zhao, X.; Li, Z.; Yu, T.; Zou, Z. Angew. Chem. Int. Ed. 52, 11016 (2013)

[10] Cao,D.; Luo, W.; Feng, J.; Zhao, X.; Li, Z.; Zou, Z. Energy Environ. Sci. 7, 752 (2014)

[11] Zhao, X.; Luo, W.; Feng, J. ; Li, M. ; Li, Z.; Yu, T.; Zou, Z. Adv. Energy Mater. 4, 1301785 (2014)

9560-34, Session 11

Hydrogen production from water by thermal and photo-excited methods (Keynote Presentation)

Hicham Idriss, SABIC (Saudi Arabia)

Hydrogen production from water is at the essence of the energy system needed for a sustainable economy. Many methods for making hydrogen from water are pursued. Among the most promising of them are thermaland photo-reactions. In thermal reactions the main challenge is making reducible materials at temperatures low enough to warrant applications while in photoreactions the main challenge is in the developments of photocatalytic materials with charge carriers' life time long enough affording high rates of electron transfers to and from the valence and conduction bands of the semiconductor.

In this work we are discussing our recent progress on both fronts. For thermal reactions a case study of the effect of doping CeO2 with metal cations on its reducibility and therefore activity based on experimental and computational results is presented. The incorporation of iso-valent metal cations of similar size to Ce4+ can enhance the reduction of CeO2 due to charge transfer and not to size effect. We correlate the extent of reduction of CeO2 to its redox/activity for hydrogen production using core level spectroscopy and thermal gravimetric analyses. For photo-catalytic reactions we focus in particular on the effect of metal particle size and dispersion (Au and Pd) on the reaction rate. We have found for example a finite range for metal coverages affecting the rate of reaction by over an order of magnitude. These may be linked to charge transfer properties increasing/decreasing the charge carriers' life time and therefore the rate of reaction.

9560-35, Session 11

Functional NiOx catalyst protected small band gap semiconductors for efficient and stable solar driven water oxidation (Invited Paper)

Ke Sun, Nathan S. Lewis, California Institute of Technology (United States)

One promising strategy for the development of an integrated artificial photosynthetic device involves the protection of traditional, high-efficiency small band-gap semiconductors, such as Si, Group II-VI and Group III-V compound semiconductors, for use in fuel-forming half reactions such as the oxidation of water or the reduction of H2O or H2O/CO2 to useful fuels. Stabilization of technologically important semiconductors against photocorrosion and photopassivation would have a significant impact on photoelectrochemical energy conversion, and could enable the development of a new generation of robust integrated devices for efficient solar-driven water splitting and solar-driven CO2 reduction. Previous efforts have been extensively dedicated on elongating the lifetime of semiconductors under harsh fuel forming reaction conditions especially during the water oxidation half reaction. To date, the energy conversion performances (energy conversion figure-of-merit < 1%) and stability (<100 h) were limited on these systems, obscuring the realization of integrated solar fuel devices. In this work, we presented our recent effort on the preparation of a functional NiOx catalyst, which provides multiple important functions on semiconductor photoelectrodes surfaces as a window layer, including chemical/corrosion protection, electrically conducting, optically transparent/antireflective, and inherent electrocatalytic active. The combination of the extraordinary film properties has resulted benchmark performances and stability on Si photoanodes. We also demonstrated that this strategy can be also used on other group II-VI and group III-V semiconductors that have never been able to be protected in relevant water oxidation conditions before. Results presented here indicated a viable strategy that is a promising approach and should be readily applied to other otherwise unstable semiconductors to achieve the long-term stability for use in solar fuel applications.

9560-36, Session 12

Synthesis and assembly of 1D inorganic semiconductor for solar energy conversion (Invited Paper)

Xinjian Feng, Suzhou Institute of Nano-tech and Nanobionics (China)

Nanoscale inorganic semiconductors have become promising low-cost high surface area electrode materials for solar cell and solar fuel productions. Charge transport within electrode materials is a major determinant of these device performances. However, high surface area electrode is normally associated with small size of randomly packed nanoparticles (NPs) and exhibits significantly low electron mobility. To address these challenges, we fabricated ordered single-crystal 1D TiO2 nanowire (NW) arrays. We first demonstrated that their electron transport is 200-fold higher than that in NP films.1 Although 1D NW arrays have marked improved electron transport, the large volume of free space between NWs limits its surface area. We have reported the fabrication of oriented assembled TiO2 hierarchical nanoarrays consisting of 1D branch epitaxially grown from the primary trunk. The 3D NW arrays show 71% higher surface area related to 1D NW arrays, which leads to 52% improvement in solar convention efficiency without affecting electron collection2. To further increase the surface area, we fabricated [10-10] oriented multichannel ZnO NW arrays. The NW exhibits 2-3 orders of magnitude faster electron transport rate than that in NP films. Moreover, the surface area of the as-prepared NW arrays is comparable to that of commonly used NP films3. The high surface area and rapid charge transport properties make these NW arrays ideal electrode structures for future various optoelectronic device applications.

1. X.J. Feng, K. Zhu, A. J. Frank, C. A. Grimes, and T.E. Mallouk, Angew. Chem. Int. Ed. 51, 2727, 2012.



2. X. Sheng, D. Q. He, J. Yang, K. Zhu, and X. J. Feng, Nano Letter 14, 1848, 2014.

3. D. Q. He, X. Sheng, J. Yang, L. P. Chen, K. Zhu, X. J. Feng, J. Am. Chem. Soc. 136, 16772, 2014.

9560-38, Session 12

Photoelectrochemical water splitting and hydrogen generation using InGaN/GaN nanowires grown directly on Si (Invited Paper)

Zetian Mi, Bandar M. AlOtaibi, Shizhao Fan, McGill Univ. (Canada)

Hydrogen generation under sunlight offers great potential for a sustainable fuel production system. Here we report on the design, fabrication, and performance characterization of multi-band InGaN/GaN nanowire photoelectrodes. InGaN/GaN core/shell nanowire arrays on Si can function as a double band photoanode in acidic solution, and relatively high incident-photon-to-current-conversion efficiency (up to 37%) is measured under ultraviolet and visible light irradiation. We have further developed p-type InGaN/GaN nanowire photocathodes, which are monolithically integrated on n-type Si substrate through a polarization-enhanced tunnel junction. The devices exhibit relatively stable hydrogen generation under simulated sunlight illumination.

9560-39, Session 12

Design of inorganic hybrid structures for photocatalytic energy conversion (Invited Paper)

Yujie Xiong, Univ. of Science and Technology of China (China)

Mastery over the surface of a nanocrystal enables control of its properties in molecular adsorption and activation, and enhances its usefulness for catalytic applications. On the other hand, hybrid systems based on semiconductors and noble metals may exhibit improved performance in photocatalysis such as water splitting, mainly determined by the efficiency in generating carriers. In the systems, perfect interface is certainly the key to efficient carrier separation and transport. Taken together, the surface and interface modulation holds the key to materials design for photocatalytic applications. Here, we will demonstrate several different approaches to designing nanocrystal-based systems with improved photocatalytic performance. For instance, a semiconductor-metal-graphene design has been implemented to efficiently extract photoexcited electrons through the graphene nanosheets, separating electron-hole pairs. Ultrafast spectroscopy characterizations exclusively demonstrate that the charge recombination occurring at interfacial defects can be substantially avoided, enabling superior efficiency in water splitting. It is anticipated that this series of works open a new window to rationally designing hybrid systems for photoinduced applications.

9560-7, Session 13

Electrophoretic deposition of composition-tunable (Cu2Sn)xZn3(1-x) S3 nanocrystal films as efficient photocathodes for photoelectrochemical water splitting

Yubin Chen, Zhixiao Qin, Liejin Guo, Xi'an Jiaotong Univ. (China) P-type semiconductor Cu2ZnSnS4 has been considered as one of the most promising light-absorbing materials for solar energy conversion due to its high absorption coefficient, suitable band gap, low toxicity, and elemental abundance. Herein, we apply a low-cost electrophoretic film preparation method to develop composition-tunable (Cu2Sn)xZn3(1-x) S3 films as efficient photocathodes for photoelectrochemical (PEC) water splitting. Firstly, a series of (Cu2Sn)xZn3(1-x)S3 ($0 \le x \le 0.75$) guaternary nanocrystals with tunable optical band gaps are synthesized. Morphologies including particles, rods, and wires are obtained by tuning the composition of the nanocrystals. (Cu2Sn)0.75Zn0.75S3 (Cu2ZnSnS4) has a pure kesterite structure but an increase in the Zn content results in a kesterite-wurtzite polytypism. Subsequently, (Cu2Sn)xZn3(1-x)S3 films are fabricated from their colloidal solutions via electrophoretic deposition and the PEC properties of these films with p-type character have been examined under water splitting conditions. It is shown that the photocurrent varies as a function of film thickness as well as chemical composition. The produced (Cu2Sn)0.45Zn1.65S3 (x = 0.45) film has the highest photocurrent. Furthermore, n-type metal oxide layer is deposited on top of (Cu2Sn) xZn3(1-x)S3 film to modify the surface structure. By forming the efficient p-n junction, photogenerated charge separation is effectively promoted, leading to the much enhanced PEC activity.

9560-40, Session 13

Complex composition and shape materials for renewable energy applications (Keynote Presentation)

(Reynole Fresentation)

Gunnar Westin, Uppsala Univ. (Sweden)

The demands on catalysts for solar fuels, solar cells and photo-assisted water and air cleaning are becoming more complex in composition and structure with design requirements down to a few nm to utilise quantum size effects. This put great demands on the precision of the preparation routes. At the same time the process and materials have to be of very cost for any societal impact to occur. For such tough demands solution based routes are often the best suited. Here solution based processing routes to doped and non-doped oxide nano-particles, thin- and ultra thin films are presented. The oxide systems involve doped and non-doped Fe2O3, TiO2, ZnO, WO3, spinel and perovskite nano-particles, films and ultra-thin films, as well as metal nano-particles and ultra-thin films. The synthesis and products are described by a wide array of techniques including; SEM, TEM, XRD, TGA, DSC/DTA, IR-, Raman and UV-Vis-NIR spectroscopy.

9560-41, Session 13

New III-V semiconductor alloys for solar hydrogen production (Invited Paper)

Mahendra K. Sunkara, Harry B. Russell, Alejandro Garcia, Swathi Sunkara, Jacek B. Jasinksi, Univ. of Louisville (United States); Madhusudan K. Menon, Univ. of Kentucky (United States)

Dilute III-V alloys have garnered immense interest as suitable materials for solar hydrogen generation due to their compositional tunable band gaps, high carrier mobilities and high absorption coefficients. Till date there are no III-V materials that can satisfy all the stringent criteria for photoelectrochemical water splitting. In this presentation, we report two new III-V materials GaSbN and GaSbP that addresses current materials bottleneck for photoelectrochemical water splitting is developed for photoelectrochemical water splitting. Applicability of the Ga(Sbx)N1?x alloys for practical realization of photoelectrochemical water splitting is investigated using first-principles density functional theory and experiments. Theoretical results predict that Ga(Sbx)N1?x , GaSbP alloys with 2 eV band gaps straddle the potential window at moderate to low pH values, thus indicating that dilute Ga(Sbx)N1?x alloys could be potential candidates for splitting water under visible light irradiation.1,2 Theoretical computations with Sb composition beyond 7% change the electronic band gap from direct to indirect. In the case of GaSbP a small amount of Sb incorporation will



change the indirect GaP band gap to direct band gap.3

Experimental synthesis is carried out using metal organic chemical vapor deposition using trimethyl gallium (TMGa) and Trimethyl Antimony (TMSb) and ammonia. Crystalline GaSbxN1-x films were obtained at x values ranging from 0-5%. The synthesis was carried out on different planar substrates and GaN nanowires. Optical measurements confirm that severe band gap reduction occurs with incorporation of antimony in to GaN as predicted by the theoretical calculations. X-Ray Diffraction (XRD) results confirm the lattice expansion at small concentrations of antimony. This work is the first successful attempt on the experimental synthesis of crystalline GaN and GaP based alloy in the low antimonide regime and photoelectrochemical data on activity, band edge energetics and stability show high suitability for direct solar water splitting. The fundamental insights gained from this work on the growth mechanisms and formation of stacking faults can be extended to other ternary alloy nanowires of interest. From a scientific point of view, the large band gap bowing and corresponding optical properties with very small alloying compositions is interesting and can be exploited for band gap engineering. This presentation will highlight our results with both synthesis and photoelectrochemical characterization of GaSbN and GaSbP alloys.

Acknowledgements: Financial support from US Department of Energy (DE-FG02-07ER46375) and NSF (DMS1125909).

I. R.M. Sheetz, E. Richter, A.N. Andriotis, C. Pendyala, M.K. Sunkara and M. Menon, "Visible light absorption and large band gap bowing in dilute alloys of gallium nitride with antimony", Phys. Rev. B, 84, 075304 (2011)

2. S. Sunkara, V.K. Vendra, J.B. Jasinski, T. Deutsch, A.N. Andriotis, K. Rajan and M.K. Sunkara, "New Visible Light Absorbing Materials for Solar Fuels, Ga(Sbx)N1-x", Adv. Mater., 26 (18), 2878-2882 (2014).

3. H.B. Russell, A.N. Andriotis, M.Menon, J. Jasinski and M.K. Sunkara, "Direct Band Gap Gallium Antimony Phosphide (GaSbxP1-x) Alloys", Submitted (2015).

9560-43, Session 13

Plasmonic metal nanostructures as photosensitizers (Invited Paper)

Nianqiang Wu, West Virginia Univ. (United States)

To data, no single semiconductors can meet the requirements of photocatalysis. Generally semiconductors with narrow band gap have a wide sunlight absorption spectral range but suffer from instability in photocatalysis. In contrast, semiconductors with wide band gap exhibit good stability but have a narrow spectral light absorption range. Organic dyes and quantum dots have been used as photosensitizer to extend the spectral range of light absorption. However, instability and band alignment constraints limit the practical use of organic dyes and quantum dots in photosensitization. Recently, plasmonic metal nanostructures emerged as a new type of photosensitizers. Compared to conventional photosensitizers, plasmonic metal nanostructures are stable and have a large light absorption cross-section and are able to transfer the solar energy to plasmonic energy. The critical issue is how to efficiently transfer the plasmonic energy from the metallic photosensitizer to the semiconductor. This talk will present the underlying mechanism and the strategy of the plasmonic energy transfer from a metallic photosensitizer to a semiconductor.

9560-44, Session 14

Ag-Au bimetallic nanocubes with excellent SERS activity and chemical stability (Invited Paper)

Dong Qin, Yin Yang, Xiaojun Sun, Jiawei Zhang, Georgia Institute of Technology (United States)

Silver nanocrystals have fascinating optical properties known as localized surface plasmon resonance (LSPR), which is essential to applications in surface-enhanced Raman scattering (SERS), optical sensing, and biomedical imaging. Silver nanocubes, in particular, have strong electromagnetic field enhancements at their sharp corners, which can drastically increase the Raman scattering cross sections of molecules at these sites for ultrasensitive detection and imaging. However, the susceptibility of elemental Ag to oxidation often leads to corner truncation and thus deterioration of SERS activity. One potential solution to improve the chemical stability of Ag nanocrystals is to form alloys with a more stable metal such as Au. In this talk, I will begin with a co-reduction strategy for transforming Ag nanocubes into Ag-Au hollow nanocubes with enrichment of Ag on their surfaces to greatly enhance their SERS activity. Additionally, I will discuss a new approach to the fabrication of Ag@Au core-shell nanocubes with superb SERS activity and chemical stability. The success relies on the introduction of a fast reduction by ascorbic acid at pH 11.6 to compete with and thereby block the galvanic reaction. An ultrathin Au shell of only 0.6 nm thick was able to protect the Ag in the core from dissolution in an oxidative environment such as 2.3% aqueous H2O2. Significantly, the core-shell nanocubes exhibited LSPR properties essentially identical to those of the original Ag nanocubes while the SERS activity showed an additional 5.4-fold increase owing to the improvement in chemical enhancement.

9560-45, Session 14

Experimental and numerical study on an annular fluidized-bed photocatalytic reactor (Invited Paper)

Dengwei Jing, Xi'an Jiaotong Univ. (China)

Photocatalytic technology has received increasing attention owing to its various advantages. In this work, we designed a fluidized-bed photocatalytic reactor using model reaction of H2S simultaneously employed as the bubbling gas for catalyst suspension and the feed for hydrogen production. The photocatalyst distribution was simulated by CFD with an Eulerian model. The simulation results indicated that the fluidizing time showed a linear relationship with the inlet gas velocity and that the optimal inlet gas velocity was between 30 and 50 mL/min. Further, light energy absorption characteristics, in both homogeneous and heterogeneous media, were simulated by the Monte Carlo method. Our study showed that light energy absorption is affected by the nonuniform distribution of the catalyst particles and that finding the optimum optical thickness in chemical reaction space and the optimal height for catalyst fluidization is essential for reactor design. Based on these numerical simulation results, experimental studies were conducted. Hydrogen productions in a batch photocatalytic reactor (BPR) and a fluidized-bed photocatalytic reactor with H2S bubbling (FBPR) were compared. The reaction rate constant was 1.12 for the FBPR, whereas it was only 0.083 for the BPR case. The similar hydrogen productions and significant difference in reaction rate constants for the two reactors indicates that an increase in the effective initial reactant concentration in FBPR is essential. In this regard, a circulating fluidized bed with recycling use of H2S gas is preferred. Our study is expected to provide useful guidance for the development of a direct photocatalytic H2S decomposition technology.

9560-46, Session 14

Hydrogen storage in high surface area materials: Amorphous graphene oxide and hybrid nanoporous oxides (Invited Paper)

Vassilios D. Binas, Foundation for Research and Technology-Hellas (Greece) and Univ. of Crete (Greece)

Until now, the main energy source was fossil fuels. The last 30 years have appeared the following unpleasant prospects: 1st petroleum stocks will be exhausted within the next few decades, and the reason is the continuous growth of the global population and the continued growth of the industry in developing Eastern European and East Asian countries, which has resulted in the continued increase in the consumption of these sources. 2nd the environmental pollution has increased to dangerous levels. The public health is adversely affected by the emission of smoke, dangerous gases (sulfur dioxide, nitrogen oxides, carbon monoxide and ozone) and the temperature of the earth rises from the increasing concentration of carbon dioxide in the



atmosphere (global emissions).

Hydrogen storage is one of the key issues for the realization of fuel-cell powered vehicles using hydrogen as the energy carrier. Porous carbon materials are a candidate for hydrogen storage and attracted extensive attention as a result of the advantages associated with its light weight, fast kinetics, complete reversibility, low cost, and high surface area.

We present here a high surface area materials and espessially Amorphous Graphene Oxide and Hybrid Nanoporous Oxides. All this materials were successfully synthesized using solvothermal method and characterized with XRD, FT-IR, RAMAN, BET, SEM, TEM, and TGA.. Also we study the gas sorption properties of H2 in different temperatures.

Conference 9561: Thin Films for Solar and Energy Technology VII

Sunday - Monday 9 -10 August 2015 Part of Proceedings of SPIE Vol. 9561 Thin Films for Solar and Energy Technology VII

9561-1, Session 1

A combined optical-electrical finiteelement simulation of nonhomogeneous thin-film solar cells

Tom H. Anderson, The Univ. of Edinburgh (United Kingdom); Muhammad Faryad, Lahore Univ. of Management Sciences (Pakistan); Tom G. Mackay, The Univ. of Edinburgh (United Kingdom); Akhlesh Lakhtakia, The Pennsylvania State Univ. (United States)

A two-dimensional finite-element model has been developed to simulate the optical and electrical properties of thin-film p-i-n junction solar cells. In the thickness direction, the i-type layers for these solar cells are optically and electrically nonhomogeneous. In the simulation, this nonhomogeneity is engineered by varying the fractional composition of an amorphous-silicongermanium alloy. An empirical model relates the energy-gap of the alloy to its complex permittivity. A transparent conducting-oxide layer is welded to the p-type layer, and the n-type layer is backed by a corrugated metallic back reflector which is periodic perpendicular to the thickness direction. Periodic boundary conditions consistent with Floquet theory simulate thin-film solar cells which are unbounded in directions perpendicular to the thickness. Multiple surface-plasmon-polariton waves as well as waveguide modes are excited in the solar cell, thereby increasing the generation rate of electron-hole pairs. A nonhomogeneous drift-diffusion model provides the charge-carrier distribution at steady state. For example, the effective electric field acting on the electrons includes a contribution from the electron affinity of the alloy, while the effective electric field acting on the holes includes contributions both from the electron affinity and the bandgap of the alloy. High-field compatible expressions for the electron and hole mobilities are used. Mid-band Shockley-Read-Hall, Auger and radiative recombination rates are taken to be the dominant methods of carrier recombination. The current density-voltage characteristics of the solar cell are determined, and the maximum efficiency point of the nonhomogenous cell may then be compared to that of a related homogeneous cell.

9561-2, Session 1

Theoretical limits of the multistacked 1-D and 2-D microstructured inorganic solar cells

Emre Yengel, Çankaya Univ. (Turkey); Hakan Karaagac, Istanbul Technical Univ. (Turkey); Logeeswaran Veerayah Jayaraman, M. Saif Islam, Univ. of California, Davis (United States)

Recent studies in monocrystalline semiconductor solar cells are focused on mechanically stacking multiple cells from different materials to increase the power conversion efficiency. Although, the results show promising increase in the device performance, the cost remains as the main drawback. In this study, we calculated the theoretical limits of multi-stacked 1D and 2D microstructered inorganic monocrstalline solar cells. This system is studied for Si and Ge material pair. The results show promising improvements in the surface reflection due to enhanced light trapping caused by photon-microstructures interactions. The theoretical results are also supported with surface reflection and angular dependent power conversion efficiency measurements of 2D axial microwall solar cells. We address the challenge of cost reduction by proposing to use our recently reported mass-manufacturable fracture-transfer- printing method which enables the use of a monocrystalline substrate wafer for repeated fabrication of devices by consuming only few microns of materials in each layer of devices. We calculated thickness dependent power conversion efficiencies of multistacked Si/Ge microstructured solar cells and found the power conversion efficiency to saturate at %26 with a combined device thickness of 30 ?m. Besides having benefits of fabricating low-cost, light weight, flexible, semi-transparent, and highly efficient devices, the proposed fabrication method is applicable for other III-V materials and compounds to further increase the power conversion efficiency above 35% range.

9561-3, Session 1

On the broadband continuous excitation of surface-plasmon-polariton waves in an amorphous silicon solar cell

Mahmoud Atalla, The Pennsylvania State Univ. (United States)

Currently, the surface-plasmon-polariton (SPP) waves can be excited only at certain wavelength and certain incidence angle. It is remarkably noticed that the wavenumber of the SPP waves decreases as the incident wavelength increases. This stands against the continuous excitation of SPP waves at certain incidence angle using a practical grating configuration. We hypothesized that the theoretical modeling of SPP waves guided by the interface of a dielectric grating and a metal will help to solve that problem. The aim of the study is to prove that the proposed grating/metal configuration has propensity of guiding SPP waves of relative wavenumber that increases as the incident electromagnetic wavelength increases. This may enable the continuous excitation of SPP waves. The successful attempt of proving the aim of this study will validate the excitation of SPP waves at certain incidence angle but at wider range of incident wavelength. This result will have a great impact on the communication and energy harvesting applications.

The rigorous coupled wave analysis (RCWA) is used to solve the Maxwell equations in its differential form. The Newton-Raphson method is used to solve the dispersion equation at the grating/metal interface for the SPP wavenumber. This provides the wavenumber of the SPP waves that can propagate at the grating metal interface. A study for the SPP wave energy decay will also be made through the calculation of the Poynting vector, and show that the propagating SPP waves decay away from the grating/metal interface, which infers the surfacing property of the propagating waves.

9561-6, Session 2

+1 360 676 3290 · help@spie.org

Manipulate the grain size and crystallinity of hybrid perovskite films for device efficiency and stability improvement

Jinsong Huang, Univ. of Nebraska-Lincoln (United States)

Large aspect ratio grains with minimal surface defects are needed in polycrystalline thin-film solar cells for reduced charge recombination at grain boundaries, however small grain size in organolead trihalide perovskite (OTP) films is generally observed, and the surfaces are generally rich in charge trap states. Here we report two strategies in reducing the charge recombination at OTP surface and grain boundaries.

First, we demonstrated that charge extraction length in CH3NH3PbI3 without CI can also be increased to above 1 μm by a solvent-annealing process, which increases both the grain size and crystallinity of perovskite films to the film thickness. The average grain sizes were increased to be comparable to film thickness so that most photo-generated charges can be extracted within single grain without crossing grain boundaries. The device efficiency was increased to 15.6% under one sun illumination, and kept above 14.5% when the thickness is increased to 1 μm .

Second, we will introduce a new method to increase the grain lateral size to be more than ten times of the film thickness so that total grain boundary area is dramatically reduced. It effectively reduces the total trap density in the device by 10-100 times to the level in OTP single crystals, and



Conference 9561: Thin Films for Solar and Energy Technology VII



increased the device efficiency to 19% in low-temperature processed planarheterojunction OTP devices. The charge trap passivation at grain boundaries and film surface by the double fullerene layers also effectively reduced the trap density, contributing the elimination of the photocurrent notorious hysteresis.

1. Solvent-Annealing of Perovskite Induced Crystal Growth for Photovoltaic Device Efficiency Enhancement Zhengguo Xiao, Qingfeng Dong, Cheng Bi, Yuchuan Shao, Yongbo Yuan and Jinsong Huang*., Advanced Materials, 26, 6503-6509(2014)

2. Large Fill-Factor Bilayer Iodine Perovskite Solar Cells Fabricated by Low-Temperature Solution-Process Qi Wang, Yuchuan Shao, Qingfeng Dong, Zhengguo Xiao, Yongbo Yuan and Jinsong Huang*, Energy and Enviromental Science, I7, 2359-2365 (2014) (Q.W, Y.S and Q.D contributed to this work equally) ?

3. Origin and Elimination of Photocurrent Hysteresis by Fullerene Passivation in CH3NH3PbI3 Planar Heterojunction Solar Cells

Yuchuan Shao, Zhengguo Xiao, Cheng Bi, Yongbo Yuan, and Jinsong Huang^{*}. Nature Communications, In Press (2014)

9561-7, Session 2

Novel materials for stable perovskite solar cells

Antonio Abate, Ecole Polytechnique Fédérale de Lausanne (Switzerland)

Organic-inorganic perovskites are quickly overrunning research activities in new materials for cost-effective and high-efficiency photovoltaic technologies. Since the first demonstration from Kojima and co-workers in 2009, several perovskite-based solar cells have been reported and certified with rapidly improving power conversion efficiency. Recent reports demonstrate that perovskites can compete with the most efficient inorganic materials, while they still allow processing from solution as potential advantage to deliver a cost-effective solar technology.

Compare to the impressive progress in power conversion efficiency, stability studies are rather poor and often controversial. An intrinsic complication comes from the fact that the stability of perovskite solar cells is strongly affected by any small difference in the device architecture, preparation procedure, materials composition and testing procedure.

In the present talk we will focus on the stability of perovskite solar cells in working condition. We will discuss a measuring protocol to extract reliable and reproducible ageing data. We will present new materials and preparation procedures which improve the device lifetime without giving up on high power conversion efficiency.

9561-8, Session 2

Investigation of degradation mechanisms of perovskite-based photovoltaic devices using LBIC mapping

Zhaoning Song, Suneth C. Watthage, Adam B. Phillips, Brandon L. Tompkins, Randy J. Ellingson, Michael J. Heben, The Univ. of Toledo (United States)

Solution processed thin film photovoltaic devices incorporating organohalide perovskites have progressed rapidly in recent years and achieved more than 20% energy conversion efficiencies. However, an important issue limiting their commercialization is that device efficiency often drops within the first few hundred hours plausibly due to the presence of moisture. To explore the origin of device degradation and failure in perovskite solar cells, we investigate the homogeneity evolution at different stages of aging using two-dimensional laser beam induced current (LBIC) mapping. We demonstrate that local decomposition of perovskites due to moisture is likely responsible for early device degradation by comparing photocurrent collection of perovskite devices in different controlled environments. We show that the addition of a poly(methyl methacrylate)/ single-wall carbon nanotube (PMMA/SWNT) encapsulation layer prevents degradation of the device in moist air. This suggests a route toward perovskite solar cells with improved operational stability and moisture resistance.

9561-4, Session 3

A novel method for mapping open-circuit voltage in solar cells with nanoscale resolution

Elizabeth Tennyson, Joseph L. Garrett, Univ. of Maryland, College Park (United States); Jesse A. Frantz, Jason D. Myers, Robel Y. Bekele, U.S. Naval Research Lab. (United States); Jasbinder S. Sanghera, Univ. Research Foundation (United States); Jeremy N. Munday, Marina S. Leite, Univ. of Maryland, College Park (United States)

The electrical characteristics of thin-film compound semiconductor solar cells have been successfully probed by scanning probe microscopy. Nevertheless, a direct relationship between the measured signals and the figures of merit that define the device performance is still missing. Here we present a novel method to image and spatially resolve the Voc of solar cells with truly nanoscale resolution (<100 nm), based on a variant of illuminated Kelvin probe force microscopy (KPFM) [1]. We map the Voc by measuring the difference between the contact potential difference under illumination and in the dark, which is equal to the photo-generated voltage of the device (and is proportional to the Fermi level splitting). We complement our new metrology by applying scanning photocurrent microscopy using near-field scanning microscopy (NSOM) probes as a local source of excitation to image local variations in Jsc within the material, also with nanoscale resolution. Further, we spatially and spectrally resolve the external quantum efficiency (EQE) within the devices, also with nanoscale resolution, while mimicking the power density operation conditions of real devices [2]. Combined, these new tools provide a complete picture of the local optoelectric characteristics of PV devices, including an indirect measurement of the centers for non-radiative recombination, and a direct mapping of the local collection properties of the material, respectively. We apply our novel metrology to polycrystalline solar cells, where we find Voc local variations of >200 mV.

[1] E.M. Tennyson et al., Nature Commun., in review; [2] M.S. Leite et al., ACS Nano. 11, 11883 (2014).

9561-5, Session 3

Robust measurement of thin-film photovoltaic modules exhibiting lightinduced transients

Michael G. Deceglie, Timothy J. Silverman, Bill Marion, Sarah R. Kurtz, National Renewable Energy Lab. (United States)

Light-induced changes to the current-voltage characteristic of thin-film photovoltaic modules (i.e. light-soaking effects) frustrate the repeatable measurement of their operating power. We describe best practices for mitigating, or stabilizing, light-soaking effects for both CdTe and CIGS modules to enable robust, repeatable, and relevant power measurements. We motivate the practices by detailing how modules react to changes in different stabilization methods. For example we find that a 20°C variation in temperature during light soaking can cause > 5% variation in measured power.

Reliable measurements of module power are critical for qualification testing, reliability testing, and power rating. Thus we developed a two-stage light-soaking method. It begins with an extended, loosely controlled, light exposure to saturate most of the transient. This step is complete when module power is changing by less than 1% per 20 kWh m-2; we describe how this can be reliably determined even in variable outdoor conditions. The second step is a tightly temperature-controlled uninterrupted 5-hour



light exposure to ensure the stabilization concludes with the module in a repeatable state.

We also describe a method for validating alternate stabilization procedures, such as those involving forward bias in the dark, to ensure they result in an outdoor-relevant module state. We have found that alternate procedures, when not applied carefully, can overestimate the light-exposed state power production of a module by as much as 10%. To prevent this, we present a validation method based on subsequent light exposure and power measurement to ensure that a relevant state has been reached.

9561-9, Session 3

sol-gel deposition and plasma treatment of intrinsic, aluminum-doped and galliumdoped zinc oxide thin films as transparent conductive electrodes

Zhaozhao Zhu, Trent Mankowski, Kaushik Balakrishnan, College of Optical Sciences, The Univ. of Arizona (United States); Ali Sehpar Shikoh, Farid Touati, Mohieddine A. Benammar, Qatar Univ. (Qatar); Masud Mansuripur, Charles M. Falco, College of Optical Sciences, The Univ. of Arizona (United States)

We have fabricated transparent conductive electrodes (TCEs) using sol-gel deposition of Aluminum Zinc Oxide (AZO) thin films followed by thermal annealing and plasma treatment. These TCEs exhibit high optical transmittance (over 90%) and good electrical conductivity (sheet resistance below 100 ohms/square). The dopant concentration and film thickness as well as pre- and post-annealing conditions are adjusted for optimum transparency and electrical conductivity. Plasma treatment is found to enhance the desirable characteristics of our fabricated TCEs. The measured optical transmittance spectra are in good agreement with calculations that account for interference effects arising from the TCE's layered structure as well as its index-mismatch with the substrate. We also assembled functioning solar cells using our AZO thin films as the transparent conductive electrode.

9561-10, Session 3

Cd-Zn-O-S alloys for optimal buffer layers in thin-film photovoltaics

Joel B. Varley, Lawrence Livermore National Lab. (United States); Xiaoqing He, Univ. of Illinois at Urbana-Champaign (United States); Neil Mackie, MiaSolé Hi-Tech Corp. (United States); Angus A. Rockett, Univ. of Illinois at Urbana-Champaign (United States); Vincenzo Lordi, Lawrence Livermore National Lab. (United States)

Advances in thin-film photovoltaics have largely focused on modifying the absorber layer(s), while the choices for other layers in the solar cell stack have remained somewhat limited. In particular, cadmium sulfide (CdS) is widely used as the buffer layer in typical record devices utilizing absorbers like Cu(In,Ga)Se2 (CIGSe) or Cu2ZnSnS4 (CZTS) despite leading to a loss of solar photocurrent due to its band gap of 2.4 eV. While different buffers such as Zn(S,O,OH) are beginning to become competitive with CdS, the identification of additional wider-band gap alternatives with electrical properties comparable to or better than CdS is highly desirable.

Here we use hybrid density functional calculations to characterize CdxZn1xOyS1-y candidate buffer layers in the quaternary phase space composed by Cd, Zn, O, and S. We focus on the band gaps and band offsets of the alloys to assess strategies for improving absorption losses from conventional CdS buffers while maintaining similar conduction band offsets known to facilitate good device performance. We also consider additional criteria such as lattice matching to identify regions in the composition space that may provide improved epitaxy to CIGSe and CZTS absorbers. Lastly, we incorporate our calculated alloy properties into device model simulations of typical CIGSe devices to identify the CdxZn1-xOyS1-y buffer compositions that lead to the best performance.

This work performed under the auspices of the U.S. Department of Energy by Lawrence Livermore National Laboratory under Contract DE-AC52-07NA27344 and funded by the Department of Energy office of Energy Efficiency & Renewable Energy (EERE) through the SunShot Bridging Research Interactions through collaborative Development Grants in Energy (BRIDGE) program.

9561-11, Session 3

Eco-friendly spray coating of organic solar cells through water-based nanoparticles ink

Jeroen Stryckers, Lien D'Olieslaeger, Jean Manca, Univ. Hasselt (Belgium) and IMEC (Belgium); Anitha Ethirajan, Univ. Hasselt (Belgium) and IMEC (Belgium); Wim Deferme, Univ. Hasselt (Belgium) and IMEC (Belgium)

Ultrasonic spray coating is currently proven to be a reliable, flexible and cost efficient fabrication method for printed electronics [1-2]. Ultrasonic nozzles are by design especially well-suited to deposit nano-suspension dispersions. Due to the ultrasonic vibration of the nozzle, droplets having a median diameter of 20 μm are created in a homogeneous droplet cloud and directed towards the substrate. When one prepares an ink having the right wetting properties, thin and homogeneous layers, fully covering the surface, can be achieved. Together with conjugated polymer nanoparticles (NPs), emerging as a new class of nanomaterials, [3] it opens possibilities towards eco-friendly roll-to-roll processing of state-of-the-art organic bulk heterojunction solar cells.

A ultrasonic spray coater was used to print the conjugated polymer NP layers under different conditions. A first optimization of the spray coater settings (flow rate, spray speed and temperature) and the ink formulation (water and co-solvent mixture and NP content) was performed for polystyrene particles dissolved in a water-ethanol mixture. As a next step, the low bandgap donor polymer poly[[9-(1-octylnonyl)-9H-carbazole-2,7diyl]-2,5-thiophenediyl-2,1,3-benzothiadiazole-4,7-diyl-2,5-thiophene-diyl] (PCDTBT) [4] and the fullerene acceptor phenyl-C71-butyric acid methyl ester (PCBM[70]) were combined in a water-based blend NP dispersion which was prepared using the mini-emulsion technique. [5,6] Optical Microscopy, profilometry and Scanning Electron Microscopy (SEM) are performed to study the roughness, surface structure, thickness and coverage of the spray coated layers. Finally the printed NP layers are integrated in organic bulk heterojunction solar cells and compared to spin coated reference devices.

[1] Koen Gilissen et al. Toward fully spray coated organic light emitting devices, Proc. of SPIE Vol. 9183, 918311 2014

[2] K.X. Steirer et al. / Solar Energy Materials & Solar Cells 93 (2009) 447-453

[3] Andersen et al. Aqueous Processing of Low-Band-Gap Polymer Solar Cells Using Roll-to-Roll Methods, American Chemical Society VOL. 5, NO. 5, 4188–4196, 2011

[4] S. Wakim, S. Beaupré, N. Blouin, B. Aich, S. Rodman, R. Gaudiana, M. Leclerc J. Mater. Chem. 2009, 19, 5351.

[5] K. Landfester, Angew. Chem. Int Ed. 2009, 48, 4488.

[6] A. Ethirajan, K. Landfester, Chem. Eur. J. 2010, 16, 9398.

9561-12, Session 4

On the interplay of light trapping and plasmonic losses in honeycomb textured silicon thin film solar cells

Asman Tamang, Jacobs Univ. Bremen (Germany); Hitoshi



Sai, National Institute of Advanced Industrial Science and Technology (Japan); Vladislav Jovanov, Jacobs Univ. Bremen (Germany); Koji Matsubara, National Institute of Advanced Industrial Science and Technology (Japan); Dietmar Knipp, Jacobs Univ. Bremen (Germany)

Microcrystalline silicon thin film solar cells on honeycomb textured substrates exhibit short circuit currents exceeding 30 mA/cm2 and energy conversion efficiencies exceeding 10 % [1]. In this study the manufacturing process and the light trapping of the honeycomb textured solar cells was investigated by numerical simulations. The interface morphologies of the individual layers of the solar cells were modeled by an etching and growth model [2]. By controlling the fabrication process the period and height of the honeycomb texture can be varied. The influence of the manufacturing process on the silver back reflector morphology and the quantum efficiency was determined. The optical wave propagation was calculated in 3D by Finite Difference Time Domain (FDTD) simulations. A very good agreement between the optical simulations and the experimental results was obtained. The short circuit current is maximized if the period of the honeycomb texture is approximately equal to the thickness of the solar cell. The short circuit current increases with increasing height up to a height/period ratio of 1/4. For larger height/period ratios the short circuit current and plasmonic losses of the silver back reflector remain unchanged.

 H. Sai, K. Saito, N. Hozuki, M. Kondo, Appl. Phys. Lett. 102, 053509 (2013).
 V. Jovanov, X. Xu, S. Shrestha, M. Schulte, J. Hüpkes, M. Zeman, D. Knipp, Solar Energy Mat. & Solar Cells 112, 182–189 (2013).

9561-14, Session 4

Light trapping enhancement in elliptical nanohole array thin film silicon solar cell

Zihuan Xia, Yonggang Wu, Yongdong Pan, Xuefei Qin, Jian Zhou, Zhongyi Zhang, Tongji Univ. (China)

Various structures employing nanorod or nanohole provide promising approaches to trap and absorb incident light in a semiconductor layer. Nanohole arrays have been found comparable to or even better than nanorod counterparts in terms of light absorption, and exhibit superior mechanical robustness in comparison with the latter. Here, we propose a perpendicular elliptical silicon nanohole (PE-SiNH) array for light absorption in thin film silicon solar cells. The lattice spacing of the array is chosen to be 500 nm, and the overall thickness of the Si thin film is fixed at 2.33?m. The major axis of each elliptical nanohole is perpendicular to that of the four nearest ones. Rsoft DiffractMod module based on rigorous coupled wave analysis (RCWA) is used in the simulation. Results show that an ultimate efficiency of 29.4 % is achieved for the optimal PE-SiNH array, which is 17.4 % and 10.8 % higher than that of the circular SiNH array with the same fill fraction and the optimal circular SiNH array respectively. Fourier analysis reveals that the optimal PE-SiNH structure show additional (11) and (22) components compared with the circular SiNH structure of the same fill fraction, which helps to couple incident light into slow Bloch modes and therefore contribute to the light trapping enhancement in the wavelength region between 700 and 1100 nm. The light trapping property of the nanohole arrays below the wavelength corresponding to the lattice spacing is dominated by the Mie scattering. It is found that high eccentricity of the elliptical nanohole is in favor of the reduction of the back scattering and therefore enhances the light trapping in this wavelength region. The relative low absorption of the optimal PE-SiNH array in the short wavelength range is partly compensated by the low transmission in the long wavelength range, though the optimal PE-SiNH array show less coupling of incident light into channeling modes than the circular SiNH one does between 500 and 730 nm.

9561-15, Session 4

Design of broadband omnidirectional antireflection coatings using ant colony algorithm

Xia Guo, Beijing Univ. of Technology (China)

Optimization method which is based on the ant colony algorithm (ACA) is described to optimize antireflection (AR) coating system with broadband omnidirectional characteristics for silicon solar cells incorporated with the solar spectrum (AM1.5 radiation). It's the first time to use ACA method for optimizing the AR coating system. In this paper, for the wavelength range from 400 nm to 1100 nm, the optimized three-layer AR coating system could provide an average reflectance of 2.98% for incident angles from 0° to 80° and 6.56% for incident angles from 0 to 90.

9561-16, Session 4

Efficiency enhancement of semitransparent organic solar cells by using printed dielectric mirrors

Carina Bronnbauer, Karen K. Forberich, Fei Guo, Nicola Gasparini, Christoph J. Brabec, iMEET (Germany)

Building integrated thin film solar cells are a strategy for future eco-friendly power generation. Such solar cells have to be semi-transparent, long-term stable and show the potential to be fabricated by a low-cost production process. Organic photovoltaics are a potential candidate because an absorber material with its main absorption in the infrared spectral region where the human eye is not sensitive can be chosen. We can increase the number of absorbed photons, at the same time, keep the transparency almost constant by using a dielectric, wavelength-selective mirror. The mirror reflects only in the absorption regime of the active layer material and shows high transparencies in the spectral region around 550 nm where the human eye is most sensitive. We doctor bladed a fully solution processed dielectric mirror at low temperatures below 80 °C. Both inks, which are printed alternatingly are based on nanoparticles and have a refractive index of 1.29 or 1.98, respectively, at 500 nm. The position and the intensity of the main reflection peak can be easily shifted and thus adjusted to the solar cell absorption spectrum. Eventually, the dielectric mirror was combined with different organic solar cells. For instance, the current increases by 20.6 % while the transparency decreases by 23.7 % for the low band gap absorber DPP and silver nanowires as top electrode. Moreover we proved via experiment and optical simulations, that a variation of the active layer thickness and the position of the main reflection peak affect the transparency and the increase in current.

9561-201,

Status and challenges of CdTe photovoltaics

Wyatt K. Metzger, National Renewable Energy Lab. (United States)

Current research in CdTe solar cells is targeting 24% efficiency to drive cost to less than 40 cents/W, displace silicon market share, and reach grid parity. By maximizing photocurrent, CdTe cell efficiency has recently reached 21.5% and surpassed multicrystalline silicon. There is still headroom to increase performance further by improving hole density, lifetime, and thereby photovoltage. However, this will require changing a stubborn defect chemistry that has caused photovoltage to be stagnant for decades. We will describe new work on single-crystal and polycrystalline CdTe designed to understand and overcome this challenge.



9561-18, Session PMon

Influence of Se interlayer in CIGS absorption layer for solar cell devices

Suthan Kissinger Nallathambi Jones, Jubail Univ. College (Saudi Arabia); Jae Kwan Sim, Cheul-Ro Lee, Chonbuk National Univ. (Korea, Republic of)

A CIGS absorber layer with high gallium contents in the space-charge region can reduce the carrier recombination and improve the open circuit voltage Voc. Therefore, controlling Ga grading on top of CIGS thin film solar cells is the main objective of this experiment. To reduce Selenium (Se) vacancy, it is important that the diffusion of Ga elements into Se vacancy between Mo back contact and CIGS absorption layer would be controlled. In order to reduce Se vacancy and confirm Ga inter-diffusion, two CIGS solar cells were fabricated by converting CIG precursor with and without Se interlayer. The copper-indium metallic precursors were fabricated corresponding to the sequence Culn/In/Mo/STS on stainless steel (STS) substrates by sequential direct current magnetron sputtering and Se layer was evaporated by rapid thermal annealing (RTA) system to obtain a Se/CuIn/In/Mo/STS stack. CuGa precursor layer was also fabricated on the Se/CuIn/In/Mo/STS stack. Finally, both CuGa/Se/CuIn/In/Mo/STS and CuGa/CuIn/In/Mo/STS stacks were selenized at 500? for 1 hour. It is observed from the secondary ion mass spectroscopy (SIMS) and X-ray diffraction (XRD), there is a change between the fabricated CIGS absorption layers and the amount of Ga elements. Furthermore, the Ga elements gradually decrease from the top to bottom layer of the CIGS absorption layer. We also discussed the effect of Se interlayer in CIGS absorption layer and its influence on the solar cell performance.

9561-19, Session PMon

Simple 'one step' spray process for CuInS2 / In2S3 heterojunctions on flexible substrates for photovoltaic applications

Titu Thomas, K. P. Vijayakumar, Cochin Univ. of Science & Technology (India)

Flexible semiconducting devices as solar cells and displays have been a recent attraction. Unlike heavy, brittle glass substrates, plastics and metallic foils have advantage of flexibility. This allows a low cost mass production of devices by roll-to-roll processes. Among these, metal foils have added advantages like good thermal stability and high melting point. In this paper we present a very simple method for the growth of CuInS2 (CIS) thin films on flexible Cu foil. CIS is one of the leading candidates for photovoltaic applications due to its optimum band gap and higher absorption coefficient. Interestingly, in the present work, we prepared CIS films by depositing merely InS directly over the Cu foil using simple and economical chemical spray pyrolysis technique. The effects of volume of precursor solution on structural, optical and electrical properties of the films were studied. Improvement in crystallinity and morphology was observed for higher volumes. All the films showed good diode characteristics. Thus for the first time with a single spray, a diode is obtained and this could be the first step towards the fabrication of flexible solar cells with the structure of Cu foil/ CuInS2/InS/Ag. Photo voltaic activity of the device can be expected by optimizing the deposition parameters.

9561-20, Session PMon

A comparison between Zn rich and Zn poor Cu2ZnSnS4 thin film solar cells fabricated by one step electrodeposition method

Ye Chan Kim, Gwangju Institute of Science and Technology (Korea, Republic of); Ho Jung Jeong, Guk Jin Jeon, Gwangju Institute of Science and Technology (Korea, Republic of); Jae Hyung Jang, Gwangju Institute of Science and Technology (Korea, Republic of)

Cu2ZnSnS-4 (CZTS) thin film has received a lot of attention in the recent years due to its great potential for eco-friendly and low-cost absorber materials. Various deposition techniques have been investigated to realize high quality CZTS materials, and they include vacuum and non-vacuum methods such as spray pyrolysis, electrodeposition and sol-gel process. The electrodeposition technique is one of the most promising methods to manufacture low cost manufacturing of CZTS based thin film photovoltaic devices.

In this report, the CZTS thin films were synthesized by one step electrodeposition method on Mo coated soda-lime-glass. The as-deposited CZTS films were subsequently annealed in Ar ambiance at 550? without any other toxic gases to crystalize CZTS films. The resulting film exhibited Zn/(Cu+Sn) ratio varying between 0.15 to 0.60. The structural and optical properties of the Zn rich and Zn poor CZTS thin film were investigated by using Energy dispersive spectroscopy, X-ray diffraction, scanning electron microscopy, atomic force microscopy, and UV-VIS spectrometer. The quality of films was improved as the Zn/(Cu+Sn) ratio was increased. However, the excessive Zn composition resulted in aggravation of performance of CZTS solar cells due to the formation of secondary phase.

Finally, both types of films were utilized to fabricate CdS/CZTS solar cells and the resulting solar power conversion efficiency was measured. The highest efficiency of 2.1 % was achieved from the single step deposited CZTS film.

This work was supported by the Core Technology Development Program for Next-generation Solar Cells of Research Institute for Solar and Sustainable Energies (RISE), GIST.

9561-21, Session PMon

Characterization of Cu2ZnSnS4 thin films prepared by the sulfurization of cosputtered metal precursors

Mohamed Abusnina, Univ. of Denver (United States) and National Renewable Energy Lab. (United States); Mohammad Matin, Univ. of Denver (United States); Helio R. Moutinho, Mowafak M. Al-Jassim, National Renewable Energy Lab. (United States)

In this work, we report the synthesis and characterization of Cu2ZnSnS4 (CZTS) thin films prepared by annealing of co-sputtered metal precursors in sulfur atmosphere. Radio frequency magnetron sputtering was applied to deposit the metal layers from single metal targets on Mo-coated sodalime glass substrates. The chemical composition of the precursors was controlled by varying the sputtering working power resulting in films with various compositions. X-ray fluorescence (XRF) was used to determine the elemental concentration of these metal films. The metal precursors were thereafter converted into CZTS in a tube furnace using different sulfurization conditions in order to investigate the effect of the annealing process on the properties of the final CZTS films. The composition of the CZTS films was carried out by XRF and energy-dispersive spectroscopy (EDS). Film structural characterization and phase identification results were supported by X-ray diffraction (XRD) and Raman spectroscopy. Surface and crosssectional film morphology was carried out by scanning electron microscopy (SEM). For the sulfurized films, XRF showed significant Sn loss which was successfully controlled by depositing precursors with excess of Sn. After optimizing the composition of the metal precursor, XRD and Raman scattering results revealed single-phase CZTS films without clear signs of the existence of secondary phases. SEM showed improved morphology in form of dense structures and smooth surface for the films sulfurized at 600 °C. Our first solar cell, based on CZTS film originated from a precursor sulfurized at 550 °C for 60 min, showed an open-circuit voltage of 471 mV, a short-circuit current density of 9.92 mA/cm-2, a fill factor of 36.9%, and an efficiency of 1.72%.



9561-23, Session PMon

Tunability of graphene: Utilizing multilayered nanoclusters

Shivani Bhardwaj, Alok Ji Shukla, Nilesh Patak, R. P. Sharma, Indian Institute of Technology Delhi (India)

Graphene plays influencive role to the coupling of the electromagnetic field to sub wavelengths structure and this field further may be merge to a thin film for various applications. Here we have studied using in quasi-static electricity, to expose coupling at nanoscales, the Aluminium, Silver and Gold nanoparticles (NPs) support localised surface plasmon resonance (LSPR) which can be resonantly coupled to a system and seizes enhanced local field, tuned reflective losses at the thin film/air interfaces, total transmittance and controlled resonant band width and height. The thickness of single layer graphene film, size of NPs and multi layered core shell thickness/multi layered dielectric core shell thickness were varied to understand the coupling of the electromagnetic field to sub wavelengths and applicability of such systems.

The optical parameters were studied from ultraviolet domain to near infrared domain, which steer a wide range of bandwidth that may suit distinct applications. The increased size of NPs or multilayered system, red shifts the resonance occurs due to damping effects and graphene facilitaty. The conductivity of the graphene is highly tuneable parameter due to the tunability of thickness of graphene since the graphene itself is having plasmonic as well as semiconductor properties. This model was developed using effective medium theory and conductivity of two dimension single layer graphene. The study of such coupled system is useful to understand the physics and may guide the experimental aspects. Without graphene, LSPRs of NPs do not show appreciable shift in resonance wave lengths as well as broad band width and height, which supporting the role of graphene as an electromagnetic field coupling agent.

9561-24, Session PMon

Device characteristics of antenna-coupled metal-insulator-metal diodes (rectenna) using Al2O3, TiO2 and Cr2O3 as insulator layer for energy harvesting applications

Mesut Inac, Atia Shafique, Meriç Özcan, Yasar Gurbuz, Sabanci Univ. (Turkey)

Demand for the inexpensive devices operating at room temperature for broadband sensing and imaging applications are increasing in the last years. Due to the small sizes and the integration capabilities, antenna coupled metal-insulator-metal (MIM) diodes are one of the potential candidates for sensing, imaging and energy harvesting in IR and solar range of spectrum. The antenna coupled diodes are already illustrated in the literature for energy harvesting applications, wireless power transmission and detection. As matter of fact, functionality of MIM diodes based on quantum tunneling leads to device time constant in the order of femtoseconds. The smaller sizes of these devices enable to place more pixels in detectors and harvesters. Due to speed and size of these devices, antenna-coupled MIM diode is thought to be a better choice as an ultrafast and highly responsive harvesting device; these devices can be an alternative to low efficiency energy harvesters: photovoltaic (PV) and thermo-photovoltaic (TPV) devices.

In this work, it is aimed to design and develop a device that can operate in the IR regime of light spectrum. The model formation is based on electron tunneling in MIM diode devices. It includes three different insulators (Al2O3, Cr2O3 and TiO2) and different sizes of devices. First the preliminary DC characterization of individual MIM diodes have been carried out, afterwards, joint characterization of antenna along with diode has been performed. Device characteristics such as responsivity and I-V results are reported.

9561-25, Session PMon

The electrodeposition of multilayers on a polymeric substrate in flexible organic photovoltaic solar cells

Andre Guedes, Idaulo Cunha, Simone Tartari, Vilmar P. Guedes, Monica L. Souza, INTELLECTOS (Brazil)

Flexible organic photovoltaic solar cells have drawn intense attention due to their advantages over competing solar cell technologies. The method utilized to deposit as well as to integrate solutions and processed materials, manufacturing organic solar cells by the Electrodeposition System, has been presented in this research. In addition, we have demonstrated a successful integration of a process for manufacturing the flexible organic solar cell prototype and we have discussed on the factors that make this process possible. The maximum process temperature was 120°C, which corresponds to the baking of the active polymeric layer. Moreover, the new process of the Electrodeposition of complementary active layer is based on the application of voltage versus time in order to obtain a homogeneous layer with thin film. This thin film was not only obtained by the electrodeposition of PANI-X1 on P3HT/PCBM Blend, but also prepared in perchloric acid solution. Furthermore, these flexible organic photovoltaic solar cells presented power conversion efficiency of 12% and the inclusion of the PANI-X1 layer reduced the effects of degradation on these organic photovoltaic panels induced by solar irradiation. Thus, in the Scanning Electron Microscopy (SEM), these studies have revealed that the surface of PANI-X1 layers is strongly conditioned by the dielectric surface morphology.

Monday - Wednesday 10-12 August 2015

Part of Proceedings of SPIE Vol. 9562 Next Generation Technologies for Solar Energy Conversion VI

9562-202,

Photochemical upconversion of light for renewable energy and more

Timothy W. Schmidt, The Univ. of New South Wales (Australia)

It has been abundantly demonstrated that certain molecular compositions are capable of photochemical upconversion (PUC), where lower energy photons are converted to higher energy photons, sometimes with quantum efficiencies approaching 50%. PUC has been applied to solar cells, increasing the EQE of the devices in the region below the bandgap of the device. There remain challenges, though, to the realisation of efficient photochemical upconversion under low levels of incident light, and the incorporation of a liquid upconversion medium into a device. This talk will address these challenges and our progress towards meeting them.

9562-23, Session PMon

Theoretical calculation of light trapping enhancement in Si SiO2 core shell nanowires

Weijian Chen, Jianfeng Yang, Santosh Shrestha, Shujuan Huang, Gavin Conibeer, The Univ. of New South Wales (Australia)

Nanophotonic light trapping for photovoltaics cell is of extensive interest recently. Semiconductor nanowires could act as optical cavity and strongly promote light trapping on certain wavelength. However, as ray theory is not applicable in nanophotonic, one central problem in nanostructure design is how to accurately analyze light trapping enhancement without making the actual cell. We apply two rigorous models to the Si-SiO2 core-shell nanowire on light trapping property compared to single crystalline Si nanowire. The first model is based on the statistical temporal couple-mode theory which is popular in analyzing planar structure but rarely applied to the core-shell cylinder configuration. In this method the enhancement factor is calculated by specifying the all resonant modes and the coupling between each resonant mode and total channels. Meanwhile, the local density of states (LDOS) elucidates the filed behavior and field-matter interaction in the nanostructure. It has been proposed that the LDOS can be a critical figure of merit in nanoscale light management. In this second model, the eigenmodes of the proposed structure are calculated by finite element method. The light trapping enhancement can be calculated by the product of the LDOS and modal occupation numbers. The results from the two models will be carefully discussed, as well as the needed calculation power. Large light trapping enhancement from the core-shell nanowires is expected and the results within reasonable error range from the two models are anticipated. The optimization of nanowires structure will be further reported in the SPIE conference.

9562-24, Session PMon

Analysis of metallic nanoantennas for solar energy conversion

Brhayllan Mora Ventura, Univ. de Guadalajara (Mexico); Ramón Díaz de León, Univ. Autónoma de San Luis Potosí (Mexico); Guillermo Garcia-Torales, Jorge L. Flores-Nuñez, Univ. de Guadalajara (Mexico); Javier Alda, Univ. Complutense de Madrid (Spain); Francisco Javier González, Univ. Autónoma de San Luis Potosí (Mexico) Recently thermo-electrical nanoantennas, also known as Seebeck nanoantennas, have been proposed as an alternative for solar energy harvesting applications. In this work we present the optical and thermal analysis of metallic nanoantennas operating at infrared wavelengths, this study is performed by numerical simulations using COMSOL Multiphysics. Several different nanoantenna designs were analyzed including dipoles, bowties and square spiral antennas. Results show that metallic nanoantennas can be tuned to absorb at thermal-infrared wavelengths, and that numerical simulation can be useful in optimizing the performance of these types of nanoantennas at optical and infrared wavelengths

SPIE. PHOTONICS+

OPTICS+PHOTONICS

FOR SUSTAINABLE ENERGY

9562-25, Session PMon

Charge recombination dynamics of perovskite solar cells

Hee Won Shin, Tae Kyu Ahn, Sungkyunkwan Univ. (Korea, Republic of)

Perovskite materials are promising candidates for realizing efficient, flexible, and lightweight solar cells. Herein, we present the fabrication of perovskite solar cells consisting of mesoporous TiO2, blocking layer, and hole transport materials (HTM), and also explain the excellence of solar cell performance in terms of the charge recombination and extraction times which verified by several spectroscopic techniques. First of all, in order to confirm the dynamics of the transient species, we have used the nanosecond transient absorption (TA) which consists of nanosecond pulse and Xe lamp as the pump and probes lights, respectively. Second, we have utilized the timeresolved photoluminescence (TRPL) to understand the excited charged carrier behaviors such as exciton generation, charge separation, and recombination which depend on the nanostructure and composition of the devices. Finally, the transient photovoltage (TPV) and transient photocurrent (TPC) techniques have been applied to directly get the recombination and extraction times in the devices. In case of TPV, nanosecond pulse and Xe lamp were used for small perturbation light source and bias light one, respectively. The device was directly connected to a digital oscilloscope and the input impedance of the oscilloscope was set to 1 M? for open circuit condition. Bias light intensity was controlled by neutral density filters for various open circuit voltages (Voc) and laser pulse was strongly attenuated to not exceed 30 mV of voltage transient (?V). Overall analysis of spectroscopic results, we can conclude that slow recombination and fast extraction rates are indispensable for highly efficient solar cells.

9562-26, Session PMon

Mie-resonance-mediated enhanced light trapping in Si nanopillar arrays

Eunah Kim, Yunae Cho, Ahrum Sohn, Ewha Womans Univ. (Korea, Republic of); Hyeong-Ho Park, Korea Advanced Nano Fab Ctr. (Korea, Republic of); Joondong Kim, Incheon National Univ. (Korea, Republic of); Dong-Wook Kim, Ewha Womans Univ. (Korea, Republic of)

Si-wafer based solar cells show predominant photovoltaic (PV) market share. The advantages of Si, as an active material for a PV device, include abundance on earth, very competitive fabrication cost, and superior device performance. Further efforts to lower the cost to generate electricity have led to light trapping strategies to improve optical absorption in Si. Nanostructures have exhibited quite remarkable absorption enhancement. We have investigated optical characteristics of Si nanopillar (NP) array surface patterns, fabricated by e-beam lithography and dry etching. Optical reflectance measurements were carried out for NP arrays with various diameter and period. The reflectance spectra showed that the NP array exhibited remarkable antireflection effects in broad wavelength range. The finite-difference time-domain (FDTD) simulations and analyses showed that



lowering of the effective refractive index, diffraction, and Mie resonance enabled the improved light trapping. It is very important to design desirable nanostructures to realize both enhanced light trapping and carrier collection capability. Surface photovoltage (SPV) behaviors of the NPs were compared with those of a planar counterpart by Kelvin probe force microscopy measurements. Surface or defect states can trap carriers and cause band bending at surface. Perturbation by light illumination changes the surface band profile, inducing SPV. The SPV studies could help to improve collection efficiency of photo-excited carriers.

9562-1, Session 1

On the road to hot carrier solar cells (*Invited Paper*)

P. Craig Taylor, Reuben T. Collins, Colorado School of Mines (United States)

Standard solar cells have limitations on their theoretical efficiencies in part due to the fact that carriers excited by light with energies above the semiconductor's band gap guickly lose some of their energy to heat, which can be overcome by collecting the carriers before they thermalize. However, since carriers thermalize over very short times and distances, one must employ a nanostructured morphology. We report results that provide a new paradigm for solar cells that uses a nanostructured crystalline silicon in an amorphous absorber matrix (hydrogenated amorphous silicon). Previously amorphous absorbers have received no serious consideration because of their low carrier mobilities. We demonstrate that carriers generated in the amorphous region are transported out of this region before losing their energy to heat. This result establishes the possibility of using a wide range of nanostructured amorphous matrices to dramatically increase the efficiencies of solar cells. Since hot carrier solar cells ultimately rely on selective collectors that pick off the excited carriers at the peak of their energetic distribution, the task is difficult with crystalline semiconductors where momentum and energy must be conserved during the transfer but easier for amorphous absorbers where crystal momentum is not applicable. Therefore, the use of an amorphous absorber provides a highly desirable and flexible approach to producing low-cost, hot carrier solar cells. Since amorphous materials can be grown over a much wider composition space than crystalline materials, this result greatly broadens the absorbing materials that can be used to dramatically increase the efficiencies of solar cells.

9562-2, Session 1

Carrier multiplication and energy dissipation in Si and Ge nanocrystals (Invited Paper)

Tom Gregorkiewicz, Saba Saeed, Univ. van Amsterdam (Netherlands)

Carrier-carrier and carrier-phonon scattering in semiconductors involves multiple physical processes which become seriously modified in nanocrystals. In particular quantum confinement strongly affects properties of hot carriers, enhancing their effective lifetime – by reduction of phonon emission, and promoting impact excitation rates – by enabling multiple exciton generation and energy transfers to the outside of the nanostructure. In my presentation, I will discuss some results of investigations of these effects in Si and Ge nanocrystals embedded in large bandgap solid state matrices. The motivation for these investigations is provided by possible application of Si and Ge nanocrystals for modification of solar spectrum with an eye on future, highly efficient photovoltaics.

In particular, I will review the most recent progress in following specific subjects:

1. Carrier multiplication in Si nanocrystals. Here I will present results as obtained by calibrated ultrafast transient absorption and advanced photoluminescence quantum yield spectroscopies. These will be supported by theoretical modeling of the relevant energy transfer processes. I will also discuss the on-going investigations towards a spectral finger fingerprint of the carrier multiplication process.

2. Energy recycling process for hot carrier in Si nanocrystals. This effect is enabled by simultaneous occurrence of impact excitation and Auger recombination of multiple excitons co-localized within the same nanostructure.

3. Energy exchange between neighboring Si nanocrystals, leading to peculiarities in the exciton lifetime and offering potential of long-range energy diffusion.

4. Excitation of Er emitters by hot carriers generated in Si nanocrystals upon absorption of highly energetic photons. I will demonstrate that this energy transfer path is sufficiently efficient to overcome hot carrier cooling by phonon emission.

[1] M.T. Trinh et al., Nature Photonics 6, 316-321 (2012).

[2] S. Saeed et al., Nature Communications 5:4665 (2014)

[3] F. Priolo, T. Gregorkiewicz, M. Galli, and T. Krauss, Nature Nanotechnology 9, 19 (2014)

[4] S. Saeed et al., NPG Light: Science and Applications, 4, e251 (2015)

9562-3, Session 1

Ultrafast carrier dynamics study in zirconium nitride

Neeti Gupta, Xiaoming Wen, Shujuan Huang, Simon Chung, Santosh Shrestha, Gavin Conibeer, The Univ. of New South Wales (Australia)

Hot carrier solar cell (HCSC) is a promising third generation photovoltaic device and potentially able to overcome the Shockley-Queisser limit. HCSC aims to circumvent the fundamental loss mechanism by extracting carriers before thermalization also minimize the non-absorbed sub-bandgap losses. The theoretical efficiency for an ideal HCSC is predicted to be 65% under 1 sun solar radiation or 85% under maximal concentration. HCSCs have potential advantage of consisting of only few layers of materials and therefore can conceptually be made relatively simply compared to a multijunction solar cell possibly. Moreover, the HCSC can potentially be made from abundant and non-toxic materials using low cost, high throughput thin film fabrication techniques. HCSC has two main parts: An absorber and an energy selective contact. A critical requirement of the absorber is to slow down the cooling rate of photoexcited hot carriers, from few ps to hundreds of ps or a few ns. ZrN theoretically have a large phononic bandgap and thus a much slowed cooling rate may be expected. In this investigation ZrN thin films were deposited by RF sputtering and characterized by a range of techniques. The carrier dynamics have been studied using ultrafast transient absorption (TA) experiments which shows excited state absorption peaks in visible and near infrared regions. Hundreds of ps cooling time were observed in ZrN by fitting TA spectra. The slowed thermalization process in ZrN suggests that it is a promising material for use as a HCSC absorber.

9562-4, Session 1

Photovoltage transients in GaAs/InGaAs solar cells

Roman Holubenko, Artem Yakovliev, Sergey V. Kondratenko, National Taras Shevchenko Univ. of Kyiv (Ukraine)

A study of the photovoltaic properties of the GaAs-based solar cells with InGaAs quantum wire had been conducted. The research included the investigation of the photovoltage rise and decay transients, spectral photovoltage dependences at different temperatures. The objects investigated were GaAs-based solar cells with InGaAs quantum wire (QWR) embedded into space-charge-region of p-i-n junction. Samples with different In content and size of InGaAs nanoobjects had been created using molecular beam epitaxy. Unlike the reference cell, the ones containing the InGaAs QWR had shown higher sensitivity in the energy range 1.2 – 1.38 eV. This is caused by the spatial separation of electron-hole (e-h) pairs excited



in the QWR due to band-to-band transition. Under selective excitation of the e-h pairs only in the InGaAs quantum wire the photovoltage rise transient is slower compared to the e-h generation in GaAs. This effect is explained by charge carriers release from the InGaAs quantum well into delocalized states of the surrounding GaAs. It was determined that the InGaAs quantum wires increase the recombination rate of the non-equilibrium carriers in the temperature range 80 to 290 K, which means that the quantum wires are the additional recombination centers.

9562-5, Session 2

Quantifying energy transfer in semiconductor nanocrystals using coherent phonon manipulation and ultrafast spectroscopy (Invited Paper)

Bryan T. Spann, U.S. Naval Research Lab. (United States) and Purdue Univ. (United States); Xianfan Xu, Purdue Univ. (United States)

One potential way to increase photovoltaic efficiency is to take advantage of hot-carriers. Nanocrystal based solar cells aim to take advantage of hot-carrier capture to boost device performance. The crucial parameter for gauging a given nanocrystal material for this application is the electron-phonon coupling. The electron-phonon coupling will dictate the thermalization time of hot-carriers. In this study we demonstrate a method of quantifying the electron-phonon coupling in semiconductor nanocrystals. By employing ultrafast transient absorption spectroscopy with temporal pulse shaping, we manipulate coherent phonons in $CdTe_{1?x}Se_{x}$ nanocrystals to quantify the efficiency of the electron-phonon coupling. The Raman active longitudinal optical phonon (LO) modes were excited and probed as a function of time. Using a temporal pulse shaper, we were able to control pump pulse pairs to coherently excite and cancel coherent phonons in the CdTe_{1?x}Se_{x} nanocrystals, and estimate the relative amount of optical energy that is coupled to the coherent CdSe LO mode which is the dominant thermalization pathway for the hot-electrons in this system.

9562-6, Session 2

Hot carrier solar cell absorbers: Investigation of phonon properties of candidate materials (Invited Paper)

Gavin Conibeer, Santosh Shrestha, Shujuan Huang, Robert Patterson, Hongze Xia, Yu Feng, Suntrana Smyth, Simon Chung, Neeti Gupta, Yi Zhang, Jianfeng Yang, Weijian Chen, Xi Dai, The Univ. of New South Wales (Australia)

The key property for a hot carrier absorber is to slow the rate of carrier cooling from the picosecond timescale to at least 100s of ps, but preferably ns to be similar to the rate of radiative recombination. Hot carriers cool primarily by emission of LO phonons. The general properties of phonons and carriers required of a hot carrier absorber have been defined. Materials and structures that exhibit some of these properties fall into three categories:

(a) Bulk materials with large difference in mass between constituent atoms such that there is a large difference between optical and acoustic phonon energies. These suppress the main carrier cooling mechanism of decay of optical phonons. Hence information on phonon dispersion across all momenta is critical to deeper understanding and prediction of appropriate materials.

(b) Low dimensional multiple quantum well (MQW) systems have also been shown to have lower carrier cooling rates. Theories vary as to the importance of carrier or of phonon confinement in this effect. Information on folded phonon modes would help to distinguish between them.

(c) Nanoparticles have also exhibited long hot carrier lifetimes. This is due to confinement of optical phonons and folding of acoustic phonon modes leading to restriction in the allowed decay paths for hot optical phonon populations. These result in longer hot carrier lifetimes.

Knowledge of the phonon energies and dispersion with momentum in these materials is important to understand phonon interaction with carriers. Measurement of these is challenging as very few techniques can map phonon energies across the whole Brillouin zone. Raman spectroscopy is used to measure close to zone centre phonon energies, principally optical phonons; FTIR is used to measure zone edge energies, primarily acoustic phonons. But for the whole zone only inelastic X-ray scattering or neutron scattering have a wide enough range of momentum. In order to achieve required momenta, very high energy photons are required, only available in 4th generation synchrotron and hence in very few beamlines.

Results on phonon dispersion are presented comparing Raman, FTIR and IXS data on a range of bulk, MQW and QD samples. The implications for appropriate application as hot carrier absorbers is discussed.

9562-7, Session 2

Surface passivated colloidal Culn(S,Se)2 quantum dots for quantum dot heterojunction solar cells

Emre Yassitepe, Univ. Estadual de Campinas (Brazil); Oleksandr Voznyy, Edward Sargent, Univ. of Toronto (Canada); Ana Flavia F. Nogueira, Univ. Estadual de Campinas (Brazil)

Colloidal quantum dot heterojunction thin film solar cells (CQD-TFSC) utilize facile thin film deposition methods and promise high photon conversion efficiencies (PCE) to cost ratio which is highly desired for commercialization. So far, surface passivated PbS CQD-TFSCs show the highest PCE results, reaching 9.2% with good stability. Among other potential candidates, CuInSe2 CQDs stand out as a non-toxic material with high potential for performance, judging on bulk Cu(Ga,In)(S,Se)2 TFSCs reaching 20% PCE, with high stability. CuInSe2 CQDs has advantage over bulk films, mainly the much less expensive manufacturing cost of uniform deposition on large areas. Ga is known to cause phase separation in the bulk CIGS system. In a CQD form, CuInSe2 band gap can be tuned between 1 to 1.6 eV by quantum confinement without need for Ga and this eliminates the phase separation issue. Within our best knowledge, there are no reports on surface trap passivated CuInSe2 CQD-TFSCs. However Cu(In,Ga)(S,Se)2 colloidal particles were cast in thin film form and fused to form bulk-like crystals by various annealing conditions for solar cell devices.

In this work, we investigated well-passivated CuInSe2 CQDs on n-type TiO2 and ZnO layers to form depleted heterojunction structure. We prepared luminescent CuInSe2 CQDs by synthetic wet chemistry methods and passivated the surface with 3-mercaptopropionic acid or tetrabutylammonium iodide using solid-state ligand exchange. X-ray photoelectron spectroscopy was used to confirm the ligand boding and surface coverage of the quantum dots. We will present the effect of synthesis and thin film preparation conditions on the solar cell device performance

9562-8, Session 2

Charge carriers recombination and photogeneration in p-i-n solar cells with InAs quantum dots grown on GaAs substrate

Artem Yakovliev, Sergiy V. Kondratenko, Roman Holubenko, National Taras Shevchenko Univ. of Kyiv (Ukraine)

Experimental results of electric and photovoltaic studying of p-i-n solar cells with InAs quantum dots grown on GaAs substrate are presented. The GaAs intrinsic region contains 20 stacks of quantum dots, separated by a GaAs spacer layer and Si dopants giving 0 – 24 electrons per quantum dot, carried out during quantum dots growth. Photovoltage spectra of samples give information about main types of electron-hole photogeneration in the



structure: band-to-band transitions through states of InAs quantum dots, weighting layer and GaAs substrate. Photovoltage transients of samples were measured at 80 – 290K temperature range using excitations by quanta with different energy. The decay time was found to be higher for samples with higher doping level. Dark and light current-voltage characteristics as well as photovoltage spectra give information about the mechanisms of charge carriers recombination and photogeneration in solar cells.

9562-9, Session 3

Quasi-random nanopatterns in Blu-ray movie discs for photon management (*Invited Paper*)

Jiaxing Huang, Northwestern Univ. (United States)

Quasi-random nanostructures have generated great interest for photon management in recent years. Such patterns typically require expensive fabrication processes to create pre-designed, sub-wavelength nanostructures. Interestingly, these patterns can also be found in Blu-ray movie discs, a low-cost consumer product that is mass-produced and readily available. We have discovered that the patterns on all pre-written Blu-ray movie discs are surprisingly well suited for light trapping applications due to their guasi-random nature. The algorithms that encode data found on such Blu-ray discs were developed in order to optimize data compression and error-tolerance. These algorithms coincidentally also create guasirandom arrangements of islands and pits on the final media discs, which are are optimized for photon management over the entire solar spectrum, regardless of the information stored on the discs. As a proof-of-concept, we imprinted polymer solar cells with the Blu-ray patterns, yielding devices with increased absorption and power conversion efficiencies. Simulation suggests that Blu-ray patterns could be broadly applied for the enhancement of solar cells made of many other photoactive materials.

9562-10, Session 3

High efficiency photonic nanostructures for thin film solar cells

Xiaowei Guo, Jia Liu, Univ. of Electronic Science and Technology of China (China)

Enhanced light absorption is a requirement to realize cost-effective photovoltaics. To absorb light more efficiently, thin film solar cells strongly rely on light-trapping schemes. The simplest light-trapping scheme was realized by building solar cells on top of randomly textured substrates capable of redirecting incident sunlight into the plane of the semiconductor. For this scheme it is often hard to predict the performance of a solar cell. Light-trapping scheme employing plasmonic nanostructures has gained significant attentions over the past decade due to their strong light concentration and scattering properties. However, there are only a limited number of cases where the beneficial impact has been experimentally demonstrated on realistic cell designs. More recently, high-index insulating and semiconducting photonic nanostructures were introduced into solar cells to achieve significant absorption enhancement. When properly sized and shaped, they can also exhibit very strong optical resonances that can further boost light-matter interaction compared with bulk materials. The PV community has started engineering these resonances with the aim to improve solar cell performance. Some typical periodic lattice structures such as triangular, square, and hexagonal were proposed as the light trapping lavers.

To further improve our ability to trap light in this scheme, it is important to understand which scattering nanostructures are optimal and how they are best arranged spatially on the cell surface. So far, this question remains unanswered. In this paper, we present a method to design high efficiency photonic nanostructures for thin film solar cells based on the coupled mode theory. Using this method, we predicted the absorption limits for solar cells with different lattice light trapping structures. It was demonstrated triangular lattice exhibits highest absorption enhancement. Then we explored the optimal spatial arrangement of unit cell. Our results show that the pentagon-block-like spatial arrangement inside a solar cell promises good absorption, approaching the predicted limit.

9562-11, Session 3

Singlet-based photon upconversion in multichromophore organic thin films

Daniel H. Weingarten, Univ. of Colorado at Boulder (United States); Michael LaCount, Colorado School of Mines (United States); Garry Rumbles, Jao van de Lagemaat, National Renewable Energy Lab. (United States); Mark T. Lusk, Colorado School of Mines (United States); Sean E. Shaheen, Univ. of Colorado at Boulder (United States)

Solid-state energy upconversion has many potential applications, from nonlinear photonics and biophotonics to expanding the spectrum available for solar energy harvest. In organic molecular systems, upconversion is frequently done in solution to mitigate aggregation-induced photoluminescence quenching or to facilitate the diffusion of triplet donors in Triplet-Triplet Annihilation (TTA) systems. Here we demonstrate an organic thin film upconversion system utilizing two-photon absorption (TPA) properties to improve upconversion efficiency. In blend films of Stilbene-420 and Rhodamine 6G we observe a tenfold increase in upconverted fluorescence compared to the fluorescence yield of TPA in pristine stilbene films. While TPA normally has quadratic dependence on excitation intensity, these blend films exhibit sub-quadratic intensity dependence, indicating a combination of linear and guadratic upconversion processes and dramatically improving upconversion efficiency at lower excitation intensities. This improvement in intensity dependence allows for relatively efficient upconversion upon excitation by a nanosecond laser pulse, in contrast to the more expensive femtosecond lasers generally required for excitation in TPA microscopy and similar systems. Timeresolved photoluminescence decay measurements reveal that all excited states involved in this upconversion process are singlets, which indicates the potential for reduced energy losses when compared to TTA upconversion systems and their inherent intersystem-crossing energy losses. We observe emission from both the Rhodamine 6G donor molecules and Stilbene-420 acceptor molecules, indicating the presence of prompt fluorescence from the donor as well as upconversion to the acceptor, and FRET losses from acceptor back to donor. By fitting to a kinetic model we extract rates for these competing processes.

9562-12, Session 3

Surface plasmon enhanced infrared absorption in P3HT-based organic solar cells: The effect of infrared sensitizer

Sungmo Ahn, Univ. of Colorado at Boulder (United States); Alexandre M. Nardes, National Renewable Energy Lab. (United States); Devin Rourke, Univ. of Colorado at Boulder (United States); Jao van de Lagemaat, Nikos Kopidakis, National Renewable Energy Lab. (United States); Wounjhang Park, Univ. of Colorado at Boulder (United States)

We have theoretically and experimentally investigated the effects of Aggrating electrode on the performance of polymer:fullerene based bulk heterojunction organic solar cells. First, an integrated numerical model has been developed, which is capable of describing both the optical and the electrical properties simultaneously. The Ag-grating patterned back electrode was then designed to enhance the absorption in sub-bandgap region of P3HT:PCBM binary devices. Laser interference lithography and metal lift-off technique were adopted to realize highly-uniform and largearea nanograting patterns. We measured almost 5 times enhancement of the external quantum efficiency at the surface plasmon resonance wavelength. However, the overall improvement in power conversion

efficiency was not significant due to the low intrinsic absorption of active layer in this sub-bandgap region. We, then, investigated about the effect of surface plasmon on the ternary device of P3HT:Si-PCPDTBT:ICBA. It was demonstrated that the infrared absorption by the Si-PCPDTBT sensitizer can be substantially enhanced by matching the surface plasmon resonance to the sensitizer absorption band. Besides, we also observed an additional enhancement in the visible range which is due to the scattering effect of the gratings. An overall short-circuit current enhancement of up to 40% was predicted numerically. We have then fabricated the device by the lamination technique and observed a 30% increase in the short circuit current. Plasmon enhancement of sensitized organic solar cell presents a promising pathway to high-efficiency, broadband-absorbing polymer:fullerene bulk heterojunction organic solar cells.

9562-13, Session 3

Novel down-converter architecture for Sibased solar efficiency enhancement based on silicon-carbon-oxynitride (SiCxOyNz) nanowire arrays

Vasileios Nikas, Brian Ford, Natasha Tabassum, Mengbing Huang, John G. Hartley, Alain E. Kaloyeros, Spyros Gallis, SUNY CNSE/SUNYIT (United States)

A significant source of efficiency losses in Si-based solar cells is associated to thermalization of high-energy absorbed photons in the ultraviolet (UV)blue range. An approach to improve this spectral mismatch and enhance the efficiency is to use high-efficiency wavelength-conversion materials to better match the solar cell's bandgap to the radiation spectrum of the sun. The present authors have shown that silicon-oxycarbide (SiCxOy) thin films synthesized by thermal chemical vapor deposition (TCVD) can intensively luminescence upon UV-blue excitation in a broad visible (VIS) and even near-infrared spectral range, when doped with erbium. Herein, we report the design, fabrication and optical characteristics of sub-100nm TCVDgrown silicon-carbon-oxynitride (SiCxOyNz) nanowire (NW) array systems fabricated by e-beam lithography and reactive ion etching. Studies on their structural and optical characteristics with UV-VIS spectroscopic ellipsometry, Fourier transform infrared and photoluminescence (PL) spectroscopies showed enhanced light emission tunability of such SiCxOyNz nanosystems (480 - 700 nm), which also exhibited high UV/ thermal stability (150 oC, 100 W/cm2) and a blue-shifted broad absorption (230 - 430 nm) allowing a high efficient down-conversion of UV-blue photons. Pertaining to furthering the efficiency yield, we fabricated a one-dimensional (1D) photonic lattice constructed by periodically arranging SiCxOyNz (C:12%; O:53%; N:1%) 1D-NW arrays on a Si substrate. Compared to its thin film counterpart, the integrated PL yield of the 1D-NW architecture exhibited a ~four-fold enhancement. Our spectral-conversion approach based on nontoxic SiCxOyNz NWs may offer an alternative pathway for high solarefficiency enhancement with potential reduced process complexity, cost and environmental impact.

9562-14, Session 4

Embedding solar cell materials with onboard integrated energy storage for loadleveling and dark power delivery

Cary L. Pint, Andrew S. Westover, Adam P. Cohn, William R. Erwin, Keith Share, Thomas Metke, Rizia Bardhan, Vanderbilt Univ. (United States)

This work will discuss our recent advances focused on integrating high power energy storage directly into the native materials of both conventional photovoltaics (PV) and dye-sensitized solar cells (DSSCs). In the first case (PV), we demonstrate the ability to etch high surface-area porous silicon charge storage interfaces directly into the backside of a conventional polycrystalline silicon photovoltaic device exhibiting over 14% efficiency. These high surface area materials are then coupled with solid-state ionic liquid-polymer electrolytes to produce solid-state fully integrated devices where the PV device can directly inject charge into an on-board supercapacitor that can be separately discharged under dark conditions with a Coulombic efficiency of 84%. In a similar manner, we further demonstrate that surface engineered silicon materials can be utilized to replace Pt counterelectrodes in conventional DSSC energy conversion devices. As the silicon counterelectrodes rely strictly on surface Faradaic chemical reactions with the electrolyte on one side of the wafer electrode, we demonstrate double-sided processing of electrodes that enables dualfunction of the material for simultaneous energy storage and conversion, each on opposing sides. In both of these devices, we demonstrate the ability to produce an all-silicon coupled energy conversion and storage system through the common ability to convert unused silicon in solar cells into high power silicon-based supercapacitors. Beyond the proof-of-concept design and performance of this integrated solar-storage system, this talk will conclude with a brief discussion of the hurdles and challenges that we envision for this emerging area both from a fundamental and technological viewpoint.

SPIE. PHOTONICS

OPTICS+PHOTONICS FOR SUSTAINABLE ENERGY

9562-15, Session 4

Organic photovoltaic devices with concurrent solar energy harvesting and charge storage capability

Arash Takshi, Anand K. Santhanakrishna, Tete Tevi, Houman Yaghoubi, Univ. of South Florida (United States)

Due to large variation of the solar energy availability in a day, energy storage is required in many applications when solar cells are used. However, application of external energy storage devices, such as batteries and supercapacitors, increases the cost of solar energy systems and requires additional charging circuitry. This combination is bulky and relatively expensive which is not ideal for many applications. In this work, a novel idea is presented for making two-terminal electrochemical devices with dual properties of solar energy harvesting and internal charge storage. The device is essentially a supercapacitor with a photoactive electrode. Energy harvesting occurs through light absorption at one of the electrodes made of a composite of a conducting polymer (i.e. PEDOT:PSS) and a Porphyrin dye. Upon exposure to AM1.0 solar irradiation, an open circuit voltage as large as 0.49 V was achieved across a cell with ~1 mF capacitance. The device showed a reasonable charge stability in dark when it took more than 30 min to drop the voltage. A short circuit current density of 0.12 mA/cm2 was obtained under illumination. The device characteristics can be tuned to be more efficient in light absorption or enhance the capacitance by changing the ratio of the polymer and dye molecules in the composite film. Our study shows a great potential of this approach for concurrent solar energy harvesting and charge storage in a two-terminal device.

9562-16, Session 4

Monolithically self-assembled organic active materials integrated with thermoelectric for large spectrum solar harvesting system

Tito L. Busani, Olga Lavrova, Matthew Erdman, Julio Martinez, The Univ. of New Mexico (United States)

We designed and studied a radial junction composed by a photovoltaic and thermoelectric array based on ZnO and CdTe nanowires surrounded by an absorbing organic self assembled in order to efficiently convert UV-visible and IR energy into electricity.

The hot anode of n-type ZnO nanowires was fabricated using a thermal process on pre-seeded layer and results to be crystalline with a transmittance up to 92 % and a bandgap of ~ 3.32 eV. Conductivity measurements reveal diode-like behavior for the ZnO nanowires.

The organic layer was deposited between the anode and cathode at room temperature The organic layer is composed of oppositely charged porphyrin



metal (Zn(II) and Sn(IV)(OH)2) derivatives that are separately water soluble, but when combined form a virtually insoluble solid. The electron donor/ acceptor properties (energy levels, band gaps) of the solid can be controlled by the choice of metals and the nature of the peripheral substituent groups of the porphyrin ring. A defect free sub nanometer deposition was achieved using a layer-by-layer deposition onto both ZnO and Bi2Te3 nanowires.

The highly thermoelectric structure, which acts as a cold cathode, is composed of p-type Bi2Te3 nanowires with a thermoelectric efficiency (ZT) between ~0.7 to 1, values that are twice that expected for bulk Bi2Te3.

Optoelectronic and structural properties shows that with 6 nm of organic layer it is possible to form a 3% efficient solar device with an enhanced thermo electric effected with a temperature gradient of 300 C.

9562-17, Session 5

Hot-phonon bottleneck in lead iodide perovskites (Invited Paper)

Matthew C. Beard, Ye Yang, National Renewable Energy Lab. (United States)

Carriers with excess kinetic energy (hot-carriers) are generated from absorption of photons with energy larger than the semiconductor bandgap. In a typical semiconductor, the excess kinetic energy is quickly dissipated as carriers thermalize to the lattice and this process accounts for ~50% of the free-energy loss in current solar energy conversion strategies. Gaining control and preventing such thermalization could result in ~doubling of the limiting efficiencies for solar energy conversion technologies. We found an efficient hot-phonon bottleneck in planar Pb iodide perovskite films using transient absorption (TA) spectroscopy. The hot-phonon bottleneck occurs above a critical injection carrier density of ~5x1017 cm-3, an order of magnitude lower than found in GaAs and thermalization times increase by 3-4 orders of magnitude beyond that found in GaAs. The hot-phonon bottleneck found here is of similar magnitude to that found in highly engineered III-V based multiple quantum wells.

9562-18, Session 5

Plasmonic enhancement of mesoporous solar cells with shape controlled nanostructures

Rizia Bardhan, Vanderbilt Univ. (United States)

Next generation mesoporous solar cells (MSCs) including dye-sensitized solar cells (DSSCs) and perovskite-sensitized solar cells (PSSCs) have rapidly emerged with efficiencies reported up to 13% for DSSCs and 19% for PSSCs. Current efforts to improve the performance of MSCs are focused on altering the photoanode morphology, and manipulating the sensitizer composition. In contrast to these approaches that often lead to incremental improvement tailored to each MSC system, plasmonic enhancement provides a universal route applicable to the whole family of MSCs that can significantly boost the optical absorption and carrier generation. Through small additions of metal nanoparticles to MSCs (< 2%), the amount of sensitizer required to achieve high efficiency can be drastically reduced enabling thin film architectures. Here we demonstrate enhanced light harvesting in both DSSCs and PSSCs by embedding silica-coated gold nanocubes (Au@SiO2-NCs) in the photoanodes. In DSSCs Au@SiO2-NCs led to 7.8% efficiency relative to 5.8% for reference (no nanocubes) devices, resulting in 34% improvement in performance; while in PSSCs Au@SiO2-NCs resulted in 8.6 % efficiency relative to 7.5 % for reference devices giving rise to 16% enhancement. Photocurrent and IPCE spectra revealed that device performance in MSCs is controlled by particle density of Au@SiO2-NCs and monotonically decreases at high concentrations. FDTD simulations demonstrated that the nanocubes predominantly absorb incident light giving rise to lightning rod-effect which results in intense electromagnetic fields at the edges and corners. These intense fields increase the plasmonic-sensitizer coupling, amplifying carrier generation in MSCs. This work shows that shape-controlled plasmonic nanostructures can be employed as a universal platform for enhanced lighttrapping in a range of solar devices.

9562-19, Session 5

Ultrafast time-resolved spectroscopy of lead halide Perovskite films

Mopelola A. Idowu, Federal Univ. of Agriculture (Nigeria) and Univ. of Michigan (United States); Oleg P. Varnavski, Theodore G. Goodson III, Univ. of Michigan (United States)

Recently, lead halide perovskites which are organic-inorganic hybrid structures, have been discovered to be highly efficient as light absorbers in solar cells [1]. They exhibit broad absorption below 800 nm and have an absorption coefficient far greater than conventional organometallic dyes used in dye sensitized solar cells [2,3]. Non-stoichiometric precursor formed lead halide perovskites grown by the inter-diffusion method were investigated to probe their fundamental excited state dynamics and emission properties using steady-state and time-resolved spectroscopic measurements. The use of a non-stoichiometric precursor solution ratio resulted in films with good morphology and better ultrafast measurement results. Steady state fluorescence was observed at ~ 760 nm for the perovskites with a weaker emission observed at 820 nm when the perovskite was excited at the band edge. Femtosecond transient absorption experiments revealed spectral features of the perovskite material. Excited state absorption was observed within the first 1 ps of the transient [4]. This was followed by a bleach with a short rise time. The long lived bleach process also had another shorter rise time feature which was observed. Measurements of the femtosecond photoluminescence upconversion were also carried out with the perovskite films of varying ratios of the precursor solution.

References

[1] Burschka, J., Pellet, N., Moon, S.J., Humphry-Baker, R., Gao, P., Nazeeruddin, M.K., and Grätzel, M., "Sequential deposition as a route to highperformance perovskite-sensitized solar cells.," Nature 499 (7458),316–319 (2013).

[2] Wang, Q., Shao, Y., Dong, Q., Xiao, Z., Yuan, Y., and Huang, J., "Large fill-factor bilayer iodine perovskite solar cells fabricated by a low-temperature solution-process.," Energy Environ. Sci., 7, 2359-2365 (2014).

[3] Lee, M.M., Teuscher, J., Miyasaka,T.N., Murakami H., and Snaith, J., "Efficient Hybrid Solar cells based on meso-superstructured organometal halide perovskites.," Science, 338, 643-647 (2012).

 $\ensuremath{\left[4\right]}$ Idowu, M.A., M.M., Varnavski, O., and Goodson III,
T., Manuscript in preparation

9562-20, Session 6

Emitter thickness optimization for GaSb thermophotovoltaic cells grown by molecular beam epitaxy

Shaimaa A. Abdallah, Daniel J. Herrera, Nassim Rahimi, Luke F. Lester, Virginia Polytechnic Institute and State Univ. (United States)

Thermophotovoltaic (TPV) cells can convert long-wavelength radiation from a variety of sources into an electrical current. Among the potential materials for TPV diodes, GaSb grown via the Molecular Beam Epitaxy (MBE) method is a promising candidate due to its relative simplicity as a binary semiconductor compared to InGaAs or InGaAsSb. However, MBE growth of GaSb with low shunt defect density over a large area is still relatively challenging, which can limit TPV device performance. In particular, the emitter thickness (de) in MBE-grown GaSb TPVs is a crucial point that is not well studied. MBE-grown GaSb TPVs with a 5E18/cm3 p-type emitter were fabricated with a de of approximately 0.5 ?m. The as-grown de was chosen to be sufficiently thin to avoid shunt defect formation and thick enough to prevent the emitter ohmic contacts from shorting the pn junction and to provide low emitter sheet resistance. However, further reduction of de is necessary to minimize the transit length of the minority electrons through the short carrier lifetime emitter. Therefore, initial AM1.5 simulations were performed to find the particular de that maximizes the short circuit current



density. These simulations indicated an optimal de = 0.2 ?m at which a maximum short-circuit current density around 35 mA/cm2 can be achieved. The theoretical results for AM1.5 and longer wavelength radiation will be compared to experimental data including quantum efficiency, short circuit current density and open circuit voltage from fabricated GaSb TPVs in which the emitter is incrementally etched and characterized at each de.

9562-21, Session 6

Performance comparison of frontside silver pastes using polyalkylene carbonates for cleaner burning binder system

Richard Stephenson, Stephenson & Associates, Inc. (United States); Peter Ferraro, Empower Materials, Inc. (United States)

Extensive work has been done over the last fifteen years toward improving efficiencies, capacities, and reliability of solar cells. Rapid decline in the cost per watt has promoted increased deployment. Given the significance of metallization process and its potential to improve solar cell efficiency and reliability, work has been done with formulations of silver bearing pastes for front side printing of conductive lines for these solar applications. This paper presents a comparison of functional qualities of silver bearing pastes made with a polyalkylene carbonate, cleaner burning binder and organic components. Adhesion strengths and microstructure are presented to show differences in obtainable reliability and resistive losses by using cleaner burning binder system.

9562-22, Session 6

Optimizing the energy band alignment at the CdS/Cu2ZnSnS4 heterojunction by Nickel Incorporation

Hui Ju Chen, National Cheng Kung Univ. (Taiwan)

The key issue when it comes to the CZTS based photovoltaics is the cliff-like conduction band offset (CBO), which has limited the power conversion efficiency resulted from the open circuit voltage deficit. Thus, optimizing the electronic structures at the CdS/CZTS heterojunction is necessary to achieve high-performance CZTS solar devices. This study proposes a new concept in which incorporates the appropriate Ni content into CZTS absorbers to fabricate the Cu2(Zn,Ni)SnS4 [C(Z,N)TS] absorbers, contacted with the CdS buffer to realize the ideal p-n heteroiunction at the interface. Three samples of CdS/C(Z,N)TS heterojunction are investigated (different Ni content, [Ni]/[CZTS] = 0, 0.1% and 0.3%, respectively). The study is investigated by ultraviolet photoelectron spectroscopy (UPS), high resolution x-ray photoelectron spectroscopy (HRXPS), optical absorption spectroscopy and photoluminescence analysis. The Ni composition dependent bandgap energy of the C(Z,N)TS absorbers is revealed. The bandgap energy decreases from wide bandgap of 1.43 eV to narrow bandgap of 1.28 eV as the Ni content of [Ni]/[CZTS] increases from 0 to 0.3%. The valence band offset (VBO) of the CdS/C(Z,N)TS heterojunction with various Ni content have been measured by two approaches, directly method using UPS and indirectly method using HRXPS. Hence, the conduction band offset (CBO) between the CdS buffer and each C(Z,N)TS absorbers could be estimated involving the use of the VBO values together with the known bandgap energy of the C(Z,N)TS absorbers. The work exhibits the CBO at the CdS/C(Z,N)TS interface switches from original cliff type to spike type while adjusting appropriate Ni content. The ideal spike CBO inhibits interface recombination and results in the increase of Voc and PCE.

The study successfully modifies the band offsets at the CdS/C(Z,N)TS interface through the control of the Ni compositions. Note the Ni ions with the valence state of 2+ substitutes to the Zn2+ ions within the C(Z,N)TS thin films.

Conference 9563: Reliability of Photovoltaic Cells, Modules, Components, and Systems VIII



Sunday - Monday 9 -10 August 2015

Part of Proceedings of SPIE Vol. 9563 Reliability of Photovoltaic Cells, Modules, Components, and Systems VIII

9563-1, Session 1

Development of a resistivity standard for polymeric materials used in photovoltaic modules (*Invited Paper*)

Michael D. Kempe, David C. Miller, Dylan L. Nobles, National Renewable Energy Lab. (United States); Keichiro Sakurai, National Institute of Advanced Industrial Science and Technology (Japan); John Tucker, Keithley Instruments, Inc. (United States); Jayesh G. Bokria, Specialized Technology Resources, Inc. (United States); Tsuyoshi Shioda, Mitsui Chemicals, Inc. (Japan); Kumar Nanjundiah, The Dow Chemical Co. (United States); Toshio Yoshihara, Dai Nippon Printing Co., Ltd. (Japan); Jeff Birchmier, DNP America, LLC (United States); Oihana Zubillaga, TECNALIA (Spain); John H. Wohlgemuth, National Renewable Energy Lab. (United States)

Photovoltaic modules, which operate at high voltages and elevated temperatures, are known to degrade because of stray current going to or from ground. These degradation processes involve electrochemical degradation and/or charge build-up in thin layers. For these mechanisms, the use of polymeric materials with a high resistivity is known to reduce the rate of aging. Because of this, materials suppliers are placing increased importance on the bulk resistivity, but there is not yet an accepted method for this measurement. The measurement time has been shown to greatly affect the apparent resistivity, with an increase as great as 100X for different measurement times. We have performed a number of exploratory and round-robin tests to establish a representative and reproducible method for determining the bulk resistivity of polymeric materials, including encapsulation, backsheet, edge seals, and adhesives. The standard has developed to use measurements alternating between an "on" and "off" voltage state with a weighted averaging function and cycle times of an hour.

9563-2, Session 1

Application of new measurement technologies to backsheet durability testing to improve correlation of accelerated exposures to fielded modules (Invited Paper)

Thomas C. Felder, William J. Gambogi Jr., Katherine M. Stika, Alexander Z. Bradley, Lucas Amspacher, Bao-Ling Yu, Babak Hamzavytehrany, R. Scott Peacock, DuPont (United States); Hongjie Hu, DuPont (China) Research & Development and Management Co., Ltd. (China); Lucie A. G. Garreau-Illes, DuPont International Operations Sarl (Switzerland)

We have previously reported good correlation of FTIR spectra between accelerated tests and field measurements. The availability of portable FTIR spectrometers has made measurement in the field convenient and reliable.

Recently, nano-indentation has shown promise to correlate changes in backsheet mechanical properties. A precisely shaped stylus is pressed into a sample, load vs displacement recorded and mechanical properties of interest calculated in a nondestructive test. Finally, we will discuss optical profilometery. In this technique a white light interferogram of a surface is Fourier transformed to produce a three-dimensional image. Height differences from 1 nm to 5 mm can be detected over an area of a few cm. This technique can be used to determine crack and defect dimensions. Results will be presented correlating accelerated tests with fielded modules covering spectroscopic, mechanical, and morphological changes.

9563-3, Session 1

Cracking and delamination behaviours of photovoltaic backsheet after accelerated laboratory weathering

Chiao-Chi Lin, Yadong Lyu, Donald L. Hunston, Jae Hyun Kim, Kai-Tak Wan, Deborah L. Stanley, Xiaohong Gu, National Institute of Standards and Technology (United States)

The channel crack and delamination phenomena that occurred during tensile tests were utilized to study adhesion properties of a multilayered backsheet. A model sample of commercial PPE backsheet, namely polyethylene terephthalate/polyethylene terephthalate/ethylene vinyl acetate (PET/PET/ EVA), was aged on the NIST SPHERE (Simulated Photodegradation via High Energy Radiant Exposure) with the UV irradiance at 170 W/m2 (300 nm to 400 nm) under accelerated weathering conditions of 85 °C and two relative humidity (R.H.) levels of 5% and 60%. A complementary aging experiment on NIST SPHERE without UV was also carried out as a control. Film stresses were analyzed experimentally based on an exact closed-form solution of multilayer bending. An asymptotic solution was used to solve the stress singularity of interfacial crack formation and therefore, the critical debond energy of the backsheet was investigated before and after aging. Furthermore, the effect of residual stress caused by thermal cycling on backsheet delamination was investigated by substituting thermal mismatch for elastic mismatch in the film stress analysis of the multilayer material.

9563-4, Session 1

Depth profiling of chemical and mechanical degradation for PV backsheets after UV exposure

Xiaohong Gu, Chiao-Chi Lin, Peter J. Krommenhoek, Stephanie S. Watson, National Institute of Standards and Technology (United States)

Polymeric backsheets protect the photovoltaic modules from damage of moisture and ultraviolet (UV) while providing electrical insulation. Due to the complication of multilayer structures, the properties of the innerlayers of the backsheets, including their interfaces, during weathering are not well known. In this study, a commercial type of PPE (polyethylene terephthalate (PET)/PET/ethylene vinyl acetate (EVA)) backsheet films was selected as a model system for a depth profiling study of chemical and mechanical properties of a backsheet film during UV exposure. Cryo-microtomy was used to obtain cross-sectional PPE samples. The NIST SPHERE (Simulated Photodegradation via High Energy Radiant Exposure) was used for the accelerated laboratory exposure of the materials with UV at 85°C and two relative humidities (RH) of 5 % (dry) and 60 % (wet). Chemical and mechanical depth profiling of the aged and unaged samples was conducted by Raman microscopic mapping and nanoindentation. The results indicate that the PPE backsheet films are comprised of five main layers, including pigmented-PET, core PET, inner EVA, pigmented-EVA and outer EVA, along with their interfacial regions and two adhesive layers. Both UV and moisture are key environmental factors for backsheet degradation. It is also found that the deterioration of adhesion layers and the residual internal stress resulted from non-uniform degradation of the multilayer can lead to the

 PHOTONICS OPTICS+PHOTONICS FOR SUSTAINABLE ENERGY

delamination of interlayers. Besides, the relationship between the chemical and mechanical degradation is discussed.

9563-5, Session 2

UV-DH-TC and UV-DML-HF-DH sequential tests for PV modules (Invited Paper)

Takuya Doi, National Institute of Advanced Industrial Science and Technology (Japan); Hideyuki Morita, Takao Amioka, Toray Industries, Inc. (Japan); Atsushi Masuda, National Institute of Advanced Industrial Science and Technology (Japan)

As a test for confirming a long time reliability of PV modules, a sequential test including the stress which gives the effect of expansion and contraction (thermal cycling test, dynamic mechanical load test, etc.) is considered necessary. Therefore, we have been conducting the UV-damp heat-thermal cycling (UV-DH-TC) sequential test and the UV-dynamic mechanical load-humidity freeze-DH (UV-DML-HF-DH) sequential test using 4 cells minimodule. The purpose of this study is to clarify the relationship between degradation and UV exposure testing, and to acquire basic data which contribute to the decision of the appropriate testing condition.

Light source is xenon lamp with intensity of UV 90 W/m2 at 300-400 nm, chamber temperature 65 degrees Celsius, no humidity control (2 to 10 %RH). Major materials of samples are as follows; multicrystalline silicon solar cell (156 x 156 mm), EVA (fast cure type), backsheet (polyolefin-PET), tempered and embossed glass (400 x 400 mm, t=3.2 mm).

The results of UV 1314h-DH 500h-TC 100c-DH 500h-TC 100c sequential test; the drop in Pmax was little (<5%) until first DH 500h-TC 100c, afterward it increased dramatically in the following sequence, and it was finally 22 to 24%. The possibility of accelerating the degradation of the series resistance increase mode by combining UV exposure test with the DH test, was suggested.

As for UV-DML-HF-DH sequential test, after UV exposure (as for a parameter, 500, 1000, 1500, 2000h), the following sequence of DML 1000c-HF 10c-DH 1000h has been going now. In addition, this result will be also reported.

9563-6, Session 2

Effects of current injection during damp heat tests on thin film photovoltaic modules (Invited Paper)

Keiichiro Sakurai, National Institute of Advanced Industrial Science and Technology (Japan) and Photovoltaic Power Generation Technology Research Association (Japan); Akihiro Takano, Photovoltaic Power Generation Technology Research Association (Japan); Masaaki Yamamichi, National Institute of Advanced Industrial Science and Technology (Japan) and Photovoltaic Power Generation Technology Research Association (Japan); Hiroko Saito, Masayoshi Takani, Photovoltaic Power Generation Technology Research Association (Japan)

It have been reported that some degradations observed in field on some flexible thin film photovoltaic (PV) modules can be reproduced better with current injected damp heat (CDH) tests [1]. If this is true for other types of flexible products, it may be worth amending the current IEC standards for testing thin film modules. To investigate the needs for an amended test standard, we have investigated the effects of current injection during conventional damp heat (DH) tests or dry-heat tests, on multiple kinds of thin film flexible modules. So far, we have tested thin film silicon flexible modules and CIGS flexible modules. At least one type of CIGS flexible modules sold in the market showed a clear difference in EL images Concurrently, I-V characteristics may degrading faster with current injection, though the data shows a large dispersion and requires confirmation. Results of destructive analysis by TEM, EDX, SCM, FT-IR and ICP will be presented. Further investigations on other types of thin film modules may also follow as well.

9563-7, Session 2

Experimental and computational investigation of microcrack behavior under combined environments in monocrystalline Si

Wei-Jie Huang, Stefan Bringuier, Kelly Simmons-Potter, Krishna Muralidharan, Barrett G. Potter Jr., The Univ. of Arizona (United States)

An investigation of microindenter-induced crack evolution with independent variation of both temperature and relative humidity has been pursued. Environmental temperatures from 25 to 60 C and atmospheric water contents from 5 to 30 g/m3 were produced over periods of up to 20 hours. Under static tensile strain conditions, a clear increase in sub-critical crack elongation with increasing atmospheric water content was observed. Moreover, elevated temperature is found to enhance this water sensitivity, supporting an interpretation of a thermally activated transport and reaction mechanism contributing to microcrack development under these conditions. To provide further insight into the potential physical and chemical conditions at the microcrack tip, micro-Raman measurements were performed. Preliminary results, now under investigation, indicate a spatially dependent variation in the frequency of the 520 cm-1 vibrational resonance in the region of the indenter and the crack tip that are associated with local stress state.

Simultaneously, to characterize atomic-scale mechanisms that govern microcrack growth, the experimental effort is paired with molecular dynamics (MD) investigations of microcrack evolution in single crystal Si. An examination of the MD results shows that the crack-tip dynamics is intimately related to the crack orientation with respect to the principal crystallographic axis, which in turn, determines the elastic strain energy release rate and the stress-strain response. Further, MD-derived mechanical parameters serve as inputs for a coarser-grained peridynamics model for crack propagation, enabling a closer correspondence to the experimental effort.

9563-8, Session 2

Environmental aging in polycrystalline-Si photovoltaic modules: Comparison of chamber-based accelerated degradation studies with field-test data

Kelly Simmons-Potter, Teh Lai, Ryan P. Biggie, Adria Brooks, Barrett G. Potter Jr., The Univ. of Arizona (United States)

Lifecycle degradation testing of photovoltaic (PV) modules in accelerateddegradation chambers can enable the prediction both of PV performance lifetimes and of return-on-investment for installations of PV systems. With degradation results strongly dependent on chamber test parameters, the validity of such studies relative to fielded, installed PV systems must be determined. In the present work, accelerated aging of a Trina Solar 250 W polycrystalline silicon module is compared to real-time performance degradation in a similar, fielded, PV technology that has been operating since October 2013. Investigation of environmental aging effects are performed in a full-scale environmental chamber equipped with single-sun irradiance capability providing illumination uniformity of 98% over a 2 x 1.6 m area. Time-dependent, photovoltaic performance (J-V) is evaluated over a recurring, compressed night-day cycle providing representative local daily solar insolation for the southwestern United States, followed by dark (night) cycling. This cycle is synchronized with thermal and humidity

Conference 9563: Reliability of Photovoltaic Cells, **SPIE**, OPTICS+ Modules, Components, and Systems VIII

PHOTONICS OPTICS+PHOTONICS FOR SUSTAINABLE ENERGY

environmental variations that are designed to mimic, as closely as possible, test-yard conditions for the fielded system. Early results confirm the impact of environmental conditions on the module long-term performance. While the effects of temperature de-rating can be clearly seen in the data, removal of these effects enables the clear interpretation of module efficiency degradation with time and environmental exposure. Analysis of PV module efficiency degradation for the chamber-tested system shows good comparison to the field-tested system with <1% degradation following an equivalent year of testing.

9563-9, Session 3

PID: From material properties to outdoor performance and quality control counter measures (Invited Paper)

Juliane Berghold, Simon Koch, PI Berlin AG (Germany); Sebastian Pingel, PI Solar Technology GmbH (Germany); Paul Grunow, PI Berlin AG (Germany)

PID is a topic with major interest and it is increasingly evident in field (Figure 1).

Figure 1: PID affected power plants with involvement of PI Berlin

Although the main root causes and referring counter measures for PID are known, a significant part of the industrial modules are still found to be PID sensitive in PID testing.

This paper is discussing field occurrence of PID with respect to environmental conditions and material properties.

One aspect for the avoidance of PID is the encapsulation material. Quality control measures were developed for the verification, whether the encapsulant (in industrial modules) is according to the 'certified' BOM.

Examples are given for the correlation of PID lab tests of a (commercial) BOM with real outdoor degradation.

Furthermore, result from outdoor experiments (Figure 2) are presented for samples at different locations (e.g. Berlin, Cyprus) with different climates and referring parameters (radiation, temperature, surface conductivity etc.) and compared with real PID field findings in power plants.

Figure 2: PID degradation (monitored by Rsh (blue, red)) for samples in Berlin and Cyprus.

Radiation (yellow) and surface conductivity (green).

Simulated potential distrbutions (Figure 3) of a solar module are presented for different conditions and materials and discussed in terms of real outdoor findings.

Figure 3: Potential distribution for different conditions (left: 'wet' versus 'dry') and with different encapsulation materials (right: ,high resistivity' versus ,low resistivity).

PID lab test result at different conditions are presented and comapred to PID field findings at different climates and conditions.

Module M, ?P=-75% Module N, ?P=-55% Module O, ?P=-46%

Figure 4: PID field degradation in PV power plant at a ,hot & humid' location and near the coast.

9563-10, Session 3

Survey of potential-induced degradation in thin film modules (Invited Paper)

Peter Hacke, Kent Terwilliger, Stephen H. Glick, Greg Perrin, Sarah R. Kurtz, National Renewable Energy Lab. (United States)

Two each CdTe and CIGS type modules were tested for degradation to system voltage stress with positive and negative 1000 V bias in an 85°C, 85% relative humidity damp heat environment. Both CdTe (currently not in production) module types exhibited degradation of about 20% power

in 500 h under negative bias, although I-V curve data indicated one type was affected more prominently by series resistance losses, the other by recombination losses. One CdTe module type showed signatures of transparent conductive oxide delamination from the glass after about 750 h of stress testing. Performance of CIGS modules differed depending on the generation of technology. Under negative bias, the older module design showed an initial 12% (relative) improvement, possibly because of the influx of sodium ions that has been reported to benefit the electrical properties, followed by severe degradation with continued stress testing. The newer design CIGS module exhibited the best stability of the four thin film types tested with less than 5% (relative) power drop after 1200 h of test, and had around one order of magnitude lower leakage current from the biased active absorber layer to ground as well. Relative rates of leakage current to ground between chamber tests and modules placed outdoors under system voltage stress will be compared to extrapolate anticipated coulombs accumulated because of leakage over the lifetime of the module.

9563-11, Session 3

A modeling framework for potential induced degradation and soiling in PV modules

Peter Bermel, Reza Asadpour, Muhammad A. Alam, Purdue Univ. (United States)

Two major sources of performance degradation for glass-encapsulated PV modules are potential-induced degradation (PID) and soiling-induced efficiency loss, due to dust accumulation, precipitation, and abrasion. Recent studies have shown that thin-film modules operating in damp heat at -600 V are vulnerable to large amounts of degradation, potentially exceeding more than half the original power output. Similarly, the deterioration of glass transmission under adverse soiling conditions has been shown to reduce short circuit currents up to 40%. To improve module reliability and restore power production in the presence of PID and soiling, a fundamental rethinking of accelerated testing is needed. This in turn will require an improved understanding of technology choices made early in development that impact PID and soiling much later.

In this talk, we will present an integrated approach of modeling, characterization, and validation to address these problems. A hierarchical modeling framework will allows us to clarify the mechanisms of PID and soiling. We will employ a physics-based compact model of the cell, topology of electrode interconnection, geometry of the packaging stack, and operating conditions to predict the current, voltage, and temperature distributions in PV modules correlated with the acceleration of specific degradation modes. A self-consistent solution will capture the essential complexity of the technology-specific acceleration of TFPV-PID and soiling as a function of illumination, ambient temperature, relative humidity, and dust properties. This will yield data suitable for direct comparison with indoor and outdoor experiments, and could play a significant role in developing novel accelerated lifetime tests.

9563-12, Session 4

In-situ monitoring of moisture ingress in PV modules (Invited Paper)

Laure-Emmanuelle Perret-Aebi, Federico Galliano, Ctr. Suisse d'Electronique et de Microtechnique SA (Switzerland); Fanny Sculati-Meillaud, Eleonora Annigoni, Ecole Polytechnique Fédérale de Lausanne (Switzerland); Heng-Yu Li, Ctr. Suisse d'Electronique et de Microtechnique SA (Switzerland); Marko Jankovec, Univ. of Ljubljana (Slovenia); Christophe Ballif, Ctr. Suisse d'Electronique et de Microtechnique SA (Switzerland)

One of the key factors for photovoltaic (PV) installations capable to produce energy for more than 25 years with limited degradation is the resistance of PV modules to varying outdoor conditions. Moisture, temperature cycling,



UV irradiation, static and dynamic mechanical loads represent the main environmental factors that affect the module reliability and their effects often superpose in an interdependent way.

Moisture ingress is in particular affecting the performance degradation and can be strongly affected by the choice of PV encapsulant, PV module configuration and exposure location. The moisture ingress behaviour of a PV module can be indirectly predicted by means of Finite Element Modelling (FEM) diffusion modelling, provided that the properties of moisture diffusion and solubility are precisely known for the given materials. However a robust and reliable direct monitoring of the moisture ingress in PV modules is still lacking.

In this work we will present an "in-situ" monitoring technique of relative humidity (RH) by means of miniaturized humidity/temperature sensors embedded in the PV encapsulant. Based on a digital data acquisition the system provides an extremely reliable and low-noise signal of RH and T.

In the experiments the technique has been successfully used on both highly permeable (Glass/Backsheet) and low permeable (Glass/Glass) PV module configurations and using EVA as encapsulant. By parallel monitoring up to 10 sensors spatially distributed in Glass/Glass modules we could show that in steady conditions of T and RH (Damp Heat 85°C and 85 % RH) the moisture ingress in the PV module follows the expected Fickian penetration profile. The diffusion coefficient of moisture in EVA as extrapolated from these tests is within close agreement with the value obtained from permeation tests on the same encapsulant material.

The monitoring of Glass/Backsheet PV modules allowed following the rapid ingress of moisture through the backsheet into the encapsulant. In DH conditions and using a commercial PET based backsheet the encapsulant is completely water saturated after approximately 3 days. The Water Vapor Transmission Rate (WVTR) of the backsheet could be extracted and it was found to be in the same order of magnitude with that obtained from permeation tests.

Finally preliminary results from outdoor monitoring will be showed where different humidity sensors will be used at the same time as a localized weather station at the back of the module and as in situ moisture monitoring embedded in the encapsulant. The measured are compared to the prediction obtained from FEM modelling.

9563-13, Session 4

Investigation of power values of PV rooftop systems based on heat gain reduction (Invited Paper)

Tanokkorn Chenvidhya, King Mongkut's Univ. of Technology Thonburi (Thailand); Manit Seapan, King Mongkut's Univ. of Technology Thonburi (Thailand); Panom Parinya, King Mongkut's Univ. of Technology Thonburi (Thailand); Buntoon Wiengmoon, Naresuan Univ. (Thailand); Dhirayut Chenvidhya, Roongrojana Songprakorp, Chamnan Limsakul, Yaowanee Sangpongsanont, King Mongkut's Univ. of Technology Thonburi (Thailand)

PV rooftop system can generally be installed to produce electricity for the domestic house, office, small enterprise as well as factory. Such a system has direct useful for reducing peak load, meanwhile it also provides shaded area on the roof and hence the heat gain into the building is reduced. This study aims to investigate the shading effect on reduction of heat transfer into the building. The 49 kWp of PV rooftop system has been installed on the deck of the office building located in the middle of Thailand where the latitude of 14 ° above the equator. The estimation of heat gain into the building due to the solar irradiation throughout a day for one year has been carried out, before and after the installation of the PV rooftop system. Then the Newton's law of cooling is applied to calculate the heat gain. The calculation and the measurement of the heat reduction is compared. Finally, the indirect benefit of the PV rooftop system installed is evaluated in terms of power value.

9563-14, Session 4

Partial illumination stress test for thin-film photovoltaic modules

Timothy J. Silverman, Michael G. Deceglie, Chris Deline, Sarah R. Kurtz, National Renewable Energy Lab. (United States)

PV cells can be permanently damaged by exposure to reverse-bias conditions, which can lead to reverse breakdown and the associated very high current density and high operating temperature. This can occur in monolithic thin-film PV modules under simple conditions of partial illumination, when cells that are not fully illuminated may be forced to operate in reverse bias due to mismatch with the illuminated cells.

The IEC standard qualification test for thin-film PV modules includes a hot-spot test that identifies major visual defects, which may pose a safety concern, resulting from partial illumination. But a test is needed to identify serious, permanent loss in performance resulting from partial illumination that may occur in the field.

In this work, we propose a partial illumination stress test for thin-film PV modules that quantifies permanent performance loss. We designed the test with the aid of a computer model that predicts the local voltage, current and temperature stress that result from partial illumination. The model predicts the module-scale interactions among the illumination pattern, the electrical properties of the photovoltaic material and the thermal properties of the module package. The test reproduces shading and loading conditions that may occur in the field. It accounts for reversible light-induced performance changes and for additional stress that may be introduced by light-enhanced reverse breakdown. We present simulated and experimental results from the application of the proposed test.

9563-15, Session 4

PV industry growth and module reliability in Thailand

Dhirayut Chenvidhya, King Mongkut's Univ. of Technology Thonburi (Thailand); Manit Seapan, King Mongkut's Univ. of Technology Thonburi (Thailand); Yaowanee Sangpongsanont, Tanokkorn Chenvidhya, Chamnan Limsakul, Roongrojana Songprakorp, King Mongkut's Univ. of Technology Thonburi (Thailand)

The cumulative PV installations in Thailand are now over 1.2 GWp. This is a result from implementation of the National Renewable Energy Programs and Targets. In the latest Alternative Energy Development Plan (AEDP), the PV electricity production target has increased from 2 GWp to 3 GWp. According to the rapid growth, PV modules have been tested over one thousand modules per annum since 2012. The test purposes include type approval test according to TIS standards, acceptance test and testing for local product development. For type test, the failed test modules were mostly found in a damp heat test. For annual performance evaluation test, power degradation and delamination were found in the modules obtained from various plants. For c-Si PV modules, the degradation of power were in range of 0-4% from its nameplate after 0-5 year operation in the field. For thin-film modules, the degradation and delamination were found in range of 0-13% (about 5% in average) from its nameplate of the modules operated less than 5 years. However, the power degradation of the modules which have been operated at our reference site on campus around 12 years was in range of 10-15% relating to their nameplates.

9563-16, Session 5

The impact of atmospheric species on CIGS solar cells (Invited Paper)

Mirjam Theelen, TNO (Netherlands) and Technische Univ.

Conference 9563: Reliability of Photovoltaic Cells, **SPIE**, OPTICS+ Modules, Components, and Systems VIII

PHOTONICS OPTICS+PHOTONICS FOR SUSTAINABLE ENERGY

Delft (Netherlands); Christopher Foster, Zeger Vroon, TNO (Netherlands); Nicolas Barreau, Institut des Matériaux Jean Rouxel (France); Miro Zeman, TNO (Netherlands) and Technische Univ. Delft (Netherlands)

CIGS solar cells were exposed to liquid water purged with the atmospheric gases carbon dioxide (CO2), oxygen (O2), nitrogen (N2) and air in order to investigate their chemical degradation behavior. The samples were analysed by electrical, compositional and optical measurements before, during and after exposure in order to follow the degradation behavior of these solar cells in time.

The solar cells showed a rapid decrease in conversion efficiency when exposed to water purged with a combination of CO2 and N2 as well as to water purged with air, while their efficiency was slowly reduced in unpurged water and water purged with N2 or O2. Cross-section SEM showed that the exposure of samples to H2O with large concentrations of CO2 led to the dissolution of the ZnO:Al layer, likely starting from the grain boundaries. This resulted in an increased series resistance, which is likely related to an increase in resistivity of the ZnO:Al layer. It also led to a very rapid decrease of the short circuit current of these samples. Therefore, the conversion efficiency was rapidly lost.

9563-17, Session 5

Activities of the PVQAT Thin Film Module Reliability Group 8

Neelkanth G. Dhere, Univ. of Central Florida (United States)

Photovoltaic module qualifications tests such as IEC 61215 and 61646 help in minimizing infant mortality. However, they do not guarantee useful lifetime over the warranty period. Highly accelerated stress testing (HAST) can be useful in exposing design and component weaknesses and consequently increasing the margin of the design. However, they do not duplicate the conditions experienced by the module and hence cannot be used for assuring the desired useful lifetime. Other attempts were concentrated on extending the existing tests such as damp heat test of 1000 hours at 85 OC and 85% RH. However, even though extending the test to 1250 hours may detect flaws that may occur in during field deployment, extending the test to 2000 and 3000 hours may cause failures that are not observed in the field. Therefore, the PV Module Quality Assurance Task Force (PVQAT) is trying to formulate accelerated tests that will be useful towards achieving the ultimate goal of assuring useful lifetime over the warranty period. Examples of accelerated stress tests and the failure modes that can be detected by them in crystalline silicon modules are as follows: damp heat test: corrosion, delamination, junction box adhesion; humidity freeze: delamination, junction box adhesion, insufficiently cured encapsulant; thermal cycles: broken interconnect, broken cells, electrical bond failure, junction box adhesion, potential for arcing. There are 12 groups working under the PVQAT. Of these the Group 8 deals with the Thin Film Module Reliability. It works on the following degradation issues that have been identified for Thin Film PV: corrosion including system voltage induced degradation, semiconductor junction diffusion, cell-to-cell; cell-to-outside interconnections and delamination (structural - macro & micro). The activities of Thin Film Module Reliability Group 8 will be presented.

9563-18, Session 5

Thin film PV standing tall side-by-side with mx-Si, also in terms of reliability

Neelkanth G. Dhere, Univ. of Central Florida (United States)

The UniSolar triple junction a-Si:H always showed exceptionally good reliability and durability. Early generation CIGS and CdTe PV modules had a different qualification standard 61646 as compared to 61215 for c-Si PV modules. This with small vulnerability in harsh climates was used to create doubts about their reliability. Recently CdTe and CIGS glass-to-

glass modules have passed the rigorous accelerated tests. Moreover, the thin film and c-Si PV modules would soon undergo a unified qualification test protocol. Thus there is basis to rate thin film PV modules as lacking in terms of reliability. CdTe PV modules have shown the lowest production cost without subsidies. CIGS and CdTe cell and module have been showing efficiencies equal or greater than those of mx-Si PV modules. Now it can be stated without any hesitation that also in terms of the reliability and durability all the thin film PV modules stand tall and compare favorably mx-Si. Now they should be judged on the basis their suitability for the specific application and market place will decide their ranking.

9563-19, Session 5

Numerical simulation of wind flow over a photovoltaic solar panel using RANS equations

Andre L. Rezende, Instituto Militar de Engenharia (Brazil); Neelkanth G. Dhere, Univ. of Central Florida (United States)

The aim of this study is the numerical simulation of wind flow over solar photovoltaic panels. At present there are 113 schools in Florida that use similar 10-kW photovoltaic (PV) solar energy systems installeds on their campus. The PV electricity is fed to the grid and reduces the consumption of grid electericity of the schools. Moreover, these schools serve as disaster relief shelters. During hurricanes or other disasters the grid electricity to the shelters may be cut for few weeks. The PV electricity can then serve to provide the minimum critical necessities during such periods. Because of strong winds and hurricanes in this region, it is essential to study the effect of flow of wind on photovoltaic panels. Such study can also be useful to design efficient protectors and supports to guard the panels.

Typicals flows phenomena such as vortex shedding and boundary layer separation may influence the distribution of wind load on PV panels. Because of the similar PV system design and construction, the geometry of the solar panel installations and wind conditions would be similar in the PV systems in 113 Florida schools. The wind speed in critical conditions can reach 50 m/s.

This work consists of a steady state and incompressible flow numerical simulation through the Reynolds Averaged Navier-Stokes equations (RANS). The turbulence closure model uses the shear stress transport (SST) k-w.

The main results of the simulations are the pressure and velocity fields that are involved in loads that panels are being subjected to.

9563-20, Session 5

Analysis of PV modules based on thin films solar cells by dark measurements technique

Kamel Agroui, Unite de Developpement de la Technologie du Silicium (Algeria); Michelle Pelegrino, Flaminio Giovanni, ENEA (Italy)

A number of analytical and characterization methods are conventionally employed to measure and determine the PV module performances. For example, current-voltage (I-V), quantum efficiency (QE), photoluminescence (PL) and electroluminescence (EL) measurements are used to allow a direct evaluation of the quality of the solar cells or mini-modules. These methods are in general complementary.

In comparison, impedance spectroscopy (IS) under dark measurements is well known to be highly suitable for analyzing a variety of R-C circuits corresponding to a large number of physical materials and devices. Specifically, IS measurements can readily allow a quantitative evaluation of the electrical property of a solar cell's p-n junction, which is typically represented by an equivalent circuit of a parallel resistor and capacitor (R-C circuit model), and its series resistance. Briefly, in a simplest form of the IS measurements, a small amplitude sinusoidal AC signal is applied to

PHOTONICS
 OPTICS+PHOTONICS
 FOR SUSTAINABLE ENERGY

the PV module over a range of frequency. The PV module responses can be identified by mapping the real and imaginary parts of their complex impedance as a function of the frequency of the applied external electric field.

The goal of this paper is to estimate the PV module performances based on 1J:a-Si and 3J:a-Si amorphous silicon solar cells. The possibility to introduce the IS measurements to more understand the amorphous PV module behavior, as a complimentary non-destructive analysis, will be examined. The frequency and voltage dependent characteristics of PV module are determined by IS technique and frequency response analysis based on sinusoidal and periodic signals.

9563-21, Session 6

Rapid field measurement of cells performance within PV modules (Invited Paper)

Alessandra Colli, Klaus Attenkofer, Brookhaven National Lab. (United States)

To develop an alternative energy economy in which solar energy plays a major role, the risks of system failure have to be understood and quantitative models developed to estimate lifetime and efficiency. The lack of these models is caused by the complexity of the underlying processes in actual operating environments, and the absence of tools which allow the fundamental PV cell parameters to be determined, such as shunt resistivity, connection resistivity, and cell capacity, in an inexpensive, non-intrusive, and non-destructive way. The presentation focuses on a method and tool to collect the essential electric variables of PV cells within a module with no destructive approach. The achievable areal resolution of about 15 mm2 and the modular building concept allows optimizing the system to all commercially relevant solar panel designs. Such tool is expected to provide the information useful to fill the existing gap between applied PV system engineering and PV material physics and analysis, ultimately providing device lifetime information useful to improve the system design and the manufacturing process of PV modules and cells. It can be used to determine: (i) the equivalent electrical parameters of the PV cell and module circuit, linking to material analysis needs, (ii) the degradation pathways, (iii) the lifetime expectations of PV cells module, (iv) the quality status (performance and reliability) of aging installations to meet the energy production expectations and set the financial value of the installation, and (v) the effects of the installation design (e.g. string positioning and grounding system) on degradation.

9563-22, Session 6

PV system reliability program at Sandia National Labs: From material-level to system-level analysis (Invited Paper)

Olga Lavrova, Sandia National Labs. (United States)

No Abstract Available

9563-23, Session 6

When PV modules are becoming real building elements: White solar module, a revolution for BIPV

Laure-Emmanuelle Perret-Aebi, Jordi Escarré, Heng-Yu Li, Laurent Sansonnens, Federico Galliano, Gianluca Cattaneo, Patrick Heinstein, Sylvain Nicolay, Julien Bailat, Ctr. Suisse d'Electronique et de Microtechnique SA (Switzerland); Sébastien Eberhard, Solaxess SA (Switzerland); Christophe Ballif, Ctr. Suisse d'Electronique et de Microtechnique SA

(Switzerland)

The use of photovoltaic (PV) is not anymore an option but a real need in the construction of nearly zero energy buildings. To date, the lack of PV products specifically designed for building integration, considering aesthetics and architectural aspects, is one important limiting factor allowing a massive deployment of PV in the built environment. Architects are continuously asking for new solutions to customize the colour of PV elements to better integrate them into the building skin. Among these colours, white is especially attractive as it is widely used in architecture for its elegance, versatility and fresh look. Until now, white solar modules were not considered to be an option and even never been though to be a technological possibility.

Nonetheless, CSEM recently developed a new technology to make white solar modules a reality. Furthermore, the new Swiss company called Solaxess is now working on the industrialisation of this very innovative technology and the first products are expecting to be on the market at the end of 2015. The technology is based on the combination of two different elements: a solar cell able to convert solar infrared light into electricity and a selective filter which reflects and diffuse the whole visible spectrum.

Any PV technology based on crystalline silicon can be used as they have a good response in the infrared. Approximately 55% of the current generated under standard test conditions comes from the infrared leading to conversion efficiencies above 11%.

We will demonstrate, that thanks to this very innovative technology PV modules can become attractive and real active building elements and therefore meets the requirements of any future energy management through advanced building skins.

9563-24, Session 6

Photovoltaic Reliability Group activities in USA and Brazil

Neelkanth G. Dhere, Univ. of Central Florida (United States); Leila R. O. Cruz, Instituto Militar de Engenharia (Brazil)

Recently prices of photovoltaic (PV) systems have been reduced considerably and may continue to be reduced making them attractive. If these systems provide electricity over the stipulated warranty period, it would be possible attain socket parity within the next few years. Current photovoltaic module qualifications tests help in minimizing infant mortality but do not guarantee useful lifetime over the warranty period. The PV Module Quality Assurance Task Force (PVQAT) is trying to formulate accelerated tests that will be useful towards achieving the ultimate goal of assuring useful lifetime over the warranty period as well as to assure manufacturing quality. Unfortunately, assuring the manufacturing quality may require 24/7 presence. Alternatively, collecting data on the performance of fielded systems would assist in assuring manufacturing quality. Here PV systems installed by home-owners and small businesses can constitute as an important untapped source of data. The volunteer group, PV - Reliable, Safe and Sustainable Quality! (PVRessQ!) is providing valuable service to small PV system owners. Photovoltaic Reliability Group (PVRG) is initiating activities in USA and Brazil to assist home owners and small businesses in monitoring photovoltaic (PV) module performance and enforcing warranty. It will work in collaboration with small PV system owners, consumer protection agencies. Brazil is endowed with excellent solar irradiance making it attractive for installation of PV systems. Participating owners of small PV systems would instruct inverter manufacturers to copy the daily e-mails to PVRG and as necessary, will authorize the PVRG to carry out review of PV systems. The presentation will consist of overall activities of PVRG in USA and Brazil.

9563-203,

The importance of reliability to the SunShot Initiative

Rebecca Jones-Albertus, U.S. Dept. of Energy (United States)

The U.S. Department of Energy's SunShot Initiative was launched in 2011 to make subsidy-free solar electricity cost competitive with conventional energy sources by the end of the decade. Research in reliability can play a major role in realizing the SunShot goal of \$0.06/kWh. By improving photovoltaic module lifetime and reducing degradation rates, a system's lifetime energy output is increased. Increasing confidence in photovoltaic performance prediction can lower perceived investment risk and thus the cost of capital. Accordingly, in 2015, SunShot expects to award more than \$40 million through its SunShot National Laboratory Multiyear Partnership (SuNLaMP) and Physics of Reliability: Evaluating Design Insights for Component Technologies in Solar (PREDICTS) 2 funding programs, for research into reliability topics such as determining acceleration factors, modeling degradation rates and failure mechanisms, improving predictive performance models, and developing new test methods and instrumentation.

9563-25, Session PMon

Analysis of aluminum nano-grating assisted light reflection reduction in metalsemiconductor-metal photodetectors

Xiaohu Han, Yahui Su, Huayong Zhang, Anhui Univ. (China); Xiaohu Han, Anhui Univ (China)

We report homogeneous and high aspect ratio nanogratings fabricated on crystalline GaAs surface exploiting femtosecond laser ablation. An optimum nano-grating height and period for the Homogeneous Nanograting (HNGs) were obtained by Finite-difference Time Domain (FDTD) simulation.The results show that the reflection loss of homogeneous shaped nano-grating structure ,which has a 250 nm grating period and a 630 nm height , is about 34% less than that of flat type GaAs substrates. Then a simple two-step femtosecond ablation process was used to control the nanoscale energy deposition that should be developed through the excitation of Surface Plasmon Polaritons (SPPs) during the fs-laser surface interaction. It is found that the height and shape of the HNGs, can be controlled by changing single pulse energy F and the superimposed shot number N of fs-laser pulses. With increasing the N of low-fluence fs-laser pulses, the periodic nanostructure develops through the bonding structure change of GaAs. Depending upon the experimental parameters nano-grating sizes varied in the range of 150~320nm. The experimental results indicate that the proposed approach can achieve homogeneous and high aspect ratio nanogratings with lower reflection compared to the polished GaAs surface. These nanogratings fabricated in GaAs surface may find potential applications in Photovoltaic Cells, optical recording, and other micro-optical devices.

9563-26, Session PMon

FTIR spectroscopy of silicon carbide thin films prepared by PECVD technology for solar cell application

Angela Kleinová, Polymer Institute (Slovakia)

The plasma CVD reactor with parallel plate electrodes was used for plasma enhanced chemical vapor deposition (PECVD) of silicon carbide films on Si substrates. Technological parameters for the preparation of samples were: substrate temperature was 300 oC and the gas mixture composition for the sample SA1 was (SiH4-7 ml/min., CH4-40 ml/min., Ar-10 ml/min) and for the sample SA2 (SiH4-4 ml/min., CH4-20 ml/min., Ar-10 ml/min., H2-100 ml/min.). For both samples the RF power was 150 W and the pressure was

set to 40 Pa. The concentration of the elements in films was determined by Rutherford backscattering spectrometry (RBS) and elastic recoil detection (ERD) analytical method simultaneously. The chemical compositions of the samples were analyzed by Fourier transform infrared spectroscopy (FTIR). RBS and ERD results showed that the films contain silicon, carbon, hydrogen and small amount of oxygen. FTIR results confirmed the presence of Si-C, Si-H, C-H, and Si-O bonds. From the FTIR spectra the main following vibration frequencies were determined: the band at 2800 to 3000 cm-1 is attributed to stretching vibration of the CHn group in both the sp2 (2880 cm-1) and sp3 (2920 cm-1) configurations. The band at 2100 cm-1 is due to SiHm stretching vibrations. The band at 780 cm-1 can be assigned to Si-C stretching vibration. Main features of FTIR spectra were Gaussian fitted and detailed analyses of chemical bonding in SiC films was performed. Differences between two types of SiC films were discussed with the aim to use these films in the heterojunction solar cell technology.

OPTICS+PHOTONICS FOR SUSTAINABLE ENERGY

9563-27, Session PMon

Raman spectroscopy study of SiC thin films prepared by PECVD for solar cell working in hard environment

Vlasta Sasinkova, Institute of Chemistry (Slovakia)

Amorphous silicon carbide is excellent alternative passivation layer material for silicon solar cells especially working in hard and space environment.

Amorphous silicon carbide films were deposited by PECVD technology using SiH4, CH4, H2 and N2 gas as precursors. Two types of samples were prepared: SV1- amorphous silicon carbide a-SiC:H thin film on Si substrate, SV2- N doped silicon carbide a-SiC(N):H on Si substrate. The concentration of elements in the films was determined by RBS and ERD analytical method. Raman spectroscopy study of the SiC films were performed by using a Raman microscope with 532 nm laser. Irradiation of samples with neutrons to a total fluencies A(7.9x1014 cm-2), B(5x1015 cm-2) and C(3.4x1016 cm-2) was performed. The films contain silicon, carbon, hydrogen and nitrogen. Raman spectra, especially the intensity of the lattice vibration at 520 cm-1. originates from the silicon substrate. The Raman band between 930 cm-1 and 990 cm-1 is created by acoustical and optical phonon modes of cubic or one of the hexagonal polytypes of SiC. The peak broadening is related to the damping of phonon modes due to the short range ordering of SiC crystallites and the effects of surroundings having Si, as well as C-clusters. The Raman band between 1300 cm-1 and 1700 cm-1 is assigned to diamond like carbon. Raman spectroscopy results of SiC showed decreasing of Raman band feature intensity after neutron irradiation and slightly decreased with increased neutron fluencies. Properties and differences between two types of films before and after neutron irradiation are discussed.

9563-28, Session PMon

Critical analysis on degradation mechanism of dye sensitized solar cells

Mukhzeer Mohamad Shahimin, Suriati Suhaimi, Mohamad Halim Abdul Wahid, Vithyacharan Retnasamy, Nor Azura Malini B. Ahmad Hambali, Univ. Malaysia Perlis (Malaysia); Ali Hussain Reshak, Univ. of West Bohemia (Czech Republic)

This paper reports on a précis of degradation mechanism for dye sensitized solar cell (DSSCs). The review indicates progress in the understanding of degradation mechanism, in particular the large improvement in the analysis of the materials used in DSSCs. The paper discussed on the stability issues of the dye, advancement of the photoelectrode film lifetime, changes in the electrolyte components and degradation analysis of the counter electrode. The photo electrochemical parameters were evaluated in view of the possible degradation routes. The new research trend together with the previous research has been highlighted to examine the key challenges faced for better performances solar cells and directly influenced the stability and reliability of DSSCs.



9563-30, Session PMon

Non-destructive luminescence polarization study related to recombination mechanisms and silicon material properties

Radek Stojan, Jirí Vanek, Brno Univ. of Technology (Czech Republic)

For non-destructive luminescence characterization of silicon solar cells is frequently used to standard electroluminescence (EL) diagnostic method. It's known that the EL spectrum from silicon wafer is out of visible range of the electromagnetic spectrum. The presented paper work is focused on room-temperature EL spectra and modify characteristics of polarization emission related to scientific innovation of standard luminescence diagnostic methods. In this paper will be image processing for qualitative analysis of solar cells in schematic diagnostic flow. Extended image processing allows further information to be obtained from EL images. Those details allow efficient interpretation of the results.

The polarization of the luminescence center radiation (ie. electromagnetic waves) can be viewed from the perspective of quantum mechanics. As is well known, luminescence is a radiant recombination of electrical charge in a semiconductor materials. Luminescence center incurred during this recombination can be described and approximated as quantum oscillator. Therefore we can say that the intensity of the emitted photons (which is a defining characteristic of polarization diagnostic method) is related to recombination mechanisms, material properties, optical properties and so junction voltage.

Theoretical describe of polarization emission related to change of intensity lead to additional understand of properties of defects in silicon solar cells. In this idea is potential for advance diagnostic element for better characterization of large defect in silicon structures.

9563-31, Session PMon

Characterizing different defects in multycrystalline silicon solar cells via modern imaging methods

Shishu Lou, Huishi Zhu, Peide Han, Institute of Semiconductors (China)

Defects in multicrystalline silicon solar cells such as impurities, gain boundaries, dislocations and metallic impurities have great influence to the final conversion efficiency of devices. Moreover, different kinds of defects and defects at different depth layers in multicrystalline silicon solar cell play different roles to the final performance of devices. This paper proposes a fast technique via electroluminescence imaging method and photoluminescence imaging method to distinguish different types and depths defects. Different types of defects have various influences to the distribution of extra minority carriers which would result in the distinctions in the final luminescence intensities. Therefore, we can recognize these defects via a group of PL and EL images in a few seconds. Also, we found that defects at different depths show a closely relationship with electrical breakdown which would lead to the differences on the final electroluminescence properties. The EL images under different forwardbiased and reversed-biased voltages give a clear separation of defects near the front surface, around p-n junction and in bulk material. Light beam induced current (LBIC) imaging is used to verify the methods we proposed. These modern imaging methods could become popular methods in photovoltaic testing field, and we hope our research could give some help in the study of silicon based devices.

Conference 9564: Light Manipulating Organic Materials and Devices II

Monday - Thursday 10-13 August 2015 Part of Proceedings of SPIE Vol. 9564 Light Manipulating Organic Materials and Devices II

9564-29, Session PMon

Studies on thermally induced third-order nonlinearity and optical power limiting of Aniline blue diammonium salt investigated using CW He-Ne laser at 633nm excitation

Poornesh P., Pramodini S., Manipal Univ. (India)

We present the results of thermally induced third-order optical nonlinearity and optical limiting performance of an organic dye Aniline blue diammonium salt. Single beam Z-scan technique was used to determine the sign and magnitude of the absorptive and refractive nonlinearities. Continuous wave (CW) He-Ne laser operating at 633nm was used as source of excitation. The nonlinear refractive index n2, the nonlinear absorption coefficient ?eff and the third-order optical susceptibility ?(3) were found to be of the order 10-5esu, 10-3 cm/W and 10-7esu respectively. The observed large third-optical nonlinearity in the dye is due to the presence high ϖ -electron density in the backbone of the molecular structure. Selfdiffraction rings pattern were observed in the dye and it is due to the refractive index change and thermal lensing. The dye exhibits good optical power limiting characteristics at the experimental wavelength 633nm. Optical power limiting and clamping studies were carried out at various input power levels. Optical clamping of about ~ 3mw and limiting threshold of 5~mw was observed. The nonlinear optical studies indicate that the dye investigated here materialize as a promising candidate for nonlinear optical devices applications such optical power limiters.

9564-30, Session PMon

Synthesis, growth, characterization and molecular hyperpolarizabilities of a novel NLO organic material

Ashwatha Narayana Prabhu, Vyasa Upadhyaya, Manipal Univ. (India)

A novel superior characteristic nonlinear optical (NLO) organic material, 1-(5-chlorothiophen-2-yl)-3-(2,3-dimethoxyphenyl)prop-2-en-1-one [CTDMP], has been synthesized and grown as a good-quality single crystal by the slow evaporation solution growth technique. The grown crystals were characterized by FT-IR, single-crystal X-ray diffraction (XRD), differential scanning calorimetry and UV-Visible spectroscopy. Single beam Z-scan technique was employed to study the third order NLO properties of the material. The nonlinear refractive index is found to be of the order of 10-11 cm2 W-1. The magnitude of third order susceptibility is of the order of 10-13 esu. The observed increase in the third order nonlinearity in these molecules clearly indicates the electronic origin. The compounds exhibit good optical limiting at 532 nm, is due to the substituted strong electron donor. The mechanical property of the grown crystals was studied using Vicker's micro hardness tester and the load dependence hardness was observed. CTDMP belongs to the monoclinic crystal system with space group P21/c. The morphology of CTDMP single crystal was indexed using the XRD data as input to the morphology indexing computer program (WinXMorph). To support the observed variation in the experimental NLO property the static second and third order NLO hyperpolarizabilities of the chalcone derivative was computed using semiempirical MOPAC 2012 computer program.

9564-31, Session PMon

Growth and characterization of a new nonlinear optical organic crystal: 2,4,6-Trimethylacetanilide

Vyasa Upadhyaya, Manipal Univ. (India); Sharada G. Prabhu, NMAM Institute of Technology (India)

A new nonlinear optical organic material, 2,4,6-trimethylacetanilide (246TMAA), also known as N-[2,4,6-trimethylphenyl]acetamide, has been synthesized and grown as a single crystal by the slow evaporation technique by organic solvents. The grown crystals have been characterized by morphology study. The crystals are prismatic. Surface examination shows granular dendritic pattern in optical micrograph. The Scanning Electron Micrograph shows the layered growth of the crystal. The Differential Scanning Calorimeter plot shows no phase change until melting point (219°C). The density of the crystals is 1.1g/cc and the crystals are soft. The crystals are transparent in the visible region and in the ultra-violet region till 280 nm. 246TMAA crystallizes with 2 molecules in a monoclinic unit cell in the non-centrosymmetric point group m, space group Pn [1]. Refractive indices of this optically biaxial crystal along the three crystallo-physical axes have been measured at 633 nm. The optical second harmonic generation efficiency of the crystal at 1064 nm is about half that of the urea crystal, measured by powder method using Nd:YAG laser. The results show that the 246TMAA crystal can efficiently be used for up-conversion of infrared radiation into visible green light. [1] V. Upadhyaya et al, Acta. Cryst. E58 (2002) 0997.

9564-32, Session PMon

Study of large nonlinear change phase in Hibiscus Sabdariffa

Mónica Trejo-Durán, Edgar Alvarado-Méndez, José A. Andrade-Lucio, Roberto Rojas-Laguna, M. A. Vazquez-Guevara, Univ. de Guanajuato (Mexico)

High intensities electromagnetic energy interacting with organic media gives rise to nonlinear optical effects. Hibiscus Sabdariffa is a flower whose concentrated solution presents interesting nonlinear optical properties. This organic material shows an important self-phase modulation with changes bigger than 2ϖ . We present a diffraction ring patterns study of the Hibiscus Sabdariffa solution. Numerical results of transmittance, with refraction and absorption simultaneously, is shown.

9564-33, Session PMon

Photorefractive polymer device with improved sensitizing property

Tam V. Nguyen, Ha N. Giang, Kenji Kinashi, Wataru Sakai, Naoto Tsutsumi, Kyoto Institute of Technology (Japan)

Recently, a photoconductive polymer of poly(4-(diphenylamino)benzyl acrylate) (PDAA) has been utilized for fast response photorefractive (PR) application because of a fast hole mobility. In most of previous studies, phenyl-C61-butyric acid methyl ester (PCBM) was used as the only sensitizer. In this study, a high-performance charge generator perylene bisimide (PBI) is additionally added into the composite. By using new charge generator, the sensitivity of PR material at a preferred wavelength and the PR speed can be enhanced simultaneously. PBI derivaties owing to a large core of ϖ -conjugated rings have been proven to provide a high to improve PR properties. To the best of our knowledge, it is the first time





for using a combine of PCBM and PBI to improve the performance of PDAAbased composites. 2-(4-(azepan-1-yl)benzylidene)malononitrile (7DCST) is used as a nonlinear optical chromophore. (4-diphenylamino)phenyl) methanol (TPAOH) is used as a plasticizer. Green laser with the wavelength of 532 nm is used because PBI has a strong absorption. Moreover, according to the previous study by another group, 7DCST also acts as a sensitizer at this wavelength. Surprisingly, a high diffraction efficiency of 76 % and a fast response time of 8 ms were obtained in the present composite (PDAA/7DCST/TPAOH/PBI/PCBM - 45/30/25/0.2/0.4 wt %) under the electric field of 55 V/?m. The introduction of PBI is a promising approach for photorefractive composite owning the video rate response.

9564-34, Session PMon

Effect of metal films on the photostabilities of emissive organic layers as probed by fluorescence microscopy

Sikandar Abbas, Linda A. Peteanu, Carnegie Mellon Univ. (United States)

Electroluminescent (EL) and photovoltaic (PV) devices utilizing conjugated polymers are comprised of an organic layer and metal film electrode deposited on a glass substrate. Photo-damage of emissive organic layers is one factor that decreases the overall efficiency and longevity of EL devices. Therefore, improvements in organic light emitting devices (OLEDs) and solar cells require a deep understanding of photo-chemistry at metal polymer interface and new methods to fabricate photo-stable devices. Here, the effects of metal film substrates on the emission properties of organic layers are investigated using total internal reflection (TIRF) fluorescence microscopy. MEH - PPV was spin casted over gold (Au) films of varying thickness (2 nm to 8 nm). While 8 nm gold films completely guench the MEH-PPV fluorescence, thinner gold films (~ 2 nm) cause minimal quenching. More surprisingly, the MEH-PPV layer exhibits a remarkable increase in photostability when deposited on thin gold films relative to that on glass even in the presence of molecular oxygen and under laser illumination. This is likely to be due to an observed shortening of excited singlet state lifetime of the MEH-PPV in the presence of the metal surface. Enhancing the stability of organic thin films in this manner supports the quest for highly-efficient EL and PV devices.

9564-35, Session PMon

Composition dependent structural, thermal, and mechanical properties of Sm2O3 doped zinc fluoroborate glasses

Sudha D. Kamath, Manipal Institute of Technology (India)

Glasses based on Sm3+ doped zinc fluoroborate have been synthesized and characterized. Formation of glass has been investigated in the 30 ZnF2-20 TeO2-(50-x) B2O3-x Sm2O3 matrix. Fast guenching is required to prevent melt crystallization and adequate heat treatment to diminish thermal stress, which results in an efficient amorphous material. The Differential Scanning Calorimeter (DSC), Scanning Electron Microscopy (SEM), Energy Dispersive X-ray Analysis (EDAX), stability, density and refractive index have been recorded, calculated, measured and analyzed for the glass samples with different concentrations of Sm3+ ranging between 0 to 3 moL%. Density increases as dopant concentration increases and glass transition temperature Tg ranges between 395 and 420°C. The increase of molar volume with Sm2O3 content indicates that the extension of glass network is due to the increase of the number of NBOs. The results found in this investigation showed that the refractive index of glass does not only depend on the density but also depends on the electronic polarizability of the glass. The increasing stability of the glass samples shows that they are thermally resistant. The presence of NBOs in the glass network is also approved by the decrease in glass transition Temperature (Tg). The variation of the properties with different composition of dopant plays a dominant role in determining a good host material in the field of optics and photonics.

9564-1, Session 1

Coupling J-aggregate excitons with confined photons in a strongly-coupled planar microcavity (Invited Paper)

David G. Lidzey, The Univ. of Sheffield (United Kingdom)

By placing an organic semiconductor material having a relatively narrow electronic transition into an optical microcavity, it is possible to 'mix' excitons with confined cavity photons, forming states termed 'cavity polaritons'. Here, I discuss the formation of polariton states in microcavities containing J-aggregates of two different molecular dyes (cyanine dyes), whose J-band electronic transitions are both coupled to the same cavity photon mode. Under such conditions, three polariton branches are formed, with the "middle" polariton branch composed of an admixture of the cavity photon and the two different exciton states. I show using both photoluminescence excitation spectroscopy and photoluminescence emission measurements that such "hybrid" polariton states effectively act as an energy transfer pathway, allowing energy to be transferred between the different exciton states. A model is presented that describes exciton scattering into polariton states, and the subsequent decay and energetic relaxation of polaritons. I argue that the transfer of middle-branch polaritons to the lower-lying excitonic states is an efficient process, that occurs in time-scale of less than 10 fs. I then discuss structures in which a single J-aggregated cyanine dye is placed into a microcavity in which the extended cavity path-length results in the formation of a series of closely spaced cavity photon modes. It is shown that excitons in the cavity can simultaneously undergo strong coupling with at least four cavity photonmodes, effectively forming a ladder of polariton states, with a significant polariton population found in 3 adjacent polariton branches.

9564-2, Session 1

Control of light-matter interaction using organic-inorganic hybrid excitons (Invited Paper)

Vinod M. Menon, The City College of New York (United States)

In this talk we will discuss our recent work on the formation of organic-inorganic hybrid excitons in microcavities as well as the nonlinear optical response of hybrid excitonic systems. Using thin film 3,4,7,8-napthalenetetracarboxylic dianhydride (NTCDA) and ZnO nanocrystals/nanowires we demonstrate enhanced Rabi splitting of hybrid polaritons and improved third order nonlinear optical response. In the former case, the hybrid materials are embedded in an optical microcavity.

9564-3, Session 1

Measuring optical anisotropies in organic semiconductors

Steven J. Brown, Ruth A. Schlitz, Niva A. Ran, Xiaofeng Liu, John A. Love, Christropher J. Takacs, Michael L. Chabinyc, Thuc-Quyen Nguyen, Guillermo C. Bazan, Jon A. Schuller, Univ. of California, Santa Barbara (United States)

Having a firm grasp of the optical properties of the active material is critical when designing optoelectronic devices. While proven optical characterization techniques exist for isotropic, highly crystalline inorganic materials, optical characterization of anisotropic, mesoscopically ordered organic materials is still nascent. Two critical questions need to be answered for efficient device engineering: What are the active material's optical properties, and how do those optical properties relate to film morphology and processing?

In this work we present recently developed momentum-space spectroscopy techniques that are uniquely suited to studying anisotropic optical

Conference 9564: Light Manipulating Organic Materials and Devices II



properties in thin films. Instead of using traditional "real-space" optical design, Fourier-space optics are used to control and measure light in "momentum-space". These momentum-resolved (or equivalently, angle-resolved) techniques have far superior sensitivities to out-of-plane optical properties than traditional techniques and obviate the complicated model-dependent fitting used in e.g. ellipsometry. Using momentum-resolved luminescence and absorption measurements we study polymer (P(NDI2OD-T2)) and small molecule (p-SIDT(FBTTh2)2) films with variable morphologies which depend on processing—thereby connecting structural and optical properties. The information gleaned from these spectroscopies will increase our fundamental understanding of organic materials and allow us to engineer devices and photonic architectures that maximize light-coupling efficiency in the presence of strong optical anisotropies.

9564-4, Session 1

Engineering the photophysical properties of organic semiconductors using plasmonic nanostructures (Invited Paper)

Jean-Charles Ribierre, Kyushu Univ. (Japan) and Japan Science and Technology Agency (JST), ERATO, Adachi Molecular Exciton Engineering Project (Japan) and CNRS-Ewha International Research Ctr., Ewha Womans Univ. (Korea, Republic of); Anthony D'Aléo, Aix Marseille Univ., CNRS, CINaM (France); Fabrice Mathevet, Univ. Pierre et Marie Curie (France); Chihaya Adachi, Kyushu Univ. (Japan) and Japan Science and Technology Agency (JST), ERATO, Adachi Molecular Exciton Engineering Project (Japan); Pascal André, Jeong Weon Wu, CNRS-Ewha International Research Ctr., Ewha Womans Univ. (Korea, Republic of)

In this talk, we report on the engineering of the photophysical properties of organic thin films using carefully designed plasmonic nano-structures. A battery of experimental techniques including steady-state absorption and photoluminescence spectra, time-resolved photoluminescence and femtosecond transient absorption measurements are used to investigate, in both solution and thin film, the photophysical properties of a discotic liquidcrystalline donor-acceptor dyad based on triphenylene and perylene diimide units linked by a flexible non-conjugated bridge. The characterization of the photophysical properties of the dyad film shows that photo-induced charge transfer occurs between the donor and acceptor moieties. I will then demonstrate that the dynamics of the formation of the charge transfer state and its recombination could be tuned with the use of plasmonic nano-structures. The mechanism of this process will be discussed in the frame of the Marcus theory. The influence of plasmonic nano-structures on the light-emitting properties of different organic molecules in thin films is also investigated using steady-state and time-resolved photoluminescence measurements. Overall, the results will provide new guidelines to manipulate the molecular excitonic processes taking place in organic semiconducting thin films using plasmonic nano-structures.

9564-5, Session 1

Ag nanoparticles on a cellulose nanocrystal scaffold for applications in organic photovoltaics (Invited Paper)

Nathan J. Dawson, Case Western Reserve Univ. (United States); Stephen Spinella, Anthony Maiorana, Rensselaer Polytechnic Institute (United States); Kenneth D. Singer, Case Western Reserve Univ. (United States); Richard A. Gross, Rensselaer Polytechnic Institute (United States)

We report on Ag nanoparticles attached to a cellulose nanocrystal (CNC)

scaffold which forms a nanoparticle-on-nanoparticle structure. The morphology of the cellulose scaffolds as well as the coverage and particle size are optimized. The applications to organic photovoltaics (OPV) are illustrated using a Poly(3-hexylthiophene-2,5-diyl) and [6,6]-Phenyl C60 butyric acid methyl ester (P3HT:PCBM) bulk heterojunction solar cell.

Either a poly(3,4-ethylenedioxythiophene)-poly(styrenesulfonate) (PEDOT:PSS) or a graphene oxide (GO) electron blocking layer is spincoated onto the indium-tin-oxide (ITO). The hole blocking layer is a thermally evaporated LiF layer with and without a bathocuproine (BCP) layer between the P3HT:PCBM/LiF interface. The architecture of the most common OPV used in this study was layered as ITO/GO/P3HT:PCBM/BCP/LiF/AI.

We study the effects of the Ag-CNCs introduced at both the front and rear interfaces of the bulk heterojunction with different blocking layers. The photoconversion efficiency of the solar cells is found to increase in some cases, which depends on the Ag-CNC concentration and layering conditions.

9564-6, Session 2

Universal scaling in nonlinear optical molecules (Invited Paper)

Javier Perez-Moreno, Skidmore College (United States)

In organic molecules, the strength of the linear and nonlinear optical response scales depends on the size of the structure. Power-laws that correlate the length of a structure and its nonlinear structure have been proposed by different researchers. These power-laws are described as function of the number of repeating units, and are derived from the experimental characterization of one set of homologue compounds. Typically, every set of homologues has been reported to obey a different power-law. We show how the sum rules allow to derive universal scaling power-laws that apply to all structures and are in agreement with the experimental data. Using the concept of universal scaling, we propose a classification of the scaling behavior that can be used to determine what are the best molecular paradigms for future nonlinear optical applications.

9564-7, Session 2

Design rules for quasi-linear nonlinear optical structures

Richard Lytel, Sean M. Mossman, Mark G. Kuzyk, Washington State Univ. (United States)

The maximization of the intrinsic optical nonlinearities of quantum structures for ultrafast applications requires a spectrum scaling as the square of the energy eigenstate number or faster. This is a necessary condition for an intrinsic response approaching the fundamental limits. A second condition is a design generating eigenfunctions whose ground and lowest excited state probability densities are spatially separated to produce large differences in dipole moments while maintaining a reasonable spatial overlap to produce large off?diagonal transition moments. A structure whose design meets both conditions will necessarily have large first or second hyperpolarizabilities. These two conditions are fundamental heuristics for the design of any nonlinear optical structure.

In this paper, we focus on topologies with a main linear chain and one or more side groups. We use quantum graph models to show how the judicious placement of a side group along a main chain structure can produce exactly the right phase shift in the eigenfunction along the main chain such that the required spatial separations of probability density between the lowest eigenstates along the chain are achieved. We show that if a single side group is correctly placed, additional side groups provide essentially no added increase in the nonlinearity and are not necessary. The length of the side group, as well as its position, must be meticulously selected to ensure that a large phase shift along the chain is introduced while minimizing the charge density diverted to the side group. We discuss the significance of these results for molecular design.



9564-8, Session 2

Development and characterization of thermally stable electro-optic polymers and devices (Invited Paper)

Akira Otomo, Isao Aoki, Chiyumi Yamada, Toshiki Yamada, National Institute of Information and Communications Technology (Japan)

Electro-optic (EO) polymers are key materials for next generation optical communications not only in wide area network but also in local area and storage area network because EO polymer modulator can be operated at fast speed more than 100 GHz with low energy consumption and can be miniaturized in combination with silicon photonics. In practical applications, thermal stability is one of the important issues to be considered for developing EO polymers. Since EO activity of the polymer is proportional to dipole orientation factor of the EO moieties, electric field assisted poling around glass transition temperature (Tg) of the polymer is necessary. However, the poled order of the molecules relaxes gradually at finite temperature, and then EO activity decreases after long period of time. We have successfully developed thermally stable EO polymers that have high-Tg up to 180 °C. They show excellent thermal stability with the Telcordia thermal test. Thermal stability is also characterized by thermally stimulated depolarization current (TSDC) measurement. Analyzing the TSDC, we can estimate the activation energy and relaxation time of polarization at any temperature. We will discuss thermal stability of the high-Tg EO polymers and devices.

9564-9, Session 3

Optical and magnetic probes of hot singlet exciton fission in pi-conjugated polymers for photovoltaic applications (Invited Paper)

Zeev V. Vardeny, Yaxin Zhai, Ella Olejnik, The Univ. of Utah (United States)

We used steady state and ps transient photoinduced absorption (PA), excitation dependence (EXPA(?)) spectrum of the triplet exciton PA band, and its magneto-PA (MPA(B)) response to investigate singlet fission (SF) of hot-excitons into two separated triplet excitons, in luminescent ϖ -conjugated polymers. From the high energy step in the triplet EXPA(?) spectrum of poly(dioctyloxy)-phenylenevinylene (DOO-PPV) films, we identified a hot-exciton SF (HE-SF) process having threshold energy at $E\approx 2ET$ (=2.8 eV, where ET is the energy of the lowest lying triplet exciton); which is about 0.8 eV above the lowest singlet exciton energy. The ps transient PA with 3.1 eV pump excitation shows that in DOO-PPV film triplet excitons are generated at short time; this is missing in DOO-PPV solution. The HE-SF process was confirmed by the triplet MPA(B) response for excitation at E>2ET, which shows typical SF response. The HE-SF process is missing in DOO-PPV solution, showing that it is predominantly interchain. Our work shows that the SF process in ϖ -conjugated polymers is a much more general process than thought previously.

9564-10, Session 3

Interfacial structure and dynamics at organic / metal interfaces (Invited Paper)

Oliver L. A. Monti, The Univ. of Arizona (United States)

The electronic structure of organic semiconductor interfaces presents a complex problem that is challenging for both theory and experiment. I will present recent results on unraveling factors that influence the electronic structure and dynamics at organic / metal interfaces. Using both ground and excited state photoemission spectroscopies, and based on a detailed atomistic understanding of the thin film structure, we are able to unravel the

critical aspects that influence molecule / surface coupling and its influence on interfacial dynamics. The conceptual understanding arising from this work does not only shed light on the delicate interplay of localized and delocalized states, but also has immediate impact on rational design of organic electronic devices.

9564-11, Session 3

Nonlinear coherent spectroscopy in the single molecule limit (Invited Paper)

Eric O. Potma, Univ. of California, Irvine (United States)

Detecting coherent anti-Stokes Raman scattering (CARS) signals from signal molecules is a longstanding experimental challenge. Driving the vibrational CARS response with surface plasmon fields has proven notoriously difficult due to strong background contributions, unfavorable heat dissipation and the phase dispersion of the plasmon modes in the ensemble. In this work we overcome previous experimental limitations and demonstrate time-resolved, vibrational CARS from molecules in the low copy number limit, down to the single molecule level. Our measurements, which are performed under ambient and non-electronic resonance conditions, establish that the coherent response from vibrational modes of individual molecules can be studied experimentally, opening up a new realm of molecular spectroscopic investigations.

9564-12, Session 3

Narrow band gap conjugated polymers for emergent optoelectronic technologies (Invited Paper)

Jason D. Azoulay, Benjamin A. Zhang, The Univ. of Southern Mississippi (United States); Bryan M. Wong, Univ. of California, Riverside (United States); Matthew Y. Sfeir, Brookhaven National Lab. (United States)

Conjugated polymers effectively produce and harvest visible light and find utility in a variety of commercially relevant optoelectronic technologies offering distinct manufacturing paradigms. There is currently considerable interest in expanding the scope of these materials to afford complementary functionality in the infrared (IR) and to endow functionality relevant in emergent technologies. A critical challenge stems from the need to control the frontier orbital energetics (separation, position, and alignment), ground state electronic configurations, interchain arrangements, solid-state properties, and many other molecular features with a degree of synthetic precision that has yet to be achieved. We recently demonstrated that cross-conjugated 4H-cyclopenta[2,1-b:3,4-b?]dithiophene (CPDT) structural units, in combination with strong acceptors with progressively delocalized ϖ -systems, afford modular donor-acceptor copolymers with broad and long wavelength light absorption that spans technologically relevant wavelength (?) ranges from 0.7 < ? < 3.2 ?m (Eg < 0.5 eV). These solution-processable materials possess some of the narrowest band gaps reported to date and exhibit unique optical, electrical, spin, and magnetic activities. In this contribution, we will describe the synthesis and characterization of these materials and couple these results with first-principles electronic structure calculations to highlight how incorporation of peripheral cross-conjugated substituents to a cyclic substructure within a ϖ -conjugated system provides a much more complex, versatile, and highly valuable tool for the tuning of material properties.

9564-13, Session 4

Dynamic filtering with liquid crystals (*Invited Paper*)

Timothy J. White, Air Force Research Lab. (United States); Kyung Min Lee, Air Force Research Lab. (United States)

Conference 9564: Light Manipulating Organic Materials and Devices II



and Azimuth Corp. (United States); Vincent P. Tondiglia, Air Force Research Lab. (United States) and Leidos (United States)

We report on the preparation of stimuli-responsive optical materials based on cholesteric liquid crystals capable of large range tuning of the reflection wavelength as well as control over the reflection bandwidth. The exceptional optical performance of these dynamic filters is enabled by polymer stabilization and the exploitation of a ionic-based, electromechanical mechanism. In this presentation, we will elucidate the fundamental optical properties of this system and contrast it to other approaches. Further, recent structure-property-performance studies relating to the properties of the polymer network will be discusses.

9564-14, Session 4

Optical switching with sign control using a nonlinear layer structure

Pengfei Wu, Nankai Univ. (China)

All-optical functions and high confinement of optical field in structures such as waveguide and photonic crystals are fundamental issues of scientific and practical importance in the fields of photonic technology [1,2]. Nonlinear optical effects like the intensity dependency of the refractive index can be used in designed structures to all-optically control or self-confine the optical field and thus offer exciting perspectives to control the flow of light beams by purely optical means [3-4]. The unique properties of nonlinear optical structures allow us to build small, low cost and fast all-optical functionalized elements such as all-optical switch to replace currently-used complex electro-optical systems for applications in the next generation of all-optical networks.

In this study, we demonstrate an all-optical switching device with a nonlinear waveguide-like structure containing liquid-crystal nonlinear material. We observe that the light field coupling out the device cladding surface has interesting intensity-depended property which furnishes the device with an additional feature that the switching sign is controllable from positive to negative. The results are unique and may be useful for photonic applications in all-optical communication and optical sensing. The negative switching feature is also useful for power limiting applications to protect the optical sensors. In our study, the device is operated at low light intensity and the switching response time of the device is as fast as nanoseconds.

References:

[1] D. N. Christodoulides, F. Lederer, and Y. Silberberg, Nature, 424, 817-823 (2003)

[2] J. Yang, Q. Zhou, and R. T. Chen, Appl. Phys. Lett. 81, 2947-2949 (2002)[3] T. T. Alkeskjold, J. Lægsgaard, A. Bjarklev, D. S. Hermann, Anawati, J.

Broeng, J. Li and S.-T. Wu, Opt. Express, 12, 5857-5871 (2004)

[4] M. A. Bader, G. Marowsky, A. Bahtiar, K. Koynov, C. Bubeck, H. Tillmann, H.-H. Hörhold, S. Pereira, J. Opt. Soc. Am. B 19, 2250-2262 (2002)

9564-15, Session 4

From nonlinear magneto-optics to magnetism in conducting polymers (Invited Paper)

André P. Persoons, Katholieke Univ. Leuven (Belgium); Palash Gangopadhyay, College of Optical Sciences, The Univ. of Arizona (United States); Philippe Dubois, Olivier Coulembier, Nicolas Delbosc, Univ. de Mons (Belgium); Thierry Verbiest, Guy Koeckelberghs, Katholieke Univ. Leuven (Belgium)

An overview is given on synthesis of ϖ -conjugated macrocycles based upon regioregular poly(3-hexyl)thiophenes. The latest macrocycles obtained, with about 30 thiophene-units, are fully conjugated with closure of the ring by an

ethenyl bridge enabling also the interruption of the conjugation by simple chemical reduction. To understand the magnetic effects observed in these organic macrocycles and cyclic structures the hypothesis is forwarded that persistent currents are present in these macrocycles. Detailed calculations and simulations on the ϖ -electron distribution in macrocycles of these cyclic poly(3-hexyl)thiophenes will be presented and related to possible fluctuating or persistent currents - as previously shown to be present in mesoscopic rings of (not superconducting) metals.. SQUID measurements on these macrocycles are undertaken to investigate experimentally the presence of fluctuating magnetic moments generated by ring currents in these new molecular structures This could be the cause of giant Faraday rotation observed, as well as the ferromagnetic transition observed in regioregular poly(3-dodecyl)thiophene at cryogenic temperatures. The possible correlation between magnetic properties of macrocycles of ϖ -conjugated thiophene rings and chirality of the macrocyles will be discussed; the wide synthetic possibilites of organics allows to study experimentally these fascinating properties.

Experimental results on Faraday rotation studies from thin films of various polythiophene macrocycles with high degree of regioregularity, but with achiral and chiral alkyl sidechains will be presented. Possible correlations of the Faraday rotation and the supramolecular organization within these thin films will be discussed.

When appropriate, we will discuss some applications, e.g. various magnetooptic devices, or suggest directions for further research.

9564-16, Session 5

Thermoreversible networks for moldable photo-responsive elastomers (*Invited Paper*)

Julia A. Kornfield, California Institute of Technology (United States); Zuleikha Kurji, Washington State Univ. (United States)

Soft-solids that retain the responsive optical anisotropy of liquid crystals (LC) can be used as mechano-optical, electro-optical and electromechanical elements. We use self-assembly of block copolymers to create reversible LC gels and elastomers that flow at elevated temperatures and physically cross link upon cooling. In the melt, they can be spun, coated or molded. Segregation of the end-blocks forms uniform and uniformly spaced crosslinks. Matched sets of block copolymers are synthesized from a single "prepolymer." Specifically, we begin with polymers having polystyrene (PS) end blocks and a poly(1,2-butadiene) midblock. The pendant vinyl groups along the backbone of the midblock are used to graft mesogens, converting it to a side-group LC polymer (SGLCP). In the present case, cyanobiphenyl groups are used as the nonphotoresponsive mesogens and azobenzene groups are used as photoresponsive mesogens. Here we show that matched pairs of block copolymers, with and without photo-responsive mesogens, provide model systems in which the optical density can be adjusted while holding other properties fixed (cross-link density, modulus, birefringence, isotropic-nematic transition temperature). For example, a triblock in which the SGLCP block has 95% cyanobiphenyl and 5% azo side groups is miscible with one having 100% cyanobiphenyl side groups. Simply blending the two gives a series of LC elastomers that have from 0 to 5% azo, while having all other physical properties matched. Results will be presented that show the outcomesof this approach to systematic and largely independent control of optical density and photo-mechanical sensitivity.

9564-17, Session 5

Model photo-responsive elastomers based on the self-assembly of side group liquid crystal triblock copolymers

Zuleikha Kurji, Washington State Univ. (United States) and California Institute of Technology (United States); Julia A. Kornfield, California Institute of Technology (United

Conference 9564: Light Manipulating Organic Materials and Devices II



States); Mark G. Kuzyk, Washington State Univ. (United States)

We report the synthesis of azobenzene-containing coil-liquid crystal-coil triblock copolymers that form uniform and highly reproducible elastomers by self-assembly. To serve as actuators to (non-invasively) steer a fiber optic, for example in deep brain stimulation, the polymers are designed to become monodomain "single liquid crystal" elastomers during the fiber-draw process and to have a large stress/strain response to stimulation with either light or heat. A fundamental scientific question that we seek to answer is how the interplay between the concentration of photoresponsive mesogens and the proximity to the nematic-isotropic transition governs the sensitivity of the material to stimuli. Specifically, a matched pair of polymers, one with ~5% azobenzene-containing side groups (~95% cyanobiphenyl side groups) and the other with 100% cyanobiphenyl side groups were synthesized from identical triblock pre-polymers (with polystyerene end blocks and 1,2-polybutadiene midblocks). These can be blended in various ratios to prepare a series of elastomers that are precisely matched in terms of the backbone length between physical crosslinks (because each polymer is derived from the same pre-polymer), while differing in % azobenzene side groups, allowing the effect of concentration of photoresponsive groups to be unambiguously determined.

9564-18, Session 5

On photomigration in azo-polymers

Zouheir Sekkat, Moroccan Foundation for Advanced Science, Innovation and Research (Morocco)

Photoisomerizable polymers, namely azo-polymers, have attracted much attention because of their tremendous importance in a large spectrum of adjacent research fields, including photochemistry, polymer science and engineering, chemical engineering, optics and nonlinear optics, and so on, Photo-induced patterns of surface deformations in azobenzene containing polymer films have attracted much attention because of possible applications in optical data storage and in nano-fabrication; and it is well known that such patterns reflect the state of the incident light polarization and the light intensity distribution. The photoinduced patterns are due to light induced mass movement of the polymer chains which, in turn, is triggered by the photoisomerization of the azo-chromophores. The polymer moves from high to low intensity regions in the direction of light polarization, and the trans-cis photoselective isomerization plays an important roles in the deformation process. There are studies to theoretically describe photoisomerization induced mass movement in polymers, and till now there is no theoretical model that fully describes the phenomenon, taking into account the combined aspects of photochemistry and photoselection and polymer science and molecular mobility. This is what will be discussed in this presentation.

9564-19, Session 5

Study on visible-light-curable polycarprolactone and poly(ethylene glycol) diacrylate for LCD-projected maskless additive manufacturing system

Yih-Lin Cheng, Hao-Lun Kao, National Taiwan Univ. of Science and Technology (Taiwan)

Photopolymers have been applied in many Additive Manufacturing (AM) systems and mostly are cured by UV light. Biodegradable photo-curable polymers are very limited and are not commercially available. DLP-projected maskless AM systems become more and more popular nowadays, but its working area is limited if the part resolution is required. For larger working envelope purpose, liquid crystal display (LCD) panel has great potentials, and LCD's resolution has been improved significantly in the past few years due to the smart phone application. Therefore, in this research, LCD panel is used to replace DLP for a maskless AM system to cure biodegradable materials, Polycarprolactone (PCL) and Poly(ethylene glycol) diacrylate

(PEG-DA). Due to the characteristics of LCD panel, the material systems should be sensitive and photo-polymerized in visible-light range, particularly in RGB. In this study, various percentages of visible-light photoinitiator, Irgacure 784, in the material systems were investigated. Differential scanning calorimetry (DSC) and thermogravimetric analysis (TGA) were utilized to characterize cured biomaterials. Because of the use of photoinitiator, the biocompatibility of the cured materials was also concerned, and hence, MTT assay tests were performed. The preliminary tests of fabrication, using the LCD-projected maskless AM system, cured grid patterns to illustrate the feasibility. The visible-light-curable PCL and PEG-DA will be able to be adopted in tissue engineering scaffold applications in the future.

9564-20, Session 5

Light manipulating vector polyphotochromatic behavior in organic polarization-sensitive materials

Irakli Chaganava, Barbara N. Kilosanidze, George Kakauridze, Institute of Cybernetics (Georgia) and Georgian Technical Univ. (Georgia)

The phenomenon of vector polyphotochromism within a wide spectral range is revealed in organic polarization-sensitive materials when material is illuminated with linearly polarized actinic light. The effect has a purely vector nature, while the transmission spectrum of the exposed material essentially changes in case of observing between crossed polarizers and the change in the spectrum unambiguously depends on the energy exposure. A significant dependence of the kinetic of the vector polyphotochromism induction on the power density of linearly polarized actinic light (445 nm) is shown for probing beam of 635 nm. It is also shown that the kinetics of the effect depends on the degree of integration of the component molecules of the material by the cohesion of both ways the electrostatic forces (by use mineral electrolytes and polyelectrolytes) and the covalent bonds (azopolymers based on different chromophores), as well as on the photosensitive layer thickness and the concentration of the chromophore. The mechanism of the phenomenon is discussed. Considering the fact that the change in the spectral characteristics occurs throughout the full visible range, this effect may be used for creating the spectrally selective dynamic polarization holographic gratings, displays based on new physical principles, and also for creating modulators and dynamic polarization spectral filters controlled by light.

9564-21, Session 6

Visible light responsive systems based on metastable-state photoacids (Invited Paper)

Yi Liao, Florida Institute of Technology (United States)

Proton transfer is one of the most fundamental processes in nature. Metastable-state photoacids can reversibly generate a large proton concentration under visible light with moderate intensity. which provides a general approach to control various proton transfer processes. The potential of metastable-state photoacids in controlling polymer interactions and properties, supramolecular assemblies, acid catalyzed reactions, and microbial fuel cell have been demonstrated by different groups recently. They have also been used to develop anti-bacterial materials, odorant release materials, cationic sensors and molecular switches. In this talk, the mechanism, structure design, and applications of metastable-state photoacids are introduced. Recent development of different types of metastable-state photoacids is presented. Challenges and future work are also discussed.



9564-22, Session 6

Characterization of photomechanical elastomers for device applications

Elizabeth A. Bernhardt, Joseph T. Lanska, Nathan F. Rasmussen, Chad M. Garrison, Mark G. Kuzyk, Washington State Univ. (United States); Mykhailo Y. Pevnyi, Fred Minkowski, Peter Palffy-Muhoray, Kent State Univ. (United States); Zuleikha Kurji, California Institute of Technology (United States) and Washington State Univ. (United States); Julia A. Kornfield, California Institute of Technology (United States)

Characterizing the photomechanical properties of novel materials and developing a theoretical model for their response functions is a crucial prerequisite for designing devices for medical applications. We present a rigorous determination of several properties of photomechanical elastomers to be used to control placement of a brain stimulation device.

High intensity laser stimulation induces stress in dye-doped photomechanical elastomers, causing a length change. Using principles of nonlinear optics and continuum mechanics, we develop a theoretical model quantifying how these elastomers react to laser stimulation. The model evaluates the quality of the response using a photomechanical coefficient, such that a larger coefficient means a larger stress, and hence a more highly photoresponsive material. We are able to determine the photoresponsiveness as a function of pre-strain, laser intensity, strain history, and other properties. Furthermore, we test our model with various types of elastomers, as well as different dyes and doping agents.

Utilizing commonly available components, we designed and implemented a methodology for characterizing the photomechanical properties of lightactivated materials. We discuss the technical specs of our apparatus as well as its design.

We thank the National Science Foundation (EFRI-??ODISSEI:1332271) for supporting this work.

9564-23, Session 6

Fabrication and modeling of fiber Bragg grating device networks in photomechanical polymer optical fibers

Joseph T. Lanska, Mark G. Kuzyk, Washington State Univ. (United States); Dennis M. Sullivan, Univ. of Idaho (United States)

Glass fiber Bragg gratings (FBGs) have found widespread use in telecommunications and optoelectronics; however, polymer fibers have lower Young's moduli (allowing for easier stretching and wavelength tuning), larger nonlinear optical susceptibilities, and larger photomechanical effects. We report on the fabrication of FBG networks in poly(methyl methacrylate) (PMMA) polymer fibers doped with azo dyes. Our target is the development of Photomechanical Optical Devices (PODs), comprised of two FBGs in series, separated by a Fabry-Perot cavity of photomechanical material. PODs exhibit photomechanical multi-stability, with the capacity to access multiple length states for the same optical input when a mechanical shock is applied.

Using finite-difference time-domain (FDTD) numerical methods, we modeled the photomechanical response of coupled networks of Bragg gratings in a single polymer optical fiber. Our model incorporates material response time, nonlinear susceptibility, intensity-dependent mechanical strain, and coherence length. Our model correctly predicts the essential optical features of FBGs, including narrow reflectance at the Bragg wavelength, as well as the photomechanical multi-stability of nonlinear Fabry-Perot cavity-based PODs. In addition, a POD can act as memory, and its response can depend on input history.

Networks of PODs may provide a framework for smart shape-shifting materials and very fast optical computation where the decision process is

distributed over the entire network. Our models inform and will accelerate targeted development of novel Bragg grating-based polymer fiber device networks for a variety of applications in optical computing and smart materials.

9564-24, Session 6

Adaptable and dynamic soft colloidal photonics

Alexander J. C. Kuehne, Dennis Go, DWI an der RWTH Aachen e.V. (Germany)

Existent photonic systems are highly integrated with the active component being completely isolated from the environment as a result of their complex format. There are almost no example for periodic photonic materials, which can interact with their environment by being sensitive to external stimuli while providing the corresponding photonic response. Due to this lack of interaction with the outside world, smart optical components, which are self-healing or adaptable, are almost impossible to achieve.

I am going to present an aqueous colloidal system, consisting of core-shell particles with a solid core and a soft shell, bearing both negatively and positively charged groups. The described soft colloids exhibit like charges over a broad range of pH, where they repel each other resulting in a pefect and defect-free photonic crystal. In the absence of a net charge the colloids acquire the arrangement of an amorphous photonic glass.

We showcase the applicability of our colloidal system for photonic applications by temporal programming of the photonic system and dynamic switching between ordered and amorphous particle arrangements. We can decrease the pH slowly allowing the particles to transit from negative through neutral to positive, and have them arrange accordingly from crystalline to amorphous and back to crystalline. Thus, we achieve a preprogrammable and autonomous dynamic modulation of the crystallinity of the colloidal arrays and their photonic response.

References

[1] Go, D., Kodger, T. E., Sprakel, J., & Kuehne, A. J.C. Soft matter. 2014, 10(40), 8060-8065.

9564-25, Session 7

Advances in photorefractive polymers and applications (Invited Paper)

Pierre-Alexandre J. Blanche, Brittany Lynn, Robert A. Norwood, Nasser N. Peyghambarian, College of Optical Sciences, The Univ. of Arizona (United States)

Photorefractive (PR) polymers change their index of refraction upon illumination through a series of electronic phenomena that makes these materials one of the most complex organic systems known. The refractive index change is dynamic and fully reversible, making PR materials very interesting for a large variety of applications.

In this talk I will introduce the PR effect in polymers and the different mechanisms that ultimately lead to the index modulation. I will present some of the most recent developments in molecular dopants such as sensitizer molecules. Their function is to absorb the photons and convert them into mobile charges. The mechanism involves the creation of an exciton, the charge must then go over the coulomb barrier and ultimately transfer to the photoconducting polymer. This indicates that HOMO/LUMO energy levels of these molecules should match each other and recombination rates should be as low as possible. In the past, variation of C60 molecules such as PCBM have been used, but most recently advances in functionalized reduced graphene oxide and perylene imide molecules have shown promising development.

At the other end of the PR effect is the chromophore alignment that leads to the index modulation. We used a multiphoton microscope to directly observe the chromophore orientation in the non-homogenous electric field created by coplanar electrodes. This type of electrode geometry, introduced



recently by our group, does not require the sample to be tilted with respect to the writing beams to record the hologram. This is a significant advantage for some applications such as the holographic 3D display we developed.

9564-26, Session 7

Electrostatic modification of ITO/ ZnSe interface in polymer-nematogen composite and its impact on photorefractive hologram

Jingwen Zhang, Jiayin Fu, Hua Zhao, Harbin Institute of Technology (China)

To meet imminent needs in real time holographic updatable display fast response photorefractive (PR) polymeric composites were designed and studied in the past years [1,2]. In further studying selected PR films made of polymer-nematogen composite: poly (N-vinylcarbazole + pentylcyanobiphenyl + fullerene (C60), with excellent photoconducting ZnSe thin films as interlayers, we observed 2D diffraction patterns emerging from the polymeric film when only two incident laser beams of small cross angle were used, without any additional feedback employed in the systems discussed in [3]. It was found that there were distinctly a bulk grating and a surface grating formed in the film, and that the latter was behind the 2D diffraction pattern observed and the accompanying energy transferring direction switching, both beyond the reach of conventional PR picture. The origin of the findings seems rooted in the electrostatic modification of the interface due to electric field applied on the polymeric film [4]. Surface plasmon polaritions (SPPs) were evidently excited near the interface due to blueshift of the plasma frequency of ZnSe via electrostatic modification and this proposed picture elucidates all the findings. The interface electrostatic modification and the SPP involvement deserve further investigation in similar PR systems.

1. P.-A. Blanche, et al. Nature, 468, 80-83 (2010).

2. H. Zhao, C. Lian, X. Sun and J. W. Zhang, Optics Express, 19, 12496-12502 (2011).

3. M. C. Cross, and P. C. Hohenberg, Rev. Mod. Phys. 65, 851-1112 (1993).

4. E. Feigenbaum, K. Diest, and H. A. Atwater, Nano Lett. 10, 2111 (2010).

9564-27, Session 7

Photopolymerizable polymer nanocomposites incorporated with hyperbranched polymer having ultrahigh index of refraction for holographic light manipulation

Yasuo Tomita, Hiroshi Urano, Taka-aki Fukamizu, Yasuhiro Kametani, The Univ. of Electro-Communications (Japan); Naoya Nishimura, Keisuke Odoi, Nissan Chemical Industries, Ltd. (Japan)

Holographic dry photopolymers have received much attention owing to their light-manipulating capability in diffractive optics, optical data storage and optical communications. But simultaneously satisfying requirements for large refractive index modulation and dimensional stability are difficult to achieve in conventional photopolymers owing to their limited refractiveindex range and inherent polymerization shrinkage. In this work we report on the diffraction properties of volume gratings recorded in a new type of photopolymerizable polymer nanocomposites that incorporate hyperbranched polymer (HBP) acting as transporting organic nanoparticles. The HBP was prepared by the polycondensation of a diamine monomer with 2, 4, 6-trichloro-1, 3, 5-triazine in N, N-dimethylacetamide, followed by the end-capping reaction with aniline. The synthesized HBP exhibits ultrahigh index of refraction (> 1.8) since it possesses triazine and aromatic ring units. Its average size and heterogeneity are approximately 10 nm and 4.4, respectively. In order to obtain high dispersion of HBP in monomer, we mixed HBPs with solvents used for a plasticizer. This syrup was further mixed with a photoinitiator titanocene and multi-functional acrylate monomer to prepare photopolymerizable polymer nanocomposite films for holographic measurements. We used a two-beam interference setup to write an unslanted transmission volume grating at grating spacing of 1?m and at a wavelength of 532 nm. We show that a volume grating with the refractive index change as large as 0.02 can be recorded at the HBP concentration of 25 vol.%. The out-of-plane thickness change due to polymerization shrinkage, measured by a holographic method, can also be reduced below 2 % at the HBP concentration of 25 vol.%.

9564-28, Session 7

Photorefractive amplification of moving light signals by photoconductive ferroelectric liquid crystal blends

Takeo Sasaki, Masanori Yoshino, Tokyo Univ. of Science (Japan)

Dynamic amplification of optical signal was demonstrated using a photorefractive ferroelectric liquid crystal blend. Ter-thiophene compounds with chiral structures were chosen as the photoconductive chiral compounds, and they were mixed with an achiral smectic C liquid crystal. The mixtures exhibit the ferroelectric chiral smectic C phase. The photorefractivity of the mixtures was investigated by two-beam coupling experiments. It was found that the ferroelectric liquid crystals containing the photoconductive chiral compound exhibit a large gain coefficient of over 1200 cm-1 and a fast response time of 1 ms. Real-time dynamic amplification of an optical image signal of over 30 fps using the photorefractive ferroelectric liquid crystal was demonstrated.

Conference 9565: Liquid Crystals XIX

Sunday - Monday 9 -10 August 2015 Part of Proceedings of SPIE Vol. 9565 Liquid Crystals XIX

9565-1, Session 1

Electrically tunable selective reflection of light by heliconical cholesteric structures *(Keynote Presentation)*

Oleg D. Lavrentovich, Jie Xiang, Sergij V. Shiyanovskii, Quan Li, Kent State Univ. (United States)

Cholesteric liquid crystals with helicoidal molecular architecture are known for their ability to selectively reflect light with the wavelength that is determined by the periodicity of molecular orientations. Resulting interference colors are highly saturated, they add like colored lights and produce a color gamut greater than that obtained with inks, dyes, and pigments. The periodicity of the helical structure and thus the wavelength of the reflected light can be controlled by chemical composition and sometimes by temperature, but tuning with the electric field has been so far elusive. Here we demonstrate that by using a cholesteric with oblique helicoidal (heliconical) structure, as opposed to the classic "right-angle" helicoid, one can vary the wavelength of selectively reflected light in a broad spectral range, by simply adjusting the electric field applied parallel to the helicoidal axis. The effect can enable many applications that require dynamically controlled transmission and reflection of light, from energysaving smart windows to tunable organic lasers, and transparent "seethrough" displays. Since the material is non-absorbing and transparent everywhere except the electrically preselected reflection band, the effect can be used in creating multilayered structures with a dynamic additive mixture of colors.

9565-2, Session 1

Light-driven motion of micro-particles by means of photoisomerization of azobenzene groups as molecular motor on a liguid crystalline film (Invited Paper)

Seiji Kurihara, Yutaka Kuwahara, Sunnam Kim, Tomonari Ogata, Kumamoto Univ. (Japan)

Light-driven micro-particles (MPs) were prepared by modification of photoresponsive azobenzene(Azo) groups as molecular motors. In a nematic liquid crystal, 5CB, we have achieved remote control of the Azo-modified MPs (Azo/MPs), which constructed with glass spheres (GSs) or rod-like glass particles (GRs) as MPs, by light stimuli. As results of photo-induced isomerization from UV-visible extinction spectroscopy and from phase evaluation under microscope observation, the motion behavior suggest to be correlated with the generation of micro-sized isotropic phase (I-phase) regions, which could be caused by disorganization of the 5CB molecules in the nematic phase (N-phase) due to photo-induced continuous isomerization of Azo groups.

9565-3, Session 1

Liquid crystal based adaptive holography for optical sensing applications (Invited Paper)

Arnaud Peigné, Thales Underwater Systems (France); Umberto Bortolozzo, INLN, Univ. de Nice Sophia Antipolis, CNRS (France); Stéphanie Molin, Daniel Dolfi, Thales Research & Technology (France); Jean-Pierre Huignard, Jphopto (France); Stefania Residori, INLN, Univ. de Nice Sophia Antipolis, CNRS (France) even in noisy environments and with strongly distorted optical wavefronts. We report examples of adaptive holographic systems based on liquid crystals, such as optically addressed liquid crystal spatial light modulator [1] and digital holography with an LCOS spatial light modulator [2]. Thanks to a beam-coupling process, a refractive index grating is written in the LC medium by a reference and signal beam. The induced hologram follows dynamically the low frequency variations undergone by the signal beam, with the frequency bandwidth B of the adaptive adjustment related to the response time of the medium. Indeed, at low frequency (< B) the phase information stored in the hologram is cancelled by the self-diffraction because of the automatic compensation of the phase conjugate components [3]. Thanks to this property, low frequency (< B) noise is rejected while high frequency (>B) phase modulations are transmitted to the diffracted orders and can be directly measured as intensity variations at the output of the hologram.

OPTICS+

PHOTONICS

ELECTRONICS

ORGANIC PHOTONICS+

[1.] U. Bortolozzo, S. Residori, and J.P. Huignard, Materials 5, 1546, (2012).

[2.] U. Bortolozzo, D. Dolfi, J.P. Huignard, S. Molin, A. Peigné, and S. Residori "Self-adaptive vibrometry with CMOS-LCOS digital holography", submitted to Opt. Lett. 2015.

[3.] U. Bortolozzo, S. Residori, and J.P. Huignard, Opt. Lett. 34, 2006 (2009).

9565-4, Session 1

Photodeformation of azobenzene containing liquid crystalline polymer networks (Invited Paper)

Vladimir P. Toshchevikov, Leibniz-Institut für Polymerforschung Dresdene e.V. (Germany) and Institute of Macromolecular Compounds (Russian Federation); Tatiana Petrova, Leibniz-Institut für Polymerforschung Dresdene e.V. (Germany) and Cherepovets State Univ. (Russian Federation); Marina Saphiannikova, Leibniz-Institut für Polymerforschung Dresdene e.V. (Germany)

Azobenzene containing polymers due to their ability to deform under light irradiation have a fascinating potential for technical applications serving as artificial muscles, sensors, microrobots, actuators, etc. Further development of these materials is determined by the understanding of the mechanism of the light-induced deformation. Recently we have shown that reorientation of chromophores perpendicular to the polarization direction of the light E (caused by multiple trans-cis-trans photoisomerization) induces the mechanical stress which is large enough to deform azobenzene polymers [1, 2].

The present theoretical study is devoted to the light-induced deformation of two-component polymer networks containing azobenzene chromophores and liquid crystalline (LC) mesogens. We show that reorientation of chromophores under light irradiation leads to the reorientation of the mesogens due to LC interactions between the components and results in the light-induced deformation of the polymer network. The sign of deformation (expansion / contraction with respect to the vector E) depends on the orientation distribution of the mesogens and chromophores inside the network strands. The magnitude of deformation increases with increase of the volume fraction of chromophores and the strength of LC interactions between the components. Influence of the bent cis-isomers of the azobenzene on the light-induced deformation is discussed.

Acknowledgements: The financial support of the DFG grant GR 3725/2-2 is gratefully acknowledged.

References:

[1] V. Toshchevikov, M. Saphiannikova, G. Heinrich. J. Phys. Chem. B 2009, 113, 5032; 2012, 116, 913; J. Chem. Phys. 2012, 137, 024903.

[2] V. Toshchevikov, M. Saphiannikova. J. Phys. Chem. B 2014, 118, 12297.

Self-adaptive holography allows measuring small optical phase modulations



9565-5, Session 1

Studies of the underlying mechanisms for optical nonlinearities of blue phase liquid crystals

Chun-Wei Chen, National Sun Yat-Sen Univ. (Taiwan); Iam Choon Khoo, Shuo Zhao, The Pennsylvania State Univ. (United States); Tsung-Hsien Lin, National Sun Yat-Sen Univ. (Taiwan); Tsung-Jui Ho, The Pennsylvania State Univ. (United States)

We have investigated the mechanisms responsible for nonlinear optical processes occurring in azobenzene-doped blue phase liquid crystals (BPLC), which exhibit two thermodynamically stable BPs: BPI and BPII. In coherent two wave-mixing experiments, a slow (minutes) and a fast (few milliseconds) side diffractions are observed. The underlying mechanisms were disclosed by monitoring the dynamics of grating formation and relaxation as well as by some supplementary experiments. We found the photothermal indexing and dye/LC intermolecular torque leading to lattice distortion to be the dominant mechanisms for the observed nonlinear response in BPLC. Moreover, the response time of the nonlinear optical process varied with operating phase. The rise time of the thermal indexing process was in good agreement with our findings on the temperature dependence of BP refractive index: ?(ISO) > ?(BPI) > ?(BPII). The relaxation time of the torque-induced lattice distortion was analogue to its electrostriction counterpart: ?'(BPI) > ?'(BPII). In a separate experiment, lattice swelling with selective reflection of <110> direction changed from green to red was also observed. This was attributable to the isomerizationinduced change in cholesteric pitch, which directly affects the lattice spacing. The phenomenon was confirmed by measuring the optical rotatory power of the BPLC.

9565-6, Session 1

Recent results on the heliconical nematic phase

Eva D. Korblova, Alyssa Scarbrough, Mark Moran, Lee Foley, Michael Tuchband, Min Shuai, Renfan Shao, Joseph E. Maclennan, Matthew A. Glaser, Noel A. Clark, David M. Walba, Univ. of Colorado at Boulder (United States)

In 2012 the basic argument for the existence of a new nematic phase exhibiting spontaneous reflection symmetry breaking, the Heliconical Nematic (HN, also known as the Twist-Bend Nematic, or NTB phase) began to get traction, and in 2013 the very tight helical pitch of the prototype HN phase was directly observed by freeze-fracture TEM by the Boulder LC group. Since then, work on this extremely novel phase has accelerated. Organic design and synthesis, including new structured exhibiting the HN phase, theoretical simulations, optical microscopy, and electron and probe microscopy experiments aimed at developing a fundamental understanding of the microscopic origins of the HN phase and emergent mesoscopic properties, will be described.

9565-7, Session 2

Tailoring complex optical fields via anisotropic microstructures (Keynote Presentation)

Yan-Qing Lu, Wei Hu, Guo-Xin Cui, Nanjing Univ. (China)

In recent years, complex optical fields with spatially inhomogeneous phases, polarizations and optical singularities have drawn many research interests. Many novel effects have been predicted and demonstrated for light beams with these unconventional states in both linear and nonlinear optics regimes. Although local optical phase could be controlled directly or through

hologram structures in isotropic materials such as glasses, optical anisotropy is still required for manipulating polarization states and wavelengths. The anisotropy could be either intrinsic such as in crystals/liquid crystals (LCs) or the induced birefringence from dielectric or metallic structures. In this talk, we will briefly review some of our attempts in tailoring complex optical fields via anisotropic microstructures. We developed a micro-photopatterning system that could generate complex micro-images then further guides the arbitrary local LC directors. Due to the electro-optically (EO) tunable anisotropy of LC, various reconfigurable complex optical fields such as optical vortices (OVs), multiplexed OVs, OV array, Airy beams and vector beams are obtained. Different LC modes such as homogeneous alignment nematic, hybrid alignment nematic and even blue phase LCs are adopted to optimize the static and dynamic beam characteristics depending on application circumstances. We are also trying to extend our approaches to new wavelength bands, such as mid-infrared and even THz ranges. Some preliminary results are obtained. In addition, based on our recently developed local poling techniques for ferroelectric crystals, we will also discuss and demonstrate the nonlinear complex optical field conversion in Lithium Niobate wafers with patterned ferroelectric domain structures.

9565-8, Session 2

Electrical induction and optical erasure of birefringence in the isotropic liquid phase of a dichiral azobenzene liquid-crystalline compound (Invited Paper)

Takahiro Yamamoto, National Institute of Advanced Industrial Science and Technology (Japan); Isa Nishiyama, DIC Corp. (Japan)

Liquid crystal is a representative soft matter, which has physical properties between those of conventional liquid and those of crystal in a temperature range above a melting point. A liquid-crystal display (LCD) employs the response of the liquid-crystal alignment to the electric field and is a key device of an information display. For common LCDs, the precise control of the initial alignment of LC molecules is needed so that a good dark state, thus a high contrast ratio, can be obtained. If the birefringence can be induced in the liquid phase by the application of electric field, it is of great use as a material for the LCD application. In this study, we will report a unique property of dichiral azobenzene liquid crystals: an electric induction of birefringence in a liquid phase of an antiferroelectric dichiral azobenzene liquid crystal. The optically isotropic texture changes into the homogenous birefringent texture by the application of the in-plane electric field above the clearing temperature of the liquid crystal. We find that one of the possible reasons of the induction of the birefringence in the isotropic phase is the electrically-induced increase of the phase transition temperature between the antiferroelectric liquid-crystalline and "liquid" phases, i.e., increase in the clearing temperature. The resulting birefringence can be disappeared by the irradiation of UV light, due to the photoinduced isomerization of the azobenzene compound, thus dual control of the birefringent structure, by the irradiation of light and/or by the application of the electric field, is achieved.

9565-9, Session 2

Low voltage driving and ultra-fast switching of SmC* on the slippery interfaces

Jun Yamamoto, Kyoto Univ. (Japan); Isa Nishiyama, DIC Corp. (Japan)

Homeotropic SmC* phase shows the fast electro-optic response against the in-plane electric field, because the molecular tilt direction (C-director) is rotated due to coupling between the spontaneous polarization and the electric field. Perfect orientation and smooth ultra-fast switching (10-100 micro sec) can be achieved. But it is problem for the flat panel application that the driving voltage of the switching is extremely high (>100V/10



micro meter) compare to the conventional nematic and the surface stabilized homogeneous SmC*. In this paper, we demonstrated that the drastic reduction of the driving voltage (<1 order ~10V/10micro meter) by introducing the slippery interface of the liquid walls under interdigitated in-plane electrodes keeping the nature of the ultra-fast switching dynamics. Slippery interfaces are artificially designed and spontaneously realized by the macroscopic phase separation due to the solvent effects on the liquid crystals. Smooth motion of the C-director is originated by the lubrication of the nolecular motion on the slippery liquid interfaces. We have identified the clear change of the mechanism of the electro-optic response of SmC* related to helix motion by analyzing the motion of the Cano's wedge by polarizing microscope. We discussed about the switching dynamics of SmC* on the slippery interfaces both intra and inter helix unwinding/rewinding motions.

9565-10, Session 2

Shape programming with light: Voxelated liquid crystal elastomers (Invited Paper)

Timothy J. White, Air Force Research Lab. (United States); Taylor H. Ware, Air Force Research Lab. (United States) and Azimuth Corp. (United States); Michael E. McConney, Air Force Research Lab. (United States); Jeong Jae Wie, Air Force Research Lab. (United States) and Azimuth Corp. (United States); Vincent P. Tondiglia, Air Force Research Lab. (United States) and Leidos (United States)

Shape can be a functional property of devices. Shape is derived topology and is designed as evident in the planar fold lines of a cardboard box or the mechanical anisotropy of certain natural structures. Here, we report on the use of light to pattern the alignment of liquid crystal elastomers. We report on the development of a facile chemistry platform that is for the first time conducive to photoalignment. Derived from the inherent spatio-temporal control afforded to light, we report on the preparation of topologically blueprinted liquid crystal elastomers that show exceptional properties as actuators and self-folding (deploying) structures.

9565-11, Session 3

Manipulating lipid membrane architecture by liquid crystal-analog curvature elasticity (Keynote Presentation)

Sin-Doo Lee, Seoul National Univ. (Korea, Republic of)

Soft matters such as liquid crystals and biological molecules exhibit a variety of interesting physical phenomena as well as new applications. Recently, in mimicking biological systems that have the ability to sense, regulate, grow, react, and regenerate in a highly responsive and self-adaptive manner, the significance of the liquid crystal order in living organisms, for example, a biological membrane possessing the lamellar order, is widely recognized from the viewpoints of physics and chemistry of interfaces and membrane biophysics. Lipid bilayers, resembling cell membranes, provide primary functions for the transport of biological components of ions and molecules in various cellular activities, including vesicle budding and membrane fusion, through lateral organization of the membrane components such as proteins. In this lecture, I will describe how the liquid crystal-analog curvature elasticity of a lipid bilayer plays a critical role in developing a new platform for understanding diverse biological functions at a cellular level. The key concept is to manipulate the local curvature at an interface between a solid substrate and a model membrane. Two representative examples will be demonstrated: one of them is the topographic control of lipid rafts in a combinatorial array where the ligand-receptor binding event occurs and the other concerns the reconstitution of a ring-type lipid raft in bud-mimicking architecture within the framework of the curvature elasticity.

9565-12, Session 3

Liquid crystals under the spotlight: Light based measurements of electrical and flow properties of liquid crystals (Invited Paper)

Giampaolo D'Alessandro, Thomas P. Bennett, Matthew B. Proctor, Malgosia Kaczmarek, Univ. of Southampton (United Kingdom)

Many liquid crystal devices consist of a thin layer of liquid crystal sandwiched between two transparent plates, normally coated with metal and polymer layers. The first allows the application of an electric field. The second not only gives a preferred orientation to the liquid crystal, but can also play an active role in the cell dynamics. In a photorefractive cell, for example, a photoconducting layer modulates the electric field as a function of the light intensity, thus making them ideal component of optical light modulators.

The performance of such devices depends strongly on the mechanical, electrical and flow properties of their liquid crystal constituents, but also on those of the polymer layers. It is therefore essential for the development of new devices, to be able to characterize as many liquid crystal and polymer parameters as possible in the simplest way. In this paper we generalize a standard cross-polarized intensity experiment to measure cell thickness, pretilt, anchoring energy, elastic constants, rotational viscosity and some of the Leslie viscosities, and also the relative dielectric permittivity and resistivity of the liquid crystal and polymer layers as a function of voltage and light intensity. We are able to do this by using the amplitude and frequency of the applied AC voltage and the intensity and wavelength of the incident light as control parameters. The advantage of using light for all these combined measurements is that we can also create a map of the cell surface and identify areas of anomalous pretilt and anchoring energy.

9565-13, Session 3

Nematic and blue phase liquid crystals for temperature stabilization and active optical tuning of silicon photonic devices (Invited Paper)

Joanna N. Ptasinski, Space and Naval Warfare Systems Ctr. Pacific (United States); Iam Choon Khoo, The Pennsylvania State Univ. (United States); Yeshaiahu Fainman, Univ. of California, San Diego (United States)

We describe the underlying theories and experimental demonstrations of passive temperature stabilization of silicon photonic devices clad in nematic liquid crystal mixtures, and active optical tuning of silicon photonic resonant structures combined with dye-doped nematic and blue phase liquid crystals. We show how modifications to the resonator device geometry allow for not only enhanced tuning of the resonator response, but also aid in achieving complete athermal operations of silicon photonic circuits. [Ref: I.C. Khoo, "DC-field-assisted grating formation and nonlinear diffractions in methylred dye-doped blue phase liquid crystals," Opt. Lett. 40, 60-63 (2015); J. Ptasinski, I.C. Khoo, and Y. Fainman, "Enhanced optical tuning of modified-geometry resonators clad in blue phase liquid crystals," Opt. Lett. 39, 5435-5438 (2014); J. Ptasinski, I.C. Khoo, and Y. Fainman, "Passive Temperature Stabilization of Silicon Photonic Devices Using Liquid Crystals," Materials 7(3), 2229-2241 (2014)].

9565-14, Session 3

Photoalignment control for photonic and mechanical applications (Invited Paper)

Atsushi Shishido, Tokyo Institute of Technology (Japan)

Light-control over molecular alignment has attracted particular interest,



for potential applications such as photonic elements and photomechanical energy conversion. We introduce our recent progress on photoalignment control for optical switching and photomechanics. Dye-doped polymerstabilized liquid crystals decreased the threshold intensity to cause photoinduced molecular reorientation.

9565-15, Session 3

Enhanced electro-optical properties of liquid crystal microlens: Low driving voltage and large dynamic operating range

Yun-Tzu Lin, National Taipei Univ. of Technology (Taiwan); Guan-Jhong Lin, National Taiwan Univ. (Taiwan); Yen-Hsing Lin, Tien-Jung Chen, National Taipei Univ. of Technology (Taiwan); Ying-Jay Yang, National Taiwan Univ. (Taiwan); Chung-Ping Chen, Jin-Jei Wu, National Taipei Univ. of Technology (Taiwan)

In this study, liquid crystal microlens with different radii of hole-pattern electrode and cell gap was simulated and discussed in detail. The fringefield was generated by hole-pattern electrode. The top substrate is a hole-pattern electrode and the bottom is a planar ITO glass. The structure is less affecting factor and easier to discuss. A liquid crystal microlens with large dynamic focal length range at low operating voltage is demonstrated. As the voltage is increased, the phase retardation resulting from the center and edge is decreased and an effective focal length can be obtained. With different radii and cell gap, there is various range of focal length when adjusting the applied voltage. This proposed structure can benefit the electro-optical properties of liquid crystal microlens in the analysis.

9565-16, Session 3

Strengthened nonlinearity in liquid crystal panel with ZnSe aligning layers due to surface charge accumulation

Jingwen Zhang, Tingyu Xue, Hua Zhao, Harbin Institute of Technology (China)

With excellent photoconducting zinc selenide thin films as aligning layers in fabricating liquid crystal (LC) panel with pentyl-cyanobiphenyl doped with fullerene (C60), the response time in writing erasable holograms was shortened further to milliseconds [1-2]. 2D diffraction patterns were observed when two coherent laser beams were overlapped in the LC panel [3], along with intriguing findings. The energy transferring direction and strength between the two beams was found LC laver thickness, incidence face, applied voltage and polarity dependent, so was the exponential gain coefficients by employing hybrid LC panels. The surface dominant grating behind the 2D diffraction patterns was found resulting from electric field induced surface charge accumulation, which pushing the plasma response of ZnSe layer towards visible regime. The dynamics of 2D diffraction patterns and all related findings can be explained well in a proposed picture based on the excitation of surface plasmon polaritons in the interfaces. The elimination of polar aligning layer and phase grating mediation SPP excitation make this LC system promising in designing photonics devices [4].

1. H. Zhao, C. Lian, F. Huang, T. Xue, X. Sun, Y. K. Zou and J. Zhang, Appl. Phys. Lett. 101, 211118 (2012)

2. C. Lian, H. Zhao, Y. Pei, X. Sun, and J. Zhang, Opt. Express, 20, 14, 15843-15852 (2012)

3. T. Xue, H. Zhao, C. Meng, J. Fu, and J. Zhang, Opt. Express, 22, 20964-20972 (2014).

4. K. R. Daly, S. Abbott, G. D'Alessandro, D. C. Smith, and M. Kaczmarek, J. Opt. Soc. Am. B, 28, 1874-1881 (2011).

9565-17, Session 4

Hysteresis on a liquid crystal and polymer composite film (Invited Paper)

Yi-Hsin Lin, Ming-Syuan Chen, National Chiao Tung Univ. (Taiwan); Chun-Yu Hsu, National Tsing Hua Univ. (Taiwan); Jing-Yi Wang, National Chiao Tung Univ. (Taiwan)

We have been developed and studied a liquid crystal and polymer composite film (LCPCF) whose surface properties are electrically switchable resulting from orientations of liquid crystal molecules. Many applications are also developed, such as displays, ophthalmic lenses, sperm testers, and biosensing devices of high-density lipoprotein (HDL) in human serum. In experiments, the hysteresis of LCPCF, defined as the difference between the advancing angle and the receding angle, changes with the applied electric fields which also affects the motion of droplet on LCPCF. In this paper, we investigate how LC orientation and surface morphologies affect the hysteresis of the LCPCF and then affect the motion of the droplet. The droplet on LCPCF has to overcome the hysteresis of LCPCF to move which depends on an oscillation between two sides of the contact angles of a droplet on LCPCF. When the hysteresis of the LCPCF under applied electric fields is low enough, the droplet moves without oscillation. When interfacial interaction between fluid and LC molecules is considered, the hysteresis of LCPCF changes because the LC molecules are realigned by such an interaction which turns out different droplet movement. This study can help us to understand why the droplet can move easily on LCPCF even though the surface free energy of LCPCF does not change dramatically with the applied electric fields.

9565-18, Session 4

Structural dynamics in azobenzene liquid crystal polymer films studied by microscopic and time-resolved techniques (Invited Paper)

Kenji Katayama, Shota Kuwahara, Tomiki Ikeda, Chuo Univ. (Japan)

In the last 20 years, various liquid crystalline (LC) polymer materials including photoresposive molecules have been developed, which have varieties of functions. They are subject to deformation, shape change, even motion, and have been applied for rewritable holograms and grating formation. In such materials, azobenzene included cross-linked liquid crystalline polymers have shown promising results, such as macroscopic bending or motion, and these films can be bent by a UV light and be returned back by a visible light. In this moiety, azobenzene connected to the mesogen is subject to photo-isomerization, causing the polymer chain contraction to induce the macroscopic transformation.

Here, we studied the photo-induced structural dynamics in a LC polymer film including azobenzene by using a time-resolved and a microscopic technique. The film was confined in a liquid crystal cell, while it is a photomobile film under a free standing condition, which is triggered by the photoisomerization of azobenezene. From the result of the time-resolved measurements, the change inside the film induced by UV irradiation was highly anisotropic polarization change, and the induced change was largest when the temperature was optimized for bending. Microscopic observation revealed that the film was consisted of ordered and disordered region with a patched structure, and the UV induced change was travelled in the ordered region on the order of seconds.

9565-19, Session 4

Thermoelectricity in liquid crystals (Invited Paper)

Suhana B. Mohd Said, Norbani Abdullah, Abdul Rahman



Nordin, Univ. of Malaya (Malaysia)

The thermoelectric effect, also known as the Seebeck effect, describes the conversion of a temperature gradient into electricity. A Figure of Merit (ZT) is used to describe the thermoelectric ability of a material. It is directly dependent on its Seebeck coefficient and electrical conductivity, and inversely dependent on its thermal conductivity [1]. There is usually a compromise between these parameters, which limit the performance of thermoelectric materials. The current achievement for ZT-2.2 falls short of the expected threshold of ZT=3 to allow its viability in commercial applications.

In recent times, advances in organic thermoelectrics been significant, improving by over 3 orders of magnitude over a period of about 10 years. Liquid crystals are newly investigated as candidate thermoelectric materials, given their low thermal conductivity, inherent ordering, and in some cases, reasonable electrical conductivity. In this work the thermoelectric behaviour of a discotic liquid crystal, is discussed. The DLC was filled into cells coated with a charge injector, and an alignment of the columnar axis perpendicular to the substrate was allowed to form. This thermoelectric behavior can be explained in terms of the carrier concentration, carrier mobility and orderdisorder transition [3]. A reasonable thermoelectric power in the liquid crystal temperature regime was noted, together with hysteresis effects between the heating and the cooling curves. The following thermoelectric phenomena are unique to liquid crystals: anisotropy, hysteresis effects, and correlation between liquid crystal morphology and thermoelectric behavior, and temperature switching. In summary, thermoelectric liquid crystals may have the potential to be utilised in flexible devices, as a standalone power source

9565-20, Session 4

A composite lens by integrating a polarization switch of ferroelectric liquid crystals with a passively anisotropic polymeric lens for ultrafast laser system

Chia-Ming Chang, Yu-Jen Wang, Hung-Shan Chen, Yi-Hsin Lin, National Chiao Tung Univ. (Taiwan); Abhishek K. Srivastava, Vladimir G. Chigrinov, Hong Kong Univ. of Science and Technology (China)

We recently have developed a bistable negative lens by integrating a polarization switch of ferroelectric liquid crystals (FLCs) with a passively anisotropic focusing element. The proposed lens not only exhibits electrically tunable bistability but also fast response time of sub-milliseconds which leads to good candidate of optical component in ultra-fast laser system for medical applications. In this paper, we redesign and demonstrate a lens with two bistable lens powers of positive and negative lens based on polarization switch of FLC. The focusing properties and electro-optical performance at wavelength of 1064nm are measured and discussed. The damage threshold of the lens and the depth of focus are measured as well. Instead of conventional lenses with mechanical movement in the medical laser system, the electrically tunable focusing lens with fast response time and high damage threshold exhibits precise adjustment. The electrically bistable lenses are also useful in the applications of portable devices, wearable devices and colored ophthalmic lenses.

9565-21, Session 4

Programable lattices of optical vortices in nematic liquid crystal (*Invited Paper*)

Marcel G. Clerc, Univ. de Chile (Chile); Stefania Residori, Umberto Bortolozzo, Institut Non Linéaire de Nice Sophia Antipolis (France) and Univ. de Nice Sophia Antipolis (France); Raouf Barboza, Estefania Vidal-Henriquez, Univ. de Chile (Chile); Gaetano Assanto, Univ. degli Studi di Roma Tre (Italy) Using self-induced vortex-like defects in the nematic liquid crystal layer of a light valve with photo-sensible wall, we demonstrate the realization of programable optical vortices lattices with arbitrary configuration in space.

On each lattice site, every matter vortex acts as a photonic spin-to-orbital momentum coupler and an array of circularly polarized input beams is converted into an output array of vortex beams with topological charges consistent with the vortex matter lattice. The vortex arrangements are explained the basis of light-induced matter defects and topological rules.

9565-22, Session 5

Recent advances in IR liquid crystal spatial light modulators (Keynote Presentation)

Fenglin Peng, CREOL, The College of Optics and Photonics, Univ. of Central Florida (United States); Robert J. Twieg, Kent State Univ. (United States); Shin-Tson Wu, CREOL, The College of Optics and Photonics, Univ. of Central Florida (United States)

Liquid crystal (LC) is an amazing class of electro-optic media; its applications span from visible to infrared, millimeter wave, and terahertz regions. In the visible and short-wavelength infrared (SWIR) regions, most LCs are highly transparent. However, to extend the electro-optic application of LCs into MWIR and LWIR, several key technical challenges have to be overcome: (1) low absorption loss, (2) high birefringence, (3) low operation voltage, and (4) fast response time. In the MWIR and LWIR regions, several fundamental molecular vibration bands and overtones exist, which contribute to high absorption loss. The absorbed light turns to heat and then alters the birefringence locally, which in turns causes spatially nonuniform phase modulation. To suppress the optical loss, several approaches have been investigated: (1) Employing thin cell gap by choosing a high birefringence LC mixture; (2) Shifting the absorption bands outside the spectral region of interest by deuteration, fluorination, or chlorination; (3) Reducing the overtone absorption by using a short alkyl chain. In this paper, we report some recently developed chlorinated LC compounds and mixtures with low absorption loss in the SWIR and MWIR regions. To achieve fast response time, we demonstrated a polymer network liquid crystal with 2-pi phase change at MWIR and response time less than 5 ms.

9565-23, Session 5

Vortex grating diffractive waveplate

Gary F. Walsh, Brian R. Kimball, U.S. Army Natick Soldier Research, Development and Engineering Ctr. (United States); Nelson V. Tabiryan, BEAM Engineering for Advanced Measurements Co. (United States)

Diffractive waveplates (DWP) have recently demonstrated unique optical properties including the creation of high order vortex beams, circular polarization selective diffraction, and complete suppression of zero order diffraction. These devices, which are part of a larger class known as metasurfaces, consist of patterned liquid crystal orientations and have been shown to operate over a broad spectral range. We present DWP gratings that couple incident light perfectly into specific diffraction orders. The continuous non-uniform liquid crystal director patterns for these gratings are constructed from an array of axial waveplate vortex singularities. A mathematical formulation of a grating structure with prefect translation symmetry has been developed. Selection of grating orders is accomplished through design of the vortex topological charge distribution. Switching between diffractive orders can be actuated with a variable phase retarder. We present results from designed arrays showing selective excitation of specific diffraction orders. This device could be used in beam steering and switching applications.



9565-24, Session 5

Imaging in natural light with nematic liquid crystals (Invited Paper)

Tigran V. Galstian, Univ. Laval (Canada)

Nametic liquid crystals (NLC) are most commonly used liquid crystal (LC) materials in various light modulators [1], displays [2] and lenses [3]. However those materials have a fundamental limitation: they are polarization sensitive since the refractive index modulation here is achieved by the electric field induced reorientation of their local anisotropy axis. Thus, the standard imaging optical systems (used in consumer electronic products and dealing with natural light sources [4]) have to use double NLC structures in a cross oriented way and in rather requiring geometrical conditions.

We describe a simple but very efficient optical device that allows the dynamic focusing of unpolarized light using a single NLC layer. The operation principle of the proposed device is based on the combination of an electrically variable "single layer lens" with two fixed optical elements for light reflection and 90? polarization flip. Such an approach is made possible thanks to the close integration of thin film wave plate and mirror. Preliminary experimental studies of the obtained electrically variable mirror show very promising results.

Several standard camera geometries, using the double layer approach, and possible new geometries, using the reflective approach, will be described. References

1. Gordon D. Love, Wave-front correction and production of Zernike modes with a liquid-crystal spatial light modulator, Applied Optics, Vol. 36, Issue 7, pp. 1517-1524 (1997).

2. P. Yeh and C. Gu, Optics of Liquid Crystal Displays, Wiley, 1999.

3. T. Galstian, Smart Mini-Cameras, CRC Press, Taylor & Francis group, 2013. 4. www.lensvector.com

9565-25, Session 5

Device and material technologies for advanced flexible liquid crystal displays (Invited Paper)

Hideo Fujikake, Takahiro Ishinabe, Tohoku Univ. (Japan)

Device and material technologies of our recent researches are discussed for advanced high-guality and large-sized flexible liquid crystal displays. As next-generation displays, flexible displays will create innovative usages and human interfaces due to excellent storability and portability. The features of flexible displays are enhanced as display screen size increases. The flexible liquid crystal displays using plastic substrates instead of glass plates have the great advantages of ease in large-size fabrication, excellent operation reliability and low cost fabrication, in comparison with other flexible displays using organic light emitting diodes formed on plastic substrate. We have researched the molecular-aligned polymer wall spacers, made from a molecular-aligned solution layer of monomer and liquid crystal, for keeping the substrate gap constant and for not disordering liquid crystal alignment. The blue phase liquid crystal layer, which had difficulty in keeping liquid crystal alignment structure, could be stabilized by polymer walls and networks in flexible devices using plastic substrates. Even when using plastic substrates, for maintaining high contrast ratio and wide viewing angle properties, we have been also developing the optical compensation technologies for vertically-aligned and in-plain switching liquid crystal displays based on precise measurement of optical anisotropy for various plastic substrates with different formation methods. We are now researching a flexible local-dimming backlight system by using a segmentdriven polymer-dispersed liquid crystal devices as a thin light-guide plate for flexible displays.

9565-26, Session 5

Bent LC molecules with a 60° central core that can form B7 and B2 phases (Invited Paper)

Junji Watanabe, Tokyo Institute of Technology (Japan)

We synthesized small-angle bent-core liquid-crystalline (LC) molecules based on a 1,2-bis(phenylethylene) benzene central core, containing seven aromatic rings and alkoxy tails with carbon numbers of 12, 16 and 18. This ortho-bistolane central core offers a 60o bend angle. Irrespective of this unusually small angle, these molecules can form banana smectic phases with a ferroelectric B7-antiferroelectric B2 phase sequence upon cooling as clarified from the micoscopic, X-ray and opto-electric observations. This indicates that despite of the low bend angle of 60o, these are able to be still packed into a layer with the polar bent direction parallel to the layer like ordinal banana molecules. The present result is striking since it had been believed that banana phases can only be stabilized when the bending angle is in the range from 110-140o, providing additional insight into the nature of banana-shaped molecules.

9565-27, Session 5

Nonlinear doped liquid crystals for dynamic holographic displays (Invited Paper)

Yikai Su, Shanghai Jiao Tong Univ. (China)

We study nonlinear performances of doped liquid crystals employing azo dye (DR1) and quantum dots. The nonlinear mechanisms include thermal effect, space-charge induced electric field, photo-isomerization, and optical-field induced molecular polarization. Our preliminary investigations reveal that these doped liquid crystals are dominated by different nonlinear mechanisms. In particular, we find that For dye-doped LC, the response time is generally robust to temperature variation but the diffraction efficiency is temperature-sensitive. Whereas, the QD-doped LC remains robust for both characteristics around room temperature. We also demonstrate dynamic holographic displays using these doped liquid crystals at a video rate of 60 Hz.

9565-28, Session 6

Reflective-emissive liquid-crystal displays constructed from AIE luminogens (Keynote Presentation)

Ben Zhong Tang, Dongyu Zhao, Hong Kong Univ. of Science and Technology (Hong Kong, China); Anjun Qin, Hong Kong Univ. of Science and Technology (China)

The chiral nematic liquid crystal (N*-LC) has plenty of prospective applications in LC display (LCD) owing to the selective reflection and circular dichroism. The molecules in the N*-LC are aligned forming a helically twisted structure and the specific wavelength of incident light is reflected by the periodically varying refractive index in the N*-LC plane without the aid of a polarizer or color filter. However, N*-LC do not emit light which restricts its application in the dark environment. Moreover, the view angle of N*-LC display device was severe limited due to the strong viewing angle dependence of the structure color of the one dimensional photonic crystal of a N*-LC. In order to overcome these weaknesses, we have synthesized a luminescent liquid crystalline compound consisting of a tetraphenylethene (TPE) core, TPE-PPE, as a luminogen with mesogenic moieties. TPE-PPE exhibits both the aggregate-induced emission (AIE) and thermotropic liquid crystalline characteristics. By dissolving a little amount of TPE-PPE into N*-LC host, a circular polarized emission was obtained on the unidirectional orientated LC cell. Utilizing the circular polarized luminescence property of the LC mixture, we fabricated a photoluminescent liquid crystal display



(PL-LCD) device which can work under both dark and sunlit conditions. This approach has simplified the device design, lowered the energy consumption and increased brightness and application of the LCD.

9565-29, Session 6

Computational chemistry modeling and design of photoswitchable alignment materials for optically addressable liquid crystal devices (Invited Paper)

Kenneth L. Marshall, Emily R. Sekera, Kyle Xiao, Univ. of Rochester (United States)

Photoalignment technology has received great interest as an alternative to buffed alignment layers for generating high-quality uniform molecular alignment in liquid crystal (LC) devices. The 1054 nm laser damage resistance of coumarin photoalignment layers (up to 60 J/cm2, 1 ns pulse) approaches that of fused silica, making these materials prime candidates for use in photoaligned LC optics for high peak power lasers. Opticallyswitchable azobenzene "command surfaces" have 1054-nm laser-damage thresholds comparable to coumarin materials, and have been proposed for use in an "optically driven" LC spatial beam shaper for high peak power laser applications. Spatially-varying the LC molecules between two alignment states in this device is achieved using low-energy polarized UV/visible incident light, providing the in-system write/erase flexibility of electro-optical LC spatial beam shapers while eliminating conductive coatings and electrical interconnects that reduce laser-damage threshold and increase device fragility and complexity, respectively. Beyond azobenzenes, relatively little has been done to develop photoswitchable alignment layers based on other photosensitive materials, and such development has been guided largely by an empirical approach. Applying computational chemistry methods to photoswitchable alignment materials design presents itself as a unprecedented opportunity to develop predictive capabilities that will lead to materials with low switching energies, enhanced bistability, and resistance to both write/erase fatigue and laser damage. To this end, we will describe our recent efforts to apply Density Functional Theory (DFT) computational methods in determining the effect of molecular structure and functional groups on the optical switching state energies of novel photoswitchable alignment materials composed of acrylate and methacrylate polymer backbones functionalized with azobenzene and spiropyran pendants.

9565-30, Session 6

Photonic band-gap modulation of blue phase liquid crystal (Invited Paper)

Tsung-Hsien Lin, National Sun Yat-Sen Univ. (Taiwan)

Blue phase liquid crystals (BPLCs) are self-assembled 3D photonic crystals exhibiting high susceptibility to external stimuli. Two methods for the photonic bandgap tuning of BPs were demonstrated in this work. Introducing a chiral azobenzene into a cholesteric liquid crystal could formulate a photoresponsive BPLC. Under violet irradiation, the azo dye experiences trans-cis isomerization, which leads to lattice swelling as well as phase transition in different stages of the process. Ultrawide reversible tuning of the BP photonic bandgap from ultraviolet to near infrared has been achieved. The tuning is reversible and nonvolatile. We will then demonstract the electric field-induced bandgap tuning in polymer-stabilized BPLCs. Under different BPLCs material preparation conditions, both red-shift and broadening of the photonic bandgaps have been achieved respectively. The stop band can be shifted over 100 nm. The bandwidth can be expanded from ~ 30 nm to ~ 250 nm covering nearly the full visible range. It is believed that the developed approaches could strongly promote the use of BPLC in photonic applications.

9565-31, Session 6

Asymmetrical phase difference distribution properties of a liquid-crystal microlens array with tetragonally-patterned electrodes

Marenori Kawamura, Kento Nakamura, Akita Univ. (Japan); Susumu Sato, LC-Lens Institute (Japan)

Liquid crystal (LC) materials have a large birefringence property and they are widely used not only for display devices but tunable optical devices. The LC device such as an LC lens with a radially-varying refractive gradient-index distribution can be realized by the LC molecular reorientation caused by an axially symmetrical electric field in the circularly hole-patterned electrode. The LC micro-lens arrays (LC-MLAs) with two-faced circularly holepatterned electrodes have been proposed based on the orientation effects of LC molecules in inhomogeneous electric fields. By controlling the applied voltage on the LC-MLAs, their optical property such as focal length can be electrically varied. The authors also proposed an LC-MLA with two-divided and tetragonally-patterned electrodes for varying a focal length and a beam deflection angle estimated by the induced refractive index distributions.

In this study, the spatial distributions of the re-orientated LC directors in the tetragonal region of the LC-MLA are calculated by a finite difference method for analyzing the static behaviors of the LC directors. The calculated and experimental results are discussed. The phase difference distribution in the tetragonal region can be estimated and its phase profile such as asymmetrical phase difference distribution properties can be predicted fairly well by the calculation.

9565-32, Session 7

Complex topological structures of frustrated liquid crystals with potential for optics and photonics (Keynote Presentation)

Slobodan ?umer, Univ. of Ljubljana (Slovenia) and Jo?ef Stefan Institute (Slovenia); Miha Cancula, Simon Copar, Miha Ravnik, Univ. of Ljubljana (Slovenia)

Geometrical constrains and intrinsic chirality in nematic mesophases enable formation of stable and metastable complex defect structures. Recently selected knotted and linked disclinations have been formed using laser manipulation of nematic braids entangling colloidal particles in nematic colloids [Tkalec et al., Science 2011; Copar et al., PNAS 2015]. In unwinded chiral nematic phases stable and metastable toron and hopfion defects have been implemented by laser tweezers [Smalyukh et al., Nature Materials 2010; Chen et al., PRL2013] and in chiral nematic colloids particles dressed by solitonic deformations [Porenta et al., Sci. Rep. 2014]. Modelling studies based on the numerical minimisation of the phenomenological free energy, supported with the adapted topological theory [Copar & Zumer, PRL 2011; Copar, Phys. Rep. 2014] allow describing the observed nematic defect structures and also predicting numerous structures in confined blue phases [Fukuda & Zumer, Nature Comms 2011 and PRL 2011] and stable knotted disclinations in cholesteric droplets with homeotropic boundary [Sec et al., Nature Comms 2014]. Coupling the modeling with finite difference time domain light field computation enables understanding of light propagation and light induced restructuring in these mesophases. The method was recently demonstrated for the description of low intensity light beam changes during the propagation along disclination lines [Brasselet et al., PRL 2009; Cancula et al., PRE 2014]. Allowing also high intensity light an order restructuring is induced [Porenta et al., Soft Matter 2012; Cancula et al., 2015]. These approaches help to uncover the potential of topological structures for beyond-display optical and photonic applications.



9565-33, Session 7

Acquiring three dimensional images based on electronically controlled liquid crystal micro lens array

Hui Li, Fan Pan, Wuhan Institute of Technology (China); Kan Liu, Wuhan Institute of Physics and Mathematics (China); Yuntao Wu, Yanduo Zhang, Wuhan Institute of Technology (China); Xiaolin Xie, Huazhong Univ. of Science and Technology (China)

In this paper, we will present a novel method based on an electrically controlled liquid crystal (LC) micro lens array (MLA) to acquire threedimensional (3D) image, which is extremely different from the other existing 3D imaging methods. This proposed method doesn't need any mechanical movements because of adapting the proposed LC-MLA as a key imaging element to compose a 3D imaging system. The 3D imaging system based on LC-MLA, which is smart, light and cheap, can be realized to solve that common problem in conventional 3D imaging systems. The LC-MLA with 128?128 elements is fabricated by the methods of photolithography and hydrochloric acid etching. Its top patterned electrode is composed of 128?128 micro-circular holes. The diameter of each micro-circular hole is 50?m, and the center-to-center distance between neighboring lenses is 150?m, and the thickness of LC layer is 20?m. The LC-MLA has 50?m hole-pattern electrodes, the operating voltage as low as 0.2Vrms, focal length range of 50?m-400?m, millisecond response time, and the optical consistency between neighbor elements of 9%. In order to present its 3D imaging feature, an interesting imaging experiment based on LC-MLA is set up. In the experiment, the two-dimensional (2D) images under different perspectives and magnifications are respectively got by tuning the external applied voltage from 0.2 to 5.0Vrms at 0.5Vrms/step, and then a ray back projection algorithm is applied to process those 2D images in order to reconstruct the 3D image of the target object. This 3D imaging system is novel for compactness and smart, so this kind of proposed imaging system is very attractive in many applications, such as 3D TVs, games, and movies.

9565-34, Session 7

Digital confocal microscopy through a multimode fiber (Invited Paper)

Christophe Moser, Damien Loterie, Salma Farahi, Demetri Psaltis, Ecole Polytechnique Fédérale de Lausanne (Switzerland)

Confocal microscopy is an important tool in biological imaging, because it substantially improves the contrast of images compared to wide field microscopy. The principle is based on a double filtering operation: a volume inside the sample is selectively illuminated by a focused beam, and light originating from this focal volume is selectively observed using a pinhole in the detection pathway. We propose to extend the concept to imaging with a multimode fiber for which its transmission matrix (TM) is first measured. Then, by using wavefront shaping and the knowledge of the TM, sharp focus spots are scanned at the distal end of the fiber and the light fields propagating in the reverse direction through the multimode fiber are decoded with the matrix. Then, we implement the double filtering required for confocal microscopy, but in the digital domain. We demonstrate that this leads to a significant increase in imaging contrast in spot-scanned images. A correlation-based filtering technique is also introduced, which offers similar performance for a significantly reduced computational cost.

9565-35, Session 7

The helical nanofilament phase as a host for creation of aligned, nanostructured composites (Invited Paper)

David M. Walba, Rebecca A. Callahan, Eva D. Korblova, Dong Chen, Yongqiang Shen, Michael Tuchband, Eric Carlson, Univ. of Colorado at Boulder (United States); Hanim Kim, KAIST (Korea, Republic of); Garry Rumbles, National Renewable Energy Lab. (United States); Sean E. Shaheen, Univ. of Colorado at Boulder (United States); Dong Ki Yoon, KAIST (Korea, Republic of); Noel A. Clark, Univ. of Colorado at Boulder (United States)

The helical nanofilament (HNF) liquid crystal phase is a member of an unusual class of thermotropic phases with lamellar structures dominated by a tendency towards developing negative Gaussian curvature of the layers. Members of this family are sometimes termed "dark conglomerates," due to their behavior in polarized light microscopy. These include a fluid phases - the high temperature dark conglomerate phase, which is a kind of sponge phase, and the low temperature dark conglomerate phase, also seemingly a sponge phase with structural details currently under investigation. The HNF phase, also a "dark conglomerate," seems to be unique in the family, since slow conformational dynamics indicate a quasi-crystalline structure within layers, but no long range positional correlations across layers. We have been exploring possible applications of the HNF phase, which is highly porous, as a host for the formation of alignable composites for photovoltaics and other organic semiconductor applications. Recent results regarding the structure of these composites, including data suggesting a remarkably elegant nanostructure for HNF-chiral nematic composites, will be discussed.

9565-36, Session 7

Liquid-crystal-based immunodetection beyond texture observations (Invited Paper)

Mon-Juan Lee, Chang Jung Christian Univ. (Taiwan); Chi-Hao Lin, Wei Lee, National Chiao Tung Univ. (Taiwan)

Immunodetection of cancer biomarkers is an essential procedure in early screening and diagnosis of cancer. Going beyond the optical texture observation, this work aims at the development of label-free and array-based multiplex immunodetection techniques by exploiting the high sensitivity of liquid crystal (LC) orientation toward the formation of antigenantibody immunocomplexes. Results from our previous studies suggested that, by applying a nematic LC with large birefringence (?n = 0.33) and by UV modification of the monolayer of N,N-dimethyl-n-octadecyl-3aminopropyltrimethoxysilyl chloride (DMOAP) as the alignment layer, the sensitivity of LC-based immunodetection is drastically enhanced. As a matter of fact, the core technology involved in our previous research still stemmed from the conventional and widely adopted method; i.e., by texture observations, which made quantitative measurements difficult.

In this invited paper, we report on our attempt to further improve the LC-based immunoassay technique through the analysis of some cancer biomarkers commonly used in clinical cancer screening, including carcinogenic antigen 125 (CA125). We propose to overcome the technical limitations in the quantitative analysis of LC-based immunodetection. By means of the induced changes in dielectric and electro-optical properties of LCs, which are expected to change in the presence of different types and concentrations of cancer biomarkers, novel quantitative techniques specific for LC-based immunodetection are developed.



9565-37, Session 7

Revealing pathologies in the liquid crystalline structures of the brain by polarimetric studies

Karen Bakhshetyan, Gurgen G. Melkonyan, Tigran V. Galstian, Armen Saghatelyan, Univ. Laval (Canada)

Natural or "self" alignment of molecular complexes in living tissue represents many similarities with liquid crystals (LC), which are anisotropic liquids. The orientational characteristics of those complexes may be related to many important functional parameters and their study may reveal important pathologies. The know-how, accumulated thanks to the study of LC materials, may thus be used to this end. One of the traditionally used methods, to characterize those materials, is the polarized light imaging (PLI) that allows for label-free analysis of anisotropic structures in the brain tissue and can be used, for example, for the analysis of myelinated fiber bundles.

In the current work, we first attempted to apply the PLI on the mouse histological brain sections to create a map of anisotropic structures using cross-polarizer transmission light. Then we implemented the PLI for comparative study of histological sections of human postmortem brain samples under normal and pathological conditions, such as Parkinson's disease (PD).

Imaging the coronal, sagittal and horizontal sections of mouse brain allowed us to create a false color-coded fiber orientation map under polarized light. In human brain datasets for both control and PD groups we measured the pixel intensities in myelin-rich subregions of internal capsule and normalized these to non-myelinated background signal from putamen and caudate nucleus. Quantification of intensities revealed a statistically significant reduction of fiber intensity of PD compared to control subjects (2.801 \pm 0.303 and 3.724 \pm 0.07 respectively; *p < 0.05).

Our study confirms the validity of PLI method for visualizing myelinated axonal fibers. This relatively simple technique can become a promising tool for study of neurodegenerative diseases where labeling-free imaging is an important benefit.

9565-38, Session 8

The next horizon for diffractive waveplate technology (Keynote Presentation)

Nelson V. Tabiryan, BEAM Engineering for Advanced Measurements Co. (United States); Diane Steeves, Brian Kimball, U.S. Army Natick Soldier Research, Development and Engineering Ctr. (United States)

Thin liquid crystal polymer films coated on a variety of substrates, glass or plastic, planar or curved, solid or flexible, can perform many of the functions of conventional optics -- deflecting, reflecting, focusing, and shaping light beams -- by appropriately patterning their optical axis orientation in the plane of the film. We will discuss this state of the art technology, its current and anticipated capabilities, and opportunities for replacing and augmenting conventional optical elements in photonics and display systems. Novel optical functions due to the full use of the unique combination of mechanical, optical and electro-optical properties of such diffractive waveplate systems will be presented.

9565-39, Session 8

One- and two-dimensional liquid crystal structures for lasing applications (*Invited Paper*)

Inge Nys, Jeroen Beeckman, Kristiaan Neyts, Univ. Gent (Belgium)

Combining liquid crystals with light emitting materials offers interesting

possibilities for lighting and lasing applications. Liquid crystal lasers have great potential as small size, low-cost, widely tunable lasers. Dye-doped chiral nematic liquid crystals are often used as active laser media since a photonic bandgap for visible light is spontaneously formed. In recent years, we have investigated different cases of light emission from one- and two-dimensional liquid crystal-containing structures.

Non-chiral nematic liquid crystals have been used to make electrically tunable lasers with a slope efficiency up to 30%. The laser performance strongly depends on the thickness of the cell and the reflectivity of the substrates.

Chiral nematic liquid crystals are frequently used to make out-of-plane emitting lasers with a one-dimensional structure but they can also be used to develop in-plane emitting liquid crystal lasers with a two-dimensional structure. These lasers have the potential to achieve low threshold lasing and they are suited for integration in a lab-on-chip environment. Compared to the conventional out-of-plane emitting liquid crystal lasers, in-plane emitting lasers with a lying helix structure are more difficult to obtain experimentally and to study theoretically. We investigated different techniques to obtain an in-plane lying helix structure. The accurate modeling of light generation in in-plane liquid crystal lasers is difficult because the structure is two-dimensional and the optical properties are anisotropic. We combine a liquid crystal simulation tool with finite-element calculations to simulate the optical modes.

9565-40, Session 8

Photopatterning of complex molecular orientation fields in liquid crystals

Qi-Huo Wei, Yubing Guo, Miao Jiang, Kent State Univ. (United States); Kai Sun, Univ. of Michigan (United States); Chenhui Peng, Kent State Univ. (United States); Oleg V. Yaroshchuk, National Academy of Sciences of Ukraine (Ukraine); Oleg D. Lavrentovich, Kent State Univ. (United States)

This talk will present a new technique for photopatterning molecular oridentational ordering in liquid crystalline materials. The technique is based on new designs of plasmonic photomasks which, when illuminated with broadband non-polarized light, can generate light with predesigned polarization patterns. Photo-active materials exposed by light with polarization patterns induce spatial-varying molecular orientations of liquid crystal molecules or mesogens with predesigned director fields. This new technique is scalable and inexpensive for large scale manufacturing, and holds a large potential for applications in various liquid crystal device manufacturing. Detailed mask designs and fabrication procedures, and their applications in defining various topological defect combinations or arrays in nematic liquid crystals will be discussed.

9565-41, Session 8

Study of liquid crystal formation of graphene oxide flakes

Ji Hyun Park, Min Jae Kim, HyeRan Jo, Kieup Lee, YoungBeom Jo, Seoul National Univ. (Korea, Republic of); Stephane Campidelli, CEA-IRAMIS (France); Jun Yamamoto, Kyoto Univ. (Japan); Youn Sang Kim, Seoul National Univ. (Korea, Republic of); Giusy Scalia, Seoul National Univ. (Korea, Republic of) and Univ. du Luxembourg (Luxembourg)

Graphene can be produced with chemical method and this process goes through the formation of an oxidative form of graphene, called graphene oxide (GO), useful for mass production of graphene, obtained by reduction. Interestingly, graphene oxide is dispersible in water due to its hydrophilic functional groups and this allows the formation of liquid crystal phases

Conference 9565: Liquid Crystals XIX



above certain threshold concentration. GO shows a discotic nematic phase above a certain concentration threshold. Due to the diversity of GO flake average size, as a result of variations in production methods, the value of the threshold and the width of the region of coexistence of the isotropic and liquid crystal phase can strongly vary from samples to samples. We have observed the appearance of a nematic liquid crystal phase at very low concentration and a co-existence region form 0.1mg/ml to 1.0mg/ml by final GO obtained from synthesis. We have controlled the size of the flakes by ultra-sonication. With smaller flakes the transition concentration shifted towards much higher concentrations since the aspect ratio of the flakes has decreased. We report a detailed study of the size distribution of the GO flakes, together with UV-VIS spectroscopic and polarized dynamic light scattering, for understanding the liquid crystal phase formation.

9565-42, Session 8

Tunable Bragg extraction of light in photonic quasi crystals: Dispersed liquid crystalline metamaterials (*Invited Paper*)

Massimo Rippa, Rossella Capasso, Consiglio Nazionale delle Ricerche (Italy); Cesare Umeton, Univ. della Calabria (Italy); Lucia Petti, Consiglio Nazionale delle Ricerche (Italy)

Metamaterials (MTMs) and Photonic Quasi-Crystals (PQCs) have attracted the attention of the scientific community in the last few years due to their ability to control the electromagnetic (EM) field in an unusual way. The performances of such artificial materials are determined by their engineered configuration; Electromagnetic properties of PCs and PQCs can be controlled by properly designing their geometry: almost each single parameter of these structures, related to periodicity or aperiodicity, shape, material, etc., can be managed to achieve a desired propagation or extraction property. Thus, it is, in general, hard to reconfigure the MTMs or control their extraction properties without redesigning them and repeating the entire fabrication process, so that, transforming these passive optical elements into devices that can be actively controlled or, more in details, fabricating MTMs that are reconfigurable/switchable, represents a new challenge. In this communication, we report on the realization and characterization of a switchable photonic device, working in the visible range, based on nanostructured PQCs, layered with a photo-responsive LC. Both experimental characterization and numerical simulations show that extraction spectra can be controlled by applying an external voltage or by means of a laser light. In our opinion, these results represent a breakthrough in the realization of innovative MTMS based active photonic devices.

9565-43, Session PMon

Analysis of selective reflection spectrum in cholesteric liquid crystal cells for solar-ray controller

Akifumi Ogiwara, Kobe City College of Technology (Japan); Hiroshi Kakiuchida, National Institute of Advanced Industrial Science and Technology (Japan)

If a nematic liquid crystal is doped with a concentration of chiral materials, then cholesteric liquid crystal (CLC) is formed with a certain helical pitch in a chiral nematic phase. Because the CLC cells have attracted features such as periodic helical structure, wavelength selective reflection of circularly polarized light, and tunable reflection wavelength, they have been widely used for modern electro-optic applications. The pitch length of the helix corresponding to a molecular rotation is determined by the concentration of the chiral dopant, decreasing with increasing the fraction of the chiral dopant. The central wavelength and bandwidth of selective reflection spectrum in CLC cells is characterized by the chiral dopant molecules and the polymer network structure formed by photopolymerization. The bandwidth of the selective reflection spectrum in CLC cells is affected by doping liquid crystal (LC) diacrylate monomers which define a macroscopic helical twisting power in photopolymerization.

We investigated the effects of modulation of the selective reflection spectrum in CLC cells on the visible and infrared lights in spectral solar irradiance. The CLC cells are fabricated by varying the concentration of various chiral dopants and liquid crystal (LC) diacrylate monomers. The central wavelength and bandwidth of selective reflection spectrum in CLC cells are evaluated by a spectroscopic analysis. The spectral solar irradiance for air mass 1.5 and the standard luminous efficiency function for photopic vision are analyzed to estimate the performance for a solar-ray controller based on the results. The optical characteristics achieved in CLC cells are confirmed to be applicable as a novel optical device for a solar-ray controller.

9565-44, Session PMon

LCD

Dongyu Zhao, Beijing Univ. of Aeronautics and Astronautics (China)

Twisted nematic (TN) liquid crystal devices doped with flower-type CuS nanoparticles were fabricated. The effects of CuS nanoparticles on the drive voltage, contrast ratio and response time of TN liquid crystal devices were investigated. It was found that addition of flower-type CuS nanoparticles remarkably decreased the drive voltage as well as response time and significantly increased the contrast ratio. The reason was deeply analyzed. Firstly, through doping of CuS nanoparticles, the movement of charged ions in liquid crystal is limited and the gather of charged ions on both sides of the electrodes is effectively inhibited, which reduces the shielding effect of charged ions and leads to decline of the drive voltage and the response time.

Furthermore, the orientation of liquid crystal molecules nearby is influenced by the orientation of CuS nanoparticles. They cannot form distorted arrangement ideally, and the light transmittance in the off state dropped significantly and light transmittance in the open state have elevated. Owing to the above two reasons, the contrast ratio increases strikingly. After doping 0.05% CuS nanoparticles, Vth and Vsat of TN liquid crystal cells fall to the minimum value. Moreover, contrast ratio of LCs increases distinctly. From the above discussion, the conclusion can be reached that with the doping of flower-type CuS nanoparticle, twisted nematic LCD modes have better electro-optical performances. Considerable work, hopefully, will be done in this area.

9565-45, Session PMon

Multifocal liquid-crystal-lens properties with additional ring-electrodes

Marenori Kawamura, Kensuke Tamura, Makoto Chida, Akita Univ. (Japan); Susumu Sato, LC-Lens Institute (Japan)

Many types of optical devices using nematic liquid crystal (LC) materials with a large birefringence and dielectric anisotropy have been developed. S.Sato et al. reported an optical device such as an LC lens with a circularly hole-patterned electrode for tuning a focal length without any mechanical movements. The LC lens with a wide variable range from a concave (negative) lens property to convex (positive) lens property has been reported. The low-driving-voltage LC lens was realized by using a highly resistive thin-film with the appropriate sheet resistivity.

In this study, we propose a low-driving-voltage multifocal LC lens, such as a concave lens inside a convex lens or a convex lens inside a concave lens. The multifocal LC lens is prepared using a circularly hole-patterned ITO electrode (15mm in diameter), inner electrode and additional ring electrodes inside the patterned-hole. A highly resistive transparent film on an insulating polymer film is laminated on these ITO electrodes. A polyimide (PI) alignment film is coated on the high resistance film and rubbed unidirectionally. Then, nematic LC material is sandwiched between the electrode and other transparent ITO electrode coated by a PI alignment film.

The multifocal lens properties, such as a ring-shaped concave-lens of about 3.5 mm width outside a convex-lens at a diameter of 8 mm or a convex-lens



outside a concave-lens with the same size, are attained. Each focal length of the concave lens and/or convex lens properties can be changed by applying low voltages to the electrodes.

9565-46, Session PMon

Three-dimensional imaging system by using a low-voltage-driving LC lens

Marenori Kawamura, Shunsuke Ishikuro, Akita Univ. (Japan)

There are many types of optical devices by using nematic liquid crystal (LC) materials with a large birefringence and dielectric anisotropy. S. Sato et. al. reported LC devices with functions of a variable focusing. An LC lens with a wide variable range from a concave (negative) lens property to convex (positive) lens property has been already reported. In this study, we propose a three-dimensional imaging system with a low-voltage-driving LC lens for obtaining all-focused image and depth mapping properties by processing an image digital filter from continuous focal images.

The position of the focused plane varies by adjusting the voltage applied to electrodes of the LC lens with circularly hole-patterned electrode and external transparent electrode above the threshold voltage. The continuous images are taken by changing the position of the focal plane. The sharp and clear all-focused image and the depth mapping image of the sample target as the test chart can be obtained by our proposed digital filter from continuous focal images. The acquisition times of this LC lens system without any mechanical movements must be faster than those of the conventional all-focused imaging system with mechanical movements such as a piezoelectric motor or stepping motor.

9565-47, Session PMon

Bragg diffraction for normal and obliquely circularly polarized light due a new chiral mixture

Paola Castro-Garay, Jesus Manzanares-Martinez, Adalberto Corella-Madueño, Arturo Rosas-Burgos, Marielena Clark, Josue Lizola-Leon, Lillian Gracia, Univ. de Sonora (Mexico)

We have found theoretically and experimentally the reflectance and transmittance of normal and obliquely incident circularly polarized light due to new chiral mixture that was distorted by electric field. The chiral mixture was achieved by mixtures of two nematic liquid crystals (50CB and 5CB) and S-1-bromo-2-methylbutane. We have found a regime of circular Bragg diffraction for certain values of concentrations and thickness. Optical difraction phenomenon have received particular attention in research for optical and electrooptical applications, such as low -voltage modulators, reflective phase gratings and smart reflectors.

The chiral mixture was sandwiched between two glass substrates with indium tin oxide (ITO) electrodes. The electrodes were coated with PVA and Trichloro(octadecyl)silane for planar and homeotropic aligment layer, respectively. Two types of rubbing aligment were adopted , one was parallel and the other was antiparallel.

The chiral mixture was irradiated with circularly polarized light. When the concentration of chiral component is increased one circularly polarized component is reflected, while the other circularly polarized component is transmitted unattenuated. Visual Observation and spectroscopy measurement prove that, if the chiral component concentration is decreased, transitions from Granjean to focal conic textures are found and selective reflection disappears.

Using the configuration of an cholesteric liquid cristal we have found the solution of the boundary-value problem for the reflection and transmission of incident optical waves. The appearance of nested band gaps of both handednesses during the sorting mixed chiral process is also obtained.

9565-48, Session PMon

An optical image stabilization using a droplet manipulation on a liquid crystal and polymer composite film

Yu-Jen Wang, Chia-Ming Chang, Yu-Shih Tsou, Ming-Syuan Chen, Hung-Shan Chen, Yi-Hsin Lin, National Chiao Tung Univ. (Taiwan)

Motion blur is one of the major factors which decrease the image quality of a hand-held image system while the image system is under shakes or vibrations during exposure. Opical image stabilization (OIS) is a technique to reduce such a blurring. The basic principle of OIS is to stabilize the recorded image in a camera by varying the optical path to the sensor under shakes or vibrations during exposure. In this paper, we demonstrate an optical image stabilization (OIS) for an image system using a droplet manipulation on a liquid crystal and polymer composite film (LCPCF) which reduces the motion blur. The mechanism is based on manipulation of curvature and position of the liquid lens on LCPCF according to electrically tunable orientations of liquid crystals. The change of curvature of the liquid lens results in a tunable focus of the system; meanwhile, the change of the position of the liquid lens compensates the deviation of light when the image system is under a handshake vibration. Therefore, the image system forms a clear image with different focal length to overcome handshake vibration. Several factors related to the image performance, such as moving speed and applied voltage, were discussed. The concept in this paper can also be extended to design other optical components for modulating the direction of light.

9565-49, Session PMon

Thermodielectric effect in dual-frequency cholesteric liquid crystals

Yu Cheng Hsiao, Wei Lee, National Chiao Tung Univ. (Taiwan)

Dual-frequency nematic liquid crystals (DFNLCs) exhibit an attractive property that their dielectric anisotropy ?? changes from positive to negative with increasing frequency beyond the crossover frequency fc. Based on this feature, DFNLCs have been suggested for uses in fastswitching optical devices. Additionally, dual-frequency cholesteric liquid crystals (DFCLCs), made of mixtures of DFNLCs and chiral dopants (CDs), hold great promise for photonic applications. Conventionally, the switching from the optically stable, transparent planar (P) state to the

light-scattering focal conic (FC) state in a cholesteric liquid crystal is achieved by applying an AC voltage pulse. Unfortunately, the transition from the FC to P state cannot be directly achieved but requires an intermediate state. Recently, we have demonstrated the direct two-way switching between the P and FC states in DFCLCs, characterized by a much shorter transition time for potential applications as light shutters and color reflective displays. However, it is a pity that DFCLC devices suffer from one common problem—high operation voltage. In this work, we explore the thermodielectric physics in a DFCLC system and employ this thermodielectric effect to switch the cell from the P to the FC or H state by a lower voltage.

9565-50, Session PMon

Field induced lattice reorientation, deformation, and optical nonlinearities in blue phase liquid crystals

lam Choon Khoo, Tsung-Jui Ho, Shuo Zhao, The Pennsylvania State Univ. (United States); Chun-Wei Chen, Tsung-Hsien Lin, National Sun Yat-Sen Univ. (Taiwan)



We have studied the transmission/reflection spectra and the nonlinear optical responses of Blue Phase liquid crystals (BPI and BPII) under the action of an external applied AC and DC fields. Significant reorientation and deformation of the photonic bandgap, and changes in the resulting transmission/reflection spectra of the samples are observed for applied field strengths on the order of a few volts/micron. For samples doped with photosensitive dyes such as methyl-red, unusually large optical nonlinearities are observed at well-defined applied DC voltage regions corresponding to the occurrence of major lattice deformation/reorientation. These nonlinearities exhibit transient as well as persistent components similar to methyl-red doped nematics; however, the observed effects are independent of the light polarization and direction of incidence [Opt. Lett. 40, 60-63 (2015)].

Conference 9566: Solution Solu

Sunday - Tuesday 9 -11 August 2015

Part of Proceedings of SPIE Vol. 9566 Organic Light Emitting Materials and Devices XIX

9566-1, Session 1

The development of materials and architectures for light-emitting diodes (Invited Paper)

Paul L. Burn, Ross Jansen-van Vuuren, Fatemah Maasoumi, Paul Meredith, Ebinazar Namdas, The Univ. of Queensland (Australia)

Innovation in materials and device architectures has played a crucial role in development of organic light-emitting diodes. Most research has concentrated either on small organic molecules or conjugated polymers. We have pursued an alternative approach to solution processable materials for LEDs based on conjugated dendrimers. Dendrimers consist of a core, conjugated dendrons (branches) and surface groups, and by suitable choice of these components, efficient solution-processed LEDs can be made. In this presentation we will discuss our recent developments on light-emitting materials and/or device architectures. A combination of synthesis, physical, photophysical measurements, and/or device fabrication and testing will be described.

9566-2, Session 1

Novel emission types in organic molecules: TADF and biluminescence (Invited Paper)

Sebastian Reineke, Technische Univ. Dresden (Germany)

Organic semiconductors possess two fundamental excited states, namely the singlet (S1) and triplet (T1) states, which are differentiated by their total spin, i.e. either 0 or 1, respectively. Generally, only the singlet state gives rise to emission, i.e. fluorescence. In OLEDs however, the vast share (75%) of excitons generated are triplets introducing severe losses. Here, thermally activated delayed fluorescence (TADF) has proven recently to overcome this spin problem. Biluminescence, where both singlet and triplet states contribute significantly and efficiently to the luminescence of a molecule, has only been observed in rare occasions. Once broadly available, it could be the platform of many different applications, such as ultra-broadband emitters, sensors, and energy manipulators. In this talk, I will discuss our recent efforts on the development and understanding of both TADF and biluminescent emitters. In the first part, I will summarize the development of novel blue TADF-based OLED emitters from molecular design to device implementation. In the second part, I will discuss organic materials with biluminescent properties, i.e. lumophores that act as dual state emitters and relate their special character to potential future applications in organic electronics.

9566-3, Session 1

Excimer formation and AIE effect in blue fluorescence core-side materials (Invited Paper)

Jongwook Park, Seungho Kim, Jaehyun Lee, Hyocheol Jung, The Catholic Univ. of Korea (Korea, Republic of); Daisuke Yokoyama, Yamagata Univ. (Japan); Chihaya Adachi, Kyushu Univ. (Japan)

We recently reported the syntheses of new multi-core chromophore materials containing anthracene and pyrene (AP dual core) that exhibit high PL and EL efficiencies. In this study, highly efficient blue emitting materials consisting of triple core derivatives with side group based on anthracene and pyrene moieties were designed and synthesized. Of the synthesized compounds, 1,6 DAP-TP was found to exhibit unusual excimer band with two sharp strong peaks which are a molecular emission peak at 455 nm and an excimer emission peak at 591 nm. Single molecular white emission of CIE (0.37, 0.31), very close to pure white, was obtained by introducing a terphenyl side group into a highly twisted core chromophore. This could be explained by the molecular orientation in the film state suitable for excimer formation. Also, when electron push and pull moieties were introduced into anthracene core, AIE effect providing highly efficient green emission of 18 cd/A with 19,000hrs (Lt50) was found.

OPTICS+

PHOTONICS

ELECTRONICS

ORGANIC PHOTONICS+

9566-4, Session 1

High efficiency blue fluorescent organic light-emitting diodes (Invited Paper)

Jun Yeob Lee, Sang Kyu Jeon, Wook Song, Sungkyunkwan Univ. (Korea, Republic of)

For the last decade, there has been a big progress of the quantum efficiency of blue organic light-emitting diodes by developing blue phosphorescent materials. However, recent development demonstrated that the quantum efficiency of the blue fluorescent devices can show high quantum efficiency. In this presentation, we present high quantum efficiency blue thermally activated delayed fluorescent and blue fluorescent organic lightemitting diodes which can show comparable quantum efficiency to blue phosphorescent organic light-emitting diodes. We developed new blue thermally activated delayed fluorescent emitter derived from acridine and carbazole, and could achieve close to 20% external quantum efficiency in blue thermally activated delayed fluorescent and blue fluorescent organic light-emitting diodes.

9566-5, Session 1

Highly efficient exciplex-based OLEDs (*Invited Paper*)

Ken-Tsung Wong, National Taiwan Univ. (Taiwan)

There are different approaches for harvesting the electro-generated triplet excitons in organic light-emitting devices (OLEDs). The invention of transition metal-centered phosphors has achieved great success due to the inherent strong spin-orbit coupling effect. More recently, highly efficient OLEDs employing pure organic emitter with thermally activated delayed fluorescence (TADF) behavior has emerged as the potential alternative because of the cost-effective material preparations. To perform efficient TADF, the excited molecule needs to perform efficient reverse intersystem crossing (RISC) process, in which a small energy difference (?EST) between the singlet and triplet excited states is necessary. Efficient TADF emitters can be achieved with tailor-made molecules comprising of electrondonating and -accepting substructures to perform sufficient intramolecular charge transfer (ICT). Alternatively, the excited states with small ?EST can also be achieved by the formation of exciplex via intermolecular charge transfer between physically blended electronic donor and acceptor molecules. The physical properties of exciplex can be manipulated by the judicious combination of hole-transporting (HT) and electron-transporting (ET) materials. In this conference, our efforts of developing new HT and/ or ET materials for generating efficient exciplexe OLEDs will be reported. In addition, the applications of exciplex as host material for highly efficient OLEDs and a new strategy for giving high efficiency (> 10%) pure fluorescence white OLED will also be presented.



9566-6, Session 1

Novel conjugated polymer colloids with applications in photonics (Invited Paper)

Alexander J. Kuehne, DWI an der RWTH Aachen e.V. (Germany)

Polymer colloids are auspicious candidates for the generation of printable and large area photonic materials via solvent-processing and self-assembly. Synthetics procedures have been developed to generate monodisperse particles from dielectric materials such as polystyrene and PMMA; however, well-defined and monodisperse colloids of semiconducting polymers, which would form excellent building blocks for self-assembled photonic materials, are not readily available.

I will present novel synthetic pathways affording monodisperse colloids, which are entirely composed of pi-conjugated polymers. Several palladiumcatalyzed and metal-free dispersion polymerization procedures leading to perfectly spherical particles will be presented. By adjusting the synthetic conditions also anisotropic particles and core-shell geometries can be produced. These monodisperse conjugated polymer particles readily assemble into photonic crystals exhibiting both photonic and electronic characteristics and unprecedented photonic properties.

Through incorporation of switchable molecular units, the electronic bandgap of the pi-conjugated material can be changed leading to responsive photonic materials. Additionally, post-modification of the colloidal particles through thiol-yne click-chemistry enables functionalization with bio-medical recognition motifs. The resulting particles can be applied as imaging probes for detection and labelling of tumor cells.

9566-7, Session 2

New trends in the design of transitionmetal OLED phosphors (Invited Paper)

Yun Chi, National Tsing Hua Univ. (Taiwan)

Luminescent third-row transition metal Os(II), Ir(III) and Pt(II) based complexes, particularly those with cyclometalating chelates and equivalents, play a key role in the recent development of optoelectronic technologies such as organic light emitting diode (OLED), light emitting electrochemical cells, and solid-state organic lighting applications. Their attractiveness comes from their higher chemical stability due to the strong metal-ligand bonding interaction, as well as the longer excitation lifetimes and higher emission quantum yields. Furthermore, the strong spin-orbit coupling induced by the central metal ion promotes an efficient intersystem crossing from the singlet to the triplet excited state manifold, which then facilitates strong electroluminescence by harnessing both singlet and triplet excitons of the as-fabricated optoelectronic devices. As a result, syntheses of these metal complexes were extensively examined. In this presentation, the recently development of new OLED phosphors, particularly those constructed with tridentate chromophores, with functional diimine, NHC carbene, azolate and even biazolate chelates, as well as those have showed bright blue phosphorescence, will be elaborated in a systematic manner.

9566-8, Session 2

Towards printed organic light-emitting devices: A solution-stable, highly soluble Cu(I)-NHetPHOS-complex for inkjet processing (Invited Paper)

Daniel Volz, Charlotte Fléchon, cynora GmbH (Germany); Manuela Wallesch, Karlsruher Institut für Technologie (Germany); Thomas Baumann, cynora GmbH (Germany)

In the last three years, great progress has been made on the field of iridium-free OLEDs. Extraordinary high device performance by using thermally activated delayed fluorescence – or singlet harvesting – instead

of phosphorescence has been demonstrated with devices exhibiting more than 20% external quantum efficiency. This puts both organic and coppercontaining emitters on eye level with modern iridium materials in terms of efficiency.

However, the release of first prototypes with printed displays emphasizes a weakness of current TADF-emitters: there are only limited results regarding the printing of such materials. While there are at least basic results with copper complexes employing lab-scale processing techniques like spin-coating, most purely organic TADF-emitters are very insoluble. Consequently, there are only a handful of organic emitters being soluble enough for solution processing.

We present the first printed TADF-OLED prototypes, moving one step further towards large-area printed TADF-OLEDs. Several new NHetPHOStype copper emitters were developed, showing a solubility of more than 100 mg mL-1 in various printing-solvents. While this is usually achieved by introducing very long, potentially insulating, alkyl chains, we demonstrate a new strategy to achieve this goal.

Unlike other copper complexes, which dissociate and decompose readily in solution, we were able to proof that these materials are considerably more stable with advanced X-ray absorption spectroscopy on the Cu-K-edge and other techniques. Consequently, the high performance of a device prepared by spin-coating under nitrogen is maintained when processing the emission layer by inkjet printing under ambient conditions.

9566-9, Session 2

Facial and meridional N-heterocyclic carbene iridium complexes enable deep blue organic light-emitting diodes

Jaesang Lee, Univ. of Michigan (United States); Hsiao-Fan Chen, The Univ. of Southern California (United States); Xiao Liu, Caleb Coburn, Univ. of Michigan (United States); Peter I. Djurovich, Mark E. Thompson, The Univ. of Southern California (United States); Stephen R. Forrest, Univ. of Michigan (United States)

We present efficient deep blue phosphorescent organic light-emitting diodes (PHOLEDs) based on facial (fac-) and meridional (mer-) isomers of the N-heterocyclic carbene (NHC) Ir complex, Ir(pmp)3. PHOLEDs using fac- and mer-Ir(pmp)3 have chromaticity coordinates of CIE = [0.16, 0.09] and [0.16, 0.15], respectively, independent of brightness. Further, These devices achieve maximum external quantum efficiencies of EQE = 10.1 ± 0.2 and 14.4 ± 0.3 % at low luminance, and that decreases by only 50% at very high luminance of 8,200 ± 400 and 23,000 ± 600 cd/m2, respectively (corresponding to current densities of J50% = 170 \pm 10 and 220 \pm 10 mA/cm2). The J50% are at least a factor of three greater than those of previously reported deep blue PHOLEDs. In addition, it is notable that mer-Ir(pmp)3 based PHOLED is more efficient than the fac-isomer, which is in a striking contrast with the conventional fac- and mer-isomers of red- and green-emitting tris-cyclometalated Ir(C^N)3 complexes. We discuss this difference in terms of the distinct energetic and electronic properties of the NHC ligands, and verify our theoretical analysis with temperature- and solution-dependent photoluminescence of fac- and mer-Ir(pmp)3.

9566-10, Session 3

Organic light-emitting diodes: Multiscale charge transport simulation and fabrication of new thermally activated delayed fluorescence (TADF) materials (Invited Paper)

Hironori Kaji, Katsuyuki Shizu, Furitsu Suzuki, Tatsuya Fukushima, Katsuaki Suzuki, Kyoto Univ. (Japan); Chihaya Adachi, Kyushu Univ. (Japan)

Conference 9566: Organic Light Emitting Materials and Devices XIX



(1) We have reported new type of organic light-emitting diodes exploiting reverse intersystem crossing (rISC). By designing light-emitting materials with small energy gap between singlet (S1) and triplet excited state (T1), electrically excited triplet excitons can be effectively up-converted to singlet excitons via rISC, which results in efficient thermally activated delayed fluorescence (TADF). Here, we show several recently-developed new TADF materials and the device performances.

(2) Charge transports in amorphous thin films with 100 nm thickness are investigated in silico by explicitly considering organic molecules. The amorphous layer of organic molecules was constructed using molecular dynamics simulations. The rate constants for charge hopping between two organic molecules, extracted from the amorphous layers, were calculated based on Quantum Chemical Calculations. The hopping transport in amorphous layers was simulated using a Monte Carlo method. The Monte Carlo simulation clearly shows that diffusion transport is dominant at low applied electric fields and that contribution of drift transport increases at high electric fields. The simulation in this study enable us to reveal molecular origin of charge transport. The details will be shown in the presentation.

9566-11, Session 3

N-type organic luminescent materials based on AIE-active siloles (Invited Paper)

Han Nie, Zujin Zhao, South China Univ. of Technology (China); Ben Zhong Tang, Hong Kong Univ. of Science and Technology (Hong Kong, China)

Simplifying the configurations of OLEDs without sacrificing device performances is of practical importance to shorten fabrication procedures and cut down cost. In view of this, organic active materials for OLEDs are anticipated to possess multiple functions, including high solid-state emission efficiency, efficient hole- and/or electron transport ability, etc. In this work, we report a series of bifunctional materials consisting of a silole core and electron-transporting functional groups, such as imidazole derivatives. These silole-based luminogens show aggregation-induced emission (AIE) characteristics and afford high emission efficiencies in the solid films. The presence of electron-withdrawing imidazole substituents lowers the LUMO energy levels as revealed by theoretical calculation and cyclic voltammetry, and allows for efficient electron transport ability of the luminogens. The bilayer OLEDs fabricated using these silole derivatives as lightemitting and electron-transporting layers simultaneously show excellent electroluminescence performances, which are better than those of trilayer OLEDs with an additional electron-transporting layer (TPBi), revealing that they are excellent n-type light emitters. These results demonstrate that the combination of AIE-active luminogens with charge transport groups at molecular level is a promising design for multifunctional solid-state light emitters.

9566-12, Session 3

High efficiency quantum dot based lightemitting devices (Invited Paper)

Weiran Cao, Univ. of Florida (United States); Huaibin Shen, Univ. of Florida (United States) and Henan Univ. (China); Nathan T. Shewmon, Univ. of Florida (United States); Paul Holloway, Univ. of Florida (United States) and NanoPhotonica, Inc. (United States); Lin Song Li, Henan Univ. (China); Jiangeng Xue, Univ. of Florida (United States)

Quantum-dot based light-emitting devices (QD-LEDs) have attracted great attention in recent years for their potential applications in solid-sate lighting and flat-panel displays. Here we will present our recent work on solutionprocessed, multilayer QD-LEDs incorporating a ZnO nanoparticle based electron transport layer. External quantum efficiencies exceeding 12% have been achieved for blue, green, and red emitting devices. We will describe the importance of surface ligand and the detailed nanostructure in the quantum dots. Our device structure also ensures good device stability, with extrapolated operating lifetime of 100,000 h (at 100 cd/m2) achieved for green and red devices.

9566-13, Session 3

Multi-stacked quantum dot light-emitting diodes and full-color displays by dry pickand-place transfer (*Invited Paper*)

Tae-Ho Kim, Samsung Advanced Institute of Technology (Korea, Republic of)

The Light-emitting diodes (LEDs) with quantum dot (QD) luminophores show promise in the development of next-generation displays, because quantum dot luminophores demonstrate high quantum yields, extremely narrow emission, spectral tunability and high stability. Layered assembly structures composed of nanomaterials, such as quantum dots, have attracted considerable attention as promising candidates for new functional devices, whose optical, electromagnetic, and electronic behaviors are determined by the spatial arrangement of component elements. In this talk, we report a pick-and-place-based transfer printing technique which enables 3D heterogeneous multi-stacking of QD monolayers as well as fine patterning of QD films in a large area. We demonstrate a large-area full-color quantum dot display, including in flexible form, using optimized QD films by pick-and-place transfer, with control of the nano-interfaces and charge behavior. We also demonstrate 3D multi-stacked nanostructures composed of quantum dot monolayers with different sizes. This solventfree transfer utilizes a lifting layer and allows the reliable transfer of a QD monolayer even onto flexible plastic substrates, enabling layer-by-layer design. With the controlled multi-stacking of different bandgap QD layers, we are able to probe the interlayer energy transfer among different QD monolayers. By controlling the emission spectrum through such designed monolayer stacking, we have achieved white emission with stable optoelectronic properties. The technology proposed here is versatile in its applicability over a wide range of materials and also provides routes toward developing various artificial solids as functional structures for application in large-scale flexible optoelectronic and electromagnetic devices.

9566-14, Session 4

Tandem organic light-emitting devices fabricated by solution-processes (Invited Paper)

Yong-Jin Pu, Yamagata Univ. (Japan)

We report the fabrication of a tandem-OLED comprising two ligh-emittingunits (LEUs) and a charge generation layer (CGL) between the anode and cathode using only solution-based processes. The individual components, 1st-LEU and 2nd-LEU are also fabricated independently. The ZnO/ polyethyleneimine bilayer is used as the EIL in 1st-LEU and a molybdic acid derivative is used as the electron acceptor of the CGL. Appropriate choice of solvents during spin coating of each layer ensures that a nine-layered structure is readily fabricated using only solution-based processes. The driving voltage and efficiency of the fabricated multi-OLED are the sums of corresponding values of the component LEUs. These results demonstrate that the solution-processed CGL successfully generated electrons and holes and that the generated electrons and holes were injected into 1st-LEU and 2nd-LEU, respectively, when a voltage was applied, resulting in charge recombinations in each LEU.

9566-15, Session 4

Solution-processed flexible organic light emitting diodes (Invited Paper)

Jiajie Liang, Shu-Yu Charlotte Chou, Fangchao Zhao, Lu Li,

Conference 9566: Organic Light Emitting Materials and Devices XIX



Qibing Pei, Univ. of California, Los Angeles (United States)

Flexible OLEDs tend to exhibit low performance thanks to the low surface conductivity, transmittance, and surface smoothness of ITO/PET as compared to ITO/glass. We are developing a flexible nanocomposite electrode comprising silver nanowires and light scattering nanoparticles that exhibit figures of merit exceeding ITO/glass. Light extraction efficiency of OLEDs employing the solution-processed transparent electrode is substantially higher than those on ITO/glass. Multiple-layer OLED structures using solution-processed small molecules and polymers have been fabricated on the new integrated substrate. Flexible OLEDs with high external quantum efficiency and luminous efficacy have been demonstrated and are being investigated for solid state lighting application.

9566-16, Session 4

Advantages and disadvantages of vacuumand solution-processed OLED films: Differences in molecular orientation, thermal stability, and interfacial mixing (Invited Paper)

Daisuke Yokoyama, Maki Shibata, Yoshiya Sakai, Yamagata Univ. (Japan)

Most of commercialized OLEDs are currently based on vacuum-processed films because vacuum process enables us to fabricate ideal multilayer structures with a very high purity. On the other hand, the use of solutionprocessed films of OLED materials has recently drawn increasing attention to realize a low-cost fabrication of large-are devices. Each process has advantages and disadvantages when compared to the other. Thus, when we select an appropriate process for production of OLED displays or lighting according to the demand of the situation, it is very important to know what is the advantages and disadvantages of each film systematically and quantitatively from a viewpoint of physical properties of the films.

In this presentation, we will show systematic comparisons of the physical properties of (a) vacuum-processed small-molecule films, (b) solutionprocessed small-molecule films, and (c) solution-processed polymer films. In particular, three properties are focused on. The first is molecular orientation, which of emitters and transporters significantly affect outcoupling efficiency and charge transport, respectively [1]. Although vacuum-deposited small molecules can be highly oriented in the horizontal direction by choosing an appropriate molecular structure, we found that spin-coated small molecules tend to be randomly oriented regardless of experimental conditions. Thus, when we use small molecules in solution processes, we have to take into account the possible loss of the benefit from the horizontal orientation. The second is thermal stability. We found that glass transition of spin-coated films occurs at the temperature lower than that for transition of vacuumdeposited films. In particular, it should be noted that molecular orientation and glass transition temperature of spin-coated films are identical to those of the "deteriorated" vacuum-deposited films that experienced transition through thermal annealing. The third is interfacial mixing. We demonstrated that it is possible to analyze interfaces between layers of many kinds of OLED materials non-destructively by laboratory-scale experiments using ellipsometry. The difference of interfaces is also important to understand device characteristics. Through the comparisons of mainly these three factors, the advantages and disadvantages of each film will be discussed comprehensively.

[1] D. Yokoyama, J. Mater. Chem. 21, 19187 (2011).

9566-17, Session 4

Charge generation layers for all-solution processed organic tandem light emitting diodes with regular device architecture

Stefan Hoefle, Christoph Bernhard, Michael Bruns, Christian Kuebel, Torsten Scherer, Alexander Colsmann,

Karlsruher Institut für Technologie (Germany)

We present multi-photon OLEDs where enhanced light emission was achieved by stacking two OLEDs utilizing a regular device architecture (top cathode) and an intermediate charge carrier generation layer (CGL) for monolithic device interconnection. With respect to future printing processes for organic optoelectronic devices, all functional layers were deposited from solution. The CGL comprises a low-work function zinc oxide layer that was applied from solution under ambient conditions and at moderate processing temperatures and a high-work function interlayer that was realized from various solution processable precursor-based metal oxides, like molybdenum-, vanadium- and tungsten-oxide. Since every injected electron-hole pair generates two photons, the luminance and the current efficiency of the tandem OLED at a given device current are doubled while the power efficiency remains constant. At a given luminance, the lower operating current in the tandem device reduces electrical stress and improves the device life-time. ToF-SIMS, TEM/FIB and EDX analyses provided evidence of a distinct layer sequence without intermixing upon solution deposition.

9566-18, Session 4

R2R processed flexible OLEDs for lighting and their mechanical stress testing

Takashi Minakata, Mitsuru Tanamura, Yasuhiro Mitamura, Masayuki Imashiro, Akira Horiguchi, Akira Sugimoto, Masahiko Yamashita, Yukito Yada, Nobuki Ibaraki, Hiroshi Tomiyasu, CEREBA (Japan)

Recently flexible OLEDs attracts significant attentions for emerging lighting applications.

In addition, R2R process is considered to be an ultimate goal for flexible device fabrication.

The authors have successfully fabricated flexible OLEDs by fully R2R process, which started from film washing, gas-barrier layer deposition, planarization, vacuum depositions of core-layers and finally encapsulated with film lamination.

Influence of fabrication conditions on OLEDs performance has been studied and R2R fabricated OLEDs showed good performance almost comparable with sheet to sheet (S2S) processed OLEDs by controlling fabrication conditions. This indicates that reduction of device performance caused by the fabrication process has been minimized.

In order to confirm this, effects of mechanical stress on device performance has been studied.

Other important issues such as encapsulation, protection for moisture permeation and R2R related process damages will be discussed at the conference.

9566-50, Session 4

High-index substrates with optical haze as a low-cost platform for efficient flexible OLEDs: Joint theoretical and experimental study (Invited Paper)

Eunhye Kim, Jinouk Song, Seunghyup Yoo, KAIST (Korea, Republic of)

Industrial grade PEN (I-PEN) substrates are studied as a simple, ideal platform enabling highly efficient flexible OLEDs at low cost. Their high refractive index (-1.75) and built-in optical haze (20-50%) are utilized to outcouple the light that would otherwise be confined as waveguide modes or substrate-confined modes. With an index-matched planarization layer and low-temperature-annealed indium zinc oxide (IZO) deposited on its top, total internal reflections occurring at the IZO/substrate interface are effectively suppressed, delivering most of the internally generated light into the bulk of I-PEN substrates. Those delivered to a substrate are then



extracted efficiently with the help of scattering from nano-scale particles already embedded inside I-PEN substrates during manufacturing.

With the proposed strategy, external quantum efficiency reaching -40% is demonstrated for flexible OLEDs without any additional lenticular structure or internal patterning. An equivalent-model based on Henyey-Greenstein phase function and a full microscopic model based on a Mie-scattering are both employed, respectively, to account for the effect of scattering in the trans-scale optical simulation, which explains the structure-dependent enhancement and provides a guideline for further optimization, all in both qualitative and quantitative fashions.

9566-55, Session 4

Direct observation of surface anions relaxed by spontaneous orientation polarization in OLED films by high sensitivity photoemission (Invited Paper)

Hiroumi Kinjo, Tomoya Sato, Junki Yamazaki, Chiba Univ. (Japan); Yutaka Noguchi, Meiji Univ. (Japan); Yasuo Nakayama, Hisao Ishii, Chiba Univ. (Japan)

OLED materials often show spontaneous orientation polarization in evaporated films with giant surface potential (GSP). This polarization induces positive and negative fixed charges on both ends of the polarized layer. Due to this fixed charge, OLED films often contain surface/interface carriers that play important role in device performance. This is a kind of self-field effect carrier doping. In this study, we will report on the direct observation of anions fixed by GSP for various OLED materials by using high-sensitivity photoemission. The spectra for Alq3, alpha-NPB, TPBi, and BCP show unusual low energy photoemission in visible or near UV photon energy. The relaxation of anion states of these materials will be discussed in relation to injection properties. This method can be also applied to measure the electron affinity of organic semiconductors.

The above materials are often used as electron transporting material in OLED, and as buffer layer in organic solar cell. In both cases, the orientation polarization will capture some carrier and relaxed their energy. This relaxation should be a key to understand the role of such buffer layer. The relation between the observed electronic structure and device performance will be also discussed.

9566-19, Session 5

Triplet related losses in organic thin film lasers (*Invited Paper*)

Thomas Riedl, Bergische Univ. Wuppertal (Germany)

Organic solid state lasers (OSL) based on semiconducting polymers or small molecules progressed enormously over the past decade. A range of highly efficient organic gain media enable OSLs optically pumped by simple inorganic laser diodes or even LEDs. Still continuous wave (cw) or electrical operation remain challenges yet to be achieved. Both are impeded by losses that are associated with the particular photo-physics of organic gain media. In the quest to find strategies to overcome these losses, it is essential to careful analyze the underlying photo-physical mechanisms.

As an example, OSL pumped under cw conditions or long pulses stop lasing within 10 ns. This is a general phenomenon found in various gain media. It can be show that triplet state absorption and triplet singlet annihilation are the key processes that explain the dynamics of OSLs. We present techniques that allow us to measure the density, the spectral absorption and the lifetime of triplet excitons at room temperature in a number of neat and host gain-media. It turns out that in low-threshold guest-host systems, the lifetime of triplet excitons trapped on the dopant molecules. Various concepts to overcome triplet related losses will be discussed. In addition, we will present evidence that there exist gain-media in which the optical gain is spectrally separated from the triplet-related absorption This opens an avenue to cw-lasing in organic thin films.

9566-20, Session 5

Solid-state fluorescent protein as a novel optical gain material for lasers and amplifiers (Invited Paper)

Malte C. Gather, Univ. of St. Andrews (United Kingdom)

Most currently used solid-state luminescent materials are based on inorganic semiconductors, phosphors and quantum dots or consist of synthetic hydrocarbon compounds. Here, we describe a distinctly different, novel class of solid-state emitters offering unique optical properties - the biologically produced fluorescent proteins. In contrast to many organic dyes, the special molecular structure of these proteins ensures that in solid-state the protein fluorophores have a fixed interspacing of 3-4 nm. This suppresses concentration guenching and enables strong optical amplification (g = 22cm-1) in thin protein films. We use protein films to fabricate efficient solidstate vertical cavity surface emitting micro-lasers with thresholds below 100 pJ and single-frequency operation. We also demonstrate a self-assembly scheme to fabricate protein ring resonator lasers. Moreover, we find that solid-state blends of proteins emitting light of different color support strong Förster resonance energy transfer (FRET). The sensitivity of self-quenching and FRET to the intermolecular distance allows all-optical sensing. Our results demonstrate that the naturally optimized, unique structure of fluorescent proteins can be harnessed in various settings, and provide bioinspiration for further improvement of synthetic luminescent molecules or nanoparticles.

9566-21, Session 5

Laser nanostructuring for highperformance organic optoelectronic devices (Invited Paper)

Hong-Bo Sun, Jing Feng, Yue-Feng Liu, Jilin Univ. (China)

Organic optoelectronic devices particularly organic light-emitting devices (OLEDs) and organic photovoltaics (OPVs) have been attracting increasing attention owing to their advantages of being thin, lightweight, and portable. High efficiency is a key issue for their commercial applications. While a very low light extraction efficiency of less than 20% is a stumbling block for high efficiency of OLEDs. More than 80% photons produced by exciton decay are trapped inside OLEDs in the form of waveguide (WG) modes in organic/ ITO layers, surface plasmon-polariton (SPP) modes, and substrate modes from total internal reflection at the glass substrate/air interface. In the other hands, the organic film has to be very thin due to its short exciton-diffusion length and low carrier mobility, which results in low light absorption efficiency and limited the conversion efficiency of the OPVs.

In our work, integration of nanostructures into OLEDs and OPVs have been demonstrated not only an effective approach to out-couple WG and SPP modes within OLEDs but also improve the light absorption by coupling SPP resonance in OPVs. The nanostructures have been fabricated by holographic lithography and laser ablation, which are simple approach with high controllability and reproducibility. Both experimental and numerical results show and support obvious enhancement in efficiency of OLEDs and OPVs compared to those of the conventional planar devices. In conclusion, we have confirmed that laser nanostructuring is an efficient method to realize organic optoelectronic devices with high performance, which are promising candidates for commercial application in display, lighting and energy harvesting devices.



9566-22, Session 5

Solution-processable, photo-stable, low-threshold, and broadly tunable thin film organic lasers based on novel highperforming laser dyes (Invited Paper)

Maria A. Diaz-Garcia, Marta Morales-Vidal, Manuel G. Ramirez, Jose M. Villalvilla, Pedro G. Boj, Jose A. Quintana, Univ. de Alicante (Spain); Aritz Retolaza, Santos Merino, Tekniker (Spain)

Thin film organic lasers represent a new generation of inexpensive, mechanically flexible devices for spectroscopy, optical communications and sensing requiring an organic, efficient, stable, wavelength-tunable and solution-processable laser material. In this presentation we will report amplified spontaneous emission (ASE) and distributed feedback (DFB) laser applications of novel high performing materials of two different classes, both dispersed in polystyrene (inert matrix): perylenediimide (PDI) dyes and oligo-p-phenylenevinylenes (OPVs). Films containing a new baysubstituted PDI compound show efficient ASE emission at wavelengths between 610 and 630 nm, widening the use of PDIs in laser applications, up to now restricted to bay-unsubstituted PDIs, all with ASE at around 579 nm. We will also show results for a new class of OPVs, which undergo ASE from 385 nm to 583 nm, depending on the oligomer length, with remarkably low threshold and high photostability. Second-order DFB lasers with standard gratings (single period), have shown single mode emission, wavelength tunability across the visible spectrum, long operational lifetimes of >105 pump pulses, outstandingly larger than previously reported PPV compounds, and thresholds close to pumping requirements with lightemitting diodes, i.e. only 0.7 kW/cm2, which is among the lowest values reported to date for dye-doped materials. It is also remarkable that the two types of materials discussed show high thermal stability, thus allowing the use of thermal nanoimprint lithography to engrave the DFB resonators directly onto the active films. This constitutes an important aspect for the prospect of preparing mechanically flexible inexpensive devices.

9566-23, Session 5

Coherence measurements of organic lightemitting diodes and lasers (*Invited Paper*)

Ifor D. Samuel, Univ. of St. Andrews (United Kingdom)

Organic semiconductors are compact and convenient light courses for displays and lighting. However, can they also exhibit significant coherence, and can it be controlled? This is a topic that has received very little attention and yet is a fundamental property of light and highly relevant to shaping light emission from such sources to make "structured light." We describe a method for the quantitative measurement of the coherence of organic light sources. The results of spatial coherence measurements of organic lightemitting diodes (OLEDs) and lasers will be reported and compared. We also explore the effect of wavelength scale microstructure on the coherence of light emission from OLEDs.

9566-24, Session 5

Photonic lattices in organic microcavities: Bloch states and control of lasing

Andreas Mischok, Robert Brückner, Hartmut Fröb, Vadim G. Lyssenko, Karl Leo, Technische Univ. Dresden (Germany)

Organic microcavities comprising the host:guest emitter system Alq3:DCM offer an interesting playground to experimentally study the full dispersion characteristics of laterally patterned microlasers due to the broad emission spectrum and large oscillator strength of the organic dye.

By structuring of metallic or dielectric sublayers directly on top of the bottom mirror, we precisely manipulate the mode structure and influence

the coherent emission properties of the device. Embedding silver layers into a microcavity leads to an interaction of the optical cavity-state in the organic layer and the neighbouring metal which red-shifts the cavity resonance, creating a Tamm-Plasmon-Polariton state. A patterning of the metal can in turn be exploited to fabricate deep photonic wells of micronsize, that efficiently confine light in the lateral direction. In periodic arrays of silver wires we create a Kronig-Penney-like optical potential in the cavity and in turn observe optical Bloch states spanning over several photonic wires. We modify the Kronig-Penney theory to analytically describe the full far-field emission dispersion of our cavities and show the emergence of either zero -, pi-, or 2pi- phase-locking in the system. By investigating periodic SiO2 patterns, we experimentally observe stimulated emission from the ground and different excited discrete states at room temperature and are able to directly control the laser emission from both extended and confined modes of the photonic wires.

The introduction of defects in the periodicity further opens the possibilities of photon confinement in three dimensions as well as studying the analogy between crystal- and photonic lattices.

9566-25, Session 6

AC quantum efficiency harmonic analysis of exciton annihilation in organic light emitting diodes (Invited Paper)

Noel C. Giebink, The Pennsylvania State Univ. (United States)

Exciton annihilation processes impact both the lifetime and efficiency roll-off of organic light emitting diodes (OLEDs), however it is notoriously difficult to identify the dominant mode of annihilation in operating devices (exciton-exciton vs. exciton-charge carrier) and subsequently to disentangle its magnitude from competing roll-off processes such as charge imbalance. Here, we introduce a simple analytical method to directly identify and extract OLED annihilation rates from standard light-current-voltage (LIV) measurement data.

The foundation of this approach lies in a frequency domain EQE analysis and is most easily understood in analogy to impedance spectroscopy, where in this case both the current (J) and electroluminescence intensity (L) are measured using a lock-in amplifier at different harmonics of the sinusoidal dither superimposed on the DC device bias. In the presence of annihilation, the relationship between recombination current and light output (proportional to exciton density) becomes nonlinear, thereby mixing the different EQE harmonics in a manner that depends uniquely on the type and magnitude of annihilation.

We derive simple expressions to extract different annihilation rate coefficients and apply this technique to a variety of OLEDs. For example, in devices dominated by triplet-triplet annihilation, the annihilation rate coefficient, K_TT, is obtained directly from the linear slope that results from plotting EQE_DC-EQE_1? versus L_DC (2EQE_1?-EQE_DC). We go not show that, in certain cases it is sufficient to calculate EQE_1? directly from the slope of the DC light versus current curve [i.e. via (dL_DC)/(dJ_DC)], thus enabling this analysis to be conducted solely from common LIV measurement data.

9566-26, Session 6

Degradation of wide band-gap electrolumienscent materials by excitonpolaron interactions (Invited Paper)

Hany Aziz, Qi Wang, Univ. of Waterloo (Canada)

The limited performance stability and gradual loss in the electroluminescence efficiency of OLEDs utilizing wide band-gap materials, such as blue-emitting phosphorescent and fluorescent devices, continues to be a challenge for wider technology adoption. We recently found that interactions between excitons and polarons play an important role in the aging behavior of electroluminescent materials, and that a correlation



exists between the susceptibility of these materials to this aging mode and their band-gap. This degradation mode is also found to be often associated with the emergence of new bands – at longer wavelength - in the electroluminescence spectra of the materials, that can often be detected after prolonged electrical driving. Such bands contribute to the increased spectral broadening and color purity loss often observed in these devices over time. Exciton-polaron interactions, and the associated degradation, are also found to occur most significantly in the vicinity of device interlayer interfaces such as at the interface between the emitter layer and the electron or hole transport layers. New results obtained from investigations of these phenomena in a wide range of commonly used host and guest OLED materials will be presented.

9566-27, Session 6

Exciton formation and diffusion in OLEDs (*Invited Paper*)

Grayson L. Ingram, Zheng-Hong Lu, Univ. of Toronto (Canada)

This talk will discuss recent experiments designed to study the formation of excitons and their subsequent diffusions in OLEDs. These experimental results suggest that contrary to conventional wisdom, host singlet exciton diffusion can occur over long distances, while host triplet excitons are confined close to the exciton formation region for the archetype host and hole transport layer CBP. The exciton formation mechanism is studied and we show that the ratio of excitons formed on the host to excitons formed on the dopant varies strongly with the applied voltage. Refinements to models of efficiency roll off are discussed in light of the improve understanding of exciton formation and we suggest design guidelines to improve efficiency by engineering exciton formation.

9566-28, Session 6

Analysis of self-heating in organic semiconductor devices

Evelyne Knapp, Beat Ruhstaller, Zürcher Hochschule für Angewandte Wissenschaften (Switzerland)

So far self-heating has been of concern in large area devices where the resistive anode leads to a potential drop resulting in inhomogeneous current, brightness and temperature distributions. In this work we show that also small lab devices suffer from self-heating effects originating from the semiconductor layers. A clear indication for this is a negative capacitance value in unipolar devices. In bipolar devices other processes such as recombination or trapping can also cause a negative capacitance value. We compare the slope of the negative capacitance vs. frequency for uniand bipolar devices to quantify the different processes. The overall device structure does affect the negative capacitance. Further impacts of self-heating are discussed: in DC an increased current density is measured after the device has heated up, in dark-injection transient current experiments an increase in the current density is seen after a while.

With the aid of a Fourier method we can transform time-dependent results to the frequency domain which allows for an effortless interpretation of the negative capacitance.

We compare our results with measurements and emphasize the importance of our analysis for OLEDs and organic solar cells. In one study, a device is cooled with a copper block leading to a less negative capacitance confirming self-heating as an origin of the negative capacitance [H. Okumoto and T. Tsutsui, Appl. Phys. Express 7, 061601 (2014)].

We have provided clear evidence of self-heating of organic semiconductor devices and conclude that a comprehensive model requires the inclusion of heat conduction and heat generation in the drift-diffusion model.

9566-29, Session 7

Determining the rate-limiting steps for the purification of organic semiconductors by thermal gradient sublimation (Invited Paper)

Nathan T. Morgan, Yi Zhang, Univ. of Minnesota, Twin Cities (United States); Matthew L. Grandbois, Bruce M. Bell, The Dow Chemical Co. (United States); E. L. Cussler, Russell J. Holmes, Univ. of Minnesota, Twin Cities (United States)

Small molecule organic semiconductors have been successfully integrated into a variety of optoelectronic platforms including light-emitting devices (OLEDs), photovoltaic cells and field-effect transistors. In all cases, materials purity plays a significant role in the realization of robust devices with high performance. Most frequently, these materials are purified using thermal gradient sublimation. The successful separation of the target molecular species from its impurities relies on differences in the vapor pressure of each component in the starting material. Here, we explore the fundamental mechanisms that limit sublimation rate and control material deposition. For the archetypical hole transport materials, N,N'-bis(naphthalen-1-yl)-N,N'bis(phenyl)-benzidine (NPD) and 4,4',4"-tris(carbazol-9-yl) triphenylamine (TCTA), a combination of diffusion to the deposition zone and physical vapor deposition are shown to be rate-limiting at constant sublimation temperature. Surprisingly, diffusion within the solid feed, reaction at the feed particle surface, and mass transfer within the bed of feed particles are not limiting. Interestingly, in cases where the feed consists of a mixture of NPD and TCTA, the sublimation rate shows the same diffusive behavior, and the separation efficiency can be manipulated by engineering the temperature gradient in the collection zone. These results can be used to guide the design and operation of future large-scale purification systems, which are critical for the scale-up of materials synthesis and supply efforts.

9566-30, Session 7

Optically and electrically detected magnetic resonance (ODMR and EDMR, respectively) of phosphorescent, thermally activated delayed fluorescence (TADF), and exciplex OLEDs (Invited Paper)

Chamika Hippola, Dusan Danilovic, Min Cai, Ruth Shinar, Joseph Shinar, Iowa State Univ. of Science and Technology (United States)

It is widely recognized that nonradiative quenching of singlet excitons (SEs) by other SEs, triplet excitons (TEs), polarons, and bipolarons becomes the dominant decay mechanism of these excitons at high excitation densities. These quenching processes cause the roll-off in the efficiency of OLEDs and prevent lasing at high injection current densities, and they result in the observed ODMR and EDMR in conventional fluorescent OLEDs. A previous ODMR study on phosphorescent OLEDs has suggested that such quenching of the host SEs is also significant. This talk will focus on the ODMR and EDMR of additional phosphorescent, TADF, and exciplex OLEDs, and on the potential role of bipolarons in device degradation.

9566-31, Session 7

Kinetic Monte Carlo simulation of the efficiency roll-off, emission color, and degradation of organic light-emitting diodes (Invited Paper)

Reinder Coehoorn, Philips Research Nederland B.V. (Netherlands); Harm van Eersel, Peter A. Bobbert, Rene A.

Conference 9566: Organic Light Emitting Materials and Devices XIX



J. Janssen, Technische Univ. Eindhoven (Netherlands)

The performance of Organic Light Emitting Diodes (OLEDs) is determined by a complex interplay of the charge transport and excitonic processes in the active layer stack. We have developed a three-dimensional kinetic Monte Carlo (kMC) OLED simulation method which includes all these processes in an integral manner. The method employs a physically transparent mechanistic approach, and is based on measurable parameters. All processes can be followed with molecular-scale spatial resolution and with sub-nanosecond time resolution, for any layer structure and any mixture of materials. In the talk, applications to the efficiency roll-off, emission color and lifetime of white and monochrome phosphorescent OLEDs [1,2] are demonstrated, and a comparison with experimental results is given. The simulations show to which extent the triplet-polaron quenching (TPQ) and triplet-triplet-annihilation (TTA) contribute to the roll-off, and how the microscopic parameters describing these processes can be deduced properly from dedicated experiments. Degradation is treated as a result of the (accelerated) conversion of emitter molecules to non-emissive sites upon a triplet-polaron quenching (TPQ) process. The degradation rate, and hence the device lifetime, is shown to depend on the emitter concentration and on the precise type of TPQ process. Results for both single-doped and co-doped OLEDs are presented, revealing that the kMC simulations enable efficient simulation-assisted layer stack development.

[1] H. van Eersel et al., Appl. Phys. Lett. 105, 143303 (2014).

[2] R. Coehoorn et al., Adv. Funct. Mater. (2015), publ. online (DOI: 10.1002/ adfm.201402532)

9566-32, Session 7

Modeling of organic light emitting diodes: From molecular to device properties

(Invited Paper)

Pascal Kordt, Jeroen J. M. van der Holst, Max-Planck-Institut für Polymerforschung (Germany); Mustapha Al Helwi, BASF SE (Germany) and Technische Univ. Braunschweig (Germany); Wolfgang Kowalsky, Technische Univ. Braunschweig (Germany); Falk May, Alexander Badinski, Christian Lennartz, BASF SE (Germany); Denis Andrienko, Max-Planck-Institut für Polymerforschung (Germany)

We review the progress in modeling of charge transport in disordered organic semiconductors on various length-scales, from atomistic to macroscopic. This includes evaluation of charge transfer rates from first principles, parametrization of coarse-grained lattice and off-lattice models, and solving the master and drift-diffusion equations. Special attention is paid to linking the length-scales and improving the efficiency of the methods. All techniques are illustrated on an amorphous organic semiconductor, DPBIC, a hole conductor and electron blocker used in state of the art organic light emitting diodes (OLEDs). The outlined multiscale scheme can be used to predict OLED properties without fitting parameters, starting from chemical structures of compounds.

Reference: Advanced Functional Materials, 2015, doi: 10.1002/ adfm 201403004

9566-33. Session 7

Development of operationally stable inverted organic light-emitting diode prepared without using alkali metals (Invited Paper)

Hirohiko Fukagawa, NHK Japan Broadcasting Corp. (Japan); Katsuyuki Morii, Munehiro Hasegawa, Shun Gouda, NIPPON SHOKUBAI CO., LTD. (Japan); Toshimitsu Tsuzuki, Takahisa Shimizu, Toshihiro Yamamoto, NHK Japan Broadcasting Corp. (Japan)

The OLED is one of the key devices for realizing future flexible displays and lightings. One of the biggest challenges left for the OLED fabricated on a flexible substrate is the improvement of its resistance to oxygen and moisture. A high barrier layer [a water vapor transmission rate (WVTR) of about 10-6 g/m2/day] is proposed to be necessary for the encapsulation of conventional OLEDs. Some flexible high barrier layers have recently been demonstrated; however, such high barrier layers require a complex process, which makes flexible OLEDs expensive. If an OLED is prepared without using air-sensitive materials such as alkali metals, no stringent encapsulation is necessary for such an OLED. In this presentation, we will discuss our continuing efforts to develop an inverted OLED (iOLED) prepared without using alkali metals. iOLEDs with a bottom cathode are considered to be effective for realizing air-stable OLEDs since the electron injection layer (EIL) can be prepared by fabrication processes that might damage the organic layers, resulting in the enhanced range of materials suitable for EILs. We have demonstrated that a highly efficient and relatively air-stable iOLED can be realized by employing poly(ethyleneimine) as an EIL. Dark spot formation was not observed after 250 days in the poly(ethyleneimine)based iOLED encapsulated by a barrier film with a WVTR of 10-4 g/m2/day. In addition, we have demonstrated the fabrication of a highly operational stable iOLED utilizing a newly developed EIL. The iOLED exhibits an expected half-lifetime of over 10,000 h from an initial luminance of 1,000 cd/m2.

9566-34, Session 8

Next generation organic light-emitting materials and devices (Invited Paper)

Bernard Kippelen, Georgia Institute of Technology (United States)

In this talk, we will discuss recent innovations in organic light-emitting materials and devices. First, we will report on organic light-emitting diodes (OLEDs) based on thermally activated delayed fluorescence (TADF). We will show that devices based on the emitter 4CzIPN doped in a novel ambipolar host can yield a current efficacy of 81 cd/A and a maximum external quantum efficiency of 26.5%. These devices exhibit a low turnon voltage of 3.2 V at 10 cd/m2, as well as reduced efficiency roll-off at high current densities. The performance of these devices is comparable to that of electrophosphorescent devices based on organic-metallic compounds that contain precious metals such as Iridium. In a second part we will report on highly efficient green-emitting organic light-emitting diodes (OLEDs) fabricated on shape memory polymer (SMP) substrates for flexible electronic applications. SMPs are a class of mechanically active materials that can change and store shape upon activation by a stimulus. The combination of the unique properties of SMP substrates with the light-emitting properties of OLEDs pave to the way for new applications, including conformable smart skin devices, minimally invasive biomedical devices, and flexible lighting/display technologies. Finally, we will present OLEDs fabricated on substrates made from cellulose nanocrystals (CNC) and discuss how such substrates can reduce the environmental footprint of printable organic electronics.

9566-35, Session 8

Construction of charge generation laver for high efficiency tandem organic lightemitting diodes (Invited Paper)

Dongge Ma, Changchun Institute of Applied Chemistry (China)

Tandem or stacked OLED is a promising device structure that can potentially achieve both high efficiency and long operating hours. A typical tandem OLED is fabricated by vertically connecting several individual electroluminescent (EL) units together in series via the so-called charge

Conference 9566: Organic Light Emitting Materials and Devices XIX



generation layer (CGL), with the entire device driven by a single power source. When certain voltage is applied on the electrodes, each EL lights up individually under the same current that flow through the whole device. Since tandem OLED can obtain the same brightness under several folds of lower current density, its lifetime can be significantly lengthened. Furthermore, the tandem structure provides the feasibility that EL units of different colors can be vertically stacked together for color tuning and white emission. In tandem OLEDs, the CGL obviously plays a very important role. Therefore, how to construct an effective CGL become a key in the fabrication of high efficiency tandem OLEDs.

Here, we presented an effective organic heterojunction CGL composed of a p-type organic material 4,4',4"-Tris(N-3-methylphenyl-Nphenylamino) triphenylamine (m-MTDATA) and an n-type organic material 1,4,5,8,9,12-hexaazatriphenylene -hexacarbonitrile (HAT-CN) bilayer and fabricated an ultra-high efficiency tandem OLED based on it as CGL. The maximum power efficiency reaches 120 lm/W, and yet remains 110.3 lm/W at 1000 cd/m2, which is greatly enhanced from the corresponding optimized green single-unit device. Also its maximum current efficiency and external quantum efficiency is as high as 201cd/A and 54.5%, all among the best result published by now. Furthermore, the working principles of the organic heterojunction as CGL are studied in detail and well explained by using a Zener tunneling model.

9566-36, Session 8

Ultraflexible high-efficiency organic lightemitting diodes using graphene anode (Invited Paper)

Tae-Woo Lee, Tae-Hee Han, Min-Ho Park, Sung-Joo Kwon, Pohang Univ. of Science and Technology (Korea, Republic of); Sang-Hoo Bae, Yonsei Univ. (Korea, Republic of); Hong-Kyu Seo, Pohang Univ. of Science and Technology (Korea, Republic of); Jong-Hyun Ahn, Yonsei Univ. (Korea, Republic of)

Organic light-emitting diodes (OLEDs) have been considered as devices for next-generation flexible displays and solid-state-lighting. However, mostly used indium-tin-oxide (ITO) electrode has poor tolerance to the mechanical stress. Therefore, brittle ITO electrode should be replaced with flexible transparent conducting electrodes to realize flexible organic opto-electronic devices. In this point of view, the use of graphene electrode in flexible OLEDs has been increasingly studied because graphene exhibits excellent electrical and mechanical properties. To approach toward ultimate flexible OLEDs, device should have i) ultra-high efficiency, ii) low efficiency roll-off characteristics at high luminance and iii) excellent flexibility for practical applications of flexible electronics. . Here, we fabricated flexible tandem OLEDs by stacking two electroluminescent (EL) units vertically on the graphene anode to enhance the luminous efficiency of flexible OLEDs. To avoid thermal damage of flexible plastic substrate which has low thermal resistance, we inserted low-temperature processable charge generation layer which is suitably developed for flexible OLEDs between two EL units. Flexible tandem OLEDs with graphene anode showed ultra-high efficiency (205.9 cd/A and 45.2 %) with low efficiency roll-off characteristics. By using hemi-spherical lens to improve light out-coupling, significantly enhanced current efficiency (396.4 cd/A) and external quantum efficiency (~87.3 %) were achieved in flexible OLEDs with graphene anode. Furthermore, the flexible tandem OLEDs with graphene anode showed excellent flexibility against bending stress up to ~7% of bending strain. Our results provide a significant step toward the next generation flexible displays and solid-stateliahtina.

9566-94, Session 8

Emitting dipole orientation of iridium complexes in OLEDs (Invited Paper)

Jang-Joo Kim, Kwon-Hyeon Kim, Chang-Ki Moon, Seoul National Univ. (Korea, Republic of); Jae-yeol Ma, Yun-Hi

Kim, Gyeongsang National Univ. (Korea, Republic of)

Phosphorescent iridium complexes have long been thought to have random orientation when doped in an emitting layer due to their octahedron structures. Recently, however, some heteroleptic iridium complexes which have the ancillary ligands of ?-diketonate or picolate have been reported to have preferred orientation of emission dipoles along horizontal direction (parallel to substrates). The outcoupling efficiency of the emitted light from the horizontally oriented emitting dipoles in an OLED can reach 45% which is much higher than isotropically oriented transition dipoles.[1] However, the origin of the preferred emitting dipole orientation (EDO) and the factors influencing the orientation have not been studied much.

In this presentations we will report the recent findings on the emitting dipole orientation of iridium complexes, which can be summarized as follows: (1) Heteroleptic iridium complexes are more likely to have preferred orientation in host materials than homoleptic iridium complexes. (2) Tetramethylheptadionate (tmd) ancillary ligand results in higher horizontal EDO than acetylacetonate (acac). (3) There is a linear correlation between the EDO in films and the orientation of the transition dipole moments against the C2 axis of the heteroleptic Ir complexes. (4) The EDO of the heteroleptic Ir-complex varies from horizontal to isotropic, or even to vertical direction depending on host molecules. (5) The preferred molecular orientation of the host molecules does not induce the preferred molecular orientation of the dopant molecules. (6) Intermolecular interaction between complex dopants and the aromatic rings in the host molecules induces preferred orientation of dopant molecules. (7) The preferred horizontal orientation of dopant emitting dipoles is due to the formation of planarstructure supra-molecular assemblies of host and dopant molecules. (8) The vertical EDO is induced when they interact repulsively during the film deposition to form non-linear binding geometry.

9566-46, Session PMon

High thermal conducting diamond/goldgrids as transparent electrode for organic light emitting diodes

Koen Gilissen, Univ. Hasselt (Belgium) and IMEC (Belgium); Pieter Robaeys, Univ. Hasselt (Belgium); Matthew Mcdonald, Emilie Bourgeois, Jan D'Haen, Univ. Hasselt (Belgium) and IMEC (Belgium); Zdenek Remes, Institute of Physics of the ASCR, v.v.i. (Czech Republic); Ken Haenen, Jean V. Manca, Michael Daenen, Milos Nesladek, Wim Deferme, Univ. Hasselt (Belgium) and IMEC (Belgium)

Since the discovery of organic light-emitting diodes (OLEDs), indium tin oxide (ITO) is the most commonly used transparent electrode due to its high optical transparency and excellent electrical properties. However, indium is scarce, expensive and has the tendency to diffuse into the active layer. Furthermore, ITO is unstable at high temperatures and has a poor thermal conductivity. In this work the thermal conductivity and the local heat generation and dissipation of organic light-emitting diodes (OLEDs) are investigated, by comparing OLEDs, with equal luminous power efficiency, utilizing ITO and heavily boron doped nanocrystalline diamond (BNCD) embedded with a gold (Au) grid as anode material. It is shown that the BNCD: Au grid anode OLEDs, under operation, have a lower temperature increase due to a more efficient heat dissipation. Furthermore it is also shown that the thermal decay of the localized hotspots generated during operation is much faster for the BNCD:Au grid anode OLEDs compared to the ITO anode OLEDs. With these excellent thermal properties and the outstanding chemical stability of diamond, increased lifetimes are expected.



9566-47, Session PMon

Hybrid structure of AgNWs-graphene-PEDOT as anode for organic light-emitting diodes

Xiaoqing Du, Chongqing Univ. (China)

The advent of graphene, with its combination of high transparency, electron mobility and chemical stability, opens the possibility of metalfree all-organic light-emitting devices. Howerver, graphene has higher sheet resistance and lower work function comparable to tranditional ITO as anode electrodes. Therefore, graphene-based electrodes need to be performance improved to meet the combination requirements of high optical transparency, electrical conductivity and current injection efficiency for OLEDs application.

A hybrid structure of silver nanowires(AgNWs)-graphene-PEDOT on PET was adopted to act as the anode of FOLEDs. AgNWs can decrease the resitivity of graphene significantly for AgNWs provide a large number of free electrons and effective conductive path network. The work function of PEDOT can be at 5.1eV, which is about 0.5eV higher than the work function of graphene. AgNWs film was firstly coated on PET by spin-coating, and then CVD-grown graphene was tranferred from copper substrate to the AgNWs film by PMMA-aided transfer technology. Subsequently, PEDOT with 30nm thicknes was spin-coated on the graphene. The hole transport layer(HTL), light-emitting layer(LEL), electron transport layer(ETL) and cathode were coated by vacuum evaporation to form a whole device. Our experiments show that the optical transmittance and electrical conductivity of the hybrid structure can be optimized by adjusting the thickness of AgNWs film. The hybrid structure with AgNWs-graphene-PEDOT can achieve the lowest sheet resistivity and highest hole injection current compared with single graphene, AgNWs and PEDOT. The OLED with the hybrid electrode has the best uniform current spreading and the lowest turn-on voltage.

9566-48, Session PMon

Influence of electrode materials on current characteristic of flexible organic electroluminescent devices

Jun Bao, Xiaoqing Du, Chongqing Univ. (China)

• Flexible organic electroluminescent devices (FOLEDs) have recently attracted a considerable amount of attention because of their potential applications in foldable screen. Compared with traditional OLEDs, FOLEDs need flexible electrode such as carbon nanotubes(CNTs), silver nanowire netwoks or graphene. These electrode materials have relative high resistivity due to their thin thickness, which often results in non-uniformity of luminescence and reduction of efficiency.

• An equivalent impedance model and current spread model were setup to describe the current-voltage(I-V) characteristics and current uniformity of FOLEDs respectively. The influences of resistivity, work function and contactresistance of electrode materials on current characteristics of FOLEDs were analyzed. The Finite element method and PSPICE were used to simulate the current distribution in three dimensions and the I-V characteristics FOLEDs, respectively.

• By quantitatively comparing the current characteristics of FOLEDs with different flexible electrode materials, which includes PEDOT:PSS, PANI, CNTs, graphene, silver nanowires and graphene-silver nanowire hybrid, we find the FOLED with the graphene-silver nanowire hybrid electrode has the best uniform current spreading and the lowest turn-on voltage due to its lower resistivity and contactresistance.

9566-49, Session PMon

High-efficiency flexible organic lightemitting diodes with novel light outcoupling structures

Jianxin Tang, Yan-Qing Li, Lei Zhou, Hengyang Xiang, Soochow Univ. (China)

Because of their mechanical flexibility, organic light-emitting diodes (OLEDs) hold great promise as a leading technology for display and lighting applications in wearable electronics. The development of flexible OLEDs requires high-quality transparent conductive electrodes with superior bendability and roll-to-roll manufacturing compatibility to replace indium tin oxide (ITO) anodes. Here we present a flexible transparent conductor on plastic with embedded silver networks which is used to achieve flexible, highly power-efficient large-area green and white OLEDs. By combining an improved outcoupling structure for simultaneously extracting light in waveguide and substrate modes and reducing the surface plasmonic losses, flexible white OLEDs exhibit a power efficiency of 106 lm/W at 1000 cd/ m2 with angular color stability, which is significantly higher than all other reports of flexible white OLEDs. These results represent an exciting step towards the realization of ITO-free, high-efficiency OLEDs for use in a wide variety of high-performance flexible applications.

9566-52, Session PMon

Control of the orientation of the lightemitting molecules in spin-coated glassy organic films

Li Zhao, Kyushu Univ. (Japan); Takeshi Komino, Kyushu Univ. (Japan) and Japan Science and Technology Agency (Japan); Munetomo Inoue, Ju-Hyung Kim, Kyushu Univ. (Japan); Jean-Charles Ribierre, Kyushu Univ. (Japan) and Japan Science and Technology Agency (Japan); Chihaya Adachi, Kyushu Univ. (Japan) and Japan Science and Technology Agency (Japan)

Horizontal molecular orientation in organic light-emitting diode (OLED) materials has been already reported in a variety of vacuum-deposited glassy thin films. It is now well-established that such a horizontal molecular orientation is essential to improve the light outcoupling efficiency and the overall performance of the light-emitting devices. However, this preferential orientation has not been observed so far in spin-coated glassy organic films. Because of the current need to develop high performance solutionprocessed OLEDs for low cost and large area applications, control of the molecular orientation in spin-coated glassy organic thin films would be very significant to the field. Here, we show that the horizontal orientation of light-emitting molecules can be obtained in spin-coated glassy thin films based on a blend of a heptafluorene derivative in a 4,4'- bis(N-carbazolyl)-1,1'-biphenyl (CBP) host. Variable angle spectroscopic ellipsometry and angle dependent photoluminescence measurements are carried out to investigate the molecular orientation in heptafluorene neat film and in CBP blends. In particular, influence of the concentration of the heptafluorene molecules in the CBP blend is studied to provide information on the mechanism of these molecular orientational processes. Solution-processed fluorescent OLEDs with horizontally oriented heptafluorene emitters are then fabricated and exhibit deep blue electroluminescence with an external quantum efficiency as high as 5.3 %.

9566-53, Session PMon

Photopolymerizable fluorescent small molecule-based materials: An all-in approach for solution-processed OLEDs

Simon Olivier, Commissariat à l'Énergie Atomique (France)



and Univ. de Nantes (France); Lionel Derue, Bernard Geffroy, Ecole Polytechnique (France) and CEA Saclay (France); Eléna Ishow, Univ. de Nantes (France); Tony Maindron, CEA Grenoble (France)

The elaboration of organic light-emitting diodes (OLEDs) has been boosted by the use of charge transporting and emissive small molecules, leading to multilayer devices through successive steps of thermal vacuum evaporation. Although small molecule-based OLEDs display higher performances compared to those involving polymers, the vacuum evaporation of small molecules faces strong technical constraints like shadow mask handling, scaling up to large substrate and is usually associated with large product waste. In order to address these issues, wet deposition processes implying small molecules have been proposed so that to full OLED architectures [1]. Yet, they appeared quite troublesome due to high solubility of the resulting thin layers, making successive depositions very difficult.

In order to conjugate the performances of small molecules with the structural stability of polymerized layers, we have synthesized a series of novel promising fluorescent materials that successfully photopolymerize after wet deposition. These compounds show various emission colors (blue, green and orange) and high fluorescence quantum yields in the solid state before (0.40), even after photopolymerization (0.32), and form stable amorphous materials without crystallites or aggregates. After photopolymerization, the thin film becomes totally insoluble in common organic solvents, allowing for the deposition of the subsequent layer following a wet process. By associating these fluorescent compounds with photopolymerizable charge carriers like QUPD [2], we have been able to build a multi-layered OLED through a wet process without using orthogonal solvents.

Duan, L. et al J. Mat. Chem. 2010, 20, 6392.
 Müller, D. et al Synth. Met. 2000, 111–112, 31.

9566-56, Session PMon

Highly transparent and low resistance ZnO/Ag/ZnO multilayer electrodes for organic photovoltaic devices

Jun Ho Kim, Dae-Hyun Kim, Jae-Ho Kim, Korea Univ. (Korea, Republic of); Young-Zo Yoo, Duksan Hi-Metal Co., Ltd. (Korea, Republic of); Tae-Yeon Seong, Korea Univ. (Korea, Republic of)

Transparent conducting electrodes (TCEs) are of technological importance because of their application in optoelectronic and photonic devices. These devices require high transmittance and low resistance. ITO is most frequently used as a TCE in optoelectronic applications because of low resistivity and high transmittance. However, due to the limited supply of indium, dielectric/metal/dielectric (D/M/D) multilayers have been extensively studied to replace ITO. Thin Ag is commonly used as the middle layer for D/M/D multilayers because of its low resistance and high transmittance. In this work, we investigated the effect of ZnO layer thickness on the optical and electrical properties of ZnO/Ag/ZnO multilayer films deposited on glass substrates. It was shown that the transmission window became wider and shifted toward lower energies with increasing ZnO thickness. The ZnO/Ag/ZnO (40 nm/18.8 nm/40 nm) multilayer sample showed a transmittance of ~96% at 550 nm. As the ZnO thickness increased from 8 to 80 nm the carrier concentration gradually decreased from 1.74 x 1022 to 4.33 x 1021 cm-3, while the charge mobility varied from 23.8 to 24.8 cm2/Vs. With increasing ZnO thickness, the samples exhibited similar sheet resistances of 3.6 - 3.9 ohm/sq, but the resistivity increased by a factor of 4.58. The samples showed smooth surfaces with a root mean square roughness in the range of 0.47 - 0.94 nm. Haacke's figure of merit (FOM) was calculated for all the samples; the ZnO (40 nm)/Ag (18.8 nm)/ZnO (40 nm) multilayer produced the highest FOM of 148.9 x 10-3 ohm-1.

9566-57, Session PMon

Singlet harvesting technology for OLED applications

Daniel M. Zink, Charlotte Fléchon, Thomas Baumann, cynora GmbH (Germany)

Luminescent materials for optoelectronic applications based on the Singlet Harvesting technology are more and more becoming a serious competitor for current state-of-the-art Iridium-based emitter systems. These new materials evoke high industrial interest because of their straightforward chemical accessibility, their high efficiency and versatility. In addition, Singlet Harvesting materials can be color-tuned from red to deep-blue, modified for solution-processing as well as evaporation and are therefore suitable for a wide range of OLED application and production processes.

Singlet Harvesting is based on thermally-activated delayed fluorescence and means that both triplet and singlet excitons can be used, which leads to internal efficiencies up to 100%. Different classes of materials can be used: copper complexes as well as pure organic materials are currently in the focus of science and industry. The use of such emitter systems results in device efficiencies comparable with the state-of-the-art iridium-based OLEDs, by achieving external quantum efficiencies well above 20%.

Due to smart molecular engineering, several new and highly potent emitter systems for displays, lighting and smart packaging applications have been developed by CYNORA and are presented in this paper. The high versatility of these molecules leads to very efficient OLED devices and demonstrates how Singlet Harvesting materials are competitive in today's market.

9566-58, Session PMon

Synthesis and characterization of red phosphorescent iridium(III) complexes based on electron-acceptor modulation of main ligand for high efficiency organic light-emitting diodes

Sang Yong Park, Hongik Univ. (Korea, Republic of)

A new series of red phosphorescent iridium(?) complexes, (PT-TFP)2Ir(tmd), (PT-P)2Ir(tmd), and (PT-MP)2Ir(tmd) were synthesized for highly efficient red emitter of the organic light-emitting diodes (OLEDs). The main ligands consisted of electron-donor (phenanthren) and electron-acceptor (trifluoromethyl pyridine, pyridine, and methyl pyridine) were synthesized by Suzuki coupling reaction. The iridium(?) complexes based on main ligands and 2,2,6,6-tetramethyl-3,5-heptanedione(tmd) ancillary ligand were synthesized by Nonoyama reaction. Their luminescence properties were investigated by UV-visible spectroscopy and photoluminescence (PL) spectroscopy. The OLEDs devices were manufactured by vacuum deposition and their configuration was indium tin oxide (ITO)/PEDOT:PSS (40 nm)/HTL (17 nm)/RH-35:red dopant (5%, 10%, 40 nm)/HCL (5 nm)/ SNABH 205: 6s-12 (5%, 15 nm)/TPBi (20 nm)/LiF (1 nm)/Al(100 nm). These OLEDs devices were characterized by investigation of current density-voltage-luminance (J-V-L), current efficiency, power efficiency, external quantum efficiency (EQE), EL spectrum. The Iridium(?) complexes will be used as a solution process dopant for the hybrid OLED devices.

9566-60, Session PMon

Development of the efficient deep-blue organic emitters exhibiting thermally activated delayed fluorescence: Design, experimental, and theoretical studies

Nadzeya A. Kukhta, Juozas V. Grazulevicius, Kaunas Univ. of Technology (Lithuania)



The development of the highly efficient and stable deep-blue phosphorescent materials has proved to be a big challenge in the last decades [1]. An efficient triplet harvesting method that uses thermally activated up-conversion of triplet into singlet states, giving thermally activated delayed fluorescence (TADF), has been reported [2]. In order to design a promising deep-blue TADF emitter a thermally accessible gap between the lowest singlet and triplet excited states [3], high and stable triplet charge transfer state and spatially separated HOMO and LUMO orbitals are required.

In current work we present design and synthesis of new bipolar carbazole derivatives with 1,3,5-triphenylbenzene backbone. The influence of the substituent orientation on the photophysical characteristics of the compounds was investigated. The enhancement of the photoluminescence quantum yield (from 0.80 to 0.99 in oxygen-free conditions) was observed. DFT calculations revealed small energy difference ?EST (0.04-0.27 eV) and spatially separated HOMO and LUMO orbitals with a slight overlap.

[1] Yang X., Xu X., Zhou G. J. Mater. Chem. C 2015, Advance Article DOI:10.1039/C4TC02474E.

[2] Dias F. B., Bourdakos K. N., Jankus V. et al. Adv. Mater. 2013, 25, 3707-3714.

[3] Zhang Q., Li B., Huang Sh. et al. Nature Photonics 2014, 8, 326-332.

9566-61, Session PMon

Dependent of light outcoupling in organic light-emitting devices on ITO thickness and roughness

Yingjie Zhang, Hany Aziz, Univ. of Waterloo (Canada)

The efficiency of organic light-emitting devices (OLEDs) is shown to significantly depend on both the thickness and roughness of the indium tin oxide (ITO) anode. The effects of changing the ITO thickness from 45 nm to 130 nm are found to be able to vary the current efficiency by 40%. The underlying mechanism is studied and revealed to be related to microcavity effects. The transmittance of the ITO substrate changes significantly with the ITO thickness, resulting in variations in microcavity, and thus light outcoupling efficiency. On the other hand, the effects of increasing the ITO roughness (rms) from 3.3 nm to 8.5 nm are found to increase light scattering at the ITO/organic interface, thus improving extraction of light trapped in the organic/ITO wave-guided mode. In addition to the enhancement in current efficiency, the device fabricated on rough ITO shows similar driving voltage to that made on smooth ITO, indicating that change balance is not altered by ITO roughness. Contrary to common belief in the community, the lifetime of the OLED is not affected when using rough ITO. Finally, by optimizing the ITO thickness and roughness, an OLED that exhibits very high current efficiency at a remarkably high brightness, demonstrating 56 cd/A at 105 cd/m2 without any external light outcoupling techniques, is obtained. The results demonstrate the significant efficiency benefits of using ITO with optimal thicknesses and higher roughness in OLEDs.

9566-62, Session PMon

High performance inverted top-emitting organic light-emitting diodes with enhanced intrinsic quantum yield

Yu-Kun Wu, Runda Guo, Hongbo Wang, Zhensong Zhang, Yi Zhao, Jilin Univ. (China)

Top-emitting organic light-emitting diodes (TEOLEDs) have attracted considerable interest in recent years, owning to their intrinsic merit that they are more suitable for high resolution active matrix full color displays. It is advantageous to invert the TEOLEDs for integrating with the n-channel amorphous silicon thin film transistors (a-Si TFTs) which cannot produce adequate p-channel TFTs.

In this work, inverted top-emitting organic light-emitting diodes (ITOLEDs) with aluminum as cathode and semitransparent silver as anode are

investigated. Iridium complex of bis(4,6-(difluorophenyl)pyridinato-N,C2)picolinate iridium(III) (FIrpic), fac-tris(2-phenylpyridine)iridium(III) (Ir(ppy)3), bis(2-methyldibenzo[f,h]quinoxaline)(acetylacetonate) iridium(III) (Ir(MDQ)2acac) are used as blue, green and red phosphor emitters, respectively. The basic ITOLED structure is: Si/SiO2/Al/electron injection layer (EIL)/electron transport layer (ETL)/ /emission layer (EML)/ electron blocking layer (EBL)/hole transport layer (HTL)/hole injection layer (HIL) /Ag (20 nm), and the control bottom-emitting organic light-emitting diodes (BEOLEDs) with the basic structure of glass substrate/indium tin oxide (ITO)/HIL/HTL/EBL/EML/ETL/EIL/AI (100 nm).

We pleasantly find that the red ITOLED exhibits a higher external quantum efficiencies (EQEs) nearly twice as that of the bottom-emitting counterpart, 18.1% vs. 8.7% at ~2mA/cm2, while EQEs of green ITOLEDs and BEOLEDs at ~1.5mA/cm2 are 15.2% vs. 13.5% and that of blue devices at ~1mA/cm2 are 12.9% vs. 11.3% respectively. We explain that the role of the strong microcavity effect improved the spontaneous emission of emitters in all ITOLEDs, what's more, only the intrinsic quantum yield (IQY) of the red emitters is improved due to its comparable radiative and nonradiative decay rates.

9566-63, Session PMon

An electro-optical characteristics test equipment for OLED lighting panels with homogeneity and non-uniformity test function

Hector H. Y. Lin, Gilbert C. W. Chen, Jamie J. M. Liu, Paul B. Y. Wu, MPI Corp. (Taiwan); Chih-Ming Lai, Wen-Yung Yeh, Chi-Yi Leu, Chao-Feng Sung, Mei-Ju Lee, Industrial Technology Research Institute (Taiwan)

To meet the testing requirement of OLED lighting panels listed on the datasheet, a test equipment capable of searching panel driving current under constant luminance (for example 1000cd/m2) has been developed. The OLED test equipment has two station. Non-uniformity, homogeneity, output luminance and operation current of OLED lighting panel is tested by first station using an imaging photometer. Luminous flux, power efficiency and chromaticity parameters is then tested by the second station in integrating sphere by spectrometer with driving current obtained from constant luminance measurement.

A comparison of homogeneity and non-uniformity from test results of 8cm?8cm light emitting area hybrid tandem white OLED lighting panels is investigated. OLED lighting panels fabricated by ITRI OLED lighting baseline has power efficiency 40 lm/W, CCT about 4,000 K, CRI>85. Panel homogeneity H(?) is calculated based on finding the largest luminance gradient with ?=0.5 suggested by CIE TC-2 68 committe. For most of OLED lighting manufactures, the luminance non-uniformity within 15% is suggested. However, there is no data about their panel homogeneity. Our test result shows that H(?=0.5) is about 0.65~0.70 when luminance non-uniformity is 15%. Interestingly, these panels can just be classified as homogeneous. In general, human eyes cannot detect luminance variation when non-uniformity smaller than 5%, and the related H(?=0.5) is about 0.88. Moreover, non-uniformity of OLED lighting panels should at least lower than 8% to be classified as very homogeneous H(?=0.5) > 0.8. OLED lighting panels will be classified as inhomogeneous H(?=0.5) < 0.6 when non-uniformity higher than 18%.

9566-64, Session PMon

OLED microdisplay in 0.35 um complementary metal-oxide semiconductor technologies for wearable electronic display applications

Chih Hsiang Chang, Po-Tsun Liu, National Chiao Tung Univ. (Taiwan)



The demand of head-mounted and wearable display is predicted in the next decades covering application areas such as sport, security and entertainment. Microdisplay technologies for near-to-eye applications mostly use a complementary metal-oxide semiconductor (CMOS) processing on top of the CMOS chip to deposit organic LED or liquid crystal display. In this paper TEOLED (Top-emitting Organic Light-Emitting Diode) for the microdisplay based on the CMOS integrated circuit substrate will be adopted. The microdisplays are implemented in a standard 0.35 um CMOS processing. The presented microdisplays offer a cost effective alternative to conventional LC and OLED based displays.

9566-65, Session PMon

Precise color-tuning using solution processed LECs in a hybrid device architecture

Serpil Tekoglu, Karlsruher Institut für Technologie (Germany) and InnovationLab GmbH (Germany); Martin Petzoldt, Ruprecht-Karls-Univ. Heidelberg (Germany) and InnovationLab GmbH (Germany); Sebastian Stolz, Karlsruher Institut für Technologie (Germany) and InnovationLab GmbH (Germany); Uli Lemmer, Karlsruher Institut für Technologie (Germany); Manuel Hamburger, Ruprecht-Karls-Univ. Heidelberg (Germany) and InnovationLab GmbH (Germany); Gerardo Hernandez-Sosa, Karlsruher Institut für Technologie (Germany) and InnovationLab GmbH (Germany);

Organic light-emitting devices are promising elements for display and artificial lighting technologies. In the fabrication of full color displays, one of the challenges is complex device fabrication to get full-color emission containing red, green, blue emissions in small areas. Furthermore, three color displays can be used to get white light emission via complicated methods. In this perspective, color-tuning have always drawn significant attention of the researchers in the field either to achieve white light, multior full-color devices. A simple light-emitting device which can emit a wide range of colors is always desirable to simplify the fabrication techniques.

In our work, color-tunable organic light emitting devices (OLEDs) were fabricated using a hybrid device architecture combining polymer organic light emitting diode (PLED) and light emitting electrochemical cells (LEC) characteristics in one structure. A novel water-soluble quaternized polyfluorene (PFO) was utilized as polyelectrolyte in a single component LEC layer on top of a conventional PLED stack. Depending on the thickness of the PFO layer, we obtained a fine tuning in the emission color of OLEDs. The luminance-current density-voltage, the lifetime and the electroluminescence characteristic of the organic light emitting devices were defined. The solution processed bilayer hybrid device showed a maximum luminance of ~ 500 cd/m2 with CIE chromaticity coordinates x=0.29, y=0.43. We highlight this new method as a strategy for white or multi-color organic light emitting devices.

9566-66, Session PMon

Computer simulation of OLED devices: From chemical structures to drift-diffusion equations

Pascal Kordt, Max-Planck-Institut für Polymerforschung (Germany); Sven Stodtmann, Mustapha Al Helwi, Alexander Badinski, BASF SE (Germany); Denis Andrienko, Max-Planck-Institut für Polymerforschung (Germany)

Drift-diffusion equations coupled to the Gaussian disorder lattice models [1] have been successfully used to study OLED devices, e.g. spacecharge formation, charge density-mobility relations, and current-voltage characteristics [2]. In order to provide parameter-free description of amorphous organic semiconductors, here we couple drift-diffusion equations to a multiscale approach which combines density functional theory, molecular dynamics, stochastic modeling, and kinetic Monte Carlo simulations [3]. We thus establish a link between underlying chemical structures and current-voltage characteristics of OLED devices. Our approach is verified against experimentally measured current-voltage characteristics of an amorphous layer of DPBIC, a hole-conductor used in blue phosphorescent OLEDs.

[1] M. Bouhassoune et al.: Organic Electronics 10, 437-445 (2009)

[2] S. Stodtmann et al.: J. Appl. Phys. 112 11409 (2012)

[3] P. Kordt et al.: Adv. Func. Mater., published online, doi: 10.1002/ adfm.201403004 (2015)

9566-67, Session PMon

To enhancement illuminance efficiency of OLED by thin film included microparticle

Chuang-Hung Chiu, Chunghwa Picture Tubes, Ltd. (Taiwan); Chao-Heng Chien, Jen-Chi Lee, Wei-Cheng Chien, Tatung Univ. (Taiwan)

The main purpose of this study is to enhance OLED illuminance. The PDMS is used to be as the enhanced illuminance film material and has a refractive index of 1.48 to be similar as the OLED glass substrate of 1.5. Two metal oxidation microparticles are doped into PDMS film, the refractive index are 1.7 and 2.4 for each other. All of particles size are 2?m and concentration of 2%.

The illuminometer (DX-200) is applied to measure the illuminance of the OLED light. The OLED is located at the center of sphere which has the radius of 30cm, and the illuminance is measured on the different location around the surface of the sphere.

The peak value of illuminance either in the X-axis or Y-axis is the light emitting angle at 90 degrees.

The original OLED forward illuminance is 4.2 lux. The enhanced illuminance film attached to the OLED, the illuminanc is 6.2 lux. OLED half-power angle is 65 degree. The enhanced illuminance film attached to the OLED, the Lambertian emission patterns is 55 degree. In this study, the optical film attached to the OLED, the Lambertian emission patterns of 10 degrees will reduce, but it can enhance the illuminance of more than 45%. Therefore to be understood that the film has a concentrator effect.

Summary:

An enhanced optical film to increase the illuminance of OLED was successful to be presented. The PDMS was chosen as the substrate material for the optical film, and including the two kinds of the micro particles. The optical film is applied on the LOED light lamp to enhance the illuminance up to 45%.

9566-68, Session PMon

Photophysical studies of the thermallyactivated delayed fluorescence of a highly luminescent mononuclear copper(I) compound

Larissa Bergmann, cynora GmbH (Germany); Gordon J. Hedley, Univ. of St. Andrews (United Kingdom); Thomas Baumann, cynora GmbH (Germany); Ifor D. W. Samuel, Univ. of St. Andrews (United Kingdom)

Efficient emitting materials for organic light-emitting diodes are a continued focus of academic and industrial research. A broad variety of luminescent copper(I) complexes for OLED applications was developed in recent years, as high material and processing costs of nowadays used iridium and platinum materials led to the search for easier accessible and solution-printable OLED materials. Although copper(I) exhibits only a small spin-



orbit coupling constant when compared to iridium(III), its complexes can harvest both triplet and singlet excitons for the emission of light and achieve internal quantum efficiencies of 100% by utilizing the smaller spin-orbit coupling for thermally activated delayed fluorescence (TADF). Furthermore, the concept of TADF enables short emission decay times for emitting materials with small spin-orbit coupling.

In contrast to photophysical studies on organic TADF compounds, which gain increasing interest in the last few years, there are only few publications about the electronic processes occurring after excitation in luminescent copper(1) compounds which are characterized by thermally-activated delayed fluorescence behavior. We studied the thermally-activated delayed fluorescence behavior of a mononuclear neutral copper(1) complex by time-resolved spectroscopy. The intersystem crossing (ISC) rate from excited singlet to triplet states was determined in the solid state for the first time, and thus, better understanding of the excited state processes and mechanisms that ensure TADF has been explored.

9566-69, Session PMon

Study on cadmium sulphide nanoparticles on blue and green light emitting polymers

Pradeep Chandran, Cochin Univ. of Science and Technology (India); Mathew Sebastian, Cochin Univ. of Science & Technology (India); Manoj A. G. Namboothiry, Indian Institute of Science Education and Research (India); C. P. G. Vallabhan, Cochin Univ. of Science & Technology (India); P. Radhakrishnan, International School of Photonics (India); V. P. N. Nampoori, Cochin Univ. of Science & Technology (India)

Cadmium Sulphide nanoparticles have been the focus of recent scientific research due to their electroluminescent and conductive properties. As a transition metal chalcogenide (II-VI) semiconductor, this material has been largely investigated in optical filters, photo detectors, solar cells, light emitting devices, thin film field effect transistors, photocatalysis etc. The material properties essentially depend on the optical bandgap, morphological and structural features, and hence require extensive and elaborative research to understand the underlying mechanism in light emitting devices. With the difficulty of making thin films from nanoparticles, these material could easily be embedded in polymers to make hybrid (organic-inorganic) light emitting diodes. Such diodes combine the advantageous of processing flexibility of polymers and the semiconducting properties of the nanoparticles.

In this paper we investigate the electroluminescence emission performance from light emitting polymers doped in cadmium sulphide nanoparticles. The nanoparticles were synthesized by precipitation technique and obtained nanoparticles of size 10 nm. The blue emitting PFO [Poly(9,9-di-n-octylfluorenyl-2,7-diyl)] and green emitting F8BT [Poly(9,9-dioctylfluorene-alt-benzothiadiazole)] were doped with CdS nanoparticles and used as active emissive layer in polymer light emitting diodes. We see a decrease in the turn on voltage in both polymers and increase in the brightness in green emitting polymer. We present and discuss the possible mechanism for the improved performance due to the incorporation of CdS nanoparticles in light emitting polymers.

9566-70, Session PMon

Measurement of charge balance and its effect on electrophosphorecent organic light emitting device lifetime

Caleb Coburn, Stephen R. Forrest, Univ. of Michigan (United States)

The long term operational lifetime of phosphorescent organic lightemitting diodes (PHOLED), particularly in the blue spectral region, remains a barrier to their widespread adoption in displays and solid state lighting. PHOLED degradation can be attributed to multiple pathways, including the loss of charge balance, molecular degradation due to high energy bimolecular recombination reactions, and delamination. We present studies on the contribution of charge balance to degradation of high efficiency PHOLEDs. For this, we introduce a technique that allows for a quantitative measurement of charge imbalance over time. We use this technique to probe charge and exciton leakage from the emissive layer of blue emitting PHOLEDs as a function of current density. The measured charge balance together with luminance loss, voltage rise, and time-resolved external quantum efficiency characteristics are used to model mechanisms leading to the degradation of PHOLEDs. For example, we calculate the relative importance of each degradation mode, namely charge balance, nonradiative recombination, and quenching on deep trap sites formed by molecular degradation in the emissive layer. Finally, the efficacy of electron/ exciton blocking layers over the device lifetime is examined.

9566-71, Session PMon

A systematic comparison of the effect of joule heating vs thermal annealing on the morphology of typical hole transport layers in organic light emitting devices

Tyler Davidson-Hall, Hany Aziz, Univ. of Waterloo (Canada)

It is well-known that hole transport layers (HTLs) in organic light emitting devices (OLEDs) are more sensitive to morphological changes than other organic layers due to lower glass transition temperatures. A high operational temperature can alter the HTL morphology, severely impacting OLED performance and stability. Although joule heating is a known factor affecting OLED stability during operation, its effect in experimental studies is typically simulated through thermal annealing of the devices rather than applying current. In this work, a systematic comparison of the effects of joule heating vs thermal annealing on the morphological stability of a N,N'-di(1-naphthyl)-N,N'-diphenylbenzidine (NPB) HTL and the impact this has on OLED performance is investigated. While thermal annealing of an OLED is a good first-order approximation of joule heating, the temperature distribution profile of the OLED is different under the two stress conditions and thus can impact the morphology of the HTL differently. However, joule heating introduces a confounding factor whereby the OLEDs experience intrinsic degradation by the flow of current, aside from thermal stress. Our recent investigations show that electrical stress can bring about morphological changes induced by polaron-exciton interations independent of those induced by thermal effects. Therefore, in this work, polaron-exciton interactions are decoupled from the findings by studying joule heating in unipolar devices that comprise solely of a NPB organic layer. Device IVL, lifetime and morphology as a function of temperature for both joule heating and thermal annealing are presented as a means to evaluate stability and performance.

9566-72, Session PMon

Vacuum nano-hole array embedded organic light emitting diodes with high efficiency

Sohee Jeon, Korea Institute of Machinery & Materials (Korea, Republic of)

OLEDs intrinsically provide higher energy efficiency than other light sources, and this efficiency has been increased significantly through the use of phosphorescent emitters and charge transport materials. As the OLED had an ultrahigh external quantum efficiency (EQE) of 29.1%, the internal quantum efficiency had almost reached the theoretical limit. However, 70% of the internal light was still wasted by the substrate, the organic layers, and the transparent electrode even in the case of the highest EQE of 29.1% which equates with an internal efficiency of 100%.

Here, high-efficiency organic light emitting diodes (OLEDs) with an EQE of greater than 50% and low roll-off were produced by inserting a vacuum



nanohole array (VNHA) into phosphorescent OLEDs (PhOLEDs). The VNHA substrate was fabricated using a novel process called robust reverse-transfer (R2T). The R2T process was utilized to generate the nanohole array, which was then inserted to the PhOLED in a vacuum to maximize the refractive index (RI) contrast of the PhC slab for a given background material of high RI. The VNHA substrate obtained by the proposed R2T process has a smooth surface that is comparable to the surface roughness of polished silicon wafers, and thereby leads to a negligible electrical loss, which indicates that the experimental results can be compared with those from optical modeling. The resultant extraction enhancement was guantified in terms of EQE by comparing experimentally measured results with those produced from optical modeling analysis, assuming almost perfect electric characteristics of the device. The measured performance of the VNHA OLEDs was compared with optical modeling analysis results, and the VNHA was verified to extracts the entire waveguide loss into the air. The EQE obtained in this study is the highest value obtained for bottom-emitting OLEDs to date.

9566-73, Session PMon

Correlation of carrier mobility with energetic disorder of host molecules in p-doped amorphous organic semiconductors

Seung-Jun Yoo, Seoul National Univ. (Korea, Republic of); Jeong-Hwan Lee, Seoul National Univ. (Korea, Republic of) and IMEC (Belgium); Jae-Min Kim, Jang-Joo Kim, Seoul National Univ. (Korea, Republic of)

Electrical doping in organic semiconductors (OSs) has been actively investigated to enhance the conductivity of bulk organic films. Despite of wide use of dopants in OSs, the charge generation efficiency (CGE) is obviously smaller than 100%. The low CGE is dominated by the dissociation process, since the transferred carriers mostly bound to the mutual ionized dopant by a strong Coulombic binding energy due to the low dielectric permittivity of about 3 in OSs. Therefore, the Coulomb trap induced by the ionized dopant will give a significant effect on the charge transport in OSs. In order to understand the effect of Coulomb trap on the charge transport in doped OSs, it is necessary to systematically analyze the correlation of carrier mobility with energetic disorder of hosts.

In this work, the effect of Coulomb traps on hole mobility was investigated using various p?doped OSs possessing different CGE and energetic disorder of hosts. The hole mobility was analyzed in the Ohmic current region to minimize the effect of the injected carrier density on the carrier mobility. Even though the hole mobility of pristine OSs has a big difference by a few orders of magnitude, that of p?doped OSs is almost same, indicating that the majority of doping-induced holes are localized in Coulomb traps caused by negatively ionized p?dopants. However, the doping-concentrationdependent hole mobility has a specific tendency, depending on the magnitude of the energetic disorder of the hosts. These phenomena are interpreted by calculating the effective density-of-states distribution of p?doped OSs and by measuring the activation energy of conductivity.

9566-74, Session PMon

Controlling orientation of emitting dipoles of iridium complexes for highly efficient phosphorescent organic light-emitting diodes

Kwon-Hyeon Kim, Seoul National Univ. (Korea, Republic of); Jae-yeol Ma, Gyeongsang National Univ. (Korea, Republic of); Chang-Ki Moon, Seoul National Univ. (Korea, Republic of); Yun-Hi Kim, Gyeongsang National Univ. (Korea, Republic of); Jang-Joo Kim, Seoul National Univ. (Korea, Republic of) It has been recently discovered that orientation of phosphorescent emission dipoles is a crucial factor influencing the efficiency of phosphorescent organic light-emitting diodes (PhOLEDs) because higher efficiency than 30% can be obtained from OLEDs if emission dipoles are oriented along horizontal direction (parallel to the substrates). We recently reported that the preferred emitting dipole orientation of iridium complexes originates from preferred direction of the triplet transition dipole moment of the molecules along a specific direction and strong supramolecular arrangement between iridium complexes and host molecules in an EML. And, we demonstrated high efficiency OLEDs with external quantum efficiency of 32% for green ad 36% using red using iridium based phosphorescent dyes with preferred horizontal orientation of emission dipoles. However, the relationship between structure of phosphorescent dyes and orientation of emission dipoles, and the factors influencing the orientation of emission dipoles of phosphorescent iridium complexes in doped films are little studied yet to our best knowledge. Besides, it has yet to be identified how to increase the ratio of horizontal dipoles of phosphorescent dyes and resultantly the EQE of OLEDs. Here, we report that the orientation of emission dipoles of heteroleptic iridium complexes doped in an emission layer is linearly proportional to the angle of the transition dipole moments against the C2 axis of the dyes using a newly synthesized series of materials. We also demonstrated unprecedented high efficiency of green OLEDs using a new emitter.

9566-75, Session PMon

Introducing a thermally activated delayed fluorescence emitter for a highly efficient blue fluorescent organic light emitting diode

Jin-Won Sun, Kwon-Hyun Kim, Seoul National Univ. (Korea, Republic of); Yun-Hi Kim, Gyeongsang National Univ. (Korea, Republic of); Jang-Joo Kim, Seoul National Univ. (Korea, Republic of)

Enhancing electroluminescence (EL) efficiency might be a never ending pursuit from displays to lightings where organic light emitting diodes (OLEDs) are being used as sources. For past years, phosphorescent OLEDs (PhOLEDs) based on heavy metal complexes have been considered as an only solution to realize high efficiencies by harvesting both singlet and triplet excitons as light. However, recent progress utilizing delayed fluorescence challenges the conventional idea of achieving high EL efficiencies. Fluorescent material showing thermally activated delayed fluorescence (TADF) phenomenon enables additional harvest of triplet excitons as well as singlet excitons via reverse intersystem crossing (RISC) from triplet (T1) to singlet (S1) state due to thermal activation and small energy gap between the two excited states.

In order to enhance EL efficiency for blue fluorescent OLEDs, a blue TADF emitter has been newly synthesized for this work. Spatial spearation of the highest occupied molecular orbital (HOMO) and lowest unoccupied molecular orbital (LUMO) of the emitter led to small exchange energy that enhances RISC.

The balanced device structure implementing a mixed co-host system and the blue TADF emitter exhibited unprecedented external quantum efficiency (EQE) for blue fluorescent OLEDs.

9566-76, Session PMon

Efficiency loss in solution processed organic light emitting diodes

Szuheng Ho, Ying Chen, Franky So, Univ. of Florida (United States)

Efficiency loss in solution processed organic light emitting diodes (OLEDs) compared to vacuum deposited counterpart is studied in a highly efficient phosphorescent OLED system. The molecular packing is examined with ellipsometry measurements. The refractive index is extracted from the data.



It reveals that compared to thermally evaporated film, solution processed counterpart is less dense. Besides, the packing of solution processed film can be closer to that in the evaporated one if higher solute concentration and higher spin speed are used in spin-casting process. The influence of molecular packing on carrier transport was also verified by the current density-voltage characteristics of single carrier devices. A relative vacuum level shift and expansion of band tail states in solution processed devices were observed. This might lead to worse charge confinement and impair device performance. The substitution of electron transport layer (ETL) with deeper highest occupied molecular orbital (HOMO) level can ameliorate this situation. A solution processed OLED with extremely high efficiency (external quantum efficiency of 28.9%) is achieved by employing ETL with deep HOMO level, which significantly suppresses the efficiency loss due to transport variation and interfacial energy level shift.

9566-77, Session PMon

Organic light emitting diodes with enhanced out-coupling efficiency and operational stability due to spontaneously formed corrugated structure within active layers

Cheng Peng, Xiangyu Fu, Shuyi Liu, Ying Chen, Franky So, Univ. of Florida (United States)

Spontaneously formed corrugated structure is realized in an all-organic system. The morphology of the corrugated structure is characterized with atomic force microscopy (AFM) technique. The results show that the corrugation can be well controlled by material choice, layer thickness and treatment conditions. Furthermore, this corrugated structure can be realized directly inside organic light emitting devices (OLEDs) with similar treatments and it can serve both as the functional layers of the OLED and the out-coupling enhancing layer. We applied this technique to OLED active layers and fabricated corrugated devices. Compared with the control device, which is a planar OLED with the same composition and thickness of each layer, the corrugated OLED shows a more than 35% enhancement in current efficiency. In addition, the corrugated OLED also has a greatly improved operational stability. The lifetime LT90 at 1000cd/m2 is improved as much as 40 times in the corrugated OLED. The enhancement in efficiency is the result of improved out-coupling of electroluminescence (EL), since the corrugated structure leads to reduced EL loss in surface plasma mode. The simplicity of the treatments and the significant enhancements in both device efficiency and operational lifetime demonstrate the potential of this technique in pursuing low-cost and high-performance OLEDs.

9566-78, Session PMon

Passivation of metal oxides surfaces for high performance organic and hybrid optoelectronic devices

Franky So, Shuyi Liu, Szuheng Ho, Ying Chen, Univ. of Florida (United States)

The exciton quenching properties of solution-processed nickel oxide (NiOx) and vanadium oxide (VOx) are studied by measuring the photoluminescence (PL) of a thin emitting layer (EML) deposited on top of the metal oxides. Strong exciton quenching is evidenced at the metal oxide/EML interface, which is proved to be detrimental to the performance of optoelectronic devices. With a thin polymer passivation polymer adsorbed on top of metal oxides, the PL quenching is found to be effectively suppressed. A short UV-O3 treatment on top of the polymer passivated metal oxides turns out to be a key procedure to trigger the chemical binding between the passivation polymer and the metal oxide surface species, resulting in substantially improved hole injection and extraction for organic light emitting diodes (OLEDs) and solar cell devices, respectively. With the passivation layer followed by UV-O3 treatment, the OLEDs incorporating NiOx as a hole transport layer (HTL) shows a record current efficiency of 91 Cd A-1 with

significantly suppressed efficiency roll-off, the OLEDs incorporating VOx as a hole injection layer (HIL) also shows higher current efficiencies at higher luminescence. Both perovskite solar cells and polymer solar cells incorporating passivated NiOx HTL also shows an enhancement of 60% due to passivation.

9566-80, Session PMon

Delayed fluorescence on triazine phenothiazine derivative

Ikbal Marghad, Ecole Polytechnique (France)

Since the report of the OLED's third generation based on the hyperfluorescent materials thermally activated delayed fluorescence (TADF) [1], a large number of TADF materials have been synthesized such as the Phenothiazine-Triphenytriazine (PTZ-TRZ) [2]. We propose a novel TADF material which is a (PTZ-TRZ) derivative. The latter is the 2,4 bis 3-thienyl 1, 3, 5-triazine 6-phenyl phenothiazine featuring donor-acceptor parts. The donor part is the phenyl phenothiazine and the acceptor one is the 2,4 bis-3 thienyl 1, 3, 5 triazine. The distribution of the HOMO and LUMO suggests a well separation of the donor and acceptor parts which are localized on the HOMO and LUMO energetic levels respectively. The properties of this material have been studied and exhibits TADF proprieties. Moreover, the substitution of 2,4 bis-phenyl on the donor part of the (PTZ-TRZ) by the 2,4 bis 3-thienyl indicate new proprieties.

[1] Hiroki Uoyama et al Highly efficient organic light-emitting diodes from delayed fluorescence 2234 | NATURE | VOL 492 | 13 DECEMBER 2012

[2] Hiroyuki Tanaka et al Dual Intramolecular Charge-Transfer Fluorescence J. Phys. Chem. C, 2014, 118 (29), pp 15985–15994

9566-81, Session PMon

Optical effect of graphene electrodes on organic light-emitting diodes

Hyunsu Cho, Jin-Wook Shin, Nam Sung Cho, Jaehyun Moon, Jun-Han Han, Electronics and Telecommunications Research Institute (Korea, Republic of); Young-Duck Kwon, Seungmin Cho, SAMSUNG Techwin Co., Ltd. (Korea, Republic of); Jeong-Ik Jeong-Ik, Electronics and Telecommunications Research Institute (Korea, Republic of)

Graphene films have been probed as a transparent electrode because it suggests a solution to overcome the drawback of ITO electrode, mechanical brittleness making it difficult to apply in flexible or stretchable electronics. In organic light-emitting diode (OLED) applications, graphene electrode has been achieved noteworthy efficiencies not only in monochromatic but also in white colors. The physical thickness of single layer graphene is about 0.34nm. The refractive index (n) of it ranges as 2.3 ~ 3.0 and the extinction coefficient (k) is bigger than 1 in the visible range. Regarding this aspect, the optical importance of graphene film as a transparent electrode in OLEDs needs to be confirmed.

In this study, we performed both optical simulations and experiments to investigate an optical effect of graphene electrodes on efficiencies and spectral emission properties of OLEDs. Simulation results suggest that graphene electrode attenuates the oscillatory behavior in efficiency of OLEDs for different organic layer thicknesses. In experiments, the current efficiency of OLEDs with graphene anode is only varied from 39 cd/A to 46 cd/A, though that of ITO anode is varied from 36 cd/A to 45 dd/A in the same variation in organic layer thickness. In addition, emission spectra distribution of graphene anode OLEDs showed weak dependency on the organic layer thickness as well as the viewing angles.



9566-82, Session PMon

Efficient OLEDs based on embedded silver grid electrodes for flexible lighting applications

Jaeho Lee, KAIST (Korea, Republic of); Jee-Hoon Seo, HANA Microelectronics, Inc. (Korea, Republic of); Sungyeon Kim, Jin Chung, Eunhye Kim, Sunghee Park, Eungjun Kim, Seung S. Lee, Seunghyup Yoo, KAIST (Korea, Republic of)

Organic light-emitting diodes (OLEDs) are being regarded as a nextgeneration lighting source due to their form-factor and cost advantages as well as their large-area compatibility. To fully utilize their potential benefits, it is critical to secure scalable and affordable transparent electrode (TE) technologies that are compatible with flexible devices and exhibit high performance (e.g. low sheet resistance and high transmittance). However, indium tin oxide (ITO), which is a TE typically used in OLEDs, is known to have a poor mechanical flexibility, being subject to bending-induced fracture and increase in Rs. Relatively high cost and high process temperature can also be limiting factors in realizing low-cost and/or flexible OLEDs.

In this study, we present large-area and/or flexible OLEDs built with a hybrid TE based on Ag grids engraved onto a plastic substrate and highconductivity-grade PEDOT:PSS layers (Clevious PH1000 with DMSO 5 wt%) covering the grids. The proposed hybrid TEs exhibit a sheet resistance of 9.7 ohm/sq. and transmittance of 87.1% (at 550 nm), yielding the effective DC to optical conductivity ratio of 302.1, which is comparable to that of ITO. OLEDs based on these hybrid TEs show a stable, leak-free operation and external quantum efficiency as high as 22.3%. Furthermore, these devices turn out to be highly flexible, exhibiting no degradation even after 1000-time bending at a radius curvature of 7.9 mm. In addition, we demonstrate a large-area OLED (50 mm ? 25 mm) that shows uniform surface emission characteristics and compare it with a PSPICE model that analyzes the area scaling behavior of local luminance distribution in consideration of TE sheet resistance and the equivalent diode characteristics of an OLED under study.

9566-83, Session PMon

Photophysical Properties of Thermally Activated Delayed Fluorescence from OLED Materials

DaSom Kim, Hee Won Shin, Tae Kyu Ahn, Sungkyunkwan Univ. (Korea, Republic of)

Improving the efficiency and lifetime of blue organic light-emitting diodes (OLEDs) are vital toward a success of OLEDs as a replacement for LCD technology. So, considerable researches have been explored to develop OLEDs with high external quantum efficiency. External quantum efficiency values of 20% and 19% have been reported for red (625 nm) and green (530 nm) diodes. However, blue diodes (430 nm) have only been able to achieve maximum external quantum efficiencies in the range of 4% to 6%. In order to realize the high blue electroluminescence efficiency in OLEDs, we adopt e?cient thermally activated delayed fluorescence (TADF) which have long operational lifetime with excited-state intermolecular proton-transfer (ESIPT) process. We explored the ESIPT molecules with charge-transporting functional groups, hydroxyl-substituted tetraphenylimidazole (HPI) derivatives to have longer lifetime component up to microsecond order.

In this study, we measured the time-resolved photoluminescent (PL) decay and transient photovoltage curves of HPI derivatives with a nanosecond pulsed laser (Quanta-Ray INDI Nd:YAG Laser, Spectra-Physics). Therefore, we proved non-negligible contribution of the delayed fluorescence in the total emission. Our study provides the design information of the dynamical behaviors of photocarriers to develop high-efficiency blue electroluminescence OLEDs.

9566-84, Session PMon

Hollow-core polymeric nanoparticles for the enhancement of OLED outcoupling efficiency

Jun-Hwan Park, Pusan National Univ. (Korea, Republic of)

Since the half of light was trapped in organic/ITO layer, the most efficient way to enhance the outcoupling efficiency was to insert an optical scattering structure close proximity to the ITO layer. Various optical elements such as a diffraction grating, scattering particles and scattering grid had been incorporated in the OLED device. In this work, hollow-core nanoparticles (HCNPs) dispersed polymer layer was inserted under the ITO layer to scatter the light more efficiently. Due to the high index contrast between the hollow nanoparticle and a host polymer. HCNPs increased the optical scattering efficiency. The efficiency also depends on the size and the volume fraction of the HCNPs in the polymer solution, together with the refractive index and the thickness of the polymer layer. For investigating the effect of these parameters, finite difference time domain (FDTD) numerical method was used. It was shown that HCNPs dispersed in a polymer layer could enhance the EQE by a factor of 2.5 with the optimum size range of 200 ~ 400 nm. The HCNPs was easily obtainable from a polystyrene/silica nano-composite. In order to synthesize the HCNPs, microfluidic synthesis method was introduced due to the advantage of smaller size dispersion and in-line production based on flow-through self-assembly process. It utilizes the interfacial reaction obtained from laminar flow and self-assembly of polymers in a microchannel. 400 nm-thick PVA film containing HCNPs with a size distributed in the range of 100 ~ 800 nm was obtained in our preliminary experiment.

9566-85, Session PMon

Highly enhanced green phosphorescent organic light-emitting diodes with cesium fluoride doped electron injection layer

Jongseok Han, Yongwon Kwon, Changhee Lee, Seoul National Univ. (Korea, Republic of)

Organic light emitting diodes (OLEDs) have attracted a lot of interest because of their potential applications in solid state lightings and displays. In order to improve device performance, one of critical issues which should be studied carefully is efficient electron injection between metal cathode and organic layer. In recent years, electrical doping has been extensively utilized in improving electron injection and transport. It decreases the operating voltage and improves power efficiency by increasing conductivity. For instance, alkali metals, including cesium and lithium, etc., as a low-work function n-type dopants in electron injection layers (EILs) can facilitate electron injection effectively and reduce ohmic losses. However, some of these derivatives have disadvantages such as their high sensitivity to oxygen or moisture and complicated evaporation process. In this work, we systematically studied doping effect of cesium fluoride (CsF) on the device performance of green phosphorescent OLEDs because CsF can be used as a stable n-type dopant due to its low chemical reactivity and simple deposition process. We confirmed that CsF could be employed as an effective n-type dopant based on experimental studies of optical absorption spectroscopy in thin films of 3,3'-[5'-[3-(3-Pyridinyl)phenyl] [1,1':3',1"-terphenyl]-3,3"-diyl]bispyridine (TmPyPB) doped with CsF at various concentrations and impedance spectroscopy in an electron only device (EOD) with CsF-doped TmPyPB. Owing to high electrical property of CsF-doped TmPyPB EIL, green phosphorescent OLEDs showed significantly lower voltage and considerably enhanced efficiency. The device with 30 vol% CsF-doped TmPyPB showed power efficiency of 28.1 lm/W at 1000 cd/ m2, whereas the device with undoped EIL exhibited 13.8 lm/W.



9566-86, Session PMon

Numerical characteristics of the intensity distribution for a white organic lightemitting diode

Henglong Yang, Wei-Cheng Li, National Taipei Univ. of Technology (Taiwan)

A feasible numerical model capable of characterizing the unique intensity distribution of a planar white organic light-emitting diodes (WOLED) as a lighting source was theoretically investigated by fitting our experimental data obtained by microscopic goniometer (MG) system associated with an energy analyzer to a statistical distribution function with three adjustable parameters. The WOLED is one of the upcoming lighting sources with planar device structure without additional optical components. The intensity characteristic of a lighting source is crucial for practical purpose. The procedure of an optical design usually requires proper numerical tools to satisfy specific application by adjusting parameters. Relatively uniform intensity distribution of a planar lighting source is needed for a specific lighting application such as back-lighting (BL) for liquid-crystal displays (LCD) in which Regular white LED's (WLED) and light-guide plate are assembled as a planar module after proper optical design. However, our intensity measurement of a WOLED revealed an unique distribution pattern in which the relative intensities near central area are higher than that near the edge of the emissive area. A practical numerical model is required to characterize this unique intensity distribution pattern exclusively for optical design tool. Our preliminary result of finding a feasible numerical model to characterize the intensity distribution of a WOLED was established by fitting experimental data to the Gaussian statistical distribution function with amplitude, average, and standard deviation as adjustable parameters. This parametric model may be used as a potential optical design tool for WOLED in the future.

9566-87, Session PMon

Improved light out-coupling efficiency of organic light emitting diodes with a simple processed light-extraction layer

Jae-Hyun Lee, Chur-Hyun Shin, Min-Hoi Kim, Yoonseuk Choi, Hanbat National Univ. (Korea, Republic of)

Organic light emitting diodes (OLEDs) are now widely commercialized in the display market due to many advantages such as possibility of making thin or flexible devices. Nevertheless there are still several things to obtain the high quality flexible OLEDs, one of the most important issues is the light extraction efficiency of the device. Since flexible OLEDs are composed of many sub-organic layers with different refractive indices and plastic substrate, it is known that flexible OLEDs have the typical light loss such as the waveguide loss, plasmon absorption loss and internal total reflection, et al.

In this presentation, we demonstrate the one-step processed light scattering films with aluminum oxide nanoparticles and polystyrene matrix composite. Light scattering films was directly fabricated by the spin-coating process on the opposite side of green phosphorescent flexible OLED devices consisting of PEN/indium zinc oxide (IZO)/molybdenum oxide (MoO3, 10 nm)/N,N'-dicarbazolyl-4,4'-biphenyl (CBP, 40 nm)/6 wt% tris-(2-phenylpyridyl) iridium(III) (Ir(ppy)3) doped CBP (15 nm)/1,3,5-tris(N-phenylbenzimidazole-2-yl)benzene (TPBi, 55 nm)/aluminum (100 nm). Especially the low annealing temperature (65?) of the light scattering film was adaptable to the plastic substrate and OLED devices.

We found that the maximized light extraction efficiency can be obtained by optimizing the size and concentration of nanoparticles. This approach shows that it can simply increase the total emission of OLEDs up to 65% with simple fabrication process. We believe this technique could be highly applicable for large size OLED application such as the lighting system.

9566-88, Session PMon

Delayed electroluminescence studies of emission mechanism in quantum dot light emitting devices with a phosphorescent sensitizer

Hossein Zamani Siboni, Hany Aziz, Univ. of Waterloo (Canada)

Quantum Dot light emitting devices (QDLEDs) have attracted significant attentions in recent years due to their ability of producing very pure emission colors. The uniquely narrow linewidth emission and size-controlled emission wavelength of nano-crystalline quantum dots make them a superior emitter material for display panels. However, in comparison to other electroluminescent technologies (i.e. inorganic and organic LEDs (OLED)), QDLEDs exhibit very low efficiency. The lower efficiency in QDLEDs is mainly caused by the misalignment of the QD energy levels with those of the adjacent charge transport layers, particularly the hole transport layer, since QDs generally have very deep conduction and valence bands. In this work we demonstrate efficient and bright hybrid organic QDLED with the use of a phosphorescent sensitizer. Results show that the thickness of the QD layer plays an important role in the efficiency enhancement by Forster resonance energy transfer (FRET) from the phosphorescent sensitizer. Using delayed EL measurements we find that the extent of efficiency enhancement by FRET is also dependent on the concentration of the phosphorescent sensitizer, where very high sensitizer concentrations reduce triplet-polaron quenching at the QD/sensitizer layer interface. In this case, efficiency enhancement in the QD layer is attributed to both an increased e-h recombination in the sensitizer layer and efficient FRET.

9566-89, Session PMon

Shape-memory polymer resonators for novel continuously tunable organic distributed feedback lasers

Senta Schauer, Xin Liu, Matthias Worgull, Uli Lemmer, Hendrik Hölscher, Karlsruher Institut für Technologie (Germany)

We introduce shape-memory polymers (SMPs) as novel materials for the fabrication of tunable diffractive optical elements. Diffractive phase gratings are important tools for many applications in optics and photonics. For instance they serve as Bragg resonators in organic semiconductor distributed feedback (DFB) lasers. SMPs are a class of smart polymers which are able to remember a predefined shape and recover it even after strong deformations, if they are triggered by a proper stimulus like heat. The SMP we used is the thermally triggered thermoplastic polyurethane Tecoflex®. To replicate nanometer scale 2nd order Bragg gratings into the surface of SMP foils we utilized the hot embossing technique. After stretching, these gratings feature increased periods which shrink back to their original length as long as a thermal stimulus is applied. In order to demonstrate the practical applicability of these gratings as useful components for photonics, we successfully fabricated continuously tunable DFB lasers based on SMP resonators with the organic semiconductor Alq3:DCM serving as laser active material. The device consisting of a pre-stretched SMP substrate covered with organic material is optically pumped and then heated with a thermoelectric element to initialize the recovery process. To evaluate our novel device we quantified the lasing threshold to about 140µJcm⁻² and the lifetime to >10^7 pulses. By changing the resonator's period via the shape-memory effect we achieved a continuously tunable and adjustable shift in the emission wavelength of about 30nm. Furthermore, our tunable devices can be integrated in Lab-on-Chips to enable various applications for point-of-care analysis.



9566-90, Session PMon

Towards fully solution processed OLEDs: Introducing a novel amino-functionalized polyfluorene as electron injection layer

Sebastian Stolz, Karlsruher Institut für Technologie (Germany) and InnovationLab GmbH (Germany); Martin Petzoldt, Ruprecht-Karls-Univ. Heidelberg (Germany) and InnovationLab GmbH (Germany); Uli Lemmer, Karlsruher Institut für Technologie (Germany); Manuel Hamburger, Ruprecht-Karls-Univ. Heidelberg (Germany) and InnovationLab GmbH (Germany); Gerardo Hernandez-Sosa, Karlsruher Institut für Technologie (Germany) and InnovationLab GmbH (Germany)

The fabrication of OLEDs by high throughput printing techniques requires the development of solution processable electron injection layers. In this context, two classes of organic materials, aliphatic amines such as polyethylenimine (PEI) and amino-functionalized polyfluorenes such as PFN, have raised interest. However, processing of PEI poses a big challenge as films need to be very thin (-5 nm) in order to reach a high device performance [1,2]. In contrast, processing of PFN is easier but OLEDs that use it as electron injection layer exhibit limited power efficiencies due to high operational voltages [3,4].

In this work, we present a novel polyfluorene hybrid material, consisting of multiple PEI-like tertiary amine side-chains connected to the polyfluorene backbone via an amide. As a result of its molecular structure, layer thicknesses of up to 15 nm can be used in OLEDs while low operational voltages are maintained.

We solution process OLEDs that use a PPV derivative as emitting layer and either PEI, PFN or the hybrid material in combination with silver as cathode layer. OLEDs that use our new material exhibit a current efficiency of ~ 7.5 cd/A compared to ~ 7 cd/A for both PFN and PEI. At the same time, operational voltages are lowered by more than 1 V compared to PFN.

These results can be correlated to KP measurements that show that the hybrid material reduces the work-function of silver substrates by ~ 1eV, exceeding the reduction observed for PFN and PEI by ~ 0.5 and 0.2 eV, respectively.

[1] Zhou et al., Science 2012, 336:327-332, 2012.

[2] Stolz et al., ACS Applied Materials and Interfaces 2014, 6:6616-6622, 2014.

[3] Zeng et al., Advanced Materials 2007, 19: 810-814

[4] Zheng et al., Nature Communications 2013,4:1971

9566-91, Session PMon

The effect of plasmonic nanostructure at the interface of optoelectronics

Seong Jun Kang, Kyung Hee Univ. (Korea, Republic of)

In this presentation, we would like to demonstrate the plasmon effect on quantum-dot light emitting diodes (QLEDs) and transparent phototransistors. Plasmon-enhanced QLEDs were fabricated by inserting gold (Au) nanorods at the interface of the QLEDs. The length of the nanorods was 60 nm, which corresponds to the plasmonic absorption of wavelengths in the range of 630 to 670 nm. CdSe/ZnS quantum-dots (QDs) were used as emission layers with additional hole injection, transport, and electron transport layers. The maximum emission was observed at 630 nm, which is in the range of the plasmon resonance of Au nanorods. The QLEDs with Au nanorods showed enhanced electroluminescent properties compared to the devices without the plasmonic nano-structure. A 172% increase in electroluminescent intensity was observed due to the plasmon coupling effect. Also, silver nanoparticles were prepared to study the plasmon effect on the phototransistors. The Ag NPs effectively absorbed light in the wavelength range of 500 and 600 nm, which corresponds to the plasmonic effect. Due to the plasmon resonance of Ag NPs, a significantly

enhanced photocurrent was observed on the devices. The current increased by 348% with exposure to light when the Ag NPs were formed at the interface between the 10-nm-thick oxide semiconductor film and SiO2 substrate. The increased photocurrent revealed the presence of strong coupling between the localized plasmon and electrical carrier of the devices. The device characteristics and origin of the improvement will be presented in detail.

9566-92, Session PMon

Solution-processed sodium hydroxide as electron injection layer in inverted bottomemitting organic light-emitting diodes

Hongmei Zhang, Nanjing Univ. of Posts and Telecommunications (China)

The challenge of building IBOLEDs is to explore an effective approach to make the bottom electrode (ITO) easy for electron injection, i.e. reduce the electron injection barrier (EIB) from ITO (4.7 eV) to the lowest unoccupied molecular orbital (LUMO) level of organic electron transport layer (ETL). Modifying the organic/metal interface is an efficient method to reduce the EIB between organic active layer and metal cathode. Various modifications at the organic/metal interface have been reported, including the deposition of an ultrathin layer of alkali metals, alkaline-earth metals, metals and metallic compounds with low work function, as well as organic self-assembled monolayer.

Here, we present inverted bottom-emitting organic light-emitting diodes (IBOLEDs), consisting of tris-(8-hydroxyquinoline) aluminum (Alq3) as the emissive layer and an ultrathin layer of sodium hydroxide (NaOH) on top of indium tin oxide (ITO) as the electron injection layer. The devices with NaOH treated by water vapor and CO2 and annealing show higher current efficiency than those with NaOH untreated. The current efficiency (6 cd/A) of the optimal devices with Treated NaOH layer is improved. The enhancement is attributed to the reduction in barrier height for electron injection due to the dipole formation caused by the conversion of NaOH to sodium carbonate.

9566-93, Session PMon

Organic/inorganic (F8T2/p-GaN) whitelight emitting device

Yen-Ju Wu, Cheng-Yi Liu, National Central Univ. (Taiwan)

We report a stable white-light emitting device, which is an organic/inorganic (F8T2/p-GaN epi-layers) interface. F8T2 is poly (9,9-dioctylfluoreneco-bithiophene). Two possible mechanisms to produce white light are electroluminescence (EL) and photoluminescence (PL). We found that the primary mechanism for this white-light emission is EL. The white-light emission attributes to the combination of two major EL emission peaks, which are 464 nm and a broad EL emission peak ranging from 521 nm to 580 nm. The 464 nm EL emission peak is contributed from the GaN LED and broad EL emission peak comes from F8T2. The International Commission on Illumination (CIE) coordinate of the white-light emission from the present device is at (0.28, 0.30), which is very close to the standard white light (0.33, 0.33). The detail optical and electrical characterization of this whitelight organic/inorganic (F8T2/p-GaN epi-layers) device would be present and discussed in this talk.

9566-95, Session PMon

Near-infrared microlasers based on whispering-gallery mode microresonators of self-assembled organic hemispheres

Hongbing Fu, Xuedong Wang, Institute of Chemistry (China)



Near-infrared (NIR) lasers are key components for applications, such as telecommunication, spectroscopy, display, and biomedical tissue imaging. Inorganic III-V semiconductor (GaAs) NIR lasers have achieved great successes,1 but require expensive and sophisticated device fabrication techniques. Organic semiconductors exhibit chemically tunable optoelectronic properties together with self-assembling features that are well suitable for low-temperature solution processing.3-5 Major blocks in realizing NIR organic lasing include low stimulated emission of narrowbandgap molecules due to fast nonradiative decay, and exciton-exciton annihilation which is considered as a main loss channel of population inversion for organic lasers under high carrier densities.6 Here, we designed and synthesized the small organic molecule 3-[(4-(N,N-di(p-tolyl)amino) phenyl)-1-(2-hydroxynaphthyl)prop-2-en-1-one (DPHP) with amphiphilic nature, which elaborately self-assembles into micrometer-sized hemispheres than simultaneously serves as the NIR emission medium with a moderate quantum-efficiency of ~15.2%, and the high-Q (~1.4?103) whispering-gallerymode microcavity. Moreover, the radiative rate of DPHP hemispheres is enhanced up to ~1.98 ns-1 on account of the exciton-vibrational coupling, and meanwhile the exciton-exciton annihilation process is eliminated. As a result, NIR lasing with a low threshold of ~610 nJ/cm2 is achieved in the single DPHP hemisphere at room temperature. Our demonstration is a major step towards incorporating the organic coherent light sources into the compact optoelectronic devices,7 which have been applied as a lab-on-achip for high-sensitivity explosive detection.

9566-96, Session PMon

Long-lived highly efficient green and blue phosphorescent emitters and device architectures for OLED displays

Christian Eickhoff, Peter Murer, Thomas Gessner, Jan Birnstock, Michael Kröger, Zungsun Choi, Soichi Watanabe, Minlu Zhang, Falk May, Christian Lennartz, Ilona Stengel, Ingo Münster, Klaus Kahle, Gerhard G. Wagenblast, Hannah Mangold, BASF SE (Germany)

The development of phosphorescent emitters started in the late 1990s, aiming to combine outstanding efficiencies with high diode lifetimes. Since that time the green emitter Ir(ppy)3 has been the reference material for OLED research and development. In 2001, BASF started to develop a new class of OLED emitter materials based on iridium carbene complexes. These complexes have several properties that make them attractive when compared to phenyl pyridine complexes: outstanding stability due to the absence of weak coordinative N-metal bonds, straight forward synthetic approach and outstanding photophysical properties, even in the deep blue regime, where carbene emitters have proven to be the most stable emitter class. Lifetimes of deep blue phosphorescent diodes can be further boosted by a concept that we call hyperphosphorescence [1].

In this talk, device architectures, materials and performance data will be presented showing that carbene type emitters have the potential to also outperform established phosphorescent green emitters both in terms of lifetime and efficiency.

The specific class of green emitters under investigation shows much larger electron affinities (2.1 to 2.5 eV) and ionization potentials (5.6 to 5.8 eV) than the standard emitter Ir(ppy)3 (5.0/1.6 eV). That difference in energy levels requires an adopted OLED design, in particular with respect to emitter hosts and blocking layers. Consequently, in the diode setup presented here, the emitter species is electron transporting or electron trapping.

For said green carbene emitters, the typical peak wavelength is 525 nm yielding CIE color coordinates of (x=0.33, y=0.62). Device data of green OLEDs will be shown with EQEs exceeding 26%. Driving voltage at 1000 cd/m? is below 3V. In an optimized stack, a device lifetime of LT97 = 4100h (1000 cd/m?) have been reached, thus fulfilling AMOLED display requirements (fig. 1).

[1] Talk by C. Lennartz (BASF SE), 249th ACS National Meeting, March 22-26, 2015

9566-301,

Current status of high efficiency OLEDs based on delayed fluorescence

Chihaya Adachi, Kyushu Univ. (Japan)

In recent years, we have reported a series of highly efficient thermally activated delayed fluorescence (TADF) molecules and their OLED performance. We clarified that a large delocalization of the highest occupied molecular orbital (HOMO) and lowest unoccupied molecular orbital (LUMO) in charge transfer compounds provides a small energy gap between singlet and triplet excited states (?EST < 0.2 eV). Simultaneously, even when there is a small overlap between the two wavefunctions, we can successfully keep rather high radiative decay rate (kr) by inducing a large oscillator strength (f). Thus, compatibility of both small ?EST and large kr is fundamental for high efficiency delayed fluorescence. Based on this design concept, we systematically synthesized a wide variety of TADF molecules and demonstrated high efficiency OLEDs with maximum external quantum efficiencies of ~20%. In this talk, we review material design, synthesis, photophysics and OLED performance and discuss the future prospects.

9566-37, Session 9

Light emitting transistors: A new route for display pixels (Invited Paper)

Ebinazar B. Namdas, The Univ. of Queensland (Australia)

Organic light emitting transistors (LEFETs) are an emerging class of light emitting devices that have been successfully demonstrated in single-layer [1] and mutil-layer device structures [2]. LEFETs can simultaneously execute light-emission and standard logic functions (ON/OFF) of a transistor in a single device architecture [1]. This dual functionality of LEFETs has a potential to offer a new route to simplify fabrication of display pixels. However, the key problem of existing LEFETs thus far has been their low external quantum efficiency (EQE) at high brightness, poor ON/OFF ratio, and mobility. More recently, hybrid light emitting transistors [3-4], consisting of solution processed n-type metal oxide (inorganic) as the charge transport layer and light emitting conjugated polymer (organic), have been used to achieve higher mobility, ON/OFF ratio and brightness. In this talk, I will discuss the various factors that currently influence device performance in LEFETs, and will provide insights into our recent progress in developing high-performance hybrid LEFETs.

References:

(1). E. B. Namdas, J. S. Swensen, P. Ledochowitsch, J. D. Yuen, D. Moses, A. J. Heeger, Adv. Mater., 20, 1321 (2008).

(2). M. Ullah, K. Tandy, S. D. Yambem, M. Aljada, P. L. Burn, P. Meredith, E. B. Namdas. Adv. Mater. 25, 6213–6218 (2013).

(3). B. Walker, M. Ullah, G. J. Chae, P. L Burn, S. Cho, J. Y. Kim, E. B. Namdas, J. H. Seo. Appl Phys Lett, 105, 183302 (2014).

(4). K. Muhieddine, M. Ullah, B. N. Pal, P. Burn, E. B. Namdas, Adv. Mater. 26, 6410 (2014).

9566-38, Session 9

OLEDs: Light-emitting thin film thermistors revealing advanced self-heating effects (*Invited Paper*)

Axel Fischer, Technische Univ. Dresden (Germany); Thomas Koprucki, Annegret Glitzky, Matthias Liero, Weierstrass-Institut für Angewandte Analysis und Stochastik (Germany); Klaus Gärtner, Univ. della Svizzera italiana (Switzerland); Jacqueline Hauptmann, Fraunhofer-Einrichtung für Organik, Materialien und Elektronische Bauelemente COMEDD (Germany); Sebastian Reineke,



Daniel Kasemann, Technische Univ. Dresden (Germany); Björn Lüssem, Kent State Univ. (United States); Karl Leo, Reinhard Scholz, Technische Univ. Dresden (Germany)

For lighting applications, OLEDs need much higher brightness than for displays, causing substantial self-heating accompanied by unpleasant brightness inhomogeneities. Although the relevance of electrothermal interplay has been recognized, the fundamental understanding is still missing. For example, there is no explanation why regions with the highest temperatures shift to the device borders albeit the heat conduction is worst at the center of the substrate. Furthermore, large area OLED panels can show a saturation of brightness around their mid position at elevated selfheating (Fischer et al., Adv. Funct. Mater. 2014, 24).

Recently, we have shown that the temperature-activated transport in C60 devices favors thermal runaway as a result of negative differential resistance (NDR) of 'S'-shape type. The effect can be explained by purely electrothermal effects arising from the positive feedback loop between the temperature dependent conductivity and the power dissipation. Such a behavior is well-known for thermistor devices with a negative temperature coefficient (NTC), but has not been shown for organic semiconductor devices.

Here, we show by experiment and simulation that due to electrothermal feedback in OLEDs, 'S'-shaped NDR occurs as well. For increasing voltage applied to the contacts, self-heating combined with the series resistance of the transparent electrode produces regions with decreasing voltage across the organic layers. Furthermore, due to the laterally extended geometry novel effects take place, like regions in which the current is switched back while the total current increases.

Our work shows that an accurate understanding of nonlinear electrothermal feedback is essential for proper device function at elevated temperatures.

9566-39, Session 9

Highly transparent electrodes for flexible electronics: Ultra-thin metal, 2D materials and their hybrid structures (*Invited Paper*)

Illhwan Lee, Pohang Univ. of Science and Technology (Korea, Republic of); Ki Chang Kwon, Chung-Ang Univ. (Korea, Republic of); Juyoung Ham, Seung O Gim, Pohang Univ. of Science and Technology (Korea, Republic of); Soo Young Kim, Chung-Ang Univ. (Korea, Republic of); Jong-Lam Lee, Pohang Univ. of Science and Technology (Korea, Republic of)

Transparent electrodes are crucial for opto-electronic devices such as organic light-emitting diodes, solar cells, and liquid-crystal displays. Conventionally, indium tin oxide (ITO) has been widely used as the electrodes, but the increasing cost of indium and its brittleness make it unsuitable for future opto-electronic devices. Therefore, it is desirable to develop alternative transparent electrodes. In recent years significant research efforts have been directed towards replacing the ITO.

In this work, we present a novel way to produce the transparent electrode would be to incorporate ultra-thin metal electrode. We show that merely a minute-plasma treatment on the glass before the deposition of Ag layer leads to significantly improved growth homogeneity. These ultra-thin Ag electrodes have very high optical transparency and sheet resistance that are comparable to or better that those of ITO electrode. In addition, their mechanical property is appropriate for flexible devices.

We also demonstrate the transparent electrode using graphene and 2D material. Graphene has shown considerable potential as a replacement for ITO because of its theoretically excellent optical, electrical, and mechanical properties. Despite graphene's ideal properties, pristine graphene films have relatively low work function, high sheet resistance and low chemical stability. We demonstrated a multilayered structure of a graphene electrode sandwiched between metal oxides, which has high stability and superior optical properties. The metal oxide over-coated graphene showed enhanced stability to air exposure and maintained the sheet resistance. Furthermore,

we demonstrated hybrid structure which was highly air stable structure comparing to PEDOT:PSS using graphene and 2D material.

9566-54, Session 9

Efficient inverted organic light-emitting devices by amine-based solvent treatment (Invited Paper)

Myoung Hoon Song, Kyoung-Jin Choi, Ulsan National Institute of Science and Technology (Korea, Republic of)

The efficiency of inverted polymer light-emitting diodes (iPLEDs) were remarkably enhanced by introducing spontaneously formed ripple-shaped nanostructure of ZnO (ZnO-R) and amine-based polar solvent treatment using 2-methoxyethanol and ethanolamine (2-ME+EA) co-solvents on ZnO-R. The ripple-shape nanostructure of ZnO layer fabricated by solution process with optimal rate of annealing temperature improves the extraction of wave guide modes inside the device structure, and 2-ME+EA interlayer enhances the electron injection and hole blocking and reduces exciton quenching between polar solvent treated ZnO-R and emissive layer. As a result, our optimized iPLEDs show the luminous efficiency (LE) of 61.6 cd A-1, power efficiency (PE) of 19.4 lm W-1 and external quantum efficiency (EQE) of 17.8 %. This method provides a promising method, and opens new possibilities for not only organic light-emitting diodes (OLEDs) but also other organic optoelectronic devices such as organic photovoltaics, organic thin film transistors, and electrically driven organic diode laser.

9566-40, Session 10

Enhanced light extraction from organic light-emitting devices using a sub-anode grid

Yue Qu, Michael Slootsky, Stephen R. Forrest, Univ. of Michigan (United States)

We demonstrate a method for extracting waveguided light trapped in the organic and indium tin oxide layers of bottom emission organic light emitting devices (OLEDs) using a patterned planar grid layer (sub-anode grid) between the anode and the substrate. The scattering layer consists of two transparent materials with different refractive indices on a period sufficiently large to avoid diffraction and other unwanted wavelengthdependent effects. The position of the sub-anode grid outside of the OLED active region allows complete freedom in varying its dimensions and materials from which it is made without impacting the electrical characteristics of the device itself. Full wave electromagnetic simulation is used to study the efficiency dependence on refractive indices and geometric parameters of the grid. We show the fabrication process and characterization of OLEDs with two different grids: a buried sub-anode grid consisting of two dielectric materials, and an air sub-anode grid consisting of a dielectric material and gridline voids. Using a sub-anode grid, substrate plus air modes quantum efficiency of an OLED is enhanced from (33±2)% to (40±2)%, resulting in an increase in external quantum efficiency from (14±1)% to (18±1)%, with identical electrical characteristics to that of a conventional device. By varying the thickness of the electron transport layer (ETL) of sub-anode grid OLEDs, we find that all power launched into the waveguide modes is scattered into substrate. We also demonstrate a subanode grid combined with a thick ETL significantly reduces surface plasmon polaritons, and results in an increase in substrate plus air modes by a >50% compared with a conventional OLED. The wavelength, viewing angle and molecular orientational independence provided by this approach make this an attractive and general solution to the problem of extracting waveguided light and reducing plasmon losses in OLEDs.



9566-41, Session 10

Extracting and directing light out of organic light emitting diodes (Invited Paper)

Uli Lemmer, Amos Egel, Matthias Hecht, Jan B. Preinfalk, Guillaume Gomard, Karlsruher Institut für Technologie (Germany)

Light extraction from organic light emitting diodes (OLEDs) is attracting considerable interest as being crucial for enhancing the energy efficiency in lighting applications. Light extraction can be realized by lithographically defined internal diffraction gratings or stochastic scattering centers. The former approach needs in addition an external optical layer for scrambling the angularly dependent emission spectra in order to avoid color shifts []]. Micro lens arrays cannot only be used for fulfilling this task but they can also be used for enhancing the luminosity into a specific direction. We demonstrate recent advances towards high efficiency OLEDs with high directionality. In addition to the relevant technologies we have also developed a comprehensive simulation software for the quantitative challenging task is the description of multiple and coherent optical scattering. We have recently developed a software for the exact simulation based on a scattering matrix formalism [2].

[1] T. Bocksrocker, J. B. Preinfalk, J. Asche-Tauscher, A. Pargner, C. Eschenbaum, F. Maier-Flaig and U. Lemmer, White organic light emitting diodes with enhanced internal and external outcoupling for ultra-efficient light extraction and Lambertian emission Opt. Expr. 20, A932 (2012).

[2] A. Egel, U. Lemmer, Dipole emission in stratified media with multiple spherical scatterers: Enhanced outcoupling from OLEDs, Journal of Quantitative Spectroscopy and Radiative Transfer 148, 165 (2014).

9566-42, Session 10

Outcoupling enhancement of ITO-free white organic light-emitting diodes with an air void-mediated scattering layer (Invited Paper)

Tae-Wook Koh, Joshua Spechler, Craig B. Arnold, Barry P. Rand, Princeton Univ. (United States)

White organic light-emitting diodes (WOLEDs) are one of the most promising technologies to realize future solid-state lighting (SSL) that require high power efficiency, excellent color quality and novel form factors. One major bottleneck in realizing such WOLED lighting is the limited outcoupling efficiency, with most light generated in the device either being evanescently coupled to metal surface plasmon modes, or trapped within the substrate or organic/transparent electrode stacks.

Hence to solve this low outcoupling efficiency we suggest two innovative ideas including (1) scattering layers with air voids embedded in transparent plastic films to reduce substrate-trapped mode loss, and (2) Ag nanowire-based transparent conductive electrode embedded in a high refractive index planarization layer. Air voids in the plastic substrate take advantage of the refractive index contrast between air and the plastic host medium to effectively scatter the substrate-trapped light, while absorption in those voids is virtually zero. Also, refractive index matching from the internal organic active layers to the planarization layer that is incorporating networks of Ag nanowire electrodes helps to convert conventional waveguided mode in organic layers to the substrate-trapped mode, which maximizes the effect of the scattering layer. These approaches were then integrated to demonstrate ITO-free WOLEDs on flexible substrates, with processes and materials that are upscalable and compatible to low-cost mass production of WOLED lighting.

9566-43, Session 10

Simple fabrication of a three-dimensional porous polymer film as a diffuser for microcavity OLEDs (Invited Paper)

Min Chul Suh, Kyung Hee Univ. (Korea, Republic of)

We used a porous polymer film with ?40% optical haze as a diffuser. It was fabricated by a simple spin-coating process during continuous water mist supply by a humidifier. The pores were created by the elastic bouncing mechanism (rather than the thermocapillary convection mechanism) of the supplied water droplets. The shapes and sizes of the caves formed near the polymer surface are randomly distributed, with a relatively narrow pore size distribution (300-500 nm). Specifically, we focused on controlling the surface morphology to give a three-dimensional (3D) multi-stacked nanocave structure because we had already learnt that twodimensional nanoporous structures showed serious loss of luminance in the forward direction. Using this approach, we found that the 3D nanoporous polymer film can effectively reduce the viewing angle dependency of strong microcavity OLEDs without any considerable decrease in the total intensity of the out-coupled light. We applied this porous polymer film to microcavity OLEDs to investigate the possibility of using it as a diffuser layer. The resulting porous polymer film effectively reduced the viewing angle dependency of the microcavity OLEDs, although a pixel blurring phenomenon occurred. Despite its negative effects, such as the drop in efficiency in the forward direction and the pixel blurring, the introduction of a porous polymer film as a scattering medium on the back side of the glass substrate eliminated the viewing angle dependency. Thus, this approach is a promising method to overcome the serious drawbacks of microcavity OLEDS.

9566-44, Session 10

Anisotropy in OLEDs (Invited Paper)

Michiel Callens, Kristiaan Neyts, Univ. Gent (Belgium); Daisuke Yokoyama, Yamagata Univ. (Japan)

Small-molecule OLEDs, deposited using thermal evaporation, allow for precise control over layer thicknesses. This enables good control over the optical behaviour of the stack which ultimately determines the outcoupling efficiency. In terms of optical outcoupling there are limits to the efficiency by which the generated electromagnetic radiation can be extracted from the stack. These limitations are linked to the refractive indices of the individual layers. Values for maximum outcoupling efficiency are sometimes calculated under the implicit assumptions that the OLED stack is planar, that all layers are isotropic with a certain refractive index and that emitters are not preferentially oriented. In reality it is known that these assumptions are not always valid, be it intentional or unintentional.

In our work we transcend these limiting assumptions and look at different forms of anisotropy in OLEDs. Anisotropy in OLEDs comes in three distinct flavours; 1. Spatial anisotropy, where one thinks of gratings, lenses or other internal or external scattering centres, 2. Anisotropic emitters, where the orientation significantly influences the direction in which radiation is emitted and 3. Anisotropic layers, where the anistropic nature of the layers breaks with the customary assumption of isotropic layers. We investigate the effect of these anisotropic features on outcoupling efficiency and ultimately, external quantum efficiency (EQE).

9566-45, Session 10

Extracting and shaping the light of OLED devices

Daniel Riedel, OSRAM Opto Semiconductors GmbH (Germany) and Friedrich-Alexander-Univ. Erlangen-Nürnberg (Germany); Thomas Wehlus, OSRAM Opto Semiconductors GmbH (Germany); Christoph J. Brabec,



Friedrich-Alexander-Univ. Erlangen-Nürnberg (Germany)

Before the market entry of OLEDs in the field of general illumination can take place, limitations in lifetime, luminous efficacy and cost needs to be overcome. Additional requirements for OLEDs used in general illumination may be imposed by workplace regulations for glare reduction that e.g. limit the luminance for high viewing angles. These requirements are in contrast to the typically Lambertian emission characteristic of OLEDs having internal extraction layers, which results in the same luminance levels for all emission angles. As a consequence, without additional measures, glare reduction could limit the maximum possible luminance of Lambertian OLEDs to relatively low levels. On the other hand, high luminance levels are desirable to get high light output. We are presenting solutions to overcome this possible limitation.

Therefore this work is focused on internal light extraction layers and light shaping structures for OLEDs. Simulations of beam shaping structures and shapes as well as the verification of the simulations with experimental measurements of the most promising structures are presented. An evaluation of the loss channels has been carried out and the overall optical system efficiency was evaluated for all structures. The most promising beam shaping structures achieve system efficiencies up to 80%, close to the theoretical limit derived from étendue calculations.

Finally, a general illumination application scenario has been simulated. The number of OLEDs needed to illuminate an office room has been deduced from this scenario. By using light-shaping structures for OLEDs, the number of OLEDs needed to reach the mandatory illuminance level for a workplace environment can be reduced to one third compared to Lambertian OLEDs

Conference 9567: Organic Photovoltaics XVI

Monday - Thursday 10-13 August 2015

Part of Proceedings of SPIE Vol. 9567 Organic Photovoltaics XVI

9567-49, Session PMon

Interface trap density effect on efficiency of Fullerene organic Schottky diode

Mebarka Daoudi, Univ. Tahri Mohammed Béchar (Algeria)

The growing demands for environmental protection and clean energy urge scientists to create new techniques and materials for a sustainable energy. The interest for Organic Electronics has dramatically increased over these past years, not only in academic research, but also in an industrial perspective. Key efforts to the success include the development of device prototype design and scale-up. The complications of these processes pose significant challenges. The main reasons for focused interest in this field is the opportunity to produce low cost devices on plastic substrates on large areas, opening, indeed, an entire new market segment. One of the fundamental points in determining the electrical performances in organic devices is that, even though they are usually thought as macroscopic devices, their behavior is strongly driven by interfacial phenomena taking place in the nano-scale.

In this work, we are going to study the electronic transport in organic thin films which is strongly affected by interfacial phenomena. For example, the scattering of conduction electrons at grain boundaries or at planar interfaces defined by the top and bottom surfaces of the film can contribute significantly to the efficiency of device [1,2]. So, in order to optimize the device performance it is very important to have knowledge about intrinsic properties, particularly the charge transport and charge injection properties. One of the basic methods to investigate the charge transport in interface metal/organic semiconductors is to determine the dark I-V characteristics, where the important effects which describe that transport mechanism are the space charge, trapping and schottky effects [3]. These are obtained from the dependence of observables on the temperature, electric field and trap density.

The interface trap density effect on dark I-V characteristics for fullerene (C60) schottky diode is investigated here for different electrodes (AI, Au, Ag).

Reference

 M. Schwoerer , H. C. Wolf: Organic Molecular Solids. Wiley-VCH, 2006
 J.C. Scott, G.G. Malliaras: Charge injection and recombination at the metal/organic interface. Chem. Phys. Lett. Vol. 299, N°2, 115–119 (1999)
 S. M. Sze: Physics of Semiconductor Devices. John Wiley and Sons, 1981

9567-50, Session PMon

Conformation modulated quinoxalinebased low band gap polymers with non-covalent Coulomb interaction for photovoltaic cells with efficiency of 8%

Yuxiang Li, Pusan National Univ. (Korea, Republic of); Seojin Ko, Jin Young Kim, Ulsan National Institute of Science and Technology (Korea, Republic of); Han Young Woo, Pusan National Univ. (Korea, Republic of)

A series of fluorinated quinoxaline-based ϖ -conjugated polymers with non-covalent conformational locks was designed and synthesized by considering the solubility, planarity, chain curvature and intramolecular steric hindrance for applications in polymer solar cells (PSCs). Insertion of different number of the axis symmetrical thiophene (as a donor moiety in a polymer backbone) allows fine-adjusting not only absorption range, the frontier energy levels, but also accompanied with the symmetrical changes. The molecular geometry, bulk film morphology and ordered film structure were investigated in detail by density function theory (DFT) calculations, atomic force microscopy (AFM) and grazing-incidence wide-angle X-ray scattering (GIWAX) analysis. Via rational design of semi-crystalline photovoltaic polymers considering chain planarity, noncovalent intra- and inter-molecular coulomb interactions and molecular geometry, the optimized photovoltaic cell based on PDFQx3T:PC70BM achieved power conversion efficiency (PCE) of 8% with an open-circuit voltage (Voc) of 0.74 V, a short-circuit current (Jsc) of 17.19 mA/cm2 and a fill factor (FF) of 63% at ~270 nm thick active layer. Most previous PSCs show the best PCE at the film thickness on the order of 100 nm. However it is not currently viable to fabricate defect-free and homogeneous films by industrial casting techniques. Our photovoltaic data at the thicker active layer suggest a great potential for industrial mass production of printed PSCs. The markedly high efficiency is most likely attributed to rationally modulated molecular geometry and highly ordered polymer structure in the active layer, in which the axis symmetry conformation of molecular, the short ϖ - ϖ stacking distance (3.6 Å) with favorable face-on orientation were achieved, also formed well interpenetrated networked morphology. We also found that quite high hole mobility with balanced h/e mobility ratio, proper miscibility and phase separation are the main reasons for high IPCE (83%) and FF (63%) at ~270 nm thick active layer. This study provides an insight into rational molecular design for efficient semi-crystalline photovoltaic structures with non-covalent conformation lock.

9567-51, Session PMon

Verification of effect of electric field on electron transport in TiO2 electrode

Kai-Ling Chuang, Ming-Show Wong, Yi-Jia Chen, Chih-Hung Tsai, National Dong Hwa Univ. (Taiwan); Hong Syuan Ling, Chien Chin Wang, National Dong Hwa Univ. (Taiwan)

We demonstrated that the dense TiO2 planar negative electrode is an effective electron transport material in the perovskite solar cells. The highest Voc is 900 mV using negative electrode with a dense TiO2 layer of 400 nm plus a mesoporous TiO2 layer of 500 nm. For conventional dye-sensitized solar cells (DSSCs) the thickness of the mesoporous negative electrode is around 15 ?m. The ideal range of film thickness in DSSCs is usually 12~16 ?m, suggesting that the electron has comparable diffusion length in the mesoporous negative electrode such that the electron recombination is insignificant below 15 um. However, design of thicker mesoporous TiO2 negative electrode in perovskite solar cells is not usually encouraged as the solar cell efficiency decreases with electrode thickness greater than 500 nm. In this study, we would like to verify if the efficiency decrease of perovskite solar cells with electrode thickness is really due to the increase of thickness of TiO2 electrode itself or some consequences that come with the increase of thickness, such as increased roughness. We will report the solar cell efficiency dependence on the thickness of dense TiO2 layer in negative electrode so to verify if the electric field does play a role in electron transport in the TiO2 electrode. With this understanding, we will be able to design a novel structure of TiO2 electrode that is suitable for perovskite solar cells.

9567-52, Session PMon

Structure-property correlations of merocyanines and their application in organic solar cells

Julian Krumrain, Univ. zu Köln (Germany); Alhama Arjona-Esteban, Julius-Maximilians-Univ. Würzburg (Germany); Selina Olthof, Dirk Hertel, Univ. zu Köln (Germany); Matthias Stolte, Frank Würthner, Julius-Maximilians-Univ. Würzburg (Germany); Klaus Meerholz, Univ. zu Köln (Germany)

Organic photovoltaics based on donor-acceptor heterojunctions using conjugated polymers or small molecules as donor component have recently achieved power conversion efficiencies of up to 9% in single junctions.





[1,2] Of particular interest is the establishment of small molecules as donor material in organic solar cells due to their simplified, large-scale synthesis and purification in comparison to conjugated polymers. However, predictable correlations between the molecular structure, molecular properties and the device performance rarely exist, but they are needed to further drive the progress in this area.

Here we demonstrate that single crystalline merocyanines show zero to three dimensional patterns which correlate with the device performance. We have characterized several merocyanines as thin films and single crystals with X-ray diffraction and ultraviolet photoemission spectroscopy. Additionally, we have studied the temperature and light dependence of the current-voltage response of planar as well as bulk heterojunction solar cells.

The power conversion efficiencies of the studied solar cells range from 1% to 5%, depending on the dimensionality of the aggregation pattern. By comparing the planar and bulk heterojunction solar cells, we demonstrate that the often reported temperature dependence of the ideality factor is caused by deep lying trap states. Our results on the temperature dependence of the open-circuit voltage complete and bring together previous studies, where either only bulk or planar heterojunctions were investigated.[3,4] Furthermore, we show that by doing precise analysis of temperature dependent current-voltage characteristics, it is possible to determine losses in the open-circuit voltage within a solar cell.

References:

1. Chen, J.-D. et al. Single-Junction Polymer Solar Cells Exceeding 10% Power Conversion Efficiency. Adv. Mater. (2014). doi:10.1002/adma.201404535

2. Subbiah, J. et al. Organic Solar Cells Using a High-Molecular-Weight Benzodithiophene-Benzothiadiazole Copolymer with an Efficiency of 9.4%. Adv. Mater. (2014). doi:10.1002/adma.201403080

3. Widmer, J., Tietze, M., Leo, K. & Riede, M. Open-Circuit Voltage and Effective Gap of Organic Solar Cells. Adv. Funct. Mater. 23, 5814–5821 (2013).

4. Hörmann, U. et al. Quantification of energy losses in organic solar cells from temperature-dependent device characteristics. Phys. Rev. B 88, 235307 (2013).

9567-53, Session PMon

Femtosecond transient absorption spectroscopy of thienylenevinylenephthalimide copolymer and of bulk heterojunction blend with PC71BM

In-Sik Kim, Seong-Hoon Kwon, Juhwan Kim, Dong-Yu Kim, Do-Kyeong Ko, Gwangju Institute of Science and Technology (Korea, Republic of)

For an enhancement of power conversion efficiency in organic solar cell, low band gap polymers are a prerequisite because the low band gap polymers can absorb a broad range of solar spectrum and induce much charge carriers. Arranging electron-rich and electron-deficient moieties alternately is one of the appropriate technics for tuning the band gap of polymers, since orbital mixing between two moieties promotes the formation of an intramolecular charge transfer state which is involved in an additional absorption band. Moreover, the band gap tuning by such structure can be useful to achieve deep-lying highest occupied molecular orbital (HOMO) level for high open circuit voltage as well.

We have developed donor-acceptor alternating copolymer which was based on alkyl-substituted thienylenevinylene and phthalimide units, and the copolymer:fullerene derivative performed intense visible absorption and the open circuit voltage of >0.8 V. In this study, we present the photoinduced carrier dynamics of the copolymer by using the femtosecond transient absorption (TA) measurement. By introducing the copolymer as a donor and [6,6]-phenyl-C71-butylic acid methyl ester (PC71BM) as an acceptor, effective charge separation in bulk heterojunction (BHJ) blend was measured from the TA. Also, the effect of processing additive for improved photovoltaic performance of this BHJ was revealed with this femtosecond TA measurement.

9567-54, Session PMon

Criteria for stabilizing polymer and small molecule solar cells

Rongrong Cheacharoen, William R. Mateker, I. T. Sachs-Quintana, Thomas Heumüller, Michael D. McGehee, Stanford Univ. (United States)

We study the degradation of organic solar cells (OSCs) and find that stability can be improved on both short and long time scales by careful material selection and operating OSCs in an oxygen-free environment. In the first 60 hours of operation, more crystalline regioregular P3HT and ZZ115 solar cells lose 10% of starting efficiency, mostly due to loss in open circuit voltage (Voc) and fill factor (FF), while more amorphous PCDTBT and regiorandom P3HT lose 25%. We find that photo-induced Voc loss is caused by a change in the density of states, while recombination dynamics remain unchanged. This effect is minimized in crystalline materials. We further demonstrate no photoinduced burn-in in highly crystalline T1 small molecule solar cells. While T1 solar cells show photostability, their efficiency degrades at elevated temperatures, and work is ongoing to better understand thermal degradation in small molecule solar cells. We further compare crystalline and amorphous films in photobleaching experiments in air and find that increased crystallinity of materials show slower photochemical degradation. For example, crystalline rubrene photobleaches three order of magnitudes slower than amorphous films. We also investigate solar cells on long time scales. We have monitored PCDTBT for 7500 hours in an oxygen free environment and extrapolate lifetimes to more than 20 years. We are also investigating the stability of molecules and polymers with power conversion efficiency approaching 10%. As these materials are highly crystalline, we are hopeful to show promising stability.

9567-55, Session PMon

Effect of thermal annealing on charge transfer states and exciton dissociation in PCDTBT: PC70BM bulk heterojunction solar cells

Iordania Constantinou, Tzung-Han Lai, Erik D. Klump, Univ. of Florida (United States); Hsien-Yi Hsu, The Univ. of Texas System (United States); Kirk S. Schanze, Franky So, Univ. of Florida (United States)

The effect of thermal annealing on charge generation was investigated for PCDTBT:PC70BM devices. Photocurrent spectral response and transient photoluminescence measurements were used to confirm that device annealing leads to more effective carrier generation due to a higher degree of charge transfer (CT) exciton delocalization. The delocalization of CT excitons was also accompanied by an increase in the dielectric constant of the blend. Even though no obvious difference in the film morphology was observed, the solar cell performance changed significantly after thermal treatment mostly due to a decrease in the device fill factor (FF). It was shown that even though the photocurrent generated for the annealed PCDTBT:PC70BM device is higher due to delocalization, a larger amount of generated photo-carriers are lost to recombination and do not contribute to the output current. Energetic disorder measurements along with recombination measurements at short and open circuit revealed a negligible bimolecular recombination for both devices. Finally, the decrease in FF was found to be due to an increase in the concentration of deep level traps causing an increase in Shockley-Read-Hall recombination. Our findings suggest that thermal annealing can not only cause significant changes in the film morphology and packing but also in the photo-generation process in organic bulk heterojunction solar cells.



9567-56, Session PMon

Probing the organic-inorganic interfaces of organic photovoltaic devices

Andrew J. Clulow, Hui Jin, Mike Hambsch, Jake A. McEwan, Paul L. Burn, Ian R. Gentle, Paul Meredith, The Univ. of Queensland (Australia)

Whilst a great deal of attention has been directed at optimising the properties of the active layers of organic photovoltaic (OPV) devices, interactions at the interface are of equal importance. The accumulation or depletion of active organic materials at the electrode interface during device manufacture and operation has the potential to greatly influence device performance by altering the electrical contacts. In recent years molybdenum oxide (MoOx) has been widely used as an interlayer to modify the work function of metallic electrodes and as an active component in transparent electrodes. Insulator/metal/insulator stacks containing MoOx have been shown to be flexible and have lower sheet resistances than indium tin oxide, making them promising transparent conducting electrode candidates.

We have used neutron reflectometry to study the buried interfaces present in the layered transparent electrode stacks and between OPV active layers and MoOx. The influence of typical thermal annealing protocols and prolonged exposure to ambient atmosphere were recorded. It was found that the use of zinc sulphide in place of MoOx as the capping material for the electrode stacks increases their stability towards exposure to ambient atmosphere and subsequent thermal annealing. The organic-inorganic interface between P3HT:PC61BM and PCDTBT:PC71BM bulk heterojunctions and MoOx was monitored in situ during thermal annealing and this revealed that the accumulation of the fullerene phase observed previously at the P3HT:PC61BM/SiO2 interface is not a common feature of oxide surfaces.

9567-57, Session PMon

Time-resolved terahertz spectroscopy (TRTS) of conducting metal-organic frameworks (MOFs) doped with redox active species

Brian G. Alberding, Edwin Heilweil, National Institute of Standards and Technology (United States)

Metal-Organic Frameworks (MOFs) are three-dimensional coordination polymers that are well known for large pore surface area and their ability to adsorb molecules from both the gaseous and solution phases. In general, MOFs are electrically insulating, but promising opportunities for tuning the electronic structure exist because MOFs possess synthetic versatility; the metal and organic ligand subunits can be exchanged or dopant molecules can be introduced into the pore space. Two such MOFs with demonstrated electrical conductivity are Cu3(1,3,5-benzenetricarboxylate)2, a.k.a HKUST-1, and Cu[Ni(1,4-pyrazinedithiolate)2]. Herein, these two MOFs have been infiltrated with the redox active species 7,7,8,8-tetracyanoquinodimethane (TCNQ) and iodine under solution phase conditions and shown to produce redox products within the MOF pore space. Vibrational bands assignable to TCNQ anion and triiodide anion have been observed in the Mid-IR and Terahertz ranges using FTIR Spectroscopy. The MOF samples have been further investigated by Time-Resolved Terehertz Spectroscopy (TRTS). Using this technique, the charge mobility, separation, and recombination dynamics have been followed on the picosecond time scale following photoexcitation with visible radiation. The preliminary results show that the MOF samples have small inherent photoconductivity with charge separation lifetimes on the order of a few picoseconds. In the case of HKUST-1, the MOF can also be supported by a TiO2 film and initial results show that charge injection into the TiO2 layer occurs with a comparable efficiency to the N3 dye sensitizer and therefore this MOF has potential as a new light absorbing and charge conducting material in photovoltaic devices.

9567-58, Session PMon

Plasmon-induced selectively chemical growth of flexible and transparent silver nano-network electrode for organic optoelectronic devices

Haifei Lu, The Chinese Univ. of Hong Kong (Hong Kong, China); Di Zhang, Xingang Ren, The Univ. of Hong Kong (Hong Kong, China); Jian Liu, Univ of Hong Kong (Hong Kong, China); Wallace C. H. Choy, The Univ. of Hong Kong (Hong Kong, China)

While great efforts have been devoted to develop enabling nanowire electrodes, reduce contact resistance of the metal nanowires and improve the electrical stability under continuous bias operation are the key issues for practical applications in flexible optoelectronics. Here, we propose and demonstrate a novel approach of selective nucleation and growth of silver nanoparticles at the junctions of silver nanowires at room temperature and atmosphere for chemically forming a silver nano-network. The selective integration of silver nanoparticles at the junctions of silver nanowires is realized through plasmon-induced chemical growth under a very low power density of light irradiation (as low as 5 mW/cm2) without using sophisticated equipment and expensive material. As a result, silver nanonetworks with very good electrical conductivity and optical transmittance are obtained. Compared to the silver nanowire electrodes treated with thermal annealing, our nano-networks from the selective integration of in situ grown silver nanoparticles with silver nanowires exhibit better electrical stability under continuous external bias. In addition, the silver conductive nano-network peels off itself from the substrate when immersed in water, which can be easily transferred to other substrate s for versatile applications. To conceptually demonstrate the potential application of our silver nano-network, semitransparent P3HT:PCBM organic solar cell is fabricated by using silver nano-network as the top electrodes and performances are close to reference device [1]. Consequently, silver nanonetwork formed through our novel approach has exhibited great potential as highly conductive transparent electrode with the attractive features of low cost and high operational stability which are desirable in practical optoelectronic and electronic applications.

[1] H. Lu, D. Zhang, X. Ren, J. Liu, W. C. H. Choy, ACS Nano, vol. 8, pp 10980-10987, 2014.

9567-60, Session PMon

ZnO:Al films modified by Zn1-xMgxO:Al surface layer as low work function transparent electrodes

Grzegorz Luka, Institute of Physics (Poland); Wojciech Lisowski, Janusz W. Sobczak, Aleksander Jablonski, Institute of Physical Chemistry (Poland); Petro S. Smertenko, V.E. Lashkaryov Institute of Semiconductor Physics (Ukraine)

Electrode work functions and their proper adjustment have an impact on the performance of organic solar cells. So far widely used metals like magnesium, calcium, lithium, or their alloys are chemically reactive and sensitive to oxygen. The commonly used indium tin oxide (ITO) material for transparent electrode applications typically has the work function of 4.2 - 4.8 eV. Aluminum-doped zinc oxide (ZnO:Al, AZO) films, which are becoming very competitive to ITO, have the work function of about 4.1 eV. This promotes their use as transparent electrodes in inverted type organic devices. By alloying AZO films with magnesium, a further decrease of the work function is achieved. Such films, however, have higher resistivities comparing to ITO or non-alloyed AZO films.

We covered AZO films with very thin (~5 nm) Zn1-xMgxO:Al layers grown by atomic layer deposition. A highly conductive state of the AZO film was combined with a lower work function of the electrode due to the



alloyed layer at the AZO surface. Depending on the growth conditions, the magnesium content at the film surface varied from x = 0 to x = 0.6. This gave a work function decrease up to 0.6 eV and resulted in a decrease of the reverse currents (by 1-2 orders of magnitude) and a rectification improvement of the prepared organic single layer devices. Based on current-voltage measurements and a differential approach, we analyzed carrier injection properties of the so-obtained electrodes.

The research was supported by The National Science Centre (NCN, Poland) under decision DEC-2012/07/D/ST3/02145.

9567-61, Session PMon

Understanding the degradation of polymer solar cells: A comparative study realized on working devices

Mario Prosa, Istituto per lo Studio dei Materiali Nanostrutturati (Italy); Mirko Seri, Istituto per la Sintesi Organica e la Fotoreattività (Italy); Marta Tessarolo, Istituto per lo Studio dei Materiali Nanostrutturati (Italy)

Over recent years, scientific interest gradually converged to Bulk Heterojunction (BHJ) solar cells since sustainable and economic benefits are simultaneously achieved. Despite worldwide research lead to interesting power conversion efficiencies greater than 10%, the rather limited stability of the devices slowed down the commercialization of this technology. In this view, a deeper understanding of the issues concerning the device stability is required. Recent publications highlight the detrimental role of light and temperature on encapsulate devices but, most of the works focus the attention mainly on a single layer or a particular interface. However, it is well known that the mechanisms inducing the degradation are not limited to a specific layer (interface) nevertheless the investigation of a complete working device is not trivial. Here, we present a complete description on the stability of BHJ solar cells in which spectroscopic as well as microscopic techniques are combined to study working devices and, an overall understanding of degradation mechanisms involved in complete solar cells is provided. Moreover, we show how a single interface (layer) contributes to the losses of performances. In particular, different i) active layers, ii) interfacial layers and iii) device architectures were combined to show the role of each layer (interface) and its influence to the lifetime of the resulting device under thermal and light soaking degradation tests. Finally, guidelines for the fabrication of time stable BHJ solar cells are presented.

9567-63, Session PMon

Efficient perovskite solar cells and their application to semitransparent devices

Hoyeon Kim, Jaewon Ha, KAIST (Korea, Republic of); Hui-Seon Kim, Nam-Gyu Park, Sungkyunkwan Univ. (Korea, Republic of); Seunghyup Yoo, KAIST (Korea, Republic of)

Advent of photovoltaic (PV) cells utilizing inorganic-organic lead halide perovskites has recently gained a great attention and led the community to put intensive efforts on boosting their overall performance. As a result, their power conversion efficiency showed a rapid increase reaching the value close to 20%, demonstrating their great potential for next-generation PV technologies balanced with both high performance and affordability. However, the geometry of highly efficient devices has been limited to a few configurations and reports on realization of efficient perovskite semitransparent PV cells were relatively scarce.

In this work, we demonstrate efficient perovskite solar cells in which nano-porous TiO2 layers are prepared on ITO substrates instead of FTO substrates, which are more commonly adopted in perovskite research. In the anode side, expensive Au or Ag top electrodes are also replaced with MoO3/Al electrodes without performance tradeoff. As a result, devices having power conversion efficiency of avg. 16.4% (champion cell with 17.3%) under 100mW/cm2 (AM 1.5G) are demonstrated with reverse voltage sweep (from forward bias to short circuit) at scan rate of 0.2V/s. Hysteresis on

the current-voltage curve and external quantum efficiency on both AC and DC measurement modes are examined. Furthermore, efficient see-through perovskite solar cells are achieved with little optical haze thanks to the high optical quality of ITO electrodes. With a top semitransparent Ag electrode capped with a high-index MoOx layer, semitransparent MAPbI3-based perovskite photovoltaic devices are shown to exhibit the power conversion efficiency of avg. 10%. Optical analysis based on transfer matrix formalism is also presented to elucidate the competition between device efficiency and transparency.

9567-64, Session PMon

Thiazolo [5,4-d]thiazole based D-A-D type Chromophore with furan spacer for BHJ organic solar cells

Mohammed Nazim, Sadia Ameen, Mohammed S. Akhtar, Hyung Kee Seo, Hyung Shik Shin, Chonbuk National Univ. (Korea, Republic of)

Organic small molecule containing thiazolo[5,4-d]thiazole-core acceptor with furan spacer (RFTzR) was designed, synthesized and applied as electron donor material for solution-processed bulk-heterojunction (BHJ) small molecule organic solar cells (SMOSCs). The synthesized small molecule had a good thermal stability of >350 and crystalline nature also. It also has shown the self-assembly behaviour due to the presence of terminal alkyl chains. It has shown a good absorption band about ~473 nm in chloroform solvent. The introduction of furan spacer improved its absorption and solubility in the common organic solvents. RFTzR exhibited a good oxidation stability with HOMO and LUMO energy levels of -5.36 eV and -3.14 eV, respectively. The solution-processed organic solar cell devices of RFTzR were optimized with PCBM in different donor:acceptor blend ratios (1:1, 2:1, 3:1, w/w). Low value of FF affects adversely on the solar cell devices which is responsible for lowering the efficiency than the expected one. The fabricated cells of RFTzR (donor) and PC60BM (acceptor) as photoactive materials showed relatively smooth thin film morphology of devices which gives a maximum PCE of 2.72% (RFTzR:PC60BM, 2:1, w/w) optimized ratio with good open-circuit voltage of 0.756 V and high photocurrent density of 10.13 mA/cm2. This study makes a way for the furan bridged chromophores in small molecule organic solar cells.

9567-65, Session PMon

Optimization of interfacial layer for double and triple junction polymer solar cell

Abu Mitul, South Dakota State Univ. (United States)

Solution processed tandem polymer solar cell has drawn a great deal of attention due its low cost, ease of production and capability of harvesting solar energy more efficiently. In solution processed tandem polymer solar cell, the most challenging part is the optimization of interfacial layer. In this work, we have investigated the robustness of PEDOT:PSS/AZO/PEIE interfacial layer to develop tandem polymer solar cell. While developing triple junction polymer solar cell, temperature of second interfacial layer has also a great impact on overall device performance. Here, the performance of tandem polymer solar cell was investigated on different temperature of interfacial layer. Triple junction polymer solar cell was able temperature of interfacial layer. Voc of 1.4 V was achieved in triple junction polymer solar cell while single junction Voc was 0.6 V. Optimization of thickness and more robust PEDOT:PSS/AZO/PEIE interfacial layer can overcome the losses in triple junction polymer solar cell.



9567-66, Session PMon

Non-oligoacence molecules exhibiting singlet fission in organic photovoltaic devices

Yong-Jin Pu, Yamagata Univ. (Japan)

We demonstrate singlet fission phenomena in a series of thienoquinoidal compounds by magnetic field dependence of photocurrent in OPVs. In the three thienoquinoidal compounds, thiophene (Th), thieno[3,2-b] thiophene (TTh), and bithiophene (BTh) are incorporated as a core between two fluorene (BF) units with double bonds, respectively: ThBF, TThBF, and BThBF. The thienoquinoidal structure leads a biradical character, and consequently their E(T1) decreases. TD-DFT calculations using the singlecrystal structure of the compounds indicated that the E(T1) of TThBF and BThBF are lower than half of the E(S1). We fabricated OPV devices using the thienoquinoidal compounds as a donor, C60 and PDIF-CN2 as an acceptor, respectively. With PDIF-CN2 having enough deep LUMO level for charge separation of triplet excitons in the donor, the photocurrents obtained by the excitation of the donor decreased with increasing magnetic field. This result indicates that the magnetic field suppressed singlet fission rate because of Zeeman splitting of triplet state, resulting in the reduction of the triplet excitons and the photocurrent from their charge separation. On the other hand, in devices with C60, the photocurrents under the excitation of the donor increased with increasing magnetic field. This result is because suppression of the singlet fission by magnetic field reduced the triplet excitons that cannot be separated to charges because of shallow LUMO level of C60.

9567-67, Session PMon

Hybrid perovskite solar cells based on zinc oxide scaffolds synthesized by different methods

Fangzhou Liu, Qi Dong, Man Kwong Wong, Aleksandra B. Djuri?i?, The Univ. of Hong Kong (Hong Kong, China); Annie Ng, Charles Surya, The Hong Kong Polytechnic Univ. (Hong Kong, China); Wai Kin Chan, The Univ. of Hong Kong (Hong Kong, China)

Investigations on solid-state organic-inorganic perovskite based solar cells have drawn worldwide attention in the recent years. Considerably high power conversion efficiencies have been achieved in the cells with TiO2 employed as the electron-selective contact or mesoporous scaffold.1 On the other hand, regarding that TiO2 materials unavoidably require high temperature processing at 450oC-500oC, research efforts have been made to explore other alternatives allowing low-temperature processing with desirable efficiencies. ZnO, with its comparable energy levels and higher electron mobility than TiO2, is a potential alternative to TiO2 for the applications in hybrid perovskite based solar cells. ZnO also possesses a variety of its nanoscaled morphologies and processing methods which provides numerous possibilities for device design. Preliminary efforts on this research topic have been made so far with considerable efficiencies achieved in perovskite solar cells based on ZnO nanorods.2

Due to the richness in morphologies and synthesis approaches, similar ZnO nanostructures can be prepared using different methods, and the properties of the as-grown materials are largely affected by synthesizing methods. In this work, we studied the perovskite solar cells with ZnO as the electronselecting and mesoporous scaffold materials prepared by different methods, including hydrothermal growth, vapor-phase deposition, and electron beam deposition. The power converting efficiencies with optimized cell structures are compared and their correlations to other material properties are discussed.

References

1. Jung, H. S. and Park, N.-G., Small 11(1), 10-25 (2014).

2. Son, D.-Y., Im, J.-H., Kim, H.-S. and Park, N.-G., J. Phys. Chem. C 118, 16567?16573 (2014).

9567-69, Session PMon

Sn/Pb binary perovskite solar cells with improved stability in air and organic amine-free perovskite solar cells with improved stability against light exposure

Koji Nishinaka, Yuhei Ogomi, Kyushu Institute of Technology (Japan); Qing Shen, The Univ. of Electro-Communications (Japan); Kosei Fujiwara, Keita Sakaguchi, Kyushu Institute of Technology (Japan); Taro Toyoda, The Univ. of Electro-Communications (Japan); Shuzi Hayase, Kyushu Institute of Technology (Japan)

Perovskite solar cells have recently attracted interest because of the high efficiency reaching 20 %. The perovskite works as light absorber and the light absorption spectrum edge for MAPbI3 (MAPbI, MA: mechylammonium cation) was 800 nm. It has been reported that Sn halide perovskites have the light absorption up to 1200nm. However, it has been reported that CH3NH3SnI3 (MASnI) was too unstable to handle in air. We found that the Sn halide perovskite became stable in air when Pb halide perovskite was added. This prompted us to evaluate binary Sn/Pb perovskite solar cells. We have already reported the binary MASnPbI3 with 4.18 % efficiency1-3. In this report we discuss photovoltaic performances for binary MASnPbI perovskite solar cells with gradient structure from the bottom to the top. The gradient structure was given by the slower diffusion of PbI2 than SnI2 into nanopores of porous titania layers and the structure gave unique long carrier life time with msec order. We also reported organic amine free-CsPbI solar cells with about 2 % efficiency, expecting enhanced stability toward light exposure. Hysteresis I-V curves were observed for the CsPbI solar cells. Therefore, we concluded that dipole of MA is not sole cause for the hysteresis. Urbach energy measurement suggested that decrease in defect density of the binary MASnPbI and CsPbI perovskite solar cells are needed for enhancing the efficiency. In this report, we show the potential for amine free CsPbI and binary MASnPbI solar cells with improved stability.

1. Y. Ogomi, S. Hayase, et al., J. Phys. Chem. C, 2014, 118, 16651-16659; 2. Y. Ogomi, S. Hayase, et al., J. Phys.Chem. Lett. 2014, 5, 1004-1011; 3. Y. Ogomi, S. Hayase et al., Chem. Phys. Chem. 2014, 15, 1062-1069.

9567-70, Session PMon

Overcoming the "light-soaking" issue in organic solar cells

Sara Trost, Bergische Univ. Wuppertal (Germany); Philip Reckers, Thomas Mayer, Technische Univ. Darmstadt (Germany); Tim Becker, Andreas Behrendt, Andreas Polywka, Ralf Heiderhoff, Patrick Görrn, Thomas Riedl, Bergische Univ. Wuppertal (Germany)

It is a general phenomenon that organic solar cells (OSCs) using TiOx or ZnO as electron extraction layers require "activation" by UV light . Otherwise, poor, s-shaped I/V characteristics with low fill-factors and overall low power conversion efficiency are found. In principle the AM1.5 solar spectrum provides enough UV radiation to activate TiOx or ZnO. However, in cases where the UV-spectral region of the solar spectrum is missing (e.g. with UV-blocking substrates, down-shifting concepts, indoor PV, multijunction cells) OSCs with interlayers of TiOx or ZnO will remain inefficient. Thus, the development of charge extraction materials that do not rely on UV activation is a critical challenge to achieve highly efficient and long term stable OSCs.

We will unveil the root cause of the "light-soaking" phenomenon using photoelectron spectroscopy and kelvin probe analysis. We will show that UV activation can be avoided by using electrically doped metal-oxides (e.g. Al:ZnO)[1] or by the application of plasmonic sensitization of the metaloxides, by introducing silver nanoparticles in the immediate vicinity of the metal-oxide/organic interface.[2] Very recently, we discovered that pristine SnOx as electron extraction layer, prepared at temperatures as low as 80°C, provides a facile avenue to light soaking-free OSCs. The work-function of



these SnOx layers is low (4.1eV) even without illumination. The absence of an electron extraction barrier is verified for a range of organic photo-active systems.

[1] S. Trost et al. Adv Energy Mater 2013, 3, 1437.[2] S. Trost et al. Sci. Rep. 2015, 5, 7765.

9567-71, Session PMon

Effects of organic and inorganic templating layers on phthalocyanine/C60 planar and bulk heterojunction organic solar cells

Sibi Sutty, Hany Aziz, Univ. of Waterloo (Canada)

Various templating layers have been used to control the molecular orientation of organic solar cell (OSC) materials and fabricate planar heterojunction (PHJ) OSCs. The templating layer forces the donor molecules of a PHJ OSC to lie flat on the substrate, which improves its absorption and charge transport properties. As a result, templated PHJ OSCs have higher efficiencies due to improved short-circuit current and fill-factor. Several organic and inorganic templating layers such as perylene-3,4,9,10tetracarboxylic dianhydride (PTCDA) and copper iodide (CuI) respectively have been used to improve OSC performance to date. However, there are no studies comparing the effects of the different types of templating layers on the morphology and molecular orientation of a donor material and the associated impacts on OSC performance. Furthermore, the suitability of organic and inorganic templating layers for various donor materials has also not been studied. In our work, we assess the key differences between organic and inorganic templating layers. First, we study the differences in morphology and molecular orientation of various metal substituted phthalocyanine donor materials deposited on these two types of templating layers. Then, we analyze the subsequent effects on the performance of phthalocyanine/C60 PHJ and bulk heterojunction (BHJ) OSCs. Finally, we correlate changes in morphology and molecular orientation to OSC performance and determine the best templating layer for each metalphthalocyanine/C60 PHJ or BHJ OSC.

9567-72, Session PMon

Advanced imaging characterization and modelling of defects in organic solar cells

Roland Rösch, Daniel Fluhr, Rolf Öttking, Burhan Muhsin, Harald Hoppe, Technische Univ. Ilmenau (Germany)

Lifetime and production yield remains a challange of organic photovoltaics (OPV). Various degradation scenarios exist, for example shunting due to impurities or electromigration. Furthermore photooxidation and morphological decomposition of the active layer materials, corrosion of the metal electrodes or deposition mismatch can strongly affect device performance.

Finite element models (FEM) enables studyingcurrent pathways and resistive losses in laterally extended organic solar cells.

The FEM calculations yield spatial distributions of current densities and according resistive power losses. The peaking current distribution within the shunting defect is locally resolved, however, considerable currents are still spread over the entire device area.

From the resulting resistive loss patterns, the heat distribution and emission was derived and directly compared with lock-in thermography imaging.

On the opposite, so-called pinholes within the metal back electrode offer pathways for ingress of water and oxygen. These attack the metalorganic interface, introducing delamination through the formation of insulating metal oxides. As charge injection and extraction is suppressed at delaminated areas, the active device area is reduced and so is the overall efficiency.

The reduction of the active area is experimentally investigated concerning the influence of different environmental conditions. Imaging experiments

provide information on location and size of insulated areas induced by pinholes in the metal back contact. Time resolved measurements during degradation of the devices reveal the dynamics and rate of growth of these individual defects.

Overall, imaging in combination with simulation offers advanced defect analysis, promoting OPV market introduction.

9567-74, Session PMon

Multiscale analysis of the effect of micro phase separation on the charge transfer at the PEDOT:PSS and P3HT:PCBM layer interface

Min Huang, Tongji Univ. (China)

The influence of micro phase behavior on the charge transfer at the interface between PEDOT:PSS and P3HT:PCBM layers was studied using multiscale analysis. Calculated Flory-Huggins parameters indicated that the PEDOT attracts P3HT and repulses PCBM that agrees well with the experimental observation of the development of P3HT rich interface during the BHJ layer formation. Based on the calculated Flory-Huggins parameters, mesoscale DPD simulations were conducted for PEDOT:PSS and P3HT:PCBM layers. Results were mapped to the CG (coarse grained) and then atomistic scales where atomistic details of the interface were studied. The density of nonbonding close contacts including that from reorientation between PEDOT and P3HT was quantified, vibronic coupling and carrier transfer efficiency were discussed.

9567-76, Session PMon

Control of ultrafast singlet exciton fission in antradithiophene derivatives: From 1 exciton to 2 exciton generation

Chaw Keong Yong, Olga Bubnova, Stavros Athanasopoulos, Univ. of Cambridge (United Kingdom); Jenny Clark, The Univ. of Sheffield (United Kingdom); John Anthony, Univ. of Kentucky (United States); Henning Sirringhaus, Univ. of Cambridge (United Kingdom)

Singlet exciton fission is a process that occurs in certain organic materials whereby one singlet exciton splits into two independent triplet excitons. In photovoltaic devices these two triplet excitons can each generate an electron, producing quantum yields per photon of >100%. We use ultrafast transient absorption spectroscopy to study the singlet fission dynamics in the thin film of antradithiophene derivatives. By controlling the intermolecular packing in the film via various solution processing routes and molecular side-chain engineering, we provide direct evidence for the control of the singlet exciton fission rate in the antradiothiophene neat films over a broad range from 10ps to 2ns, and eventually, no singlet exciton fission is observed in the amorphous neat film. Temperature dependent photoluminescence characterization further reveals peculiar radiative recombination rate. While singlet exciton fission is dominant at room temperature, the photoluminescence is dominated by the triplet-triplet annihilation and exhibits excimer-like spectra. The radiative recombination rate decreases as the substrate temperature is reduced to 120K. When the substrate temperature is further reduced to 5K, the photoluminescence is dominated by superradiance with the radiative recombination rate enhanced by a factor of 46, with respect to the radiative recombination rate observed at 120K. This work provides the foundation for ways to tailor the multicarrier generation in organic semiconductor by controlling the intermolecular interaction via solution processing routes and molecular side-chain engineering.



9567-77, Session PMon

Copper (I) oxide (Cu2O) as a hole transport layer for inverted perovskite solar cells

Rodrigo Szostak, Ivo B. Freitas, Ana Flavia Nogueira, Univ. Estadual de Campinas (Brazil)

Perovskite solar cells emerged six years ago with an efficiency of 3,0% and today an efficiency of 15% is easily achieved, reaching up to 20%. Several materials have been used in perovskite solar cells seeking high efficiency and low cost. Copper (I) oxide (Cu2O) is a p-type semiconductor, non-toxic, abundant and readily available. Cu2O can be synthesized easily by thermal oxidation of metallic copper. In this work, we report for the first time the introduction of Cu2O as hole transport layer in inverted perovskite solar cells with the ITO/Cu2O/CH3NH3PbI3/PC71BM/AI configuration. A thin layer of copper metal was deposited on ITO by thermal evaporation and the film is oxidized in air at room temperature. Perovskite was deposited by a twostep method. The band gap of the Cu2O film 2.52 eV. P-type conductivity and hole density in the order of 1017 cm-3 were determined from the Hall measurements. Valence-band of Cu2O is very close to the perovskite CH3NH3PbI3, so a comparable open circuit voltage (Voc) is expected. The inverted solar cells exhibited Voc of 0.83V and 0.74 V, Jcs of 0.34 and 0.32 mA/cm2, FF of 34.9 and 37.2%, in both forward and reverse bias with a delay time of 50 ms.

9567-78, Session PMon

Understanding the photo current generation in organic tandem solar cells utilizing a 3-terminal device architecture

Daniel Bahro, Manuel Koppitz, Adrian Mertens, Konstantin Glaser, Jan Mescher, Alexander Colsmann, Karlsruher Institut für Technologie (Germany)

Tandem architectures are one of the most promising concepts to boost organic solar cells towards competitive power conversion efficiencies. To develop a better understanding of the charge carrier generation and extraction mechanisms in organic tandem solar cells, it is of pivotal importance to access the subcells of the tandem device and to monitor their spectral response. Therefore we built 3-terminal devices with direct electric access to the PEDOT:PSS/ZnO recombination zone. By introducing this fully operational intermediate contact we overcome many drawbacks of previously published methods. By carefully choosing the thickness of the intermediate electrode, we maintain the optical field distribution and the optoelectronic properties and power conversion efficiencies (> 7%) of the corresponding 2-terminal device architectures. Utilizing this method, we developed models for the photovoltaic properties and the EQE under normal and oblique light incidence. To demonstrate the power of this approach, we focused on homo-tandem solar cells, which require more advanced optical characterization.

9567-79, Session PMon

Automated spray deposition for plastic electronics

Kirsty A. Roy, James Bannock, Neil Treat, John de Mello, Martyn McLachlan, Imperial College London (United Kingdom)

Spray deposition is a promising technique for the solution processing of plastic electronic devices, owing to the potential for high-speed, large-scale device fabrication using low capital cost equipment. To date most reports of spray-deposited electronic devices have used ultrasonic systems for film deposition to minimise surface roughness, but such systems suffer from low materials throughput, and are consequently ill-suited to industrial

manufacturing. Pressure-driven spray heads enable higher throughput materials delivery but typically result in an unacceptably rough film due to the hard-impact nature of the deposition system.

Here we describe a new automated pressure-driven spray coater for the controlled deposition of a broad variety of solution processed electronic materials, which overcomes many of the disadvantages of conventional pressure-driven spray coaters. Key features of the system include: a novel, high performance 3D-printed spray-head for the generation of ultrafine sprays; full-three dimensional position and velocity control of the spray-head; integrated temperature control, and independent control of solution and gas rates.

The system allows for the controlled fabrication of thin film semiconducting polymers from non-chlorinated solvents. We investigate the influence of deposition variables such as solution carrier gas pressure, solvent composition and substrate temperature as well as post deposition treatments on the properties of the polymer films. We also demonstrate sequential deposition of oxide and organic materials, solvent annealing of polymer films and gradient doping of both organic and inorganic films.

9567-80, Session PMon

Selective non-contact modification of the polymer chain orientation and morphology in conducting polymers by femtosecond laser writing

Hyo Jung Kim, Sang Min Chae, See Wo Lee, Pusan National Univ. (Korea, Republic of); Jiyeon Choi, Korea Institute of Machinery & Materials (Korea, Republic of); Hyun Hwi Lee, Pohang Univ. of Science and Technology (Korea, Republic of)

We propose a novel direct writing technique with a femtosecond laser enabling selective modification of not only the morphology of conducting polymer thin films but also the orientation and alignment of the polymer crystals. Surface relief gratings resulting from photoexpansion on poly(3hexylthiophene)(P3HT):[6,6]-phenyl-C61-butlyric methyl ester (PCBM) thin films were fabricated by a femtosecond laser direct writing. The photoexpansion was induced at laser fluence below the ablation threshold of the thin film. The morphology (size and shape) of photoexpansion could be quantitatively controlled by laser writing parameters such as focused beam size, writing speed, and laser fluence. Grazing incidence x-ray scsattering results showed that the amount of face-on P3HT crystals were largely increased in the photoexpansion in comparison with pristine region of the thin film. In addition, the P3HT polymer chains in the photoexpansion were highly aligned along the polarization of the laser. The micro-RAMAN spectra confirmed that neither chemical composition change nor the polymer chain breaking was observable after femtosecond laser irradiation. We believe that this laser direct writing technique opens a new door to the fabrication of more efficient organic semiconductor devices via non-contact, toxic-free approach.

9567-81, Session PMon

Study of PEDOT: PSS and BCP thicknesses effect on SubPc/C60 organic solar cell efficiency

Nesrine Zoulikha Mendil, Mebarka Daoudi, Zakarya Berkai, Abderrahmane Belghachi, Univ. Tahri Mohammed Béchar (Algeria)

Most of the power generated nowadays is produced using fossil fuels, which emit tons of carbon dioxide and other pollution every second [1]. In order to make the development of our civilization sustainable and cause less harm to our environment, scientific people are looking for new source of substitute clean energy. The photovoltaic solar energy industry is one of the fastest growing forces in the market; therefore, the research of new



technology which uses cheap photovoltaic materials as well as fabrication methods to collect solar energy becomes more and more important. In 1986, the first organic thin-film solar cell with reasonable efficiency (up to 1%) was created and reported by Tang [1]. Since then, great interest has been devoted to the advantages of using organic materials in the solar cells field. The performance of organic solar cells depends on many parameters, such as absorption, charge transport, the diffusion length excitant, the status of interfaces, etc.

The choice of photo-active materials and metal electrodes is required to achieve good conversion efficiency. The latter can be improved by using organic semiconductor having a high absorption coefficient, good electrical conductivity and an adequate structuring of the photo-active layer, as well as the use of interpenetrating network concept in forming the cell. In this context, we chose the Fullerene (C60) used as the organic electron-acceptor for its high stability and high carrier mobility with a0=1.42nm and energy gap about 1.5eV [2]and Boron Subphthalocyanine Chloride (SubPc) as the electron-donor due to its high peak absorption coefficient (2.12?105cm-1 at -590 nm) and with a0=1.2nm and energy gap about 2eV at ambient conditions[3]. The cell that we studied is composed of the following structure: ITO(30nm)/PEDOT:PSS(xnm)/SubPc(25nm)/C60(35nm)/BCP(ynm)/Al(30nm), with different value of x=5,10,12,15,20 nm and y=8,10,12,14,16. So, the aim of our work is to investigate the effect of PEDOT: PSS and BCP thicknesses on the efficiency of this organic solar cell.

9567-82, Session PMon

Bulk-heterojunction morphologies of solution processed BODIPY solar cells

Alexander Colsmann, Jens Ludwig, Martin Hochberg, Karlsruher Institut für Technologie (Germany); Alexandre Cheminal, Jérémy Léonard, Univ. de Strasbourg (France); Stefan Haacke, Univ. de Strasbourg (France); Laure Biniek, Martin Brinkmann, Institut Charles Sadron (France); Nicolas Leclerc, Antoine Mirloup, Raymond Ziessel, Univ. de Strasbourg (France); Markus Kohlstädt, Uli Würfel, Nils Hofmann, Fraunhofer-Institut für Solare Energiesysteme (Germany); Patrick Lévêque, Univ. de Strasbourg (France); Thomas Heiser, Univ. de Strasbourg (France)

Because of reproducible syntheses and high material purities, light harvesting molecules with low molecular weight may enable organic solar cells with improved long-term stability. In contrast to polymers, however, low molecular weight organic compounds often show poor film forming properties due to strong molecular aggregation. In this work, we present 5% organic solar cells and corresponding mini-modules, fabricated from solution, comprising light harvesting BODIPY molecules. The devices exhibit long-time stable bulk-heterojunction morphologies and hence enhanced device life-time. The morphology can be adjusted by applying proper processing temperatures or suitable additives. We investigated the bulkheterojunction morphology and performance by means of AFM, KPFM and conductive AFM. Photophysical investigations revealed the charge carrier dynamics within the active layer.

9567-83, Session PMon

Using hydrogen-bond mediated supramolecular self-assembly to direct the formation of organic bulk heterojunction

Jiangeng Xue, Ronald K. Castellano, Nathan T. Shewmon, Davita L. Watkins, Weiran Cao, Benjamin M. Schulze, Xueying Zhao, Scott S. Perry, Johan F. Galindo, Adrian E. Roitberg, Univ. of Florida (United States)

Intermixing the organic donor and acceptor materials to form the socalled bulk heterojunction (BHJ) helps to circumvent the exciton diffusion bottleneck; however the overall photovoltaic properties critically depends on the BHJ morphology, which often is irregular and is hard to predict due to the complex interplay between thermodynamics and kinetics. Minor changes in molecular structures or processing conditions could lead to significant changes in morphology and device performance. Here, we report a supramolecular self-assembly approach to control the morphology of bulk hetejunctions to yield optimal charge generation and transport simultaneously. The design is based on convalently linking an appropriate hydrogen bonding unit to a donor chromophore, which directs the formation of star-shaped trimer rosettes through self-complementary H-bonding, as confirmed by both computation and STM characterization. Using grazing incidence X-ray scattering, we confirmed that the donor trimers preferentially stack along the substrate normal. The surface of the mixed film of H-bonding modified oligothiophene donor and C60 does not show any apparent lateral phase separation under AFM, further confirming the existence of one-dimensional donor columns and the interdigitated BHJ morphology. Compared to comparator molecules that do not enable intermolecular H-bonding, these H-bonding enabled molecules result in near doubling in the external quantum efficiency in solar cells, which coupled with the red-shifted absorption as a result of enhanced stacking leads to a more than two-fold increase in the overall power conversion efficiency. We expect that this H-bonding mediated supramolecular assembly approach could be a general platform to separately optimize the morphology of BHJs and the optoelectronic properties of the donor chromophores.

9567-85, Session PMon

Study of electrical transport properties of P3HT using impedance spectroscopy

Camilo A. Otalora, Andres F. Loaiza, Gerardo Gordillo, Univ. Nacional de Colombia (Colombia)

In this work the electrical transport properties of devices with structure ITO/P3HT/M (M=AI or Ag) were studied using impedance spectroscopy. It was found that P3HT forms ohmic contacts with ITO and Ag while Schottky contact was observed with AI. The concentration of aceptor impurities in P3HT was determined; this proved to be about of 5,2x1016cm-3 in samples exposed to air for a short time, while an increment was observed by increasing the time of exposition. A study of the influence of the solvent type used to prepare the P3HT samples on the mobility of minority carriers (electrons) and majority carriers (hole) was additionally done. The higher mobilities were obtained on samples prepared using mesitylene; these have electron mobilities around 3,6x10-3 cm2V-1s-1 for electrons and 6,04x10-6 cm2V-1s-1 for hole. It was also determined that the charge carrier mobility strongly decreases with increasing exposure time.

9567-86, Session PMon

Accurate correlation between panchromaticity and power conversion efficiencies in small molecule organic photovoltaic devices

Chenyu Zheng, Anirudh Raju Penmetcha, Brandon Cona, Jeremy Cody, Christopher J. Collison, Rochester Institute of Technology (United States)

Squaraines are targeted for application with bulk heterojunction devices since they can easily be chemically tailored while maintaining reproducibility in manufacturing compared to polymers, based on their singular molecular weight distribution.

Squaraines in solution have very narrow absorption spectra with very high extinction coefficients but are particularly attractive for photovoltaic application because of the substantial panchromaticity in the thin film, such that extinction coefficients are maintained over a very broad region of the solar spectrum. However, despite the promise of very high short circuit currents that would accompany broad absorption efficiency, large power conversion efficiencies have not materialized.

In this work we will present a full description of the excited state



populations and broadening mechanisms that give rise to the spectra of blended squaraine:PCBM active layers. The assignments of monomers and aggregates will be made for optical data from (i) mixed solvent nanoparticle studies, (ii) solid solution spectroscopy and (iii) comparisons before and after annealing of films. We will further confirm assignments with theoretical validation.

Given that aggregate states can be manipulated through choice of squaraine and processing conditions, we can probe the charge transfer process at the bulk heterojunction interface. Beyond panchromaticity, we describe how excited states must be predictably managed to positively influence the mechanism for improved efficiencies.

9567-87, Session PMon

Nanostructure control in crystalline polymer-fullerene blends and its impact on the charge carrier dynamics in bulk heterojunction solar cells

Swaminathan Venkatesan, Qiquan Qiao, Devendra Khatiwada, Cheng Zhang, South Dakota State Univ. (United States); Jihua Chen, Oak Ridge National Lab. (United States)

High boiling point selective solvent additives are widely used for tailoring the nanomorphology in bulk heterojunction solar cells consisting of either crystalline or amorphous donor polymers. This study focuses and differentiates the role of solid additive namely 2,3-Pyridinediol (PD) on tailoring the nanostructure of bulk heterojunction solar cells consisting of donor polymers which are able to crystallize during film formation. Blend films cast from solutions consisting PD lead to formation of smaller domains and finer phase segregation between donor and acceptor as observed from AFM topography, phase and kelvin probe force microscopy (KPFM) images. Such a morphology leads to efficient solar cells attributed to significant enhancement in fill factor. However when PD is added to blend solutions consisting of amorphous polymers such as PBDTTT-C-T, the performance is drastically reduced compared to devices processed without any additive or with DIO additive. The importance of domain aggregation and phase separation for charge transport (mobility, carrier density and bimolecular recombination) will be highlighted for both crystalline and amorphous donor polymer-fullerene blends using photo-CELIV spectroscopy.Detailed understanding on the working mechanism of solid and liquid additive in film formation will also be shown. EFTEM and GIWAXS of blend films with liquid and solid additive will be compared to provide more insight on domain mixing, crystallization and orientation in several donor-acceptor blends.

9567-88, Session PMon

Thermal and photo-stability of non-halide lead precursors in perovskite material

Fadi Kamal Aldibaja, Univ. degli Studi di Roma La Sapienza (Italy); Eva Unger, Lund Univ. (Sweden)

We present the use of halide (PbCl2) and non-halide lead precursors (Pb(OAc)2 (OAc=CH3CH2COO-), Pb(NO3)2, Pb(acac)2 (acac=(CH3COCHCOCH3)-) and PbCO3) for the preparation of perovskite solar cells. We have confirmed by X-ray diffraction the growth of CH3NH3PbI3 in all the analyzed cases, except for PbCO3, independently of the lead precursor used for the synthesis of the perovskite. In addition, different cell configurations, thin film and mesoporous scaffolds, TiO2 or Al2O3, have also been prepared. We have observed that the lead precursor influences strongly in the structural properties of perovskite (grain size), as well as on the solar cell performance. Photovoltaic conversion efficiencies comparable to those achieved when using the commonly employed PbCl2 have been obtained with Pb(OAc)2 as lead source. Stability studies of the perovskite films and devices have also been carried out; demonstrating that the lead precursor also influences this aspect. Stability is strongly affected by atmosphere and illumination conditions, but also by the lead precursor employed for the perovskite synthesis, detecting higher stability when using PbCl2 instead of Pb(OAc)2. These results highlight that other lead sources, different to the commonly used PbCl2 and Pbl2, are also suitable for the development of PSCs, opening a new way for device performance optimization.

9567-89, Session PMon

The comparison of photoinduced excited energy transfer and electron transfer in organic-inorganic compound

Wenping Yin, Yan Cui, Hee-won Shin, Jungwoon Yang, Sungkyunkwan Univ. (Korea, Republic of); Arkady P. Yartsev, Lund Univ. (Sweden); Tae Kyu Ahn, Sungkyunkwan Univ. (Korea, Republic of)

A family of ZnP-Tri-SWNT conjugates as Donor-Linkage-Acceptor (D-L-A) photosynthetic mimics was designed and synthesized, achieving efficient intramolecular excited energy transfer (EET), as well as deeper understanding of the competition between energy transfer (ENT) and electron transfer (ET) dynamics.

We composited Znic(II)-porphyrin(ZnP) with different single walled carbon nanotube(SWNT) via high selective copper-catalyze azide-alkyne cycloaddition (CuAAC) reaction— with a single change in their connection without excessive destroy the delocalized electron structure in SWNT. Due to the D-L-A systems store energy mainly according to the drive of higher net electron transfer rate, achieving long term charge separate state, which can be severely affected by the linkage different. We demonstrated phenyl (ZnP-ph-SWNT) and bi-phenyl (ZnP-biph-SWNT) linkage dependent photoinduced excited energy transfer in each sample according to XPS, Streak Camera and femto-second Transient Absorption (fsTA) analysis.

In order to get rid of the possibility of non-covalent effect between ZnP and SWNT, we mixt ZnP and SWNT using physical method. Although both of non-covalent and covalent showed PL quenching effect, with about 20% and 80-90%. ZnP-SWNT has a much faster delay life time, less than 10ps, which comes from photoinduced EET. Uv-vis and NIR fsTA proved the ion pair exsit more than 300ps after electron transfer from ZnP to SWNT. We also tried to follow the kinetic change of porphyrin fluorescence peak at 660nm in fsTA, which showed more information of electron injection of each sample.

The variation in charge separation and charge recombination dynamics is mainly associated with the electronic properties of the conjugates, including orbital energies, electron affinity and the energies of the excited states. The charge of the electronic coupling is in turn, a consequence of the different connectivity patterns at the triazole moieties. Excited energy transfer is correlation with the length of linkage, as the basic for bond but not space electron transfer. Our study in ENT and ET comparative analysis is not only used in the energy since, but also used in industrial research, such as the nonlinearity of CNT itself, and even in clinical medicine.

9567-91, Session PMon

Sterically protected small molecules as novel donors for efficient bulk heterojunction solar cells

Swaminathan Venkatesan, Qiquan Qiao, South Dakota State Univ. (United States); Jihua Chen, Oak Ridge National Lab. (United States); Cheng Zhang, South Dakota State Univ. (United States)

The effect of steric ring protection on the morphology, structural, optical and device performance of a previously reported small molecular semiconductor is investigated and compared to small molecule without ring protection. Pristine films show significant large domains and surface roughness for small molecules without ring protection (SC371). Further



XRD and optical measurements show high aggregation and ordering of polymer in edge on orientation for small molecules thin films without ring protections. Films consisting of small molecule with ring protection (SC354) show smaller domains, smoother surface and completely amorphous nature. When blended with fullerene and cast as films similar properties are observed as in the case of pristine films. Bulk heterojunction solar cells consisting of SC371:PCBM active layer show high fill factor owing to interconnected pathways for electron and hole transport. SC354:PCBM cells show enhanced short circuit current density and open circuit voltage compared to SC371:PCBM cells attributed to higher extent of intermixing and finer phase separation. When 0.3% DIO is used as a solvent additive SC354:PCBM devices show comparable efficiency (~2.5%). Further charge carrier mobility, density and device stability of the two blends will be compared and evaluated. Sterically protecting organic semiconductors can serve as an effective strategy to tailor molecular structure for isotropic charge transport in low temperature processed organic electronics.

9567-92, Session PMon

Impact of the Poole-Frenkel effect on charge transport in PDTSiTzTz:PCBM based photovoltaic devices

Oleksiy Slobodyan, Kelly Liang, Eric Danielson, Marlene Gutierrez, Sarah Moench, Bradley Holliday, David Vanden Bout, Ananth Dodabalapur, The Univ. of Texas at Austin (United States)

While organic solar cell (OSC) power conversion efficiencies >10% are a crucial threshold for industrial viability, active industrial scale production will likely require active material thickness greater than typically reported in literature. Of many of donor-acceptor copolymers, bulk heterojunction (BHJ) with (2-ethylhexyl)dithieno [3,2-b:2',3'-d] silole)-2,6-diyl-alt-(2,5-bis 3-tetradecylthiophen-2-yl thiazolo 5,4-d thiazole)-2,5diyl] (PDTSiTzTz) is one of the rare few reported to maintain high fill factors with thick active lavers. The performance of PDTSiTzTz-containing OSCs coupled with its tolerance for higher layer thicknesses, make it an attractive materials system to study transport and recombination physics. We have extensively studied transport and recombination in PDTSiTzTz:PCBM using lateral photovoltaic structures. This materials system displays strongly reduced bimolecular recombination, with a bimolecular reduction factor <10-2, From our measurements, we obtain both electron and hole mobilities, and show that these values are carrier concentration dependent. Most unusually. the electron mobility displays a negative Poole-Frenkel effect. Numerical modeling of the lateral structure shows that accounting for the Poole-Frenkel behavior has a significant effect on charge carrier behavior within the active material channel. Applying numerical modeling to the vertical OSC structure demonstrates that results from lateral structures also provide insight into charge carrier transport in structures employed for collecting sunlight, thereby highlighting the importance of considering the Poole-Frenkel effect these photovoltaic devices.

9567-93, Session PMon

Efficient perovskite solar cells employing polymers as effective hole transport layer

Ashish Dubey, Nirmal Adhikari, Swaminathan Venkatesan, Devendra Khatiwada, Qiquan Qiao, South Dakota State Univ. (United States)

Perovskite based solar cells have shown to be an highly efficient solution processable device, because of its broad band light absorbing property and high charge diffusion length. However, a long term stable perovskites still remains a challenge, yet to overcome. Perovskite, inherently absorbs moisture, and its solar cell device design utilizes most widely used hole transport layer, spiro-OMeTAD, which is doped with lithium salt and tert-butyl pyridine, causing further degradation. Herein, we report stable perovskite thin film and top electrode. In this work we have optimized the

device structure by studying the perovskite film morphology with varying annealing time, varying polymer concentration and hole transport layer thickness. These low temperature solution processed polymer film showed excellent photovoltaic properties with power conversion efficiency greater than 8%. With further optimization in device design, by introducing effective interfacial layers can enhance extraction of electrons and holes from the solar cell leading to high PCE.

9567-94, Session PMon

Surface modification of electron selective metal oxide thin films in organic solar cells for enhanced efficiency and stability

Swaminathan Venkatesan, Evan C. Ngo, Qiquan Qiao, Cheng Zhang, South Dakota State Univ. (United States)

P3HT:PCBM solar cells with bi-layer interfaces consisting of metal oxide thin films with cationic polymer modification namely Polyethylenimine ethoxylated (PEIE) showed enhanced lifetime compared to bare metal oxide interfaces. The device characteristics are periodically investigated in illuminated and dark conditions for 180 days. It is found that performance of devices with zinc oxide (ZnO) and aluminum doped zinc oxide (AZO) drops to 56% of initial efficiency after ageing. While the devices with PEIE modification showed above 75% of their initial efficiency after 180 days of ageing. The higher degradation in ZnO and AZO based devices arises mainly due to lower fill factor. Kelvin probe measurement show small reduction in work function of the bare oxide films. Kelvin probe microscopic images show a significant reduction in surface potential of bare ZnO with 7 days of ageing. The reduction in surface potential is shown to be due to surface oxidation which leads to p-type of doping of of metal oxide. This oxidative doping leads to higher trap assisted recombination between P3HT-ZnO interface detrimental to the device lifetime. Hence passivation of charge selective interfaces is crucial to enhance the bulk heterojunction solar cell's stability and paves path to a low cost solution based approach for large scale roll to roll processing.

9567-95, Session PMon

Inkjet printing of organic photovoltaics using a water-based active layer ink

Anirudh Penmetcha, James Sinka, Chenyu Zheng, Christopher J. Collison, Rochester Institute of Technology (United States)

Chlorinated and Aromatic solvents typically used for the processing of Organic Photovoltaics, may not be used in large scale manufacturing of OPVs as they pose serious risks towards human health and the environment. Thus there is a need to develop a medium by which the OPV materials may be processed safely.

In this study, we focus on improving the processability of the active layer materials (P3HT:PCBM). By using a miniemulsion process, we fabricated and dispersed P3HT:PCBM nanoparticles in a "safe" solvent i.e water. We choose P3HT:PCBM the materials of choice due to them being benchmark materials in literature. Blend ratios of the P3HT:PCBM nanoparticles are characterized using UV-Vis and Fluorescence spectroscopy; we show that the blend ratio of the nanoparticle can be optimized (1:0.8) by modifying the initial concentrations of the donor and acceptor in the miniemulsion phase.

We modified the nanoparticle dispersion's surface tension to convert them into inks for inkjet printing; we improve the wettability of the ink on the PEDOT:PSS layer of the OPV. The nanoparticle ink was printed onto PEDOT:PSS coated ITO slides. Aluminum cathodes were evaporated ontop of the printed active layer to complete the OPV device structure. The OPVs were characterized for their Power Conversion Efficiency; the best device had a PCE of 0.07%. This proof of concept result is very promising as it is a stepping stone between lab-based prototype devices and large scale manufacturing.



9567-96, Session PMon

Photo-stability of crystalline large-grain planar perovskite solar cell

Wanyi Nie, Hsinhan Tsai, Amanda Neukirch, Jean-Christophe Blancon, Hsing-Lin Wang, Jared Crochet, Gautam Gupta, Los Alamos National Lab. (United States); Muhammad Alam, Purdue Univ. (United States); Sergei Tretiak, Aditya Mohite, Los Alamos National Lab. (United States)

Organometallic perovskite based planar solar cell have emerged the most promising thin film solar cell technology largely due to high power conversion efficiency. However, photo-stability of perovskite solar cells under constant illumination for several hours of outdoor operation is yet to be realized. Here, we demonstrate the synthesis of large grain size (mms) perovskite solar cells and study the photo-stability of these devices. We measured the JSC, VOC and FF under constant illumination with device maintained at A) open circuit B) short circuit and C) at forward bias with no illumination and record the J-V scan under one-Sun illumination. The results show that the VOC does not degrade for all conditions. However, under open-circuit condition, there is a degradation of the JSC by ~40%, whereas at short-circuit condition ~10% degradation in JSC is observed. All the figures of merit return to their original value, when the device is maintained in dark (>60 mins) suggesting that the large grain perovskite crystal structure does not degrade with long-term illumination. We attribute the degradation in the JSC to photo charging of the device by the filling of subgap trap states, which accumulate at open circuit and cause degradation in JSC under flat band condition. However, under short circuit condition, photo-generated charges can drift out of these states due to the build-in potential thus preventing charge accumulation and no significant loss in the JSC. Under dark (C point), the captured free carrier can drift out, which in complete recovery of the key parameters. We validate our observation using Capacitance-Voltage measurement by extracting the charge density profile. We also demonstrate that by operating at a certain desired power point results in relatively photo-stable perovskite solar cells.

9567-97, Session PMon

Efficient vacuum-deposited tandem organic solar cells with fill factor higher than single junction subcells

Hyun-Sub Shim, Seoul National Univ. (Korea, Republic of); Francis Lin, National Taiwan Univ. (Taiwan); Jihun Kim, Bomi Sim, Tae-Min Kim, Chang-Ki Moon, Yongsok Seo, Seoul National Univ. (Korea, Republic of); Chun-Kai Wang, Ken-Tsung Wong, National Taiwan Univ. (Taiwan); Jang-Joo Kim, Seoul National Univ. (Korea, Republic of)

Tandem structures have been used to enhance device performance because of the use of broader solar spectra converted into the current. Moreover, open circuit voltage (VOC) or short circuit current density (JSC) can be increased if the sub-cells are connected in the series or parallel structures, respectively.

The vacuum deposition have several advantages such as the ease of purification via the sublimation, no use of solvents which might damage pre-deposited layer and the precise control of the thickness of layers in the nanometer scale. Despite of these advantages, most vacuum-deposited OPVs show lower efficiency compared with solution-processed OPVs due to the difficulty in forming charge transporting path in the blended active layer, resulting in the lower JSC and fill factor (FF).

In this paper, we demonstrates efficient vacuum-deposited tandem OPVs whose device structures are 80 nm-thick sub-cells connected by the interconnection unit (ICU) composed of electron-transporting layer (ETL)/ metal/p-doped hole-transporting layer (p-HTL). The p-doped layer in the ICU enables tuning the sub-cell position in the devices to have the maximum optical field distribution for increasing JSC without any electrical loss.

Moreover, it enhances FF due to the reduction of the contact resistance caused by the p-doped layer in the ICU. As a result, power conversion efficiency (PCE) of 9.2% with JSC of 8.7 mA/cm2 and VOC of 1.7 V is obtained. FF of 0.62 is achieved, which is higher than the one of the single junctions although the thickness of the sub-cells is relatively thick with 80 nm.

9567-98, Session PMon

Application of metal nanoparticleconducting polymer composite to organic based solar cells

Sungho Woo, Wook Hyun Kim, Shi-Joon Sung, Daegu Gyeongbuk Institute of Science & Technology (Korea, Republic of)

Recently, organic based solar cells, those are using organic light absorption materials such as organic solar cells (OSCs) and dye-sensitized solar cells (DSSCs), have attracted a lot of attention due to their unique advantages including low cost, solution processability, and mechanical flexibility. Although their power conversion efficiencies (PCE) have been improved dramatically, there are still many limitations for practical applications.

In OSCs, the difficulty of increasing the active layer thickness due to the limitation of the exciton diffusion length and the poor charge transport property leads to insufficient absorption of incident light. To improve light absorption in the organic photoactive layer, the application of surface plasmons (SPs) based on metal nanoparticles (NPs) has been reported.

In flexible DSSCs, the thermally reduced Pt counter electrode (CE) should be replaced by low temperature process and material, because most flexible plastic substrates cannot bear at high temperature up to 400 ?. Hence it is strongly required to develop a process that can reduce the annealing temperature.

Here, we made metal NPs generated via in-situ method inside PEDOT:PSS conducting polymer solutions. The prepared Ag or Au NPs-PEDOT:PSS composite was applied to hole transport layer in OSCs, and Pt NPs-PEDOT:PSS composite was applied to CE in DSSCs. The improvement of device performance was mainly attributed to the high specific surface area and catalytic activity due to the support of small amounts of metal NPs incorporated in the PEDOT:PSS media.

9567-99, Session PMon

Dye anchoring functional groups on performance of dye sensitized solar cells: Comparison between alkoxysilyl and carboxyl groups

Sri Kasi V N R. Matta, RMIT Univ. (Australia); Yasuhiro Tachibana, RMIT Univ. (Australia) and Osaka Univ. (Japan); Kenji Kakiage, Yano Toru, Adeka Corp. (Japan)

Performance of dye sensitized solar cells (DSSCs) is driven by photoinduced charge transfer processes mimicking natural photosynthetic reaction systems. Following excitation of a dye sensitizer, efficient forward and slow reverse charge transfer processes are required. These reaction kinetics are controlled at the interfaces of materials and charge transport processes in the cell. Interfacial material design is therefore crucial to improve the performance of DSSCs.

Herewith, two dye anchoring functional groups, alkoxysilyl and carboxyl groups, were compared to investigate their influence on the performance of DSSCs. Dimethylaminoazobenzene was selected as a chromophore possessing a donor-accepter transition for the light absorption. Electrochemical and optical measurements were performed for 4-dimethylaminoazobenzene-4'-carboxylic acid and 4-dimethylaminoazobenzene-4'-triethoxysilane attached TiO2 films. Electrochemical measurements and DFT calculation indicated almost identical potential energy levels and electron density of HOMO and LUMO



states between these two dyes. Solar cell APCE spectra and charge recombination kinetics at the dye/TiO2 interface revealed almost identical charge transfer rates/yields from and to the dye. The difference observed on improvement of an open circuit photovoltage (Voc) by 60 mV and on the lifetimes of an electron in the TiO2 conduction band for the dye with the alkoxysilyl functional group, suggesting that an alkoxysilyl functional group is more attractive to retard the charge recombination reaction between an electron in the TiO2 conduction band an oxidized form of an electrolyte redox couple. The highest solar energy conversion efficiency of 2.6 % was achieved for DSSCs based on an azobenzene dye sensitizer under AM1.5G, one sun condition.

9567-100, Session PMon

Improved hole transport layers in perovskite solar cells based on functionalized carbon nanostructures doped P3HT

Teresa Gatti, Univ. degli Studi di Padova (Italy); Simone Casaluci, Univ. degli Studi di Roma "Tor Vergata" (Italy) and Ctr. for Hybrid and Organic Photovoltaics (Italy); Aldo Di Carlo, Univ. degli Studi di Roma "Tor Vergata" (Italy); Enzo Menna, Univ. degli Studi di Padova (Italy)

Perovskite solar cells (PSCs) fabricated with two step deposition have been prepared and tested using P3HT as hole transport layer (HTL). P3HT was dissolved in chlorobenzene and blended with single walled carbon nanotubes (SWCNTs) and rGO graphene nanoplatelets (GNPs) bearing on the external surface covalently bound para-methoxyphenyl substituents, aimed at improving their homogeneous mixing with the semiconducting polymer. The SWCNTs and GNPs used for P3HT doping have been functionalized using aryl diazonium chemistry, keeping the amount of functionalities in a range which allows to gain better solubility but do not affect their electronic properties. Caution was taken in order to obtain blends with no insoluble GNPs residues, by applying a thorough protocol of sonication/centrifugation steps before spin coating the HTL on top of the hybrid junctions. Different weight percentages of functionalized GNPs/ P3HT were deposited, in order to determine the optimum percentage. Such doping of the P3HT layer resulted in increased efficiencies and prolonged stabilities of the resulting PSCs with respect to devices with undoped P3HT HTLs. The best solar cells showed a power conversion efficiency (PCE) up to 11.7 %. These promising results prompted us to test the effect of functionalized SWCNTs and GNPs doping on other hole-conductors, such as spiro-OMeTAD, in order to improve results of stability tests.

9567-101, Session PMon

High-performance planar-heterojunction perovskite solar cell using surface modified hole-transport layer

Santanu Bag, UES, Inc. (United States); Michael F. Durstock, Air Force Research Lab. (United States)

Perovskite solar cells based on organic/inorganic hybrid methylammonium lead trihalide absorber materials are attractive for low-cost energy harvesting because of their advantages in solution processability, mechanical flexibility, rapid improvement of power conversion efficiencies to greater than 15%, and lack of rare elements. However, fabrication of most high-performance perovskite solar cells often involves use of compact or mesoporous metal-oxides as charge-selective layers that require high temperature (>400°C) sintering and prevent their applicability to flexible plastic based devices. Thus, perovskite device structures devoid of metal-oxide interlayers are highly desirable for integration of devices into flexible form factors. Among various alternatives, poly(3,4ethylenedioxythiophene):poly(4-styrenesulfonate) (PEDOT:PSS) is an attractive hole-transporting interlayer (HTL) material due to its lowtemperature solution processability, commercial availability, tunable conductivity and extraordinary bending property. Although promising, the perovskite film growth on PEDOT:PSS has to overcome certain challenges in a planar heterojunction architecture in order to achieve higher efficiencies. Formation of crystallite islands of perovskite on top of PEDOT:PSS often leads to pinhole generation and incomplete surface coverage resulting in low device performance. Here we will demonstrate a new surface passivation strategy to improve the perovskite film coverage on PEDOT:PSS hole-transport layer and thereby increase the photovoltaic power conversion efficiencies. A simple passivation method based on thiourea treatment on a very thin PEDOT:PSS layer in a glass/ITO/PEDOT:PSS/CH3NH3PbI3/PCBM/ C60/Al device structure shows enhanced efficiency close to 10%. These findings highlight the importance of surface modification for achieving high performance metal-oxide free solution processed perovskite solar cells.

9567-102, Session PMon

Harnessing atomic layer deposition to directly map the morphology of organic photovoltaic bulk heterojunctions

Stas Obuchovsky, Gitti Frey, Technion-Israel Institute of Technology (Israel)

Investigating the morphology of OPV BHJ is extremely challenging, as no direct high-resolution characterization methods are available for such systems. We show that atomic layer deposition (ALD), a conventional thin-film processing technique, can be used as a characterization tool to directly map the morphology of OPV BHJs. ALD is commonly used for producing conformal coatings on top of a given substrate. However, when applying metal-oxide ALD onto organic materials with no surface reactivity, the precursors diffuse into the organic film and generate a sub-surface deposition of the metal oxide.

Here we demonstrate the use of ALD for studying OPV BHJ morphology by ZnO precursor diffusion and in-situ conversion in P3HT:PCBM blends. We find that PCBM and ZnO compete over the amorphous domains of P3HT, mapping the location of ZnO by HRSEM can be used to identify the vertical distribution and solubility limit of PCBM in P3HT. We find that during film processing PCBM segregates to the bottom interface, its solubility in P3HT is -17%. This study demonstrates a new, alternative and general method for the visual characterization of organic functional blends.

9567-304,

Recent progress on hybrid organicinorganic and perovskite-based solar cells

Yang Yang, Univ. of California, Los Angeles (United States)

By combining the attributes from both organic and inorganic species, the light-harvesting hybrid perovskite (e.g. CH3NH3PbI3) materials possess amazing physical properties that led to high performance solar cells within only a few years of research. Film formation and interface engineering of perovskite materials are crucial parameters that determine the resulting solar cell efficiency. Besides single junction perovskite-based solar cells, research has turned to the tandem devices that combine another low band gap material such as Si in order to achieve even higher efficiency. My presentation will summarize recent progress in this field and report on new results from UCLA (e.g. interface engineering, perovskite-based photodetectors and tandem solar cells).

9567-1, Session 1

To live and let die: The role of excitons in the life of organic devices (Keynote Presentation)

Stephen R. Forrest, Univ. of Michigan (United States)

No Abstract Available



9567-3, Session 1

Design principles in polymer-fullerene bulk-heterojunction solar cells: A focus on PBDTTPD and wide-bandgap analogs (Invited Paper)

Pierre M. Beaujuge, King Abdullah Univ. of Science and Technology (Saudi Arabia)

With published power conversion efficiencies (PCE) >8% in bulkheterojunction (BHJ) solar cells with fullerene acceptors (single cells), and PCEs >10% in tandem devices, solution-processable m-conjugated polymers continue to garner much interest across the PV community. In this context, forging a better understanding of the critical material parameters that impact BHJ device performance is of paramount importance. Our recent work with poly(benzo[1,2-b:4,5-b']dithiophene-thieno[3,4-c] pyrrole-4,6-dione) (PBDTTPD) and wide-bandgap analogs blended with phenyl-C61/71-butyric acid methyl ester (PCBM) sheds light on several structural parameters that critically impact polymer performance, such as the combination of side-chain substituents and the identity of the functional groups appended to the main chain.[1-11] In many instances, morphological aspects are convoluted with the unique pattern of electronic and selfassembling properties of the polymer donor, and broader systematic analyses can help improve our understanding of those correlated effects. [1-11] In parallel, our recent developments show that PBDTTPD and widebandgap analogs (harvesting sunlight in the range 400-650 nm) are some of the most promising systems for use in the high-band-gap cell of tandem and triple-junction solar cells. High-efficiency wide band-gap polymers are required in order to continue improving upon currently reported PCEs in multi-junction solar cells.

[1] Beaujuge, P. M.; Fréchet, J. M. J. JACS 2011, 133, 20009-20029. [2] Piliego, C.; Holcombe, T. W.; Douglas, J. D.; Woo, C. H.; Beaujuge, P. M.; Fréchet; J. M. J. JACS 2010, 132, 7595-7597. [3] Cabanetos, C.; El Labban, A.; Bartelt, J. A.; Douglas, J. D.; Mateker, W. R.; Fréchet, J. M. J.; McGehee, M. D.; Beaujuge, P. M. JACS 2013, 135, 4656-4659. [4] Bartelt, J. A.; Douglas, J. D.; Mateker, W. R.; El Labban, A.; Tassone, C. J.; Toney, M. F.; Fréchet, J. M. J.; Beaujuge, P. M.; McGehee, M. D. Adv. Energy Mater. 2014, 4, 1301733. [5] Warnan, J.; Cabanetos, C.; Bude, R.; El Labban, A.; Li, L.; Beaujuge, P. M. Chem. Mater. 2014, 26, 2829-2835. [6] Warnan, J.; El Labban, A.; Cabanetos, C.; Hoke, E.; Risko, C.; Brédas, J-L.; McGehee, M. D.; Beaujuge, P. M. Chem. Mater. 2014, 26, 2299-2306. [7] Warnan, J.; Cabanetos, C.; El Labban, A.; Hansen, M. R.; Tassone, C.; Toney, M. F.; Beaujuge, P. M. Adv. Mater. 2014, 26, 4357-4362. [8] Graham, K. R.; Cabanetos, C.; Jahnke, J. P.; Idso, M. N.; El Labban, A.; Ngongang Ndjawa, G. O.; Chmelka, B. F.; Amassian, A.; Beaujuge, P. M.; McGehee, M. D. JACS 2014, 136, 9608-9618. [9] El Labban, A.; Warnan, J.; Cabanetos, C.; Ratel, O.; Tassone, C. J.; Toney, M. F.; Beaujuge; P. M. ACS Appl. Mater. & Interfaces 2015, 6, 19477-19481. [10] Dyer-Smith, C.; Howard, I. A.; Cabanetos, C.; El Labban, A.; Beaujuge, P. M.; Laquai, F. Adv. Energy Mater. 2015, Accepted. [11] Wolf, J.; Cruciani, F.; El Labban, A.; Beaujuge, P. M. 2015, Submitted.

9567-4, Session 1

Aggregation and morphology control enables polymer solar cells with efficiencies near 11.5%

He Yan, Hong Kong Univ. of Science and Technology (Hong Kong, China)

Current high-efficiency (>9.0%) PSCs are restricted to materials combinations that are based on limited donor polymers and only one specific fullerene acceptor, PC7IBM. Furthermore, best-efficiency PSCs are mostly based on relatively thin (100 nm) active layers. Here we first report multiple cases of high-performance thick-film (300 nm) PSCs (efficiencies up to 10.8%, fill factors up to 77%) based on conventional PCBM and many non-PCBM fullerenes. Our simple aggregation control and materials design rules allowed us to develop, within a short time, three new donor polymer, six fullerenes (including C60-based fullerenes), and over ten polymer:fullerene combinations, all of which yielded higher efficiency than previous state of art devices (~9.5%). The common structural feature of the three new donor polymers, the 2-octyldodecyl (20D) alkyl chains sitting on quaterthiophene, causes a temperature-dependent aggregation behavior that allows for the processing of the polymer solutions at moderately elevated temperature, and more importantly, controlled aggregation and strong crystallization of the polymer during the film cooling and drying process. This results in a well-controlled and near-ideal polymer:fullerene morphology (containing highly crystalline, preferentially orientated, yet small polymer domains) that is controlled by polymer aggregation during warm casting and thus insensitive to the choice of fullerenes. The 20D structural motif is then further applied to several other polymer backbones and produces three additional polymers with efficiencies between 10-11.5%. Our best efficiency (11.5%) is achieved via the combination of new structural designs, interface and optical engineering and optimizations on the solvents and additives of the polymer:fullerene solution.

9567-44, Session 1

Poly(sulfobetaine methacrylate)s as electrode modifiers for inverted solar cells (*Invited Paper*)

Hyunbok Lee, Egle Puodziukynaite, Todd Emrick, Alejandro L. Briseño, Univ. of Massachusetts Amherst (United States)

We demonstrate the use of polymeric zwitterions, namely, poly(sulfobetaine methacrylate) (PSBMA), as solution-processable work function reducers for inverted organic electronic devices. A notable feature of PSBMA is orthogonal solubility relative to solvents typically employed in the processing of organic semiconductors. A strong permanent dipole moment on the sulfobetaine moiety was calculated by density functional theory. PSBMA interlayers reduced the work function of a broad range of electrodes [indium tin oxide (ITO), Au, Ag, poly(3,4-ethylenedioxythiophene):poly(st yrenesulfonate) (PEDOT:PSS), Cu, Al, and even graphene] by over 1 eV. By employing an ultrathin interlayer of PSBMA, one can reduce the electron injection barrier between ITO and C70 by 0.67 eV. As a result, the device performance of OPVs with PSBMA interlayers are significantly improved, and enhanced electron injection is demonstrated in electron-only devices with ITO, PEDOT:PSS and graphene electrodes. This work makes available a new class of dipole-rich, counterion-free, pH insensitive interlayers for use as strong work function reducers for any electrode.

9567-5, Session 2

Fabricating thin-film photovoltaic devices using ultra-sonic spray-coating (Invited Paper)

David G. Lidzey, The Univ. of Sheffield (United Kingdom)

The scale-up of thin-film electronic devices requires a manufacture tool set that is capable of fabricating thin films at high speed over large areas. One such technique capable of such a task is ultra-sonic spray coating. Here, a target solution is fed onto a vibrating tip that breaks the solution up into very fine droplets, with such droplets being carried to a surface by a gas stream. Such ultra-sonic coating processes are already widely used in Electronics, Medical and Displays industries to create films having excellent smoothness and homogeneity.

In this talk, I describe the use of ultra-sonic spray-coating to deposit a range of materials for thin-film optoelectronics. As our spray-coating system operates in air, it was first necessary to explore the relative sensitivity of various conjugated polymer / fullerene blends to an air-based process route. It is found that carbazole based co-polymers are particularly stable, and can be processed in air (by spin-coating) into organic photovoltaic devices (OPV) without any apparent loss in device efficiency. I then show that spray-coating can be used to deposit a range of semiconductor materials into smooth, thin-films, including PEDOT:PSS, MoOx (from a precursor) and



a series of polymer:fullerene blends. Using such a technique, we are able to scale up an array of devices having an area of 7 cm2, and using a PBDTTT-EFT:PC70BM blend, obtain OPVs having a power conversion efficiency (PCE) of 8.7%. I then discuss spray-coating as a method to fabricate photovoltaic devices based on CH3NH3PbI(3-x)Clx perovskite films. Here, by optimization of deposition parameters, devices are created having a PCE of 11.1%.

9567-6, Session 2

Activating grain boundaries for highperformance hybrid perovskite solar cells

Bin Yang, Oak Ridge National Lab. (United States); Ondrej Dyck, The Univ. of Tennessee Knoxville (United States); Jonathan Poplawsky, Jong Keum, Alexander Puretzky, Oak Ridge National Lab. (United States); Sanjib Das, The Univ. of Tennessee Knoxville (United States); Ilia Ivanov, Christopher Rouleau, Oak Ridge National Lab. (United States); Gerd Duscher, The Univ. of Tennessee Knoxville (United States); David Geohegan, Kai Xiao, Oak Ridge National Lab. (United States)

Grain boundaries (GBs) in the crystal structure detrimentally decrease power conversion efficiency (PCE) in hybrid organometal halide-perovskite solar cells, where defects, traps as well as energetic disorder cause significant non-radiative recombination energy loss. In this talk, we will show that, rather attempting to passivate or eliminate GBs, we activate GBs as active carrier collection channels for increased carrier collection efficiency.1 Space-charge-regions between each grain can suppress nonradiative recombination and enhance carrier collection efficiency. Solar cells with activated GBs yielded average PCE of 16.3±0.9%, comparable to the best solution-processed perovskite devices. Optimizing the morphology and activating the GBs of perovskite solar cells appears to be a promising pathway toward theoretical maximum PCE through industrially realistic processing techniques.

This research was conducted at the Center for Nanophase Materials Sciences ((CNMS)), which is a DOE Office of Science User Facility.

References:

1. B. Yang, et al. Submitted, (2015).

9567-7, Session 2

Additive controlled solution process for high efficiency perovskite solar cells (Invited Paper)

Kai Zhu, National Renewable Energy Lab. (United States)

Methylammonium lead halide perovskites represent a novel class of absorbers for solar conversion applications. Solar conversion efficiencies over 15%–17% have been demonstrated by multiple groups. Various perovskite absorbers (e.g., CH3NH3PbI3, CH3NH3PbI3-xClx, and CH3NH3PbBr3) and device architectures (e.g., mesoporous and planar cell configurations) have been examined with promising results by using either solution processing or thermal evaporation. Controlling the morphology and composition of the perovskite layer has been found critical for developing high-performance perovskite solar cells. Here we demonstrate that the use of chemical additive (e.g., CH3NH3CI) in the precursor affects strongly the perovskite crystallization kinetics and film formation process for both the one-step and two-step sequential solution deposition approaches. For one-step deposition, the additive primarily serves as a glue or soft template to control the initial formation of a solid solution of precursor film. A subsequent thermal decomposition process leads to the formation of perovskite films with good surface coverage and device characteristics. The thermal decomposition process is also found beneficial for accelerating Pbl2-to-perovskite conversion for two-step sequential deposition. The effect of using additive on the structural, optical, and electronic properties

of perovskite films and device characteristics of perovskite solar cells are reported.

9567-9, Session 2

Perovskite thin film formation during solution processing: An In situ timeresolved multiprobe investigation (Invited Paper)

Aram Amassian, King Abdullah Univ. of Science and Technology (Saudi Arabia)

The efficiency of perovskite solar cells has risen at a remarkable pace in recent years. The solution-to-solid phase transformation process leading to the formation of the light harvesting perovskite layer is universally acknowledged as being important to control to achieve efficient perovskite solar cells and has understandably been the subject of several ex situ investigations looking at understanding the perovskite conversion process and the influence of processing conditions, formulations, environmental conditions and surface modifications on the nucleation and growth of perovskite thin films. Yet, despite this great interest in the phase transformation process there are important technical challenges which have prevented in situ time-resolved investigations during the actual solution process (e.g., spin-coating, blade-coating or spray-coating).

We have successfully performed time-resolved in situ grazing incidence wide angle x-ray scattering (GIWAXS) measurements during the spincoating and subsequent thermal annealing of planar and mesostructured perovskite thin films based on three different halides (chlorine, bromine and iodine). The GIWAXS measurements are complemented by in situ optical reflectometry and transmission measurements which can also be performed during spin-coating, making it possible to estimate the solvent evaporation rate, the time-evolution of solution concentration and link the onset of nucleation and subsequent growth of perovskite phases (as detected by GIWAXS and/or UV-vis absorption) to the solution drying process. We will discuss our findings with respect to perovskite thin film formation kinetics and mechanisms for different halides, solution compositions, environmental conditions and substrates.

9567-14, Session 3

Sub-ns triplet state formation in polymer:fullerene photovoltaic blends (Invited Paper)

Frédéric Laquai, Max Planck Institute for Polymer Research (Germany)

I will present recent results on charge generation, recombination, and triplet state formation in various bulk heterojunction photovoltaic blends investigated by femto- to microsecond broadband Vis-NIR transient absorption (TA) pump-probe spectroscopy. Specifically, we looked into the processes following exciton dissociation in low-bandgap polymer and small molecule solar cells using either fullerene or non-fullerene acceptors. As a first example I will show results obtained on the donor-acceptor copolymers PCPDTBT and its silicon-substituted analogue PSBTBT.[1] Here, broadband TA experiments in combination with sophisticated data analyses techniques such as evolving factor analysis (EFA) and multivariate curve resolution with alternating least squares (MCR-ALS) [2] revealed that after exciton dissociation and free charge formation is completed fast subnanosecond non-geminate recombination occurs and leads to a substantial population of the polymer's triplet state. The extent to which triplet states are formed depends on the initial concentration of free charges, which itself is controlled by the microstructure of the blend, especially in case of PCPDTBT:PC60BM. Interestingly, PSBTBT:PC70BM blends showed a higher charge generation efficiency, but less triplet state formation at similar free charge carrier concentrations. This indicates that the solid-state morphology and interfacial structure of PSBTBT:PC70BM blends reduce non-geminate recombination and thus triplet state formation, leading to increased



device performance compared to optimized PCPDTBT:PC60BM blends. Based on the aforementioned observations I will extend the discussion to other material systems relevant for organic photovoltaic devices such as PBDTTPD:PCBM,[3] PBDTTT-C:PCBM and DPP-based copolymers.

9567-15, Session 3

2D- and trap-assisted 2D-Langevin recombination in polymer:fullerene blends

Mathias Nyman, Oskar J. Sandberg, Ronald Österbacka, Åbo Akademi Univ. (Finland)

We have clarified the impact of trapping on the recombination dynamics in polymer:fullerene blends using the highly ordered bulk heterojunction blend poly[2,5-bis(3-tetradecylthiophen-2-yl)thieno[3,2-b]thiophene] (PBTTT) and [6,6]-phenyl-C61-butyric acid methyl ester (PCBM) at different weight ratios as a model system. The recombination dynamics are determined using both transient charge extraction and steady state techniques. In addition, the theory of 2-dimensional Langevin recombination is extended to the case with high trap density.

Using photo-CELIV we show that both the recombination dynamics and the recombination reduction factor in PBTTT:PCBM at a 1:4 weight ratio are consistent with 2D-Langevin. In a 1:1 weight ratio, however, the recombination is much less reduced although the dynamics still roughly follow a \uparrow -3/2 dependence. In order to further elucidate the recombination mechanisms the so called light ideality factor is a useful tool. The light ideality factor describes the slope of the exponential dependence of the recombination mechanisms. Systems displaying 2D-Langevin should have a light ideality factor m = 0.8 whereas m = 1 is expected in the 3D-Langevin case. We measured m = 0.87 in the 1:4 case and m = 1.15 in the 1:1 case.

The recombination capture coefficients are derived both for trap-assisted and band-to-band recombination and it can be seen that anisotropic charge transport reduces the capture coefficients in both cases resulting in a reduced overall recombination.

9567-16, Session 3

Manipulation of the dielectric constant of non-fullerene organic semiconductors (Invited Paper)

Paul L. Burn, Jenny Donaghey, Ardalan Armin, Paul Meredith, The Univ. of Queensland (Australia)

Inorganic (crystalline) semiconductors used in solar cells have a high dielectric constant (?r > 10) that results in a low exciton binding energy (C.f. Si: 15.0 meV; GaAs: 4.2 meV; CdTe: 10.5 meV). Such low binding energies make inorganic devices operate in a 'non-excitonic' regime at room temperature. Conversely, organic semiconductors have typically low dielectric constants (?r < 4) and exciton binding energies of several hundreds meV. Thus, homojunction organic diodes tend to have low efficiency as neither thermal activation nor external electric field are sufficient to efficiently overcome the strong Coulombic interaction of the excitons. Recently, Hummelen et al have shown that the introduction of triethylene glycol monoethyl ether (TEG) chains to fulleropyrrolidines resulted in a 46% increase in dielectric constant [1]. In this presentation we discuss how non-fullerene acceptors can be engineered to give high film dielectric constants and how the dielectric constant affects the optoelectronic properties.

[1] Jahani, F.,Torabi, S.,Chiechi, R. C.,Koster, L. J. A.,Hummelen, J. C. Chem. Commun. 2014, 50, 10645.

9567-17, Session 3

Exciton binding energy limitations in organic materials and potentials for improvements

Stefan Kraner, Reinhard Scholz, Technische Univ. Dresden (Germany); Eric Müller, Martin Knupfer, Leibniz-Institut für Festkörper- und Werkstoffforschung Dresden (Germany); Christian Koerner, Karl Leo, Technische Univ. Dresden (Germany)

In current organic photovoltaic devices, the loss in energy caused by the inevitable charge transfer step leads to a low open circuit voltage, which is one of the main reasons for rather low power conversion efficiencies. A possible approach to avoid these losses is to tune the exciton binding energy below 25 meV, which would lead to free charges upon absorption of a photon, and therefore increase the power conversion efficiency towards the Shockley Queisser limit for inorganic solar cells. We determine the size of the excitons for different one-dimensional organic small molecules or polymers by electron energy loss spectroscopy (EELS) measurements and by DFT calculations. Using the measured dielectric constant and exciton extension, the exciton binding energy is calculated for the investigated molecules, leading to a lower limit of the exciton binding energy for laddertype polymers. We discuss and propose potential ways to increase the ionic and electronic part of the dielectric function in order to further lower the limit of the exciton binding energy in organic materials. Furthermore, the influence of charge transfer states on the exciton size and its binding energy is calculated with DFT methods for the ladder-type polymer poly(benzimida zobenzophenanthroline) (BBL) in a dimer configuration.

9567-18, Session 3

Conditions for charge transport without recombination in low mobility organic solar cells and photodiodes

Martin Stolterfoht, Ardalan Armin, The Univ. of Queensland (Australia); Bronson Philippa, Ronald D. White, James Cook Univ. (Australia); Paul L. Burn, Paul Meredith, The Univ. of Queensland (Australia); Gytis Ju?ka, Vilnius Univ. (Lithuania); Almantas Pivrikas, The Univ. of Queensland (Australia)

Organic semiconductors typically possess low charge carrier mobilities and Langevin-type recombination dynamics, which both negatively impact the performance of organic solar cells and photodetectors. Charge transport in organic solar cells is usually characterized by the mobility-lifetime product. Using newly developed transient and steady state photocurrent measurement techniques we show that the onset of efficiency limiting photocarrier recombination is determined by the charge that can be stored on the electrodes of the device. It is shown that significant photocarrier recombination can be avoided when the total charge inside the device, defined by the trapped, doping-induced and mobile charge carriers, is less than the electrode charge. Based upon this physics we propose the mobilityrecombination coefficient product as an alternative and more convenient figure of merit to minimize the recombination losses. We validate the results in 3 different organic semiconductor-based light harvesting systems with very different charge transport properties. The findings allow the determination of the charge collection efficiency in fully operational devices. In turn, knowing the conditions under which non-geminate recombination is eliminated enables one to quantify the generation efficiency of free charge carriers. The results are relevant to a wide range of light harvesting systems, particularly those based upon disordered semiconductors, and require a rethink of the critical parameters for charge transport.



9567-10, Session 4

Colored ultra-thin hybrid photovoltaics with high quantum efficiency for decorative PV applications (Invited Paper)

L. Jay Guo, Univ. of Michigan (United States)

This talk will describe an approach to create architecturally compatible and decorative thin-film-based hybrid photovoltaics [1]. Most current solar panels are fabricated via complex processes using expensive semiconductor materials, and they are rigid and heavy with a dull, black appearance. As a result of their non-aesthetic appearance and weight, they are primarily installed on rooftops to minimize their negative impact on building appearance. Recently we introduced dual-function solar cells based on ultra-thin dopant-free amorphous silicon embedded in an optical cavity that not only efficiently extract the photogenerated carriers but also display distinctive colors with the desired angle-insensitive appearances [1,2]. The angle-insensitive behavior is the result of an interesting phase cancellation effect in the optical cavity with respect to angle of light propagation [3]. In order to produce the desired optical effect, the semiconductor layer should be ultra-thin and the traditional doped layers need to be eliminated. We adopted the approach of employing charge transport/blocking layers used in organic solar cells to meet this demand. We showed that the ultra-thin (6 to 31 nm) undoped amorphous silicon/organic hybrid solar cell can transmit desired wavelength of light and that most of the absorbed photons in the undoped a-Si layer contributed to the extracted electric charges. This is because the a-Si layer thickness is smaller than the charge diffusion length, therefore the electron-hole recombination is strongly suppressed in such ultra-thin layer. Reflective colored PVs can be made in a similar fashion. Light-energy-harvesting colored signage was demonstrated. Furthermore, a cascaded photovoltaics scheme based on tunable spectrum splitting can be employed to increase power efficiency by absorbing a broader band of light energy. Our work provides a guideline for optimizing a photoactive layer thickness in high efficiency hybrid PV design, which can be adopted by other material systems as well. Based on these understandings, we have also developed colored perovskite PV by integrating an optical cavity with the perovskite semiconductors [4]. The principle and experimental results will be presented.

1. J. Y. Lee, K. T. Lee, S.Y. Seo, L. J. Guo, "Decorative power generating panels creating angle insensitive transmissive colors," Sci. Rep. 4, 4192, 2014.

2. K. T. Lee, J.Y. Lee, S.-Y. Seo, and L. J. Guo, "Colored ultra-thin hybrid photovoltaics with high quantum efficiency," Light: Science & Applications, 3, e215, 2014.

3. K. T. Lee, S.-Y. Seo, J.Y. Lee, and L. J. Guo, "Ultrathin metal-semiconductormetal resonator for angle invariant visible band transmission filters," Appl. Phys. Lett. 104, 231112, (2014); and "Strong resonance effect in a lossy medium-based optical cavity for angle robust spectrum filters," Adv. Mater, 26, 6324–6328, 2014.

4. K. T. Lee, M. Fukuda, L. J. Guo, "Colored, see-through perovskite solar cells employing an optical cavity," Submitted, 2015

9567-11, Session 4

Nano-photonic organic solar cell architecture for advanced light management utilizing dual photonic crystals (Invited Paper)

Akshit Peer, Rana Biswas, Iowa State Univ. (United States) and Ames Lab. (United States)

Organic solar cells have rapidly increasing efficiencies, but typically absorb less than half of the incident solar spectrum. To increase broadband light absorption, we rigorously design experimentally realizable solar cell architectures based on dual photonic crystals. Our optimized architecture consists of a polymer microlens at the air-glass interface, coupled with a photonic-plasmonic crystal at the metal cathode. The microlens focuses light on the periodic nanostructure that generates strong light diffraction. Waveguiding modes and surface plasmon modes together enhance long wavelength absorption in P3HT-PCBM. The architecture has a period of 500 nm, with absorption and photocurrent enhancement of 49% and 58%, respectively.

9567-13, Session 4

Nanophotonic light management strategies for ultrathin solar cells (Invited Paper)

Mark L. Brongersma, Geballe Lab. for Advanced Materials (GLAM) (United States)

Nanophotonics is an exciting new field of science and technology that is directed towards making the smallest possible structures and devices that can manipulate light. In this presentation, I will start by showing how semiconductor and metallic nanostructures can mold the flow of light well below the free-space wavelength of light. I will then discuss how dense arrays of such nanostructures can effectively enhance light absorption in ultrathin solar cells, especially when the size and spacing between the structures is at a deep-subwavelength scale. The use of subwavelength arrays is distinct from conventional light trapping strategies that are aimed at coupling sunlight to quasi-guided modes of the high-index semiconductor layer(s) of a solar cell. I will explain how the size, shape and arrangement of nanostructures can be engineered to achieve near-unity absorption across a broad spectrum.

9567-19, Session 5

Photocurrent hysteresis and switchable organometal trihalide perovskite photovoltaic

Jinsong Huang, Univ. of Nebraska-Lincoln (United States)

The large photocurrent hysteresis observed in many organometal trihalide perovskite (OTP) solar cells has become a major hindrance impairing the ultimate performance and stability of these devices. Here we will report two device structures with completely different behaviors upon photocurrent scanning: one with eliminated photocurrent hysteresis (1), and the other with completely switchable photocurrent direction (2).

We showed the trap states on the surface and grain boundaries of the perovskite materials to be the origin of photocurrent hysteresis and that the fullerene layers deposited on perovskites can effectively passivate these charge trap states and eliminate the notorious photocurrent hysteresis. Fullerenes deposited on the top of the perovskites reduce the trap density by two orders of magnitude and double the power conversion efficiency of CH3NH3PbI3 solar cells to near 19%. The elucidation of the origin of photocurrent hysteresis and its elimination by trap passivation in perovskite solar cells provides important directions for enhancements to device efficiency.

In another device structure without fullerene, we showed that in OTPbased photovoltaic devices with vertical and lateral cell configurations, the photocurrent direction can be switched repeatedly by applying a small electric field of <1 V ?m?1. The switchable photocurrent, generally observed in devices based on ferroelectric materials, reached 20.1 mA cm?2 under one sun illumination in OTP devices with a vertical architecture, which is four orders of magnitude larger than that measured in other ferroelectric photovoltaic devices. This field-switchable photovoltaic effect can be explained by the formation of reversible p-i-n structures induced by ion drift in the perovskite layer.

1. Origin and Elimination of Photocurrent Hysteresis by Fullerene Passivation in CH3NH3PbI3 Planar Heterojunction Solar Cells, Yuchuan Shao, Zhengguo Xiao, Cheng Bi, Yongbo Yuan, and Jinsong Huang^{*}. Nature Communications, In Press (2014)

2. Giant Switchable Photovoltaic Effect in Organometal Trihalide Perovskite Devices, Zhengguo Xiao, Yongbo Yuan, Yuchuan Shao, Qi Wang,Qingfeng Dong, Cheng Bi, Pankaj Sharma, Alexei Gruverman, and Jinsong Huang*. Nature Materials, In Press (2015)



9567-20, Session 5

A comparison of perovskite and colloidal quantum dot solar cells (Invited Paper)

Brandon R. Sutherland, Edward H. Sargent, Univ. of Toronto (Canada)

In this talk, we review the progress of perovskite and colloidal quantum dot solar cells and discuss their future prospects. We detail the fundamental differences in these two materials, the current challenges that they face and must overcome, as well as discuss their potential synergy in new and exciting architectures.

9567-21, Session 5

Hysteresis-free, stable and efficient perovskite solar cells achieved by vacuumtreated thermal annealing of CH3NH3PbI3

Feng-Xian Xie, Di Zhang, Wallace C. H. Choy, The Univ. of Hong Kong (Hong Kong, China)

CH3NH3I and PbCI2 mixture are the most commonly used materials in the deposition solution in one step planar structures. Since the crystallization process of CH3NH3PbI3 can be controlled during the phase of forming intermediate organometal mixed halide, the photovoltaic properties of the perovskite films are typically superior to those of films formed directly in one step precipitation process from a CH3NH3I and PbI2 mixture. Nevertheless, controlling the crystallization process of perovskite films remains a challenging issue. The CH3NH3PbI3 perovskite crystallization is strongly affected by the ambient, which in turn can compromise the performance and reproducibility of the perovskite device. Therefore, an effective approach for enhancing the morphology of perovskite films through controlling their crystallization process is highly desired.

Here, we propose a vacuum-assisted thermal annealing method for providing favorable environment for effectively controlling the crystallization of the perovskite films. Besides confirming the generation of MACI byproduct, our studies indicate that MACI plays a critical role during the perovskite film formation and device degradation. By promoting the release of MACI and suppressing residual MACI in the film through the vacuum-assisted thermal annealing, we are able to obtain pore-free and well crystallized pure triiodide (CH3NH3PbI3) perovskite films that contained no residual chloride species. As a result, we realize highly stable and efficient solar cells displaying excellent reproducibility (15.60 ± 0.92% among 60 devices; highest PCE: 14.52%) and a very small photocurrent hysteresis effect [1]. We believe that this approach will also enable further improvements in the performance of related perovskite materials.

[1] F.X. Xie, D. Zhang, H. Su, X. Ren, K.S. Wong, M. Grätzel, W.C.H. Choy, "Vacuum-Assisted Thermal Annealing of CH3NH3PbI3 for Highly Stable and Efficient Perovskite Solar Cells", ACS Nano, in press.

9567-22, Session 6

Charge generation and charge transfer processes in organic and hybrid (organicinorganic) solar cell materials (Invited Paper)

Natalie Banerji, Univ. de Fribourg (Switzerland)

The generation of free charge carriers is a key in the functioning of any solar cell. In all-organic polymer:fullerene materials, excitons are generated by light absorption and they must be dissociated by charge separation between the electron donor (polymer) and the electron acceptor (fullerene). We will address our recent advances in understanding the charge generation process in a variety of polymer:fullerene blends, where the phase morphology and microstructure were carefully controlled during

film processing. Ultrafast transient absorption, electro-absorption (Stark effect) and fluorescence spectroscopies were used. We will also present preliminary results about charge transfer from methyl ammonium lead iodide to conjugated polymers, revealing information about the nature and generation of charges in the highly efficient perovskite materials.

9567-23, Session 6

The role of charge transfer states in organic photovoltaic blends

Remco W. Havenith, Hilde D. de Gier, Ria Broer, Univ. of Groningen (Netherlands)

Charge separation in organic photovoltaic blends occurs at the donor/ acceptor interface. In these blends, a manifold of charge transfer (CT) states exists, and it is not clear whether the lowest charge transfer states are involved in charge carrier generation, or act as trap states.

We discuss here how we model these blends using a combined quantum mechanical and molecular dynamics approach, and present results on the nature of the different CT states, their dependence on the size of the model used, and how the environment influences them. The first two studies will show whether delocalisation effects are important in charge carrier generation. The latter study demonstrates how the local environment, which can be modified by the introduction of dipoles or polarisable groups, influences charge separation.

Furthermore, electronic couplings between the initially excited state on the polymer and the various CT states are calculated to estimate the rates of electron transfer to the different target CT states. From these rates, we can determine which of the states are involved in the charge separation process. These couplings are studied as a function of chemical composition of the blends, and for various conformations. The results of this study show how the charge transfer process is influenced by the local structure of the donor/ acceptor interface. It will also reveal whether the lowest CT states act as trap states, and how that can be circumvented. This information is used in the design of the next generation organic photovoltaic blends with a higher efficiency.

9567-24, Session 6

Charge transfer and triplet states in OPV materials and devices (Invited Paper)

Vladimir Dyakonov, Julius-Maximilians-Univ. Würzburg (Germany)

Electron back transfer (EBT), potentially occurring after electron transfer from donor to acceptor may populate the lower lying donor or acceptor triplet state and serve as recombination channel.[1] Here we report on studies of charge transfer and triplet states in blends of highly efficient benzodithiophene PTB7 polymer in combination with the fullerenederivative PC71BM using the spin sensitive optically detected magnetic resonance (ODMR) technique and compare the results with those obtained in P3HT (poly(3- hexylthiophene):PC61BM blends. Although PTB7:PC71BM absorbers yield much higher power conversion efficiencies in solar cells exceeding 7%, we found a significant increase of triplet exciton generation, which was absent in the P3HT based blends. We discuss this observation within the EBT scenario with the emphasis on the influence of morphology, fullerene load, HOMO/LUMO energy and presence of additives (DIO). Suppressing the EBT process by morphology and/or energetics of polymer and molecules is important to achieve the full potential of highly efficient OPV materials. [1] M. Liedtke, et al., JACS 133, 9088 (2011).



9567-25, Session 6

Charge transfer states as traps in organic solar cells

Andreas Arndt, Karlsruher Institut für Technologie (Germany); Marina Gerhard, Philipps-Univ. Marburg (Germany); Aina Quintilla, Ian Howard, Karlsruher Institut für Technologie (Germany); Martin Koch, Philipps-Univ. Marburg (Germany); Uli Lemmer, Karlsruher Institut für Technologie (Germany)

We investigate the NIR time-resolved photoluminescence of a series of P3HT:PC61BM solar cells with varying blend ratios after preferential excitation of the PC61BM and P3HT components respectively.

Besides the rapid and diffusion-limited quenching of singlet excitons we resolve a weak emission feature in the near-infrared that our measurements confirm comes from interfacial charge-transfer (CT) states. This CT state emission becomes stronger for samples with an excess of PC6IBM, and also after selective excitation of the PC6IBM component. In this way, we show that these NIR time-resolved photoluminescence measurements provide an accurate method of observing subtle changes in the formation and dynamics of CT states at organic heterojunctions due to its high selectivity, and suggest that PC6IBM excitons are more likely to lead to geminately recombining CT states than are the excitons created on P3HT.

We also measure the temperature dependence of the transient NIR photoluminescence and find that while the intensity of the NIR emission is temperature dependent, its lifetime is not. This interesting observation suggests that the CT states we observe are formed through a precursor state which can either form separated charges or CT states, and that the relative yield of these two pools is temperature dependent. Furthermore, it indicates that charges within these relaxed CT states are trapped at the donor-acceptor interface and cannot contribute to free-charge generation via thermal activation anymore.

9567-26, Session 6

Charge-transfer absorption, emission, and the open-circuit voltage of organic solar cells (Invited Paper)

Koen Vandewal, Technische Univ. Dresden (Germany)

Electronic processes at the organic hetero-interface limit the photocurrent and photovoltage of organic solar cells. While devices with incidentphoton-to-extracted-charge conversion yields of over 85%, and absorbed photon-to-extracted-charge conversion yields of 90-100% have been achieved, the difference between the optical gap of main absorber and open-circuit voltage (Voc) is much larger than for inorganic solar cells. The main improvements in the Voc of organic solar cells have so far been made by tailoring the donor-acceptor interfacial energetics, taking advantage of well-known principles of molecular design. Nevertheless, for most material systems we consistently find a large (>0.55 eV) difference between eVoc and the energy of the intermolecular charge transfer (CT) state. We present experimental evidence that this difference can be reduced by reducing the physical interfacial area available for free carrier recombination. We quantify this by analyzing the strength of the interfacial CT state absorption and emission signal at photon energies below the optical gap of the neat materials. We further discuss the influence of the measured electronic coupling, molecular reorganization and non-radiative recombination pathways on Voc. This work opens up unexplored possibilities for increasing the Voc of organic solar cells, bringing it closer to the optical gap of the main absorber.

9567-27, Session 6

Theory and assignment of intermolecular charge transfer states in squaraines and their impact on efficiency in bulk heterojunction solar cells

Christopher J. Collison, Chenyu Zheng, Rochester Institute of Technology (United States); Nicholas Hestand, Temple Univ. (United States); Brandon Cona, Anirudh Penmetcha, Susan Spencer, Jeremy Cody, Rochester Institute of Technology (United States); Frank Spano, Temple Univ. (United States)

Squaraines are targeted for organic photovoltaic devices because of their high extinction coefficients over a broad wavelength range from visible to near infra-red (NIR). Moreover, their side groups can be changed with profound effects upon their ability to crystallize, leading to improvements in charge mobility and exciton diffusion.

The broadening in squaraine absorption is often qualitatively attributed to H- and J-aggregates based on the exciton model, proposed by Kasha. However, such assignment is misleading considering that spectral shifts can arise from sources other than excitonic coupling. Our group has shown that packing structure influences the rate of charge transfer; thus a complete and accurate reassessment of the excited states must be completed before the true charge transfer mechanism can be confirmed.

In this work, we will show how squaraine H-aggregates can pack in complete vertical stacks or slipped vertical stacks depending upon sidegroups and processing conditions. Hence, we uncover the contribution of an intermolecular charge transfer (IMCT) state through essential states modeling validated by spectroscopic and X-Ray diffraction data.

We further show external quantum efficiency data that describe the influence of the IMCT state on the efficiency of our devices.

This comprehensive understanding of squaraine aggregates drives the development of more efficient organic photovoltaic devices, leading towards a prescription for derivatives that can be tailored for optimized exciton diffusion, charge transfer, higher mobilities and reduced recombination in small molecule OPV devices.

9567-28, Session 7

Rational material, interface, and device engineering for high-performance polymer and perovskite solar cells (Invited Paper)

Alex K-Y Jen, Univ. of Washington (United States)

The performance of polymer and hybrid solar cells is also strongly dependent on their efficiency in harvesting light, exciton dissociation, charge transport, and charge collection at the metal/organic/metal oxide or the metal/perovskite/metal oxide interfaces. Our laboratory employs a molecular engineering approach to develop processible low bandgap polymers with high charge carrier mobility that can enhance power conversion efficiency of the single junction solar cells to values as high as ~11%. We have also developed several innovative strategies to modify the interface of bulk-heterojunction devices and create new device architectures to fully explore their potential for solar applications.

In this talk, the integrated approach of combining material design, interface, and device engineering to significantly improve the performance of polymer and hybrid perovskite photovoltaic cells will be discussed. Specific emphasis will be placed on the development of low band-gap polymers with reduced reorganizational energy and proper energy levels, formation of optimized morphology of active layer, and minimized interfacial energy barriers using functional conductive surfactants. At the end, several new device architectures and optical engineering strategies to make tandem cells and semitransparent solar cells will be discussed to explore the full promise of polymer and perovskite hybrid solar cells.



9567-29, Session 7

Vacuum deposited triple absorber organic solar cells (OSCs)

Karsten Walzer, Heliatek GmbH (Germany)

Thanks to the availability of doped hole and electron transport layers, which allow the fabrication of nearly loss-free charge transport and charge conversion layers, vacuum deposited organic solar cells (OSCs) can be easily stacked as monolithically connected multiple devices, such as tandem or triple OSCs.

We report on triple absorber layer devices as a route to reliable and production relevant OSC stacks. Already in early 2013, Heliatek achieved an independently certified 12% efficiency device, which used using twice the same orange-red broad-band absorber in combination with an efficient green absorber. Recently, we found a class of infrared absorbers that can extend the solar harvesting of vacuum processable OSCs to the near infrared beyond 900 nm, which gives access to triple absorber devices using three different absorbers. Thus, both the energy rich visible and the NIR part of the solar spectrum can be absorbed by the OSC. We will report about the latest developments in such devices, as well as giving a brief update about the current status of the vacuum-based roll-to-roll volume production of small molecule tandem OSCs.

9567-30, Session 7

High performance x-ray imaging detectors on foil using solution-processed organic photodiodes with extremely low dark leakage current

Abhishek Kumar, Date Moet, Jan Laurens van der Steen, Albert van Breemen, Santhosh Shanmugam, Jan Gilot, Ronn Andriessen, Holst Ctr. (Netherlands); Matthias Simon, Philips Research (Netherlands); Walter Ruetten, Alexander Douglas, Philips Research (Netherlands); Rob Raaijmakers, Philips Healthcare (Netherlands); Pawel E. Malinowski, Kris Myny, IMEC (Belgium); Gerwin Gelinck, Holst Ctr. (Netherlands) and Technische Univ. Eindhoven (Netherlands)

We demonstrate high performance X-ray imaging detectors on foil suitable for medical grade X-ray imaging applications. The detectors are based on solution-processed organic photodiodes forming bulk-heterojunctions from photovoltaic donor and acceptor blend. The organic photodiodes are deposited using an industrially compatible slot die coating technique with end of line processing temperature below 100° C. These photodiodes have extremely low dark leakage current density of 10-7 mA/cm2 at -2V bias with very high yield and have peak absorption around 550 nm wavelength. We combine these organic photodiodes with high mobility metal oxide semiconductor based thin film transistor arrays with high pixel resolution of 200ppi on thin plastic substrate. When combined with a typical CsI(TI) scintillator material on top, they are well suited for low dose X-ray imaging applications. The optical crosstalk is insignificant upto resolution of 200 ppi despite the fact that the photodiode layer is one continuous layer and is non-pixelated. Low processing temperatures are another key advantage since they can be fabricated on plastic substrate. This implies that we can make X-ray detectors on flexible foil. Those detectors can be mechanically more robust and light weight when compared to amorphous Si based detectors fabricated on glass substrate.

9567-31, Session 7

High performance all polymer solar cells fabricated via non-halogenated solvents

Yan Zhou, Zhenan Bao, Stanford Univ. (United States)

The performance of organic solar cells consisting of a donor/acceptor bulk heterojunction (BHJ) has rapidly improved over the past few years.1. Major efforts have been focused on developing a variety of donor materials to gain access to different regions of the solar spectrum as well as to improve carrier transport properties.2 On the other hand, the most utilized acceptors are still restricted to the fullerene family, which includes PC61BM, PC71BM and ICBA.2b, 3 All-polymer solar cells, consisting of polymers for both the donor and acceptor, gained significantly increased interests recently, because of their ease of solution processing, potentially low cost, versatility in molecular design, and their potential for good chemical and morphological stability due to entanglement of polymers. Unlike small molecular fullerene acceptors, polymer acceptors can benefit from the high mobility of intra-chain charge transport and exciton generation by both donor and acceptor.

Despite extensive efforts on all-polymer solar cells in the past decade, the fundamental understanding of all-polymer solar cells is still in its inceptive stage regarding both the materials chemistry and structure physics.4 Thus, rational design rules must be utilized to enable fundamental materials understanding of the all polymer solar cells.

We report high performance all-polymer solar cells employing polymeric donors based on isoindigo and acceptor based on pervlenedicarboximide. The phase separation domain length scale correlates well with the JSC and is found to be highly sensitive to the aromatic co-monomer structures used in the crystalline donor polymers. With the PS polymer side chain engineering, the phase separation domain length scale decreased by more than 45%. The PCE and JSC of the devices increased accordingly by more than 20%. A JSC as high as 10.0 mA cm?2 is obtained with the donoracceptor pair despite of a low LUMO-LUMO energy offset of less than 0.1 eV. All the factors such as crystallinity, surface roughness, charge carrier mobility, and absorptions of the polymers blends are found irrelevant to the performance of these all polymer solar cells. This work demonstrates that a better understanding of tuning polymer phase separation domain size provides an important path towards high performance, all-polymer solar cells. The use of polymer side-chain engineering provides an effective molecular engineering approach that may be combined with additional processing parameter control to further elevate the performance of allpolymer solar cells. We obtained a record PCE of 4.8% (avarage from 20 devices), with an average JSC of 9.8 mA cm-2. The highest PCE shoots to 5.1%, with JSC as high as 10.2 mA cm-2, and VOC of 1.02 V. It is the highest performance ever published for an all-polymer solar cell.4

1. Li, G.; Zhu, R.; Yang, Y., Nat. Photon. 2012, 6 , 153-161.

2. (a) Nelson, J., Mater. Today 2011, 14 , 462-470; (b) Lin, Y.; Li, Y.; Zhan, X., Chem. Soc. Rev. 2012, 41, 4245-4272; (c) Chen, J.; Cao, Y., Acc. Chem. Res. 2009, 42, 1709-1718.

Sonar, P.; Fong Lim, J. P.; Chan, K. L., Energy Environ. Sci. 2011, 4, 1558.
 Facchetti, A., Mater. Today 2013, 16, 123-132.

9567-32, Session 7

Design of low band gap small molecules with alkyldicyanovinyl acceptor and different donor groups for efficient bulk heterojunction organic solar cells

Sergey A. Ponomarenko, Institute of Synthetic Polymeric Materials (Russian Federation) and Lomonosov Moscow State Univ. (Russian Federation); Yuriy N. Luponosov, Institute of Synthetic Polymeric Materials (Russian Federation); Jie Min, Friedrich-Alexander-Univ. Erlangen-Nürnberg (Germany); Alexander N. Solodukhin, Maxim A. Shcherbina, Sergey N. Chvalun, Institute of Synthetic Polymeric Materials (Russian Federation); Tayebeh Ameri, Friedrich-Alexander-Univ. Erlangen-Nürnberg (Germany); Christoph J. Brabec, Friedrich-Alexander-Univ. Erlangen-Nürnberg (Germany) and Bayerisches Zentrum für Angewandte Energieforschung e.V. (Germany)



Nowadays soluble small molecule organic semiconductors play a significant role in organic photovoltaics, leading to highly efficient solution-processable devices. In this work an approach to creation of a library of low band gap small molecules with alkyldicyanovinyl acceptor linked through (oligo) thiophene conjugated spacers to different donor groups, including but not limited to triphenylamine, tris(2-methoxyphenyl)amine or dithienosilole units, was elaborated. Due to intramolecular charge transfer and aggregation in the solid state they absorb the solar light in a wide spectral range, from 300-400 to 650-900 nm. Alkyldicyanovinyl groups differ from regular dicyanovinyl groups by better solubility and higher stability due to the absence of acidic proton. Systematic variations of the alkyl chain length and the number of conjugated thiophene rings in the molecules allowed to elucidate the relationship between their molecular structure and different physical properties, including their solubility, absorption spectra, phase behavior, morphology and structure in thin films, as well as semiconducting and photovoltaic properties. Bulk heterojunction organic solar cells (BHJ OSC) prepared from these molecules as donors and PCBM[70] as acceptor by solution processing showed power conversion efficiency up to 5.4 -6.3%. The peculiarities of these molecules in BHJ OSC are high open circuit voltage Voc, up to 0.96 – 1.08 V, and relatively high fill factor FF, up to 54 - 69%, which can be achieved by special interface design or solvent vapor annealing. Some of these molecules form columnar mesophases, which bring an additional factor for further improving their efficiencies by possible ordering of the bulk heterojunction structure.

9567-33, Session 8

Harnessing the diffusion of small molecules in OPV films for processing and characterization of BHJs (Invited Paper)

Gitti Frey, Technion-Israel Institute of Technology (Israel)

The efficiency of OPVs critically depends on the nano- and mesoscale morphology of the donor: acceptor BHJ which is directed by the phase separation and mutual solubility of both constituents. The "soft" characteristics of the BHJ allows kinetic and/or thermodynamic modulations of the morphology. For example, it is post-processing thermal and solvent annealing are common processing protocols. Here we show how the tendency of small molecules to diffuse through "soft" materials can also be harnessed to direct and even study the morphology of OPV BHJs. This approach is demonstrated in two systems: i) the spontaneous migration of selected additives from within the active layers to form interlayers at the organic/metal interface. Using a plethora of techniques, we show that the migration, which occurs during the metal evaporation process, is driven by the metal-additives interactions and can enhance the Voc and device efficiency. ii) the diffusion of atomic layer deposition (ALD) precursors into the active layer can be used to directly map the morphology of OPV BHJs and to fabricate new hybrid PV structures. More specifically, we use the ALD of ZnO inside OPV films to spatially map the amorphous and crystalline domain of P3HT, the distribution of PCBM; and to fabricate new hybrid PV devices.

9567-34, Session 8

Impact of molecular mixing on open circuit voltage of bulk heterojunction solar cells

Swaminathan Venkatesan, Qiquan Qiao, Cheng Zhang, South Dakota State Univ. (United States); Wei Chen, Argonne National Lab. (United States); Jihua Chen, Oak Ridge National Lab. (United States)

Role of donor-acceptor ratios on the morphology and charge transport in bulk heterojunction solar cells consisting of highly self-ordered semiconducting polymers are studied. It is found that the open circuit voltage linearly increases when fullerene loading is increased from 1:1 to 1:4 donor-acceptor mixing ratio. The active layer morphology is characterized using AFM topography, phase, Kelvin probe force microscopy (KPFM) and energy filtered transmission electron microscopy (EFTEM). With higher fullerene mixing ratios smaller domains and finer phase separation is observed. Surface potential distribution from KPFM images reveal that higher fullerene loading leads to higher surface potential variation (higher FWHM). EFTEM results showed higher polymer aggregation in blends having 1:1 and 1:2 donor acceptor ratios. Further films were also characterized using grazing incidence wide angle x-ray scattering (GIWAXS) which showed highly ordered polymer domains having edge on orientation in 1:1 and 1:2 blend films. When fullerene loading was increased to 1:3 and 1:4, smaller crystallites of polymer domains are observed which orient in random directions. Device performance was studied for six different blend ratios and 1:4 ratio was found to be optimum for achieving best photovoltaic performance. Further photo-generated charge carrier extraction using linearly increasing voltage (P-CELIV) measurements show that the optimum mixing ratio leads to the highest charge carrier density, mobility and lowest bimolecular recombination. These results indicate the crucial role of fullerene loading for achieving the ideal morphology and avoiding polymer aggregation during film formation for efficient photovoltaic devices.

9567-35, Session 8

Morphology control for efficient and stable small molecule organic solar cells

Hideyuki Tanaka, Eiichi Nakamura, The Univ. of Tokyo (Japan)

Printable organic solar cells (OSCs) have received much attention because of their attractive advantage such as large scale, lightweight, low cost and facile fabrication process. In these solution-processable OSCs, bicontinuous network structure of phase-separated electron donor and acceptor materials in nanoscale becomes most crucial factor to realize high power conversion efficiency (PCE). The phase separation has been widely investigated with the bulk-heterojunction (BHJ) concept by use of pi-conjugated polymer and fullerene derivative. Small molecular materials also can be a good candidate material for the solution-processable OSCs, however, there are very few reports due to the difficulty constructing the nano scale phase separation despite it has practical advantages such as ease purification and high stability. Here, we demonstrate the new approach for fabricating efficient small molecular OSCs through controlling of phase-separation of binary blend of donor molecules and non-active soft materials. We found that the limited molecular diffusion of donor molecules within highly viscous soft matrix play a key role for the nano-scale phase separation. A 20-30 nm sized BP crystal can be created within a highly viscous matrix (TCTA), and that provides efficient charge carrier generation system showing high PCE of 7.8%.

9567-36, Session 8

Morphological study on small molecule acceptor-based organic solar cells with efficiencies beyond 7%

Wei Ma, Xi'an Jiaotong Univ. (China); He Yan, Hong Kong Univ. of Science and Technology (Hong Kong, China)

Despite the essential role of fullerenes in achieving best-performance organic solar cells (OSCs), fullerene acceptors have several drawbacks including poor light absorption, high-cost production and purification. For this reason, small molecule acceptor (SMA)-based OSCs have attracted much attention due to the easy tunability of electronic and optical properties of SMA materials. In this study, polymers with temperature dependent aggregation behaviors are combined with various small molecule acceptor materials, which lead to impressive power conversion efficiencies of up to 7.3%. The morphological and aggregation properties of the polymer:small molecule blends are studied in details. It is found that the temperature-dependent aggregation behavior of polymers allows for the processing of the polymer solutions at moderately elevated temperature, and more importantly, controlled aggregation and strong crystallization of the polymer during the film cooling and drying process. This results in a well-controlled and near-ideal polymer:small molecule morphology that is



controlled by polymer aggregation during warm casting and thus insensitive to the choice of small molecules. As a result, several cases of highly efficient (PCE between 6-7.3%) SMA OSCs are achieved. The second part of this presentation will describe the morphology of a new small molecule acceptor with a unique 3D structure. The relationship between molecular structure and morphology is revealed.

9567-37, Session 8

Mechanical stability of organic solar cells: Molecular and microstructural determinants

Darren J. Lipomi, Suchol Savagatrup, Adam D. Printz, Timothy F. O'Connor, Aliaksandr V. Zaretski, Univ. of California, San Diego (United States)

The mechanical properties of organic semiconductors and the mechanical failure mechanisms of devices play critical roles in the yield of modules in roll-to-roll manufacturing and the operational stability of organic solar cells (OSCs) in portable and outdoor applications. This talk begins by reviewing the mechanical properties-principally stiffness and brittleness-of pure films of organic semiconductors. It identifies several determinants of the mechanical properties including molecular structures, polymorphism, and microstructure and texture. Next, a discussion of the mechanical properties of polymer:fullerene bulk heterojunction blends reveals the strong influence of the size and purity of the fullerenes, the effect of processing additives as plasticizers, and the details of molecular mixing-i.e., the extent of intercalation of fullerene molecules between the side chains of the polymer. Mechanical strain in principle affects the photovoltaic output of devices in several ways, from strain-evolved changes in alignment of chains, degree of crystallinity, and orientation of texture, to debonding, cohesive failure, and cracking, which dominate changes in the high-strain regime. These conclusions highlight the importance of mechanical properties and mechanical effects on the viability of OSCs during manufacture and in operational environments. The talk-whose focus is on molecular and microstructural determinants of mechanical properties-concludes by suggesting several potential routes to maximize both mechanical resilience and photovoltaic performance for improving the lifetime of devices in the near term and enabling devices that require extreme deformation (i.e., stretchability and ultra-flexibility) in the future.

9567-38, Session 8

Ultrashort-pulsed laser processing and solution based coating in roll-to-roll manufacturing of organic photovoltaics

Christian J. Hördemann, Katrin Hirschfelder, Moritz Schäfer, Arnold Gillner, Fraunhofer-Institut für Lasertechnik (Germany)

The breakthrough of flexible organic electronics and especially organic photovoltaics is highly dependent on cost-efficient production technologies. Roll-2-Roll processes show potential for a promising solution in terms of high throughput and low-cost production of thin film organic components. Solution based material deposition and integrated laser patterning processes offer new possibilities for versatile production lines. The use of flexible polymeric substrates brings along difficulties in laser patterning which have to be overcome. One main challenge when patterning transparent conductive layers on polymeric substrates are material bulges at the edges of the ablated area. Bulges can lead to short circuits in the laver system leading to device failure. Therefore following layers have to have a sufficient thickness to cover and smooth the ridge. In order to minimize the bulging height, a study has been carried out on transparent conductive ITO layers on flexible PET substrates. Ablation results using different beam shapes, such as Gaussian beam, Top-Hat beam and Donutshaped beam, as well as multi-pass scribing and double-pulsed ablation are compared. Furthermore, lab scale methods for cleaning the patterned

layer and eliminating bulges are contrasted to the use of additional water based sacrificial layers in order to obtain an alternative procedure suitable for large scale Roll-2-Roll manufacturing. Besides progress in research, ongoing transfer of the process into a Roll-2-Roll demonstrator is illustrated. By using fixed optical elements in combination with a galvanometric scanner, scribing, variable patterning and edge deletion can be performed individually.

9567-39, Session 9

Dominant degradation mechanisms of organic photovoltaic devices (Invited Paper)

Thomas Heumueller, Markus Biele, Friedrich-Alexander-Univ. Erlangen-Nürnberg (Germany); Jens Adams, Bayerisches Zentrum für Angewandte Energieforschung e.V. (Germany); Timothy Burke, William Mateker, Stanford Univ. (United States); Michael Salvador, Friedrich-Alexander-Univ. Erlangen-Nürnberg (Germany); Andreas Distler, BELECTRIC OPV (Germany); Hans-Joachim Egelhaaf, Energie Campus Nürnberg (Germany) and BELECTRIC OPV (Germany) and Bayerisches Zentrum für Angewandte Energieforschung e.V. (Germany); Michael McGehee, Stanford Univ. (United States); Christoph J. Brabec, Friedrich-Alexander-Univ. Erlangen-Nürnberg (Germany) and Bayerisches Zentrum für Angewandte Energieforschung e.V. (Germany) and Energie Campus Nürnberg (Germany)

We have studied the stability of a variety of organic photovoltaic (OPV) materials and observe three dominant intrinsic degradation mechanisms: Disorder induced Voc losses, dimerization related Jsc losses and FF losses due to interface defects. Alleviating those mechanisms we demonstrate lifetimes in excess of 10 years.

Using charge extraction and photocurrent spectroscopy we identify an increase of energetic disorder in aged solar cells. This increased energetic disorder lowers the open-circuit voltage by broadening the density of states. Both, the temperature and light intensity dependence of those disorder induced Voc losses can be described with an analytical model using only one fit parameter.

Fullerene dimerization is observed to cause short circuit current losses in organic solar cells. We show that this reaction depends on the fullerene morphology and thus only happens under certain circumstances. Changing the operating conditions of the investigated solar cell from Voc to Jsc significantly reduces the amount of dimerization related performance losses and illustrates the role of excited species in the degradation mechanism.

In several different systems a direct correlation between fill factor losses and interface defects at the contacts is observed. Solar cells with ZnO as interface material clearly show how contact deterioration primarily causes FF losses. An additional Ba(OH)2 layer on top of ZnO is able to stabilize the interface and prevent FF losses. For solar cells with standard architecture we replace the metal electrode after degradation and observe that the fill factor is being restored while the open circuit voltage stays low.

9567-40, Session 9

Degradation mechanism of planar perovskite solar cells

Chuanjiang Qin, Toshinori Matsushima, Chihaya Adachi, Kyushu Univ. (Japan)

Organic-inorganic hybrid halide perovskites are an interesting class of materials that have excellent semiconductor properties, and demonstrated promising applications on many fields, such as solar cells, water photolysis,



light emitting diodes, and amplified spontaneous emission. So far, the device lifetime is still short, and this is an important key issue faced for all researchers in this field.[1] The deep understanding of their durability and degradation mechanism is critical and necessary toward future applications.

Towards development of efficient and long-term stable perovskite solar cells (PSCs), we firstly studied the relationship between crystallization, morphology, device architecture, efficiency and durability of encapsulated PSCs. Furthermore, the degradation mechanism of the devices was elucidated by different experimental methods. The well crystallized and fully covered perovskite layer improves not only power conversion efficiency but also long-time durability. Compared to a widely used silver counter electrode, lithium fluoride/aluminum and gold electrode-based PSCs demonstrated better durability owing to less chemical degradation and interface changing. We also confirmed that the amount of accumulated charge carriers induces the degradation of the PSCs, which was proved by a thermally stimulated current technique. Finally, we realized a planar PSC with excellent durability by improving device encapsulation and optimizing device structures.

Reference:

1. M. Grätzel, Nature Materials 2014, 13, 838-842.

9567-41, Session 9

Predicting thermal stability of organic solar cells through real-time capacitive techniques

Marta Tessarolo, Istituto per lo Studio dei Materiali Nanostrutturati (Italy); Antonio Guerrero, Univ. Jaume I (Spain); Mirko Seri, Istituto per la Sintesi Organica e la Fotoreattività (Italy); Mario Prosa, Istituto per lo Studio dei Materiali Nanostrutturati (Italy); Margherita Bolognesi, Consiglio Nazionale delle Ricerche (Italy); Germà Garcia Belmonte, Univ. Jaume I (Spain)

Bulk Heterojunction (BHJ) solar cells have reached Power Conversion Efficiencies (PCE) over 10% but to be a competitive product long lifetimes are mandatory. In this view, guidelines for the prediction and optimization of the device stability are crucial to generate improved materials for efficient and stable BHJ devices. For encapsulated cells, degradation mechanisms can be mainly ascribed to external agents such as light and temperature. In particular, thermal degradation appears to be related not only to the BHJ morphology but also to the adjacent interfaces. Therefore, in order to have a complete description of the thermal stability of a BHJ cell, it is necessary to consider the entire stack degradation processes by using techniques enabling a direct investigation on working devices.

Here, five different donor polymers were selected and the OPV performance of the corresponding BHJ devices were monitored during the thermal degradation at 85°C, showing an exponential decay of the corresponding PCEs. In parallel, we measured the geometrical capacitance of analogous OPV devices as a function of temperature and we observed that at a defined temperature (TMAX), typical for each polymer-based device, the capacitance starts to decrease. Combining all these results we found an evident and direct correlation between TMAX and the PCE decay parameters (obtained from capacitance-temperature an thermal measurements, respectively). This implies that the capacitance-method here presented is a fast, reliable and relatively simple method to predict the thermal stability of BHJ solar cells without the need to perform time-consuming thermal degradation tests.

9567-42, Session 9

Perovskite solar cells: From device fabrication to device degradation (Invited Paper)

Jinli Yang, Dianyi Liu, Braden Siempelkamp, Timothy Kelly,

Univ. of Saskatchewan (Canada)

Solar cells based on CH3NH3PbI3 have recently emerged at the forefront of solution-processable photovoltaic devices, with power conversion efficiencies as high as 20.1% having now been certified. In this presentation, I will discuss our research group's work in the area of perovskite solar cells. Our early work demonstrated that room temperature solution-processing techniques can be used to prepare devices on flexible substrates while retaining excellent power conversion efficiencies. Since then, we have examined issues related to charge carrier diffusion, interfacial contacts, and device flexibility, with our most recent efforts focusing on probing device failure mechanisms using in situ synchrotron-based techniques.

9567-43, Session 9

High-efficiency perovskite solar cells with long operation lifetime

Chenchen Yang, Weiran Cao, Nathan T. Shewmon, Jiangeng Xue, Univ. of Florida (United States)

Perovskite solar cells have attracted tremendous attention for their outstanding energy conversion efficiency in the past few years. Due to the development of active materials, device architectures and processing methods, power conversion efficiency (PCE) of perovskite solar cells is now growing up to 20%. Beyond the efficiency, to get rid of Lead, the widely-used toxic element in the perovskite layers, as well as to improve the device/ module operation lifetime are the other two major challenges that need to be solved before their commercialization.

Here, we apply a layer of ZnO nanoparticles onto to a planar perovskite solar cell, which can not only improve the electron transport/extraction in the devices but highly improve the device operation lifetime. The devices were fabricated by spin-coating a poly(3,4-ethylenedioxythuiphene):poly styrene sulfonate (PEDOT:PSS) layer onto a glass/ITO substrate, followed by the deposition of a perovskite layer from a lead chloride (PbCl2) and methyl ammonium iodine (MAI) blend precursor solution. After that, a layer of [6,6]-phenyl-C61-butyric acid methyl ester (PCBM) and a layer of ZnO nanoparticles were successively deposited as the electron transport layers, and the device was finished by thermally evaporation AI as the cathode. Such planar perovskite solar cell with ZnO NPs exhibits a maximum PCE of up to 14.1%, which is about 35% higher than that without the ZnO layer. Moreover, the device remains 80% of its initial PCE after 2500 hours under 1 sum illumination, majorly due to the protection of ZnO layer that prevent the diffusion of oxygen and moisture molecules into the perovskite layers as revealed by x-ray photoelectron spectroscopy studies.

9567-2, Session 10

Photoactive and interfacial materials for flexible photovoltaic devices (Invited Paper)

Antonio F. Facchetti, Polyera Corp. (United States)

In this presentation we will report the molecular design by DFT computations, synthesis, and molecular and structural characterization of a new polymeric building block based on aromatic sulfonamides as donor for organic photovoltaic cells. Furthermore, we report results on using self-assembled interlayers and metal oxide blends with fine tuning of the conduction band to replace conventional spin-coated materials enabling improved performance or enable new functions. Finally, we will show recent studies on device performance achieved upon ambient processing and lifetime stability test under light soaking. Our results demonstrate that single-junction OPV cell with efficiencies surpassing 10% are possible and can exhibit considerable stability.



9567-45, Session 10

Polymer solar cells with efficiency >10% enabled via a facile solution-processed Aldoped ZnO electron transporting layer

Lethy K. Jagadamma, Mohammed Al-Senani, Aram Amassian, King Abdullah Univ. of Science and Technology (Saudi Arabia)

The present work details a facile and low-temperature (125C) solutionprocessed Al-doped ZnO (AZO) buffer layer functioning very effectively as electron accepting/hole blocking layer for a wide range of polymer:fullerene bulk heterojunction systems, and yielding power conversion efficiency in excess of 10% (8%) on glass (plastic) substrates. We show that ammonia addition to the aqueous AZO nanoparticle solution is a critically important step toward producing compact and smooth thin films which partially retain the aluminum doping and crystalline order of the starting AZO nanocrystals. The ammonia treatment appears to reduce the native defects via nitrogen incorporation, making the AZO film a very good electron transporter and energetically matched with the fullerene acceptor. Importantly, highly efficient solar cells are achieved without the need for additional surface chemical passivation or modification, which has become an increasingly common route to improving the performance of evaporated or solutionprocessed ZnO ETLs in solar cells.

9567-46, Session 10

Polymer-facilitated low temperature fusing of spray-coated silver nanowire networks as transparent top and bottom electrodes in small molecule organic photovoltaics

Franz Selzer, Nelli Weiß, David Kneppe, Ludwig Bormann, Christoph Sachse, Nikolai Gaponik, Alexander Eychmüller, Karl Leo, Lars Müller-Meskamp, Technische Univ. Dresden (Germany)

Networks of silver nanowires (AgNWs) are promising candidates for transparent conducting electrodes in organic photovoltaics (OPV), as they achieve similar performance as the commonly used indium tin oxide (ITO) at lower cost and increased flexibility. The initial sheet resistance (Rs) of AgNW electrodes typically needs to be reduced by a post-annealing step (90 min@200 °C), being detrimental for processing on polymeric substrates.

We present novel low temperature-based methods to integrate AgNWs in organic small molecule-based photovoltaics, either as transparent and highly conductive bottom-electrode or, for the first time, as spray-coated AgNW top-electrode. The bottom-electrodes are prepared by organic matrix assisted low-temperature fusing. Here, selected polymers are coated below the AgNWs to increase the interaction between NWs and substrate. In comparison to networks without these polymeric sublayers, the Rs is reduced by two orders of magnitude.

AgNW top-electrodes are realized by dispersing modified high-quality AgNWs in inert solvents, which do not damage small molecule layers. Accordingly, our AgNW dispersion can be spray-coated onto all kind of OPV devices. Both bottom- and top-electrodes show a Rs of <11 ?/? at >87 % transparency directly after spray-coating at very low substrate temperatures of <80 °C. We also demonstrate the implementation of our AgNW electrodes in organic solar cells. The corresponding devices show almost identical performance compared to organic solar cells exploiting ITO as bottom or thermally evaporated thin-metal as top-electrode.

9567-47, Session 10

A solution-doped small molecule hole transport layer for efficient ITO-free organic solar cells

Ludwig Bormann, Franz Selzer, Karl Leo, Lars Mueller-Meskamp, Technische Univ. Dresden (Germany)

Indium-tin-oxide-free (ITO-free) organic solar cells are an important, emerging research field because ITO transparent electrodes are a bottleneck for cheap large area devices on flexible substrates. Among highly conductive PEDOT:PSS and metal grids, percolation networks made of silver nanowires (AgNW) with a diameter in the nanoscale show a huge potential due to easy processing (e.g. spray coating), high aspect ratios and excellent electrical and optical properties like 15 Ohm/sq with a transmission of 83.5 % including the substrate.

However, the inherent surface roughness of the AgNW film impedes the implementation as bottom electrode in organic devices, especially fully vacuum deposited ones, where often shunts are obtained.

Here, we report about the solution processing of a small molecule hole transport layer (s-HTL) comprising N,N'-((Diphenyl-N,N'-bis)9,9,-dimethyl-fluoren-2-yl)-benzidine (BF-DPB, host material) and the proprietary NDP9 (p-dopant) deposited from tetrahydrofuran (THF) as non-halogenated, "green" solvent. We show, that the doping process already takes place in solution and that conductivities, achieved with this process at high doping efficiencies (4 * 10'-4 S/cm at 10 wt% doping concentration), are comparable to thermal co-evaporation of BF-DPB:NDP9 under high vacuum, which is the proven deposition method for doped small molecule films.

Applying this s-HTL to AgNW films leads to well smoothened electrodes, ready for application in organic devices.

Vacuum-deposited organic p-i-n solar cells with DCV2-5T-Me(3:3):C60 as active layer show a power conversion efficiency of 4.4% and 3.7% on AgNW electrode with 35nm and 90 nm wire diameter, compared to 4.1% on ITO with the s-HTL.

9567-48, Session 10

Transparent conductive thin-film encapsulation layers

Andreas Behrendt, Tobias Gahlmann, Sara Trost, Andreas Polywka, Patrick Görrn, Thomas Riedl, Bergische Univ. Wuppertal (Germany)

Gas diffusion barriers (GDB) are inevitable to protect sensitive organic materials or devices against ambient gases. Typically, thin-film gas diffusion barriers are insulators, e.g. Al2O3 or multilayers of Al2O3/ZrO2, etc.. A wide range of applications would require GDB which are at the same time transparent and electrically conductive. They could serve as electrode and moisture barrier simultaneously, thereby simplifying production. As of yet, work on transparent conductive GDB (TCGDBs) is very limited. TCGDBs based on ZnO prepared by atomic layer deposition (ALD) have been reported. Due to the chemical instability of ZnO, it turns out that their electrical conductivity severely deteriorates by orders of magnitude upon exposure to damp heat conditions after very short time. We will show that these issues can be overcome by the use of tin oxide (SnO2). Conductivities of up to 300 S/cm and extremely low water vapor transmission rates (WVTR) on the order of 10-6 g/(m2 day) can been achieved in SnOx layers prepared by ALD at low temperatures (<150°C). A sandwich of SnOx/Ag/ SnOx is shown to provide an average transmittance of 82% and a low sheet resistance of 9 Ohm/sq. At the same time the resulting electrodes are extremely robust. E.g., while unprotected Cu and Ag electrodes degrade within a few minutes at 85°C/85%rH (e.g. Cu lost 7 orders of magnitude in electrical conductivity), sandwich structures of SnOx/(Cu or Ag)/SnOx remain virtually unchanged even after 100 h. The SnOx in this work will also provide corrosion protection for the metal in case of harsh processing steps on top these electodes (e.g. acidic). We demonstrate the application of these TCGDBs as electrodes for organic solar cells and OLEDs.



Monday - Wednesday 10-12 August 2015

Part of Proceedings of SPIE Vol. 9568 Organic Field-Effect Transistors XIV; and Organic Sensors and Bioelectronics VIII

9568-101, Session 1

OFET surface treatments on copper and silver source and drain electrodes (*Invited Paper*)

Zhang Jia, Columbia Univ. (United States); Chang-Hyun Kim, Yvan Bonnassieux, Gilles Horowitz, Ecole Polytechnique (France); Luca Floreano, Alberto Verdini, INFM (Italy); Dean Cvetko, Ljubljana Univ. (Slovenia); Alberto Morgante, INFM (Italy); Ioannis Kymissis, Columbia Univ. (United States)

Organic field effect transistors (OFETs) offer a number of potential advantages for large area, low thermal budget, and flexible electronic systems. As the channel transconductance and current density in OFETs has improved over the past decade, the performance of transistor contacts has become a primary concern.

There is an increasing interest in the use of alternative metals to gold for transistor contacts. It is possible to engineer surface treatments for silver and copper electrodes that deliver similar advantages to surface treatments developed for use on gold electrodes. We will review how the understanding of surface treatments has evolved over the past decade, and in particular, discuss the use of photocurrent, structural analysis, and energy resolved X-ray techniques to understand surface treatment performance on device behavior. We will also discuss analysis of many of the same surface treatment strategies on silver and copper electrodes using printed and lithographic approaches, opening the door to potentially lower cost, higher throughput fabrication of OFETs with improved contact performance.

9568-102, Session 1

Scaling effects of organic thin-film transistors

Anita Risteska, Jacobs Univ. Bremen (Germany); Kris Myny, Sören Steudel, IMEC (Belgium); Masakazu Nakamura, Nara Institute of Science and Technology (Japan); Dietmar Knipp, Jacobs Univ. Bremen (Germany)

The influence of scaling of organic thin-film transistors on the operation of organic digital circuits was studied. Particularly, the influence of drain and source contact resistance on the static and the dynamic behaviour of the circuits was investigated. An analytical model describing the voltage transfer characteristics (static behaviour) and the propagation delay (dynamic behaviour) was developed. A static and dynamic experimentally measured data was modelled by a consistent set of data and good agreement between the model and the experiments was observed. For pentacene thin-film transistors with channel lengths in the range of few micrometers, the influence of contact effects has to be considered. Using the model, it was shown that for organic thin-film transistors with channel lengths of less than 10 ?m the contact resistance has negative influence on both, the static noise margin and the propagation delay. Scaling the lateral dimensions of the transistors down to few ?m limits the circuit performance due to contact effects, and the 1-10 MHz frequency range operation required by some applications can only be achieved by reducing the specific contact resistance, ?C, 10-100 times. This need for ?C reduction highlights the importance of improving charge injection in organic transistors that can usually be achieved by contact doping like in inorganic electronics or surface treatment with self-assembled monolayers.

9568-103, Session 1

Molecular-layer thick organic semiconductor materials and electronic devices

Liqiang Li, Suzhou Institute of Nano-Tech and Nano-Bionics (China)

Organic semiconductors (OSCs) are the key components of organic electronic devices. In conventional organic field-effect transistors (OFETs), thick organic semiconductor film (tens of nanomter) are adopted. It is known that the conductive channel (one to several molecular layers, several nanometers thick) in OFETs is located at the interface between OSCs and dielectrics, and is generally buried in the thick OSCs film. Therefore, it is difficult to characterize the conductive channel.

Molecular-layer thick OSCs ultrathin film may provide excellent model for both fundamental research and device applications, because in OFETs based on molecular layer thick OSCs ultrathin film, conductive channel is exposed. It would be favorable to investigate the structure-property relationships as well as to fabricate high performance sensors. However, the growth of such system is technologically challenging.

In our work, we demonstrated controllable growth of monolayer to multilayer organic semiconductor film in monolayer precision via dipcoating [Ref1], and further elucidated the growth mechanism for this unique phenomenon [Ref 2]. Moreover, high performance ammonia sensors were fabricated based on the ultrathin film [Ref 3].

Referenes:

[1] L.Q. Li et al. J. Am. Chem. Soc. 2010, 132, 8807. (Cover).[2] L.Q. Li et al. Angwe. Chem. Int. Ed. 2013, 52, 12530. (Hotpaper, Frontispiece)

[3] L.Q. Li et al. Adv. Mater. 2013, 25, 3419. (Back cover)

9568-104, Session 1

Operation mechanism of the organic permeable base transistor

Felix Kaschura, Institut für Angewandte Photophysik (Germany) and Technische Univ. Dresden (Germany); Axel Fischer, Markus Klinger, Institut für Angewandte Photophysik (Germany); Duy Hai Doan, Weierstrass-Institut für Angewandte Analysis und Stochastik (Germany); Klaus Gärtner, Univ. della Svizzera italiana (Switzerland); Thomas Koprucki, Annegret Glitzky, Weierstrass-Institut für Angewandte Analysis und Stochastik (Germany); Daniel Kasemann, Institut für Angewandte Photophysik (Germany); Karl Leo, Institut für Angewandte Photophysik (Germany)

The Organic Permeable Base Transistor (PBT) is a promising device concept profiting from vertical current transport and thus short channel length. A perforated and insulated Base electrode is placed between Emitter and Collector, acting as control electrode regulating the current flowing through the openings of this electrode. In order to improve the device performance and tune the properties, a detailed understanding of the operation mechanism of the PBT is required.

In this contribution, we perform three-dimensional drift-diffusion simulations, to get an insight into the processes occurring in the device. We study the effect of different semiconductor and geometry parameters on the transistor characteristics, compare the simulation data to experimental



results, and outline the importance of charge carrier accumulation at the Base electrode for the high current densities obtained in these devices.

The operation of the PBT can be divided into two major regimes: At low current densities, the applied Base potential directly controls the collector current in the PBT. Hence, the number of charges allowed to pass the opening is the current limiting factor and this regime leads to an exponential current-voltage characteristics. At higher current densities, however, the opening does not act as a bottleneck any more. Instead, the intrinsic semiconductor current in the in the on-state.

9568-105, Session 1

Hybrid light emitting transistors

Khalid Muhieddine, Mujeeb Ullah, Ebinazar B. Namdas, Paul L. Burn, The Univ. of Queensland (Australia)

Organic light-emitting diodes (OLEDs) are well studied and established in current display applications. Light-emitting transistors (LETs) have been developed to further simplify the necessary circuitry for these applications, combining the switching capabilities of a transistor with the light emitting capabilities of an OLED. Such devices have been studied using mono- and bilayer geometries and a variety of polymers [1], small organic molecules [2] and single crystals [3] within the active layers. Current devices can often suffer from low carrier mobilities and most operate in p-type mode due to a lack of suitable n-type organic charge carrier materials. Hybrid light-emitting transistors (HLETs) are a logical step to improve device performance by harnessing the charge carrier capabilities of inorganic semiconductors [4].

We present state of the art, all solution processed hybrid light-emitting transistors using a non-planar contact geometry [1, 5]. We will discuss HLETs comprised of an inorganic electron transport layer prepared from a sol-gel of zinc tin oxide and several organic emissive materials. The mobility of the devices is found between 1-5 cm2/Vs and they had on/off ratios of -105. Combined with optical brightness and efficiencies of the order of 103 cd/m2 and 10-3-10-1 %, respectively, these devices are moving towards the performance required for application in displays.

[1] M. Ullah, K. Tandy, S. D. Yambem, M. Aljada, P. L. Burn, P. Meredith, E. B. Namdas., Adv. Mater. 2013, 25, 53, 6213

[2] R. Capelli, S. Toffanin, G. Generali, H. Usta, A. Facchetti, M. Muccini, Nature Materials 2010, 9, 496

[3] T. Takenobu, S. Z. Bisri, T. Takahashi, M. Yahiro, C. Adachi, Y. Iwasa, Phys. Rev. Lett. 2008, 100, 066601

[4] H. Nakanotani, M. Yahiro, C. Adachi, K. Yano, Appl. Phys. Lett. 2007, 90, 262104

[5] K. Muhieddine, M. Ullah, B. N. Pal, P. Burn E. B. Namdas, Adv. Mater. 2014, 26,37, 6410

9568-106, Session 2

On the use of organic transistors in flexible large-area sensor arrays (Invited Paper)

Brian Cobb, Abhishek Kumar, Holst Ctr. (Netherlands)

While much of the OTFT activity has been display-centric there is no doubt that as the OTFT technology matures the number of applications will continue to increase. Using our most recent flexible X-ray detectors we will discuss the prospect and challenges of organic transistors in sensor backplanes. For these application, the current mobility of ~0.1-2 cm2/Vs of OTFTs is currently not a problem. Their low leakage currents give them a distinct advantage over competing technologies, such as amorphous silicon TFT. Yet, challenges remain and these will be discussed.

9568-107, Session 2

New polymer dielectrics for low-voltage high transconductance organic transistors

Chao Wang, Desheng Kong, Wen-Ya Lee, Zhenan Bao, Stanford Univ. (United States)

Both high gain and transconductance at low operating voltages are crucial for organic field-effect transistors (OFETs) in practical applications. Here, we describe unexpected double-layer capacitance effect in polar elastomer dielectrics despite of very low ion concentration and ion conductivity, thus, significantly enhances OFET transconductances at low-voltages. In particular, we employed a special polar elastomer as the dielectric material. We obtained transconductance per channel width at -3V gate voltage 30 times higher as compared to the same organic semiconductors on a semicrystalline polymer. Compared with the previously reported high-transconductance OFETs using double-layer capacitance effects, our dielectric materials have the advantages of compatibility with standard manufacturing processes and high stability in air and water, resulting in highly stable operation in water with low bias stress effects.

9568-108, Session 2

Top-gate organic field-effect transistors and circuits on shape-memory polymer substrates

Sangmoo Choi, Canek Fuentes-Hemandez, Cheng-Yin Wang, Georgia Institute of Technology (United States); Andrew Wei, Walter E. Voit, The Univ. of Texas at Dallas (United States); Bernard Kippelen, Georgia Institute of Technology (United States)

Organic field-effect transistors (OFETs) have been intensively developed, and their characteristics and processibility have dramatically improved: carrier mobility (?) values in OFETs are now even higher than amorphous silicon thin-film-transistors (a-Si TFTs); threshold voltage values (VTH) have decreased near zero, which enables low voltage driving of OFET circuits; high operational and environmental stability has also been reported, particularly in top bilayer gate OFET geometries; and new fabrication methods, such as inkjet-printing, have been developed.

As the basic properties of OFETs are approaching the required performance for the realization of commercially viable products, applications of OFETs have become an important topic of research. One desirable property of OFETs is the realization of flexible electronic devices, such as wearable electronics. Towards this goal, researchers have been exploring new flexible substrate materials. Among these new substrates, shape-memory polymers (SMPs) have shown unique features: a variable Young's modulus dependent on temperature; the ability to fix two or more shapes when a thermal stimulus is applied; low cure stress, and biocompatibility. These features make SMPs good candidates as substrate materials for three-dimensional shape applications like human body-embedded sensors, but also present challenges for the direct fabrication of OFETs on its surface.

Here, we report on the direct fabrication of high-performance top-gate OFETs and circuits on biocompatible, low cure stress SMP substrates, and a comparison with the performance of OFETs on conventional glass substrates. Demonstration of OFET circuits on SMP substrates opens the door to potential applications that will be discussed.

9568-109, Session 2

Organic transistors for electrophysiology (*Invited Paper*)

Jonathan Rivnay, Ecole Nationale Supérieure des Mines de Saint-Étienne (France)



Efficient local transduction of biological signals is of critical importance for mapping brain activity and diagnosing pathological conditions. Traditional devices used to record electrophysiological signals are passive electrodes that require (pre)amplification with downstream electronics. Organic electrochemical transistors (OECTs) that utilize conducting polymer films as the channel have shown considerable promise as amplifying transducers due to their stability in aqueous conditions and high transconductance (>3 mS). The materials properties and physics of such transistors, however, remains largely unexplored thus limiting their potential. Here we show that the uptake of ionic charge from an electrolyte into a poly(3,4ethylenedioxythiophene) doped with polystyrene sulfonate (PEDOT:PSS) OECT channel leads to a dependence of the effective capacitance on the entire volume of the film. Subsequently, device transconductance and time response vary with channel thickness, a defining characteristic that differentiates OECTs from field effect transistors, and provides a new degree of freedom for device engineering. Using this understanding we tailor OECTs for a variety of low (1-100 Hz) and high (1-10 kHz) frequency applications, including human electroencephalography, where high transconductance devices impart richer signal content without the need for additional amplification circuitry. We also show that the materials figure of merit OECTs is the product of hole mobility and volumetric capacitance of the channel, leading to design rules for novel high performance materials.

9568-110, Session 2

Transcap: A new integrated hybrid supercapacitor and electrolyte-gated transistor device (Invited Paper)

Clara Santato, Ecole Polytechnique de Montréal (Canada)

The boom in multifunctional, flexible, and portable electronics and the increasing need of low-energy cost and autonomy for applications ranging from wireless sensor networks for smart environments to biomedical applications are triggering research efforts towards the development of self-powered sustainable electronic devices. Within this context, the coupling of electronic devices (e.g. sensors, transistors) with small size energy storage systems (e.g. micro-batteries or micro-supercapacitors) is actively pursued.

Micro-electrochemical supercapacitors are attracting much attention in electronics for their capability of delivering short power pulses with high stability over repeated charge/discharge cycling.

For their high specific pseudocapacitance, electronically conducting polymers are well known as positive materials for hybrid supercapacitors featuring high surface carbon negative electrodes. The processability of both polymer and carbon is of great relevance for the development of flexible miniaturised devices.

Electronically conducting polymers are even well known to feature an electronic conductivity that depends on their oxidation (p-doped state) and that it is modulated by the polymer potential. This property and the related pseudocapacitive response make polymer very attracting channel materials for electrolyte-gated (EG) transistors.

Here, we propose a novel concept of "Trans-capacitor", an integrated device that exhibits the storage properties of a polymer/carbon hybrid supercapacitor and the low-voltage operation of an electrolyte-gated transistor.

9568-137, Session PMon

Well-balanced carrier mobilities of ambipolar transistors based on a low band gap small molecule semiconductor

Min Je Kim, Woonggi Kang, Sungkyunkwan Univ. (Korea, Republic of)

We synthesized a solution-processable low bandgap small molecule, SiITDPP-EE-COC6 for semiconducting channel material in organic fieldeffect transistors (FETs). The SiITDPP-EE-COC6 consisted of electron-rich thiophene-dithienosilole-thiophene (SiIT) units and electron-deficient diketopyrrolopyrrole (DPP) units. The change of the electrical properties of FETs induced by thermal annealing was systematically investigated. The hole and electron mobilities of as-spun Si1TDPP-EE-COC6 were 3.3 ? 10-4 and 1.7 ? 10-4 cm2/(Vs), respectively. A significant increase in carrier mobilities was obtained by thermal annealing at 150 °C: hole mobility of 0.003 cm2/(Vs) and electron mobility of 0.002 cm2/(Vs). This performance enhancement upon thermal annealing is strongly related with the enhanced layered edgeon structure and resulting reduced ϖ - ϖ intermolecular spacing, examined by grazing incidence X-ray diffraction (GIXD) and atomic force microscopy (AFM) measurements. Importantly, atomically-thin CVD-grown graphene source/drain electrodes led to dramatic increase in the carrier mobilities. For example, the FETs based on 150 °C-annealed SiITDPP-EE-COC6 exhibited a hole mobility of 0.011 cm2/(Vs) and electron mobility of 0.015 cm2/(Vs), which are best performance among FETs with DPP-based small molecules. The CVD-grown graphene electrodes provide a facile method to improve the FET performance based on DPP-based small molecule semiconductor.

9568-138, Session PMon

High performance ferroelectric organic field-effect transistor using soft contact process

Min-Hoi Kim, Hanbat National Univ. (Korea, Republic of); Gyu Jeong Lee, Seoul National Univ. (Korea, Republic of); Jae-Hyun Lee, Hanbat National Univ. (Korea, Republic of); Jin-Hyuk Bae, Kyungpook National Univ. (Korea, Republic of)

Nonvolatile memory based on ferroelectric organic field-effect transistors (FeOFETs) has attracted much attention due to cost effective processing compatibility. Although the device performance of the FeOFETs have been drastically improved over the past decades, low memory on-off ratio, which is caused by the low mobility, hinders the practical applications such as identification tags and memory embedded sensors. In this work, we demonstrated the high performance FeOFET with high memory on-off ratio by the simple soft-contact-process.

For a gate electrode of the FeOFETs, aluminum was thermally deposited on a cleaned glass substrate through a shadow mask. For a ferroelectric gate insulator, poly(vinylidene fluoride) copolymer with trifluoroethylene (75/25 mol %) [P(VDF-TrFE)], dissolved in cyclopentanone in 10 wt %, was spin-coated on the substrate. The samples were cured at 140 °C for 2 h. During the curing process, for the SCP-processed OFETs, the surface of the ferroelectric insulator was pressed by the elastomer, polydimethylsiloxane, under the pressure of about 9.8 N/cm2. A p-type organic semiconductor of pentacene of 50 nm and gold of 65 nm was sequentially formed on the gate insulator through a shadow mask by thermal.

Through the soft contact process, the rms roughness of the ferroelectric insulator was reduced from 15nm to 5nm. The mobility of the soft-contact-processed FeOFETs exhibits more than ten times increased mobility (0.04 cm2/Vs,), which results in the ten times increased memory on-off ratio. **This work was supported by NRF-2014R1A1A2053957.

9568-139, Session PMon

Indium gallium zinc oxide-based stretchable organic-inorganic hybrid transistors using stiff island structure

Soon-Won Jung, Jae Bon Koo, Chan Woo Park, Bock Soon Na, Ji-Young Oh, Sang Seok Lee, Electronics and Telecommunications Research Institute (Korea, Republic of)

In this study, stretchable organic-inorganic hybrid thin-film transistors (TFTs) are fabricated on a polyimide (PI) stiff-island/elastomer substrate using blends of poly(vinylidene fluoride-trifluoroethylene) [P(VDF-TrFE)] and poly(methyl methacrylate) (PMMA) and oxide semiconductor In-Ga-



Zn-O as the gate dielectric and semiconducting layer, respectively. Carrier mobility, Ion/Ioff ratio, and subthreshold swing (SS) values of 6.1 cm2V-1s-1, 107, and 0.2 V/decade, respectively, were achieved. For the hybrid TFTs, the endurable maximum strain without degradation of electrical properties was approximately 49%. These results correspond to those obtained in the first study on fabrication of stretchable hybrid-type TFTs on elastomer substrate using an organic gate insulator and oxide semiconducting active channel structure, thus indicating the feasibility of a promising device for stretchable electronic systems

9568-140, Session PMon

Improvement of micro-contact patterning fidelity of organic semiconductors through ultraviolet ozone treatment on nanoporous stamps

Hea-Lim Park, Bo-Yeon Lee, Chang-Min Keum, Se-Um Kim, Seoul National Univ. (Korea, Republic of); Min-Hoi Kim, Hanbat National Univ. (Korea, Republic of); Sin-Doo Lee, Seoul National Univ. (Korea, Republic of)

Among various kinds of organic semiconductor (OSC) materials, 6,13-bis(tr iisopropylsilylethynyl) pentacene (TIPS-PEN) has widely been investigated due to its relatively high mobility and possibility of cost-effective fabrication by solution process. In spite of these advantages, the practical application of TIPS-PEN for the large-area devices still struggles to satisfy the industrial figures of merit, since it is challenging to obtain the precise pattern together with the uniform film properties of solution-processed TIPS-PEN. It should be noted that the patterning of OSC films with high pattern fidelity is significant to eliminate the undesirable current pathway and thus to ensure the performance reliability between individual device components.

In this work, we demonstrated the effect of ultraviolet ozone (UVO) treatment of a polydimethylsiloxane (PDMS) stamp on the micro-contact patterning fidelity of TIPS-PEN film. Here, TIPS-PEN was blended with an insulating organic polymer to enhance the uniformity of TIPS-PEN films. For patterning, the UVO-treated PDMS stamp having micrometer-scale patterns was contacted with a thin film of blended TIPS-PEN uniformly coated on a substrate by spin-coating. During this process, the nanoporous PDMS stamp absorbed the TIPS-PEN monomers through the contact area, generating the complementary patterns of TIPS-PEN. It was found that the pattern fidelity was greatly improved by increasing the UVO treatment time on PDMS stamps from 0 to 30 minutes. Our approach for achieving high pattern fidelity by a simple and low-cost patterning technique will provide a useful platform for integration of solution-processed organic electronic devices.

This work was supported in part by Samsung Display, Inc.

9568-141, Session PMon

Tunable solubility parameter of poly(3hexyl thiophene) with hydrophobic sidechains to achieve rubbery semiconducting films

Mi Jang, Hyeonji Bae, Hoichang Yang, Joongyu Ahn, Inha Univ. (Korea, Republic of)

A highly ϖ -conjugated nanofibrillar network of poly(3-hexyl thiophene) (P3HT) embedded in polydimethylsiloxane (PDMS) elastomer films on dielectrics was facilely developed via solution-blending of an ultrasonicated P3HT solution with a PDMS followed by spin-casting and curing. In contrast, simple blending without ultrasonication yielded large agglomerates in cast films owing to a great difference in solubility parameter (P3HT = 9.5 cal1/2cm-3/2, PDMS = 7.3 cal1/2cm-3/2). Via ultrasonicating, P3HT could develop nanofibrils surrounded by side-chains with the same solubility parameter value as that of PDMS, yielding homogeneous P3HT/PDMS blend films. Blend films could yield high electrical properties, as well as excellent environmental stability.

9568-142, Session PMon

Air-processable silane-coupled polymers to modify a dielectric for solution-processed organic field-effect semiconductors

Mi Jang, Young Chang Yu, Ji Ho Youk, Hoichang Yang, Inha Univ. (Korea, Republic of)

Poly(styrene-r-3-methacryloxypropyltrimethoxysilane) (PSMPTS) copolymers were synthesized by the free radical polymerization of styrene and 3-methacryloxypropyltrimethoxysilane (MPTS) for use as surface modifiers. PSMPTS copolymers were spun-cast onto a hydrophilic SiO2 layer and were then annealed at 150 °C in ambient air. The polystyrene (PS)-based copolymer with approximately 30 MPTS coupling sites, was easily grafted onto the SiO2 surface after annealing periods longer than 1 min. On the untreated and polymer-treated dielectrics, spin-casting of an ultrasonicated poly(3-hexyl thiophene) solution yielded highly interconnected crystal nanofibrils. We believe that ambient-air-processable silane-coupled copolymer can be used as a solution-based surface modifier for continuous, large-scale OFET fabrication.

9568-143, Session PMon

Analysis of different deposition patterns for semiconductor at organic field-effect transistors using inkjet printing technique

Josiani Cristina Stefanelo, Lilian Soares Cardoso, Roberto Mendonça Faria, Univ. de São Paulo (Brazil)

Inkjet printing is a potential tool that can be applied to fabricate organic field-effect transistors (OFETs) because it has several advantages, such as, easiness to print well-defined patterns with deposition accuracy and in small dimensions. Moreover, it allows different materials to be deposited on the same substrate. This last advantage favors the fabrication of organic digital logic inverters, such as, organic CMOS (complementary metal oxide semiconductor). Here, we show the OFETs fabrication using the inkjet printing technique. The poly(3-hexylthiophene) (P3HT) semiconductor was printed using functional materials printer. The semiconductor was deposited using different line deposition patterns, with the same or variable dispensing direction. Patterns of parallel and perpendicular lines with respect to direction of electronic conduction were printed. This study evaluated the influence of deposition patterns in the OFETs performance, using the architecture top gate-bottom contact. Other printing parameters were kept, as well as the polymeric dielectric layer, produced via spin-casting, and the evaporated metal electrodes. High-performance OFET devices were obtained for the case which parallel lines regarding direction of electronic conduction had the same dispensing direction. These obtained devices reached on/off ratio up to 104 and swing subthreshold of 3 V/dec. In OFETs with perpendicular lines regarding electronic conduction, the performance was similar to the two types of dispensing direction. This study showed that the best performance of OFETs was obtained for the printed parallel pattern in respect to direction of electronic conduction, due to its lower channel resistance.

9568-144, Session PMon

Photo-physics and charge transport in hetero-structure organic light emitting transistors

Fatemeh Maasoumi, Mujeeb Ullah, Paul E. Shaw, The Univ. of Queensland (Australia); Jun Li, National Univ. of Singapore (Singapore); Paul L. Burn, Paul Meredith, Ebinazar B. Namdas, The Univ. of Queensland (Australia)



Organic light emitting field effect transistors (LEFETs) are multifunctional devices. They not only have the electroluminescent properties of an organic light emitting diode (OLED) but also the switching capabilities of a transistor in a single device architecture. This dual functionality of LEFETs has the potential for new applications such as simplified pixels for flat panel displays, integrated sensor architectures and potentially electrically driven lasers. They are also useful structures for basic optoelectronic studies. Although LEFET brightnesses have improved in the last decade, their electrical switching ON/OFF ratio and EQE at high brightnesses still needs to be improved [1-4]. This is due to the lack of ideal materials and LEFET design, and the absence of a comprehensive understanding of charge transport, radiative recombination processes, and light out coupling in such devices.

A useful probe for studying charge transport in light emitting organic semiconducting materials is to measure the optoelectronic characteristics as a function of temperature. In this work, we demonstrate for the first time, simultaneous probing of charge transport (for both electron and holes), charge injection, contact resistance and radiative recombination in bilayer light emitting and charge transporting polymer films in an LEFET configuration. We employed temperature dependent measurements on bilayer LEFETs consisting of charge transporting ambipolar DPP based polymer and a yellow-green emissive polymer. The bilayer LEFETs show decreases in the source-drain current, mobility (both electron and hole) and brightness with decreasing temperature. In contrast, the external quantum efficiency (EQE) was found to increase by an order of magnitude. We correlate temperature dependent mobility and drain current measurements with thermally activated processes, which is consistent with hopping charge transport in disordered semiconductors. We demonstrate that increases in EQE at low temperatures are predominately due to an increase in the recombination efficiency.

[1] J. Zaumseil, R. H. Friend and H. Sirringhaus, Spatial Control of the Recombination Zone in an Ambipolar Light-Emitting Organic Transistor. Nature Mat. 5, 69 - 74 (2006).

[2] M. Ullah, K. Tandy, S. D. Yambem, M. Aljada, P. L. Burn, P. Meredith, and E. B. Namdas . Simultaneous Enhancement of Brightness, Efficiency, and Switching in RGB Organic Light Emitting Transistors. Adv. Mater.25, 6213–6218 (2013).

[3] B. B. Y. Hsu, C. Duan, E. B. Namdas, A. Gutacker, J. D. Yuen, F. Huang, Y. Cao, G. C. Bazan, I. D. W. Samuel and A. J. Heeger. Control of Efficiency, Brightness and Recombination Zone in Light-Emitting Field Effect Transistors. Adv. Mater. 24, 1171-1175 (2012).

[4] M. Ullah, K. Tandy, J. Li, Z. Shi, P. L. Burn, P. Meredith and E. B. Namdas. High-Mobility, Heterostructure Light-Emitting Transistors and Complementary Inverters. ACS. Photonics. 1. 954?959 (2014).

9568-145, Session PMon

Gate dielectric surface treatments for performance improvement of poly(3hexylthiophene-2,5-diyl) based organic field-effect transistors

Ali Nawaz, Cristiane D. Col, Isidro C. Cruz, Univ. Federal do Parana (Brazil); Anshu Kumar, Anil Kumar, Indian Institute of Technology Bombay (India); Ivo A. Hümmelgen, Univ. Federal do Parana (Brazil)

While organic field effect transistors (OFETs) remain as the center of extensive research, several techniques are being developed for performance improvement. Correspondingly, we investigate the role of passivation of charge traps present on cross-linked poly (vinyl alcohol) (cr-PVA) surface using hexadecyltrimethylammonium bromide (CTAB), sodium dodecyl sulfate (SDS) and vitamin C (ascorbic acid) treatments in OFETs prepared using bottom-gate top-contact geometry. The OFETs constitute of cr-PVA as gate dielectric and poly(3-hexylthiophene-2,5-diyl) as channel semiconductor. CTAB and SDS are cationic and anionic surfactants respectively, known for formation of micelles with positively and negatively charged heads above critical micelle concentration (CMC), which contribute to the passivation of charge traps. Vitamin C is a reducing agent which

contributes to the passivation of positively charged defects. Without compromising the low power consumption, the passivation of charge traps present on the surface of cr-PVA results in ca. 50% higher specific dielectric capacitance and significant improvements in field-effect mobility (?FET), on/off current ratio, subthreshold swing and transconductance. ?FET of 0.35, 0.34 and 0.29 cm2 V-1.s-1 are presented for vitamin C, CTAB and SDS treated devices respectively, as compared to the ?FET of 0.09 cm2 V-1.s-1 for untreated device.

9568-146, Session PMon

Natural dielectrics in flexible organic fieldeffect transistors

Tzung-Fang Guo, Chun-Ting Yeh, Tzung-Da Tsai, National Cheng Kung Univ. (Taiwan)

Our previous study had demonstrated the fabrication of organic field-effect transistors (OFETs) and invertors by applying the chicken albumen (natural dielectrics) film directly from a fresh egg as the gate dielectrics (Adv. Mater. 2011, 23, 4077). Additionally, albumen dielectrics shows the enhanced ultraviolet fluorescence through plasmon resonance energy transfer of gold nanoparticles under the photo excitation (Sci. Rep. 2013, 3, 1505). In this presentation, the denaturation of albumen was modulated by varying the process of thermal treatment, resulting in the changes of the electrical, mechanical, and surface properties of chicken and duck albumen dielectrics and the optimization of OFET device performance.

The second part of presentation studies the OFETs fabricated with the other natural dielectrics from the porcine (pig) protein. The dielectric constant of porcine protein is approximate, 9.2-9.8, relatively higher than that of chicken albumen. The OFETs made of the porcine protein dielectrics exhibits the decent output characteristics, of an on-off ratio of roughly 10 4-10 5, a threshold voltage below -0.5 V. The porcine protein dielectrics-based complementary inverters were also fabricated in this study. A complementary inverter made of a pentacene p-channel OFET and a C60 n-channel OFET with porcine protein operated at the supply voltage (VDD) of 6 V is successfully demonstrated. The inverted output voltage is at 2.9 V as VDD of 6.0 V, in which the gain has reached a decent level of 25. Our results highlight the benefits of utilizing biomaterial dielectrics in fabricating organic and flexible electronics for applications.

9568-147, Session PMon

Dimensional extendibility in conjugation and ordering of solution-processed semiconducting polymers

Hoichang Yang, Mi Jang, Inha Univ. (Korea, Republic of); Ji-Hoon Kim, Pusan National Univ. (Korea, Republic of); Yun-Hi Kim, Gyeongsang National Univ. (Korea, Republic of); Do-Hoon Hwang, Pusan National Univ. (Korea, Republic of); Minjung Lee, Inha Univ. (Korea, Republic of)

Various conjugated polymers were synthesized with well-defined molecular weights, and their ϖ -conjugation extendibility were investigated. Crystal nanostructures of these conjugated polymers in films were controlled from rods, fibrils to percolated layers, depending on the backbone/side chains and film procedures. Electrical properties of these films in organic field-effect transistors (OFETs) supported that the both intra- and inter-molecular ϖ -conjugation of these polymers plays an important role in yielding better charge transport. Among these polymers synthesized, diketopyrrolopyrrole-based copolymers could develop highly percolated, conjugated layers on gate dielectrics, and the corresponding films showed high field-effect mobility up to 4 cm2V-1s-1 in OFETs.



9568-303,

Ultraflexible organic thin-film devices for wearable and implantable electronics

Takao Someya, The Univ. of Tokyo (Japan)

Mechanically flexible and stretchable devices are expected to open new possibilities in fields of wearable and implantable electronics. Especially, conformability, ruggedness, lightweight, biocompatibility, and large-area are all important to create new electronic applications that can be directly mounted on the surface of human skins and/or even inside the body. From this viewpoint, ultraflexible organic thin-film devices, such as organic light-emitting diodes (OLEDs), have attracted much attention recently. In this talk, we report recent progress of ultraflexible organic thin-film devices of 1?m. We will also describe emerging applications using ultraflexible and stretchable electronic systems in the fields of biomedical electronics.

9568-111, Session 3

Fundamental aspects in single crystal OFETs and large area crystalline films for applications (Invited Paper)

Marta Mas-Torrent, Freddy Del Pozo, Raphael Pfattner, Francisco Otón, Jaume Veciana, Concepció Rovira, Institut de Ciència de Materials de Barcelona (Spain)

Organic-based devices are currently attracting great attention for applications where low-cost, large area coverage and flexibility are required. In addition, the versatility of organic synthesis allows for the preparation of materials "à la carte". That is, since by chemically modifying their molecular structure and functionality, the solid state structure and the resulting macroscopic properties are altered, it is feasible to synthesize tailored materials for specific uses. Tetrethiafulvalenes (TTF) have shown to exhibit excellent OFET mobility (up to 6 cm2/Vs) as well as easy processability. Thus, TTFs offer a suitable platform to perform structuremobility correlation studies, due to the fact that their chemistry is very well-known making it possible to synthesize a large variety of very similar molecules exhibiting different solid-state organization or different electronic structure. Here we will describe our recent work related to explore the influence of crystal structure, polymorphism, electronic structure and device configuration and interfaces in TTF OFETs. Further, we demonstrate the fabrication of large area coverage devices based on solution processed blends of a TTF derivative with an inert polymer that exhibits an excellent performance and exceptionally environmental stability.

9568-112, Session 3

Polymorphism in the organic charge-transfer complex dibenzotetrathiafulvalene-7,7,8,8tetracyanoquinodimethane (DBTTF-TCNQ) and its effect on optical and electrical properties

Katelyn P. Goetz, Wake Forest Univ. (United States); Jun Ya Tsutsumi, National Institute of Advanced Industrial Science and Technology (Japan); Sujitra Pookpanratana, National Institute of Standards and Technology (United States); Jihua Chen, Oak Ridge National Lab. (United States); Tatsuo Hasegawa, National Institute of Advanced Industrial Science and Technology (Japan) and The Univ. of Tokyo (Japan); Oana D. Jurchescu, Wake Forest Univ. (United States) We present the structural, optical, and electronic properties of two polymorphs of the charge-transfer complex dibenzotetrathiafulvalene-7,7,8,8-tetracyanoquinodimethane (DBTTF-TCNQ). The structures were resolved using electron diffraction. One is a rectangular-shaped platelet and exhibits ambipolar transport with gold contacts in organic field-effect transistors (OFETs). The second polymorph grows as a thin, circular platelet and shows p-type transport within the same OFET structure. The difference in electrical characteristics originates from two factors. First, the position of the HOMO level of the rectangular polymorph lies 0.07 eV below that of the circular polymorph, as determined by ultraviolet photoelectron spectroscopy (UPS). Second, using X-Ray photoelectron and Raman spectroscopies we find that the degree of charge transfer between the donor DBTTF and acceptor TCNQ varies from 0.4e ± 0.1e for the rectangular crystals to 0.1e ± 0.1e for the circular crystals. Additional differences between the two polymorphs arise when measuring the absorbance of the crystals. First, the peak corresponding to intermolecular charge transfer is offset by 0.05 eV between the two polymorphs, in agreement with UPS measurements. Additionally, the polarization angle dependence of the intermolecular CT band for the rectangular crystal is shifted by 60deg with respect to the angle dependence of the intramolecular transition. In contrast, this shift was only 20deg for the circular polymorph. These angle dependences allowed us to couple the anisotropy of the electrical characteristics to the optical measurements. Our results demonstrate how slight modifications in crystal structure yield drastic differences in optical and electrical properties in organic semiconducting materials.

9568-113, Session 3

Fabrication of water-stable organic transistors using crystalline rubrene thinfilm and polymer-treated dielectric

Jaejoon Kim, KAIST (Korea, Republic of); Hyoek Moo Lee, LG Chem, Ltd. (Korea, Republic of); Sung Oh Cho, KAIST (Korea, Republic of)

For the real application of organic electronics, stable operation of electronic devices in humid or aqueous condition is essential and desirable. However, most of organic semiconductors were very weak to the oxygen or water and especially, cannot be operated well in aqueous condition without an encapsulation.

Here, we present water-stable organic thin-film transistors with highly crystallized rubrene and polymer-treated dielectrics. These high water-stability could be achieved by two factors. First, rubrene, a well-known p-type semiconducting material, showed high air and water stability after the crystallization of 'abrupt heating'. By the fabrication and aqueous operation of rubrene thin film transistor, we could show the water stability of crystallized thin-film rubrene. Such high environmental stability is attributed to the fact that rubrene has comparatively low HOMO level of -5.4 eV and large bandgap energy of 3.2 eV and that the rubrene thin-film is composed of well-interconnected orthorhombic rubrene crystals.

Second, the polymer-treatment of dielectrics can enhance long-term water stability of fabricated rubrene thin-film transistor. By the complete immersion test of transistors, we could characterize the increase of waterstability after the treatment of dielectrics with cross-linked polymer. For this purpose, polystyrene is cross-linked by electron irradiation and the water penetration into semiconductor/dielectric interface was decreased due to the decreased surface energy of polymer dielectric compared to the SiO?.

The fabricated rubrene thin-film transistors showed a field-effect mobility of ~0.5 cm?V??s?? and long-term stability under ambient and aqueous conditions. Also, we investigated their potential applications in chemical or bio sensors.



9568-114, Session 3

Charge transport and device physics of layered-crystalline organic semiconductors (Invited Paper)

Tatsuo Hasegawa, The Univ. of Tokyo (Japan)

Here we present and discuss our recent investigations into the understanding of microscopic charge transport, novel film processing technologies, and a development of layered-crystalline organic semiconductors for high performance OTFTs. We first discuss the microscopic charge transport in the OTFTs, as investigated by field-induced electron spin resonance spectroscopy. The technique can detect signals due to tiny amount of field-induced carriers, accumulated at the semiconductorinsulator interfaces. Following aspects are presented and discussed: 1) Carrier motion within the crystalline domains can be understood in terms of the trap-and-release transport, 2) charge trap states are spatially extended over several sites depending on the trap levels, and 3) the intraand inter-domain transport can be discriminated by anisotropic electron spin resonance measurements. Next we discuss novel print production technologies for organic semiconductors showing high layered crystallinity. The concept of "printed electronics" is now regarded as a realistic paradigm to manufacture light-weight, thin, and impact-resistant electronics devices, although production of highly crystalline semiconductor films may be incompatible with conventional printing process. We here present printing techniques for manufacturing high performance OTFTs; 1) double-shot inkjet printing for small-molecule-based semiconductors, and 2) push-coating for semiconducting polymers. We demonstrate that both processes are useful to manufacture high quality semiconductor layers with the high layered crvstallinity.

9568-115, Session 4

Characterizing the channel properties and operation of organic transistors with nonideal behavior (Invited Paper)

David J. Gundlach, National Institute of Standards and Technology (United States)

Field effect transistors based on organic semiconductor thin films (OTFTs) are of interest for a number of electronic applications where mechanical ruggedness, flexibility, and specific functionality is required. Continued improvement in materials design and novel processing have yielded several impressive technological demonstrations, and more recently, OTFTs with electrical properties significantly improved from previous reports. In this presentation, we examine device operation and critical electronic parameters by using impedance spectroscopy and quasi-static capacitancevoltage to disentangle and guantify the contributions of the contacts and channel as a function of applied voltage. To remove ambiguity associated with film formation and resulting microstructure we fabricated and characterized organic single crystal field effect transistors using the wellstudied organic semiconductor Rubrene. Rubrene single crystals were grown by vapor transport and laminated on top of oxidized silicon substrates with source and drain electrodes patterned by using photolithograpy, thermal evaporation, and lift-off process. Capacitance-voltage analysis was used to investigate channel accumulation and threshold voltage, and classical transmission line theory and modeling was used to quantify the contact and channel properties along with their response to the applied gate bias. The findings are compared with commonly employed DC electrical measurements to provide greater insight into intrinsic channel properties and highlight caveats in parameterizing the electronic properties of OTFTs which exhibit non-ideal electronic behavior.

9568-116, Session 4

Charge transport and device operation mechanisms in field-effect transistors with high mobility donor-acceptor polymer semiconductors (Invited Paper)

Takayuki Okachi, Tomoya Kashiki, Kenichiro Ohya, Sumitomo Chemical Co., Ltd. (Japan)

The field-effect transistors based on our donor-acceptor alternating polymer semiconductor were fabricated and the charge transport mechanisms were investigated. It was found that the electric field and the temperature dependences of the mobility can be fitted by a Poole-Frenkel model of charge transport. The mobility was increased with decreasing the channel length of the devices i.e., with increasing the lateral electric field, due to its small contact resistance. The mobility of higher than 1 cm²/Vs was achieved at room temperature with the channel length of smaller than 10 um. Although an apparent "band-like" negative temperature coefficient of the mobility has not been observed, an almost temperature independent mobility was observed in the transistors with a channel length of 5 um and the high mobility as large as 0.4 cm²/Vs was obtained even at 4 K due to its very low activation energy. Based on this material, the next generation polymer semiconductor with higher mobility and higher air stability has been successfully developed. The device operation mechanism of the transistors with high mobility donor-acceptor alternating polymers will be also discussed. It was revealed that the trapped electrons injected from the drain electrode prevent complete pinch-off in the saturation region in p-type transistors and can cause an inaccurate estimation of the intrinsic mobility.

9568-117, Session 4

Study on contact and channel resistance of pentacene-based ambipolar organic thin-film transistors

Tsung Jun Ho, Horng-Long Cheng, Guo En Yan, National Cheng Kung Univ. (Taiwan)

In this work, we investigated the electrical characteristics of pentacenebased ambipolar organic thin-film transistors (OTFTs) by modifying the channel length. We fabricated a top contact device structure with sliver as the source and drain electrodes and heavy doped p-type silicon wafer as the gate electrode. The channel length of the pentacene-based ambipolar OTFTs are 50, 100, 250, and 400 μ m; the channel width is fixed. The output current of the n-channel and p-channel decreases with increasing channel length. The saturated mobility and threshold voltage of both channels increase with the increase in channel length. The increase rate of saturated mobility and threshold voltage of the n-channel is larger than that of the p-channel. The influence of channel length on the electrical properties of the p-channel and n-channel is different. Furthermore, we utilized the gatedtransfer length method to study the contact resistance between sliver and pentacene and the channel resistance of pentacene. Contact and channel resistance decrease with the increase in gate voltage in the saturation region. The total resistance of pentacene-based ambipolar OTFTs increases with channel length at a fixed gate voltage. However, n-channel total resistance has stronger gate voltage and channel length dependence than p-channel total resistance. This result reveals that electron transport in the device channel requires a larger driving voltage than in the hole. Selecting a suitable channel length is critical to obtain a well-balanced performance of the dual carriers that transport ambipolar OTFTs and to avoid a large loss in injection barrier.

9568-118, Session 4

Charge transport physics of high mobility conjugated polymers (Invited Paper)

Deepak Venkateshvaran, Univ. of Cambridge (United Kingdom)



Over recent years there has been tremendous progress in developing low-temperature, solution-processible organic semiconductors that provide high charge carrier mobilities for both n-type and p-type device operation, good operational stability and other functionalities such as efficient electroluminescene, sensing or memory functions for a variety of applications. Here we are interested in understanding the charge transport physics of high mobility conjugated polymers and the relationship between molecular structure, polymer microstructure and charge transport. Many of the recently discovered high mobility polymers, in particular donor-acceptor copolymers, are characterised by a puzzling lack of pronounced crystalline order. In this presentation we will present our current understanding of the transport physics of these materials and of the reasons why these materials exhibit such high carrier mobilities.

9568-119, Session 5

Sub-15-nm patterning of asymmetric metal electrodes and devices by adhesion lithography (Invited Paper)

David Beesley, Thomas D. Anthopoulos, John C. de Mello, Imperial College London (United Kingdom)

Coplanar electrodes formed from asymmetric metals separated on the nanometre length scale are essential elements of nanoscale photonic and electronic devices. Existing fabrication methods typically involve electronbeam lithography—a technique that enables high fidelity patterning but suffers from significant limitations in terms of low throughput, poor scalability to large areas and restrictive choice of substrate and electrode materials. Here, we describe a versatile method for the rapid fabrication of asymmetric nanogap electrodes that exploits the ability of selected self-assembled monolayers to attach conformally to a prepatterned metal layer and thereby weaken adhesion to a subsequently deposited metal film. The method may be carried out under ambient conditions using simple equipment and a minimum of processing steps, enabling the rapid fabrication of nanogap electrodes and optoelectronic devices with aspect ratios in excess of 100,000.

9568-120, Session 5

Fabrication of a high-resolution roll for gravure printing of 2 μm features

Gerd Grau, Rungrot Kitsomboonloha, Vivek Subramanian, Univ. of California, Berkeley (United States)

High-resolution features are key to achieve high performance printed electronics devices such as transistors. Gravure printing is very promising to achieve high resolution in combination with high printing speeds on the order of 1m/s. High-speed gravure has recently been shown to print high resolution features down to linewidths and spacing of 2µm. Whilst this was a tremendous improvement over previous reports, these results had been obtained using silicon printing plates. These silicon printing plates are fabricated using microfabrication techniques which offers several advantages over traditional metal gravure cylinders where the features are defined by techniques such as stylus engraving, laser engraving or etching. This offers much greater precision and design freedom in terms of feature size, surface roughness, cell placement and cell shape. However, rigid silicon printing plates cannot be used in a roll-to-roll printing process that would truly enable low-cost printed electronics. Here we demonstrate for the first time a gravure printing roll that combines the precision of silicon printing plates with the form factor of a metal cylinder.

The fabrication process starts with a silicon master whose pattern is replicated by polymer molding. The actual metal printing plate is then built up on the polymer negative of the pattern by a combination of electroless and electroplating. After separation of the polymer and the metal, the metal printing plate can be mounted on a magnetic roll for printing. Printing of highly scaled 2μ m features is demonstrated. Different metal surfaces were explored to optimize printing performance and wear during printing.

9568-121, Session 5

Orthogonal lithography and doped organic semiconductors and their application in organic transistors

Daniel Kasemann, Alrun Günther, Xuhai Liu, Technische Univ. Dresden (Germany); Björn Lüssem, Kent State Univ. (United States); Karl Leo, Technische Univ. Dresden (Germany)

Organic field effect transistors (OFET) have been in the focus of research for more than two decades and their performance increases steadily. However, due to a lack of performance, flexibility in parameter design, and issues with upscaling the current processing techniques, they have not yet left the prototype stage for applications. In this contribution, we demonstrate the realization of novel organic transistor concepts to overcome the current limitations of OFET.

The performance of organic transistors as well as the potential for upscaling to large-area processing can be significantly enhanced by improved device geometry and structuring techniques. The transconductance and cut-off frequency of horizontal OFET are substantially limited by the charge carrier mobility and channel length, requiring channel lengths in the range of 1 µm. While difficult to realize in planar devices, we demonstrate that these dimensions can be easily achieved in vertical devices like vertical organic field effect transistors (VOFET)[1, 2] and organic permeable base transistors (PBT)[3]. In these devices, the contacts and the organic semiconductor are structured by a novel orthogonal photolithography [4], allowing for a precise vertical alignment as well as an upscaling to large areas. Furthermore, the controlled deposition of molecular dopants for selective manipulation of the semiconductor fermi level and a reduction of contact resistance.

[1] H. Kleemann et al, Org. Electron. 13, 506 (2012)

[2] H. Kleemann et al, Small 9, 21 (2013)

[3] A. Fischer et al, Appl. Phys. Lett. 101, 213303 (2012)

[4] S. Krotkus et al, Adv Optical Mater. 2(11), 1043 (2014)

9568-122, Session 5

The study for hydrogen bond rich dendron as dielectric layer for N-type OTFTs device

You-Yi Syu, National Taiwan Univ. (Taiwan)

A series of hydrogen bond rich (malonamide linkaged) dendrons were served as dielectric layer in organic thin-film transistors (OTFTs) device. The intramolecular hydrogen bond were generated between the malonamide linkage and imide linkage from the dendrons (as dielectric layer) and naphthalene diimide derivatives (NDI-R) (n-type semiconductor). The molecular packing of NDI-R were induced and enhanced during vacuum deposition process because of the intermolecular hydrogenbonded interaction. The interaction of hydrogen-bonded interface was characterized by ATR-FTIR, DSC and contact angle. The investigation of thin film morphology were performed by AFM and GIWAXS, the better enhanced regularity for NDI-R molecules could be found when G1 as dielectric layer. The mobility of those OTFTs were in the range of of 10-4-10-3 cm2/V•s. The properties are better than the standard device made by octadecyltrimethoxysilane (ODTS) as modification layer. The best performance is G1 as dielectric layer (mobility was 3.24x10-3 cm2/V•s, onoff current ratio was 3.1x104, and the threshold voltage was 22.59 V). In this study, the interaction between the dielectric layer and semiconducting layer can be enhanced by hydrogen-bonded dendrons. Modification of molecular generation will fine tune the electrical properties of OTFTs. Semiconducting layer with specific linkage for forming hydrogen bond will expect useful for this concept.



9568-123, Session 5

Fully printed flexible thin film transistor arrays (*Invited Paper*)

Adrien Pierre, Mahsa Sadeghi, Ana Claudia Arias, Univ. of California, Berkeley (United States)

Blade coating and slot die coating are alternative thin film deposition methods to inkjet printing that enable higher throughputs at the expense of inherently being a one-dimensional coating method. We have developed printing methods and optimized material formulations for the fabrication of fully printed and flexible arrays of organic thin film transistors (OTFTs). In our work, all layers are processed from solution and deposited and patterned by printing. These printed devices exhibit high reliability, low variability, ideal electrical behaviour and good mechanical properties. Blade coating on surface energy patterned (SEP) plastic substrates combines the scalable properties of a roll-to-roll compatible printing technique used to fabricate high quality homogeneous thin films with the practicality of generating two-dimensional patterns.

Using this technique, scalable self-aligned blade-coated source and drain (SD) electrodes with minimal variability can be very reliably printed. The high reliability and good performance of these arrays was achieved by characterizing the printability of each layer on the OTFT stack. The high yields combined with high device performance indicate that SEP blade coating is a scalable and robust technique which can be used to design electronic circuits where device reliability is required and could lead to all-printed systems on plastic.

9568-124, Session 6

Higher-dimensional organic semiconductors (Invited Paper)

John E. Anthony, Thilanga Liyanage, Anthony Petty, Univ. of Kentucky (United States)

The majority of high-performance organic semiconductors used in thin-film transistors are comprised of linearly-fused aromatic or heteroaromatic units, comprising a one-ring-wide ribbon of conjugated surface. While perylene derivatives are near-ubiquitous in organic electronics, other fused-ring systems with widths greater than one ring are much less common, typically due to the difficulties in synthesis of these types of compounds. In this talk, I will discuss our approach to wider aromatic ribbons, their scalable synthesis, their crystal engineering, and the evaluation of their stability and charge-transport properties.

9568-125, Session 6

Novel nature-inspired conjugated polymers for high performance transistors and solar cells (Invited Paper)

Hugo A. Bronstein, Kealan Falon, Univ. College London (United Kingdom); Nir Yaacobi-Gross, Raja Shahid Ashraf, Iain McCulloch, Thomas D. Anthopoulos, Imperial College London (United Kingdom)

Novel, extremely narrow band-gap polymer with a structure based on natural indigo has been synthesised and exhibits high crystallinity, high ambipolar transport in OFET devices, and OPV device efficiencies up to 2.35% with light absorbance up to 950 nm, demonstrating potential in near-IR photovoltaics. We demonstrate that the use of a potentially bio-sustainable monomer unit in a conjugated polymer can give balanced ambipolar OFET mobilities in excess of 0.5 cm2/Vs. This novel monomer, and polymers are synthesized by rigidifying the structure of indigo by condensation with an aromatic acidic acid. The materials display high crystallinity which can be further enhanced by annealing and demonstrate that it can be used as a potentially biosustainable alternative to the commonly used DPP and iso-indigo monomers. We believe this is the first attempt to tackle the issue of sustainability in conjugated polymer synthesis.

9568-126, Session 6

Controlling conjugation and solubility of diketopyrrolopyrrole derivative copolymers for organic field-effect transistors

Mi Jang, Inha Univ. (Korea, Republic of); Ji-Hoon Kim, Do-Hoon Hwang, Pusan National Univ. (Korea, Republic of); Hoichang Yang, Inha Univ. (Korea, Republic of)

Diketopyrrolopyrrole (DPP)-based copolymers, including poly[2,5-bis(2-octyldodecyl)pyrrolo[3,4-c]pyrrole-1,4(2H,5H)-dione-alt-(E)-1,2-di(2,2'-bithiophen-5-yl)ethene (PDDBE) and poly[2,5-bis(2-octyldodecyl) pyrrolo[3,4-c]pyrrole-1,4(2H,5H)-dione-alt-(E)-1,2-bis(6-hexylthieno[3,2-b] thiophene-2-yl)ethene (PDTE), were synthesized by alternating a DPP-derivative acceptor (A) block with different donor (D) blocks, such as (E)-1,2-di(2,2'-bithiophene-5-yl)ethene and (E)-1,2-bis(6-hexylthieno[3,2-b] thiophene-2-yl)ethene. These copolymers had drastically different crystal structures on polymer-grafted SiO2 dielectrics. Multiple-layered crystallites of PDDBE had a long-range, ϖ -conjugated extension but a wide conjugated distance, d(010), of 3.71 Å, originating from the alternating structures of the DPP derivative with slightly different D blocks. The corresponding crystallites yielded a wide range of mobilities from 0.01 to 1.40 cm2V-ls-1 in the OFETs.

9568-127, Session 6

Intertwined co-assemblies in liquidcrystalline semi-conducting materials: Towards a new class of nanostructured supramolecular organic semiconductors

Fabrice Mathevet, Yiming Xiao, Danli Zeng, Univ. Pierre et Marie Curie (France); Martin Brinkmann, Institut Charles Sadron (France); Benoît Heinrich, Bertrand Donnio, Institut de Physique et Chimie des Matériaux de Strasbourg (France); Jeong Weon Wu, Jean-Charles Ribierre, Ewha Womans Univ. (Korea, Republic of); Emmanuelle Lacaze, David Kreher, André-Jean Attias, Univ. Pierre et Marie Curie (France)

The self-organization of ϖ -conjugated organic materials forming highly ordered supramolecular architectures has been extensively investigated in the last two decades in view of optoelectronic applications. Indeed, the control of both the mesoscopic and nanoscale organization within thin semiconducting films is the key issue for the improvement of charge transport properties and achievement of high charge carrier mobilities. These well-ordered materials are currently either self-organized semiconducting polymers or liquid crystals.

In this context, we endeavored to investigate the self-organization of semiconducting liquid crystalline materials incorporating different kind of ϖ -conjugated systems in unique molecular or macromolecular architectures. Here we describe the design and synthesis of (i) dyads and triads combining discotic or calamitic ϖ -conjugated mesogens, and (ii) side-chain liquid crystal semiconducting polymers where the backbone is a ϖ -conjugated polymer and the side groups are ϖ -conjugated discotic mesogens.

In this work, we will give the details on the synthesis, structural characterization and morphology studied by Polarized-light Optical Microscopy (POM), Differential Scanning Calorimetry (DSC), Temperature-dependent small-angle X-ray diffraction, Grazing-incidence X-ray scattering (GIXS) and Atomic Force Microscopy (AFM). Moreover, their charge transport properties studied in OFET configuration will also be depicted.



9568-128, Session 6

Printable semiconductors for all-polymer transistors and circuits (*Invited Paper*)

Antonio F. Facchetti, Polyera Corp. (United States)

In this presentation we will describe the design rationale, synthesis, characterization, of several organic semiconducting polymers for printed thin-film transistors (TFTs) and understand their charge-transport characteristics as a function of the device architecture. Furthermore, we will disclose new interfacial modifications dramatically enhancing the electron injection efficiency. Finally we will report the realization of printed organic TFTs and complementary circuits with high charge carrier mobilities where all the TFT components are polymers.

9568-129, Session 7

Charge transport in highly aligned conjugated polymers (Invited Paper)

Brendan O'Connor, Xiao Xue, Tianlei Sun, North Carolina State Univ. (United States)

Charge transport in conjugated polymers has a complex dependence on film morphology. Aligning the polymer chains in the plane of the film simplifies the morphology of the system allowing for insight into the morphological dependence of charge transport. Highly aligned conjugated polymers have also been shown to lead to among the highest reported field effect mobilities in these materials to date. In this talk, a comparison will be made between aligned polymer films processed using two primary methods, nanostructured substrate assisted growth and mechanical strain. A number of polymer systems including P3HT, pBTTT, N2200, and PCDTPT are considered, and the processed films are analyzed in detail with optical spectroscopy, AFM, TEM, and X-ray scattering providing insight into the molecular features that allow for effective alignment. By contrasting the morphology of these films, several insights into underlying charge transport limitations can be made. A number of key morphological features that lead to high field effect mobility and charge transport anisotropy in these films will be discussed. In addition, several unique features of organic thin film transistor device behavior in these systems will be examined including the commonly observed gate voltage dependence of saturated field effect mobility.

9568-130, Session 7

Percolation, tie-molecules, and microstructural origins of charge transport in semicrystalline conjugated polymers

Sonya A. Mollinger, Brad Krajina, Stanford Univ. (United States); Rodrigo J. Noriega-Manez, Univ. of California, Berkeley (United States); Alberto Salleo, Andrew J. Spakowitz, Stanford Univ. (United States)

Semiconducting polymers play an important role in a wide range of optical and electronic material applications. Polymer thin films that result in the highest performance typically have a complex semicrystalline morphology, indicating that considerable device improvement can be achieved through optimization of microstructural properties. However, the connection between molecular ordering and device performance is difficult to predict due to the current need for a mathematical theory of the physics that dictates charge transport in semiconducting polymers. It is experimentally suggested that efficient transport in such films occurs via connected networks of crystallites. We present an analytical and computational description of semicrystalline conjugated polymer materials that captures the impact of polymer conformation on charge transport in heterogeneous thin films. We first develop an analytical theory for the statistical behavior of a polymer emanating from a crystallite and predict the average distance to the first kink in the chain that traps a charge. We use this analysis to define the conditions for percolation and the consequent efficient transport through a semicrystalline material. We then establish a charge transport model using Monte Carlo simulations that predicts the multi-scale charge transport and crystallite connections. We approximate the thin film as a two-dimensional grid of crystallites embedded in amorphous polymer. The chain conformations in the amorphous region are determined by the wormlike chain model, and the crystallites are assigned fixed mobilities. We use this model to identify limits of charge transport at various time scales for varying fraction of crystallinity.

9568-131, Session 7

Organic blend semiconductors and transistors with hole mobility exceeding 10 cm2/Vs

Alexandra F. Paterson, Thomas D. Anthopoulos, Imperial College London (United Kingdom)

Plastic electronics that can be manufactured using solution-based methods are the subject of great research interest due to their potential for lowcost, large-area electronic applications. The interest in this field has led to considerable research and subsequent advances in device performance. To this end solution-processed organic thin-film transistors (OTFTs) have shown impressive improvements in recent years through the increasing values of charge carrier mobility. Here we report the development of next generation organic blend materials for OTFTs with hole mobilities of 10 cm2/Vs. These high performance devices have been achieved using a novel semiconducting blend system comprising of an amorphous-like conjugated polymer and a high mobility small molecule. The combination of a highly crystalline small molecule with the polymer binder aids the formation of uniform films as well as enables an element of control over the nucleation and growth of the small molecule. The polymer binders investigated belongs to the family of indacenodithiophene-based copolymers which are renowned for their high carrier mobilities regardless of their apparent structural disorder. The addition of the polymer with carefully chosen small molecules is found to further increase the hole mobility of the resulting blend OTFT to over 10 cm2/Vs. These organic devices provide an interesting insight into this rather complex blend system, highlighting the correlation between the morphology developed following solution processing and device performance, as well as exploring the role of each of the two components in the blend in terms of their contribution to charge transport.

9568-132, Session 7

Decoupling the semiconductor crystallization from the coating process to the benefit of solution-processed smallmolecule organic thin film transistors (Invited Paper)

Aram Amassian, King Abdullah Univ. of Science and Technology (Saudi Arabia)

Recent progress in the design and processing of organic semiconductors (OSC) has made it easier to routinely fabricate high performance organic thin film transistors (OTFTs) with carrier mobility in the 1-10 cm2/ Vs range. Here, we take a closer look at the crystallization behavior of small molecule OSCs with respect to the solvent evaporation behavior in different processes and reveal - in certain circumstances - a surprising new mechanism of nucleation reminiscent of two-step nucleation previously only seen in proteins, colloids and other soft matter, whereby an intermediate disordered phase of the solute forms prior to crystallization. The two-step nucleation in effect decouples the solvent drying and film formation from the crystallization process, leading to dramatically improved microstructure and morphology which can be credited with substantially improved performance. We demonstrate the universality of this method for a wide range of OSCs and OSC-polymer blends. We also take this idea to the next



level wherein we demonstrate how it can be exploited in the case of certain OSCs to induce crystallization on demand according to predetermined patterns, e.g., along the channel of an OTFT, with significant benefit to performance and to its spread.

9568-133, Session 8

Thermocleavable side chains: A gateway to new processing routes for semiconducting polymers (Invited Paper)

Bob C. Schroeder, Zhenan Bao, Stanford Univ. (United States)

Solubilising side chains are an essential part of semiconducting polymers and their engineering has shifted into focus over the last couple of years. The solution processability of conjugated polymers is one of the major advantages over silicon based semiconductors and would not be possible without the use of solubilising side chains. However with ongoing research, it became apparent that by careful side chain engineering certain properties of the conjugated backbone could be enhanced or supressed depending on the application. Nowadays side chain design is crucial to achieve high performing organic field effect transistors (OFET) and often significant synthetic efforts are taken to balance the semiconducting properties of conjugated polymers by means of side chain engineering. Despite their importance, side chains do not actively contribute to the semiconducting properties of the polymer. Their electrically insulating character could actually hinder charge transport between adjacent polymer chains and if poorly designed disrupt the solid state packing in the material.

To circumvent these problems, we developed thermocleavable side chains. This allows us to deposit the polymer from conventional organic solvents and to remove the side chains by post-deposition thermal annealing. By taking this two-step approach, we are able to maintain the advantages of solution processability, but at the same time allow the polymer chains to pack closely to achieve superior charge transport characteristics. Furthermore, stripping the polymer of its side chains significantly alters its solubility, making the use of orthogonal solvents for subsequent layer unnecessary, thus open-up new and potentially "greener" processing routes.

9568-134, Session 8

Oligothiophene-based monolayer OFETs by Langmuir techniques

Sergey A. Ponomarenko, Institute of Synthetic Polymeric Materials (Russian Federation) and Lomonosov Moscow State Univ. (Russian Federation); Elena V. Agina, Alexey S. Sizov, Institute of Synthetic Polymeric Materials (Russian Federation); Daniil S. Anisimov, Lomonosov Moscow State Univ. (Russian Federation); Oleg V. Borshchev, Maxim A. Shcherbina, Institute of Synthetic Polymeric Materials (Russian Federation); Sergey N. Chvalun, Institute of Synthetic Polymeric Materials (Russian Federation); Dmitry Y. Paraschuk, Lomonosov Moscow State Univ. (Russian Federation)

Nowadays development of efficient self-assembled monolayer field-effect transistors (SAMFETs) is a challenge of organic electronics. SAMFETs could provide a significant reduction of rather expensive organic semiconducting materials consumption without the device performance degradation. The known technique for SAMFET fabrication is a self-assembly from solution [E.C.P.Smits, et all, Nature, 2008, 455, 956] that requires highly reactive functional semiconducting molecules and inert atmosphere, it takes at least ten hours and could not be applied in industry.

Herein, we report a novel fast, easily processible and highly reproducible approach to oligothiophene-based SAMFETs fabrication by Langmuir, Langmuir-Blodgett (LB) and Langmuir-Schaefer (LS) techniques. It was shown that LB and LS techniques allow successful fabrication of 2D

crystalline semiconducting monolayers based on various organosilicon derivatives of oligothiophenes. An influence of conjugation length and anchor group chemistry of the semiconducting self-assembling molecules on the monolayer structure and electric performance of the SAMFETs was systematically investigated and optimal conditions of SAMFETs fabrication were determined. The efficient SAMFETs with charge carrier mobilities up to 0.01 cm²/Vs and on/off ratio up to 10⁶ based on chlorosilane and disiloxane derivatives of oligothiophenes were fabricated and their functionality in integrated circuits under normal air conditions were demonstrated [Appl. Phys. Lett. 2013, 103, 043310; Langmuir, 2014, 30, 15327]. The performance of the reported SAMFETs is close to those of the SAMFETs prepared by self-assembly from solution. The results obtained demonstrate that the presence of covalent bonds between a semiconducting monolayer and a substrate is not crucial for the monolayer OFETs performance.

9568-135, Session 8

Organic vertical field effect transistors: Achieving high on-off ratio and vertical integration with OLEDs

Hyukyun Kwon, Mincheol Kim, Hyunsu Cho, Seunghyup Yoo, KAIST (Korea, Republic of)

Organic vertical field effect transistors (VFETs) have been explored to enhance the output current level and device operation speed due to the inherent low carrier mobility of organic semiconductors. However, most of VFETs reported to date involve a complex source electrode patterning process owing to their operation mechanism. Here, we investigate on VFETs based on C60 that do not require complex source electrode patterning process by insulting the top surface of a source electrode embedded in C60 layer [1]. In a VFET structure studied in this work, current flow is controlled by the electric field between a gate and a source electrode embedded within an active layer which is called bottom active layer. Based on its operation mechanism, several geometrical parameters such as (i) bottom active layer thickness; (ii) presence of a charge blocking layer and its thickness ensuring insulating properties; and (iii) the width of electrodes are identified as key factors influencing device performance. Through the device optimization with these parameters, the proposed organic VFETs exhibit a large on/off ratio of 6?10⁵ and output current that is greater than that of a conventional C60 based OTFT with a similar device dimension. In order to show the benefit of VFETs, a single-pixel organic light-emitting diode (OLED) is integrated vertically with the VFETs under study.

9568-136, Session 8

Sub-threshold charge transport in polymer/organic field-effect transistor (Invited Paper)

Seohee Kim, The Univ. of Texas at Austin (United States); Tae-Jun Ha, Kwangwoon Univ. (Korea, Republic of); Prashant M. Sonar, Queensland Univ. of Technology (Australia); Ananth Dodabalapur, The Univ. of Texas at Austin (United States)

Polymer field-effect transistors have been highlighted in the past two decades due to their promising properties and potential for use in large-area electronics and displays. Along with the advance of performance, a detailed understanding on charge carrier transport in polymer field-effect transistors has become more important. In this presentation we provide methods to distinguish between the various modes of conduction and preset a detailed analysis and interpretation of charge transport in the sub-threshold drift-limited regime.

Our experimental results are based on the diketopyrrolopyrrole (DPP) core based polymer transistors which have received a lot of attention especially for their large mobilities exceeding 2 cm2/Vs. Similarly to the other transistors which have a lot of disorder, sub-threshold regime conduction



is critical in polymer field-effect transistors even at high gate voltages and should be analyzed separately from above threshold conduction. In this work, we present the modeling process for the DPP core based co-polymer field-effect transistors. A separate modeling of conduction in the sub-threshold regime provides us a lot of meaningful information. The accurate calculation method for the density of trap states (DOS) in polymer transistors, which is the one of the key methods in describing charge carrier transport phenomena in transistors, will be presented. In addition, a subthreshold behavior of polymer transistors, such as the separation of subthreshold regime into two different regimes and the dominant charge carrier transport mechanism in each regime of polymer transistors with varying temperature, will be analyzed in detail.

Conference 9569: Printed Memory and Circuits

Monday - Thursday 10-13 August 2015

SPIE. PHOTONICS ORGANIC PHOTONICS+ ELECTRONICS

Part of Proceedings of SPIE Vol. 9569 Printed Memory and Circuits

9569-17, Session PMon

Frequency dependent learning achieved using a type of semiconducting polymer/ electrolyte composite

Wenshuai Dong, Fei Zeng, Tsinghua Univ. (China)

Frequency dependent learning, i.e., the conventional spike-rate-dependentplasticity learning model (SRDP), has been achieved using semiconducting polymer/electrolyte composite cells of Pt/MEH-PPV/ PEO+Li^+/Pt. These cells responded to depression at low frequency stimulation and to potentiation at high frequency stimulation. This frequency selection displayed a long term memory up to hours and was a unidirectional behavior, which occurred only when applied positive bias but not negative ones. The transition threshold ?m from depression to potentiation varied depending on the previous stimulations. The consumption of this device can be very low compared to other existed artificial synaptic systems, as the current inside it is just tens of nA. Using mixture of semiconducting polymer and electrolytes, i.e., light-emitting electrochemical cells, could simplify fabrication of artificial synapse and related neuromorphic circuits, giving a future that intelligentization of image cognition, photon detection and light emitting could be integrated in a single LEC based circuit. A random channel model was proposed based on the SEM images, to describe ionic kinetics at polymer/electrolyte interface during and after stimulations with various frequencies, and gave a reasonable explanation of our frequency dependent learning behavior.

9569-18, Session PMon

Band-pass filtering phenomenon of a semiconducting polymer/electrolyte composite

Xiaojun Li, Wenshuai Dong, Fei Zeng, Tsinghua Univ. (China)

We reported here a band-pass filtering phenomenon of MEH-PPV/PEO+Cs+ composite, which had been studied as a promise planar light source, i.e., light-emitting electrochemical cells (LECs). Pt/MEH-PPV/PEO+Cs+/Ag cell (Cs-LEC) and Pt/PEO+Cs+/Ag cell (Cs-PEO) were fabricated. Pulse responses were studied by using rectangular pulse with amplitude of 0.5 V, width of 5 ms and varied frequencies. It was found that the charging and discharging peaks varied with input frequency. The weights of responses to various frequencies were calculated by using the responses to 1 Hz as baseline. The responses of Cs-LEC were depressed with a weight modification by 30% between frequency ranges of 50 to 100 Hz, which were irrelative to input sign and types of electrodes. This demonstrated that signal could be transferred bi-directionally. The observed results were repeatable and stable. After exposed under environment of 65% humidity and 25oC for a period of two months, the Cs-LECs displayed moderate degradation. However, the weight of responses of Cs-PEO was found to be potentiated after 50 Hz frequency. The state of Cs ionic pairs in PEO and migration cross polymer/electrolyte interface might play important roles in our observation. Our study gives a strong confidence in uses of LECs for information handling and synaptic computation.

9569-19, Session PMon

Conjugated polymer nanoparticles as nano floating gate electrets for high performance non-volatile organic transistor memory devices

Chien-Chung Shih, Wen-Chang Chen, Wen-Ya Lee, Yu-

Cheng Chiu, Jung-Yao Chen, National Taiwan Univ. (Taiwan)

We developed a molecular nano-floating gate of pentacene based transistor memory devices using conjugated polymer nanoparticles (CPN) as the discrete trapping sites embedded in an insulating polymer, Poly (methacrylic acid)(PMAA). The nanoparticles of polyfluorene (PF) and poly(fluorene-altbenzo[2,1,3]thiadiazole (PFBT) with average diameters of around 50-70 nm were used as a charge-trapping sites, while hydrophilic PMAA served as a matrix and a tunneling layer. By inserting PF nanoparticles as the floating gates, the transistor memory device revealed a controllable threshold voltage shift, indicating effectively electron-trapping by the PF CPN. The electron-storage capability could be further improved using the PFBTbased NFG since their lower LUMO level was beneficial for stabilization of the trapped charges, leading a large memory window (35 V), retention time longer than 104 s with a high ON/OFF ratio of >104. In addition, the memory device performance using conjugated polymer nanoparticle NFG was much higher than that of the corresponding polymer blend thin films of PF/polystyrene (PS). It suggested that the discrete polymer nanoparticles could be effectively covered by tunneling layer, PMAA, to achieve the superior memory characteristics. Besides, the beta phase formation was observed in the conjugated polymer nanoparticles but not in blend system. PF nanoparticles with the beta phase may provide more stable energy state to store electrons than in the PF/PS blend. Our proposed nano-floating conjugated nanoparticles as charge storage sites provides a promising potential route towards the solution-processed organic transistor memories.

9569-20, Session PMon

Oligosaccharide dielectrics towards high performance non-volatile transistor memory devices

Yu-Cheng Chiu, Han-Sheng Sun, Wen-Ya Lee, National Taiwan Univ. (Taiwan); Halila Sami, Redouane Borsali, Ctr. de Recherches sur les Macromolécules Végétales (France); Wen-Chang Chen, National Taiwan Univ. (Taiwan)

Natural-polymers have the potential applications as the substrate or dielectric materials for next-generation green electronics. Herein, we employ the glucose-based oligosaccharides as the gate dielectric to control the threshold voltage of organic field-effect transistor (OFET) based memory devices. The green dielectric, maltoheptaose (MH) and pentacene are employed as the charge-trapping layer and the p-type semiconductor, respectively. The device with the bottom-gate-top-contact configuration exhibits outstanding write-once-read-many (WORM)-type behavior, attributed to the irreversibly electrochemical reaction on the hydroxy groups. The OFET memory device using the MH charge storage layer shows a significant memory window (39.9 V), a high ON/OFF current ratio (>106) and an excellent retention time over 15 days, which is comparable (or even better) to that of the state-of-the-art nano-floating gate memory devices reported in the literature. Moreover, the high-k MH layer can effectively decrease the operation voltage of memory down to the drain voltage of -4 V and maintain the high ON/OFF ratio. The operating mechanism for the dielectric is clarified by an analog device with N-type semiconductor as the active layer and further probed by Kelvin force microscopy. Another two polysaccharides containing the glucose segments are also shown similar results to those of the MH based OFET memory device, revealing the promising application of oligosaccharides for green electronics.

9569-21, Session PMon

Inkjet-printing of non-volatile organic resistive devices and crossbar array structures

Stefan Sax, Sebastian Nau, Alexander Blümel, Karl Popovic,



NanoTecCenter Weiz Forschungsgesellschaft mbH (Austria); Emil J. W. List-Kratochvil, NanoTecCenter Weiz Forschungsgesellschaft mbH (Austria) and Technische Univ. Graz (Austria)

Due to the increasing demand for storage capacity in various electronic gadgets like mobile phones or tablets new types of non-volatile memory devices have gained a lot of attention over the last years. Especially multilevel conductance switching elements based on organic semiconductors are of great interest due to their relatively simple device architecture and their small device feature size. Since organic semiconductors combine the electronic properties of inorganic materials with the mechanical characteristics of polymers, this class of materials are suitable for solution based large area device preparation techniques. Consequently, ink jet based deposition techniques are highly capable to face all preparation related requirements.

In this contribution we present a route towards the first all ink jet printed organic resistive switching memory device. In a detailed study the influence of ink jet printing on the device performance was demonstrated by the stepwise replacement of each functional layer.

A distinct impact to the IV – characteristics was found and analyzed. Along these lines the integration of ink jet printed devices into a fully functional crossbar array structures is reported.

9569-22, Session PMon

Recent progress in printed 2/3D electronic devices

Andreas Klug, Karl Popovic, Alexander Blümel, Stefan Sax, Emil J. W. List-Kratochvil, NanoTecCenter Weiz Forschungsgesellschaft mbH (Austria)

New, energy-saving, efficient and cost-effective processing technologies such as 2D and 3D inkjet printing (JJP) for the production and integration of intelligent components will be opening up very interesting possibilities for industrial applications of molecular materials in the near future. Beyond the use of home and office based printers, "inkjet printing technology" allows for the additive structured deposition of photonic and electronic materials on a wide variety of substrates such as textiles, plastics, wood, stone, tiles or cardboard. Great interest also exists in applying IJP in industrial manufacturing such as the manufacturing of PCBs, of solar cells, printed organic electronics and medical products. In all these cases inkjet printing is a flexible (digital), additive, selective and cost-efficient material deposition method. Due to these advantages, there is the prospect that up to now used standard processes can be replaced through this innovative material deposition technique.

A main issue in this research area is the formulation of novel functional inks or the adaptation of commercially available inks for specific industrial applications and/or processes. In this contribution we report on the design, realization and characterization of novel active and passive inkjet printed electronic and photonic devices such as sensors and memory devices and the heterogeneous integration in printed 3D packages and demonstrators. The main emphasis of this presentation will be on how to convert scientific inkjet knowledge into industrially relevant processes and applications.

9569-23, Session PMon

Optical memory effect in ZnO nanowire based organic bulk heterojunction devices

Arash Takshi, Anand K. Santhanakrishna, Univ. of South Florida (United States)

Due to the required stablished field to separate photogenerated electrons and holes, the current- voltage (I-V) characteristic in almost all photovoltaic devices in dark is an exponential curve. Upon illumination, the shape of the curve remains almost the same, but the current shifts due to the photocurrent. Also, because of the lack of any storage mechanism, the I-V curve returns to the dark characteristic immediately after cessation of the light. Here, we are reporting a photo-electric memory effect in an organic bulk hetrojuction device made of ZnO nanowires as the electron transport layer. The study of the I-V characteristic in dark and light showed a unique change from a rectifying response in dark to a resistive behavior in light. Additionally, after cessation of light, it was observed that the transition from the resistive to rectifying response occurred very slowly, taking about 270 minutes to fully return to the original characteristic in the dark. To our best of the knowledge, such a long opto-electric memory effect has not been observed before in any organic photovoltaic devices. Repeatability of the memory effect was tested by illuminating the cell and measuring the I-V characteristics in several cycles. Also, the impedance study of the device showed a significant change in the dark and light responses. For practical applications as a photo memory device, further experiments are required to gain a better understanding of the mechanism behind the observed memory effect.

9569-24, Session PMon

Flash memory based on solution processed hafnium dioxide charge trapping layer

Jiaqing Zhuang, Su-Ting Han, Ye Zhou, Roy Vellaisamy, City Univ. of Hong Kong (Hong Kong, China)

Hafnium dioxide (HfO2) film prepared by the sol-gel technique has been used as a charge trapping layer in organic flash memory. The thickness, crystallinity and morphology of HfO2 fabricated under various conditions were investigated. X-ray diffraction (XRD) patterns indicated the formation of monoclinic HfO2 crystals with increasing annealing temperature. Atomic force microscopy (AFM) images showed relatively smooth films of HfO2 growth. The annealing temperature-dependent effects on the memory window as well as data retention properties have been discussed. A large memory window and long data retention time have been achieved for the pentacene-based flash memory. The results demonstrate that solution processed HfO2 film could be a promising candidate as a charge trapping layer in printable flash memory.

9569-25, Session PMon

Cellulose-based material as dielectric layer in organic complementary inverters

Barbara Stadlober, Alexander Fian, JOANNEUM RESEARCH Forschungsgesellschaft mbH (Austria); Archim Wolfberger, Thomas Grießer, Montan Univ. Leoben (Austria); Mihai Irimia-Vladu, Andreas Petritz, JOANNEUM RESEARCH Forschungsgesellschaft mbH (Austria)

We report on Trimethylsilylcellulose (TMSC), a natural source based material, as ultrathin dielectric layer for organic thin film transistors and complementary inverters. Dielectric films of about 30 nm are used as gate dielectric on 28 nm thick alumina generated by anodization of the aluminum gate electrode. These thin inorganic/organic bilayer dielectrics exhibit low gate leakage currents of 10-9 A/cm2 at an electric field of 3.0 MV/cm2. Pentacene and C60 based transistors are fabricated using this bilayer dielectric and implemented in organic complementary inverters. The fabricated inverters show excellent performance with respect to high gains up to 1600, high noise margin values of 92.5 % for a supply voltage as low as 4 V.

All measurements within a period of 45 days show noise margin values above 87% for a supply voltage as low as 4 V, indicating a good electrical stability thus making these inverters highly suitable for complex electronic circuits.



9569-1, Session 1

Printed organic nanowire synaptic transistors (Invited Paper)

Wentao Xu, Sung-Yong Min, Hyunsang Hwang, Tae-Woo Lee, Pohang Univ. of Science and Technology (Korea, Republic of)

A human brain consumes only as much energy as household light bulb, but can overperform a super computer in many aspects. This ability is realized by a dense network of 1012 neurons and 1015 synapses, where synapses play an important role in human-brain computation and memory. Recently, great efforts have been made to develop synapse-emulating electronic devices, which have reduced energy consumption per synaptic event to picoloules. However, reducing it to the femtoloule level that is comparable to biological synapses is still a challenge. Here, we demonstrated here organic nanowire (ONW) synaptic transistors. The devices emulated functions of a biological synapse, including presynaptic-spike-induced excitatory postsynaptic current (EPSC), inhibitory post-synaptic current (IPSC), short-term plasticity and long-term plasticity. The active channels are composed of highly-aligned ONWs that have a semiconducting polymer inner core in an insulating polymer sheath. These ONW STs consume ~43 fJ per synaptic event, which is so far the lowest among currently available synaptic devices. The ultra-low-energy consuming nanoscale-dimension ONW STs with highly aligned ONW active channels exhibited great promise for realizing intelligent electronics and assembling soft neuromorphic systems with nano-feature size.

9569-2, Session 1

Unraveling the role of space-charge switch mechanism in hybrid non-volatile memory devices

Giovanni Ligorio, Marco Vittorio Nardi, Humboldt-Univ. zu Berlin (Germany); Martin Brinkmann, Institut Charles Sadron (France); Dieter Neher, Univ. Potsdam (Germany); Norbert Koch, Humboldt-Univ. zu Berlin (Germany) and Helmholtz-Zentrum Berlin für Materialien und Energie GmbH (Germany)

The increasing interest in non-volatile memory devices has extended the exploration towards new materials, such as organic-inorganic hybrids. Devices based on organic semiconductors and embedded metal nanoparticles (MNPs) were found to display resistive bistability, suitable for programmable electronic applications.

Different models were developed to explain the resistive switching mechanism occurring in the devices. Charging/de-charging of MNPs and concomitant resistivity changes was mainly proposed as mechanism, despite the lack of solid experimental evidence.

In this contribution we report on the role of the space-charge field due to charged MNPs in two-terminal devices, via electrical characterization. Devices comprise 4,4-bis[N-(1-naphthyl)-N-phenyl-amino]diphenyl (?-NPD) with embedded gold nanoparticles (AuNPs). The electrical characterization (current vs bias) of the devices was conducted with and without illumination during operation. Due to the energy level alignment of the chosen materials, the AuNPs behave as deep charge carrier traps. The induced space-charge spontaneously sets the device to the low conductivity state. The de-charging of the AuNPs can then be dynamically induced through illumination, setting the device to a high conductivity state.

Despite the ability to optically control the charging state of the AuNPs, the devices do not display any bistability. This finding provides evidence that the commonly proposed MNPs charging/de-charging mechanism can be excluded as the cause for electrical bistability in two-terminal devices, and that other mechanisms, such as filament formation, should be evoked.

9569-3, Session 1

Electroforming and resistive switching in alkalihalide - polymer diodes

Stefan C. J. Meskers, Benjamin F. Bory, Technische Univ. Eindhoven (Netherlands); Paulo Rocha, Max-Planck-Institut für Polymerforschung (Germany); Henrique L. Gomes, Univ. do Algarve (Portugal); Dago M. de Leeuw, Max-Planck-Institut für Polymerforschung (Germany)

Organic-Inorganic hybrid diodes containing alkali halide and semiconducting polymer layers, show non-volatile resistive switching after electroforming. The resistive switching is due to voltage-induced changes in the effective work function of the combined alkalihalide and metal contact layer in the diodes . Electroluminescence measurements show that the diodes are electrically bistable and can switch between hole-only and bipolar charge transport configurations.

Before the diodes show non-volatile memory effects, they need to be electroformed. Electroforming involves Frenkel defect formation in the alkalihalide layers of the diodes and results from application of bias voltage exceeding the bandgap of the alkali halide. The electroforming process is completed when the defect density exceeds a critical limit (estimated at $10^{25}/m^{3}$). The resistive switching after electroforming results from changes in the ionization state of the defects in the alkali halide layers.

9569-4, Session 1

Characterizing filamentary switching in resistive memories (Invited Paper)

Yan Busby, Jean-Jacques Pireaux, Univ. of Namur (Belgium)

Characterizing filamentary switching in resistive memories

For many organic, inorganic and hybrid memory devices the resistive switching mechanism is well known to rely on filament formation [1]. This implies that localized conductive paths are established between the two terminal electrodes during the forming step. This filaments sustain the current flow when the memory is in the low conductive state and they can be ruptured and possibly re-formed for more than hundreds of I-V cycles.

The nature and morphology of filaments has been long time debated especially for organic memories. The filament size, density and formation mechanism have been very challenging to be characterized, and need appropriate experimental techniques. However, filaments in organic memories have been recently identified and characterized by cross-section transmission electron microscopy (TEM), conductive-AFM, AFM-tomography and through depth profile analysis combining Time-of-flight secondary ions mass spectrometry (SIMS) and X-ray photoelectron spectroscopy (XPS).

In particular, 3D spectroscopic images obtained with ToF-SIMS give access for the first time to filament formation process and rupture mechanism. From these results, a clear picture of the filament(s) dynamics during memory operation can be drawn.

In this contribution, recent results showing filaments in memories based on different structures and architectures will be discussed. The memories are based on insulating polymers (polystyrene [2] and poly methyl methacrylate [3]), conductive polymers/nanocomposites (polyera N1400 with metal NPs [4]), and small semiconducting molecules (Tris(8hydroxyquinolinato)aluminium - Alq3 [5]). The results show that resistive switching clearly involves the inhomogeneous metal diffusion in the organic layer taking place during the top electrode deposition and during memory operation. This may be of great relevance in many other organic electronics applications.

REFERENCES

S. Nau, S. Sax, E.J.W. List-Kratochvil, Adv. Mater. 2014, 26, 2508–2513.
 Y. Busby, N. Crespo-Monteiro, M. Girleanu, M. Brinkmann, O. Ersen, J.-J. Pireaux, Organic Electronics 2015, 16, 40–45.

[3] C. Wolf, S. Nau, S. Sax, Y. Busby, J.-J. Pireaux, E.J.W. List-Kratochvil



(under submission).

[4] G. Casula, P. Cosseddu, Y. Busby, J.-J. Pireaux, M. Rosowski, B. Tkacz Szczesna, K. Soliwoda, G. Celichowski, J. Grobelny, J. Novák, R. Banerjee, F. Schreiber, A. Bonfiglio, Organic Electronics, 2015, 18, 17-23.

[5] Y. Busby, S. Nau, S. Sax, E.J.W. List- Kratochvil, J. Novak, R. Banerjee, F. Schreiber, J.-J. Pireaux, (under submission)

9569-5, Session 2

Flexible non volatile memory devices based on organic semiconductors (Invited Paper)

Piero Cosseddu, Giulia Casula, Stefano Lai, Annalisa Bonfiglio, Univ. degli Studi di Cagliari (Italy)

The possibility of developing fully organic electronic circuits is critically dependent on the ability to realize a full set of electronic functionalities based on organic devices. In order to complete the scene, a fundamental element is still missing, i.e. reliable data storage. Over the past few years, a considerable effort has been spent on the development and optimization of organic polymer based memory elements. Among several possible solutions, transistor-based memories and resistive switching-based memories are attracting a great interest in the scientific community. In this presentation an overview of these two approaches for achieving well performing non volatile memory (NVM) devices will be given.

At first, we will show that inkjet printing can be used for the fabrication of highly flexible Organic Thin Film Transistors, and that they can be eventually employed, by properly engineering their dielectric and/or active layers, as non volatile memory devices with high retention time.

A different interesting solution for the realization of high retention time NVM elements consists in the fabrication of bi-stable resistive devices. Each memory element can be obtained by sandwiching a hybrid organic/ inorganic active layer between two metal electrodes. Also in this case, the possibility of employing solution-processable materials and inkjet printing as fabrication process will be addressed.

Moreover, it will be shown, for both cases, that such devices can be easily integrated with electrical sensors enabling the development of a wide range of applications, from artificial skin to smart packaging.

9569-6, Session 2

Ion-dependent frequency selectivity and learning of semiconducting polymer/ electrolyte composites

Fei Zeng, Siheng Lu, Wenshuai Dong, Xiaojun Li, Ao Liu, Tsinghua Univ. (China)

Studies on pulse responses have been performed on several semiconducting polymer/electrolyte composites. Frequency selectivity and learning were found and dependent on the types of ions and polymer/electrolyte interfaces. In a Pt/P3HT/PEO+X+ (X=Li, Mg, Nd)/Pt hetero junction, the system response was depressed to low-frequency stimulations (10~50 Hz) but was potentiated to high-frequency stimulations (higher than 80 Hz). Long term memory and learning was realized when the semiconducting polymer was changed to MEH-PPV. Conventional spike-rate-dependent plasticity (SRDP), i.e., BCM learning rule, was realized. The microstructures suitable for frequency selectivity were examined and confirmed by SEM images. Bi-directional signal transportation could be realized by simple connection or using semiconductor/electrolyte mixtures. It was found that input frequency could modulate ionic doping, de-doping and redoping at the semiconducting polymer/electrolyte interface. Thus, we established a random channel model to describe dynamic processes at the semiconducting polymer/electrolyte interface and explain the observed learning phenomena. We suggest that semiconducting polymer/electrolyte composites will be useful and powerful in mimicking plasticity and learning of bio- synapses, constructing neuromorphic circuits and information computation.

9569-7, Session 2

Non-volatile resistive photo-switches for flexible image detector arrays

Sebastian Nau, Christoph Wolf, Stefan Sax, NanoTecCenter Weiz Forschungsgesellschaft mbH (Austria); Emil J. W. List-Kratochvil, NanoTecCenter Weiz Forschungsgesellschaft mbH (Austria) and Technische Univ. Graz (Austria)

The increasing quest for lightweight, conformable or flexible image detectors for machine vision or medical imaging brings organic electronics into the spotlight for these fields of application. Here were we introduce a unique imaging device concept and its utilization in an organic, flexible detector array with a simple passive matrix wiring.

Along these lines, the origin of unipolar resistive switching in organic electronic devices is unraveled by utilizing the photovoltaic effect: For the first time it is unambiguously possible to rule out most models which are held to be responsible for switching in organic devices. It is shown that the memory behavior is due to the formation and rupture of a localized conductive pathway ('filament') rather than any other claimed effect.

With this knowledge, we present a flexible organic image detector array built up from non-volatile resistive multi-bit photo-switchable elements. This unique realization is based on an organic photodiode combined with an organic resistive memory device wired in a simple crossbar configuration. The presented concept exhibits significant advantages compared to present organic and inorganic detector array technologies, facilitating the detection and simultaneous storage of the image information in one detector pixel, yet also allowing for simple read-out of the information from a simple passive-matrix crossbar wiring. This concept is demonstrated for single photo-switchable pixels as well as for arrays with sizes up to 32 by 32 pixels (1024 bit). The presented results pave the way for a versatile flexible and easy-to-fabricate sensor array technology.

9569-8, Session 2

Design rules and prototype examples for additive printing of organic complementary circuits (Invited Paper)

Tse Nga Ng, David E. Schwartz, Ping Mei, Brent S. Krusor, Sivheng Kor, Janos Veres, PARC, A Xerox Co. (United States)

With the recent improvements in printed devices, it is now possible to build integrated circuit systems out of printed devices. The combination of sensor, logic, and rewritable memory will greatly enhance the functionalities of printed electronics. Non-volatile ferroelectric memory in passive or active matrix arrays has been demonstrated (Sekitani, et al., Science, 326 (2009) 1516–1519; Naber, et al., Adv. Mater., 22 (2010) 933–945; Ng, et al., Org. Electron., 12 (2011) 2012–2018). The addition of addressing logic is necessary for these arrays to be scalable (Ng, et al., Sci Rep., doi:10.1038/srep00585): a binary logic decoder allows 2^N rows in an array to be controlled with just N-bit lines. In addition to scaling memory arrays, the decoder logic is also widely applicable to arrayed sensor and display applications.

At Palo Alto Research Center (PARC), we have demonstrated organic complementary circuits by inkjet printing. An example is a printed decoder for handling 3-bit address lines to an array of ferroelectric capacitors. Another example is a temperature sensor tag, in which the control circuit is triggered to generate a pulse to write into the memory when the thermistor temperature exceeds a preset threshold. For these examples, simulation models are developed for the organic transistors to achieve circuit designs that tolerate the variations in printed devices, as well as to determine the minimum performance requirements for reliable digital logic circuits. I will discuss how we tackle the challenges of device variations and in printed transistors and the design rules we learned in the course of developing these circuits.



9569-9, Session 3

Large area formation of self-aligned crystalline domains of organic semiconductors on transistor channels using CONNECT (Invited Paper)

Steve Park, Stanford Univ. (United States) and Columbia Univ. (United States)

The electronic properties of solution-processable small molecule organic semiconductors (OSCs) have rapidly improved in recent years, rendering them highly promising for various low-cost large area electronic applications such as active matrix displays, radio frequency identification tags, and integrated logic circuits. However, practical applications of organic electronics requires patterned and precisely registered OSC film within the transistor channel region with uniform electrical properties over a large area, a task that remains a significant challenge. Here we present a novel technique known as CONNECT (Controlled OSC NucleatioN and Extension for CircuiTs), which utilizes differential surface energy and solution shearing to simultaneously generate self-patterned and self-registered OSC film within the channel region and with aligned crystalline domains, resulting in low device-to-device variability. We have fabricated transistor density as high as 840 dpi, with a yield of 99%. We have successfully built various logic gates and a 2-bit half adder circuit, demonstrating the practical applicability of our technique for large-scale circuit fabrication. CONNECT was expanded to use with inkjet printed silver electrodes, showing the versatility of our method to accommodate various solution deposition and fabrication methods.

9569-10, Session 3

High-resolution gravure printed lines: Proximity effects and design rules

Gerd Grau, William J. Scheideler, Vivek Subramanian, Univ. of California, Berkeley (United States)

Gravure printing is a very promising method for printed electronics because it combines high throughput with high resolution. Recently, printed lines with $2\mu m$ resolution have been demonstrated at printing speeds on the order of 1m/s. Here we build on these results to study how more complex patterns can be printed that will ultimately lead to printed circuits. We study how the drag-out effect leads to proximity effects in gravure when multiple lines are printed close to each other. Drag-out occurs as the doctor blade passes over the roll surface to remove excess ink from the land areas in between the cells that make up the pattern. In addition to this desirable removal of excess ink, some ink from the cells also wicks up the doctor blade and is removed from the cells. This ink is subsequently deposited on the land area behind the cells leading to characteristic drag-out tails. If multiple lines, oriented perpendicular to the print direction, are printed close to each other, the ink that has wicked up the doctor blade from the first line will affect the drag-out process for subsequent lines. Here we show how this effect can be used to enhance print quality of lines as well as how it can deteriorate print quality. Important variables that will determine the regime for printing optimization are ink viscosity, printing speed, cell size, cell spacing and relative placement of lines. Considering these factors carefully allows one to determine design rules for optimal printing results.

9569-11, Session 3

Inkjet printed carbon nanotubes and zinc tin oxide based thin-film complementary circuits

Bongjun Kim, The Univ. of Texas at Austin (United States); Michael L. Geier, Mark C. Hersam, Northwestern Univ. (United States); Ananth Dodabalapur, The Univ. of Texas at Austin (United States) Inkjet printing is one of the most promising techniques for low-cost, largearea, and flexible electronics due to its capability for direct patterning. Among many printable semiconducting materials, sorted single-walled carbon nanotubes (SWCNTs) and amorphous zinc tin oxide (ZTO) are some of the most attractive materials for p- and n-type semiconductors, respectively, since they exhibit superior electrical properties. Combination of these two materials makes possible realization of high performance complementary circuits. Such circuits, which are composed of both n- and p-type semiconductors, are essential for low power applications.

In this work, we demonstrate high performance hybrid complementary circuits based on inkjet printed SWCNTs and ZTO semiconductors. These circuits include inverters, ring oscillators, and D flip-flops. Solution processed high-k dielectric layer permits these circuits to operate at low voltages. The complementary inverters show high DC gain and low static power consumption. Five-stage ring oscillators based on these inverters show the highest operating frequencies among previously reported printed-semiconductor based ring oscillators. Positive edge-triggered D flip-flops, which are basic building blocks in sequential logic circuits, operate well at high clock frequencies.

In addition, novel voltage-controlled oscillators are demonstrated by employing double-gate structures. In this structure, an applied gate bias can control transistor threshold voltage and tune oscillation frequencies of the circuit. Such functional block will enable realization of printed analog-todigital converters.

9569-12, Session 3

Flexible thin film circuitry enabling ubiquitous electronics via post-fabrication customization (Invited Paper)

Brian Cobb, Holst Ctr. (Netherlands)

For decades, the electronics industry has been accurately described by Moore's Law, where the march towards increasing density and smaller feature sizes has enabled continuous cost reductions and performance improvements. With flexible electronics, this perpetual scaling is not foreseen to occur. Instead, the industry will be dominated by Wright's Law, first proposed in 1936, where increasing demand for high volumes of product will drive costs down. We have demonstrated thin film based circuitry compatible with flexible substrates with high levels of functionality designed for such a high volume industry. This includes a generic 8-bit microprocessor totaling more than 3.5k TFTs operating at 2.1 kHz. We have also developed a post fabrication programming technique via inkjet printing of conductive spots to form a one-time programmable instruction generator, allowing customization of the processor for a specific task. The combination demonstrates the possibility to achieve the high volume production of identical products necessary to reap the benefits promised by Wright's Law, while still retaining the individualization necessary for application differentiation. This is of particular importance in the area of item level identification via RFID, where low cost and individualized identification are necessary. Remotely powered RFID tags have been fabricated using an oxide semiconductor based TFT process. This process is compatible with the post-fabrication printing process to detail individual identification codes, with the goal of producing low cost, high volume flexible tags. The goal is to produce tags compatible with existing NFC communication protocols in order to communicate with readers that are already ubiquitous in the market.

9569-13, Session 4

Flexible low-voltage organic integrated circuits with megahertz switching frequencies (Invited Paper)

Ute Zschieschang, Max-Planck-Institut für Festkörperforschung (Germany); Kazuo Takimiya, RIKEN Ctr. for Emergent Matter Science (Japan); Tarek Zaki, Univ. Stuttgart (Germany); Florian Letzkus, Harald



Richter, Joachim N. Burghartz, Institut für Mikroelektronik Stuttgart (Germany); Hagen Klauk, Max-Planck-Institut für Festkörperforschung (Germany)

A process for the fabrication of integrated circuits based on bottom-gate, top-contact organic thin-film transistors (TFTs) with channel lengths as short as 1 µm on flexible plastic substrates has been developed. In this process, all TFT layers (gate electrodes, organic semiconductors, source/ drain contacts) are patterned with the help of high-resolution silicon stencil masks, thus eliminating the need for subtractive patterning and avoiding the exposure of the organic semiconductors to potentially harmful organic solvents or resists. The TFTs employ a low-temperature-processed gate dielectric that is sufficiently thin to allow the TFTs and circuits to operate with voltages of about 3 V. Using the vacuum-deposited small-molecule organic semiconductor 2,9-didecyl-dinaphtho[2,3-b:2',3'-f]thieno[3,2-b] thiophene (C10 DNTT), TFTs with an effective field-effect mobility of 1.2 cm2/Vs, an on/off current ratio of 107, a width-normalized transconductance of 1.2 S/m (with a standard deviation of 6%), and a signal propagation delay (measured in 11-stage ring oscillators) of 420 nsec per stage at a supply voltage of 3 V have been obtained. To our knowledge, this is the first time that megahertz operation has been achieved in flexible organic transistors at supply voltages of less than 10 V. In addition to flexible ring oscillators, we have also demonstrated a 6-bit digital-to-analog converter (DAC) in a binary-weighted current-steering architecture, based on TFTs with a channel length of 4 µm and fabricated on a glass substrate. This DAC has a supply voltage of 3.3 V, a circuit area of 2.6? 4.6 mm2, and a maximum sampling rate of 100 kS/s.

9569-14, Session 4

Fully printed 2-bit shift register based on organic electrochemical transistors

Philipp C. Hütter, Thomas Rothländer, Gregor Scheipl, Barbara Stadlober, JOANNEUM RESEARCH Forschungsgesellschaft mbH (Austria)

Organic electrochemical transistors (OECTs) have received considerable attention in recent years due to their numerous advantages. Prominent examples are their simple design allowing for a fabrication by additive printing technique, their low operating voltage, the compatibility with flexible substrates and their possibility to conduct both ionic and electronic charge carriers. Developing circuitry based on organic materials benefiting from those advantages is, in our view, an aim worth pursuing.

We report on entirely screen printed logic gates based on OECTs. The transistors are fabricated from poly(3,4-ethylenedioxithiophene) poly(styrenesulfonate) (PEDOT:PSS), a polymer electrolyte and a conductive carbon screen printing paste. They operate at a voltage of 1.5 V and exhibit an on/off current ratio of 104. The resistors needed to expand the OECTs range of use to logic gates are screen printed PEDOT:PSS resistors. Both, transistors and resistors, show highly reproducible characteristics and are combined to integrated logic gates. In total only five different screen printable materials, including the ones needed for wiring, are utilized to fabricate inverters, NAND gates, flipflops and a 2-bit shift register. The obtained logic gates are characterized by dynamic measurements, revealing a very high reproducibility of the devices' output signals. These very promising results clearly indicate the high uniformity and reproducibility of the screen printed transistors and resistors, emphasizing their applicability for higher integrated circuitry.

9569-15, Session 4

Field-effect memory transistors based on arrays of nanowires of a ferroelectric polymer

Ronggang Cai, Hailu G. Kassa, Univ. Catholique de Louvain (Belgium); Alessio Marrani, Solvay Specialty Polymers Italy S.P.A. (Italy); Albert J. van Breemen, Gerwin H. Gelinck, Holst Ctr. (Netherlands); Bernard L. Nysten, Univ. Catholique de Louvain (Belgium); Zhijun Hu, Soochow Univ. (China); Alain M. Jonas, Univ. Catholique de Louvain (Belgium)

Ferroelectric poly(vinylidene fluoride-co-trifluoroethylene), P(VDF-TrFE), is attracting renewed interest for use in organic non-volatile memory devices, e.g., in ferroelectric field effect transistors (FeFETs). In a FeFET, information is stored in two different permanent polarization states of a ferroelectric film, associated to bits 1 and 0; the reading capability is realized by detecting the source-drain current flowing through a film of a semiconducting material stacked over the ferroelectrics, which is modulated by the permanent polarization state of the ferroelectrics.

Recently, we have developed nanoimprint lithography as a tool to shape ferroelectric P(VDF-TrFE) into arrays of nanowires; as a side benefit of this process, preferential crystal orientation occurs, resulting in improved ferroelectric performance. Here, we report on FeFETs integrating such arrays of ferroelectric polymer nanowires. Two different original architectures are tested, the first one consisting of stacked P(VDF-TrFE) nanowires placed over a continuous semiconducting polymer film; the second one consisting of a nanostriped blend layer wherein the semiconducting and ferroelectric components alternate regularly, leading to lateral electrostatic coupling (as opposed to the usual vertical coupling of standard FeFETs).

Such devices exhibit significant reversible memory effects, with operating voltages reduced compared to their continuous film equivalent. Piezoresponse Force Microscopy (PFM) experiments reveal that the two memory states correspond to a polarized and a depolarized state, with different possible geometries of the channels of free charge carriers accumulating in the semiconductor. The advantages and drawbacks of each coupling geometry will be discussed, as well as their potential for further miniaturization.

9569-16, Session 4

Printed circuits and their applications: Which way forward? (Invited Paper)

Eugenio Cantatore, Technische Univ. Eindhoven (Netherlands)

The continuous advancements in Printed Electronics make nowadays feasible the design of printed circuits which enable meaningful applications. Examples include ultra-low cost sensors embedded in food packaging, large-area sensing surfaces and biomedical assays.

This invited paper will offer an overview of state-of-the-art printed electronics circuits, including sensor front-ends and data converters for sensor applications.

Further, the bottlenecks that still hamper a full exploitation of the potential of printed technologies to build circuits will be analyzed. Finally, the most relevant research directions in the field of technology, device modeling, and circuit design for improved performance, yield and robustness will be discussed.

Conference 9570: The Nature of Light: What are Photons? VI



Monday - Thursday 10-13 August 2015

Part of Proceedings of SPIE Vol. 9570 The Nature of Light: What are Photons? VI

9570-1, Session 1

Quantum theory as a description of robust experiments: application to Stern-Gerlach and Einstein-Podolsky-Rosen-Bohm experiments (Invited Paper)

Hans De Raedt, Univ. of Groningen (Netherlands); Mikhail I. Katsnelson, Hylke C. Donker, Radboud Univ. Nijmegen (Netherlands); Kristel F. Michielsen, Forschungszentrum Jülich GmbH (Germany)

It is shown that the probability distribution of quantum systems in the singlet state emerges from the requirement that (i) space is isotropic, (ii) the observed events are logically independent, and (iii) the data generated by Einstein-Podolsky-Rosen-Bohm experiments is robust with respect to small changes in the conditions under which the experiment is carried out.

The derivation is based on general principles of logical inference which have been shown to lead to the Schr"odinger and Pauli equation, without taking recourse to any concept of quantum theory.

This analysis suggests that quantum theory follows from logical inference applied to a well-defined class of experiments, without any commitment to further notions of reality.

It is shown how the mathematical structure of quantum theory follows from the desire to organize experimental data such that it untangles as much as possible, the description of the system under scrutiny from the description of the probes used to acquire the data.

9570-3, Session 1

A convergence: Special relativity, zitterbewegung, and new models for the subcomponent structure of quantum particles

Michael J. Mobley, Grand Canyon Univ. (United States) and The Biodesign Institute, Arizona State Univ. (United States)

Hestenes has presented an integration of Schrödinger's zitterbewegung with the spin matrices of the Dirac equation, suggesting the electron can be modeled by a rapidly rotating dipole moment and a frequency related to the de Broglie frequency. He presents an elegant spacetime algebra that provides a reformulation of the Dirac equation that incorporates these real spin characteristics. A similar model for quantum particles has been derived by this author from a different, guasi-classical premise: That the most fundamental subcomponents of quantum particles all travel at a constant speed of light. Time is equated with the spatial displacement of these subcomponents - the speed of light is the speed of time. This approach suggests a means of integrating special relativity and quantum mechanics with the same concept of time. The relativistic transformation of spinning quantum particles create the appearance of additional, compactified spatial dimensions that can be correlated with the complex phase of the spin matrices as in the Dirac formalism. This paper further examines the convergence on such new models for quantum particles built on this rapid motion of particle subcomponents. The modeling leverages a string-like heuristic for particle subcomponents and a revised description for the wavelike properties of particles. This examination provides useful insights to the real spatial geometries and interactions of electrons and photons.

9570-4, Session 1

Classical explanations of results of quantum mechanics

Albrecht Giese, Consultant (Germany)

In present physics there is a great conviction in favour of the necessity and ability of quantum mechanics to describe our physical world. This is considerably caused by those experimental results which seem to be in clear conflict with classical physics. Topics well known in this sense are the particle-wave paradox and e.g. the quantisation of the spin and of the magnetic moment.

In the view of the particle model presented separately in the meeting, and in the view of Lorentzian relativity as a replacement of Einstein's relativity, several of these observations can in fact be classically explained, at least to a certain extent. Some of these cases are not new but can be traced back to Louis de Broglie and partially also to Albert Einstein.

We will give an overview about the present situation of these phenomena. And we will discuss whether certain restrictions caused by the present understanding of QM can be alleviated.

Points in view:

- Determination of particle mass
- Particle-wave
- Non-emptiness of vacuum
- Virtual particles
- Bohr Magneton + Landé factor
- Quantisation of spin (absolute)
- Quantisation of angular momentum
- Quantisation of magnetic moment (Stern-Gerlach)
- Casimir effect
- Missing radiation in atomic orbits
- Pauli principle
- Unification of strong force and weak force
- Quantum gravity.

9570-5, Session 1

Photons as observer transitions in the event-oriented world view

Wolfgang Baer, Nascent Systems Inc. (United States)

This paper shows how the physical phase of an observing activity cycle can be described as a field of classic systems. When this field exists in a state of dynamic equilibrium, the observable experience of empty space is produced. Small enough oscillations around the dynamic equilibrium are shown to correspond to deBroglie waves, satisfy the Schrödinger equation, and represent the content of space. Larger disturbances can create or destroy the field of systems that underlie the observation of empty space.

This possibility points to the existence of an Event Theory of Reality from which quantum mechanics can be derived as a linear approximation. Such a theory would describes reality as a set of interacting action cycles. Hilbert space would be identified with detector/activator arrays that form the von Neumann cut between physical and observational phases of action cycles. If such arrays are conceived as charge and mass densities then the physical phase is characterized by gravito-inertial influences between the masses and electro-magnetic influences between the charges while the observational phase is characterized by forces that hold charge and mass together. A disturbance in either electromagnetic or gravito-inertial fields would be coupled to each other and therefore light quanta can only transfer from one cycle to another when matched equilibrium eigenstate allow



absorption and emission by mass-charge structures defining the detector/ activator arrays. While electromagnetic fields provide a global propensity to transition quasi-random gravito-inertial influences would occasionally satisfy the equilibrium condition that allows quantized amounts of action to actually make the transfer.

9570-6, Session 2

Genesis of quantization of matter and radiation field (Invited Paper)

Luis de la Peña, Univ. Nacional Autónoma de México (Mexico); Ana María Cetto, Univ. Nacional Autónoma de Mexico (Mexico)

Are we to accept quantization as a fundamental property of nature, the origin of which does not require or accept further investigation?

To get an insight into this question we consider atomic systems as open systems, since they are by necessity in contact with the electromagnetic radiation field. This includes not only photonic radiation, but, more importantly for our purposes, the random zero-point or nonthermal radiation that pervades the Universe. The Heisenberg inequalities, atomic stability and the existence of discrete solutions are explained as a result of the permanent action of this field upon matter and the balance between absorbed and emitted powers in the equilibrium regime. A detailed study carried out along the years has led to the usual quantum-mechanical formalism as a powerful and revealing statistical description of the behavior of matter in the radiationless approximation, as well as to the radiative corrections of QED. The theory presented gives thus a response to the question posed above, within a local, realist and objective framework: quantization appears as an emergent phenomenon due to the matter-field interaction.

9570-7, Session 2

Urgency of evolution-process congruent thinking in physics

Chandrasekhar Roychoudhuri, Univ. of Connecticut (United States)

The prevailing mode of doing physics can be briefly summarized as establishing some conceptual continuity among inter-related but diverse observations by constructing some postulates to bring some logical congruency between the same observations. The postulates become new ad hoc "knowledge" whose reasonable-ness is first established further through coherent mathematical logics (the constructed theory) and then validated through acquisition of experimental data. This trend has been very successful for over several centuries. This approach can be characterized as the Measurable Data Modeling Epistemology (MDM-E). Unfortunately, MDM-E does not guide us to visualize the invisible interaction processes that are behind the emergence of data. Accordingly, such theories do not provide direct guidance to engineers to become better innovators. So, my proposal is to consciously add Interaction Process Mapping Epistemology (IPM-E) to complement the currently successful MDM-E. Consider the facts that the theories for photoelectric effect and the stimulated emission were proposed by Einstein by the first and the second decade of the twentieth century. But, our engineers did not succeed in establishing the Knowledge Age through Global Internet until the late twentieth century. Let us further, acknowledge that the establishment of the fiber optic network required four engineering processes - generation, modulation, propagation and detection - of two fundamental entities in the universe -electrons and photons. However, no physicists would dare to claim that we really understand what the photons and the electrons really are. But, our technological evolution is continuing un-interrupted. We can now utilize the Global Internet to engage a very large segment of our global smart engineers to start spending a portion of their time to figure out how to slow down the rate of the scary "Sixth Extinction"!

9570-8, Session 2

What is a photon?

A. F. Kracklauer, Consultant (Germany)

The central technical point of this presentation is that EPR-B type experiments preclude a direct, single event, measurement of the intensity of a pulse. In stead, repeated measurements for which the ratio of detections to the total number of possible events is used to determine intensity. This constraint, results in a distortion of the statistics involved. Analysis of the interplay of the consequences of these factors will be presented.

9570-9, Session 2

Did Planck, Einstein, Bose count indivisible photons, or discrete emission/absorption processes in a black-body cavity?

Michael Ambroselli, Chandrasekhar Roychoudhuri, Univ. of Connecticut (United States)

Planck, Einstein and Bose all had to introduce statistics, and thus counting, in order to successfully derive an equation for the energy distribution within the black-body radiation spectrum. The statistical result from this we now call Bose-Einstein statistics. Some of the details involved in the counting procedure may vary while still giving the same result. Similarly, the interpretation of what we count may differ dramatically from one another (as, for example, between Planck and Bose), without impacting the final, mathematical result. We demonstrate here a further alternative, which varies both, in the details of the counting, as well as in the interpretation, while still producing the same well known statistics. This approach puts the "quantumness" back into the radiation emission/absorption process, possibly dispensing with the requirement of quantized light, at least in the context of black-body radiation.

9570-10, Session 3

Spatial photon localization and magnetic monopoles (Invited Paper)

Ole Keller, Aalborg Univ. (Denmark)

A wave-packet photon from an atom (or a mesoscopic particle) is born in the so-called rim (Lorenz) zone of matter. This weakly spatial localizability of the photon has enabled us to gain deeper insight in e.g. evanescent fields, photon tunneling, entanglement, and near-field electrodynamics as such. After a brief review of certain aspects of the spatial localization problem, I discuss how magnetic monopoles (so far not observed!) might change the photon mediated interaction between magnetic and electric monopoles in rim-zone contact. Special attention is devoted to the photon wave mechanical picture, and its field-quantized extension.

9570-11, Session 3

Light dispersion in space

Luiz C. Barbosa, Univ. Estadual de Campinas (Brazil)

Abstract Considering an idea of F. Arago in 1853 regarding light dispersion through the light ether in the interstellar space, this paper presents a new idea on an alternative interpretation of the cosmological red shift of the galaxies in the universe. The model is based on an analogy with the temporal material dispersion that occurs with light in the optical fiber core. Since intergalactic space is transparent, according to the model, this phenomenon is related to the gravitational potential existing in the whole space. Thus, it is possible to find a new interpretation to Hubble's constant. In space, light undergoes a dispersion process in its path, which is interpreted by a special red shift equation, with a constante that is similar with Hubble constant. We observe that this "constant" is governed by three

Conference 9570: The Nature of Light: What are Photons? VI



new parameters. Light traveling the intergalactic space undergoes red shift due to this mechanism, while light amplitude decreases with time, and the wavelength always increases, thus producing the same type of behavior given by Hubble's Law. It can be demonstrated that the dark matter phenomenon is produced by the apparent speed of light of the stars on the periphery of the galaxies, without the existence of dark energy. Based on this new idea, the model of the universe is static, lacking expansion. Other phenomena may be interpreted based on this new model of the universe. We have what we call temporal gravitational dispersion of light in space produced by the variations of the speed of light, due to the presence of the gravitational potential in the whole space

.Keywords: alternative cosmology, alternative red shift.

9570-12, Session 3

The photon: EM fields, electrical potentials, and AC charge

Andrew Meulenberg Jr., Hi Pi Consulting (United States); Robert W. Hudgins, Science for Humanity Trust, Inc. (United States); Ralph F. Penland Jr., Science for Humanity Trust, Inc. (India)

Continued analysis of the interference of two converging parallel laser beams and the resultant standing wave has led to further thoughts on the forces and potentials developed in the interaction between photons. A number of papers have raised the issue of oscillating charge as the source of the alternating electric and magnetic fields composing the photon. Since the known (accepted) minimum charge is that of the electron and positron (leptons) with their minimum mass and energy, such a model is untenable. Nevertheless, E- and B-Fields without source charge(s) are not generally accepted today. Since Maxwell did not have that preconceived limitation and his equations still hold, these classical ideas are explored in the attempt to better understand the standing waves that exist within and between photons.

Photons are here considered to be resonant oscillations (solitons) in four dimensions of an undefined 'field' otherwise generally existing at a local energy minimum. The photons' constituent EM fields are modes of this oscillation and result in elevated energy and therefore potentials. It is in the context of the standing waves of photons that the EM fields and potentials lead to a description of alternating (AC) 'currents' (of some form) of unquantized alternating 'charge' (of some sort). The main topic of this paper is the alternating charge.

9570-13, Session 3

Electrons are spin 1/2 charged photons generating the de Broglie wavelength

Richard Gauthier, Santa Rosa Junior College (United States)

A charged photon and its light-speed helical trajectory form a surprising new solution to the relativistic electron's energy-momentum equation E $^2 = p^2 c^2 + m^2 c^4$. This charged photon is a new model for the electron, and quantitatively resembles the light-speed electron described by Dirac. His relativistic guantum mechanical equation for the electron was partly derived from the above energy-momentum equation. While the electron's energy is $E = gamma mc^2$, the charged photon's energy is E =gamma mc 2 = hf . The electron's relativistic momentum p = gamma mv is the longitudinal component of the charged photon's helically circulating momentum p total = gamma mc. At any electron speed, the charged photon has an internally circulating transverse momentum p trans = mc , which at the helical radius Ro = L Compton / $4pi = 1.93 \times 10^{-13} m$ for a slowly-moving electron produces the z-component hbar/ 2 of the electron's spin. The right and left turning directions of the charged photon's helical trajectory correspond to a spin up (sz = +hbar /2) and spin down (sz = -hbar /2) electron. The negative and positive possible charges of the charged photon correspond to the electron and the positron. Using the wave vector k of the circulating charged photon of momentum p=gamma

mc, where the wave vector k makes an angle theta given by cos (theta)=v/c with the electron's velocity v, the relativistic de Broglie wavelength of an electron LdeBroglie = h/(gamma mv) is easily derived from the charged photon model. This gives further support for the charged photon model of the electron. The charged photon model for an electron suggests a new interpretation of quantum mechanics where atomic and molecular electrons as well as free electrons are all charged photons. Bound charged photon mode an atom have discrete energy levels given by the Schrodinger and Dirac equations, and a charged photon moves from one atomic or molecular energy level to another. Wave-particle duality can be understood better with the charged photon model of the electron, since electrons have wave properties because they are charged photons.

9570-14, Session 3

A study of the nature of light by comparing real and digital universes (Invited Paper)

Luping Shi, Tsinghua Univ. (China)

The nature of light has been puzzling us for more than a century. The modern theory of quantum mechanics came to picture light as both a particle and a wave. In this talk, the nature of light is studied by comparisons between the real and digital worlds. Together with analysis of theoretical and experiments results, we discuss the possibility that a photon has structure. A possible photon model with internal structure is proposed and discussed. The model can be used to explain not only all of the experiment phenomena, but also the wave particle dualism of light. It can provide clear pictures of both polarization and coherency of light. It can also explain that there are two spin states of 1 and -1. It should be noted that C.N.Yang and R. Mills have generalized electromagnetism, as a U(1) bundle theory, to a very beautiful non-abelian gauge theory as a natural mathematical extension. This theory has not been accepted by the physics community because it requires the existence of massless charged particles. However it might be useful for studying the force within a photon of the proposed photon model. The possible experiments that could be used to prove the model are also addressed.

9570-16, Session 4

Biomimetic antennas for light (Invited Paper)

Dmitri V. Voronine, Texas A&M Univ. (United States)

Light-matter interactions play an important role in nature. For example, first steps of photosynthesis involve capture of photons and conversion into useful work. Natural light-harvesting complexes can be described as quantum heat engines and can be used to develop similar bioinspired artificial devices. Processes that are important for optimizing the performance of such biomimetic antennas will be discussed and analyzed from the point of view of recent quantum biology experiments. The nature of light will be considered in order to improve the understanding of these processes.

9570-17, Session 4

Are there photons in fact?

Sergey A. Rashkovskiy, A. Ishlinsky Institute for Problems in Mechanics (Russian Federation)

There are two opposing points of view on the nature of light: the first one manifests the wave-particle duality as a fundamental property of the nature; the second one claims that photons do not exist and the light is a continuous classical wave field, while the so-called "quantum" properties of this field appear only as a result of its interaction with matter.

Conference 9570: The Nature of Light: What are Photons? VI



In this paper we show that many quantum phenomena which are traditionally described by quantum electrodynamics can be described if light is considered within the limits of classical electrodynamics without quantization of the radiation. These include the photoelectric effect, Compton effect, Lamb shift, radiative effects, spontaneous emission, etc. We show that this point of view allows explaining the "quantum" behavior of light in all optical experiments. In particular we give the purely wave description of "the wave-particle duality" of light in the double-slit experiments and in Wiener experiments with standing waves. We show that the Born's rule for light should be replaced by more general rule which follows from wave nature of light from which, the Born's rule can be obtained as an approximation for low intensity of light.

We show that the Heisenberg uncertainty principle for "photons" has a simple classical sense and cannot be considered as a limitation of experimental accuracy. Within the limits of proposed concept we give a purely wave explanation of Hanbury Brown and Twiss experiments and Aspect's experiments with entangled "photons". We show that these experiments demonstrate the purely optical phenomena.

9570-18, Session 4

Electron-positron annihilation and absorption models

Randy T. Dorn, Independent Researcher (United States)

An experimentally verified mathematical model that precisely describes the attraction and motion between an electron and positron does not yet exist. Although there have been no direct experimental measurements of the particle velocity when the distance between the two particles approaches zero, the basic inverse square model used for point charges is thought to be inadequate because it would predict speeds in excess of c, the speed of light. Modifications to this basic model have been made by theorizing a variable velocity dependent relativistic mass or a velocity dependent force. These more complex models predict a particle velocity of approximately c as these particles undergo the particle - antiparticle collisions that result in photon production. This assumption, that the electron and positron both attain a velocity of approximately c during their annihilation collision results in a very compelling model of a photon as an electron and positron in a two body orbital union traveling through space. However, models based on this assumption show that the photon translational velocity must have some dependence on the photon wavelength. Although this dispersion is well known for photons traveling through a medium, it is objectionable to those who insist that in a vacuum every photon travels with a velocity of c regardless of its wavelength. In this paper it is shown that the basic inverse square model of electron - positron attraction actually predicts the basic two body photon model with no wavelength dependent dispersion. Careful measurement and study of two body photon properties may make it possible to develop a more accurate electron-positron annihilation model.

9570-19, Session 4

An epitaph for all photons: thou revealest thyself in thy demise (Invited Paper)

Chary Rangacharyulu, Univ. of Saskatchewan (Canada)

Photon interactions with matter, either scattering or absorption processes, involve disappearance of the photon. It is to be stressed that photon scattering is not a process in which a photon changes its direction and momentum etc during the scattering. Here, a secondary photon appears in the final state, necessarily satisfying all the conservation laws. This property of photon interactions, that original photon is always lost leaving no trace of itself except for the partner material entities carrying that information, is very unique to them and not shared by any other subatomic entity. We infer the birth of a photon by experimental arrangements and energy/momentum conservation principles. We may even assign a direction of propagation if an associated particle accompanies the photon. We cannot track a photon as it goes on its endless voyage till it meets its demise. A photon may pass through great distances in vacuum and materials without leaving a trace of its existence. It is only when a photon interacts within a sensitive detector volume, marking the end of its travel, we deduce the photon properties. Thus, a photon is not seen at birth, nor during its long voyage. But, it is "seen" as it ends its life. So, we can only write an epitaph but no birthday songs nor celebrations commemorating its life. This presentation will focus on this peculiarity of photons and its implications to particles and interactions.

9570-20, Session 5

Harnessing infrared photons in optical antenna (Invited Paper)

Debashis Chanda, Univ. of Central Florida (United States)

The open scientific question is can we detect infrared radiation in the same way radio frequency (RF) is detected by RF antennas? Such optical antenna will be the ideal solution to address both cooling and color imaging/ detection limitations of present infrared detectors where direct excitation of current on the antenna element avoids cooling requirement and simple dimensional scaling enables frequency tunability. However, all previous efforts based on optical dipole antenna in conjunction with rectifying diode (in combination called "optical rectenna") produced very low IR to electrical conversion efficiencies (~1%) primarily due to very high metal plasma loss at optical frequencies and low antenna IR absorption cross-section. Here we propose a two-element optical antenna array comprised of a perforated metallic (gold) hole array coupled with an underneath disk array which functions as a "light funnel" to trap incident radiation as dipole currents. The sub-wavelength hole-disk antenna array when coupled with a ground plane results in extraordinary transmission through the hole array and zero back reflection. The energy is dissipated as electron plasma loss on the holedisk system inducing perfect ~100% absorption of the incident radiation captured from a much larger area than the physical dimensions. Further the absorption band is shown to tune over the entire mid-IR band by tuning dipolar coupling between two antenna elements by changing element dimensions or array spacing. Compare to other loss mechanisms electron plasma loss offers the advantage of direct detection via an electronic biasing circuit with high signal to noise ratio.

9570-21, Session 5

Visualizing electrons and photons

Azizul Haque, Independent Researcher (United States); Adam Haque, Univ. of California, Los Angeles (United States)

At the dawn of twentieth century scientists discovered a negatively charged fundamental particle called electron. In addition, particles properties of light were observed in photo-electric effect. Properties that are well established for these light particles (photons), electrons, are their charges, spin magnetic moment and inertia. Nature endows electrons with half-integer spin and photons with integer spin. Positron, an antiparticle of electron, also has half-integer spin, but differ from electron due to its positive charge. At present, all half-integer elementary particles are called fermions and the integer spin particles are called bosons. Unlike fermions, photons are charge neutral. Electrons and positrons are known to annihilate each other on contact. Their annihilation creates photons. Again, high energy photons are found to dissociate into electrons and positrons. Fermions participate in forming atoms and nuclei. Fermions absorb and emit photons. In spite of this, fermions are treated as point particles. Through interference experiments, fermions are found to possess wave property. Our investigation shows that the wave property associated with fermions imply its finite size. However, the existing quantum formulations are based on point particle concept. This is due to the fact that, quantum theories for finite sized charged particles, fail to maintain relativistic invariance. Quantum uncertainty also introduces finite size in all elementary particles. Recently, we have developed a theory to understand the quantum properties of finite sized fermions and bosons that is consistent with special relativity and the quantum uncertainty principle. Using this theory, we are able to demonstrate theoretically the physical appearances of the bosons and fermions. Understanding of the physical structure of photons and electrons will definitely help us advance our technology.



9570-22, Session 5

Wave interference: mechanics of the standing wave component and the illusion of 'which way' information?

Robert W. Hudgins, Science for Humanity Trust, Inc. (United States); Andrew Meulenberg Jr., Hi Pi Consulting (India); Ralph F. Penland Jr., Science for Humanity Trust, Inc. (India)

Two identical, coherent, light beams, 180 degrees out of phase, traveling adjacent parallel paths remain visibly separated by the null (dark) zone produced by their interference. Each part of the interference pattern can be traced to one of the beams. Does such an experiment provide "which way" knowledge in contravention of quantum theory? It is a common and convenient practice, to apply Maxwell's very successful superposition principle to predict the patterns produced by converging wave trains. It uses only the abstract values of wave amplitudes (or even probabilities). As abstractions, waves can pass through each other without interacting and cancel each other without explanation. But waves are not abstractions. They are physical entities. As such, all waves carry energy, momentum, force and mass (effective mass in the case of light), and therefore cannot pass through each other like ghosts or cancel each other without violating conservation laws. Importantly, we have proposed that a standing wave component is intrinsic to the formation of interference phenomenon. Geometric analyses of the mechanical processes that generate standing waves in water, an electric circuit, and in light demonstrated that analogous physical interactions in each type of standing wave create null zones where the equal energies of opposing waves reflect off each other, causing an exchange of momentum. Standing wave analysis of the experimental interference between the two parallel laser beams proved that such a continuous interaction across the null zone between them makes it impossible to provide "which way" knowledge.

9570-23, Session 5

Detection of superposition effects of polarized light by Photo-EMF detectors

Narasimha S. Prasad, NASA Langley Research Ctr. (United States)

We use photo-emf, in contrast to photo-voltaic detection method to analyze the two- beam fringe visibility due to a pair of polarized beams through a Mach-Zehnder interferometer. Measured data and our formulation of the superposition effect demonstrate that the observed effect is carried out by the polarized molecules of the photo-emf detector. The two polarized wave amplitudes do not sum themselves into a new resultant E-vector prior to

stimulating the photo-emf detecting molecules; which are discernible by mathematical models. Our observations conforms to Roychouduri's generalized formulation of Non-Interaction of Waves (or the NIW- property).

Photo-emf detectors based on CdTe single crystals are being used for sensitive vibration measurements. In one configuration, a photo-emf detector is used in a Mach-Zehnder interferometer (MZ) in which two beams from a laser are made to interfere at the detector surface to form fringes. Fringe motion generates electrical current corresponding to vibrations encountered in one its beam paths. In this paper, the role of a photo-emf detector will be explored to underscore that waves by themselves do not interfere. The Mach-Zhender interferometer with variable polarizers withinits beam paths is used to investigate the fringe characteristics. The polarized detecting molecules, physically constrained to oscillate only along the optical axis of the crystal, accept simultaneous stimulations by the two cosine-projected E vector components of the two incident beams along this optical axis. By rotating the two polarizers within the MZ with respect to the detector's optical axis, while keeping the angle between them fixed; one can demonstrate that the detecting molecules actively execute the summation of the stimulations due to the waves; rather than the waves summing themselves. The energy transfer is the square modulus of the sum of the two cosine-projected E-vector stimulations of the detecting molecules. This

experiment re-validates the Non-Interaction of Waves (NIW) property.

Using a photo-emf the two- beam fringe visibility due to a pair of polarized beams through a Mach-Zehnder interferometer is demonstrated. Measured data and our formulation of the superposition effect demonstrate that the observed effect is carried out by the polarized molecules of the photoemf detector. The two polarized wave amplitudes do not sum themselves into a new resultant E-vector prior to stimulating the photo-emf detecting molecules; which are discernible by mathematical models. This experiment re-validates the Non-Interaction of Waves (NIW) property.

9570-24, Session 6

Mysterious quantum Cheshire cat: an illusion resulting from interference (Invited Paper)

Kristel F. Michielsen, Forschungszentrum Jülich GmbH (Germany); Hans De Raedt, Univ. of Groningen (Netherlands)

The quantum Cheshire cat was introduced by Aharonov et al. [New J. Phys. 15, 113015 (2013)] in the form of a circularly polarized photon whereby the photon represents the cat and its polarization state the grin, realizing the mysterious behavior of the grinning Cheshire cat in the novel "Alice's Adventures in Wonderland" by Lewis Carroll.

We show that an event-based simulation model [H. De Raedt et al., Quantum Matter 1, 20 - 40 (2012)] reproduces all the reported data of the quantum Cheshire cat interference experiment of Denkmayer et al. [Nature Comm. 5, 4492 (2014)].

As the simulation does not rely on concepts of quantum theory and reproduces all the experimental observations, the latter can be explained without introducing concepts such as particle-wave duality or weak measurements.

Moreover it is explicit that the equivalent of the cat and grin never separate. In other words, the quantum Cheshire cat is an illusion.

9570-25, Session 6

New experiments call for a continuous absorption alternative to the photon model

Eric S. Reiter, Unquantum Lab. (United States)

A famous beam-split coincidence test of the photon model was performed with gamma-rays instead of visible light. A similar test was performed to split alpha-rays. In both tests, coincidence rates greatly exceed chance, leading to an unquantum effect. Details of these tests are described. In contradiction to quantum theory and the photon model, these new results are strong evidence of the long abandoned accumulation hypothesis, also known as the loading theory. Attention will be drawn to assumptions applied to past key experiments that led to quantum mechanics.

9570-26, Session 6

Quantum physics and the beam splitter mystery

François B. Hénault, Institut de Planétologie et d'Astrophysique de Grenoble (France)

Optical lossless beam splitters are frequently encountered in fundamental physics experiments regarding the nature of light, including "which-way" determination or the EPR paradox. Although they look as common optical components at first glance, their behaviour remains somewhat mysterious. In this communication are examined and discussed some basic properties of these beamssplitters, both from a classical optics and quantum physics



point of view. Herein the most evident contradictions are highlighted, and a new experimental set-up enabling to discriminate the two types of theory is described. Alternative empirical optical models are also proposed.

9570-27, Session 6

Photon diffraction described by momentum exchange theory: what more can edge diffraction tell us?

Michael J. Mobley, Grand Canyon Univ. (United States) and The Biodesign Institute, Arizona State Univ. (United States)

Previous papers have presented an alternative picture for photon diffraction based on a distribution of photon paths through guantized momentum exchange with probabilities defined at the location of scattering, not the point of detection. This contrasted with the picture from classical optical wave theory that describes diffraction in terms of the Huygens-Fresnel principle and sums the phased contributions of electromagnetic waves at the location of detection to determine probabilities. This alternative picture was termed "Momentum Exchange Theory" (MET), replacing the concept of Huygens wavelets with photon scattering (positive and negative dispersions) through momentum exchange with the scattering lattice. MET assumes a momentum representation for diffracted particles and has been applied to several different optical diffraction experimental configurations. Straight edge diffraction has been a particularly revealing experimental configuration as it provides significant clues to the geometric parameters controlling exchange probabilities. Diffraction by an opaque disc is examined to provide further insight to negative (attractive) dispersions. This analysis indicates that the "diffraction force" is an integration of momentum exchange field interactions to derive an exchange probability at interaction points along the photon path - resembling aspects of the QED path integral formulation for particle interactions.

9570-28, Session 6

The photon to electron/positron-pair transition

Andrew Meulenberg Jr., Hi Pi Consulting (United States); Ralph F. Penland Jr., Science for Humanity Trust, Inc. (India); Robert W. Hudgins, Science for Humanity Trust, Inc. (United States)

Our prior work has discussed the solitonic nature and interference of photons and light. This paper addresses the interference of photons with themselves and the conditions under which a specific resonance creates the entangled electron/positron pair. Analysis of the forces and potentials in the interaction between photons has raised the issue of oscillating charge as the source of the alternating electric and magnetic fields comprising the photon. Since the photon is net neutral yet is composed of electric fields, the object of this paper is to explore the physical mechanism(s) describing how the alternating fields of the photon can be 'rectified' to produce the separated opposite charges of the electron and positron pair.

Physics spent more than 50 years deciding that the electron mass is entirely electromagnetic. Nevertheless, the concept of the electron being a self-bound photon has never been acceptable. Since photons are here considered to be resonant oscillations (solitons) of an undefined 'field' in four dimensions, we must also look to the 4th dimension to resolve the charge separation. The photons' constituent EM fields are modes of this oscillation. It is in the context of the standing waves of photons that the EM fields and potentials lead to a description of alternating (AC) 'currents' (of some form) of unquantized alternating 'charge' (of some sort) that can be rectified (twisted) into two coupled (at least initially) resonant bodies with opposite charge and, now, with restmass.

9570-29, Session 6

Matter in the form of toroidal electromagnetic vortices

Wilhelm F. Hagen, Consultant (Germany)

The creation of charged elementary particles e± from neutral photons g is explained as a conversion process of electromagnetic energy from linear to circular motion at the speed of light into two localized, toroidal shaped vortices of trapped electromagnetic energy with opposite charges (EM-vortices or Energiewirbel). The photon can be represented as a superposition of left and right circular polarized transverse electric fields of opposite polarity. If these components are separated by interaction with a strong field (nucleon) they would curl up into two electromagnetic vortices (EMV) due to longitudinal magnetic field components forming toroids. These vortices resist change of motion, perceptible as particles with inertia and hence mass. The opposite electrical fields of the photon can be envisioned as originating from a common zero potential axis, the optical axis of the photon. This leads to opposite potentials at the surface of the toroids perceptible as opposite charged elementary particles e± from neutral photons g. These spinning toroids generate extended oscillating fields that interact with stationary field oscillations. The velocity-dependent frequency differences cause beat signals equivalent to matter waves, leading to interference. The extended fields entangled with every particle explain wave particle duality issues. Spin and magnetic moment are the natural outcome of these gyrating particles. As the energy and hence mass of the electron increases with acceleration so does its size shrink proportional to its reduced wavelength. The mysteries about the weak and strong nuclear forces can be easily explained as different manifestations of the intermediate electromagnetic forces. The unstable neutron consists of a proton surrounded by a contracted and captured electron. The associated radial electromagnetic forces are the source of the weak nuclear force. The deuteron consists of two axially separated protons held together by a centrally captured electron. The axial electromagnetic forces are the source of the strong nuclear force, providing stability for "neutrons" only within nucleons.

The same principles were applied to determine the geometries of forcebalanced nuclei. The alpha particle emerges as a very compact symmetric cuboid that provides a unique building block to assemble the isotopic chart. Exotic neutron-4 appears viable which may explain dark matter. The recognition that all heavy particles, including the protons, are related to electrons via muons and pions explains the identity of all charges to within 10–36. Greater deviations would overpower gravitation and may explain the accelerating inflation of the universe based on mismatched charges. Such explanations would render the invention of dark energy obsolete. Gravitation is envisioned as residual force of standing electromagnetic (SEM) waves generated by interacting particles that experience SEM quantum jumps as observed with slow neutrons. Correlating gravity to microscopic quantities leads to the age of the universe of 13.5 b-years. There is no need to invent complex quarks, gluons, strings, virtual particles or multiverses. Reality is simple and beautiful.

9570-101,

The photon: From Newton and Maxwell to Einstein and Schwinger (Keynote Presentation)

Marlan O. Scully, Texas A&M Univ. (United States) and Princeton Univ. (United States) and Baylor Univ. (United States)

The photon concept has a strange history. From the beginning there has been debate whether light is particle-like as Newton suggested or wave-like as Young showed. This debate continued up to modern times and was in particular illuminated by Einstein's discussion the fluctuations and entropy of electromagnetic radiation. Based on thermodynamic reasoning he came to the conclusion that light has both a particle and a wave side. In the mid '20's quantum mechanics in the Heisenberg-Schrödinger form came into being and the first papers on quantum electrodynamics (which really blends

Conference 9570: The Nature of Light: What are Photons? VI



both the particle and the wave nature of light) were put forth by people like Born, Heisenberg, and Jordan in the famous dreimaennerarbeit and Dirac's quantization of the electromagnetic field. It was however later in the early '30's that Fermi wrote his famous Reviews of Modern Physics paper and put the quantum theory of radiation on solid footing. Simultaneously, the electron was being investigated both from the point of view of quantum field theory and the Schrödinger wave equation and it was shown that the Schrödinger equation is in a real sense the wave rendition of the quantum field theoretic description of the electron.

One then naturally asks and the great minds like Kramers (think WKB, that Kramers), asks the question "how far and how exactly can we consistently compare the radiation field with an ensemble of independent particles?" He goes on to note that wave phenomena are now being applied to the electron, e.g., and says "now that wave mechanics has become a consistent formalism one could ask whether it is possible to consider the Maxwell equations to be a kind of Schrödinger equation for light particles instead of considering them up to now to be classical equations of motion which formally look like a wave equation and which are quantized only later. In our book on guantum optics, Zubairy and I show that it is possible to develop a theory in which the photon and the neutrino are very analogous; and show that the photon wave function obeys Maxwell's equations which can be written as a Dirac equation for the photon much like the Dirac equation for the neutrino. Both are massless particles and we are talking in the single photon and single neutrino limit. In this way, we see that the photon wave function has many points in common with the matter wave function. It is however important to note that there are differences associated with for example, the fact that the electromagnetic field, i.e., the photon is transverse in the present study and this is one example of how the photon wave function is different from a nonrelativistic massless particle. In general, there is much to be said for taking the literal point of view that a photon is what a photon detector detects. Following this philosophy we arrive at the wave function for a photon coming from the perspective of quantum field theory.

9570-30, Session 7

Could space be considered as the inertial rest frame?

Chandrasekhar Roychoudhuri, Michael Ambroselli, Univ. of Connecticut (United States)

Separability of Doppler Effect: Analysis of spontaneous and stimulated emissions by excited Ne-atoms with different velocities inside a He-Ne laser tube help us appreciate that emitter and detector velocities are separately identifiable with separate Doppler effects accommodated by quantum mechanics. Optical Doppler Effect should not be explained as due to a single relative velocity between the source and the detector. When this understanding is applied to distant stellar spectra; we can start separating out various components of spectral frequency shifts. The line broadening taking place within the stellar atmosphere is due to Maxwell's velocity distribution of hot molecules. The physical line-center frequency shift happens separately due to the vectorial velocity of the entire star (collectively, the same vectorial velocity of all the gas molecules). Then the detecting star's velocity (the Sun holding our earth-based detector) introduces another apparent Doppler shift. Clever experiments would be able to discern these Doppler shifts and hence the different velocities in the inertial space.

Ether drag experiments: We will present arguments to explain the three key ether-drag experiments viz., (i) Fresnel Drag results (positive and negative from two-way and one-way interferometers), (ii) Bradley (always positive) telescope aberration and (iii) Michelson-Morley (essentially) negative results. We will present our arguments by positing space as a Complex Tension Field (CTF). EM waves are linear excitations of this CTF and hence must always propagate away from the generating source. The stable particles are localized resonant complex non-linear excitations of the same stationary CTF; hence their movement will always require some potential gradients (forces) produced around the particles due to their complex oscillations.

Running time is not a measurable physical parameter of any object. Both classical and quantum physics have modeled and analyzed diverse types of classical and quantized oscillators and under what conditions the characteristic frequencies can be altered. Thus, frequency has the status as

a primary physical parameter that can be altered by altering the physical condition of the oscillator. We can derive a secondary parameter, one period or a time interval, by inverting the primary parameter, the frequency. We assign the measurability to our conceptually derived running time by multiplying the period (inverse of the frequency) by counting larger and larger number of oscillation frequency or the period. This conceptually defined mathematical tertiary parameter, the running time, cannot undergo any physical changes, except through physical changes imposed on the frequency of the primary physical oscillator; which may represent the experimental clock.

References:

[1] C. Roychoudhuri, "Causal Physics: Photon Model by Non-Interaction of Waves", CRC/Taylor & Francis, 2014. See Ch.11 and Ch.12.

[2] Reginald Cahill and Valerie V. Dvoeglazov, "Process Physics: From Information Theory to Quantum Space and Matter"; Feb 21, 2012.

[3] Joseph Levy and Michael Ciaran Duffy, "Ether space-time and cosmology: new insights into a key physical medium"; C. Roy Keys, Inc., 2009.

9570-31, Session 7

Is the natural linewidth due to spontaneous emission life-times or due to time-finite envelopes of the emitted-wave packets?

Negussie Tirfessa, Manchester Community College (United States); Chandrasekhar Roychoudhuri, Michael Ambroselli, Univ. of Connecticut (United States)

We have achieved a great success with the standard model of elementary particles but we also understand that it does not give us a complete picture of our universe. The photon concept is more than a century old but both classical and quantum theories of radiation do not provide us with a prescription for modeling the shape and structure of an EM radiation emitted or absorbed by atoms and dipoles. The quantum theory of interaction between matter and field, Quantum Electrodynamics (QED), has been successfully applied to matter and field interactions. Despite the great success of QED in predicting matter field interactions outcomes, QED does not provide us with the nature and structure of a photon. QED does not also give us guidelines for localizing photons. Semi-classical radiation theory has also been successfully used in predicting experimental results but there are disagreements in some of the experimental results. Our experimental data are guided and dictated by the interaction process between atoms, dipoles and fields. Atoms and dipoles as detectors guide our observation of emission and absorption processes. Developing a model of the emission process requires visualization of the invisible interaction process during emission.

Most of the measured spontaneous emission life times are ?t ~ ns. Conventional method gives a natural linewidth of 1/?t ~ GHz by using Fourier Transform. This is in agreement with experimental results of linewidth. Some metastable atomic emission life times are longer ?t ~ ?s which gives a natural linewidth of 1/?t ~ MHz. Fourier transform techniques is a great mathematical tool that gives results that coincides with experiments but it gives us guidance on the representation of the emission process or on how to model the emitted photon.

In a previous papers and book, we have proposed that photons are diffractively evolving classical wave packet as a propagating undulation of the Complex Cosmic Tension Field (C2TF) after the excess energies are released by atomic or molecular dipoles as perturbations of the C2TF. The carrier frequency of the pulse exactly matches the quantum condition ?Emn= h?mn and the temporal envelope function creates the Lorentzian broadening of the measured spectral lines. In this paper we will use our photon model to match experimentally measured spectral lines of atoms and use it to compute linewidth .



9570-32, Session 7

Phase shift between Michelson two beam due to propagation in an optical waveguide

Octavio N. Sanchez, Manuel Fernández-Guasti, Univ. Autónoma Metropolitana-Unidad Iztapalapa (Mexico)

The electromagnetic energy within the interference fringes of two crossing coherent light beams poses important conceptual problems. In the standard electromagnetic description, the energy is redistributed from the dark to the bright fringes. No clear mechanism has been stated regarding this energy redistribution. However, if the two beams no longer overlap, each beam should regain their initial features. Efforts to measure the two beams after the interference region have been elusive due to diffraction.

An alternative indirect measurement explored here, is to feed the interfering fields into an optical fibre. Due to the different incidence angle of each beam, they can propagate in different waveguide modes. Since modes have different velocities, the relative phase between the two fields should change. A relative phase retardation of the two interfering beams, will produce a displacement of the interference maxima and minima at the fibre output with respect to these extrema at the input.

To this end, a Michelson interferometer was set up and a small portion of a fringe was selected. This wave front was subsequently split, one beam focused into an optical fibre while the other was used as reference. The interferometer mirror was scanned so that fringes were displaced at the output. The two intensities, before and after the fibre, were registered as a function of scanning. A phase shift of 29 mrad was obtained between the two signals. These results indicate that there are two fields propagating in the fibre in different modes. Thus the two fields are still present after their interference at the interferometer output.

9570-33, Session 7

Light and harmonicity: the golden section

Dionysios G. Raftopoulos, Independent Researcher (Greece)

Adhering to Werner Heisenberg's and the school of Copenhagen's natural philosophy we introduce the localized observer as an absolutely necessary element of a consistent physical description of nature. Thus we have synthesized the theory of the harmonicity of the field of light, which attempts to present a new approach to the events in the human perceptible space. It is an axiomatic theory based on the selection of the projective space as the geometrical space of choice and its first fundamental hypothesis is none other than special relativity theory's second hypothesis properly modified. The result is that all our observations and measurements of physical entities always refer not to their present state but rather to a previous one, a conclusion evocative of the "shadows" paradigm in Plato's cave allegory. In the kinematics of a material point this previous state we call "conjugate position", which has been called the "retarded position" by Richard Feynman. We prove that the relation of the present position with its conjugate is ruled by a harmonic tetrad. Thus the relation of the elements of the geometrical (noetic) and the perceptible space is harmonic. In this work we show a consequence of this harmonic relation: the golden section.

Keywords: Perceptible and geometrical projective space, theory of the harmonicity of the field of light, golden section.

9570-34, Session 8

Can the photon be described by a general particle model?

Albrecht Giese, Consultant (Germany)

Particle physics deal with a few basic particle types: Leptons, Quarks, Photons.

Most of the particles we know are either leptons or are built by quarks (as e.g. mesons and nucleons). A special place occupies the photon which seems to be independent. And, among other aspects, it has twice the spin of leptons and quarks.

Using the properties of particles such as their mass, spin, and magnetic moment, and from the relativistic behaviour of matter – which can be derived from the 'zitterbewegung' of the electron – we can draw up a model, in which a particle is composed of a pair of sub-particles which orbit each other. This model conforms largely to the quantum mechanical concepts of Louis de Broglie. It replaces the idea of particle-wave-duality as manifested by the Copenhagen interpretation of GM. And this model allows for a description of particle properties with high precision on the basic of classical physics.

This particle model, which was developed for leptons and quarks, is also a candidate for the description of the photon. The consequences for an understanding of the photon are an essential topic of this talk. Most of the properties of the photon can be explained by the model, some aspects need further evaluation.

This model explains for the first time the famous relation E=h*?. It has also the capability to explain open issues like cosmological inflation, dark energy, and dark matter. And in contrast to the way as Albert Einstein has done it, relativity has not to be founded on 'principles' but follows from the structure of fields and particles and gets in this way a real physical basis.

9570-35, Session 8

Quantum mechanical probability current as electromagnetic 4-current from topological EM fields

Martin B. van der Mark, Philips Research Nederland B.V. (Netherlands)

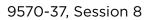
Starting from a complex 4-potential A=?d? we show that the 4-current density in electromagnetism and the probability current density in relativistic quantum mechanics are of identical form. With the Dirac-Clifford algebra Cl(1,3) as mathematical basis, the given 4-potential allows topological solutions of the fields, quite similar to Bateman's approach, but with a double field solution that was overlooked previously. A more general null-vector condition is found and wave-functions of charged and neutral particles appear as topological configurations of the electromagnetic fields. The description of electron-positron annihilation into two photons requires a seamless integration of the Maxwell and Dirac equations, which may be shown as an example.

9570-36, Session 8

On a heuristic framework for modeling the fundamental particles and interactions

Ted Silverman, IIAS (United States)

A quasi-constructive model of the vacuum is presented in a 3-space plus 1-time dimensional framework. Space is represented as a continuum with a dynamical density. Particles are localized, harmonic oscillations of spatial density, which interact via their extended scalar fields. Density gradients manifest in the space surrounding particles, as well as in the ambient space of scalar fields generally, and these gradients comprise, collectively, the metric field. Newton's constant is deduced from first principles and is given by a simple expression in terms of the Planck and fine structure constants, in a form analogous to that in which the electric charge is represented in quantum electrodynamics. In particular, the photon emerges as a kinematic effect - relativistic modulation of the electron's extended scalar field.



Quantum mechanics beyond Gaussians: from coarse graining to tower of scales

Antonina N. Fedorova, Michael G. Zeitlin, Institute of Problems of Mechanical Engineering (Russian Federation)

We construct some universal picture for re-consideration of base states and generic phenomena, like entanglement, in Quantum Mechanical set-up.

Our main goal is related to the analytical continuation of the standard zoo of solutions/base states from trivial ones, like plane waves or gaussians to novel states, possibly realizable, which permit more realistic (re) interpretation of the base folklore of Quantum Mechanics as well as more proper analytical/numerical modeling on the whole qualitative scale from entanglement to decoherence. Definitely, there is a set of experimental features as well as theoretical prerequisites demanding the appearance of new usefulness images.

We start from some simple categorification procedure allowing to consider generic states as sheaves but not functions, after that we look for internal hidden symmetries on the level of the underlying "categorified" Hilbert space of extended states. The orbits of these symmetries create the arena where we can model the novel features of our generalization of Quantum Mechanics. The analytical instruments allowing us to model both qualitative and quantitative aspects are Nonlinear Local Harmonic

Analysis on the representations of orbits of hidden symmetries of underlying generalized Hilbertian spaces and variational principles which permit the algebraization of the subsequent control of the type of behaviour.

It seems that reasonable extension of the zoo of possible (realizable) states can simplify the search of prototypes for realizable quantum devices as well as provide the more realistic (re)interpretation of the long-living standard "quantum folklore".

9570-38, Session 9

The fine structure constant alpha: relevant for a model of a self-propelling photon and for particle masses (*Invited Paper*)

Karl Otto Greulich, Fritz Lipmann Institute (Germany)

A model for a self propelling (i.e. massless) photon (K.O. Greulich Proc SPIE 8832-43) is based on oscillations of a charge amounting to elementary charge / SQRT alpha, where alpha is the fine structure (Sommerfeld) constant (1/137, 036). When one assumes a similar model for particles which do have rest mass (i.e. non- self propelling), alpha plays also a role in elementary particles.

Indeed all fundamental elementary particles can be described by the alpha / beta rule --? m(particle) = alpha power to – n * beta power to m* 27.2 eV / c2 ?-- where beta is the proton to electron mass ratio 1836.12 and n= 0....14, m= -1,0 or 1 (K.O. Greulich, Spring meeting 2014 German Physical Society T 99.4). Thus, photons and particle masses are intimately related to the fine structure constant. If the latter would not have been strictly constant throughout all times, this would have had consequences for the nature of light and for all masses including those of elementary particles.

9570-39, Session 9

The electron as a confined photon

Charles G. Akins, Akins Enterprises LLC (United States)

A new topological study is presented of a semi classical quantized model for the electron, consisting of a circularly bound monochromatic photon. This model for the electron includes a topologically created elementary charge, point-like behavior in high-energy scattering events, half-integral spin, and the magnetic moment of the electron. We will also present evidence for the causes of: 1) the fine structure constant, 2) the magnetic moment anomaly of the electron, 3) the elementary charge, 4) a binding force which allows a photon to be confined to become and electron, 5) the property of inherent inertial mass in the electron, and 6) Relativity. Within this context we propose that all matter is composed of EM waves, and that Relativity and Quantum Mechanics are the simple result of the behavior of those EM waves. For the most part we will use simple scalar mathematics to support this premise, because most of the problems have relatively simple solutions. However we will also submit that new formulations are needed for field equations. The following is a "thought experiment" intended to explore the architecture and topology of the electron.

SPIE. OPTICS+ PHOTONICS

OPTICAL ENGINEERING+

APPLICATIONS

9570-40, Session 9

The nature of the photon and the electron (*Invited Paper*)

John G. Williamson, Univ. of Glasgow (United Kingdom)

A linear, first order, extension of the classical theory of electromagnetism has been developed. A wave-function has been derived which is a solution to the first order, free-space Maxwell equation. Allowed propagating field only solutions are in some respects quantised in that they come in "lumps" and are associated with an integral angular momentum. The new solutions encompass all the fields of the photon, just and no more, properly describe the components in each and every Lorentz frame, and hence embody the relativistic transformations. These are photon-like solutions of the classical Maxwell equations.

Including a dynamical rest-mass term gives a mechanism for the selfconfinement of the elements of the extended electromagnetism into qualitatively new kinds of solutions. Though charge is not introduced, the confinement mechanism forces the new solutions into a re-configuration of the fields, exhibiting a quantised charge. For the simplest configuration, this may be readily estimated and is found to be close to the elementary charge. The spin may also be calculated and is found to be half-integral. Just as is the case with the, related but simpler, Dirac equation, there are four and only four such solutions. These are identified with the spin up and spin down electron and positron. Experimental tests of the new theory lie in high energy laser experiments, spin-polarised scattering experiments and in cosmology.

The new theory, because it describes light and matter on the same footing, may be expected to offer unprecedented opportunities in developing new materials, devices and technologies.

9570-41, Session 9

Absolute relativity and the quantisation of light

John G. Williamson, Univ. of Glasgow (United Kingdom)

A new theory has been developed to describe both light and material particles. A surprising consequence is that field only solutions –light – are necessarily quantised.

A principle, called here absolute relativity, is implemented using a physical mathematics based only on the proper relativistic properties of the four dimensions of space-time.

Processes corresponding to multiplication, division and differentiation are defined. In addition to the 4 unit vector quantities this leads to twelve further unit elements, each encapsulating precisely a proper relativistic form: a Lorentz invariant unit point, six unit planes transforming as the elements of the electromagnetic field, four volumes, transforming like an angular momentum density, and a unit hyper-volume which squares to negative unity.

A set of coupled linear differential equations have been derived. These simplify to the free-space Maxwell equations in the pure-field case. A new, relativistic, field-only wave-function is proposed describing packets of energy of any magnitude but all with the same angular momentum: photons. It is concluded that the "quantisation" of light arises as a result of the rigorous consideration of the properties of space and time in special relativity. The new theory predicts that the "quantisation" is not intrinsic,



but arises from the nature of the emitter and absorber. The near-field should remain continuous. It predicts a series of "photons" with relative energies of the squares of the natural numbers. Phat photons. It is predicted that, in the fractional Quantum Hall regime, fractionally quantised "photons" may be possible.

9570-42, Session 9

A meta-analyzer for circular polarization resolved spectroscopy (Invited Paper)

Din Ping Tsai, Academia Sinica (Taiwan) and National Taiwan Univ. (Taiwan); Wei-Yi Tsai, Chun Yen Liao, Wei Ting Chen, Pei Ru Wu, National Taiwan Univ. (Taiwan); Greg Sun, Univ. of Massachusetts Boston (United States); Peter Török, Imperial College London (United Kingdom)

Distinguishing from a right-handed (RCP) or left-handed circularly polarized (LCP) wave in both spatial and spectral domain by a conventional method is less efficient since the most materials in nature exhibit similar optical properties under a RCP or LCP illumination. The metasurfaces, an array of sub-wavelength antenna with varying sizes, shapes and orientations enable us to design the devices with tailored optical properties [1, 2]. Here, we present a multifunctional metasurface working in visible region, which integrating the functionalities of grating, mirror and circular polarization splitter into a single micro-device. Using gold nano-rods with varying orientations as building blocks to construct our device with -?/4 thickness, different wavelengths and handed circular polarizations of incident wave can be distinguished through diffraction angles. The spatial resolution of angular dispersion is about 0.025 degree per unit wavelength. This work paves the road to a wide range of applications such as polarization analyser and plasmon-enhanced circular dichroism spectroscopy.

The authors acknowledge financial support from Ministry of Science and Technology, Taiwan (Grant Nos. 103-2745-M-002-004-ASP, 102-2745-M-002-005-ASP, 102-2911-I-002-505, 100-2112-M-019-003-MY3, and 100- 2923-M-002-007-MY3) and Academia Sinica (Grant No. AS-103-TP-A06). They are also grateful to National Center for Theoretical Sciences, Taipei Office, Molecular Imaging Center of National Taiwan University, National Center for High-Performance Computing, Taiwan, and Research Center for Applied Sciences, Academia Sinica, Taiwan for their supports.

9570-44, Session 10

Discovery of dynamical space: experiments and theory (*Invited Paper*)

Reginald T. Cahill, Flinders Univ. (Australia)

Recently the existence of space as a complex dynamical system was discovered, based on various experiments going back to 1887. The early experiments by Michelson and Morley 1887, and Miller 1925, used light speed anisotropy detected with interferometers. Only in 2002 was the calibration theory first derived. More recently there have been other experimental techniques, including Doppler shift effects detected by NASA using spacecraft earth flybys. The most recent technique uses current fluctuations through the nanotechnology reverse biased Zener diode barrier potential, by using two detectors and measuring the time delay in correlations to determine speed and direction of the space flow. Physics has never had a knowledge of this dynamical space, and the theory is well developed, and is now known to explain the origin of gravity, quantum fluctuations, bore hole g anomalies, galactic rotations, galactic lensing of light, universe dynamics, laboratory G measurements, GPS, and more. This dynamical space supports a coordinate system, and it was this that was originally thought to be space itself.

9570-45, Session 10

Energetic spacetime: the new aether

John A. Macken, Macken Instruments Inc. (United States)

This work builds on the spacetime-based photon model initially presented at The Nature of Light V conference. Previously it was shown that a proposed "charge conversion constant" with units of meters/Coulomb was capable of converting charge, electric field and the impedance of free space into quantifiable properties of spacetime. Since the impedance of free space (Zo \approx 377 ohms) converts to the impedance of spacetime (c^3/G), the implication is that photons are a quantized wave propagation in the "spacetime field" which was also described.

Now this model is expanded further to show that it meets several other properties required of a photon model. First, this wave-based model is shown to explain Compton scattering better than the particle models of a photon. Second, the proposed model satisfies the Feynman path integral formulation. Rather than a photon having a single trajectory between the emission and absorption points, the model produces a sum over an infinity of trajectories to achieve a quantum amplitude determining the probability of absorption. Third, the model explains the wave-particle duality of photons. A photon does not have quantized energy because a photon can lose energy in Compton scattering or redshift and the phopton continues to exist. The photon's particle-like properties are shown to be the result of angular momentum being quantized. Finally, the angular momentum of a linearly polarized photon is examined and found to possess predictable angular momentum which is hard to detect. An experiment is suggested to test this contention

9570-46, Session 10

Modelling superposition of many polarized beams on an isotropic photo detector

Chandrasekhar Roychoudhuri, Michael Ambroselli, Univ. of Connecticut (United States)

In a previous paper [SPIE Proc.Vol.7063, paper #4 (2008)], we have modeled possible modes of excitations that detecting dipoles carry out before absorbing a quantum cupful of energy out of two simultaneously stimulating EM waves along with experimental validation; basically corroborating Malus' law. For the two beam case, the cos? factor, ? being the angle between the two polarization vectors, is too simple a case to directly extrapolate the model to possible complex behavior of quantum dipoles stimulated simultaneously by N-polarized beams. This paper presents possible models for simultaneous stimulation by N-polarized beams and the follow-on energy absorption. We then propose experiments for the particular case of three polarized beams. Comparison with literature will be presented. We will also compare the behaviors of energy absorbed by an anisotropic photo detector with that of the energy transmitted by a transparent polarized crystal. The comparison should be interesting because photo detection is a quantum process; but transmission by a crystal is a classical bulk process. We will also discuss helicity of "photons" in the context of "chirality" of materials (molecules) while interacting with polarized beams.

9570-47, Session 10

Tabletop demonstration of non-Interaction of photons and non-interference of waves

Narasimha S. Prasad, NASA Langley Research Ctr. (United States); Chandra Roychoudhuri, Univ. of Connecticut (United States)

Recently, Non- Interaction of Waves or the NIW property has been proposed as a generic property of all propagating electromagnetic waves by one of the authors (CR). In other words, optical beams do not interact with each other to modify or distribute their field energy distribution in the

Conference 9570: The Nature of Light: What are Photons? VI



absence of interacting materials. This paper plans to re-create CR's original demonstration of the NIW-property as an on-site table-top experiment. We will use a tilted Fabry-Perot etalon to generate a set of spatially separate parallel beams out of an incident laser beam; which will then be focused on a one-sided ground glass, the flat side being towards the etalon. This flat side reflects back all the incident beams as fanning out independent laser beams, remaining unperturbed even though they are reflecting out of a common superposed spot. It is clear that there are neither "interference between different photons", nor "a photon interferes with itself", even within a region of superposed beams. In contrast, the ground glass surface (same silica molecules but granular or lumpy) generates a set of spatial fringes on its surface. Clearly, granulated individual silica lumps are responding simultaneously to the local resultant E-vectors due to all the superposed beams and are scattering energy proportional to the square modulus of the sum of all the simultaneous dipolar amplitude stimulations. The dark fringe locations imply zero resultant amplitude stimulation and hence no scattering. Are the fundamental physics behind the generation of superposition fringes by photo detectors different from those due to aground glass? We will discuss our views.

9570-48, Session 11

Clock time is absolute and universal (*Invited Paper*)

Xinhang Shen, NAC Geographic Products Inc. (Canada)

A physical clock can never directly measure time, but can only record the result of a physical process during a period of time such as the number of cycles of oscillation which is the multiplication of time and the frequency of oscillation. After Lorentz Transformation, time expands by a factor gamma, but the frequency decreases by the same factor gamma, and the resulting multiplication i.e. the displayed time of a moving clock remains unchanged. That is, the displayed time of any physical clock is an invariant of Lorentz Transformation. The Lorentz invariance of the displayed times of clocks can further prove within the framework of Special Relativity our earth based standard physical time is absolute, universal and independent of inertial reference frames as confirmed by the universal synchronization of clocks on the GPS satellites and clocks on the earth.

9570-49, Session 11

Special relativity from observer's mathematics point of view

Boris Khots, Dmitriy Khots, Compressor Controls Corp. (United States)

When we create mathematical models for quantum theory of light we assume that the mathematical apparatus used in modeling, at least the simplest mathematical apparatus, is infallible. In particular, this relates to the use of "infinitely small" and "infinitely large" quantities in arithmetic and the use of Newton – Cauchy definitions of a limit and derivative in analysis. We believe that is where the main problem lies in contemporary study of nature. We have introduced a new concept of Observer's Mathematics (see www.mathrelativity.com). Observer's Mathematics creates new arithmetic, algebra, geometry, topology, analysis and logic which do not contain the concept of continuum, but locally coincide with the standard fields.

We use Einstein special relativity principles and get the analogue of classical Lorentz transformation. This work considers this transformation from Observer's Mathematics point of view.

Keywords: Observer, arithmetic, derivative, probability, quantum mechanics, quantum theory of light

9570-52, Session 11

Quantum mechanics via sheaves and schemes: on the route to categorification

Michael G. Zeitlin, Antonina N. Fedorova, Institute of Problems of Mechanical Engineering (Russian Federation)

Sheafification together with microlocalization and the subsequent analysis of quantum dynamics on orbits with special, so-called MRAfiltrations (generating a full tower of the underlying internal hidden scales), considered in the companion paper, are the starting points of our attempt of Categorification Program for Quantum Mechanics and/or General Local Quantum Field Theory.

In some sense, we may hope on the same breakthrough as in the golden era of Algebraic Topology and Algebraic Geometry in the 50s and 60s of the 20th Century, which was concluded by Grothendieck's approach and provided the universal description for a variety of long standing problems. Roughly speaking, in (Quantum) Physics such an approach provides useful, constructive and universal methods to glue the complex local data into the general picture by power machinery taking into account the topological and (algebraical) geometrical data of the underlying hidden internal structures.

Definitely, the simple linear algebra of structureless Hilbert spaces cannot describe the whole rich world of quantum phenomena. Our approach introduces (Grothendieck's) Schemes instead of varieties/ manifolds as generic quantum objects, naturally encoded the full zoo of phenomenological things discussed in Quantum Mechanics. The key ingredient of such an approach is the bridge between the von Neumann description of measurement together with the Gelfand ideal of the state and GNS (Gelfand-Naimark-Segal)-construction on one side of the river and locally ringed space, structure scheaf and (affine) scheme on the opposite (categorificated) side.

9570-53, Session 11

On the nature of "stuff" and the hierarchy of forces

Martin B. van der Mark, Philips Research Nederland B.V. (Netherlands)

From super clusters of galaxies down to the quarks in the proton, at all length scales the structure of matter is the result of a balance of forces. In this paper it is argued that with decreasing size there must necessarily be an increase of the fraction of kinetic and binding energy with respect to the total energy. Smaller sizes require stronger forces which represent more of the energy available. The smallest possible size of granularity is found to be where the internal kinetic energy and total energy become comparable, which occurs at the size of the proton. We infer that the proton is the smallest stable particle, being a light speed circulation of energy.

9570-54, Session 11

The electrostatic to gravitational force ratio within the electro-gravi-magnetic (EGM) construct

Riccardo C. Storti, Delta Group Engineering, P/L (Australia)

The Electro-Gravi-Magnetic (EGM) construct is a derived methodology based upon the Polarizable Vacuum (PV) model of gravity and Buckingham Pi Theory (BPT). Their union has produced impressive experimentally verified results consistent with the Standard Models of Particle-Physics and Cosmology. The body of research in this paper is based on the fundamental EGM prediction that Photons are quantized massive propagating units of matter such that, when standard engineering scaling and similarity techniques are applied, the "Many Orders of Magnitude" problem between



ElectroStatic and Gravitational Forces is reconciled as a function of Cosmological Expansion.

9570-100,

Are electrons oscillating photons; or, oscillating "vacuum"; or, something else? -The 2015 Panel discussion

Chandrasekhar Roychoudhuri, Univ. of Connecticut (United States) and Femto Macro Continuum (United States); Charles G. Akins, Akins Enterprises LLC (United States); John G. Williamson, Univ. of Glasgow (United Kingdom); John A. Macken, Macken Instruments Inc. (United States); David Mathes, Parsec (United States); Richard Gauthier, Santa Rosa Junior College (United States); Martin B. van der Mark, Philips Research Nederland B.V. (Netherlands)

What physical attributes separate EM waves, of the enormous band of radio to visible to x-ray, from the high energy narrow band of gammaray? From radio to visible to x-ray, telescopes are designed based upon the optical imaging theory; which is an extension of the Huygens-Fresnel diffraction integral. Do we understand the physical properties of gamma rays that defy us to manipulate them similarly? One demonstrated unique property of gamma rays is that they can be converted to elementary particles (electron and positron pair); or a particle-antiparticle pair can be converted into gamma rays. Thus, EM waves and elementary particles, being inter-convertible; we cannot expect to understand the deeper nature of light without succeeding to find structural inter-relationship between photons and particles. This topic is directly relevant to develop a deeper understanding of the nature of light; which will, in turn, help our engineers to invent better optical instruments.

Conference 9571: Fourteenth International Conference on Solid State Lighting and LED-based Illumination Systems

Wednesday - Thursday 12-13 August 2015

Part of Proceedings of SPIE Vol. 9571 Fourteenth International Conference on Solid State Lighting and LEDbased Illumination Systems

9571-1, Session 1

Semiconductor lasers (VCSEL, laser diode, and LEDs) characterization

Mahmoud Gadalla, Tanta Univ. (Egypt)

This paper includes some experimental results and theoretical explanation about VCSEL, Laser Diode (LD) and LEDs. It explains the power-current (P-I) relation with temperature effect, and then goes briefly to discuss VCSEL and LD emission pattern and their spectrum temperature dependence. Finally a number of LEDs will be examined from the point of view of emission pattern and spectrum analysis.

9571-2, Session 1

Next-generation glass-base phosphorconverted laser light engine

Jin-Kai Chang, National Sun Yat-Sen Univ. (Taiwan); Wei-Chih Cheng, Taiwan Color Optics, Inc. (Taiwan); Yi-Yin Kuo, National Sun Yat-Sen Univ. (Taiwan); Chun-Chin Tsai, Far East Univ. (Taiwan); Yung-Peng Chang, Taiwan Color Optics, Inc. (Taiwan); Yi-Chung Huang, Brogent Technologies, Inc. (Taiwan); Li-Yin Chen, National Sun Yat-Sen Univ. (Taiwan); Wood-Hi Cheng, National Chung Hsing Univ. (Taiwan)

We report the first experimental demonstrating a novel high-reliable laser light engine (LLE) employing employing Ce:YAG and Ce:LAG-doped glass. The LLE module consisted of a color wheel and a 10 W blue light laser array. The color wheel included two color conversion layers and a micro motor. The conversion layers of the yellow and green phosphors were bonded on an aluminum substrate and placed on a micro-motor. The laser array source was used to excite the color wheel which would create yellow and green lights. The combination of blue, yellow, and green lights will produce high-purity white light for use in laser light engines.

A common type of phosphor-converted color wheel consisted of a GaNbased semiconductor chip and phosphor-doped silicone as a phosphorconverted layer. The silicone is a key component in conventional LLEs. However, the high heat flux radiating from the laser focus point may make the silicone yellow and decreasing the transmittance. In recent years, glassbased phosphors have been discussed as the solution of carrier material for high-power white LEDs due to much higher thermal stability than siliconebased phosphors.

In this study, we present a novel LLE employing glass-based phosphor. The luminance and chromaticity measurements of the LLEs including luminous efficacy, quantum efficiency, color purity, correlated color temperature, and chromaticity coordinates will be presented. A better thermal stability of glass-based phosphor-converted color wheel may be beneficial to the many applications where the LLE modules with high power and high reliability are demanded for use in the next-generation LLEs.

9571-3, Session 1

Extraction efficiency enhancement in ultra-violet LEDs based on spin on glass microlenses

Chi-min Liu, National Taiwan University (Taiwan); Guo-

Dung J. Su, National Taiwan Univ. (Taiwan)

Currently, light emitting diodes (LEDs) technology is widely applied to many aspects in daily life. We developed a new method to enhance the ultra-violet LEDs efficiency. A new fabrication method of a microlens is proposed that can be easily applied to ultraviolet light-emitting diodes (UV LEDs) and microlens system. We demonstrated a self-assembled microlens on top of UV LEDs based on self-surface tension and hydrophilic confinement effect to improve extraction efficiency. The microlens was made of transparent negative photoresist SU-8 and self-surface tension. This approach is cost effective and low time-consuming. Integrated with UV LEDs, microlens can improve extraction efficiency 5% in total power.

9571-4, Session 1

Standardization of UV LED measurements

George P. Eppeldauer, Thomas C. Larason, Howard W. Yoon, National Institute of Standards and Technology (United States)

Traditionally used source spectral-distribution or detector spectral-response based standards cannot be applied for accurate UV LED measurements. The most popular LEDs in the UV range have peaks at 405 nm, 395 nm, 385 nm, and 365 nm. These LEDs produce broadband radiation and their peaks can change about +/- 5 nm. The spectral bandwidths of the LEDs can be different as well. The detectors used for the measurement of these LEDs also have different spectral bandwidths. The CIE standardized squareshape spectral response function for UV measurements cannot be realized with small spectral mismatch when using filtered detectors. E.g., for the measurement of 365 nm peak LEDs, the realized UV-A meters have different response functions producing large measurement errors even if the same LED is measured. In these broadband UV measurements, the signal is equal to the spectral product of the source distribution and the spectral response of the LED-measuring detector/meter. In order to perform uniform LED measurements, instead of the traditional source and detector standards, the signal measurement procedure is standardized here. In the present example, LEDs with 365 nm peak are applied for fluorescent crack-recognition using liquid penetrant (non-destructive) inspection. Using the traditional standards and measurement methods, the broadband UV measurement errors can be several times ten percent or larger. The requirement from the standard signal-measurement procedure is to obtain invariance in the measured output signal for variations in both the peak and the spectral width of the source. The spectral-shape of the meter response has to be chosen broad and flat enough to obtain the same signal for the different LEDs or LED groups with the required low measurement uncertainty. As a first step of the new standard procedure, the UV source is standardized. Instead of traditionally used Hg lamps, environment friendly UV LED sources are used. The peak changes and the spectrum-half-width can be maximized according to the spectral flatness of the detector in the spectral range determined by the LED sources to be measured. The UV LED source can be calibrated against an FEL lamp standard to determine its spectral irradiance. In a second step, the measurement procedure is standardized. The spectral irradiance responsivity of a reference UV detector/meter is calibrated. The output signal of the reference UV meter is calculated from the calibrated spectral function of the UV source and the calibrated spectral response of the reference UV meter. The maximum allowed peak wavelength changes of the source (using the measured response function of the reference meter) can be calculated from the expected uncertainty of the output signal measurement. From the output signal, both the integrated irradiance (in the reference plane of the reference meter) and the integrated responsivity of the reference meter can be determined. Test UV meters can be substituted for the reference UV meter in the same irradiance, and the ratio of the output signals can be used as the calibration factor for the test meter. From the calibration factor and the integrated response of the reference

356



Conference 9571: Fourteenth International Conference on Solid State Lighting and LED-based Illumination Systems



meter, the integrated response of the test meter can be determined. When the calibrated test meter measures the signal from a field UV source, the integrated irradiance from the field source can be determined. In the given LED-365 nm example, this irradiance level is standardized by the ASTM-E1417 and it shall be at least 1 mW/cm2 at a distance of 40 cm from the source. UV damage-free nitrided Si detectors were used in the here developed reference UV irradiance meters with fluorescence-free band-pass filters attached to the front. The realized spectral response function was broad and flat (constant) enough, compared to the source distributions, to obtain small enough output signal variations as a result of using the standard procedure. When the measurements are extended for a wider wavelength range (using more different UV LEDs) pyroelectric detectors with low noise-equivalent-power (NEP) can be used as reference detectors. The low-NEP is needed to calibrate the detector for spectral response at the output of a monochromator. The scale transfer to field UV LED measurements can be made with filtered UV quantum detectors. The measurement uncertainty obtained using the LED-365 source standard and the standard broadband UV measurement procedure, was 5 % (k=2), significantly lower than the measurement errors obtained using traditional standards. Improving the spectral flatness of the reference meter, the uncertainty of the reference UV LED measurements can be decreased to the couple of percent (k=2) level.

9571-5, Session 2

Thermoresponsive scattering coating for smart white LEDs

Hugo J. Cornelissen, Joan Yu, Giovanni Cennini, Philips Research (Netherlands); Jurica Bauer, Paul P. C. Verbunt, Cees W. M. Bastiaansen, Dick J. Broer, Technische Univ. Eindhoven (Netherlands)

In this paper we present a novel smart LED system, based on single white emitting LEDs, able to adjust the CCT of the emitted light in response to electrical current. The smart LEDs are based on a thermoresponsive material, coated on top of LEDs, that uses the heat generated by the LED to switch between a scattering and a transparent state, in turn causing a change in the CCT of the light emitted by the device. Furthermore, by tuning the design of the LED we were able to develop an LED system that automatically changes the CCT of the emitted light in the range between 2900 and 4150 K upon changing the current applied to the LED. Due to the presence of two different phosphors in the LED package, the chromaticity of the light emitted by the LED system remains within the 5-steps MacAdam ellipses from the black body line at all currents and CCTs, rendering this LED system applicable in the lighting industry.

9571-6, Session 2

High efficient packaging structure with high concentration phosphor matrix

Yu-Yu Chang, Hsin-Ying Lin, Zi-Yan Ting, Tsung-Hsun Yang, Ching-Cherng Sun, National Central Univ. (Taiwan)

In this paper, we propose and demonstrate a high efficient packaging structure of pcW-LED. In the packaging structure, a high reflective cup is used for a higher photon recycling and phosphor matrix is used for a higher light extraction for blue light without scattering effect. Accordingly, to minimize the loss blue light and to maximize the white light efficiency can be fulfilled at the same time. With a high concentration phosphor optical model, phosphor which is coated on a transparent substrate can be simulated to optimize the coating area and spacing. In simulation, a full coated phosphor substrate is analyzed first, and a specific thickness of phosphor layer will be chosen for a maximum light output of yellow light. Therefore, the spacing of phosphor matrix can be analyzed and optimized to extract more blue light for a certain correlated color temperature which is fixed at 6500K in this paper. In simulation, the best result is 71.6% in packaging efficiency with the phosphor particle size is center at 6 ?m in the radius. The result shows a 4% enhancement compared with a remote

hemisphere packaging structure which is the best result of the previous simulation. In experiment, when the CCT is 6590K, the best packaging efficiency of the phosphor matrix structure can be 68% which is much higher than 62.4% of the remote hemisphere package. Therefore, with the same spectrum, the luminous efficacy could be 18 lm/W more. This packaging structure can be realized and closer to the boundary of 75% in packaging efficiency at 6500K which can be a breakthrough for a high efficient package in pcW-LED.

9571-7, Session 2

Direct growth and controlled coalescence of thick AIN template on circle patterned-Si substrate

Tinh Binh Tran, Hideki Hirayama, Shiro Toyoda, Noritoshi Maeda, RIKEN (Japan)

AlGaN-based deep ultraviolet light emitting diodes (UV-LEDs) have attracted considerable attention due to their wide range of applications in air, water purification, disinfection, non-line-of-sight communication, etc. AlGaN-based deep UV-LEDs on sapphire substrates have been already commercialization. However, the growth of AlGaN/AlN on silicon substrates for deep UV-LED applications have been extensively studied due to lots of challenges such as a large lattice mismatch between AlN and Si (111) (-19%) will lead to high-dislocation density and crack initiating stress, the presence of an oxide on the Si substrate also leads to low coherence between AlN template and the Si substrate, or the low growth rate, etc. Thus, conventional bulk AlN grows on Si is troublesome for researchers.

In this work, we report on the fabrication and investigation of thick AIN templates grown directly on circle patterned-Si(111) substrates using NH3 pulse-flow multilayer with epitaxial lateral overgrowth (ELO) for further use in AlGaN-based deep UV-LED applications. The effect V/III ratio on the growth rate and the growth temperature on the crystalline quality of thick AIN templates were mainly studied. A -8 μ m-thick AIN template with XRD FWHM of about -840 arcsec and 1350 aresec for (002) and (102) reflection planes were obtained, respectively. Low roughness surface and dislocation density were also confirmed by using AFM (atomic force microscope) and TEM (transmission electron microscopy) techniques. The achievement of high quality and crack free with a uniform thickness of AIN film on 2-inch Si(111) substrate is of great interest for AIN-based deep UV-LED applications.

9571-8, Session 3

Köhler integration in color mixing collimators

Oliver Dross, Philips Research (Netherlands)

No Abstract Available

9571-9, Session 3

Selecting "pleasing" correlated color temperature for illumination of outdoor environments

Andrius Petrulis, Pranci?kus Vitta, Rimantas Vaicekauskas, Arturas ?ukauskas, Vilnius Univ. (Lithuania)

Commonly, subjects prefer higher illuminances irrespectively of the correlated color temperature (CCT). However in outdoor environments, energy saving, light pollution, and circadian disruption issues require limiting the illuminance to particular levels. To that end, finding the most appropriate lighting conditions can be performed by the selection of the most "pleasing" CCT. In this work, subjective judgments on the most "pleasing" CCT were investigated in outdoor environments using a tetrachromatic solid-state light engine with tunable CCT and high-fidelity color rendition. Using a

Conference 9571: Fourteenth International Conference on Solid State Lighting and LED-based Illumination Systems

remote control (smart phone with application software), subjects were asked to adjust CCT within the 1850-10,000 K range in several outdoor environments (medieval courtyard, park area, and modern city). Typically, the normal distributions of the widely scattered selections were observed on the reciprocal CCT scale. Despite a wide scatter of individual judgments, the mean selected CCT of 3000±200 K and 3500±250 K was established for constant illuminances of 5 lx and 50 lx, respectively, almost independently of the viewed scene. In addition, when instantaneous dimming was applied in order to maintain constant circadian irradiance with increasing CCT, subjects selected even lower CCTs at low illuminances in order to maintain visibility and sacrificed a part of high illuminance of the ranges of "pleasing" CCT for outdoor environments with limited illuminance and resolve the ambiguity of the Kruithof rule in that it is not invariant in respect of adjustable variables (illuminance and CCT).

9571-10, Session 3

A color management system for multicolored LED lighting

Maumita Chakrabarti, Anders Thorseth, Jørgen Jepsen, Dennis D. Corell, Carsten Dam-Hansen, DTU Fotonik (Denmark)

The LED color mixing systems, widely used in different lighting applications, often suffer from poor color rendering and color instability. In order to overcome these problems without sacrificing efficiency, we present an approach to obtain controlled chromaticity and stability over short and long term from a set of initially optimized settings.

A new color control system is described and implemented for a five-color LED light engine, covering a wide white gamut. The system provides intelligent control of the individual LED color arrays to produce high quality white light ranging in correlated color temperatures (CCT) between 3000 K and 5800 K. A feed-back control system combines a new way of using pre-calibrated look-up tables and a rule-based optimization of chromaticity distance from the Planckian locus (Duv) for each CCT with a calibrated color sensor for chromaticity control. A pre-calibrated look-up table is generated using a new algorithm, called Ideal White Light Radiator-guided search algorithm (IWLiR) which can provide spectral mixtures characterized by a high general color rendering index (CRI) Ra > 85 and specific CRI R9 > 40 for rendering the strong red objects e.g. skin tones. The calibrated color sensor monitors the chromaticity of the mixed light and also provides the correction factor for the current driver by using the look-up table. The long term stability and accuracy of the system will be experimentally investigated with a target tolerance within a circle radius 0.0011 in the uniform chromaticity diagram (CIE 1976).

9571-11, Session 3

The stability of spectrum reproduction by LEDs

Hua Yang, Jing Li, Ran Yao, Pengzhi Lu, Yanrong Pei, Institute of Semiconductors (China)

Reconstruction natural light spectrum by reasonable method is an important branch when fabricating LED-based products for general illumination, especially to the needs of health lighting. But as is well-known, although mixed LED sources have a higher theoretical maximum efficiency and allow for dynamic control, it generally have less color consistency both initially and over time because of different LEDs are not stable by operating conditions and operating temperature. So while there are many methods to realize the spectrum simulation, the complexity of manufacture progress and color quality of products is key consideration when evaluating these methods.

In order to find some method for evaluating the quality of spectral reconstruction, this article fabricate the white-light LED systems that simulated the natural light and analyze the methods that the basics spectral power distribution simulation and mainly color issues that related

to such as color consistency and constancy that is inherent in the design and manufacturing process. The model with 3, 4, 6 and more primary LEDs based on the real measured spectrum and theoretical spectrum are analyzed. The spectral power sensitivity relation between the LEDs with different wavelength and color characteristic is analyzed. The degree of fitting is over 0.99, and color constancy is acceptable. These researches simplified the method of visible spectrum reconstruction and make it possible for the light simulators used in general lighting in a cost effective way.

SPIE. PHOTONICS

OPTICAL ENGINEERING+

APPLICATIONS

9571-12, Session 3

Experimental investigation of analog and digital dimming techniques on photometric performance of an indoor Visible Light Communication (VLC) system

Fahad Zafar, Vineetha Kalavally, Monash Univ. Malaysia (Malaysia); Masuduzzaman Bakaul, Monash University Malaysia (Malaysia); Rajendran Parthiban, Monash Univ. Malaysia (Malaysia)

For making commercial implementation of light emitting diode (LED) based visible light communication (VLC) systems feasible, it is necessary to incorporate it with dimming schemes which will provide energy savings, moods and increase the aesthetic value of the places using this technology. There are two general methods which are used to dim LEDs commonly categorized as analog and digital dimming. Incorporating fast data transmission with these techniques is a key challenge in VLC. In this paper, digital and analog dimming for a 10 Mb/s non return to zero on-off keying (NRZ-OOK) based VLC system is experimentally investigated considering both photometric and communicative parameters. A spectrophotometer was used for photometric analysis and a line of sight (LOS) configuration in the presence of ambient light was used for analyzing communication parameters. Based on the experimental results, it was determined that digital dimming scheme is preferable for use in indoor VLC systems requiring high dimming precision and data transmission at lower brightness levels. On the other hand, analog dimming scheme is a cost effective solution for high speed systems where dimming precision is insignificant.

9571-13, Session 4

Necessity of mixed-level simulations for optical modeling of light-emitting diodes with patterned substrates

Mayank Bahl, Synopsys, Inc. (United States); Alexander Linkov, OSRAM Opto Semiconductors GmbH (Germany); Evan Heller, Synopsys, Inc. (United States); Georg Rossbach, OSRAM Opto Semiconductors GmbH (Germany); William Cassarly, Robert Scarmozzino, Synopsys, Inc. (United States)

Extensive research has been conducted to improve the design of lightemitting diodes (LEDs) so as to enhance the light extraction efficiency, and improve beam shaping, through techniques such as the use of photonic crystal gratings, patterned substrates, surface textures and back reflectors. Increasingly complex designs have necessitated the use of computational simulations which have provided numerous insights for improving LED performance. Ray optics based techniques such as Monte Carlo ray-tracing or rigorous electromagnetic (EM) wave optics based techniques such as finite-difference time-domain (FDTD) and rigorous coupled wave analysis (RCWA) are commonly applied for optical modeling of LEDs. Whether ray-optic or wave-optic techniques are used for the numerical simulation is usually based on the focus of the design and the geometric scale of the structures involved in the problem. This paper compares the optical responses of prototypical periodically-patterned substrate examples with varying lateral periods and dimensions computed with both methods. It

Conference 9571: Fourteenth International Conference on Solid State Lighting and LED-based Illumination Systems



is shown that these results may differ even when the grating periods are much larger than the wavelength, especially when the considered surface is in a realistic LED chip environment. Such results indicate that to accurately model LEDs involving periodically-patterned features a standalone rayoptics approach may be insufficient even at large structure sizes. We have recently proposed a mixed-level simulation approach combining rigorous EM wave based tools (RCWA and/or FDTD) and ray-optic tools. Here, we demonstrate cases where this approach is necessary to comprehensively model the light extraction in modern LED designs.

9571-14, Session 4

A novel design for high-performance dental lamp based on white-LEDs

Jhih-You Cai, National Central Univ. (Taiwan); Hsin-Yang Ho, Witslight Technology Group (Taiwan); Wei-Ting Chien, National Central Univ. (Taiwan) and Witslight Technology Group (Taiwan); Ching-Cherng Sun, National Central Univ. (Taiwan)

In our research, we propose a novel design for the dental lamp based on white-light LEDs. In general, the uniform illumination, low glare, high colorrendering index, and shadowless performance are needed consideration in the design of dental lamp. Traditionally, the halogen is used in the dental light, the light source is wasted energy caused by the low efficacy. Furthermore, the patient is in danger and uncomfortableness caused by the UV and IR radiation, respectively. LEDs can solve the problems, which we talk above. In our design, the concept is easy. The LEDs with high colorrendering index are used in our design. To avoid the glare happening, the LEDs are put in the center with a tilt angle, and the light is emitted in the opposite direction of dental lamp. The secondary optical elements, such as reflector, are used in our design. The reflector can reflect the light toward the oral cavity of the patient. We optimize the surface of the reflector, and make uniform illumination with high illuminance. Finally, we make a prototype to verify our design. The prototype produces high performance lighting in dental light.

9571-16, Session 4

LED streetlight analysis from outer space

Ivan Moreno, José Samuel Pérez Huerta, Tonatiuh Saucedo Anaya, Univ. Autónoma de Zacatecas (Mexico); Daniel Luis, Univ Autonoma de Zacatecas (Mexico)

Photographs of the Earth at night are a valuable source of freely available online information of streetlights. And since 2012 two new spaceborne imaging detectors may be used for city lighting photometry because they have higher spatial resolution and radiometric precision. Data from these detectors have sufficient resolution to identify and measure sources of waste light, such as streetlights, airports, harbors, leisure, stadiums and city centers. We retrieve data from imagery of these new instruments to analyze LED street lighting. In particular we propose a method to measure and analyze light pollution. Also, color image processing is used for approximate identification or discrimination of lighting technology types: high intensity discharge (HID), fluorescent, and LED lamps.

9571-17, Session 4

Freeform TIR lens design by sampling LED's intensity distribution in multiple Cartesian coordinate systems: A composite ray mapping method

Donglin Ma, College of Optical Sciences, The Univ. of Arizona (United States); Zexin Feng, The Univ. of Arizona (United States); Rongguang Liang, College of Optical Sciences, The Univ. of Arizona (United States)

A composite ray mapping method by combining uv ray mapping and ?? ray mapping method has been proposed to design a freefrom TIR lens for rectangular illumination, where the source's intensity distribution is tailored in hybrid coordinate system consisting of uv spherical coordinate system and ?? spherical coordinate system. In this paper, we are going to extend the composite ray mapping method to multiple xy coordinate systems. In the method, we sample the ray's intensity distribution into plenty of rectangular grids, which have the best topological match to those rectangular grids on the target surface. With the multiple-to-one corresponding relationships between the source's intensity distribution and target's irradiance distribution, we can finally construct the freeform TIR surfaces and freeform refractive surface using Snell's law. Compared to our previous design using uv- ?? composite ray mapping method, this design approach is expected to have much less surface error and improve the illumination uniformity in a further step due to the better topological match. Moreover, this design method can only have flat surfaces to work as the flux acceptance surface inside and all of freeform surfaces are located outside. As a result, it can greatly reduce the difficulties of fabrication. In addition, due to the overlapping mechanism by multiple-to-one ray mapping, the method could lead to a more robust freeform optics compared to traditional freeform optics designs.

9571-18, Session 4

LEDs-based multiwavelength photoreactor for photocatalysis applications

Luis Armando Díaz-Torres, Ctr. de Investigaciones en Óptica, A.C. (Mexico); Daniel Berrones, Carlos R. García, Univ. Autonoma de Coahuila (Mexico); Jorge Roberto Oliva-Uc, Ctr. de Investigaciones en Óptica, A.C. (Mexico); Raul Ochoa-Valiente, Univ. Autonoma de Coahuila (Mexico)

In this work, a low cost photoreactor based on LEDs technology was designed, constructed and characterized for photocatalysis applications. The photoreactor was designed with cylindrical configuration; its dimensions were 15.3 cm and 26 cm for diameter and height respectively. The maximum volume of solution for controlled photocatalysis experiments using this reactor is 600 ml. Arrangements of three low-cost LEDs (365nm, 395 nm and 420 nm) were placed in triangular configuration in order to optimize the density of energy at the center of the photoreactor. The different LEDs' arrangements were connected with independent and tunable electronic circuits. In addition, a cooling system (low-cost fan) was installed on top of the photoreactor to keep constant the temperature during the photocatalysis experiments. The temperature inside of photoreactor was monitored by measuring the temperature of 600 ml. of deionized water into the reactor and under the UV light during 180 min, which simulates a photocatalysis experiment. The maximum temperatures obtained inside the reactor when the LEDs of 365 nm, 395 nm and 420 nm are operating were 26°±2°C, 17.2°±1C, 18±0.5°C, respectively. Finally, the spectral radiance and the optical power were characterized at the center of the photoreactor for the different LEDs systems for optimization purposes. Due to the good stability of temperature as a function of time and the high optical power emitted by the LEDs at the center of the photoreactor, this design can be very suitable for controlled photocatalysis experiments.

9571-27, Session PWed

High performance near-ultraviolet flipchip light-emitting diodes with distributed Bragg reflector

II-Gyun Choi, Geun-Mo Jin, Jun-Cheon Park, Soo-Kun Jeon, Eun-Hyun Park, Semicon Light Co., Ltd. (Korea, Republic of)

Conference 9571: Fourteenth International Conference SPIE. OPTICS+ on Solid State Lighting and LED-based Illumination Systems



Ultraviolet (UV) light-emitting diodes (LEDs) usually have very low external guantum efficiency (EQE) and high forward voltage due to poor light extraction efficiency and high contact resistance. Thus, to enhance the performance of UV flip-chip LEDs, p-type electrodes should be good reflectors having high reflectance, low contact resistance and thermal stability. For GaN-based flip-chip LEDs, metal-based reflectors, such as Ag- and Al-based schemes, have been widely used so as to increase the light extraction. Unlike Al reflector, however, Ag is subject to thermal degradation, such as agglomeration and the formation of voids. In addition, the reflectance of Ag contact drop rapidly in the near-UV region. On the other hand, reflectance of AI is also kept in the UV region but, AI has a small work function and so serves as an electrode for n-type GaN. Therefore, in this work, we have fabricated the near-UV flip-chip LEDs with the high EQE using distributed Bragg reflectors (DBRs). A DBR is a highly reflective mirror which consists of alternating layers of high- and low-index materials, each having a quarter-wavelength thickness to generate constructive interference. In conventional DBR structures are composed of two different materials which have high-index contrast, such as TiO2 and SiO2. However, to achieve high-performance near-UV flip-chip LEDs, we used Ta2O5 instead of TiO2 that absorbs lights of UV region. Thus, we have designed a DBR composed of twenty pairs of Ta2O5 and SiO2 using optical coating design software. The DBR designed by our group achieves a reflectance of ~100 % in the near-UV region, which is much better than reflectance of Ag and Al. The difference of reflectance between DBR and metals will be more increased in the real device due to above mentioned issues.

9571-28, Session PWed

High performance GaN based blue flipchip light-emitting diodes

Geun Mo Jin, IL-Gyun Choi, Jun-Cheon Park, Soo-Kun Jeon, Eun-Hyun Park, Semicon Light Co., Ltd. (Korea, Republic of)

In this study, high performance nitride-based flip-chip (FC)l ight-emitting diodes (LEDs) were investigated and fabricated. The availability of high brightness, high power, and large area of GaN-based light-emitting diodes (LEDs) has enabled their applications in exterior automotive lightings, outdoor displays, backlights for liquid crystal display (LCD) TV. Recently ,the FC LEDs has been used to contain such high-performance products. In general, the use of silver as a p ohmic contact metal and a highly reflective material of the flip chip. However, silver has a problem in the manufacturing process and the reliability due to agglomeration or migration. Therefore, to solve this problem, was used instead of Ag reflector Distributed Bragg Reflectors(DBR) to improve the EQE. Further, ITO was used as a p ohmic layer in order to stabilize the voltage. A DBR is a highly reflective mirror which consists of alternating layers of high- and low-index materials, each having a quarter-wavelength thickness to generate constructive interference. In conventional DBR structures are composed of two different materials which have high-index contrast, such as TiO2 and SiO2. DBR is designed 99% or more reflectivity for normal incidence in the visible region of 400nm ~ 700nm, in consideration of the oblique angle of incidence. FC LEDs fabricated of a reflector having a better reflectance than the silver will have a high-performance, high-reliability.

9571-30. Session PWed

White LED motorcycle headlamp design

Wen-Shing Sun, National Central Univ. (Taiwan)

The motorcycle headlamp is composed of a white LED module, an elliptical reflector, a parabolic reflector and a toric lens. We use non-sequential ray to improve the optical efficiency of the compound reflectors. Using the toric lens can meet ECE_113 regulation and obtain a good uniformity.

9571-31, Session PWed

Trap-assisted tunneling contributions to subthreshold forward current in InGaN/ **GaN light-emitting diodes**

Marco Mandurrino, Michele Goano, Stefano Dominici, Marco Vallone, Francesco Bertazzi, Giovanni Ghione, Politecnico di Torino (Italy); Mario Bernabei, Luigi Rovati, Giovanni Verzellesi, Univ. degli Studi di Modena e Reggio Emilia (Italy); Matteo Meneghini, Gaudenzio Meneghesso, Enrico Zanoni, Univ. degli Studi di Padova (Italy)

Improving the physical understanding of the subthreshold forward current in GaN-based LED is important for LED technology optimization purposes. This current is actually a sensitive marker of device growth qualit. Its increase is a signature of device degradation induced by accelerated stresses. Moreover, it is governed by trap-assisted tunneling mechanisms, that may also play a role in the efficiency droop phenomenon at high driving currents.

In this work, we presents results from a simulation-based investigation of the subthreshold forward current in blue InGaN/GaN single-quantumwell LEDs. We specifically show that the excess forward leakage currents in InGaN/GaN LEDs grown on different substrate materials (SiC, Si) can be explained by the combined effect of trap-assisted, electron and hole tunneling "under the quantum well", i.e. electron tunneling from the n-doped LED region into traps located in the spacer and EBL regions and hole tunneling from the p-doped EBL into traps located in the n-doped GaN region. Non-local tunneling-to-trap currents and attendant recombination with free carriers are accounted for in the adopted simulation code selfconsistently with Poisson's and charge transport equations, so that their impact on subthreshold IV curves can be assessed quantitatively for LED structures realistically described at both material and technology level. The sensitivity of the electron and hole tunneling currents to trap parameters (energy, donor/acceptor type) is analyzed in detail for the possible correlations with trap characterization data available in the literature and the information it can provide on the role played by extended or point defects.

9571-32, Session PWed

RGB color sensor implemented with LEDs

José David Filoteo, Julián Móises Estudillo-Ayala, Univ. de Guanajuato (Mexico); Juan Carlos Hernández-Garcia, Consejo Nacional de Ciencia y Tecnología (Mexico); Mónica Trejo-Durán, Alberto Muñoz Lopez, Daniel Jauregui-Vázquez, Roberto Rojas-Laguna, Univ. de Guanajuato (Mexico)

In this paper is present the design and implementation of an optical sensor to detect color changes in objects through reflection of incident light from a white light source, with the purpose of use it in measuring the ripeness of fruit and applications in industrial and / or agriculture. The system is constituted by an RGB LED array, a photodetector, a current source and a plastic optical fiber. The multimode optical fiber has the characteristics of a numerical aperture of 0.51, a diameter of 1mm, an interval of transmission in the visible. Using a graphical interface designed in Labview ®, it is possible control the power of the diodes in a digital form mixing colors using different intensities achieving a white light source that will serve as a source for the color sensor. We use a microcontroller ATmega2560 as data acquisition device to monitor the colors obtained using Matlab® and showing the result with the RGB color model of 8 bits. We show tests with guava fruits with two different maturity stages. Observing the evolution of color change of the skin of the fruit to conditions to over-maturity. The results obtained with instrument show a precision error of 3% average to detect changes color when compared to samples of digital images by 11 days test.

9571-33, Session PWed

Numerical and experimental study on the evaluation of light collecting performance of the bio-fluorescence sensor

Bonghyun Jo, YiSeul Jo, Sun-Seok Byeon, Hee Won Shin, Tae Kyu Ahn, Sungkyunkwan Univ. (Korea, Republic of); Jong-Chul Lee, Gangneung-Wonju National Univ. (Korea, Republic of); Youn-Jea Kim, Sungkyunkwan Univ. (Korea, Republic of)

Bio-fluorescence sensor using deep UV LED (Light Emitting Diode) has been explored and developed to detect tactical biological agent against biological aerosol attacks. The LED as excitation source adopted in bio-fluorescence sensor introduces lightweight, low cost, low electrical power consumption. However, LED is generally difficult to be focused in small area and to induce fluorescence that distinguishes between bioparticles and non-bioparticles (i.e. abiotics) because emitted at a large divergence angle. In order to enhance the detection efficiency in bio-fluorescence sensor capitalized on LED, light collecting is an important problem. We have performed several numerical studies on three types of optical lens such as aspheric, ball, and bi-objective lens using the commercial software. LightTools (Synopsys Inc.), which is used to analyze illumination characteristics from LED. The estimated losses are reported to be 20%, 25%, and 17% for aspheric, ball, and bi-objectice lens, respectively. The values and distributions of irradiance were compared with various types of optical lens to evaluate light collecting performance in detection area.

9571-34, Session PWed

Design of high power LED-based UVA emission system and a photosensitive substance for clinical application in corneal radiation

Alessandro D. Mota, André M. Cestari, Opto Eletrônica S.A. (Brazil); André Orlandi, Univ. de São Paulo (Brazil); Anselmo G. Oliveira, Cristina H. B. Terruggi, Univ. Estadual Paulista "Júlio de Mesquita Filho" (Brazil); Giuliano Rossi, Opto Eletrônica S.A. (Brazil); Jarbas C. Castro Neto, Univ. de São Paulo (Brazil); João P. B. Ligabô, Opto Eletrônica S.A. (Brazil); Tiago A. Ortega, Univ. de São Paulo (Brazil); Tiago Rosa, Opto Eletrônica S.A. (Brazil)

An alternative treatment to keratoconus disease is a procedure called crosslinking. This disease weakens the corneal cell structure, leading the corneal to a conical shape, and the consequence is the lost of visual acuity. The standard technique consists of administration of a photosensitive substance called riboflavin in corneal tissue, which penetration is possible by removing corneal epithelium, and a dose of 5.4 J/cm2 of homogeneous UV light is fired on corneal surface for 30 minutes. The UV light exposure leads to a modification of corneal collagen fibers, becoming it more rigid and dense, which will contain the advance of the disease. This work presents an optoelectronic equipment that permit the reduction of treatment duration in up to 2 minutes by increasing UV power up to 45mw/cm2, and keeping the total well established accumulated energy of 5.4J/cm2. It consists of one UV LED source (365nm), one projection optical system to patient's cornea on a circular area of 11mm diameter, and a microcontrolled electronic system for controlling output power by using a system based on PID (proportional, integrative, and derivative controller in a closed loop) in software. This system results in constant output power and in uniform power distribution, with less than 10% of variation in both cases. Additionally, the main advantages of the system presented are: fast treatment procedure, low risk of infection (no epithelium remove), painless procedure, and reduction of treatment costs because there is no demand to controlled operating room.

9571-35, Session PWed

Process research of LED full-color display matrix with small pixel

SPIE. PHOTONICS

OPTICAL ENGINEERING+ APPLICATIONS

Jing Li, Hua Yang, Ran Yao, Institute of Semiconductors (China)

Besides lighting, Light-emitting diode (LED) is offer a wide range of potential applications including display. In contrast with LCD, LEDs display has better contrast ratio, higher response rate etc which makes LEDs along with other self-illumination technologies an ideal candidate in making display panel. Due to the popularization of HD and Ultra HD standard, display panel with better image quality is needed which means the number of pixels of the panel needs to be increased while the size of each pixel needs to be minimized. In this paper, we demonstrated a LED full-color display panel based on a 32?32 LED matrix with typical pixel size of 0.5mm. Benefit from the application of flip-chip bonding, LED full-color display array with small pixel was obtained by mounting red LEDs, green LEDs and blue LEDs directly onto an isolating substrate. The isolation layer consists of a SiO2 layer of 800nm and polyimide layer of 2700nm. Polyimide as an important electrical insulating layer, we study some properties of it, such as :PI amination rate as a function of the curing temperature, PI resistivity as a function of the curing temperature and the punction electric field intensity of PI as a function of the film thickness of PI.In addition, the substrate has metalized pads and connection before the matrix was connected to control unit. Comparable brightness of the LED matrix emitting at different color was achieved by adjusting the input current.

9571-36, Session PWed

Inline arrayed beam spot lighting in agriculture based on a guided-wave beam splitter

Hong-Shik Lee, Jin Hwan Lee, Jae Hyoung Ryu, Korea Institute of Lighting Technology (Korea, Republic of)

With the increasing attention towards the fusion of green-IT and agriculture in the recent days, the light-emitting-diode (LED) plant factory has been receiving tremendous attention. Miniaturization of such LED based illumination products will enable them to be used in relatively small space. In addition to that, due to their low power consumption and low heat dissipation, those products can be used for a long period of time. However, For the economic efficiency of the photosynthetic efficiency of the LED lighting facilities may be required to increase the specific light distribution technology light irradiation efficiency of the plant. In this paper, we propose and implemented an inline arrayed beam spot lighting in agriculture based on a guided-wave beam splitter, in order to achieve a particular light distribution. We primarily endeavored to create an inline arrayed beam spot lighting based on an integrated optic guided wave beam splitter drawing upon silica waveguides, where the guided beam emerge from the corresponding 5 ports with a power ratio determined by the design configuration. The beam splitter is constituted of an integrated-optic 1 ? 5 beam splitter and a beam forming lens configuration. The splitter is designed with a tree-shaped geometry in which one straight waveguide at the input end branches out into 5 waveguides at the output end using Y-junctions. The ratio of power distributed among the 5 output waveguides was calculated to be 0.17:0.22:1:0.22:0.17, with the power normalized to the output of central waveguide.

9571-19, Session 5

Carrier-distribution studies in GaN-based light-emitting-diodes

Dinh Chuong Nguyen, David Vaufrey, CEA Grenoble (France); Mathieu Leroux, Ctr. de Recherche sur l'Hétéro-Epitaxie et ses Applications (France)

Conference 9571: Fourteenth International Conference on Solid State Lighting and LED-based Illumination Systems



Carrier injection in GaN-based light-emitting-diodes (LEDs) is studied by means of simulation. Initially, two LED structures were optically and electrically characterized: the first one has a single-stripe-like cathode (SC) and the second one has multiple-stripe-like cathodes (MC). The experiments revealed an internal-quantum-efficiency (IQE) improvement in the MC structure: its IQE's peak value and the related current-density are both higher than their counterparts in the SC structure. Based on these results, those multiple-quantum-well LEDs were modeled with the carrier leakage and the Auger recombination being specifically focused. The simulations show a similar IQE enhancement in the MC structure and an unbalanced distribution of electrons and holes at the edges of the active region in both models. The disparity is even more pronounced in the SC structure. Furthermore, several parameters at the MC structure's active-region-p-side interface, such as the injected-hole concentration, can be up to as seven times higher as that in the SC structure. Meanwhile, the difference is smaller for the corresponding parameters at the active-region-n-side interface, such as the injected-electron concentration. This may suggest that the p-type layer play an important role in carrier-concentration balancing and further studies on the p-GaN properties are then needed.

The simulation results imply that the disparity between electron and hole injections may be related to the LED efficiency-loss. The injection ratio between these two types of carrier is currently being studied by the ongoing pulsed-electroluminescence experiments. Its results will be communicated later.

9571-20, Session 5

Design analysis of InGaN-GaNAs active region for long wavelength visible emission

Chee-Keong Tan, Nelson Tansu, Lehigh Univ. (United States)

Charge separation issue in III-Nitride InGaN light-emitting diodes (LEDs) becomes more severe with higher In-content due to polarization field in the QW, hampering the development of high efficiency long-wavelength InGaN LEDs. Critical implementation of approaches such as semipolar/nonpolar QW and staggered QW have been successfully adopted to address the charge separation issue in the blue and green LEDs. Nonetheless realizing a high In-content InGaN QW active region for long wavelength emission especially in the red spectral regime remains a fundamental barrier for current approaches, primarily due to the difficulty in high quality crystal growth of the InGaN QW. The strategy of probing the high In-content use and charge separation issue through active region design is thus essential for future development in high efficiency GaN-based long wavelength LEDs.

In this work we present a GaN-based active region through the formation of InGaN / GaNAs QW to achieve long wavelength emission from green to red spectral regime in the LEDs. Dilute-As GaNAs alloy has been recognized as a potential candidate for GaN-based LEDs in long wavelength spectral regime. The characteristics of InGaN / GaNAs QW active region are analyzed as follow: (a) transition energy, (b) wavefunction overlap and (c) spontaneous emission rate. Our finding demonstrates significant enhancement of electron-hole wavefunction overlap and thus improved spontaneous emission rate by the use of InGaN / GaNAs QW as compared to the conventional InGaN QW. The comparison of the characteristics between the conventional InGaN QW and InGaN / GaNAs QW will be discussed.

9571-21, Session 5

Effect of barrier materials on the polarization field in the active region of blue InGaN LED using Sentaurus

Karunavani Sarukunaselan, Vithyacharan Retnasamy, Zaliman Sauli, Mukhzeer Mohamad Shahimin, Steven Taniselass, Sarveshvaran Suppiah, Kamarudin Hussin, Univ. Malaysia Perlis (Malaysia) This paper addresses the barrier material of the structural design of a blue InGaN light emitting diode (LED) in order to analyze the polarization effect occurred in the active region by carrying out a simulation using Sentaurus Synopsys. It was observed that the traditional GaN barrier had the highest polarization field due to high lattice mismatch between the wells and barriers. When InGaN or AlInGaN were employed as barrier, the band diagram showed a lower polarization effect. This was attributed to the overlapping of electrons and holes wave functions.

9571-22, Session 5

Quantum well thickness variation investigation on optical and thermal performances of GaN LEDs

Karunavani Sarukunaselan, Vithyacharan Retnasamy, Zaliman Sauli, Mukhzeer Mohamad Shahimin, Steven Taniselass, Sarveshvaran Suppiah, Kamarudin Hussin, Univ. Malaysia Perlis (Malaysia)

Blue InGaN LED suffers from a severe efficiency droop at high current density and electron leakage is believed to be one of the primary cause of it. In this study, InGaN LED was simulated using Sentaurus TCAD. The effects of thickness of the quantum wells on the device performances when were examined through simulation. Results of the simulations suggested that to achieve a low efficiency droop, the wells have to be thick.

9571-23, Session 6

Understanding the dopant activation for improved manufacturing yield in InGaN based light emitting diodes

Nicholas A. Lacroce, Guangyu Liu, Chee-Keong Tan, Lehigh Univ. (United States); Ronald A. Arif, Soo Min Lee, Veeco Instruments Inc. (United States); Nelson Tansu, Lehigh Univ. (United States)

Manufacturing efficiency of InGaN-based light-emitting diodes (LEDs) depends heavily on growth uniformity and control of dopant levels. Effectively controlling dopant activation and the variables which affect it are critical for large scale manufacturing. Without a controlled manufacturing environment, device characteristics vary greatly with position on the fabricated wafer. Specifically, the post-growth annealing used for activating the Mg+ acceptor dopant in the p-type AlGaN and p-GaN layers of the LEDs is very sensitive to the annealing environment of the wafer. Within the reaction chamber however, annealing temperature varies with position causing large non-uniformity in dopant activation and device characteristics. Thus, understanding how the Mg acceptor activation of the p-GaN and AlGaN layers alters the device properties is a critical step in understanding the way these temperature changes affect the device quality of commercially produced LEDs.

In this work we examine both numerically and experimentally the effect of varying p-type doping levels in the p-GaN layers as well as the AlGaN electron blocking layers of the LED devices. Specifically, the device properties of the LEDs are investigated which include the internal quantum efficiency, output power, band profile, and carrier concentration as functions of current density. In addition, the contribution of the dopant activation in the individual p-GaN and AlGaN layers to the variation of device characteristics is discussed. The temperature-dependent dopant activation issues will be clarified by better understanding the effect of the p-type GaN doping levels on the relevant device characteristics.



Efficiency improvement of the lightemitting diodes by the lateral overgrowth GaN on an ALN nanorod template

Wen-Yi Lan, Yu-Feng Yin, Chen-Hung Tsai, National Taiwan Univ. (Taiwan); Mu-Xin Ma, National Cheng Kung Univ. (Taiwan); Hsiang-Wei Li, National Taiwan Univ. (Taiwan); Wei-Chi Lai, National Cheng Kung Univ. (Taiwan); Jian-Jang Huang, National Taiwan Univ. (Taiwan)

In recent years, light-emitting diodes (LEDs) have played a critical role in the areas of backlights for flat panel displays, optical communications and general lightings. Despite their superior light emitting efficiency, there is still demand for better performance so that LEDs can achieve a higher penetration rate to general lighting market. In the past, GaN epi-layers were grown directly on the planar sapphire substrate by metal-organic chemical vapor deposition (MOCVD). However, the quality of GaN epi-layers suffers from a high threading dislocation density due to the large lattice mismatch (13%) and thermal expansion coefficient misfit (62%). In this work, we propose an AIN nanostructure template on the sapphire substrate to decrease the defect density in GaN epi-layers. The AIN naonstructure was synthesized by vapor-liquid-solid (VLS) mechanism. VLS is considered as a cost-effective and fast growth way to fabricate high quality nanostructures. We characterize the GaN LED epi-structure by its luminescence efficiency along with the extraction of internal quantum efficiency (IQE) of the InGaN/ GaN quantum wells. The corresponding material quality is investigated by Raman spectra and transmission electron microscopy (TEM) images near the voids of the AIN rods. As a result, IQE of the device with the proposed AIN nanorod template increases by 12.2% as compared with the reference sample without AIN rod.

9571-25, Session 6

Optoelectronic and structural properties of InGaN nanostructures grown by plasmaassisted MOCVD

Daniel Seidlitz, Matara K. I. Senevirathna, Yohannes Abate, Nikolaus Dietz, Georgia State Univ. (United States); Axel Hoffmann, Technische Univ. Berlin (Germany)

This contribution reports on the optoelectronic and structural layer characteristics of InN and InGaN epilayers grown on sapphire templates with an AIN buffer layer by Plasma Assisted Metal Organic Chemical Vapor Deposition (PA-MOCVD).

In-situ characterization during the PA-MOCVD enables essential insight of the remote plasma composition and the epitaxial growth process. Analyzed Plasma Emission Spectroscopy (PES) and UV Absorption Spectroscopy (UVAS) provide detection and concentrations of plasma generated active species (N*/NH*/NH*). Nitrogen (N2) as well as hydrogen (H2) or ammonia (NH3) precursors have been used to assess the nitrogen-active fragments that are directed from the hollow cathode plasma tube to the growth surface. Normal Incidence Reflection Spectroscopy (NI-RS) is utilized to obtain real-time information about be nucleation and overgrowth process as well as the growth evolution and film thickness of InGaN layers deposited on sapphire substrates with various high-/low temperature AIN buffer layers.

The in-situ diagnostics results are supplemented with ex-situ materials structures investigation results of nanoscale structures using Scanning Near-field Optical Microscopy (SNOM). The structural properties have been analyzed by Raman spectroscopy and Fourier Transform Infrared Reflectance (FTIR). The Optoelectronic and optical properties were extracted by modeling the FTIR reflectance (e.g. free carrier concentration, high frequency dielectric constant, mobility) and optical absorption spectroscopy. The correlation and comparison between the in-situ metrology results with the ex-situ nano-structural and optoelectronic layer properties provide insight into the growth mechanism on how plasma-activated nitrogen-fragments can be utilized as nitrogen precursor in group

III-nitride MOCVD. The here assessed growth process parameter focus on the reactor pressure, substrate temperature and composition of plasma generated reactive species.

SPIE. PHOTONICS

OPTICAL ENGINEERING+ APPLICATIONS

9571-26, Session 6

Quantum barrier thickness study on blue InGaN LED optical performance using Sentaurus

Karunavani Sarukunaselan, Vithyacharan Retnasamy, Zaliman Sauli, Mukhzeer Mohamad Shahimin, Steven Taniselass, Sarveshvaran Suppiah, Kamarudin Hussin, Univ. Malaysia Perlis (Malaysia)

Blue InGaN LEDs have a drawback whereby it suffers from efficiency droop at high current injection levels. One of the major factors of this droop behaviour is contributed by electron leakage. The aim of this study is to suppress electron leakage in the device by understanding how barrier thickness affects the carrier distribution in the device as well as the device performances. Simulation results obtained showed that thinner barrier increased the device's efficiency since there was better electron confinement and tunnelling effect.

Conference 9572: Nonimaging Optics: Efficient Design for Illumination and Solar Concentration XII

Sunday - Monday 9 -10 August 2015

Part of Proceedings of SPIE Vol. 9572 Nonimaging Optics: Efficient Design for Illumination and Solar Concentration XII

9572-1, Session 1

String method of nonimaging optics from a radiation theory perspective

Benaz Colabewala, Roland Winston, Lun Jiang, Univ. of California, Merced (United States)

String method of Nonimaging Optics from a Radiation Theory Perspective

9572-2, Session 1

Asymmetric design for compound elliptical concentrators (CEC)

Lun Jiang, Roland Winston, Univ. of California, Merced (United States)

It has been known that asymmetric design for nonimaging concentrators can be realized by the string method for infinitely far away source. In this paper we present and prove that the string method can also be used for a finite source and any convex absorber even when it is positioned asymmetrically. This prompts the question of whether there exists an ideal concentrator for any source-absorber pair naturally. This also produces the curious question of whether the SMS method can be implemented for asymmetric cases.

9572-3, Session 1

All fiber actively mode-locked fiber laser emitting cylindrical vector beam

Yong Zhou, An-Ting Wang, Chun Gu, Lixin Xu, Hai Ming, Univ. of Science and Technology of China (China)

We demonstrated an all fiber actively mode-locked pulse laser emitting cylindrical vector beam. A few-mode fiber Bragg grating is adopted to achieve mode selecting and spectrum filtering. An offset splicing of single mode fiber with four mode fiber is utilized as a mode coupler in the laser cavity. A LiNbO3 Mach-Zehnder modulator , which is controlled by an electric signal, is utilized to achieve active mode locking in the laser cavity. The laser emits mode-locked pulses with 1-ns duration and 12.06 MHz repetition and operates at 1547nm with 30 dB spectrum width of 0.3nm. We built a mechanical polarization controller in the laser cavity to adjust the polarization in the laser cavity, both radially and azimuthally polarized beams have been obtained with with very good modal symmetry. An optical circulator is utilized in the ring fiber laser to connect with the few-mode fiber Bragg grating and ensure unidirectional propagation of the light.

9572-4, Session 1

Improved and customized secondary optics for solar concentrators

Daniel Vázquez, Antonio A. Fernandez-Balbuena, Univ. Complutense de Madrid (Spain); Angel Garcia-Botella, Univ. Politécnica de Madrid (Spain); Javier Alda, Univ. Complutense de Madrid (Spain)

In this contribution the line flow method is applied to an optimized

secondary optics in a photovoltaic concentration system where the primary optics is already defined and characterized. This method is a particular application of photic field theory. This method uses the parameterization of a given primary optics, including actual tolerances of the manufacturing process. The design of the secondary optics is constrained by the selection of primary optics and maximizes the concentration at a previously specified collection area. The geometry of the secondary element is calculated by using a virtual source, which sends light in a first concentration step. This allows us to calculate the line flow for this specific case. This concept allows designing more compact and efficient secondary optics of photovoltaic systems.

9572-5, Session 2

Dielectric totally internally reflecting concentrator structure for vertical bifacial photovoltaic receivers

Elizabeth Thomsen, Matthew Stocks, Andrew W. Blakers, The Australian National Univ. (Australia)

A new dielectric total internal reflective concentrator (DTIRC) design has been developed for use with bifacial photovoltaic cells. The structure incorporates the bifacial cell standing vertically at the base of the structure, immersed in dielectric.

DTIRC structures have several advantages including having no losses at the sidewalls (unlike mirrors), being able to manufacture the entire structure from one material, and being shorter and more compact than comparable compound parabolic concentrator (CPC) structures.

DTIRC structures with single-sided photovoltaic receivers, like CPC structures, are designed using the paths of the edge rays to calculate the sidewalls. If these rays successfully hit the receiver then all rays at lower angles will also hit the receiver.

In a vertical DTIRC structure, it is not just the edge rays which need to be taken into account in designing the structure. Around the bifacial receiver, rays at normal and close to normal incidence are the hardest to totally internally reflect onto the receiver. Once outside the area closest to the receiver, a modification of the maximum concentration method can be used to design the remainder of the sidewalls.

Ray tracing has been performed to confirm that the vertical DTIRC structure concentrates light as expected. The structure gives a lower concentration than a CPC with vertical bifacial receiver, however it is also a shorter structure with more uniform flux distribution over the receiver (leading to lower losses in the photovoltaic receiver).

9572-6, Session 2

Advances in luminescent and microtracking solar concentration (Invited Paper)

Noel C. Giebink, The Pennsylvania State Univ. (United States)

Sunlight is a diffuse energy resource and thus all methods of solar energy conversion and use by society share one feature in common – concentration. Optical concentration offers a route to lower the cost of high efficiency photovoltaics, but this typically requires bulky mechanical tracking that is incompatible with rooftop installation and on geometric optics that cannot harvest the diffuse solar component. This talk will focus on recent developments in quasi-static microtracking and luminescent solar



Conference 9572: Nonimaging Optics: Efficient Design for Illumination and Solar Concentration XII



concentration that address these respective challenges.

Whereas étendue conservation limits geometric concentration of diffuse light in a dielectric slab depending on its refractive index to -5x, luminescent concentration has the potential to reach higher concentration ratio >100x. We are exploring a new opportunity to boost luminescent concentrator performance by photonically controlling the luminescent étendue, leveraging highly directional emission within the framework of nonimaging optics to demonstrate >3x secondary geometric gain that has applications ranging from photovoltaics to scintillator-based radiation detection.

Recent efforts in high efficiency concentrating photovoltaics (CPV) will also be discussed, focusing on a new paradigm that combines microscale solar cells with wide-angle microtracking to enable >200x concentration ratio CPV panels < 1 cm thick that accomplish full-day tracking with < 1 cm lateral translation at fixed latitude tilt. This approach is experimentally validated outdoors for a small-scale panel prototype featuring 3D-printed plastic lenslet arrays and GaAs microcell photovoltaics, representing a step toward the goal of embedded CPV systems that can be integrated on building rooftops in the form factor of standard fixed panel PV.

9572-7, Session 3

Hybrid solar collector using nonimaging optics and photovoltaic components (Invited Paper)

Eli Yablonovitch, Gregg Scranton, Univ. of California, Berkeley (United States); Roland Winston, Lun Jiang, Bennett K. Widyolar, Univ. of California, Merced (United States); David Cygan, Alexandr Kozlov, Gas Technology Institute (United States)

The project team of Gas Technology Institute, University of California at Merced (UC-M) and Dr. Eli Yablonovitch of University of California at Berkeley are developing a hybrid solar collector using non-imaging optics and photovoltaic components integrated with particle laden gas as thermal transfer and storage media, to simultaneously generate electricity and high temperature dispatchable heat. The collector uses the spectral selectivity property of Gallium arsenide (GaAs) cells to maximize the exergy output of the system, resulting in an estimated exergy efficiency of 48%. The thermal media is composed of fine particles of high melting point material in an inert gas that increases heat transfer and effectively stores excess heat in hot particles for later on-demand use.

9572-8, Session 3

A new optical concentrator design and analysis for rooftop solar applications

Cheng Zheng, Qiyuan Li, Evatt Hawkes, The Univ. of New South Wales (Australia); Gary Rosengarten, RMIT Univ. (Australia); Robert A. Taylor, The Univ. of New South Wales (Australia)

Nearly one half of our global energy consumption is associated with meeting thermal requirements for buildings and industrial processes. This is a huge market for thermal energy – a market which is currently powered by natural gas. Alternatively, solar energy technology can potentially provide a cleaner and more sustainable way to deliver some of that thermal energy. We propose that compact, roof-integrated solar thermal systems are critically underdeveloped since they represent a viable alternative for providing industrial heat in a diversified energy portfolio. In order to produce high quality thermal energy for industrial processes (e.g. > 200 oC), concentration of sunlight is needed. In order to avoid wind loading issues, low-profile collectors are desirable. In this paper, a linear focus, linear tracking, catadioptric concentrator system is proposed and indoor optical experiments are conducted to validate this design. The performance is analyzed using both optical simulation software (Zemax) and indoor laser experiments. The developed concentrator proposed has a focal distance of <

10cm and relatively high concentration ratio (4.5 - 5.9 X). The concentrator is capable of achieving up to 75% optical efficiency (at normal incidence) and operates effectively during the middle 6 hours of a sunny day (e.g. under a global irradiance of 1,000W/m2). Overall, we hope this paper will catalyze dialogue on rooftop solar thermal concentrators with form factors similar to PV panels.

9572-9, Session 3

Self-tracking concentrator based on switchable transparency and rejected-ray recycling

Harry N. Apostoleris, Matteo Chiesa, Masdar Institute of Science & Technology (United Arab Emirates); Marco Stefancich, National Research Council (Italy)

We present a solar concentrator with a reactive tracking mechanism based on light-activated transparency switching. The system is composed of a CPC whose exit aperture contains a solar cell and whose entrance aperture is covered by a transparency switching material (TSM). A lens focuses incident light onto the entrance surface, inducing a localized transparency switch in the TSM, a phenomenon which has been demonstrated in paraffin-silicone composites. The localized switching produces a moving aperture that follows the position of the focal spot, which changes with the variation in the solar angle. Because the entrance surface is mostly reflective, rays rejected by the by the concentrator on first incidence have a high probability of being trapped by a second reflection at the entrance. In this way rejected rays are recycled multiple times through the concentrator, increasing the probability of absorption. This tracking-trapping mechanism essentially rotates the acceptance cone of the concentrator to follow the sun, increasing the effective acceptance angle of the concentrator without the corresponding decrease in concentration required by thermodynamics for a fully static concentrator. By theorectical analysis based on statistical ray optics and rigorous ray-tracing simulation we demonstrate the capabilities and limits of the system in terms of flux concentration and acceptance angle. Preliminary experimental results including proof-of-concept demonstrations of the concentrator and the moving aperture component will be presented.

9572-10, Session 3

Design of a solar collector system formed by a Fresnel lens and a CEC coupled to plastic fibers

Perla M. Viera-Gonzalez, Guillermo E. Sánchez-Guerrero, Daniel E. Ceballos-Herrera, Romeo J. Selvas-Aguilar, Univ. Autónoma de Nuevo León (Mexico)

One of the main challenges for systems based in solar concentrators and plastic optical fibers (POF) is the accuracy needed for the solar tracking. One approach to overcome these requirements is increasing tolerances to angular misalignments by using systems composed by Fresnel lens and compound elliptical concentrators (CEC), however this technique is effective for photovoltaic applications, it is not clear for systems coupled to POF for indoor illumination. On this subject, it is presented a numerical analysis of a solar collector formed by a Fresnel lens combined with a CEC coupled to POF in order to compare its performance under angular misalignments and also to show a trade-off analysis for different Fresnel lens shapes used in the collector system. The description of the Fresnel lenses and its designs are included, in addition to the focal point areas with space and angular distribution profiles considering the optimal alignment with the source and maximum permissible misalignments for each case. For the two systems the coupling between the optical components is analyzed and the total performance is calculated, having as result a comparison between an Imaging and a Nonimaging system for building illumination.

9572-11, Session 4

Experimental flux mapping for linear solar concentrators

Cameron C. Stanley, Ahmad Mojiri, Gary Rosengarten, RMIT Univ. (Australia)

Silicon photovoltaic cells typically convert 15-20% of the incident solar energy into electrical power, with the majority of the remaining energy dissipated as heat. Photovoltaic-thermal (PV/T) solar receivers attempt to utilise this wasted energy and are capable of simultaneously producing both thermal energy and electricity. A fluid flowing adjacent to the photovoltaic cells is used to capture the wasted heat and also actively cool the photovoltaic cells. However, in practice the maximum temperature of the fluid is limited to around 70°C by the direct thermal coupling between the PV cells and the thermal channel, and the dependence of the cells performance on temperature.

We have developed a hybrid PVT receiver for linear concentrating systems, such as parabolic troughs or linear Fresnel mirrors, which utilises spectral beam splitting to thermally decouple the PV cells from the thermal absorber. Incident solar energy is decomposed into different wavelength bands, with wavelengths above 1100nm and less than 700nm absorbed directly as heat whilst the remaining wavelengths are directed to the silicon PV cells. By doing so, we have effectively decoupled the thermal absorber from the PV cells and achieved thermal output temperatures up to 150°C concurrently with electrical conversion efficiency of around 9%.

This work reports on experimental flux mapping performed for the hybrid PVT receiver to determine the optimal receiver design. This was done using a close range radiometry technique together with a swept point-source measurement technique. Radiant flux distribution across the thermal absorber and the photovoltaic cells were measured and are discussed.

9572-12, Session 4

Fundamentally new classes of aplanatic lenses (Invited Paper)

Heylal Mashaal, Daniel Feuermann, Jeffrey M. Gordon, Ben-Gurion Univ. of the Negev (Israel)

We identify fundamentally new classes of aplanatic lenses where the focus resides inside the lens. These new aplanatic designs comprise a primary contoured dielectric entry and a secondary contoured profile where the secondary surface can, in general, be mirrored, but, in these puredielectric devices, are required to satisfy total internal reflection. We show that, in analogy to their dual-mirror counterparts, these aplanatic lenses engender 8 basic, distinct design categories. Only a minority of categories is found to have the potential to yield viable lenses from realistic materials. Flux concentration of far-field small-angle sources such as the sun and, conversely, narrow-field collimation of wide-angle emitting light sources can approach the thermodynamic limit. Losses due to chromatic aberration are smaller than in conventional lenses of comparable f-number, primarily due to the focus being embedded in the lens. By the same token, exit numerical aperture can be increased by a factor of n (the dielectric's refractive index) - and hence flux concentration can be increased by a factor of n² - relative to common lenses where the focus resides outside the lens.

9572-13, Session 4

Design and optical analysis of solar dish and linear secondary concentrator for photovoltaics

Nicholas W. Fette, Arizona State Univ. (United States); Herb Hayden, Tyler Beeney, Chao-han Lin, Southwest Solar Technology, LLC (United States); Zihan Zhang, Exa Corp. (United States) A high efficiency, commercial scale (54 m2) concentrating solar energy system using high flux photovoltaic cells and a unique concentrator design has been developed, analyzed, and tested. The development for a dish primary concentrator and linear secondary optic was previously reported. In continued technical development, the team has applied new materials for thermal, optical, and mechanical performance; new optical design of primary concentrator for increased flux uniformity under optical aberration; and new workflow and tools for computer aided design, engineering analysis, and manufacture of the dish and secondary optical components. For the secondary optic and cell encapsulant, materials selection is driven by need for thermal stability. As a result, fused silica components with high clarity and low thermal expansion have been manufactured via two processes for comparison: molding and negative machining from off-the-shelf rods. A more stable encapsulant has also been applied to reduce effects of off-gassing that damage TIR surfaces. For the primary concentrator dish, a novel overlay design has been developed, including software to automatically generate a massive number of surfaces for direct import into CAD models. In this approach, multiple mirrors panels attached to a single mirror facet fill the same target area with light, similar to a heliostat system. This overlay design shows potential for reducing flux non-uniformity due to manufacture tolerances, and the implemented design matches the incoming flux in position and angle space to the acceptance profile of the secondary optical array. Operation of the system is ongoing.

SPIE. PHOTONICS

OPTICAL ENGINEERING+

APPLICATIONS

9572-14, Session 5

Six-primary laser-phosphor illuminator for cinema projector

Junejei Huang, Yuchang Wang, Delta Electronics, Inc. (Taiwan)

To meet the high performance requirement of cinema projector, a laserphosphor illuminator with 6 primary colors is proposed. The six primary colors are divided into two groups and include colors of R1, R2, G1, G2, B1 and B2. Colors of B1, B2 and R2 come from lasers of wavelengths 440 nm, 465 nm and 639 nm. A second B1 laser alternately pumps G-phosphor to get G1 and pumps Y-phosphor to get G2 and R1. The illuminator comprises collimating and condensing lenses, green and yellow reflectors, phosphorwheel and integration rod. The G-phosphor and Y-phosphor are deposited on two rings of the phosphor-wheel. For each phosphor, half ring is occupied and the other half is mirror or transparent. A taper rod is used as integration rod and connected to the illumination path of the projector. Two groups of colors are sequentially switched by the rotation of the phosphor-wheel. Two sequences of three colors are sent to the 3-chip cinema projector and synchronized with frame rate of 120Hz. In 2D mode, six primary colors get a wide color gamut. In 3D mode, two groups of three primary colors provide two groups of images that received by left and right eyes. All lasers in a refrigerator are connected to the lamp module by optical fibers. The lamp module is compact and suitable for retro-fit market. By replacing the conventional UHP lamp in the existing 0.95" DMD 3-chip engine with this lamp module, an equivalent brightness can be achieved both in 3D and 2D mode.

9572-15, Session 5

Efficient color mixing through etendue conservation using freeform optics

Simone Sorgato, Light Prescriptions Innovators Europe, S. L. (Spain) and Vrije Univ. Brussel (Belgium); Julio C. P. Chaves, Rubén Mohedano, Aleksandra Cvetkovic, Maikel Hernandez, Light Prescriptions Innovators Europe, S. L. (Spain); Juan Carlos Miñano, Pablo Benitez, Light Prescriptions Innovators Europe, S. L. (United States); Hugo Thienpont, Brussels Photonics Team, Vrije Univ. Brussel (Belgium); Fabian Duerr, Vrije Univ. Brussel (Belgium)

Conference 9572: Nonimaging Optics: Efficient Design for Illumination and Solar Concentration XII

Today's SSL illumination market shows a clear trend to high flux packages with higher efficiency and higher CRI, realized by means of multiple color chips and phosphors. Such light sources require the optics to provide both near- and far-field color mixing. This design problem is particularly challenging for collimated luminaries, since traditional diffusers cannot be employed without enlarging the exit aperture and reducing brightness. Furthermore, diffusers compromise the light output ratio (efficiency) of the lamps to which they are applied.

A solution, based on Köhler integration, consisting of a spherical cap comprising spherical microlenses on both its interior and exterior sides was presented in 2012. The diameter of this so-called Shell-Mixer was 3 times that of the chip-array footprint, which makes it not fully compatible with luminaires with tight geometrical/mechanical constraints. A new version of the Shell-Mixer, based on Nonimaging Optics principles, where neither the outer shape of the cap nor the surfaces of the lenses are constrained to spheres or 2D Cartesian ovals will be shown in this work. The new shell is free-form, only twice as large as the original chip-array and equals the original model in terms of uniformity and brightness.

9572-16, Session 5

Illumination system design with random optimization

Simon Magarill, William Cassarly, Synopsys, Inc. (United States)

Automatic optimization algorithms can be used when designing illumination systems. Illumination system optimization using merit functions that are adjusted to match a given design setup can provide improved system performance. For systems with many design variables, we present a multi-step optimization process method. At each step, different variables and/or merit functions are used. We have found that this approach can sometimes leads to more efficient solutions. In this paper we illustrate the effectiveness of a multi-step approach using several different examples.

9572-17, Session 5

Light extraction method for mixing rods based in grooves with elliptical shape

Guillermo E. Sánchez-Guerrero, Perla M. Viera-González, Daniel E. Ceballos-Herrera, Romeo J. Selvas-Aguilar, Univ. Autónoma de Nuevo León (Mexico)

Homogenize light is the principal purpose of mixing rods. Light extraction from mixing rods is proposed by changing the shape of the face, the rod or a combination of both for many applications. Light extraction also can be done by its lateral face by cutting the Mixing rod. In this work a simulation of square and hexagonal poly(methyl methacrylate) (PMMA) mixing rods were made in Zemax® OpticStudio designed with an elliptical transversal cut to extract light from a lateral face. The cut is specular for rays that fulfill the total internal reflection condition, the reflected rays are deviated and the Total Internal Reflection (TIR) condition broken, then, extracted. An advantage of this cut is that it can be controlled in depth to extract the amount of light required and the remaining light used for other purposes. Also it can reduce the size of the mixing rods and optical components. For the simulation an LED light were used as source, the light were homogenized by the mixing rod and due to it, the light extracted is also homogenous. The candela map, radiant intensity and color of the light extracted are presented and compared in both mixing rods.

9572-18, Session 5

Etendue-squeezing light injector

Julio C. Chaves, Simone Sorgato, Light Prescriptions Innovators Europe, S. L. (Spain); Pablo Benitez, Juan Carlos Miñano, Light Prescriptions Innovators, LLC (United



States) and Univ. Politécnica de Madrid (Spain); Waqidi Falicoff, Light Prescriptions Innovators, LLC (United States); Ruben Mohedano, Light Prescriptions Innovators Europe, S. L. (Spain)

There is a need to make portable devices, such as smartphones or tablets, thin and light weight. All components in these devices need to be small and closely packed, and this is also true of backlights, one of the largest components in these devices. Very thin backlights, however, may lead to situations in which the backlight is thinner than the LED illuminating it, leading to a need to inject light from a relatively large LED into a thin light guide. This cannot be done by simply placing the LED next to the light guide, as a considerable amount of light would be lost. There is, therefore, the need for a coupling optic between LED and light guide.

For a horizontal light guide, one possible way to achieve a good coupling is by dividing the LED emitter horizontally into several sections, each of which is the same height as the thickness of the light guide. Then, an optic is designed to bring the light emitted from these different LED sections to the same height as the light guide. This is achieved in a two-step process in which the light from each LED section is first shifted sideways and then shifted up or down to bring it to the same level as the light guide. This process is called etendue squeezing and it transforms a tall LED light source into a wide but thin light source, whose height matches the thickness of the light guide, making the optical coupling possible.

9572-19, Session 6

Design of diffractive optical surfaces within the SMS design method (*Invited Paper*)

João Mendes-Lopes, Pablo Benítez, Juan Carlos Miñano, Univ. Politécnica de Madrid (Spain)

The Simultaneous Multiple Surfaces (SMS) was developed as a design method in Nonimaging Optics during the 90s. Later, the method was extended for designing Imaging Optics. The SMS method involves the simultaneous calculation of N optical surfaces (refractive or reflective) using N one-parameter wavefronts for which specific conditions are imposed. The relationship between degrees of freedom (N optical surfaces) and constrains (N wavefronts) is not exactly one to one. For simplicity in our explanation we will consider that it is so. When designing an nonimaging optical system, these conditions comprise coupling of every one of these N wavefronts to other wavefronts with prescribed conditons.

This paper shows an extension of the SMS method to diffractive surfaces. Using this method, diffractive kinoform surfaces are calculated simultaneously and through a direct method, i. e. it is not based in multiparametric optimization techniques. Using the phase-shift properties of diffractive surfaces as an extra degree of freedom, only N/2 surfaces are needed to perfectly couple N one parameter wavefronts. Wavefronts of different wavelengths can also be coupled, hence chromatic aberration can be corrected in SMS-based systems. This method can be used by combining and calculating simultaneously both reflective, refractive and diffractive surfaces, through direct calculation of phase and refractive/reflective profiles. Representative diffractive systems designed by the SMS method are presented.

9572-20, Session 6

Exact wavefront surface refracted by a smooth arbitrary surface considering a plane wavefront incident

Maximino M. Avendaño-Alejo, Univ. Nacional Autónoma de México (Mexico)

We study the formation of wavefront produced by smooth arbitrary surfaces with symmetry of revolution considering a plane wavefront propagating parallel to the optical axis and impinging on the refracting surface. The

Conference 9572: Nonimaging Optics: Efficient Design for Illumination and Solar Concentration XII

wavefronts are obtained by using the Huygens' principle; we have already seen that the shape of the caustic and wavefront surfaces are related through Malus-Dupin theorem and they represent the monochromatic aberrations which can be called image errors, furthermore their shapes could be modified by changing the parameters of the lens in such a way that if a caustic surface is vanished the optical system produces a perfect image, on the other hand for a caustic possessing a large area it could be applied to design no-imaging optical systems. The shape of the wavefront depends only on the indices of refraction and geometrical properties of the refracting surface such as the first and second derivatives. This analytic formula has potential applications in the microscopy field, illumination or corrector plates.

9572-21, Session 6

Freeform aplanatic concentrators

Bharathwaj Narasimhan, Pablo Benitez, Dejan Grabovickic, Juan Carlos Miñano, Milena I. Nikolic, Jose M. Infante Herrero, Univ. Politécnica de Madrid (Spain)

Axisymmetric aplanatic concentrators have been used in the past for solar concentrators and condensers (Gordon et. al, 2004; Winston et. al, 2012). It is well know that such a system must be stigmatic and satisfy the Abbe sine condition. This problem is well known (Schwartlitz, 1906) to be solvable with two aspherics when the system has rotational symmetry.

However, some of those axisymmetric solution have intrinsically shading losses when using mirrors, which can be prevented if freeform optical surfaces are used (Benitez, 2007).

In this paper, we explore the design of freeform surfaces to obtain full aplanatic systems. Here we prove that a rigorous solution to the general non-symmetric problem needs at least three free form surfaces, which are solutions of a system of partial differential equations (PDE). We present here that the solutions of the said system of PDE can be found using optimization. The merit function for such an optimization includes the spatial and angular deviation of the rays from the target rays according to the aplanatic condition. Therefore, the value of the merit function at the "exact" solution will be zero. The examples considered have one plane of symmetry, where a consistent 2D solution is used as a boundary condition for the 3D problem. We have used the x-y polynomial representations for all the surfaces, and the optimization has shown very fast convergence. As an example, an aplanatic freeform concentrator compose by two mirrors and a single-sided lens is shown.

9572-22, Session 6

Freeform reflector construction by ray mapping method in modified double pole coordinate system

Donglin Ma, Zexin Feng, Rongguang Liang, College of Optical Sciences, The Univ. of Arizona (United States)

With the broad application of freeform optics in the field of LED illumination engineering, people have developed various kinds of methods to design freeform reflectors. These methodologies include supporting ellipsoids, trial and error approaches, simultaneous multiple surfaces (SMS) method solving corresponding Monge-Ampere equation, and geometrical ray mapping method and so on. The main drawback for the trial and error method is too much computing time required due to the costly ray tracing techniques. The method of supporting ellipsoids also requires of a number of optimization steps and iterations for the generation of each ellipsoid, which is also very time consuming. The SMS method usually requires at least one pair of surfaces and is not suitable to design the reflector with only one single surface. For the Monge-Ampere method, the derivation and solving of the partial differential equation is very tedious and time consuming. In a word, among all of these methods the geometrical ray mapping method is the most efficient in freeform optics design. However, this method cannot guarantee that the derived freeform surface can satisfy the integrability condition. Therefore, the key task is to find a diffeomorphism ("ray



mapping") so that the transformed irradiance distribution matches the design target and the constructed surface satisfies the so called integrability condition. In this presentation, we will introduce a new ray mapping method to sample the source's intensity distribution in the modified double pole coordinate system to realize the "perfect" match between the source and target.

9572-23, Session 6

Diffraction effects in freeform optics

Melissa N. Ricketts, Roland Winston, Univ. of California, Merced (United States); Vladimir I. Oliker, Emory Univ. (United States)

Freeform optics is a relatively new field that addresses the methods necessary to describe surfaces lacking symmetry, and/or surfaces that create non-symmetrical irradiance distributions. The Supporting Quadrics Method (SQM) developed by Oliker uses envelopes of quadrics to create prescribed irradiance distributions. These optical systems are tested in ray trace software, which does not take into account diffraction effects. It is important to understand what diffraction effects are present when moving from the ray trace stage to the prototype stage. Here we study the diffraction effects of Supporting Quadrics Method.

9572-24, Session PMon

Development of daylighting systems with non-imaging concentrator

Seoyong Shin, Myongji Univ. (Korea, Republic of)

Recently, it is found that more consideration has been given to the interaction between energy, buildings, and the environment. As buildings are the main source of energy use and greenhouse gas emissions, davlighting serves for both to improve indoor environment as well as to save energy utilization in buildings. Fiber-based daylighting systems have been shown to be a promising and e?ective way to transmit sunlight in the interior space. To increase efficiency, the current need is to illuminate optical fibers with uniform light flux so that uniform light can be delivered in the interior of the building. We propose a method for achieving uniform illumination over the fiber-bundle and distributing uniform light in the interior. Light is collected through a concentrator and focused toward a collimating device, which inserts the light over the trough compound parabolic concentrator to illuminate array of optical fibers with uniform light flux. An optics diffusing structure, which includes a combination of lenses to achieve high average illuminance and illuminance uniformity, is utilized to spread the light in the interior. The results clearly reveal that the efficiency in terms of uniform illumination, which also reduces the heat problem for optical fibers, is improved. Furthermore, a comparison study is conducted between current and previous approaches. Finally, the proposed daylighting system turns out convenient in terms of energy saving and reduction in greenhouse gas emissions.



9572-25, Session PMon

Day lightening system with fibre optics using non imaging concentrator

Shivaji B. Sadale, Pratika G. Patil, Sanskruti J. Powar, Madhavi N. Nikam, Shivaji Univ. (India)

Energy crisis is one of the biggest challenges before mankind. The electric lightening for domestic and industrial use is a major portion of the total energy demand. On a normal bright day usually there is excess intensity of light outdoors but in large building still there is a need of lightening. We have investigated the indoor day lightening with solar light using fiber optics. The outdoor sunlight can be used to provide light inside the building during daytime. Day light is always in superior to artificial light for everyday tasks. We have developed an effective day lighting device comprising a concentrator and optical fiber with a view to harness maximum solar lighting, eliminate the dark area lighting problem in various domestic as well as commercial building. The concentrator has been designed using non imaging techniques particularly edge ray principle. We have studied the concentration of light outdoor with our device and transport of light from outdoor to the interiors of the building through optical fiber cable. The rays falling on the device are reflected and then focused at one end of optical fiber. The intensity of light is measured for visibility, and losses.

Conference 9573: Optomechanical Engineering 2015



Monday - Wednesday 10-12 August 2015 Part of Proceedings of SPIE Vol. 9573 Optomechanical Engineering 2015

9573-4, Session PMon

Aligning and measuring the curvature and thickness of high-precision lens

Kun-Huan Wu, Shenq-Tsong Chang, Ming-Ying Hsu, Ting-Ming Huang, Wei-Yao Hsu, Shih-Feng Tseng, Instrument Technology Research Ctr. (Taiwan)

The radius of curvature is one of the most important specifications for spherical optics. There are several methods and devices currently on the market that can be used to measure it, including optical level, noncontact laser interferometer (Interferometer), a probe-contact profiler (Profilometer), the centering machine and three-point contact ball diameter meter (Spherometer). The amount that can be measured with a radius of curvature of the lens aperture range depends on the interferometer standard lens f / number and lens of R / number (radius of curvature divided by the clear aperture of the spherical surface ratio between them). Unfortunately, for lens with diameter greater than 300 mm, the device is limited by the size of the holding fixture lenses or space. This paper aims to provide a novel surface contour detection method and machine, named "CMM spherometry by probe compensation," to measure the radius and thickness of the curvature of the optical surface by a coordinate measurement machine (CMM). In order to obtain more accurate optimization results, we used probe and temperature compensation to discuss the effect. The trace samples and the measurement results of CMM and the centering machine, which has top and bottom autocollimators, are compared.

9573-30, Session PMon

Analysis investigation of supporting and restraint conditions on the surface deformation of a collimator primary mirror

Chia-Yen Chan, Instrument Technology Research Ctr. (Taiwan); Zhen-Ting You, Bo-Kai Huang, Yi-Cheng Chen, National Central Univ. (Taiwan); Ting-Ming Huang, Instrument Technology Research Ctr. (Taiwan)

For meeting the requirements of the high-precision telescopes, the design of collimator is essential. The diameter of the collimator should be larger than that of the target for the using of alignment. Special supporting structures are demanded to reduce the deformation of gravity and to control the surface deformation induced by the mounting force when inspecting large-aperture primary mirrors.

9573-31, Session PMon

Development of 1-m primary mirror for a spaceborne camera

Hagyong Kihm, Korea Research Institute of Standards and Science (Korea, Republic of)

We present the development of a 1-m lightweight mirror system for a spaceborne electro-optical camera. The mirror design was optimized to satisfy the performance requirements under launch loads and space environment. The mirror made of Zerodur* has pockets at the back surface and three square bosses at the rim. Metallic bipod flexures support the mirror at the bosses and adjust the mirror's surface distortion due to gravity. We also show an analytical formulation of the bipod flexure, where compliance and stiffness matrices of the bipod flexure are derived to estimate theoretical performance and to make initial design guidelines. Optomechanical performances such as surface distortions due to gravity,

assembly, isothermal loads, and moisture absorption are explained. Environmental verification of the mirror is achieved by vibration and thermal vacuum tests.

9573-1, Session 1

ICESat-2 ATLAS telescope testing and integration

Tyler C. Evans, SGT, Inc. (United States)

Many lessons were learned in the comprehensive testing of the one meter Beryllium flight telescope for the ICESat-2 mission. This paper will focus on testing areas of encircled energy analysis and boresight alignment of fiber optic cables. Several tests were able to be performed on the telescope itself, helping drive down risk, cost, and schedule during the integration phase of the telescope onto the instrument and box structure. The main ICESat-2 instrument is the Advanced Topographic Laser Altimeter System (ATLAS). It measures ice elevation by transmitting laser pulses, and collecting the reflection in a telescope. Because so few photons return from each pulse, the alignment of each receiver channel fiber is critical as well as minimizing the distortion.

A one meter parabola collimator system with a point source fiber-coupled 532nm laser and a CCD detector was used to feed collimated light into the telescope that was recorded with a CCD detector in the telescope focal plane. Fiber optic cables were also used to back-illuminate the telescope and image in the collimator focal plane. The telescope was mounted in a gimbal that allowed for three degrees of rotational freedom allowing the telescope to be steered to each respective science field point. The setup worked well for accomplishing the testing. Through well written procedures and prior experience, the testing was carried out according to plan and on schedule despite obstacles along the way such as late ground support equipment and tests that needed to be repeated.

9573-2, Session 1

In-situ mitigation of radiation-induced attenuation in optical fiber used for sensing at nuclear facilities

Reinhold Povilaitis, Keith E. Holbert, Arizona State Univ. (United States)

Modern high-bandwidth fiber optics are good candidates for use in sensing applications at nuclear waste facilities and generating stations. Though many exhibit good radiation hardness, radiation-induced attenuation may represent a significant challenge in maintaining signal quality over the operational lifetime of such sensing systems. Use of higher power light sources at operational wavelengths has been shown to reduce transmission loss caused by radiation.

Tests by Holbert et al. to determine radiation-induced attenuation (RIA) of fiber optics at 850 nm subjected to 0.8 and 7 Mrad of gamma radiation have been extended to assess the extent to which the RIA may be mitigated. Cable sections approximately 85 m in length are irradiated up to a total dose of 2-3 Mrad at room temperature. Optical power measurements are logged by a fiber optic sensor module by way of a 1?W LED light source. After absorbing the desired dose the cables are removed from the radiation environment and allowed to anneal at room temperature for >24 hours. Photobleaching is accomplished using the same 850 nm light source used for measuring attenuation. The intensity of the LED light source is incrementally increased to a max output of 1 mW while transmission loss recovery is recorded. We seek to determine the optimum light intensity and treatment interval for in-situ healing as well as the periodicity for ensuring that attenuation remains manageable without intolerable degradation of the fiber optic cable due to the episodic application of this RIA mitigation strategy.



9573-3, Session 1

ZERODUR(R): new stress corrosion data improve strength fatigue prediction

Peter Hartmann, SCHOTT AG (Germany); Günter Kleer, Fraunhofer-Institut für Werkstoffmechanik (Germany)

The extremely low thermal expansion glass ceramic ZERODUR[®] finds more and more applications as sophisticated light weight structures with thin ribs or as thin shells. Quite often they will be subject to higher mechanical loads such as rocket launches or modulating wobbling vibrations. Designing such structures requires calculation methods and data taking into account their long term fatigue. With brittle materials fatigue is not only given by the material itself but to a high extent also by its surface condition and the environmental media especially humidity. This work extends the new data and information gathered on the bending strength of ZERODUR[®] with new results concerning its long term behavior under tensile stress.

The parameter needed for prediction calculations which combines the influences of time and environmental media is the stress corrosion constant n. Results from the past differ significantly from each other. In order to obtain more reliable data the stress corrosion constant has been measured with the method comparing the breakage statistical distributions at different stress increase rates. For better significance the stress increase rate was varied over four orders of magnitude from 0.004 MPa/s to 40 MPa/s. Experiments were performed under normal humidity for long term earth bound applications and under nitrogen atmosphere as equivalent to dry environment occurring for example with telescopes in deserts and also equivalent to vacuum for space applications.

As shown earlier diamond ground surfaces of ZERODUR® can be represented with a three parameter Weibull distribution. Predictions on the long term strength change of ZERODUR® structures under tensile stress are possible with reduced uncertainty if Weibull threshold strength values are considered and better reliable stress corrosion constant data are applied.

9573-5, Session 1

Effect of major factors on damage threshold of optical rectification crystals

Qinglong Meng, Zhuolin Su, Junli Yu, Bin Zhang, Sichuan Univ. (China)

The crystal material would be damaged under the high-power femtosecond laser radiation during the generation of terahertz in optical rectification, limiting the further increase of the generation efficiency of terahertz radiation. It remains a big challenge to theoretically predict the material removal mechanism in femtosecond laser damage. In this paper, the prediction model of crystal damage threshold under femtosecond laser based on the two-temperature model has been built up. On the basis, the influence of the major parameters of the femtosecond laser on the damage threshold has been analyzed quantitatively. For comparison, the experimental results have also been presented. The results show that, for the given peak power density of femtosecond laser, the damage threshold of the optical rectification crystal increases with the increasing of pulses duration for the case of the relatively small pulse duration, whereas decreases for the case of the relatively large pulse duration. The experimental results are consistent quite well with the theoretical results.

9573-6, Session 2

Optomechanical performance of 3D-printed mirrors with embedded cooling channels and substructures

Joni Mici, Paul Zorabedian, Saatyan S. Zalawadia, David M. Stubbs, Lockheed Martin Space Systems Co. (United States) Advances in additive manufacturing increasingly allow for manufacture of topologically complex parts not otherwise feasible through conventional manufacturing methods. Maturing metal and ceramic additive manufacturing technologies are becoming more adept at printing topologically complex mirror substrates. Reflective optics used in high energy laser (HEL) systems require materials with low coefficient of thermal expansion (CTE), high specific stiffness, and most importantly high thermal conductivity to effectively dissipate heat from the optical surface. Currently, the limits of conventional manufacturing dictate the topology of HEL optics to be monolithic structures which rely on passive cooling mechanisms and high reflectivity coatings to withstand laser damage. Additive manufacturing enables the printing of embedded cooling channels in metallic mirror substrates to allow for (1) active cooling and (2) tunable cooling. This paper analyzes the performance improvement possibilities of HEL mirrors with embedded cooling channels using finite element methods and analytical approximations.

9573-7, Session 2

Extended volume and surface scatterometer for characterization of 3D-printed optical elements

Florian Dannenberg, Cornelius F. Hahlweg, bbw Hochschule (Germany)

The use of 3d printing technology seems to be a promising way for low cost prototyping of optical components or systems. It is especially useful in applications where customized equipment repeatedly is subject to immediate destruction, as in experimental detonics and the like. Due to the nature of the 3d printing process, there is a certain inner texture and therefore inhomogeneous optical behaviour to be taken into account. Recent investigations are dedicated to quantification of optical properties of such printed bodies and derivation of corresponding optimization strategies for the prinitng process. Beside mounting and alignment means, also refractive and reflective elements are subject to investigation. The measurements are based on an imaging nearfield scatterometer for combined volume and surface scatter measurements as proposed in previous papers. The device has been extended for observation of photoelasticity effects and therefore homogeneity of polarization behaviour. Such optical properties are of interest not only for light guiding elements, but also for mounts and other supporting parts, which have to be characterized regarding to their absorption and scatter behaviour. Practical examples from current research studies are included.

9573-8, Session 2

Fabrication of light-weighted 3D-printed mirrors

Harrison Herzog, Richard Bates, Alyssa De La Torre, Jacob Calis, Jacob Segal, Jeremy Smith, The Univ. of Arizona (United States)

Direct Metal Laser Sintering (DMLS) and Electron Beam Melting (EBM) 3D printing technologies are being utilized to create lightweight, optical grade mirrors out of AlSi10Mg aluminum and Ti6Al4V titanium alloys at the University of Arizona. The mirror prototypes are polished to meet the ?/20 RMS and ?/4 P-V visible optical requirements.

The senior interdisciplinary design team is comprised of six University of Arizona engineering students that within three different major disciplines. The students are tasked to design a mirror that is fully optimized for low mass and maximum stiffness, using topological optimization algorithms. The mirror must endure the polishing process with the necessary stiffness to eliminate print-through. The challenge for the team is to reduce porosity within the 3D printed mirror and determine the best polishing methods to meet the optical requirements. The prototypes will undergo hot isostatic press (HIP) and heat treatment to improve density, eliminate porosity, and relieve stress.

Conference 9573: Optomechanical Engineering 2015



Metal 3D printing allows for nearly unlimited constraints on design and eliminates the need for a machine shop when creating an optical mirror. This research can lead to an increase in mirror mounting support complexity in the manufacturing of lightweight mirrors and improve specific properties of the mirror substrate. Additionally, the project aspires to have many future applications of light-weighted 3D printed mirrors, such as spaceflight.

This paper covers the design/fab/polish/test of the 3D printed mirrors, the thermal/structural finite element analysis, and the results.

9573-9, Session 2

3D-additive manufactured optical mount

Paul V. Mammini, Lockheed Martin Space Systems Co. (United States); David Ciscel, John Wooten, CalRAM Inc. (United States)

The Area Defense Anti-Munitions (ADAM) is a low cost and effective high power laser weapon system. It's designed to address and negate important threats such as short-range rockets, UAVs, and small boats. Many critical optical components operate in the system. The optics and mounts must accommodate thermal and mechanical stresses, plus maintain an exceptional wavefront during operation.

Lockheed Martin Space Systems Company (LMSSC) developed, designed, and currently operates ADAM.

This paper covers the design and development of a key monolithic, flexured titanium mirror mount that was manufactured by CalRAM using additive processes.

9573-10, Session 3

Leveraging semiconductor lithography technology for projection lens applications (Invited Paper)

Brian M. McMaster, Corning Tropel Corp. (United States)

The materials, tooling and processing developed for lithograph lenses is now being applied to commercial high power projection lenses after decades of technology development. These technologies include lens suspensions, adhesives and alignments. Lens suspension techniques for low stress & large temperature ranges will be presented as well as the unique adhesives used. A discussion of different methods of individual lens alignments of individual components, lens stacks and the technology selection for positioning of multiple moving lens groups motion will be reviewed. Finally, an overview how some of these technologies were selected by using DFMA.

9573-11, Session 3

Elliptically framed tip-tilt mirror optimized for stellar tracking

James H. Clark III, U.S. Naval Research Lab. (United States); F. Ernesto Penado, Jeremy Petak, Northern Arizona Univ. (United States)

We compare a design innovation of an elliptically framed tip-tilt optical tracker with an existing circularly framed tracker for the Navy Precision Optical Interferometer. The tracker stabilizes a 12.5 cm stellar beam on a target hundreds of meters away and requires an increase in operational frequency. We reduced mass and size by integrating an elliptical mirror as one of the rotating components, which eliminated a rotating frame. We used the same materials as the existing tracker; however, light-weighted both the aluminum frame and Zerodur® mirror. We generated a computer-aided design, converted it into a finite element model, and performed modal analysis on two load cases. In load case 1, we tied down three points on the bottom surface of the tracker that correspond to the tie-down points of the comparison tracker. This reveals a first mode of frequency of 140 Hz, a factor

of two over the current tracker's first mode of frequency of 67 Hz. In load case 2, we tied down the four corners of the tracker base in addition to the three tie-down points, simulating a firmly bolted and secured mount. The first mode of vibration for this case is 203 Hz, an increase over load case 1 by a factor of 1.45 and more than three times the fundamental frequency of the existing tracker. We conclude that these geometrical changes with the additional tie-down bolts are a viable solution path forward to improve steering speed and recommend a continuation with this effort.

9573-12, Session 3

Contamination and UV lasers: lessons learned

John G. Daly, Vector Engineering (United States)

Laser Induced damage to optical elements has been a subject of significant research, development, and improvement, since the first lasers were built over the last 50 years. Better materials, with less absorption, impurities, and defects are available, as well as surface coatings with higher laser damage resistance. However, the presence of contamination (particles, surface deposition films, or airborne) can reduce the threshold for damage by several orders of magnitude. A brief review of the anticipated laser energy levels for damage free operation is presented as a lead into the problems associated with contamination for ultraviolet (UV) laser systems. As UV lasers become more common in applications especially in areas such as lithography, these problems have been costly. This has been characterized as Airborne Molecular Contamination (AMC) in many published reports. Normal engineering guidelines such as screening materials within the optical compartment for low outgassing levels is the first step. The use of the NASA outgassing database (or similar test methods) with low Total Mass Loss (TML) and Collected Volatile Condensable Materials (CVCM) is a good baseline. Energetic UV photons are capable of chemical bond scission and interaction with surface contaminant or airborne materials results in deposition of obscuring film laser footprints that continue to degrade laser system performance. Laser systems with average powers less than 5 mW exhibit aggressive degradation. Lessons learned over the past 15 years with UV laser contamination and steps to reduce risk will be presented.

9573-13, Session 4

Criteria to asses production readiness of complex optical systems (Keynote Presentation)

Anees Ahmad, Nathan Tenney, Raytheon Missile Systems (United States)

The product development cycle consists of many phases with increasing levels of design and production maturity. These days there is a much greater emphasis on affordability and producibility of complex space and military systems because of the reduced budgets. Therefore, it is important to evaluate the production readiness of complex systems to ensure smooth transition to the production phase. NASA and Department of Defense commonly use the Technology Readiness Levels (TRLs) and the Engineering Manufacturing Readiness Levels (EMRLs) to determine the technical maturity and production readiness of complex systems at various stages of development.

The EMRL assessment is a good method of concisely and effectively assessing and communicating the degree to which a product is producible, reliable, and affordable. It is objective measure of product or program maturity and progress during design, development, and production phases. The EMRLs capture the knowledge required to successfully transition from technology development phase to the engineering manufacturing development and into production phase with minimal risk. The EMRLs consist of six levels (0-5) and twenty criteria and metrics including such items as technology, engineering, manufacturing, quality, reliability, test, logistics, safety, contracts, funding, and cost. Each EMRL is matched to an established product development milestone or gate and provides a concise, easy to use metric of product maturity against the maturity required for

Conference 9573: Optomechanical Engineering 2015



the desired milestone. The EMRLs have proven to be effective and efficient in measuring product maturity and readiness for transition from one phase to the next. A system must be able to satisfy EMRL-4 criteria before it is deemed to be ready for full rate production. This presentation will describe the level of system's maturity required for each of the 20 EMRL-4 criteria before it is deemed ready for full rate production.

9573-14, Session 5

Cost-optimized methods extending the solution space of lightweight spaceborne monolithic ZERODUR(R) mirrors to larger sizes

Antoine Leys, SCHOTT AG (Germany); Tony B. Hull, The Univ. of New Mexico (United States); Thomas Westerhoff, SCHOTT AG (Germany)

We address the problem that larger spaceborne mirrors require greater sectional thickness to achieve a sufficient first eigenfrequency that is resilient to launch loads, and to be stable during optical telescope assembly integration and test, this added thickness results in unacceptable added mass if we simply scale up solutions for smaller mirrors. Special features, like cathedral ribs, arch, chamfers, and back-side following the contour of the mirror face have been considered for these studies. For computational efficiency, we have conducted detailed analysis on various configurations of a 800 mm hexagonal segment and of a 1.2-m mirror, in a manner that they can be constrained by manufacturing parameters as would be a 4-m mirror. Furthermore each model considered also has been constrained by cost-effective machining practice as defined in the SCHOTT Mainz factory. Analysis on variants of this 1.2-m mirror has shown an optimal configuration. We have then scaled this optimal configuration to 4-m aperture. We discuss resulting parameters of cost-optimized 4-m mirrors. We also discuss the advantages and disadvantages this analysis reveals of going to cathedral rib architecture on 1-m class mirror substrates.

9573-15, Session 5

Selection considerations between ZERODUR and silicon carbide for dimensionally-stable spaceborne optical telescopes in low-earth-orbit

Tony B. Hull, The Univ. of New Mexico (United States); Antoine Leys, Thomas Westerhoff, SCHOTT AG (Germany)

A principal consideration for spaceborne optical telescope assemblies is material dimensional stability under realistic varying thermal boundary conditions. Candidate materials for spaceborne mirrors fall into two groups, those with low coefficient of thermal expansion and low thermal diffusivity, and those with high coefficient of thermal expansion and high thermal diffusivity. An example of the former is ZERODUR® and of the latter is Silicon Carbide (SiC). Cases are analyzed comparing how examples of ZERODUR® based systems and SiC based systems will distort as each system is exposed to thermal stimuli varying in both direction and amplitude. Such time domain thermal variation is typical of low-earth-orbit surveillance platforms, where not only view factors relative to the sun and earth change considerably in short time intervals, but also the location-specific thermal attributes of the earth below may enter the optical telescope assembly. The thermal figures-of-merit are minimal distortion of the optics, and minimal perturbations of the six-degree-of-freedom solid body alignments between mirrors, focal plane and pointing systems. Factors of selection other than thermal are considered, including optical finishing, heritage, stiffness and mass, ground testing, driven complexity of the system, cost and schedule.

9573-16, Session 5

Evolving design criteria for very large aperture space-based telescopes and their influence on the need for intergrated tools in the optimization process

William R. Arnold Sr., NASA Marshall Space Flight Ctr. (United States)

NASA's Advanced Mirror Technology Development (AMTD) program has been developing the means to design and build the future generations of space based telescopes. With the nearing completion of the James Webb Space Telescope (JWST), the astrophysics community is already starting to define the requirements for follow on observatories. The restrictions of available launch vehicles and the possibilities of planned future vehicles have fueled the competition between monolithic primaries (with better optical quality) and segmented primaries (with larger apertures, but with diffraction, costs and figure control issues). Regardless of the current shroud sizes and lift capacities, these competing architectures share the need for rapid design tools. As part of the AMTD program a number of tools have been developed and tested to speed up the design process. Starting with the Arnold Mirror Modeler (which creates Finite Element Models (FEM) for structural analysis) and now also feeds these models into thermal stability analyses. They share common file formats and interchangeable results. During the development of the program, numerous trade studies were created for 4 meter and 8 meter monolithic primaries, complete with support systems. Evaluation of these results has led to a better understanding of how the specification drives the results. This paper will show some of the early trade studies for typical specification requirements such as lowest mirror bending frequency and suspension system lowest frequency. The results use representative allowable stress values for each mirror substrate material and construction method and generic material properties. These studies lead to some interesting relationships between feasible designs and the realities of actually trying to build these mirrors. Much of the traditional specifications were developed for much smaller systems, where the mass and volume of the primary where a small portion of the overall satellite. JWST shows us that as the aperture grows, the primary takes up the majority of the mass and volume and the established rules need to be adjusted. For example, a small change in lowest frequency requirement can change the cost by millions of dollars.

The paper uses numerous trade studies created during the software development phase of the Arnold Mirror Modeler to illustrate the influences of system specifications on the design space. The future telescopes will require better performance, stability and documented feasibility to meet the hurdles of today's budget and schedules realities. AMTD is developing the tools, but the basic system planning mentality also has to adopt to the requirements of these very large and complex physical structures.

9573-17, Session 5

Recent updates to the Arnold Mirror Modeler and integration into the evolving NASA overall design system for large space-based optical systems

William R. Arnold Sr., NASA Marshall Space Flight Ctr. (United States)

Since last year, a number of expanded capabilities have been added to the modeler. The support the integration with thermal modeling, the program can now produce simplified thermal models with the same geometric parameters as the more detailed dynamic and even more refined stress models. The local mesh refinement and mesh improvement tools have been expanded and more user friendly.

The goal is to provide a means of evaluating both monolithic and segmented mirrors to the same level of fidelity and loading conditions at reasonable man-power efforts. The paper will demonstrate most of these new capabilities.



9573-18, Session 6

Novel applications of active mirror analysis

Victor L. Genberg, Gregory J. Michels, Sigmadyne, Inc. (United States)

Active and adaptive mirrors are commonly used to improve the performance of telescopes and other high performance optical systems. This paper will address the use of this analysis capability to solve a variety of other optomechanical problems. Examples will include:

1) Finding best coating thickness to minimize surface error

- 2) Understanding perplexing test results
- 3) Correlation of test and analysis results

4) Determining CTE variation within an optic

9573-19, Session 6

Shear stresses in cemented and bonded optics due to temperature changes

Paul R. Yoder Jr., Consultant (United States); Daniel Vukobratovich, Raytheon Missile Systems (United States)

This paper applies analytical means previously published by Chen and Nelson (1979) to estimate the shear stresses developed within the joints between typical cemented optical components and within opto-mechanical subassemblies made of materials with significantly different coefficients of thermal expansion (CTEs) when exposed to extreme ambient temperatures. Two cemented doublet examples, one involving glasses with a large CTE mismatch and another with more equal CTEs, are analyzed. An example involving a prism made of fused silica bonded with epoxy to a titanium base also is considered.

9573-20, Session 6

Unified optomechanical modeling: Thermo-elastic stability of a fiber optic diffractive encoding system

Alson E. Hatheway, Alson E. Hatheway Inc. (United States)

A challenge for optomechanical engineers is to make the structure sufficiently stiff to support the optical elements and stabilize the image on the detector. A complementary challenge, in an existing design, is to determine which elements need more stiffness and which others are satisfactory.

When presented with evidence (either empirical or analytical) that the image is unstable it is often not obvious which optical elements are the prime offenders. The uncertainty arises because both the elements' motions and their optical properties contribute the image motions. Since both the motions and the properties may vary by orders of magnitude in a particular design, neither one is a reliable guide for identifying major contributors to the problem.

Unified optomechanical modeling provides a vehicle for tracing offending image motions to particular optical elements and their supporting structure. The unified modeling method imports the optical elements' properties into a finite element structural model of optical system. It convolves the elements' motions and their optical properties in a single optomechanical modeling medium. This provides the engineer with a tool that discloses each element's contribution to the offending motions of the image on the detector.

This paper describes the use of the unified modeling technique to optimize the structure of an infrared imaging system.

9573-21, Session 6

Light source heat absorption analysis of a Dyson type lithography lens

Ming-Ying Hsu, Cheng-Fong Ho, Shenq-Tsong Chang, Ting-Ming Huang, Instrument Technology Research Ctr. (Taiwan)

The lithography system in high energy light source, the system refractive lens is absorption the heat from light source. The light source power is uniform distribution in mask side. The incident rays power density is calculated by radiometry in each lens surface. The lens heat absorption ratio is depending on optical glass species, quality and wave length. The optical glass higher internal transmittance means less heat absorption. Meanwhile, the optical glass in different temperature condition, the lens refractive index will change with temperature.

There is publish paper trying to calculate lens temperature distribution; the lens heat is absorbed from high energy light source. This study is applying FEM, radiometry and ray tracing solved lens temperature distribution. The each incident ray path is separate into many sections, the each section calculate the heat generated from heat absorption in the lens. Therefore, the heat generated in incident rays sections are weighting to finite element grids, and solving temperature distribution. The lens non-uniform temperature distribution will cause incident rays Optical Path Difference (OPD). The each incident rays OPD can fit by Zernike polynomials, the fitting results bring into optical software can be used to evaluate the thermal effect on lens heat absorption.

9573-22, Session 7

Techniques for analyzing lens manufacturing data with optical design applications (Invited Paper)

Morris I. Kaufman, National Security Technologies, LLC (United States); Brandon B. Light, Optimax Systems, Inc. (United States); Robert M. Malone, National Security Technologies, LLC (United States); Michael K. Gregory, Optimax Systems, Inc. (United States)

Optical designers assume a mathematically derived statistical distribution of the relevant design parameters for their Monte Carlo tolerancing simulations. However, there may be significant differences between the assumed distributions and the likely outcomes from manufacturing. Of particular interest for this study are the data analysis techniques and how they may be applied to optical and mechanical tolerance decisions. The effect of geometric factors and mechanical glass properties on lens manufacturability will be also be presented. Although the present work concerns lens grinding and polishing, some of the concepts and analysis techniques could also be applied to other processes such molding and single-point diamond turning.

9573-23, Session 7

Dependency between removal characteristics and defined measurement categories of pellet-tools

Christian Vogt, Rolf Rascher, Christine Wuensche, Hochschule Deggendorf (Germany)

Optical surfaces are usually machined by grinding and polishing. To achieve short polishing times it is intended to grind with best possible form accuracy and with low sub-surface damages. This leads to the use of very fine-grained grinding tools for the finishing process. These often show timedependent problems regarding cutting ability in conjunction with tool wear.

Fine grinding tools for manufacturing of optics are often comprised of

Conference 9573: Optomechanical Engineering 2015



grinding pellets. For a successful grinding process the tools must show a constant self-sharpening performance. A constant, at least predictable wear and cutting behavior is crucial for a deterministic machining.

This work describes a method to determine the characteristics of pellet grinding tools by tests conducted with a single pellet. The determination of the effective material removal rate and the derivation of the G-ratio are carried out here. Especially their change from the newly dressed via the quasi-stationary to the worn status of the tool is followed up. By recording the achieved roughness with the single pellet, a conclusion is possible for the expected roughness from a series pellet tool made of the same pellet specification.

From the results of these tests the usability of a pellet grinding tool for a special grinding task can be determined without testing a comparatively expensive serial tool.

The results are verified by a production test with a serial tool under series conditions.

The collected data can be stored and used in an appropriate data base for tool characteristics and be combined with useful applications.

9573-24, Session 7

Q-switched 1064nm laser source for photomechanical ablation in obsidianus lapis

Alfredo I. Aguilar-Morales, José Alfredo Álvarez-Chávez, A J. Morales-Ramírez, Ctr. de Investigación e Innovación Tecnológica (Mexico); Moises A. Ortega Delgado, Michael Panzner, Fraunhofer IWS Dresden (Germany)

The process of ablation in obsidianus lapis is mainly governed by laser pulse energy and scanning speed. The rate of material ablation is influenced by its chemical and physical properties. In this work, laser energy at 1064nm, the main commercially available wavelength for this application, has been used for ablation behavior in Q-switch regime. A >40W, CW Nd:YAG source with energy pulses ranging from 2.0mJ to nearly 7mJ, achieved surface damages up to 160 μ m of depth. Photo-mechanical ablation in terms of scanning speed showed a maximum depth of nearly 500 μ m at 130mm/s, and the maximum pulse energy of 8mJ was required for a 170 μ m depth. Highly efficient ablation in obsidianus lapis for artistic work is an interesting field of application.

9573-25, Session 7

The aspherical plastic lens molding stress residue and OPD analysis

Ming-Ying Hsu, Instrument Technology Research Ctr. (Taiwan)

The large size aspherical plastic lens is widely use in commercial optical product. The lens warpage and stress residue will introduce optical aberration into optical system. This paper is trying to link mould flow and optical design software by opto-mechanical analysis. Mold flow software is generally used in injection molding simulation to calculate the plastic lens stress residue of the injection process. Meanwhile, the optical ray path through the lens can be calculated by optical software. The stress residue results can be weighted to the optical ray path, and to evaluate the stress Optical Path Different (OPD) in each ray path. Each ray path OPD can be transformed to an optical axis sag, giving feedback on optical software estimate stress residue effect lens optical performance, and optimizing the injection model design.

9573-26, Session 7

A high-contrast 400- to 2500-nm hyperspectral checkerboard consisting of Acktar material cut with a femtosecond laser

Janos C. Keresztes, KU Leuven (Belgium); Anne Henrottin, Laser Engineering Applications S.A. (Belgium); Mohammad Goodarzi, Niels Wouters, Jeroen Van Roy, Wouter Saeys, KU Leuven (Belgium)

Visible-near infrared (Vis-NIR) and short wave infrared (SWIR) hyperspectral imaging (HSI) are gaining interest in the food sorting industry. As for traditional machine vision (MV), spectral image registration is an important step which affects the quality of the sorting system. Unfortunately, it currently still remains challenging to accurately register the images acquired with the different imagers as this requires a reference with good contrast over the full measurement range. Therefore, the objective of this work was to provide an accurate high contrast checkerboard over the full spectral range. From the investigated white and dark materials, Teflon and Acktar were found to present very good contrast over the full spectral range from 400 to 2500 nm, with a difference of 60%. The Metal Velvet selfadhesive coating from Acktar was selected as it also provides high specular absorbance. This was taped onto a near Lambertian polished Teflon plate, with further one out of two square removed after laser cutting the dark coating with an accuracy below 0.1 mm. As standard technologies such as nano-second pulsed lasers generated unwanted damages on both materials, a pulsed femto-second laser setup from Lasea with 60 um accuracy was used to manufacture the checkerboard. This pattern was monitored with an Imec Vis-NIR and a Headwall SWIR HSI line scanners. The camera intrinsic parameters were further extracted from the acquired images using computer vision. The contrast and effective focal length for different wavebands of each HSI are presented.

9573-27, Session 8

Unit moment analysis as a guide to mirror mount design

Daniel Vukobratovich, Patrick A. Coronato, Raytheon Missile Systems (United States)

Unit moment analysis minimizes the computational overhead associated with mirror mount design. Since mirrors operate in the linear domain with respect to stress/strain, it is possible to use the principle of superposition to determine overall optical surface deflection from a variety of sources. Surface deflection is calculated by FEA (finite element analysis) when applying unit loads at single mounting point. Deflection coefficients relating moments with surface deflection can be derived from the results of this analysis. These deflection coefficients are then applied, using the principle of superposition, to find the maximum tolerable moments associated with the mirror mount. Finally, manufacturing tolerances as well as environmental effects can be included to determine the required mirror mount compliance. This design approach is applicable to a wide range of mounting types, including classical kinematic and flexure mounts.

9573-28, Session 8

Mechanical design of a precision linear flexural stage for 3D x-ray diffraction microscope at the Advanced Photon Source

Deming Shu, Wenjun Liu, Argonne National Lab. (United States); Steven Kearney, Argonne National Lab. (United States) and Univ. of Illinois at Chicago (United States);



Jonathan Z. Tischler, Argonne National Lab. (United States)

The 3-D X-ray diffraction microscope is a new nondestructive tool for the three-dimensional characterization of mesoscopic materials structure. A flexural-pivot-based precision linear stage has been designed to perform a wire scan as a differential aperture for the 3-D diffraction microscope at the Advanced Photon Source, Argonne National Laboratory. The mechanical design and finite element analyses of the flexural stage, as well as its initial mechanical test results with laser interferometer are described in this paper.

* Work supported by the U.S. Department of Energy, Office of Science, under Contract No. DE-AC02-06CH11357.

9573-29, Session 8

Pre-construction of giant steerable science mirror for TMT

Fei Yang, Haibo Jiang, Qichang An, Hongchao Zhao, Peng Guo, Changchun Institute of Optics, Fine Mechanics and Physics (China)

The Changchun Institute of Optics, Fine Mechanics and Physics (CIOMP) team is developing the Giant Steerable Science Mirror (GSSM) for Thirty Meter Telescope (TMT) which will get into the preliminary design phase in 2016. To develop the passive support structure system for the largest elliptic-plano flat mirror, the smoothest tracking mechanism for the gravityinvariant condition, CIOMP is designing and building a 1/4 scale, functionally accurate version of the GSSM prototype. The prototype will incorporate the same opto-mechanical system and electric control system as the GSSM. The size of the prototype mirror is 898.5mm?634mm?12 mm with ellipticplano figure and will be supported by 18 points whiffletree on axial and 12 points whiffletree on lateral. The mirror surface figure will be evaluated by SlopeRMS which is the final evaluation method used in the actual GSSM. The prototype allows the mirror point to and be tested in five specified gravity orientations and meet the requirements of SlopeRMS. The prototype testing platform will have the interfaces with direct drive systems. The jitter testing will be implemented on the prototype system to verify the bearing, the encoder, the servo control algorithm in the low speed up to 5 arcsecond per second. The total prototype system configured mirror surface figure will be better than 1 micro radian SlopeRMS in each tested orientation. The positioner jitter will be less than 0.1 arcsecond RMS for tilt and rotator axis respectively and will be analysed with frequency domain to meet the requirements of the TMT adaptive optics system. The pre-construction will be completed at the beginning of 2016 and provide the technical support to the preliminary design of GSSM.

Monday - Thursday 10-13 August 2015

Part of Proceedings of SPIE Vol. 9574 Material Technologies and Applications to Optics, Structures, Components, and Sub-Systems II

9574-25, Session PMon

Numerically modeling diffraction efficiency of holographic volume grating formatted in photopolymer materials

Haoyu Li, Yue Qi, Ra'ed Malallah, John T. Sheridan, Univ. College Dublin (Ireland)

Based on the developed three-dimensional nonlocal photo-polymerization driven diffusion (NPDD), the non-linear response between the light intensity and material polymerization has been significantly presented in photopolymer material layer. The resulting spatial distribution of grating refractive index is not ideal sinusoidal as exposing pattern. Thus we denote that the harmonics of orders for the refractive index should not be just the zero and first order. In this paper we calculate the periodical distribution refractive index using the Lorentz-Lorentz relation and expanding it as four orders Fourier series. Then an effective first harmonic refractive index modulation which is time and space varying to describe the formatted volume grating is introduced. To do so the effects of the distortion effects produced by higher harmonics of refractive index can be considered into the refractive index modulation. The predictions are examined numerically for different physical conditions. The experimentally obtained deviation that the grating diffraction efficiency cannot reach the theoretical maximum value (2max = 100%) and the minimum value (2min = 0%) corresponding to the typical "sin2" curve during modulation and over-modulation exposure time, can be explained applying this model assumed in an acrylamide/polyvinyl alcohol (AA/PVA) photopolymer material.

9574-26, Session PMon

White-emitting SrAl2O4:Ce3+ phosphor for solid-state lighting

Luis Armando Díaz-Torres, Ctr. de Investigaciones en Óptica, A.C. (Mexico); David A. Chávez, Univ. Autónoma de Coahuila (Mexico); Carlos R. García, Maria T. Romero, Univ. Autonoma de Coahuila (Mexico); Jorge Oliva, Ctr. de Investigaciones Ópticas (Mexico)

Pure and Ce3+ doped SrAl2O4 phosphors were obtained by a combustion synthesis followed by a post-annealing process in reductive atmosphere at high temperature. The Ce3+ doping molar concentrations (x) were varied as follows x = 0.0, 0.5, 1.0, 2.0, 3.0, 5.0 and 10.0 mol%. Structural, morphological, optical and luminescent characterizations were performed by means X-ray diffraction, scanning electron microscopy, diffuse reflectance and photoluminescence spectroscopy, respectively. X-ray diffraction analysis showed a single monoclinic phase SrAI2O4 even for higher Ce3+ doping concentrations, suggesting that the Ce3+ ions are well incorporated into the host lattice. SEM micrographs show irregular micro-grains with sizes in the range of 1-100 μ m. A broadband white emission from 390 nm to 650 nm, with a maximum peak at lambda1=435 nm and a strong shoulder at lambda2= 520 nm, is observed when the phosphor is excited with UV light at lambdaexc= 351 nm. The maximum peak observed is attributed to the 5d-4f allowed transitions of Ce3+ ions substituted in the Sr sites within the SrAl2O4 monoclinic lattice. The excitation spectrum depicted a broadband profile from 250 nm to 400 nm, showing that the SrAl2O4:Ce3+ phosphors can be excited by near UV LEDs. The higher luminescent intensity was achieve by the x= 0.5 mol% doped SrAl2O4 phosphor. Due to this feature the SrAI2O4:Ce3+ phosphors are good candidates for white light generation LEDs technology.

9574-27, Session PMon

Focus tunable device actuator based on ionic polymer metal composite

Yi Wei Zhang, Guo-Dung J. Su, National Taiwan Univ. (Taiwan)

The voice coil motors (VCMs) are widely used in autofocus cameras in electronic portable devices recently. In this paper, we used ionic polymer metallic composite (IPMC) to replace VCMs because of its light weight and low driving voltage. To lower the driving voltage, we used silver as electrodes and demonstrated that silver can be deposited by either electroor electroless-plating. The IPMC made of silver electrode required 30% less driving voltage and the response speed could also improve almost 2 times in comparison with traditional platinum electrodes. Furthermore, the light-weighted microlens arrays with 0.7 mm in diameter made by micromachining technology can be moved by the IPMC actuators proposed in this paper. The modeling of this IPMC is presented as well. We believe the lower operating voltage and the relatively fast response speed of Ag-IPMC could be used in various optical applications.

9574-1, Session 1

Design and manufacturing considerations for 0.25-1.5 meter beryllium telescopes for current and future space missions

Mike N. Sweeney, Mark R. Warren, Joseph Ho, Jeff Calvert, Jeff Ruzan, General Dynamics Corp. (United States)

Recently there has been resurging interest in beryllium telescopes ranging in aperture from 0.25-1.5 meter for various NASA space missions. The central design feature for each mission currently under consideration is an axially symmetric, all beryllium telescope.

Design considerations include achieving minimized mass simultaneous with demanding structural, thermal, and optical requirements on orbit after sustaining the rigors of space launch. Modern analysis tools and modeling techniques enable simulation of telescope wavefront errors resulting from environmental effects and the influences of bi-metallic bending. Manufacturing considerations include diamond point turning, coordinate measurement machine profilometry, computerized grinding and polishing, brazing of complex beryllium structures, very thin electroless nickel plating, and other advanced manufacturing technologies imperative to successful visible-NIR optical performance. Current design and manufacturing efforts on 0.60, 0.80, and 1.0 meter beryllium telescopes are profiled to illuminate the confluence of applicable design and manufacturing technologies.

9574-2, Session 1

+1 360 676 3290 · help@spie.org

New decade of shaped beryllium blanks

Don Hashiguchi, Jeffrey Campbell, Materion Brush Beryllium & Composites (United States); Aaron Sayer, Amanda Morales, Materion Corp. (United States)

Near-net-shape powder consolidation technology has been developing over the past 30+ years. One relatively recent example is production of hexagonal shaped beryllium mirror blanks made for the James Webb Space Telescope. More cost saving examples, specifically from the past decade, utilizing growing experience and lesson's learned whether from a mirror substrate or structure will be discussed to show the latitude of production



technology. Powder consolidation techniques include Hot Isostatic Pressing (HIP) for either round or shaped blanks and Vacuum Hot Pressing (VHP) consolidation for round blanks. The range of sizes will be presented to further illustrate the latitude of current production capability.

9574-3, Session 1

Design and manufacturing considerations for high-performance gimbals used for land, sea, air, and space

Mike N. Sweeney, Lafe Redd, Tom Vettese, David Uchida, General Dynamics Corp. (United States)

High performance stabilized EO/IR surveillance and targeting systems are in demand for a wide variety of military, law enforcement, and commercial assets for land, sea, air, and space. Operating ranges, wavelengths, and angular resolution capabilities define the requirements for EO/IR optics and sensors, and line of sight stabilization. Many materials and design configurations are available for EO/IR pointing gimbals depending on trade-offs of size, weight, power, performance, and cost. Space and high performance military aircraft applications are often driven toward expensive but exceptionally performing beryllium and aluminum beryllium components. Commercial applications often rely on aluminum and composite materials.

Gimbal design considerations include achieving minimized mass and inertia simultaneous with demanding structural, thermal, optical, and scene stabilization requirements when operating in dynamic operational environments. Manufacturing considerations include precision lapping and honing of ball bearing interfaces, brazing, welding, and casting of complex aluminum and beryllium alloy structures, and molding of composite structures. Several notional and previously developed EO/IR gimbal platforms are profiled that exemplify applicable design and manufacturing technologies.

9574-4, Session 1

Fabrication of stable lightweight Be-38Al optics and optical support structures

Robert Hardesty, Kelsey Parker, Peregrine Falcon Corp. (United States)

This paper will describe recent aerospace applications where Be-38Al (AlBeMet) has been successfully applied to produce optics and stable support structures. The information presented will touch on historical uses of beryllium and beryllium-aluminum in satellite optical systems, and then address the latest developments in regards to Be-38Al and its application to optical substrates and stable support structures. Peregrine has ongoing development activities and will provide the latest progress concerning pertinent applications and designs from Be-38Al.

9574-5, Session 1

Application and testing of additive manufacturing for mirrors and precision structures

Mike N. Sweeney, Martyn Acreman, Tom Vettese, Ray Myatt, Mike Thompson, General Dynamics Corp. (United States)

Additive Manufacturing (aka AM, and 3-D printing) is widely touted in the media as the next industrial revolution. Beneath the hype, AM does offer profound advantages in lead-time, dramatically reduced consumption of expensive raw materials, while enabling new and innovative design forms that cannot be produced by other means. General Dynamics and industry partners have begun to challenge and embrace this technology

for mirrors and precision structures used in the aerospace, defense, and precision instrumentation industries. Aggressively light-weighted, open and closed back mirror designs, 75-150 mm in size, were first produced by AM. Subsequent optical finishing and test experiments have exceeded expectations for density, surface finish, dimensional stability and isotropy of thermal expansion on the optical scale of measurement. Materials currently under examination include aluminum, titanium, beryllium, AlBe MMC, Inconel, stainless bronze, and PEKK polymer.

SPIE. PHOTONICS

OPTICAL ENGINEERING+

APPLICATIONS

Design considerations for AM include the expanding availability of material choices, producible wall thicknesses, build overhang criteria, and powder removal considerations. Manufacturing considerations include scaffolding during build processes, heat treat, thermal cycling, hot isostatic pressing diamond point turning, optical polishing, The finished specimen were then subjected to thermal cycles to verify dimensional stability at room temperature and then measured under vacuum at hot and cold temperature excursions using laser interferometry. Both flat and spherical optical reference surfaces were used to differentiate longitudinal and transverse effects.

9574-6, Session 2

Structured surfaces on metal optics

Ralf Steinkopf, Johannes Hartung, Andreas Gebhardt, Stefan Risse, Ramona Eberhardt, Fraunhofer-Institut für Angewandte Optik und Feinmechanik (Germany)

Diamond machining of metal optics is an excellent way to manufacture structured elements on different surface geometries. Especially curved substrates such as spheres, aspheres, or freeforms in combination with structured elements enable innovative products like headlights of automobiles or spectrometers of telescopes in space applications. With diamond turning, servo turning, milling, and shaping, different technologies for almost any geometry are available. The addressed wavelengths are typically in the range of IR and NIR optical applications. Applying additional finishing processes, diamond machining is also used for optics applicable down to the EUV spectral range. The materials used for metal optics provide an additional advantage. Caused by manufacturing the mirror substrate and the mirror frame from materials with the same thermal expansion coefficient and even the same material, respectively, the completed optical systems are very robust and operationally stable within a wide temperature range. To achieve athermal optics, the alloy components are especially designed to match certain material components of the optical system. An exemplary model is the presented combination of AlSi42 and NiP.

Due to the complexity of the process chain for manufacturing freeform elements and structured surfaces, it is important to think about the right technologies from the beginning and to choose designs for series productions with time and cost effective processes, respectively. The paper shows the background to the effective use of manufacturing processes derived from the optical design and concentrates on the technologies for diamond machining of structured surfaces.

9574-7, Session 2

Physical and mechanical properties of LoVAR: a new lightweight particlereinforced Fe-36Ni alloy

Robert Michel, Materion Brush Beryllium & Composites (United States); Andrew Tarrant, Materion Aerospace Metal Composites Ltd. (United Kingdom); Jason R. Clune, Materion Brush Beryllium & Composites (United States); David Tricker, Materion Aerospace Metal Composites Ltd. (United Kingdom); Tim A. Stephenson, NASA Goddard Space Flight Ctr. (United States)

Because of its low thermal expansion, Fe-36Ni is the alloy of choice for optical, instrument and electrical applications where dimensional stability is critical. This paper will outline the development of a particle-reinforced



Fe-36Ni MMC that offers reduced density, lower CTE, improved temporal stability and greater specific stiffness compared to the conventional wrought alloy. A summary of processing capability will be given relating the composition and microstructure to mechanical and physical properties.

9574-8, Session 2

Advanced thermal control for spacecraft applications

Robert Hardesty, Kelsey Parker, Peregrine Falcon Corp. (United States)

In optical, infrared and advanced systems just like all other space borne systems, thermal control plays an important role. In fact, most advanced designs are plagued with volume constraints that further complicate the thermal control challenges for even the most experienced systems engineers. Peregrine will present advances in satellite thermal control based upon passive heat transfer technologies to dissipate large thermal loads. This will address the use of high thermal conducting products that are at least five times better than aluminum on a specific basis providing enabling thermal control while maintaining structural support.

9574-9, Session 3

New polishable R-SiC layer on ultralightweighted SiC substrates

Eric Ruch, REOSC (France)

Silicon Carbide is a material of high interest in the design and manufacturing of space telescopes, thanks to its mechanical and thermal properties. Since many years, Reosc has gathered a large experience in the polishing, testing, integration and coating of large size Silicon Carbide mirrors and also in the integration of full SiC TMAs.

Reosc has manufactured the 3 TMAs of the NIRSpec instrument that will take place on board JWST. Reosc has also polished 2 sets of mirrors for the Japanese HISUI instruments. Reosc has also polished the 1.5m primary mirrors of the GAIA instrument and currently polishing the scan mirrors of the MTG telescope and the 1,3m diameter primary mirror of the EUCLID instrument.

Based on this experience, Reosc is still improving its capability in the field of SiC mirrors. Two main activities are currently on-going:

1. replacement of CVD SiC by a new polishable layer R-SiC

2. development of ultra-lightweighted SiC mirror

The polishing of usual SiC mirrors does not provide very low microroughness. This is why it is required to coat the mirror with a layer that allows the polishing with a low micro-roughness (typically < 1nm RMS). The current process uses CVD SiC that has some drawbacks, mainly in terms of sizability to very large mirrors. This is why Reosc has developed an alternative material for polishing layers, R-SiC. The main requirements (low micro-roughness polishing, CTE compatibility with substrate, environment compatibility) have been successfully demonstrated. The next phase of the technology research program run in collaboration with ESA was to manufacture a 300mm demonstrator.

Reosc has successfully polished two ultra-lightweighted SiC mirrors, with R-SiC polishable layer, with an areal density of 20kg/m?. The design and the manufacturing process are representative of a 1.5 to 2m diameter mirror class. The goal is to develop the process and the tools allowing the polishing of this mirror including the quilting conditions.

9574-10, Session 3

RAP paper

Flemming Tinker, Aperture Optical Sciences Inc. (United States)

No Abstract Available

9574-11, Session 3

Low-stress silicon cladding made by pulsed-ion-assisted evaporation

David A. Sheikh, ZeCoat Corp. (United States)

ZeCoat Corporation has developed a low-stress silicon cladding process, which is super-polishable for meter-class SiC mirrors. The coating process is based on a low temperature, ion-assisted, evaporation technique (IAD), whereby the coating stress of a silicon film may be reversed periodically from compressive to tensile, in order to produce a near-zero net stress for the complete layer. A cladding with little intrinsic stress is essential to minimize bending that would otherwise distort the figure of very lightweight mirrors. ZeCoat has demonstrated silicon claddings 100-microns thick, with less than 50 MPa of compressive stress.

Large silicon carbide (SiC) mirrors (4+-meters in diameter) are being considered for future space-based UVOIR astronomy missions. These lightweight mirrors may require a highly-polishable layer of silicon (10 to 100-microns) applied on top of a SiC mirror substrate. A relatively thick layer of Si is desirable for the purpose of reducing figuring time and for achieving a super-polished surface, suitable for UV astronomy.

This paper presents coating stress data and polishing results for silicon claddings manufactured by the pulsed ion-assist process.

9574-12, Session 4

Trade-off study of all-SiC lightweight primary mirror and metering structure for spaceborne telescope (Invited Paper)

Haeng Bok Lee, Agency for Defense Development (Korea, Republic of); Jinyoung SUK, Chungnam National Univ. (Korea, Republic of); Jongin BAE, Hanwhathales (Korea, Republic of)

Silicon carbide is the best material for various telescope mirrors since it is high stiffness, low density, high thermal stability and fine surface optical quality. This paper describes a conceptual design trade studies that explores the structural views for the lightweight primary mirror made by SiC as well s the metering structure in half-metric GSD class telescope for space application.

9574-13, Session 4

T300HoneySiC: a new near-zero CTE molded C/SiC material

William A. Goodman, Trex Enterprises Corp. (United States); Mehrdad N Ghasemi-Nejhad, University of Hawaii (United States); Stan Wright, Ultracor Inc (United States); Darren Welson, Starfire Systems Inc (United States)

Trex enterprises and teammates were successful in producing a 12-inch by 12-inch by 0.5-inch vented, lightweight,Honeycomb C/SiC panel which had a density relative to bulk silicon carbide of 11% (89% lightweighting). The so-called T300/HoneySiC panel and facesheet stock material were fabricated into ASTM standard coupons and tested at Southern Research



Institute to obtain basic materials properties data. The materials properties data showed that we had made a near-zero coefficient of thermal expansion (CTE, from -196 to +24 deg C = -0.22 ppm/degC) ceramic matrix composite (CMC) C/SiC material with good strength. This material will be ideal for space opto-mechanical structures and optical benches due to it's near Zero-CTE and lightweight. The material is initially molded and then converted to a C/SiC ceramic matrix composite. Thus the fabrication time can be less than 3 weeks from start to finish, resulting in low cost.

9574-14, Session 4

Fabrication of extreme light-weighted ceramic mirrors

Matthias Krödel, ECM Engineered Ceramic Materials GmbH (Germany); Daniel Waechter, Fraunhofer-Institut für Produktionstechnologie (Germany); Frank Stahr, FAP Plasmatechnik GmbH (Germany); Claus-Peter Soose, fineoptix GmbH (Germany)

This paper will present the recent development achievements of a German SME supply chain to manufacture super light-weighted HB-Cesic mirrors for IR to visible applications. We will present recent design developments for achieving extreme light-weighted mirror substrates with extremely high stiffness and performance and in the second part the newly established German supply chain for the manufacturing of such extreme light-weighted mirror substrates.

9574-15, Session 4

Extreme stable and complex structures for optomechanical application

Matthias Krödel, ECM Engineered Ceramic Materials GmbH (Germany)

This paper will present the possibility to design and fabricate extreme stable and complex structure for opto-mechanical space application. Due to the fabrication features of our technology it is possible to fabricate complex light weighted structures for different thermal environments. We will present the complete process starting from the design up to the qualification of such structures. Finally we present some successful fabricated structures for such applications.

9574-16, Session 5

GRIN and homogeneous infrared materials for compact broadband IR imagers (Invited Paper)

Daniel J. Gibson, Shyam Bayya, Vinh Q. Nguyen, Jasbinder S. Sanghera, U.S. Naval Research Lab. (United States); Mikhail Kotov, Sotera Defense Solutions, Inc. (United States); Gryphon Drake, Univ. Research Foundation (United States)

The increasing reliance on simultaneous imaging in two or more spectral bands (visible, shortwave, mid-wave and long-wave infrared) on military platforms and technological advances in focal plane arrays (FPAs) highlight the need for compact multi-spectral IR imagers. Multi-spectral imagers based on reflective optics are typically large and limited to narrow field of view (FOV) applications. The small number of refractive materials that simultaneously transmit the SWIR, MWIR and LWIR wavelength regions imposes design constraints on multi-band imagers and the resulting designs can contain many elements making them heavy and complex with very tight tolerances. At the Naval Research Laboratory (NRL) we are developing new technologies for multispectral optics: new homogeneous broadband IR materials and IR gradient index (IR-GRIN) optical materials. This paper will present the latest progress in the development of these materials including their properties, and availability. Topics include refractive index, dispersion, index and dispersion gradients, design space guidelines and preliminary mechanical properties.

9574-17, Session 5

Homogeneity of material and optical properties in HEM grown sappire

Melissa Stout, Douglas L. Hibbard, II-VI Optical Systems (United States)

Sapphire crystal boules, approximately 34 cm in diameter and 22 cm tall, grown by the Heat Exchanger Method (HEM) are currently being sliced, ground and polished for use as window substrates in a variety of aerospace applications. As the need for larger volumes of higher quality material increases, it is necessary to evaluate and understand the homogeneity of optical and material properties within sapphire boules to ensure the needs of the industry can be met. The optical homogeneity throughout the full useable thickness of a representative sapphire boule was evaluated by measuring the transmitted wavefront error of multiple thin slices. This approach allowed the creation of a full-volume three-dimensional homogeneity map. Additionally, the uniformity of other critical characteristics of the material was evaluated at multiple locations within a boule. Specific properties investigated were equibiaxial flexural strength, index of refraction, Knoop hardness, coefficient of thermal expansion and modulus of elasticity. The results of those evaluations will be reported.

9574-18, Session 5

Strength of Zerodur(R) for mirror applications

Stephanie Behar-Lafenetre, Thales Alenia Space (France); Laurence Cornillon, Thales Alenia Space (France); Sonia Ait Zaid, Ctr. National d'Études Spatiales (France)

Zerodur[®] is a well-known glass-ceramic used for optical components because of its unequalled dimensional stability under thermal environment. In particular it has been used since decades in Thales Alenia Space's optical payloads for space telescopes, especially for mirrors. The drawback of Zerodur[®] is however its quite low strength, but the relatively small size of mirrors in the past had made it unnecessary to further investigate this aspect, although elementary tests have always shown higher failure strength. As performance of space telescopes is increasing, the size of mirrors increases accordingly, and an optimization of the design is necessary, mainly for mass saving. Therefore the question of the effective strength of Zerodur[®] has become a real issue.

Thales Alenia Space has investigated the application of the Weibull law and associated size effects on Zerodur[®] in 2014, under CNES funding, through a thorough test campaign with a high number of samples (300) of various types. The purpose was to accurately determine the parameters of the Weibull law for Zerodur[®] when machined in the same conditions as mirrors.

The proposed paper will discuss the obtained results, in the light of the Weibull theory. The applicability of the 2-parameter and 3-parameter (with threshold strength) laws will be compared. The expected size effect has not been evidenced therefore some investigations are led to determine the reasons of this result, from the test implementation quality to the data post-processing methodology. Eventually, the reliability of a proposed new allowable value for the studied surface finish will be discussed.

9574-19, Session 5

Low-temperature GRISM direct bonding

Gerhard Kalkowski, Gerd Harnisch, André L. Matthes, Uwe D. Zeitner, Stefan Risse, Fraunhofer-Institut für Angewandte Optik und Feinmechanik (Germany)

For high resolution spectroscopy in space, grating prism (GRISM) designs have been developed /1/ and are gaining increasing relevance. Common manufacturing proceeds either by directly "ruling" the grating structure into the prism surface, or by sophisticated high temperature diffusion bonding of a grating to a prism (to avoid the drawbacks of adhesive interlayers in the optical path).

We currently investigate an alternative approach for GRISM production, by using hydrophilic direct bonding at low temperatures /2/ to join gratings and prisms. Fig. 1 shows exemplary results of bonding lithographically structured fused silica glass plates of dimensions 25x35x6.35 mm? to right angle prisms of edge length 25 mm at temperatures of about 200°C in vacuum. The glass plates were furnished with binary gratings of size about 20x30 mm? in the bonding area and periods of about 600 nm. Flatness and roughness of both bonding surfaces are decisive for successful bonding. Our contribution describes the bonding process and characterizes bonding strength and optical performance of selected specimen.

This work was supported by $\mathsf{BMWI}/\mathsf{DLR}$ (Germany) under contract No. 55EE1204.

References:

1. T. Greene. C. Beichman, D. Eisenstein, S. Horner, D. Kelly, Y. Mao, M. Meyer, M. Rieke, F. Shi, Observing exoplanets with the JWST NIRCam grisms, Proc. SPIE Vol. 6693 (2007) 66930G

2. G. Kalkowski, S. Risse, U. Zeitner, F. Fuchs, R. Eberhardt, A, Tünnermann, Glass-Glass Direct Bonding, ECS Transactions, Vol. 64 (5) 3-11 (2014).

9574-20, Session 5

Polymers with customizable optical and rheological properties based on an epoxy acrylate based host-guest system

Uwe Gleissner, Thomas Hanemann, Jost Hobmaier, Univ. of Freiburg (Germany)

We report an easy way to tune the optical refractive index and viscosity of an epoxy acrylate-based host-guest system which can be used for the fabrication of optical waveguides. This allows fast and precise modification of the material system for different replication methods like hot embossing, inkjet printing or spin coating.

To modify the refractive index n, an electron-rich organic dopant such as phenanthrene is added to a commercially available reactive polymer based resin. Moreover, changes in viscosity can be achieved by using a comonomer with suitable properties like benzyl methacrylate (BMA).

We used a commercially available UV-curable epoxy acrylate based polymer matrix to investigate both the influence of phenanthrene and of benzyl methacrylate. First, mixtures of the pure polymer and benzyl methacrylate with a ratio of 30, 50, and 80 wt% benzyl methacrylate were produced. Second, phenanthrene was added with 5 and 10 wt%, respectively. All components were mixed and then polymerized by UV-irradiation and with a thermal postcure.

Characterization of the system with respect to viscosity, refractive index, Abbe number, glass transition temperature and optical damping was performed.

The viscosity of the mixtures decreased at 20°C linearly from 1.5 Pa•s (30 wt%) to 8 mPa•s (80 wt%), whereas the refractive index decreased at the same time by a small amount from 1.570 to 1.568 (@589 nm, 20°C). By adding phenanthrene refractive index increased to a maximum of n = 1.586 (50 wt% BMA, 10 wt% phenanthrene). Abbe numbers for the compositions without phenanthrene ranged from 35 to 38.

9574-21, Session 5

Low-strain laser-based solder joining of mounted lenses

Thomas Burkhardt, Marcel Hornaff, Andreas Kamm, Diana Burkhardt, Erik Schmidt, Erik Beckert, Ramona Eberhardt, Andreas Tünnermann, Fraunhofer-Institut für Angewandte Optik und Feinmechanik (Germany)

A novel laser based soldering technique - Solderjet Bumping - using liquid solder droplets in a flux-free process with only localized heating is demonstrating the all inorganic, adhesive free bonding of optical components and support structures that is suitable for optical assemblies and instruments under harsh environmental conditions. Low strain bonding with a following high precision adjustment turning process is presented, addressing components and subsystems for objectives for high power and short wavelengths. The discussed case study will show large aperture transmissive optics (diameter approx. 80 mm) made of fused silica and LAK9G15, a radiation resistant glass, bonded to thermally matched metallic mounts. The process chain of Solderjet Bumping - cleaning, solderable metallization, handling, bonding and inspection - is discussed. This multi-material approach requires numerical modelling for dimensioning according to thermal and mechanical loads. The findings of numerical modelling, process parametrization and environmental testing (thermal and vibrational loads) are presented. Stress and strain introduced into optical components as well as deformation of optical surfaces can significantly deteriorate the wave front of passing light and therefore reduce system performance significantly. The optical performance with respect to stress/ strain and surface deformation during bonding and environmental testing are evaluated using non-contact optical techniques: polarimetry and interferometry, respectively.

9574-22, Session 6

State-of-the-art cryogenic CTE measurements of ultra-low thermal expansion materials (Invited Paper)

Thomas Middelmann, Alexander Walkov, René Schödel, Physikalisch-Technische Bundesanstalt (Germany)

Absolute length measurements performed by imaging phase stepping interferometry allow for investigation of dimensional properties such as thermal expansion, length relaxation and long term stability with highest accuracy. The accurate knowledge of these properties is essential for development and characterization of ultra stable materials needed e.g. in the semiconductor industry or for aerospace applications. Accurate data on the coefficient of thermal Expansion (CTE) at cryogenic temperatures are especially important for construction and operation of space-borne telescopes as the Herschel Space Observatory or the James Webb Space Telescope of the European Space Agency, where large diameter mirrors are used at cryogenic temperatures.

Inside the extended measurements pathway of PTB's ultra precision interferometer the temperature can be varied from 7 K to 293 K. We have measured the absolute length of two samples made from different sorts of silicon nitride ceramics. We use these measurements to determine the CTE with an uncertainty below 5E-9/K in the temperature range from 10 K to 290 K. The CTE is defined via the derivative of the length with respect to temperature. To obtain the derivative the functional dependence of length versus temperature needs to be known. For this we fitted a physically motivated model to the length data. This model supports a low uncertainty by a low number of fit parameters. The physically motivated model is appropriate above 45 K but fails at lower temperatures. Thus in the temperature range from 7 K to 45 K we use a 5th order polynomial fit instead.





9574-23, Session 6

Next-generation dilatometer for highest accuracy thermal expansion measurement of ZERODUR(R)

Ralf Jedamzik, Axel Engel, Clemens Kunisch, Gerhard Westenberger, Peter Fischer, Thomas Westerhoff, SCHOTT AG (Germany)

In the recent years, the ever tighter tolerance for the Coefficient of thermal expansion (CTE) of IC Lithography component materials is requesting significant progress in the metrology accuracy to determine this property as requested.

ZERODUR* is known for its extremely low CTE between 0°C to 50°C. The current measurement of the thermal expansion coefficient is done using push rod dilatometer measurement systems developed at SCHOTT. In recent years measurements have been published showing the excellent CTE homogeneity of ZERODUR* in the one-digit ppb/K range using these systems. The verifiable homogeneity was limited by the CTE(0°C,50°C) measurement repeatability in the range of +- 1.2 ppb/K of the current improved push rod dilatometer setup using an optical interferometer as detector instead of an inductive coil.

With ZERODUR* TAILORED, SCHOTT introduced a low thermal expansion material grade that can be adapted to individual customer application temperature profiles. The basis for this product is a model that has been developed in 2010 for better understanding of the thermal expansion behavior under given temperature versus time conditions. In the ideal case, this model should match with real thermal expansions measurements. For this purpose a dilatometer setup is required with excellent stability and accuracy over long measurement times of several days.

In the past few years SCHOTT spent a lot of effort to drive a dilatometer measurement technology based on the push rod setup to its limit, to fulfill the continuously demand for higher CTE accuracy and deeper material knowledge of ZERODUR[®]. This paper reports on the status of the dilatometer technology development at SCHOTT.

9574-24, Session 6

Measurement of an optical surface roughness by of optical gradient waveguide method

Nikolai D. Espinosa, Univ. de las Fuerzas Armadas (Ecuador)

Theoretically and experimentally, we measured and analysis the scattering spectrum of the roughness optical surface using the multimodes optical planar gradient waveguide method. Described the method of preparation of prototypes (gradient waveguides) and the used methodology to perform the corresponding measurements.

With the acquired parameters (scattering spectrum) we proceed to perform recovery of the surface roughness. Analysis of experimental results is made and compared with the theoretical results.



Sunday - Tuesday 9 -11 August 2015

Part of Proceedings of SPIE Vol. 9575 Optical Manufacturing and Testing XI

9575-1, Session 1

Examination of the quality of 120 degree silicon double mirror for a micro-optical laser gyroscope

Thalke Niesel, Ingmar Leber, Andreas H. Dietzel, Technische Univ. Braunschweig (Germany)

For use in a novel micro optical laser gyroscope, 120° silicon double mirrors have been developed in order to maximize the robustness of the sensor design against alignment errors. The idea being pursued to the use of double mirrors with an angle between these two mirrors that is intrinsically defined by silicon crystallography and with a total reflection angle that is robust against misalignment. As a consequence, measurement errors can be minimized.

In this work the manufacturing of the special mirror elements were described. For the fabrication of these mirrors silicon wafers are used which are almost in [100] orientation but are tilted by 5.3 ° towards [011] direction and, therefore, provide an etching facet with a slope of 60° by KOH/IPA wet chemical etching. Two wafers structured in such way are connected by silicon direct bonding and then cut into small mirror elements which are mounted onto the gyroscope micro platform. Subsequently, the quality of the mirror surface is examined to confirm their suitability for the micro optical gyroscope. In addition, the angle accuracy of the elements and the stability after reflection at several elements is measured. Finally, the current sensor design is described and an outlook is given.

9575-2, Session 1

INAF-OAB deflectometry facility calibration

Giorgia Sironi, Rodolfo Canestrari, INAF - Osservatorio Astronomico di Brera (Italy)

A deflectometrical facility was developed at Italian National Institute for Astrophysics – OAB in the context of the ASTRI project to characterize free-form segments for Cherenkov optics. Our setup allows performing an inverse Ronchi test, it works illuminating the reflecting surface with a known light pattern and observing how the surface local shape error acts warping the reflected image. Knowing the geometry of the system it is possible to convert this optical test, classically adopted as a qualitative test, in quantitative surface slope error. The test suitability for Cherenkov mirrors characterization was proved comparing directly the mirror PSF with the PSF expected by a mirror with the measured surface errors.

In this paper we present the INAF-OAB facility calibration obtained testing the components of the system and comparing the measurements obtained on sample optics with coordinate measurements machine data.

9575-3, Session 1

JWST pathfinder telescope optical alignment, integration, and test program

Gary W. Matthews, Scott Kennard, Ronald Broccolo, John Amon, Stephen Mt.Pleasant, James Ellis, Walter Hahn, Exelis Inc. (United States); Lee D. Feinberg, NASA Goddard Space Flight Ctr. (United States)

The James Webb Space Telescope (JWST) is a 6.5m, segmented, IR telescope that will explore the first light of the universe after the big bang. In 2014, a major risk reduction effort related to the Alignment, Integration, and Test (AI&T) of the segmented telescope was completed. The Pathfinder

telescope was built at the Goddard Space Flight Center SSDIF which includes integrating two Primary Mirror Segment Assemblies (PMSA's) and the Secondary Mirror Assembly (SMA) onto a flight-like composite telescope backplane. This pathfinder allowed the JWST team to assess the alignment process and to better understand the various error sources that need to be accommodated in the flight build. The successful completion of the Pathfinder Telescope provides a final integration roadmap for the flight operations that will start in August 2015.

9575-4, Session 1

JWST pathfinder telescope risk reduction cryo test program

Gary W. Matthews, Thomas R. Scorse, John Spina, Exelis Inc. (United States); Ritva A. Keski-Kuha, Juli A. Lander, Mark F. Voyton, Lee D. Feinberg, NASA Goddard Space Flight Ctr. (United States); Carl A. Reis, NASA Johnson Space Ctr. (United States); Tony L. Whitman, Exelis Inc. (United States)

The James Webb Space Telescope (JWST) is a 6.5m, segmented, IR telescope that will explore the first light of the universe after the big bang. In 2014, the Optical Ground Support Equipment was integrated into the large cryo vacuum chamber at Johnson Space Center (JSC) and an initial Chamber Commissioning Test was completed. This insured that the support equipment was ready for the three Pathfinder telescope cryo tests. The Pathfinder telescope which consists of two primary mirror segment assemblies and the secondary mirror was delivered to JSC in February 2015 in support of this critical risk reduction test program prior to the flight hardware. This paper will detail the Chamber Commissioning and first optical test of the JWST Pathfinder telescope.

9575-5, Session 2

Optomechanical design and tolerance of a microscope objective at 121.6 nm

Derek S. Keyes, Thiago S. Jota, Weichuan Gao, Dakota Luepke, Victor E. Densmore, Thomas D. Milster, College of Optical Sciences, The Univ. of Arizona (United States); Gun Hee Kim, Korea Basic Science Institute (Korea, Republic of)

Utilizing the Hydrogen-Lyman-? (HLA) source at 121.6 nm we hope to achieve an intrinsic resolution of 247 nm at 0.3 NA and 92 nm at 0.8 NA. The motivation for 121.6 nm microscopy is a transparent window in the air absorption spectrum, which allows for the sample to be in air while the microscope is in an enclosed environment of nitrogen. The microscope objective consists of two reflective optics and a LiF window, and has been designed to demonstrate diffraction limited performance over a 160µm full field at 121.6 nm. The optomechanical design consists of mechanical subcells for each optical component, precision spacers and a barrel bore, which allows for submicron control of tolerance parameters.

9575-6, Session 2

Thermal optical metrology development for large lightweight UV to IR mirrors and future space observatory missions

Ron Eng, Markus A. Baker, William D. Hogue, Jeffrey R.



Kegley, Richard D. Siler, H. Philip Stahl, John M. Tucker, Ernest R. Wright, NASA Marshall Space Flight Ctr. (United States)

Optical metrology in an active thermal controlled environment plays a critical mission enabling role for future exoplanet and astrophysics exploration programs. The optical metrology results will validate concurrent integrated thermal, structural, and optical performance modeling effort. This paper summarizes the objectives and development effort in order to test different mirror architectures currently being developed by industry and government partners for NASA's Advanced Mirror Technology Development program. These lightweight mirror systems will be tested at the Marshall Space Flight Center's X-Ray & Cryogenic Facility, and the facility is currently being modified for testing mirrors up to 6 meters in diameter with metrology instruments housed inside the thermal vacuum test chamber.

9575-7, Session 2

Metrology requirements for the serial production of ELT primary mirror segments

Paul C. T. Rees, Caroline Gray, Glyndwr Univ. (United Kingdom)

The manufacture of the next generation of large astronomical telescopes, the extremely large telescopes (ELT), requires the rapid manufacture of greater than 500 1.44m hexagonal segments for the primary mirror of each telescope. Both leading projects, the Thirty Meter Telescope (TMT) and the European Extremely Large Telescope (E-ELT), have set highly demanding technical requirements for each fabricated segment. These technical requirements, when combined with the anticipated construction schedule for each telescope, suggest that more than one optical fabricator will be involved in the delivery of the primary mirror segments in order to meet the project schedule. For one supplier, the technical specification is challenging and requires highly consistent control of metrology in close coordination with the polishing technologies used in order to optimise production rates. For production using multiple suppliers, however the supply chain is structured, consistent control of metrology along the supply chain will be required. This requires a broader pattern of independent verification than is the case of a single supplier.

This paper outlines the metrology requirements for a single supplier throughout all stages of the fabrication process. We identify and outline those areas where metrology accuracy and duration have a significant impact on production efficiency. We use the challenging ESO E-ELT technical specification as an example of our treatment, including actual process data. We further develop this model for the case of a supply chain consisting of multiple suppliers. Here, we emphasise the need to control metrology throughout the supply chain in order to optimise net production efficiency.

9575-9, Session 2

Functionalization of UV-curing adhesives for surface-integrated single-mode polymer optical fibers

Bechir M. Hachicha, Ludger Overmeyer, Leibniz Univ. Hannover (Germany)

Polymer optical waveguides, especially single-mode waveguides are increasingly used for short distance communication, as well as for sensing applications. In this context, we are investigating an automated integration method of single-mode POF onto metallic substrates. Using microdispensing process, we functionalize UV-curing adhesives as cladding for single-mode optical cores. Furthermore, the adhesives are used for inherent bonding to the substrate. In this paper we pinpoint the necessary optical and mechanical characterization of these adhesives. Based on experiment results we inferred limits and opportunities, which this method offers.

9575-10, Session 3

Surface roughness when diamond turning RSA 905 optical aluminium

Timothy Otieno, Khaled Abou-El-Hossein, Nelson Mandela Metropolitan Univ. (South Africa); Wei-Yao Hsu, Yuan -Chieh Cheng, Instrument Technology Research Ctr. (Taiwan); Zwelinzima Mkoko, Nelson Mandela Metropolitan Univ. (South Africa)

Ultra-high precision machining is used intensively in the photonics industry for the production of various optical components. Aluminium alloys have proven to be advantageous and are most commonly used over other optical materials. Recently, the increasing demands from optical systems have led to the development of newly modified grades of aluminium alloys produced by rapid solidification during foundry process, characterised by finer microstructures and refined mechanical and physical properties. Their machining database is very limited and more research is still required in their machining performance when these modified aluminium alloys are diamond turned. This work investigates the machinability of rapidly solidified aluminium RSA 905 by varying cutting parameters and measuring the surface roughness over a cutting distance of 4 km. The machining parameters varied were cutting speed, feed rate and depth of cut. Statistical analysis was performed and a model was developed to predict the surface roughness from the cutting parameters. The results showed a common trend of decrease in surface roughness with increasing cutting distance. The lowest Ra result obtained after 4 km was 3.2 nm, where the parameters were cutting speed 1750 rpm, feed rate 5 mm/min and depth of cut 25 μ m. The results showed that cutting speed to be the most influential parameter on resulting surface roughness, while depth of cut was the least influential. Contour maps were developed to determine zones where the cutting parameters would produce the best surface quality.

9575-11, Session 3

Aspects of ultra-high-precision diamond machining of RSA443 optical aluminium

Zwelinzima Mkoko, Khaled Abou-El-Hossein, Nelson Mandela Metropolitan Univ. (South Africa)

Optical aluminium alloys such as 6061-T6 are traditionally used in ultrahigh precision manufacturing for making optical mirrors for aerospace and other applications. However, the optics industry has recently witnessed the development of more advanced optical aluminium grades that are capable of addressing some of the issues encountered when turning with single-point natural monocrystalline diamond cutters. The advent of rapidly solidified aluminium (RSA) grades has generally opened up new possibilities for ultra-high precision manufacturing of optical components. In this study, experiments were conducted with single-point diamond cutters on rapidly solidified aluminium RSA 443 material. The objective of this study is to observe the effects of depth of cut, feed rate and rotational speed on the tool wear rate and resulting surface roughness of diamond turned specimen. This is done to gain further understanding of the rate of wear on the diamond cutters versus the surface texture generated on RSA 443 material. Results obtained thus far have yielded machined surfaces which are less reflective but with consistent surface roughness values. Cutting tools were observed for wear through scanning microscopy; relatively significant wear pattern was evident on the cutters that were subjected to higher depth of cut and increased feed rate

9575-12, Session 3

The role of robotics in computercontrolled polishing of large and small optics

David D. Walker, Zeeko Research Ltd. (United Kingdom)



and Univ. College London (United Kingdom) and Glyndwr Univ. (United Kingdom); Matthew Bibby, Zeeko Research Ltd. (United Kingdom); Guoyu Yu, Caroline Gray, Paul C. T. Rees, Glyndwr Univ. (United Kingdom); Hsing Yu Wu, Univ. College London (United Kingdom); Xiao Zheng, Peng Zhang, Glyndwr Univ. (United Kingdom); Christina R. Dunn, Univ. College London (United Kingdom)

Following formal acceptance by ESO of three 1.4m hexagonal offaxis prototype mirror segments for the E-ELT produced at OpTIC, and certification of the optical test facility including 1.5m Master Spherical Segment, we summarise the state-of-the-art and then turn our attention to the challenge of segment mass-production.

In particular, we focus on the role of industrial robots in this and similar process-chains, particularly involving aspheric and free-form surfaces. We highlight the complementarity of robots and Zeeko machines, particularly regarding the inferior positional precision but higher motion-speeds delivered by robots. We have previously reported on pseudo-random tool-paths that fill any aperture but cross themselves nowhere – which avoids the double removals when paths cross. These paths are appropriate for the relatively slow tool-path motions of CNC machines. However, the high-speed motions that robots can deliver, open a new paradigm where the tool does not follow rectilinear or spiral tracks, but curved paths that cross for effective smoothing, and present experimental results to justify this.

We then report on progress in an adventurous project that is marrying robots and Zeeko machines to automate currently manual operations on the Zeeko platform, such as changing tools, changing (smaller) parts, deploying on-machine metrology instrumentation, and washing-down prior to metrology. We demonstrate how automating such operations in a unified software environment, constitute important steps towards our future vision of the fully autonomous manufacturing cell.

We conclude by showing how the combination of robotic processing per se, and robotic automation of CNC machines, are expected to have significant impact throughout the optical manufacturing community and beyond.

9575-13, Session 3

Evaluation and control of spatial frequency errors in reflective telescopes

Xue-jun Zhang, Li-gong Zheng, Xuefeng Zeng, Changchun Institute of Optics, Fine Mechanics and Physics (China)

In this paper, the influence on the image quality of manufacturing residual errors was studied. By analyzing the statistical distribution characteristics of the residual errors and their effects on PSF and MTF, we divided those errors into low, middle and high frequency domains using the unit "cycles per aperture". For current deterministic polishing processes, such as MRF or IBF, there are two types of mid-frequency errors, the algorithm intrinsic and the tool path induced. We studied several deconvolution algorithms and their contributions to so called "ringing effect", and proposed a conformal transform approach to pre-process the data map prior to deconvolution operation. It was found that the algorithm intrinsic mid-frequency errors could be reduced. Finally, tool path optimization methods in MRF or IBF process were presented.

9575-14, Session 3

Combined fabrication technique for ultraprecision optical surfaces

Hao Hu, Wenlin Liao, Yifan Dai, Feng Shi, Guilin Wang, National Univ. of Defense Technology (China)

The specifications of surface accuracy and surface smoothness made on optical components are becoming more and more stringent with the performance improvement of modern optical systems. Nowadays, deterministic figuring technologies are developed to meet the growing demands of such high-precision optical components. This presentation will report the fabrication process for ultra-precision optical surfaces in our laboratory, which combines magnetorheological finishing (MRF), smoothing polishing (SP) and ion beam figuring (IBF). We will highlight their applications for the nanometer/sub-nanometer fabrication of highperformance optics.

IBF is a highly deterministic, highly stable, non-contact method, and can provide an ultra-precise fabrication method for optical surfaces. All these advantages distinguish IBF as the final procedure for high precision optics manufacture. However, there are still some issues existing in IBF for high precision surfaces, such as its low material removal rate and sensitivity to mid-to-high frequency surface errors. Fortunately, MRF is a deterministic method with very high convergence and high material removal rates and SP is excellent in eliminating mid-to-high spatial frequency surface ripples and high slope errors. These two polishing methods just can overcome the disadvantages of the IBF process. Consequently, the combined fabrication technique is developed to fabricate the ultra-precision optical surfaces with high machining efficiency. Additionally, ultra-smooth surfaces are also vitally important for these high-performance optical components. The complex microscopic morphology evolution is investigated to improve the surface smoothness during the combined polishing process. The final experiments made on some spherical and aspherical samples will validate the highefficiency of this combined fabrication technique for ultra-precision and ultra-smooth optical surfaces.

9575-57, Session 3

Correction of mid-spatial-frequency errors by smoothing in spin motion for CCOS

Yizhong Zhang, Chaoyang Wei, Jianda Shao, Xueke Xu, Shijie Liu, Chen Hu, Haichao Zhang, Haojin Gu, Shanghai Institute of Optics and Fine Mechanics (China)

Smoothing is a convenient and efficient way to correct mid-spatialfrequency errors. Quantifying the smoothing effect allows improvements in efficiency for finishing precision optics. A series experiments in spin motion are performed to study the smoothing effects about correcting mid-spatial-frequency errors. Some of them use a same pitch tool at different spinning speed, and others at a same spinning speed with different tools. Introduced and improved Shu's model to describe and compare the smoothing efficiency with different spinning speed and different tools. From the experimental results, the mid-spatial-frequency errors on the initial surface were nearly smoothed out after the process in spin motion and the number of smoothing times can be estimated by the model before the process. Meanwhile this method was also applied to smooth the aspherical component, which has an obvious mid-spatial-frequency errors after Magnetorheological Finishing processing. As a result, a high precision aspheric optical component was obtained with PV=0.1? and RMS=0.02?.

9575-15, Session 4

Spectral characteristics and control of machining errors of KDP optical elements in ultra-precision turning

Guilin Wang, Feng Shi, Shengyi Li, Wenlin Liao, Furen Li, National Univ. of Defense Technology (China)

The laser induced damage threshold of optical elements can be reduced by the machining errors, and the performances of high-power laser system will be badly influenced. Therefore, the magnitude and the distributing features of machining errors must be strictly controlled. The ultra-precision turning technology is suitable for manufacturing KDP optical elements which are used as frequency switching unit in high-power laser system, but the machining stripes are easily to be found after ultra-precision turning, and this can introduce the working damage of KDP elements. In the presentation, the machining characteristics and the error morphology of KDP elements are analyzed in the process of ultra-precision turning,



and the measuring results show that low frequency errors are dominant on the machining surface. The relation between machining parameters and error spectrum are studied by using the power spectral density (PSD). The results show that the feeding rate and the spindle speed have obvious influences on the PSD of surface errors, the cutting depth has hardly any influence on the spectrum of PSD, but it will clearly affect the magnitude of PSD. Furthermore, the reasonable machining parameters are given for ultra-precision turning of KDP elements. Taking a typical KDP element as machining object, the distributing features and the microscopic evolution of surface errors are investigated. The PSD of low frequency errors is controlled within 103 nm2•mm by using the compensating turning method, the PSD of mid-to-high frequency errors is under "Not-to-Exceed" line applied in national ignition facility which is presented by Lawrence Livermore National Laboratory, and the working requirements for high-power laser system can be well satisfied.

9575-16, Session 4

Monolithical freeform element

Sven R. Kiontke, asphericon GmbH (Germany)

For 10 years there has been the asphere as one of the new products to be accepted by the market. All parts of the chain design, production and measurement needed to lear how to treat the asphere and what it is helpful for. The aspherical optical element now is established and accepted as an equal optical element between other as a fast growing part of all the optical elements.

Now we are focusing onto the next new element with a lot of potential, the optical freeform surface. Manufacturing results will be shown for fully tolerance optic including manufacturing, setup and optics configurations including measurement setup. The element itself is a monolith consisting of several optical surfaces that have to be aligned properly to each other. All surfaces are measured for surface form tolerance (irregularity, slope, Zernike, pv). In addition roughness will be qualified as well as reference surfaces.

9575-17, Session 4

The fabrication of freeform optics

Todd Blalock, Kate Medicus, Jessica D. Nelson, Optimax Systems, Inc. (United States)

Freeform surfaces on optical components have become an important design tool for optical designers. Non-rotationally symmetric optical surfaces have made solving complex optical problems easier. The manufacturing and testing of these surfaces has been the technical hurdle in freeform optic's wide-spread use. CNC optics manufacturing technology has made the fabrication of optical components more deterministic and streamlined for traditional optics and aspheres. Optimax has developed a robust freeform optical fabrication CNC process that includes generation, high speed VIBE polishing, sub-aperture figure correction, surface smoothing and testing of freeform surfaces. Two of the main benefits of the VIBE process are the high speed associated with the process and the ability to maintain the form introduced during generation. The process flow consists of

CNC Generate --> Pre-Polish --> Measurement --> Deterministic Figure Correction --> VIBE Smoothing

The VIBE polishing process is shown to work well with freeform surface by the full-aperture tooling and optimized compliant layers on the tool. The stiffness of the compliant layer is selected for optimal figure correction. The VIBE polishing process then removes the mid-spatial frequencies. This process has been shown to limit the amount of mid-spatial frequency surface error on the optic. We will show the reduction of mid-spatial frequencies and form error in a variety of freeform optical shapes using specialized tooling and processes.

9575-19, Session 4

Ion beam figuring of glass moulds for the integration of x-ray optics

Mauro Ghigo, Gabriele Valsecchi, Stefano Basso, Marta Civitani, Enrico G. Mattaini, Giovanni Pareschi, Giorgia Sironi, INAF - Osservatorio Astronomico di Brera (Italy)

The INAF-Astronomical Observatory of Brera (INAF-OAB) is studying the glass technology needed to reach the 5 arcsec requested to the ATHENA telescope optics, currently approved by ESA. During this study we have developed a direct hot slumping technique assisted by pressure, in which the glass optical surface is in contact with a ceramic mould and a pressure is applied in order to force the glass to copy the mould shape. After this step, the integration of the slumped glass foils is made by means of the IMA, a purpose built machine, able to stack the foils and create the X-ray Optical Unit, the building block of the final optical module. During this phase the foils are held in position and pressed against an integration mould made of glass, with a very precise shape since it controls the final optical performances of the individual glass segments. To improve the optical figure of these moulds, we foresee the use of the Ion Beam Figuring that is available internally in OAB. The institute has two facilities, one for large optics up to 1.4 meters in diameter and a second one for relatively small optics, up to 350 mm. The aim of this work is to bring the optical accuracy of the present moulds from 5-6 arcsec down to 2 arcsec HEW. Since the moulds are made in BK7 and it is known that this material can suffer distortions deriving from the thermal load from the ion source beam, this issue must be taken into account properly. In this paper we describe the achieved results in the correction of the integration moulds, and the steps implemented to mitigate the thermal load.

9575-49, Session 4

Measuring skew in average surface roughness as a function of surface preparation

Mark T. Stahl, NASA Marshall Space Flight Ctr. (United States)

Characterizing surface roughness is important for predicting optical performance. Better measurement of surface roughness reduces polishing time, saves money and allows the science requirements to be better defined. This study characterizes statistics of average surface roughness as a function of processing time. Average surface roughness is measured at 81 locations using a Zygo white light interferometer at regular intervals during the polishing process. Each data set is fit with various Normal and Largest Extreme Value (LEV) distributions; then tested for goodness of fit. We show that the skew in the data changes as a function of polishing time.

9575-20, Session 5

Development of practical Ge immersion grating

Takashi Sukegawa, Takeshi Suzuki, Yukinobu Okura, Yukiya Enokida, Canon Inc. (Japan)

Immersion grating is a powerful optical device for the infrared highresolution spectroscope.(Marsh et al.(2007),Kuzmenko et al.(2006)) Ge is the best material for a mid-infrared immersion grating because of Ge has very large reflective index (n=4.0). On the other hands, there is no practical Ge immersion grating around 5um use. Our original free-forming machine has accuracy of a few nano-meter in positioning and stability. We already fabricated the large CdZnTe immersion grating with groove area (77mm x 21mm) which was found to have the scattered energy loss at 5 um was 0.07 %, the ghost intensity ratio at 5 um was < 0.0026%. We are developing Ge immersion grating that can be a good solution for high-resolution



infrared spectroscopy with the large ground-based / space telescopes and laser frequency comb. Our first Ge immersion grating has the entrance clear aperture of 19mm x 19mm, grooved area of 75mm(ruled direction) x 19mm(groove width), the groove pitch of 144.44um and the blaze angle of 75 degrees. Even this small size, the theoretical spectral resolution is 120,000 at 5um. And second Ge immersion grating has the groove pitch of 91.74um. The typical grooves performance are the spacing accuracy of <5nmRMS, the surface roughness of <2nmRMS and the surface irregularity of 52nm(PV) / 12nm(RMS) at first grating and 45nm(PV) / 5nm(RMS) at second grating. In this paper, we report our development of practical Ge immersion grating especially optical performance results and also discuss further development for larger size (> 100mm) and productivity.

9575-21, Session 5

Status of the Advanced Mirror Technology Development (AMTD) phase 2 1.5m ULE mirror

Robert M. Egerman, Gary W. Matthews, Albert J. Ferland, Matthew Johnson, Exelis Inc. (United States)

The Decadal Survey stated that an advanced large-aperture ultraviolet, optical, near-infrared (UVOIR) telescope is required to enable the next generation of compelling astrophysics and exoplanet science; and, that present technology is not mature enough to affordably build and launch any potential UVOIR mission concept. Under Science and Technology funding, NASA's Marshall Space Flight Center (MSFC) and Exelis have developed a more cost effective process to make up to 4m monolithic spaceflight UV quality, low areal density, thermally and dynamically stable primary mirrors. Under a Phase I program, a proof of concept mirror was completed at Exelis and tested down to 250K at MSFC which would allow imaging out to 2.5 microns. In 2014, Exelis and NASA started a Phase II program to design and build a 1.5m mirror to demonstrate lateral scalability to a 4m monolithic primary mirror. The current status of the Phase II development program will be provided along with a Phase II program summary

9575-22, Session 5

Improving profitability through slurry management: A look at the impact of slurry pH on various glass types

Abigail R. Hooper, Harry W. Sarkas, Nathan Hoffmann, Kevin Cureton, Nanophase Technologies Corp. (United States)

When building an optical system, optical fabricators and designers meticulously choose the glass type for their application knowing that each one will have different chemical, thermal and mechanical properties. As the requirements for new optical systems have grown more demanding, the range of available glass types has vastly expanded and the specifications on the produced products have grown tighter. In an attempt to simplify processes and streamline consumable purchases, optical polishing houses often rely on one polishing slurry to manage these vast array of glass types. An unforeseen consequence of these practices can be a reduction in productivity by reduced removal rate, poor yields and frequent re-work all translating into higher costs and reduced profitability.

In this paper, the authors will examine the impact slurry pH has on glass types of different compositions and chemical, thermal and mechanical properties when using a double-sided polishing process. Experiments will use material removal rate, surface quality and surface figure to provide insight into improving process control of changing glass types. Further guidance will be provided on how simple on-site monitoring and adjustment can deliver improved profitability on challenging substrates.

9575-23, Session 5

Material removal characteristics of orthogonal velocity polishing tool for efficient fabrication of CVD SiC mirror surfaces

Hyunju Seo, Yonsei Univ. (Korea, Republic of) and Korea Astronomy and Space Science Institute (Korea, Republic of); Jeong-Yeol Han, Korea Astronomy and Space Science Institute (Korea, Republic of); Sug-Whan Kim, Yonsei Univ. (Korea, Republic of); Sehyun Seong, SphereDyne Co., Ltd. (Korea, Republic of) and Yonsei Univ. (Korea, Republic of); Siyoung Yoon, Kyungmook Lee, Samsung Thales Co., Ltd. (Korea, Republic of); Haengbok Lee, Agency for Defense Development (Korea, Republic of)

Today, CVD SiC mirrors of small and medium sizes are available in the market. However, it is well known to the community that the key surface fabrication processes and, in particular, the material removal characteristics of the CVD SiC mirror surface varies sensitively depending on the shop floor polishing and figuring conditions. We investigated the material removal characteristics of CVD SiC mirror surfaces using a new and patented polishing tool called orthogonal velocity tool (OVT) that employs two orthogonal velocity fields generated simultaneously during polishing and figuring machine runs. We built an in-house OVT machine and its operating principle allows for generation of pseudo Gaussian shapes of material removal from the target surface. The shapes are very similar to the tool influence functions (TIFs) of other polishing machine such as IRP series polishing machines from Zeeko. Using two CVD SiC mirrors of 150 mm in diameter and flat surface, we ran trial material removal experiments over the machine run parameter ranges from 12.901 to 25.867 psi in pressure, 0.086 m/sec to 0.147 m/sec in tool linear velocity, and 5 to 15 sec in dwell time. An in-house developed data analysis program was used to obtain a number of Gaussian shaped TIFs and the resulting material removal coefficient varies from 3.124 to 11.954 um/psi hour m/sec with the mean value to 6.140 ± 1.377(standard deviation). We report the technical details of the new OVT machine and the data analysis program, of the experiments and the results together with the implications to the future development of the machine and process for large CVD SiC mirror surfaces.

9575-24, Session 5

Surface errors in the course of machining precision optics

Rolf Rascher, Christine Wuensche, Heiko Biskup, Alexander Haberl, Hochschule Deggendorf Technologiecampus Teisnach (Germany)

Precision optical components are usually machined by grinding and polishing in several steps with increasing accuracy. Spherical surfaces will be finished in a last step with large tools to smooth the surface. The requested surface accuracy of non-spherical surfaces only can be achieved with tools in point contact to the surface. So called mid-frequency errors MSFE accumulate with zonal processes.

This work is on the formation of spatial errors from grinding to polishing by conducting an analysis of the surfaces in their machining steps by contact and non-contact interferometric methods. In both cases all describing data of the surface are collected as far as the technology allows. The errors on the surface can be distinguished as described in DIN 4760. 3rd order errors are usually so called MSFE.

By appropriate filtering of the measured data frequencies of errors can be suppressed in a manner that only defined spatial frequencies will be shown in the surface plot. It can be observed that some frequencies already may be formed in the early machining steps like grinding and main-polishing. Additionally it is known that MSFE can be produced by the process itself and other side effects.

Beside a description of spatial errors based on the limits of measurement technologies, different formation mechanisms for selected spatial



frequencies are presented. A correction may be only possible by tools that have a lateral size below half of the wavelength of the error structure. The presented considerations may be used to develop proposals to handle spatial errors.

9575-59, Session 5

The effect of HF etching on the surface quality and figure of fused silica optics

Jiafeng Xu, Xueke Xu, Chaoyang Wei, Wenlan Gao, Minghong Yang, Jianda Shao, Shijie Liu, Shanghai Institute of Optics and Fine Mechanics (China)

Impurity cation in polishing layer contributes to the deposition of etching product. Residual micron grinding cracks and submicron crack pits are etched into digs which are not more than 1?m deep. These digs worsen the surface roughness. Digs also frosts the sample. Abrasives of large size or the agglomeration of abrasives creates submillimeter scratches. These short scratches appear as sparkling points under the high power lamp when they are exposed through etching. The average total length of millimeter scratches on single surface is over 200 mm. Not all millimeter scratches can be exposed until removal depth of up to 2?m. Etching on the edge of the upper surface of samples placed horizontally goes faster than on the inside parts, and the surface of samples placed vertically assume a more complicated removal distribution, which can be both explained in terms of "fringe tip effect" and the diffusion of etching product and acid. How surface PV evolves is dependent of the initial surface figure feature as well as the etching removal distribution.

9575-26, Session 6

Using frictional power to model LSST removal with conventional abrasives

Richard G. Allen, William H. Hubler, The Univ. of Arizona (United States)

The stressed lap on the Large Polishing Machine (LPM) at the Steward Observatory Mirror Lab has recently been used to polish the M1 and M3 surfaces of the 8.4-m mirror for the Large Synoptic Survey Telescope (LSST). Loadcells in the three 4-bar links that connect this lap to the spindle of the machine allow the translational forces and torque on the lap to be measured once a second. These force readings and all other available machine parameters are sent to a history file that can be used to create 2-D removal maps after the stroke is finished. While the Preston equation has been used for many years to predict removal in conventional polishing processes, we have adopted a new equation that assumes that removal is proportional to the energy that is transferred from the lap to the substrate via friction. Specifically, the instantaneous removal rate at any point is defined to be the product of four parameters - an energy conversion factor called the Allen constant, the coefficient of friction, the lap pressure, and the speed of the lap. The Allen constant is the ratio of volumetric removal to frictional energy for a particular combination of pad material, abrasive, and substrate. Because the removal calculations take into account changes in the coefficient of friction between the lap and mirror, our 2-D maps usually correlate well with optical data. Removal maps for future polishing strokes are created in simulations that track the position and speed of individual lap pads.

9575-27, Session 6

Influence of coolant on ductile mode processing of binderless nanocrystalline tungsten carbide through ultraprecision diamond turning

Marius Doetz, Fritz Klocke, Olaf Dambon, Fraunhofer-

Institut für Produktionstechnologie (Germany); Oliver W. Fähnle, FISBA OPTIK AG (Switzerland)

Molds made of tungsten carbide are typically used for the replicative mass production of glass lenses by precision glass molding due to their high temperature hardness and the chemical behavior of the material in contact with glass. For the manufacturing of these inserts, the ultraprecision grinding process with a subsequent manual polishing operation is conventionally applied. These processes are time consuming and have a relatively low reproducibility.

An alternative manufacturing technology, with a high predictability and efficiency, which additionally allows a higher geometrical flexibility, is the diamond turning technique. However, the extreme hardness and the chemical properties of tungsten carbide lead to significant tool wear and therefore the impossibility of machining the work pieces in an economical way. One approach to enlarge the tool life is to affect the contact zone between tool and work piece by the use of special cutting fluids.

This publication emphasizes on the most recent investigations and results in direct machining of nano-grained tungsten carbide with mono crystal diamonds under the influence of various kinds of cutting fluids. Therefore basic ruling experiments were performed, where the tool performed a linear movement with a steadily increasing depth of cut. As the ductile cutting mechanism is a prerequisite for the optical manufacturing of tungsten carbide these experiments serve the purpose for establish the influence of different cutting fluid characteristics on the cutting performance of mono crystal diamonds.

9575-28, Session 6

Optimizing computer control ball polishing of spherical surfaces

Rasool Koosha, Peiman Mosaddegh, Hosein Hashemi, Isfahan Univ. of Technology (Iran, Islamic Republic of)

About half a century ago, computer controlled-polishing (CCP) was represented as a respond to great demand for precision glass manufacturing. Since then, CCP is developed to challenge the difficulties of manufacturing of more complex optical components. Simulation of polishing process and optimization of dwell time are the most prominent key factors of CCP in which numerous papers are published. In this paper, a new model based on discretizing tool path with sub-millimeter distances in length is presented to simulate polishing process. As a result, complex polishing tool path as spiral or epicyclical tool path can be easily and precisely modeled with 50-100 micron accuracy. Converting continuous tool path to discrete points with small steps would improve surface quality in an optimum time and it also reduces fluctuation in tool feed rate. This smooth gradient in feed rate can improve final quality and prevent any damage to polishing machine. Then, a fuzzy algorithm is programmed to optimize the dwell time of polishing process. Considering initial surface error under tool positions and tool influence removal rate, the method calculates optimum dwell time distribution to reduce surface roughness in a short period of time. Both polishing simulation and dwell time fuzzy optimization algorithms are easy to program and could be conducted to operate the CCP on a 3 axis CNC machine. The methodology developed in this study is used for ball polishing of spherical lenses. To establish the authenticity of represented method, a BK7 flat lens with 130 mm in diameter and 320 mm radius in curvature was selected to perform CCP process. The result of initial surface measurement shows 1.114 μ m of surface roughness for PV (Peak to Valley) and 175 nm for rms (Root Mean Square). The represented method was applied to calculate the optimum dwell time distribution over a spiral tool path with 1 mm in step over. Based on the simulation results, the 3axis CNC machine was programmed to operate polishing process. Based on the final surface measurement, the surface roughness was reduced to 394 nm for PV and 74 nm for RMS. The experimental results show that surface error declined by 64% in PV and 57% in rms which are in good agreement with the modeling.



9575-58, Session 6

The effect of the pad groove feature on the material removal rate and mid-spatial frequency error in CCOS

Jianwei Ji, Chaoyang Wei, Shijie Liu, Xueke Xu, Jianda Shao, Shanghai Institute of Optics and Fine Mechanics (China)

One of important factors that influencing the polishing results is pad groove feature in the process of CCOS(Computer Controlled Optical Surfacing). A comparative study has been done on material removal rate and midspatial frequency error with pads which have different groove feature. Firstly, derive the removal functions in the smooth running mode and carried out the experiments according to suitable parameters with pads which have different groove feature, and the experimental results were explained. Furthermore, a series of simulations about mid-spatial frequency error which were caused by pads groove were done using the numerical superposition method in the smooth running mode, the groove feature including groove patterns, groove width, and groove intensive degree , and the simulation results consistent with the experimental results. This lay the foundation for NC machining which have high material removal rate and low mid-spatial frequency error.

9575-60, Session 6

Influence of temperature distribution in the workpiece-lap interface on surface figure controlling during continuous polishing

Meijuan Hong, Xueke Xu, Minghong Yang, Chaoyang Wei, Shijie Liu, Jianda Shao, Shanghai Institute of Optics and Fine Mechanics (China)

During continuous polishing, temperature is the main source of processing uncertainty. However, few scholars have studied the temperature distribution in the workpiece-lap interface, most of their attention are paid to the environment temperature and its variation. It's our main approach to achieve deterministic processing that we study the temperature distribution in the workpiece-lap interface and find out its influence on surface figure controlling. Hence, we explored the temperature distribution in the workpiece-lap interface by simulation and actual measurement using infrared thermal imager. And, simulations have been done to research the diversity response to temperature distribution of different material workpieces, which coincides with the experiments. We find that since when temperature changes, the workpieces will have different deformation, even though they are all well matched to the lap (which means, by this time, they have the same surface figure), when they are done of polishing and off the lap, the temperature changes, they will have different deformation (or we can call it shrink), which results in different surface figure. The temperature distribution in the Workpiece-lap Interface plays a crucial role in surface figure controlling. To achieve Deterministic processing, we attempted many methods to decrease the effects of temperature distribution, such as circulation slurry injection, broaden and deepen the Groove-Scale, which have been tested in our experiments and turned out to be useful.

9575-25, Session PMon

Influence of different rigid tool groove in polishing process

Kai Meng, Fan Wu, Yongjian Wan, Institute of Optics and Electronics (China); Hsing Yu Wu, Univ. College London (United Kingdom)

During optical polishing process, there are a lot of factors which affect

the polishing results like material removal rate and surface roughness. According to Preston equation, the pressure between tool and processed surface affects the material removal rate effectively. However, different tool has different groove which causes different tool deformation and pressure distribution. This paper mainly focuses on the deformation and pressure of rigid tool using Finite Element Method (FEM) and statistical analysis. Four kinds of tool groove pattern types are investigated on this paper: non-groove, grid grove, annular groove and radial groove and each tool has two different loading conditions. Firstly, the different tool deformation and pressure models are built using FEM. Secondly, we got the deformation and pressure data on contact regions. Thirdly, data on different part faces and edges of the groove are separated. Finally, these separated data are analyzed using statistical method, which indicates that the tool groove needs more optimization and the edge effects of groove needs more attention and research as edge tool influence function control.

9575-45, Session PMon

Investigation of rapidly-solidified aluminum with diamond turning and magnetorheological finishing (MRF) process

Yuan-Chieh Cheng, Wei-Yao Hsu, Ching-Hsiang Kuo, Instrument Technology Research Ctr. (Taiwan); Khaled Abou-El-Hossein, Timothy Otieno, Nelson Mandela Metropolitan Univ. (South Africa)

The metal mirror has been widely used in optical application for a longtime. Especially the aluminum 6061 is often considered the preferred material for manufacturing optical components for ground-based astronomical applications. One reason for using this material is its high specific stiffness and excellent thermal properties. However, a large amount of data exists for this material and commercially available aluminum 6061 using single point diamond turning (SPDT) and polishing process can achieve surface roughness values of approximately 2 to 4 nm, which is adequate for applications that involve the infrared spectral range, but not for the shorter spectral range. A novel aluminum material, fabricated using a rapid solidification process that is equivalent to the conventional aluminum 6061 alloy grade has been used in optical applications in recent years because of its smaller grain size. In this study, the surface quality of the rapid solidification aluminum after single point diamond turning and followed by magnetorheological finish (MRF) process is investigated and compared with conventional aluminum 6061. Both the surface roughness Ra and power spectral density (PSD) were evaluated using white light interferometers. Finally, indicators such as optimal fabrication parameter combination and optical performance are discussed.

9575-46, Session PMon

Optical diffraction interpretation: an alternative to interferometers

Stephane Bouillet, Commissariat à l'Énergie Atomique (France)

The Laser MégaJoule (LMJ) is a French high power laser project that requires thousands of large optical components. The wavefront performances of all those optics are critical to achieve the desired focal spot shape and to limit the hot spots that could damage the components. Fizeau interferometers and interferometric microscopes are the most commonly used tools to cover the whole range of interesting spatial frequencies. Anyway, in some particular cases like diffractive and/or coated and/or aspheric optics, an interferometric set-up becomes very expensive with the need to build a costly reference component or a specific to-the-wavelength designed interferometer. Despite the increasing spatial resolution of Fizeau interferometers, it may even not do the job, if you are trying to access the highest spatial frequencies of a transmitted wavefront for instance. The method we developed is based upon laser beam diffraction intermediate



field measurements and their interpretation with a Fourier analysis and the Talbot effect theory. We demonstrated in previous papers that it is a credible alternative to classical methods. In this paper we go further by analyzing main error sources (source, pupil shape and position, ghost light...) and discussing main practical difficulties. We also show a qualification of the method thanks to cross-measurements with a Fizeau interferometer.

9575-47, Session PMon

Effect of aging on photoelectrical properties of AlInGaP LEDs

Donatas Me?kauskas, Laurynas Daba?inskas, Arturas ?ukauskas, Vilnius Univ. (Lithuania)

One of the advantages of light-emitting diodes (LEDs) against conventional sources of light is a slow degradation rather an abrupt burn-out. However, the physical reasons of the degradation of LEDs are not completely understood so far and require searching for new approaches to the characterization of LEDs. In this work we present results on the effect of aging on photoelectrical properties of AlGaInP LEDs (short-circuit photocurrent and photoconductivity sampled from differential photovoltage under excitation by modulated light). Commercial high-power AlGaInP LEDs with the peak wavelength of 640 nm were investigated during the stress by rated forward current. At the interruptions of the aging process, the photoelectrical properties of the LEDs were investigated using photoexcitation by shorter-wavelength radiation. Also, common I-V and L-I characteristics were measured. After about three hours of aging, the LEDs exhibited a minimum of short-circuit photocurrent, the highest effect of photoconductivity on the reduction of series resistance, the highest value of the ideality factor, and a drop of radiant output at low forward currents. Within the subsequent 1000 hours, these parameters restored to their initial values. The observed non-monotonous behavior of the photoelectrical properties of LEDs under aging was attributed to the rearrangement of defects in the semiconductor structure due to self-annealing caused by electrical, thermal and photo-induced processes. Our results indicate on the usefulness of photoelectrical properties for understanding the aging effects of LEDs.

9575-48, Session PMon

Noninvasive method for determination of parameters of cemented doublet

Petr Pokorn?, Antonín Mik?, Jirí Novák, Pavel Novák, Czech Technical Univ. in Prague (Czech Republic)

A cemented doublet is a very frequently used optical element in the design of various optical systems, which is composed of two lenses cemented together where the second radius of curvature of the first lens and the first radius of curvature of the second lens is identical. In practice it is often needed to analyze the unknown geometrical and optical parameters of the cemented doublet in a non-destructive way without a separation of individual lenses of the doublet.

In our work we propose and analyze an experimental method for the determination of internal parameters of the doublet on a basis of measurement external geometric parameters and paraxial properties and aberrations of the doublet. We describe a procedure for the calculation of unknown parameters of the doublet from experimentally measured geometrical and optical parameters of the doublet using an optimization method. The method calculates unknown parameters (central thicknesses, refractive indices, and second radius of curvature) in such a way that it corresponds to experimentally measured parameters of the doublet. It is also analyzed an influence of individual measured input parameters on uncertainties in calculated geometrical and optical parameters of the doublet. This method is nondestructive and one can determine internal parameters of the doublet without any damage to the doublet. The proposed method and analysis can be also used for the determination of parameters of fluidic lenses with a variable focal length. The method is presented on several examples.

9575-50, Session PMon

Detection of subsurface defects and measurement of thickness of screen layers made of graphene and carbon nanotubes with application of full-field optical coherence tomography in Linnik configuration

Paulina Mlynarska, Slawomir Tomczewski, Anna Paku?a, Grzegorz Wróblewski, Marcin Sloma, Leszek Salbut, Warsaw Univ. of Technology (Poland)

Optical coherence tomography (OCT) is a noncontact and a nondestructive interferometric method which allows visualization of an internal structure of investigated sample. Till now it has found many applications in measurements of biological tissues, technical materials and conservation of art. Optical coherence tomography in full-field configuration is a great technique for visualization of subsurface structures of measured sample with high resolution. In this technique en-face data acquisition is applied, enabled by application of high numerical aperture microscope objectives therefore the depth of focus. Microscopes objectives allow obtaining ultra high transverse resolution like in traditional microscopy. Additionally light source with broad spectrum, like cheap incandescent lamps, allow obtaining micrometer scale axial resolution.

In this paper authors present application of full-field optical coherence tomography with Linnik microscope for measurement of thickness of screen layers made of graphene and carbone nanotubes. Thickness has a huge impact on a layer resistivity. There is a direct correlation between the thickness of graphene layer and its electrical resistance. Graphene is a new and very promising material, which is durable, flexible and has a good adhesion to diverse substrates. It gives a theoretical possibility to create flexible electronics, such as graphene bendable screens. The aim is to obtain uniformly luminous surface - that means a surface of constant resistance. To reach this goal a method of precise measurement of the graphene layer thickness is required. Using proposed OCT setup we can evaluate the quality of printed layer and detect subsurface damages.

9575-51, Session PMon

Subsurface damage characterization with nonlinear high-numerical microscopy

Phat Lu, Thomas D. Milster, The Univ. of Arizona (United States)

Sub-surface damage characterization occurs in semiconductor device fabrication, like diamond turning and milling. Third harmonic generation (THG) microscopy can help to characterize subsurface damage, because nanometer sized asperities caused by defects amplify the THG signal. The goal is to investigate the theory of the THG field of enhancement due to the defects, as well as the possibility to apply the theory in surface and subsurface characterization. With the use of solid immersion lens, a higher resolution can be achieve at the same time.

9575-52, Session PMon

Comparison of experimental and simulation results of pupil plane polarization effects in a 1.6 numerical aperture solid immersion lens microscope from surface and subsurface damage

Victor E. Densmore, Phat Lu, Young-Sik Kim, The Univ. of Arizona (United States); Geon-Hee Kim, Korea Basic Science Institute (Korea, Republic of); Thomas D. Milster,



The Univ. of Arizona (United States)

Precision fabrication of brittle material surfaces is an important aspect of many high-technology products. These fabrication techniques often produce some amount of surface microstructure and sub-surface damage, both of which can be detrimental to device performance. Therefore, testing for surface variations and subsurface damage is critical for the successful production of high-performance devices. A solid immersion lens microscope (NA=1.6) has been designed to provide a means for high resolution, nondestructive testing of optical surfaces by using pupil plane polarimetry. Relationships between the defect geometries and polarization effects in the pupil plane are not known a priori. As such, simulation methods adapting rigorously coupled wave theory are explored and compared to experimental data. Reference samples are precision fabricated with nano-features from a focused ion beam machine to serve as a baseline and validate the high-NA solid immersion lens microscope in conjunction with polarization modulated pupil plane imaging as a means for surface and subsurface damage detection in optical materials.

9575-53, Session PMon

Designing null phase screens to test a fast plano-convex aspheric lens

Jesús DelOImo-Márquez, Diana N. Castán-Ricaño, Maximino M. Avendaño-Alejo, Jose Rufino Díaz-Uribe, Univ. Nacional Autónoma de México (Mexico)

We have obtained a formula to represent the wavefront produced by a plano-convex aspheric lens with symmetry of revolution considering a plane wavefront propagating parallel to the optical axis and impinging on the refracting surface, it is called a phase-zero wavefront. As is well know the phase-zero wavefront is the first wavefront to be out of the optical system. Using a concept of differential geometry called parallel curves it is possible to obtain an analytic formula to represent the wavefront propagated at arbitrary distances through the optical axis. We modify an interferometer Tywman-Green in order to evaluate guantitatively a plano-convex aspheric lens as follow: In the reference beam we use a plane mirror and the test beam we use a light spatial modulator SLM to compensate the phase produced by the lens under test. It will be called a null phase interferometer. The main idea is to recombine both wavefronts in order to get a null interferogram, otherwise we will associate the patterns of the interferogram to deformations of the lens under test. The null phase screens are formed with concentric circumferences assuming different gray levels printed on SLM.

9575-54, Session PMon

Null screens type Hartmann to test simple lenses

Alfredo Gozález-Galindo, Gabriel Castillo-Santiago, Maximino M. Avendaño-Alejo, Jose Rufino Díaz-Uribe, Univ. Nacional Autónoma de México (Mexico)

In order to evaluate either qualitative or quantitatively the shape of fast plano-convex aspheric lenses, a method to design null screens type Ronchi-Hartmann is proposed. The null screens are formed with non-uniform spots, which allow us to have uniform images at detection's plane. The screens are printed on a foil sheet and placed in front of the lens under test, they are illuminated with a collimated monochromatic beam propagating along the optical axis, in such a way that through the process of refraction will form a uniform spot patterns which are recorded at a predefined plane of detection, finally processing its image recorded we could be able to get a quantitative evaluation of the lens under test. The designs of these null screens are based on the equations of the caustic surface produced by refraction. The null screens can be printed in gray levels on a foil sheet. A preliminary test for a fast plano-convex aspheric lens with F/# = 0:8 is presented in this work. This method also could be applied to alignment of optical systems.

9575-55, Session PMon

Fringe projection method to evaluate the quality of the shape of a parabolic solar collector

Agustín Santiago-Alvarado, Univ. Tecnológica de la Mixteca (Mexico); Eduardo Torres Moreno, Victor I. Moreno-Oliva, Univ. del Istmo (Mexico); Moisés E. Ramírez Guzmán, Cuauhtémoc H. Castañeda Roldan, Ángel S. Cruz-Félix, Univ. Tecnológica de la Mixteca (Mexico)

Fringe projection technique has been widely used for 3D objects reconstruction and some of the reported applications of this technique include the digitalization of museum archeological pieces and the evaluation of reflective surfaces. In this work we apply this technique to evaluate the surface shape of a parabolic trough solar collector that employs wind turbines and are used in low power aerogenerators. The evaluation process consist in the projection of lines over the surface under study and to capture the reflexion of such lines by means of a CCD, later a pre-processing method is performed for the smoothing, thinning, skeletonization and discretization of the captured image fringes. Finally, the spot centroids are found to perform the integration of the information in order to obtain the surface shape. We apply genetic algorithms and linear programming to obtain the analytical form of the best fit shape. We show preliminary results.

9575-56, Session PMon

Estimation of optimal parameters of material removal by milling to minimize the surface roughness

Agustín Santiago-Alvarado, Orquídea Sánchez López, Ignacio Hernández Castillo, Cuauhtémoc H. Castañeda Roldán, Ángel S. Cruz-Félix, Univ. Tecnológica de la Mixteca (Mexico)

Different processes of material removal are used in the manufacture of industrial components and milling by computerized numerical control (CNC) is one of the most used; several machining milling parameters have to be considered such like the cut velocity, feed rate, work piece material and coating of the cutting tool among others. The election of the parameter have influence in the surface quality of the finished piece, and they determine the manufacture cost. In this work we determine the optimal values of the following milling parameters: cut velocity, cut depth and feed rate. We employ stainless steel as machine tool and we used the surface response method and genetic algorithms in order to obtain mathematical models to estimate surface roughness. On the other hand, we employed an interferometric test and a profilometer for the measurement of the roughness of the finished piece.

9575-30, Session 7

Measuring the tilt and decenter of biaspheric lenses

Scott DeFisher, Mitchell Sedore, David E. Mohring, OptiPro Systems (United States)

Wedge and centration are common measures for optical lenses and are characterized using accurate spindles and run-out indicators. These parameters are both defined relative to the edge of a lens. Tilt and decenter are defined as a relationship between the upper and lower optical surfaces regardless of the edge. A technique will be presented in this paper to measure and calculate the tilt and decenter of bi-aspheric lenses using contact and non-contact profilometry. The method employs a specially designed kinematic mount. The bi-aspheric lens is fixed in the center with both optical surfaces exposed. Three spheres on the perimeter of the mount



are used as the reference for each measured trace. The tilt, decenter, form error, and thickness between of the two aspheric surfaces are calculated with a registration and alignment algorithm. Multiple diametral traces are recorded for each aspheric surface to ensure tilt and decenter are calculated in two dimensions. A standard contact profilometer with a programmable rotation and translation stage were used to perform the measurements. In-addition, the methodology was implemented on a multi-axis, non-contact metrology system for nearly automatic operation. The contact profilometer employs stylus with a micron sized diamond tip or millimeter sized ruby sphere. The non-contact system measures with a single point chromatic confocal sensor. Results will be presented from both contact and noncontact metrology systems.

9575-31, Session 7

Bamboo book stitching interferometer

Po-Chih Lin, Chao-Wen Liang, Yi-Chun Chen, Hung-Sheng Chang, Jia-Wei Chen, National Central Univ. (Taiwan)

Aspherical optical surface testing has always been considered a crucial challenge. There are several methods being used to evaluate this task such as stylus profiler, null optics, CGH and subaperture stitching interferometer (SSI). Among of them, the SSI has been proved to be the only method to be non-contact, flexible, high dynamic range, and high precision. However, it still has limitation for measuring steep aspherical surface since the fringe resolvable region of the subaperture can be small. In order to stitch the adjacent sub-aperture taken in SSI measurement, the number of sub-apertures must to be increased at the cost increasing number of sub apertures and thus time. Or, one can use the auxiliary null optics to null the sub aperture aberration for maximum resolvable fringe area.

In this research, we utilize the vibration modulated interferometer to acquire the interference phase while the tested lens is rotating. Instead of nulling the fringe over the complete sub-aperture as before, we null the fringe only along the tangential and sagittal directions. By nulling the fringe along a line, the capability of aspherical surface measuring of the vibration interferometer is significantly increased. After the line interference phase is recovered, the line phases of different directions are stitched in to a complete tested surface in a similar way as the ancient Chinese bamboo book.

9575-32, Session 7

Subaperture stitching surface errors due to noise in a circular subaperture ring

Greg A. Smith, James H. Burge, The Univ. of Arizona (United States)

Subaperture stitching is a popular method for extending small, subaperture interferometer measurements to cover large-aperture optics. The method is simple in that there are only two steps: 1) make multiple measurements across the surface and 2) use well-established software techniques to merge the individual measurements into one surface estimate. Because parts of the system must move between measurements, small misalignments between subapertures are unavoidable, but easily accommodated within the software. Unfortunately this process has the potential to introduce errors.

In this work, we show how random noise in a circular ring of subapertures creates artifacts in low-order surface shape estimates. The magnitude of these errors depends on setup parameters such as the number of subapertures and their overlap, as well as the measurement noise within a single subaperture. Understanding the relationships between subaperture stitching configuration and surface artifacts is important when designing high-accuracy metrology systems which rely on stitching. This work will help metrology system designers incorporate subaperture stitching into error budgets and tolerances.

9575-33, Session 7

An iterative subaperture position correction algorithm

Weng-Hou Lo, Po-Chih Lin, Yi-Chun Chen, National Central Univ. (Taiwan)

??The subaperture stitching interferometry is a technique suitable for testing high numerical-aperture optics, large-diameter spherical lenses and aspheric optics. In the stitching process, each subaperture has to be placed at its correct position in the global coordinate, and the positioning precision would affect the accuracy of stitching result. However, the mechanical limitations in the alignment process as well as vibrations during the measurement would induce inevitable subaperture position uncertainties.

??In our previous study, a rotational scanning subaperture stitching interferometer has been constructed. This paper provides an iterative algorithm to correct the subaperture position without altering the interferometer configuration. Each subaperture is first placed at its geometric position estimated with the F number of reference lens, the measurement null angle and the number of pixels along the width of subaperture. By using the concept of differentiation, a shift compensator along the radial direction of the global coordinate is added into the stitching algorithm. The algorithm is divided into two parts: one with four compensators of piston, two direction tilts and defocus, and the other with the shift compensator. The two parts are computed iteratively to minimize the phase differences in the overlapped regions of subapertures on a least-squares sense. The simulation results demonstrate that the proposed method works to the precision of rounding errors both for the single-ring and multiple-ring measuring configurations. Preliminary verification with single-ring experimental data also shows the effectiveness of the algorithm. Further studies on multiple-ring experimental data are underway.

9575-38, Session 7

Wavefront analysis of a large sic mirror of 700 mm in diameter due to the surface figure error

Jinsuk Hong, Samsung Thales Co., Ltd. (Korea, Republic of)

SiC is very interesting material for mirror and structure for a large optical system working in a severe condition due to its thermal stability. However when manufacturing this material in a mirror form requires a lot of new techniques and analysis. We have been designed the system with SiC material and manufacturing SiC mirrors in various form up to 700mm in diameter. We've performed structural and optical analysis of the mirror itself and the system. We can confirm the manufacturability of the components assigning proper WFE budget to each component. We present the result of the wavefront error analysis in the component level as well as the system level.

9575-34, Session 8

Direct light scattering characterization of optical components

Sven Schröder, Alexander von Finck, Angela Duparré, Fraunhofer-Institut für Angewandte Optik und Feinmechanik (Germany)

Surface roughness is a critical parameter for the specification of an optical component in order to ensure a certain performance. The main reason is that even the smallest levels of residual surface roughness give rise to light scattering which degrades the imaging properties and reduces the throughput. However, surface defects, subsurface damage, interference effects caused by dielectric coatings, photonic structures, and rough absorbing structures also produce light scattering which is usually much



more complicated to describe. For some applications, scattering properties must therefore be carefully specified and measured directly. Bidirectional Reflectance and Transmittance Distribution Functions (BRDF / BTDF) are used to quantify the angle resolved scattering properties. The data can be used as an input for optical engineering software like FRED, ASAP, or ZEMAX for stray light modeling. In addition, analysis of the scattered light can provide valuable information about the relevant imperfections. The presentation provides an overview of instrumentation for light scattering measurements at wavelengths ranging from the visible to the extreme ultraviolet and the infrared spectral regions. Examples of applications will be discussed ranging from superpolished mirrors to diffraction gratings, interference coatings, and black absorbing coatings.

9575-35, Session 8

Roughness, homogeneity, and defect characterization using light scattering techniques

Sven Schröder, Marcus Trost, Tobias Herffurth, Angela Duparré, Fraunhofer-Institut für Angewandte Optik und Feinmechanik (Germany)

The assessment of surface properties like roughness, homogeneity, and the distribution of defects gains more and more importance in particular close to, or even in, manufacturing processes. Light scattering is a fast, non-contact, extremely robust, and at the same time highly sensitive approach to meeting this challenging requirement. Several tools will be presented that enable measurements to be performed even on very large (diameter > 600 mm) and curved surfaces with 100% coverage of the surface. Examples are discussed ranging from smooth mirrors to structured surfaces. Surface power spectral densities and surface roughness are determined from the scattering results and compared to results obtained by white light interferometry and atomic force microscopy. In addition to laboratory instruments, compact table-top tools and sensors are presented that can be used close to or even during manufacturing.

9575-36, Session 8

Measuring and quantifying scatter from non-isotropic sources

John C. Stover, The Scatter Works Inc. (United States)

The usual definition for BRDF assumes that the illuminated surface is isotropic. This is why when the primary source of scatter is a surface pit or particle the differential scattering cross-section is used to quantify scatter. In these cases the DSC is independent of changes in illumination spot size and thus is a more meaningful characterization than the measured BRDF. The same thing is true for other situations. These include scatter from isolated scratches, non-isotropic roughness (such as a rolled surface) and scatter from the edge or corner of a surface. In these situations the measurements may be done differently and the quantified scatter often has different units – such as area/sr or 1/deg instead of the common 1/sr associated with BRDF. If the data is being taken for use in one of the stray radiation codes this can cause problems. This paper reviews these situations for both measurement and analysis issues.

9575-37, Session 8

Fabrication and qualification of roughness reference samples for industrial testing of surface roughness levels below 0.5 nm Sq

Oliver W. Fähnle, Eckhard Langenbach, Frank Zygalsky, FISBA OPTIK AG (Switzerland); Frank Frost, Renate Fechner, Axel Schindler, Leibniz-Institut für Oberflächenmodifizierung e.V. (Germany); Matthias Cumme, Carl Zeiss Jena GmbH (Germany); Christine Wuensche, Heiko Biskup, Rolf Rascher, Technische Hochschule Deggendorf (Germany)

Applying reactive ion beam etching (RIBE) processes at the Leibniz Institute of Surface Modification (IOM), several reference samples to be used in industry for calibrating of roughness testing equipment have been generated with the smoothest sample featuring 0.1 nm rms Sq. Subsequently these reference samples have been measured cross-site in industry applying atomic force microscopy (AFM), white light interferometry (WLI), Nomarski microscopy (NM) and scatterometry (iTIRM) determining the appropriate range of measurable rms surface roughness for each industrial measuring device. This paper reports on the newly developed fabrication process to generate reference samples with sub-nanometer level of surface roughness in Si wafers. Especially the capability of generating different samples featuring the same level of roughness while differing in the generated surface spatial wavelength (e.g. 2 nm rms with 2, 4 and 10 micron waviness, respectively) is very useful for the calibration of measurement equipment. Their use as calibration samples has been demonstrated by carrying out cross-site tests in R&D and industry achieving good compliances between AFM, WLI, Nomarski and iTIRM.

9575-39, Session 9

Integrated Ray Tracing (IRT) simulation of SCOTS measurement of GMT fast steering mirror surface

Ji Nyeong Choi, Yonsei Univ (Korea, Republic of); Dongok Ryu, Sug-Whan Kim, Yonsei Univ. (Korea, Republic of); Dae Wook Kim, Peng Su, Run Huang, College of Optical Sciences, The Univ. of Arizona (United States)

Software Configurable Optical Testing System (SCOTS) is one of new testing methods for large mirror surfaces. Integrated Ray Tracing (IRT) technique can be applicable to the SCOTS simulation by performing end-to-end ray tracing in the real scale. In this study, we construct IRT SCOTS simulation model for Fast Steering Mirror (FSM) surface of Giant Magellan Telescope (GMT). GMT FSM is off-axis ellipsoidal concave mirror of 1064 mm diameter and PV 1.7 mm in aspheric departure. The surface error requirement is less than 20 nm rms. The screen is modeled as an array of 500 by 500 screen pixels of 0.2 mm in pitch size. The screen is considered as a lambertian scattering surface. The camera model has an iris of 1mm diameter, singlet in BK and a detector as an array of 125 by 125 pixels of 40 ?m in pitch size. The screen and the camera are positioned 4378 mm away from the mirror and separated by 70 mm from each other. Light source is 10 cycles of sinusoidal patterns generated by ten million rays per one screen pixel. 0.1 % of initially generated rays are finally received by the camera's detector and contribute to form distorted pattern images. These images are used and converted to the slope and height of the mirror surface. As a result, the height difference between input surface and reconstructed surface is 10.74 nm rms. The study also shows that the same SCOTS setup also useful to GMT FSM for measurement of the surface error from 10 nm to 1.0 ?m rms. Finally, this study shows applicability of IRT model to SCOTS simulation with nanometer level numerical accuracy.

9575-40, Session 9

Oil defect detection of electrowetting display

Hou-Chi Chiang, National Chiao Tung Univ. (Taiwan); Yu-Hsiang Tsai, Industrial Technology Research Institute (Taiwan); Yung-Jhe Yan, Ting-Wei Huang, Ou-Yang Mang, National Chiao Tung Univ. (Taiwan)

In recent years, transparent display is an emerging topic in display technologies. Apply in many fields just like mobile device, shopping or advertising window, and etc. Electrowetting Display (EWD) is one kind of



potential transparent display technology advantages of high transmittance, fast response time, high contrast and rich color with pigment based oil system. In mass production process of Electrowetting Display, oil defects should be found by Automated Optical Inspection (AOI) detection system. It is useful in determination of panel defects for quality control. According to the research of our group, we proposed a mechanism of AOI detection system detecting the different kinds of oil defects. This mechanism can detect different kinds of oil defect caused by oil overflow or material deteriorated after oil coating or driving. We had experimented our mechanism with a 6-inch Electrowetting Display panel from ITRI, using an Epson V750 scanner with 1200 dpi resolution. Two AOI algorithms were developed, which were high speed method and high precision method. In high precision method, oil jumping or non-recovered can be detected successfully. This mechanism of AOI detection system can be used to evaluate the oil uniformity in EWD panel process. In the future, our AOI detection system can be used in quality control of panel manufacturing for mass production.

9575-41, Session 9

Deflectometry measurement of Daniel K. Inouye Solar Telescope primary mirror

Run Huang, Peng Su, James H. Burge, The Univ. of Arizona (United States)

SCOTS (software configurable optical test system) is a high-precision slope measurement technique based on deflectometry. It utilizes well calibrated commercial LCD screen and diffraction limited camera to provide high dynamic range, non-contact and full field metrology of reflective/refractive optics at high accuracy but low cost. Recently, we applied this metrology method on the fabrication of the primary mirror of Daniel K. Inouye Solar Telescope (DKIST), which is a 4.2 meter off-axis parabolic segment with more than 9 mm peak-to-valley aspheric departure. Sophisticated calibrations and compensation including camera aperture, camera distortion and screen shape bending were performed to achieve high accuracy measurement results. Benefiting from the combination of phase shifting and line scanning method, the absolute slope of each mirror pixel can be calculated with short measurement time. By measuring the mirror at different orientations, non-symmetrical systematic errors are eliminated. The metrology system also includes dual cameras that provide verification test. The measurement results are being used to guide the fabrication process.

9575-42, Session 9

The use of diffractive imitator optics as calibration artefacts

Paul C. T. Rees, John B. Mitchell, Glyndwr Univ. (United Kingdom); Andy Volkov, Nanomobile Ltd. (United Kingdom); Jean-Michel Asfour, Frank Weidner, Dioptic GmbH (Germany); Alexander G. Poleshchuk, Ruslan K. Nasyrov, Institute of Automation and Electrometry (Russian Federation)

The testing of highly aspheric optics often requires complex test arrangements. Optical test systems designed for testing aspherical optical surfaces can be multi-element and will have both fabrication and alignment errors present in the test wavefront. It may not be feasible to calibrate such systems with conventional optical shop practice. The use of diffractive imitator optics, with carefully controlled fabrication uncertainties, can be used to characterise these systems.

We describe the use of reflective imitator CGH optics as calibration artefacts in the calibration of an optical test system used to test ELT primary mirror segments. The optical test system is designed to have two operational modes: one to measure a spherical reference optic; and one to measure the primary mirror segment. The use of diffractive imitators in this test system is designed to provide traceability between these two operational configurations, to quantify residual alignment aberrations, and to quantify fabrication errors in part of the test system. We outline the design of the optical test system, the design of three imitator CGH artefacts required to provide traceability between the two optical test modes, and our calibration approach.

We demonstrate the calibration performance achieved with this approach. Without the use of these imitator artefacts, the absolute accuracy of the optical test is estimated to be 136 nm RMS wavefront, of which 57 nm RMS is attributed to midspatial wavefront errors and 116 nm RMS is attributed to alignment and prescription errors. The repeatability of this calibration has been established as better than 7 nm wavefront standard deviation, with an absolute accuracy of 19 nm RMS wavefront.

9575-43, Session 9

Local frequency estimation from intensity gradients in spatial carrier fringe pattern analysis

Ruihua Zhang, Hongwei Guo, Shanghai Univ. (China)

Spatial carrier fringe pattern analysis is an effective tool in optical measurement, e.g. in interferometry and fringe projection technique. With it, the very large phase deformations in a spatial carrier fringe pattern may increases the bandwidth of fringe component thus leading to difficulties in retrieving its phase map. In order to overcome this problem, many localadaptive methods have been developed for processing the spatial carrier fringe pattern with large phase variations, and in fact the local spatial frequency estimation is central to these methods. This paper introduces a simple algorithm for estimating the local frequencies of a fringe pattern with spatial carrier. First, the intensity gradients of the fringe pattern are calculated, and then the standard deviations (SDs) of the intensity gradients at each pixel are estimated from its neighborhood. Finally the local frequencies are estimated from the SDs just calculated simply using an arccosine function. This algorithm is potential in developing effective techniques for retrieving phases from a spatial carrier fringe pattern with large phase variations. For example, we can recover the phase map by directly integrating the local frequencies or by use of an adaptive spatial carrier phase shifting algorithm (SCPS) with the local frequencies being the local phase shifts. It can also be used in Fourier transform method for exactly determining the carrier frequencies, or for extrapolating aperture in order to reduce the boundary effect. Combined with time-frequency techniques such as windowed Fourier transform and wavelet transform methods, it is helpful for alleviating the computational burdens.

9575-44, Session 9

Triple-wavelength phase unwrapping for dispersive objects

Behnam Tayebi, Yonsei Univ. (Korea, Republic of)

Here, we present a novel triple-wavelength unwrapping technique to measure phase of the dispersive objects without using unwrapping algorithms. Dual- wavelength method can unwrap phase of the reflective objects, successfully. However, for unwrapping transparent dispersive objects it is failed. Adding another wavelength and Cauchy equation allow us to unwrap dispersive objects without using numerical techniques. The feasibility of this technique is demonstrated experimentally.

Conference 9576: Applied Advanced Optical Metrology Solutions

Monday - Wednesday 10-12 August 2015 Part of Proceedings of SPIE Vol. 9576 Applied Advanced Optical Metrology Solutions

9576-23, Session PMon

Study of high-contrast mark used for imprint lithography alignment

Liang Wang, Li Ding, Jin Qin, Univ. of Science and Technology of China (China)

Moiré fringes for overlay used two sets of gratings with slightly different periods, which can magnify the tiny misalignment to an observable quantum. During imprint lithography alignment process, imprint resist will deteriorate the intensity and contrast of the Moiré fringes which is a drawback for high precision alignment. This paper proposed a novel high contrast alignment mark used for imprint lithography. Through coating optically dens materials inside or on the surface of the imprint mask and changing the material and thickness of coating, high contrast Moiré patterns can be obtained. Simulations based on Rigorous coupled-wave analysis (RCWA) are performed to calculate the reflection efficiency and contrast of the obtained Moiré fringes. We found that the coating material, thickness, etching depth and pitch size of grating all have significant influence on the reflection efficiency and contrast of alignment pattern. Optimized alignment marks were fabricated and measured to verify the findings. Experiments demonstrated that the simulation results are correct and feasible.

9576-25, Session PMon

Rapid three-dimensional chromoscan system of body surface based on digital fringe projection

Bin Wei, Jin Liang, Xi'an Jiaotong Univ. (China); Jie Li, Shijiazhuang Information Engineering Vocational College (China); Maodong Ren, Xi'an Jiaotong Univ. (China)

This paper proposes a rapid body scanning system that uses optical digital fringe projection method. Twelve cameras and four digital projectors are placed around the human body from four different directions, so that the body surface three-dimensional(3D) point cloud data can be scanned in 5~8 seconds. It can overcome many difficulties in a traditional measurement method, such as laser scanning causes damage to human eve and low splicing accuracy using structured white light scanning system. First, an accurate calibration method based on close-range photogrammetry, is proposed and verified for calibrating the twelve cameras and the four digital projectors simultaneously, where a 1m?2m plate as calibration target with feature points pasted on its two-sides is used. An experiment indicates that the proposed calibration method, with a re-projection error less than 0.05 pixels, has a considerable accuracy. The whole 3D body surface color point cloud data can be measured without splice different views of point cloud, because of the high accuracy calibration results. Then, in order to measure the whole body point cloud data with high accuracy, a combination of single and stereo camera measuring method, based on digital fringe projection, has presented to calculating 3D point cloud data. At last, a novel body chromoscan system is developed and a human body 3D digital model was scanned, by which a physical body model was manufactured using 3D printing technology.

9576-26, Session PMon

Two-detector digital holographic smart camera for holographic imaging and digital holographic interferometry

Jakub P. Zak, Michal Józwik, Malgorzata Kujawi?ska, Warsaw Univ. of Technology (Poland) Although digital holographic camera may be a versatile tool and digital holography itself experiences growing interest and development, it is still fairly limited. The most crucial problems are resolution and the size of a single pixel in available detectors. These parameters limit the size of an object that can be registered and its viewing angle. Also, the functionality and flexibility of the system in use for different 3D objects or scenes are strongly limited.

SPIE. PHOTONICS

OPTICAL ENGINEERING+

APPLICATIONS

In this paper we present the design and proof of concept of functionality of a monochromatic holographic camera system consisting of two matrix detectors and Liquid Crystal on Silicon Spatial Light Modulator. The device allows capturing both Fresnel and Fourier holograms in flexible configuration, matched to an object/scene requirements. The two detectors are meant to increase the viewing angle of the camera or even to create synthetic aperture holograms for static objects. The SLM serves as an active element in the reference arm of the system. The use of LCOS SLM enables:

- formation and modification of the reference beam(s) through designing and displaying a diffractive element in full or divided SLM aperture,

- execution of the Temporal Phase Shifting algorithm or introducing carrier frequency

A model of the camera was tested for a variety of engineering objects (loaded cylinder, a distributed group of objects under different load conditions) in imaging and DHI modes.

9576-27, Session PMon

Uncertainties in strain measurements with birefringence

José G. Suárez-Romero, Instituto Tecnológico de Querétaro (Mexico); Eduardo Hernandez-Gomez, Instituto Tecnologico de Queretaro (Mexico)

Strain is an important test applied to materials in order to measure its mechanical properties and to evaluate the suitability of mechanical components. There are many experimental methods to measure strain, for example by use of strain gages, by measure of capacitance changes, by moire methods and others, but a very accepted method is by birefringence. Birefringence has the characteristic that it can show the whole strain distribution of the tested piece in a visual way. Other methods measure strain only in a small region and give a mean value. In the case of birefringence can be properly used to validate numerical modulations in engineering, where techniques like finite element are used to model the mechanical performance of designs. Validation of numerical calculations is a procedure where the numerical results are compared with another accepted method whose reproducibility and uncertainty are known.

Therefore in this work the possible errors and uncertainties are analyzed. Between the possible errors introduced in the method is the difference of the poisson coefficient of the material to be analyzed and the poisson coefficient of the material used in the birefringence test. The difference between both coefficients is a source of error in the reproducibility of the results. The uncertainties considered are due to thinness of material, wavelength, the material optical constant and the order of diffraction. The most important source of uncertainty is the order of diffraction, when the orders take values close to one.

9576-28, Session PMon

Evaluation of optical surfaces using heuristic techniques in the information integration stage

Agustín Santiago-Alvarado, Moisés E. Ramírez Guzmán, Erik G. Ramos Pérez, José Y. Luis-García, Ángel S. Cruz-

Conference 9576: Applied Advanced Optical Metrology Solutions



Félix, Univ. Tecnológica de la Mixteca (Mexico)

There exist a large amount of interferometric methods that are used to evaluate optical surfaces and several of them use the implementation of an optical device that is placed right in the area where light is concentrated. However, when the optical surface does not concentrate the light in a single spot, these methods are impossible to use and alternative techniques are developed in order to being used in such cases. By means of certain implemented measurements, these techniques acquire a set of points coordinates over the surface under study and then an integration process is performed in order to obtain the surface profile. In this work, several heuristic techniques are studied in order to know which of them perform a best integration process of the set of points to obtain the surface profile. The time on which the process is done to evaluate the surface is analyzed as the precision achieved of each one of them. The obtained results and analysis from the evaluation of the surface of a parabolic solar collector are presented

9576-29, Session PMon

A model to perform bandwidth-spectralcorrection in spectrophotometers

Juan B. Hurtado-Ramos, Paulina Arrieta-Navarro, Instituto Politécnico Nacional (Mexico); José G. Suárez-Romero, Instituto Tecnológico de Querétaro (Mexico)

Two functions for modeling a spectrophotometer line-spread characteristic function are analyzed. These models are used to calculate the corrected spectral transmittance of holmium oxide and didymium oxide, which are often used as calibration standards. Correction is carried out through Fourier transform techniques; we show a comparison between the spectral transmittance measured with a 4 nm bandwidth spectrophotometer corrected with our technique, and the spectral transmittance measured with a 0.1 nm bandwidth spectrophotometer.

9576-30, Session PMon

Auto-elimination of fiber optical pathlength drift in a frequency scanning interferometer for absolute distance measurements

Long Tao, Zhigang Liu, Weibo Zhang, Xi'an Jiaotong Univ. (China)

Because of its compact size and portability, optical fiber has been wildly used as optical paths in frequency-scanning interferometers for highprecision absolute distance measurements. However, since the fiber is sensitive to ambient temperature, its length and refractive index change with temperature, resulting in an optical path length drift that influences the repeatability of measurements. To improve the thermal stability of the measurement system, a novel frequency-scanning interferometer composed of two Michelson-type interferometers sharing a common fiber optical path is proposed. One interferometer defined as origin interferometer is used to monitor the drift of the measurement origin due to the optical path length drift of the optical fiber under on-site environment. The other interferometer defined as measurement interferometer is used to measure the distance to the target. Because the optical path length drift of the fiber appears in both interferometers, its influence can be eliminated by subtracting the optical path difference of the origin interferometer from the optical path difference of the measurement interferometer. A prototype interferometer was developed in our research, and experimental results demonstrate its robustness and stability. Under on-site environment, an accuracy about 4 ?m was achieved for a distance of about 1 m.

9576-1, Session 1

A rugged stereoscopical device for surface inspection

Florian Dannenberg, Cornelius F. Hahlweg, bbw Hochschule (Germany); Lukas Pescoller, Peret GmbH (Italy)

The paper is understood as a continuation of a series of papers on surface metrology for application in quality control of printed matter. A stereoscopic method for extremely rugged applications, expecially in quality controk in printing industry, is presented. The deivce developed is based on variable tilted delay elements, which allow the use of a single imaging sensor and robust definition of parallax shift. Variable orthogonal delay elements were already used for variation of plane of focus in surface inspection, as described in previous papers. The method can be applied for macroscopical as well as for microscopical imaging. Beside mechanical design issues, the theoretical descirption, geometrical-optical approaches, Fourier-optical aspects, polarization issues, and especially the treatment of the dispersion problem are discussed. Experimental results are included.

9576-2, Session 1

In-line roll-to-roll metrology for flexible electronics

Bradley T. Kimbrough, 4D Technology Corp. (United States)

The flexible electronics market continues to grow at a rapid pace. Increasing numbers of applications employ the flexible components including displays, biomedical devices, smart apparel, and advanced sensors. To maintain performance and lifetime, many characteristics of the substrate and deposited layers must be monitored. This includes defects, surface roughness, and feature alignment. Ideally, in-situ metrology can be employed in roll-to-roll (R2R) equipment to allow for real-time process control. This presents the necessary three-dimensional metrology system with several challenging requirements: high vertical and transverse resolution, large field-of-view, extremely fast measurement times, and robust vibration immunity.

This paper will discuss the design and performance of a compact, low-cost, large-field interferometric probe for in-situ measurement of R2R substrates. Samples with a variety of known and unknown features and roughnesses will be measured to characterize the performance of the system. Static and moving substrates will be measured to examine effects on results. Optimization of processing to allow for on-board analysis will be examined. Lastly, the paper will discuss how such probes may be arrayed to provide a high degree of areal coverage of the flexible substrate under test.

9576-3, Session 1

Three-dimensional speckle imaging employing a frequency-locked tunable diode laser

Bret D. Cannon, Bruce E. Bernacki, John T. Schiffern, Albert M. Mendoza, Pacific Northwest National Lab. (United States)

We describe a high accuracy frequency stepping method for a tunable diode laser to improve a three dimensional (3D) imaging approach based upon interferometric speckle imaging. The approach, modeled after Takeda, exploits tuning an illumination laser in frequency as speckle interferograms of the object (specklegrams) are acquired at each frequency in a Michelson interferometer. The resulting 3D hypercube of specklegrams encode spatial information in the x-y plane of each image with laser fourier Transformation (FFT) along the z-axis of the hypercube and the center of the peak in



the resulting power spectrum for each pixel encodes its surface height. Alternatively, Takeda's method can be followed which uses the phase of the FFT, unwraps it, and determines the surface height encoded in the slope of a line fitted to the phase. Wraparound of modulations above the Nyquist limit results in ambiguity in the optical path difference (OPD) between test and reference surfaces. Wraparound also amplifies measurement noise caused by errors and jitter in frequency stepping the illumination laser. By locking the laser frequency to successive cavity modes of a reference confocal interferometer, tuning is precisely controlled resulting in dramatically improved imaging accuracy. We present laboratory data of before and after results showing enhanced 3D imaging resulting from precise laser frequency control.

9576-4, Session 1

Aperiodic sinusoidal fringes in comparison to phase-shifted sinusoidal fringes for high-speed three-dimensional shape measurement

Stefan Heist, Peter Lutzke, Peter Kühmstedt, Fraunhofer-Institut für Angewandte Optik und Feinmechanik (Germany); Gunther Notni, Technische Univ. Ilmenau (Germany)

Reconstructing the three-dimensional (3D) surface shape of moving objects or deformation processes has become an important task in many application areas, such as in-line quality control or medical sciences. Structured-light 3D scanners are well-established for performing these measurements since they allow full-field measurement and contactless operation. However, their measurement speed is limited by both camera and projector frame rate. Whereas high-speed cameras have been commercially available for some time, efforts are still necessary to develop high-speed projectors.

In previous contributions, we presented an array projector, enabling projection frame rates of several 10 kHz. In contrast to a large number of 3D sensors, instead of projecting well-known phase-shifted sinusoidal fringes, aperiodic sinusoidal fringes are projected onto the measurement object and observed by two cameras. Instead of comparing phase values, homologous pixels are found by cross-correlation.

In this contribution, we want to analyze the similarities and differences between both approaches. In particular, this includes theoretical considerations on designing a sequence of aperiodic sinusoidal fringes that leads to an accuracy as well as completeness of the 3D point cloud as high as possible. The results of extensive simulations of a specific 3D sensor setup are presented, and the achievable accuracy of both pattern approaches is compared.

The subsequent experimental investigations are based on the simulated sensor setup and include comparative measurements of different test specimens. The experimental results are discussed and compared with the simulated results. The main purposes are to derive criteria for the design of optimal sequences of aperiodic sinusoidal fringes and to compare the number of patterns of both approaches necessary for comparable accuracies.

9576-5, Session 1

Development of three-dimensional speckle deformation measurement method with same sensitivities in three directions

Yasuhiko Arai, Kansai Univ. (Japan)

The speckle interferometry is a useful optical deformation measurement method concerning the object with rough surfaces. The speckle interferometry has been improved to the electronic speckle pattern interferometry, ESPI, by introducing some TV technologies. Furthermore, the high resolution deformation measurement methods have been developed by using fringe scanning methods in the 1980s. The deformation measurement method by using only two speckle pattern has also been proposed in ESPI by using Fourier transform. Then, the method can perform not only the out-of-plane but also the in-plane deformation measurement of the objects with rough surfaces in high resolution. The methods can also measure three-dimensional deformation. Some kinds of the three-dimensional deformation measurement methods based on the speckle interferometry have been proposed. However, the sensibilities of ordinary methods in three directions are not always same. Generally, the parameters in sensibility matrices of these methods are not same in each direction. In this paper, the novel analysis method of which sensibilities in three directions are same is proposed. The optical system is set up under the idea of the proposed method. The multi-recording technology of the signals of the deformations in three dimensional using one camera is employed.

The feature of the measurement based on the multi-recording technology of the signals is investigated. Then, it is confirmed that there is not difference between the single and the multi recording-methods in the measuring accuracy. From the experimental results, the validity of the novel method is confirmed.

9576-6, Session 1

3D interferometric microscope: visualization of sample in real color appearance benefits industrial samples assessment

Joanna Schmit, Matt Novak, Bruker Nano Surfaces, Inc. (United States)

3D microscopes based on white light interference [1] which scan vertically for height data collection provide excellent vertical resolution and very good lateral resolution for surface topography measurements in industry.

Besides the precise measurement of a sample, often the display of an object in its true colors, as observed under white light illumination, is desired [2,3,4]. Color images are not only appealing to the eye and great for presentations, but also may provide a very useful and quick evaluation of certain characteristics of the sample, such as defects, delamination, or deposition of different materials.

In order to digitally observe a sample in its natural color, at minimum white light illumination and a color camera are needed, or a combination of RGB (three) cameras and a white light or RGB source. Separate RGB illumination sources and a B&W camera also can be used. Some considerations need to be made when choosing the illumination-camera combination as different options affect the lateral or vertical system resolution, add system cost or increase the system to a much larger size. Some choices also may significantly slow down the measurement if, for example, RGB illumination is sequential.

Interferometric objectives deliver excellent 3D topography, but good quality color determination is not straightforward as in the use of standard bright-field objectives[2,3,4]. There are a few main issues that need to be overcome in acquisition of images using an interferometric objective, namely: the presence of interference fringes, poor color quality and low visibility of object features. The first issue is that fringes present at the best focus obscure the view of the sample and must be removed (e.g., by frames averaging around the best focus). The second issue is that interferometric objectives introduce additional background intensity from the reference mirror causing the image of low reflectivity samples to have low saturation and low contrast colors.

To illustrate these issues, the image of a paper sample as observed with a color camera and using a 5X Michelson interferometric objective under white light LED illumination can be examined. In standard scanning interferometric microscopes, such a sample exhibits little color content due to low reflectivity and the small numerical aperture of the objective. In addition, the sample itself is difficult to see under observation. However, enhanced interferometric color imaging can provide quality 3D mapping in a single interferometric scan and result in a satisfactory 3D color image.

We will show that 3D microscopes based on white light interferometry have color imaging capabilities similar to an ordinary microscope. This color imaging and precise surface topography measurement capability, along



with different degrees of process automation, makes 3D microscopes based on WLI a very attractive metrology tool for different automotive, medical or printing industry areas, where color images can also provide valuable information to the user.

[1] P. J. Caber, "Interferometric Profiler for Rough Surfaces", Appl. Opt. 32(19), 3438-3441 (1993).

[2] M. K. Kim, L. Yu, US Patent 7317540 Method of Full-Color Optical Coherence Tomography, 2008

[3] T. Machleidt, D. Kollhoff, O. Dathe, D. Kapusi, R. Nestler, K.-H. Franke ", Application of Color Cameras for 3D Surface Measurements with White Light Interferometers", 14th SpectroNet Collaboration Forum AM 05.09.2012 in Jena

[4] J. L. Beverage, X. Colonna De Lega, M. F. Fay, "Interferometric Microscope with True Color Imaging", Proceedings of SPIE Vol. 9203, 92030S (2014)

9576-7, Session 2

Binary pseudorandom test standard to determine the modulation transfer function of optical microscopes

Ian Lacey, Valeriy V. Yashchuk, Erik H. Anderson, Nikolay A. Artemiev, Lawrence Berkeley National Lab. (United States); Christophe Peroz, Sergey Babin, Guiseppe Calafiore, Abeam Technologies, Inc. (United States); Elaine R. Chan, Stefano Cabrini, Lawrence Berkeley National Lab. (United States); Peter Z. Takacs, Brookhaven National Lab. (United States)

This work reports on the development of a binary pseudo-random test sample optimized to calibrate the MTF of optical microscopes. The sample consists of a number of 1-D and 2-D patterns, with different minimum sizes of spatial artifacts from 300 nm to 2 microns. We describe the mathematical background, fabrication process, data acquisition and analysis procedure to return spatial frequency based instrument calibration. We show that the developed samples satisfy the characteristics of a test standard: functionality, ease of specification and fabrication, reproducibility, and low sensitivity to manufacturing error. This work was supported in part by the UC Office of the President, Proof of Concept Grant ID No. 268826 and by the U.S. Department of Energy Office of Science, Office of Basic Energy Sciences Energy Small Business Technology Transfer (STTR) program under Award Number DE-SC0011352, and by the U. S. Department of Energy under contract number DE-AC02-05CH11231.

9576-8, Session 2

Performance analysis of a full-field fullrange swept-source OCT system

Johann Krauter, Institut für Technische Optik (Germany)

The optical coherence tomography (OCT) is an optical measurement technique that has been developed for ophthalmological applications at first. However, in dermatology the default analysis technique of malign tissues is still the traditional biopsy, whose drawback is a long diagnosis time and its invasiveness. Recent, OCT systems are also emerging in the traditional field of dermatology and permit non-invasive 3D optical biopsies of skin. In the research project VIAMOS (Vertically Integrated Array-type Mirau-based OCT System) an approach for a new generation of sensor systems for the skin analysis is developed. Micro-Opto-Electro-Mechanical Systems (MOEMS) enable a low-cost, miniaturized and hand-held OCT device. This concept combines swept-source OCT, full-field detection, phase-shifting interferometry and MOEMS, providing 3D tomograms of the human skin from a volume of 8 x 8 x 0.5 mm? with an axial and transverse resolution of 6 µm. The key component of this system is a wafer stacked 4 x 4 array detector. Each measurement channel consists of an active Mirau interferometer with an oscillating reference mirror, which introduces an

additional phase shift between the reference and object path.

A prototype OCT setup is developed in a laboratory environment based on the same design parameters as the final VIAMOS system. This reference setup uses a Linnik interferometer microscope with a swept-source, operating in the 850 nm range with a full-tuning range of 50 nm and a minimal linewidth of one single wavelength of 0.05 nm. The Linnik interferometer uses two equally infinity-corrected microscope objective lenses, where the reference path is mounted together with a Piezo-driven actuator for phase shifting.

This paper presents performance analysis of the signal detection process, focusing on the improvement of decreasing the complex conjugate artifact and system sensitivity analysis. At first, the sensor performance under ideal conditions is simulated and measured using the experimental setup. Furthermore influence of phase-shifter instabilities and a discussion of the system limitations are presented. The key figure of merit for OCT is the system sensitivity and resolution. For biological tissues the target values for sensitivity are more than 80 dB and a lateral and axial resolution of 5 μ m.

9576-9, Session 2

Framework for removal of outliers in highspeed fringe projection profilometry

Shijie Feng, Yuzhen Zhang, Qian Chen, Chao Zuo, Nanjing Univ. of Science and Technology (China)

Fringe projection profilometry combining with the temporal phase unwrapping is widely used for high-speed, real-time acquisition of threedimensional shapes. However, when the object is not motionless during the acquisition process, some unreliable results may emerge, especially around the contours of the measured object. The main reason for this is that the same point in the projected pattern sequence can map to different points within the camera images resulting from depth changes over time. We present a novel framework to identify those invalid pixels affected by such an error. By carefully examining the captured fringe pattern, comparing two modulation maps, utilizing the phase relationship between two neighboring pixels, and employing a Gaussian filter to detect the protruding points, the bad measurement pixels (outliers) can be detected and filtered out effectively. The whole procedure is of low computational complexity because of the introduced lookup table based fast data processing method. Some experimental results are presented to verify the validity of our method.

9576-10, Session 2

Geometric superresolution using an optical mask

Ihtsham U. Haq, Pakistan Council of Scientific & Industrial Research (Pakistan) and Pakistan Institute of Engineering and Applied Sciences (Pakistan); Asloob A. Mudassar, Pakistan Institute of Engineering and Applied Sciences (Pakistan); Ihtram U. Haq, A. Ikram, Univ. of Karachi (Pakistan); A. Haleem, S. Raja, Pakistan Council of Scientific and Industrial Research (PCSIR) (Pakistan)

Today, in everyday imaging in science and research, a digital imager – despite of its lower resolution than conventional film camera, is the first choice due to its obvious advantages. Assuming the imaging system to be diffraction limited, this low resolution is due to two geometrical characteristics of the detector array (CCD/CMOS) used in it at image plane. These two characteristics are pitch and non-zero pixel size – which do sampling and averaging of optical information over pixel spatial area respectively and dictates geometric resolution limit of digital imager.

In this paper, we are proposing an efficient optical mask for achieving geometric super-resolution – having high SNR. Keeping the target-imager relatively static, the mask is scanned over CCD by one pixel in subpixel steps. The mask optically codes the image. The resulting coded digital images are then decoded computationally to get a superresolved image –



enhanced in resolution by subpixel step factor N. By this, each CCD-pixel is virtually resolved into a matrix of subpixels. The proposed mask has an intelligent profile design that lead to high SNR, quick computation, always stable and solvable solution. The mathematical model developed for the proposed scanning methodology is efficient enough to calculate result quickly in just one mathematical step.

The 2D simulation results are presented – showing an improvement in resolution by given super-resolution factor - in both x and y directions. Increasing the super-resolution factor more makes the result more close to original. The given superresolution technique can be applied to microscopy, medical imaging, machine vision, industrial inspection, metrology (specifically dimensional metrology), defense, satellite imaging and astronomy.

9576-11, Session 3

Digital focusing schlieren imaging

Benjamin D. Buckner, Spectabit Optics, LLC (United States); James D. Trolinger, MetroLaser, Inc. (United States); Drew M. L'Esperance, Spectabit Optics, LLC (United States) and Pomona College (United States)

Since its invention in the 19th century, schlieren imaging has been an essential method for studying many aerodynamic effects, particularly convection and shock waves, but the classical method using parabolic mirrors is extremely difficult to set up and very expensive for large fields of view. Focusing schlieren methods have made large- area schlieren more feasible but have tended to be difficult to align and set up, limiting their utility in many applications We recently developed an alternative approach which utilizes recent advances in digital display technology to produce simpler schlieren system that yields similar sensitivity with greater flexibility.

The digital schlieren concept combines analog optical components, most significantly a cutoff grid (usually a Ronchi ruling), with a digital display device such as a flat screen television or digital projector. A portable computer and digital camera measure the transmission of the cutoff grid and compute a complementary display in the background. This digital measurement step obviates many of the long-standing problems with focusing schlieren techniques that are associated with precisely matching the cutoff grid to the background light pattern. Because the system is digital, the control software has great freedom to perform real-time image enhancement as well. Consequently, the most severe hardware production and alignment restrictions are now software problems that are solved continuously, quickly, and inexpensively in real time. This capability enables the system to compute and compensate for imperfect windows and optics, optical aberrations, misalignments, and temporal changes in the system and subject.

9576-12, Session 3

Digital speckle-based stereo microscope strain measurement system for forming limit diagram prediction by hydraulic bulge tests

Maodong Ren, Jin Liang, Lizhong Wang, Bin Wei, Xi'an Jiaotong Univ. (China)

A digital speckle based stereo microscope strain measurement system is developed to investigate the forming limit diagram (FLD) of miniature sheet metal under hydraulic bulge testing conditions. A stochastic speckle pattern is sprayed on the surface of the tested metal before forming. A series of images are recorded by two cameras mounted on a binocular stereo microscope during the hydroforming process. The critical major and minor strains are then calculated and plotted to construct the forming limit curve. The key technologies applied in the system are discussed in detail, including stereo microscope calibration and large deformation strain filed determination. First, considering complex optical paths and high magnification of the stereo microscope, an accurate orthogonal projection model is proposed to optimize the intrinsic and extrinsic parameters of the stereo microscope. Then, to solve the problem of strain measurement of the tested metal in large deformation situation, a three dimensional strain calculation method is specially used to calculate the full-field strains. And an algorithm of limit strain determination based on spline model is proposed to calculate the critical strains at the onset of plastic instability. Finally, with our self-developed stereo microscope imaging system and sheet metal hydraulic bulging setup, FLD determination tests are conducted to validate the performance of the system. And the measured FLD is compared with the traditional experimental FLD as well as with that predicted by the finite element method. The simulation and experimental results confirm that the proposed system is feasible to measure the full-field strain during the whole bulging processes and provides a better solution for forming limit diagram prediction.

9576-13, Session 3

Background-oriented schlieren for the study of large flow fields

James D. Trolinger, MetroLaser, Inc. (United States); Benjamin D. Buckner, Spectabit Optics, LLC (United States)

Flow fields around large structures are difficult to observe because of the size of optics typically employed with conventional flow visualization systems like shadowgraph, schlieren, and interferometry. More recently, digital imaging and processing methods have allowed extending these methods to cover much larger fields of view. Background oriented schlieren imaging enables analysis of refractive index gradients in large fields of view by observing the effects on an image of a background structure behind the field. This is achieved computationally by subtracting reference backgrounds from the distorted background images and inverting the difference to extract information about the refractive index field. The background can be a natural structure, such as a cloudy sky, mountains, trees, or the ground or in some cases a specially designed backdrop. Applications include observing flow fields associated with full sized aircraft, helicopters, automobiles, explosives, and buildings. This paper presents some of the applications and measurement capabilities in aero optics and explosives testing.

9576-14, Session 3

Interferometric strain measurements with a fiber-optic probe

Ethan D. Burnham-Fay, Douglas Jacobs-Perkins, Jonathan D. Ellis, Univ. of Rochester (United States)

Experience at the Laboratory for Laser Energetics has shown that broadband base vibrations presents difficulty in positioning cryogenic inertial confinement fusion targets. These effects must be mitigated for National Ignition Facility scale targets; to this end an active vibration stabilization system is proposed. A single mode optical fiber strain probe and a novel fiber contained heterodyne interferometer have been developed as a position feedback sensor for the vibration control system. A resolution limit of \$54.5\$-n\$epsilon\$ is measured with the optical strain gauge, limited by the Lock In Amplifier. Experimental measurements of the sensor are presented, which show good agreement with reference resistive strain gauge measurements.

9576-15, Session 3

An iterative approach to measuring twodimensional gradient-index profiles based on external measurements of laser beam deflection

Di Lin, James R. Leger, Univ. of Minnesota, Twin Cities (United States)



We present a numerical method for calculating the refractive index profile of two-dimensional gradient-index optical materials. Using boundary values of ray position and angle obtained by deflectometry to approximate trajectories for the measured interrogating rays, we show that the inverse problem can be reduced to a sparse linear system. The linear system is subsequently inverted using the LSQR method to obtain the refractive index distribution. We demonstrate our method through simulation and reconstruct the index profile of a hypothetical rectangular gradient-index medium, where RMS index errors below 0.5% of the index range (n_max-n_ min) are achieved if boundary values of the refractive index are measured. If the boundary values of the refractive index are unknown, we take an iterative approach to obtain a solution that is consistent with Snell's law of refraction at the boundaries of the gradient-index medium. We demonstrate our technique in simulation and reconstruct the test index distribution from ray angles measured outside the gradient-index medium, resulting in RMS index errors below 1% of the index range. In addition, the approximate ray trajectories used initially for solving the inverse problem are corrected through an iterative ray trace procedure until the solution becomes consistent with the ray equation of geometric optics. Furthermore, we identify three primary sources of error contributing to the inversion process and assess the importance of data redundancy and system conditioning in accurate reconstructions of the index distribution. The principles developed in our method are fully extendable to three-dimensions as well as more complex geometries.

9576-16, Session 4

Three-dimensional digital holographic aperture synthesis for rapid and highlyaccurate large-volume metrology

Randy R. Reibel, Brant M. Kaylor, Stephen Crouch, Bridger Photonics, Inc. (United States); Zeb Barber, Montana State Univ. (United States)

Currently large volume, high accuracy three-dimensional (3D) metrology is dominated by laser trackers, which typically utilize a laser scanner and cooperative reflector to estimate points on a given surface. The dependency upon the placement of cooperative targets dramatically inhibits the speed at which metrology can be conducted. To increase speed, laser scanners or structured illumination systems can be used directly on the surface of interest. Both approaches are restricted in their axial and lateral resolution at longer stand-off distances due to the diffraction limit of the optics used. Holographic aperture ladar (HAL) and synthetic aperture ladar (SAL) can enhance the lateral resolution of an imaging system by synthesizing much larger apertures by digitally combining measurements from multiple smaller apertures. Both of these approaches only produce two-dimensional imagery and are therefore not suitable for large-volume 3D metrology. We combined the SAL and HAL approaches to create a swept frequency digital holographic 3D imaging system that provides rapid measurement speed for surface coverage with unprecedented axial and lateral resolution at longer standoff ranges. The technique yields a "data cube" of Fourier domain data, which can be processed with a 3D Fourier transform to reveal a 3D estimate of the surface. In this talk, we will outline the theoretical background for the technique and show experimental results based on an ultra-wideband frequency modulated continuous wave (FMCW) chirped heterodyne ranging system showing sub-100 micron lateral and axial precisions at >10m standoff distances.

9576-17, Session 4

Development of a non-contact center thickness optical metrology system

Peter Roos, Michael Thorpe, Jason Brasseur, Bridger Photonics, Inc. (United States)

The last place an optics manufacturer wants to physically touch a lens is at the center. However, this is precisely what is currently done to measure center thickness of lenses. Using contact methods, the question is not whether the optic is damaged, it is whether the resulting damage is acceptably low. At Bridger Photonics, we have proven the feasibility of a non-contact center thickness metrology system to address this need. The apparatus uses a technique similar to swept-frequency optical coherence tomography to measure both physical thickness and optical thickness. From these measurements, the group index of refraction can also be determined. Moreover, the phase index can be determined, given the Sellmeier coefficients. In this presentation, we will report our demonstrated measurement range of 75 mm optical thickness (larger possible), as low as 20 nm precision, and group index of refraction determined to better than 5 parts is 10°5. We believe the metrology system resulting from these proof-of-principle demonstrations will be a valuable tool for precision optics manufacturing.

9576-18, Session 4

Moire interferometry patterns for rotational alignment of structures

Esmaeil Heidari, Kevin G. Harding, GE Global Research (United States)

In some manufacturing applications the alignment of fine structures formed on the surface of a part such as micro-scribed patterns on solar panels can be critical to the panel performance. Variations in pattern uniformity may degrade the efficiency of the solar panel if the pattern deviates significantly from designed parameters. This paper will explore the use of moire patterns to interpret the angular alignment of such structures on 3 dimensional nonplanar shapes. The moire interferometry pattern creates a beat between the scribed pattern and a reference pattern that is a function of both the shape of the part as well as the shape of the scribed pattern. Both the part shape variations and the patterns of interest are typically much smaller than can be seen visually. Similar challenges exist when inspecting specular models or testing low quality optics. The moire effect allows small displacements to be measured from patterns that are well below the resolution of the camera systems that are used to view the patterns. Issues such as the separation of the shape of the part from the alignment of the fine structure as well as resolution and robustness of the technique will be explored in this paper.

9576-19, Session 4

Digital holography microscopic array for measuring of mechanical properties on biological samples

Cesar G. Tavera, J. M. Flores, Ctr. de Investigaciones en Óptica, A.C. (Mexico)

Nowadays, the different areas of biomedical science are eager to indeed comprehend internal organic structures as a whole and foreseeing its behavior under specific controlled excitation signals and stimuli. The development of imaging reconstruction by optical techniques, such as Digital Holographic Microscopy (DHM), has allowed determination of shape and measuring of deformations on different kind of materials.

Since cells and organic structures of biological organisms can be viewed as liquid-liquid or liquid-air interfaces, in this work we use a DHM technique to be implemented in a Mach-Zehnder interferometer in order to observe not only the shape, but also, to characterize mechanical and thermal properties on organic material by non-destructive excitation. This measurements are possible by taking advantage from interfacial models on "thermal lensing" [1-3] and "optical pressure radiation" over liquid-liquid interfaces [4]. By using non-contact excitation methods, [5,6] it would be possible (to be proved) to determine some opto-mechanical parameters (i.e. refraction index, group velocity, surface tension, etc.) by quantifying the thermal and optical pressure phenomena. The level of murky samples will represent the discriminating element to make measuring on total or local areas of the element under study. This testing is performed over fields of view of hundreds of microns. Deformations are in the order of a few nanometers of resolution. Numerical algorithms will be adapted and employed for reconstruction and processing of the recorded holographic images. This



information will be valuable for engineering design of antibiotics, control of cellular growing and in bio-chemical science.

9576-20, Session 4

A novel extrinsic calibration method of ToF cameras based on a virtual multi-cubes shaped object

Lei Ao, Yongqi Liu, Xin Dong, Ze Zhang, Chinese Academy of Sciences (China)

In recent years, due to their ability to capture 3D range data at video framerate, time-of-flight (ToF) cameras have been widely used in many fields, such as mobile robotics, automotive engineering and industrial engineering. Researchers concentrate on extrinsic calibration methods used to eliminate the measurement errors which is typically caused by the disparity between the world coordinate system and the measurement coordinate system. Generally, calibration accuracy is affected by accumulated errors which are generated by recognition of objects with multi-characteristics such as checkerboard. Thus, in this paper, we propose a novel extrinsic calibration method of ToF cameras with a virtual multi-cubes shaped object. First, we establish the motion model of a 3-axis translation stage composed of three linear translation stages which are orthogonal to each other. Then, a virtual multi-cubes shaped object with multi-characteristics is generated from an optimized combination of multi-motions of the 3-axis translation stage. The proposed extrinsic calibration of ToF cameras is accomplished by recognizing corner characteristics of this multi-cubes shaped object and performing least square adjustment method. Experiment results show that the measurement accuracy of a ToF camera is improved from ±10mm to 6.85mm, which is much better than that of the conventional method based on a 2D plane checkerboard. The proposed method is very simple and has the ability to improve calibration accuracy to a high level. It may find great potential applications in many fields.

9576-21, Session 4

Fiber coupler end face wavefront surface metrology

David C. Compertore, Filipp V. Ignatovich, Michael A. Marcus, Lumetrics, Inc. (United States)

Despite significant technological advances in the field of fiber optic communications, one area remains surprisingly 'low-tech': fiber termination. In many instances it involves manual labor and subjective visual inspection. At the same time, high quality fiber connections are one of the most critical parameters in constructing an efficient communication link. The shape and finish of the fiber end faces determines the efficiency of a connection comprised of coupled fiber end faces. The importance of fiber end face quality becomes even more critical for fiber connection arrays and for in the field applications.

Here we propose and demonstrate a quantitative inspection method for the fiber connectors using reflected wavefront technology. The manufactured and polished fiber tip is illuminated by a collimated light from a microscope objective. The reflected light is collected by the objective and is directed to a Shack-Hartmann wavefront sensor. A set of lenses is used to create the image of the fiber tip on the surface of the sensor. The wavefront is analyzed by the sensor, and the measured parameters are used to obtain surface properties of the fiber tip, and estimate connection loss. For example, defocus components in the reflected light indicate the presence of bow in the fiber end face.

This inspection method provides a contact-free approach for quantitative inspection of fiber end faces and for estimating the connection loss, and can potentially be integrated into a feedback system for automated inspection and polishing of fiber tips and fiber tip arrays.

9576-22, Session 4

Optical range finder using semiconductor laser frequency noise

Takahiro Saito, Katsuki Kondo, Yuuya Tokutake, Shinya Maehara, Niigata Univ. (Japan); Kohei Doi, Tokyo Univ. (Japan); Hideaki Arai, Takashi Sato, Masashi Ohkawa, Yasuo Ohdaira, Shuichi Sakamoto, Niigata Univ. (Japan)

Semiconductor laser range-finder systems use so-called "time-of-flight" methods, in which we need to modulate semiconductor laser's intensity or frequency and detect those of reflected lights in order to compare optical paths to the reference and the target. But, accurate measurement requires both high-speed modulation and detection systems. Taking advantage of semiconductor lasers' broad- spectrum frequency noise, which has a range of up to a few GHz, and converting it to intensity noise; we were able to generate a set of high-speed physical random numbers that we used, to precisely measure the distance.

We tuned the semiconductor laser's oscillation frequency loosely to frequency discriminators, such as Rb absorption lines, and converted laser's frequency noise to intensity noise in the transmitted light. Observed through a frequency discriminator, beams traveling along two different paths will share intensity noise patterns, but there is a time lag. We compare these two signals and calculate their cross-correlation by sweeping the time lag of two signals. The time lag, at which the highest correlation was observed, was that corresponding to the distance between two optical paths.

Through our experiments, we confirmed that the system was accurate to a distance of up to 50 m, at a resolution of 0.03 m, when the sampling rate was adjusted to 0.2 ns.

SPIE. OPTICS+ PHOTONICS Conference 9577: **Optical Modeling and Performance Predictions VII**

Monday - Thursday 10-13 August 2015

Part of Proceedings of SPIE Vol. 9577 Optical Modeling and Performance Predictions VII

9577-21, Session PMon

Laser generation of ultrasound in adhesively-bonded multilayered structure

Yan Zhao, Bixing Zhang, Liping Xue, Nanjing Univ. of Science and Technology (China)

An analytical model for the pulsed laser generation of ultrasound in an adhesively bonded multilayered structure is presented. The model gives the time domain displacement of the structure as a function of laser characteristics and materials properties. Simulation of ultrasonic wave motion in multilayered structures is solved here with the finite element analysis. Detailed descriptions of ultrasonic waves are presented. The simulation allows a better understanding of generation and propagation by creating a window of observation in the multilayered structure.

9577-22, Session PMon

Sensitivity of a capillary fiber resonator for measuring the fluid pressure and humidity

Duber A. Avila Padilla, Univ. Popular del Cesar (Colombia) and Univ. de Sucre (Colombia); César O. Torres Moreno, Univ. Popular del Cesar (Colombia)

In this work studied and compared the sensitivity of a micro-resonator capillary fiber made of a polymer (PMMA) for measuring fluid pressure and humidity of the environment. In the measurement we obtained and compared measurements of sensitivities from the coupling of the field of a Taper fiber. During the coupling of the field within the device, the resonance peaks device moved with the change in pressure and humidity of the environment. We conclude that there may be cross-sensitivity when the device is subjected to large changes in pressure and humidity of the environment simultaneously.

9577-23, Session PMon

Modeling of waveguide-couplers for the use in a micro-optical laser gyroscope

Ingmar Leber, Thalke Niesel, Andreas H. Dietzel, Technische Univ. Braunschweig (Germany)

A new concept for the realization of a micro optical laser gyroscope was developed. This new concept consists of a passive free space ring resonator in which the light is circulating by reflections at three double mirrors. An external light source will be used to activate the resonator. To couple the light in and out of the resonator there will be waveguide-couplers used. This paper reports on simulations of these waveguide-coupler structures. The modeled coupler structures consist of two parallel waveguides. Both waveguides have a rectangular profile. They are in close proximity over a certain path length and separated by a narrow gap. The influence of the gap width (1?m to 5?m), the proximity path length and the size (maximum profile edge length: 50?m) of the waveguides are systematically investigated. Furthermore there have been micro fabricated waveguidecoupler structures optically characterized. These experimental results are compared to the results of the simulation.

It can be ascribed to the fabrication process of the couplers that for narrow gaps waveguide material remains in these gaps. Thus in some structures there is a connection between the two parallel waveguides. Neither the experimental results nor the simulations show a considerable coupling effect when there is a great cap (maximum 5?m) and no waveguide material links the two waveguides. Thus the comparison shows that for an efficient coupling within the scope of the tested waveguide sizes there have to be a

connection. These results will be used to determine the best geometry of the coupler structure for the use in the new gyroscope.

OPTICAL ENGINEERING+

APPLICATIONS

9577-1, Session 1

Using integrated modeling to assess performance of the Transiting Exoplanet **Survey Satellite**

Gerhard P. Stoeckel, Keith B. Doyle, MIT Lincoln Lab. (United States)

The Transiting Exoplanet Survey Satellite (TESS) is an instrument consisting of four wide field-of-view CCD cameras dedicated to the discovery of exoplanets around the brightest stars, and understanding the diversity of planets and planetary systems in our galaxy. Each camera utilizes a sevenelement lens assembly with low-power and low-noise CCD electronics. The system orbits the Earth in a highly eccentric orbit. Using internally developed integrated modeling software, the point spread function is computed for multiple field points over the orbit and used to predict pointing errors for each of the four cameras. The pointing errors are caused by thermoelastic distortions of the structure and optics, and thermally induced variations in refractive index of lenses. These errors are then compared against the requirement for the maximum allowable angular rate of change, and design modifications are implemented to ensure top-level performance requirements of the TESS instrument are met.

9577-2, Session 1

Advanced Mirror Technology Development (AMTD) thermal trade studies

Thomas Brooks, H. Philip Stahl, NASA Marshall Space Flight Ctr. (United States); William R. Arnold Sr., a.i. solutions, Inc. (United States); Brent Knight, Mike R. Effinger, W. Scott Smith, NASA Marshall Space Flight Ctr. (United States)

Advanced Mirror Technology Development (AMTD) is being done at Marshall Space Flight Center (MSFC) in preparation for the next large aperture UVOIR space observatory. A key science mission of that observatory is the detection and characterization of 'Earth-like' exoplanets. Direct exoplanet observation requires a telescope to see a planet which will be 10^-10 times dimmer than its host star. To accomplish this using an internal coronagraph requires a telescope with an ultra-stable wavefront error (WFE). This paper investigates parametric relationships between primary mirror physical parameters and thermal WFE stability.

Candidate mirrors are designed as a mesh and placed into a thermal analysis model to determine the temperature distribution in the mirror when it is placed inside of an actively controlled cylindrical shroud at Lagrange point 2. Thermal strains resulting from the temperature distribution are found and an estimation of WFE is found to characterize the effect that thermal inputs have on the optical quality of the mirror. This process is repeated for several mirror material properties, material types, and mirror designs to determine how to design a mirror for thermal stability.

9577-3, Session 1

AMTD: Advanced mirror technology development in mechanical stability

Joseph B. Knight, NASA Marshall Space Flight Ctr. (United States)

Conference 9577: Optical Modeling and Performance Predictions VII



Analytical tools and processes are being developed at NASA Marshal Space Flight Center in support of Advanced Mirror Technology Development (AMTD) efforts. One facet of optical performance is the mechanical stability of a mirror system. Dynamic inputs into the optical system, such as navigational maneuvers and reaction wheel or antenna motion, will potentially result in mirror deformations due to modal responses that would roll into the total Wave Front Error (WFE). The analytical process/tool reported herein makes pertinent predictions for a case study mirror design and the corresponding results. The utility of such results include being the basis for spacecraft vibration isolation systems derived performance requirements, prediction of the time required for modal responses to diminish, and contributing to the overall systems WFE predictions.

9577-4, Session 1

Unified optomechanical modeling: Stabilizing the line-of-sight of an IR imager

Alson E. Hatheway, Alson E. Hatheway Inc. (United States)

A challenge for optomechanical engineers is to make the structure sufficiently stiff to support the optical elements and stabilize the image on the detector. A complementary challenge, in an existing design, is to determine which elements need more stiffness and which others are satisfactory.

When presented with evidence (either empirical or analytical) that the image is unstable it is often not obvious which optical elements are the prime offenders. The uncertainty arises because both the elements' motions and their optical properties contribute the image motions. Since both the motions and the properties may vary by orders of magnitude in a particular design, neither one is a reliable guide for identifying major contributors to the problem.

Unified optomechanical modeling provides a vehicle for tracing offending image motions to particular optical elements and their supporting structure. The unified modeling method imports the optical elements' properties into a finite element structural model of optical system. It convolves the elements' motions and their optical properties in a single optomechanical modeling medium. This provides the engineer with a tool that discloses each element's contribution to the offending motions of the image on the detector.

This paper presents the theory of unified optomechanical modeling as used in Nastran finite element codes. The steps used in developing a unified optomechanical model will be described in detail. Comparisons of the unified modeling technique to both analytical and empirical validation studies are shown.

9577-5, Session 1

Research on model identification of ultraprecision motion stage

Sheng Qiang, Bin Wang, Harbin Institute of Technology (China)

Lithography is a high-precision manufacturing equipment of electromechanical integration, involving precision machinery, precision control, precision measurement and other subjects. It is limited by the development of optical properties, electrical properties, measurement resolution, machining capabilities, control performance, etc. The performance of lithography can be improved by the design of controllers that can ensure the high speed and high precision. The core devices of lithography is wafer stage and reticle stage, which is composed of coarse and fine motion stage with gas-lubricated bearings. Permanent magnet linear motor and voice coil motor drive the coarse and fine motion stage respectively, so as to achieve six degrees of freedom motion. For optimizing the mechanical structure and validating of advanced control methods, it is necessary to identify the ultra-precision motion platform model with resonance characteristics.

This paper analyzes the structure of precision motion platform and builds mathematical model of linear motors and voice coil motors, thereby SDOF

macro-micro coupling theoretical models and 6-DOF mechanical model are established, which can reflect the combined effect of multiple motors motion characteristics. Theoretical model is the basis of model identification. The unknown parameters of the SDOF macro-micro coupling theoretical model are identified by adaptive real-coded genetic algorithm. Considering the great disturbance generated by mechanical resonance, the mechanical resonance model is built, and the parameters of the model are identified based on the hierarchical identification principle. Then the notch filter that can be used to suppress the mechanical resonance is designed to improve the dynamic response of the system. Validity of the precision motion platform model has been verified. The model will bring great convenience in designing and debugging of lithograph control system.

9577-6, Session 1

Integrated modeling: a look back

Clark Briggs, ATA Engineering, Inc. (United States)

Applications and implementation approaches for integrated modeling of structural systems with optics over the past 30 years will be provided. While much of the development work focused on control system design, significant contributions were made in system modelling and computer aided environments. Early work appended handmade line of sight models to traditional finite element models, such as the HALO spacecraft concept from the ACOSS program. The IDEAS2 computational environment built in support of Space Station collected a wider variety of existing tools around a parametric database. Later, IMOS supported interferometer and large telescope mission studies at JPL with Matlab modeling of structural dynamics, thermal analysis and geometric optics. IMOS's predecessor was a simple FORTRAN command line interpreter for LQG controller design with additional functions that built state space FEM models. Specialized language systems such as CASEY were formulated to provide more complex object oriented functions suited to control structure interaction. A more recent example of optical modeling directly in mechanical CAD is used to illustrate possible future directions. While the value of directly posing the optical metric in the system dynamics terms is well understood today, the eventual payoff will be illustrated briefly via project-based examples.

9577-7, Session 2

The different (yet similar) realms of illumination and stray light modeling

Edward Freniere, Michael A. Gauvin, Lambda Research Corp. (United States); Richard N. Youngworth, Riyo LLC (United States)

The field of non-imaging optics is a currently a diverse and fertile ground for innovation and analysis. Modeling systems for illumination and stray light effects influences a wide variety of electrical, optical, mechanical, material science, and system design decisions. Applications are also diverse in nonimaging including not only modeling of effects in imaging systems, but also important technologies such as solar energy, illumination, and projection systems, to name just a few areas of interest. In this paper, two optical engineers meet for the first time. One engineer is an expert illumination system designer. The other engineer is a stray light analysis expert. Both engineers have been pure in their disciplines. Hence, before they meet neither of them knows anything about the other engineer's world of modeling non-imaging effects. Through their interaction, an understanding of the differences and similarities in modeling these two different (yet alike) fields is covered in detail.



9577-8, Session 2

Simulating the 2D PSF of multiplereflection optical systems with rough surfaces

Kashmira Tayabaly, INAF - Osservatorio Astronomico di Brera (Italy) and Politecnico di Milano (Italy); Daniele Spiga, Giorgia Sironi, Rodolfo Canestrari, Giovanni Pareschi, Paolo Conconni, INAF - Osservatorio Astronomico di Brera (Italy)

The Point Spread Function (PSF) is a key figure of merit for specifying optical systems' angular resolution. As the demand for higher and higher angular resolution increases, surface finishing must be seriously considered even in optical telescopes. From the instrument's optical design, wellestablished ray-tracing routines allow computing and display of the PSF based on geometrical optics but does not directly account for the scattering caused by surface microroughness, which is interferential in nature. Although the scattering effect can be separately modeled, its inclusion in the ray-tracing routine requires assumptions that are difficult to verify. Therefore, a purely physical optics approach is more appropriate as it remains valid regardless of the shape and size of the defects appearing on the optical surface. Such a computation, when performed in twodimensional consideration, is memory and time consuming as it requires processing a surface map with a few micron resolution, and this becomes even more complicated for multi-reflection optical systems. Fortunately, in the far-field configuration, the computation comes down to calculate Fourier Transforms. However, to date this method was used only to study the PSF for single reflection systems. In this paper, we extend this method to multiple reflections layouts, accounting for physical optics effects. As a test case, we simulate the PSF of an ASTRI Cherenkov telescope mirror panel using physical optics approach, including measured surface defects, and we compare the result with the corresponding simulation obtained from raytracing and the experimental image observed in the laboratory.

9577-9, Session 2

General physically-realistic BRDF models for computing stray light from arbitrary isotropic surfaces

Alan W. Greynolds, Retired (United States)

Proposed twenty-five years ago specifically for stray light computations, a general BRDF model that automatically enforces continuity, positivity, reciprocity, and isotropic surface symmetry over all possible input/output directions has been implemented in commercial optical analysis codes. It was originally motivated by the need to fit (and possibly catalogue) measured BRDFs of everything from polished optical surfaces to rough diffuse blacks, reasonably extend in-plane only data to out-of-plane, reduce hundreds or thousands of measurement points to a relatively small number of parameters (like glass dispersion formulas), and cleanup "sloppy" data or models that violate physical constraints. However, there is no attempt to relate the BRDF to any actual surface structure or statistics (the inverse problem). As application examples, the model successfully fits several thousand measured data points on a "glossy" anodized Aluminum sample to a 100-coefficient form and several dozen measured data points on Aeroglaze Z306 diffuse black paint to a general 20-coefficient form then a simpler 2-parameter model. Variations and other general BRDF models are also proposed.

9577-10, Session 2

Optomechanical analysis of diffractive optical elements

Gregory J. Michels, Victor L. Genberg, Sigmadyne, Inc. (United States)

Diffractive optical elements are important components to many high precision optical systems. When such systems are subjected to mechanical loading these optical components yield performance degradation contributions quite different from non-diffractive optical components. It is of interest to predict by analysis such performance degradations for the purposes of development of the optomechanical design for relevant optical systems. While non-diffractive optical surfaces contribute to optical performance degradation through changes in surface shape as might be characterized by deformation normal to the surface or parallel to the optical axis of the surface, diffractive optical surfaces contribute additional optical errors due to the change in phase properties associated with deformations in directions tangent to the optical surface. Such tangent deformations cause changes in spacing on linear gratings or changes in phase profiles on more complex diffractive elements. The developments of this paper are to characterize the changes in phase due to such deformations as predicted by the finite element method and represent them in optical analysis alongside characterizations of surface shape changes.

9577-11, Session 3

Minimize polarization aberrations to use all of the photons all of the time

James B. Breckinridge, California Institute of Technology (United States) and The Univ. of Arizona (United States); Wal Sze T. Lam, College of Optical Sciences, The Univ. of Arizona (United States); Russell A. Chipman, The Univ. of Arizona (United States)

The image of the point spread function (PSF) for astronomical telescopes and instruments depends not only on geometric aberrations and scalar wave diffraction, but also on those wavefront errors introduced by the physical optics or polarization properties of reflecting and transmission surfaces within the optical system. These vector wave aberrations are called polarization aberrations and result from two sources: 1 The mirror coatings necessary to make the highly reflecting mirror surfaces and 2. The optomechanical packaging. Here, I discuss polarization aberrations, provide the analytical tools to calculate the PSF images and give examples of how astronomical image data may be affected.

Our findings are: 1. The image plane irradiance distribution is the linear superposition of four PSF images: One for each of the two orthogonal polarizations and one for each of two cross-product polarization terms. 2. The PSF image is brighter by 9% for one polarization component compared to its orthogonal state. 3. The image of the PSF for orthogonal polarization components are shifted with respect to each other, causing the PSF image for astronomical sources (polarized or unpolarized) to become slightly elongated (elliptical) with a centroid separation of about 0.6 masec. This is important for both astrometry and coronagraph applications. 3. The orthogonally polarized components of unpolarized sources contain different wavefront aberrations, which are separated by approximately 32 milliwaves. This implies that a wavefront correction system cannot optimally correct the aberrations for all polarizations simultaneously. 4. The polarization aberrations couple small parts of each polarization component of the light (~1E-4) into the orthogonal polarization to create highly distorted secondary, or "ghost" PSF image. 5. The radius of the spatial extent of the 90% encircled energy of this ghost PSF image is twice as large as the Airy diffraction pattern. Methods to mitigate polarization aberrations are discussed.

9577-12, Session 3

Simultaneous and independent optical impairments monitoring using singular spectrum analysis of asynchronouslysampled signal amplitudes

Latifa Guesmi, Mourad Menif, SUP'COM (Tunisia)

Fiber optic communication has been tremendous growth over the last

Conference 9577: Optical Modeling and Performance Predictions VII



decade fueled mainly by the continuous and relentless demand for high capacity. Besides, transmission of high data rates over long distances is limited by the impairments in an optical fiber, like chromatic dispersion (CD), polarization mode dispersion (PMD) and optical signal-to-noise ratio (OSNR) as well as in other network components. These impairments have a significant impact of the performance of optical networks operating at data rates in excess of 40Gbps.

Thus, optical performance monitoring (OPM) is an enabling technologies for the management and maintenance of future high-speed reconfigurable optical networks. In the other hand, advanced optical modulation formats offering high spectral efficiencies have been successfully employed by analyzing the asynchronously sampled amplitude.

Based on the previous studies, this paper proposes a novel technique for independent and simultaneous multi-impairment monitoring of CD, OSNR, first-order PMD and Q-factor, where we propose the use of singular spectrum analysis (SSA) of time series analysis and prediction. It has proven their usefulness in the temporal and spatio-temporal analysis of short and noisy time series in several fields of some disciplines. This technique is based on the singular value decomposition (SVD) of a specific matrix constructed upon the time series.

The SSA forecasting method consists of two stages: decomposition and reconstruction of time series representing various optical impairments at different bit rates and modulation formats.

Numerical simulations are performed to investigate the applicability of this methods in the monitoring of phase-modulated optical signals and the prediction of OSNR, CD, PMD and Q-factor for advanced modulation formats signals at high bit rates: 100 Gbps NRZ-DP-QPSK and 160 Gbps DP-64QAM.

It is obvious from the results that the proposed technique enables large monitoring ranges. In particular, the CD monitoring ranges of 0-800 ps/nm and 0-500 ps/nm for 100 Gbps NRZ-DP-QPSK and 160 Gbps DP-64QAM systems, respectively, and also the DGD up 20 ps is monitored. We could accurately monitor the OSNR in the range of 5-30 dB with monitoring error remains less than 1 dB in the presence of large accumulated CD.

The proposed SSA-based technique proves a good monitoring accuracies of optical impairments without requiring any information about the modulation format and signals bit rates during the monitoring process.

9577-13, Session 3

Combining topology optimization and computational lithography for micro-/ nano-device design

Mingdong Zhou, Technical Univ. of Denmark (Denmark) and Dassault Systèmes Deutschland GmbH (Germany); Boyan S. Lazarov, Ole Sigmund, Technical Univ. of Denmark (Denmark)

A unified approach combining topology optimization and computational lithography is presented for the design of micro- / nano- devices fabricated by optical projection lithography. By solving a topology optimization problem and simultaneously considering the manufacturing process, it yields an effective source and a binary mask, which can be sent directly to manufacturing without additional Optical Proximity Correction (OPC). At the same time, the performance of the device, which is simulated using finite element analysis, is optimized and robust w.r.t. process variations, such as lens defocus or photo-resist / dose variations. The proposed computational framework can be applied to design micro- / nano- devices for various physical problems. A micro-compliant mechanism design example is presented to show the potential of this solution.

9577-14, Session 4

System simulation method for fiber-based homodyne multiple target interferometers using short coherence length laser sources

Maik Fox, Thorsten Beuth, Karlsruher Institut für Technologie (Germany); Andreas Streck, ELOVIS GmbH (Germany); Wilhelm Stork, Karlsruher Institut für Technologie (Germany)

Homodyne laser interferometers for velocimetry are well-known optical systems used in many applications. While the detector power output signal of such a system, using a long coherence length laser and a single target, is easily modelled using the Doppler shift, scenarios with a short coherence length source, e.g. an unstabilized semiconductor laser, and multiple weak targets demand a more elaborated approach for simulation. Especially when using fiber components, the actual setup is an important factor for system performance, as effects like return losses and multiple way propagation have to be taken into account. If the power received from the targets is in the same region as stray light created in the fiber setup, a complete system simulation becomes a necessity.

In previous work, an amplitude based signal simulation approach for interferometers based on short coherence length laser sources has been evaluated. To facilitate the use of the signal simulation, a fiber component ray tracer has since been developed that allows the creation of input files for the signal simulation environment. The software uses object oriented MATLAB code, simplifying the entry of different fiber setups and the extension of the ray tracer.

Thus, a seamless way from a system description based on arbitrarily interconnected fiber components to a signal simulation for different target scenarios has been established. The ray tracer and signal simulation are being used for the evaluation of interferometer concepts incorporating delay lines to compensate for short coherence length.

Future work will include modelling of free space optics effects in the ray tracing component.

9577-15, Session 4

Calculation of detection efficiency of the fiber-optic sensor to measure radioactive contamination using MCNP simulation

Hanyoung Joo, Arim Lee, Chan Hee Park, Rinah Kim, Joo Hyun Moon, Dongguk Univ. (Korea, Republic of)

The residual radioactivity in soil at nuclear facility site shall be measured after complete decommissioning of it. This study developed a fiber-optic sensor for measurement of gamma radiation from contaminated soil. The fiber-optic sensor consisted of Lyso scintillator, epoxy resin, and optical fiber. The epoxy resin was manufactured in trapezoid pillar shape. The small end-side of epoxy resin was connected with an optical fiber, and its other end-side was connected to a bundle of LYSO scintillator with 3 mm in diameter.

To confirm if the fiber-optic sensor has a good capability to measure gamma radiation, it was set to measure gamma radiations from Cs-137 source (1.1 ?Ci) in a disk shape for 600, 1000, and 1,800 seconds, respectively. Also, MCNP simulation was performed for the same geometry and compositions as that in the experimental setup. Comparison between measurements by the fiber-optic sensor and MCNP simulation showed that its detection efficiency was about 20%. The fiber-optic radiation sensor is expected to be useful in measuring gamma radiations from the radioactive soil at nuclear facility site.



Numerical investigation of the high spatial frequency gratings in photopolymer materials

Haoyu Li, Yue Qi, Ra'ed Malallah, John T. Sheridan, Univ. College Dublin (Ireland)

When a Solid-State Crystal laser source at ? nm is used for holographic recording in photopolymer materials, the maximal spatial frequency formatted theoretically is less than about 2/? nm-1 for formatting transmission gratings. To overcome the restriction of the laser wavelength achieving a higher spatial frequency, a multiply phase exposure method is introduced, by making use of the non-linear response of the photopolymer materials to the exposure intensity. By theoretical modeling, typical high spatial frequency transmission gratings are produced in an acrylamide/ polyvinyl alcohol (AA/PVA) photopolymer material, which can reach by twice previously produced maximal spatial frequency. The simulations are also carried out to calculate the holographic characterizations of the resulting high spatial frequency gratings. By doing so, the maximal holographic memory capacity for the materials can be improved.

9577-17, Session 5

Experimental study on high-brightness semiconductor laser based on spectral beam combining

Hao Tan, China Academy of Engineering Physics (China)

Based on the spectral beam combining technology, use the wavelength selection characteristic of the grating and the feedback by external cavity , to simultaneously control each element of The Diode Laser Array (DLA) to emit a different wavelength and to overlap the individual beams in the near and far fields. The spectral combined beam has the same beam quality as the beam of single element of the DLA, greatly improve the beam quality of the output beam. The conventional CM-Bar with 19 emitters is apllied, The period of the CM-Bar is 500 um and the width of emitters is 100 um. With a maximum continuous injection current of 70.00A, obtain a continuous 44.90W laser output ,The beam quality of slow and fast axes after spectral beam combining , respectively are 1.52mm * mrad and 5.00mm * mrad, spectral broadening is 3.24nm and electro-optic conversion efficiency of 36% are achieved. The output spot brightness is about 36.92MW / cm?-str.

9577-18, Session 5

Spectral beam combining of four fiber lasers based on a pair of parallel diffraction gratings

Fei Tian, Hong Yan, Gengcheng Xie, Jianmin Li, Shufeng Wang, Institute of Applied Electronics (China)

Spectral beam combining (SBC) is believed to be a feasible method to combine multiple fiber outputs with high beam quality, which attracts broad attentions in recent years. In a single diffraction grating SBC system?the requirement for laser parameters is restrict , which limits the development of high power beam combination system. In this paper, we described a theoretical and experimental investigation on the SBC of four fiber lasers based on a pair of parallel diffraction gratings. The wavelengths of the four fiber lasers are 1060 nm, 1062 nm, 1064 nm and 1066 nm, respectively, and the beam quality of each one is approximately diffraction limited. With spectral beam combining, the output power of 1.62 kW was achieved with beam quality M2 as high as 1.4, while the combining efficiency was about 92.2%. Both theoretical and experimental results illustrated that SBC based on a pair of parallel diffraction gratings could be useful for multiple fiber output combination while maintain high beam quality.

9577-19, Session 5

Temperature sensing on tapered singlemode fibre using mechanically-induced long-period fibre gratings

SPIE. PHOTONICS

OPTICAL ENGINEERING+

APPLICATIONS

Sigifredo Marrujo-García, Ernesto González-Ocaña, Jesus Salvador Velazquez-Gonzalez, Fernando Martínez-Piñón, Maria Guadalupe Pulido-Navarro, Ctr. de Investigación e Innovación Tecnológica (Mexico); Daniel Enrique Ceballos-Herrera, Univ. Autónoma de Nuevo León (Mexico)

The modeling of a temperature optical fibre sensor is proposed and experimentally demonstrated in this work. The suggested structure to obtain the sensing temperature characteristics is by the use of a mechanically induced long period fiber grating on a tapered single mode optical fibre. The optical taper is made by applying heat using a butane flame burner and stretching the single mode fibre whose coating has been removed. The resulting geometry of the device is important to analyze the coupling from the core mode to the taper cladding, and this will determine whether the fibre taper is adiabatic or nonadiabatic. The sensor is tested from room temperature up to 600 OC showing high sensitivity of nearly 50 pm/OC around the resonant wavelength of 1550 nm.

9577-20, Session 5

Low-cost and high-resolution interrogation scheme for LPG temperature sensor

Venkata Reddy Mamidi, Srimannarayana Kamineni, National Institute of Technology, Warangal (India)

In this article we present a low-cost and high resolution interrogation scheme for a long-period fiber grating (LPG) temperature sensor, with adjustable temperature range. In general LPG is used as an optical edge filter to interrogate the wavelength encoded signal from sensors such as fiber Bragg grating (FBG) by converting it into intensity modulated signal. But the interrogation of LPG sensors using FBG is a bit novel and is to be studied experimentally. In this study an LPG drawn by using CO2 laser has been used as sensing element for temperature measurement over a range of 15-450°C. The sensor works based on measurement of shift in attenuation band of LPG corresponding to the temperature. The wavelength information form the LPG sensor is measured using an optical spectrum analyser (OSA). Further the bulk and expensive OSA is replaced with a low cost interrogation system employed a fiber Bragg grating (FBG), photodiode and a transimpedance amplifier (TIA). The light signal from LPG is reflected by the FBG of suitable Bragg wavelength and thus converted into an intensity modulated signal. This intensity signal is captured by a photodiode accompanied with TIA. The designed interrogation scheme made the system low-cost and fast in response, and also enhanced its resolution to 0.1°C. But the scheme has reduced the range of temperature measurement to 120°C. However this range can be shifted within 15-450°C by means of adjusting the Bragg wavelength of FBG.

Conference 9578: Current Developments in Lens Design and Optical Engineering XVI



Monday - Tuesday 10-11 August 2015

Part of Proceedings of SPIE Vol. 9578 Current Developments in Lens Design and Optical Engineering XVI

9578-1, Session 1

Simulation of the optical performance of refractive elements to mimic the human eye focusing

Gerardo Diaz-Gonzalez, Agustín Santiago-Alvarado, Ángel S. Cruz-Félix, Univ. Tecnológica de la Mixteca (Mexico)

Refractive optics has evolved and incorporated new elements in optical systems every day, such as conventional lenses, tunable lenses, GRIN lenses, Fresnel lenses, diffractive lenses, intraocular lenses, etc. Some of these elements are reported in the literature together with different proposed models of the human eye. In this work, optical properties of each of these lenses will be studied, and simulations of their behavior will be done in order to analyze which one is better for imaging process. Such lenses will be incorporated in an optical system that mimics the human eye behavior. Analysis and obtained results are reported, as well as the proposed optical system. Finally, we present the conclusions of the work.

9578-2, Session 1

The point spread function in paraxial optics

Russell A. Chipman, Wai Sze T. Lam, College of Optical Sciences, The Univ. of Arizona (United States)

Paraxial optics is generally regarded as yielding ideal spherical wavefronts. These spherical wavefronts should yield ideal Point Spread Functions. But small polarization deviations from uniformly polarized input occur across the exit pupil in paraxial optics for skew rays. The cause of this polarization rotation, known as skew aberrations, is related to the Berry phase. These polarization variations yield additional cross-polarized components in the PSF. The form of these PSF components are related to the derivative of the PSF. These PSF components, which although very small, are nevertheless not zero. Since they occur within paraxial optics they are thus intrinsically interesting.

9578-3, Session 1

Fast robust non-sequential optical raytracing with implicit algebraic surfaces

Alan W. Greynolds, Retired (United States)

The fastest, most robust, general technique for non-sequentially raytracing a large class of imaging and non-imaging optical systems is by geometric modeling with algebraic (i.e. polynomial) implicit surfaces. The basic theory of these surfaces with special attention to optimizing their precise intersection with a ray (even at grazing incidence) is outlined for an admittedly limited software implementation. On a couple of "tame" examples, a 64-bit Windows 7 version is significantly faster than the fastest commercial design software (all multi-threaded). Non-sequential ray-surface interactions approaching 30M/sec are achieved on a 12-core 2.67 GHz Mac Pro desktop computer. For a more exotic example of a 6th degree Wood's horn beam dump (light trap), a 32-bit Windows single thread version traces rays at least 3 times faster than the commercial ASAP software's implicit algebraic surface and over 10 times faster than its equivalent NURBS surface. However, implicit surfaces don't play well with most CAD systems and thus unfortunately, don't easily fit into a modern workflow. 9578-4, Session 1

Mathematical modeling and analysis for self-radiation stray light of infrared imaging system

Jian Du, Beijing Simulation Ctr. (China)

Stray light is the non-imaging beam arriving at the detector. Due to its existence, detector's SNR (Signal Noise Ratio) is depressed and the whole optical system's detecting and recognizing ability is also affected. So the ability to suppress stray light is the key to improve the detecting ability of systems for a certain photoelectric sensor of the detector. In visible light range, optical systems only channel off the beams but not emit stray light. While the infrared optical systems shelter and absorb the incident stray light and emit thermal radiation at the same times.

In this thesis?a novel way to quantitatively analyze and calculate the nearfield stray radiation of infrared system is proposed. The main contents are:

Firstly, by analyzing and researching the source and transmitted process of self-radiation stray light, it is found that the reflection and refraction are the main factors but the scattering and diffraction are subordination ones. So the self-radiation stray light is researched in deterministic way, and the result is evaluated with the distribution of radiant illumination.

Secondly, a mathematical model based on geometrical optics of selfradiation stray light is built. The coordinate of the intersection point of the light and the imaging plane is calculated with the method of certain directional differential and sequent ray tracing, and the energy distribution is exported with energy count matrix.

Thirdly, a self-radiation stray light of infrared imaging system analysis software is developed. Based on the basic principle of radiation energy and power, a detailed project of radiation source and entrance pupil sampling of self-radiation analysis is proposed, giving the calculating formula with the assistance of MATLAB.

9578-5, Session 1

Comparison of geometrical and diffraction optical transfer functions (Invited Paper)

Virendra N. Mahajan, College of Optical Sciences, The Univ. of Arizona (United States); José Antonio Diaz Navas, Univ. de Granada (Spain)

In an earlier paper, we reviewed and compared the geometrical and diffraction point-spread functions of an optical imaging system [V. N. Mahajan, "Comparison of geometrical and diffraction point-spread functions," SPIE Proc. 3729, 434-445 (1999)]. In this paper, we review and compare its corresponding optical transfer functions. While the truth lies with the diffraction OTF, it is considered easier and quicker to calculate the geometrical OTF, especially for large aberrations. We describe the theory of the two OTFs, and explore the range of spatial frequencies and the magnitude of the primary aberrations over which the geometrical OTF may provide a reasonable approximation of the diffraction OTF.

9578-6, Session 2

Integration design of endoscopes with different viewing directions (Invited Paper)

Dewen Cheng, Yongtian Wang, Beijing Institute of Technology (China)

Endoscopic optical systems for different viewing directions of 0°, 12°, 30°, 45°, 70° and 90° are designed and fabricated. Effort is made to use a



similar set of lenses in the designs of the objectives of these endoscopes in order to reduce the fabrication cost. However, the stop surface is located at different positions for different viewing directions, as the obstruction of the light should always be avoided when different folding prisms are used. In our design results, two of the objective lenses are different, and the space distances between the objective lenses are set as zoom parameters in order to improve the imaging quality of different systems for different viewing angles. The six endoscopes are set up as a multi-configuration system and optimized as a whole. The design and prototype results show that the imaging performance of the systems are fine enough for medical usage. We further introduce freeform surfaces into the design of the endoscopic objectives, which can greatly simplify the structure of the systems.

9578-7, Session 2

Recent experience with design and manufacture of cine lenses

Michael D. Thorpe, Kristy Dalzell, Raytheon ELCAN Optical Technologies (Canada)

Modern cine lenses require a high degree of aberration correction over a large and ever expanding image size. It would be difficult if not impossible to achieve this correction in a lightweight and compact lens package without the use of aspheric surfaces and the modern glasses that have been developed in recent years. The nominal compact design using high index glass is then typically very tolerance sensitive, not least of these tolerances are the aspheric surface and aspheric surface alignment tolerances. Some assembly strategy including compensators must be selected to achieve an acceptable level of performance in a medium volume production environment. The compensation strategy is critical to the manufacturability of the lens as it defines the tolerance band for both optics and mechanics. For instance use of a decenter compensator may offer the attractive prospect of much looser element decenter and wedge tolerances.

In this paper we first review the toleranced performance characteristics of some modern cine designs both our own internal designs and from the patent literature. The critical tolerances and tolerance uncertainties are reviewed as well as the development of particular aberrations with build errors. Several potential compensation schemes are proposed and assessed with impact on tolerances. We then present some statistical data on production lens performance relative to a particular tolerance and compensation model.

9578-8, Session 2

Ultra-compact hourglass lens for integrated cameras

Mohsen Rezaei, Hooman Mohseni, Northwestern Univ. (United States)

Producing a high field of view (FOV) sub-millimeter lens for ultra-low dimensional cameras is still a considerable challenge. Here we introduced a new design for an ultra-compact lens with special frequency of -200 cycle/mm (MTF=0.5), at FOV= $\pm 30^{\circ}$. A part of our work is to produce a micro-machined assembly holder for such lens. Conventional assembly methods are not suitable for these dimensions - nor are traditional micro-processed lenses due to the high aspect ratios needed. We developed micromachining technique to make a holder with volumes below 0.6?0.6?0.6 mm3. The main goal of this work is realization of ultra-compact high-resolution optics with large FOV for ultra-thin 2D and 3D imagers. Point spread function (PSF) for this lens will be extracted using direct imaging on imager arrays with small (-1.2um) pixel pitch, as well as measurement of beam shape with costume designed scanning confocal microscopy.

9578-9, Session 2

Landsat-swath imaging spectrometer: optical design

Pantazis Mouroulis, Robert O. Green, Byron E. Van Gorp, Lori Moore, Jet Propulsion Lab. (United States)

We describe the optical design of a high-throughput pushbroom imaging spectrometer and telescope system capable of Landsat swath and resolution, while providing better than 10 nm per pixel spectral resolution. The design is based on a 3200 element x 18 ?m pixel size focal plane array, two of which are utilized to provide the full swath. At an optical speed of F/1.8, the system is the fastest proposed to date to our knowledge. The utilization of only two spectrometer modules fed from the same telescope reduces system complexity while providing a solution within reachable detector technology.

9578-10, Session 3

Testing and alignment of freeform-based multi-mirror telescopes (Invited Paper)

Xue-jun Zhang, Donglin Xue, Ming Li, Changchun Institute of Optics, Fine Mechanics and Physics (China)

Three Mirror Anastigmat (TMA) systems including both on-axis and offaxis configurations have been widely used in space applications. In some designs, correction for high-order aberrations and realization of large FOV, freeform surfaces are used to provide more design freedoms. This trend brings challenges to optical manufacturing and testing community. In this paper, the design principle and aberration fields of freeform-based multi-mirror telescopes are discussed. Since testing is critical to make highly accurate aspheres and freeform surfaces, the paper also addresses Computer Generated Hologram (CGH) design and implementation to measure large freeform mirrors. In particular, the design of a multifunctional CGH element simultaneously used for individual mirror testing and system alignment is introduced. Finally, CGH assisted alignment procedure for TMA telescopes are discussed in detail.

9578-11, Session 3

Tolerancing an optical freeform surface: an optical fabricator's perspective

Jessica D. Nelson, Kate Medicus, Michael P. Mandina, Optimax Systems, Inc. (United States)

Freeform optical shapes or optical surfaces that are designed with non-symmetric features are gaining popularity with lens designers and optical system integrators. Tolerances on a freeform optical design influence the optical fabrication process. Case studies and soft tolerancing limits for easier fabrication of these freeform surfaces will be discussed. Freeform optical manufacturing is similar to high departure and complex aspheres, which implies that many of the same tolerancing limits apply, such as a minimum local concave radius and maximum sag to allow for tool clearances. Measurement is also a gating item. Initial work shows that various measurement platforms correlate, but discrepancies at low orders remain. Although significant progress has been made in this area, additional research is ongoing in order to ensure the capability of fractional wave freeform surfaces. In addition to reducing freeform measurement uncertainty, questions have arisen around specifying and controlling the surface form. A few of these questions include: How is radius error separated from irregularity? How is alignment error separated from irregularity? How is wedge defined for a freeform? How is thickness measured and defined? These questions along with others regarding optical tolerancing of freeforms will be addressed in this paper.



9578-12, Session 3

Manufacture and analysis of a refractive surface with variable asphericity to model the human cornea

Ángel S. Cruz-Félix, Agustin Santiago Alvarado, Fernando Iturbide Jiménez, Univ. Tecnológica de la Mixteca (Mexico); Eduardo Tepichín-Rodríguez, Estela López-Olazagasti, Instituto Nacional de Astrofísica, Óptica y Electrónica (Mexico)

The cornea contributes substantially to the performance of the human eye and obtaining the shape of the corneal surface is crucial for ophthalmic applications such as manufacture of contact lenses and visual laser correction. In this direction, there exist a large amount of theoretical models which describe the shape of the corneal surface. A previous model of the anterior corneal surface using high-order aspherics have been reported in the literature, and one of the main features of this model is that it has been shown to accurate reproduce the clinical data. In this work we design a refractive surface with variable asphericity using the model mentioned above by means of finite element software, and once the design was obtained we proceeded to manufacture the optical surface made of a polymer known as PDMS. Also an interferometric analysis with a Mach-Zehnder interferometer was performed in order to obtain its wavefront aberration function. The main application of this optical surface is to be used as a substitute of a corneal surface within an optomechanical system to mimic the performance of the human eye.

9578-13, Session 3

Research on the collimators' position method for nanometer accuracy aberration inspection with Shack-Hartmann method

Jiani Su, Zengxiong Lu, Yuejing Qi, Guangyi Liu, Qingbin Meng, Academy of Opto-Electronics (China)

The accurate position of the collimator before the sensor is one key factor for lithographic lens aberration inspection with nanometer accuracy based on the method of Shack-Hartmann.

Based on the wave-front reconstruction with Zernike polynomials, in this paper, an optical alignment method for acquiring the positional displacements of collimator is presented. The function between the Zernike coefficients and the displacements with multi-degree-of-freedom is used, a matrix in the function is obtained from the Zernike coefficients variations for collimator's different positions, and then the collimator's positional displacements were acquired. The accurate position of collimator is solved by this method.

Based on the aberration inspection with Shack-Hartmann method, an engineering model of 193nm NA 0.75 projection lens in commercial simulating software (ZEMAX) was established, analyzed the influence of measurement accuracy toward the positional displacement of collimator, and the distribution map of positional displacement was acquired.

9578-14, Session 4

The design of spherical aberration free multi-layer lenses for the K- and W-bands

Alex Orange, David Schurig, The Univ. of Utah (United States)

In the context of designing microwave and millimeter focusing optics, we explore the optimization of a multilayer lens design with arbitrary (azimuthally symmetric) surfaces and interfaces to reduce geometric aberrations and reflection over moderate bandwidth. In these wavelength ranges arbitrary surface fabrication and mating is possible with standard machining techniques. Optimizations are performed using ray optical path length, with confirmation and diffraction effects provided by FDTD simulations. Test lenses are machined from commercially available polymers and measured with a K-band and W-band free-space, scanning measurement system.

Prior work has focused on the use of power series to describe the surfaces of a lens system and eliminate a finite set of aberrations. This work provides a method to describe the final surface to be added to any lens system that compensates for all spherical aberrations. The resulting surface is the solution to a quadratic equation that satisfies the condition that all optical path lengths are the same. As such the surface is analytic. We use this formulation to specify the final surface of a multi-layered lens. Using multiple, properly chosen, layers reduces both reflections and aberrations. These extra layers are free surfaces and can be used to reduce or eliminate other aberrations (i.e. coma, astigmatism, distortion, field curvature and others of higher order). Raytracing confirms the lack of spherical aberrations. Preliminary electromagnetic simulations using FDTD have shown that this provides a focal intensity of 5.22 compared to 4.44 for a spherical surface (with a 20 wavelength aperture).

9578-15, Session 4

Rainbow station via geometric phase holograms

Jihwan Kim, North Carolina State Univ. (United States)

Wavefront control over the optical geometric phase is a completely new way of beam shaping beyond a spatial control of classical optics based on the optical path differences. Optical elements that are based on spatial control of the geometric phase have been studied but prior studies were limited by the fact there were no practical method to realize spatially varying optical elements with arbitrary polarization patterns. Here we report an effective way to generate geometric phase holograms (GPHs), which are formed as thin films of liquid crystal that can control the angle and color dispersion of lightwaves with very high efficiency. This paper shows various examples of the GPHs including recent high-tech demonstration of the elements working as a rainbow maker onto one of the Amsterdam Central Station's 45 by 25 meter roof arches. This demonstration comes courtesy of artist Daan Roosegaarde and researchers in NC State University, Leiden University, and ImagineOptix Corporation, in celebration of the 125th anniversary of the station's opening and the start of the UNESCO International Year of Light 2015.

9578-16, Session 4

Assessment of technological need and availability to use optical imaging devices in augmented reality devices for cancer detection and improved removal

Rose Ann M. Haft, MUIH (United States)

Cancerous cells are larger and smaller than normal cells, with nuclei that are either enlarged or smaller. They also emit a different wavelength than normal cells, which can be detected using optical detectors sensing between 1226 and 1370 nm with a resolution of <0.5mm that to be able to tell the difference between cancerous and noncancerous cells without having to worry about the pixel size of cameras or sensors. Current augmented reality systems have very small screens and various degrees of resolution and pixel to pixel mapping onto the surface to be used before and during surgery to help make informed decisions during procedures. An overview of the state of science and directly applicable technology is given to understand the feasibility, challenges and benefits of using optical technology combined with augmented reality to help improve the cancer detection and removal process.



9578-17, Session 4

Reducing chromatic aberrations of a multichannel multiresolution imaging system using hybrid lenses

Gebirie Y. Belay, Heidi Ottevaere, Michael Vervaeke, Jürgen Van Erps, Youri Meuret, Hugo Thienpont, Vrije Univ. Brussel (Belgium)

Conventional multichannel imaging systems comprise of many channels having similar imaging properties, namely field-of-view (FOV) and angular resolution/magnification. We demonstrated that the different channels can be designed such that each channel captures a different FOV and angular resolution compared to its neighboring channels. We designed and experimentally demonstrated a three-channel multiresolution imaging system where the first channel has the narrowest FOV (7°) and highest angular resolution (0.0096°) and the third channel has the widest FOV (80°) and lowest angular resolution (0.078°). The second channel has intermediate properties. The performance of the demonstrated threechannel imaging system however was affected by chromatic aberrations as it was designed for a single wavelength of 587.6 nm. The first channel was largely influenced by longitudinal chromatic aberration and the third channel by lateral chromatic aberration. Therefore, we have replaced the aspherical refractive lenses by hybrid lenses, which contain diffractive structures on top of their refractive surfaces, in the three-channel multiresolution imaging system to reduce its chromatic aberrations. The performance of the three channels with hybrid lenses is compared with those of the corresponding channels without hybrid lenses. The longitudinal color aberration of the first channel has been reduced from 1.7 mm to 0.2 mm; whereas the lateral color aberration of the third channel has been reduced from 250 μm to 14 $\mu m.$ In conclusion, the hybrid lenses have reduced the chromatic aberrations of the three channels and extended the operating spectral range of the imaging system in the visible wavelength range.

9578-26, Session PMon

Laser-strength interference coatings at 1540-2100 nm

Vladimir V. Novopashin, Alexsandr V. Shestakov, JSC "Research Institute" POLYUS "them. M.F. Stelmaha" (Russian Federation)

The development of laser technologies defined the novel quality demands to optical interference coatings. Among various film parameters, laser strength to laser irradiation is the most importance. It is necessary to note, that laser damage at spectral range 1540-2100nm has some peculiarities in comparison with 1064 nm. We can added, that almost perfect film structure without porous must be obtained in both cases, but in range 1540-2100nm water molecule can be present in micro-porous structure. Thin-film microstructure has strongly affects on optical coatings performance in harsh environments and is complex function of arrival energy of film atoms, growth rate and temperature, surface preparation and topography, residual gases and ion bombardment [1, 2]. By no means, optical films with low losses and high laser strength can be produced by ion-beam evaporation materials or electron ion assisted beam evaporation. Advantages and deficiency of both methods will be discussed. All films in this work were produced by electron-beam evaporation with ion assistance. The effect of ion-beam influence at grate extent displayed during evaporation oxide materials. Besides, influence of active ions Ar +and O2+ and substrate temperature is considered to be the factor of densification film structure. Various regime of ion source that impact on laser strength were investigated. Ion energy from less than 100 eV to a few hundred eV is generally sufficient for surface cleaning without significant damage. Based on these technological effects experimental processes were produced. Precleaning pure substrate by the ion-beam of Ar+ before the evaporation and also after each layer was important to produce mirrors for Y3Al5O12 +Ho3+ lasers in 2088 nm. Moreover, this effect revealed when oxide materials with d-electron orbital were used. To such materials can be regarded TiO2, Ta2O5, Nb2O5 which possess the possibility to have various valences of

metals. For this reason the connection metal – O2 can be disturbed, and empty appear on film structure. Influence of active Ar+ +O2+ ions in this case led to formation almost perfectly surface. Anti-reflection, output and high reflection coatings were examined. High reflection mirrors at 1540 nm have laser damage 3.0 – 3.5 GW/cm2 with pulse 20ns. At 2088nm laser damage for output mirror with anti-reflection coating and high reflection mirror was 30 – 40 J/cm2 with pulse 600 μ s in laser spot 2.5 mm. References

1. V.V.Novopashin, E.A. Levchuk, A.V. Shestakov Interference polarizers for high power solid- state lasers and laser components, Conference on Laser Optics, St. Pertersburg 2008.

2. V.V. Novopashin, E.A. Levchuk, A.V. Shestakov, High performance dielectric interference coatings in a broad spectral range, Conference on Laser Optics, St. Petersburg 2012.

9578-27, Session PMon

Microresonator based on a polymer capillary fiber PMMA for the measurement of humidity

Duber A. Avila Padilla, Univ. Popular del Cesar (Colombia) and Univ. de Sucre (Colombia); César O. Torres Moreno, Univ. Popular del Cesar (Colombia)

In this paper the properties of a polymer fiber capillary PMMA for measuring the humidity of the environment is studied. Polymer fiber capillary has a reduced size and acts as a microresonador where the field is coupled through a fiber Taper reaching WGMS excitation of modes within the cylindrical cavity. The sensitivity of the device is measured and calculated from a simplified theoretical model being able to obtain similar results. The sensitivity of the device depends on the geometric parameters such as wall thickness and outer diameter.

9578-28, Session PMon

All-reflective zoom system based on foveae technology

Jun Chang, Ke Zhang, YiFan Huang, Jing Chen, Jian Yang, Beijing Institute of Technology (China)

Reflective zoom optical system has many advantages, such as light weighted, no influence of chromatic aberration, and high thermal stability, which can be widely used in many fields. This paper is based on the foveae principle to design a new reflective zoom system with several different mirrors, respectively presents the simulation, optimization, and image quality evaluation. Finally, through the analysis of aberration and structural performance, the new concept system was introduced to improve the balance capacity for optical aberration; we obtained the off-axis threemirror system based on foveae concept, this kind of new systems is of good technical reference for the use of different special area.

9578-29, Session PMon

Design considerations for an unconventional infrared prism with a 90-degree ray deviation

Beyza Akarca, Goktug G. Artan, TÜBITAK SAGE (Turkey)

In this study, the optical performance of a 90 degree prism working in the mid-wave infrared region with the purpose of carrying a beam of light from one optical system to another in an unconventional way is discussed. First, a group of mirrors is considered as a design alternative to lower the overall cost of the system. However, using mirrors greatly increases the diameter of the beam due to the rays coming from wide field of view angles.

Conference 9578: Current Developments in Lens Design and Optical Engineering XVI

Another drawback of mirrors is that having separate mirrors requires precise alignment for the system to work at full performance which is difficult for the given application. However, these alignment issues are not valid for a single piece prism. Therefore, a single piece prism is the preferred option and has been taken into account in this study. Material selection is important, especially in the mid-wave infrared region where the index of refraction differs greatly from material to material. Silicon and Germanium are the materials preferred because of their high index of refraction and transmission characteristics. Aside from optical properties, these materials are also considered in terms of manufacturability. Also, options for the coatings to be applied to reflecting surfaces of the prism are discussed with regard to the transmission loss within the system. In order to have total internal reflection within a prism, coatings must be chosen carefully to handle transmission loss at the reflecting surfaces. All of the system parameters are examined using sequential and non-sequential modes of ZEMAX OpticStudio software.

9578-30, Session PMon

Optical modeling with precise spatialchromatic light distribution in phosphorconverted white LEDs

Ching-Cherng Sun, Yu-Yu Chang, Yu-Huan Wang, Ching-Yi Chen, Yi-Chien Lo, Han-Hsiang Cheng, National Central Univ. (Taiwan)

In this paper, a new modeling algorithm for use in phosphor-converted white light-emitting diodes (pcW-LEDs) is proposed, which is aimed to perform accurate simulation for color appearance. Furthermore, the algorithm can be potentially enabling optical designers to remove yellowish/ bluish spots in LED lighting. The modeling process begins by conducting ray tracing of the light emissions from the active layer of a blue die. The blue light then penetrates the phosphor volume with absorption for reemitting yellow light, or redistributes through Mie scattering. The yellow light is from isotropic radiation caused by the yellow phosphor and is redistributed through Mie scattering. After verifying key parameters, namely the absorption coefficient and conversion efficiency of the phosphor, the blue and yellow light distributions can be precisely simulated. Accordingly, the proposed modeling method was applied to simulate a pcW-LED without an encapsulation lens, and subsequently, a pcW-LED with a hemispherical lens. Both simulations accurately predicted the blue and yellow light distribution. The model was further verified by applying a total internal reflector lens to the pcW-LED. In the midfield region, the blue and yellow light distribution exhibited large variations as the observation distance changed; this varying light pattern for both the blue and yellow lights can be accurately predicted using the proposed model. The developed optical model will be helpful to facilitate designing a pcW-LED that features high-quality illumination and higher color uniformity in practical.

9578-31, Session PMon

Analysis of three-element zoom systems for laser beam expanders with tunablefocus lenses

Pavel Kulmon, Antonín Mik?, Pavel Novák, Ji?í Novák, Czech Technical Univ. in Prague (Czech Republic)

Lasers are widely used in many areas of science and technology. Since a laser beam has specific optical properties, there are required special optical systems for transformation of laser beams. Common optical systems used both in classical imaging optics and laser optics are beam expanders. In case of transformation of a homocentric light beam simple telescopic systems are being used for the beam expansion. In case of a laser beam the input Gaussian beam has to be transformed into output Gaussian beam with a different waist diameter and divergence. Thus, the design of the optical system of a laser beam expander is different because of different formulas are valid for the transformation of the Gaussian laser beam. The properties of the Gaussian beam has to be considered during the design of such laser



beam expanders. In practice zoom optical systems are frequently required in various applications. For the case of classical homocentric beams the problem of an analysis and design of zoom systems is described thoroughly in literature.

Our work is focused on the problem of a theoretical analysis of imaging properties and initial optical design of the three-element zoom optical system for laser beam expanders using lenses with a tunable focal length. Equations that enable to calculate basic paraxial properties and parameters of such optical systems are derived. Finally, the derived equations are applied on an example of calculation of parameters of the three-element zoom system for the laser beam expander.

9578-32, Session PMon

Recovery of objects on move with digital holographic techniques

Martin Hernández-Romo, Pedro Soto-López, Alfonso Padilla-Vivanco, Univ. Politécnica de Tulancingo (Mexico)

A digital holographic recorder setup based on off-axis interferometer is presented. The holographic recording makes use of illumination by reflection in order to get some holograms from samples with disturbance induced by mechanical vibrations. Moreover, the Gabor Wavelet transform and the impulse response technique are used to compute the numerical diffraction pattern distributions, which both are compared with the angular spectrum method. This last method allows to retrieval the phase distribution in short reconstruction distances down to zero and with flexibility in the control of image noise. Finally, the phase retrieval algorithms are completed with the two dimensional unwrapping phase method based on a reference hologram for the purpose of compensate the optical aberrations introduced by the digital holographic recorder system. On other hand, due to the samples have high scattering surfaces it is important to use a retrieval algorithm that is previously calibrated. Experimental results are presented.

9578-33, Session PMon

The fractional Fourier transform of the aperidic and fractal functions

Alfonso Padilla-Vivanco, Aldo Yuck-Franco, Univ. Politécnica de Tulancingo (Mexico)

In this work the fractional Fourier transform (FRFT) from aperiodic and fractal functions have been computed to obtain the physical properties of some optical elements. One of most promising candidates in optical imaging is the Fibonacci grid. In this paper, the diffraction patterns of Fibonacci gratings (FBG) are computed, which are typical examples of aperiodic devices. These kinds of optical devices have some novel features such as redundancy and robustness, maintaining their imaging features intact even when there is significant loss of information. FBGs also contain fractal signatures and are characterized by a fractal dimension. Our study suggests that non-periodic gratings may be better than their counterparts the fractal-based technologies. Also we can identify the characteristics that define the frequency. We investigate the analysis of a digital-optical information system based on the architecture of the Fractional Fourier transform. We describe the intensity retrieval process by Fourier-type filters. A mathematical analysis and an optical-digital setup is shown. Experimental results are shown.

9578-34, Session PMon

Design and fabrication of a tunable solid elastic lens

Agustín Santiago-Alvarado, Univ. Tecnológica de la Mixteca (Mexico); Emilio Reyes Pérez, Univ. Technológica de la Mixteca (Mexico); Daniel Arriaga Martínez, Fernando



Iturbide Jiménez, Ángel S. Cruz Félix, Jorge González García, Enrique A. López López, Univ. Tecnológica de la Mixteca (Mexico)

The development of a tunable Solid Elastic Lens (SEL) involves the design of an electromechanical system that will be used to modify some of its geometrical parameters. The raw material used for the fabrication of the SEL is the polymer known as PDMS due to its excellent mechanical and optical properties which are desirable for a particular application. Nevertheless, the presence of air bubbles formed within the main body during the process of curing of these kinds of lenses is a recurring problem; additionally the jaws do not exert pressure or tension uniform on the lens body, extra optical aberrations are introduced to the overall optical system because of the mentioned problems. We describe in this work a new methodology to fabricate SELs made of PDMS without air bubbles and the use of a mechanical system of uniform actuation is presented in order to reduce optical aberrations.

9578-35, Session PMon

Design of an optical system that mimics the human eye image formation

Agustín Santiago-Alvarado, Cristian Á. Domínguez Osante, Ángel S. Cruz Félix, Univ. Tecnológica de la Mixteca (Mexico)

The eye is one of the most complex organs in the human body and constantly is being under study in order to fully describe its objective performance and its characteristics. Several theoretical models have been proposed to describe it and even functional models using fixed elements to describe the iris and the crystalline lens can be found in the literature, however, these result in a restricted version of the actual eye and are mainly used for educational purposes. In this work, we present the design of an optical system that mimic the optical behavior of the human eye for image formation. We include a dynamical aperture diaphragm to emulate the iris and a tunable lens is used to emulate the crystalline lens in order to achieve focus objects at different focal distances. Results and simulation analysis of the opto-mechanical performance of the proposed optical system is presented.

9578-36, Session PMon

Extending the depth-of-field for microscopic imaging by means of digital image fusion

Alfonso Padilla-Vivanco, Carina Toxqui-Quitl, Roman Hurtado-Perez, Univ. Politécnica de Tulancingo (Mexico)

In optical microscopy, the depth of field (DOF) is limited by the physical characteristics of the image-forming systems. Taking a focused picture with all the field of view can be impossible to reach in optical microscopy. So that, we have to use some digital image techniques to produce a complete focused image from all the field of view. In order to extend the DOF in an optical microscopic system, this paper propose a method based on image fusion and in the module of the gradient color planes. The procedure is to move the microscope stage in the paraxial Z-axis taking several color images to fuse them in a single composite image. The lighting technique used is by means of the bright field in reflection. Our results are obtained by using real samples and also any post-processing steps are performed to merge a final fused image. The proposed method is simple, fast and virtually free of artifacts or false color. Experimental results are presented.

9578-37, Session PMon

Optical model of optical volume diffusion plate: polycarbonate plate doped with silicon dioxide micro particle

Yeh-Wei Yu, Yu-Heng Chen, Ming Le, Ching-Cherng Sun, National Central Univ. (Taiwan); Jong-Wu Chen, Plastic Industry Development Ctr. (Taiwan); Chih-Yuan Cheng, National Central Univ. (Taiwan)

High-efficiency diffusers play important roles in modern optical industry. The applications include back-light of television, uniform lighting, glare suppression, lighting decoration, and so on. In this paper, we develop optical volume diffusion plate using polycarbonate (PC) plate doped with silicon dioxide (SiO2) micro particle. In order to predict the optical performance of the diffuser with different particle concentration and micro particle size, we use Monte-Carlo ray-tracing with Mie-scattering model to build up the optical model. Because particles distribution is not uniform inside the volume diffusion plate, we use particle space as a tuning factor in the Mie-scattering model. Finally, we use the high speed measurement system screen imaging synthesis (SIS) system to measure the BSDF of each diffuser and demonstrate the optical model.

9578-38, Session PMon

Coaxial fundus camera for opthalmology

Jarbas C. Castro Neto, Univ. de São Paulo (Brazil)

A Fundus Camera for ophthalmology is a high definition device which needs to meet low light illumination of the human retina, high resolution in the retina and reflection free image. Those constraints make its optical design very sophisticated, but the most difficult to comply with is the reflection free illumination and the final alignment due to the high number of non coaxial optical components in the system. The reflection of the illumination, both in the objective and at the cornea, mask the quality of the image, and a poor alignment make the sophisticated optical design useless. In this work we developed a totally axial optical system for a non-midriatic Fundus Camera. The illumination is performed by a LED ring, coaxial with the optical system and composed of IR of visible LEDs. The illumination ring is projected by the objective lens in the cornea. The Objective, LED illuminator, CCD lens are coaxial making the final alignment easily to perform. The CCD lens is a CCTV camera with autofocus and Zoom built in, making the system easily operated and very compact.

9578-18, Session 5

Temperature-dependent refractive index measurements of L-BBH2 glass for the Subaru CHARIS integral field spectrograph

Douglas B. Leviton, Leviton Metrology Solutions, Inc. (United States); Kevin H. Miller, Manuel A. Quijada, NASA Goddard Space Flight Ctr. (United States); Tyler D. Groff, Princeton Univ. (United States)

Using the Cryogenic High Accuracy Refraction Measuring System (CHARMS) at NASA's Goddard Space Flight Center, we have made the first cryogenic measurements of absolute refractive index for Ohara L-BBH2 glass to enable the design of a prism for the Coronagraphic High Angular Resolution Imaging Spectrograph (CHARIS) at the Subaru telescope. L-BBH2 is employed in CHARIS's prism design for improving the spectrograph's dispersion uniformity. Index measurements were made at temperatures from 115 to 305 K at wavelengths from 0.46 to 3.16 microns. We report absolute refractive index, dispersion, and thermo-optic coefficient for this material. We provide temperature-dependent Sellmeier coefficients based on our data to allow accurate interpolation of index to other wavelengths and temperatures. This paper also speaks of the challenges in measuring



index for a material which is not available in sufficient thickness to fabricate a typical prism for measurement in CHARMS. Under this circumstance, designing a prism which will produce accessible beam deviations, has adequately large refracting face area (which affects signal levels), and is also manufacturable with adequately accurate refracting faces is non-trivial. The tailoring of the index prism's design that allowed index measurements to be made and the remarkable results obtained from that prism for this practical infrared material are discussed. (Please see related paper on the optical design for CHARIS by Tyler Groff in session OP405.)

9578-19, Session 5

The need for accurate cryo refractive indices and mechanical properties of optical materials (Lithosil 3001, CaF2 and S-FTM16 for EUCLID NISP)

Frank U. Grupp, Univ.-Sternwarte München (Germany) and Max-Planck-Institut für extraterrestrische Physik (Germany); Douglas B. Leviton, Manuel A. Quijada, Kevin H. Miller, NASA Goddard Space Flight Ctr. (United States); Hans D. Thiele, OHB-System AG (Germany); Ralf Bender, Max-Planck-Institut für extraterrestrische Physik (Germany)

No Abstract Available

9578-20, Session 5

Cryogenic refractive indices of S-LAH55, S-LAH55V, S-LAH59, S-LAM3, S-NBM51, S-NPH2, S-PHM52, and S-TIH14 Glasses

Kevin H. Miller, Manuel A. Quijada, NASA Goddard Space Flight Ctr. (United States); Douglas B. Leviton, Genesis Engineering Solutions, Inc. (United States)

The Transiting Exoplanet Survey Satellite (TESS) is an explorer-class planet finder, whose principal goal is to detect small planets with bright host starts in the solar neighborhood. The TESS payload consists of four identical cameras and a Data Handling Unit (DHU) fitted with CCD detectors and associated electronics. Each camera consist of a lens assembly with seven optical elements that include various types of Ohara glass substrates. The successful implementation of a panchromatic and a thermal lens assembly design for these cameras requires a fairly accurate (up to 1e-6) knowledge of the temperature- and wavelength-dependent of the refractive index in the wavelength and temperature range of operation. Hence, this paper is devoted to report on measurements of the refractive index over the wavelength range of 0.42–1.15 um and temperature range of 110–300 K for the following Ohara glasses: S-LAH55, S-LAH55V, S-LAH59, S-LAM3, S-NBM51, S-NPH2, S-PHM52, and S-TIH14. The measurements were performed utilizing the Cryogenic High Accuracy Refraction Measuring System (CHARMS) facility at NASA's Goddard Space Flight Center. A dense coverage of the absolute refractive index for all these substrates in the aforementioned wavelength and temperature ranges was used to determine the thermo-optic coefficient (dn/dT) and dispersion relation (dn/d?) as a function of wavelength and temperature. A comparison of the measured indices with literature values, specifically the temperature-dependent refractive indices of S-PHM52 and S-TIH14 reported by Yamamuro et al. [Yamamuro et al., Opt. Eng. 45(8), 083401 (2006)], will be presented.

9578-21, Session 5

Temperature-dependent refractive index measurements of CaF2, Suprasil 3001, and S-FTM16 for the Euclid Near-Infrared Spectrometer and Photometer

Douglas B. Leviton, Leviton Metrology Solutions, Inc. (United States); Kevin H. Miller, Manuel A. Quijada, NASA Goddard Space Flight Ctr. (United States); Frank U. Grupp, Max-Planck-Institut für extraterrestrische Physik (Germany)

Using the Cryogenic High Accuracy Refraction Measuring System (CHARMS) at NASA's Goddard Space Flight Center, we measured absolute refractive indices at temperatures from 110 to 300 K at wavelengths from 0.42 to 2.72 microns for CaF2, Suprasil 3001 fused silica, and S-FTM16 glass in support of lens designs for the Near Infrared Spectrometer and Photometer (NISP) for ESA's Euclid dark energy mission. We report absolute refractive index, dispersion (dn/d?), and thermo-optic coefficient (dn/dT) for these materials. In this study, materials from different melts were procured to understand index variability in each material. Inter-melt variability study is further enabled by comparisons with our measurements of these material types for previous projects. We provide temperature-dependent Sellmeier coefficients based on our data to allow accurate interpolation of index to other wavelengths and temperatures. (Please see companion paper on the need for accurate cryo refractive indices and mechanical properties of optical materials for Euclid NISP by Frank Grupp in session OP401.)

9578-22, Session 6

Laser-activated remote phosphor light engine for projection applications

Martin Daniels, OSRAM GmbH (Germany)

Laser-activated remote phosphor light engine for projection applications

Recent developments in blue laser sources enable attractive solutions in projection applications using phosphors for efficient light conversion with very high luminance levels. Various commercially available projectors incorporating this technology have entered the market in the past years. Luminous flux levels are currently still comparable to lamp-based systems, while lifetime expectations of classical lamp systems are exceeded by far. OSRAM has been exploring this technology for several years now and has introduced the PHASER* brand name (Phosphor + Laser).

Various optical system design approaches and laser/phosphor architectures will be discussed. State-of-the-art is a rotating phosphor wheel to deliver the necessary primary colors either sequentially for single-imager projection engines or simultaneously for 3-panel systems. The PHASER® technology enables flux and luminance scaling, which allows for smaller imagers and therefore cost-efficient projection solutions.

The resulting overall efficiency and ANSI lumen specification at the projection screen of these systems is significantly determined by the target color gamut and the transmission of the projection system. With increasing power and flux level demand, thermal issues, especially phosphor conversion related, dominate the opto-mechanical system design requirements. These flux levels are a great challenge for all components of an SSL-projection system. OSRAM's PHASER* light engine platform is constantly expanded to higher luminous flux levels and also to higher luminance levels for various applications. Recent experiments employ blue laser pump power of multiple 100 Watts to excite various color phosphors resulting in luminous flux levels of more than 40 klm.



9578-23, Session 6

Complex visible scene projection technology

Hong Yu, Beijing Simulation Ctr. (China)

The first and most essential capability a visible scene projection system must have is low background and high contrast during dynamic simulation. A complex visible scene projection system was developed to meet the above requirements. The complex visible scene projection system mainly consists of the optical fiber subsystem, LCD (Liquid Crystal Display) subsystem, multiple focal plane coupler and the collimation objective. There are three channels which represent a target and two different star field simulations in optical fiber subsystem. 9 fibers arranged in 3?3 array to display the simulated target which comes from far to near, the center fiber is lighted when the target is far, the peripheral fibers are then lighted gradually and become brighter and brighter when the target approaching. Thaler prism polarizers were used as attenuator in each of 9 fibers, motor driving one of the pair of the polarizer to change the energy timely in each of 9 fibers. In the star field simulations, two different star field patterns can be displayed. There are 7 fibers fixed in 7 holes respectively on a star board in each of two star field simulations, so a star field pattern of 7 stars at most can be simulated, and the star field patterns were determined in advanced. Polarizers were used as attenuator in each of 14 star fibers. Manually rotate one of the pair of the polarizer to change the output energy. 23 fibers in all in the optical fiber subsystem were connected with an integral sphere to obtain the uniform light. The LCD subsystem consists of illumination, LCD module and imaging objective. 1024?1024 of 1920?1080 LCD array were used to display dynamic visible scene. because the sizes of the 1024?1024 LCD array and the above star boards are different, so the imaging objective were used to project the original 1024?1024 LCD array to an image with the same size as the star board. Multiple focal plane coupler is responsible for coupling the 4 focal planes of 3?3 target fibers, two star boards and the LCD image. A prism was used as beam combination element to transmit the target fibers through and reflect the rest of three. Two star boards and the LCD image can be reflected optionally by rotating the prism to make the reflection surface facing at it. The collimation objective projects any one or two of combination of 4 focal plane to infinity. The size and weight of the whole system was confined to be suitable to mount on flight motion table.

9578-24, Session 6

LED collimation optics for large sources

Yasmín Berenice Alcántara-Pérez, Univ. de Guanajuato (Mexico); Ivan Moreno, Univ. Autónoma de Zacatecas (Mexico)

Trending chip-on-board (COB) and multichip LEDs are extended light sources that significantly increase flux output. However, a large light source can be a nightmare when dealing with compact and high efficiency collimation optics. Here we analyze nonimaging optics that concentrates the light of an extended source into a small cone. We discuss the foundations of nonimaging collimators, and the primary architectures that have been exploited for developing collimators with large LEDs. Considerations on collimating optics such as optical efficiency, beam divergence angle, and performance optimization are also discussed. We review some important methods and designs from the specialized literature, proposing a new design method for optimized directional lighting with large LEDs, which directly considers the extended source without beginning with a point source approximation.

9578-25, Session 6

High-performance LED luminaire for sports hall

Xuan Hao Lee, Jin-Tsung Yang, National Central Univ. (Taiwan); Wei-Ting Chien, Jung-Hsuan Chang, National Central Univ. (Taiwan) and WitsLight Technology Group (Taiwan); Yi-Chien Lo, Che-Chu Lin, Ching-Cherng Sun, National Central Univ. (Taiwan)

In this paper, we present a luminaire design with anti-glare and energysaving effects for sports hall. Compared with traditional lamps using in a badminton court, the average illuminance on the ground of the proposed LED luminaire is enhanced about 300%. Besides, the uniformity is obviously enhanced and improved. The switch-on speed of lighting in sports hall is greatly reduced from 5-10 minutes to 1 second. The simulation analysis and the corresponding experiment results are demonstrated.

Monday - Wednesday 10-12 August 2015

Part of Proceedings of SPIE Vol. 9579 Novel Optical Systems Design and Optimization XVIII

9579-23, Session PMon

An optical filter with angular selectivity of the light transmission

Rustam S. Zakirullin, Orenburg State Univ. (Russian Federation)

Features of the application of a novel optical filter with angular selectivity of the light transmission to architectural glazing are considered. The filter consists of a sheet transparent substrate with thin-film grating layers on both surfaces. The gratings formed by directionally transmissive strips, alternating with absorptive, reflective, or scattering strips. Their relative position on the input and output surfaces provides angular selectivity of the directional light transmission – as the incidence angle changes, the proportion of radiation that passes through both gratings of the filter also changes. Chromogenic materials currently used in the laminated smart windows, providing control over the intensity and spectrum of the transmitted solar radiation, cannot achieve the selective regulation on the ranges of incidence angles. Such a regulation requires the use of additional daylight-redirecting devices, especially blinds, to dynamically adapt to the position of the sun. The grating optical filter provides angular selectivity of the light transmission of a window without such devices. The features of using this filter in the single and double glazed windows are described. A graphic-analytical calculation method is proposed for estimating the effect of geometrical and optical parameters of the filter on the angular characteristics of the light transmission. An algorithm to optimize filtering solar radiation taking into account the geographical coordinates of terrain, time of day and year and the orientation of the window to the cardinal is set. An algorithm to calculating geometrical parameters of the filter with pre-specified characteristics of the light transmission is obtained.

9579-24, Session PMon

Analysis in the allocation of bandwidth applied to the concept of flexible optical networks

William S. Puche, Univ. Pontificia Bolivariana (Colombia) and Politécnico Colombiano Jaime Isaza Cadavid (Colombia); Javier E. Sierra, Corporación Univ. del Caribe (Colombia); Ferney O. Amaya-Fernández, Univ. Pontificia Bolivariana (Colombia)

The continued increase in the capabilities and performance in fiber optic networks today require more robust network designs to allow high consumption of information and thus enable users to have greater capacity and data content. That's why we in the task of analyzing and implementing the concept of flexible optical networks to optimize the use of bandwidth at high transmission rates and improved spectral efficiency, which represents the industry an effective economy, and energy.

9579-25, Session PMon

Design and verifications of an eye model fitted with contact lenses for wavefront measurement systems

Yuan-Chieh Cheng, National Tsing Hua Univ. (Taiwan) and Instrument Technology Research Ctr. (Taiwan); Jia-Hong Chen, Rong-Jie Chang, Chung-Yen Wang, National Tsing Hua Univ. (Taiwan); Wei-Yao Hsu, Instrument Technology Research Ctr. (Taiwan); Pei-Jen Wang, National Tsing Hua Univ. (Taiwan) Contact lenses are measured by liquid-immersed box method due to large optical power from small anterior central curve radius (ACCR) though the Back Vertex Power of contact lenses may be small. In this study, an optical measurement system based on Shack-Hartmann wavefront principle has been established for investigation of the aberrations of soft contact lenses. By mimicking the fitting conditions, optical design of an eye model with various topographical shapes in anterior cornea are studied. Initially, it is essential to measure samples of contact lens not only by conventional method but also fitted with various topographical corneal shapes fitted on the model. In addition, optics simulation program has been employed for evaluation of sources of errors and accuracy of the system. Finally, with various Diopters of in samples of soft contact lenses, both the simulations and experiments have confirmed the controversial issues in the measurement method by eye-model fitted contact lenses. More importantly, the results have concluded aberrations of contact lenses could be measured with the proposed system.

9579-26, Session PMon

Plenoptic camera based on a liquid crystal microlens array

Yu Lei, Huazhong Univ. of Science and Technology (China) and Shijiazhuang Tiedao Univ. (China); Qing Tong, Xinyu Zhang, Hongshi Sang, Changsheng Xie, Huazhong Univ. of Science and Technology (China)

The plenoptic camera is an innovation of photography which can acquire the three-dimensional radiance of a scene by inserting a silica microlens array between the main lens and the image sensor of the traditional camera. In this paper, we propose to substitute a liquid crystal microlens array (LCMLA) with electrically tunable focal length for the silica microlens array in the plenoptic camera to adjust the depth of field (DOF). The LCMLA we fabricated is mainly composed of an aluminum patterned silica electrode and an indium-tin-oxide coated planar silica electrode with liquid crystals injected between them. The pattern etched in the aluminum silica electrode is an array of circular holes with a diameter of 128 ?m and a hole pitch of 160 ?m. When a certain alternating current voltage signal is applied over the two electrodes, symmetrical inhomogeneous electric fields in each holes will be generated and an array of liquid crystal microlenses with gradient refractive index are formed for converging incident rays. The focal length of the microlens can be changed by adjusting the voltage signal between the electrodes. We integrated the LCMLA with an image sensor to construct a plenoptic camera prototype based on LCMLA. Several raw images are acquired using our plenoptic camera and rendered images are also presented after image processing. Our experiments proved that it is feasible to apply a LCMLA in plenoptic cameras and the DOF of the LCMLA-based plenoptic camera can be adjusted by changing the applied voltage signals.

9579-27, Session PMon

Performance analysis of NRZ, RZ, raised cosine and Gaussian modulation formats in 32x10 Gbps WDM system with different compensation techniques

Hardeep Singh, Thapar Univ. (India); Nivedita Mishra, Thapar Univ. (India) and Thapar University, Patiala(Punjab), India (India)

In this paper, four modulation techniques are studied along with different dispersion compensation techniques namely, pre compensation, postcompensation and symmetric compensation technique. The performance of NRZ, RZ, Gaussian and Raised cosine at 10 Gb/s for 32 channel WDM optical communication system is analysed. The performance evaluation is





being done graphically in terms of maximum received Quality factor. The transmitter section consists of the data source (PBRS), electrical driver, CW laser source and Mach-Zehnder modulator. The data source is generating signal of 10 Gbps with random sequence and CW laser source generates 32 laser beams from 192.1 THz to 195.3 THz at 100 GHz spacing. After multiplexing, signals are sent onto fiber transmission link which is designed considering the fiber parameters of DCF and SSMF so that the first-order dispersion is compensated exactly (D=0). Link consists of 5 spans of standard single mode fiber (SSMF) of 50 km each and 10 km of dispersion compensating fiber whose placement depends upon type of compensation used. In the receiver the signal is demultiplexed, detected by PIN detector, passed through the filter and 3R regenerator.

We investigated pre, post-compensation and symmetrical or hybridcompensation in the presence of fiber nonlinearities with NRZ, RZ, Raised Cosine and Gaussian modulation formats for 32x10 Gbps system in this work. Analysis is done taking Quality factor and eye diagram at receiver. The simulation results showed that for all the modulation formats as the signal input power increases up to certain limit Q value first increases and then starts decreasing. The symmetric compensation scheme performs better than pre and post compensation techniques for all type of modulation formats except in case of Gaussian format at input signal power 0 dBm. It is also found out that NRZ performs better for lower input signal power and RZ performs better at high input signal powers for symmetric compensation.

9579-28, Session PMon

Enhanced and heralded single-photon source models for quantum applications

Attia Moez, Amor Gueddana, Rihab Chatta, SUP'COM (Tunisia)

This work addresses a comparison study between two kinds of Single Photon Sources (SPS). The first SPS is an Enhanced SPS (ESPS), which consists of an association between InAs/GaAs Quantum Dot (QD) and an optical microcavity. The fundamental mode of the QD emits a single photon at 1550 nm. To exclude the other photons being on other modes, we show that the QD has to be embedded in an optical microcavity with resonant mode at 1550 nm. The resonant performances of three different optical microcavities are highlighted, they are the microdisk, the microgear and the Photonic Crystal (PC), which are all based on GaAs material. We show that the PC microcavity used with QD provides the best resonant and coupling performances, which allows to obtain a probability P1 to get a single photon at 1550 nm around 0,7. The second SPS is the Heralded SPS (HSPS) and based on active two-dimensional PC over LiNbO3. When PC is excited by a pump laser source at 980 nm, it emits two single photons at 1310 nm and 1550 nm. These photons are separated spatially using a demultiplexer. The photon at 1550 nm, called idler photon is delayed and the photon at 1310 nm, called signal photon, informs about the coming of the idler photon and triggers it's detection mechanism. According to the physical parameters of this architecture, including photons generation, photons loss and the detection process, we demonstrate that the probability to obtain a HSPS at 1550 nm is closed to 0,57. Finally, we address a comparison study between ESPS and HSPS when they are used in an application of quantum communication.

9579-29, Session PMon

Optical sensor for detection of the level of liquids or liquefied gases in tanks without the use of moving parts

Cicero L. Omegna, Jonas Fontes Garcia, Luxtec Sistemas Ópticos LTDA (Brazil); Roddy E Ramos-Gonzales, Luxtec Sistemas Ópticos LTDA (Brazil) and Luxtec Optical Systems (Brazil); Luiz C. Barbosa, Luxtec Sistemas Ópticos LTDA (Brazil) This study aims to build a prototype of a new device for measuring by optics, the level of liquids or liquefied gases in tanks without the use of moving parts for general applications, stationary or not, industrial and chemical vehicles. There are a lot of optical devices for measuring liquid level and various settings and runs, some devices with buildings and sophisticated technologies, complicated and more simple, but none of these devices has the configuration (provision and operation), for measuring by optical means, the level of liquids in tanks and reservoirs. That is a simple, efficient and cost effective device.

9579-30, Session PMon

Chemical resistance of optical plastics and resin for level detectors

Cicero L. Omegna, Jonas Fontes Garcia, Roddy E. Ramos-Gonzales, Luiz C. Barbosa, Luxtec Sistemas Ópticos LTDA (Brazil)

A test method was developed to find the ideal optical material that supports the chemical reaction of some fuels. Optical plastics and resin were submerged for long periods of time in reservoirs of ethanol, gasoline, diesel and biodiesel. The dimensional change and weight change of the submerged samples was measured. A special resin successfully supported the chemical attack of fuels. Samples of acrylic polymer and polycarbonate were used as type of optical plastic.

9579-31, Session PMon

One-mirror and two-mirror laser scanners with variable focus lens

Petr Pokorn?, Antonín Mik?, Ji?í Novák, Pavel Novák, Czech Technical Univ. in Prague (Czech Republic)

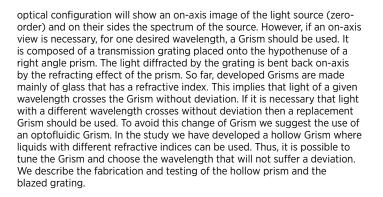
A disadvantage of the present state of laser scanners is that their parameters cannot be continuously and adaptively changed. Active optical components such as variable focal lenses make possible to design new types of adaptive scanners. The work presents formulas for a ray tracing in the optical system of a one-mirror and two-mirror laser scanner with a variable focus lens. The procedures for modeling of one-mirror and twomirror systems, which are used frequently in practice, are described. The result of the analysis describes a general calculation of the position of the laser beam spot in the detection plane with respect to deflection angles of scanner mirrors. Furthermore, equations for the calculation of the focal length which ensure focusing of a beam at the desired point in a detection plane are derived. The chosen vector approach is general. Thus, the application of the formulas in various configurations of the optical systems is possible. An uncertainty analysis of the position of the laser beam spot in the detection plane is performed. Using derived formulas one can calculate deflection angles of scanner mirrors and required focal length of the variable focus lens provided that the position of the focused beam in space is given with a required tolerance. Computer simulations are performed on examples of one-mirror and two mirror laser scanners with a variable focus lens.

9579-33, Session PMon

An optofluidic grism

Sergio Calixto-Carrera, Ctr. de Investigaciones en Óptica, A.C. (Mexico); Martha Rosete-Aguilar, Univ. Nacional Autónoma de México (Mexico); Guillermo Garnica, Ismael Torres-Gomez, Ctr. de Investigaciones en Óptica, A.C. (Mexico)

For some type of instrumentation transmission gratings are needed instead of reflection gratings. For example it is possible to convert cameras or telescopes into spectrographs by placing a grating in front of the lens. This



9579-34, Session PMon

Analysis and compensation of moiré effects in fiber-coupled image sensors

Salman Karbasi, Ashkan Arianpour, Nojan Motamedi, Joseph Ford, Univ. of California, San Diego (United States)

Imaging fiber bundles can relay a curved image surface to a conventional flat focal plane, effectively providing the curved image sensor needed for some high performance lenses. If the fiber bundle period or image sensor pitch are very different, the system resolution is determined by the oversampled fiber or sensor feature. But crosstalk imposes an approximately 2µm minimum waveguide pitch, and light collection and fabrication constraints imposes a limit of 1-2µm for the sensor pitch. Maximizing image information leads to some degree of aliasing, which appears in the form of moiré pattern on the raw sensed image. For example, a 30 Mpixel 120° field of view imager using a $1.75\mu m$ Bayer filtered CMOS focal plane with $2.5\mu m$ pitch fiber bundle yielded images with visible moiré, which was mitigated by sensor response calibration. Here we present a study of moiré effects in fiber-coupled image sensors, including a method for quantitative analysis of moiré, and experimental characterization of color and monochrome sensors with 1.1µm pixel pitch, the highest spatial resolution in commercially available focal plane arrays. We investigate the effect of temperature, angle of incidence of collimated light, and imaging lens F/# on the raw moiré pattern strength, and on the calibrated final image. We also examine the behavior of the sensor by varying exposure times, source irradiance and color. This study provides a guideline for optimization and operation of high resolution fiber-coupled imagers.

9579-1, Session 1

Nonlinear multi-photon laser wave-mixing optical detection in microarrays and microchips for ultrasensitive detection and separation of biomarkers for cancer and neurodegenerative diseases

Manna Iwabuchi, Marcel Hetu, Eric Maxwell, Sebastien Pradel, Sashary Ramos, William G. Tong, San Diego State Univ. (United States)

Multi-photon degenerate four-wave mixing is demonstrated as an ultrasensitive absorption-based optical method for detection, separation and identification of biomarker proteins in the development of early diagnostic methods for HIV-1, cancer and neurodegenerative diseases using compact, portable microarrays and capillary- or microchip-based chemical separation systems that offer high chemical specificity levels. The wave-mixing signal has a quadratic dependence on concentration, and hence, it allows more reliable monitoring of smaller changes in analyte properties. Our wave-mixing detection sensitivity is comparable or better than those of current methods including enzyme-linked immunoassay for clinical diagnostic and screening. Detection sensitivity is excellent since the wave-mixing signal is a coherent laser-like beam that can be collected with virtually 100% collection efficiency with high S/N. Our analysis time is short (1-15 minutes) for molecular weight-based protein separation as compared to that of a conventional separation technique, e.g., sodium dodecyl sulfate-polyacrylamide gel electrophoresis (SDS-PAGE). When ultrasensitive wave-mixing detection is paired with high-resolution capillaryor microchip-based separation systems, biomarkers can be separated and identified at the zepto- and yocto-mole levels for a wide range of analytes. Specific analytes can be captured in a microchannel through the use of antibody-antigen interactions that provide better chemical specificity as compared to size-based separation alone. The technique can also be combined with immune-precipitation and a multi-channel capillary array for high-throughput analysis of more complex protein samples. Wave mixing allows the use of chromophores and absorption-modifying tags, in addition to conventional fluorophores, for online detection of immune-complexes related to cancer.

SPIE. PHOTONICS

OPTICAL ENGINEERING+ APPLICATIONS

9579-2, Session 1

A compact, efficient, and lightweight laser head for CARLO: integration, performance, and benefits

Waldemar Deibel, Adrian Schneider, Univ. Basel (Switzerland); Marcello Augello, Univ. Hospital Basel (Switzerland); Alfredo E. Bruno, AOT AG (Switzerland); Philipp Jürgens, Univ. Hospital Basel (Switzerland); Philippe C. Cattin, Univ. Basel (Switzerland)

Ever since the first functional lasers were built about 50 years ago, researchers and doctors have dreamed of a medical use for such systems. Today's technology is finally advanced enough to realize these ambitions in a variety of medical fields. There are well-established laser based systems in ophthalmology, dental applications, treatment of kidney stones, and many more. The Er:YAG laser presents more than just an alternative to conventional methods for osteotomies. It offers less tissue damage, faster healing times, comparable intervention duration and in the consequence improves postoperative treatment of patients. However, there are a few factors that limit routine applications. These technical drawbacks include missing depth control and safely guiding the laser beam. But those drawbacks can be overcome. This paper presents the engineering and integration of a miniaturized laser head for a computer assisted and robotguided laser osteotome (CARLO), which is developed in the University of Basel Spin-off AOT AG. The CARLO device ensures a safe and precise guidance of the laser beam. Such guidance also enables new opportunities and methods, e.g. free geometrical functional cuts, which have the potential to revolutionize bone surgery. The laser head is optimized for beam shaping, target conditioning, compactness and the integration of all other parts needed for the CARLO device, e.g. CCD-Camera for referencing, a visible guidance laser, etc. The beam coming out of the laser system is conditioned in shape, energy properties and working distance with an optical arrangement to achieve the desired cutting performance. Here also parameters like optical losses, operating mode, optics materials and longterm stability have are taken into account.

9579-3, Session 1

Multispectral digital holographic microscopy with applications in water quality assessment

Farnoud Kazemzadeh, Chao Jin, Iman Khodadad, Robert Amelard, Shahid A. Haider, Simarjeet S. Saini, Monica B. Emelko, Univ. of Waterloo (Canada); David A Clausi, Univ of Waterloo (Canada); Alexander Wong, Univ. of Waterloo (Canada)

Safe drinking water is essential for human health, yet over a billion people



worldwide do not have access to safe drinking water. Due to the presence and accumulation of bio-contaminates in the natural water sources, (e.g. pathogenic microorganisms, neurotoxin, hepatotoxin or cytotoxin released due to algal bloom), it is increasingly challenging to provide safe drinking water supply around the world. One of the biggest challenges in water quality assessment is the speed and accuracy of quantitative analysis at reasonable costs. Traditional laboratory methods are costly, time consuming and require well trained experts to conduct the sample analysis. It is not financially feasible and practical to monitor and quantify water quality frequently enough to identify the potential health risk due to contamination, especially in developing countries. We propose a low-cost, small-profile multispectral (MS) system based on Digital Holographic Microscopy (DHM) and investigate methods for rapidly capturing holographic data of natural water samples. We have developed a test-bed for an MSDHM instrument to produce and capture holographic data of the sample at different wavelengths in the visible and the near Infra-red spectral region, allowing for resolution improvement in the reconstructed images. Additionally, we have developed high-speed statistical signal processing and analysis techniques to facilitate rapid reconstruction and assessment of the MS holographic data being captured by the MSDHM instrument. The proposed system is used to examine cyanobacteria as well as Cryptosporidium parvum which are the main concerns in the natural water sources globally.

9579-4, Session 1

Concurrent fluorescence macro-imaging across multiple spectral regions in the visible and the near infrared

Farnoud Kazemzadeh, Shahid A. Haider, Chao Jin, David A. Clausi, Alexander Wong, Univ. of Waterloo (Canada)

Fluorescent imaging, often synonymous with microscopic imaging, is an imaging modality whereby various features of a target are observed based on assignment of chemical labels. These labels are in most cases indirect tracers of specific structures or chemical compounds which cannot be otherwise identified. The tracers are excited by an illuminating source and they in turn emit light at specific wavelengths. This light is then captured by an imaging device and represented as an indirect observation of the specific feature in the sample. The process of excitation and imaging of the emitted light is performed sequentially and is proportional to the number of tracers or fluorescence species present in the sample. We present an imaging system that can image fluorescent tracers, in the visible and the near Infra-red, simultaneously. This system is capable of illuminating the target with different excitation light sources and capture the corresponding fluorescence images in one snapshot using a series of mirrors to capture different views of the sample. The simultaneously captured image are fused using a computational reconstruction process to present a coherent multispectral fluorescence image. The system is proposed for use in applications where the rapid enumeration of fluorescent species in a large field of view is paramount as opposed to their microscopic image of in a narrow field of view. The system was tested using a controlled cocktail solution of four different types fluorescent microspheres and was able to enumerate the microspheres based on their different fluorescent signatures as captured by the system.

9579-5, Session 1

Endoscopic system for automated high dynamic range inspection of moving periodic structures

Cornelius F. Hahlweg, bbw Hochschule (Germany); Hendrik Rothe, Helmut-Schmidt Univ. (Germany)

In the current paper an advanced endoscopic system for high resolution and high dynamic range inspection of persiodic structures in rotating machines is presented. We address the system architecture, short time illumination, special optical problems, such as exclusion of the specular reflex, image processing, forward velocity prediction and metrological image processing. There are several special requirements to be met, such as the thermal stability above 100 °C, robustness of the image field, illumination in view direction and the separation of metallic surface diffuse scatter. To find a compromise between image resolution and frame rate, an external sensor system was applied for synchronization with the moving target. The system originally was intended for inspection of thermal engines, but turned out to be of a more general use. Beside the theoretical part and dimensioning issues, practical examples and measurement results are included.

9579-101,

Democratization of next-generation imaging, sensing, and diagnostics tools through computational photonics

Aydogan Ozcan, Univ. of California, Los Angeles (United States) and California NanoSystems Institute (United States)

My research focuses on the use of computation/algorithms to create new optical microscopy, sensing, and diagnostic techniques, significantly improving existing tools for probing micro- and nano-objects while also simplifying the designs of these analysis tools. In this presentation, I will introduce a new set of computational microscopes which use lens-free onchip imaging to replace traditional lenses with holographic reconstruction algorithms. Basically, 3D images of specimens are reconstructed from their "shadows" providing considerably improved field-of-view (FOV) and depth-of-field, thus enabling large sample volumes to be rapidly imaged, even at nanoscale. These new computational microscopes routinely generate >1-2 billion pixels (giga-pixels), where even single viruses can be detected with a FOV that is >100 fold wider than other techniques. At the heart of this leapfrog performance lie self-assembled liquid nano-lenses that are computationally imaged on a chip. These self-assembled nanolenses are stable for >1 hour at room temperature, and are composed of a biocompatible buffer that prevents nano-particle aggregation while also acting as a spatial "phase mask." The field-of-view of these computational microscopes is equal to the active-area of the sensor-array, easily reaching, for example, >20 mm2 or >10 cm2 by employing state-of-the-art CMOS or CCD imaging chips, respectively.

In addition to this remarkable increase in throughput, another major benefit of this technology is that it lends itself to field-portable and cost-effective designs which easily integrate with smartphones to conduct giga-pixel telepathology and microscopy even in resource-poor and remote settings where traditional techniques are difficult to implement and sustain, thus opening the door to various telemedicine applications in global health. Some other examples of these smartphone-based biomedical tools that I will describe include imaging flow cytometers, immunochromatographic diagnostic test readers, bacteria/pathogen sensors, blood analyzers for complete blood count, and allergen detectors. Through the development of similar computational imagers, I will also report the discovery of new 3D swimming patterns observed in human and animal sperm. One of this newly discovered and extremely rare motion is in the form of "chiral ribbons" where the planar swings of the sperm head occur on an osculating plane creating in some cases a helical ribbon and in some others a twisted ribbon. Shedding light onto the statistics and biophysics of various micro-swimmers' 3D motion, these results provide an important example of how biomedical imaging significantly benefits from emerging computational algorithms/theories, revolutionizing existing tools for observing various micro- and nano-scale phenomena in innovative, high-throughput, and yet cost-effective ways.

9579-102,

Restocking the optical designers' toolbox for next-generation wearable displays

Bernard C. Kress, Google (United States)

Three years ago, industry and consumers learned that there was more to Head Mounted Displays (HMDs) than the long-lasting but steady market for defense or the market for gadget video player headsets: the first versions



of Smart Glasses were introduced to the public. Since then, most major consumer electronics companies unveiled their own versions of Connected Glasses, Smart Glasses or Smart Eyewear, AR (Augmented Reality) and VR (Virtual Reality) headsets. This rush resulted in the build-up of a formidable zoo of optical technologies, each claiming to be best suited for the task on hand. Today, the question is not so much anymore "will the Smart Glass market happen?" but rather "which optical technologies will be best fitted for the various declinations of the existing wearable display market," one of the main declination being the Smart Glasses market.

9579-6, Session 2

Development features of nuclear CCTV systems for reactors' internal surfaces surveillance

Sergei L. Pervov, Radda A. Iureva, Nadezhda K. Maltseva, Michael E. Fedosovsky, National Research Univ. of Information Technologies, Mechanics and Optics (Russian Federation)

Special devices with high tolerance to radiation and certification for tolerance to a certain level and nature of radiation exposure are required to service an existing nuclear power plant (NPP).

Some part of system will be a subject to radiation exposure's maximum. A good solution to reduce the net cost of an element base under radiation exposure's maximum is to remove a part of camera's elements to an external unit, also located at a distance from a radiation source. This solution not only provides an opportunity to reduce an amount of components, receiving the highest dose of radiation, but also helps to reduce the size and weight of a camera and allows to simplify the design and circuit of the device operating under constant negative radiation exposure. Thus, only lens, vidicon and minimum of electronic circuits have to be located in camera unit in order to achieve maximum of radiation tolerance. The main part of electronic circuits is removed to television system remote unit located outside radiation exposure.

As for an optical part of a system, thanks to special circuit design and use of rad-tolerant vidicon as light-to-signal transducer it provides excellent image quality and sharpness in high radiation fields. All lenses are made of rad-tolerant glass, not darkening under radiation exposure.

Rad-tolerant TV camera, minimization of electronic circuits, exposed to radiation, specialized software for receiving, processing and recording images contribute to implementation of the above mentioned features and operation of rad-tolerant CCTV systems twenty four by seven.

9579-7, Session 2

Dynamic noise corrected hyperspectral radiometric calibration in the SWIR 1000-2300 nm using a supercontinuum laser

Janos C. Keresztes, Ben Aernouts, KU Leuven (Belgium); R. John Koshel, College of Optical Sciences, The Univ. of Arizona (United States); Wouter Saeys, KU Leuven (Belgium)

As line scanning short wave infrared (SWIR) hyperspectral imaging (HSI) is a growing field in the food industry, it is important to select efficient illumination designs to image contaminants with high contrast and low noise. Spectral radiometric measurements onto an illuminated lambertian target can be performed to compare SWIR light systems. Those imagers can be calibrated in spectral radiometric units using a supercontinuum laser setup. However, as those measurements can be time consuming, InGaAs based sensors being very sensitive to noise, the dark current should be sampled frequently to avoid noise time drifts. Additionally, fluctuations of the laser power can occur, which may bias the radiometric model. To correct for source fluctuations, an optical system consisting of a supercontinuum laser, a monochromator, a second order filter and a gold-coated integrating

sphere (IS) setup is proposed. The input laser power is first measured using a power meter coupled with a thermal sensor. A high sensitivity photodiode and the HSI are further placed at different ports of the IS to measure synchronously the monochromatic light during calibration. For each spectral band, the radiance observed by the imager corresponding to a line is detected using image analysis, while the remainder of the image is used to sample the noise of the sensor. This approach allowed to correct for 6% of noise temporal fluctuations. A per-pixel linear radiometric model was fitted with an R? of 0.94 \pm 0.3, and used to measure a halogen spot light distribution with and without a diffuser using the calibrated SWIR HSI.

9579-8, Session 2

Risley prism universal pointing system

John P. Dixon, James R. Engel, Robert Vaillancourt, Craig Schwarze, Kevin Potter, OPTRA, Inc. (United States)

OPTRA is currently developing a Risley Prism Universal Pointing System (RPUPS): a highly customizable cued beamsteering system. The RPUPS consists of a visible or infrared cueing imager co-aligned with an optical beam steering system's pointing-field-of-regard. The cueing imager is used to identify a region-of-interest within its wide field-of-view, via a wireless tablet device. The tablet user can choose to manually or automatically, identify and track regions-of-interest. The optical beam steering system uses a matched pair of Risley Prisms to direct an interrogating optical system's instantaneous-field-of-view onto the identified region-of-interest. The tablet updates the user with real time information from both the cueing imager and the interrogating optical system. Risley prism material and geometry choices provide operating wavelength, aperture size, and field-of-regard flexibility for this front-end pointing component. Back-end components may be receive-only, transmit-only, or transmit/receive combinations. The flexibility of the RPUPS allows for mission specific customization where applications include but are not limited to: synthetic foveated imaging, spectroscopic probes and laser (LIDAR) ranging and tracking. This paper will focus on the design and anticipated applications of the RPUPS.

9579-9, Session 2

Further development of imaging near-field scatterometer

Denise Uebeler, Florian Dannenberg, Cornelius F. Hahlweg, bbw Hochschule (Germany)

In continuation of last years paper on the use of near field imaging, which basically is a reflective shadowgraph method, for characterization of glossy surfaces like printed matter or laminated material, further developments are discussed. Beside the identification of several types of surfaces and related features, for which the method is applicable, several refinements are introduced. First, the theory of the method is extended, based on a mixed fourier-optical and geometrical approach. Further, cross and parallel polarization techniques are applied for separation of the shadow image and the image of the near field distribution of the diffuse reflective part of the shadowing areas. Variation of plane of focus and incident angle are used for reconstruction of the surface unter test. Finally, latest measurement results and examples are included.

9579-10, Session 2

Object silhouettes and surface directions through stereo matching image processing

Akira Akiyama, Kanazawa Technical College (Japan); Hideo Kumagai, Tamagawa Seiki Co., Ltd. (Japan)

We have studied the object silhouettes and surface directions through the stereo matching image processing to recognize the occupation position, size and direction of the object.



When we work for the stereo matching image processing by using a pair of the good contrast captured images, we can only match the object component areas between a pair of image. And the extraction of the object silhouette is difficult under using a pair of the good contrast images only when the object boundary intensity is smoothly close to the other objects and the background.

We usually need the object silhouette to realize the object body as a whole. We note that the tendency of the object intensity change near the good contrast focus position is more stable than the tendency of other objects intensity change under not good contrast focus position.

Therefore we use several images near the good contrast focus position to extract the object silhouette. We can extract the object silhouette by computing the intensity change with respect to each pixel, arranging the pixel intensity change into the pixel intensity change distribution form large to small order as a half normal distribution, extending it as a whole normal distribution, computing its standard deviation and selecting the small intensity change pixel by the computed standard deviation. The group of the selected small intensity change pixel becomes the object silhouette candidate.

We use the pixel numbers of a pair of object component area and the projection cosine rule to find the surface direction followed by the stereo matching image processing.

9579-11, Session 3

Advancements in transformation opticsenabled gradient-index lens design

Sawyer D. Campbell, Donovan E. Brocker, Jogender Nagar, Pingjuan L. Werner, Douglas H. Werner, The Pennsylvania State Univ. (United States)

Transformation Optics (TO) provides the mathematical framework for representing the behavior of electromagnetic radiation in a given geometry by "transforming" it to an alternative, usually more desirable, geometry through an appropriate mapping of the constituent material parameters. Using a quasi-conformal mapping, the restrictions on the required material parameters can be relaxed allowing isotropic inhomogeneous all-dielectric materials to be employed. This approach has led to the development of a new and powerful design tool for gradient-index (GRIN) optical systems. Using TO, aspherical lenses can be transformed to simpler spherical and flat geometries or even rotationally-asymmetric shapes which result in true 3D GRIN profiles. TO can also potentially be extended to collapse an entire lens system into a representative GRIN profile thus reducing its physical dimensions while retaining the optical performance of the original system. However, dispersion effects of the constituent materials often limit the bandwidth of metamaterial and TO structures thus restricting their potential applicability. Nonetheless, with the proper pairing of GRIN profile and lens geometry to a given material system, chromatic aberrations can be minimized. To aid in the GRIN construction, we employ advanced multiobjective optimization algorithms which allow the designer to explicitly view the trade-offs between all design objectives such as RMS spot size, field-of-view (FOV), lens thickness, ?n, and focal drift due to chromatic aberrations. We present an overview of our TO-enabled GRIN lens design process and analysis techniques while demonstrating designs which minimize the presence of mono- and polychromatic aberrations and discuss their requisite material systems.

9579-12, Session 3

Simulating optical system performance with three-dimensional scenes

William J. Duncan, Jim Schwiegerling, The Univ. of Arizona (United States)

A variety of techniques with varying levels of accuracy have been developed to simulate images that are produced by optical systems. In the simplest approximation, the Point Spread Function (PSF) is assumed invariant over

the field of view of the system. This leads to a simulated image which is simply the convolution of the PSF with the appropriately-scale version of the object scene. The next level of approximation samples the PSF at multiple points in the field and uses this information to interpolate the PSF at an arbitrary field point. The simulated image is then assembled from the individual PSFs. Both of these techniques inherently assume a 2D planar object. In this effort, we develop techniques for extending the image simulations to 3D scenes. In general, the PSF will now be dependent both on the location of a point in the field as well as the distance to the point is object space. We investigate the image simulation for standardized scenes and compare to similar scenes captured photographically. In addition, we examine approximations to simulating the blurred 3D scene which include assuming the scene is composed of discrete planes at different distances, as well as ignoring higher order aberrations in cases where defocus is the dominant aberration. These approximations facilitate a reduction in computation time.

9579-13, Session 3

Curved fiber bundles for monocentric lens imaging (*Invited Paper*)

Salman Karbasi, Igor Stamenov, Nojan Motamedi, Ashkan Arianpour, Univ. of California, San Diego (United States); Adam Johnson, Ron Stack, Rick Morrison, Distant Focus Corp. (United States); Ilya Agurok, Distant Focus Corp. (United States) and Univ. of California, San Diego (United States); Joseph Ford, Univ. of California, San Diego (United States)

Monocentric lenses allow high resolution panoramic imaging, where imaging fiber bundles transport the hemispherical image surface to conventional focal planes. Refraction at the curved image surface limits the field of view coupled through a single bundle of straight fibers to less than +/-34°, even for NA 1 fibers. Previously we have demonstrated a nearly continuous 128° field of view using a single lens and multiple adjacent straight fiber coupled image sensors, but this imposes mechanical complexity of fiber bundle shaping and integration. However, a 3-D waveguide structure with internally curved optical fiber pathways can couple the full continuous field of view onto a single focal plane. Here we demonstrate how the 3D bundle can be formed from a tapered fiber bundle, and show that it can be used for relaying a 128° field of view from a curved input to the planar output face. We numerically show the coupling efficiency of light to the tapered bundle for different field of views depends on the taper ratio of the bundle as well as center of the curvature chosen for polishing of the fiber bundle facet. We characterize a tapered fiber bundle by measuring the angle dependent impulse response and the divergence angle of the light propagating from the output end of the fiber. Finally, we demonstrate wide-field imaging using a monocentric lens and the curved fiber bundle.

9579-14, Session 4

Optical transfer function optimization based on linear expansions

Jim Schwiegerling, The Univ. of Arizona (United States)

The Optical Transfer Function (OTF) and its modulus the Modulation Transfer Function (MTF) are metrics of optical system performance. However in system optimization, calculation times for the OTF are often substantially longer than more traditional optimization targets such as wavefront error or transverse ray error. The OTF is typically calculated as either the autocorrelation of the complex pupil function or as the Fourier transform of the Point Spread Function. We recently demonstrated that the on-axis OTF can be represented as a linear combination of analytical functions where the weighting terms are directly related to the wavefront error coefficients and apodization of the complex pupil function. Here, we extend this technique to the off-axis case. Strategies for fast and stable calculation of the expansion terms, as well as examples of OTF optimization of traditional imaging systems and extended depth of focus systems will



be illustrated. The expansion technique offers a potential for accelerating OTF optimization in lens design, as well as insight into the interaction of aberrations with components of the OTF.

9579-15, Session 4

Illumination design using computer experiments

Janos C. Keresztes, Bart De Ketelaere, Jan Audenaert, KU Leuven (Belgium); R. John Koshel, College of Optical Sciences, The Univ. of Arizona (United States); Wouter Saeys, KU Leuven (Belgium)

Illumination design becomes crucial when designing cost-effective machine vision systems. Local optimization methods, such as the down hill simplex optimization (simplex), often result in an optimal solution that is influenced by the starting point by converging to a local minima, especially when dealing with high dimensional designs or nonlinear merit spaces. This work suggests a novel non-linear optimization approach, based on computer experiments. The methodology is first illustrated with a 2D case study on four lights symmetrically positioned along a fixed arc in order to obtain optimal irradiance uniformity on a flat Lambertian reflecting target. The first step consists to choose angular positions with no overlap between sources using a fast flexible space filling design. Ray tracing simulations are then performed at the found design space points and a merit function is used for each configuration to quantify the homogeneity of the irradiance at the target. The screening points and their response are further used as input to a Gaussian kriging model (GKM), which models the merit space. Global optimization is performed on the GKM providing an estimate optimum. Next, the light positioning case study is further investigated by varying the radius of the arc, and by adding two spots symmetrically positioned along an arc diametrically opposed to the first one. The added value of computer experiments with regard to the performance in convergence is compared to simplex. Experimental validation is performed using a short-wavelength infrared (SWIR) hyperspectral imager monitoring a Spectralon panel illuminated by tungsten halogen sources.

9579-16, Session 4

Comparative analysis of optimization with freeform orthogonal polynomials for rectangular apertures

Milena I. Nikolic, Univ. Polítecnica de Madrid (Spain); Pablo Benítez, Juan Carlos Miñano, Univ. Politécnica de Madrid (Spain) and Light Prescriptions Innovators, LLC (United States); Jiayao Liu, Dejan Grabovickic, Bharathwaj Narasimhan, Marina Buljan, Univ. Politécnica de Madrid (Spain)

Interest in optical systems that use freeform surfaces is rapidly increasing with the development of new manufacturing techniques. With the investigation of novel applications new issues constantly appear. Since freeform surfaces tend to be used in a non-conventional optical systems, like off-axis systems or high aspect ratio systems, a study of non-circular apertures is of potential relevance.

First non-circular aperture shape that one can be interested in due to tessellation or various folds system is the rectangular one. This paper covers the comparative analysis of a simple local optimization of one design example using different orthogonalized representations of our freeform surface for the rectangular aperture.

A very simple single surface off-axis mirror is chosen as a starting system. The surface is fitted to the desired polynomial representation, and the whole system is then optimized with the only constraint being the effective focal length. The process is repeated for different surface representations, amongst which there are some defined inside a circle, like Zernike or Forbes polynomials, and others that can be defined inside a rectangle like Legendre and new calculated Legendre type polynomials orthogonal in the gradient.

It can be observed that with Legendre or this new calculated polynomial type there is a faster convergence to a deeper minimum compared to defined-inside-a-circle polynomials. The average MTF values across 17 field points also show clear benefits in using the polynomials that adapted more accurately to the aperture used in the system.

9579-17, Session 4

Design of three freeform mirror aplanats

Bharathwaj Narasimhan, Pablo Benitez, Dejan Grabovickic, Juan C. Miñano, Milena Nikolic, Jose Infante, Univ. Politécnica de Madrid (Spain)

Freeform optical surfaces have been in much demand recently due to improved techniques in their manufacturability and design methodology, and the degrees of freedom it gives the designers. Specifically in the case of off-axis mirror systems, freeforms can considerably reduce the number of surfaces and compensate for some of the higher order aberrations as well, which improves the overall system performance.

In this paper, we explore the design of freeform surfaces to obtain full aplanatic mirror system, i.e, free of spherical aberration and circular coma of all orders. It is well know that such a system must be stigmatic and satisfy the Abbe sine condition. This problem is well known (Schwartlitz, 1906) to be solvable with two aspherics when the system has rotational symmetry. Here we prove that a rigorous solution to the general non-symmetric problem needs at least three free form surfaces, which are solutions of a system of partial differential equations.

We present here that the three mirror solutions of said system of PDE can be found using optimization. The merit function for such an optimization includes the spatial and angular deviation of the rays sampled in the pupil from the aplanatic condition. Therefore, the value of the merit function at the exact solution will be zero. The examples considered have one plane of symmetry, where a consistent 2D solution is used as boundary condition for the 3D problem. We have used the x-y polynomial representations for all the surfaces, and the optimization has shown fast convergence.

9579-18, Session 4

A method to improve the image reconstruction quality in a coded aperture compressive imaging system

Ouyang Yao, Jing Chen, Beijing Institute of Technology (China)

Compressive imaging is one of the emerging novel research areas based on compressive sensing theory. The first successful compressive imaging application is the single pixel camera designed by Rice University which used only one detector for image sensing. Another promising compressive imaging device is based on a coded aperture system called coded aperture compressive imaging designed by Duke University which embodied its advantages in reducing imaging time compared with single pixel camera. To make coded aperture compressive imaging method become a practical imaging system, several optical system parameters have to been considered and optimized. Therefore in this paper we simulated a coded aperture compressive imaging system using optical simulation software and described an optimized design of coded aperture mask to improve the performance of reconstructed image.

The contribution of this paper includes three parts. First, we simulated a coded aperture compressive imaging system by utilizing ZEMAX and quantified the relationship between the image reconstruction error and optical parameters, such as defocus distance, F number of lens, mask position and fill-factor of mask. Second, for coded aperture compressive imaging system the projection matrix was generated from the coded aperture mask. According to compressive sensing theory, the sparse dictionary and projection matrix have a great influence on the quality of reconstructed image. Therefore we used an optimization method that based



on equiangular tight frame (ETF) design to minimize the mutual coherence between projection matrix and sparse dictionary. From this optimized projection matrix, we derived a better coded aperture mask pattern. Experimental results show that the mutual coherence coefficient between projection matrix and the sparse basis was reduced more than 15% and the retrieved image error was decreased significantly.

9579-19, Session 5

120-view autostereoscopic display

Junejei Huang, Yuchang Wang, Delta Electronics, Inc. (Taiwan)

A 120-view autostereoscopic display using angle-magnifying screen is proposed. The angle-magnifying screen comprises a double-lenticular main part and a micro-deflector attaching part. With the micro-deflector, small angles eixting from the aperture of the projection lens is deflected into four angle ranges. With the double-lenticular, four ranges of small angles incident into the screen are magnified into a large field of view for the observer. The scanning angles are realized by the vibration of Galvomirror that synchronizing with the frame rate of the DMD and reflecting the laser illuminator to the scanning angles. For one cycle of vibration of Galvo-mirror, 8 and 7steps of reflections happen on going and returning paths. A frame is divided into two viewing frames of odd or even lines. For each viewing position, 48 viewing frames with odd or even lines per second are provided. Two aperture-relay lenses are used to double the aperture of the projection lens and viewing frame of of odd or even lines is selected for each aperture. On the exit pupil, a scanning 30 spots of light source is realized. The double-lenticular is covered with two micro-deflector sheets of (+1,-1) and (+2,-2) deflecting angles. The defecting directions of two sheets are perpendicular to each other. Each elements of the micro-deflector are aligned with the pixels that imaged on the screen. When a scanning of 30 spots passes different deflecting elements of 4 pixels, the scanning is deflected to four angle ranges and 120 viewing zones are formed after the screen magnification.

9579-20, Session 5

Color and brightness uniformity compensation of a multi-projection 3D display

Jin-Ho Lee, Juyong Park, Dongkyung Nam, Du-Sik Park, SAMSUNG Electronics Co., Ltd. (Korea, Republic of)

Light-field displays are good candidates in the field of glasses-free 3D display for showing real 3D images without decreasing the image resolution. To acquire a large number of light-field rays, the projector arrays could be used. But, in the multi-projection display system, the compensation is very critical due to slightly different characteristics and arrangement positions of the projectors. In this paper, we present an enhanced 55-inch, 100-Mpixel multi-projection 3D display consisting of 96 micro projectors for immersive natural 3D viewing in medical and educational applications. To achieve enhanced image quality, color and brightness uniformity compensation method are utilized along with an improved projector configuration design and a real-time calibration process of projector alignment. In the color compensation method, the reference images from each projector are captured by a camera arranged in front of the screen, and then a number of pixels depending on color intensities of the captured images are calculated, and the distributions of the RGB colors are corrected based on a maximum value of the color intensity. In the brightness compensation method, each light-field ray emitted from a screen pixel is modeled by a radial basis function, and then compensating weights of each screen pixel are calculated for the desired uniformity distribution. Compensating weights are transferred to the projection images by the mapping relationship between the screen and projector coordinates. Finally, brightness compensated images are rendered for each projector. Consequently, the display shows improved color and brightness uniformity, and consistent, exceptional 3D image quality.

9579-21, Session 5

3M miniature projection optical system design

Zhisheng Yun, Andrew Ouderkirk, Stephen J. Willett, 3M Co. (United States)

This paper describes the pros and cons of designing a miniature projection system with the emphasis on efficiency (Im/w) with respect to maximum brightness (Im) on screen. In particular, this paper will discuss how to design a miniature optical system to achieve high efficiency and how to design the optical system to get maximum brightness on screen. This paper will present a couple of optical system design examples to explain the findings by the authors.

9579-22, Session 5

Convertible 2D-3D display using an edgelit light guide plate based on integral imaging

Zi Wang, An-Ting Wang, Chun Gu, Lixin Xu, Hai Ming, Univ. of Science and Technology of China (China)

A thin and lensless two-dimensional (2D) to three-dimensional (3D) convertible display based on integral imaging using an edge-lit light guide plate (LGP) is proposed with improved optical efficiency. The proposed system is composed of a general flat backlight and an edge-lit LGP which is commonly used in the backlight of LCD and a LC panel. The edge-lit LGP is a waveguide (an acrylic sheet) that is drilled by laser to form a diffuser dot array at the bottom and edge illuminated with LEDs. Light from the LEDs is channeled through the waveguide to the opposite side except where it encounters the diffuser dots, which scatter light and cause bright spots to appear. A point light source array for 3D mode is created then. A general flat backlight behind the transparent LGP is turned on for 2D mode meanwhile edge-lit light is turned off. The 2D and the 3D display modes can be simply modulated by turning on different light source. The explanation of the proposed system is provided and the experimental results are also presented.

Conference 9580: Zoom Lenses V

Monday - Thursday 10–13 August 2015 Part of Proceedings of SPIE Vol. 9580 Zoom Lenses V

9580-23, Session PMon

A liquid lens actuated using dielectric polymer

Boya Jin, Jihyeon Lee, Zuowei Zhou, Sangwoo Park, Changwoon Nah, Hongwen Ren, Chonbuk National Univ. (Korea, Republic of)

Adaptive liquid lenses have been studied intensively in the past decades. They have potential applications in machine vision, target tracking, image surveillance systems, and portable electronic devices. Owing to the optical isotropy, these liquid lenses can obtain the highest optical performances. Various approaches, such as mechanical actuation, stimuli-responsive hydrogel, ferrofluidic, acoustic, electrowetting, dielectrophoretic effect, and dielectric polymer (DEP) actuation were demonstrated. Each approach has its own strengths and limitations. In contrast to other approaches, a liquid lens based on DEP owns the advantages of scalable lens aperture, a large focus power change, and voltage actuation. The major challenge of the demonstrated DEP lenses is the bulky system.

In this report, an adaptive liquid lens actuated using a DEP film is demonstrated. Different from previous method, we integrate a DEP film and a liquid droplet to form a lens system. Therefore, our lens system is very compact. The DEP film has a circular hole, and the liquid droplet is fixed in the hole. The droplet has a lens character. When a DC voltage is applied to the DEP film, the aperture of the DEP hole is changed due to the pressure of the generated Maxwell force. The changed aperture can cause the surface profile of the droplet to vary. As a result, the focal length of the liquid lens has to change. In this work, we demonstrated a DEP liquid lens with a miniature aperture size, the focal length of the lens is measured and the optical performances of the lens are evaluated. Our lens can present a high performance with a large dynamic range for imaging. Our DEP liquid lens has potential applications in image processing, machine vision, biotechnology, and other lab-on-a-chip devices.

9580-1, Session 1

Challenges of designing a zoom lens for planetarium projection (Invited Paper)

Marco Hanft, Dirk Döring, Carl Zeiss AG (Germany)

The optical design of zoom lenses for projection applications is a task which has to take many different aspects into consideration. The optical designer has to achieve a demanding specification with respect to monochromatic and polychromatic aberrations across a significant magnification range.

Besides the requirements on image quality there are usually numerous constraints deriving from fixed mechanical interfaces that already have an impact in the very early design stages of the paraxial and monochromatic design.

It has been proven essential to also include cost targets in the figure of merit during the design work.

This paper will outline a systematic process for projection zoom lenses design.

A solid specification of the design task in terms of magnification range, image quality therein, mechanical and cost requirements is necessary as starting point.

Paraxial considerations are helpful to gain insight into the design problem and choose the appropriate zoom design type for further design work.

Intermediate designs, which are only monochromatically corrected, proofed invaluable while considering mechanical design requirements.

As soon the basic design requirements are fulfilled it makes sense to correct chromatic aberrations.

Outstanding color correction requires extensive use of expensive glasses for secondary color correction.

In order to find an ideal compromise between potential cost of an optical

design and image quality achieved therewith, we employ tools to identify cost drivers as well as tools to simulate the perceived imaging performance. Together these tools also enable us to efficiently discuss specifications that drive cost without aiding perceived image quality.

9580-2, Session 1

"Perfect Zoom System" which enables both a zoom ratio of 25:1 and a highresolution in stereo microscope (Invited Paper)

Norio Miyake, Masahiro Mizuta, Nobuhiro Shinada, Hiroaki Nakayama, Yumiko Ohuchi, Nikon Corp. (Japan)

A stereo microscope can stereoscopically observe an object with protrusions and recesses as if the object is viewed by both eyes. In such a stereo microscope, an optical system of the luminous flux entering left and right eyes is at least partially separated to cause the optical axes to intersect over the surface of the object to obtain a parallax for stereoscopically observing the object. Enlarged images of the object viewed from different directions are created, and the images are observed through an eyepiece to stereoscopically view a minute object. Each of the observation optical systems usually includes a variable magnification mechanism which will be called a zoom lens system.

In recent years, a demand for a stereo microscope capable of observing a wide variable magnification range by one microscope is increasing along with the diversification of applications.

However, there are no stereo microscope zoom lenses with high resolution and large zoom ratio. We developed Perfect Zoom System, which can reduce the light flux diameter going through the objective lens in the lowpower state. In the Perfect Zoom System, the zoom lens groups move along not only the optical axes but also perpendicular to the axes. Therefore, it made the objective lens smaller by decentering both the second group lens G2 and the third lens group G3 in zoom lens group. We achieved a high resolution and a zoom ratio of 25:1.

9580-3, Session 1

Understanding how entrance and exit pupils have determined the evolution of the modern zoom lens design (Invited Paper)

Ellis Betensky, Consultant (Canada)

Stated simply, a zoom lens is an imaging device that allows for a continuously variable image scale without the need to refocus. Usually a zoom lens is further defined according the zoom ratio (range of magnification change), the size of the object covered, the image size, and the relative aperture. However, while the details of the entrance and exit pupils, particularly their locations and stability during zooming, have always played an important role in the design, they are rarely mentioned in the description of the lens. In this tutorial the position of the aperture stop, rather than the number of moving groups, will be used as a means of examining the design characteristics, and explaining how new designs have evolved. In addition to lens diameters, as determined by paraxial locations and the effects of aberration of the pupils, the position of the pupils, and their shapes as a function of zooming will be examined. The primary objective of the tutorial is to provide insight and a better understanding of zoom lens fundamentals, towards the selection of a design starting point; whether from an existing design, or from basic principles.





9580-4, Session 2

Toward a paraxial pre-design of zoom lenses (Invited Paper)

Thomas Milde, Carl Zeiss AG (Germany)

Optimizing the power distribution of fixed and moved lens groups as well as the motions of the latter, is typically a challenging part of the whole zoom lens optical design task. Once, the merit function is formulated to optimize an initial approach, the paraxial moving equations are solved implicitly in local optima. Hence, finding local optima becomes an ill posed problem when these equations cannot be solved uniquely for certain zoom configurations. Furthermore, an inappropriate initial power distribution can lead to large overall lengths, sensitive lens groups, small zoom ranges, induced aberrations and much more disadvantageous effects. From these reasons it appears as a logical consequence to first consider a paraxial pre-design of the zoom lens. This paper shows how first order aberrations, centering sensitivities as well as all common paraxial requirements can be analyzed and formulated as a merit function for finding power distributions and (zooming) air spaces. In particular, the benefit of formulating zoom invariants as constraints in order to apply the Sequential Quadratic Programming (SQP) is shown. Based on a variation approach, an optimizable characteristic is introduced for control of the uniqueness of the moving equations. Global optimization methods like e.g. Differential Evolution can be used to obtain an initial paraxial approach. This approach can be improved using the SQP or the Damped Least Squares (DLS) method. Finally, the generation of an initial real lens system is described.

9580-5, Session 2

New tools for finding first-order zoom lens solutions and the analysis of zoom lenses during the design process

Anthony J. Yee, Gustavo A. Gandara-Montano, Daniel J. L. Williams, Peter McCarthy, Julie Bentley, Duncan T. Moore, Univ. of Rochester (United States)

We developed software design tools in MATLAB that are compatible with CodeV for supporting the process of designing zoom lenses. These tools simplify the process of finding paraxial solutions and evaluating intermediary design steps. Paraxial solutions are found through a partially random search for four group zoom systems with moving second and third groups. It requires several user-specified system parameters and then randomly assigns powers to each group. This process of randomly assigning powers is done a set number of times and only the valid solutions where no lenses crash are considered for further use. The valid designs are plotted over different design criteria and can then be selected to retrieve the first order design parameters. For the intermediate design process, the software displays lens specifications and diagnostic results across zoom for the entire lens as well as the individual groups. Systematic evaluation of the intermediate design steps is useful in determining how to proceed and improve the design. The design process is described for two different zoom lenses to show the efficiency and utility of these tools. The two zoom lenses are a 16x surveillance camera zoom lens working in the visible and a 3x zoom lens working in the visible and short wave infrared. The design procedure for these lenses covers finding the paraxial solutions to evaluating the lens for further improvement.

9580-6, Session 2

Modular optical design for flexible beam expansion

Ulrike Fuchs, Sven Wickenhagen, asphericon GmbH (Germany)

In complex laser systems, such as those for material processing, and in basically all laboratory applications passive optical components are

indispensable. Matching beam diameters is a common task, where Galileo type telescopes are preferred for beam expansion. Nevertheless, researches and customers have found various limitations when using these systems. Some of them are complicated adjustment, very small diameter for the incoming beam (1/e?), fixed and non-modifiable magnifications. Above that, diffraction-limited performance is often only assured within the optical design. Additionally, one often would like to have a system that can be adapted to the wavelength used without varying the magnification.

A monolithic solution, which is based on the usage of only one aspheric component, will be presented. Systems are designed for four basic wavelengths (532, 632, 780 1064nm) and allow for a remarkable input aperture of up to 14.7mm. If various magnification levels (1.5x, 1.75x, 2.0x) are combined with each other in a cascade, one can achieve 230 possible overall enlargements. Experimental data on the performance of cascades with up to five monolithic elements with diffraction-limited wavefronts will be shown. Additionally, we present an add-on element, which allows for wavelength tuning and adaption of divergence of the incoming beam without changing the beam diameter. This allows for the usage of the monolithic beam expanders over the complete wavelength range from 500nm up to 1600nm. Furthermore, another module – a zoom lens - is introduced. Adding this element overcomes the discreet incrementation and allows for continuous enlargement from 1x to 32x.

9580-7, Session 2

Zoom lens design for tilted objects

Robert M. Malone, Daniel K. Frayer, Morris I. Kaufman, Heather R. Leffler, Alfred Meidinger, National Security Technologies, LLC (United States)

When a zoom lens views a tilted finite conjugate object, its image plane is both tilted and distorted depending on magnification. Our image plane design has six degrees of freedom; only one moving doublet lens is required to change magnification. Two lens design models were analyzed. The first required the optical and mechanical axes to be collinear, resulting in a tilted stop. The second allowed the optical axis to be tilted from the lens mechanical axis with an untilted stop moving along the mechanical axis. Both designs produced useful zoom lenses with excellent resolution for a distorted image. For both lens designs, the stop was anchored to the moving doublet and its diameter is unchanged throughout magnification changes. This unusual outcome allows the light level at each camera pixel to remain constant, independent of magnification. As-built tolerance analysis is used to compare both optical models.

The design application is for proton radiography. At the end of an accelerator, protons exit an aluminum vacuum window producing a shadowgraph image onto an LYSO (lutetium yttrium orthosilicate) scintillator. The 5? square scintillator emission reflects off a pellicle and is collected by the zoom lenses located 24? away. Four zoom lenses will view the same pellicle at different alpha and beta angles. Blue emission from the scintillator is viewed at an alpha angle of -14° or -23° and beta angles of $\pm 9^{\circ}$ or $\pm 25^{\circ}$. The pellicle directs the light backwards to a zone where adequate shielding of the cameras can be achieved against radiation scattered from the aluminum window.

9580-8, Session 2

Compensator selection considerations for a zoom lens

John R. Rogers, Synopsys, Inc. (United States)

The selection of compensators for a cam-driven zoom lens is more complex than for a prime lens, because tolerances cause the back focal distance to shift by different amounts in different zoom positions, i.e, the system loses parfocality. Adjustment of the back focal distance can bring one, but not all, of the zoom positions back into focus. Furthermore, compensator selection is more complex because it is usually desirable to avoid adjustments within the moving groups. If moving groups are to be adjusted, it is often desirable to restrict the adjustments to shifting entire groups rather than changing



spacings within the moving groups.

In this paper, we examine the effects of tolerances and compensators on a photographic-format zoom lens. We begin by assigning reasonable tolerances to all surfaces, materials, and groups, and then examine in detail how these tolerances affect the image quality. We determine the relative amount of degradation caused by transverse tolerances (decenters and tilts) compared to rotationally symmetric tolerances (power, index, thicknesses and spacings). For the rotationally symmetric tolerances, we examine the efficacy of the following compensators (which we list approximately in order of decreasing desirability): shifting the detector, shifting the fixed groups, respacing elements within the fixed groups, shifting the moving groups. Similarly, for the transverse tolerances, we examine the efficacy of implementing decenter compensators within the fixed groups, and then examine the additional performance gain achieved by implementing decenter compensators inside the moving groups.

9580-9, Session 2

To zoom or not to zoom: do we have enough pixels?

Richard N. Youngworth, Riyo LLC (United States); Eric Herman, The Aerospace Corp. (United States)

Common lexicon in imaging systems includes the commonly used term digital zoom. Of course this term is a complete misnomer as there is no zooming in such systems. Instead, digital zoom is a term describing the illusion of zoom that comes with an image rewriting or reprinting that is more accurately described cropping and enlarging an image (a pixel remapping) for viewing or printing. The essential question, pondered and manipulated since the advent of digital image science, really becomes "do we have enough pixels to not zoom." This paper will summarize known imaging factors in detail, most notably resolution considerations. The paper includes examples and information useful to the greater consumer, technical, and business community who all have an interest in understanding the key technical details that have driven the amazing technology and development of zoom lenses.

Ideas on nice things to possibly include:

- Space mapping out for zoom versus resolution (needs more thought)
- Examples will include cases where zoom MUST be used
- Another way to look at it: "Justifying zoom"

- Pixels are useful for other purposes – good point to make. Should any pixels be used to avoid zoom?

- Include zooming up and down types of cases

- Ask basic yet useful question here and provide a good summary of something that is not always understood by even technical people and certainly not the public

- Focus factors
- Pupil size changes

9580-10, Session 3

Increasing dual band infrared zoom ranges (Invited Paper)

Jay N. Vizgaitis, Arthur Hastings Jr., optX imaging system (United States)

Complexity in infrared zoom lenses is increased with the broadening of the spectral band. Trying to find ways to increase the zoom range for multi-spectral infrared systems without the overburdening of the optical train with significantly more elements or reduced performance can involve applying a combination of known methods. Traditionally zoom lenses generally take one of two forms...continuous zoom or discrete zoom. Continuous zoom lenses are generally built as all refractive solutions which require multiple

moving groups to achieve good performance over large magnification ranges. Discrete zoom lenses can be built in a similar method, be all reflective, or utilize combined reflective/refractive approaches for larger magnification ranges. Scaling pixel sizes for any given focal length also effectively zoom a lens by changing its instantaneous field of view. The concept and performance impact of combining all these concepts into a single zoom lens to significantly increase the zoom range of a dual band infrared system is explored in this paper.

9580-11, Session 3

Optical design study and prototyping of a dual-field zoom lens imaging in the 1-5 micron infrared waveband

Dmitry Reshidko, The Univ. of Arizona (United States); Pavel Reshidko, Ran Carmeli, RP Optical Lab. Ltd. (Israel); Jose Sasian, The Univ. of Arizona (United States)

Some optical systems can benefit from simultaneous imaging in several spectral bands. A new generation of focal plane arrays allow detection in more than one spectral region. The design of a refractive imaging lens for such detector is particularly challenging: the aberrations should be balanced over the wide range of wavelengths. On the other hand, the selection of available optical materials and coatings is limited.

We show a dual-field zoom lens designed for a cooled detector sensing from short-wave infra-red (SWIR) to mid-wave infra-red (MWIR) spectral bands (continuous imaging for 1-5 micron). The zoom lens has 75 mm focal length in the wide mode (horizontal field-of-view (HFOV) of 7.6 degrees) and 250mm focal length in the narrow mode (HFOV of 2.22 degrees), operating at f/4.7. The lens is designed to work in thermal environments from -20C to +70C. We present the optical design methodology, discuss the selection of materials and coatings for the optical elements, and analyze the transmission of the lens and optical performance. A prototype system has been manufactured and assembled. We validate our design with the experimental data.

9580-12, Session 3

Optical design study of a VIS-SWIR 3X zoom lens

Rebecca E. Berman, James A. Corsetti, Keija Fang, Eryn Fennig, Peter McCarthy, Greg R. Schmidt, Anthony J. Visconti, Daniel J. L. Williams, Anthony J. Yee, Yang Zhao, Julie Bentley, Duncan T. Moore, Univ. of Rochester (United States); Craig Olson, L-3 Communications (United States)

A design study is compiled for a VIS-SWIR dual band 3x zoom lens. The initial first order design study investigated zoom motion, power in each lens group, and aperture stop location. All designs were constrained to have both the first and last lens groups fixed, with two middle moving groups. The first order solutions were filtered based on zoom motion, performance. and size constraints, and were then modified to thick lens solutions for the SWIR spectrum. Successful solutions in the SWIR were next extended to the VIS-SWIR. The resulting nine solutions are all nearly diffraction limited using either PNNP or PNPZ ("Z" indicating the fourth group has a near-zero power) design forms with two moving groups. Solutions were found with the aperture stop in each of the four lens groups. Fixed f-number solutions exist when the aperture stop is located at the first and last lens groups, while varying f-number solutions occur when it is placed at either of the middle moving groups. Design exploration included trade-offs between parameters such as diameter, overall length, back focal length, number of elements, materials, and performance.



9580-13, Session 3

Chromatic correction for a VIS-SWIR zoom lens using optical glasses

Yang Zhao, Daniel J. L. Williams, Peter McCarthy, Anthony J. Visconti, Julie L. Bentley, Duncan T. Moore, Univ. of Rochester (United States)

With the advancement in sensors, hyperspectral imaging in short wave infrared (SWIR 0.9 ?m to 1.7 ?m) now has wide applications, including night vision, haze-penetrating imaging etc. Most conventional optical glasses can be material candidates for designing in the SWIR as they transmit up to 2.2 ?m. However, since SWIR is in the middle of the glasses' major absorption wavebands in UV and IR, the flint glasses in SWIR are less dispersive than in the visible spectrum. As a result, the glass map in the SWIR is highly compressed, with crowns and flints all clustering together. Thus correcting for chromatic aberration is more challenging in the SWIR, since the Abbe number ratio of the same glass combination is reduced. Conventionally, fluorides, such as CaF2 and BaF2, are widely used in designing SWIR system due to their unique dispersion properties, even though they are notorious for poor manufacturability or even high toxicity. For lens elements in a zoom system, the ray bundle samples different sections of the each lens aperture as the lens zooms. This creates extra uncertainty in correcting chromatic aberrations. This paper focuses on using only commercially available optical glasses to color-correct a 3X dual-band zoom lens system in the VIS-SWIR. The design tools and techniques are detailed in terms of material selections to minimize the chromatic aberrations in such a large spectrum band and all zoom positions. Examples are discussed for designs with different aperture stop locations, which considerably affect the material choices.

9580-14, Session 4

Cine-servo lens technology for 4K broadcast and cinematography (Invited Paper)

Ryuji Nurishi, Tsuyoshi Wakazono, Fumiaki Usui, Canon Inc. (Japan)

Along with the rapid evolution of 4K image capturing technology in the past few years, usage of large-format cameras with Super35mm Single Sensors has increased in TV production for diverse shows such as dramas, documentaries, wildlife, and sports. While large format image capturing has been the standard in the cinema world for a long time, the recent trend seen in the broadcast industry has revealed various differences in the requirements of large format lenses as compared to the cinema industry. A typical requirement for a broadcast lens is higher zoom ratio in order to avoid changing lenses in the middle of a live event, which is mostly not the case for traditional cinema productions. Another example would be the need for compact size, light weight and servo operability for a single camera operator shooting in a shoulder-mount ENG style. On the other hand, there are new requirements that are common to both worlds, such as smooth and seamless change in angle of view throughout the long zoom range, which could lead to a new image expression that never existed in the past.

This paper will discuss the requirements from both industries, cinema and broadcast, while at the same time introducing the new technologies and new optical design concepts applied to our latest "CINE-SERVO" lens series which consists of the two models, CN7x17KAS-H and CN20x50IAS-H.

It will further explain how Canon has realized 4K optical performance and fast servo control while achieving compact size, light weight and high zoom ratio at the same time, by referring to patent-pending technologies such as the optical power layout, lens construction, and glass material combinations.

9580-15, Session 4

Extreme retrofocus zoom lens for singleshot single-lens HDR photography and video

Anthony Vella, Julie L. Bentley, Univ. of Rochester (United States)

Traditional high dynamic range (HDR) photography is performed by capturing multiple images of the same scene with different exposure times, which are then digitally combined to produce an image with great detail in both its light and dark areas. However, this method is not viable for moving subjects since the multiple exposures are not captured simultaneously. Recently an alternative method has been developed in which beamsplitters are utilized to simultaneously record the same image on three identical sensors at different illumination levels. This process enables single-shot HDR photography as well as continuous HDR video. This paper describes the design of a 2.5x zoom lens for use in this application. The design satisfies the challenging working distance and ray angle constraints imposed by the placement of two beamsplitters between the lens and the image plane. The particular importance of first-order layout when designing a retrofocus zoom lens is also discussed.

9580-16, Session 4

All-reflective optical power zoom objectives (Invited Paper)

Jens Knobbe, Heinrich Grueger, Fraunhofer-Institut für Photonische Mikrosysteme (Germany); Kristof Seidl, Fraunhofer-Institut für Photonische Mikorsysteme (Germany)

Over the past decades zoom lenses have become an important type of objective. Due to their ability to dynamically change magnification or field angle they are being used in many fields of application. Most zoom lenses consist of a number of lenses or lens groups. The magnification can be changed by axially shifting some of these lens groups with a more or less complicated moving function.

However, in principle it should be possible to construct zoom lenses that do not rely on the movement of some of their components. Instead, the change in magnification is achieved by changing the optical power of at least two lenses within the system (optical power zoom (OPZ)). Moreover, for broadband applications it is highly favourable to use mirrors instead of lenses due to the absence of chromatic aberrations.

Based on a "Schiefspiegler" approach a 3x reflective OPZ objective consisting of four mirrors has been designed. Two mirrors are assumed to have a variable radius of curvature for changing optical power. During aberration correction special consideration has been given to the reduction of field curvature, since the optical power change strongly influences field curvature for different zoom positions. The simulation shows adequate image quality for photographic applications over the whole zooming range.

For the realization of such a OPZ objective deformable mirrors with a comparatively large stroke are needed. Before starting a complex development of such devices three setups with different fixed focal lengths were built as a prove of concept.

9580-17, Session 4

Design of a zoom lens with a large field-ofview and better solutions with asphere

Takanori Yamanashi, Theta Optical LLC (United States)

It is known that a wide angle zoom lens can include "wild asphere". It must be interesting to know how aspheres are influenced by aberration correction. Even if there are zoom lenses of positive lead and negative lead,



the latter one is commonly used for the wide angle zoom lens. In this paper different types of zoom lens are introduced and discussed, in terms of the optical design with the same specifications. Then possible ways on how to modify the asphere is suggested. In comparison a solution of all spherical version is also described.

9580-18, Session 5

Change of optical design thought about focusing of zoom lens (Invited Paper)

Hitoshi Hagimori, Panasonic Corp. (Japan)

Zoom lens has accomplished most various evolution as interchangeable lens attached to single-lens camera system to be differentiation from a fixed focal lens.

The interchangeable lens with zoom function put up a first cry around 1960 and so far many lenses with various specifications, from standard type to high zoom ratio type, has been sent out in the market by the innovation of optics type to change focal length continually.

When I move the eye to a camera body of single-lens system ,it may be said that the evolution of camera's function has been the history of the automation. most especially the auto focus alignment function evolved in by an appearance of phase difference AF method dramatically.

In late years contrast AF method with the imaging sensor comes up in digitization and auto focusing came to be made in the case of not only still image but also movie.

On the other hand, in the zoom lens for interchangeable system, new and original design thought about zooming and focusing that matched each AF method of this camera body was brought about and led to the development of the zoom lens.

In this report I introduce the design thought of optics about zooming and focusing of interchangeable zoom lens that evolved to the change of camera body AF method mentioned above. Also I say associated technique such as actuator and lens control, in addition introduce one end about directionality of the evolution of the future zoom lens.

9580-19, Session 5

Multi-channel compact optical zoom module by using microlenses

Wei-Hsiang Liao, Guo-Dung Su, National Taiwan Univ. (Taiwan)

Nowadays mobile cell phones are a few millimeters thickness. It becomes challenging to achieve optical zoom function in such a small device. In this paper, we propose a multi-channel imaging system which combines the principles of insect's compound eyes and optical zoom. The proposed optical system could reduce the total track length of optical zoom imaging device and has potential for compact mobile phone. The optical zoom is achieved by adjusting distance between two aspherical lenses to change effective focal length of the optical zoom system and insect's compound eye (multi-channel structure) is made by a curved hexgonal microlens array. By the curved hexgonal microlens array, we can get the same effect when using the lens group to make our system thinner. The thickness is about 8 mm and the zoom ratio is about 2X.

9580-20, Session 5

Design study for a 16x zoom lens system for visible surveillance camera

Anthony Vella, Heng Li, Yang Zhao, Isaac Trumper, Gustavo A. Gandara-Montano, Di Xu, Daniel K. Nikolov, Changchen Chen, Andres Guevara-Torres, Nicolas S. Brown, Hae Won Jung, Jacob Reimers, Julie L. Bentley, Univ. of Rochester (United States)

High zoom ratio zoom lenses have extensive applications in broadcasting, cinema and surveillance. Here, we present a design study on a 16x zoom lens with 4 groups (including two internal moving groups), designed for, but not limited to, a visible spectrum surveillance camera. Fifteen different solutions were discovered with nearly diffraction limited performance, using PNPX or PNNP design forms with the stop located in either the third or fourth group. Some interesting patterns and trends in the summarized results include the following: (a) in designs with such a large zoom ratio, the potential of locating the aperture stop in the front half of the system is limited, with ray height variations through zoom necessitating a very large lens diameter; (b) in many cases, the lens zoom motion has significant freedom to vary due to near zero total power in the middle two groups; and (c) we discuss the trade-offs between zoom configuration, stop location, packaging factors, and zoom group aberration sensitivity.

9580-21, Session 5

Novel optical system for very thin zoom lenses

Akira Yabe, Consultant (Japan)

In this report a novel optical system for very thin zoom lenses is shown. This system is expected to be used in the mobile phone camera.

This system has a prism or a mirror as the first element to bend the optical axis 90 degrees. The key point of this system is the use of the intermediate image. The system consists of 3 lens groups with the positive optical power. The first group makes the intermediate image. The second group is put around the intermediate image to reduce the height of rays from the off-axis object points. The third group relays the intermediate image to the image plane.

The possibility of the zooming and focusing types is investigated, as well as the possibility of the power distribution of 3 lens groups. If all the groups are moved for the zooming, this has the largest freedom of the design. By fixing one group or connecting two groups, the system is simplified. 6 different zooming types can realize the good performance.

Finally the procedure to realize such an unprecedented optical system is shown. The thin lens model with the intrinsic aberration coefficients is used to construct the zooming system. Then thin lenses are replaced to real lenses. This is the starting point of the optimization with the real ray trace. Global optimization is applied and the best solution is chosen.

9580-22, Session 5

Optical design of optical zoom optics with intermediate image

Yi-Chin Fang, National Kaohsiung First Univ. of Science and Technology (Taiwan)

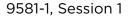
This study designs a 6x zoom lens which is compounded by two groups of lens with 6x zoom ratio and another fixed focal optics. A real image (e.g., intermediate image) is shown between two zoom lens groups. The effect of the intermediate image makes the power of two group of lens independently, which can assign a lower power in the front lens group to alleviate the diameter of lens elements. The traditional zoom ratio is defined by Mtotal = ftele/fwid, where fwid is the effective focal length (EFL) with wide-angle and ftele is the EFL for telescope. Figure 1 illustrates the total zoom ratio for intermediate image.

The specification of the proposal is shown in Table 1. The CCD size is 1/2.7" and its diagonal distance is 6.592mm. Since the proposed zoom lens is symmetrical, the half diagonal distance of CCD size (that is 3.296mm) is used to evaluate the performance in Code V.

Conference 9581: Laser Beam Shaping XVI

Monday 10-10 August 2015

Part of Proceedings of SPIE Vol. 9581 Laser Beam Shaping XVI



Self-healing of light beams: a wave-optics approach (Invited Paper)

Andrea Aiello, Max-Planck-Institut für die Physik des Lichts (Germany); Girish S. Agarwal, Oklahoma State Univ. (United States)

Contrarily to common beliefs, almost all beams of light possesses somehow the ability to "reconstruct themselves" after hitting an obstacle [1-3]. The celebrated Arago spot phenomenon is nothing but a manifestation of this property. In this work we analyze the self-healing mechanism from a wave-optics point of view [4]. This leads to a novel expression for the minimum reconstruction distance, which is valid for any kind of beam, including Gaussian ones [5]. Finally, a witness function that quantifies the self-reconstruction capability of a beam is proposed and tested. Our results represent a step forward in the understanding of the physics underlying self-healing mechanism in optical beams.

REFERENCES:

 F. O. Fahrbach, P. Simon, and A. Rohrbach, Nat. Phot. 4, 780 (2010).
 M. McLaren, T. Mhlanga, M. J. Padgett, F. S. Roux, and A. Forbes, Nat. Commun. 5, 3248 (2014)

[3] X. Chu, and W. Wen, Opt. Exp. 22, 6899 (2014)

[4] A. Aiello, G. S. Agarwal, Opt. Lett. 39, 6819 (2014)

[5] A. Aiello, G. S. Agarwal, arXiv:1501.05722 [physics.optics] (2015)

9581-2, Session 1

Angular accelerating white light

Angela Dudley, CSIR National Laser Ctr. (South Africa); Christian Vetter, Alexander Szameit, Friedrich-Schiller-Univ. Jena (Germany); Andrew Forbes, Univ. of the Witwatersrand (South Africa)

Significant interest has been devoted to tailoring optical fields that transversely accelerate during propagation in the form of Airy, Weber and Mathieu beams. In this work, we introduce a new type of optical field that exhibits controlled angular acceleration during propagation which is achieved by superpositions of Bessel beams with non-canonical phase functions. We demonstrate these angular accelerating fields by modulating the phase and amplitude of a supercontinuum source with the use of a phase-only spatial light modulator (SLM). We illustrate that by considering only the first diffraction order when the SLM is encoded with a blazed grating, the SLM is capable of tailoring the spatial profile of broadband sources without any wavelength dependence. By digitally simulating freespace propagation on the SLM, we compare the effects of real and digital propagation on the angular rotation rates of the resulting optical fields for various wavelengths. The development of controlled angular accelerating optical fields will be useful in areas such as particle manipulation, plasma control, material processing and non-linear optics.

9581-3, Session 1

Self-healing of Hermite-Gauss and Ince-Gauss beams

Dilia Aguirre-Olivas, Gabriel Mellado-Villaseñor, Victor Arrizón, Sabino Chávez-Cerda, Instituto Nacional de Astrofísica, Óptica y Electrónica (Mexico)

An optical beam that is subject to a partial obstruction propagates showing certain degree of self-reconstruction in the obstruction domain. This phenomenon is known as self-healing (SH) of the beam. The SH has been

widely studied in propagation invariant beams like Bessel, Airy, Mathieu and Weber.

Nevertheless, there is a family of beams whose transverse profile remains invariant under propagation, changing only the scale. This beams are solution of the paraxial wave equation in three different coordinate systems, Hermite-gauss (HG) beam in rectangular coordinates, Ince-gauss (IG) beam in elliptical-cylindrical coordinates and Laguerre-gauss (LG) beam in cylindrical coordinates.

In this work we report numerically and experimentally the SH effect in HG and IG beams with an opaque obstruction.

First, a semi-analytical analysis is made by means of a figure of merit named signal to noise intensity ratio. This figure of merit is based on analytical diffraction formulas and is explicitly dependent on the features of the beam and the obstruction applied to it.

We demonstrate the SH effect by numerical simulation and experimentally. Numerical simulations were made with analytic expression for HG and IG beams. Experimental generation of the beams under test we employ amplitude computer-generated holograms (CGHs), displayed in a twisted nematic liquid crystal (TNLC) spatial light modulator (SLM). A significant detail is that the holograms were designed including the obstruction as a feature of the generated fields.

Finally, as a complement of the semi-analytical analysis, a quantitative evaluation of the SH effect in HG and IG beams was made employing the Root Mean Square deviation and the similarity function.

This phenomenon is known as self-healing (SH) of the beam. The SH has been widely studied in propagation invariant beams like Bessel, Airy, Mathieu and Weber.

Nevertheless, there is a family of beams whose transverse profile remains invariant under propagation, changing only the scale. This beams are solution of the paraxial wave equation in three different coordinate systems, Hermite-gauss (HG) beam in rectangular coordinates, Ince-gauss (IG) beam in elliptical-cylindrical coordinates and Laguerre-gauss (LG) beam in cylindrical coordinates.

In this work we report numerically and experimentally the SH effect in HG and IG beams with an opaque obstruction.

First, a semi-analytical analysis is made by means of a figure of merit named signal to noise intensity ratio. This figure of merit is based on analytical diffraction formulas and is explicitly dependent on the features of the beam and the obstruction applied to it.

We demonstrate the SH effect by numerical simulation and experimentally. Numerical simulations were made with analytic expression for HG and IG beams. For experimental generation of the beams under test we employ amplitude computer-generated holograms (CGHs), displayed in a twisted nematic liquid crystal (TNLC) spatial light modulator (SLM). A significant detail is that the holograms were designed including the obstruction as a feature of the generated fields.

Finally, as a complement of the semi-analytical analysis, a quantitative evaluation of the SH effect in HG and IG beams was made employing the Root Mean Square deviation and the similarity function.

9581-4, Session 1

Classical entanglement of vector vortex beams

Melanie McLaren, Univ. of the Witwatersrand (South Africa); Thomas Konrad, Univ. of KwaZulu-Natal (South Africa); Andrew Forbes, Univ. of the Witwatersrand (South Africa) and CSIR National Laser Ctr. (South Africa)

Vector beams are defined by spatially inhomogeneous states of polarization, that is, the spatial distribution and polarization state of the beam are non-separable. These beams have found interest in a variety of optical fields such as microscopy, interferometry and optical tweezing. It is therefore important to determine the degree to which these beams are non-separable or to determine the "vectorness" of such beams. We show that the non-





separability of vector beams is analogous to that of entangled quantum states and as such, we use traditionally quantum techniques such as a Bell inequality, to determine the vectorness of our generated vector vortex beams.

9581-5, Session 1

Generating non-diffraction beams using DMD

Yongdong Wang, Nanyang Technological Univ. (Singapore); Yilei Zhang, Nanyang Technological Univ (Singapore)

Non-diffraction beams, such as the Airy beam and the Bessel beam, have attracted more and more attension due to their unique properties, such as non-diffraction, self-healing. Digital Micromirror Device (DMD) is a powerful tool using microfabricated mirrors to control light reflection, which could be used for laser beam shaping. Well designed holographic or structural patterns could be loaded in DMD to control micromirror reflection and generated desired non-diffraction beams. Wavefronts of the generated non-diffraction beams are measured using a Mach-Zehnder interferometer method. Both wavefront and profile of the generated beams agree with theoretical calculation, which proof the successful construction of the non-diffraction beams. This powerful and straightforward DMD based method could also be applied to generate other beams for engineering and biological applications.

9581-6, Session 2

2 um intra- and extra-cavity beam shaping (*Invited Paper*)

Igor A. Litvin, Council for Scientific and Industrial Research (South Africa); Hencharl Strauss, Gary King, CSIR National Laser Ctr. (South Africa)

In this work, the new techniques for intra- and extra-cavity laser beam shaping were proposed and tested. The intra-cavity beam shaping techniques was implemented to Tm:YLF slab laser. The method based on DOE and cylindrical lenses retransformation of intra-cavity oscillation field to fit rectangular like pump beam. The method allows the increasing of output laser brightness dramatically. Moreover we propose a new technique for extra-cavity laser beam shaping namely the reshaping of the laser beam into a desirable beam profile by the use of a laser amplifier with a pump beam that has a modified intensity profile. One the advantages of this method are the ability to reshape multimode beams as the method relies only on the transverse intensity of the beams. All techniques were verified experimentally for 2 μ m lasers and laser beams.

9581-7, Session 2

High-brightness fiber-coupled laser-diode beam-shaping design based on right-angle prism array

Junhong Yu, Haitian (China)

A new beam shaping technique that twists the emitters of laser-diode bar and rearranges the twisted emitters abutted against each other is proposed considering a right-angle prism array and a distributed cylinderlens stack. By using this innovative beam shaping technique, the coupling of 12 mini-bars to a fiber with a 100 ?m core diameter and 0.15 NA is is demonstrated both by simulation and experiment . The proposed coupling system is very effective and compact for coupling the laser-diode into fibers. The simulation and experiment results indicate that the right-angle prism stack and the distributed cylinder-lens stack successfully eliminate the lightless area and equalize the beam quality of the mini-bar. With the availability of output power above 400 watts and high brightness above 71.5 MW/ (cm2•sr?, much wider applications of fiber-coupled laser-diode are anticipated.

9581-8, Session 2

Intracavity beam shaping using an SLM

Liesl Burger, Council for Scientific and Industrial Research (South Africa) and Stellenbosch Univ. (South Africa); Igor Litvin, Sandile Ngcobo, Council for Scientific and Industrial Research (South Africa); Andrew Forbes, CSIR National Laser Ctr. (South Africa)

Spatial light modulators (SLMs) are phase-modulating liquid crystal display devices, and are widely used for beam-shaping of laser beam for applications like micro-machining, advanced microscopy, and the creation of novel beams. Coherent light is modulated by passing through reflectively-coated electrically-addressed liquid crystal (LC) cells, which are each programmed by means of a grey-scale bitmap displayed on the LCD screen. In standard operation incident light is reflected once off the SLM, but we replace the back reflector of a simple folded resonator with a SLM in order to exploit its phase modulating properties. In this configuration the light circulating in the resonator is subject on each pass to a phase modulation which is calculated to produce a specific desired laser beam profile using known techniques.

A prototype system revealed that although SLMs are said to be phaseonly, that SLMs containing twisted nematic LCs have a small degree of amplitude modulation together with the expected phase modulation. This effect, although small and negligible in the traditional single-reflection configuration, is amplified when the SLM is in the intracavity configuration. We show that as a result, a phase-only SLM behaves as a phase modulating element inside the resonator. An investigation of LC properties predicts that the new generation of SLMs containing parallel aligned LCs have a negligibly small amplitude modulation, which is confirmed by experiment, and which allows these SLMs to function as per our original idea.

A number of chosen laser beam profiles produced by our two prototypes are shown to illustrate the versatility of the system.

9581-9, Session 2

Selective excitation and detection of higher-order doughnut laser modes as an incoherent superposition of two petals modes in a digital laser resonator

Sandile S. Ngcobo, Igor Litvin, Council for Scientific and Industrial Research (South Africa); Darryl Naidoo, CSIR National Laser Ctr. (South Africa); Kamel Ait-Ameur, Ecole Nationale Supérieure d'Ingenieurs de Caen et Ctr. de Recherche (France); Andrew Forbes, CSIR National Laser Ctr. (South Africa)

Higher-order Laguerre-Gaussian beams with zero radial index and nonzero azimuthal index are known to carry orbital angular momentum (OAM), and they are routinely created external to laser cavities. Previous reports on the generation of such modes from laser cavities suffer from inconclusive evidence of the real electromagnetic field. In this paper we demonstrate a simple method of selectively generating higher-order doughnut modes using a digital laser and we show that an observed doughnut beam from a laser cavity may not be a pure Laguerre-Gaussian azimuthal mode but can be an incoherent sum of petal modes, which do not carry OAM. We also demonstrate a method that could be used for future analysis of such fields from laser resonators.



9581-10, Session 3

C-shaped structured electron beams: design and experimental production

Michael Mousley, Jun Yuan, Mohamed Babiker, Gnanavel Thirunavukkarasu, The Univ. of York (United Kingdom)

Computer generated holograms (CGHs) have been designed to create structured illumination with a C shape. The structured illumination is based on a vortex state, however the inclusion of radial phase gradients leads to non integer topological charge and a redistribution of intensity in the far field diffraction pattern. By analysing the phase gradients present in the wavefunction the structured illumination pattern can be predicted and independent control of the radius and opening angle is possible. C shaped illumination is experimentally produced in an electron microscope showing two different opening angles, using two different CGH mask types an amplitude mask and a phase mask. C-shaped structured illumination offers interesting particle interactions and trapping possibilities with the ability to control the size of the gap between trapped particles at the ends of the intensity curve. A spatial light modulator would allow for the real time opening and closing of the C shape whilst interacting with particles. C shaped illumination promises potential applications both in the optical and electron beam lithography of metamaterials which utilise split ring structures and dimensions as small as nanometres can be achieved in the electron beam case.

9581-11, Session 3

Shaping sinusoidal phase contrast holograms (SPCH) for highly-efficient electron vortex beams

Gnanavel Thirunavukkarasu, Michael Mousley, Mohamed Barbiker, Jun Yuan, The Univ. of York (United Kingdom)

Generation of electron vortex (EV) beams with high efficiency is a much discussed topic following the experimental realizations of EV beams in a TEM. The initial realization was based on searching graphite flakes in a randomly stacked graphite thin films sheet to locate a staircase like spiral structure which produces the required 2ϖ phase variation around their point of intersection [1]. Shaping the wave function using this method is very difficult; nonetheless, it initiated the search for alternative, more efficient ways of producing electron vortex beams in a reasonably controlled manner. Consequently, a well-known optical computer generated hologram (CGH) method is adopted and successfully demonstrated for the production of EV beams [2,3]. Using this binarized CGH method one can easily realize EV beams, however, half of the beams incident intensity is blocked by the relatively thick binarized hologram grating and half of the remaining 50% is concentrated on the center beams that possess no angular momentum. Thus there is 25% left for the orders containing angular momentum limiting each first orders to a maximum of close to 10% of the total intensity incident on the hologram.

Increasing the efficiency of a particular order of this CGH generated beams is beneficial for future EV applications. Here, we demonstrate a way of increasing the efficiency of first order beams by tuning the thickness profile. The phase variation between the thicker and thinner regions of the hologram gratings follows a sinusoidal variation with the number of forks endowed at its center representing the topological charge of the beams. By manipulating the phase in this way, we experimentally demonstrate a transmitted diffraction efficiency (intensity of the first order beam divided by the transmitted intensity) of the first order vortex beams (I = \pm 1) of 30% for a sinusoidal phase variation between 0 and 1.2ω . Theoretically a phase variation of 0 to 1.18ω is required to obtain the maximum diffraction efficiency of 33.8% for the I = ±1 beams of this SPCH. The absolute diffraction efficiency, (intensity of the first order beam divided by the incident beam intensity), of this SPCH is calculated to be 11.6% using electron energy loss spectroscopy (EELS). The deviation of absolute efficiency from its theoretical maximum diffraction efficiency is mainly attributed to the loss of intensity by inelastic scattering due to the thick support films.

[1] M. Uchida and A. Tonomura, "Generation of electron beams carrying orbital angular momentum.," Nature, vol. 464, no. 7289, pp. 737–9, Apr. 2010.

[2] J. Verbeeck, H. Tian, and P. Schattschneider, "Production and application of electron vortex beams.," Nature, vol. 467, no. 7313, pp. 301–4, Sep. 2010.

[3] B. J. McMorran, A. Agrawal, I. M. Anderson, A. a Herzing, H. J. Lezec, J. J. McClelland, and J. Unguris, "Electron vortex beams with high quanta of orbital angular momentum.," Science, vol. 331, no. 6014, pp. 192–5, Jan. 2011.

9581-12, Session 3

Electronically-controlled optical tweezing using space-time-wavelength mapping

Shah Rahman, Rasul Torun, Qiancheng Zhao, Tuva Atasever, Ozdal Boyraz, University of California, Irvine (United States)

We propose electronically controlled optical tweezing based on timespace-wavelength mapping technology. Space-time-wavelength mapping technology has been proven to be useful in arbitrary waveform generation in RF photonics and wide-field real time imaging in microscopy. Here we show that the same technology can be applied to optical tweezing. By using time-domain modulation, the location and the polarity of force hot-spots created by Lorentz force (gradient force) can be controlled. In this preliminary study we use 150 fs optical pulses that are dispersed in time and space to achieve a focused elliptical beam that is ~30 ?m long and ~2 ?m wide. We use an electro-optic modulator to modulate power spectral distribution of the femtosecond beam after temporal dispersion and hence change the intensity gradient along the beam at the focal spot. The results show that we can achieve ±200 pN forces on nano objects (~100 nm) without mechanical beam steering. The intensity of wavelengths along the spectrum can be manipulated by using different RF waveforms to create a desired intensity gradient profile at the focal plane. By choosing the appropriate RF waveform, it is possible to create force fields for cell stretching and compression as well as multiple hot spots for attractive or repulsive forces. 2D space-time-wavelength mapping can also be utilized to create tunable 2D force field distributions.

9581-13, Session 3

Encoding information using Laguerre Gaussian modes

Abderrahmen Trichili, SUP'COM (Tunisia); Angela Dudley, CSIR National Laser Ctr. (South Africa); Mourad Zghal, SUP'COM (Tunisia); Andrew Forbes, CSIR National Laser Ctr. (South Africa)

Over the last few years, there has been considerable interest in mode division multiplexing for data transmission in optical fibers and free space optical links. Using the spatial modes of light increases the overall capacity of the communication systems by several orders of magnitude.

In this context, we experimentally demonstrate an information encoding protocol using Laguerre Gaussian modes having different radial and azimuthal components. A detailed method, based on digital holography, for information encoding and decoding using different data transmission scenarios is presented. The effects of the atmospheric turbulence introduced in free space communication is discussed as well. We are convinced that this technique will find uses in the commercial free space communication systems and in mode de-multiplexers in optical fibers.



9581-14, Session 4

Experimental generation of Hermite-Gauss and Ince-Gauss beams through kinoform phase holograms

Gabriel Mellado-Villaseñor, Dilia Aguirre-Olivas, David Sánchez-de-la-Llave, Victor Arrizón, Instituto Nacional de Astrofísica, Óptica y Electrónica (Mexico)

Hermite-Gauss (HG) and Ince-Gauss (IG) functions are exact solutions of the scalar paraxial wave equation in cartesian and in elliptic cylindrical coordinates, respectively. Each of them forms a complete orthogonal basis under which any function can be represented. Both of them, together with the Laguerre-Gauss functions, which are exact solutions to the paraxial wave equation in free space in circular cylindrical coordinates, can be classified in the family of structurally stable optical fields. Consequently, they are also self-transforming fields under the Fourier transform operation. Recently, the Kinoform Phase Hologram (KPH) codification technique was reported in the generation of Laguerre-Gauss beams. However, the KPH has not been investigated for the efficient and accurate generation of HG and IG beams. In this work, we propose to employ KPHs to efficiently and accurately synthesize the structurally stable Hermite-Gauss and Ince-Gauss beams. Also, we review the mathematical description of the Hermite-Gauss and Ince-Gauss functions and define the KPH transmittance. The KPH codification technique consists on taking the phase of the field to be synthesized as the hologram transmittance. We give an explanation for the high efficiency and accuracy of the kinoform technique for synthesizing these fields. In order to provide a guantitative evaluation of the performance of the KPHs, we employed the root mean square deviation. We described the experimental setup, which contains a reflective phase-only spatial light modulator for codifying the KPHs transmittance. Experimental and numerical results are presented and compared.

9581-15, Session 4

New approach for laser beam formation by means of deformable mirrors

Alexis V. Kudryashov, Julia Sheldakova, Anna Lylova, Vadim Samarkin, Active Optics Night N Ltd. (Russian Federation)

No Abstract Available

9581-16, Session 4

Polarization design of high-efficiency diffractive optics

Michael A. Golub, Tel Aviv Univ. (Israel)

Polarization shaping of laser beams can be performed with subwavelength structures based on effective index technique at zero diffraction order. Resorting to different diffraction orders of diffractive structures provides further degrees of freedom in the polarization control, albeit shows cumbersome coupling to power distribution between diffractive elements, polarization control is uncoupled from inter-order power distributions. We proposed an effective grating method for transformation of light beam polarization in the first diffraction order of dense transmission binary surface-relief diffractive elements with 80-100% efficiency.

We resorted to a combination of rigorous vector diffraction approaches for periodic medium and surface relief gratings, to derive analytical closed form "effective grating" equations that generalize effective index. A polarization of a diffracted beam, under general three-dimensional angles of incidence, was related to a complete set of incident beam and grating parameters in the resonance domain of diffraction. It was shown that in two-wave diffracted negime, when incident beam essentially converts to the diffracted one, incident polarization states will be straightforwardly coupled to polarization of the 1st order diffracted wave. Also shown that generalized TE and TM polarizations are uncoupled in both wave equations and boundary conditions and differ from those of classical diffraction. Pure, either TE or TM, polarizations provide up to 100% diffraction efficiency, whereas mixed TE and TM polarizations cannot reach such.

A powerful tool for rigorous design of polarization controlling diffractive beam shapers with spectroscopic scale periods is now enabled.

9581-17, Session 4

Closed-loop adaptive optics system for laser beam shaping

Javier Garces, Pedro Escarate, Mario Castro, Sebastian Zuniga, Univ. Técnica Federico Santa María (Chile); Andres Guesalaga, Pontificia Univ. Católica de Chile (Chile)

Adaptive Optics systems are rapidly becoming the norm on high-level astronomical installations. New technology development has allowed for deformable mirrors and related instruments which can allow higher precision and resolution on astronomical measurements. However, the performance of the AO system is highly dependent on the calibration process.

In order to correct the light distortion caused by the atmosphere, a wavefront reference is required by the AO system. Often, bright stars are used for this purpose, however, these are not available in all parts of the sky, and so artificial stars created through the use of laser beams are used instead. Since the laser beam is subject to atmospheric distortion on the way up, a beam shaping concept is introduced to counteract this distortion, improving the quality of the laser guide stars, and as such, improving the system's performance.

The beam shaping process is based on an optical setup with two deformable mirrors through which the laser beam is introduced before launch. The phase distortions to be applied by each deformable mirror are estimated through a phase retrieval method. The first mirror's purpose is to correct the amplitude distortions during propagation in the near-field, while the second mirror corrects phase aberrations.

A closed-loop control approach for the deformable mirrors' arrangement is investigated, based on a model for the optical setup elements and evaluation for different control techniques. The purpose for this approach is to obtain a faster and more robust response for the system regarding the open loop results, which have been previously investigated and presented.

The system's performance is examined through simulations, in order to obtain graphical results of amplitude and phase correction, compare the benefits of different control techniques, observe improvements regarding the open loop approach, and analyze different parameters' influence on the system (such as distance and size of the beam shaping system's elements). Following this analysis, the method is implemented on a laboratory bench, adjusting the system for the specific instruments on the optical set-up, and obtaining graphical results with comparison purposes regarding the simulated results.

9581-18, Session 4

Square shaped flat-top beam in refractive beam shapers

Alexander V. Laskin, Vadim V. Laskin, AdlOptica Optical Systems GmbH (Germany); Aleksei B. Ostrun, National Research Univ. of Information Technologies, Mechanics and Optics (Russian Federation)

Lossless transformation of round Gaussian to square shaped flat-top collimated beam is important in building high-power solid state laser systems to improve optical pumping or amplification. There are industrial micromachining applications like scribing, display repair, which performance is improved when a square shaped spot with uniform intensity is created.



Proved beam shaping solutions to these techniques are refractive field mapping beam shapers having some important features: flatness of output phase front, small output divergence, high transmittance, extended depth of field, operation with TEMOO and multimode lasers.

Usual approach to design refractive beam shapers implies that input and output beams have round cross-section, therefore the only way to create a square shaped output beam is using a square mask, which leads to essential losses. When polarized input laser beam it is suggested to generate square shaped flat-top output by applying beam shaper lenses from birefringent materials or by using additional birefringent components. Due to birefringence there is introduced phase retardation in beam parts and is realized a square shaped interference pattern at the beam shaper output. Realization of this approach requires small phase retardation, therefore weak birefringence effect is enough and birefringent optical components, operating in convergent or divergent beams, can be made from refractive materials, which crystal optical axis is parallel to optical axis of entire beam shaper optical system.

There will be considered design features of beam shapers creating square shaped flat-top beams. Examples of real implementations and experimental results will be presented as well.

9581-19, Session 4

Beam shaping concepts with aspheric surfaces

Ulrike Fuchs, asphericon GmbH (Germany)

Employing aspherical lenses to reduce aberrations to improve focusing qualities is a well-known concept. But the potpourri of aspheric surfaces offers way more possibilities, even the chance for flexible beam shaping setups. Since these are refractive optical elements the beam shaping is robust with respect to wavelength changes.

Being able to generate ring shaped light distributions is interesting for various applications. Here the most uncommon aspheric surface - an axicon - is utilized. Axicons are glass cones, which convert the incoming light into Bessel beams. Those are characterized by their concentric ring structure and long depth of focus, which makes them very interesting for material processing. Above that, combining such an axicon with a focusing lens leads to a ring focus. Its size is not only determined by the choice of the axicon angle and the lens properties, but also through the diameter of the incoming beam. Thus, for optimal usage a flexible beam expander, which leaves the beam quality unaltered is mandatory. The remarkable properties of these beam shaping set-ups are shown in theory and experimentally. Furthermore, a configuration consisting of two axicons and interchangeable focusing lenses is presented. For one thing, this set-up allows for tuning of the working distance in any required way for optimal material processing. For another thing, the induced chromatic focal shift of the focusing lens that occurs by a change of wavelength can be compensated for by adapting the distance of the axicons and leaving the working distance unchanged.

9581-20, Session PMon

A new error compensation strategy on laser displacement sensor in freeform surface measurement

Bin Sun, Bing Li, Xi'an Jiaotong Univ. (China)

The Laser Displacement Sensor (LDS) is designed according to the principle of laser triangulation. It is a precise geometric measurement sensor, and it is characterized by non-contact, large measuring range and high measuring efficiency. Therefore it is widely used in the field of industrial inspection and reverse engineering. However, the measurement accuracy of the LDS is easy to be influenced by other factors, such as the workpiece surface color, roughness and the inclination angle of the surface, especially for free-form surface, the incidence angle has greater impact on measurement accuracy and the research is relatively less. The paper proposes a new error compensation strategy, this strategy is an approximate mathematical model which can be quantified. By inclination error compensation, it can effectively improve the measurement accuracy of free-form surfaces.

The paper analyzes the geometry of the laser light path system in detail according to the principle of direct laser triangulation measurement. The study found that the change of laser light path leads to the change of light centroid, thus producing non-linear relationship between object and image. Depending on the cause inclination error generated, a quantifiable approximate mathematical model is deduced. Subsequently, the paper verifies the correctness and reliability of the error model by using high precision Renishaw XL-80 Laser Interferometer and Sine Gauge.

By measuring the aero-engine blade surfaces, the appropriate measurement path is planned in accordance with the characteristics of the blade, and the calculation method of measuring point inclination angle is presented. After the measurement data of the blade are compensated with error model proposed, the experiment indicated that the measurement accuracy is less than 10?m. The result shows that the proposed inclination angle error compensation method can effectively improve the measurement accuracy of the LDS, and the model has certain popularize and use value in engineering applications.

9581-21, Session PMon

Scanning in the optical vortex microscope

Agnieszka Popio?ek-Masajada, ?ukasz P?ócienniczak, Jan Masajada, S?awomir Drobczy?ski, Wroclaw Univ. of Technology (Poland)

We propose a microscopic system in which the Gaussian beam with embedded optical vortex is used. The special helical phase plate is illuminated by the Gaussian beam and then focused by the microscope objective into the sample plane. Such a beam carries the optical vortex - the zero intensity point around which the phase gradient becomes infinitely large. By moving the phase plate within the Gaussian beam, the singular point in the sample plane can be moved and such configuration can be used for scanning the sample. We found in our previous works that moving the phase plate along a straight line causes a movement of the optical vortex also along straight line. The angle of the vortex trajectory however depends on the observation plane position. There is a plane in which the trajectory is perpendicular to the phase plate shift. In this plane the core region of a vortex beam is extremely sensitive to any phase imperfections introduced into the beam. The analytical formula for the complex amplitude of the focused spot with off-axis vortex was calculated in order to calibrate the microscopic system. In this presentation the theoretical fundamentals of microscope are discussed. The conclusions are verified experimentally

9581-22, Session PMon

Orbital angular momentum mode coupling in fibers

Bienvenu I. Ndagano, Melanie McLaren, Univ. of the Witwatersrand (South Africa); Andrew Forbes, Univ. of the Witwatersrand (South Africa) and CSIR National Laser Ctr. (South Africa)

Orbital angular momentum (OAM) of light has become, over the years, the focus of intensive research worldwide. We are particularly interested in the additional degrees of freedom OAM provides for optical communication. To this end, we built an optical setup to generate and detect OAM modes. To overcome the issue of turbulence, which is detrimental to the formation and propagation of OAM modes, we propagated the generated OAM modes through an optical fibre. We demonstrate that using spatial light modulators we can not only generate specific beams carrying OAM but also decompose them in terms of orthogonal azimuthal functions characteristic of OAM modes. This decomposition technique, referred to as mode decomposition or spatial correlation, can be used to detect OAM modes. Using our optical setup we show that OAM is maintained as the modes propagate through the fibre. We first perform our analysis using scalar Laguerre – Gaussian (LG) and linearly polarised (LP) modes, where the latter approximates the natural fibre modes. We repeated the analysis using the true fibre modes,



the cylindrical vector (CV) modes which exhibit azimuthal symmetry of field distribution and polarisation. We demonstrate a novel method of generating CV modes using a q-plate and show that CV modes are better suited to carry OAM through fibres as opposed to LG and LP modes.

9581-23, Session PMon

Practical implementation of propagationinvariant laser beams

Michael G. Soskind, Rose Soskind, Rutgers, The State Univ. of New Jersey (United States); Yakov Soskind, DHPC Technologies (United States)

Due to their several unique properties, propagation invariant laser beams are playing an increasingly important role in several photonics applications. This paper describes several practical aspects of producing propagation invariant laser beams with different symmetries and structured light field distributions. Both intra-cavity and extra-cavity schemes are discussed. In the case of extra-cavity implementations, we show several practical layouts of anamorphic optical systems for shaping propagation-invariant laser beams based on the size and waist locations of the input laser beams.

The influence of components' misalignments and optical imperfections on the spatial characteristics of the produced output beams is presented as well.

9581-24, Session PMon

Fabrication and characterization of a non-zero dispersion-shifted mechanicallyinduced long-period grating for optical fiber sensing

Eloisa Gallegos-Arellano, Ruth I. Mata-Chavez, Eduardo H. Huerta-Mascotte, Julian M. Estudillo-Ayala, Ana D. Guzman-Chavez, Everardo Vargas-Rodriguez, Juan M. Sierra-Hernandez, Roberto Rojas-Laguna, Igor Guryev, Univ. de Guanajuato (Mexico)

We present the fabrication and characterization of a mechanically induced long period grating (MILPG) using a grating period of 400 μm and 1m of NZ-DSF. Pressure is gradually applied up to 120 Lb at different angles like 0, 30, 45 and 60 degrees. An attenuation band is observed centered at a wavelength around 1064nm using a fiber position of 30 degrees with respect to the grating's metal plate and a maximum pressure of 145 Lb. The loss band presents a maximum depth of 22dB and a bandwidth of approximately 10nm. Torsion and curvature characterizations did not change the output spectrum of the optical grating. However, temperature characterization depicted a small shifting which could be insignificant for some applications. Still, there is a 10dB attenuation as temperature increases in a range from room temperature up to 200 °C. These preliminary studies show that this 1064 nm centered wavelength MILPG might be used in a very low dynamic range with temperature as a temperature sensor.

9581-25, Session PMon

Closed-Loop control for tip-tilt compensation

Mario A. Castro R., Pedro Escárate, Javier Garcés, Sebastián Zuñiga, Univ. Técnica Federico Santa María (Chile); Andrés Guesalaga, Pontificia Univ. Católica de Chile (Chile)

Adaptive optics (AO) is a well-known technology that compensates image distortions induced by atmospheric turbulences and low frequency vibrations. Currently the vast majority of 8 meters class telescopes are now equipped with adaptive optics systems and will be an integral component in the next generation of telescopes and astronomical instruments.

Despite the significant advances in astronomical instrumentation and adaptive optics, some problems still persist during the operations. In particular, achieving a satisfactory performance in front of mechanical vibrations progressively more important.

The vibrations effects, acting in the propagation of the science light, strongly affects the performance of the AO systems, often producing an additional image jitter. These perturbations mainly affect lower aberration modes (Piston, Tip, Tilt, Defocus), but possibly higher modes (e.g.: Coma). Also, these perturbations can corrupt the Wavefront Sensor (WFS) path or generate jitter in the laser projection system beacons on the sky, producing the AO system to correct for disturbances that actually have no effect on the science path. Moreover, vibration often occurs at frequency near or beyond the AO Bandwidth, and thus, may be poorly corrected.

This work presents a laboratory validation of a vibration mitigation system of tip-tilt modes using closed-loop control, inducing vibrations on the test bench by a motor with controllable frequency, in order to simulate the mechanical vibrations mentioned above. The tip-tilt aberrations were measured using the centroid position of laser spot. The control action is carried out by a Fast Steering Mirror (FSM).

Finally, we conclude discussing the technological limitations and possible improvements of the demonstration and its implementation on a telescope.

9581-26, Session PMon

Low-loss selective excitation of higherorder modes in a diode-pumped solidstate digital laser

Sandile Ngcobo, Teboho J. Bell, CSIR National Laser Ctr. (South Africa); Kamel Ait-Ameur, Ecole Nationale Supérieure d'Ingenieurs de Caen et Ctr. de Recherche (France); Andrew Forbes, CSIR National Laser Ctr. (South Africa)

In this paper we experimentally demonstrate intra-cavity selective excitation of Higher-Order Laguerre-Gaussian modes with nonzero radial index and zero azimuthal index using a simple absorbing ring implemented on a digital laser. We show selective excitation of modes with radial order of zero to five using a non-segment absorbing rings. We then reduce the losses associated with the absorbing ring by cutting it into segments and then experimentally demonstrate that excited modes using segmented absorbing rings have a lower threshold compared to using a full ring while at the same time maintaining mode volume, purity and slope efficient of the laser.

Conference 9582: Optical System Alignment, Tolerancing, and Verification IX

Sunday - Monday 9 -10 August 2015

Part of Proceedings of SPIE Vol. 9582 Optical System Alignment, Tolerancing, and Verification IX

9582-1, Session 1

New freeform standard in ISO 10110

Sven R. Kiontke, asphericon GmbH (Germany)

For 10 years there has been the asphere as one of the new products to be accepted by the market. All parts of the chain design, production and measurement needed to lear how to treat the asphere and what it is helpful for. The aspherical optical element now is established and accepted as an equal optical element between other as a fast growing part of all the optical elements.

Now we are focusing onto the next new element with a lot of potential, the optical freeform surface. First manufacturing has been show successfully and the ISO 10110 will soon launch four standards helping the industry.

A big part of the ISO results will be shown. There under for instance the description of freeform surfaces, as well as their tolerancing like centration, surface form deviation (irregularity, slope, Zernike, pv, pvr). Furthermore how to analyze the measurement results including some data handling and many more.

9582-2, Session 1

Scanning pupil approach to aspheric surface slope error tolerancing in head-up display optics

Viktor P. Sivokon, Raytheon ELCAN Optical Technologies (Canada)

We present a novel approach to tolerancing slope errors of aspheric surfaces in relay optics of typical avionics head-up displays (HUD). In these systems about 5mm diameter light beam entering the pilot eye occupies only a tiny fraction of HUD entrance pupil/eyebox with typical diameter of 125mm. Consequently the beam footprint on any HUD optical surface is a small fraction of its clear aperture. This presents challenges to HUD tolerancing which is typically based on parallax (angular difference in line of sight between left and right eyes) analysis. Aspheric surfaces manufactured by sub-aperture grinding/polishing techniques inherently have structured residual artifacts and add another source of errors - surface slope errors. This type of error can not only degrade image quality of observed HUD symbology but lead to "waviness" and "floating" especially noticeable when the pilot moves his head within the HUD eyebox. The suggested approach allows tolerancing of aspheric surface slope errors and guarantees acceptable level of symbology "waviness". Narrow light beam is traced from certain pilot eye position backwards through HUD optics until it hits the light source plane. Due to small beam size slope error of aspheric surface acts primarily as overall tilt/wedge that deviates the beam and causes it to shift. Slope error is acceptable when this shift is less that certain fraction of symbol linewidth. Eye is scanned over entire eyebox and field of view and slope error tolerance is established for several zones in aspheric surface clear aperture. Procedure is then repeated for each aspheric surface.

9582-3, Session 1

The need for fiducials on freeform optical surfaces

Kate Medicus, Jessica D. Nelson, Matthew Brunelle, Optimax Systems, Inc. (United States)

The evolution from spherical, to aspheric, to freeform optics is quickly progressing towards more complex freeform surfaces. Freeform surfaces typically have little to no symmetry making the alignment of the surfaces difficult. The alignment of such freeform surfaces relative to the other

features on the optic has been little considered. A typical alignment specification like wedge (edge thickness difference) is not well defined for freeform optics, nor is the wedge measurement. We show that by using fiducials during the manufacturing of freeform surfaces, the alignment and locating of the freeform surface can be specified and measured.

Fiducials are features on the optic that can be accessed during the measurement, manufacturing, and alignment processes. Fiducials can be optical or mechanical features such as flats, spheres, or diameters. Fiducial design and placement must be considered early in the design process to permit fiducial usage during the full manufacturing process. Depending on customer need, the fiducials could be removed after manufacturing is complete or they could remain on the part to assist in the alignment process.

We will show examples of freeform parts made with fiducials that demonstrate the wedge measurement and a measurement of locating two freeform surfaces relative to each other that is not feasible without fiducials. In addition, we will show how using the fiducials will allow us to separate center thickness errors and radius errors of freeform surfaces, which is not feasible without fiducials.

9582-4, Session 1

Tolerancing aspheric surfaces in optical design

Ulrike Fuchs, asphericon GmbH (Germany)

Aspheres are becoming more and more popular in optical design of lens systems. This trend is caused by the demand for reducing size and weight or even novel optical performance, which cannot be obtained with spherical designs only. This demand leads to innovative manufacturing processes for serial production of aspherical surfaces of high quality. Unfortunately, due to the type of surface form deviation introduced by CNC based grinding and polishing processes, tolerancing an optical system with aspherical surfaces becomes very complicated. Especially for serial production it is critical to know just how "good" an asphere has to be in order to guarantee the optical performance needed without overdoing it. Later one is a delicate issue to cost.

Due to the full contact polishing process spheres have surface form deviations, which can be described well with low order Zernike polynomials. Thus, common optical design software can simulate manufacturing tolerances by adding these terms to the optical surface and analyze the change in performance. Polishing aspherical surfaces is always a local process and therefore introduces a whole new type of surface form deviation, which cannot be modeled properly for tolerancing process in common optical design software.

Additionally, tolerancing of aspheres involves a complete new type of surface form deviation – slope errors. As one can imagine, depending on the slope errors introduced, this can make all the difference in performance, especially when wavefront quality is a criteria. It will be demonstrated how to overcome this limitation up to a certain level.

9582-5, Session 2

Slope sensitivities for optical surfaces

John R. Rogers, Synopsys, Inc. (United States)

Setting a tolerance for the slope errors of an optical surface (e.g., surface form errors of the "mid-spatial-frequencies") requires some knowledge of how those surface errors affect the final image of the system. While excellent tools exist for simulating those effects on a surface-by-surface basis, considerable insight may be gained by examining, for each surface, a simple sensitivity parameter that relates the slope error on the surface to the ray displacement at the final image plane.

Snell's law gives a relationship between the slope errors of a surface and



Conference 9582: Optical System Alignment, Tolerancing, and Verification IX



the angular deviations of the rays emerging from the surface. For a singlet or a thin doublet acting by itself, these angular deviations are related to ray deviations at the image plane by the focal length of the lens. However, for optical surfaces inside an optical system having a substantial axial extent, the focal length of the system is not the correct multiplier, as the sensitivity is influenced by the optical surfaces that follow.

In this paper, a simple expression is derived that relates the slope errors at an arbitrary optical surface to the ray deviation at the image plane. This expression is experimentally verified by comparison to a real-ray perturbation analysis. The sensitivity parameter relates the RMS slope errors to the RMS spot radius, and also relates the peak slope error to the 100% spot radius, and may be used to create an RSS error budget for slope error. Application to various types of system are shown and discussed.

9582-6, Session 2

Tolerance analysis of optical systems using the Nijboer-Zernike approach (*Invited Paper*)

Marco Hanft, Carl Zeiss AG (Germany)

Optical systems are designed to provide a specific functionality. The system is defined by the characteristic and location of its surfaces. Based on ray tracing and analysis routines (e.g. PSF or MTF) we know the performance of an optical system. But an built optical system will show some deviation from the nominal performance. Every component and assembling them will deviate from the original description. Tolerances are defined to control deviations caused by manufacturing process. The sensitivity analysis considers the influence of each tolerance to the performance of the optical system. In many cases the wave front itself can be used to describe the system performance. This talk will demonstrate the tolerance process using Nijboer-Zernike polynomials as expression for wave front aberrations. Nijboer-Zernike polynomials are a special form of well-known circle polynomials developed by Zernike. They are orthogonal and have an automatic balancing of aberrations of various orders. The degradation of the Strehl Ratio can be estimated very easily for every single aberration using the value of the specific coefficient. This property is very beneficial for the definition of a tolerance budget. Furthermore a sensitivity analysis with Nijboer-Zernike approach is a very clear basis to choose compensators for the alignment.

The talk will show the following steps on exemplary systems:

- Analysis with initial tolerances,
- Choice of compensators,
- Relaxation or tightening of tolerances,

- Final error budget and adjustment proposal.

9582-7, Session 2

Design and tolerance analysis of a transmission sphere by interferometer model

Wei-Jei Peng, Cheng-Fong Ho, Wen-Lung Lin, Zong-Ru Yu, Chien-Yao Huang, Wei-Yao Hsu, Instrument Technology Research Ctr. (Taiwan)

The design of a 6-in, f/2.2 transmission sphere for Fizeau interferometry is presented. To predict the actual performance during design phase, we build an interferometer model combined with tolerance analysis in Zemax. The transmission sphere belongs to double-pass system, it's not enough to only evaluate focus imaging. Thus, we study the interferometer model that includes system error, wavefronts reflected from reference surface and tested surface. Firstly, we generate a deformation map of the tested surface. Because of multiple configurations in Zemax, we can get the test wavefront and the reference surface of transmission sphere respectively. According to the theory of interferometry, we subtract both wavefront to acquire the phase

of tested surface. Zernike polynomial is applied to transfer the map from phase to sag and to remove piston, tilt and power. The result is the same as original map; because of no system error exists. Secondly, tolerances including fabrication of lenses and assembly are considered. The system error occurs because the test and reference beam are no longer common path perfectly. The calculated map is inaccurate while the system error is added. Although the system error can be subtracted by calibration, it should be controlled within a small range to avoid calibration error. Generally the system error of 6-in transmission sphere is measured within peak-to-valley (PV) 0.1? (?=0.6328 um), which is not easy to approach. Consequently, it's necessary and worth to evaluate the system error before fabrication. Finally, a prototype is developed and tested by a reference spherical surface with PV less than 0.1? irregularity.

9582-8, Session 3

Characterization of cryo-vacuum chamber windows for NIRCam instrument alignment and testing

Paul F. Schweiger, Torben B. Andersen, Lockheed Martin Space Systems Co. (United States)

The Near Infrared Camera (NIRCam) instrument used to align and obtain science data for NASA's James Webb Space Telescope (JWST) was tested at the module level at flight-like cryogenic temperature. This paper explains the innovative techniques used to measure the precise location and orientation of the modules. A laser tracker was used to precision locate the instrument, using a flat reference mirror/reticle surface on the modules inside a chamber through its port windows. This technique established 5 degrees of freedom of position and orientation. The accuracy achieved was on the order of 20 microns in position and 5 arc-seconds in angular orientation.

9582-9, Session 3

Measuring NIRCam's position and orientation in 6 DOF using one reference mirror surface inside an environmental chamber

Paul F. Schweiger, Torben B. Andersen, Lockheed Martin Space Systems Co. (United States)

The Near Infrared Camera (NIRCam) instrument used to align and obtain science data for NASA's James Webb Space Telescope (JWST) was tested at the module level at flight-like cryogenic temperature. This paper explains the background that created the innovative techniques used to measure NIRCam's modules alignments in 6 degrees of freedom (DOF) inside a thermal vacuum chamber. All 6 DOF were measured remotely, through a single chamber window port, using only a flat reference mirror/reticle surface mounted on each module. This measured orientation was then used to determine the optical input axis and entrance pupil for each module. The accuracy achieved was on the order of 20 microns in position and 5 arc seconds in angular orientation.

9582-10, Session 3

Dynamic alignment, tolerances, and metrology fundamentals at the nano and micro scales (Invited Paper)

Donn M. Silberman, PI (Physik Instrumente) L.P. (United States)

Although the terms "micropositioning" and "nanopositioning" refer to different classes of positioning systems, "nanopositioning" is often used mistakenly to describe micropositioning systems. Micropositioning systems

Conference 9582: Optical System Alignment, Tolerancing, and Verification IX



are typically motor-driven stages with travel ranges of a few millimeters up to a few hundred millimeters. Because the guiding systems in such stages — usually bearings of some kind — generate frictional forces, their resolution and repeatability are typically limited to 0.1 μm . The guiding system working principle also adds errors that are typically in the micrometer range. Nanopositioning systems are typically based on frictionless drives and guiding systems such as piezo actuators and flexures. These systems can achieve resolutions and guiding accuracies down to the sub-nanometer level.

Both of these classes of precision positioning and motion systems are used extensively in precision optical and photonic systems to achieve desired performance specifications of instruments and experimental research projects. Currently, many precision positioning and motion systems have been design and implemented to cross over from the micro to the nano ranges with excellent results. This paper will describe some of the fundamental performance parameters and tolerances typical of these systems, some of the metrology used to confirm specifications and a few high end applications of general interest.

9582-11, Session 3

1um adjustment-tolerance for highprecision helical laser drilling

Frank Zibner, Christian Fornaroli, Arnold Gillner, Jens Holtkamp, Fraunhofer-Institut für Lasertechnik (Germany)

High-precision micro laser drilling with high aspect ratios requires laser imaging effects such as optical double rotation. Optical double rotation is an effect where the laser beam is guided through any optical elements with a total amount of reflections that remains uneven. Those optical elements need to be mounted in a rotary stage that spins the elements with a certain velocity. In an ideal case the optical axis is identically with the rotational axis. Few optical elements such as the Dove-prism show the effect that the beam is rotated in itself while it is moving on a helical path. That offers an independency of the beam profile. However the Dove-prism alone can not be adjusted in a way that the two axis match. This is based on geometrical errors of the Dove-prism due to manufacturing technologies. Certain deviation in length and angle lead to a helical error. Additional optical elements can compensate this effect. Alignment that only takes place in one 2D plane (e.g. the focal plane) leads most likely to a cross-over of both axes (x-alignment) in that one plane. In order to match both axes the alignment needs to be done at least in two 2D planes. That requires the opportunity to both influence the optical angle and the optical position (parallel shift) in both planes. The highly complex optical alignment method as well as the mechanical storage of the optical elements will be shown in this paper. Additionally an alternative system based on a Smidt-Pechan-prism will be presented where its alignment requires precise placement of the prisms to each other.

9582-13, Session 4

State estimation in optical system alignment using monochromatic beam imaging

Joyce Fang, Dmitry Savransky, Cornell Univ. (United States)

Automated alignment of optical systems saves the time and energy needed for manual alignment and is required in cases where manual intervention is impossible. This research discusses the state estimation of the misalignment of a reimaging system using a focal plane sensor. We control multiple moving lenses and achieve high precision alignments by feeding back state estimates calculated from images from a CCD camera. A batch estimator and a Kalman filter are used to estimate the misalignment of the lenses, and we describe a closed-loop control experiment with monochromatic laser light to demonstrate the performance of the state estimation process. The result of using a Kalman filter converges to the misalignment parameters obtained from a batch estimator. The efficiency and accuracy of both methods is compared and discussed. Moving the lenses independently allows us to break degeneracies in the effects of misalignments of two lenses. The automated alignment technique can be extended to reconfigurable systems with multiple lenses and other optical components.

9582-14, Session 4

Alignment estimation performance analysis of new MDCO algorithm for a TMA optical system

Hyukmo Kang, Yonsei Univ. (Korea, Republic of); Eunsong Oh, Korea Institute of Ocean Science & Technology (Korea, Republic of); Sug-Whan Kim, Yonsei Univ. (Korea, Republic of)

In this study, we studied alignment state estimation simulations and compared the performance between two CAA algorithms i.e. 'Merit function regression (MFR)' and 'Multiple design configuration optimization (MDCO).' The former minimizes the merit function using multi-field wavefront error measurements from single configuration, while the latter minimizes the merit function using single-field wavefront error measurements from multi configurations. The target optical system used is an unobscured threemirror anastigmat (TMA) optical system of 70mm in diameter, and F/5.0 designed for an unmanned aerial vehicle for coastal water remote sensing. The TMA consists of two aspherical mirrors (concave primary mirror, M1, and convex secondary mirror, M2), and one spherical mirror (tertiary mirror, M3) designated as the compensator. Because of its spherical mirror characteristic of M3, we used two degrees of freedom of M3 (tilt X, tilt Y) to compensate wavefront error. For the simulation, we defined deliberate misalignment to M3 (decenter X, Y: 0.1mm, tilt X, Y: 0.06mrad), and it is five times larger than the assembly tolerance of 0.02mm in decenter X, Y, and 0.12mrad in tilt X, Y. After one alignment simulation step, both algorithms can meet the alignment requirement (1/15? RMS wavefront error at 633nm) without further iteration. Both algorithms are similar in terms of alignment state estimation performance. However, MDCO is more practical than MFR as it requires for single-field wavefront error measurements only. Using MDCO, we then investigated how the misalignments of M1 and M2, the surface fabrication error, the wavefront measurement uncertainty, and the control uncertainty can affect alignment estimation performance. The computational details and simulation results are presented together with implications.

9582-15, Session 4

Alignment state estimation performance of Merit Function Regression(MFR) method under mirror fabrication error

Dongok Ryu, Sug-Whan Kim, Yonsei Univ. (Korea, Republic of)

We report alignment state estimation of compact and high performance optical instrument that is disturbed by fabrication uncertainty; i.e. power, astigmatism and other low-order fabrication errors. Even high-order terms are likely to cause uncertainty in tight error budget condition. In this study, we simulated alignment state estimation for a hypothetic 3 mirror F/10 Korch-type telescope with 800mm aperture. The Merit Function Regression (MFR) method determined alignment state estimation for 2 cases of fabrication statements. The first is designed condition which denoted no fabrication error. The case 2 used increasing surface errors up to 1/10 lambda with randomly generated Zernike polynomials which terms from 4th to 37th. The 1000 times statistic result calculations of alignment state estimation are represented and compared with no error case. The detailed progress, simulations and implications are presented together with input fabrication errors and alignment state estimation solutions.



9582-20, Session 4

Disruptive advancement in precision lens mounting

Frédéric Lamontagne, Nichola Desnoyers, Michel Doucet, Patrice Côté, Jonny Gauvin, Geneviève Anctil, INO (Canada)

No Abstract Available

9582-16, Session PMon

Analysis of alignment tolerance of focal plane assembly of a telescope

Shenq-Tsong Chang, Yu-Chuan Lin, Ming-Ying Hsu, Ting-Ming Huang, Fong-Zhi Chen, Instrument Technology Research Ctr. (Taiwan)

Focal plane assembly (FPA) is an important component for modern remote sensing instruments. Array or linear CCD or CMOS detectors are usually applied. Linear detectors are often used in the space project to have a wider swath. In a remote-sensing project, five spectral ranges are desired. The spectral ranges are designated to be Panchromatic (450-700 nm), B1 (455-515 nm), B2 (525-595 nm), B3 (630-690 nm), and B4 (765-900 nm). Pixel size of the Panchromatic band (Pan) is 10 ?m, and those for B1~B4 (multispectral, MS) are 20 ?m. Pixel numbers are 12000 and 6000 for Pan band and MS bands, respectively. The FPA is consisted of a filter with five stripe band-pass thin films, filter mask and a five-line detector. The arrangement of the detector is B1, B2, Pan, B3 and B4 from the top to the bottom. In order to give the alignment tolerance, an analysis of the parameters of each component in FPA has been performed. Ray tracing method has been applied to have a image projection onto the plane where thin films are located. Spread sheet computation was adopted to simulate the situations when the design parameters were changed. According to the analysis, some supplement wideness to the stripe thin films has to be added to have a satisfied alignment tolerance.

9582-17, Session PMon

An optomechanical tolerance simulation for a four-group zoom lens

Chen-Chin Cheng, Industrial Technology Research Institute (Taiwan); John D. Griffith, Moondog Optics, Inc. (United States)

The zoom lens is a typical optical system. In general, opto-mechanical design plays as important role as optical design does in the optical system design. The results of optical tolerance analysis of a zoom lens carried out by optical design software usually consist of the tolerance budgets of lens tilt, lens decenter, lens position, group tilt, group decenter, grout position and image sensor tilt. However, in real world these tolerance budgets are achieved by lens fabrication process, mechanical design, mechanical manufacturing process, and assembly sequence. Mechanical engineer must consider the capabilities of a real manufacturing process and variations caused by the tolerances of optical and mechanical components that occur in the assembly process. Only when the components and assembly variations are calculated and simulated, can the performance of a zoom lens be predicted. In this study, an opto-mechanical tolerance simulation was implemented by VSA-3D? software to calculate the tilt, decenter and despace of the lens elements and groups of a four-group zoom lens. The simulation was carried out by Monte Carlo method and the results were conducted by descriptive statistics. The results indicate that the tolerance budgets of a zoom lens requested by optical designer can be verified through the manufacturing variations of lenses, mechanical parts, and assembly method. As a result, the performance of a zoom lens system can be predicted before mass production.

9582-18, Session PMon

Development of a FSMP mirror assembly

Jihun Kim, Young-Soo Kim, Je Heon Song, Korea Astronomy and Space Science Institute (Korea, Republic of); Myung Cho, National Optical Astronomy Observatory (United States); Ho-Soon Yang, Joohyung Lee, Korea Research Institute of Standards and Science (Korea, Republic of); Ho-Sang Kim, Kyoung-Don Lee, Institute for Advanced Engineering (Korea, Republic of); Won Hyun Park, National Optical Astronomy Observatory (United States) and The Univ. of Arizona (United States); Byeong-Gon Park, Korea Astronomy and Space Science Institute (Korea, Republic of)

Fast-steering Secondary Mirror Prototype (FSMP) of the Giant Magellan Telescope (GMT) has been developed by the consortium consisting of institutes in Korea and the US. In 2014 we have finalized the FSMP project by combining two sub-systems, the mirror fabricated by Korea Research Institute of Standards and Science (KRISS) and the mirror cell with tip-tilt controlling system developed by Institute for Advanced Engineering (IAE), in the KRISS facility. We have developed an assembly procedure in which we have identified potential difficulties such as handling without contacting mirror surface, optimizing bonding process, and elsewhere. As the solutions of the difficulties we developed supporting jigs and optimized bonding procedures. The assembled FSMP system was installed in the test tower in KRISS, and we confirmed the stability of the system. For the future works, the performance of FSMP system will be evaluated in static and dynamic environments for the validation of the FSMP system operation.

9582-19, Session PMon

Multiple sensor fusion into a single optical instrument

Oren Aharon, Duma Optronics Ltd. (Israel); Itai Vishnia, PLX Inc. (United States)

The reality of accurate optical measurements is that instruments are tailored to specific applications, resulting in the need for multiple devices in order to perform a system characterization. Many applications require the use of multiple optical elements in combination with laser beams and optical axis orientations. These applications dictate a need for a better integrative measurement tool. For example, the Electronic Autocollimator is a high precision angle measurement instrument, capable of measuring angle deviations with sub arc second accuracies. However it lacks the capability of measuring optical axis deviations, as well as comparing angle deviations from laser beam directions. This article presents a sensor fusion technology that combines the power of accurate electronics and optics into a measuring instrument. This allows performing electronic auto-collimation, laser beam characterization, laser alignment to mechanical and optical axis, and many more. Specifically, by providing the new instrument with a cooperative reflective target, additional characteristics are feasible, such as optical line deviation measurement, distances to target and remote examination of parts. An integral part of the process is the integration of Monolithic Optical Structure Technology, which allows for much greater stability, resulting in greater accuracy. This new fusion sensor technology substantially increases lab measurement capabilities, offering intricate measurements to be performed on lasers, high-power laser beams, mechanical datum stability and alignment with one single instrument.

Conference 9583: An Optical Believe It or Not: Key Lessons Learned IV



Monday 10-10 August 2015

Part of Proceedings of SPIE Vol. 9583 An Optical Believe It or Not: Key Lessons Learned IV

9583-1, Session 1

Why most strategic plans don't work

Robert W. Bradford, Ctr. for Simplified Strategic Planning, Inc. (United States)

Are you thinking strategically – or just going through the motions? Robert will discuss where he has seen plans go awry and how you can get more out of your planning process.

9583-2, Session 1

Acquisitions: 8 steps to success

Denise A Harrison, Spex, Inc.; Strategic Planning and Execution (United States)

Often companies try and grow from within – when should you look outside? What are some pitfalls that can be prevented as you look to the outside to complement your company's internal capabilities?

9583-3, Session 1

Everyone knows execution is important: so why do we fail to execute?

Robert W. Bradford, Ctr. for Simplified Strategic Planning, Inc. (United States); Denise A. Harrison, Spex, Inc. (United States)

Developing the strategy comes first. Implementing it in the organization is the real challenge. What causes execution train wrecks and how can you prevent them? Robert and Denise will present their findings based on their experience working with hundreds of companies.

9583-4, Session 1

Lessons learned in aligning an organization: two-way communication is key

Denise A Harrison, Strategic Planning and Execution; Spex, Inc. (United States)

Do you ever have the feeling that you aren't getting through to your employees? Listen to how this CEO found that she wasn't communicating to her employees and how she turned the situation around.

9583-5, Session 2

They never said anything about this in school: lessons from the engineering front line

Jonathan W. Arenberg, Northrop Grumman Aerospace Systems (United States)

Engineering cutting edge systems is simultaneously, a fulfilling intellectual endeavor and a contact team sport. Creating and managing a fun and successful career requires more than simply course work. This talk will present the top missing lessons learned by the author, gleaned from several decades of experience learning it the hard way. 9583-6, Session 2

Root cause analysis: shutting down the alligator farm

Anthony J. DeMarinis, Consultant (United States)

Many companies realize the importance or root cause analysis and correcting problems. However, there is still much confusion and many problems continue to recur.

Inadequate Failure Investigation, Recurring Problems and Inadequate Documentation are often cited by auditors, and many presentations focus on the regulatory requirements and how to do and document these investigations. However, few focus on the environmental and cultural factors that prevent people from seeing and addressing the true root cause in the systems that enable and spawn these problems. This presentation addresses those barriers to real root cause analysis and enables the participant to see and overcome these barriers during their investigation activities. We will use thoughtful discussion and humorous analogies to distinguish between the true root cause and other common imposters. Emphasis will be placed on realizing system interactions and the cultural environment that often lies at the root of the problem and prevents true root cause analysis, and we will include concepts and practical advice on how to identify cultural and environmental obstacles to root cause analysis and organizational improvement. It will also review the basic tools and analytical methods needed to objectively identify the true root cause and prevent recurrence.

9583-20, Session 2

What do you do when your critical to quality features (CTQs) turn into what the flig (is happening)!? (WTFs) (Invited Paper)

Lance B Coleman, Full Moon Consulting (United States)

At the heart of every lean, six sigma and continuous improvement project is one thing – root cause analysis. Root cause analysis can be used to determine why a process is not performing as expected, or to determine significant factors that may lead to process improvement. Conversely, faulty root cause analysis is often the reason why problems keep occurring over and over again and why continuous improvement sometimes seems an elusive concept at best. This session will teach attendees how to accurately determine root cause as a first step in implementing effective improvement initiatives, capturing lessons learned and mitigating risk.

When analyzing complex processes, potential root causes can be identified through root cause analysis (RCA) and then Design of Experiments (DOE) or General Linear Modeling (GLM) can be used to determine the truly significant input factors to a process. Alternatively, once a significant factor has been determined through use of DOE or GLM, then RCA can be performed to help determine why the factor is significant. Whether you utilize RCA before or after DOE or GLM, the offshoot of the RCA process is to use the information discovered to create effective preventative, corrective, and/or improvement actions.

Key takeaways are:

• Learning how RCA is interconnected with both continuous improvement and risk management

• Determining root cause – tools and methods – 5WHYs, Ishikawa Diagrams, IS/IS NOT

- Effective RCA training methods
- Using root cause analysis to capture lessons learned
- Understanding the root cause analysis and corrective action process



9583-7, Session 3

Lessons learned over the last thirty years

Richard C. Juergens, Raytheon Missile Systems (United States)

This talk discusses some mistakes, goofs, and misjudgments I have come across over the last thirty years, and the lessons learned from them. The experiences cover several different disciplines, including optical design and engineering, stray light, and polarization issues, and includes both design and hardware examples.

9583-8, Session 3

Lessons not to make light of (when designing optical systems for space)

Stephen E. Kendrick, Consultant (United States)

There is a range of lessons learned when taking an optical system from design through deployment in space. I will summarize some key lessons and observations related to both airborne and spaceborne optical systems with an emphasis on lightweighted optics and space telescopes. Areas discussed encompass 1) the initial architecture and system trades as constrained by system error budgets, 2) manufacturing considerations, 3) testing implications, and 4) real and perceived cost impacts.

9583-9, Session 3

Requirements management lessons learned: fuzzy "most likely" versus clean shaven "not to exceed"

Paul A. Lightsey, Ball Aerospace & Technologies Corp. (United States)

Mission objectives often have a level of imprecision that lends itself to a fuzzy logic approach, even though the more traditional approach is to flow down bimodal pass/fail "not to exceed" type of requirements. Examples will be given for large astronomical telescope applications involving optical performance, active wave front and control, and radiometric/stray light controls demonstrating the pros and cons of the two contrasting strategies.

9583-11, Session 3

How to raise a teenage instrument: building and flying the Orbiting Carbon Observatory-2 (OCO-2)

David Crisp, Jet Propulsion Lab. (United States)

The NASA Orbiting Carbon Observatory-2 carries a 3-channel imaging grating spectrometer that was designed to make space based measurements of atmospheric carbon dioxide with unprecedented precision, accuracy, resolution, and coverage. When embarking on the development of a high performance flight instrument of this kind, it is always best practice to limit risk, to the extent possible, by adopting (and freezing) a conservative design based on high heritage parts, with ample cost, schedule, and performance margins. What happens when those practices encounter the reality of a highly competitive, cost-capped opportunity embedded in a rapidly evolving programmatic environment characterized by funding delays, team changes, delivery delays, performance shortfalls, and obsolescence of "high heritage" parts, and ever growing expectations for the instrument's performance from your customers in the science community and beyond? Is it possible to deliver and operate an instrument, 14 years after it was conceived, which still exceeds its requirements and redefines the state of the art in spite of a few quirks and idiosyncratic features? Somehow, we managed to surmount these and

other hurdles and deliver and launch OCO-2, a NASA Earth Science mission that is now collecting hundreds of thousands of precise carbon dioxide measurements over the sunlit hemisphere of the Earth each day. Here, I will summarize a few of the key technical challenges, frustrations, and surprises encountered on this long odyssey, and try to remember how we got through it all.

9583-12, Session 3

The beam rotation that almost was in the National Ignition Facility

R. Edward English Jr., L-3/Cincinnati Electronics (United States) and REE Optical Systems, LLC (United States)

How might an optical design change in the final optics assembly couple with the spherical geometry required for beam delivery to the target chamber to cause the 40 cm beam to be rotated by more than several design teams had thought, and not be discovered until the final design stage for the beam enclosure and structures?

9583-13, Session 3

Four big mistakes in developing photonics-enabled medical devices

David Hill, Krista McEuen, Zygo Corporation (United States)

Photonics components have become key enablers in the design and development of next-generation medical devices and diagnostics. This trend has its roots in mature imaging technologies like optical microscopy and endoscopy/colonoscopy, and is poised to accelerate through emerging applications such as optogenetics, laser ablation therapy, and optical coherence tomography (OCT), among many others. This white paper identifies four of the most common mistakes we see medical device manufacturers make when attempting to incorporate optics and photonics into their designs — and how to avoid them.

9583-10, Session 4

The art of planning for optical systems integration and alignment

Joseph F. Sullivan, Ball Aerospace & Technologies Corp. (United States)

This will address Lessons Learned on the approaches that worked or did not work over various programs when integrating and aligning elements into fairly complex optical systems. The appropriate planning can prevent many unnecessary headaches and achieve the desired optical performance while optimizing integration efficiency.

9583-15, Session 4

Trials and tribulations of optical manufacturing: asphere edition (Invited Paper)

Gregory Frisch, Kate Medicus, Mark E. Schickler, Brandon B. Light, Jessica DeGroote Nelson, Optimax Systems, Inc. (United States)

With the ongoing advancements in aspheric manufacturing and metrology, companies have to overcome processing challenges and from time to time learn costly lessons along the way. Optimax Systems, Inc., a leader in quick delivery prototype optics, has been manufacturing aspheric lenses for over



20 years. Along the way, we have learned many lessons, some the hard way. In this paper, I will share a few stories of how aspheres have humbled us, how we overcame the problem, and provide takeaways for other manufactures and designers.

9583-16, Session 4

Polarimeter calibration error gets far out of control

Russell A. Chipman, College of Optical Sciences, The Univ. of Arizona (United States)

This is a sad story about a polarization calibration error gone amuck. A simple laboratory mistake was mistaken for a new phenomena. Aggressive management did their job and sold the fictitious idea very effectively and substantial funding followed. Questions were raised and a Government lab tried to recreate the breakthrough. The results were unpleasant and the field developed a bad reputation for several years.

9583-17, Session 4

A quintuple of painful lessons from surface inspection to high-speed imaging

Cornelius F. Hahlweg, bbw Hochschule (Germany); Cornelia Weyer, G&S Gesundheit für Betriebe GmbH (Germany)

The paper delivers interesting short stories from about two decades of research and development in the field of surface inspection, hyper spectral imaging, high speed techniques and endoscopy. The papers covers problems with an import restricted SWIR sensor, which turned out to be creatively calibrated, the repeatedly ignored need for IR filters, the self-sustaining diffraction order, if you don't understand it ... shoot it visualization plans which ended up at the Shooting range, and the desire for substituting filament bulbs in colorimetry. From todays point of view a set tirivialities, at their time thwarting factors of monstrous dimension, the problems discussed are squezed into short chapters, which hopefully will be good for some fun without unnecessary lengthy elaboration. The presentation will contain exemplary footage and visualization.

9583-18, Session 4

From SDI to tactical battlefield lasers: myths, legends, and facts. Reflections of a "Star Warrior"

James A. Horkovich, Schafer Corp. (United States)

This talk presents a history of missile defense and the "Star Wars" program and its' evolution to today's tactical battlefield laser systems, marking the 30th anniversary of President Ronald Reagan's "Star Wars" speech. Since Archimedes' "Burning Glass" at the siege of Syracuse 212 B.C. through the development of the LASER man has been fascinated with the idea of using directed energy weapons. But nothing did more to focus this effort than the threat posed by Mutually Assured Destruction. Under Reagan's "Star Wars" plan years and billions of dollars were invested in making high energy laser systems a reality. This presentation reviews the fundamentals of laser physics and traces the development of these systems in the USA, the USSR. and across the world from the Gas Dynamic LASER laboratory in the 1960s and the USAF Airborne Laser Laboratory of 1981 through the SDI era and up to today. In reflecting on the effort invested in developing this technology, this interdisciplinary talk addresses the role that this technology played in changing the geopolitical state of the cold war and continues to play in international defense efforts today.

9583-19, Session 5

The sage on the stage - and the audience is texting

Judith F. Donnelly, Three Rivers Community College (United States)

As it is, the professors give too many lectures and the students listen to too many. Or pretend to; really they do not listen, however attentive and orderly they may be. ... They reproduce the lecture in recitations like the phonograph, mechanically and faithfully, but with the tempo and timbre so changed that the speaker would like to disown his remarks if he could. (Slossen, 1910)

SPIE. OPTICS+ PHOTONICS **Conference 9584:** Ultrafast Nonlinear Imaging and Spectroscopy III

Sunday - Monday 9 -10 August 2015

Part of Proceedings of SPIE Vol. 9584 Ultrafast Nonlinear Imaging and Spectroscopy III

9584-1, Session 1

A beamline for attosecond pump-probe experiments: Mapping ultrafast electron dynamics in atoms and molecules

Emma R. Simpson, Simon E. E. Hutchinson, Thomas Siegel, Zsolt Diveki, Alvaro Sanchez-Gonzalez, Christian S. Struber, Lukas Miseikis, Dane R. Austin, Jon P. Marangos, Imperial College London (United Kingdom)

We present a versatile beamline for attosecond pump-probe experiments using the techniques of attosecond transient absorption spectroscopy (ATAS) and extreme ultra-violet (XUV) initiated high harmonic generation (XiHHG) to probe ultrafast electron dynamics on the attosecond timescale. Utilising a non-colinear geometry we split our incident beam into two arms, one of which generates high harmonics that can act as either the pump or the probe. A controllable delay is introduced between the two arms using a voltage-controlled piezo. The non-colinear pump-probe arrangement enables individual control over the parameters of each arm such as intensity, polarisation and ellipticity allowing these variables to be scanned as functions of delay. The recombined pump and probe arms are re-imaged in an interaction chamber using a toroidal mirror before a flatfield spectrometer with micro-channel plate (MCP) and camera assembly to detect and record the resultant harmonics.

Preliminary results from ATAS in laser dressed helium indicate we can achieve a temporal resolution better than 250as between the pump and probe arms through the use of post-processing temporal correction to account for long-term thermal drifts in the system. Delay-dependent modulations in the absorption for both the above and below ionisation potential (Ip) harmonics at even multiples of the driving field wavelength have been observed and the results are in the process of being analysed. Using a commercial optical parametric amplifier (OPA) we are extending our driving wavelength to access higher ponderomotive energy in order to look for XiHHG and ATAS from 3d ionisation in Krypton (around 93eV).

9584-2, Session 1

Ultrafast electron diffraction from laseraligned carbon disulfide molecules (Invited Paper)

Jie Yang, Martin Centurion, Univ. of Nebraska-Lincoln (United States)

In conventional gas-phase electron diffraction (GED), only one-dimensional structural information can be accessed due to the random orientation of molecules in the gas phase. The method ultrafast electron diffraction from laser-aligned molecules (UEDAM) can resolve the three-dimensional molecular structure with atomic resolution. Previously, we have used this method to image the structure of the ground state of the CF3I molecule. In this work, we use UEDAM to investigate the dynamics of carbon disulfide (CS2) molecules following the interaction with an intense femtosecond IR laser pulse. Two-dimensional molecular images with atomic resolution are recorded under different laser intensities. An upper limit of degree of alignment is found with the increase of laser intensity. At higher intensity, structural deformation and dissociation are observed. We have found a diffraction-difference method that allows us to access only the 3% most aligned molecules. With this method, we're able to measure the atomic positions in transient state structures with 0.03Å precision and 1ps temporal resolution. This proof-of-principle work demonstrates the capability of studying molecular dynamics with high spatial and temporal resolution using UEDAM.

9584-3. Session 1

Imaging molecules with sub-angstrom resolution using femtosecond electron pulses (Invited Paper)

OPTICAL ENGINEERING+

APPLICATIONS

Omid Zandi, Univ. of Nebraska-Lincoln (United States); Alice DeSimone, Kyle Wilkin, Jie Yang, Martin Centurion, Univ. of Nebraska-Lincoln (United States)

Ultrafast electron diffraction can provide time resolved images of molecules with atomic resolution. In this talk, we will present recent results on ultrafast imaging of molecules and describe recent improvements in sources and new experimental setups designed to reach femtosecond temporal resolution. In particular, a photoelectron gun coupled with an RF cavity has been implemented to compress 100 keV electron pulses. The duration of the electron pulses is measured in-situ using a streak camera that can reach a resolution of 200 fs. Even with short electron pulses, the resolution in gas phase experiments can be degraded by the fact that laser and electron pulse traverse the sample with different velocities. We use a tilted laser pulse to match the velocity of the sub-relativistic electrons as they traverse the sample. Other approaches to achieve femtosecond resolution are to use relativistic electron pulses with MeV energy that minimize the effect of velocity mismatch. These can be generated with RF electron guns or with laser-accelerated electrons.

9584-4. Session 1

Transient chromatic aberrations at discrete energies in ultrafast electron microscopy (Invited Paper)

David J. Flannigan, Dayne A. Plemmons, Univ. of Minnesota, Twin Cities (United States)

In ultrafast electron microscopy (UEM), extension of the capabilities of transmission electron microscopy to the ultrafast domain allows for visualization of non-equilibrium structural and electronic phenomena. The operating principle of UEM requires spatiotemporal overlap of the fs photon pulse and electron packet at the specimen. At time zero, photon absorption by the electrons occurs, and peaks at integer multiples of the photon energy can be observed in electron-energy spectra. In this talk, I will discuss considerations for isolating inherent artifacts of the highly non-linear near-field interactions from the actual packet characteristics. Using theory developed to describe these interactions, I will discuss how temporal cross sections of peaks in the electron-energy spectra corresponding to highorder transitions are expected to exhibit the true temporal behavior of the electron packets. The portion of the pump laser pulse capable of initiating such transitions results in temporal widths converging to the electron packet duration. Additionally, photon absorption by electrons focused on the edge of a nanostructure suggests the resulting energy distribution may produce well-defined chromatic aberrations in bright-field images arising from the velocity dependence of the Lorentz force. I will discuss the prospect for detecting these discrete aberrations and their potential as a means of determining the UEM instrument response without the need for a spectrometer. Appropriate interpretation of observed spectroscopic and image features should in principle enable systematic temporal and spatial deconvolution allowing for a more accurate depiction of intrinsic ultrafast dynamics, especially as UEM capabilities advance toward angstrom-scale, real-space fs imaging.



9584-5, Session 1

Ultrafast probe using femtosecond electron pulses (Invited Paper)

Jianming Cao, Florida State Univ. (United States)

In recent years, femtosecond electron pulses have emerged as a powerful tool to probe ultrafast dynamics in matter. They have been used in ultrafast diffraction to reveal the atomic-detail structural dynamics in real time, covering a wide range of applications such as monitoring phase transitions in physics and materials science, and examining dynamics of reactions in chemistry and biology. They have also been used in ultrafast electron shadow imaging and deflection measurement to monitor the transient electron field and plasma dynamics. In this talk, I will focus on the development of ultrafast electron probe and its application in our research, ultrafast photo-induced demagnetization in ferromagnetic materials, photo-induced phase transition in correlated electron materials and the dynamics of warm dense matter.

9584-6, Session 1

MeV ultrafast electron diffraction and imaging at SLAC (Invited Paper)

Xijie Wang, SLAC National Accelerator Lab. (United States)

The SLAC UED&UEM facility will take advantage of the recent developments in high-brightness ultrafast electron sources, high-field magnets and electron detection. It will provide direct access to atomic coordinates with temporal resolution down to 100 fs and even below in the diffraction (UED) mode. The ultrafast imaging capabilities of the SLAC UEM will represent a paradigm shift compared to present day facilities, and it can achieve 10-nanometer and 10-picosecond resolution in single-shot mode. To realize high temporal resolution required for the SLAC UED&UEM facility, a MeV high-brightness electron beam generated by a photocathode RF gun will be employed. This allows more electrons to be packed into each bunch, offering single-shot capabilities similar to those of x-rays from LCLS. A further important advantage of relativistic beams is that they eliminate the velocity mismatch between the electromagnetic pump pulses and the electron probe beam. This mismatch limits the time resolution of ultrafast dynamics for dilute samples, such as gas and liquid samples. In addition to the higher temporal resolution, MeV electrons can penetrate thicker samples. Finally, the higher electron beam energy leads to a larger elastic scattering cross section and a decrease in the inelastic scattering cross sections, increasing the diffraction signal and reducing inelastic scattering.

9584-7, Session 2

True surface spectra from sum-frequency vibrational spectroscopy of nonpolar media (Invited Paper)

Chuanshan Tian, Fudan Univ. (China)

In the past decades, sum-frequency vibrational spectroscopy (SFVS) has been well established as a powerful technique for surface studies. It is based on the idea that under the electric dipole (ED) approximation, SF generation originates only from the surface or interface where the inversion symmetry is broken. There is, however, always a lingering doubt that the electricquadrupole (EQ) bulk contribution to surface SF generation may not be negligible. The problem is particularly important for SFVS application to media that do not have a surface layer of strongly polar-oriented molecules, although it has been largely ignored by many practitioners of SFVS. Despite many theoretical and experimental studies in the past, a comprehensive picture supported by experiment is still missing.

Following our theoretical understanding, we designed an experiment and used benzene as an example to show that for the first time, we can separately obtain EQ bulk spectra and surface spectra from SFVS of a medium composed of nonpolar (symmetric) molecules. The true bulk spectra with no contribution from the surface were directly measured by transmission SFVS, and the true surface spectra with no bulk contribution was deduced from reflection SFVS through proper spectral analysis. The results also provide guidelines for evaluation of the importance of bulk contribution to SFVS when applied to media of polar molecules. This work is supported by NSFC and NCET.

9584-8, Session 2

Chiral sum frequency generation microscopy by using polarization manipulation (Invited Paper)

Ziheng Ji, Peking Univ. (China); Kebin Shi, Peking Univ. (China) and State Key Lab. for Mesoscopic Physics (China) and Collaborative Innovation Ctr. of Quantum Matter (China)

Chiral sum-frequency generation (C-SFG) is an electric-dipole allowed non-degenerate second order nonlinear process which could be used to probe the chiral component of second order nonlinear susceptibility in chiral interface and chiral bulk media. Being chemical and chiral selective, C-SFG imaging and spectroscopy technique are capable for label-free, achiral background free, in situ and realtime characterization of biomolecule and bioengineering sample. Due to the sub-micron dimension of biofunctional structure. C-SFG microscopic and micro-spectroscopic toolsare often needed. Efforts have been made to adapt the classical non-paraxial configuration directly into a microscopic configuration. In this paper, we propose a new microscopic setup to manipulate the polarization state of the laser beam in order to avoid the non-paraxial arrangement. As a result, higher resolution and larger effective imaging area can be achieved. Our results also show the capabilities to combine the proposed approach with confocal microscopy or other existed imaging technique.Simulation is performed by using vector diffraction theory and Green's function formulation to calculate the structure of focal field, the generation and the propagation of C-SFG signal. The results indicate the feasibility and promising application of polarization manipulated C-SFG microscopy in practical bioengineering and biomedical research.

9584-9, Session 2

Bond models of linear and nonlinear optics (*Invited Paper*)

David E. Aspnes, North Carolina State Univ. (United States)

Bond models have a long history in optics, originating with the largely forgotten Ewald-Oseen Extinction Theorem of linear optics (Ewald, 1912; Oseen, 1915) and being used in the 1960's and early 1970's to calculate nonlinear-optical (NLO) susceptibilities in the static limit. Interest revived with the recent work of Powell et al., who showed that an anisotropic version enormously simplified the interpretation of second-harmonic-generation (SHG) data for Si-SiO2 interfaces. These models are based on fundamental physics instead of phenomenology, and describe optical responses in terms of processes that occur on the atomic scale, in real time. Also, since crystal structure is incorporated at the atomic level, tensor components emerge automatically. For linear optics, the four steps involved constitute a difficult problem in self-consistency, but for NLO, where the emerging radiation is orders of magnitude weaker and occurs at a different wavelength, all four steps can be treated independently and calculations are straightforward.

I discuss the use of bond models to identify the four basic contributions to SHG: bond anharmonicity, spatial dispersion, retardation, and magnetism, all of which can be understood in this framework in simple physical terms. I then discuss various applications, including surface and interface analysis by SHG. Other applications include third- and fourth-harmonic generation (THG, FHG), dipole-forbidden NLO processes in the bulk of amorphous



materials and crystals with inversion symmetry, and following the surface chemistry of Si oxidation under uniaxial strain.

9584-10, Session 3

Leveraging higher-order nonlinearities in optical transient absorption for microscopic imaging contrast (Invited Paper)

Jesse W. Wilson, Jong Kang Park, Miguel Anderson, Martin C. Fischer, Warren S. Warren, Duke Univ. (United States)

The transient absorption response of melanin is a promising opticallyaccessible biomarker for distinguishing malignant melanoma from benign pigmented lesions, as demonstrated by earlier experiments on thin sections from biopsied tissue. The technique has also been demonstrated in vivo, but the higher optical intensity required for detecting these signals from backscattered light introduces higher-order nonlinearities in the transient response of melanin. These components that are quadratic with respect to the pump or the probe introduce intensity-dependent changes to the overall response that complicate data analysis. However, our data also suggest these nonlinearities might be advantageous to in vivo imaging, in that different types of melanins have different nonlinear responses. Therefore, methods to separate linear from nonlinear components in transient absorption measurements might provide additional information to aid in the diagnosis of melanoma.

We will discuss numerical methods for analyzing the various nonlinear contributions to pump-probe signals, and our progress toward realtime analysis with digital signal processing techniques. To that end, we have replaced the lock-in amplifier in our pump-probe microscope with a high-speed data acquisition board, and reprogrammed the coprocessor field-programmable gate array (FPGA) to perform lock-in detection. The FPGA lock-in offers better performance than the commercial instrument, in terms of both signal to noise ratio and speed. In addition, the flexibility of the digital signal processing approach enables demodulation of more complicated waveforms, such as spread-spectrum sequences, which has the potential to accelerate microscopy methods that rely on slow relaxation phenomena, such as photothermal and phosphorescence lifetime imaging.

9584-11, Session 3

Optimization of mid-IR photothermal imaging for tissue analysis (Invited Paper)

Atcha Totachawattana, Shyamsunder Erramilli, Michelle Y. Sander, Boston Univ. (United States)

Photothermal imaging in the mid-infrared allows highly sensitive, labelfree microscopy by relying on bond-specific material characterization of the samples. In a pump-probe configuration, the mid-IR pump laser is tuned to characteristic vibrational molecular modes and thermally induces changes in the refractive index. The shorter wavelength probe scatter can be detected with lock-in technology, utilizing highly sensitive detectors at telecommunication wavelengths. This mitigates the need of complex detector technology as required for traditional infrared spectroscopy/ Fourier Transform infrared spectroscopy.

Our system features a high brightness quantum cascade laser that can be tuned continuously over a spectrum of interest. This is combined with fiber laser technology for the probe laser which features a compact footprint, robust performance metrics and reduced sensitivity to environmental perturbations compared to free-space laser configurations. In systematic spectroscopy studies where the probe laser parameters were modified, we demonstrate that the signal-to-noise ratio can be significantly increased by utilizing a mode-locked laser configuration instead of a continuous-wave laser.

With a raster-scanning approach, the photothermal spectroscopy system can be extended to a label-free mid-infrared microscope. By tuning the pump laser to the amide-I absorption band around 1650cm-1 in biological tissue samples, whose spectral characteristics can provide insight into the secondary structure of proteins (e.g. amyloid plaques; alpha-helix, beta-sheet), we can combine spectral content with localized sample details. We will present the versatility of the mid-IR photothermal system for analyzing histopathological tissue sections of e.g. cancerous tissue in a non-contact, non-destructive approach with good sensitivity.

9584-12, Session 3

Multifunctional diagnostic, nanothermometer, and photothermal nano-devices (Invited Paper)

Shuang Fang Lim, Kory Green, Janina Wirth M.D., North Carolina State Univ. (United States)

In this study, the known therapeutic capabilities of gold nanorods (AuNRs) have been combined with the diagnostic and nanothermometer abilities of upconversion nanoparticles (UCNPs) to develop a system for simultaneous biological imaging, photothermal therapy, and nanothermal sensing. Both the excitation of UCNPs and the finely tuned longitudinal surface plasmon resonance (LSPR) mode of AuNRs lay in a window of relatively high light penetration of tissue in the infra-red. The nanothermometer property of the UCNPs allows direct quantification of the localized temperature of the photothermally heated AuNRs chemically adsorbed to their surface and is free from the bleaching problems inherent in dye thermal sensing systems, especially at high laser fluences required to kill tissue. Spectroscopy on single particles, verified by transmission electron microscopy (TEM), has been performed at varying temperatures to confirm 1) the thermal sensing properties of UCNPs and 2) to finely tune their upconversion enhancement arising from the LSPR coupling of the AuNRs. Simultaneously measurement of the emission of two thermally coupled states in the UCNP Erbium ions, enables quantification of the localized temperature of photothermally heated AuNRs. HeLa cell viability studies have also been performed to ensure that cell death accompanying particle incubation at various concentrations and fluence dosing are the direct result of the photothermally heated AuNRs and not a result of cytotoxicity of the particle composites or absorptive properties of the medium itself.

9584-13, Session 3

Multiscale diffusion of single molecules in crowded environments (Invited Paper)

Ahmed A. Heikal, Univ. of Minnesota, Duluth (United States)

Living cells are crowded with organelles, biomembranes, and macromolecules such as proteins, DNA, RNA, and actin filaments. Such macromolecular crowding is believed to influence biomolecular diffusion, protein-protein interactions, protein-substrate interaction, and protein folding. In this project, we elucidate crowding effects on the diffusion of a rhodamine green (RhG), nonspecific binding and the heterogeneity of microviscosity in a crowded environment of macromolecules. For biomimetic crowding, Ficoll-70, BSA, and ovalbumin were used as crowding agents at biologically relevant concentrations and compared with glycerol-rich solutions as a continuum. The rotational (ps-ns) and translational (ms-s) diffusion of RhG was investigated using time-resolved fluorescence anisotropy (TRA) and fluorescence correlation spectroscopy (FCS), respectively, as a function of crowding. Our results suggest that the multi-scale diffusion of RhG can be described using the Stokes-Einstein model only in a continuum (e.g., glycerol) environment. Rotational diffusion measurements indicate non-specific binding between RhG and proteins (BSA and Ovalbumin), which explains the deviation from the Stokes-Einstein model in a protein-crowded environment. The equilibrium constant and changes in standard free energy of such non-specific binding were calculated using TRA results. The local microviscosity experienced during the rotational and translational diffusion of RhG agrees with the bulk viscosity over the 1-20 cP range. In Ficoll-70, BSA, and ovalbumin-crowded environments, however, the microviscosity differs from the corresponding

Conference 9584: Ultrafast Nonlinear Imaging and Spectroscopy III



bulk viscosity depending on the nature (i.e., proteins versus polymers) and concentration of crowding agents. Our findings provide a foundation for multi-scale diffusion studies of biomolecules in the crowded milieu of living cells using fluorescence spectroscopy.

9584-14, Session 3

Optical imaging for digital biosensing (*Invited Paper*)

Zhenyu Li, The George Washington Univ. (United States)

Digital biosensors enable absolute counting of individual target biomolecules in a given sample without a calibration curve. Such sensing modalities with single molecule resolution has proved powerful in both ultrasensitive medical diagnostics and fundamental biological research. A variety of optical imaging techniques are particularly suited for digital biosensing. In the talk, I will discuss the general requirements for digital biosensing and how a number of optical imaging techniques can provide such capabilities, in some cases with low cost setup and small system foot print.

9584-15, Session 4

Adaptive control of waveguide modes in a few-mode fiber network (Invited Paper)

Yong Xu, Peng Lu, Matthew Shipton, Brennan Thews, Anbo Wang, Virginia Polytechnic Institute and State Univ. (United States)

We report an adaptive optics (AO) method that can be used to control the form of optical waves in a few-mode fiber (FMF) network. Our method relies on the incorporation of fiber Bragg gratings (FBGs) within the FMF network for model control. Since different guided modes possess different propagation constants, a typical FBG should produce different transmission / reflection responses for different guided modes. Therefore, by using optical signals reflected / transmitted by the FBG as feedback, we can utilize a simple AO algorithm to control the form of optical waves at the FBG location. This feasibility of this approach is confirmed through direct comparison with guided wave profiles captured by a CCD camera. By incorporating multiple FBGs in the FMF network, we should be able to achieve mode control in the FMF network in a quasi-distributed manner.

9584-16, Session 4

Transmission of femtosecond pulses through multimode fibers (Invited Paper)

Demetri Psaltis, Ecole Polytechnique Fédérale de Lausanne (Switzerland)

Multimode fibers have been investigated recently for imaging and communications. In this presentation we will explore how femtosecond pulse propagate through multi-mode fibers and discuss applications.

9584-17, Session 4

Delivery of ultrashort spatially focused pulses through a multimode fiber (*Invited Paper*)

Christophe Moser, Edgar E. Morales, Demetri Psaltis, Salma Farahi, Ecole Polytechnique Fédérale de Lausanne (Switzerland)

Multimode optical fibers potentially allow the transmission of larger

amounts of information than their single mode counterparts because of their high number of supported modes. However, propagation of a light pulse through a multimode optical fiber suffers from spatial distortions due to superposition of the various exited modes and from time broadening due to modal dispersion.

We present a method to selectively excite specific optical fiber modes in a multimode fiber that follow similar optical paths as they travel through the fiber. In this way, they can interfere constructively at the fiber output generating an ultrashort spatially focused pulse. The excitation of a limited number of modes following similar optical paths limits modal dispersion, allowing the transmission of the ultrashort pulse. Digital scanning of the spatially focused pulse without movable elements is shown.

We also demonstrate that the intensity of the pulse delivered as a focused spot on the other end of the fiber is enough to excite two-photon fluorescence of a fluorescent dye whose spectral absorption peak occurs at half the wavelength of the delivered pulse.

We have experimentally demonstrated the delivery of a focused pulse through a 30 cm , 200 micrometer core multimode fiber with a duration of approximately 500 fs. This study adds two-photon imaging capability for endoscopy using commercial multimode fibers.

9584-18, Session 5

Effects of quantum confinement and environment on exciton dynamics of monolayer and few-layers molybdenum disulphide (Invited Paper)

Hongyan Shi, Harbin Institute of Technology (China) and Key Lab. of Micro-Optics and Photonic Technology (China); Xuan Li, Ruihuan Tian, Yan Ling, Harbin Institute of Technology (China); Xiudong Sun, Harbin Institute of Technology (China) and Key Lab. of Micro-Optics and Photonic Technology (China)

Two-dimension transition metal dichalcogenide monolayer and fewlayers, i. e. MoS2, are emerging as promising potential for exploring 2D semiconductor optoelectronic devices. How exactly quantum confinement and surrounding environment affect excitonic properties of monolayer MoS2 is still currently under heated debate. We perform laser scanning transient absorption microscopy (TAM) to study optical properties and exciton dynamics in monolayer and few-layers MoS2 supported on different substrates. The novel laser scanning TAM setup allows the direct tracking of excitation propagation in space and time with ultrafast temporal resolution and sub-diffraction limited spatial resolution by scanning the probe beam relative to the pump at the focus of a microscope with a galvanometer scanner. The resulting time-dependent dynamics reveals the influence of quantum confinement and surrounding environment on exciton resonance and energy relaxation related to many-body interactions and screening due to dielectric screening of Coulomb interactions.

9584-19, Session 5

Lithography-free super absorbing metasurfaces for surface enhanced nonlinear optics (Invited Paper)

Kai Liu, Tianmu Zhang, Dengxin Ji, Joseph Murphy, Haomin Song, Tim Thomay, Univ. at Buffalo (United States); Kebin Shi, Peking Univ. (China); Qiaoqiang Gan, Alexander Cartwright, Univ. at Buffalo (United States)

Nanoplasmonic metamaterials are effective platforms to create ultra-compact on-chip optical devices through deep-subwavelength concentration of electromagnetic fields. These strongly localized fields are particularly promising to enhance inherently weak nonlinear optical responses of materials. Recently, lithography-fabricated periodic plasmonic/

Conference 9584: Ultrafast Nonlinear Imaging and Spectroscopy III



metamaterial structures were employed to enhance nonlinear optical responses, yet imposing a cost barrier for practical applications. Here we will employ a lithography-fee low-cost metasurface to demonstrate its application on surface enhanced second harmonic generation (SHG). The proposed metasurface absorber consists of a monolayer of silver (Ag) nanoparticles (NPs), a SiO2 spacer layer and an optically thick Ag ground plate. A super absorption peak of 68% was achieved in the metasurface at the wavelength of 830 nm which was aligned well with our pump wavelength at 800 nm. Only ~25% absorption peaks was observed in the control sample (i.e. AgNPs on a glass substrate with no nanocavity enhancement). Simulation results revealed a strongly confined electric field between the Ag ground plate and the AgNP, contributing to the enhanced nonlinear optical response of those metal NPs. SHG measurement results show an obvious signal at the wavelength of 400 nm generated from the designed metasurface absorber, while no substantial SHG signal was observed from the control sample even under higher pump power conditions. Compared with previously reported lithography-fabricated matematerials for enhanced nonlinear optics processes, our lithographyfree metasurface is low-cost, large-area and amenable to develop practical applications.

9584-20, Session 5

Ultrafast pump-probe spectroscopy with force detection (Invited Paper)

Eric O. Potma, Univ. of California, Irvine (United States)

A very important class of nonlinear optical techniques is pump-probe spectroscopy, in which the sample is optically excited by a pump pulse and the ensuing excitation dynamics is followed by a time-delayed probe pulse. As pump-probe techniques, which were originally developed for macroscopic ensemble measurements, are finding their way into single molecule applications, proper descriptions are required to interpret the pump-probe signal at the spatial scales relevant to individual molecules. In this presentation, we will discuss the pump-probe interaction in the nearfield in various excita- tion geometries, and how the near-field interaction is manifested in the far-field. Based on a general description of the pumpprobe signal, we examine two detection strategies of the light-matter interaction: optical detection and force detection. We will show that, besides the more conventional optical detection approach, non-optical methods such as force detection offer a viable route towards exploring ultrafast single molecule dynamics at the nanoscale.

9584-21, Session 5

An exciton's transformation in a semiconducting polymer: How absorption and emission relate in an anisotropic solid (Invited Paper)

Kenan Gundogdu, Bhoj Gautham, Harald W. Ade, North Carolina State Univ. (United States); Natalie Stingelin, Imperial College London (United Kingdom); Robert Younts, North Carolina State Univ. (United States); Christoph Hellmann, Imperial College London (United Kingdom)

Due to the heterogeneity of the solid-state structure of semiconducting polymers, the understanding of their electronic and opto-electronic characteristics continues to be incomplete - despite extensive investigations and considerable technological potential of these materials. As isolated chains, the one-dimensional optoelectronic structure of the conjugated backbone can be considered molecular in character. In the complex solid state, H- or J-like coupling of certain polymer segments ('chromophores') can occur, which imparts an anisotropic 2D opto-electronic character (with the third dimension being inactive) and significantly modifies the absorption and emission spectrum compared to the molecularly isolated state. Despite the effective 2D nature of the materials, the fluorescence state with lifetimes

of 100s of ps following the much faster absorption is currently thought to be a result of the continuous evolution of the same quantum mechanical state. Through spectroscopic studies of the ubiquitous semiconductor poly(3-hexylthiophene) (P3HT), whose H- and J-coupling has been manipulated, we show that even in cases where the absorption spectrum exhibits intrachain excitonic line shapes (J-like), intramonomer repulsive forces and the anisotropic coupling along and transverse to the polymer chains drive formation of interchain excitons, which radiatively recombine to generate H-like emission spectra. Our time resolved studies show that this transformation is discontinuous and that photogenerated excitons seem to first form an intermediate dark polaron-pair prior to forming an interchain exciton.

9584-22, Session 5

Nano-imaging and spectroscopy with optical antennas (Invited Paper)

Joanna M. Atkin, Univ. of Colorado at Boulder (United States) and The Univ. of North Carolina at Chapel Hill (United States)

Many materials classes show some of mesoscale spatial heterogeneity that is important for functional properties, ranging from biological structurefunction relations to domain formation in strongly correlated electron materials. Optical and IR spectroscopic techniques are important for accessing electronic and vibrational properties, but these approaches are diffraction limited and therefore have low spatial resolution.

The use of ultrasharp scanning probe tips as optical antennas provides a means to overcome the diffraction limit and extend optical spectroscopy to the nanoscale, in order to investigate the causes and effects of spatial heterogeneities. This approach is compatible with a broad range of optical modalities, including ultrafast and nonlinear implementations, enabling the study of sub-ensemble and sub-domain behavior. I will discuss several of our recent results in ultrafast scattering scanning near-field optical microscopy (s-SNOM) that have demonstrated an unprecedented degree of specificity. sensitivity, and selectivity in probing nanoscale systems. With femtosecond vibrational s-SNOM spectroscopy we can directly access homogeneous sub-ensemble dynamics within polymer systems, revealing novel coherence behavior. Pump-probe implementations allow us to investigate the impact of defects and localized strain in even nominally homogeneous microcrystal structures, while nonlinear approaches such as second-harmonic generation and four-wave mixing enable us to resolve nanometer-scale crystallographic and ferroic domain structures, with modified near-field selection rules. I will also discuss novel antenna concepts for background-free nanometer spatial and femtosecond temporal control.

9584-23, Session 6

Raman sensing in microresonators

Corey Janisch, Alexander Cocking, The Pennsylvania State Univ. (United States); Lan Yang, Washington Univ. in St. Louis (United States); Zhiwen Liu, The Pennsylvania State Univ. (United States)

High-quality whispering-gallery-mode optical resonators have garnered interest in particle sensing for a variety of applications. By utilizing high quality cavity modes to enhance the light-matter interaction between the resonant mode and the particle, several microresonator based approaches have been developed for single-particle detection by monitoring changes to the resonant mode. Here, we further explore the idea of using ultrahigh quality microresonators to enhance single-particle detection and identification by monitoring the Raman scattering from a particle adhered to a silica micro-sphere. A tunable diode laser is critically coupled into a resonant mode of the micro-sphere resonator, allowing circulating power to build up within the cavity for enhanced interaction with the attached particle. Experimental results of single particle Raman scattering in high-Q microsphere resonators will be presented.



9584-24, Session 6

UV resonance Raman signatures of phonon-allowed absorptions and phonondriven bubble formation (Invited Paper)

Hans D. Hallen, North Carolina State Univ. (United States); Adam H. Willitsford, Johns Hopkins Univ. Applied Physics Lab., LLC (United States); Reagan Weeks, C. Russell Philbrick, North Carolina State Univ. (United States)

We have measured UV resonance Raman near and at the resonance phonon-allowed absorption lines of several liquid species. Resonance absorption with excitation on the symmetry-forbidden but strongly phonon coupled bands in the 230-290 nm spectral band present enhancement corresponding to the vapor phase absorptions rather than those of the liquid phase. This effect is related to the coherence forced by the internal molecular resonance required to absorb light at this energy. Large resonance gains (~1000x) reflect the narrower vapor phase lines. At the low laser fluence used, bubble formation is observed when the excitation energy corresponds to the maximum in Raman signal generation, not at the wavelength of maximum absorption in the liquid sample, which is several nanometers away.

9584-25, Session 6

G-Fresnel cellphone spectrometer

Chenji Zhang, The Pennsylvania State Univ. (United States); Perry S. Edwards, Atoptix, LLC (United States); Zhiwen Liu, The Pennsylvania State Univ. (United States)

The G-Fresnel cellphone spectrometer covering visible wavelength range has been demonstrated previously by our group. The previously demonstrated design however, relies on a two-sided diffractive element design, which poses inconveniences for large scale fabrication. Additionally, the fabrication process imposes limitations on the efficiency of the device. In this work, a holographic fabrication procedure is developed to produce a single-sided G-Fresnel device with improved optical efficiency. The interference lithography setup is described which produces a singlesided device with the desired dual focusing and dispersion functions. Replication of the device by using PDMS soft lithography is also discussed. A spectrophotometer is constructed using the fabricated holographic G-Fresnel and its performance is demonstrated through experimental measurements. The improved sensitivity due to the new device design can enable many applications in biomedical sensing.

9584-26, Session 6

Smartphone spectroscopy for non-invasive point-of-care diagnostics (Invited Paper)

Perry S. Edwards, Atoptix, LLC (United States); Zhiwen Liu, The Pennsylvania State Univ. (United States)

An ultra-compact, visible/near-infrared optical spectrometer is demonstrated as an add-on attachment to a smartphone for noninvasive point-of care applications. Spectra captured by the smartphone spectrometer are transferred to a cloud based server and processed using spectral analysis algorithms, which provide near real-time results of vital health information back to the user. The noninvasive, mobile measurement capability shows great promise for improving monitoring and treatment for several health concerns. Our current development of the smartphone spectrometer system for point-of-care applications as well as future development directions will be discussed.

9584-27, Session 7

Axial slice light sheet microscopy with micro mirror array

Yizhu Chen, Mingda Zhou, Yiqiu Xia, Ding Ma, Siyang Zheng, Zhiwen Liu, The Pennsylvania State Univ. (United States)

A novel axial slice light sheet microscopy technique will be presented, which can simultaneously image an axial cross section slice of a specimen by using an array of long-aspect-ratio micro mirrors. The imaging principle, the design and fabrication of micro mirrors will be discussed. Preliminary experimental demonstration will also be presented.

9584-28, Session 7

Compressive sensing in CARS holography

Alexander Cocking, Nikhil Mehta, Zhiwen Liu, The Pennsylvania State Univ. (United States)

Coherent anti-Stokes Raman scattering (CARS) holography has been demonstrated successfully as a single shot, label-free, chemically selective 3D imaging technique. It is well known that hologram samples only very small subset in the k-space describing the 3D image and hence has poor axial resolution. Due to this, images reconstructed using digital holography based on Fresnel kernel suffer from diffraction noise, i.e. out-of-focus background. To help improve the quality of reconstructed 3D images by reducing this noise, we present compressive CARS holography, a numerical technique based on the novel concept of compressive sensing. Compressive sensing is a powerful technique for estimation of sparse signals using relatively few measurements. By applying compressive sensing to our single shot CARS hologram, we demonstrate nearly noise-free retrieval of multiple microspheres within an imaging volume which is nearly 15 um along 'z' at every 1 um axial depth. In particular, we use the two step iterative shrinkage threshold (TwIST) algorithm along with I1 normalization to iteratively minimize the system objective function and retrieve an image in each depth slice. Thus the use of compressive CARS holography enhances the powerful CARS holography technique by reducing noise and thereby effectively emulating higher axial resolution using only single shot hologram.

9584-29, Session 7

Fast acquisition for wide field of view high-resolution phase microscopy (Invited Paper)

Laura Waller, Lei Tian, Ziji Liu, Univ. of California, Berkeley (United States); Chenguang Ma, Tsinghua Univ. (China); Simon Li, Kannan Ramchandran, Univ. of California, Berkeley (United States)

This talk will describe new methods for rapid acquisition of 3D and highresolution phase images across large volumes, in a commercial microscope with partially coherent illumination. We show connections between Fourier Ptychography and light field imaging for 3D complex-field recovery and discuss optimization of coding strategies for fast capture of large-scale large volume image datasets. Such computational approaches to optical microscopy add significant new capabilities to commercial microscopes without much cost or hardware modification.



9584-30, Session 7

Watching photons on the fly by compressed ultrafast photography (Invited Paper)

Liang S. Gao, Washington Univ. in St. Louis (United States)

Video recording of ultrafast phenomena using a detector array based on the CCD or CMOS technologies is fundamentally limited by the sensor's on-chip storage and data transfer speed. To get around this problem, the most practical approach is to utilize a streak camera. However, the resultant image is normally one dimensional—only a line of the scene can be seen at a time. Acquiring a two-dimensional image thus requires mechanical scanning across the entire field of view. This requirement poses severe restrictions on the applicable scenes because the event itself must be repetitive.

To overcome these limitations, we have developed a new computational ultrafast imaging method, referred to as compressed ultrafast photography (CUP), which can capture two-dimensional dynamic scenes at up to 100 billion frames per second. Based on the concept of compressed sensing, CUP works by encoding the input scene with a random binary pattern in the spatial domain, followed by shearing the resultant image in a streak camera with a fully-opened entrance slit. The image reconstruction is the solution of the inverse problem of above processes. Given sparsity in the spatiotemporal domain, the original event datacube can be reasonably estimated by employing a two-step iterative shrinkage/thresholding algorithm.

To demonstrate CUP, we imaged light reflection, refraction, and racing in two different media (air and resin). Our technique, for the first time, enables video recording of photon propagation at a temporal resolution down to tens of picoseconds. Moreover, to further expand CUP's functionality, we added a color separation unit to the system, thereby allowing simultaneous acquisition of a four-dimensional datacube (x,y,t,?), where ? is wavelength, within a single camera snapshot.

9584-31, Session 7

Advances in the optical delivery architecture for femtosecond micromachining systems that employ simultaneous spatial and temporal focusing (Invited Paper)

Jeffrey A. Squier, Colorado School of Mines (United States)

Simultaneous spatial and temporal focusing (SSTF) has been demonstrated to have many attractive features as applied to micromachining with femtosecond lasers. These include 1) the ability to use low numerical aperture beams that are not compromised by nonlinear effects, 2) an improved depth-of-field as compared to a standard focus with the same lateral spot size, and 3), the ability to create a pulse-front-tilt that can be exploited in terms of material modification in novel ways. To fully exploit this range of features optical delivery systems that are integrated within a chirped pulse amplification architecture are highly desirable. We will present a series of these systems. The first is a novel single grating compressor that can be used in a guartic- or guintic phase limited chirped pulse amplification system in lieu of a standard double-pass grating compressor. The new compressor allows smooth variation of the beam aspect ratio of the SSTF beam. This enables control over the achievable depth of focus and the pulse front tilt. Indeed, with this system the compressor can be varied between a standard focus and an SSTF focus. Next, we demonstrate an optical delivery system that employs in-line refractive optics that facilitates micromachining especially in industrial and medical environments. This type of delivery system is difficult to achieve with a standard focus, and is one of the advantages of SSTF: energetic, femtosecond pulses can travel through extensive path lengths of material without significant degradation in the focus as a result of the accumulation of nonlinear phase shifts.

9584-32, Session 7

Three-color two-photon three-axis digital scanned light-sheet microscopy (3c2p3a-DSLM) (Invited Paper)

Liangyi Chen, Weijian Zong, Aimin Wang, Peking Univ. (China)

We demonstrate a new two-photon light-sheet microscopy with three-color excitation, diffraction-limited thickness and tailorable illumination area, capable of multi-color multi-scale live imaging in one setup.

9584-33, Session 7

Nonlinear tomographic spatial frequency modulated imaging (Invited Paper)

Randy A. Bartels, Colorado State Univ. (United States)

In this talk, we will discuss nonlinear spatial frequency modulated imaging. This approach opens new imaging capabilities, with benefits of high speed and large volume imaging. Super-resolution and tomographic imaging modes will be presented.

9584-34, Session 8

Photonic-crystal-fiber platform for highpower multi-wavelength ultrashort-pulse sources and its applications (Invited Paper)

Minglie Hu, Tianjin Univ. (China)

It has been shown by intensive research activities in the laser and photonics fields that many novel properties unimaginable with conventional optical fibers can result from the photonic crystal fibers (PCFs). PCF is a new class of optical fiber based on the properties of photonic crystal, which features micro/nano air hole array or higher-index rode array in the fiber cladding. With its huge degree of design freedom, the propagation properties of PCF can be tailored for any needs. Recently, based on some of these properties, photonic crystal fiber has been successfully applied in femtosecond laser technology and greatly improve the performance of femtosecond laser. A brief review of recent work on high power femtosecond laser based on PCF is demonstrated. Furthermore, garmonic generation, optical parametric process based on the high power femtosecond fiber laser can generate new wavelengths of femtosecond pulses from the ultraviolet to mid-infrared. And the wavelength tunable femtosecond laser have a tremendous impact on physics in subwavelength structure, Chemics and Bioglogy.

9584-35, Session 8

Ultrafast nonlinear THz emission and electrodynamics in low dimensions (Invited Paper)

Jigang Wang, Iowa State Univ. (United States) and Ames Lab. (United States)

Nonlinear and non-equilibrium properties of low-dimensional quantum matter are fundamental in nanoscale science yet transformative in nonlinear imaging/photonic technology today. These have been poorly addressed in many nanomaterials despite of their well-established equilibrium optical and transport properties. The development of ultrafast THz sources and nonlinear spectroscopy tools facilitates understanding these issues and reveals a wide range of novel nonlinear quantum phenomena that are not expected in bulk solids or atoms. In this talk, I will discuss our recent discoveries in two model photonic and electronic nanostructures to solve some puzzling questions: (1) how to create nonlinear broadband terahertz



emitters using deeply subwavelength nanoscale meta-atom resonators? (2) How to access one-dimensional dark excitons and their non-equilibrium correlated states in single-walled carbon nanotubes? Finally, I will also discuss their significance for quantum phase discoveries and other nonlinear imaging/spectroscopy applications.

9584-36, Session 8

Ultrafast THz and mid-IR studies of nanoscale charge dynamics and electronic correlations (Invited Paper)

Giacomo Coslovich, Ryan P. Smith, Jan H. Buss, Sascha Behl, Bernhard Huber, Lawrence Berkeley National Lab. (United States); Takao Sasagawa, Tokyo Institute of Technology (Japan); Hans A. Bechtel, Michael C. Martin, Robert A. Kaindl, Lawrence Berkeley National Lab. (United States)

We will present our recent experiments employing broadband THz and mid-IR pulses to explore ultrafast charge dynamics and interactions in correlated and nanoscale materials. Transition-metal oxides exhibit an intriguing self-organization of charges into 1D stripes and other atomic-scale patterns, whose complex and dynamic driving forces may be central to understanding high Tc superconductivity. By exploring the mid-IR response of stripe-phase nickelates, we resolve femtosecond charge localization and transient electron-phonon coupling, revealing their precursor role in stripe formation. In turn, the Ni-O bending vibration around 11 THz exhibits a splitting arising from long-range stripe order, while a broad background results from the opening of the electronic pseudogap. Employing optical pump multi-THz probe spectroscopy with high energy resolution allows us to resolve the dynamic modulation of the order-induced phonon splitting and the localization dynamics, thus capturing both the short- and the longrange order dynamics within the single spectrum of a THz pulse. Finally, we will discuss experiments that track the optical conductivity in graphene and transition-metal dichalcogenides via ultra-broadband THz spectroscopy, exposing the high-frequency transport of non-equilbrium Dirac fermions and photo-excited electron-hole pairs.

9584-37, Session PMon

Optical parametric oscillation in synchronously pumped MgO-doped periodically poled lithium niobate

leva Pipinyte, Agne Marcinkeviciute, Rimantas Grigonis, Valdas Sirutkaitis, Vilnius Univ. (Lithuania)

Femtosecond laser pulses tunable in wide spectral range are valuable instruments for investigation of various ultrafast processes or nonlinear imaging. Synchronously pumping optical parametric oscillator (SPOPO) allows generation of tunable radiation at low pump energies and high pulse repetition rate. We present experimental data obtained during investigation of synchronously pumped optical parametric oscillator (SPOPO) pumped by fundamental (1030 nm) radiation of mode-locked Yb:KGW laser, providing 105 fs pulses at 76 MHz repetition rate with an average power of 4 W. We used a 1.5 mm long MgO:PPLN crystal as nonlinear material, which was placed in a four- mirror linear resonator. Spectral tuning and power characteristics of this SPOPO was investigated, while keeping the temperature of MgO:PPLN crystal fixed. Generation of signal pulses tunable in 1.38 - 1.82 ?m spectral range was obtained by changing grating period of the crystal and a cavity length. Temporal characteristics of SPOPO were investigated by using the constructed multi-shot intensity correlator. Furthermore, the group delay dispersion of flat mirrors of resonator was measured by the white light interferometer due to it can have an important influence for temporal properties of SPOPO radiation.

9584-38, Session PMon

Wavelet analysis of polarization maps of the myocardium tissue microscopic images in the diagnosis of the causes of death

Alexander Ushenko, Yuriy Fedkovych Chernivtsi National Univ. (Ukraine)

By tradition, the processes of transforming optical radiation of phaseinhomogeneous objects and media are considered, as a rule, in a statistical approach (theory of radiation transfer, Monte-Carlo modeling). Among the most spread traditional methods for studying the scattered light fields, one can separate the following independent directions: "scalar" (photometry and spectrophotometry) and "vector" (polarization nephelometry, Muellermatrix optics). Using these approaches, determined are interrelations between the sets of statistical moments of the 1-st to 4-th orders, correlation functions, fractal dimensionalities that characterize phaseinhomogeneous or rough surfaces and coordinate distributions for phases, azimuths and ellipticity of polarization in their laser images.

In parallel with traditional statistical investigations, formed in recent 10 to 15 years is the new optical approach to describe a structure of polarizationally inhomogeneous fields in the case of scattered coherent radiation. The main feature of this approach is the analysis of definite polarization states to determine the whole structure of coordinate distributions for azimuths and ellipticities of polarization.

This work is aimed at ascertaining the possibilities to diagnose and classify phase-inhomogeneous layers (PhIL) of myocardium of the patients who died of coronary artery disease (CAD) and acute coronary insufficiency (ACI) by determination values and ranges for changing the statistical (moments of the 1-st to 4-th orders), correlation (autocorrelation functions) and fractal (logarithmic dependences for power spectra) parameters that characterize coordinate distributions for polarization-singular states in PhIL laser images.

1. Analyzed in this work are the main physical mechanisms providing formation of polarization singularities in laser images of PhIL with surface, subsurface and bulk light scattering.

2. Offered are statistical, wavelet, correlation and fractal parameters for polarization-singular estimating the optical properties inherent to PhIL of all types.

3. Determined are the ranges for changing the set of criteria that characterize distributions of the amount of polarization-singular states in laser images, which enabled us to realize both "intergroup" classification and differentiation of optical properties related to PhIL of various types.

4. We have demonstrated diagnostic efficiency of the wavelet analysis applied to coordinate distributions for polarization maps in laser images of patients with CAD and ACI.

9584-39, Session PMon

System of polarization correlometry of polycrystalline layers of urine in the differentiation stage of diabetes

Olexander V. Dubolazov, Yuriy Ushenko, Yuriy Fedkovych Chernivtsi National Univ. (Ukraine)

Among diverse optical-physical methods of diagnosing the structure and properties of the optical-anisotropic component of various biological objects a specific trend has separated – multidimensional laser polarimetry

Our research is aimed at designing the experimental method of Fourier's laser polarimetry of human urine polycrystalline layers for the sake of diagnosing and differentiating cholelithiasis with underlying chronic cholecystitis and diabetes mellitus of degree II by means of the statistical analysis of the polarization filtered out scattered coherent radiation in a distant (Fourier) zone of diffraction with due regard for linear and circular birefringence of biological crystals.

A model of generalized optical anisotropy of human urine polycrystalline

Conference 9584: Ultrafast Nonlinear Imaging and Spectroscopy III



layers is suggested and a method of polarimetric of the module and phase Fourier of the image of the field of laser radiation is analytically substantiated, that is generated by the mechanisms of linear (a phase shift between the orthogonal components of the amplitude of a laser wave) and circular (the angle of rotation of the polarization plane) birefringence of polycrystalline networks with a wavelet - diagnosis and differentiation of stage of diabetes.

A set of diagnostic criteria and diagnosis and differentiation of stage of diabetes is identified and substantiated:

- statistical moments of the 3rd and 4th orders, which characterize the distributions of wavelet coefficients of Fourier phase of the image of a polarization inhomogeneous laser image of polycrystalline network of urine.

9584-40, Session PMon

Confocal fluorescence microscopy for diagnostic of the bone grafts

Pavel E. Timchenko, Elena V. Timchenko, Larisa A. Zherdeva (Taskina), Samara State Aerospace Univ. (Russian Federation); Larisa T. Volova, Samara State Medical Univ. (Russian Federation); Nikolay V. Belousov, Samara State Aerospace Univ. (Russian Federation)

Microscopic analysis of cell osseointegration in the lyophilized bioimplants, made of human connective tissues by «Lioplast»* technology, was conducted. The analysis was carried out using a system of laser confocal fluorescence microscopy, assembled on the basis of Olympus IX71 microscope and ANDOR laser harvester. This system provides the high-speed scanning of up to 25 layers per second and the resolution of up to 400 nm. Processing of the received images was performed using the ANDOR software.

The dynamics of the different cells in the model environment was investigated. Shown, that the cells have a significantly greater length, surface area and form a monolayer in the model environment, unlike the cells in the natural environment. As a result, the image has a low contrast in the confocal mode (no more than 0.2 - 0.3), that is not able to identify the internal structure of cells. Using propidium iodide fluorophore (Ex. wavelength of 488 nm) allows to raise the image contrast up to 0.9 and to register the dynamics of cell growth. The cell integration in bone grafts with different time of demineralization was investigated. Analysis of the micrographs suggests that the cells penetrate into the graft and settle in the inner surface. The average sectional area of the cell in control model environment is 26 μ m2, the average diameter – 6 μ m.

As a consequence, the method of confocal fluorescence microscopy identifies the viable cells in the composition of cellular-tissue graft, and therefore allows to conduct the quality control of produced grafts.

9584-41, Session PMon

Optical methods for the demineralization control of bone tissues

Elena V. Timchenko, Larisa A. Zherdeva (Taskina), Pavel E. Timchenko, Samara State Aerospace Univ. (Russian Federation); Larisa T. Volova, Samara State Medical Univ. (Russian Federation); Julia V. Ponomareva, Samara Medicine Univ. (Russian Federation)

The important step in obtaining of the bone biomaterial for defect substitution is a bone demineralization process - processing in an acidic solution, which leads to loss of most of the mineral components, while maintaining the proportion of collagen and proteins necessary for regeneration. Correctly selected of demineralization degree provides the perfect combination of osteoinductive and osteoconductive properties for successful bone regeneration.

Samples of cortical and cancellous bone tissue of «Lioplast» [®] technology with different degrees of demineralization were used as objects of study.

Raman spectroscopy (RS) was used to control of the demineralization degree of research objects. Change of mineral composition in experimental samples also was monitored by scanning electron microscopy.

The change of Raman band intensity at 1284 cm-1 (amide III region) and 2840 cm-1 (CH3 stretching vibration region) in the process of demineralization experimentally established. Using the spectrum deconvolution, the changes in the region 1200-1500 cm-1 (amide III), 1600-1700 cm-1 (amide I) and 900-1100 cm-1 (RO43- and SO32-) also were detected.

As a result, the demineralization process can be controlled using the ratio of ??43- and amide I, as well as the ratio of ??32- substitution B- and A-type. Raman spectroscopy results of change in the content of the mineral component with demineralization degree were compared with the results of scanning electron microscopy.

9584-42, Session PMon

Spectrally tunable femto-second Erbium fiber laser based on an all-normal-dispersion cavity

Zhiqiang Lv, Zibo Gong, Xing Lu, Peking Univ. (China); Kebin Shi, Peking Univ. (China) and Collaborative Innovation Ctr. of Quantum Matter (China)

Compared with solid state ultrafast lasers, femto-second fiber lasers possess unique properties such as compact, reliable, efficient and low-cost. However, the lacking of spectral tunability greatly limits its using in many applications. Recently fiber laser oscillators with all-normal-dispersion cavity have brought increasing interests due to their capability of avoiding wave-breaking under large nonlinear phase accumulation and consequently supporting higher pulse energy than those in dispersion-managed-soliton configurations. Pulse formations essentially undergo dissipative processes in all-normal-dispersion cavity where chirped pulse spectral filtering mechanism is necessarily adapted for stabilizing the mode-locking. Allnormal-dispersion ytterbium fiber lasers operating at ~1?m spectral range were previously studied by utilizing different spectral filtering schemes such as birefringent filters and gratings. The works of erbium fiber oscillator is later published, but there is few work to use the gratings as a filter as well as the benefits of them are not fully developed in the works above. In this work, we report on a spectrally tunable erbium fiber oscillator by using grating based spectral filter consist of a grating and a fiber collimator. The center wavelength and the spectral bandwidth of the laser can be continuously tuned by translating collimator along the perpendicular direction of the grating output and varying the free space distance between the grating and collimator respectively.

9584-43, Session PMon

Ultrafast lattice dynamics in L10 phase FePt nanoparticles measured by MeV electron diffraction

Xiaozhe Shen, SLAC National Accelerator Lab. (United States)

We studied the ultrafast lattice dynamics of a next generation magnetic data storage material FePt using MeV electron diffraction. The sample studied was a free-standing 10nm thick film of aligned FePt grains in the L10 phase separated by Carbon segregants. Each grain is approximately 10nm in diameter, with the c axis orientated perpendicular to the film plane. Lattice dynamics was excited by a 50 fs laser of 800 nm wavelength, and probed by MeV electron pulses with 100 fs bunch length and 100 fC beam charge. The individual Bragg reflections of the electron beam from the FePt grains were resolved as a result of the high degree of alignment between grains. The transient response of (020), (111), (131), and (202) Bragg reflections was measured. It is determined that the thermal expansion along the c axis is an order of magnitude smaller than that along the a and b axes. The transient response can be separated into two characteristic motions

Conference 9584: Ultrafast Nonlinear Imaging and Spectroscopy III



of the grain: a large anisotropic volume expansion, which occurs primarily in the film plane, followed by a volume conserving bulk oscillation. The resolved three dimensional ultrafast lattice dynamics in FePt nanoparticles provides important insight in electronic and lattice heat transport in this technologically important material. In addition, this experiment demonstrates the technique of MeV electron diffraction for high resolution time-resolved measurement of ultrafast lattice dynamics.

9584-44, Session PMon

Determination of radionucluides concentrations in concrete raw materials via analytical technique

Mohamed M. ElFaham, Banha Univ. (Egypt); Osama M. Khalil, MIT Univ. (Egypt); Asmaa Elhassan, Tenth of Ramadan Institute (Egypt)

The presence of natural radionuclides in raw materials used in cement manufacturing was determined by using analytical methods to analyze the principle components of cement in order to achieve precise chemical proportions. The Raw materials used are limestone, clay, slag, and gypsum, which can be used with different concentration in cement production. The obtained data from our study is important for the development of standards materials and will be guidelines for use and the processing of these materials in cement production to assure high indoor air quality and to show that there is no significant radiological hazards arising from using the cement in house constructions.

9584-45, Session PMon

Coherent interference of a number of filaments as a step to superfilamentation

Daniil Shipilo, Vera Andreeva, Nicolay Panov, Olga G. Kosareva, Lomonosov Moscow State Univ. (Russian Federation); See Leang Chin, Laval Univ. (Canada)

Femtosecond filament is a unique nonlinear medium due to highly localized extended channel of radiation with the peak intensity of about 5.10^13 W/cm². However, it is quite complicated to overcome the clamped intensity in the filament. The possibility has been shown recently both theoretically and in the experiment. Theoretically, a fusion of two filaments has been predicted and intensity increase by 20% has been attained as compared with a single filament case [Laser Physics 19, 1776 (2009)]. In the experiment [Physical Review Letters 112, 223902 (2014)], 3 cm loosely focused beam with the peak power of about 200 critical powers for selffocusing has formed tens of filaments, which, after the merging, increased the electron density by a factor of 10 as compared with a single filament case. In the present work, the collision of four and more coherent filaments is considered. Such task is an intermediate step between relatively simple case of two filaments collision and complicated case of multi-terawatt beam. This task, on the one hand, allows us to reproduce the experiment qualitatively and, on the other hand, is relatively simple to analyze. Using Forward Maxwell Equation, we show that the collision of a several coherent filaments leads to intensity increase by 40% and the plasma density increase by 400%. Moreover, we demonstrate a significant (about 10 nm) blue shift of the frequency spectrum maximum from its original position at 800 nm.

SPIE. OPTICS+ PHOTONICS **Conference 9585: Terahertz Emitters, Receivers, and Applications VI**

Sunday - Monday 9 -10 August 2015

Part of Proceedings of SPIE Vol. 9585 Terahertz Emitters, Receivers, and Applications VI

9585-1, Session 1

To be announced (Invited Paper)

Manijeh Razeghi, Northwestern Univ. (United States)

No Abstract Available

9585-2, Session 1

Merging THz with optical waveguides for stabilization and modulation of quantum cascade lasers (Invited Paper)

Maria Amanti, Margaux Renaudat St-Jean, Univ. Paris 7-Denis Diderot (France); Alfredo Bismuto, Mattias Beck, Jérôme Faist, ETH Zürich (Switzerland); Carlo Sirtori, Univ. Paris 7-Denis Diderot (France)

In this work we present stabilization of the inter-mode separation of a quantum cascade laser (QCL) emitting at 9 ?m, via integration of the laser cavity with a double metal THz waveguide. Quantum cascade lasers are today very attractive powerful semiconductor light sources in a wide frequency range, spanning from the THz region up to 3?m wavelength in the mid-infrared. High frequency modulation and microwave injection at the round trip frequency of these sources are extremely interesting for application as free space communications and high resolution spectroscopy. In this work we present the design of QC laser dielectric guide embedded in a double metal line. In this structure the modulation field oscillating at GHz experiences reduced losses and it has an improved overlap with the optical mode respect to standard lasers. We present experimental results on direct modulation of these devices demonstrating a flat frequency response up to 14 GHz. We present the locking of the laser inter-mode spacing to an external stable source and its tuning in the MHz range. Properties of self stabilization of these cavities are also studied: narrow beating signal at the round trip frequency are presented with typical width of less than 100 kHz, more than one order of magnitude lower than in standard guide. This phenomenon will be presented in the frame of a nonlinear formalism based on the cascading of two second order susceptibilities. This process is demonstrated to be enhanced respect to other cavities by the specific double metal design presented in this work.

9585-3. Session 1

Recent progress of THz-quantum cascade lasers using nitride-based materials (Invited Paper)

Hideki Hirayama, Wataru Terashima, RIKEN (Japan)

We demonstrate the first lasing action of III-nitride-based quantum cascade lasers (QCLs). Nitride-based semiconductor is a material having a potential for realizing wide frequency range of QCL, i.e., 3-20 THz and 40-300 THz $(1-8 \mu m)$ including the unexplored frequency range from 5 to 12 THz, as well as for realizing room temperature operation of THz-QCL, owing to high longitudinal optical phonon energies (ELO ?90 meV) and large band offset (1.8 eV). We fabricated GaN/AlGaN THz-QCLs with active layers consisting of 100-periods of 2 quantum well (QW) by molecular beam epitaxy (MBE) on a sapphire/AIN templates. Low threading-dislocation density (TDD) AIN templates were grown by metal-organic chemical-vapor deposition (MOCVD), which have been developed for use as deep-UV LEDs. A novel pure-3-level scheme design was introduced as an active layer, in order to obtain lasing from targeted levels. A single metal waveguide structure using Cu metal was fabricated. The cavity length and width were approximately 1.5 mm and 100 μ m, respectively. A 5.5 THz lasing was obtained from the

QCL measured under pulsed current injection at operating temperature of 5.6 K. The threshold current density (Jth) and the applying voltage (Vth) were 1.7 KA/cm2 and 16 V, respectively. We also fabricated GaN/AlGaN QCL by using MOCVD, and obtained 6.97 THz lasing measured at 5.2 K. The Jth of the QCL fabricated by MOCVD were 0.75 KA/cm2.

OPTICAL ENGINEERING+

APPLICATIONS

9585-4, Session 2

Electrically pumped semiconductor lasers with monolithic control of circular polarization (Invited Paper)

Federico Capasso, Harvard School of Engineering and Applied Sciences (United States)

As powerful semiconductor sources of mid-infrared and terahertz radiation open up new possibilities for the realization of compact and versatile spectroscopy and detection systems, monolithic control of the laser output characteristics becomes essential. While engineering of spectral characteristics and beam shape has reached a high level of maturity, manipulation of the polarization state remains a challenge. We present a method for monolithic control of the degree of circular polarization by aperture antennas forming a surface emitting grating on a semiconductor laser cavity, and demonstrate its realization for a terahertz quantum cascade laser [1] Our approach is not limited to the terahertz regime, and paves the way to an increased functionality and customizability of monolithic semiconductor laser sources for a variety of applications (e.g. vibrational circular dichroism spectroscopy).

[1] P. Rauter et al. PNAS 111, E5623-E5632 (2015)

9585-5, Session 2

Broadband and enhanced-output-power terahertz-wave emitter based on slotantenna-integrated uni-traveling-carrier photodiode

Hiroshi Ito, Kitasato Univ. (Japan); Toshihide Yoshimatsu, Nippon Telegraph and Telephone Corp. (Japan); Hiroshi Yamamoto, Kitasato Univ. (Japan); Tadao Ishibashi, NTT Electronics Corp. (Japan)

Photomixing is a promising technique for generating continuous terahertz (THz) waves due to its superior features, such as extremely-wide frequency tunability, very narrow line-width, good frequency stability, and the capability of low-loss signal transmissions through flexible optical fibers. To further increase output powers of the photonic THz-wave emitter, implementation of a resonant antenna is effective. However, the resonant design usually deteriorates the bandwidth of the antenna, so the broadband feature of the photomixer is not effectively utilized. In this work, we integrated two types of slot antennas having relatively weak resonant characteristics with uni-traveling-carrier photodiodes (UTC-PDs) for increasing the THz-wave output powers while maintaining relatively large bandwidths. The fabricated devices were assembled in compact quasi-optical packages, and their output powers were compared with those for a broadband (non-resonant) bowtie-antenna-integrated device. The output powers of the slot-antenna-integrated devices were confirmed to be about two to three times larger at their peak frequencies than those of the broadband device. The output powers were enhanced at frequencies from 350 to 850 GHz for a wider-slot device and from 900 GHz to 1.6 THz for a narrower-slot device. These results agreed well with numerical analysis based on the HFSS. The typical output powers were 28 uW at 700 GHz and 3.5 uW at 1.25 THz both for a photocurrent of 10 mA with a bias voltage of only -0.4 V.



TeraFermi: The THz beamline at the FERMI Free Electron Laser

Cristian Svetina, Nicola Mahne, Lorenzo Raimondi, Andrea Perucchi, P. Di Pietro, Elettra-Sincrotrone Trieste S.C.p.A. (Italy); Marco Zangrando, Elettra-Sincrotrone Trieste S.C.p.A. (Italy) and IOM-CNR Lab. TASC (Italy)

TeraFERMI is the THz beamline for pump-probe studies on the femtosecond time-scale, under construction at the FERMI Free Electron Laser (FEL) facility in Trieste (Italy). The beamline will take advantage use of the coherent radiation emitted by the electrons already spent from the FEL undulators, before being dumped. This will result in short, coherent, high power THz pulses to be used as a "pump" beam, in order to modulate structural properties of matter, thereby inducing phase transitions. The intense THz pulses are also associated with a remarkably large transient magnetic field, to be used for controlling and manipulating magnetic structures and the corresponding changes induced to the ionic and magnetic structures of application of TeraFERMI will cover a wide range of fields from solid-state physics to biochemistry. We discuss here the source, the optical layout as well as the expected performances of the novel TeraFERMI beamline.

9585-7, Session 3

Negative differential resistance devices for generation of terahertz radiation (*Invited Paper*)

Heribert Eisele, Univ. of Leeds (United Kingdom)

In 1970, Esaki and Tsu proposed a unipolar device structure where Bragg reflection of miniband electrons in a semiconductor superlattice (SL) creates regions of negative differential velocity [1]. Superlattice electronic devices (SLEDs) utilize this effect. They have received much attention since the 1990s [2] because the underlying Bloch effect is associated with much shorter time constants than those of the transferred-electron effect in, for example, GaAs Gunn devices [3].

GaAs/AlAs SLEDs on integral heat sinks were evaluated from wafers grown at Cambridge and at Leeds [5]. The structures grown at Leeds were designed for estimated miniband widths [4] of more than 100 meV and had lengths suitable to achieve operation in D-band (110-170 GHz). SLED fabrication and packaging followed the same procedures as described in [5] except for some changes to facilitate much higher operating frequencies. The same type of top-hat WR-6 waveguide cavity was employed as was previously with fundamental-mode InP Gunn devices [6]. Examples of measured record output powers are 5.0 mW at 123.3 GHz, 2.2 mW at 134.9 GHz, 0.62 mW at 151.5 GHz, and 1.1 mW at 155.1 GHz, all in the fundamental mode, and 0.52 mW at 252.8 GHz in a second-harmonic mode.

Fundamental-mode operation at D-band frequencies was fully confirmed with second-harmonic power extraction and by testing tuneability. The above oscillation frequencies are the highest reported to date and approximately twice as high as those observed with GaAs Gunn devices [7]. Futhermore, these oscillation frequencies exceed those of InGaAs/InAIAs SLEDs [8] and the output powers around 150 GHz are also higher than those in [8]. This superior performance confirms the strong potential of SLEDs for achieving power generation up to at least 1 THz [5]. Substantial increases in output power are expected from optimized thermal management.

Tunnel injection transit-time diodes and Gunn devices have also been investigated for extraction of harmonics, in particular, third and higher harmonics [9]. One example is an oscillator at 480 GHz with an InP Gunn device [9], [10]. More recent measurements show that such third-harmonic power extraction from InP Gunn devices is feasible above 500 GHz [10].

[1] L. Esaki and R. Tsu, IBM J. Res. Develop., vol. 14, no. 1, pp. 61–65, Jan. 1970.

[2] E. Schomburg, et al., Appl. Phys. Lett., vol. 74, no. 15, pp. 2179–2181, Apr. 1999.

[3] R. Scheuerer, et al., Appl. Phys. Lett., vol. 81, no. 8, pp. 1515–1517, Aug. 2002.

SPIE. PHOTONICS

OPTICAL ENGINEERING+

APPLICATIONS

[4] G. Bastard, Phys. Rev. B, vol. 24, no. 10, pp. 5693–5697, Nov. 1981.

[5] H. Eisele, S. P. Khanna, and E. H. Linfield, Appl. Phys. Lett., vol. 96, no. 7, Feb. 2010, pp. 072101-1-3.

[6] H. Eisele and G. I. Haddad, IEEE Microw. Guid. Wave Lett., vol. 5, no. 11, Nov. 1995, pp. 385–387.

[7] H. Eisele and G. I. Haddad, in Modern Semiconductor Devices, S. M. Sze, Ed., Ch. 6, John Wiley & Sons, New York, 1997, pp. 343-407.

[8] E. Schomburg, et al., Electron. Lett., vol. 35, no. 17, pp. 1491–1492, Aug. 1999.

[9] H. Eisele, in Special Supplement on "Terahertz Technology," Electron. Lett., 46, 2010, pp. S8–S11.

[10] H. Eisele, in Encyclopedia of Electrical and Electronics Engineering (2nd Edition, J. G. Webster, ed.), John Wiley & Sons, New York, 2014.

9585-8, Session 3

The study of gas species on THz generation from laser-induced air plasma

Ji Zhao, Yuejin Zhao, Beijing Institute of Technology (China); Xiaomei Yu, Peking University (China)

Intense Terahertz waves generated from air-induced plasma and serving as broadband THz source provide a promising broadband source for innovative technology. Terahertz generation in selected gases has attracted more and more researchers' interests in recent years. In this research, the THz emission from different atoms is described, such as nitrogen, argon and helium in Michelson. The THz radiation is detected by a Golay Cell equipped with a 6-mm-diameter diamond-inputting window. It can be seen in the first time that when the pump power lies at a stable level, the THz generation created by the femtosecond laser focusing on the nitrogen is higher than which focusing on the helium, and lower than that produced in the argon gas environment. We believe that the THz intensity is Ar > N > Ne because of its atomic mass, which is Ar > N > Ne as well. It is clear that the Gas molecular decides the release of free electrons ionized from ultra short femtosecond laser through the electronic dynamic analysis. The higher the gas mass is, the stronger the terahertz emission will be. We further explore the THz emission at the different laser power levels, and the experimental results can be commendably guadratic fitted. It can be inferred that THz emission under different gas medium environment still complies with the law of four-wave mixing (FWM) process and has nothing to do with the gas environment: the radiation energy is proportional to the quadratic of incident laser power.

9585-9, Session 3

TE and TM THz intervalence band polaritons and antipolaritons

Mauro F. Pereira, Inuwa A. Faragai, Sheffield Hallam Univ. (United Kingdom)

The interaction of THz cavity modes with intervalence transitions can improve the quantum efficiency of THz-polaritonics devices. These devices have strong potential for applications in spectroscopy, imaging and improved data transmission in communications and ultra-strong coupling of THz radiation with intersubband transitions which can further improve the applicability of polaritonics. Conduction band-based polariton coupling is restricted to the TM mode. However, the fact that valence subband transitions can be coupled with both TE and TM modes polarized cavity modes, stimulated us to extend our studies of TE valence band polaritons [M.F. Pereira and I. A. Faragay, Optics Express 22, 3439 (2014).] by comparing results obtained for THz polaritons and antipolaritons for the two possible modes. Both cases are investigated for different cavities and excitation conditions and the possibility of switching between one mode to the other with a large change in resonant frequency and polariton splittings are discussed. The strong nonparabolicity and k-dependence of the



transition dipole moment has a very strong role in the shifting of effective resonance frequencies between TE and TM modes for the same transition. The numerical results presented can stimulate further experimental investigations for a deeper understanding of the valence band coupling scenario and have potential for applications in which a simple design with two possible outputs with different polarizations and resonant frequencies could be of relevance.

9585-10, Session 3

Research on Output Characteristics of optically pumped THz gas laser

Xiaoyang Guo, Renshuai Huang, Qinglong Meng, Bin Zhang, Sichuan Univ. (China)

The model of the output of optically pumped THz gas laser has been established on the basis of the rate equations theory. And the influence of the Two-Photon light shift (TPLS) on the THz frequency has been analyzed theoretically. The effect of various factors on the output power and frequency of the optically pumped THz gas laser has been discussed numerically and theoretically. Results indicate that, the output THz power increases first and then decreases gradually with the increasing pressure of the gas, while it continues to grow due to the increasing pumping power within certain range. However, increasing the pump laser power may degrade the THz frequency stability to some extent. With given pump laser power, the THz frequency shift caused by TPLS increases first and then decreases with the increasing pump laser frequency offset drifting from the vibrational transition line-center. In addition, the THz frequency shift may be reduced gradually by increasing the pressure of the gas and the operating temperature. Results provide significant guidance for improving energy conversion efficiency and frequency stability in optically pumped THz gas laser.

9585-11, Session 3

Terahertz generation via asymmetric Cherenkov radiation in LiNbO3

Elena V. Svinkina, N.I. Lobachevsky State Univ. of Nizhni Novgorod (Russian Federation)

One of the most efficient optical-to-terahertz converters is the structure consisting of a layer (30-50 μm thick) of LiNbO_3 (LN) attached to a Siprism outcoupler. A femtosecond laser pulse propagates in the LN layer as a guided mode and produces nonlinear polarization, which emits terahertz Cherenkov radiation to the Si prism. An inherent disadvantage of the converter is a dip in the generated terahertz spectrum originating from the destructive interference of the terahertz waves emitted to the Si prism from the LN layer directly and after reflections from the layer boundaries.

We propose to remove the spectral dip by using the spatial asymmetry of the Cherenkov radiation from a moving nonlinear polarization, which is tilted with respect to the direction of motion.

The crystallographic axes in LN can be arranged in such a way that the line-like nonlinear polarization, produced by a focused-to-a-line pump laser pulse, will be almost orthogonal to the electric field E (tilted with respect to the displacement D) on a half of the Cherenkov wedge. As a result, this halfwedge will be practically not generated.

We propose to apply this phenomenon to suppressing the interference effects in one of the most efficient optical-to-terahertz converters. A null in the emission spectrum of the converter, which limits its application possibilities, can be eliminated.

9585-12, Session 4

Microscopic view on carrier dynamics in Landau-quantized graphene (Invited Paper)

Ermin Malic, Chalmers Univ. of Technology (Sweden); Florian Wendler, Andreas Knorr, Technische Univ. Berlin (Germany); Martin Mittendorff, Stephan F. Winnerl, Manfred Helm, Helmholtz-Zentrum Dresden-Rossendorf e. V. (Germany)

We present a microscopic view on the time-resolved carrier dynamics in Landau-quantized graphene. In the presence of a strong magnetic field, graphene exhibits non-equidistant Landau levels. Due to specific optical selection rules, single Landau-level transitions can be selectively excited and probed with circularly polarized light

Based on the density matrix formalism, we derive graphene Bloch equations allowing us to resolve the efficiency of Coulomb- and phonon-induced relaxation channels determining the inter-Landau-level dynamics [1-4]. Surprisingly, our calculations reveal that Auger scattering plays the crucial role despite the non-equidistant spacing between the Landau levels [1]. In most cases, scattering with optical phonons is strongly suppressed due to the mismatch of the phonon energy and the Landau-level separation [2]. In contrast, Auger scattering is highly efficient and can lead to a significant carrier multiplication [3]. Furthermore, we show that Auger-induced depopulation of Landau levels can even be faster than the optical pumping resulting in unexpected features in polarization-resolved pump-probe spectra [1]. Finally, we demonstrate that Auger scattering can be even exploited to generate a population inversion in Landau-quantized graphene suggesting the design of novel Landau level lasers that can be tuned over a wide spectral range [4].

[1] M. Mittendorff, F. Wendler, E. Malic et al., Nat. Phys. 11, 75 (2015).

- [2] F. Wendler, A. Knorr, and E. Malic, Appl. Phys. Lett. 103, 253117 (2013).
- [3] F. Wendler, A. Knorr, and E. Malic., Nat. Commun. 5, 3703 (2014).

[4] F. Wendler and E. Malic, arXiv:1410.2080.

9585-13, Session 4

Microscopic theory for the optical properties of dilute semiconductors

Mauro F. Pereira, Chijioke I. Oriaku, Sheffield Hallam Univ. (United Kingdom)

Dilute semiconductors have a strong potential for THz generation, with an extra degree of freedom with controllable fundamental gaps and effective masses at both valence and conduction band methods. However, before intersubband designs that can reach THz frequencies can be delivered, the properties of bulk materials must be fully understood. This paper explains hitherto not clearly understood features in the luminescence spectra of dilute nitrides, bismides and antimonides structures through a combination of many body and inhomogeneous broadening effects, as well as the unexpected influence of strain in samples expected to be relaxed. A seemingly anomalous temperature dependence of the luminescence peak emission is explained and that can have a strong impact in the design of future sources and detectors for the far infrared including interband Mid Infrared and intersubband THz sources. The simple and accurate analytical approximations delivered can be easily programmed and include the main many body effects required to describe bulk semiconductors. The luminescence is connected to the nonlinear absorption and gain and the expressions delivered reduce exactly to Elliott's formula in the low density limit. This leads to a very powerful tool to investigate new materials, starting e.g. from ab initio calculations and has potential for a major impact in the development of new bulk materials for efficient solar cells and for mid infrared radiation generation and detection. The level of agreement between the theory and experimental data clearly demonstrates the power and accuracy of the approach.



9585-14, Session 4

Development of low dielectric loss Nb-SiO2-Nb superconducting microstrips for the SPT-3G experiment

Chrystian M. Posada, Argonne National Lab. (United States); Brad A. Benson, The Univ. of Chicago (United States); Jason E. Austermann, Univ. of Colorado at Boulder (United States); Amy Bender, Argonne National Lab. (United States); John E. Carlstrom, The Univ. of Chicago (United States); Clarence L. Chang, Argonne National Lab. (United States); Thomas M. Crawford, The Univ. of Chicago (United States); Ari Cukierman, Univ. of California, Berkeley (United States); Junjia Ding, Argonne National Lab. (United States); Tijmen de Haan, Matthew Adam Dobbs, McGill Univ. (Canada); Daniel Dutcher, The Univ. of Chicago (United States); Wenderline Everett, Nils W. Halverson, Univ. of Colorado at Boulder (United States); Nicholas L. Harrington, Kaori Hattori, Univ. of California, Berkeley (United States); Jason W. Henning, The Univ. of Chicago (United States); Gene C. Hilton, National Institute of Standards and Technology (United States); William L. Holzapfel, Univ. of California, Berkeley (United States); Johannes Hubmayr, National Institute of Standards and Technology (United States); Donna Kubik, Fermi National Accelerator Lab. (United States); Chao-Lin Kuo, Stanford Univ. (United States); Adrian T. Lee, Michael J. Myers, Univ. of California, Berkeley (United States); Tyler J. Natoli, The Univ. of Chicago (United States); Hogan Nguyen, Fermi National Accelerator Lab. (United States); Valentine Novosad, Argonne National Lab. (United States); Zhaodi Pan, The Univ. of Chicago (United States); John E. Pearson, Argonne National Lab. (United States); John E. Ruhl, Benjamin Saliwanchik, Case Western Reserve Univ. (United States); Erik D. Shirokoff, The Univ. of Chicago (United States); Aritoki Suzuki, Univ. of California, Berkeley (United States); Keith L. Thompson, Stanford Univ. (United States); Keith Vanderlinde, Univ. of Toronto (Canada); Joaquin D. Vieira, Univ. of Illinois at Urbana-Champaign (United States); Gensheng Wang, Volodymyr Yefremenko, Argonne National Lab. (United States); Ki Won Yoon, Stanford Univ. (United States)

Since its discovery, the cosmic microwave background (CMB) has played a pivotal role in cosmology and particle physics. As such, CMB science is led by detector innovation. The frontier of CMB detector development is focused on improving bolometric detectors based on Transition Edge Sensors (TES). Currently, the most competitive CMB detector technologies utilize superconducting microstrip lines to couple radiation on to TES bolometers. Developing low loss microstrip technology makes possible to use in-line filters to define optical detector pass bands, allowing for the fabrication of multi-chroic pixels. In this sense, this work presents the development and characterization of low loss superconducting Nb microstrips to support the fabrication of mm-wave multi-chroic pixels for the upcoming SPT-3G experiment.

To characterize the microstrip loss, a series of half-wavelength microstrip resonators capacitively coupled to a Coplanar Waveguide feedline (CPW) have been fabricated. These resonators consist of 300 nm thick Nb ground plane, 500 nm thick silicon dioxide dielectric spacer, and a 300 nm thick Nb transmission layer. The Nb ground layer and Nb microstrip are deposited by DC magnetron sputtering, whereas SiO2 films deposited both by reactive sputtering and by plasma enhanced chemical vapor deposition (PECVD) are evaluated. The microstrip loss at a few GHz frequencies is determined by measuring the shift in a resonator's resonance frequency as a function

of temperature. The measured loss tangent for Nb microstrips deposited on sputtered silicon dioxide is 1.3 x 10-3. Microstrips deposited on PECVD SiO2 films showed a loss tangent as low as $2.1 \times 10-3$.

9585-15, Session 4

Relativistic Doppler frequency upconversion of terahertz pulses via reflection from photo-induced plasma fronts in solid-state media (Invited Paper)

Mark D. Thomson, Fanqi Meng, Hartmut G. Roskos, Johann Wolfgang Goethe-Univ. Frankfurt am Main (Germany)

We present experimental and theoretical results concerning the use of the relativistic Doppler effect to induce a frequency up-shift for terahertz pulses, reflecting from a charge-carrier plasma front in solid-state media. The plasma front is excited with femtosecond amplifier-laser pulses, and we focus on conventional semiconductors, such as undoped Si and GaAs. Besides offering a possible scheme for extending the bandwidth of existing high-field THz sources, the Doppler geometry constitutes a novel approach to probe the initial charge-carrier dynamics, as any up-shifted radiation arises chiefly due to interaction with the plasma front. This is demonstrated in our Doppler experiments on Si, where the data can be reconciled by assuming an effective Drude scattering time well below 10 fs, i.e. much shorter than that found for the thermalized plasma (-20 fs), which we determined vs. excitation density in additional pump-probe experiments with ultra-broadband THz-mid-infrared probe pulses.

The impact of these charge-carrier dynamics, as well as optical excitation parameters, on the Doppler interaction is investigated with a series of finite-difference time-domain (FDTD) simulations which allow a detailed description of the spatio-temporal interaction between the counterpropagating pump and probe pulses. We also discuss other material systems which might allow one to enhance the performance of the Doppler up-shift, or where the Doppler geometry could offer a unique probe of the photoexcitations.

9585-16, Session 5

TERA-MIR radiation: Materials, generation, detection, and applications (Invited Paper)

Mauro F. Pereira, Sheffield Hallam Univ. (United Kingdom)

This paper summarizes the joint progress in different projects in the THz field achieved by the teams in COST ACTION MP1204: TERA-MIR radiation: materials, generation, detection and applications. The results achieved benefit from the unique networking and capacity-building capabilities provided by the COST framework to unify these two spectral domains from their common aspects of sources, detectors, materials and applications. We are building a platform to investigate interdisciplinary topics in Physics, Electrical Engineering and Technology, Applied Chemistry, Materials Sciences and Biology and Radio Astronomy. In this sense THz and MIR are considered jointly, the driving force for both regimes being applications. The main emphasis of the research presented here is on new fundamental material properties, concepts and device designs that are likely to open the way to new products or to the exploitation of new technologies in the fields of sensing, healthcare, biology, and industrial applications. End users are: research centres, academic, well-established and start-up companies and hospitals. The strong coupling of THz radiation and material excitations has potential to improve the quantum efficiency of THz devices.



9585-17, Session 5

High effective algorithm of the detection and identification of substance using the noisy reflected THz pulse

Vyacheslav A. Trofimov, Svetlana A. Varentsova, Vladislav V. Trofimov, Lomonosov Moscow State Univ. (Russian Federation)

We demonstrate principal limitations of standard approach of TDS based on broadband THz pulse for the detection and identification of substance To avoid of these limitations we propose new high effective algorithm for this purpose. We demonstrate its applicability in real situation forvarious substances under consideration.

9585-18, Session 5

Development of ultra-broadband terahertz time domain ellipsometry (*Invited Paper*)

Masatsugu Yamashita, Chiko Otani, RIKEN (Japan)

We present a reflection-type ultra-broadband terahertz (THz) time-domain spectroscopic ellipsometry (THz-TDSE) system covering the frequency range of 0.5–30 THz. GaP (110) and z-cut GaSe crystals are used as emitters to generate the THz and mid-infrared pulses, respectively, and a photoconductive antenna switch using a low-temperature grown GaAs epitaxial layer transferred on Si substrate was used as a detector. By changing the emitter between the GaP and GaSe crystals, the measurable frequency range without additional optical alignment. We demonstrated the measurement of the dielectric function in a p-type InAs wafer and the optical conductivity of an indium tin oxide (ITO) thin film. The obtained carrier density and the mobility of the ITO thin film show good agreement with that obtained by the Hall measurement.

9585-19, Session 5

Numerical analysis of a terahertz transmission line resonator for heterodyne photomixing

Lars Juul, Inverto Digital Labs (Luxembourg); Martin Mikuli?, Forschungszentrum Jülich GmbH (Germany); Michel Marso, Univ. du Luxembourg (Luxembourg); Mauro F. Pereira, Sheffield Hallam Univ. (United Kingdom)

Substantial progress has been achieved in the area of CW terahertz sources over the last decade, including highly effective Quantum Cascade Lasers, negative differential resistance devices and terahertz multipliers, but heterodyne photomixing remains far from obsolete. THz photomixers have become commercially available for CW spectroscopy applications and are still among the simplest methods for THz-generation in terms of device complexity and fabrication. In addition, stacked InGaAs and InAlAs quantum well structures have been shown to have a low carrier lifetime and a band gap of 1.55um enabling the use of less costly optical sources.

Using the numerical method presented in [Juul et al, Optical and Quantum Electronics, DOI 10.1007/s11082-014-0048-3], we present a novel and tantalisingly simple terahertz photomixer structure based on a conventional photoconductor driving a coplanar stripline (CPS) terminated with a multilayer capacitance and RF-chokes doubling as bond pads for the photoconductor bias circuit. The transmission line is a better and more compact inductive reactance element than a comparable uniplanar meander structure and contributes to a higher radiation resistance of the resonant circuit.

The design leads to a predicted a radiated power of close to 15 uW at 0.85 THz, which is a five fold improvement over [Duffy et al, IEEE Transactions

on Microwave Theory and Techniques 49(6):1032–1038, 2001]. The current distribution on the transmission line indicates a linear polarisation of the radiated power.

The layout features of the design are intentionally conservative and can be produced with conventional, inexpensive photolithographic methods.

9585-20, Session 5

High transmittance silicon terahertz polarizer using wafer bonding technology

Ting-Yang Yu, Hsin-Cheng Tsai, National Chiao Tung Univ. (Taiwan); Shiang-Yu Wang, Academia Sinica (Taiwan); Chih-Wei Luo, Kuan-Neng Chen, National Chiao Tung Univ. (Taiwan)

Increasing the efficiency of THz system with reduced cost is still the most essential task, because of the difficulties in fabricating robust THz optical components with low Fresnel reflection loss. In this report, a new low cost THz polarizer with robust structure is proposed and demonstrated. This new THz wire grid polarizer was based on single anti-reflection layers fabricated with low temperature metal bonding and deep reactive-ion etching (DRIE). After patterning Cu wire gratings and the corresponding In/Sn solder ring on the individual silicon wafers, the inner gratings were sealed by the Cu to In/Sn wafer bonding guard ring providing the protection of humidity oxidation and corrosion. With the low eutectic melting point of In/Sn solder, wafers could be bonded face to face below 150°C. Two anti-reflection layers on both outward surfaces were fabricated by DRIE. With the mixing of empty holes and silicon, the effective refractive index was designed to be the square root of the silicon refractive index. The central frequency of the anti-reflection layers was designed between 0.5THz to 2THz with bandwidth about 0.5THz. The samples were measured with a commercial free-standing wire grid polarizer by a THz time domain spectroscopy from 0.3THz to 2THz. The power transmittance of the sample is close to 100% at central frequency. Extinction ratio of the polarizer is between 20dB to 40dB depending on the frequency and the Cu wire pitch. The advantages of this new polarizer include high transmittance, robust structure, low cost and no precision alignment required.

9585-21, Session 6

Terahertz detector arrays based on nanometer field effect transistors (Invited Paper)

Wojciech Knap, Univ. Montpellier 2 (France); J. Marczewski, Institute of Electron Technology (Poland); Dmytro B. But, Univ. Montpellier 2 (France); Nina V. Dyakonova-Cywinski, Institute of High Pressure Physics (Poland); Maciej Sypek, Warsaw Univ. of Technology (Poland)

We propose an overview of some recent results concerning THz detection related to plasma nonlinearities in nanometer field effect transistors[1,2]. The subjects were selected in a way to show physics related limitations and advantages rather than purely technological/engineering improvements of nanometer Field Effect transistors (FETs) working as Terahertz detectors. We address the basic physics related problems like temperature dependence, of the response [3], helicity sensitive detection [4] and nonlinear/saturation response at high incident power [5]. We present also the first results on new THz detectors based on Si junction-less FETs [6]. The results will be discussed in view of the physical and technical limitations of THz detector arrays based on Field Effect Transistors [7].

The observed high incident power photoresponse nonlinearity is explained by nonlinearity/saturation of the transistor channel current. The theoretical model of terahertz field effect transistor photoresponse at high intensity was developed.

The results show that dynamic range of field effect transistors is very high and can extend over more than six orders of magnitudes of power densities

Conference 9585: Terahertz Emitters, Receivers, and Applications VI



(from ~0.5 mW/cm2 to ~5 kW/cm2). Nonlinear and saturation regions of detections are seen for intensities above 1kW/cm2.

Silicon based FETs are the most promising for THz focal plane arrays. Standard technology Si -MOSFETS have an important responsivity limitation related to the p-n junction capacitance short-circuiting the incoming THz signals. The new junction-less Si technology transistors based THz detectors will be presented. They show amazingly high signal to noise ratio and unusual – still unexplained-THz responsivity versus gate voltage dependence [6]. We will present also recent results on arrays of GaN and GaAs FET based THZ detectors in view of their applications to on-line nondestructive testing and imaging [7].

Acknowledgements: This work was partially supported by the National Centre for Research and Development in Poland (grant no. PBS1/ A9/11/2012), by the National Science Centre in Poland (DEC-2013/10/M/ ST3/00705) and by CNRS France via LIA –TERAMIR project.

REFERENCES

1. W. Knap and M. I. Dyakonov, 'Field effect transistors for terahertz applications' in D. Saeedkia, Handbook of terahertz technology for imaging, sensing and communications, Cambridge, Woodhead Publishing, 121-155(2013)

2. W Knap, et al Nanometer size field effect transistors for terahertz detectors Nanotechnology 24 (2013)

3. O.Klimenko et al Temperature enhancement of terahertz FETs responsivity J. Appl. Phys. 112, 014506 (2012)

4. C.Drexler et al Helicity sensitive terahertz radiation detection by FETs J. Appl. Phys. 111 124504 (2012)]

5. D.But et al Power dependence of THz photoresponse of field effect transistors J.Appl .Phys. 115, 164514 (2014);

6. J.Marczewski, W.Knap, D. Tomaszewski, M. Zaborowski, P. Zagrajek Silicon junction less FETs as room temperature THz detectors submitted to J. of Applied Phys – Jan. (2015)

7. J. Suszek et al 3-D-printed flat optics for THz linear scanners , Terahertz Science and Technology, IEEE Transactions on , vol.PP, no.99, pp.1,3 Feb. (2015)

9585-22, Session 6

On-chip integration solutions of compact optics and detectors in room-temperature terahertz imaging systems

Gintaras Valu?is, Linas Minkevi?ius, Vincas Tamo?i?nas, Irmantas Ka?alynas, Rimvydas Venckevi?ius, Karolis Madeikis, Bogdan Voisiat, Dalius Seliuta, Gediminas Ra?iukaitis, Ctr. for Physical Sciences and Technology (Lithuania)

Reduction of dimensions in room-temperature terahertz (THz) imaging systems remains one of the most challenging tasks in employment them for direct practical applications.

In this communication, we discuss solutions in miniaturization of the THz image recording setup employing compact optics based on zone plates [1] and their on-chip integration with InGaAs-based bow-tie THz detectors [2].

Conventional, inverted and combined zone plates with integrated bandpass filters [1] were designed numerically using the 3D finite-difference time-domain method and produced using laser direct writing technique. Performance of the plates was studied experimentally comparing results with simulated ones. Spatial profiles of the concentrated radiation in the focal plane at the resonant frequency of 0.6 THz are demonstrated and focal depth influence is considered. To investigate the effect of Fabry-Perot resonances phase zone plate made on the silicon substrate was studied in the same experiments.

We demonstrate one order of magnitude detection enhancement of bow-tie-shaped InGaAs-based terahertz detectors at 0.76 THz by on-chip incorporation of the secondary diffractive optics [3].

Good correlation of the experimental and theoretical results shows that the

observed enhancement is resulting from the focusing performance of the zone plate rather than by the sensitivity of the single detector.

[1] L. Minkevi?ius et al, Electron. Lett. 49, 49 (2013).

[2] I. Ka?alynas et al, IEEE Sensors Journal 13, 50 (2013).

[3] L. Minkevi?ius et al, Electron. Lett. 50, 1367 (2014)

9585-23, Session 6

Plasmonic enhancement of sensitivity in terahertz (THz) photo-conductive detectors

Oleg Mitrofanov, Univ. College London (United Kingdom) and Sandia National Labs. (United States); Ting Shan Luk, Igal Brener, John Reno, Sandia National Labs. (United States)

We demonstrate enhancement of sensitivity in terahertz photoconductive detectors achieved by incorporation of plasmonic structures into the photo-conductive region of the detector. Auston switches based on low-temperature grown GaAs (LT GaAs) have been reliably used for detection of THz pulses over two decades. This material exhibits high electron mobility with sub-picosecond carrier lifetimes and high dark resistivity. This combination is difficult to achieve in other materials. Application of LT GaAs in THz devices is nevertheless limited due to absorption characteristics of this material. Plasmonic structures can be employed to modify the distribution of the optical field in the photoconductive region and hence modify the response of the THz photoconductive detectors.

We will discuss design of plasmonic structures to enhance the response of THz detectors based on LT GaAs and demonstrate incorporation of such structures into THz detectors. We also apply the developed design in integrated photo-conductive probes for THz near-field microscopy, where the enhancement of the material absorption translates into an increase of the detector sensitivity and an improvement in spatial resolution. Performance on these near-field probes that provide a spatial resolution of 3-5 micrometers (~1/100 of the wavelength) will be discussed and demonstrated.

9585-24, Session 6

Theoretical and experimental study on the response of Golay detector to the pulsed light

Weitao Wang, Zhenhua Cong, Xiaohan Chen, Xingyu Zhang, Zengguang Qin, Guanqi Tang, Ning Li, Qiang Fu, Shiqi Jiang, Shandong Univ. (China)

Golay Cells are generally applied to measure the average powers and the pulse energies of the light sources from the ultraviolet to the THz and millimeter waves due to their widely response wavelength range and high efficiency. The manufacturers provide their power responsivities to the continuous wave light signals, while the calibration of their energy responsivities for short pulses is rarely investigated and pendent. In this paper we present a theoretical and experimental study on the response of a Golay Cell (GC-1D, TYDEX) to the pulsed light.

The theoretical expression for the Frequency Transfer Function (FTF) of the Golay Cell together with the oscilloscope with AC-coupling (Tek, TDS 5052B) is first derived. It can be expressed as the function of a wavelength-dependent parameter K and two time parameters T1 and T2. By using the experimental results of an incident 1064 nm step signal, three parameters are determined to be K = 0.101 MV/W, T1 = 0.029 s and T2 = 0.485 s. The response of the Golay Cell to the light pulse is then calculated based on the verified FTF. It is found that, for pulses whose duration is much smaller than T1 and T2, if the response voltage u is defined as the voltage difference between the beginning of the pulse and the maximum value in the waveform, the energy responsivity Rp (the ratio of u to the pulse energy)



E) will be (1/T1-1/T2)K. It is independent of the pulse duration and repetition frequency. The experimental results agree well with the calculated results. For THz waves, K is different while T1 and T2 keep the same.

9585-34, Session 6

Coherent detection for continuous terahertz wave

Hui Yuan, Tielin Lu, Yuejin Zhao, Beijing Institute of Technology (China); LiangLiang Zhang, Cunlin Zhang, Capital Normal Univ. (China)

We demonstrate a coherent raster-scan imaging system that can acquire phase information based on continuous terahertz imaging. It mixes the terahertz with a femtosecond laser at a electro-optic zinc telluride(ZnTe) crystal to make a hybrid modulation on the ZnTe crystal to achieve continuous terahertz detection. It can not only propagate for a long distance but also achieve phase detection for continuous terahertz imaging. The surface images of objects that are under test can be obtain with a BWO(backward-wave oscillator) output power of 10mW at 205.994GHz and a MaiTai laser output power of 1W and 100fs pulse light at 800nm with repetition frequency of 80MHz. The images can achieve diffraction-limited resolution approximately. And the results show that the system can obtain phase imaging of test objects based on continuous terahertz source. And it has significant meaning for coherent detection of continuous terahertz source. And it makes significance for development of coherent detection for continuous terahertz wave.

9585-25, Session 7

Multifrequency high precise subTHz-THz_IR spectroscopy for exhaled breath research (Invited Paper)

Vladimir L. Vaks, Institute for Physics of Microstructures (Russian Federation) and N.I. Lobachevsky State Univ. of Nizhni Novgorod (Russian Federation)

Nowadays the development of analytical spectroscopy with high performance, sensitivity and spectral resolution for exhaled breath research is attended. The method of two-frequency high precise THz spectroscopy and the method of high precise subTHz-THz-IR spectroscopy are presented. Development of a subTHz-THz-IR gas analyzer increases the number of gases that can be identified and the reliability of the detection by confirming the signature in both THz and MIR ranges. The testing measurements have testified this new direction of analytical spectroscopy to open widespread trends of its using for various problems of medicine and biology. First of all, there are laboratory investigations of the processes in exhaled breath and studying of their dynamics. Besides, the methods presented can be applied for detecting intermediate and short time living products of reactions in exhaled breath. The spectrometers have been employed for investigations of acetone, methanol and ethanol in the breath samples of healthy volunteers and diabetes patients. The results have demonstrated an increased concentration of acetone in breath of diabetes patients. The dynamic of changing the acetone concentration before and after taking the medicines is discovered. The potential markers of pre-cancer states and oncological diseases of gastrointestinal tract organs have been detected. The changes in the NO concentration in exhaled breath of cancer patients during radiotherapy as well as increase of the NH3 concentration at gastrointestinal diseases have been revealed. The preliminary investigations of biomarkers in three frequency ranges have demonstrated the advantages of the multifrequency high precise spectroscopy for noninvasive medical diagnostics.

9585-26, Session 7

Toward THz imaging of human eye: Direct mapping of corneal tissue water content with THz imaging

Shijun Sung, Somporn Chantra, Neha Bajwa, Ryan McCurdy, Gintare Kerezyte, James Garritano, Jean-Pierre Hubschman, Univ. of California, Los Angeles (United States); Sohpie X. Deng, Univ. California, Los Angeles (United States); Warren Grundfest, Zachary Taylor, Univ. of California, Los Angeles (United States)

THz imaging applied in ocular tissue water content sensing can address shortfalls in current clinical challenges of accurately measuring corneal hydration. Hydration sensing ability in THz band can also be a powerful tool in ophthalmologic science, as many pathologies such as Fuchs' endothelial Dystrophy, and pseudophakic bullous keratopathy result in increased corneal tissue water content (CTWC).

This paper presents a pilot study of edema an in vivo rabbit model and demonstrates a significant difference between THz reflectivity in the control group and treatment group in which the water content of the cornea was perturbed through surgical means.

The endothelium of the cornea was surgically excised and the resulting increase in corneal tissue water content was monitored by a non-contact THz imaging system and compared with current clinical standard of corneal pachymetry (central corneal thickness measurement). We demonstrate direct measurement of CTWC in in-vivo is possible with ~ 2mm spatial resolution. The technique is robust, sensitive, and does not rely on assumptions of healthy cornea central thicknesses. This allows the technology to be robust to physiologic variation and feasible to be translated into clinical application. Imaging system design and optical engineering challenges associated with ophthalmologic applications are also presented.

9585-27, Session 7

New way for both quality enhancement of THz images and detection of concealed objects

Vyacheslav A. Trofimov, Vladislav V. Trofimov, Lomonosov Moscow State Univ. (Russian Federation)

We developed new real-time algorithm, based on the correlation function, for the detection of concealed objects by using computer processing of the passive THz images without their viewing. This algorithm allows us to make a conclusion about presence of forbidden objects on the human body. To see this object with high quality we propose one more algorithm which allows to increase the image quality. Current approach for computer processing of the THz images differs from approaches developed by us early.

We apply new algorithms with success to the images captured by passive THz camera TS4 manufactured by ThruVision Inc. The distance between the camera and person is changed from 4 to 10 metres.

9585-28, Session 7

Ultrafast field-resolved multi-THz spectroscopy on the sub-nanoparticle scale (Invited Paper)

Tyler L. Cocker, Max Eisele, Markus A. Huber, Markus Plankl, Univ. Regensburg (Germany); Leonardo Viti, Daniele Ercolani, Lucia Sorba, Miriam S. Vitiello, Scuola Normale Superiore (Italy); Rupert Huber, Univ. Regensburg (Germany)

Conference 9585: Terahertz Emitters, Receivers, and Applications VI



Over the past 20 years, terahertz and multi-terahertz spectroscopy have provided valuable insights into ultrafast carrier dynamics in nanomaterials. Nevertheless, researchers have had to contend with various effective medium theories to extract nanoscale information, and have been limited to studying ensembles of nano-objects. Conversely, scattering-type near-field scanning optical microscopy (s-NSOM) in the mid-infrared can measure the dielectric properties of surface features as small as 10 nm. Until very recently, though, ultrafast near-field studies in the infrared had not been reported. Here, we demonstrate a combination of ultrafast multi-terahertz spectroscopy with s-NSOM that achieves simultaneous sub-cycle temporal resolution and 10 nm spatial resolution: Phase-stable multi-terahertz pulses are coupled to the tip of the s-NSOM and the scattered electric near-field is detected by electro-optic sampling. The broad phase-matching bandwidth of the GaSe detection crystal ensures that the oscillating electric near field is recorded with a time resolution defined by the duration of the electro-optic gate pulse (10 fs). Meanwhile, the 10 nm spatial resolution of our nanospectroscopy is given by the radius of curvature of the s-NSOM tip apex, which was confirmed by electro-optic line scans. We have applied our novel microscope to the study of photoinduced carrier dynamics in isolated InAs nanowires. Ultrafast imaging provides a map of the photoinduced carrier density, while nano-spectroscopy reveals the local evolution of the plasma frequency. Finally, by using the tapping amplitude of the s-NSOM tip to control the nano-spectroscopy probing volume, we observe the build-up of a carrier depletion layer on the nanowire surface.

9585-29, Session 7

Exploration of burn wound induction parameters on wound edema

Neha Bajwa, Ctr. for Advanced Surgical and Interventional Technology (United States); Shijun Sung, James Garritano, Ctr. for Advanced Surgical & Interventional Technology (United States); Michael Fishbein, Univ. of California, Los Angeles (United States); Warren Grundfest, Zachary Taylor, Ctr. for Advanced Surgical & Interventional Technology (United States)

The high contrast resolution afforded by terahertz (1 THz = 1012 Hz) imaging of physiologic tissue continues to drive explorations into the utility of THz technology for burn wound detection. Although we have previously reported the use of a novel, reflective THz imaging technology to sense spatiotemporal differences in reflectivity between partial and full thickness burn wounds, no evidence exists of a one-to-one correlation between structural damage observed in histological assessments of burn severity and THz signal. For example, varying burn induction methods may all result in a particular burn classification, however, burn features observed in parallel THz imagery may not be identical. Successful clinical translation of THz technology as a comprehensive burn guidance tool, therefore, necessitates an understanding of THz signal and its relation to wound pathophysiology. This work aims to perform THz imaging of in vivo rat burn wounds (n=4) induced using multiple brands (~ 20 mm x 4 mm rectangular brass heads with varying topology on the inferior side) to investigate the effects of contact brand geometry on THz reflectivity signal. Steps toward exploring the sensitivity of THz imaging to varying burn tissue boundaries (rigid vs curved) will help define the ultimate potential of the technology as well as lead to better design of instrumentation and analytical techniques to delineate tissue regions for effective and accurate prognosis.

9585-30, Session 7

Investigation of pharmaceutical drugs and caffeine-containing foods using Fourier and terahertz time-domain spectroscopy

Gintaras Valu?is, Mindaugas Karali?nas, Rimvydas Venckevi?ius, Irmantas Ka?alynas, Ctr. for Physical Sciences and Technology (Lithuania); Uro? Puc, Andreja Abina, Anton Jegli?, Aleksander Zidan?ek, Jo?ef Stefan Institute (Slovenia)

Feature of terahertz (THz) radiation to penetrate through paper- or plastic-based packaging can be not only used in development of security systems to observe hidden objects via THz imaging, but also be served as a powerful tool for identification of various materials employing spectroscopic approaches.

In this work, several pharmaceutical drugs like ascorbic acid, melatonin, etc. as well as caffeine-containing foods were tested using terahertz timedomain spectroscopy (TDS) and Fourier spectroscopy (FS).

The dry powder of pharmaceutical drugs was mixed with polyethylene and pressed into the pellets using hydraulic press. The coffee grounds were also pressed into the pellets after ball-milling and mixing with polyethylene powders. The caffeine-containing liquid foods were dried out on the paper strips of various stacking.

TDS experiments were carried out employing T-Spec (Teravil Ltd) commercial spectrometer in combination with a femtosecond laser (Toptica, Femto Fiber Pro) having 800 nm emission wavelength, less than 90 fs pulse duration and 80 MHz repetition rate for THz generation and detection. Additionally, TDS system based on organic electrooptic crystals was used [1]. Samples transmission spectra at frequency range of 0.3-10 THz with the resolution of 1 cm-1 were measured by the Fourier spectrometer with vacuum option.

Experiments allowed one to determine characteristic spectral signatures within THz range of the objects under test. Spectroscopic THz imaging approach [2] was considered as possible option to identify packaged pharmaceutical drugs.

[1] A. Abina et al, Polymer Testing 32, 739 (2013).

[2] I. Ka?alynas et al, IEEE Sensors Journal 13, 50 (2013).

9585-31, Session 8

Quantum spin dynamics at terahertz frequencies in 2D hole gases and improper ferroelectrics (Invited Paper)

James Lloyd-Hughes, The Univ. of Warwick (United Kingdom)

Terahertz time-domain spectroscopy permits the excitations of novel materials to be examined with exquisite precision. Improper ferroelectric materials such as cupric oxide (CuO) exhibit complex magnetic ground states. CuO is antiferromagnetic below 213K, but has an incommensurate cycloidal magnetic phase between 213K and 230K. Remarkably, the cycloidal magnetic phase drives ferroelectricity, where the material becomes polar. Such improper multiferroics are of great contemporary interest, as a better understanding of the science of magnetoelectric materials may lead to their application in actuators, sensors and solid state memories. Improper multiferroics also have novel quasiparticle excitations: electromagnons form when spin-waves become electric-dipole active. By examining the dynamic response of spins as they interact with THz radiation we gain insights into the underlying physics of multiferroics.

In contrast to improper ferroelectrics, where magnetism drives structural inversion asymmetry (SIA), two-dimensional electronic systems can exhibit non-degenerate spin states as a consequence of SIA created by strain and/ or electric fields. We identify and explore the influence of the Rashba spin-orbit interaction upon cyclotron resonance at terahertz frequencies in high-mobility 2D hole gases in germanium quantum wells. An enhanced Rashba spin-orbit interaction can be linked to the strain of the quantum well, while a time-frequency decomposition method permitted the dynamical formation and decay of spin-split cyclotron resonances to be tracked on picosecond timescales. Long spin-decherence times concurrent with high hole mobilities highlight the potential of Ge quantum wells in spintronics.



9585-32, Session 8

THz polarization difference imaging of aqueous targets

Shijun Sung, Neha Bajwa, Ryan McCurdy, Gintare Kerezyte, James Garritano, Warren Grundfest, Zachary Taylor, Univ. of California, Los Angeles (United States)

This paper describes the basic design, implementation, and testing of a polarization difference imaging system for use on aqueous targets. The ultimate performance limitation of THz imaging in many active areas of research is clutter from surface geometry. While the signal to nose ratio (SNR) of standard THz imaging systems are quite large, the signal to clutter ratio (SCR) often faced in an imaging application is orders of magnitude lower and, in many cases, lower than the contrast to noise (CNR) resulting in imagery where the contrast mechanism of interest does not significantly contribute to the overall observed contrast.

To overcome these limitations we developed a system that uses a circularly polarized source, polarization demultiplexer, and linearly polarized detectors to resolve the transverse electric (TE) and transverse magnetic (TM) reflectivities of a target simultaneously. The targets were illuminated at an oblique incidence angle thus creating a difference in reflectivities of the two polarizations and enabling a differential measurement.

Tissue mimicking phantoms were fabricated using hydrogels with spatially varying water content and modified with a range of surface topologies and surface roughness. The results indicated that the imaging field clutter affected both polarization channels nearly equally allowing the system to resolve differences in phantom water content. This design holds significant promise for clinical translation where patient imaging is dominated by clutter.

9585-33, Session 8

Nonlinear dynamics in THz metamaterials: From impact ionization to field emission (Invited Paper)

Richard D. Averitt, Univ. of California, San Diego (United States)

Recent advances in the generation of picosecond high-field terahertz pulses enables novel studies of nonlinear dynamics in materials ranging from semiconductors to correlated electron materials. Suitably designed metamaterials localize and enhance the electric and magnetic fields of incident terahertz pulse pulses. This talk will describe our recent results in this area which includes creating superconducting perfect absorbers and terahertz induced field emission in metamaterials. In particular, we have created YBCO superconducting split ring resonators and configured them into a perfect absorber geometry. We observe a nonlinear response as a function of the incident THz field strength in these metamaterial structures. In separate experiments, we have measured the THz induced field emission current across the capacitive gap of field enhanced metamaterials structures.

9585-35, Session PMon

Silicon based active terahertz metamaterial devices

Hyun-Woong Kim, Jeong Min Woo, Sung-Min Hong, Jae-Hyung Jang, Gwangju Institute of Science and Technology (Korea, Republic of)

Terahertz (THz) modulators based on active metamaterials have conventionally been realized on compound semiconductors. Spectral responses of metamaterials realized on semiconductors were controlled by optical pumping, electrical power, or thermal power to demonstrate the intensity modulation of the transmitted THz wave. In this study, silicon (Si) based THz modulator which can be controlled by the electrical power input is reported. All the fabrication processes are compatible with the conventional Si integrated circuit technologies. Metamaterials composed of metallic slot array was formed on top of silicon on insulator (SOI) substrates. The metamaterial structure is used as an anode electrode and the other cathode electrode has been placed beside the anode electrode by forming ohmic contact to the doped Si layer. When electrical bias is applied to the devices, the current flowing through the diode structure elevates the lattice temperature of the silicon layer. At the elevated temperature, the mobility of carriers in the Si layer is dramatically decreased meanwhile the carrier density in the Si layer is preserved. The decreased mobility of the carriers in Si layer leads to the increased resistance in the slot structures, and the quality factor of the slot is increasing. By controlling the quality factor of the metamaterial structures, the transmission of THz waves was successfully controlled. The resulting modulation depth calculated by the change of transmittance over the maximum transmittance was 42% with the highest bias voltage of 12 V. This work is supported by National Research Foundation of Korea through a grant (No. 20110017603).

9585-36, Session PMon

Development of magnetic system with high-anisotropy localized magnetic field for terahertz time-domain spectroscopy

Solveyga E. Azbite, Mikhail K. Khodzitsky, National Research Univ. of Information Technologies, Mechanics and Optics (Russian Federation)

At the present time researches of biological objects spectra in terahertz frequency range attract the widespread interest, because in this frequency range there are vibrational and rotational transition frequencies for many molecules. The THz setups need for magnetic systems to improve THz radiation generation. At this moment there are three types of magnetic systems for THz time-domain spectrometers, namely the superconductor ones operating at low temperatures, the electromagnet systems including an optional power source and permanent magnetic ones. The 1st and 2nd ones produce strong magnetic field, and the last one has a small field.

In this paper magnetic system with a localized high-intensity magnetic field due to giant magnetic anisotropy magnets was proposed for THz timedomain spectroscopy. The design consists of two pairs of conical magnets, which form two semi-spheres[1]. Each pair of cones (apart from the central one) was divided into some equal sectors. The stray strong magnetic field is localized at the center of semi-sphere. Such two semi-spheres design will be used for an improvement of THz generation, it turns direction of dipole radiation pattern. One semi-sphere will be used for investigation of spectral and optical properties of an object at strong magnetic field.

The proposed magnetic system was numerically calculated in COMSOL MultiPhysics using AC/DC Module. Stray magnetic field for various geometrical parameters of system and different magnetic materials was analytically evaluated. These results may be used for development of real magnetic THz time-domain spectroscopy system.

[1] Samofalov V. N. et. al. Physics-Uspekhi. 2013 V. 56(3)pp.269-288.

Conference 9586: Photonic Fiber and Crystal Devices: Advances in Materials and Innovations in Device Applications IX



Sunday - Monday 9 -10 August 2015 Part of Proceedings of SPIE Vol. 9586 Photonic Fiber and Crystal Devices: Advances in Materials and Innovations in Device Applications IX

9586-1, Session 1

Polymer-inorganic nanocomposite thin film emitters, optoelectronic chemical sensors, and energy harvesters produced by multiple-beam pulsed laser deposition

Abdalla M. Darwish, Dillard Univ. (United States); Sergey Sarkisov, SSS Optical Technologies, LLC (United States); Darayas Patel, Oakwood Univ. (United States); Allan Burkett, Simeon Wilson, Ashley Blackwell, Dillard Univ. (United States); Brent Koplitz, Tulane Univ. (United States)

Huge variety of new photonic devices, including light emitters, chemical sensors, and energy harvesters, can be made of the polymer-inorganic nanocomposite thin films produced by the new multiple-beam pulsed laser deposition process (MB-PLD). We describe the PLD system and the film deposition process itself, particularly the multiple-beam matrix assisted pulsed laser evaporation (MB-MAPLE) version. We also report on the results of the investigation of optical, electrical, morphological, and performance characteristics of the three types of the fabricated nanocomposite thin film photonic devices: upconversion light emitters, chemical (ammonia) sensors, and thermo-electric energy harvesters. The emitters were made of poly(methyl methacrylate) (PMMA) film impregnated with nanoparticles of rare-earth (RE) fluorides such as NaYF4: Yb3+, Er3+, NaYF4: Yb3+, Ho3+, and NaYF4: Yb3+, Tm3+. They demonstrated the quantum yield of upconversion visible emission approaching one percent when being pimped with 980-nm infra-red laser. The same films, but doped with an indicator dye, were tested as ammonia sensors. They demonstrated the drop of upconversion emission (registered by a photodetector) due to the rise of the optical absorption of the indicator dye affected by ammonia. The capability of detecting fractions of one percent (by volume) of ammonia was established. The thermo-eclectic energy harvesting films (useful for concentrated solar power) were made of aluminum-zinc-oxide with nanodefects produced my polymer dopants. The role of nanodefects was to disrupt the phonon-related thermoconductivity while maintain electroconductivity high in order to enhance the Seebeck effect figure-ofmerit (make it greater than one).

9586-2, Session 1

Negative differential resistance behaviors in SnO2 thin film

Chih-Yi Hsieh, Cheng-Yi Liu, National Central Univ. (Taiwan)

Negative differential resistance (NDR) characteristics is usually observed in tunneling diode. In this work, we found NDR characteristics in a single undoped SnO2 thin film. The highest peak-to-valley current ratio (PVCR) is estimated to be 4.54. In addition, the overall transmittance of undoped SnO2 thin films is higher than 90% in the visible region. The undoped SnO2 thin films were deposited on the glass substrates by the magnetron sputtering system. The NDR characteristics of the undoped SnO2 thin films only observed under oxygen-rich ambient during the sputtering process. Also, NDR behavior depends on the size of the probe (or the size of the contact pad). The NDR characteristics are used on the applications on tunnel diode, and resonant tunnel diode. Therefore, the mechanism of the NDR characteristic of the undoped SnO2 thin films is very interested to be understood. In this talk, we will discuss the mechanism of the NDR characteristic of the undoped SnO2 thin films. X-ray diffraction, X-ray photoelectron spectroscopy and uv-visible spectroscopy analysis on the undoped SnO2 thin films also would be reported.

9586-3, Session 1

Orientation dependence of dispersion and band gap of PIMNT single crystal

Chongjun He, Nanjing Univ. of Aeronautics and Astronautics (China); Hongbing Chen, Ningbo Univ. (China); Jiming Wang, Xiaorong Gu, Tong Wu, Youwen Liu, Nanjing Univ. of Aeronautics and Astronautics (China)

Refractive indices and optical transmission of PIMNT single crystal with three orientations have been measured. Their Sellmeier dispersion equations of the refractive indices were obtained through least square fitting. After poled, optical transmission of [011] oriented crystal is much higher than that of [001] and [111] oriented crystals. The optical band gap was determined from absorption coefficient spectra. These results provide an important basis for further theoretical study and practical device fabrications based on PIMNT single crystal.

9586-4, Session 1

Significant near-IR light transmission asymmetry demonstrated in an alldielectric (1+2)-dimensional photonic crystals

Lukasz Zinkiewicz, Univ. of Warsaw (Poland); Jakub Haberko, AGH Univ. of Science and Technology (Poland); Piotr Wasylczyk, Univ. of Warsaw (Poland)

We demonstrate the design, optimization, fabrication and characterization of an all-dielectric photonic structure with a significant, broadband asymmetry in transmission of the near-infrared radiation for opposite propagation directions. Our approach is based on a two-layer crystal made of a quarter wavelength stack (Bragg mirror) topped with a transmission phase diffraction grating consisting of a series of parallel lines. The structure performance can qualitatively be understood as follows. If a light beam of properly chosen frequency impinges at normal incidence from the dielectric stack side, it will be transmitted with high efficiency and afterwards will be diffracted on the grating, while the sum of all diffraction orders contributes to the total transmitted intensity. However, if the same wave arrives at the structure from the other side, first illuminating the grating of an optimized lines geometry, a significant fraction of energy may be transformed into higher orders, now propagating in the stack at different angles, so that it is highly reflective and thus total light transmission is significantly smaller. The asymmetry, defined as the difference between the intensity transmission coefficients, reaches 0.72±0.06 for a single wavelength and exceeds 0.2 over a spectral range spanning from 700-850 nm for one incident polarization and 750-800 nm for both polarizations. The experimental results are consistent with the numerical model of light propagation in the structure. This concept can be directly adopted at shorter wavelengths, covering the visible and near UV regions.

9586-5, Session 1

Polarization holograms in gold nanoparticle-doped PQ/PMMA photopolymer

Liangcai Cao, Chengmingyue Li, Zheng Wang, Guofan Jin, Tsinghua Univ. (China)

Conference 9586: Photonic Fiber and Crystal Devices: Advances in Materials and Innovations in Device Applications IX



Thick phenanthrenequinonedoped poly (methyl methacrylate) (PQ/ PMMA) photopolymer was reported as an attractive candidate for volume polarization holographic recording [1]. When doping the gold nanoparticles, a strong absorption grating could be introduced as a result of localized surface plasmon resonance effect of gold nanoparticles and the multicomponent diffusion process. The linear photoinduced birefringence of the gold nanoparticle-doped PQ/PMMA photopolymer is observed experimentally to be increased, compared with the pure PQ/PMMA photopolymer [2]. The volume polarization gratings could be recorded and even multiplexed with the orthogonal circular polarized beams. The principles of the polarization gratings are investigated to achieve a better dynamic range and material sensitivity for the volume holographic material. Based on above analyses and volume holographic performance of the gold nanoparticle-doped PQ/PMMA photopolymer, a polarization multiplexing holographic memory for higher density and lower crosstalk is designed and experimentally demonstrated

Acknowledgements:

This work is supported by National Basic Research Program of China (2013CB328803), Nature Science

Foundation of China (61361160418, 61275013).

1. Shiuan Huei Lin, Sheng-Lung Cho, Shin-Fu Chou, June Hua Lin, Chih Min Lin, Sien Chi, and Ken Yuh Hsu, "Volume polarization holographic recording in thick photopolymer for optical memory," Optics Express 22, 14944-14957 (2014).

2. Chengmingyue Li, Liangcai Cao*, Zheng Wang, and Guofan Jin, "Hybrid polarization-angle multiplexing for volume holography in gold nanoparticle-doped photopolymer," Optics Letters, 39, 6891-6894 (2014).

9586-6, Session 1

Terahertz electrical and optical properties of LiNbO3 single crystal thin films

Moumita Dutta, Xomalin G. Peralta, Carol Ellis, Amar S. Bhalla, Ruyan Guo, The Univ. of Texas at San Antonio (United States)

Lithium niobate crystals are known to have important applications as acousto-optic, pyro-electric, electro-optic, SAW, signal processing and many more. In this work we report the electrical and optical properties ranging from terahertz to optical frequencies. The techniques used include terahertz time domain spectroscopy, Raman spectroscopy, optical spectrometer, ellipsometry and vibrometry. While bulk crystals have been extensively studied, LiNbO3 thin films, especially the single crystal thin films (<700nm in thickness), have been seldom reported. This work focuses on the single crystal LiNbO3 thin films to present a comparative study with that of bulk crystals. Both the orientation of the films and the configuration of the filminterlayer-substrate systems are studied to explore suitable configuration for high speed and efficient modulator applications in wide range of frequencies including terahertz.

9586-7, Session 1

Magneto-acoustic-electroporation (MAEP): In-vitro visualization and numerical characterization

Soutik Betal, Binita Shrestha, The Univ. of Texas at San Antonio (United States); Luiz F. Cotica, Univ. Estadual de Maringá (Brazil); Liang Tang, Kelly L. Nash, Amar S. Bhalla, Ruyan Guo, The Univ. of Texas at San Antonio (United States)

Magneto-Acoustic-Electroporation (MAEP) is a magnetically controlled acoustic-electroporation observed while core-shell Magneto-electric nanoparticles interact with Biological Cells. The surface polarity change of the piezoelectric coating (BaTiO3) due to absorption of pressure created due magneto-striction of core (CoFe2O4) in AC magnetic field results in electric field (Uext) change at the external vicinity of the cell membrane when nanoparticles are nearby. This results in transmembrane Voltage (Um) change which is basically the difference in Cell's internal potential (Uint) and external potential. The nonlinear permeability change of cell membrane due to change in Um opens the nano-pores on the membrane. The magnetic moment of the nanoparticles further helps in penetration of the Magnetoelectric nanoparticles inside the cell through these magneto-electrically controlled newly opened nano-pores on cell's membrane. MAEP is analyzed through in-vitro analysis and Mathematical equations are formulated for numerically expressing its fundamental effect. TEM imaging, XRD analysis, Zeta-potentiometer measurement and AFM imaging are confirming the coating of the piezoelectric layer on Magneto-stricitve nanoparticles, Acoustic measurements confirms the photo-acoustic and magneto-acoustic property of CoFe2O4 nanoparticles and Fluorescence microscopy as well as Confocal microscopy are confirming the penetration of particle inside the Human Epithelial cells (HEP2). These particles can be used as nano-probes for electroporation experiments and Cell membrane permeability study & exploring this mechanism can introduce a new level of remotely controlled efficient treatment of various diseases by accurate & efficient targeted delivery of drug into the infected cells.

9586-8, Session 1

Design and development of a high sensitive low cost fiber optic refractometer

Vayunandana Kishore Pabbisetti, National Institute of Technology, Warangal (India)

A simple and low-cost fiber optic refractometer is designed and demonstrated. The sensor is configured by etching a short region of a standard single-mode circularly bent fiber. Circularly bent three fiber loops are etched in equal lengths and arranged parallel to each other. The working principle of the sensor is evanescent field modulation with respect to the change in ambient refractive index at the sensing region. In the present study sugar solution with various concentrations, possessing different refractive indices is chosen as the ambient.

There have been many efforts to show that bent and etched optical fiber sensors have increased sensing capabilities but they are very much prone to fracture and breakage. The proposed sensor is stable showing very less tendency towards any breakage or fracture. Light from a broad band light source is coupled to the sensor and the output is detected by using a photo detector. The sensitivity of the sensor is tested for various sugar concentrations. It is evident from the experimental results that with the increase of sugar concentration the output intensity of the sensor is decreased linearly. The effect of number of fiber loops, diameter of the fiber loop and length of the etched region on the sensitivity of the sensor will be investigated. The proposed sensor may find applications in detecting various chemical species, biochemical testing and many other fields.

9586-9, Session 1

Study of P-type TiO2 thin film and transparent p-n junction device

Chia-Hua Lin, National Central Univ. (Taiwan)

This study reports a transparent p-type TiO2 thin film by DC reactive magnetron sputtering method under oxygen rich ambient. The p-type TiO2 thin film has a low resistivity (about 0.8 ?·cm) and a high hole concentration (about 4.6?1019 cm-3). The p-type conduction was also confirmed by Seebeck effect. In addition, the overall transmittance of the p-type TiO2 thin film is higher than 80% in the visible region. P-type conduction of TiO2 thin film is believed to be achieved by the so-called "self-substitution reaction", which means that the Ti ions with a low valence number in the TiO2 thin film substitute the Ti ions with higher valence number. For example, Ti3+-Ti4+ and Ti2+-Ti4+ substitution reactions are the two possible self-substitution reaction in the TiO2 thin film. These two substitution reactions have been verified by XPS analysis. Using the produced p-type TiO2 thin film, transparent p-TiO2/n-ITO p-n junctions were fabricated. The I-V characteristics of the p-TiO2/n-ITO junction exhibit distinct diode

characteristics. The transparent p-TiO2/n-ITO diode can be further applied in invisible electronics.

9586-10, Session 2

Formation of ultrashort parabolic pulses via passive nonlinear reshaping in normal dispersive optical fibers at 1550 nm

Igor A. Sukhoivanov, Univ. de Guanajuato (Mexico); Sergii O. lakushev, Kharkiv National Univ. of Radio Electronics (Ukraine); Oleksiy V. Shulika, Erick R. Baca Montero, Alejandro Barrientos García, Luis A. Herrera Piad, Igor V. Guryev, José A. Andrade Lucio, Univ. de Guanajuato (Mexico)

We have investigated ultrashort parabolic pulse formation via passive nonlinear reshaping in normal dispersive optical fibers at 1550 nm in the transient-state regime and in the steady-state regime. Numerical simulations have been made based on generalized nonlinear Schrödinger equation taking into account high-order dispersion terms (third-order dispersion) and high order nonlinear terms such as self-steepening and the intrapulse Raman scattering. The impact of initial pulse parameters such as initial pulse shape, pulse energy and chirp on the pulse reshaping were investigated. It was found the areas of parameters providing the formation of parabolic pulses in available commercial fibers with normal dispersion at 1550 nm. It was found that small amount of positive second-order dispersion and quite sufficient third-order dispersion can restrict strongly the formation of parabolic pulses at 1550 nm. The most suitable fiber for pulse reshaping has been found. We have shown that femtosecond parabolic pulses can be formed as short as 200-300 fs in the transient-state regime and 700-800 fs in the steady-state regime. In the first case shorter parabolic pulses can be obtained but they are not stable during further propagation in the fiber. Whereas in the steady-state regime the duration of parabolic pulses is larger, but they remain the parabolic shape during subsequent propagation in the fiber. Such parabolic pulses can be used for pulse amplification and compression as well as in many optical communications applications such as optical regeneration, pulse re-timing, and mitigation of the linear waveform distortions.

9586-11, Session 2

A novel As2S5-tellurite hybrid photonic crystal fiber for long mid-IR supercontinuum fiber lasers

Mbaye Diouf, Univ. Cheikh Anta Diop (Senegal); Amine Ben Salem, Rim Cherif, National Engineering School of Communication of Tunis (Tunisia); Ahmadou Wague, Univ. Cheikh Anta Diop (Senegal); Mourad Zghal, National Engineering School of Communication of Tunis (Tunisia)

Recently, non-silica glasses like Tellurite and chalcogenide have been extensively studied owing to their wide transparency in the mid-IR region as well as their intrinsic and strong nonlinearities. By combining these characteristics with ultra-small waveguide structures like photonic crystal fibers, the waveguiding properties are enhanced through the large contrast difference between the core and the cladding refractive index. Thus, major and important effects on the nonlinear response of the waveguide are expected.

In this work, we numerically demonstrate the supercontinuum (SC) generation in a novel chalcogenide As2S5 nanowire embedded-core into Tellurite photonic crystal fiber (PCF). This hybrid As2S5-tellurite small core PCF has a pitch of 0.7 μ m and air hole diameter of 0.2 μ m. It exhibits a zero dispersion wavelength (ZDW) of $3.25 \,\mu m$ with an overall highly engineered group velocity dispersion (GVD) shifted to the mid-IR wavelengths region. By injecting 100 fs hyperbolic-secant input pulses delivered by available tunable optical parametric oscillator (OPO) system at the pump wavelength of 3.389 μ m, we obtain a broadband coherent mid-IR SC generated in only 1 mm-long PCF with a peak power of 9 kW. An ultra-large mid-IR bandwidth extending from 1000 to 7300 nm is generated with more than 60% of the total power which is available beyond 3 µm. The proposed hybrid PCF structure shows to be very promising for designing new compact, stable and powerful SC fiber laser sources in the long mid-IR wavelength region.

OPTICAL ENGINEERING+

APPLICATIONS

9586-12, Session 2

The impacts of ageing effects due to radiation burden on optical fiber couplers

Frantisek Perecar, V?B-Technical Univ. of Ostrava (Czech Republic); Ondrej Marcinka, Research Ctr. Rez (Czech Republic); Lukas Bednarek, V?B-Technical Univ. of Ostrava (Czech Republic); Michal Lucki, Czech Technical Univ. in Prague (Czech Republic); Andrej Liner, Lukas Hajek, Martin Papes, Jakub Jaros, Vladimir Vasinek, V?B-Technical Univ. of Ostrava (Czech Republic)

This article focuses on applied research and experimental development of resources for safety operation of optical networks since monitoring of ageing substantially contributes to its security. It addresses issues of accelerated ageing of optical fiber elements in their burdened with gamma radiation. How does radiation energy of gamma radiation influence optical network elements? This effect is explored just very little bit and is yet another unanswered question. In addition to the destruction of coating materials, gamma radiation has its effect on the internal structure of the optical fiber. It is necessary to specify the changes in the optical coupler and find out why these changes occur. This article contains experimental measurement of the impact of gamma radiation Cobalt-60 on the optical couplers of various split performance ratio. Optical passive components, couplers, were exposed to gradually increasing doses of 60Co. Measurements are focused on the overall distribution of the energy of LP01 mode in the core and cladding various branches of SM optical fiber couplers. Graphical and mathematical detect changes in the dissemination of energy coupler after single doses of gamma radiation are useful to understand the phenomenon of accelerated ageing elements of optical networks in environments with an increased incidence of radiation energy.

9586-13, Session 2

Improve the light power of InP based 100nm tunable AMQW lasers using forced electrical confinement method

Hesham M. Enshasy, King Faisal Univ. (Saudi Arabia)

100 nm Broadly tunable InGaAsP/InP asymmetric multiple quantum well (AMQW) ridge waveguide laser diodes has limited applications because of its low output power problem. The current injection efficiency of such lasers in average is 18 %. A FlexPDE simulation model showed that the main reason for this poor current injection efficiency is the ridge structure. Since the ridge structure is an essential part of these type of laser diodes, we proposed a forced electrical confinement method to improve current injection efficiency of these lasers. The simulation data for the proposed method showed that it is possible to increase the current injection efficiency up to 90 %. The simulation data also, showed a reduction of nearly 10°C in the maximum temperature of these devices compared with original AMQW devices. This temperature improvement is significant and can lead to a significant improvement of the laser output power. Experimental data however, give less optimistic results. The experimental data did show improvement in the current injection efficiency but also showed creation of recombination centers that reduce the temperature and power improvement. The proposed method can be efficient but a passivation technique needs to be developed for these devices.

9586-14, Session 2

Design and analysis of rectangular photonic crystal fiber for supercontinuum generation

Than Singh Saini, Ajeet Kumar, Rim Cherif, Ravindra K. Sinha, Mourad Zghal, Delhi Technological Univ. (India)

Now-a-days the mid-infrared supercontinuum generation (SCG) is one of the most exciting research topics due to its major impact on spectroscopy and molecular sensing. SCG is a process in which ultra-short pulses of laser light evolves into the light with a broadband spectrum. It happens when optical pulses pass through a highly nonlinear optical medium. The spectral brightness of supercontinuum is million times brighter than the conventional light sources. The mid-infrared spectral domain is particularly important because of not only it contains two important window in which the earth's atmosphere is relatively transparent but also the strong characteristic vibrational transitions of most of the molecules in this domain. Mid-infrared molecular 'fingerprint region' is applicable in various important applications in different diverse fields such as medical, industry and security. In this work, we present numerical modeling of mid-infrared supercontinuum generation using a new design of rectangular-core photonic crystal fiber pumped with 50 fs optical pulses of 500 W peak power at 2800 nm. Proposed design of photonic crystal fiber offers nonlinear coefficient as high as 20956 W-1km-1 with effective mode area of 2.57 ?m² at pump wavelength. Supercontinuum spectra spanning 1480 - 9990 nm [which covers the atmospheric transparent windows $(3 - 5 \mu m)$ in mid-infrared domain] have been generated using only 4 mm long proposed photonic crystal fiber. Proposed design of rectangular-core photonic crystal fiber has potential applications in gas sensing, food quality control and early cancer diagnostics.

9586-15, Session 2

Design of single mode single polarization large mode area photonic crystal fiber

Kishor D. Naik, Than Singh Saini, Ajeet Kumar, Ravindra K. Sinha, Delhi Technological Univ. (India)

Recently, Photonic crystal fibers have attracted significant attention for their applications in optical communication systems. In polarization sensitive applications photonic crystal fibers with single mode and single polarization are highly desirable. In this paper a rectangular core large mode area photonic crystal fiber has been designed for single mode and single polarization. Large mode area with effective single mode operation is achieved based on higher order mode filtering. Single polarization is obtained by introducing a very large confinement loss for one polarization and very low confinement loss for other polarization of fundamental mode. All the simulations have been performed by using a full vectorial finite element method with anisotropic perfectly matched layer. The variations of confinement loss and effective mode area of x and y-polarization of fundamental mode have been observed by varying the structural parameters of proposed photonic crystal fiber design. At optimized parameters the confinement loss and effective mode area is obtained as 0.9 dB/m and 927 µm2 respectively for x-polarization of fundamental mode. While, the confinement loss is as large as 12.53 dB/m for y-polarized fundamental mode at 1.55 μ m. Therefore, only 1.6 m length of fiber will be sufficient to get x-polarized fundamental mode with effective mode area as large as 927 µm2.

9586-16, Session 2

Design and development of hightemperature sensor using FBG

Venkata Reddy Mamidi, Venkatappa Rao Thumu, National Institute of Technology, Warangal (India) In this article we present design and development of a fiber Bragg grating (FBG)-based novel high-temperature sensor that measures temperature from 20°C to 1500°C. FBGs are the most attractive sensing elements for temperature. For many years, a large quantity of development and research have been reported in the field of FBG low-temperature sensing, but the area of high-temperature sensing is comparatively immature. The standard Type-I FBGs imprinted by weak and strong excimer laser survive up to 450°C and 700°C respectively, beyond the limit the gratings get erased if they are directly subjected to the temperature. However, Fs-IR laser induced Type-II gratings and regenerated gratings are proved to withstand higher-temperature up to 1000°C, they are observed to have short term stability. It is therefore necessary to have an alternative design/technique to stabilize and to enhance the temperature range beyond 1000°C. The designed FBG temperature sensor works based on measurement of the shift in Bragg wavelength that corresponds to the temperature induced strain by making use of a transducer. The transducing element provides temperature dependent strain on FBG by means of differential linear thermal expansion of ceramic alumina and silicon carbide. A Type-I FBG is glued on transducer, and experienced an induced strain of 3.15 x10-6 for increase of each 1°C. In response to this temperature induced strain the Bragg wavelength is found to be shifted at 3.78 pm/°C, over the range of 20-1500 °C. The achieved resolution of the sensor is 1°C.

SPIE. PHOTONICS

OPTICAL ENGINEERING+ APPLICATIONS

9586-17, Session 2

Investigation of electrical, optical and structural properties of sputtered indium tin oxide thin film

Md. Tanvir Hasan, Amar S. Bhalla, Ruyan Guo, The Univ. of Texas at San Antonio (United States)

Transparent and conductive Indium Tin Oxide (ITO) films were grown on borosilicate glass substrate by radio frequency (RF) magnetron sputtering process. The effects of changing sputtering parameters e.g. substrate temperature and RF power on electrical, optical and structural properties were delved. The results showed that films crystallinity, conductivity and transparency were greatly influenced by substrate temperature. It has also been noted that surface roughness and grain size of the films were affected by changing substrate temperature. For the case of 200?C substrate temperature the measured thickness and bandgap of the film was 130.18 nm and 3.66eV respectively. In the visible region, optical transmission for this film was found as ~ 80%. At 200?C, it showed the best electrical and optical properties. By changing the RF power and keeping other deposition parameters as constant, it's been found that the conductivity of the films were increased significantly by increasing the RF power. Just by changing the RF power (35W to 80W) and without applying any substrate temperature it's been seen that the films were still amorphous. By varying the RF power the change in film thickness, surface roughness, grain size and optical transmission were also observed.

9586-18, Session 2

Developing of 2D helical waves in semiconductor under the action of femtosecond laser pulse and external electric field

Vyacheslav A. Trofimov, Vladimir A. Egorenkov, Mariya M. Loginova, Lomonosov Moscow State Univ. (Russian Federation)

We analyze laser-induced periodic structure developing in a semiconductor under the condition of both optical bistability existence and action of 2D external electric field. Optical bistability occurs because of nonlinear dependence of semiconductor absorption coefficient on charged particles concentration. The electron mobility, diffusion of electrons, and laserinduced electric field are taken into account for laser pulse propagation analyzing. 2D external electric field together with electric field of free

Conference 9586: Photonic Fiber and Crystal Devices: **SPIE**, PHOTONICS Advances in Materials and Innovations in **Device Applications IX**



electrons and ionized donors governs the electron motion. Under certain conditions the additional positive inverse loop between electron motion and electric field caused by redistribution of free charged particles appears. As a result, the helical wave for free charged particle concentration of electronhole plasma in semiconductor develops under action of the electric field.

For computer simulation of a problem under consideration, a new finitedifference scheme is proposed. The main feature of proposed methods consists in constructed iterative process.

9586-20, Session 3

Massive orbital angular momentum channels for high capacity optical communication using Dammann gratings

Ting Lei, Shenzhen Univ. (China); Meng Zhang, Nankai Univ. (China); Yuru Li, Zhaohui Li, Jinan Univ. (China); Xiaocong Yuan, Shenzhen Univ. (China)

The orbital angular momentum (OAM) in optical vortex (OV) beams has recently been shown to dramatically increase the data transmission rate in both free-space optical (FSO) and fiber optical communication systems. However, practical applications of massive OAM channels in optical communications still represent significant challenges from the receiver end, namely the parallel detection of multiple OAM states.

In this work, we propose and demonstrate a robust and efficient mechanism, by which collinear OV beams carrying multiple individually modulated OAM states can be demultiplexed and detected in a parallel manner with a Dammann optical vortex grating (DOVG). This contrasts with the previously demonstrated OAM-based communication systems using spiral phase planes or spatial light modulators by enabling simultaneous detection of massive OAM states. Additionally, our proposed scheme only requires two sets of gratings rather than bulky optics setup and expensive opto-electronic devices. In the experiment, we have achieved real-time data detections of 80Tbit/s QPSK signals and off-line detections of 160Tbit/s 16-QAM signals from 1,600 independent channels by demultiplexing 10 OAM states along with 80 wavelengths and two polarizations. We also demonstrate OAM based optical interconnect functions, such as reconfigurable switching, broadcasting and filtering of the communication channels using a digital micromirror device. The DOVG as the key component are capable of further increasing numbers of available OAM channels from tens to hundreds by a straightforward extension to a two-dimensional DOVG. The DOVG also enables uniform power distributions across all the OAM channels removing the power non-uniformity constraint of conventional diffraction gratings.

9586-21, Session 3

Global sensitivity analysis for fine-tuning the dispersion properties of photonic crystal fibers

Igor V. Guryev, Igor A. Sukhoivanov, Jose A. Andrade Lucio, Everardo Vargas Rodrigues, Oleksiy V. Shulika, Univ. de Guanajuato (Mexico)

In the work, we have applied the global sensitivity analysis technique to photonic crystal fibers to investigate the sensitivity of the wavelength of dispersion maximum as well as its absolute value as respect to fiber parameters variation. Namely, we have considered two structures. The first one was hexagonal-symmetric fiber with constant radii within a single ring which has given 5 parameters (pitch, 1st ring radii, 2nd ring radii, 3rd ring radii and radii of external rings). The second structure was hexagonal-symmetric fiber with radii varying within a single ring which has given 7 parameters. According to global sensitivity analysis, in each case, the position and the absolute value of fiber dispersion was computed for random set of the parameter. Then the sensitivity characteristics has been analyzed. The sensitivities obtained in this manner have been used for finetuning the fiber dispersion.

To make the realization of the technique possible, the dispersion characteristics of the photonic crystal fiber have been computed using plane wave expansion (PWE) method. It is not as accurate as, for instance, finite elements method (FEM). However, in case of strongly localized field as is observed in fibers it gives satisfactory results. Moreover, the computation of a single dispersion characteristic using the PWE method takes several minutes while the FEM gives the same result in about 10 hours which is essential when about 1000 computations are required.

The method has been verified by tuning the dispersion characteristic of the fiber presented in previous works.

9586-22, Session 3

Break-through of the spatial bandwidth product limit of digital holographic image detection by a light pipe

Yeh-Wei Yu, Ting-Wei Lin, Ching-Cherng Sun, National Central Univ. (Taiwan)

For the application of digital holographic imaging detection, the spatial bandwidth product is limited by the total pixels number of the image sensor. The product of the field of view (FOV) and the spatial frequency of the target is thus limited. In this paper, we break the spatial bandwidth product limit of a digital holographic microscope with the aid of a light pipe. The light pipe is put between the target and the image sensor and is used to replace the objective lens. When laser beam passes through target, the diffracted light with small diffracting angle illuminates the image sensor directly, the diffracted light with large diffracting angle is also directed to the image sensor by the light pipe. Thus, all of the signal are superposed on the image sensor. In order to retrieve the target, we develop a mirroringmatrix reconstruction method. In our simulation and experiment, we not only demonstrate the enhancement of FOV with constant resolution but also demonstrate the enhancement of resolution with constant FOV. Accordingly, we demonstrate the break-through of the spatial bandwidth product.

9586-23, Session 3

Numerical investigation of silicon nitride trench waveguide

Qiancheng Zhao, Yuewang Huang, Rasul Torun, Shah Rahman, Tuva C. Atasever, Ozdal Boyraz, Univ. of California, Irvine (United States)

We numerically investigated optical properties, including effective refractive index, dispersion coefficient, mode confinement, mode area, and nonlinear parameter, of the sub wavelength silicon nitride trench waveguides fabricated by using conventional lithography. The waveguides are etched 3.5 ?m deep by potassium hydroxide for triangle and trapezoidal waveguides or by plasma etching for rectangular waveguides, then followed by 3 ?m thermal oxidation and 725 nm silicon nitride deposition. 7 trapezoidal and rectangular waveguide structures with different waveguide widths are studied. Simulation reveals that waveguide modes, which are guided in the valley of the trench, are sensitive to waveguide structure. Narrower waveguides can support both TE and TM modes, whereas wider waveguides can support only TE mode. TM mode has higher refractive index in triangular and trapezoidal waveguides, while TE mode has higher refractive index in rectangular waveguides. All waveguides have small dispersion parameter |D| < 100 ps/(nm?km) in the wavelength range from 1350 nm to 1650 nm. The wider the waveguide width, the smaller the absolute value of dispersion parameter is. On the contrary to triangle and trapezoidal waveguides which have normal dispersion, rectangular waveguides are in anomalous dispersion regime. The triangular trench waveguide has 2.73 ?m2 mode area for TE mode and 2.32 ?m2 for TM mode at 1550 nm. The mode area decreases with increasing waveguide width. Waveguides fabricated by dry etching offer larger confinement factor (> 0.5) than wet etching counterparts. However, larger evanescent modes of the waveguides fabricated by wet etching offer higher efficiency in sensing applications. In addition, the calculated nonlinear parameter ? = 0.21 W-1/m for TE



mode and 0.25 W-1/m in triangular trench waveguide indicates promising applications in nonlinear optics.

9586-24, Session 3

Slow light generated via Brillouin scattering in small core chalcogenide photonic crystal fiber

Amira Baili, Rim Cherif, Amine Ben Salem, Ajeet Kumar, Ravindra Kumar Sinha, Mourad Zghal, SUP'COM (Tunisia)

Stimulated brillouin scattering (SBS) is a third-order nonlinear process arising from the interaction between propagating optical and acoustic waves. Nonlinear coupling between traveling-wave photons and phonons through SBS has been widely exploited in many applications, such as optical frequency conversion, radio frequency signal processing, fiber amplifiers and lasers, distributed fiber sensors and slow light. Slowing down the group velocity of light has been recognized as a key technology in future optical communication and microwave photonics systems for its potential applications such as optical delay, data synchronization, optical buffering, and pattern correlation. This technique, based on SBS in optical fibers, has recently attracted interest of many researchers.

In our contribution, we report on full modal analysis of the SBS in newly designed As2Se3-based chalcogenide photonic crystal fibers. Such fibers have drawn much interest because of their capacity of increasing the SBS gain and thus decrease the required input power. A Brillouin gain coefficient, gB, of 9.055 10-9 m.W-1 is found around the acoustic frequency of 8.087 GHz and 1.67 10-10 m.W-1 around 8.347 GHz in 1.69 µm core diameter. The calculated effective mode area is 1.5µm2 at 1550 nm. The Brillouin threshold Pth is evaluated to be 0.82 mW for a 10 m long fiber. A time delay of 94 ns can be achieved using only 1.15 mW pump power in 10 m As2Se3-based chalcogenide photonic crystal fiber.

9586-25, Session 3

Angular interrogation of evanescent wave absorption spectroscopy based sensors for harsh environment sensing applications

Paul R. Ohodnicki Jr., Michael P. Buric, Zsolt L. Poole, National Energy Technology Lab. (United States)

Evanescent wave absorption based spectroscopy (EWAS) sensors offer a number of unique advantages which include compatibility with remote optical sensing, simplicity of sensor design, low cost of sensing elements, and compatibility with harsh environment sensing applications. This presentation will focus on a detailed comparison between modeling of wave propagation in EWAS based sensors and measured transmitted intensity in selected sensors for harsh environment applications as a function of both launch and collection optics.

In particular, EWAS sensors that employ functional sensing elements of metal oxides and nanocomposite sensing layers targeted for ambient and high temperature H2 sensing will be investigated. Experimentally derived optical transmission spectra as a function of light launch conditions as well as collection optics will be directly compared with theoretically derived results using a single-layer waveguide model that permits finite film thickness relevant for the sensor layers under investigation. Based upon the results obtained, the potential for sensing response optimization using advanced interrogation approaches in this unique class of sensors will be demonstrated and critically discussed.

9586-26, Session 3

Simultaneous multi-parametric sensing in phase-shifted waveguide gratings

Renilkumar Mudachathi, Takuo Tanaka, RIKEN (Japan);

Manoj M. Varma, Indian Institute of Science (India)

The emerging customized point of care (POC) and home health care diagnostic applications demand the development of highly integrated, compact, smart and low cost biosensors. The recent advances in the integrated silicon photonics have stimulated research around the globe on the development of such label free chemical and biosensing platform using photonic resonant structures. We present a scheme for multi parametric sensing based on phase-shifted waveguide grating.

The device is a grated waveguide with a defect at the center, in which multiple transmission modes could be excited containing defect mode and band edge transmissions. These transmission modes respond differently for different parameters such as surrounding refractive index change, temperature gradient and strain. That is, the same sensor element produces multiple signals; each carries separate information of the measurands. A semi-analytical model of the device in the general framework of transfer matrix method has shown that the wavelength of defect mode transmission depends only on the defect layer and those of band edge transmission on the bulk grating properties, providing a means for simultaneous multiparametric sensing. Several devices with and without defect layer have been fabricated on SOI wafer using the micro-fabrication technique. The presence of multiple transmission modes with defect mode wavelength at 1545nm and band edge mode wavelengths at 1510nm and 1565nm providing a wide dynamic range of about 50nm was confirmed. In the presentation, the simultaneous multi-parametric sensing experiment will be demonstrated.

9586-27, Session 3

Digital holographic interferometer with a self-pumped phase conjugating mirror

Prathan Buranasiri, King Mongkut's Institute of Technology Ladkrabang (Thailand)

A digital holographic interferometer having a self-pumped phase conjugating mirror using cerium doped barium titanate crystal is demonstrated. The self-pumped phase conjugate beam is readily generated from stimulated photorefractive scattering and four-wave mixing inside the crystal. First, the fringe patterns obtained from the interferometer have been investigated. Then, the interferometer has been used to exploring a fingerprint pattern on a plain mirror. In both experiments, the images recorded on CMOS camera have been reconstructed by using numerical process. Finally, the experimental image results are compared with the image results that get from the conventional interferometer with regular mirrors.

9586-28, Session 4

Nanosecond speed KTN beam deflector

Shizhuo Yin, Juhung Chao, Wenbin Zhu, Chao Wang, The Pennsylvania State Univ. (United States); Robert Hoffman, U.S. Army Research Lab. (United States)

In this paper, a nanosecond speed KTN beam deflector is presented. The beam deflector is based on the combination of pre-injected space charge field and high speed (nanosecond) switching field. A beam deflection speed <= 1 ns was demonstrated, which was faster than the speed predicted previously (on the order of several hundred MHz). The experimentally results confirmed that the speed limitation of KTN beam deflector was not limited by the EO effect itself but the driving electric source and circuit. With a faster speed driving source and circuit, it is possible to develop GHz frequency beam deflector.

9586-29, Session 4

Fibre optic sensors for load-displacement measurements and its comparisons to piezo sensor based electromechanical admittance signatures

Muneesh Maheshwari, Venu Gopal M. Annamdas, John H. L. Pang, Swee Chuan Tjin, Anand K. Asundi, Nanyang Technological Univ. (Singapore)

Structural health monitoring techniques using smart materials are on rise to meet the ever ending demand due to increased construction and manufacturing activities worldwide. The civil-structural components such as slabs, beams and columns and aero-components such as wings are constantly subjected to some or the other forms of external loading. This article thus focuses on strain measurement due to loading-unloading cycle for a simply supported aluminum beam using multiple smart materials. On the specimen, fibre optic polarimetric sensor (FOPS) and fibre Bragg grating (FBG) sensors were glued. Piezoelectric wafer active sensor (PWAS) was also bonded at the centre of the specimen. FOPS and FBG provided the global and local strain measurements respectively whereas, PWAS predicted boundary condition variations by electromechanical admittance signatures. Thus these multiple smart materials together successfully assessed the condition of structure for loading and unloading tests.

9586-30, Session 4

Supersymmetric mode converters

Matthias Heinrich, Friedrich-Schiller-Univ. Jena (Germany); Mohammad-Ali Miri, CREOL, The College of Optics and Photonics, Univ. of Central Florida (United States); Simon Stützer, Stefan Nolte, Alexander Szameit, Friedrich-Schiller-Univ. Jena (Germany); Demetrios N. Christodoulides, CREOL, The College of Optics and Photonics, Univ. of Central Florida (United States)

In recent years, the ever-increasing demand for high-capacity transmission systems has driven remarkable advances in technologies that encode information on an optical signal. Mode-division multiplexing makes use of individual modes supported by an optical waveguide as mutually orthogonal channels. The key requirement in this approach is the capability to selectively populate and extract specific modes. Optical supersymmetry (SUSY) has recently been proposed as a particularly elegant way to resolve this design challenge in a manner that is inherently scalable, and at the same time maintains compatibility with existing multiplexing strategies.

Supersymmetric partners of multimode waveguides are characterized by the fact that they share all of their effective indices with the original waveguide. The crucial exception is the fundamental mode, which is absent from the spectrum of the partner waveguide. Here, we demonstrate experimentally how this global phase-matching property can be exploited for efficient mode conversion. Multimode structures and their superpartners are experimentally realized in coupled networks of femtosecond laser-written waveguides, and the corresponding light dynamics are directly observed by means of fluorescence microscopy. We show that SUSY transformations can readily facilitate the removal of the fundamental mode from multimode optical structures. In turn, hierarchical sequences of such SUSY partners naturally implement the conversion between modes of adjacent order. Our experiments illustrate just one of the many possibilities of how SUSY may serve as a building block for integrated mode-division multiplexing arrangements. Supersymmetric notions may enrich and expand integrated photonics by versatile optical components and desirable, yet previously unattainable, functionalities.

9586-31, Session 4

Design and implementation of super broadband high speed waveguide switches

OPTICAL ENGINEERING+

APPLICATIONS

Shizhuo Yin, Wenbin Zhu, Juhung Chao, Chao Wang, Jimmy Yao, The Pennsylvania State Univ. (United States)

In this paper, based on the theory of dynamic waveguiding effect in nanodisordered KTN crystals, a detailed design and implementation of a super broadband 1x2 high speed waveguide switch is presented. The important waveguide parameters, including the dimension, the refractive index distribution, and the electric field distribution within the waveguide are quantitatively simulated and analyzed. An experimental verification of switching effect based on the design is also conducted, which confirmed the design. The broadband and high speed nature of such kind of switch can play a key role in data center networks and cloud computing, which needs low power consumption and high speed switches.

9586-32, Session 4

Slow light effect in pinch waveguide in photonic crystal

Ravindra K. Sinha, Preeti Rani, Yogita Kalra, Delhi Technological Univ. (India)

Recently, photonic crystal has attracted wide attention due to its feasibility for slow light effect. Till now various designs has been proposed for the slow light effect in photonic crystal based waveguides. In this paper, we have proposed slow light effect in pinch waveguide created in photonic crystal. The proposed design consists of two dimensional (2D) triangular arrangement of air holes in silicon on insulator (SOI) substrate with the radius of air holes, r=0.3a, where 'a' is the lattice constant. The 2D effective refractive index method has been used to estimate the properties of slow light. Initially a row of air holes has been removed from the bulk arrangement and a pinch waveguide has been created by joining a row of air holes with the air slots. The pinch photonic crystal waveguide leads to the enhancement of localized fields than those of the traditional slot or photonic crystal waveguide structures. The size and shape of the pinch waveguide has been optimized to get the slow light effect. For the proposed structure the group index and group velocity dispersion (GVD) has been calculated from the dispersion relation of the pinch waveguide structure. From the calculations it has been found out that for the proposed structure the group index is high and GVD is low, which are the basic requirements for the slow light effect. The confinement of light in the pinch waveguide with slow light can be useful for sensor applications.

9586-33, Session 4

Investigation the effects of dispersion and intensity on supercontinuum spectrum

Abolfazl Safaei, Mohammad Agha Bolorizadeh, Aliasghar Zakerifar, Graduate Univ. of Advanced Technology -Kerman (Iran, Islamic Republic of)

When a light pulse is launched into a highly nonlinear fiber, the frequency broadening is observed due to dispersive and nonlinear effects, known as Supercontinuum Generation. One of the most significant current discussions in this course (SC) is supercontinuum generation in photonic crystal fiber.

This article provides numerically study of the nonlinear effects on a light pulse that is launched into a Photonic crystal fiber. The basic theory on SC generation process is explained briefly and more than that the physics behind the SC mechanisms is introduced. Also the higher order dispersion effects on Supercontinuum (SC) generation in microstructure fibers are analyzed by studying the temporal and frequency dependence of the ejected pulse via numerical study. As each dispersion coefficient cause a deformation in pulse shape, we work out to consider the effect of higher order dispersion on pulse shape.

Conference 9586: Photonic Fiber and Crystal Devices: Advances in Materials and Innovations in Device Applications IX



The equation that governs supercontinuum generation is generalized nonlinear equation. The solution of this equation is Soliton that have different orders (N). However, there are a myriad of numerical methods to solve the equation, in this essay, Split Step Fourier method is applied to reach the aims.

To sum up, we investigate the higher order dispersion effects on supercontinuum (SC) generation in microstructure fibers. We also investigate the Soliton formation and spectrum broadening spectrum. In these processes, we observed dispersive wave generated due to Soliton fission. Here, we solve nonlinear Schrodinger equation by Split Step Fourier method.

9586-19, Session PMon

Integrated Ti:lithium niobate digital optical switch (DOS) for quantum information processing

Richard S. Kim, Eunsung Shin, Attila Szep, Michael Fanto, Paul M. Alsing, Air Force Research Lab. (United States); Antao Chen, Beckman Coulter, Inc. (United States)

Integrated photonic switches have been extensively researched for a long time in photonic communications to develop large-capacity optical cross connections or add/drop multiplexers. Digital optical switch (DOS) has several advantages including its high insensitivity to wavelength, refractive index, polarization, and temperature. Due to its step-like switch response to an applied voltage, DOS can be an effective tool to switch or distribute simultaneously its output power of both TM and TE modes with certain splitting ratios; for example, 100%:0% for TM wave and 66%:33% for TE wave. In this work, a novel design of 1x2 Y-branch DOS based on Ti:LiNbO3 optical waveguide operating at a wavelength of 810nm is simulated based on the BEAMPROP, and fabricated for application of simultaneous switching of both modes in quantum information processing (QIP). Its optical crosstalk, optical loss, tuning ability of splitting ratio, and required driving power are experimentally carried out and its potentials for manipulating modal qubits in photonic quantum circuit are discussed.

9586-34, Session PMon

Post-shaping optical fiber taper filters

Alejandro Martínez-Rios, Guillermo Salceda-Delgado, Ctr. de Investigaciones en Óptica, A.C. (Mexico); Romeo Selvas-Aguilar, Univ. Autónoma de Nuevo León (Mexico); Gilberto Anzueto-Sanchez, Univ. Autónoma del Estado de Morelos (Mexico); Victor Manuel Duran-Ramirez, Univ. de Guadalajara (Mexico); Daniel Toral-Acosta, Univ. Autónoma de Nuevo León (Mexico)

Geometrical shaping of non-adiabatic single tapers is used to modify the filtering characteristics. The fiber tapers are shaped by successive tapering. The taper shaping produces deeper rejection bands. As an application of the shaped tapers, fluidic temperature sensing cells were fabricated. In a first case, the wavelength shift of a single rejection band was monitored, showing a nonlinear response and low sensitivity to temperature changes. In a second case, a shaped taper fluidic cell containing two rejection bands was used, and the wavelength shift of the half intensity points of the transmission band (between the rejection bands) was taken as a measure of the temperature change. In this case, the fluidic cell showed a linear sensitivity of 481.9 pm/°C in a temperature range of 25°C-60°C.

9586-35, Session PMon

3 x 3 free-space optical router based on crossbar network and its control algorithm

Peipei Hou, Jianfeng Sun, Zhou Yu, Wei Lu, Lijuan Wang, Liren Liu, Shanghai Institute of Optics and Fine Mechanics (China)

A 3 ? 3 free-space optical router, which comprises optical switches and polarizing beam splitter (PBS) and based on crossbar network, is proposed in this paper. A control algorithm for the 3 ? 3 free-space optical router is also developed to achieve rapid control without rearrangement. In order to test the performance of the network based on 3 ? 3 freespace optical router and that of the algorithm developed for the optical router, experiments are designed. The experiment results show that the interconnection network based on the 3 ? 3 free-space optical router has low cross talk, fast connection speed. Under the control of the algorithm developed, a non-block and real free interconnection network is obtained based on the 3 ? 3 free-space optical router we proposed.

9586-36, Session PMon

According to difference by poly styreneblock-poly-2-vinyl pyridine of molecular weight and swelling solution change, color difference in particle of photonic crystal

Jin Youb Lim, Hongik Univ. (Korea, Republic of)

Commonly unidimensional construct has restriction of viewing angle. We report a new facile strategy to Particle Photonic Crystal which is ellipsoidal block copolymer nanoparticles. it has a wider viewing angle as well as easy to make. We made particle of photonic crystal based on Poly Styrene-block-Poly-2-Vinyl Pyridine(PS-b-P2VP) in chloroform. After using Poly Vinyl Alcohol(PVA), It was in state of emulsion and self assembly method was followed by. In a first step, we observed particle structure variation according to difference in molecular weight such as 25k-25k, 52k-57k, 75k-66.5k. After wards, we exhibited how particle structure changed by swelling solution of difference which is Alcohol. The molecular structure of particle photonic crystal was investigated by Transmission Electron Microscope and Dynamic Light Scattering. The color was measured by color-difference meter.

9586-37, Session PMon

According to diblock copolymer photonic film of various molecular weight, difference of wavelength change

Sang Wook Lee, Hongik Univ. (Korea, Republic of)

Optical properties of photonic crystal film were investigated by tuning photonic band gap (PBG). The lamellar-forming photonic films were prepared by nearly symmetric poly(styrene-b-2-vinyl pyridine) (PS-b-P2VP) block copolymers. Molecular weight of PS-P2VP is 25k-25k, 52k-57k, 57k-57k, 75k-66.5k, 190k-190k(g/mol), respectively. The lamellar stacks, which are alternating layers of hydrophilic and hydrophobic moiety of PSb-P2VP, are obtained by exposing the spin coated film under chloroform vapor. The band gaps of the lamellar films interestingly varied after immersion into the quaternizing solvents containing 5wt% of iodomethane solubilized in n-hexane. Reflection color of photonic film was measured by uv-vis spectrophotometer. The change of pH gradation, metal ions and solvents of films can be changing the photonic band gap by molecular weight of PS-b-P2VP. The methods of control of reflection color show the shift of wavelength which is red shift or blue shift. 9586-38, Session PMon

The ageing process of optical couplers by gamma irradiation

Lukas Bednarek, V?B-Technical Univ. of Ostrava (Czech Republic); Ondrej Marcinka, Research Ctr. Rez (Czech Republic); Frantisek Perecar, Martin Papes, Lukas Hajek, Jan Nedoma, Vladimir Vasinek, V?B-Technical Univ. of Ostrava (Czech Republic)

Scientists have recently discovered that the ageing process of optical elements is faster than it was originally anticipated. It is mostly due to the multiple increase of the optical power in optical components, the introduction of wavelength division multiplexers and, overall, the increased flow of traffic in optical communications. This article examines the ageing process of optical couplers and it focuses on their performance parameters. It describes the measurement procedure followed by the evaluation of the measurement results. To accelerate the ageing process, gamma irradiation from 60Co was used. The results of the measurements of the optical coupler with one input and eight outputs (1:8) were summarized. The results gained by measuring of the optical coupler with one input and four outputs (1:4) as well as of the optical couplers with one input and two outputs (1:2) with different dividing ratios were also processed. The optical powers were measured on the input and the outputs of each branch of each optical coupler at the wavelengths of 1310 nm and 1550 nm. The parameters of the optical couplers were subsequently calculated according to the appropriate formulas. These parameters were the insertion loss of the individual branches, split ratio, total losses, homogeneity of the losses and directionalities alias cross-talk between the individual output branches. The gathered data were summarized before and after the first irradiation when the configuration of the couplers was 1:8 and 1:4. The data were summarized after the second irradiation when the configuration of the couplers was 1:2.

9586-39, Session PMon

DLC and AIN thin films influence the thermal conduction of HPLED light

Ming Seng Hsu, Chinese Military Academy (Taiwan); Ching Yao Hsu, Cantwell-Sacred Heart of Mary High School (United States); Jen Wei Huang, Feng Lin Shyu, Chinese Military Academy (Taiwan)

Thermal dissipation had an important influence in the effect and life of light emitting diodes (LED) because it enables transfer the heat away from electric device to the aluminum plate that can be used for heat removal. In the industrial processing, the quality of the thermal dissipation decides by the gumming technique between the PCB and aluminum plate. In this study, we fabricated double layer ceramic thin films of diamond like carbon (DLC) and alumina nitride (AIN) by vacuum sputtering soldered the substrate of high power light emitting diodes (HPLED) light to check the heat conduction. The ceramic dielectric coatings were characterized by several subsequent analyses, especially the measurement of real work temperature. The X-Ray diffraction (XRD) patterns reveal those ceramic phases were successfully grown onto the substrate. The work temperatures show DLC and AIN thin film coating had limited the heat transfer by the lower thermal conductivity, 3.5 Wm-1K-1, of DLC. Obviously, it hadn't transferred heat and limited work temperature of HPLED better than AIN thin film only.

9586-40, Session PMon

S-band multi-wavelength Brillouin Raman fiber laser utilizing FBG and Raman amplifier in the ring cavity

Nor Azura Malini B. Ahmad Hambali, Nur Elina B. Anwar, Muhammad Halim B. Abdul Wahid, Mukhzeer B. Mohamad Shahimin, Mohd Azarulsani B. Md. Azidin, Amira Zakiah B. Malek, Roshidah B. Yusof, Univ. Malaysia Perlis (Malaysia)

OPTICAL ENGINEERING+

APPLICATIONS

This paper is focusing on simulates and evaluates the performance for S-band multiwavelength Brillouin-Raman fiber laser (MBRFL) utilizing Fiber Bragg Grating (FBG) and Raman Amplifier in ring cavity using Optisystem software. Raman amplifier- average power model is employed for signals amplification. This laser system is operates in S-band wavelength region (1566 nm to 1620 nm) due to vast demanding on transmitting the information. Multiwavelength fiber lasers based on hybrid Brillouin-Raman gain configuration supported by Rayleigh scattering effect have attracted significant research interest due to the large numbers of channel generation from a single light source. When narrow bandwidth Brillouin gain combines with broad bandwidth Raman gains, hundreds of channels would be generated. In MBRFL configuration, single mode fiber (SMF) is utilized as the nonlinear gain media. When a single laser launches into a distributed Raman gain area, it grows very fast through stimulated Raman scattering, and when it acquires threshold condition, it is back-scattered through nonlinear Brillouin and Rayleigh effects, inelastically and elastically inside the gain media respectively. From output results, the output coupling ratio of 90% provides the higher output Stokes power at input power at 20 dBm and Raman pump power is at 14dBm. The average output powers are around 20 dBm to 45dBm. As the input power increases, the number of Stokes signals also increases, because there will be more than enough power to overcome the SBS threshold. Meanwhile, the total number of the number of Stokes signal produces is 7.

9586-41, Session PMon

Two-center recording in LiNbO3:Fe:Ru and LiNbO3:Ce:Ru crystals

Zhifang Chai, East China Normal Univ. (China)

To realize nonvolatile photorefractive holograms, Buse et al., proposed a two-center holographic recording method in doubly doped LiNbO3:Fe:Mn crystals in 1998. The key point of this technique is that two different dopants are used to provide shallower and deeper centers in LiNbO3 crystals. From 1998, the development of new materials with different dopants has become an important direction for two-center recording, so that the optimized performance can be obtained. Doubly-doped LiNbO3 crystals, such as LiNbO3:Fe:Cu, LiNbO3:Ce:Cu, and LiNbO3:Ce:Mn et al., are reported to perform two-center recording effectively. Low holographic scatter noise and high fixed diffraction efficiency can be obtained in LiNbO3:Ce:Cu crystals.

Ru can be used as the deep center in doubly doped LiNbO3 crystals, and LiNbO3:Fe:Ru and LiNbO3:Ce:Ru crystals can be used to realize twocenter recording effectively, too. In this paper, the two-center recording with 633nm recording and 404nm sensitizing is performed in oxidized LiNbO3:Fe:Ru and LiNbO3:Ce:Ru crystals, respectively. Performance measures, such as dynamic range, recording sensitivity and holographic scatter noise, are calculated and compared according to the time evolution curves of diffraction efficiency. The results show that the high recording sensitivity and dynamic range can be obtained in LiNbO3:Fe:Ru crystal. However, the low scattering noise can be observed in LiNbO3:Ce:Ru crystals. At last, the theoretical analysis is carried out based on jointly solving the two-center material equations and the coupled-wave equations.

9586-42, Session PMon

Photon management assisted by surface modes on a photonic crystal platform

Angelo Angelini, Politecnico di Torino (Italy); Luca Boarino, Istituto Nazionale di Ricerca Metrologica (Italy); Peter Munzert, Fraunhofer-Institut für Angewandte Optik und Feinmechanik (Germany); Natascia De Leo, Istituto Nazionale di Ricerca Metrologica (Italy); Emiliano Descrovi, Politecnico di Torino (Italv)

The ability of modifying the radiation pattern of emitters is gaining attention

Conference 9586: Photonic Fiber and Crystal Devices: Advances in Materials and Innovations in Device Applications IX



in a variety of applications related to nanophotonics, such as few-molecule and quantum emitters detection. In this framework, Surface Plasmon Coupled Emission (SPCE) has demonstrated to be an effective way to address this issue. Generally, plasmonic-based mechanisms exploit a nearfield transfer of energy from the emitters to plasmonic modes. However, the main drawback in using plasmons on metal is represented by ohmic losses, producing broad resonances and absorption of useful signal.

An effect similar to SPCE occurs on properly tailored one dimensional photonic crystals (1DPC). 1DPC can indeed sustain resonant surface electromagnetic modes, that we call Bloch Surface Waves (BSWs), at the truncation interface of the dielectric stack.

Due to the low absorption coefficient of the 1DCP materials, BSW-coupled fluorescence can propagate for longer distances as compared to plasmons. In addition, the use of dielectric structures offers interesting advantages such as a wide spectral tunability (from UV to IR), the possibility to have either TE or TM polarized BSW and higher Q-factors.

By properly structuring the surface of 1DPC, light coupled to BSWs can be manipulated in several ways (e.g. diffracted, guided, focused). In particular, spontaneous emission of emitters lying on the surface of 1DPC can be efficiently beamed out in arbitrary directions with low divergence by employing surface relief diffraction gratings.

An implementation of a biosensing platform based on such fluorescence beaming effect is provided, showing an enhancement factor of the detected fluorescence of about 100 if compared with the signal detected on a simple glass coverslip using an equal numerical aperture collection system.

9586-43, Session PMon

A tunable wavelength erbium doped fiber ring laser based on mechanically induced long-period fiber gratings

Miguel Perez Maciel, Yanelis López Dieguez, Roberto Rojas Laguna, Eduardo H. Huerta Masscote, Daniel Jauregui Vazquez, Juan M. Sierra Hernández, José Alejandro Montenegro Orenday, Julián Móises Estudillo Ayala, Univ. de Guanajuato (Mexico)

In this work, a tunable wavelength erbium doped fiber ring laser is proposed and demonstrated; the ring fiber laser is based on mechanically induced long-period fiber gratings (LPFG). In the scheme a semiconductor laser of 980nm is pumped in the cavity, where 4.30 meters of erbium doped fiber is used like active medium, the signal laser is monitoring by using a coupler 90/10, here the 90% of the signal is feedback into the cavity and only the 10% is analyzed by the optical spectrum analyzer (OSA); by using an insulator the light in the cavity has a single direction. In order to, tuning the laser, a controlled load was applied to the mechanical long period grating as a result the transmission spectrum change. The load was applied by pressing a plate with periodic grooves against a short length and controlled by using a digital torque tester. The grooves used in the plates have a period around 630 μ m. However, this set-up, can be easily reconfigurable to tuned other wavelengths by a simple modification on the groves. Moreover, control polarization was set in the cavity to provided stability and by changing the polarization of our system the single line emission can be tuned in the L-band telecommunications, where the laser line presents high stability in the room temperature. Furthermore, the mechanical long-period fiber gratings implemented in this work offers unique advantages, they are tunable, erasable, reconfigurable and exhibit transmission spectra and high thermal stability, similar to photoinduced LPFG's. This laser present a stability of 60 minutes and can be tuned by applying a .05lbf.

9586-44, Session PMon

A cylindrical structure fiber-optic amplifier with broad-side pump coupling

Steven R. Laxton, Tyler Bravo, Christi K. Madsen, Texas A&M Univ. (United States) We propose a unique physical structure for coupling a low brightness source to a dual-clad fiber for amplification. A pumped-cylindrical structure is used to greatly enhance the area for pump coupling over standard end-fiber coupling into a dual-clad fiber. In addition, it provides a compact volume for fiber amplification. Pump signal is inserted by photonic broadside coupling into the external surface area of the coil. We will discuss the basic coupling mechanism, simulations and prototype fabrication overview. Our first experimental results will employ a 980nm pump laser and 1550nm for the amplified signal. We will then test using a broadband source and compare to the pump laser results. Excess losses, mainly due to bend loss, are characterized across the wavelength range of interest.

9586-45, Session PMon

Investigation of the laser energy parameters for laser initiation

Natalia Korobova, Veniamin A. Vodopyanov, Evgeny Paderin, Evgeny Sholokhov, Sergey P. Timoshenkov, Valeri Timoshenkov, National Research Univ. of Electronic Technology (Russian Federation)

Insensitivity light detonators to electromagnetic interference and static electricity charges have been used as one of the advantages of laser initiation. High level of light detonator insulation from the false pulse has been done, as in the optical range there were no random sources with sufficient power to undermine the detonator. Pulse energy density was determined using Yb fiber laser with Ho3+ gate which worked in a Q-switched modulation. The calculations of the mode change field, power density and energy density according to the distance from the fiber end at the maximum pump current have been presented. Composite materials with thickness 0.3 to 0.5 mm were used as samples of polymeric matrix and reinforced by nanocarbon particles. During the study of the sample pulse characteristics focusing node input was using and sample was placed in the focus. This scheme actually complicates the design of the input node radiation, but at the same time potentially allows for greater energy per pulse correctly focused beam. For the beam at the output of focusing input node and the maximum pump current we had the following values: mode field diameter at the fiber end 9.88 um, mode field area of 7.66•10-7 cm2, power density (irradiance) in the beam 5.22 •106 W/cm2, energy density at the output of the focusing input node 261 mJ/cm2. It was experimentally established that burning time order of several milliseconds can be achieved by the correct selection of the focus radiation. Recommendations for the design input node of radiation to initiate known types of explosives have been done

9586-46, Session PMon

Sputtered germanium/silicon devices for photonics applications

Naga Korivi, Melvin DeBerry, Nabila Nujhat, Jean-Pierre Papouloute, Li Jiang, Tuskegee Univ. (United States)

We report on the ongoing investigation of germanium (Ge)/silicon (Si) photodetector devices for photonics applications. The devices are made by depositing Ge and in some cases, Si layers by radio frequency and direct current magnetron sputtering and patterning them by standard ultra-violet light photolithography. The development of Ge/Si devices has till date involved methods such as molecular beam epitaxy to deposit Ge on Si and SOI wafers. The sputtering-based developments in our present research are expected to provide for a flexible and economically viable manufacturing process for such devices.

In this work, photodetector devices with diode type structures and heterojunctions integrated with sputtered Si waveguides are being investigated. The devices and waveguide structures are made by sputtering Ge and Si layers on a substrate, followed by a combination of photolithographic patterning and rapid thermal annealing to impart a polycrystalline nature to the sputtered materials. All sputtering processes are done at an elevated temperature (450-500 °C). The annealing is done in nitrogen ambient at Conference 9586: Photonic Fiber and Crystal Devices: **SPIE**, PHOTONICS Advances in Materials and Innovations in **Device Applications IX**



temperatures of more than 600 °C. Initial prototypes of sputtered Ge/Si diodes have been developed, while fabrication of heterojunction field effect transistors is in progress. Stand-alone Si waveguides have been fabricated with a polymeric cladding. The fabricated devices and waveguides have been evaluated for response to 1500 nm wavelength light through an externally mounted optical fiber. A significant difference is observed in current-voltage behavior under the dark and illuminated conditions, indicating a clear response to 1550 nm light.

9586-47, Session PMon

Memristor memory element based on ZnO thin film structures

Armen R. Poghosyan, Elbak Y. Elbakyan, Institute for Physical Research (Armenia); Ruyan Guo, The Univ. of Texas at San Antonio (United States); Ruben K. Hovsepyan, Institute for Physical Research (Armenia)

The memristor element for random access memory (resistance random access memory - ReRAM) has been developed and studied. The developed structure consists of a Schottky diode (1D) based on ZnO:Ga/ ZnO:Li/ZnO heterostructure and memristor (1R) based Pt/ZnO/ZnO:Li/ Al heterostructure. Thus the unipolar memristor memory element of 1D1R type has been obtained. The heterostructures were made by the electronbeam vacuum deposition method. The laboratory samples of the memory elements have been prepared and their characteristics have been studied. The proposed device has a high stability and withstands 1000 switching cycles without derating.

9586-48, Session PMon

80 channels HDTV signal transmission using optical carrier suppression scheme and injection-locked FPLDs

Ardhendu S. Patra, Sidho-Kanho-Birsha Univ. (India)

A novel bidirectional ROF configuration has been proposed and developed to transmit 80 channels HDTV signal of datat-rate 1.25 Gbps over 80 km SMF integrating mutually injection locking, optical carrier suppression (OCS) and reflective semiconductor optical amplifier (RSOA) based remodulation techniques. The RSOA is deployed at the user end to reuse and remodulate the downstream HDTV signal to upstream transportation over same 80km fiber-link. Noise due to the Rayleigh backscattering and Fresnel backreflection are the main limitation for the RSOA based configurations. To reduce these effects and the power consumption in the transmission the OCS scheme has been used in the ROF designs. As the power consumption is reduced by the suppressing carrier mode the effects of backscattering is also degraded. Therefore the crosstalk and inter-symbol interference are also mitigated. Dual-arm LiNbO3 Mach-Zehnder modulator which is biased at $V\varpi$ and driven by two complementary RF signals of 30GHz is used at transmitter end to realize the OCS scheme. To make cost-effective, the scheme of mutually injection locking of FPLDs has been used. The uplink and downlink transmission performances are observed and analyzed by excellent eye-diagram and low bit error rate values. The received optical power is recorded as -21dBm and -18dBm at the BER of 10-9 order for downlink and uplink transmission respectively. At the 80 km length of SMF the power penalty is 3dB between the uplink and downlink transmission. This architecture can play an important role in the future broadband access network to transmit HDTV signals over long-haul SMF.

9586-49, Session PMon

Bidirectional and simultaneous FTTX/ Ethernet services using RSOA based remodulation and polarization multiplexing technique

Ardhendu S. Patra, Anindya Sundar Das, Sidho-Kanho-Birsha Univ. (India)

A bidirectional WDM-PON architecture has been investigated for simultaneous transmission of 2.5 Gbps and 10 Gbps over 50 km single mode fiber employing polarization multiplexing (POLMUX) technique at OLT and ONU. POLMUX technique has been introduced to minimize the cost and complication of the multi-service provider systems. This scheme is based on equally splitting an optical field into two components and employs them as optical carrier to transmit simultaneously independent data-rates over same wavelength and increases the spectral efficiency and transmission capacity of the system. The POLMUX technique is embraced by polarization beam splitters and polarization beam combiners in the system. Unlike the previous works RSOA have been used for reusing and remodulation of 2.5 Gbps and 10 Gbps at the same time in upstream transmission over the same 50km SMF. The downlink and uplink transmission performances are observed by eye diagrams and bit error rate (BER) values, obtained at BER analyzer. The clear eye diagrams, low BER values and low power penalties are observed at downlink and uplink and prove that the proposed configuration is suitable to provide the FTTH, Ethernet services simultaneously to the user. Using of single source for different services have reduced the cost of the system and increases the spectral efficiency of configuration. The transmission capacity is also increased as our proposed architecture have successfully transmitted 10 Gbps to 50 km reach in uplink, which is much better than the previous works. Therefore this configuration will be suitable for the next generation high speed networks.

9586-50, Session PMon

Gray-level encoded fringe projection for profile measurements

Wei-Hung Su, Bo-Chin Huang, National Sun Yat-Sen Univ. (Taiwan)

An encoding algorithm to identify the fringe orders for Fourier transform profilometry is described. Phase unwrapping is then performed with reference to the encoding algorithm. Even though the inspected object is colorful or sensitive to the reflectance variation, unwrapping can be performed without ambiguity. The computation cost is very low, and its unwrapped errors can be confined in a local area.

9586-51, Session PMon

Projected fringe profilometry for metal surfaces

Wei-Hung Su, Bo-Chin Huang, National Sun Yat-Sen Univ. (Taiwan)

A non-scanning fringe projection method to describe the 3D profile of a metal surface is proposed. Fringes projected on the inspected surfaces are formed by launching a laser beam into a hologram. The size of the hologram is large enough that fringes on the surface are collected from various diffraction directions. Shinny or specular reflection can be efficiently reduced. This makes it possible to inspect the entire metal surface at a desirable viewpoint.



9586-52, Session PMon

Three-dimensional shape measurements using endoscopes

Wei-Hung Su, Tzu-Chien Hsu, Cho-Yo Kuo, National Sun Yat-Sen Univ. (Taiwan)

We present a structured light illumination system embedded into an endoscope to describe the absolute shape of an inspected object. A fringe pattern generated by launching incoherent light waves into a volume hologram is projected on the inspected surface. The endoscope observes the projected fringes at another point of view. Fringes on the obtained image are deformed both by the topography of the object, and are analyzable to retrieve the 3D shape.

9586-53, Session PMon

A reliable image processing algorithm using the scanning fringe projection for 3D profile measurements

Wei-Hung Su, National Sun Yat-Sen Univ. (Taiwan); Nai-Jen Cheng, National Kaohsiung Univ. of Applied Sciences (Taiwan)

A reliable image processing method is provided to enhance the accuracy of the scanning fringe projection technique. Noises and errors for surfaces on the edge area can be efficiently detected and reduced. To accurately describe the shape of a complicated object is available.

Conference 9587: Optical Data Storage 2015

Sunday 9 -9 August 2015

Part of Proceedings of SPIE Vol. 9587 Optical Data Storage 2015

9587-1, Session 1

Multi-terabit/in2 holographic data storage demonstration (Invited Paper)

Mark R. Ayres, Ken E. Anderson, Fred Askham, Brad Sissom, Adam C. Urness, Akonia Holographics, LLC (United States)

Holographic data storage (HDS) employs the physics of holography to record digital data in three dimensions in a highly stable photopolymer medium. As such, it enjoys a substantial density advantage over rival technologies which are fundamentally two-dimensional. We have previously reported results using a demonstrator designed to implement dynamic aperture multiplexing, quadrature homodyne detection, and phase quadrature holographic multiplexing in a monocular architecture. In this presentation, we report on further progress and recording density results.

The Akonia API demonstrator previously achieved a raw recording density of 1.5 Tbit/in2, easily exceeding that of commercially available technologies. This result was accomplished using the new DRED high-dynamic range recording medium formulation and the new technique of dynamic aperture holographic multiplexing. However, the coherent channel techniques were not yet incorporated. The first coherent channel technique, quadrature homodyne detection, enables the use of phase shift keying (PSK) for signal encoding, which dramatically improves recording intensity homogeneity and increases SNR. The second, phase quadrature holographic multiplexing, further doubles density by recording pairs of holograms in quadrature (QPSK encoding).

We report on the incorporation of these coherent channel techniques into the AP1 demonstrator, and on the results of recording experiments.

9587-2, Session 1

Numerical evaluation of multilayer holographic data storage with a varifocal lens generated with a spatial light modulator

Teruyoshi Nobukawa, Takanori Nomura, Wakayama Univ. (Japan)

The feasibility of multilayer recording in holographic data storage have been studied. Multilayer recording allows to use the dynamic range of a recording medium effectively and improve a recording density. Conventional multilayer recording, however, requires a movable stage for shifting a recording medium along an optical axis. This makes an optical setup complicated and large. In order to solve the problem, we propose the multilayer recording with a varifocal lens generated with a phase-only spatial light modulator. In the proposed method, a focal plane is shifted by adding a spherical phase to a phase modulation pattern which consists of a random phase mask and a computer-generated reference pattern. We investigate the shift selectivity along an optical axis in the proposed method and perform multiplexed recording with a numerical simulation. In the numerical simulation, calculation for a propagation is based on a scalar diffraction theory, and an optical setup is assumed to be a coaxial holographic data storage. The numerical results show that the proposed method enables us to implement multilayer recording without moving both a stage and a recording medium. We believe that the proposed method contributes the realization of compact and high-density multilayer recording holographic storage.

9587-3, Session 1

Design of binary data page with a phase mask for high-density holographic recording

Daisuke Barada, Shigeo Kawata, Toyohiko Yatagai, Utsunomiya Univ. (Japan)

Holographic memory is expected for a storage with large data capacity and high data transfer rate because two dimensional coding pattern called data page can be recorded onto the volume of a recording medium. The data page is given to a signal beam by a spatial light modulator (SLM). To realize high data transfer rate, ferroelectric liquid crystal spatial light modulator (FLC-SLM) is used. The FLC-SLM modulates a light to two states so that binary pattern is used as the data page. The data page pattern is focused by a lens and the Fourier pattern is illuminated onto a recording medium. In order to limit the recording area of the medium, a rectangular aperture is used. Then, the resolution of the SLM is limited because the rectangular aperture plays the role of a spatial frequency filter. In this study, a binary data page coding method was proposed with a phase mask. When the rectangular aperture size is not enough corresponding to the resolution of the SLM, the pattern from a pixel becomes broaden and interpixel cross-talk noise is increased in reconstruction. In our proposed method, the cross-talk effect is aggressively utilized. The complex value of a pixel with a designed phase mask can be switched to two constant vectors on the complex plane. By superposing some constant vectors, arbitrary vector can be expressed. The interpixel superposition is realized by limiting the size of the aperture. In reconstruction, the complex value is measured by phase-shifting algorithm and the data is extracted from the complex value. It was numerically confirmed that the noise level can be suppressed by using our proposed method in the case of decreasing the aperture size.

9587-4, Session 1

Optimization of holographic data storage system based on Seidel aberrations reduction

Ren-Chung Liu, National Chiao Tung Univ. (Taiwan)

Volume holographic data storage is regarded as a potential technology for next generation optical storage in the era of cloud computing. It has attracted intense research effort from both academia and industries. Storage capacity (SC) and bit-error-rate (BER) are two parameters that are often used to evaluate the performance of holographic data storage systems. Bit errors can be induced by many factors such as material scattering, device imperfections, system misalignment, intra-page cross-talk between pixels of the same page, inter-page cross-talk between different pages, and optical aberrations, etc. When bit error occurs, it will require more error correction codes and thus the storage capacity will be degraded. In this talk, we consider the influence of optical aberrations on BER and SC of holographic data storage systems. A system model for holographic data storage system (HDSS) with multiple lenses is proposed, and the point spread function (PSF) for the system is derived. The PSF is used to investigate the influence of aberrations on the probability density function (PDF) of the retrieved data from the HDSS, and thus the SC and BER are developed. Then, parametric studies on numerical apertures and Seidel aberration on SC and BER of HDSS are performed. Tolerances of Seidel aberrations with different NA are obtained. Performance improvement and optimization of HDSS for achieving lower BER and higher SC will be presented. We also consider further improvement of HDSS by using circular spatial light modulator for displaying the data pages.





9587-5, Session 2

Recent progress towards practical holographic digital data storage system (Invited Paper)

Yuzuru Takashima, The Univ. of Arizona (United States)

No Abstract Available

9587-6, Session 2

Quantitative roadmap of holographic media performance (Invited Paper)

Benjamin A. Kowalski, Robert R. McLeod, Univ. of Colorado at Boulder (United States)

We calculate the theoretically achievable refractive index modulation for a broad range of commercially and academically interesting holographic media. In each case, a comparison of this theoretical upper limit to the reported performance reveals that a significant fraction of the writing chemistry is wasted due to unwanted reactions. Design strategies to reduce this wasted fraction are evaluated, leading to a quantitative roadmap of the performance improvements that can be expected in state-of-the-art media. Finally, we derive additional theoretical bounds on media performance from fundamental scaling relationships between recording-induced scatter (typically the dominant noise term) and index modulation and sensitivity.

9587-7, Session 2

High dynamic range holographic data storage media

Mark R. Ayres, Fred Askham, Adam C. Urness, Akonia Holographics, LLC (United States)

Photopolymer based photonic materials find relevance in a wide range of applications including holographic data storage, display holography, holographic and graded refractive index (GRIN) optical elements, waveguides, etc. Their importance stems from an ability to respond to a patterned light intensity by forming a corresponding permanent refractive index structure within the material. The effectiveness of a particular material derives largely from the maximum contrast which can be achieved as the initially homogeneous material is induced to separate into volumes of high and low refractive index.

Previous strategies for producing materials with greater dynamic range have included widening the difference in refractive index between monomer and matrix by judicious choice of their compositional elements, or simply increasing the initial concentration of the writing monomer. While these methods have achieved some success, practical constraints due to recording induced physical shrinkage, solubility and expense limit the degree to which they can be employed.

In contrast, Akonia's DRED technology provides a new method which increases the efficiency with which the monomer is used, thereby leading to large increases in the dynamic range performance of these materials. This technology employs a class of compounds (termed "Dynamic Range Enhancing Dopants") having defined reactivity features that dramatically increase the medium's dynamic range when added in small amounts to existing formulations. In some embodiments, a quintupling of the material's M/# performance has been achieved without an increase in recording induced shrinkage.

We report details on these materials and their holographic recording performance characteristics.

9587-8, Session 2

Proposal for one-beam microholographic recording using radially polarized light beam

Ryuichi Katayama, Fukuoka Institute of Technology (Japan)

Microholographic recording is promising for realizing next-generation optical data storage systems because of its affinity with conventional optical disk systems. However, there is a problem in the microholographic recording that two beams facing each other in between the recording medium are necessary for recording, which makes the optical configuration complicated. This paper proposes a novel microholographic recording using only one beam for recording.

In the recording process, a radially polarized light beam is used. When the radially polarized light beam is focused, lights from two parts located symmetrically with respect to the optical axis interfere with each other. As a result, a microhologram whose grating vector is perpendicular to the optical axis is formed in the recording medium, in contrast to the conventional microholographic recording in which the grating vector of the microhologram is parallel to the optical axis.

In the readout process, a circularly polarized Laguerre Gaussian light beam is used. A radially polarized light beam can be generated by synthesizing two circularly polarized Laguerre Gaussian light beams whose handednesses are opposite to each other. Therefore, if a right-handed circularly polarized Laguerre Gaussian light beam is focused on the microhologram, a lefthanded circularly polarized Laguerre Gaussian light beam is generated as a diffracted light beam. Here, the diffracted light beam is generated in the transmission direction, in contrast to the conventional microholographic recording in which it is generated in the reflection direction. The diffracted light beam is detected and discriminated from a non-diffracted light beam using their different handednesses.

9587-9, Session 3

Metasurface: Where meta, microfluidic, and tunable meet? (Invited Paper)

Wei Zhang, Nanyang Technological Univ. (Singapore); D. T. Tsai, National Taiwan Univ. (Taiwan); Zhen Chuan Yang, Xing Zhu, Peking Univ. (China); Federico Capasso, Harvard School of Engineering and Applied Sciences (United States); Ai Qun Liu, Nanyang Technological Univ. (Singapore)

A perfect absorber, which fully absorbs the incoming electromagnetic (EM) wave and transfers it into other forms of energy, is intensively studied for its wide applications in energy harvesting, military defense, EM wave modulation and communications, etc. The metamaterial, an artificial material consisting of subwavelength meta-atoms, has been designed for perfect absorption by utilizing the impedance matched meta-atoms. Although successfully demonstrated, they are usually limited in a narrow working bandwidth. The rigid structure of the design also hampers its real life applications that require all-directional absorption. In this talk, a soft metamaterial is proposed to realize the perfect absorption in microwave regime, which can be easily deformed to face to different directions. The polymer polydimethylsiloxane (PDMS) is used as the soft substrate, which is filled with the most common material in nature, i.e. water. Due to the extremely high dielectric constant and high absorption by its polar molecules in microwave regime, water is a perfect candidate for perfect absorption. By properly patterning the PDMS channels, which are filled with water, the microwave across a wide band is well confined and fully absorbed. The perfect absorption is further manipulated in two aspects: first, the absorption band is shifted by deforming the water pattern under different inlet water pressures applied in the PDMS channel. Second, the absorption coefficient of the soft metamaterial can be effectively controlled by mixing water with other organic solvent, such as ethanol in this work. By controlling the volume ratio of the water and ethanol, the tunability



from zero absorption to full absorption is realized. With the wideband and tunable capability, the proposed perfect metamaterial absorber gives a promising applications in energy harvesting, stealth system and microwave communications.

9587-10, Session 3

Potential of multi-photon reading and writing for optical data storage systems (Invited Paper)

Thomas D. Milster, Phat Lu, Khanh Kieu, College of Optical Sciences, The Univ. of Arizona (United States)

Several examples of multi-photon (MP) media for optical data storage (ODS) include the Call/Recall fluorescent disc, vitreous silica, MP excitable resins, photorefractive polymers, bulk glass, molecular glasses, highly linked polymers, sapphire, and others. These media all utilize MP interaction to form data bits. In addition, some readout systems use MP interactions to limit inter-layer crosstalk. Typically, a 2-photon interaction is the basis for writing data. That is, the polarization of the illuminated material responds to the square of the electric field amplitude, which has the effect of localizing the interaction to a very small volume near the tightly focused laser beam. Higher-order interactions, if possible, could limit the interaction volume to much smaller dimensions. For example, in the laboratory, tenth-order voids in glass have been demonstrated. The lasers used to generate the femto-second pulses and kW peak powers necessary for writing MP data have dramatically reduced in size and cost in just the last few years. It is now possible to purchase a hand-held femto-second laser operating at 1560nm that produces over 1nJ per pulse. Near-term advances in this laser technology promise to provide smaller footprints, higher powers and a wide selection of wavelengths. Lastly, we will discuss a new mechanism of MP field enhancement that may be useful to increase the contrast of ODS readout signals. We have demonstrated a third-harmonic generation signal enhancement factor of 8 when scanning a laser beam over a structured surface.

9587-11, Session 3

Roll-to-roll fabrication of multilayer polymer films for high capacity optical data storage (Invited Paper)

Kenneth D. Singer, Cory W. Christenson, Anuj Saini, Case Western Reserve Univ. (United States); Christopher J. Ryan, Heather Mirletz, Irina Shiyanovskaya, Folio Photonics LLC (United States); Kezhen Yin, Eric Baer, Case Western Reserve Univ. (United States)

Multilayer optical data storage is a promising approach for realizing archival optical discs with terabyte capacity for applications in enterprise data storage. We report on the fabrication of optical discs containing dozens of layers from a high-scalable multilayer polymer film co-extrusion process.

Polymer co-extrusion is a well-established roll-to-roll manufacturing process with applications as diverse as food packaging and high performance optical filters. We have adapted this to produce films with up to dozens of layers of photo-patternable material. The film is easily fabricated into optical discs with the potential capacity of several terabytes.

Data is stored in voxels defined by photobleaching a fluorescent dye contained in writable layers of 200-300nm thickness separated by inert layers of 2-3 microns. We have shown that at short pulse durations of a pulse-modulated commercial BDXL laser, the nonlinear writing process within the absorption band of the dye exhibits a distinct threshold, thus promising low crosstalk and sub-diffraction limit bit patterns. The writing process exhibits a crossover from a linear to nonlinear regime at pulse durations of a few hundred microseconds. We describe the physics of the writing process in terms of a thermal diffusion.

We have recently demonstrated that data can be written and read using

a modestly adapted commercial BDXL pick-up. The confocal optical configuration for reading suggests that the drive developed for our discs could be backward compatible with earlier commercial optical discs. Studies of photostability and defect density suggest the suitability of this technology for long-term, high-performance enterprise archival data storage.

9587-12, Session 3

Air gap control and residual aberration compensation in a Hyper Blu-Ray Disc (NA=1.4) objective

Victor E. Densmore, Young-Sik Kim, Thomas D. Milster, College of Optical Sciences, The Univ. of Arizona (United States); Matthew C. Watson, Dolaphine Kwok, The Univ. of Arizona (United States)

Nano-scale resolution in miniature optical systems has been realized in the optical data storage industry. Numerical apertures greater than unity have been achieved in by utilizing the high index material of a hemispherical Solid Immersion Lens (SIL), which increases the resolution of the backing objective by a factor that is related to the refractive index of the SIL. In this research, a custom Hyper-Blu-Disc (HBD) NA=1.4 SIL objective is utilized for high-fidelity readout of data pits beneath a 100?m thick cover layer on an optical Blu-Ray Disc. If realized commercially, the increase in data density could be 3X today's Blu-Ray technology. A distinct difference between this work and other work with SILs in optical data storage is the data storage capacity improvement is made using the current Blu-Ray Disc structure that uses a 100?m thick cover layer. In this report, a phase plate is designed to compensate for residual aberrations resulting from non-ideal cover layer thicknesses and a method for controlling the air gap height of the SIL-cover layer region is proposed.

9587-13, Session 3

Optimized six-dimensional optical storage: A practicable way to large capacity and fast throughputs

Shangqing Liu, Willow Optics Corp. (Canada)

An optimized six-dimensional optical storage system has been designed and investigated theoretically. This system uses multiple beams with different wavelengths, coded polarizations and graded intensities to create multiple and overlapped micro gratings as each storage cell. Because the storage cell capacity depends exponentially on the write beam wavelength number, and the data are written and read by the multiple beams simultaneously, this system can have large storage capacity and fast data throughputs.

By two-photon absorption writing, up to 180 data layers can be created in a DVD sized disk. Also by optical coherence tomography reading, the stored data can be retrieved with high signal-to-noise ratio of over 66 dB. Furthermore, the superresolving pupil filters are used to optimize the system. By reducing the beam focus diameters, the storage cell density can be increased obviously, resulting in larger storage capacity (over 1 Pbyte per DVD sized disk and -60 Pbytes per disk is potential) and faster data throughputs (reading speed is over 117 Gbits/s).

In addition, the storage cell sizes (~ 1?m ? 6?m) of this system are much larger than those (less than several tens of nm) required for the large capacity three-dimensional storage system, which can greatly reduce the huge difficulties for creating and addressing the tiny data spots.

This system structure is very like a standard drive, and so has good compatibility with the CD and DVD disks.

These comprehensive advantages will make this technology become an actually practicable one for extra-large capacity and extra-fast throughputs optical storage.



9587-14, Session 4

Modeling and measures against the effect of mechanical instabilities on holographic data storage system (Invited Paper)

Kenichi Shimada, Toshiki Ishii, Taku Hoshizawa, Hitachi, Ltd. (Japan); Yuzuru Takashima, The Univ. of Arizona (United States)

The volume of worldwide digital data is expanding exponentially and will reach 44ZB (1ZB = 10^9 TB) in 2020. Under the circumstances, the significance of Optical Data Storage (ODS) as archival data storage is affirmed because of their lower bit cost and longer archival life. Holographic Data Storage System (HDSS) has been considered as one of promising candidates for future ODS due to its abilities of high density recording and fast transfer rate. However, in a HDSS, tolerance of vibrations caused by mechanical instabilities is subject to become severe in return for their high density recording. Thus, it is crucial to understand effects of vibrations on HDSS in order to make recording density of the system enlarged maximally. We analytically formulated the effects on the HDSS by incorporating the concept of a Time-Averaged Holography. Mechanical parameters such as amplitude and frequency of mechanical oscillation are related to optical parameters such as amplitude and phase of reference and signal beams in the formalization. Based on the formalization, we analyzed how the effects are related to system performances and developed write mode control technique to prevent data transfer rate decrease in writing holograms. Then, the analytical formulation led to a new technique of optical and post compensation for mechanical instability during recording hologram. These techniques enable a robust implementation of HDSS against mechanical instabilities.

9587-15, Session 4

Enhancement of data rates by single and double cavity holographic recording

Bo E. Miller, Yuzuru Takashima, College of Optical Sciences, The Univ. of Arizona (United States)

To satisfy the growing need for faster archival data storage and retrieval, we proposed an improvement to the read and write data transfer rates of Holographic Data Storage Systems (HDSS). Conventionally, reading and writing of data utilize only a fraction of the available light. Our techniques apply a resonator cavity to the readout and recording of holograms so that more of the available light is used. Functionally, more power is used than what is provided without violating energy conservation. Thus, data rates and/or capacities can be increased due to enhanced power. These improvements are also inversely related to the diffraction efficiency of a hologram, which makes these cavity enhanced techniques well suited to HDSS where large numbers of multiplexed holograms require low diffraction efficiencies.

Previously, we presented the theory of Cavity Enhanced HDSS and the results of enhanced readout upon diffraction efficiency and Bragg selectivity. We have now formalized the enhancement in writing power and experimentally evaluated the improvement in writing speed over conventional means for writing a single plane wave hologram in Fe:LiNbO3 with a 532 nm wavelength, CW, single mode, DPSS, Nd:YAG, laser with a cavity on one of the writing arms. The diffraction efficiency was read during the recording by using a 632.8 nm wavelength HeNe Laser. We found that the enhancement of recording power for this configuration asymptotically approaches a factor of two, while the use of cavities in both writing arms provides a power enhancement which is limited only by the losses in the cavities.

9587-16, Session 4

Optimized aperture for collinear holographic data storage system

Jinqiu Liu, Yan Zhao, Liangcai Cao, Hao Zhang, Guofan Jin, Tsinghua Univ. (China)

The quality of the reconstructed data pages is an important factor representing the performance of the collinear holographic data storage system [1]. It is primarily determined by the quality of the source, the input data page. In our collinear holographic data storage system, the input data page is uploaded by a spatial light modulator, which has a micron-size pixel structure. Both the object beam and reference beam are converged into the objective lens through a set of relay lens [2-3]. The quality of the input data page is highly influenced by the aperture in the Fourier plane of the relay lens. Limited size of the aperture causes the interpixel cross talk, which reduces the signal-to-noise ratio (SNR). In this work, an spectrum model for the imaging of the pages from the spatial light modulator are proposed in the collinear holographic data storage system. It can be used to analyze the impact of the aperture on the input image quality on the recording media. Experiments are conducted to evaluate the effects of different diffracted orders in the Fourier plane. Simulated and experimental results show that higher SNR can be achieved by optimized apertures for different kinds of image patterns. This work provides a simple and practical method for improving the SNR of the reconstructed data page. The understanding of the spatial spectrum of the input data page offers one of the guidelines for the design of the collinear holographic system.

Acknowledgement:

This work is supported by National Natural Science Foundation of China (61275013), National Basic Research Program of China (2013CB328803), and Tsinghua University Initiative Scientific Research Program. References:

[1] T. Nobukawa and T. Nomura, "Coaxial holographic memory with designed reference pattern on the basis of nyquist aperture for high density recording," Jpn. J. Appl. Phys. 52, 09LD09 (2013).

[2] Jianhua Li, Liangcai Cao, Huarong Gu, Xiaodi Tan, Qingsheng He, and Guofan Jin, "Orthogonal-reference-pattern-modulated shift multiplexing for collinear holographic data storage," Optics Letters, 37, 936-938 (2012).

[3] Liangcai Cao, Jinqiu Liu, Jianhua Li, Qingsheng He, and Guofan Jin, "Orthogonal reference pattern multiplexing for collinear holographic data storage," Applied Optics, 53, 1-8 (2014).



9587-17, Session 4

Volume holography with Bessel-like reference beams

Raphael A. Guerrero, Jonathan P. Manigo, Ateneo de Manila Univ. (Philippines)

We report volume holographic recording and reconstruction of plane waves using reference beams with Bessel-like propagation properties. A photorefractive lithium niobate crystal (0.05% Fe:LiNbO3) is employed as the holographic medium in a two-wave mixing set-up. Our light source is a 4 mW HeNe laser operating at a wavelength of 543.5 nm. The laser output is collimated and split into an unmodified plane wave object beam and a Bessel-like reference beam. A Bessel-like beam is generated by an annular slit, with diameter = 0.75 mm and slit width = 0.15mm, placed at the back focal plane of a lens with focal length = 50 cm. Recording time is set at 5 minutes. Reconstructed images are captured with a CCD camera positioned at increasing distances from the crystal starting at 10 cm. The reconstructed plane wave has the same appearance as a Bessel beam, displaying a central maximum and concentric rings. Over a propagation range of 10 to 50 cm, the central intensity is observed to oscillate between maximum and zero intensity. Taking into account the well-established self-healing nature of Bessel beams, we also examine the effects of using a partially blocked reference beam. A small obstruction with width = 0.5 mm is placed 2.5 cm after the lens used to produce the Bessel-like beam. The reconstructed wave initially appears altered but recovers its original intensity profile after propagating 40 cm. The propagation properties of the beam reconstructed via our method have potential utility in holographic storage and optical trapping.

Conference 9588: Advances in X-Ray/EUV Optics and Components X

Tuesday - Wednesday 11-12 August 2015 Part of Proceedings of SPIE Vol. 9588 Advances in X-Ray/EUV Optics and Components X

9588-1, Session 1

Multilayer coatings for free-electron laser sources

Alain J. Corso, Paola Zuppella, Davide Bacco, Enrico Tessarolo, Marco Nardello, Francesca Gerlin, Univ. degli Studi di Padova (Italy); Emiliano Principi, Erika Giangrisostomi, Filippo Bencivenga, Alessandro Gessini, Claudio Masciovecchio, Angelo Giglia, Stefano Nannarone, Elettra-Sincrotrone Trieste S.C.p.A. (Italy); Maria G. Pelizzo, Univ. degli Studi di Padova (Italy)

Extreme ultraviolet (EUV) multilayer (ML) technology has been intensively applied in many scientific and technological fields such as solar physics and photolithography. More recently, the advent of free electron lasers (FEL) emitting bright sub-ps pulses with very high quality in term of intensity stability, coherence and temporal shape has encouraged the usage of multilayer coatings also in the transport and manipulation of FEL radiation. In fact, conventional single layers coated mirrors provide negligible reflectance in the EUV spectral range whereas ML mirrors can reach high efficiency at normal incidence without affecting the pulses characteristics. Such optical elements have been also exploited at FERMI@ELETTRA FEL where novel multilayer coatings specifically conceived for pump and probe experiment and ultrafast absorption spectroscopy have been designed. The main results are reported.

9588-2, Session 1

Graded multilayers for figured Kirkpatrick-Baez mirrors on the new ESRF end station ID16A

Christian Morawe, Raymond Barrett, Peter Cloetens, Benjamin Lantelme, Jean-Christophe Peffen, Amparo Vivo, ESRF - The European Synchrotron (France)

The upgraded ESRF end station ID16A was equipped with a new Kirkpatrick-Baez (KB) nano-focusing setup. The figured KB mirrors were coated with steeply graded W/B4C multilayers to account for the variable angle of reflection along the beam footprint. The multilayers were deposited at the ESRF Multilayer Facilities by DC magnetron sputtering in dynamic mode, where the substrates move in front of the sputter cathodes. The present work deals with the design, the fabrication, and the characterization of the coatings. First results obtained during commissioning experiments on ID16A complement the report.

9588-3, Session 1

In-situ GISAXS monitoring of ultrashort period W/B4C multilayer x-ray mirror growth

Martin Hodas, Peter ?iffalovi?, Yuriy Halahovets, Marco Pelletta, Karol Vegso, Matej Jergel, Eva Majkova, Institute of Physics SAS (Slovakia)

Ultrashort period multilayer X-ray mirrors with the layer thickness down to 1 nm or less represent a technological challenge. Here, the layer thickness becomes comparable to the interface roughness and discontinuous layers producing strong diffuse scattering may appear. The grazing-incidence small-angle X-ray scattering (GISAXS) is a unique nondestructive technique to probe the mirror quality in terms of the statistical interface roughness and its correlation properties. We present the first in situ laboratory GISAXS experiments of monitoring the multilayer mirror growth in order to better understand and optimize the deposition process. A microfocus X-ray source IuS with focusing Montel optics (Incoatec) and 2D X-ray detector Pilatus 200K (Dectris) were mounted on a custom-designed dual-ion beam sputtering apparatus (Bestec). Two W/B4C mirrors with 15 periods of 1.8 nm and 2.1 nm were prepared as determined from the post-deposition specular X-ray reflectivity measurements. The in situ GISAXS tracking was done by a fast repeated collection of the GISAXS frames with the integration time of 8 s at the incidence angle of 0.25 degree. Two distinct features along qz at qy=0, namely Yoneda and Bragg-like (BL) multilayer peaks evolved in the GISAXS pattern. Oscillatory behavior of the latter in terms of intensity and FWHM was observed after the initial stage. Lateral cuts of the diffuse scattering concentration stripes surrounding BL peaks in particular GISAXS frames provided temporal evolution of the correlation and fractal interface parameters. Their potential for tailoring the multilayer properties is discussed.

9588-4, Session 1

Multilayer optics for monochromatic highresolution x-ray imaging

Philippe P. Troussel, Berenice Loupias, Vincent dervieux, Ludovic Lecherbourg, Dominique Gontier, Commissariat à l'Énergie Atomique (France); Alexandre DO, Sophie D. Baton, Frédéric Perez, Ecole Polytechnique (France) and Ctr. National de la Recherche Scientifique (France); David Dennetiere, Synchrotron SOLEIL (France)

Within the framework of its researche on Inertial Confinement Fusion (ICF), the "Commissariat à l'Énergie Atomique et aux Énergies Alternatives" (CEA) studies and designs advanced X-ray diagnostics in order to probe dense plasmas produced by Laser facilities.

We have chosen to present two types of advanced High Resolution X-ray Imaging (HRXI) microscopes who have high spatial resolution capability (3-6 μ m) and high efficiency for monochromatic focusing x-ray radiation.

The first microscope consists of two toroïdals mirrors mounted into a Wolter type geometry and working at grazing incidence. Non-periodic multilayer (depth graded) mirrors were developed with special coatings designed to provide broadband X-ray reflectance and to be use in the 1-22 keV energy range. Mainly, a high resolution, high X-ray photon energy involving state-of-the-art toroïdal mirror and W/Si multilayer mirrors coating are detailed. Associated to this Wolter microscope a potential monochromatic third mirror coated with a multilayer stack can be used for monochromatic application in that range.

The second microscope is composed of a transmission gold Fresnel Phase Zone plate (FPZP) and of a very narrow bandwidth multilayer mirror. We present an experimental study with X-ray plasma-source. We show the interest in the case of broadband source imaging (plasma source) associated with the FPZP a multilayer mirror.

Potentialities (a few μm spatial resolution monochromatic images) and complementarity of these two monochromatic HRXI are discussed.

The multilayer mirrors and sub-nanoscale layers characterization were detailed.

9588-21, Session 1

help@spie.org

+1 360 676 3290 ·

High-reflectance La/B-based multilayer mirror for 6.x-nm wavelength

Dmitry S. Kuznetsov, Marko Sturm, Robbert W. E. van de Kruijs, Andrey E. Yakshin, Eric Louis, Fred Bijkerk, MESA+ Institute for Nanotechnology (Netherlands)





For future photolithography processes, the wavelength of 6 nm can be considered. The perspective of this chip fabrication technique however, will depend essentially on the performance of multilayer reflective mirrors, which will need to be based on La/B. One of the issues is formation of LaxBy compounds at the interfaces, which decreases the optical contrast and therefore dramatically reduces the reflectivity. To prevent such chemical interaction, passivation of Lay nitrogen has been investigated. We successfully synthesized LaN layers that resulted in a new world record reflectivity of 64% at 6.6 nm at near normal incidence. This reduces the gap to the target of 70% desired for a possible next generation lithography.

9588-5, Session 2

Development of an adaptive K-B mirror for hard x-ray nanofocusing using piezoelectric deformable mirrors

Takumi Goto, Satoshi Matsuyama, Osaka Univ (Japan); Hiroki Nakamori, JTEC Corp. (Japan); Takashi Kimura, Hokkaido Univ. (Japan); Yasuhisa Sano, Osaka Univ (Japan); Yoshiki Kohmura, Makina Yabashi, Tetsuya Ishikawa, RIKEN/SPring-8 (Japan); Kazuto Yamauchi, Osaka Univ (Japan)

We have been developing an adaptive x-ray focusing optical system that consists of two-stage Kirkpatrick-Baez deformable mirrors. The optical system can provide focused x-ray beam with controlled beam size in diffraction-limited condition at the fixed focal point. To realize the optical system, we developed an ultraprecise deformable mirror with a piezoelectric bimorph structure. It consists of a quartz glass substrate, four piezoelectric actuators and 18 electrodes on each actuators. The substrate has dimensions of 50?100?t5 mm3. The four actuators, which have dimensions of 17.5?100?t1 mm3, were attached to face and back sides of the substrate. To investigate the performance of the optical system, we performed a two-dimensional focusing test by using an adaptive K-B mirrors at the EH3 of BL29XUL of SPring-8 using 10keV X-rays. To deform the mirrors to the required elliptical shape, first, the mirror is deformed by applying initial voltages that has been predetermined by performing a deformation test with an optical interferometer. Then, to correct deformation errors, we adjusted supply voltages according to the measured mirror shape by pencil-beam scanning. As a result, the deformation accuracy of 2 nm (peak-to-valley) was achieved. In addition, a focused beam with full width at half maximum of 110 ? 65 nm2 (V ? H) was obtained.

9588-6, Session 2

MZP design and fabrication for efficient hard x-ray nano-focusing and imaging

Christian Eberl, Florian Döring, Hans-Ulrich Krebs, Markus Osterhoff, Georg-August-Univ. Göttingen (Germany)

Efficient focusing optics are a key ingredient for high-resolution (few nano metre) hard x-ray imaging. In recent years, a combined optical scheme uses prefocusing to match the coherent fraction of the synchrotron beam to a high-resolution multilayer zone plate (MZP) has been presented. This scheme allows for sub-5?nm focusing of hard x-rays in two dimensions.

We present latest optimisations achieved in both design and fabrication of high-resolution MZPs. First lenses produced by Pulsed Laser Deposition from alternating W and Si layers suffered from droplet formation during an unfavourable growth process. The material combination has been changed to Ta2O5 and ZrO2, allowing for much faster and more accurate layer growth. The initial roughness of the central core has been minimised by using a pulled glass fibre, bringing the focusing efficiency close to seven per cent (+1st order).

C. Eberl et al., Appl. Surf. Sci. 307, 638 (2014)

9588-7, Session 2

Adaptive optics at the angstrom scale: from discrete to continuous surface manipulation

Benjamin J. Wylie-van Eerd, Univ. Twente (Netherlands); Bram Krijnen, DEMCON (Netherlands); Fred Bijkerk, Guus J. H. M. Rijnders, Eric Louis, Univ. Twente (Netherlands)

Adaptive optics are of great utility in increasing the performance of optical systems. However, they are not currently widely used in EUV, X-ray and higher energy ranges due to the difficulties of surface manipulation with angstrom scale precision.

In this presentation we will show progress in creating an piezoelectric based adaptive optic system suitable for correcting wave fronts at EUV and X-ray wavelengths. In particular, novel technology allowing wave front correction by continuous rather than discrete manipulation of surface elements will be demonstrated. The theoretical concept behind this technology and experimental proof will both be shown.

The continuous surface manipulation technique is capable of creating surfaces much better suited to wave front correction than individual discrete elements while still benefiting from the speed and precision of piezoelectric materials. The current state of the technology, advantages of its use and the outstanding challenges will be discussed.

Such a technology can be used for example in EUV lithography systems, to increase tolerances for imperfections elsewhere in the multiple mirror system. This allows leeway for a challenging problem in the optical system, and accelerates the technology towards market readiness.

9588-8, Session 2

Evaluation of surface figure error profile of ultra-precise ellipsoidal mirror for soft x-ray focusing

Yoko Takeo, Takahiro Saito, Hidekazu Mimura, The Univ. of Tokyo (Japan)

Soft X-ray nanofocusing with high efficiency and no chromatic aberration is possible by using the ultra-precise ellipsoidal mirror. Surface figure metrology is key for improving surface figure accuracy. In this research, we use ptychographic phase retrieval using a visible light laser for measuring surface figure error profiles of ellipsoidal mirrors. Recently, the measurement accuracy has been further increased by employing advanced calculation methods and improving the experiment system. In this presentation, we will explain the method in detail and show the measurement performance of the developed system.

9588-9, Session 3

Profile-coating of x-ray optics using the new magnetron sputtering deposition system

Bing Shi, Jun Qian, Raymond Conley, Argonne National Lab. (United States)

X-ray mirrors and multilayer optics for synchrotron beamlines have been fabricated using the newly developed magnetron sputtering system at the Optics Group at Advanced Photon Source (APS). This new linear deposition system has two cathodes with DC power supplies. It has been equipped recently and used in the fabrication of multilayers and profile-coating mirrors. The commissioning of this machine, the fabrication of x-ray mirrors using profile-coating technique, the results of the mirrors fabricated, the coating materials testing for thin film optics stress reduction, the existing issues, and the future plan will be presented.



This work supported by the DOE office of Science, Office of Basic energy Sciences, under Contract No. DE-AC02-06CH11357 and under Contract No. DE-AC-02-98CH10886

9588-10, Session 3

Recent advances in multilayer Laue lens fabrication techniques

Raymond Conley Jr., Argonne National Lab. (United States) and Brookhaven National Lab. (United States); Nathalie Bouet, Juan Zhou, Hanfei Yan, Xiaojing Huang, Kenneth Lauer, Evgeny Nazaretski, Matthew Vescovi, Brookhaven National Lab. (United States); Adam Kubec, Fraunhofer IWS Dresden (Germany); Albert T. Macrander, Jörg Maser, Bing Shi, Argonne National Lab. (United States); Yong S. Chu, Brookhaven National Lab. (United States)

Multilayer Laue lens (MLL) fabrication techniques have gradually matured from providing only limited production of small "proof of concept" devices to true nanofocusing optics ready for beamline deployment. New multilayer material systems and deposition techniques that offer both larger aperture growths and higher optical performance are introduced. Wedged MLL, where the individual layers within the stack are both depth-graded and laterally graded in thickness, have been produced with apertures greater than 30?m. Initial synchrotron results at beamlines 1-BM and 34-ID at the Advanced Photon Source on tilted and wedged large aperture MLLs indicate clear performance increases and point the way towards the next fabrication challenges to overcome.

Work at Argonne National Laboratory was supported by the Department of Energy, Office of Basic Energy Sciences under contract DE-AC-02-06CH11357. Work at Brookhaven National Laboratory was supported by the Department of Energy, Office of Basic Energy Sciences under contract DE-AC-02-98CH10886.

9588-11, Session 3

Development of polycapillary x-ray optics for synchrotron spectroscopy

Daniel Bennis, Incom Inc. (United States)

A new spectrometer design that will result in a highly efficient, easy to handle, low-cost, high-resolution spectroscopy system with excellent background suppression is being developed for the NSLS-II Inner-Shell Spectroscopy beamline. This system utilizes non-diffractive optics comprised of fused and directed glass capillary tubes that will be used to collect and pre-collimate fluorescence photons. There are several advantages enabled by this design; a large energy range is accessible without modifying the system, a large collection angle is achieved per detection unit: 4-5% of the full solid angle, easy integration in complex and harsh environments is enabled due to the use of a pre-collimation system as a secondary source for the spectrometer, and background from a complex sample environment can be easily and efficiently suppressed.

Development of the polycapillary x-ray focusing optics for this application will be presented. This includes simulation of key design parameters of x-ray optics to guide optimization efforts, improvement in manufacturing methods of polycapillary structure for x-ray optics, forming the polycapillary structure to produce x-ray optics to achieve the required solid angle collection and transmission efficiency, and measurement of x-ray focusing properties of the optics using an x-ray tube source.

9588-12, Session 3

RXR: a new experimental station for 2D and 3D micro-XRF based on polycapillary optics

Claudia Polese, Istituto Nazionale di Fisica Nucleare (Italy) and Sapienza Univ. di Roma (Italy); Andrea Liedl, Dariush Hampai, Istituto Nazionale di Fisica Nucleare (Italy); Sultan B. Dabagov, Istituto Nazionale di Fisica Nucleare (Italy) and Russian Academy of Sciences (Russian Federation) and National Research Nuclear Univ. MEPhI (Russian Federation); Francesco Taccetti, Istituto Nazionale di Fisica Nucleare (Italy)

XRF imaging spectrometry is a powerful tool for materials characterization, for example in the cultural heritage field. A high spatial resolution is often required, in order to appreciate very tiny details of the studied object. With respect to simple pinholes, polycapillary optics allows much more intense fluxes to be achieved. This is fundamental to detect elements in trace and to strongly reduce the global acquisition time that is actually among the main reasons, in addition to radioprotection issues, affecting the competitiveness of XRF imaging with respect to other faster imaging techniques such as multispectral imaging. Unlike other well-known X-ray optics, principally employed for high brilliant radiation source such as synchrotron facilities, polyCO can be efficiently coupled also with conventional X-ray tubes. All these aspects make them the most suitable choice to realize portable, safe and high performing μ XRF spectrometers.

In this work the first results achieved with a novel 2D and 3D XRF facility, Rainbow X-Ray (RXR), are reported, with particular attention to the spatial and energy resolution achieved. RXR is based on the confocal arrangement of three polycapillary lenses, one focusing the primary beam and the other two capturing the fluorescence signal. The detection system is split in two couples of lens-detector in order to cover a wider energy range. The entire device is a laboratory user-friendly facility and, though it allows measurements on medium size objects, its dimensions do not preclude it to be transported for in situ analysis on request, thanks also to a proper shielded cabinet.

9588-13, Session 3

Large-area kapton x-ray windows

Mikhail A. Antimonov, Univ. of Illinois at Chicago (United States); Ali M. Khounsary, X-ray Optics, Inc. (United States) and Illinois Institute of Technology (United States); Steven J. Weigand, Jack Rix, Denis T. Keane, Jim Grudzinski, W. Jansma, Argonne National Lab. (United States); Zhenwen Zhou, Univ. of Illinois at Chicago (United States); A. Johnson, Bowling Green State Univ. (United States)

Some X-ray instruments require the utilization of large-area windows to provide vacuum barriers. The necessary attributes of the window material include transparency to X-rays, low scattering, and possession of suitable mechanical properties for reliable long-term performance. Kapton is one such material except that it is a polymer and a large window made from Kapton undergoes substantial deformation at room temperature under a pressure difference of the order of the atmospheric pressure.

In this paper, we report on the mechanical testing of sample Kapton foils including creep, comparison with published data, and use this data and analytical/numerical models to predict the changing profile of Kapton windows over time, showing good correlation with experimental measurements.

Acknowledgements

Portions of this work were performed at the DuPont-Northwestern-Dow Collaborative Access Team (DND-CAT) located at Sector 5 of the Advanced Photon Source (APS). DND-CAT is supported by Northwestern University, E.I. DuPont de Nemours & Co., and The Dow Chemical Company.

Conference 9588: Advances in X-Ray/EUV Optics and Components X



This research used, in part, the resources of the Department of Civil and Materials Engineering (CME) at the University of Illinois, Chicago (UIC) and of Argonne National Laboratory (ANL) and the Advanced Photon Source (APS), a U.S. Department of Energy (DOE) Office of Science User Facility operated for the DOE Office of Science by ANL under Contract No. DE-AC02-06CH1357. Fruitful discussions with Dr. A. Chudnovsky at UIC/CME, the technical staff at DuPont, and Ben Stillwell at APS are graciously acknowledged.

9588-14, Session 4

Effect of beamline optics vibration on the source size and divergence for synchrotron radiation

Shunji Goto, Japan Synchrotron Radiation Research Institute (Japan)

Suppression of the beamline optics vibration is crucial particularly for a low-emittance storage ring. Reflection optics such as mirror and crystal monochromator affect light source size and divergence virtually due to the optics vibration. Minute vibrations result in degradation of synchrotron radiation beam quality: photon flux density, focusing property, averaged coherence.

Variations of the beam size and divergence were formulated using a simple geometrical model. The vibration effect was involved in the phase space. An angular vibration effect was examined for source size, source divergence, beam size at the sample position, and also distance between light source beam waist and optics. A typical arrangement of the SPring-8 beamline was assumed with the primary reflection optics at 40 m from the source. The vertical source size increase is significant compared with the other values for vertical-deflection optics. Suppression of the angular vibration less than 0.1 micro-radians (rms), for example, is required to maintain the 5-micron beam with less than 10% increase.

9588-15, Session 4

Development of split-delay optics with wide range of photon energy for XFEL pump/XFEL probe experiments

Takashi Hirano, Taito Osaka, Osaka Univ. (Japan); Yuichi Inubushi, Japan Synchrotron Radiation Research Institute (Japan); Yasuhisa Sano, Satoshi Matsuyama, Osaka Univ. (Japan); Kensuke Tono, Tetsuo Katayama, Japan Synchrotron Radiation Research Institute (Japan); Tetsuya Ishikawa, RIKEN/SPring-8 (Japan); Kazuto Yamauchi, Osaka Univ. (Japan); Makina Yabashi, RIKEN/SPring-8 (Japan)

Ultra-intense transversely-coherent, and ultrafast hard x-ray pulses provided from x-ray free-electron laser (XFEL) sources, such as SPring-8 Angstrom Compact free-electron LAser (SACLA) in Japan are powerful tools to explore ultrafast science with hard x-rays. Development of a split-delay optics (SDO), which provides two replica XFEL pulses with time delay precisely controlled, is essential for XFEL pump/XFEL probe experiments. An SDO based on Bragg diffraction of Si(220) single crystals consists of sub 10-umthick beam splitter/mixer crystals, two beam reflectors (thick crystals), and a pair of channel-cut crystals, thus it yields high throughput and is applicable in wide ranges of delay time and photon energies. The SDO is contemplated in combination with a focusing system to realize high power density field, hence the replica XFEL pulses need to be overlapped each other onto the focal plane where samples are set in experiments. In order to achieve not only spatial overlap of the replica pulses but also high throughput, precise parallelization of the two beams is required. A tolerated error in crystal angle of ±0.2 urad was calculated by ray trace calculations. We devised a simple and precise alignment procedure and have demonstrated it at SPring-8. We obtained well-overlapped two-dimensionally focal profiles and

the world's highest throughput of ~25%, its collinearity was evaluated to be 0.03 urad (H) ? 0.24 urad (V). In the presentation we report about the test at SPring-8 and commissioning at SACLA performed on May in this year.

9588-16, Session 4

0.1-meV-resolution broadband imaging spectrographs for inelastic x-ray scattering

Yuri V. Shvyd'ko, Argonne National Lab. (United States)

A spectrograph is an optical instrument that disperses photons of different energies into distinct directions and space locations, and images photon spectra on a position-sensitive detector. Spectrographs consist of collimating, angular dispersive, and focusing optical elements. Feasibility of hard x-ray spectrographs with an ultra-high spectral resolution (0.1-meV resolution) has been experimentally demonstrated recently [1]. Bragg reflecting crystals arranged in an asymmetric scattering geometry are used as the dispersing elements. The spectral window of imaging in the demonstrated device, however, was narrow, only 0.45 meV. Here we show that the ultra-high-resolution spectrographs with a significantly increased spectral window of imaging of up to a few tens of meVs are feasible and can be efficiently applied for inelastic x-ray scattering (IXS) spectroscopy [2]. Such spectrographs, equivalent to an IXS spectrometer with more than hundred 0.1-meV resolution analyzers, will enable IXS spectroscopy with the ultra-high resolution and very high efficiency, applicable both at synchrotron and x-ray free-electron laser facilities.

1. Yu. Shvyd'ko, S. Stoupin, K. Mundboth, and J.-H. Kim "Hard-x-ray spectrographs with resolution beyond 100 micro-eV," Phys. Rev. A, 87, (2013) 043835

2. Yu. Shvyd'ko, "Theory of angular dispersive imaging hard x-ray spectrographs", arXiv:1501.05052, (2015)

9588-17, Session 4

Virtual x-ray differential phase contrast imaging system simulator

Young-Sik Kim, Chris Summitt, Sunglin Wang, The Univ. of Arizona (United States); Yin Yuen, Charles Qi, Lambertus Hesselink, Stanford Univ. (United States); Yuzuru Takashima, The Univ. of Arizona (United States)

X-ray differential phase contrast (DPC) imaging system consisting of source amplitude grating (G0), phase grating (G1), and analyzer amplitude grating (G2) is widely adopted because of its compatibility with low brilliance and incoherent X-ray sources, high detection sensitivity of index of refraction (< 1E-6) while having reasonably short system size (~1m), and is expected to be used for security screening applications as luggage inspections. For such applications, object of interest is surrounded by various kinds of and randomly oriented clutter which alters amplitude, spectra and phase of X-ray detected by detector. Such effects ideally have to be taken into account during the design phase of the X-ray DPC imaging modalities. Thus, we developed an integrated and end-to-end simulation environment to systematically optimize and predict imaging performances of X-ray DPC imaging systems. The simulation environment consists of two off-the-shelf modules, such as 3D CAD and Optical Ray-trace Code, as well as a custom physical optics module to simulate polychromatic fringe formation. Each module are interfaced to pipeline data so that the 3D CAD data of the object under inspection and clutter is exported to Ray-trace Code. The Ray-trace Code calculates shift of monochromatic fringes by non-sequential raytracing though objects and clutter. Finally the ray-trace data is interfaced to the physical optics module to obtain signal from scanned G2 grating. The virtual X-ray DPC simulator enables optimizing the system parameters. design energy, X-ray tube voltage and beam hardening while taking into account practical objects and clutter. We also present comparison of simulation results with experimental results for objects surrounded by clutter.



9588-18, Session 5

Waveguiding, mode filtering, and polarization control at extreme-ultraviolet frequencies

Sergey Zayko, Georg-August-Univ. Göttingen (Germany)

Lensless imaging techniques have a unique potential for direct investigation of the field distributions, governed by the nanoscale structures, in the spectral ranges where applicability of the conventional optical elements is limited. Here, we present a study of the extreme ultraviolet wave propagation in the nanoscale designed masks by means of coherent diffractive imaging (CDI) utilizing high-harmonic generation source. Exit surface waves, scattered from the objects, are reconstructed from their far field diffraction patterns using iterative phase retrieval algorithm. Reconstructions are susceptible to multiple scattering within the depth of the object and demonstrate pronounced waveguiding entailing strong high order modes suppression and substantial transmission contrast for varying light polarization. The observed phenomena are reproduced in semianalytical and numerical simulations indicating the potential of designing new optical elements such as mode filters, wave plates and polarizers for extreme-ultraviolet spectral range.

9588-19, Session 5

Development of ellipsoidal focusing mirror for soft x-ray and EUV

Hidekazu Mimura, Yoshinori Takei, Takahiro Saito, Takehiro Kume, Hiroto Motoyama, Satoru Egawa, Yoko Takeo, Takahiro Higashi, The Univ. of Tokyo (Japan)

Ellipsoidal mirror is one of promising focusing optics for soft X-ray and EUV. We have been developing the manufacturing system of ultra-precise ellipsoidal mirrors for 4 years. This system consists of mandrel fabrication, electroforming, wavefront measurement and additional deposition. We successfully fabricated an ellipsoidal mirror with 50 nm-level figure accuracy and evaluated its focusing performance using EUV light produced by a high order harmonic generation. In this presentation, we will introduce fabrication process and show the focusing performance of the ellipsoidal mirror.

9588-20, Session PWed

X-ray crystal optic fabrication process of the OPT Group of the X-ray Science Division at the Advanced Photon Source of Argonne National Laboratory

Michael Wieczorek, Xianrong Huang, Elina Kasman, Lahsen Assoufid, Argonne National Lab. (United States)

One of the missions of the OPT group of the X-ray Science Division at Argonne National Laboratory is to fabricate crystal-based X-ray optics from materials such as Silicon, Germanium, Quartz, and Sapphire, which is a unique capability in the USA for the synchrotron light source community. Some of these finished optics include single-bounce monochromators, channel-cut crystals, analyzers, and other devices. These optics are placed in the beamlines of the Advanced Photon Source to provide users with useful X-ray data in conjunction with electro-mechanical systems and measurement electronics. The steps involved in making these optics include slicing, cropping, grinding, crystal plane orienting, ultrasonic milling, wet chemical etching, and polishing. This poster illustrates these steps so the viewer may obtain a better understanding and appreciation of how X-ray optics are fabricated.

SPIE. PHOTONICS **Conference 9589: X-Ray Lasers and Coherent** X-Ray Sources: Development and Applications XI

Wednesday - Thursday 12-13 August 2015

Part of Proceedings of SPIE Vol. 9589 X-Ray Lasers and Coherent X-Ray Sources: Development and Applications XI

9589-1. Session 1

Observation of dynamics and modification of solid surface using a picosecond soft x-ray laser (Invited Paper)

Masaharu Nishikino, Tetsuya Kawachi, Noboru Hasegawa, Masahiko Ishino, Japan Atomic Energy Agency (Japan); Takuro Tomita, Univ. of Tokushima (Japan); Naofumi Ohnishi, Tohoku Univ. (Japan); Atsushi M. Ito, National Institute for Fusion Science (Japan); Takashi Eyama, Naoya Kakimoto, Rui Idutsu, Univ. of Tokushima (Japan); Yasuo Minami, Yokohama National Univ. (Japan); Tohru Suemoto, The Univ. of Tokyo (Japan); Anatoly Y. Faenov, Osaka Univ. (Japan); Nail A. Inogamov, Russian Academy of Sciences (Russian Federation); Mitsuru Yamagiwa, Japan Atomic Energy Agency (Japan)

Short pulse x-ray sources are widely used as probing beams for new material development and non-destructive x-ray imaging. The high quality soft x-ray laser (SXRL) source enables us to achieve quite high spatialresolution as a probe and quite intense x-ray as a pump. As an application using the SXRL, we have observed the spallative ablation process by the interaction with SXRL or femto-second (fs) laser. The dynamical processes of the SXRL and/or the fs laser-induced surface modifications come to attract much attention for the micro processing. However, it is difficult to observe the spallative ablation dynamics, because of non-repetitive, irreversible and rapid phenomena in a small feature size. In the case with SXRL irradiation (13.9 nm, 7 ps, 60 mJ/cm²), we have observed the damage structures and the optical emission from the ablated materials. When focused SXRL pulses were have been irradiated onto the metal surface, we have confirmed damage structures, however no optical emission signal during SXRL ablation could be observed. The electron temperature is estimated to be around a few eV at the ablated surface. In the case with fs laser irradiation (795 nm, 80 fs, 1.5 J/cm²), we have observed the surface morphology of fs laser ablation by the SXRL interferometer and SXRL reflectometer. The time resolved image of nano-scaled ablation dynamics of the sample surface was observed. The numerical simulation study is underway by using a molecular dynamics code. These results lead to understanding the full process of the interaction with the SXRL and/or fs laser.

9589-2, Session 1

An overview of the application of extreme ultra-violet lasers in plasma heating and diagnosis

Gregory J. Tallents, Valentin Aslanyan, Andrew K. Rossall, Sarah Wilson, The Univ. of York (United Kingdom)

Laser-plasma studies have been undertaken for over 50 years now using infra-red, visible and ultra-violet lasers. The critical density at infra-red to ultra-violet wavelengths is below the density of free electrons in a solid resulting in infra-red to ultra-violet lasers interacting with a solid target predominantly by collective absorption effects at densities up to a critical electron density which is typically at a material density 2 - 3 orders-ofmagnitude below the solid density. With pulse durations > 1 ps, the incoming laser interacts with an expanding plume of plasma formed by early components of the laser pulse and does not penetrate to the solid target surface. Extreme ultra-violet radiation (wavelength < 50 nm) has a critical electron density well-above any electron density formed by ionization at solid material density and so potentially can penetrate to a much greater

depth into a solid density plasma. We explore in this talk the importance of this penetration in ablating solid targets, in creating novel warm dense matter and in the diagnosis of plasmas. We show that a new regime of extreme ultra-violet laser-produced plasmas are created and explore some of their properties.

OPTICAL ENGINEERING+

APPLICATIONS

9589-3, Session 1

Low electron temperature in ablating materials formed by picosecond soft x-ray laser pulses

Masahiko Ishino, Noboru Hasegawa, Masaharu Nishikino, Japan Atomic Energy Agency (Japan); Tatiana A. Pikuz, Russian Academy of Sciences (Russian Federation) and Osaka Univ. (Japan); Igor Y. Skobelev, Russian Academy of Sciences (Russian Federation) and National Research Nuclear Univ. MEPhI (Russian Federation); Anatoly Y. Faenov, Russian Academy of Sciences (Russian Federation) and Osaka Univ. (Japan); Nail A. Inogamov, Russian Academy of Sciences (Russian Federation); Tetsuya Kawachi, Mitsuru Yamagiwa, Japan Atomic Energy Agency (Japan)

To study the ablation process induced by the soft x-ray laser pulse, we investigated the electron temperature of the ablating material. Focused soft x-ray laser pulses having a wavelength of 13.9 nm and duration of 7 ps were irradiated onto the LiF, AI, and Cu targets, and we observed the optical emission from the surfaces by use of an optical camera. On target surfaces, we could confirm damage structures, but no emission signal in the visible spectral range during ablation could be observed. Then, we estimated the electron temperature in the ablating matter. To consider the radiation from a heated layer, we supposed a black-body radiator as an object. The calculation result was that the electron temperature was estimated to be lower than 1 eV and the process duration was shorter than 1000 ps. The theoretical model calculation suggests the spallative ablation for the interaction between the soft x-ray laser and materials. The driving force for the spallation is an increasing pressure appearing in the heated layer, and the change of the surface is considered to be due to a splash of a molten layer. The model calculation predicts that the soft x-ray laser with the fluence around the ablation threshold can create an electron temperature around 1 eV in a material. The experimental result is in good accordance with the theoretical prediction. Our investigation implies that the spallative ablation occurs in the low electron temperature region of a non-equilibrium state of warm dense matter.

9589-4, Session 1

Advances in nanoscale 3D molecular imaging by soft x-ray laser ablation mass spectrometry

Ilya Kuznetsov, Jorge Filevich, Mark R. Woolston, Tyler Green, Colorado State Univ. (United States); David Carlton, Weilun Chao, Eric Anderson, Lawrence Berkeley National Lab. (United States); Elliot Bernstein, Dean Crick, Debbie Crans, Colorado State Univ. (United States); Valentin Aslanyan, Andrew Rossall, Greg Tallents, The Univ. of York (United Kingdom); Tomas Burian, Libor Juha, Institute of Physics of the ASCR, v.v.i. (Czech Republic); Jorge Rocca,



Carmen Menoni, Colorado State Univ. (United States)

Laser ablation and ionization combined with mass spectrometry (MS) forms the basis of one of the most widely exploited analytical tools of the solid state. This paper describes advances in three dimensional (3D) molecular composition imaging with nanoscale spatial resolution by soft x-ray (SXR) laser ablation time of flight (TOF) MS. The use of the SXR laser light of 46.9 nm wavelength from a compact capillary discharge laser makes it possible to ablate craters with diameters as small as 120 nm and a depth of 3.5 nm in organic materials. Moreover, the single shot ablation of organic materials produces craters with none or little sign of thermal damage to the surroundings of the focal spot. Both positive and negative ion extraction modes provide single shot detection of intact analyte molecules from probing volumes down to 50 zL. We have applied SXR TOF MS to the chemical analysis of antibiotics, aminoacids, organic dyes, and dielectrics. The corresponding mass spectra show protonation is the dominant ionization mechanism in positive extraction mode while electron attachment is predominant in negative mode. The high sensitivity and spatial resolution of SXR TOF MS has enabled the demonstration of composition imaging in organic samples with nanoscale lateral - 75 nm and depth - 20 nm resolutions, without compromising mass resolution. SXR TOF MSI is specifically suited in analysis and imaging of insoluble solid state compounds with low ionization efficiency in ultraviolet range.

9589-5, Session 1

XUV/x-ray laser-induced irreversible changes in solids (Invited Paper)

Libor Juha, Institute of Physics of the ASCR, v.v.i. (Czech Republic)

Although irreversible changes occurring in solids exposed to high fluxes of energetic photons (i.e., extreme ultraviolet, soft x-ray and x-ray radiation) were first studied almost forty years ago, particular processes responsible for material alteration were investigated in detail only infrequently until now. Let us consider material removal (erosion) as the most illustrative case of XUV/x-ray-induced irreversible substantial changes in a certain material. The XUV/x-ray sources commonly used for the studies of material removal emit at either low peak power (e.g., synchrotron radiation sources) or high peak power (e.g., free-electron lasers and various sources based on short-lived hot dense plasmas): (a) With low-peak-power sources, material is removed by photon-induced desorption from the irradiated sample surface. (b) High-peak-power sources make possible to expose material to a high local dose of radiation in a short period of time, i.e., at a very high dose rate. It produces an overheated, fragmented region of the sample which tends to blow off (ablate) into the vacuum. Investigating these processes with short-wavelength radiation delivered by various sources, we observed both desorption- and ablation-like behavior. A phenomenological desorptionablation model has been developed. An influence of wavelength, pulse duration, angle of incidence, and other beam parameters on a course of the above-mentioned phenomena will be treated and summarized in this contribution. Recent results obtained with numerous materials of a very different kind, i.e., from ionic crystals to (bio)molecular solids, will be presented. The role of thermal and non-thermal processes will be discussed.

9589-6, Session 2

Multilayer optics for coherent EUV/X-ray laser sources (Invited Paper)

Franck Delmotte, Charles Bourassin-Bouchet, Sébastien de Rossi, Evgueni Meltchakov, Maël Dehlinger, Lab. Charles Fabry (France)

The development of new sources and related applications in the EUV and soft X-ray spectral domain, raises more stringent requirements on the quality of multilayer mirrors. Mirrors with high efficiency, good stability, enhanced selectivity and/or broad bandwidth and phase controlled are key components to manipulate the pulses generated by coherent EUV/X-ray laser sources like X-ray lasers, High Harmonic Generation or X-ray Free

Electron Laser sources.

After a brief description of the theoretical principles and history of multilayer mirrors, we present the state of the art of multilayer optics for coherent EUV/X-ray laser sources. First, we focus on the specificities of multilayer mirrors for pico- and femto-second sources, in terms of reflectivity, selectivity and stability. Then, we report the recent advances in the design, deposition and characterization of multilayer mirrors for attosecond sources. Phase controlled multilayer mirrors provide a powerful tool towards transporting or even compressing attosecond pulses. Pulse compression down to sub-50 as duration has already been demonstrated in the extreme ultraviolet (EUV) domain (30 – 100 eV). The design and the phase characterization of such mirrors in the soft X-ray domain (100 – 500 eV) remain challenging and will be discussed.

9589-7, Session 2

X-ray diffractive optics (Invited Paper)

Anne E. Sakdinawat, Sharon Oh, Chieh Chang, Jeongwon Park, SLAC National Accelerator Lab. (United States); Michael J. Rooks, Yale Univ. (United States); Richard C. Tiberio, Stanford Univ. (United States)

X-ray diffractive optics provide one of the most versatile ways to shape and manipulate an x-ray beam which is important for areas such as x-ray imaging. One of the barriers to practical use of x-ray diffractive optics, especially for the hard x-ray region, is the low efficiency of these optics, stemming from the difficulty in fabricating very high aspect ratio, high resolution dense features. We will describe the use of metal assisted chemical etching schemes to address and solve problems in the area of x-ray optics.

9589-8, Session 3

EUV laser photoelectron spectroscopy of mass selected neutral clusters (Invited Paper)

Elliot R. Bernstein, Shi Yin, Colorado State Univ. (United States)

A long standing set of goals for the study of a system of inhomogeneous, neutral clusters (e.g., MmXn or (molecule)p) has been to mass sort and select them individually for determination of physical and chemical properties of each neutral cluster by spectroscopic techniques. We have constructed appropriate instrumentation to achieve these important goals employing photoelectron spectroscopy (PES), driven by both visible (for MmXn -) and EUV (for MmXn0) radiation. Our 26.5 eV/photon EUV laser can ionize any neutral cluster or molecule (EUV PES) that can be identified and isolated. The algorithm includes the following steps: 1. generation of cluster negative ions in a laser ablation supersonic source with the addition, as required, of low energy electrons from a Y2O3 disk; 2. separation of these anionic clusters in a reflectron time of flight mass spectrometer (RTOFMS); 3. selection and slowing of specific, chosen clusters in a mass gate/momentum deceleration stage; 4. threshold photo-detachment of the sorted and selected negative ion clusters with a tunable VIS/UV laser to generate neutral, isolated clusters; and 5. EUV PES of these neutral clusters. Such studies generate vibrational and structural information on the ground states of the neutral clusters (through VIS/UV PES), and information on the ion states of the clusters (through EUV PES). The presentation will include PES results on various metal oxides, sulfides, and other cluster systems and molecules.



9589-9, Session 3

The observation of a transient surface morphology in the femtosecond laser ablation process by using the soft x-ray laser probe

Noboru Hasegawa, Masaharu Nishikino, Masahiko Ishino, Japan Atomic Energy Agency (Japan); Takuro Tomita, The Univ. of Tokushima (Japan); Naofumi Ohnishi, Tohoku Univ. (Japan); Atsushi M. Ito, National Institute for Fusion Science (Japan); Takashi Eyama, Naoya Kakimoto, Rui Idutsu, The Univ. of Tokushima (Japan); Yasuo Minami, The Univ. of Tokyo (Japan); Motoyoshi Baba, Tohru Suemoto, The Univ. of Tokyo (Japan); Anatoly Y. Faenov, Osaka Univ. (Japan); Nail A. Inogamov, Russian Academy of Sciences (Russian Federation); Tetsuya Kawachi, Mitsuru Yamagiwa, Japan Atomic Energy Agency (Japan)

The dynamics of the femto-second laser ablation process is a key issue for the understanding of the sub-micron scale processing. In previous works, the formation of an expansion front with a thin filmy structure outer the ablating surface (= ablation front) was observed by using a probe laser at the wavelength of 400 nm. However the details of both the fronts were not observed because they were covered with plasmas, which interrupted the penetration of the probe beam. We have succeeded in simultaneous observation of the expansion front and the ablation front of the gold which was irradiated by Ti:Sapphire laser with 80 fs duration by using the 13.9 nm soft x-ray laser interferometer. The dynamics of the ablation front was obtained by using the soft X-ray interferometer. The surface roughness of the ablation front was better than a few nm until t = 1 ns of the laser irradiation, and the height of it increased to only 30 nm. The dynamics of the expansion front was obtained from the Newton's rings generated between both the fronts within the time of 200 ~ 800 ps. It implies the expansion front worked as the soft X-ray beam splitter. The expansion speed of the expansion front strongly depended on the local fluence of the pump laser. These results implies that the potential of the expansion front as the novel transient soft x-ray optics because the spatial profile of the expansion front will be controlled by the spatial profile of the pump laser.

9589-10, Session 3

Overview of warm dense matter experiments at SLAC (Invited Paper)

Eric C. Galtier, SLAC National Accelerator Lab. (United States)

Warm dense matter (WDM) is found in numerous astrophysical systems, from giant planets to Brown dwarves or cool dense stars. Being this intermediate regime where condensed matter or plasma theories do not apply, it is produced in all laser produced plasma experiments on earth. As a consequence, understanding its properties is fundamental and the whole community is investigating this extreme state of matter.

With the advent of the 4th generation of light sources, namely the Free Electron Lasers (FELs), a new way of producing and diagnosing warm dense matter becomes available. In 2009, the Linac Coherent Light Source (LCLS) at SLAC was the first FEL to produce X-ray photons to be used by the user community.

Since then, various experiments took place at LCLS to produce and measure specific physical properties of warm dense matter. In this talk, we will present an overview of these experiments as well as ongoing efforts. The LCLS has been used in a variety of configuration: as a principle heating mechanism, as a probe or both at the same time. When used as a probe, high power lasers have been used to shock matter and excite it into the WDM regime. Results will be presented.

The end of the talk will describe exciting perspectives on the WDM research, as the LCLS-II will become available in a 5 years time scale.

9589-11, Session 3

Generation of strongly-coupled plasma using Argon-based capillary discharge lasers

Andrew K. Rossall, Valentin Aslanyan, Sarah Wilson, Gregory J. Tallents, The Univ. of York (United Kingdom)

Argon based capillary discharge lasers operate in the extreme ultra violet (EUV) at 46.9 nm with an output of up to 0.5mJ energy per pulse and up to a 10 Hz repetition rate. Focussed irradiances of up to 10^12 W cm^-2 are achievable and can be used to generate plasma in the warm dense matter regime by irradiating solid material. To model the interaction between such an EUV laser and solid material, the 2D radiative-hydrodynamic code POLLUX has been modified to include absorption via direct photo-ionisation, a super-configuration model to describe the ionisation dependant electronic configurations and a calculation of plasma refractive indices for ray tracing of the incident EUV laser radiation. A simulation study is presented, demonstrating how capillary discharge lasers of 1.2ns pulse duration can be used to generate strongly coupled plasma at close to solid density with temperatures of a few eV and energy densities up to 1?10^5 J cm^-3.

Plasmas produced by EUV laser irradiation are shown to be useful for examining the equation-of-state properties of warm dense matter. One difficulty with this technique is the reduction of the strong temperature and density gradients which are produced during the interaction. Methods to inhibit and control these gradients will be examined.

9589-12, Session 4

Development of an ultrashort plasmabased soft x-ray laser (*Invited Paper*)

Adrien Depresseux, Lab. d'Optique Appliquée (France); Eduardo Oliva, Lab. de Physique des Gaz et des Plasmas (France); Julien Gautier, Fabien Tissandier, Lab. d'Optique Appliquée (France); Jaroslav Nejdl, Michaela Kozlova, Institute of Physics of the ASCR, v.v.i. (Czech Republic); Gilles Maynard, Lab. de Physique des Gaz et des Plasmas (France); Jean-Philippe Goddet, Amar Tafzi, Agustin Lifschitz, Lab. d'Optique Appliquée (France); Hyung Taek Kim, Gwangju Institute of Science and Technology (Korea, Republic of) and Institute for Basic Science (Korea, Republic of); Sylvie Jacquemot, Lab. pour l'Utilisation des Lasers Intenses (France) and Commissariat à l'Energie Atomique et aux Energies Alternatives (France); Victor Malka, Kim Ta Phuoc, Cédric Thaury, Pascal Rousseau, Thierry Lefrou, Gregory Iaquaniello, Alessandro Flacco, Boris Vodungbo, Guillaume Lambert, Antoine Rousse, Philippe Zeitoun, Stéphane Sebban, Lab. d'Optique Appliquée (France)

The development of x-ray free electron lasers allowed a myriad of innovative applications notably in biology, requiring high-energy and ultrashort pulse duration in the femtosecond-range to probe the ultra-fast dynamics of matter in the nanometre scale.

Alongside those large-scale and expensive high-brilliance sources, compact and cheap plasma-based x-ray lasers arouse great interest, notably due to their ability to deliver the highest demonstrated energy per pulse [1] within a narrow linewidth. But also because they display excellent optical properties when seeded with a high-harmonic source [2].

However, those sources have been limited to the picosecond range [3] for more than a decade, which restrained the scope of applications.

We proposed and implemented an original technique, named "Collisional lonization Gating", which allowed us not only to achieve femtosecond pulse



duration for the first time, but also to report a boost in output energy. The combination of those made possible a remarkable enhancement of total peak intensity by about two orders of magnitude compared to the present state of the art.

Our scheme relies on increasing the plasma density to quench the gain duration of the plasma amplifier, which also leads to an increase in saturation intensity and laser gain [4]. At the reported high densities, guiding techniques prove to be pivotal to counterbalance refraction [5].

The demonstrated plasma-based soft x-ray laser was implemented focusing an ultra-intense IR pule into a krypton gas and pumping the atomic transition of Ni-like species at 32.8nm [6].

Tailoring the plasma waveguide for higher densities and longer amplifiers holds great promises to further outdistance previous performances of plasma-based soft x-ray lasers.

[1] Rus, B. et al., Phys. Rev. A. 66, 063806 (2002).

[2] Goddet, J. P. et al. Opt. Lett. 34, 16 (2009).

[3] Wang Y. et al. Nat. Phot. 2, 94-98 (2008).

[4] Mocek, T. et al., Phys. Rev. A. 95, 173902 (2005).

[5] Chou, M. C. et al., Phys. Rev. Lett. 99, 063904 (2007).

[6] Zeitoun, P. et al, Nature 431, 426-429 (2004).

9589-13, Session 4

Modeling of dense injection-seeded Ni-like Krypton plasma amplifiers

Eduardo Oliva, Univ. Politécnica de Madrid (Spain); Adrien Depresseux, Fabien Tissandier, Julien Gautier, Stéphane Sebban, Lab. d'Optique Appliquée (France); Gilles Maynard, Lab. de Physique des Gaz et des Plasmas (France)

Plasma amplifiers seeded with High Order Harmonics have demonstrated to be a high-repetition rate, table top source of short (picosecond or less), intense and coherent soft X-ray beams. In the quest for shorter (100 fs or less) and more energetic pulses (several microJoules at least), increasing the density of the amplifier promises to fulfill both goals.

In this work we will present modeling results of the recent experiments using the 60 TW laser "Salle Jaune" at LOA. In these experiments, the lasing ion (Ni-like Krypton) is created by Optical Field Ionization in a dense plasma. To ensure the propagation of the IR pulse through the plasma column, the ignitor+heater technique is used to create a plasma channel that acts as a waveguide, compensating the the defocusing and guiding the pulse over several Rayleigh lengths. Once the population inversion is created via collisional excitation, the 25th harmonic of the driving laser is seeded to be amplified when passing through the plasma.

The propagation of the IR pulse through the plasma channel was modeled using the Particle In Cell code WAKE-EP. The results uncover a selfregulating mechanism between the overionization induced refraction at the central part of the channel and the focusing at the channel borders. The amplification of the seeded harmonic is modeled with our Maxwell-Bloch model DeepOne. The code is benchmarked over a huge range of electron densities, confirming the unprecedented duration of 64 fs FWHM (123 fs RMS). DeepOne also gives information about the polarization of the amplified beam.

9589-14, Session 4

FEL seeding at FERMI: a root to table-top laser-like FEL performance (Invited Paper)

Miltcho B. Danailov, Paolo Cinquegrana, Alexander A. Demidovich, Gabor Kurdi, Ivaylo P. Nikolov, Paolo Sigalotti, Elettra-Sincrotrone Trieste S.C.p.A. (Italy)

Free Electron Lasers (FELs) have made remarkable progress in the last

decades. In this paper we show that one important direction of the Extreme UV and Soft X-ray FEL development, i.e. the use of seeding by an external laser, is already allowing to generate pulses having the high coherence, stability of the pulse intensity, wavelength and timing of table-top ultrafast lasers. This work presents some of the novel schemes developed and under development at the FERMI FEL. The work will first describe some key points in the use of High Gain Harmonic Generation (HGHG) seeding at FERMI that have led to the generation of highly stable nearly transform limited FEL pulses. We then concentrate on the recently developed modalities allowing pump-probe experiments with practically no litter between the pump and probe pulses. One of the presented techniques relies on the use of pulses generated by the seed laser, optically transported to the experimental stations. the seed laser light for pump-probe experiments. We are presenting the design of a scheme implementing this idea at the FERMI FEL. Another new technique described is based on the use of twin-seed pulses and delivers twin FEL pulses with tunable time delay and wavelengths. Some examples from pump-probe measurements based on the above two approaches will be presented and near future development will be discussed.

9589-15, Session 4

Chirped-pulse amplification in x-ray freeelectron lasers

Benoît Mahieu, Hugo Dacasa, Lab. d'Optique Appliquée (France); Marta Fajardo, Instituto Superior Técnico (Portugal); Thuy T. T. Le, Lab. d'Optique Appliquée (France); Lu Li, Queen's Univ. Belfast (Ireland); Eduardo Oliva, Univ. Politécnica de Madrid (Spain); Philippe Zeitoun, Lab. d'Optique Appliquée (France)

X-ray Free-Electron Lasers (FEL's) are powerful tools for probing matter properties down to sub-nanometer scales with femtosecond dynamics, allowing a growing number of physical, chemical, biological and medical investigations to be carried out. FEL's operating in seeding mode intrinsically present enhanced temporal coherence properties with respect to those relying on the self-amplified spontaneous emission process. They are however limited, for the moment, to extreme-ultraviolet wavelengths, or with hardness to soft X-rays, and durations of tens of femtoseconds. We studied how these limits can be overcome by means of X-ray chirped-pulse amplification schemes, inspired from infrared lasers.

As a matter of fact, the use of a seed enables a fine control of the chirp and a spectro-temporal shaping of the FEL emission. Moreover, ultrashort wavelengths can be envisaged through high-gain harmonic generation and echo-enabled harmonic generation configurations. We will present FEL simulations coupled with the design of stretcher/compressor in both classical and conical diffraction geometries.

9589-16, Session 4

EIS-TIMER, mini-TIMER, and nano-TIMER: present and future experimental facilities for VUV/soft x-ray transient grating experiments

Cristian Svetina, Nicola Mahne, Lorenzo Raimondi, Filippo Bencivenga, Riccardo Cucini, Flavio Capotondi, Elettra-Sincrotrone Trieste S.C.p.A. (Italy); Andrea Battistoni, Elettra-Sincrotrone Trieste S.C.p.A. (Italy) and Univ. degli Studi di Trieste (Italy); Riccardo Mincigrucci, Elettra-Sincrotrone Trieste S.C.p.A. (Italy) and Univ. degli Studi di Perugia (Italy); Erika Giangrisostomi, Elettra-Sincrotrone Trieste S.C.p.A. (Italy) and Univ. degli Studi di Trieste (Italy); Alessandro Gessini, Michele Manfredda, Ivaylo Petrov Nikolov, Emanuele Pedersoli, Emiliano Principi, P.



Parisse, F. Casolari, Miltcho B. Danailov, Maya Kiskinova, Claudio Masciovecchio, Elettra-Sincrotrone Trieste S.C.p.A. (Italy); Marco Zangrando, Elettra-Sincrotrone Trieste S.C.p.A. (Italy) and IOM-CNR Lab. TASC (Italy)

FERMI, the Italian Free Electron Laser user facility, provides VUV/soft x-ray photons pulses with unprecedented high brilliance and coherence. The EIS-TIMER beamline is foreseen to be installed in 2015-2016 and will be dedicated to perform transient grating experiments. The unique design of EIS-TIMER is conceived to exploit such kind of non-linear coherent experiments to probe collective vibrational and electronic properties of matter at the nanoscale. Lately a proof of principle experiment has been successfully carried out at the DiProl beamline employing a simplified and compact setup: the "mini-TIMER". Meanwhile we are studying a new and even more compact optical configuration (the "nano-TIMER") able to extend this approach to a wider wavevector range and to employ ultra-short FEL pulses.

In this seminar we will briefly describe the FERMI user facility, the EIS-TIMER beamline and its scientific case. We will also report on the experimental results obtained with "mini-TIMER" and will focus to the "nano-TIMER" set-up.

9589-35, Session PWed

Design challenges to photon diagnostics and beam line components under highrepetition-rate x-ray FEL operation

Yiping Feng, SLAC National Accelerator Lab. (United States)

Future high repetition rate X-ray FEL's such as the European XFEL and LCLS-II presents new challenges to photon diagnostics as well as essential beamline components. In addition to these devices having to sustain the high peak power of a single-pulse FEL radiation, they must also be capable of handling the enormous power density of tens to hundreds of watts over a small area as small as 0.1 mm2. In this talk, I will discuss the potential impact of high power FEL operation on performance of a gas attenuator and the design challenges to beam intercepting components such as a collimator or stopper.

9589-36, Session PWed

Soft x-ray source based on the highcurrent capillary-discharge system

Jiri Schmidt, Karel Kolacek, Oleksandr Frolov, Jaroslav Straus, Institute of Plasma Physics of the ASCR, v.v.i. (Czech Republic)

Our department has been studying high-current capillary discharge as a prospective XUV laser source since 1998. Among others we have built two experimental apparatuses CAPEX (since 1998) and CAPEX-U (since 2005). On both these devices we have observed lasing at 46.9 nm (Ne-like argon line). While the experimental apparatus CAPEX-U has laser-triggered spark gap, which enables exact synchronization with diagnostics or with other attached experiments, the apparatus CAPEX is capable to run at a higher repetition rate (up to ~ 1 Hz). Some laser beam characteristics have already been measured (e.g. laser pulse energy, laser beam profile and divergence). However, these devices are not only lasing at 46.9 nm, but also they are used for testing a possibility of amplification at the wavelength below 20 nm, that have more practical applications.

Nowadays, the fast high-current capillary-discharge experiments with nitrogen-filled capillary are in progress as well. In this paper the recent results obtained from both these discharge systems (argon-, nitrogen-filled capillaries) will be presented.

Acknowledgement.

This work was performed under auspices and with the support of the Grant

Agency of the Czech Republic (contract 14-29772S) and of the Ministry of Education, Youth, and Sports, CR (contract LG13029).

9589-37, Session PWed

Ultra-broadband ptychography with selfconsistent coherence estimation from a high harmonic source

Michal Odstr?il, Univ. of Southampton (United Kingdom) and RWTH Aachen Univ. (Germany); Peter Baksh, Univ. of Southampton (United Kingdom); Hyun-su Kim, RWTH Aachen Univ. (Germany) and Univ. of Southampton (United Kingdom); William S. Brocklesby, Jeremy G. Frey, Univ. of Southampton (United Kingdom)

The ptychography method for coherent diffractive imaging (CDI) is gaining significant popularity over the last few years in the synchrotron science community because of its advantages over simpler CDI schemes. However, for imaging applications in the extreme ultraviolet (XUV), the ability to perform ptychography with table top setups is limited by requirements on coherence and overall beam quality.

With the aim of improving imaging using table top XUV apparatus, we demonstrate an improved ptychography method that can tolerate a relative bandwidth of -20% for achromatic objects. Further, our algorithm is able to reconstruct diffraction patterns blurred by low beam pointing stability. The coherence and blurring properties of the illumination probe are automatically identified during the ptychographic reconstruction. This improved method allows the use of fewer monochromating optics, obtaining higher flux at the sample and reaching higher resolution for semi-opaque objects. This is critical in the case of ptychography when a large number of diffraction patterns needs to be collected compared to the standard coherent diffraction method with compactness constraints. Our method is tested on reconstruct on for partly transparent samples to show the improved reconstruct quality.

9589-17, Session 5

Towards milliwatt average power table-top soft x-ray lasers (Invited Paper)

Jorge J. Rocca, Brendan Reagan, Cory Baumgarten, Yong Wang, Shoujun Wang, Alex Rockwood, Liang Yin, Mario Marconi, Vyacheslav Shlyaptsev, Carmen Menoni, Colorado State Univ. (United States)

We will discuss advances in the development of high repetition rate, tabletop soft x-ray lasers operating at wavelengths between 10 nm and 20 nm. Combining newly developed diode-pumped high energy ultra-short pulse laser technology with efficient plasma generation techniques we have demonstrated a new generation of compact high average power soft x-ray lasers. Recent results include the first table-top soft x-ray lasers to operate at 100 Hz repetition rate, that have made possible the generation of record 0.2 mW average power at ? = 18.9 nm, 0.1 mW at ? = 13.9nm, and 20 ?W at ? = 11.9nm. These lasers are enabled by a compact chirped pulse amplification laser based on diode-pumped, cryogenically-cooled Yb:YAG power amplifiers that produces 1 Joule, 5 ps FWHM duration pulses at 100 Hz repetition rate. Operation of these lasers with rotating targets has allowed the uninterrupted high repetition rate operation of the ? = 18.9nm soft x-ray laser for hundreds of thousands of consecutive shots, making it suitable for applications in nanoscience and nanotechnology that require high photon flux at short wavelengths. A high energy Ti:Sa driver laser to pump sub-10 nm table top lasers at multi-Hz repetition ray will also be discussed.



9589-18, Session 5

Single-shot phase-controlled diffraction imaging using an Ag x-ray laser at 13.9 nm

Kyoung Hwan Lee, Hyeok Yun, Institute for Basic Science (Korea, Republic of); Jae Hee Sung, Seong Ku Lee, Institute for Basic Science (Korea, Republic of) and Advanced Photonics Research Institute (Korea, Republic of); Hwang Woon Lee, Institute for Basic Science (Korea, Republic of); Hyung Taek Kim, Institute for Basic Science (Korea, Republic of) and Advanced Photonics Research Institute (Korea, Republic of); Chang Hee Nam, Institute for Basic Science (Korea, Republic of) and Gwangju Institute of Science & Technology (Korea, Republic of)

Single-shot x-ray coherent diffraction imaging (CDI) is an emerging technology developed to observe the ultrafast dynamics of nanometer-scale objects without objective lenses. In spite of the potential to achieve wavelength-limited single-shot CDI, the spatial resolution of the CDI has been limited due to practical reasons of illumination flux, the dynamic range of x-ray detectors, noise, and the steep scaling of diffraction signal. Through a detailed analysis of factors limiting the spatial resolution of single-shot CDI, we could substantially improve the achievable spatial resolution of CDI by the sharp phase edges.

We devised a new method to improve the spatial resolution of x-ray CDI by implementing the sharp phase variation in a sample. In our experiment, the spatial resolution of 22 nm was achieved using a single Ag X-ray laser pulse, very close to the diffraction-limited resolution of 21 nm. The achieved spatial resolution was only 1.5 times the wavelength, 13.9 nm, of the x-ray laser. The introduction of the sharp phase edge modified the power scaling of the diffraction signal by inducing an asymmetric diffraction pattern, efficiently extending the diffraction signal to the region of high spatial frequencies. We also performed a simulation to examine the experimental result and confirmed that the sharp phase edge enhanced the resolution compared to the case of a pure absorption edge. Since this phase controlled CDI makes use of a fundamental phenomenon of diffraction, it is a general approach applicable to other lensless imaging methods.

9589-19, Session 5

X-ray characterization of short-pulse laser illuminated hydrogen storage alloys having very high performance

Hiroyuki Daido, Japan Atomic Energy Agency (Japan)

At present, hydrogen starage alloys are more and more important in the fields of electric energy production and strage, automobiles and so on. The initial rates of hydrogen absorption and desorption of a hydrogen storage alloy are one of the important performances to be improved. On the basis of the previous experimental study using accelerators (1), charged particles cause surface modifications on the alloys resulting in improvement of the hydrogen absorption rate while these machines also cause radioactivity. The vacancies introduced into a hydrogen absorption alloy are found to be positive effect on the improvement of the initial hydrogen absorption rate. We also have made improvement of the absorption rate using an ultra-high intensity laser driven proton beam (2). Here, we report on the characterization of the hydrogen absorption rate using direct illumination technique with a femoto second laser as well as nano second laser instead of rather complicated bigger illumination sytems. A laser illuminates the whole surface sequentially on a tip of a few cm sequre LaNi4.6AlO.4 alloy resulting in significant improvement of the hydrogen absorption rate. The expected scenario of this improvement is following. Firstly, the laser hits the surface with appropirate laser intensity and duration, next the ablation occurs. The strong pressure applied to the interior of the sample makes suitable defects in the surface layer of the sample. In order to characterize the surface layer, we perform x-ray diffraction experiment using SPring-8 synchrotron radiation facility. We also discuss useful x-ray techniques for understading the mechnism.

References

1) H. Abe, S. Aone, R. Morimoto and H. Uchida, J. Alloys Comp., 580 (2013) 5219.

2) H. Abe, S. Orimo, M. Kishimoto, S. Aone, H. Uchida, H. Daido and T. Ohshima, Nucl. Inst. Meth. B 307 (2013) 218.

9589-20, Session 5

Coherent diffractive imaging employing a laboratory-scale, spatially partiallycoherent discharge plasma EUV light source

Jan Bussmann, Forschungszentrum Jülich GmbH (Germany) and RWTH Aachen Univ. (Germany) and JARA-Fundamentals of Future Information Technology (Germany); Michal Odstr?il, Univ. of Southampton (United Kingdom) and RWTH Aachen Univ. (Germany); Raoul Bresenitz, Forschungszentrum Jülich GmbH (Germany) and JARA-Fundamentals of Future Information Technology (Germany) and RWTH Aachen Univ. (Germany); Denis Rudolf, Forschungszentrum Jülich GmbH (Germany); William S. Brocklesby, Univ. of Southampton (United Kingdom); Jianwei Miao, Univ. of California, Los Angeles (United States) and California NanoSystems Institute (United States); Detlev Grützmacher, Forschungszentrum Jülich GmbH (Germany); Larissa Juschkin, RWTH Aachen Univ. (Germany) and Forschungszentrum Jülich GmbH (Germany)

Diffraction limited microscopy in the EUV and soft X-ray spectral region requires expensive either low roughness reflective optics or diffractive optics structured on the nanometer scale. Alternatively, coherent diffraction imaging (CDI) offers the possibility to replace the optics completely by image reconstruction algorithms.

Experimentally, a sufficiently coherent beam shines on the test object which diffraction pattern is recorded on the detector. Then, the object can be reconstructed from its diffraction pattern down to the diffraction limit by means of phase retrieval techniques.

So far, most experiments were performed at synchrotron and free electron laser facilities. Only few laboratory based CDI experiments employing either a high harmonic or a soft X-ray laser source were conducted so far. In our work, we demonstrate CDI with laboratory based high radiance plasma sources with partial spatially coherence developed for EUV lithography. Experimentally, a 10 μm cross-like structured silicon nitride sample is imaged with light of the O VI emission line (17.3 nm). To account for spatial and temporal incoherence a dynamical adapting deblurring kernel is used during reconstruction. This modified modulus constraint method in combination with the small bandwidth of the plasma emission line, allows spectral filtering without transmission filters and only by one multilayer mirror. Steps to push the resolution closer to the diffraction limit and utilizing multiple wavelength will be presented.

9589-21, Session 5

3D nanoscale imaging of biological samples with laboratory-based soft x-ray sources

Aurélie Dehlinger, Berlin Lab. for Innovative X-ray Technologies (Germany) and Technische Univ. Berlin (Germany) and Max-Born-Institut (Germany); Anne Blechschmidt, Technische Univ. Berlin (Germany); Birgit Kanngießer, Technische Univ. Berlin (Germany) and Berlin

Conference 9589: X-Ray Lasers and Coherent X-Ray Sources: Development and Applications XI



Lab. for Innovative X-ray Technologies (Germany); Martina C. Meinke, Fiorenza Rancan, Charité Universitätsmedizin Berlin (Germany); Kai Reineke, Leibniz-Institut für Agrartechnik Potsdam-Bornim e.V. (Germany); Christian Seim, Berlin Lab. for Innovative X-ray Technologies (Germany) and Max-Born-Institut für Nichtlineare Optik und Kurzzeitspektroskopie (Germany); Holger Stiel, Berlin Lab. for Innovative X-ray Technologies (Germany); Stephan Werner, Helmholtz-Zentrum Berlin für Materialien und Energie GmbH (Germany)

In microscopy, where the theoretical resolution limit depends on the wavelength of the probing light, radiation in the soft X-ray regime can be used to analyze samples that cannot be resolved with visible light microscopes. In the case of soft X-ray microscopy in the water-window, the energy range of the radiation lies between the absorption edges of carbon and oxygen. As a result, carbon-based structures, such as biological samples, possess a strong absorption, whereas e.g. water is more transparent to this radiation. Microscopy in the water-window therefore allows the structural investigation of aqueous samples with resolutions of a few ten nanometers and a penetration depth of up to 10 μ m.

In this contribution we present a Laboratory Transmission X-ray Microscope (LTXM) which runs with a laser produced nitrogen plasma that emits radiation at 500 eV. The mentioned high penetration depth can be exploited to analyze biological samples in their natural state and with several projection angles. The obtained tomogram is the key to a more precise and global analysis of samples originating from various fields of life science. The application of this method for the investigation of nanoparticles in human skin and of high-pressure treated bacterial endospores will be presented.

In conclusion we compare our results with other nanoscale imaging methods using coherent laboratory based sources like plasma based X-ray lasers or radiation from high harmonic generation.

9589-22, Session 6

Output beam polarisation of x-ray lasers with transient inversion (Invited Paper)

Karol A. Janulewicz, Gwangju Institute of Science and Technology (Korea, Republic of); Chul Min Kim, Gwangju Institute of Science and Technology (Korea, Republic of) and Institute of Basic Science (Korea, Republic of); Holger Stiel, Max-Born-Institut für Nichtlineare Optik und Kurzzeitspektroskopie (Germany); Tetsuya Kawachi, Masaharu Nishikino, Noboru Hasegawa, Japan Atomic Energy Agency (Japan)

Polarisation of the generated radiation is a parameter of paramount importance for application of any radiation source. X-ray lasers work nearly exclusively in the regime of amplified spontaneous emission (ASE) and it is frequently expected that the polarization state of the output radiation should stay undefined. A few attempts to clear the situation did not put much light on the effect giving contradictory conclusions. In fact, it is little consideration on how the amplification process changes the polarization state. The theoretical analysis within the uniform (singlemode) approximation, focusing on the dynamics of X-ray laser generation, suggested that in such a case the output radiation should show some level of polarization but randomly changing from shot-to-shot. To verify this hypothesis we have conducted relevant experiment using traditional double-pulse scheme of transient inversion and a membrane beamsplitter as a polarization selector. It was found that the output radiation has a significant, but fluctuating as far as its amplitude is concerned, s-polarisation component (parallel to the target surface) in each shot. However, it was also found that this result does not gives ultimate answer due to simplified measurement technique and the traditional formula used to determine the degree of polarisation (DOP). The expression, used also in other experiments, is under conditions of these experiments no more valid. More detailed analysis shows that the correlations between the mutually

perpendicular components generated in the amplification process are responsible for this fact. This justification will be explained in detail, along with the relation between both treatments.

9589-23, Session 6

Spectral interferometric methods for the complete characterization of femtosecond extreme-ultraviolet pulses

Benoît Mahieu, Hugo Dacasa, Lab. d'Optique Appliquée (France); Lu Li, Queen's Univ. Belfast (Ireland); Eduardo Oliva, Univ. Politécnica de Madrid (France); Philippe Zeitoun, Lab. d'Optique Appliquée (France)

The advent of powerful extreme-ultraviolet coherent sources such as freeelectron lasers, high-order harmonic generation or plasma-based lasers is opening opportunities in numerous applications at temporal femtosecond and spatial nanometer resolutions. For these applications, spectral phase and temporal intensity profile are precious pieces of information of the source. Nevertheless, they are regrettably lacking. This is mainly due to the strong absorption of extreme-ultraviolet light in crystals, commonly used at longer wavelengths for pulse characterization.

In this presentation, we will show how spectral interferometric methods have the potential to overcome this barrier. Since a spectrum measurement represents an accessible task, the possibility to encode the complete spectro-temporal information in the frequency domain represents an attractive solution. We will discuss three possible methods relying on the same basis. First, Fourier-transform spectral interferometry using a reference pulse; second, spectral phase interferometry for direct electric field reconstruction applied to seeded free-electron lasers; third, twodimensional beatings of spatially-shifted replicas. Principle, simulations and first experimental results will be shown.

9589-24, Session 6

Influence of the partial temporal coherence of XUV laser pulses on the measurement of their spectral properties

Andréa Le Marec, Institut des Sciences Moléculaires d'Orsay (France) and Ctr. National de la Recherche Scientifique (France); Olivier A. Guilbaud, Univ. Paris-Sud 11 (France) and Ctr. National de la Recherche Scientifique (France); Pierre Chavel, Ctr. National de la Recherche Scientifique (France) and Univ. Paris-Sud II (France); Olivier Larroche, Commissariat à l'Énergie Atomique (France); Annie Klisnick, Univ. Paris-Sud 11 (France)

The temporal coherence and related spectral properties of the four types of collisional XUV lasers currently operational worldwide were experimentally characterized in the past few years. This comprehensive work has been carried out using the same instrument, a variable pathdifference interferometer. The coherence time was inferred from a linear autocorrelation of the XUV pulse, by measuring the variation of the fringe visibility with the path difference, which yields the modulus of the degree of coherence. The spectral profile and the associated linewidth of the XUV laser is obtained through a Fourier transform of the degree of coherence, following the Wiener-Khintchin theorem.

In this work we investigate the role of the partial temporal coherence of the XUV pulse on the measurements. More specifically we will present numerical simulations that help to understand how the partial coherence of the pulse, represented by the ratio of the coherence time to the pulse duration, can influence the measured fringe visibility curve and affect the estimation of the coherence time.



9589-25, Session 6

Wigner distribution measurement of the spatial coherence properties of FELs

Tobias Mey, Bernd Schäfer, Klaus Mann, Laser-Lab. Göttingen e.V. (Germany); Barbara Keitel, Elke Plönjes, Marion Kuhlmann, Deutsches Elektronen-Synchrotron (Germany)

Free-electron lasers deliver VUV and soft x-ray pulses with the best brilliance available and a high degree of spatial coherence. Users of such facilities have high demands on phase and coherence properties of the beam, for instance when working with coherent diffractive imaging. Thus, detailed knowledge of these parameters is of great importance and provides the possibility for advanced machine studies.

The Wigner distribution function (WDF) describes the entire propagation properties of an electromagnetic beam including all information on its spatial coherence. It can be reconstructed from beam profiles taken at different positions along its propagation direction. Here, we present measurements of the WDF conducted at the Free-electron laser FLASH at DESY. As a result, we derive the entire four-dimensional mutual coherence function, the coherence lengths and the global degree of coherence. Additionally, we provide an estimation of the possible error that our algorithm might produce for the derived quantities.

In comparison to existing studies that characterize the photon beam of FLASH, we find significantly lower values for the global degree of coherence. This difference cannot be explained by our error estimation. We explore the possible reasons for this discrepancy and their effect on the value of the global degree of coherence.

9589-26, Session 6

Cross-correlation measurement of femtosecond hard x-ray pulses from a laser plasma source: approaching 100 fs benchmark

Mazhar Iqbal, Muhammad Ijaz, Gwangju Institute of Science and Technology (Korea, Republic of); Holger Stiel, Max-Born-Institut für Nichtlineare Optik und Kurzzeitspektroskopie (Germany); Do Young Noh, Karol A. Janulewicz, Gwangju Institute of Science and Technology (Korea, Republic of)

X-ray pulse duration measurement from laser plasma source is done using cross correlation scheme exploiting ultrafast response of x-ray absorption in Ni metal. We measured the shortest pulse duration of 110 \pm 6 fs for high energy bremsstrahlung fulfilling the theoretical prediction of 100 fs.

9589-27, Session 7

Applications of EUV high-harmonics for probing molecular structure and ultrafast dynamics (Invited Paper)

Chang Hee Nam, Institute for Basic Science (Korea, Republic of) and Gwangju Institute of Science and Technology (Korea, Republic of); Hyeok Yun, Institute for Basic Science (Korea, Republic of); Hyung Taek Kim, Kyung Taec Kim, Institute for Basic Science (Korea, Republic of) and Gwangju Institute of Science and Technology (Korea, Republic of)

High harmonic light sources possess unique characteristics of attosecond duration in the EUV and soft x-ray spectral range. High harmonic light

sources can be applied to probe ultrafast dynamics of atoms and molecules. By tuning harmonic wavelength a specific state of an atom or molecule can be excited, which can be further excited or ionized by applying a timedelayed femtosecond laser pulse. This process of combining harmonic pulses and time-delayed femtosecond laser pulses can reveal the dynamics of photoexcitation and photoionization processes. In addition highharmonic radiation generated from molecules contains the information on the structure of molecules. When multiple molecular orbitals are exposed to a strong laser field, the highest-occupied molecular orbital (HOMO) is mostly ionized and thus emits strong high-harmonic radiation containing the characteristics of HOMO. The radiation from the energetically lowerlying molecular orbital (HOMO-1) is often too weak in investigating the characteristics of the HOMO-1, necessitating special techniques to observe the radiation from the HOMO-1. In the case of CO2 the ϖ g symmetry of the HOMO does not exhibit directional dependence along either the molecular axis or its perpendicular direction. In order to resolve multiple orbitals of such molecules we employ two-dimensional high-harmonic spectroscopy (HHS) by applying an orthogonally polarized two-color laser field, consisting of the fundamental frequency (1?) and its second harmonic (2?). In this case odd and even harmonics carry the characteristics of the HOMO and HOMO-1, respectively. The multi-orbital characteristics are thus revealed in the twodimensional spectroscopy employing the two-color laser field.

9589-28, Session 7

The MEL-X project at the Lawrence Livermore National Laboratory: a multilayer delay line for x-rays

Tommaso Pardini, Randolph M. Hill, Jennifer B. Alameda, Regina Soufli, Lawrence Livermore National Lab. (United States); Andy Aquila, Sébastien Boutet, SLAC National Accelerator Lab. (United States); Stefan P. Hau-Riege, Lawrence Livermore National Lab. (United States)

At the Lawrence Livermore National Laboratory we are developing a multilayer delay line for x-rays (MEL-X) to enable all-x-ray pump-and-probe experiments at Free Electron Lasers (FELs). The goal of this project is the development and deployment of a proof-of-principle delay line featuring coated x-ray optics. The four- mirror design of the MEL-X is motivated by the need for ease of alignment and use. In order to simplify the overlap of the pump and the probe beam after each delay time change, a scheme involving super-polished rails and mirror-to-motor decoupling has been adopted. The MEL-X features a high intensity pump beam. Its Iridium coating allows it to work at soft and hard x-ray energies all the way up to 9keV, with a probe beam transmission as high as 35% at 8keV, and 14% at 9keV. The delay time can be tailored to each particular experiment, with a nominal range of 70 - 350 fs for this prototype. The MEL-X, combined with established techniques such as x-ray diffraction, absorption or emission, could provide new insights on ultra-fast transitions in highly excited states of matter.

This work was performed under the auspices of the U.S. Department of Energy by Lawrence

Livermore National Laboratory under Contract DE-AC52-07NA27344. Document Release Number LLNL-ABS-666376

9589-29, Session 7

High-harmonics generation and applications (Invited Paper)

Jens Biegert, Seth L. Cousin, Stephan Teichmann, Michael Hemmer, Barbara Buades, Noslen Suarez, Francisco Silva, Nicola Di Palo, ICFO - Institut de Ciències Fotòniques (Spain)

Isolated attosecond pulses at the Carbon K-edge (284 eV) hold the promise to image, probe and control the most fundamental electronic processes with



extreme temporal and spatial resolution. Extension of current attosecond pulse generation techniques into the so called water window (284-543 eV) is possible by ponderomotive scaling of the generated attosecond bursts in high-harmonic generation using an intense long wavelength driving laser. We demonstrate for the first time the attosecond lighthouse effect at 300 eV in neon to isolate an attosecond pulse at the water window. The attosecond lighthouse is then compared with spectrally filtered high harmonic generation, which reveals that given the same driving laser both techniques lead to comparable photon flux in conditions leading to isolated attosecond pulses. We will also demonstrate the first near-edge x-ray absorption fine-structure (NEXAFS) measurement in the solid state on a 200 nm free-standing polyimide film at the carbon K-shell edge with our source. The individual fine structure peaks with the known orbitals in polyimide are identified and are in good agreement with state of the art synchrotron data. These results are a first decisive step towards attosecond time resolved soft-X-ray spectroscopy with element selectivity for the condensed phase [1].

[1] S. L. Cousin, F. Silva, S. Teichmann, M. Hemmer, B. Buades, and J. Biegert, Optics Letters 39, 18, 5383 (2014).

9589-30, Session 7

Scalings of high-order harmonics from relativistic electron cusps

Alexander S. Pirozhkov, Masaki Kando, Timur Z. Esirkepov, Japan Atomic Energy Agency (Japan); Tatiana A. Pikuz, Photon Pioneers Ctr. in Osaka Univ. (Japan) and Joint Institute for High Temperatures of the Russian Academy of Sciences (JIHT RAS) (Russian Federation); Anatoly Ya. Faenov, Osaka Univ. (Japan); Koichi Ogura, Yukio Hayashi, Hideyuki Kotaki, Japan Atomic Energy Agency (Japan); Eugene N Ragozin, P.N. Lebedev Physical Institute (Russian Federation) and Moscow Institute of Physics and Technology (Russian Federation); David Neely, STFC Rutherford Appleton Lab. (United Kingdom) and Univ. of Strathclyde (United Kingdom); Hiromitsu Kiriyama, James K. Koga, Yuji Fukuda, Akito Sagisaka, Masaharu Nishikino, Takashi Imazono, Noboru Hasegawa, Tetsuya Kawachi, Hiroyuki Daido, Japan Atomic Energy Agency (Japan); Yoshiaki Kato, The Graduate School for the Creation of New Photonics Industries (Japan); Paul R. Bolton, Sergei V. Bulanov, Kiminori Kondo, Japan Atomic Energy Agency (Japan)

Relativistic laser plasma is a known source of XUV and x-ray radiation generated via various mechanisms. We have recently discovered high-order harmonic emission from gas jet targets driven by relativistic-irradiance multi-terawatt femtosecond lasers [Phys. Rev. Lett. 108, 135004 (2012); New J. Phys. 16, 093003 (2014)]. The harmonics constitute short-pulse highfrequency coherent radiation, desirable for many applications. According to the model developed on the basis of catastrophe theory corroborated by 3D and 2D PIC simulations using the REMP code [Comput. Phys. Comm. 135, 144 (2001)], the harmonics are emitted by structurally stable, oscillating electron spikes (cusps), which are the density singularities resulting from catastrophes of a multi-stream relativistic plasma flow [Phys. Rev. Lett. 101, 265001 (2008)]. In this presentation we report results of experiments performed with the J-KAREN laser [Opt. Lett. 35, 1497 (2010)]. We measured dependences of the harmonic yield on several parameters, including the gas jet density and laser pulse energy. We also found a very steep dependence of the yield on the focal spot quality.

9589-31, Session 8

Attosecond pulses formation via switching of resonant interaction by tunnel ionization (Invited Paper)

Timur R. Akhmedzhanov, Texas A&M Univ. (United States); Vladimir A. Antonov, Institute of Applied Physics (Russian Federation); Yevgeny V. Radeonychev, Institute of Applied Physics (Russian Federation) and Russian Academy of Sciences (Russian Federation); Olga Kocharovskaya, Texas A&M Univ. (United States)

We investigate a new method to produce attosecond pulses from resonant XUV radiation in an atomic gas which is simultaneously irradiated by an IR laser field. Around the crests of IR field all the excited atomic energy levels are strongly broadened due to rapid tunnel ionization from the corresponding excited states and atoms are not able to resonantly absorb the incident vacuum ultraviolet radiation. Vice verse, around zeroes of IR field, ionization is slow and atoms effectively absorb the vacuum ultraviolet radiation. As a result, interaction between atoms and XUV field is switched on and off resulting in formation of attosecond pulses.

We present analytically solvable model of ultrashort pulses formation using two-level at-om and stepwise ionization time dependence approximations. Using many-level atomic model and tunneling ionization rates, we also numerically calculate the result of propagation of XUV field through the optically thin layer of atomic gas (H, He and Ne). Finally, we perform numerical solution of full time-dependent Schrodinger equation for IR-dressed He atoms interacting with quasi-resonant XUV radiation. The results of all three approaches prove the possibility of formation of trains of pulses with a pulse duration in the range of hundreds of attoseconds.

9589-32, Session 8

Using the XFEL to drive the gain of innershell x-ray lasers using photo-ionization and photo-excitation processes

Joseph Nilsen, Lawrence Livermore National Lab. (United States)

For the last four decades many photo-pumped X-ray laser schemes have been proposed but demonstrating these schemes in the laboratory has proved to be elusive because of the difficulty of finding a strong resonant pump line or X-ray source. With the availability of the X-ray free electron lasers (X-FEL) at several facilities a tunable X-ray laser source can be used to replace the pump line or X-ray source in previously proposed laser schemes and allow researchers to study the physics and feasibility of photopumped laser schemes. Many of these photo-pumped schemes are driven by photo-excitation from a resonant line source but others are driven by photo-ionization from a strong non-resonant X-ray source.

Three years ago an inner-shell X-ray laser was demonstrated at 849 eV in singly ionized neon gas using the LCLS X-FEL at 960 eV to photo-ionize the 1s electron in neutral neon followed by lasing on the 2p – 1s transition in singly-ionized neon. It took many decades to demonstrate this scheme because it required a very strong X-ray source that could photo-ionize the 1s (K shell) electrons in neon on a time scale comparable to the intrinsic auger lifetime in the neon, which is typically 2 fsec.

In this work we model the neon inner shell X-ray laser under similar conditions to those used at LCLS and investigate how we can improve the efficiency of the neon laser and reduce the drive requirements by tuning the X-FEL to the 1s-3p transition in neutral neon in order to create gain on the 2p-1s line in neutral neon. We also explore using the XFEL to drive gain on 3-2 transitions in singly-ionized Ar and Cu plasmas.



9589-33, Session 8

Enhancement of laser-driven betatron radiation (Invited Paper)

Liming Chen, The Institue of Physics (China)

A new method is demonstrated for generating intense betatron x-rays using a clustering gas target irradiated with an ultra-high contrast laser of 3 TW only [1]. The yield of the Ar x-ray betatron emission has been measured to be 2?10^8 photons/pulse, which is over ten-fold enhancement compared to the emission yield produced by using a normal gas target. Simulations point to the existence of clustering as a contributor to the DLA mechanism, thereby finally enhancing the betatron x-ray photons and improving conversion efficiency over 40 times. Another concept of generation of bright betatron radiation during electron acceleration was newly studied [2]. Two electron bunches with different qualities were injected sequentially into the wakefield driven by a super-intense laser pulse. The first one is a monoenergetic electron bunch with peak energy of GeV level, and the second one is injected continuously with large charge and performs transverse oscillation with large amplitude during the subsequent acceleration. The enhancement of transverse resonant oscillation of the inonization injected electron bunch which results in the betatron radiation would lead to Gamma-ray photon energy and peak brilliance beyond that of 3rd generation synchrotron facilities [3].

[1] Sci. Reports 3, 1912(2013)

[2] PNAS 111, 5825(2014)

[3] K. Huang, L. M. Chen et al, (to be submitted)

9589-34, Session 8

Multi-stage Auger pumping of atomic EUV lasers in Xe and Kr by a soft x-ray freeelectron laser

Laurent Mercadier, Clemens Weninger, Ctr. for Free-Electron Laser Science (Germany) and Max-Planck-Institut für Physik komplexer Systeme (Germany); Sven Bernitt, Michael Blessenohl, Hendrick Bekker, Stepan Dobrodey, Max-Planck-Institut für Kernphysik (Germany); Alvaro Sanchez-Gonzalez, Imperial College London (United Kingdom); Cedric Bomme, Deutsches Elektronen-Synchrotron (Germany); Benjamin Erk, Deutsches Elektronen-Synchrotron (Germany); Philipp Schmidt, Martin Wilke, Andre Knie, Univ. Kassel (Germany); Wen Te Liao, Ctr. for Free-Electron Laser Science (Germany) and Max-Planck-Institut für Physik komplexer Systeme (Germany): Artem Rudenko, Kansas State Univ. (United States); Jan P. Müller, Technische Univ. Berlin (Germany); Zhong Yin, Deutsches Elektronen-Synchrotron (Germany); Rebecca Boll, Evgeny Savelyev, Rolf Treusch, Andrey Sorokin, Deutsches Elektronen-Synchrotron (Germany); Daniel Rolles, Deutsches Elektronen-Synchrotron (Germany): Arno Ehresmann, Univ. Kassel (Germany): Jose R. Crespo Lopez-Urrutia, René Steinbrügge, Max-Planck-Institut für Kernphysik (Germany); Nina Rohringer, Ctr. for Free-Electron Laser Science (Germany) and Max-Planck-Institut für Physik komplexer Systeme (Germany)

The advent of X-ray free-electron lasers (FELs) makes it possible to pump new atomic x-ray lasers with short pulse duration, extreme spectral brightness and full temporal coherence. One of the advantages of such a laser is the spectral stability as compared to the self-amplified spontaneous emission (SASE) used to generate it. We present results on Auger-decay pumping of EUV lasing emission of highly charged Xe and Kr ions. We use a soft x-ray FEL with photon energy between 72 eV and 100 eV to photoionize the inner shells of Xe (4d) and Kr (3d) in an elongated gaseous medium with pressures ranging from 1 mbar to almost 1 atmosphere. Using high-resolution spectroscopy, we observe several lasing lines for both gases, ranging from 56 nm to 120 nm. These lines arise from population inversions of highly charged ions after a sequence of inner-shell photoionization events and Auger decays. Varying the pump-photon energy in the range of the giant 4d and 3d resonances in Xe and Kr allows the change of ionization rates, so that plasmas of different ionic charge-state distributions can be created and certain emission lines can be quenched, others enhanced. We measure a strong dependence of the emission-line strength on both pulse energy and pressure, and find an optimum pressure close to 6 mbar. Bleaching and the large variation of the intensity along the strongly diverging focus of the FEL beam result in a highly nonuniform plasma. This in turn results in different line-emissions along the elongated plasma channel.

Conference 9590: Advances in Laboratory-based X-Ray Sources, Optics, and Applications IV



Monday 10-10 August 2015

Part of Proceedings of SPIE Vol. 9590 Advances in Laboratory-based X-Ray Sources, Optics, and

Applications IV

9590-1, Session 1

Hard x-rays from a table-top all-laserdriven synchrotron light source (Invited Paper)

Donald P Umstadter, Univ. of Nebraska-Lincoln (United States)

We discuss the experimental development of a compact, tunable hard x-ray light source. The repetitive petawatt-class Diocles laser system at the University of Nebraska, Lincoln, serves dual purposes. First, it drives a laser-plasma wakefield when it is focused to high intensity (I ~ 10^19W/cm^2) onto a gas jet. The electrostatic field of the relativistically propagating laser-wakefield accelerates electrons to highly relativistic energy, up to 0.5 GeV. Another high intensity laser pulse (I ~ 10^17W/cm^2), from the same laser system, is focused in a counter-propagating direction onto the relativistic electron beam, which generates x-rays by inverse Compton scattering. This is the first all-laser-driven hard x-ray source with a peaked photon spectrum. It is shown to be tunable from 70 keV to 9 MeV, and thus suitable for both atomic and nuclear research and applications. Femtosecond x-ray pulse duration also makes this novel light source suitable for research into ultrafast phenomena.

9590-2, Session 1

The compact light source: A miniature synchrotron producing x-rays via inverse Compton scattering (Invited Paper)

Ronald D. Ruth, SLAC National Accelerator Lab. (United States) and Lyncean Technologies, Inc. (United States); Rod Loewen, Lyncean Technologies, Inc. (United States)

The Compact Light Source concept was first developed as a spin off from work at Stanford Linear Accelerator Center towards very small electron storage rings for beam cooling in linear colliders.[1] Later, further research at SLAC explored a miniature storage ring and high-finesse cavity optimized for the hard x-ray regime.[2] These studies led to the formation of a corporation, Lyncean Technologies, Inc., which developed the Compact Light Source (CLS) [3]. The CLS is a near-monochromatic, tunable, homelab-size x-ray source with beamlines that can be used like the x-ray beamlines at the synchrotrons--but it is about 200 times smaller than a conventional synchrotron light source. The compact size is achieved using a "laser undulator" and a miniature electron-beam storage ring. In other words, the x-rays are produced via inverse Compton scattering of electrons circulating in a miniature storage ring interacting with an IR photon pulse stored in a high-finesse cavity. The CLS can produce a photon flux on sample that is comparable to highly-productive synchrotron beamlines. The productionprototype CLS and the Beta CLS operated for many years at Lyncean Technologies, Inc.[3]. The first delivery and commissioning of a commercial CLS took place in the spring of 2015. This presentation will introduce the Compact Light Source showing the injector, linac, storage ring and laser/ cavity system. We then present selected results of grating-based imaging and tomography experiments.[4]

[1] Z. Huang and R. D. Ruth, "Laser-Electron Storage Ring", Phys. Rev. Lett., 80:976-979 (1998).

[2] R. Loewen, Ph.D. Dissertation: "A compact light source: design and technical feasibility study of a laser electron storage ring x-ray source," R.J. Loewen, SLAC/Stanford University, SLAC-R-632 (2003).

[3] Supported by the NIGMS and NCRR, the National Institutes of Health,

Grant numbers: R44-GM66511, R44- GM074437, U54-GM074961, and R43-RR025730, and the Department of Energy, Grant number: DE-SC0009622 [4] References at www.lynceantech.com

9590-3, Session 1

Liquid-metal-jet and ultra-high resolution x-ray tube technology including microscopy applications (Invited Paper)

Emil Espes, Björn A. M. Hansson, Oscar Hemberg, Mikael Otendal, Per Takman, Tomi Tuohimaa, Excillum AB (Sweden)

The power and brightness of electron-impact micro-focus X-ray tubes have long been limited by thermal damage in the anode. This limit is overcome by the liquid-metal-jet anode (MetalJet) technology that has previously demonstrated brightness in the range of one order of magnitude above current state-of-the art sources. This is possible due to the regenerative nature of this anode and the fact that the anode is already molten, which allows for significantly higher e-beam power density than on conventional solid anodes.

Over the last years, the MetalJet technology has developed from prototypes into fully operational and stable X-ray tubes running in many labs over the world. Key applications include X-ray diffraction and scattering.

To be able to benefit from the higher power-loading capability of the liquidmetal-jet anode, advanced electron optics had to be developed. Based on this advanced electron optics, a new nanofocus x-ray tube (NanoTube) is under development. The foundation of the NanoTube is the advanced electron optics, combined with a tungsten coated diamond transmission target. The NanoTube is designed to reach spot sizes of 100 nm, and by doing so, achieving line-spacing resolution of 50 nm.

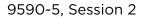
This presentation will review the current status of the MetalJet technology specifically in terms of stability, lifetime, flux and brightness. It will also discuss details of the liquid-metal-jet technology with a focus on the fundamental limitations of the technology and refer to some recent data from relevant applications. Furthermore, it will review the state of the development of the NanoTube.

9590-4, Session 1

A novel technique to produce x-rays for XRF, medical, and scientific purposes (Invited Paper)

Carlos Camara, Tribogenics (United States)

Since the discovery of X-rays by Wilhelm Roentgen in 1895 X-ray have been produced in basically the same way, using a high voltage power supply attached to an X-ray vacuum tube. In 2008 Seth Putterman, Carlos Camara, Jonathan Hird and Juan Escobar discovered that one could generate enough X-rays to capture an image by peeling scotch tape inside a vacuum. This lead to the formation of Tribogenics in 2011. Since then we have improved our technology by 6 orders of magnitude. Currently we are focused on our first commercial product, a hand held X-ray fluorescence (XRF) instrument. This is the first step towards the development of other x-ray solutions utilizing our technology. We will discuss this new method for producing X-rays, the challenges we face, and some of the products that will be enabled by our efforts.



From incoherent to coherent x-rays with **ICS sources** (Invited Paper)

Emilio Alessandro Nanni, Massachusetts Institute of Technology (United States)

No Abstract Available

9590-6, Session 2

Current challenges in diagnostic x-ray source and how they can be met

J. Scott Price, GE Global Research (United States)

No Abstract Available

9590-7, Session 2

Development of an adaptable shield wall design for the CSU Linac

Joel Williams, Tejas Doshi, Madhuri Ravikumar, Jeff Ngyn, Sandra G. Biedron, Stephen V. Milton, Josh Einstein, Colorado State Univ. (United States)

When designing an accelerator radiation enclosure, both current demands and any future modifications must be taken into account. At CSU, the initial design for radiation shielding calls for protection from the radiation produced by a 6 MeV electron beam with a current of 1.2188A. In order to ensure the design of the accelerator meets government regulatory specifications for radiation safety under all operational scenarios, we have ran simulations to estimate the necessary shielding required. After determining the ideal materials, we proceeded to design a CAD model and reiterate through the design to ensure all guidelines are still followed. Further, we are planning for upgrades for additional accelerator engineering tests, including a compact light source device. Discussions of the facility and its light source test will be discussed.

9590-8, Session 2

Liquid jet target x-ray tube with field emission cathode

Gennadiv Karpinskiv, Siemens Russia (Russian Federation) and National Research Nuclear Univ. MEPhI (Russian Federation); Taras Bondarenko, Stepan Polikhov, Siemens Russia (Russian Federation); Alexandra Botyachkova, Siemens Russia (Russian Federation) and National Research Nuclear Univ. MEPhI (Russian Federation); Sergev Frolov, Vvacheslav Ivanov, N.N. Semenov Institute of Chemical Physics (Russian Federation); Andreas Geisler, Oliver Heid, Siemens AG (Germany)

Over the last years microfocus X-ray sources faced two main restrictions that substantially limited the enhancement of their performances. The first one is a limited brightness of the electron source and the second is a limitation concerned with anode thermal loads. Our research is concerned with the development of high power X-ray source that is based on the carbon nanostructure field emission cathode as an electron source and high speed liquid metal jet as a target for X-ray generation to solve both these restrictions. The liquid jet of the source is based on the alloys of two metals: heavy atom weight and light atom weight. Besides the high thermal load durability this alloys allows to obtain high characteristics spectrum relative to bremsstrahlung X-ray. CFD simulations were performed to

estimate break-up length and behavior of a micrometer jet at velocities up to 500 m/s. High brightness cold emission electron source based on carbon nanostructures and electrostatic extraction grid is designed. Electron beam dynamics simulations are performed. To verify the electron beam dynamics calculations the experimental setup with bulk metal anode is designed and under construction now. The experimental setup for verification of the jet dynamics simulation is as well designed and built. This setup also implies the mounting of the conventional electron gun to analyze the generation of the X-ray radiation from the jet.

OPTICS+

OPTICAL ENGINEERING+ APPLICATIONS

SPIE. PHOTONICS

9590-9, Session 3

A review of formed optics for lab-based x-ray systems (Invited Paper)

Ladislav Pina, Czech Technical Univ. in Prague (Czech Republic)

Imaging in EUV and X-ray region plays important role in radiography, tomography, spectroscop and lithography. Imaging includes also collectors of radiation working as condensers for sample illumination or for intermediate focus formation in EUV lithography exposure systems. One class of optics consist of electroformed mirrors and mechanically bent multifoil mirrors. Formed optical systems and their main characteristics are presented. Comparison of theoretical results obtained by ray-tracing with experimental results is presented. Examples of various optical systems and their applications in the field of X-ray microscopy and tomography, EUV metrology, lithography and spectroscopy are presented.

9590-10, Session 3

Beam conditioning multilayer optics for laboratory x-ray sources

Yuriy Ya, Platonov, Boris Verman, Licai Jiang, Bonglea Kim, Rigaku Innovative Technologies, Inc. (United States)

Multilaver optics for collimating and focusing of X-ray radiation from laboratory-based sources will be discussed.

9590-11. Session 3

NanoCT imaging with a prototype nanofocus source

Mark Müller, Simone Ferstl, Sebastian Allner, Martin Dierolf, Technische Univ. München (Germany); Björn Hansson, Tomi Tuohimaa, Per Takman, Excillum AB (Sweden); Franz Pfeiffer, Technische Univ. München (Germany)

n the last decade X-ray microCT (μ CT) has gained importance in many research domains and is becoming a routine microscopy technique. Due to the recent development of transmission X-ray tubes with very small focal spot sizes, laboratory-based CT imaging with submicron resolution is possible nowadays.

We present a novel microCT setup featuring a prototype nanofocus X-ray source and a single-photon counting detector. The system relies on mere geometrical magnification and can reach resolutions around 300 nm at its current state.

The nanofocus X-ray tube (Excillum AB, Sweden) consists of a tungsten transmission target on a diamond layer and can so far reach focal spot sizes down to about 300 nm.

The X-ray camera is a PILATUS 300K-W 20Hz detector with a 1000 μm silicon sensor, 1475 x 195 pixels, and a pixel size of 172 x 172 ?m?.

First results demonstrate that the focal spot of the tube is stable enough to permit CT imaging with submicron resolution. The small focal spot size also results in sufficient spatial coherence to exploit edge enhancement effects



and to apply phase contrast imaging methods.

Moreover, the first images indicate that image acquisition with a practically noise-free photon counting detector combined with a low-flux nanofocus tube can result in enhanced contrast compared to similar setups.

We will show first applications comprising stained soft tissue samples as well as bone and tooth samples; e.g. a 3D data set of a piece of tooth, where the dentin tubules, are clearly resolved.

9590-12, Session 3

The best of both worlds: automated CMP polishing of channel-cut monochromators

Elina Kasman, Argonne National Lab. (United States)

The use of a channel-cut monochromator is the most straightforward method to ensure that the two reflection surfaces maintain alignment between crystallographic planes without the need for complicated alignment mechanisms. Three basic characteristics that affect monochromator performance are: subsurface damage which contaminates spectral purity; surface roughness which reduces efficiency due to scattering; and surface figure error which imparts intensity structure and coherence distortion in the beam. Standard chemical-mechanical polishing processes and equipment are used when the reflecting surface is easily accessible, such as for single-bounce monochromators. Due to the inaccessibly of the surfaces inside a channel-cut monochromator for polishing, these optics are generally wet-etched for their final processing. This results in minimal subsurface damage, but very poor roughness and figure error. A new CMP channel polishing instrument design is presented which allows the internal reflecting surface quality of channel-cut crystals to approach that of conventional single-bounce monochromators.

9590-13, Session 3

Possibility for new PolyCO imaging: stroboscopic imaging based on vibrating capillary optics

Andrea Liedl, Univ. degli Studi di Roma Tre (Italy) and Infn-LNF (Italy); Dariush Hampai, Istituto Nazionale di Fisica Nucleare (Italy); Sultan B. Dabagov, Istituto Nazionale di Fisica Nucleare (Italy) and P.N. Lebedev Physical Institute (Russian Federation) and National Research Nuclear Univ. MEPhI (Russian Federation); Claudia Polese, Istituto Nazionale di Fisica Nucleare (Italy) and Univ. degli Studi di Roma La Sapienza (Italy)

Polycapillary lenses are a well known optical devices for radiation and charged particles. These lenses consist of thousands channels through which the signal is transmitted by Total External Reflection phenomenon. Their application have made possible technical improvements in different fields such as Imaging, Fluorescence analysis, channeling studies etc...

In particular, application of this optics coupled on conventional sources such as x-ray tube has open a new season for potential application of desktop instrumentation. For instance, usage of lenses has enhanced spatial coherence and brilliance over the sample allowing better resolution and contrast for imaging purpose. Likewise improved focusing power and confocal configuration of more lenses has improved resolution, from energy and spatial point of view, in fluorescence mapping analysis.

Recent work has studied the behavior of transmitted radiation through a single capillary in vibrating regime. In this work a utilization of vibrating capillary for stroboscopic imaging is presented. A sample characterized by a known periodic event is studied with synchronized vibrating capillary.

The same sample is then analyzed, without optics, by synchronization of detector image acquisition. A comparison between these two results is discussed.

9590-14, Session 4

A triboelectric closed loop band system for the generation of x-rays

Eli Van Cleve, Zach Ganlieli, Ben Lucas, Dan Cudra, Eric W. Wong, Mark Valentine, Pedro Cortes Jr., David Kamkar, Gilberto Jimenez, Andreas Magnusson, Rebecka Jacobsson, Timothy Baxendale, Nikhil Mehta, Jon Fong, Steve Hansen, Andy Kotowski, Dale Fox, Carlos Camra, Justen Harper, Tribogenics (United States)

In 2008 Seth Putterman, Carlos Camara, Jonathan Hird and Juan Escobar discovered that one could generate X-rays by peeling scotch tape inside a vacuum. Since, Tribogenics has developed multiple architectures to generate X-rays from tribocharging. One such design is realized by sliding a polymer band across a metal cylinder and using a target to collect the triboelectric generated electrons from the polymer to generate X-rays. This new architecture is capable of generating x-rays for the purposes of X-ray fluorescence (XRF). In this talk we will describe this architecture and discuss important insights into the generation of x-rays through tribocharging that has resulted from the development of the device.

9590-15, Session 4

Thermal analysis of high-power microfocus x-ray target-scaling effect

Xi Zhang, Vance Robinson, Mark Frontera, GE Global Research (United States)

High resolution X-ray systems require small focal spots which, depending on the application, range from 1 ?m for defect detection to 1 mm for medical CT. Often in opposition to the demand for small spot sizes is the need for faster scan times. The high X-ray flux required for fast scan times and small focal spots required for high resolution result in extremely high power densities and temperature at the focal spot. This is critical because the focal spot temperature is often the limiting factor in both performance and life of imaging system. In this paper, a finite element model is developed to compute the temperature of a stationary x-ray target. This model is used to demonstrate the effect of focal spot size - diameter, on the heat dissipation capability. As the spot size reduces, a higher power density may be sustained by the target. This effect is explained by increased in-plane heat conduction. The peak temperature of a small focal spot also becomes more sensitive to the current density distribution of the incident electron beam. The relationship of the peak power and electron beam profile, power deposition inside the X-ray target and focal spot aspect ratio are discussed. Some experimental data demonstrating such scaling effects is included. General design rules for higher-flux capable targets leveraging these scaling effects are also proposed.

9590-16, Session 4

X-ray tube thermal management

Ali M. Khounsary, Illinois Institute of Technology (United States)

This paper presents an overview of the various fixed X-ray tube designs and the target's thermal management challenges that limit the intensity of the generated X-ray beams. Analytical and numerical results for various sources size/power are presented and methods to further increase the beam intensity are discussed.



9590-17, Session 4

Table-top-analyzer-based phase contrast imaging system optimization

Jovan G. Brankov, Wei Zhou, Illinois Institute of Technology (United States); Boris Verman, Rigaku Innovative Technologies, Inc. (United States)

No Abstract Available

9590-18, Session 4

Low-dose high-contrast x-ray radiography with tunable narrow-bandwidth x-rays

Shouyuan Chen, Univ. of Nebraska-Lincoln (United States)

No Abstract Available

SPIE. PHOTONICS **Conference 9591: Target Diagnostics Physics** and Engineering for Inertial Confinement Fusion IV

Wednesday - Thursday 12-13 August 2015

Part of Proceedings of SPIE Vol. 9591 Target Diagnostics Physics and Engineering for Inertial Confinement Fusion IV

9591-1. Session 1

Fundamental performance differences of CMOS and CCD imagers: part VI (Invited Paper)

James R. Janesick, Tom Elliott, James Andrews, John Tower, SRI International Sarnoff (United States)

Past papers delivered have demonstrated progress made on developing scientific PMOS/NMOS CMOS imagers that match or exceed CCD performance. New data and discussions presented in this paper continue to show further advancements that include: 1). 1 h+ read noise data with detailed understandings for how noise can be further reduced, 2). digital correlated double sampling (dCDS) fundamentals in response to RTN and 1/f noise sources, 3). performance and radiation damage test data for NASA/NRL's SoloHi/WISPR 2k x 2k x 10 um pixel CMOS imagers, 4). performance and thinning data produced by BSI SoloHi and BSI 1k x 1k x 16 um pixel CMOS imagers, 5). PMOS versus NMOS design and fabrication considerations behind a stitched Mk x Nk x 10 um pixel imager, 6). data and simulation comparisons for a new class of night vision CMOS imagers.

9591-2, Session 1

Complete time-resolved polarimetry of scattered light on the NIF (Invited Paper)

David Turnbull, Joseph E. Ralph, Robert Chow, Pierre A. Michel, Gene Frieders, Robin L. Hibbard, Kenn M. Knittel, Joel R. Stanley, James L. Vickers, Ziad M. Zeid, John D. Moody, Lawrence Livermore National Lab. (United States)

The polarization of 3? scattered light has been measured in the full aperture backscatter (FABS) diagnostic on a 30° incidence quad at the National Ignition Facility (NIF) since June 2013. The initial scoping stage was capable of measuring the time-integrated Jones vector of the collected signal. Two key insights were derived from early experiments. First, laser "glint" (a specular reflection from the inner hohlraum wall), which could cause early time capsule imprint and has been found to seed stimulated Brillouin scattering (SBS) later in time, is observed in near-vacuum hohlraums. Second, the polarizations of the incident laser beam and its backscatter are affected by crossed-beam energy transfer (CBET) in gas-filled hohlraums, and backscatter polarization might therefore serve as a quantitative CBET diagnostic. To more definitively assess the latter possibility, the diagnostic is currently being upgraded to complete time-resolved polarimetry, which means it will measure the full Stokes vector and its evolution over time. Insights derived to date, as well as the new diagnostic design, will be presented. Time-resolved polarimetry will also be used to diagnose Faraday rotation induced by magnetic fields in collisionless shock experiments that are planned this year.

9591-3. Session 2

Upgrades to the VISAR-streaked optical pyrometer (SOP) system on NIF

Anastacia M. Manuel, Marius Millot, Peter M. Celliers, Eugene O. Vergel de Dios, Glen James, Philip Datte, Lynn G. Seppala, Lawrence Livermore National Lab. (United States)

The Velocity Interferometer System for Any Reflector (VISAR) is a critical diagnostic in Inertial Confinement Fusion and High Energy Density research as it allows the ability to track shock fronts or interfaces moving 0.1-100 km/s with great accuracy. At the National Ignition Facility (NIF), the VISAR has recently been used successfully for implosion tuning and equation of state measurements. However, the initial design of the companion streaked optical pyrometer (SOP) to measure spectral radiance - hence shock temperature - suffers from large background levels and poor spatial resolution. The SOP upgrade improves spatial resolution in the 560-640nm band by using custom lenses and K-mirrors, and a gating-circuit for the streak camera to reduce background signal. The upgraded SOP now allows high quality data collection matching NIF VISAR's standards.

OPTICAL ENGINEERING+

APPLICATIONS

Auspices or Acknowledgment

This work performed under the auspices of the U.S. Department of Energy by Lawrence Livermore National Laboratory under Contract DE-AC52-07NA27344.

9591-4, Session 2

Radiation test results for a megapixel CMOS charge dump and read camera at the National Ignition Facility

Joseph R. Kimbrough, Perry M. Bell, Alexander A. Lumbard, Mai S. Thao, Lawrence Livermore National Lab. (United States)

A prototype radiation tolerant camera based on a 2k by 2k CMV4000 sensor from CMOSIS Inc. was tested for total dose and neutron damage effects at the National Ignition Facility. Camera electronic parts were selected to operate up to 10 krad(Si). The CMOS based camera incorporate a fast charge and dump of the sensor, followed by image readout. This allows dumping the charge in the pixel due to the prompt radiation and then readout of the longer persistence phosphor image from the x-ray streak camera or gated imaging detector. Characterization results of the camera's performance before and after the radiation test are compared

Lawrence Livermore National Laboratory is operated by Lawrence Livermore National Security, LLC, for the U.S. Department of Energy, National Nuclear Security Administration under Contract DE-AC52-07NA27344. LLNL-ABS-666586

9591-5, Session 2

Design and implementation of a gatedlaser entrance hole imaging diagnostic (G-LEH-1) at NIF

Nathan E. Palmer, Hui Chen, Jarom Nelson, Joe Kimbrough, Marilyn B. Schneider, Perry M. Bell, Lawrence Livermore National Lab. (United States); Eric Huffman, National Security Technologies, LLC (United States); John L. Porter, Marcos O. Sanchez, Liam D. Claus, Mark W. Kimmel, Sandia National Labs. (United States); John W. Stahoviak, Sandia Staffing Alliance, LLC (United States); Terance J. Hilsabeck, Joseph D. Kilkenny, General Atomics (United States)

Gated x-ray images through the laser entrance hole (LEH) of a hohlraum can provide critical information for ICF experiments at the National Ignition Facility (NIF), such as the size of the LEH vs time, the growth of the gold bubble [1], and the change in the brightness of inner beam spots due to time-varying cross beam energy transfer [2]. Incorporating a high-speed multi-frame CMOS x-ray imager developed by Sandia National Laboratories [3] into the existing Static X-ray Imager (SXI) diagnostic [4] at NIF, the new Gated LEH Imager #1 (G-LEH-1) diagnostic is capable of capturing two to



four LEH images per shot on its 1024x448 pixel photo detector array, with integration times as low as 2 ns per frame. The design of this diagnostic and its implementation on NIF will be presented.

This work was performed under the auspices of the U.S. Department of Energy by Lawrence Livermore National Security, LLC, (LLNS) under Contract No. DE-AC52- 07NA27344. LLNL-ABS-666596. Sandia National Laboratories is a multi-program laboratory managed and operated by Sandia Corporation, a wholly owned subsidiary of Lockheed Martin Corporation, for the U.S. Department of Energy's National Nuclear Security Administration under Contract No. DE-AC04-94AL85000.

[1] M. Schneider, et al., Proceeding of the 8th International Conference on Inertial Fusion Sciences and Applications (IFSA 2013), Japan

[2] S. MacLaren, M. Schneider, K. Widmann, et al., Phys. Rev. Lett. 112, 105003 (2014)

[3] J. Porter, The 20th Topical Conference on High Temperature Plasma Diagnostics, 1-5 June 2014, Atlanta, Georgia, USA

[4] M. Schneider, O. Jones, N. Meezan, et al., Rev. Sci. Instruments 81, 10E538 (2010)

9591-6, Session 2

Gated x-ray camera microchannel plate gain droop investigation

Bart Beeman, Jorge Carrera, John M. Chesser, John B. Lugten, Fred V. Allen, Alex A. Lumbard, Charles G. Brown Jr., Joe P. Holder, Joseph R. Kimbrough, Lawrence Livermore National Lab. (United States)

We present measurements and modeling results of the electrical conductor "strips" deposited on microchannel plate (MCP) x-ray detectors. Short pulse mode response of the MCP is extremely sensitive with the output intensity related to the applied voltage by up to V23. Thus any voltage drop as the pulse travels along the strip due to conductor losses, surface roughness, etc. leads to significant changes in recorded signal intensity. This is commonly referred to as gain droop with typical variations of >3x over a 7mm x 34mm strip (3% change in voltage -2x change in gain). In an effort to minimize this gain droop we investigate electrode material choice, material thickness, and effects of annealing on the DC ohmic loss of the strip.

Additionally any reflected energy due to impedance mismatches at the output of the MCP, or crosstalk between strips, may superimpose on the incident voltage pulse, again causing gain variations. Impedance matching measurement tools and techniques for ~10ohm MCP's will be discussed.

Lawrence Livermore National Laboratory is operated by Lawrence Livermore National Security, LLC, for the U.S. Department of Energy, National Nuclear Security Administration under Contract DE-AC52-07NA27344.

9591-7, Session 2

Mirrored low-energy channel for the MiniXRD

Eric C. Dutra, Larwence P. MacNeil, National Security Technologies, LLC (United States); Steven M. Compton, Barry A. Jacoby, Lawrence Livermore National Lab. (United States); Mark L. Raphaelian, National Security Technologies, LLC (United States)

X-ray Diodes (XRD) are currently used for spectroscopic measurements, measuring x-ray flux, and estimating spectral shape of the VUV to soft x-ray spectrum. A niche exists for an inexpensive, robust x-ray diode that can be used for experiments in hostile environments on multiple platforms, including explosively driven experiments that have the potential for destroying the diode during the experiment. A multiple channel stacked filtered array was developed with a small field of view where a wider parallel array could not be used, but filtered channels for energies lower than 1000 eV were too fragile to deploy under normal conditions. To achieve both the robustness and the required low-energy detection ability, we designed a small low-energy mirrored channel with a spectral sensitivity from 30 to 1000 eV. The stacked MiniXRD x-ray diode system design incorporates the mirrored low-energy channel on the front of the stacked filtered channels to allow the system to work within a small field of view. We will present results that demonstrate this is a promising solution for low-energy spectrum measurements.

This work was done by National Security Technologies, LLC, under Contract No. DE-AC52-06NA25946 with the U.S. Department of Energy and supported by the Site-Directed Research and Development Program. DOE/ NV/25946--2316

9591-8, Session 3

Disposable blast shields for use on NIF imaging diagnostics

Cal A. Smith, Lawrence Livermore National Lab. (United States); Karen M. Wang, Lawrence Livermore National Lab. (United States) and Stanford Univ. (United States); Marion J. Ayers, Robbin L. Hibbard, Kim Christensen, Nathan D. Masters, Lawrence Livermore National Lab. (United States)

The 192 lasers deliver 2MJ of energy to Target Chamber Center (TCC) that produces an intense amount of energy to a single small volume. Along with The National Ignition Facilities (NIF) scientific experimental results come the harsh consequences to the experimental equipment and supporting diagnostic structures, which include hohlraums, support packages, target positioners, diagnostic equipment, and laser optics. Of these, the hohlraum and support packages are typically quickly vaporized and are transformed into an expanding spherical shell of high-hypersonic gases referred to as "Debris Wind". During an experimental event, such as fusion implosion, the target diagnostic components used to measure key observables on NIF are subjected to extreme pressures and impact shocks due to incident "Debris Wind" loading. As diagnostics are positioned closer to TCC, the diagnostic pinhole stacks, and other components along the diagnostic structure are become more likely to be at or above the yield strength of the materials commonly used. Of these, the pinhole stack components and data recording instruments behind the pinholes are the most costly to replace. A conceptual configuration for a pinhole shield has been proposed, analyzed and tested with the hopes that it will be able to mitigate damage to the pinhole stack and imaging equipment and allow immediate re-use of the diagnostic equipment. The shield would be a single use, disposable window that could be replaced guickly by inserting and removing it before and after each experimental laser shot. This will allow NIF to benefit from significant material and labor costs.

9591-9, Session 3

3? beam timing diagnostic for the OMEGA laser facility

Joseph D. Katz, W. Donaldson, R. Huff, E. Hill, J. Kelly, J. Kwiatkowski, R. Brannon, Univ. of Rochester (United States)

The OMEGA laser at the University of Rochester's Laboratory for Laser Energetics is a 60-beam system used for inertial confinement fusion (ICF) experiments. Uniform drive of the target surface requires precise beam timing to achieve accurate power balance. A new diagnostic has been implemented to measure the relative beam-to-beam time of arrival of each of the 60 beamlines. An 860-?m spherical diffuser placed at the target chamber center serves as a quasi-isotropic scattering source, making it possible for a fixed optical detector to view light from of any individual beamline. During a beam-timing run, the OMEGA laser is configured to generate frequency-tripled, 351-nm, ultraviolet (UV) pulses with energies of ~100 pJ at a repetition rate of 5 Hz. Light from the scattering target is optically relayed to a fast photomultiplier tube and recorded on a digital oscilloscope. A portion of the original infrared (IR) seed pulse is fiber

Conference 9591: Target Diagnostics Physics and Engineering for Inertial Confinement Fusion IV



optically delivered the beam-timing oscilloscope and recorded using a photodiode. By recording the scattered UV pulse and the IR seed on the same oscilloscope trace, a jitter-free measurement of the beam arrival time can be made. Discrepancies in beam timing are corrected by adjusting the total optical path length of the beamlines. Typical variation in the measured arrival times of all 60 OMEGA beams after adjustment is 5-ps rms (root mean square).

9591-10, Session 3

Digitizer architecture analysis for target diagnostics on the National Ignition Facility

Arthur Carpenter, Todd J. Clancy, Bart Beeman, Perry Bell, Lawrence Livermore National Lab. (United States)

This paper covers a systems engineering analysis of existing scope-based Target Diagnostics (TD) on the National Ignition Facility (NIF) at Lawrence Livermore National Laboratory (LLNL), for the purpose of selecting standard digitizer architectures for NIFs future use. Key performance criteria and a summary of test results is presented.

Currently of the 60+ Target Diagnostics, at least fifteen use a type of high speed electrical signal data read-out device leading to over 200 digitization channels spread over six types of CRT and digital oscilloscopes, each with multiple models and versions. The proposed standard architectures discussed in this paper allow the NIF to efficiently and reliably operate digitizers that meet the required performance metrics for the lifetime of the NIF.

The systems engineering analysis identifies key stakeholders for multiple subsets of scope-based diagnostics including but not limited to the nToFs (neutron Time of Flight), DANTE a broadband, time-resolved x-ray spectrometer, SPBT (South Pole Bang Time), GRH (Gamma Reaction History), and FFLEX (Filter Fluorescer Diagnostic). From these stakeholders, key performance metrics are derived and drive a test plan that evaluates different digitizers and architectures. The results of this work allows for the selection of several architectures to be used in future diagnostics.

This work was performed under the auspices of the U.S. Department of Energy by Lawrence Livermore National Laboratory under Contract DE-AC52-07NA27344.

9591-11, Session 3

Materials characterization of irradiated spectralon from the NIF target chamber

Robert Chow, Gene Frieders, Wayne Jensen, Mark Pearson, Phil Datte, Lawrence Livermore National Lab. (United States)

The Near Backscatter Imager (NBI) participates in nearly every kind of experiment conducted at NIF and measures backscatter, the result of the interaction between incident laser light and plasma waves at a target. Large Spectralon plates, on the order of a hundreds of mm per side, are used as Lambertian scatter components for the NBI diagnostics. The plates were deployed in 2009 and replaced in April of 2014. All NBI assemblies suffered reflectivity degradation, and some changes were spatially localized. The growth of some defects was correlated to the cumulative fusion energy and the cumulative neutron yield created from the Deuterium-Tritium target shots.

Spectralon plates were extracted from the NIF target chamber in April of 2014 after irradiation to a cumulative neutron fluence of 3.53E8 neutrons/ mm2 and cumulative total fusion energy from energetic particles of 0.92 mJ/mm2. These plates were characterized for materials and mechanical changes with the following techniques: RBS, FTIR, XPS, SEM, EDX and tensile tests. These tests indicate that the bulk Spectralon has not degraded but there are the defects created that significantly change the reflectivity of the Spectralon. The analysis shows that the surface loses F atoms and the C bonds to H, O, N and other C-F molecules.

Auspices

Lawrence Livermore National Laboratory is operated by Lawrence Livermore National Security, LLC, for the U.S. Department of Energy, National Nuclear Security Administration under Contract DE-AC52-07NA27344.

9591-12, Session 3

Gated photocathode design for the P510 electron tube used in the National Ignition Facility (NIF) optical streak cameras (Invited Paper)

Philip S Datte, Glen James, Daniel Kalantar, Gene Vergel de Dios, Lawrence Livermore National Lab. (United States)

The optical streak cameras currently used at the National Ignition Facility (NIF) implement the P510 electron tube from Photonis1. The existing high voltage electronics provide DC bias voltages to the cathode, slot, and focusing electrodes. The sweep deflection plates are driven by a ramp voltage. This configuration has been very successful for the majority of measurements required at NIF. New experiments require that the photocathode be gated or blanked to reduce the effects of undesirable scattered light competing with low light level experimental data. The required 2300V gate voltage is applied between the photocathode and the slot electrode in response to an external trigger, to allow the electrons to flow. Otherwise the slot electronde is held at near the same potential as the photocathode, preventing electron flow. This article reviews the implementation and performance of the gating circuit that applies an electronic gate to the photocathode with a nominal 50ns rise and fall time, and a pulse width between 50ns and 2000ns.

9591-13, Session 4

Multi-axis neutron imaging at the National Ignition Facility (Invited Paper)

David N. Fittinghoff, Gary P. Grim, Robin L. Hibbard, Donald R. Jedlovec, Lawrence Livermore National Lab. (United States); Frank E. Merrill, Petr L. Volegov, Carl H. Wilde, Los Alamos National Lab. (United States)

Inertial Containment Fusion (ICF) experiments at the National Ignition Facility (NIF) rely on a Neutron Imager (NI) to measure the 2D size and shape of the neutrons produced by the burning deuterium-tritium plasma. Since the NI is located on the equator of the NIF chamber, it provides only one view of the plasma, which complicates understanding the inherently three-dimensional nature of the implosion. Attempts to use x-ray images combined with the neutron image to improve our understanding of the 3D neutron-burn volume have proved to be inconsistent with the fuel mass. This result is understandable since neutrons and x-rays are not produced or propagated in the same manner. Thus, it is desirable to use multiple NIs, and we are designing two NIs nearly orthogonal to the current imager, one near the pole of the chamber and one near the equator, for fielding on the NIF in the next five years. In this paper, we will discuss the current designs, including the resolution, field of view and placement in the facility as well as the analysis that will be required to use the three orthogonal neutron imagers to measure the neutron burn volume of plasmas at NIF. Prepared by LLNL under Contract DE-AC52-07NA27344.

9591-14, Session 4

Upgrades to the Radiochemistry Analysis of Gas Samples (RAGS) diagnostic at the National Ignition Facility

Donald R. Jedlovec, Kim Christensen, Lawrence Livermore National Security, LLC (United States); Carol Velsko,



William Cassata, Wolfgang Stoeffl, Dawn Shaughnessy, Lawrence Livermore National Security, LLC (United States)

The Radiochemical Analysis of Gaseous Samples (RAGS) diagnostic apparatus operates at the National Ignition Facility (NIF). At the NIF, Xenon is: injected into the target chamber as a tracer, is used as an analyte in the NIF targets, and is also generated as a fission product from fast 14Mev neutron fission of uranium contained in the NIF hohlraum. Following a NIF shot, the RAGS is used to collect the gas from the NIF target chamber and then to cryogenically fractionate Xenon gas. Radio Xenon and other collected activation products are counted via gamma spectroscopy, with the results used to determine critical physics parameters including: capsule areal density, fuel-ablator mix, and nuclear cross sections.

We will discuss the following performance upgrades to the system:

1) Modification of the Xenon fractionator to allow collection of Krypton. Krypton is an important target analyte and is also generated as fission gas in NIF shots. We have modified the cryostat to enable fractionation of Xenon, Krypton, or both, and

2), a translatable detector for quantification of the Xenon activity. An in situ Germanium detector is used to count the radio isotopes collected on the cold head. NIF shots that incorporate uranium in the hohlraum generate large amounts of fission gas, the radioactivity of which swamps the detector. We have designed a system that will adjust the detector to cold head distance based upon either the count rate or the time after the NIF shot.

9591-15, Session 4

Vast Area Detection for Experimental Radiochemistry (VADER) at the National Ignition Facility

Justin D. Galbraith, Ron Bettencourt, Dawn Shaughnessy, Bahram Talison, Kevin Morris, Lawrence Livermore National Lab. (United States)

At the National Ignition Facility (NIF), the flux of neutrons and charged particles at peak burn in an inertial confinement fusion capsule induces measureable concentrations of nuclear reaction products in the target material. Radiochemistry analysis of post-shot debris can be used to determine diagnostic parameters associated with implosion of the capsule, including fuel areal density and ablator-fuel mixing. Additionally, analysis of debris from specially doped targets can provide realistic debris samples for nuclear forensics.

We have developed and are deploying the Vast Area Detection for Experimental Radiochemistry (VADER) diagnostic to collect shot debris at the NIF. VADER uses quick release collector panels that are easily reconfigured for different collector materials and geometry. The VADER collectors are located 50 cm from the NIF target; each of nine collectors views approximately 25 square degrees solid angle. Dynamic loading of the NIF target debris field was modelled using LS-DYNA. Three dimensional printing was utilized to expedite the design process. Model-based manufacturing was used throughout.

We will describe the design and operation of this diagnostic as well as some initial results.

This work was performed under the auspices of the U.S. Department of Energy by Lawrence Livermore National Laboratory under Contract DE-AC52-07NA27344.

LLNL-ABS-666600

9591-16, Session 4

Implementation of an enhanced permanently-installed neutron activation diagnostic hardware in NIF

Donald R. Jedlovec, Lawrence Livermore National Security. LLC (United States); Charles B. Yeamans, Ellen R. Edwards, Jorge A. Carrera, Lawrence Livermore National Security, LLC (United States)

Neutron activation diagnostics are commonly employed as baseline neutron yield and flux measurement instruments. Much insight into implosion performance has been gained by deployment of up to 19 identical activation diagnostic samples distributed around the target chamber at unique angular locations. Their relative simplicity and traceability provide neutron facilities with a diagnostic platform that is easy to implement and verify. However, the current NIF implementation relies on removable activation samples, creating a 1-2 week data turn-around time and considerable labor costs. The system described here utilized a commercially-available lanthanum bromide (cerium-doped) scintillator with integrated MCA emulator as the counting system and a machined zirconium-702 cap as the activation medium. The device is installed within the target bay and monitored remotely. Yield values are returned within 10 minutes after a NIF shot. Additionally, this system allows the placement of any activation medium tailored to the specific measurement needs. We discuss the design and function of a standalone and permanently installed neutron activation detector unit to measure the yield and average energy of a nominal 14 MeV neutron source with a pulse length less than 1 nanosecond.

9591-17, Session 5

Design of a spectrometer for opacity experiments at the National Ignition Facility (Invited Paper)

Patrick W. Ross, Jeffrey A. Koch, Michael J. Haugh, Wayne C. Stolte, National Security Technologies, LLC (United States); Robert F. Heeter, Marilyn B. Schneider, Duane A. Liedahl, Theodore S. Perry, Lawrence Livermore National Lab. (United States); Greg S. Dunham, Sandia National Labs. (United States)

The National Ignition Facility (NIF) Opacity Spectrometer (OpSpec) is a modular spectrometer designed initially for opacity experiments on NIF. The design of the OpSpec will be presented in light of the requirements and constraints. Potential dispersing elements and detector configurations will be presented, and the advantages and disadvantages of each configuration will be discussed. The full OpSpec design covers the energy range from approximately 550 eV to 2 keV. The energy resolution of the OpSpec is E/?E > 500. Applications of the OpSpec will be discussed, including relevant astrophysical applications for NIF experiments, and will compliment recently published work on the Z machine. (Bailey, et al., Nature 517, 56-59 (2015).)

This work was done by National Security Technologies, LLC, under Contract No. DE-AC52-06NA25946 with the U.S. Department of Energy.

9591-18, Session 5

Calibration results for first NIF Kirkpatrick-Baez diagnostic

Nicolai F. Brejnholt, Louisa A. Pickworth, Jay J. Ayers, David K. Bradley, Todd A. Decker, Stefan P. Hau-Riege, Randolph M. Hill, Thomas J. McCarville, Tommaso Pardini, Julia K. Vogel, Chris C. Walton, Lawrence Livermore National Lab. (United States)

The Lawrence Livermore National Laboratory (LLNL) has been developing a series of novel x-ray imagers for the National Ignition Facility (NIF) utilizing Kirkpatrick-Baez (KB) geometry. A fully assembled imager contains four KB optic pairs featuring cylindrical mirrors with custom-designed single or multi-layer coatings applied to them. Multiple interchangeable mirror packs have been commissioned for various experimental campaigns, with spatial resolution as low as 5 ?m at the center of the field of view and 12x magnification.

Tight tolerances on the grazing angles of the x-ray mirrors require precision



alignment of each component via a coordinate measuring machine (CMM), and a comprehensive off-line calibration of each optic pair at x-ray wavelengths. The first fully assembled imager is currently being aligned and tested. The main goals of the calibration are to validate the CMM alignment of the optic pairs, and measure the spatial resolution as a function of position in the field of view. Here we report first results of the calibration effort.

This work was performed under the auspices of the U.S. Department of Energy by Lawrence Livermore National Laboratory under Contract DE-AC52-07NA27344. LLNL-ABS-666488

9591-19, Session 5

Determining the diffraction properties of a cylindrically-bent KAP crystal from 1 to 4.5 keV

Michael J. Haugh, National Security Technologies, LLC (United States); Ming Wu, Sandia National Labs. (United States); Kenneth D. Jacoby, Cindy Christensen, National Security Technologies, LLC (United States); Joshua J. Lee, National Security Technologies, LLC (United States) and Sandia National Labs. (United States)

Bent KAP crystals are frequently used in spectroscopic diagnostics for plasma studies on the Z machine at Sandia National Laboratories and the National Ignition Facility at the Lawrence Livermore National Laboratory. For an anisotropic crystal, like KAP, bending the crystal can produce distortions of the planar spacing in other directions. The bending can alter the diffraction properties significantly compared to the corresponding flat crystals. These diffraction properties affect the throughput and the resolving power of the spectrometer. The KAP crystal is a valuable tool for the X-ray spectral energy range from 500 to 5000 eV, and a better understanding of the effect of bending will be valuable to spectrometer designers and users. We have measured reflectivity curves for cylindrically bent KAP crystals for the energy range from 1000 to 5000 eV for bent crystals that range from 5 to 23 cm radii of curvature. The measurements were made using the NSTec dual goniometer X-ray source, with a flat KAP crystal as the monochromator. The method used to analyze the data and the conclusions obtained will be presented.

9591-20, Session 5

Optimizing the input and output transmission lines that gate the microchannel plate in a high-speed x-ray framing camera

John B. Lugten, Charles G. Brown Jr., Bart V. Beeman, Alex A. Lumbard, Fred V. Allen, Douglas R. Kittle, Lawrence Livermore National Lab. (United States)

We present new designs for the launch and receiver boards used in a high speed x-ray framing camera at the National Ignition Facility. The new launch board uses a Klopfenstein taper to match the 50 ohm input impedance to the -10 ohm microchannel plate. The new receiver board incorporates design changes resulting in an output monitor pulse shape that more accurately reproduces the pulse shape at the input and across the microchannel plate; this is valuable for assessing and monitoring the electrical performance of the assembled framing camera head. The launch and receiver boards maximize power coupling to the microchannel plate, minimize cross talk between channels, and minimize reflections. We discuss some of the design tradeoffs we explored, and present modeling results and measured performance. We also present our methods for dealing with the non-ideal behavior of coupling capacitors and terminating resistors. We compare the performance of these new designs to that of some earlier designs.

9591-21, Session 6

Exploration of high Miller index Ge crystals in flat and bent geometries for imaging high-energy x-rays (Invited Paper)

Joshua J. Lee, Michael J. Haugh, Jeffery A. Koch, National Security Technologies, LLC (United States)

Near normal-incidence spherically-bent crystals are used as x-ray imaging optics for a variety of applications at HEDP (high-energy-density physics) facilities worldwide. The combination of constraints from geometric optics, requiring operating near normal incidence, as well as limited inter-atomic spacings, typically at least several angstroms, limits the upper useful energy range to several keV. Accessing energies in excess of 10 keV have been achieved by using higher-order reflections where the 2d lattice spacing happens to match an integral number of wavelengths. We propose using high Miller-index crystals, operated in the first diffraction order, as an alternative to high-order reflections from low Miller-index crystals. We have tested a Ge (15, 7, 7) crystal for integrated reflectivity and will present comparisons of experimental results to theoretical predictions for both flat and cylindrically-bent geometries. This work was done by National Security Technologies, LLC, under Contract No. DE-AC52-06NA25946 with the U.S. Department of Energy.

9591-22, Session 6

Shot-time photography at the National Ignition Facility

Donald R. Jedlovec, Kim Christensen, Lawrence Livermore National Lab. (United States)

The Nation Ignition Facility (NIF) conducts a variety of experiments to study matter at the extremes, including studies of material properties, hydrodynamics, and the interaction of intense radiation fields with matter. The NIF supports the users by operating twenty-four hours a day, with a laser shot rate averages roughly one per day.

We have developed a shot time camera that has the capability to provide an image of each shot for the users. While initially more of promotional tool, recent improvements show potential as a shot diagnostic. The shot time camera is a time integrated, shot- triggered, digital camera that images visible light generated at shot time in the NIF target chamber. It is selectable by the user and operates automatically with the NIF shot cycle. We will discuss the system design, recent results, and plans for the future.

9591-23, Session 6

Precision fabrication of large-area siliconbased geometrically-enhanced x-ray photocathodes using plasma etching

Yekaterina P. Opachich, National Security Technologies, LLC (United States); Ning Chen, Ashwini Gopal, Salah Uddin, Nanoshift, LLC (United States); Eric Huffman, Jeffrey A. Koch, National Security Technologies, LLC (United States); Andrew MacPhee, Lawrence Livermore National Lab. (United States); Terance J. Hilsabeck, General Atomics (United States); Sabrina R. Nagel, Perry M. Bell, David K. Bradley, Otto L. Landen, Lawrence Livermore National Lab. (United States)

Geometrically enhanced photocathodes are currently being developed for use in applications that seek to improve detector efficiency in the visible to X-ray ranges. Various photocathode surface geometries are typically chosen based on the detector operational wavelength region, along with requirements such as spatial resolution, temporal resolution and dynamic



range. Recently, a potential structure has been identified for use in the X-ray region. This anisotropic high aspect ratio structure has been produced in silicon using inductively coupled plasma (ICP) etching technology. The process is specifically developed with respect to the pattern density and geometry of the photocathode chip to achieve the desired sidewall profile angle. The tapered sidewall profile angle precision has been demonstrated to be within $\pm 2.5^{\circ}$ for a ~12° wall angle, with feature sizes that range between 4-9 µm in diameter and 10-25 µm depth. Here we present the method used to produce a set of geometrically enhanced high yield X-ray photocathodes in silicon.

9591-24, Session 6

An overview of the Ultrafast X-ray Imager (UXI) program at Sandia Labs

Liam Claus, Lu Fang, Mark W. Kimmel, Joel Long, John L. Porter, Gideon Robertson, Marcos Sanchez, Sandia National Labs. (United States); Douglas Trotter, Douglas Trotter Consulting (United States); Randolph R. Kay, Sandia National Labs. (United States)

The Ultra-Fast X-ray Imager (UXI) program is an ongoing effort at Sandia National Laboratories to create high speed, multi-frame, time gated Readout Integrated Circuits (ROICs), and a corresponding suite of photodetectors to image a wide variety of High Energy Density (HED) physics experiments on both Sandia's Z-Machine and National Ignition Facility (NIF). The program is currently fielding a 1024 x 448 prototype camera with 25 ?m pixel spatial resolution, 2 frames of in-pixel storage and the possibility of exchanging spatial resolution to achieve 4 or 8 frames of storage. The camera's minimum integration time is 2 ns. Minimum signal target is 1500 e- rms and full well is 1.5 million e-. The design and initial characterization results will be presented as well as a description of future imagers.

Sandia is a multiprogram laboratory operated by Sandia Corporation, a Lockheed Martin Company, for the United States Department of Energy's National Nuclear Security Administration under contract DE-AC04-94AL85000. SAND2015-0304C

Conference 9592: X-Ray Nanoimaging: Instruments and Methods II

Wednesday - Thursday 12-13 August 2015

Part of Proceedings of SPIE Vol. 9592 X-Ray Nanoimaging: Instruments and Methods II

9592-1, Session 1

Science capabilities of the Hard X-ray Nanoprobe (HXN) at NSLS-II (Invited Paper)

Yong S. Chu, Hanfei Yan, Xiaojing Huang, Sebastian Kalbfleisch, Evgeny Nazaretski, Nathalie Bouet, Juan Zhou, Li Li, Weihe Xu, Hui Yan, Kenneth Lauer, Kazimierz J. Gofron, Brian Mullany, Dennis Kuhne, James Biancarosa, Michael Maklary, Nikolaos Simos, Brookhaven National Lab. (United States)

The Hard X-ray Nanoprobe (HXN) beamline at the NSLS-II has been designed and constructed to explore new frontier of the x-ray microscopy, by offering a suite of scanning microscopy techniques at an initial spatial resolution of 10 nm. The designed scanning microscopy techniques include x-ray fluorescence, x-ray diffraction, x-ray absorption, x-ray scattering, phase-contrast imaging, spectroscopy, and ptychography. Aggressive R&D on multilayer Laue lens and nanopositioning have resulted in instrument capabilities to focus hard x-rays down to 11 nm and to perform scanning x-ray microscopy experiments with excellent precision. Innovative approaches have been implemented in the beamline design to achieve required stability for x-ray beam and experiment environment. Commissioning measurements provide preliminary evidences that the HXN beamline is performing as designed. Presentation will summarize key instrument designs supporting the science capabilities and commissioning data.

9592-2, Session 1

Fast scanning multi-technique imaging and tomography at Nanoscopium (Synchrotron Soleil)

Andrea Somogyi, Kadda Medjoubi, Gil Baranton, François A. Polack, Jean-Pierre Samama, Synchrotron SOLEIL (France)

The 155 m long Nanoscopium beamline of Synchrotron Soleil is dedicated to scanning multi-technique hard X-ray imaging and tomography. It aims to reach 30-200 nm resolution in the 5-20 keV energy range for routine user experiments. The beamline design tackles the tight stability requirements of such a scanning nano-probe by creating an overfilled secondary source, implementing all horizontally reflecting main beamline optics, applying high mechanical stability equipments and constructing a dedicated high stability building envelope. The beamline aims to provide high sensitivity elemental and sample morphology mapping by fast scanning spectro-microscopy combined with absorption, differential phase contrast and dark field imaging and electron density mapping by coherent imaging techniques.

The typical scientific fields to be covered by the beamline are biology and life sciences, earth- and environmental sciences, geo-biology and bionanotechnology. The beamline is especially well suited for studies seeking information about highly heterogeneous systems at multiple length scales also in natural or in operando conditions. In this presentation we report on the optical design of Nanoscopium and the measured operational characteristics. Then we present the proof of principle multimodal fast scanning imaging and 3D tomography experiments performed with ms/pixel dwell time.

References:

Medjoubi K, Leclercq N, Langlois F, Buteau A, Lé S, Poirier S, Mercère P, Sforna MC, Kewish CM, Somogyi A (2013). J Synch Rad 20:293–299. Somogyi A, Polack F, Moreno T, (2010). SRI 2009, 10th International Conference on Radiation Instrumentation. AIP Conference Proceedings 1234:395-398.

Somogyi A, Medjoubi K, Kewish CM, Le Roux V, Ribbens M, Baranton G, Polack F, Samama J P (2013). SPIE 8851, X-Ray Nanoimaging: Instruments and Methods, 885104

9592-3, Session 1

Hard x-ray nanoprobe by Montel KB mirrors at Taiwan Photon Source

Gung-Chian Yin, Shi-Hung Chang, Bo-Yi Chen, Huang-Yeh Chen, Bi-Hsuan Lin, Shao-Chin Tseng, Chien-Yu Lee, Jian-Xing Wu, National Synchrotron Radiation Research Ctr. (Taiwan); Shao-Yun Wu, National Tsing Hua Univ. (Taiwan); Mau-Tsu Tang, National Synchrotron Radiation Research Ctr. (Taiwan)

The hard X-ray nanoprobe beamline at TPS acquires a large numerical aperture by utilizing a pair of diffraction-limited Montel nested Kirkpatrick-Baez mirrors. The beamline, despite with a moderate length of 69 meters, can accordingly achieve similar performances compared to those beamlines longer than 100 meters. The Montel KB mirrors made of silica are places symmetrically with a 45 degrees cut to reduce the gap and unintentional crack between the mirrors. The size and the divergence of the focus spot are simulated to be less than 40 nm and 6.29 mrad, respectively, as the slope errors for the mirrors are expected less than 0.05 ?rad. An ultra precise ten-axis mirror holder is designed and fabricated to meet the critical requirement for the mirror alignment.

The beamline optics, thus designed to take the advantage of the geometry of Motel mirrors, brings about a symmetrical focal spot at the sample. The design feature of the beamline optics includes a horizontal double crystal monochromator, and a two stage horizontally focusing mirrors before the Montel mirrors.

For the endstation, multimodal probes will be provided, including XRF, XAS, XEOL, XRD, CDI, etc. An SEM in close cooperation with laser interferometers is equipped to precisely position the samples and perform the fly scanning. The updated progress of the endstation will be reported in the presentation.

9592-4, Session 1

A next-generation in-situ nanoprobe beamline at the APS MBA lattice

Jörg Maser, Barry Lai, Argonne National Lab. (United States); Mariana Bertoni, Arizona State Univ. (United States); Tonio Buonassisi, Massachusetts Institute of Technology (United States); Si Chen, Lydia Finney, Sophie-Charlotte Gleber, Ross Harder, Curt Preissner, Ruben Reininger, Chris Roehrig, Xianbo Shi, Volker Rose, Deming Shu, David Vine, Stefan Vogt, Argonne National Lab. (United States)

The Upgrade of the Advanced Photon Source's Storage Ring with a multibend achromat (MBA) magnetic lattice will yield a 4th Generation Hard X-ray Synchrotron with massively increased brilliance and source dimensions perfectly suited for nanofocusing and coherent imaging. To exploit the new source's 100x increase in coherent hard x-ray flux and its almost symmetric x-ray shape, we are developing a new flagship hard x-ray microscopy beamline, the In-Situ Nanoprobe (ISN).[1] The ISN is dedicated to the study of materials and devices for generation, storage and transmission of energy, such as photovoltaic systems,[2] batteries[3] and fuel cells. The ISN will provide in-situ and operando characterization of advanced materials and devices under change of temperature, gases, and under applied fields, at

SPIE. PHOTONICS OPTICAL ENGINEERING+ APPLICATIONS

Conference 9592: X-Ray Nanoimaging: Instruments and Methods II



previously unattainable spatial resolution and throughput. The ISN will use nanofocusing mirrors to focus hard x-rays into a probe of as small as 20 nm size. Use of mirror as nanofocusing optics will yield an increase in focused flux to 1.6?1011 Phot/s at 25 keV, into an energy band of $\Delta E/E$ = 10-4. The achromatic properties of mirror optics will allow fast spectroscopic studies at very high spatial resolution. To fully exploit the powerful source properties, the ISN beamline will have a length of approximately 180 m. This will yield large working distances of around 50 mm at a resolution of 20 nm, critical to deploying a wide variety of in-situ environments. The combination of very large focused flux and flux density, nano-spectroscopy and large working distance will enable very high-speed scanning of complex materials and devices at physically relevant time scales, and characterization through multidimensional parameter spaces. This will, for example, enable materials discovery and materials or device optimization efforts. To enable the potential of the ISN, the beamline will be designed with view to user friendliness, batch-scan capability and efficiency of operation. We will present the conceptual design of the ISN beamline, and discuss initial studies of advanced photovoltaic systems.

[1] J. Maser, B. Lai, T. Buonassisi, Z. Cai, S.Chen, L. Finney, S. Gleber, C. Jacobsen, C. Preissner, C. Roehrig, V. Rose, D. Shu, D. Vine, S. Vogt, Metall. Mater. Trans. A 45 (1), 85-97 (2014).

[2] M. Bertoni, D. Fenning, M. Rinio, V. Rose, M. Holt, J. Maser, T. Buonassisi: Energy Environ. Sci., 2011, vol. 4, 4252-4257

[3] A. Ulvestad et al., Nano Lett. 14 (9), 5123-5127 (2014).

9592-5, Session 1

High-speed x-ray mapping using the FalconX4 at extremely-high count rates

Peter Grudberg, XIA LLC (United States); Paul A. Scoullar, Southern Innovation (Australia)

As synchrotron fluxes continue to increase and the beam spot size decreases at nanoscale beam lines, there is unprecedented need for the ability to perform very high rate X-ray spectroscopy with the ability to do very fast mapping. The FalconX4 (with family members FalconX1 and FalconX8) is the latest of the next generation pulse processors that allow for extremely high throughput while maintaining good resolution; the FalconX4 offers a highly flexibly control architecture that allows for high-speed mapping with a wide range of different detectors and control signals. We present the results of a variety of sample experiments, illustrating what can be done with this new technology.

9592-6, Session 2

Resolution limits of projection x-ray microscopy and tomography

Michael Feser, Carl Zeiss X-ray Microscopy, Inc. (United States)

High-resolution x-ray microscopy can be realized by projection microscopy or by use of x-ray lenses to produce magnified images. Both types of microscopes suffer fundamental and practical limitations to the resolution achievable. Contrary to intuition, the limit to the resolution of both types of microscopes is given by the diffraction limit. In the projection microscope this takes the form of blurring due to propagation Fresnel diffraction. This effect is energy dependent and gets severe at low x-ray energies which are preferred for high-resolution imaging due to the increased contrast. In many practical cases this establishes the resolution limit for projection microscopy. X-ray lens based microscopes on the other hand are limited by the diffraction limit of the optics employed putting more emphasis on the ability of manufacturing these optics. The role of practical limitations such as imaging time and sample working distance to realize tomographic or in-situ imaging are discussed and it is shown that for practical purposes for most cases below one micrometer spatial resolution it is preferable to use a x-ray lens based microscope. The reason for this are the requirement for sufficient sample working distance to carry out measurements and the requirements for practical exposure times to conduct the experiments.

9592-7, Session 2

Development of achromatic full-field hard x-ray microscopy with two monolithic imaging mirrors

Satoshi Matsuyama, Hidetoshi Kino, Shuhei Yasuda, Osaka Univ. (Japan); Yoshiki Kohmura, RIKEN/SPring-8 (Japan); Hiromi Okada, JTEC Corp. (Japan); Tetsuya Ishikawa, RIKEN/SPring-8 (Japan); Kazuto Yamauchi, Osaka Univ. (Japan)

We developed an achromatic and high-resolution full-field hard X-ray microscope based on advanced Kirkpatrick-Baez mirror optics that comprises two monolithic one-dimensional Wolter mirrors. The monolithic imaging mirrors were figured to have an elliptical shape and a hyperbolic shape on a single substrate, which can function as a one-dimensional imaging optics. The monolithic structure of the imaging mirror can make the mirror alignment easy, leading to keep the arrangement very stable. The mirror fabrication was performed with a shape accuracy of 2 nm using our home-built techniques of elastic emission machining (EEM), microstitching interferometry (MSI) and relative-angle-determinable stitching interferometry (RADSI). The constructed microscope consists of a polycapillary lens as a condenser, the imaging mirrors as an objective and a CMOS camera coupled with a phosphor screen and a relay lens. It has a numerical aperture of ~1.5 and magnification of 634x and 195x in vertical and horizontal directions, respectively. The first performance test, in which a Siemens star chart with a 100-nm pattern was observed at an X-ray energy around 10 keV, was performed at BL29XUL of SPring-8. The 100-nm pattern was clearly observed. The contrast analysis revealed that the microscope achieved the spatial resolution less than 100 nm.

9592-8, Session 2

FXI: a full-field x-ray imaging beamline at NSLS-II

Wah-Keat Lee, William Loo, Yong S. Chu, Jun Wang, Richard Gambella, Zhong Zhong, Brookhaven National Lab. (United States); Ruben Reininger, Argonne National Lab. (United States)

The Full Field X-ray Imaging (FXI) beamline at the NSLS-II will enable x-ray microscopy with 30 nm spatial resolution and very high speed image acquisition, using a Transmission X-ray Microscope (TXM). The TXM will operate in the 5-11 keV range and the data collection time for a complete 3D tomographic data set will be < 1 minute. Single image acquisition times will be < 100 ms. The TXM has also been designed with nano-XANES capability, incorporating automated alignment during nano-XANES measurements. The beamline has been designed to tackle the very high power loads from the NSLS-II damping wigglers, with the sole purpose of delivering maximum photon flux for the TXM to enable high speed data acquisition. This paper will discuss the technical details of the FXI beamline.

9592-9, Session 3

Ptychographic x-ray nanotomography at the Swiss Light Source (Invited Paper)

Manuel Guizar-Sicairos, Ana Diaz, Mirko Holler, Julio C. da Silva, Oliver Bunk, Andreas Menzel, Paul Scherrer Institut (Switzerland)

Ptychography combines elements of scanning probe microscopy with coherent diffractive imaging and has been developed to be a robust highresolution imaging technique that finds today applications in X-ray, electron and optical microscopy. It provides reconstructions of the beam and the specimen's complex-valued transmissivity which allows for instance to

Conference 9592: X-Ray Nanoimaging: Instruments and Methods II



fully characterize focused X-ray beams, images with elemental specificity, quantify mixtures of known components, or combine with fluorescence microscopy for complementary imaging contrast.

The extension of ptychography to 3D, often named ptychographic X-ray computed tomography (PXCT), was originally demonstrated at the Swiss Light Source (SLS) in 2010. This technique provides a nanoscale 3D map of the sample's complex-valued refractive index. It is amenable for use with hard X-rays which gives access to the interior of samples with several tens of microns thickness and has great potential for high-resolution due to the high sensitive phase contrast and the small wavelength below 1 nm.

We present here progress in reconstruction and post-processing algorithms as well as implementation and development of dedicated instrumentation for fast and precise 3D scanning at the SLS. Compared to the first demonstration in 2010, such developments have already allowed an improvement of one order of magnitude in resolution and two orders of magnitude in imaging speed. We showcase results of in situ measurements under varying environmental conditions, quantitative imaging of bio-mineralized specimens, frozen hydrated cells, and nanoscale characterization of catalyst materials.

9592-10, Session 3

Development of a soft x-ray ptychography beamline at SSRL and its application in the study of energy storage materials

Anna M. Wise, Hendrik Ohldag, SLAC National Accelerator Lab. (United States); William Chueh, Stanford Univ. (United States); Joshua J. Turner, Michael F. Toney, Johanna L. Nelson Weker, SLAC National Accelerator Lab. (United States)

Ptychography is an emerging high resolution coherent imaging technique which can improve the resolution of scanning transmission X-ray microscopy (STXM) by over ten-fold. Development of this capability is underway at SSRL to establish sub-5 nm resolution in situ ptychography with near-edge X-ray absorption fine structure (NEXAFS) imaging. This is being achieved via an upgrade of the current soft X-ray STXM chamber on beamline 13-1, involving the installation of an area detector and an interferometer system for high precision sample motor control. The undulator source on beamline 13-1 provides the spatially and temporally coherent X-ray beam required for ptychographic imaging in the energy range 500 - 1200 eV. This energy range allows access to the oxygen chemistry and the valence states of 3d transition metals found in energy storage materials, making soft x-ray ptychography a particularly powerful tool to study the chemical states and structure of battery materials at relevant length scales. The implementation of in situ ptychographic imaging can therefore provide a wealth of additional information on battery operation and failure, with measurements possible at comparable imaging resolutions to TEM with a lower radiation dose. The development of this in situ ptychography capability will be described, along with its application to the study of energy storage materials.

9592-11, Session 3

Imaging strain in SiGe thin films at the nanoscale by x-ray Bragg ptychography

Wen Hu, Xiaojing Huang, Brookhaven National Lab. (United States); Conal E.. Murray, IBM Thomas J. Watson Research Ctr. (United States); Zhonghou Cai, Argonne National Lab. (United States); Evgeny Nazaretski, Yong S. Chu, Brookhaven National Lab. (United States); Hanfei Yan, National Synchrotron Light Source II, Brookhaven National Lab. (United States)

Strain is known to play a crucial role in determining the performance of semiconductor devices, thereby the control of strain is a key issue in their

design and fabrication. Conventional x-ray diffraction techniques, although capable of measuring strain at very high accuracy, do not offer the spatial resolution needed for microelectronics. X-ray Bragg ptychography is a new emerging technique to image strain noninvasively in an extended crystalline specimen with a resolution better than the beam size of the x-ray probe, ultimately enabling a 3D strain measurement at the nanoscale. In this work, we present a theoretical study on the effects of partial coherence, the overlap ratio and position uncertainty in Bragg Ptychography, using synthetic data generated from forward simulation. The convergence of the reconstruction and the detection sensitivity of the strain field under various conditions are discussed. We also report a Bragg Ptychography experiment on a SiGe thin film feature for 3D strain reconstruction by performing spiral 2D scans at different rocking angles. Reconstructed strains are compared to previously reported values and results obtained from theoretical modeling. Issues and challenges in the reconstruction are discussed as well.

9592-29, Session 3

Fast strain mapping of nanoLED devices using nano-focused x-ray beams

Tomas Stankevic, Univ. of Copenhagen (Denmark); Dmitry Dzhigaev, Max Rose, Anatoly Shabalin, Deutsches Elektronen-Synchrotron (Germany); Zhaoxia Bi, Lund Univ. (Sweden); Juliane Reinhardt, Deutsches Elektronen-Synchrotron (Germany); Anders Mikkelsen, Lars Samuelson, Lund Univ. (Sweden); Gerald Falkenberg, Ivan A. Vartanyants, Deutsches Elektronen-Synchrotron (Germany); Robert K. Feidenhans'l, Univ. of Copenhagen (Denmark)

Strain engineering applied on the semiconductor core-shell nanowires opens new possibilities in the fields of solid state lightning and nanoelectronics. Better elastic strain relaxation in 3D geometry allows growing heterostructures of lattice mismatched materials without introducing misfit dislocations. It is crucial to be able to measure local strain variations in each individual nanodevice with nanometer resolution. X-rays are the only tool that provides such possibility and can be used on the samples thicker than 200 nm. In this paper we show results of the nanoscale strain mapping performed on a single, 400 nm thick and 2µm long core-shell InGaN/GaN nanowire. The thickness of the shell with 30% In concentration was 25 nm thick, which highly exceeds the critical dimensions for such heterostructure and thus both plastic and elastic strain relaxation was expected. We scanned the sample with 40 nm steps in the X-ray beam, focused down to 100 nm at full width at half maximum. At each step diffraction pattern was measured, which contained signals from the core and the shell of the nanowire. By measuring positions of the Bragg peaks we were able to extract local strain and tilt of the crystal planes. We observed inhomogeneous strain distribution caused by the asymmetric strain relaxation of the InGaN shell. One side of the shell was still fully strained with respect to the core, while the other was nearly fully relaxed. Moreover, large tilt and strain gradients were seen at the interface with the substrate.

9592-13, Session 4

Progress on multi-order hard x-ray imaging with multilayer zone plates (*Invited Paper*)

Markus Osterhoff, Christian Eberl, Robin Wilke, Jesper Wallentin, Florian Döring, Hans-Ulrich Krebs, Georg-August-Univ. Göttingen (Germany); Michael Sprung, Deutsches Elektronen-Synchrotron (Germany); Tim Salditt, Georg-August-Univ. Göttingen (Germany)

Today's technical developments and challenges often involve particles and phaenomena on the nano metre scale. In the field of x-ray imaging, a wide variety of techniques has been developed to gather highly resolved data on shape, density distribution, local order, or x-ray induced changes in the

Conference 9592: X-Ray Nanoimaging: Instruments and Methods II

sample. While techniques like ptychography overcome the resolution limit on beam size, other contrast mechanisms like fluorescent maps, local stimuli, or nano-diffraction are limited by the quality and size of the probing beam.

We present our latest results in hard x-ray imaging using multilayer zone plates (MZPs) that can focus down well below 10?nm in two dimensions. A combined optics set-up constisting of prefocusing optics (by, e.g., Kirkpatrick-Baez mirrors or compound refractive lenses) that adapt the coherence area of synchrotron radiation (depending on beamline and energy, about 50 to 500?micro metre) to the MZP diameter, about 1.5 to 15?micro metre in our case.

With the experience of first imaging experiments using high-resolution MZPs at 18?keV, we identify and tackle challenges in the experimental set-up and the imaging experiment itself. The experimental side is accompanied by recent developments in data analysis methods.

M. Osterhoff et al., J. Appl. Crystallogr. (accepted, 2015)

9592-14, Session 4

High-resolution high-efficiency multilayer Fresnel zone plates for soft and hard x-rays

Umut T. Sanli, Kahraman Keskinbora, Corinne Grévent, Max-Planck-Institut für Intelligente Systeme (Germany); Keith Gregorczyk, CIC nanoGUNE Consolider (Spain); Mato Knez, CIC nanoGUNE Consolider (Spain) and IKERBASQUE, Basque Foundation for Science (Spain); Gisela Schütz, Max-Planck-Institut für Intelligente Systeme (Germany)

X-ray microscopy enables high spatial resolutions, high penetration depths and characterization of a broad range of materials. Calculations show that nanometer range resolution is achievable in the hard X-ray regime by using Fresnel zone plates (FZPs) if certain conditions are satisfied. However, this requires, among other things, aspect ratios of several thousands. The multilayer (ML) type FZPs, having virtually unlimited aspect ratios, are strong candidates to achieve single nanometer resolutions. Our research is focused on the fabrication of ML-FZPs which encompasses deposition of multi-layers over a glass fiber via the atomic layer deposition (ALD), which is subsequently sliced in the optimum thickness for the X-ray energy by a focused ion beam (FIB). We recently achieved aberration free imaging with an efficiency of up to 12.5 % and resolved 21 nm features. This is the highest imaging resolution achieved by an ML-FZP. We also showed efficient focusing of 7.9 keV X-rays down to 30 nm focal spot size (FWHM). For resolutions below ~10 nm, efficiencies would decrease significantly due to wave coupling effects. To compensate this effect high efficiency, low stress materials have to be researched, as lower intrinsic stresses will allow fabrication of larger FZPs with higher number of zones, leading to larger light collecting area. As a first step we fabricated an ML-FZP with a diameter of 62 μ m, an outermost zone width of 12 nm and over 400 active zones. Further strategies for fabrication of high resolution high efficiency multilayer FZPs will also be discussed.

9592-15, Session 4

Stacking multiple zone plates for efficient hard x-ray focusing at the Advanced **Photon Source**

Michael Wojcik, Sophie-Charlotte Gleber, Deming Shu, Christian Roehrig, Barry Lai, David J. Vine, Stefan Vogt, Argonne National Lab. (United States)

Zone plates are diffractive focusing optics capable of nanometer focusing but limited focusing efficiency at hard x-ray energy. A smaller focus spot is possible by reducing the outer zone width (OZW) while increasing the zone height will generally increase focusing efficiency. The combination

of thick zones with small outer zone width, or high aspect ratio, for better performing zone plates is not feasible with state-of-the-art fabrication methods and requires other methods to achieve the aspect ratio desired.

OPTICS+

OPTICAL ENGINEERING+ APPLICATIONS

SPIE. PHOTONICS

Near field stacking involves two zone plates with the same dimensions and aligning them within the depth of focus in the beam direction and one third of the OZW in the transverse direction. Due to the depth of focus limitation, stacking more than 2 zone plates is extremely difficult, so a new method was proposed and developed to stack zone plates in the intermediate field. Zone plates were designed for intermediate field stacking and fabricated. Multiple stacking apparatuses were assembled and tested. We will report on results from stacking up to 6 zone plates with sub-100-nm OZW, e.g. 28% focusing efficiency at 27 keV x-ray energy, as well as applications using the stacking apparatus.

This research used resources of the Advanced Photon Source and Center for Nanoscale Materials, U.S. Department of Energy (DOE) Office of Science User Facilities operated for the DOE Office of Science by Argonne National Laboratory under Contract No. DE-AC02-06CH11357.

9592-16, Session 4

Fabrication and x-ray testing of true kinoform lenses with high efficiency

Kahraman Keskinbora, Umut T. Sanli, Corinne Grévent, Gisela Schütz, Max-Planck-Institut für Intelligente Systeme (Germany)

Fresnel zone plates have been very successful in focusing of X-rays enabling high resolution X-ray microscopy. However, FZPs are limited to a theoretical maximum of 40 % diffraction efficiency and in practice much less efficient than this. However, a refractive/diffractive optical device with a three dimensional surface structure called the kinoform lens enables focusing X-rays with a theoretical diffraction efficiency of 100 %. The fabrication of kinoform type lenses have been pursued by utilizing step-approximated geometries via gray scale optical lithography or overlay electron lithography among other methods, while the realization of true continuous kinoform surface remained elusive. Recently, we have succeeded in fabricating true kinoforms with an effective gray scale ion beam lithography route. The fabricated kinoforms showed high focusing efficiencies (>14 % absolute and ~ 90 % relative) and were used for imaging in a scanning soft X-ray microscope. Results demonstrate that almost ideal kinoform profile was achieved through this process and the efficiency was dominated by absorption of soft X-rays which was used for testing. Efficiency calculations show that the kinoforms can reach very high efficiencies at EUV and hard X-ray energies. Especially in the hard X-ray range where the absorption is low kinoforms can in principle achieve tremendous focusing efficiencies when the material constraints are satisfied. We also discuss, the prospects and challenges of kinoform lenses including materials issues and microstructural design, efficiency considerations at low and high energies and possible applications as focusing optics in laboratory sources where efficiency is crucial.

9592-26, Session PWed

Extending x-ray imaging with current nanofabrication techniques for fabrication of high-yield Fresnel zone plate optics

Robert Peters, Mirwais Aktary, Luis Gutierrez-Rivera, Cameron Horvath, Applied NanoTools Inc. (Canada)

Advances in sources for x-ray nanoimaging have led to an increased demand for focusing optics that can provide both nanoscale resolution and high efficiency. Nanofabrication challenges in producing x-ray optics are one of the limitations in furthering the widespread reception of x-ray nano-imaging. Fresnel zone plates in particular, due to the requirements for nanoscale features with high aspect ratios on nano-thin membranes, can suffer from low yield, high-costs, and short lifetimes, especially for hard x-ray designs. We demonstrate a fabrication process that allows

Conference 9592: X-Ray Nanoimaging: Instruments and Methods II



for the production of low-cost, high yield, and increased-lifetime zone plates. Diffraction efficiency experiments have been shown to provide near theoretical efficiency for the first order along with high resolution imaging. A several micrometer thick gold central stop process also significantly improves contrast in imaging by limiting the Oth order light, while adding structural integrity to the fragile membrane without additional film stress, reducing the risk of damaging the optics during handling and imaging. Nanofabrication methods, including cold development with vibration regulation, and anti-charging films have extended the normal capabilities of traditional nanofabrication of Fresnel zone plates. These techniques have allowed the fabrication of zone plates with high resolution for soft to hard x-ray imaging. Work involving state-of-the art reactive ion etching to further increase the aspect ratio for 20 keV energies and above is also presented.

9592-27, Session PWed

High-resolution strain mapping of single nanowires with x-ray Bragg ptychography

Dmitry Dzhigaev, Deutsches Elektronen-Synchrotron (Germany); Tomas Stankevic, Univ. of Copenhagen (Denmark); Zhaoxia Bi, Lund Univ. (Sweden); Max Rose, Anatoly Shabalin, Juliane Reinhardt, Deutsches Elektronen-Synchrotron (Germany); Anders Mikkelsen, Lund Univ. (Sweden); Ulf Lorenz, Univ. Potsdam (Germany); Ruslan Kurta, European XFEL GmbH (Germany); Andrei Singer, Univ. of California, San Diego (United States); Frank Seiboth, Technische Univ. Dresden (Germany); Lars Samuelson, Lund Univ. (Sweden); Christian G. Schroer, Deutsches Elektronen-Synchrotron (Germany); Robert Fedenhans'l, Univ. of Copenhagen (Denmark); Ivan A. Vartanyants, Deutsches Elektronen-Synchrotron (Germany)

Strain analysis at the nanoscales is crucial for understanding physical, electrical, and photonic properties and fabrication processes of crystalline structures such as nanowires. For structural studies we considered individual nanowires. These were InP nanowire with applications in solar cells technology and core-shell GaN/InGaN nanowire with applications in light emitting diodes. Diameters of investigated samples were 100 nm and 400 nm, respectively.

Recently developed X-ray Bragg ptychography technique allows reconstruction of the crystal displacement field from coherently scattered intensities by solving the phase problem iteratively. Bragg ptychography experiments were performed at PO6 nanoprobe end-station of PETRA III synchrotron source. By using X-ray nano-beam with the size below 100 nm (FWHM) it was possible to map quantitatively the internal strain field of a single InP and GaN/InGaN core-shell nanowires without destructive sample preparation.

Our results show inhomogeneous strain distribution in the core of the NW, which is caused by asymmetric strain relaxation in the shell. Finite Element Model (FEM) simulations based on the elasticity theory were performed in order to ensure the reliability of experiments. Values and profiles of the strain field from FEM simulations are consistent with the experimental results. This technique permitted a non-destructive determination of strain with a spatial resolution better than 20 nm.

Presented results extend the possibilities of nano-crystals in situ characterization in order to improve the efficiency of fabrication and performance of the future nanowire-based devices.

9592-28, Session PWed

Transmission x-ray microscopy at Diamond Light Source I13 Beamline

Joan Vila Comamala, Diamond Light Source Ltd. (United Kingdom); Jeroen Borgra, Paul Scherrer Institut (Switzerland); David S. Eastwood, The Univ. of Manchester (United Kingdom) and Research Complex at Harwell (United Kingdom); Ulrich H. Wagner, Andrew J. Bodey, Miryam Garcia-Fernandez, Diamond Light Source Ltd. (United Kingdom); Christian David, Paul Scherrer Institut (Switzerland); Christoph Rau, Diamond Light Source Ltd. (United Kingdom)

To date, full-field Transmission X-ray Microscopy (TXM) has shown to be a powerful method for obtaining quantitative internal structural and chemical information from materials at the nanoscale. The installation of a full-field TXM station will extend the current microtomographic capabilities of Diamond-Manchester BL-I13 Beamline Imaging Branch at Diamond Light Source into the sub-100 nm spatial resolution range using photon energies from 8 to 15 keV. Preliminary full-field TXM experiments demonstrate a spatial resolution of about 50 nm in both transmission and Zernike phase contrast modes at 8.3 keV photon energy. The tomographic capabilities using Zernike phase contrast were tested using a Nickel particle from a solid oxide fuel cell (courtesy of R. Bradley, University of Manchester) and the fibres of a coir-based supercapacitor material (courtesy of C. P. Gray and N. Trease, University of Cambridge). The dedicated Full-Field TXM station will be built in-house with the contributions of Diamond Light Source support divisions in collaboration of the X-ray Optics Group of the Paul Scherrer Institut (Switzerland) developing state-of-the-art diffractive X-ray optical elements. The full-field TXM will become an important direct imaging asset for material science, energy science and biology at the nanoscale at the Diamond Light Source.

9592-30, Session PWed

Fly-scan ptychography

Junjing Deng, Northwestern Univ. (United States); Youssef S. G. Nashed, Si Chen, Argonne National Lab. (United States); Nicholas W. Phillips, La Trobe Univ. (Australia); Tom Peterka, Rob Ross, Stefan Vogt, Argonne National Lab. (United States); Chris J. Jacobsen, Northwestern Univ. (United States); David J. Vine, Argonne National Lab. (United States)

Ptychography is a coherent diffraction imaging method which offers powerful tools to image extended objects at a spatial resolution limited only by the scattering strength of the object and the detector geometry. Most ptychography experiments to date employ a move-settle-measure mode for data acquisition, which is often referred as step-scan mode. In this mode, data acquisition can be very slow when the move and settle steps take longer to complete than the measure step. We describe here the use of a continuous "fly-scan" mode for ptychographic data collection in which the sample is moved continuously for fast scan, while multiple probe mode reconstruction methods are used to obtain the sample complex transmission function as well as the illumination functions. We show in simulations, and in x-ray imaging experiments, some of the characteristics of fly-scan ptychography, including the reduction in the data acquisition time. This approach will become increasingly important as brighter x-ray sources are developed, such as diffraction limited storage rings.

9592-31, Session PWed

Layer tilt analyses of MLLs using diffraction efficiency versus rocking angle for defect mapping

Adam Kubec, Fraunhofer IWS Dresden (Germany) and Argonne National Lab. (United States); Raymond Conley, Argonne National Lab. (United States) and Brookhaven National Lab. (United States); Nathalie Bouet, Hanfei Yan, Juan Zhou, Brookhaven National Lab. (United States);



Albert T. Macrander, Jörg Maser, Argonne National Lab. (United States)

With new and improved fabrication of Multilayer Laue lenses (MLL) analyses of these structures becomes more important to identify remaining challenges in the fabrication. This is especially necessary when large aperture and wedged MLLs are introduced as their fabrication must meet increasingly stringent precision requirements.

We have developed a method to quantitatively determine defects in an MLL structure such as local bending, twisting, possible discontinuities, or local delamination. Using Coupled-Wave-Theory, we calculated expected diffraction patterns for a particular lens. These are then compared to measured diffraction data. The results show absolute bending in a lens structure, where the resolution is only limited by instrumentation parameters. We used a representation of the data, where diffracted intensity is shown as a function of the rocking angle.

9592-32, Session PWed

MAPStoTomoPy: a workflow for synchrotron-based fluorescence tomography

Young Pyo Hong, Northwestern Univ. (United States); Si Chen, Advanced Photon Source, Argonne National Lab. (United States); Chris Jacobsen, Northwestern Univ. (United States) and Advanced Photon Source, Argonne National Lab. (United States)

Analyzing fluorescence tomographic data aquired from 2IDE and BioNanoprobe(BNP) was rather complex and time-consuming. One had to collect per-pixel-fitted data from MAPS, align the dataset respect to common rotation axis, do the reconstruction, and attain visualization of the data. There was no dedicated program for the dataset from the beamlines. Moreover, most of the users of beamlines are experts on their fields but had a little knowledge about 3d reconstruction. Thus, users had to wait for beamline scientists to analyzing 3d tomographic data while beamline scientists other workloads. Consequently, we developed a program, MapsToTomoPy, that provides a workflow from image registration to reconstruction.

The program would take an output of MAPS as an input and generates slices of a reconstructed 3d image by utilizing TomoPy. While some users of the beamlines are also interested in the process of image registration and reconstruction, most of users are interested in reconstructed data rather than the process. The goal of the program is to provide a comprehensive 3d tomographic data analyzing tool even for the users with a little knowledge of how image registration and/or reconstruction works.

9592-33, Session PWed

Refractive lens-based full-field x-ray imaging at 50 keV with sub-micron resolution

Sarvjit D. Shastri, Peter Kenesei, Argonne National Lab. (United States); Robert M. Suter, Carnegie Mellon Univ. (United States)

Combining sub-micron resolution imaging with the penetration property of high-energy x-rays (> 50 keV) offers numerous applications, such as the ability to examine cracks and voids associated with the onset of failure in engineering materials. Progress on the development of this method at the Advanced Photon Source beamline 1-ID is reported. A tested configuration having approximately 20x imaging magnification with compound refractive lenses placed 1.7 m after the specimen, and a two-dimensional detector located 32-37 m further downstream, gave sub-micron resolution with 50 keV x-rays. The subsequent goal of achieving tomographic capability, while compacting the full set-up to a more practical length of a few meters, is discussed.

9592-17, Session 5

Simultaneous x-ray nano-ptychographic and fluorescence microscopy at the bionanoprobe (Invited Paper)

Si Chen, Argonne National Lab. (United States); Junjing Deng, Northwestern Univ. (United States); David J. Vine, Youssef Nashed, Argonne National Lab. (United States); Qiaoling Jin, Northwestern Univ. (United States); Stefan Vogt, Argonne National Lab. (United States); Chris J. Jacobsen, Argonne National Lab. (United States) and Northwestern Univ. (United States)

Hard x-ray fluorescence microscopy (XFM) offers unparalleled sensitivity for quantitative analysis of most of the trace elements in biological samples, such as Fe, Cu, and Zn. These trace elements play critical roles in many biological processes. With the advanced nano-focusing optics, nowadays one can focus hard x-rays down to 30 nm or below and probe the trace elements within subcellular compartments. However, XFM does not usually show much ultrastructural information, because main constituents of biomaterials, i.e. H. C. N. and O. have low fluorescence vield and little absorption contrast at multi-keV x-ray energies. An alternative technique for imaging ultrastructure is ptychography. One can record diffraction patterns from a coherently-illuminated sample, and then reconstruct the complex transmission function of the sample. In theory the spatial resolution of ptychography can reach the wavelength limit. In the presentation, we will describe the implementation of ptychography at the Bionanoprobe (a recently development hard x-ray fluorescence nanoprobe at the Advanced Photon Source) and demonstrate simultaneous ptychographic and fluorescence imaging of a frozen green algae cell. This method allows one to locate trace elements within the ultrastructure of biological samples with high spatial resolution. Additionally, both ptychography and fluorescence are compatible with tomographic approach for 3D imaging.

9592-18, Session 5

The hard x-ray nanoprobe beamline and electron microscopy facility at Diamond

Paul Quinn, Julia Parker, Fernando Cacho-Neri, Andrew Peach, Guy Wilkin, Diamond Light Source Ltd. (United Kingdom)

Diamond is currently constructing a new microscopy and imaging facility which will house a hard X-ray nanoprobe beamline (I14) and a new electron microscopy facility.

The I14 nanoprobe beamline is a 185m long beamline which will use a nanofocussing KB system with cryogenic sample handling capabilities for 2D and 3D scanning X-ray fluorescence, X-ray spectroscopy and imaging applications in a range of areas.

The microscopy centre provide 4 electron microscope suites which serve two facilities:

The Electron imaging centre for biology which will provide two cryo electron microscopes and offer single particle analysis of biological macromolecules and cellular tomography, as well as electron crystallography. These techniques will complement the atomic mapping possible with the macromolecular crystallography beamlines, the elemental mapping in cells provided by the X-ray nanoprobe and the larger scale cell imaging capability of the new Full Field Cryo Transmission X-ray Microscope (B24 cryo-TXM). In addition the facility will provide extensive range of cryogenic sample preparation tools.

The Electron microscopy centre for physical sciences which will be used look at the ordering and chemical state of atoms in the sample, through EDX, EELS, atomic scale imaging, and electron diffraction and should also compliment the nanoprobe beamline.

This facility combines staff and expertise from a number of different areas which we believe we will allow us to make exciting progress in correlative

Conference 9592: X-Ray Nanoimaging: Instruments and Methods II



x-ray, optical and electron microscopy studies. Details of the facilities and plans for correlative experimental studies will be discussed.

9592-19, Session 5

Development of differential analysis techniques for multivariate imaging data analysis

Zhonghou Cai, Argonne National Lab. (United States)

Recent technological advances in X-ray detectors and diffraction limited synchrotron storage ring will allow the chemical element, structure, and energy state of a material to be imaged through fast X-ray microscopy with fluorescence emission, diffraction, and spectroscopy. It is anticipated that the fast X-ray microscopy will particularly enable imaging studies of heterogeneous materials that often are of multi-element, multi-phase, and multi-energy state and are complex spatially and compositionally. Once merging multimodal imaging data across various contrasts, the dimension of the imaging variable space increases quickly. When the variances of the imaging variables are widely dispersed, the degree of the image complexity will be beyond the processing capability of a human brain through visual recognition of features. This poses a great challenge on analyzing and extracting scientific information from multivariate imaging data. We are developing at the Advanced Photon Source multivariate descriptive statistical analysis tools that hierarchically differentiate image pixels based on their composition in the multivariable space and differentiate imaging variables based on their associations with principal components along which the image pixels exhibit statistically significant variances. These numerical methods can sensitively summarize all meaningful composition features in images with the level of differentiation controllable to as small as that of noise and reveal inherent relations among imaging variables of elemental contents, phases concentrations, and energy states. Since it imposes no limitation in the dimension of the variable space, the developed tools are particularly suited for data analysis across different imaging platforms. We will present the differential analysis method, demonstrate its applications, and discuss the direction of future development.

9592-20, Session 5

Chemical speciation imaging at environmentally-relevant concentrations using x-ray fluorescence microscopy

David J. Paterson, Daryl L. Howard, Martin D. de Jonge, Kathryn M. Spiers, Australian Synchrotron (Australia); Chris G Ryan, Robin Kirkham, CSIRO (Australia); Barbara E. Etschmann, Monash Univ. (Australia); Enzo Lombi, Erica Donner, Univ. of South Australia (Australia); Peter M. Kopittke, The Univ. of Queensland (Australia)

X-ray fluorescence microscopy (XFM) can be used for elemental and chemical microanalysis across length scales ranging from millimeter to nanometer. XFM is ideally suited to quantitatively map trace elements within whole plant and other biological specimens, environmental and soil samples. The elemental sensitivity of the X-ray fluorescence probe provides valuable information for investigations in a diversity of environmental sciences, and the high penetration of hard X-rays enables measurement of whole cells and tissue sections with a minimum of preparation.

Advances in X-ray fluorescence detection methods such as the Maia detector now enable high definition images at mega-pixel per hour rates. The ability to rapidly acquire 2D images enables 3D information such as fluorescence tomography to be obtained in realistic times. Chemical speciation (valence) imaging (CSI) is a 3D technique where the third dimension is spectroscopic detail. CSI produces an X-ray Absorption Near Edge Structure (XANES) spectra from the X-ray fluorescence signal at each pixel in the spatial image. Fitting of spectra with incident X?ray beam energy tracking has been developed in GeoPIXE software using the Dynamic Analysis method.

CSI has been demonstrated at the Australian Synchrotron XFM beamline with micron resolution and moderate definition (10K pixels) across a diverse range of sciences and applications from environmental chemistry to arsenic toxicity in crop production. Recent studies probing and optimising the efficiency and sensitivity of the CSI technique to achieve measurements at environmentally relevant concentrations will be presented.

9592-25, Session 5

Nano Investigator: a versatile tool for nmscale spatial resolution x-ray imaging with MLL nanofocusing optics

Evgeny Nazaretski, Brookhaven National Lab. (United States)

The Hard X-ray Nanoprobe (HXN) beamline at the NSLS-II has been designed and constructed to address questions related to scientific and technological challenges at the nm-scale. The HXN X-ray Microscope is a key instrument for the beamline, providing a suite of experimental capabilities which includes scanning fluorescence, diffraction, differential phase contrast and ptychography utilizing Multilayer Laue Lenses (MLL) and zoneplate (ZP) as nanofocusing optics. To enable higher impact and explore the phase space in materials research studies, the instrument is equipped with a temperature regulation system capable of varying specimen temperature between 100 K and 1000 K. During this presentation, different phases of the x-ray microscope development process will be discussed, various prototype systems designed and constructed will be reviewed. Preliminary data demonstrating nm-scale spatial resolution imaging using MLL optics will be presented.

9592-21, Session 6

Chemical and tomographic microscopy of energy materials in action (Invited Paper)

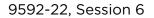
Johanna L. Nelson Weker, Yijin Liu, Joy C. Andrews, SLAC National Accelerator Lab. (United States)

Using the rapid imaging rate and penetrative power of full-field hard X-ray transmission microscopy (TXM), we are able to track morphological [1] and chemical [2] changes of energy materials under realistic conditions. High resolution, in situ microscopy allows the visualization of dynamic systems in time, capturing a wealth of information inaccessible to ex situ imaging methods. In situ TXM is fundamental to understanding of the standard operation and failure mechanisms of energy materials such as catalysts and battery electrodes, as well as the nucleation and growth of nanostructures, which directly affect the properties of the final structure. In addition to in situ microscopy, energy materials benefit greatly from mapping elemental and chemical information in 3D. By mapping this information, the surface chemistry, which often dominates the functionality of these materials, can be visualized and understood.

We will discuss recent results on battery electrodes tracking the morphological and chemical changes in 2D and density and volume changes in 3D. Additionally, we will present and discuss results on visualizing the nucleation and growth of nanostructures with unique electrical, optoelectronic and luminescent properties. Finally we will show our latest results of in situ and ex situ imaging on catalytic materials used in petroleum refinery.

[1] J. Nelson Weker, and M. F. Toney, "Emerging In Situ and Operando Nanoscale X-Ray Imaging Techniques for Energy Storage Materials," Advanced Functional Materials, (2015).

[2] J. C. Andrews, and B. M. Weckhuysen, "Hard X-ray Spectroscopic Nano-Imaging of Hierarchical Functional Materials at Work," ChemPhysChem, 14(16), 3655-66 (2013).



Synchrotron-based transmission x-ray microscopy for improved extraction in shale during hydraulic fracturing

Andrew M. Kiss, Adam D. Jew, Stanford Synchrotron Radiation Lightsource (United States); Claresta Joe-Wong, Stanford Univ. (United States); Kate M. Maher, Yijin Liu, Gordon E. Brown, John Bargar, Stanford Synchrotron Radiation Lightsource (United States)

Engineering topics which span a range of length and time scales present a unique challenge to researchers. Hydraulic fracturing (fracking) of oil shales is one of these challenges and provides an opportunity to use multiple research tools to thoroughly investigate a topic. Currently, the extraction efficiency for hydrocarbons from source rock is low but can be improved by carefully studying the processes at the micro- and nano-scale. Fracture fluid induces chemical changes in the shale which can have significant effects on the microstructure morphology, permeability, and chemical composition. These phenomena occur at length scales from nanometer to hundreds of microns and times from days to months which require different instrumentation to properly study. Synchrotron-based techniques such as fluorescence tomography provide high sensitivity elemental mapping and an in situ micro-tomography system records morphological changes with time. Since typical pores sizes can be less than 100 nm, the transmission X-ray microscope (TXM) at the Stanford Synchrotron Radiation Lightsource (SSRL) beamline 6-2 is utilized to collect a nano-scale three-dimensional representation of the sample morphology with elemental and chemical sensitivity. We present the study of model shale system containing quartz and pyrite, in which particles are mixed and exposed to oxidizing solution, to establish the basic understanding of the more complex geology-relevant oxidation reaction. The spatial distribution of the production of the oxidation reaction, ferrihydrite, is retrieved via full-field XANES tomography showing the reaction pathway. Further correlation between the high resolution TXM data and the high sensitivity micro-probe data provides insight into potential morphology changes which can decrease permeability and limit hydrocarbon recovery.

9592-23, Session 6

Magnetic contrast nanotomography

Robert P. Winarski, Argonne National Lab. (United States)

We are using the X-ray polarization selectivity (linear, right and left circularly polarized) available at the Hard X-ray Nanoprobe Beamline to examine magnetic materials in three dimensions using magnetism as a contrast mechanism [1,2,3]. X-ray magnetic circular dichroism (XMCD) refers to the differential absorption of left and right circularly polarized (LCP and RCP) X-rays, induced in a sample by an applied magnetic field. By closely analyzing the difference in the XMCD absorption spectra, information can be obtained on the magnetic moments. Differences in the system, such as spin and orbital magnetic moments. Differences in spin densities of the unoccupied electron bands in the sample. We are measuring these differences in absorption contrast while controlling the polarization during nanotomography acquisition.

[1] Winarski, R. P., Holt, M. V., Rose, V., Fuesz, P., Carbaugh, D., Benson, C., Shu, D., Kline, D., Stephenson, G. B., McNulty, I. and Maser, J. (2012), A hard X-ray nanoprobe beamline for nanoscale microscopy. Jnl of Synchrotron Radiation, 19: 1056–1060. doi: 10.1107/S0909049512036783

[2] J. C. Lang and G. Srajer, Rev. Sci. Instrum. 66, 1540 (1995).

[3] G. Schütz, W. Wagner, W. Wilhelm, P. Kienle, R. Zeller, R. Frahm, and G. Materlik, Phys. Rev. Lett. 58, 737

9592-24, Session 6

X-ray microscopy for in situ characterization of 3D microstructure evolution in the laboratory

Benjamin Hornberger, Hrishikesh Bale, Arno Merkle, Michael Feser, William Harris, Carl Zeiss X-ray Microscopy, Inc. (United States)

SPIE. OPTICS+ PHOTONICS

OPTICAL ENGINEERING+ APPLICATIONS

X-ray microscopy (XRM) has emerged as a powerful technique that reveals 3D images and guantitative information of interior structures. XRM executed both in the laboratory and at the synchrotron have demonstrated critical analysis and materials characterization on meso-, micro-, and nanoscales, with spatial resolution down to 50nm in laboratory systems. The nondestructive nature of X-rays has made the technique widely appealing, with potential for "4D" characterization, delivering 3D micro- and nanostructural information on the same sample as a function of sequential processing or experimental conditions. Understanding volumetric and nanostructural changes, such as solid deformation, pore evolution, and crack propagation are fundamental to understanding how materials form, deform, and perform. We will present recent instrumentation developments in laboratory based XRM including a novel in situ nanomechanical testing stage. These developments bridge the gap between existing in situ stages for micro scale XRM, and SEM/TEM techniques that offer nanometer resolution but are limited to analysis of surfaces or extremely thin samples whose behavior is strongly influenced by surface effects. Several applications will be presented including 3D-characterization and in situ mechanical testing of polymers, metal alloys, composites and biomaterials. They span multiple length scales from the micro- to the nanoscale and different mechanical testing modes such as compression, indentation and tension.

Conference 9593: Hard X-Ray, Gamma-Ray, and Neutron Detector Physics XVII

Monday - Wednesday 10-12 August 2015

Part of Proceedings of SPIE Vol. 9593 Hard X-Ray, Gamma-Ray, and Neutron Detector Physics XVII

9593-1, Session 1

Physics of spectral resolution in gammaray scintillator detectors (Invited Paper)

Stephen A. Payne, Nerine J. Cherepy, Steven L. Hunter, Erik L. Swanberg, Patrick R. Beck, Zachary M. Seeley, Lawrence Livermore National Lab. (United States)

For scintillators, the fundamental limit to achieving better spectral resolution is due to the so-called nonproportionality. To understand this limit better, we have recorded hundreds of curves of the light yield against the energy of a single high-energy electron injected into the scintillator (using an instrument known as SLYNCI). By employing this single high-energy electron we are able to measure and model the interplay between the electron stopping behavior (which mediates the initial carrier concentration) and the subsequent dynamics where the electrons and holes can form excitons, annihilate or be trapped, and can be captured by activators to lead to luminescence. Scintillators including binary halides and oxides and ternary compounds have been characterized, as well as organics (crystals, liquids, plastics). Further studies of the impact of codopants, temperature variation and atmospheric processing conditions have been conducted. These experimental data have been modeled to fit the light yield curves versus the electron energy and to predict the resolution. We also attended to the formation of delta-rays, resulting from high-energy collisions between electrons, and to the initial distribution of electrons (rather than a single electron) arising from gamma excitation of scintillators (i.e. from photoelectric absorption and Compton scattering). We compare the gamma and electron nonproportionality curves, as well as their measured and predicted values of resolution.

9593-2, Session 1

Co-doping effects in halide scintillators: density-functional calculations

Koushik Biswas, Arkansas State Univ. (United States); Richard T. Williams, Wake Forest Univ. (United States)

Understanding the behavior of dopants and codopants and their consequences on material properties is an important area in scientific research. Recently aliovalent doping or codoping of activated scintillator crystals has generated substantial interest. Some scintillators showed remarkable improvement in energy resolution e.g., LaBr3:Ce (Sr, Ca), while others did not produce desired outcome, Srl2:Eu (La). We report our density functional theory based studies of codoping in scintillator materials and their interactions with other defect centers.

9593-3, Session 1

Linearity response of Ca2+-doped CeBr3 as a function of gamma-ray energy

Paul P. Guss, National Security Technologies, LLC (United States); Michael E. Foster, Sandia National Labs. (United States); Bryan M. Wong, Univ. of California, Riverside (United States); F. P. Doty, Sandia National Labs. (United States); Kanai S. Shah, Michael R. Squillante, Urmila Shirwadkar, Rastgo Hawrami, Joshua P. Tower, Radiation Monitoring Devices, Inc. (United States); Thomas G. Stampahar, Sanjoy Mukhopadhyay, National Security Technologies, LLC (United States)

An aliovalently calcium-doped cerium tribromide (CeBr3:Ca2+) crystal was

prepared with a gamma-energy resolution (FWHM) of 3.2% at the 137Cs 662 keV gamma energy. We completed a crystal assessment and calculated the predictive performance and physical characteristics using density functional theory (DFT) formalism. Detector performance, characteristics, calcium doping concentration, and crystal strength are reported. The structural, electronic, and optical properties of CeBr3 crystals were investigated using the DFT within generalized gradient approximation. Specifically, we see excellent linearity of photons per unit energy with the aliovalent CeBr3:Ca2+ crystal. Proportionality of light yield is one area of performance in which Cedoped and Ce-based lanthanide halides excel. Maintaining proportionality is the key to producing a strong, high-performance scintillator. Relative light yield proportionality was measured for both doped and undoped samples of CeBr3 to ensure no loss in performance was incurred by doping. The light output and proportionality for doped CeBr3, however, appears to be similar to that of undoped CeBr3. The new crystal was subjected to additional testing and evaluation, including a benchmark spectroscopy assessment. Results, which present energy resolution as a function of energy, are summarized. Typical spectroscopy results using a 137Cs radiation source are shown for our crystallites with diameters <1 cm. We obtain energy resolution of 3.2% before packing the crystallite in a sealed detector container and 4.5% after packing. Spectra were also obtained for 241Am, 60Co, 228Th, and background to illustrate the spectrosocopic quality of CeBr3:Ca2+ over a broader energy range.

9593-4, Session 1

Versatile rate equation and transport model for proportionality of light yield in electron tracks: undoped and TI-doped CsI at 295 K, undoped CsI at 100 K, and YAP:Ce vs [Ce] (Invited Paper)

Richard T. Williams, Xinfu Lu, James L. Drewery, Wake Forest Univ. (United States); Gregory A. Bizarri, Lawrence Berkeley National Lab. (United States); Samuel Donnald, The Univ. of Tennessee (United States) and Agile Technologies (United States); Jason Hayward, Merry Koschan, Charles L. Melcher, The Univ. of Tennessee Knoxville (United States); Kan Yang, Saint-Gobain Crystals (United States); Michael Mayhugh, Saint-Gobain Crystals (United States) and Faceted Development, LLC (United States); Peter R. Menge, Saint-Gobain Crystals (United States)

We describe validation tests in pure and TI-doped CsI vs temperature and in YAP:Ce vs Ce concentration of a versatile numerical model of scintillator nonproportionality based on rate equations including electron, hole, and exciton mutual interaction and transport, solved by a finite element method appropriate to the geometry of electron tracks. The coupled rate equations include hot and thermalized carrier transport as well as charge separation and resulting space charge fields, carrier capture on activators and defects, bimolecular formation of excitons. Auger and dipole-dipole quenching. Coefficients in the equations are physical rate constants and transport coefficients, most of which can be determined from experiments independent of scintillation. The solution of coupled diffusion-limited rate equations for untrapped and trapped electrons, holes, and excitons is combined with Geant4 Monte Carlo simulation of electron tracks to model electron energy response. The employed protocol for testing the model is to first fit the measured proportionality curve of the undoped host at room temperature with most of the rate and transport coefficients set at published values from interband laser z-scan, picosecond absorption, transport, and luminescence lifetime measurements or calculations. The pure-host parameters so determined are then held fixed for modeling the activator-doped host with input from ps absorption, thermoluminescence,



Conference 9593: Hard X-Ray, Gamma-Ray, and Neutron Detector Physics XVII



and/or calculation. Temperature dependence of proportionality and light yield in undoped CsI, the different mechanisms determining proportionality, light yield, and decay time between pure CsI and CsI:TI, and Ce-concentration dependence in YAP:Ce are accounted for with measured and/ or physically supportable fitting parameters.

Acknowledgment: WFU and LBNL acknowledge support from the National Nuclear Security Administration (NNSA), Office of Defense Nuclear Nonproliferation Research and Development (DNN R&D) under Contract LB15-V-GammaDetMater-PD2Jf, and WFU from the US Department of Homeland Security, Domestic Nuclear Detection Office (DNDO), and NSF Academic Research Initiative (ARI) Grant 2014-DN-077-ARI-077. UTK acknowledges NNSA DNN R&D award #DE-NA0000473 and the Center for Materials Processing at the University of Tennessee. This support does not constitute an express or implied endorsement on the part of the Government. We thank Qi Li, M. Moszynski, L. Swiderski, A. Syntfeld-Kazuch, S. Gridin, and A. V. Gektin for helpful discussions.

9593-5, Session 2

Crystallographic defects in detector-grade CZT crystals: exploring their properties using synchrotron facilities (Invited Paper)

Anwar Hossain, Aleksey Bolotnikov, Giuseppe Camarda, Yonggang Cui, Rubi Gul, Utpal Roy, Ge Yang, Ralph James, Brookhaven National Lab. (United States)

At the present status of CZT detector technology, it is true to state that the advancement and commercialization of these technologies mostly depends on the guality of the detector crystals. Over the past decade, many problems have been identified and resolved, taking this technology to a more advanced stage. The remaining critical defects in CZT crystals can mostly be attributed to stress-related sub-grain boundaries or dislocation walls and crystallographic strains, which cause non-uniformities in detector response and eventually degrade the performance of the fabricated detectors. We carried out experiments to identify and understand the roles of such defects in commercial-grade CZT crystals. We employed state-ofthe-art tools including high spatial resolution X-ray spectroscopy, microdiffraction and micro-tomography techniques at the National Synchrotron Light Source (NSLS-I & II) and at the Advanced Light Source (ALS). In this presentation, we describe in detail our acquired data of the material defects, their influence on the detector's performance, and discuss possible resolutions.

9593-6, Session 2

Control of electric field in CdZnTe radiation detectors by above-bandgap light

Jan Franc, Václav Dedic, Martin Rejhon, Charles Univ. in Prague (Czech Republic)

We have studied in details the high-flux induced polarization and above bandgap light induced depolarization in planar CdZnTe detector. We have observed the depolarization of the detector under simultaneous cathodesite illumination with excitation LED at 910nm and above bangap LED at 640nm caused by trapping of drifting photogenerated electrons. Although the detector current is quite high during this depolarization, we have shown that it decreases within ~5ms to its initial value after switching off the depolarizing light. In order to get detailed information about physical processes present during polarization and depolarization and, moreover, about associated deep levels, we have performed the series of infrared spectral scanning measurements of detector without illumination and under illumination in polarized and optically depolarized states. Three deep levels participating on polarization and depolarization have been found. Level at energy Ec-1.13 eV is associated with a strong optical transition of the electrons to the conduction band forming positive space charge. The photogenerated electrons coming from above bandgap light illumination

drifting from cathode towards anode fill the electron trap localized at energy Ec-0.88 eV and cause the formation of the negative space charge and the depolarization of the detector operating under high flux. Weaker electron trapping happens also at midgap level with energy Ev+0.75 eV which mainly interacts with the valence band as the hole trap causing polarization of the detector irradiated with high-flux X-rays.

9593-7, Session 2

Study of point defects in As-grown and annealed bridgman grown CZT crystals and their effects on ?-product and resistivity

Rubi Gul, Brookhaven National Lab. (United States) and Alabama A&M Univ. (United States); Stephen Egarievwe, Alabama A&M Univ. (United States); Georgios Prekas, Uri El-Hanany, Redlen Technologies (Canada); Aleksey E. Bolotnikov, Giuseppe Camarda, Yonggang Cui, Anwar Hossain, Utpal Roy, Ge Yang, Brookhaven National Lab. (United States); Adam Densmore, Redlen Technologies (Canada); Ralph B. James, Brookhaven National Lab. (United States)

In this research, we report on the presence of point defects and their abundance in as-grown and annealed CdZnTe radiation detectors grown under different conditions using travelling heater method (THM). We used Deep Level Transient Spectroscopy (I-DLTS) to determine the activation energy, capture cross-section, and density for different traps. The deepest observed trap has a binding energy of around 1.1 eV, and the shallowest is at a few meV. 1.1 eV trap and Cadmium vacancies are extensively studied in the detectors, before and after different annealing processes. The electrical resistivity and carrier-transport properties (??? of the detectors are studied as a function of the concentration for the 1.1-eV trap. The knowledge gained from the DLTS of point defects and ??-products is used to understand the effects of traps on the performance of CdZnTe detectors. The results indicate that the concentration of 1.1-eV trap causes non-uniformity in the E-field, and also causes a change in the resistivity and the ??e-product, and hence, it is a dominant feature in the degradation of detector performance.

9593-8, Session 2

Correcting response inhomogeneity of CdZnTe detectors

Aleksey E. Bolotnikov, Giuseppe S. Camarda, Yonggang Cui, Gianluigi De Geronimo, Jack Fried, Anwar Hossain, Utpal N. Roy, Emerson Vernon, Ge Yang, Ralph B. James, Brookhaven National Lab. (United States)

We describe the techniques for correcting the charge losses caused by defects in CdZnTe (CZT) detectors fabricated from unselected off-theshelve CZT crystals. The techniques are based on implementing a correction method for high-granularity position-sensitive detectors to enhance their performance by dividing the active volumes of the detectors into small voxels and applying corrections to the charge-signals generated from them. We present the results obtained from testing position-sensitive virtual Frisch-grid detectors and 3D position-sensitive pixelated detectors with small pixel sizes.



9593-9, Session 2

Towards a post-growth annealing approach to mitigate material defects: case analysis of CdZnTe, CdMnTe, and CdTeSe

Ge Yang, Aleksey E. Bolotnikov, Yonggang Cui, Giuseppe S. Camarda, Anwar Hossain, Utpal N. Roy, Rubi Gul, Ralph B. James, Brookhaven National Lab. (United States)

In this work, we investigate post-growth annealing to improve the properties of CdZnTe, CdMnTe and CdTeSe crystals. Defect structures and opto-electronic properties of as-grown and annealed CZT crystals are characterized by IR transmission microscopy, white X-ray beam diffraction topography, current-voltage measurements, and low-temperature photoluminescence spectroscopy. New results from recent long-term annealing experiments at lower temperatures will be presented and discussed.

9593-10, Session 3

Investigations of 6Liln(1-x)Ga(x)Se2 semiinsulating crystals for neutron detection

Brenden Wiggins, Vanderbilt Univ. (United States); Arnold Burger, Fisk Univ. (United States); Keivan G. Stassun, Vanderbilt Univ. (United States); Ashley C. Stowe, Y-12 National Security Complex (United States)

Neutron detectors are used for illicit material detection, neutron radiography, compositional analysis of stellar bodies, and nuclear power monitoring. Li-containing chalcogenides have the potential to replace 3He detectors for thermal neutron detection. The high density of lithium-6 in the 6LiInSe2 crystal results in high intrinsic thermal neutron efficiency; however, the effective efficiency is limited to 80% due to an 115In neutron capture reaction. In order to improve the overall detection efficiency, gallium has been systematically substituted for indium in the crystal lattice yielding 6LiIn1-xGaxSe2. In addition, gallium addition will be tested as a scintillation activator. A comparison of crystal quality and radiation response will be presented.

9593-12, Session 3

Thermal neutron detectors based on hexagonal boron nitride epilayers

Hongxing Jiang, Jingyu Lin, Texas Tech Univ. (United States)

Solid-state thermal neutron detectors with improved detection efficiencies are highly sought after for the detection of fissile materials. Due to low emission of neutrons by a potential fissile materials as well as decreasing of neutron flux with square of distance, it is difficult in many cases to detect neutron signal at a reasonable distance. A large size high efficiency detector is desired to improve the detector performance and to provide a relatively high counting rate.

Wafer-scale hexagonal boron nitride (h-BN) semiconducting epilayers with a thickness up to 4.5 um have been successfully synthesized by MOCVD on sapphire substrates. Metal-semiconductor-metal thermal neutron detectors with size up to 1.5 cm x 1.5 cm were fabricated. The reaction product pulse-height spectra were measured under thermal neutron irradiation produced by a 252Cf source moderated by high density polyethylene block. The measured pulse-height spectra revealed distinguishable peaks corresponding to the product energies of 10B and neutron reaction. The results indicate that h-BN semiconductor detectors are very sensitive in resolving energies of specific reaction products and have a negligible response to gamma photons produced by 137Cs decay at 0.662 MeV. Our results indicate that h-BN are highly promising for realizing sensitive solid-state thermal neutron detectors with expected advantages resulting from semiconductor technologies, including compact size, light weight, low operating voltage, and low cost.

9593-13, Session 3

Neutron detection with LiInSe2 (Invited Paper)

Zane W. Bell, Oak Ridge National Lab. (United States); Arnold Burger, Fisk Univ. (United States); Ashley C. Stowe, Y-12 National Security Complex (United States); Joshua P. Tower, Radiation Monitoring Devices, Inc. (United States); Liviu Matei, Michael Groza, Fisk Univ. (United States); Alireza Kargar, Huicong Hong, Radiation Monitoring Devices, Inc. (United States)

The detection of thermal neutrons has traditionally been accomplished with 3He-tubes, but with the recent shortage of 3He, much research has gone into finding suitable replacements. Both relatively inefficient 10B- and 6LiF-coated silicon diodes and HgI2 have been known for many years, and engineered structures in Si that have been filled with 10B and 6LiF have shown promise. These devices are intended to realize an optimal juxtaposition of neutron-sensitive material and semiconductor and thereby simulate a semiconductor containing B or Li. Such material has been realized for the first time in the form of 6LilnSe2 in which collectable charge from the 6Li(n,t) reaction indicates a neutron event. In this paper, we report neutron, gamma, and alpha responses of 6LiInSe2, Monte Carlo simulations of the responses, and compare the simulations to the measured data. We show pulse height spectra from pure gamma sources and from a thermal neutron source, and the effects of threshold on the separation of neutron and gamma events. We derive the mu-tau product from the position of spectral features as a function of bias voltage. In addition, we demonstrate the observation of the beta decay of 116mIn in samples exposed to thermal neutrons. This feature of the response serves as a confirmation of exposure to neutrons.

This work has been supported by the US Department of Homeland Security, Domestic Nuclear Detection Office, under competitively awarded Cooperative Agreement 2013-DN-077-ER00002. This support does not constitute an express or implied endorsement on the part of the Government.

9593-14, Session 4

Towards stable thallium bromide devices for long-term use (Invited Paper)

Amlan Datta, CapeSym, Inc. (United States); Piotr Becla, CapeSym, Inc. (United States) and Massachusetts Institute of Technology (United States); Shariar Motakef, CapeSym, Inc. (United States)

Thallium Bromide (TIBr) is a wide bandgap, compound semiconductor with high gamma-ray stopping power and promising physical properties. However, performance degradation and the eventual irreversible failure of TIBr devices occurs due to ionic polarization. Along with polarization, there are a number of scarcely explored processes which renders the devices unusable for practical purposes. This includes but are not limited to degradation of the electrodes with time, changes in residual stress of the TIBr crystals, and variations in the surface chemistry. Several of these issues will be explored in detail and potential solutions will be provided. For example, we have observed that the reaction of anode metal with Br decreases the lifetime of the device significantly. Different anode materials were tested to find the most resilient candidate. Several other modifications to the TIBr device fabrication techniques were also made and their effects on the long term performance was evaluated. A uniform electric field in TIBr devices is a necessary condition for device stability. We will also present results of direction observation of changes in the electric field for



an extended time in a TIBr, and relate it to residual stresses. We will present most recent lifetime results that we have obtained by employing a number of techniques to stabilize the semiconductor-metal interface. This is an invited paper.

This is an invited paper.

9593-15, Session 4

Impact of heat treatment on the electrical characteristics and charge collection efficiency of metal-GaAs:Cr-metal x-ray sensors

Anton V. Tyazhev, Andrei N. Zarubin, Vladimir A. Novikov, Oleg P. Tolbanov, Anastasiya D. Lozinskaya, David L. Budnitsky, Maxim S. Skakunov, National Research Tomsk State Univ. (Russian Federation)

The paper presents the results of experimental studies of the resistivity, electron mobility, charge collection efficiency, (mu*tau)n product and the IV characteristics of "metal-GaAs:Cr-metal" X-ray sensors dependences on the heat treatment. Experimental samples were pad sensors with an active area of 0.1-0.25 cm2 and a thickness in the range of 400 - 500 microns.

Resistivity measurements were carried out using both classical methods (Hall measurements) as well as a non-contact measurement technique.

The values of (mu*tau)n were evaluated from measurements of the charge collection efficiency dependences on the bias voltage when exposed to gamma rays from the source of 241Am.

It is shown that the heat treatment in the temperature range 200-500? C does not lead to significant degradation of characteristics of "metal-GaAs: Cr-metal" sensors and can be used in technology of ionizing radiation GaAs:Cr pixel sensors.

9593-16, Session 4

Novel semiconductor radiation detector based on mercurous halides (Invited Paper)

Henry Chen, Joo-Soo Kim, Proyanthi Amarasinghe, Feng Jin, Sudhir B. Trivedi, Brimrose Technology Corp. (United States); Arnold Burger, Fisk Univ. (United States); Jarrod Marsh, Marc S. Litz, U.S. Army Research Lab. (United States); James O. Jensen, U.S. Army Edgewood Chemical Biological Ctr. (United States)

The three most important desirable features in the search for RTSD candidate as an alternative material to current COTS material for gamma and/or thermal neutron detection are: low cost, high performance and long term stability. This is especially important for pager form application in homeland security. Yet, despite years of research, no explored RTSD candidate so far can satisfy the above 3 features simultaneously. In this work, we show that mercurous halide materials Hg2X2 (X= I, Cl, Br) is a new class of innovative compound semiconductors that can deliver breakthrough advances to COTS radiation detector materials. These materials are much easier to grow thicker crystals. They can detect gamma and potentially neutron radiation making it possible to detect two types of radiation with just one crystal material. The materials have a wider bandgap meaning higher resistivity and lower leakage current, making this new technology more compatible with available microelectronics. The materials also have higher atomic number and density leading to higher stopping power and better detector sensitivity/efficiency. They are not hazardous so there are no environmental and health concerns during manufacturing and are more stable making them more practical for commercial deployment. Focus will be on Hg2l2. Material characterization and detector performance will be presented and discussed. Initial results show that an energy resolution of 2.45% @ 59.6 keV gamma from Am-241 can be achieved at room temperature.

9593-17, Session 4

Neutron Detection with Noble Gas Scintillation: A Review of Recent Results

Christopher M. Lavelle, Johns Hopkins Univ. Applied Physics Lab., LLC (United States); Michael Coplan, Univ. of Maryland, College Park (United States); Eric C. Miller, Johns Hopkins Univ. Applied Physics Lab., LLC (United States); Alan K. Thompson, National Institute of Standards and Technology (United States); Alex Kowler, Univ. of Maryland, College Park (United States); Rob Vest, Andrew Yue, National Institute of Standards and Technology (United States); Tim Koeth, Johns Hopkins Univ. Applied Physics Lab., LLC (United States) and Univ. of Maryland, College Park (United States); Mohammad Al-Sheikhly, Univ. of Maryland, College Park (United States); Charles Clark, National Institute of Standards and Technology (United States)

Thermal neutron detection is of vital importance to many disciplines, including neutron scattering, workplace monitoring, and homeland protection. We survey recent results from our collaboration which couple low pressure noble gas scintillation with novel approaches to neutron absorbing materials and geometries to achieve potentially advantageous detector concepts. Noble gas scintillators were used for neutron detection as early as the late 1950's. Modern use of noble gas scintillation includes liquid and solid forms of argon and xenon in the dark matter and neutron physics experiments and commercially available high pressure applications have achieved high resolution gamma ray spectroscopy. Little attention has been paid to the overlap between low pressure noble gas scintillation and thermal neutron detection, for which there are many potential benefits. Approaches currently under study include multiple thin films of boron-10, boron carbide dispersed in an open cell foam, and transparent neutron absorbing materials. Experiments have been conducting using neutron beams at the NIST Center for Neutron Research.

9593-58, Session 4

High-barrier Schottky contact on n-type 4H-SiC epitaxial layer and investigation of defect levels by deep level transient spectroscopy (DLTS)

Khai V. Nguyen, Rahmi O. Pak, Cihan Oner, Mohammad A. Mannan, Krishna C. Mandal, Univ. of South Carolina (United States)

High barrier Schottky contact has been fabricated on 20 um n-type 4H-SiC epitaxial layers grown on 350 um thick substrate 4 degrees off-cut towards the [112 0] direction. The 4H-SiC epitaxial wafer was diced into 8 x 8 mm2 samples. The metal-semiconductor junctions were fabricated by photolithography and dc sputtering with metals of various work functions. The junction properties were characterized through current-voltage (I-V) and capacitance-voltage (C-V) measurements. Detectors were characterized by alpha spectroscopy measurements in terms of energy resolution and charge collection efficiency using a 0.1 uCi 241Am radiation source. It was found that detectors fabricated from high work function rare transition metal demonstrated very low leakage current and significant improvement of detector performance. Defect characterization of the epitaxial layers was conducted by deep level transient spectroscopy (DLTS) to thoroughly investigate the defect levels in the active region. The presence of a new defect level induced by this rare transition metal-semiconductor interface has been identified and characterized.



9593-18, Session 5

Novel highly-stable and rugged contact on CdTe-based materials for radiation detector applications (Invited Paper)

Utpal N. Roy, Aleksey E. Bolotnikov, Giuseppe S. Camarda, Yonggang Cui, Rubi Gul, Anwar Hossain, Ge Yang, Ralph B. James, Brookhaven National Lab. (United States); Aswini K. Pradhan, Rajeh Mundle, Norfolk State Univ. (United States)

Mechanical degradation of contacts and their poor adhesion to CdZnTe and CdTe is a major and long-standing technological problem for use of this material for detector applications. The contact interfacial layer plays a vital role in detector performance. The main reason for the contact degradation is the large differences in the thermal expansion coefficients of the common metals used for contacts and the CdZnTe. The stress between the contact and CdZnTe causes mechanical degradation and thus affects adversely the detector performance and aging. In this presentation the advantages of a novel contact and the performance of devices with the novel contact for radiation detector applications will be discussed.

9593-19, Session 5

Growth characterization of CdTeSe-based materials and fabrication of devices for radiation detector applications

Utpal N. Roy, Aleksey E. Bolotnikov, Giuseppe S. Camarda, Yonggang Cui, Rubi Gul, Anwar Hossain, Ryan Tappero, Ge Yang, Ralph B. James, Brookhaven National Lab. (United States)

Selenium in the CdTe matrix was found to be very effective in reduction of various defects such as sub-grain boundary networks and the concentration of secondary phases. In addition, the concentration of electrically active defects were also found to be reduced drastically in the CdTe matrix after alloying with Se. Growth of CdTeSe and CdZnTeSe crystals and the effects of Se on the structural defects and the concentration of electrically active defects will be discussed. The charge transport characteristics and the correlation with the electrically active defects will be presented. Finally, preliminary results of the device performance for radiation detector applications will be reported.

9593-20, Session 5

Xenon gamma-ray spectrometer in the experiment Signal on board the spacecraft Interhelioprobe

Alexander S. Novikov, Sergey E. Ulin, Valery V. Dmitrenko, Victor M. Grachev, Viktor N. Stekhanov, Konstantin F. Vlasik, Ziyaetdin M. Uteshev, Irina V. Chernysheva, Alexander E. Shustov, Denis V. Petrenko, National Research Nuclear Univ. MEPhI (Russian Federation)

In the experiment SIGNAL, which is planned to take place on board spacecraft INTERHELIOPROBE, a xenon gamma-ray spectrometer is to be used. The gamma-ray spectrometer in question has been chosen because of its characteristics permitting detailed study of solar gamma-radiation under rough experimental conditions. The equipment is able to provide: high energy resolution (5-6-fold better than that of scintillation detectors), performance at high temperatures, steady operation under significant vibroacoustic load, and high radiation resistance of the working medium. The aforesaid properties of the xenon gamma-ray spectrometer meet goals and objectives of the experiment SIGNAL. The description of ballistics

scenario and operation orbit of the spacecraft $\ensuremath{\mathsf{INTERHELIOPROBE}}$ are presented.

Currently development of the scientific equipment SIGNAL is in the stage of preparation of design documentation and SIGNAL device model manufacturing. The equipment in question is being developed at NRNU MEPHI. The established deadline is October 2015.

9593-21, Session 5

First principles studies of the stability and Shottky barriers of metal/CdTe(111) interfaces

Zhen Liu, Dorj Odkhuu, Maosheng Miao, Nicholas Kioussis, California State Univ., Northridge (United States); Suleyman Tari, Fikri Aqariden, Yong Chang, Sivananthan Labs., Inc. (United States); Christoph H. Grein, Univ. of Illinois at Chicago (United States)

CdZnTe and CdTe based semiconductor X-Ray and Gamma-Ray detectors have been intensively studied recently due to their promising potentials for achieving high-resolution, high signal-to-noise ratios and low leakage current, all are desirable features in applications ranging from medical diagnostics to homeland security. Understanding the atomic and electronic structures of the metal/semiconductor interfaces is essential for the further improvements of performance. Using density functional calculations, we systematically studied the stability, the atomic and electronic structures of the interfaces between CdTe (111) surfaces (Te- and Cd- terminated) and the selected metals (Al, Cu and Pt). We also calculated the Schottky barrier height (SBH) by aligning the electrostatic potentials in semiconductor and metal regions. Our calculations revealed the importance of intermixing between semiconductor and metal layers and the formation of Te-metal alloys at the interface. The obtained SBH does not depend much on the choice of metals despite the large variation of the work functions. On the other hand, the interface structure is found to have large effect to the SBH, which is attributed to the metal induced states in the gap. The position of such states is insensitive to the metal work functions, as revealed by the analysis of the electronic structures.

9593-22, Session 6

Potassium-based halide scintillators with high-energy resolution (*Invited Paper*)

Mariya Zhuravleva, Luis Stand, Eric D. Lukosi, Charles L. Melcher, The Univ. of Tennessee Knoxville (United States)

Our goal is to discover and develop low-cost, effective new scintillators that can be used for the detection of illicit radioactive materials. In order to unambiguously identify the specific gamma-ray signatures of radioactive elements, scintillator materials must possess energy resolution approaching 2% at 662 keV. Currently available radiation sensors have either inadequate energy resolution (NaI:TI), unacceptably high cost (CZT and LaBr3:Ce), or limiting operational burden (HPGe).

We present a summary of crystal growth and scintillation properties of new high-resolution scintillators that were discovered by our group during the past two years. When activated with Eu2+, ternary compounds that belong to the KA2X5 and K2AI4 (A = Sr, Ba; X = I, Br) compositional families demonstrate excellent combinations of scintillation light yield and proportionality. Light yields up to -95,000 photons/MeV and energy resolution as good as 2.4% at 662 keV were measured. Several of the new compounds display very proportional photon and electron responses. The effect of intrinsic radioactivity due to 40K on their performance in nuclear security applications was evaluated.

Using the vertical Bridgman method, we have demonstrated that KSr2X5:Eu scintillator crystals can be successfully grown at fast pulling rates (up to 10 mm/h) and can have low growth defect density and uniform scintillation performance even for relatively large samples (~1 inch3). We further improved the purity of the raw materials via zone refining and melt-aging.

Conference 9593: Hard X-Ray, Gamma-Ray, and Neutron Detector Physics XVII



Improvements of phase homogeneity of K2AI4:Eu crystals via optimization of growth parameters and using off-stoichiometric melt compositions are reported. In order to improve crystal quality and scintillation performance, we implemented co-doping and solid solutions.

9593-23, Session 6

Organic-inorganic scintillator detectors for radiation detection

Nathan T. Shewmon, Paul M. Johns, Weiran Cao, Daken Starkenburg, Shinyoung Yeo, James E. Baciak Jr., Juan C. Nino, Jiangeng Xue, Univ. of Florida (United States)

Organic photodiodes (OPDs) coupled to inorganic scintillator crystals can improve upon photocathode and photomultiplier tube systems to provide low cost, low power consumption, and high collection efficiency photodiodes for portable scintillator radiation detectors. Over the last two decades, developments in organic, polymer-based, semiconductor technology has spurred tremendous interest in their applications for photovoltaics, lighting, and circuitry. In this work we present the coupling of OPDs with nuclear electronic technology to drive the development of scintillator detectors with improved characteristics compared to those used currently. The design and development of integrated scintillator and OPD systems is presented in the context of building detection systems for medical radiology and national security applications.

OPDs fabricated on scintillator crystals offer the design advantages of flexibility, conformability to the morphology of the crystal, and a relative ease of fabrication. In this work, results from the design and analysis of OPDs coupled to scintillators will be presented along with the challenges of integrating organic-inorganic components. By careful selection of device structure and processing, we demonstrate highly sensitive OPDs with specific detectivity (D⁺) of >1013 Jones as a result of low leakage current <5 nA/cm2 and high responsivity >300 mA/W within a wavelength range that is tunable across the near UV through the full visible spectrum by selection of appropriate photoactive organic materials. Further, we show how OPD compositions can be selected to maximize the absorption efficiency of the device at wavelengths that match the emission range of alkali-halide scintillator crystals.

Highlights of the work presented include results from coupling the organic photodetectors to the surface of CsI(TI) scintillator crystals, as well as the electronic response of the device from external stimulus sources. The capability for using organic photodetectors in pulse mode operation for the collection and analysis of signals will also be presented for future work on resolving gamma ray spectra.

9593-24, Session 6

Transparent ceramic scintillators (Invited Paper)

Nerine J. Cherepy, Zachary M. Seeley, Stephen A. Payne, Patrick R. Beck, Erik L. Swanberg, Brian Wihl, Steven Hunter, Scott E. Fisher, Peter A. Thelin, Daniel J. Schneberk, Gary F. Stone, Randall Thompson, Lawrence Livermore National Lab. (United States); Todd Stefanik, Nanocerox, Inc. (United States); Joel Kindem, Cokiya, Inc. (United States)

Transparent ceramics fabrication offers a new pathway to high melting point oxide scintillators previously considered ungrowable. Fabrication of transparent ceramics begins with high purity oxide nanopowders, consolidated by pressing and sintering to full density to produce a purephase polycrystalline optic with no residual porosity. We report here on progress in scaleup and instrumentation of Cerium-doped Gadolinium Yttrium Gallium Aluminum Garnet, or GYGAG(Ce). The Ce-doped GYGAG ceramic scintillators are mechanically rugged and stable in air while providing good light yield (-50,000 Ph/MeV) with an emission peak centered at 550 nm. We have fabricated optically transparent GYGAG(Ce) ceramics as large as 5.3 in3 for PMT-based detectors. The mechanical ruggedness of the GYGAG(Ce) ceramic lends itself to pixelation, as it is readily cut and polished with high yield. A gamma spectrometer incorporating 1024 GYGAG(Ce) pixels, mounted on a photodiode array, offers energy resolution at 662 keV of 3.3% for single pixels, 3.6% for the summed histogram of our 32 best pixels, and 4.0% for a sum of 220 pixels. Another transparent ceramic scintillator, Gd0.3Lu1.6Eu0.103, or "GLO," offers excellent x-ray stopping, due to its Zeff = 68 and density of 9.1 g/cm3. We have recently fabricated a transparent ceramic GLO scintillator plate 11.5" in diameter by 0.1" thick for high energy radiography, and we will report here on its performance in a 9 MeV imager.

9593-25, Session 6

Degradation of deliquescent halide scintillators

Mariya Zhuravleva, Luis Stand, Hua Wei, The Univ. of Tennessee Knoxville (United States); Lynn A. Boatner, Oak Ridge National Lab. (United States); Kanai Shah, Radiation Monitoring Devices, Inc. (United States); Arnold Burger, Fisk Univ. (United States); Charles L. Melcher, The Univ. of Tennessee Knoxville (United States)

Most high-performance inorganic scintillators are halide compounds, which exhibit hygroscopic, or even deliquescent, behavior. Scintillator crystals react with oxygen and moisture from an ambient atmosphere, which results in rapid deterioration of their physical form and is accompanied by degradation of the scintillation properties. The knowledge of relative hygroscopicity alone is not sufficient to in order to assess the requirements for protective packaging.

The goal of this work is to provide a better understanding of the complex mechanisms of hydration and degradation of scintillation performance of various multicomponent scintillators such as SrI2:Eu, CsBa2I5:Eu, KSr2I5:Eu, LaBr3:Eu, CsSrI3:Eu, and Cs2LiYCl6:Ce. We present real-time observations of physical degradation and show that the degradation rate and morphology development are correlated with the composition, crystal structure, and sample history. We have also developed a technique to measure the water solubility of ternary compounds by allowing the samples to absorb moisture from the atmosphere and monitoring their weight in dynamic equilibrium under controlled conditions. The results suggest that dissolution is accompanied with the formation of intermediate decomposition products, and that water solubility is not a quantitative representation of hygroscopicity. We have also studied the effect of surface roughness on physical decomposition and light collection efficiency. The results for various metal halide scintillators are compared with standard commercial scintillators such as Nal:Tl and CeBr3.

9593-26, Session 7

Challenges and future directions for planetary gamma ray and neutron spectroscopy (Invited Paper)

Thomas H. Prettyman, Planetary Science Institute (United States); Arnold Burger, Fisk Univ. (United States); James L. Lambert, Julie Castillo-Rogez, Jet Propulsion Lab. (United States); Naoyuki Yamashita, Planetary Science Institute (United States)

The elemental composition of planetary surfaces can be determined using nuclear spectroscopy. Cosmic-ray interactions with planetary surfaces and atmospheres make gamma rays and neutrons, some of which escape into space. Gamma rays are also produced by the decay of long-lived radioelements. The emitted radiation provides a chemical fingerprint from which the concentration of major elements in silicate minerals, selected trace elements and volatiles can be determined. In situ and close-proximity orbital measurements are possible. The origins of planetary gamma ray and

Conference 9593: Hard X-Ray, Gamma-Ray, and Neutron Detector Physics XVII



neutron spectroscopy date back to Ranger and Apollo. Nuclear methods were used to characterize the surface composition of the terrestrial planets, the near-Earth asteroid Eros, and the main-belt asteroid Vesta. Nevertheless, rapid developments in other fields have rendered some of the technology obsolete. This is a natural consequence of extreme challenges facing the development of flight hardware, which must survive launch and acquire data in harsh environments. The technology gap for scintillators for gamma ray spectroscopy is striking. Scintillators fill a niche for planetary applications requiring rugged, compact, and low-power sensors. New technologies such as LaBr3, CeBr3, and Srl2 must undergo rigorous testing and demonstrate a competitive edge over heritage technology in order to be considered for flight. Opportunities for more frequent, low-cost missions with miniaturized satellites may help bring new technologies to maturity at a rapid pace, providing planetary scientists with a better selection of tools for composition analysis. The fundamentals of planetary nuclear spectroscopy, the state-of-the-art in instrumentation, current challenges and possibilities for future development are presented.

9593-27, Session 7

Radiation anomaly detection algorithms for field acquired gamma energy spectra

Sanjoy Mukhopadhyay, Richard J. Maurer, Ronald S. Wolff, Paul P. Guss, Stephen E. Mitchell, National Security Technologies, LLC (United States)

The Remote Sensing Laboratory (RSL) is developing a tactical, networked radiation detection system that will be agile, reconfigurable, and capable of rapid threat assessment with high degree of fidelity and certainty. Our design is driven by the needs of users such as law enforcement personnel who must make decisions by evaluating threat signatures in urban settings. The most efficient tool available to identify the nature of the threat object is real-time gamma spectroscopic analysis, as it is fast and has a very low probability of producing false positive alarm conditions. Urban radiological

searches are inherently challenged by the rapid and large spatial variation of background gamma radiation, the presence of benign radioactive materials in terms of the normally occurring radioactive materials (NORM), and shielded and/or masked threat sources. Multiple spectral anomaly detection algorithms have been developed by national laboratories and commercial vendors. For example, the Gamma Detector Response and Analysis Software (GADRAS) a one-dimensional deterministic radiation transport software capable of calculating gamma ray spectra using physics-based detector response functions was developed at Sandia National Laboratories. The nuisance-rejection spectral comparison ratio anomaly detection algorithm (or N-SCRAD), developed at Pacific Northwest National Laboratory, uses spectral comparison ratios to detect deviation from benign medical and NORM radiation source and can work in spite of strong presence of NORM and or medical sources. RSL has developed its own wavelet-based gamma energy spectral anomaly detection algorithm called WAVRAD. Test results and relative merits of these different algorithms will be discussed and demonstrated.

9593-28, Session 7

The next generation of crystal detectors for future HEP experiments

Ren-Yuan Zhu, California Institute of Technology (United States)

Crystal detectors have been used widely in high energy and nuclear physics experiments, medical instruments and homeland security applications. Novel crystal detectors are continuously being discovered and developed in academia and in industry. In high energy and nuclear physics experiments, total absorption electromagnetic calorimeters (ECAL) made of inorganic crystals are known for their superb energy resolution and detection efficiency for photon and electron measurements. A crystal ECAL is thus the choice for those experiments where precision measurements of photons and electrons are crucial for their physics missions. For future HEP experiments at the energy and intensity frontiers, however, the crystal detectors used in current ECALs are either not bright and fast enough, or not radiation hard enough. Crystal detectors have also been proposed to build a Homogeneous Hadron Calorimeter (HHCAL) to achieve unprecedented jet mass resolution by duel readout of both Cherenkov and scintillation light, where development of cost-effective crystal detectors is a crucial issue because of the huge crystal volume required. This paper discusses several R&D directions for the next generation of crystal detectors for future HEP experiments at all frontiers.

9593-29, Session 7

Measurements on scintillators and semiconductor detectors at the Advanced Light Source (ALS)

Giuseppe S. Camarda, Aleksey E. Bolotnikov, Yonggang Cui, Rubi Gul, Anwar Hossain, Utpal Roy, Ge Yang, Ralph B. James, Brookhaven National Lab. (United States)

During the transition period between closure of Beamline X27B at BNL's NSLS and opening of Beamline MID at NSLS-II, we began operation of LBNL's ALS Beamline 3.3.2 to carry out our radiation detection materials R&D. Measurements performed at this Beamline include, X-ray Detector Response Mapping and White Beam X-ray Diffraction Topography (WBXDT), among others. We will introduce the capabilities of the Beamline and present the most recent results obtained on CdZnTe and multiple scintillators. The goal of the studies on CdZnTe is to understand the origin and effects of subgrain boundaries and help to visualize the presence of a higher concentration of impurities, which might be responsible for the deterioration of the energy resolution and response uniformity.

9593-30, Session 7

Development of NEUANCE: the neutron detector array at DANCE

Marian Jandel, Bayar Baramsai, Aaron Couture, Shea M. Mosby, Gencho Y. Rusev, John L. Ullmann, Carrie L. Walker, Los Alamos National Lab. (United States)

The Detector for Advanced Neutron Capture Experiments (DANCE) at Los Alamos Neutron Science Center (LANSCE) has been successfully used for numerous measurements of capture cross sections. The DANCE array is a gamma ray calorimeter that consists of 160 BaF2 scintillation arranged in 4ϖ geometry. In recent years, we have carried out also measurements on neutron-induced fission and new results on emission of prompt-fission gamma rays were obtained. To enhance the capabilities of the DANCE array, we are designing a smaller segmented array from liquid scintillators that fits inside a central cavity of the DANCE array. Using a pulse shape discrimination, we have additional information on the gamma-rays and neutrons emitted from neutron-induced fission. Preliminary results from the first experiments at DANCE with the prototype of NEUANCE will be presented for U-235 neutron-induced reactions and Cf-252 spontaneous fission.

We gratefully acknowledge the support of the U.S. Department of Energy through the LANL/LDRD Program. Part of this work was also supported by the U.S. Department of Energy, Office of Science, Nuclear Physics under the Early Career Award No. LANL20135009.

9593-31, Session 8

Hard X-ray camera (HXC) for the FFAST mission

Hiroshi Tsunemi, Kiyoshi Hayashida, Hiroshi Nakajima, Naohisa Anabuki, Ryo Nagino, Osaka Univ. (Japan);



Masanobu Ozaki, Japan Aerospace Exploration Agency (Japan)

We have developed the Hard X-ray Camera (HXC) for the FFAST mission. FFAST is proposed to observe a large sky region to search for heavily obscured AGN. It will cover larger sky region than that by Nustar and detect fainter AGNs than those by Swift/BAT. It consists of two small satellites in formation flight with a 12m distance. One satellite carries a super mirror and the other carries the HXC, which forms a space telescope covering the energy range up to 80 keV. The HXC is similar in structure to that of the CCD camera (SXI) for ASTRO-H. They employ similar type of CCDs. CCDs for HXC is added a thin plate of scintillator attached to the CCD that is called a SDCCD. The soft X-ray (below 15 keV) is absorbed in the CCD while hard X-ray, passing through the CCD, is absorbed in the scintillator. The HXC body is similar to that of the SXI. The SXI employs two mechanical cooler to keep the working temperature around -110C while the HXC employs one mechanical cooler to keep the working temperature around -70C. Surrounding electronics for both cameras are also similar to each other. We will report the results of the radiation hardness, performance results both for X-rays and for charged particles. Various tests have been done so far. ASTRO-H will go in the 2015FY while FFAST is proposing to the scientific small satellite mission.

9593-32, Session 8

A low-noise wide-dynamic-range eventdriven detector using SOI pixel technology for high-energy particle imaging

Sumeet Shrestha, Hiroki Kamehama, Keita Yasutomi, Keiichiro Kagawa, Shizuoka Univ. (Japan); Ayaki Takeda, Takeshi G. Tsuru, Kyoto Univ. (Japan); Yasuo Arai, High Energy Accelerator Research Organization, KEK (Japan); Shoji Kawahito, Shizuoka Univ. (Japan)

This paper presents a low-noise wide-dynamic-range pixel design for high-energy particle detector in astronomical application. Silicon on insulator (SOI) based detector is used for the detection of wide range of high energy particle (both soft and hard X-ray). The sensor has thin layer of CMOS readout circuitry and thick layer of high-resistivity detector vertically stacked in a single chip. Pixel circuits are divided into two parts; signal sensing circuit and event detection circuit. Event detection circuit consisting of a comparator and logic circuits detects the incidence of high energy particle, categorizes it into two energy groups using an appropriate energy threshold and generates a two-bit code for an event and energy level. The code for energy level is then used for selection of the gain of the in-pixel amplifier for the detected signal, providing a function of high-dynamicrange signal measurement. The two-bit code for the event and energy level is scanned in the event scanning block and the signals from the hit pixels only are read out. The variable-gain in-pixel amplifier uses a continuous integrator and integration-time control for the variable gain. The proposed design allows the small signal detection and wide dynamic range due to the adaptive gain technique and capability of correlated double sampling (CDS) technique of kTC noise canceling of the charge detector. An experimental chip with an 8 x 8 pixel array designed with the SOI pixel technology is being manufactured and the results of the first sample will be presented at the meeting.

9593-33, Session 8

X-CELIV: X-ray-excited charge extraction by linearly increasing voltage: a new method for the electrical charge transport characterization of x-ray detectors

Moses Richter, Friedrich-Alexander-Univ. Erlangen-Nürnberg (Germany); Patric Büchele, Siemens AG (Germany); Gebhard J. Matt, Friedrich-Alexander-Univ. Erlangen-Nürnberg (Germany); Sandro F. Tedde, Oliver Schmidt, Siemens AG (Germany); Christoph J. Brabec, Friedrich-Alexander-Univ. Erlangen-Nürnberg (Germany)

A novel generation of hybrid X-ray detector, comprising an active material composition of terbium doped gadolinium oxysulfide (GOS) scintillator particles dispersed in a blend of the organic semiconductor poly-3-hexylthiophene (P3HT) and a fullerene derivative (PCBM) is investigated. The active layer is easily processed from solution, e.g. by spraycoating or printing. The achieved X-ray conversion efficiencies are comparable to well established direct converting semiconductors such as a-Se.

Upon X-ray irradiation the GOS scintillator emits green light which is reabsorbed by the P3HT:PCBM blend, where free electron-hole pairs are generated. The electrons (holes) are extracted by an applied electrical field along the PCBM (P3HT) phase. The conversion efficiency of the detector is a trade-off between higher X-ray absorption (i.e. increased GOS content) and the charge carrier extraction efficiency over the organic matrix. The latter is greatly influenced by the layer morphology and thickness. Therefore, key parameters, such as the charge carrier mobility μ and life time ?, are of high interest to optimize the active hybrid blend.

We here demonstrate a new adaptation of the charge extraction by linearly increased voltage method in combination with X-ray excitation (X-CELIV) as a versatile characterization technique for (any) X-ray detector technology. It allows the quantitative device investigation under real operational conditions, meaning a homogeneous excitation of the photo-conducting P3HT:PCBM blend. The measured mobilites agree very well to the literature values for P3HT and PCBM. The lifetime ? is determined by delayed charge extraction and the conversion rate simultaneously derived from the integrated signal.

9593-34, Session 8

Photon counting 3D x-ray CT as a input device for 3D-printers

Toru Aoki, Univ. of Shizuoka (Japan); Akifumi Koike, ANSeeN, Inc. (Japan) and Univ. of Shizuoka (Japan); Kiryu Sugiyama, Univ. of Shizuoka (Japan)

Photon counting X-ray CT has been developed by using CdTe photon counting sensor. We have already reported Photon counting X-ray CT system for material identification system by using dual- and/or multienergy X-ray CT. In this paper, we have evaluated this system as a input device for 3D-printers. 3D-printers are required the simple binary data for each of voxel without half tone. We have compared with two CdTe detectors system, one is the current integration detector, and the other is the photon counting detector. Photon counting CT shows very high contrast, and it could be separate cross-sectional images by materials. The results data is very suitable for input data for 3D-printer.

9593-35, Session 8

Spectral x-ray imaging performance of a hybrid pixel detector working in data driven read out mode

Erik Fröjdh, Rafael Ballabriga Sune, Jerome Alozy, Michael Campbell, Erik H. M. Heijne, Xavier Llopart, Tuomas Poikela, Lukas Tlustos, Winnie S. Wong, CERN (Switzerland)

Timepix3 is a new hybrid pixel detector readout chip working in data driven read out mode, capable of simultaneously measuring energy and time of arrival of each impinging photon. The pixel size is 55×55 um2 and the matrix consists of 256 x 256 pixels. Immediately after a pixel is hit a data packet with the pixel coordinates, the time over threshold (energy) and time of arrival is sent out. The maximum hit rate of Timepix3 is 85.3 Mhits/s/ chip. The chip is designed with a super pixel structure, consisting of 2 x 4 pixels. Each super pixel has one 640 MHz oscillator which is activated when

Conference 9593: Hard X-Ray, Gamma-Ray, and Neutron Detector Physics XVII



the signal on any of the 8 pixels crosses the analogue threshold, providing a timestamp with a step size of 1.56 ns. The noise of the front end is $-60 e^{-1}$ and with a silicon sensor the energy resolution in time over threshold mode has been measured to be 4.07 keV at 60 keV (all cluster sizes included).

In this work we investigate the spectral imagining performance of Timepix3 with both CdTe and silicon sensors. Having the energy and time information of each hit enables new correction algorithms for sensor defect and image reconstruction. Results are compared to the Medipix3RX chip, which provides analogue charge summing and four thresholds but not energy information for individual hits. Timepix3 can also be used as a platform for detailed sensor characterization since the time information is detailed enough to resolve the charge drift time for most sensor materials..

9593-36, Session 9

Growth and characterization of selfactivated scintillator for dual gamma- and neutron- detector applications

Utpal N. Roy, Aleksey E. Bolotnikov, Giuseppe S. Camarda, Yonggang Cui, Rubi Gul, Anwar Hossain, Ge Yang, Ralph B. James, Brookhaven National Lab. (United States)

Most present-day scintillators are activated by doping with foreign elements that engender striations or a concentration gradient along the direction of growth, so rendering the host non-uniform, and thus degrading the uniformity and energy resolution for large-volume devices. The resolution for doped scintillators suffers serious degradation with increasing volume, thus lowering the yield and increase in the cost of large-volume detectors. Self-activated scintillators possibly are the best choice to resolve this problem. Growth and characterization of self-activated scintillator for dual gamma- and neutron- detector applications will be presented.

9593-37, Session 9

Synthesis of transparent nanocomposite monoliths for gamma scintillation

Yunxia Jin, Chao Liu, Tibor J. Hajagos, David Kishpaugh, Yi Chen, Qibing Pei, Univ. of California, Los Angeles (United States)

Heavy element loaded polymer composites have long been proposed to detect high energy X- and ?-rays via scintillation. The previously reported composite scintillation monoliths have achieved limited success because of the diminished light output resulting from fluorescence quenching and opacity. We report the synthesis of transparent nanocomposite monoliths comprising high-Z nanocrystals uniformly dispersed in polymer matrix at high loading content. The strategies to avoid luminescence quenching and opacity in the nanocomposite have produced transparent monoliths with high loading of nanocrystals while retaining the light yield of the neat polymer matrix. Photoelectric peak for Cs-137 gamma (662 keV) can be obtained from the monoliths.

9593-38, Session 9

Characterization and testing of EJ309 liquid scintillator detector

Bayarbadrakh Baramsai, Marian Jandel, Todd A. Bredeweg, Aaron Couture, Shea Mosby, Gencho Rusev, John L. Ullmann, Carrie L. Walker, Los Alamos National Lab. (United States)

LA-UR-15-21671

This work is part of a new neutron detector array (NEUANCE) development project.

NEUANCE is installed in the central cavity of the 4pi gamma-ray array DANCE located at Los Alamos Neutron Science Center. The detector system with simultaneous neutron and gamma-ray detection capability will provide data to investigate neutron induced capture and fission theory and it's applications.

The EJ309 scintillator was tested with different geometries, each coupled to a Hamamatsu photomultiplier tube (PMT) or a Silicon photomultiplier (SiPM) for the test measurements with standard gamma-ray and {252}Cf sources. GEANT4 was used to understand the light output and the optical photon transport in the scintillator. The detector geometry and optimum parameters for the data acquisition system were determined based on the test results and the simulations.

We gratefully acknowledge the support of the U.S. Department of Energy through the LANL/LDRD Program for the work. Part of this work was also supported by the Department of Energy, Office of Science, Nuclear Physics under the Early Career Award No. LANL20135009.

9593-39, Session 9

Development of a thin scintillation film fission-fragment detector and a novel neutron source

Gencho Y. Rusev, Marian Jandel, Evelyn M. Bond, Audrey R. Roman, Jaimie K. Daum, Rebecca K. Springs, Los Alamos National Lab. (United States)

Investigation of prompt fission and neutron-capture gamma rays from fissile actinide samples at the Detector for Advanced Neutron Capture Experiments (DANCE) requires use of a fission-fragment detector to provide a trigger or a veto signal. Development and testing of a Thin scintillation Film Detector (TFD) will be presented. A layered TFD detector composed of multiple U-235 samples, which served as an active target, has been tested at DANCE with a white-source neutron beam produced at the Los Alamos Neutron Science Center. Results from a systematic study of the performance of this detector will be reported.

In addition, a novel neutron source with fast neutron-emission timing has been designed in help with the TFD characterization. The development and the performance of the neutron source will also be presented.

We gratefully acknowledge the support of the U.S. Department of Energy through the LANL/LDRD Program and the U.S. Department of Energy, Office of Science, Nuclear Physics under the Early Career Award No. LANL20135009.

9593-40, Session 9

Electronic properties of ternary alkalialkaline earth halide scintillators

Koushik Biswas, Changming Fang, Arkansas State Univ. (United States); Sanjoy Mukhopadhyay, National Security Technologies, LLC (United States)

A class of scintillators comprising of alkali and alkaline earth metal halides having the general formula AiBjXk, where A (alkali metal) = Na, K, Cs; B (alkali earth metal) = Ca, Sr, Ba; and X (halogen) = Cl, Br, I are of interest. Here i-j-k are typically 1-2-5 or 2-1-4 (for charge neutrality). However, basic understanding about these ternary compounds is incomplete. Here, we present the results of a systematic first-principles study on the crystal structures and electronic properties of these halides employing both the standard density-functional theory (DFT) within the local density approximation (LDA) or the generalized gradient approximation (GGA), and 'beyond DFT' methods using hybrid functionals. Role of activator doping (Eu2+) will be discussed.



9593-41, Session PWed

Networked gamma radiation detection system for tactical deployment

Sanjoy Mukhopadhyay, Richard J. Maurer, Ronald S. Wolff, Paul P. Guss, Ethan X. Smith, Stephen E. Mitchell, National Security Technologies, LLC (United States)

A networked gamma radiation detection system with directional sensitivity and energy spectral data acquisition capability is being developed by the National Security Technologies, LLC, Remote Sensing Laboratory to support the close and intense tactical engagement of law enforcement who carry out counterterrorism missions. In the proposed design, three clusters of 2"? 4"? 16" sodium iodide crystals ?4 each? with digiBASE-E ?for list mode data collection? would be placed at four corners of a minivan. To enhance localization and facilitate rapid identification of isotopes, advanced smart real-time localization and radioisotope identification algorithms like WAVRAD and NSCRAD will be incorporated. We will test a collection of algorithms and analysis that centers around the problem of radiation detection with a distributed sensor network.

We will study the basic characteristics of a radiation sensor network and focus on the trade-offs between false positive alarm rates, true positive alarm rates, and time to detect multiple radiation sources in a large area. Empirical and simulation analyses of critical system parameters, such as number of sensors, sensor placement, and sensor response functions, will be examined. This networked system will provide an integrated radiation detection architecture and framework with (i) a large nationally recognized search database equivalent that would help generate a common operational picture in a major radiological crisis; (ii) a robust reachback connectivity for integrating search data from multi-agency responders.

9593-42, Session PWed

Possibility of gated silicon drift detector detecting hard x-ray

Hideharu Matsuura, Shinya Fukushima, Shungo Sakurai, Shohei Ishikawa, Akinobu Takeshita, Atsuki Hidaka, Osaka Electro-Communication Univ. (Japan)

One of the authors has proposed a simple-structure Silicon X-ray detector (Gated Silicon Drift Detector: GSDD), whose structure is much simpler than a commercial Silicon Drift Detector (SDD). SDDs contain multiple built-in metal-oxide-semiconductor field-effect transistors (MOSFETs) or implanted resistors whose fabrication processes lower the yield rate of detectors, and require at least two high-voltage sources. On the other hand, GSDDs do not contain the MOSFETs or implanted resistors. Although GSDDs contain multiple gates instead of p-rings in SDDs, no extra fabrication processes are required to form the gates because the metal gates are formed on the passivating oxide layer during the metallization of the anode and the p-ring. Moreover, GSDDs require only one high-voltage source. Therefore, GSDDs greatly reduce the cost of the X-ray detection system.

We fabricate prototype GSDDs that contained 0.625-mm-thick Si substrates with an active area of 18 mm2 operated by Peltier cooling and a single voltage source. Its energy resolution at 5.9 keV from an 55Fe source is 145 eV at -38 $^\circ$ C and -90 V.

The thicker the Si substrate is, the higher the absorption of X-rays by it is. We design GSDDs to detect X-ray photons with energies up to 80 keV for X-ray absorbance higher than 15%. We simulate the electric potential distribution in GSDDs with Si thicknesses from 0.5 to 3.0 mm. We obtain an adequate electric potential distribution in the thickness of 3.0 mm, and the capacitance of the GSDD remains small and its X-ray count rate remain high.

9593-43, Session PWed

Response function of planar Cd(Zn)Te detectors to beta-radiation

Alexandr A. Zakharchenko, Alexandr V. Rybka, Leonid N. Davydov, Vladimir E. Kutny, Manap A. Khazhmuradov, National Science Ctr. Kharkov Institute of Physics and Technology (Ukraine); Petro M. Fochuk, Yuriy Fedkovych Chernivtsi National Univ. (Ukraine); Aleksey E. Bolotnikov, Ralph B. James, Brookhaven National Lab. (United States)

We investigated the response function of a planar CdZnTe detector designed for measurement of electron energy spectra and experimentally measured the response of CdZnTe detector to radiation of 90Sr/90Y reference radiation source. The model of the wide gap semiconductor gamma-ray detector, developed earlier, was used for the simulation of CdZnTe detector response functions by Monte-Carlo method. The simulated response functions of a CdZnTe detector agree well with the experimentally measured one with the use in the detector model of only two fitting parameters: products of mobility and average lifetime for electrons and holes. Other parameters of the model (bias voltage, equivalent noise charge, shaping time, detector unit geometry) correspond to the actual characteristics of the measuring channel. This agreement allows abandoning the measurements and using instead the proposed simulated response functions when the mu-tau products are known. It is expedient in the problem of obtaining beta radiation spectra from the mixed beta and gamma fields (e.g., at in situ determination of 137Cs and 90Sr sources activity). Some insignificant divergences between spectra were explained by a high enough level of noise of the preamplifier in which we did not apply temperature stabilization. The simulation has shown that the increase in the discrimination threshold largely eliminates divergences between measurement and simulation data. A similar effect is achieved at the application of thin metal filters. When exact determination of beta spectra for energy less than 100 keV is needed, it is necessary to use a measuring channel with noise level of 10 keV and below.

9593-44, Session PWed

The effect/influence of crystal thickness on the electrical characteristics of Cd(Zn) Te detectors

Valerii M. Sklyarchuk, Petro M. Fochuk, Ilarii Rarenko, Zinajida Zakharuk, Yuriy Fedkovych Chernivtsi National Univ. (Ukraine); Aleksey E. Bolotnikov, Ralph B. James, Brookhaven National Lab. (United States)

The electrical characteristics of Cd(Zn)Te detectors with rectifying contacts and varying thickness were studied. It was established that the geometric dimensions affect the electrical properties. We find that the maximum value of the operating bias voltage and the electric field in the detector for moderate values of dark current can be achieved at a certain optimum crystal thickness. This observation is due to the combined effect of generation-recombination in the space-charge region and space-charge limited currents. Results of this study will be presented.

9593-45, Session PWed

Temperature-dependent electrical properties of high-resistivity CdTe

Petro M. Fochuk, Yuriy Fedkovych Chernivtsi National Univ. (Ukraine); Yevhen Nykoniuk, National Univ. of Water Management and Natural Resources Application (Ukraine); Valerii M. Sklyarchuk, Zinajida Zakharuk, Serhii Dremlyuzhenko, Ilarii Rarenko, Yuriy Fedkovych Chernivtsi

Conference 9593: Hard X-Ray, Gamma-Ray, and Neutron Detector Physics XVII



National Univ. (Ukraine); Aleksey E. Bolotnikov, Ralph B. James, Brookhaven National Lab. (United States)

High-resistivity CdTe crystals were grown by a modified technology. The temperature dependences of the charge-carrier density, ionization energy of the donors, degree of compensation, and dependency of the photo-characteristics of the material on the photo-excitation level were studied. The role of spatial micro-scale inhomogeneities on the electrical properties was identified. Samples showed a high detection resolution for Am-241.

9593-46, Session PWed

Regularities of melting and crystallization in CdTe-Al alloys

Andriy I. Kanak, Oleh Kopach, Petro M. Fochuk, Larysa P. Shcherbak, Igor Nakonechnyj, Yuriy Fedkovych Chernivtsi National Univ. (Ukraine); Aleksey E. Bolotnikov, Ralph B. James, Brookhaven National Lab. (United States)

The differential thermal analysis was used to study CdTe-Al system. We investigated parameters of melting and crystallization processes of this system. Three alloys with different content of aluminum (2, 4 and 6 mol. % Al) were synthesized. Research was conducted by cyclic heating and cooling with isothermal holding during 10-, 30- and 60 minutes. Aluminum concentration on the CdTe phase transitions parameters' was established.

9593-47, Session PWed

Development of wide-band-gap AlGaAs photodiodes for scintillation-based radiation detection applications

Xiao Jie Chen, Erik B. Johnson, Chad M. Whitney, Radiation Monitoring Devices, Inc. (United States); Taehoon Kang, Michigan State Univ. (United States); Mark D. Hammig, Univ. of Michigan (United States); James F. Christian, Radiation Monitoring Devices, Inc. (United States)

The development of high-performance scintillation materials that emit light below 400 nm has prompted the development of improved solidstate UV photodetectors. While silicon provides a mature context for UV photodetectors, the high dark current due to its low band-gap (1.1eV) limits the signal-to-noise performance as the detector is scaled to large areas. Photodetectors fabricated in materials with a larger band-gap have the potential to surmount the performance limitations experienced by silicon. AlGaAs is a material that provides a band gap from 1.55eV to 2.13 eV, depending on Al concentration. Using high Al concentration AlGaAs to engineer a wider bandgap >2eV is very desirable in terms of reducing dark noise, however, due to its strong absorption of UV-light at the material surface, it may limit the quantum efficiency <400 nm due to surface effects. By introducing surface layers that have a longer penetration depth for UV photons, promises a boost in quantum efficiency in the UV while maintaining low dark current

This work describes the development of photodiodes fabricated in AlGaAs. It presents the design of the photodiodes, simulations of their performance, the fabrication process, along with characterization data of fabricated photodiode samples. We report on the surface effects of high aluminum concentrated AlGaAs to provide a high quantum efficiency for photons below 400 nm, providing information on reflectivity and charge collection.

9593-48, Session PWed

Gamma radiation sensor by using Si implanted SONOS device

Wen-Ching Hsieh, Minghsin Univ. of Science and

Technology (Taiwan); Fuh-Cheng Jong, Southern Taiwan Univ. of Science & Technology (Taiwan); Shich-Chuan Wu, National Nano Device Labs. (Taiwan)

The Si implantation silicon -oxide-nitride-oxide-silicon (hereafter Si-SONOS) can be candidates for nonvolatile gamma radiation sensors. In the case of Si-SONOS gamma radiation sensors, the gamma radiation induces a significant decrease of threshold voltage VT. The change of threshold voltage for Si-SONOS after gamma irradiation has a strong correlation to the dose of gamma ray exposure as well. The Si-SONOS capacitor device in this study has demonstrated the better feasibility for non-volatile gamma radiation sensing in the future.

EXPERIMENTAL

In this paper, the changes of VT between SONOS & Si-SONOS after Gamma ray expose were compared. N-type SONOS capacitor structures were fabricated on p-type resistivity 15-25ohm-cm Si <100> substrate. We use thermal SiO2 for tunneling oxide, CVD Si3N4 or Si implanted CVD Si3N4 for trapping layer, CVD TEOS SiO2 for blocking oxide of ONO gate dielectric. The SiO2- Si3N4- SiO2 (hereafter ONO) gate stack consists of a 200 Å ~300 Å thick silicon nitride trapping layer and 50 Å ~100 Å bottom and top silicon oxides. To write data on these SONOS & Si-SONOS capacity devices, gamma radiation was exposed on these SONOS & Si-SONOS capacity devices. For the data read, the change of VT in this case can be correlated to the exposure dosage of gamma radiation as well. These trapped charges can be always accumulated in gate dielectric layer, so dose record can't be destroyed by data write and read.

RESULTS AND DISCUSSIONS

As illustrated in figure 3 it can be seen that the capacity to voltage curves (C-V curve) of Si-SONOS shifted far to the left after 10 Mrad of gamma irradiation. This implies that gamma radiation induces a significant decrease of VT for Si-SONOS. The amount of decrease of VT is about 2.5 volts. It is considered that the change is due to significant increase of net positive trapped charges in the Si implantation ONO (hereafter Si-ONO) gate dielectric layer after gamma irradiation. From figure 4, it also can be seen that C-V curve of SONOS shifted to the left after 10 Mrad of gamma irradiation. The amount of decrease of VT is up to about 2 volts. As shown in the experiment data, the change of VT for Si-SONOS is more than that for SONOS after 10Mrad TID of gamma irradiation. The dependence of VT shift on radiation dose for Si-SONOS is more than that for SONOS after gamma irradiation. It can be explained that the amount of net positive trapped charges in the Si-ONO gate dielectric is greater than that in the ONO gate dielectric after gamma irradiation. These radiation-induced shifts in the irradiated device are a combination of two effects; the first effect is a result from the loss of stored charge in the ONO trapping layer and the second effect is due to a build-up of positive charge resulted from asymmetric trapping of electrons and holes in the ONO trapping layer. These two combined effects cause a large threshold voltage shift in the Si-SONOS but create a smaller threshold voltage shift in the SONOS. In figure 5, it further shows the threshold voltage change as a function of TID of gamma radiation for Si-SONOS. The decrease of threshold voltage for Si-SONOS are plotted against the TID of gamma ray radiation received. The decrease of gate threshold voltage in this case can be correlated to the increase of positive trapped charges in the insulator and the increase of exposure dosage for gamma radiation as well. In figure 6, it further shows the VT change as a function of TID of gamma radiation for SONOS. The decrease of VT for SONOS are plotted against the TID of gamma ray radiation received. As shown in the experiment data, the effect of gamma ray dosage on the VT of the Si-SONOS device is more than that of SONOS device after 10 Mrad TID of gamma ray irradiation. This capacity device with Si-ONO gate dielectric in this study has demonstrated the better feasibility of using Si-SONOS capacity device for the application of gamma ray dosimeter.

9593-49, Session PWed

Bismuth- and lithium-loaded plastic scintillators for gamma and neutron detection

H. Paul Martinez, Nerine J. Cherepy, Robert D. Sanner, Thomas T. Tillotson, Patrick R. Beck, Erik L. Swanberg,

Conference 9593: Hard X-Ray, Gamma-Ray, and Neutron Detector Physics XVII



Stephen A. Payne, Lawrence Livermore National Lab. (United States)

Plastic scintillators are widely deployed for ionizing radiation detection, as they can be fabricated in large sizes, for high detection efficiency, however commercial plastics are limited in use for gamma spectroscopy, since their photopeak is too weak, due to low Z, and neutron detection, since proton recoils are indistinguishable from other ionizing radiation absorption events in standard plastics. We are working on fabrication of transparent plastic scintillators based on polyvinyltoluene (PVT) with high loading of bismuth metallorganics for gamma spectroscopy, and with lithium metallorganics for neutron detection. When activated with Iridium complex fluors, PVT scintillators containing 22 wt% bismuth provide energy resolution of 10% at 662 keV. A PVT plastic formulation including 1.3 wt% lithium-6 provides a neutron capture peak at 525 keVee, with 11% resolution and 90% efficiency for thermal neutron capture in 2mm thickness.

9593-50, Session PWed

Comparative study of CdMnTe crystals grown by three different methods

Anwar Hossain, Aleksey Bolotnikov, Giuseppe Camarda, Yonggang Cui, Rubi Gul, Brookhaven National Lab. (United States); Kihyun Kim, Korea Univ. College of Health Sciences (Korea, Republic of); Utpal Roy, Ge Yang, Ralph James, Brookhaven National Lab. (United States)

CdMnTe has several potential advantages over CdZnTe as a roomtemperature gamma-ray detector. However, there remain many shortcomings in the growth process of CdMnTe that limit the yield of large-volume single crystals with high resistivity and high electron-lifetimes. We recently characterized various bulk defects in the material, including Te inclusions, twins, and dislocations, as well as differences in the electrical properties of CdMnTe crystals grown by three different methods: The travelling heater method (THM), the modified floating zone (MFZ), and the Bridgman method (BM). In this presentation, we outline in detail our comparative findings and assessment of the three differently grown crystals.

9593-51, Session PWed

Ionizing radiation detection by Yb-doped silica optical fibers

Cristina De Mattia, Ivan Veronese, Univ. degli Studi di Milano (Italy); Mauro Fasoli, Norberto Chiodini, Univ. degli Studi di Milano-Bicocca (Italy); Eleonora Mones, Azienda Ospedaliera Maggiore della Carità (Italy); Marie Claire Cantone, Simone Cialdi, Marco Gargano, Nicola Ludwig, Letizia Bonizzoni, Univ. degli Studi di Milano (Italy); Anna Vedda, Univ. degli Studi di Milano-Bicocca (Italy)

Rare earths-doped silica optical fibers have shown promising results for ionizing radiation monitoring, thanks to their radio-luminescence (RL) properties. However, the use of these systems for accurate and precise dosimetric measurements in radiation fields above the Cerenkov energy threshold, like those employed in radiation therapy, is still challenging, since a spurious luminescence, namely the "stem effect," is also generated in the passive fiber portion exposed to radiation. The spurious signal mainly occurs in the UV-VIS region, therefore a dopant emitting in the near infrared may be suitable for an optical discrimination of the stem effect.

In this work, the RL and dosimetric properties of Yb-doped silica optical fibers, produced by sol-gel technique, are studied, together with the methods and instruments to achieve an efficient optical detection the Yb3+ emission, characterized by a sharp line at about 975 nm.

The results demonstrate that the RL of Yb3+ is free from any spectral superposition with the spurious luminescence. This aspect, in addition with the suitable linearity, reproducibility, and sensitivity properties of the Yb-

doped fibers, paves the way to their use in applications where an efficient stem effect removal is required.

9593-55, Session PWed

Isochronal annealing and passivation studies on 50 um 4H-SiC epitaxial layers

Mohammad A. Mannan, Khai V. Nguyen, Rahmi O. Pak, Cihan Oner, Krishna C. Mandal, Univ. of South Carolina (United States)

Schottky barrier radiation detectors were fabricated on the Si-face of 50 µm thick detector grade n-type 4H-SiC epitaxial layers. The junction properties of the fabricated detectors were investigated by current-voltage (I-V) and capacitance-voltage (C-V) measurements. The radiation detector performances were evaluated by alpha pulse height spectroscopy using a 0.1 µCi 241Am radiation source. Deep level transient spectroscopy (DLTS) measurements were carried out to identify and characterize the electrically active defect levels present in the epitaxial layers. The performance of the detector was found to be limited by the presence of electrically active defect centers in the epilayer. Deep level defects were reduced significantly by isochronal annealing and by using a new passivation method. Energy resolution of the detector was found to have improved following the reduction of the life time killing defects that were responsible for preventing full charge collection. Systematic and thorough C-DLTS studies were conducted prior and subsequent to isochronal annealing to observe evolution of the deep level defects.

9593-56, Session PWed

Investigation of metal contacts on highresistivity amorphous selenium alloy films

Krishna C. Mandal, Rahmi O. Pak, Mohammad A. Mannan, Khai V. Nguyen, Cihan Oner, Univ. of South Carolina (United States)

Amorphous selenium (a-Se) alloy materials with arsenic and chlorine doping were synthesized for room temperature nuclear radiation detection applications using an optimized alloy composition for enhanced charge transport properties. A two-step synthesis process has been implemented to first synthesize the a-Se (As) and a-Se (CI) master alloys from zonerefined Se (~7N), and then synthesize the final mixed alloy used in thin-film deposition on oxidized aluminum and indium tin oxide (ITO) coated glass substrates. Material purity, morphology, and compositional characteristics of the a-Se alloy materials were confirmed using glow discharge mass spectroscopy (GDMS), x-ray diffraction (XRD), differential scanning calorimetry (DSC), and x-ray photoelectron spectroscopy (XPS). Eight metals of various work functions (Ni, W, Au, Pd, In, Cu, Sn, and Mo) were selected for Schottky detector performance studies. Current-voltage (I-V), capacitance voltage (C-V), and current transient measurements were performed at different temperatures to investigate the contact behavior and stability characteristics. Single and multi-element detectors with and without various blocking contacts (electron and holes) have been fabricated and tested and the results show promising characteristics for x-ray and high energy nuclear radiations with its high dark resistivity (1012 - 1013 ?-cm) and large area scalability.



9593-57, Session PWed

Defect characterization of nuclear detector grade Cd0.9Zn0.1Te crystals using electron beam induced current (EBIC) imaging, thermally stimulated current (TSC), and deep level transient spectroscopy (DLTS)

Rahmi O. Pak, Khai V. Nguyen, Cihan Oner, Mohammad A. Mannan, Krishna C. Mandal, Univ. of South Carolina (United States)

Semi-insulating Cd0.9Zn0.1Te nuclear detector grade crystals were grown by the tellurium solvent method from zone refined (7N) precursor materials. The processed crystals from the grown ingot were thoroughly characterized using electron beam induced current (EBIC) contrast imaging. The EBIC results were correlated with the infrared (IR) transmittance mapping, which confirms the variation of contrasts in EBIC is due to non-uniform distribution of tellurium precipitates in the grown CZT crystal. Electrical characteristics of defect regions in the fabricated detectors were further investigated using I-V measurements, spreading resistance microscopy (SSRM), deep level transient spectroscopy (DLTS), and thermally stimulated current (TSC) measurements. Finally, to demonstrate the high quality of the grown CZT crystals using the low temperature tellurium solvent method, pulse height spectra (PHS) measurements were carried out using gamma radiation sources of 241Am and 137Cs and the results will be presented.

9593-59, Session PWed

Feasibility studies of icosahedral boron arsenide (B12As2) for thermal neutron detection

Yonggang Cui, Aleksey E. Bolotnikov, Giuseppe S. Camarda, Rubi Gul, Anwar Hossain, Utpal N. Roy, Ge Yang, Brookhaven National Lab. (United States); James H. Edgar, Ugochukwu Nwagwu, Kansas State Univ. (United States); Ralph B. James, Brookhaven National Lab. (United States)

The global shortage of 3He has motivated researchers to seek alternative materials for thermal neutron detection. Among them, solid-state detectors, which have potential advantages of compact size, light-weight, easy maintenance and low cost, are of special interest. Boron compound semiconductors are excellent candidates because the B-10 isotope has large thermal neutron capture cross-section (3840 barns) and is readily abundant (20% of natural boron). Currently we are investigating the feasibility of icosahedral boron arsenide (B12As2) materials as thermal neutron detectors. We studied both bulk materials grown from a metal flux solution and thin films produced by a chemical vapor deposition (CVD) process. In addition, we explored electron beam physical vapor deposition (EBPVD) process to produce B12As2 thin-film materials. For material characterization, we measured the photocurrent response of the materials with blue light and used Hall-effect measurements to determine the charge carrier type and its mobility. We also fabricated planar devices and conducted electrical characterization by measuring low- temperature, and above- room temperature I-V characteristic plots. In this presentation, we will discuss the characterization of the materials and devices and present our test results.

9593-60, Session PWed

Interface modification of CdZnTe-based radiation detectors by glancing angle ion sputtering

Stephen Babalola, Jonathan Lassiter, David Brown, Charles Payton, Tsige Zergaw, Alabama A&M Univ. (United States); Anwar Hossain, Brookhaven National Lab. (United States)

CdZnTe has been well investigated as a top choice for room temperature radiation detectors due to its attractive physical and opto-electronic properties and room-temperature operation capabilities. The bulk of CdZnTe has been extensively studied, understoon and improved upon, hence the device fabrication factors are becoming more prominent and need to be addressed in order to obtain high performance detector devices. The main problem with current devices are charge trapping at surfaces and interfaces, which cause charge loss, distortion of near-surface electric field, high leakage current and deteriorates device performance. The surface and interfacial states of the metal-semiconductor interface formed affects the performance of CdZnTe nuclear detectors.. In this work we have modified CZT crystal surface, and hence the metal-semiconductor interface, by adding a surface preparation step of cleansing the surfaces of the CZT crystals with argon ion at a glancing angle in high vacuum, followed by gold contact sputtering using the Ion-Beam-Assisted Deposition (IBAD) technique. We went further to deposit a thin layer of nickel followed by sputtered gold and compared the interface properties. We characterized the ion-cleansed detectors and compared the interface properties with those of un-cleansed detectors. Results showing improvement of surface leakeage current and detector performance due to the additional step are presented.

Conference 9594: Medical Applications of Radiation Detectors V

Thursday 13-13 August 2015

Part of Proceedings of SPIE Vol. 9594 Medical Applications of Radiation Detectors V

9594-1, Session 1

Dual-energy x-ray computed tomography system using a cadmium telluride detector and its application to gadolinium imaging

Yasuhiro Miura, Eiichi Sato, Yasuyuki Oda, Satoshi Yamaguchi, Iwate Medical Univ. (Japan); Osahiko Hagiwara, Hiroshi Matsukiyo, Manabu Watanabe, Shinya Kusachi, Toho Univ. (Japan)

To obtain two tomograms with two different-photon-energy ranges simultaneously, we performed dual-energy X-ray photon counting using a cadmium telluride (CdTe) detector, two comparators, two frequencyvoltage converters (FVCs), and an analog digital converter (ADC). X-ray photons are detected using the CdTe detector with an energy resolution of 1% at 122 keV, and the event pulses from a shaping amplifier are sent to two comparators simultaneously to regulate two thresholds of photon energy. The logical pulses from a comparator are sent to an FVC to convert count rates into voltages. The smoothed outputs from the two FVCs are input to a personal computer through the ADC to carry out dual-energy imaging. The DE-CT was performed using gadolinium (Gd) contrast media with the Gd-K-edge energy of 50.2 keV. To observe contrast variations with changes in the energy range, we performed energy-dispersive computed tomography utilizing the dual-energy photon counting at a tube voltage of 80 kV. Two threshold energies were 30.0 and 50.2 keV, and two-differentenergy tomograms were obtained simultaneously with two energy ranges of 30.0-50.2 keV and 50.2-80.0 keV. The maximum count rate was below 10 kilocounts per second with energies ranging from 30.0 to 80.0 keV, and the exposure time for tomography was 10 min.

9594-2, Session 1

Exploring the feasibility of traditional image querying tasks for industrial radiographs

Edward S. Jimenez Jr., Sandia National Labs. (United States)

N/A

9594-3, Session 1

X-ray imaging with scintillator-sensitized hybrid organic photodetectors

Patric Büchele, Siemens AG (Germany) and Karlsruhe Institute of Technology (Germany); Genesis N. Ankah, Leibniz-Institut für Neue Materialien GmbH (Germany); Moses Richter, Friedrich-Alexander-Univ. Erlangen-Nürnberg (Germany); Sandro F. Tedde, Rene Fischer, Barbara Wegler, Wilhelm Metzger, Markus Biele, Siemens AG (Germany); Gebhard J. Matt, Friedrich-Alexander-Univ. Erlangen-Nürnberg (Germany); Samuele Lilliu, Masdar Institute of Science & Technology (United Arab Emirates); Christoph J. Brabec, Friedrich-Alexander-Univ. Erlangen-Nürnberg (Germany); Tobias Kraus, Leibniz-Institut für Neue Materialien GmbH (Germany); Oliver Schmidt, Siemens AG (Germany)

Medical imaging requires large area X-ray detectors due to the limited

ability to focus X-ray radiation. Most detectors today are realized by stacking a scintillating layer on top of an amorphous silicon (a-Si:H) photodetector array. These scintillators convert the incoming X-ray photons into visible light, which then can be detected by the photodiodes. Several concepts have been proposed recently to leverage the advantages of organic semiconductors in the field of flat panel X-ray detectors. The organic photodetector (OPD) technology is based on an interpenetrating donor-acceptor network of e.g. phenyl-C61-butyric acid methyl ester (PCBM) and poly(3-hexylthiophen-2,5-diyl) (P3HT), which is known as bulk heterojunction (BHJ). Solution-processed photodetectors provide exiting new opportunities for the realization of flat panel X-ray detectors as they can be processed from the solution phase on large areas at low cost. In combination with incorporated X-ray absorbing scintillators like terbium doped gadolinium oxysulfide (GOS:Tb) inside of the BHJ, a quasidirect X-ray detection scheme has been realized. Significant advances towards cost-effective high resolution x-ray imaging are expected from this technology. These hybrid-organic photodiodes (HPDs) promise to achieve a modulation transfer function (MTF) that is as high as in direct converting materials such as amorphous selenium. Here we will demonstrate flat panel X-ray imaging detectors with a hybrid-organic photoactive layer, deposited by high throughput spraycoating. The a-Si:H TFT backplane has a pixel array of 256x256 pixels (pixel pitch of 98 μ m). The emitted light from an X-ray excited GOS:Tb with a diameter of ~1.8 μ m is absorbed within 300nm in the BHJ. This leads to an optical crosstalk, which is negligible compared to the pixel pitch. A comparison of HPDs with different thicknesses and GOS:Tb contents will be presented. Investigations include sample preparation and characterization by 3D profilometry and scanning electron microscopy (SEM) cross-sections, morphological data from grazing incidence wide angle X-ray scattering (GIWAXS) measurements. Optoelectronical data contains IV characteristics, X-ray conversion rates and mobility measurements from X-ray charge extraction by linearly increasing voltage (X-CELIV). X-ray images will demonstrate the feasibility on system level.

SPIE. PHOTONICS

OPTICAL ENGINEERING+

APPLICATIONS

9594-4, Session 1

Monochromatic x-ray photon counting using a microcomputer and its application to iodine imaging

Yasuyuki Oda, Eiichi Sato, Satoshi Yamaguchi, Iwate Medical Univ. (Japan); Osahiko Hagiwara, Hiroshi Matsukiyo, Manabu Watanabe, Shinya Kusachi, Toho Univ. (Japan)

To perform quasi-monochromatic imaging, a photon-energy range should be selected by determining both the energy level and the width. Currently, the energy range for energy dispersive computed tomography (ED-CT) can be selected using a multichannel analyzer. However, the photon-count subtraction using a computer program is necessary using two comparators for determining two threshold energies for subtraction. Without the program, a microcomputer is useful for counting X-ray photons between two threshold energies. The monochromatic photon counting was performed using two comparators and a microcomputer. The low and highthreshold energies are determined using low and high-energy comparators, respectively. The microcomputer produces a single logical pulse when only a logical pulse from a low-energy comparator is input to the microcomputer. Next, the microcomputer does not produce the pulse when two pulses from low and high comparators are input to the microcomputer, simultaneously. The logical pulses from the microcomputer are input to a frequency-voltage converter (FVC) to convert count rates into voltages; the rate is proportion to the voltage. The output voltage from the FVC is sent to a personal computer through an analog-digital converter to reconstruct tomograms. The X-ray projection curves for tomography are obtained by repeated linear scans and rotations of the object, and the scanning is conducted in both directions of its movement. Iodine (I) K-edge CT was performed using I contrast media and X-ray photons with an energy range from 35 to 55 keV, since photons with energies just beyond I-K-edge energy 33.2 keV are absorbed effectively by I toms.



9594-5, Session 1

Si-strip photon counting detectors for contrast-enhanced spectral mammography (Invited Paper)

Buxin Chen, Ingrid Reiser, The Univ. of Chicago (United States); Jan C. Wessel, DxRay Inc. (United States) and Interon AS (Norway); Nail Malakhov, Gregor Wawrzyniak, Interon AS (Norway); Neal E. Hartsough, Thulasidharan Gandhi, DxRay Inc. (United States); Chin-Tu Chen, The Univ. of Chicago (United States); Einar Nygard, Interon AS (Norway); Jan S. Iwanczyk, DxRay, Inc. (United States); William C. Barber, DxRay, Inc. (United States) and Interon AS (Norway)

We report on the development of silicon (Si) strip detectors for energyresolved clinical mammography. Typically, X-ray integrating detectors based on scintillating cesium iodide CsI(TI) or amorphous selenium (a-Se) are used in most commercial systems. Recently, mammography instrumentation has been introduced based on photon counting Si strip detectors. The required performance for mammography in terms of the output count rate (OCR), spatial resolution, and dynamic range must be obtained with sufficient field of view (FOV) for the application, thus requiring the tiling of pixel arrays and particular scanning techniques. Room temperature Si strip detector, operating as direct conversion x-ray sensors, can provide the required speed when connected to application specific integrated circuits (ASICs) operating at fast peaking times with multiple fixed thresholds per pixel, provided that the sensors are designed for rapid signal formation across the X-ray energy ranges of the application. We present our methods and results from the optimization of Si-strip detectors for contrast enhanced spectral mammography. We describe the detector optimization methods that provide the required spatial resolution, low noise, high count rate capabilities, and minimal power consumption. We further describe the method being developed for guantifying iodine contrast using the energyresolved detector with fixed thresholds. We demonstrate the feasibility of the method by scanning an iodine phantom with clinically relevant contrast levels.

9594-6, Session 2

Advances in molecular breast imaging (Invited Paper)

Haris Kudrolli, Timothy R. Garcia, Aleksandr Kivenson, Gamma Medica, Inc. (United States)

We will present the advances in Molecular Breast Imaging (MBI) instrumentation that allow for detection of breast cancer with high sensitivity, high specificity and low radiation exposure to the patient. In MBI, a patient is injected with Tc-99m labeled radiotracer that is preferential taken up by breast lesions and is detected using two planar arrays of cadmium zinc telluride (CZT) detectors in close proximity to the breast. Modifications to the collimator from a traditional hexagonal shaped collimator to tungsten collimator registered to the CZT pixels and optimized for breast imaging configuration has allowed the reduction of patient dose from 20 mCi to 8 mCi of Tc-99m-sestamibi. We will present our ongoing efforts to further reduce the injected dose by optimizations to the collimator and improvements to CZT detector performance. Development of the biopsy guidance capability with MBI will also be presented.

9594-7, Session 2

Integration of hardware and estimation methods in the design process for solid-state detectors

Esen Salcin, College of Optical Sciences, The Univ. of

Arizona (United States); Lars R Furenlid, The Univ. of Arizona (United States)

In a traditional detector design process, guestions about how the detector signals will be processed or what estimation algorithms will be used to extract imaged source attributes usually do not enter as part of the development stage. Generally the hardware and the estimation algorithms, which we will refer to as simply the "software" of the system, are developed separately by independent teams who have little visibility for each other's process. The development is focused on designing the hardware first and the software is appended later that is made to work on the existing platform. For example, in an imaging semiconductor detector with pixel geometry, the simplest algorithm to estimate the x-ray/gamma-ray photon interaction location is to identify the pixel with the largest amplitude and assign the event to that pixel. In this case, the smallest resolution element becomes the pixel element itself and it is not possible to distinguish changes in the event locations smaller than the pixel size. It follows that, the decision of employing such an estimation algorithm drives the hardware design in a way to make pixels as small as possible.

In this work, we propose the idea of integrating the detector hardware and software design and development flows based on the expectation that the detector system can perform the best when the hardware is optimized for the algorithms that are running on it. Designing hardware for the estimators that take into account signal statistics can open a way to engineer detector signals, which are perhaps not intuitive and different from the current designs, but ultimately provide increased performance. We investigate this development methodology on an example system; a double-sided strip CdTe detector. We use Fisher Information as a "recipe" on our understanding of how the detector signals should be shaped in order to obtain large signal separation for small differences in x-ray/gamma-ray event attributes we are interested in. By identifying the physical detector parameters that have influence on Fisher Information, we propose a list of detector parameters and their potential specifications based on this new methodology. We compare how the hardware design specifications change with the employment of different estimation algorithms.

9594-8, Session 2

Where have we been and where are we going: a look into the past and future of preclinical imaging (Invited Paper)

Kevin B. Parnham, Hein P. Haas, JoAnn Zhang, James M. Masciotti, TriFoil Imaging (United States)

No Abstract Available

9594-9, Session 2

Optimization of an adaptive SPECT system with the scanning linear estimator

Nasrin Ghanbari, Eric Clarkson, Matthew A. Kupinski, The Univ. of Arizona (United States)

Optimization of an Adaptive SPECT System with the Scanning Linear Estimator

The adaptive single-photon emission computed tomography (SPECT) system studied here acquires an initial scout image to obtain preliminary information about the object and then adjusts the configuration by selecting the size of the pinhole and the magnification that optimize system performance on an ensemble of virtual objects generated to be consistent with the scout data. In this study the object is a lumpy background that contains a Gaussian signal with a known width and amplitude. The virtual objects in the ensemble are imaged by all of the available configurations and the subsequent images are evaluated with the scanning linear estimator to obtain an estimate of the signal width and amplitude. The EMSE on the virtual ensemble between the estimated and the true parameters serves as the performance figure of merit for selecting the optimum configuration.



The results indicate that variability in the original object background and signal parameters leads to a specific optimum configuration in each case. A statistical study carried out for a number of objects show that the adaptive system on average performs better than its non-adaptive counterpart.

9594-10, Session 2

Fisher information analysis of digital pulse timing

Maria D. Ruiz-Gonzalez, Lars R. Furenlid, The Univ. of Arizona (United States)

In PET imaging with digital estimation of pulse timing, there is a trade-off between the sampling rate, the amount of data acquired, and the resulting timing resolution of a detector. In order to develop an efficient data acquisition system, the acquired data reported should be be the minimum number of digital samples that contains the information needed to achieve desired temporal resolution. We have written a simulation package that performs a Fisher Information analysis of simulated scintillation pulses with arbitrary decay times, shaper support, and A/D conversion rates. The results obtained in this work allow us to determine which parts of the digitized waveform are most needed for maximum likelihood timing analysis.

9594-11, Session 3

Properties of transparent (Gd,Lu)3(Al,Ga)5012:Ce ceramic with Ca and Mg co-dopants (Invited Paper)

Yimin Wang, Gary Baldoni, William H. Rhodes, Urmila Shirwadkar, Charles Brecher, Chuncheng Ji, Jarek Glodo, Kanai S. Shah, Radiation Monitoring Devices, Inc. (United States)

Mixed lutetium/gadolinium and gallium/aluminum based garnets have a great potential as host structures for scintillation materials for medical imaging due to their cubic structure, high density, chemical radiation stability as well as high degree of transparency. The isotropic optical properties of garnets allow the fabrication of fully transparent, high-performance polycrystalline ceramic scintillator materials. Lutetium/ Gadolinium aluminum/gallium garnets ((Gd,Lu)3(Al,Ga)5012:Ce (GLuGAG:Ce, Gd3(Al,Ga)5012:Ce (GGAG:Ce)) feature high effective atomic number and good light yield, which make them particularly attractive for Positron Emission Tomography (PET) and other ?-ray detection applications. The ceramic processing route offers an attractive alternative to single crystal growth for obtaining scintillator materials at relatively low temperature and reasonable cost with flexibility in dimension control as well as activator concentration adjustment.

For PET application, the decay and time resolution are critical for achieving the better resolution of the scan. The main decay component of most Cedoped mixed garnet materials such as GLuGAG:Ce is about 80 ns. It has been reported co-doping GGAG:Ce (Gd3(Ga,AI)5O12:Ce) single crystal with different co-dopant such as Ca and B can effectively improve the decay of GGAG:Ce single crystal. In this study, Ce doped (Gd,Lu)3(Al,Ga)5O12 ceramic was co-doped with Ca, Mg and additional Ce to improve the scintillation properties. Transparent polycrystalline (Gd, Lu)3(Al,Ga)5O12:Ce ceramics with Ca, Mg co-dopant and additional Ce dopant were prepared by the sintering-HIP approach. The properties and microstructures of the ceramics were controlled by varying the processing parameters during sintering. The scintillation decay and light yield under gamma-ray excitation was investigated by using 137Cs excitation sources. The results shows the decay time of the sample with Ca co-dopant decreases from 80 ns to 39 ns with increasing Ca dopant level. Increasing Ce dopant level from 0.6 at% to 1.8 at% (with respect to (Gd+Lu)) slightly decreases the light yield of the ceramic without influence on decay. The transmission and excitation spectra were also measured and used to explain the results. The results shows the decay of the GLuGAG:Ce ceramic can be effectively tailored and improved by co-doping the ceramic for future PET applications.

9594-12, Session 3

Biomimetic-integrated surface nanostructures for medical imaging scintillation radiation

Ya Sha Yi, Univ. of Michigan (United States)

Inorganic scintillators are widely used in modern medical imaging modalities as converter for the x-rays and ?-radiation; they are also used to obtain information about the interior of the body, like x-ray, CT and PET scan. Most of the high-density scintillators have a high refractive index, so when the light travels from inside the crystal to the air, the total reflection critical angle is small, most of light is trapped in the crystal, only 10-30% of the light from the scintillator can enter into the photodetector, the majority of light couldn't be effectively extracted, which seriously affected the detection system's efficiency and detection sensitivity. The use of micro and nano photonics can help us to explore new structural flashing material, such as artificial micro-nano structures, photonic crystals, optical microcavity, and surface plasmon materials. Artificial micro-nano structure can improve the extraction efficiency of light-emitting materials (LED) and is becoming more mature. However, the idea to apply this novel photonic structure for scintillator has just started. In this work, we have investigated a novel class of nano scale devices based on photonic structures that function as efficient light extraction devices for scintillator detectors. We have studied the light output enhancement characteristics of Lu2SiO5:Ce thin film scintillator devices, similar mechanism can be extended to various types of scintillator detectors, such as ?-Cul single crystal and doped Tb3+ glass. We have designed light extraction structures based on their optical properties by using numerical simulation and optimized the sample preparation process, so that the overall efficiency of these scintillator detectors is increased significantly.

9594-13, Session 3

Efficient high-resolution hard x-ray imaging with transparent Lu2O3:Eu scintillator thin films (Invited Paper)

Zsolt Marton, Stuart R. Miller, Charles Brecher, Radiation Monitoring Devices, Inc. (United States); Peter Kenesei, Matthew D. Moore, Russell Woods, Jonathon D. Almer, Antonino Miceli, Argonne National Lab. (United States); Vivek V. Nagarkar, Radiation Monitoring Devices, Inc. (United States)

No Abstract Available

9594-14, Session 3

Development of an LSO-MPPC x-ray spectrometer and its application to highcount-rate energy-dispersive computed tomography using a high-speed linear scanner

Eiichi Sato, Yasuyuki Oda, Satoshi Yamaguchi, Iwate Medical Univ. (Japan); Osahiko Hagiwara, Hiroshi Matsukiyo, Toho Univ. (Japan); Manabu Watanabe, Iwate Medical Univ. (Japan) and Toho Univ. (Japan); Shinya Kusachi, Toho Univ. (Japan)

To measure X-ray and gamma-ray spectra with high count rates, we developed an LSO-MPPC spectrometer. Photocurrents flowing through an MPPC are converted into voltages and amplified using a high-speed current-voltage (I-V) amplifier. Event pulses from the amplifier are sent to a multichannel analyzer (MCA) to measure spectra. The maximum energy

Conference 9594: Medical Applications of Radiation Detectors V



increased with increasing tube voltage. In contrast, the bremsstrahlung peak energy increased with the increase in the tube voltage and the insertion of a 5.0-mm-thick aluminum filter. The energy-dispersive computed tomography (ED-CT) system consists of following main components: an X-ray generator, a turn table, a high-speed linear X-ray scanner, comparators, frequency voltage converters, an analog-digital converter (ADC), and a personal computer (PC). The X-ray projection curves for tomography are obtained by repeated linear scans and rotations of the object, and the scanning is conducted in both directions of its movement. The event pulses from the spectrometer are input to comparators, and the count rates are converted into voltages and sent to the PC through the ADC. The maximum count rate was approximately 1 Mcps, and the scan velocity was beyond 100 mm/s.

9594-15, Session 4

GPU programming for biomedical imaging (*Invited Paper*)

Luca Caucci, Lars R. Furenlid, The Univ. of Arizona (United States)

Driven by the insatiable demand for real-time high-definition 3D graphics, programmable graphics processing units (or GPUs) have evolved into highly parallel, multithreaded, manycore processors with tremendous computational horsepower. No longer confined to the entertainment industry, GPU technology has found applications in many scientific fields, ranging from signal processing to medical imaging, and from life sciences to fluid dynamics. This paper summarized the basic concepts of GPU programming and provides introductory details about the CUDA computing platform. CUDA is a minimal extension to the C/C++ programming language that allows the development of parallel algorithms that can run on modern GPUs. We consider two concrete examples of GPU programming related to the field of medical imaging. In the first example, we discuss a real-time maximum-likelihood algorithm for the estimation of gamma-ray photon parameters from photomultiplier (PMT) tube data. In the second example, we examine a possible GPU implementation of the maximum-likelihood expectation-maximization (MLEM) algorithm. These examples have the dual intent of 1) showing how highly parallelizable algorithms can be implemented in CUDA; and 2) illustrating the unique capabilities (such as texture and constant memory spaces) of today's GPU devices. We conclude this paper by arguing that GPU technology will enable the development of new detector concepts---such as photon-processing detectors---capable of performing maximum-likelihood estimation of parameters (such as position, energy, time of arrival, direction of propagation, etc.) on a photon-byphoton basis.

9594-16, Session 4

Design of photonic-channeled x-ray detector array for single-grating x-ray differential phase contrast imaging system

Yuzuru Takashima, Young-Sik Kim, Chris Summitt, Sunglin Wang, The Univ. of Arizona (United States)

Grating based X-ray differential phase contrast (DPC) imaging systems employing an incoherent X-ray source are widely adopted for medical imaging applications. Thanks to the grating-based source, the overall length of the system is on the order of meters, which is substantially shorter compared to other system employing sources such as synchrotron radiation light sources or propagation based detection methods which typically requires more than tens of meters of propagation distance. On the other hand, the limited absorption of the source and detector gratings impose a trade-off between the signal contrast and field-of-view. Thus grating less source and detectors are highly desirable to overcome the limitations. We propose a grating less detector, Photonic-channeled X-ray Detector Array (PcXDA). The PcXDA is an X-ray and visible hybrid detector concept which eliminates high aspect ratio gratings. X-ray fringe pattern is converted to photon fringe pattern by a scintillator and is forming a three dimensional and incoherent volumetric secondary light sources. The volumetric light pattern is detected by micro optics array which operates in a similar manner to confocal microscopy. As a key optical device, phase plate is incorporated to increase the depth of field of the micro optics based confocal detection so that the three dimensional light sources effectively creates signal contrast. Complete ray trace model of PCXDA along with physical optics based X-ray DPC imaging system provides an enhanced performance for X-ray DPC imaging system which enables high contrast and wide field of view detection.

9594-17, Session 4

A grating-based x-ray phase-contrast imaging simulation

Edward S. Jimenez Jr., Amber L. Young, Sandia National Labs. (United States)

No Abstract Available

9594-18, Session 4

Portable LED-induced autofluorescence imager with a probe of L shape for oral cancer diagnosis

Ting-Wei Huang, Nai-Lun Cheng, Yung-Jhe Yan, Hou-Chi Chiang, Jin-Chern Chiou, Ou-Yang Mang, National Chiao Tung Univ. (Taiwan)

Many researches utilize the autofluorescence of cells and tissue to diagnose oral cancer. The difference of spectral distribution between lesions of epithelial cells and normal cells after excited fluorescence is one of methods for the cancer diagnosis. We developed the hyperspectral and multispectral techniques for oral cancer diagnosis in three generations. In our previous work of the third generation, we proposed a portable LED Induced autofluorescence imager that can acquire the image of specific spectrum in vivo for oral cancer diagnosis. Our portable system for detection of oral cancer has a probe in front of the lens for fixing the object distance. The shape of the probe is cone, and it is not convenient for doctor to capture the oral image. Therefore, a probe of L shape containing a mirror is proposed in this paper, it is easy for doctors to capture the images from different angles. Besides, a glass plate is placed in front of LED to prevent the liquid entering in the body. The radiance intensity of LED is enhanced. Therefore, we can capture clearer oral images of the specific wavelength via fluorescence reaction. The recent experiments show that the specificity and sensitivity of the system are better than previous results.

9594-19, Session 4

Natural radioactivity in scintillators

H. Bradford Barber, The Univ. of Arizona (United States)

Recently, many new scintillators have been developed with novel properties relevant to PET or SPECT imaging. Examples include: LSO:Ce, LYSO:Ce, Cs2LiLaBr6:Ce and LaBr3:Ce. Some of these scintillators include elements with naturally-occurring radionuclides (e.g. Lu-176 in LYSO:Ce). We review these materials and discuss the implications of radioactive decay for gamma-ray spectroscopy and imaging.

Conference 9595: Radiation Detectors: Systems and Applications XVI



Wednesday 12-12 August 2015

Part of Proceedings of SPIE Vol. 9595 Radiation Detectors: Systems and Applications XVI

9595-1, Session 1

Maximum likelihood source localization using elpasolite crystals as a dual gamma neutron directional detector

Paul P. Guss, Thomas G. Stampahar, Sanjoy Mukhopadhyay, National Security Technologies, LLC (United States); Alexander Barzilov, Amber Guckes, Univ. of Nevada, Las Vegas (United States)

The problem of accurately detecting extremely low levels of nuclear radiation is rapidly increasing in importance in nuclear counter-proliferation, verification, and environmental and waste management. Because the 239Pu gamma signature may be weak, for instance, even when compared to the natural terrestrial background, coincidence counting with the 239Pu neutron signature may improve overall 239Pu detection sensitivity. However, systems with sufficient multiple-particle detectors require demonstration that the increased sensitivity be sufficiently high to overcome added cost and weight. We report the results of measurements and calculations to determine sensitivity that can be gained in detecting low levels of nuclear radiation from use of a relatively new detector technology based on elpasolite crystals. We have performed investigations exploring cerium (Ce3+)-doped elpasolites Cs2LiYCl6:Ce3+0.5% (CLYC) and Cs2LiLa(Br6) 90%(Cl6)10%:Ce3+0.5% (CLLBC:Ce). These materials can provide energy resolution (r(E) = 2.35?(E)/E) as good as 2.9% at 662 keV (FWHM). The crystals show an excellent neutron and gamma radiation response. The goals of the investigation were to set up the neutron/gamma pulse shape discrimination electronics for elpasolite detectors; perform limited static source benchmarking, testing and evaluation to validate system performance; and explore application of a maximum likelihood algorithm for source location. Data were measured and processed through a maximum likelihood estimation algorithm providing a direction to the radioactive source for each individual position. The estimated directions were good representations for the actual directions to the radioactive source. This paper summarizes the maximum likelihood results for our elpasolite system.

9595-2, Session 1

Imaging system for dynamic x-ray diffraction and radiographic diagnostics from 17 to 25 keV

Dane V. Morgan, National Security Technologies, LLC (United States)

X-ray imaging systems in the energy range of 17-25 keV are commonly used with short-pulse radiographic and x-ray diffraction (XRD) diagnostics for dynamic materials experiments. For the x-ray imaging system described, scintillators were directly coupled to a fiber-optic taper, and the image was transmitted to a CCD camera via coherent fiber-optic bundle. We have characterized the resolution and signal-to-noise ratio of P-43, P-47, and LSO scintillators in this configuration, using a 35-stage Marx bank to generate a 400 kV, 30 ns x-ray pulse from a molybdenum anode. Design considerations for the x-ray imaging system also include the spectral response, x-ray shielding, and blast protection. This imaging system is an integral part of a novel single-pulse XRD diagnostic developed for nanosecond studies of shocked polycrystalline materials. The diagnostic has been used to observe phase transformations, grain size distribution, texture, and the presence of inelastic behavior in single crystals. We describe a series of high explosivesdriven zirconium shock experiments at 5.6-5.8 GPa uniaxial interface stress, with a thin, vitreous carbon window for sample shock loading. The experiments consistently have shown the presence of a broad diffraction peak, which is indicative of an amorphous structure within the shocked material.

9595-3, Session 1

Microsystem for remote sensing of high-energy radiation with associated extremely-low photon flux densities

Vijay K. Jain, Alex Otten, Univ. of South Florida (United States)

This paper presents a microsystem for remote sensing of high energy radiation in extremely low flux density conditions. With wide deployment in mind, potential applications range from nuclear non-proliferation, to hospital radiation-safety. At smaller scales, on the other hand, potential applications include bio-sensing at small-sample and even single-cell levels. The daunting challenge is the low level of photon flux densities – emerging from a Scintillation Crystal (SC) on to a -1 mm-square detector, which are a factor of 10000 or so lower than those acceptable to recently reported photonic chips (including 'single-photon detection' chips), due to a combination of low LUX, small detector size, and the short SC output pulse widths – on the order of 1 micro-s each. These challenges are overcome by effective coupling from the SC to the photodetector at each stage through: SC geometry, multiple layers of PTFE wrapping, efficient optical coupling, and most of all high detector sensitivity achieved in a microchip.

Basic overview of system: The system consists of a CsI(TI) SC and an application specific IC (ASIC), which houses a 0.6mm?1.2mm, n+ diff p-epi photodiode (PD), as well as the associated analog amplification circuitry fabricated in 0.5micron, 3-metal 2-poly CMOS technology. The amplification, together with pulse-shaping of the photocurrent-induced voltage signal, is achieved through a tandem of two capacitively coupled, double-cascode amplifiers, with an observed overall-small-signal gain of up to 13,000. Acknowledgment: NNSA/DNN R&D

9595-4, Session 1

Measuring x-ray spectra of flash radiographic sources

Amanda E. Gehring, Michelle A. Espy, Todd J. Haines, Robert Sedillo, Los Alamos National Lab. (United States)

A Compton spectrometer has been re-commissioned for measurements of flash radiographic sources. The determination of the energy spectrum of these sources is difficult due to the high count rates and short nature of the pulses (-50 ns). The spectrometer is a 300 kg neodymium-iron magnet which measures spectra in the <1 MeV to 20 MeV energy range. Incoming x-rays are collimated into a narrow beam incident on a converter foil. The ejected Compton electrons are collimated so that the forward-directed electrons enter the magnetic field region of the spectrometer. The position of the electrons at the magnet's focal plane is a function of their momentum, allowing the x-ray spectrum to be reconstructed. Recent measurements of flash sources and continuous sources will be presented.

9595-5, Session 1

Auger compositional depth profiling of the metal contact-TIBr interface

Art J. Nelson, Erik L. Swanberg, Lars F. Voss, Robert T. Graff, Adam M. Conway, Stephen A. Payne, Lawrence Livermore National Lab. (United States); Hadong Kim, Leonard J. Cirignano, Kanai S. Shah, Radiation Monitoring Devices, Inc. (United States)

Degradation of room temperature operation of TIBr radiation detectors

Conference 9595: Radiation Detectors: Systems and Applications XVI



with time is thought to be due to electromigration of TI and Br vacancies within the crystal as well as the metal contacts migrating into the TIBr crystal itself due to electrochemical reactions at the metal/TIBr interface. Scanning Auger electron spectroscopy (AES) in combination with sputter depth profiling was used to investigate the metal contact surface/interfacial structure on TIBr devices. Device-grade TIBr was polished and subjected to a 32% HCI etch to remove surface damage and create a TIBr1-xCIx surface layer prior to Pt contact deposition. Auger compositional depth profiling results reveal non-equilibrium interfacial diffusion before and after device operation in both air and N2 at ambient temperature. These results improve our understanding of contact/device degradation versus operating environment for further enhancing radiation detector performance.

9595-6, Session 1

Design and optimization of a radiation detector for ground- and spaced-based exposure

Dileon Saint-Jean, Louisiana Tech Univ. (United States); Kazim R. Abbot, Darnel D. Williams, Grambling State Univ. (United States); Pedro Derosa, Lee Sawyer, Dilip K. Jana, Louisiana Tech Univ. (United States)

This project aims to construct a detector capable of analyzing the effects of radiation on different biological samples for ground and space-based expeditions. The device will measure the amount of radiation that reaches DNA, a result that if correlated with the observed damage will help in assessing human survival under those radiation conditions. In order to optimize the design of the detector, simulations were run using the Monte Carlo technique as implemented in GEANT4; a toolkit for the simulation of particles through matter.

The detection system design places the sample between glasses and a series of scintillator fiber arrays above and below to track radiation before and after hitting the sample. Two designs, one with 3 fiber layers above and below and a second model with 4 fiber layers were tested. A proton beam was fired with energies between 5 MeV and 200MeV.

Simulation results show that below 40MeV, protons are absorbed before reaching the last fiber layers and thus outgoing direction cannot be determined, protons of even lower energy are fully absorbed in the top fiber not reaching the sample. It is observed that the energy deposited in the sample peaks for protons between 40-50 MeV.

9595-7, Session 2

Detector blur associated with MeV radiographic imaging systems (Invited Paper)

Stuart A. Baker, Kristina K. Brown, Duane D Smalley, Russell A. Howe, Stephen E. Mitchell, National Security Technologies, LLC (United States); Stephen S. Lutz, Keystone International, Inc. (United States); Rachel M Posner, National Security Technologies, LLC (United States); Timothy J. Webb, Sandia National Labs. (United States); Jeremy Danielson, Todd J. Haines, Los Alamos National Lab. (United States)

We are investigating scintillator performance in radiographic imaging systems at x-ray energies from 2.3 to 8 MeV in single-pulse x-ray machines. The trade-offs for brightness versus resolution in monolithic scintillators thickness is being examined. A custom large-format lens relays the scintillator image to be recorded on an integrating high-resolution CCD camera. Previous discussion1 has reviewed energy absorption and efficiency of various imaging scintillators with the 2.3 MeV Cygnus source. The 2.3 MeV data is supplemented with some higher-energy x-ray efficiency data. The focal point of our study is how scintillator blur contribution affects

overall image quality. Monolithic LYSO:Ce (cerium-doped lutetium yttrium orthosilicate) is being studied to understand brightness and resolution trade-offs to a range of micro-columnar CsI:TI (thallium-doped cesium iodide) scintillator screens. The micro-columnar scintillator structure exhibits an optical gain mechanism that results in brighter signals from thinner samples. For higher-energy x-rays, thicker materials generally produce brighter signal due to greater x-ray absorption and the optical emission properties of the material. However with the scintillator image produced throughout its thickness, blur begins to dominate imaging quality due to the volume image generated in the scintillator depth. We investigate imaging LYSO:Ce at thickness from 3 mm to 10 mm. Results are compared with micro-columnar CsI:TI screens less than 1 mm thick.

9595-8, Session 2

Quantitative criteria for assessment of gamma-ray imager performance

Hans Malik, Stephen R. Gottesman, Kristi Keller, Northrop Grumman Electronic Systems (United States)

In recent years gamma ray imagers such as the GammaCam[™] and Polaris have demonstrated good imaging performance in the field. Imager performance is often summarized as "resolution", either angular, or spatial at some distance from the imager, however the definition of resolution is not always related to the ability to image an object. It is difficult to quantitatively compare imagers without a common definition of image quality. This paper examines three categories of definition: point source; line source; and area source. It discusses the details of those definitions and which ones are more relevant for different situations. Metrics such as Full Width Half Maximum (FWHM), variations on the Rayleigh criterion, and some analogous to National Imagery Interpretability Rating Scale (NIIRS) are discussed. The performance against these metrics is evaluated for a high resolution coded aperture imager modeled using Monte Carlo N-Particle (MCNP), and for a medium resolution imager measured in the lab.

9595-9, Session 2

Physical basis for signal separation for remote sensing of multiple high-energy radiation sources

Vijay K. Jain, John Richards, Univ. of South Florida (United States)

In 'radiation remote sensing' multiple unknown high energy sources are generally involved. The detectors, upon sensing the corresponding mixed signals, must separate their contributions blindly for further analysis. With wide deployment in mind, potential applications range from nuclear nonproliferation, to hospital radiation-safety. An effective way to perform this separation is through Independent Component Analysis algorithm. However, the challenges faced are the low level of photon flux densities emerging from a Scintillation Crystal (SC) on to a ~1 mm-square detector, and the fact that theoretically there is no correlation among events, even those arising from the same source. We overcome the latter by use of a thin barrier and by taking into account the detector pulse shape. The radiation events that interact with the barrier take a longer time to reach the detector due to their increased path length. They also lose energy, which makes them increasingly prone to capture in the barrier once they have scattered. These observations are confirmed through Monte-Carlo simulations upon Gamma-radiation sources. This includes modeling of isotropic sources of 662 keV radiation impinging upon a thin tungsten barrier (0 to 0.5mm to 5mm), while using the Klein-Nishina formula to precisely follow the track of each Gamma-ray from each source. Normalized cross-covariance ranging from 0.02 to 0.22 was found, and conveniently controllable by the duration of the detector shaping-pulse. Finally, the application of the ICA approach is demonstrated to demix, or separate, the individual contributions of the sources to the observed detector signals.



9595-10, Session 2

Design of x-ray differential phase contrast imaging system for high energy and incoherent x-ray sources

Yuzuru Takashima, Young-Sik Kim, Jihun Kim, The Univ. of Arizona (United States)

A grating based Talbot-Lau interferometer, differential phase contrast (DPC) imaging employing a low brilliance X-ray source is actively researched in medical imaging community. A grating in front of the incoherent source (GO) produces an array of partially coherent line sources. Each line sources forms a Talbot image by the second grating (G2). Deformation of a wave front induced by an object distorts the Talbot image. The distortion is detected by the third grating (G2) placed in front of detector array. Recently the X-ray DPC imaging for aviation security purpose becomes of interest because it provides richer information enabling detection of potentially hazardous materials. For the purpose, a higher X-ray photon energy is needed so that X-ray can penetrate deeply into the object. For the higher X-ray energy applications, more careful understanding of the signal formation mechanism is required since the X-ray DPC optics is not achromatized, but the source spectrum becomes wider.

We optimized X-ray DPC imaging system based on a physical optics modeling while taking into account source and absorption spectrum of X-ray optical components. The optimum design energy maximizing signal contrast is independent to X-ray photon spectrum, and is about 40KeV. The smaller absorption of the G0 and G2 is one of the limiting factors to apply the X-ray DPC system for the higher energy applications. The result suggests a grating-less sources and detectors are highly preferable to utilize higher X-ray photon while increasing the field of view of the system.

9595-11, Session 3

Co-linear neutron and x-ray imaging at the National Ignition Facility (*Invited Paper*)

Frank E. Merrill, Los Alamos National Lab. (United States); Kim Christensen, Lawrence Livermore National Lab. (United States); Christopher R. Danly, Valerie Fatherley, Los Alamos National Lab. (United States); David N. Fittinghoff, Lawrence Livermore National Lab. (United States); Jeffrey R. Griego, Los Alamos National Lab. (United States); Gary P. Grim, Nobuhiko Izumi, Lawrence Livermore National Lab. (United States); Donald R. Jedlovec, Lawrence Livermore National Lab. (United States) and Los Alamos National Lab. (United States); Raspberry Simpson, Los Alamos National Lab. (United States); Kenneth M. Skulina, Lawrence Livermore National Lab. (United States); Petr L. Volegov, Carl H. Wilde, Los Alamos National Lab. (United States)

Neutron and x-ray imagers are standard diagnostics for Inertial Containment Fusion (ICF) experiments at the National Ignition Facility (NIF). Since neutrons are produced by deuterium-tritium fusion, neutron images show burning regions of the deuterium-tritium plasma, and since any sufficiently hot regions of the plasma produce x-rays, x-ray images are sensitive to the electron temperature, density and atomic composition of plasma. While neutron and x-ray images from imploding fusion capsules may appear to be similar in many 2D calculations and in some experiments, recent 3D simulations and some experiments at the NIF indicate that asymmetric or 3D behavior of the implosion may produce neutron and x-ray images that are significantly different. Since the current neutron imager and x-ray imagers at NIF are located at different polar or azimuthal angles around target chamber, we are developing the ability to obtain a time-integrated x-ray image on the same line of sight as the current neutron imager to allow us to look for asymmetry effects in the imploding capsules. In this paper, we will discuss the current designs, including the resolution, field of view and potential co-registration of the neutron and x-ray images.

9595-12, Session 3

Testing of the gamma-ray imaging system with a mono-energetic gamma source at HIGS

Daniel A Lemieux, College of Optical Sciences, The Univ. of Arizona (United States)

A gamma ray imaging system was designed for use at the National Ignition Facility. Previous testing of this system used a broad spectrum of 50-300 keV X-rays but not the 4.44 MeV gammas the system is designed to image. Consequently the system was taken to Duke University where the High Intensity Gamma Source (HIGS) was used as a 4.44 MeV monoenergetic source to radiograph tungsten targets. These targets consisted of simple shapes and coded aperture images that were simulated to represent 180-micron shells similar to those used at the National Ignition Facility. These coded images were reconstructed using a Maximum Likelihood Estimation method and characterized using Legendre Polynomials.

9595-13, Session 4

The challenge of building large-area highprecision tracking detectors for upgrading the ATLAS Muon Spectrometer for the LHC high-luminosity phase (Invited Paper)

Oliver Stelzer-Chilton, TRIUMF (Canada)

The current innermost stations of the Atlas endcap muon tracking system must be upgraded in 2018 and 2019 to retain the good precision tracking and trigger capabilities in the high background environment expected with the upcoming luminosity increase of the LHC. The upgraded detector will consist of 2 detectors technologies, Micromegas (MICRO-MEsh-GAseous Structure) and sTGC (small-strip Thin Gap Chamber) modules, 2 to 3m2 in size, and totalling an active area each of 1200 m2. In order to achieve a 15% transverse momentum resolution for 1TeV muons, and take benefit of the very good position resolution of the detectors, the position of each strip must be known with an accuracy of 30 μ m along the precision coordinate and 80 μm along the beam. On such large area detectors, the mechanical precision is a key point and then must be controlled and monitored all along the process of construction and integration. Design and construction methods of large area Micromegas and sTGC modules will be presented together with studies of thermo-mechanical deformations. The methods for quality control of modules and the system for strip alignment in the detection layers will be also reported, together with prototype results from test beam measurements.

9595-14, Session 4

Spatial response characterization of He-4 scintillation detectors

Ryan P. Kelley, Noah Steinberg, Univ. of Florida (United States); David Murer, Arktis Radiation Detectors Ltd. (Switzerland); Heather Ray, Kelly A. Jordan, Univ. of Florida (United States)

Helium-4 detectors are a new technological development with demonstrated energy discrimination and gamma rejection capabilities. These detectors take advantage of the high He-4 cross section for elastic scattering at fast neutron energies. A neutron elastically scattering in the detector volume results in the production of helium scintillation light, which is counted by photomultiplier tubes (PMTs) at either end of the detector. The amount of light detected by the PMTs for a given event is proportional to the neutron energy.

For this work a collimator was designed and built using polyethylene and lead to confine the flux from an isotropic Cf-252 spontaneous fission source

Conference 9595: Radiation Detectors: Systems and Applications XVI



into a narrow beam. Measurements were conducted with this beam focused at various points along the axis of the He-4 detector's active volume, and the resulting light responses were compared. The results show that the position of particle interaction along the axis of the active volume has a measurable effect on the scintillation light response of the detector, and therefore this characterization is directly applicable to efforts to unfold the neutron energy spectrum from the detector light output distribution. Additionally, the count rate at each beam position was also measured and compared in order to assess the detection sensitivity along the tube axis.

By analyzing each PMT trace independently of the other, the two-sided PMT readout allowed for the calculation of the "centroid" of each event by computing the ratio of light measured between the two PMTs. This metric provided the relative position of particle interaction along the detector axis.

An algorithm was developed using the distribution of these centroid measurements to estimate the direction to the neutron source with respect to the detector. A Cf-252 source was moved through a 180-degree arc around the detector while being kept at a fixed distance. Obviously, measurements with the source position closer to one PMT resulted in a higher fraction of centroid measurements near that PMT, but it was also demonstrated that a reverse application of this principle could be used to predict the direction to the source based on the distribution of centroids detected by the He-4 system. In a cargo-scanning scenario, this principle could be applied to reduce uncertainty regarding the position of special nuclear material (SNM) within a sealed container prior to opening it for search.

All measurements described above were further supported by MCNPX-PoliMi simulations modeling the neutron transport characteristics between the source and detector. In summary, these simulations and measurements were used to characterize the spatial sensitivity of the He-4 fast neutron scintillation detector, the spatial response with respect to the scintillation light output, and to develop a new method of source localization. Combined with their demonstrated neutron energy sensitivity and gamma rejection abilities, these results expand the potential for these new He-4 detectors to be implemented as powerful instruments for the detection of hidden shielded nuclear material.

9595-15, Session 4

ENGA: a novel large area neutron detector

Marian Jandel, Gencho Y. Rusev, Terry N. Taddeucci, Los Alamos National Lab. (United States)

A large area neutron detector prototype was developed and tested at Los Alamos National Laboratory [1]. The detector consists of two walls of five plastic scintillation detectors, each with the dimensions 10 cm x10 cm x1m, and Cadmium (Cd) foils placed around it and in between.

Fission neutrons from special nuclear material (SNM) slow down in plastic material until they are absorbed in Cd material via the neutron capture reaction. After neutron capture, a cascade of energetic gamma rays is emitted and detected in the detector system within 20-40 ns narrow coincidence windows. The neutron capture event is then determined from the two dimensional multiplicity and total deposited energy information. The detector sensitivity to fission neutrons was determined to be superior to existing technology with a high signal-to-background (STB) ratio of 5-to-1 and confirmed by series of benchmark measurements. The STB ratio was determined for the neutrons detected from Cf-252 (1uCi) source at 20 cm from the ENGA detector to a number of cosmic neutrons at Los Alamos altitude of 7300 feet above the sea level.

The detection sensitivity in terms of amounts of SNM and the interrogation time length were determined. A significant advantage of this detector system is its scalability to larger areas at low costs. The internal efficiency to detect one fission neutron is as high as 15% for the smaller prototype, which was confirmed experimentally. With the different materials that would provide better efficiency and resolution for the detecting gamma-rays, highly efficient detectors can be developed, superseding the He-3 based systems, and providing both gamma-ray and neutron detection capabilities in one box.

[1] M. Jandel, G. Rusev, T. N. Taddeucci, "System for Detecting Special Nuclear Materials", LANL Patent Application, Docket Number S-121, 360, filed on March 4, 2013 (pending)

9595-16, Session 4

Operational performance of a high-speed neutron detector using CLYC

Erik B. Johnson, Chad M. Whitney, Sam Vogel, Radiation Monitoring Devices, Inc. (United States); Keith E. Holbert, Premkumar Chandhran, Arizona State Univ. (United States); Joshua P. Tower, Patrick J. O'Dougherty, Craig Hines, James F. Christian, Radiation Monitoring Devices, Inc. (United States)

A replacement for He-3 neutron measurement is CLYC (Cs2LiYCl6), a scintillation material that has a pulse shape that depends on the linear energy transfer producing the event, e.g., electrons from gamma rays versus charged ions from neutrons. Pulse shape discrimination of neutrons and gamma rays with CLYC has shown an eight FWHM separation. The drawback to CLYC is the long emission time, where using traditional charge comparison methods (i.e., integration of a fast component compared to the integration of a slow component) will fail beyond event rates exceeding 100 kHz. We have developed algorithms that handle the pulse pileup and provide both gamma-neutron discrimination and gamma energy, where one of these algorithms has demonstrated discrimination greater than two FWHM beyond an event rate of 1 MHz. A prototype detector system was built using a 250 MSPS, 12-bit ADC and read out with a Zyng system-on-achip (SOC), which was mounted on a development board (microZed). The prototype consisted of a 1-cm cube of CLYC coupled to a photomultiplier tube, and the system operated from +5 V. The detector was tested at RMD using an AmBe source and was tested at Idaho National Laboratories with reactor grade Pu. This paper provides a review of the operational performance of the prototype CLYC detector.

9595-17, Session 4

Time-gating for energy selection and scatter rejection: high-energy pulsed neutron imaging at LANSCE

Alicia L. Swift, Los Alamos National Lab. (United States) and The Univ. of Tennessee (United States); Richard C. Schirato, Edward A. McKigney, James F. Hunter, Brian Temple, Los Alamos National Lab. (United States)

The Los Alamos Neutron Science Center (LANSCE) is a linear accelerator in Los Alamos, New Mexico that accelerates a proton beam to 800 MeV, which then produces spallation neutron beams. Flight path FP15R uses a tungsten target to generate neutrons of energy ranging from several hundred keV to ~600 MeV. The beam structure has micropulses of sub-ns width and period of 1.784 ns, and macropulses of 625 ?s width and frequency of either 50 Hz or 100 Hz. This corresponds to 347 micropulses per macropulse, or 1.74 x 104 micropulses per second when operating at 50 Hz. Using a very fast, cooled ICCD camera (Princeton Instruments PI-Max 4), gated images of various objects were obtained on FP15R in January 2015. Objects imaged included blocks of lead and borated polyethylene; a tungsten sphere; and a tungsten, polyethylene, and steel cylinder. Images were obtained in 36 min or less, with some in as little as 6 min. This is novel because the gate widths (some as narrow as 10 ns) were selected to reject scatter and other signal not of interest (e.g. the gamma flash that precedes the neutron pulse), which has not been demonstrated at energies above 14 MeV. This proof-of-principle experiment shows that time gating is possible above 14MeV and is useful for selecting neutron energy and reducing scatter, thus forming clearer images. Future work (simulation and experimental) is being undertaken to improve camera shielding and system design and to precisely determine optical properties of the imaging system.



9595-18, Session PWed

Evaluation of a gamma camera system for the RITS-6 accelerator using the selfmagnetic pinch diode

Timothy J. Webb, Mark L. Kiefer, Sandia National Labs. (United States); Raymond Gignac, Stuart A. Baker, National Security Technologies, LLC (United States)

The self-magnetic pinch (SMP) diode1 is an intense radiographic source fielded on the Radiographic Integrated Test Stand (RITS-6) accelerator at Sandia National Laboratories in Albuquerque, NM. The accelerator is an inductive voltage adder (IVA) that can operate from 2-10 MV with currents up to 160 kA (at 7 MV). The SMP diode consists of an annular cathode separated from a flat anode, holding the bremsstrahlung conversion target, by a vacuum gap. The resulting spot size or x-ray source distribution is characterized by the analysis of the radiograph of a thick "L" rolled edge with both time-resolved and time-integrated diagnostics. It has been found that the spot size and dose varies according to the diode geometry (cathode size and A-K gap) and diode materials but similar minimum spot sizes are achievable independent of voltage.

* Sandia National Laboratories is a multi-program laboratory managed and operated by Sandia Corporation, a wholly owned subsidiary of Lockheed Martin Corporation, for the U.S. Department of Energy's National Nuclear Security Administration under contract DE-AC04-94AL85000.

9595-19, Session PWed

Influence of tailed-current on UXO prospecting

Linlin Zhang, Shuang Zhang, Shudong Chen, Haoyang Fu, Jilin Univ. (China)

Time-domain electromagnetic method used in unexploded ordnance detection has always faced the problem of losing early-time response due to tailed-current. In this article, the response of UXO like targets with different tailed-current is calculated and measured, and the influence of tailed-current on UXO prospecting is talked. The targets include a sphere, an iron pipe and a shell, and the tailed-current is set with cut-off time varies from 0 μ s to 250 μ s. According to magnetic surface modes(MSM), the step response of a compact steel target exhibits an early algebraic regime wherein the response transitions from t-1/2 to t-3/2 decay, followed by a late regime characterized by an exponentially decay. In fact, the transmitting current cannot be turned off immediately, especially for system with multi-turn coil and large current. The cut-off process is decided by system parameters such as coil induction, resister and maximum voltage across the coil.

The target response of tailed-current is calculated through a convolution algorithm and measured with a specially designed system. The result shows that the response of UXO like targets is influenced by the tailed-current in two ways. Firstly, the primary response of the tailed-current will lead to signal saturation in the early times. Secondly, the off-time response of UXO like targets is distorted by the tailed-current. All the influences will affect the system ability on detecting and discriminating the UXO like targets. An extra-fast switch-off system and deconvolution strategies are good advices to solve the problems of the response.

9595-20, Session PWed

An improved RF circuit for overhauser magnetometer excitation

Di Zheng, Shuang Zhang, Xin Guo, Haoyang Fu, Jilin Univ. (China)

Overhauser magnetometer is a high-precision device for magnetostatic field measurement, which can be used in a wide variety of purposes: UXO detection, pipeline mapping and other engineering and environmental

applications. Traditional proton magnetometer adopts DC polarization, suffering from low polarization efficiency, high power consumption and low signal noise ratio (SNR). Compared with the traditional proton magnetometer, nitroxide free radicals are used for dynamic nuclear polarization (DNP) to enhance nuclear magnetic resonance (NMR). RF excitation is very important for electron resonance in nitrogen oxygen free radical solution, and it is primarily significant for the obtention of high SNR signal and high sensitive field observation. Therefore, RF excitation source plays a crucial role in the development of Overhauser magnetometer.

In this paper, an improved design of a RF circuit is discussed. The new RF excitation circuit consists of two parts: Quartz crystal oscillator circuit and RF power amplifier circuit. Simulation and optimization designs for power amplifier circuit based on software ADS are presented. Finally we achieve a continuous and stable sine wave of 60MHz with 1- 2.5 W output power, and the second harmonic suppression is close to -20dBc. The improved RF circuit has many merits such as small size, low-power consumption and high efficiency, and it can be applied to Overhauser magnetometer to obtain high sensitive field observation.

9595-21, Session PWed

Stacked filtered multi-channel x-ray diode array

Lawrence P. MacNeil, Eric C. Dutra, National Security Technologies, LLC (United States); Steven M. Compton, Barry A. Jacoby, Lawrence Livermore National Lab. (United States); Mark L. Raphaelian, National Security Technologies, LLC (United States)

There are many types of X-ray diodes that are used for X-ray flux or spectroscopic measurements and estimating the spectral shape of the VUV to soft X-ray spectrum. However, a need arose for a low cost, robust X-ray diode to use for experiments in hostile environments on multiple platforms, and for explosively driven experiments that may potentially destroy the diode(s). Since the typical use required a small size with a minimal single line-of-sight, a parallel array could not be used. So, a stacked, filtered multi-channel X-ray diode array was developed, called the MiniXRD. To achieve significant cost savings while maintaining robustness and ease of field setup, repair, and replacement, we designed the system to be modular. The filters were manufactured in-house and cover the range from 900 eV to 5000 eV. To achieve the line-of-sight accuracy needed, we developed mounts and laser alignment techniques. We modeled and tested elements of the diode design at NSTec Livermore Operations to determine temporal response and dynamic range, leading to diode shape and circuitry changes to optimize impedance and charge storage. We deployed individual and stacked systems at several national facilities to test and improve the design usability. We present results on MiniXRD sensitivity, individual diode comparisons and multiple-system correlations. The system performance supports consideration of the MiniXRD as a viable low-cost alternative for multiple-channel low-energy X-ray measurements.

This work was done by National Security Technologies, LLC, under Contract No. DE-AC52-06NA25946 with the U.S. Department of Energy and supported by the Site-Directed Research and Development Program.

9595-22, Session PWed

The short line of sight neutron imaging diagnostic at the National Ignition Facility

Raspberry Simpson, Frank E. Merrill, Christopher R. Danly, Petr L. Volegov, Carl H. Wilde, Los Alamos National Lab. (United States); David N. Fittinghoff, Nobuhiko Izumi, Kim Christensen, Kenneth M. Skulina, Donald R. Jedlovec, Lawrence Livermore National Lab. (United States)

The Neutron Imaging System (NIS) at NIF is an important diagnostic tool for understanding characteristics of DT implosions at ignition. The NIS is positioned 28m from the NIF target chamber center to produce

Conference 9595: Radiation Detectors: Systems and Applications XVI



the appropriate imaging magnification and resolution. However, recent testing of a short line of sight neutron imaging system has proven to be a promising technique to preserve the source reconstruction capabilities of the existing NIS at 10 m. Therefore, multiple neutron imaging diagnostics can be positioned at a shorter detector distance providing additional views of the target and improved diagnostics of implosion asymmetries and failures. The system is primarily composed of stacks of 2mm thick highdensity polyethylene converter material followed by a phosphorous image plate. Neutrons generated from the DT reaction pass through a pinhole aperture array located 32.5 cm from TCC, enter the converter material, interacts with a proton, which recoils and deposits its energy on the image plate. We present details of the measurement scheme for this novel technique to produce energy-integrated neutron images as well as its source reconstruction results.

Conference 9596: Signal and Data Processing of Small Targets 2015

Wednesday - Thursday 12-13 August 2015

Part of Proceedings of SPIE Vol. 9596 Signal and Data Processing of Small Targets 2015

9596-1, Session 1

Infrared moving target detection algorithm based on improved multiscale codebook model

Lei Liu, Yayun Zhou, Nanjing Univ. of Science and Technology (China)

With the continuous development of science and technology, infrared sensor technology has played an important role in national defense, medical, transportation and other areas. The tracking technology of small infrared target is an important branch of infrared imaging technology, which has not only very important scientific research value, but also has broad application prospect in the military and civil area.

Nowadays, different algorithms have been proposed for infrared target tracking. However, under complex backgrounds, such as clutter, varying illumination, and occlusion, the traditional tracking method often loses the real infrared small target.

To cope with these problems, in this paper we have present a novel infrared moving target detection algorithm based on multiscale codebook model according to the characteristics of small target in infrared images. The basic principles and the implementing procedure of these algorithms for target tracking are described. Firstly, the infrared video is stratified by Gauss Pyramid. Secondly, codebook model is built for each layer image and the moving target in infrared video is detected according to model. Finally, each layer results are combined and the final detection result is get. The experimental results show that, compared with traditional detection effects, richer target information and lower false detection rate. This algorithm can not only be used in the field of image fusion, in order to improve the fusion effect, but also be used in security surveillance, night vision surveillance and other civil and military fields.

9596-2, Session 1

Enhanced accuracy of heart-rate measurement using the green light diode laser and infrared reflection model from Taipei, Taiwan

Yen-Hsing Lin, National Taipei Univ. of Technology (Taiwan); Guan-Jhong Lin, National Taiwan Univ. (Taiwan); Chung-Ping Chen, National Taipei Univ. of Technology (Taiwan)

In order to improve the accuracy of the heart rate measurement, the system combining a green light diode laser with an infrared reflection model is developed. With this configuration, the R-wave detection accuracy is significantly enhanced around 99%, and the analysis of heart rate variability to get the user's fatigue level and the degree of pressure is also implemented. In addition, the measurement error occurring between the stable state and the motion state is also investigated. This system not only builds an interface for user to monitor body status, but also constructs a backend platform with a data base for a long time monitoring.

9596-3, Session 1

Small and dim target detection by background modeling

Jing Hu, Yi Yu, Fan Liu, Huazhong Univ. of Science and Technology (China)

For images with complicated background and low signal-to-noise ratio, it's a challenge to detect small and dim moving point target. In the paper an effective method for small and dim target detection in complicated background is proposed. It takes advantage of the Non-local means filter, and applies a novel weight calculation model based on circular mask to the original background modeling method. We name it R-NLM algorithm.

SPIE. PHOTONICS

OPTICAL ENGINEERING+

APPLICATIONS

By associating similarity of grayscale distribution of the images with temporal information, the extended method estimates the complicated background precisely and extracts point target successfully. It's robust to low and fast target velocities, moreover, it need neither prior knowledge nor learning and training procedure. Owing to its effectiveness and implementability, the proposed method is well adapted to target detection system, where it outperforms significantly conventional spatio-temporal filters. Furthermore, by applying this new weight model within single frame, the method can be robust to large background motions and work well even without images accumulation.

More than 1000 frames of images with different complicated backgrounds and different intensity of targets are used in the experiment. To compare existing target detection methods with the proposed one, signal-to-clutter ratio gain (SCRG) and background suppression factor (BSF) are employed for spatial performance comparison, and receiver operating characteristics (ROC) is used for detection-performance comparison of the target trajectory. Experimental results demonstrate good performance of the proposed method for images in complicated scene, especially for low signalto-noise ratio images. This work was supported by the fund of CAST under Grant 2014A06.

9596-4, Session 1

Raman laser spectrometer adaptive processing for Mars exploration

Carlos Diaz Cano, Andoni G. Moral Inza, Carlos Pérez Canora, INTA Instituto Nacional de Técnica Aeroespacial (Spain); Guillermo López Reyes, Univ. de Valladolid (Spain); Eva Díaz Catalá, INTA Instituto Nacional de Técnica Aeroespacial (Spain) and INTA (Spain); Fernando Rull, Universidad de Valladolid (Spain); Gonzalo Ramos Zapata, INTA Instituto Nacional de Técnica Aeroespacial (Spain); Maria Colombo, INTA (Spain); Jose Antonio Rodriguez, ISDEFE, S.A. (Spain)

The Raman Laser Spectrometer (RLS) is one of the Pasteur Payload instruments, within the ESA's Aurora Exploration Programme, ExoMars mission. Particularly, the RLS scientific objectives are as follows: identify organic compound and search for life; identify the mineral products and indicators of biologic activities; characterize mineral phases produced by water-related processes; characterize igneous minerals and their alteration products; characterise water/geochemical environment as a function of depth in the shallow subsurface A flexible operational concept has been designed to accomodate scientific return to the sample nature and available resources (energy, time and data bandwidth).

The nature of the materials being analysed makes the measurement differ one to the other, based on the fluorescence, background and Raman efficiency. The acquisition of the spectra from different materials shall be, therefore, adaptative and dynamic to the sample. This, plus the restricted and changing communication bandwidth, makes mandatory the development of means to perform on-board: estimation of acquisition parameters, dynamic time-distribution, adaptative size of images and number of spots within the sample to be analysed. Currently, development of Phase C is on going and it is expected to deliver a functional model end 2015. RLS will perform Raman spectroscopy on crushed powdered samples inside the Rover's Analytical Laboratory Drawer.

Conclusions: RLS complete and flexible operation concept is neccesary to make benefit of the full potential of the instrument.



9596-5, Session 1

Numerical study of the statistical characteristics of range-resolved sea clutter

Jianing Wang, Xiaojian Xu, BeiHang Univ. (China)

Knowledge of sea clutter is of great significance in marine target detection and discrimination, especially for small targets where false alarms caused by sea spikes easily happen. To assist with the target detection algorithm test and the marine surveillance radar system design, the simulation of rangeresolved sea clutter data and the analysis of its statistical characteristics have been performed by Toporkov et al. based on 1-D sea surfaces. In this paper, the range-resolved sea clutter data of 2-D sea surfaces are numerically simulated and studied. The linear sea surfaces, the Creamer (2) sea surfaces and the choppy wave model (CWM) sea surfaces are used. The wideband backscattering fields of the sea surfaces are calculated employing the weighted curvature approximation (WCA) method. A large number of Monte Carlo trials are performed under different range-resolutions, grazing angles, beam widths, and azimuth angles to investigate the influences of radar parameters on amplitude statistics of the range-resolved sea clutter. It is found from our studies that the sea clutter tends to be spikier with finer radar resolution, lower grazing angle, and narrower beam width. Sea spikes are also more likely to appear when the radar sight is parallel with the wind direction. Meanwhile, different distribution models are adopted to fit with the sea clutter distribution and the Pareto distribution is found to describe the amplitude statistics of sea clutter better. In addition, comparison between sea clutter data from different sea surface models suggests that the nonlinear effect between sea waves is one factor causing the sea spikes.

9596-6, Session 1

Research on the algorithm of infrared target detection based on the frame difference and background subtraction method

Yun Liu, Yuejin Zhao, Ming Liu, Liquan Dong, Mei Hui, Xiaohua Liu, Beijing Institute of Technology (China)

As an important branch of infrared imaging technology, infrared target tracking and detection has a very important scientific value and a wide range of applications in both military and civilian areas. For the infrared image which is characterized by low SNR and serious disturbance of background noise, an innovative and effective target detection algorithm is proposed in this paper, according to the correlation of moving target frame-to-frame and the irrelevance of noise in sequential images based on OpenCV. Firstly, since the temporal differencing and background subtraction are very complementary, we use a combined detection method of three frame difference and background subtraction which is based on adaptive background updating. Results indicate that it is simple and can extract the foreground moving target from the video sequencestably. For the background updating mechanism continuously updating each pixel, we can detect the infrared moving target more accurately. It paves the way for eventually realizing real-time infrared target detection and tracking, when transplanting the algorithms on OpenCV to the DSP platform. Afterwards, the adaptive threshold method of image segmentation is adopted. It transforms the gray images to black-white images in order to provide a better condition for the image sequences detection. In this way, it can adapt to the changes in various scenes better. Finally, according to the relevance of moving objects between different frames and mathematical morphology processing, we can eliminate noise, decrease he area, and smooth region boundaries. Experimental results proves that our algorithm precisely achieve the purpose of rapid detection of small infrared target.

9596-7, Session 1

Contour detect of objects in the image by shearlet transform

Luis Cadena, Nikolai D. Espinosa, Escuela Politecnica del Ejercito (Ecuador); Grigory Okhotnikov, Siberian Federal Univ. (Russian Federation); Franklin Cadena, Colegio Nacional Eloy Alfaro (Ecuador); Jesus Vila, Univ. Pais Vasco (Spain)

Contour detect of objects in the image. The investigation algorithm FFST revealed that the contours of objects can be obtained as the sum of the coefficients shearlet transform a fixed value for the last scale and the of all possible values of the shift parameter.

The results of this task using a modified algorithm FFST for data processing tomography is show. In the results of the corresponding calculations for some images and a comparison with filters Sobel and Prewitt.

Shows the relevant calculations for some images and a comparison with Sobel and Prewitt filters respectively.

9596-20, Session PWed

Detection of bone fragment embedded in de-boned chicken meat using nearinfrared hyperspectral reflectance imaging technique

Jongguk Lim, Giyoung Kim, Changyeun Mo, Rural Development Administration (Korea, Republic of)

White meat such as chicken meat is considered a healthy and beneficial food because of low contents of fat and cholesterol, and abundant proteins, mineral salt, and vitamins compared to red meat. The safety and quality of chicken meat is related to physical, chemical, and biological conditions. The presence of foreign materials in agricultural products and food should be removed because they are food hazards to consumers. If someone inadvertently eats bone fragments contained in boneless chicken meat, it will cause serious damage to the teeth and mouth. In recent years, hyperspectral imaging technique has been regarded as an emerging spectroscopy technology attainable a large amount of imaging and continuous spectrum information for agricultural products and food. In this study, near-infrared (NIR) hyperspectral reflectance imaging technique was investigated whether it can discriminate the embedded bone fragment in chicken meat. The boneless and skinless breast chicken breast of 1? thick and 5 bone fragments of 2 ? long were used for this experiment. The reflectance spectra of 5 bone fragments under the chicken breast in the wavelength range from 1,000 nm to 1,700 nm are collected from hyperspectral reflectance images obtained using guartz-tungsten halogen illumination. The discrimination result was able to detect 100% of bone fragments in chicken breast especially with a ratio image of 1061/1480 nm. Thus, NIR hyperspectral reflectance imaging technique showed considerable potential for the discrimination of bone fragments in chicken meat.

9596-21, Session PWed

A survey of maneuvering target tracking: Part VId: sampling-based nonlinear filters

Xiao-Rong Li, Vesselin P. Jilkov, Univ. of New Orleans (United States)

This paper is Part VId of a comprehensive survey of maneuvering target tracking without addressing the so-called measurement-origin uncertainty. It provides an in-depth coverage of various sampling-based nonlinear filters, commonly referred to as particle filters, developed particularly for handling the uncertainties induced by potential target maneuvers as well as nonlinearities in the dynamical systems commonly encountered in target

tracking. Various implementations and tracking applications are reviewed. Some computational issues, such as different resampling schemes and parallel processing are addressed.

9596-22, Session PWed

Detecting ground moving objects using panoramic system

Fu-yuan Xu, Guohua Gu, Nanjing Univ of Science and Technology (China); Jing Wang, LiShui MinFeng Town Bank (China)

The moving objects detection is an essential issue in many computer vision and video processing tasks. In this paper, a detecting moving objects method using a panoramic system is proposed. It can detect ground moving objects when the camera is rotated, so it is called the moving objects detection in rotation (MODIR). The detection area and flexible of the panoramic system are be enhanced by MODIR. The background and moving objects are moving in image when the camera is rotated. Compare with the traditional methods, the aim of MODIR is to segment the isolated entities out according to the motions in the video whether imaging platform is moving or not. Firstly, the corresponding relations between the images captured from two different views is deduced from the multi-view geometric. The moving objects and stationary background in the images are distinguished by this corresponding relations. Secondly, the moving object detection framework base on multi-frame is established. This detection framework can reduce the impacts of the image matching error and cumulative error on the moving objects detection. In the experiment, an evaluation metrics method is used to compare the performance of MODIR with the traditional methods. And a lot of videos captured by the panoramic system are processed by MODIR to demonstrate its good performance in practice.

9596-23, Session PWed

A new geometric constraint method of moving object detection using moving camera

Wei Yang, Nanjing Univ of Science and Technology (China); Guohua Gu, Nanjing Univ. of Science and Technology (China); Wenjuan Wang, Nanjing Panda Handa Technology Company Limited (China)

The ground motion object detection is an essential issue in many computer vision and video processing tasks, such as vision-based motion analysis, intelligent surveillance and regional defense. The epipolar constraint is a commonly method for the motion object detection using a moving camera. Indeed, there is a special plane where the epipolar constraint cannot detect the motion object which moves on. This phenomenon is called "surface degradation". In order to overcome the surface degradation of the epipolar constraint, a new three-view constraint for the motion object detection using a moving camera is proposed. The feature points in the video sequence can distinguished into background and motion object by applying the epipolar constraint and the new three-view constraint which called the "Three-view Distance Constraint". The three-view distance constraint, being the main contribution of this paper, is derived from the relative camera poses in three different views and implemented within the detection framework. Unlike the epipolar constraint, the three-view distance constraint modifies the surface degradation to the line degradation. The three-view distance constraint is capable of detecting the motion object followed by a moving camera in the same direction. We evaluate the proposed method with several video sequences to demonstrate the effectiveness and robustness of the three-view distance constraint

9596-24, Session PWed

Motion object tracking algorithm using multi-cameras

Xiao-fang Kong, Qian Chen, Nanjing University of Science and Technology (China); Guohua Gu, Nanjing Univ. of Science and Technology (China)

SPIE. PHOTONICS

OPTICAL ENGINEERING+ APPLICATIONS

Motion object tracking is one of the most important research directions in the field of computer vision. Challenges in designing a robust tracking method are usually caused by partial or complete occlusions on targets. However, motion object tracking algorithm based on multiple cameras according to the homography relation in three views can deal with this issue more effectively since the information combining from multiple cameras in different views can make the target more complete and accurate. In this paper, a robust visual tracking algorithm based on the homography relations of three cameras in different views is presented to cope with the occlusion. First of all, being the main contribution of this paper, the motion object tracking algorithm based on the low-rank matrix representation under the framework of the particle filter is applied to track the same target in the public region respectively in different views. The target model and the occlusion model are established and an alternating optimization algorithm is utilized to solve the proposed optimization formulation while tracking. Then, we confirm the plane in which the target has the largest occlusion weight to be the principal plane and calculate the homography to find out the mapping relations between different views. Finally, the images of the other two views are projected into the main plane. By making use of the homography relation between different views, the information of the occluded target can be obtained completely. The proposed algorithm has been examined throughout several challenging image sequences, and experiments show that it overcomes the failure of the motion tracking especially under the situation of the occlusion. Besides, the proposed algorithm improves the accuracy of the motion tracking comparing with other state-of-the-art algorithms.

9596-8, Session 2

Track-to-track association for object matching in an inter-vehicle communication system

Ting Yuan, Tobias Roth, Qi Chen, Mercedes-Benz Research & Development North America, Inc. (United States); Jacob Breu, Miro Bogdanovic, Christian Weiss, Mercedes-Benz Research & Development North America, Inc. (Germany)

Dedicated Short Range Communication (DSRC), serving as an inter-vehicle communication systems, can provide information processing center (on host vehicle) the information of surrounding remote vehicles. The transmitted data, including real-time kinematic observations, current driving status and past trajectory histories, are containing beneficial information for advanced driver assistant systems. However, in a heavy vehicle traffic, there is a matching uncertainty issue (object identity problem), i.e., which DSRC sender is identical with which Radar observed object. If the DSRC data are associated with the corresponding host vehicle Radar observations, the useful remote vehicle information can be used to enhance host vehicle environment perceiving capability.

This paper presents a track-to-track association approach for associating the DSRC information with the corresponding Radar information. In this study, only GPS position data from remote vehicle are used in host vehicle information processing center for object matching purpose. The association between remote vehicle GPS position information via DSRC and the host vehicle locally perceived Radar information is examined, with the help of statistical tools. The challenge lies in high uncertainties of the heterogeneous-source data that belong to a same remote vehicle (i.e., the target) in complicated driving scenarios. The uncertainties lead to significant difficulties in matching decision if one uses directly the raw observations. Based on Kalman filtering techniques, we present a track-to-track association (T2TA) approach and build a real-time driving

Conference 9596: Signal and Data Processing of Small Targets 2015



system for on-road scenario object matching. The matching results show a promising potential for DSRC systems as an important/reliable enhancement component in advanced driver assistant systems.

9596-9, Session 2

Relationship between fractional calculus and fractional Fourier transform

Yan-Shan Zhang, Feng Zhang, Mingfeng Lu, Beijing Institute of Technology (China)

The Fractional calculus (FC) deals with integrals and derivatives of arbitrary (i.e., non-integer) order, and shares its origins with classical integral and differential calculus. The fractional Fourier transform (FRFT), which has been found having many applications in optics and other areas, is a generalization of the usual Fourier transform. The FC and the FRFT are two of the most interesting and useful fractional areas. In recent years, it appears many papers on the FC and FRFT, however, few of them discuss the connection of the two fractional areas. We study the relationship between the FC and the FRFT. The relational expression between them is deduced. It is a very nice result. The expectation of interdisciplinary cross fertilization is our motivation. For example, we can use the properties of the FC (non-locality, etc.) to solve the problem which is difficult to be solved by the FRFT in optical engineering; we can also through the physical meaning of the FRFT optical implementation to explain the physical meaning of the FC. Therefore, the FC and FRFT approaches can be transposed each other in the two fractional areas. It makes that the success of the fractional methodology is unquestionable with a lot of applications, namely in nonlinear and complex system dynamics and image processing.

9596-14, Session 2

Implementation and performance comparison of FPGA-accelerated particle flow and particle filters

Jiande Wu, Vesselin P. Jilkov, Dimitrios Charalampidis, Univ. of New Orleans (United States)

The Particle filter (PF) and particle flow filter (PFF) are powerful methods for nonlinear filtering but their computation is intense and may be prohibitive for real-time applications. This paper proposes design and program implementation of a parallel PF and a PFF using a field-programmable gate array (FPGA) as a parallel environment to speedup the computation. Simulation results from a nonlinear filtering problem for performance evaluation and comparison are presented. It is demonstrated that using FPGA can dramatically accelerate both particle filters and particle flow filters through parallelization at the expense of a tolerable loss in accuracy as compared to nonparallel implementation.

9596-16, Session 3

Dim target trajectory-associated detection in bright earth limb background

Penghui Chen, Xiaojian Xu, Xiaoyu He, Yuesong Jiang, BeiHang Univ. (China)

The intensive emission of earth limb in the field of view of sensors contributes much to the observation images. Due to the low signalto-clutter ratio, it is a challenge to detect small targets in earth limb background, especially for the detection of point-like targets from a single frame. To improve the target detection, track before detection based on the frame sequence is performed.

In this paper, a new technique is proposed to determine target trajectories, which jointly deploys background removing, maximum value projection (MVP) and modified Hough transform (HT). First, the background of earth

and its limb are estimated and eliminated based on the contour. Second, MVP is carried out to generate a synthetic image from the residual images. Thus, the pixels indicating targets are collected into one image. Third, if targets' motion can be considered to be linear in a short time interval, HT is implemented for the residual image to find target trajectories from locationassociated pixels. Therefore, line segments are extracted including the target trajectory and some texture of clutter and noise. Finally, to discriminate true trajectories, extra information from MVP recording the frame serial number for each pixel in the synthetic image is employed. For a moving target, the corresponding pixels in the MVP image are shifting approximately regularly in time sequence. And the target trajectory is determined according to the pixel characteristics of the target and the clutter and noise.

Comparing with traditional frame-by-frame methods, determining associated trajectories from MVP reduces the computation load. Meanwhile, the modified HT method has a better performance to overcome the target pixel shift. Numerical simulations are presented to demonstrate the effectiveness and efficiency of the approach proposed in this paper.

9596-17, Session 4

Action windows with resource limits

David D Sworder, Univ of California San Diego (United States); John Boyd, Cubic Defense Applications, Inc. (United States)

An assurance region at level p, Ap, is an area in motion space that contains the target with assigned probability p. It is on the basis of Ap that an action is taken or a decision made. Common model-based trackers generate a notional distribution function for the kinematic state of the target. Unfortunately, this distribution is very coarse, and the resulting Ap lack credibility.

Let us consider an engagement in which a target of uncertain intent is detected. The defender must illuminate the target to infer its purpose. The defender will focus on a small area to increase the interrogation accuracy. In another engagement, the defender recognizes a target with hostile intent and must neutralize the target. In the latter case, the defender may use a directed energy weapon (DEW) focused at the current position. Or the weapon may use ballistic particles focused on a future location of the target.

In what follows we will investigate the ability of a defender to place an action window about a target, either concurrently or predictively. If the target is within the action window, it is counted as a hit. If the target is outside the action window, it is counted as a miss. In either of the above engagements, proper defense requires that we hit the target a specified fraction of the time.

It is shown that a map-enhanced, multiple model algorithm reduces the tracking error and leads to a compact assurance region. The algorithm minimizes the expenditure of defensive assets.

9596-18, Session 4

Implementation and evaluation of a detector of clutter embedded resolved targets in optical and infrared maritime video

Martin Jaszewski, Eric Hallenborg, Space and Naval Warfare Systems Ctr. Pacific (United States)

We implement the method proposed in 2014 by Stotts and Hoff (SH14) [1] to automatically detect resolved targets embedded in background clutter. The SH14 method provides a test statistic which emphasizes comparing apparent contrast rather than signal to noise ratio. The SH14 authors demonstrated through analysis and simulations that their method can detect low or even zero contrast targets in clutter if the background variance is greater than the common system noise variance.

We apply this detector to the maritime domain in which marine vessels are typically found amid clutter such as waves, glint, whitecaps, wakes, port

Conference 9596: Signal and Data Processing of Small Targets 2015



and harbor infrastructure, etc. Our implementation provides an estimate of the common system noise variance whereas SH14 uses a fixed value in their theoretical validation. We estimate the system noise from the video directly without any prior knowledge of the imaging sensor parameters. After considering several noise models with different assumptions about the spatiotemporal variance of system noise we will compare the results to justify our model selection. Further, we provide a means to compute the background statistics needed by the SH14 detector, following the approach in [2] by using a sliding annulus with a guard band and distinct background mean and variance estimation bands.

Finally, we will evaluate the detection accuracy of our implementation of the SH14 detector using a video dataset depicting marine vessels in real world maritime environments using the PASCAL VOC Challenge evaluation framework. We will analyze the computational performance of our detector as a function of various input parameters.

References:

[1] Stotts, L. B. and Hoff, L. E., "Statistical detection of resolved targets in background clutter using optical/infrared imagery," Applied Optics, 53(22), 5042-5052 (2014).

[2] Matteoli, S., Diani, M. and Theiler, J., "An overview of background modeling for detection of targets and anomalies in hyperspectral remotely sensed imagery," IEEE Journal of Selected Topics in Applied Earth Observations and Remote Sensing, 7(6), 2317-2336 (2014).

9596-19, Session 4

Revisit of estimation and decision methods with insufficient apriori information

Oliver Drummond, CyberRnD, Inc. (United States)

No Abstract Available

Conference 9597: Wavelets and Sparsity XVI

Monday - Wednesday 10-12 August 2015

Part of Proceedings of SPIE Vol. 9597 Wavelets and Sparsity XVI

9597-1, Session 1

Off-the-grid recovery of piecewise constant MR images

Mathews Jacob, The Univ. of Iowa (United States)

We introduce a novel piecewise polynomial continuous model, whose discontinuities are localized to the zero level-sets of band-limited curves, to represent MR images. We show that such images can be perfectly recovered from their very few Fourier coefficients. Unlike current compressed sensing recovery schemes, the proposed approach is completely off-the-grid; this approach generalizes Prony-like methods that are widely used in signal processing. We also introduce efficient algorithms and demonstrate their application to recovery of MR images from Fourier samples.

9597-2, Session 1

Learning sparsifying filter banks

Luke Pfister, Yoram Bresler, Univ. of Illinois at Urbana-Champaign (United States)

Recent years have numerous algorithms to learn a sparse synthesis or analysis model from data. Recently, a generalized analysis model called the 'transform model' has been proposed. Data following the transform model is approximately sparsified when acted on by a linear operator called a sparsifying transform.

While existing transform learning algorithms can learn a transform for any vectorized data, they are most often used to learn a model for overlapping image patches. However, these approaches do not exploit the redundant nature of this data and scale poorly with the dimensionality of the data and size of patches.

We propose a new sparsifying transform learning framework where the transform acts on entire images rather than on patches. We illustrate the connection between existing patch-based transform learning approaches and the theory of block transforms, then develop a new transform learning framework where the transforms have the structure of an undecimated filter bank with short filters.

Unlike previous work on transform learning, the filter length can be chosen independently of the number of filter bank channels.

Learning is accelerated using Forward-Backward Splitting and convolution is implemented using the overlap-add algorithm. The resulting algorithm scales gracefully to high dimensional data and long filters.

Numerical results show our new model sparsifies images better than earlier patch-based transforms.

Image denoising experiments show our method to be competitive with state-of-the-art analysis operator learning methods. While our experiments utilize a set of training images, our framework can also learn a model from a single noisy image.

9597-3, Session 1

Advanced image reconstruction strategies for 4D prostate DCE-MRI: steps toward clinical practicality

Eric G. Stinson, Eric A. Borisch, Adam T. Froemming M.D., Akira Kawashima M.D., Brent A. Warndahl, Roger C. Grimm, Stephen J. Riederer, Joshua D. Trzasko, Mayo Clinic (United States)

No Abstract Available

9597-4, Session 1

Imaging industry expectations for compressed sensing in MRI

Kevin F. King, GE Healthcare (United States)

No Abstract Available

9597-5, Session 2

PDE-free variational imaging methods based on sparse representations

Julia Dobrosotskaya, Case Western Reserve Univ. (United States)

No Abstract Available

9597-6, Session 2

Dictionary learning for compressive parameter mapping in magnetic resonance imaging

Benjamin P. Berman, Mahesh B. Keerthivasan, Zhitao Li, The Univ. of Arizona (United States); Diego R. Martin, The Univ. of Arizona College of Medicine (United States); Maria I. Altbach, Ali Bilgin, The Univ. of Arizona (United States)

No Abstract Available

9597-7, Session 2

Semi-supervised high dimensional clustering by tight wavelet frames

Bin Dong, Peking Univ. (China); Ning Hao, The Univ. of Arizona (United States)

No Abstract Available

9597-8, Session 2

Smooth affine shear tight frames: digitization and applications

Xiaosheng Zhuang, City Univ. of Hong Kong (Hong Kong, China)

No Abstract Available

9597-9, Session 2

A fast algorithm for reconstruction of spectrally sparse signals in superresolution

Jian-Feng Cai, Suhui Liu, Weiyu Xu, The Univ. of Iowa (United States)





We propose a fast algorithm to reconstruct a spectrally sparse signal from a small number of randomly observed time domain samples. In conventional compressed sensing setting, the frequencies are usually discretized, and it suffers from basis-mismatch caused by the resolution of the discretization. In this talk, we consider the super-resolution case where the frequencies can be any values in the nomalized continous frequency domain [0,1]. Under

this setting, the problem of reconstruct a specatrally sparse signal can be solved by convex optimizations such as atomic norm minimization and enhanced matrix completion. However, in these methods, the optimization is performed in an N²-dimensional space for signals of size N. Thus, large scale problems are prohibited. To relieve this, we propose an efficient algorithm for large-scale super-resolution of spectrally sparse signals. The signal recovery problem is first converted into a low rank Hankel matrix completion problem. Then, we employ an efficient feasible point algorithm named projected gradient algorithm(PGA). Since each iteration is either a Hankel or a low-rank matrix, our proposed algorithm can handel largescale problems. By using the Kurdyka-Lojasiewicz property, we give the convergence analysis of the algorithm. The algorithm can be significantly accelerated by the FISTA-like technique. Numerical experiments are provided to illustrate the effectiveness of our proposed algorithm.

9597-10, Session 3

Algebraic and geometric spread in finite frames

Emily J. King, Univ. Bremen (Germany)

When searching for finite unit norm tight frames (FUNTFs) of \$M\$ vectors in \$mathbb{F}^N\$ which yield robust representations, one is concerned with finding frames consisting of frame vectors which are in some sense as spread apart as possible. Algebraic spread and geometric spread are the two most commonly used measures of spread. A frame with optimal algebraic spread is called full spark and is such that any subcollection of \$N\$ frame vectors is a basis for \$mathbb{F}^N\$. A Grassmannian frame is a FUNTF which satisfies the Grassmannian packing problem; that is, the frame vectors are optimally geometrically spread given fixed \$M\$ and \$N\$. A particular example of a Grassmannian frame is an equiangular frame, which is such that the absolute value of all inner products of distinct vectors is equal. The relationship between these two types of optimal spread is complicated. The folk knowledge for many years was that equiangular frames were full spark; however, this is now known not to hold for an infinite class of equiangular frames. The exact relationship between these types of spread will be further explored in this talk, as well as Pl"ucker coordinates and mutual coherence, which are measures of how much a frame misses being optimally algebraically or geometrically spread.

9597-11, Session 3

Compressive classification and the rare eclipse problem

Dustin G. Mixon, Air Force Institute of Technology (United States)

No Abstract Available

9597-12, Session 3

Gabor fusion frames generated by difference sets

Irena Bojarovska, Technische Univ. Berlin (Germany); Victoria Paternostro, Univ. de Buenos Aires (Argentina)

No Abstract Available

9597-13, Session 3

The null space property of compressed sensing

Xuemei Chen, Univ. of Missouri (United States); Rongrong Wang, The Univ. of British Columbia (Canada)

No Abstract Available

9597-14, Session 3

Generalized Steiner equiangular tight frames

John D. Jasper, Univ. of Oregon (United States); Matthew Fickus, Dustin G. Mixon, Jesse D. Peterson, Air Force Institute of Technology (United States)

No Abstract Available

9597-15, Session 3

Sparse frame representation in DOA estimations under severe noise

Cao Zeng, Xidian Univ. (China); Shidong Li, San Francisco State Univ. (United States); Guisheng Liao, Xidian Univ. (China)

Direction of arrival (DOA) estimation has been one of the main topics of array signal processing, which is widely encountered in application platforms such as radar, communication, navigation and sonar et al [1]. Subspace-based methods such as multiple signal classifications (MUSIC) [2] and estimations of signal parameters via rotation invariance techniques (ESPRIT) [3] can achieve relatively high resolution with enough snapshots under moderately high signal-to-noise ratio (SNR). These methods also require that the source number is precisely known and the sources are not strongly correlated.

Among new techniques, sparse-representation-based (SR) methods perform relatively well when observations carry high signal-to-noise ratio (SNR). Typical techniques in these new methods are, e.g., ?1-norm based convex optimization (?1-min) [4], orthogonal matching pursuit (OMP) [5], and various variations. However, performances of these methods degrade substantially under typically very noisy observations in DOA application platforms. The method of ?1-based singular value decomposition (?1-SVD) [6] can improve the performance of SR-based methods in low SNR circumstances. The cost, however, is its rather time-consuming computational complexities.

In this report, a fast and super-resolution DOA estimation approach based on a crucial correlation operation and sparse-representations is proposed. Typical DOA formulations by a sparse frame representations or compressed sensing with frames suffer seriously under severe noisy measurement which is common in the platform of DOA applications. To mitigate low SNR issue in typical DOA application, a crucial and effective correlation operation is proposed from the sparse frame representation point of view. The proposed DOA recovery technique is based on a new iterative null space tuning method with feedbacks (NST+FB) [7]. An improvement to the adaptive scheme of the NST+FB is also proposed to estimate the source number dynamically, by a technique of thresholding differences. Simulation results demonstrate apparent advantages of the proposed technique over known approaches. The proposed method has the characteristics of simultaneous high resolution, robustness to noise, and effectiveness at estimating the number of sources. The algorithm is also computationally efficient.



9597-16, Session 4

Registration using the shearlet transform

Glenn R. Easley, The MITRE Corp. (United States); Demetrio Labate, Univ. of Houston (United States)

In this paper, we present an algorithm for image registration utilizing the shearlet representation. The shearlet representation allows one to collect multi-scale and multi-directional feature information that can be used to combine a synthesized feature graph for a more accurate registration. We will demonstrate our proposed algorithm on various medical databases.

9597-17, Session 4

Shearlet-domain task-driven postprocessing and filtering of CT noise

Bart Goossens, Jan Aelterman, Hiêp Q. Luong, Aleksandra Pi?urica, Wilfried Philips, Univ. Gent (Belgium)

No Abstract Available

9597-18, Session 4

Geometry and dimensionality reduction of feature spaces in primary visual cortex

Davide Barbieri, Univ. Autónoma de Madrid (Spain)

No Abstract Available

9597-19, Session 4

Shearlets-based regularization in fan-beam ROI-CT problems

Tatiana A. Bubba, Univ. of Ferrara (Italy); Silvia Bonettini, Univ. degli Studi di Ferrara (Italy); Demetrio Labate, Univ. of Houston (United States); Gaetano Zanghirati, Univ. degli Studi di Ferrara (Italy)

This talk is invited by special session organizer prof. D. Labate.

Region-of-interest Computed Tomography (ROI CT) is a challenging problem, currently receiving increasing attention due to a wide range of applications, especially in biomedical imaging. It has the potential to significantly reduce the X-ray radiation dose and shorten the scanning time. However, due to the truncation of projection images, the ROI reconstruction problem is severely ill-posed in general and naive local reconstruction algorithms may be very unstable. In order to obtain a stable reconstruction, the ROI CT can be modelled as a convex optimization problem with a regularized functional and solved using an iterative algorithm. In this study, we consider different regularization approaches, based on wavelets or shearlets, and possibly coupled with a Total Variation (TV) regularization term. For our numerical solution, we propose and analyse an iterative approach based on the scaled gradient projection method (SGP). We compare the reconstruction performance of our algorithm under different regularization conditions in the case of fan-beam CT using both simulated and real data. One major advantage of our approach is that - in contrast to many existing methods - no assumptions are made either on the size or on the location of the ROL

9597-20, Session 4

Directional ratio based on parabolic molecules and its applications to tubular structure detection

Manos Papadakis, Burcin Ozcan, Univ. of Houston (United States); Fernanda Laezza, The Univ. of Texas Medical Branch (United States); Demetrio Labate, Univ. of Houston (United States)

No Abstract Available

9597-21, Session 4

Investigating the impact of blood pressure increase to the brain using high resolution serial histology and image processing

Frédéric Lesage, Baoqiang Li, Alexandre Castonguay, Pramod Avti, Joel Lefebvre, Ecole Polytechnique de Montréal (Canada)

We recently developed a combined serial OCT/confocal scanner to image large sections of biological tissues at microscopic resolution. Embedding organs in agarose blocks and cutting through tissue using a vibratome enabled serial high resolution imaging. The vibratome is integrated in the microscopic platform to sequentially cuts slices in order to reveal new tissue to image, overcoming limited light penetration encountered in microscopy. In this work, the mechanisms of white matter properties change by inducing transverse, between carotids, aortic constriction (TAC) in healthy WT mice are investigated in relation with microvasculature properties. At sacrifice, mice were transcardially perfused with a FITC containing gel. The dual imaging capability of the system allowed to reveal different contrast information: OCT imaging reveals changes in refractive indices giving contrast between white and grey matter in the mouse brain, while transcardial perfusion of a FITC shows microsvasculature in the brain with confocal imaging. We then describe a method to enhance microvessels from confocal images using curvelets and compare to Frangi's vesselness filter. These are then used to correlate white matter and microvasculature changes.

9597-58, Session 4

Estimating brain's functional graph from the structural graph's Laplacian

Farras Abdelnour, Michael Dayan, Weill Cornell Medical College (United States); Orrin Devinsky, Thomas Thesen, New York Univ. Langone Medical Ctr. (United States); Ashish Raj, Weill Cornell Medical College (United States)

The relationship between anatomic connectivity of large-scale brain networks and their functional connectivity is of immense importance and an area of ongoing research. Previous attempts have required complex simulations which model the dynamic of each cortical region, and explore the coupling between regions as derived by anatomic connections. While much insight is gained from these nonlinear simulations, they can be computationally taxing tools for predicting functional from anatomic conductivities. We show that a simple linear model based on the Laplacian of the structural graph adjacency matrix can predict the brain's functional network.



9597-22, Session 5

Phase retrieval by projections

Peter G. Casazza, Univ. of Missouri-Columbia (United States)

Over the 100 year history of phase retrieval, it

has had broad application to x-ray crystallography, electron microscopy, diffractive imaging, DNA, x-ray tomography and much more. Phase retrieval will even be needed to align the mirrors of the new James Webb Space Telescope scheduled for launch in 2018. Recently, in crystal twinning and related areas, a variation of standard phase

retrieval called phase retrieval by projections has arisen. We will look at recent advances in the mathematics of phase retrieval by projections, including the surprising result that in the real case, phase retrieval can be done with 2n-1 arbitrary rank projections in an n-dimensional Hilbert space.

9597-23, Session 5

Frame and compressed sensing quantization with exponential accuracy

Ozgur Yilmaz, The Univ. of British Columbia (Canada)

No Abstract Available

9597-24, Session 5

Scalable filter banks

Kasso A. Okoudjou, Univ. of Maryland, College Park (United States); Youngmi Hur, Yonsei Univ. (Korea, Republic of)

No Abstract Available

9597-25, Session 5

Self-calibration and biconvex compressive sensing

Thomas Strohmer, Shuyang Ling, Univ. of California, Davis (United States)

The design of high-precision sensing devises becomes ever more difficult and expensive.

At the same time, the need for precise calibration of these devices (ranging from tiny sensors to space telescopes) manifests itself as a major roadblock in many scientific and technological endeavors.

To achieve optimal performance of advanced high-performance sensors one must carefully calibrate them, which is often difficult or even impossible to do in practice. In this work we bring together three seemingly unrelated concepts, namely Self-Calibration, Compressive Sensing, and Biconvex Optimization.

The idea behind self-calibration is to equip a hardware device with a smart algorithm that can compensate automatically for the lack of calibration.

We show how several self-calibration problems can be treated efficiently within the framework of biconvex compressive sensing via a new method called SparseLift. More specifically, we consider a linear system of equations y = DAx, where both x and the diagonal matrix D (which models the calibration error) are unknown. By ``lifting'' this biconvex inverse problem we arrive at a convex optimization problem. By exploiting sparsity in the signal model, we derive explicit theoretical guarantees under which both x and D can be recovered exactly, robustly, and numerically efficiently via linear programming.

Applications in array calibration and wireless communications are discussed and numerical simulations are presented, confirming and complementing our theoretical analysis. This talk is invited by special session organizers Radu Balan, Bernhard Bodmann, and Gitta Kutyniok.

9597-26, Session 5

Perturbations of frame sequences and the effect on their duals

Friedrich Philipp, Technische Univ. Berlin (Germany); Victoria Paternostro, Univ. de Buenos Aires (Argentina)

No Abstract Available

9597-27, Session 5

Performance bounds in the phase retrieval problem

Radu V. Balan, Univ. of Maryland, College Park (United States)

No Abstract Available

9597-28, Session 6

Mesocopic and macrosocpic fluorescence molecular optical tomography enhanced by sparsity

Xavier Intes, Rensselaer Polytechnic Institute (United States)

No Abstract Available

9597-29, Session 6

Fast live cell imaging at nanometer scale using spare recovery

Junhong Min, KAIST (Korea, Republic of); Michael Unser, Suliana Manley, Ecole Polytechnique Fédérale de Lausanne (Switzerland); Jong Chul Ye, KAIST (Korea, Republic of)

Super resolution microscopy such as STORM/PALM can achieves nanoscale spatial resolution by iterative localization of sparse subset of fluorescence molecules. However, this basic scheme generally leads to a long acquisition time which is critical limitation for investigating live cell dynamics. Imaging of densely activated molecules can accelerate temporal resolution by incorporating advanced localization algorithms to deal with overlapping point spread functions (PSFs). Recently, we introduced localization algorithm called FALCON using continuous localization model to deal with this issue. Specifically, it combines a sparsity-promoting deconvolution formulation with Taylor approximation of PSF for refining positions of localization on a continuous space. Our localization model is not only accurate, showing minimum localization bias, but also computationally advantageous. In addition, it can be implemented in a computationally efficient way by utilizing fast sparse recovery algorithms such as ADMM. Furthermore, we extended our approach to fast 3D super-resolution imaging which is more challenging than 2D case since PSFs are often far more similar along the axial dimension than the lateral dimensions. Therefore, we considered the hybrid system that is implemented by combining astigmatic and biplane imaging. Using mutual coherence analysis of model PSFs, we validated that the hybrid system is more suitable than astigmatic or biplane imaging alone for 3D localization of high-density data. We also successfully demonstrated fluorescent-protein-based 3D live cell imaging with a temporal resolution of just 3 seconds which is, to our best knowledge, currently the fastest 3D localization microscopy.



9597-30, Session 6

Light propagation via B-spline discretizedconvolutions: examples of use

Nikhil Chacko, Univ. of California, Santa Barbara (United States); Michael Liebling, Idiap Research Institute (Switzerland) and The Univ. of California, Santa Barbara (United States)

No Abstract Available

9597-31, Session 6

Biological image denoising via compressed sensing

Jean-Christophe Olivo-Marin, William Meiniel, Institut Pasteur (France); Elsa D. Angelini, Columbia Univ. (United States)

No Abstract Available

9597-32, Session 6

PSF super-resolution using sparsity and low rank matrices constraint

Fred Ngole, Jean-Luc Starck, Commissariat à l'Énergie Atomique (France)

In large scale spatial surveys such as the forthcoming ESA Euclid mission, images may be undersampled due to the optical sensors sizes. Therefore, one may consider using a super-resolution (SR) method to recover aliased frequencies, prior to further analysis. This is particularly relevant for point source images which provide direct measurements of the instrument point spread function (PSF). We propose a sparsity-based SR approach. Assuming that different shifted low resolution (LR) versions of the same PSF are available, we show that our method provides significant improvements over existing SR methods.

In practice, even if the PSF varies slowly across the instrument field of view, strictly speaking, one only has a single LR observation of the PSF at a given position in the field. Therefore we propose to jointly super-resolve a PSF field, exploiting the fact that the PSFs are randomly shifted on the sensor grid, and are similar to each other. This global prior translates into a low rank matrix constraint on the whole set of super-resolved PSFs.

9597-33, Session Key

The dark side of imaging: emerging methods in photon-limited image reconstruction (Invited Paper)

Rebecca M. Willett, Univ. of Wisconsin-Madison (United States)

No Abstract Available

9597-34, Session 7

Low-rank modeling of local k-space neighborhoods: from phase and support constraints to structured sparsity

Justin P. Haldar, The Univ. of Southern California (United States)

No Abstract Available

9597-35, Session 7

Sparse methods for quantitative susceptibility mapping (QSM)

Berkin Bilgic, Athinoula A. Martinos Ctr. for Biomedical Imaging (United States)

No Abstract Available

9597-36, Session 7

Real-time MRI of speech in multiple planes using a novel custom upper airway coil, golden angle spirals, and temporal regularization

Sajan Goud Lingala, Krishna S. Nayak, The Univ. of Southern California (United States)

No Abstract Available

9597-37, Session 7

Better and faster imaging and reconstruction by transform-based blind compressed sensing

Saiprasad Ravishankar, Yoram Bresler, Univ. of Illinois at Urbana-Champaign (United States)

No Abstract Available

9597-38, Session 7

Diffusion tensor MR imaging denoising with image and eigen-value sparsity constraint

Xi Peng, Dong Liang, Shenzhen Institutes of Advanced Technology (China)

No Abstract Available

9597-39, Session 7

Magnetic resonance fingerprinting

Mark Griswold, Case Western Reserve Univ. (United States)

No Abstract Available



9597-40, Session 8

Weaving Hilbert space frames

Richard G. Lynch, Peter G. Casazza, Univ. of Missouri (United States)

No Abstract Available

9597-41, Session 8

Bayesian wavelet change point detection

Darrin Speegle, Saint Louis Univ. (United States); Robert Steward, Saint Louis Univ. (United States) and National Geospatial-Intelligence Agency (United States)

A Bayesian-wavelet techinque is developed to analyze statistical change point problems, primarily a change in mean, in one and in low dimensions. This technique in low dimensions is combined with dimension reduction to analyze statistical change point problems in high dimensions. Examples are provided of the technique applied to sequences of images. In these examples, various types of changes in the images are detected. This talk is invited by special session organizers Pete Cassaza and Matt Fickus.

9597-42, Session 8

Block-circulant constructions for robust and efficient phase retrieval

Mark Iwen, Aditya Viswanathan, Michigan State Univ. (United States); Yang Wang, Hong Kong Univ. of Science and Technology (Hong Kong, China)

No Abstract Available

9597-43, Session 9

Detailing the equivalence between real equiangular tight frames and certain strongly regular graphs

Matthew Fickus, Air Force Institute of Technology (United States)

No Abstract Available

9597-44, Session 9

Connectivity of spaces of finite unit-norm tight frames

Nathaniel Strawn, Jameson Cahill, Duke Univ. (United States); Dustin G. Mixon, Air Force Institute of Technology (United States)

By constructing liftings of paths in the space of eigensteps, we demonstrate that the spaces of Finite Unit-Norm Tight Frames are path connected. After some refinements of this technique, we also show that these spaces are irreducible as algebraic varieties.

9597-45, Session 9

The generalized lasso with non-linear measurements

Yaniv Plan, The Univ. of British Columbia (Canada); Roman Vershynin, Univ. of Michigan (United States)

No Abstract Available

9597-46, Session 10

Geometric muli-resolution analysis for dictionary learning

Nathaniel Strawn, Mauro Maggioni, Duke Univ. (United States); Stanislav Minsker, Wells Fargo (United States)

In this talk, we demonstrate an extended theory for the Geometric Multi-Resolution Analysis method developed by Allard, Chen, and Maggioni. In particular, we prove a finite-sample error bound, develop a general theory for "noisy" manifold models, and discuss applications.

9597-47, Session 10

Geometric multi-resolution analysis and data-driven convolutions

Nathaniel Strawn, Duke Univ. (United States)

Using the Geometric Multi-Resolution Analysis procedure of Allard, Chen, and Maggioni, we construct data-driven convolutional filters and discuss various applications. This talk is invited by special session organizers Radu Balan, Bernard Bodman, and Gitta Kutyniok.

9597-48, Session 10

Higher-order graph wavelets and sparsity on circulant graphs

Madeleine S. Kotzagiannidis, Pier Luigi Dragotti, Imperial College London (United Kingdom)

The notion of a graph wavelet gives rise to a more advanced processing of data on graphs due to its ability to operate in a localized manner, across newly arising data-dependency structures, with respect to the graph signal and underlying graph structure, thereby taking into consideration the inherent geometry of the data. In this work, we tackle the problem of creating graph wavelet filterbanks on circulant graphs for a sparse representation of certain classes of graph signals, lying on the vertices of such graphs, in the graph wavelet domain. Hereby, we consider scenarios in which the underlying graph is data-driven as well as fixed, for applications including image processing and social network theory, whereby clusters can be modelled as circulant graphs, respectively. We present a set of novel graph wavelet filterbank constructions, which annihilate higher-order polynomial graph signals defined on the vertices of undirected, circulant graphs and are localized in the vertex domain. Their design is based on a generalization of the annihilation property of the corresponding graph Laplacian matrix, which is shown to have two vanishing moments for a sufficiently small bandwidth. The derivation is conducted through spectral factorization, using similar methods as in the traditional domain; we additionally present constructions using matrix theory. We give preliminary results on their performance for non-linear approximation. Furthermore, we provide extensions to our previously developed segmentationinspired graph wavelet framework for non-linear image approximation, by incorporating notions of smoothness and vanishing moments, which further improve performance compared to traditional methods.



9597-49, Session Key

Applied and computational harmonic analysis on graphs and networks (Keynote Presentation)

Naoki Saito, Univ. of California, Davis (United States)

In recent years, the advent of new sensor technologies and social network infrastructure has provided huge opportunities and challenges for analyzing data recorded on such networks. For analyzing data recorded on regular lattices, computational harmonic analysis tools such as the Fourier and wavelet transforms have well-developed theories and proven track records of success. It is therefore quite important to extend such tools from the classical setting of regular lattices to the more general setting of graphs and networks.

In this talk, I will first review basics of Laplacian matrices of a graph whose eigenpairs are often interpreted as the frequencies and the Fourier basis vectors on a given graph. I will point out, however, that such an interpretation is misleading unless the underlying graph is unweighted path or cycle. I will then discuss our recent effort of constructing multiscale basis dictionaries on a graph including the Hierarchical Graph Laplacian Eigenbasis Dictionary and the Generalized Haar-Walsh Wavelet Packet Dictionary, which are viewed as the generalization of the classical hierarchical block DCTs and the Haar-Walsh wavelet packets for the graph setting. If time permits, I will also discuss how to generalize those constructions for directed graphs.

9597-50, Session 11

Multiresolution matrix factorization

Risi Kondor, The Univ. of Chicago (United States)

No Abstract Available

9597-51, Session 11

Randomized Kaczmarz algorithms: dynamics in the large system limit

Chuang Wang, Yue M. Lu, Harvard Univ. (United States)

No Abstract Available.

9597-53, Session 12

Directed brain graphs from autoregressive models

Fabrizio De Vico Fallani, Institut National de Recherche en Informatique et en Automatique (France) and L'Institut du Cerveau et de la Moelle épinière (France)

In the last decade, the sparse representation of the brain as a graph, consisting of nodes and links, has allowed to visualize functional brain networks and describe their non-trivial topological properties in a compact and objective way.

Nowadays, the use of graph analysis in neuroscience has become essential to quantify the physiological brain organization and pathological dysfunctions in terms of aberrant reconfiguration of functional brain

networks. After defining the brain nodes, which usually correspond to different brain regions, assigning the inks between them is the subsequent crucial modeling step.

In functional neuroimaging the links of a brain graph are given by evaluating the similarity between the activities of the two brain regions, through functional connectivity (FC) measures. FC methods fall into two broad categories: those measuring symmetric mutual interaction (undirected weighted links) and those measuring asymmetric information propagation (directed weighted links).

In the present talk, I will focus on the construction of directed brain graphs from a given set of signals representing the activities recorded in different brain regions. Specifically, I will introduce the use of autoregressive models to build directed graph links that code Granger-causality between different brain areas. Also, I will present some applications to real data ranging from electroencephalography (EEG) in healthy and diseased subjects to calcium imaging signals optically recorded from the spinal cord of the zebrafish.

Finally, I will conclude by highlighting current limitations and open issues related to the construction, analysis and interpretation of directed brain graphs.

9597-54, Session 12

Graph spectroscopy

Paul Expert, King's College London (United Kingdom); Renaud Lambiotte, Sarah de Nigris, Univ. of Namur (Belgium); Taro Takaguchi, National Institute of Informatics (Japan)

No Abstract Available

9597-55, Session 12

Classification of fMRI data using Gaussian graphical models

Aude Costard, Sophie Achard, Olivier Michel, GIPSA-lab (France); Pierre Borgnat, Patrice Abry, Lab. de Physique (France) and Ecole Normale Supérieure de Lyon (France)

No Abstract Available

9597-56, Session 12

Statistical methods for comparing brain connectomes at different scales

Djalel-Eddine Meskaldji, Univ. of Genéva (Switzerland); Stephan Morgenthaler, Ecole Polytechnique Fédérale de Lausanne (Switzerland); Dimitri Van De Ville, Ecole Polytechnique Fédérale de Lausanne (Switzerland) and Univ. of Genéva (Switzerland)

No Abstract Available

Conference 9598: Optics and Photonics for Information Processing IX

Monday - Wednesday 10-12 August 2015 Part of Proceedings of SPIE Vol. 9598 Optics and Photonics for Information Processing IX

9598-1, Session 1

3D imaging of amplitude objects embedded in phase objects using transport of intensity

Mahmudunnabi Basunia, Univ. of Dayton (United States); Partha Banerjee, University of Dayton (United States)

The amplitude and phase of the complex optical field in the Helmholtz equation obey a pair of coupled equations, arising from equating the real and imaginary parts. The imaginary part yields the transport of intensity equation (TIE), which can be used to derive the phase distribution at the observation plane. If a phase object is approximately imaged on the recording plane(s), TIE yields the phase without the need for phase unwrapping. In our experiment, we recover the 3D image of an amplitude object embedded in a phase object. The phase object is created by heating a liquid, comprising a solution of red dye in alcohol, using a focused 514 nm laser beam to the point where self-phase modulation of the beam is observed. The optical intensities are recorded are various planes during propagation of a low power 633 nm laser beam through the liquid. In the process of applying TIE to derive the phase at the observation plane, the real part of the complex equation is also examined as a cross-check of our calculations. Our work can find applications in, for instance, referenceless 3D imaging of debris in a fireball, and is well suited for moving objects.

9598-2, Session 1

Linear fitting interpolation based on FOV division for correcting wide angle fish-eye lens distortion

An Li, Yisi Wu, Chi Chen, Zhenrong Zheng, Zhejiang Univ. (China)

The wide angle lens, like fish eye lens, suffers great optical distortion that causes severe deformation of the real world. A method to correct the strong distortion was presented in this work. Due to the nonlinear distribution of the distortion, linear algorithms are generally not under consideration to establish the math model of distorted-to-ideal images. However, this method employed the calibration pattern that comprised of regular array of dots to divides the full field of view (FOV) to subsections, each subsection is a small FOV, the mapping parameters between the distorted image and ideal image in each small FOV can be calculated by employing the very simple linear polynomial. Thus, applying the determined parameters to their corresponding sub-FOVs, respectively, all the ideal pixel coordinates of the distorted image can be obtained. The method employed linear polynomial characterizes the geometric deformation between the distorted and ideal images directly. Therefore, it contains both of radial distortion and tangential distortion and there is no need of concerning any intrinsic or extrinsic parameters of the optical systems. So, this algorithm reliefs the computational work that employed by conventional radial models and other mathematical models. Experiments performed on off-axis optical systems which exist complicated distortion, such as the head mounted displays (HMDs), had already yielded accurate correcting results. Likewise, in this paper, the experiments refer to the fish-eye lens also verified the effectiveness and flexibility of this method.

9598-3, Session 1

Real-time sine transform of images based on volume holographic optical correlator

+1 360 676 3290 ·

help@spie.org

Fanglin Liu, Liangcai Cao, Dezhao Kong, Guofan Jin, Tsinghua Univ. (China) Volume holographic correlator (VHC) is a multi-channel optical correlator with the merits of high speed, high storage density and parallel computing [1]. It presents the potential in areas where fast computing and massive capacity are acquired [2, 3]. In this work, the two-dimensional discrete sine transform based on this optical method is proposed. More than two thousand data pages standing for the orthogonal sine transform functions are recorded in a photorefractive crystal by angle multiplexing [4]. During the transform process, an input image is uploaded to the optical path through a spatial light modulator. VHC calculates the inner products between the input image and all the pre-recorded data pages in parallel. All the angle-multiplexed reference beams are simultaneously reconstructed and the intensities of correlation spots are detected by a CCD. The transform coefficient of each transform function can be retrieved according to the intensities in the center of each correlation spot. These transform coefficients can also be used to reconstruct the original input image. Because the transform time for optical method is only the light propagation time and the computing is finished in parallel, the VHC has a great advantage over the purely electronic method. The real-time sine transform using an automatic optical correlator is demonstrated.

Acknowledgement:

This work is supported by National Natural Science Foundation of China (61177001, 61327902), and Tsinghua University Initiative Scientific Research Program.

References

[1] G. W. Burr, "Holography for information storage and processing," Proc. SPIE 5181, 70-84 (2003).

[2] Qiang Ma, Kai Ni, Qingsheng He, Liangcai Cao, and Guofan Jin, "Fast associative filtering based on two-dimensional discrete Walsh transform by a volume holographic correlator," Opt. Express 17,838–843 (2009).

[3] Yao Yi, Liangcai Cao*, Wei Guo, Yaping Luo, Jianjiang Feng, Qingsheng He, and Guofan Jin, "Optical fingerprint recognition based on local minutiae structure coding," Opt. Express 21, 17108-17121(2013).

[4] Tianxiang Zheng, Liangcai Cao^{*}, Qingsheng He, and Guofan Jin, "Fullrange in-plane rotation measurement for image recognition with hybrid digital-optical correlator," Opt. Eng. 53, 011003 (2014).

9598-4, Session 1

Modeling for space-based visible imaging characteristics of space object

Cheng-Ming Sun, Academy of Opto-Electronics (China); Yan Yuan, BeiHang Univ. (China); Zhiliang Zhou, Academy of Opto-Electronics (China)

With the development of space technology, the number of space objects dramatically increases in recent years. The miniaturization, diversification and complication of space objects pose new challenges for their detection. Space-based visible imaging detection, which is flexible and intuitive, gradually becomes an important means for space object detection. As the theoretical foundation and technical support for the schematic design and performance analysis of imaging detection systems, an imaging detection model should synthetically involve the physical parameters of the object, the performance parameters of the detector, and the orbit parameters of the sun, object and detector.

In order to enhance the capability of space-based surveillance, the detailed modeling for visible imaging characteristics of space object is described in this paper. Firstly, a space-based imaging detection model is built based on the scattering visible radiation from space object. The model consists of radiation transmission based on the bidirectional reflectance distribution function (BRDF) and grayscale transformation. Then, according to the position of the sun, object and detector, the imaging conditions such as imaging angle and size are analyzed. Finally, the grayscale images of the HuanJing-1 satellite are simulated. It shows the grayscales for the different regions of the object appear great difference, indicating that the space-





based detector needs a larger dynamic range. The simulation results can provide reference basis for space object detection.

9598-57, Session 1

The fast Fresnel diffraction algorithm: from the ray matrix approach to experimental virtual propagation systems (Invited Paper)

Jeffrey A Davis, Don M. Cottrell, Cassidy A. Berg, Christopher Li Freeman, Adriana Carmona, William Debenham, San Diego State Univ. (United States); Ignacio Moreno, Univ. Miguel Hernández de Elche (Spain)

In this paper the fast Fresnel diffracion algorithm is reviewed from different non-standard points of view and applied to some novel applications. The algorithm (also named the angular spectrum method) is a very powerful numerical technique that has been employed for years in the calculation of diffraction patterns. It utilizes two Fourier transform operations, thus becoming computationally much faster than the conventional approach. We analyze the practical implementation with spatial light modulators (SLM).

First, the ray matrix approach is applied to derive and reexamine the technique. This approach permits to easily find explicit expressions for the distances over which the algorithm is accurate. Then, we describe its practical implementation to encode Fresnel propagated masks onto a SLM. We discuss the limitations caused by the Nyquist limit.

Finally, we apply the technique to create an experimental virtual optical beam propagator system. This system uses one SLM and allows the experimental study of beam propagation without physically moving any element. This laboratory propagator system can be extremely useful to build compact optical architectures or to emulate beam propagation without misalignments caused by moving elements.

As examples, we design holograms producing different patterns at different distances, and we can change the effective plane of observation by changing the encoded propagation. Other multiplexed patterns are designed to create azimuthal multiple beam interference effects by applying different propagation distances to different vortex generating maks. The technique can find applications in many different contexts, including the analysis of propagation dynamics of nondiffracting beams, and Airy beams.

9598-5, Session 2

Image quality improvement of digital holography by use of various rectangle apertures

Takanori Nomura, Takahiko Fukuoka, Yutaka Mori, Wakayama Univ. (Japan)

Digital holography is a useful technique for recording the fully complex field of a wavefront. In line with advances in imaging devices such as charge coupled devices, digital holography is available. Digital holography has been used for lots of applications including display, encryption and threedimensional object recognition. However, the quality of a reconstructed image of a digital hologram is not good, because it is suffering from speckles. Compared with a conventional film hologram, the extent of a digital hologram is small. This is why the reconstructed image has noticeable speckles, because, the speckle size of reconstructed image is in inverse proportion to the image sensor size. Therefore, the synthetic aperture digital holography was proposed to decrease the size of speckles. If a huge size image sensor is used, the size of speckles is enough small to ignore. However, it is not practical.

Then we propose a speckle reduction method in digital holography using various rectangular apertures. In the proposed method, different-sized rectangular apertures are applied for the hologram. Furthermore, the position of the aperture is arbitrary. Owing to the various size and position, the generated speckles have the various sizes and patterns. By averaging the speckle, the speckle noise can be reduced.

Some reconstructed images based on the experimental results are shown to confirm the proposed method. For quantitative evaluation, the speckle contrast is also shown.

9598-6, Session 2

Static and dynamic effects of flicker in phase multilevel elements on LCoS devices

Andrés Márquez, Francisco J. Martínez-Gaurdioloa, Sergi Gallego, Manuel Ortuño, Jorge Francés, Augusto Beléndez, Inmaculada Pascual, Univ. de Alicante (Spain)

Phase-only modulation is necessary in a great number of modern spatial light modulation applications, and the spatial light modulator (SLM) technology of choice is usually the parallel-aligned liquid crystal on silicon (PA-LCoS) microdisplay. Various degradation effects have been analyzed in the literature which may be introduced by SLMs and whose quantitative knowledge enables to select the best working conditions and/or to design specific compensation strategies to diminish negative effects. In this paper we concentrate on the phase flicker typically produced by PA-LCoS devices. The availability of a recent polarimetric-based method, the average Stokes polarimetric technique, to measure the linear retardance and its flicker amplitude eases the capability to simulate the performance of spatially varying phase multilevel elements typically addressed onto PA-LCoS. A representative element is the blazed grating. We analyse both their average diffraction efficiency, "static" analysis, and its associated time fluctuation, "dynamic" analysis, under a wide set of conditions. We obtain a good agreement between simulation and experiment, thus further demonstrating the predictive capability of the calibration provided by the average Stokes polarimetric technique. An interesting result is that, in general, the influence of flicker greatly diminishes when the number of quantization levels in the optical element increases, thus limiting to acceptable levels the effects introduced by the phase flicker.

9598-7, Session 2

Incoherent holography to obtain depth information by a rotational shearing interferometer

Kaho Watanabe, Takanori Nomura, Wakayama Univ. (Japan)

The possibility of incoherent holography has been widely studied. It enables us to record hologram without coherent illumination such as a laser. We have proposed the system to record incoherent Fourier hologram of an object (incoherently illuminated or self-luminous object) using a rotational shearing interferometer. The system can record incoherent hologram by self-interference of the two coherent object points created by the beam splitter from one object point. The Fourier hologram has the advantage of increasing space-bandwidth product performance. However, no depth information is obtained. In general, rotational shearing interferometer cannot reproduce any depth information. The reason is indicated that the shear by rotational shearing interferometer is a purely lateral shear orthogonal to the optical axis by Bryngdahl and Lohmann. In this paper, we propose the system of incoherent holography which can record depth information using a rotational shearing interferometer. The system has a lens for the shear which is parallel to the optical axis. This is because we can obtain depth information by a rotational shearing interferometer. A preliminary experiment was performed to confirm our method. A liquid crystal display with a LED backlight was used as an incoherent object. The Fresnel zone-like intensity was recorded from a circular object pattern. We reconstructed recorded incoherent hologram by a Fresnel diffraction integral at some reconstruction distances. We obtained reconstructed images which defocus and focus on the incoherent object. These experimental results confirm the proposed system of incoherent holography to obtain depth information using a rotational shearing interferometer.



9598-8, Session 2

Spectral characterization and tuning with liquid-crystal retarders

María del Mar Sánchez-López, Ignacio Moreno, Univ. Miguel Hernández de Elche (Spain); Asticio V. Vargas, Univ. de la Frontera (Chile); Pascuala García-Martínez, Univ. de València (Spain)

We present an accurate and simple technique to characterize the spectral retardance of a liquid-crystal retarder (LCR), including multiple-beam Fabry-Perot (FP) interferences. Interference effects occur in LCR devices devoid of an antireflective coating and must be considered in applications that require a fine control of the phase or the polarization.

The proposed technique is based on a simple physical model with few parameters, namely: absorption losses, the complex transmission coefficients in the extraordinary and ordinary axes accounting for the FP interference in the liquid crystal layer, and the phase shifts introduced by the compensator layer present in most devices. Considering that the retarder is illuminated under normal incidence, the wavelength dependence of the model parameters is first retrieved by characterizing the LCR in the offstate. Then, we apply a voltage transfer fuction valid in the spectral range of characterization. As a result of this procedure, a full description of the LCR spectral modulation properties is obtained.

By tilting the LCR we extend the former analysis to illumination under nonnormal angles of incidence. This situation is relevant for liquid crystal on silicon (LCoS) displays, which are often illuminated under oblique incidence to avoid the use of beam splitters. With this technique we can retrieve the ordinary and extraordinary spectral phase delays and distinguish between fast and slow axis. This allows us to use the stationary phase-time approach and discuss the arising of superluminal and slow-light group delay regimes for the LCR inserted between linear polarizers. It is also useful to design optical architectures to achieve full spectral control.

9598-9, Session 2

Z-domain modeling and analysis of vertically coupled triple asymmetrical optical micro ring resonator (VCTAOMRR)

Sanjoy Mandal, Suchita Lakra, Indian School of Mines (India)

Theoretical modeling of a carefully designed vertically coupled triple asymmetrical optical micro ring resonator(VCTAOMRR) is developed using delay line signal processing approach. Overall transfer function of the proposed VCTAOMRR is determined in Z-domain using signal flow graph and Mason's rule. Vertically coupled triple micro ring resonator(VCTMRR) of two symmetrical ring was successfully modeled in Z-domain by S Mandal et.al.[1] where its performance in terms of free spectral range (FSR) and crosstalk of the VCTMRR with two symmetric rings is compared with previously published results, and found to be in very close agreement.

Frequency response , group delay and dispersion characteristics of the proposed VCTAOMRR are evaluated in MATLAB environment. Performance in terms of free spectral range (FSR) and crosstalk of the VCTAOMRR is determined from the frequency response characteristics. The Vernier principle is used to expand the FSR when optical triple micro ring resonators with unequal radii are combined so that the passbands overlap only once in several periods. The proposed VCTAOMRR can produce very wide FSR around 80 nm. The design provides frequency response characteristics where crosstalk at the interstitial frequencies that lie between the extended FSR is adequately suppressed. Dispersion causes broadening of signal pulses around the resonant peaks. Dispersion characteristics is evaluated from group delay characteristics of the proposed VCTAOMRR.

Reference:

[1] Modeling and performance analysis of vertically coupled triple micro ring resonator in Z-domain, S Mandal et.al.December 2014 / Vol. 53, No. 36 / APPLIED OPTICS,pp 8381-8388

9598-10, Session 3

Measurement of repetitive surface displacement modulation induced by illuminating femto-second laser pulses

Ryoma Tozawa, Daisuke Barada, Shigeo Kawata, Utsunomiya Univ. (Japan)

When an opaque object is illuminated by femto-second laser pulses, an acoustic wave is generated. The fundamental frequency of the acoustic wave seems depend on the repetition frequency of the laser pulse. It is considered that the acoustic wave is generated by repetitive surface displacement modulation. In this study, momentary optical phase modulation of another continuous wave laser beam was investigated and the repetitive phase modulation was measured by interferometry. In experiments, Ti: Sapphire laser pulses with a central wavelength of 780 nm were illuminated onto a mirror used as a sample from the back. The pulse width and repetition frequency was set to tens femtoseconds and 1 kHz, respectively. In order to confirm the spatial effect, the femto-second laser pulse was spatially modulated by a liquid crystal spatial light modulator. A He-Ne laser beam was used as a probe beam. The He-Ne laser beam was split to two beams by a beam splitter and illuminated onto the sample mirror and the reference mirror. The two reflected beams were superposed onto a CMOS image sensor and the interference fringe was obtained with a frame rate of 100,000 fps. In order to block the femto-second pulses, a low pass filter was put on a front of CMOS image sensor. Then, it was observed that the interference fringe is periodically changed with a frequency of 1kHz by temporal Fourier transform pattern at each pixel. By extracting the 1kHz signal from all pixels, the phase modulation distribution was visualized.

9598-11, Session 3

Phase correction method for leastsquares wavefront calculation in statistical generalized phase-shifting digital holography

Nobukazu Yoshikawa, Kazuki Kajihara, Saitama Univ. (Japan)

The continuous fringe scanning scheme offers some advantages such as short measurement time, high phase stability and high noise tolerance. However, it may be difficult to generate a constant phase-shift using a low-cost system because it requires accurate synchronization between an image sensor and phase-shifter. On the other hand, the generalized phase-shifting method does not require a specific phase-shift value such as the integral multiples of $\varpi/2$ phase shift. Therefore, there is no difficulty in implementation of the continuous fringe scanning scheme.

In this study, we propose statistical generalized phase-shifting digital holography using continuous fringe scanning scheme and the phase-shift estimation method using a least-squares algorithm. The phase-shifts are generated by a continuous fringe scanning technique, and time-varying interference fringes are detected sequentially by an image sensor without synchronizing a phase-shifter. Integrations of the time-varying intensity in the interference fringe produce an arbitrary phase-shifted digital hologram. Since there is no wait time for phase stabilization unlike the step fringe scanning technique, many phase-shifted interference fringes can be obtained in a short time. Signed phase-shift values are estimated by the statistical approach and then the object wave is obtained by the least-squares algorithm. The proposed method does not require precise control and calibration of the phase shifter and synchronization between the image sensor and phase shifter. Experiments demonstrate the validity of the proposed method. The practical digital holography system with high accuracy can be implemented at low cost.



9598-12, Session 3

A hybrid MEMS-planar waveguide optical signal processor

Dwayne Macik, Russell J. Howe, Christi K. Madsen, Texas A&M Univ. (United States)

An optical signal processor is proposed that performs a direct signal-filter convolution without the use of Fourier Transformed filter multiplication. The convolution operation is carried out utilizing electro-optical components to generate and steer an optical beam to a digital micro-mirror device. Input signal in the form of a collimated optical beam is scanned through an imaging optic across a micro-mirror array that presents a 1-D spatial filter function. The filter function is shifted spatially with changing row or column to carry out a convolution operation. Filter "bit depth" is determined by the mirror pattern in the local spot zone giving a ratio of 'on' state to 'off' state area. The reflected signal returns along the original path through the imaging lens and is read by a receiver following a beam splitter. Design feasibility is presented along with laboratory setup results. Functionality limits based on component selection are considered.

9598-13, Session 3

The solution spectroellipsometry objectives for environmental monitoring

Ferdenant A. Mkrtchyan, Institute of Radio Engineering and Electronics (Russian Federation)

Ellipsometry is an optical technique that uses the change in the state of polarization of light upon reflection and refraction for the in-situ and realtime characterization of surfaces, interfaces, thin films in the physics, and liquid solutions in the hydrochemical investigations. Spectroellipsometry methods are used for the undestroying investigation of chemical and physical characteristics of solid materials and liquid solutions. These methods are based on the registration of optical polarization effects appearing under reflection or deformation of the light wave as a result of its interaction with studied object. In the solid physics, spectroellipsometry gives possibility to measure simultaneously amplitude and phase characteristics of studied object and allows the precise definition of the film thickness and optical constants for film material. The diagnostics of liquids gives possibility to assess the concentration of chemicals dissolved and weighed in the liquid as well as to determine the spots of pollutants on the water surface.

In this paper the task of liquid solutions identification is considered basing on the measurement data of optical characteristics delivered by the multi-channel spectroellipsometer. Learning decision making system is proposed. Four algorithms are proposed and analyzed for this task solution. These algorithms are based on different procedures for the spectral image recognition. Comparative empirical assessments are given for precision of these algorithms and dependence of index for identification reliability on the solution concentration is shown. Efficiency of proposed algorithms is shown by means of the examples of diagnostics of water systems located in South Vietnam.

The reported study was partially supported by RFBR, research project No. 13-07-00146.

9598-15, Session 4

Measuring refractive index of glass by using two captures under speckle field illumination

Changliang Guo, Univ. College Dublin (Ireland); Dayan Li, Institut Langevin (France) and Ecole Supérieure de Physique et de Chimie Industrielles de la Ville de Paris (France); Damien P. Kelly, Technische Univ. Ilmenau

(Germany); John T. Sheridan, Univ. College Dublin (Ireland)

Measurement of the refractive index of regular shaped glass by speckle correlation is reported. One intensity image in the diffraction field of a speckle-illuminated sample is captured by a CCD before the presence of glass sample and another intensity image is captured after the presence of glass sample. As the position of peak correlation coefficient is quantitatively related to the change in optical path length arising due to the presence of glass, the refractive index of the glass can be evaluated by the correlation of the intensity image before and after the glass insertion. The theoretical correlation function is first derived that describes the relationship between optical path length change and speckle decorrelation. In experiment, various regular shaped glasses are measured to demonstrate the accuracy and robustness of the proposed technique.

9598-16, Session 4

Compressive sensing based ptychography image encryption

Nitin Rawat, Gwangju Institute of Science and Technology (Korea, Republic of) and Analog and Mixed Signal Integrated Circuit Design Lab. (Korea, Republic of)

A compressive sensing (CS) based ptychography combined with an optical image encryption is proposed. The diffraction pattern is recorded through ptychography technique further compressed by non-uniform sampling via CS framework. The system requires much less encrypted data and provides high security. The diffraction pattern as well as the lesser measurements of the encrypted samples serves as a secret key which make the intruder attacks more difficult. Furthermore, CS shows that the linearly projected few random samples have adequate information for decryption with a dramatic volume reduction. Experimental results validate the feasibility and effectiveness of our proposed technique compared with the existing techniques. The retrieved images do not reveal any information with the original information. In addition, the proposed system can be robust even with partial encryption and under brute-force attacks. To the best of our knowledge, this is the first report on an optical encryption ptychography integrating with CS.

9598-17, Session 4

Research on signal-to-noise ratio characteristics and image restoration for wavefront coding

Yijian Wu, Yuejin Zhao, Liquan Dong, Xiaohu Guo, Wei Jia, Ji Zhao, Beijing Institute of Technology (China)

Wavefront coding, a technique of optical-digital hybrid image, can be used to extend the depth of the field. However, it sacrifices the signal-to-noise ratio (SNR) of system at a certain degree, especially on focus situation. The on-focus modulation transfer function (MTF) of wavefront coding system is much lower than that of generally traditional optical system. And the noise will be amplified in the digital image processing. This paper analyzes characteristics of the SNR of the wavefront coding system in the frequency domain and calculates the rate of noise amplification in the digital processing. It also explains the influence of the image detector noise severely reducing the restored quality of images. In order to reduce noise amplification in the process of image restoration, we propose a modified wiener filter which is more suitable for restoration in consideration of noise suppression. The simulation experiment demonstrates that the modified wiener filter, compared with traditional wiener filter, has much better performance for wavefront coding system and the restored images having much higher SNR in the whole depth of the field.



9598-18, Session 4

Fractional Fourier transform of non-integer vortex beams

Yaqin Zhao, Xin Zhong, Guanghui Ren, Zhilu Wu, Harbin Institute of Technology (China)

In these two decades, optical vortices with orbital angular momentum have gained a lot of attention in physics, information science and so on. Most of the researches focus on the beams with integer topological charges, because these beams are spatially orthogonal with each other. Nevertheless, some researches have shown that vortex beams with fractional topological charges also have great potential in the areas of particle manipulation, communications and so on. Fractional Fourier transform (FrFT) is a powerful tool to analyze and process both electric and optical signals and it has the potential to process non-integer vortex beams.

The properties of vortex beams with fractional topological charges when propagating through fractional Fourier planes are analyzed. Based on the FrFT, the theoretical formula is derived to analyze the effects of the parameters of non-integer vortex beams. Numerical results of the evolution of non-integer vortex beams through different fractional Fourier planes are illustrated. The results show that the fractional order of the FrFT has great influence on the normalized intensity distribution properties of non-integer vortex beams. The beams show the same evolution trend, but different shapes.

9598-19, Session 5

Characterization of dynamic speckle sequences using principal component analysis and image descriptors

José Manuel López-Alonso, Univ. Complutense de Madrid (Spain); Eduardo Grumel, Ctr. de Investigaciones Ópticas (Argentina); Nelly L. Cap, Centro de Investigaciones Opticas (Argentina); Hector J. Rabal, Marcelo Trivi, Ctr. de Investigaciones Ópticas (Argentina); Javier Alda, Univ. Complutense de Madrid (Spain)

Speckle is being used as a characterization tool for the analysis of the dynamic of slow varying phenomena ocurring in biological and industrial samples. The retrieved data takes the form of a sequence of speckle images. The analysis of these images should reveal the inner dynamic of the biological or physical proccess taking place in the sample. Very recently, it has been shown that principal component analysis is able to split the original data set in a collection of clasess. These classes can be related with the dynamic of the observed phenomena. At the same time, statistical descriptors of biospeckle images have been used to retrieve information on the characteristics of the sample. These statistical descriptors can be calculated in real time and provides a fast monitoring of the sample. On the other hand, principal component analysis requires longer computation time but the results contain more information related with spatial-temporal pattern that can be identified with physical proccess. This contribution merges both descriptions and uses principal component analysis as a preprocessing tool to obtain a collection of filtered images where a simpler statistical descriptor can be calculated. The method has been applied to slow-varying biological processes

9598-20, Session 5

Edge extraction of optical subaperture based on fractal dimension method

Yunqi Wang, Mei Hui, Ming Liu, Liquan Dong, Xiaohua Liu, Yuejin Zhao, Beijing Institute of Technology (China)

The main problem of optical synthetic aperture imaging system is to achieve

cophasing between each subaperture, it is necessary to detect edge phase of subaperture. The edge of optical synthetic aperture imaging system is more complex than that of traditional optical imaging system. For largeaperture optical component, the steep-slope in edge region leads to quite dense interference fringe. So it is significant to extract edge phase of subaperture to avoid the loss of effective frequency.

The anti-jamming capability is weak for traditional edge extraction algorithm, such as Sobel, Roberts, Prewitt, LOG, Canny and Laplacian. They may mistakenly identify noise as edge phase, resulting in the loss of effective frequency.

Fractal dimension as a measure method of image surface irregularities can not only statistically evaluate the complexity but also carry the invariant properties of multi-scale and multi-resolution. It is consistent with human visual image perception of rough surface texture. Fractal theory is based on self-similarity of image, and has a certain suppression effect on noise. Therefore, fractal dimension provides a powerful tool to describe surface characteristics of image.

For edge detection, the box-counting dimension was used to calculate fractal dimension of the whole image. Then the calculated fractal dimension is mapped to grayscale image. The region with large fractal dimension represents a sharper change of the gray scale in original image, which was accurately extracted as the edge region of optical subaperture.

9598-21, Session 5

Low crosstalk optical hierarchical authentication with a fixed random phase lock based on two beams interference

Dajiang Lu, Wenqi He, Xiang Peng, Shenzhen Univ. (China)

We propose a novel method to achieve the purpose of hierarchical authentication based on two beams interference. In this method, different target images indicating different authentication levels are analytically encoded into corresponding phase-only masks (phase keys) and amplitudeonly masks (amplitude keys) with the help of a random phase mask, which is created in advance and acts as the fixed lock of this authentication system. For the authentication process, a legal user can obtain a specified target image at the output plane if his/her phase key, and amplitude key, which should be settled close against the fixed internal phase lock, are respectively illuminated by two coherent beams. By comparing the target image with all the standard certification images in the database, the system can thus verify the user's identity. In simple terms, this system can not only confirm the legality of a user but also distinguish his/her identity level. Moreover, in despite of the internal phase lock of this system being fixed, the crosstalk between different target images is low. Theoretical analysis and numerical simulation are both provided to demonstrate the validity of this method.

9598-22, Session 5

Variants of light modulation for MINACE filter implementation in 4-F correlators

Dmitry V. Shaulskiy, Nikolay N. Evtikhiev, Evgenie Y. Zlokazov, Sergey N. Starikov, Rostislav S. Starikov, Elizaveta K. Petrova, National Research Nuclear Univ. MEPhI (Russian Federation)

We address the recognition problem of grayscale images of object subjected to out-of-plane rotation distortion. We compare filter realization as computer generated hologram and filter projection on modulator domain. Our study results of filter discriminating characteristic analysis are shown. The results of filter implementation modeling in 4-f correlator and initial experimental resuls are represented.



9598-23, Session 5

A fast decoding of Reed-Solomon code with p-polynomial and look-up table method

Yan-Haw Chen, Chong-Dao Lee, Trieu-Kien Truong, I-Shou Univ. (Taiwan); Ching-Fu Huang, I-Shou University (Taiwan)

An efficient lookup table method for evaluating syndrome needed in the RS decoder is presented in this paper. It can also be applied to data storage of RAID, 2D bar code, DVD, and CD decoder, which are based on p-polynomial and lookup table method. The method can evaluate the 2t syndromes that can be simplified by the iteration method of P-polynomial and lookup table method. It can reduce the decoding time by fifty-percent only using the p-polynomial method, and thus the speed is much faster than Horner's rule. Finally, the proposed syndrome evaluation method for RS codes is suitable to software implementations on DSP systems.

Summary

In this paper, the decoding of RS codes has been performed by precomputing lookup table method and efficiently evaluating p-polynomial method. Regarding the complexity of the developed method, table lookup time for evaluating syndromes are only O(2t(n-2)/n). Whereas, the computational complexity of the Horner rule with the same table can provide more efficient scheme for speeding up the decoding syndrome evaluation in RS codes. Furthermore, the experimental results show that the proposed method for decoding of RS codes is more effective than the previous methods, such as traditional p-polynomial and Horner's rule.

9598-56, Session 5

Novel cellular recurrent deep network for image registration

Mahbubul Alam, L. Vidyaratne, Khan M. Iftekharuddin, Old Dominion Univ. (United States)

Image registration is a geometric transformation process where two images (source image and target image) of the same scene with different viewpoints are overlaid to match the alignment. In a rigid registration, the source image is translated, rotated or scaled to spatially align its coordinate locations to those of a target image. Biological evidence suggests that registration is an integral part of human visual system. However, image registration utilizing Artificial Neural Network (ANN) remains a challenging learning task. Registration can be posed as a two-step problem: parameter estimation and actual alignment/transformation. To date ANN based image registration techniques only perform the parameter estimation, while the actual transformation is done using affine equations. In this paper, we propose a novel deep ANN based image rigid registration technique that combines parameter estimation and transformation as a simultaneous learning task. Image transformation represents complex topological mappings. Our previous work shows that a complex universal approximator known as Cellular Simultaneous Recurrent Network (CSRN) can successfully approximate affine transformations with known transformation parameters. This study introduces a deep ANN that combines a feed forward network with a CSRN to perform full rigid registration. A layer wise training approach is followed to pretrain the feed forward network for parameter estimation and the CSRN for transformation. The deep network is then fine-tuned to perform the final registration task. The novel deep ANN based architecture is inspired by deep neural network based classification where the feature extraction step is replaced by parameter estimation and the classification step is replaced by transformation. Our result shows that the deep ANN architecture achieves comparable registration accuracy to that of a usual image affine transformation using CSRN where the parameters are known. We also demonstrate the efficacy of our novel deep architecture by a performance comparison with a deep clustered MLP.

9598-24, Session 6

Video annotations of Mexican nature in a collaborative environment

Lester Arturo Oropesa Morales, Abraham Montoya Obeso, Ctr. de Investigación y Desarrollo de Tecnología Digital (Mexico); Rosaura Hernández García, Escuela Superior en Cómputo (Mexico); Sara Ivonne Cocolán Almeda, MIRAL R&D&I (United States); Mireya Saraí García Vázquez, Ctr. de Investigación y Desarrollo de Tecnología Digital (Mexico); Jenny Benois-Pineau, Bordeaux Univ. (France); Luis Miguel Zamudio Fuentes, Ctr. de Investigación y Desarrollo de Tecnología Digital (Mexico); Jesús A. Martinez Nuño, Escuela Superior de Cómputo (Mexico); Alejandro Alvaro Ramírez Acosta, MIRAL R&D&I (United States)

Multimedia content production and storage in repositories are now an increasingly widespread practice. The index concepts for search in multimedia libraries are very useful for users at the repositories. However the search tools of content based on automatic video tagging, still do not have great consistency. Regardless of how these systems are implemented, it is vital importance possess lots of videos that have concepts tagged with ground truth (training and testing sets). This paper describes a novel methodology to make complex annotation on video resources through ELAN software. These concepts are annotated and related to Mexican nature in a High Level Features (HLF) from development set of TRECVID 2014 on a collaborative environment. Base on this set, each nature concept observed is tagged on each video shots using concepts of the TRECVid 2014 set also we propose new concepts, like tropical settings, urban scenes, actions, events, weather, places for name a few and propose specific concepts that best describe video content of Mexican culture. We have been careful to get the database tagged with concept of nature and ground truth. It is clear evident that a collaborative environment is more suitable for annotated concepts related to ground truth and nature. As a result a Mexican nature database was built also is the basis for test and train sets to classify automatically new multimedia contents of Mexican nature.

9598-25, Session 6

Detecting fiducials affected by Trombone delay in ARC and the main laser alignment at the National Ignition Facility

Abdul A. S. Awwal, Richard R. Leach Jr., Randy S. Roberts, Karl Wilhelmsen, Victoria J. Miller-Kamm, Roger R. Lowe-Webb, Lawrence Livermore National Lab. (United States)

Four of the 192 beams of the National Ignition Facility (NIF) are diverted for use in the Advanced Radiographic Capability (ARC) system to generate a sequence of short (1-50 picoseconds) laser pulses. These beams generate pulses of high energy x-rays that illuminate and penetrate the imploding fuel plasma during ignition scale experiments. The transmitted x-rays imaged with x-ray diagnostics will create a movie of radiographs that is expected to provide unprecedented insight into the implosion dynamics and serve as a diagnostic for tuning the experimental parameters for successful fusion reaction. Beam delay is introduced into the ARC beamlets via independent, free-space optical trombones to stagger these eight pulses responsible for creating the x-ray movie. However, this beam delay causes optical distortion of various beam alignment fiducials used in both in the main laser and the ARC system. This work describes how these alignment fiducials are detected and position estimated in the presence of distortion.



9598-26, Session 6

Robust estimators for speech enhancement in real environments

Yuma Sandoval Ibarra, Víctor H. Díaz-Ramírez, Ctr. de Investigación y Desarrollo de Tecnología Digital (Mexico); Vitaly Kober, Ctr. de Investigación Científica y de Educación Superior de Ensenada B.C. (Mexico)

Common statistical estimators for speech enhancement rely on several assumptions about stationary of speech signals and noise. For instance, it is assumed that the Fourier coefficients (real and imaginary parts) of speech and noise processes are zero-mean independent Gaussian random variables: the variance of the Fourier coefficients is time-variant; and the speech is guasi-stationary within a short time interval. In real-life applications, these assumptions may not always valid. In this work, we propose new estimators based on existing estimators such as maximum likelihood (ML) and minimum mean-squared-error (MMSE) by incorporation of rank-order statistics. It is known that rank-order statistics-based filters are robust and able to preserve high frequency details of the processed signals. In speech enhancement, this feature helps to suppress additive noise while preserving speech intelligibility. The estimators proposed in the present work are better adapted to non-stationary characteristics of speech signals and noise. Through computer simulations we show that the proposed estimators yield a better performance than known estimators in terms of objective metrics of intelligibility when speech signals are contaminated with babble and street noise. The proposed estimators are implemented in FPGA.

9598-27, Session 6

Automatic alignment of the Advanced Radiographic Capability at the National Ignition Facility

Randy S. Roberts, Abdul A. S. Awwal, Erlan S. Bliss, Richard R. Leach Jr., Charles D. Orth, Michael C. Rushford, Roger R. Lowe-Webb, Karl Wilhelmsen, Lawrence Livermore National Lab. (United States)

The Advanced Radiographic Capability (ARC) at the National Ignition Facility (NIF) is a pettawatt-class, short-pulse laser system designed to provide x-ray backlighting of NIF targets. ARC uses four NIF beamlines to produce eight beamlets to create a sequence of eight images of imploding fuel capsules using backlighting targets and diagnostic instrumentation. ARC employs a specially designed master oscillator which produces two pulses, disperses the pulses in wavelength, and then injects the pulses into two halves of each of four NIF beamlines. These pulses are amplified by NIF pre- and main amplifiers and transported to compressor vessels located in the NIF target area. The pulses are then compressed and pointed into the NIF target chamber where they impinge upon an array of backlighters. The interaction of the ARC laser pulses and the backlighting material produces bursts of high-energy x-rays that illuminate an imploding fuel capsule. The transmitted x-rays are imaged by diagnostic instrumentation to produce a sequence of images. A key component of the success of ARC is the automatic alignment system that accomplishes the precise alignment of the beamlets to avoid damaging equipment and to ensure that the beamlets are directed onto the tens-of-microns scale backlighters. In this paper, we describe the ARC automatic alignment system, with emphasis on control loops used to align the beampaths. We also provide a detailed discussion of the alignment image processing, because it plays a critical role in providing beam centering and pointing information for the control loops.

9598-28, Session 6

Annotations of Mexican bullfighting videos for semantic index

Abraham Montoya Obeso, Lester Arturo Oropesa Morales,

Ctr. de Investigación y Desarrollo de Tecnología Digital (Mexico); Luis Fernando Vazquez, Instituto Politécnico Nacional (Mexico); Sara Ivonne Cocolán Almeda, MIRAL R&D&I (United States); Andrei Stoian, Conservatoire National des Arts et Metiers (France); Mireya Saraí García Vázquez, Luis Miguel Zamudio Fuentes, Ctr. de Investigación y Desarrollo de Tecnología Digital (Mexico); Jesús Yaljá Montiel Pérez, Saúl A. de La O Torres, Instituto Politécnico Nacional (Mexico) and Escuela Superior en Cómputo (Mexico); Alejandro Álvaro Ramírez Acosta, MIRAL R&D&I (United States)

The video annotation is extremely important. Due this, it allows to obtain a content descriptors that permit an automatic index and classification from the same kind of files. Therefore, it is necessary generate a database with semantic index that represents the digital content of the Mexican bullfighting atmosphere. This paper proposes a scheme to make complex annotations in a video. Each video is partitioned using our segmentation algorithm that creates shots of different length and different number of frames. In order to make complex annotations about the video we are using the ELAN software. These annotations are done in two steps: First, we took note about the whole content in each shot. Second, we wrote down the actions with parameters regarding to the camera like direction, position and deepness, as a consequence we obtained a more complete descriptor of every action. In both cases we used the concepts of the TRECVid 2014 set also we propose new concepts. This methodology generated a database with the information necessary to create descriptors and algorithms capable of detect actions in order to automatically index and classify new bullfighting multimedia content. It is important to have a database of concise annotations that represents the "ground truth" about the videos already annotated, the quality of the descriptors and algorithms based on that information increase, therefore the entire system improves too.

9598-500, Session Plen

Visual Signal Analysis: Focus on Texture Similarity

Thrasyvoulos N. Pappas, Northwestern Univ. (United States)

Texture is an important visual attribute both for human perception and image analysis systems. We present new structural texture similarity metrics and applications that critically depend on such metrics, with emphasis on image compression and content-based retrieval. The new metrics account for human visual perception and the stochastic nature of textures. They rely entirely on local image statistics and allow substantial point-by-point deviations between textures that according to human judgment are similar or essentially identical.

We also present new testing procedures for objective texture similarity metrics. We identify three operating domains for evaluating the performance of such similarity metrics: the top of the similarity scale, where a monotonic relationship between metric values and subjective scores is desired; the ability to distinguish between perceptually similar and dissimilar textures; and the ability to retrieve "identical" textures. Each domain has different performance goals and requires different testing procedures. Experimental results demonstrate both the performance of the proposed metrics and the effectiveness of the proposed subjective testing procedures.

9598-29, Session 7

Mathematical model for classification of EEG signals

Victor Hugo Ortiz Flores, Instituto Politécnico Nacional (Mexico) and Ctr. de Investigación y Desarrollo de Tecnología Digital (Mexico); Juan Jose Tapia Armenta,

Conference 9598: Optics and Photonics for Information Processing IX



Ctr. de Investigación y Desarrollo de Tecnología Digital (Mexico) and Instituto Politécnico Nacional (Mexico)

A mathematical model to filter and classify brain signals from a brain machine interface is developed. The mathematical model classifies the signals from the different lobes of the brain to differentiate the signals: alpha, beta, gamma and theta, besides the signals from vision, speech, and orientation. The model to develop further eliminates noise signals that occur in the process of signal acquisition. This mathematical model can be used on different platforms interfaces for rehabilitation of physically handicapped persons.

9598-30, Session 7

Luminance and contrast ideal balancing based tone mapping algorithm

Amine Besrour, SUP'COM (Tunisia) and Univ. de Technologie Troyes (France); Mohamed Siala, Fatma Abdelkefi, SUP'COM (Tunisia); Hichem Snoussi, Univ. de Technologie Troyes (France)

Despite the recentness of the tone mapping researches, a number of surveys summarizing the current solutions have been published. In general, the tone mapping can be considered as a technique depending on time and it is dedicated to process time independent sequences. It is especially developed to handle static images. Also, there are different algorithms attempting to model certain characteristics of the human visual system and others representing pure image processing transforming an image into another.

On the other hand, a final classification takes into account the fact that the same mapping function is used for all the pixels (global operators), or if the mapping function deals with random variables given in a vicinity of the pixel that is often dependent on modeling the spatial adaptation (local operators). In this paper, we are concerned by the local ones. Indeed, the local tone mapping methods are more efficient in terms of the compression for high dynamic range images. In fact, they perceive the neighborhood of the given pixel and assign the suitable function of local compression. This paper proposes a design of a recent tone mapping operator used in a high dynamic range imaging system. The proposed operator represents a local method which uses an adaptable factor combining the average neighboring contrast and the brightness difference. Thanks to that, this solution provides good results with better brightness, contrast, and visibility without producing undesired artifacts neither halo effects.

9598-31, Session 7

A 3D approach for object recognition in illuminated scenes with adaptive correlation filters

Kenia Picos, Víctor H. Díaz-Ramírez, Ctr. de Investigación y Desarrollo de Tecnología Digital (Mexico)

Object recognition is a computer vision task that is needed in several applications to improve human activities, such as surveillance, automotive navigation, medical image processing, among others. However, to obtain an accurate object recognition system is very challenging, due to several factors that compromise its performance. In a real-life images, the presence of noise, geometrical distortions of objects, occlusion, and the influence of several light sources are some issues that make object recognition a complex task. These issues modify the appearance of an object of interest with respect an observation point. Due to this problem, we analyze the physical phenomena implied in the visualization of the geometrical distortions and the interaction of light of 3D objects. To solve target recognition of an object in a scene we use a correlation filtering method. Correlation filtering possesses an accurate performance, however for a 3D object recognition approach becomes expensive to compute. The current proposal focuses on improving the algorithm execution using a combination of data parallelism and task parallelism taking advantage of a CPU/GPU

architecture. Computer simulations results are obtained in order to evaluate the performance of the proposed system in terms on recognition accuracy, computational efficiency and tolerance to illumination.

9598-32, Session 7

Robust modulation formats recognition technique using wavelet transform for high speed optical networks

Latifa Guesmi, Abir Hraghi, Mourad Menif, SUP'COM (Tunisia)

The rapid growth of capacity demand on wavelength division multiplexing (WDM) system and orthogonal frequency division multiplexing (OFDM) has caused considerable interest in alternative multi-carrier modulation format that can increase the capacity of communication system. Moreover, high speed optical networks are nowadays becoming more heterogeneous, supporting a plethora of services with different modulation formats. Therefore, in recent years, to enable a real-time information about the signal modulation format and discuss the pattern recognition approach, much interest by academic and military research institutes has focused around the research and development of modulation format recognition (MFR) algorithms.

In this paper, we present a new achievement of MFR technique, where we propose the use of wavelet transform and statistical parameters of the detected signal in conjunction with the artificial neural network (ANN) algorithm at high bit rates using direct detection and coherent detection.

In order to investigate the validity of the proposed technique for a no prior knowledge of the transmitted signal, numerical simulation have been performed for four optical modulation schemes namely NRZ-OOK as a single-carrier format, DC-PDM-QPSK, OFDM DP-16QAM, and WDM Nyquist NRZ-DP-QPSK as a multi-carrier formats at high data rate.

The proposed technique is shown to be capable of recognizing the modulation scheme with high accuracy under different transmission impairments such as chromatic dispersion (CD), differential group delay (DGD) and accumulated Amplified Spontaneous Emission (ASE). This technique allows us the estimation of the optical signal to-noise ratio (OSNR) in the range of 10-30 dB, chromatic dispersion (CD) in the range of 0-15 ps.

The results of numerical simulation demonstrate successful recognition of all modulation formats from a known bit rates with a higher estimation accuracy.

9598-33, Session 7

Real-time image dehazing using local adaptive neighborhoods and darkchannel-prior

Jesus A. Valderrama, Víctor H. Díaz-Ramírez, Ctr. de Investigación y Desarrollo de Tecnología Digital (Mexico); Enrique Hernandez, Ctr. de Investigación Científica y de Educación Superior de Ensenada (Mexico); Vitaly Kober, Ctr. de Investigación Científica y de Educación Superior de Ensenada B.C. (Mexico)

A real-time algorithm for single image dehazing is presented. The algorithm is based on calculation of local neighborhoods of a hazed image inside a moving window. Next the dark-channel-prior is applied to local neighborhoods to estimate the scene

transmission without any refining algorithm. To achieve high-rate signal processing the algorithm is implemented in parallel on a graphics processing unit (GPU). Computer simulation results are carried out to test the performance of the algorithm in terms of dehazing e?ciency and speed of processing. These results are analyzed and compared with those obtained with existing dehazing algorithms.



9598-34, Session 7

Development of a polarimetric experimental setup for surface profiling based on a microscopy application

Alejandra Serrano Trujillo, Univ Autónoma de Baja California (Mexico); Adriana Nava, Univ. Autónoma de Baja California (Mexico); Victor Ruiz-Cortes, Ctr. de Investigación Científica y de Educación Superior de Ensenada B.C. (Mexico)

The experimental setups for recovering an object's surface according to the polarimetric and fringe projection approaches are implemented. Both experiments are carried under the use of coherent light and over a reference testing piece. Fringe projection images are processed using standard phase wrapping and unwrapping routines, while an algorithm for analysis of the Stokes parameters is implemented for the polarization images. An analysis of the resulting 3D surface from both techniques is done, comparing the features that each method was able to detect, relating them to the properties of the projected light. In this contribution we deduce the characteristics required by an algorithm to deliver a detailed surface reconstruction, based on the two tested methods.

9598-35, Session PWed

High dynamic range imaging for shiny surface with single-shot raw data of the color camera

Yongkai Yin, Shandong Univ. (China) and Univ. of Wollongong (Australia); Jiangtao Xi, Univ. of Wollongong (Australia); Zewei Cai, Shenzhen Univ. (China); Yanguang Yu, Univ. of Wollongong (Australia); Xiang Peng, Shenzhen Univ. (China)

Fringe projection profilometry (FPP) has been widely applied in many industrial sectors in recent years, such as reverse engineering, product design and garment industry and so on so forth. Although traditional FPP performs well to ordinary diffuse surface of objects, it still remains a challenging issue to get satisfied results in terms of 3D imaging for shiny surface, e.g. the surface of metal and porcelain. The difficulty mainly arises from the wide variation of surface reflectivity, which results in the high dynamic range of the deformed fringe image reflected form the surface. Therefore, FPP for shiny surfaces usually needs high dynamic range imaging (HDRI) technique. Existing HDRI for shiny surface focuses on the approach of multiple exposures, leading to an unavoidable extra time expense. To overcome this disadvantage, HDRI with single-shot raw data of the color camera is presented in this paper. A fringe pattern is projected based on monochromatic illumination and the deformed fringe image is captured in single-shot fashion using a color camera. From the single-shot raw data, three monochrome images corresponding to R, G and B channels can be separated respectively. The three images have different intensity attenuation because the guantum efficiency of R, G and B channels are guite different for specific wavelength. After the attenuation ratios corresponding to R, G and B channels are calibrated, a higher dynamic range image can be synthesized with the three images. Experiments demonstrate the validity of proposed method for shiny surface.

9598-36, Session PWed

Automated counting of morphologically normal red blood cells by using digital holographic microscopy and statistical methods

Inkyu Moon, Faliu Yi, Chosun Univ. (Korea, Republic of)

The fully automated morphologically normal red blood cells (RBCs) counting method can be helpful in computer-aided-diagnosis and beneficial to the medical doctor for effectively analyzing the RBCs relevant disease. In this paper we overview an automated approach to count morphologically normal RBCs with the three-dimensional morphological and biophysical parameters of mature RBCs such as projected surface area, average phase value, mean corpuscular hemoglobin (MCH), perimeter, MCH surface density (MCHSD), circularity, mean phase of center part, sphericity coefficient, elongation, and pallor. The fully automated RBCs counting method is based on the integration of digital holographic microscopic imaging system and multivariate statistical method. This technique can be easily extended to the classification of different kinds of cells representing a promising diagnosis tool.

9598-37, Session PWed

3D face recognition based on matching of facial surfaces

Beatriz A. Echeagaray Patrón, Vitaly Kober, Ctr. de Investigación Científica y de Educación Superior de Ensenada B.C. (Mexico)

Face Recognition is a problem that has remained relevant in pattern recognition and computer vision in recent years due to its wide range of applications such as access control, surveillance, human-computer interaction and biometric identification systems. Despite the variety of techniques that have been developed, the problem remains open: accurate and robust face recognition still offers a number of challenges, especially under unconstrained environments. This work introduces a method for 3D face recognition in presence of facial expression, pose and illumination variations. The proposed approach uses 3D shape data without color or texture information. Before face recognition techniques are applied, the surfaces are standardized and aligned. Next step is extraction from face regions which are almost expression-invariant. Finally, a new matching algorithm based on conformal and isometric mapping of original facial surfaces onto a Riemannian manifold followed by a comparison of conformal and isometric invariants computed in the manifold is proposed. This approach preserves angles and geodesic distances in the original face surface while simplifies the correspondence problem in 3D. Experimental results are presented using common 3D face databases that contain significant amount of expression and pose variations.

9598-38, Session PWed

Illumination-invariant hand gesture recognition

América I. Mendoza-Morales, CICESE (Mexico); Daniel Miramontes-Jaramillo, Vitaly Kober, Ctr. de Investigación Científica y de Educación Superior de Ensenada B.C. (Mexico)

In recent years, human-computer interaction (HCI) has received increased interest in industry and science because it provides new ways to interact with a wide variety of devices through voice, body, and facial/hand gestures. Applications range from accessibility to entertainment. Hand gesture recognition is a particularly interesting problem because the shape and dynamic of hands are complex and flexible to codify many different signs. In this work we propose a three step algorithm: first, detection of hands in the current frame is carried out; second, hand tracking across the video sequence is performed; finally, robust recognition of gestures across subsequent frames is made. Recognition rate highly depends on nonuniform illumination of the scene and occlusion of hands. In order to overcome these issues we use two Microsoft Kinect devices utilizing combined information from RGB and infrared sensors. The algorithm performance is tested in terms of recognition rate and processing time. Finally, our algorithm is compared with other state-of-the-art hand gesture recognition algorithms.



9598-39, Session PWed

Research on the high-precision noncontact optical detection technology for banknotes

Xiaofeng Jin, Shanghai Institute of Optics and Fine Mechanics (China); Tiancai Liang, Pengfeng Luo, GRG Banking Equipment Co., Ltd. (China); Jianfeng Sun, Shanghai Institute of Optics and Fine Mechanics (China)

The technology of high-precision laser interferometry was introduced for optical measurement of the banknotes in this paper. Taking advantage of laser short wavelength and high sensitivity, information of adhesive tape and cavity about the banknotes could be checked efficiently. Compared with current measurement devices, including mechanical wheel measurement device, Infrared measurement device, ultrasonic measurement device, the laser interferometry measurement has higher precision and reliability. This will improve the ability of banknotes feature information in financial electronic equipment.

9598-40, Session PWed

The research of measurements mode of optical spectra by spectral device based on acousto-optic tunable filter

Georgy Korol, Saint- Petersburg State Univ. of Aerospace Instrumentation (Russian Federation)

Optical spectral device, based on acousto-optic tunable filter (AOTF), is very promising to spectral analysis problems solving, where analyzed optical radiation is very narrow-band emission approximate to monochromatic. Spectral analysis problem is the optical harmonics resolution and their levels measuring. With particular interest is spectrum spread function width of the spectral device, which determines its resolution. The formula, describing the spectrum spread function of the spectral device based AOTF, was obtained previously (Proc. of SPIE Vol. 9216 92161F-1-11). This spectrum spread function is expressed in terms of Fresnel integrals and contains complex depending on the following parameters: average frequency and rate of change of frequency control of electrical oscillations, the deviation of frequency of the optical radiation from the average mean of band of analyzed frequencies. These parameters determine the form of spectrum spread function depending on the mode analysis of the optical spectrums. The purpose of this paper is broad mathematical modeling of the spectrum spread function of spectral device on the basis of AOTF in various modes of analysis to solve the problem of optimizing the process of spectral measurements.

9598-41, Session PWed

Objects tracking with adaptive correlation filters and Kalman filtering

Sergio E. Ontiveros Gallardo, Vitaly Kober, Ctr. de Investigación Científica y de Educación Superior de Ensenada B.C. (Mexico)

Object tracking is commonly used for applications such as video surveillance, motion based recognition, and vehicle navigation. In this work, a tracking system using adaptive correlation filters and robust Kalman's prediction of target locations is proposed. Tracking is performed by means of multiple object detections in reduced frame areas. A bank of filters is designed from multiple views of a target using synthetic discriminant functions. An adaptive algorithm is used to improve discrimination capability of the synthesized filters. The bank of filters allows adapting the filters to multiple types of backgrounds. The number of filters in the bank can be controlled to guarantee a prescribed tracking accuracy. With the help of computer simulation the performance of the proposed algorithm is evaluated and compared with that of state-of-art algorithms in terms of detection efficiency and accuracy of object tracking.

9598-42, Session PWed

Optical image encryption based on phasetruncated Fresnel diffraction

Chenggong Zhang, Wenqi He, Xiang Peng, Dajiang Lu, Shenzhen Univ. (China)

A novel optical cryptosystem based on phase-truncated Fresnel diffraction (PTFD) and transport of intensity equation (TIE) is proposed. By using of the phase truncation technique, a phase-encoded plaintext could be encrypted into a real-valued noise-like intensity distribution by employing a random amplitude mask (RAM) and a random phase mask (RPM), which are regarded as two secret keys. For decryption, a generalized amplitude-phase retrieval (GAPR) algorithm combined with the TIE method are adopted to obtain the plaintext with the help of two keys. Different from the current phase-truncated-based optical cryptosystems which need record the truncated phase as decryption keys, our scheme have no need of the truncated phase because of the introducing of the TIE method. Moreover, the proposed scheme is expected to against existing attacks. A set of numerical simulation results show the feasibility and security of the proposed method.

9598-43, Session PWed

Optical hierarchical identity authentication based on hash function and moiré effect of nonlinear gratings

Meihua Liao, Wenqi He, Dajiang Lu, Jiachen Wu, Xiang Peng, Shenzhen Univ. (China)

A new optical identity authentication scheme based on the phase modulation of moiré effect in the phase-space optics is proposed. The information of standard authentication image can be hidden into the phase function of two gratings by using of the phase modulation of optical moiré effect. One of the gratings settled into the authentication system is designed as the "Authentication lock", and the other will be held by a legal user. The authentication procedure is performed by optical setup. The evaluation of the identity authentication relies on the correlation coefficient between moiré pattern of the two designed gratings superposition and the standard authentication image. Theoretical analysis and simulation experiments are both provided to verify the feasibility and effectiveness of the proposed scheme.

9598-44, Session PWed

Evolution of optical pulses in the optical fiber as basis of spectral devices

Ilya ?. Osmakov, Oleg D. Moskaletz, Saint- Petersburg State Univ. of Aerospace Instrumentation (Russian Federation)

Optical pulse evolution in the form cutting monochromatic optical radiation at it's propagation in optical fiber as dispersive system is considered. Ratio between the duration of the input pulse, and differential group delay in a dispersive system which provides that distorted form of the input pulse which is proportional to its spectrum is determined. This result defines a complex spectrum spread function of the optical device. That complex spectrum spread function is its exhaustive characteristic of spectral device. Complex spectrum spread function is the kernel of the integral operator witch sets the ratio of the input-output spectral device for complex spectra. In the process of researching the evolution the deviation of pulse distortion of the spread function from the ideal spectral device performing the Fourier transform of the segment monochromatic oscillations is investigated.

Conference 9598: Optics and Photonics for Information Processing IX



Analysis method using a single segment of optical fiber provides a spectrum non-real-time, which leads to loss of information about the analyzed optical radiation. For this loss information excluding the question of multi-channel fiber-optic system to measure the optical spectrum for a long period of time by forming a sequence of short optical pulses is considered. The optical fiber must have a different length.

Result of the measurement in the optical range is power spectrum of optical radiation. To obtain an estimate of the power spectrum of optical radiation in each optical fiber channel, which is part of the spectral device, photodetection is applied. After then the total sum from photodections results is preformed.

9598-45, Session PWed

Influence of lens system aperture on optical information processing

Sergey N. Mosentsov, Vasily Kazakov, Oleg D. Moskaletz, Saint- Petersburg State Univ. of Aerospace Instrumentation (Russian Federation)

Any optical information system is characterized by sizes of input aperture, lengths of free space layers and the lens system apertures.

In terms of constructions, an important issue is relationship between the sizes of input aperture and the lens system aperture.

Simple optical system is considered, which including:

- input aperture of finite size, on which supplied optical signal;

- free space layer, described by Fresnel's diffraction;

- lens system with own finite aperture, larger than the size of input aperture.

This simple optical system is considered as element of more complex optical information systems.

Known mathematical analysis of optical systems suggests that the lenses system has infinite size. But, the real construction of any optical system suggests the presence of a lens system with finite size aperture. This results to occurrence of errors, affecting on further processing diffractive optical field. Assessment of error based on the analysis of piece of optical radiation, which partially extends beyond the lens system.

Transmission of optical radiation through finite aperture of the lens systems expressed in form the Fresnel's integrals. Mathematical modeling of such a system is based on the Fresnel integrals expansion in asymptotic series with large values of the argument. Results of the calculation are to definition the minimum size of the lens aperture, considering the allowable loss of optical radiation due to the finite size of the aperture.

9598-46, Session PWed

Correlation measurements in optical range

Aleksey Orlov, Oleg D. Moskaletz, Saint-Petersburg State Univ. of Aerospace Instrumentation (Russian Federation); Dmitry O. Moskaletz, Saint Petersburg Electrotechnical Univ. "LETI" (Russian Federation)

Three variants of the possible implementation of the measurement time correlation functions of optical radiation:

- multichannel correlation measurements of optical radiation with delay lines in the optical fiber cuts form (optical correlator analogue RF) ;

- refined consideration of correlator of optical radiation in the form of a Michelson's interferometer;

- correlation measurement of optical radiation on the basis of the analysis of instantaneous complex spectra.

Mathematical basis for calculating of correlation functions of pulsed optical radiation on the basis of an analysis of its instantaneous complex spectrum is given. The proposed mathematical apparatus is based on the theorem of Wiener - Paley and the theory of integral operators with reproducing kernels.

Algorithm for computing of correlation functions of pulsed optical radiation is based on the basis of calculating the instantaneous complex spectrum of optical radiation. These instantaneous spectra can be obtained using diffractive optical spectral devices. New definition of the instantaneous spectrum is given into account the specifics of measuring diffraction spectral devices.

This algorithm is implemented in the system including two complex spectrum analyzers, the adder, the squaring unit, the spatial integrator.

The estimation of advantages and disadvantages for each option of possible implementation of measurements time correlation functions of optical radiation is discussed. Method of calculating the correlation function on the basis of analysis of instantaneous spectra is especially important in the context of intense development of physics and technology of femtosecond pulses.

9598-47, Session PWed

Power spectrum estimation of optical radiation by multichannel resonant spectral device

Artur Paraskun, Oleg D. Moskaletz, Saint-Petersburg State Univ. of Aerospace Instrumentation (Russian Federation)

The estimating problem of power spectrum in optical range via new type of optical spectral device constructed on the basis of resonance phenomenon in narrow-band interference filters which performs parallel analysis of the optical spectrum is solved.

Such device is based on phenomenon resonance in narrowband interference filters.

Spectral decomposition of the optical radiation is performed by multichannel resonant optical system. That device includes forming optics, fiber-optic beam; optical system of narrowband interference filters, each filter is connected in series with the photodetector.

One of main aspects from statistical measurement is power spectrum assessment of stationary random processes. Optical radiation is the one such process. Therefore, main attention is given to photodetection and properties of power spectrum resulting estimates.

However, since all channels spectral device are identical, the process for estimation of power spectrum is considered in one channel. Two detection modes of photodetection operations are considered.

The equivalent circuit of the first mode includes a quadratic photodetector and integrator completed by system of integration result reset. It has been established that the thus obtained evaluation is good. In the case of the second mode equivalent circuit includes quadratic photodetector and lowpass filter. Thus, this system operates in continuously mode evaluating of power spectrum.

The comparison of photodetection on two modes is completed.

9598-48, Session PWed

The conception and implementation of a local HDR fusion algorithm depending on contrast and luminosity parameters

Amine Besrour, SUP'COM (Tunisia) and Univ. de Technologie Troyes (France); Fatma Abdelkefi, Mohamed Siala, SUP'COM (Tunisia); Hichem Snoussi, Univ. de Technologie Troyes (France)

Nowadays, the high dynamic range (HDR) imaging represents the subject of the most researches. The major problem lies in the implementation of the best algorithm to acquire the best video quality. In fact, the major constraint is manifested in the need to implement a fusion algorithm fast enough to meet the rapid movement of video frames. The implemented merging algorithms were not quick enough to reconstitute the HDR video. In this paper, we detail each of the previous existed works before detailing



our algorithm and presenting results from the acquired HDR images, tone mapped with various techniques. This algorithm represents a more enhanced and faster solution than the existing ones. In fact, it has the ability to calculate the saturation matrix representing the saturation rate of the neighboring pixels. The computed coefficients are affected respectively to each picture from the tested ones. This analyze provides faster and more efficient results in terms of quality and brightness. The originality of our work remains on its processing method including the pixels saturation in the totality of the captured pictures and their combination in order to obtain the best pictures illustrating all the possible details. These parameters are computed for each zone depending on the contrast and the luminosity of the current pixel and its neighboring. The final HDR image's coefficients are calculated dynamically ensuring the best image quality equilibrating the brightness and contrast values and making the perfect final image.

9598-49, Session PWed

Study of the index matching for different photopolymers

Roberto Fernández, Sergi Gallego, Univ. de Alicante (Spain); Andrés Márquez, Univ de Alicante (Spain); manuel Ortuño, Stephan Marini, Inmaculada Pascual, Augusto Beléndez, Univ. de Alicante (Spain)

Photopolymers enable modulation of the electrical permittivity and thickness, are self processing, layers with a wide range of thicknesses and properties can be fabricated on demand. Various index matching components have introduced and analyzed to improve the characterization and the conservation of different photopolymers with polyvinyl alcohol (PVA) as a binder and different main monomer, one have acrylamide and the second one sodium acrylate. We have recorded very low diffractive optical elements and we have studied their conservation.

9598-50, Session PWed

Correlations filters used for object recognition and tracking in UAV's applications

Francisco Javier Ramirez-Arias, Univ. Autónoma de Baja California (Mexico); Víctor H. Díaz-Ramírez, Ctr. de Investigación y Desarrollo de Tecnología Digital (Mexico); Antonio Gomez Roa, Univ. Autónoma de Baja California (Mexico)

One of the most attended problems within unmanned aerial vehicles is the optimization of the control system module to operate under different environments. Coupled with this human perception and the operator skills play an important role to perform tasks of specific purpose those are assigned to these vehicles. The trend in these applications is the recognition and tracking objects are offline due to computational cost off this algorithms and the limited resources in these vehicles, therefore develop algorithms that are optimal from a computational point of view is important. The correlation filters are considered a viable option for use in unmanned aerial vehicles for their results presented in applications for recognition and tracking of objects when the opto-electronic sensor is fixed and the computational cost is optimal, because these algorithms are based on the fast Fourier transform. In this work the opto-electronic sensor is in the unmanned aerial vehicle therefore it is considered dynamic. Evaluate the performance of correlation filters for tracking and object recognition becomes important due to applications that can be derived from the used of these filters. Besides the recognition and tracking of objects is desirable to develop efficient algorithms for implementing these with good response time to be implemented on computers that are on board of the unmanned aerial vehicles. Basically, we are interested in developing new techniques for digital image processing, while performing practical implementations of these techniques.

9598-51, Session PWed

Numerical analysis of holographic tomography with different reconstruction algorithms in the presence of noise

Andrey V. Belashov, National Research Univ. of Information Technologies, Mechanics and Optics (Russian Federation) and Ioffe Physical-Technical Institute (Russian Federation); Nikolay V. Petrov, National Research Univ. of Information Technologies, Mechanics and Optics (Russian Federation); Irina V. Semenova, Ioffe Physical-Technical Institute (Russian Federation); Igor A. Shevkunov, National Research Univ. of Information Technologies, Mechanics and Optics (Russian Federation)

Due to the rapid progress in computer technologies and development of digital cameras digital methods of hologram processing become an important instrument for investigations of physical objects and phenomena. Digital holography allows one to reconstruct a wave front of a light beam interacted with an object under study. If the object is transparent one can detect an integral phase shift gained by the light passed through it. An interpretation of the acquired information in the case of complex objects, such as for instance biological tissues, can be difficult, since it is hard to understand to what extent each domain inside the object shifts the phase of the wave front. One can however extract the necessary data from a set of phase images recorded at various angles to the object. We analyze the performance of holographic tomography technique depending upon the number of digital holograms and sampling degree. The procedure is as follows. First we simulated a process of hologram recording from different positions in a presence of noise. Then a set of integral phase shift images were obtained from these holograms using different reconstruction algorithms. Afterwards a spatial distribution of refractive index variations has been obtained using the inverse radon transformation.

9598-52, Session PWed

Alignment mask design and image processing for the Advanced Radiographic Capability (ARC) at the National Ignition Facility

Richard R. Leach Jr., Abdul A. S. Awwal, Simon J. Cohen, Roger R. Lowe-Webb, Randy S. Roberts, Joseph T. Salmon, David A. Smauley, Karl Wilhelmsen, Lawrence Livermore National Lab. (United States)

The Advance Radiographic Capability (ARC) at the National Ignition Facility (NIF) is a laser system that employs up to four petawatt (PW) lasers to produce a sequence of short pulses that generate X-rays which backlight high-density inertial confinement fusion (ICF) targets. ARC is designed to produce multiple, sequential X-ray images by using up to eight backlighters. The images will be used to examine the compression and ignition of a cryogenic deuterium-tritium target with tens-of-picosecond temporal resolution during the critical phases of an ICF shot. Multi-frame, hard-X-ray radiography of imploding NIF capsules is a capability which is critical to the success of NIF's missions. As in the NIF system, ARC requires an optical alignment mask that can be inserted and removed as needed for precise positioning of the beam. Due to ARC's split beam design, inserting the nominal NIF main laser alignment mask in ARC produced a partial blockage of the mask pattern. Requirements for a new mask design were needed. In this paper we describe the ARC mask requirements, the resulting mask design pattern, and the image analysis algorithms used to detect and identify the beam and reference centers required for ARC alignment.



9598-53, Session PWed

Object recognition via MINACE filter trained on synthetic 3D model

Dmitry V. Shaulskiy, Maxim V. Konstantinov, Rostislav S. Starikov, National Research Nuclear Univ. MEPhI (Russian Federation)

Paper presents study results of MINACE filter implementation to recognition problem of object subjected to out-of-plane rotation distortion and captured as raster image. Filter training conducted by images acquired from synthetic 3D object model. Dependence of recognition results from 3D model illumination type is showen.

9598-54, Session PWed

High-speed and large accepted incidence area for a self-pumped phase conjugate mirror

Che-Chu Lin, Yeh-Wei Yu, Ching-Cherng Sun, National Central Univ. (Taiwan)

In this Letter, a study for the incidence geometry to extend the accepted incidence position is presented and demonstrated. High-guality selfpumped phase conjugate mirror (SPPCM) can be formed with a counterdirection incidence with respect to the master light for the Cat-SPPCM. The study starts from changing the incidence position from the other in-plane three faces. The incident direction along the c axis or in the reverse direction cannot form the Kitty-SPPCM effectively. The situation depends on the coupling strength of the grating for the four-wave mixing across the fanning loops. When the incident light is sent into the crystal in the counter direction of the master light, effective Kitty-SPPCM can be observed. According to the forming of the Kitty-SPPCM, the position acceptance can be divided into three regions. In such a matter, we can find that the incidence on the other face rather than the usual Kitty-SPPCM can generate three different SPPCMs, where the first is a counter-direction Kitty-SPPCM, the second is the high-pass Kitty-SPPCM and the third is similar to Bridge-SPPCM. The discovery of these three SPPCMs is helpful to apply the SPPCM in various applications.

9598-55, Session PWed

Simultaneous transmission of accurate time and stable frequency through bidirectional channel over telecommunication infrastructure with excessive spans

Josef Vojtěch, Vladimir Smotlacha, CESNET z.s.p.o. (Czech Republic)

Very accurate time or timing is essential for broad range of fields, e.g. sensing, metrology, navigation, geodesy, radio-astronomy, seismology, fundamental physics, etc. The optical time transfer undergoes increased interest in recent years. It eliminates usage of antennas in case of global navigation satellite systems (e.g. GPS). Furthermore, it delivers accuracy in the order of tens of picosecond compared with both IEEE 1588 and satellite systems. Typical challenge of long haul accurate time of frequency transfer over fiber is single bidirectional optical path including optical amplifiers in order to achieve the best available accuracy. The main obstacle of this bidirectional lies in missing optical isolators, widely used in data communications to avoid propagation of back-scattering and reflections. Majority of accurate time transfer projects aim at decreasing of reflection as much as possible and operate bidirectional optical amplifiers in low gain mode to avoid line lase. Demand of low gain determines fiber spans with excessive attenuation must be split into the more spans with lower

attenuation. We establish simultaneous transmission of accurate time and stable frequency over of 310 km (192 mi) long path with two excessive segments of attenuation over 28 dB. This paper will describe results including path stability and operational issues of services over such path.

SPIE. PHOTONICS Conference 9599: Applications of Digital Image Processing XXXVIII

Monday - Thursday 10-13 August 2015 Part of Proceedings of SPIE Vol. 9599 Applications of Digital Image Processing XXXVIII

9599-1, Session 1

Sparse reconstruction of compressed sensing multispectral data using a crossspectral multilayered conditional random field model

Edward Li, Mohammad Javad Shafiee, Farnoud Kazemzadeh, Alexander Wong, Univ. of Waterloo (Canada)

The broadband spectrum contains more information than what the human eye can detect. Spectral information from different wavelengths can provide unique information about the intrinsic properties of an object. Recently, compressed sensing imaging systems with low acquisition time have been introduced. These systems capture a sparse, under-sampled, set of measurements which is sufficiently representative of the target being observed. To utilize compressed sensing strategies, strong reconstruction algorithms that can reconstruct a complete signal from sparse observations are required. This work proposes a Cross-Spectral Multilayered Conditional Random Field (CS-MCRF) approach for sparse reconstruction of multispectral compressive sensing data in multispectral vision and imaging systems. The CS-MCRF will use information between neighboring spectral bands to better utilize available information for a more robust reconstruction of each independent spectral band image. This method was evaluated using simulated compressed sensing multispectral acquisitions. Results show improvement over existing techniques in preserving spectral fidelity while effectively inferring missing information from sparsely available observations. The availability of such reconstruction algorithms will enable fast acquisition of multispectral data with reduced imaging hardware cost and complexity.

9599-2, Session 1

Optical character recognition of cameracaptured images based on phase features

Julia Diaz, Vitaly Kober, Ctr. de Investigación Científica y de Educación Superior de Ensenada B.C. (Mexico)

Nowadays most of digital information is obtained using mobile devices specially smartphones. In particular, it brings the opportunity for character recognition (OCR) in camera-captured images. For this reason many recognition applications have been recently developed, for example: license plates, business cards, receipts and street signal recognition; document classification; augmented reality; language translator; etc. But also new challenges are appeared. Camera-captured images are usually affected by geometric distortions, nonuniform illumination, shadows, noise, etc., which make difficult the recognition task of existing systems. It is well known that the Fourier phase contains a lot of important information regardless of Fourier intensities. So, in this work we propose to use a phase-based recognition system. First we use a pre-processing stage to remove sensors noise and to align the text. Then we use phase-congruency features to provide illumination/scale invariance. The algorithm performance is tested in terms of miss classifications and false alarms. Finally, computer simulation results obtained with the proposed system are presented and discussed.

9599-3, Session 1

Performance evaluation of correlation filters for target tracking

Leopoldo N. Gaxiola, Víctor H. Díaz-Ramírez, Juan Jose Tapia Armenta, Ctr. de Investigación y Desarrollo de Tecnología Digital (Mexico); Pascuala García-Martínez,

Univ. de València (Spain); Andres Cuevas, CITEDI-IPN (Mexico)

OPTICAL ENGINEERING+

APPLICATIONS

The use of correlation filters for target tracking has increased in recent years. This is because these filters can estimate with high accuracy the position of a moving target in noisy scenes. Additionally, correlation filters are robust to noise and yield low computational complexity. In this work, we present a performance evaluation of several state-of-the-art correlation filters within the context of target tracking. The filters are tested using an introduced algorithm that is adapted online using information of current and past scene frames of the scene. The suggested algorithm achieves a high-rate operation by focusing signal processing only on a small fragment of every frame. For performance evaluation, the algorithm is tested in several video test sequences that contain geometric modifications of the target, partial occlusions and clutter. The performance of the tested filters is presented and discussed in terms of detection efficiency, tracking accuracy, and computational complexity. The results obtained with the suggested algorithm based on correlation filtering are discussed compared with those obtained with existing state-of-the-art target tracking algorithms in terms of objective metrics.

9599-4, Session 1

Shearlet-based edge detection: flame fronts and tidal flats

Emily J. King, Rafael Reisenhofer, Univ. Bremen (Germany)

Shearlets are wavelet-like systems which are better suited for handling geometric features in multi-dimensional data than traditional wavelets. A novel method for edge detection which is in the spirit of phase congruency but is based on a complex shearlet transform will be presented. This approach to edge detection yields an approximate tangent direction of detected edges as a byproduct of the edge measure computation.

Two applications of the edge detection method will be discussed. First, the tracking and classification of flame fronts is a critical component of research in technical thermodynamics. Quite often, the flame fronts are transient or weak and the images are noisy. The standard methods used in the field for the detection of flame fronts do not handle such data well. Fortunately, using the shearlet-based edge measure yields dramatically better results.

Second, the Wadden tidal flats are a biodiverse region along the North Sea coast. One approach to surveying the delicate region and tracking the topographical changes is to use pre-existing Synthetic Aperture Radar (SAR) images. Unfortunately, SAR data suffers from multiplicative noise as well as sensitivity to environmental factors. The first large-scale mapping project of that type showed good results but only with a tremendous amount of manual interaction because there are many edges in the data which are not boundaries of the tidal flats but are edges of features like fields or islands. A method using a combination of the shearlet-based edge measure with a diffusion-based image segmentation will be presented.

9599-5, Session 1

The impact of privacy protection filters on deep learning-based gender recognition by machines and crowdsourced evaluation by humans

Pavel Korshunov, Ecole Polytechnique Fédérale de Lausanne (Switzerland); Natacha Rachaud, EURECOM (France); Anne-Flore Perrin, Ecole Polytechnique Fédérale de Lausanne (Switzerland); Grigory Antipov, Jean-Luc Dugelay, EURECOM (France); Touradj Ebrahimi, Ecole Polytechnique Fédérale de Lausanne (Switzerland)



Deep learning-based algorithms are becoming increasingly efficient in recognition and detection tasks, especially when using large-scale datasets. Such recent success has led to a speculation that deep learning methods are comparable or even outperform human visual system in its ability to detect and recognize objects and their features. In this paper, we focus on the task of gender recognition in images when they have been processed by privacy protection filters (e.g., blurring, masking, pixelization) applied at different strengths. Assuming a privacy protection scenario, we compare the performance of state of the art deep learning algorithms with a subjective evaluation obtained via a crowdsourcing evaluation to understand how privacy protection filters affect both computer vision and human vision.

9599-6, Session 1

Detection of smoke plume for a landbased early forest fire detection system

John A. Saghri, California Polytechnic State Univ., San Luis Obispo (United States); John T. Jacobs, Timothy M. Davenport, Raytheon Space and Airborne Systems (United States); David Garges, California Polytechnic State Univ., San Luis Obispo (United States)

This paper examines several processing schemes to detect early forest fire via a 24/7 monitoring infrared and visible video data. Both the temporal and the spectral signatures of fire and smoke plume are exploited. The methods include principle component transformation and clustering of the spectral and temporal imagery data. The methods are compared based on video data from several staged test forest fries. It is shown that the resulting difference images can be effectively exploited to detect and classify heat plumes which are expelled at the early stages of the forest fire.

9599-7, Session 1

Localization of tumors using edge detectors

Felipe Lopez-Velez, Univ. EAFIT (Colombia)

The edge of an image is a set of points organized in a curved line, where in each of these points the brightness of the image changes abruptly, or has discontinuities, in order to find these edges there will be four different mathematical methods to be used and later on compared with its peers, this is with the aim of finding which of the methods is the one that can find the edges of any given image.

In this paper these four methods will be used for medical purposes in order to find which one is capable of finding the edges of a scanned image more accurately than the others.

The problem consists in analyzing the following two biomedical images. One of them represents a brain tumor and the other one a liver tumor.

These images will be analyzed with the help of the four methods described and the the results will be compared in order to determine the best method to be used.

It was decide to use different algorithms of edges detection in order to obtain the results shown below; Bessel algorithm, Morse algorithm, Hermite algorithm, Weibull algorithm and Sobel algorithm.

After analyzing the appliance of each of the methods to both images it impossible to determine that in each case the better method changed, i.e., for the brain tumor image it can be noticed that the Morse method was the best at finding the edges of the image but for the liver tumor image it was the Hermite method.

Making further observations it is found that Hermite and Morse have for these two cases the lowest standard deviations, concluding that these two are the most accurate method to find the edges in analysis of biomedical images.

9599-8, Session 1

Inpaiting using Airy diffusion

Sara Lourduy-Hernandez, Univ. EAFIT (Colombia)

One inpainting procedure based on Airy diffusion is proposed, implemented via Maple and applied to some digital images. Airy diffusion is a partial differential equation with spatial derivatives of third order in contrast with the usual diffusion with spatial derivatives of second order. Airy diffusion generates the Airy semigroup in terms of the Airy functions which can be rewritten in terms of Bessel functions. The Airy diffusion can be used to smooth an image with the corresponding noise elimination via convolution. Also the Airy diffusion can be used to erase objects from an image. We build an algorithm using the Maple package ImageTools and such algorithm is tested using some images. Our results using Airy diffusion are compared with the similar results using standard diffusion. We observe that Airy diffusion generates powerful filters for image processing which could be incorporated in the usual packages for image processing such as ImageJ and photoshop. Also is interesting to consider the possibility to incorporate the Airy filters as applications for smartphones and smart-glasses.

9599-10, Session 2

Performance and complexity of color gamut scalable coding

Yuwen He, Yan Ye, Xiaoyu Xiu, InterDigital, Inc. (United States)

Wide color gamut such as BT.2020 allows pictures to be rendered with sharper details and more vivid colors. It is considered an essential video parameter for next generation content generation, and has drawn significant commercial interests recently. As the upgrading cycle of content production work flow and consumer displays takes place, current generation and next generation video content are expected to co-exist. Thus, maintaining backward compatibility becomes an important consideration for efficient content delivery systems. The Scalable Extension of HEVC (SHVC) was recently finalized in the second version of the HEVC specifications. SHVC provides a color mapping tool to improve scalable coding efficiency when the base layer and the enhancement layer video signals are in different color spaces. The SHVC color mapping tool uses a 3D Look-Up Table (3D LUT) based cross-color linear model to efficiently convert the video in base layer color space into enhancement layer color space. Due to complexity concerns, certain limitations, including limiting the maximum 3D LUT size to 8x2x2, were applied to the color mapping process in SHVC. In this paper, we investigate the complexity and performance trade-off of the 3D LUT based color mapping process. Specifically, we explore the performance benefits of enlarging the size of the 3D LUT. In order to reduce computational complexity, we use a simplified cross-color linear model within each 3D LUT partition. Simulation results are provided to detail the various performance vs complexity trade-offs achievable in the proposed design.

9599-11, Session 2

Implication of high dynamic range and wide color gamut content distribution

Taoran Lu, Fangjun Pu, Peng Yin, Tao Chen, Walter J. Husak, Dolby Labs., Inc. (United States)

High Dynamic Range (HDR) and Wider Color Gamut (WCG) content represents a greater range of luminance levels and a more complete reproduction of colors found in real-world scenes. The current video distribution environments deliver Standard Dynamic Range (SDR) signal, typically created to represent a range of brightness of around 0.1 to 100 cd/m2 and a color gamut defined by BT. 709. Compared to SDR, new HDR and WCG content may cover a luminance range of 0.005 to 10000 cd/m2, and significantly wider color gamut (e.g. BT. 2020). Therefore, there might be some significant implication on today's end-to-end ecosystem from content creation to distribution and finally to consumption. One strong



candidate for HDR/WCG signal compression is the state-of-the-art video compression standard - HEVC main 10 profile, which requires the input to be in 10-bit and 4:2:0 chroma sampling format. For SDR content, the common practice is to apply compression on Y'CbCr 4:2:0 using gamma transfer function and non-constant luminance 4:2:0 chroma subsampling. For HDR and WCG content, it is desirable to examine if such signal format still works well for compression, and it is interesting to know if the overall system performance can be further improved by exploring different signal formats and processing workflows. In this paper, we will provide some of our insight into those problems. Specifically, we will focus on the compression performance using different color space containers and with various chroma resampling workflows, and present analysis on their possible implication to the overall system.

9599-12, Session 2

HEVC for high dynamic range services

Seung-Hwan Kim, Jie Zhao, Kiran M. Misra, Andrew Segall, Sharp Labs. of America, Inc. (United States)

Displays capable of showing a greater range of luminance values can render content containing high dynamic range information in a way such that the viewers have a more immersive experience. This paper considers the endto-end design and performance aspects of a high dynamic range (HDR) system. Specifically, we examine the performance of critical components in the HDR processing chain including the design of the opto-electrical transfer function, compression codec, electro-optical transfer function and the tone mapping and rendering operation of a display. We then propose a method to extend the existing high efficiency video coding (HEVC) framework to compress and render HDR video content on an HDR capable display. Additionally, the method supports the rendering of HDR video content on a display capable of showing only a lower range of luminance values; thereby allowing existing and future deployments of standard dynamic range (SDR) displays to render HDR content while preserving much of the content authors intended viewing experience. Results are presented comparing the efficiency of the current approach versus simulcast of HDR and SDR content to a display.

9599-13, Session 2

Chroma sampling and modulation techniques in high dynamic range video coding

Pankaj Topiwala, Wei Dai, Madhu Krishnan, FastVDO Inc. (United States)

High Dynamic Range (HDR) and Wide Color Gamut (WCG) video presents an interesting new challenge in media communication, and in presentation. Existing solutions for compression and communication of video, such as the ITU/H.265 | ISO/IEC High Efficiency Video Coding (HEVC) Standard, apply mainly to Standard Dynamic Range video sources, and to standard color gamuts (such as Rec. 709). In HDR/WCG, both of these dimensions are broadened, and new tools may be required to efficiently represent such data in compressed form. In this paper, we explore several novel techniques of color spaces, chroma sampling, and luminosity scaling, to compress such data efficiently. Such innovations, built on top of the existing HEVC infrastructure, can provide state of the art performance in the compression and representation of such video, while also providing valuable backwards compatibility with existing infrastructure based on the Main and Main 10 Profiles of HEVC.

9599-14, Session 2

High dynamic range and wide color gamut in HEVC Main10

Chad Fogg, MovieLabs (United States); Bill Mandel,

Universal Pictures (United States); James L. Helman, MovieLabs (United States)

In Spring of 2013, five Motion picture studios launched an industry initiative to find near-term technical solutions that deliver the High Dynamic Range (HDR) and Wide Color Gamut (WCG) aspects of Ultra High Definition (UHD) video content to end consumers. The first platform is Blu-Ray 2.0. Some over the top (OTT) services have already begun HDR services, customized to traditional gamma transfer functions that are hardwired into the display driver DAC's of traditional flat panel monitor designs. This paper describes the experiments and solutions explored during this project, and an analysis of bitstream efficiency sensitive system elements, including workflow steps far upstream from the codec, and downstream from the decoder, that interact to affect the rendered outcome. It was discovered that the system philosophy of HDR/WCG that best describes the independence of major variables are those expressed by the existing Video Usability Information (VUI) metadata dimensions present in most AVC and HEVC bitstreams. The key role of the transfer function is to map the conceptual floatingpoint linear video sensor signal into integer video with visually uniform quantization steps steps, at least in luminance, in which video encoders best traditionally work. The color space derivation from the primary signal, such as YCbCr, has also been motivated for compression efficiency. Benefits from alternative spaces, that have been found to be more ideal in human and machine vision such as La*b*, were overshadowed by desirable properties intentionally designed into the simpler color difference equations. This interacts well with the residual block transform coder's deadzone quantizer to eliminate minor, but costly noise in color prediction errors. This paper is a technical background of the short, high-level summary of the solution provided in the May 2015 IEEE CVST paper "HDR and WCG Video Coding in HEVC: Status and Potential Future Enhancements."

9599-15, Session 2

On metrics for objective and subjective evaluation of high dynamic range video

Koohyar Minoo, Zhouye Gu, David Baylon, Ajay Luthra, ARRIS Group, Inc. (United States)

In High Dynamic Range (HDR) video, it is possible to represent a wider range of intensities and contrasts compared to the current Standard Dynamic Range (SDR) video. HDR video can simultaneously preserve details in very bright and very dark areas of a scene whereas these details become lost or washed out in SDR video. Because the perceived quality due to this increased fidelity may not fit the same model of perceived quality in the SDR video, it is not clear whether the objective metrics that have been widely used and studied for SDR visual experience are reasonably accurate for HDR cases, in terms of correlation with subjective measurement for HDR video quality. This paper investigates several objective metrics (e.g. PSNR, weighted-MSE, VIF, HDR-VDP2) and their correlation to subjective quality for a variety of HDR video content. For some metrics, attention is given to the domain in which they are applied, such as color space and linear vs. nonlinear domains. Results are given for the case of HDR content compressed after using different transfer functions and quantization parameters. In addition to rating the relevance of each objective metric in terms of its correlation to the subjective measurements, comparisons are also presented to show how closely different objective metrics can predict the results obtained by subjective quality assessment in terms of coding efficiency provided by different coding tools or processes.

9599-16, Session 2

Towards high dynamic range extensions of HEVC: subjective evaluation of potential coding technologies

Philippe Hanhart, Touradj Ebrahimi, Ecole Polytechnique Federale de Lausanne (Switzerland); Martin ?e?ábek, Anne-Flore Perrin, Ecole Polytechnique Fédérale de Lausanne (Switzerland)



Since the completion of the first edition of the High Efficiency Video Coding (HEVC) standard, several key extensions of its capabilities have been developed to address the needs of an even broader range of applications. Recognizing the rise of High Dynamic Range (HDR) applications and the lack of a corresponding video coding standard, the Moving Picture Experts Group (MPEG) has released in February 2015 a Call for Evidence (CfE) for HDR and Wide Colour Gamut (WCG) video coding. The purpose of this CfE is to explore whether the coding efficiency and/or the functionality of HEVC can be significantly improved for HDR and WCG content. This paper describes the details and the results of the subjective quality evaluation performed to benchmark the potential coding technologiessubmitted in response to the CfE.

9599-17, Session 3

Digital signal processing of light in holographic 3D imaging (Invited Paper)

Kyoji Matsushima, Kansai Univ. (Japan)

Techniques in digital holography are gradually evolved over a past decade. Recently, the techniques allow us to capture wide spatial information of light and handle it as digital data that includes not only optical intensity distribution like conventional digital imaging but also phase distribution. This can be interpreted as A/D conversion of light. Recent techniques in computer holography also make it possible to generate real light from digital data. This provides D/A conversion of light. This means that the both ends of common digital processing are now available in the field of holography. In this report, we present several techniques for holographic digital signal processing of light, which is specialized for 3D imaging.

Holographic 3D imaging, however, has the problem of an enormous spaceband product. This is caused by the requirement for optical reconstruction with a wide screen and large viewing-angle. Therefore, the techniques presented include (a) capturing optical wave fields in extremely highdefinition, e.g. more than billion samplings, (b) creation of high-definition computer-generated holograms (CGH), also composed of more than billion pixels, and (c) numerical techniques for various field-propagations of this gigantic wave field, which provide basic signal processing of light.

Some of actual high-definition CGHs created by using the techniques is demonstrated for verifying the techniques. These high-definition CGHs can reconstruct impressive fine 3D images that give strong sensation of depth to viewers.

9599-18, Session 3

Compression of digital holographic data: an overview

Frederic Dufaux, Yafei Xing, Beatrice Pesquet-Popescu, Télécom ParisTech (France); Peter Schelkens, Vrije Univ. Brussel (Belgium) and iMinds (Belgium)

Existing 3D video systems based on the principle of stereoscopic vision exploit limited depth cues. In addition, the accommodation/vergence conflict is an inherent limitation of such solutions. In contrast, by fully reconstructing the object wavefront, holography offers all depth cues. It has therefore the potential to become the ultimate 3D experience. Nevertheless, in order to achieve practical working systems, major scientific and technological challenges have to be tackled.

In particular, as digital holographic data represents a huge amount of information, the development of efficient compression techniques is a key component. This problem has gain significant attention by the research community during the last 10 years. In this paper, we will review and analyze past and on-going work in the compression of digital holographic data.

9599-19, Session 3

Fast generation of complex modulation video holograms using temporal redundancy compression and hybrid pointsource/wave-field approaches

Antonin Gilles, Institut de recherche technologique B-Com (France); Patrick Gioia, Institut de recherche technologique B-Com (France) and Orange SA (France); Rémi Cozot, Institut de recherche technologique B-Com (France) and Univ. de Rennes 1 (France); Luce Morin, Institut de recherche technologique B-Com (France) and Institut National des Sciences Appliquées de Rennes (France)

Hybrid point-source/wave-field method is a newly proposed approach for Computer-Generated Hologram (CGH) calculation, based on the slicing of the scene into several depth layers parallel to the hologram plane. The complex wave scattered by each depth layer is then computed either using a wave-field or a point-source approach according to a threshold criterion on the number of points within the layer. Finally, the complex waves scattered by all the depth layers are summed up in order to obtain the final CGH.

Although outperforming both point-source and wave-field methods without producing any visible artifact, this approach has not yet been used for animated holograms, and the possible exploitation of temporal redundancies has not been studied. In this paper, we propose a fast computation of video holograms by taking into account those redundancies. Our algorithm consists of three steps. First, intensity and depth data of the current frame of the 3D video are extracted and compared with those of the previous frame in order to remove temporally redundant data. Then the CGH pattern for this compressed frame is generated using the hybrid pointsource/wave-field approach. The resulting CGH pattern is finally transmitted to the video output as well as stored in the previous frame buffer. Experimental results reveal that our proposed method is able to produce video holograms at interactive rates without producing any visible artifact.

9599-20, Session 3

Evaluation inter- and intra-channel correlations of representations for the compression of holograms

Ayyoub Ahar, David Blinder, Tim Bruylants, Colas Schretter, Adrian Munteanu, Peter Schelkens, Vrije Univ. Brussel (Belgium)

The signal properties of holograms differ considerably from natural photographs, which causes conventional image codecs to perform sub-optimally on this type of data. In this paper, we investigate how to effectively code interference patterns in the hologram domain. The complex amplitudes can be encoded using various multi-channel representations such as real-imaginary, amplitude-phase, and off-axis real-valued or multiple phase-shifted hologram recordings. The specific choice of representation significantly affects the compressibility of the signal when compressing fringes in the hologram domain. For this purpose, we analyzed both inter-and intra-channel correlations for each representation. We encode several holograms using a JPEG 2000-based image codec that supports additional wavelet packet decompositions and directional transforms. Finally, we evaluate how the various compression settings affect the quality of the hologram, both in the image as well as in the reconstruction domain.



9599-22, Session 4

The image registration of multi-band images by geometrical optics

Yung-Jhe Yan, Hou-Chi Chiang, National Chiao Tung Univ. (Taiwan); Yu-Hsiang Tsai, Industrial Technology Research Institute (Taiwan); Ting-Wei Huang, Ou-Yang Mang, National Chiao Tung Univ. (Taiwan)

The image fusion is combination of two or more images into one image. The fusion of multi-band spectral image has been in many applications, such as thermal system, remote sensing, medical treatment, etc. Before fusion, these images are mostly taken from different camera modules. If camera modules take an image from the different optical path in the same time, it must be in different position. It comes into the problem of the image registration. Because the images are in different field of views, also called FOV, different resolution and different view angles. It is important to build the relationship of view point in one image to the other image.

In this paper, we focus on the problem of different field of views and different resolution for two non-pinhole camera modules. The affine transformation between a 2-D image and the 3-D real world can be derived from the geometrical optics of the camera modules. In the other word, the geometrical affine function of two image are also derived from the intrinsic and extrinsic parameter of two camera modules. Through deriving the affine function, the overlap of the FOV in two images can be calculated and resample two images in the same resolution. Finally, we construct the image registration model by the affine function. It merge images for different camera sensors. And, camera sensors absorb different wavebands of electromagnetic spectrum at different position in the same time.

9599-23, Session 4

Restoration of remotely sensed images through bilevel multiobjectives programming

Soo Mee Wong, National Space Agency (ANGKASA) (Malaysia); Chee Seng Chan, Univ. of Malaya (Malaysia)

Finding a compromise between regularity to remove noise and preserving image fidelity for remotely sensed imagery is unarguably a non-trivial problem. This paper proposes a new image restoration algorithm that executes an optimal tradeoff between sharpness and noise to warrant an acceptable result of image restoration based on bilevel multiobjectives programming. The algorithm demands two objective functions for the lower-level problem; to derive the degradation function and to perform denoising on the degraded image, while the upper-level problem with ultimate objective function that is to obtain restored image by performing deblurring to the denoised image using the knowledge of the degradation function. Points of sharp variations and discontinuities are two important properties for analyzing an image or signal. Due to this consideration, in the lower-level problem, curvelet multiscale transform is employed to decompose degraded image into different scale, where the low and high frequency sub-band are used to derive the degradation function and remove image noise, respectively. Ideally the denoised image from lower level problem will contain no noise; however, in practice it will always contain some noise, therefore, the upper-level objective must be regularized. The upper-level problem is solved using an improved empirical Wiener filter to attenuate the leaked noise if any. Experiment was conducted for natural and synthetically blurred satellite imagery. The experimental result shows that the algorithm successfully restores image detail. Numerical measurements of the image quality reveal that the algorithm is comparable with other state-of-the-art methods and has advantage for image contrast and preserving edge strength.

9599-24, Session 4

Quick matching of binary images

Adnan A. Mustafa, Kuwait Univ. (Kuwait)

Matching images is a central problem in image processing. The most common technique used to compare binary images is to calculate the correlation between two images or simply to subtract them. Both of these methods require some type of similarity operation to be applied to the whole image, i.e. they are image size dependent. This implies that as image size increases, more processing time is required. However, with image sizes already exceeding 20 mega-pixels and standard image sizes doubling every five years, the need to find a size invariant image matching method is becoming crucial. In this paper, we present a faster way to compare and match binary images by using the Probabilistic Matching Model (PMM) that is image size invariant. We present two simple image size invariant algorithms based on PMM: one for fast detection of dissimilar binary images and another for matching binary images. For detecting dissimilar binary images we introduce the Dissimilar Detection via Mapping method (DDM). We compare DDM to other popular methods used in the image processing arena and show that DDM is magnitudes faster than any other method. For binary image matching, we use DDM as a preprocessor for other popular methods to speed up their matching speed. In particular, we use DDM with cross correlation to speed it up. Results are shown with real images varying in size from 16k images to 10 mega-pixel images to show the method's size invariance.

9599-25, Session 4

Airy-Kaup-Kupershmidt filters applied to image processing

Laura Hoyos, Univ. EAFIT (Colombia)

The Kaup-Kupershmidt operator is applied to the two-dimensional solution of the Airy-diffusion equation and the resulting filter is applied via convolution to image processing. The full procedure is implemented using Maple code with the package ImageTools. Some experiments were performed using a wide category of images including biomedical images generated by magnetic resonance, computarized axial tomography, positron emission tomography, infrared and photon diffusion. The Airy-Kaup-Kupershmidt filter can be used as a powerful edge detector and as powerful enhancement tool in image processing. It is expected that the Airy-Kaup-Kupershmidt could be incorporated in standard programs for image processing such as ImageJ.

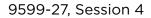
9599-26, Session 4

Compression and denoising in image processing via SVD on the Fourier domain using computer algebra

Felipe Díaz Jaramillo, Ana M. Ospina-Duque, Univ. EAFIT (Colombia)

Magnetic resonance (MR) data reconstruction can be computationally a challenging task. The signal-noise ratio might also present complications, especially with high-resolution images. In this sense, data compression can be useful not only for reducing the complexity and memory requirements, but also to reduce noise, even to allow eliminate spurious components.

This paper proposes the use of a system based on singular value decomposition of low order for noise reconstruction and reduction in MR imaging system. The Akaike information criterion is used to estimate the model order, which is used to remove noise components and reduce the amount of data processed and stored. The proposed method is evaluated using in vivo MRI data. Rebuilt images with less than 20% of the original data and with similar quality in terms of visual inspection are presented. Also a quantitative evaluation of the method is presented. The full procedure is implemented using Computer Algebra, specifically the Maple package Image Tools.



An adaptive spatio-temporal bilateral filter for video denoising

Ehsan Nadernejad, Apical (United Kingdom); Sara Saravi, Eran A. Edirisinghe, Loughborough Univ. (United Kingdom)

In image processing and computer vision, denoising is one of the most important topics. A bilateral filter is a non-linear filter, which the intensity of each pixel in an image replaces by a weight average of intensity values from neighboring pixels. This paper presents a new denoising algorithm that exploits the characteristics of the spatial and temporal frames.

The bilateral filter is extended for noise reduction in noisy video sequences. To increase the correlation between pixels, the surrounding frames are motion compensated before applying spatio-temporal bilateral filter. To obtain accurate motion vectors, an adaptive bilateral filter enhances each frame before motion estimation phase. Next, the spatio-temporal filter is applied to a set w (window size) of spatio-temporal surrounding pixels.

For denoising, all spread parameters (spatial, intensity and time) of the filter should be chosen carefully to ovoid over-smoothing in the texture regions and to preserve edges. The spread parameters are proportional with noise level, which is calculated using patch based noise level estimation method by employing principal component analysis.

First an adaptive bilateral filter is applied to the current, previous and next frames. Next, motion compensation is applied to the previous and next frames. The motion vectors are estimated by exhaustive search block matching algorithm with Half-Pel accuracy. Finally, the spatio-temporal bilateral filter is applied to a three dimensional image to remove the noise.

Experimental results indicate that the performance of the proposed approach is competitive when compared to state-of-the-art video denoising algorithms based on objective evaluations.

9599-28, Session 5

Effects of display rendering on HDR image quality assessment

Emin Zerman, Giuseppe Valenzise, Télécom ParisTech (France); Francesco Banterle, Consiglio Nazionale delle Ricerche (Italy); Francesca De Simone, Frederic Dufaux, Télécom ParisTech (France)

The quality of experience of High Dynamic Range (HDR) content is influenced by many factors, such as the way pictures are generated and displayed. For the same acquisition and rendering conditions, HDR pictures of diverse scenes may actually entail a radically different visual experience, depending on the content of the scene. In order to select video content for the evaluation of HDR processing techniques, it is therefore necessary to develop computational methods able to measure the HDR characteristics of a scene, similarly to what the Spatial Information (SI) or Temporal Information (TI) do for LDR spatial and temporal complexity, respectively. In this paper we propose a dynamic range index (DRI) which quantifies the characteristics related to the dynamic range of HDR video sequences.

9599-29, Session 5

Color transfer between high-dynamicrange images

Hristina Hristova, Remi Cozot, Olivier Le Meur, Kadi Bouatouch, Univ. de Rennes 1 (France)

Color transfer domain aims at transferring the color and light features of a reference image to a source image. So far, the proposed color transfer methods have been limited to LDR images. Unlike LDR images, which are display-dependent, HDR images contain real physical values and are able to capture high luminance variations and finer details of real world scenes. Therefore, there exists a strong discrepancy between the two types of images. In this paper, we introduce the first solution for bridging the gap between HDR imaging and the existing LDR color transfer methods. We propose a framework which tackles the main issues of applying a color transfer between two HDR images. First, to address the nature of light and color distributions in the context of HDR imaging, we carry out modifications of traditional color spaces. Furthermore, our framework ensures high precision in the quantization of the dynamic range for histogram computations. As image clustering (based on light and colors) proved to be an important aspect of color transfer, we analyze and adapt it to the HDR domain. Our framework has been applied to several stateof-the-art color transfer methods. Qualitative experiments have shown that results obtained with the proposed adaptation approach exhibit less artifacts and are visually more pleasing than results obtained when applying straightforwardly existing color transfer methods to HDR images.

SPIE. PHOTONICS

OPTICAL ENGINEERING+ APPLICATIONS

9599-30, Session 5

The JPEG XT suite of standards: status and future plans

Thomas Richter, Univ. Stuttgart (Germany); Tim Bruylants, Peter Schelkens, Vrije Univ. Brussel (Belgium) and iMinds (Belgium); Touradj Ebrahimi, Ecole Polytechnique Fédérale de Lausanne (Switzerland)

The JPEG standard has known an enormous market adoption. Daily, billions of pictures are created, stored and exchanged in this format. The JPEG committee acknowledges this success and spends continued efforts in maintaining and expanding the standard specification. JPEG XT is a standardization effort that targets the expansion of the JPEG functionality, enabling support for high dynamic range imaging, lossless and nearlossless coding and alpha channel coding while guaranteeing backward compatibility with JPEG legacy decoders.

This paper gives an overview of the current status of the JPEG XT standards suite. It discusses the JPEG legacy specification, and details how higher dynamic range support is facilitated both for integer and floating-point color representations. JPEG XT includes support for lossless and near-lossless coding of low and high dynamic range images, while providing backward JPEG compatibility. In addition, the extensible boxed-based JPEG XT file format on which all following and future extensions of JPEG will be based on is introduced. This article also details how the lossy and lossless representation of alpha channels, thus enabling the coding of transparency information and coding of arbitrarily shaped images, is supported. Finally, this paper concludes with giving prospects on future JPEG standardization initiatives.

9599-31, Session 5

Live HDR video streaming on commodity hardware

Alan Chalmers, Joshua McNamee, Jon Hatchett, Kurt Debattista, The Univ. of Warwick (United Kingdom)

High Dynamic Range (HDR) video provides a step change in viewing experience, for example the ability to clearly see the football when it is kicked from the shadow of the stadium into sunshine. To achieve the full potential of HDR video, so-called true-HDR, it is crucial that all the dynamic range that was captured or generated is delivered to the display device and tone mapping does not occur anywhere in the pipeline prior to the display. This paper describes a system for capturing, encoding and streaming high-definition HDR video in real-time to a variety of displays using only commodity hardware.



9599-32, Session 5

Study of high dynamic range video quality assessment

Manish Narwaria, Matthieu Perreira Da Silva, Patrick Le Callet, Institut de Recherche en Communications et en Cybernétique de Nantes (France)

In recent years, High Dynamic Range (HDR) imaging has attracted significant attention from industry and academia. As a result, there are currently several on-going efforts towards standardization and benchmarking of existing tools for HDR image and video. However, one key aspect that has probably not received enough attention is that HDR visual quality measurement (both subjective and objective approaches). This paper aims to fill that gap by first identifying the key challenges in the said area and discuss few existing solutions. Specifically, the paper targets three main aspects of HDR quality assessment. First, we discuss a few important practical aspects that make HDR video quality measurement potentially challenging. Second, we report our recent efforts towards developing HDR datasets that have been subjectively annotated for visual quality. Finally, we analyze and compare the effectiveness of existing solutions for objective quality prediction.

9599-33, Session 5

Automatic HDR merging algorithm based on GPU-assisted optimization for technical vision applications

Igor V. Guryev, Cesar Alejandro Martinez Hernandez, Natalia Gurieva, Carlos Rodriguez Doñate, Eduardo Cabal Yepez, Univ. de Guanajuato (Mexico)

In the work, there has been proposed a highly-tunable algorithm for creating an HDR image. The algorithm is based on main principles of manual image rendering. It does not involve image recognition techniques and implements weighted patches summation based on their histograms only. For an automation of an HDR merging it has been proposed the algorithm involving four parameters. The parameters are optimized using the genetic algorithm. An optimization criterion is based on the final image histogram analysis.

To avoid the color and intensity confusion another criterion has been introduced. Namely, the intensities of each pixel of the final image as respect to the average intensity of surrounding pixels should be close to the ones of the image with normal exposition. This criterion is introduced into an algorithm as a multiplication by the number of pixels where the intensity relation is inverted.

Because of high picture resolution on modern cameras even a single HDR merging takes minutes. An optimization procedure always requires hundreds of steps which makes this idea unreal. Therefore we have introduced several simplifications and assumptions to accelerate the process. Namely, when the image does not contain small essential details its histogram as well as intensities distribution is similar to the one with lower resolution. We run an optimization procedure for low-resolution image and after this apply the same parameters to generate high-resolution image.

After this we have implemented the algorithm using GPU parallelization, the optimization had become several timer faster with the same result quality.

9599-34, Session 5

Rendering of HDR content on LDR displays: an objective approach

Luká? Krasula, Czech Technical Univ. in Prague (Czech Republic) and Institut de Recherche en Communications et en Cybernétique de Nantes (France); Manish Narwaria, Institut de Recherche en Communications et en Cybernétique de Nantes (France); Karel Fliegel, Czech Technical Univ. in Prague (Czech Republic); Patrick Le Callet, Institut de Recherche en Communications et en Cybernétique de Nantes (France)

Dynamic range compression (or tone mapping) of HDR content is a an essential step towards rendering them on traditional LDR displays in a meaningful way. This is however non-trivial and one of the reasons is that tone mapping operators (TMOs) usually need content-specific parameters to achieve the said goal. While subjective TMO parameter adjustment is the most accurate, it may not be easy deployable in many practical applications. Thus, there is need for objective TMO parameter selection to automate the rendering process. To that end, we investigate into a new objective method for TMO parameters optimization. Our method is based on quantification of contrast reversal and naturalness. As an important advantage, it does not require any prior knowledge about the input HDR image and works for both global and local TMOs. Experimental results using a variety of HDR images and several popular TMOs demonstrate the value of our method in comparison to default TMO parameter settings.

9599-35, Session 6

Objective video presentation QoE predictor for smart adaptive video streaming

Zhou Wang, Kai Zeng, Abdul Rehman, Hojatollah Yeganeh, Shiqi Wang, Univ. of Waterloo (Canada)

How to deliver videos to consumers over the network for optimal qualityof-experience (QoE) has been the central goal of modern video delivery services. Surprisingly, regardless of the large volume of videos being delivered everyday through various systems attempting to improve visual QoE, the actual QoE of end consumers is not properly assessed, not to say using QoE as the key factor in making critical decisions at the video hosting, network and receiving sites. Real-world video streaming systems typically use bitrate as the main video presentation quality indicator, but using the same bitrate to encode different video content could result in drastically different visual QoE, which is further affected by the display device and viewing condition of each individual consumer who receives the video. To correct this, we have to put QoE back to the driver's seat and redesign the video delivery system. To achieve this goal, a major challenge is to find an objective video presentation QoE predictor that is accurate, fast, easy-touse, display device adaptive, and provides meaningful QoE predictions across resolution and content. We propose to use the newly developed SSIMplus index (https://ece.uwaterloo.ca/~z70wang/research/ssimplus/) for this role. We demonstrate that based on SSIMplus, one can develop a smart adaptive video streaming strategy that leads to much smoother visual QoE impossible to achieve using existing adaptive bitrate video streaming approaches. Furthermore, SSIMplus finds many more applications, in live and file-based quality monitoring, in benchmarking video encoders and transcoders, and in guiding network resource allocations.

9599-36, Session 6

Experimental design and analysis of JND test on coded image/video

YuChieh Lin, Lina Jin, Sudeng Hu, The Univ. of Southern California (United States); Ioannis Katsavounidis, Zhi Li, Anne M. Aaron, Netflix, Inc. (United States); C.-C. Jay Kuo, The Univ. of Southern California (United States)

The Just-Noticeable-Difference (JND) metric is characterized by the detectable minimum amount of two stimuli. JND has been used to enhance perceptual video quality in the context of image/video compression. For the context video coding, given a set of coding parameters, a video JND test is designed to determine the JND level against a reference video, which is called the anchor video. In other words, the JND metric can be used to save



coding bit rates by exploiting the special characteristics of the human visual system (HVS). The task of video JND testing is labor and time intensive. In this work, we present a novel human-computer interactive method for video JND test.

The proposed JND test is based on two alternative forced choice, which is a commonly used psychophysical method to discriminate the difference in perception. The assessors are asked to compare video pairs and determine the impairment of each pair. A ladder-climbing process is designed to help assessors find the pair with the smallest difference and terminate the test. The video pairs are seamlessly combined and presented so that assessors are confident in their decisions. We will show some statistics to demonstrate the efficiency of the proposed video JND test.

9599-37, Session 6

Predicting the visibility of dynamic DCT distortion in natural videos

Jeremy P. Evert, Md Mushfiqul Alam, Damon M. Chandler, Oklahoma State Univ. (United States)

Compression has enabled years of exponential growth in global video consumption, providing video everywhere we live, with few perceptible artifacts.

A key enabler of compression is automated Video Quality Assessment (VQA).

However, current VQA algorithms are hindered by a limited understanding of artifact visibility, based mainly on a few idealized psychophysical experiments or popular still image compression heuristics.

An extremely limited number of studies quantify artifact detection in still images (e.g., Chandler and Hemami JOSA 2003, Alam et al. JOV 2014), and only our recent studies have quantified video masked compression-artifact visibility (Evert and Chandler ACSSC 2013, Pending submission: Evert and Chandler JEI 2015).

Experiment result analyses show both target properties and video content affect artifact visibility, and existing VQA models have limited artifact visibility threshold prediction capability.

Here we present new data showing a positively correlated relationship between video contrast and artifact visibility thresholds.

Increasing video contrast amplifies differences between video masking abilities, and artifact visibility is still a function of artifact spatiotemporal frequencies.

Based on our data, we suggest a contrast-gain-control VQA model, with target spatiotemporal property weighting, to overcome performance limitations of previous VQA.

We demonstrate how using our data can tune various objective VQA algorithms, including ViS3, MOVIE, and VQM, for improved artifact threshold predictions.

This paper provides much needed data on the relationship between natural video mask contrast and artifact visibility, and provides important insights for improving existing VQA algorithms for better compression artifact visibility prediction in the high-quality regime

9599-38, Session 6

A time-varying subjective quality model for mobile streaming videos with stalling events

Deepti Ghadiyaram, Janice Pan, Alan C. Bovik, The Univ. of Texas at Austin (United States)

Over-the-top mobile video streaming is invariably influenced by volatile network conditions which cause playback interruptions (stalling events) and impair a viewer's quality of experience (QoE). The ability to accurately predict a viewer's QoE can help in the design of efficient solutions for video streaming networks that can reduce network operational costs while still delivering high-quality video content to customers. Existing objective models that predict QoE are based on simple, global video features, such as the number of stall events and their lengths, and are trained and validated on a small pool of ad hoc video datasets, most of which are not publicly available. Aside from these aforementioned global features, the model we propose in this work differs from previous models as it also accounts for the fundamental effect that a viewer's recent level of satisfaction or dissatisfaction has on their overall viewing experience. In other words, the proposed model accounts for and adapts to the recency, or the hysteresis effect caused by a stall event in addition to accounting for the lengths, frequency of occurrence, and the positions of stall events - all factors which interact complexly and affect a user's QoE. We train and validate our model on the recently created LIVE-Avvasi Mobile Video Database, which consists of 180 distorted videos of varied content that are afflicted solely with over 25 unique realistic stalling events.

9599-39, Session 6

The effect of texture granularity on texture synthesis quality

S. Alireza Golestaneh, Mahesh M. Subedar, Lina J. Karam, Arizona State Univ. (United States)

Natural and artificial textures occur frequently in images and in video sequences. In a general framework for imagevideo coding based on texture synthesis, the input image or a frame of video is first segmented into texture and non-texture regions. The texture regions are further analyzed to extract the data needed for texture synthesis. This data may be constraint parameters in parametric texture synthesis approaches or it could be seed-pixel regions in exemplar-based synthesis approaches. The guality assessment unit uses the synthesized and the original texture to estimate the fidelity of the synthesized texture. The texture synthesis process is repeated in an iterative manner until a prescribed quality is met. Existing objective visual quality assessment methods do not perform satisfactorily when predicting the synthesized texture quality. In our previous work, we showed that texture regularity can be used as an attribute for estimating the quality of synthesized textures. In this paper, we study the effect of another texture attribute, namely texture granularity, on the quality of synthesized textures. For this purpose, subjective studies are conducted to assess the quality of synthesized textures with different levels (low, medium, high) of perceived texture granularity using different types of texture synthesis methods.

9599-40, Session 6

Objective video quality for video on mobile devices

Louis J. Kerofsky, Yuriy A. Reznik, Rahul Vanam, InterDigital, Inc. (United States)

Background on visual models and influence of viewing distance and ambient light on visibility of high frequency detail. Description of critical viewing frequency and associated low-pass filter. Extension of objective image quality metrics by modification of test and reference images based on viewing conditions. We evaluate the PSNR, SSIM, MS-SSIM under changing viewing conditions. A subjective study examines the visibility of compression artifacts on a mobile device under changing viewing conditions.

9599-41, Session 6

Neurophysiological assessment of perceived image quality using steady-state visual evoked potentials

Sebastian Bosse, Fraunhofer-Institut für



Nachrichtentechnik Heinrich-Hertz-Institut (Germany); Laura Aqualagna, Anne K. Porbadnigk, Technische Univ. Berlin (Germany); Gabriel Curio, Univ. Berlin, Charite (Germany); Klaus-Robert Müller, Technische Univ. Berlin (Germany) and Korea Univ. (Korea, Republic of); Benjamin Blankertz, Technische Univ. Berlin (Germany); Thomas Wiegand, Fraunhofer-Institut für Nachrichtentechnik Heinrich-Hertz-Institut (Germany)

A neurophysiological approach of assessing the perceived quality of images exploiting steady state visual evoked potentials (SSVEP) as neural correlates of quality changes is proposed. We presented images degraded through compression by High Efficiency Video Coding (HEVC) at different distortion level in rapid alternation with the original uncompressed images to 16 observers. In this setting, SSVEPs are evoked as neural markers of perceived image quality objectively indicating visual perception of the image quality. We find the MOS values of the presented images significantly correlated to the neural response at presentation frequency and its harmonics. Our findings are in line with neurophysiology.

9599-42, Session 6

Optimal sequence duration for subjective video quality assessment

Felix J. Mercer Moss, Fan Zhang, Ke Wang, Roland Baddeley, David Bull, Univ. of Bristol (United Kingdom)

Subjective quality assessment is an essential component of modern image and video processing, both for the validation of objective metrics and for the comparison of coding methods. However, the standard procedures used to collect data can be prohibitively time-consuming. One way of increasing the efficiency of data collection is to reduce the duration of test sequences from the 10 second length currently used in most subjective video quality assessment experiments. Here, we explore the impact of reducing sequence length upon perceptual performance when identifying compression artefacts. A group of four reference sequences, together with five levels of HEVC distortion, are used to compare the subjective ratings of viewers watching videos between 1.5 and 10 seconds long. We identify a smooth function indicating that perceptual performance increases linearly as the length of the sequences increases from 1.5 seconds to 7 seconds. However, the performance of observers viewing 10 second sequences was not significantly superior to observers viewing 7, 5 or 3 second sequences. We argue that sequences between 3 seconds and 10 seconds produce satisfactory levels of human performance but the practical benefits of acquiring more data lead us to recommend the use shorter sequences for future subjective video quality assessment studies.

9599-114, Session 6

3D meshes compression performance benchmarking

Christian Tulvan, Télécom SudParis (France); Lazar M. Bivolarski, Albena Technologes Ltd. (United Kingdom)

In this paper we discuss the benchmarking of 3D mesh encoders compression performance. The tested encoders are the MPEG-SC3DMC codec (Scalable Complexity 3D Mesh Compression) based on the TFAN codec (Open3DGC implementation) and also we discuss the benchmarking of OpenCTM (Open Compressed Triangle Mesh) implementation. The geometry is compressed to a fraction of comparable file formats (3DS, STL, VRML, COLLADA...), and the format is easily accessible through a simple, portable API. The OpenCTM is a file format for storing 3D triangle meshes and is not for handling scenes, which make it versatile and widely used from online e-shopping system to game engines, and medical application to phone widgets. In comparison the 3D scene formats tend to be application specific.

9599-43, Session 7

Video streaming with SHVC to HEVC transcoding

Srinivas Gudumasu, Aricent, Inc. (India); Yuwen He, Yan Ye, Xiaoyu Xiu, InterDigital, Inc. (United States)

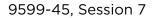
Adaptive streaming is a popular solution for video on-demand services, but requires the server to store multiple copies (bit-rate, resolution, etc) of the same content, which increases server storage cost severely. To reduce server storage requirement, one can store only the highest quality stream and apply real-time video transcoding to convert the content to a suitable lower quality stream as requested by the client. However, transcoding can also put significant computational burden on the servers. In order to properly balance computational load and storage cost, we propose a joint strategy of scalable HEVC video coding and fast SHVC to HEVC transcoding. In particular, the representation with basic guality settings is coded as the base layer, and higher quality representations are coded as enhancement layers. When the basic quality stream is requested, it is simply extracted without the need for transcoding. When a higher quality stream is requested, transcoding is applied to convert the scalable bit-stream into a single layer bit-stream to reduce the scalable coding overhead. The proposed transcoding algorithm reuses and refines the quadtree depth, mode and motion information of each coding unit available in the scalable bit-stream to ease computational load. Different transcoding strategies are applied according to coding modes to increase the speed further. Simulation results confirm that significant speed-up can be achieved with satisfactory rate distortion performance.

9599-44, Session 7

A perceptual quantization strategy for HEVC based on a convolutional neural network trained on natural videos

Md Mushfiqul Alam, Tuan Nguyen, Damon M. Chandler, Oklahoma State Univ. (United States)

A crucial requirement for effective video coding is the ability to accurately and efficiently predict the local visibility of coding artifacts. Such predictions could help guide the allocation of bits or the determination of quality for each spatiotemporal region. However, previous approaches to predicting artifact visibility exhibit two primary shortcomings. First, they are based on heuristics from overly controlled psychophysical studies using unnatural videos. Second, and more importantly, they are largely impractical for real-time applications due to prohibitive computational/memory demands. Thus, predicting artifact visibility in a manner which is simultaneously more accurate and more efficient than existing models remains an open research challenge. Here, we propose an HEVC-based guantization scheme based on a fast model of local artifact visibility designed specifically for natural videos. The model uses a convolutional-neural-network (CNN) architecture for predicting local artifact visibility and quality of each spatiotemporal region of a video. We trained the CNN model using our recently published database of local masking and quality in natural scenes (Alam et al. JOV 2014 and Alam et al. HVEI 2015, respectively). When coupled with an HEVC encoder, our results provide 5-10% more compression over baseline HEVC when matched in visual quality, while requiring almost half the computational time and memory footprint of an equivalent gain control model. We demonstrate how by integrating a fast model of artifact visibility within natural videos lead to better compression efficiency for the same guality. Our work opens the doors for similar techniques which may work for different forthcoming compression standards.



Performance analysis of HEVC and its format range and screen content coding extensions

Bin Li, Microsoft Corp. (United States); Jizheng Xu, Microsoft Research Asia (China); Gary J. Sullivan, Microsoft Corp. (United States)

No Abstract Available

9599-46. Session 7

Smart pattern-based full-pel search strategies in the context of HEVC

Georg Maier, Fraunhofer-Institut für Optronik, Systemtechnik und Bildauswertung (Germany); Benjamin Bross, Dan Grois, Detlev Marpe, Heiko Schwarz, Fraunhofer-Institut für Nachrichtentechnik Heinrich-Hertz-Institut (Germany); R.C. Veltkamp, Utrecht Univ. (Netherlands); Thomas Wiegand, Fraunhofer-Institut für Nachrichtentechnik Heinrich-Hertz-Institut (Germany)

No Abstract Available

9599-47, Session 7

Coding tools investigation for next generation video coding based on HEVC

Jianle Chen, Ying Chen, Marta Karczewicz, Hongbin Liu, Li Zhang, Xin Zhao, Qualcomm Inc. (United States)

No Abstract Available

9599-48, Session 7

Coding efficiency improvements beyond **HEVC with known tools**

Alexander Alshin, Elena A. Alshina, SAMSUNG Electronics Co., Ltd. (Korea, Republic of); Madhukar Budagavi, SAMSUNG Telecommunications America Inc. (United States); SeungSoo Jeong, SAMSUNG Electronics Co., Ltd. (Korea, Republic of); Junghye Min, SAMSUNG Electronics Co, Ltd. (Korea, Republic of); Ankur Saxena, SAMSUNG Electronics Co., Ltd. (Korea, Republic of)

No Abstract Available

9599-49, Session 7

Improved block copy and motion search methods for HEVC screen content coding

Krishna Rapaka, Qualcomm Inc. (United States); Chao Pang, Sole Joel, Qualcomm Technologies, Inc. (United States); Marta Karczewicz, Qualcomm Inc. (United States); Jizheng Xu, Microsoft Research Asia (China); Bin Li, Microsoft Corp. (United States)

No Abstract Available

9599-58, Session PWed

Classification for skin cancer using the intensity-based, texture-based and fractalbased features with optical coherence tomography

OPTICS+

OPTICAL ENGINEERING+ APPLICATIONS

SPIE. PHOTONICS

Wei Gao, Valery P. Zakharov, Oleg O. Myakinin, Ivan A. Bratchenko, Dmitry N. Artemyev, Dmitry V. Kornilin, Samara State Aerospace Univ. (Russian Federation)

Optical coherence tomography (OCT) is employed in the diagnosis of skin tumors. Particularly, quantitative image features extracted from OCT images might be used as indicators to classify skin tumors. In the present paper, we investigated intensity-based, texture-based and fractal-based features for automatically differentiating the melanomas from basal cell carcinomas and pigment nevi. Generalized estimating equations were used to test for differences between the skin tumors. A modified p value of <0.001 was considered statistically significant. Significant increase of mean and median of intensity and significant decrease of mean and median of absolute gradient were observed in basal cell carcinomas and pigment nevi as compared with melanomas. Significant decrease of contrast, entropy and fractal dimension were also observed in basal cell carcinomas and pigment nevi as compared with melanomas. Our results suggest that the selected quantitative image features of OCT images could provide useful information to differentiate melanomas from basal cell carcinomas and pigment nevi. Further research is warranted to determine how this approach may be used to improve the classification of skin tumors.

9599-59, Session PWed

A novel teaching-learning-based optimization for image enhancement

Xiaojun Bi, Harbin Engineering Univ. (China)

Image enhancement is considered as a complex optimization problem. In order to make the enhancement of the image more suitable than the original image from the perceptual viewpoint of human, a novel teachingleaching based optimization (TLBO) for image enhancement is proposed to enhance gray-level images. Firstly a transformation function which combines local information and global information of the image is used to convert the original image into the enhanced image. Then, TLBO algorithm is applied to maximize the objective function of measuring image enhancement in order to enhance the image contrast by maximizing the parameters like edge intensity, edge pixels and entropy of the enhanced image. The main goal of us is to achieve the best enhanced image according to the objective function through optimizing the parameters used in the transformation function with the help of TLBO. Finally experimental results are compared with the state-of-the-art approaches such as particle swarm optimization for image enhancement and differential evolution for image enhancement and TLBO for image enhancement has obtained better image contrast.

9599-60. Session PWed

Registration of point cloud data for HDD stamped base inspection

Sungho Suh, Hansang Cho, SAMSUNG Electro-Mechanics (Korea, Republic of)

As part of the HDD manufacturing process, HDD stamped base, an exterior container, is one of the most essential components in which various parts become assembled to compose a hard disk drive (HDD). Because it is designed by a stamping method, height errors that are caused by pressing, breaking or cracking can occur on the base. In order to detect these height errors, the inspection process is essential in production fields. In the current industry, CMM (Coordinate Measurement Machine) is one of the most widely used inspection machines that inspect certain areas on a product.



This machine examines a designated point with a probe and finds defects by comparing its height with the originally designed height. However, this method takes a long time to inspect each designated point resulting in total of 17 minutes In order to reduce this total inspection time, we propose an inspection method using 3D point cloud data acquired from a holographic sensor. To compare the height from the acquired 3D point cloud data with the one from the originally designed CAD data, the exact registration of point cloud data is important.

The difference between 2D image registration and 3D point cloud registration is that the latter requires that three things be considered: translation on each plane, rotation and tilt. The relationship between the acquired 3D point cloud data and the originally designed CAD data can be known by Affine transformation. If Affine transformation matrix between 3D point cloud data and the CAD data is obtained, 3D point cloud data registration can be performed.

In order to calculate 3D Affine transformation matrix, corresponding points between 3D point cloud data and CAD data are required. To find corresponding points, we use the height map which is projected from 3D point cloud data onto the XY plane. The height map has pixel intensity from the height value of each point. If the height map from 3D point cloud data and CAD data are matched, corresponding points can be known.

In this paper, we find the corresponding points between 3D point cloud data and CAD data using circle fitting since there are multiple circles on the base, and obtain 2D Affine transformation matrix from these corresponding points. By applying 2D Affine transformation matrix to the height map, the corresponding points on the 3D coordinate can be obtained. Using such points, we propose the method designed to achieve 3D Affine transformation matrix. To find the proper 3D Affine transformation matrix, we formulate a cost function which uses the relationship of corresponding points. Also the proper 3D Affine transformation matrix can be calculated by minimizing this cost function. Then the 3D point cloud data can be matched to CAD data and the height values of each point of 3D point cloud can be compared to those of CAD data. The experiment result shows two types of errors: (1) error observed by comparing CAD data with artificially transformed data, (2) error observed by comparing CAD data with the actual 3D point cloud data. The average error observed by comparing CAD data with artificially transformed data is 0.2557, but the average error by the proposed method is 0.0005. Considering this result, the average error is dramatically decreased. Additionally, we compare the proposed method to the other methods. The experiment result shows that the proposed method gives better performance.

9599-61, Session PWed

Robust illumination-invariant tracking algorithm based on HOGs

Daniel Miramontes-Jaramillo, Vitaly Kober, Ctr. de Investigación Científica y de Educación Superior de Ensenada B.C. (Mexico); Víctor H. Díaz-Ramírez, Ctr. de Investigación y Desarrollo de Tecnología Digital (Mexico)

Common tracking systems are usually affected by environmental and technical interferences such as nonuniform illumination, sensors' noise, geometrical scene distortion, etc. Among these issues, the former is particularly interesting because it destroys important spatial characteristics of objects in observed scenes. A poor illumination of a scene hides edges and texture which are essential for tracking of a target in video sequence. Actually, real applications such as video surveillance, robot vision, automated manufacturing and augmented and virtual reality are very sensible to nonuniform illumination of scenes. We propose a two-step tracking algorithm: first, a preprocessing locally normalizes the illumination difference between the target object and observed frames; second, the normalized object is tracked by means of a designed template structure based on histograms of oriented gradients and kinematic prediction model. The algorithm performance is tested in terms of recognition and localization errors in real scenarios. In order to achieve high rate of the processing, we use GPU parallel processing technologies. Finally, our algorithm is compared with other state-of-the-art trackers.

9599-62, Session PWed

Adaptive codebook selection schemes for image classification in correlated channels

Chia-Chang Hu, Xiang-Lian Liu, Kuan-Fu Liu, National Chung Cheng Univ. (Taiwan)

The multiple-input multiple-output (MIMO) system with the use of transmit and receive antenna arrays achieves diversity and array gains via transmit beamforming. Due to the absence of full channel state information (CSI) at the transmitter, the transmit beamforming vector can be quantized at the receiver and sent back to the transmitter by a low-rate feedback channel, called limited feedback beamforming. One of the key roles of Vector Quantization (VQ) is how to generate a good codebook such that the distortion between the original image and the reconstructed image is the minimized. In this paper, a novel adaptive codebook selection scheme for image classification is proposed with taking both spatial and temporal correlation inherent in the channel into consideration. The new codebook selection algorithm is developed to select two codebooks from the discrete Fourier transform (DFT) codebook, the generalized Lloyd algorithm (GLA) codebook and the Grassmannian codebook to be combined and used as candidates of the original image and the reconstructed image for image transmission. The channel is estimated and divided into four regions based on the spatial and temporal correlation of the channel and an appropriate codebook is assigned to each region. The proposed method can efficiently reduce the required information of feedback under the spatially and temporally correlated channels, where each region is adaptively. Simulation results show that in the case of temporally and spatially correlated channels, the bit-error-rate (BER) performance can be improved substantially by the proposed algorithm compared to the one with only single codebook.

9599-63, Session PWed

Research of improved sparse grid nonuniformity correction technologies for infrared resistor array

Huijie Du, Beijing Simulation Ctr. (China)

Abstract: Infrared resistor arrays perform a vital role in the hardware in the loop testing of infrared seekers. Infrared resistor arrays composed of large numbers of suspended resistor elements are commonly used to produce dynamic two-dimensional images of infrared radiation. Due to inconsistencies in the fabrication process of the resistor arrays, the temperature each resistor elements reaches for a given input voltage is variable and this leads to more significant radiance differences, these differences result in spatially-distributed radiance non-uniformity. Therefore, in order to obtain an available infrared image, non-uniformity correction (NUC) is necessary. In this paper, the non-uniformity characters of the infrared resistor arrays are analyzed base on measured data and then an improved sparse grid method for engineering are discussed and analyzed. First of all, the NUC camera has a strong influence on the effectiveness of the infrared resistor arrays NUC procedure. According to the actual fact and the laboratory condition, we presented an alternative method for collecting resistor arrays intended to reduce the influence causing by the NUC camera. Secondly, based on the measured non-uniformity data, we obtain the response characteristics of the infrared resistor arrays. In each gray level, we take two points or several points correction algorithm to calculate the gain data and the offset data, and then the linear look-up table is established. Finally, through MATLAB we develop the correction software, and we can obtain the driving output conveniently. The result shows that the image quality has a remarkable improvement after non-uniformity correction, the non-uniformity correction flow and algorithm preferably satisfies the requirement of the high confidence infrared imaging simulation.



9599-64, Session PWed

Digital image database processing to simulate image formation in ideal lightning conditions of the human eye

Jessica Castañeda Santos, Univ. Technológica de la Mixteca (Mexico); Agustín Santiago-Alvarado, Angel S. Cruz-Félix, Arturo Hernández Méndez, Univ. Tecnológica de la Mixteca (Mexico)

The pupil size of the human eye has a large effect in the image quality due to inherent aberrations. Several studies have been performed to calculate its size relative to the luminance as well as considering other factors, i.e., age, size of the adapting field and mono and binocular vision. Moreover, ideal lighting conditions are known, but software suited to our specific requirements, low cost and low computational consumption, in order to simulate radiation adaptation and image formation in the retina with ideal lighting conditions has not yet been developed. In this work, a database is created in the course of three days consisting of 70 photographs corresponding to the same scene with a fixed target at different times of the day with a span of 30 minutes between each photograph. By using this database, characteristics of the photographs are obtained by measuring the luminance average initial threshold value of each photograph by means of an image histogram. Also, we present the implementation of a digital filter for both, image processing on the threshold values of our database and generating output images with the threshold values reported for the human eye in ideal cases. Some potential applications for this kind of filters may be used in artificial vision systems.

9599-65, Session PWed

Inverse ill-posed problems in sensing with terahertz pulsed spectroscopy: from nondestructive evaluation of materials to noninvasive diagnosis of dysplastic skin nevi

Egor Yakovlev, Kirill I. Zaytsev, Nikita V. Chernomyrdin, Arsenii A. Gavdush, Irina N. Dolganova, Stanislav O. Yurchenko, Bauman Moscow State Technical Univ. (Russian Federation)

Terahertz pulsed spectroscopy (TPS) recently attracts considerable interest as a perspective instrument of applied physics. TPS allows solving the problems of remote sensing, non-destructive evaluations of materials and constructions, material characterization and studying of the phase transitions in media, and non-invasive medical diagnosis. Many factors could impact on the process of sensing, including noises in TPS waveforms and various instabilities of TPS set-up parameters. All factors should be considered during the processing of TPS data. Thus, development of novel techniques for accurately solution of the TPS inverse ill-posed problems, as well as studying the accuracy of TPS inverse problem solution are very important tasks for all applications of TPS. In our work we consider some novel results in sensing with TPS. We show the results of non-destructive evaluations of composite materials at the stages of material processing and exploitation. Moreover, we study the ability for non-invasive medical diagnosis of dysplastic skin nevi. Dysplastic nevus of the skin is a precursor of melanoma, which is reported to be the most dangerous skin cancer. We discuss the ability to study phase transitions and glassing of media via TPS. Finally the problems of TPS signal processing, related to the applications listed above, are considered in this work.

9599-66, Session PWed

A position, rotation, and scale invariant image descriptor based on rays and circular paths

Selene Solorza, Univ. Autónoma de Baja California (Mexico)

In this paper a rotation, scale and translation (RST) invariant gray-level image descriptor based on 1D signatures is presented. The position invariant is achieved from the amplitude spectrum of the Fourier transform of the given image. The Fourier's amplitude spectrum is introduced in the analytical Fourier-Mellin (AFM) transform. This transform is not scale invariance yet. The AFM transform is normalized by its dc-value to obtain an amplitude spectrum invariant to scale. From the normalized AFM amplitude spectrum two 1D signatures are constructed. The first 1D signature is obtained from circle path binary masks. The circle masks are used to filter the normalized AFM amplitude spectrum, by this manner to build the 1D circle signature. The second 1D signature results from ray path binary masks that filter the normalized AFM amplitude spectrum. These two 1D signatures are rotation, scale and translation invariant image descriptors. In the descriptor training phase, confidence intervals of 95% for the instantaneous amplitude of the 1D RST signatures are built using the statistical method of bootstrap with constant replacement B=1000 and normal distribution. Those confidence intervals are utilized to generate a single classifier output plane, reducing in this form the comparison cost time in the classification step. The Latin alphabet letters in Arial font style were employed to test the descriptor efficiency obtaining a confidence level at least of 95%.

9599-67, Session PWed

ROI-preserving 3D video compression method utilizing depth information analysis

Chunli Ti, Guodong Xu, Yudong Guan, Yidan Teng, Harbin Institute of Technology (China)

The demand of extra information to render or directly display several different views simultaneously is becoming a key challenge in the field of three dimensional (3D) TV. The 2D plus depth representation occupies a lower bandwidth than most 3D video representations; besides the depth information in it can provide convenience for region of interest (ROI) selection. In this paper, we proposed a ROI-preserving compression method for the 2D plus depth representation to ensure visual effects of viewerconcerned parts at a higher overall compression ratio. The main contribution of this work is introducing an automatic ROI extraction method via processing the depth map which is a valuable index of the visual attention model and not fully developed by the methods mentioned earlier. By meanshift based image segmenting of the depth map, the foreground of the 3D video is obtained. For its higher degree of color contrast, texture richness movement details, the foreground attracts more attention in the Human Visual System (HVS). Then the depth mutation region, which contains significant high frequency information of 2D video and its depth perception, is determined utilizing the edge detection and morphological filtering of the depth map. After the ROI extraction, a ROI based preprocessing filter is applied to both 2D video and the depth map to be compatible with existing video channel. Experiments show obvious effects on ROI preserving in a lower bit rate both visually and statistically. And the result of ROI selection is more reasonable than the conventional approaches.

9599-68, Session PWed

New visual sensitivity based error concealment algorithm in wireless stereo video communication

Yue Sun, Mei Yu, Keseng Yan, Gangyi Jiang, Ningbo Univ. (China)



Coding techniques may result in reducing stereo video transmission fault tolerance due to network congestion and channel disturbance, when the packet loss or bit error portion, affect directly the quality of decoded image at the receiver. In this paper, a new visual sensitivity based error concealment algorithm is proposed for partially lost macroblocks (MBs) in wireless stereo video communication. The characteristics of coding structure and temporal, spatial and interview relativities in stereo video coding are firstly analyzed. The lost MBs are classified into obscured and non-obscured boundary MBs according to MB's occlusion characteristics, and the nonobscured boundary MBs are further defined into moving MBs and static MBs according to their moving ability. Binocular just noticeable distortion (BJND) indicates that human being cannot perceive some distortions when watching a stereo image if the distortions of one view are less than the BJND value. The characteristics of MBs' BJND values are computed and used to analyze the lost MBs and stereo image. Then, on the basis of human visual sensitivity and texture characteristics of stereo image, the moving MBs are divided into sensitive and insensitive MBs, texture and smooth MBs, respectively. Finally, adaptive error concealment operations with different types of lost MBs are given and used to recover the lost MB according to MB's characteristic analyses. Experimental results with classical test stereo videos show that the proposed algorithm can effectively improve the subjective and objective quality of the error stereo videos compared with other state-of-the-art error concealment methods.

9599-69, Session PWed

Korteweg-de Vries-Kuramoto-Sivashinsky filters for image processing

Juan C Arango, Universidad EAFIT (Colombia)

The Kuramoto- Sivashinsky operator is applied to the two-dimensional solution of the Korteweg-de Vries equation and the resulting filter is applied via convolution to image processing. The full procedure is implemented using an algorithm: prototyped with the Maple package named Image Tools. Some experiments were performed using biomedical images, infrared images obtained with smartphones and images generated by photon diffusion. The results from these experiments show that the Kuramoto-Sivashinsky-Korteweg-de Vries Filters are excellent tools for enhancement of images with interesting applications in image processing at general and biomedical image processing in particular. It is expected that the incorporation of the Kuramoto-Sivashinsky-Korteweg-de Vries Filters in standard programs for image processing will led to important improvements in various fields of optical engineering.

9599-70, Session PWed

System of scale-selective tomography of myocardium birefringence

Alexander G. Ushenko, Yuriy Fedkovych Chernivtsi National Univ. (Ukraine)

Laser polarimetry enabling to obtain information about optical anisotropy of biological tissues (BT) is an important direction of non-invasive diagnostics of organic phase-heterogeneous layers. For statistic analysis of such polarimetric information a model approach has been worked out based on the following conditions:

• morphological structure of BT is regarded as a two-component amorphous-crystalline one;

• the crystalline component or extracellular matrix is formed by the network of optically uniaxial birefringent protein (collagen, myosin, elastine, etc.) fibrils or biological liguid crystals;

A new approach to description of the BT laser images based on the analysis of coordinate distributions of polarization singularities (linearly (S-points) and circularly (C-points) polarized states; - the fourth parameter of the Stokes vector) became developed the above mentioned statistical.

Three groups of histological sections of the myocardium tissue were used as the objects of investigation:

• biopsy of the myocardium tissue of deaths from cancer (type "A");

• biopsy of the myocardium tissue of deaths from coronary heart disease (type "B");

• biopsy of the myocardium tissue of deaths from acute coronary insufficiency (type "C").

Analytical conditions of forming the singularity elements of Jones matrix of birefringent liquid crystal networks of biological tissues are determined. Correlation between the coordinate locations of characteristic points of 2D elements of Mueller matrix of optically thin layer of myocardium tissue and the network of S- and C-points in its laser image is defined.

9599-71, Session PWed

Mueller-matrix invariants of optical anisotropy of the bile polycrystalline films in the diagnosis of human liver pathologies

Olexander V. Dubolazov, Vladimir A. Ushenko, Yuriy Fedkovych Chernivtsi National Univ. (Ukraine)

Biological tissues and liguids represent structurally inhomogeneous optically anisotropic media with absorption. To describe the interaction of polarized light with such sophisticated systems, more general approximation based on Mueller-matrix formalism is required. Nowadays many practical techniques based on measuring and analyzing the Mueller-matrices of the samples under investigation are being used in biological and medical researches. During recent 10-15 years a separate direction – laser polarimetry – has been formed in matrix optics. On its basis the interconnections between the set of statistical moments of the 1st-4th order, correlation, fractal parameters were determined, which characterize the distributions of Mueller matrix elements and the parameters of linear birefringence of fibrillar protein networks of human biological tissues. The diagnostics of pathological changes of skin derma, epithelial and connective tissues of the women's reproductive organs, etc. was realized on this basis.

This research work is focused on determining the potentialities of diagnostics of pathological changes in human liver basing on polarization analysis of Mueller – matrix images of polycrystalline networks of blood plasma albumins and globulins.

1. The model of blood plasma layer considering the mechanisms of optically anisotropic absorption – linear and circular dichroism of protein networks was suggested.

2. Mueller-matrix rotation invariants characterizing polarization manifestations of biological network optical anisotropy are determined.

3. The interconnections between the statistical, correlation and fractal parameters characterizing the Mueller-matrix images of blood plasma layer and the peculiarities of the mechanisms of optically anisotropic absorption biological crystals network were found.

9599-72, Session PWed

Autofluorescent polarimetry of bile films in the liver pathology differentiation

Olexander V. Dubolazov, Yuriy A. Ushenko, Yuriy Fedkovych Chernivtsi National Univ. (Ukraine)

Biological tissues represent structurally inhomogeneous optically anisotropic media with absorption. To describe the interaction of polarized light with such sophisticated systems, more general approximation based on Mueller-matrix formalism are required. Nowadays many practical techniques based on measuring and analyzing the Mueller-matrices of the samples under investigation are being used in biological and medical researches. At the same time there practically no data concerning polarization manifestations of fluorescence effects in biological tissues in modern literature. Therefore, the task of complex uniting the diagnostic potentialities of the techniques of laser polarimetry and laser fluorescence proves to be topical.

In this research the model of complex optical anisotropy, possessed by protein networks of the tissues of liver is suggested, and on this ground the



method of Mueller-matrix mapping of laser polarization fluorescence of bile films is developed.

1. The model of laser polarization fluorescence of biological tissues and fluids considering the mechanisms of optically anisotropic absorption – linear and circular dichroism of optical anisotropic networks was suggested.

2. Mueller-matrix rotation invariants characterizing polarization manifestations of laser fluorescence are determined.

3. The interconnections between the statistical, correlation and fractal parameters characterizing the Mueller-matrix images of laser polarization fluorescence and the peculiarities of the mechanisms of optically anisotropic absorption of bile films were found.

9599-73, Session PWed

Polarization-correlation microscopy of human liquid polycrystalline films in infertility diagnosis

Olexander V. Dubolazov, Artem O. Karachevtsev, Yuriy Fedkovych Chernivtsi National Univ. (Ukraine)

Among the methods of optical diagnostics of human biological tissues the techniques of laser polarimetry diagnostics of their optical anisotropic structure became widely spread. The main information for these methods is obtained from coordinate distributions of polarization azimuths and ellipticity (polarization maps) with the following correlation (auto- and mutually correlation functions and fractal dimensions analysis). As a result, several techniques of early diagnostics and differentiation of pathological changes in biological tissue (BT) structure with their degenerative, dystrophic and oncological changes were developed.

Besides, there is a widely spread group of optically anisotropic biological objects, for which the techniques of laser polarimetry diagnostics are not efficient enough. Optically thin layers of different biological fluids (bile, urine, liquor, synovial fluid, blood plasma, etc.) belong to such objects.

This research is focused on the analysis of potentiality of diagnostics infertility by means of new technique of polarization correlometry of human blood plasma layers laser images.

1. A new technique of estimating the structure of laser images based on measuring coordinate distributions of mutual polarization degree is suggested that characterizes the homogeneity of optically isotropic and optically anisotropic components in biochemical composition of blood plasma.

2. The statistical (mean, dispersion, asymmetry and excess), correlation (correlation area of distribution of mutual polarization degree values) and fractal (dispersion of extremes of log-log dependencies of power spectra of mutual polarization degree values distribution) criteria of polarization-correlation diagnostics of all groups of blood plasma layers.

9599-75, Session PWed

Volumetric liquid flow measurement through thermography to simulate blood flow in an artery

Carlos Villaseñor-Mora, Adela Rabell-Montiel, Arturo González-Vega, Gerardo Gutierrez-Juarez, Univ. de Guanajuato (Mexico)

Exist a variety of methods to measure the flow of a liquid through a conduit; however, most of those methods significantly interfere with the flow, which affects the measurement. In medical applications the measurement of blood flow is essential when peripheral artery disease want to diagnose. The use of non-invasive techniques for flow measurement has been developed very little, especially which are based on infrared thermography that has not shown significant improvement. In this work is developed a methodology to measure flow in a conduit, based on thermal images acquired with an infrared camera in the middle infrared range adjusted at ambient characteristics. The experimental setup proposed was studied at external disturbances such as: ambient temperature and humidity, and infrared camera stability in order to find their error contribution during the measurement. To study the sensitivity of the measurement system, it was used a flow control capable of causing small changes in this, allowing to measure flows with a resolution of milliliters per second with the proposed setup. It is analyzed and discussed how the variations in flow due to changes in temperature or vice versa affect the thermal images acquired, which could lead to an incorrect interpretation of the flow velocity. Additionally, it is discussed how the effects of turbulence produced by curved hoses, and the change in the emissivity of the conduit as a function of the temperature can also affect the measurement.

9599-76, Session PWed

Multifunctional polarization tomography of optical anisotropy biological layers in diagnosis of endometriosis

Olexander V. Dubolazov, Yuriy A. Ushenko, Artem O. Karachevtsev, Yuriy Fedkovych Chernivtsi National Univ. (Ukraine)

Among the various optic and physical methods of diagnosing the structure and properties of the optical anisotropic component of various biological objects a specific trend has been singled out - multidimensional laser polarimetry of microscopic images of the biological tissues with the following statistic, correlative and fractal analysis of the coordinate distributions of the azimuths and ellipticity of polarization in approximating of linear birefringence polycrystalline protein networks. At the same time, in most cases, experimental obtaining of tissue sample is a traumatic biopsy operation. In addition, the mechanisms of transformation of the state of polarization of laser radiation by means of the optic anisotropic biological structures are more varied (optical dichroism, circular birefringence). Here at, real polycrystalline networks can be formed by different types, both in size and optical properties of biological crystals.

Our research is aimed at developing experimental method of the Fourier polarimetry and a spatial-frequency selection for distributions of the azimuth and the ellipticity polarization of blood plasma laser images with a view of diagnosing prostate cancer.

A method of polarization mapping of the optic-anisotropic polycrystalline networks of the blood plasma albumin and globulin proteins with adjusted spatial-frequency filtering of the coordinate distributions of the azimuth and ellipticity of the polarization of laser radiation in the Fourier plane is proposed and substantiated.

Comparative studies of the effectiveness of direct methods of mapping and a spatial-frequency selection in differentiating polarization azimuth and ellipticity maps of the field of laser radiation converted by the networks of albumin - globulin crystals of the blood plasma in healthy people and patients with prostate cancer have been carried out.

A set of criteria of diagnosing prostate cancer based on the statistical (statistical moments of the 1st - 4th orders), correlation (correlation moments) and fractal (the slope of approximating curves and the dispersion of the distribution of extreme log - log dependences of power spectra) analysis of the spatial - frequency filtered polarization distributions generated by dendritic networks of albumin and globulin and spherolithic networks has been detected and substantiated.

9599-77, Session PWed

Spectrometry techniques of differential diagnosis of benign and malignant prostate tumor

Sergey B. Yermolenko, Yuriy Fedkovych Chernivtsi National Univ. (Ukraine); Olexander Fedoruk, Dmytro Voloshynskyi, Bukovinian State Medical Univ. (Ukraine)



Medical and social problems of modern urology is the prevalence of various pathologies of the prostate, such as cancer and benign prostatic hyperplasia (BPH). BPH has become one of the most common diseases of the elderly men. In the structure of cancer diceases prostate cancer in a number of some countries takes the 2-3 rd place after stomach cancer, and in the USA and Sweden it takes the 1st place. There are many works devoted to the comparison of histological studies in the evaluation of prostate biopsies and tissue samples after transurethral resection (TUR) of the prostate. We discuss the relevance of different morphological parameters in assessing the prognosis of benign and malignant tumors of the prostate. According to this, an important problem is the standardization of histological studies. Leading role in the objectification diagnosis of the pathological processes of prostate cancer can play spectrometric studies of prostate that can make the conclusion that the development of spectrometry methods may be relevant for solving above mentioned problems.

The aim of this work is to develop spectrometric criteria of differential diagnosis in patients with benign and malignant tumors of the prostate through conducting a comparative evaluation of clinical, laboratory and biophysical studies.

We will present the results of diagnostic possibilities of the spectrometry method in benign and malignant tumors of the prostate; determine the diagnostic value of PSA in the blood; develope spectrometric diagnostic criteria.

9599-78, Session PWed

Explicit solutions of one-dimensional total variation problem

Artyom Makovetskii, Sergei Voronin, Chelyabinsk State Univ. (Russian Federation); Vitaly Kober, Ctr. de Investigación Científica y de Educación Superior de Ensenada B.C. (Mexico)

In this work we consider denosing of a one-dimensional signal corrupted by additive white Gaussian noise. A common way to solve the problem is to utilize the total variation (TV) method. Basically, the TV regularization minimizes a functional that consists of the sum of fidelity and regularization terms. We derive explicit solutions of the one-dimensional TV regularization problem that help us to better understand how the TV regularization restores signals. On the base of the solutions, a non-iterative algorithm for the one-dimensional TV can be obtained. The one-dimensional TV algorithm is extended for denoising of images degraded by additive Gaussian noise. In this case topological and metrical characteristics of the degraded image are used. The topological characteristics of a function of two variables are linear variations. Computer simulation results are provided to illustrate the performance of the proposed algorithm for restoration of noisy images.

9599-79, Session PWed

Performance evaluation of image deconvolution techniques in spacevariant astronomical imaging systems with nonlinearities

Karel Fliegel, Petr Janout, Jan Bednar, Czech Technical Univ. in Prague (Czech Republic); Jan Švihlík, Faculty of Chemical Technology (Czech Republic); Lukáš Krasula, Stanislav Vítek, Petr Páta, Czech Technical Univ. in Prague (Czech Republic)

There are various deconvolution methods for suppression of blur in images. In this paper a survey of image deconvolution techniques is presented with focus on methods designed to handle images acquired with wide-field astronomical imaging systems. Image blur present in such images is spacevariant especially due to space-variant nature of the lens. In special cases, an imaging system contains non-linear electro-optical elements. Analysis of non-linear and space-variant imaging systems is usually simplified so that the system is considered as LSI (Linear and Space-Invariant) under specific constraints. Performance analysis of selected image deconvolution methods is presented in this paper, while considering space-variant nature of wide-field astronomical imaging system. Impact of nonlinearity on the overall performance of image deconvolution technique is also analyzed. Artificially generated test images and images obtained from the real astronomical imaging system are used for the performance analysis. The real astronomical imaging system, used as a source of test image data, contains space-variant wide-field input lens and non-linear image intensifier.

9599-80, Session PWed

Implementation of cost-effective diffuse light source mechanism to reduce specular reflection and halo effects for resistorimage processing

Yung-Sheng Chen, Jeng-Yau Wang, Yuan Ze Univ. (Taiwan)

Light source plays a significant role to acquire a gualified image from objects for facilitating the image processing and pattern recognition. For objects possessing specular surface, the phenomena of reflection and halo appear in the acquired image will increase the difficulty of information processing. Such a situation may be improved by the assistance of valuable diffuse light source. Consider reading resistor via computer vision, due to the resistor's specular reflective surface it will face with a severe non-uniform luminous intensity on image yielding a higher error rate in recognition without a well-controlled light source. A measurement system including mainly a digital microscope embedded in a replaceable diffuse cover, a ring-type LED embedded onto a small pad carrying a resistor for evaluation, and an Arduino microcontroller connected with PC, is presented in this paper. Several replaceable cost-effective diffuse covers made by paper bowl, cup and box inside pasted with white paper are presented for reducing specular reflection and halo effects and compared with a commercial diffuse some. The ring-type LED can be flexibly configured to be a full or partial lighting based on the application. For each self-made diffuse cover, a set of resistors with 4 or 5 color bands are captured via digital microscope for experiments. The signal-to-noise ratio from the thresholded resistor-image is used for performance evaluation. The detected principal axis of resistor body is used for the partial LED configuration to further improve the lighting condition. Experimental results confirm that the proposed mechanism can not only evaluate the cost-effective diffuse light source but also be extended as an automatic recognition system for resistor reading.

9599-81, Session PWed

A fusion algorithm for building threedimensional maps

Aleksandr Vokhmintcev, Artyom Makovetskii, Chelyabinsk State Univ. (Russian Federation); Vitaly Kober, Ctr. de Investigación Científica y de Educación Superior de Ensenada B.C. (Mexico); Ilya Sochenkov, Russian Academy of Sciences (Russian Federation); Vladislav Kuznetsov, Rambler (Russian Federation)

Dense three-dimensional maps of indoor environments have various applications in navigation, manipulation and semantic mapping. In this work we use a Kinect camera that captures RGB images along with per-pixel depth information for building dense three-dimensional maps of indoor environments. Commonly three-dimensional mapping systems contain three components, that is, first, the spatial alignment of consecutive data frames; second, the detection of loop closures; and third, the globally consistent alignment of the complete data sequence. It is known that three-dimensional point clouds are well suited for frame-to-frame alignment and for dense three-dimensional reconstruction; however, they ignore valuable information contained in images. Color cameras capture visual information and are very suitable for loop closure detection. A novel fusion



algorithm combining visual features and depth information for view-based loop closure detection followed by pose optimization to achieve globally consistent maps is proposed. The performance of the proposed system is tested in real indoor environments and discussed.

9599-82, Session PWed

Mueller imaging of white blood cells

Shirsendu Sarkar, Ajay Ghosh, Univ. of Calcutta (India)

Mueller imaging of white blood cells for medical purposes is presented here. Based on the input and output Stokes vectors of the interaction of polarized light with elements which can change its state of polarization, Mueller matrix is the transfer function of optical system such as linear media described by 4x4 real matrix. Development of optical techniques using polarized light has received considerable recent attention because the polarization properties of photons contain morphological and functional information of potential bio-medical importance and additional diagnostic information on linear media which cannot be achieved from polarization blind measurements. Defected white blood cells contain the morphological information with optically active birefringent property. The 36 different intensity states obtained from experimental results are used for the construction of the Mueller matrix in each pixel. The elements of that matrix corresponding to that pixel of the final image will show functional as well as diagnostic information which has medical importance. It is interesting to note that using this imaging technique, white blood cells are also detected and blood cell size is also determined.

9599-83, Session PWed

Dermoscopy analysis of RGB-images based on comparative features

Oleg O. Myakinin, Valery P. Zakharov, Ivan A. Bratchenko, Dmitry N. Artemyev, Samara State Aerospace Univ. (Russian Federation); Evgeny Y. Neretin, Sergey V. Kozlov, Samara State Medical Univ. (Russian Federation)

In this paper, we propose an algorithm for color and texture analysis for dermoscopic images of human skin based on Haar wavelets, Local Binary Patterns (LBP) and Histogram Analysis. This approach is a modification of «7-point checklist» clinical method. Thus, that is an "absolute" diagnostic method because one is using only features extracted from tumor's ROI (Region of Interest), which can be selected manually and/or using a special algorithm. We propose additional features extracted from the same image for comparative analysis of tumor and healthy skin. We used Euclidean distance, Cosine similarity, and Tanimoto coefficient as comparison metrics between color and texture features extracted from tumor's and healthy skin's ROI separately. A classifier for separating melanoma images from other tumors has been built by SVM (Support Vector Machine) algorithm. Classification's errors with and without comparative features between skin and tumor have been analyzed. Significant increase of recognition quality with comparative features has been demonstrated. Moreover, we analyzed two modes (manual and automatic) for ROI selecting on tumor and healthy skin areas. We have reached 91% of sensitivity using comparative features in contrast with 77% of sensitivity using the only "absolute" method. The specificity was the invariable (94%) in both cases.

9599-84, Session PWed

Meteor localization via statistical analysis of spatially: temporal fluctuations in image sequences

Jaromír Kukal, Institute of Chemical Technology (Czech Republic); Martin Klimt, Czech Technical Univ. in Prague (Czech Republic); Jan Švihlík, Institute of Chemical Technology (Czech Republic); Karel Fliegel, Czech Technical Univ. in Prague (Czech Republic)

Meteor detection is one of the most important procedure in astronomical imaging. Meteor path in Earth's atmosphere is traditionally reconstructed from double station video observation system generating 2D image sequences.

However, the atmospheric turbulences and other factors cause spatially temporal fluctuations of image background, which makes the localization of meteor path more difficult. Our approach is based on non-linear preprocessing of image intensity using Box-Cox and logarithmic transform as its particular case. The transformed image sequences are then differentiated along discrete coordinates to obtain statistical description of sky background fluctuations, which can be modeled by multivariate normal distribution. After verification and hypothesis testing, we use the statistical model for outlier detection. Meanwhile the isolated outlier points are ignored, the compact cluster of outliers indicates the presence of meteoroids after ignition.

9599-85, Session PWed

Virtual spectral multiplexing for applications in in-situ imaging microscopy of transient phenomena

Farnoud Kazemzadeh, Mohammad Javad Shafiee, Jason Deglint, Edward Li, Iman Khodadad, Simarjeet S. Saini, Alexander Wong, David A. Clausi, Univ. of Waterloo (Canada)

Multispectral sensing is specifically designed to provide quantitative spectral information about various materials or scenes. Using spectral informatio, various properties of objects can be measured and analysed. Microscopy, or observing and imaging objects at the micron- or nano-scale is one application where multispectral sensing can help tremendously, as there are many fields of science and research that use microscopy that would benefit from observing a specimen in multiple wavelengths. Multispectral microscopy is available but often requires the operator of the device to switch filters which is a labor intensive process. Furthermore, the need for filter switching makes such systems particularly limiting in cases where the sample contains live species that are constantly moving or exhibit transient phenomena. Direct methods for capturing multispectral data simultaneously of a live sample can also be challenging for microscopy applications as it requires elaborate optical systems design using beamsplitters and a number of detectors, proportional to the number of bands sought after. Such devices can therefore be quite costly to build and difficult to maintain, particularly for microscopy. Here, we present the concept of virtual spectral multiplexing imaging (VSMI) microscopy for low-cost, in-situ multispectral microscopy of transient phenomena. In VSMI microscopy, the spectral response of a color detector in the microscope is characterized and virtual spectral multiplexing is performed on the simultaneously-acquired detector measurements based on the developed spectral characterization model to produce microscopic imagery at multiple wavelengths. The proposed VSMI microscope was used to observe nano-reflectors at various wavelengths simultaneously to illustrate its efficacy.

9599-86, Session PWed

Additive discrete 1D linear canonical transform

Liang T. Zhao, John J. Healy, John T. Sheridan, Univ. College Dublin (Ireland)

The continuous linear canonical transforms (LCT) can describe a wide variety of wave field propagations through paraxial first order optical systems. Digital algorithms to numerically calculate the LCT are therefore important in modelling scalar wave field propagations and are also of interest for many digital signal processing applications. The continuous



LCTs are additive, but discretization can remove this property. In this paper we discuss several special cases of the LCT for which constraints can be identified to ensure the DLCTs are additive.

9599-87, Session PWed

Color normalization for robust evaluation of microscopy images

Jan Švihlík, Jan Kybic, Czech Technical Univ. in Prague (Czech Republic); David Habart, Institute for Clinical and Experimental Medicine (Czech Republic)

This paper deals with color normalization of microscopy images of Langerhans islets to increase robustness of the islet segmentation to illumination changes. The main application is automatic quantitative evaluation of the islet parameters, useful for determining the feasibility of islet transplantation in diabetes. The microscopy image intended for color normalization is firstly normalized due to nonuniform profile of illumination. It means that we have to find background profile for all color channels. We found that image background could be fitted by second order polynomial. Hence, the islets must be approximately identified by preliminary mask created as a preliminary segmentation of image. The mask areas where the islets were identified are interpolated to obtain smooth background surface.

Color normalization were done in logarithmic RGB and l-alpha-beta color spaces. We consider color normalization for two classes (islet and background). The method normalizes colors of two classes in source image according to colors of corresponding classes in reference images. To identify classes we used mask created by k-means algorithm. The classifier based on logistic regression was trained using 46 images and corresponding fully manual segmentation (ground truth).

There are 141 clinical images (Z set) in our database taken under different light conditions. Approximately 17% images from this database cannot be segmented satisfactorily using trained classifier. Hence, we apply color normalization to selected clinical images, where the fully manual segmentations were created. ROC curve computed for images normalized in color showed considerable improvement of segmentation results.

9599-88, Session PWed

Inference of dense spectral reflectance images from sparse reflectance measurement using non-linear regression modeling

Jason Deglint, Farnoud Kazemzadeh, Alexander Wong, David A. Clausi, Univ. of Waterloo (Canada)

One method to acquire multispectral images is to sequentially capture a series of images where each image contains information from a different bandwidth of light. Another method is to use a series of beamsplitters and dichroic filters to guide different bandwidths of light onto different cameras. However, these methods are very time consuming and expensive and perform poorly in dynamic scenes or when observing transient phenomena. An alternative strategy to capturing multispectral data is to infer this data using sparse spectral reflectance measurements captured using an imaging device with overlapping bandpass filters, such as a consumer digital camera using a Bayer filter pattern. Currently the only method of inferring dense reflectance spectra is the Wiener adaptive filter, which makes Gaussian assumptions about the data. However, these assumptions may not always hold true for all data. We propose a new technique to infer dense reflectance spectra from sparse spectral measurements through the use of a non-linear regression model. The non-linear regression model used in this technique is the random forest model, which is an ensemble of decision trees and trained via the spectral characterization of the optical imaging system and spectral data pair generation. This model is then evaluated by spectrally characterizing different patches on the Macbeth color chart, as well as by reconstructing virtual multispectral images. Results show that the proposed technique can produce inferred dense reflectance spectra that

correlate well with the true dense reflectance spectra, which illustrates the merits of the technique.

9599-89, Session PWed

A digital architecture for striping noise compensation in push-broom hyperspectral cameras

Wladimir Valenzuela, Miguel Figueroa, Jorge E. Pezoa Nunez, Univ. de Concepción (Chile)

We present a striping noise compensation architecture for hyperspectral push-broom cameras, implemented on a Field-Programmable Gate Array (FPGA). The circuit is fast, compact, low power, and is capable of eliminating the striping noise in-line during the image acquisition process

The architecture implements a multidimensional neural-network algorithm for striping noise compensation previously reported by our group. The algorithm relies on the assumption that the amount of light impinging at the neighboring photo-detectors is approximately the same in the spatial and spectral dimensions. Under this assumption, two striping noise parameters are estimated using spatial and spectral information from the raw data.

We implemented the circuit on a Xilinx ZYNQ XC7Z2010 FPGA and tested it with images obtained from a NIR N17E push-broom camera, with a frame rate of 25fps and a band-pixel rate of 1.888 MHz. The setup consists of a loop of 320 samples of 320 spatial lines and 236 spectral bands between 900 and 1700 nanometers, in laboratory condition, captured with a rigid push-broom controller. The computation core can run at 100 MHZ and consumes less than 25mW of dynamic power, using less than 10% of the logic resources available on the chip. It also uses one of two ARM processors available on the FPGA for data acquisition and communication purposes.

9599-90, Session PWed

Blind identification of linear degradation operators in the Fourier domain

Victor N. Karnaukhov, Vitaly Kober, Institute for Information Transmission Problems (Russian Federation)

Digital images are often affected by environmental and technical interferences such as linear homogeneous distortion, nonuniform illumination, sensors' noise, geometrical scene distortion, etc. Among these issues, the former is particularly interesting because various physical problems can be modeled by such degradations. In this work we propose a blind algorithm for identification of the linear distortion operator based on the analysis of zero-crossings and phase distribution of the distorted image spectrum. The proposed blind identification algorithm is tested with common real linear distortion operators and its identification rate is discussed.

9599-92, Session PWed

Support plane method applied to ground objects recognition using modelled SAR images

Denis A. Zherdev, Vladimir A. Fursov, Samara State Aerospace Univ. (Russian Federation) and Image Processing Systems Institute (Russian Federation)

The solution of electromagnetic scattering radiation problem is very important and has a wide application in practice, e.g. in navigation systems, in problem of target type determining. We can interpret radar system measuring in different manner such as making 1D radar cross section diagram or making 2D synthetic aperture radar (SAR) image. In this investigation we are concentrate our discuss on a target recognition



using modelled SAR images. We are using the same FDTD method for electromagnetic scattering modelling which is presented at work [1]. In our work, we are modelling airborne SAR image scenario of ground objects electromagnetic field scattering. The modelling approach is very useful in a target recognition problem, when we do not exactly known about the electromagnetic properties of the underlying surface. In this study, we are show recognition quality of support plane method [2] and discuss the results.

[1] Calvin Le; Traian Dogaru, "Synthetic aperture radar imaging of a twostory building" Proc. SPIE 8361, Radar Sensor Technology XVI, 83610J; 2012; doi: 10.1117/12.919923.

[2] Denis A. Zherdev, Vladimir A. Fursov, "Pattern recognition of electromagnetic field scattering from anthropogenic objects on underlying surface" Proc. SPIE 9216, Optics and Photonics for Information Processing VIII, 92160Z, 2014; doi:10.1117/12.2061354.

9599-94, Session PWed

A custom hardware classifier for bruised apple detection in hyperspectral images

Javier Cárdenas, Miguel Figueroa, Jorge E. Pezoa Nunez, Univ. de Concepción (Chile)

We present a custom digital architecture for bruised apple classification using hyperspectral images in the near infrared (NIR) spectrum. The algorithm classifies each pixel in an image into one of three classes: bruised, non bruised, and background. We extract two 5-element feature vectors for each pixel using only 10 out of the 236 spectral bands provided by the hyperspectral camera, which greatly reduces the requirements of the imager and the computational complexity of the algorithm. We then use two linearkernel support vector machines (SVMs) to classify each pixel. Each SVM was trained with 504 17x17-pixel windows taken from 14 hyperspectral images of 320x320 pixels each, for each class. The architecture then computes the percentage of bruised pixels in each apple in order to adequately classify the fruit.

We implemented the architecture on a Xilinx ZYNQ XC7Z210 Field-Programmable Gate Array (FPGA) and tested it on images from a NIR N17E push-broom camera with a frame rate of 25fps, a band-pixel rate of 1.888 MHz, and 236 spectral bands between 900 and 1700 nanometers in laboratory conditions. Using 12-bit fixed-point arithmetic, the circuit accurately discriminates 95.2% of the pixels corresponding to an apple, 81% of the pixels corresponding to a bruised apple, and 93.4% of the background. With the default threshold settings, the highest false-positive for a bruised apple is 18.7%. The circuit operates at the native frame rate of the camera, consumes 88mW of dynamic power, and uses less than 20% of the logic resources on the FPGA.

9599-95, Session PWed

GPU accelerated processing of astronomical high frame-rate videosequences

Stanislav Vítek, Czech Technical Univ. in Prague (Czech Republic); Jan Švihlík, Faculty of Chemical Technology (Czech Republic); Lukáš Krasula, Karel Fliegel, Petr Páta, Czech Technical Univ. in Prague (Czech Republic)

This work deals with GPU accelerated processing of high frame-rate astronomical video-sequences, mostly originating from experiment MAIA. MAIA (Meteor Automatic Imager and Analyser) is an double station system primarily focused to observing of faint meteoric events with a high time resolution. Using the double station data of the meteor we can calculate its atmospheric trajectory and the heliocentric orbit. The meteor light curve provides us with information about the mass of the original particle. Both the shape of this curves as well as the height interval where the meteor radiates correspond to the structure of the parent meteoroid.The instrument with price bellow 2000 euro consists of image intensifier (typical gain is about 30000 to 60000 lm/lm) and gigabite ethernet camera with resolution 767x576 pixels running at 61 fps. The biggest bottleneck of the device is built-in automatic gain control of the image intensifier - gain is rapidly decreasing if any bright stellar object appears in the field of view. With resolution better than VGA the system produces up to 2TB of possible scientifically valuable video data on both stations. Main goal of the paper is to propose and evaluate parallel GPU algorithms able to classify huge amount of video-sequences in order to delete all uninteresting data – there is limited storage capacity on the station. Paper shows that it is possible to reduce algorithms' complexity and process the data in almost real-time.

9599-96, Session PWed

Pattern recognition descriptor using the Z-Fisher transform

Carolina Barajas-Garcia, Selene Solorza-Calderón, Univ. Autónoma de Baja California (Mexico); Josué Álvarez-Borrego, Ctr. de Investigación Científica y de Educación Superior de Ensenada B.C. (Mexico)

In this work a pattern recognition digital image descriptor invariant to rotation, scale and translation (RST), which classify images using the Z-Fisher transform is presented. The descriptor uses binary rings masks obtained from the Fourier transform (called Fourier masks) to build 1D signatures. In this manner the computational cost time is reduced because the relevant data is contained in a vector (the 1D signature) instead of a matrix (an image). The 1D signature is invariant to rotation, scale and translation. The descriptor uses the amplitude spectrum of the Fourier transform, which is translation invariance. The amplitude spectrum of the normalized analytic Fourier-Mellin transform (AFM) is utilized in the scale invariance. The rings masks filter this normalized AFM amplitude spectrum to achieve the rotation invariance. The comparisons of the signatures were calculated using the normalized linear correlation, that is, the Pearson correlation coefficient (PCC). If the PCC value of a problem image is similar to the PCC value of the target image, then the problem image is the same as the target otherwise they are different. In general, those PCC values do not satisfy a normal distribution, hence the Fisher's Z distribution is employed to determine the confidence level of the RST invariant descriptor. A Matlab program was develop to classify gray-scale digital images of fossil diatoms. Those images were selected due to the similarity in their morphology. The descriptor presents a confidence level of 95%; moreover it works when the images have some noise or non-homogeneous illumination.

9599-97, Session PWed

Fourier based detection of microcalcifications in mammograms

Elizabeth López Meléndez, Luis David Lara-Rodríguez, Gonzalo Urcid, Instituto Nacional de Astrofísica, Óptica y Electrónica (Mexico)

This paper presents a Fourier transform approach to detect microcalcifications in digital mammograms. The basic idea consists in the design of parametric Butterworth bandpass filters in the Fourier domain used to extract sharpened border like structures that correspond to detected mammographic microcalcifications. Image thresholding of the filtered image is accomplished, first by homogenizing the background (fibroglandular tissue) with a median filter, after which a gamma correction is applied to change the global contrast. Second, by postprocessing the resulting image using histogram based local and global criteria we obtain a properly binarized image that signals the desired objects (microcalcifications) and final segmentation is achieved using a sequence of morphological binary operations. Several illustrative examples taken from a clinical database are included to demonstrate the capability of the proposed approach in comparison with other edge detection techniques such as the difference of Gaussians (DOG) and the Laplacian of a Gaussian (LOG).



9599-98, Session PWed

A dendritic lattice neural network for color image segmentation

Gonzalo Urcid, Luis David Lara-Rodríguez, Elizabeth López Meléndez, Instituto Nacional de Astrofísica, Óptica y Electrónica (Mexico)

A two-layer dendritic lattice neural network is proposed to segment color images in RGB space. The two layer neural network is a fully interconnected feedforward net consisting of an input layer that recieves color pixel values, an intermediate layer that computes pixel interdistances, and an output layer used to classify colors by hetero-association. The two-layer net is first initialized with a finite small subset of the colors present in the input image. These colors are obtained by means of an automatic clustering procedure such as k-means, fuzzy c-means, or as derived from the column vectors and main diagonals of the dual lattice min and max auto-associative memories. In the second stage the color image is scanned on a pixel by pixel basis where each picture element is treated as a vector and feeded into the network. For illustration purposes we use public domain color images to show the performance of our proposed image segmentation technique.

9599-99, Session PWed

True-color image encoding technique for segmented RF transmission using limited bandwidth

Yuriy Kotsarenko, Gustavo Urquiza, Svetlana V. Koshevaya, Univ. Autónoma del Estado de Morelos (Mexico)

In this work a new technique for encoding true-color image data is described, where individual segments of color pixels provided in one of perceptually accurate color spaces are encoded into digital bits suitable for RF transmission over long distances such as volcano monitoring or highaltitude photography. The data in its simplest form can be taken linearly or by using certain patterns such as Hilbert curve to improve overall image recovery in case of data loss or corruption. Color information is encoded into bits by allocating higher bandwidth to overall brightness while still providing limited amount of color information sufficient to reconstruct the image with decent visual quality after transmission. Experimental results are provided, where different high-quality images are processed using the described technique, including noise and data loss simulation, comparing and analyzing the resulting images with their original counterparts. Performance benchmarks are also provided running on a variety of embedded and desktop hardware compared with other classical encoding techniques such as JPEG and YUYV. The resulting experiments show that the proposed technique provides reasonable balance between image quality, bandwidth usage and real-time performance, while also being tolerant to data loss and corruption during transmission.

9599-100, Session PWed

Analysis of the palm vein distribution for people recognition

Raúl Castro-Ortega, Carina Toxqui-Quitl, Univ. Politécnica de Tulancingo (Mexico); Gabriel Cristóbal Perez, Instituto de Óptica "Daza de Valdés" (Spain) and Consejo Superior de Investigaciones Científicas (Spain); José Victor Marcos-Martín, Instituto de Óptica "Daza de Valdés" (Spain); Alfonso Padilla-Vivanco, Univ. Politécnica de Tulancingo (Mexico)

The shape of the hand vascular pattern contains useful and unique features that can be used for identifying and authenticating people, with applications in access control, medicine and financial services. In this work,

an optical system for the image acquisition of the hand vascular pattern is implemented. It consists of a CCD camera with sensitivity in the IR and a light source with emission in the 880 nm. The IR radiation interacts with the desoxyhemoglobin, hemoglobin and water present in the blood of the veins, making possible to see the vein pattern underneath skin. The segmentation of the Region Of Interest (ROI) is achieved using geometrical moments locating the centroid of each image. To enhancement the image of the vein pattern, a preprocessing step is given by spatial filtering that remove unnecessary information such as body hair and skinfolds. After that, a method of adaptive thresholding and mathematical morphology operations are used in order to get a binary image. A feature extraction method based on subsampled binary image is proposed. The classification task is achieved using K-Nearest Neighbors (KNN) and Artificial Neural Networks (ANN). Experimental results using the PolyU Multispectral Palmprint database show a percentage of correct classification, higher of 97% with KNN and ANN for 2,400 images of 200 people with 12 versions each one.

9599-101, Session PWed

Correlation peak analysis applied to a sequence of images using two different filters

Veronica Patron, Univ. de Sonora (Mexico); Josué Álvarez-Borrego, Ctr. de Investigación Científica y de Educación Superior de Ensenada B.C. (Mexico); Ángel Coronel Beltrán, Univ. de Sonora (Mexico)

Eye tracking has many useful applications that range from biometrics to face recognition and human-computer interaction. The analysis of the characteristics of the eyes has become one of the methods to accomplish the location of the eyes and the tracking of the point of gaze. Characteristics such as the contrast between the iris and the sclera, the shape, and distribution of colors and dark/light zones in the area, are the starting point for these analyses. In this work, we will focus on the contrast between the iris and the sclera, performing a correlation in the frequency domain. The images are acquired with an ordinary camera, with the aid of thirty volunteers. The reference image is an image of the subjects looking to a point in front of them at 0° angle. Then sequences of images are taken with the subject looking at different angles. These images are processed in MATLAB, obtaining the correlation peak maximum for each image, using two different filters. Each filter is analyzed and then we selected the filter that gives us the best performance in terms of the utility of the data, which is displayed in graphs that shows us the decay of the correlation peak as the eye moves progressively at different angle. This data will be used to obtain a mathematical model or function that establishes a relationship between the angle of vision and the correlation peak. This model will be tested using different input images than the ones used to create the initial database. being able to predict angle of vision using the correlation peak maximum data.

9599-102, Session PWed

Robust template matching using runlength encoding

Hunsue Lee, Sungho Suh, Hansang Cho, SAMSUNG Electro-Mechanics (Korea, Republic of)

In this paper, we introduce a template matching algorithm using Run-length Encoding (RLE). In manufacturing process, visual inspection is essential to prevent customers from receiving defective products. Since template matching is the fundamental step for visual inspection, the procedure should be not only fast but also accurate. Conventionally, our template matching approach was based on the convolution which is fast, relatively accurate, and easy to apply on greyscale images. However, due to variations in real products, cases where template images are mismatched or not found in captured images can occur.

As a description for the problem, we assumed as follows: 1) Only one



template image exists in the region of interest (ROI), 2) There are differences between the template image and the captured image in size, shape, and other features due to the factors such as manufacturing processes.

The matching procedures are as follows. First, the template image is blurred by a 5x5 box filter. Second, two sets of accumulated data, both foreground and background of the blurred image, are generated. Third, make RLE data from these data. Finally, find each offset that minimizes the cost function.

We verified the performance of the proposed algorithm by comparing it with the pattern matching function provided by Matrox Imaging Library (MIL). As a result, the processing duration was almost the same. However, the proposed algorithm was able to find several templates in the images whereas MIL was not. Consequently, our proposed algorithm was verified more promising results than the conventional template matching method for visual inspection.

9599-103, Session PWed

Discrete Wigner distribution function of a circular aperture displaced of the origin of space coordinates using coherent light

Sergio Mejia-Romero, Luis Raúl Berriel-Valdos, Instituto Nacional de Astrofísica, Óptica y Electrónica (Mexico)

In this work we have applied the experimental Discrete Wigner Distribution Function (DWD) to a circular aperture in order to know the behavior of the Quasi-Point Sources (QPS) placed outside of the origin over the object space. In the experimental setup we placed the circle aperture with radius a in the object space. This aperture is coherently illuminated. Then the optical system form the DWD resultant in the focal image plane which is detected by the CCD sensor. The aperture is displaced over the object space and the DWD is observed in real-time for each point of object space. When the DWD has been captured with the CCD sensor we digitally verified the positivity criterion, thus we can assess if the object is a QPS for the optical system used in the experimental setup. For the computational simulation we use the numerical aperture (NA) of the optical system. From NA obtained, we evaluate the Airy disc. This information allows us to calculate the maximum radius of the circular aperture that still supports this aperture act as QPS. Finally, we compared both theoretical and experimental results thus discard systematic errors in the experiment.

This analysis of the experimental results allows us to conclude that if a circular aperture is a QPS in the origin then the same circular aperture can be a QPS in any point of the object space. Otherwise, if it is proved that the circular aperture in the origin is not a QPS then neither will be in any other point of the object space.

9599-104, Session PWed

Reconstruction of digital holograms from three intensity measurements

Liang T. Zhao, Univ. College Dublin (Ireland); Yang Wu, Damien P. Kelly, Technische Univ. Ilmenau (Germany); John T. Sheridan, Univ. College Dublin (Ireland)

In this paper, we develop a new practical technique based on digital holography for the reconstruction of a wave front from three intensity recordings. Combining the off-axis Fourier filtering technique with boundary detection and iterative phase retrieval algorithm, it is shown how problems such as elimination of the twin image can be achieved. Our proposed method overcomes the issues of feasibility and accuracy associated with off-axis Fourier filtering, cost and alignment associated with Phase shifting interferometry, and also the issues associated with working with diffuser objects. In order to further test the performance of our proposed method, simulation results for both non-diffuser and diffuser objects are presented.

9599-105, Session PWed

Non-destructively reading out information embedded inside real objects by using farinfrared light

Ayumi Okada, Masahiro Suzuki, Hideyuki Torii, Kazutake Uehira, Kanagawa Institute of Technology (Japan); Youichi Takashima, Nippon Telegraph and Telephone Corp. (Japan)

This paper presents a technique that can non-destructively read out information embedded inside real objects by using far-infrared light. We proposed a technique that could protect the copyrights of digital content for homemade products using digital fabrication technologies such as those in 3D printers. It embeds information on copyrights inside real objects produced by 3D printers by forming fine structures inside the objects as a watermark that cannot be observed from the outside. Fine structure is formed near the surface inside the real object during its fabrication. Information embedded inside the real object is required to be read out non-destructively. We used a technique that can non-destructively read out information from inside real objects by using far-infrared light. We conducted experiments where we structured fine cavities inside the objects. The disposition of the fine domain expressed information. We used the flat and curved surface of the object. The results obtained from the experiments demonstrated that the disposition pattern of fine structure was appeared on the surface of the object as temperature profile when irradiating farinfrared light on the surface of the object. Embedded information could be read out successfully by analyzing temperature profile image of the surface of the object that is captured with thermography. These results demonstrated the feasibility of the technique we propose.

9599-106, Session PWed

Information embedding in real object image using temporally brightnessmodulated light

Piyarat Silapasuphakornwong, Hiroshi Unno, Kazutake Uehira, Kanagawa Institute of Technology (Japan)

We propose a new technology that can embed information invisibly into the image of the object in a real space that is captured with video camera. This technique uses illumination that invisibly contains some information. As the illumination for the object contains information, the image of the object taken by the video camera also contains information although it cannot be seen. This information can be extracted by image processing. It uses temporally luminance modulated pattern as invisible information. Amplitude of the modulation is too small to perceive. Frequency of modulation is the same as the frame frequency of the projector that is used as a lighting device. Frame images over some period are added up after changing the sign of the even- or odd-numbered frames. Brightness changes by modulation in each frame are accumulated over the frames used in addition. On the other hand, the object and background image is removed because the even and odd frame are opposite in a sign. AS a result, the patterns become visible. We conducted experiment and the results from these revealed that invisible patterns could be read out extremely accurately. Moreover, we evaluated invisibility of the embedded pattern and confirmed that there existed conditions where both invisibility and readability of the patterns were satisfied at the same time. This paper also describes some application of this technique such as invisible QR code that is on the real object.

9599-107, Session PWed

Tutte polynomial applied to processing of functional magnetic resonance images

Marlly Garcia-Castillon, Univ. EAFIT (Colombia)

Conference 9599: Applications of Digital Image Processing XXXVIII



Methods of graph theory are applied to the processing of functional magnetic resonance images. Specifically the Tutte polynomial is used to analyze such kind of images. Functional Magnetic Resonance Imaging provide us connectivity networks in the brain which are represented by graphs and the Tutte polynomial will be applied. The problem of computing the Tutte polynomial for a given graph is #P-hard even for planar graphs. For a practical application the maple packages "GraphTheory" and "SpecialGraphs" will be used. We will consider certain diagram which is depicting functional connectivity, specifically between frontal and posterior areas, in autism during an inferential text comprehension task. The Tutte polynomial for the resulting neural networks will be obtained. Our results show that the Tutte polynomial is a powerful tool to analyze and characterize the networks obtained from functional magnetic resonance imaging.

9599-108, Session PWed

Detecting curvatures in digital images using filters derived from differential geometry

Juanita Toro-Giraldo, Univ. EAFIT (Colombia)

Detection of curvature in digital images is an important theoretical and practical problem in image processing. Many important features in an image are associated with curvature and the detection of such features is reduced to detection and characterization of curvatures. Differential geometry studies many kinds of curvature operators and from these curvature operators is possible to derive powerful filters for image processing which are able to detect curvature in digital images and videos. The curvature operators are formulated in terms of partial differential operators which can be applied to images via convolution with gaussian kernels. We present an algorithm for detection of curvature in digital images which is implemented using the Maple package ImageTools. Some experiments were performed and the results we very good. We compare the results using gaussian derivatives with the results obtained using Airy derivatives. It is claimed that the resulting curvature detectors could be incorporated in standard programs for image processing.

9599-109, Session PWed

An image registration technique based on BWB mask

Ihtsham U. Haq, Pakistan Council of Scientific & Industrial Research (Pakistan) and Pakistan Institute of Engineering and Applied Sciences (Pakistan); Asloob A. Mudassar, Pakistan Institute of Engineering and Applied Sciences (Pakistan)

Image registration has now become a pre-processing stage in many of the image processing tasks such as geometric super-resolution, image reconstruction, ... etc – having applications in the field of medical imaging, machine vision, industrial inspection, metrology, motion detection,...etc.

In this paper, we are presenting a registration technique for indoor targets – whose digital images are collected from a digital imager under jittering or motion. For this a Black-White-Black (BWB) mask is pasted over a region of less or no interest on the target. This BWB mask is made by pasting a white sticker concentric over a wider black sticker – having nearly same width of these three regions. Minimum mask widths required for this are described in paper.

The masked object/target is then imaged through a jittering/moving camera and many images are recorded. For registering these images, the subpixally equivalent digital images are first discarded. The rest of the unique images are then detected for BWB mark in them. The relative contrast in x and y direction within the BWB images of the selected images are then sorted in ascending or descending order. The images are then ordered corresponding to these sorted contrasts. This yields us a subpixally-ordered registered set of images. Simulation results are presented. This technique can be applied to indoor and remote targets as well – which have inherent relatively-immovable high contrast marks/objects in it – assuming any of them as equivalent BWB mask. On this assumption, the applications of this technique can be extended to remote targets also – such as defense, astronomy, image mosaicing, space imaging, mobile imaging.

9599-110, Session PWed

Face recognition using the most representative sift images

Issam J. Dagher, Univ. of Balamand (Lebanon)

In this paper, face recognition using the most representative SIFT images is presented. It is based on obtaining the SIFT (SCALE INVARIANT FEATURE TRANSFORM) features in different regions of each training image. Those regions were obtained using the K-means clustering algorithm applied on the key-points obtained from the SIFT algorithm. Based on these features, an algorithm which will get the most representative images of each face is presented. In the test phase, an unknown face image is recognized according to those representative images. This algorithm is compared to other algorithms for different databases.

9599-111, Session PWed

Improvements for hot pixels in digital imagers using lossless approximation techniques

Ofer Hadar, Ariel Shleifer, Ben-Gurion Univ. of the Negev (Israel)

During the last twenty years, digital imagers have spread into industrial and everyday devices such as satellites, security cameras, cell phones, laptops and more. "hot pixels" are the main defects in remote digital cameras. Previous studies led by Prof. Israel Koren, have shown that these defects are permanent, their number increases continuously over the sensor's lifetime, and they eventually manifest themselves in all captured images and reduce significantly the image quality.

We will show improvements in the prediction of the pixel using lossless compression techniques.

We shall use the study of Prof. Koren as our basis.

These defects pose a serious problem for applications that demand high image quality. The defect rate was shown to increase dramatically as the pixel size falls from 2 microns. Prof. Koren's group developed a Bayesian technique for detecting and tracing defects based on a series of images taken by the imager.

A linear correction technique presented is able to correct a large percentage of the hot pixels up to the level of the noise floor using exposure time, illumination and an average of the neighboring pixels.

We shall use known prediction methods on top of the algorithm, namely the CALIC algorithm, which shows the greatest accuracy in the prediction of the pixel. Still, all of the lossless algorithms assume input of pixels in the way of a raster scan but we can use the entire information from the image except for one hot pixel. Thus we intend to re-engineer the lossless algorithm to use all the surrounding pixels.

9599-50, Session 8

An overview of new video coding tools under consideration for VP10: the successor to VP9

Debargha Mukherjee, Google (United States)

Google has recently embarked on an ambitious open-source project to develop a next generation royalty-free video codec VP10 that achieves at

Conference 9599: Applications of Digital Image Processing XXXVIII



least 30-40% bit-rate reduction over the current generation codec VP9. While the project is still in early stages, a set of new coding tools has been added to baseline VP9 to achieve at least about 6% coding gain already over a large enough test set. This talk will provide an in-depth technical overview of these coding tools, along with information on how other parties can be involved in this project.

9599-51, Session 8

Cyber attack/defense algorithms based on data hiding in compressed video stream

Ofer Hadar, Y. Amsalem, Ben-Gurion Univ. of the Negev (Israel)

This research presents several algorithms to generate a fast, robust, sophisticated and hard to detect cyber attack/defense over trusted video streams.

More specifically, we focus on H.264 coded video over MPEG2 Transport Stream (ISO/IEC standard 13818-1 or ITU-T Rec. H.222.0), which is the most common protocol for video streaming now days.

Those video streams are very attractive access points (for attackers) into organizations internal secured network, and they highly compromise the network security.

Main research outcomes:

• Defense tool - which proactively defends against incoming cyber-attacks. This tool is based on causing random location damage to the original Image/Video, such that the probability of damaging the embedded malicious code will be high enough to destroy its capabilities in one hand, on the other hand causing only unnoticeable degradation of the image or video quality.

The tool will be located next to the network gateway.

• Attack tool - which embeds malicious shell code into the video payload (establishing a covert channel), injects malicious malware into a highly sensitive network, extracts the hacker shell code from the video payload on the victim servers and executing it.

Those tools are based on data hiding algorithms that was developed exclusively for purposes of attacking/defending the information system through compressed video streams.

9599-52, Session 8

Vision-based driver assistance systems using looking-in and looking-out framework

Ravi Kumar Satzoda, Univ. of California, San Diego (United States)

No Abstract Available

9599-53, Session 8

Overview of MPEG internet video coding

Ronggang Wang, Sang-hyo Park, Peking Univ. (China); Jae-Gon Kim, Korea Aerospace Univ. (Korea, Republic of); Tie-jun Huang, Peking Univ. (China); Euee S. Jang, Hanyang Univ. (Korea, Republic of); Wen Gao, Peking Univ. (China)

MPEG has produced standards that have provided the industry with the best video compression technologies. In order to address the diversified needs of the Internet, MPEG issued the Call for Proposals (CfP) for internet video coding in July, 2011 and April, 2013. It is anticipated that any patent declaration associated with the Baseline Profile of this standard will indicate

that the patent owner is prepared to grant a free of charge license to an unrestricted number of applicants on a worldwide, non-discriminatory basis and under other reasonable terms and conditions to make, use, and sell implementations of the Baseline Profile of this standard in accordance with the ITU-T/ITU-R/ISO/IEC Common Patent Policy. There three different codecs responded to the above requirements, which are WVC, VCB and IVC. WVC was proposed jointly by Apple, Cisco, Fraunhofer HHI, Magnum Semiconductor, Polycom and RIM etc. it's in fact AVC baseline. VCB was proposed by Google, and it's in fact VP8. IVC was proposed by several Universities (Peking University, Tsinghua University, Zhejiang University, HKUST, Hanyang University etc.) and its coding tools was developed from Zero. In this paper, we give an overview of the developing process, coding tools and IPR analysis of IVC, and evaluate its performance by comparing it with other competitors of WVC and VCB.

9599-54, Session 8

Privacy protection by transmorphing JPEG images

Touradj Ebrahimi, Lin Yuan, Ecole Polytechnique Fédérale de Lausanne (Switzerland)

The work presented in this paper deals with privacy protection of JPEG compressed images using a new approach called transmorphing. As opposed to scrambling, transmorphing now only protects selected regions of an image but also provide pictures that look pleasant. We present a working system composed of an application running on a mobile phone and a cloud service similar to Instagram where images can be share in a secure and privacy friendly way, and at the same time with the possibility of sharing such images in social networks such as Facebook. The paper in particular also includes results of an evaluation study that compared transmorphing with scrambling from various points of views.

9599-55, Session 8

Frequency Doman methods for demosaicking images sampled using arbitrary color filter array patterns

Hasib A. Siddiqui, Kalin Attanassov, Qualcomm Inc. (United States)

No Abstract Available

9599-57, Session 8

Compressed data organization for high throughput parallel entropy coding

Amir Said, Qualcomm Inc. (United States); Abo-Talib Mahfoodh, Michigan State Univ. (United States); Sehoon Yea, LG Electronics Inc. (Korea, Republic of)

No Abstract Available

9599-112, Session 8

3D objects sensing and coding for real virtual reality applications in the IoT and future media internet

Lazar Bivolarsky, Albena Technologies Ltd. (United Kingdom)

Deep learning is motivated by neuroscience and has a significant impact on

Conference 9599: Applications of Digital Image Processing XXXVIII



various applications such as computer vision. The multidisciplinary nature of deep learning led to advances in learning architectures and coding models. Artificial intelligence has gone through some dismal periods in the past, but now is not one of those times. The current excitement about AI stems, in great part, from groundbreaking advances in the areas involving neural networks. This machine learning technique promises dramatic improvements in computer vision exploring the bridge between bits and atoms aimed to make a path between the digital world and the physical one we populate, turning the environment we occupy into a digital model what connects virtual reality, augmented reality and reality. The future of IoT is in the coexistence of the physical world, cyber world and the machinehuman interface. The possibilities of virtual reality and IoT are in next step of information sharing and the evolution immersive video environments that allows for even more social experiences of ubiquitous applications that move beyond the computer, tablet and smartphone and into everything else. The future of computing lays into the new understanding of an intelligent data objects that interact with each other and the environment, including virtual and augmented reality, wearables, and collaboration applications.

9599-113, Session 8

Objective and subjective quality assessment of geometry compression of reconstructed 3D humans in a 3D virtual room

Rufael N Mekuria, Pablo Cesar, Centrum Wiskunde en Informatica (Netherlands); Ioannis Doumanis, CTVC (United Kingdom); Antonella Frisiello, ISMB Instituto Superiore Mario Boella (Italy)

Compression of 3D object based video is relevant for 3D Immersive applications.

Nevertheless, the perceptual aspects of the degradation introduced by codecs for meshes and point clouds are not well understood.

In this paper we evaluate the subjective and objective degradations introduced by such codecs in a state of art 3D immersive virtual room.

In the 3D immersive virtual room users are captured with multiple cameras, and their surfaces are reconstructed as photorealistic colored/textured 3D Meshes or point clouds.

To test the perceptual effect of compression and transmission, we render degraded versions with different frame rates in the scene in different contexts (near/far). The results show that simplified surfaces do not degrade the quality.

SPIE. PHOTONICS **Conference 9600:** Image Reconstruction from Incomplete Data VIII

Tuesday - Wednesday 11-12 August 2015

Part of Proceedings of SPIE Vol. 9600 Image Reconstruction from Incomplete Data VIII

9600-1, Session 1

Image reconstruction in serial femtosecond nanocrystallography using x-ray free-electron lasers (Invited Paper)

Rick P. Millane, Romain Arnal, Joe Chen, David Wojtas, Philip J. Bones, Univ. of Canterbury (New Zealand); Rick Kirian, Arizona State Univ. (United States); Ken Beyerlein, Richard Bean, Henry N. Chapman, Ctr. for Free-Electron Laser Science (Germany); John C. H. Spence, Arizona State Univ. (United States)

Serial femtosecond nanocrystallography (SFX) is a form of x-ray coherent diffraction imaging that utilises a stream of tiny nanocrystals of the biological assembly under study, in contrast to the larger crystals used in conventional x-ray crystallography using conventional x-ray synchrotron x-ray sources. Nanocrystallography utilises the extremely brief and intense x-ray pulses that are obtained from an x-ray free-electron laser (XFEL). A key advantage is that some biological macromolecules, such as membrane proteins for example, do not easily form large crystals, but spontaneously form nanocrystals. There is therefore an opportunity for structure determination for biological molecules that are inaccessible using conventional x-ray crystallography. Nanocrystallography introduces a number of interesting image reconstruction problems. Weak diffraction patterns are recorded from hundreds of thousands of nancocrystals in unknown orientations, and these data have to be assembled and merged into a 3D intensity dataset. The diffracted intensities can also be affected by the surface structure of the crystals that can contain incomplete unit cells. Furthermore, the small crystal size means that there is potentially access to diffraction information between the crystalline Bragg peaks. With this information, phase retrieval is possible without resorting to the collection of additional experimental data as is necessary in conventional protein crystallography. We report recent work on the diffraction characteristics of nanocrystals and the resulting reconstruction algorithms.

9600-2, Session 1

Dynamic optically multiplexed imaging

Yaron Rachlin, Vinay Shah, R. Hamilton Shepard, Tina Shih, MIT Lincoln Lab. (United States)

Optically multiplexed imagers overcome the tradeoff between field of view and resolution by superimposing images from multiple fields of view on a single focal plane. In this paper, imaging modes enabled by dynamically modified encoding of each field of view with high precision are investigated. Dynamic encoding functions allow for both the reconstruction of sparse scenes from a snapshot, compressive measurement, as well as the reconstruction of temporally varying dense scenes by capturing a sequence of encoded frames. The image quality and frame rate of a dynamic optically multiplexed imager are compared to conventional methods for achieving high resolution over a wide field of view. To demonstrate the feasibility of the sensor concept, a compact pupil-division multiplexed sensor capable of precisely changing its encoding functions was prototyped. Experimental results obtained with this sensor are presented.

9600-3, Session 1

Restoration of defocused images using quasi-point sources which are detected with coherent light

Rosalinda Ortiz Sosa, Luis Raúl Berriel-Valdos, J. Félix

Aguilar, Instituto Nacional de Astrofísica, Óptica y Electrónica (Mexico)

Since the intensity point spread function (ipsf) characterizes an imaging optical system (OS), it contains all the possible present aberrations in the image. However, the ipsf is an abstraction, useful for modeling the image formation process, but it cannot be experimentally realizable. Instead, the characterization of the OS could be estimated by means of the image of a quasi point source (qps), this is an aperture so small that cannot be resolved by the OS.

OPTICAL ENGINEERING+

APPLICATIONS

In this work, the use of the image of a qps illuminated with coherent light for restoring out-of-focus images detected with incoherent light is presented. An optical-digital method for the restoration is implemented, and consists of the characterization of the OS (which in this case is a conventional microscope), with a qps is illuminated with coherent light and detected outof-focus. The obtained image is then introduced in the Wiener filter for the deconvolution of the image of an extended object, provided this has been detected with the same amount of defocus but illuminated with incoherent light. The results of the restored images are shown and compared with those images restored when the qps is illuminated with incoherent light. Finally, a numerical evaluation of the quality of the restoration, using the RMSD (root mean square deviation) method, was made for both cases.

9600-4, Session 1

United estimation of blur distribution for space-variant rotation motion deblurring

Ziyi Shen, Tingfa Xu, Ziwei Liu, Hongqing Wang, Guokai Shi, Beijing Institute of Technology (China)

In recent years, many successful image deblurring algorithms have been proposed. A single kernel just has to be estimated in the situation of spaceinvariant deblurring. However, considering the space-variant blurs taken by nonlinear motion, such as influenced by the camera linear shaken and rotation, we could not estimate a kernel for the whole image and deblur it accurately, for a majority of models in our real situation, uniform deblurring is not usable or practical. In this paper, we present a method for estimating the space-varying kernel for rotation motion. After dividing several sector modules of the motion blur image into such blocks with different size, we estimate the rotary direction and the movement for each block in Fourier domain. An improved optimization for both direction and scale of different parts around the rotation center we estimated with the same radius, through a constraint of United Least square Filter is taken in our algorithm to structure the blur path accurately. Aiming at the different position of the rotary region, combining the blur distribution estimated with an operator which we create related to the spatial location, character and degree of rotation motion, we build a model to estimate a space-varying kernel for the rotation motion which is replaced by such pixels on the motion-blur-path with uniform and separate influence during the exposure in the original algorithm, it also could be used for space-variant deblurring. Experimental results for synthetic and real images demonstrate the effectiveness of this algorithm.

9600-5, Session 1

Geometric superresolution using double rect mask

Ihtsham U. Haq, National Physical and Standard Lab. (Pakistan) and Pakistan Institute of Engineering and Applied Sciences (Pakistan) and Pakistan Council of Scientific and Industrial Research (Pakistan); Asloob A. Mudassar, Pakistan Institute of Engineering and Applied Sciences (Pakistan); Ihtram U. Haq, Univ. of Karachi



(Pakistan); Asma A. Mirza, Federal Urdu Univ. of Arts, Sciences and Technology (Pakistan); Shakeel A. Khan, Government College Jaranwala, Faisalabad (Pakistan); A. Ikram, Univ. of Karachi (Pakistan); E. Hameed, Space and Upper Atmosphere Research Commission of Pakistan (Pakistan)

Today, in everyday imaging in science and research, a digital imager – despite of its lower resolution than conventional film camera, is the first choice due to its obvious advantages. Assuming the imaging system to be diffraction limited, this low resolution is due to two geometrical characteristics of the detector array (CCD/CMOS) used in it at image plane. These two characteristics are pitch and non-zero pixel size – which do sampling and averaging of optical information over pixel spatial area respectively and dictates geometric resolution limit of digital imager.

In this paper, we are proposing a geometric superresolution technique based on Double Rect Mask (DRM) – which are scanned over CCD by a half pixel in subpixel steps. The width of DRM are made relative to pixel such that max SNR is achieved keeping the system deterministic. DRM codes the image optically – which is then decoded computationally to get a superresolved image – spatially enhanced in resolution by subpixel factor. This virtually replaces each CCD pixel by a matrix of subpixels. The decoding process is executed in just one mathematical step.

The 2D simulation results are presented – showing an improvement in resolution by given super-resolution factor - in both x and y directions. Increasing the super-resolution factor more makes the result more close to original. The given superresolution technique can be applied to microscopy, medical imaging, machine vision, industrial inspection, metrology (dimensional metrology, optical metrology), defense, satellite imaging and astronomy.

9600-6, Session 2

Phase estimation for magnetic resonance imaging near metal prostheses

Philip J. Bones, Laura J. King, Rick P. Millane, Univ. of Canterbury (New Zealand)

Magnetic resonance imaging (MRI) has the potential to be the best technique for assessing complications in patients with metal orthopedic implants. The presence of fat can obscure definition of the other soft tissues in MRI images, so fat suppression is often required. However, the performance of existing fat suppression techniques is inadequate near metal, due to very large magnetic field perturbations induced by the implant. The three-point Dixon technique is potentially a method of choice as it is able to suppress fat in inhomogeneous magnetic fields, but the success of this technique depends on being able to accurately calculate the phase shift. This is generally done using phase unwrapping or iterative reconstruction algorithms. Most current techniques assume that the phase function is slowly varying and phase differences between adjacent points are limited to less than \$pi\$ radians in magnitude. Much greater phase differences can be present near metal prostheses. We present our experience with three phase estimation techniques which have been adapted to use prior knowledge of the implant. Two methods use phase unwrapping, with the first method identifying phase discontinuities before recovering the phase along paths through the image. Method 2 employs a transform to find the least squares solution to the unwrapped phase. The third method uses an iterative reconstruction technique which is assisted by prior knowledge. Simulation results indicate that all three methods show promise. Initial results obtained with image data acquired from a metal implant, oil and water phantom are presented as well.

9600-7, Session 2

Phase retrieval for multiple objects and undersampled intensity data

Rick P. Millane, Romain Arnal, Joe Chen, Univ. of Canterbury (New Zealand)

The phase retrieval problem for a single object is known to have a unique solution in two or more dimensions, and iterative projection algorithms are generally an effective reconstruction method. More difficult situations can arise however if it is necessary to retrieve phases when there are multiple objects or when the diffraction intensities are undersampled. These situations can arise if weak diffraction data are recorded from a small set of different kinds of object, and the intensities need to be averaged to increase the snr. The data can be undersampled if the object is crystalline. In both of these cases, the solvability, or uniqueness, of the problem can be characterised by an appropriate calculation of the "constraint ratio," that measures the independent data-to-parameter ratio. We show that uniqueness in such cases depends on the nature of the supports of the different objects and their dimensionality. For crystalline objects, uniqueness depends on an interplay between the object support and dimensionality, and the crystal symmetry. In cases where the solution is unique, iterative projection algorithms can be appropriately adapted to invert the data. Uniqueness results will be illustrated by examples and reconstruction algorithms by simulation. Specific applications in coherent diffraction imaging will be described.

9600-8, Session 2

A phase-space approach to imaging from limited data

Markus E. Testorf, Dartmouth College (United States)

The performance of imaging methods is inherently limited by the amount and type of data, which can be used for image reconstruction. Physical constraints may limit the access to information critical for the reconstruction process. Equally critical is the need to consider the amount of data stored, transmitted, and processed with an acceptable amount of resources.

In this contribution a system theory based on a phase-space description of optical signals is developed which provides a framework to analyze and compare imaging techniques, and which serves as the basis to develop efficient numerical image reconstruction algorithms.

This phase-space approach is based on the optical instrument function, where each optical detector is described by a function, and the measurement process by an overlap integral with the optical signal. A phase-space interpretation allows one to interpret the instrument function of optical detectors as an incoherent superposition of individual point detectors. Instruments are analyzed by tracing the detector function to the input plane of the optical instrument, where the measured signal is calculated as the phase-space overlap integral.

This framework provides the basis to analyze both coherent and incoherent imaging systems. Shack-Hartman sensors, plenoptic cameras, and phase retrieval, and compressive imaging methods are shown to measure domains in phase-space of finite size and finite resolution. It is demonstrated, how a sufficient diversity between measurements minimizes the number of data points required for solving a particular imaging problems. Both analytic as well as numeric methods for optimizing imaging methods from limited data sets are discussed. 9600-9, Session 2

Combination of genetic algorithms and FSD applied to fringe pattern demodulation

Ulises H. Rodríguez-Marmolejo, Univ. de Guadalajara (Mexico) and Instituto Tecnológico de Aguascalientes (Mexico); Tania A. Ramirez del Real, Jesús Muñoz-Maciel, Miguel Mora-González, Univ. de Guadalajara (Mexico)

In optical interferometry are several optimization methods applied to estimate the phase of a closed fringe pattern. There are several optimization techniques which play an important role in finding the phase interferogram parameters. In this work, a Genetic Algorithm in combination with Frequency guided Sequential Demodulation are implemented to estimation the phase of synthetic fringe pattern. The method gives good results in demodulation of closed fringe patterns. Results in processing time are similar to traditional optimization techniques, but the method presents computer simplifications to others algorithms.

9600-10, Session 3

Exploiting reciprocity for imaging

Morteza Karami, Michael A. Fiddy, The Univ. of North Carolina at Charlotte (United States)

We have considered the scattering and conversion of high spatial frequency (evanescent) waves into propagating waves by a complex scattering structure originally conceived as a metamaterial. The scattering structure thus serves as an encoder of that information. A metamaterial designed to have complementary scattering characteristics can be made to serve as a decoder. We explain how this structure might be used remotely to provide the reconstruction or decoding scattering mechanism to recover high resolution information, without the need for intermediate detection and numerical time reversal. We have investigated the application of the generalized reciprocity theorem to design complementary structures. Reciprocity in wave propagation refers to symmetry of the propagation under the interchange of the source and the observer. The dielectric tensors of the medium must satisfy certain symmetry properties for this to be true. S matrix methods show that reciprocity with or without evanescent waves is equivalent to time reversal invariance provided there are no losses. Reciprocity with losses is possible but is then not invariant under time reversal. We present some metamaterial designs which produce scattered fields that are phase conjugates of each other and relate this to time reversal and reciprocal scattering. These structures are then investigated to illustrate their use for remote imaging.

9600-11, Session 3

Joint sparse recovery in inverse scattering

Ok Kyun Lee, Jong Chul Ye, KAIST (Korea, Republic of)

Inverse scattering problems of various bio and medical imaging applications are required to solve the nonlinear integral equations accompanied with the nonlinear coupling between the target of recovery and the unknown data. Conventionally, linear approximation or iterative approach has been widely used to solve this non-linearity, however, they suffer from the approximation error or the computational burden, respectively. In this abstract, we propose a novel reconstruction method that solves the non-linearity in the inverse scattering problem using a joint sparsity in the compressed sensing theory. Based on the assumption that the target is sparse, the nonlinear coupling discussed above rather gives a clue to change the original inverse scattering problem into the joint sparse recovery problem under the multiple source and fixed detector geometry. Now, the entire procedure of the sparse target and the coupled nonlinear signal are estimated from the joint sparse recovery, and then they are utilized to estimate the unknown

data using the recursive nature of the forward problem formulation. Finally, the target is reconstructed based on the previous results. Neither approximation nor the time consuming iterative approach is necessary in the proposed method, therefore, we can expect more accurate and faster recovery compared to conventional approaches. We will show how it works for specific imaging techniques such as diffuse optical tomography and electrical impedance tomography.

SPIE. PHOTONICS

OPTICAL ENGINEERING+ APPLICATIONS

9600-12, Session 3

Superresolution imaging from nonlinear inverse scattering

Richard S. Ritter, Olivet Nazarene Univ. (United States); Michael A. Fiddy, The Univ. of North Carolina at Charlotte (United States)

Imaging from scattered fields is inherently a nonlinear problem unless weak or single scattering approximations (first Born or Rytov) can be made. Image reconstruction quality also clearly depends on the nature of the illumination used and number of scattered field measurements taken. We have developed a fast inversion method based on cepstral filtering in which an image of the scattering structure can be separated numerically from the associated total internal scattered fields [1]. The ability to do this depends on some prior knowledge of the maximum index or permittivity of the object in order to determine the number of degrees of freedom associated with the scattering-imaging problem. Having done this and recovered an image, we routinely see subwavelength scale features of the scattering object. This effect has been reported as far back as 1998 (Chew) and we have routinely observed it. We have conducted a series of numerical experiments using cepstral inversion for a cluster of discrete scatterers which together constitute a strong scatterer and investigated the trade-offs between the calculated number of degrees of freedom and the resolution achievable. The consequences of this study have importance not only for coherent diffraction imaging and superresolution imaging in general, but also for synthesis problems. The design of subwavelength-scale features in a scattering target can be used to define far field properties.

[1] Fiddy, M. A. and Ritter, R. S., Introduction to Imaging from Scattered Fields, CRC Press/Taylor and Francis, November 2014, ISBN-13: 978-1-4665-6958-4

9600-13, Session 4

Feature extraction for 3D object detection from integral imaging data (Invited Paper)

Doron Aloni, Yitzhak Yitzhaky, Ben-Gurion Univ. of the Negev (Israel)

Detecting the location of objects in a 3D scene is an interesting challenge, and can be useful for various applications of computer-vision. Recently, a new method was developed for locating objects in a 3D space using computationally-reconstructed integral imaging. In computationallyreconstructed integral imaging, using the multi-view images (recorded at slightly different angles), confocal images of depth planes are computationally reconstructed. In each reconstructed plane, the images of objects located at the depth of that plane appear sharp, while objects at other depths appear blurred, according to their distance from the reconstructed depth. The method for 3D object detection, finds the most focused regions in the reconstructed planes (D. Aloni, Y. Yitzhaky: "Detection of object existence from a single reconstructed plane obtained by integral imaging", IEEE Phot. Tech. Lett., 2014), and occurrence of objects at the depth axis (J.-H. Jung , D. Aloni, Y. Yitzhaky, E. Peli: "Active confocal imaging for visual prostheses", Vision Research, 2014). The features extracted and used in the object detection process are edges. Edges are informative and efficient descriptors of objects. Their efficiency results from the small number of edge pixels (relative to the whole intensity image) used in the detection process. In this work we analyze and compare different edge extraction methods for the purpose of 3D object detection and representation. Considerations include: the effect of the edge detection on

Conference 9600: Image Reconstruction from Incomplete Data VIII

the quality of the object detection, the appearance of the detected objects (i.e., how the edge features characterize the detected object) and the computational complexity.

9600-14, Session 4

Charactering heterogeneity among virus particles by stochastic 3D signal reconstruction

Peter C. Doerschuk, Nan Xu, Yunye Gong, Cornell Univ. (United States); Qiu Wang, Siemens AG (United States); Yili Zheng, Lawrence Berkeley National Lab. (United States)

No Abstract Available

9600-15, Session 4

Alternative techniques for high-resolution spectral estimation of spectrally encoded endoscopy

Mahta Mousavi, Univ. of California, San Diego (United States); Lian Duan, Stanford Univ. (United States); Tara Javidi, Univ. of California, San Diego (United States); Audrey K. Ellerbee, Stanford Univ. (United States)

Spectrally encoded endoscopy (SEE) is a minimally invasive optical imaging modality capable of fast confocal imaging of internal tissue structures. Modern SEE systems use coherent sources to image deep within the tissue and data are processed similar to optical coherence tomography (OCT); however, standard processing of SEE data via the Fast Fourier Transform (FFT) leads to degradation of the axial resolution as the bandwidth of the source shrinks, resulting in a well-known trade-off between speed and axial resolution. Recognizing the limitation of the FFT as a general spectral estimation algorithm to only take into account samples collected by the detector, in this work we investigate alternative high-resolution spectral estimation algorithms that exploit information such as sparsity and the general region position of the bulk sample to improve the axial resolution of processed SEE data. Moreover, we demonstrate the ability of high sampling-rate systems to exploit oversampling to yield higher quality A-scans extracted from averaging of sub-sampled datasets. We validate the performance of these algorithms using both MATLAB simulations and analysis of experimental results generated from a home-built SEE system. We also discuss guidelines to design new SEE systems ideally suited for various kinds of SEE data. Our results open a new door towards using non-FFT algorithms to generate higher quality (i.e., higher resolution) SEE images at correspondingly fast scan rates, resulting in systems that are more accurate and more comfortable for patients due to the reduced image time.

9600-16, Session 4

FPGA acceleration by asynchronous parallelization for simultaneous image reconstruction and segmentation based on the Mumford-Shah regularization

Wentai Zhang, Guojie Luo, Li Shen, Peking Univ. (China); Thomas Page, Univ. Bremen (Germany); Peng Li, Univ. of California, Los Angeles (United States); Ming Jiang, Peking Univ. (China); Peter Maass, Univ. Bremen (Germany); Jason Cong, Univ. of California, Los Angeles (United States)

X-ray computed tomography (XCT) is an important technique for clinical diagnose. In many applications a number of image processing steps

are needed before the image features of interests are available. Image segmentation is one of such processing steps to generate the edge and structural features of regions of interests. The conventional flow is to first reconstruct images and then apply image segmentation methods on reconstructed images. Recently, an emerging technique is to obtain the tomographic image and segmentation simultaneously, especially in the case of limited data. The Mumford-Shah regularization for image reconstruction provides such an approach. With this approach, it does not only enable the simultaneous reconstructions of tomographic images and their segmentations, but also utilizes the interaction between the edge indicator function for segmentation and the tomographic image to enhance both reconstructions. However, the computation involves an NP-hard problem and is computationally expensive. By the Gamma-convergence approximation, we have established an iterative method for simultaneous reconstruction and segmentation with Mumford-Shah regularization. In this work, to find an energy-efficient solution with the field programmable gate array (FPGA) technology, we propose an asynchronous parallel algorithm to accelerate the implementation in FPGA. Experimental results show that the FPGA implementation achieves a 1.2X speedup with an energy efficiency as great as 58X, over the GPU implementation.

SPIE. OPTICS+ PHOTONICS

APPLICATIONS

OPTICAL ENGINEERING+

9600-17, Session 5

Imaging fields through heavily scattering random media with speckle correlations over source position (Invited Paper)

Jason A. Newman, Kevin J. Webb, Purdue Univ. (United States)

We describe a method whereby coherent optical fields can be imaged on the other side of a randomly scattering medium by recording speckle intensity patterns as a function of the spatially scanned incident beam position. Two constrained phase reconstructions are required to obtain the fields from the measured data. We show example patterned beam reconstruction results to demonstrate the concept. Extensions of this description lead to a method to image moving objects in scattering media. While several methods exist for imaging through thin opaque materials, coherent imaging and sensing in these extreme limits has not been previously possible. Furthermore, through the use of speckle correlations as a function of object position, we are able to exploit the speckled images to provide motion sensitivity on a wavelength scale. Such spatial speckle image correlations should prove valuable for non-ionizing high resolution medical imaging, sensing is heavily cluttered environments, and coherent imaging in and through opaque materials. At a more general level, our work provides a new framework for communication and characterization of scattering media. Natural motion can be exploited, and the approach can be extended to other geometries.

9600-19, Session 5

Imaging through scattering media via Hadamard Illumination and single-pixel detection

Vicente Durán, Chalmers Univ. of Technology (Sweden); Fernando Soldevila Torres, Esther Irles, Pedro J. Clemente Pesudo, Enrique Tajahuerce, Univ. Jaume I (Spain); Pedro Andrés Bou, Univ. de València (Spain); Jesús S. Lancis, Univ. Jaume I (Spain)

One challenge that has long held the attention of scientists is that of clearly seeing objects hidden by turbid media, as smoke, fog or biological tissue, which has major implications in fields such as remote sensing or early diagnosis of diseases.

Photons propagating through a turbid medium experience a certain number of scattering events and, as a result, part of the emerging radiation follows a completely uncorrelated direction. The intensity of the unscattered light component falls off with the medium thickness. As a consequence, imaging



begins to be difficult or unfeasible at a penetration depth larger than the tissue transport mean free path (TMFP), a measurement of the mean distance that photons travel before they completely 'forget' their initial direction.

We present a novel imaging technique, based on the concept of single-pixel camera which enables to image objects embedded at a depth of several times the TMFP of the tissue. Our results demonstrate transillumination imaging of an object embedded within a 6-mm thick sample of chicken breast, light penetration depth of about 3 times the TMFP. A sequence of microstructured light patterns implemented onto a digital micromirror device is launched onto an object completely embedded in the turbid medium. Single-pixel detectors allow us to operate at illumination power levels that are three orders of magnitude lower than the tissue damage threshold. Our technique is noninvasive, does not require coherent sources, raster scanning nor time-gated detection, works without increasing the cost and system complexity, and benefits from the compressive sensing strategy.

9600-24, Session 5

Online submillimeter three dimensional imaging of magnetic and paramagnetic contaminants flow rate in multiphase flow pipelines using magnetic particle imaging technique

K. Bin Said, Mahmoud Meribout, The Petroleum Institute (United Arab Emirates)

In oil fields, crude oil is transported over steel?made pipeline which may carry paramagnetic contaminants (e.g. iron sulfide), generated from corrosion and erosion phenomena, in addition to other diamagnetic organic scales such as naphthenic, acids, and paraffin. For example, practically all oil export pipelines transport can carry up to 0.1% of magnetic contaminants. In addition of causing wrong readings of the actual crude oil flows, these contaminants may gather at various downstream locations causing a drop of production throughput. The online devices used so far for multiphase flow metering do not consider the existence of such contaminants which indeed can provide significant over readings of the meter. Accurately measuring the flow rate of such contaminants will not only compensate the readings of the multiphase flow meters but also can mitigate their source, avoid process shutdown and prevent offline cleanings.

In this paper, submillimeter three dimensional tomography imaging of paramagnetic contaminants flow rate in multiphase flow pipelines is presented. The device, which is based on Magnetic Particle Imaging (MPI), consists of an array of twelve coils and a pair of permanent magnets and is not influenced with the other phases that constitute the crude oil (e.g. oil, water, sand, and gas) and which are mainly diamagnetic materials. The concentration of the paramagnetic particles can be measured in a three dimensional volumetric space with high spatial and temporal sensitivities which are proportional to the strength of the applied magnetic field. This is also influenced by the size and distribution of the particles and the anisotropy of the permanent magnet. To increase the sensitivity and improve the spatio encoding field, a two dimensional Linear Field Scanning (LFS) technique coupled with a two dimensional excitation field is proposed. The results demonstrate that the technique would constitute a breakthrough in the area of solid flow measurements.

9600-21, Session 6

Inter-trial alignment of EEG data and highfrequency phase-locking

Markus E. Testorf, Peter Horak, Andy Connolly, Dartmouth College (United States); Gregory L. Holmes M.D., The Univ. of Vermont (United States); Barbara C. Jobst, Darmouth College (United States)

Neuro-scientific studies typically try to correlate the behavior of

human subjects to changes of functional signals, such as fMRI and electroencephalogram (EEG) recordings. Images of brain activity are derived from statistical evaluations of multiple trials time synchronized to a repeated external stimulus.

Even in well-designed experiments the signal component of interest may be recorded in each trial with a different time lag relative to the stimulus. This may be caused by an uncontrolled latency of the equipment. For complex brain activities the response time may also depend on brain processes unrelated to the external stimulus.

This is particularly critical for EEG data. While events manifesting in low frequency bands (<10Hz) may tolerate a time jitter of the order of 100ms, higher frequency signals may be desynchonized by time delays of less than 1ms. This is even more important if the phase of a discrete frequency is compared across trials.

In this contribution we investigate methods for aligning trials based on the recorded signal itself. Cross-correlations between trials serve as the baseline to consider various algorithms, including wavelet based algorithms and iterative optimization algorithms. The bias potentially introduced into the signal recovery process by using the same data for alignment as well as subsequent ensemble averaging will be addressed by the selection of recording sites in the brain.

The trial alignment will be applied to the evaluation of phase-locking across trials. The frequency resolved phase-locking will be computed from intercranial EEG data recorded in a clinical setting.

9600-22, Session 6

Precoding design of compressive sensing data based on singular value decomposition criterion

Chia-Chang Hu, Kang-Tsao Tang, Bo-Hung Chen, National Chung Cheng Univ. (Taiwan)

In this paper, joint relay and source precoders for image transmission is proposed for a multiple-input multiple-output (MIMO) multiple-relays system. In mobile devices powered by battery, reducing the sensor's compression energy consumption is critical to extend its lifetime. A novel antenna selection scheme based on the singular value decomposition (SVD) is proposed in order to decrease energy consumption and computational complexity in image transmission. The main purpose of the proposed algorithm is to suppress noise, preserve image details, and have low computational complexity, which are very difficult to achieve simultaneously. It is noticed that the SVD-based joint design of relay-and-source precoders in conjunction with the antenna selection mechanism is capable of achieving superior bit-error-rate (BER) and MSE performance.

9600-23, Session 6

Implementation of an adaptive ictal spike detection algorithm

Stephen Meisenhelter, Peter C. Horak, Andrew Connolly, Barbara C. Jobst, Dartmouth Hitchcock Medical Ctr. (United States)

The identification of epileptiform activity and recording artifacts is crucial for the analysis of electroencephalogram (EEG) data. For imaging the study of human brain activity, for clinical diagnostics, and study of epilepsy, it is desirable to detect and classify spikes and other epilepsy related signals automatically. For many neuro-scientific studies, the removal of these waveforms is an indispensable pre-processing step. In humans, automatic detection and classification of epileptiform activity remains difficult, since the signal components in question vary considerably between patients. However, epileptiform activity is usually consistent within patients.

Currently, the detection of interictal spikes and other epileptiform activity in clinical EEG data is almost always carried out manually by trained neurologists. This introduces considerable variability in the accuracy of spike

Conference 9600: Image Reconstruction from Incomplete Data VIII



detection from reviewer to reviewer. The problem is further complicated by the lack of a consensus among neurologists on the features which define a spike. Discrepancies in review are explained by subjective variance.

In this study, we demonstrate a clustering-based interictal spike detection algorithm. This algorithm improves upon an earlier method of creating patient-specific pattern matching templates by clustering the results of a generic pattern matching analysis (Nonclerq et al., 2010). This method was extended by expanding the generic pattern matching step and the clustering method. This improved algorithm was evaluated using hippocampal EEG recordings from 11 epilepsy patients.

Conference 9601: UV, X-Ray, and Gamma-Ray Space Instrumentation for Astronomy XIX



Sunday - Monday 9 -10 August 2015

Part of Proceedings of SPIE Vol. 9601 UV, X-Ray, and Gamma-Ray Space Instrumentation for Astronomy XIX

9601-1, Session 1

Generation of response matrix for multipixel CZT detectors

Tanmoy Chattopadhyay, Santosh V. Vadawale, Physical Research Lab. (India); A. R. Rao, Tata Institute of Fundamental Research (India)

Cadmium Zinc Telluride (CZT) detectors have been the workhorse in hard X-ray astronomy for a decade now, implemented in many X-ray observatories e.g. SWIFT, NuSTAR and more recently in ASTROSAT. Response matrix for pixelated CZT detectors requires precise modelling of the X-ray lines as a function of energy. Instead of showing simple Gaussian feature, these lines exhibit a long tail at lower energies because of trapping of the charge carriers due to their low mobility (μ) and lifetime (?). This effect is found to be more significant for high energy photons as the probability of charge loss increases with the depth of interaction. Therefore, precise line modelling in case of CZT detectors needs accurate measurement of µ? values for electrons and holes. For pixelated detectors, other significant components in the line modelling come from the crosstalk between pixels due to charge sharing, fluorescence photons and Compton scattering. Here we present experimental measurements of mobility and lifetime for 4 cm X 4 cm and 5 mm thick CZT detectors with pixel dimension of 2.5 mm X 2.5 mm, procured from Orbotech Medical Solutions (similar to the modules used in CZTI, Astrosat). Here we independently generate pixel-wise response matrix for the CZT modules and test in laboratory by fitting a known continuum spectra in 20 - 50 kev using a X-ray gun. We also draw a comparison between the µ? response matrix involving all physical processes and a Gaussian response matrix using the same continuum source of radiation.

9601-2, Session 1

CdTe focal plane detector for hard x-ray focusing optics

Paul Seller, Matthew D. Wilson, Matthew C. Veale, Andreas Schneider, STFC Rutherford Appleton Lab. (United Kingdom); Jessica A. Gaskin, Colleen Wilson-Hodge, NASA Marshall Space Flight Ctr. (United States); Steven D. Christe, Albert Y. Shih, NASA Goddard Space Flight Ctr. (United States)

The demand for higher resolution x-ray optics (a few arcseconds or better) in the areas of astrophysics and solar science has, in turn, driven the development of complementary detectors. These detectors should have fine pixels, necessary to appropriately oversample the optics at a given focal length, and an energy response also matched to that of the optics. At Rutherford Appleton Laboratory, we have developed a 3-side abuttable, 20mm x 20mm CdTe-based detector with 250 micron square pixels (80x80 pixels) which achieves 1keV FWHM @60keV and gives full spectroscopy between 5keV and 200keV. An added advantage of these detectors is that they have a full-frame readout rate of 10 kHz. Working with NASA Goddard Space Flight Center and Marshall Space Flight Center, we have tiled 4 of these 1mm-thick CdTe detectors into a 2x2 array for use at the focal plane of a balloon-borne hard-x-ray telescope, and are considering configurations suitable for astrophysics and solar space-based missions. This effort encompasses the fabrication and testing of flight-suitable front-end electronics and calibration of the assembled detector arrays. We explain the operation of the pixelated ASIC readout and measurements, front-end electronics development, preliminary X-ray imaging and spectral performance, and plans for full calibration of the detector assemblies. Work done in conjunction with the NASA Centers is funded through the NASA Science Mission Directorate Astrophysics Research and Analysis Program.

9601-3, Session 1

First results from the OGRESS sounding rocket payload

Thomas D. Rogers, Univ. of Colorado at Boulder (United States); Ted B. Schultz, James H. Tutt, Jake McCoy, Drew M. Miles, Randall L. McEntaffer, The Univ. of Iowa (United States)

The Off-plane Grating Rocket for Extended Source Spectroscopy (OGRESS) is a soft x-ray spectrograph designed to observe diffuse sources such as Supernova Remnants and large gas clouds with significantly increased resolving power over current state-of-the-art. OGRESS's large field of view and off-plane diffraction gratings will produce a spatially integrated spectrum of the entire Cygnus Loop with the highest resolving power ever achieved between 300 - 1000 eV. OGRESS uses Gaseous Electron Multiplier (GEM) detectors. OGRESS, scheduled to launch in the spring of 2015, will demonstrate the first comprehensive success of GEM spaceflight.

9601-4, Session 1

Technological developments with the OGRE focal plane array

James H. Tutt, Randall L. McEntaffer, Casey T. DeRoo, Ted B. Schultz, The Univ. of Iowa (United States); Andrew D. Holland, Neil J. Murray, The Open Univ. (United Kingdom); Karen Holland, David Colebrook, David Farn, XCAM Ltd. (United Kingdom); Daniel P. Weatherill, The Open Univ. (United Kingdom); Anthony M. Evagora, XCAM Ltd. (United Kingdom); Drew M. Miles, The Univ. of Iowa (United States); William W. Zhang, NASA Goddard Space Flight Ctr. (United States)

The Off-plane Grating Rocket Experiment (OGRE) is a suborbital rocket payload designed to test the spectral resolution performance of an instrument based on off-plane reflection grating technology. Through the combination of silicon based optics, blazed and radially groove off-plane gratings and Electron Multiplying Charge-Coupled Devices (EM-CCDs), an instrument with resolution in excess of 1500 across the soft X-ray bandpass is possible within a suborbital payload.

Using the design of OGRE's optics (focusing and grating) along with specifications on readout speed and signal-to-noise, an EM-CCD camera array was baselined for the focal plane array (CCD207-40). This detector has a large imaging area and, due to the use of multiplication gain, can be read out quickly with a sub-electron readout noise. The decision to use this detector on OGRE defined the aspects that the mechanical, vacuum and cooling systems needed to include.

A prototype for the camera has been developed using the similar but more commercially available CCD207-10. This prototype has allowed the designs for the final camera system to be optimised in preparation of the construction of the flight camera.

This paper analyses the optical design of OGRE and how this led to the decision to use EM-CCDs on the focal plane. The requirements that this decision put on the mechanical, thermal and electrical properties of the camera are then covered before looking at the progress made with the prototype system.



9601-5, Session 1

A primer for telemetry interfacing in accordance with NASA standards using low cost FPGAs

Jake A. McCoy, Ted B. Schultz, The Univ. of Iowa (United States); Thomas D. Rogers, Univ. of Colorado at Boulder (United States); James H. Tutt, Drew M. Miles, Thomas J. Peterson, Randall L. McEntaffer, The Univ. of Iowa (United States)

X-ray detector systems on sounding rocket payloads often require interfacing asynchronous outputs with a synchronously clocked telemetry stream. Though this can be handled with an on-board computer, there are several low cost alternatives including custom hardware, microcontrollers, and Field-Programmable Gate Arrays (FPGAs). FPGAs have the advantage of being highly flexible and reconfigurable while also having low power consumption and a small printed circuit board footprint. This paper outlines how a telemetry interface for detectors on a sounding rocket with asynchronous parallel digital output can be implemented using FPGAs and minimal custom hardware. It also serves as a guide for working with Pulse Code Modulation (PCM) formatted telemetry encoding and the Inter-Range Instrumentation Group (IRIG) Chapter 10 digital recording standard. Additionally, methods for testing the telemetry interface with a simulated telemetry chain in the small laboratory setting are discussed. This includes using FPGAs as detector simulators and recording data according to the IRIG Chapter 10 format using a PCM processor and data acquisition software. Finally, this paper discusses specifically how the telemetry interface is integrated into the electronics assembly of the Off-plane Grating Rocket for Extended Source Spectroscopy (OGRESS) with the associated custom hardware.

9601-6, Session 2

Modeling contamination migration on the Chandra X-ray Observatory: III

Stephen L. O'Dell, Douglas A. Swartz, NASA Marshall Space Flight Ctr. (United States); Neil W. Tice, Massachusetts Institute of Technology (United States); Paul P. Plucinsky, Smithsonian Astrophysical Observatory (United States); Catherine E. Grant, Herman L. Marshall, Massachusetts Institute of Technology (United States); Alexey A. Vikhlinin, Smithsonian Astrophysical Observatory (United States); Allyn F. Tennant, NASA Marshall Space Flight Ctr. (United States)

During its first 16 years of operation, the cold (about -60°C) optical blocking filter of the Advanced CCD Imaging Spectrometer (ACIS), aboard the Chandra X-ray Observatory, has accumulated a growing layer of molecular contamination that attenuates low-energy x rays. Over the past few years, the accumulation rate, spatial distribution, and composition have changed. This evolution has motivated further analysis of contamination migration within and near the ACIS cavity. To this end, the current study employs a high-fidelity geometric model of the ACIS cavity, detailed thermal modeling based upon temperature data, and a refined model of the molecular transport.

9601-7, Session 2

Soft x-ray, UV, and optical transmission of the contamination blocking filer for the soft x-ray imager (SXI) on board ASTRO-H

Takayoshi Kohmura, Yuta Sato, Koki Tamasawa, Shoma Tanno, Yuma Yoshino, Shintaro Kuwano, Masato Ando, Kenta Kaneko, Tokyo Univ. of Science (Japan); Tadayasu Dotani, Masanobu Ozaki, Hiroshi Tomida, Masashi Kimura, Keisuke Kondo, Japan Aerospace Exploration Agency (Japan); Hiroshi Tsunemi, Kiyoshi Hayashida, Naohisa Anabuki, Hiroshi Nakajima, Ryo Nagino, Juyong Kim, Ritsuko Imatani, Hiroyuki Kurubi, Osaka Univ. (Japan)

The X-ray detectors, such as cooled X-ray CCD, onboard satellite are contaminated by the outgas which is produced from organic material used in satellites. This contamination causes to a significant reduction of detection sensitivity of X-ray detectors. We have developed Contamination Blocking Filter (CBF), which is consisted with 120nm thick Aluminum and 200nm thick Polyimide, to prevent the contamination to Back-Illuminated-CCD (BI-CCD) for Soft X-ray Imager (SXI) onboard ASTRO-H. The CBF plays important role to block UV and optical as well as to prevent the contamination to SXI.

We carried out UV and optical transmission measurement and obtained their transmission to be <10^-3 at 40eV and <10-5 at 500nm, respectively. As these results, we confirmed the shading performance of CBF was as expected from its design thickness.

The quantum efficiency of SXI is determined by the X-ray transmission of CBF especially in the soft X-ray energy range below 2keV therefore to measure the soft X-ray transmission of CBF is necessary. Therefore we measured soft X-ray transmission of CBF at the High Energy Accelerator Research Organization (KEK), and obtained the X-ray transmission of CBF in the energy from 0.02 to 2.2keV by 1eV step and obtained its high X-ray transmission to be ?60% at 0.5keV. In this measurement, we also measured the absorption edges around C-K, O-K, Al-K, and N-K, including X-ray absorption fine structure (XAFS).

We will report X-ray, UV, and optical transmission in detail.

9601-8, Session 2

The optical blocking filter for the ATHENA wide field imager: baselign design and preliminary performance evaluation

Marco Barbera, Univ. degli Studi di Palermo (Italy) and INAF - Osservatorio Astronomico di Palermo Giuseppe S. Vaiana (Italy); Graziella Branduardi-Raymont, Univ. College London (United Kingdom); Alfonso Collura, INAF - Osservatorio Astronomico di Palermo Giuseppe S. Vaiana (Italy); Andrea Comastri, INAF - Osservatorio Astronomico di Bologna (Italy); Tadeusz Kamisi?ski, AGH Univ. of Science and Technology (Poland); Ugo Lo Cicero, INAF - Osservatorio Astronomico di Palermo Giuseppe S. Vaiana (Italy); Norbert Meidinger, Max-Planck-Institut für extraterrestrische Physik (Germany); Teresa Mineo, INAF -Istituto di Astrofisica Spaziale e Fisica Cosmica di Palermo (Italy); Silvano Molendi, INAF - IASF Milano (Italy); Adam Pilch, AGH Univ. of Science and Technology (Poland); Luigi Piro, INAF - IASF Roma (Italy); Miroslaw Rataj, Space Research Ctr. (Poland); Gregor Rauw, Univ. de Liège (Belgium); Luisa Sciortino, Univ. degli studi di Palermo (Italy); Salvatore Sciortino, INAF - Istituto di Astrofisica Spaziale e Fisica Cosmica di Palermo (Italy); Piotr Wawer, Space Research Ctr. (Poland)

ATHENA is an advanced X-ray observatory designed to pursue the science theme "Hot and Energetic Universe" selected by ESA for the L2 mission within the Cosmic Vision science programme (launch scheduled in 2028). One of the key instruments of ATHENA is the Wide Field Imager (WFI) which will provide imaging in the 0.1-15 keV band over a 40' diameter field of view, simultaneously with spectrally and time-resolved photon counting.

The WFI camera, based on arrays of DEPFET active pixels, is also sensitive



to UV/VIS photons, with an electron-hole pair production efficiency in the UV/VIS that is larger than for X-ray photons. Optically generated photoelectrons may degrade the spectral resolution as well as change the energy scale by introducing a signal offset. For this reason, the use of an X-ray transparent optical blocking filter is needed to allow the observation of all type of X-ray sources that present a UV/Visible bright counterpart.

We present the filter baseline design, which includes the use of an Aluminum layer directly deposited on-chip and an external filter mounted on a filter wheel, we show the performances based on simulations and preliminary measurements conducted on test samples, and discuss criticalities to reach TRL 5-6 during the instrument technology development phase.

9601-9, Session 2

Development of the strontium iodide coded aperture (SICA) instrument

Lee Mitchell, Bernard F. Phlips, U.S. Naval Research Lab. (United States)

Europium-doped strontium iodide (Srl2:Eu) detectors have recently become available and the material is a strong candidate to replace existing detector technology currently used for space-based gamma-ray astrophysics research. The detectors have a typical energy resolution of 3.2% at 662 keV, a significant improvement over the 6.5% energy resolution of thalliumdoped sodium iodide (NaI(TI)). SrI2:Eu is comparable to lanthanum bromide (LaBr3) in both energy resolution and density, but LaBr3 has an added internal background due to natural occurring 138La. With a density of 4.59 g/cm and a Zeff of 49 SrI2:Eu has a high efficiency for MeV gamma ray detection. Coupling this with recent improvements in silicon photomultiplier technology (i.e. no bulky photomultiplier tubes) creates high density, large area, low power detector arrays with good energy resolution. The Naval Research Laboratory is in the process of developing a prototype array of SrI2:Eu that would consist of an 8x8 array of pixels, each read out by a silicon photomultiplier. The array would be used to demonstrate coded aperture imaging performance and to perform Compton imaging tests in combination with silicon detectors. The energy resolution of SrI2:Eu makes it ideal for use in as the backplane of a Compton telescope or a coded aperture imager. A discussion on the overall design, simulations used to optimize the design, and initial tests of the electronic components will be presented.

9601-10, Session 3

The speedster-EXD: a new event-triggered hybrid CMOS x-ray detector

Christopher V. Griffith, Abe D. Falcone, Zachary R. Prieskorn, David N. Burrows, The Pennsylvania State Univ. (United States)

We present the characterization of a new event driven x-ray hybrid CMOS detector developed by Penn State University in collaboration with Teledyne Imaging Sensors. Along with its low susceptibility to radiation damage, low power consumption, and fast read-out time to avoid pile-up, the Speedster-EXD has been designed with the capability to limit its readout to only those pixels containing charge, thus enabling even faster effective frame rates. The threshold for the comparator in each pixel can be set by the user so that only pixels with signal above the set threshold are read out. The Speedster-EXD hybrid CMOS detector also has two new in-pixel features that reduce noise from known noise sources: (1) a low-noise, high-gain CTIA amplifier to eliminate interpixel capacitance crosstalk and (2) in-pixel CDS subtraction to reduce kTC noise. We present the read noise, dark current, interpixel capacitance, energy resolution, and gain variation measurements of two Speedster-EXD detectors.

9601-11, Session 3

Soft x-ray quantum efficiency and other characteristics of x-ray sensitive Si hybrid CMOS detectors

Zachary R. Prieskorn, The Pennsylvania State Univ. (United States); Stephen D. Bongiorno, Johns Hopkins Univ. (United States); David N. Burrows, Abraham D. Falcone, Christopher V. Griffith, The Pennsylvania State Univ. (United States); Jonathan A. Nikoleyczik, Univ. of Maryland, College Park (United States)

X-ray sensitive Si Hybrid CMOS detectors (HCDs) will potentially replace X-ray CCDs in the focal planes of future X-ray observatories. HCDs improve on the performance of CCDs in numerous areas: faster read out time, windowed read out modes, less susceptibility to radiation & micrometeoroid damage, and lower power consumption. Understanding detector quantum efficiency (QE) is critical for estimating the sensitivity of an X-ray instrument. We report on QE across the soft X-ray band for four Teledyne Imaging Sensors HyViSI HCDs. These detectors have AI optical blocking filters deposited directly on the Si substrate; these filters vary in thickness from 180 – 1000 Å. We estimate the QE with a 1D slab absorption model and find good agreement between the model and our results across an energy range from 0.677 – 8.05 keV. We will also describe upcoming work to measure the sub-pixel QE of these detectors using the Penn State 47 m X-ray facility and give a broad overview of the current capabilities and development plans for X-ray sensitive HCDs.

9601-12, Session 3

Recent progress in the development of Kyoto's x-ray astronomical SOI pixel sensor

Takeshi G. Tsuru, Hideaki Matsumura, Ayaki Takeda, Takaaki Tanaka, Kyoto Univ. (Japan); Shinya Nakashima, Institute of Space and Astronautical Science (Japan); Yasuo Arai, High Energy Accelerator Research Organization, KEK (Japan); Koji Mori, Ryota Takenaka, Yusuke Nishioka, Univ. of Miyazaki (Japan); Takayoshi Kohmura, Tokyo Univ. of Science (Japan); Takayoshi Kohmura, Tokyo Univ. of Science (Japan); Takaki Hatsui, Yoshiki Kohmura, RIKEN SPring-8 Ctr. (Japan); Takashi Kameshima, Japan Synchrotron Radiation Research Institute (Japan); Dai Takei, RIKEN SPring-8 Ctr. (Japan); Shoji Kawahito, Keiichiro Kagawa, Keita Yasutomi, Hiroki Kamehama, Sumeet Shrestha, Shizuoka Univ. (Japan)

We have been developing monolithic active pixel sensors, X-ray SOIPIXs, based on the Silicon-On-Insulator (SOI) CMOS technology for nextgeneration X-ray astronomy satellites. The event trigger output function implemented in each pixel offers a high time resolution of ~micro sec, which allows us to reduce non-X-ray background dominating the high X-ray energy band above 5-10 keV by adopting anti-coincidence technique. We reported in the previous SPIE conference (AS14) that we achieved the depletion layer thickness of 500 micron and the energy resolution of 300 eV (FWHM) at 6keV. In this paper, we give recent progress from the development. (1) In the previously developed device, a significant tail component was seen in the X-ray spectral response due to non-uniformity of the charge collection efficiency. We realized in-pixel circuitry disturbs the electric fields in the depletion layer through which signal charge is collected. We successfully solved the non-uniformity problem by modifying the placement of the inpixel circuitry. (2) We developed a new device equipped with programable gain amplifiers and differential amplifiers are implemented (see paper in OP318 by Shrestha for details on the device description). We report the X-ray performances of the device. (3) We introduce the status of the development of a larger size device with the imaging area of 22mm x 14mm towards practical use.



9601-13, Session 3

The soft x-ray imager (SXI) for the ASTRO-H Mission

Takaaki Tanaka, Kyoto Univ. (Japan); Hiroshi Tsunemi, Kiyoshi Hayashida, Osaka Univ. (Japan); Takeshi G. Tsuru, Kyoto Univ. (Japan); Tadayasu Dotani, Institute of Space and Astronautical Science (Japan); Hiroshi Nakajima, Naohisa Anabuki, Ryo Nagino, Shutaro Ueda, Osaka Univ. (Japan); Hiroyuki Uchida, Masayoshi Nobukawa, Kyoto Univ. (Japan); Masanobu Ozaki, Japan Aerospace Exploration Agency (Japan); Chikara Natsukari, Institute of Space and Astronautical Science (Japan); Hiroshi Tomida, Masashi Kimura, Japan Aerospace Exploration Agency (Japan); Junko S. Hiraga, The Univ. of Tokyo (Japan); Takayoshi Kohmura, Tokyo Univ. of Science (Japan); Hiroshi Murakami, Tohoku Gakuin Univ. (Japan); Koji Mori, Makoto Yamauchi, Isamu Hatukade, Yusuke Nishioka, Univ. of Miyazaki (Japan); Aya Bamba, Aoyama Gakuin Univ. (Japan); John P. Doty, Nogsi Aerospace, Ltd. (United States)

The Soft X-ray Imager (SXI) is an X-ray CCD camera onboard the ASTRO-H X-ray observatory, which is scheduled to be launched in Japanese fiscal year 2015. The SXI consists of four CCD chips with an imaging area of 31 mm by 31 mm arranged in a 2 by 2 grid so that it covers a large field-of-view of 38 arcmin by 38 arcmin. The CCDs are P-channel back-illumination type with a depletion layer of 200 micron, with which the SXI covers the energy range between 0.4 keV and 12 keV. The CCD chips are cooled down to -110 degrees Celsius or below by using a Stirling cooler. As is done for the CCD camera onboard the Suzaku satellite, artificial charges are injected to selected rows of the CCDs in order to recover charge transfer inefficiency due to radiation damage caused by in-orbit cosmic rays.

We completed the flight model fabrication and performed an end-to-end verification test and on-ground calibration. Through the tests, we verified the functionality and performance of the SXI system and obtained an energy resolution of ~ 160 eV (FWHM) for 5.9 keV X-rays. The same level of the energy resolution was also obtained with the SXI onboard the satellite during the first integration test. We then carried out vibration, acoustic, and thermal-vacuum tests before the final integration and testing. In the presentation, we will report the status of the SXI and the detector performance expected in orbit.

9601-14, Session 3

Initial results from a cryogenic proton irradiation of a p-channel CCD

Jason P. D. Gow, David J. Hall, Ben J. Dryer, Simeon Barber, Andrew D. Holland, Neil J. Murray, The Open Univ. (United Kingdom)

The displacement damage hardness that can be achieved using p-channel charged coupled devices (CCD) was originally demonstrated in 1997 and since then a number of other studies have demonstrated an improved tolerance to radiation-induced CTI when compared to n-channel CCDs. A number of recent studies have also shown that the temperature history of the device after the irradiation impacts the performance of the detector, linked to the mobility of defects at different temperatures. This study describes the initial results from an e2v technologies p-channel CCD204 irradiated at 153 K with a 10 MeV equivalent proton fluences of 4.0?109 and 8.0?109 protons.cm-2. The number of defects identified using trap pumping, oharge transfer efficiency and dark current immediately after irradiation, over a period of time with the device held at 153 K and then after different periods of time at room temperature are described.

9601-15, Session 4

Hard x-ray polarimetry with Astrosat-CZTI

Tanmoy Chattopadhyay, Santosh V. Vadawale, Physical Research Lab. (India); A. R. Rao, Tata Institute of Fundamental Research (India)

Astrosat is the forthcoming Indian satellite dedicated for astronomical studies. CdZnTe Imager (CZTI), one of the five instruments in Astrosat, is a pixelated spectroscopic instrument sensitive in 20-150 kev range. Because of its pixilation nature and significant Compton scattering efficiency at energies beyond 100 kev, it is possible to measure polarization in X-rays exploiting the Compton scattering technique at energies beyond its primary energy range. The simulation and experimental results clearly show that the flight configuration of Astrosat-CZTI will be capable of polarisation measurement in hard X-rays in 100 -300 keV. Detailed polarimetric background analysis and therefrom the polarimetric sensitivity estimations show that CZTI will be able to measure polarization for few highly polarized bright hard X-ray sources, e.g. CygX1 - black hole source, Crab pulsar including any new transient sources in Astrosat lifetime . We discuss the possibility of constraining various possible hard X-ray emission mechanisms in black hole sources and emission geometries in X-ray pulsars with CZTI polarimetry.

9601-16, Session 4

Development of the wide field imager for Athena

Norbert Meidinger, Kirpal Nandra, Arne Rau, Markus Plattner, Max-Planck-Institut für extraterrestrische Physik (Germany); Joern Wilms, Friedrich-Alexander-Univ. Erlangen-Nürnberg (Germany); Marco Barbera, Univ. degli Studi di Palermo (Italy)

The WFI (Wide Field Imager) instrument is planned to be one of two complementary focal plane cameras on ESA's Athena satellite.

It combines unprecedented survey power through its large field of view of 40 arcmin with a high count-rate capability (> 1 Crab). The energy resolution of the silicon sensor is state-of-the-art in the energy band of interest from 0.1 keV to 15 keV. At energy of 6 keV for example, the full width at half maximum of the line shall be not worse than 150 eV until the end of the mission.

The performance is accomplished by a set of DEPFET active pixel sensor matrices with a pixel size well suited to the angular resolution of 5 arc sec (on-axis) of the mirror system.

Each DEPFET pixel is a combined detector-amplifier structure with a MOSFET integrated onto a fully depleted 450 micron thick silicon bulk.

Two different types of DEPFET sensors are planned for the WFI instrument: A set of large-area sensors to cover the physical size of 14 cm x 14 cm in the focal plane and a single gateable DEPFET sensor matrix optimized for the high count rate capability of the instrument.

An overview will be given about the presently developed instrument concept and design, the status of the technology development, and the expected performance. An outline of the project organization, the model philosophy as well as the schedule will complete the presentation about the Wide Field Imager for Athena.

9601-17, Session 4

LAMP: a micro-satellite based soft x-ray polarimeter for astrophysics

Rui She, Hua Feng, Tsinghua Univ. (China); Paolo Soffitta, Fabio Muleri, INAF - IASF Roma (Italy); Renxin Xu, Peking Univ. (China); Hong Li, Tsinghua Univ. (China); Ronaldo

Conference 9601: UV, X-Ray, and Gamma-Ray Space Instrumentation for Astronomy XIX



Bellazzini, Istituto Nazionale di Fisica Nucleare (Italy); Zhanshan Wang, Tongji Univ. (China); Daniele Spiga, Giovanni Pareschi, Gianpiero Tagliaferri, Kashmira Tayabaly, Bianca Salmaso, INAF - Osservatorio Astronomico di Brera (Italy); Yafeng Zhan, Jianhua Lu, Tsinghua Univ. (China)

The Lightweight Asymmetry and Magnetism Probe (LAMP) is microsatellite mission concept dedicated for astronomical X-ray polarimetry and is currently under early phase study. It consists of segmented paraboloidal multilayer mirrors with a collecting area of about 1300 cm2 to reflect and focus 250 eV X-rays, which will be detected by position sensitive detectors at the focal plane. The primary targets of LAMP include the thermal emission from the surface of pulsars and synchrotron emission produced by relativistic jets in blazars. The expected sensitivity of LAMP will allow us to detect polarization or place a tight upper limit from about 10 pulsars and 20 blazars. In addition to measuring magnetic structures in these objects, LAMP will also enable us to discover bare quark stars if they exist, whose thermal emission is expected to be zero polarized, while the thermal emission from neutron stars is thought to be highly polarized. Here we present an overview of the mission concept, its science objectives and simulated observational results.

9601-18, Session 4

NASA x-ray surveyor mission: a concept study

Jessica A. Gaskin, NASA Marshall Space Flight Ctr. (United States); Alexey Vikhlinin, Harvard-Smithsonian Ctr. for Astrophysics (United States); Martin Weisskopf, NASA Marshall Space Flight Ctr. (United States); Harvey Tananbaum, Harvard-Smithsonian Ctr. for Astrophysics (United States)

Over the past 16 years, NASA's Chandra X-ray Observatory has provided an unparalleled means for exploring the high-energy universe with its half-arcsecond angular resolution. Chandra studies have deepened our understanding of galaxy clusters, active galactic nuclei, galaxies, supernova remnants, neutron stars, black holes, and solar system objects. As we look beyond Chandra, it is clear that comparable or even better angular resolution with greatly increased photon throughput is essential to address ever more demanding science questions-such as formation and subsequent growth of black hole seeds at very high redshifts; emergence of the first galaxy groups; and details of feedback over a large range of scales from galaxies to galaxy clusters. Recently, we initiated a concept study for such a mission. This concept study starts from a strawman payload comprising a high-resolution mirror assembly and an instrument set, which may include an X-ray calorimeter, a wide-field imager, and a dispersive grating spectrometer and its readout. The mirror assembly would consist of highly nested, thin, grazing-incidence mirrors, for which a number of technical approaches are currently under development-including adjustable X-ray optics, differential deposition, and modern polishing techniques applied to a variety of substrates. This study benefits from previous studies of large-area missions carried out over the past two decades and, in most areas, points to mission requirements no more stringent than those of Chandra.

9601-19, Session 4

The eROSITA X-ray Observatory

Vadim Burwitz, Peter Predehl, Max-Planck-Institut für extraterrestrische Physik (Germany)

In 2016 the X-ray observatory eROSITA will be launched on board the Russian Spectrum-RG mission from Baikonur. eROSITA with its 7 even X-ray telescopes will first be used to perform eight all-sky surveys over a period of 4 years continuing with a 3 year pointed observation phase. With the impending launch date on the horizon, the hardware phase is coming to an end, therefore the thorough testing of the cameras, electronics, and mirrors is in high gears. These tests will then culminate with an end to end

test at MPEs PANTER X-ray test facility before shipment to Russia. Here we describe the status of the Observatory and yield insights into the challenges we faced while making eROSITA.

9601-34, Session 4

ATHENA: system design and implementation for a next generation x-ray telescope

Mark R. Ayre, Marcos Bavdaz, Ivo Ferreira, Martin Linder, Eric Wille, David H. Lumb, European Space Agency (Netherlands)

ATHENA, Europe's next generation x-ray telescope, has recently been selected for the 'L2' slot in ESA's Cosmic Vision Programme, with a mandate to address the 'Hot and Energetic Universe' Cosmic Vision science theme. The mission is currently in the Assessment/Definition Phase (A/B1), with a view to formal adoption after a successful System Requirements Review in 2019. This paper will describe the reference mission architecture and spacecraft design produced during Phase 0 by the ESA Concurrent Design Facility (CDF), in response to the challenging technical requirements and programmatic boundary conditions.

The main technical requirements and their mapping to resulting design choices will be presented, at both mission and spacecraft level. An overview of the spacecraft design down to subsystem level will then be presented (including the telescope and instruments), touching upon the criticallyenabling technologies where appropriate. Finally, a programmatic overview will be given of the on-going Assessment Phase, and a snapshot of the prospects for securing the 'as-proposed' mission within the cost envelope will be given.

9601-20, Session 5

Fireball-2: a UV multi-object spectrograph for detecting the low z circumgalactic medium

D. Christopher Martin, Erika T. Hamden, California Institute of Technology (United States); David Schiminovich, Columbia Univ. (United States); Bruno Milliard, Robert Grange, Lab. d'Astrophysique de Marseille (France); Shouleh Nikzad, Jet Propulsion Lab. (United States); Lauren Corlies, Columbia Univ. (United States); Robert Crabill, California Institute of Technology (United States); Didier Ferrand, Lab. d'Astrophysique de Marseille (France); Albert Gomes, Ctr. National d'Études Spatiales (France); Anne-Sophie Hutter, Marc Jaguet, Lab. d'Astrophysique de Marseille (France); April Jewell, Jet Propulsion Lab. (United States); Gillian Kyne, California Institute of Technology (United States); Vincent Lamande, Gerard Lemaitre, Lab. d'Astrophysique de Marseille (France); Michele Limon, Columbia Univ. (United States); Nicole Lingner, California Institute of Technology (United States); Marc Llored, Lab. d'Astrophysique de Marseille (France); Mateusz Matuszewski, California Institute of Technology (United States); Pierre Mege, Lab. d'Astrophysique de Marseille (France); Frederi Mirc, Ctr. National d'Études Spatiales (France); Patrick Morrissey, California Institute of Technology (United States); Hwei Ru Ong, Columbia Univ. (United States); Alain Origne, Sandrine Pascal, Celine Peroux, Samuel Quiret, Didier Vibert, Lab. d'Astrophysique de Marseille (France); Jose M. Zorrilla, Columbia Univ. (United States)

Conference 9601: UV, X-Ray, and Gamma-Ray Space Instrumentation for Astronomy XIX



The Faint Intergalactic Redshifted Emission Balloon (FIREBall-2) is a joint NASA/CNES collaboration that will launch in 2016. FIREBall-2 is a balloonborn ultraviolet (UV) multi-object spectrograph designed to detect faint emission from the circumgalactic medium (CGM) around low z galaxies. This emission is visible via a narrow atmospheric window (195-225 nm) accessible at balloon altitudes (40km). FIREBall-2 builds on the existing gondola and large optics of FIREBall-1, which launched in 2007 and 2009. The new spectrograph for FIREBall-2 has been extensively redesigned to improve performance by over an order of magnitude. To improve instrument throughput, a photon-counting delta-doped electron multiplying chargecoupled device (EMCCD) has replaced the Galaxy Evolution Explorer (GALEX) spare near-UV microchannel plate. Custom red blocking coatings minimize out-of-band light and improve in-band transmission. A set of field correcting optics has been added to increase the field of view, and a suite of slit masks yield up to 50 objects per field. Here we discuss the final flight design along with ongoing integration and testing in Marseille. We describe expected performance in flight, the detection limits we anticipate given our instrument model, and potential targets for our flight in 2016.

9601-21, Session 5

Detector performance for FIREBall's UV experiment

April D. Jewell, Jet Propulsion Lab. (United States); Erika T. Hamden, California Institute of Technology (United States); Timothy M. Goodsall, Charles A. Shapiro, Samuel R. Cheng, Todd J. Jones, Alexander G. Carver, Michael E. Hoenk, Jet Propulsion Lab. (United States); David Schiminovich, Columbia Univ. (United States); D. Christopher Martin, California Institute of Technology (United States); Shouleh Nikzad, Jet Propulsion Lab. (United States)

We present an overview of the detector for the upcoming Faint Intergalactic Red-shifted Emission Balloon (FIREBall-2) experiment, with a particular focus on the development of device-integrated optical coatings and detector quantum efficiency (QE). FIREBall-2 is designed to measure emission from the strong resonance lines of HI, OVI, and CIV, all red-shifted to 195-225 nm window; its detector is a delta-doped electron multiplying charge-coupled device (EM-CCD). Delta-doped arrays, invented at JPL, achieve 100% internal QE from the UV through the visible. External losses due to reflection (~70% in some UV regions) can be mitigated with antireflection (AR) coatings. Using atomic layer deposition (ALD) thin-film optical filters are incorporated with existing detector technologies. ALD offers nanometer-scale control over film thickness and interface quality, allowing for precision growth of multilayer films. Several AR coatings, including single and multi-layer designs, were tested for FIREBall-2. QE measurements match modeled transmittance behavior remarkably well, showing improved performance in the target wavelength range. Also under development are ALD coatings to enhance QE for a variety of spectral regions throughout the UV (90-320) and visible (320-1000 nm) range both for space-based imaging and spectroscopy as well as for ground-based telescopes.

9601-22, Session 5

Noise and dark performance for FIREBall-2 EMCCD delta-doped CCD detector

Erika T. Hamden, Nicole Lingner, Gillian Kyne, Patrick Morrissey, D. Christopher Martin, California Institute of Technology (United States)

The Faint Intergalactic Redshifted Emission Balloon (FIREBall-2) is an experiment designed to observe low-density emission from HI, CIV, and OVI in the circum-galactic medium (CGM) around low-redshift galaxies (z=0.3-1.0). To detect this diffuse emission, we have chosen to use a high-efficiency photon-counting EMCCD as part of FIREBall-2's detector system. The flight camera system includes a custom PC board, a mechanical

cryo-cooler (stirling engine), zeolite and charcoal getters, and a NUVU controller, for fast read-out speeds. Here we report on overall detector system performance, including pressure and temperature stability. We describe our characterization of detector noise from a delta-doped, anti-reflection-coated, electron-multiplying e2v CCD201-20. We describe our use of a NUVU controller to create custom waveforms that reduce clock-induced charge (CIC). We detail the clock frequencies, waveform shapes, and well depths required to reduce parallel and serial CIC to acceptable levels for our application (~10-3 events/pix/frame), at a range of substrate voltages. We also describe dark current measurements at several temperatures, including at our operating temperature of -125°C, with the flight set-up. Finally, we examine the overall performance for photon counting and the expected signal to noise for this experiment.

9601-23, Session 5

Solar glint suppression in compact planetary ultraviolet spectrographs

Michael W. Davis, G. Randall Gladstone, Cesare Grava, Thomas K. Greathouse, Kurt D. Retherford, Southwest Research Institute (United States)

Solar glint suppression is an important consideration in the design of compact photon-counting ultraviolet spectrographs. Southwest Research Institute developed the Lyman Alpha Mapping Project for the Lunar Reconnaissance Orbiter (launch in 2009), and the Ultraviolet Spectrograph on Juno (Juno-UVS, launch in 2011). Both of these compact spectrographs revealed minor solar glints in flight that did not appear in pre-launch analyses. These glints only appeared when their respective spacecraft were operating outside primary science mission parameters. Post-facto scattered light analysis verifies the geometries at which these glints occurred and why they were not caught during ground testing or nominal mission operations. The limitations of standard baffle design at near-grazing angles are discussed, as well as the importance of including surface scatter properties in standard stray light analyses when determining solar keep-out regions. In particular, the scattered light analysis of these two instruments shows that standard "one bounce" assumptions in baffle design are not always enough to prevent scattered sunlight from reaching the instrument focal plane. Future builds, such as JUICE-UVS, will implement improved scattered and stray light modeling early in the design phase to enhance capabilities in extended mission science phases, as well as optimize solar keep out volume.

9601-24, Session 5

Characterizing, managing, and correcting distortions in the HST/COS FUV detector

David J. Sahnow, George Dana Becker, John H. Debes, Justin Ely, Sean A. Lockwood, Derck Massa, Cristina M. Oliveira, Steven V. Penton, Charles Proffitt, Julia Roman-Duval, Hugues Sana, Paule Sonnentrucker, Joanna Taylor, Space Telescope Science Institute (United States)

The Far Ultraviolet (FUV) detector on the Cosmic Origins Spectrograph (COS) of the Hubble Space Telescope (HST) is subject to a variety of distortions due to its analog nature. Thermal variations of the detector and electronics stretch and shift the active area. Geometric distortions on a range of spatial scales warp the two-dimensional spectral image. Changes to detector walk - the dependence of detected position on pulse height – add distortions that change as a function of time. The CalCOS calibration pipeline includes corrections for each of these effects in the calibrated spectra, but these are imperfect, and they do not help with the target acquisition process, which uses raw detector coordinates.

We discuss these distortions and their effect on the data, our attempts to mitigate them, the current pipeline corrections and their success at removing the effects, and possible improvements to improve the data quality in the future.



9601-25, Session 6

New UV instrumentation enabled by enhanced broadband lithium fluoride coatings

Brian T. Fleming, Univ. of Colorado at Boulder (United States); Manuel A. Quijada, NASA Goddard Space Flight Ctr. (United States); Kevin France, Univ. of Colorado at Boulder (United States)

We present the results of a preliminary aging study of new enhanced broadband reflectivity lithium fluoride mirror coatings under development at the thin films laboratory at GSFC. These coatings have demonstrated greater than 80% reflectivity from the Lyman ultraviolet (-1040 Angstroms) to the optical, and have the potential to revolutionize FUV instrument design and capabilities. This work is part of a concept study in preparation for the flight qualification of these new coatings in a working astronomical environment. We outline the timeline for TRL advancement, and discuss the FUV science enabled by these high reflectivity broadband coatings on proposed or planned space missions. We also present the early design of the first space experiment to utilize these coatings, the proposed University of Colorado sounding rocket payload SISTINE, and show how these new coatings make the science goals of SISTINE attainable on a suborbital platform.

9601-26, Session 6

Characterization of borosilicate microchannel plates functionalized by atomic layer deposition

Camden D. Ertley, Oswald H. W. Siegmund, Jason McPhate, Anton Tremsin, John V. Vallerga, Space Sciences Lab. (United States); Henry J. Frisch, The Univ. of Chicago (United States); Jeffrey W. Elam, Anil U. Mane, Robert G. Wagner, Argonne National Lab. (United States); Michael J. Minot, Aileen O'Mahony, Christoher A. Craven, Mark Popecki, Incom Inc. (United States)

Glass capillary arrays (GCAs) have been functionalized through Atomic Layer Deposition (ALD) to produce robust microchannel plates (MCPs) with improved performance characteristics over traditional MCPs. The GCA substrates, made from a Borosilicate glass, have many advantages over traditional MCP lead glass, including the ability to be fabricated in large areas (currently at 400 cm2). The Borosilicate substrates have a lower radioactive content, meaning a lower background, can withstand higher temperatures during processing, and have a low outgassing. Using ALD to functionalize the substrate decouples the two and provides the opportunity to explore many new materials. Preliminary results indicate that using an MgO secondary electron emitting layer could provide stable high gains (-1x104 @ 900V) for orders of magnitude longer than standard MCPs (5 C cm-2). Also in contrast to standard devices only a very short burn in period (<0.05 C cm-2 vs. 0.25 C cm-2) seems to be required, and the gain rises during this period.

9601-27, Session 6

Performance and characteristics of the FUV microchannel plate detector for icon

Oswald H. W. Siegmund, Jason McPhate, Nate Darling, Travis Curtis, Sharon R. Jelinsky, Univ. of California, Berkeley (United States)

No Abstract Available

9601-28, Session 6

Design and characterization of the ICON FUV CCD cameras

Erik Syrstad, Brian C. Thompson, Robert Burt, Mitch Whiteley, Space Dynamics Lab. (United States)

The Far Ultraviolet Imaging Spectrograph (FUV) on the upcoming lonospheric Connection Explorer (ICON) mission uses dual image-intensified CCD camera systems, capable of detecting individual UV photons from both spectrometer channels (135.6 and 155 nm). Incident photons are converted to visible light using a sealed tube UV converter (described in an accompanying paper). The converter output is coupled to the CCD active area using a bonded fiber optic taper. The CCD (Teledyne DALSA FTT1010M) is a 1024x1024 frame transfer architecture. The camera readout electronics provide video imagery to the spacecraft over a 21 bit serialized LVDS interface, nominally at 10 frames per second and in 512x512 format (2x2 pixel binning). The CCD and primary electronics assembly reside in separate thermal zones, to minimize dark current without active cooling.

An engineering model camera system has been assembled, integrated, and tested. The CCD camera has been fully characterized with both visible light (prior to integration with the UV converter) and UV photons (following system integration). Measured parameters include camera dark current, read noise, linearity, gain, pulse height distribution, dynamic range, charge transfer efficiency, resolution, and full well capacity. Functional testing demonstrates that over a range of microchannel plate (MCP) voltages, camera performance will meet the critical FUV dynamic range requirements.

Flight model cameras will be fabricated and tested, followed by integration with the FUV instrument and sensor calibration in Summer 2015. Camera design and full performance data for the engineering and flight model cameras will be presented.

9601-29, Session PMon

A transmissive x-ray polarimeter conception for hard x-ray focusing telescopes

Hong Li, Hua Feng, Jianfeng Ji, Zhi Deng, Li He, Ming Zeng, Tenglin Li, Yinong Liu, Peiying Heng, Qiong Wu, Dong Han, Tsinghua Univ. (China); Yongwei Dong, Fangjun Lu, Shuangnan Zhang, Institute of High Energy Physics (China)

The X-ray Timing and Polarization (XTP) is a mission concept for a future space borne X-ray observatory and is currently selected for early phase study. We present a new design of X-ray polarimeter based on the time projection gas chamber. The polarimeter, placed above the focal plane, has an additional rear window that allows hard X-rays to penetrate (a transmission of nearly 80% at 6 keV) and reach the focal plane detector of focusing telescopes. Such a design is to compensate the low detection efficiency of gas detectors, at a negligible cost of sensitivity, and can maximize the science return of multilayer hard X-ray telescopes without the risk of moving focal plane instruments. The sensitivity in terms of minimum detectable polarization, based on current instrument configuration, is expected to be 3% for a ImCrab source given an observing time of 10⁵ s. We present preliminary test results, including photoelectron tracks and modulation curves, using a test chamber and polarized X-ray source in the lab.

9601-30, Session PMon

Characterization of single photon operation of AIO.8GaO.2As Geiger photodiodes

Xiao Jie Chen, Erik B. Johnson, Chad M. Whitney, Radiation

Conference 9601: UV, X-Ray, and Gamma-Ray Space Instrumentation for Astronomy XIX



Monitoring Devices, Inc. (United States); Min Ren, Yaojia Chen, Joe C. Campbell, Univ. of Virginia (United States); James F. Christian, Radiation Monitoring Devices, Inc. (United States)

Solid-state photomultipliers (SSPM) are high gain photodetectors composed of Geiger photodiodes (GPD) operating above device breakdown voltage. In scintillation based detection applications, SSPMs fabricated using silicon (SiPMs, MPPCs, etc) provide a compact, low cost alternative to photomultiplier tubes (PMTs), however, the high dark count rate due to its low band-gap (1.1eV) limits the signal-to-noise performance as the silicon SSPM is scaled to large areas. SSPMs fabricated in materials with a larger band-gap have the potential to surmount the performance limitations experienced by silicon. AlGaAs is a material that provides a bandgap from 1.55eV to 2.13 eV, depending on Al concentration. Using high Al concentration AlGaAs to engineer a wide-band-gap (>2eV) SSPM is very desirable in terms of reducing dark noise, which promises better signal-tonoise performances when large detector areas is needed.

This work describes the development of Geiger photodiodes (GPDs), the individual elements of a SSPM, fabricated in AlGaAs with 80% Al concentration. It presents the design of the GPDs, simulations of their performance, the fabrication process, along with characterization data of fabricated GPD samples. We show that with proper surface and sidewall passivation, high material quality, extremely low dark count rate GPD and SSPMs can be realized in this wide-band-gap material.

9601-31, Session PMon

Current progress in the characterization of atomic layer deposited metal fluorides for future astronomical ultraviolet mirror coatings

Christopher S. Moore, Univ. of Colorado at Boulder (United States); John Hennessy, April D. Jewell, Shouleh Nikzad, Jet Propulsion Lab. (United States); Kevin France, Univ. of Colorado at Boulder (United States)

Astronomical reflective aluminum (AI) mirrors are traditionally protected by a transmissive overcoat. The optical, mechanical and chemical properties of this overcoat material strongly effect the spectral reflective properties and durability of the mirror system. We are developing atomic layer deposited metal fluorides and assessing their applicability for future astronomical space missions in the ultraviolet and visible wavelengths. In this paper we present reflectance, environmental storage, surface roughness and chemical stability results.

9601-32, Session PMon

Silicon photomultipliers for next generation high-energy space telescopes

Karine Lacombe, Jürgen Knödlseder, Simon Delaigue, Maël Galliano, Baptiste Houret, Pascale Ramon, Gilbert Rouaix, Institut de Recherche en Astrophysique et Planétologie (France); Cédric Virmontois, Ctr. National d'Études Spatiales (France)

Photon detection is a central element of any high-energy astronomy instrumentation. One classical setup that has proven successful in many missions is the combination of photomultiplier tubes (PMTs) with scintillators, converting incoming high-energy photons into visible light, which in turn is converted in an electrical impulse. Although being extremely sensitive and rapid, PMTs have the drawback of being bulky, fragile, and requiring a high-voltage power supply of up to several thousand volts. Recent technological advances in the development of silicon photomultipliers (SiPM) make them a promising alternative to PMTs in essentially all their applications. We have started a R&D program to assess the possibility of using SiPMs for space-based applications in the domain of high-energy astronomy. We will present first results of our characterization studies of SiPMs from several manufacturers. Each SiPM has been tested inside a vacuum chamber and at low temperature to assess its performance in a space environment. After comparison, we will select a baseline detector with to design a dedicated front-end electronics and mechanical system. Furthermore, we plan to develop a specific low noise voltage power supply that ensures the stability of the SiPMs. Our ultimate goal is to qualify the system for a Technical Readiness Level of 5.

9601-33, Session PMon

VUV testing of science cameras at MSFC: QE measurement of the clasp flight cameras

Patrick R. Champey, The Univ. of Alabama in Huntsville (United States); Ken Kobayashi, Amy R. Winebarger, Jonathan W. Cirtain, David W. Hyde, Bryan A. Robertson, Brent L. Beabout, Dyana L. Beabout, NASA Marshall Space Flight Ctr. (United States); Mike Stewart, The Univ. of Alabama in Huntsville (United States)

The NASA Marshall Space Flight Center (MSFC) has developed a science camera suitable for sub-orbital missions for observations in the UV, EUV and soft X-ray. Six cameras were built and tested for the Chromospheric Lyman-Alpha Spectro-Polarimeter (CLASP), a joint National Astronomical Observatory of Japan (NAOJ) and MSFC sounding rocket mission. The CLASP camera design includes a frame-transfer e2v CCD57-10 512x512 detector, dual channel analog readout electronics and an internally mounted cold block. At the fight operating temperature of -20 C, the CLASP cameras achieved the low-noise performance requirements (≤25 e- read noise and ≤10 e-/sec/pixel dark current), in addition to maintaining a stable gain of -2.0 e-/DN. The e2v CCD57-10 detectors were coated with Lumogen-E to improve quantum efficiency (QE) at the Lyman-alpha wavelength. A vacuum ultraviolet (VUV) monochromator and a NIST calibrated photodiode were employed to measure the QE of each camera. Four fight-like cameras were tested in a high-vacuum chamber, which was configured to operate several tests intended to measure the QE, gain, read noise, dark current and residual non-linearity of the CCD. We present and discuss the QE measurements performed on the CLASP cameras. We also discuss the high-vacuum system outfitted for testing of UV and EUV science cameras at MSFC.

9601-35, Session PMon

The UV multi-object slit-spectrograph FireBALL-2 simulator

Pierre Mège, Sandrine Pascal, Samuel Quiret, Lab. d'Astrophysique de Marseille (France); Lauren Corlies, Columbia Univ. (United States); Didier Vibert, Robert Grange, Bruno Milliard, Lab. d'Astrophysique de Marseille (France)

The FIREBall-2 Instrument Model (FIREBallIMO) is a piece of software aiming at reproducing the optical behaviour of the Multi-Object Two-Curved Schmidt Slit Spectograph of FIREBall-2 (Faint Intergalactic Redshifted Emission BALLoon), a balloon-flight space mission (40 km in alt.) designed to perform a direct detection of the Circum Galactic Medium (CGM) in emission around low-z galaxies (c.f. 9601-20 conference). The spectrograph is optimized to operate in a narrow UV band [195-225] nanometers, the so-called the atmospheric sweet spot, where the sky background presents no emission lines and can be considered approximately flat, a value of 500 continnum units, seen through an optical transmission of a 50 at an atmospheric pressure of 3 millibars. This paper gives an overview of the software current modular architecture after a year of productive effort (in terms of parametric model space definition, associated data cubes and digital processing) from the instrument initial optical model designed under Zemax software to the final 2D-detected image. A special emphasis



is put on the design of a cython-wrapped driver able to retrieve dense raysampled PSFs out of the Zemax box efficiently. The optical mappings and distortions from the sky to the spectrograph entrance slit plane and from the sky to the detection plane are presented, as well as some end-to-end simulations leading to Signal-to-Noise Ratio estimates from artificial pointlike or extended test sources.

Sunday - Monday 9 -10 August 2015

Part of Proceedings of SPIE Vol. 9602 UV/Optical/IR Space Telescopes and Instruments: Innovative Technologies and Concepts VII

9602-1, Session 1

The JWST science instrument payload: mission context and status

Matthew A Greenhouse, NASA Goddard Space Flight Ctr. (United States)

Status of the Integrated Science Instrument Module (ISIM) of the James Webb Space Telescope (JWST) is discussed from a systems perspective with emphasis on integration and test. The ISIM is the science instrument payload of the JWST and is one of three elements that comprise the JWST space vehicle. It is in the final stage of space simulation testing ahead of delivery for integration with the telescope at the end of this year.

9602-2, Session 1

Beyond JWST: a technology path to the next great UVOIR space telescope

David C. Redding, Jet Propulsion Lab. (United States); David Schiminovich, Columbia Univ. (United States); Sara Seager, Massachusetts Institute of Technology (United States); Julianne Dalcanton, Univ. of Washington (United States); Suzanne Aigrain, Oxford Univ. (United Kingdom); Steven J. Battel, Battel Engineering, Inc. (United States); Niel Brandt, The Pennsylvania State Univ. (United States); Charles Conroy, Univ. of California, Santa Cruz (United States); Lee D. Feinberg, NASA Goddard Space Flight Ctr. (United States); Suvi Gezari, Univ. of Maryland, College Park (United States); Olivier Guyon, Subaru Telescope, National Astronomical Observatory of Japan (United States); Walter Harris, The Univ. of Arizona (United States); Christopher M. Hirata, The Ohio State Univ. (United States); John C. Mather, NASA Goddard Space Flight Ctr. (United States); Marc Postman, Space Telescope Science Institute (United States); H. Philip Stahl, NASA Marshall Space Flight Ctr. (United States); Jason Tumlinson, Space Telescope Science Institute (United States)

We report on the AURA "Beyond JWST" committee's considerations and conclusions regarding technology paths for the development of a large UVOIR observatory, to be launched following JWST and WFIRST-AFTA. The ambitious science goals for this mission include the discovery and spectral characterization of exo-earth candidates; the study of galaxies and stellar populations at spatial resolutions of 100 parsec at any redshift in the UV and visible universe; and multi-object spectroscopy up to R of 50,000, especially in the UV, to probe the chemical evolution and gas kinematics in and around galaxies both near and far. Requirements for aperture size, starlight suppression efficiency, and sensitivity at Far-UV wavelengths, all present significant technology challenges - but challenges that are within reach, building incrementally on current NASA investments and progress within the community. WFIRST-AFTA is pioneering new methods for coronagraphs that work with obscured apertures - work that can be extended to include larger segmented apertures. Exoplanet Program investments in starshade technologies for smaller telescopes inform choices for larger apertures. Cosmic Origins Program and non-NASA investments in mirrors, coatings and detectors already enable a range of telescope and scientific instrument architectures. We will present the consensus recommendations of the AURA committee on both the current readiness levels of these key technologies

and on the additional steps needed to support a viable flight concept for a future large UVOIR space telescope.

9602-3, Session 1

TECHBREAK: a technology foresight activity for the European Space Agency points the way to future space telescopes

Colin Cunningham, UK Astronomy Technology Ctr. (United Kingdom); Martin J. Cullum, European Southern Observatory (Germany); Emmanouil Detsis, European Science Foundation (France); Paul Kamoun, Thales Alenia Space (Belgium); Jean-Pierre Swings, Univ. de Liège (Belgium); Jean-Jacques Tortora, Eurospace (France); Jean-Claude Worms, European Science Foundation (France)

We report on a joint European Science Foundation-ESA "Forward Look" project called TECHBREAK aimed at identifying technological breakthroughs for space originating in the non-space sector. We show how some of the technologies highlighted may impact future space programmes, in particular novel ideas to enable future long-life large telescopes to be deployed. The goals of the study, which reported to ESA's High level Science Policy Advisory Committee (HISPAC) in late 2014, were to forecast the development of breakthrough technologies to enable novel space missions in the 2030-2050 timeframe, and to identify related partnerships through synergies with non-space specialists. Rather than be a definitive guide for very specific technologies to be developed for future space missions, it aims to flag up the main developments in technological and scientific areas outside space that may hold promise for use in the space domain, by identifying the current status of research for each technology domain, asserting the development horizon for each technology and providing links to key European experts and institutions with knowledge. The identification of problems and solutions specific to the space area led to focus the discussion around the concept of "Overwhelming Drivers" for space research and exploration, i.e. long-term goals that can be transposed into technological development goals. Two of these drivers are directly relevant to ambitious future telescope projects, and we will show how some of the technologies we identified such as biomimetic structures, nanophotonics, novel materials and additive manufacturing could be combined to enable revolutionary new concepts for space telescopes.

9602-4, Session 1

A future large-aperture UVOIR space observatory: reference designs

Norman Rioux, Lee D. Feinberg, NASA Goddard Space Flight Ctr. (United States); David C. Redding, Jet Propulsion Lab. (United States); H. Philip Stahl, NASA Marshall Space Flight Ctr. (United States)

Our joint NASA GSFC/JPL/MSFC/STScI study team has used communityprovided science goals to derive mission needs, requirements, and candidate mission architectures for a future large-aperture UVOIR space observatory. Reference designs have been developed for non-cryogenic telescopes that span UVOIR wavelengths. We describe the assessment we are conducting on the requirements and feasibility of system thermal and dynamic stability for supporting coronagraphy. The observatory is in a Sun-Earth L2 orbit providing a stable thermal environment and excellent





field of regard. ATLAST has developed a reference design for a 36-segment 9.2 m aperture telescope that stows within a five meter diameter launch vehicle fairing. Compatibility with three different launch vehicles mitigates programmatic risk. A deployed, three-layer, flat stray light shield oriented perpendicular to the sun provides stray light protection and benefits thermal stability. The telescope and instruments are dynamically isolated from spacecraft disturbance sources and the secondary mirror is actively controlled. The team has also assessed an 11.2 m aperture that required a different method of deploying the secondary mirror support structure and has evaluated some on-orbit assembly options. Options for a monolithic primary mirror up to 8 meters in diameter are also in the trade space. The performance needs developed under the study are traceable to a variety of reference designs. The observatory reference concepts are designed to be serviceable for potential life extension and upgrades, but do not require servicing for mission success. The details of these reference designs will be presented.

9602-5, Session 1

SLS launched missions concept studies for LUVOIR Mission

H. Philip Stahl, Randall Hopkins, NASA Marshall Space Flight Ctr. (United States)

The "Enduring Quests Daring Visions: NASA Astrophysics in the Next Three Decades" report calls for a Large UV-Optical-IR (LUVOIR) Surveyor mission to enable ultra-high-contrast spectroscopic and coronagraphic studies. A key technical challenge is how to get a 'large' telescope into space. The JWST design was severely constrained by the mass and volume capacities of its launch vehicle. Using an SLS (Space Launch System) rocket with its 10-m diameter x 30-m tall fairing and 45 mt payload to SE-L2, allows considerable design margin. This paper reports on concept studies of missions launch using an SLS (Space Launch System) rocket.

9602-6, Session 1

An evolvable space telescope for future astronomical missions: 2015 update

Ronald S. Polidan, Northrop Grumman Aerospace Systems (United States); James B. Breckinridge, Breckinridge Associates, LLC (United States); Charles F. Lillie, Lillie Consulting, LLC (United States); Howard A. MacEwen, Reviresco LLC (United States); Martin R. Flannery, Dean R. Dailey, Northrop Grumman Aerospace Systems (United States)

Astronomical flagship missions after the James Webb Space Telescope (JWST) will require lower cost space telescopes and science instruments. Innovative spacecraft-electro-opto-mechanical system architectures matched to the science requirements are needed for observations for exoplanet characterization, cosmology, dark energy, galactic evolution formation of stars and planets, and many other research areas. The needs and requirements to perform this science will continue to drive us toward larger and larger apertures.

Recent technology developments in precision station keeping of spacecraft, interplanetary transfer orbits, wavefront/sensing and control, laser engineering, macroscopic application of nano-technology, lossless optical designs, deployed structures, thermal management, interferometry, detectors and signal processing enable innovative telescope/system architectures with break-through performance.

Unfortunately, NASA's budget for Astrophysics is unlikely to be able to support the funding required for the 8-m to 16-m telescopes that have been studied for the follow-on to JWST using similar development/ assembly approaches without accounting for too large of a portion of the Astrophysics Division's budget. Consequently, we have been examining the feasibility of developing an "Evolvable Space Telescope" that would be 3 to 4-m when placed on orbit and then periodically augmented with additional

mirror segments, structures, and newer instruments to evolve the telescope and achieve the performance of a 16-m space telescope.

This paper provides an update to the 2014 SPIE paper discussing the technologies required for such a mission, candidate architecture approaches, and discusses different science measurement objectives for the stages of the architectures.

9602-7, Session 2

Overview and accomplishments of advanced mirror technology development phase 2 (AMTD-2) project

H. Philip Stahl, NASA Marshall Space Flight Ctr. (United States)

The Advance Mirror Technology Development (AMTD) project is a multiyear effort initiated in FY12 to mature technologies required to enable 4 to 8 meter (or larger) UVOIR space telescope primary mirror assemblies for both general astrophysics and ultra-high contrast observations of exoplanets. AMTD Phase 1 completed all of its goals and accomplished all of its milestones. AMTD Phase 2 started in 2014. Key accomplishments include deriving primary mirror engineering specifications from science requirements; developing integrated modeling tools and using those tools to perform parametric design trades; and demonstrating new mirror technologies via sub-scale fabrication and test. AMTD-1 demonstrated the stacked core technique by making a 43-cm diameter 400 mm thick 'biscuitcut' of a 4-m class mirror. AMTD-2 is demonstrating lateral scalability of the stacked core method by making a 1.5 meter 1/3rd scale model of a 4-m class mirror.

9602-8, Session 2

Technology development for the Advanced Technology Large Aperture Space Telescope (ATLAST) as a candidate large UV-Optical-Infrared (LUVOIR) surveyor

Matthew R. Bolcar, NASA Goddard Space Flight Ctr. (United States); Kunji Balasubramanian, Jet Propulsion Lab. (United States); Mark Clampin, Julie A. Crooke, Lee D. Feinberg, NASA Goddard Space Flight Ctr. (United States); Marc Postman, Space Telescope Science Institute (United States); Manuel A. Quijada, Bernard J. Rauscher, NASA Goddard Space Flight Ctr. (United States); David C. Redding, Jet Propulsion Lab. (United States); Norman Rioux, NASA Goddard Space Flight Ctr. (United States); Stuart B. Shaklan, Jet Propulsion Lab. (United States); H. Philip Stahl, NASA Marshall Space Flight Ctr. (United States); Carl M. Stahle, Harley A. Thronson Jr., NASA Goddard Space Flight Ctr. (United States)

We have identified six key technologies that will enable the Advanced Technology Large Aperture Space Telescope (ATLAST), a candidate architecture for the future large-aperture ultraviolet/optical/infrared (LUVOIR) space observatory envisioned by the NASA Astrophysics 30-year roadmap, "Enduring Quests, Daring Visions". The science goals of ATLAST address a broad range of astrophysical questions from early galaxy and star formation to the processes that contributed to the formation of life on Earth, combining general astrophysics with direct-imaging and spectroscopy of habitable exoplanets. The key technologies are: starlight suppression systems, lightweight mirrors, sensing and control systems, ultra-stable structures, detectors, and mirror coatings. Selected technology performance goals include: 1x10°-10 raw contrast at an inner working angle of 35 mas, wavefront error stability of 10 pm per 10 minutes, autonomous on-board sensing & control, and zero read noise photon-counting detectors spanning wavelengths from 300 nm to 1.8 μ m. Development of these technologies



will provide significant advances over current and planned observatories in terms of sensitivity, angular resolution, stability, and high-contrast imaging. The science goals of ATLAST are presented and flowed down to top-level telescope and instrument performance requirements in the context of a reference architecture: a 10 meter class, segmented aperture telescope operating at room temperature (-290 K) at the sun-Earth L2 point. For each technology area, we define best estimates of required capabilities, current state-of-the-art performance, and current Technology Readiness Level (TRL) – thus identifying the current technology gap. We report on current, planned, or recommended efforts to develop each technology to TRL 5.

9602-9, Session 2

ATLAST ULE mirror segment performance analytical predictions based on thermally induced distortions

Michael J. Eisenhower, Lester M. Cohen, Smithsonian Astrophysical Observatory (United States); Lee D. Feinberg, NASA Goddard Space Flight Ctr. (United States); Gary W. Matthews, Exelis Inc. (United States); Joel A. Nissen, Jet Propulsion Lab. (United States); Sang C. Park, Smithsonian Astrophysical Observatory (United States); Hume L. Peabody, NASA Goddard Space Flight Ctr. (United States)

The Advanced Technology Large-Aperture Space Telescope (ATLAST) is a concept for a 9.2 m aperture space-borne observatory operating across the UV/Optical/NIR spectra. The primary mirror for ATLAST is a segmented architecture with pico-meter class wavefront stability. Due to its extraordinarily low coefficient of thermal expansion a leading candidate for the primary mirror substrate is Corning's ULE® titaniasilicate glass. The ATLAST ULE® mirror substrates will be maintained at 'room temperature' during on orbit flight operations minimizing the need for compensation of mirror deformation between the manufacturing temperature and the operational temperatures. This approach requires active thermal management to maintain operational temperature while on orbit. Furthermore, the active thermal control must be sufficiently stable to prevent time-varying thermally induced distortions in the mirror substrates. This paper describes a conceptual thermal management system for the ATLAST 9.2m segmented mirror architecture that maintains the surface distortion to less than 10 pico-meters/10 minutes RMS. Thermal and finite-element models, analytical techniques, accuracies involved in solving the mirror figure errors, and early findings from the thermal and thermaldistortion analyses are presented.

9602-10, Session 2

Correction of large aperture active space telescope mirror using a gradient approach and a secondary deformable mirror

Matthew R. Allen, Jae Jun Kim, Brij N. Agrawal, Naval Postgraduate School (United States)

High development cost is a challenge for space telescopes and imaging satellites. One of the primary reasons for this high cost is the development of the primary mirror, which is required to meet diffraction limit surface figure requirements. Recent efforts have been made to develop lower cost, lightweight, replicable primary mirrors to include SiC actuated hybrid mirrors and carbon fiber mirrors. The SiC and carbon fiber mirrors at the Naval Postgraduate School do not meet the surface quality required for an optical telescope due to high spatial frequency residual surface errors. A technique under investigation at the Naval Postgraduate School is to correct the residue surface figure error by incorporating a deformable mirror in the optical path. This approach could result in significant reduction in development cost of the primary mirror by reducing surface figure

requirements and provide an on orbit correction capability.

The Naval Postgraduate School's Segmented Mirror Telescope (SMT) test bed uses 1-meter silicon carbide (SiC) active mirror segments to form a six-segment deployable 3-meter telescope. The active segments suffer from residual surface figure errors after a correction is applied. This research adds an additional deformable mirror to the optical path and uses a single closed loop adaptive gradient feedback controller to actively control the SMT segment and the secondary deformable mirror. The SMT segment surface figure error is characterized and a closed loop adaptive gradient controller is demonstrated by simulation and experiment. Simulation and experimental results are presented.

9602-11, Session 2

Optical design of camera for transiting exoplanet survey satellite (TESS)

Michael Chrisp, Kristin E. Clark, Brian C. Primeau, Michael Dalpiaz, Joseph Lennon, MIT Lincoln Lab. (United States)

This paper covers the design of a wide field of view refractive camera system, one of four identical cameras which form the TESS scientific payload. Photometry performed by these cameras requires maximum light gathering power, so the optical design was optimized to provide the fastest f-number (f/1.4) given the volume and weight available for the cameras. The cameras are designed with no vignetting, unlike most fast lens systems. The final design evolved from a starting Petzval design form, and has seven lenses, two of which have aspheric surfaces. This design was developed to make maximum use of the correction of the aspheric surfaces. The resulting design has an intermediate pair of negative lenses lessening the field curvature needed to be corrected by the field lens group. Forbes aspheres were used during the optimization process, with search methods used to establish which surfaces the two aspheres should be placed on for maximum performance improvement. Interestingly, these were better than those from CODEV's asphere expert module. The aspheres in the design reduce the average spot size by 60% compared with an all spherical design. The tolerancing of the system is described together with the current tolerance set, which shows the feasibility of building the system.

9602-12, Session 2

Detector requirements for coronagraphic biosignature characterization

Bernard J. Rauscher, NASA Goddard Space Flight Ctr. (United States)

Are we alone? Answering this ageless question, by searching for habitable worlds, will be a major focus for astrophysics in the 2020s. Our primary tools will be unprecedentedly powerful UV-Optical-IR space telescopes coupled with coronagraphs and/or starshades. Yet, these incredible facilities will not accomplish their objectives without better detectors than we have today.

Biosignature gases include oxygen, ozone, water vapor, and methane. Other non-biological gases, including carbon monoxide and carbon dioxide, can discriminate false positives. All imprint spectroscopic features in the UV-Optical-IR that can be characterized at low spectral resolution, R > 70, to constrain atmospheric chemistry and determine the likelihood of biological processes.

Even assuming an observatory like the Large UV-Optical-IR (LUVOIR) Surveyor described in NASA's "Enduring Quests Daring Visions" 30-year roadmap and recently recommended to NASA by the "BJWST" study, the detector requirements are beyond today's state-of-the-art. Essentially noiseless detection from the UV through at least near-IR is required with QE >- 80%. At the expected ~0.003 photon/s/pix flux, likely requirements include read noise << 1 e-, dark current <- 0.0003 e-/s, and negligible noise from other instrumental sources. Moreover, the detectors must withstand the rigors of space including the L2 radiation environment for a notional >- 5 yrs.



To inform detector development, we provide a broad overview of the detector requirements, and their scientific rationale, for spectroscopic characterization of atmospheric biosignature gasses using a LUVOIR. Where existing detector technologies are close to meeting requirements, we comment on where improvement would be most beneficial.

9602-13, Session 3

Orbiting rainbows: NIAC phase II progress

Scott A. Basinger, Marco B. Quadrelli, Jet Propulsion Lab. (United States); Grover A. Swartzlander Jr., Xiaopeng Peng, Rochester Institute of Technology (United States); Alexandra Artusio, Rochester State Rocks (United States); Darmin D. Arumugam, Jet Propulsion Lab. (United States)

"Orbiting Rainbows" is a Phase II NASA Innovative Advanced Concepts (NIAC) study that is looking twenty years into the future of creating a spacebased observatory from granular media. "Granular matter" is considered to be the fifth state of matter; this investigation draws from recent research on disordered lenses and turbid lens imaging. The investigators are performing fundamental research and developing the technology roadmap to construct an optical system in space using nonlinear optical properties of a cloud of micron-sized particles, shaped into a specific surface by light pressure, to form a very large and lightweight aperture of an optical system. This "cloud optic" will be relatively simple to package, transport, and deploy. It is reconfigurable and can be re-targeted; the focal length is variable and it will be self-healing and ultimately disposable. The concept, in which the aperture does not need to be continuous and monolithic, will allow the aperture size to be several times larger than currently envisioned observatories such as ATLAST and a fraction of the mass and cost. The ultimate cloud optic could be several tens of meters in diameter, and multiple clouds can be combined to create kilometer-class apertures. The concept also relies heavily on computational optics to deconvolve objects from non-deal imagery. Simulations and experiments have been positive using speckle interferometry techniques together with blind image deconvolution using a sparse, specular media for a primary mirror of an optical system. This talk will give a brief overview of the Orbiting Rainbows concept and presents ground-based subscale experimental results.

9602-15, Session 3

Design and test of the new generation solar imaging telescope

Olha V. Asmolova, Geoff Andersen, U.S. Air Force Academy (United States)

We describe imaging capabilities of a 0.2 m membrane diffractive primary (DOE) used as a key element in FalconSat-7, a space-based solar telescope. Its mission is to take an image of the Sun at the H-alpha wavelength (656nm) over a narrow bandwidth while in orbit. In this case the DOE is a photon sieve which consists of billions of tiny holes, with the focusing ability dependent on an underlying Fresnel zone geometry. Uniform radial expansion/contraction of the substrate due to temperature or relative humidity change will result in a shift in focal length without introducing errors in phase of the transmitted wavefront and without a decrease in efficiency. We will also show that while ideally the DOE surface should be held flat to within 5.25 microns, an opto-mechanical analysis showed that local deformations up to 32 microns are possible without significantly degrading the image quality.

9602-17, Session 4

Characterization of Euclid-like H2RG IR detectors for the NISP instrument

Benoît Serra, Aurélia Secroun, Anne Ealet, Jean Claude Clémens, Philippe Lagier, Mathieu Niclas, Ctr. de Physique des Particules de Marseille (France); remi Barbier, Eric Chabanat, Bogna Kubik, Institut de Physique Nucléaire de Lyon (France); Michael I. Andersen, Niels Bohr Institute (Denmark); Thierry Maciaszek, Lab. d'Astrophysique de Marseille (France); Anton Norup Sørensen, Niels Bohr Institute (Denmark); Eric Prieto, Lab. d'Astrophysique de Marseille (France); Gérard Smadja, Institut de Physique Nucléaire de Lyon (France)

The success of the Euclid's NISP (Near-Infrared Spectro-Photometer) survey requires very high performance detectors for which tight specifications have been defined. These must be verified over more than 95% of the focal plane: typically a dark current lower than 0.07 e-/s, a total noise lower than 13 e- in spectroscopic mode and 9 e- in photometric mode or a persistence signal lower than 0.05e-/s after 5 hours. The detectors are a procurement of ESA under a contract of NASA who will deliver to us selected flight detectors under Euclid specifications. 16 of Teledyne's 2.3 μ m cutoff 2048x2048 pixels H2RG infrared detectors will fill the NISP focal plane and must be fully characterized at the pixel level: this is CPPM's responsibility.

This characterization is crucial to the future processing and in-flight calibration and may be quite challenging: for instance, measuring very low level dark currents – as low as 10^{-3} e-/s – or persistence signals, which implies alternating dark current measurements with flat field strong illumination. This has led to the definition of a thorough test plan and to the development of dedicated facilities, analysis methods and software tools. First tests of high performance engineering grade detectors show the quality of our characterization chain and will be presented, including dark current, total noise, both CDS and science modes, conversion gain and persistence. A pilot run is foreseen at the end of the year to validate the test plan. Next step will be the characterization of flight detectors expected to start in Spring 2016.

9602-18, Session 4

Preliminary results on the EUCLID NISP stray-light and ghost analysis

Frank U. Grupp, Univ.-Sternwarte München (Germany) and Max-Planck-Institut für extraterrestrische Physik (Germany); Norbert Geis, Ralf Bender, Max-Planck-Institut für extraterrestrische Physik (Germany)

No Abstract Available

9602-19, Session 5

Coatings for UVOIR telescope mirrors

Kunjithapatham Balasubramanian, John Hennessy, Shouleh Nikzad, Nasrat A. Raouf, Michael E. Ayala, Jet Propulsion Lab. (United States); Javier G. Del Hoyo, Manuel A. Quijada, NASA Goddard Space Flight Ctr. (United States)

NASA Cosmic Origins Program initiatives call for large telescope architectures with high throughput from far UV to near IR to enable efficient gathering of light with important spectral signatures including those in far UV region down to 90nm. Typical Aluminum mirrors protected with MgF2 fall short of the requirements below 120nm. Therefore new and improved coatings are sought to protect aluminum from oxidation that causes severe absorption. Besides choice of materials, the process of applying coatings has to be optimized and controlled accurately and reliably to ensure the coatings preserve the expected optical characteristics. This challenge is addressed here with experimental investigations at JPL and at GSFC. We present the progress achieved to date and discuss the path forward to achieve 90% reflectance in the spectral region from 90 to 130nm without degrading performance in the visible and NIR regions taking into account durability concerns when the mirrors are exposed to normal laboratory conditions.



9602-20, Session 5

Carbon nanotube optical mirrors

Peter C. Chen, NASA Goddard Space Flight Ctr. (United States) and The Catholic Univ. of America (United States); Douglas M. Rabin, NASA Goddard Space Flight Ctr. (United States)

We report the fabrication of imaging quality optical mirrors with smooth and super-smooth surfaces using carbon nanotubes (CNT) embedded in an epoxy matrix. CNT/epoxy is a multifunctional composite material that has sensing capabilities and can be made to incorporate self-actuation. As the precursor is a low density liquid, large and lightweight mirrors can be fabricated by non-traditional processes such as replication, spincasting, and additive manufacturing. With the infusion of advanced numerical modeling techniques such as topology optimization and state of the art 3D printing, CNT/E technology is a promising candidate for the development of a new generation of lightweight, compact "smart" telescope mirrors and structures with figure sensing, active optics, adaptive optics, athermal construction, and in-space fabrication capabilities. We report on measurements made of optical and mechanical characteristics, active optics experiments, and numerical modeling. We discuss possible paths for future development.

9602-21, Session 5

A global shutter CMOS image sensor with in-pixel CDS for hyperspectral imaging

Ben J. Dryer, Konstantin D. Stefanov, David J. Hall, The Open Univ. (United Kingdom); Jérôme Pratlong, Martin Fryer, Andrew Pike, e2v technologies plc (United Kingdom)

Hyperspectral imaging has been providing vital information on the Earth landscape in response to the changing environment, land use and natural phenomena. While conventional hyperspectral imaging instruments have typically used rows of linescan CCDs, CMOS imaging sensors (CIS) have been slowly penetrating space instrumentation for the past decade, and Earth Observation (EO) is no exception. CIS provide distinct advantages over CCDs that are relevant to EO hyperspectral imaging. The lack of charge transfer through the array allows the reduction of cross talk usually present in CCDs due to imperfect charge transfer efficiency, and random pixel addressing makes variable integration time possible, and thus improves the camera sensitivity and dynamic range.

e2v technologies has developed a 10T pixel design that integrates a pinned photodiode with global shutter (to reduce blurring of the 'broom') and in-pixel CDS to increase the signal to noise ratio in less intense spectral regimes, allowing for both high resolution and low noise hyperspectral imaging for EO. This paper details the characterisation of a test device, providing baseline performance measurements of the array such as noise, responsivity, dark current and global shutter efficiency, and also discussing benchmark hyperspectral imaging requirements such as dynamic range, pixel crosstalk, and image lag.

9602-22, Session 5

Testing simple models for dynamic correlated charge collection effects in thick CCDs

Daniel P. Weatherill, Konstantin D. Stefanov, Andrew D. Holland, The Open Univ. (United Kingdom); Douglas Jordan, e2v technologies plc (United Kingdom); Ivan V. Kotov, Brookhaven National Lab. (United States)

The subject of dynamic charge collection effects in thick CCDs has received great interest in recent years, due to the major performance and calibration

consequences implied for precision optical astronomy, in both ground-based (e.g. LSST) and space-based (e.g. EUCLID) missions. These phenomena are observed as both the "brighter - fatter" effect, causing measured asymmetry in the PSF of a CCD, and as statistical correlations visible in the photon transfer curve and spatial autocorrelation measurements of the device.

It is widely accepted that the dynamic effects are caused due to the changing geometry and magnitude of the electric fields in the pixels as the collecting potential wells are filled. Several models have been proposed based on this which are able to calculate ancillary pixel data to aid in correcting for the effect in device calibration and data reduction.

In this paper we present validation results using flat-field calibration data from an e2v CCD250 for a simple model, based on analytical solutions of the Poisson equation. The model is not intended to provide detailed correction data for a specific device, but as an estimator for predicting sensor performance based on design parameters.

9602-23, Session 5

Proton-induced random telegraph signal in the CMOS imaging sensor for JANUS, the visible imaging telescope on JUICE

George P. Winstone, Matthew R. Soman, Andrew D. Holland, Jason P. D. Gow, Konstantin D. Stefanov, Mark Leese, The Open Univ. (United Kingdom)

JUpiter ICy moons Explorer (JUICE) is an ESA L class mission due for launch in 2022 as part of the agency's Cosmic Vision program. The primary science goal is to explore and characterise Jupiter and several of its potentially habitable icy moons, particularly Ganymede, Europa and Callisto.

The JANUS instrument is designated to be the scientific imager on-board the spacecraft with a wavelength range between 400 nm and 1000 nm and consists of a catoptric telescope coupled to a CMOS detector, specifically the CIS115 monolithic active pixel sensor supplied by e2v technologies. A CMOS sensor has been chosen due to a combination of the high radiation tolerance required for all systems aboard the spacecraft and its capability of operating with integration times as low as 1 ms, which is required to prevent blur when imaging the moons at fast ground velocities since the camera has no mechanical shutter. However, an important consideration of using CMOS in high radiation environments is the generation of defects or defect clusters that result in pixels exhibiting Random Telegraph Signal (RTS).

A study of RTS effects in the CIS115 has been undertaken, and the method applied to identify pixels in the array that display RTS behaviour is discussed and individual RTS exhibiting pixels are characterised. The changes observed in RTS behaviour following irradiation of the CIS115 with protons will be presented and the temperature dependence of the RTS behaviour is studied. The implications on the camera design and imaging requirements of the mission are examined.

9602-24, Session 5

Radiation qualification of the CIS115 for the JUICE mission

Matthew Soman, Andrew D. Holland, George P. Winstone, Jason P. D. Gow, Konstantin D. Stefanov, Mark Leese, The Open Univ. (United Kingdom)

The CIS115 is one of the latest CMOS Imaging Sensors designed by e2v technologies, with 1504x2000 pixels on a 7 μm pitch. Each pixel in the array is a pinned photodiode with a 4T architecture, achieving an average dark current of 22 electrons/pixel/s at 21°C. The sensor aims for high optical sensitivity by utilising e2v's back-thinning and processing capabilities, providing a sensitive silicon thickness approximately 9 μm to 12 μm thick with a tuned anti-reflective coating.

The sensor operates in a rolling shutter mode incorporating reset level subtraction resulting in a mean pixel readout noise of 4.25 electrons rms.



The full well has been measured to be 34000 electrons, resulting in a dynamic range of up to 8000. These performance characteristics have led to the CIS115 being chosen for JANUS, the high-resolution and wide angle optical camera on the JUpiter ICy moon Explorer (JUICE).

The three year science phase of JUICE is in the harsh radiation environment of the Jovian magnetosphere, primarily studying Jupiter and its icy moons. Analysis of the expected radiation environment and shielding levels from the spacecraft and instrument design predict the End of Life (EOL) displacement and ionising damage for the CIS115 to be equivalent to 10^10 10 MeV protons cm⁻2 and 100 krad(Si) respectively. Characterisation results following proton and gamma irradiations will be presented, detailing the initial phase of space qualification of the CIS115. Results will be compared to the pre-irradiation performance and the instrument specifications and further qualification plans will be outlined.

9602-36, Session 5

A low noise, high QE, large format CCD camera system for the MIGHTI instrument on the NASA ICON mission

Jed J. Hancock, Joel G. Cardon, Michael Watson, Space Dynamics Lab. (United States); James Cook, Utah State Univ. (United States); Mitch Whiteley, James Beukers, Space Dynamics Lab. (United States); Christoph R. Englert, Charles M. Brown, U.S. Naval Research Lab. (United States); John M. Harlander, St. Cloud State Univ. (United States); Stewart E. Harris, Univ. of California, Berkeley (United States)

The Michelson Interferometer for Global High-resolution Thermospheric Imaging (MIGHTI) instrument is part of the NASA lonospheric Connection Explorer (ICON) mission designed to uncover the mysteries of the extreme variability of the Earth's ionosphere. MIGHTI consists of two identical units positioned to observe the Earth's low latitude thermosphere from perpendicular viewing directions. The MIGHTI instrument is a spatial heterodyne spectrometer and requires a low noise, high QE, large format camera system to detect slight phase changes in the fringe patterns which reveal the neutral wind velocity.

The MIGHTI camera system uses a single control electronics box to operate two identical CCD camera heads and communicate with the ICON Instrument Control Package (ICP) electronics. The control electronics are carefully designed for a low noise implementation of CCD biases, clocking, and CCD output digitization. The camera heads use a 2k by 2K, back-illuminated, frame transfer CCD provided by e2v. The CCD's are both TEC cooled and have butcher-block interference filters mounted in close proximity to the active area. The CCDs are nominally operated in binned mode, the control electronics register-settings provide flexibility for binning and gain control. An engineering model of the camera system has been assembled and tested. The EM camera system characterization meets all performance requirements. Performance highlights include a measured read noise of 5.7 electrons and dark current of less than 0.01 electrons/ pixel/second. The camera system design and characterization results are discussed.

9602-25, Session 6

Optical design and tolerance analysis of a reflecting telescope for CubeSat

Ching-Wei Chen, Chia-Ray Chen, National Space Organization (Taiwan)

Optical design of a small reflecting telescope for use in a 3U CubeSat mission is reported in this study. The off-axis segmented method for earth observation techniques based on a Ritchey-Chrétien type telescope is adopted in this design. The primary mirror and secondary mirror are circular apertures with 70-mm and 22-mm in diameter. The effective focal length

is 685-mm operated at 450-km altitude. A commercial 1928 ? 1084 CCD image sensor with a pixel size of 7.4-?m ? 7.4-?m is applied, which capture a 9.2-km ? 5.3-km swath area. The ground resolution is moderate to be 4.86-m for CubeSat application. The MTF is expected to be about 0.4 at camera resolution at 67.6-lp/mm. The tolerance analysis is performed for further understanding on fabrication and assembly errors. This telescope shows a reasonable design to obtain a more detailed image with a CubeSat. These results will be used in space exploration with CubeSat missions.

9602-26, Session 6

Analysis of an optical relay system and integration into a satellite imager

Louahab Noui, Surrey Satellite Technology Ltd. (United Kingdom)

A description of an optical relay subsystem used in a high resolution earth observation satellite imager is presented. Tolerance and thermal analysis showed that very tight tolerances are required to achieve diffraction limited performance. The tolerancing methodology of the optical system is described and compared to the actual build process. Alignment of optical elements is critical for the successful build of the relay system, and ground support equipment was developed for this purpose. The alignment technique and verification of the build of different components are presented. Typical results of the alignment process together with predicted performance are reported.

Optical characterisation of the relay subsystem in terms of wavefront analysis is described and it is shown that some tolerances were not practically achievable. To achieve diffraction limited performance an optical correction method was developed and implemented. The description of the methodology adopted to measure the optical performance of the relay system and to calculate the corresponding wavefront correction is discussed. The implementation of free-form surface figuring is also presented. The successful practical implementation of wavefront correction to achieve diffraction limited space telescope system is demonstrated.

9602-27, Session 6

Focal plane actuation for the development of a high resolution suborbital telescope

Alexander D. Miller, Paul A. Scowen, Arizona State Univ. (United States); Todd J. Veach, NASA Goddard Space Flight Ctr. (United States)

We present a hexapod stabilized focal plane as the key instrument for a proposed suborbital balloon mission. Balloon gondolas currently achieve 1-2 arcsecond pointing error, but cannot correct for unavoidable jitter movements (~50 microns at 20hz) caused by wind rushing over balloon surfaces, thermal variations, cryocoolers, and reaction wheels. The jitter causes image blur during exposures and is the limiting resolution of the system. To solve this, the hexapod system actuates the focal plane to counteract the jitter through real-time closed loop feedback from startrackers. Removal of this final jitter term decreases pointing error by an order of magnitude and allows for true diffraction-limited observation. This boost in resolution will allow for Hubble-quality imaging for a fraction of the cost. Tip-tilt pointing systems have been used for these purposes in the past, but require additional optics and introduce multiple reflections. The hexapod system, rather, is compact and can be plugged into the focal point of nearly any configuration. The design also thermally isolates the hexapod from the cryogenic focal plane enabling the use of well-established noncryogenic hexapod technology.

High-resolution time domain multispectral imaging of the gas giant outer planets, especially in the UV range, is of particular interest to the planetary community, and a suborbital telescope with the hexapod stabilization in place would provide a wealth of new data. On an Antarctic ~100-day Long-Duration-Balloon mission the continued high-resolution imaging of gas giant storm systems would provide cloud formation and evolution data second to only a Flagship orbiter.

9602-28, Session 6

Low cost visible imaging and IR spectroscopy from stratospheric telescopes

Eliot F. Young, Southwest Research Institute (United States); Charles A. Hibbitts, Andrew F. Cheng, Johns Hopkins Univ. Applied Physics Lab., LLC (United States); Robert A. Woodruff, Lockheed Martin Corp. (United States)

NASA's Balloon Office regularly supports missions in which stratospheric telescopes make observations from altitudes of 33 - 38 km, above 99.3% - 99.6% of the Earth's atmosphere. These missions are much cheaper than spacecraft missions while providing two key advantages over ground-based facilities: the potential for diffraction-limited imaging in UV-visible wavelengths and nearly complete access to the infrared spectrum.

The BOPPS mission (Balloon Observation Platform for Planetary Science) flew 0.8-m telescope on September 25, 2014 for a 20-hour flight. BOPPS carried an infrared camera (0.8-5 μm) to image targets that are normally obscured from the ground by telluric species and a guide camera/fast steering mirror to stabilize the focal plane at the sub-0.1" level.

Prospects for upcoming balloon missions are promising: NASA is testing large super-pressure balloons for 100-day circumglobal flights. These missions will nominally provide 1000 hours of dark-time from a near-space environment, comparable to the ~3000 hours that HST awards annually to science observations. Furthermore, several recent payloads (including BOPPS) have stabilized telescopes at the level of a few arc seconds or better, with fine steering systems able to maintain pointing at the diffraction limit. Finally, recent work suggests that passive thermal shielding can lower telescope temperatures to less than 180 K to reduce thermal self-emission below the sky background levels from 1 - 4.8 microns.

These capabilities potentially make scientific balloon platforms as productive as space telescopes for certain science applications, but with distinct advantages such as low cost, re-usability and short timescales from proposal to flight.

9602-30, Session 7

Thermal shield with high soft x-ray transparency

Bruce M. Lairson, Heidi Lopez, David Grove, Travis Ayers, Luxel Corp. (United States)

Thermal shields are required for cryogenic sensors, cooled imaging arrays, and the interior of spacecraft. We present a hybrid metal grid/metal membrane with improved blocking of thermal infrared photons, with high EUV and soft X-ray transmittance. In some cases, infrared blocking can be 10X higher for the hybrid structure compared with superposition of separate membranes and grids. We present infrared thermal shielding of grid-supported freestanding aluminum membranes between 15nm and 50nm thick, as well as membranes supported by both a grid and by ultrathin polyimide.

9602-31, Session 7

Challenges in photon-starved space astronomy in a harsh radiation environment using CCDs

David J. Hall, Nathan L. Bush, Neil J. Murray, Jason P. D. Gow, Andrew S. Clarke, Ross Burgon, Andrew D. Holland, The Open Univ. (United Kingdom)

The Charge Coupled Device (CCD) has a long heritage for imaging and

spectroscopy in many space astronomy missions. However, the harsh radiation environment experienced in orbit creates defects in the silicon that capture the signal being transferred through the CCD. This radiation damage has a detrimental impact on the detector performance and requires carefully planned mitigation strategies.

SPIE. PHOTONICS

OPTICAL ENGINEERING+ APPLICATIONS

The ESA Gaia mission uses 106 CCDs, now orbiting around the second Lagrange point as part of the largest focal-plane ever launched. Following readout, signal electrons will be affected by the traps generated in the devices from the radiation environment and this degradation will be corrected for using a charge distortion model. ESA's Euclid mission will also contain a focal plane of CCDs in the VIS instrument. Moving further forwards, the World Space Observatory (WSO) UV spectrographs and the WFIRST-AFTA coronagraph intend to look at very faint sources in which mitigating the impact of traps on the transfer of single electron signals will be of great interest.

Following the development of novel experimental and analysis techniques, one is now able to study the impact of radiation on the detector to new levels of detail. Through a combination of TCAD simulations, defect studies and device testing, we are now probing the interaction of single electrons with individual radiation-induced traps to analyse the impact of radiation in photon-starved applications.

9602-32, Session 7

Optical tolerancing and predicted performance of the Wide-Field InfraRed Survey Telescope / Astrophysics Focused Telescope Assets (WFIRST/AFTA) widefield instrument

Bert A. Pasquale, Catherine T. Marx, David A. Content, Jeffrey W. Kruk, Qian Gong, Joseph M. Howard, Alden S. Jurling, J. Eric Mentzell, NASA Goddard Space Flight Ctr. (United States); Nerses V. Armani, Arthur L. Whipple, Martina S. Atanassova, Cliffton E. Jackson, SGT, Inc. (United States); Thomas M. Casey, Sigma Space Corp. (United States); Carl A. Blaurock, Nightsky Systems, Inc. (United States)

The optical design of the Wide-Field InfraRed Survey Telescope (WFIRST) Wide-Field Channel (WFC) continues to evolve through design and analysis cycles. While the as-designed performance has been discussed in previous publications, ultimately it is the as-built on-orbit performance that must satisfy the scientific requirements. The 2.37-meter diameter (Hubble-Class) aperture Three Mirror Anastigmat (TMA) -based optical design has been analyzed for fabrication, alignment, and stability budgets. We have taken into account the Integration and Testing (I&T) plan, Integrated Modeling (IM) and Structural / Thermal / Optical (STOP) analysis. The WFC is predicted to maintain diffraction-limited performance over a focal plane of 300 million pixels. Its instantaneous field of view coverage of 0.282 degrees at 0.11 arcsecond pixel scale will operates in six panchromatic bands between $0.7 - 2.0\mu$ m, or in spectrographic imaging mode from 1.35-1.95 μ m.

9602-33, Session 7

Wide-Field InfraRed Survey Telescope/ Astrophysics Focused Telescope Assets (WFIRST/AFTA) grism spectrometer

Qian Gong, NASA Goddard Space Flight Ctr. (United States); Thomas Casey, Sigma Space Corp. (United States); David A. Content, Margaret Z. Dominguez, Jeffrey W. Kruk, Catherine Marx, Bert A. Pasquale, Thomas E. Wallace, Arthur O. Whipple, NASA Goddard Space Flight Ctr. (United States)



The Grism spectrometer plays an important role in WFIRST/AFTA mission for the survey of emission-line galaxies. This presentation discusses the challenges and solutions of the optical design, as well as its potential to further expand the wavelength range and accommodate any Field Of View (FOV) change for future design cycles. However, the emphasis of this presentation is the progress of the grism prototype: the design, fabrication, and test of the complicated diffractive optical elements and powered prism and current status. It also addresses the cryogenic test plan: to test the designed infrared diffractive elements using a visible interferometer and to test whole grism assembly using phase retrieval at the designed wavelength range. Finally, the optical alignment, tolerance, and mechanical design will be discussed.

9602-34, Session 7

Spectral performance of WFIRST/AFTA bandpass filter prototypes

Manuel A. Quijada, David A. Content, Jeffrey W. Kruk, Kevin H. Miller, NASA Goddard Space Flight Ctr. (United States)

The current pre-formulation baseline for the Wide Field Infrared Survey Telescope Astrophysics Focused Telescope Assets (WFIRST/AFTA) consists of a single wide field channel instrument with 0.28 deg2 active field of view for both imaging and spectroscopy. The only routinely moving part during scientific observations for this wide field channel is the element wheel (EW) assembly. This filter wheel assembly will have 8 positions that will be populated with 6 different bandpass coatings, a blank position, and a Grism that will consist of 3 element assembly that disperses with the central wavelength undeviated for galaxy redshift surveys. All elements in the EW assembly will have ~110 mm diameter fused silica substrates that will have the appropriate band-pass coatings according to the filter designations (Z087, Y106, J129, H158, F184, W149 and Grism). This paper will present and discuss spectral performance (including spectral transmission and surface figure wavefront errors) for a subset of the band-pass coatings for the filter types Z087, W149, and Grism. These filter coatings have been procured from three different vendors to address the most challenging aspects in terms of the in-band throughput (>95%), Out of band rejection (<10^E-05), uniformity (< 1% transmission level) and the cut-on and cut-off slopes (3% for the filters and 0.3% for the Grism coatings).

9602-16, Session PMon

Demonstrator model: a first demonstration of the NISP detection system

Jean Claude Clémens, Aurélia Secroun, Benoît Serra, Anne Ealet, Ctr. de Physique des Particules de Marseille (France); Rémi Barbier, Institut de Physique Nucléaire de Lyon (France); Florent Beaumont, Lab. d'Astrophysique de Marseille (France); Eric Chabanat, Institut de Physique Nucléaire de Lyon (France); Christophe Fabron, José Garcia, Emmanuel Grassi, Lab. d'Astrophysique de Marseille (France); Bogna Kubik, Institut de Physique Nucléaire de Lyon (France); Thierry Maciaszek, Eric Prieto, Lab. d'Astrophysique de Marseille (France); Gérard Smadja, Institut de Physique Nucléaire de Lyon (France)

CPPM is in charge of the characterization and integration into the focal plane of EUCLID's NISP (Near-Infrared Spectro-Photometer) 2.3 μ m cutoff 2048 x 2048 pixel H2RG infrared detectors. NISP's focal plane array (FPA) contains a matrix of 16 detectors acquired simultaneously. Before delivering the full instrument to ESA after the detectors characterization, several test models will have to demonstrate the performances of the detector system.

The first test model, the Demonstrator Model (DM), has been integrated at LAM and tested in dedicated facilities. The aim was to validate both the integration process and the simultaneous acquisition of four detectors and their EMC behavior. In order to validate the science acquisition modes, a series of dark measurements has been acquired to assess the stability and the good performances of the detectors. Dark levels down to 10^-2 electrons/second were measured without using a dark lid onto the FPA. Dark current peak-to-peak oscillations at the level of 3.10^-2 were observed for acquisitions of 560s and confirmed later on. Moreover noise studies in various acquisition configurations showed that total noise is quite independent of the configuration.

Measurements and analysis done using the data acquired during the DM tests will be described. In addition, a study on cosmic ray impact on detectors has been conducted and initial results will be shown. Tests and data will be used for next sessions of test models that will come before the delivery of the NISP instrument to ESA in 2017.

9602-35, Session PMon

ACCESS: integration and pre-launch performance

Mary E. Kaiser, Matthew J. Morris, Johns Hopkins Univ. (United States); Jeffrey W. Kruk, Bernard J. Rauscher, Randy A. Kimble, NASA Goddard Space Flight Ctr. (United States); Edward L. Wright, Univ. of California, Los Angeles (United States); Stephan R. McCandliss, Russell Pelton, Lauren N. Aldoroty, Grant O. Peacock, Paul D. Feldman, Henry W. Moos, Johns Hopkins Univ. (United States); Adam G. Riess, Johns Hopkins Univ. (United States) and Space Telescope Science Institute (United States); Dominic J. Benford, Jonathan P. Gardner, NASA Goddard Space Flight Ctr. (United States); Ralph C. Bohlin, Susana E. Deustua, William V. Dixon, David J. Sahnow, Space Telescope Science Institute (United States); Robert Kurucz, Harvard-Smithsonian Ctr. for Astrophysics (United States); Michael Lampton, Space Sciences Lab. (United States); Saul Perlmutter, Lawrence Berkeley National Lab. (United States)

ACCESS, Absolute Color Calibration Experiment for Standard Stars, is a series of rocket-borne sub-orbital missions and ground-based experiments that will leverage the significant technological advances in detectors, instruments, and the precision of the fundamental laboratory standards used to calibrate these instruments to enable improvements in the precision of the astrophysical flux scale through the transfer of absolute laboratory detector standards from the National Institute of Standards and Technology (NIST) to a network of stellar standards with a calibration accuracy of 1% and a spectral resolving power of 500 across the 0.35 to 1.7 micron bandpass.

Achieving a calibration accuracy of 1% precision is important for understanding scientific phenomena such as dark energy where a reduction in the cross-color calibration systematic errors associated with SNeIa photometry is needed to distinguish between dark energy models

The ACCESS Cassegrain telescope feeds a compact (Rowland circle design) spectrograph with a cross dispersing Fery prism and HST/WFC3 heritage 1024x1024 HgCdTe detector. The telescope, spectrograph, and avionics system are currently being fabricated, assembled, and integrated. Subsystem testing of flight components is ongoing. Detector characterization is in progress. Flight software is under test. The detector telemetry interface has been written and stand-alone tested. Thermal vacuum testing of the detector, controller and flight computer has been successful.

Integration and test results will be presented in addition to the calibration strategy and status. Launch is expected within the year. NASA sounding rocket grant NNX08AI65G supports this work.

Conference 9603: Optics for EUV, X-Ray, and Gamma-Ray Astronomy VII

Monday - Thursday 10-13 August 2015

Part of Proceedings of SPIE Vol. 9603 Optics for EUV, X-Ray, and Gamma-Ray Astronomy VII

9603-59, Session PMon

Coarse alignment of thin-shell, segmented mirrors for Wolter telescopes

Benjamin D. Donovan, The Univ. of Iowa (United States); Edward Hertz, Vanessa Marquez, Stuart McMuldroch, Paul B. Reid, Ryan Allured, Harvard-Smithsonian Ctr. for Astrophysics (United States)

The alignment of thin-shell, segmented mirrors for Wolter I telescopes frequently involves the use of a Hartmann test. In order to get optical throughput in the Hartmann test, the mirrors must first be coarsely aligned to one another and to the entire optical system. In the past, the coarse alignment of these mirrors at the Smithsonian Astrophysical Observatory has largely relied upon component machine tolerances and contact measurements with a coordinate measurement machine (CMM). This process takes time and does not produce reliable, nor repeatable results. Thus, methods were developed to allow for the quick and reliable coarse alignment of thin-shell, segmented mirrors, with the mirrors supported at their final locations in the mirror assembly. We present the coarse alignment system developed at the Smithsonian Astrophysical Observatory and its use in the alignment of thin-shell, segmented mirrors for the adjustable X-ray optics program.

9603-60, Session PMon

Addressing the problem of glass thickness variation in the indirect slumping technology

Laura Proserpio, Elias Breunig, Peter Friedrich, Anita Winter, Max-Planck-Institut für extraterrestrische Physik (Germany); Christoph Wellnhofer, Max-Planck-Institut für extraterrestrische Physik (Germany) and Institut für Werkstoffwissenschaft und Werkstoffmechanik (Germany)

The indirect hot slumping technology is being developed at Max-Planck-Institute for extraterrestrial Physics (MPE) for the manufacturing of lightweight astronomical X-ray telescopes. To obtain mirror segments of high optical quality, the optimization of the slumping thermal cycle itself is of fundamental importance, but also the starting materials, primarily the mould and the glass foils, play a major role. This paper will review the MPE latest results in the slumping technology and will then concentrate on the selection of the initial glass, with particular regards to the problem of glass foils thickness variation.

9603-61, Session PMon

Off-plane x-ray diffraction grating fabrication

Thomas J. Peterson, Casey T. DeRoo, Randall L. McEntaffer, The Univ. of Iowa (United States)

High performance X-ray diffraction gratings are essential for achieving key astrophysical science goals. Off-plane X-ray diffraction gratings with precision groove profiles at the submicron scale are necessary for next generation X-ray spectrometers. Such gratings will be used on a current NASA suborbital rocket mission, the Off-plane Grating Rocket Experiment (OGRE), and have application for future grating missions. The fabrication of these gratings does not come without challenges. High performance off-plane gratings must be fabricated with precise radial grating patterns, optically flat surfaces, and specific facet angles. Such gratings can be made

using a series of common microfabrication techniques. First, the radial groove pattern is written into a resist/Cr coated fused silica plate using e-beam lithography. The pattern is then transferred into a silicon wafer using DUV immersion lithography and subsequent reactive ion etching. Creating the angled facets involves nanoimprinting the grating pattern onto a Si wafer of specific crystallographic orientation that has been nitride coated, followed by reactive ion etching through the nitride. An anisotropic chemical wet etch is then employed to form blazed triangular facets. This pattern is then replicated into a resist-coated fused silica substrate, which is optically flat, and UV cured. This process is highly customizable, making it useful for different mission architectures, as well as capable of low surface roughness over the grating facets, which is ideal for X-ray Spectrometers.

9603-62, Session PMon

Design and implementation of an x-ray reflectometer system for testing x-ray optics coatings

Danielle Gurgew, The Univ. of Alabama in Huntsville (United States) and NASA Marshall Space Flight Ctr. (United States); Brian D. Ramsey, Mikhail V. Gubarev, David Broadway, NASA Marshall Space Flight Ctr. (United States)

We have developed an X-ray reflectometer (XRR) system for the characterization of various soft and hard X-ray optic coatings being developed at Marshall Space Flight Center. The XRR system generates X-ray radiation with a high-output Rigaku rotating anode source (RAS), operational at a voltage range of 5 - 40 kV, a current range of 10-450 mA. A series of precision slits, adjustable down to approximately 20 micrometers, positioned in the beam path limit the extent of the x-ray beam and control the resolution of the XRR measurement while a goniometer consisting of two precision rotary stages controls the angular position of the coating sample and X-ray detector with respect to the beam. With the high count rate capability of the RAS, a very-high-speed silicon drift detector, the Amptek Fast SDD, is implemented to achieve good count rate efficiency and improve reflectivity measurements of coatings at larger graze angles. The coating sample can be adjusted using a series of linear and tipping stages to perfectly align the center of the sample with the center of the incident X-ray beam. These stages in conjunction with the goniometer components are integrated through original control software resulting in full automation of the XRR system. We will show some initial XRR measurements of both single and multilayer coatings made with this system. These results and future measurements are used to characterize potential X-ray optic coatings culminating in the production of highly reflective coatings operational at a large range of X-ray energies.

9603-63, Session PMon

The development of a deflectometer for accurate surface figure metrology

Mikhail V. Gubarev, Brian Ramsey, NASA Marshall Space Flight Ctr. (United States); Carolyn Atkins, The Univ. of Alabama in Huntsville (United States)

With the recent introduction of optical surface error correction methods, such as differential deposition and smart optics, the availability of in situ surface figure metrology methods becomes crucial for the development of the high-resolution, optics needed for future Astrophysics Missions. A surface-figure-metrology instrument based on an optical deflectometer scheme is under development at the Marshall Space Flight Center (MSFC). This presentation will detail the current status of the program and the expected capability of the instrument.





9603-64, Session PMon

Development of an x-ray telescope with a large effective area for the iron K line band

Hironori Matsumoto, Sasagu Tachibana, Shun Yoshikawa, Keisuke Tamura, Hideyuki Mori, Kojun Yamashita, Ikuyuki Mitsuishi, Yuzuru Tawara, Hideyo Kunieda, Nagoya Univ. (Japan)

X-ray micro-calorimeters such as the Soft X-ray Spectrometer (SXS) on board ASTRO-H will enable precise spectroscopy of iron K lines even for spatially extended objects. To exploit the full power of the high-energy resolution, X-ray telescopes with a large effective area around 6 keV are essentially important. Conventional X-ray telescopes aimed at X-rays below 10 keV have used the principle of total reflection to collect the X-rays. Enlarging the diameter of this type of telescopes is not effective to obtain the large effective area, since the incident angle of X-rays for the outer part of the telescope exceeds the critical angle and few X-rays are reflected from the outer part of the telescope. Therefore we are developing a multilayer mirror to enhance the effective area at around 6 keV by using Bragg reflection. We assumed that the diameter of our telescope is 110 cm and the focal length is 6 m, which can be launched by the epsilon rocket of ISAS/ JAXA. When the mirror surface is covered with a multi-layer of Ir/C, our simulation suggests that the effective area averaged in the 5.7--7.7 keV band could be 2000 cm2. This area is comparable to the effective area of Athena, which will be launched in 2028 by European Space Agency (ESA).

9603-65, Session PMon

Development of an x-ray telescope using the carbon fiber reinforced plastic

Hironori Matsumoto, Toshihiro Iwase, Masato Maejima, Nagoya Univ. (Japan); Hisamitsu Awaki, Ehime Univ. (Japan); Hideyo Kunieda, Nagoya Univ. (Japan); Naoki Ishida, Tamagawa Engineering Co., Ltd. (Japan); Satoshi Sugita, Ehime Univ. (Japan); Takuya Miyazawa, Naoki Shima, Ikuyuki Mitsuishi, Yuzuru Tawara, Nagoya Univ. (Japan)

Conventional X-ray telescopes utilize the Wolter-I optics which consist of parabolic mirrors followed by hyperbolic mirrors. X-ray telescopes on board Japanese satellites such as ASTRO-H have used many thin-foil mirrors to obtain large aperture efficiency and a large effective area. However, the mirrors are conically approximated. Moreover,

it is difficult to keep the shape of mirrors good and the mirrors are conically approximated. Therefore the angular resolution of this type of telescope has been limited. We are developing an X-ray mirror using the carbon fiber reinforced plastic (CFRP) as substrate in order to improve the angular resolution; the CFRP has a high strength-to-weight ratio and can be used to realize the quadratic surface of the Wolter-I optics. We have fabricated the reflection surface of Pt on the CFRP substrate by the epoxy-replication method by which we made the Hard X-ray Telescope of the ASTRO-H. We found that curing the epoxy at the room temperature is effective to suppress the print through. We were able to make mirrors whose shape accuracy is 3–5 um and roughness is ~4A. Characterization at the synchrotron facility SPring-8 using the X-ray pencil beam of 20 keV showed that the angular resolution was 3–5 arcmin as a whole, but can reach to 20 arcsec locally.

9603-1, Session 1

An overview on mirrors for Cherenkov telescopes manufactured by glass coldshaping technology

Rodolfo Canestrari, INAF - Osservatorio Astronomico di

Brera (Italy); Enrico Giro, INAF - Osservatorio Astronomico di Padova (Italy); Giacomo Bonnoli, Giuseppe Crimi, INAF - Osservatorio Astronomico di Brera (Italy); Mauro Fiorini, INAF - Istituto di Astrofisica Spaziale e Fisica Cosmica di Palermo (Italy); Giovanni Pareschi, INAF - Osservatorio Astronomico di Brera (Italy); Gabriele Rodeghiero, INAF -Osservatorio Astronomico di Padova (Italy); Giorgia Sironi, INAF - Osservatorio Astronomico di Brera (Italy)

The cold glass-slumping technique is a low cost processing developed at INAF-Osservatorio Astronomico di Brera (INAF-OAB) for the manufacturing of mirrors for Cherenkov telescopes. This technology is based on the shaping of thin glass foils by means of bending at room temperature. The glass foils are thus assembled into a sandwich structure for retaining the imposed shape by the use of a honeycomb core. These mirrors employ commercial of-the-shelf materials thus allowing a competitive cost and production time. They show very low weight, rigidity and environmental robustness.

In this paper we give an overview on the most recent results achieved from the adoption of the cold-shaping technology to different projects of Cherenkov telescopes. We show the variety of optical shapes implemented ranging from those spherical with long radius of curvature up to the most curved free form ones.

9603-2, Session 1

The ASTRI SST-2M prototype for the Cherenkov Telescope Array: optomechanical test results

Rodolfo Canestrari, INAF - Osservatorio Astronomico di Brera (Italy); Enrico Giro, Gabriele Rodeghiero, INAF -Osservatorio Astronomico di Padova (Italy); Giorgia Sironi, INAF - Osservatorio Astronomico di Brera (Italy)

The Cherenkov Telescope Array (CTA) observatory, with a combination of large-, medium-, and small-scale telescopes (LST, MST, SST, respectively), will represent the next generation of Imaging Atmospheric Cherenkov Telescopes. It will explore the Very High Energy domain from a few tens of GeV up to few hundreds of TeV with unprecedented sensitivity, angular resolution and imaging quality.

In this framework, the Italian ASTRI program, led by the Italian National Institute of Astrophysics (INAF), is currently developing a scientific and technological SST prototype named ASTRI SST-2M. It is a 4-meter class telescope; it adopts an aplanatic, wide-field, double-reflection optical layout in a Schwarzschild-Couder configuration.

In this contribution we report about the on-site erection and the latest results on the opto-mechanical performance test conducted soon after the telescope installation.

9603-3, Session 1

ASTRI primary mirrors characterization by deflectometry

Giorgia Sironi, Rodolfo Canestrari, INAF - Osservatorio Astronomico di Brera (Italy)

In 2014 the Italian National Institute for Astrophysics for the ASTRI collaboration realized an end-to-end Cherenkov dual mirror prototypal telescope and installed it at Serra La Nave (Italy). In this project the Brera Astronomical Observatory was in charge for the primary mirror realization and testing. The ASTRI telescope primary mirror has an aperture of ~ 4 mm, a polynomial design and is tasselled in 18 hexagons. These characteristics lead to necessity of realize and test panels with a typical size of ~1 m and with an aspheric component up to millimeters.

The manufacturing of the segments was performed by assembling sandwich

Conference 9603: Optics for EUV, X-Ray, and Gamma-Ray Astronomy VII



of thin glass foils bended at room temperature to reach the desired shape. While for the characterization we realized an ad-hoc deflectometry facility than works as an inverse Ronchi interacting with a ray-tracing.

In this paper we report the results of the deflectometry metrological campaign realized on the primary mirror segments of the ASTRI dual mirror telescope. The expected PSF and the contributions to the image quality degradation are studied.

9603-4, Session 1

Towards the construction of a medium size prototype Schwarzschild-Couder telescope for CTA

Julien Rousselle, Univ. of California, Los Angeles (United States)

The US members of the Cherenkov Telescope Array (CTA) consortium will start the construction of a 10-m prototype Schwarzschild-Couder telescope (pSCT) in summer 2015 at the Fred Lawrence Whipple Observatory in Southern Arizona.

Compared to traditional Davies-Cotton telescopes, this novel instrument with aplanatic two-mirror optical system will offer a wider field-of-view and improved angular resolution. In addition, the reduced plate scale at the camera allows the use of highly-integrated photon detectors such as silicon photo multipliers. As part of CTA, this design has the potential to greatly improve the performance of the next generation ground-based observatory for very high-energy (E>100 GeV) gamma-ray astronomy.

In this contribution we present the final design of the optical system and optical support structure, as well as the telescope assembly and construction plan.

9603-5, Session 1

Results and developments from the 12m Davies-Cotton MST prototype for CTA

Louise Oakes, Humboldt-Univ. zu Berlin (Germany); Markus Garczarcyk, Stefan Schlenstedt, DESY Zeuthen (Germany); Ullrich Schwanke, Humboldt-Univ. zu Berlin (Germany)

The Cherenkov Telescope Array (CTA) will be the next generation groundbased observatory for gamma-ray astronomy, covering an energy range from a few tens of GeV to a few hundred TeV. The CTA project is currently in the design and prototyping phase, the start of construction is planned for 2016. The planned sensitivity of CTA improves on current ground based Cherenkov telescope experiments by about an order of magnitude. In the core energy range this sensitivity will be dominated by up to 40 Medium-Sized Telescopes. These telescopes, of a modified Davies-Cotton mount type with a reflector diameter of 12 m, are currently being prototyped.

A full-size mechanical prototype MST has been operating in Berlin since 2012. Several types of prototype mirrors have been developed and tested, and are mounted on the telescope. CCD cameras with various lenses are mounted on the prototype for studying deformation of the structure, testing alignment techniques, and telescope pointing using astrometry methods. The report will focus on results of more than two years of optical and structural measurements, commissioning and testing of the MST prototype in Berlin, as well as the final design plans for the Davies-Cotton MSTs for CTA.

9603-6, Session 1

Roughness tolerances for Cherenkov telescope mirrors

Kashmira Tayabaly, INAF - Osservatorio Astronomico di Brera (Italy) and Politecnico di Milano (Italy); Daniele Spiga, Giacomo Bonnoli, Rodolfo Canestrari, Giorgia Sironi, Giovanni Pareschi, INAF - Osservatorio Astronomico di Brera (Italy)

The Cherenkov Telescope Array (CTA) is a forthcoming international ground-based observatory for very high-energy gamma rays. Its goal is to reach sensitivity five to ten times better than existing Cherenkov telescopes such as VERITAS, H.E.S.S. or MAGIC and extend the range of observation to energies down to few tens of GeV and beyond 100 TeV. To achieve this goal, an array of about 100 telescopes is required, meaning a total reflective surface of several thousands of m2. Thence, the optimal technology used for CTA mirrors' manufacture should be both low-cost (~1000euros/m2) and allow high optical performances over a [300nm-600nm] wavelength range: a reflectivity higher than 85% and a PSF diameter smaller than 1mrad. Surface roughness can significantly contribute to PSF broadening and limit telescope performances; but, it can also be easily controlled during mirrors' manufacturing so that surface roughness does not dominate other sources of scatter (surface defects, dust particles deposition,...). This paper determines first order surface finish tolerances based on a surface microroughness characterization campaign, using Phase Shift Interferometry. That allows us to compute the roughness contribution to Cherenkov telescope's point spread function. This study is performed for diverse mirror candidates (MAGIC-I and II, ASTRI, MST and FACT) varying in manufacture technologies, selected materials and taking into account the degradation over time due to environmental hazards.

9603-7, Session 2

Hard x-rays broad band Laue lenses (80 - 600 keV): building methods and performances

Enrico Virgilli, Filippo Frontera, Piero Rosati, Vittore Carassiti, Univ. degli Studi di Ferrara (Italy); Stefano Squerzanti, Istituto Nazionale di Fisica Nucleare (Italy); Ezio Caroli, John Stephen, Natalia Auricchio, Angelo Basili, Stefano Silvestri, INAF - IASF Bologna (Italy); Ferdinando Cassese, Luca Recanatesi, DTM Srl (Italy)

Soft gamma-ray astrophysics (> 80 keV) is expected to undergo a big leap ahead thanks to the introduction of focusing instruments replacing the currently used direct-view telescopes. Thanks to the technological progress of the last years, Laue lenses appear to be good candidates to fulfill such a role, considerably improving both the sensitivity and the angular resolution with respect to the conventional non-focusing instruments.

With the final goal of building a 20 m focal length Laue lens (80-600 keV), in the framework of the LAUE project, a set of bent crystals are being properly oriented and positioned on a lens petal frame, to focus radiation from 100 to 300 keV. Before bent crystals have never been used for this purpose, and we expect a great enhancement in terms of point spread function with respect to the flat mosaic crystals. We expect to present for the first time the energy response of the lens petal prototype and the achieved accuracy thanks to the adopted mounting method. We will also compare the measured results with the theoretical expectations both in laboratory with a divergent beam and in the case of parallel beam as that expected in space operation.

9603-8, Session 2

Rapid and accurate assembly method for a new Laue lens prototype

Colin Wade, Univ. College Dublin (Ireland); Nicolas M. Barrière, cosine Research B.V. (Netherlands); Lorraine Hanlon, Univ. College Dublin (Ireland); Steven E. Boggs, Space Sciences Lab. (United States); Nicolai F. Brejnholt, Lawrence Livermore National Lab. (United States); Sonny Massahi, Univ. of California, Berkeley (United States); John



A. Tomsick, Space Sciences Lab. (United States); Peter von Ballmoos, Institut de Recherche en Astrophysique et Planétologie (France)

The Laue lens is a technology for gamma-ray astrophysics whereby gamma-rays of particular energies can be brought to a focus by a suitable arrangement of crystals. The Laue lens assembly station at UC Berkeley was used to build a technological demonstrator addressing the key questions of crystal mounting speed, crystal position and orientation accuracy, and crystal reflectivity. The new prototype is a lens segment containing a total of 48 5x5mm2 crystals - 36 Iron and 12 Aluminium. The segment is composed of 8 partial rings, each of which is aligned to diffract an energy between 95 and 130 keV.

The system now in place demonstrates that a technique to quickly and accurately construct a Laue lens is now well established. The use of glue that cures under UV exposure has reduced the time needed to fix a crystal by a factor of -200 compared to previous iterations. With this improvement, constructing a full lens with hundreds or even thousands of crystals becomes a far more achievable goal. This represents a great leap forward for Laue lens construction. Preliminary results are presented which demonstrate the performance of the system using the new assembly method.

9603-9, Session 2

Bending of crystals using carbon fiber films

Vincenzo Guidi, Riccardo Camattari, Valerio Bellucci, Gianfranco Paternò, Andrea Mazzolari, Enrico Virgilli, Univ. degli Studi di Ferrara (Italy)

Bent crystals are used or planned to be used in modern physics experiments based on coherent interactions of particles or e.m. radiation with crystals, such as for steering charged-particle beams and for focusing hard X-rays and soft ?-rays. Bent crystals are capable of deflecting X-rays through Bragg diffraction at high efficiency and with high-focusing power. For this reason, self-standing bent crystals are considered good candidates as optical elements for an X-ray concentrator, e.g. for a Laue lens. Thick crystals may be desirable because the efficiency of a Laue lens is proportional to the crystal thickness. Moreover, using large crystals implies that a relatively small number of samples is required for filling the lens. However, manufacturing of self-standing bent thick crystals is not simple, and the maximum thickness obtainable with several techniques does not exceed 2 mm. Recently, a method involving the use of carbon fiber as a tensile film was developed to manufacture self-standing bent samples up to 5 mm thick, with the curvature being homogeneous and suitable for X-ray diffraction. The samples have been manufactured as part of the INFN-LOGOS project, in collaboration with the Sensor and Semiconductor Laboratory, Ferrara (Italy) and RI-BA Composites, Faenza (Italy). The bent crystals were characterized with hard X-rays at ESRF and ILL, Grenoble (France). Further tests are being planned at LARIX, Ferrara (Italy). Here we report in details the procedure for realizing bent and quasi-mosaic crystals using carbon fiber as a tensile film, the film thickness being up to some hundreds of microns.

9603-10, Session 2

Development of self-focusing Si Laue components (SiLCs) for high performance Laue lenses

Nicolas M. Barrière, cosine Research B.V. (Netherlands) and Univ. of California, Berkeley (United States); Abdelhakim Chatbi, Maximilien Collon, Ramses Guenther, cosine Research B.V. (Netherlands); Lorraine Hanlon, Univ. College Dublin (Ireland); Giuseppe Vacanti, Mark Vervest, cosine Research B.V. (Netherlands); Peter von Ballmoos, Institut de Recherche en Astrophysique et Planétologie (France); Colin Wade, Univ. College Dublin (Ireland); Alexei Yanson,

cosine Research B.V. (Netherlands)

In the soft gamma-ray domain, a Laue lens telescope could efficiently complement wide field of view instruments (like a compact Compton telescope for instance) by providing enhanced sensitivity and angular resolution in a selection of relatively narrow energy bands. The observation of nuclear decay lines from supernovae, novae or supernovae remnants, the study of the hard tails from compact objects are areas for which a Laue lens telescope would provide unmatched performance.

Cosine, in collaboration with the University of California at Berkeley, has been developing Silicon Laue Components (SiLCs): curved stacks of wedged crystalline Si plates held together by direct Si bonding, resulting in selfstanding diffracting elements that focus both radially and azimuthally. These elements can be assembled into a high performance Laue lens, where for the first time, the size of the point spread function is decoupled from the size of the diffracting elements. A synchrotron run at the APS validated the concept and provided data to refine models. In this talk, we will present the development status of SiLCs, and refined estimates of the performance they could deliver.

9603-11, Session 3

Status of ART-XC / SRG instrument

Mikhail N. Pavlinsky, Valeriy Akimov, Vasiliy Levin, Igor Lapshov, Alexey Tkachenko, Nikolay Semena, Mikhail Buntov, Alexander Glushenko, Vadim Arefiev, Alexander Yaskovich, Space Research Institute (Russian Federation); Rashid Sunyaev, Eugene Churazov, Marat Gilfanov, Space Research Institute (Russian Federation) and Max-Planck-Institut für Astrophysik (Germany); Sergei Grebenev, Sergey Sazonov, Mikhail Revnivtsev, Alexander Lutovinov, Sergey Molkov, Mikhail Kudelin, Tatyana Drozdova, Space Research Institute (Russian Federation); Sergey Garanin, Sergey Grigorovich, Dmitriy Litvin, Valeriy Lazarchuk, Igor Roiz, Mikhail Garin, Russian Federal Nuclear Ctr. -All-Russian Research Institute of Experimental Physics (Russian Federation); Vladimir Babyshkin, Ilya Lomakin, Alexander Menderov, NPO Lavochkin (Russian Federation); Mikhail Gubarev, Brian Ramsey, Kiranmayee Kilaru, Stephen O'Dell, Jeffery Kolodziejczak, Ronald Elsner, NASA Marshall Space Flight Ctr. (United States)

Spectrum Roentgen Gamma (SRG) is an X-ray astrophysical observatory, developed by Russia in collaboration with Germany. The mission will be launched in March 2016 from Baikonur, by a Zenit rocket with a Fregat booster and placed in a 6-month-period halo orbit around L2. The scientific payload consists of two independent telescopes – a soft-x-ray survey instrument, eROSITA, being provided by Germany and a medium-x-ray-energy survey instrument ART-XC being developed by Russia. ART-XC will consist of seven independent, but co-aligned, telescope modules. The ART-XC flight mirror modules has been developed and fabricated at the NASA Marshall Space Flight Center (MSFC). Each mirror module will be aligned with a focal plane CdTe double-sided strip detector which will operate over the energy range of 6-30 keV, with an angular resolution of <1?, a field of view of -34? and an expected energy resolution of about 10% at 14 keV. The current status of the ART-XC/SRG instrument will be presented.

9603-12, Session 3

Ultra high throughput four-reflection x-ray telescope for high resolution spectroscopy

Yuzuru Tawara, Ikuyuki Mitsuishi, Yasunori Babazaki, Ren Nakamichi, Ayako Bandai, Nagoya Univ. (Japan)

The first application of four-times reflection X-ray optics was used for the

Conference 9603: Optics for EUV, X-Ray, and Gamma-Ray Astronomy VII



DIOS mission, where very soft X-ray observation is planned. On the other hand, effective area of the telescope for higher X-ray energy (E < 10 keV) including iron K emission lines has been so far limited to about 1000 cm2 assumig several meter focal length. However, if we introduce four-reflection optics to this energy range, we can get several times large effective area for single telescope with same several meter focal length. To prove this possibility, we performed ray tracing simulation for four-relection telescope with 6 m focal length and found that effective area of 3000 cm2 at 6 keV can be obtained for single telescope. In this paper, we will discuss about other telescope performances, mechanical properties and application to fine spectroscopic mission using X-ray microcalorimeter.

9603-13, Session 3

Development of the four-stage x-ray telescope (FXT) for the DIOS mission (2)

Ikuyuki Mitsuishi, Yasunori Babazaki, Ren Nakamichi, Ayako Bandai, Yuzuru Tawara, Ikuya Sakurai, Tatsuharu Torii, Kenji Tachibana, Takefumi Onishi, Nagoya Univ. (Japan); Satoshi Sugita, Ehime Univ. (Japan); Naomichi Kikuchi, Toshiki Sato, Tokyo Metropolitan Univ. (Japan); Takayuki Hayashi, Japan Aerospace Exploration Agency (Japan); Ryo Iizuka, Yoshitomo Maeda, Institute of Space and Astronautical Science (Japan) and Japan Aerospace Exploration Agency (Japan)

A Four-stage X-ray Telescope (FXT) has been developed for a small satellite mission, the Diffuse Intergalactic Oxygen Surveyor (DIOS), designed for mapping the warm-hot intergalactic medium in the nearby Universe located at z < 0.3 using redshifted highly-ionized oxygen emission lines. The FXT is a key component to achieve the scientific goal by realizing a large field of view (~50 arcmin in radius) and grasp (~100 deg2 cm2). A conventional replica foil method is employed to fabricate the FXT mirrors based on conically-approximated Wolter type I design (Tawara et al. 2014 SPIE).

We made the third FXT demonstration model and conducted both optical and X-ray measurements to investigate its performance. A thickness of the aluminum foil mirrors was changed from 0.15 mm to 0.2 mm to improve stiffness and 10 sets of 4 stage mirrors with a diameter of about 500 mm were arranged close together in a quadrant housing to reproduce a final configuration. Even though resultant angular resolution is approximately two times worse than that of the requirement, the angular resolution is reduced down to ~9 arcmin in half power diameter at 1.5 keV. We confirmed that resulting field of view is almost consistent with the expected values from simulations. In this conference, we will report on detailed results of the irradiation tests such as error budget analysis and recent status of our developments.

9603-14, Session 4

New ray-tracing capabilities for the development of silicon pore optics

Giuseppe Vacanti, Nicols Barrière, Abdelhakim Chatbi, cosine Science & Computing B.V. (Netherlands); Maximilien Collon, cosine Research B.V. (Netherlands); Ramses Günther, Alexei Yanson, Mark Vervest, cosine Science & Computing B.V. (Netherlands); Marcos Bavdaz, Eric Wille, European Space Agency (Netherlands)

The Geant4 based ray-tracer used to support the development of Silicon Pore Optics has been extended to take into account more subtle effects that affect the performance of the optics, like thermo-mechanical stresses and detailed surface metrology. Its performance has also been increased to make it possible to simulate rapidly and in detail the optics of Athena so that various possible configurations can be explored and characterized providing important feedback to the development and system teams. In this paper we report on the state of the development. Details of the geometrical objects used, and the interfaces to FEM/thermal output will be given. Preliminary performances will also be discussed.

9603-15, Session 4

Analytical computation of stray light in nested mirror modules for X-ray telescopes

Daniele Spiga, INAF - Osservatorio Astronomico di Brera (Italy)

Stray light in X-ray telescopes is a well-known issue. Unlike rays focused via a double reflection by usual grazing-incidence geometries such as the Wolter-I, stray rays coming from off-axis sources are reflected only once by either parabolic or hyperbolic segment. Although not focused, stray light may represent a major source of background and ghost images especially when observing a field of faint sources in the vicinity of a more intense source just outside the field of view of the telescope. The stray-light problem is addressed by mounting a pre-collimator in front of the mirror module, in order to shade a part of the reflective surfaces that may give rise to singly-reflected rays. Studying the expected stray-light impact, and consequently designing a pre-collimator, is a typical ray-tracing problem, usually time and computation consuming, especially if we consider that rays propagate throughout a densely nested structure. This in turn requires one to pay attention to all possible obstructions, increasing the complexity of the simulation. In contrast, approaching the problems of mirror module design and stray-light calculation from an analytical viewpoint largely simplifies the problem, and also eases the task of designing an effective precollimator. In this work we describe an analytical formalism that can be used to compute the stray light in a nested optical module, in a fast and effective way and accounting for obstruction effects. We also show how the design of the X-ray mirror module can be optimized to return the desired field of view and at the same time minimize the stray-light effect.

9603-16, Session 4

On the statistical error of the half energy width

Giuseppe Vacanti, cosine Science & Computing B.V. (Netherlands)

The half energy width (HEW) is the all powerful performance parameter used to characterize and compare X-ray optics. Values of HEW are always reported without an error bar or confidence interval, suggesting that the statistical error associated with such estimates are neglegible. Is this true? And if it is, could one characterize the optics more quickly accepting a nonneglegible but still acceptable statistical error in the estimate of the HEW? We try to answer these questions with the use of non-parametric statistical methods. The answers obtained will be compared to the results obtained through numerical simulations.

Standard non-parametric techniques like the bootstrap can be used to answer the questions.

9603-17, Session 5

The Athena optics

Marcos Bavdaz, Eric Wille, Brian Shortt, Sebastiaan Fransen, European Space Agency (Netherlands); Maximilien Collon, cosine Research B.V. (Netherlands); Giuseppe Vacanti, Ramses Guenther, Alexei Yanson, Mark Vervest, cosine Science & Computing B.V. (Netherlands); Jeroen Haneveld, Micronit Microfluidics B.V. (Netherlands); Coen van Baren, SRON Netherlands Institute for Space Research (Netherlands); Karl-Heinz Zuknik, OHB-System AG (Germany); Finn E. Christensen, DTU Space



(Denmark); Michael Krumrey, Physikalisch-Technische Bundesanstalt (Germany); Vadim Burwitz, Max-Planck-Institut für extraterrestrische Physik (Germany); Giovanni Pareschi, INAF - Osservatorio Astronomico di Brera (Italy); Giuseppe Valsecchi, Media Lario Technologies S.r.l. (Italy)

The Advanced Telescope for High ENergy Astrophysics (Athena) was selected in 2014 as the second large class mission (L2) of the ESA Cosmic Vision Science Programme, and system studies and technology preparation activities are on-going.

The core enabling technology for the high performance mirror is the Silicon Pore Optics (SPO), a modular X-ray optics technology, which utilises processes and equipment developed for the semiconductor industry.

The paper will provide an overview of the programmatic background, the status of SPO technology and give an outline of the development roadmap and activities undertaken and planned by ESA.

9603-18, Session 5

Silicon pore optics development for ATHENA

Maximilien Collon, cosine Research B.V. (Netherlands); Ramses Günther, Alexei Yanson, Abdelhakim Chatbi, Giuseppe Vacanti, Mark Vervest, Nicolas M. Barrière, cosine Science & Computing B.V. (Netherlands); Marco W. Beijersbergen, cosine Research B.V (Netherlands); Marcos Bavdaz, Eric Wille, European Space Agency (Netherlands); Jeroen Haneveld, Arenda Koelewijn, Micronit Microfluidics B.V. (Netherlands); Coen van Baren, SRON Netherlands Institute for Space Research (Netherlands); Peter Müller, Michael Krumrey, Physikalisch-Technische Bundesanstalt (Germany); Vadim Burwitz, Max-Planck-Institut für extraterrestrische Physik (Germany); Finn E. Christensen, DTU Space (Denmark); Giovanni Pareschi, Paolo Conconi, INAF - Osservatorio Astronomico di Brera (Italy)

The ATHENA mission, a European large (L) class X-ray observatory to be launched in 2028, will essentially consist of an X-ray lens and two focal plane instruments. The lens, based on a Wolter-I type double reflection grazing incidence angle design, will be very large (~ 3 m in diameter) to meet the science requirements of large effective area (1-2 m2 at a few keV) at a focal length of 12 m. To meet the high angular resolution (5 arc seconds) requirement the X-ray lens will also need to be very accurate.

Silicon Pore Optics (SPO) technology has been invented to enable building such a lens and thus enabling the ATHENA mission. We will report in this paper on the latest status of the development, including details of X-ray test campaigns.

9603-19, Session 5

Silicon pore optics mirror modules for inner and outer radii

Eric Wille, Marcos Bavdaz, Tim Oosterbroek, European Space Research and Technology Ctr. (Netherlands); Maximilien Collon, Marcelo D. Ackermann, cosine Research B.V. (Netherlands); Ramses Guenther, Giuseppe Vacanti, Mark Vervest, Alexei Yanson, cosine Science & Computing B.V. (Netherlands); Coen van Baren, SRON Netherlands Institute for Space Research (Netherlands); Jeroen Haneveld, Arenda Koelewijn, Anne Leenstra, Micronit Microfluidics B.V. (Netherlands); Giovanni Pareschi, Marta Civitani, Paolo Conconi, Daniele Spiga, INAF - Osservatorio Astronomico di Brera (Italy); Giuseppe Valsecchi, Fabio Marioni, Media Lario Technologies S.r.I. (Italy); Mario Schweitzer, Karl-Heinz Zuknik, OHB-System AG (Germany)

Athena (Advanced Telescope for High Energy Astrophysics) is an x-ray observatory using a Silicon Pore Optics telescope and was selected as ESA's second L-class science mission for a launch in 2028. The x-ray telescope consists of several hundreds of mirror modules distributed over about 15-20 radial rings. The radius of curvature and the module sizes vary among the different radial positions of the rings resulting in different technical challenges for mirror modules for inner and outer radii.

We present first results of demonstrating Silicon Pore Optics for the extreme radial positions of the Athena telescope. For the inner most radii (0.25 m) a new mirror plate design is shown which overcomes the challenges of larger curvatures, higher stress values and bigger plates. Preliminary designs for the mounting system and its mechanical properties are discussed for mirror modules covering all other radial positions up to the most outer radius of the Athena telescope.

9603-20, Session 5

Multilayer coated SPO stack: Production and test

Sonny Massahi, Anders C. Jakobsen, David Girou, Finn E. Christensen, DTU Space (Denmark); Brian Shortt, European Space Research and Technology Ctr. (Netherlands); Maximilien Collon, cosine Research B.V. (Netherlands); Michael Krumrey, Levent Cibik, Stefanie Langner, Physikalisch-Technische Bundesanstalt (Germany)

As part of the ongoing effort to optimize the throughput of the Athena optics we have produced an SPO stack with optimized linearly graded Ir/B4C multilayer coatings. The paper describes the coating development and qualification as well as studies related to the photolithographic process, the stacking and subsequent X-ray tests at the PTB laboratory at the BESSY synchrotron radiation facility.

9603-21, Session 6

An alternative solution for ATHENA mission: preliminary design of the mirror modules and mirror assembly based on the slumped glass

Stefano Basso, Marta M. Civitani, Giovanni Pareschi, Enrico Buratti, INAF - Osservatorio Astronomico di Brera (Italy); Josef Eder, Peter Friedrich, Maria Fürmetz, Max-Planck-Institut für extraterrestrische Physik (Germany)

The Athena mission was selected for the second large-class mission, due for launch in 2028, in ESA's Cosmic Vision program. The current solution for the optics is based on the Silicon Pore Optics (SPO) technology with the goal of 2m2 effective area at 1keV (aperture about 3m diameter) with a focal length of 12m. The SPO advantages are the compactness along the axial direction and the high conductivity of the Silicon. Recent development in the fabrication of mirror shells based on the Slumped Glass Optics (SGO) makes this technology a competitive and attractive solution for the mirror modules for Athena or similar telescopes. The SGO advantages are a potential high collecting area due to the lower shadowing and the aptitude to curve the glass plates up to small radius of curvature. This study shows an alternative mirror design based on SGO technology, tailored for Athena needs. The main challenges are the optimization of the manufacturing technology with respect to the required accuracy and the thermal control of the large surface in conjunction with the low conductivity of the glass. A concept has been elaborated which considers the specific benefits of the SGO technology and provides an efficient thermal control. The output of the study is a preliminary design substantiated by analyses and technological



studies. The study proposes interfaces and predicts performances and budgets. It describes also how such a mirror system could be implemented as an alternative or as a backup solution for the SPO mirror system.

9603-22, Session 6

Slumped glass optics for x-ray telescopes: advances in the hot slumping assisted by pressure

Bianca Salmaso, Claudia Brizzolari, Stefano Basso, Marta Civitani, Mauro Ghigo, Giovanni Pareschi, Daniele Spiga, Gianpiero Tagliaferri, INAF - Osservatorio Astronomico di Brera (Italy)

Slumped Glass Optics are a viable solution to build future X-ray telescopes, such as ATHENA, with large effective area (Aeff ~ 2 m2 at 1 keV) and angular resolution better than 5 arcsec. In our laboratories we use a direct hot slumping approach assisted by pressure, in which the glass optical surface is in contact with the mould, and a pressure is applied to enforce the replication of the mould shape on the glass optical surface. Several prototypes have been already produced and tested in X-rays, showing a continuous improvement in our technology. In this paper, we present the results obtained introducing several improvements in our setup, with the use of Eagle XG glass type and Zerodur K20 material for the mould. We present a critical analysis correlating the changes in the process to the improvements in different spatial frequency ranges encompassing the profile and roughness measurements. The slumped glass foils giving the best results were integrated in a new prototype tested in X-ray at the PANTER facility. Finally, we obtained further improvements in the glass foils quality by introducing a re-polished K20 cylindrical mould, with the goal to improve the mid- to high-frequency region of the Power Spectral Density. This work presents all the relevant steps forward, in the hot slumping assisted by pressure technology, aimed at reaching angular resolutions of 5 arcsec HEW.

9603-23, Session 6

Slumped glass optics based on thin hot formed glass segments and interfacing ribs for high angular resolution x-ray astronomy: performances and development status

Marta M. Civitani, Stefano Basso, Mauro Ghigo, Bianca Salmaso, Daniele Spiga, Gianpiero Tagliaferri, Gabriele Vecchi, INAF - Osservatorio Astronomico di Brera (Italy); Gisela D. Hartner, Benedikt Menz, Vadim Burwitz, Max-Planck-Institut Röntgen Testanlage PANTER (Germany); Giovanni Pareschi, INAF - Osservatorio Astronomico di Brera (Italy)

The Slumped Glass Optics technology, developed at INAF/OAB since a few years, is becoming a competitive solution for the realization of the future X-ray telescopes with a very large collecting area, as e.g. the proposed Athena, with more than 2 m2 effective area at 1 keV and with a high angular resolution (5" HEW). The developed technique is based on modular elements, named X-ray Optical Units (XOUs), made of several layers of thin foils of glass, previously formed by direct hot slumping in cylindrical configuration, and then stacked in a Wolter-I configuration, through interfacing ribs. The achievable global angular resolution of the optics relies on the surface shape accuracy of the slumped foils, on the smoothness of the mirror segments achieved with a dedicated Integration Machine (IMA). In this paper we provide an update of the project development, reporting on the last results achieved. In particular, we will present the results obtained with full illumination X-ray tests for the last developed prototypes.

9603-24, Session 6

Lightweight and high-resolution x-ray optics for astronomy

William W. Zhang, NASA Goddard Space Flight Ctr. (United States)

In this paper we will report our work of developing lightweight and highresolution x-ray optics for astronomical applications. Our work has four technical elements: substrate fabrication, coating, alignment, and bonding. Each of these four elements presents unique challenges. Our strategy is to tackle all four in parallel such that each meet its own requirements. We regularly combine the four elements to make and test mirror modules consist 3 pairs of Wolter-I mirror segments. As of January 2015, all these elements are such that we can consistently produce modules that achieve full-illumination x-ray images of 8 arc-seconds half-power diameter. Our near term (next two years) objective is to be able to build modules better than 5 arc-seconds, and long term (next five years) objective to build modules better than 1 arc-second, while demonstrably preserving lightweight and low production cost of the approach.

9603-25, Session 6

Progress report on air bearing slumping of thin glass mirrors for x-ray telescopes

Mark L. Schattenburg, MIT Kavli Institute for Astrophysics and Space Research (United States); Brandon Chalifoux, Massachusetts Institute of Technology (United States); Michael D. DeTienne, Ralf Heilmann, Heng Zuo, MIT Kavli Institute for Astrophysics and Space Research (United States)

Thermal shaping (or slumping) of thin glass sheets onto high precision mandrels was used by the GSFC team to fabricate the NASA NuSTAR telescope with spectacular success. While mirrors generated by this process can have good resolution (<10 arc sec), they require very long thermal cycles. Furthermore, the required anti-stick mandrel coatings produce mid-range spatial frequency errors, slowing progress below 5 arc sec. Over the last several years we have developed a new slumping process which utilizes a pair of porous air bearing mandrels through which compressed nitrogen is forced. The glass sheet floats on a thin layer (<50 microns) of nitrogen during the thermal cycle. This results in glass with reduced midrange spatial frequency errors and can be accomplished in much shorter thermal cycles. Recent progress has focused on improvements to a tool which slumps mirrors in a horizontal orientation. This configuration results in an unstable mirror in the bearing which must be actively controlled. Recent work has developed improved fiber sensing techniques to measure the glass location and improved Inconel bellows which control the apparatus tilt using compressed nitrogen. We report on the design and testing of this improved slumping tool.

9603-26, Session 6

Indirect glass slumping for future x-ray missions: overview, status and progress

Anita Winter, Elias Breunig, Peter Friedrich, Laura Proserpio, Max-Planck-Institut für extraterrestrische Physik (Germany); Thorsten Döhring, Hochschule Aschaffenburg (Germany)

Future X-ray telescopes aim for large effective area within the given mass limits of the launcher. A promising method is the hot shaping of thin glass sheets via a thermal slumping process. This paper presents the status and progress of the indirect glass slumping technology developed at MPE. Recent developments in our research include the successful use of the mould material Cesic under vacuum, as well as the fabrication of a high-

Conference 9603: Optics for EUV, X-Ray, and Gamma-Ray Astronomy VII



precision slumping mould, which meets the requirements of large, high angular resolution missions like ATHENA. The way forward to optimise the slumping process on these materials is reviewed, and the application process for a separation layer on the slumping mould to avoid sticking is described.

Furthermore we present the recent progress on the MPE integration system. The concept of force-free integration and the implementation in the laboratory are described. A real-time measurement system for detecting deformations in the mirror surface during integration has been developed and implemented. Finally the concept for an integrated mirror module segment will be presented.

In addition we have started tests and measurements on the application of a reflective coating. In collaboration with the Hochschule Aschaffenburg first tests with a sputtering facility have been performed, and the test results and analysis will be described. Additionally we present future plans for the next steps in the coating development at MPE.

9603-27, Session 7

Development of precision Wolter mirrors for future solar x-ray observations

Taro Sakao, Japan Aerospace Exploration Agency (Japan) and The Graduate Univ. for Advanced Studies (Japan); Satoshi Matsuyama, Ayumi Kime, Takumi Goto, Akihiko Nishihara, Hiroki Nakamori, Kazuto Yamauchi, Osaka Univ. (Japan); Yoshiki Kohmura, RIKEN SPring-8 Ctr. (Japan); Yoshinori Suematsu, Noriyuki Narukage, National Astronomical Observatory of Japan (Japan)

High resolution imagery of solar X-ray corona provides a crucial key to understand dynamics and heating processes of plasma particles there. However, X-ray imagery of the Sun with sub-arcsecond resolution has yet to be conducted due to severe technical difficulty in fabricating precision Wolter mirrors.

For future X-ray observations of the solar corona, we are attempting to realize precision Wolter mirrors with sub-arcsecond resolution by adopting advanced surface polish and measurement methods based on nano-technology to sector mirrors which consist of a portion of an entire circle.

Evaluation on the X-ray focusing performance at 8-10 keV of the first engineering Wolter mirror was conducted in 2013 using BL29XUL coherent X-ray beam line at SPring-8 synchrotron facility. While X-rays were focused within -0.3" in the sagittal direction of the mirror, the focus profile was extended by -30" in the meridional direction due mainly to residual figure ripples of amplitude -10 nm with spatial frequency -1 /mm.

Based on these results, we devised a systematic approach for the improvement of the precise surface polish. The final polish of the second engineering mirror was completed recently with its figure error <1 nm rms at spatial frequency around 1/mm. Wave-optical estimate indicates that the mirror would have 0.5" FWHM spot size at 8 keV. Another X-ray evaluation at SPring-8 is scheduled in February 2015. Development activities for precision Wolter mirrors will be introduced including some measurement results.

9603-28, Session 7

Direct fabrication of full-shell x-ray optics

Mikhail V. Gubarev, NASA Marshall Space Flight Ctr. (United States); Brian Ramsey, NASA Marshall Space Flight Ctr (United States); W. Scott Smith, Jeffery Kolodziejczak, Jacqueline Roche, William Jones, William Arnold, NASA Marshall Space Flight Ctr. (United States); Carolyn Atkins, The Univ. of Alabama in Huntsville (United States)

The next generation of astrophysical missions will require fabrication technology capable of producing high angular resolution x-ray mirrors.

A full-shell direct fabrication approach using modern robotic polishing machines has the potential for producing stiff and light-weight shells that can be heavily nested, to produce large collecting areas, and are easier to mount, align and assemble, giving improved angular resolution. This approach to mirror fabrication, is being pursued at MSFC. Methods for the mirror metrology, mirror-shell mounting and support during fabrication, and mirror surface figuring using a seven degrees of freedom computer-controlled polishing machine will be presented.

9603-29, Session 7

Fabrication of high resolution and lightweight monocrystalline silicon x-ray mirrors

Raul E. Riveros, Univ. of Maryland, Baltimore County (United States); Linette D. Kolos, NASA Goddard Space Flight Ctr. (United States); James R. Mazzarella, Kevin P. McKeon, SGT, Inc. (United States); William W. Zhang, NASA Goddard Space Flight Ctr. (United States)

Monocrystalline silicon as an X-ray mirror substrate material promises significant improvements over the X-ray mirror technologies used to date, since it is mechanically stiff, stress-free, highly thermally conductive, and widely commercially available. Producing highly accurate and lightweight X-ray mirrors from monocrystalline silicon requires a unique and specialized manufacturing process capable of producing mirrors quickly and cost effectively. The identification, development, and testing of this process is the focus of the work described in this proceeding. Monocrystalline silicon blocks were obtained, and a variety of processes (wire electro-discharge machining, etching, polishing) were applied to generate an accurate and stress-free cylindrical or Wolter-I mirror surface. The mirror surface is then sliced off at a thickness of 0.5 mm and further processed to yield an X-ray mirror segment with < 3" slope errors. Furthermore, our experiments suggest that this mirror production process requires only four days to produce a mirror segment and is easily integrated into a cost-reducing parallel processing scheme. Presently, there is strong evidence that the mirror production process described in this paper will meet the stringent requirements of future X-ray missions.

9603-30, Session 7

Development of light weight replicated x-ray optics

Suzanne E. Romaine, Ricardo Bruni, Harvard-Smithsonian Ctr. for Astrophysics (United States); Brian Choi, Christopher Jensen, ReliaCoat Technologies, LLC (United States); Brian D. Ramsey, National Space Science and Technology Ctr. (United States); Sanjay Sampath, ReliaCoat Technologies, LLC (United States)

NASA'S future X-ray astronomy missions will require X-ray optics that have large effective area while remaining lightweight, and cost effective. Some X-ray missions, such as XMM-Newton , and the upcoming Spectrum-Röntgen-Gamma mission use an electroformed nickel replication (ENR) process to fabricate the nested grazing incidence X-ray telescope mirror shells for an array of moderate resolution, moderate effective area telescopes. We are developing a process to fabricate metal-ceramic replicated optics which will be lighter weight than current nickel replicated technology. Our technology development takes full advantage of the replication technique by fabricating large diameter mirrors with thin cross sections allowing maximum nesting and increase in collecting area. This will lead to future cost effective missions with large effective area and lightweight optics with good angular resolution.

Recent results on fabrication and testing of these optics are presented.



9603-31, Session 8

Alignment, bonding, and testing of lightweight x-ray mirrors

Kai-Wing Chan, Michael P. Biskach, Joseph Bonafede, Linette D. Kolos, James R. Mazzarella, NASA Goddard Space Flight Ctr. (United States); Ryan S. McClelland, Kevin P. McKeon, SGT, Inc. (United States); Jason Niemeyer, Raul E. Riveros, Timo T. Saha, NASA Goddard Space Flight Ctr. (United States); Mark J. Schofield, SGT, Inc. (United States); Marton V. Sharpe, William W. Zhang, NASA Goddard Space Flight Ctr. (United States)

Lightweight, high-resolution, high throughput optics for x-ray astronomy requires fabrication and integration of thin mirrors segments with arcsecond precision. In this paper, we present recent advance on alignment, bonding and testing lightweight glass and silicon mirrors developed at NASA/Goddard Space Flight Center. We address techniques of alignment and bonding of such thin mirrors that produce segmented mirror modules with angular resolution better than 10 arc-seconds. Critical opto-mechanical and thermal issues related to integrating such high resolution mirrors are addressed. We show that the bonded-in mirrors are stable and survive thermal excursion that modules may encounter in a flight mission.

9603-32, Session 8

Cold shaping of thin glass foils: a fast and cost-effective solution for making lightweight astronomical x-ray optics

Marta M. Civitani, Stefano Basso, Oberto Citterio, Mauro Ghigo, Bianca Salmaso, Gianpiero Tagliaferri, Giovanni Pareschi, INAF - Osservatorio Astronomico di Brera (Italy)

Recent advancements in thin glass materials allowed the development and the mass production of very thin glass foils, like e.g. the Willow glass (thickness of 0.1-0.2 mm) produced by Corning or AF32 produced by by Schott (thickness of 0.055 mm). The thickness, strength and flexibility of these glass foils allow bending them up to very small radius of curvature without breaks. This feature, together with the very low micro-roughness, makes this kind of materials ideal candidates for pursuing a cold replication approach for cost-effective and fast making of grazing incidence astronomical optics. Starting from the very thin flat glass sheets, the process under development foresees to bond them onto the supporting structure while they are wrapped around reference mandrels. The assembly concept, based on the use of Wolter-I counter-form moulds, is also based on the use of reinforcing ribs that connect pairs of consecutive foils in the final assembly. The ribs do not only play the role of mechanical connectors, they keep the shape and increase the structural stiffness. Indeed, the ribs constrain the foil profile to the correct shape during the bonding, damping the low-frequency residuals with respect to the Wolter I configuration. This approach is particularly interesting because of their low weight and cost. They could e.g be used for the production of high throughput optics as those needed for the Chines XTP mission, in which the requirements on the angular resolution are not too tight. In fact, a Half Energy Width in the range of 20-60 arcsec is compatible with the expected residual error due to the spring back of the glass sheets. In this paper we provide an overview of the project, the expected performances and presents the first preliminary results.

9603-33, Session 8

JIM: a joint integrated module of glass x-ray optics for astronomical telescopes

Laura Proserpio, Max-Planck-Institut für extraterrestrische Physik (Germany); Stefano Basso, INAF - Osservatorio Astronomico di Brera (Italy); Elias Breunig, Max-Planck-Institut für extraterrestrische Physik (Germany); Enrico Buratti, INAF - Osservatorio Astronomico di Brera (Italy); Vadim Burwitz, Max-Planck-Institut für extraterrestrische Physik (Germany); Marta Civitani, INAF - Osservatorio Astronomico di Brera (Italy); Josef Eder, Peter Friedrich, Gisela D. Hartner, Benedikt Menz, Christian Rohé, Anita Winter, Max-Planck-Institut für extraterrestrische Physik (Germany)

Since several years, the Max-Planck-Institute for extraterrestrial Physics in Germany (MPE) and the Astronomical Observatory of Brera in Italy (INAF-OAB) have been studying the slumping technology for the manufacturing of segmented glass X-ray optics for astronomy. Despite some differences in their specific approaches, the synergy of the two institutes has always been fruitful, focusing on the common goal of developing a technology able to meet the challenging requirements for future X-ray telescopes: i.e. large collecting areas, low mass and good angular resolution. In the last year, this synergy has resulted in an active collaboration for the production of a Joint Integrated Module (JIM) that puts together the expertise of the two research groups. In particular, the indirect slumping approach of MPE has been employed for the manufacturing of X-ray mirror segments, which has then been integrated into an X-ray Optical Unit following the approach developed at INAF-OAB; at this purpose, the appositely designed and developed Integration Machine (IMA) has been employed. The module has finally been tested in X-ray at the MPE PANTER facility, in Neuried. The several steps and the results of this joint activity are reviewed and discussed in this paper.

9603-34, Session 8

Liquid metal actuators: correctable mounting and assembly of thin-shell x-ray telescope mirrors

Alexander R. Bruccoleri, Martin L. Klingensmith, Brandon D. Chalifoux, Ralf K. Heilmann, Mark L. Schattenburg, Massachusetts Institute of Technology (United States)

An ideal bonding agent for thin-shell x-ray mirrors could be quickly applied to joints and set with deterministic and stable properties. Unfortunately, mirror assembly methods have typically utilized various epoxy formulations which are messy, slow to apply and cure, and far from deterministic or stable. Problems include shrinkage, creep and high thermal and humidity sensitivity. Once the bond is set errors are frozen in and can't be corrected. We are developing a new method for bonding thin-foil mirrors that has the potential to solve these problems. Our process to bond mirrors to housing reference points is achieved via small beads of a low-melting-point bonding agent (such as solder or thermoset). The mirror is bonded to small contact surface points under real-time metrology. If the position of the mirror needs to be adjusted after bonding, a small force is applied normal to the contact surface and a pulsed fiber laser is used to melt an ultrathin layer of the solder for a very short time. The joint is then compressed or stretched while molten before refreezing in a new position, enabling repeatable and stable mirror position adjustments along the direction of the force in nmlevel steps with minimal heat input. We present results from our prototype apparatus demonstrating proof of principle. The initial experiment includes developing a technique to bond D263 glass to invar, designing and building a one-dimensional stage to precisely apply force, and applying an infrared laser to heat the joint while measuring position and force.

9603-35, Session 9

High-efficiency blazed transmission gratings for high-resolution soft x-ray spectroscopy

Ralf K. Heilmann, MIT Kavli Institute for Astrophysics and Space Research (United States); Alexander R. Bruccoleri,



Izentis, LLC (United States); Mark L. Schattenburg, MIT Kavli Institute for Astrophysics and Space Research (United States)

High-resolution spectroscopy of astrophysical sources is the key to gaining a quantitative understanding of the history, dynamics, and current conditions of the cosmos. A large-area (> 1,000 cm2), high resolving power (R =lambda/Dlambda > 3,000) soft x-ray grating spectrometer that covers the lines of C, N, O, Ne and Fe ions is the ideal tool to address a number of high-priority sciences questions from the 2010 Decadal Survey, such as the connection between super-massive black holes and large-scale structure via cosmic feedback, the evolution of large-scale structure, the behavior of matter at high densities, and the conditions close to black holes. However, no grating missions or instruments are currently approved. To improve the chances for future soft x-ray grating spectroscopy missions, grating technology has to progress and advance to higher TRLs. We have developed Critical-Angle Transmission (CAT) gratings that combine the advantages of blazed reflection gratings (high efficiency, use of higher diffraction orders) with those of conventional transmission gratings (low mass, relaxed alignment tolerances and temperature requirements, transparent at higher energies). A CAT grating-based spectrometer can provide performance 1-2 orders of magnitude better than current grating instruments on Chandra and Newton-XMM with minimal resource requirements. We have fabricated large-area free-standing CAT gratings with minimal integrated support structures from silicon-on-insulator wafers using advanced lithography and a combination of deep reactive-ion and wet etching, and will present our latest x-ray test results showing record high diffraction efficiencies in blazed orders.

9603-36, Session 9

X-ray and optical alignment approaches to off-plane reflection gratings

Ryan Allured, Harvard-Smithsonian Ctr. for Astrophysics (United States); Benjamin D. Donovan, The Univ. of Iowa (United States); Vadim Burwitz, Max-Planck-Institut für Astrophysik (Germany); Peter N. Cheimets, Harvard-Smithsonian Ctr. for Astrophysics (United States); Casey T. DeRoo, The Univ. of Iowa (United States); Gisela Hartner, Max-Planck-Institut für Astrophysik (Germany); Hannah R. Marlowe, The Univ. of Iowa (United States); Randall L. McEntaffer, The Univ. of Iowa (United States); Edward Hertz, Harvard-Smithsonian Ctr. for Astrophysics (United States); Benedikt Menz, Max-Planck-Institut für Astrophysik (Germany); Randall K. Smith, Harvard-Smithsonian Ctr. for Astrophysics (United States); James H. Tutt, The Univ. of Iowa (United States)

Off-plane reflection gratings offer the potential for high-resolution, high-throughput x-ray spectroscopy on future missions. Most mission concepts, such as Arcus or SMART-X, involve gratings placed in the path of a converging x-ray beam from an x-ray telescope. In the off-plane reflection grating case, these gratings must be co-aligned such that their diffracted spectra overlap at the focal plane. Misalignments degrade spectral resolution and effective area. In-situ x-ray alignment of a pair of off-plane reflection gratings in the path of an SPO module has recently been performed at the PANTER beamline in Germany. The diffracted spectra achieved spectral overlap to within the quality of the SPO point spread function. For a flight-like mission concept, however, in-situ x-ray alignment may not be feasible. In that event, optical methods must be developed to achieve spectral alignment. We have designed and fabricated a flight-like grating module for integration with an SPO module. Metrology techniques have been developed and used to populate the grating module and align it to the SPO. Finally, the combined SPO and grating modules have been taken to PANTER for x-ray performance testing.

9603-37, Session 9

Diffraction efficiency measurements of radially-profiled off-plane gratings

Drew M. Miles, Hannah R. Marlowe, Jake A. McCoy, Randall L. McEntaffer, Thomas J. Peterson, Ted B. Schultz, James H. Tutt, The Univ. of Iowa (United States); Thomas D. Rogers, Univ. of Colorado at Boulder (United States); Christian Laubis, Frank Scholze, Physikalisch-Technische Bundesanstalt (Germany)

Future X-ray missions will require gratings with high throughput and high spectral resolution. Blazed off-plane reflection gratings are capable of meeting these demands. A blazed grating profile optimizes grating efficiency, providing higher throughput to one side of zero-order on the arc of diffraction. This paper presents efficiency measurements made in the 0.3 - 1.5 keV energy band at the Physikalisch-Technische Bundesanstalt (PTB) BESSY II facility for three radially-profiled, holographically-ruled gratings, two of which are blazed. Each blazed grating was tested in both the Littrow configuration and anti-Littrow configuration in order to test the alignment sensitivity of these gratings with regard to throughput. In addition, efficiency measurements are provided on all three gratings with incoming light parallel to the groove direction. This paper will outline the procedure of the grating experiment performed at BESSY II and discuss the resulting efficiency measurements across various energies. Experimental results were generally consistent with theory and demonstrate that the blaze does increase throughput to one side of zero-order. However, the total efficiency of the non-blazed, sinusoidal grating is greater than that of the blazed gratings, which suggests that the method of manufacturing these blazed profiles fails to produce facets with the desired level of precision. Finally, efficiency models for the two grating arrays that will fly on board the suborbital rocket payload, Off-plane Grating Rocket for Extended Source Spectroscopy (OGRESS), will be presented along with an analysis of the grating performance from the mission.

9603-38, Session 10

Polarization sensitivity of blazed, off-plane reflection gratings in the soft x-ray regime

Hannah R. Marlowe, James H. Tutt, Casey T. DeRoo, Drew M. Miles, Randal L. McEntaffer, The Univ. of Iowa (United States); Frank Scholze, Christian Laubis, Physikalisch-Technische Bundesanstalt (Germany)

X-ray diffraction gratings in the off-plane, or conical mount, are able to achieve higher spectral resolution and efficiency than their in-plane counterparts. They also offer favorable packing geometries and are able to reach very large absolute efficiencies at high orders. In addition to these benefits, efficiency calculations show that unlike in the in-plane configuration, gratings in the off-plane mount have noticeable efficiency variations between TM and TE waves which can be exploited to extract polarization information of incident radiation. Therefore, these gratings have the potential to enable and support next generation X-ray polarimetry missions. We present expectations and results of the polarization sensitivity of blazed, off-plane reflection gratings in the 30-1800 eV regime taken at the BESSY II synchrotron using the PTB beamline. In addition, specific instrument applications in the context of current mission concepts will be discussed.

9603-39, Session 10

New laterally graded multilayer mirrors for soft x-ray polarimetry

Herman L. Marshall, Norbert S. Schulz, Massachusetts Institute of Technology (United States); David L. Windt,

Conference 9603: Optics for EUV, X-Ray, and Gamma-Ray Astronomy VII



Reflective X-Ray Optics LLC (United States); Eric M. Gullikson, Lawrence Berkeley National Lab. (United States); Eric Blake, Univ. of Massachusetts Lowell (United States); Dan Getty, Massachusetts Institute of Technology (United States); Zane McInturff, Univ. of Wisconsin-Madison (United States); John A. Clarke, Massachusetts Institute of Technology (United States)

We present continued development of laterally graded multilayer-coated mirrors (LGMMs) for a telescope design capable of measuring linear X-ray polarization over a broad X-ray band. The multilayer-coated mirrors are used as Bragg reflectors at the Brewster angle. By matching to the dispersion of a spectrometer, one may take advantage of high multilayer reflectivities and achieve polarization modulation factors over 50% over the entire 0.2-0.8 keV band. Previously, we demonstrated that the polarimetry beam-line provides 100% polarized X-rays at 0.525 keV (Marshall et al. 2013). Recently, we augmented the system using a LGMM to create a source of polarized X-rays at energies from 180 eV to 525 eV. Here, we will present results from continued development that includes LGMMs of new material combinations (C/CrCo and La/B4C) with high efficiencies in different soft X-ray bands. We have also sponsored the development of new gratings and anticipate showing results from testing these new gratings.

Support for this work was provided by the National Aeronautics and Space Administration through grant NNX12AH12G and by Research Investment Grants from the MIT Kavli Institute.

9603-40, Session 10

High efficiency carbon-based multilayers for LAMP at 250 eV

Mingwu Wen, Qiushi Huang, Tongji Univ. (China); Rui She, Tsinghua Univ. (China); Li Jiang, Zhong Zhang, Zhanshan Wang, Tongji Univ. (China); Hua Feng, Tsinghua Univ. (China); Daniele Spiga, INAF - Osservatorio Astronomico di Brera (Italy)

X-ray reflection near the Brewster's angle by multilayer mirrors can be used to detect the polarization from X-ray sources. The photon spectra from some isolated neutron stars and AGN/blazars etc. show that their emission is peaked at low energies near 250eV, which is just below carbon K-absorption edge. The Lightweight Asymmetry and Magnetism Probe (LAMP) is proposed as a micro-satellite mission dedicated for astronomical X-ray polarimetry working at 250 eV and is currently under early phase study. Different carbon-based multilayers including Co/C, Cr/C, and Co8Cr2/C are selected and designed at the energy near 250eV with a grazing incident angle of 45°. The carbon layer thickness ratio is optimized to get the highest integral reflectivity which means more effective signals in the astrophysics observation. The multilayer coatings are manufactured by direct current magnetron sputtering and characterized using Grazing incidence X-ray reflectometry (GIXR) at 8keV. Different base vacuum pressures were investigated to study the influence of e.g. oxygen and nitrogen in the vacuum. Reactive sputtering with 2%, 4%, 6% and 8% nitrogen, respectively, were also used to improve the Co/C multilayer interfaces. The fittings to GIXR results and atomic force microscopy (AFM) measurements show that both the interlayer and surface roughness can be reduced using reactive sputtering.

9603-41, Session 10

Testing multilayer-coated nickel mirrors for the LAMP x-ray polarimetric telescope

Daniele Spiga, INAF - Osservatorio Astronomico di Brera (Italy); Zhanshan Wang, Tongji Univ. (China); Robert Banham, Media Lario Technologies S.r.l. (Italy); Enrico Costa, INAF - Istituto di Astrofisica e Planetologia Spaziali (Italy); Hua Feng, Tsinghua Univ. (China); Angelo Giglia, Elettra-Sincrotrone Trieste S.C.p.A. (Italy); Qiushi Huang, Tongji Univ. (China); Fabio Muleri, INAF - Istituto di Astrofisica e Planetologia Spaziali (Italy); Giovanni Pareschi, Bianca Salmaso, INAF - Osservatorio Astronomico di Brera (Italy); Rui She, Tsinghua Univ. (China); Paolo Soffitta, INAF - Istituto di Astrofisica e Planetologia Spaziali (Italy); Gianpiero Tagliaferri, INAF - Osservatorio Astronomico di Brera (Italy); Kashmira Tayabaly, Politecnico di Milano (Italy) and INAF -Osservatorio Astronomico di Brera (Italy); Giuseppe Valsecchi, Media Lario Technologies S.r.l. (Italy); Mingwu Wen, Tongji Univ. (China)

The LAMP (Lightweight Asymmetry and Magnetism Probe) polarimetric X-ray telescope is a mission concept to analyze the polarization of X-ray sources in the Universe at 250 eV via focusing mirrors near the Brewster angle, i.e., at angles of 40 to 50 deg. Hence it will require the adoption of multilayer coatings with a few nanometers d-spacing in order to enhance the reflectivity. The Nickel electroforming technology has already been successfully used to fabricate the high angular resolution imaging mirrors of the X-ray telescopes SAX, XMM-Newton, and Swift/XRT. We are investigating this consolidated technology as a possible technique to manufacture focusing mirrors for LAMP. Although the very good reflectivity performances of this kind of mirrors were fully demonstrated in grazing incidence, the reflectivity and scattering properties have not yet been tested directly at the unusual large 45 deg angle. In this paper we present the results of the X-ray reflectivity campaign performed at the BEAR beamline at ELETTRA Sincrotrone Trieste on 12 electroformed Nickel samples with multilayer coatings of various composition (Cr/C, Co/C, Fe/C), using polarized X-rays at 250 eV. We deal with an analysis of the reflectivity curves in order to derive the polarizing properties, the multilayer structure, and the roughness/diffuseness characteristics. We also perform a comparison of the results with the expectations obtained from the roughness measured by Atomic Force Microscopy.

9603-42, Session 11

Advancements in hard x-ray multilayers for x-ray astronomy

David L. Windt, Reflective X-Ray Optics LLC (United States)

The development in recent years of nanometer-scale X-ray multilayer coatings that provide high reflectance over a broad spectral band at energies above 10 keV, in combination with the simultaneous development of thin-shell cylindrical mirror substrates, has enabled the construction of efficient, light-weight, hard X-ray astronomical telescopes, embodied most notably in the NuSTAR instrument launched in 2012. This new hard X-ray optics capability has in turn led to ground-breaking observations of a variety of Galactic and extra-Galactic objects.

Future X-ray astronomy missions currently being formulated that will use multilayer X-ray optics technology will require performance that exceeds what can be achieved at present. In particular, there is a need for new X-ray multilayer coatings that have higher reflectance, and that operate at even higher energies than the W- and Pt-based multilayer coatings used for NuSTAR. Furthermore, as the angular resolution of the thin-shell mirror substrates approaches one arc-second and beyond, achieving near-zero multilayer film stress will become an increasingly important requirement, in order to avoid stress-driven substrate deformations that would otherwise degrade angular resolution.

In this presentation, recent investigations into a variety of new multilayer designs, materials combinations, film deposition techniques, and film characterization techniques will be described. The overarching goal of these investigations is the development of high-performance, low-stress, hard X-ray multilayer coatings for use in future X-ray astronomy missions.



9603-43, Session 11

Development of Ni-based multilayers for future focusing soft gamma ray telescopes

David Girou, Erlend Sleire, Sonny Massahi, Finn E. Christensen, Anders C. Jakobsen, DTU Space (Denmark)

The hard X-ray focusing telescopes on the NuSTAR mission and to be flown on the ASTRO-H mission uses depth graded multilayer coatings to extend the energy bandwidth to the hard X-ray range. For both missions the upper energy range is limited to 79.4 keV by the Pt-K absorption edge of the constituent heavy material. One possible solution for extending the energy bandwidth into the soft gamma ray range of several hundred keV is to use Ni as the heavy element in the multilayer as this material does not have absorption edges in hard X-ray/soft gamma ray range. This paper reports on our current status of developing these coatings in the DC magnetron sputtering facility at DTU-space including the combined methods of collimation, reactive sputtering using Nitrogen and heating of the substrates.

9603-44, Session 11

A soft gamma-ray concentrator using thinfilm multilayer structures

Peter F. Bloser, Paul Aliotta, Olof Echt, James Krzanowski, Jason S. Legere, Mark L. McConnell, Farzane Shirazi, John Tsavalas, Emily Wong, The Univ. of New Hampshire (United States)

We have begun to investigate the use of thin-film, multilayer structures to form optics capable of concentrating soft gamma rays with energies greater than 100 keV, beyond the reach of current grazing-incidence hard X-ray mirrors. Alternating layers of low- and high-density materials (e.g., polymers and metals) will channel soft gamma-ray photons via total external reflection. A suitable arrangement of bent structures will then concentrate the incident radiation to a point. Gamma-ray optics made in this way offer the potential for soft gamma-ray telescopes with focal lengths of less than 10 m, removing the need for formation flying spacecraft and opening the field up to balloon-borne instruments. Building on initial investigations at Los Alamos National Laboratory, we are investigating whether it is possible to grow such flexible multi-layer structures with the required thicknesses and smoothness using magnetron sputter and pulsed laser deposition techniques. We will present the initial results of tests aimed at fabricating such structures using both spin coating and pulsed laser deposition, and demonstrating gamma-ray channeling of 122 keV photons in the laboratory. If successful, this technology offers the potential for transformational increases in sensitivity while dramatically improving the system-level performance of future high-energy astronomy missions through reduced mass and complexity.

9603-45, Session 12

Progress in differential deposition for improving the figures of full-shell astronomical grazing incidence x-ray optics

Kiranmayee Kilaru, NASA Marshall Space Flight Ctr. (United States); Carolyn Atkins, The Univ. of Alabama in Huntsville (United States); Brian D. Ramsey, Mikhail V. Gubarev, David M. Broadway, NASA Marshall Space Flight Ctr. (United States)

One of the developments at MSFC that is underway to meet the demand of high-resolution X-ray optics for the support of future X-ray astronomy missions is the 'differential deposition' technique. This process corrects the axial figure profile of optics by selectively depositing material onto the mirror's surface. The process relies on accurate metrology achieved using a long trace profiler whose slope resolution is better than 1µrad. From these metrology data an error map is generated that shows the profile of material to be deposited to correct the optic's figure. A computer-controlled deposition system then applies this corrective coating.

Simulations show that substantial improvements in angular resolution are possible. To date, custom coating systems have been developed and corrections of full-shell optics are underway. This presentation gives an overview of the program and results obtained to date.

9603-46, Session 12

Differential deposition correction of segmented glass x-ray optics

Carolyn Atkins, The Univ. of Alabama in Huntsville (United States); Kiranmayee Kilaru, Brian D. Ramsey, David M. Broadway, Jessica A. Gaskin, Mikhail V. Gubarev, Stephen L. O'Dell, NASA Marshall Space Flight Ctr. (United States); William W. Zhang, NASA Goddard Space Flight Ctr. (United States)

One of the challenges faced within the astronomical X-ray community is how to produce lightweight high angular resolution optics for a future X-ray mission capable of probing the early X-ray universe. To this end, the differential deposition project at NASA's MSFC is looking to improve current X-ray optic technology by applying a corrective coatings with a goal of achieving arc-second-level resolution. Recently at MSFC we have commissioned two new vacuum deposition chambers explicitly for this research. One chamber corrects the full shell NiCo mirrors fabricated at the MSFC and the other corrects the segmented glass optics fabricated by GSFC.

This paper will focus on the correction of the segmented glass optics and the paper will highlight: the design of the chamber and internal mechanics; the algorithm used to perform the correction; metrology of the glass segments; and the improvement in resolution post correction that has been achieved to date.

9603-47, Session 12

Two-dimensional differential deposition for figure correction of thin-shell mirror substrates for x-ray astronomy

David L. Windt, Reflective X-Ray Optics LLC (United States); Raymond Conley Jr., Argonne National Lab. (United States)

Future X-ray astronomy missions will likely use light-weight X-ray telescopes constructed from thin-shell mirror segments. To realize angular resolution of 1" or better, figure errors in the mirror substrates must be sufficiently controlled over all relevant spatial frequencies. In particular, axial mid-frequency surface-height errors (i.e., with lateral scales in the range 1 – 10 mm) must be controlled to better than -0.5 nm in order to achieve 1" resolution.

We describe a new technique for correction of mid-frequency, surfaceheight errors in thin-shell mirror segments. The technique is based on the differential deposition concept, wherein material is added to the substrate surface (e.g., using magnetron sputtering) so as to fill in the 'valleys' and thus reduce the magnitude of surface-height errors. Other differential deposition techniques currently being pursued for figure correction modulate the velocity of the substrate as it moves past a fixed-width aperture placed over the sputter source, providing one-dimensional film thickness control. In contrast, our new approach provides two-dimensional control of film thickness so that surface-height errors along adjacent strips spanning the entire substrate surface can be corrected simultaneously. We use a constant substrate velocity in conjunction with an array of -5-mmwide dynamically-actuated apertures: as the substrate moves past the



sputter source, each of the apertures is modulated individually, in real-time, in accord with a pre-measured surface-height map. Preliminary results will be presented on the development of the necessary film deposition and surface metrology techniques, including the crucial development of dynamically-actuated apertures suitable for use with magnetron sputtering.

9603-49, Session 13

Compensating for piezo-electric materials processing stresses in adjustable x-ray optics

Katie Ames, Ricardo Bruni, Paul B. Reid, Suzanne E. Romaine, Harvard-Smithsonian Ctr. for Astrophysics (United States)

Adjustable X-ray optics represent an enabling technology for simultaneously achieving large effective area and high angular resolution. The adjustable optics employ a bimorph mirror composed of a thin (1.5 um) film of piezoelectric material deposited on the back of a 0.4 mm thick conical mirror segment.

The application of localized electric fields in the piezoelectric material, normal to the mirror surface, result in localized deformations in mirror shape. Thus, mirror fabrication and mounting induced figure errors can be corrected, without the need for a massive reaction structure. A problem encountered with this approach is that film stresses in the piezoelectric layer, resulting from deposition, crystallization, and differences in coefficient of thermal expansion, can distort the mirror. The large relative thickness of the piezoelectric material means that even 100MPa stresses can result in significant distortions.

We have examined compensating for the piezoelectric processing related distortions by the deposition of controlled stress iridium films on the front surface of the mirror. We describe our experiments to balance the stress resulting from the piezoelectric layer. We also evaluated the repeatability of this deposition process, and the robustness of the iridium coating.

9603-50, Session 13

Stress manipulated coating: a new surface correction method for light weight x-ray optics

Youwei Yao, Xiaoli Wang, Jian Cao, Michael E. Graham, Semyon Vaynman, Shannon E. Grogans, Yifang Cao, Melville P. Ulmer, Northwestern Univ. (United States)

We present a stress manipulated coating method for light weight X-ray optics to improve the figure quality. The principle of this idea is to produce local stress in coating on the non-reflecting surface of the mirror to correct the surface profile. In order to demonstrate a proof of concept, a standard magnetron sputtering system was modified. First, a mask with a slit has been fixed under the sputtering source to restrict the flow of coating material. Second, the sample holder was put on a translation stage which was mounted below the mask. Then, an adjustable bias circuit was attached to the sample holder. The result was a set up that allowed us to vary locally the coating stress. To demonstrate repeatability of stress with a set bias, 5 test glass pieces (20mm by 5mm by 0.2mm) were coated with a 100nm Cr layer under a constant bias of -62.5V. The curvatures of the samples before and after coating were measured by a Dektak profilometer. The results suggest that the method could improve the surface profile by factor of over 160 down to slope errors of below 1 arc second. In addition, a sinusoidal waviness over the length scale of 10mm was produced on a test glass piece to demonstrate the feasibility of manipulating the surface figure via a changing stress. The measured profile was consistent with our FEA simulation. These results suggest the method has a promising future for reducing the cost of high quality (arc second) X-ray optics.

9603-51, Session 13

Ion implantation for figure correction of segmented x-ray telescope mirror substrates

Brandon D. Chalifoux, Graham Wright, Ralf K. Heilmann, Mark L. Schattenburg, Massachusetts Institute of Technology (United States)

Figure correction of x-ray telescope mirrors may be critical for future missions that require high resolution and large collecting areas. Ion implantation offers a method of correcting figure errors by imparting sub-surface strain in a controllable magnitude and location. In this paper, we demonstrate that sufficient strain can be applied to achieve significant figure correction in D-263 glass, Eagle XG glass, and silicon. Figure correction with equibiaxial strain applied to the surface, regardless of how the strain is applied, requires large strain at high spatial frequency to provide substantial figure correction. In contrast, if a general strain can be applied to the surface, then nearly exact correction can be made using small strains at low spatial frequencies. We show that in some materials, such as D-263 glass, substantial anisotropic strain can be generated. This may provide substantial improvement in the ability to correct figure errors. We will also report on progress to build a vacuum chamber capable of imposing non-uniform ion dose distributions on a mirror substrate.

9603-52, Session 14

Development of adjustable x-ray optics with 0.5 arcsec resolution: a status update

Paul B. Reid, Ryan Allured, Sagi Ben-Ami, Vincenzo Cotroneo, Harvard-Smithsonian Ctr. for Astrophysics (United States); Edward Hertz, Smithsonian Astrophysical Observatory (United States); Raegan L. Johnson-Wilke, Sandia National Labs. (United States); Vanessa Marquez, Smithsonian Astrophysical Observatory (United States); Stuart McMuldroch, Daniel A. Schwartz, Harvey D. Tananbaum, Harvard-Smithsonian Ctr. for Astrophysics (United States); Susan Trolier-McKinstry, The Pennsylvania State Univ. (United States); Alexey A. Vikhlinin, Harvard-Smithsonian Ctr. for Astrophysics (United States); Margeaux L. Wallace, The Pennsylvania State Univ. (United States); Rudeger H. T. Wilke, Sandia National Labs. (United States)

Adjustable grazing incidence X-ray optics represent a candidate technology for the development of the successor to the Chandra X-ray Observatory. The adjustable optics, produced by depositing a thin film of piezoelectric material on the back surface of a Wolter mirror segment, represents a way in which mirror figure errors resulting from fabrication and mounting can be corrected once on the ground. After launch, it may also be feasible to make on-orbit corrections for figure changes due to thermal effects. This powerful technology does not require massive reaction structures, and will make possible the simultaneous achievement of very large effective area and subarcsecond X-ray imaging.

We describe recent progress in our continuing development of adjustable X-ray optics. We discuss improvements in piezoelectric lifetime and yield, development of a mirror segment alignment approach consistent with subarcsecond imaging, demonstration of deterministic figure correction on flat test mirrors, and progress towards X-ray testing of a mounted, aligned, and corrected pair of mirrors.



9603-53, Session 14

Improved control and characterization of adjustable x-ray optics

Ryan Allured, Sagi Ben-Ami, Vincenzo Cotroneo, Vanessa Marquez, Stuart McMuldroch, Paul B. Reid, Daniel A. Schwartz, Harvard-Smithsonian Ctr. for Astrophysics (United States); Susan Trolier-McKinstry, The Pennsylvania State Univ. (United States); Alexey A. Vikhlinin, Harvard-Smithsonian Ctr. for Astrophysics (United States); Margeaux L. Wallace, The Pennsylvania State Univ. (United States)

We report on significant improvements on the metrology systems and control systems for piezoelectrically adjustable X-ray optics. In the past, an optical profilometer and Shack-Hartmann wavefront sensor have been used to measure several influence functions for a flat adjustable mirror. We have since performed a full calibration of a flat mirror and used a multi-channel DAC to induce pre-determined figure changes to the mirror, representing our first attempt at figure control of a full mirror. Furthermore, we have adapted our metrology systems to a cylindrical geometry, allowing characterization of Wolter-type mirrors. We review measurements of figure, roughness, and influence functions of a cylindrical mirror and finally discuss implications for future work.

9603-54, Session 14

Manufacturing and testing a thin glass mirror shell with piezoelectric active control

Daniele Spiga, INAF - Osservatorio Astronomico di Brera (Italy); Marco Barbera, Univ. degli Studi di Palermo (Italy); Stefano Basso, Marta Civitani, INAF - Osservatorio Astronomico di Brera (Italy); Alfonso Collura, Ugo Lo Cicero, INAF - Osservatorio Astronomico di Palermo Giuseppe S. Vaiana (Italy); Giuseppe Lullo, Univ. degli Studi di Palermo (Italy); Carlo Pelliciari, Marco Riva, Bianca Salmaso, INAF - Osservatorio Astronomico di Brera (Italy); Luisa Sciortino, Univ. degli Studi di Palermo (Italy)

Optics for future X-ray telescopes will be characterized by very large aperture and focal length, and will be made of lightweight materials like glass or Silicon in order to keep the total mass within acceptable limits. Optical modules based on thin slumped glass foils are being developed at various institutes, aiming at improving the angular resolution to a few arcsec HEW. Thin mirrors are prone to deform, so they require a careful integration to avoid deformations and even correct forming errors. On the other hand, this offers the opportunity to actively correct the residual deformation: a viable possibility to improve the mirror figure is the application of piezoelectric actuators onto the non-optical side of the mirrors, and several groups are already at work on this approach. The concept we are developing consists of actively integrating thin glass foils with piezoelectric patches, fed by voltages driven by the feedback provided by X-rays. The actuators are commercial components, while the tension signals are carried by a printed circuit obtained by photolithography, and the driving electronic is a multichannel low power consumption voltage supply developed in-house. Finally, the shape detection and the consequent voltage signal to be provided to the piezoelectric array are determined in X-rays, in intra-focal setup at the XACT facility at INAF/OAPA. In this work, we describe the manufacturing steps to obtain a first active mirror prototype and the first test performed in X-rays.

9603-55, Session 14

Investigation of magnetically smart films applied to correct the surface profile of light weight x-ray optics in two directions

Xiaoli Wang, Youwei Yao, Jian Cao, Michael E. Graham, Semyon Vaynman, Tianchen Liu, Melville P. Ulmer, Northwestern Univ. (United States)

Our goal is to improve initially fabricated X-ray optics figures by applying a magnetic field to drive a magnetic smart material (MSM) coating on the backside of the mirror. The consequent deformation of the surface should be three-dimensional. Here we will report on the results of working with a glass sample of 50x50x0.2 mm that has been coated with MSMs. The coated glass can be deformed in 3 dimensions and its surface profile will be measured under our Zygo NewView white light interferometer (WLI). The driving magnetic field will be produced via a pseudo-magnetic write head made up of two permanent magnet posts. The magnet posts can be moved around the glass sample with a 3-d computer controlled translation stage. The system allows four degrees of freedom of motion, i.e., up and down, side to side, back and forth, and rotation of the posts (3 mm diameter) about the vertical axis to allow us to change the orientation of the magnetic field in the (horizontal) plane of the sample. Key features of the design are that the positions can be controlled and recorded by a computer, and that the device is compact enough so the surface deflections of the shaped piece can be measured in situ with WLI. We will establish a FEA model to predict deformations and compare with the observed results in order to demonstrate that magnetically controlled MSMs can be used to improve X-ray optics figures.

9603-56, Session 15

BEaTriX: an expanded soft x-ray beam facility for test of focusing optics, an update

Carlo Pelliciari, Daniele Spiga, Giovanni Pareschi, Gianpiero Tagliaferri, INAF - Osservatorio Astronomico di Brera (Italy)

The BEaTRiX X-ray facility has been designed to test modular optics with very high angular resolution (FWHM < 3 arcsec). The main components of the facility are bremsstrahlung X-ray tubes, a parabolic mirror, a multi-reflection monochromator, an asymmetric Si(220) crystal to enlarge the beam and a CCD positioned in the focal plane (12 m). The setup is expected to generate a beam with a collimation of better than 1.8 arcsec and a section of 60x200 mm2. Other crystals and geometrical configuration are under study in order to extend the range to lower energies (1.5 keV). Simulation, Beatrix design and optical system are illustrated.

9603-57, Session 15

A Fresnel zone plate collimator: potential and aberrations

Benedikt Menz, Heinrich Brauninger, Vadim Burwitz, Gisela D. Hartner, Peter Predehl, Max-Planck-Institut für extraterrestrische Physik (Germany)

A collimator, that parallelizes an X-ray beam, provides a significant improvement of the metrology to characterize X-ray optics for satellite experiments at MPEs PANTER X-ray test facility. A Fresnel zone plate was selected as a collimating optic, as it meets a good angular resolution < 0.1" combined with a large active area > 10 cm^2.

Such an optic is ideally suited to illuminate Silicon Pore Optic (SPO) modules as proposed for ATHENA.

This paper provides the theoretic description of such a Fresnel zone plate



especially considering resolution and efficiency. Based on the theoretic results the collimator setup performance is analyzed and requirements for fabrication and alignment are calculated.

9603-58, Session 15

The characterization of mirror module for the qualification model of the ART-XC/SRG instrument

Alexey Tkachenko, Mikhail N. Pavlinsky, Alexander Yaskovich, Igor Y. Lapshov, Vladimir A. Oleynikov, Space Research Institute (Russian Federation); Sergey V. Grigorovich, Dmitriy Litvin, Valeriy P. Lazarchuk, Igor Roiz, Mikhail Garin, Russian Federal Nuclear Ctr. - All-Russian Research Institute of Experimental Physics (Russian Federation)

The Astronomical Roentgen Telescope – X-Ray Concentrator (ART-XC) is a medium-x-ray-energy survey instrument to be launched on board of the Spectrum Roentgen Gamma (SRG) Mission. The instrument consists of seven identical mirror modules coupled with seven CdTe strip focal-plane detectors. The ART-XC flight mirror modules have been developed and manufactured at the Marshall Space Flight Center (MSFC). VNIIEF (Sarov, Russia) has manufactured seven mirror modules for ART-XC qualification model. Some of these qualification mirror modules have been tested in x-rays at the Space Research Institute (Moscow, Russia) Stray Light Facility in order to develop measurement techniques and to clarify characteristics of mirror modules for fine-tuning technologies in future projects. Details of the characterization procedure and an overview of the obtained results are presented here.

Conference 9604: Solar Physics and Space Weather Instrumentation VI

Sunday - Monday 9 -10 August 2015

Part of Proceedings of SPIE Vol. 9604 Solar Physics and Space Weather Instrumentation VI

9604-1, Session 1

SSUSI-Lite : a far-ultraviolet hyper-spectral imager for space weather remote sensing (Invited Paper)

Bernard S. Ogorzalek, Steve N. Osterman, John E. Hicks, Larry J. Paxton, Matthew P. Grey, Johns Hopkins Univ. Applied Physics Lab., LLC (United States)

SSUSI-Lite is a far-ultraviolet hyper-spectral imager for monitoring space weather. SSUSI-Lite is a refresh of the Special Sensor Ultraviolet Spectrographic Imager (SSUSI) that has flown on DMSP spacecraft FI6 through F19. SSUSI-Lite maintains the same optical layout as the DMSP SSUSI, includes updates to key functional elements, and reduces the sensor volume, mass, and power requirements. We describe the re-design of the sensor, the improvements that have been made, and its measurement capabilities.

SSUSI-Lite generates images of the Earth's airglow in the far-ultraviolet by sweeping a mirror from horizon to horizon in the cross track direction at the input to the spectrograph. SSUSI-Lite contains an improved scanner design, which uses a pair of limited angle DC motors. The detector processing electronics, including pulse shaping and event binning, has been changed to all digital circuitry. The largest decrease in volume, mass, and power from the DMSP SSUSI has been obtained by consolidating all electronics into one data processing unit.

9604-2, Session 1

Stellar calibration of the special sensor ultraviolet limb imager (SSULI) on the DMSP spacecraft

Peter Walker, Computational Physics, Inc. (United States); Andrew C. Nicholas, Scott A. Budzien, Kenneth F. Dymond, Andrew W. Stephan, U.S. Naval Research Lab. (United States)

The SSULI (Special Sensor Ultraviolet Limb Imager) is a limb-scanning far- and extreme-ultraviolet spectrometer designed to fly on the Defense Meteorological Satellite Program (DMSP). The sensor sensitivity is tracked through the mission life by taking advantage of serendipitous stellar apparitions which, over the course of several days, track across the sensor's field of view, allowing for not only the production of a sensitivity curve when compared against the known stellar spectra, but additionally pointing information and field-of-view information can be gleaned from comparing the star's expected and observed positions. Most notably, because the star's apparition traces across the field of view predictably in one axis, and randomly in another, multiple apparitions of these point sources can be used to map out the gain on the detector's entire surface, revealing the existence and extent of localized gain sags. Additionally, multiple, routinized, and scheduled calibrations can be used to track sensor behavior through the mission life, including effects like a detector scrub, photocathode performance, and possible optics contamination. Results from the SSULI 002/DMSP F18 and SSULI 005/DMSP F19 stellar calibrations are presented.

9604-3, Session 1

WINCS on-orbit performance results

Andrew C. Nicholas, U.S. Naval Research Lab. (United States); Fred Herrero, Space Systems Research Corp. (United States); Andrew W. Stephan, Theodore Finne, U.S. Naval Research Lab. (United States) The Winds-Ions-Neutral Composition Suite (WINCS) instrument, also know as the Small Wind and Temperature Spectrometer (SWATS), was designed and developed jointly by the Naval Research Laboratory (NRL) and NASA/ Goddard Space Flight Center (GSFC) for ionosphere-thermosphere investigations in orbit between 120 and 550 km altitude. The CubeSat compatible WINCS design provides the following measurements in a single package with a low Size, Weight, and Power (SWaP), 7.6 x 7.6 x 7.1 cm outer dimensions, 0.75 kg total mass, and about 1.3 Watt total power: neutral winds, neutral temperature, neutral density, neutral composition, ion drifts, ion temperature, ion density and ion composition. The instrument is currently operating on the International Space Station (Sep. 2013) and on the STP-Sat3 spacecraft (Nov. 2013). On-orbit results of the instrument will be presented along with a summary of future flight manifests.

SPIE. PHOTONICS

OPTICAL ENGINEERING+

APPLICATIONS

9604-5, Session 1

Proton-electron discrimination detector (PEDD) for space weather monitoring

Chad M. Whitney, Erik B. Johnson, Xiao J. Chen, Christopher Stapels, Sam Vogel, James F. Christian, Radiation Monitoring Devices, Inc. (United States)

Electronics used for space applications (e.g. communication satellites) are susceptible to space weather, primarily consisting of electrons and protons. As more critical equipment is used in space, a comprehensive monitoring network is needed to mitigate risks associated with radiation damage. Compact detectors suited for this requirement have been too complicated or do not provide sufficient information. As the damage from electrons (e.g. total ionizing dose effects) is significantly different compared to protons (e.g. displacement damage effects), monitors that can provide unique measurements of the dose and/or spectral information for electrons and protons separately are necessary for mission assessment to determine strategies for maintaining function. Previously, we demonstrated that the Proton-Electron Discrimination Detector (PEDD) is space-compatible and can discriminate fast electrons from protons using a diphenylanthrecene (DPA) scintillator coupled to a CMOS solid-state photomultiplier (SSPM). The SSPM has a temperature dependence, and we will present a solution to this issue, providing a stable response as a function of temperature. The PEDD detector is scheduled to participate on the RHEME experiment to be flown on the ISS, scheduled for launch in 2016. The system will go live once powered, and we anticipate transmitting the acquired data from an FPGA system to the ISS in the form of 3, 32-bit integers per event containing information on the waveform integrals for proton-electron discrimination, event number, sensor temperature, and trigger amplitude. The latest results presented here expand on our previous work to include space-compatible packaging, temperature compensation for the SSPM, readout circuit design and specifications, and FPGA implementation.

9604-6, Session 1

South Atlantic anomaly and CubeSat design considerations

Judy A. Fennelly, William R. Johnston, Daniel M. Ober, Gordon R. Wilson, Air Force Research Lab. (United States); T. Paul O'Brien, The Aerospace Corp. (United States); Stuart L. Huston, Atmospheric and Environmental Research, Inc. (United States)

Effects of the South Atlantic Anomaly (SAA) on spacecraft in low Earth orbit (LEO) are well known and documented. The SAA exposes spacecraft in LEO to high doses of ionizing radiation as well as higher than normal rates of Single Event Upsets (SEU) and Single Event Latch-ups (SEL). CubeSats, spacecraft built around 10 x 10 cm cubes, are even more susceptible to

Conference 9604: Solar Physics and Space Weather Instrumentation VI



SEUs and SELs due to the use of commercial off-the-shelf components for electronics and payload instrumentation. Examination of the SAA using both data from the Defense Meteorological Satellite Program (DMSP) and a new set of models for the flux of particles is presented. The models, AE9, AP9, and SPM for energetic electrons, energetic protons and space plasma were developed for use in space system design. These models introduce data-based statistical constraints on the uncertainties from measurements and climatological variability. Discussion of the models' capabilities and limitations with regard to LEO CubSat design is presented.

9604-17, Session 2

Study of solar wind ions implantation effects in optical coatings in view of solar orbiter space mission operation

Davide Bacco, Alain Jody Corso, Univ. degli Studi di Padova (Italy); Enrico Tessarolo, IFN-CNR LUXOR Lab. (Italy); Enrico Napolitani, Univ. degli Studi di Padova (Italy); Paola Zuppella, IFN-CNR LUXOR Lab. (Italy); Francesca Gerlin, Marco Nardello, Univ. degli Studi di Padova (Italy); Silvano Fineschi, Ester Antonucci, INAF - Osservatorio Astronomico di Torino (Italy); Maria Guglielmina Pelizzo, IFN-CNR LUXOR Lab. (Italy)

Low energy ions coming from the quite solar wind are considered among causes of potential damage of the optical instrumentation and components on board of ESA Solar Orbiter. Predictions of space radiation parameters are available for instruments on board of such mission. Accelerators are commonly used to reproduce the particle irradiation on a spacecraft during its lifetime at the ground level. By selecting energies and equivalent doses it is possible to replicate the damage induced on space components. Implantation of Helium ions has been carried out on different single layer thin films at LEI facility at Forschungszentrum Dresden-Rossendorf varying the total dose. Profile of the implanted samples has been experimentally recovered by SIMS measurements. The change in reflectance performances of such coatings has been experimentally evaluated and modelled. The outcomes have been used to verify the potential impact on the METIS instrument and to drive the optimization of the MO mirror coating.

9604-23, Session 2

Fabrication and testing of the Daniel K. Inouye Solar Telescope polarization optics

Erika K. Petrak, Meadowlark Optics, Inc. (United States); Stacey R. Sueoka, College of Optical Sciences, The Univ. of Arizona (United States); Thomas G. Baur, Meadowlark Optics, Inc. (United States)

Monitoring solar magnetic activity is an important function of the DKIST. This will be done by measuring the Stokes parameters with high polarimetric accuracy and precision over a broad wavelength range using polarization optics built at Meadowlark Optics. Six polarization assemblies, each 120mm in diameter, will measure these complex magnetic fields over 380nm-5,000nm. These assemblies are divided into three sub-spectrum specific pairs comprised of an achromatic calibration retarder and a poly-achromatic polarization modulator.

Each assembly contains six quartz or magnesium fluoride crystal waveplates. The optics' large aperture and materials choices enable full use of the 4-meter telescope's light collection but present a fabrication challenge. We have fine-tuned processes for precisely orienting and slicing magnesium fluoride needed for infrared polarimetry, and rigorously tested coupling materials that will minimize heating of these thermally sensitive, delicate crystals under the high solar flux of the DKIST. We have also developed techniques necessary to polish the assertive crystal symmetry of magnesium fluoride to difficult aspect ratios while maintaining required optical uniformity. We have achieved retardance uniformity of +0.01 waves

Our final assembly process ensures rotational alignment of all component waveplates to + 0.3 ?with low beam deviation and transmitted wavefront distortion. To validate the polarization performance of the optical assemblies, NSO will conduct Mueller matrix measurements at a number of wavelengths using a laboratory spectro-polarimeter. With these measurements we determine the performance of the retarders as calibration and modulator optics.

9604-25, Session 2

Investigation of contamination of thinfilm aluminum filters by MMH-NTO plumes exposed to UV radiation

Vaibhav Gupta, Seth Wieman, Leonid Didkovsky, Space Sciences Ctr. (United States); Ralf Haiges, Wei Wu, Yuhan yao, Mike Gruntman, Dan Erwin, The Univ. of Southern California (United States)

Filter degradation accounts for 90% or more of the reduction in sensitivity that the EUV Spectrophotometer (ESP) onboard of the Solar Dynamics Observatory's (SDO) EUV Variability Experiment (EVE) and the Solar EUV Monitor (SEM) onboard of the Solar and Heliospheric Observatory (SOHO) have experienced in space. A possible cause for deterioration of the used thin-film Aluminum filters is contamination of their surfaces from plumes coming from periodic firing of their satellite's Monomethylhydrazine (MMH) - Nitrogen Tetroxide (NTO) thrusters. When adsorbed by the filters these contaminant molecules exposed to solar irradiance could lead to two possible compositions. First, they could get polymerized leading to a permanent hydrocarbon layer buildup on the filter's surface. Second, they could accelerate oxidation of filter's bulk Aluminum material internal to its most outer layers. To study the phenomenon we experimentally replicate contamination of such filters in a simulated environment by MMH-NTO plumes. We apply Atomic Force/Scanning Electron Microscopy and Raman/ FTIR spectroscopy to characterize the physical and chemical changes on these contaminated sample filter surfaces and their layers. We then examine the processes involved in these interactions, specifically the role the UV radiation from our lab source plays in facilitating some underlying mechanisms. In addition, we present our first analysis of the effects of additional protective layer coatings based on self-assembled fluorinated Carbon monolayers for Aluminum filters. This coverage can significantly decrease these filter's susceptibility to contamination and reduce the overall degradation of filter based EUV instruments over their mission life.

9604-30, Session 2

First sub-arcsecond spectra covering solar chromosphere to corona: results from VERIS

Samuel D. Tun Beltran, Clarence M. Korendyke, Damien Chua, U.S. Naval Research Lab. (United States); Angelos Vourlidas, Applied Physics Lab. (United States)

We present the first results from the U.S. Naval Research Laboratory's (NRL's) VEry high angular Resolution Imaging Spectrometer (VERIS), launched from the White Sands Missile Range in New Mexico on August 8, 2013. It has obtained the first ever sub-arcsecond (0.2 arcsecond/ pixel) spectrally pure images of transition region and coronal structures, directly addressing unresolved issues relating to interconnections of various temperature solar plasmas. VERIS' novel two-element, normal-incidence optical design with highly reflective EUV coatings give access to a spectral range with broad temperature range (0.03-15 MK) and density-sensitive lines emitted from the chromosphere to the corona. We discuss the instrument design, launch, and analysis of the He I (584 Å) slit-spectrum and 10x150 arcsecond image.



9604-7, Session 3

Design and modelisation of ASPIICS optics

Yvan G. Stockman, Camille Galy, Cedric Thizy, Etienne Renotte, Jean-Sébastien Servaye, Univ. de Liège (Belgium)

In the framework of development of ASPIICS (Association of Spacecraft for Polarimetric and Imaging Investigation of the Corona of the Sun), the Centre Spatial de Liege is responsible of the optical design of the coronagraph and the optics are manufactured by TOPTEC.

The particularity of this coronagraph is to have an external occulter located 150 m ahead a first imaging lens. This external occulter is re-imaged on an internal occulter. The function of this internal occulter is, as in a classical Lyot coronagraph, to block the sun light diffracted by the external Occulter and to reduce the straylight on the detector. The selection of this configuration is driven by the requirement to observe the corona as close as possible to the solar limb (i.e. 1 Rsun) without imaging the limb itself; a requirement of 1.08 Rsun is specified while 1.15 Rsun is the best performance currently reached by other space coronagraphs. The instrument is designed to have a field of view of 1.6° x 1.6° with a plate scale of 2.8 arcsec/pixel. Its performances are limited by diffraction in a 540 – 570 nm wavelength range.

This paper presents the optical design and demonstrates that the requirements are fulfilled by design and within the misalignment, manufacturing and thermo-elastic distortion errors.

9604-8, Session 3

Design status of ASPIICS, an externally occulted coronagraph for PROBA-3

Etienne Renotte, Andres Alia, Univ. de Liège (Belgium); Alessandro Bemporad, INAF - Osservatorio Astronomico di Torino (Italy); Joseph Bernier, Univ. de Liège (Belgium); Cristina Bramanti, European Space Research and Technology Ctr. (Netherlands); Steve Buckley, SensL (Ireland); Gerardo Capobianco, INAF -Osservatorio Astrofisico di Torino (Italy); Ileana Cernica, National Institute for Research and Development in Microtechnologies (Romania); Vladimir Dániel, Serenum a.s. (Czech Republic); Radoslav Darakchiev, Astri Polska Sp.z.o.o. (Poland); Marcin Darmetko, Centrum Bada? Kosmicznych Polskiej Akademii Nauk (Poland); Arnaud Debaize, François Denis, Univ. de Liège (Belgium); Richard Desselle, Univ. de Liège (Belgium); Lieve De Vos, OIP N.V. (Belgium); Adrian Dinescu, National Institute for Research and Development in Microtechnologies (Romania); Silvano Fineschi, INAF - Osservatorio Astronomico di Torino (Italy); Karl Fleury-Frenette, Univ. de Liège (Belgium); Mauro Focardi, INAF - Osservatorio Astrofisico di Arcetri (Italy); Aurélie Fumel, Univ. de Liège (Belgium); Damien Galano, European Space Research and Technology Ctr. (Netherlands); Jean-Marie Gillis, Univ. de Liège (Belgium); Tomasz Górski, Creotech Instruments S.A. (Poland); Estelle Graas, Univ. de Liège (Belgium); Rafal Graczyk, Centrum Bada? Kosmicznych Polskiej Akademii Nauk (Poland); Konrad Grochowski, N7 Mobile sp. z o.o. (Poland); Jean-Philippe A. Halain, Aline Hermans, Univ. de Liège (Belgium); Ron Howard, Institut d'Astrophysique de Paris (France); Carl Jackson, SensL (Ireland); Emmanuel Janssen, Univ. de Liège (Belgium); Hubert Kasprzyk, Astri Polska Sp.z.o.o. (Poland); Jacek Kosiec, Creotech Instruments S.A. (Poland); S. Koutchmy, U.S. Naval Research Lab. (United States); Jana Kovacicinova, Institute of Plasma Physics of the ASCR, v.v.i. (Czech Republic); Nektarios Kranitis, National and Kapodistrian Univ. of Athens (Greece); Micha? Kurowski, N7 Mobile sp. z o.o. (Poland); Micha? ?adno, Centrum Bada? Kosmicznych Polskiej Akademii Nauk (Poland); Philippe L. Lamy, Lab. d'Astrophysique de Marseille (France); Federico Landini, INAF - Osservatorio Astrofisico di Arcetri (Italy); Radek Lapá?ek, Serenum a.s. (Czech Republic); Vít Lédl, Institute of Plasma Physics of the ASCR, v.v.i. (Czech Republic); Sylvie Liebecq, Univ. de Liège (Belgium); Davide Loreggia, INAF - Osservatorio Astronomico di Torino (Italy); Brian McGarvey, SensL (Ireland); Giuseppe Massone, INAF - Osservatorio Astronomico di Torino (Italy); Radek Melich, Institute of Plasma Physics of the ASCR, v.v.i. (Czech Republic); Agnes Mestreau-Garreau, European Space Research and Technology Ctr. (Netherlands); Dominique Mollet, OIP N.V. (Belgium); ?ukasz Mosdorf, Micha? Mosdorf, N7 Mobile sp. z o.o. (Poland); Mateusz Mroczkowski, Astri Polska Sp.z.o.o. (Poland); Raluca Muller, National Institute for Research and Development in Microtechnologies (Romania); Gianalfredo Nicolini, INAF - Osservatorio Astrofisico di Torino (Italy); Bogdan Nicula, Royal Observatory of Belgium (Belgium); Kevin O'Neill, SensL (Ireland); Piotr Orlea?ski, Centrum Bada? Kosmicznych Polskiej Akademii Nauk (Poland); Marie-Catherine Palau, Astri Polska Sp.z.o.o. (Poland); Maurizio Pancrazzi. INAF - Osservatorio Astrofisico di Arcetri (Italy); Antonios Paschalis, National and Kapodistrian Univ. of Athens (Greece); Karel Pato?ka, Institute of Plasma Physics of the ASCR, v.v.i. (Czech Republic); Radek Peresty, Serenum a.s. (Czech Republic); Irina Popescu, National Institute for Research and Development in Microtechnologies (Romania); Pavel Psota, Institute of Plasma Physics of the ASCR, v.v.i. (Czech Republic); Miroslaw Rataj, Centrum Bada? Kosmicznych Polskiej Akademii Nauk (Poland); Jan Rautakoski, European Space Research and Technology Ctr. (Netherlands); Marco Romoli, Univ. degli Studi di Firenze (Italy); Roman Rybeck?, Serenum a.s., (Czech Republic); Lucas Salvador, Jean-Sébastien Servaye, Univ. de Liège (Belgium); Cornel Solomon, AE Electronics S.A. (Romania); Yvan G. Stockman, Univ. de Liège (Belgium); Arkadiusz Swat, Solaris Optics S.A. (Poland); Cédric Thizy, Michel Thome, Univ. de Liège (Belgium); Kanaris Tsinganos, National and Kapodistrian Univ. of Athens (Greece); Jim Van der Meulen, Nico Van Vooren, OIP N.V. (Belgium); Tomá? Vit, Institute of Plasma Physics of the ASCR, v.v.i. (Czech Republic); Tomasz Walczak, Alicja Zarzycka, PCO S.A. (Poland); Joe Zender, European Space Research and Technology Ctr. (Netherlands); Andrei N. Zhukov, Royal Observatory of Belgium (Belgium)

The "sonic region" of the Sun corona remains extremely difficult to observe with spatial resolution and sensitivity sufficient to understand the fine scale phenomena that govern the quiescent solar corona, as well as phenomena that lead to coronal mass ejections (CMEs), which influence space weather. Improvement on this front requires eclipse-like conditions over long observation times. The space-borne coronagraphs flown so far provided a continuous coverage of the external parts of the corona but their overocculting system did not permit to analyse the part of the white-light corona where the main coronal mass is concentrated. The proposed PROBA-3 Coronagraph System, also known as ASPIICS (Association of Spacecraft for Polarimetric and Imaging Investigation of the Corona of the Sun), with its

Conference 9604: Solar Physics and Space Weather Instrumentation VI



novel design, will be the first space coronagraph to cover the range of radial distances between 1.08 and 3 solar radii where the magnetic field plays a crucial role in the coronal dynamics, thus providing continuous observational conditions very close to those during a total solar eclipse.

PROBA-3 is first a mission devoted to the in-orbit demonstration of precise formation flying techniques and technologies for future European missions, which will fly ASPIICS as primary payload. The instrument is distributed over two satellites flying in formation (approx. 150m apart) to form a giant coronagraph capable of producing a nearly perfect eclipse allowing to observe the sun corona closer to the rim than ever before.

The coronagraph instrument is developed by a large European consortium including about 20 partners from 7 countries under the auspices of the European Space Agency. This paper is reviewing the recent improvements and design updates of the ASPIICS instrument as it is stepping into the detailed design phase.

9604-9, Session 3

The shadow positioning sensors (SPS) for formation flying metrology on-board the ESA-PROBA3 mission

Alessandro Bemporad, INAF - Osservatorio Astronomico di Torino (Italy); Gerardo Capobianco, INAF - Osservatorio Astrofisico di Torino (Italy); Silvano Fineschi, INAF - Osservatorio Astronomico di Torino (Italy); Mauro Focardi, Univ. of Florence (Italy) and INAF - Osservatorio Astrofisico di Arcetri (Italy); Federico Landini, INAF -Osservatorio Astrofisico di Arcetri (Italy); Davide Loreggia, Giuseppe Massone, INAF - Osservatorio Astronomico di Torino (Italy); Gianalfredo Nicolini, INAF - Osservatorio Astrofisico di Torino (Italy); Vladimiro Noce, INAF -Osservatorio Astrofisico di Arcetri (Italy); Maurizio Pancrazzi, Univ. of Florence (Italy); Marco Romoli, INAF - Osservatorio Astrofisico di Arcetri (Italy); Steve Buckley, Kevin O'Neill, SensL (Ireland)

PROBA3 is an ESA technology mission devoted to in-orbit demonstration of the formation flight (FF) technique, with two satellites kept at an average inter-distance by about 144 m. The ASPIIC instrument on-board PROBA3 will be the first ever space-based coronagraph working on one satellite and having the external occulter located on the second satellite, thus allowing observations of the inner solar corona with unprecedented reduction of stray light. During the observational periods, the FF configuration will be implemented: the use of Shadow Positioning Sensors (SPS) located on the Coronagraph Spacecraft (diodes measuring the penumbral light intensity on the entrance pupil plane) and the use of Occulter Position Sensor LEDs (OPSE) located on the back side of the Occulter Spacecraft. This paper will review the main instrumental requirements on the SPS needed to determine the 3-dimensional relative positioning of the two PROBA3 satellites with the high precision and frequency.

9604-10, Session 3

Formation flying metrology for the ESA-PROBA3 Mission: the shadow positioning sensors (SPS) silicon photomultipliers (SiPMs) readout electronics

Mauro Focardi, INAF - Osservatorio Astrofisico di Arcetri (Italy); Alessandro Bemporad, INAF - Osservatorio Astronomico di Torino (Italy); Steve Buckley, Kevin O'Neill, SensL (Ireland); Silvano Fineschi, INAF - Osservatorio Astronomico di Torino (Italy); Maurizio Pancrazzi, Federico Landini, Vladimiro Noce, Gerardo Capobianco, INAF -Osservatorio Astrofisico di Arcetri (Italy); Marco Romoli, Univ. degli Studi di Firenze (Italy); Davide Loreggia, Giuseppe Massone, INAF - Osservatorio Astronomico di Torino (Italy); Gianalfredo Nicolini, INAF - Osservatorio Astrofisico di Torino (Italy); Cedric Thizy, Etienne Renotte, Univ. de Liège (Belgium)

The European Space Agency is planning to launch in 2018 the PROBA3 Mission, designed to demonstrate the in-orbit formation flight (FF) attitude capability of its two satellites and to observe the inner part of the visible solar corona at the same time. The solar corona will be observed thanks to the presence on the first satellite facing the Sun of an external occulter producing an artificial eclipse of the Sun disk. The second satellite will carry on the coronagraph telescope and the digital camera system in order to perform imaging of the inner part of the corona, from 1.08 RSun up to about 3 RSun.

One of the main spacecraft devices used to control and to maintain the relative (i.e. between the two satellites) and absolute (i.e. with respect to the Sun) FF attitude is the Shadow Positioning Sensor (SPS) subsystem. It is composed of eight micro arrays of silicon photomultipliers (SiPMs) able to measure with the required sensitivity and dynamic range the penumbral light intensity on the Coronagraph entrance pupil. This paper will describe the overall SPS subsystem and its capability to satisfy the mission requirements from the light conversion process on board the silicon-based SPS devices up to the digital signal readout following both the amplification and analog to digital conversion stages.

9604-11, Session 3

Significance of the occulter diffraction for the PROBA3/ASPIICS formation flight metrology

Federico Landini, INAF - Osservatorio Astrofisico di Arcetri (Italy); Alessandro Bemporad, INAF - Osservatorio Astronomico di Torino (Italy); Mauro Focardi, INAF -Osservatorio Astrofisico di Arcetri (Italy); Silvano Fineschi, INAF - Osservatorio Astrofisico di Torino (Italy); Marco Romoli, Univ. degli Studi di Firenze (Italy); Maurizio Pancrazzi, INAF - Osservatorio Astrofisico di Arcetri (Italy); Gerardo Capobianco, Davide Loreggia, Gianalfredo Nicolini, INAF - Osservatorio Astrofisico di Torino (Italy); Giuseppe Massone, INAF - Osservatorio Astrofisico di Torino (Italy); Giuseppe Massone, INAF - Osservatorio Astrofisico di Arcetri Astrofisico di Arcetri (Italy); Cédric Thizy, Etienne Renotte, Univ. de Liège (Belgium)

 $\mathsf{PROBA3/ASPIICS}$ is a formation flight coronagraph selected by ESA and currently in phase C/D.

It is constituted by two spacecrafts (one with the occulter, diameter 142 cm, and one with the telescope) separated by 144 m, kept in strict alignment by means of an active custom system. The alignment active system most critical components are the Shadow Positioning Sensors (SPS), a series of Si-PM (Silicon Photomultiplier) disposed around the telescope entrance aperture and measuring the pen-umbra generated by the occulter. The position of the SPSs is defined as a trade-off between mechanical constraints and maximum sensitivity to misalignments.

The diffraction generated by the occulter on the plane of the SPSs is not negligible respect to the pen-umbra intensity, and is mandatory to carefully evaluate its impact in order to refine the active alignment adjustment algorithm.

This work is dedicated to the description of the dedicated investigation that has been performed in order to evaluate the impact of the diffraction on the signal detected by the SPSs.



9604-13, Session 4

The extreme UV imager telescope onboard the Solar Orbiter Mission: overview of phase C and D

Jean-Philippe A. Halain, Pierre L. Rochus, Etienne Renotte, Aline Hermans, Lionel Jacques, Univ. de Liège (Belgium); Frédéric Auchère, Institut d'Astrophysique Spatiale (France); David Berghmans, Royal Observatory of Belgium (Belgium); Louise K. Harra, Mullard Space Science Lab. (United Kingdom); Udo H. Schühle, Max-Planck-Institut für Sonnensystemforschung (Germany); Werner K. Schmutz, Physikalisch-Meteorologisches Observatorium Davos (Switzerland); Andrei N. Zhukov, Royal Observatory of Belgium (Belgium); Regina Aznar Cuadrado, Max-Planck-Institut für Sonnensystemforschung (Germany); Franck Delmotte, Institut d'Optique Graduate School (France); Cydalise Dumesnil, Institut d'Astrophysique Spatiale (France); Manfred Gyo, Physikalisch-Meteorologisches Observatorium Davos (Switzerland); Thomas E. Kennedy, Philip J. Smith, Jason A. Tandy, Mullard Space Science Lab. (United Kingdom); Raymond F. Mercier, Institut d'Optique Graduate School (France); Francis Verbeeck, Royal Observatory of Belgium (Belgium)

The Solar Orbiter mission is composed of ten scientific instruments dedicated to the observation of the Sun's atmosphere and its heliosphere, taking advantage of an out-of ecliptic orbit and at perihelion reaching a proximity close to 0.28 A.U.

On board Solar Orbiter, the Extreme Ultraviolet Imager (EUI) will provide full-Sun image sequences of the solar corona in the extreme ultraviolet (17.1 nm and 30.4 nm), and high-resolution image sequences of the solar disk in the extreme ultraviolet (17.1 nm) and in the vacuum ultraviolet (121.6 nm).

The EUI concept uses heritage from previous similar extreme ultraviolet instrument. Additional constraints from the specific orbit (thermal and radiation environment, limited telemetry download) however required dedicated technologies to achieve the scientific objectives of the mission. We report on the development of CMOS-APS detectors, high reflectivity mirror coatings, heat pipe and highly efficient heat-rejection entrance baffles, data compression and prioritization, and re-closable door mechanisms.

The development phase C of the instrument and its sub-systems has been successfully completed, including thermo-mechanical and electrical design validations with the Structural Thermal Model (STM) and the Engineering Model (EM).

The instrument STM and EM units have been integrated on the respective spacecraft models and will undergo the system level tests. In parallel, the Phase D has been started with the sub-system qualifications and the flight part manufacturing.

The next step of the EUI development will be the instrument Qualification Model (QM) integration and qualification tests. The Flight Model (FM) instrument activities will then follow with the acceptance tests and calibration campaigns.

9604-14, Session 4

The extreme ultraviolet imager of solar orbiter: optical design and alignment scheme

Jean-Philippe A. Halain, Alexandra Mazzoli, Univ. de Liège (Belgium); Stefan Meining, Max-Planck-Institut für Sonnensystemforschung (Germany); Pierre L. Rochus, Etienne Renotte, Univ. de Liège (Belgium); Frédéric Auchère, Institut d'Astrophysique Spatiale (France); Udo H. Schühle, Max-Planck-Institut für Sonnensystemforschung (Germany); Franck Delmotte, Institut d'Optique Graduate School (France); Anne Philippon, Institut d'Astrophysique Spatiale (France); Raymond F. Mercier, Institut d'Optique Graduate School (France); Aline Hermans, Univ. de Liège (Belgium)

The Extreme Ultraviolet Imager (EUI) is one of the remote sensing instruments on-board the Solar Orbiter mission. It will provide dual-band full-Sun images of the solar corona in the extreme ultraviolet (17.1 nm and 30.4 nm), and high-resolution images of the solar disk in both extreme ultraviolet (17.1 nm) and vacuum ultraviolet (Lyman-alpha 121.6 nm).

The EUI optical design takes heritage of previous similar instruments. The Full Sun Imager (FSI) channel is a single-mirror Herschel design telescope. The two High Resolution Imager (HRI) channels are based on a two-mirror optical refractive scheme, one Ritchey-Chretien and one Gregory optical design for the EUV and the Lyman-alpha channels, respectively.

The spectral performances of the EUI channels are obtained thanks to dedicated mirror multilayer coatings and specific band-pass filters. The FSI channel uses a dual-band mirror coating combined with aluminum and zirconium band-pass filters. The HRI channels use optimized band-pass selection mirror coatings combined with aluminum band-pass filters and narrow band interference filters for Lyman-alpha.

The optical performances result from accurate mirror manufacturing tolerances and from a two-step alignment procedure. The primary mirrors are first co-aligned. The HRI secondary mirrors and focal planes positions are then adjusted to have an optimum interferometric cavity in each of these two channels. For that purpose a dedicated alignment test setup has been prepared, composed of a dummy focal plane assembly representing the detector position.

Before the alignment on the flight optical bench, the overall alignment method has been validated on a dummy bench using flight spare optics that then be aligned on the Qualification Model to be used for the system verification test and qualifications.

9604-15, Session 4

Off-pointing stray light effects analysis on solar orbiter/METIS coronagraph

Marco Romoli, Univ. degli Studi di Firenze (Italy); Federico Landini, INAF - Osservatorio Astrofisico di Arcetri (Italy); Silvano Fineschi, Ester Antonucci, INAF - Osservatorio Astronomico di Torino (Italy); John D. Moses, U.S. Naval Research Lab. (United States); Mauro Focardi, Maurizio Pancrazzi, INAF - Osservatorio Astrofisico di Arcetri (Italy); Giampiero Naletto, Univ. degli Studi di Padova (Italy); Gianalfredo Nicolini, INAF - Osservatorio Astrofisico di Torino (Italy); Daniele Spadaro, INAF - Osservatorio Astrofisico di Catania (Italy); Vincenzo Andretta, INAF -Osservatorio Astronomico di Capodimonte (Italy)

The METIS coronagraph will provide a measurement of the linear polarization of the visible corona and imaging in the Ly-a HI 121.6 nm line. Furthermore, being the only instrument to provide full imaging of the solar corona, METIS will constitute a context reference for the whole mission. Coronagraphs are designed to operate Sun center pointed and, given Solar Orbiter limited mass and power budget, METIS cannot be equipped with a re-pointing mechanism. Therefore, the spacecraft off-pointings may have an impact on the instrument performance, ranging from a slight disturbance in the stray light pattern up to a complete observation inability.

A comprehensive analysis has been conducted on the impact of offpointings on the METIS performance. After the definition of the tolerable off-pointing ranges for METIS and their influence on the instrument performance, an experimental activity was conducted on a METIS prototype in order to understand the dependence of the stray light pattern change on the off-pointing conditions.



9604-16, Session 4

Dependence of the polarimetric efficiencies of a polarization modulator based on liquid crystal variable retarder on angle of incidence for the solar orbiter mission

Pilar García Parejo, Alberto Alvarez-Herrero, INTA Instituto Nacional de Técnica Aeroespacial (Spain)

Liquid Crystals Variable Retarders used as light polarization modulators in ground-based polarimeters and ellipsometers is a well-known and mature technology. In aerospace applications, they present many advantages with respect to the traditional rotatory retardance plates, as they avoid the use of mechanisms and present low mass and low power consumption. LCVRs will be used in the polarization modulation packages of the instruments SO/PHI (Polarimetric and Helioseismic Imager) and METIS/COR (Multi Element Telescope for Imaging and Spectroscopy, Coronagraph) for the Solar Orbiter Mission of ESA. Coronagraphs are characterized by having wide field-of-views (FOV) compared to instruments designed to study solar magnetic structures which involves large incidence angles through the entire instrument. Specifically, the METIS polarization modulation package will have to work with collimated rays and angles of incidence up to ±7.0 deg. Polarization optics, in particular retarders, are sensitive to the angle of incidence as their retardance changes with the incident angle. Since the retardances during the polarization modulations are optimized for a particular angle of incidence, other angles reduce the signal-to-noise ratio of the instrument and therefore the polarimetric sensitivity. For this reason, a configuration of double-cell has been selected for the METIS polarization modulator allowing wide acceptance angles. In this work, the demodulation efficiencies of the METIS polarization modulation package based on LCVRs have been measured at the incident angles of METIS coronagraph in order to quantify the polarimetric efficiencies across the Field of View and hence the polarimetric sensitivity as result of using different angles of incidence.

9604-27, Session 4

Polarimetric visible-light imaging with the METIS coronagraph on solar orbiter

Silvano Fineschi, INAF - Osservatorio Astronomico di Torino (Italy); Gerardo Capobianco, INAF - Osservatorio Astrofisico di Torino (Italy); Matteo Marmonti, Optec S.p.A. (Italy); Paolo Sandri, CGS S.p.A. (Italy); Ester Antonucci, INAF - Osservatorio Astronomico di Torino (Italy); Marco Romoli, Univ. degli Studi di Firenze (Italy); Giampiero Naletto, Univ. degli Studi di Padova (Italy); Daniele Spadaro, INAF - Osservatorio Astrofisico di Catania (Italy)

The METIS coronagraph onboard the Solar Orbiter mission will have the unique opportunity of observing the solar outer atmosphere as close to the Sun as 0.3 A.U., and from up to 35? out-of-ecliptic. The telescope design of the METIS coronagraph includes two optical paths for i) broad-band imaging of the full corona in linearly polarized visible-light (VL: 580-640 nm); ii) narrow-band imaging of the full corona in the ultraviolet (UV) Lyman ? (121.6 nm).

The original METIS optical design departs from the classical optical design for visible-light, solar coronagraphs by combining an all-reflective telescope for both UV and VL imaging, and an inverted external occultation for minimizing the Sun-disk thermal load.

This presentation describes the optical design of the imaging polarimeter for the METIS VL paths. The linearly polarized brightness (pB) images of the K-corona are used to derive the density distribution of the coronal electrons. The pB modulation is performed with an electro-optic polarimeter based on liquid crystals. The requirements on the polarization sensitivity, and instrumental polarization control are described. The expected performances of the VL path are also presented.

9604-29, Session 4

Stray-light analyses of the METIS coronagraph on solar orbiter

Paolo Sandri, CGS S.p.A. (Italy); Silvano Fineschi, INAF -Osservatorio Astronomico di Torino (Italy); Marco Romoli, Univ. degli Studi di Firenze (Italy); Federico Landini, INAF -Osservatorio Astrofisico di Arcetri (Italy); Vania Da Deppo, IFN-CNR LUXOR Lab. (Italy); Fabio Frassetto, CNR-IFN UoS Padova (Italy); Giampiero Naletto, Univ. degli Studi di Padova (Italy); D. Moreau, CGS S.p.A. (Italy); Ester Antonucci, INAF - Osservatorio Astronomico di Torino (Italy); Daniele Spadaro, INAF - Osservatorio Astrofisico di Catania (Italy); Vincenzo Andretta, INAF - Osservatorio Astronomico di Capodimonte (Italy)

The METIS coronagraph on board the Solar Orbiter mission will have the unique opportunity of observing the solar outer atmosphere as close to the Sun as 0.28 A.U., and from up to 35? out-of-ecliptic. The telescope design of the METIS coronagraph includes two optical paths for i) broad-band imaging of the full corona in linearly polarized visible-light (VL: 580-640 nm); ii) narrow-band imaging of the full corona in the ultraviolet (UV) Lyman ? (121.6 nm).

The original METIS optical design departs from the classical optical design for visible-light, solar coronagraphs by combining an all-reflective telescope for both UV and VL imaging, and an inverted external occultation for minimizing the Sun-disk thermal load.

This presentation describes the stray-light analysis performed on the UV and VL channels of the METIS Telescope with the non-sequential modality of the software Zemax. A detailed opto-mechanical model of the METIS Telescope is simulated by placing the CAD parts of all the sub-assemblies, including the UV photocathode with its protective window, at the nominal position. Each surface, mechanical and optical, is provided with a property of reflection and/or transmission, absorption and scattering. The values inserted in the model reproduce the optical and the diffusing properties measured on representative samples.

The model allows for the verification of the correct functioning of the blocking elements inside the telescope. These elements are the baffle at the Shield Entrance Aperture (SEA), the Sun-disk light rejection mirror (MO=, the Lyot Stop, the Field Stop, the Internal Occulter and the annular diaphragm of the Collimating Doublet of the Polarimeter. These elements are in the most critical positions for the generation of diffuse light, with the Sun simulated at the distance of 0.28 AU from the instrument. The model allows also for an evaluation of the stray-light level on the sensitive area of the VL detector and of the UV detector. The results of the simulations are compared to the requirements of stray-light levels.

A simple model for including the effects of the diffraction off the inner edge of the IEO on the plane of the IO is also presented. In spite of the limitation to few millions of rays in the standard ray-tracing simulation, the model allows for an useful insight in the expected performances of the instrument. The results of this analysis compare well with those performed also with the ASAP optical software.

9604-18, Session 5

New scheme of international task shares of the Solar-C Mission

Tetsuya Watanabe, National Astronomical Observatory of Japan (Japan); Kiyoshi Ichimoto, Kyoto Univ. Hida Observatory (Japan); Kanya Kusano, Nagoya Univ. (Japan); Toshifumi Shimizu, Japan Aerospace Exploration Agency (Japan); Hirohisa Hara, National Astronomical Observatory of Japan (Japan); Taro Sakao, Japan Aerospace Exploration Agency (Japan); Yoshinori Suematsu, Yukio Katsukawa, National Astronomical Observatory of Japan

Conference 9604: Solar Physics and Space Weather Instrumentation VI



(Japan); Keisuke Yoshihara, Japan Aerospace Exploration Agency (Japan)

Solar-C is a Japanese-led international solar observing mission designed to answer some of the most important questions in solar physics. Recent progress achieved by space missions like Hinode has revealed that the different parts of the magnetized solar atmosphere are essentially coupled and has defined the spatial scales and temperature regimes that need to be observed in order to achieve a comprehensive physical understanding of this coupling. Solar-C will have on board a carefully coordinated suite of three major complementary instruments: the Solar Ultra-violet Visible and IR Telescope (SUVIT), accommodating three focal plane instruments; Spectropolarimeter (SP), Filtergraph (FG), and UV-Blue Imaging Spectrometer (UBIS), the High-throughput EUV Spectroscopic Telescope (EUVST) with an Irradiance Monitor, and a High-resolution Coronal Imager (HCI). The science of Solar-C will greatly advance our understanding of the Sun, of basic physical processes operating throughout the universe, and of how the Sun influences the Earth and other planets in our solar system.

9604-19, Session 5

Magnetic activity of the solar corona (MASC)

Frédéric Auchère, Institut d'Astrophysique Spatiale (France); Hui Li, Purple Mountain Observatory (China)

MASC is designed to answer the following top-level scientific questions: 1. What is the global magnetic field configuration in the corona?

 What is the role of the magnetic field in the triggering of flares and CMEs?
 What is the role of the magnetic field in the acceleration mechanisms of the solar winds?

4. What is the energy spectrum and in particular what are the highest energies to which charged particles can be accelerated in the solar corona?

MASC will address these fundamental questions with a suite of instruments composed of an X-ray spectrometer, a UV / EUV imager, and a coronagraph working in the visible and at Lyman alpha. The spectrometer will provide information on the energetics of solar flares, in particular at very high energies of accelerated particles. The UV / EUV imager will provide constraints on the temperature of the flaring and non-flaring corona. The coronagraph will provide the number density of free electrons in the corona, maps of the outflow velocity of neutral hydrogen, and measurements will be performed at all steps of the flare-CME processes, thus providing a detailed picture of the solar coronal dynamics in the quiet and eruptive periods.

9604-20, Session 5

Coronal and heliospheric imagers for solar wind phenomena

Kevin F. Middleton, Jackie A. Davies, Chris J. Eyles, Doug K. Griffin, Richard A. Harrison, S. James Tappin, Ian A. J. Tosh, Nick R. Waltham, STFC Rutherford Appleton Lab. (United Kingdom)

RAL Space is enhancing its programme to lead the development of European capabilities in visible-light coronal and heliospheric imaging instrumentation in the light of emerging opportunities such as the European Space Agency's Space Situational Awareness programme and S2 smallmission call. Visible-light coronal and heliospheric imaging of solar wind phenomena, such as coronal mass ejections and interaction regions, is of critical importance to space weather, both operationally and in terms of enabling the underpinning science. This work draws on heritage from scientific instruments such as LASCO (Large Angle and Spectrometric Coronagraph) on the SOHO spacecraft, the SMEI (Solar Mass Ejection Imager) on the Coriolis spacecraft and the HI (Heliospheric Imager) instruments on STEREO. Observation of solar wind structures relies on the detection of sunlight that has been Thomson-scattered from electrons (the so-called K-corona). The Thomson-scattered signal must be extracted from other signals that can be many orders of magnitude greater (such as that from the F-corona and the solar disc itself) and this places stringent constraints on stray-light rejection, as well as pointing stability and accuracy. We discuss the determination of instrument requirements, key design tradeoffs and the evolution of base-line designs for the coronal and heliospheric regimes. We explain how the next generation of instruments will build on this heritage while also, in some cases, meeting the challenges on resources imposed on operational space weather imagers. In particular, we discuss the optical engineering challenges involved in the design of these instruments.

9604-21, Session 5

ASO-S: advanced space-based solar observatory

Weiqun Gan, Purple Mountain Observatory (China)

ASO-S is the mission proposed for the next solar maximum by the Chinese solar community. The scientific objectives are to study the relationships among solar magnetic field, solar flares, and coronal mass ejections. ASO-S is now undertaking the phase-B study. The talk will give a brief introduction of the mission.

9604-22, Session 5

The Bragg solar x-ray spectrometer SolpeX

Daniel ?cis?owski, Janusz Sylwester, Stefan P?ocieniak, Jaros?aw B?ka?a, ?aneta Szaforz, Marek St??licki, Miros?aw Kowali?ski, Piotr Podgórski, Jose Hernandez, Witold Trzebi?ski, Space Research Ctr. (Poland); Sergey V. Kuzin, Sergey V. Shestov, P.N. Lebedev Physical Institute (Russian Federation)

Detection of polarization and spectra of X-ray solar flare emission are indispensable in improving our understanding of the processes releasing energy of these most energetic phenomena in the solar system. We shall present some details of the construction of SolpeX - an innovative Bragg soft X-ray flare polarimeter and spectrometer. The instrument is a part of KORTES – Russian instrument complex to be mounted aboard the science module to be attached to the International Space Station (2017/2018).

The SolpeX will be composed of three individual measuring units: the soft X-ray polarimeter with 1-2% linear polarization detection threshold, a fast-rotating flat crystal X-ray spectrometer with a very high time resolution (0.1s) and a simple pin-hole soft X-ray imager-spectrometer with a moderate spatial (-20arcsec), spectral (0.5 keV) and high time resolution (0.1s). Having a fast rotating unit to be served with power, telemetry and "intelligence" poses a challenge for the designer. Some of the solutions to this challenge will be provided and described.

9604-24, Session 5

EUV multilayer coatings for solar imaging and spectroscopy

David L. Windt, Reflective X-Ray Optics LLC (United States)

Nanometer-scale multilayer coatings that provide high reflectance at normal incidence in the EUV have proven extremely valuable to current spacebased solar research targeting this scientifically-important spectral region. EUV multilayers now constitute an essential, mission-enabling technology that is widely used for both imaging and spectroscopy. Multilayer-based instruments have been used in a number of major satellite instruments over the past two decades, and have flown in numerous sounding rocket experiments as well.

Conference 9604: Solar Physics and Space Weather Instrumentation VI

To successfully address the unresolved physics underlying coronal activity, future solar missions targeting the EUV that are now being formulated will require even higher spatial resolution and better signal-to-noise than has been achieved thus far in any satellite instrument, while supporting the exposure times and cadences necessary to capture the evolution of flares, jets, CMEs and other dynamic processes in the solar atmosphere. To meet these science requirements, new multilayer coatings will be needed that have higher reflectance, and either better spectral selectivity for narrow-band imaging, or broad spectral response for spectroscopy.

I will describe recent progress, and future prospects, in the development of new EUV multilayer coatings for solar physics. Specifically, I will describe the development of a variety of new high-performance multilayers for narrowband EUV imaging, as well as the development of aperiodic multilayer coatings that can provide broad spectral response at normal incidence for EUV spectroscopy.

9604-26, Session 5

Hydrogen Lyman-alpha polarimeter for SCORE

Silvano Fineschi, INAF - Osservatorio Astronomico di Torino (Italy); John D. Moses, U.S. Naval Research Lab. (United States); Juan Ignacio Larruquert, Instituto de Óptica "Daza de Valdés" (Spain)

The linear polarization by resonance scattering of coronal permitted lineemission in the ultraviolet (UV) can be modified by magnetic fields through the Hanle effect. Space-based UV spectro-polarimeters would provide an additional tool for the diagnostics of coronal magnetism. As a case study of space-borne UV spectro-polarimeters, this presentation will describe the future upgrade of the Sounding-rocket Coronagraphic Experiment (SCORE) to include the capability of imaging polarimetry of the HI Lyman-?, 121.6 nm. SCORE is a multi-wavelength imager for the emission-lines, Hell 30.4 nm and HI 121.6 nm, and visible-light broad-band emission of the polarized K-corona.

SCORE has flown successfully in 2009. This presentation will describe how in future reflights SCORE could observe the expected Hanle effect in corona with a HI Lyman-? polarimeter. This UV polarimeter comprises a novel transmissive analyser with a narrow-band UV polarization coating. The polarization modulation is achieved by mechanically rotating a MgF2 half-wave plate.

9604-28, Session 5

Waves and magnetism in the solar atmosphere (WAMIS)

John D. Moses, Yuan-Kuen Ko, J. Martin Laming, Leonard Strachan, U.S. Naval Research Lab. (United States); Steven Tomczyk, National Ctr. for Atmospheric Research (United States); Frédéric Auchère, Institut d'Astrophysique Spatiale (France); Roberto Casini, National Ctr. for Atmospheric Research (United States); Silvano Fineschi, INAF - Osservatorio Astronomico di Torino (Italy); Sarah E. Gibson, Michael Knoelker, National Ctr. for Atmospheric Research (United States); Clarence M. Korendyke, U.S. Naval Research Lab. (United States); Scott McIntosh, National Ctr. for Atmospheric Research (United States); Marco Romoli, Univ. degli Studi di Firenze (Italy); Jan Rybak, Astronomical Institute (Slovakia); Dennis George Socker, U.S. Naval Research Lab. (United States); Angelos Vourlidas, Johns Hopkins Univ. (United States); Qian Wu, National Ctr. for Atmospheric Research (United States)

Since the advent of SOHO followed by TRACE and SDO, the solar

atmosphere has come to be appreciated as an increasingly dynamic and complex environment. Waves play a much larger role in shaping the plasma properties than hitherto assumed and can have non-negligible energy densities compared to the thermal gas in the low ??corona. Various oscillation modes of coronal loops have been identified in observations. Compressive waves connected to slow mode or fast mode waves, or their analogs in non-homogeneous media, have been readily detected, but the non-compressive Alfvén wave has proven more elusive. Even so, the realization that Alfvén or fast mode (collectively referred to as 'Alfvénic') waves are ubiquitous in the solar upper atmosphere signifies an important new development with profound consequences for our understanding of the corona and solar wind. Comprehensive measurements of magnetic fields in the solar corona have a longer history as an important scientific goal. Besides being crucial to understanding and predicting the Sun's generation of space weather, direct measurement of its strength and direction is also a crucial step in understanding observed wave motions. In this regard, the remote sensing instrumentation used to make magnetic field measurements is well suited to measuring the Doppler signature of waves in the solar structures. In this paper, we describe the design and scientific values of the WAMIS (Waves and Magnetism in the Solar Atmosphere) investigation. WAMIS, taking advantage of greatly improved infrared (IR) detectors, forward models, advanced diagnostic tools and inversion codes, is a longduration high-altitude balloon payload designed to obtain a breakthrough in the measurement of coronal magnetic fields and in the understanding of the interaction of these fields with space plasmas. It consists of a 20 cm aperture coronagraph with an IR spectro-polarimeter focal plane assembly. The balloon altitude will provide minimum atmospheric absorption and scattering at the IR wavelengths in which these observations are made. WAMIS will obtain continuous measurements over at least two weeks of the strength and direction of coronal magnetic fields. These measurements will be made over a large field-of-view and at the spatial and temporal resolutions required to address several outstanding problems in coronal physics. Additionally, WAMIS will obtain near simultaneous observations of the electron scattered K-corona for context and to establish electron density. These comprehensive observations are not provided by any current single ground-based or space observatory.

SPIE. PHOTONICS

OPTICAL ENGINEERING+

APPLICATIONS

9604-12, Session PMon

OPSE metrology system onboard of the PROBA3 mission of ESA

Davide Loreggia, Alessandro Bemporad, INAF -Osservatorio Astronomico di Torino (Italy); Gerardo Capobianco, Silvano Fineschi, INAF - Osservatorio Astrofisico di Torino (Italy); Mauro Focardi, Federico Landini, INAF - Osservatorio Astrofisico di Arcetri (Italy); Giuseppe Massone, Gianalfredo Nicolini, INAF - Osservatorio Astrofisico di Torino (Italy); Maurizio Pancrazi, INAF - Osservatorio Astrofisico di Arcetri (Italy); Marco Romoli, INAF - Osservatorio Astrofisico di Arcetri (Italy); Marco Romoli, INAF - Osservatorio Astronomico di Arcetri (Italy); Ileana Cernica, Munizer G. Purica, Elena Budianu, National Institute for Research and Development in Microtechnologies (Romania); Cedric Thizy, Etienne Renotte, Jean-Sébastien Servaye, CSL - Centre Spatial de Liège (Belgium)

In recent years, ESA has assessed several mission involving formation flying (FF). The great interest in this topic is mainly driven by the need for moving from ground to space the location of next generation astronomical telescopes overcoming most of the critical problems, as example the construction of huge baselines for interferometry. In this scenario, metrology systems play a critical role. PROBA3 is an ESA technology mission devoted to in-orbit demonstration of the FF technique, with two satellites, an occulter and a main satellite housing a coronagraph named ASPIICS, kept at an average inter-distance by about 144m, with micron scale accuracy. The guiding proposal is to test several metrology solution for spacecraft alignment, with the important scientific return of having observation of Corona at never reached before angular field. The Shadow Position Sensors (SPS), and the Optical Position Emitters Sensors (OPSE)



are two of the systems used for FF fine tracking. The SPS are finalized to monitor the position of the two spacecraft with respect to the Sun and are discussed in dedicated papers presented in this conference. The OPSE will monitor the relative position of the two satellites and consists of 3 emitters positioned on the rear surface of the occulter, that will be observed by the coronagraph itself. By following the evolution of the emitters images at the focal plane the alignment of the two spacecrafts is retrieved via dedicated centroiding algoritm. We present an overview of the OPSE system and of the centroiding approach.

Monday - Thursday 10-13 August 2015

Part of Proceedings of SPIE Vol. 9605 Techniques and Instrumentation for Detection of Exoplanets VII

9605-60, Session PMon

Fluoride fiber thermal emission study for SPIRou @ CFHT

Yoan Micheau, Marc Bouyé, Observatoire Midi-Pyrénées (France); Jérôme Parisot, Observatoire de Paris à Meudon (France); Driss Kouach, Observatoire Midi-Pyrénées (France)

SPIRou is a near-IR (0.98-2.35?m), echelle spectropolarimeter / high precision velocimeter being designed as a next-generation instrument for the 3.6m Canada-France-Hawaii Telescope on Mauna Kea, Hawaii, with the main goal of detecting Earth-like planets around low mass stars and magnetic fields of forming stars.

The SPIRou science fiber, which connects the polarimeter unit to the cryogenic spectrograph unit (35 meter apart), emits an undesirable thermal flux into the spectrograph, due to its intrinsic absorption.

This may degrade the signal to noise ratio and then the sensitivity of the instrument for the reddest wavelengths.

For verifying the calculation model used to predict the thermal emission from the SPIRou science fiber, a test bench is set-up at LESIA (Observatory of Paris).

In this paper, we described the experimental approach to measure the thermal emission from a 30 meter long fluoride fiber $@3\mu$ m. Experimental results are then compared to those predicted by the theoretical model.

9605-61, Session PMon

A new fiber slit assembly for the foces spectrograph

Hanna Kellermann, Univ.-Sternwarte München (Germany); Frank U. Grupp, Univ.-Sternwarte München (Germany) and Max-Planck-Institut für extraterrestrische Physik (Germany); Christian Franik, Univ.-Sternwarte München (Germany); Anna Brucalassi, Max-Planck-Institut für extraterrestrische Physik (Germany); Florian Lang-Bardl, Ulrich Hopp, Univ.-Sternwarte München (Germany); Ralf Bender, Max-Planck-Institut für extraterrestrische Physik (Germany)

The R=70000 Echelle spectrograph at Wendelstein observatory will be equipped with a multi fibre slit allowing simultaneous calibration utilizing a Laser Frequency Comb as wavelength normal. The slit assembly consists of two multi-mode and two sigle-mode fibres. We will present fibre scrambling and optical image quality of the slit assembly. The four fibres will allow to test the spectrograph in the normal astronomical working condition with multi mode fibre coupling, and at the same time allow to test without fibre modal noise in the mono-mode configuration. As fibre modal noise is one of the dominant sources of insecurity in high precision radial velocity and planet detection spectroscopy the availability of mono-mode fibres allows to test the hardware chain in absence of modal noise.

9605-62, Session PMon

The replicable high-resolution exoplanet and asteroseismology (RHEA) spectrograph

Tobias Feger, Macquarie Univ. (Australia); Alexander Arriola Martiarena, Macquarie Univ. (Australia) and Ctr. for Ultrahigh Bandwidth Devices for Optical Systems (Australia); Izabela Spaleniak, Heriot-Watt Univ. (United Kingdom); Simon Gross, Macquarie Univ. (Australia) and Ctr. for Ultrahigh Bandwidth Devices for Optical Systems (Australia); Michael Ireland, The Australian National Univ. (Australia); David W. Coutts, Macquarie Univ. (Australia); Christian Schwab, Macquarie Univ. (Australia) and Australian Astronomical Observatory (Australia); Joao Bento, Macquarie Univ. (Australia)

SPIE. PHOTONICS

OPTICAL ENGINEERING+

APPLICATIONS

RHEA is a compact single-mode spectrograph, designed to be used at modern-sized 0.2-1m class robotic telescopes, where long-term dedicated projects are feasible. The instrument will be primarily used for accurate radial velocity (RV) studies of low to intermediate-mass giant stars for the purpose of searching for hot Jupiters and using asteroseismology to simultaneously measure the host star parameters and de-correlate stellar pulsations. RHEA comprises a near-Littrow configuration and is mainly composed from off-the-shelf items with the aim of creating an inexpensive and replicable unit. The echelle format covers 47 spectral orders, spanning a wavelength range of 430-670 nm with minimum order separation of ?180 ?m. This separation allows the integration of a photonic lantern (PL) that converts incoherent light from a few-mode fiber into a series of 6 isolated diffraction-limited outputs. The PL chip eliminates modal noise and forms the entrance slit of the spectrograph. This enables an efficient and inherently stable instrument that Nyquist samples the line-spread function (LSF). In this paper we present a brief characterization of the laser-inscribed PL chip followed by results from on-sky testing at the Macquarie University Observatory.

9605-63, Session PMon

A white super-stable source for the metrology of astronomical photometers

François Wildi, Adrien Deline, Bruno Chazelas, Observatoire de Genève (Switzerland)

In the frame of the CHEOPS photometric transits mission, a calibration system has been developed that will allow measuring the absolute stability of the payload to a few ppm. One key element of this system is a white light source that is extremely accurately stabilized in flux.

This patent pending novel device is a very versatile building block that has applications in the characterization of all kind of photometers but is especially useful to test the performance of astronomical instruments dedicated to the photometric transit search. This paper addresses the design, the operation and the measured performance of this super-stable source.

9605-64, Session PMon

Design of the iLocater acquisition camera for the LBT

Andrew Bechter, Jonathan Crass, Ryan Ketterer, Justin R. Crepp, Univ. of Notre Dame (United States); David M. P. King, Univ. of Cambridge (United Kingdom); Robert O. Reynolds, Phil M. Hinz, The Univ. of Arizona (United States); Jack Brooks, Eric Bechter, Univ. of Notre Dame (United States); Bo Zhao, Univ. of Florida (United States); Christopher Matthews, Univ. of Notre Dame (United States)

Existing radial velocity instruments for planet detection are limited by



systematic errors resulting from their seeing-limited design. iLocater is an ultra-precise spectrometer that operates at the diffraction limit. Officially approved for installation at the Large Binocular Telescope, iLocater will search for Earth-like planets orbiting the nearest stars. We present the optical and mechanical design for iLocater's acquisition camera, which uses separate adaptive optics systems from two 8.4m telescopes to feed starlight into single mode fibers.

9605-65, Session PMon

Numerically designed phase-mask for stellar coronagraph

Naoshi Baba, Naoshi Murakami, Hokkaido Univ. (Japan); Noriaki Miura, Kitami Institute of Technology (Japan); Motohide Tamura, The Univ. of Tokyo (Japan)

Phase-mask coronagraph holds the ability to detect exoplanets at a distance of around 1 lambda/D from their parent star. Phase masks like a four-quadrant, an eight-octant, and a vortex types are shown to completely extinguish starlight for circular aperture telescopes. The problem here is that ordinary telescopes do not have perfect circular apertures but shades of a secondary mirror and spiders. It is known that shades of a secondary mirror and spiders. It is known that shades of a secondary mirror and spiders. The problem here is the deterioration. There have been proposed several ideas to overcome the deterioration. A pupil-remapping optical element is used to convert a secondary mirror obscured aperture to a clear circular one. A multistage vortex coronagraph is proposed to reduce the deterioration. Apodization to an entrance pupil has been shown effective to avoid the deterioration. However, these ideas are based on using theoretically established phasemasks.

We report a new kind of phase mask that performs the contrast ratio of more than the tenth power of 10 for a circular aperture with shades of a secondary mirror and spiders. The phase distribution of the phase mask is numerically obtained by letting the leaked light outside the transparent part of the pupil. The Lyot filter employed here is the same shape of the entrance pupil without any margin. We applied the hybrid input-output algorithm, one of phase retrieval methods, to find the phase distribution of the phase mask. We show the characteristics of thus obtained phase mask.

9605-66, Session PMon

Sparse aperture mask for low order wavefront sensing

Hari Subedi, Neil T. Zimmerman, N. Jeremy Kasdin, A. J. E. Riggs, Princeton Univ. (United States); Kathleen Cavanagh, SciTec, Inc. (United States)

A high contrast is required for direct imaging of exoplanets. Ideally, the level of contrast required for direct imaging of exoplanets can be achieved by coronagraphic imaging, but in practice, the contrast is degraded by wavefront aberrations. To achieve the required contrast, low-order wavefront aberrations such as tip-tilt, defocus and coma must be determined and corrected. In this paper, we present a technique that integrates a sparseaperture mask (SAM) with a shaped pupil coronagraph (SPC) to make precise estimations of these low-order aberrations. Starlight rejected by the coronagraph's focal plane stop is collimated to a relay pupil, where the mask forms an interference fringe pattern on a detector. Using numerical simulations, we show that the SAM with optimized parameters: number of sub apertures, their radii and location can estimate rapidly varying tip-tilt errors in space telescopes arising from line-of-sight pointing oscillations as well as other higher order modes. At Princeton's High Contrast Imaging Laboratory, we have recently created a testbed devoted to low-order wavefront sensing experiments. The testbed incorporates custom-fabricated masks (shaped pupil, focal plane, and sparse aperture) with a deformable mirror and a CCD camera to demonstrate the estimation and correction of low-order aberrations. Our first experiments aim to replicate the results of the SAM WFS Fourier propagation models.

9605-67, Session PMon

Coronagraphic image analysis for tiptilt retrieval applied to the vector vortex phase mask

Elsa Huby, Univ. de Liège (Belgium); Pierre Baudoz, Observatoire de Paris (France); Olivier Absil, Univ. de Liège (Belgium); Dimitri Mawet, California Institute of Technology (United States) and European Southern Observatory (Chile); Aïssa Jolivet, Univ. de Liège (Belgium); Garreth J. Ruane, Rochester Institute of Technology (United States); Brunella Carlomagno, Pierre Piron, Jean Surdej, Univ. de Liège (Belgium)

Small inner-working angle coronagraphs (1 to 4 lambda/D), such as the vector vortex phase mask, are very sensitive to low-order aberrations. In particular, decentering errors (tip-tilt aberrations) lead to leakage of the central star light and thus to a reduction of the contrast performance close to the star. Such pointing errors are often a consequence of mechanical flexures due to temperature variations, and may result in slow drifts that are not sensed by the AO system (non-common path errors). In order to improve the on-sky performance of these coronagraphs, we intend to implement post-coronagraphic low-order aberration sensing by direct analysis of coronagraphic images. This technique has been initially described by Mas et al. 2012 for retrieving the tip-tilt amount in the case of the four quadrant phase mask coronagraph. The asymmetry of the coronagraphic PSF is quantified by measuring the flux in four quadrants of the image plane detector and the differential flux along two orthogonal directions is derived. In the case of the vortex phase mask, we show that these quantities are directly linked to the amount of tip-tilt affecting the beam upstream of the coronagraphic mask. For that purpose, we have developed a Zernikebased analysis to model the response of the coronagraph in presence of aberrations. We present simulations and experimental results that validate this method in the case of an unobstructed circular pupil. This promising technique will be soon implemented on-sky, in the Keck/NIRC2 instrument for instance, where an AGPM vortex phase mask will be integrated in Spring 2015.

9605-68, Session PMon

High-contrast coronagraph performance in the presence of DM actuator defects

Erkin Sidick, Stuart B. Shaklan, Eric Cady, Jet Propulsion Lab. (United States)

Deformable Mirrors are critical elements in high contrast coronagraphs, requiring precision and stability measured in picometers to enable detection of Earth-like exoplanets. Occasionally DM actuators or their associated cables or electronics fail, requiring the wavefront control algorithm to compensate for actuators that may be displaced from their neighbors by hundreds of nanometers or more. We have carried out experiments on the HCIT testbed to study the impact of failed actuators in partial fulfilment of the Terrestrial Planet Finder Coronagraph optical model validation milestone. We show that the wavefront control algorithm adapts to several broken actuators and maintains dark hole contrast in broadband light.

9605-69, Session PMon

Development of focal plane phase masks for PIAACMC

Kevin E. Newman, Olivier Guyon, The Univ. of Arizona (United States); James W. Conway, Stanford Univ. (United States); Ruslan Belikov, NASA Ames Research Ctr. (United States)



The Phase Induced Amplitude Apodization Complex Mask Coronagraph (PIAACMC) is an architecture for directly observing extrasolar planets, and can achieve performance near the theoretical limits for any direct-detection instrument. PIAACMC can be designed for centrally-obscured and segmented apertures, which is particularly useful for next-generation telescopes. The PIAACMC architecture includes aspheric PIAA optics, and a complex phase-shifting focal plane mask that provides a pi phase shift to a portion of the on-axis starlight. The phase-shifted starlight is forced to interfere destructively with the un-shifted starlight, causing the starlight to be eliminated, and allowing a region for high-contrast imaging near the star.

The PIAACMC focal plane mask is composed of zones that are optimized for broadband operation. We discuss various mask design and optimization strategies, with an emphasis on choosing designs that are more favorable for the manufacturing process. We include a discussion of mask manufacturing techniques, manufacturing limits, and their impact on potential coronagraph performance. We show laboratory results from fabricated masks, and propose the next steps for developing broadband achromatic phase masks for coronagraphy.

9605-70, Session PMon

High performance PIAACMC-type coronagraph designs for centrally obscured and segmented apertures

Olivier Guyon, The Univ. of Arizona (United States); Brian D. Kern, Jet Propulsion Lab. (United States); Ruslan Belikov, Kevin E. Newman, Eugene A. Pluzhnik, NASA Ames Research Ctr. (United States)

The Phase-Induced Amplitude Apodization Complex Mask Coronagraph (PIAACMC) combines lossless pupil apodization by beam shaping with a complex amplitude circular focal plane mask. The focal plane is realized as a multi-zone mirror or transmissive optical element, allowing design optimization for broadband operation. We describe the design process for the PIAACMC, and show that it can be simultaneously optimized for broadband operation and tip-tilt jitter sensitivity. The second optimization is especially important on large telescopes, as nearby stars are partially resolved. The design process takes into account chromatic diffraction by the aperture's edges (spiders, gap between segments).

We show that PIAACMC is fully compatible with pupil shapes previously thought to be "unfriendly" for coronagraphs, and illustrate its potential with two example. First, we describe the 3rd generation PIAACMC for the centrally obscured 2.4m WFIRST-AFTA telescope, and discuss its technology maturity and expected scientific yield. Second, we show a PIAACMC design for a large segmented aperture representative of what a future large telescope aimed at characterizing habitable exoplanets. We also briefly discuss PIAACMC designs for less challenging ground-based applications.

9605-71, Session PMon

In-lab performance of the latest AGPMs (angular groove phase mask) and recent development of VODCA (vortex optical demonstrator for coronagraphic applications)

Aïssa Jolivet, Elsa Huby, Olivier Absil, Univ. de Liège (Belgium); Christian Delacroix, Ctr. de Recherche Astrophysique de Lyon (France); Serge Habraken, Univ. de Liège (Belgium); Dimitri Mawet, European Southern Observatory (Chile); Pierre Piron, Jean Surdej, Univ. de Liège (Belgium)

We first present in this poster coronagraphic test results obtained with the latest AGPMs (Angular Groove Phase Masks), the charge two vortex phase masks made of circular sub-wavelength gratings in diamond.

Some of the tests were performed at the JPL (Jet Propulsion Laboratory) on IRCT (Infrared Coronagraphic Testbed). Other tests were carried out at the Observatoire de Paris, on YACADIRE (the coronagraphic bench of LESIA).

We detail here some of the tests and corresponding results especially about the peak attenuation in the infrared. These AGPMs were optimized in the L-band (wavelengths between 3 and 4 μ m).

In the last part, we also present the most recent developments of VODCA (Vortex Optical Demonstrator for Coronagraphic Applications), an optical bench designed at the University of Liège (Belgium) to operate in near- to mid-infrared wavelengths (1-5 μ m).

This bench is dedicated to the future characterization of Vortex phase masks. In order to improve starlight cancellation, we shall implement different pre- and/or post-coronagraphic concepts, such as optimal apodisation and wavefront control by coronagraphic image analysis.

9605-72, Session PMon

Design of off-axis PIAACMC mirrors

Eugene A. Pluzhnik, NASA Ames Research Ctr. (United States); Olivier Guyon, The Univ. of Arizona (United States) and Subaru Telescope, National Astronomical Observatory of Japan (United States); Ruslan Belikov, Eduardo Bendek, NASA Ames Research Ctr. (United States)

The Phase-Induced Amplitude Apodization Complex Mask Coronagraph (PIAACMC) provides an efficient way to control diffraction propagation effects caused by the central obstruction/segmented mirrors of the telescope. The PIAACMC can be optimized in a way that takes into account both chromatic diffraction effects caused by the telescope aperture and tip/tilt sensitivity of the coronagraph. As a result, in comparison with the original PIAA design, the PIAACMC mirror shapes appear to be asymmetric even for an on-axis coronagraph and require more care in calculating real off-axis shapes.

A method to design off-axis PIAA optics given known on-axis mirror shapes and remapping function is presented. The algorithm is based on geometrical ray tracing and is able to calculate off-axis PIAA mirror shapes for an arbitrary geometry of the input and output beams. The method is demonstrated with the third generation of the PIAACMC for WFIRST-AFTA telescope. Geometrical optics design issues related to the off-axis diffraction propagation effects are also discussed.

9605-73, Session PMon

Design and performance simulations of mid-IR AGPMs for ELT/METIS applications

Brunella Carlomagno, Univ. de Liège (Belgium); Christian Delacroix, Ctr. de Recherche Astrophysique de Lyon (France); Elsa Huby, Olivier Absil, Univ. de Liège (Belgium); Dimitri Mawet, European Southern Observatory (Chile); Aïssa Jolivet, Univ. de Liège (Belgium); Mikael Karlsson, Pontus Forsberg, Ernesto Vargas, Uppsala Univ. (Sweden); Serge Habraken, Jean Surdej, Univ. de Liège (Belgium)

The direct detection of exoplanets requires the use of dedicated, high contrast imaging instruments. In this context, vector vortex coronagraphs (VVCs) are considered to be among the most promising solutions to reach high contrast at small angular separations. They feature a small inner working angle (down to 0.9 lambda/D), high throughput, clear off-axis 360° discovery space, and are simple to implement. The AGPM (Annular Groove Phase Mask) is an implementation of the vortex phase mask, which provides achromaticity over an appreciable spectral range thanks to the use of sub-wavelength gratings. The grating profile can be optimized based on the rigorous coupled wave analysis (RCWA) to achieve a quasi-achromatic phase shift up to a very broad band (L+M band: 3.5-5.1µm). These devices have been manufactured onto CVD diamond substrates, using reactive ion etching. In this communication, I will first present the latest RCWA



simulations performed in the L, M and N spectral bands, and for some combinations of these bands. The resulting optimized AGPMs could be perfectly integrated in the E-ELT/METIS instrument, which aims at detecting and characterizing exoplanets by direct imaging. The target contrast for METIS is <1e-4 at 2 lambda/D (-40 mas in L band), which translates into a peak rejection rate of few hundreds for the AGPMs. Secondly, the optical propagation within the METIS instrument will be studied to determine the performances of a vortex coronagraph at the focus of METIS. In particular, the effect of the central obstruction, spiders, missing E-ELT segments, and pointing jitter will be analysed, together with the sensitivity to tip-tilt. Finally, the atmosphere and the AO contributions will be considered to obtain more realistic results.

9605-74, Session PMon

PISCES: high contrast integral field spectrograph simulations and data reduction pipeline

Jorge Domingo Llop Sayson, The Catholic Univ. of America (United States); Nargess Memarsadeghi, Michael McElwain, NASA Goddard Space Flight Ctr. (United States); Marshall Perrin, Space Telescope Science Institute (United States); Qian Gong, NASA Goddard Space Flight Ctr. (United States); Bryan Grammer, SGT, Inc. (United States) and NASA Goddard Space Flight Ctr. (United States); Bradford W. Greeley, NASA Goddard Space Flight Ctr. (United States); George M. Hilton, Universities Space Research Association (United States) and NASA Goddard Space Flight Ctr. (United States); Catherine T. Marx, NASA Goddard Space Flight Ctr. (United States)

PISCES (Prototype Imaging Spectrograph for Coronagraphic Exoplanet Studies) is a lenslet array based integral field spectrograph (IFS) meant to advance the technology readiness of the WFIRST/AFTA high contrast Coronagraph Instrument. An optical simulator based on the IDL-based PROPER library for PISCES, as well as the Data Reduction Pipeline (DRP) are presented. The IFS simulations of the propagation of light are designed to probe the ability to preserve high contrast in the final data product. The DRP enables transformation of IFS data to calibrated spectral data cubes that are used to both validate the instrument requirements and predict the instrument performance.

9605-75, Session PMon

Maturing CCD photon counting technology for space flight

Udayan Mallik, Richard G. Lyon, Michael McElwain, Dominic J. Benford, Mark Clampin, Brian A. HIcks, NASA Goddard Space Flight Ctr. (United States)

Exo-planets are ultra low-light objects in space. Reflected terrestrial exoplanet light is 10^10-10^11 times fainter than the light of its parent star over a targeted spectral range of 450-950nm. This wavelength spectrum is of interest for spectroscopic characterization of exo-planet atmospheres. A space-based ~10 m aperture telescope will collect light from a terrestrial sized exo-planet around a nearby star at the rate of ~0.1photon/sec. Coronagraphic instruments are used to suppress starlight and image planet light with single photon counting cameras. A Visible Nulling Coronagraph (VNC) is an interferometric system for directly imaging exo-planets. It uses a high-speed, image feedback based active control system to sense and suppress residual starlight to a level below the brightness of the exo-planet. Imaging terrestrial exo-planets using a VNC, therefore, requires the ability to image single photon events at high frame-rates.

Electron Multiplying Charge Coupled Devices (EMCCDs) have a high Quantum Efficiency and low Read Noise. They are good detector candidates for instruments that image exo-planets. EMCCDs, however, suffer from a phenomenon called Clock Induced Charge (CIC) where energy from clock signals knock off valence electrons into the signal chain and generate an image signal which was not the result of integration of light. This effect is amplified in high-speed cameras. Herein, we present results from a shaped clock signal generator for EMCCDs which can control the energy distribution of the clock signal and limit CIC. The presented clock generator architecture can be easily modified for space by using appropriately qualified parts.

9605-76, Session PMon

Technological progress of a ferrofluid deformable mirror with tunable nominal optical power for high-contrast imaging

Aaron J. Lemmer, Tyler D. Groff, N. Jeremy Kasdin, Princeton Univ. (United States)

The success of a space-borne direct-imaging mission pursuing earthsized exoplanets in the habitable zone hinges on the ability to achieve high contrast over a maximum field of view. Coronagraphic instruments designed to address this challenge suffer from optical aberrations and rely on focal-plane wavefront control to suppress the resulting speckles and widen the search area. Even small-featured quasi-static speckles---which may obscure or be confused with a planet---must be suppressed to the order of \$10^{-10}\$ over the search region, placing extreme demands on the deformable mirrors (DMs) used to implement the closed-loop control, both in wavefront requirements and actuation resolution. The ideal DM for focalplane wavefront control has high surface quality and is capable of highprecision, low-stroke actuation. Conventional mirror technologies such as MEMS DMs, with heritage in ground-based adaptive optics instruments that correct for dynamic atmosphere-induced aberrations, are nominally flat and provide high-stroke, high-resolution control but at a cost of precision and surface quality. We present a new technology currently under development at Princeton, which features a ferrofluid-supported optical surface with local magnetic actuation. The actuation is transferred to the optical surface through a liquid medium which continuously supports it, decoupling the nominal surface profile from the actuator configuration and eliminating quilting. Additionally, the device carries nominal optical power via pneumatic control of the ferrofluid pressure, permitting a degree of highfidelity low-order wavefront control impossible with current instrumentation. We report on the continuing technological growth of the prototype device, including progress with actuation, metrology, and modeling of the DM response.

9605-77, Session PMon

Wavefront sensing with pupil diversity using science hardware

Anand Sivaramakrishnan, Space Telescope Science Institute (United States); Alexandra Z. Greenbaum, Johns Hopkins Univ. (United States)

We combine in-focus images through a full pupil and a non-redundant mask (NRM) to provide a wavefront sensor (WFS). Utilizing filters and pupil masks designed solely for science, we create a WFS for future space telescopes, and obviate the necessity of flying some specialized WFS hardware. We use JWST's NIRISS NRM geometry and a full circular pupil in our demonstration, which includes photon noise, the fundamental limiting factor of this approach.

We also quantitatively investigate Fizeau-based approaches to a photon noise-limited wavefront stability monitor. The latter may be useful for very high contrast coronagraphic observations that utilize a bright WFS star prior to observing a coronagraphic target.



9605-78, Session PMon

Two DM probe test for high-contrast wavefront estimation

Christopher C. Veto, A. J. Eldorado Riggs, Neil T. Zimmerman, Tyler D. Groff, N. Jeremy Kasdin, Princeton Univ. (United States)

Motivated by the success of transit surveys such as Kepler, ground-based instruments for imaging warm, Jupiter-sized exoplanets, and the upcoming WFIRST/AFTA mission, progress towards a space-based coronagraph system that can create extremely dark, high-contrast regions in the PSF where Super-Earths to mini-Neptunes may be observed has accelerated. All coronagraphs require wavefront correction to re-gain regions of high star-to-plant contrast by correcting for aberrations in the electric field using estimation and control logic. Most current lab tests use model-based deformable mirror (DM) diversity type algorithms for wavefront estimation. Unfortunately, model uncertainties in the system (including assuming incorrect spatial frequencies which may cause energy to be unintendedly distributed) and in each DM's influence function shape limit the estimation accuracy. This paper presents a new approach for in situ calibration of the DM surface models. Assuming two sequential DMs for control, we refine the actuator-voltage-to-surface-map of each DM by iterating back and forth between which DM is probed and measure the resulting change in the electric field. By alternating DMs and iterating, there is sufficient information to accurately model the change in electric field for each shape applied to the deformable mirrors. The resulting field can then be used in the same estimation and control algorithms, resulting in more accurate estimates and more effective control. Here we present the results of our calibration algorithm in both simulation and experiment.

9605-79, Session PMon

Zernike wavefront sensor (ZWFS) modeling development for low order wavefront sensing (LOWFS) on widefield IR space telescope (WFIRST) / astrophysics focused telescope assets (AFTA)

Xu Wang, J.Kent Wallace, Fang Shi, Jet Propulsion Lab. (United States)

WFIRST/AFTA design makes use of an existing 2.4m telescope for direct imaging of exoplanets. To keep the high contrast needed for the coronagraph, wavefront error (WFE) of the optical system needs to be continuously sensed and controlled. LOWFS uses the rejected starlight from an intermediate focal plane to sense wavefront changes (mostly thermally induced low order WFE) by combining the LOWFS mask (a phase plate located at the small center region with reflective layer) with the starlight rejection masks, i.e. Hybrid Lyot Coronagraph (HLC)'s occulter or Shaped Pupil Coronagraph (SPC)'s field stop. ZWFS measures phase via the phasecontrast method and is known to be photon noise optimal for measuring low order aberrations. Recently, ZWFS was selected as the baseline LOWFS technology on WFIST/AFTA for its good sensitivity, accuracy, and its easy integration with the starlight rejection mask. In this paper, we review the theory of ZWFS operation, describe the ZWFS algorithm development, and summarize various numerical sensitivity studies as well as WFS performance with AFTA pupil configurations (HLC/SPC) and the baseline CCD camera (CCD39 from E2V). We also show preliminary ZWFS model validation experiment results from the fabricated ZWFS phase mask on a stand-alone LOWFS testbed.

9605-80, Session PMon

Deconvolution of differential OTF (dOTF) to measure high-resolution wavefront structure

Justin M. Knight, Kelsey L. Miller, Alexander T. Rodack, Johanan L. Codona, Olivier Guyon, The Univ. of Arizona (United States)

Differential OTF [Codona, Opt. Eng. 0001;52(9):097105-097105. doi:10.1117/1. OE.52.9.097105] uses two images taken with a telescope pupil modification between them to measure the complex field over most of the pupil. If the pupil modification involves a non-negligible region of the pupil, the dOTF field is blurred by convolution with the complex conjugate of the pupil field change. In some cases, such as using actuation of a primary mirror segment to make the measurement, the blurring can be significant [Codona & Doble, JATIS, 2015]. We explore using deconvolution to recover a higher-resolution measurement of the complex pupil field. We show that by masking off the redundant and overlapping parts of the dOTF and Fourier transforming back into image space, we have the complex diffraction field from the full pupil multiplied by the conjugate of the diffraction field from the modified part of the pupil. By assuming we know something about the area and nature of the difference field, we can construct a Wiener filter that gives a better estimate of the pupil field. We explore the use of constraints, such as zero dOTF amplitude beyond the edge of the pupil, to achieve a more robust result. We will present the theory, numerical simulations, and laboratory experiments to demonstrate the method. Our results for this paper are appropriate for narrowband measurements where the proportional radial blurring can be ignored over the entire dOTF result. We will show the effect of naively using this technique on a broadband dOTF measurement.

9605-81, Session PMon

UA wavefront control lab: design overview and implementation of new wavefront sensing techniques

Kelsey L. Miller, Justin M. Knight, Alexander T. Rodack, Johanan L. Codona, Olivier Guyon, The Univ. of Arizona, Steward Observatory (United States)

We present a new testbed designed to study coronagraphic imaging and wavefront control using a variety of pupil and coronagraph architectures. The testbed is designed to explore optimal use of starlight (including starlight rejected by the coronagraph) for wavefront control, system selfcalibration, and point spread function (PSF) calibration. It is also compatible with coronagraph designs for centrally obscured and segmented apertures, and includes shaped or apodized pupils, a range of focal plane masks and Lyot stops of multiple sizes, and an optional PIAA apodizing stage. Starlight is reflected and imaged from the focal plane mask and Lyot stop for low-order wavefront sensing. Both a segmented and a continuous sheet MEMS DM are included to simulate segmented telescope pupils, apply known test phase patterns, and implement a controllable phase apodization coronagraph. The testbed is flexible and is used for exploring new and innovative techniques in wavefront sensing and PSF calibration, and coronagraph design. We describe how the testbed is currently being used to investigate three different techniques: (1) low-order wavefront sensing (LOWFS) using the light rejected by a hybrid-Lyot coronagraph, (2) linear dark field control (LDFC), and (3) the differential optical transfer function (dOTF) using displacements of the pupil segments to correct aberrations and enhance coronagraph performance.

9605-82, Session PMon

Adaptive optics self-calibration using differential OTF (dOTF)

Alexander T. Rodack, Justin M. Knight, Kelsey L. Miller,



Johanan L. Codona, The Univ. of Arizona (United States); Olivier Guyon, Subaru Telescope, National Astronomical Observatory of Japan (United States)

We demonstrate self-calibration of an adaptive optical system using Differential OTF [Codona JL; Opt. Eng. 0001;52(9):097105-097105. doi:10.1117/1.OE.52.9.097105]. We use a deformable mirror (DM) along with science camera focal plane images to implement a closed-loop servo that both flattens the DM and corrects for non-common-path aberrations within the telescope. The pupil field modification required for the dOTF measurement is introduced by displacing actuators near the edge of the illuminated pupil. We tested both an Iris AO hexagonal segmented MEMS DM and a Boston Micromachines continuous sheet MEMS DM. We normally compute the actuator correction updates directly from the phase of the dOTF measurements, reading out displacements and slopes at segment and actuator positions. We also note that since the dOTF is a linear combination of unmodified and modified pupil plane images, it is possible to build a reconstructor matrix that directly takes a vector of pixel values and outputs actuator updates. We explore the effectiveness of these techniques for a variety of bandwidths and number of photons collected in each dOTF exposure pair. We also explore the possibility of using the DM to intentionally add defocus during calibration to allow more photons to be captured in a single exposure without saturation.

9605-83, Session PMon

Control design for momentumcompensated fast steering mirror for WFIRST/AFTA coronagraph instrument

Brent E. Tweddle, Keith Patterson, Joel F. Shields, Xu Wang, Paul B. Brugarolas, Fang Shi, Jet Propulsion Lab. (United States)

This poster will present results of the feedback control design for JPL's Fast Steering Mirror (FSM) for the WFIRST/AFTA coronagraph instrument. The objective of this controller is to cancel jitter disturbances in the beam from the spacecraft to a pointing stability of 0.4 masec over the duration of the observation using a momentum-compensated FSM. The plant model for the FSM was characterized experimentally, and the sensor model is based on simulated results. The controller was designed using discrete-time pole placement techniques and simulated in Matlab with both feedback and disturbance feedforward control. This poster will present all aspects of the controller design, simulation and testing. Estimations of coronagraph contrast performance improvement based on a sensitivities model will also be presented.

9605-84, Session PMon

Design of a laboratory tesbed for external occulters at flight Fresnel numbers

Yunjong Kim, Michael Galvin, N. Jeremy Kasdin, Robert J. Vanderbei, Princeton Univ. (United States); Dongok Ryu, Sug-Whan Kim, Yonsei Univ. (Korea, Republic of); Dan Sirbu, NASA Ames Research Ctr. (United States)

Most extra planets are detected by using indirect observation such as the radial velocity method, transit photometry, and microlensing. There is increasing interest lately in the atmospheric composition of extra planets and in the discovery of bio-signatures. Information about extra planets can be obtained by direct observation. However, the main problem with the direct observation of extra planets is that the planet is 10^10 fainter than the parent star and the angular separation between the extra planet star and the parent star and the parent star. An external occulter is a spacecraft flown along the line-of-sight of a space telescope to suppress starlight and enable high-contrast direct imaging of exoplanets. Laboratory verification of occulter designs

is necessary to validate the optical models used to design and predict occulter performance. At Princeton, we are designing and building a testbed that allows verification of scaled occulter designs whose suppressed shadow is mathematically identical to that of space occulters. Here, we present a sample design operating at a flight Fresnel number and is thus representative of a realistic space mission. We will present the mechanical design of the testbed and simulations predicted the ultimate contrast performance. We will also present progress in implementation and preliminary results.

9605-85, Session PMon

External occulter edge scattering control using metamaterials for exoplanet detection

Eduardo A. Bendek, Dan Sirbu, NASA Ames Research Ctr. (United States); Zhaowei Liu, Univ. of California, San Diego (United States); Stefan R. Martin, Jet Propulsion Lab. (United States)

Direct imaging of earth-like exoplanets in the Habitable Zone of sun-like stars requires image contrast of ~10^10 at angular separations of around a hundred milliarcseconds. One approach for achieving this performance is to fly a starshade at a long distance in front of the telescope, shading the telescope from the direct starlight, but allowing planets around the star to be seen. The starshade is positioned so that sunlight falls on the surface away from the telescope, so it is not directly illuminated by the sun. However, sunlight scattered from the starshade edge can enter the telescope, raising the background light level and potentially preventing the starshade from delivering the required contrast. As a result, starshade edge design has been identified as one of the highest priority technology gaps for external occulter missions in the NASAs Exoplanet Exploration Program Technology Plan 2013. To reduce the sunlight edge scatter to an acceptable level, the edge radius of curvature (ROC) should be 1?m or less (commercial razor blades have ROC of a few hundred nanometer). This poses a challenging manufacturing requirement and may make the occulter difficult to handle. In this paper we propose an alternative approach to controlling the edge scattering by applying a flexible metamaterial to the occulter edge. Metamaterials are artificially structured materials, which have been designed to display properties not found in natural materials. Metamaterials can be designed to direct the scatter at planned incident angles away from the space telescope, thereby directly decreasing the contaminating background light.Reduction of the background light translates into shorter integration time to characterize a target planet and therefore improves the efficiency of the observations. As an additional benefit, metamaterials also have potential to produce increased tolerance to edge defects.

9605-86, Session PMon

Scaling relation for occulter manufacturing errors

Dan Sirbu, NASA Ames Research Ctr. (United States); N. Jeremy Kasdin, Robert J. Vanderbei, Princeton Univ. (United States)

An external occulter, or a starshade, is a spacecraft flown along the line-ofsight of a space telescope to suppress starlight and enable high-contrast direct imaging of exoplanets. The shape of an external occulter must be specially designed to optimally suppress starlight and deviations from the ideal shape due to manufacturing errors can result loss of suppression of the shadow. Due to the large dimensions involved for a space occulter, laboratory testing is conducted with scaled versions of occulters. Using numerical simulations for a flight Fresnel occulter design, we investigate suppression and contrast performance scaling for various levels of fixed feature-sizes.



9605-87, Session PMon

Astrometry with JWST-NIRISS AMI cryovac data

Deepashri Thatte, Space Telescope Science Institute (United States); Alexandra Z. Greenbaum, Johns Hopkins Univ. (United States); André R. Martel, Space Telescope Science Institute (United States); Étienne Artigau, Univ. de Montréal (Canada); Anand Sivaramakrishnan, Space Telescope Science Institute (United States)

JWST/NIRISS has a non-redundant aperture mask (NRM) for use with its F380M, F430M, F480M and F277W filters. In addition to high-resolution imaging with moderate contrast, the NRM provides better astrometric accuracy over a wide field than regular imaging. We investigate the accuracy achievable with the NRM by using an image-plane algorithm to analyze the PSFs of a point source that were obtained at a fixed pixel with sub-pixel dithers during the second Cryo-Vacuum test campaign. Astrometry of brown dwarfs with the NRM will be sensitive to terrestrial planets and used to probe the architecture of planetary systems around these objects.

9605-88, Session PMon

A method to directly image exoplanets in multi-star systems such as Alpha-Centauri

Sandrine J. Thomas, Ruslan Belikov, Eduardo A. Bendek, NASA Ames Research Ctr. (United States)

During the past year, extra-solar planets hunters witnessed the deployment and commissioning of the first generation of specialized ground-based exoplanets direct imaging instruments such as the Gemini Planet Imager and SPHERE. These systems allow detection and characterization of Jupiter-like planets 107 times fainter than their host star. Obtaining such contrast level and beyond requires a coronagraph to suppress light coming from the host star, a wavefront control system including a deformable mirror (DM) to remove residual light or speckles.

However, all these current as well as future systems focus on detecting faint planets around a single or unresolved binaries/multiples star systems in within a very small field of view (-2"). The limitations are (1) the incoherent light pollution of the companion(s) in the region of interest; (2) the degrees of freedom of the correcting devices are thought to be unable to correct for such polluting light.

Several planet candidates though are located around binary stars such as our neighboring star Alpha Centauri.

We showed in a previous SPIE paper our capability of creating a dark region around a single star outside the control region of the DM (beyond its half-Nyquist frequency), by taking advantage of aliasing effects. In this paper, we present a method to simultaneously correct aberrations and diffraction of light coming from the target star as well as its companion star in order to reveal planets orbiting the target star, both in within and outside the half-Nyquist region.

9605-89, Session PMon

Modeling of planetary signal detection through ray-tracing based beam propagation

Dongok Ryu, Sug-Whan Kim, Yonsei Univ. (Korea, Republic of)

High contrast images of exoplanet are limited by diffraction from optical and opto-mechanical components of instrumentation. Therefore it needs optimized solution of these components design with accurate estimation of its optical performance. We are developing model of planetary signal detection through ray-tracing related beam propagation. Sun-like G-star with 695,500km in radius is light source that emitting rays towards a planet and an instrument model. Earth-like planet with 6,400km in radius is composed with atmosphere, land and ocean optical scattering model. The star and Earthlike planet is located 10 parsec away from hypothetic instrument model that has 6.5 meter diameter and F/20 telescope with spiders and Lyot coronagraph. Total 100,000,000 rays per spectral unit are emitted inside of the star surface and traced to directly instrument aperture or reflected and scattered through earth-like planetary model. The rays from emission to instrument aperture through star and planet model are traced by geometric optics condition. Then the rays passing through aperture in telescope model are traced with 8 additional para-basal rays that calculate beam propagation in order to wave optics properties. The model allows for simultaneous evaluations of the beam propagated imaging and radiometric performances for planetary signal detection with some cases of simulation. This simulation results would evaluate valuable information improving estimates space optical instrument in all phases of a space mission.

9605-90, Session PMon

Initial look at the technology gap for direct imaging of exo-earths

Rhonda M. Morgan, Nicholas Siegler, Jet Propulsion Lab. (United States)

The NASA Astrophysics division intends to begin studies in 2016 of candidate flagship missions for proposal to the 2020 decadal survey. One of the anticipated candidates is an exo-earth direct imaging mission. The observation of an exo-earth requires a space telescope with 10e-10 suppression of the host star's light. While technologically challenging, the goal is not impossible. Many of the required technologies are TRL 1-3. After the successful on-orbit operation of WFIRST-AFTA, some of the technologies will be TRL 5-9. This paper summarizes the needed technologies and their development status in the context of current state of the art and expected maturity post-WFIRST-AFTA.

9605-1, Session 1

Requirements and design reference mission for the WFIRST-AFTA coronagraph instrument

Richard Demers, Frank G. Dekens, Robert J. Calvet, Zensheu Chang, Robert T. Effinger, Eric M. Ek, Laura Jones, Anthony Loc, Bijan Nemati, Martin Charley Noecker, Timothy Neville, Hung Pham, Hong Tang, Jet Propulsion Lab. (United States); Juan Villalvazo, Applied Sciences Lab. Inc. (United States)

The WFIRST-AFTA coronagraph instrument takes advantage of AFTAs 2.4-meter aperture to provide novel exoplanet imaging science at approximately the same cost as an Explorer mission. The AFTA coronagraph also matures direct imaging technologies to high TRL for an Exo-Earth Imager in the next decade. The coronagraph Design Reference Mission (DRM) optical design is based on the highly successful High Contrast Imaging Testbed (HCIT), with modifications to accommodate the AFTA telescope design, service-ability, volume constraints, and the addition of an Integral Field Spectrograph (IFS). In order to optimally satisfy the three science objectives of planet imaging, planet spectral characterization and dust debris imaging, the coronagraph or Shaped Pupil Coronagraph. Active mechanisms change pupil masks, focal plane masks, Lyot masks, and bandpass filters to shift between modes. A single optical beam train can thus operate alternatively as two different coronagraphs.

Structural Thermal Optical Performance (STOP) analysis predicts the instrument contrast with the Low Order Wave Front Control loop closed. The STOP analysis was also used to verify that the optical/structural/thermal design provides the extreme stability required for planet characterization in the presence of thermal disturbances expected in a typical observing



scenario. This paper describes the instrument design and the flow down from science requirements to high level engineering requirements.

9605-2, Session 1

WFIRST/AFTA coronagraph technology development: component maturation and testbed validation

Ilya Poberezhskiy, Jet Propulsion Lab. (United States)

NASA's WFIRST/AFTA mission study includes the first high-contrast stellar coronagraph in space. This coronagraph will be capable of imaging and spectrally characterizing giant exoplanets similar to Neptune and Jupiter and possibly super-Earths, as well as circumstellar disks. The selected primary design called the Occulting Mask Coronagraph (OMC) combines two starlight suppression approaches, Shaped Pupil and Hybrid Lyot, in one instrument. The Phase-Induced Amplitude Apodization Complex Mask Coronagraph (PIAA-CMC) was selected as the backup design.

NASA set the objective of maturing the WFIRST/AFTA coronagraph to Technology Readiness Level (TRL) 5 by October 1, 2016, with 9 milestones to track the technology development progress along the way. Substantial advances have been made since the technology development plan was formulated in February of 2014, including successful fabrication of starlight suppression masks for all 3 selected coronagraph types and the testbed demonstration of better than 10⁻⁸ contrast for the obscured AFTA pupil. We will present the milestone status and the recent technical results, including:

• Fabrication and characterization of coronagraph pupil plane and focal plane masks designed to work with the existing AFTA telescope.

• Experimental results demonstrating high contrast achieved on coronagraph testbeds in narrowband and broadband light.

• Status of the key coronagraph components and subsystems, including the deformable mirrors and the low-order wavefront sensing and control subsystem, which uses rejected starlight to sense and correct both the pointing jitter and low order wavefront aberrations. This subsystem will be integrated with the OMC coronagraph in 2015 for the next phase of starlight suppression experiments with dynamic input wavefront.

9605-3, Session 1

The WFIRST/AFTA coronagraph instrument optical design

Hong Tang, Jet Propulsion Lab. (United States)

The most recent concept for the Wide Field Infrared Survey Telescope (WFIRST) flight mission features an instrument that will perform exoplanet detection via coronagraphy of the host star. This observatory is based on the existing Astrophysics Focused Telescope Assets (AFTA) 2.4-meter telescope. The WFIRST/AFTA Coronagraph Instrument combines the Hybrid Lyot and Shaped Pupil Coronagraphs to meet the mission requirements. The optical layout Cycle 5 design fits the required enclosure and accommodates both coronagraphic techniques. We present the optical performances that include throughputs of the imaging channel and the IFS channel, the wavefront errors at the first pupil and the imaging channel, and polarization effects from optical coatings.

9605-4, Session 1

An overview of WFIRST/AFTA coronagraph optical modeling

John Krist, Gary Gutt, Jeffrey Jewell, Brian Kern, Bijan Nemati, David C. Palacios, Jet Propulsion Lab. (United States); A. J. Eldorado Riggs, Princeton Univ. (United States); Erkin Sidick, Hanying Zhou, Jet Propulsion Lab.

(United States)

The WFIRST/AFTA 2.4 m space telescope currently under study includes a stellar coronagraph for the imaging and spectral characterization of extrasolar planets. Based largely on performance predictions from end-toend optical propagation modeling, promising coronagraphic methods were selected in late 2013 for further consideration for use on AFTA. Since those downselect analyses further modeling work has been done on evaluating refined coronagraph designs, wavefront sensing and control, detector representation, and time-dependent effects. Thermal, structural, ray trace, and diffraction propagation models are used in these studies. Presented here is the progress to date and plans for future analyses.

9605-5, Session 1

Effect of DM actuator gain errors on the WFIRST/AFTA coronagraph contrast performance

Erkin Sidick, Fang Shi, Jet Propulsion Lab. (United States)

The WFIRST/AFTA 2.4 m space telescope currently under study includes a stellar coronagraph for the imaging and the spectral characterization of extrasolar planets. The coronagraph employs sequential deformable mirrors (DMs) to compensate for phase and amplitude errors in creating dark holes. DMs are critical elements in high contrast coronagraphs, requiring precision and stability measured in picometers to enable detection of Earth-like exoplanets. Working with the low-order wavefront-sensor (LOWFS) the DM that is conjugate to a pupil can also be used to correct low-order wavefront drift during a scientific observation. However, not all actuators in a DM have the same gain. When using such a DM in low-order wavefront sensing and control (LOWFSC), the actuator gain errors introduce high-spatial frequency error to the DM surface and thus worsen the contrast performance of the coronagraph. We have investigated the effect of actuator gain errors on the contrast performance of the coronagraph through modeling and simulations, and will present our results in this paper.

9605-6, Session 1

Wavefront correction with Kalman filtering for the WFIRST/AFTA coronagraph instrument

A. J. Eldorado Riggs, N. Jeremy Kasdin, Tyler D. Groff, Princeton Univ. (United States)

The only way to characterize most exoplanets spectrally is via direct imaging. For example, the Coronagraph Instrument (CGI) on the proposed Wide-Field Infrared Survey Telescope-Astrophysics Focused Telescope Assets (WFIRST/AFTA) mission plans to image and characterize several cool gas giants around nearby stars. The integration time on these faint exoplanets will be many hours to days. A crucial assumption for mission planning is that the time required to dig a dark hole (a region of high starto-planet contrast) with deformable mirrors is small compared to science integration time. The science camera must be used as the wavefront sensor to avoid non-common path aberrations, but this approach can be quite time intensive. Several estimation images are required to build an estimate of the starlight electric field before it can be partially corrected, and this process is repeated iteratively until high contrast is reached. Here we compare simulated and experimental results of recursive wavefront estimation schemes. In particular, we test a Kalman filter and an extended Kalman filter (EKF) to reduce the total estimation exposure time and improve the robustness of the wavefront correction. We then put our results in the context of the WFIRST/AFTA CGI to predict the improved science yield from spending less time on wavefront correction. An EKF or other nonlinear filter also allows recursive, real-time estimation of sources incoherent with the star, such as exoplanets and disks, and may therefore reduce detection uncertainty.



Current best estimates of planet populations (*Invited Paper*)

Leslie A. Rogers, California Institute of Technology (United States)

Exoplanets are revolutionizing planetary science by enabling statistical studies of a large number of planets. Empirical measurements of planet occurrence rates inform our understanding of the ubiquity and efficiency of planet formation, while the identification of sub-populations and trends in the distribution of observed exoplanet properties provides insights into the formation and evolution processes that are sculpting distant Solar Systems. In this talk, I will review the current best estimates of planet populations. I will focus in particular on eta_Earth, the occurrence rate of habitable zone rocky planets, since this factor strongly influences the design of future space based exoplanet direct detection missions.

9605-8, Session 2

Low order wavefront sensing and control for WFIRST/AFTA coronagraph

Fang Shi, Kunjithapatham Balasubramanian, Randall D. Bartos, Randall C. Hein, Brian D. Kern, John Krist, Raymond K. Lam, James Moore, Keith Patterson, Joel F. Shields, Ilya Poberezhskiy, Erkin Sidick, Hong Tang, Tuan Truong, Brent Tweddle, J.Kent Wallace, Xu Wang, Jet Propulsion Lab. (United States)

NASA's WFIRST-AFTA Coronagraph will be capable of directly imaging and spectrally characterizing giant exoplanets similar to Neptune and Jupiter, and possibly even super-Earths, around nearby stars. To maintain the required coronagraph performance in a realistic space environment, a Low Order Wavefront Sensing and Control (LOWFS/C) subsystem is necessary. The LOWFS/C will use the rejected stellar light to sense and suppress the telescope pointing drift and jitter as well as low order wavefront errors due to the changes in thermal loading of the telescope and the rest of the observatory. The measured wavefront information will also be used for the coronagraph data post-processing (PSF subtraction) needed to further remove the speckle field and enhance the contrast. The WFIRST/AFTA LOWFS/C uses a Zernike phase contrast wavefront sensor with the phase shifting disk combined with the stellar light rejecting occulting mask, a key concept to minimize the non-common path error. Developed as a part of the Dynamic High Contrast Imaging Testbed (DHCIT), the LOWFS/C subsystem also consists of an Optical Telescope Assembly (OTA) Simulator to simulate the realistic wavefront error from WFIRST-AFTA telescope's jitter and thermal drift. The entire LOWFS/C subsystem will be integrated, calibrated, and tested in a dedicated LOWFS/C testbed before being integrated into DHCIT. In this paper we will present the LOWFS/C subsystem design. performance analysis, and LOWFS/C testbed integration and test (I&T) plan. We will also report the LOWFS/C testbed I&T status and some preliminary test results.

9605-9, Session 2

Shaped pupil Lyot coronagraph designs for WFIRST/AFTA

Neil T. Zimmerman, A. J. E. Riggs, N. Jeremy Kasdin, Princeton Univ. (United States); Alexis Carlotti, Institut de Planétologie et d'Astrophysique de Grenoble (France); Robert J. Vanderbei, Princeton Univ. (United States)

The exoplanet imaging campaign of WFIRST/AFTA will require a starlight suppression system surpassing 10⁻⁸ contrast at angular separation 0.2 arcsec from the host star. The baseline instrument configuration includes several shaped pupil coronagraphs to meet these requirements across a

range of observing modes. Our latest designs integrate the shaped pupil mask optimization with a Lyot architecture to yield deeper contrast and smaller inner working angle. By selecting distinct tradeoffs in contrast, working angle, azimuthal span, bandwidth, and throughput, we arrive at three mask configurations. Each one accommodates a major scientific goal: spectroscopic characterization, survey/imaging, and debris disk observations. Our Fourier propagation models incorporate wavefront control to predict the performance in the final image plane. We also analyze the sensitivity to low-order aberrations, alignment, and fabrication errors.

SPIE. PHOTONICS

APPLICATIONS

OPTICAL ENGINEERING+

9605-10, Session 2

Laboratory performance of the shaped pupil coronagraphic architecture for the WFIRST/AFTA coronagraph

Eric Cady, Camilo A. Mejia Prada, Xin An, Kunjithapatham Balasubramanian, Rosemary T. Diaz, Jeffrey Jewell, Jet Propulsion Lab. (United States) and California Institute of Technology (United States); N. Jeremy Kasdin, Princeton Univ. (United States); Brian D. Kern, Andreas Kuhnert, Bijan Nemati, Keith Patterson, Ilya Poberezhskiy, Jet Propulsion Lab. (United States) and California Institute of Technology (United States); A. J. Eldorado Riggs, Princeton Univ. (United States); Daniel J. Ryan, Hanying Zhou, Robert P. Zimmer, Jet Propulsion Lab. (United States) and California Institute of Technology (United States); Neil T. Zimmerman, Princeton Univ. (United States)

One of the two primary architectures being tested for the WFIRST/AFTA coronagraph instrument is the shaped pupil coronagraph, which uses a binary aperture in a pupil plane to create localized regions of high contrast in a subsequent focal plane. The aperture shapes are determined by optimization, and can be designed to work in the presence of secondary obscurations and spiders---an important consideration for coronagraphy with WFIRST/AFTA. We present the current performance of the shaped pupil testbed, including the results of AFTA Milestone 2, in which 6e-9 contrast was achieved in three independent runs starting from a neutral setting.

9605-11, Session 3

PIAACMC coronagraphic occulting mask fabrication, characterization, and modeling

Brian D. Kern, Daniel W. Wilson, Jet Propulsion Lab. (United States); Olivier Guyon, Subaru Telescope, National Astronomical Observatory of Japan (United States); Richard E. Muller, Kunjithapatham Balasubramanian, Erkin Sidick, Ilya Poberezhskiy, Jet Propulsion Lab. (United States); Ruslan Belikov, NASA Ames Research Ctr. (United States)

PIAACMC is a coronagraph architecture suited for high-contrast, small-IWA coronagraphy with high bandwidths (20%). The PIAACMC designs proposed for near-term implementation differ from PIAA architectures with testbed heritage in the inclusion of a phase-only occulting mask, allowing simpler (less aspheric) PIAA mirror shapes and smaller IWAs. The PIAACMC architecture also allows operation on obscured apertures, such as segmented and centrally-obstructed mirrors.

A high-performance PIAACMC mask design has been fabricated and measured at JPL's Micro Devices Lab. The design, measurements, and modeled performance are presented here, with particular attention to application on the WFIRST-AFTA coronagraph instrument. The conclusion is that the current fabrication capabilities at JPL's MDL are sufficient to deliver PIAACMC masks that would perform well in a planet characterization mission.



9605-12, Session 3

AFTA coronagraph performance: feedback from post-processing studies to overall design

Bertrand Mennesson, Jet Propulsion Lab. (United States)

The AFTA Coronagraph aims at forming direct images and measuring the first spectra of exoplanets in orbit around main sequence stars. An important aspect of the instrument is the ability to remove residual stellar speckles to improve the detectability of such planets. Based on detailed simulations and early laboratory tests, we present here some first estimates of the contrast gain expected from advanced post-processing treatments of AFTA-like coronagraphic images. We further discuss their impact on the overall design of the instrument, including its anticipated observing methodology.

9605-13, Session 3

The impact of radiation damage on photon counting with an EM-CCD for the WFIRST-AFTA coronagraph

Nathan L. Bush, David J. Hall, Andrew D. Holland, Ross Burgon, Neil J. Murray, Jason P. D. Gow, Matthew R. Soman, The Open Univ. (United Kingdom); Douglas Jordan, e2v technologies (UK) Ltd. (United Kingdom); Richard Demers, Leon K. Harding, Michael E. Hoenk, Darren Michaels, Bijan Nemati, Pavani Peddada, Jet Propulsion Lab. (United States)

The Wide Field Infra-Red Survey Telescope (WFIRST) is a NASA observatory designed to perform wide-field surveys of the near-infrared sky and direct imaging of exoplanets in the visible. Two instruments are on board. The Wide Field Instrument offers Hubble quality imaging over a 0.28 square degree field of view and will investigate the nature of Dark Energy and its relation to cosmological expansion. The second instrument is a high contrast coronagraph that will carry out the direct imaging and spectroscopic analysis of exoplanets, providing a means to probe the structure and composition of planetary systems.

Since the WFIRST coronagraph is expected to operate in low photon flux for long integration times, all noise sources must be kept to a minimum. In order to satisfy the coronagraph low noise requirements, the Electron Multiplication (EM)-CCD has been baselined for both the imaging and spectrograph cameras. The EM-CCD was selected in comparison with other candidates because of its low effective electronic read noise at sub-electron values with appropriate multiplication gain setting. The presence of other noise sources, however, such as thermal dark signal and Clock Induced Charge (CIC), need to be characterized and mitigated. In addition, operation within a space environment will subject the device to radiation damage that will degrade the Charge Transfer efficiency (CTE) of the device throughout the mission lifetime.

Here we present our latest results from pre-and post- irradiation test of the e2v CCD201-20 BI EM-CCD sensor, baselined for the WFIRST-AFTA coronagraph instrument.

9605-14, Session 3

Electron multiplication CCD detector technology advancement for the WFIRST-AFTA coronagraph integral field spectrograph

Leon K. Harding, Michael Cherng, Richard Demers, Michael E. Hoenk, Darren Michaels, Bijan Nemati, Pavani Peddada,

Jet Propulsion Lab. (United States)

The WFIRST-AFTA mission is a 2.4 meter-class space telescope that will be used across a swath of astrophysical research domains, including dark energy, extrasolar planet exploration and galactic/extragalactic surveys. The observatory will host two major astronomical instruments: a short wave infrared Wide Field Instrument (WFI) provided by GSFC and a High Contrast Imaging Coronagraph provided by JPL. The Coronagraph will include an Integral Field Spectrograph (IFS), capable of spectral characterization of exoplanets. The expected science photon flux on the IFS sensor is extremely low given that the exoplanet targets will reflect light of intensity 109 lower than that of the parent star. Furthermore, in the IFS, light from the target point spread function will be spread over multiple sensor pixels for spectral dispersion. In order to achieve the extremely low noise performance required to detect planets under such low flux conditions, the Electron Multiplication CCD (EMCCD) has been baselined for both of the Coronagraph's sensors; the imaging camera and IFS. EMCCDs have the capability of amplifying signal at the single photon level via avalanche multiplication in the EM register - an additional stage after the conventional CCD register. JPL has established an EMCCD test laboratory in order to advance EMCCD maturity to TRL-6. This plan includes full sensor characterization with the WFIRST life-span and space environment in mind. Test parameters include read noise, dark current, and clock induced charge. In addition, by considering the unique challenges of the space environment, JPL will assess degradation to the sensor's charge transfer efficiency, as a result of damage from high energy particles such as protons, electrons and cosmic rays. Under JPL's guidance, science-grade CCD201-20 EMCCD sensors have been irradiated to a proton fluence that reflect the projected WFIRST orbit. Performance degradation due to radiation displacement damage is reported. In addition, the results of techniques intended to mitigate radiation-induced electron trapping such as charge injection, thermal cycling and clocking patterns are discussed.

9605-15, Session 3

Prototype imaging spectrograph for coronagraphic exoplanet studies (PISCES) for WFIRST/AFTA

Qian Gong, Michael Mcelwain, Bradford Greeley, Bryan Grammer, Catherine Marx, Nargess Memarsadeghi, George Hilton, NASA Goddard Space Flight Ctr. (United States); Marshall Perrin, Space Telescope Science Institute (United States); Jorge Domingo Llop Sayson, Karl Stapelfeldt, NASA Goddard Space Flight Ctr. (United States); Richard Demers, Hong Tang, Brian Kern, Janan Ferdosi, Jet Propulsion Lab. (United States)

PISCES is a prototype lenslet array based integral field spectrograph (IFS) designed for high contrast imaging of extrasolar planets. PISCES will be used to advance the technology readiness of the high contrast IFS baselined on the WFIRST/AFTA Coronagraph Instrument. PISCES will be integrated into the high contrast imaging testbed (HCIT) at the Jet Propulsion Laboratory and will work with both the Hybrid Lyot Coronagraph (HLC) and the Shaped Pupil Coronagraph (SPC). We will present the PISCES optical design, including the similarities and differences of lenslet based IFSs to normal spectrometers, the trade-off between a refractive design and reflective design, as well as the compatibility to upgrade from the current 1k x 1k detector array to 4k x 4k detector array. The optical analysis, alignment plan, and mechanical design of the instrument will be addressed.

9605-16, Session 4

Studies of the effects of control bandwidth and dark-hole size on the HCIT contrast performance

Erkin Sidick, Stuart B. Shaklan, Kunjithapatham



Balasubramanian, Eric Cady, Jet Propulsion Lab. (United States)

We have carried out both theoretical and experimental studies of the sensitivity of dark hole contrast to the control bandwidth and dark-hole dimensions in high-contrast broadband stellar coronagraphy. We have evaluated the performance of DM actuator solutions in the presence of occulting mask defects using one to five 2%-wide bands spanning a 10% bandpasss. We have also investigated the dependence of the HCIT contrast performance on the size of dark-hole area including large dark holes formed at the Nyquist limit of the DM.

9605-17, Session 4

High-contrast imager for complex aperture telescopes (HiCAT): 3. First laboratory results including wavefront control

Mamadou N'Diaye, Élodie Choquet, Johan Mazoyer, Space Telescope Science Institute (United States); Alexis Carlotti, Institut de Planétologie et d'Astrophysique de Grenoble (France); Laurent A. Pueyo, Space Telescope Science Institute (United States); Sylvain Egron, Lucie Leboulleux, Olivier Levecg, Institut d'Optique Graduate School (France); Marshall D. Perrin, Space Telescope Science Institute (United States); J.Kent Wallace, Jet Propulsion Lab. (United States); Chris A. Long, Rachel Lajoie, Charles-Philippe Lajoie, Space Telescope Science Institute (United States); A. J. Eldorado Riggs, Neil T. Zimmerman, Robert J. Vanderbei, Tyler D. Groff, N. Jeremy Kasdin, Princeton Univ. (United States); Dimitri Mawet, California Institute of Technology (United States); Bruce A. Macintosh, Stanford Univ. (United States); Stuart B. Shaklan, Jet Propulsion Lab. (United States); Rémi Soummer, Space Telescope Science Institute (United States)

HiCAT is a high-contrast imaging testbed designed to provide complete solutions in wavefront sensing, control and starlight suppression with complex aperture telescopes. The pupil geometry of such observatories includes primary mirror segmentation, central obstruction, and spider vanes, which make direct imaging of habitable worlds very challenging. The testbed alignment was completed in the summer of 2014, exceeding specifications with a total wavefront error of 12nm rms over a 18mm pupil. The installation of two deformable mirrors for wavefront control is to be completed in the winter of 2015. In this communication, we report on the first testbed results using a classical Lyot coronagraph. We also present the coronagraph design for HiCAT geometry, based on our recent development of Apodized Pupil Lyot Coronagraph (APLC) with shaped-pupil type optimizations. These new APLC-type solutions using two-dimensional shaped-pupil apodizer render the system guasi-insensitive to jitter and low-order aberrations, while improving the performance in terms of inner working angle, bandpass and contrast over a classical APLC.

9605-18, Session 4

EXCEDE technology development III: demonstration of polychromatic contrast in vacuum at 1.2 L/D

Dan Sirbu, Sandrine J. Thomas, Ruslan Belikov, NASA Ames Research Ctr. (United States); Julien Lozi, National Astronomical Observatory of Japan (United States); Eduardo A. Bendek, Eugene A. Pluzhnik, Dana Lynch, NASA Ames Research Ctr. (United States); Troy T. Hix, Lockheed Martin Space Systems Co. (United States); Peter T. Zell, NASA Ames Research Ctr. (United States); Glenn H. Schneider, The Univ. of Arizona (United States); Olivier Guyon, National Astronomical Observatory of Japan (United States)

Exoplanetary Circumstellar Environments and Disk Explorer (EXCEDE) is a proposed Explorer-class NASA space mission. It uses a 0.7-m diameter telescope with a Phase Induced Amplitude Apodization (PIAA) Coronograph and a Deformable Mirror (DM) to create a "dark-hole" or a region of high-contrast starlight suppression at the focal plane to allow direct imaging of debris disks and exoplanets. EXCEDE will also serve as a technological and scientific precursor for an exo-Earth imaging mission. The PIAA coronagraph allows for an aggressive inner working angle of 1.2 I/D for imaging in the habitable zone with high throughput. We have been developing the EXCEDE starlight suppression system technology for high-contrast imaging capability in polychromatic light in vacuum at the Lockheed Martin Advanced Technology Center. In this paper, we present the latest of these results, including high contrast demonstrations in vacuum at inner working angles of 1.2 I/D.

9605-19, Session 4

Broadband results with the visible nulling coronagraph

Brian A. Hicks, Richard G. Lyon, NASA Goddard Space Flight Ctr. (United States); Peter Petrone III, Sigma Space Corp. (United States); Ian J. Miller, LightMachinery Inc. (Canada); Matthew R. Bolcar, Mark Clampin, NASA Goddard Space Flight Ctr. (United States); Michael A. Helmbrecht, Iris AO, Inc. (United States); Udayan Mallik, NASA Goddard Space Flight Ctr. (United States)

The key to broadband operation of the Visible Nulling Coronagraph (VNC) is introducing an achromatic field inversion between interfering beams. Here we present broadband results using Fresnel rhombs in each arm as orthogonally aligned half wave phase retarders, the goal being a demonstration of 1x10⁻⁹ at 2 lambda/D over a 40 nm bandpass centered at 633 nm. In practice, the challenge with this approach is meeting arcsecond level fabrication and alignment requirements between rhombs in a pair and between pairs relative to the instrument, as well as the sub-arcminute requirement on orthogonality between pairs. A multi-step approach to alignment using coarse positioners for each rhomb and each rhomb pair is used to get within range of piezos used for fine positioning. Adapting the narrowband sensing and control approach to include positioning of the piezo-mounted rhombs is described.

9605-20, Session 4

Fabrication and characterization of exoplanet coronagraph shaped pupil masks and laboratory scale star-shade masks

Kunjithapatham Balasubramanian, Victor E. White, Karl Y. Yee, Pierre M. Echternach, Richard Muller, Matthew R. Dickie, Eric Cady, Daniel J. Ryan, Jet Propulsion Lab. (United States); A. J. Eldorado Riggs, Neil T. Zimmerman, N. Jeremy Kasdin, Princeton Univ. (United States)

NASA WFIRST/AFTA mission proposes to include a coronagraph to find and characterize earth like exoplanets. Masks are needed to suppress the host star light to about 10-10 level contrast over a broad bandwidth to enable the coronagraph mission objectives. Such masks for high contrast internal as well as external coronagraphic imaging require various fabrication technologies to meet a wide range of specifications, including precise shapes, micron scale island features, ultra-low reflectivity regions,



uniformity, wave front quality, etc. We present the approaches employed at JPL to produce pupil plane and image plane coronagraph masks, and labscale external occulter masks by combining electron beam, ion beam, deep reactive ion etching, and black silicon technologies with illustrative examples of each, highlighting accomplishments from the high contrast imaging testbed (HCIL) at JPL and from the high contrast imaging lab (HCIL) at Princeton University.

9605-21, Session 5

Active correction of aperture discontinuities for high contrast imaging: parametrical analysis

Johan Mazoyer, Laurent A. Pueyo, Space Telescope Science Institute (United States); Colin A. Norman, Johns Hopkins Univ. (United States); Marshall D. Perrin, Rémi Soummer, Mamadou N'Diaye, Élodie Choquet, Space Telescope Science Institute (United States); Alexis Carlotti, Institut de Planétologie et d'Astrophysique de Grenoble (France); Dimitri Mawet, European Southern Observatory (Chile)

As the performance of coronagraphs improves, the achievable contrast is more and more dependent of the shape of the pupil. The future generation of space and ground based coronagraphic instruments will have to achieve high contrast levels on on-axis and/or segmented telescopes. To correct for the high amplitude aberrations introduced by secondary mirror structures and segmentations of the primary mirror, we explore a two deformable mirror (DM) method. The major difficulty of several DM methods is the non-linear relation linking actuator strokes to the point spread function in the coronagraph focal plane. The Active Compensation of Aperture Discontinuities (ACAD) method is achieving this minimization by solving a non linear differential Monge Ampere equation. Once this open loop method have reached the minimum, a close-loop stroke minimization method can be applied to correct for phase and amplitude aberrations to achieve the ultimate contrast. In this paper we will first describe the recent developments in the end to end propagation simulations of the two DM correction. These propagation simulations will be then use to explore the performance of the ACAD + stroke minimization method for apertures varying on a large space of parameters (width and number of secondary support structures, size of the secondary mirror, number of missing segments, ...). Finally, we will test this method on several known space telescope apertures (JWST, WFIRST, ATLAST).

9605-22, Session 5

Managing the optical wavefront for exoplanet imaging with a space coronagraph

John T. Trauger, Dwight C. Moody, John Krist, Jet Propulsion Lab. (United States)

We update the designs, demonstrations, and science prospects for the direct imaging and spectroscopic characterization of exoplanetary systems with the hybrid Lyot coronagraph. We update our model predictions for exoplanet science performance with the flagship AFTA/WFIRST mission as well as dedicated smaller-class space observatories. Together with a pair of deformable mirrors for optical wavefront control, the hybrid Lyot coronagraph creates high contrast dark fields of view extending to within angular separations of 2.5 lambda/D from the central star at visible wavelengths. Performance metrics and design trades are presented, including image contrast, spectral bandwidth, overall efficiency and throughput, and model-validating laboratory demonstrations.

9605-23, Session 5

Estimation of chromatic errors from broadband images for high contrast imaging

Dan Sirbu, Ruslan Belikov, NASA Ames Research Ctr. (United States)

Usage of an internal coronagraph with an adaptive optical system for wavefront correction for direct imaging of exoplanets is currently being considered as an instrument addition to the AFTA mission to follow the James Web Space Telescope, and many other mission concepts. The main technical challenge associated with direct imaging of exoplanets is to effectively control both the diffraction and scattered light from the star so that the dim planetary companion can be seen. For the deformable mirror (DM) to recover a dark hole region with sufficiently high contrast in the image plane, wavefront errors are usually estimated using probes on the DM. To date, most broadband lab demonstrations use narrowband filters to estimate the chromaticity of the wavefront error, but this reduces the photon flux per filter and requires a filter system. Here, we propose a method to estimate the chromaticity of wavefront errors using only a broadband image. This is achieved by using special DM probes that have sufficient chromatic diversity. We also examine and quantify the integration time performance gains that can be obtained by using such chromatic probes in broadband light to directly estimate the electric field.

9605-24, Session 5

Preliminary analysis of effect of random segment errors on coronagraph performance

Mark T. Stahl, H. Philip Stahl, NASA Marshall Space Flight Ctr. (United States); Stuart B. Shaklan, Jet Propulsion Lab. (United States)

Comparative exo-Earth planetology requires the ability to characterize dozens of planets. Based on current design reference missions, a telescope with an aperture as large as 12 to 16 meters may be required. Obviously such a telescope will need to be segmented. But, temporal rigid-body motion of individual segments can result in leakage which reduces contrast. To fully characterize exo-Earths requires contrast stability of 10^-11. This paper reports a preliminary investigation of the sensitivity of contrast stability to segment rigid-body motion stability.

9605-25, Session 5

Linearized dark field control (LDFC) and self-calibration for high contrast imaging

Olivier Guyon, Johanan L. Codona, The Univ. of Arizona (United States); Brian D. Kern, Jet Propulsion Lab. (United States); Ruslan Belikov, NASA Ames Research Ctr. (United States)

High contrast imaging systems aimed at detecting and characterizing exoplanets must reach deep contrast levels over part of the focal plane image. This is achieved by iteratively cancelling diffracted starlight in a predefined region, in which exoplanets can be imaged and characterized. Each iteration requires several images, each with a different deformable mirror shape (probes), to be acquired in order to solve for the complex amplitude field (dark field) in the dark region. This approach is slow (several images need to be acquired, each with sufficiently long exposure to measure speckles), disruptive (the optimal dark field solution must be periodically broken to measure speckles) and prone to errors due to imperfect knowledge of the DM-to-speckles relationship.

We present two techniques that significantly improve on the conventional



approach described above:

- We show that a model-free self-calibration of the system response matrix can be performed by moving small groups of actuators sequentially and using a non-linear solver.

- We show that the dark field complex amplitude is linearly coupled with brighter speckles lying outside the geometric control region, and with speckles outside the control spectral band. It is therefore possible to control dark field speckles with a fast model-free linear controller using brighter starlight. By utilizing light outside the dark hole (both spatially and spectrally), the control loop is significantly simpler, faster, and more sensitive. It also does not require a model of the system, as the linear relationship can be easily and quickly measured. This approach enables full utilization of the available observing time for science observations, and is more robust to non-ideal deformable mirror behaviours, such as hysteresis.

The Linearized Dark Field Control (LDFC) is also a powerful aid to PSF calibration, as the residual dark field speckles can be inferred from the intensity of the brighter speckles used as the input to the LDFC loop.

9605-26, Session 5

Blind source separation approaches for exoplanet signal extraction

Dmitry Savransky, Cornell Univ. (United States)

While the next generation of exoplanet direct-imaging instrumentation that is currently coming online is making remarkable strides in increasing achievable contrast levels, post-processing still plays a crucial role in the detection of exoplanets. The current state of the art involves extracting the planet signal from the noisy background using a variety of techniques, several of which (including all variations on principal component analysis) belong to a general class of algorithms called Blind Source Separation (BSS). Here we demonstrate the application of other BSS algorithms that have previously not been tested on exoplanet imaging data, including independent component analysis, common spatial pattern filtering, and stationary subspace analysis. We utilize both synthetic and real imaging data and discuss the strengths and weaknesses of each approach (as well as available degrees of freedom in their implementation) as a function of the correlation and relative magnitude of various noise sources commonly found in exoplanet imaging data.

9605-27, Session 5

Point spread function subtraction methods for high-contrast imaging in the context of future space-based coronagraph instruments

Marie Ygouf, Rémi Soummer, Marshall D. Perrin, Laurent A. Pueyo, Space Telescope Science Institute (United States); Bruce A. Macintosh, Stanford Univ. (United States)

Direct detection and characterization of Earth-like exoplanets with contrasts of 10⁻⁹ require space-based instruments optimized for high-contrast imaging. In this context, the Wide-Field Infrared Survey Telescope -Astrophysics Focused Telescope Assets (WFIRST-AFTA) project will reach contrasts of about 10⁻⁸, using state-of-the-art starlight suppression and wavefront control techniques. A ten-fold contrast improvement to reach the required contrast of 10⁻⁹ is expected to come from post-processing techniques. But the methods of point spread function (PSF) subtraction currently used on both ground-based and space-based instruments have not yet been demonstrated at such high contrast level.

In this communication, we explore new ways of implementing postprocessing methods on AFTA-like simulated images, taking into account the presence of deformable mirrors, coronagraph and an IFS. Among all the existing PSF subtraction techniques, the Karunhen-Loève Image Projection (KLIP) algorithm is one of the most promising for the future space-based coronagraphic instruments. This method has been applied successfully on real ground-based and space-based images with a contrast up to 10⁻⁶. But its performances have to be demonstrated at the high contrast level of WFIRST-AFTA. In this communication, we perform a sensitivity analysis of KLIP on AFTA-like simulated images and we assess the preliminary performance of the algorithm in terms of contrast.

9605-28, Session 6

Exo-C: a probe-scale space observatory for direct imaging and spectroscopy of extrasolar planetary systems (Invited Paper)

Karl Stapelfeldt, NASA Goddard Space Flight Ctr. (United States); Frank G. Dekens, Michael P. Brenner, Keith R. Warfield, Jet Propulsion Lab. (United States) and California Institute of Technology (United States); Ruslan Belikov, NASA Ames Research Ctr. (United States); Paul B. Brugarolas, Geoffrey Bryden, Jet Propulsion Lab. (United States) and California Institute of Technology (United States); Kerri L. Cahoy, Massachusetts Institute of Technology (United States); Supriya Chakrabarti, Univ. of Massachusetts Lowell (United States); Serge Dubovitsky, Robert T. Effinger, Casey Heeg, Brian Hirsch, Andrew Kissil, John Krist, Jared J. Lang, Jet Propulsion Lab. (United States) and California Institute of Technology (United States); Mark S. Marley, NASA Ames Research Ctr. (United States); Michael McElwain, NASA Goddard Space Flight Ctr. (United States); Victoria Meadows, Univ. of Washington (United States); Joel A. Nissen, Jeffrey M. Oseas, Christopher Pong, Eugene Serabyn, Eric T. Sunada, John T. Trauger, Jet Propulsion Lab. (United States) and California Institute of Technology (United States)

"Exo-C" is NASA's first community study of a modest aperture space telescope optimized for high contrast observations of exoplanetary systems. The mission will be capable of taking optical spectra of nearby exoplanets in reflected light, discovering previously undetected planets, and imaging structure in a large sample of circumstellar disks. It will obtain unique science results on planets down to super-Earth sizes and serve as a technology pathfinder toward an eventual flagship-class mission to find and characterize habitable Earth-like exoplanets. We present the mission/ payload design and its science yield, highlighting steps to reduce mission cost/risk relative to previous mission concepts. Key elements are an 1.4 m unobscured telescope aperture, an internal coronagraph with deformable mirrors for precise wavefront control, and an orbit and observatory design chosen for high thermal stability. Exo-C has a similar telescope aperture, orbit, lifetime, and spacecraft bus requirements to the highly successful Kepler mission (which is our cost reference). The needed technology development is on-course to support a mission start in 2017, should NASA decide to proceed. This paper summarizes the study final report completed in February 2015. Key accomplishments include excellent modeled telescope stability, a telescope and instrument design that is optimal for dual polarization throughput, and fitting the mission into the prescibed cost cap.

9605-29, Session 6

Ultra-stable thermal-optical performance from the Exo-C design study

Joel A. Nissen, Robert T. Effinger, Andrew Kissil, Jet Propulsion Lab. (United States)

Space-based coronagraphs offer the promise of direct observations of exoplanets, ultimately within the habitable zone of many stars. In order to take full advantage of the 10-9 contrast achievable at the inner working



angle, the observatory will require unprecedented wavefront stability. For reasons of observing efficiency and in order to pull a dim planet from the coronagraph speckle, it is also highly desirable that the wavefront is stable at the picometer level during observing maneuvers. Exo-C is a design study for a space-based internal coronagraph with a 1.4 meter unobscured aperture that achieves this goal maintaining contrast drift below 10-10. To achieve this stability, a systems level approach is necessary, starting with the choice of a Kepler-like Earth trailing orbit. In this orbit, the only thermal disturbances are the Sun and the power dissipation inside the spacecraft. To take full advantage of the stable environment of the earth trailing orbit, the sunshade fully covers the Exo-C optical barrel on the Sun-facing side and is flat so that when the spacecraft is rolled around the optical axis, from +15° to -15°, the solar load on the optical barrel is unchanged. A combination of low CTE materials and 29 thermal control zones on the optical barrel ensures that the primary-secondary mirror spacing drifts are under a nanometer. Thermal disturbances resulting from heat dissipation in the spacecraft bus are managed with passive and active thermal control of the interface. This paper details the modeling and design strategies that result in an ultra-stable coronagraph.

9605-30, Session 6

PIAA coronagraph design for the Exo-C Mission concept

Ruslan Belikov, NASA Ames Research Ctr. (United States); John Krist, Jet Propulsion Lab. (United States); Karl Stapelfeldt, NASA Goddard Space Flight Ctr. (United States)

The Exoplanet Coronagraph (Exo-C) mission concept consists of a 1.4m space telescope equipped with a high performance coronagraph to directly image exoplanets and disks around many nearby stars. One of the coronagraphs under consideration to be used for this mission is the highly efficient Phase-Induced Amplitude Apodization (PIAA) coronagraph. This paper presents and describes: (a) the PIAA design for Exo-C; (b) an end-toend performance analysis including sensitivity to jitter, and (c) the expected science yield of Exo-C with PIAA. The design is a "classic" PIAA, which is made possible by the unobstructed aperture. It consists of a pair of forward and inverse PIAA optics and a simple hard-edge focal plane mask. A mild binary pre-apodizer relaxes the radius of curvature on the PIAA mirrors to be easier than typical PIAA mirrors manufactured to date. This design has been optimized for high performance while being relatively insensitive to low order aberrations. The throughput is 90% relative to telescope PSF, while the inner working angle is 2.1 I/D and the contrast is ~1e-9 in a full 360-degree field of view (after wavefront control with two DMs), all for a 20% spectral band centered around 550nm. The design also has good tolerance to jitter: contrast at 1.6mas jitter is still within a factor of a few of 1e-9.

9605-31, Session 7

The Exo-S Probe Class Starshade Mission (*Invited Paper*)

Sara Seager, Massachusetts Institute of Technology (United States); Margaret C. Turnbull, Global Science Institute (United States); William B. Sparks, Space Telescope Science Institute (United States); Mark Thomson, Stuart B. Shaklan, Jet Propulsion Lab. (United States); Aki Roberge, Marc J. Kuchner, NASA Goddard Space Flight Ctr. (United States); N. Jeremy Kasdin, Princeton Univ. (United States); Shawn Domagal-Goldman, NASA Goddard Space Flight Ctr. (United States); Webster Cash, Univ. of Colorado at Boulder (United States); Keith R. Warfield, Douglas Lisman, Daniel P. Scharf, David R. Webb, Rachel Trabert, Stefan R. Martin, Eric Cady, Cate Heneghan, Jet Propulsion Lab. (United States) Exo-S is a direct imaging space-based mission to discover and characterize exoplanets. With its modest size, Exo-S bridges the gap between census missions like Kepler and a future space-based flagship direct imaging exoplanet mission. With the ability to reach down to Earth-size planets in the habitable zones of nearly two dozen nearby stars, Exo-S is a powerful first step in the search for and identification of Earth-like planets. Compelling science can be returned at the same time as the technological and scientific framework is developed for a larger flagship mission.

The Exo-S Science and Technology Definition Team studied two viable and compelling starshade-telescope missions for exoplanet direct imaging, targeted to the \$1B cost guideline. The first Exo-S mission concept is a starshade and telescope system dedicated to each other for the sole purpose of direct imaging for exoplanets (The "Starshade Dedicated Mission"). The starshade and commercial, 1.1-m diameter telescope co-launch, sharing the same low-cost launch vehicle, conserving cost. The Dedicated mission orbits in a heliocentric, Earth leading, Earth-drift away orbit. The telescope has a conventional instrument package that includes the planet camera, a basic spectrometer, and a guide camera.

The second Exo-S mission concept is a starshade that launches separately to rendezvous with an existing on orbit space telescope (the "Starshade Rendezvous Mission"). The existing telescope adopted for the study is the WFIRST-AFTA (Wide-Field Infrared Survey Telescope Astrophysics Focused Telescope Asset). The WFIRST-AFTA 2.4-m telescope is assumed to have previously launched to a Halo orbit about the Earth-Sun L2 point, away from the gravity gradient of Earth orbit which is unsuitable for formation flying of the starshade and telescope. The impact on WFIRST/AFTA for starshade readiness is minimized; the existing coronagraph instrument performs as the starshade science instrument, formation guidance is handled by the existing coronagraph focal planes with minimal modification, and an added transceiver.

9605-32, Session 7

Optical instrumentation for science and formation flying with a starshade observatory

Stefan R. Martin, Eric Cady, Stuart B. Shaklan, Daniel P. Scharf, Hong Tang, Jet Propulsion Lab. (United States)

In conjunction with a space telescope of modest size, a starshade enables observation of small exoplanets close to the parent star by blocking the direct starlight while the planet light remains unobscured. The starshade will be flown some tens of thousands of kilometers ahead of the telescope and maintained in the direct line of sight to the star to an accuracy of a meter or so. Using the optical telescope as part of the sensor, we show how this alignment can be maintained by observing out of band starlight that leaks around the starshade. Science instruments may include a wide field camera for imaging the target exoplanetary system as well as an integral field spectrometer for characterization of exoplanets. We discuss the preliminary designs of the optical instruments for observatories such as Exo-S and a starshade-ready WFIRST/AFTA and show how a compact, standalone instrument package could be developed as an add-on to future space telescopes. We discuss observation times for exoplanets, formation flying and control, retargeting maneuvers and other aspects of the mission.

This work was conducted at the Jet Propulsion Laboratory, California Institute of Technology, under contract with the National Aeronautics and Space Administration. © 2014 California Institute of Technology. Government sponsorship acknowledged. All rights reserved.

9605-33, Session 7

Design reference missions for the Exoplanet Starshade (Exo-S) Probe-Class study

Rachel Trabert, Stuart B. Shaklan, Douglas Lisman, Jet Propulsion Lab. (United States); Aki Roberge, NASA



Goddard Space Flight Ctr. (United States); Margaret C. Turnbull, Global Science Institute (United States); Shawn Domagal-Goldman, Christopher C. Stark, NASA Goddard Space Flight Ctr. (United States)

Exo-S is a direct imaging space-based mission to discover and characterize exoplanets. The mission is comprised of two formation-flying spacecraft – a starlight suppressing starshade and a telescope separated by -30,000 km. To align the starshade between the target star and telescope, one of the two spacecraft must perform a retargeting slew. This drives the need for a sophisticated program to help optimize this path to maximize target yield within mission constraints such as solar and earth avoidance angles, thrust and fuel limitations, and target scheduling for previously-discovered known giant planets. The Design Reference Mission (DRM) describes the sequence of observations to be performed and estimates the number of planets that will be detected and characterized. It is executed with a Matlab-based tool developed for the Exo-S Study. Here we show analyze three case studies:

• Case 1: Starshade with a 1.1m dedicated telescope focused on searching for earths in the Habitable Zone (HZ).

• Case 2: Starshade with a 1.1m dedicated telescope focused on maximizing planet harvest return and characterization.

 \bullet Case 3: Starshade that rendezvous with a 2.4 m shared telescope focused on searching for earths in the HZ.

Previous starshade DRM tools have been reported in the literature, all of them focused on detection and/or characterization of Earth-twins in the habitable zone. This study has taken then next step and focused on total planet harvest including known Gas Giants, Earths in the Habitable Zone and elsewhere, super-earths, sub-Neptunes, and Jupiters. The DRM employs a hierarchical approach: an observation schedule of known radial velocity gas giants, whose availabilities for observation are known form their orbital parameters, forms a "framework" of observation that have a high probability of success. Between these observations, the next highest priority stars are scheduled and these in turn form the framework for the next observational tier. We report the expected observational completeness, planet yields, and planet characterizations for the three case studies.

9605-34, Session 7

Error budgets for the Exoplanet Starshade (Exo-S) Probe-Class Mission study

Stuart B. Shaklan, Luis Marchen, Eric Cady, Douglas Lisman, Stefan R. Martin, Mark Thomson, Jet Propulsion Lab. (United States)

Exo-S is a probe-class mission study that includes the Dedicated mission, a 30 m starshade co-launched with a 1.1 m commercial telescope in an Earth-leading deep-space orbit, and the Rendezvous mission, a 34 m starshade indended two work with a 2.4 m telescope in an Earth-Sun L2 orbit. This paper presents error budgets for the detection of Earth-like planets with each of these missions. The budgets include manufacture and deployment tolerances, the allowed thermal fluctuations and dynamic motions, formation flying alignment requirements, surface and edge reflectivity requirements, and the allowed transmission due to micrometeoroid damage. The budget is created through electric field propagation modeling of a variety of perturbations to the starshade design under consideration.

9605-35, Session 7

The Exo-S Starshade mechanical design

Mark Thomson, David R. Webb, Brian Hirsch, Brian P. Trease, Vinh M. Bach, Brian Y. Lim, Jet Propulsion Lab. (United States)

The mechanical and structural design of a 34-meter diameter deployable externally occulting starshade for the Exoplanet Rendezvous Mission (ERM) described in the Exo-S Final Report is detailed. This starshade is being developed at JPL with funding from NASA SMD Astrophysics under the

TDEMs and Exoplanet Program Office.

The JPL starshade has grown in an environment of mechanical engineering prototype development in collaboration with optical, and systems engineers. This collaboration has yielded realistically achievable requirements, designs and hardware that will provide deployment and maintenance of the shape and stability needed for suppression of visible starlight to at least 10E-10 with inner working angles sufficient to image Earth-like exoplanets in the habitable zone using a 2.86-meter conventional telescope, or smaller.

Various aspects of the JPL starshade design will be presented including how the structural architecture supports the optical design with adequate in-plane precision and stability. Mechanical design heritage, the deployment sequence and petal, inner disk structure, perimeter truss ring structure, spoke, hub, petal and inner disc optical shield designs will be outlined.

9605-37, Session 8

Fully achromatic nulling interferometer (FANI) for high SNR exoplanet characterization

François B. Hénault, Institut de Planétologie et d'Astrophysique de Grenoble (France)

Space-borne nulling interferometers have long been considered as the best option for characterizing extra-solar planets. Solutions for achieving deep starlight extinction are now numerous and well demonstrated. However they essentially aim at realizing an achromatic central null. In this communication is described a major improvement of the technique, where the achromatization process is extended to the entire fringe pattern. The basic principle of this Fully achromatic nulling interferometer consists in inserting dispersive elements along the arms of the interferometer. Herein this principle is explained and illustrated by a preliminary optical design.

9605-38, Session 8

A 4-telescope linear nuller based on an integrated optics beam combiner

Ronny Errmann, Romina Diener, Stefano Minardi, Friedrich-Schiller-Univ. Jena (Germany); Lucas Labadie, Univ. zu Köln (Germany); Felix Dreisow, Stefan Nolte, Thomas Pertsch, Matthias Heinrich, Friedrich-Schiller-Univ. Jena (Germany)

Nulling interferometry is a coronographic technique particularly powerful at long infrared wavelengths (-3-10 microns) where it combines efficient starlight suppression and high angular resolution to resolve and characterize spectroscopically the thermal emission of exoplanets orbiting a nearby Sun like star. This technique has been technically explored in details during the last decade in the context of space projects such as Darwin, TPF or FKSI. While nulling interferometry in space is still hampered by high costs and by the lack of technological maturity of some sub-systems, ground-based nulling with the LBTI and Keck has shown the power of the technique to study the circumstellar environment of nearby solar-type stars.

An important aspect to minimize residual stellar leaks being transmitted by the interferometer is to combine the beams of more than two or three telescopes in order to broaden the central null. Several configurations have been proposed on paper to reach a broader dark fringe. To verify the experimental validity of these options, we have conducted a specific laboratory study of the so-called Angel's scheme (Angel & Wolf 1997) that foresees the combination of four telescopes to produce a null with a theta⁻⁶ shape. The novelty is in the use of an integrated optics beam combiner to implement a cascaded 4-telescope nulling scheme able to significantly broaden the central null. We report on the properties of the beam combiner, on the polynomial dependance of the produced null, and on the promising characterization results obtained at visible wavelengths. We also draw new perspectives to extend this approach to the mid-infrared in the context of our ALSI project, which aims at delivering optimized IO combiners for the 3-10 microns range.



9605-39, Session 8

A pareto-optimal characterization of small-scale distributed occulter/telescope systems

Adam W. Koenig, Simone D'Amico, Bruce A. Macintosh, Stanford Univ. (United States)

Distributed occulter/telescope systems are a promising candidate to enable direct imaging of exoplanets. However, proposed missions using this concept such as NASA's New Worlds Observer are exceptionally large with occulter diameters of tens of meters and inter-spacecraft separations of tens of megameters, requiring deployment in deep space. The costs associated with these concepts are estimated to be in the billions of dollars. In this work, we assess the feasibility of shrinking the occulter and telescope to a size compatible with microsatellites or nanosatellites and reducing the spacecraft separation by several orders of magnitude in order to allow deployment in Earth orbit, drastically reducing mission costs. We will use the convex optimization formulation introduced by previous authors with an improved objective function and an additional shadow recovery constraint to generate a pareto-optimal relationship between the performance specifications of the system (angular resolution, shadow size, shadow depth, shadow bandwidth, etc.) in the microsatellite and nanosatellite size regimes over a wide range of operating wavelengths. In addition, this work will assess the performance penalty incurred by enforcing engineering constraints (monotonically shrinking petals, solid core) presented by previous authors. Finally, the resulting pareto-optimal performance set will be compared to the performance requirements for imaging exoplanet classes of scientific interest. The result of this work will be a comprehensive trade of the capabilities of small-scale occulter/telescope systems, providing a valuable methodology and performance guidelines for future occulter/ telescope designs.

9605-40, Session 9

Space telescope design to directly image the habitable zone of Alpha Centauri

Eduardo A. Bendek, Ruslan Belikov, Sandrine J. Thomas, NASA Ames Research Ctr. (United States); Julien Lozi, Subaru Telescope, National Astronomical Observatory of Japan (United States); Jared R. Males, The Univ. of Arizona (United States)

The inner edge of Alpha Cen A&B Habitable Zone is found at exceptionally large angular separations of 0.7" and 0.4" respectively. This enables direct imaging of the system with a 30cm class telescope. Contrast ratios in the order of 1010 are needed to image Earth-brightness planets. Low-resolution (5-band) spectra of all planets, will allow establishing the presence and amount of an atmosphere. This star system configuration is optimal for an specialized small, and stable space telescope, that can achieve high-contrast but has limited resolution. This paper describes an innovative instrument design and a mission concept based on a full Silicon Carbide off-axis telescope, which has a Phase Induce Amplitude Apodization coronagraph embedded in the telescope. This architecture maximizes stability and throughput. The Multi-Star Wave Front algorithm is implemented to drive a deformable mirror controlling simultaneously diffracted light from the on-axis and binary companion star. The instrument has a Focal Plane Occulter to reject starlight into a Low Order Wavefront Sensor that delivers high-precision pointing control. Finally we utilize the ODI post-processing method that takes advantage of a highly stable environment (Earth-trailing orbit) and a continuous sequence of images spanning 2 years, to reduce the final noise floor in post processing to ~2e-11 levels, enabling high confidence and at least 90% completeness detections of Earth-like planets.

9605-41, Session 9

How to directly image a habitable planet around Alpha Centauri with a ~30-45cm space telescope

Ruslan Belikov, Eduardo A. Bendek, Sandrine J. Thomas, NASA Ames Research Ctr. (United States); Jared R. Males, The Univ. of Arizona (United States); Julien Lozi, Subaru Telescope, National Astronomical Observatory of Japan (United States)

Several mission concepts are being studied to directly image planets around nearby stars. It is commonly thought that directly imaging a potentially habitable exoplanet around a Sun-like star requires space telescopes with apertures of at least 1m. A notable exception to this is Alpha Centauri (A and B), which is an extreme outlier among FGKM stars in terms of apparent habitable zone size: the habitable zones are ~3x wider in apparent size than around any other FGKM star. This enables a ~30-45cm visible light space telescope equipped with a modern high performance coronagraph or starshade to resolve the habitable zone at high contrast and directly image any potentially habitable planet that may exist in the system. The raw contrast requirements for such an instrument can be relaxed to 1e-8 if the mission spends 2 years collecting tens of thousands of images on the same target, enabling a factor of 500-1000 speckle suppression in post processing using a new technique called Orbital Difference Imaging (ODI). The raw light leak from both stars is controllable with a special wavefront control algorithm known as Multi-Star Wavefront Control (MSWC), which independently suppresses diffraction and aberrations from both stars using independent modes on the deformable mirror. This paper will present an analysis of the challenges involved with direct imaging of Alpha Centauri with a small telescope and how the above technologies are used together to solve them. We also show examples of small coronagraphic mission concepts currently being developed to take advantage of this opportunity.

9605-42, Session 9

Orbital difference imaging: a new highcontrast post-processing technique for direct imaging of exoplanets

Jared R. Males, The Univ. of Arizona (United States); Ruslan Belikov, Eduardo A. Bendek, NASA Ames Research Ctr. (United States)

Current post-processing techniques in high contrast imaging depend on some source of diversity between the exoplanet signal and the residual star light at that location. The two main techniques are angular differential imaging (ADI), which makes use of parallactic sky rotation to separate planet from star light, and spectral differential imaging (SDI), which makes use of differences in the spectrum of planet and star light and the wavelength dependence of the point spread function (PSF). Here we introduce our technique for exploiting another source of diversity: orbital motion. Given repeated observations of an exoplanetary system with sufficiently short orbital periods, the motion of the planets allows us to discriminate them from the PSF. In addition to using powerful PSF subtraction algorithms, such an observing strategy enables temporal filtering. Once an orbit is determined, the planet can be ``de-orbited" to further increase the signal-to-noise ratio. We call this collection of techniques Orbital Difference Imaging (ODI). Here we present the motivation for this technique, present a noise model, and present results from simulations. We believe ODI will be an enabling technique for imaging Earth-like planets in the habitable zone with dedicated space missions.



9605-43, Session 9

The low-order wavefront sensor for the PICTURE-C exoplanetary imaging balloon mission

Christopher B. Mendillo, Glenn A. Howe, Timothy A. Cook, Univ. of Massachusetts Lowell (United States); Ewan S. Douglas, Boston Univ. (United States); Susanna C. Finn, Kuravi Hewasawam, Jason Martel, Supriya Chakrabarti, Univ. of Massachusetts Lowell (United States)

The PICTURE-C mission will fly a 60 cm off-axis unobscured telescope and two high-contrast coronagraphs in successive flights with the goal of directly imaging and spectrally characterizing visible scattered light from exozodiacal dust in the interior 1-10 AU of nearby exoplanetary systems. The first flight in 2017 will use a 10⁻⁴ visible nulling coronagraph (previously flown on the PICTURE-B sounding rocket) and the second flight in 2019 will use a 10^-7 vector vortex coronagraph. A low-order wavefront corrector (LOWC) will be used in both flights to remove time-varying aberrations from the coronagraph wavefront. The LOWC actuator is a 76 channel high-stroke deformable mirror packaged on top of a tip-tilt stage. This paper will detail the selection of a high-speed low-order wavefront sensor (LOWFS) for the mission. The relative performance and feasibility of several LOWFS designs will be compared including the Shack-Hartmann, CLOWFS, pyramid, and Zernike phase mask. To model the LOWFS input, a model of the timevarying wavefront is used. This model is driven by measured pointing data and thermal and inertial dynamics models that predict the optical alignment and optical surface deformation in the balloon environment.

9605-44, Session 9

End-to-end simulation of high-contrast imaging systems: methods and results for the PICTURE Mission family

Ewan S. Douglas, Boston Univ. (United States); Kuravi Hewasawam, Christopher B. Mendillo, Univ. of Massachusetts Lowell (United States); Kerri L. Cahoy, Massachusetts Institute of Technology (United States); Timothy A. Cook, Susanna C. Finn, Glenn A. Howe, Univ. of Massachusetts Lowell (United States); Marc J. Kuchner, NASA Goddard Space Flight Ctr. (United States); Nikole K. Lewis, Space Telescope Science Institute (United States); Anne D. Marinan, Massachusetts Institute of Technology (United States); Dimitri Mawet, Jet Propulsion Lab. (United States) and European Southern Observatory (Chile); Supriya Chakrabarti, Univ. of Massachusetts Lowell (United States)

Mission design for high-contrast imaging requires accurate numerical wavefront error propagation to ensure accurate component specifications. For constructed instruments, accurate wavelength and angle dependent throughput and contrast models allow detailed simulations of science observations, allowing mission planners to target the most productive targets.

The PICTURE family of missions seek to quantify the optical brightness of scattered light from extrasolar debris disks via several high contrast imaging techniques; a sounding rocket (the Planet Imaging Concept Testbed Using a Rocket Experiment) and balloon flight of a visible nulling coronagraph, as well as a balloon flight of a vector vortex coronagraph (the Planetary Imaging Concept Testbed Using a Recoverable Experiment - Coronagraph, PICTURE-C). The rocket mission employs an on-axis 0.5m Gregorian, while the balloon flights will share an unobstructed off-axis 0.6m Gregorian design.

We describe the flexible approach to polychromatic, end-to-end physical optics simulation used for both the balloon and rocket missions. We show

the PICTURE-C coronagraph design will achieve 10⁻⁷ contrast with postprocessing, illustrated by predicted observations of realistic science targets.

9605-45, Session 9

On-ground calibration of the CHEOPS payload

François Wildi, Bruno Chazelas, Adrien Deline, Mirsad Sarajlic , Michael Sordet, Observatoire de Genève (Switzerland)

CHEOPS is a small ESA mission, which purpose is to do extra-solar planets characterization using the photometric transit technique. It is the first ESA S-class mission and will be able to switch from target to target unlike KEPLER or COROT. (http://cheops.unibe.ch/). We are developing a comprehensive support equipment to test, validate and also calibrate the CHEOPS payload before launch. This equipment is quite sophisticated because it has to goal to allow the characterization of the photometric performance of CHEOPS below the 20ppm precision of CHEOPS itself. This paper addresses the goal of the CHEOPS on-ground calibrations as well as the design, performance budget and verification plan of the CHEOPS calibration system.

9605-46, Session 10

The CHARIS IFS for high contrast imaging at Subaru

Tyler D. Groff, N. Jeremy Kasdin, Mary Anne Peters-Limbach, Michael Galvin, Michael A. Carr, Gillian R. Knapp, Princeton Univ. (United States); Timothy D. Brandt, Institute for Advanced Study (United States); Craig Loomis, Norman Jarosik, Princeton Univ. (United States); Kyle Mede, The Univ. of Tokyo (Japan); Michael McElwain, NASA Goddard Space Flight Ctr. (United States); Douglas B. Leviton, Leviton Metrology Solutions (United States); Kevin H. Miller, Manuel A. Quijada, NASA Goddard Space Flight Ctr. (United States); Olivier Guyon, Nemanja Jovanovic, Naruhisa Takato, Subaru Telescope, National Astronomical Observatory of Japan (United States); Masahiko Hayashi, Subaru Telescope, National Astronomical Observatory of Japan)

The Coronagraphic High Angular Resolution Imaging Spectrograph (CHARIS) is an integral field spectrograph (IFS) being built for the Subaru telescope. CHARIS will take spectra of brown dwarfs and hot Jovian planets in the coronagraphic image provided by the Subaru Coronagraphic Extreme Adaptive Optics (SCExAO) and AO188 adaptive optics systems. The system is designed to detect objects five orders of magnitude dimmer than their parent star down to an 80 milliarcsecond inner working angle. For characterization, CHARIS has a 'high-resolution' prism providing an average spectral resolution of R82, R69, and R82 in J, H, and K bands respectively. The so-called discovery mode uses a second 'low-resolution' prism with an average spectral resolution of R19 spanning 1.15-2.37 microns (J+H+K bands). This is unique compared to other high contrast IFS designs. It augments low inner working angle performance by reducing the separation at which we can rely on spectral differential imaging. The principal challenge for a high-contrast IFS is quasi-static speckles, which cause undue levels of spectral crosstalk. CHARIS has addressed this through several key design aspects that should constrain crosstalk between adjacent spectral features to be below 1%. Sitting on the Nasmyth platform, the alignment between the lenslet array, prism, and detector will be highly stable, key for the performance of the data pipeline. Nearly every component has arrived and the project is entering its final build phase. Here we review the science case, the resulting design, status of final construction, and lessons learned that are directly applicable to future exoplanet instruments.



9605-47, Session 10

Arizona lenslet for exoplanet spectroscopy (ALES): an AO-fed 3-5 micron optimized integral field spectrograph for the LBT

Andrew J. Skemer, Phil M. Hinz, Manny Montoya, The Univ. of Arizona (United States); Olivier Durney, Univ. of Arizona (United States); Michael F. Skrutskie, John C. Wilson, Matt J. Nelson, Univ. of Virginia (United States); Jarron M. Leisenring, The Univ. of Arizona (United States); Charles E. Woodward, Univ. of Minnesota (United States); Denis Defrere, Vanessa P. Bailey, The Univ. of Arizona (United States)

Integral field spectrographs are an important technology for exoplanet imaging, due to their ability to take spectra in a high-contrast environment, and improve planet detection sensitivity through spectral differential imaging. ALES is the first integral field spectrograph capable of imaging exoplanets from 3-5 microns, and will extend our ability to characterize self-luminous exoplanets into a range where they peak in brightness. ALES is installed inside LBTI/LMIRcam on the Large Binocular Telescope, taking advantage of existing AO systems, camera optics, and a Hawaii-2RG detector. The new optics that comprise ALES are a Keplerian magnifier, a silicon lenslet array with diffraction suppressing pinholes, a direct vision prism, and calibration optics. All of these components are installed in filter wheels making ALES a completely modular design.

9605-48, Session 10

High contrast imaging from the ground with combined visible light extreme-AO and fast near-IR speckle control

Olivier Guyon, Nemanja Jovanovic, Julien Lozi, Subaru Telescope, National Astronomical Observatory of Japan (United States); Jared R. Males, The Univ. of Arizona (United States); Garima Singh, Subaru Telescope, National Astronomical Observatory of Japan (United States); Benjamin A. Mazin, Univ. of California, Santa Barbara (United States); Frantz Martinache, Observatoire de la Côte d'Azur (France); Tomoyuki Kudo, Prashant Pathak, Subaru Telescope, National Astronomical Observatory of Japan (United States); Sean Goebel, Univ. of Hawai'i (United States) and Subaru Telescope, National Astronomical Observatory of Japan (United States)

The current generation of Extreme-AO systems is based on high speed visible-light extreme adaptive optics combined with near-IR PSF calibration techniques. In this architecture, the main contributors to residual speckles

are (1) time-lag speckles due to the limited speed of the visible light correction loop, (2) non-common path errors which may be static or slowly varying and (3) chromatic wavefront terms. While these three terms are not strong contributors to the overall wavefront error budget, they create slow speckles that do not average well over typical integration times, and limit current systems' ability to reach high contrast at small angular separations.

We show that by combining a fast (>kHz sampling) visible-light high sensitivity WFS with a fast (~kHz) near-IR post-coronagraphic speckle control loop, all three terms are significantly reduced, allowing 1e-8 contrast to be reached at 50-100 mas on an 8m telescope around bright nearby stars. Predictive control can further improve/extend system performance. This is the strategy adopted by the Subaru Coronagraphic Extreme-AO (SCEXAO) system, which combines a 3.5 kHz visible light non-modulated Pyramid WFS using a deep depletion EMCCD with a kHz near-IR speckle control loop using a photon-counting wavelength-resolving MKIDs detector. The same approach, when deployed on Extremely Large Telescopes, will allow direct imaging and spectroscopic characterization of habitable planets around nearby M-type stars.

9605-49, Session 10

An update on the VORTEX project

Olivier Absil, Univ. de Liège (Belgium); Dimitri Mawet, California Institute of Technology (United States); Mikael Karlsson, Uppsala Univ. (Sweden); Serge Habraken, Jean Surdej, Univ. de Liège (Belgium); Pierre-Antoine Absil, Univ. Catholique de Louvain (Belgium); Brunella Carlomagno, Univ. de Liège (Belgium); Valentin Christiaens, Univ. de Chile (Chile) and Univ. de Liège (Belgium); Denis Defrère, The Univ. of Arizona (United States); Pontus Forsberg, Uppsala Univ. (Sweden); Julien H. V. Girard, European Southern Observatory (Chile); Carlos A. Gomez Gonzalez, Univ. de Liège (Belgium); Philip M. Hinz, The Univ. of Arizona (United States); Elsa Huby, Aïssa Jolivet, Univ. de Liège (Belgium); Julien Milli, European Southern Observatory (Chile); Eric J. Pantin, CEA-Ctr. de SACLAY (France); Garreth J. Ruane, Rochester Institute of Technology (United States); Eugene Serabyn, Jet Propulsion Lab. (United States); Marc Van Droogenbroeck, Univ. de Liège (Belgium); Ernesto Vargas Catalan, Uppsala Univ. (Sweden); Olivier Wertz, Univ. de Liège (Belgium)

In this talk, we will review the on-going activities within the VORTEX team at the University of Liège and Uppsala University. The VORTEX project aims to design, manufacture, test, and exploit vector vortex phase masks made of sub-wavelength gratings (aka the Annular Groove Phase Mask, AGPM) for the direct detection and characterization of extrasolar planets. This talk will specifically report on the commissioning of several AGPMs on infrared cameras equipping 10-m class telescopes, including the VLT, the LBT and the Keck. We will describe the in-lab and on-sky performance of the AGPMs, and discuss first scientific observations. We will also report on the lessons learned from the on-sky operation of our vortices, and discuss ways to improve their performance. The potential of our coronagraphic devices in the context of future extremely large telescopes and space missions will also be addressed.

9605-50, Session 11

Exoplanet science with the LBTI: instrument status and plans

Denis Defrère, Philip M. Hinz, Andrew J. Skemer, Vanessa P. Bailey, Elwood C. Downey, Olivier Durney, John M. Hill, William F. Hoffmann, Jarron M. Leisenring, The Univ. of Arizona (United States); Bertrand Mennesson, Jet Propulsion Lab. (United States); Rafael Millan-Gabet, Infrared Processing and Analysis Ctr. (United States); Manny Montoya, The Univ. of Arizona (United States); Michael F. Skrutskie, Univ. of Virginia (United States); Eckhart Spalding, Amali Vaz, The Univ. of Arizona (United States)

The Large Binocular Telescope Interferometer (LBTI) is a strategic instrument of the LBT designed for high-sensitivity, high-contrast, and high-resolution infrared imaging of nearby planetary systems, operating at infrared wavelengths (1.5 to 13 ?m). To carry out a wide range of high-spatial resolution observations, it can combine the two AO-corrected 8.4-m apertures of the LBT in various ways including direct (non-interferometric) imaging, coronagraphy, Fizeau imaging, non-redundant aperture masking,



and nulling interferometry; and has broadband, narrowband or spectrally dispersed capabilities. In this paper, we review the performance of these modes in terms of exoplanet science capabilities and describe recent instrumental milestones such as first-light Fizeau images (with the angular resolution of an equivalent 22.7-m telescope) and interferometric nulling observations.

9605-51, Session 11

Post processing for direct imaging: characterizing noise properties and astrophysical sources in modern ground based coronagraphs

Laurent A. Pueyo, Space Telescope Science Institute (United States)

In this paper we present recent progress on data analysis of modern ground based coronagraph aimed at detecting and characterizing exo-planets. We first discuss the overall architecture of such instruments, that combine an Extreme Adaptive Optics system, an optimized coronagraph, low and high-order wavefront sensors and use an Integral Field Spectrograph. In this context we quantify the temporal and chromatic properties of the residual noise associated with imperfections in the optics, their correlation with wavefront sensing and control performances. We discuss post-processing strategies to subtract these speckles in order to detect exo-plantes and circumstellar structures buried under the diffracted stellar light. We then describe the intricacies associated with spectroscopy and astrometry estimation and present two recent algorithms. The first one retrieves the stellar focal plane position when the star is occulted by a coronagraphic stop. The second one yields precise astrometry and spectro-photometry estimates of faint point sources even when they are initially buried in the speckle noise. We finally highlight recent scientific results obtained using these methods.

9605-52, Session 11

Optimized pupil and focal plane phase elements for vortex coronagraphs on telescopes with obstructed apertures

Garreth J. Ruane, Rochester Institute of Technology (United States); Elsa Huby, Univ. de Liège (Belgium); Christian Delacroix, Ctr. de Recherche Astrophysique de Lyon (France); Dimitri Mawet, Jet Propulsion Lab. (United States); Olivier Absil, Univ. de Liège (Belgium); Grover A. Swartzlander Jr., Rochester Institute of Technology (United States)

We present a technique for optimizing pupil and focal plane phase elements for vortex coronagraphs on telescopes with obstructed apertures. The phase elements are calculated numerically using a point-by-point iterative phase retrieval algorithm. Two example designs for the future European Extremely Large Telescope (E-ELT) and the Thirty Meter Telescope (TMT) are described. The first design applies a phase correction to the focal plane element in order to improve the starlight suppression of a conventional vortex coronagraph. The second design introduces a phase element after the Lyot stop to modify the residual on-axis point spread function and improve the contrast in a pre-defined region of the image plane. We analyze the performance of these designs in terms of contrast and off-axis image quality. Limitations set by chromatic effects and manufacturing constraints are also explored.

9605-53, Session 11

A Mach-Zehnder interferometer based on orbital angular momentum for improved vortex coronagraph efficiency

Pierre Piron, Univ. de Liège (Belgium); Christian Delacroix, Ctr. de Recherche Astrophysique de Lyon (France); Elsa Huby, Univ. de Liège (Belgium); Dimitri Mawet, Jet Propulsion Lab. (United States); Aïssa Jolivet, Brunella Carlomagno, Serge Habraken, Olivier Absil, Jean Surdej, Univ. de Liège (Belgium)

When used as coronagraphs, vortex phase masks provide a continuous helical phase ramp for on-axis input light, which leads to the creation of orbital angular momentum (OAM). Thanks to that helical phase, the intensity of the central source is rejected outside the geometrical pupil in a subsequent pupil plane, while off-axis sources located beyond an angular distance of lambda/D are mostly unaffected. However, due to wave front imperfections, the on-axis light rejection is not perfect. To improve on-axis light rejection, a Mach-Zehnder interferometer containing Dove prisms differently oriented has recently been proposed to sort photons based on their OAM (Riaud 2014).

In this paper, we will develop the mathematical model of the wave front propagation in the Mach-Zehnder interferometer using the Jones formalism. Based on our model, we show that the performance of this setup is limited to a 10-fold increase in the on-axis light rejection due the Dove prism birefringence. We propose and evaluate possible ways to improve the interferometer performance, including the addition of a birefringent wave-plate in each arms to compensate for the Dove prism birefringence. The effect of the birefringent plate is mathematically described and used to reassess the performance. Finally, we discuss the sensitivity of the interferometer performance to several experimental conditions, such as the central obstruction and the imperfections of the AGPM.

9605-54, Session 11

A family of subwavelength grating vortex coronagraphs (SGVCs) with higher topological charge

Christian Delacroix, Ctr. de Recherche Astrophysique de Lyon (France); Pontus Forsberg, Uppsala Univ. (Sweden); Pierre Piron, Univ. de Liège (Belgium); Garreth J. Ruane, Rochester Institute of Technology (United States); Elsa Huby, Brunella Carlomagno, Aïssa Jolivet, Univ. de Liège (Belgium); Ernesto Vargas, Uppsala Univ. (Sweden); Olivier Absil, Univ. de Liège (Belgium); Dimitri Mawet, European Southern Observatory (Chile); Mikael Karlsson, Uppsala Univ. (Sweden); Jean Surdej, Serge Habraken, Univ. de Liège (Belgium)

The subwavelength grating vortex coronagraph (SGVC) is a focal-plane spiral-like phase mask whose key benefit is to allow high contrast imaging at small angles. Directly etched onto a CVD diamond substrate, it is well suited to perform in the mid-infrared domain. It provides a continuous helical phase ramp with a dark singularity in its center, and is characterized by its number of phase revolutions, called the topological charge. Over the past two years, we have manufactured several charge-2 SGVCs (a.k.a. annular groove phase masks) and successfully demonstrated their performances on 10-m class telescopes (LBT, VLT/NaCo, VLT/VISIR). To prevent stellar leakage on future 30-m class telescopes (E-ELT, TMT, GMT), a broader off-axis extinction is required, which can be achieved by increasing the topological charge. We have recently proposed an original design for a charge-4 SGVC allowing less starlight to leak through the coronagraph, at the cost of a degraded inner working angle. In this talk, we report on our latest development of higher charge SGVCs. From 3D rigorous numerical simulations using a finite-difference time-domain (FDTD) algorithm, we



have derived a family of coronagraphs with higher topological charge (SGVC4/6/8). Our new optimization method addresses the principal limitation of such space-variant polarization state manipulation, i.e., the inconvenient discontinuities in the discrete grating pattern. The resulting gratings offer improved precision to the phase modulation compared to previous designs. Finally, we present our preliminary manufacturing and metrology results for infrared components down to the K-band.

9605-55, Session 11

ExTrA

Jose Manuel Almenara, Xavier Bonfils, Laurent Jocou, Institut de Planétologie et d'Astrophysique de Grenoble (France); Anael Wunsche, Institut d'Informatique et Mathématiques Appliquées de Grenoble (France); Pierre Kern, Alain Delboulbé, Philippe Feautrier, Laurence Gluck, Sylvain Lafrasse, Yves Magnard, Didier Maurel, Thibaut Moulin, Felipe Murgas, Patrick Rabou, Sylvain Rochat, Alain Roux, Eric Stadler, Institut de Planétologie et d'Astrophysique de Grenoble (France)

ExTrA is an ERC-funded project offering a novel method to dramatically improve on the precision of ground based photometry and more efficiently search for exo-Earths orbiting cool stars. The method makes use of a multiobject spectrograph to add the spectroscopic resolution to the traditional differential photometry method. We will discuss how this shall enable the fine correction of color-dependent systematics (atmospheric variations, instrument and detector errors) that would otherwise hinder ground-based observations.

ExTrA aims to develop this method with a new facility composed of three small telescopes (60cm in diameter) and a near-infrared spectrograph (R<500, lbda=0.8-1.6 ?m). Near-infrared observations will boost the efficiency of its cool-star observations, such that ExTrA might become the most sensitive survey for Earth-size planets transiting nearby planets. It shall yield dozens exo-Earths amenable to atmospheric characterization, including several exo-Earths in the habitable zone, which may provide our first peek into an exolife laboratory. In addition, ExTrA might prove to be powerful in following-up K2, TESS and PLATO candidates.

In this talk, we shall discuss all aspects of ExTrA from its concept to the expected exoplanet yield, passing by its design, feasibility laboratory tests, and implementation.

9605-56, Session 12

iLocater: a high-resolution, near-infrared Doppler spectrometer for the large binocular telescope

Justin R. Crepp, Eric Bechter, Erica Gonzales, Edward Kielb, Andrew Bechter, Jonathan Crass, Jay Carroll, Ryan Ketterer, John Brooks, Univ. of Notre Dame (United States); Robert O. Reynolds, Large Binocular Telescope Observatory (United States); Phil M. Hinz, The Univ. of Arizona (United States); Michael F. Skrutskie, Univ. of Virginia (United States); Joshua Eisner, The Univ. of Arizona (United States); Louis G. Fantano, NASA Goddard Space Flight Ctr. (United States); B. Scott Gaudi, The Ohio State Univ. (United States); David Go, John Kearns, Univ. of Notre Dame (United States); David M. P. King, Univ. of Cambridge (United States); Corina Koca, NASA Goddard Space Flight Ctr. (United States); Kaitlin Kratter, The Univ. of Arizona (United States); Christopher Matthews, Univ. of Notre Dame (United States); Giuseppina Micela, INAF -Osservatorio Astronomico di Palermo Giuseppe S. Vaiana

(Italy); Andreas Quirrenbach, Landessternwarte Heidelberg (Germany); Alessandro Sozzetti, INAF - Osservatorio Astronomico di Torino (Italy); Karl Stapelfeldt, NASA Goddard Space Flight Ctr. (United States); Darren Williams, The Pennsylvania State Univ. (United States); Charles E. Woodward, Univ. of Minnesota, Twin Cities (United States); Bo Zhao, Univ. of Florida (United States); Isabella Pagano, INAF - Osservatorio Astrofisico di Catania (Italy)

iLocater will soon become the world's first diffraction-limited Doppler spectrometer. An infrared-optimized, high resolution planet-finding spectrograph recently approved for construction at the Large Binocular Telescope, iLocater is the first radial velocity instrument that will use "extreme" adaptive optics to inject starlight into single mode optical fibers. In addition to completely eliminating modal noise, iLocater will also reduce background contamination from OH-emission lines by two orders of magnitude compared to seeing-limited instruments, use an Invar design to relax temperature control requirements by an order of magnitude, and use two 8.4m telescope dishes simultaneously to monitor and remove internal velocity errors. In this presentation, we discuss iLocater's expected performance and science return.

9605-57, Session 12

First results of instrumental stability using an astro frequency comb at the foces spectrograph

Frank U. Grupp, Univ.-Sternwarte München (Germany) and Max-Planck-Institut für extraterrestrische Physik (Germany); Anna Brucalassi, Max-Planck-Institut für extraterrestrische Physik (Germany); Hanna Kellermann, Univ.-Sternwarte München (Germany); Ronald Holzwarth, Tilo Steinmetz, Menlo Systems GmbH (Germany); Ulrich Hopp, Univ-Sternwarte München (Germany); Ralf Bender, Max-Planck-Institut für extraterrestrische Physik (Germany)

Since January 2015 the R=70000 FOCES Echelle spectrograph is equipped by an Astro Frequency COMB. With this paper we present first results on the instrument stability measured by this "perfect calibrator". As FOCES is equipped with temperature and pressure stabilization, the Frequency Comb allows to test the stability models and predictions of pressure and temperature sensitivity. In addition, the stability of the thermo-electrically cooled FOCES CCD system will be presented.

9605-58, Session 12

Effects of fiber manipulation methods on optical fiber properties

Robert O. Reynolds, Large Binocular Telescope Observatory (United States)

Optical fibers are now routinely used to couple high-resolution spectrographs to modern telescopes, enabling important advantages in areas such as the search for extrasolar planets using spectroscopic radial velocity measurements of candidate stars. Optical fibers partially scramble the input illumination, and this phenomenon enables a fiber feed to provide more uniform illumination to the spectrograph optics, thereby reducing systematic errors in radial velocity measurements. Current instruments now achieve a precision of ~1m/s using fiber-feeds, but greater precision approaching 10cm/s is required to detect terrestrial planets orbiting sunlike stars. A primary limiting factor in multimode fiber coupling is modal noise, a measurement uncertainty caused by inherent properties of optical fibers, evident as a varying spatial intensity at the fiber exit plane. Many



instruments utilize the strategy of agitating the fiber during an observation to reduce modal noise, and squeezing of the fiber and dynamical optical diffusers have been tested as alternatives to agitation. However, deformation of the fiber can lead to light loss, and diffusers may be suitable only for calibration sources due to known losses. The technique of stretching or varying the length of the fiber has been shown to offer advantages over other approaches, but effects of stretching on fiber parameters such as total transmission and focal ratio degradation have not been adequately studied. In this paper we present results of measurement of transmission loss and focal ratio degradation in a stretched fiber, along with discussion of possible consequences.

9605-59, Session 13

Archival legacy investigation of circumstellar environments (ALICE): statistical analysis of high-contrast images of 400 stars with HST-NICMOS

Élodie Choquet, Rémi Soummer, Laurent A. Pueyo, J. Brendan Hagan, Elena Gofas-Salas, Marshall D. Perrin, Christine Chen, John H. Debes, David A. Golimowski, Dean C. Hines, Space Telescope Science Institute (United States); Glenn H. Schneider, The Univ. of Arizona (United States); Amaya Moro-Martin, Space Telescope Science Institute (United States); Christian Marois, NRC-Dominion Astrophysical Observatory (Canada); Dimitri Mawet, European Southern Observatory (Chile); Mamadou N'Diaye, Space Telescope Science Institute (United States); Abhijith Rajan, Arizona State Univ. (United States); Schuyler G. Wolff, Jonathan Aguilar, Alexandra Z. Greenbaum, Johns Hopkins Univ. (United States); Bin Ren, Johns Hopkins Univ. (United States)

We are currently conducting a comprehensive and consistent re-processing of archival HST-NICMOS coronagraphic surveys using advanced PSF subtraction methods, entitled the Archival Legacy Investigation of Circumstellar Environments program (ALICE, HST/AR 12652). This virtual campaign of about 400 stars observed between 1998 and 2008 has already produced numerous new detections of previously unidentified point sources and circumstellar structures (both protoplanetary disks and debris disks). We present an overview of the objects detected as part of this program and report on follow-up status for the companion candidates, and characterization status for the circumstellar disks. We also estimate the number of exoplanets in our candidate sample, based on background source probability from stellar population models. Finally, we discuss the preliminary statistical constraints ALICE places on the occurrence of brown dwarf and exoplanet companions around nearby stars. Since the methods developed as part of ALICE are directly applicable to future missions (JWST, AFTA coronagraph) we emphasize the importance of devising optimal PSF subtraction methods for upcoming coronagraphic imaging missions. We describe efforts in defining direct imaging high-level science product (HLSP) standards that can be applicable to other coronagraphic campaigns, including ground-based (e.g., Gemini Planet Imager, SPHERE, ELTs), and future space instruments (e.g., JWST).

Conference 9606: Instruments, Methods, and Missions for Astrobiology XVII

Sunday - Tuesday 9 -11 August 2015

Part of Proceedings of SPIE Vol. 9606 Instruments, Methods, and Missions for Astrobiology XVII

9606-1, Session 1

The centenary of the birth of Fred Hoyle, a landmark event in astrobiology

Chandra N. Wickramasinghe, The Univ. of Buckingham (United Kingdom) and Institute for the Study of Panspermia and Astroeconomics (Japan) and Univ. of Peradeniya (Sri Lanka); G. Tokoro, Institute for the Study of Panspermia and Astroeconomics (Japan); Brig Klyce, Astrobiology Research Trust (United States)

The setting up of the Institute for the Study of Panspermia and Astroeconomics (ISPA) in Japan in the centenary year of Fred Hoyle marks an important step in the progress of a field of study pioneered by Hoyle. Panspermia theory in the form it was developed by Hoyle and one of the present authors (NCW) has recently been gaining support from a wide range of studies, but is still being resisted to varying degrees by mainstream science. The website managed by one of us (BK) has attempted to record the new data and chronicle the ensuing debate. The aim of ISPA will be monitor the stratosphere with balloon-borne detectors for viruses and bacteria that might unequivocally demonstrate their space origin. The present tendency to ignore data that supports panspermia appears to be deep-rooted in economic incentives to maintain the status quo. With the arrival of more data a paradigm shift from Earth-centred to cosmic-centred life will become increasingly likely. The present year is already bringing a wealth of new supportive data for panspermia.

9606-2, Session 2

Is life supernatural? (Invited Paper)

Gilbert V. Levin, Arizona State Univ. (United States)

The big question of the origin of life is examined. The paradox of Pasteur's dictum "Life only comes from life," and the need for spontaneous generation is explored. This seemingly dead end conundrum contrasts sharply with the great progress we have made in understanding the evolution of the species since Darwin's revolutionary insight. The conditions that promoted non-living molecules and compounds to cross the sharp line from inert to life is contemplated. Future prospects for solving this penultimate mystery, with some suggestions for experiments, are conjectured with the objective of promoting much needed discussion on this key issue.

9606-3, Session 2

Oparin's coacervates as an important milestone in chemical evolution (Invited Paper)

Vera M. Kolb, Univ. of Wisconsin-Parkside (United States)

We summarize first some traditional views on the milestones in chemical evolution which led to life. Then we focus on Oparin's coacervates as one such milestone. We review our recent work in which we have shown that Oparin's coacervates can serve as prebiotic chemical reactors. We then present Oparin's views on chemical evolution via his coacervates, and show that they are still valid. He has pointed out a competition between coacervates for "food", namely chemicals from the prebiotic soup, a selection process which gives advantage to coacervates which have useful catalysts that enable them to synthesize their own "food", and finally more sophisticated coacervates which ultimately acquire capability to synthesize primitive information molecules that will preserve chemical knowledge of the system.

+1 360 676 3290 ·

help@spie.org

9606-4, Session 2

Philosophy of astrobiology: Some recent developments

Vera M. Kolb, Univ. of Wisconsin-Parkside (United States)

We present some recent developments in philosophy of astrobiology to illustrate usefulness of philosophy to astrobiology. Our examples include philosophical applications to the definition of life and chemical evolution. We include Aristotelian views, dialetheism, and the philosophical analysis by Iris Fry about the beginning of natural selection in prebiotic world.

9606-5, Session 2

How to survive a late heavy bombardment

Gregory A. Konesky, National Nanotech Inc. (United States)

The disparity of the radiometric age of the Earth and the age of the oldest rock formations was addressed by the Apollo Lunar samples which strongly supported the idea of a Late Heavy Bombardment which essentially resurfaced the Earth. Zircon mineral grains, which predate the LHB, grow by concretion and occasionally entrap samples of their immediate environment as inclusions, and reveal the presence of oceans on Earth prior to the LHB. Suppose life originated prior to the LHB, but any microfossil evidence of it would have been erased by that event. While the oldest microfossils, as evidenced by carbon-13 depletion relative to carbon-12, might suggest a recurrent origination of life, we consider how still earlier life could have survived in the deep hot biosphere and re-emerged at the end of the LHB, reestablishing life on the surface of the Earth. We review the deep hot biosphere as it exists today and consider the dynamics of the LHB in terms of frequency and size of impacts to show that the putative "first" life to originate prior to the LHB could have survived this event. Indeed, we consider the environment of the early pre-LHB Earth and find it more favorable to the origination of life than the post-LHB.

9606-6, Session 3

Bioluminescent bacteria grown under modelled gravity of different astronomical bodies in the solar system (Invited Paper)

Santosh Bhaskaran, Vivekanand Education Society College of Arts, Science and Commerce (India) and Savitribai Phule Pune Univ. (India); Rohan D. Dudhale, P.E.S. Modern College of Arts, Science and Commerce (India) and Haffkine Institute (India); Jyotsana P. Dixit, P.E.S. Modern College of Arts, Science and Commerce (India) and Savitribai Phule Pune Univ. (India); Ajit N. Sahasrabuddhe, P.E.S. Modern College of Arts, Science and Commerce (India) and Serum Institute of India (India); Pandit B. Vidyasagar, Savitribai Phule Pune Univ. (India) and Swami Ramanand Teerth Marathwada Univ. (India)

Vibrio harveyi (strain NB0903), a bioluminescent bacterium, were exposed to modelled gravity conditions viz. Microgravity (Space), 0.16 g (Lunar), 0.38 g (Martian), 1 g (Earth) as dynamic control and 2.5 g (Jovian) for 15 hours using a clinostat-centrifuge system. The suspension culture was adjusted to OD = 0.2 (approx. $5x10^9$ cells/ml) and 1% inoculum added to sterile BOSS broth (Klein et al., 1998) in each of four identical glass vessels specially designed for the system. Two of these cultures were exposed to altered gravity. The other two cultures acted as static controls. At regular



Conference 9606: Instruments, Methods, and Missions for Astrobiology XVII



intervals of one hour, aliquots were taken for measuring optical density at 590 nm using a digital colorimeter. Both control and test vessels were shaken well before taking the aliquots so that the cultures were well-mixed. All experiments were carried out at room temperature (25±1 °C). Each experiment was repeated three times and consistent results were obtained.

Comparison of OD showed maximum growth in modelled lunar gravity followed by modelled microgravity compared to static control. This was followed by modelled Martian gravity, Earth's gravity/ dynamic control and Jovian gravity compared to static control. Thus modelled Lunar gravity appears to be most favourable for the growth of Vibrio harveyi. Similar studies on mammalian cells are important, since they will provide an insight as to how our physiological systems will adapt to such gravity conditions. This can be used in industry to get maximum output from micro-organisms just by optimising the value of g in addition to pH, temperature, etc.

9606-7, Session 3

Exomoon habitability

Gregory A. Konesky, National Nanotech Inc. (United States)

The highly successful transit method for detecting exoplanets can also provide evidence for the possible presence of exomoons by variations in the transit timing, caused by the motions of exomoons around the host exoplanet. We consider two categories of habitable exomoons. One is where the exomoon/exoplanet system in within the habitable zone of the host star, even though the exoplanet itself may be unsuitable for life, such as a gas giant. Another category of habitable exomoon is where the habitable conditions are maintained by tidal heating as it orbits the host exoplanet. Such habitability is independent of illumination from the host star. In the early phases of the formation of a solar system, large numbers of planets may form which, through gravitational encounters with each other, have been ejected from the solar system, and today wander interstellar space, far from any host star. Yet exomoons orbiting these wandering or "rogue" planets may remain habitable due to tidal heating. It is estimated that the number of rogue planets exceeds the number of stars in our galaxy by at least an order of magnitude. We also consider the role of Earth's Moon in establishing and maintaining conditions for the development of advanced life forms. When viewed over interstellar distances, the Earth-Moon system might well be considered a double or binary planet. If this is a necessary criterion for the development of advanced life forms, then simple basic life may be quite common in the universe, but advanced forms may be exceedingly rare.

9606-8, Session 4

The search for extra-terrestrial intelligence: current status and future prospects (Invited Paper)

Stuart Bowyer, Univ. of California, Berkeley (United States)

The idea that credible searches for Extra-Terrestrial Intelligence (ETI) could be carried out using the radio band were laid out in detail in a classic paper by Morrison and Cocconi (1959). Since then radio searches have been carried out by over sixty different groups. No signals from ETIs have been identified. Most searches did not have high sensitivity so it is not surprising that no ETI signals were detected. Within the last few years, important new ideas regarding the existence of ETI have evolved. New radio instrumentation with greatly superior sensitivity has been developed, new information on the existence of possible sites for ETI (especially in regards to planetary sites) has been found, and new types of searches have been suggested. A major discovery of import was the detection of a surprising number of planetary systems. This increases the potential locations for extraterrestrial intelligence. However, the systems that have been discovered show that the formation of planetary systems is complex and results in many systems that are unstable. In a worst case scenario for the Search for Extra-Terestrial Intelligence (SETI), there will be far more stars with planetary systems but few planets with appropriate orbits. An additional complexity is the requirement, based on very general grounds, that water

is a necessity for the development of life. But the origin of water on Earth is unclear and may not occur in other planets. Despite these uncertainties most workers in the field continue to be optimistic regarding the possibility of eventually detecting an ETI signal. In this paper I review these issues.

9606-9, Session 4

The next phases of SETI@home

Eric J. Korpela, Andrew P. V. Siemion, Dan Werthimer, Univ. of California, Berkeley (United States); Matt Lebofsky, Space Sciences Lab. (United States); Jeff Cobb, Univ. of California, Berkeley (United States)

The SETI@home project, which has been underway since May 1999 is the largest volunteer computing project in existence. Over 9 million people have signed up since its introduction. Since its release, multiple enhancements have been made which better utilize the capabilities of the computers running SETI@home including ports to graphics processing units (GPU) and ports to Android devices including mobile phones. We are preparing a new release of SETI@home entirely reweritten. It will include full stokes parameterization of signals, and RFI rejection using cross polarization and cross beam techniques. It will, whenever possible, be data source agnostic. I will describe the state of development and plans for its release.

9606-10, Session 5

The universal alien and the case for our Martian origins (Invited Paper)

Steven Albert Benner, The Foundation For Applied Molecular Evolution (United States)

A survey of ongoing activities seeking to understand the origin of life on Earth finds today much that would have been familiar half a century ago to Leslie Orgel, Jim Ferris, Stanley Miller, and other heroes of the field. Pathways are still being sought to get simple biological molecules (amino acids, nucleosides and nucleotides) from a "prebiotic soup" containing the same organic building blocks that have been identified for years. Laboratories are still attempting to get RNA to be synthesized on template RNA from activated building blocks, much as Orgel attempted in the 1960s. The same kinds of lipids are being sought to create much the same compartments as were sought in the classical era of "origins". Today's experiments are, of course, easier because of recent advances in technology. However, the fact that the questions being asked would be familiar to those who asked them a half-century ago is disappointing, and is prompting many organizations, including the John Templeton Foundation, to seek research directions that embody new concepts.

One new concept recognizes that the terran biochemistry need not be universal. Work in synthetic biology has taught us that other biopolymers can perform the roles that DNA, RNA, and proteins perform in the life that we know here on Earth. Accordingly, it is necessary to extract general principles about how Darwinian evolution might be done in life that does not share a common ancestry with life on Earth. This concept of the "universal alien" must then be extended to origins as well. Here, the universal rules of chemistry create suggest some paradoxes. For example, water appears to be a particularly good solvent for life. At the same time, the biopolymers that we know in life on Earth are easily corroded by water. The only reason why we survive today in water is because we have repair systems that constantly fix the damage that water is doing to our nucleic acids and proteins.

Those repair systems almost certainly did not arise together with the first Darwinian systems. Further, the inventory of water on early Earth appears to be too excessive to permit many of the chemical reactions that we most favor to create the first life forms. Interestingly, the inventory of water on Mars was never as high, and Mars contains certain minerals (including those containing elements such as boron) that could function in a semi arid environment, but never on a flooded planet.

This talk will present the case to the layperson for a universal biochemistry, and the possibility that it could have been established on Mars, only to come



from Mars to Earth to be our ancestors after it was safely established.

9606-11, Session 5

Prebiotic reactions in superheated water

Vera M. Kolb, Univ. of Wisconsin-Parkside (United States)

Water changes its properties when superheated and behaves more like an organic solvent. Thus, numerous organic reactions occur in superheated water, which do not occur readily in water under normal conditions. Functional group transformations which occur in water at elevated temperatures and pressures are directly related to the chemical syntheses in hydrothermal vents. We review key properties of superheated water and select the reactions which occur readily in this medium and which are of prebiotic importance.

9606-12, Session 5

The bioinformatics of nucleotide sequence coding for proteins requiring metal coenzymes and proteins embedded with metals (Invited Paper)

George Tremberger Jr., Sunil Dehipawala, Andrew Nguyen, Todd Holden, David Lieberman, Tak D. Cheung, Queensborough Community College (United States)

All metallo-proteins (proteins embedded with metals) require posttranslation metal incorporation in order to perform their functions. The measurement of isotope ratios of iron, copper, and zinc has emerged as an important tool in the fields of physiology and oncology. The random nature in which metals are assimilated in proteins can be studied in terms of nucleotide sequence complexity. The inside-out theory for the emergence of eukaryotic cells via bleb formation as proposed by Baum (BMC Bio 2014 Oct 28) has been found to be consistent with the view that the activity of metals are critical for the evolution of life. The isotope ratio of Carbon-12 to Carbon-13 has been used to bolster support for a recent theory that establishes the origin of life on Earth at 4 billion years BP. The hypothesis that early methanogens would favor releasing Carbon-12 while retaining Carbon-13 finds support in the isotope ratio results reported in physiology and oncology studies. The nickel-containing F430 is the prosthetic group of the enzyme methyl coenzyme M reductase, which catalyzes the release of methane in the final step of methanogenesis. Sequences requiring metalembedded coenzymes have also been studied in terms of bioinformatics complexity as measured by fractal dimension and entropy. The results are consistent with the idea that metal-embedded coenzymes could act as life switches. The evolutionary advantage of metallo-proteins and proteins with metal-embedded coenzymes in the contexts of molecular crowding and the RNA granule dynamical cytoplasm is also discussed.

9606-13, Session 5

The advantage of dynamic, covalent bonds in the formation and evolution of proto-RNA (Invited Paper)

Nicholas V. Hud, Georgia Institute of Technology (United States)

The RNA World hypothesis remains popular among many origins of life researchers. However, a prebiotic synthesis of RNA has not been demonstrated. Significant challenges facing the prebiotic formation of RNA polymers include nucleobase selection, sugar selection, nucleoside bond formation, and nucleotide polymerization. We are investigating the hypothesis that RNA was preceded by a polymer that would have assembled more easily than RNA, a hypothetical polymer that we refer to as proto-RNA. This primitive genetic polymer (or polymers) would have had a different backbone and different nucleobases. Each component of proto-RNA would have been changed over the course of time by chemical and biological evolution, most likely through a series of intermediate pre-RNAs. In support of this hypothesis, recent advances in our laboratory have revealed that alternative, plausibly prebiotic nucleobases can self-assemble in water and readily form nucleosides with ribose, two properties not observed with the nucleobases currently found in RNA. In addition to molecular selection by noncovalent interactions, which is common in self-assembly, we are also finding that dynamic, covalent bonds allow for the selection of molecules and structures that could have facilitated and greatly accelerated the emergence and evolution of the first biopolymers.

9606-14, Session 6

Ribosome dynamics and the evolutionary history of ribosomes (*Invited Paper*)

George E. Fox, Maxim Paci, Quyen Tran, Univ. of Houston (United States)

The modern ribosome is a dynamic nanomachine responsible for coded peptide synthesis in modern cells. The major ribosomal subsystems were essentially in place at the time of the last universal common ancestor (LUCA) and ribosome evolutionary history thus provides a window into the pre-LUCA world. The large ribosomal RNAs (rRNAs) grew in size over time and recent studies show that the growth mechanisms were likely the same in the pre- and post-LUCA time periods. This understanding has allowed development of a detailed model for the relative age of each helical segment in the rRNAs. A key ribosomal component is the transfer RNAs that bring activated amino acids into the ribosomal A-site. There is a hinge like structure (pivot point) in each tRNA that allows it to rotate from the A- site, to the P- site and ultimately the E site from which it exits the ribosome. Large numbers of high resolution ribosome structures and ribosomal subunits in different states are now available. We have used this information to identify the location of 21 additional pivot points in the large rRNAs. When examined in the context of helix age, these pivots appear to have been added in a similar time period, which likely was after the addition of the tRNA hinge. In particular, there appears to be a portion of the small subunit RNA that may be inherently flexible. The addition of this segment and the tRNA hinge would have made mRNA moment and hence coded peptide synthesis possible.

9606-15, Session 6

The complexity of genetic sequences modified by horizontal gene transfer

George Tremberger Jr., Sunil Dehipawala, Andrew Nguyen, Todd Holden, David Lieberman, Tak D. Cheung, Queensborough Community College (United States)

Horizontal gene transfer is an important and efficient means of moving genetic material among living species and could serve as a pathway for the incorporation of non-coding DNA into a genome. Our previous study of Inc-RNA sequence complexity using fractal dimension and information entropy analysis shows a strongly regulated trend among the studied genes in numerous diseases. Sequence complexity due to retrovirus-related horizontal gene transfer has been investigated in several symbiotic species living within the mealybug (www.cell.com/abstract/ S0092-8674%2813%2900646-6). A recent study on Gamma Ray Bursts, which suggests that a redshift of z < 0.5 is the earliest time when life could emerge in the universe, proposes that radiation resistance in genomes is of foremost importance (On the role of GRBs on life extinction in the Universe, Phys. Rev. Lett. 113, 231102, 2014). Research supporting the view that the origin of asteroids is the result of planet formation strengthens a solarorigin hypothesis for the emergence of a radiation resistance gene at time z<0.5. The interpretation that non-coding gene transcription differences in Deinococcus radiodurans exposed to ionizing radiation would give rise to global gene regulation (Transcriptional Analysis of Deinococcus radiodurans Reveal Novel sRNAs that are Differentially Expressed under

lonizing Radiation. Appl Environ Microbiol. 2014 Dec 29) is analyzed from a bioinformatics perspective in this project. The likelihood that DR radiation repair sequences underwent horizontal gene transfer is also discussed.

9606-16, Session 6

Mutation, but not random

Brig Klyce, Astrobiology Research Trust (United States)

The strongest version of panspermia holds that life on Earth comes from elsewhere, and all the genetic programs for evolution to higher life forms likewise must ultimately come from elsewhere. Once the programs are supplied, darwinian mutation-and-selection can test and optimise them. The needed mutations can be sped up by stress; this process is called adaptive mutation. If the mutations are confined to appropriate DNA segments, as usual, that is called directed mutation. But for significant evolutionary progress, horizontal gene transfer is essential. New evidence suggests that some bacteria can actively induce other species to donate their genes to the inducers. In these ways, evolution benefits from mutations that are far from random.

9606-17, Session 7

Possible effects of diagenesis on the stable isotope composition of amino acids in carbonaceous meteorites (Invited Paper)

Michael H. Engel, The Univ. of Oklahoma (United States)

The initial report of indigenous, non-racemic protein amino acids (L-enantiomer excess) in the Murchison meteorite was based on the fact that only eight of the 20 amino acids characteristic of all life on Earth was present in this stone (Engel and Nagy, 1982). The absence of the other protein amino acids indicated that contamination subsequent to impact was highly unlikely. The development of new techniques for determining the stable isotope composition of individual amino acid enantiomers in the Murchison meteorite further documented the extraterrestrial origins of these compounds (Engel et al., 1990; Engel and Macko, 1997). The stable isotope approach continues to be used to document the occurrence of an extraterrestrial L-enantiomer excess of protein amino acids in other carbonaceous meteorites (e.g. Glavin et al., 2012). It has been suggested that this L-enantiomer excess may result from aqueous reprocessing on meteorite parent bodies (e.g. Engel, 2012; Glavin et al., 2012). Preliminary results of simulation experiments are presented that are used to determine the extent to which the stable isotope compositions of amino acid constituents of carbonaceous meteorites may have been altered by these types of diagenetic processes subsequent to synthesis.

9606-18, Session 7

Carbonaceous structures in the Tissint Martian Meteorite: evidence of a biogenetic origin (Invited Paper)

Jamie H. Wallis, Cardiff Univ. (United Kingdom); Nalin Chandra Wickramasinghe, Daryl H. Wallis, The Univ. of Buckingham (United Kingdom); Norimune Miyake, Chiba Institute of Technology (Japan); Max K. Wallis, The Univ. of Buckingham (United Kingdom); Richard B. Hoover, The Univ. of Buckingham (United Kingdom) and Athens State Univ. (United States)

We report for the first time in situ observations of $5-50\mu$ m spherical carbonaceous structures in the Tissint Martian meteorite comprising of pyrite (FeS2) cores and carbonaceous outer coatings. The structures are characterized as smooth immiscible spheres with curved boundaries occasionally following the contours of the pyrite inclusion. The structures

bear striking resemblance to similar-sized immiscible carbonaceous spheres found in hydrothermal calcite vein deposits in the Mullaghwornia Quarry in central Ireland. Similar structures have been reported in Proterozoic and Ordovician sandstones from Canada as well as in a variety of astronomical sources including carbonaceous chondrites, chondritic IDPs and primitive chondritic meteorites. SEM and X-Ray elemental mapping confirmed the presence of organic carbon filling the crack and cleavage space in the pyroxene substrate, with further evidence of pyrite acting as an attractive substrate for the collection of organic matter. The detection of precipitated carbon collecting around pyrite grains is at variance with an igneous origin as proposed for the reduced organic component in Tissint, and is more consistent with a biogenetic origin.

SPIE. PHOTONICS+

APPLICATIONS

OPTICAL ENGINEERING+

9606-19, Session 7

Chemical and structural composition of organic carbonaceous structures in Tissint: evidence for a biogenetic origin

Jamie H. Wallis, Cardiff Univ. (United Kingdom); N. C. Wickramasinghe, Daryl H. Wallis, The Univ. of Buckingham (United Kingdom); Norimune Miyake, Chiba Institute of Technology (Japan); Max K. Wallis, The Univ. of Buckingham (United Kingdom); Richard Hoover, The Univ. of Buckingham (United Kingdom) and Athens State Univ. (United States)

Earlier studies of the Tissint Martian meteorite identified the presence of a number of 5-50µm carbonaceous spherical structures. SEM and EDS elemental spectra for 11 selected structures confirmed that they comprise of a carbonaceous outer coating with a inner core of FeS2 (pyrite) and are characterised as immiscible globules with curved boundaries. Here we report on the results of Raman spectroscopic studies that unambiguously confirm the mantle as comprising of 'disordered carbonaceous material' R1 = ID/IG against ?D (cm-1) band parameter plots of the carbonaceous coatings imply a complex precursor carbon inventory comparable to the precursor carbon component of materials of known biotic source (plants, algae, fungi, crustaceans, prokaryotes). Correlation between peak metamorphic temperatures and Raman D-band (?D) parameters further indicate the carbonaceous component was subjected to a peak temperature of ~250 OC suggesting a possible link with the hydrothermal precipitation processes responsible for the formation of similar globules observed in hydrothermal calcite veins in central Ireland. ? G (cm-1), ?G (cm-1), ? D (cm-1) and ?D (cm-1) parameters further imply a level of crystallinity and disorder of the carbon component consistent with carbonaceous material recovered from a variety of non-terrestrial sources. Cl, N, O and S to C elemental ratios are typical of high volatility bituminous coals and distinctly higher than equivalent graphite standards.

9606-20, Session 7

Microbiological investigation of two chondrite meteorites: Murchison and Polonnaruwa

Elena V. Pikuta, Athens State Univ. (United States); Paul A. Lawson, Nisha Patel, The Univ. of Oklahoma (United States); William B. Whitman, The Univ. of Georgia (United States); Jacob Hagel, Daniel Easters, Geneviev LaBrake, Athens State Univ. (United States); Chandra N. Wickramasinghe, The Univ. of Buckingham (United Kingdom); Richard B. Hoover, Athens State Univ. (United States) and The Univ. of Buckingham (United Kingdom)

The problem of contamination of meteorites by modern environmental microorganisms is a serious issue that appears during interpretation of results of electron microscopy. Even so, the recently established marker



of nitrogen spectra (element spectrometry), which is low or absent in indigenous fossil material of a meteorite but significant in all modern contamination's cells, skepticism on the authenticity of these samples remains. Several investigations conducted by geologists found that environmental microorganisms could colonize the internal parts of meteorites with subsequent growth of Cyanobacteria being reported.

The purpose of this study is to demonstrate if any microbial contamination from the environment (geographical place where meteorites were found) would be present in the internal part of a meteorite. The possibility to metabolize organic matter of a meteorite as a major or supplemental substrate or growth factor by the bacteria from our laboratory culture collection will be checked. Potential toxic or inhibitory effects also will be tested on living cultures. UV exposure of the meteorites under investigation will be followed by the aseptic extraction of internal material that will be inoculated into growth media. All viable cells cultivated will be subjected to the study of physiology, molecular (16SrRNA sequencing) and microscopic investigation.

9606-21, Session 8

Instruments and methods to search for viable extraterrestrial microorganisms

Richard B. Hoover, The Univ. of Buckingham (United Kingdom) and Athens State Univ. (United States)

Is Life restricted to the Planet Earth? or Do living organisms exist today elsewhere in the Cosmos? The question of extant extraterrestrial life forms even more difficult and restrictive than the question of whether life forms that may have once inhabited the oceans of ancient Mars, comets, waterbearing asteroids or other cosmic bodies. During the past half century, microbiological studies have provided clear and convincing evidence that microbial extremophiles inhabit virtually every niche of planet Earth where water, energy, and a small suite of life-critical biogenic elements co-exist. No scientific rationale has ever been advanced to suggest that these essential requirements for life (as we know it) does not exist widely throughout the Universe. Furthermore, numerous independent studies have yielded a large body of imaging and spectral evidence for the remains of filamentous cyanobacteria and other prokaryotic and eukaryotic microorganisms in a variety of carbonaceous and SNC meteorites. Recent contamination is ruled out by the absence of detectable levels of nitrogen in the fossilized filaments. Recent contamination by living or dead modern terrestrial microbes is also excluded by the fact that the many independent meteoriticists who have studied these samples have failed to detect numerous essential life-critical biomolecules (unstable amino acids, nucleobases, ATP, chlorins, etc.) in the same meteorites (e.g., Orgueil, Murchison) that contain the fossils and are likely of cometary origin. The red, purple, green and blue-green regimes in high-resolution images of comet 67P/Churyumov-Gerasimenko are consistent with the phycoerythrin and phycocyanin photosynthetic pigments of cyanobacteria, and enhance the need for high resolution multi-spectral and fluorescence studies of these regions to search for biomolecular pigments.

The Viking Labeled Release Experiment results were consistent with metabolic activity possibly associated with viable microorganisms in the Mars regolith. However, the Viking results were dismissed on grounds that may have been erroneous. No life-detection experiment has been flown on any NASA Mars mission post-Viking. The confirmation of sporadic release of methane on Mars is consistent with possible metabolic activity of methanogenic archaea living today in the martian permafrost. It is now known that extremophiles can remain viable for thousands to millions of years while cryopreserved in ice and permafrost. This paper will discuss problems and consider some methods and instruments that may be used to remotely or directly obtain physical, chemical, biomolecular, or spectroscopic evidence for extant microorganisms on Mars, comets, waterbearing asteroids, or dwarf planets.

9606-23, Session 8

Raman laser spectrometer for ExoMars 2018 (Invited Paper)

Andoni G. Moral, Carlos Pérez Canora, INTA Instituto Nacional de Técnica Aeroespacial (Spain)

The Raman Laser Spectrometer (RLS) is one of the Pasteur Payload instruments, within the ESA's Aurora Exploration Programme, ExoMars mission.

 $\mathsf{ExoMars}$ 2018 main Scientific objective is "Searching for evidence of past and present life on Mars".

Raman Spectroscopy is used to analyze the vibrational modes of a substance either in the solid, liquid or gas state. It relies on the inelastic scattering (Raman Scattering) of monochromatic light produced by atoms and molecules. The radiation-matter interaction results in the energy of the exciting photons to be shifted up or down. The shift in energy appears as a spectral distribution and therefore provides an unique fingerprint by which the substances can be identified and structurally analyzed.

The RLS is being developed by an European Consortium composed by Spanish, UK, French and German partners. It will perform Raman spectroscopy on crushed powdered samples, obtained from 2 meters depth under Mars surface, inside the Rover's Analytical Laboratory Drawer.

After a wide campaign for evaluating Instrument performances by means of simulation tools and development of an instrument prototype, Instrument Structural and Thermal Model has been successfully delivered on February 2015, and the Engineering and Qualification Model is expected to be manufactured by June 2015 for its delivery after a testing campaign by end of 2015.

A summary of main Instrument performances may be obtained during the following months, achieving high levels of spectral resolution and accuracy in the obtained spectra.

9606-24, Session 8

CRIRES+: the ESO/VLT planet hunter in the NIR

Ulf Seemann, Georg-August-Univ. Göttingen (Germany)

ESO's flagship high-resolution NIR spectrograph, CRIRES, is currently undergoing a major instrument upgrade. The project, through a consortium of five European institutions, transforms the latest of the first generation VLT instruments into "CRIRES+", adding capabilities such as crossdispersion, polarimetry, large state-of-the-art detector mosaics, and a suite of new calibration techniques. CRIRES+ will be a premier instrument tailored for high-precision radial velocimetry on the sub-3m/s level, exoplanet athmosphere characterization, solar system studies and many others in the 1-5um domain at high spectral (R=1e5) and spacial (AO-assisted) resolution. CRIRES+ offers an observing efficiency boosted by more than an order of magnitude by its large simultaneous wavelength coverage, rendering it ideal for molecular spectroscopy.

In this talk, I will give an overview of the project and the lessons learned up to the current final design phase, and highlight the instrumental details as well as the performance related to the detection and characterization of (exo-)planets at first-light in 2017. A particular focus of the talk will be the set of calibration techniques, including a newly designed Fabry-Perot etalon system for reliable wavelength calibration of CRIRES+.

9606-26, Session 9

Terrain and biology of Comet 67P/ Churyumov-Gerasimenko (Invited Paper)

Chandra N. Wickramasinghe, The Univ. of Buckingham (United Kingdom) and Institute for the Study of Panspermia and Astroeconomics (Japan) and Univ.

Conference 9606: Instruments, Methods, and Missions for Astrobiology XVII



of Peradeniya (Sri Lanka); Max K. Wallis, The Univ. of Buckingham (United Kingdom); Milton Wainwright, The Univ. of Sheffield (United Kingdom); G. Tokoro, Institute for the Study of Panspermia and Astroeconomics (Japan)

We examine a wide range of data from the Rosetta Mission all of which can be interpreted as pointing indirectly to microbiological activity in Comet 67P/Churyumov-Gerasimenko. The largest sea ('Cheops' Sea, 600 x 800m) curves around one lobe of the 4km-diameter comet, and the crater lakes extending to ~150m across are re-frozen bodies of water overlain with organic-rich sublimation lag of order 10 cm. The parallel furrows are seen that relate to flexing of a asymmetric and spinning two-lobe body, which generates fractures in an underlying body of ice. We draw attention to the existence of recently resealed cracks and fissures on smooth surface terrain as well as ongoing outgassing activity all of which are consistent with the presence of subsurface lakes. Within nutrient-rich watery domains biological activity builds up high pressures of volatile gases that sporadically leads to a rupturing of a frozen icy crust. The detection of a high abundance of complex organic molecules throughout the comet's surface by Philae combined with 3-D imaging of dust in the nm-?m size range from the MIDAS instrument aboard Rosetta also point to ongoing microbiology. The possibility of significant fluxes of nanometre-sized particles (of viral sizes) emanating from comets will be examined.

9606-27, Session 9

Big bang nucleosynthesis, comets and life

Robert B. Sheldon, NASA Marshall Space Flight Ctr. (United States)

The origin-of-life (OOL) consensus holds that life began 3.65-3.85Gya after Earth had cooled, or <100Mya since the molten Hadean. If true, OOL would populate planets multiple times de novo, but instead, every extraterrestrial fossil discovery is remarkably similar. We suggest comets not only are infected and transport life, but make up the ~70% dark matter of the galaxy, so that the entire galaxy is one connected biosphere ~12Gya. Although comets have all the right properties for dark matter, cosmologists argue that the Big Bang Nucleosynthesis (BBN) produces only hydrogen, helium and minute amounts of lithium. These BBN models, however, are 1-D, homogeneous, isotropic and without magnetic fields. In this paper we modify a state-of-the-art BBN model to include chaotic magnetic fields with a corresponding change to the equation of state. This not only creates Carbon-Oxygen to make primeval ice grains and comets that accelerate galaxy formation, but also the magnetized dust that may explain dark energy. We discuss how gamma-ray telescopes can observe the gravitational lensing of background light sources caused by this cometary fraction of dark matter. Thus the bioengineering of comets by life also affects cosmic evolution, providing a feedback from the very smallest to the very largest scales of the universe. In this sense, the universe is a coherent, low-entropy system designed for life.

9606-28, Session 9

Arrhenius reconsidered: astrophysical jets and the spread of spores

Malkah I. Sheldon, Covenant Christian Academy (United States); Robert B. Sheldon, NASA Marshall Space Flight Ctr. (United States)

In 1871, Lord Kelvin suggested that the fossil record could be an account of bacterial arrivals on comets. In 1903, Svante Arrhenius suggested that spores could be transported on stellar winds without comets. In 1984, Sir Fred Hoyle claimed to see the infrared signature of vast clouds of dried bacteria and diatoms. In 2012, the Polonnaruwa carbonaceous chondrite revealed fossilized diatoms apparently living on a comet. However, Arrhenius' spores were thought to perish in the long transit between stars. Those calculations, however, assume that maximum velocities are limited by solar winds to ~300 km/s. Herbig-Haro objects, however, are young stars with jets of near-relativistic speed, -3000km/s. The central engine of astrophysical jets is not presently understood, but we argue it is a kinetic plasma instability of a charged central magnetic body. We show how to make a bipolar jet in a belljar. The instability is non-linear, and thus very robust to scaling laws that map from microquasars to active galactic nuclei. We scale up to stellar sizes and recalculate the viability/transit-time for spores carried by supersonic jets, to show the viability of the Arrhenius mechanism.

9606-29, Session 9

Hydro-gravitational-dynamics cosmology is crucial to astrobiology and the biological big bang at two million years

Carl H. Gibson, Univ. of California, San Diego (United States)

Collisional fluid mechanics and modern stratified turbulence theory is applied to the evolution of structures in self gravitational systems, starting with the cosmological big bang. Planck-Kerr turbulent combustion powers this event, producing a fireball quenched by gluon viscosity at 10^-27 seconds, and inflation. Fossils of big bang turbulence persist in the cosmic microwave background at scales > 10^25 meters. The baryon plasma fragments at galaxy scales at 10^12 s, producing weak turbulence. Earth mass gas planets in clumps of a trillion fragment at 10^13 s. Stars form by planet mergers, and explode. DNA life forms at two million years.

See journalofcosmology.com for details about HGD cosmology. HGD is crucial to understanding the formation of the 30,000,000 hydrogen planets that exist on average per star in all galaxies (not ~ 8 as usually assumed). These dark matter planets in clumps of a trillion have hosted life as we see it. All stars form by planet mergers within the dark matter clumps. If all planets in a clump merge to form stars, the clump is a globular star cluster. If the stars overfeed on planets, they explode to release carbon, oxygen and nitrogen as oxides. These are reduced to organic chemicals by the hydrogen to form water atmospheres of the hot planets (3000K). First iron, nickel and rocks condense to form planet cores. At 2 million years liquid water oceans to form larger planets and stars, and RNA and DNA life as we know it is inevitable.

9606-30, Session 10

Link between organic life and hydrocarbons on comets and asteroids (eg. CCs): evolution of biogenic hydrocarbon source rocks and oil & gas on Mars, Earth, and other solar system planets (and their respective moons) (Invited Paper)

Prasanta K. Mukhopadhyay , Global Geoenergy Research Ltd. (Canada)

Previous data on various carbonaceous chondrites (CC) and comet dust by various scientists since the 1960s, recent findings on the abundance of hydrocarbon-like organic molecules in various moons of Saturn or Jupiter and comets (including the Comet 67P) and the key geological features and the abundance of methane on Mars may suggest the presence of abundant biologically derived thermogenic petroleum hydrocarbons within our Solar System . Recent geochemical and other analytical data of various CCs indicate that they are organic rich with abundant kerogens and oil like extractable biomarkers. They closely resemble terrestrial hydrocarbon source rock kerogen and bitumen usually observed in shale and carbonates on Earth. The bacteriomorphic microstructures preserved in these CCs closely resemble microbial (prokaryotic and archaeoprokaryotic) ecosystems established on Earth over 3.85 to 4 Ga years ago. The early geology of both planet Mars and Earth are quite similar. They both contain abundant water



and bacterial or algal derived organic components possibly suggesting a common link for the origin of life and the presence of hydrocarbons in planets (and their moons) within the Solar System. This data indicates that the hydrocarbon molecules that were originated from a organic life on CCs and Comets (as seen in Comet 67P) from a 'geopolymer'(PAHs like complex macromolecule) via a stage of "biopolymer" (bacterial and algal rich complex in mineral matrix). They were later transported in sediments to Mars, Earth, and other planets during the early formation of the Solar System along with the life forming elements and organic molecules.

Consequently, the Solar system possibly represents a connected biosphere with life transfer (originated in Comet and carbonaceous Asteroids) that has been continuously taking place on dynamic timescales for at least the last 4.5 Ga of years. Now the question before us is how life has been transported to various planets in the Solar System. It was suggested that life could be transported in the planets in the Solar System as a result of: (a) purging of the primordial "comet dust" or (b) slow impact of carbonaceous meteoritic showers. Both of them contain both life forming organic molecules and hydrocarbons. Life cannot have originated from a violent and high temperature impact by asteroid or comet.

9606-32, Session 10

Evidence of ancient microbial activity on Mars

Jamie H. Wallis, Cardiff Univ. (United Kingdom); N. C. Wickramasinghe, The Univ. of Buckingham (United Kingdom); Daryl Wallis, Cardiff Univ. (United Kingdom) and The Univ. of Buckingham (United Kingdom); Norimune Miyake, Chiba Institute of Technology (Japan); Max K. Wallis, The Univ. of Buckingham (United Kingdom); Richard B. Hoover, The Univ. of Buckingham (United Kingdom) and Athens State Univ. (United States)

We report for the first time in situ observations of a relatively rare secondary iron arsenate-sulphate mineral named bukovsk?ite - Fe3+2(As5+O4) (S6+O4)(OH)•7(H2O) - found in a shock melt vein of the Tissint Martian meteorite. It is hypothesised that the mineral formed when high concentrations of aqueous H+, Fe(III), SO4 and AsO4 were maintained for long periods of time in microenvironments created within wet subsurface Martian clays. The aqueous H+, Fe(III), SO4 and AsO4 species arose from the microbial oxidation of FeS2 with concurrent release of sequestrated As. The availability of aqueous AsO4 would also be complemented by dissolution by-products of the microbial reduction of Fe-oxides influenced by dissolved organic matter that alters the redox state and the complexation of As, thus shifting As partitioning in favour of the solute phase. This hypothesis is substantially supported by SEM analysis of a 15µm spherical structure comprising of a carbonaceous outer coating with a inner core of FeS2 (pyrite) that showed the pyrite surface with spherical pits, and chains of pits, with morphologies distinct from abiotic alteration features. The pits and channels have a clustered, geometric distribution, typical of microbial activity, and are closely comparable to biologically mediated microstructures created by Fe- and S-oxidising microbes in the laboratory. These microstructures are interpreted as trace fossils resulting from the attachment of bacteria to the pyrite surfaces.

9606-33, Session 11

Microorganisms in extreme environments with a view to astrobiology in the outer solar system (Invited Paper)

Joseph Seckbach, The Hebrew Univ. of Jerusalem (Israel); Julian Chela-Flores, The Abdus Salam International Ctr. for Theoretical Physics (Italy)

Life exists almost all over Earth environments. We are mainly familiar with the "normal" conditions where we find most of the living organisms.

However, there are various prokaryotic microbes and a smaller number of eukaryotes that can tolerate and thrive in very severe places on Earth. These organisms that live at the edge of life are the extremophiles. Some of them are not able to tolerate the "normal" environments, while other "normal" organisms do not survive the extreme conditions.

Among the extremophiles are thermophiles thriving in high temperatures and psycrophiles in severe cold environments. In the ranges of pH are the acidophiles and the Alkaliphiles. The halophiles thrive in high solution of salt, a saline environment which can reach >30% dissolved salts. We know about prokaryotes and eukaryotes that flourish in niches with very low levels or absence of oxygen (anaerobes). Among the extremophiles, we also include those who tolerate dormancy and desiccation for long periods of time. Many extremophiles grow under more than a single stress factor; they are the Polyextremophiles.

A special discussion will be devoted to extremophiles and Astrobiology.

9606-34, Session 11

Molecular study of anaerobic strains from Antarctica and their taxonomic identifications

Zhe Lyu, William B. Whitman, The Univ. of Georgia (United States); Jacob Hagel, Daniel Easters, Geneviev LaBrake, Elena V. Pikuta, Athens State Univ. (United States)

Our previous study of phenotypic properties and 16SrRNA gene sequences demonstrated that two novel anaerobic strains from Antarctica have very close similarity with known species of the genera Halolactibacillus and Sanguibacter. To determine if these strains belong to separate novel species or differ just on a subspecies level, an additional molecular comparison was performed. Primers for a specific protein encoding genes were designed to conduct PCR amplification and sequencing. This method allows much higher resolution of the taxonomic affiliation than traditional sequencing the 16S rRNA gene.

Here we describe this molecular analysis with details regarding the PCR procedure, and the phylogenetic similarity of studied novel strains to the species (within Halolactibacillus and Sanguibacter genera) that were isolated from other continents.

9606-35, Session 11

Searching for the algorithm of genes distribution during the process of microbial evolution (Invited Paper)

Elena V. Pikuta, Athens State Univ. (United States)

Previous 2&3D graph analysis of Archaea and Bacteria demonstrated specific geometry in the function of a hyperboloid for physiological/ environmental distribution of major microbial groups. Function of a two-sheet hyperboloid covered all known biological groups, and therefore, could be applied for the entire evolution of life on Earth. The vector of evolution was indicated from point of HyperthermophilyExtreme acidityLow salinity to the point of Low temperatureAlkalinityHigh salinity.

According to this vector, the following groups were chosen in the gene screening analysis: For the vector "High-Temperature ? Low-Temperature" within extreme acidic pH (0-3) Hyperthermophilic Crenarchaeota – order Sulfolobales, moderately thermophilic Euryarchaeota - Class Thermoplasmata, and mesophilic acidophiles- genus Thiobacillus and others. For the vector "Low pH ? High pH" the following groups of microorganisms were checked in three Temperature arias: a) Hyperthermophilic Archaea and Eubacteria; b) moderately thermophilic – representatives of the genera Anaerobacter and Anoxybacillus; and c) mesophilic haloalkaliphiles (Eubacteria and Archaea). The genes associated with acidophily (H+ pump), chemolitho-autotrophy (proteins of biochemichal cycles), polymerases, his tones were checked for the first vector, and for the second vector the genes associated with alkaliphily (K+/Na+ pumps), organotrophy (sugar- &



protein- metabolizing cycles), and others were screened.

Here, we present the results of tracing several evolutionary key genes associated with characters of physiological features of microorganisms. The search was performed by comparison of genome-draft sequences of representatives of major physiological groups of Archaea, Eubacteria, and Protozoa available in databases.

9606-36, Session 12

How can parasites promote life? Group behaviors and the 'Gangen' hypothesis (Invited Paper)

Luis Villarreal, Univ. of California, Irvine (United States)

Viruses are inherently dependent on others for replication so how can they be involved in the origin of life? Surely, cells must have evolved before virus. However, such dependency can also include other viruses, establishing some tendency for viruses to cooperate. Lytic viruses have long been thought to kill the most numerous host (i.e., kill the winner). But persisting viruses/ defectives can also protect against viruses, especially in a ubiquitous virosphere. In 1991, Yarmolinsky et al. discovered the addiction modules of P1 phage, in which opposing toxic and protective functions stabilize viral persistence. Subsequently, I proposed that lytic and persisting cryptic virus also provide addiction modules that promote cooperation and group identity. In eukaryotes (and the RNA world), a distinct RNA virus-host relationship exists. Retrovirurses/retroposons are major contributors to eukaryotic genomes. Eukaryotic complexity appears to be mostly mediated by regulatory complexity involving noncoding retroposon-derived RNA. RNA viruses evolve via quasispecies, which contain cooperating, minority, and even opposing RNA types. Quasispecies can also demonstrate group preclusion (e.g., hepatitis C), thus quasispecies show both cooperation and group identity. Stem-loop RNA domains are found in long terminal repeats (and viral RNA) and are core mediators of viral regulation/identity. Thus, stem-loop RNAs may be ancestral regulators for all viruses. I here consider the RNA (ribozyme) world scenario from the perspective of addiction modules and cooperating RNA quasispecies (i.e., subfunctional agents that establish group identity). Such an RNA collective resembles a "gang" but requires the simultaneous emergence of endonuclease, ligase, cooperative catalysis, group identity, and history markers (RNA). I call such a collective a 'gangen' (pathway to gang) and suggest that a consortial group identity is needed for life to emerge.

9606-37, Session 12

Bioinformatics comparison of sulfatereducing metabolism nucleotide sequences

George Tremberger Jr., Sunil Dehipawala, Andrew Nguyen, Todd Holden, David Lieberman, Tak D. Cheung, Queensborough Community College (United States)

Sulfate-reducing bacteria can be traced back to 3.5 billion years ago. The thermodynamics of the sulfur cycle has been well documented. A recent report with Genbank nucleotide data has been analyzed in terms of the sulfite reductase (dsrAB) needed its metabolism via fractal dimension and entropy and free energy values (Robator, Jungbluth, et al , 2015 Jan, Front. Microbiol) Archaea and bacteria 16S RNA has also been compared. The hypothesis of sulfate-reducing bacteria in the vicinity of organism that consume oxygen has been examined in terms of the metal requirement and competition, as a model for Sulfur Cycle (www.ncbi.nlm. nih.gov/pubmed/19426853) and photosynthesis adaptation in the Early Earth environment. Our results suggest that the clustering of the studied sequences in the Entropy-Fractal Dimension Diagram is consistent with an initial uniform distribution which then experienced a linear transformation indicative of a simple evolutionary pressure selection process. The sulfatereducing bacteria in arctic (Robador, Brüchert, and Jørgensen, Environ Microbiol. 2009) and Psychrobacter metabolism nucleotide sequence difference is also discussed

9606-38, Session 12

Biological entities isolated from the stratosphere-evidence for a space origin

Milton Wainwright, Chandra N. Wickramasinghe, The Univ. of Buckingham (United Kingdom)

Since late 2013, we have reported scanning electron images (SEM) of biological entities (BEs) isolated from the stratosphere using a balloonlaunched sampler. These reports provide evidence for a limited number, but wide variety of BEs which EDX analysis shows are not inorganic particles comprised of elements such as silicon, calcium and iron, but are instead comprise only carbon and oxygen, i.e. they have an organic composition. We suggest, based on the following, that these biological particles are incoming to Earth from space:

1) The BEs occur in very low numbers as isolated particles on the carbon sampling stubs which were exposed to the stratosphere. With the exception of a single diatom frustule fragment, known terrestrial organisms commonly found on Earth (e.g. grass seeds and pollen) are however, not sampled from this source. In addition material having the typical morphology and EDX signature of volcanic dust has never been seen on the sampling stubs.

2) The observed stratosphere-derived BEs is unusual and (with the exception of the diatom fragment) cannot be identified, by us, as terrestrial organisms (e.g. marine or terrestrial alga or protozoa).

3) The bimorphs are often associated with impact craters caused by inorganic, space-derived cosmic dust.

4) Some of the BEs themselves also produced impact craters on the carbon sampling stubs, again suggesting that they are incoming to Earth from space.

5) The BEs, and/or the inorganic masses on which they are found, exceed 5 microns, the size limit above which it is generally assumed that particles cannot be transported from the troposphere to the stratosphere. Finally we report evidence for the presence of biological entities comprised of nanoparticles which stain positive for DNA. We conclude that the biological entities we have isolated are continually arriving to Earth from space

9606-39, Session 12

Eukaryotes in oldest rocks of Earth and meteorites

Alexei Yu. Rozanov, Paleontological Institute (Russian Federation); Richard B. Hoover, Athens State Univ. (United States)

No Abstract Available

9606-40, Session 12

Phytoplankton and the Archean Earth system (Invited Paper)

Stanley M. Awramik, David J. Chapman, Univ. of California, Santa Barbara (United States)

The Archean Earth was significantly different from younger times. It was characterized by elevated surface temperatures (20oC to as much as 70oC), reduced solar luminosity, elevated CO2 and CH4 in the atmosphere, chemically insignificant atmospheric O2, UV radiation striking the surface, and an Earth spin rate almost double that of today. Hadley cells were probably more compact and severe, producing significant turbulence in the upper part of the water column. Higher surface temperatures could have resulted in increased salinity through evaporation and thus a higher density of seawater.

An unusual aspect of some Archean microfossils is their large size. Solitary, unicellular spindle or flanged-shaped microfossils from the ~3.4 Ga Strelley Pool Formation are up to 105 um in size and similar fossils in the



-3.3 Ga Kromberg Formation up to 135 um in size. The -3.2 Ga Moodies Group contains spheroids up to 298 um in diameter. These large solitary microfossils are likely plankton, presumably phytoplankton. Such large size in pre-Phanerozoic microfossils is usually attributed to eukaryotes. However, eukaryotes did not arise until after the great oxidation event, 2.4 Ga. Thus, large size had some selective advantage in planktonic prokaryotes early in their history. But, were these vegetative cells, reproductive cells, or preserved envelopes containing many cells? The advantages for large size for prokaryotes in the Archean remain elusive but is probably tied to the Archean Earth system.

Conference 9607: Earth Observing Systems XX

Monday - Thursday 10-13 August 2015

Part of Proceedings of SPIE Vol. 9607 Earth Observing Systems XX



9607-1, Session 1

Measuring atmospheric carbon dioxide from space with the Orbiting Carbon Observatory-2 (OCO-2)

David Crisp, Jet Propulsion Lab. (United States)

Fossil fuel combustion, deforestation, and other human activities are now adding almost 40 billion tons of carbon dioxide (CO2) to the atmosphere each year. This is enough to increase the atmospheric CO2 abundance by more than 1% per year. Interestingly, as these emissions have increased over time, natural "sinks" in land biosphere and oceans have absorbed roughly half of this CO2, reducing the rate of atmospheric buildup by a factor of two. Measurements of the increasing acidity (pH) of seawater indicate that the ocean absorbs one guarter of this CO2. Another guarter is apparently being absorbed by the land biosphere, but the identity and location of these natural sinks are still unknown. The existing ground-based greenhouse gas monitoring network provides an accurate record of the atmospheric buildup, but still does not have the spatial resolution or coverage needed to identify or quantify CO2 sources and sinks. One way to address this need is to retrieve precise, spatially-resolved, global estimates of the column-averaged CO2 dry air mole fraction (XCO2) from space based measurements. The Orbiting Carbon Observatory-2 (OCO-2) is this first NASA satellite designed for this purpose. OCO-2 was launched from Vandenberg Air Force Base on 2 July 2014, and joined the 705 km Afternoon Constellation a month later. Its primary instrument, a 3-channel imaging grating spectrometer, was then cooled to its operating temperatures and began collecting about one million soundings over the sunlit hemisphere each day. This presentation will provide a brief overview of the preliminary results from this mission.

9607-2, Session 1

Toward consistent radiometric calibration of the NOAA AVHRR visible and nearinfrared data record

Rajendra Bhatt, Science Systems and Applications, Inc. (United States); David R. Doelling, NASA Langley Research Ctr. (United States); Benjamin R. Scarino, Arun Gopalan, Conor O. Haney, Science Systems and Applications, Inc. (United States)

The 35-year Advanced Very High Resolution Radiometer (AVHRR) satelliteinstrument data record is critical for studying decadal climate change, provided that the AVHRR sensors are consistently calibrated. Owing to the lack of onboard calibration capability, the AVHRR data need to be adjusted using vicarious approaches. One of the greatest challenges plaguing these vicarious calibration techniques, however, is the degrading orbits of the NOAA satellites that house the instruments, or, more specifically, the fact that the satellites eventually drift into a terminator orbit several years after launch. This paper presents a uniform sensor calibration approach for the AVHRR visible (VIS) and near-infrared (NIR) records using specifically designed NOAA-16 AVHRR-based, top-of-atmosphere (TOA) calibration models that take into account orbit degradation. These models are based on multiple invariant Earth targets, including Saharan deserts, polar ice scenes, and tropical deep-convective clouds. All invariant targets are referenced to the Aqua-MODIS Collection-6 calibration via transfer of the Aqua-MODIS calibration to NOAA-16 AVHRR using simultaneous nadir overpass (SNO) comparisons over the North Pole. A spectral band adjustment factor, based on SCanning Imaging Absorption SpectroMeter for Atmospheric CartograpHY (SCIAMACHY) spectral radiances, is used to account for the spectrally-induced biases caused by the spectral response function (SRF) differences of the AVHRR and MODIS sensors. Validation of the AVHRR Earth target calibration is performed by comparisons with contemporary MODIS SNOs. Calibration consistency between Earth targets validates the historical AVHRR record.

9607-3, Session 1

Geometric effects in SeaWiFs lunar observations

Robert E. Eplee Jr., Frederick S. Patt, Gerhard Meister, NASA Goddard Space Flight Ctr. (United States)

SeaWiFS made 204 lunar observatios over its 13-year mission. 145 radiometric trending observations were made at low phase angles (-8 to -6 degrees and +5 to +10 degrees). 59 additional observations were made at high phase angles (-26 to -49 degrees and +27 to +66 degrees). The NASA Ocean Biology Processing Group has undertaken a reanalysis of geometric effects in the SeaWiFS lunar data set with the final radiometric trend corrections applied. At high phase angles an increased uncertainty in the oversampling corrections of the lunar images gives rise to greater uncertainties in the lunar irradiances. Ratios of SeaWiFS observations to USGS ROLO photometric model predctions were fit with a quadratic function of phase angle and linear functions of sub-spacecraft point libration longitude and latitude angles. The phase and libration fit coefficients have been used as additional geometric corrections for the SeaWiFS lunar observations. For Band 1 (412 nm) and -50 degrees phase the phase correction is 1.8% and the libration correction is 0.7%. At +/- 7 degrees phase, the phase correction is 0.14% and the libration correction is 0.33%. At +50 degrees phase the phase correction is 0.3% and the libration correction is 0.7%. The long-term stability of the full data set is 0.058%, while the stability for the low phase angle data is 0.047%. These geometric corrections have reduced the overall scatter in the lunar observations, bringing the high phase angle data into family with the low phase angle measurements without impacting the time dependence of the low phase angle observations.

9607-4, Session 1

Cross radiometric calibration for GF-1 WFVs

Yong Xie, Institute of Remote Sensing and Digital Earth (China)

The Gaofen 1 (GF-1) satellite, the first satellite in Chinese high-resolution Earth Observation System (CHEOS), was launched successfully from Jiuquan Launch Centre on April 26, 2013. Except a 2m/8m Panchromatic Multi-spectral Sensor, a wide field of view (WFV) sensor is also installed on GF-1 platform, which is comprised of 4 cameras, namely WFV1, WFV2, WFV3, and WFV4, with the same nadir spatial resolution of 16m. The swath of each WFV camera is 200km and can reach to an 800km large swath by merging four cameras. Due to its high spatial resolution and wide swath, the GF-1 WFV image has been widely used in land and resources, agriculture, environmental protection, and surveying and mapping. In order to enhance the wideness and deepness of the quantitative remote sensing applications, it is crucial to implement the comprehensive post-launch calibration and validation to ensure the radiometric accuracy and consistency of GF-1 WFV cameras.

Since no on-board calibrator is equipped for GF-1 WFV, the cross-sensor radiometric calibration approach is one of effective ways to achieve the calibration coefficients. However, although the characteristics of four cameras are theoretically identical, the minute radiometric differences intrinsically exist. The separate radiometric calibration for each WFV camera is necessary. Furthermore, due to four WFV cameras are not independent and frequently used together, separate cross-sensor calibration with one reference sensor can cause large errors and cannot guarantee the consistency among cameras.

In this paper, we firstly plan to use the cross-sensor calibration method to achieve the accurate calibration coefficient for one of camera with the well-calibrated MODIS as the reference. After our statistical analysis, the amount of effective image pairs between WFV4 camera and MODIS over Dunhuang calibration site is the most, hence, WFV4 is chosen to perform the cross-sensor calibration to obtain the calibration coefficients. Secondly,



with the overlapping area between cameras, an inter-cross radiometric calibration method is proposed to carry out in-flight radiometric calibration for other WFV cameras with the reference of WFV4. Taken WFV3 and WFV4 camera as an example, the feasibility and precision of this method are performed. In this method, the correlation models of Digital Number and top of atmosphere radiances between WFV3 and WFV4 cameras are applied to implement the relative radiometric correction and get the absolute radiometric calibration coefficients of WFV3. Finally, the absolute radiometric calibration accuracy of the both cross-sensor and inter-cross calibration results and the radiometric inconsistency between cameras are validated

9607-5, Session 1

Preliminary evaluation of AHI L1b products

Xiangqian Wu, National Oceanic and Atmospheric Administration (United States); Hidehiko Murata, Japan Meteorological Agency (Japan); Fangfang Yu, ERT, Inc. (United States); Arata Okuyama, Japan Meteorological Agency (Japan); Michael Grotenhuis, ERT, Inc. (United States); Kotaro Bessho, Japan Meteorological Agency (Japan); Aaron Pearlman, Michael Chu, ERT, Inc. (United States)

The Advanced Himawari Imager (AHI) was successfully launched onboard Himawari-8 on October 7, 2014 for Japan Meteorological Agency (JMA). Level 1b (L1b) products have been generated from AHI since the first image on December 18, 2014. AHI is very similar to the Advanced Baseline Imager (ABI); both are of a new generation of geostationary imager developed by the U. S. for gathering environmental intelligence. ABI will be launched onboard GOES-R in 2016 for the U. S. National Oceanic and Atmospheric Administration (NOAA). NOAA and JMA are exchanging AHI data and the evaluation of its on-orbit performance. The data from and experience with AHI, 18 months before the ABI launch, provides a significant benefit in risk reduction for NOAA. We will present a preliminary evaluation of AHI L1b products. The exchange of information will enhance the usefulness of data from the JMA and NOAA systems for users worldwide.

9607-6, Session 1

Building vectorization inside a favela utilizing lidar spot elevation

Plinio Temba, Marcelo A. Nero, Lucas M. R. Botelho, Matheus E. C. Lopes, Univ. Federal de Minas Gerais (Brazil)

Brazil - officially the Federal Republic of Brazil, is the largest country in South America. It is the world's fifth largest country, both by geographical area and by population with over 192 million in habitant. Brazil is also home to a diversity of wildlife and extensive natural resources The Brazilian economy is the eighth largest by purchasing power parity. Despite the economic success, it is still a country with a high inequality rate wich is responsible for 25% of the big cities population living live in favelas (portuguese term for irregular settlements - IS). IS is a collection of shacks and poor quality housing system which often lack electricity or sewage disposal. Settlements Global Planning guides the local authorities for intervention in the IS and establishes priorities for implementing the actions and deeds. The diagnosis and proposals are analyzed in an integrated way through three lines of action: urban-environmental recovery; land regularization and development socio-organizational. This article describes the first stage to determining the SGP, which becomes the fisical property registry. The building registration process is determined with a developed algorithm in Matlab using the point cloud of the DSM and targets all points that lie on the roof of the building and the neighboring regions, then using models that analyze the operation of the laser sensor determines the centroid of the polygon. Furthermore, it discusses the advantages / disadvantages in terms of quality and runtime when compared with photogrammetric techniques.

9607-7, Session 1

Optimizing urban growth modeling based on land use/cover changes and road network by using agent-based cellular automata

Yousef Khajavigodellou, Salahaddin Univ.-Hawler (Iraq); Ali A. Alesheikh, K.N. Toosi Univ. of Technology (Iran, Islamic Republic of); Kamran Chapi, Univ. of Kurdistan (Iran, Islamic Republic of); Farshad Hakimpour, Univ. of Tehran (Iran, Islamic Republic of)

A city is considered as a complex system. It consists of numerous interactive sub-systems and is affected by diverse factors including governmental land policies, population growth, and transportation system. Urban modeling is a valuable tool for explaining mutual relation of the artificial and natural environment to help urban planners in complex situations. In this paper Patterns of Road Network, Type of Transportation systems and Land Use/ Cover Changes are considered as the three most important subsystems determining urban form and structure in the long term.

The CA – ABM model with spatiotemporal allocation criterions was shown effectiveness in simulation. Calibration of the Agent Base Cellular Automata model is one of the challenging issues in urban extension simulation. Complexity of urban development process, numerous variables, and various rules have made the calibration a difficult and sensitive stage within the modeling process. This paper presents a new version of CA and ABM models which parameterized for EMA and explores how factors such as road network, build-up area, green space, elevation, slope and types of transportation system can influence urban expansion.

CA model couldn't completely simulate the rules of agent, because after 2000s Erbil has shown rapid expansion based on agents. A few policy scenarios for baseline development, rapid development and green land protection under the influences of the behaviors and decision modes of regional authority agents, real estate developer agents, resident agents and future agents and their interactions must be apply to predict the future development patterns of the Erbil metropolitan region.

9607-8, Session 2

Design of an ultra-portable field transfer radiometer supporting automated vicarious calibration

Nikolaus J. Anderson, The Univ. of Arizona (United States); Kurtis Thome, NASA Goddard Space Flight Ctr. (United States); Jeffrey Czapla-Myers, Stuart Biggar, The Univ. of Arizona (United States)

The University of Arizona Remote Sensing Group (RSG) began outfitting the radiometric calibration test site (RadCaTS) at Railroad Valley Nevada in 2004 for automated vicarious calibration of Earth-observing sensors. RadCaTS was upgraded to use RSG custom 8-band ground viewing radiometers (GVRs) beginning in 2011 and currently four GVRs are deployed providing an average reflectance for the test site. This measurement of ground reflectance is the most critical component of vicarious calibration using the reflectance-based method. In order to ensure the quality of these measurements, RSG has been exploring more efficient and accurate methods of on-site calibration evaluation.

This work describes the design of, and initial results from, a small portable transfer radiometer for the purpose of GVR calibration validation on site. Prior to deployment, RSG uses high accuracy laboratory calibration methods in order to provide radiance calibrations with low uncertainties for each GVR. After deployment, a solar radiation based calibration has typically been used. The method is highly dependent on a clear, stable atmosphere, requires at least two people to perform, is time consuming in post processing, and is dependent on several large pieces of equipment. In order to provide more regular and more accurate calibration monitoring, the small



portable transfer radiometer is designed for quick, one-person operation and on-site field calibration comparison results. The radiometer is also suited for laboratory calibration use and thus could be used as the primary calibration standard for ground viewing radiometers of a RadCalNet site.

9607-9, Session 2

Atmospheric measurement analysis for the radiometric calibration test site (RadCaTS)

Jeffrey S. Czapla-Myers, The Univ. of Arizona (United States)

The Radiometric Calibration Test Site (RadCaTS) was developed by the University of Arizona in the early 2000s to collect ground-based data in support of the calibration and validation of Earth-observing sensors. It uses the reflectance-based approach, which requires measurements of the atmosphere and surface reflectance. These measurements are used in MODTRAN to determine the at-sensor radiance for a given time and date. In the traditional reflectance-based approach, on-site personnel use automated solar radiometers (ASR) to measure the atmospheric attenuation, but in the case of RadCaTS, and AERONET Cimel sun photometer is used to make atmospheric measurements. This work presents a comparison between the Cimel-derived atmospheric characteristics such as aerosol optical depth, the Angstrom exponent, and the columnar water vapor, to those derived using the traditional ASR. The top-of-atmosphere radiance derived using the Cimel and ASR are compared using Landsat 8 OLI for the period 2013-2014 to determine if any biases exist between the two methodologies.

9607-10, Session 2

Requirements for online resource for earth-observing satellite sensor calibration

Joel McCorkel, NASA Goddard Space Flight Ctr. (United States); Jeffrey S. Czapla-Myers, College of Optical Sciences, The Univ. of Arizona (United States); Brian Wenny, Science Systems and Applications, Inc. (United States); Kurtis J. Thome, NASA Goddard Space Flight Ctr. (United States)

The Radiometric Calibration Test Site (RadCaTS) at Railroad Valley Playa in Nevada is being developed by the University of Arizona to enable improved accuracy and consistency for satellite sensor calibration. Primary instrumentation at the site consists of ground-viewing radiometers, a sun photometer, and a meteorological station. Measurements made by these instruments are used to calculate surface reflectance, atmospheric properties and a prediction for top-of-atmosphere radiance. This work will leverage research for RadCaTS presented at this conference and describe the requirements for an online database, associated data formats and quality control, and processing levels.

9607-11, Session 2

Radiometric calibration of GLiHT's imaging spectrometer using GLAMR for satellite sensor intercalibration

Amit Angal, Science Systems and Applications, Inc. (United States); Joel McCorkel, NASA Goddard Space Flight Ctr. (United States)

NASA Goddard's Lidar, Hyperspectral and Thermal Imager (GLiHT) facilitates simultaneous measurements beneficial to variety of applications. Of the suite of "off-the shelf" instruments of GLiHT, the Visible Near-Infrared (VNIR) Imaging Spectrometer acquires high resolution spectral measurements (1.5 nm resolution) from 0.4 to 1 μ m. Goddard Space Flight Center's Laser for Absolute Measurement of Response (GLAMR) was used

to measure the absolute spectral response (ASR) of the GLiHT's imaging spectrometer. Continuously tunable lasers coupled to an integrating sphere allow a radiance-based calibration for the detectors at reflective solar wavelengths. GLAMR measurements, covering a wavelength range from 0.58 to 0.99 μ m were acquired between July 30 to August 2, 2013. In order to account for the large field-of-view (50°), GLiHT was rotated in 2 degree increments so that the same area of the sphere is viewed by all detectors. Using this data along with the coincident Silicon trap radiometer measurements, the ASR was computed. The derived calibration parameters for GLiHT's Imaging Spectrometer are to be transferred to near-simultaneous measurements of Landsat sensors. Calibration uncertainty of GLiHT is 1-3% depending spectral region and transferring this traceability to coincident satellite sensors has 3-5% depending on spectral region.

9607-12, Session 3

Preliminary study for improving the VIIRS DNB low light calibration accuracy with ground based active light source

Changyong Cao, NOAA National Environmental Satellite, Data, and Information Service (United States); Yuqing Zong, National Institute of Standards and Technology (United States); Xi Shao, Yan Bai, Univ. of Maryland, College Park (United States)

There is a great interest in the science and user community in the Visible Infrared Imaging Radiometer Suite (VIIRS) Day/Night Band (DNB) low light detection capabilities at night for quantitative applications such as airglow, geophysical retrievals under lunar illumination, light power estimation, search and rescue, energy use, urban expansion and other human activities. This leads to a pressing need for improving the calibration stability and absolute accuracy of the DNB at low radiances. The low light calibration uncertainty was estimated to be at approximately 15% while the long-term stability has yet to be characterized. This study investigates the feasibility of accurate nightlight source at radiance levels near 3 nW?cm^?2?sr^?1, which potentially can be installed at selected sites for VIIRS DNB calibration/ validation. Suomi NPP VIIRS observations from selected point sources are analyzed as examples. The illumination geometry, surrounding environment, as well as atmospheric effects are discussed. The uncertainties of the ground based light source are estimated. This study will contribute to the understanding of how the Earth's atmosphere and surface variability affect the stability of the DNB measured radiances; how to separate them from instrument calibration stability; whether or not SI traceable active light sources can be designed and installed at selected sites to monitor the calibration stability, radiometric and geolocation accuracy, and point spread functions of the DNB. Finally, it is also hoped to address whether or not active light sources can be used for detecting environmental changes, such as aerosols.

9607-13, Session 3

On-orbit calibration of S-NPP VIIRS daynight band and M bands using ground reference targets of Libya 4 and dome C sites

Xuexia Chen, Aisheng Wu, Science Systems and Applications, Inc. (United States); Xiaoxiong Xiong, NASA Goddard Space Flight Ctr. (United States)

This paper provides methodologies developed and implemented by the NASA VIIRS Calibration Support Team (VCST) to evaluate the S-NPP VIIRS Day-Night Band (DNB) on-orbit performance by monitoring the long term radiance and reflectance trends of DNB measurement over radiometrically stable ground sites. The DNB and M bands Sensor Data Records produced by the Interface Data Processing Segment (IDPS) and NASA Land Product Evaluation and Algorithm Testing Element (PEATE) are acquired nearly



nadir overpass for the Libya 4 desert and Dome C snow surfaces. The top of atmosphere radiance and reflectance long term trends are generated and the simulated DNB radiance values from the aggregated M bands (M4, M5, and M7) are compared with the simultaneously-observed DNB radiances. Our results show that since launch the DNB modulated RSR could have up to 4% influence on the DNB average solar spectral irradiances and the M bands influence have been less than 0.065%. After excluding some early mission data points, the results derived using IDPS DNB data show a general upward trend (about 10% - 16%) in both radiance and reflectance. These trends are likely caused by inconsistent calibration used in the IDPS forward data processing, including the use of different SDSM screen transmission and algorithms, and RSR degradation coefficients. On the other hand, the IDPS M4, M5, and M7 did not show obvious upward trends. By comparison, the long-term trends derived from the Land PEATE DNB and M bands data over Libya 4 and Dome C have been very stable.

9607-14, Session 3

Multiimage matching for lunar surface reconstruction from orbital images

Ahmed Elaksher, New Mexico State Univ. (United States)

The last three Apollo lunar missions (15, 16, and 17) carried an integrated photogrammetric mapping system of a Metric Camera (MC), a highresolution Panoramic Camera, a Star Camera, and a Laser Altimeter. Recently images taken by the MC were scanned by Arizona State University (ASU); these images contain valuable information for scientific exploration, engineering analysis, and visualization of the moon's surface. In this article, we took advantage of the large overlaps, the multi viewing, and the high ground resolution of the images taken by the Apollo MC in generating an accurate and reliable surface of the moon. We started by computing the relative positions and orientations of the exposure stations through a rigorous photogrammetric bundle adjustment process. We then generated a surface model using a hierarchical correlation-based matching algorithm. The matching algorithm was implemented in a multi-photo scheme and permits the exclusion of obscured pixels. The generated surface model was registered with LOLA topographic data and the comparison between the two surfaces yielded an average absolute difference of 36 meters. These results look very promising and demonstrate the effectiveness of the proposed algorithm in accounting for depth discontinuities, occlusions, and noises.

9607-15, Session 3

Remote sensing of 'APEC blue' skies in China

Xingfa Gu, Ying Wang, Tianhai Cheng, Hao Chen, Hong Guo, Xiangqin Wei, Bin Li, Chinese Academy of Sciences (China)

Air pollution is more frequent and durative in China. During the Asia-Pacific Economic Cooperation summit (APEC) in early November, 2014, Beijing and adjacent provinces reduced pollutant emissions, yielding the 'APEC Blue' skies. As the visibility is largely concerned with the concentration of atmospheric aerosols (Dockery and Pope, 1996), we detected the Aerosol Optical Depth (AOD) using MODIS data during four periods - November 6-12, 2013, October 6-12, 2014, November 6-12, 2014 and December 6-12, 2014. We used lookup table method to retrieve AOD of 1 km resolution, during which MOD09 surface reflectance products were adopted and clustered aerosol models derived from AERONET measurements of Eastern Asia were used (Chen et al. 2013). Then we convert AOD values to PM2.5 concentration based on the linear relationship of ground-based PM2.5 measurements and AOD values. We found that: (1) the concentration of PM2.5 over Beijing in November 6-12, 2014 reduced by 47.8% compared with that in November 6-12, 2013; (2) the concentration of PM2.5 over Beijing-Tianjin-Hebei region in November 6-12, 2014 declined by 69.6% and 56.7% compared with that in October 6-12, 2014 and December 6-12, 2014; (3) the concentration of PM2.5 over Shandong province during APEC increased by 20.6% compared with that in 2013.

References

[1] D. Dockery and A. Pope, Epidemiology of Acute Health Effects: Summary of Time-series Studies. In: Wilson, R., Spengler, J.D., (Eds.), Particles in Our Air: Concentration and Health Effects. Cambridge, MA, USA: Harvard University Press, 1996, pp.123-147.

[2] H. Chen, X. Gu, T. Cheng, T. Yu and Z. Li. 2013. Characteristics of aerosol types over China. Journal of Remote Sensing, 17(6): 1559-1571.

9607-16, Session 3

Cross calibration of GF-1 satellite PMS sensor using Landsat 8 OLI

Hailiang Gao, Institute of Remote Sensing and Digital Earth (China) and Chinese Academy of Sciences (China)

This paper presents the radiometric cross calibration of PMS sensor (Panchromatic and Multi-Spectral) aboard on Chinese GF-1 satellite using Landsat 8 OLI (Operational Land Imager). Two different SBAF factors (Spectral Band Adjustment Factor) were calculated using MODTRAN radiation transfer model, respectively. One is based on TOA radiance and the other is based on TOA reflectance. The cross calibration coefficients of these two SBAF factors are calculated and compared with office calibration coefficient. Then the uncertainty of cross calibration was analyzed. The results show that these two SBAF factor can be used for cross calibration.

9607-17, Session 4

Results from CrIS/ATMS obtained using an "AIRS version-6 like" retrieval algorithm

Joel Susskind, NASA Goddard Space Flight Ctr. (United States)

AIRS was launched on EOS Aqua in May 2002, together with AMSU-A to form a next generation polar orbiting infrared and microwave atmospheric sounding system. A main objective of AIRS/AMSU was to provide accurate unbiased sounding products with good spatial coverage that are used to generate stable multi-year climate data sets. AIRS/AMSU data for all time periods have been processed using the state of the art AIRS Science Team Version-6 retrieval methodology. The Suomi-NPP mission was launched in October 2011 as part of a sequence of LEO satellite missions under JPSS. NPP carries CrIS and ATMS, which are advanced infra-red and microwave atmospheric sounders that were designed as follow-ons to the AIRS and AMSU instruments. The objective of this work is to generate a long term climate data set of products derived from CrIS/ATMS to serve as a continuation of the AIRS/AMSU products. To achieve this, it is desirable for CrIS/ATMS to be processed using an algorithm similar to, or at least comparable with. AIRS Version-6. We have modified the AIRS Version-6 retrieval algorithm for use with CrIS/ATMS data and have been conducting research to optimize CrIS/ATMS products derived using this approach. As demonstrated on two different days in different seasons, CrIS/ATMS temperature and water vapor profiles retrievals are of very good quality, and are of comparable quality to and consistent with those retrieved from AIRS, as are other CrIS derived products. AIRS and CrIS products will be compared on daily, monthly mean, and interannual difference bases.

9607-18, Session 4

Comparison of AIRS and CrIS using synthetic principle component analysis

Hartmut H. Aumann, Evan M. Manning, Jet Propulsion Lab. (United States)

The algorithm used for the simulation of data is basically the forward algorithm used in the retrieval process. Inconsistencies between the observed data and simulated (expected) data can result in retrieval artifacts.



Synthetic Eigenvectors (SEV) are based on simulated data. Empirical Eigenvectors (EEV) are created from the data from the instrument. The residuals of data reconstruction from EEV show internal consistency, may be used to evaluate how many PC are needed to reproduce the data at the noise level and for noise filtering. They are not as useful for comparisons of two instruments. AIRS (grating array spectrometer) and CrIS (Fourier Spectrometer) respond different to spatial inhomogeneities due to the presence of clouds.

9607-19, Session 4

Improving AIRS radiance spectra in cloudy scenes using MODIS

Thomas S. Pagano, Hartmut H. Aumann, Denis A. Elliott, Evan M. Manning, Jet Propulsion Lab. (United States); Steven E Broberg, Jet Propulsion Lab (United States)

The Atmospheric Infrared Sounder (AIRS) on the EOS Aqua Spacecraft was launched on May 4, 2002. AIRS acquires hyperspectral infrared radiances in 2378 channels ranging in wavelength from 3.7-15.4 um with spectral resolution of better than 1200, and spatial resolution of 13.5 km with global daily coverage. The AIRS was designed to measure temperature and water vapor profiles for improvement in weather forecast and improved parameterization of climate processes. Currently the AIRS Level 1B Radiance Products are assimilated by NWP centers worldwide and have shown considerable forecast improvement. AIRS L1 and L2 products are widely used for studying critical climate processes related to water vapor feedback, atmospheric transport and cloud properties. AIRS trace gas products include ozone profiles, carbon monxide, and mid-tropospheric carbon dioxide. The global daily coverage of AIRS allows scientists to follow the transport of these gases to aid in validation of chemical/weather transport models.

The AIRS radiances are calibrated using a uniform on-board blackbody and full aperture space view. For this reason, all radiometric measurements assume a uniform scene. As with most instruments, the AIRS 2D spatial response functions (tophat functions) are not flat for all channels, nor are they the same. When viewing a non-uniform scene, this causes a radiometric error that is scene dependent and cannot be removed without knowledge of the scene response. The magnitude of the error depends on the nonuniformity of the AIRS spatial response and the non-uniformity of the scene, but typically only affects about 1% of the data.

In this effort we use data from the MODIS instrument to provide information on the scene uniformity that can be used to correct the AIRS data. Early results show we can match the AIRS and MODIS radiances to about 0.6K when we include the AIRS tophat functions in the normalization of the MODIS data (Elliott, Proc SPIE 6296, 2006). The method requires use of different infrared bands in MODIS depending on the channels of AIRS being corrected. Resulting improvement in noise and bias will be presented by comparing to the new AIRS Level 1C product that uses PC techniques to correct impacted channels. The method can be used to recover impacted channels, validate the Level 1C product, and identify scene conditions where the error is most significant.

9607-20, Session 4

Enhanced simultaneous Nadir observations for IR sounder evaluation and comparison

Evan M. Manning, Hartmut H. Aumann, Jet Propulsion Lab. (United States)

Simultaneous Nadir Observations (SNO) contain thousands of pairs of observations taken within 8 km and 10 minutes. SNO have been very useful for comparisons in polar conditions. But SNO pairing criteria alone are not close enough in time and space for assessing small effects, like tropical cases with cloud, where the number of SNO is much more limited. We introduce a modified methodology, which finds pairs of matched spectra using looser spatio-temporal matching criteria but adding radiometric matching criteria. We illustrate this with AIRS and CrIS data. An AIRS FOV

which is 45% cloudy will be matched to a CrIS FOV with a similar cloudiness, even though they are not the physically closest pair. Insight into instrument differences is gained from statistical distributions of the residual differences between the matched pairs. Sample analyses include comparisons of AIRS and CrIS spectra as function of cloudiness and comparisons of CrIS spectra from different FOVs. The proposed method may be applicable to matchups of other sensors on different spacecraft.

9607-21, Session 4

Usability, calibration, and data analysis issues in modern infrared spectrometers using large detector arrays

Denis A. Elliott, Hartmut H. Aumann, Jet Propulsion Lab. (United States)

Modern infrared spectrometers contain many detectors. The Moderate Resolution Imaging Spectrometer (MODIS) has 320 detectors. The Atmospheric Infrared Sounder (AIRS) has 4482 detectors. The Cross-track Infrared Sounder (CrIS) has only 27. This paper examines issues related to large arrays in multi-detector instruments and describes their impact on calibration and data analysis, using examples from AIRS and CrIS. Note that GIFTS was proposed with 2x256x256 channels and MISTIC is proposed with one 512x512 channel array. The potential differences among detectors are not limited to dead channels. They can include: noise characteristics, spatial response, illumination through the optical system, aging, and exposure to radiation. The more detectors in an instrument, the more important it is for both the hardware and data analysis software designers to be prepared to handle such differences. Techniques used on AIRS to mitigate these effects will be described.

9607-74, Session PMon

Intercomparison calibration study of Terra ASTER and MODIS

Karen Y. Yuan, Kurtis J. Thome, Joel McCorkel, NASA Goddard Space Flight Ctr. (United States)

Terra, the Earth-Observing System flagship, has reached a milestone with over 15 years of highly calibrated datasets. The value of these datasets will continue to grow and improve our understanding on the health of this planet. The present calibration study compares at sensor radiance between ASTER and MODIS with the latest calibration tables. Although ASTER and MODIS are on the same platform, they are not spectrally identical. To compensate this spectral difference, spectral correction is applied by using seasonal average from a hyperspectral sensor with 240 bands that cover from 420 - 2400 nm.

9607-75, Session PMon

Implementation of electronic crosstalk correction for terra MODIS PV LWIR bands

Xu Geng, Sriharsha Madhavan, Na Chen, Science Systems and Applications, Inc. (United States); Xiaoxiong J. Xiong, NASA Goddard Space Flight Ctr. (United States)

The MODerate-resolution Imaging Spectroradiometer (MODIS) is one of the primary instruments in the fleet of NASA's Earth Observing Systems (EOS) in space. Terra MODIS has completed 15 years of operation far exceeding its design lifetime of 6 years. The MODIS Level 1B (L1B) processing is the first in the process chain for deriving various higher level science products. These products are used mainly in understanding the geophysical changes occurring in the Earth's land, ocean, and atmosphere. The L1B code is designed to carefully calibrate the responses of all the detectors of the 36 spectral bands of MODIS and provide accurate L1B radiances (also



reflectances in the case of Reflective Solar Bands). To fulfill this purpose, Look Up Tables (LUTs), that contain calibration coefficients derived from both on-board calibrators and Earth-view characterized responses, are used in the L1B processing. In this paper, we present the implementation mechanism of the electronic crosstalk correction in the Photo Voltaic (PV) Long Wave InfraRed (LWIR) bands (Bands 27-30). The crosstalk correction involves two vital components. First, a crosstalk correction modular is implemented in the L1B code to correct the on-board Blackbody and Earthview digital number (dn) responses using a linear correction model. Second, the correction coefficients, derived from the scheduled lunar observations, are supplied in the form of LUTs. Further, the LUTs contain time stamps reflecting to the change in the coefficients assessed using the Noise Equivalent difference Temperature (NEdT) trending. With the algorithms applied in the MODIS L1B processing it is demonstrated that these corrections indeed restore the radiometric balance for each of the affected bands and substantially reduce the striping noise in the processed images.

9607-76, Session PMon

Precise pre-launch radiometric calibration of VIIRS

Leonid A. Mikheenko, Volodymyr N. Borovytsky, Andrii V. Fesenko, National Technical Univ. of Ukraine (Ukraine)

The paper presents the new approach that includes technique, scheme and instruments for precise calibration of space-borne and airborne visible infrared imaging radiometers (VIIRs). The key component of this technique is the precise uniform light source based on optically- interconnected integrating spheres. Its principal advantages are high photometric and metrological characteristics. The light source contains several (5...11) primary integrating spheres of small diameters which are installed on a secondary integrating sphere of bigger diameter. The initial light sources - halogen lamps or light emitted diodes are installed inside the primary integrating spheres. These spheres are mounted on the secondary integrating sphere. The radiation comes from the primary integrating spheres to the secondary one through diaphragms which diameters can be varied. The secondary integrating sphere has an output aperture where uniform radiance emits. As a result the output radiance can be varied in extremely wide range – up to 600 W/(st•m2) with dynamic range 1 000 000 - without any change of spectral characteristics. Non-uniformity of the radiance throughout the output aperture can be small as 0.5 % because the secondary integrating sphere is illuminated uniformly and it does not contains lamps inside. The paper discusses the requirements to calibration system, the application of this light source in calibration procedures, metrological aspects of calibration and absolutization of measurements in radiometry.

9607-77, Session PMon

Assessment of scan-angle dependent bias of Suomi-NPP VIIRS day/night band from bridge light observations

Yan Bai, Univ. of Maryland, College Park (United States); Changyong Cao, National Oceanic and Atmospheric Administration (United States); Xi Shao, Univ. of Maryland, College Park (United States)

The low gain stage of the Visible Infrared Imaging Radiometer Suite (VIIRS) Day/Night Band (DNB) on Suomi National Polar-orbiting Partnership (NPP) is calibrated using an onboard solar diffuser. The calibration is then transferred to the medium and high gain stages of DNB based on the gain ratios determined from data collected in the solar terminator region. The calibration transfer causes increase of uncertainties and affects the accuracy of the low light radiances observed by DNB at night. Since there are 32 aggregation zones from nadir to the edge of the scan for DNB and each zone has its own calibration, the calibration versus scan angle of DNB needs to be independently assessed. This study presents preliminary analysis of the scan-angle dependence of the light intensity from lights at the San Mateo bridge observed by VIIRS DNB during 2014 in different aggregation zones. Cloud screening was done using VIIRS cloud masks. Effects of aggregation mode, aggregation mode dependent point spread functions, atmospheric path length, and potential traffic light at the time of observation, associated with scan angles are analyzed. The effect of lunar illumination is also taken into account based on model simulations. This study will be especially useful for JPSS J1 VIIRS, which is known to have a large nonlinearity across aggregation zones and new aggregation modes are being developed. The methodology developed will be very useful for the longterm vicarious monitoring the VIIRS/DNB performance and will be potentially useful for monitoring environmental changes such as aerosols.

9607-78, Session PMon

Noise characteristics research of Overhauser magnetometer sensor

Tala Liu, Lingjia Gu, Shuang Zhang, Haoyang Fu, Jilin Univ. (China)

Overhauser magnetometer, a kind of weak-magnetic measurement system based on the Overhauser effect, has been widely used in satellite magnetic survey, aeromagnetic survey and other engineering and environmental applications. Overhauser magnetometer plays an important role in the application of magnetic field measurement for its advantages of low power consumption and high accuracy. Weak field magnetic resonance is usually limited by the signal to noise ratio (SNR). In order to improve the SNR of Overhauser magnetometer, noise characteristics of Overhauser magnetometer sensor are researched in this paper. A background noise model of Overhauser magnetometer sensor is established. The calculated results indicate that the noise power spectrum destiny presents a bandlimited white noise characteristic, and the maximum spectrum destiny observed at the resonant frequency is approximately equivalent to thermal noise of the matched resistance. The correlation between the SNR and the matched resistance is investigated by using the noise model. The calculated results demonstrate that large matched resistance is beneficial to improve the SNR of the sensor, although it generates more noise. When matched resistance is larger than 200k?, the SNR tends to be a constant. On the premise of ensuring proper bandwidth, the sensor will achieve the optimal SNR when the matched resistance is in the range of 80k?-100k?. The measured results coincide with the theoretical calculation, so the noise model is verified to be correct. This investigation is beneficial to improve noise performance of Overhauser magnetometer sensor.

9607-79, Session PMon

An improved proton magnetometer for Earth's magnetic field observation

Chengyu Xiao, Shuang Zhang, Xin Guo, Haoyang Fu, Jilin Univ. (China)

As a precision instrument to measure the earth magnetic field, proton magnetometer is widely used on different fields such as geological survey, buried objects detection and earth field variations. Due to poor signal to noise ratio (SNR) of the system, proton magnetometer suffers from low sensitivity which directly affects the performance. In order to increase the sensitivity, we present an improved proton magnetometer. First, the effect of matching resistance on Q value is discussed to enhance SNR, and high matching resistance has been chosen to improve the Q value of the resonant circuit. Second, noise induced by pre-amplifier is investigated in order to obtain low noise signal, and we adopt the JFET with noise figure less than 0.5dB as the pre-amplifier. Third, by using band-pass filter, low-noise output signal is obtained. Fourth, the method of period measurement based on CPLD is employed to measure frequency of the square wave shaped from the output sinusoidal signal. High precision temperature compensate crystal oscillator (TCXO) has been used to improve the frequency measurement accuracy. Last, experimental data are obtained through field measurements. By calculating the standard deviation, the sensitivity of the improved proton magnetometer is 0.15nT for Earth's magnetic field observation. Experimental results show that the new magnetometer is sensitive to the earth field.



9607-81, Session PMon

GOCI in-orbit radiometric calibration status after four-year operation

Seongick Cho, Kibeom Ahn, Eunsong Oh, Korea Institute of Ocean Science & Technology (Korea, Republic of) and Yonsei Univ. (Korea, Republic of); YoungJe Park, Korea Institute of Ocean Science & Technology (Korea, Republic of); Sug-Whan Kim, Yonsei Univ. (Korea, Republic of)

The first spaceborne imager for ocean color remote sensing in Geostationary Earth Orbit (GEO), GOCI (Geostationary Ocean Color Imager)/COMS (Communication, Ocean and Meteorological Satellite), is successfully operated over the four years since its launch in June 2010. In order to fulfill the ocean color monitoring mission in geostationary orbit, GOCI implements 2D CMOS FPA (Focal Plane Array) with 2 million pixels, which enables staring capture method with 700km x 700km IFOV (Instantaneous Field of View) and 500m GSD (Ground Sampling Distance) over the center of the coverage area (130°E, 36°N) which corresponds to 380m GSD over the nadir. GOCI can observe Korea, Japan, and coastal region of China with 4 x 4 slot image acquisitions. One slot image of GOCI is equivalent to IFOV, and size of coverage area with 4 x 4 slot images is 2,500km x 2,500km including overlap area among adjacent slot images. GOCI equips 8 spectral bands. In visible wavelength region from 402nm to 685nm, 6 spectral bands are implemented on GOCI with the bandwidth of 20nm (for B1 ~B5) or 10nm (for B6, central wavelength at 680nm). Two spectral bands located in NIR wavelength region with band center at 745nm and 865nm are mainly used for the atmospheric correction.

In-orbit calibration method of GOCI is solar calibration using onboard Solar Diffuser (SD) and Diffuser Aging Monitoring Device (DAMD) equipped in the Shutter Wheel Assembly (SWA) on the top panel of the instrument. DAMD for the purpose of monitoring the in-orbit performance degradation of SD is identical to SD except for the size. The diameter of SD and DAMD are 14cm and 7cm, respectively. GOCI radiometric model which converts raw data recorded in DN (Digital Number) to physical unit (in the case of GOCI, it is radiance with the unit of W/m2/?m/sr) is defined with 3rd order polynomial with no quadratic term. Linear gain (G) and 3rd order non-linear gain (b) in GOCI radiometric model can be acquired from the calibration images observed with SD and DAMD at local night time. In this paper, we present the in-orbit radiometric calibration status of GOCI during first three years of operation. Annual sinusoidal variation of GOCI radiometric gains due to the diffuser transmittance variation with respect to the solar incident angle on azimuth direction is mainly discussed. Existing in-orbit calibration data shows that GOCI radiometric performance is stable with about 0.12% variation per year after the correction of annual diffuser variation in terms of solar incident angle.

9607-82, Session PMon

Assessment of the collection 6 Terra and Aqua MODIS bands 1 and 2 calibration performance

Aisheng Wu, Xuexia Chen, Amit Angal, Yonghong Li, Science Systems and Applications, Inc. (United States); Xiaoxiong Xiong, NASA Goddard Space Flight Ctr. (United States)

MODIS (Moderate Resolution Imaging Spectroradiometer) is a key sensor aboard the Terra (EOS AM) and Aqua (EOS PM) satellites. MODIS collects data in 36 spectral bands and generates many data products for land, atmosphere, cryosphere and oceans. MODIS bands 1 and 2 have nadir spatial resolution of 250 m, compared with 500 m for bands 3 to 7 and 1000 m for all the remaining bands, and their measurements are crucial to derive key land surface products. This study evaluates the performance of the Collection-6 (C6) L1B calibrations of both Terra and Aqua MODIS bands 1 and 2 using three vicarious approaches. The first and second approaches focus on stability assessment using data collected from two pseudo-invariant sites on the Libya-4 desert and Antarctic Dome C snow surface over the entire mission. The third approach examines the relative stability between Terra and Aqua in reference to a third sensor from a series of NOAA 15-19 AVHRR (The Advanced Very High Resolution Radiometer). The comparison is based on measurements from MODIS and AVHRR Simultaneous Nadir Overpasses (SNO) over a thirteen-year period from 2002 to 2015. Results from this study provide a quantitative assessment of Terra and Aqua MODIS bands 1 and 2 calibration stability and the relative differences between the two sensors.

9607-83, Session PMon

Radiometric performance assessment of Suomi NPP VIIRS SWIR band (2.25 μ m)

Sirish Uprety, Colorado State Univ. (United States); Changyong Cao, NOAA National Environmental Satellite, Data, and Information Service (United States)

Suomi NPP VIIRS SWIR band M11 (2.25 µm) has larger radiometric uncertainty compared to rest of the reflective solar bands. This could be due to a number of reasons including prelaunch calibration. One of the most commonly used technique of verifying the radiometric stability and accuracy of VIIRS is by intercomparing it with other well calibrated radiometers such as MODIS. One of the limitations of using MODIS is that VIIRS band M11 RSR doesn't overlap with MODIS bands at all. Thus the accuracy of intercomparison relies completely on how well the spectral differences are analyzed over the given target. Since desert sites have higher reflectance and more flat spectra, this study uses desert sites to analyze M11 radiometric performance. In order to better match the RSR between instruments, we have chosen Landsat-8 OLI SWIR band 2 (2.2 um) to perform intercomparison. This is mainly because OLI SWIR band 2 fully covers the VIIRS band M11 even though OLI has much wider RSR compared to VIIRS. The study suggests that there exists large radiometric inconsistency between VIIRS M11 and OLI, on the order of 5%. The impact due to spectral differences is estimated and accounted using EO-1 Hyperion observations and MODTRAN.

9607-84, Session PMon

Measured polarized transmittance of JPSS J1 VIIRS using the NIST T-SIRCUS

Jeffrey McIntire, Science Systems and Applications, Inc. (United States); James B. Young, Stellar Solutions Inc. (United States); David I. Moyer, The Aerospace Corp. (United States); Eugene Waluschka, Xiaoxiong J. Xiong, NASA Goddard Space Flight Ctr. (United States)

Recent pre-launch measurements performed on the Joint Polar Satellite System (JPSS) J1 Visible Infrared Imaging Radiometer Suite (VIIRS) using the NIST T-SIRCUS monochromatic source have provided wavelength dependent polarization sensitivity for select spectral bands and viewing conditions. Measurements were made at a number of input linear polarization states (thirteen in total) and initially over thirteen wavelengths. Using the source radiance information collected by an external monitor, a spectral responsivity function was constructed for each input linear polarization state. Additionally, an unpolarized spectral responsivity function was derived from these polarized measurements. An investigation of how the centroid, bandwidth, and detector responsivity vary with polarization state was weighted with a number of model input spectra to simulate both ground measurements as well as expected on-orbit conditions. These measurements will enhance our understanding of VIIRS polarization sensitivity, improve the design for future flight models, and provide valuable data to enhance products quality in the post-launch phase.



9607-85, Session PMon

Preliminary validation of Himawari-8/AHI navigation and calibration

Arata Okuyama, Akiyoshi Andou, Masaya Takahashi, Kenji Date, Tasuku Tabata, Keita Hosaka, Hidehiko Murata, Nobutaka Mori, Japan Meteorological Agency (Japan); Ryoko Yoshino, Japan Aerospace Exploration Agency (Japan); Kotaro Bessho, Japan Meteorological Agency (Japan)

The next-generation geostationary meteorological satellite of the Japan Meteorological Agency (JMA), Himawari-8, was successfully launched on 7 October 2014. The satellite will start operation in middle of 2015 after the completion of in-orbit testing and checking of the overall system. Himawari-8 features a new imager, Advanced Himawari Imager (AHI), with 16 bands. The imager's spatial resolution is double that of its predecessor satellites, MTSAT series. Full-disk imagery is obtained every 10 minutes. Rapid scanning with 2.5-minute interval is also conducted. These significant improvements will bring unprecedented levels of performance in nowcasting services and short-range weather forecasting systems. To bring out potential of the advanced imager sufficiently, precise navigation and accurate radiometric calibration are essential. This presentation will report navigation and calibration status of AHI.

Himawari-8 is equipped with three sensors onboard, the star tracker, the inertia reference unit and the angular rate sensor to realize accurate image navigation. The navigation and co-registration accuracy is validated by landmark analysis. As to radiometric calibration, AHI has a blackbody for infrared bands and a solar diffuser for visible and near infrared bands as on-board calibration references. We have a plan to perform inter-calibration and vicarious calibration in some approaches to improve its reliability. Our approach refers MTSAT observation, hyper-sounders observation such as AIRS, NPP/VIIRS observation, lunar model and simulated radiance by radiative transfer model. In the conference, the analysis based on preoperational half year AHI data will be introduced.

9607-86, Session PMon

Comparison of JPSS-1 VIIRS VisNIR responsivities measured with monochromatic and broadband sources

Thomas Schwarting, Qiang Ji, Jeffrey McIntire, Hassan Oudrari, Science Systems and Applications, Inc. (United States); Xiaoxiong J. Xiong, NASA Goddard Space Flight Ctr. (United States)

NIST's laser-based traveling SIRCUS test facility was used to characterize the spectral response of the JPSS-1 VIIRS VisNIR bands after the conclusion of environmental testing in December 2014. The SIRCUS facility uses tunable lasers fed into an integrating sphere that is concurrently viewed by VIIRS and a calibrated reference detector which allows for a measurement of spectral response and the responsivity of the band through integrating the series of monochromatic measurements over the bandpass. Presented are the responsivities compared to those calculated via the traditional test method with a discussion of the impact of crosstalk to each measurement set.

9607-87, Session PMon

Extracting information on urban impervious surface from GF-1 data in Tianjin City of China

Bin Li, Institute of Remote Sensing and Digital Earth (China); Qingyan Meng, Jun Wu, Xingfa Gu, Chinese Academy of Sciences (China) ?1?Based on the spectral signatures of Tianjin's different surface features, Tianjin's surface coverage types can be divided in to 4 basic types, including vegetation, soil, high albedo and low albedo, and the linear model consisting of 4 endmembers selected by this study can well express the spectral signatures of Tianjin's different surface features. Then, solved by least square method without limited conditions of band correlations, coverage diagram of Tianjin's 4 endmember components was obtained. At last, after removing water body areas, impervious surface can be expressed as the overlay of high reflectance endmember coverage and low reflectance endmember coverage depending on the relationship among high albedo, low albedo and impervious surface. The estimation of Tianjin's impervious surface was verified by high resolution image data of remote sensing. In general, Tianjin has a relatively high impervious surface coverage, particularly Tianjin's central area and coastal area which have coverage of more than 65%.

?2?From the fig of Tianjin's impervious coverage, it can be found that the impervious coverage of Tianjin's coverage reaches up to 65%, while that the impervious coverage of Hongkong and some American cities is only 60% and 40% respectively. It is obvious that the overall ecological environment of Tianjin is poorer than Hongkong and some American cities, because of its high density of buildings and its small urban green space in its city system.

?3?When calculating the Tianjin's impervious surface coverage depending on linear spectral decomposition model, estimation accuracy is often influenced by water body shadow, spectral decomposition accuracy, high and low albedo. For example, the effect of removing water body will be influenced by the choice of method of water mask and the threshold value of binarization processing and low albedo of some areas will be increased by some shadow such as northwestern part of Wuqing District.

9607-88, Session PMon

Vicarious validation of straylight correction for VIIRS day/night band using Dome-C

Shi Qiu, Xi Shao, Univ. of Maryland, College Park (United States); Changyong Cao, Wenhui Wang, NOAA National Environmental Satellite, Data, and Information Service (United States)

The Day/Night Band (DNB) of the Visible Infrared Imaging Radiometer Suite (VIIRS) onboard Suomi National Polar-orbiting Partnership (Suomi-NPP) represents a major advancement in night time imaging capabilities. However, the VIIRS DNB sensor is affected by stray light, which is due to solar illumination entering the optical path when the satellite passes through the day-night terminator at the spacecraft. The straylight results in an overall increase in the recorded radiance values. This effect is more significant during solstice. After launch of Suomi-NPP in October 2011 it was found that there is a gray haze in radiance images observed by DNB due to straylight and a straylight correction has been implemented to remove this effect. This study performs vicarious validation of straylight correction for VIIRS DNB band using Dome-C in Antarctic. Nadir observations of these high latitude regions by VIIRS are selected during perpetual night season, i.e. from April to July during the year 2014 under various lunar phases. The lunar spectral irradiance model, as a function of Sun-Earth-Moon distances and lunar phase, is used to determine the top-of atmosphere (TOA) reflectance at the vicarious site. The comparison of observed radiance and model predictions for different lunar phases are shown in this paper. In addition, the crosscomparison between DNB observations for events with/without straylight is also demonstrated. The VIIRS DNB data from two sources such as IDPS and NASA Land Peate are compared, which revealed some differences possibly due to difference in the calibration algorithm implementation.

9607-89, Session PMon

Ray tracing based ISRD (inter-slot radiometric discrepancy) simulation tool for GOCI

Ki-Beom Ahn, Seongick Cho, Eunsong Oh, Korea Institute



of Ocean Science & Technology (Korea, Republic of) and Yonsei Univ. (Korea, Republic of); Young Je Park, Korea Institute of Ocean Science & Technology (Korea, Republic of); Sug-Whan Kim, Yonsei Univ. (Korea, Republic of)

Geostationary Ocean Color Imager (GOCI) is the world's first geostationary satellite for ocean color remote sensing mission. It observes coastal and ocean region around the Korean Peninsula, Japan, and East China with a spatial resolution of 500 meters.

GOCI uses step-stare imaging technique by the implementation of 2D detector array (1413 x 1430) and 2-axis pointing mechanism. It enables multiple image acquisitions for the same location of FOR (Field Of Regard) at sixty-minute intervals during daytime (8 images per day in nominal operation). Because GOCI IFOV is about a sixteenth of GOCI FOR, an image acquisition and processing sequence for GOCI FOR consists 16 (4 x 4) slot image acquisitions which correspond to GOCI IFOV and image processing to combine 16 slot images into one image for GOCI FOR.

Inter Solar Radiometric Discrepancy (ISRD) of GOCI means the radiance (i.e. digital count) discrepancy in the overlapped area between adjacent slot images. This is mainly derived by the difference of solar zenith angle by the gap of acquisition time between slots with overlapped area. Due to the boustrophedonic pattern of GOCI slot image acquisition sequence, maximum difference of acquisition time is about 12 minutes. After the normalization processing in terms of solar zenith angle for the reduction of ISRD, early in GOCI on-orbit operation, systematic residual ISRD about 3% discrepancy was observed for B6 (680nm) and B8 (865nm), where optical ghost/straylight in the southern part of a slot image was found to cause ISRD in the overlapped area between southern part of upper slot and northern part of lower slot.

For the qualitative and quantitative analyses of ISRD and the development of ISRD correction algorithm, end-to-end ISRD simulation tool based on ray tracing technique is developed. This also can be used for ISRD analysis of GOCI-II which is planned to be launched in late 2018. In this paper, we present the verification result of end-to-end ISRD simulation tool by comparing with pre-flight straylight/ghost test results, and development status of correction algorithm of systematic ISRD induced by straylight/ ghost.

9607-90, Session PMon

How much particles outburst is responsible to Geomagnetism rise during SME of certain solar activity?

Umesh P Verma, Patna Science College (India); Sergy Pullinet, Academy of Russian academy,space science resdearch , (Russian Federation) and Spcae science research directorate (Russian Federation); Madhurendra Nath Sinha, Patna Science College (India)

X-ray flux fluctuation observant during particle outburst of most of common SME has been noticed through the GOES13-15 Satellite monitoring of NOAA and IPS Australia. In numerous instances X-ray have been observed to rise associated with the K index scaling 3to 6 level of D,C, and M class solar wind. Interaction of these cosmic particles consisting of electrons and protons and other radioactive particles have excited the ionospheres' environment resulting geomagnetism rise Facts are indicated by k index rise and scaling index reflective in the magneto gram recorded by Goes13 and 15 satellites link. Rise in x-ray flux are propitiating the proton flux and reciprocating electron flux on the site of observation of global map. Rise in geomagnetism is the consequent feature displayed by X-ray rise and other electromagnetic parameters fluctuation and variation. Our study notices interesting feature of k index rise of different class of solar mass ejection associating geomagnetism rise confusing about seismic activity at the site of observation. The doubt is clarified by D components of geomagnetism rise. X-ray observed by 13 and 15 have similar to some extent but differ in some respect.

9607-22, Session 5

Radiometric calibration and stability of the Landsat-8 operational land imager (OLI)

Brian L. Markham, NASA Goddard Space Flight Ctr. (United States); Julia A. Barsi, Edward Kaita, Lawrence Ong, Science Systems and Applications, Inc. (United States); Ron A. Morfitt, U.S. Geological Survey (United States); Md. Obaidul Haque, SGT, Inc. (United States); Jeffrey S. Czapla-Myers, College of Optical Sciences, The Univ. of Arizona (United States); Dennis L. Helder, Nischal Mishra, South Dakota State Univ. (United States)

Landsat-8 has been operating on on-orbit for two years with its two Earth imaging sensors: the Operational Land Imager (OLI) and the Thermal InfraRed Sensor (TIRS). This paper discusses the OLI, the reflective band instrument. The OLI has 9 spectral bands spanning from 443 nm to 2300 nm. The OLI has been extremely stable radiometrically since launch: the shortest wavelength band (443 nm) has degraded about 1% in responsivity over 2 years; all other bands have changed less than 0.3%. Multiple on-board calibration systems (3 lamps, 2 solar diffusers) as well as the moon and Earth targets are used at different revisit frequencies to aid in separating calibrator degradation from instrument degradation. The on-board and lunar techniques all show band average trends in responsivity consistent to within 0.3%, distinctly better than prior Landsat sensors. Comparisons to ground vicarious measurements and other sensors (MODIS Aqua, MODIS Terra, Landsat-7 ETM+) are generally within 5% for both reflectance and radiance.

9607-23, Session 5

OLI relative radiometric calibration

Julia A. Barsi, Brian L. Markham, NASA Goddard Space Flight Ctr. (United States)

The Operational Land Imager (OLI), on board the Landsat-8 satellite, is a pushbroom sensor with nearly 7000 detectors per band, divided between 14 separate arrays. While rigorously characterized prior to launch, the shear number of individual detectors presents a challenge to maintaining the relative calibration such that stripes, bands and other artifacts are minimized in the final image products.

On-orbit relative calibration of the OLI is primarily monitored and corrected using observations of the primary solar diffuser panel. The panel is the most uniform target available to the OLI. Just after launch, coefficients were derived to flat-field the solar diffuser data, both for individual detectors as well as across the 14 arrays. The discontinuities between arrays and the detector-to-detector uniformity continue to be monitored on a weekly basis.

Changes to the relative calibration since launch are thought to be changes in the calibration of individual detectors. Since launch the Coastal/Aerosol and Blue bands have shown the most change in relative calibration over time, with many detectors showing a slow drift of about 0.2% per year. However, larger changes have been seen in the SWIR bands, where individual detectors' responses change suddenly by as much as 1.5%.

The mechanisms behind these changes are not well understood but in order to minimize impact to the users, the OLI relative calibration is updated on a quarterly basis in order to capture changes in time.

9607-24, Session 5

Assessing OLI stray light and contamination changes with lunar observations

Raviv Levy, NASA Goddard Space Flight Ctr. (United States) and Science Systems and Applications, Inc. (United States); Philip W. Dabney, Brian L. Markham, NASA



Goddard Space Flight Ctr. (United States)

The Operational Land Imager (OLI) aboard the LDCM satellite was rigorously characterized prior to launch to assure stray light and ghosting artifacts are at an acceptable level for science needs. On orbit dedicated calibration collects are being made to continue monitor the OLI stray light performance. In this paper we report on the use of OLI on-orbit Lunar collects and subsequent processing that extracts and trends the stray light isolation level.

9607-25, Session 5

TIRS stray light correction: algorithms and performance

Aaron D. Gerace, Matthew Montanaro, Rochester Institute of Technology (United States); Julia A. Barsi, NASA Goddard Space Flight Ctr. (United States); Tim Beckmann, U.S. Geological Survey (United States); Victoria Scholl, Jiang Fu, Rochester Institute of Technology (United States)

The Thermal Infrared Sensor (TIRS) onboard Landsat 8 was tasked with continuing thermal band measurements of the Earth as part of the Landsat program. From first light in early 2013, there were obvious indications that stray light was contaminating the thermal image data collected from the instrument. Traditional calibration techniques did not perform adequately as non-uniform banding was evident in the corrected data and error in absolute estimates of temperature over trusted buoys sites varied seasonally and, in worst cases, exceeded 9 K error. The development of an operational technique to remove the effects of the stray light has become a high priority to enhance the utility of the TIRS data.

This paper introduces the current algorithm being tested by Landsat's calibration and validation team to remove stray light from TIRS image data. The integration of the algorithm into the EROS test system is discussed with strategies for operationalizing the method emphasized. Techniques for assessing the methodologies used are presented and potential refinements to the algorithm are suggested. Initial results indicate that the proposed algorithm significantly removes stray light artifacts from the algorithm practically, visual and quantitative evidence suggests that the algorithm practically eliminates banding in the image data. Additionally, the seasonal variation in absolute errors is flattened and, in the worst case, errors of over 9 K are reduced to within 2 K. Future work focuses on refining the algorithm based on these findings and applying traditional calibration techniques to enhance the final image product.

9607-26, Session 5

Atmospheric correction for Landsat 8 over case 2 waters

Javier A. Concha, John R. Schott, Rochester Institute of Technology (United States)

Landsat 8 is a promising candidate to address the remote sensing of inland and coastal waters (Case 2 waters) due to its improved signal-to-noise ratio (SNR), spectral resolution, bit quantization, and high spatial resolution. Atmospheric correction is essential for remote sensing of water since the signal from the water reaching the sensor is small compared to atmospheric scattering. Standard atmospheric correction algorithms fail over highly turbid Case 2 waters because the black pixel assumption, i.e. the signal leaving the water is zero beyond near infrared (NIR), is not always satisfied. We develop a new atmospheric correction algorithm for Landsat 8 imagery based on the empirical line method (ELM) that does not rely on the black pixel assumption. This algorithm uses pseudo-invariant features (PIF) from the image, ground-truth data, and water-leaving reflectances from an inwater radiative transfer model to determine reflectance and radiance values of the bright and dark pixels used in the ELM method. We compare the results with in situ remote sensing reflectance measurements for different water bodies that exhibit a range of optical properties. We calculate reflectance errors for each band taking the in situ data as ground-truth,

and then compare them to results from standard atmospheric correction algorithms. These reflectance errors are small in all the visible bands for a wide range of concentrations. These results show that our atmospheric correction algorithm allows one to use Landsat 8 to study Case 2 waters as an alternative to traditional ocean color satellites (e.g. MODIS, SeaWiFS).

9607-27, Session 5

Requirement sensitivity studies for a future Landsat sensor

Matthew Montanaro, Aaron D. Gerace, John R. Schott, Rochester Institute of Technology (United States); Brian L. Markham, NASA Goddard Space Flight Ctr. (United States)

The Landsat program has collected imagery of the Earth for the past 40 vears. Although both Landsat 7 and 8 are currently operating on-orbit, the next generation Landsat mission is already being planned. Concept studies for this mission include reproducing the Landsat 8 design (mainly pushbroom imaging architecture). The definition of science requirements is an important step towards the development of instrument specifications. At this early stage, a re-evaluation of the Landsat requirements is beneficial since they might be flexible enough to relax in some areas to possibly save on manufacturing costs or may need to be tightened in other areas to produce better science products. The investigations presented here focused on spatial aliasing and spectral banding effects. The specifications of these two key performance requirements were taken from the Landsat 8 Operational Land Imager (OLI) sensor as a starting point for the analyses. They were then adjusted to determine their effects on the final image products through the use of standard radiometry equations and synthetic Earth scene data. The results of the modeling efforts for these two requirements concepts are presented here and could be used as a template for future instrument studies.

9607-28, Session 6

Assessment of the clouds and the Earth's radiant energy system (CERES) instrument performance and stability on the Aqua, Terra, and S-NPP spacecraft

Nathaniel P. Smith, Susan Thomas, Mohan Shankar, Phillip C. Hess, Natividad M. Smith, Dale R. Walikainen, Robert S. Wilson, Science Systems and Applications, Inc. (United States); Kory J. Priestley, NASA Langley Research Ctr. (United States)

The Clouds and the Earth's Radiant Energy System (CERES) scanning radiometer is designed to measure reflected solar radiation and thermal radiation emitted by the Earth. Five CERES instruments are currently taking active measurements in-orbit with two aboard the Terra spacecraft (FM1 and FM2), two aboard the Aqua spacecraft (FM3 and FM4), and one aboard the S-NPP spacecraft (FM5). The CERES instrument uses three scanning thermistor bolometers to make broadband radiance measurements in the shortwave (0.3 - 5.0 micrometers), total (0.3 - >100 micrometers) and water vapor window (8 - 12 micrometer) regions. An internal calibration module (ICM) used for in-flight calibration is built into the CERES instrument package consisting of an anodized aluminum blackbody source for calibrating the total and window sensors, and a shortwave internal calibration source (SWICS) for the shortwave sensor. The ICM sources, along with a solar diffusor called the Mirror Attenuator Mosaic (MAM), are used to define shifts or drifts in the sensor response over the life of the mission. In addition, validation studies are conducted to understand any spectral changes that may occur with the sensors and assess the pointing accuracy of the instrument, allowing for corrections to be made to the radiance calculations in CERES data products. This paper covers the observed trends in the internal and solar calibration data, discusses the latest techniques used to correct for sensor response, and explains the validation studies used to assess the performance and stability of the instrument.



9607-29, Session 6

Evaluating the impact of cold focal plane temperature on Aqua MODIS thermal emissive photoconductive band calibration

Yonghong Li, Aisheng Wu, Brian Wenny, Science Systems and Applications, Inc. (United States); Xiaoxiong J. Xiong, NASA Goddard Space Flight Ctr. (United States)

Aqua MODIS, the second MODIS instrument of NASA Earth Observation System, has operated for over twelve years since launch in 2002. MODIS has sixteen thermal emissive bands (TEBs) located on two separate cold focal plane assemblies (CFPA). The TEB are calibrated using onboard blackbody and space view observations. MODIS CFPA temperature is controlled by a passive radiative cooler in order to maintain detector gain stability. Beginning in 2006, the CFPA temperature gradually varies from its designed operating temperature with increasing orbital and seasonal fluctuations. In Aqua Collection 6 (C6), a correction to the detector gain due to the CFPA temperature variation is applied for data after mid-2012, with the largest observed impacts on the TEB photoconductive (PC) bands. This paper evaluates the impact of the CFPA temperature variation on the TEB PC band calibration through comparisons with simultaneous nadir overpasses (SNO) measurements from the Infrared Atmospheric Sounding Interferometer (IASI) and Atmospheric Infrared Sounder (AIRS). Our analysis shows that the current L1B product from mid-2011 to mid-2012 is affected by the CFPA temperature fluctuation. The MODIS-IASI comparison results show that no drift is observed in PC bands over the CFPA temperature variation range, except band 33. In the MODIS-AIRS comparison, bands 31-32 show flat trends over the range of CFPA temperature while a slight drift in band 33 and relatively larger fluctuation in bands 34-36 are seen from the comparison results.

9607-30, Session 6

Electronic crosstalk in Terra MODIS thermal emissive bands

Junqiang Sun, National Oceanie and Atmospheric Administration (United States) and Global Science & Technology, Inc. (United States); Sriharsha Madhavan, Science Systems and Applications, Inc. (United States); Xiaoxiong Xiong, NASA Goddard Space Flight Ctr. (United States); Menghua Wang, NOAA National Environmental Satellite, Data, and Information Service (United States)

The MODerate-resolution Imaging Spectroradiometer (MODIS) is one of the primary instruments in the National Aeronautics and Space Administration (NASA) Earth Observing System (EOS). The first MODIS instrument was launched in December 1999 on board the Terra spacecraft. MODIS has 36 bands, among which bands 20-25 and bands 27-36 are thermal emissive bands covering a wavelength range from 3.7 ?m to 14.2 ?m. It has been found that there are severe contaminations in Terra bands 27-30 (6.7 μ m - 9.73 μ m) due to crosstalk of signals among them. The crosstalk effect induces strong striping in the earth view (EV) images and causes large long-term drift in the EV brightness temperature (BT) in these bands. An algorithm using a linear approximation derived from on-orbit lunar observations has been developed to correct the crosstalk effect for them. It was demonstrated that the crosstalk correction can substantially reduce the striping in the EV images and significantly remove the long-term drift in the EV BT in bands 27 and 28. In this paper, the crosstalk correction algorithm previously developed is applied to correct the crosstalk effect in bands 29 and 30. The crosstalk correction successfully reduces the striping in the EV images and removes long-term drifts in the EV BT in bands 29-30 as was done similarly for bands 27-28. The crosstalk correction algorithm can thus substantially improve both the image guality and the radiometric accuracy of the LWIR PV bands, bands 27-30, Level 1B (L1B) products. It is also shown that other Terra MODIS thermal emissive bands are contaminated by the crosstalk effect and that the algorithm can be applied to these bands for crosstalk correction.

9607-31, Session 6

Electronic crosstalk characterization of Terra MODIS long wave infrared channels

Sriharsha Madhavan, Science Systems and Applications, Inc. (United States); Xiaoxiong J. Xiong, NASA Goddard Space Flight Ctr. (United States); Junqiang Sun, Global Science & Technology, Inc. (United States) and National Oceanic and Atmospheric Administration (United States); Aisheng Wu, Science Systems and Applications, Inc. (United States)

Terra (T) MODerate-resolution Imaging Spectroradiometer (MODIS), a heritage Earth observing sensor has completed 15 years of operation as of December 18 2014. T-MODIS has 36 spectral channels designed to monitor the land, ocean, and atmosphere. The long term climate data record from T-MODIS is an important dataset for global change monitoring. Sixteen of the spectral channels fall in the Mid (M) $(3.7-4.5\mu m)$ to Long (L) (6.7-14.1) μ m) Wave InfraRed (M/LWIR) wavelengths, which are also referred to as the Thermal Emissive Bands (TEBs). To date the TEBs have very satisfactory performance which is attributed to the scan-by-scan calibration using an onboard BlackBody whose temperature is traceable to the NIST temperature standards. However, with an aging instrument, it was observed from 2010 onwards that the Photo Voltaic LWIR channels (Bands 27-30) have suffered significantly from electronic crosstalk. This is mainly due to the deterioration of the electronic circuits of the relevant bands in the LWIR Focal Plane Array (FPA). In this paper, we report the characterization of the electronic crosstalk in the above-mentioned bands using the scheduled sensor observations of the lunar surface, as well as from the Earth-view responses. Such characterization can be used to reduce the effects of crosstalk when implemented in the future Level 1B reprocessing and thereby increasing the radiometric fidelity of the concerned bands.

9607-32, Session 7

Solar diffusers in earth observation instruments with an illumination angle of up to 70°: design and verification of performance in BSDF

Bilgehan Gür, Hans Bol, TNO Science and Industry (Netherlands); Pengmei Xu, Bicen Li, Beijing Institute of Space Mechanics and Electricity (China)

An important part of an earth observation instrument is the onboard calibration unit. This unit ensures through its calibrating and monitoring functionality accurate performances and thus accurate scientific observations of an instrument during its lifetime in orbit. One critical optical element in this unit is the so-called solar diffuser, which is illuminated by the sun as an irradiance source. The diffusers performance is expressed through its scattering properties, the Bi-Directional Scattering

Function BSDF. The BSDF depends on several parameters, such as surface properties, angle of incidence and detection and further.

This paper describes the challenging diffuser design and verification activities of TNO under contract of a customer for an earth observation instrument with observation conditions that require feasible BSDF under large angles of incidence of up to 70° with respect to the surface normal.

Not only the design though but also the verification of the diffuser performance under such angles including "out-of-plane", i.e. angle theta detection of the scattered light, was an essential activity to be executed. A representative measurement set-up was realized in the "Absolute Radiometric Calibration Facility ARCF" at TNO Delft in the Netherlands, a unique facility for the characterization and calibration of optical components for space applications.



In this paper we will summarize the R&D activities with respect to diffuser design and verification that were recently carried out at TNO and present its applicability to current and future earth observation missions with challenging observation conditions and thus challenging diffuser requirements under high illumination angles.

9607-33, Session 7

Characterization and application of a LEDdriven integrating sphere source

Leibo Ding, Science Systems and Applications, Inc. (United States); Elena M. Georgieva, NASA Langley Research Ctr. (United States); James J. Butler, NASA Goddard Space Flight Ctr. (United States); Georgi T. Georgiev, John W. Cooper, Gilbert R. Smith, Science Systems and Applications, Inc. (United States)

A Light-Emitting Diode (LED)-driven integrating sphere light source has been fabricated and assembled in the NASA Goddard Space Flight Center (GSFC) Code 618 Biospheric Sciences Laboratory's Calibration Facility. This light source is a 30.5 cm diameter integrating sphere lined with Spectralon. A set of four LEDs of different wavelengths are mounted on the integrating sphere's wall ports. A National Institute of Standards and Technology (NIST) characterized Si detector is mounted on a port to provide realtime monitoring data for reference. The measurement results presented here include the short-term and long-term stability and polarization characterization of the output from this LED-driven integrating sphere light source. As part of its application, this light source is used to characterize detector/pre-amplifier gain linearity in light detection systems. The measurement results will be presented and discussed.

9607-34, Session 7

Improved thermal-vacuum compatible flat plate radiometric source for system-level testing of optical sensors

Mark A. Schwarz, Craig J. Kent, Stellar Solutions Inc. (United States); Steven W. Brown, National Institute of Standards and Technology (United States); Robert Bousquet, Genesis Engineering Solutions, Inc. (United States)

In this work, development of a fiber-optically coupled, vacuumcompatible, flat plate radiometric source applicable to the characterization and calibration of remote sensing optical sensors in situ in a thermal vacuum chamber is described. The original flat plate radiometric source configuration's performance was presented at the 2009 SPIEI. Following the original effort, design upgrades were incorporated in order to improve radiometric throughput and uniformity. Results of ambient and thermalvacuum testing of a remote sensing optical sensor, with incorporated upgrades, of a flat plate illumination source are presented.

Keywords: Calibration, radiometry, remote sensing, source.

9607-35, Session 7

JPSS-1 VIIRS pre-launch radiometric performance

Hassan Oudrari, Jeff McIntire, Science Systems and Applications, Inc. (United States); Xiaoxiong Xiong, James Butler, NASA Goddard Space Flight Ctr. (United States); Boryana Efremova, Qiang Ji, Science Systems and Applications, Inc. (United States); Shihyan Lee, Contractor (United States); Tom Schwarting, Science Systems and

Applications, Inc. (United States)

The Visible-Infrared Imaging Radiometer Suite (VIIRS) is a key instrument onboard the Joint Polar Satellite System (JPSS) spacecraft. The JPSS-1 (J1) mission is scheduled to launch in January 2017, and will be very similar to the Suomi-National Polar-orbiting Partnership (SNPP) mission. VIIRS instrument was designed to provide measurements of the globe twice daily. It is a wide-swath (3,040 km) cross-track scanning radiometer with spatial resolutions of 370 and 740 m at nadir for imaging and moderate bands, respectively. It has 22 spectral bands covering the spectrum between 0.412 μ m and 12.01 μ m, including 14 reflective solar bands (RSB), 7 thermal emissive bands (TEB), and 1 day-night band (DNB). VIIRS observations are used to generate 22 environmental data products (EDRs). This paper will briefly describe J1 VIIRS characterization and calibration performance and strategies executed during the pre-launch testing phases by the independent government team, to generate the at-launch baseline radiometric performance, and the metrics needed to populate the Look-Up-Tables (LUTs). This paper will also provide an assessment of the sensor pre-launch radiometric performance, such as the sensor signal to noise ratios (SNRs), dual gain transition verification, dynamic range, reflective and emissive bands calibration, bands spectral performance, response-vsscan (RVS), and near-field-response. A comprehensive set of performance metrics generated during the pre-launch testing program will be compared to the SNPP VIIRS pre-launch performance.

9607-36, Session 7

JPSS-1 VIIRS pre-launch spectral characterization and performance

Christopher Moeller, Univ. of Wisconsin-Madison (United States); Thomas Schwarting, Jeffrey McIntire, Science Systems and Applications, Inc. (United States); Dave I. Moyer, The Aerospace Corp. (United States)

The pre-launch sensor level test program for the JPSS-1 VIIRS instrument, the second in the series (SNPP VIIRS launched in 2011), was completed in 2015 at the Raytheon El Segundo facility. The pre-launch test program provides characterization for all elements of sensor performance, populating the Sensor Data Record (SDR) algorithm lookup tables, and establishing compliance on performance metrics. During the pre-TVAC and TVAC phases, in-band and out-of-band measurements were collected to characterize the spectral performance of all VIIRS Moderate ("M"), Imager ("I") and Day-Night ("DNB") bands. The warm focal plane bands (M1-M7, I1, I2, DNB) were measured at ambient temperature using the Spectral Measurement Assembly (SpMA) with a tungsten source while the cold bands (M8-M16, 13-15) were cooled to their nominal on-orbit operational temperature in a thermal vacuum environment and measured using a combination of the SpMA tungsten and heated ceramic element sources. A slit oriented along the length of the focal plane axis constrains the illumination to the 16 (32) detectors of an M-band (I-band) to prevent electrical or optical influences from other bands influencing the spectral characterization.

The spectral measurements have been analyzed by Raytheon analysts with oversight from subject matter experts (SME) on the VIIRS Data Analysis Working Group (DAWG), as well as independently analyzed by the DAWG spectral SMEs. The effort shows that all bands are well characterized, with minor non-compliances in a few bands similar to those seen on SNPP VIIRS. Significant non-compliant out-of-band response found in SNPP VIIRS warm focal plane bands has been largely eliminated by a redesign of the optical filters. Corrections for signal attenuation by absorbing gases in the ambient portion of the measurement environment are found to materially alter the RSR shape of two bands, M9 and M13. Comparisons of SNPP VIIRS RSR to those of JPSS-1 will be presented. The DAWG will be releasing JPSS-1 RSR products to the user community in the first quarter of 2015 with subsequent updates planned.



9607-37, Session 8

VIIRS/J1 Polarization Narrative

Eugene Waluschka, NASA Goddard Space Flight Ctr. (United States); Steven W. Brown, National Institute of Standards and Technology (United States); James J. Butler, NASA Goddard Space Flight Ctr. (United States): Eric C. Fest. Raytheon Missile Systems (United States); Keith R. Lykke, National Institute of Standards and Technology (United States); Brendan McAndrew, Joel McCorkel, NASA Goddard Space Flight Ctr. (United States); Jeffrey McIntire, Sigma Space Corp. (United States); Gerhard Meister, NASA Goddard Space Flight Ctr. (United States); Eslim O. Monroy, Raytheon Space and Airborne Systems (United States); David I. Moyer, The Aerospace Corp. (United States); Kevin Terpie, Kurtis J. Thome, NASA Goddard Space Flight Ctr. (United States); Tung R. Wang, Raytheon Space and Airborne Systems (United States); James B. Young, Stellar Solutions Inc. (United States)

The second Visible/Infrared Imager/Radiometer Suite (VIIRS) instrument, just as the first instrument, has a requirement that its polarization sensitivity not exceed 2.5% or 3% (depending on wavelength band). But, unlike the first instrument, the second instrument does exceed its requirement in four of its spectral bands. Needless to say, this was not welcome news which resulted in a careful look at the requirement and its uncertainty, at the polarization model and additional polarization measurements using broadband and monochromatic light. The following sections document the activities associated with the polarization model and the model results, the role of the focal plane filters, the polarizers, the use of NIST's T-SIRCUS for polarization testing and associated analyses.

9607-38, Session 8

Analysis of JPSS J1 VIIRS polarization sensitivity using the NIST T-SIRCUS

Jeffrey McIntire, Science Systems and Applications, Inc. (United States); James B. Young, Stellar Solutions Inc. (United States); David I. Moyer, The Aerospace Corp. (United States); Eugene Waluschka, NASA Goddard Space Flight Ctr. (United States); Hassan Oudrari, Science Systems and Applications, Inc. (United States); Xiaoxiong J. Xiong, NASA Goddard Space Flight Ctr. (United States)

The polarization sensitivity of the Joint Polar Satellite System (JPSS) J1 Visible Infrared Imaging Radiometer Suite (VIIRS) measured pre-launch using a broadband source was observed to be larger than expected for many reflective bands. Ray trace modeling predicted that the observed polarization sensitivity was the result of larger diattenuation at the edges of the focal plane filter spectral bandpass. Additional ground measurements were performed using a monochromatic source (the NIST T-SIRCUS) to input linearly polarized light at a number of wavelengths across the bandpass of two VIIRS spectral bands and two scan angles. This work describes the data processing, analysis, and results derived from the T-SIRCUS measurements, comparing them with broadband measurements. Results have shown that the observed degree of linear polarization, when weighted by the sensor's spectral response function, is generally larger on the edges and smaller in the center of the spectral bandpass, as predicted. However, particularly phase angle changes in the center of the bandpass differ between model and measurement. Integration of the monochromatic polarization sensitivity over wavelength produced results consistent with the broadband source measurements, for all cases considered.

9607-39, Session 8

Impacts of VIIRS polarization sensitivity on non-ocean scenes

Timothy S. Wilkinson, The Aerospace Corp. (United States)

The Visible and Infrared Imaging Radiometer Suite (VIIRS) collects Earth science data continually in a sun-synchronous orbit. VIIRS raw data records (RDRs) are processed by ground software to generate a variety of environmental data records (EDRs). Over open ocean, ground software produces measurements of chlorophyll concentration based on subsurface reflectance estimates. Considering that about 90% of the top of the atmosphere (TOA) radiance reaching a sensor over open ocean can be attributed to atmosphere or surface reflectance, it is possible to introduce large chlorophyll estimate errors by ignoring ordinarily small contributions due to polarization sensitivity. For chlorophyll determination, instrument polarization sensitivity measurements are used in combination with atmospheric models to compensate for polarization phenomenon. VIIRS ground software does not compensate for polarization phenomenon when processing land scenes. It is therefore natural to consider the impacts of ignoring VIIRS polarization phenomenon for land surface reflectance estimates. In this work, pre-flight polarization sensitivity characterization data is used in conjunction with a polarized atmospheric propagation model to analyze potential impacts on retrieved TOA reflectance. Impacts are analyzed across several collection conditions, including ground surface type, atmospheric visibility, general atmospheric profile and collection geometry. Actual pre-flight characterization data is used for both NPP and J1 VIIRS.

9607-40, Session 8

JPSS solar diffuser stability monitor response to sun angle of incidence

Vijay Murgai, Kristie Yu, Neil R. Nelson, Raytheon Space and Airborne Systems (United States); James K. McCarthy, Stellar Solutions Inc. (United States)

The Visible/Infrared Imaging Radiometer Suite (VIIRS) is a key sensor on the Suomi National Polar-orbiting Partnership (NPP) satellite in orbit as well as for the upcoming Joint Polar Satellite System (JPSS). VIIRS collects Earth radiometry and imagery in 22 spectral from 0.4 to 12.5 ?m. Radiometric calibration of the reflective bands in the 0.4 to 2.5 ?m wavelength range is performed by measuring the sunlight reflectance from Solar Diffuser Assembly (diffuser is Spectralon®). Spectralon® is known to solarize due to sun UV exposure at the blue end of the spectrum (-0.4 - 0.6+?m) as seen by laboratory tests as well as on orbit data from MODIS and NPP. VIIRS uses a Solar Diffuser Stability Monitor (SDSM) to monitor the change in the Solar Diffuser reflectance in the 0.4 - 0.94 ?m wavelength range to correct the calibration constants. The SDSM measures the ratio of sun light reflecting from the Solar Diffuser to a direct view of the sun. As the intensity of the light reaching the SDSM in both Solar Diffuser view and sun view is a function of the sun's angle of incidence (AOI), the SDSM response to sun AOI has to be characterized.

This paper presents details of the test setup including an extended collimated source simulating the sun across all SDSM bands. The prelaunch characterization results for the J1 SDSM are presented. Comparison with NPP on orbit yaw maneuver SDSM results shows similar behavior demonstrating that the J1 test successfully characterized the SDSM response to sun AOI.

9607-41, Session 9

JPSS-1 VIIRS pre-launch day/night band radiometric calibration

Thomas Schwarting, Science Systems and Applications, Inc. (United States); ShihYan Lee, ERT, Inc. (United States); Jeffrey McIntire, Science Systems and Applications, Inc.



(United States); Xiaoxiong J. Xiong, NASA Goddard Space Flight Ctr. (United States)

JPSS-1 VIIRS, like its predecessor SNPP-VIIRS, features the panchromatic, three gain stage, Day/Night Band (DNB) capable of imaging the Earth under illumination conditions ranging from direct sunlight to reflected moonlight. The DNB CCDs use 32 different modes of time-delay integration and sub-pixel aggregation to achieve high SNR in low light conditions whilst maintaining roughly constant spatial resolution across scan. In the pre-launch test program these 32 different aggregation modes are separately calibrated over a dynamic range covering 7 orders of magnitude through a series of tests designed to generate initial calibration coefficients for the Sensor Data Record (SDR) algorithm lookup tables, assess radiometric performance, and determine compliance with the sensor specification.

Early in environmental testing at Raytheon El Segundo non-linear behavior was discovered in the DNB aggregation modes used at the end of scan for low signal levels. In response to this non-linearity, which was not present in SNPP VIIRS, the test program was modified to characterize the radiometric performance both in the baseline configuration and with a modified aggregation scheme that eliminates the modes used at the end of scan, replacing them with the unaffected adjacent mode and trading off spatial resolution for improved linearity. Presented is the radiometric performance under both sensor configurations including dynamic range, sensitivity, radiometric uncertainty and non-linearity along with a discussion of the potential impacts to on-orbit calibration and SDR performance.

9607-42, Session 9

JPSS-1 VIIRS DNB/SWIR non-linearity and its impact on SDR calibration

ShihYan Lee, Wenhui Wang, ERT, Inc. (United States); Chengyong Cao, NOAA National Environmental Satellite, Data, and Information Service (United States)

During JPSS-1 VIIRS testing at Raytheon El Segundo, non-linear behaviors were discovered in the low radiance levels of the SWIR band and DNB. In addition, the DNB non-linearity is aggregation mode dependent, where the most severe non-linear behavior are the aggregation modes used at high scan angles (>49 degree). A modified test program was conducted to characterize this non-linear behavior. Based on the characterized non-linear behavior, we explored options in modified on-orbit calibration strategy to improve SDR accuracy in the non-linear regions. The potential performance with the baseline (NPP) calibration strategy. The options in SDR code and Look Up Tables (LUTs) modifications are also presented with a discussion of calibration efficiency and on-orbit operation.

9607-43, Session 9

Preliminary results of J1 VIIRS ground geometric testing

Guoqing Lin, Science Systems and Applications, Inc. (United States); Robert E. Wolfe, NASA Goddard Space Flight Ctr. (United States); Masahiro Nishihama, Science Systems and Applications, Inc. (United States)

Following the successful operations of the first Visible Infrared Imaging Radiometer Suite (VIIRS) instrument on-board the Suomi National Polar?orbiting Partnership (SNPP) spacecraft since launch in October 2011, a second VIIRS instrument to be on-board the first Joint Polar Satellite System (JPSS-1) satellite has been fabricated. Ground testing at the sensor level has been completed in December 2014, which included geometric functional performance testing. The instrument geometric performance includes sensor (detector) spatial response, band-to-band co-registration (BBR) and pointing stability. They parameters have been calibrated and characterized through ground testing under ambient and thermal vacuum conditions, and numerical modeling and analysis. This paper summarizes the preliminary results, along with anomaly investigations. VIIRS sensor spatial response is measured by line spread functions (LSFs) in the scan and track directions for every detector. We parameterize the LSFs by: 1) dynamic field of view (DFOV) in the scan direction and instantaneous FOV (IFOV) in the track direction; and 2) modulation transfer function (MTF) for the 17 moderate resolution bands (M-bands) and for the five imagery bands (I-bands). We define VIIRS BBR for M-bands and I-bands as the overlapped fractional area of angular pixel sizes from the corresponding detectors in a band pair, including nested I-bands with M-bands. The ground tests result in static BBR matrices. VIIRS pointing stability includes scan plane tilt, scan rate and scan start position variations, and thermally induced pointing variations with respect to orbital position. These will be tracked or corrected in on-orbit operations.

9607-44, Session 9

A robust method for determining VIIRS calibration coefficients in solar reflective bands

Qiang Ji, Boryana V. Efremova, Thomas Schwarting, Jeffrey McIntire, Hassan Oudrari, Science Systems and Applications, Inc. (United States); Xiaoxiong J. Xiong, NASA Goddard Space Flight Ctr. (United States)

This paper presents a method for determining the JPSS J1 VIIRS RSB calibration coefficients and their uncertainties in quadratic calibration equation. Similar to a historical "attenuator method," our method is based on all measurements with and without an attenuator deployed. Different from other polynomial curve fitting techniques, which fit multiple coefficients in a complex nonlinear equation, our method breaks the fitting into two parts. The first part is a quadratic equation for the transmittance of attenuator, which can be solved analytically on four sets of measurements. The second part is a reformed calibration equation, which is linear for the zeroth-order to first-order and the second-order to first-order coefficient ratios once the transmittance is known. For both parts a non-parametric technique (Theil-Sen estimator) yields robust solutions using all combinations of measurements. After the two coefficient ratios are determined, the first-order coefficient is given in the calibration equation. In short, our method is numerically stable, and the analysis of uncertainty is straightforward. To demonstrate the results, examples using the recent JPSS J1 VIIRS pre-launch tests data are shown.

9607-45, Session 9

Modeling spectrally varying resolution in broadband imaging systems

Stephen A. Cota, Scott L. Schnee, Adam L. Loverro, The Aerospace Corp. (United States)

No Abstract Available

9607-46, Session 9

Simple techniques for modeling wavefront error in imaging systems

Scott L. Schnee, Stephen A. Cota, The Aerospace Corp. (United States)

No Abstract Available



9607-47, Session 10

Demonstrating the error budget for the climate absolute radiance and refractivity observatory through solar irradiance measurements

Kurtis J. Thome, Joel McCorkel, Brendan McAndrew, NASA Goddard Space Flight Ctr. (United States)

The Climate Absolute Radiance and Refractivity Observatory (CLARREO) mission addresses the need to observe high-accuracy, long-term climate change trends and to use decadal change observations as a method to determine the accuracy of climate change. A CLARREO objective is to improve the accuracy of SI-traceable, absolute calibration at infrared and reflected solar wavelengths to reach on-orbit accuracies required to allow climate change observations to survive data gaps and observe climate change at the limit of natural variability. Such an effort will also demonstrate NIST approaches for use in future spaceborne instruments.

9607-48, Session 10

Development of the next geostationary ocean color imager, GOCI-II

Seongick Cho, YoungJe Park, Kibeom Ahn, Eunsong Oh, Yu-Hwan Ahn, Korea Institute of Ocean Science & Technology (Korea, Republic of)

After the successful launch and operation of Geostationary Ocean Color Imager (GOCI), the first pathfinder of ocean color remote sensing in geostationary orbit from 2010, necessity of succession of GOCI mission after the expected lifetime by 2018, is gradually increasing into the international ocean color remote sensing users as well as domestic users in Korea.

As a successor of GOCI, development of GOCI-II has been started in 2012 with a planned launch in 2018. The mission and user requirements of GOCI-II are defined by Korea Institute of Ocean Science and Technology (KIOST) and international GOCI PI (Principal Investigators). GOCI-II will be able to monitor the nearly full Earth disk area on 128.2°E longitude in geostationary orbit, and to acquire the local area(observation region can be freely definable by user) image with 250m spatial resolution at nadir with 12 spectral bands from visible to NIR (370~885nm). These enhanced features will enable the monitoring and research of long-term ocean environment change with better image quality. Additional 4 spectral bands are added to improve the accuracy of data products such as chlorophyll concentration, total suspended sediments, dissolved organic matters, enhancement of atmospheric correction, and to have a novel capability such as PFT (Phytoplankton Functional Type) which enables to discriminate harmful algae bloom. Newly implemented panchromatic band with 402~885nm bandwidth is expected to enable star imaging for the geometric correction of GOCI-II images.

Full Disk(FD) and user-definable local area observation mode to be implemented for GOCI-II will satisfy the user requests such as ocean observation over clear sky without clouds and special ocean event area over specific region in anytime and anywhere. We are expecting this new capability will produce more applicable data products about special event area such as typhoon, oil spill, green algae bloom, and etc. GOCI- II will perform 10 LA observations per day. This is two more LA observations per day than the number of daily LA observations of GOCI (8 times per day). Additionally, a daily global observation is planned for GOCI-II for the research of long-term climate change in ocean.

In order to develop the GOCI-II with the full satisfaction of user requirements and to develop the data processing technique based on the actual GOCI-II on-ground test results, two research scientists are working together as Joint Development Team (JDT) with Airbus Defence & Space, and KARI (Korea Aerospace Research Institute). Airbus DS is the GOCI-II main developer according to the contract signed in July 2013. In this workshop, we present the development status of GOCI-II and principal enhancement of GOCI-II comparing with GOCI.

9607-49, Session 10

New polishable R-SiC layer on ultra lightweighted SiC substrates for space applications

Eric Ruch, REOSC (France)

Silicon Carbide is a material of high interest in the design and manufacturing of space telescopes, thanks to its mechanical and thermal properties.

Reosc has manufactured the 3 TMAs of the NIRSpec instrument that will take place on board JWST. Reosc has also polished 2 sets of mirrors for the Japanese HISUI instruments. Reosc has also polished the 1.5m primary mirrors of the GAIA instrument and currently polishing the scan mirrors of the MTG telescope and the 1,3m diameter primary mirror of the EUCLID instrument.

Based on this experience, Reosc is still improving its capability in the field of SiC mirrors. Two main activities are currently on-going:

1. replacement of CVD SiC by a new polishable layer R-SiC

2. development of ultra-lightweighted SiC mirror

The polishing of usual SiC mirrors does not provide very low microroughness. The current process uses CVD SiC that has some drawbacks, mainly in terms of sizability to very large mirrors. This is why Reosc has developed an alternative material for polishing layers, R-SiC. The main requirements (low micro-roughness polishing, CTE compatibility with substrate, environment compatibility) have been successfully demonstrated. The next phase of the technology research program run in collaboration with ESA was to manufacture a 300mm demonstrator.

Reosc has successfully polished two ultra-lightweighted SiC mirrors, with R-SiC polishable layer, with an areal density of 20kg/m?. The design and the manufacturing process are representative of a 1.5 to 2m diameter mirror class. The goal is to develop the process and the tools allowing the polishing of this mirror including the quilting conditions.

9607-50, Session 10

Novel compound parabolic concentrator for broadband radiometric measurement of ratio of reflected to incoming solar radiations around L1 halo orbit

Sehyun Seong, Sug-Whan Kim, Yonsei Univ. (Korea, Republic of); Michael Lockwood, The Univ. of Reading (United Kingdom)

The broadband scanning radiometer concept using compound parabolic concentrator (CPC) was proposed for measurement of ratio of reflected to incoming solar radiations to the measurement uncertainty better than ± 0.28 %, at around the L1 halo orbit. We present the optical performance evaluation of a new CPC designed to satisfy required optical efficiency and spectral flatness over 0.2 to 4.0 ?m in shortwave (SW) radiation wavelength range. The CPC was manufactured with electroless nickel plating aluminum. It has 23° in acceptance angle, 4.45 mm in focal length of parabola, 26.83 \pm 0.05 mm in overall length, 8.19 \pm 0.01 mm and 3.20 \pm 0.01 mm in radii of entrance and exit apertures, respectively. Its parabolic surface was finished to the surface roughness of less than 3 nm Ra and coated with protected aluminum for average reflectance over 80 % in the wavelength range. The test setup was constructed as distant small source (DSS) configuration using quartz tungsten halogen (QTH) lamps, infrared emitters, collimators, filters and the NIST traceable calibrated sensors. Within the CPC acceptance angle and wavelength range, the CPC optical efficiency and spectral flatness were measured. It implies that the measurement uncertainty corresponds to less than ± 0.28 %. The study proves that the new CPC can be used in measurement of ratio of reflected to incoming solar radiations around the L1 halo orbit.



9607-51, Session 11

Development of low optical cross talk filters for VIIRS for JPSS

Vijay Murgai, Derek Hendry, Raytheon Space and Airborne Systems (United States); Kevin R. Downing, Dave Carbone, Materion Barr Precision Optics & Thin Film Coatings (United States)

The Visible/Infrared Imaging Radiometer Suite (VIIRS) is a key sensor on Suomi National Polar-orbiting Partnership (NPP) satellite launched on October 28, 2011 into a polar orbit of 824 km nominal altitude and the JPSS sensors currently being built. VIIRS collects radiometric and imagery data of the Earth's atmosphere, oceans, and land surfaces in 22 spectral bands spanning the visible and infrared spectrum from 0.4 to 12.5 ?m. Interference filters assembled in 'butcher-block' arrays are used close to focal plane arrays for spectral definition. Out-of-band signal and out-of-band optical cross-talk was observed for bands in the 0.4 to 1 ?m range in testing of VIIRS for NPP. Optical cross-talk is in-band or out-of-band light incident on an adjacent filter or adjacent region of the same filter reaching the detector. Out-of-band optical cross-talk results in spectral and spatial 'impurities' in the signal and consequent errors in the calculated environmental parameters such as ocean color that rely on calculations based on combinations of signals from more than one band.

This paper presents results of characterization, specification, and coating process improvements that enabled production of filters with significantly reduced out of band light for JPSS J1 and subsequent sensors. Total transmission and scatter measurements at a wavelength within the pass band can successfully characterize filter performance prior to cutting and assembling into the butcher block assemblies. Coating and process development demonstrated performance on test samples followed by production of filters for J1 and J2. Results for J1 and J2 filters will be presented.

9607-52, Session 11

An update on EUMETSAT programmes and plans

K. Dieter Klaes, Kenneth Holmlund, EUMETSAT (Germany)

EUMETSAT as an inter governmental organisation representing 30 European Member States and one cooperating state is contributing space based observations for operational meteorology and climate monitoring. These observations are collected from the geostationary and sun-synchronous polar orbits though satellites systems developed and operated in the frame of mandatory programmes. In the frame of optional programmes further observations for altimetry and oceanography are provided. Through third party programmes, EUMETSAT provides data from other agencies' satellites to the user community. In summer 2015 EUMETSAT plans to launch MSG-4, which will complement the current operational fleet of operational geostationary spacecraft, namely the Meteosat-7, which is the last satellite of the first generation and the three satellites of the Second Generation of Meteosat (Meteosat Second Generation (MSG-1, MSG-2 and MSG-3)), Meteosat-8, Meteorsat-9 and Meteosat-10. MSG-4 will be stored in orbit after successful commissioning. The MSG Programme has been developed in co-operation between EUMETSAT and ESA. Two satellites of the EUMETSAT Polar System (EPS) are currently in orbit. Metop-B, the second of a series of three satellites, was launched in September 2012 and is the prime operational satellite. Metop-A, the first of the series is in orbit since October 2006. The satellites provide operational services in parallel operations from the mid-morning polar orbit. They belong to the Initial Joint Polar System (IJPS) with the US. The EUMETSAT Advanced Retransmission Service (EARS) provides observations from partner HRPT (High Resolution Picture Transmission) stations. EUMETSAT's first optional programme exploits the data from the Jason-2 satellite. Operational Ocean Surface Topography information services are provided since summer 2008. Jason-2 is a joint programme with CNES, NOAA and NASA. In a follow on Jason-3 optional programme the Jason-3 satellite is prepared for a lunch in summer 2015. To assure continuity development of Meteosat Third Generation

(MTG) and the preparations for EPS-SG (EPS Second Generation) are ongoing. The MTG programme is now in Phase C and the development is proceeding. EPS-SG is currently in phase B under a preparatory programme and the full programme approval is expected in 2015. In the frame of the Copernicus Programme (formerly GMES (Global Monitoring for Environment and Security)) EUMETSAT will operate the marine part of the Sentinel-3 satellites.

9607-53, Session 11

The convergence of earth science and applications from space: it's not your grandparents' R2O

Philip E. Ardanuy, Raytheon Intelligence & Information Systems (United States); Molly K. Macauley, Resources for the Future (United States); William B. Gail, Global Weather Corp. (United States); William H. Hooke, American Meteorological Society (United States)

Fifty-five years after the first weather satellite was launched into orbit, constellations and trains of meteorological and environmental satellites are now enabling routine Earth System Science from space. In addition to the tremendous advances in core science obtained from NASA, NOAA, USGS, and international-partner Earth observations, the Earth System Science community has had extraordinary success in building applications of significant societal value that leverage these data. Indeed, the applications science community has achieved a critically important milestone. It has successfully completed its incubation phase, characterized by efforts to educate mission planners and end-users about the benefits of applications along with the skills and tools required to obtain those benefits. Compelling evidence shows the community has transitioned to the demand phase, in which its investment has begun to succeed, its value is becoming well recognized, and its services are increasingly demanded. Demand for societal use of Earth information is growing rapidly, in some cases perhaps faster than the funding of basic Earth System Science itself. This transition requires fundamental changes in how the pure science research and applied research/scientific applications organizations operate virtually as a single enterprise in order to properly serve the rapidly growing need for their services. We are entering an era where research, operations, and applications are becoming an integrated system rather than distinct disciplines. This implies a need for profoundly improved interfaces between these three areas of our enterprise.

9607-54, Session 11

Collaboration tools for optimizing 'operational' climate monitoring from space

Douglas B. Helmuth, Lockheed Martin Corp. (United States)

Consistently collecting the earth's critical climate signatures (atmosphere, oceans, and terrestrial) remains a priority for world governments and international scientific organizations. Architecting optimized earth observing constellation solution(s) requires transforming today's scientific missions into an optimized robust 'operational' constellation that addresses the needs of decision makers, scientific investigators and global users for trusted data.

The application of new tools offers paths forward for global architecture collaboration of Remote Sensing Platforms in Constellation. This year rule-based expert system (RBES) modeling runs have been made optimized the intended but maligned NPOESS architecture, and become a surrogate for a global operational climate monitoring architecture(s). This rule-based systems tool delivers valuable insights for Global climate architectures, through the valuations of alternatives considered and the exhaustive range of trade space explored. Results from a more complex constellation optimization for monitoring/collecting Global Essential Climate Variables (ECV's) are discussed in detail with explanations and thoughts on



appropriate rule-based valuations. This specific modeling case is a global capabilities based example of an 'operational' climate-centric case study. This science traceability optimizing tool can be used to compare the relative value for hundreds of thousands of different possible architectures.

The paper & presentation includes graphic representation(s) of the architecture trade space(s) considered and the sensor/platform combinations that suggest and support collaborative paths forward. The material is intended for audience interaction and responses from climate scientists & national/regional decision makers.

9607-55, Session 12

S-NPP VIIRS instrument telemetry and calibration data trend study

ZiPing Sun, Frank J. De Luccia, Jason C. Cardema, Gabriel Moy, The Aerospace Corp. (United States)

The Suomi National Polar Orbiting Partnership (S-NPP) VIIRS (Visible Infrared Imaging Radiometer Suite) employs a large number of temperature and voltage sensors (telemetry points) to monitor instrument health and performance. We have collected data and built tools to study telemetry and calibration parameters trends. The telemetry points are organized into groups based on locations and functionalities. Examples of the groups are: telescope motor, focal plane array (FPA), scan cavity bulkhead, radiators, solar diffuser and solar diffuser stability monitor. We have performed daily monitoring and long-term trending studies. Daily monitoring processes are automated with alarms built into the software to indicate if pre-defined limits are exceeded. Long-term trending studies focus on instrument performance and sensitivities of Sensor Data Record (SDR) products and calibration look-up tables (LUTs) to instrument temperature and voltage variations.

VIIRS uses a DC Restore (DCR) process to periodically correct the analog offsets of each detector channel of each spectral band to ensure that the FPA output signals are always within dynamic range of the Analog to Digital Converters (ADCs). The offset values are updated based on observations of the On-Board Calibrator Blackbody (OBC BB) source. We have performed long-term trend study of DCR offsets and calibration parameters to explore connections of the DCR offsets with calibration parameters. The study also shows how the instrument and calibration parameters respond to the VIIRS Petulant Mode, spacecraft (SC) anomalies and flight software updates. These studies may help to improve calibration LUTs and SDR Quality Flags.

9607-56, Session 12

Trending of SNPP ephemeris and its implications on VIIRS geometric performance

Guoqing Lin, Science Systems and Applications, Inc. (United States); Robert E. Wolfe, NASA Goddard Space Flight Ctr. (United States); Masahiro Nishihama, Science Systems and Applications, Inc. (United States)

This paper describes the trending results of the ephemeris data in the three and half years of operations of the Suomi National Polar?orbiting Partnership (SNPP) spacecraft since its launch in October 2011. The ephemeris data includes time stamped positions and velocities, which are used to derive altitudes and speeds. The orbital mean altitude has been maintained at 838.8 km through drag make-up maneuvers for. The mean speed is 7524 m/s with orbital period of 101.5 minutes. The altitude above the Equator is 829.8 km to within +/- 1 km peak-to-valley. Within an orbit, the altitude varies from 828 km to 856 km and the speed varies from 7503 m/s to 7537 m/s. The local time of ascending node drifted slowly from 13:25:24 GMT at launch to 13:23:02 in November 2012, then back to 13:33:40 as of 16 October 2014. With four inclination adjustments, the inclination angle started drifting down, probably back to and maintained around 13:25:00.

The Visible Infrared Imaging Radiometer Suite (VIIRS) instrument onboard

the SNPP satellite has a swath width of 3055 km over the Equator, making observations once a day over the Equator both in the day side and night side without under-lap from one scan to the next or from one orbit to the next. For latitude above 55 (TBR) degrees in the northern hemisphere or below -55 (TBR) degrees in the southern hemisphere, VIIRS makes daily observations two or more times, up to 14 times over the poles.

9607-57, Session 12

Mission history of reflective solar band calibration performance of VIIRS

Gabriel Moy, Kameron Rausch, Evan Haas, Timothy S. Wilkinson, Jason C. Cardema, Frank J. De Luccia, The Aerospace Corp. (United States)

The VIIRS sensor onboard Suomi-NPP has 22 bands spanning the visible and infrared wavelengths from 0.4 to 12.5 um. The 14 reflective solar bands (RSB) are calibrated using solar radiance reflected from a Solar Diffuser (SD) and a dark reference from a Space View (SV). A Solar Diffuser Stability Monitor (SDSM) tracks the degradation of SD reflectance, measured by a derived parameter known as the "H factor". The ratio between calculated SD radiance, which includes the H factor, and the VIIRS measured SD radiance is known as the "F factor". Ground processing uses the F factor and the prelaunch measured instrument characteristics on which it depends to generate calibrated radiances and reflectances contained in the Sensor Data Record (SDR).

In this paper we discuss improvements to data product quality over the mission history through Look-Up Table (LUT) and algorithmic code changes, such as automated RSB calibration (RSBAutocal). The current operational calibration uses manually derived, weekly updates of predicted F LUTs that go into operation a week after delivery. As a result, calibration data are applied one to two weeks after their collection, resulting in significant predict-ahead errors. Another consequence of the weekly LUT update process is that anomalous trend changes in F factors may not be recognized and compensated for many weeks. Once RSBAutocal is operational, calibration will occur every orbit, eliminating both predict-ahead and trend change errors and thereby improving data product quality.

9607-58, Session 12

VIIRS reflective solar bands calibration improvements with hybrid approach

Junqiang Sun, National Oceanic and Atmospheric Administration (United States) and Global Science & Technology, Inc. (United States); Menghua Wang, NOAA National Environmental Satellite, Data, and Information Service (United States)

The on-orbit calibration of the reflective solar bands (RSBs) of the Visible Infrared Imaging Radiometer Suite (VIIRS) and the result from the analysis of the up-to-date 4 years of mission data are presented. The VIIRS solar diffuser (SD) and lunar calibration methodology are discussed, and the calibration coefficients, called F-factors, for the RSBs are given for the latest reincarnation. The coefficients derived from the two calibrations are compared and the uncertainties of the calibrations are discussed. Each calibration has advantages and disadvantages. Lunar calibration can provide long-term stable calibration coefficients, while SD/SDSM calibration is feasible every orbit. By combining the calibration coefficients of SD and lunar calibration, we produce a set of lookup tables (LUTs) that is the optimal result up to date and its accuracy level is estimated at ~0.2%. This hybrid approach highlights an important progress in calibration and it is made possible by the design change in VIIRS instrument layout allowing both the SD and the Moon to be viewed by RSB to be at the same angle of incidence (AOI). We assess the improvement to the ocean color products by comparing the official output to the new result and show the significant improvement.



9607-59, Session 13

Progress in the on-orbit calibration of SNPP VIIRS for ocean data applications

Robert E. Eplee Jr., Kevin R. Turpie, Gerhard Meister, Frederick S. Patt, Bryan A. Franz, NASA Goddard Space Flight Ctr. (United States)

The NASA Ocean Biology Processing Group has continued monitoring the SNPP VIIRS on-orbit calibration since the derivation of the calibration for Reprocssing 2014.0 of the VIIRS ocean color data set, which was based on solar and lunar observations through July of 2014. The VIIRS instrument calibration model developed for Reprocessing 2014.0 continues to hold true for data obtained through July of 2015. The optimum normaliztion for the SDSM-derived H-factors used in correcting the solar diffuser BRDF degradation is the detrended SDSM channel 8 time series. The optimum fits for the solar observations are exponential plus linear function of time for bands M1-M4 and simultaneous exonential functions of time for bands M5-M7. The optimum fits for the lunar observations are simultaneous exponentials of time plus linear functions of the sub-spacecraft point libration angles. Comparison of the solar and lunar time series show that lunar-derived adjustments of the solar time series are significant for bands M1, M3, and M4. The solar calibration time series shows an RMS error per band of 0.068-0.16%. The lunar calibration time series shows an RMS error per band of 0.070-0.24%. Due to the on-orbit aggregation of the band M6 lunar data, the scatter in the lunar time series is higher for this band than for the dual gain bands. Discounting the M6 lunar calibrations, the RMS errors for the lunar data are 0.070-0.17%, which are comparable to the solar residuals. The relative differences in the two trends are 0.10-0.24%, or 0.10-0.14% discounting the band M6 observations.

9607-60, Session 13

Propagation of visible infrared imaging radiometer suite (VIIRS) calibration uncertainty trends to ocean color data

Kevin R. Turpie, Univ. of Maryland, Baltimore County (United States); Robert E. Eplee Jr., SAIC (United States); Gerhard Meister, NASA Goddard Space Flight Ctr. (United States)

During the first few years of the Suomi National Polar-orbiting Partnership (NPP) mission, the NASA Ocean Color calibration team continued to improve on their approach to the on-orbit calibration of the Visible Infrared Imaging Radiometer Suite (VIIRS). As the calibration was adjusted for changes in ocean band responsitivity, the team also estimated a theoretic residual error in the calibration trends well within a few tenths of a percent, which could be translated in to trend uncertainties in regional time series of surface reflectance and derived products, where biases as low as a few tenths of a percent in certain bands can lead to significant effects. This study looks at effects from spurious trends inherent to the calibration and biases that arise between reprocessing efforts because of extrapolation of the time-dependent calibration table. With the addition of new models for instrument and calibration system trend artifacts, new calibration trends led to improved estimates of ocean time series uncertainty. Table extrapolation biases are presented for the first time. The results further the understanding of uncertainty in measuring regional and global biospheric trends in the ocean using VIIRS, which better define the roles of such records in climate research.

9607-61, Session 13

JPSS-1 VIIRS Prelaunch RSB RVS characterization and water vapor correction

ShihYan Lee, ERT, Inc. (United States); Changyong

Cao, NOAA National Environmental Satellite, Data, and Information Service (United States)

The accuracy of pre-launch VIIRS response versus scan angle (RVS) characterization is vitally important to the quality of calibrated radiance products. The RVS correct the optical system's scan angle dependency with respect to the calibrator scan angle. In this document, we describe the methodology used in JPSS-1 RSB RVS characterization and the efficacy of MODTRAN5 in water vapor correction. The RVS is characterized using a 2nd order polynomial fit over the measured scan angles. The results show high fitting accuracy with uncertainty of 0.05% of less for all bands except for M9 due to water vapor absorption. To improve M9 RVS, MODTRAN5 is used to correction water vapor absorption variation during the RVS measurements. This correction reduced M9 RVS uncertainty from ~0.2% to ~0.07% with a RVS that is up to 0.4% difference compared with RVS prior to correction.

9607-62, Session 13

Stellar calibration of the Suomi-NPP VIIRS day-night band high gain

Jon P. Fulbright, Science Systems and Applications, Inc. (United States); Xiaoxiong Xiong, NASA Goddard Space Flight Ctr. (United States)

The Day-Night Band (DNB) of the VIIRS instrument on Suomi-NPP has a remarkable dynamic range, and its high gain stage has extreme low-light sensitivity. The specification for the low radiance limit of the high gain state of the DNB is 3x10-9 W cm-2 sr-1, which means bright stars and planets are readily detectible when the DNB is viewing deep space. In this paper we describe how these stellar measurements can be used to calibrate the highgain stage of the DNB. The process includes determining which stars are crossing the SV field-of-view at a given time, computing the stellar radiance, and the computation of the gain trending. We also describe some of the complications and limits to this method, including undersampling of the stellar image, saturation, and crowding. Most stars have minimal variability, and the stars detectible by the DNB are mostly well-studied and any known variable stars can be discarded as calibration sources. We present the relative gain trending for the duration of the mission, which includes over 4500,000 measurements of over 3500 bright stars in the first three years on-orbit. We also show how spectrophotometric flux standard stars can be used to set an absolute radiance scale for the high-gain stage. Finally, we present results from our analysis of the S-NPP VIIRS Deep Space maneuver. which includes measurements of the DNB gain linearity and gain switching point.

9607-63, Session 14

Assessment of MODIS and VIIRS solar diffuser on-orbit degradation

Xiaoxiong J. Xiong, Jim Butler, NASA Goddard Space Flight Ctr. (United States); Amit Angal, Zhipeng Wang, Science Systems and Applications, Inc. (United States)

Both MODIS and VIIRS instruments use a solar diffuser (SD) system for their reflective solar bands on-orbit calibration. On-orbit changes in its bidirectional reflectance factor is tracked by a solar diffuser stability monitor (SDSM) using its alternate measurements of direct sunlight through an attenuation screen and the sunlight diffusely reflected off the SD. The SDSM calibration data are collected by a number of filtered detectors, covering wavelengths from 0.41 to 0.94 microns. This paper provides an in-depth assessment of both Terra and Aqua MODIS and S-NPP VIIRS SD on-orbit degradation. It examines the dependency of SD on-orbit degradation on spectral wavelength as well as solar exposure time. Due to different launch dates, operation configurations, and calibration frequencies, the Terra and Aqua MODIS and S-NPP VIIRS SD have experienced quite different amount of SD degradation. In general, however, the shorter the wavelength, the larger is the SD on-orbit degradation over solar exposure time for all three



instruments. Lessons learned from this assessment will help future earth observing sensors for their SD calibration system design, on-orbit operation, and calibration.

9607-64, Session 14

Out-of-band response and the Suomi-NPP solar diffuser stability monitor

Jon P. Fulbright, Ning Lei, Zhipeng Wang, Science Systems and Applications, Inc. (United States); Xiaoxiong Xiong, NASA Goddard Space Flight Ctr. (United States)

The Suomi-NPP VIIRS Solar Diffuser Stability Monitor (SDSM) is a crucial component of the calibration of the Reflected Solar Bands (RSB). The SDSM observes the Solar Diffuser (SD) to determine the amount of degradation affecting the Bidirectional Reflectance Distribution Function (BRDF) due to on-orbit exposure to UV light. The SDSM performs measurements in eight filtered bands covering the 410 to 926 nm wavelength range. The degradation of the SD in these eight bands is quantified by the H-factor. The SDSM has performed very well over the course of the SNPP mission, but concerns have been raised about whether the filters used in the SDSM have significant out-of-band (OOB) transmission. Possible OOB effects were not fully characterized pre-launch for the VIIRS SDSM, and therefore the potential influence on the on-orbit calibration has not been included into the H-factor measurements. We present the results of our efforts to: 1) quantify the magnitude of the possible OOB effect on the H -factors, and 2) use additional VIIRS observations, such as lunar and Earth-view data, to learn more about the existence of any OOB effect.

9607-65, Session 14

Estimation of the accuracy of the SNPP VIIRS solar diffuser BRDF degradation factor determined by the on-board solar diffuser stability monitor

Ning Lei, Science Systems and Applications, Inc. (United States); Xiaoxiong Xiong, NASA Goddard Space Flight Ctr. (United States)

The radiometric calibration of the reflective solar bands of the Visible Infrared Imaging Radiometer Suite (VIIRS) aboard the Suomi National Polarorbiting Partnership (SNPP) satellite relies on observing an onboard solar diffuser (SD). Once on orbit, the SD bidirectional reflectance distribution function (BRDF) degrades over time. An onboard solar diffuser stability monitor (SDSM) is used to determine the degradation. The degradation factor is derived from the response ratio when the SDSM detectors observe the Sun through a pinhole screen and the fully solar radiation illuminated SD through another pinhole screen at almost the same time. Consequently, it is crucial to determining accurately the ratio of the SDSM screen transmittance and the product of the SD screen transmittance and the SD BRDF at the initial time when the BRDF just starts to degrade. In order to accurately determine the screen transmittances, once on orbit, satellite yaw maneuvers were performed. Previously, we determined the SDSM screen transmittance with both yaw maneuver and a small portion of regular on-orbit data. Similarly, here we use both yaw maneuver and a small portion of regular on-orbit data to determine the product of the SD screen transmittance and the SD BRDF at the initial time. Importantly, we consider the impact of the angular dependence of the BRDF degradation factor. We fit a semi-physical model to the measured degradation factor to determine the measurement accuracy.

9607-66, Session 14

Determination of the SNPP VIIRS solar diffuser BRDF degradation factor over wavelengths not covered by the SDSM detectors

Ning Lei, Science Systems and Applications, Inc. (United States); Xiaoxiong Xiong, NASA Goddard Space Flight Ctr. (United States)

Once on orbit, the bidirectional reflectance distribution function (BRDF) of the solar diffuser (SD) of the Visible Infrared Imaging Radiometer Suite (VIIRS) aboard the Suomi National Polar-orbiting Partnership (SNPP) satellite degrades over time. The degradation factor is determined by an onboard solar diffuser stability monitor (SDSM). However, the central wavelengths (412 to 926 nm) of the SDSM detectors do not cover the VIIRS short wave infrared (SWIR) bands which have central wavelengths from 1238 to 2257 nm. Although it is known that the SD BRDF degrades at a much smaller rate over longer wavelengths, the degradation over some of the SWIR bands' central wavelengths may still be large enough to be ignored since Ocean Color products often require a radiometric calibration accuracy of at least 0.1%. To address the SD BRDF degradation factor over the SWIR bands wavelength region, we investigate a phenomenological theory and apply the theory to determine the SD BRDF degradation factor over the SWIR bands wavelength region.

9607-67, Session 14

Investigation of the solar diffuser degradation non-uniformity

Junqiang Sun, National Oceanic and Atmospheric Administration (United States) and Global Science & Technology, Inc. (United States); Mike Chu, National Oceanic and Atmospheric Administration (United States) and ERT, Inc. (United States); Menghua Wang, NOAA National Environmental Satellite, Data, and Information Service (United States)

The solar diffuser (SD) is the key component of the onboard calibration of the solar reflective bands (RSB) for many global monitoring instruments. Crucial in the use of the SD in the calibration of the RSB is a working assumption that the reflectance property of the SD remains the same functional form throughout degradation apart from an overall factor. In this work, we examine the angle dependence of SD degradation in the Visible Infrared Imaging Radiometer Suite (VIIRS) onboard Suomi National Polar orbiting Partnership (SNPP) satellite as well as other satellite sensors. An important and common step in the standard radiometric calibration methodology of the RSB is the input of the SD degradation result measured by the solar diffuser stability monitor (SDSM). It has been implicitly assumed that the SD degradation measured at the angle toward the SDSM is the same as the SD degradation toward the direction of the RSB location, but non-uniform degradation can invalidate this condition given that the SDSM and the RSB are at different outgoing angles with respect to the RSB. The evidence revealed by our analysis shows a clear evolving dependency, in particular, for short-wavelength bands for all sensors examined, on the solar declination angle over time that invalidates the current practice. We present the analysis, the result and a discussion on the implication for on-orbit calibration using SD going forward.



9607-68, Session 14

Impact of the angular dependence of the SNPP VIIRS solar diffuser BRDF degradation factor on the radiometric calibration of the reflective solar bands

Ning Lei, Science Systems and Applications, Inc. (United States); Xiaoxiong Xiong, NASA Goddard Space Flight Ctr. (United States)

The Visible Infrared Imaging Radiometer Suite (VIIRS) aboard the Suomi National Polar-orbiting Partnership (SNPP) satellite carries out radiometric calibration of its reflective solar bands (RSBs) primarily through observing an onboard solar diffuser (SD). The SD optical scattering property is measured by a bidirectional reflectance distribution function (BRDF). Once on orbit, the BRDF degrades over time and the degradation factor is determined by an onboard solar diffuser stability monitor (SDSM) which observes the Sun (through a pinhole screen) and the SD (through another screen with holes) at almost the same time. We showed in a previously SPIE proceeding that the BRDF degradation factor is angle dependent. Consequently, due to that the SDSM and the VIIRS telescope SD views have different angles, applying the BRDF degradation factor determined from the SDSM without any adjustments to the VIIRS RSB calibration can result in large systematic errors. In addition, the BRDF angular dependence has impacts on the determinations of the SD attenuation screen transmittances viewed by both the SDSM detectors and the VIIRS telescope. In this proceeding, we first determine the SD attenuation screen viewed by the VIIRS telescope with the impact of the SD BRDF angular dependence, using both yaw maneuver and regular on-orbit data (we show the determination of the SD attenuation screen transmittance viewed by the SDSM elsewhere). Then we explore how we can apply the degradation factor obtained from SDSM SD observations to the VIIRS RSB radiometric calibration.

9607-69, Session 15

Calibration improvements for MODIS and VIIRS SWIR spectral bands

Xiaoxiong J. Xiong, NASA Goddard Space Flight Ctr. (United States); Amit Angal, Jon P. Fulbright, Ning Lei, Zhipeng Wang, Aisheng Wu, Science Systems and Applications, Inc. (United States)

Both MODIS and VIIRS use a solar diffuser (SD) to calibrate their reflective solar bands (RSB), covering wavelengths from 0.41 to 2.3 microns. Onorbit change of the SD bi-directional reflectance factor (BRF) is tracked by an on-board solar diffuser stability monitor (SDSM). The current SDSM design, however, only covers the spectral range from 0.41 to 0.93 microns. In general, the SD degradation is strongly wavelength dependent with larger degradation occurring at shorter wavelengths, and the degradation in the SWIR region is expected to be extremely small. As each mission continues, however, the impact due to SD degradation at SWIR needs to be carefully examined and the correction if necessary should be applied in order to maintain the calibration quality. For Terra MODIS, alternative approaches have been developed and used to estimate the SD degradation for its band 5 (1.24 microns) and a time-dependent correction has already been applied to the current level 1B (L1B) collection 6 (C6). In this paper, we will describe different methodologies that can be used to examine the SD degradation and their applications for both Terra and Aqua MODIS and S-NPP VIIRS SWIR calibration. These methodologies include but not limited to the use of lunar observations, Pseudo Invariant Calibration Sites (PICS), band-to-band relative calibration, and a differential approach.

9607-70, Session 15

Update on the performance of Suomi-NPP VIIRS lunar calibration

Zhipeng Wang, Jon Fulbright, Science Systems and Applications, Inc. (United States); Xiaoxiong Xiong, NASA Goddard Space Flight Ctr. (United States)

Lunar observations have been regularly scheduled for the Visible Infrared Imaging Radiometer Suite (VIIRS) instrument aboard the Suomi National Polar-orbiting Partnership (S-NPP) satellite since its launch on October 28th, 2011. In reference to the ROLO irradiance model, the detector gain coefficient or F-factor can be derived from these lunar observations for the reflective solar bands (RSB). Unlike its predecessor Moderate Resolution Imaging Spectro-radiometer (MODIS), the Moon and the on-board solar diffuser (SD) are viewed by VIIRS detectors at the same angle of incidence (AOI) to the half angle mirror (HAM). Eliminating the impact from the variation in the instrument response to the HAM AOI, this design allows the detector gain changes tracked by the Moon and the SD to be directly compared. In this paper, we update the lunar F-factors from the scheduled lunar calibration. The long-term trends of the lunar F-factor trending and the SD F-factor trending still agree in general for all RSBs. We also calculate the lunar F-factor at detector level and compare the detector dependency of the lunar F-factor and the SD F-factor. For a few RSBs at shorter wavelengths, a bias of up to 1% between the two has been identified. Using the detectordependent lunar F-factors will decrease the retrieved Earth view radiance of lower-number detectors in relative to higher-number detectors than the SD F-factors. The inconsistency indicates systematic bias between the lunar and SD calibration approaches.

9607-71, Session 15

Improved VIIRS offset correction during lunar intrusion into space view

Peter J. Isaacson, Frank J. De Luccia, Gabriel Moy, Nicholas R. Vandermierden, The Aerospace Corp. (United States)

The Suomi NPP VIIRS is a scanning radiometer designed to collect measurements that support a diverse range of operational and science applications. VIIRS radiometric calibration requires a zero radiance source to determine the background level. This background level, due to both dark current and electronic offsets, must be removed from the instrument digital output to determine the contribution from the earth scene radiance of interest.

The VIIRS space view (SV) is employed to determine the background level. The space view digital output is applied as an additive (offset) term in the VIIRS radiometric calibration. However, the SV is occasionally "contaminated" by viewing the Moon, which leads to substantially higher SV counts than would be expected for cold space. The VIIRS calibration algorithms have a catch for this situation, but it is conservative, leading to "false positives" in which scans are flagged as contaminated when they actually view cold space. Furthermore, when scans are flagged as lunar contaminated, the VIIRS calibration algorithms use alternate data sources as substitute SV observations, and the data are flagged as poor quality.

In this work, we present a new technique for evaluating the lunar contamination of VIIRS scans. For scans that are only partially contaminated (that "see" both lunar contamination and cold space), this technique enables calculation of the zero radiance offset from the same scan, rather than relying on alternate sources. This approach could potentially reduce the need to flag scans for which the Moon contaminates the SV as lower quality.



9607-72, Session 15

An improved algorithm for VIIRS bandto-band registration characterization with lunar observation

Zhipeng Wang, Science Systems and Applications, Inc. (United States); Xiaoxiong J. Xiong, NASA Goddard Space Flight Ctr. (United States); Yonghong Li, Science Systems and Applications, Inc. (United States)

Since launch, lunar observations have been performed on a regular basis for the Visible Infrared Imaging Radiometer Suite (VIIRS) instrument aboard the Suomi National Polar-orbiting Partnership (S-NPP) satellite. Unlike its predecessor Moderate Resolution Imaging Spectro-radiometer (MODIS), VIIRS has no on-board calibrator to perform the on-orbit spatial characterization. Therefore, the methodologies for spatial characterization using the Moon that have been developed for MODIS are extended for VIIRS. One of the key spatial parameters is the band-to-band registration (BBR) in both along-scan and along-track directions. While the lunar BBR results can satisfactorily show that the long-term stability of VIIRS BBR meets the design requirement specification of ±0.1 M-band pixels, seasonal oscillations have been observed in the BBR results, mostly noticeable between the visible/near infrared bands and short/middle wave infrared bands. This paper investigates the cause of this oscillation. It is found that the oscillation is correlated with the orientations of the lunar images that rotate from event to event. After figuring out an approach to quantify the rotation and compensate its impact, current BBR algorithm is improved and the seasonal oscillation in the BBR results is significantly reduced from up to ±0.05 M-band pixels to less than ±0.01 M-band pixels. With suppressed seasonal oscillation, the actual BBR can be derived and its long-term drift is easier to be identified.

9607-73, Session 15

S-NPP VIIRS TEB detector noise analysis using ICVS linear gain

Taeyoung J. Choi, NOAA National Environmental Satellite, Data, and Information Service (United States) and ERT, Inc. (United States); Changyong Cao, Fuzhong Weng, NOAA National Environmental Satellite, Data, and Information Service (United States)

The Soumi-NPP Visible Infrared Imaging Radiometer Suite (VIIRS) was launched on October 28th, 2011 and its Sensor Data Record (SDR) product was reached maturity status in March of 2014. Although the VIIRS SDR products gained the 'validated maturity' state, there were remaining issues such as residual stripings in the scan direction in some thermal bands. These horizontal striping issues in the Thermal Emissive Bands (TEBs) were reported by Sea Surface Temperature (SST) Environmental Data Record (EDR) group. The observed noise patterns had up to ± 0.2 K level especially in the band M14 and M15.

As an independent source of calibration, the Solar Diffuser (SD) is utilized in this study. The SD is originally designed for the Reflective Solar Band (RSB), however, it is assumed to be thermally stable at the time of SD observation. Residual thermal transitions are removed by applying a simple differentiation filtering. For each detector, a linear gain developed by Integrated Calibration and Validation System (ICVS) is applied to convert digital number (DN) to radiance unit. After the conversion, noise analyses are performed within the SD scan and among the scan-averaged responses.

Conference 9608: Infrared Remote Sensing and Instrumentation XXIII



Monday - Wednesday 10-12 August 2015

Part of Proceedings of SPIE Vol. 9608 Infrared Remote Sensing and Instrumentation XXIII

9608-1, Session 1

Rosetta and 67p/ Churyumov -Gerasimenko: a comet under observation (Invited Paper)

Gabriele E. Arnold, Deutsches Zentrum für Luft- und Raumfahrt e.V. (Germany)

After a ten year's expedition through the Solar system Europe's comet chaser Rosetta arrived at comet 67 P/ Churyumov-Gerasimenko in August 2014. Less than 100 kilometers from the nucleus the eleven orbiter payload instruments started to map and characterize the comet in great detail. In November 2014 Philae was the first robotic subsystem ever that landed on a cometary surface performing in situ measurements with ten instruments. The mission's scientific program following the deployment of Philae is determined by the activity of the comet, which will increase as 67P approaches perihelion in August 2015.

This paper introduces the mission goals and profile. It gives an overview of some of the preliminary results of the mission. Selected results gained during the pre-landing phase of the subsystem Philae's subsystem and the comet's escort phases are discussed.

9608-2, Session 1

VIRTIS on Rosetta: a unique technique to observe comet 67p/Churyumov -Gerasimenko: first results and prospects

Gabriele E. Arnold, Deutsches Zentrum für Luft- und Raumfahrt e.V. (Germany); Fabrizio Capaccioni, INAF -IASF Roma (Italy); Gianrico Filacchione, INAF - Istituto di Astrofisica e Planetologia Spaziali (Italy); Stéphane Erard, Lab. d'Etudes Spatiales et d'Instrumentation en Astrophysique (France); Dominique Bockelee-Morvan, Antonella Barucci, Observatoire de Paris à Meudon (France); Maria Cristina De Sanctis, Ernesto Palomba, Maria Teresa Capria, Priscilla Cerroni, INAF - IASF Roma (Italy); Pierre Drossart, Florence Henry, Cedric Leyrat, Observatoire de Paris à Meudon (France); Giuseppe Piccioni, INAF - IASF Roma (Italy); Bernard Schmitt, Lab. d'Astrophysique de l'Observatoire de Grenoble (France); Frederico Tosi, INAF - IASF Roma (Italy); Gian Paolo Tozzi, INAF - Osservatorio Astrofisico di Arcetri (Italy)

VIRTIS aboard ESA's Rosetta mission is a complex imaging spectrometer that combines three unique data channels in one compact instrument to study nucleus and coma of comet 67P/Churyumov-Gerasimenko. Two of the spectral channels are dedicated to spectral mapping (-M) at moderate spectral resolution in the range from 0.25 to 5.1 ?m. The third channel is devoted to high resolution spectroscopy (-H) between 2 and 5 ?m. The VIRTIS-H field of view is approximately centered in the middle of the -M image. The spectral sampling of VIRTIS-M is 1.8 nm/band below 1 μ m and 9.7 nm/band between 1-5 μ m, while for VIRTIS-H ?/??= 1300-3000 in the 2-5 μ m range.

This paper describes selected findings during the pre-landing phase of Philae's robotic subsystem and the comet's escort phase as well as prospects of further observations. The preliminary results include studies of surface composition, coma analyses and temperature retrieval for the nucleus surface-coma system demonstrating the capability of the instrument.

VIRTIS was developed by a consortium under the scientific direction of

the Institute for Space Astrophysics and Planetology (IAPS, INAF), in Rome (I). The consortium includes the Laboratory for Space Studies and Astrophysics Instrumentation (LESIA) of the Observatoire de Paris (F) and the DLR Institute of Planetary Research in Berlin (G). The development of the instrument was funded by the national space agencies ASI, CNES, and DLR. The authors gratefully acknowledge the support from the Rosetta and VIRTIS science, instrument, and operation teams.

9608-3, Session 1

MERTIS: geometrical calibration of thermal infrared optical system by applying diffractive optical elements

Martin Bauer, Technische Univ. Berlin (Germany) and Technische Fachhochschule Wildau (Germany)

Geometrical sensor calibration is essential for space applications based on high accuracy optical measurements, in this case for the thermal infrared push-broom imaging spectrometer MERTIS. The goal is the determination of the interior sensor orientation. A conventional method is to measure the line of sight for a subset of pixels by single pixel illumination with collimated light. To adjust angles which define the line of sight of a pixel a manipulator construction is used.

A new method for geometrical sensor calibration is using Diffractive Optical Elements (DOE) in connection with laser beam equipment. Diffractive optical elements (DOE) are optical microstructures which are used to split an incoming laser beam with a dedicated wavelength into a number of beams with well-known propagation directions. As the virtual sources of the diffracted beams are points at infinity which gives an image invariant against translation. This particular feature allows a complete geometrical sensor calibration with one image avoiding complex adjustment procedures which means a significant reduction of calibration effort.

We present a method for geometrical calibration of thermal infrared optical system. The fundamentals of this approach of infrared optical system calibration by applying diffractive optical elements are discussed. The demonstrated results underpin the consistency between simulation and real data.

9608-4, Session 1

MERTIS FM: optical performance of the thermal infrared push-broom imaging spectrometer

Martin Bauer, Technische Univ. Berlin (Germany)

The Mercury Radiometer and Thermal Infrared Spectrometer (MERTIS) onboard the BepiColombo Mercury Planetary Orbiter (MPO) is a state of the art instrument for studies of the surface composition of Mercury. MERTIS is the first spaceborne push-broom spectrometer that allows mapping the Mercury's surface mineralogy in the diagnostic mid-infrared range.

The assessment of the optical performance by optical simulation and testing is presented. Moreover, the method for geometrical calibration of the thermal infrared imaging spectrometer and the fundamentals of this approach are discussed. The demonstrated results underpin the consistency between simulation and real data.



9608-5, Session 1

VIRTIS on Venus Express: retrieval of real surface emissivity at global scales

Gabriele E. Arnold, David Kappel, Deutsches Zentrum für Luft- und Raumfahrt e.V. (Germany); Rainer Haus, Westfälische Wilhelms-Univ. Münster (Germany); Laura Tellez Pedroza, Univ. Potsdam (Germany); Giuseppe Piccioni, INAF - IASF Roma (Italy); Pierre Drossart, Observatoire de Paris à Meudon (France)

The extraction of surface emissivity data provides the data base for surface composition analysis and enables to evaluate Venus' geology. The Visible and InfraRed Thermal Imaging Spectrometer (VIRTIS) aboard ESA's Venus Express mission measured, inter alia, the nightside thermal emission of Venus in the near infrared atmospheric windows between 1.0 and 1.2 μ m. These data can be used to determine information about surface properties on global scales. This requires a sophisticated approach to understand and consider the effects and interferences of different atmospheric and surface parameters influencing the retrieved values. In the present work, results of a new technique for retrieval of the 1.0 – 1.2 μ m – surface emissivity are summarized. It includes a Multi-Window Retrieval Technique (MWT), a Multi-Spectrum Retrieval technique (MSR), and a detailed reliability analysis. The MWT bases on a detailed radiative transfer model making simultaneous use of information from different atmospheric windows of an individual spectrum. MSR regularizes the retrieval by incorporating available a priori mean values, standard deviations as well as spatial-temporal correlations of parameters to be retrieved. The capability of this method is shown for selected examples (surface target areas). Implications for geologic investigations are discussed. Based on these results the work draws conclusions for future Venus surface composition analyses on global scales using spectral remote sensing techniques. In that context, requirements for observational scenarios and instrumental performances are investigated, and recommendations are derived to optimize spectral measurements on Venus' surface studies.

9608-6, Session 1

Development of a mast or robotic armmounted infrared AOTF spectrometer for surface moon and mars probes (Invited Paper)

Oleg Korablev, Andrei Y. Ivanov, Space Research Institute (Russian Federation); Yurii K. Kalinnikov, VNIIFTRI (Russian Federation); Alexei Shapkin, Space Research Institute (Russian Federation); Sergei N. Mantsevich, Lomonosov Moscow State Univ. (Russian Federation) and Space Research Institute (Russian Federation); Anna A. Fedorova, Alexander V. Kiselev, Space Research Institute (Russian Federation)

A pencil-beam infrared AOTF spectrometer for context analyses of the surface in the vicinity of a planetary probe or a rover is being developed. One application is the ISEM (Infrared Spectrometer for ExoMars) instrument to be deployed on the mast of ExoMars Rover planned for launch in 2018. A very similar instrument LIS (Lunar Infrared Spectrometer) is planned to be flown on Russian Luna-25 (Luna Globe Lander) and Luna-27 (Luna Resource Lander) missions in 2018 and 2020 respectively. On these landers the instrument will be mounted at a robotic arm (Luna-25) or at a dedicated mast (Luna-27). The instrument covers the spectral range of 1.15-3.3 ?m with the spectral resolution of ~20 cm-1. The spectral range is selected to characterize the mineralogy; the long-wave bound allows to assess the hydration of the regolith on the Moon, and offers the ability to detect carbonates on Mars. The optical scheme includes entry optics, the TeO2 AOTF, and a Peltier-cooled InAs detector. To cover the whole spectral range the AOTF is equipped with two piezotransducers. At present the gualification prototype is being characterized. The instrument optics, and

different aspects of its characterization, including low-temperature survival qualification will be described.

9608-7, Session 1

Middle-infrared echelle cross-dispersion spectrometer ACS-MIR for the ExoMars trace gas orbiter

Alexander Y. Trokhimovsky, Oleg Korablev, Space Research Institute (Russian Federation); Yurii S. Ivanov, Ivan I. Syniavsly, National Academy of Sciences (Ukraine); Alexander V. Stepanov, Lomonosov Moscow State Univ. (Russian Federation) and Space Research Institute (Russian Federation); Andrei Y. Titov, SKB IKI (Russian Federation); Tatiana O. Kozlova, Space Research Institute (Russian Federation); Andrei S. Patrakeev, Space Research Institute (Russian Federation) and Moscow Institute of Physics and Technology (Russian Federation); Pavel P. Moiseev, Astron Electronics (Russian Federation); Anna A. Fedorova, Space Research Institute (Russian Federation); Franck Montmessin, LATMOS (France)

The middle-infrared (MIR) echelle spectrometer is one channel of the Atmospheric Chemistry Suite (ACS) package dedicated for the studies of the Martian atmosphere on board ExoMars Trace Gas Orbiter (TGO) planned for launch in 2016. The MIR channel of ACS is a cross-dispersion echelle instrument dedicated to solar occultation measurements in the range of 2.2-4.4 ?m with the resolving power of ~50,000. MIR is dedicated to sensitive measurements of trace gases. The MIR channel consists of entry optics, an echelle spectrometer with a 140x250 mm grating and twomirror collimator, a secondary steerable grating, and a cryogenically cooled MCT detector array with proximity optics. The spectrometer operates in high orders of diffraction, allowing to acquire ~20 orders at one detector frame, and to cover simultaneously ~300-nm spectral interval within the spectral range. The mechanism allows moving the secondary grating with a characteristic time of ~0.1 s, and the alternation of two positions is possible for a 1-s measurement cycle. This concept is novel for space application. The instrument is a complete block with power and data interfaces, and the overall mass of 12 kg.

At the moment of the abstract submission the integration of NIR protoflight model is being completed. The calibrated and tested instrument will be delivered to ESA in April 2015. The description of the instrument and the results of tests will be reported.

9608-8, Session 1

Near-infrared echelle-AOTF spectrometer ACS-NIR for the ExoMars trace gas orbiter

Alexander Y. Trokhimovsky, Oleg Korablev, Space Research Institute (Russian Federation); Yurii K. Kalinnikov, VNIIFTRI (Russian Federation); Anna A. Fedorova, Space Research Institute (Russian Federation); Alexander V. Stepanov, Lomonosov Moscow State Univ. (Russian Federation) and Space Research Institute (Russian Federation); Andrei Yu Titov, SKB IKI (Russian Federation); Andrei S. Patrakeev, Space Research Institute (Russian Federation) and Moscow Institute of Physics and Technology (Russian Federation); Ilya Dziuban, Space Research Institute (Russian Federation); Franck Montmessin, LATMOS (France)

The near-Infrared echelle-AOTF spectrometer is one channel of the Atmospheric Chemistry Suite (ACS) package dedicated for the studies

Conference 9608: Infrared Remote Sensing and Instrumentation XXIII



of the Martian atmosphere on board ExoMars Trace Gas Orbiter planned for launch in 2016. The near-infrared (NIR) channel of ACS is a versatile spectrometer for the spectral range of 0.7-1.6 ?m with a resolving power of ?20,000. The NIR channel is intended to measure the atmospheric water vapor, aerosols, airglows, in nadir, in solar occultation, and on the limb. The science goals of NIR are basically the same as for SPICAM IR channel presently in flight on board Mars Express ESA orbiter, but it offers significantly better spectral resolution. The instrument employs the principle of an echelle spectrometer with an acoustooptical tunable filter (AOTF) as a preselector. The same principle was employed in SOIR, working on Venus Express ESA mission in 2006-2014, and in RUSALKA, operated onboard ISS in 2009-2012. The NIR channel of ACS consists of entry optics, the AOTF, a Littrow echelle spectrometer, and an electrically cooled InGaAs detector array. It is a complete block with power and data interfaces, and the overall mass of 3.5 kg. At the moment of the abstract submission the integration of NIR protoflight model is being completed. The calibrated and tested instrument will be delivered to ESA in April 2015. The description of the instrument and the results of tests will be reported. A novel element, the AOTF in the converging beam will be also described, and some discussion on the echelle-AOTF scheme trade-offs will be presented.

9608-9, Session 1

Fourier-spectrometer ACS-TIRVIM for the ExoMars trace gas orbiter

Alexei V. Grigoriev, Boris E. Moshkin, Alexei V. Shakun, Oleg Korablev, Alexander V. Zharkov, Dmitry V. Patsaev, Fedor G. Martynovich, Andrei S. Kungurov, Oleg M. Sazonov, Igor A. Maslov, Alexander Santos-Skripko, Sergei A. Nenashev, Igor A. Stupin, Nikolai I. Ignatiev, Space Research Institute (Russian Federation)

The thermal-infrared (TIRVIM) is one channel of the Atmospheric Chemistry Suite (ACS) package dedicated for the studies of the Martian atmosphere on board ExoMars Trace Gas Orbiter (TGO) planned for launch in 2016. The TIRVIM channel is a 2-in. double pendulum Fourier-transform spectrometer for the spectral range of 1.7-17 ?m with apodized resolution of 0.2 to 1.6 cm?1, varying in function of the observing mode. TIRVIM is primarily dedicated to the monitoring of atmospheric temperatures and aerosol states in nadir, but also provides wide-range solar occultation measurements. TIRVIM optical scheme includes a sun periscope, a scanner, a blackbody simulator, an interferometer with a reference channel, and a detector with associated proximity optics. The whole spectral range is covered by one double pendulum interferometer with a KBr beamsplitter. The full (twosided) maximal optical path difference (OPD) is 12 cm, allowing to reach an apodized spectral resolution of 0.2 cm?1. The custom-made MCT detector is cooled by a Stirling machine down to 65 K. The detector is sensitive at 1.7-17 ?m (germanium window), and it is determining the LW bound of the instrument. It is employed both in nadir and in solar occultation, allowing spectral resolution of 1.6 cm?1 and 0.2 cm?1, respectively. The instrument is a complete block with power and data interfaces, and the overall mass of 12 kg. At the moment of the abstract submission the integration of the TIRVIM protoflight model is being completed. The calibrated and tested instrument will be delivered to ESA in April 2015. The description of the instrument and the results of tests will be reported.

9608-10, Session 1

M-DLS laser and heterodyne IR spectrometer for studies of the martian atmosphere from ExoMars-2018 landing platform

Alexander V. Rodin, Moscow Institute of Physics and Technology (Russian Federation) and Space Research Institute (Russian Federation); Imant I. Vinogradov, Space Research Institute (Russian Federation) and Moscow Institute of Physics and Technology (Russian Federation); V. V. Barke, Space Research Institute (Russian Federation); O. V. Benderov, D. V. Churbanov, Artem Klimchuk, Moscow Institute of Physics and Technology (Russian Federation); Yu. V. Lebedev, Space Research Institute (Russian Federation); A. A. Pereslavtseva, Z. B. Seilov, V. S. Semenov, Moscow Institute of Physics and Technology (Russian Federation); Maxim V. Spiridonov, Prokhorov General Physics Institute (Russian Federation)

We present the concept of a compact, lightweight, multichannel laser spectrometer for in situ and remote sensing of the chemical and isotopic composition of the Martian atmosphere. The instrument M-DLS (Martian Diode Laser Spectrometer) has been accepted as part of science payload of the ExoMars landing platform, whose launch is planned in 2018. After delivery of ESA's rover to Mars' surface, the platform is expected to operate as an autonomous lander at least for one Martian year. A primary goal of the experiment is highly accurate measurements of composition and structure of the Martian atmosphere, with particular focus on water vapor, isotopic ratios, and methane. Measurements will be carried out on regular basis both in situ, using a sample of ambient atmosphere, and remotely, by direct Sun observations in heterodyne channel.

The instrument employs principles of diode laser spectroscopy, with tunable distributed feedback (DFB) lasers emission frequency being controlled by temperature stabilization and pumping current. Saw-like pumping current modulation results in ramping laser frequency so that it covers a particular spectral line. Laser radiation is partially put into optical cell filled by a sample of ambient air, with another portion of radiation passing through reference cell that provides feedback for frequency modulation control. Two types of lasers are used: diode DFB lasers for 1.6 °m range, targeting H2O, H218O, CO2, 13CO2, and interband cascade lasers (ICL) for 2.76 °m (H2O, HDO) and 3.3 °m (CH4). For the sake of maximal sensitivity, an integrated cavity output spectroscopy (ICOS) technique is implemented by means of a multipass off-axis cell with highly reflective windows, which provides an effective optical path of -1.5 km.

In addition to in situ analysis of atmospheric samples by means of classical laser spectroscoly technique, M-DLS instrument implements remote sensing of the atmosphere using optical heterodyning technique. Sunlight captured by a microtelescope is coupled in a single model optical fiber with local oscillator radiation taken from tunable diode and ICL lasers, whereas beat signal is analyzed by a digital data processing block. Heterodyne technique provides such unique measurements as Doppler sounding of winds in the free atmosphere and vertical profiling of water vapor in the lower scale height. Both in situ measurements with ICOS technique and remote sensing in heterodyne channel provide comparable sensitivity of methane detection, ~70 ppt.

With numerous engineering and photonic solutions implemented for the first time in space applications, M-DLS opens a unique opportunity to monitor Martian atmosphere with unprecedented accuracy. Further implications of this approach for future missions is a promising area of infrared instrument development.

9608-11, Session 2

Infrared sensor system using robotics technology for inter-planetary mission

Hiroki Hihara, NEC TOSHIBA Space Systems Ltd. (Japan) and The Univ. of Tokyo (Japan); Yousuke Takano, NEC Corp. (Japan); Junpei Sano, Kaori Iwase, NEC TOSHIBA Space Systems Ltd. (Japan); Satoko Kawakami, NEC Space Technologies, Ltd. (Japan); Hisashi Otake, Tatsuaki Okada, Japan Aerospace Exploration Agency (Japan); Ryu Funase, The Univ. of Tokyo (Japan); Jun Takada, Tetsuya Masuda, NEC Corp. (Japan)

Infrared sensor system is a major concern for inter-planetary missions in order to investigate the nature and the formation processes of planets and

Conference 9608: Infrared Remote Sensing and Instrumentation XXIII



asteroids. Since it takes long time for the communication of inter-planetary probes, automatic and autonomous functions are essential for provisioning observation sequence including the setup procedures of peripheral equipment. Robotics technology which has been adopted on HAYABUSA 2 asteroid probe provides functions for setting up onboard equipment, sensor signal calibration, and post signal processing. HAYABUSA2 was launched successfully in 2014 for the exploration of C class near-Earth asteroid 162173 (1999JU3). An optical navigation camera with telephoto lens (ONC-T), a thermal-infrared imager (TIR), and a near infrared spectrometer (NIRS3) have been developed for the observation of geology, thermo-physical properties, and organic or hydrated materials on the asteroid. ONC-T and TIR are used for those scientific purposes as well as assessment of landing site selection and safe descent operation onto the asteroid surface for sample acquisition. NIRS3 is used to characterize the mineralogy of the asteroid surface by observing the 3-micron band, where the particular diagnostic absorption features due to hydrated minerals appear.

Modifications were required in order to apply robotics technology for the probe, because the operation of satellites is different from standard robot operation environment. The major difference is time line consideration, because the standardized robotics operation software development system is based on event driven framework. The consistency between the framework of time line and event driven was established for the automatic and autonomous operation for HAYABUSA2.

9608-13, Session 2

Measurement of the speed of light from extraterrestrial sources (Invited Paper)

Jing-shown Wu, National Taiwan Univ. (Taiwan)

We first discuss the conventional measurements of the speed of light, which were performed before the early twentieth century. Only few utilized extraterrestrial light sources and obtained the results with large uncertainty, others used the local light sources and got guite accurate value, c. Recently science and technologies have advanced very much, which provides us a great opportunity to measure the speed of light from extraterrestrial sources. Here we propose a new concept by using the well-known value, c, as the reference to measure the speed of light from extraterrestrial sources. We design a modulator at the transmitter to modulate the rays from a local infrared light source and the extraterrestrial sources simultaneously into pulses which are received by a distant receiver. We use the infrared pulses as the reference and the trigger signal. We have a local white light travelling exactly along the path of the light from the extraterrestrial sources for calibration. We used Capella, Aldebaran, and Vega as the extraterrestrial sources. We compare the travel times of these starlight pulses and the white light pulses. It is found that the travelling times of Aldebaran and Capella pulses are longer than that of Vega pulses, where Aldebaran and Capella are moving away and Vega is approaching us. The results indicate that the speeds of lights from the extraterrestrial sources are different from the wellknown value, c. We have analyzed the uncertainty of the results in details. The data obtained in 2010-2014 are guite consistent.

9608-14, Session 2

Stratospheric observatory for infrared astronomy (SOFIA): science, science instruments and observatory operations (Invited Paper)

Maureen L. Savage, SOFIA / USRA (United States)

The joint U.S. and German Stratospheric Observatory for Infrared Astronomy (SOFIA), project has been operating airborne astronomy flights from Palmdale, California since 2011. The observatory consists of a modified 747sp aircraft with a 2.5 meter telescope in the tail section. In addition to observing flights out of Palmdale, Ca. this airborne observatory has been able to take advantage of its mobility to observe in the southern hemisphere (New Zealand), to perform multi-wavelength observations of the Super Novae (SN 2014b) in 2014, and to intersect the track of a Pluto Occultation

in the southern hemisphere just a few weeks prior to the New Horizons mission fly by of the planet in summer 2015.

Science results, observatory operations, current instrument status and participation in future instrument developments, over the lifetime of the observatory will be discussed.

9608-56, Session 2

A compact, lightweight and low cost laser heterodyne IR spectrometer for greenhouse gases and wind monitoring

Artem Klimchuk, Moscow Institute of Physics and Technology (Russian Federation); Alexander V. Rodin, Moscow Institute of Physics and Technology (Russian Federation) and Space Research Institute (Russian Federation); V. S. Semenov, O. V. Benderov, D. V. Churbanov, A. A. Pereslavtseva, Z. B. Seilov, Moscow Institute of Physics and Technology (Russian Federation)

Greenhouse gases (GHG), among which most important are CO2, CH4, and N2O, are subject to monitoring from spacecraft, in situ measurements, and ground-based remote observations. One of the problem limiting development of ground networks, such as TCCON, is relatively expansive and complex Fourier transform spectrometers used for GHG monitoring. and necessity of highly skilled personnel for their maintenance. We propose a compact, lightweight and low cost instrument that provides precise in situ GHG measurements by means of tunable diode laser spectroscopy technique (TDLS) and simultaneous spectroradiometric sounding of the atmospheric column. As local oscillators the instrument uses distributed feedback (DFB) diode lasers with precisely controlled radiation frequency, modulated by pumping current. Wavelengths in the range 1.6 - 1.65 mm are chosen, so that at least one unsaturated line of GHG is covered by each laser. LO frequency is ramping around the contour of a selected spectral line, and stabilized using an off-axis multipass reference cell. Radiation of Sun passed through the atmosphere is coupled with LO signal in a single mode optical fiber. Backend data treatment is reduced to digital square detection of a noise produced by phase-decoupled mixing of sunlight with LO. Not only the resulting spectral resolution ????~108 allows highly accurate measurements of GHG column, but also provides a unique opportunity to retrieve vertical profiles of some component and to estimate vertical profile of wind velocity up to 30-50 km. Due to relatively low cost of the instrument's production and maintenance, existing ground networks of GHG monitoring and sounding may substantially expanded, which in turn may result in new insight into climate change problem.

9608-15, Session 3

Dim object detection in cluttered scenes

Chris Agh, Matt Buoni, Toyon Research Corp. (United States)

In this paper, we discuss an algorithmic approach for exploiting temporal signatures in cluttered optical data for the purpose of detecting dim, stationary objects. The cluttered scene backgrounds are substantially more intense than focal plane array noise and temporal variations in signals from dim objects. As a result, clutter estimation and rejection algorithms are performed prior to implementing object detection schemes. Even then, stationary clutter leakage may have similar spatial characteristics to, and intensities that are more than an order of magnitude higher than, those of the stationary objects of interest. We discuss here an algorithm which was developed in a track-before-detect (TrbD) framework in order to overcome these challenges. The algorithmic approach will be presented as well as results showing low-latency detection of small, stationary objects with extremely low signal-to-clutter ratios (SCRs) in cluttered images.



9608-16, Session 3

Field results from investigating potential correlations between jet engine noise and plume dynamics in the hypertemporal infrared domain

Phillip M. Cunio, Reed A. Weber, Kimberly Knobel, Air Force Research Lab. (United States)

Following up on initial research presented at SPIE Optics + Photonics 2014, a theoretical analysis of jet engine infrared signatures and potentiallydetectable characteristics of such signatures in the hypertemporal domain was used to define and carry out a systematic test campaign to detect and correlate these signatures with acoustic jet engine characteristics.

This paper describes the field campaign and its results. Test conditions and equipment are detailed, and field data is summarized. Analysis methods and results are also described, and conclusions are drawn about the correlated characteristics of temporal and acoustic signatures. Finally, follow-up work is proposed.

Detected hypertemporal signatures in association with acoustic signatures of jet engines can enable the use of a new domain in characterizing jet engine noise. This may in turn enable new methods of predicting or mitigating jet engine noise, which could lead to socioeconomic benefits for airlines and other operators of large numbers of jet engines.

9608-17, Session 3

Fractional intensity modulation of diffusely scattered light

John Kielkopf, Elijah Jensen, Univ. of Louisville (United States); Frank O. Clark, Spectral Sciences, Inc. (United States); Bradley Noyes, Wopeco Research (United States)

We report on model predictions of angular effects of fractional intensity modulation of light that is diffusely scattered from a vibrating surface, and compare these to experimental data for a few common materials. We show the predicted and observed effects of the time dependent properties of the BRDF of the material on detected fractional modulation. We suggest a few practical commercial applications of this type of measurement.

9608-18, Session 3

Remote optical interrogation of vibrations in materials inspection applications

Jason A. Cline, Ryan W. Penny, Bridget Tannian, Spectral Sciences, Inc. (United States); John Kielkopf, Univ. of Louisville (United States)

We report development of applications of remote sensing of vibration for purposes of nondestructive inspection of aerospace equipment. Remote sensing of vibration recently made headlines when it was shown that vibrations in video recorded with consumer-grade cameras can be detected and translated into audio [1]. Earlier and perhaps more quietly heralded were developments applying similar techniques to deduce structural health of bridges [2] and to survey spatial variation of materials properties [3], either by examining subtle but correlated in-scene motions that span many pixels, or through the influence of minuscule surface-normal deflections on the light reflected into the sensor. These passive stand-o? techniques have the potential to revolutionize routine inspections of mechanical and aerospace equipment by making remote vibration detection and analysis e?cient and a?ordable.

Given these observational technologies, the stand-o? inspection of materials is enabled by the principle that the propagation of vibration through a mechanical medium, as observed from its surface, depends on its internal properties. This fact is routinely employed in laser doppler velocimetry (LDV) inspections; for test articles such as sti? flat plates, the behavior is specifically described by Lamb waves. LDV interrogates one or multiple points directly for position and velocity, while in contrast the passive approach is indirect through the surface's bidirectional reflectance distribution function and its parameters (ambient light distribution, camera bistatic angle). While this external dependence might at first seem like an inconvenience, it provides the opportunity for the lighting and camera bistatic angle to be manipulated to produce the best measurement.

We present progress developing software and measurement protocols that are designed to detect and locate local anomalies in subsurface material properties (i.e., damage) as well as material boundary conditions (i.e., attachment along a bond line). We will start with our own experimental measurements on carbon-epoxy composite and other test articles and describe model data agreement.

[1] Davis, A., Rubinstein, M., Wadhwa, N., Mysore, G., Durand, F., and Freeman, W. T., "The visual microphone: Passive recovery of sound from video," ACM Transactions on Graphics (Proc. SIGGRAPH) 33(4), 79:1–79:10 (2014).

[2] Hay, J. R., Kielkopf, J. F., and Clark, F. O., "Non-contact stand-o? optical sensing of cable vibrations for monitoring structural health of the William H. Harsha Bridge," in [Proceedings of the 15th International Conference on Experimental Mechanics (IECM15)], Gomes, J. F. S. and Vaz, M. A. P., eds., Paper 3019, Edicoes INEGI (22-27 July 2012).

[3] Clark, F. O., Penny, R., Pereira, W. E., Kielkopf, K., and Cline, J., "A passive optical technique to measure physical properties of a vibrating surface," in [Proc. SPIE 9219, Infrared Remote Sensing and Instrumentation XXII], 92190G, Society of Photonics and Instrumentation Engineers (2014). doi:10.1117/12.2064366.

9608-19, Session 3

Remote optical detection of ground vibrations

Robert M. Shroll, Spectral Sciences, Inc. (United States); Benjamin St. Peter, Univ. of Massachusetts Amherst (United States); Steven C. Richtsmeier, Bridget Tannian, Spectral Sciences, Inc. (United States); Elijah Jensen, John Kielkopf, Univ. of Louisville (United States); Wellesley E. Pereira, Air Force Research Lab. (United States)

We present progress being made in the passive optical remote detection of ground surface vibration. With proper design, minute seismic surface waves may be captured using remote visible imagery. We identify factors that determine the degree of modulation, including the angle of illumination from the surface normal, the angle of scattering to the sensor, the surface tilts with respect to these directions, and for an uncollimated source, the distance of the source to the surface. We also note the dependence of the modulation on surface texture and contrast, which may be treated with a bidirectional reflectance distribution function to represent the behavior of a complex surface with unresolved structure. We present an analysis of the optical measurements of ground surfaces performed during the passing of nearby trains with discussions of the hardware, software, and detection clutter sources. The field measurements are put into context with laboratory measurements, theory, and simulation.

9608-20, Session 3

Comparative analysis of IR images degraded by lossy compression techniques

Reed A. Weber, Air Force Research Lab. (United States); William A. Toussaint, Boston College (United States)

This work addresses image degradation introduced by lossy compression techniques and the effects of such degradation on signal detection statistics for applications in fast-framing (>100 Hz) IR image analysis. As future space systems make use of increasingly higher pixel count IR focal plane arrays,



data generation rates are anticipated to become too copious for continuous download. The prevailing solution to this issue has been to compress image data prior to downlink. While this solution is application independent for lossless compression, the expected benefits of lossy compression, including higher compression ratio, necessitate several application specific trades in order to characterize preservation of critical information within the data. Current analyses via standard statistical image processing techniques following tunably lossy compression algorithms (JPEG2000, JPEG) allow for detection statistics nearly identical to analyses following standard lossless compression techniques, such as Rice and PNG, even at degradation levels offering a greater than twofold increase in compression ratio. Ongoing efforts focus on repeating the analysis for other tunably lossy compression techniques while also assessing the relative computational burden of each algorithm. Current results suggest that lossy compression techniques can preserve critical information in fast-framing IR data while either significantly reducing downlink bandwidth requirements or significantly increasing the usable focal plane array window size.

9608-21, Session 4

GOSAT operation beyond the designed lifetime (Invited Paper)

Hiroshi Suto, Akihiko Kuze, Kei Shiomi, Masakatsu Nakajima, Japan Aerospace Exploration Agency (Japan)

To observe the global column concentration of carbon dioxide (CO2) and methane (CH4) from space, the Greenhouse gases Observing SATellite (GOSAT) was launched on January 23, 2009, and has started the operational observation. Thermal and Near Infrared Sensor for Carbon Observation - Fourier Transform Spectrometer (TANSO-FTS) has been continuously measuring CO2 and CH4 distributions globally, and supporting the global carbon cycle elucidation. It is important to monitor the greenhouse gases in long time period with same quality. During 6 years operational periods, GOSAT passed the designed lifetime, which is 5 years, and some components report the change of characteristic in-orbit. The pointing mechanism, which has a capability of change a line of scene both of along track and cross track, is equipped on GOSAT. Usually, the settling time of pointing mechanism is less than 0.4sec. Recently, it is slightly longer than the expected one. To keep the quality of spectra from TANSO-FTS and try to ambitious observation plan, the pointing mechanism is switched to the backup one. The initial check with the backup pointing mechanism present that the settling time is less than 0.4 sec and the spectra is good quality. After the radiance, spectral and geometric characterization, the dataset with the backup pointing mechanism will be released. The latest status of instrument, ground processing and observation plan with refreshed pointing mechanism will be presented.

9608-22, Session 4

High resolution near infrared imaging spectrometer in CO2 detection

Xueqian Zhu, Lei Ding, Xinhua Niu, Shanghai Institute of Technical Physics (China)

The overview of the related performance indexes of the hyperspectral atmospheric CO2 imaging system has been described above. In the paper, we design and simulate a feasible imaging system, which has a big opposite aperture and small IFOV (instantaneous field of view), it results in good performance. A planar reflection grating structure is selected for beam splitting, and an appropriate image sensor is chose to cooperate to carry out the demonstration system which aims at the 1606nm channel, and with it we conduct several experimental measurements both in the library and external field. The experiment results show that, in the near-infrared band of 1606 nm, the spectral resolution of this demonstration system meets the requirements of acquiring high precise CO2 data, show us, meanwhile, which aspects should be reconsidered or improved. The future work is to implement the whole tri-channel system obeying the scheme and ameliorate it gradually.

9608-23, Session 4

Fast calculation of scattered radiance in multispectral imagery simulation

Xiaoyu He, Xiaojian Xu, BeiHang Univ. (China)

Two-stream approximation is most commonly used to calculate scattered radiance in multispectral imagery simulation. However, the typical twostream approximation is based on the plane-parallel atmosphere assumption and may not be used in the radiance calculation of scenario involving the earth-limb region without modification. In addition, if the two-stream approximation is used to calculate the scattered radiance pixel-by-pixel, it is very time-consuming to generate a large-scaled image. As a consequence, an imagery simulation model needs to make a compromise between the computational accuracy and speed.

In this paper, a fast calculation method of scattered radiance for scenario involving both earth surface region and earth-limb region is proposed. The single scattering equation of typical two-stream approximate is adapted to compute atmospheric radiative transfer under the spherical-parallel atmosphere assumption. With specified atmospheric profiles, spectral band and observation geometry, a 2-D matrix of the scattered radiance varying with incident zenith angle and viewing zenith angle are then calculated. Finally, the earth disk images are generated in different spectral bands by interpolating the calculated radiance matrices. Numerical simulation results of multispectral earth disk images for space-based earth observation sensors are presented to demonstrate the usefulness of the proposed technique for high fidelity scene where both the earth surface and the earth-limb regions are observed.

9608-24, Session 4

Radiometric calibration of the ECOSTRESS signal chain

William R. Johnson, Andre Wong, Colin Donahue, Robert Smythe, Jet Propulsion Lab. (United States)

ECOsystem Spaceborne Thermal Radiometer Experiment on Space Station (ECOSTRESS) is a NADIR viewing instrument that will provide 5 thermal infrared spectral bands across a wide swath (53 degrees) at high spatial resolution (38m along track x 64m cross track). The instrument and payload will be delivered to the JSC in early 2017 and installed on the Japanese experiment module (JEM) sometime after. ECOSTRESS will be the first thermal infrared multi-spectral imager on the space station.

The signal chain is unique, since it uses a custom read out integrated circuit (ROIC) which operates 32 output channels at high speed. This fast readout allows the high resolution spatial sampling when coupled to a telescope and scan mirror assembly. The scan mirror operates at a constant scan speed. Part of the work in completing the total dynamic signal chain was to confirm the velocity motion of the scan mirror is smooth to within a fraction of the time frame it takes to scan a ground sample distance (GSD). The signal chain uses flexible links for connectors and the noise performance was compared with an existing test dewar. It was found the system signal chain could provide enough isolation to equal the test results in the original dewar assembly. This allows the proper signal to noise performance as required.

9608-26, Session 5

Verification of gallium as thermal calibration reference in space (Invited Paper)

Gail E. Bingham, Shane Topham, Harri Latvikoski, Utah State Univ. Research Foundation (United States); Igor Podolski, Institute of Biomedical Problems (Russian Federation)

During long space flights, precision temperature calibration may be a

Conference 9608: Infrared Remote Sensing and Instrumentation XXIII



requirement that cannot be maintained using available temperature sensors. Examples of future systems that may require on-orbit calibration are missions like those of the Voyager spacecraft which may have left the solar system after being launched in 1977, the New Horizons mission to Pluto which was launched in 2006, or remotely controlled plant growth chambers to support human exploration on Mars. Another critical application is the orbital sensors that will monitor global climate change during the next few decades. Climate change remote sensors require low drift rates for their onboard thermometry, which are unattainable currently without some means of on-orbit recalibration. Phase change materials (PCM) such as those that make up the International Temperature Standard (ITS-90) standards are seen as the most reliable references on the ground and could be good candidates for orbital recalibration references.

We have been developing miniaturized phase change references for recalibration of long-duration space sensors. To determine if microgravity would affect the phase transitions of Phase change materials we recently conducted an experiment with the ITS-90 material (gallium) on the ISS. We compared gallium's phase change temperature with earth based measurements. The Ga melt cell was launched to the ISS in November 2013 returned to Kazakhstan in March 2014. The experiment measured melts and freezes of Ga using repeated six hour cycles. This presentation will provide a comparison of the preflight, flight and post flight data.

9608-27, Session 5

Absolute spectroradiometric calibration of standard stars

John T. Woodward, Keith R. Lykke, Claire E. Cramer, Gerald T. Fraser, National Institute of Standards and Technology (United States)

The SI traceability of astronomical measurements depends on measurements of Vega made at Mount Hopkins in the 1970's. More recent observations of Vega have shown it is oriented pole on, rapidly rotating, and surrounded by a debris disk. This leads to questions about its suitability as a standard star. Additionally, advances in both radiometry and measurements and modeling of the atmosphere over the past 30 years lead us to conclude that a new campaign to make SI traceable measurements of absolute, top-of-the-atmosphere, stellar spectroradiometry with <1% uncertainty is in order.

There are two primary challenges facing such a campaign: making lowuncertainty, traceable radiometric measurements in the field as opposed to a laboratory setting, and accounting for atmospheric absorption. Preliminary measurements of Vega indicate we can achieve sufficient signal to noise with a 4" refractive telescope coupled to a fiber fed spectrometer. By viewing a calibrated source -80 meters away the system can be calibrated in the field. By observing the target star as it moves through a range of airmass from -1.5 to 3.0, a variant of a Langley analysis is used to assess and correct for light lost in the atmosphere. The radiometric performance of the system is currently being tested in the Telescope Calibration Facility (TCF) at NIST. Methodologies and results from a preliminary campaign at Mount Hopkins will be presented.

9608-28, Session 5

Optical gratings and grisms: developments on straylight and polarization sensitivity improved microstructures

Peter Triebel, Torsten Diehl, Tobias Moeller, Carl Zeiss Microscopy GmbH (Germany); Alexandre Gatto, Alexander Pesch, Lars Erdmann, Matthias Burkhardt, Alexander Kalies, Carl Zeiss Jena GmbH (Germany)

Optical diffraction gratings are mainly influencing the optical performance of spectral imaging devices and optical spectrometers. Thus elements are designed and manufactured to the specific requirements of the imaging devices and optical spectrometers. The spectral sensing properties of spectral imaging devices and optical spectrometers are driven by the parameters spectral resolution and signal-to-noise ratio. The performance of diffraction gratings provides an initial way to improve instrumental resolution.

Over recent years, ZEISS has established and optimized a systematic manufacturing process to produce monolithic, real blazed gratings (transmission or reflection), based on a combination of holographic recording and ion beam etching together with in-house processing of highend grating substrates.

This paper presents recent developments on the optical design and manufacturing process of real blazed monolithic gratings. Such microstructures can be applied on substrates having flat surfaces and curved surfaces such as spherical, aspherical or free-form shapes. In order to enhance the spectral resolution of a grating, the combination with a prism-like (Grism) acting substrate is a proven method. We report on a monolithically (Grism) approach for simulating and realizing such functionality.

The optical parameters of polarization sensitivity, efficiency and straylight are the key-parameters and will be discussed on recent manufactured gratings together with its potential for optimization.

Beside of the polarization sensitivity the improvements of low scattering gratings without having ghosts is one of the important parameter to improve to system performance of spectral imaging devices and optical spectrometers. The latest results of those improvements will be reported in this paper.

9608-29, Session 5

Payload system design for reducing size weight and power of a thermal infrared Earth resource monitoring instrument

Trent Newswander, Scott Hansen, Jed Hancock, Space Dynamics Lab. (United States)

An instrument for thermal infrared Earth resource monitoring has been designed to meet stringent Landsat heritage requirements with reduced size, weight and power (SWaP). Measurement of the land surface temperatures in two long-wave infrared bands provides Earth resource monitoring. These bands are especially valuable for monitoring water resources and water use.

Stringent radiometric and spatial resolution requirements drive the instrument design increasing SWaP. Specifically the stringent radiometric requirements require tight thermal management including multiple temperature zones and cryogenic operating temperatures. Furthermore radiometric requirements necessitate an on-board calibration system and strong straylight rejection. For spatial resolution, the ground sample distance and the relative edge response slope and edge extent requirements drive the aperture size of the optical telescope assembly.

Instrument subsystems including the focal plane module subassembly, optical telescope assembly, payload electronics, thermal management system and inflight calibration system have been studied, analyzed and conceptually designed to reduce overall instrument SWaP while still meeting all requirements. Reductions in SWaP make it possible for the instrument to fit on a small satellite bus. Since mission cost historically correlates well with mass and power on-orbit, it is expected that significant cost savings will result from the predicted SWaP reductions.

9608-30, Session 6

Optimal assimilation of advanced infrared and microwave sounding data for numerical weather prediction

Chian-Yi Liu, National Central Univ. (Taiwan); Chung-Chih Liu, Minghsin Univ. of Science and Technology (Taiwan); Tang-Huang Lin, National Central Univ. (Taiwan); Agnes H.

Conference 9608: Infrared Remote Sensing and Instrumentation XXIII



N. Lim, Univ. of Wisconsin-Madison (United States)

Regional numerical weather prediction (NWP) model can handle high spatial and temporal resolutions forecast when the initial fields are in a reliable state nowadays. The meteorological satellite could provide critical data when convectional observation is not available. The advanced infrared and microwave sounders, such as the hyperspectral infrared AIRS and microwave AMSU onboard NASA's Agua satellite, could retrieve the best estimation of atmospheric thermodynamic state, which will help to improve the initial fields through data assimilation technique. However, the soundings from these two sensors have some limitation when use both of them. The AIRS could provide fine spatial resolution data than AMSU. It is anticipated the spatial gradient could retrain in AIRS. However, AMSU could provide atmospheric profiles in cloudy sky. In this presentation, we would like to discuss the optimal assimilation of both advanced infrared and microwave sounding data for improving the numerical weather prediction. It demonstrates a better handling of both hyperspectral infrared and microwave sensors data could provide positive impact over than use either sensor alone.

9608-31, Session 6

Temperature resolution enhancing of commercially available IR camera using computer processing

Vyacheslav A. Trofimov, Vladislav V. Trofimov, Lomonosov Moscow State Univ. (Russian Federation)

We use new developed computer code for computer processing of the images captured by commercially available IR camera . Using this code we demonstrate clearly changing of human body skin temperature induced by water drinking. We discuss also another experiments dealing with the person which is drinking or eating. We believe that we increase ten times (or more) the temperature resolution of such camera

Shown phenomena are very important for the detection of forbidden samples and substances cancelled inside the human body using nondestructive control without using X-rays. Early we have demonstrated such possibility using THz radiation. Carried out experiments can be used for solving of counter-terrorism problem and for medicine problems.

9608-32, Session 7

Efficient visible through SWIR focal plane MTF measurement

Neil R. Malone, Raytheon Co. (United States)

Raytheon Vision Systems (RVS) has developed an efficient method to measure MTF on Visible through SWIR small pixel FPAs. The measured data was obtained using an advanced but low cost test set with sub μ m target projection on the FPA and real time display of the LSF as the slit is walked through focus. The test set is commercially procured, maintained and calibrated, provides target and filter holders and a light source. The analysis summary includes references from simplified MTF published analysis tools and a list of artifacts to be aware of when measuring MTF. The SWIR detectors have Mesa structure geometry for improved MTF performance and the Visible has state of the art crosstalk control to provide excellent MTF measured data and shows close agreement.

9608-33, Session 7

Modern multispectral, ground, airborne and space digital focal plane technology

Neil R. Malone, Raytheon Co. (United States)

Modern focal plane (FPA) Read Out Integrated Circuitry (ROIC) includes on FPA analog to digital conversion, multiple gain states and well sizes, and

allows the hybridization of multiple detector material types with tunable Visible through LWIR performance. These revolutionary design capabilities support the next generation ground, airborne and space applications. Responsiivity, NEI and linearity Performance data is shown for SWIR, MWIR and LWIR focal planes that meets or exceeds the best performance possible using the same ROIC while hybridized to a different cutoff detector material.

9608-34, Session 7

Advancements in large-format SiPIN hybrid focal plane technology at Raytheon

Sean P. Kilcoyne, Neil Malone, Raytheon Co. (United States)

This paper presents Raytheon's recent advancements in the latest generation large format Hybrid CMOS/SiPIN focal planes. The current family of devices has very low read-noise ROICs, low detector dark current, operate with a 25 volt bias and deliver 50% mean response operability greater than 99.99%. The continuous improvement efforts in both ROIC and device processing have led to enhancements in improvements in device performance. Detectors with customized thicknesses and anti-reflective interfaces have demonstrated the ability to manipulate QE and MTF per design specifications. Improvements in the DBH hybridization capability have demonstrated 4 and 5μ m pitch capability.

9608-35, Session 7

Lifetime evaluation of large format CMOS mixed signal infrared devices

Albert W. Linder, Raytheon Co. (United States)

New large scale foundry processes continue to produce reliable products. These new large scale devices continue to use industry best practice to screen for failure mechanisms and validate their long lifetime. The Failurein-Time analysis in conjunction with foundry qualification information can be used to evaluate large format device lifetimes. This analysis is a helpful tool when zero failure life tests are typical. The reliability of the device is estimated by applying the failure rate to the use conditions. JEDEC publications continue to be the industry accepted methods.

9608-36, Session 7

Focal plane precision alignment, metrology, accuracy, knowledge and capability

Jay R. Neumann, Raytheon Co. (United States)

Focal plane alignment reduced pixel sizes and faster optical systems require enhanced precision methodology and stability. The increasing focal plane array sizes continue to drive the alignment capability. The Focal Plane flatness often requires flatness of 25 um range held over transition temperatures from ambient to cryogenic temperatures as well as maintained in an airborne or launch vibration. This paper addresses the challenge of the detector integration into the focal plane assembly, the methodology to reduce error terms, the incorporation of thermal shifts and co-registration of detectors.

The alignment methodology reduces the error terms by minimizing the measurement transfers and providing direct read options. Proper material selection using matched coefficient of expansion materials minimizes both the physical shift over temperature as well as lowering the stress induced into the detector. The co-registration of focal planes and /or slits can achieve submicron relative positioning capabilities by applying precision equipment interferometry and piezoelectric positioning stages. All measurements and characterizations maintain traceability to NIST standards. The metrology characterizes the equipment's accuracy, repeatability and precision of the measurements.



9608-37, Session 8

Cavity-enhanced AlGaAs/GaAs resonant tunneling photodetectors for telecommunication wavelength light detection at 1.3 μ m (*Invited Paper*)

Andreas Pfenning, Fabian Hartmann, Fabian Langer, Sven Höfling, Martin Kamp, Lukas Worschech, Julius-Maximilians-Univ. Würzburg (Germany)

We demonstrate a cavity-enhanced photodetector at the telecommunication wavelength of ? = 1.3 μ m based on a resonant tunneling diode (RTD). The cavity-enhanced resonant tunneling diode (RTD) photodetector consists of three integral parts: A Ga0.89In0.11N0.04As0.96 absorption layer that can be lattice-matched grown on GaAs and is light-active in the near infrared spectral region due to its reduced bandgap energy. An AlO.6GaO.4As/ GaAs double barrier RTD that serves as high gain internal amplifier of weak electric signals caused by the photo-generation of electron hole pairs within the GaInNAs absorption layer. An optical distributed Bragg reflector (DBR) cavity consisting of five top and seven bottom alternating GaAs/AlAs mirror pairs, which provides an enhanced quantum efficiency at the resonance wavelength. The samples were grown by molecular beam epitaxy and RTD mesa structures with diameters from 1 μ m up to 12 μ m were fabricated on the epitaxial layers. Ring-shaped Au-top-contacts ensure optical access and electric contact. The electro-optical properties of the RTDs were studied at room temperature. From the reflection-spectrum the optical resonance at ? = 1.29 μ m was extracted. The current-voltage characteristics were studied in the dark and under illumination and a well-pronounced photo-response was found that is attributed to accumulation of photogenerated holes in the vicinity of the resonant tunneling structure. The maximum photocurrent was found at the optical resonance of 1.29 $\mu m.$ At resonance, sensitivity up to S = 3.1 ? 10⁴ A/W were observed and photocurrent up to several pA per incident photon was measured.

9608-38, Session 8

Modulation transfer function of infrared focal plane arrays (Invited Paper)

Sarath D. Gunapala, Sir B. Rafol, David Z. Ting, Alexander Soibel, Cory J. Hill, Arezou Khoshakhlagh, John K. Liu, Jason M. Mumolo, Sam A. Keo, Linda Hoeglund, Edward M. Luong, Jet Propulsion Lab. (United States)

Modulation transfer function (MTF) is the ability of an imaging system to faithfully image a given object. The MTF of an imaging system quantifies the ability of the system to resolve or transfer spatial frequencies. In this presentation we will discuss the detail MTF measurements of 1024x1024 pixels multi-band quantum well infrared photodetector and 320x256 pixels long-wavelength InAs/GaSb superlattice infrared focal plane arrays (FPAs). Broad-band (7.5-12?m) Quantum Well Infrared Photodetector (QWIP) detector array with progressively varying light coupling gratings based on GaAs/AlGaAs material is hybridized to 1024x1024 pixel format read out integrated circuit (ROIC). Nine types of light coupling gratings were used to optimize the light coupling in efficiency of the different regions of the FPA. We measured the horizontal and vertical MTFs of the FPA as a function of spatial frequency of all nine spectral bands. The experimentally measured Noise Equivalent Temperature Differences (NE?Ts) of the nineband 1024x1024 FPA were spread from 12.1 - 13.8 mK with 300K background and f/2 cold stop at 40K FPA operating temperature. Long wavelength Complementary Barrier Infrared Detector (CBIRD) based on InAs/GaSb superlattice material is hybridized to recently designed and fabricated 320x256 pixel format ROIC. The n-type CBIRD was characterized in terms of performance and thermal stability. The experimentally measured NE?T of the 8.8?m cutoff n-CBIRD FPA was 18.6 mK with 300K background and f/2 cold stop at 78K FPA operating temperature. The horizontal and vertical MTFs of this pixel fully delineated CBIRD FPA at Nyquist frequency are 49% and 52%, respectively.

9608-39, Session 8

Alternative infrared and plasmonic materials: metal germanides and conductive oxides (Invited Paper)

Nima Nader, Air Force Research Lab. (United States) and College of Optical Sciences, The Univ. of Arizona (United States); Shivashankar Vangala, Joshua Hendrickson, Air Force Research Lab. (United States); William Streyer, Daniel Wasserman, Univ. of Illinois at Urbana-Champaign (United States); Kevin Leedy, David Look, Air Force Research Lab. (United States); Richard Soref, Univ. of Massachusetts Boston (United States); Justin Cleary, Air Force Research Lab. (United States)

In recent years, search for alternative infrared materials with applications in optics and plasmonic have been accelerated which in part is attributed to the poor performance and large losses of noble metals. Presented in this work are different classes of newly emerging materials with properties superior to that of conventional metals in applications suitable for infrared plasmonics and optics. Special emphasis has been placed in designed structures specific to sensing mechanisms.

Metal germanides are investigated as the first group of candidates in order to enable a CMOS-compatible group-IV based plasmonics technology. Different compositions were formed by electron beam evaporation of Ge and metal (Ni, Pd, Pt, Ta, and Ti) and annealing in a nitrogen purged furnace. Different characterization methods such as x-ray diffraction analysis (XRD) and x-ray photoelectron spectroscopy (XPS) are used to determine the material composition of the final films. Infrared (IR) ellipsometry is also used to determine the IR complex permittivity which is utilized to analytically determine basic plasmonic characteristics such as propagation loss and mode confinement for each composition.

Highly-doped gallium zinc oxide (ZnGaO) is also studied as a possible candidate for low-loss and widely broadband infrared material. In addition to material characterization and determination of optical constants, specifically designed 1D-grating and 2D-array structures are presented for investigation of plasmon mode excitation, extraordinary optical transmission, and light trapping. These designs can be tailored to the wavelengths of interest and utilized for capabilities in infrared sensing, enhanced sensitivity detection, signal processing, and communications.

9608-40, Session 8

Colloidal quantum dot materials for infrared optoelectronics

Susanna M. Thon, Johns Hopkins Univ. (United States)

Colloidal quantum dots (CQDs) are an attractive material for optoelectronic applications because they combine flexible, low-cost solution-phase synthesis and processing with the potential for novel functionality arising from their nanostructure. Specifically, the bandgap of films composed of arrays of CQDs can be tuned via the quantum confinement effect for tailored spectral utilization. PbS-based CQDs can be tuned throughout the near and mid-infrared wavelengths and are a promising materials system for photovoltaic devices that harvest non-visible solar radiation. The performance of CQD solar cells is currently limited by an absorptionextraction compromise, whereby photon absorption lengths in the near infrared spectral regime exceed minority carrier diffusion lengths in the bulk films. I will review several light trapping strategies for overcoming this compromise and increasing the efficiency of infrared energy harvesting. These include hierarchical geometric, nanophotonic, and plasmonic light trapping techniques, all of which enable photocurrents approaching the theoretical limits in sub-micron film thicknesses of the active material.



9608-41, Session 9

Quantum confined semiconductor nanocrystals for use in high efficiency: low cost solar energy conversion strategies (Invited Paper)

Matthew C. Beard, National Renewable Energy Lab. (United States)

Nanoscale systems as opposed to bulk or thin film versions of the same compounds exhibit some profoundly different properties and have dramatically changed the picture of how solar cells convert sunlight into free energy. In general there are two broad approaches based on nanostructures that are being explored for PV; (1) significantly reduce material usage and/ or associated final costs; and (2) target PV approaches that have a higher limiting efficiency than that determined by the Shockley-Queisser analysis. One approach to higher limiting efficiencies is the process of multiple exciton generation (MEG) where absorption of high-energy photons can lead to the production of multiple electron-hole pairs that can contribute to an enhanced photocurrent in solar cells. We have studied this process in a variety of semiconductor nanostructures and find that MEG increases with quantum confinement. I will discuss the MEG characteristics needed in order to make the largest impact on solar energy conversion technologies. We have incorporated QDs into solar cells and are developing new chemistries that can increase PLQYs and improve PV performance. I will discuss our recent progress in QD solar cells

9608-42, Session 9

Limiting efficiencies of photo-detection and solar energy conversion via internal emission of hot electrons and hot holes (Invited Paper)

Svetlana V. Boriskina, Jiawei Zhou, Wei-Chun Hsu, Bolin Liao, Gang Chen, Massachusetts Institute of Technology (United States)

Photo-detection and solar energy harvesting via photon absorption in metal nanostructures and collection of photo-generated hot electrons via the internal photoemission have been recently actively explored as promising alternatives to conventional semiconductor-based detectors and energy converters. Metals such as Au were considered as candidates for gapless photon absorbers that are potentially capable of infrared photon detection and full solar spectrum harvesting. However, the energy conversion efficiencies demonstrated to date have been extremely low, although successful photo-detection experiments have been reported. In this talk, I will discuss the efficiency and responsivity limits for infrared detection and full-spectrum harvesting of solar light that can be achieved with traditional metals such as gold, and will also introduce some alternative materials that potentially offer comparable or superior performance. In particular, I will discuss the efficiency and responsivity limits for hot electron extraction via the use of cheap, abundant and lightweight carbon-based materials such graphite and graphene. Overall, a promising photoactive material should simultaneously offer (1) high broadband photon absorption, (2) slow hot electron decay, and (3) electron density of states that yields a sizeable population of hot electrons (or hot holes) with the energies high enough to be collected across the potential barrier.

9608-43, Session 9

Nanomembranes and soft fabrication methods for high performance, low cost energy technologies (Invited Paper)

Ralph G. Nuzzo, Univ. of Illinois at Urbana-Champaign

(United States)

The fabrication of high performance integrated circuits provides examples of the most sophisticated manufacturing methods, as well as the most high performance materials, used in any area of modern technology. The advanced functional systems they provide are ones that are generally characterized by a massive integration of circuit elements within compact, rigid and essentially planar form factor devices. New means of fabrication and enabling nanomembrane materials are beginning to provide a set of means through which it is possible to lift these constraints-doing so in ways that both retain capacities for high (or altogether new forms of) performance while enabling new opportunities in technology. Our collaborative research here at the University of Illinois is providing form factors for devices with interesting but what had been to date difficult to realize features. Examples include: light weight, large area, high performance electronics, optics, and photonics; electrooptical systems with curvilinear shapes and capacities for accommodating demanding forms of mechanical flexure; new device form factors for use in sensing and imaging that integrate responsive materials in 3D with demanding nanometer design rules; functional biomaterials, and hybrid systems for lighting, energy storage, and photovoltaic energy conversion that provide a potentially transformational approach to supplant current technologies with high performance, low cost alternatives. Taken together, the results recent research and commercialization efforts illustrate important opportunities for exploiting advances in materials in synergy within additive and physical means of patterning and fabrication. In this lecture I will explore several exemplary applications taken from this work, and specifically highlight scalable approaches to high performance integrated systems for low cost photovoltaic energy conversion.

9608-44, Session 9

New concept to break the intrinsic properties of organic semiconductors for optical sensing applications (Invited Paper)

Wallace C. H. Choy, The Univ. of Hong Kong (Hong Kong, China)

The space charge limit (SCL) effect is a universal phenomenon in semiconductor devices involving light emitting diodes, solar cells, and photodetectors. Typically, the SCL will exist in the condition of (1) unbalanced hole and electron mobility; (2) thick active layer; (3) high light intensity or dense photocarriers (electrons and holes) generation; and (4) moderate reverse bias. Through the study of plasmonic organic solar cells, we will show metallic nanostructures go beyond their optical functions to control recombination, transport, and collection of photocarriers generated from active organic materials. Through spatially redistributing light absorption at the active layer, the proposed plasmonic-electrical concept is fundamentally different from the hot carrier effect where photocarriers are generated from metallic nanostructures. The new plasmonic-electrical effect not only lays a physical foundation but also upgrades electrical properties for semiconductor devices [1]. We will also design different device structures to investigate and demonstrated how plasmonic-electrical [2] and plasmonic-optical [3] effects can be used to enhance device performances such as improving the light absorption of solar cells, increasing emission efficiency of light emitting devices, reducing dark current and enhancing sensitivity of photodetector as well as intensifying the surface enhanced Raman scattering for biosensor applications. Besides the optical (plasmonic) resonances from metal nanostructure, we will also use metal nanostructures to demonstrate electrical resonance which can be used for bistable and memory devices [4]. Consequently, exploiting both plasmonic-optical and plasmonic-electrical effects via metallic nanostructures will open up a more flexible and integrated way to design high-performance optoelectronic nanodevices.

[1] W.E.I. Sha, X. Li, W.C.H. Choy, Scientific Reports, vol. 4, p. 6236 (10pp), 2014.

[2] F.X. Xie, W.C.H. Choy, W.E.I. Sha, D. Zhang, S. Zhang, X. Li, C.W. Leung, J. Hou, Energy Environ. Sci., vol. 6, pp.3372 – 3379, 2013; D. Zhang, W.C.H. Choy, F. Xie, W.E.I. Sha, X. Li, B. Ding, K. Zhang, F. Huang, and Y. Cao, Adv. Funct. Mat., vol. 23, pp.4255–4261, 2013; D.D.S. Fung, L. Qiao, W.C.H. Choy,



C.C.D. Wang, W.E.I. Sha, F. Xie, and S. He, J. Mater. Chem., vol. 21, pp. 16349 – 16356, 2011.

[3] X.H. Li, W.C. H. Choy, X. Ren, D. Zhang, H.F. Lu, Adv. Funct. Mat. DOI: 10.1002/adfm.201303384; X.H.Li, W.C.H.Choy, H.F. Lu, W.E.I. Sha, and H. P. Ho, Adv. Funct. Mat., vol.23, pp.2728–2735, 2013; X.H. Li, W. C.H. Choy, L Huo, F.X. Xie, W.E.I. Sha, B. Ding, X. Guo, Y. Li, J. Hou, J. You, Y. Yang, Adv. Mater. vol. 24, pp.3046-3052, 2012; X.H. Li, W. E.I. Sha, W.C.H. Choy, D.D.S. Fung, F. X. Xie, J. of Phys. Chem. C, vol. 116, pp.7200-7206, 2012; C.C.D. Wang, W. C. H. Choy, C. Duan, D.D.S. Fung, W.E.I. Sha, F.X. Xie, F. Huang, and Y. Cao, J. Mater. Chem., vol. 22, pp.1206–1211, 2012.

[4] T.H. Zheng, W.C.H. Choy, and Y.X. Sun, vol. 19, pp.2648-2653, 2009; T.H. Zheng, W.C.H. Choy, and Y.X. Sun, Appl. Phys. Lett, vol. 94, 123303 (pp.3), 2009.

9608-45, Session 9

Hot electron detectors and energy conversion in the UV and IR (Invited Paper)

Jeremy N. Munday, Univ. of Maryland, College Park (United States)

Semiconductor materials are well suited for power conversion when the incident photon energy is slightly larger than the bandgap energy of the semiconductor. However, for photons with energy significantly greater than the bandgap energy, power conversion efficiencies are low. Further, for photons with energy below the bandgap energy, the absence of absorption results in no power conversion. In this talk, I will discuss our recent results in photon detection and power conversion of both high energy and sub-bandgap photons using hot carrier effects. For the absorption of high-energy photons, excited electrons and holes have excess kinetic energy, which results in the generation of hot electrons and holes. Energy is typically lost through a thermalization process between the carriers and the lattice. However, collection of carriers before thermaliztion allows for reduced power loss. We have recently shown that transparent conductor - insulator - metal structures can be used to collect these hot carriers. Further, for photons with energy below the semiconductor bandgap energy, no electrons and holes are generated; however, hot carrier collection is still possible when a Schottky junction is formed at the semiconductor-metal interface. I will also discuss our recent work in IR detection based on subbandgap photon absorption.

9608-46, Session 9

2D materials for photon conversion and nanophotonics (Invited Paper)

Volker J. Sorger, Mohammad H. Tahersima, The George Washington Univ. (United States)

Recent investigations of semiconducting two-dimensional (2D) transition metal dichalcogenides have provided evidence for strong light absorption relative to its thickness attributed to high density of states. Stacking a combination of metallic, insulating, and semiconducting 2D materials enables functional devices with atomic thicknesses. While photovoltaic cells based on 2D materials have been demonstrated, the reported absorption is still just a few percent of the incident light due to their subwavelength thickness leading to low cell efficiencies. Here we show that taking advantage of the mechanical flexibility of 2D materials by rolling a molybdenum disulfide (MoS2)/graphene (Gr)/hexagonal boron nitride (hBN) stack to a spiral solar cell allows for solar absorption up to 90%. The optical absorption of a 1 um-long hetero-material spiral cell consisting of the aforementioned hetero stack is about 50% stronger compared to a planar MoS2 cell of the same thickness; although the volumetric absorbing material ratio is only 6%. We anticipate these results to provide guidance for photonic structures that take advantage of the unique properties of 2D materials in solar energy conversion applications.

9608-47, Session 10

Photothermal effects, hot plasmonic electrons and plasmonic photochemistry in hybrid nanostructures for light harvesting in the visible and infrared intervals (Invited Paper)

Alexander Govorov, Ohio Univ. (United States)

We investigate the effects of generation of heat and hot plasmonic carriers in metal nanostructures. The problem of heat release from optically-excited plasmonic nanocrystals is treated classically [1,2] whereas the hot electron problem is calculated using the quantum mechanical approach based on the equation of motion for the density matrix [3-5]. The energy distribution of optically-excited plasmonic carriers is very different in metal nanocrystals with large and small sizes. In large nanocrystals, most excited carriers have very small energies and the electron distribution resembles the case of a plasmon wave in bulk. For gold nanocrystal with smaller sizes (less than 20nm), the energy distribution of hot carriers becomes flat and has a large number of carriers with high energy [3-5]. Therefore, smaller nanocrystals are preferable for injection of plasmonic carriers into semiconductors or into molecules on the surface. The physical reason for the above behavior is non-conservation of momentum in a nanocrystal. The geometry, type of metal, and orientation of the external electric field are important to obtain high quantum efficiencies of generation and injection of plasmonic electrons [3-5]. Other important properties and limitations: (1) Intra-band transitions are preferable for generation of energetic electrons and dominate the absorption for relatively long wavelengths (approximately >600 nm), (2) inter-band transitions efficiently generate energetic holes in the d-band of gold and (3) the carrier-generation and absorption spectra can be significantly different [3-5]. The d-band hole generation can be used for efficient plasmonic photochemistry [6]. The results obtained in this study can be used to design a variety of plasmonic nanodevices based on hot electron injection for photo-catalysis, light-harvesting, and solar cells.

[1] A. Govorov and H.H. Richardson, NanoToday 2, 20 (2007).

[2] S. Baral, A. Green, M. Livshits, A. Govorov and H.H. Richardson, ACS Nano 8, 1439-1448 (2014).

[3] A. O. Govorov, H. Zhang and Y. K. Gun'ko, J. Phys. Chem. C 117, 16616 (2013).

[4] H. Zhang and A. O. Govorov, J. Phys. Chem. C 118, 7606 (2014).

[5] A.O. Govorov, H. Zhang, V. Demi, and Y. K. Gun'ko, NanoToday, 9, 85 (2014) [Editors' Highlights].

[6] L. Weng, H. Zhang, A. O. Govorov, and M. Ouyang, Nature Communications 5, 4792 (2014).

9608-48, Session 10

Refractory plasmonic metal nitrides for infrared spectral region (*Invited Paper*)

Vladimir M. Shalaev, Purdue Univ. (United States); Urcan Guler, Nano-Meta Technologies, Inc. (United States); Alexander V. Kildishev, Alexandra Boltasseva, Purdue Univ. (United States)

The use of plasmonic effects over a broad range of electromagnetic spectrum has been a challenge over the first few decades of research due to limited number of available materials. Recently, the efforts in the area has been concentrated on identifying and examining new material classes as the building blocks for optical technologies over a broader electromagnetic spectrum. Transition metal nitrides attract attention as plasmonic materials in the visible and infrared spectral regions with optical properties resembling gold. As refractory materials, nitrides can withstand heatinduced physical phenomena as well as aggressive chemical environment. Adjustable dielectric permittivity of plasmonic nitrides allows for fine-tuning of optical properties for selected applications. In addition to favorable optical, physical and chemical properties, transition metal nitrides provide

Conference 9608: Infrared Remote Sensing and Instrumentation XXIII



CMOS- and bio-compatibility. In this talk, novel designs and concepts based on refractory plasmonic materials for infrared applications will be presented. Furthermore, light confinement at the nanoscale with refractory plasmonic antennas, spectral engineering of absorption and emission with subwavelength-thin metasurfaces, and the use of colloidal solutions for a variety of applications will be discussed.

9608-49, Session 10

Enhancing selectivity of infrared absorbers and emitters through quality-factor matching (Invited Paper)

Peter Bermel, Purdue Univ. (United States)

It has recently been proposed that designing selective emitters with photonic crystals (PhCs) or plasmonic metamaterials can suppress lowenergy photon emission, while enhancing higher-energy photon emission. In this presentation, we will consider multiple approaches to designing and fabricating nanophotonic structures concentrating infrared thermal radiation at energies above a critical threshold. These are based on quality factor matching, in which one creates resonant cavities that couple light out at the same rate that the underlying materials emit it. When this quality-factor matching is done properly, emissivities can approach those of a blackbody, but only within a selected range of thermal photon energies. One potential application is for improving the conversion of heat to electricity via a thermophotovoltaic (TPV) system, by using thermal radiation to illuminate a photovoltaic (PV) diode. In this study, realistic simulations of system efficiencies are performed using finite-difference time domain (FDTD) and rigorous coupled wave analysis (RCWA) to capture both thermal radiation and PV diode absorption. We first consider a 2D molybdenum photonic crystal with a commercially-available silicon PV diode, which can yield TPV efficiencies up to 26%. Second, a 1D-periodic erbium aluminum garnet emitter with a gallium antimonide PV diode is presented, which can yield efficiencies up to 34%. Finally, a 2D tungsten photonic crystal with a 1D integrated, chirped filter can yield efficiencies up to 49.3%; however, the fabrication procedure is expected to be more challenging. The advantages and disadvantages of each strategy will be discussed, and preliminary roomtemperature characterization measurements will be presented.

9608-50, Session 10

Passive radiative cooling of terrestrial surfaces below ambient under direct sunlight (Invited Paper)

Aaswath P. Raman, Linxiao Zhu, Shanhui Fan, Stanford Univ. (United States)

Cooling is a significant end-use of energy globally and a major driver of peak electricity demand. At night, electricity-free cooling below ambient air temperature has been demonstrated using a technique known as radiative cooling or night-sky cooling, where one uses a device exposed to the sky to radiatively emit heat to outer space through a transparency window in the atmosphere between 8-13 μ m. Peak cooling demand however occurs during the daytime. Daytime radiative cooling below ambient under direct sunlight has not previously been achieved because sky access during the day results in heating of the radiative cooler by the sun.

In this talk, we first highlight the theoretical requirements necessary for daytime radiative cooling and discuss the need for a photonic approach. We then present results of the first experimental demonstration of daytime radiative cooling, where we achieve a temperature of nearly 5°C below the ambient air temperature under direct sunlight. Using a thermal photonic approach, we design and fabricate an integrated photonic solar reflector and thermal emitter consisting of 7 layers of HfO2 and SiO2 that reflects 97% of incident sunlight while emitting strongly and selectively in the mid-infrared atmospheric transparency window. Even when exposed to direct solar irradiance of greater than 850 W/m2 on a rooftop, the photonic radiative cooler achieves an average of 4.9°C below ambient air temperature over, and has a cooling power of 40.1 W/m2 at ambient. Finally, we will

briefly comment on related work on using thermal photonic approaches to passively maintain solar cells at lower temperatures, while maintaining their solar absorption.

9608-51, Session 10

Nanophotonics for energy applications (Invited Paper)

Marin Soljacic, Massachusetts Institute of Technology (United States)

Nanophotonics provides superb opportunities for tailoring the flow of light. This way, many novel physical phenomena can be enabled, as well as many important functionalities for novel energy applications. In order to make these phenomena useful for large systems, large-area nano-fabrication techniques have to be successfully implemented. In this talk, I will present some of our recent theoretical and experimental progress in exploring these opportunities.

9608-52, Session PWed

Estimation of urban surface emissivity based on sub-pixel classification of Landsat 8 imagery

Erdeneshoo Orolmaa, Mongolian Univ. of Science and Technology (Mongolia); Sanjaa Tuya, MUST (Mongolia); Jadamba Batbayar, Mongolian Univ. of Science and Technology (Mongolia)

Abstract— Information about the spatial distribution of urban surface emissivity is essential for surface temperature estimation. The latter is critical in many applications, such as estimation of surface sensible and latent heat fluxes, energy budget, urban canopy modeling, bio-climatic studies and urban planning. This study proposes an estimation of urban surface emissivity, which is primarily based on spectral mixture analysis. The urban surface is assumed to consist of three fundamental land cover components, namely vegetation, impervious and soil that refer to the urban environment. Due to the complexity of the urban environment, the impervious component is further divided into two land cover components: high-albedo and low-albedo impervious. Emissivity values are assigned to each component based on emissivity distributions derived from the Landsat 8. Following the proposed method, by combining the fraction of each cover component with a respective emissivity value, an overall emissivity for a given pixel is estimated. The methodology is applicable to visible and near infrared satellite imagery, therefore it could be used to derive emissivity maps from most multispectral satellite sensors. The proposed approach was applied to Landsat 8 multispectral data for the city of Ulaanbaatar, Mongolia. Emissivity, as well as land surface temperature maps in the spectral region of 10.6 - 11.2 ?m (Landsat8 band 10) and 11.5-12.5 (Landsat8 band 11) were derived.

9608-53, Session PWed

Intelligent image processing for vegetation classification using multispectral Landsat data

Stewart Rene Santos Arce, Jorge Luis Flores Nuñez, Guillermo Garcia-Torales, Univ. de Guadalajara (Mexico)

We propose an intelligent computational technique for analysis of vegetation imaging, which are acquired with multispectral scanner (MSS) sensor. This work is focuses on intelligent and adaptive artificial neural network (ANN) methodologies that allow segmentation and classification of spectral remote sensing (RS) signatures, in order to obtain a high resolution map, in which we can delimit the wooded areas and quantify

Conference 9608: Infrared Remote Sensing and Instrumentation XXIII



the amount of combustible materials present into these areas. This could provides information to prevent fires and deforestation of wooded areas. The spectral RS input data, acquired by the MSS sensor, are considered in a random propagation remotely sensed scene with unknown statistics for each Thematic Mapper (TM) band. Once performing high-resolution reconstruction and adding these spectral values with neighbor pixels information from each TM band, we can include contextual information into an ANN. The biggest challenge in conventional classifiers is how to reduce the number of components in the feature vector, while preserving the major information contained in the data, especially when the dimensionality of the feature space is high. Preliminary results show that this method is a promising and effective spectral method for segmentation and classification in RS images acquired with MSS sensor.

9608-54, Session PWed

Neurotransmitter identification Raman spectroscopy for sleep deprivation assessment

Raul Beltran, Univ. de Guadalajara (Mexico); G. Lopez-Armas, Ctr. de Enseñanza Técnica Industrial (Mexico); Guillermo Garcia-Torales, Verónica María Rodríguez Betancourtt, Jorge L. Flores, Univ. de Guadalajara (Mexico)

Insomnia is one of the most common sleep disorders in humans. Due to ethical and methodological difficulties involved in human research we use mice models to evaluate what has been called Paradoxical Sleep Deprivation (PSD) which is selective for Rapid eye movement (REM) sleep. By other hand brainstem cholinergic neurotransmission is involved in the generation and maintenance of rapid eye movement (REM) sleep. There is strong evidence that pontine cholinergic and cholinoceptive neurons, interacting in coordination, trigger and maintain REM sleep. So in this work we measure the content of acetylcholine and serotonin by Raman spectrophotometry and western blot technique in cerebral cortex.

9608-55, Session PWed

Terrestrial photograph spectral band analysis for shape and material by using remote sensing technique

Abdulrazak A. Mohammed, Ali Izzadin, Salahaddin Univ.-Hawler (Iraq)

One of the remote sensing technique is Photogrammetric grid system , which is the generation of processing system with an efficiency developed based on photographic spectral analysis and computer cluster parallel processing and the new development of photogrammetry has been applied on the traditional sample " Citadel -Gate of Erbil city".

9608-57, Session PWed

Recent progress of microscale IR thermography: a practical application to visual thermal analysis and microscale heat transfer

Junko Morikawa, Tokyo Institute of Technology (Japan)

As the performance of thermal detectors of infrared focal plane arrays (IR FPA), called micro-bolometers, has been developed, a practical application of microscale infrared (IR) thermography to a quantitative visual thermal analysis becomes more realistic with a smaller pixel pitch and larger pixel numbers of FPA obtaining NETD 50 mK and pixel size smaller than 17 ?m, with reducing the cost.

In order to realize the mobile type quantitative micro-scale thermography

apparatus using a micro-bolometer, we presented the following proposals;

- 1. An achromatic lens design for a micro-scale image,
- 2. A video signal superimposed for the real time emissivity correction,
- 3. A pseudo acceleration of a timeframe.

The mobile type apparatus for a quantitative micro-scale thermography using a micro-bolometer was developed based on the above original techniques. The total size of the instrument was designed as it was put in the 17 cm x 28 cm x 26 cm size carrying box.

Our next stage is to expand the recent technique to the spectroscopic thermal imaging and the flying spot method.

Conference 9609: Infrared Sensors, Devices, and Applications V



Wednesday - Thursday 12-13 August 2015

Part of Proceedings of SPIE Vol. 9609 Infrared Sensors, Devices, and Applications V

9609-1, Session 1

Semi-insulating GaAs and Au Schottky barrier photodetectors for near-infrared detection (1280 nm)

Ahmad I. Nusir, Yahia Makableh, Omar Manasreh, Univ. of Arkansas (United States)

Schottky barriers formed between metal (Au) and semiconductor (GaAs) can be used to detect photons with energy lower than the bandgap of the semiconductor. In this study, photodetectors based on Schottky barriers were fabricated and characterized for detection of light at wavelength of 1280 nm. The device structure consists of three gold fingers with 1.75 mm long and separated by 0.95 mm, creating an E shape while the middle finger is disconnected from the outer frame. When the device is biased, electric field is stretched between the middle finger and the two outermost fingers.

The device was characterized by measuring the current-voltage (I-V) curve at room temperature. This showed low dark current on the order of 10^-10 A, while the photocurrent was higher than the dark current by four orders of magnitude. The detectivity of the device at room temperature was extracted from the I-V curve and estimated to be on the order of 4.2x10^10 cm.Hz^0.5.W^-1 at bias voltage of 5 V. The step response of the device was measured from time-resolved photocurrent curve at 5 V bias with multiple on/off cycle. From which the average recovery time was estimated to be 0.63 second when the photocurrent decreases by four orders of magnitude, and the average rise time was measured to be 0.897 second. Furthermore, the spectral response spectrum of the device exhibits a strong peak at wavelength of 1280 nm, which is attributed to the internal photoemission of electrons above the Schottky barrier formed between Au and semi-insulating GaAs.

9609-2, Session 1

Dependence on the depth of the arsenic implant in planar P+-on-n SWIR HgCdTe infrared detectors

Jonathan Schuster, U.S. Army Research Lab. (United States) and Boston Univ. (United States); Roger E. DeWames, Corbin Co. (United States); Enrico Bellotti, Boston Univ. (United States); Priyalal S. Wijewarnasuriya, U.S. Army Research Lab. (United States)

Recently there has been significant interest in utilizing planar P+-on-n HgCdTe detectors for applications in the short-wave infrared (SWIR) spectral band with detector cutoff wavelengths from 2.2-2.5 microns. Such cutoff wavelengths are well beyond the optimal cutoff wavelength of the closest competing technology which is InGaAs on InP. A key design feature of the Arsenic implanted planar P+-on-n HgCdTe detector design is the depth of the Arsenic implant. Normally, these detectors are designed such that the Arsenic implant extends into the narrow-gap absorber layer. This is done to facilitate the collection of photo-carriers from the absorber layer to the contact; however, this also results in a higher dark current. Alternatively, the implant could be designed such that it resides solely in the wide-gap cap layer. The detector performance is now especially dependent on the following sensitivity parameters: implant depth, layer doping, valence band offset between the narrow- and wide-gap layers, lifetime (specifically Shockley-Reed-Hall) and detector bias. The dark current and quantum efficiency due to these sensitivity parameters is determined by performing simulations using the finite element method which simultaneously solves the carrier continuity and Poisson equations on a finite element grid. The simulations reveal that by properly designing the depletion region the implant can be confined to the wide-gap cap layer, without reducing the quantum efficiency at small reverse bias. This is due to the significantly smaller valence band offset in HgCdTe, compared to InGaAs, which does not substantially prevent the collection of photo-carriers from the absorber to the contact.

9609-3, Session 1

Compositional control of the mixed anion alloys in gallium-free InAs InAsSb superlattice materials for infrared sensing

Heather J. Haugan, Frank Szmulowicz, Gail J. Brown, Krishnamurthy Mahalingam, Air Force Research Lab. (United States); Susan L Bowers, Air Force Research Lab (United States)

The objective of this work is to establish the molecular beam epitaxy (MBE) growth processes that can produce the high quality InAs/InAsSb type-II superlattice (SL) materials tailored for the maximum Auger suppression for a band gap of 207 meV. To accomplish this goal, several series of growth optimization studies were performed using a SL structure of 77 Å InAs/35 Å InAs0.7Sb0.3 to refine the MBE growth process and optimize growth parameters. Experimental results demonstrated that the SL structure we have chosen for the studies can produce an intended energy band gap, which is an important for the infrared sensing. However, there are other growth factors that also impact material properties of the SL materials. Since compositional control of the mixed anion alloys is essential to create the high quality strain-free SL structure that meets a specific wavelength requirement, the precise control of antimony composition was demonstrated through systematic study series by manipulating Sb/As flux ratios and deposition temperature. Optimization results are reported in the context of comparative studies on the influence of the deposition temperature on the crystalline quality and antimony composition performed under a variety condition of Sb/As flux ratios, InAs growth rates, and arsenic cracking temperatures. A quantitative analysis of the lattice strain, performed at the atomic scale by aberration corrected transmission electron microscopy, provided valuable information about compositional gradient at the InAsSb and the InAs layers, which was important for optimizing the mixed anion conditions.

9609-4, Session 1

An InGaAs p-i-n photodiode focal plane array with 360 degree field of view and 100% external quantum efficiency

Dejiu Fan, Kyusang Lee, Stephen Forrest, Univ. of Michigan (United States)

InGaAs focal plane arrays (FPAs) provide excellent performance for shortwave infrared (SWIR) range imaging. However, these SWIR FPAs have a planar structure, requiring complex and costly optical systems to reduce aberration while having only a limited field of view (FOV). Achieving a very wide FOV with a simplified optical system is possible if the image sensor arrays are made flexible to conform to the focal plane of the lens system. Here, we develop a method to transfer a thin-film InGaAs p-i-n photodiode FPA from its rigid and bulky InP substrate to a flexible and light-weight Kapton substrate using a combination of epitaxial lift-off (ELO) and coldweld bonding technologies. Using these methods, we demonstrate a flexible 8 ? 100 detector FPA, which can be transformed into a cylinder to provide 360 degree FOV with ~99% fabrication yield. The array exhibits very high (~100%) external quantum efficiency (EQE) with a relatively thin InGaAs active layer by employing an integrated rear-side metal reflector that acts as a light trap. Under -1V bias, EQE = 82%, 99%, and 88% with a 5% estimated error at wavelengths of 980nm, 1300nm, and 1550nm, respectively. We also demonstrate 360 degree awareness of the array by imaging a rotating laser beam. These results suggest that flexible thin-film InGaAs p-i-n photodiode



FPAs can have improved performance compared to conventional substratebased arrays. The unique features of this FPA integrated on the flexible or conformal structure provides a practical path for many imaging applications that will be discussed.

9609-5, Session 1

High-speed and high-saturation-current Si/ Ge uni-traveling-carrier photodetector

Chong Li, Beijing Univ. of Technology (China)

A Ge-on-SOI uni-traveling carrier (UTC) photodetector was reported for high-power high-speed applications. The performances, in terms of darkcurrent, photocurrent responsivity and 3-dB bandwidth, were characterized for analog and coherent communications applications. The responsivity was 0.165 A/W at 1550 nm. The detector with a 15?m-diameter demonstrated an optical bandwidth of 10 GHz at -5V for 1550nm and dark current of 58nA at -1V. The -1dB compression photocurrent at 13GHz under -6V was about 16.2mA, the RF output power came to be 3.7 dBmw.

9609-6, Session 1

Enhancement of electron-injection detector performance by their special three-dimensional-geometry

Vala Fathipour, Hooman Mohseni, Northwestern Univ. (United States)

Sensitive short-wavelength infrared (SWIR) detectors with ultra-low noise levels and high signal-to-noise ratios are largely beneficial to a wide range of applications including astronomy, optical coherence tomography, and LIDAR. Absence of internal amplification in the mainstream InGaAs p-i-n detectors with extremely low noise levels, places stringent conditions on the read-out integrated circuit (ROIC) noise levels. Thus, a detector with a high internal amplification in addition to a low noise level could allow for ultimate sensitivity. Electron-injection detectors are based on a new single photon detection mechanism and address both above criterion. The large amplification in the detector takes advantage of the special three-dimensional geometry of the device that uses a large-scale absorbing volume and a small-scaled injector.

We have systematically studied the effect of the three-dimensional geometry on electron-injection detector's characteristics. Two different detector geometries were fabricated: Devices with same size injector and absorber diameters (type-A geometry) and devices with a smaller injector than the absorber diameters (type-B geometry). Analytical expressions were derived for the detector optical-gain to explain the significance of scaling the injector with respect to the absorber. Experimental measurement data together with our developed analytical model, confirm that the type-B device presents a larger optical-gain: ~ ten-times smaller injector area than the absorber, dark current of the type-B device is an order of magnitude lower than that of a type-A device with a similar mesa size.

9609-7, Session 1

Sensitivity advantage of using electroninjection detectors in ultra high speed 1060nm swept-source optical coherence tomography

Vala Fathipour, Hooman Mohseni, Northwestern Univ. (United States)

Optical coherence tomography (OCT) has recently become a powerful tool for non-invasive tomographic imaging in transparent and turbid specimens. Swept-source optical coherence tomography (SS-OCT) is emerging as one

of the best methods within the OCT family as it has enabled higher framerate imaging, increased signal-to-noise ratio (SNR) and resolution.

Balanced detection is a commonly used detection method for suppression of the relative intensity noise (RIN) in SS-OCT systems. With today's swept-source lasers ~ 20-25 dB common-mode-rejection is needed by the balanced-detection method to reach shot noise limited SNR. A detector with no excess-noise-factor and with an internal amplification would be able to reach the shot-noise-limited performance at lower reference powers and reduce the RIN contribution. This would ultimately enable shot-noise-limited performance with a single detector, reducing the OCT system complexity and cost.

Electron-injection detectors are a new class of detectors with high internal avalanche-free amplifications (-2000 at -3V) together with an excess-noise-factor of unity. These characteristics make electron-injection detectors a potential candidate for an OCT system. To characterize the electron-injection detector for OCT application, we used a coupler to simultaneously send the interference signal to both the electron-injection detector and a commercial p-i-n detector. Despite the larger system input noise for the electron-injection detector, as a result of probing of the device, the internal-gain of the device results in SNRs in excess of 20 dB higher than a commercial p-i-n detector at measurement frequency of 22 MHz. Although the current device is not optimized for high speed, but even at the highest beating frequency of 250 MHz, 10 dB higher SNR was measured

9609-8, Session 1

A 16.4?m InGaAs/InAIAs quantum cascade detector

Shenqiang Zhai, Junqi Liu, Fengqi Liu, Zhanguo Wang, Institute of Semiconductors (China)

Very long wave infrared (VWIR) photodetectors, covering the spectral range from 14 to 20?m, are needed for a variety of space applications, such as atmospheric temperature profile and pollution monitoring, infrared astronomy and satellite mapping. However, the infrared detectors for this range are often limited to high dark current and low work temperature. As an alternative solution, quantum cascade detectors (QCDs), a new type of photovoltaic QWIPs, operating without bias are presented. They have clear advantages on the absence of dark current, low background noise, and high operation temperature. Therefore QCD is a very competitive technology for applications in very long wave range. In a QCD, the photon-generated electrons transferred from one period to another based on a carefully designed extraction cascade, which is adapted to the longitudinal optical (LO) phonon energy. However, for very long wave detection, only few cascade steps, namely quantum well (QW)/barrier pairs, are permitted due to the small detetction energy. This will induce strong coupling between adjacent active well ground states and the associated large noise current. In this work, we present a very long wave InGaAI/InAIAs quantum cascade detector operating at 16.4?m grown by solid source molecular beam epitaxy based on miniband based electron transport mechanism. The addition of miniband can suppress leakage current and increase device resistance, overcoming the challenge in constructing QCDs for very long wavelength detection. At 15K, we observed a responsivity of 10.6mA/W and a Johnson noise limited detectivity of 1.8?1010 Jones at 16.4?m.

9609-9, Session 1

Characterization on Geiger-mode operation of deep diffused silicon APDs

Erik B. Johnson, Xiao J. Chen, Mickel McClish, Richard Farrell, James F. Christian, Radiation Monitoring Devices, Inc. (United States)

Avalanche photodiodes (APD) manufactured at RMD are fabricated using deep diffusion processes, resulting in a thick reach-through APD with excellent performance characteristics. These include a high quantum efficiency (>50% for visible photons) and low excess noise (F ~ 2). Due to the structure of the APD, the devices have very low junction capacitance

Conference 9609: Infrared Sensors, Devices, and Applications V



(~0.7pF/mm2). These devices have been made as squares or hexagons on the order of 2-4" dimensionally and require >1000 V for operation. Due to the high operating bias, studies on the Geiger behavior were dismissed, yet this structure provides unique capability to improve upon existing silicon solid-state photomultipliers. The low capacitance is conducive to developing large-area devices, and the large drift region allows for charge steering toward the high breakdown field region. These results provide initial data on the performance characteristics of RMD's APDs when operated in Geiger mode. Due to the thickness of these devices, they provide a high gain-bandwidth product for near IR single photon counting. A small area (~1 mm2) APD was biased beyond the reverse bias breakdown voltage (~1640 V at -20 C), where the device showed typical Geiger-mode behavior with a low dark count rate (<1 kHz at an excess bias of 1 V). Data on the responsivity for different incident positions on the device area will be presented, as well as a measure of the efficiency as a function of excess bias beyond the breakdown voltage.

9609-32, Session 1

Advanced EO/IR Technologies at DARPA-MTO (Invited Paper)

Jay S. Lewis, DARPA/MTO (United States); Nibir K. Dhar, U.S. Army Night Vision & Electronic Sensors Directorate (United States); Ravi Dat, Lee A. Elizondo, Booz Allen Hamilton Inc. (United States)

No Abstract Available

9609-37, Session 1

Imaging technology: What is on the horizon?

Nibir K. Dhar, U.S. Army Night Vision & Electronic Sensors Directorate (United States)

No Abstract Available

9609-10, Session 2

Determining the electrical mechanism of surface resistivity property of doped polyvinyl alcohol (pva) and pyroelectric properties of polyvinylidene difluoride (pvdf) films

Matthew E. Edwards Sr., Jemelia Polius, Padmaja Guggilla, Afef Janen, Michael Curley, Alabama A&M Univ. (United States)

Previously, we reported measurements of the temperature dependent surface resistivity of multi-wall carbon nanotube doped Polyvinyl Alcohol (PVA) thin films. In the temperature range from 22 OC to 40 OC, with a humidity control environment, we found the surface resistivity to decrease initially but to rise as the temperature continues to increases. Correspondingly, we have measured the temperature dependence of similarly doped PVDF thin films, as well, for their pyroelectric effect. While the physical mechanism of the pyroelectric phenomenon in thin films is better determined, that is not the case for surface resistivity of such films. Here, we address this concern by reporting the electrical mechanistic phenomena that contribute to surface resistivity of doped PVA thin films, and give resistivity surface effect detectivity D* and other relevant quality factor quality factor as sensors. Regarding pyroelectric effects of doped PVDF thin films, we give materials Figure of Merit for the values for our measurements. In addition, pyroelectric infrared sensors fundamentals, detector designs, unique and innovative techniques are presented.

Finally, we report temperature dependent measure of surface resistivity measurements of single-wall carbon nanotube doped PVA thin film in comparison to that of the above multi-wall doped PVA thin films

9609-11, Session 2

Analytical model of avalanche photodiode based on "low-high-low" type heterostructure with separate absorption and multiplication regions

Viacheslav A. Kholodnov, Institute of Radio Engineering and Electronics (Russian Federation); Mikhail S. Nikitin, JSC "Shvabe-Photodevice" (Russian Federation); Igor D. Burlakov, Orion Research-and-Production Association (Russian Federation)

Traditional way to describe operation of avalanche photodiodes (APD) including avalanche heterophotodiodes with separate absorption and multiplication regions (SAM AHPD) is based on numerical calculation of well-known integral relations and it is very laborious. Traditional approach is not pictorial and very difficult in use for solving related problems. Our problem is calculation of tunnel current in SAM AHPD based on direct band semiconductors. In previous work, we have proposed analytical approach for description of SAM AHPD operation. Approach includes analytical expressions for avalanche breakdown electric field of p-n heterostructure and primary band-to-band tunnel current I(tun) in it, which defines minimum noise level of SAM APD based on direct band semiconductors. Main result obtained in previous consideration is strongly non-monotonic dependence I(tun) with minimum type extremum on dopant concentration N in multiplication layer. However, with increasing N, electric field at metallurgical boundary of p-n junction increases, that narrowing differential between coefficients of impact ionization of electrons and holes. This, in turn, increases avalanche noise-factor F. Therefore, to provide simultaneously low density of tunnel current and low value of avalanche noise-factor should be used heterostructure of "low-high-low" type. In such structures wide-gap layer consists of two sub-layers. First sub-layer, adjacent to metallurgical boundary of p-n junction is rather thick and low doped (up to i - type), and second layer, bordered with light absorber, is thin and heavily doped. Doping of light absorber can be mid-level.

9609-12, Session 2

Band structure and semiconductor to semimetal transition in InAs/GaSb nanostructure mid-infrared detector superlattice

Abderrazak Boutramine, Abdelhakim Nafidi, Driss Barkissy, Abdelkrim Hannour, Ahmed Saba, Thami El Gouti, Univ. Ibn Zohr (Morocco)

We report here theoretical investigation of the electronic properties for InAs (d1=25 Å)/GaSb(d2=25 Å) type II superlattice at 300 K with an experimental valence band offset ?=570 meV. Using the envelope function formalism, we calculated the energy E(kz) and E(kp), respectively, in the direction of growth and in plane of the superlattice. We studied the effect of the InAs layer thickness d1,?, and temperature on the band gap Eg (?)= E1-HH1, correspond to the optical transition of carriers from heavy-hole HH1 to conduction E1 bands, at the center ? of the first Brillouin zone. When d1 increases, the energy E(d1, ?, 300 K) shows that the band gap decreases to zero at d1c=61? accusing a semiconductor to semimetal transition and become negative with a semimetallic conduction behavior. In our case, d1=25 Å and Eg (?, 300K) = 230 meV. With increasing ? the band gap increases, presents a maximum of 600 meV at ?=-38.4 meV and switch from being positive to negative accusing a semimetallic conduction after ?c =920 meV. In the investigated temperature range, the cut-off wavelength 4.3 $m \le c \le 5.4$ m situates this sample as mid-wavelength infrared detector



(MWIR). These results agree well with the experimental data reported in literature.

9609-13, Session 2

Indirect-direct gap transition and electronic bands properties of GaAs/ AIAs nanostructure superlattice for near infrared detection at room temperature

Driss Barkissy, Abdelhakim Nafidi, Abderrazak Boutramine, Hicham Charifi, Abdellatif Elanique, Ali Khalal, Univ. Ibn Zohr (Morocco)

We report here calculations of the electronic bands properties of GaAs(d1)/ Ga1-xAlxAs(d2) for x=1 type I superlattice performed in the envelope function formalism as a function of the well layer thickness d1, the valence band offset ? at room temperature. The transition indirect to direct band gap, of (GaAs)m/(AIAs)4 SLs consisting of m GaAs monolayers (ML) and 4 ML of AlAs with $3 \le m \le 11$ ML, takes place near m=5. The calculated fundamental band gap Eg (?)=E1-HH1 correspond to the optical transition of carriers from heavy-hole HH1 to conduction E1 bands. When the offset ? increases, this gap increases to a maximum near 1765 meV at ?=451 meV. After, it decreases parabolically. For each well thickness d1, the gap increases with the ratio d2/d1. For each ratio d2/d1, when d1 increases the gap decreases to the gap of GaAs (1424 eV at 300 K) for infinite d1. On the other hand, we have studied the temperature dependence of the direct band gap (m=9) of the GaAs (d1=2.52 nm)/AIAs (d2=1.16 nm) superlattice in the range of 6 K to 300 K. Eg decreases with temperature. Therefore, when d1 increases from 2 Å to 50 Å, Eg decreases and the corresponding cut-off wavelength ?c increases. These results are in agreement with the photoluminescence excitation (PLE) measurements of Lendentsov et al for a Kane energy Ep= 22.7 eV. In the investigated temperature range, the cut-off wavelength is 674 nm \leq ?c \leq 709 nm situates this sample as near infrared device.

9609-14, Session 3

Fabrication of resonator-QWIP FPA by inductively coupled plasma etching and projection printing

Jason N. Sun, Kwong Choi, Kimberley Olver, U.S. Army Research Lab. (United States)

Resonator-Quantum Well Infrared Photo detectors (R-QWIPs) are the next generation of QWIP detectors that use resonances to increase the quantum efficiency (QE). In order to improve thermal sensitivity, integration time, and operating temperature, a theoretical optimization of R-QWIPs has been performed. For 25 micron pitch, 10 Me- integrated charge, F/2 optics, and 9.2 micron cutoff, NETD can be 19 mK at Tint = 1.43 ms and T = 77 K. For 6 micron pitch, 6.8 Me- integrated charges, and F/1 optics, NETD = 19 mK at 4.0 ms and 77 K. To achieve the expected performance, the detector geometry must be produced in precise specification. In particular, the height of the diffractive elements (DE) and the thickness of the active resonator must be uniformly and accurately realized to within 0.05 ?m accuracy and the substrates of the detectors have to be removed totally to prevent the escape of unabsorbed light in the detectors. To achieve these specifications, two optimized inductively coupled plasma (ICP) etching processes are developed. Using these etching techniques, we have studied single detectors and fabricated FPAs with pixel pitches from 6 to 30 microns and formats from 256 x 256 to 1920 x 1080. Both contact and step and repeat projection systems were used to pattern the wafers. The detail of the FPA fabrication and their characteristics will be presented

9609-15, Session 3

High temperature operation In1-xAlxSb infrared focal plane

Yanqiu Lv, Luoyang Institute of Electro-Optical Equipment (China); Junjie Si, Xiancun Cao, Liang Zhang, Zhengyu Peng, Jiaxin Ding, Xiaolei Zhang, Luoyang Optoelectro Technology Development Ctr. (China); Valeriy Reobrazhenskiy, Institute of Semiconductor Physics (Russian Federation)

A high temperature operation mid-wavelength 128*128 infrared focal plane arrays (FPA) based on low Al component In1-xAlxSb was presented in this work. In1-xAlxSb materials were grown on InSb (100) substrates using MBE technology, which was confirmed by XRD and AFM analyses. We have designed and grown two structures with and without barrier. The pixel of the detector had a conventional PIN structure with a size of 50?m*50?m. The device fabrication process consisted of mesa etching, side-wall passivation, metallization and flip-chip hybridization with readout integrated circuit (ROIC), epoxy backfill, lap and polish. Diode resistance, imaging, NETD and operability results are presented for a progression of structures that reduce the diode leakage current as the temperature is raised above 80K, compared with a basic pin structure presented previously. These include addition of a thin region of InAISb to reduce p-contact leakage current, and construction of the whole device from InAISb to reduce thermal generation in the active region of the detector. An increase in temperature to 110K, whilst maintaining full 80K performance, is achieved. The responsivity spectra, I-V curves and blackbody current responsivity were measured at different temperature. Quantum efficiency. Pixel operability of the detector, non-uniformity, and the mean NETD values of the FPAs were measured at 110K. This gives the prospect of significant benefits for the cooling systems, including, for example, use of argon in Joule-Thomson coolers or an increase in the life and/or decrease in the cost, power consumption and cool-down time of Stirling engines by several tens of percent.

9609-16, Session 3

All optical modulator based on silicon resonator

Meir Danino, Moshe Sinvani, Zeev Zalevsky, Liron Bidani, Oded M. Baharav, Hadar Pinhas, Bar-Ilan Univ. (Israel)

In this paper we present an all-optical silicon modulator, where a silicon slab (450 μ m) thick is coated on both sides to get a Fabry-Perot resonator for laser beam at wavelength of 1550nm. Most of the modulators discussed in literature, are driven by electrical field rather than by light. We investigate new approaches regarding the dependence of the absorption of the optical signal on the control laser pulse at 532 nm having 5nm pulse width. Our silicon based Fabry-Perot resonator increases the intrinsic c-Si finesse to >10, instead of the uncoated silicon with natural finesse of 2.5. The improved finesse is shown to have significant effect on the modulation depth using a pulsed laser. A modulation of 12dB was attained. The modulation is ascribed to two different effects - The Plasma Dispersion Effect (PDE) and the Thermo-Optic Effect (TOE). The PDE causes increase in the signal absorption in silicon via the absorption of the control laser light. On top of that, the transmission of the signal can decrease dramatically in high finesse resonators due to change in the refractive index due to TOE. The changes in the signal's absorption coefficient and in the refractive index are the result of incremental change in the concentration of free carriers. The TOE gives rise to higher refractive index as opposed to the PDE which triggers a decrease in the refractive index. Finally, tradeoff considerations are presented on how to modify one effect to counter the other one, leading to an optimal device having reduced temperature dependence.



9609-17, Session 3

Design of ultra-thin metallic grating based circular polarize for near infrared

DeJiao Hu, Ping Wang, Lin Pang, Sichuan Univ. (China)

The controlling of the polarization, which is crucial in applications such as signal sensing and processing, has attracted lots of attention. In this paper, we propose an ultra-thin metallic grating based circular polarizer, which can convert any polarization into circular polarization. The ultra-thin metallic grating, which is thinner than the skin depth and is half transparent for transverse electric (TE) wave, holds for high reflection for transverse magnetic (TM) incident wave. This anomaly is attributed to the Localized surface plasmon resonance (LSPR) of a single nano-strip in the grating. We found that the grating also has anomalous modulation property for the phase of transmission coefficient for TM illumination, which can be utilize to control the phase difference between TM and TE transmitted waves and realize a guarter-wave plate. Meanwhile, a linear polarizer formed by silicon grating is applied, ensuring that the light wave arriving the quarter-wave plate is linear polarization. The angle between the metallic grating wire and the silicon grating wire is designed so that the output wave behind the metallic grating is of specific circular polarization. The designing includes two steps. Firstly, realizing a quarter-wave plate with metallic grating. Secondly, optimizing the parameters of the silicon grating to ensure that the effective wavelength range contains the operation wavelength of the guarter-wave plate. We use COMSOL Multiphysics to calculate the phase difference between TM and TE transmitted waves from the ultrathin metallic grating and choosing the parameters for the silicon grating. Our results show that the circular polarizer can convert any polarized into designed circular wave.

9609-18, Session 3

Comparison of a liquid crystal display and MEMS deformable mirror for adaptive optics compensation in a flood illuminating system

José Luis Magaña-Chávez, Sandra E. Balderas-Mata, Univ. de Guadalajara (Mexico); Gustavo Ramírez-Zavaleta, Luis Gabriel Valdivieso-González, Eduardo Tepichín-Rodriguez, Instituto Nacional de Astrofísica, Óptica y Electrónica (Mexico)

Adaptive optics (AO) has been used in the last decades to compensate the aberrations of the atmosphere as well as those of the eye, i.e., static and dynamic aberrations. In ophthalmic instruments this technique has been used to improve the lateral resolution of the retinal images. Unfortunately, Deformable Mirror devices are still quite expensive. Recently, Liquid Crystal Display (LCD) devices has been analyzed to perform the compensation task because, these are less expensive; however, they need to be characterized to perform the aberration compensation task. In this work the comparison of the performance of a Liquid Crystal Display and a MEMS deformable mirror acting as adaptive optics devices in a flood illuminating fundus camera system is presented.

9609-26, Session PWed

Angle deviation correction for symmetric slant edges in linear imaging sensor MTF measurement

Ho-Lin Tsay, Ting-Ming Huang, Instrument Technology Research Ctr. (Taiwan)

Linear imaging sensors used in space instruments and industrial applications need a proof in various functions such as response linearity, signal-to-noise

ratio, response non-uniformity, and modulation transfer function (MTF). For MTF test in imaging sensors, a tilted edge pattern was used to measure MTF in cross sensorline direction of these linear imaging sensors. Angle of tilting edge was demonstrated to be in certain range. And with knowledge of tilting angle, one can measure MTF curve convergently for different angles. In practice, we design one single tilting angle for measurement and develop signal processing algorithm for this specific angle. A misalignment between projected pattern and sensorline in relative orientation lead angle variation and therefore alter measuring result deriving by this algorithm. In this poster, we demonstrate the evolution of measuring result at different tilting angles, and development in correction of measuring result for angle

9609-27, Session PWed

Study on electron escaping mechanism of multi-alkali photocathode in the Super Gen. II image intensifier

Xiao Feng Li, North Night Vision Technology Group Co., Ltd. (China)

By measuring the multi-alkali cathode spectral reflectance and transmittance of super gen.?image intensifier, the spectral absorption was obtained through calculating by the energy conservation law. Results shows that the multi-alkali cathode spectral absorption has a long wavelength absorption limit of 915 nm. During the electronic transition process of multi-alkali cathodes after the absorption of a photon, the energy increases of transition electron is less than the energy of the incident photons, i.e. there is an "energy loss". The higher the photon energy and the higher transition electron's energy level are, the greater the energy loss is. After Na2KSb cathode film of super gen.? image intensifier was activated by Cs, the peak wavelength of the fluorescence is shift toward blue, i.e. "blue shift" phenomenon was occurred. This indicated that transition electron energy levels of Na2KSb cathode film was promoted because of surface Cs activation.

9609-28, Session PWed

The fiber grating strain sensor using in high temperature environment

Qing Shi, Zhoulu Sun, Dongli Wang, Qingsong Chen, Jiachen Ning, Beijing Research Institute of Telemetry (China)

Fiber grating strain sensors often work in the high-temperature environment in many special industries. The temperature is even higher than 400 Celsius degrees. An increase in temperature corresponds to thermal expansion of the measured materials. The high temperature impacts not only the sensing element of the fiber grating sensor, but also the properties of the other materials in the fiber grating sensor except the sensing element. Moreover, the installation of the fiber grating strain sensor which need to work under high temperature become complicated. Fiber grating strain sensors getting the measurement precisely in the high temperature environment need several special designs.

Through lots of experiments, the influential factors impacted by the temperature are studied, and the fiber grating strain sensor working in the high temperature has been presented. Especially, we introduce the approaches and notices to design this kind of sensors.

9609-29, Session PWed

Welding pool measurement using thermal array sensor

Chia Hung Cho, Yi Chen Hsieh, Hsin Yi Chen, Industrial Technology Research Institute (Taiwan)

Conference 9609: Infrared Sensors, Devices, and Applications V



Selective laser melting (SLM) is an additive manufacturing (AM) technology that uses a high-power laser beam to melt metal powder in chamber of inert gas. Melting pool was formed by using laser irradiation on metal powders which then solidified to consolidated structure. In a selective laser melting process, the variation of melt pool affects the yield of a printed threedimensional product. For three dimensional parts, the border conditions of the conductive heat transport have a very large influence on the melt pool dimensions. Therefore, melting pool is an important behavior that affects the final quality of the 3D object. To meet the temperature and geometry of the melting pool for monitoring in additive manufacturing technology. In this paper, we proposed the temperature sensing system which is composed of infrared photodiode array, band-pass filter, dichroic beam splitter and focus lens. Since the photodiode array look at the process through the 2D galvanometer scanner and f-theta lens, the temperature sensing system can be used to observe the melting pool at any time, regardless of the movement of the laser spot. In order to obtain a wide temperature detecting range, 100 °C to 2500 °C, the radiation from the melting pool to be measured is filtered into a plurality of radiation portions, and since the intensity ratio distribution of the radiation portions is calculated by using black-body radiation.

9609-30, Session PWed

Photothermal deflection of laser beam as means to characterize thermal properties of biological tissue: numerical study

Enoch Gutierrez-Herrera, Univ. Nacional Autónoma de México (Mexico) and Ctr. de Ciencias Aplicadas y Desarrollo Tecnológico (Mexico); Celia A. Sánchez Pérez, Carlos A. García-Cadena, Ctr. de Ciencias Aplicadas y Desarrollo Tecnológico (Mexico) and Univ. Nacional Autónoma de México (Mexico)

In the world, chronic diseases account for 60% of the rate of mortality. Chronic liver disease and cirrhosis (i.e. liver fibrosis) were the twelfth leading cause of death in 2010 in the U.S.A. Fibrosis refers to the accumulation of fibrous scar tissue, which is predominantly collagen. The gold standard of diagnosis for liver fibrosis continues to be biopsy sample and its corresponding histology assessment. A non-subjective and early diagnostic technique may improve clinical outcome by decreasing morbidity in patients and reducing medical costs. The build-up of collagen in the extracellular matrix of liver results in changes in density and thermal properties of tissue. We proposed to use the optical beam deflection method (OBDM) for characterization of tissue thermal properties. In this work, we evaluate numerically the feasibility of using the photothermal deflection of a laser beam that traverses a thermo-optic material in contact with liver to quantitate changes in thermal conduction. The ultimate goal is to develop an optical-integrated sensor for thermal characterization of tissue. We used the finite-difference method to model the heat transfer in liver for different fibrosis stages and to determine the refraction index gradient within an acrylic slab because of heat conduction. The response required from the optical-integrated sensor is assessed by calculating the photothermal deflection angle using ray trace. Numerical study shows the potential of the OBDM for developing an optical-integrated sensor as non-subjective diagnostic technique for liver fibrosis.

9609-19, Session 4

Remote road surface sensor using a singlewavelength light source

Chi Ruan, Yuntao Wang, Xi'an Institute of Optics and Precision Mechanics (China)

Road surface conditions are very important for traffic safety. According to statistics, the ratio of traffic accidents that occur on icy, wet and dry road surface is 4.2:1.6:1. A remote road surface sensor was developed in this paper which could identify the surface condition including dry, icy

and wet, that may be vital for preventing traffic accidents. Traditionally, multiple wavelength light from 900nm to 1700nm would be used for road face sensor, which system is complex and expensive. Such non-invasive sensor based on detecting the reflection of road surface illuminated by a single wavelength light source with 1550nm wavelength is proposed. Under different surface conditions, the power of diffuse reflection varied with incident angle was plotted in curves, and by comparing the shape, the road condition could be identified. The relationship between the detected light power and incident angle has been studied, both theoretically and experimentally. The experiment and simulation results show that the curve of received power vs. incident angle possesses certain pattern under certain road surface conditions, when incident angle is within the range of zero to seven point three degree. By using these patterns of curve, the road surface condition could be identified.. Such road sensors was tested on No. G50 highway in Chongqing, China from May. 2013. Experiment results show that the system could meet the requirements well.

9609-20, Session 4

Series-coupled fiber double-ring in Mach-Zehnder interferometer for temperature sensing

Yundong Zhang, Yongfeng Wu, Xuenan Zhang, Hui Li, Ping Yuan, Harbin Institute of Technology (China)

In this paper, we theoretically investigate the properties of the seriescoupled fiber double-ring resonator in a Mach-Zehnder interferometer as highly sensitive temperature sensor. We acquire transfer function of this system by transfer matrix theory, and numerically analyze transmission of this system. This structure can achieve sharp asymmetric line shapes by controlling phase difference between the reference arm and sensing arm of Mach-Zehnder interferometer. Sharp asymmetric line shapes result from the interference between the electromagnetically induced transparency beam propagating in the sensing arm and continuous beam propagating in the reference arm. By comparison of phase difference between two arms of Mach-Zehnder interferometer, we acquired suitable phase difference of 0.5ϖ between the reference arm and sensing arm for sharpest asymmetric line shape around the resonance wavelength. At the same time, sharpest asymmetric line shape can achieve maximum sensitivity for sensing. We also analyze the effect of parameters of this sensing system on the sensitivity and the detection limit by measuring the intensity change at a fixed wavelength. For the 30dB signal/noise system, the temperature sensitivity and the temperature detection limit can achieve 21.689/°C and 0.461?10?4°C, respectively. Furthermore, we discuss the relationship between the temperature sensitivity and the temperature detection range, which obtain the inverse relationship between the temperature sensitivity and the temperature detection range. These results indicate that this structure is suitable for highly sensitive, compact and stable sensors.

9609-21, Session 4

Integrated multi-color illumination source for lab-on-a-chip fluorescence analysis

Abdullah J. Zakariya, CREOL, The College of Optics and Photonics, Univ. of Central Florida (United States); Ishaq Mulla, Ministry of Electricity & Water (Kuwait)

We propose an integrated microfluidic optical system device design for a monolithic integration of blood plasma analysis in a single step using microfluidic channels on a tri wavelength LED source emitting wavelengths in ultraviolet, infrared and visible. The device is a miniature disposable Lab-on-a-Chipas small as 6x 1.5mm with a blood plasma reservoir volume of 2?I providing instantaneous results. The device is fabricated using minimal lithographic fabrication steps and consists of a microfluidic Polydimethylsiloxane (PDMS) layer on top of a quantum well (QW) structure. The PDMS layer has three 100?m thick microfluidic channels connected to the 2?I reservoir where the blood plasma is injected. The three microfluidic channels pass over the QW substrate which is micro fabricated

Conference 9609: Infrared Sensors, Devices, and Applications V



to produce three LEDs that emit light in three different wavelengths on a single structure. The LEDs emit light in UV, infrared and visible and can be controlled individually for specific plasma testing or can emit light simultaneously depending on the application. To operate the device, first current is injected into the LEDs to turn on light emission. Light travels within the LED structure and at the same time light is emitted through the surface. Light can be either collected from the top of the device or the output facets by focusing the channels output on a spectrometer to collect the spectra of the device and analyze the output. The device is compact in size and provides fast, low power consumption and cost effective point of care devices with minimal heat output.

9609-22, Session 4

Mechanically induced long period fiber gratings on single mode tapered optical fiber for structure sensing applications

María G. Pulido-Navarro, Sigifredo Marrujo-García, José A. Álvarez-Chávez, Jesús S. Velázquez-González, Fernando Martínez-Piñón, Ctr. de Investigación e Innovación Tecnológica (Mexico); Ponciano J. Escamilla-Ambrosio, Ctr. de Investigación en Computación (Mexico)

The modal characteristics of tapered single mode optical fibers and its tension sensing characteristics by using mechanically induced long period fiber gratings are presented in this work. Both LPG and fiber tapers are fiber devices that couple light from the core fiber into the fiber cladding modes. The mechanical LPG is made up of two plates, one flat and the other grooved. For this experiment the grooved plate was done on an acrylic slab with the help of a computer numerical control machine. The manufacturing of the tapered fiber is accomplished by applying heat using a butane flame burner and stretching it, where the protective coating has been removed. Then, a polymer-tube-package is added in order to make the sensor sufficiently stiff for the tests. The induced MLPG is accomplished by putting the tapered fiber in between the two plates, so the taper acquires the form of the grooved plate slots. Using a white light the transmission spectrum showed a large peak transmission attenuation of around -40 dB. The resultant attenuation peak wavelength in the transmission spectrum shifts with changes in tension showing a strain sensitivity of $2pm/\mu$?. This reveals an improvement on the sensitivity for structure monitoring applications compared with the use of a standard optical fiber. In addition to the experimental work, the supporting theory and numerical simulation analysis are also included.

9609-23, Session 4

PET and PVC separation system based on optical sensors

Grethell Georgina Pérez-Sánchez, Univ. Autónoma Metropolitana (Mexico); José A. Álvarez-Chávez, Ctr. de Investigación e Innovación Tecnológica (Mexico); José R. Pérez-Torres, Tecnológico de Estudios Superiores de Coacalco (Mexico); Armando Gómez-Vieyra, Univ. Autónoma Metropolitana (Mexico)

In this work experimental results of a separate PET and PVC bottles machine using optical sensors are shown.

Two aligned pump lasers diodes working at 810 nm wavelength emission and 1 Watt output power where used.

At the end of each laser a lens is allocated for generating a perpendicular line with respect to the laser emission, with this we cover a 50 cm length over a band where the plastic bottles are transported.

In the receptor, four photodetectors were used for the opto-electronic conversion, the output signal is filtered for noise reduction and amplified for later pass through an analog to digital converter.

When a PET bottle is transported, the signal is transmitted and detected, and when a PVC bottle pass, the photodetector doesn't receive a signal, then an alarm is activated in the control stage where the signal is processed for activating the electrovalves which send the PVC bottles to a second container.

The sensor design and the experimental results of the system are shown in the full article.

9609-33, Session 4

Design and development of wafer-level short wave infrared micro-camera

Ashok K. Sood, John W. Zeller, Yash R. Puri, Magnolia Optical Technologies, Inc. (United States); Harry Efsthadiatis, Pradeep Haldar, Univ. at Albany (United States); Nibir K. Dhar, U.S. Army Night Vision & Electronic Sensors Directorate (United States); Jay S. Lewis, DARPA/ MTO (United States)

Low cost IR Sensors are needed for a variety of Defense and Commercial Applications as low cost imagers for various Army and Marine missions. SiGe based IR Focal Planes offers a low cost alternative for developing waferlevel shortwave infrared micro-camera that will not require any cooling and can operate in the Visible-NIR band. The attractive features of SiGe based IRFPA's will take advantage of Silicon based technology, that promises small feature size and compatibility with the low power silicon CMOS circuits for signal processing.

SiGe technology offers a low cost alternative for developing Visible-NIR sensors that will not require any cooling and can operate from 0.4-1.7 microns. The attractive features of SiGe based IRFPA's will take advantage of Silicon based technology that can be processed on 12-inch silicon substrates, that can promise small feature size and compatibility with the Silicon CMOS circuit for signal processing.

In this paper, we will discuss the design and development of Wafer-Level Short Wave Infrared (SWIR) Micro-Camera. We will discuss manufacturing approaches and sensor configurations for short wave infrared (SWIR) focal plane arrays (FPAs) that significantly reduce the cost of SWIR FPA packaging, optics and integration into micro-systems.

9609-36, Session 4

Mid-infrared GeTe4 waveguide on silicon with ZnSe isolation layer

Vinita Mittal, James S. Wilkinson, Ganapathy S. Murugan, Univ. of Southampton (United Kingdom)

Integrated photonic devices for mid-infrared biosensing need highly sensitive planar optical waveguides for efficient and reproducible interaction of analytes with photons. GeTe4/ZnSe waveguides were designed and fabricated on silicon substrates for 2-14 μ m band of the mid-infrared spectrum. Silicon is a convenient and cheap substrate to deposit and fabricate optical waveguides. GeTe4 has a refractive index of 3.3 and it needs a lower refractive index isolation layer between the silicon substrate and the GeTe4 core to realise low loss optical waveguides. Numerical modelling was carried out to calculate the thickness of the isolation layer (ZnSe, refractive index ~2.4) required on high refractive index silicon substrate to achieve low loss waveguides. For a monomode slab waveguide of GeTe4 with a loss between 0.1 and 0.01dB/cm due to the underlying silicon, it was found that ~ 3 μm thick ZnSe film is required at 6.5 μm wavelength. ZnSe films about 3 μ m thickness were deposited on silicon and were characterised for its structure and morphology by XRD and SEM, and surface roughness was measured by AFM. Photolithography was used to fabricate channel patterns on ZnSe films using a lift-off resist and GeTe4 was deposited on the patterned sample and finally photoresist removed to form channel waveguides of various widths. Optical characterization of these waveguides is underway and the results will be presented at the conference.



Long-term infrared background compensation for faint objects and variable backgrounds: a feasibility study

Paul D. LeVan, Air Force Research Lab. (United States); Mark Stegall, Greg Pierce, SE-IR Corp. (United States)

One class of Focal Plane Array (FPA) drive and data acquisition electronics (the "SE-IR System", working with the CamIRaTM software package), has successfully operated 100s of FPA types over the years. Many of these have been configured with different types of optical systems that gather spectral images, collect high spatial resolution bandpass images, or perform other novel functions.

An emerging capability exists for an infrared camera mounted on a commercial tracking platform. These platforms, popular with amateur astronomers, now offer high levels of pointing control and include a "guider port" that accepts pulse width modulation (PWM) error signals generated by centroiding of a bright source. A variation on the use of the guider port to "dither" the tracking platform in synchronization with the continuous collection of infrared images would effectuate highly efficient background subtraction, even when spatial gradients and temporal drifts are present in the background.

We describe an embodiment of the SE-IR system that provides the dither signal to the tracking platform and tags the imagery with the polarity of the dither, to distinguish between source & background, and background-only images. Such a capability would result in high performance background subtraction over long (hours) timeframes, realizing increases in SNR for very faint (in some cases, fractional A-to-D LSB) sources.

9609-25, Session 5

High-performance near-infrared spectrally encoded microscopy by using a balanced detector

Jluling Liao, Wanrong Gao, Nanjing Univ. of Science and Technology (China)

Spectrally encoded microscopy (SEM) is a new microscopic imaging technique in which a grating is used to illuminate different positions along a line on the sample by distinct wavelengths. The size of system and the imaging time can be dramatically reduced which replaced rapid scanning by spatial spectral encoding. In this paper, a SEM device is described which is based on a swept source and a balanced detection. A near-infrared wavelength is used in our system?which central wavelength is 1302.5 nm, and the available bandwidth is over 94 nm. A fixed gain balanced detector (BD) was employed in imaging test to detect the low sample light without amplifier. Compared to conventional SEM detection method, our BD-SEM device has two significant advantages, one is its capability of suppressing common-mode noise and thermal noise, resulting in the lateral resolution is better than directly detection, the other is that it can amplify the signal intensity which is particularly helpful for tissue reflectance imaging. With the purpose of testing the actual performance of BD-SEM, the lateral resolution was measured by imaging a USAF resolution target. The images of onion cells showed that the signal noise ratio was increased. The data showed that both the lateral resolution and signal noise ratio are better than non-BD method. The method presented in this work is helpful for developing miniature endoscopic probe for in vivo tissue visualization with high acquisition speed and high imaging quality.

9609-31, Session 5

Metal bonding to enable contact to three-dimensional antenna-coupled intersubband detectors

Robert L. Brown, Alan Selewa, Sung Jun Jang, Alireza Bonakdar, Mohsen Rezaei, Hooman Mohseni, Northwestern Univ. (United States)

SPIE. PHOTONICS

OPTICAL ENGINEERING+ APPLICATIONS

III-V semiconductor-based mid- and long-wave infrared detectors are desirable due to their relatively low-cost and mature fabrication technology compared to the state-of-the art. However, these detectors are fundamentally limited by their weak absorption due to their intersubband mechanism and can never approach the performance of Mercury-Cadmium-Telluride detectors in a traditional arrangement. However, these limits can be overcome when coupling a small-volume of intersubband detector with an antenna. The small volume will greatly reduce dark current and thus noise. The antenna-coupling can effectively increase the optical area relative to the electrical area as well as boosting (or at least compensating for) quantum efficiency. Due to the prevalence of non-radiative processes in the recombination rate, the increase in local-density of states (LDOS) is negligible for this configuration.

However, the integration of a significantly small absorber with an efficientlycoupled antenna is not trivial and requires novel 3D processes. Previous attempts at this have had multiple problems including: large distance between antenna and absorber, inefficient antenna, complex wafer-transfer process, dead-space, and incompatibility with an FPA arrangement. We recently proposed an embedded antenna structure that would overcome these issues, but had difficulty making contact to these 3D structures. We propose the use of metal-to-metal bonding to directly integrate metal contacts or potentially antenna structures with infrared detectors. This offers two advantages over a once-chip solution: 1) Multiple processing steps can be done on the second substrate, eliminating some complexity. 2) Device contacts and antennas can be on a rigid surface instead of "floating" as previously proposed.

9609-34, Session 5

Development of high gain avalanche photodiodes for UV imaging applications

Ashok K. Sood, John W. Zeller, Roger E. Welser, Yash R. Puri, Magnolia Optical Technologies, Inc. (United States); Mi-He Jee, Russell D. Dupuis, Georgia Institute of Technology (United States); Nibir K. Dhar, U.S. Army Night Vision & Electronic Sensors Directorate (United States); Jay S. Lewis, DARPA/MTO (United States)

High resolution imaging in UV band has a lot of applications in Defense and commercial applications. The shortest wavelength is desired for spatial resolution which allows for small pixels and large formats. UVAPD's have been demonstrated as discrete devices demonstrating gain. The next frontier is to develop UV APD arrays with high gain to demonstrate high resolution imaging.

We will discuss model that can predict sensor performance in the UV band using APD's with various gain and other parameters for a desired UV band of interest. SNR's can be modeled from illuminated targets at various distances with high resolution under standard atmospheres in the UV band and the solar blind region using detector arrays with unity gain and with high gain APD's.

We will present recent data on the GaN based APD's for their gain, detector response, dark current noise and the 1/f noise. We will discuss various approaches and device designs that are being evaluated for developing APD's in wide band gap semiconductors. The paper will also discuss state of the art in UV APD and the future directions for small unit cell size and gain in the APD's.



9609-35, Session 5

Large format MBE HgCdTe on silicon detector development for astronomy

Brandon J. Hanold, Donald F. Figer, Joong Y. Lee, Kimberly E. Kolb, Iain Marcuson, Rochester Institute of Technology (United States); Elizabeth Corrales, Jonathan Getty, Lynn Mears, Raytheon Co. (United States)

The Center for Detectors at Rochester Institute of Technology and Raytheon Vision Systems (RVS) are leveraging RVS capabilities to produce large format, short-wave infrared HgCdTe focal plane arrays on silicon (Si) substrate wafers. MBE grown HgCdTe on Si can reduce detector fabrication costs dramatically, while keeping performance competitive with HgCdTe grown on CdZnTe. Reduction in detector costs will decrease a dominant expense for telescopes. This paper presents the characterization of 2.5µm cutoff MBE HgCdTe/Si detectors including pre- and post-thinning performance. Detector characteristics presented include dark current, read noise, spectral response, persistence, linearity, crosstalk probability, and analysis of material defects.

Conference 9610: Remote Sensing and Modeling of Ecosystems for Sustainability XII



Tuesday - Wednesday 11-12 August 2015

Part of Proceedings of SPIE Vol. 9610 Remote Sensing and Modeling of Ecosystems for Sustainability XII

9610-1, Session 1

Site suitability evaluation for ecotourism potential areas using remote sensing (RS) and geographic information system (GIS): a case study of Wadi Wurayah, Fujairah, United Arab Emirates (Invited Paper)

Ali Abou-Elnour, Ajman Univ. of Science & Technology (United Arab Emirates); Ahmad Abouelnour, Varkki Pallathucheril, American University of Sharjah (United Arab Emirates)

UAE views sustainable development as the best way to provide stability and security for all peoples of the world. One of the main approaches to achieve sustainable development was adopted by the UAE by preserving environmental sustainability and integrating environmental preservation into national planning for a diversified economy. Tourism is one of the major sector that UAE depends on to diversify and grow the economy sustainably. Based on the World Travel and Tourism Council (WTTC) in 2012 the estimated total value added generated by the UAE travel and tourism sector approximately accounting for a 14.3% share of GDP. The UAE travel and tourism sector value-added percentage share is expected to register an average annual growth rate of 5% and to reach about 16.4% of the total by 2023. As UAE features some of the most stunning landscapes and beautiful natural attractions in the region, it has been named among the top 10 fastest growing tourism hotspots in 2013, according to the United Nations World Tourism Organization (UNWTO) report. However, UAE is always dedicated to develop low-impact, eco-friendly tourism across the country, so visitors can take in the natural majesty that stretches across the country while leaving the landscape pristine and untouched.

Ecotourism helps drive conservation efforts, protecting wildlife for generations to come. The UAE includes more than 5036.24 km2 of protected area which represents 6.044 % of its total area. These protected areas are distributed in Abu Dhabi, Dubai, Sharjah, Ajman, and Fujairah. In 2006, the Government of Fujairah, Emirates Wildlife Society (EWS), and World Wide Fund (WWF) for Nature joined forces to begin conservation efforts for Wadi Wurayah in Fujairah. After three years of assessment and research, on March 16, 2009, Wadi Wurayah officially became the UAE's first protected mountain area in the United Arab Emirates in order to protect fresh water springs, pools and streams that provide its unique wildlife with a renewable and safe drinking resource. In 2010, Ramsar Convention, which is an intergovernmental treaty which commits member countries to maintaining the ecological character of their Wetlands, listed Wadi Wurayah as a Wetland of International Importance for its important freshwater catchments, which provide sustenance for a number of native species as well as migratory birds. In January 2013, the Fujairah government appointed EWS-WWF to lead the development of a management plan of Wadi Wurayah National Park and ensure environmental protection according to best international standards. In 2014, after declaring the Wadi as the UAE's first National Park, the area was also closed to the public to allow the ecosystems to revive without any interference. The current developments in Wadi Wurayah are set to take things forward to ensure active protection of the rich biodiversity and the natural and cultural resources of the area and, to deliver a unique model of how environment conservation can be economically viable.

In the last decade, Geographic Information Systems (GIS) is efficiently used in tourism as a decision supporting tool for sustainable tourism planning and tourism site selection. The aim of the present work is to identify and prioritize the potential ecotourism sites in Wadi Wurayah, Fujairah, UAE using GIS. The present work assesses the potential suitable areas for ecotourism based on bio-physical characteristics of the land ecosystems and socio-economic data. The characteristics are landscape or naturalness like visibility and land use or cover, the topography like elevation and slope, the accessibility like distance from roads, and community characteristics like settlement size. These criteria and factors were selected according to the professional expert's opinions.

After developing the list of ecotourism criteria, GIS techniques were used to measure the ranking of different sites according to the set criteria and thus identify those with the best potential. Subsequently, the land suitability map for ecotourism was created. The degree of suitability of each factor was classified as highly suitable, moderately suitable, marginally suitable, and not suitable for ecotourism. Based from the suitability map, the areas of highly ecotourism potential are located in protected areas. These areas can be used for education as well as conservation. It could serve as main ecotourism attractions but with the use of certain limitations and guidelines. The areas of moderately ecotourism potential can be developed as ecotourism destination by facilitating proper ecotourism infrastructure and services and can still be considered for ecotourism attractions. The marginally suitable areas are suitable for tourism development in general. However, the not suitable areas for ecotourism have several effects of development and degraded environment. As concerns theirs utilization, they may have some environmental problems but these are controllable. The methodology proposed was useful in identifying ecotourism sites by linking the criteria deemed important with the actual resources of the province. This study result helped to identify optimal use of the land for tourism facilities development and ecotourism resource utilization within Wadi Wurayah province in near future. GIS Additionally, it may also serve as a starting point for more complex studies in the future.

9610-2, Session 1

Evaluations of cropland representations in CMIP5 simulations (*Invited Paper*)

Min Xu, Forrest Hoffman, Oak Ridge National Lab. (United States)

Cropland is possibly the sector among earth system most affected by climate change and is the major source of carbon lost to the atmosphere and contribute directly to emissions of greenhouse gases. There is, however, large potential for cropland to reduce its carbon flux to the atmosphere and sequester soil carbon through soil and crop managements including no-tillage, perennial and/or deep root crops, irrigation, and organic fertilization etc. But these estimations over cropland remain largest uncertain among all other terrestrial biomes. In most models in CMIP5, the cropland is generally treated similarly as grassland without accounting for realistic crop phenology and physiology processes, and the managements. In this study, we will evaluate how well cropland is represented in CMIP5 simulations and how to improve the representations and reduce the uncertainties over cropland. We will compare the modeled biogeochemical variables against multiple observational data including various remote sensing products and in-situ data.

9610-3, Session 1

UV irradiance products from combined TOMS-OMI satellite and UVMRP ground measurements across the continental U.S. (Invited Paper)

Zhibin Sun, John Davis, Wei Gao, Colorado State Univ. (United States)

Increasing surface ultraviolet (UV) irradiance has been a global concern as it is harmful to humans and agriculture. There are agencies monitoring the UV irradiance by providing observational products to the public. All such products have different temporal and spatial resolutions. So far only some comparisons among them have been conducted. This study combines optimally two kinds of surface UV irradiance observations, TOMS-OMI and UVMRP (Ultraviolet-B Monitoring and Research Program), based on data



fusion methodology. The final product takes advantage of both sources, wide coverage from TOMS-OMI and more accurate ground measurement from UVMRP. Besides the four wavelengths from TOMS-OMI, the product can provide the daily surface UV irradiance across the continental U.S. for any wavelengths between 305nm and 380nm, which can be accessed for public or scientific usage.

9610-4, Session 1

Mapping the lawn in urban area using airborne LIDAR and aerial visible images

Hongbo Su, Florida Atlantic Univ. (United States); Ni-Bin Chang, Univ. of Central Florida (United States)

According to a recent study, 36 states in US anticipate local, regional or statewide water shortage. Homeowners in USA usually use 30%-70% of their water outdoor if the house doesn't use a Xeriscape landscaping design. One example is golf course which is not considered an environmental friendly land use. To get an accounting of water consumed by the lawn irrigation and to understand the ecological consequences of the lawn care, it is necessary to measure the lawn size and map their locations accurately for urban areas where we see more active anthropogenic activities. In this study, remote sensing technology and image fusion techniques are used to achieve that goal, based on the high resolution airborne Lidar images and aerial images in visible bands.

Experiments shows that using then aerial images alone is not sufficient to accurately map the lawns due to the contamination of shadow and cloud, although its spatial resolution is as high as 0.5 feet per pixel. To improve the mapping of lawn, the airborne Lidar images with an elevation accuracy of 15cm and a spatial resolution of 1.5 meter are employed in combination with the aerial visible images. A new image fusion technique based on huesaturation-intensity (HSI) transforms is developed to merge the Lidar and visible images to retrieve the lawn information. In this study, Palm Beach County in south Florida is chosen as the study area, since it is a place with a high density of golf courses which raises a concern on their environmental impact.

9610-5, Session 1

Continuous evaluation of land cover restoration of tsunami struck plains in Japan by using several kinds of optical satellite image in time series

Hideki Hashiba, Nihon Univ. (Japan)

The Mw 9.0 earthquake that struck Japan in 2011 was followed by a large-scale tsunami disaster in the Tohoku region. The damage situation of coastal plane was extensively reported by many satellite images, and ongoing evaluation of the restoration process is requested to many kind of satellites. Especially, an effective long-term monitoring is demanded for reconstructing the urban land cover and the recovering farmland, grassland and coastal forest that collapsed under the large tsunami. Moreover, modeling of changing trend of the land cover dynamics in plains after disaster using time series satellite data can be effectively used for measures at large-scale tsunami disaster of the future. However, remote satellite capture of long-term restoration processes is compromised by accumulating spatial resolution effects and seasonal influences. It is necessary to devise the data selection and the construction of data set for these reasons. In this study, the restoration process three years following the disaster in a part of Sendai plain located in northeast region in Japan was deduced from same season satellite images acquired by different optical sensors. The coastal plains struck by the tsunami were evaluated by land cover classification processing using clustering method. The changes in land cover were analyzed from time series optical images acquired by the Landsat 5/TM, 7/ETM+, 8/OLI, EO-1/ALI, and ALOS/AVNIR2 satellites. The study revealed several characteristics of the change in the inundation area and signs of artificial and natural restoration.

9610-6, Session 1

In situ hyperspectral data analysis for chlorophyll content estimation of an invasive species spartina alterniflora based on PROSAIL canopy radiative transfer model

Jinquan Ai, East China Normal Univ. (China); Wei Gao, Colorado State Univ. (United States); Runhe Shi, East China Normal Univ. (China); Zhibin Sun, Colorado State Univ. (United States); Wenhui Chen, Fujian Normal Univ. (China); Chao Zhang, Pudong Liu, Yuyan Zeng, East China Normal Univ. (China)

An accurate quantitative estimation of invasive species chlorophyll content is of great importance for monitoring ecosystem health and estimating biomass or carbon stock change by alien invasion species. This paper aims to analyze the capabilities and limitations for retrieving chlorophyll content of wetland vegetation at the canopy level. The hyperspectral reflectance of an invasive species Spartina alterniflora was measured using a Spectroradiometer with spectral range of 350-2500 nm in late autumn in a sub-tropical estuarine marsh. We used the PROSAIL canopy radiative transfer model to estimate chlorophyll content. Frist, sensitivity analysis was done to determine input parameters change and simulate canopy reflectance. Then, the best vegetation index for estimating chlorophyll content was selected from a series of hyperspectral vegetation indices. The results showed that the PROSAIL model was able to predict canopy leaf chlorophyll content of S. alterniflora with reasonable accuracy later in the growing season.

9610-7, Session 1

Monitoring forest biodiversity using imaging spectroscopy based on leaf biochemical variations in subtropical forest

YuJin Zhao, Yuan Zeng, Bingfang Wu, Qianjun Zhao, Dan Zhao, Institute of Remote Sensing and Digital Earth (China)

Forest biodiversity is a key element in the provision of ecosystem service, function and stability. Monitoring forest biodiversity is essential to the conservation and management of forest resource. In the past two decades, imaging spectrometry technique has been widely applied in forest biodiversity mapping or tree species identification. A new method called "spectranomics" that maps forest species richness based on leaf chemical and spectroscopic traits using imaging spectroscopy, has been developed. In this paper, this method would be used for detecting the relationship among the spectral, biochemical and taxonomic diversity of tree species based on 20 dominant canopy species collected in the Shennongjia National Forest Nature Reserve. Firstly, sixteen leaf biochemical components including pigments, water, Specific Leaf Area (SLA), nitrogen, phosphorus, cellulose, lignin and trace elements are standardized to indicate the unique combinations for each species. The hierarchical cluster analysis based on spectral reflectance signatures in 400-2400nm are applied to divide forest species to different clusters. Furthermore, the Constrained Partial Least Squares(PLS-PRESS) regress analysisisused to establish the relationship between biochemical and spectral signatures. Finally, a Monte-Carlo simulation model is used to find the species richness changes caused by the biochemical and spectral properties. The results show that the biochemical components could be well quantified by spectral signatures (R2>0.43, P<0.01; excluding the trace elements) for identifying the subtropical forest species richness.



9610-8, Session 1

Detecting response of rice phenology to cold and heat damages using time series analysis of MODIS images

Shenbin Yang, Shuanghe Shen, Nanjing Univ. of Information Science & Technology (China); Chunlin Shi, Jiangsu Academy of Agricultural Sciences (China)

This paper focuses on the evaluation of the capability of MODIS-EVI time series to detect the response of rice phenology to cold and heat damages during single rice season in the middle and lower reaches of Yangtze River Plain. Field experiment data and MODIS-EVI time series of 2012 and 2013 were used. At first, the slops of MODIS-EVI time series at increasing phase were analyzed with accumulated hot temperatures, and slops at decreasing phase were analyzed with accumulated cold temperatures. Then, empirical relationships were constructed by taking the accumulated cold and hot temperatures as a function of slops, respectively. Obtained empirical relationships were also classified according to the seriousness of cold and heat damages to rice phenology. Finally, based on the classification and application of the empirical relationships to all rice pixels in the study area in 2012 and 2013 respectively, the regional response of rice phenology to heat damages before flowering and cold damages after flowering were obtained. The result showed that heat damages shorten the phenology and lead to higher slops, while cold damages extend the phenology and lead to lesser slops. The estimated regional patterns of the adverse temperature damages were well consistent with the real situation, with different color representing different level of influences. Large discrepancies could be for the reason of different rice paddy management and difference in rice species. In addition, mixed rice pixels may have unpredictable results, since the changes of the slops are somehow determined by other land types instead of rice paddy. In conclusion, MODIS-EVI time series are able to detect the influence of cold and heat damages to rice phenology, but more validations have to be performed.

9610-10, Session 2

Seasonal urban heat island effect in Tampa Bay under the varying hydrological patterns (Invited Paper)

Ni-Bin Chang, Univ. of Central Florida (United States); Kaixu Bai, Univ. of Central Florida (United States) and East China Normal Univ. (China); Wei Gao, Colorado State Univ. (China)

Urban heat island effect exhibits some fundamental features of complex self-organizing systems with seasonality effect regulated by some hydrological patterns. For instance, as soil moisture is affected by both water and energy balances in the soil-vegetation-atmosphere system, it involves many complex processes in the nexus of water and thermal cycles at the surface of the urban environment. Yet soil moisture is modulated by precipitation, stormwater runoff, vegetation cover, and evapotranspiration (ET) in urban regions associated with different land use and land cover. But how these hydrological patterns affect the land surface thermal fluxes have not yet been fully explored. The advent of urban hydrology and remote sensing technologies opens new and innovative means to undertake eventbased assessment of hydrological effects in urban regions. In this study, remote sensing images related to land use and land cover, soil moisture, precipitation, ET, the Enhanced Vegetation Index (EVI), and Land Surface Temperature (LST) have been pieced together to investigate the profound impact of seasonal urban heat island effect and identify the hot spots and hot moments over time. Maximum Covariance Analysis was used to explore the spatiotemporal interactions among those relevant hydrological and geographical factors relative to LST. These designated patterns above were performed for Tampa Bay area on the 2 km x 2km grid in Florida. Finally the Extreme Learning Machine was applied to simulate the complex relationships between those associated factors and LST in urban regions as well as quantify the relative contribution of each factor to seasonal variations of LST.

9610-11, Session 2

Incorporation of crop growth models into climate weather research and forecasting model: biophysical feedbacks of maize growth to regional climate (Invited Paper)

Xin-Zhong Liang, Min Xu, Xuesong Zhang, Univ. of Maryland, College Park (United States); Wei Gao, Colorado State Univ. (United States)

A regional Climate-CROP coupled modeling system was established by implementing crop growth models with comprehensive phenology and physiology processes to the Climate Weather Research and Forecasting (CWRF) model (hereafter denotes CWRF-CROP) The crop growth models from the Crop Environmental Resource Synthesis (CERES) maize and wheat, and the GOSSYM cotton, and the Decision Support System for Agrotechnology Transfer (DSSAT) soybean growth models were reengineered following FORTRAN90 module and data structures and then incorporated into the CWRF-CROP coupled system. In this study, we will preliminary evaluate the biophysical feedbacks of maize growth in U.S. Midwest Corn Belt to present and future regional climates and future climate changes using CWRF-CROP driven by the CCSM4 global simulations under historical and future RCP8.5 emission scenarios. The key biophysical parameters including leaf and stem area index (LAI and SAI), canopy height and width, and root length density are dynamically simulated by the CERESmaize module of CWRF-CROP and are returned to the CWRF land surface component to calculate the land-atmosphere fluxes and feedbacks of crop growth to regional climate. Preliminary results indicate that the feedbacks of maize growth to regional climate are substantial, especially for surface climate, including surface air temperature, humidity, and precipitation. In future, further study will be conducted on the impacts of crop growth on regional hydrology and the mitigations of crop managements in responses to anticipated climate changes.

9610-12, Session 2

Land cover fraction estimation with global endmembers using collaborative SUnSAL

Uttam Kumar, Cristina Milesi, NASA Ames Research Ctr. (United States); S. Kumar Raja, EADS Innovation Works, Airbus Engineering Ctr. (India); Ramakrishna Nemani, NASA Ames Research Ctr. (United States); Sangram Ganguly, NASA Ames Research Ctr. (United States) and Bay Area Environmental Research Institute (BAERI) (United States); Weile Wang, California State Univ. (United States) and NASA Ames Research Ctr. (United States)

Land cover (LC) refers to the physical state of the Earth's surface such as soil, vegetation and water, etc. However, most LC features occur at spatial scales much finer than the resolution of the primary remote sensing satellites. In this paper, we explore the possibility of Collaborative Sparse Unmixing for estimation and quantification of LC classes at subpixel level to obtain abundance maps in both the unconstrained and constrained forms (with abundance nonnegativity and abundance sum-to-one constraints imposed).

Firstly, computer simulated noise-free and noisy data (Gaussian noise of different noise variance: 2, 4, 8, 16, 32, 64, 128 and 256) were unmixed with a set of global endmembers (substrate, vegetation and dark objects) in the NASA Earth Exchange. In the second set of experiments, a spectrally diverse collection of 11 cloud free scenes of Landsat-5 TM data representing an agricultural set-up in Fresno, California were unmixed and validated using ground vegetation cover. Finally, Landsat TM data for an area of San Francisco (an urbanized landscape) were used to assess the algorithm and compared with the fractional estimates of World View 2 data (2 m spatial resolution) for validation. The results were evaluated by using descriptive statistics, correlation coefficient, RMSE, probability of success, boxplot and bivariate distribution function. With computer simulated data,



both unconstrained and constrained solutions gave excellent results. For an agricultural setup mean absolute error (MAE) of vegetation fraction between actual and estimated values was 0.08 for both unconstrained and constrained case and for the urban landscape, the MAE was 0.72 (unconstrained) and 0.07 for the constrained solution.

9610-13, Session 2

Effects of errors in solar radiation inputs on ecosystem model performance

Shinichi Asao, Zhibin Sun, Wei Gao, Colorado State Univ. (United States)

Solar radiation inputs drive many processes in terrestrial ecosystem models. The processes (e.g. photosynthesis) account for most of the fluxes of carbon and water cycling in the models. It is thus clear that errors in solar radiation inputs cause key model outputs to deviate from observations, parameters to become suboptimal, and model predictions to loose confidence. However, errors in solar radiation inputs are unavoidable for most model predictions since models are often run with observations with spatial or / and temporal gaps. As modeled processes are non-linear and interacting with each other, it is unclear how much confidence most model predictions merits without examining the effects of those errors on the model performance. In this study, we examined the effects, using a terrestrial ecosystem model, DayCent, parameterized for a shortgrass prairie of US. Using observed solar radiation values, we introduced both bias and random noise to simulate the errors in solar radiation inputs. Resulting deviations in model outputs were analyzed for their relationship with the bias and the noise. The results show that biases less than 20% produced much smaller deviation in model outputs, but the deviations varied inter-annually, depending on different parameterization and environmental factors. Even a small deviation in daily fluxes accumulated to large deviation in pool sizes in long-term simulations. We conclude that small errors in solar radiation inputs reduce confidence by only a little for short-term predictions, but greatly for long-term predictions and for parameterization and application elsewhere.

9610-14, Session 2

Visualization of remote sensing image positioning uncertainty

Jiao Weili, Saiguang Ling, Yiqing Yu, Tengfei Long, Guojin He, Institute of Remote Sensing and Digital Earth (China)

It is inevitable to bring about uncertainty during the process of data acquisition. The traditional method to evaluate the geometric positioning accuracy is usually by the statistical method and represented by the root mean square errors (RMSEs) of control points. It is individual and discontinuous, so it is difficult to describe the error spatial distribution. Visualizing uncertainty is a representation method of the data quality. The purpose is to help users probe the uncertainty of original data for better understanding and using. In this paper the uncertainty range of each control point is deduced, and the uncertainty spatial distribution model between the control point and each arbitrary point is established. The distance between control points is introduced to evaluate the geometric accuracy of remote sensing image, and compared with the traditional method of RMSE. Then several visualization methods are studied to describe the geometric uncertainties of the remote sensing image, and kriging is used to visualize the geometric uncertainties as the spatial interpolation method. The uncertainties at any point in different directions are represented clearly by the contour lines and three-dimensional visualization map. The experiments show that the visualization methods can effectively and objectively represents the image geometric quality, and also can help users probe the reasons of bringing the image uncertainties.

9610-15, Session 2

Using artificial neural network and satellite data to predict rice yield in Bangladesh

Kawsar A. Akhand, The City Univ. of New York (United States); Mohammad Nizamuddin, Leonid Roytman, The City College of New York (United States); Felix Kogan, Mitch Goldberg, Ctr. for Satellite Applications and Research (United States)

Rice production in Bangladesh is a crucial part of the national economy and providing about 70 percent of an average citizen's total calorie intake. The demand for rice is constantly rising as the new populations are added in every year in Bangladesh. Due to the increase in population, the cultivation land decreases. In addition, Bangladesh is faced with production constraints such as drought, flooding, salinity, lack of irrigation facilities and lack of modern technology. To maintain self sufficiency in rice, Bangladesh will have to continue to expand rice production by increasing yield at a rate that is at least equal to the population growth until the demand of rice has stabilized. Accurate rice yield prediction is one of the most important challenges in managing supply and demand of rice as well as decision making processes. Artificial Neural Network (ANN) is used to construct a model to predict rice yield in Bangladesh. Advanced Very High Resolution Radiometer (AVHRR)-based remote sensing satellite data vegetation health (VH) indices (Vegetation Condition Index (VCI) and Temperature Condition Index (TCI)) are used as input variables and Rice yield is used as target variable for ANN prediction model. The result obtained with ANN method is encouraging and the error of prediction is less than 10%. Therefore, prediction can play an important role in planning and storing of sufficient rice to face in any future uncertainty.

9610-16, Session 2

Sensitivity analysis of canopy model parameters by EFAST method

Pudong Liu, Runhe Shi, Hong Wang, Wei Gao, East China Normal Univ. (China); Zhibin Sun, Colorado State Univ. (United States)

Abstract: Sensitivity analysis of plant canopy parameters basing on remote sensing model is a prerequisite for the inversion. As the limitation of local sensitivity analysis without considering the coupling effect among the parameters, the EFAST(Extended Fourier Amplitude Sensitivity Test) as a global sensitivity analysis method can be used not only the sensitivity of each parameter, but also the interacted influence among them. Based on PROSAIL model, the paper made a concentration to analyze the parameters' sensitivity by using EFAST method and simulated data so as to improve the inversion precision and develop the performance of model

9610-18, Session 2

A study on China's LUCC and carbon sink response with remote sensing

Zhiqiang Gao, Xiangyu Zheng, Jicai Ning, Yantai Institute of Coastal Zone Research (China); Wei Gao, Colorado State Univ. (United States)

Land use / land cover change (LUCC) is a core issue of global change research, which can not only influence regional and global climate change, but also is an important impact factor of carbon cycling. LUCC research is of great significance to expand national carbon emission space. Based on SPOT VEGETATION NDVI time-series data, multi-phase China's land use / land cover (LULC) data were extracted in this study, where land use degree method and land dynamic degree method were used to analyze the spatial and temporal change characteristics of China's land use / land cover data in the latest decade. Moreover, bookkeeping model was applied to analyze the response of China's carbon sink to vegetation cover change.



9610-19, Session 3

Long-term precipitation forecasting based on teleconnection signal propagation across North America (Invited Paper)

Ni-Bin Chang, Sanaz Imen, Univ. of Central Florida (United States); Kaixu Bai, Univ. of Central Florida (United States) and East China Normal Univ. (China)

Global sea surface temperature (SST) anomalies have a demonstrable effect on precipitation patterns throughout the continental U.S., which can be determined by statistical relationships between hydrological variables and the atmospheric-oceanic variables separated by large distances called 'hydroclimatic teleconnection'. However, the existence of non-stationary signals makes the identification of teleconnection complicated at a local scale. This means that it can hardly be analyzed by only relying on linear analysis across a wide region at sub-continental scale, and weak signals can be masked by anthropogenic effects. To address this need, this study aims to develop a method to assess the non-stationary teleconnection signals at a local scale using non-linear spectral wavelet analysis and remote sensing technology. To specify oceanic regions which have statistically significant contribution on precipitation pattern at a local scale, the pixelwise linear correlation was applied to determine the correlation between the localized variation of wavelet power and dominant modes of the Atlantic and Pacific SST and precipitation variability. After removing noisy signals from the identified teleconnection signals, nonlinear models were simulated to forecast precipitation utilizing the reconstructed signals with the aid of extreme learning machine (ELM). The developed ELM forecasting methodology on a monthly scale was applied for three sites in the Northeast, the Northwest, and the Southwest United States. This method can improve the understanding and projections of the impacts of climate change at a local scale, and reveal the contribution of the Atlantic and Pacific SST on precipitation variability over three regions in the U.S.

9610-20, Session 3

Climate change impacts on the U.S. agricultural economy (Invited Paper)

Xin-Zhong Liang, You Wu, Robert G. Chambers, Univ. of Maryland (United States); Daniel L. Schmoldt, U.S. Dept. of Agriculture (United States); Chao Sun, Univ. of Maryland (United States)

Past records have shown that climate variations play a major role on U.S. crop yields. There has been, however, a lively debate about the potential impact of climate change on the overall economic growth of U.S. agriculture. A vital measure of an agricultural economy's growth is its rate of total factor productivity (TFP) that measures aggregate output produced per unit of aggregate input used. This study will present a comprehensive analysis using the U.S. national TFP records and observed high-resolution climate (precipitation and surface air temperature) geographic maps during 1950-2010. We will demonstrate that TFPC interannual variations strongly depend on climate conditions over distinct regions of intensive agricultural productions. We will then develop a statistical model to show that future U.S. agricultural productivity will be significantly altered by substantial climate changes projected over these regions.

9610-21, Session 3

Temporal variation (seasonal and interannual) of vegetation indices of corn and soybeans across multiple years in central lowa

John H. Prueger, Jerry L. Hatfield, Agricultural Research Service (United States) Remotely sensed reflectance parameters from corn and soybean surfaces can be correlated to crop production. Surface reflectance of a typical Upper Midwest corn /soybean region in central Iowa across multiple years reveal subtle dynamics in vegetative surface response to a continually varying climate. From 2006 through 2014 remotely sensed data have been acquired over production fields of corn and soybeans in central IA, U.S.A. with the fields alternating between corn and soybeans. The data have been acquired with ground-based radiometers with 16 wavebands covering the visible, near-infrared, and shortwave infrared wavebands and combined into a series of vegetative indices. These data are collected on clear days with the goal of collecting data at a minimum of once per week from prior to planting until after the fall tillage operations. Within each field, five sites were established and sampled during the year to reduce the spatial variation and allow for an assessment of the changes in the vegetative indices during the growing season. Ancillary data collected for each crop included the phenological stage at each sampling date with biomass collected at the onset of the reproductive stage and at physiological maturity. Evaluation of the vegetative indices for the different years revealed that patterns were related to weather effects on corn and soybean growth. Remote sensing provides a method to evaluate changes within and among growing seasons to assess crop growth and development as affected by differences in weather variability.

9610-22, Session 3

Two-stage reference channel calibration for collocated UV and VIS Multi-Filter Rotating Shadowband Radiometers

Maosi Chen, John Davis, Zhibin Sun, Wei Gao, Colorado State Univ. (United States)

Multi-Filter Rotating Shadowband Radiometer (MFRSR) and its UV version (UV-MFRSR) are ground-based instruments for measuring solar UV and VIS radiation. They are usually deployed together in field at USDA UV-B Monitoring and Research Program (UVMRP) sites. The Langley Analysis (L is applied on (UV-) MFRSR channels individually to generate calibration factors at all channels. It is observed that the performance of LA varies with channels and sites. We attribute it to the monotonically changing total optical depths (TOD) in the cloud screened points. Since (1) aerosol is main source of TOD variation at the 368nm channel and (2) UV-MFRSR measures direct normal and diffuse horizontal simultaneously, we use the Radiative Transfer Model (i.e. MODTRAN) to create the look-up table (LUT) of the ratio of direct normal and diffuse (DDR) with respect to aerosol optical depth (AOD) and solar zenith angle. The LUT is used to evaluate the quality of the Langley Offset (VLO) by giving lower weights to VLO generated from points with monotonic variation in AOD. With the 368nm channel and other calibrated channels as Reference Channels (RC), the most stable points in RC are selected and LA is applied to the adjacent un-calibrated channel (TC) on those points to generate VLO in TC. The test of this method on the UVMRP site at Homestead, Florida shows that (1) The long-term trend of the original LA VLO is impacted by the monotonic changing in AOD at 368nm channel; and (2) more clustered VLO at shorter wavelength are generated compared with the original LA method.

9610-23, Session 3

Water stress detection of lilac leaves using a polarized laser

Songxin Tan, A. S. M. K. Khan, South Dakota State Univ. (United States)

Vegetation stress detection is of great importance to many agricultural and ecological studies. Vegetation water stress is commonly encountered in many areas. The accurate detection of water stress may not only save the vegetation from dying, but also may enable more efficient use of limited water resource.

Plant leaf water content is one of the primary factors indicating vegetation health condition. In this study, a linearly polarized Nd:YAG laser at 532-

Conference 9610: Remote Sensing and Modeling of Ecosystems for Sustainability XII



nm was used in the lab to study water stress from plant leaves. Leaf samples were collected and brought into the lab for measurement. An optical measurement system was built. Polarimetric measurements of the backscattered laser light were conducted as the leaf samples continued to lose water in the lab. The same measurement procedures were repeated several times until the leaf samples were almost completely dry. Preliminary study indicates that depolarization ratio is a good indicator of water stress in the studied case. In addition, an overall increasing trend of depolarization ratio under water stress condition was also observed.

9610-24, Session 3

Raman spectroscopy for the control of the atmosphere bioindicator

Elena V. Timchenko, Larisa A. Zherdeva Taskina, Nikolay V. Tregub, Pavel E. Timchenko, Ludmila A. Shamina, Samara State Aerospace Univ. (Russian Federation)

In view of ability to accumulate pollutants, plant facilities are effective markers of the ecological state of the atmosphere, which in contrast to traditional methods for measuring concentrations of pollutants express resistive functions of the biological environment to external influence, including the multiple factors and types of pollutants.

Experimental studies of the optical parameters of various bioindicators of the atmosphere (woody plants and soil types) using the method of Raman spectroscopy were presented. Changes in the optical parameters were studied for objects, under the direct influence of light, so for objects in the shadows, as well as age-appropriate bio-indicators.

The spectral characteristics of the samples were studied using experimental stand implementing the Raman method and includes a high-resolution digital spectrometer Shamrock sr-303i with a built-in cooling camera DV420A-OE, fiber-optic probe for Raman spectroscopy RPB785, combined with laser module LuxxMaster LML-785.0RB-04 (power of 150 mW, wavelength 785 nm).

The research resulted in produced the following conclusions:

- Tthe spectral characteristics of different types of biological indicators, depending on the level of illumination, experimentally established.

Shown that the ratio of the intensities of Raman wavenumbers at 730 cm-1 and 1600 cm-1 does not depend on the level of illumination for two bio-indicators - dandelion (Taraxacum) and silver birch (Betula pendula);

- Established that the statistical scatter parameters for optical bio-indicators wood ranged from 9% to 14%, and for the plant - from 4% to 8.7%.

- On the basis of the results obtained as a bio-indicator of atmospheric emissions was chosen dandelion (Taraxacum).

9610-25, Session 3

Study of emissivity changes presented by inorganic and organic soil under drying at ambient temperature

Carlos Villaseñor-Mora, Arturo Gonzalez-Vega, Haydee Hernández-Arellano, Univ. de Guanajuato (Mexico); Pablo Martinez-Torres, Univ. Michoacana de San Nicolás de Hidalgo (Mexico)

In this work, it is investigated the applicability and suitability of infrared thermography to study the degree of moisture of different kinds of soils. This technique could be applied to measure soil water content in a fast way, which could be helpful in both agricultural and environmental fields. In the first part of this study, the emissivity of the dry soils, with different and controlled content of organic matter, were characterized using an infrared camera and an integrating sphere, the emissivity was measured indirectly by reflection and absorption for the sample. To perform the experiments to measure the emissivity of the wet soils as a function of water loss, first the samples were wetted to field capacity, then, it was acquired a sequence of

thermal images in time to follow the different stages of drying of the studied samples. The content of humidity was monitored by conventional method. These measurements were compared with the infrared thermography procedure developed, and it was observed that the wet soils show different thermal emissivity behaviors when they are losing humidity. This behavior is strongly influenced by the percentage of organic matter content in the soil studied. Also, if the organic matter is predominant in the soil, the emissivity varies inversely proportional to the moisture content in the soil, however, if the soil is completely inorganic, the behavior of the emissivity is directly proportional to the moisture content in the soil.

9610-26, Session 3

Accurate extracting of moso bamboo from Landsat TM based on a constrained linear least square method

Yixiang Wang, Zhejiang Agriculture & Forestry Univ. (China) and Colorado State Univ. (United States); Zhibin Sun, Colorado State Univ. (United States); Shangbin Bai, Zhejiang Agriculture & Forestry Univ. (China) and Colorado State Univ. (United States)

Accurate extracting of moso bamboo is important for accounting its carbon sink, evaluating its expansion and predicting its implication management. Landsat TM image have been widely used for moso bamboo extracting because it covers large areas more efficiently than the traditional inventory. Using different bands from satellite data, this study applied an optimization method, constrained linear least square, to extract all moso bamboo forest image grids in Tianmu Mountain National Natural Reserve in Southern China. Ground truthing of the bamboo forest was performed by randomly locating 100 grids. Field surveys using GPS confirmed all of the grids were moso bamboo forest in this region and the bamboo distribution map was drawn for further research. This algorithm can also be applied to extract other forest types in satellite images.

9610-28, Session PWed

Rapid urban sprawl stimulated by increasing GDP and rising urban land price in east China coast from 2000 to 2009

Qingshui Lu, Yantai Institute of Coastal Zone Research (China)

Cities in east China coast have grown explosively in both number and size during the past several decades. Mapping results from satellite images indicated a vibrant urban sprawl from 2000 to 2004 with a growth rate of 74% while the expansion has slowed down to 40% from 2004 to 2009. Average urban land price in our study areas has increased 5 times during the same time period. Results of correlation and linear regression analyses suggested that rapid increase in GDP in our study area led to accelerated urban expansion, which was further promoted by the rising urban land price. Urban encroachment of agricultural land would potentially threat China's food security as eastern coastal region is one of the most productive agriculture regions in China. Wise policies are thus needed to better curtain urban development in east China coast.

9610-29, Session PWed

Evaluation of WRF physics and cumulus parameterization schemes in simulating convective precipitation over Yangtze River Delta

Yu Kan, Chaoshun Liu, Yan-an Liu, East China Normal Univ.



(China)

In order to study the impact of the parameterization schemes in the WRF model on rainstorm

simulations, a heavy rainfall on 13 September 2013 in Yangtze River Delta, China is simulated.The study was carried out with three cumulus parameterization schemes (KF, BMJ, and GD) and three physics parameterization schemes (Lin et al, WSM5 and WSM6 scheme) under a horizontal resolution of 4km. The results indicated that the Lin et al scheme, coupled with the Beetts-Miller-Janjie(BMJ) scheme, can accurately simulate the location and intensity of the heavy rainfall. The results of an analysis of temperature ,humidity and wind speed also indicated that this scheme can accurately simulate the reality of the rainfall.Generally, when coupled with the Beetts-Miller-Janjie(BMJ) scheme, this scheme is more accurate in simulating rainstorms in Yangtze River Delta.

9610-30, Session PWed

A soil heavy metal source apportionment method based on GIS

Cheng C. Fu, Chinese Academy of Sciences (China); Zhiqiang Gao, Bo H. Zhang, Shui Q. Lu, Institute of Geographic Sciences and Natural Resources Research (China)

It's an important work to analysis the soil heavy metal sources accurately and quantitatively to control and prevent heavy metal pollution in soil. In this study, a new method of soil heavy metal source apportionment based GIS was raised and discussed. The investigation of 109 soil samples was carried out in 2012 in Zhetang Town, Nanjing, and then As, Cr, Cu, for Hg, Ni and Zn was analyzed in laboratory. Using spatial-temporal variation and pollution assessment data, taking artery, river, factory and town as the most influential factors, the sources of soil heavy metals was obtained by GIS spatial analysis technology. In order to verify its feasibility, the mathematical analysis method was also carried out. The result showed that: the contribution of four factors of As were: 28%, 7%, 21% and 45%; the contribution of four factors of Cr were: 22%, 0%, 77% and 1%; the contributions of four factors of Cu were: 28%, 11%, 38% and 23%; the contributions of four factors of Ni were: 23%, 7%, 46% and 24%; the contributions of four factors of Zn were: 27%, 9%, 53% and 11%. The two methods drew a consistent conclusion, so the soil heavy metal source apportionment method based GIS is reliable and feasible.

9610-31, Session PWed

A tool for NDVI time series extraction from wide-swath remotely sensed images

Zhishan Li, Runhe Shi, Wei Gao, East China Normal Univ. (China)

Normalized Difference Vegetation Index (NDVI) is one of the most widely used indicators for monitoring the vegetation coverage in land surface. And its time series features are capable of reflecting dynamic changes of various ecosystems. Calculating NDVI via Moderate Resolution Imaging Spectrometer (MODIS) and other wide-swath remotely sensed images provide an important way to monitor large-scale NDVI spatially and temporally. However, there are some difficulties for ecologists to extract such information correctly and efficiently because of several professional processes on the original remote sensing images such as radiometric calibration, geometric correction, multiple data composition and curve smoothing. In this study, we develop an efficient and convenient online toolbox for non-remote sensing professionals who want to extract NDVI time series with a friendly graphic user interface. It is based on Java Web and Web GIS technically. Moreover, Struts, Spring, and Hibernate frameworks (SSH) are integrated in the system for the purpose of easy maintenance and expansion. Latitude, longitude and time period are the key inputs a user need to provide. Then NDVI time series are calculated automatically.

9610-32, Session PWed

Detecting harmful algal blooms using geostationary ocean color imager (GOCI) data in Bohai Sea, China

Mingzhu Xu, Institute of Geographic Sciences and Natural Resources Research (China) and Univ. of Chinese Academy of Sciences (China); Zhiqiang Gao, Institute of Geographic Sciences and Natural Resources Research (China)

Bohai Sea is a semi-enclosed inland sea with serious environmental problems. Harmful algal blooms (HABs) in Bohai Sea happen almost every year since the new century with the characteristics of pretty large area and long duration. Detecting the range of HABs in time can largely reduce economic losses and assure human safety. Remote sensing technology has the characteristics of large-scale, synchronized, rapid monitoring which is a main means to detect HABs. GOCI is the world's first Geostationary Ocean Color Imager with outstanding temporal resolution and high spatial resolution whose monitoring range include Bohai Sea. Its continuous observations increase the chance of obtaining valid data. As the red tide happens, ocean color, sea surface temperature (SST) and water-leaving radiance(LW) will changed distinct from normal sea water. So we try to use chlorophyll-a concentration, SST and several spectral indexes derived from GOCI as indicators of red tide, to find out which are better ones. Thresholds will be defined through history red tide cases studying in Bohai Sea. Valid indicators will be integrated to construct an algorithm to detect HABs. We validate the algorithm with new red tide cases in Bohai sea. Results derived from GOCI are also compared to those derived from MODIS.

9610-33, Session PWed

Spatial-temporal variability of the continental coastline in Bohai Rim

Ning Xu, Zhiqiang Gao, Yantai Institute of Coastal Zone Research (China)

Abstract

This paper is mainly focused on the continental coastline changes of Bohai Rim with a time span from 1980 to 2010. Remote sensing images of Landsat MSS, TM and ETM in the year of 1980, 1990, 2000 and 2010 were processed to extract coastlines and land use in the gap of coastline changes. Based on Remote Sensing and GIS spatial analysis techniques, the spatial and temporal changes of coastline were analyzed and the fractal dimensions of the coastlines were calculated by box-counting method. The result show that during the research period, the coastline length of the study area increased progressively and the most significant change in coastline length was found in Bohai Bay. Especially after 2000, the coastline length entered a period of rapid growth. Comparing the three sub period of the research span, a coastal reclamation is mainly focused on an urban construction and a maritime transport in the later period while focuses on aquiculture in the earlier period; the changes of continental coastline in Bohai Rim show significant temporal and spatial heterogeneity. Moreover, the fractal dimension of the coastline in Bohai Rim was increasing during the research period, however, large scale project such as ports construction, reduced tortuous degree of the coastline.

9610-34, Session PWed

Salinity and soil moisture retrieval algorithms in western Jilin province of China using passive microwave remote sensing data

Haoyang Fu, Lingjia Gu, Ruizhi Ren, Jilin Univ. (China)

Land surface features such as area, degree of salinity, soil moisture and

Conference 9610: Remote Sensing and Modeling of Ecosystems for Sustainability XII



salinity are mainly concerned in the observation of soil salinization. Although the field measurement of land surface features may provide more accurate results, it consumes a significant amount of manpower and time. That is a limitation on monitoring the soil salinization over a large area. Spectral remote sensing data is often used to observe the saline-alkali land and further obtain the information of its area and distribution. However, it is unable to detect soil moisture and salinity of saline land using spectral remote sensing data due to its spectral properties. Passive microwave remote sensing data reflects the dielectric properties of different land surfaces. Meanwhile, permittivity has high sensitivity to changes of soil moisture and salinity. As a result, passive microwave remote sensing data can be used for retrieval of surface soil moisture and salinity of saline land. Combined with the field sample data and passive microwave data, Western Jilin Province of China was selected as the study area in this paper. Through researching and analyzing the relationships between passive microwave brightness temperature, surface permittivity, soil moisture and salinity, effective retrieval algorithms of surface soil moisture and salinity of saline land was proposed.

9610-35, Session PWed

Dynamic analysis on coastline and sea reclamation in the efficient ecological economic zone of the Yellow River Delta based on 30-years satellite data

Xiangyu Zheng, Yantai Institute of Coastal Zone Research (China); ZhiQiang Gao, Jicai Ning, Qingshui Lu, Yantai Institute of Coastal Zone Research (China)

Coastline change and coastal reclamation change is one of the major environmental geological problems in the Highly Effective Ecologcal Zone of the Yellow River Delta. Grasp the changes and characteristics of evolution has important significance to implement the strategy of sustainable development. For this reason, the Highly Effective Ecologcal Zone of the Yellow River Delta's coastline and coastal reclamation change information were extracted by the means of visual interpretation and the artificial vector method, which four remote sensing images from the 1980 to 2010 period and the coastal survey data were used. On this basis,we have drawn a deep analysis to the evolution process and driving factors. The result show that: (1) The Highly Effective Ecological Zone of the Yellow River Delta's coastline showed an increasing trend in this 30 years. The change direction of it's coastline is promoting to the ocean and it was mainly induced by the deposition of sediment in the Yellow River and human factors. (2) The maximum increased of it's coastline was found during the period of 2000 to 2010 and it is espically obvious in The Yellow River Delta.(3) Coastal reclamation was mainly used for the construction of port and the breeding pool. Natural and social factors together determine the evaluation of coastal reclamation

9610-36, Session PWed

Snow depth retrieval algorithm of salinealkali land in western Jilin province of China using passive microwave remote sensing data

Mingbo Sun, Lingjia Gu, Ruizhi Ren, Haoyang Fu, Jilin Univ. (China)

Snow has extremely important influence to the natural environment and human activities. The research of snow depth retrieval has practical significance to the study of climate change. Jilin Province is located in the central part of Northeast China. It has a continental monsoon climate, winter is long and cold with heavy snowfall. The western region of Jilin Province is an important part of fragile ecological environment in Northeast China where the land salinization problem is particularly obvious. With the improvement of passive microwave remote sensing techniques, passive microwave data has become an important mean to retrieve snow depth. In this paper, the western Jilin province was selected as the study area. Furthermore, the two snow depth retrieval algorithms, including Chang algorithm and FY3B operational retrieval algorithm, were validated and analyzed in the study area using FY-3B/MWRI passive microwave remote sensing data. The main research focused on the analysis of the snow depth covered on saline-alkali land and the common land. Through the observation data for five consecutive years, the snow depth change trend of saline-alkali land and common land were analyzed. The effect of salinity on snow depth was further discussed. This research provides important information to evaluate the snow depth retrieval algorithm of saline-alkali land.

9610-37, Session PWed

The application of geo-information TuPu in coastline change study: taking coastland of Shandong province as an example

Xiangyang Liu, Zhiqiang Gao, Jicai Ning, Qingshui Lu, Yantai Institute of Coastal Zone Research (China)

With 4 periods of remote sensing images as data sources, based on Geoinformation TuPu analysis method, costaline change information mapping of Shandong province during the past 30 years is established using ArcGIS software, and then this kind of information was studied deeply. The conclusions are as follows: 1) During the past 30 years, costaline of Shandong province shows an incresing trend; the centre of increasing shifts eastward gradully; different areas have different increasing situations. 2) During the past 30 years, costaline change degree of Shandong province is basically stable, change fiercely areas concentrate on the Yellow River estuary while Zhaoyuan, Penglai and Longkou have a rather slow drgree. 3) From 1980 to 1990, costaline of Shandong province retreats to land quickly, draws back slowly from 1990 to 2000 while advances to sea rapidly entering into 21st century; Dongying has a backward trace for 30 years, Zhaoyuan and Laiyang have been basically unchanged, Yantai, Rizhao and Jiaonan have a obvious trend of advancing to sea.

9610-38, Session PWed

Analysis of scaling effect on the estimation of chlorophyll content using narrow band NDVI based on radiative transfer models

Hong Wang, Runhe Shi, Pudong Liu, East China Normal Univ. (China)

This study used particular narrow band normalized difference vegetation indices(NDVIs) to compare the estimations of chlorophyll contents at foliar level and canopy level, through a large number of simulated canopy reflectance spectra with different chlorophyll contents run on PROSPECT model and SAIL model. 10 narrow band NDVIs were selected at the identified ranges that can effectively assess foliar chlorophyll content. We firstly, analyzed the sensitivities between canopy chlorophyll contents and narrow band NDVIs, and then research the indices' resisting interferences to other parameters, aiming to evaluate the adaptation of the 10 narrow band NDVIs used in assessing the canopy chlorophyll content.

9610-39, Session PWed

Retrieving aerosol optical depth over Beijing based on Landsat8 OLI data

Lu Zhang, Runhe Shi, Long Li, East China Normal Univ. (China)

Aerosol is a significantly important factor in climate change and environmental quality, and remote sensing makes it feasible for us to do large scale aerosol monitoring. Using Operational Land Imager (OLI) images of landsat8, Aerosol Optical Depth (AOD) was retrieved over Beijing, China,



on May 15, September 4 and October 6, 2014. Look-up tables of blue and red channel were built with 6S atmospheric radiative transfer model, and the linear relationships between AOD, TOA reflectance and surface reflectance were investigated by multiple regression analyses. The AOD of dark pixels were got from OLI images by applying the regression models. After that, the spatial distribution of AOD over Beijing was figured out by using kriging interpolation method. The retrieved results were compared with AODs from ground-based measurements of AERONET. The differences between them were analyzed. It showed that when retrieved AOD using the regression models, the errors were related to the values and ranges of AOD input in the LUT. The middle values of the input AOD would have the minimum errors. From the retrieved AOD, we can find that AOD values were higher over the city areas in the middle of Beijing and lower over the forest in the northern and western Beijing. The OLI images, which have a higher resolution, can be used to reflect the detailed distributions of AOD over Beijing.

9610-40, Session PWed

Comparative analysis of land surface emissivity (LSE) retrieval methods and the impact on the land surface temperature based on Landsat-8 thermal infrared data

Zenghui Kan, Chaoshun Liu, Wei Gao, East China Normal Univ. (China)

With the deep application of remote sensing?several algorithms have been put forward for land surface temperature retrieval?However?land surface emissivity?which is one of the significant parameters in temperature retrieval?can be calculated in various ways?In this paper, two methods for estimating LSE based on TM data were introduced, one is Van's empirical formula method and the other is the mixed pixels decomposing method. The accuracy of the results are compared by 0.01 MODIS LSE product. Based on the detailed introduction to Van's empirical formula and the mixed pixels decomposing method in computing surface emissivity, Landsat-8 thermal infrared data and the radiative transfer equation method were used to obtain the land surface temperature in Taihu region?In this paper , atmospheric parameters based on real-time atmospheric profile , which reduce the LST error brought by the atmosphere profile .Two figures were acquired?which represented the LST RTE JYGS and the LST RTE HHXY respectively . The relationship between land surface temperature and land cover was also studied. It is shown that when the two surface emissivities obtained by the algorithms above are applied to the radiative transfer equation method ?the general trend is approximately the same for the two surface temperature retrieval results .

9610-41, Session PWed

Assessing the potential and actual productivity of winter wheat in the North China Plain by WOFOST model

Jialin Yang, Chaoshun Liu, East China Normal Univ. (China); Wei Gao, East China Normal Univ. (China) and Colorado State Univ. (United States)

This study simulated the potential and water limited yield of winter wheat in the North China Plain from 1993 to 2013 by using WOFOST model. The yield gaps between the actual and potential production in this region were analyzed at the same time. The aims are to reveal the yield potential and its spatial and temporal variation, identify the limiting factors affecting the growth process of winter wheat. The site simulated yield data of winter wheat were interpolated spatially to map the spatial distribution. The results showed that WOFOST model is applicable for simulating yield of Winter Wheat in the North China Plain. It describes crop photosynthesis in detail and is good at simulating crop potential growth. The potential production in North China Plain is about 8000kg/hm2 while present production achieves only about 60%-70% of this. So it is urgent to improving the way of management to increase the yield of Winter Wheat in the North China Plain.

9610-42, Session PWed

Validation of the OMI-TOMS and OMI-DOAS total ozone column data using ground-based observations over China

Ming-Liang Ma, Runhe Shi, Wei Gao, East China Normal Univ. (China)

Analysis of the accuracy and variability of total ozone columns (TOC) has been conducted by many studies. However, the differences between the TOC derived from Total Ozone Mapping Spectrometer (TOMS), the Ozone Monitoring Instrument (OMI), and the Total Ozone Unit on board the Chinese Feng Yun-3A, also the differences between the TOC of space-based sensors and ground-based sensors such as Brewer and Dobson in the recent ten years. The data of four Brewer and Dobson observation sites: Xianghe, Kunming, Waliguan and Longfengshan are analyzed. In this study, the accuracy of data from the ground-based observation sites and the satellite sensors are evaluated. The spatial and temporal variation trends of the total ozone columns in different areas of China are discovered.

9610-43, Session PWed

Remote estimation of GPP in temperate grassland: implications of the uncertainty in GPP estimation in grassland using MODIS data

Shishi Liu, Huazhong Agricultural Univ. (China); Yi Peng, Wuhan Univ. (China); Nathaniel Brunsell, University of Kansas (United States); Qingfeng Guan, China Univ. of Geosciences (China)

Many studies have pointed out that remote-sensing-based GPP models provided less accurate estimations under water stress. This study analyzed grassland GPP estimated by the Temperature and Greenness (TG) model and the MODIS algorithm along the mean precipitation gradient. The evaluation of the uniform TG model and MODIS algorithm for each site/ year demonstrated the variations of the accuracy of GPP estimates among different sites and years. GPP were overestimated at the driest site among three study sites, and during the dry years of the other semiarid site. Both models provide more accurate GPP estimates for the wet site and during the wet and normal years of the semiarid sites. Calibrating both models for each site/year showed that the parameters of both models varied among sites and years, especially for the TG model. The relationship between flux-tower GPP observations and (scaled EVI *scaled LST) for the TG model and the relationship between flux-tower GPP observations and (fPAR*PAR*Tmin scalar*VPD scalar) for the MODIS algorithm were different during green-up and dry-down period of grassland during the dry years at semiarid sites. This result implied that different relationships at different growing stages might be one of the major reasons for the overestimation of GPP by the TG model and the MODIS algorithm for semiarid grassland where water is a limiting resource. Both TG model and MODIS algorithm should be used with caution in the arid and semiarid grassland regions, particularly when grassland experiences drought events.

9610-44, Session PWed

Analysis of temporal and spatial variation in Shandong province island shoreline and land cover based on remote sensing and GIS

Ruqing Zhuo, Yantai Institute of Coastal Zone Research (China)

Island and its surrounding waters rich in resources, island is the base of

Conference 9610: Remote Sensing and Modeling of Ecosystems for Sustainability XII



human development spend long distance ocean waters and forward pivot. Island Remote sensing of domestic research mainly research in methods and theory, as well as short-term Dynamic Study on change in a small range of island, in a wide range of long time scale Dynamic Study on the island is still in the blank. In addition, the dominated monitoring target is shoreline changes, and few work of human development and utilization of dynamic change monitoring conducted, and in the region rarely comes to the island in northern China. In this article, extraction the information of the island in Shandong Province, in 1980, 1990, 2000, 2010 four periods remote sensing image through visual interpretation and computer classification, to get the island coastline and land cover thematic information, and analyze the spatial and temporal variation of the dynamic and driving force, to provide scientific guidance and data support for the relevant departments of Shandong Province to protect and develop and use island.

9610-45, Session PWed

Simulation and analysis of NDVI performance based on vegetation canopy radiative transfer model

Yuyan Zeng, Runhe Shi, Pudong Liu, Jinquan Ai, Wei Gao, East China Normal Univ. (China)

this paper uses PROSAIL model to simulate vegetation canopy reflectance under different chlorophyll contents and LAI. The changes of NDVI with different LAI and chlorophyll contents are analyzed. A simulated spectral dataset was built by using PROSIAL vegetation radiative transfer model with various vegetation chlorophyll concentrations and leaf area index. Based on the dataset, the responses of NDVI to LAI were quantitatively analyzed. A sensitivity analysis indicated that NDVI had a close relationship with LAI under different chlorophyll contents. It is concluded that the vegetation canopy biochemical parameters can be estimated efficiently by using the simulated spectrum with PROSAIL model.

?

9610-46, Session PWed

Changes on albedo after a large forest fire in Mediterranean ecosystems

Carmen Quintano, Univ. de Valladolid (Spain); Alfonso Fernández-Manso, Victor Fernández, Univ. de León (Spain); Elena Marcos, Leonor Calvo, Univ. de León (Spain)

Fires are one of the main causes of environmental alteration in forest Mediterranean ecosystems. Albedo varies spatially and evolves seasonally based on solar illumination. It is greatly influenced by changes on vegetation: vegetation growth, cutting/planting forests or forest fires. This work analyzes albedo variations due to a large forest fire which occurred on 19-21 September, 2012 in Northwestern Spain. From this area, a 1-year series of six albedo images were generated from Landsat 7 Enhanced Thematic Mapper (ETM+) data. Specifically we considered the total shortwave albedo, total-, direct-, and diffuse-visible, and near-infrared albedo. Nine to twelve weeks after fire, 111 field plots were measured (27 unburned plots, 84 burned plots). The relationship between albedo values and thematic class burned/ unburned was evaluated by a one-way analysis de variance. Our results demonstrate that albedo changes were related to burned/unburned variable with statistical significance, indicating the importance of forestry areas as regulators of land surface energy fluxes and revealing the potential of immediately post-fire albedo for assessing burned areas. Future research, however, is needed to evaluate the persistence of albedo changes. Albedo is greatly influenced by changes on vegetation: vegetation growth, cutting/ planting forests or forest fires. This work analyzes albedo variations due to a large forest fire which occurred in Northwestern Spain. A 1-year series of six albedo images were generated from Landsat 7 Enhanced Thematic Mapper data. 111 field plots were measured (27 unburned plots, 84 burned plots). The relationship between albedo values and thematic class burned/ unburned was evaluated by a one-way analysis de variance. Our results demonstrate that albedo changes were related to burned/unburned variable with statistical significance, revealing the potential of immediately post-fire albedo for assessing burned areas.

9610-47, Session PWed

Linear fractional-based filter as a preclassifier to map surface coal mining affected area

Carmen Quintano, Univ. de Valladolid (Spain); Alfonso Fernández-Manso, Univ. de León (Spain); Eduardo Cuesta, Univ. de Valladolid (Spain)

Surface coal mining techniques extract multiple coal seams by removing an area of many square kilometers and creating serious environmental problems. Information about mining activities location and dimensions is essential for environmental applications. In this work a linear fractionalbased filter is considered as pre-classifier for surface coal mining affected area estimation in three study areas in Spain. Two vegetation indexes (Normalized Difference Vegetation Index, NDVI, and Modified Soil-Adjusted Vegetation Index, MSAVI) and three reflectance bands from Landsat 7 Enhanced Thematic Mapper (ETM+) data were used as input for the proposed filter. The filtered images were classified and the accuracy of the estimates was computed by K statistic. Surface coal mining affected area perimeters measured on the ground by Global Positioning System (GPS) were used as reference truth. The results showed that the non-local filter, used as pre-classifier, allowed higher accuracy than the same inputs without filtering. A McNemar's test confirmed that such accuracy improvement had statistical significance. Surface coal mining affected areas in Spain were accurately mapped when the linear fractional-based filter proposed here was used as a pre-classifier.

9610-48, Session PWed

Data fusion of CO2 retrieved from GOSAT and AIRS using regression analysis and fixed rank kriging

Cong Zhou, Runhe Shi, East China Normal Univ. (China)

This paper proposes an improved statistical method for fusing carbon dioxide (CO2) data retrieved from two major instruments, the Greenhouse gases Observing SATellite (GOSAT) and the Atmospheric Infrared Sounder (AIRS). These two datasets were fused to obtain CO2 concentrations near the surface, which is a region that is especially important for studies on carbon sources and sinks. Overall, the CO2 monthly average values from GOSAT are all lower than those from AIRS from 2010 to 2012. The datasets show the similar seasonal cycles of carbon dioxide and show an increasing trend with a determination coefficient of 0.45. The analysis of the relationship between the climatic factors and the CO2 reveals that wind is the most significant contributing factor. A strong correlation was determined by adding the climatic factors as independent variables for regression analysis. The correlation coefficients between the CO2 values from AIRS and GOSAT significantly increased in response. The true CO2 data processes were then predicted using the fixed rank kriging method. This showed that the data-fusion CO2 product provides more reasonable information and that the corresponding mean squared prediction errors are smaller than those from the single GOSAT CO2 dataset.

9610-49, Session PWed

Study on relationship between concentration of air pollution and meteorological factor in Shanghai from 2013-2014

Jing Wang, Runhe Shi, East China Normal Univ. (China)

Conference 9610: Remote Sensing and Modeling of Ecosystems for Sustainability XII



To explore relationship of concentrations of SO2, NO2 and PM10 in the air with temperature, air pressure and relative humidity. The correlated relationship of concentration of atmospheric pollutant with meteorological element was analyzed by multiple stepwise regression.

The air concentration of SO2 was associated with the daily max atmospheric pressure, the increasing air pressure was profit to the increasing concentration of SO2, The changes of SO2 showed significantly associated with relative humidity. The air concentration of NO2 revealed to be significantly positive association with the daily max atmospheric pressure, while negative association with the daily max air temperature and the daily average relative humidity. The air concentration of PM10 showed positive correlation with the daily average atmospheric pressure, while negative association with daily average relative humidity and and the daily min relative humidity.

9610-50, Session PWed

Optical methods for control of aquatic plants under pollutant effect

Elena V. Timchenko, Larisa A. Zherdeva Taskina, Pavel E. Timchenko, Anna A. Asadova, Samara State Aerospace Univ. (Russian Federation)

Monitoring of aquatic plants by the action of various pollutants such as synthetic surface active agents (surfactants), heavy metals and agricultural emissions (different types of fertilizers) using the methods of Raman spectroscopy (RS) and confocal fluorescence microscopy was carried out.

Stand of Raman spectroscopy is made on the basis of high-resolution digital spectrometer Shamrock sr-303i with a built-in cooling camera DV420A-OE. Confocal fluorescence microscopy was performed on the basis of an inverted microscope Olympus IX71, confocal scanner Yokogawa CSU-1 with camera EMCCD iXon Andor.

The dependence of the optical parameters of aquatic plants on the concentration of pollutants experimentally established. Shown, that the under the action of pollutants changes the intensity of the Raman wavenumber at 740 cm-1 and 1522 cm-1, which are associated with a change in the concentration of chlorophyll and carotenoids.

Shown, that the under the influence of pollutants on plant tissue occurs Raman intensity decrease by 70% at wavenumber 740 cm-1, 1522 cm-1, responsible for the C=C stretching vibration in chlorophylls and carotenoids.

This feature corresponds to the "washout pigments" from plant cells and changes in the concentration of chlorophyll and carotenoids.

Introduced optical factor that determines the impact of pollutants on plants, defined as the ratio of the intensities of the Raman scattering at wave numbers 740 cm-1, 1522 cm-1 and 1435 cm-1, corresponding to a change in the concentration of chlorophyll, v(C = C) in b-carotene and arginine.

Microscopically, it is proved that the mechanism of degradation of chlorophyll in the presence of surfactants associated with the solubilizing of membrane proteins and the change of its permeability.

9610-51, Session PWed

Retrieval of water and heat flux based on fusion of LANDSAT TM/ETM+ and MODIS data

Jicai Ning, Yantai Institute of Coastal Zone Research (China); Zhiqiang Gao, Yantai Institute of Coastal Zone Research, Chinese Academy of Sciences (China)

The Moderate Resolution Imaging Spectroradiometer (MODIS) data has a high temporal resolution, which, at present, is an ideal data source in simulative monitoring of regional-scale changes in surface energy and water. However, the spatial resolution of its thermal infrared band is relatively low (1 km). The Landsat TM/ETM+ data have a high spatial resolution, but their single thermal infrared bands can lead to the fact that the inversion accuracy for the surface temperature is not high, and that the time resolution is low. This limits its application in the surface evapotranspiration (ET) monitoring. Combining TM/ETM + visible wave band with MODIS thermal infrared wave band, this paper discusses a multi-scale remote sensing method to estimate regional surface ET. On the basis of space enhancement method, the vegetation index estimated by TM/ETM + enhances the surface temperature scale with the inversion of MODIS to a 30 m resolution, which aims to improve the estimation accuracy of ET in the non-uniform surface mixed-pixel. The results show that this method has a higher accuracy of ET estimation compared with the method of only using MODIS or ETM+ data. Moreover, it can obtain a more obvious effect on scale correction in the uneven land surface or various surface covering types, and the corrected ET is close to the observation result.

Conference 9611: Imaging Spectrometry XX

Monday - Wednesday 10-12 August 2015

Part of Proceedings of SPIE Vol. 9611 Imaging Spectrometry XX

9611-1, Session 1

Compact wide swath imaging spectrometer (CWIS): alignment and laboratory calibration

Byron E. Van Gorp, Pantazis Mouroulis, Robert O. Green, Daniel W. Wilson, Jose I. Rodriguez, Elliot Liggett, Jet Propulsion Lab. (United States)

The Compact Wide Swath Imaging Spectrometer (CWIS) is a pushbroom imaging spectrometer for the solar reflected spectrum (380-2500 nm) with wide swath (1600 elements), fast optical speed (F/1.8), and high uniformity (\geq 95%). CWIS is currently under development at the Jet Propulsion Laboratory and is intended to address the need for high signal to noise ratio compact imaging spectrometer systems for the visible short wave infrared wavelength range. We give an overview of the instrument functionality, describe progress in spectrometer alignment and system integration and report laboratory data that include spatial, spectral and radiometric calibration.

9611-2, Session 1

Snow and water imaging spectrometer (SWIS): opto-mechanical and system design for a CubeSat-compatible instrument

Holly A. Bender, Pantazis Mouroulis, Byron E. Van Gorp, Jet Propulsion Lab. (United States); Christopher D. Smith, ATK Aerospace Systems (United States); Michael Eastwood, Ernesto Diaz, Colin H. Smith, Jet Propulsion Lab. (United States)

The Snow and Water Imaging Spectrometer (SWIS) is a fast, highuniformity, low-polarization sensitivity imaging spectrometer and telescope system designed for integration in a 6U CubeSat. Operating in the 350-1700nm spectral region with 5.7nm sampling, SWIS is intended to address critical science in two localized regions of the Earth: coastal zones and snow/ice covered mountains. We discuss progress in the SWIS optomechanical design, thermal analysis, and mission plan. We also describe an on-board calibration system capable of addressing the stringent radiometric stability and knowledge these missions require. The spectrometer will feature a new Teledyne CHROMA array, optimized for high temperature operation, with a linear variable anti-reflection coating to enhance quantum efficiency and minimize backscatter.

9611-3, Session 1

Technical developments toward the pre-processing and quality assessment of the upcoming EnMAP space-based hyperspectral data

André Hollstein, Karl Segl, Christian Rogass, Luis Guanter, Helmholtz-Zentrum Potsdam Deutsches GeoForschungsZentrum GFZ (Germany)

EnMAP is a German imaging spectroscopy satellite mission with the declared goal to investigate the Earth's surface with a so far surpassing quality. The key scientific questions to which EnMAP will contribute are related to climate change impacts, land cover changes and processes, natural resources, biodiversity and ecosystems, water availability and quality, geohazards and risk management.

During the current mission preparation phase, technical developments at the GFZ Potsdam (EnMAP's scientific principal investigator) are going in two separate directions. On the one hand, several ground based validation activities are planed which will allow to assess the EnMAP instrument by technical means alternative to those considered in the Ground Segment calibration and monitoring plans. In particular, a program for the quantitative evaluation of EnMAP radiance and reflectance data and their spatial accuracy along the commissioning phase and the normal mission operation period is presented. This plan proposes ground- and scene-based techniques for product evaluation to derive characteristic deviation figures for the final EnMAP products and includes the assessment of technical parameters such as spectrometer co-registration, keystone or smile.

SPIE. PHOTONICS

APPLICATIONS

OPTICAL ENGINEERING+

On the other hand is the development of pre-procseeing tools, among which is a research driven atmospheric correction scheme which allows for supervision and inclusion of additionally measured atmospheric parameters by potential end-users. This scheme will be based on the latest spectroscopic databases and accurate radiative transfer including the coupling of gaseous absorption and multiple scattering by various aerosol types and cirrus clouds. It will be made available to end-users trough the EnMAP-Box software.

9611-4, Session 1

Effect of entangled PSF/ISRF of imaging spectrometers on the retrieval of low signals over spectrally contrasting features: a case study for remote sensing of chlorophyll fluorescence

Luis Alonso, Univ. de València (Spain); Francisco Pinto, Uwe Rascher, Forschungszentrum Jülich GmbH (Germany); Jose Moreno, Univ. de València (Spain)

Imaging spectrographs records the signal by means of a bi-dimensional sensor where the spatial information is collected in one dimension while spectra is captured along the other dimension. Ideally, a monochromatic point source should produce a single pixel response. In real systems this is not the case, and the resulting signal spreads along and across the sensor matrix and the PSF and ISRF responses get entangled into a 2D monochromatic point spread function (MPSF).

Smooth spectral signals are not significantly affected. However, when spectra present neighboring bands with contrasting values, e.g. when absorption features or narrow emission peaks are resolved, the result is a transfer of energy between them that causes the high signal to decrease and the low signal to increase distorting the shape and the values.

Moreover, in regions around target edges, due to the diagonal terms in the MPSF, high signal in a band of one surface can be transferred to a neighboring band on an adjacent surface. Even very weak contributions in the PSF, in the order of 1E-4, can result in a noticeable effect that might be usually negligible, turns relevant for application where the objective is to discriminate weak signals such as vegetation's chlorophyll fluorescence.

This work presents a quantification of this effect through a theoretical analysis, a correction by means of an iterative deconvolution process and its application to the real case of HyPlant airborne hyperspectral imager for fluorescence retrieval.

9611-5, Session 1

Mapping pigment distribution in mud samples through hyperspectral imaging

Mehrube Mehrübeoglu, Cosmina Nicula, Shane W. Smith, Dustin K. Smith, Elizabeth S. Shanks, Paul V. Zimba, Texas A&M Univ. Corpus Christi (United States)



Mud samples collected from lakes and other bodies of water reveal information about the distribution of microorganisms in the local sediments. The pigment distribution associated with microorganisms can then be correlated to water and other environmental quality, which is a continuing research challenge. In this project hyperspectral imaging has been investigated as a technology to identify phototropic organisms living on sediments collected from the Texas Coastal Bend area. Hyperspectral data cubes offer both spatial and spectral data that can be used to examine organisms based on their spectral pigment profiles and spatial arrangement. High-performance Liquid Chromatography (HPLC) has been used as the ground truth for pigment content of microalgae living on the mud surface. The top pigment profiles identified through HPLC have been correlated with spectral signatures extracted from the hyperspectral data cubes of mud using Fast Fourier Transforms. Spatial distributions have also been investigated using 2D hyperspectral image processing. 2D pigment distribution maps have been created based on the highest correlation with pigments. Pigments identified using HPLC include chlorophyll (ch) a, chl b, and chl c2 in addition to the carotenoids fucoxanthin, diadinoxanthin, zeaxanthin, ?-? carotene, and lutein. Diatoms had the most abundant source of spectral signal, as indicated by the carotenoid fucoxanthin. Cyanobacteria (blue-green algae) were present as indicated by zeaxanthin and green algae by chl b and lutein.

9611-6, Session 1

Long-wavelength infrared hyperspectral data "mining" at Cuprite, NV

Steven M. Adler-Golden, Patrick F. Conforti, Lawrence S. Bernstein, Robert Sundberg, Spectral Sciences, Inc. (United States)

In recent years long-wavelength infrared (LWIR) hyperspectral imagery has significantly improved in quality and become much more widely available. sparking interest in a variety of applications involving remote sensing of surface composition. This in turn has motivated the development and study of LWIR-focused algorithms for atmospheric retrieval, temperatureemissivity separation (TES) and material detection and identification. In this paper we evaluate some algorithms for atmospheric retrieval, TES, endmember-finding and rare material detection for their utility in characterizing mineral composition in SEBASS hyperspectral imagery taken near Cuprite, NV. Atmospheric correction results using the In-Scene Atmospheric Correction (ISAC) method are compared with those from the first-principles, MODTRAN©-based FLAASH-IR method. Our covariancewhitened endmember-finding methods are observed to be very sensitive to image artifacts and cultural clutter. However, with clean data and all-natural terrain they can automatically locate and distinguish many minor mineral components, with especially high sensitivity to varieties of calcite. Not surprisingly, the major scene materials, including silicates, are best located using unwhitened techniques. Minerals that we identified in the data include calcite, guartz, alunite and kaolinite.

9611-7, Session 1

Baffling for high performance thermal imaging spectroscopy

William R. Johnson, Jonathan Mihaly, Simon J. Hook, Bjorn T. Eng, Jet Propulsion Lab. (United States)

The Hyperspectral Thermal Emission Spectrometer (HyTES) has flown on successful science and application campaigns since 2012. It currently flys on a Twin Otter aircraft at low altitude (1000m to 3000m AGL). HyTES utilizes a challenging optical design in practice, since it operates at cryogenic temperatures and has a small form factor compared to other designs. It utilizes a state-of-the-art Dyson optical configuration. The Dyson design uses a concave diffraction grating coupled to a 2-pass monolithic relay to disperse the light. It captures a 50-degree field of view in the cross track direction with 256 spectral channels between 7.5\$ mu \$m to 12.0\$ mu \$m. The instrument sensitivity per spectral channel is 0.2C. This is enough

sensitivity to discriminate trace gas plumes at ambient temperature.

Recent modifications have improved the instrument performance considerably. This includes optimal cold operational alignment, improved thermal stability/control, and advanced calibration techniques. This paper describes these improvements in brief and explores secondary baffling techniques which we've found eliminate out-of-field radiometric gradients which contaminate the cross track imagery under subtle (-few degrees) roll maneuvers. Simulation results are shown as well as actual flight data.

9611-8, Session 1

Performance status of the AIRS instrument thirteen years after launch

Denis A. Elliott, Thomas S. Pagano, Jet Propulsion Lab. (United States)

The Atmospheric Infrared Sounder (AIRS) is a hyperspectral infrared instrument on the EOS Aqua Spacecraft, launched on May 4, 2002. AIRS has 2378 infrared channels ranging from 3.7 ? m to 15.4 ? m and a 13.5 km footprint at nadir. The AIRS is a "facility" instrument developed by NASA as an experimental demonstration of advanced technology for remote sensing and the benefits of high resolution infrared spectra to science investigations. AIRS, in conjunction with the Advanced Microwave Sounding Unit (AMSU), produces temperature profiles with 1K/km accuracy on a global scale, as well as water vapor profiles and trace gas amounts for CO2 , CO, SO2 , O3 and CH4. AIRS data are used for weather forecasting, climate process studies and validating climate models. The AIRS instrument has far exceeded its required design life of 5 years, with nearly 13 years of routine science operations that began on August 31, 2002. While the instrument has performed exceptionally well, with little sign of wear, the AIRS Project continues to monitor and maintain the health of AIRS, characterize its behavior and improve performance where possible. Radiometric stability has been monitored and trending shows better than 16 mK/year stability. Spectral calibration stability is better than 1 ppm/year. At this time we expect the AIRS to continue to perform well into the next decade. This paper contains updates to previous instrument status reports, with emphasis on the last three years.

9611-9, Session 2

Retrieved products from simulated hyperspectral infrared observations of a hurricane

Joel Susskind, NASA Goddard Space Flight Ctr. (United States)

This research uses Observing System Simulation Experiments (OSSEs) to assess the impact of higher spatial and temporal resolution soundings on hurricane forecast accuracy. The simulation experiments use as truth surface and atmospheric parameters obtained from an NOAA AOML OSSE GCM model. The model, called the nature run, was run with a 1km x 1km spatial resolution and sampled every 10 minutes over a moving limited area following the track of a severe Atlantic storm. Nature run products were sampled and averaged over sounder footprints for three instrument configurations, corresponding to 15kmx15km footprints in LEO orbit, 2kmx2km footprints in LEO, and 5kmx5km footprints sampled every hour in GEO. These colocated truth files were each used to simulate radiances for an IR instrument with AIRS spectral and radiometric characteristics. We analyzed the simulated radiance data using the AIRS Science Team Version-6 retrieval algorithm. This algorithm employs empirical Neural-Net first guess coefficients trained using observed AIRS radiances. These empirical coefficients, trained using real AIRS data, worked well using our simulated AIRS radiances, even under very cloudy conditions. Accuracy of retrievals obtained using simulated AIRS radiances with a 15 km footprint was similar to that obtained using real AIRS data. Retrieval results will be shown for all three sounding scenarios. Our simulated retrievals are currently being assessed by NOAA AOML in an OSSE study to determine the impact of advanced hyperspectral infrared sounders on hurricane forecast



improvement and assess whether this impact increases with higher spatial and/or temporal resolution.

9611-10, Session 2

Observing system simulation experiments to evaluate the potential impact of new remote sensing instruments on hurricane track and intensity forecasting

Robert M. Atlas, National Oceanic and Atmospheric Administration (United States)

Observing System Simulation Experiments (OSSEs) are an important tool for evaluating the potential impact of proposed new observing systems, as well as for evaluating trade-offs in observing system design, and in developing and assessing improved methodology for assimilating new observations. Detailed OSSEs have been conducted at NASA/ GSFC and NOAA/AOML in collaboration with Simpson Weather Associates and operational data assimilation centers over the last three decades. These OSSEs determined correctly the quantitative potential for several proposed satellite observing systems to improve weather analysis and prediction prior to their launch, evaluated trade-offs in orbits, coverage and accuracy for space-based wind lidars, and were used in the development of the methodology that led to the first beneficial impacts of satellite surface winds on numerical weather prediction. In this paper, we will summarize the NOAA Hurricane OSSE system and present results from experiments to evaluate hyperspectral data from polar and geostationary orbit as well as the application of GNSS and lidar data to hurricane prediction.

9611-11, Session 3

Design of a satellite end-to-end mission performance simulator for imaging spectrometers and its application to the ESA's FLEX/Sentinel-3 tandem mission

Jorge Vicent, Neus Sabater, Carolina Tenjo, Univ. de València (Spain); Juan Acarreta, Elecnor Deimos Space S.L.U. (Spain); María Manzano, GMV Aerospace & Defence (Spain); Juan Pablo Rivera, Univ. de València (Spain); Raffaella Franco, European Space Research and Technology Ctr. (Netherlands); Jose Moreno, Univ. de València (Spain)

The performance analysis of a satellite mission requires specific tools that can simulate the behavior of the platform; its payload; and the acquisition of scientific data from synthetic scenes. These software tools, called End-to-End Mission Performance Simulators (E2ES), are promoted by the European Space Agency (ESA) with the goal of consolidating the instrument and mission requirements as well as optimizing the implemented data processing algorithms. Nevertheless, most developed E2ES are designed for a specific satellite mission and can hardly be adapted to other satellite missions. In the frame of ESA's FLEX mission activities, an E2ES is being developed based on a generic architecture for passive optical missions. FLEX E2ES implements a state-of-the-art synthetic scene generator that is coupled with dedicated algorithms that model the platform and instrument characteristics. This work will describe the flexibility of the FLEX E2ES to simulate complex synthetic scenes with a variety of land cover classes, topography and cloud cover that are observed separately by each instrument (FLORIS, OLCI and SLSTR). The implemented algorithms allows modelling the sensor behavior, i.e. the spectral/spatial resampling of the input scene; the geometry of acquisition; the sensor noises and nonuniformity effects (e.g. stray-light, spectral smile and radiometric noise); and the full retrieval scheme up to Level-2 products. It is expected that the design methodology implemented in FLEX E2ES can be used as baseline for other imaging spectrometer missions and will be further expanded towards a generic E2ES software tool.

9611-12, Session 3

Best practices for performance modeling of imaging spectrometers

Louis Zellinger, Raytheon Space and Airborne Systems (United States)

This paper provides best practices for the spectral, spatial, and radiometric performance modeling of imaging spectrometers. We propose a set of standard terminology to use when modeling imaging spectrometers. The difference between resolution and sampling is discussed for both spatial and spectral dimensions. We also outline the calculation of various radiometric sensitivity metrics and their contrast counterparts. Modeling approaches are described for both solar reflected and thermally emitted bands. Finally, we apply our approach to an example hyperspectral sensor.

9611-13, Session 3

Analysis of a LWIR HSI design concept to mitigate the impact of optical distort

Pierre V. Villeneuve, Exelis, Inc. (United States); Eric M. Moskun, Joseph G. Shanks, John F. Silny, Raytheon Space and Airborne Systems (United States); Alan D. Stocker, DRS Sensors & Targeting Systems, Inc. (United States)

This report is a summary of a recent effort to quantify the relationship between LWIR spectral distortion and data utility. A representative model scene was generated from a high-fidelity terrain material database and a MODTRAN-predicted atmosphere. An optical distortion model was derived from a notional system design concept, specifying distortion as a 2D function across the FPA surface. A signal-processing framework was developed and used to propagate scene radiance through the system model (at high spatial resolution and high spectral resolution), one frame of data at a time. The output of this initial processing framework is a prediction of sensed radiance for a given prescription of optical distortion, with data sampled onto a representative FPA native-

pixel grid. The penultimate step is to (optionally) correct for the known spectral distortion by resampling the spectral signal at each spatial element onto consistent spectral grid. The final step is then to apply 2x2 spatial-spectral binning prior to recording to disk. This 2x2 binning step is critically important for feasibility of spectral resampling. The trade-off is between a more expensive, higher-resolution detector array versus the ability to perform signal processing data correction as part of standard on-board calibration. Final analysis results are presented as RMS spectral error (microflicks) illustrating the degree to which spectral distortion can be mitigated as part of an on-board data processing chain.

9611-14, Session 4

Experimental measurement and analysis of wavelength-dependent properties of the BRDF

Samuel D. Butler, Stephen E. Nauyoks, Michael A. Marciniak, Air Force Institute of Technology (United States)

The Bidirectional Reflectance Distribution Function (BRDF) is a quantity relating reflected radiance to incident irradiance and is dependent on incident angle, outgoing angle, and wavelength. Popular BRDF models include the microfacet model and the more complex linear systems diffraction model. The microfacet model is preferred in many applications, as it is a closed form approximation to the BRDF that is relatively straightforward to use. However, the microfacet model has the disadvantage of excluding the wavelength scaling almost entirely, other than in a Fresnel term; this does not agree with experimental measurements of the BRDF. In this paper, HeNe, CO2, and tunable quantum cascade lasers were



used to measure the BRDF at multiple incident angles and for multiple materials at several wavelengths between 3.39 μm and 10.6 μm , using a Schmitt Industries Complete Angle Scatter Instrument*. These BRDF results are compared with microfacet models and a linear wavelength scaling approximation. Results from the BRDF measurements quantify the dramatic change in the specular peak and surrounding region for a variety of materials, even after accounting for differences in Fresnel reflectance as a function of wavelength, and even for surface reflecting materials such as nickel that are resistant to oxidation. These experimental results suggest that it is necessary to modify the microfacet probability distribution function as a function of wavelength, instead of only an overall linear wavelength scaling. These results are an important step toward applying the BRDF to hyperspectral remote sensing, where wavelength dependent attributes may affect the quality of material identification.

9611-15, Session 4

Comparative study of spectral diffuse-only and diffuse-specular radiative transfer models and field-collected data in the LWIR

Dimitar M. Stoyanov, Michael A. Marciniak, Air Force Institute of Technology (United States); Joseph Meola, Air Force Research Lab. (United States)

The sensitivity of hyper-spectral remote sensing to the directional reflectance of surfaces was studied using both laboratory and field measurements. Namely, the effects of the specular- and diffuse-reflectance properties of a set of eight samples, ranging from high to low in both total reflectance and specularity, on diffuse-only and diffuse-specular radiative transfer models in the long-wave infrared (LWIR, 7-14-micron wavelength) were studied. The samples were measured in the field as a set of eight panels, each in two orientations, with surface normal pointing toward zenith and tipped at 45° from zenith. The field-collected data also included down-welling spectral sky radiance at several angles from zenith to the horizon, ground spectral radiance, panel spectral radiances in both orientations, infragold® spectral radiances in both orientations near each panel location, and panel temperatures. Laboratory measurements included spectral hemispherical, specular and diffuse directional reflectance (HDR, SDR and DDR) for each sample for several reflectance angles with respect to the surface normal. The diffuse-only radiative transfer model used the HDR data, while the diffuse-specular model used the SDR and DDR data. Both calculated spectral reflected and self-emitted radiances for each panel, using the field-collected sky radiance data to avoid uncertainties associated with atmospheric models. The modeled spectral radiances were then compared to the field-collected values to quantify differences in moving from an HDR-based model to an SDR/DDR model in the LWIR for a variety of surface-reflectance types.

9611-16, Session 4

Snapshot spectral imaging for gas cloud sensing and quantification

Nathan A. Hagen, Robert T. Kester, Ryan P. Mallery, Rebellion Photonics (United States)

While the design and performance of snapshot spectral imaging systems have undergone steady development over the last two decades, it is only recently that these systems have begun to find use in commercial applications. In the case of gas cloud imaging, snapshot collection has converted an application that was previously too light starved to be commercially viable into one that has demonstrated commercial success. We provide a summary of gas cloud imaging, how the snapshot advantage transforms the problem, and provide examples of gas quantification measurements and gas cloud detection videos.

9611-17, Session 4

Improved modeling of multiple scattering in hyperspectral BRDF of coastal sediments

Charles M. Bachmann, Rochester Institute of Technology (United States)

Approximate solutions to the Radiative transfer equation for granular media have been developed [1]. To apply these models to coastal sediments, modifications are needed to account for observed phenomenology. Laboratory studies [2] using a hyperspectral goniometer in the principal plane demonstrate that the degree of optical contrast between coastal sand constituents determines whether these models accurately predict the observed bi-directional reflectance distribution function (BRDF) as geophysical parameters such as density are varied. In [2] highly contrasting constituents (translucent quartz and opaque magnetite) lead to greater reflectance as density decreased, exactly the opposite of what is observed for more uniform sand. Field measurements using a hyperspectral goniometer have demonstrated results consistent with the laboratory measurements [3] as well as with CASI-1500 airborne hyperspectral measurements. Our study uses a new highly portable hyperspectral goniometer, the Goniometer of the Rochester Institute of Technology (GRIT), that can be used in both field and laboratory settings to provide data to examine the validity of and propose alternatives to earlier model assumptions [1] concerning multiple scatter.

[1] B. W. Hapke, 2012. Theory of Reflectance and Emittance Spectroscopy, Second Edition. Cambridge, England: Cambridge University Press.

[2] C. M. Bachmann, W. Philpot, A. Abelev, D. Korwan, 2014. "Phase angle dependence of sand density observable in hyperspectral reflectance," Remote Sensing of Environment, 150:53-65, http://dx.doi.org/10.1016/j. rse.2014.03.024.

[3] C. M. Bachmann, A. Abelev, W. Philpot, K. Z. Doctor, M. J. Montes, R. Fusina, R.-R.- Li, E. van Roggen, 2014. "Retrieval of Sand Density from Hyperspectral BRDF," Proc. SPIE, Vol 9088, http://dx.doi. org/10.1117/12.2050682.

9611-18, Session 4

Determining the bilirubin concentration in bruises of human skin using spectral imaging

Marta Lange, Inga Saknite, Janis Spigulis, Univ. of Latvia (Latvia)

The aim of this research is to determine bilirubin concentration difference in the bruises of human skin, to estimate it in order to define when exactly the bruise was made or how old it is. It is very important aspect in forensic medicine where usually the assessment of the victim is done only with visual methods and experience by the medical doctor.

The instruments used in the study are multi-spectral camera and specially custom-made device with RGB optical radiation and later MatLab program to analyze the images of the bruises to assess bilirubin concentration in time.

The idea is based on the fact that image cube of the bruise is captured at different light wavelengths, taking into account that the bilirubin absorption peak is from 400..500 nm. Then the image stack is analyzed using an algorithm where the image of the healthy skin is used as a reference and the maps of chromophores of human skin: oxyhemoglobin, deoxyhemoglobin, melanin and bilirubin are calculated and imaged.

The acquired data gives a great investment in bilirubin concentration statistical estimation, taking into account that more than 400 images of bruises were taken and analyzed of various parts of the body where the properties of bruising differ. After the analysis it is possible to conclude the age of the bruise.

This research mainly will benefit forensic medicine where currently in Latvia



the only non-invasive method for bruise assessment is the visual assessment method by the medical doctor or an expert.

9611-19, Session 4

A comparative study of three vision systems for metal surface defect detection

Mehrube Mehrübeoglu, Petru-Aurelian Simionescu, Shawn Robinson, Texas A&M Univ. Corpus Christi (United States); Lifford McLauchlan, Texas A&M Univ.-Kingsville (United States)

Identifying metal surface defects requires technologies that can detect surface anomalies while maintaining the parts intact. We present a comparative analysis of three vision systems to predict defects on the surfaces of aluminum castings: a hyperspectral imaging system, thermal imager, and digital color camera have been used to inspect the metal surfaces. Hyperspectral imaging provides both spectral and spatial information. Each material produces specific spectral signatures which are also affected by surface texture. The thermal imager detects infrared radiation whereby hotspots can be investigated to identify possible trapped inclusions close to the surface, or other superficial defects. Finally, digital color images show apparent surface defects that can also be viewed with the naked eye but can be automated for fast and efficient data analysis. The surface defect locations are analyzed and predicted using the three systems, and verified by tensile testing. Tensile testing results in the breakage of the aluminum castings, thus identifying the defective or weakest areas in the metal. This paper provides a comparative analysis of results and benefits of the three technologies.

9611-20, Session 4

Relating water absorption features to soil moisture characteristics

Jia Tian, William Philpot, Cornell Univ. (United States)

Spectral reflectance of three soil samples – selected to represent a range of particle size distribution, texture, and drying characteristics – was monitored as the samples progressed from fully saturated to air dry. Band depths of water absorption features in the near and shortwave infrared were then used as indicators of the surface water content. The change in band depth at 1930 nm reached a maximum coincident with the transition from a constant to a slowing evaporation rate and coincided with a trace amount of water in the pore spaces, consistent with the transition in drying rates.

9611-21, Session 4

Application of imaging spectrometer in gas analysis by Raman scattering

Duluo Zuo, Anlan Yu, Zhe Li, Xingbing Wang, Huazhong Univ. of Science and Technology (China); Youhui Xiong, Wuhan Cubic Optoelectronics Co., Ltd. (China)

Spontaneous Raman scattering is an effective technique in the analysis of gas composition, but the detection of minor components is difficult because of the low signal level and the usually existed background. Imaging spectrometer can provide highly spatial resolved spectra, so it should be much easier to pick up Raman signal of minor components from the Raman/fluorescence background of the sample cell and transporting optics compared with the widely used fiber-coupled spectrometers. For this reason, an imaging spectrometer was constructed from transmitting volume holographic gratings, camera lens and CCD detector. When it was used to analyze the gas sample in silver-plated capillary, which is a sample cell believed with 100-fold higher enlargement of Raman signal, the background was compressed obviously. When it was used to analyze the gas sample in a sample cell including a parabolic reflector, only weak background signal was observed, as the wide separation between the gas-signal-collecting area (the focus spot of the detecting laser beam) and the wall of sample cell benefitted in the analysis by imaging spectrometer. By using the last sample cell, the signal from CO2 in ambient air can be observed in an exposure time less than 200 sec, and the signal from minor gas component in the level of 10 ppm can also be observed in a longer exposure. These results show that an imaging spectrometer paired with a well-arranged sample cell will lower the detecting limit effectively.

9611-22, Session 5

Predicted and measured properties of single-blaze and dual-blaze diamond-ruled Offner gratings for VIS-SWIR

Mohammad A. Saleh, Patrick Woodman, Lovell E. Comstock, Richard L. Wiggins, Corning Incorporated (United States)

The Offner spectrograph is a popular choice for hyperspectral imaging systems because of its wavelength simultaneity, excellent spatial-spectral resolution, ruggedness, and unmatched reproducibility. The quality of the data from Offner spectrographs is highly dependent on the quality of the convex diffraction grating. The grating is the primary driver of optical transmission, spectral resolution, and signal linearity. Mechanical ruling, holography, and e-beam lithography have all been used in attempts to make Offner gratings with ideal merit functions.

We relate the Offner optical transmission to the grating groove profile and optical coating. We examine theoretical diffraction efficiency for single-blazed, dual-blazed and phase-step gratings and compare to as-manufactured groove profiles and grating diffraction efficiency measurements from Corning's grating test stations. We present data for both aluminum and protected silver coatings. Coating reliability data is included.

We connect signal linearity to the surface figure and finish of the grating. Data includes surface roughness measurements, figure measurements, and the measured optical scatter transfer function. Data from dual-blaze and single blaze gratings is compared.

9611-23, Session 5

Standing wave integrated Fourier transform spectrometer for imaging spectrometry in the near infrared

Gaël D. Osowiecki, Ecole Polytechnique Fédérale de Lausanne (Switzerland); Mohammadreza Madi, Edoardo Alberti, Micos Engineering GmbH (Switzerland); Toralf Scharf, Hans Peter Herzig, Ecole Polytechnique Fédérale de Lausanne (Switzerland)

We show the miniaturization and parallelization of a standing wave spectrometer with a long term goal of creating a compact imaging spectrometer. In our standing wave integrated Fourier transform spectrometer, light is injected with micro-lenses into several optical polymer waveguides having a mode field diameter of around 3-4 microns. A piezo actuated mirror located at the waveguide end-facet is completing the experimental setup. The spatial distribution of the standing wave intensity inside the waveguide is scattered out of the plane by a periodic metallic grating located in the evanescent field of the wave. Electron beam lithography is used for the fabrication of these metallic scattering elements. The periodic metallic grating is imaged with a CCD camera which is recording a sampled intensity of the standing wave. By moving the mirror at the end of the waveguide the sampling frequency of the intensity of the standing wave can be increased, thus a larger spectrum can be recorded. We show how this is achieved for six adjacent waveguides simultaneously at a wavelength of 794nm.



9611-24, Session 5

Straylight analysis of a hyperspectral spectrometer using non sequential ray tracing

Jinsuk Hong, Samsung Thales Co., Ltd. (Korea, Republic of)

The designed hyperspectral spectrometer consists of two spectral channels, which are VNIR and SWIR. Both of the channels share same entrance slit, beam splitter and fore optics. Due to the co-registration requirement of the system, Slit length and width are slightly different according to the channel. Also, manufactured grating also can generate unwanted ray path. We investigate the straylight effect to evaluate the possibility to degrade the system performance. We confirmed the straylight effect and designed the baffle to minimize the effect.

9611-25, Session 5

Bae systems small form factor long wave infrared hyperspectral imager

John MacEachin, Michael J. Russo, BAE Systems (United States)

BAE Systems has developed a Small Form Factor (SFF) Long Wave Infrared (LWIR) Hyper-Spectral Imager (HSI). The Offner-based imager, developed through Internal Research and Development (IRAD) funding, incorporates design features that result in a substantially reduced Size, Weight, Power and Cost (SWAP-C) system that can be hosted on a wide variety of platforms. Predicted performance of the environmentally robust system is comparable to the most advanced LWIR HSI systems operating today and is achieved through a careful design approach. The optics project a nearly spatial and spectral distortion-free image onto a specially-designed Focal Plane Assembly (FPA). In addition, the mechanical configuration effectively limits background emission from noise sources, crucial to imaging in spectral clutter-limited conditions, yet avoids being overly complex as some competing technologies.

9611-26, Session 5

Smart CMOS sensor for wideband laser threat detection

Craig R. Schwarze, OPTRA, Inc. (United States); Sameer Sonkusale, Tufts Univ. (United States)

The proliferation of lasers has led to their widespread use in applications ranging from short range standoff chemical detection to long range Lidar sensing and target designation operating across the UV to LWIR spectrum. Recent advances in high energy lasers has renewed the development of laser weapons systems. The ability to measure and assess laser source information is important to both identify a potential threat as well as determine safety and nominal hazard zone (NHZ). Laser detection sensors are required that provide high dynamic range, wide spectral coverage, pulsed and continuous wave detection, and large field of view. OPTRA, Inc and Tufts have developed a custom ROIC smart pixel imaging sensor architecture and wavelength encoding optics for measurement of source wavelength, pulse length, pulse repetition frequency (PRF), irradiance, and angle of arrival. The smart architecture provides dual linear and logarithmic operating modes to provide 8+ orders of signal dynamic range and nanosecond pulse measurement capability that can be hybridized with the appropriate detector array to provide UV through LWIR laser sensing. Recent advances in sputtering techniques provide the capability for postprocessing CMOS dies from the foundry and patterning PbS and PbSe photoconductors directly on the chip to create a single monolithic sensor array architecture for measuring sources operating from 0.26 - 5.0 microns, 1 mW/cm2 - 2 kW/cm2.

9611-27, Session 5

Propagation of spectral characterization errors of imaging spectrometers at level-1 and its correction within a level-2 recalibration scheme

Jorge Vicent, Neus Sabater, Univ. de València (Spain); Christophe Miesch, Airbus Defence and Space (France); Stefan Kraft, European Space Operations Ctr. (Germany); Jose Moreno, Univ. de València (Spain)

The uncertainties in the knowledge of the Instrument Spectral Response Function (ISRF), barycenter of the spectral channels and bandwidth / spectral sampling (spectral resolution) are important error sources in the processing of satellite imaging spectrometers within the narrow atmospheric absorption bands. The exhaustive laboratory spectral characterization is a costly engineering process that differs from the instrument configuration in-flight given the harsh space environment and harmful launching phase. The retrieval schemes at Level-2 commonly assume a Gaussian ISRF, leading to uncorrected spectral stray-light effects and wrong characterization and correction of the spectral shift and smile. These effects produce inaccurate atmospherically corrected data and are propagated to final Level-2 mission products. Within ESA's FLEX satellite mission activities, we have analyzed the impact of the ISRF knowledge error and spectral calibration at the Level-1b products and its propagation to the Level-2 retrieved chlorophyll fluorescence. A spectral recalibration scheme has been implemented at Level-2 reducing the spectral calibration errors in the Level-1b products down to 1-2% within the Oxygen absorption bands and enhance the quality of the retrieved products. The work presented here will show how the minimization of the spectral calibration errors requires an effort both from the laboratory characterization and from the implementation of specific algorithms at Level-2.

9611-28, Session 5

The CHROMA focal plane array: a largeformat, low-noise detector optimized for imaging spectroscopy

Bradley Jones, Steven G. Bernd, Jason Herring, Jianmei Pan, Ryan S. Ries, Brian Starr, Donald L. Lee, James W. Beletic, Teledyne Imaging Sensors (United States); Elliott Liggett, Jet Propulsion Lab. (United States)

The CHROMA (Configurable Hyperspectral Readout for Multiple Applications) is an advanced Focal Plane Array (FPA) designed for visibleinfrared imaging spectroscopy. CHROMA has been delivered for use in several airborne imaging spectroscopic instruments and is planned in many instrument and mission proposals. CHROMA has a pixel pitch of 30 microns and is available in array formats ranging from 320?480 to 1600?480 pixels with a range of full well sizes that allow CHROMA to be used for VSWIR, MWIR and LWIR applications. Users typically install CHROMA in pushbroom slit spectrographs and disperse spectra down the 480 pixel-length columns with the cross-scan (spatial) direction spread over the n?160 pixel-length rows, where n=2, 4, 8, 10. The CHROMA readout integrated circuit (ROIC) has correlated double sampling (CDS) in pixel, and generates its own internal bias signals and clocks. There is one analog output port, operating at 10 MHz, for every 160 columns of the array. The full frame (480 rows) readout rate is 125 Hz with 250 Hz frame rate achieved for the 240 row readout that is typical of VSWIR applications.

This paper presents the latest performance results of the CHROMA array including results of recent radiation tests. In addition, the paper will discuss progress made in additional features including: FPA (focal plane array) packaging, linear variable anti-reflection (LVAR) coating, lower noise focal plane electronics, and the potential of a future digital CHROMA with analog-to-digital converters (ADCs) on-chip.



9611-29, Session 5

Advanced space Cryocoolers for imaging spectrometry

Ted Conrad, Brian Schaefer, Lowell A. Bellis, Ryan Yates, Michael Barr, John F. Silny, Raytheon Space and Airborne Systems (United States)

Over the last several years, Raytheon has made significant advances on two long-life cryocoolers suitable for future imaging spectrometer missions. The first is the Low-Temperature Raytheon Stirling / Pulse Tube 2-stage (LT-RSP2) hybrid cryocooler, which is capable of providing simultaneous cooling at 55 K and 10 K nominal first and second stage temperatures. The LT-RSP2 also has the unique ability to shift cooling capacity between its stages, allowing it to adjust to changing load conditions and independently control both of its stage temperatures without hardware modifications or the addition of trim heat. The second cryocooler is the Raytheon Advanced Miniature (RAM) cryocooler, a robust single stage pulse tube cooler intended for VNIR and SWIR focal planes. It is an efficient, compact and robust cryocooler designed for long life and low exported vibration. Additionally, it incorporates mechanical, thermal, and electrical interfaces specifically designed to ease integration into optomechanical systems. In this paper, aspects of both the LT-RSP2 and RAM mechanical and thermodynamic designs will be presented as well as information regarding their capabilities and performance.

9611-30, Session 6

Measurement and modeling of longwave infrared directional downwelling spectral radiance

Nathan P. Wurst, Joseph Meola, Air Force Research Lab. (United States); David L. Perry, General Dynamics Corp. (United States)

Exploitation of longwave infrared hyperspectral imagery often requires atmospheric compensation (AC) in order to retrieve intrinsic material emissivity properties. For materials possessing subtle spectral features and those with lower emissivity, downwelling radiance plays an important role in the atmospheric compensation process. Most AC algorithms use an estimate of the total downwelling radiance integrated over the hemisphere. However, for tilted surfaces and non-nadir imaging scenarios, directional downwelling radiance information may be required. This work examines collection of directional downwelling radiance measurements using a Fourier transform infrared (FTIR) spectrometer. Specifically, work is done to determine a minimum number of angles to measure for which the remainder of the directional estimates can be estimated with minimal error through the use of simple data fitting models.

9611-31, Session 6

Nonnegative matrix factorization for efficient hyperspectral image projection

Alexander S. Iacchetta, James R. Fienup, Univ. of Rochester (United States); David T. Leisawitz, Matthew R. Bolcar, NASA Goddard Space Flight Ctr. (United States)

Hyperspectral imaging for remote sensing has prompted development of hyperspectral image projectors that can characterize hyperspectral imaging cameras and techniques in the lab. One such emerging astronomical hyperspectral imaging technique is wide-field double-Fourier interferometry. NASA's current state-of-the-art, wide-field imaging interferometry testbed (WIIT) has been characterized by NASA's calibrated hyperspectral image projector (CHIP), but test scenes of complicated polychromatic astronomical sources have yet to be measured with WIIT, needed to provide a more complete understanding of wide-field double-Fourier interferometry. Given enough time, CHIP can precisely synthesize a projected field containing numerous spectrally varying targets; however, it would require a very lengthy data collection process. For accurate but time-efficient projection of complicated hyperspectral images with CHIP, the field must be decomposed both spectrally and spatially in a way that provides a trade-off between accurately projecting the image and the duration of data collection. We apply nonnegative matrix factorization (NMF) to decompose hyperspectral astronomical fields into so-called eigenspectra and eigenimages that allow time-efficient projection with CHIP. Included is a brief analysis of NMF parameters that affect accuracy, including the number of eigenspectra and eigenimages used to approximate the hyperspectral image to be projected. For the chosen field, the normalized mean squared synthesis error is under 1% with just 8 eigenspectra. NMF of hyperspectral astronomical fields better utilizes CHIP's capabilities, providing time efficient and accurate representations of astronomical scenes to be imaged with WIIT.

9611-32, Session 7

Comparison of hyperspectral change detection algorithms

Michael L. Pieper, Dimitris G. Manolakis, MIT Lincoln Lab. (United States); Thomas W. Cooley, Air Force Research Lab. (United States); Michael S. Brueggeman, Andrew J. Weisner, John Jacobson, National Air and Space Intelligence Ctr. (United States)

There are a multitude of civilian and military applications for the detection of anomalous changes in hyperspectral images. Anomalous changes occur when the material within a pixel is replaced. Environmental factors that change over time, such as illumination, will affect the radiance of all the pixels in a scene, despite the materials within remaining constant. The goal of an anomalous change detection algorithm is to suppress changes caused by the environment, and find pixels where the materials within have changed.

Anomalous change detection is a two-step process. Two co-registered images of a scene are first transformed to maximize the overall correlation between the images, and then an anomalous change detector is applied to the transformed images. The transforms maximize the correlation between the two images to attenuate the environmental differences that distract from the anomalous changes of importance. Several categories of transforms with differing optimization parameters are discussed and compared.

We apply one of two types of anomalous change detectors to the transformed images. The first anomaly (AD) uses the difference of the two transformed images. The second concatenates the spectra of two images and uses an aggregated AD. A comparison of the two anomaly detection methods and their effectiveness with the different transforms is done for the first time.

9611-33, Session 7

Ultrafast high accuracy radiative transfer modeling of cloudy atmosphere in solar spectral region

Qiguang Yang, Xu Liu, NASA Langley Research Ctr. (United States); Wan Wu, Science Systems and Applications, Inc. (United States); Ping Yang, Chenxi Wang, Texas A&M Univ. (United States)

An ultrafast radiative transfer model has been developed at NASA Langley research center for simulating the radiance and relfectance at top of atmosphere (TOA). Both thermal and solar contributions are included in our model in the wavenumber range from 1800 cm-1 to 3000 cm-1. We are expanding our results to visible and UV wavelength range. The scattering properties of the cloud have been obtained using 52-stream DISORT and stored in a 3.3 GB lookup table (LUT) and three smaller LUTs. To efficiently



use these data we compressed them to less than 1% of its original size using our recently proposed algorithm. These very small LUTs were used to simulate the radiance detected by satellite. Billions of simulations indicate that the accuracy in the TOA reflectance is excellent. Compared to 52-stream DISORT, 93.3% of the over one billion off grid cases have an error in TOA reflectance smaller than 0.001. The maximum error of 0.0337 occurred at the back scattering direction. The simulation is ultrafast, it takes only about 6 ms to simulate the infrared atmospheric sounding interferometer (IASI) radiance data from 645 cm-1 to 2760 cm-1 at fixed solar and satellite angles. The solar part alone takes only 0.52 ms. The high accuracy as well as the ultrafast nature of our algorithm make it very useful for hyperspectral remote sensing.

9611-34, Session 7

Phase correction algorithms for a snapshot hyperspectral imaging system

Victoria C. Chan, The Univ. of Arizona (United States); Michael W. Kudenov, North Carolina State Univ. (United States); Eustace L. Dereniak, The Univ. of Arizona (United States)

We present image processing algorithms that improve spatial and spectral resolution on the Snapshot Hyperspectral Imaging Fourier Transform (SHIFT) spectrometer. A 10x10 lenslet array superimposes a two-dimensional (2D) interferogram onto 100 sub-images of the scene. By arranging the sub-images in increasing optical path difference, a threedimensional (3D) interferogram cube is formed. Phase corrections are applied to the interferogram cube. Final measurements are stored in a 3D datacube containing the scene's spatial and spectral information. We discuss calibration procedures, review post-processing methods, and present preliminary results from proof-of-concept experiments.

9611-35, Session 7

Characterizing intimate mixtures of materials in hyperspectral imagery with albedo-based and kernel-based least squares and approaches

Robert S. Rand, Ronald G. Resmini, National Geospatial-Intelligence Agency (United States); David W. Allen, National Institute of Standards and Technology (United States)

Linear mixtures of materials in a scene often occur because the pixel size of a sensor is relatively large and consequently they contain patches of different materials within them. This type of mixing can be thought of as areal mixing and modeled by a linear mixture model with certain constraints on the abundances. However, there are more complex situations, such as scattering that occurs in mixtures of vegetation and soil, or intimate mixing of granular materials like soils. Such multiple scattering and microscopic mixtures within pixels have varying degrees of non-linearity. Often enough, scenes may contain cases of both linear and non-linear mixing on a pixelby-pixel basis. This study considers two approaches for un-mixing pixels in a scene. The methods are motivated by earlier studies that indicate non-linear mixtures in reflectance space are approximately linear in albedo space. The first method converts reflectance to single-scattering albedo (SSA) according to Hapke's theory assuming bidirectional scattering at nadir look angles and uses a constrained linear model on the computed albedo values. The second method is motivated by the same idea, but uses a kernel that seeks to capture the linear behavior of albedo in non-linear mixtures of materials. The behavior of the kernel method is dependent on the value of a parameter, gamma. Both methods are dependent on the endmembers and on error metrics. This study compares the two approaches and pays particular attention to these dependencies. Both laboratory and aerial collections of hyperspectral imagery are used to validate the methods.

9611-36, Session 7

Improved atmospheric retrievals of hyperspectral data using geometric constraints

Kenneth Ewald, Ball Aerospace & Technologies Corp. (United States); Emmett J. lentilucci, Rochester Institute of Technology (United States); John Jacobson, National Air and Space Intelligence Ctr. (United States); Alan T. Buswell, Ball Aerospace & Technologies Corp. (United States)

Under complex illumination conditions, such as urban environments or targets along a tree line, LIDAR data can be used to improve hyperspectral surface reflectance retrievals by accounting for per-pixel geometric effects, such as shadowing, surface tilt, and partial sky occlusions. The impact of individual surface illumination factors, including atmospheric transmission, path radiance, and direct solar and downwelled sky radiance, can vary based on a pixel's geometry. Therefore, it is important to accurately estimate each atmospheric term used to convert calibrated radiance to surface reflectance when including geometric effects in retrievals. This paper discusses techniques to use in-scene radiance data and LIDAR scene geometry to iterate on atmospheric parameters for improved reflectance retrievals using MODTRAN.

A Lambertian material's reflectance is invariant to illumination changes across the scene. Therefore, any instance of that material's retrieved reflectance should be equivalent when atmospheric and geometric considerations are properly taken into account. When incorrect atmospheric parameters are applied, the same material will exhibit differences in retrieved reflectance as a function of illumination. This is an important consideration, as requiring the reflectance of similar materials to be equivalent provides an additional constraint on which to solve for individual atmospheric parameters. These parameters can be iterated upon until the difference between the retrieved reflectivity for a material found under multiple unique illumination conditions is minimized. The overall improvements in retrieved reflectance will be evaluated, and the impacts of scene geometry assumptions and uniqueness of solution for the retrieved optimal atmospheric parameters will be investigated.

9611-37, Session 7

Hyperspectral band selection using the total dependence metric

Seyed Enayat Hosseini Aria, Massimo Menenti, Ben Gorte, Technische Univ. Delft (Netherlands)

One of the objectives of dimensionality reduction of hyperspectral images is to minimize the dependency among a selected bandset. It means that from a hyperspectral dataset a number of bands should be selected in such a way that a new bandset has the least redundant information. Band selection techniques, despite the feature extraction ones, prevent the original data from being compromised or distorted by a transformation such as PCA. However, the problem of selecting the most independent bands is the lack of a unique metric revealing the dependency in hyper-dimensional spaces. The common way for the selection is to compute the dependence between each pair of bands, making a dependency matrix, categorizing the bands, and selecting a representative band from each category. Eventually, as there has been no single metric to show the most independent bandset so far, classification accuracy has been used to assess the independent bandsets.

In this paper, a newly developed metric of dependency in hyper-dimensional spaces is introduced to show which band selection technique determines the best independent bandset. This measure, named Total Dependence (TD), is a function of the greatest eigenvalue derived from the absolute correlation matrix of the original dataset. Using TD, it is feasible to compare different bandsets with respect to dependence. In addition to the comparisons, TD is also used to select a bandset with the lowest dependence. Primary results over a hyperspectral vegetation scene show five selected bands using TD has much lower dependence than a well-known band selection method.



9611-38, Session 7

A novel anomaly detection approach based on clustering and decision-level fusion

Shengwei Zhong, Ye Zhang, Harbin Institute of Technology (China)

In hyperspectral image processing, anomaly detection is a valuable way of searching targets whose spectral characteristics are not known, and the estimation of background signals is the key procedure. On account of the high dimensionality and complexity of hyperspectral image, dimensionality reduction and background suppression is necessary. In addition, the complementarity of different anomaly detection algorithms can be utilized to improve the effectiveness of anomaly detection. In this paper, we propose a novel method of anomaly detection, which is based on clustering of Artificial Searching Swarm Algorithm (ASSA) and decision-level fusion. In our proposed method, bands with similar features are firstly clustered using the optimized k-means method based on ASSA. Secondly, dimensionality reduction is conducted using principle component analysis to reduce the amount of calculation. Then, to increase the accuracy of detection and decrease the false-alarm ratio, both Reed-Xiaoli (RX) and Kernel RX algorithm are used on processed image. Lastly, a decision-level fusion is processed on the detection results. A simulated hyperspectral image and a real hyperspectral one are both used to evaluate the performance of our proposed method. Visual analysis and quantative analysis of receiver operating characteristic (ROC) curves show that our algorithm can achieve better performance when compared with other classic approaches and state-of-the-art approaches.

9611-39, Session 7

An improved full automated endmember extraction algorithm based on endmember independence

Yiran Wang, Shengwei Zhong, Ye Zhang, Harbin Institute of Technology (China)

Current algorithms of endmember extraction generally need to determine the number of endmembers manually. However, the number of endmembers is unknown in practical application, so an automated and iterative endmember extraction algorithm is put forward in this paper to solve the problem. Firstly, due to the spectral information of endmember is similar with its neighbors but noise is independent with others, we analyze the relevance between pixels and endmember in the concentric sliding window centered at each test endmember in order to eliminate the influence of noise. Then, due to the independence among endmembers, a candidate set formed of endmembers which have been extracted is constructed. We compute the correlation between the new endmember and the candidates in the set each time, if the largest correlation is small; the new one is added to the set. If the new one fails to join the set directly, we can take it to replace the existed in the set to increase the distance among endmembers. Finally, if the endmembers in the set remain unchanged in a few times, the iteration stops. The experiment shows that the improved algorithm have a near accuracy of endmember extraction with the traditional algorithm, meanwhile it weakens the influence of noise on the endmember extraction.

9611-40, Session PWed

Random projection-based dimensionality reduction method for hyperspectral target detection

Weiyi Feng, Nanjing Univ. of Science and Technology (China)

Dimensionality reduction is a frequent preprocessing step in hyperspectral

image analysis. High-dimensional data will cause the issue of the "curse of dimensionality" in the applications of hyperspectral imagery. In this paper, a dimensionality reduction method of hyperspectral images based on random projection (RP) for target detection was investigated. In the application areas of hyperspectral imagery, e.g. target detection, the high dimensionality of the hyperspectral data would lead to burdensome computations. Random projection is attractive in this area because it is data independent and computationally more efficient than other widelyused hyperspectral dimensionality-reduction methods, such as Principal Component Analysis (PCA) or the maximum-noise-fraction (MNF) transform. In RP, the original high-dimensional data is projected onto a low dimensional subspace using a random matrix, which is very simple. Theoretical and experimental results indicated that random projections preserved the structure of the original high-dimensional data quite well without introducing significant distortion. In the experiments, Constrained Energy Minimization (CEM) was adopted as the target detector and a RPbased CEM method for hyperspectral target detection was implemented to reveal that random projections might be a good alternative as a dimensionality reduction tool of hyperspectral images to yield improved target detection with higher detection accuracy and lower computation time than other methods.

9611-41, Session PWed

Analysis of active oxygen species kinetics

Andrey Pershin, Samara State Aerospace Univ. (Russian Federation)

Reactive oxygen species play an important role in atmospheric processes, combustion in oxygen plasma, into the active environments of lasers, etc. Pulse laser photolysis of ozone used for the electronically excited molecular oxygen, oxygen atoms and vibrationally excited ozone is often. In post-photolysis zone runs a lot of chemical and energy exchange processes involving reactive oxygen species. The paper is composed kinetic scheme of these processes and the related system of nonlinear differential equations. Obtained by both analytical and numerical solutions of the equations, which are in good agreement with the experimental dependences. The ratio of the reaction channel to a relaxation for the reaction of vibrationally excited ozone and atomic oxygen.

9611-42, Session PWed

Development and testing of an imageguided FT-IR Instrument for field spectroscopy

Xiaobing Dai, State Key Lab. for Multi-Spectral Information Processing Technologies (China) and Huazhong Univ. of Science and Technology (China); Xiangyan Liu, Huazhong Univ. of Science and Technology (China)

Standoff detection, identification and guantification of chemicals require sensitive spectrometers with calibration capabilities. We have developed a compact novel instrument that can not only provide imaging capability, bust also one that provides spectral capability of the field of view (FOV) center under the image-guided. The system employs a Fourier transform infrared (FT-IR) spectrometer, coupled with chalcogenide glass optical fiber, and a specially designed infrared optic lens. A special kit provided by Bruker Optics is connected on the spectrometer to focus the infrared beam from the lens at the entry of the fiber. Its spectral range covers the infrared band from 1870cm-1 to 5000cm-1 and its spectral resolution could be chosen among five selected values 1, 2, 4, 8, 16, 32cm-1. This paper will address the issues of image-guided spectroscopy and will show how an instrument designed for specifically imaging applications can dramatically improve the performance of the system and quality of the data acquired. The benefit of these technologies in spectroscopy can be demonstrated with a system optimally designed for detecting spectral characteristics of moving targets.

Conference 9612: Lidar Remote Sensing for Environmental Monitoring XV



Wednesday - Thursday 12-13 August 2015

Part of Proceedings of SPIE Vol. 9612 Lidar Remote Sensing for Environmental Monitoring XV

9612-19, Session PWed

Parameterization of a geometrical reaction time model for two beam nacelle LIDARs

Thorsten Beuth, Maik Fox, Wilhelm Stork, Karlsruher Institut für Technologie (Germany)

The reaction time model is briefly reintroduced as published in a previous publication to explain the restrictions of detecting a horizontal homogenous wind field by two beams of a LiDAR placed on a wind turbine's nacelle that measure the line-of-sight velocity v_l and v_r in the distance l_m between an opening angle of 2?. The wind vector length V and wind angle ? can be reconstructed by ?=arctan?((f-1)/((f+1) tan??)) and $V=\sqrt{(u^2+v^2)}$ with the relationship between the measured wind speeds $f=v_l/v_r$ and the orthogonal components $u=(v_l+v_r)/(2\cos??)$ and $v=(v_l-v_r)/(2\sin??)$. In the model, the distance I_r is estimated as the minimum distance that a homogenous wind front with an angle of ? in comparison to the yaw angle has to travel between the second measuring point of a two beam nacelle LiDAR and the tip of the rotor. In a next step, this model is parameterized to get more general statements for a beneficial system design concept. This approach is based on a parameterization towards the rotor disc radius R. All other parameters, whether they are distances like the measuring length I_m or velocities like the cut-out wind speed v_co, can be expressed by the rotor disc radius R. With the consideration of the measuring frequency of the system, the computation time of the controller and the actuator reaction time, an overall reaction time can be estimated. This reaction time leads to a minimum measurement distance that the LiDAR system has to have. In the end, the requirements are matched against the commercially available LiDARs to show the necessity to advance these systems to suit the upcoming challenges of gust regulation.

9612-1, Session 1

NASA's future earth science technology capabilities: challenges and opportunities (Keynote Presentation)

George J. Komar, NASA Headquarters (United States)

A decade of technology investments has contributed to the current missions and the measurements for Earth Science, and these investments are based upon active sensing technologies, such as lasers and radars. The mid and far term measurement concepts and the technology developments supporting the science measurement capabilities are highlighted.

9612-2, Session 2

Progress in developing the CO2 sounder Lidar as a candidate for the ASCENDS Mission (Invited Paper)

James B. Abshire, Haris Riris, NASA Goddard Space Flight Ctr. (United States); Graham R. Allan, Sigma Space Corp. (United States); Jeffrey R. Chen, Anthony W. Yu, Xiaoli Sun, NASA Goddard Space Flight Ctr. (United States); Anand K. Ramanathan, Univ. of Maryland, College Park (United States)

The lidar on NASA's planned ASCENDS mission will measure atmospheric CO2 and O2 column absorption and range, allowing calculation of the atmospheric CO2 mixing ratio needed for flux estimates. The lidar approach for ASCENDS will permit, for the first time, accurate atmospheric CO2 concentration measurements to be made globally over a wide range of

conditions. These include at night, at high latitudes during all seasons, through hazy and thin cloud conditions and to cloud tops. None of these are possible using passive sensors.

The CO2 Sounder team has made significant progress in developing of the CO2 Sounder approach and laser technology for the ASCENDS lidar. The team has demonstrated their airborne CO2 lidar on flights onboard the NASA DC-8 during 2010, 2011 and 2013. The results show that airborne measurements made in 2011 and 2013 were accurate to -1 ppm for airborne altitudes between 6 and 12 km. Analysis also highlighted a new capability to measure CO2 column absorption and range both to cloud tops and the ground. Differencing the retrievals allows estimating the CO2 in the column between the ground and cloud top, which allows a direct estimate of the CO2 concentrations in the boundary layer.

The project has demonstrated several key elements needed for the space lidar. A new step-locked laser diode source and a high power fiber laser preamplifier. The high power fiber preamplifier is based on an EDFA and has produced over 350 uJ/pulse at 1572 nm. A breadboard of a laser power amplifier using an initial planar waveguide gain element has been assembled. The goal for it is to produce the 2.7 mJ/pulse needed for space. Completion is planned for late spring 2015. A new HgCdTe APD detector also developed in collaboration with DRS RSTA. Testing shows it has photon counting sensitivity, analog response, high linear dynamic range and more sensitivity than the IR-PMT detector used previously.

For the 2014 airborne campaign, the CO2 Sounder team incorporated several of these capabilities into its airborne lidar. These include the step-locked laser source and HgCdTe APD detector. Airborne measurements of column CO2 and range were made over the California Central Valley, the redwood forests along the northern California coast, and above growing agriculture in Iowa. Two flights were also made under the OCO-2 satellite track. A summary of all these results will be presented.

9612-3, Session 2

Development of double and tripled-pulsed 2-micron IPDA Lidars for column CO2 measurement (*Invited Paper*)

Upendra N. Singh, Jirong Yu, Mulugeta Petros, Tamer F. Refaat, Ruben G. Remus, NASA Langley Research Ctr. (United States); Karl Reithmaier, Science Systems and Applications, Inc. (United States)

Carbon dioxide (CO2) is an important greenhouse gas that significantly contributes to the carbon cycle and global radiation budget on Earth. CO2 role on Earth's climate is complicated due to different interactions with various climate components that include the atmosphere, the biosphere and the hydrosphere. Although extensive worldwide efforts for monitoring atmospheric CO2 through various techniques, including in-situ and passive sensors, are taking place high uncertainties exist in quantifying CO2 sources and sinks. These uncertainties are mainly due to insufficient spatial and temporal mapping of the gas. Therefore it is required to have more rapid and accurate CO2 monitoring with higher uniform coverage and higher resolution. CO2 DIAL operating in the 2-?m band offer better near-surface CO2 measurement sensitivity due to the intrinsically stronger absorption lines. For more than 15 years, NASA Langley Research Center (LaRC) contributed in developing several 2-?m CO2 DIAL systems and technologies. This paper focuses on the current development of the airborne doublepulsed and triple-pulsed 2-?m CO2 integrated path differential absorption (IPDA) lidar system at NASA LaRC. This includes the IPDA system development and integration. Results from ground and airborne CO2 IPDA testing will be presented. The potential of scaling such technology to a space mission will be addressed.



9612-5, Session 2

Optical parametric technology for methane measurements

Martha W. Dawsey, NASA Goddard Space Flight Ctr. (United States); Kenji Numata, Univ. of Maryland, College Park (United States); Stewart T. Wu, Haris Riris, NASA Goddard Space Flight Ctr. (United States)

Atmospheric methane (CH4) is the second most important anthropogenic greenhouse gas, with approximately 25 times the radiative forcing of carbon dioxide (CO2) per molecule. Yet, lack of understanding of the processes that control CH4 sources and sinks and its potential release from stored carbon reservoirs contributes significant uncertainty to our knowledge of the interaction between carbon cycle and climate change.

At Goddard Space Flight Center (GSFC) we have been developing the technology needed to remotely measure CH4 from orbit. Our concept for a CH4 lidar is a nadir viewing instrument that uses the strong laser echoes from the Earth's surface to measure CH4. The instrument uses a tunable, narrow-frequency light source and photon-sensitive detector to make continuous measurements from orbit, in sunlight and darkness, at all latitudes and can be relatively immune to errors introduced by scattering from clouds and aerosols.

Our measurement technique uses Integrated Path Differential Absorption (IPDA), which measures the absorption of laser pulses by a trace gas when tuned to a wavelength coincident with an absorption line. We have already demonstrated ground-based and airborne CH4 detection using Optical Parametric Amplifiers (OPA) at 1651 nm using a laser with approximately 10 μ J/pulse. However, with our optical parametric oscillator (OPO), we were able to obtain 210 μ J/pulse at 5 KHz with a narrow linewidth. Next, we will upgrade our OPO system to add several more wavelengths in preparation for our September 2015 airborne campaign, and expect that these upgrades will enable CH4 measurements with 1% precision (10-20 ppb).

9612-6, Session 2

Single frequency pulsed and continuous wave fiber lasers near 2 micron wavelength (Invited Paper)

Shibin Jiang, AdValue Photonics, Inc. (United States)

Single-frequency pulsed and continuous wave (CW) lasers operating in the spectral region near 2?m are highly desirable for many applications, including airborne and space-borne coherent lidar for atmospheric sensing, and nonlinear frequency conversion for the generation of narrow-band mid-infrared radiation. Although high-power pulsed single-frequency Tm- or Ho-doped crystal lasers have been demonstrated decades ago, they suffer from a complicated free-space laser cavity design with a concern of its longterm reliability. Fiber-based laser sources are much more reliable and more suitable for these applications, especially for their field deployment.

In this paper we will present our demonstration of CW single frequency fiber laser with narrow linewidth using Tm doped and Tm/Ho-co-doped fibers, all-fiber Q-switched single-frequency laser oscillator near 2 micron, and modulated single frequency fiber lasers. Pulse energy of 0.5mJ and average power of 15W were demonstrated by using our innovative large mode field diameter polarization maintaining gain fibers, which enable many new applications.

9612-7, Session 2

Monolithic high power semiconductor seed lasers near 2.05 ?m

Mahmood Bagheri, Clifford Frez, Ryan Briggs, Siamak Forouhar, Jet Propulsion Lab. (United States) We report on the development and demonstration of a compact 2-µm semiconductor laser. Our monolithic fiber-pigtailed semiconductor seed laser will greatly enhance the operability and applicability of IPDA lidar systems for high spatial and temporal resolution CO2 airborne measurements as well as future Earth-orbiting CO2 measurement missions. The frequency agility and multi-format modulation capability of the proposed technology, its small size and compatibility with standard DFB lasers at the telecom band paves the way for adoption of the attractive 2.05 ?m CO2 band in the already demonstrated lidar systems operating at the 1.57 ?m band. Furthermore, the large tuning range of the proposed semiconductor laser (>150 GHz), and their high speed modulation capability at moderate power consumption (<2 W) would enable unprecedented high vertical range-finding resolution on lidar systems and would greatly enhance the performance of current lidar systems operating at 2.05 ?m that utilize solid-state crystal lasers.

The large mode-hop free tuning range of these lasers covers multiple CO2 absorption lines. The current tuning capability enables a variety of high-speed frequency sequencing and switching formats. This is important for high precision CO2 lidar measurement schemes that require near-simultaneous measurements at multiple wavelengths in the vicinity of the target absorption line in order to infer column CO2 concentration.

9612-8, Session 3

Laser transmitter development for NASA's Global Ecosystem Dynamics Investigation (GEDI) Lidar (Invited Paper)

Donald B. Coyle, Paul R. Stysley, NASA Goddard Space Flight Ctr. (United States); Demetrios Poulios, Greg B. Clarke, Richard B. Kay, American Univ. (United States)

The Global Ecosystems Dynamics Investigation (GEDI) Lidar, to be installed aboard the International Space Station in early 2018, will use 3 NASA-developed laser transmitters to produce 14 parallel tracks of 25 m footprints on the Earth's surface. The High Output Maximum Efficiency Resonator (HOMER) diode pumped Nd:YAG laser is an oscillator-only design, producing 17 mJ pulses at 240 Hz with TEM00 12 ns pulses. The unstable resonator uses gaussian optics and thermal lensing compensation to achieve an aperture-free, TEM00 cavity with a side pumped zigzag Nd:YAG slab, typical in amplifier staging but not 4W oscillators. This basic concept allowed us to high efficiency and long lifetime, while keeping complexity and costs down. Also critical to the HOMER laser success is the minimal part count, high diode derating and low intracavity fluence. Achieving a long duration laser instrument is a GEDI priority and has been the focus of numerous efforts over the years. The 3 HOMER lasers will be used in combination with active electro-optic transmit beam dithering and diffractive optics to achieve the 16 Billion laser footprint pattern on the Earth. We were careful to keep the risk low by using only high TRL (technology readiness level) components and technologies where ever possible, and worked extensively to remove opto-mechanical distortions from impacting the relatively long (40 cm) cavity. Even with access to the Japanese Experiment Module (JEM) liquid cooling loop, the laser will see wide swings in temperatures, and thus, removing temperature dependent performance is a priority.

9612-9, Session 3

UV lifetime laser demonstrator for spacebased applications

Floyd E. Hovis, Michael Albert, Kent Puffenburger, Tom Schum, Fran Fitzpatrick, Slava Litvinovitch, Joe Rudd, Fibertek, Inc. (United States)

A long-lived UV laser is an enabling technology for a number of highpriority, space-based lidar instruments. These include a next generation cloud and aerosol lidar that incorporates a UV channel, a direct detection 3-D wind lidar, and an ozone DIAL system. In previous SBIR funded work

Conference 9612: Lidar Remote Sensing for Environmental Monitoring XV



we developed techniques for increasing the survivability of components in high power UV lasers and demonstrated improved operational lifetimes. In this Phase III ESTO funded effort we are designing and building a TRL 6 demonstrator that will have increased output power and a space-qualifiable package that is mechanically robust and thermally-stable. For full space compatibility, thermal control will be through pure conductive cooling. Contamination control processes and optical coatings will be chosen that are compatible with lifetimes in excess of 1 billion shots. The demonstration laser will incorporate a diode-pumped, single-frequency, Nd:YAG master oscillator and three diode pumped amplifier stages capable of providing over 250mJ per pulse of 1064nm light at 150Hz. The 1064nm output will be frequency tripled to provide greater than 100mJ pulses of 355nm light. After completing the laser module build in the second quarter of 2015 we will initiate lifetime, TVAC and vibration testing to demonstrate that the design is at TRL 6.

9612-10, Session 3

The cloud-aerosol transport system (CATS): a technology demonstration from the International Space Station (Invited Paper)

Matthew McGill, John Yorks, Stan Scott, NASA Goddard Space Flight Ctr. (United States); Andrew Kupchock, Patrick Selmer, Science Systems and Applications, Inc. (United States)

The Cloud-Aerosol Transport System (CATS) is a new instrument deployed to the International Space Station (ISS) in January 2015. The CATS instrument is a technology demonstration for laser remote sensing of clouds and aerosols. Utilizing high repetition rate lasers and photon-counting detectors, the CATS instrument is demonstrating multiple new technologies in-space. Measurements are downlinked via the near-continuous ISS communications links to be ingested in near-real time directly into aerosol forecast models.

Funded by the ISS Program as a demonstration of the operational science capability of the ISS, CATS is a low-cost approach to obtaining new science measurements while demonstrating new technologies. Development of CATS also served as a pathfinder for NASA, as it is the first NASA-developed payload for the Japanese Experiment Module-Exposed Facility (JEM-EF).

The ISS orbit is well suited to the science goals of CATS, as the ISS tracks over and along primary aerosol transport paths in the atmosphere. The science goals are to augment the CALIPSO data record for space-based lidar measurements, provide observational lidar data to improve operational aerosol models, and to demonstrate direct retrieval of aerosol extinction from space.

9612-11, Session 3

Fiber-based, carbon dioxide, laser transmitter development for space application

Mark A. Stephen, Anthony W. Yu, NASA Goddard Space Flight Ctr. (United States)

NASA's Goddard Space Flight Center (GSFC) is working on maturing the technology readiness of a laser transmitter designed for use in atmospheric CO2 remote-sensing. GSFC has been developing an airplane-based CO2 lidar instrument over several years to demonstrate the efficacy of the instrumentation and measurement technique and to link the science models to the instrument performance. The ultimate goal is to make space-based satellite measurements with global coverage. In order to accomplish this, we must demonstrate the technology readiness and performance of the components as well as demonstrate the required power-scaling to make the link with the required signal-to-noise-ratio (SNR). To date, all the instrument components have been shown to have the required performance with the

exception of the laser transmitter.

In this program we are working on a fiber-based MOPA laser transmitter architecture where we will develop a ruggedized package and perform the relevant environmental tests to demonstrate TRL-6. In this paper we will review our transmitter architecture and progress on the performance and packaging of the laser transmitter.

9612-12, Session 4

Lidar investigations of atmospheric dynamics and structure (Invited Paper)

C. Russell Philbrick, Hans D. Hallen, North Carolina State Univ. (United States)

Ground based lidar using Raleigh and Raman scattering, differential absorption (DIAL), and resonance fluorescence techniques are capable of providing unique signatures to study active atmospheric dynamical processes. Excellent measurements of structure in the lower atmosphere are available in time sequences of water vapor profiles from Raman and DIAL lidar. For example, water vapor profiles show the scale and motion of daytime convection cells, residual layer bursts into the planetary boundary layer (PBL), determine PBL height, study cloud formation and dissipation, observe scale size of gravity waves and turbulent eddies, as well as observe Brunt-Väisälä oscillations and Boer waves. Rayleigh lidar provide backscatter profiles in the troposphere show the PBL, but they provide more valuable temperature profiles in the stratosphere and mesosphere, where the gravity waves, stratospheric volcanic clouds and noctilucent clouds are observed. Resonance fluorescence lidar is able to profile temperature 80-100 km, and measure species concentration with resonance scattering signatures of meteoric dust metastable states deposited there, swept up by Earth's orbital motion. Lidar techniques provide the optimum technique for investigating atmospheric dynamics in atmospheric profile structure. Examples of several features forced by dynamical processes are selected to illustrate this and could be subjects for future focused investigations. Several future experiments are described that should improve our understanding of physical processes modifying atmospheric structure, determine the magnitudes of wavelike features, show the initiation of turbulence, and show other structure properties.

9612-13, Session 4

Two-component wind fields from single scanning aerosol lidar

Shane D. Mayor, Pierre Derian, Christopher F. Mauzey, California State Univ., Chico (United States)

An experiment was conducted in Chico, California, in 2013 and 2014 in order to quantify the accuracy and resolution of two-component vector wind fields resulting from the application of two motion estimation algorithms to image sequences from the REAL. A compact Doppler lidar was used to validate the remote wind estimates made by the REAL. The availability of good wind estimates at 100 m AGL in Chico is strongly correlated with the presence of coherent aerosol structures in the elastic backscatter data which is strongly linked to the diurnal cycle. In order to determine the maximum potential of the technique (in other words, the best it can do given the current state-of-the-art eye-safe elastic backscatter data), we restricted the analysis to the best 15 daytime periods containing abundant coherent aerosol features. From this data we computed 10-minute means for comparison with the Doppler lidar wind measurements and we computed spatial velocity power spectra from the velocity fields in order to estimate the filtering effect of the technique on small scale velocity perturbations. From this data subset, we found correlation coefficients with the Doppler lidar greater than 0.99. For spatial resolution, we assumed turbulent flow and a -5/3 power law dependence for velocity spectra. By comparing with the idealized spectra, we found the mean transfer function to equal 1 down to spatial scales of about 300 m. The mean transfer function rolls off towards smaller scales and is 0.88 at 205 m; 0.51 at 102 m; and 0.09 at 30 m



9612-14, Session 4

Optical autocovariance wind Lidar: aircraft test-flight history and current plans

Sara C. Tucker, Ball Aerospace & Technologies Corp. (United States)

To address mission risk and cost limitations the US has faced in putting a much needed Doppler wind lidar into space, Ball Aerospace and Technologies Corp, with support from NASA's Earth Science Technology Office (ESTO), has developed the Optical Autocovariance Wind Lidar (OAWL), designed to measure winds from aerosol backscatter at the 355 nm wavelength, although the system has recently been modified to also operate at 532 nm. Preliminary proof of concept hardware efforts started at Ball back in 2004. From 2008 to 2012, under an ESTO-funded Instrument Incubator Program, Ball incorporated the Optical Autocovariance (OA) interferometer receiver into a prototype breadboard lidar system by adding a laser, telescope, and COTS-based data system for operation at the 355 nm wavelength. In 2011, the prototype system underwent ground-based validation testing, and three months later, after hardware and software modifications to ensure autonomous operation and aircraft safety, it was flown on the NASA WB-57 aircraft. The history of the 2011 test flights are reviewed, including efforts to get the system qualified for aircraft flights, modifications made during the flight test period, and the final flight data results. We also present lessons learned and plans for the new, robust, twowavelength, aircraft system with flight demonstrations planned for Spring 2016

9612-15, Session 5

1 micron wavelength single frequency pulsed fiber lasers with mJ pulse energy

Shibin Jiang, AdValue Photonics, Inc. (United States)

Single-frequency pulsed lasers are widely used for fiber optical sensing, nonlinear frequency conversion, and coherent lidar applications. 1 micron wavelength is still the most popular one because of the availability of related components and the sensitivity of the detectors. Coherent lidar application, especially airborne and space-borne coherent lidar, requires a high pulse energy. Free-space solid state laser can offer high pulse energy, but the long-term reliability is one of the major drawbacks. Fiber-based laser sources are much more reliable and more suitable for these applications, especially for their field deployment, but the pulse energy is limited to a few hundred microjoules.

In this paper we will present our recent progress of high pulse energy single frequency fiber laser at 1 micron wavelength using our proprietary Ybdoped fibers. A polarization maintaining Yb-doped fiber with a large mode field diameter was developed to effectively suppress stimulated Brillouin scattering (SBS). A singe frequency narrow linewidth laser is modulated and amplified via MOPA configuration. A pulse energy of greater than 1mJ was demonstrated, which represents several times increase in pulse energy. Amplified fiber lasers with pulse width from 5ns to 400ns will be presented.

9612-16, Session 5

Comparison of aerosol backscatter and wind field estimates from REAL and SAMPLE

Shane D. Mayor, Christopher F. Mauzey, Paul Arpin, Shea Arceo, California State Univ., Chico (United States); Scott Higdon, Thomas Chyba, Darrell Ramsey, Spectral Sensor Solutions, LLC (United States)

The Raman-shifted Eye-safe Aerosol Lidar (REAL) at California State University Chico provides high signal-to-noise ratio elastic backscatter to several kilometers range from individual laser pulses as a result of transmitting energetic pulses (120 - 170 mJ/pulse) at a low pulse repetition frequency (10 Hz). It employs analog direct detection. This results in impressive aerosol imagery that can be used with motion estimation algorithms to deduce vector wind fields. However, the REAL is large (housed in a shipping container) thereby limiting deployment opportunities. As an alternative, the Scanning Aerosol Micro Pulse Lidar Eyesafe (SAMPLE), available through Spectral Sensor Solutions LLC, is compact and operates at the same 1.5 micron wavelength as the REAL. It is a photo-counting aerosol lidar transmitting 350 microjoule pulses at 15 KHz. At the time of this writing, a side-by-side experiment involving both the REAL and the SAMPLE is planned to be conducted in northern California in March of 2015. Results from the experiment will be presented.

9612-17, Session 5

Performance characterization of a pressure-tuned wide-angle Michelson interferometric spectral filter for high spectral resolution Lidar

Shane T. Seaman, Anthony L. Cook, Salvatore J. Scola, Chris A. Hostetler, NASA Langley Research Ctr. (United States)

High Spectral Resolution Lidar (HSRL) is typically realized using an absorption filter to separate molecular returns from particulate returns. NASA Langley Research Center has designed and built a Pressure-Tuned Wide-Angle Michelson Interferometer (PTWAMI) as an alternate means to separate the two types of returns. Absorption filters only work within certain resonance/absorption frequencies and suffer from low photon efficiency. An interferometric spectral filter can be designed for any wavelength of interest and has greater photon efficiency. The principal challenge in successfully using an interferometer as a spectral filter for HSRL in flight is that variations in temperature and pressure cause the interferometer's optical path difference to change considerably. Therefore, a tuning mechanism must be used to actively accommodate for these changes in optical path difference. The pressure-tuning mechanism employed here relies on changing the pressure in an air-filled arm of the interferometer to change the arm's refractive index, and therefore optical path length. However, tuning using pressure will not adjust for tilt, warpage, or thermally induced wavefront error, so the structural, thermal, and optical behavior of the device must be well understood and optimized prior to flight. The PTWAMI has been characterized for particulate contrast ratio, thermal tuning rate, thermal stabilization time, wavefront error, and tilt. The results from these characterizations will be presented, and their correlation with a Structural Thermal Optical Performance (STOP) model will also be discussed.



9612-18, Session 5

Multi-wavelength high efficiency laser system for Lidar applications

Christina C. Willis, Charles Culpepper, Ralph L. Burnham, Fibertek, Inc. (United States)

Motivated by the growing need for more efficient, high output power laser transmitters, we demonstrate a multi-wavelength laser system for lidarbased applications. The first stage of the system is a 1064 nm MOPA system which employs two novel ceramic Nd:YAG slab amplifiers, the structure of which is designed to improve the amplifier's thermal performance and energy extraction. Each slab has three stages of progressive Nd doping concentration. This structure enabled an extraction efficiency of 24.6%, which constitutes a 19% increase in overall extraction efficiency over previous designs. A maximum energy of 34 mJ was produced at 500 Hz with a 10.8 ns pulse duration. The second stage of the system is a non-linear conversion system which consists of a KTP ring OPO with a BBO intracavity doubler pumped with 16 ns 1064 nm pulses. The OPO generates 1571 nm signal and 3300 nm idler wavelengths. The ring cavity is designed to circulate the 1571 nm signal and double it to 756 nm with intra-cavity BBO crystal. The output 786 nm pulses are then mixed with the 1064 nm pump pulses to generate 452 nm pulses. The optical conversion efficiency of this process was 17.1%, generating 3 mJ of 452 nm pulses of 7.8 ns duration, and an M2 of < 1.7 in both axes. Pump power was limited by intra-cavity damage thresholds, and in future experiments we anticipated >20% conversion efficiency and greater pump energy.

Conference 9613: Polarization Science and Remote Sensing VII



Tuesday - Wednesday 11-12 August 2015 Part of Proceedings of SPIE Vol. 9613 Polarization Science and Remote Sensing VII

9613-1, Session 1

Polarizer-free degree of polarization computational imaging from a single speckle image

Julien Fade, Institut de Physique de Rennes (France); Muriel Roche, Institut Fresnel (France); Mehdi Alouini, Institut de Physique de Rennes (France)

Imaging of the degree of polarization (DOP) of the light backscattered by a scene can reveal contrasts invisible in conventional reflectance images. Standard DOP imaging techniques involve multiple image acquisitions through several configurations of polarization analyzers: 4 images for standard Stokes imaging setup, while simplified imaging schemes, such as Orthogonal States Contrast (OSC) imaging, involve only 2 image acquisitions. We recently theoretically investigated the performances of an alternative DOP estimation technique, based on a single image acquisition of a sample under coherent illumination, without requiring any polarization analyzing device at the reception. Relying on a local analysis of the speckle intensity statistics in the image, this extremely simple technique has the potential to reach estimation performances compatible with applications to the expense of a high resolution detector. In this work, we first report the recent experimental validation of the applicability of this imaging technique on various samples, analyze its precision and test its robustness when illumination wavelength or imaging setup geometry are varied.

Then, we theoretically investigate the ability of this snapshot approach to discriminate samples with various depolarization degrees while sharing similar reflectance properties. Such detection tasks can indeed be of great interest for industrial applications. In that perspective, we quantitatively compare the detection performances of this approach with more standard polarization imaging strategies. We show on numerical simulations that the best compromise in terms of detection vs and false alarm rates requires the implementation of a generalized likelihood ratio test, which strongly outperforms much simpler moments-based detection tests.

9613-2, Session 1

Single shot diattenuation imaging by circular polarization orthogonality breaking

Noé Ortega-Quijano, Julien Fade, Institut de Physique de Rennes (France); Emmanuel Schaub, François Parnet, Univ. de Rennes 1 (France); Mehdi Alouini, Institut de Physique de Rennes (France)

Polarimetric sensing by orthogonality breaking is a recently proposed measurement principle which enables to perform a direct characterization of sample dichroism and/or depolarization in a single measurement, with a high dynamic range and acquisition speed. It relies on the use of a specific dual-frequency dual-polarization coherent source and on the measurement of a radio-frequency intensity beatnote induced by the sample dichroism/ depolarization. In this work, we show that this approach enables to fully characterize the anisotropy parameters (magnitude and orientation angle) of a dichroic sample in a single measurement, by illuminating the sample with two orthogonal circularly-polarized modes with a slight frequency detuning. The source used in this work is based on a 40 mW commercial 488 nm monomode source that is introduced into a polarization splitting/ combining Mach-Zehnder architecture. An acousto-optic modulator in one of the arms introduces a fixed frequency shift of 80MHz between the orthogonally-polarized circular states of polarization provided at the output of the source. This dual-frequency dual-polarization coherent source is then introduced into a laser scanning microscope, which enables to acquire a 256x256 pixels image in about 4 s only. The proposed method enables to

determine diattenuation magnitude and orientation in a straightforward, fast and decoupled way. It is validated on several test samples and the potential of this technique to perform real-time dichroism imaging is explored on a synthetic imaging scenario. Moreover, this technique is easily adaptable to endoscopic systems due to its insensitivity to birefringence effects, hence representing an interesting approach for minimally-invasive tissue characterization.

9613-3, Session 1

Adaptive filters for bad pixel replacement in microgrid modulated polarimeters

Daniel A. LeMaster, Air Force Research Lab. (United States); Bradley M. Ratliff, Exelis Space Computer Corp. (United States)

Uncorrected or poorly corrected bad pixels reduce the effectiveness of polarimetric clutter suppression. The conventional approach to mitigating bad pixels for microgrid polarimetric imagers is the redundancy-based method. This method predates the literature of microgrid polarimetric image demodulation as a linear system. Furthermore, bad pixel replacement and Stokes image recovery are treated as separate steps. In this paper, we attempt to improve on the redundancy-based method by using adaptive filtering for joint bad pixel replacement and Stokes image demodulation.

9613-4, Session 1

Bandwidth and crosstalk considerations in modulated polarimeters with finite integration time

Israel J. Vaughn, Oscar G. Rodriguez-Herrera, College of Optical Sciences, The Univ. of Arizona (United States); Mohan Xu, The Univ. of Arizona (United States); J. Scott Tyo, College of Optical Sciences, The Univ. of Arizona (United States)

Recently we designed and built a portable imaging polarimeter for remote sensing applications. Polarimetric imaging operators are a class of linear systems operators in the Mueller matrix reconstruction space, resulting in a set of measurement channels. The nature of remote sensing requires channel crosstalk to be minimized for either general Mueller matrix reconstruction or task specific polarimetric remote sensing. We present a general framework which may be used for any modulated Mueller matrix reconstruction operator which minimizes channel crosstalk. We also discuss the constraints on these operators. We illustrate the framework with examples of specific spatio-temporally modulated system operators derived from our portable imaging polarimeter. Specifically channel cancellation allows increases in channel bandwidth. We also address the impact that systematic deviations from the ideal operators and i.i.d. noise have on Mueller matrix image reconstruction. We analyze the negative effects of the time-modulated polarization state generated and analyzed with dualrotating retarder polarization state generators (PSG) and analyzers (PSA) on measurements obtained with Mueller matrix polarimeters with a finite integration time detector. We present strategies to decrease these effects by performing a reduced number of measurements at specific regions of the curve described over the Poincaré sphere by the instantaneous polarization in the PSG and PSA. The strategies presented are particularly suitable for polarimeters that require a relatively long integration time, such as systems with a sub-optimal detector or analyzing weakly scattering targets.

9613-5, Session 1

On demand polarimetry using a movable microgrid polarizer

Page King, Raytheon Co. (United States); Eric C. Fest, Raytheon Missile Systems (United States)

A movable pixelated filter array is proposed to provide low cost, on demand polarimetry and wavefront sensing. With this concept, an optical system can turn polarimetry on and off by using a shutter to move a microgrid polarizer array in and out of the optical path of the system. This allows an optical system to operate in two modes, a non-polarimetric mode in which sensor range is maintained, and a polarimetric mode in which it is reduced. In implementing this concept, adequate knowledge of the position of the filter in the optical path and calibration procedures become critical topics. This paper discusses simulated and hardware-tested results of this invention.

9613-6, Session 2

The twisted universe: cosmic polarimetry at the few parts-per-billion level (Invited Paper)

Brian G. Keating, Univ. of California, San Diego (United States)

The era of Cosmic Microwave Background B-mode polarization cosmology began in March 2014 with two landmark papers released within a week of each other. The BICEP2 telescope observed from the South Pole for three seasons (2010-2012) and released results showing an excess of B-modes in the degree angular scale range with >5 sigma significance. We find that this excess could not be explained by instrumental systematics and it was confirmed in cross-correlation with BICEP1 (at 100 and 150 GHz) and preliminary data from the Keck Array. The observed B-mode power spectrum was well-fit by a lensed-LCDM cosmological model with the addition of primordial tensor fluctuations. However, it is impossible to rule out foreground contamination and we are working alongside the Planck team to resolve this matter. I will discuss the BICEP2 experiment, observations, and data analysis. One week before the BICEP2 announcement, the POLARBEAR telescope (which observed from the Atacama Desert, Chile for one season 2012-2013) announced the first evidence for B-modes at sub-degree scales caused by gravitational lensing of the CMB's E-modes by large scale structure at low-redshift. The combination of the BICEP2 and POLARBEAR results paves the way towards precision tests of inflation, foreground contamination as well as probes of other aspects of fundamental physics including measuring the number and masses of cosmological neutrinos.

9613-7, Session 2

Complete intrinsic coincident polarimetry using stacked organic photovoltaics

Subharup Gupta Roy, Omar M. Awartani, Pratik Sen, Brendan T. O'Connor, Michael W. Kudenov, North Carolina State Univ. (United States)

Measuring 2-D Stokes vector, to determine the polarization state of light, finds application in multiple areas, including the characterization of aerosol size distributions, military purposes (e,g, target sighting), quality control for evaluating the distribution of stress birefringence, resolving data channels in telecommunications, and for evaluating biological tissues in medical imaging. Conventional methods, such as channeled (CH) and division of focal plane (DoF) polarimeters, usually limit spatial resolution, while others, like division of aperture (DoA) or division of amplitude (DoA) polarimeters, have higher complexity and less compactness. To solve these issues, we developed a system that uses organic photovoltaics (OPVs) as photodetectors. The active area of the devices have strain aligned

polymer chains in a periodic arrangement, which enables the device to preferentially absorb certain polarized states of incident light, depending on the orientation of the polymer chains. Taking advantage of the cells' transparency and ease of processing compared to inorganic materials, several devices can be stacked along the optical axis. We use four stacked OPVs, where each device can measure one of the four Stokes parameters simultaneously, thereby ensuring high spatial and temporal resolution with inherent spatial registration. In this paper, the fabrication of the OPVs and the design and calibration technique is documented along with experimental data, supporting the hypothesis.

SPIE. PHOTONICS

OPTICAL ENGINEERING+ APPLICATIONS

9613-8, Session 2

Integrated computational imaging system for enhanced polarimetric measurements

Shahid A. Haider, Farnoud Kazemzadeh, Alexander Wong, David A. Clausi, Univ. of Waterloo (Canada)

Polarimetry is a common technique used in chemistry for solution characterization and analysis, giving insight into the molecular structure of a solution measured through the rotation of linearly polarized light. This rotation is characterized by the Boit-Savart's law. Without large optical path lengths, or high concentrations of solution, these optical rotations are typically very small, requiring elaborate and costly apparatuses. To ensure that the rotation measurements are accurate, these devices usually perform complex optical procedures or time-averaged point measurements to ensure that any intensity variation seen is a product of optical rotation and not from inherent noise sources in the system, such as sensor or shot noise. Time averaging is a lengthy process and rarely utilizes all of the information available on the sensor. To this end, we have developed a novel integrated, miniature, computational imaging system that enhances polarimetric measurements that takes advantage of the full spot size observed on an array detector. This computational imaging system is capable of using a single acquisition at unity gain to enhance the polarimetric measurements using a probabilistic framework, which accounts for inherent noise and optical characteristics in the acquisition process, to take advantage of spatial intensity relations. This approach is faster than time-averaging methods and can better account for any measurement uncertainties. In preliminary experiments, this system has produced comparably consistent measurements across multiple trials with the same chemical solution than time averaging techniques.

9613-9, Session 3

Snapshot retinal imaging Mueller matrix polarimeter

Yifan Wang, Michael Kudenov, North Carolina State Univ. (United States); Amir Kashani, Keck School of Medicine (United States); Jim Schwiegerling, College of Optical Sciences, The Univ. of Arizona (United States)

Glaucoma is the second leading cause of visual impairment in the world. An especially significant step for successful glaucoma treatment is early diagnosis. It has been vastly known that, through scanning laser polarimetry (SLP) and scanning laser Mueller matrix (MM) polarimetry techniques, the pathologic changes on retinal nerve fiber layer (RNFL) could be detected before complete atrophy, leading to earlier diagnosis of glaucoma. However, these techniques currently have limitations such as limited sensing region on retina and motion artifacts due to the temporal scanning nature. In this paper, we theoretically and experimentally present a snapshot Mueller Matrix Polarimeter (SMMP) fundus camera, which is able to record polarization-altering characteristics of relatively large areas on retina with a single snapshot. It is made by incorporating broad-band polarization gratings into fundus camera design as generator and analyzer of the polarization fringes. A complete Mueller Matrix data set with high temporal resolution is obtained by analyzing the polarization patterns projected onto the image plane. Thus, the measurement errors due to diattenuation and depolarization of the RNFL are minimized. We believe that the SMMP holds

Conference 9613: Polarization Science and Remote Sensing VII



great potential for being applied as a practical instrument for screening glaucoma patients in the future.

9613-10, Session 3

A polarization system for persistent chemical detection

Julia Craven-Jones, Leah Appelhans, Todd Embree, Patrick Finnegan, Sandia National Labs. (United States); Dennis Goldstein, Polaris Sensor Technologies, Inc. (United States); Charles LaCasse, Ting S. Luk, Sandia National Labs. (United States); Adoum Mahamat, College of Optical Sciences, The Univ. of Arizona (United States); Lee Massey, Anthony Tanbakuchi, Cody Washburn, Steven Vigil, Sandia National Labs. (United States)

We report on the development of a prototype polarization tag based system for detecting chemical vapors. The system primarily consists of two components, a chemically sensitive tag that experiences a change in its optical polarization properties when exposed to a specific chemical of interest, and an optical polarimeter that is used to measure the polarization properties of the tags. Although the system concept could be extended to other chemicals, for the initial system prototype presented here the tags were developed to be sensitive to hydrogen fluoride (HF) vapors. HF is used in many industrial processes but is highly toxic and thus monitoring for its presence and concentration is often of interest for personnel and environmental safety. The tags are periodic multilayer structures that are produced using standard photolithographic processes. The polarimetric imager has been designed to measure the degree of linear polarization reflected from the tags in the short wave infrared. By monitoring the change in the reflected polarization signature from the tags, the polarimeter can be used to determine if the tag was exposed to HF gas. In this paper, a review of the system development effort and preliminary test results are presented and discussed, as well as our plan for future work.

9613-11, Session 3

Full-field imaging for spectroscopic stokes parameters in all directions and its application to flaw detection

Hiroshi Hasegawa, Yukitoshi Otani, Utsunomiya Univ. (Japan)

This paper describes a spectroscopic imaging Stokes polarimeter by dual rotation retarder and analyzer on a six-axis robot arm. It is succeeded to calibrate of wavelength dependence of its retarder. To measure in all field of entire circumference, the Stokes polarimeter is attached on the robot arm. It is succeeded to measure the state of polarization of a sample from reflected light, scattered light and transmitted light from any angle in all directions. It is also applied to detect flaw detections of lenses.

9613-12, Session 4

Innovative static spectropolarimeter concept for wide spectral ranges

Martin Pertenais, Observatoire de Paris à Meudon (France) and Univ. de Toulouse (France); Coralie Neiner, Observatoire de Paris à Meudon (France); Laurent P. Parès, Observatoire Midi-Pyrénées (France) and Univ. de Toulouse (France); Pascal M. Petit, Univ. de Toulouse (France) and Institut de Recherche en Astrophysique et Planétologie (France) Developing an efficient and robust polarimeter for wide spectral ranges and space applications is a main issue in many projects. As part of the UVMag consortium created to develop UV facilities in space (e.g. the Arago mission proposed to ESA), we are studying an innovative concept of polarimeter that is robust, simple, and efficient on a wide spectral range. The idea, based on the article by Sparks et al. (2012), is to use polarization scramblers to create a spatial modulation of the polarization. Along the height of the wedges of the scramblers, the thickness of the birefringent material crossed by the light, and thus the retardance, vary continuously. This variation creates an intensity modulation of the light related to the entrance polarization state. Analyzing this modulation with a linear polarizer, and dispersing the light spectrally in the orthogonal spatial direction, enables the measurement of the full Stokes vector over the entire spectrum. This determination is made with a single-shot measurement and without any moving parts in the system.

During this talk, I will develop the theory of this concept and present the first laboratory results of our prototype. In the future, we will test and validate this concept in space environment and in the FUV range.

9613-13, Session 4

Snapshot Mueller-matrix spectropolarimeter using spectral and spatial carriers

Kazuhiko Oka, Yujin Haga, Hiroshi Michida, Hokkaido Univ. (Japan)

We report on a novel spectroscopic Mueller-matrix polarimeter based on channeled spectropolarimetry. The channeled spectropolarimetry is a method for measuring polarimetric parameters using a cosinusoidallymodulated spectrum. Although a channeled Mueller-matrix spectropolarimeter using only spectral carriers has been proposed, it requires a spectrometer with a high spectral resolution so that sixteen Mueller matrix elements can be discriminated only in the one-dimensional Fourier domain. In this work, to relax the severe requirement, we incorporate spatial as well as spectral carriers in the channeled Muellermatrix spectropolarimeter. In the developed system, light from a Xe lamp first passes through a spectral polarization state modulator, consisting of a polarizer and two high-order retarders, and is then transmitted by a sample under measurement. The light emerging from the sample is fed into a polarization state analyzer using spatial carriers, including two Savart plates, and impinges upon a spectrometer with two-dimensional CCD. The obtained two-dimensional spectrum is cosinusoidally modulated along both wavenumber- and space-axes. The two-dimensional Fourier analysis of the spectrum allows us to demodulate the wavenumber-resolved Mueller matrix of the sample. The spectropolarimeter uses no mechanical or active elements for the polarization modulation and the snapshot measurement of sixteen Mueller-matrix elements can be achieved. In addition, a spectrometer with much lower spectral resolution can be used compared to the previous method using only spectral carriers. The feasibility of the proposed implementation was experimentally demonstrated in the spectral range between 500 and 750 nm.

9613-14, Session 4

High precision stokes polarimeter for scattered light by intensity detection with high dynamic range

Yukitoshi Otani, Shuhei Shibata, Tomohiro Kiire, Yoshio Hayasaki, Toyohiko Yatagai, Utsunomiya Univ. (Japan)

This paper describes a high precision Stokes polarimeter for scattered light by a detector of high dynamic range with six ranges of neutral density (ND) filters which have different absorption ratio. A photon counting system is used to capture the intensities. Its dynamic range is achieved up to the tenth power of ten by combination of NDs. The measuring algorism of Stokes parameters are proposed a dual rotating retarder and analyzer



which can be calibrated polarization errors such as retardance error and diattenuation error. The accuracy of Stokes parameters was achieved 0.003 in transmission type. The Stokes parameters of scattered light of glass material was measured from -20° to 20° in detection angle.

9613-15, Session 4

A multi-domain full-Stokes polarization modulator that is efficient for 300-2500nm spectropolarimetry

Frans Snik, Gerard van Harten, Leiden Observatory (Netherlands); Andrey Alenin, J. Scott Tyo, College of Optical Sciences, The Univ. of Arizona (United States)

We present the design and prototyping results for an ultra-wideband rotating polarization modulator that consists of a stack of quartz plates. The plate thicknesses and orientations were optimized such that after rotation of the modulator to 6 different angles before a polarization analyzer, the full Stokes vector can be optimally determined at all wavelengths from 300 to 2500 nm. Additional optimization parameters include minimal variation of the retardance with incidence angle and temperature, and the suppression of polarized spectral fringes for a spectral resolution of 10,000. The prototype modulator's design was re-optimized after the production and measurement of each individual quartz plate. We present the performance of the as-built prototype.

To eliminate aliasing with inherent temporal variations of the source, the modulator can be used together with a polarizing beam-splitter ("dualbeam" approach). Because of the large sinusoidal spectral variations of the polarization modulation, this modulator can also be considered a "spectral modulator for channeled spectropolarimetry". Therefore, at each modulation state, spectrally resolved polarization information can also be extracted directly, although at limited spectral resolution. We use this modulator as an example of a "multi-domain polarization information in all available measurement dimensions (temporal, spatial, spectral), and rendering the overall polarization measurement independent from systematic effects in any of these dimensions.

9613-16, Session 5

Polarization aberration in astronomical telescopes

Russell A. Chipman, James B. Breckinridge, Wai Sze T. Lam, College of Optical Sciences, The Univ. of Arizona (United States)

The PSF for astronomical telescopes and instruments depends not only on geometric aberrations and scalar wave diffraction, but also on those wavefront errors introduced by the physical optics and the polarization properties of reflecting and transmitting surfaces within the optical system. These vector wave aberrations, called polarization aberrations, result from two sources the mirror coatings necessary to make the highly reflecting mirror surfaces, and the angles of incidence. The analytical tools to calculate the PSF image are described. The point spread function consists of four separate components, which include two faint components with a spatial extent about twice the size of the diffraction limited image. An example telescope system is analyzed to help understand how astronomical image data is affected by instrumental polarization.

9613-17, Session 5

Polarization modulators based on liquid crystal variable retarders for the solar orbiter mission

Alberto Alvarez-Herrero, Pilar García Parejo, Hugo Laguna, Javier Villanueva, Javier Barandiarán, Laurent Bastide, Manuel Reina, Isabel Vera, Mayte Royo, INTA Instituto Nacional de Técnica Aeroespacial (Spain)

A polarization modulator based on Liquid Crystal Variable Retarders (LCVRs) will be used in the Polarimetric and Helioseismic Imager (PHI) for the Solar Orbiter mission to measure the complete Stokes vector of the incoming light. PHI is one of the six remote sensing instruments onboard of this space mission led by the European Space Agency (ESA) with strong NASA participation. It is an imaging spectro-polarimeter that will acquire high resolution solar magnetograms. Also the LCVRs will be used in the polarization modulator of the METIS instrument (Multi Element Telescope for Imaging and Spectroscopy). METIS is a solar coronagraph that will analyze the linear polarization for observations of the visible-light K-corona.

The polarization modulators are described in this work including the optical, mechanical, thermal and electrical aspects. Both modulators will consist of two identical LCVRs with a relative azimuth orientation of 45° for PHI and parallel for the METIS modulator. In the first case, the configuration allows the analysis of the full Stokes vector with maximum polarimetric efficiencies. In the second setup, wide acceptance angles ($\leq \pm 7^\circ$) are obtained.

In this work the results obtained from the full representative prototypes after the verification and environmental test campaigns are presented. The main performances were measured and analyzed including polarimetric efficiencies, wavefront error transmission, transmittance and response times. This valuable information has allowed to finish the detailed design of these devices and to proceed to the manufacturing of the Qualification Model (QM) and Flight Models (FM).

9613-18, Session 5

The Polaris-M ray tracing program

Russell A. Chipman, Wai Sze T. Lam, College of Optical Sciences, The Univ. of Arizona (United States)

An optical design program developed at the University of Arizona incorporates many advanced polarization analysis features. At the core of the program is a three-dimensional polarization ray tracing structure used to characterize polarization effects occurring at interfaces and upon propagation through anisotropic materials. Reflection and refraction at uniaxial, biaxial, and optically active interfaces are handled rigorously, as our anisotropic grating structures. By analyzing multiple polarized wavefront components individually, one can study the complicated effects of multiple anisotropic optical elements at the image. A ray tree structure keeps track of ray doubling at anisotropic interfaces and ray multiplication at gratings. Wavefronts can be expanded into polarization aberration terms. Polarized diffraction image formation and polarization dependent optical transfer functions are included.

9613-19, Session 6

The geostationary operational environmental satellite R-series advanced baseline imager: polarization sensitivity and potential impacts

Aaron J. Pearlman, ERT, Inc. (United States) and NOAA National Environmental Satellite, Data, and Information Service (United States); Changyong Cao, NOAA National Environmental Satellite, Data, and Information Service

Conference 9613: Polarization Science and Remote Sensing VII



(United States); Xiangqian Wu, National Oceanic and Atmospheric Administration (United States)

The Advanced Baseline Imager (ABI) will fly aboard the Geostationary Operational Environmental Satellite R-Series (GOES-R). Contrary to National Oceanic and Atmospheric Administration's current imagers for operational weather forecasting, this newest version, which is planned to launch in 2016, will have six reflective solar bands - five more than currently available. These bands will be used for applications such as aerosol retrievals, which are influenced by polarization effects.

Characterizing these effects is part of the extensive pre-launch testing that has been done to ensure the high quality of Level 1b data. The vendor characterized the polarization sensitivity in the 0.47 μ m and 0.64 μ m channels by recording the ABI counts while illuminated with an integrating sphere and through a linear polarizer set to different angles. The polarizer was characterized by placing an additional polarizer in front of the ABI and repeating the measurements.

We analyzed the results using a formulation that accounts for the nonideal properties of the polarizing filter and assessed the measurement uncertainties. We also compared the measurement results with outputs from optical models produced by the instrument vendor. To estimate the radiometric performance impacts from the instrument polarization sensitivity, we simulated polarized scenes using a radiative transfer code and accounted for the instrument polarization sensitivity over its field of regard. The impacts varied with channel wavelength and aerosol model type. This work enhances our ability to diagnose and resolve polarizationrelated anomalies on-orbit and reduce calibration uncertainty for improved system performance.

The manuscript contents are solely the opinions of the authors and do not constitute a statement of policy, decision, or position on behalf of NOAA or the U.S. government.

9613-20, Session 6

Why diffractive retarders are not in common use

Russell A. Chipman, College of Optical Sciences, The Univ. of Arizona (United States)

Diffractive retarders fabricated from gratings in isotropic materials are analyzed by rigorous coupled wave analysis. The efficiency and dispersion of these gratings is compared to the conventional materials used in the majority of retarders.

9613-21, Session 7

Channeled partial Mueller matrix polarimetry

Andrey S. Alenin, J. Scott Tyo, College of Optical Sciences, The Univ. of Arizona (United States)

In prior work, we introduced methods to treat channeled systems in a way that is similar to Data Reduction Method (DRM), by focusing attention on the Fourier content of the measurement conditions. Introduction of Q enabled us to more readily extract the performance of the system and thereby optimize it to obtain reconstruction with the least noise. The analysis tools developed for that exercise can be expanded to be applicable to partial Mueller Matrix Polarimeters (pMMPs), which were a topic of prior discussion as well. In this treatment, we combine the principles involved in both of those research trajectories and identify a set of channeled pMMP families. As a result, the measurement structure of such systems is completely known and the design of a channeled pMMP intended for any given task becomes a search over a finite set of possibilities.

9613-22, Session 7

Ray tracing based path-length calculations for polarized light tomographic imaging

Rakesh Manjappa, Rajan Kanhirodan, Indian Institute of Science (India)

The amount of light absorbed inside a biological tissue gives away a lot of hidden information about the composition and dynamics inside. For example, the diffuse optical tomography (DOT) depends on fluence distribution inside the tissue to arrive at the absorption coefficient map. The study of polarized light transport through a tissue material has many biomedical applications. It provides a powerful tool to study the interaction of light with a turbid media. The degree of polarization (DOP) provides a pointer to the disease state of a tissue.

A ray tracing based path length calculation is investigated for polarized light transport in a pixel space. Tomographic imaging using polarized light transport is promising for applications in optical projection tomography of small animal imaging and samples with low scattering. Polarized light transport through a medium can have complex effects due to interactions such as optical rotation of linearly polarized light, birefringence, interior refraction etc... Here we investigate the effects of refraction of polarized light in a non-scattering medium. This step is used to obtain the initial absorption estimate. This can be used as prior in Monte Carlo methods to assist in faster convergence of the final estimate. The principle of polarization by refraction uses the fact that at certain angles of incidence (Brewster's angle) only the perpendicular component is reflected.

The transmission medium consists of regions of homogeneous refractive index (RI) values with an embedded inhomogeneity having a RI different from the homogeneous background. The proposed method takes care of refractive index mismatches at the interface and corrects for the interior ray bending. Snell's law is used to arrive at the direction after interior refraction. The reflectance for p-polarized (parallel) and s-polarized (perpendicular) are different and hence there is a difference in the intensities that reach the detector end.

The algorithm computes the length of the ray in each pixel along the refracted path and this is used to build the weight matrix. This weight matrix with corrected ray path length and the resultant intensity reaching the detector for each ray is used in the algebraic reconstruction method. The proposed method is tested with numerical phantoms for various noise levels. Refraction at interior inhomogeneities results in inaccurate reconstruction while using filtered back-projection algorithm.

It is important to note that when the refractive index mismatch is less (i.e less than 0.2 RI Units) there is no significant difference between reflection coefficients of the two polarization states of light, and the value is same as that of unpolarized light. As the refractive index mismatch between the region and inhomogeneity increases the difference between reflection coefficients Rs and Rp increases and is most prominent when the mismatch is highest.

Air bubble (with RI=1.0) inside a gel dosimeter with the surrounding medium presents such a scenario. The surrounding gel medium typically has a high refractive index of 1.35 to 1.5 depending on the material used. Similar is the case of air pockets inside tissue. Micro-CT using X-ray, has been used to image the contrast between regions of air and tissue. Here we propose to use polarization based optical techniques to quantify the contrast. Preliminary analysis and results show that polarization based imaging is promising.

The refraction errors due to regions of different refractive indices are discussed, the difference in intensities with polarization is considered. The improvements in reconstruction using corrections is presented. This is achieved by tracking the path of the ray as well as the intensity of the ray as it traverses through the medium.



9613-23, Session 7

Bandwidth and information in the design and analysis of polarimeters (Invited Paper)

J. Scott Tyo, College of Optical Sciences, The Univ. of Arizona (United States) and Univ. of New South Wales, Canberra (Australia)

Over the past decade, the Advanced Sensing Laboratory at the College of Optical Sciences has been working with several collaborating groups on improving the understanding of information content in polarimeter measurements. What began as an effort to understand noise and error in the calibration of polarimeters evolved into an understanding of how the various bandwidths available in an instrument (spatial, temporal, spectral, angle of incidence) map on to the corresponding domains of the polarization objects that are being measured. In this presentation, I will review some of key historical results from our group and from others, and show how they are all fundamentally related in considering the unique information content of the individual polarimeter measurements. Applications of these methods in microgrid polarimeters, partial Mueller polarimeters, coherence sensors, and advanced polarimeter modulation schemes will all be considered. Much of the talk will be a historical review, but special emphasis will be made on the aspects that inform current research projects that are being considered in depth in other talks at the meeting.

9613-24, Session 8

The visible-to-SWIR spectrum of skylight polarization

Laura M. Dahl, Joseph A. Shaw, Montana State Univ. (United States)

For a clear-sky atmosphere, a successive orders of scattering (SOS) radiative transfer model can estimate the degree of polarization (DoP) in the sky accurately. We previously published measurements and simulations illustrating the complex interaction of atmospheric molecular and aerosol properties with surface reflectance in determining the spectrum of skylight polarization from the visible to 1 ?m wavelength in the near infrared. Those results showed that skylight polarization can trend upward or downward, or even have unusual spectral discontinuities that arise because of sharp features in the underlying surface reflectance. The specific spectrum that is observed in any given case depends strongly on atmospheric and surface properties that vary with wavelength. In the previous study, the SOS model was fed with actual measurements of highly variable aerosol and surface properties from locations around the world. Results, however, were limited to wavelengths below 1 ?m because of the lack of appropriate satellite measurements of surface reflectance at longer wavelengths. We now report measurement-driven simulations of skylight polarization, extending from 400 nm to 2500 nm in the short-wave infrared (SWIR). Rather than relying on satellite information, the surface reflectance was measured with a ground-based spectrometer. The basic optical physics of the skylight polarization process and example results of the skylight polarization spectra for the vis-NIR-SWIR spectral region (400-2500 nm) will be presented.

9613-25, Session 8

Light scattering by roughed spheroids: a database of dust aerosols for POLDER/ PARASOL 490, 670 and 865nm channels

Jianping Liu, Ping Yang, Texas A&M Univ. (United States); Ralph Kahn, NASA Goddard Space Flight Ctr. (United States)

A database is developed containing the comprehensive single-scattering properties (namely, the 4x4 phase matrix, extinction cross section, and

single-scattering albedo) of dust aerosols for application to remote sensing based on POLDER/PARASOL 490, 670 and 865 nm channels. A roughed spheroid model is developed for the single-scattering computation with a combination of the invariant imbedding T-matrix method (IITM) and the improved geometric optics method (IGOM). Properties such as the extinction efficiency, single-scattering albedo, asymmetry factor and phase matrix are provided for a set of discretized parameters including the size parameter, the aspect ratio, the real and imaginary parts of the refractive index and the degree of roughness. Furthermore, the database is applied to the retrieval of the microphysical properties (specifically, the aspect ratio and degree of surface roughness) of dust aerosols through the comparison between the simulated polarized reflectance and POLDER/PARASOL satellite observations.

9613-26, Session 8

Morphological operators for enhanced polarimetric imaging target detection

Joao M. Romano, U.S. Army Armament Research, Development and Engineering Ctr. (United States); Dalton S. Rosario, U.S. Army Research Lab. (United States)

We introduce an algorithm of morphological filters and propose its use to the information content of classic polarization metrics for commercial or military applications requiring passive longwave infrared polarimetric remote sensing and real-time anomaly detection. The approach has shown to significantly augment the daytime and nighttime detection of weaksignal manmade objects immersed in a predominant natural background scene (foliage, terrain). The approach features a tailored sequence of signalenhancing filters, consisting of core morphological operators (dilation, erosion) and higher level morphological operations (e.g., spatial gradient, opening, closing) to achieve a desired overarching goal. Qualitatively, the goal is to effectively squeeze the variance of pixel values representing the natural clutter background, while simultaneously spreading the pixel variance within the manmade object class and separating the pixel mean averages between the two object classes (natural and manmade). Using represented data from a large database known as SPICE, where continuous data acquisition covered a 72-h time period, the results show that the approach was able to automatically and persistently detect with a high confidence level the presence of three mobile military howitzer surrogates (targets) in natural clutter, posed at three distinct aspect angles at a range of 557 m. The approach detected the targets as scene anomalies, yielding a negligible false alarm rate. The targets' heating components were mostly turned off during data acquisition, with a few exceptions. The approach yielded performance invariance toward four major sources of signature variation: diurnal cycle, mild atmospheric changes, geometry of illumination, and target's thermal operating condition.

9613-27, Session 9

Accurate spectrally modulating polarimeters for atmospheric aerosol characterization

Jeroen H. H. Rietjens, Martijn Smit, SRON Netherlands Institute for Space Research (Netherlands); Gerard van Harten, Leiden Observatory (Netherlands); Antonio Di Noia, Otto P. Hasekamp, SRON Netherlands Institute for Space Research (Netherlands); Jos de Boer, Leiden Observatory (Netherlands); Hester Volten, Rijksinstituut voor Volksgezondheid en Milieu (Netherlands); Frans Snik, Christoph U. Keller, Leiden Observatory (Netherlands)

Multi-angle spectro-polarimetry holds great potential as a remote sensing technique to derive information about aerosol suspended in the Earth's atmosphere. A consortium of Dutch research institutes has developed a spectro-polarimeter that is based on spectral polarization modulation: by encoding the polarization state of scattered sunlight in a sinusoidal



modulation in the intensity spectrum, the spectral flux and state of polarization are measured simultaneously in a single measurement of a target scene. As a consequence, this passive method enables highly accurate and reliable spectro-polarimetry.

The technique has been employed in two instrument realizations. The SPEXprototype is developed for space-based observations and is a multi-angle viewing instrument with nine fixed viewing apertures. This instrument is currently upgraded to perform aerosol characterization campaigns onboard an ER-2 research aircraft together with NASA's Research Scanning Polarimeter. Another realization, groundSPEX, has a single scanning viewing aperture and was developed specifically for air-quality observations made from the ground.

We will present lab calibration results using a recently developed polarization calibration stimulus and compare the polarimeteric accuracy of both instruments, which are better than 0.005.

Also, we will show results of ground-based multi-angle spectro-polarimetric diffuse sky measurements with both SPEX instruments at the Cabauw Experimental Site for Atmospheric Research (CESAR). Retrievals of aerosol characterization parameters (e.g. aerosol optical thickness, refractive index, and effective radii) will be intercompared and validated against products of the co-located AERONET station. The results indicate that the SPEX measurement concept has the power to deliver high quality aerosol parameters.

9613-28, Session 9

Applying a microfacet model to polarized light scattering measurements of the Earth's surface

Meredith K. Kupinski, Christine L. Bradley, College of Optical Sciences, The Univ. of Arizona (United States); David Diner, Feng Xu, Jet Propulsion Lab. (United States); Russell Chipman, College of Optical Sciences, The Univ. of Arizona (United States)

Currently, urban air quality monitoring systems rely exclusively on groundbased sun photometers, which do not provide adequate spatial or optical sampling to constrain the inverse problem of global aerosol estimation. A downward-looking polarimeter collects light from both the atmosphere and the Earth's surface and can provide information for global aerosol estimation. Currently, models of atmospheric scattering are more advanced than models of surface reflectance because the polarized light scattering from the Earth's surface is globally diverse and all analysis to date has been empirical. To extract the optical and microphysical properties of aerosols over urban areas, it is essential to have more accurate models for polarized surface reflectance coupled to atmospheric radiative transfer.

In this work, three years of observations from JPL's Ground-based Multiangle SpectroPolarimetric Imager (GroundMSPI) are used to evaluate a surface polarized bidirectional reflectance distribution function (p-BRDF) model. GroundMSPI is an eight-band spectropolarimetric camera mounted on a rotating gimbal to acquire pushbroom imagery of outdoor landscapes. The camera uses a photoelastic-modulator-based polarimetric imaging technique to measure linear Stokes parameters in three wavebands (470, 660, and 865 nm) with a 0.005 uncertainty in degree of linear polarization. Data collected during the course of the day provided a range of illumination geometries that facilitated evaluation of the p-BRDF model, which is comprised of a volumetric reflection term plus a specular reflection term generated by a randomly oriented array of Fresnel-reflecting microfacets. We report on the appropriateness of this p-BRDF model for manmade materials as compared to natural materials.

9613-29, Session 9

Spectral invariance hypothesis study of polarized reflectance with ground-based multiangle spectropolarimetric imager (GroundMSPI)

Christine L. Bradley, Meredith Kupinski, College of Optical Sciences, The Univ. of Arizona (United States); David J. Diner, Jet Propulsion Lab. (United States); Russell A. Chipman, College of Optical Sciences, The Univ. of Arizona (United States)

Many models used to represent the boundary condition for the separation of atmospheric scattering from the surface reflectance in polarized remote sensing measurements assume that the polarized surface reflectance is spectrally neutral. Though this is a common assumption in polarized bidirectional reflectance distribution (pBRDF) models, little data has been published to support this hypothesis. The Spectral Invariance Hypothesis states that the magnitude and shape of the pBRDF is equal for all wavelengths. In order to test this hypothesis, JPL's ground-based Multiangle SpectroPolarimetric Imager (GroundMSPI) is used to measure polarization information of different outdoor surface types. GroundMSPI measures the linear polarization Stokes parameters (I, Q, U), at three wavebands, 470 nm, 660 nm, and 865 nm. The camera is mounted on a two-axis gimbaled mount to accurately select the view azimuth and elevation directions. We set the instrument up on clear sky days to acquire daylong scans of scenes that contain various surface types such as grass, dirt, cement, and asphalt with a Spectralon panel in the camera field of view. Over the course of a day, the sun changes its position in the sky to provide a large range of scattering angles for this study. The pBRDF is calculated for the three wavelengths and the spectral correlation is reported. This work investigates the validity of the spectral invariance assumption for different types of materials in outdoor scenes

9613-30, Session 9

Optimal contrast enhancement in long distance snapshot polarimetric imaging through fog

Swapnesh Panigrahi, Univ. de Rennes 1 (France); Julien Fade, Mehdi Alouini, Institut de Physique de Rennes (France); Hema Ramachandran, Raman Research Institute (India)

We investigate optimal contrast enhancement of a polarized light beacon through fog over long distances, for navigation assistance and transportation safety in low visibility conditions. To this aim, we have set up a long distance imaging experiment spanning over a kilometer to obtain polarimetric images of a scene containing an incoherent linearly polarized light beacon embedded in fog. Using a Wollaston prism-based snapshot polarimetric camera, we obtain two simultaneous images of a scene in orthogonal polarizations. A suitable combination of the two acquired images is sought such that the contrast of the polarized source is maximized in the resulting image. Using a correlated Gaussian model to describe noise fluctuations in the polarimetric images, we theoretically exhibit the optimal form of such contrast-maximizing representation, and show that it simply consists of a linear combination of the two acquired images with appropriate weighting. This optimal representation differs in general from standard polarimetric image representations used in the literature and strongly depends on atmospheric/visibility conditions. The implementation of such adaptive optimal representation simply requires local estimation of the noise correlation coefficient and is therefore highly compatible with realtime constraints, even when the number and location of polarized sources in the image are unknown. Using such an information theoretical approach, we also compute the optimal gain in contrast that can be obtained by using a polarization sensitive camera in various atmospheric conditions. The optimality of this representation and the theoretical gain expected are



experimentally confirmed on various data acquisitions obtained in different atmospheric conditions.

9613-31, Session 9

Characterization of sun and sky glint from wind ruffled sea surfaces for improved estimation of polarized remote sensing reflectance

Robert Foster, Amir Ibrahim, Alex Gilerson, Ahmed El-Habashi, Carlos Carrizo, Sam Ahmed, The City College of New York (United States)

During two cruises in 2014, the polarized radiance of the ocean and the sky were continuously acquired using a HyperSAS-POL system. The system consists of 6 hyperspectral radiometric sensors, three of which (one unpolarized and two polarized) look at the water and similarly three at the sky. The system autonomously tracks the Sun position and the heading of the research vessel to which it is attached in order to maintain a fixed relative azimuth angle with respect to the Sun (i.e. 90°) and therefore avoid the specular reflection of the sunlight. For the duration of both cruises, (NASA Ship Aircraft Bio-Optical Research (SABOR), and NOAA VIIRS Validation/Calibration), in-situ inherent optical properties (IOPs) were continuously acquired using a set of instrument packages modified for underway measurement, and hyperspectral radiometric measurements were taken manually at all stations. During SABOR, an underwater polarimeter and a full Stokes polarization camera were deployed when conditions permitted. All measurements, above and below the sea surface, were combined and compared in an effort to first develop a glint (sky + Sun) correction scheme for the upwelling polarized signal from the ocean, and compare this signal with one simulated by a vector radiative transfer code using the measured IOPs as input. Further, we examine the relationship recently developed by us between the degree of linear polarization (DoLP) and the optical properties of ocean waters, specifically the ratio of the attenuation to absorption coefficients. Relationships between the DoLP and microphysics of particulates are also analyzed.

9613-32, Session 10

Material identification using polarimetric hyperspectral imagery

Jacob A. Martin, Kevin C. Gross, Air Force Institute of Technology (United States) and Oak Ridge Institute for Science and Education (United States)

Polarimetric hyperspectral imaging (P-HSI) combines two common remote sensing modalities. This work leverages the combination of these techniques to improve material classification. Classifying and identifying materials requires parameters which are invariant to changing viewing conditions, most often a materialÃ, Ts reflectivity or emissivity is used. Measuring these most often requires assumptions be made about the material and atmospheric conditions. Utilizing both polarimetric and hyperspectral imaging, we can remotely estimate the index of refraction of a material, while simultaneously solving for a handful of parameters describing the atmosphere. In general, this is an underdetermined problem because both the real and imaginary components of index of refraction are unknown at every spectral point. By modeling the spectral variation of the index of refraction using a few parameters, however, the problem can be made overdetermined. A number of different functions can be used to describe this spectral variation, and some are discussed here. Reducing the number of spectral parameters to fit allows us to add parameters which estimate atmospheric downwelling radiance and transmittance. Additionally, the object temperature is added as a fit parameter. The set of these parameters that best replicate the measured data is then found using a bounded Nelder-Mead simplex search algorithm. Other search algorithms are also examined and discussed. Results show that this technique has promise, but also some limitations, which are the subject of ongoing work.

9613-33, Session 10

Polarization-based complex index of refraction estimation with volumetric scattering consideration

Hanyu Zhan, David G. Voelz, Xifeng Xiao, New Mexico State Univ. (United States)

Abstract

The estimation or recovery of the index of refraction from optical scatter off a target's surface is a task of pivotal importance for remote sensing applications such as material classification and target recognition. Previous studies show that optical polarimetry is an effective approach for index of refraction estimation in remote sensing applications. However, straightforward polarimetric models based on Fresnel inversion are limited to specular targets and surface scattering. In this paper, we propose a method to estimate the refractive index in the presence of an unknown, unpolarized diffuse scattering component in the polarimeter measurements. The effect of the diffuse scattering is modeled following the Kubelka-Munk theory, which describes the polarization phenomena of non-specular materials including both contributions of surface and diffuse scattering. Our simulation results indicate that the recovered indices of refraction without consideration of diffuse scattering will introduce significant errors, especially for dielectric materials. Our method can accurately recover the complex index of refraction for both specular and non-specular targets in both visible and infrared spectrum involving surface and diffuse scattering.

9613-34, Session 10

Remotely sensing the photochemical reflectance index (pri)

Vern C. Vanderbilt, NASA Ames Research Ctr. (United States); Craig S. T. Daughtry, U.S. Dept. of Agriculture (United States); Robert P. Dahlgren, NASA Ames Research Ctr. (United States)

In remote sensing, the Photochemical Reflectance Index (PRI) provides insight into physiological processes occurring inside the leaves in a stand of plants. Developed by Gamon et al., (1990 and 1992), PRI evolved from laboratory measurements of the reflectance of individual leaves (Bilger et al.,1989). Yet in a remotely sensed image, a pixel measurement may include light from both reflecting and transmitting leaves.

We conducted laboratory experiments comparing values of PRI based upon polarized reflectance and transmittance measurements of water and nutrient stressed leaves. We illuminated single detached leaves using a current controlled light source (Oriel model 66881) and measured the leaf weight using an analytical balance (Mettler model AE 260) and the light reflected and transmitted by the leaf during dry down using two Analytical Spectral Devices spectroradiometers. Polarizers on the incident and reflected light beams allowed us to divide the leaf reflectance into two parts: a polarized surface reflectance and a non-polarized 'leaf interior' reflectance.

Our results underscore the importance when calculating PRI of removing the leaf surface reflection, which contains no information about physiological processes ongoing in the leaf interior. The results show that the leaf physiology information is contained in the leaf interior reflectance, not the leaf transmittance. Applied to a plant stand, these results suggest use of polarization measurements in sun-view directions that minimize the light arriving from transmitting leaves in the sensor field of view.



9613-35, Session 10

The 3MI mission: multi-viewing -channel -polarisation imager of the EUMETSAT polar system - second generation (EPS-SG) dedicated to aerosol and cloud monitoring

Thierry Marbach, European Organisation for the Exploitation of Meteorological Satellites (Germany); Jérôme Riedi, Univ. des Sciences et Technologies de Lille (France); Antoine Lacan, Peter Schluessel, European Organisation for the Exploitation of Meteorological Satellites (Germany)

The Multi-Viewing -Channel -Polarisation Imager (3MI), planned to fly on the EPS-SG platform in the time-frame 2020–2040, is a push-broom radiometer dedicated to aerosol and cloud characterisation for climate monitoring, atmospheric composition, air quality and numerical weather prediction.

The role of clouds in determining climate sensitivity to change is highly uncertain. Hence new cloud observation systems (ground-based and space-borne) are needed for cloud monitoring. Cloud remote sensing must be performed at multiple channels (from UV to microwave) using passive multi-angle observations of the intensity and polarization characteristics of reflected/transmitted radiation and also radiative fluxes inside/above/below clouds.

The purpose of the 3MI is to provide multi-spectral (from 410 to 2130 nm), multi-polarisation (-60° , 0° , and $+60^{\circ}$), and multi-angular (10 to 14 views) images of the Earth top of atmosphere (TOA) outgoing radiance. First results from the 3MI synthetic data simulator will be presented.

Although aerosol and cloud characterisation is the primary application, 3MI will further support observation of land-surface characteristics which will benefit from the enhanced directional and polarisation measurements and provide a better understanding of the Earth radiative forcing budget.

3MI will benefit from the synergy of other instruments flying also onboard EPS-SG. Measurements from thermal infrared channels will be available from the METimage and IASI-NG instruments. Furthermore, the Sentinel-5 will provide information from the ultra-violet to the short-wave infra-red, through a coarser horizontal sampling. The synergy with these instruments will also support 3MI with beneficial cross-calibration as 3MI will not have an onboard calibration and its radiometric performance will rely on vicarious calibration.

9613-36, Session PWed

System of polarization phasometry of polycrystalline blood plasma networks in mammary gland pathology diagnostics

Natalia I. Zabolotna, Vinnytsia National Technical Univ. (Ukraine); Bogdan P. Oliinychenko, Medivin (Ukraine); Kostiantyn O. Radchenko, Anastasiia K. Krasnoshchoka, Olga K. Shcherba, Vinnytsia National Technical Univ. (Ukraine)

Nowadays, laser polarimetry methods and systems that start to be used for diagnostic purposes in medicine, allow to get qualitatively new results in research into morphological and functional state of biological objects.

In this paper the effectiveness indexes of the direct polarization phasometry system are determined for diagnosing mammary gland pathology by direct phase mapping of human plasma films with the subsequent statistic, correlation, and fractal estimation of the received phase map structure. This has revealed the objective possibility of phase detection of breast pathological states by using statistical, correlation and fractal parameters characterizing optical - anisotropic component of plasma proteins.

The experiment was conducted in the traditional direct phase polarimetry system, including: He-Ne laser, quarter-wave plates, collimator optics, a polarizer and an analyzer, a micro lens, a research sample and a CCD camera

connected to the computer.

The object of research was a series of plasma stroke samples taken from three groups of patients - healthy (group 1), with mastopathy (Group 2), patients with breast cancer (group 3). Further experimental research of coordinate structure distribution of phase shifts between orthogonal states of polarization of laser microscopic images of crystallized amino albumin and globulin plasma films networks for all patient groups was performed. This study was followed by determining quantitative criteria for phase differentiation of pathological breast conditions (statistical, correlation and spectral moments of 1st - 4th orders). It has been established that spectral and correlation moments do not allow differentiating the state of the object, so it is advisable to use statistic estimation.

To characterize information content of direct phasometry method for the diagnosis of benign and malignant breast changes, primary and secondary operating characteristics: sensitivity, specificity, accuracy, positive outcome predictability, negative result predictability were defined.

High self-descriptiveness level in mapping distributions of phase shifts in plasma films by using a common statistic moment for diagnosing benign and malignant breast changes has been discovered.

From the obtained data about statistic structure of phase maps of plasma films laser images for all groups of healthy and sick patients, the unbiased opportunity for not only emergency diagnosing mammary gland pathology, but also differentiating their severity. Sensitivity and specificity of statistical moment of 2nd order phase maps made respectively: in diagnosing benign breast changes 77% and 83%; in diagnosing malignant changes in breast 91% and 86%; in differentiating benign and malignant breast changes 86% and 80%. Accordingly, a high level of reliability and validity of the proposed method has been stated.

9613-37, Session PWed

A portable imaging Mueller matrix polarimeter based on a spatio-temporal modulation approach: theory and implementation

Israel J. Vaughn, College of Optical Sciences, The Univ. of Arizona (United States); Oscar G. Rodriguez, Mohan Xu, The Univ. of Arizona (United States); J. Scott Tyo, College of Optical Sciences, The Univ. of Arizona (United States)

Imaging polarimeters have been largely used for remote sensing tasks, and most imaging polarimeters are division of time or division of space Stokes polarimeters. Imaging Mueller matrix polarimeters have just begun to be constructed which can take data quickly enough to be useful for remote sensing tasks. We have constructed a full Mueller matrix polarimeter utilizing a hybrid modulation approach (modulated in both time and space) based on a micro-polarizer array camera and rotating retarders.

We introduce a channel structure derived from the spatio-temporal modulation and optimize over control parameters to minimize channel crosstalk. We present an instrument utilizing this hybrid approach and various reconstruction schemes tailored to specific constraints. Furthermore, we present example data acquired with the instrument and some specific examples of reconstruction of that data.



9613-38, Session PWed

Polarization modulation for the Atacama Cosmology Telescope using continuously rotating half-wave plates

Jonathan T. Ward, Mark J. Devlin, Univ. of Pennsylvania (United States); Robert Thornton, West Chester Univ. of Pennsylvania (United States); Jeffrey McMahon, Kevin Coughlin, Fletcher Boone, Charles Munson, Rahul Datta, Univ. of Michigan (United States)

Among the greatest open challenges confronting the field of contemporary physics is understanding the first moments of the universe, the properties of it's contents, the formation of structure under the influence of gravity, and the nature of dark energy. A principal method of improving our understanding of these topics originates through direct measurement of the Cosmic Microwave Background (CMB). The Atacama Cosmology Telescope (ACT) makes high resolution measurements of the CMB and it's polarization. Measuring the polarization allows cosmologists to better understand the structure of the universe and the moments immediately following the Big Bang. To achieve polarization measurements at large angular scales, ACT utilizes continuously rotating half-wave plates (HWPs). The HWPs are controlled using a custom air bearing system coupled to high-performance drive motors, with position and frequency readout handled by a self-built encoder. Such measurements will allow ACT to probe the faint B-mode polarization signal created by primordial gravitational waves, a key piece of evidence for the theory of cosmological inflation. Details of the mechanical design, control system, encoder readout, and installation are discussed as well as preliminary performance tests that highlight the stability and reliability of the instrument. The optical properties and performance of the achromatic, birefringent, metamaterial, silicon HWPs are also presented. The complete system highlights innovative methods in polarization science, both in the field of cosmology and for other applications.

9613-39, Session PWed

Characterizing the kinetics of suspended cylindrical particles by polarization measurements

Ran Liao, Nan Zeng, Honghui He, Hui Ma, Tsinghua Univ. (China)

Polarization responses sensitively to the microstructures in the samples such as the tissues, and has promising potential to retrieve the information. However, for the fast changing sample such as the suspended algae in the water, the kinetics of the particles also influence the scattered polarization. The present paper will show our recent results to extract the information about the kinetics of the suspended cylindrical particles from polarization measurements. The sample is the aqueous suspension of the fiber glasses stirred by a magnetic stirrer. We measure the scattered polarization of the glass fibers by use of a simultaneous measurement system and obtain the time series of two polarization components, i.e., VV and VH. By use of correlation analysis, we obtain the correlation times of both VV and VH, which change with the concentration and the stirring speed of the sample. We find that the correlation time of VV and VH are different, which indicates that VV and VH describe different motion of the fibers. Also, the time corresponding to the maximum of the cross-correlation function of VV and VH has a shift which changes differently as we change the concentration and the stirring speed of the sample. Preliminary analysis shows that these time constants, i.e., the correlation time and the time shift, may originate from the translation and rotation kinetics of glass fibers in the flow field.

9613-40, Session PWed

Identification of soot particles in air using polarization scattering method

Da Li, Nan Zeng, Maomao Zeng, Ran Liao, Hui Ma, Tsinghua Univ. (China)

Light scattering in atmosphere can change optical polarization properties. Analysis and Measurement on interaction of polarized light with atmospheric particulates can provide important information to evaluate the atmospheric composition and conditions. In this paper, we propose a polarization character focusing on the evaluation of soot content in the air, based on our polarized photon scattering simulation program. The simulation results demonstrate how the polarization parameter at a specific scattering angle can identify the soot particles from the other air pollutants. Compared with non-polarization optical measurement, polarization characterization can enhance the contrast of distinguishing different type particles and also can be applied in a wide particle size range.

SPIE. OPTICS+ PHOTONICS **Conference 9614: Laser Communication and** Propagation through the Atmosphere and Oceans IV

Monday - Wednesday 10-12 August 2015

Part of Proceedings of SPIE Vol. 9614 Laser Communication and Propagation through the Atmosphere and Oceans IV

9614-1, Session 1

Estimation of turbulence strength, anisotropy, outer scale and spectral slope from an LED array (Invited Paper)

Max Segel, Szymon Gladysz, Christian Eisele, Rui Barros, Fraunhofer-Institut für Optronik, Systemtechnik und Bildauswertung (Germany)

Decorrelation of tip/tilt information is of fundamental importance in imaging and laser propagation through the atmosphere without a cooperative beacon on the target. Applications include laser-guide-star adaptive optics, tracking of fast-moving objects and multi-beam laser communications. We compute gradient-tilt anisoplanatism for the case of spherical-wave propagation. The model is then fitted to data obtained from an LED array observed from a 110-m distance. We show how with this data one can estimate several properties of atmospheric turbulence: turbulence strength, anisotropy, outer scale and spectral slope.

9614-2, Session 1

Blob identification algorithms applied to laser speckle to characterize optical turbulence

Galen Cauble, David T. Wayne, Space and Naval Warfare Systems Ctr. Pacific (United States)

Laser beam speckle resulting from atmospheric turbulence contains information about the propagation channel. The number and size of the speckle cells can be used to infer the spatial coherence and thus the Cn2 along a path. The challenge with this technique is the rapidly evolving speckle pattern and non-uniformity of the speckle cells. In this paper we investigate modern blob counting techniques used in biology, microscopy, and medical imaging. These methods are then applied to turbulent speckle images to estimate the number and size of the speckle cells. Speckle theory is reviewed for different beam types and different regimes of turbulence. Algorithms are generated to calculate path Cn2 from speckle information and path geometry. To test our algorithms, we use WaveProp software to generate propagation simulations with known turbulence conditions. Additionally, the algorithms are tested on speckle images from experimental data collected over a turbulent 1km path.

9614-3, Session 1

Stereo image motion monitor for atmospheric mitigation and estimation

Kristofor Gibson, SPAWAR Systems Ctr. (United States)

The knowledge of the turbulence strength in the atmosphere is important for many applications. Imagery in the atmosphere experience significant blur when the turbulence is strong. This can be automatically improved (without user intervention) if the turbulence strength is known. The performance of a high-power laser emitting in the atmosphere can be predicted if the statistics of the turbulence strength is known. If not predicted correctly, the laser may unintentionally destroy a target or fail to be able to disable a target.

In this article, we review existing methods that estimate turbulence strength, provide a more in depth error analysis, and propose a new method for estimating and mitigating turbulence in the atmosphere. We focus on methods that are passive in design in order to prevent detection in surveillance scenarios and tactical situations. We also propose a new method, stereo image motion monitor (SIMM) which is a system containing two independent apertures. Our goal in this approach is threefold: 1) We can measure r0 using the DIMM method 2) We can simultaneously estimate r0 individually for each aperture and 3) We have multiple views of the same scene thus can increase the number of frames used in turbulence mitigation methods.

OPTICAL ENGINEERING+

APPLICATIONS

9614-4, Session 1

Imaging through turbulence using a plenoptic sensor

Chensheng Wu, Jonathan Ko, Christopher C. Davis, Univ. of Marvland, College Park (United States)

Atmospheric turbulence is a natural disturbance affecting remote imaging along paths near the ground. It causes time varying inhomogeneity of the refractive index of air and therefore disrupts the propagation of optical signals from the object to the viewer. Under circumstances of deep turbulence or strong turbulence, the object is hard to recognize through direct imaging. And conventional methods will have degraded results, such as increased time for performing lucky imaging and more complicated de-blurring process at the software layer. We propose the approach of using a plenoptic sensor after a telescope for imaging remote targets through turbulence. The plenoptic sensor uses a shared objective lens and a microlens array to form a mini Keplerian telescope array. Thus, the image obtained by a conventional telescope will be separated into an array of images that contains multiple copies of the object's image and less correlated turbulence disturbances. Then a high-dimensional lucky imaging algorithm can be performed based on the collected video from the imaging camera. The corresponding algorithm will select the most stable pixels from various image cells and assemble the image of the object as if there is only a weak turbulence effect. Then, by comparing the reconstructed image with the recorded images in each MLA cell, the difference can be regarded as the turbulence effects. As a result, the retrieval of the object's image and extraction of turbulence effect can be performed simultaneously. The system structure, algorithm and experimental results will be demonstrated in this presentation.

9614-5, Session 2

Super-resolution in the scintillation imaging through turbulence

Mikhail I. Charnotskii, National Oceanic and Atmospheric Administration (United States)

Fluctuations of the images of stationary incoherent objects viewed through turbulence normally are treated as a detrimental noise, and variety of techniques have been suggested to mitigate this nuisance. In this talk we discuss the concept of the Scintillation Imaging (SI), when, instead of attempting to recover the proper object image, image fluctuations are used to gain the information about the object. It appears that due to the "third constraint" on the turbulent point spread function [Charnotskii, OE, 52, 046001, 2013] SI has differentiating properties and emphasizes the areas of the high contrast of the object. We show, that the SI can unveil the turbulence super-resolution effect that was originally discovered in [Charnotskii, et. al. JOSA A, 7, p. 1345, 1990]. The peculiarities of the SI are discussed using a simple example of a sinusoidal grating object. In this case SI consists of the uniform background and harmonic components at the double spatial frequency. The contrast of this SI is not sensitive to the contrast of the object, and amplitude of the harmonic component vanishes when target wave number exceeds the diffraction limit. However, the scintillation background persists even when the grating cannot be



resolved by the imaging aperture. This is a manifestation of the turbulent super-resolution when light scattering by turbulent eddies makes it possible for the imaging aperture to collect high spatial frequencies of the object. We will discuss possible applications of this effect for the imaging of homogeneous random textures, such agricultural and forestation landscapes.

9614-6, Session 2

Using aperture partitioning to improve scene recovery in horizontal long-path speckle imaging

Jeremy P. Bos, Air Force Research Lab. (United States); Brandoch Calef, Boeing LTS Inc. (United States)

Recently, Calef [1] showed that a novel aperture-partitioning optic could be used to vastly improve imagery of space object when in situations where the ratio of aperture size to coherence radius was very large. These situations are common when either the aperture is large or the turbulence is strong. Borrowing from the terminology of interferometry, the presence of multiple independent coherence cells across the aperture results in baseline redundancy. These redundancies further blur imagery and reduce the effectiveness of speckle imaging. Calef's partitioned aperture optic removes this redundancy by dividing aperture into annular rings; each creating a separate image. Phase estimates at each spatial frequency are acquired using the bispectrum method [2] and combined by weighting each estimate by the SNR of the estimate.

In this work, we explore the use of a similar partitioned aperture optic to improve speckle imaging in daytime horizontal imaging scenarios. In these scenarios, the turbulence is typically strong but the aperture sizes more modest. Thus, outright baseline redundancy is less severe. On the other hand, imaging through a distributed turbulence volume introduces severe anisoplantism. In some scenarios, the isoplanatic angle may be on the order of the diffraction-limit. In previous presentation at this conference [3,4,5] we successfully demonstrated the application of speckle imaging on both simulated [4] and field data [5]. In this presentation we will begin by reviewing both the reasoning and technique of aperture partitioning. Next, we will describe straightforward modifications to our horizontal imaging simulation model and show image sequences from each of the partitioned along with the image of a full aperture. After briefly describing the reconstruction process we will present examples of reconstructed images and compare results objectively via the residual MSE of image sets to a diffraction-limited reference.

[1] Calef, Brandoch. "Improving imaging through turbulence via aperture partitioning." SPIE Defense, Security, and Sensing, 2010.

[2] Roggemann, Michael C., Byron M. Welsh, and Bobby R. Hunt. Imaging through turbulence. CRC press, 1996.

[3]Bos, Jeremy P., and Michael C. Roggeman. "Simulation of extended scenes imaged through turbulence over horizontal paths." SPIE Optical Engineering+ Applications. , 2011.

[4] Bos, Jeremy P., and Michael C. Roggeman. "The effect of free parameter estimates on the reconstruction of turbulence corrupted images using the bispectrum." SPIE Optical Engineering+ Applications, 2011.

[5]Bos, Jeremy P., and Michael C. Roggemann. "Estimation of the atmospheric blurring function using blind image quality metrics." SPIE Optical Engineering+ Applications. 2012.

9614-7, Session 2

Modeling and simulation of anisoplanatic (space-variant) imaging through the atmosphere

Colin Reinhardt, Space and Naval Warfare Systems Ctr. Pacific (United States)

We wish to synthesize computer-generated images which are as physically-

realistic as possible. For terrestrial imaging scenarios we must account for the physical effects of the earth's atmospheric boundary layer on EO/ IR wave propagation between remote objects and the imaging device. These effects can vary pixel-by-pixel depending on the optical path lengths between the imager and objects subtended by each pixel instantaneous field-of-view (IFOV), on the path height above ground (or water) and the path elevation angle to the horizontal, and on the intervening atmospheric microphysical properties. When an image sensor array has a wide enough field-of-view (FOV) that there is significant variation in the optical path length to objects imaged by the different pixels, or such that the sensor full angle FOV is greater than the isoplanatic angle of the atmospheric turbulence, then the typical assumptions of linear space/shift-invariance (LSI) which allow the representation of the output image as the convolution of the input image and a single point-spread function (PSF) are no longer valid. Instead we must use the space-variant (or shift-variant) (SV) formulation. We present a physically accurate modeling and simulation algorithm which solves the SV imaging problem in a computationallyaffordable manner, with a significant increase in image fidelity. Our method includes the effects of atmospheric aerosols (extinction and multiplescatter) along the varying optical paths to objects subtended by each pixel, including slant-path geometries, and also the effects of optical turbulence under anisoplanatic imaging conditions. We also present useful uncertainty bounds on the results.

9614-8, Session 2

Propagation dynamics of optical vortices in turbulent atmosphere

Haiyan Wang, Nanjing Univ. of Science and Technology (China)

Due to the conservation of topological charges and quantum secrecy, laser beams embedded optical vortices can be widely used in Optical communication. Optical vortices may exhibit propagation dynamics similar to hydrodynamic vortex phenomena. Numerical methods are used to describe and investigate the interaction between optical vortices and the turbulence of atmosphere when laser beams propagating through turbulent atmosphere. We demonstrate that the turbulence of atmosphere may affect the orbit of optical vortices. We also describe the properties of the unsymmetrical discrete optical vortices.

9614-10, Session 3

Spread and wander of a laser beam propagating through anisotropic atmospheric turbulence

Italo Toselli, Olga Korotkova, Univ. of Miami (United States)

On propagation of a laser (TEM00) beam at high altitude it may traverse the regions of stratified turbulence, and hence may experience its anisotropic effects. Naturally such anisotropy occurs in x-z or y-z planes, where x and y are the mutually orthogonal horizontal directions and z is the vertical direction. On assuming that the beam propagates along a horizontal direction y we employ the Rytov method together with the Markov approximation for derivation of the closed-form expressions for the short and long terms of the averaged intensity of the beam and deduce its spread and wander, along directions x and z. For our derivations we use the recently introduced anisotropic non-Kolmogorov spectrum for taking into account the distribution of crude and fine structures of turbulence in addition to the anisotropy



9614-35, Session 3

Enhanced backscatter analysis for longrange optical tracking in deep turbulent conditions

Christopher A. Smith, Sara B. Belichki, Ronald L. Philips, Larry C. Andrews, Townes Laser Institute (United States) and CREOL, The College of Optics and Photonics, Univ. of Central Florida (United States); David T. Wayne, Space and Naval Warfare Systems Ctr. Pacific (United States)

The usage of long-range optical systems for tracking applications encounters regions of deep turbulence throughout propagation. Such conditions lead to the inability to remain on target for a tracked object due to scintillation. To mitigate this issue, an enhanced backscatter (EBS) optical system is utilized as a means of keeping alignment while characterizing turbulent conditions. EBS is detected through the means of image processing algorithms that capture the returning constructive interference from the target. This paper evaluates EBS optical systems using a retroreflector for both 1 kilometer and 13 kilometer ranges in order to validate theoretical models that typify atmospheric turbulence regarding low-ground and slant path propagation. Meteorological conditions are also included in the empirical data obtained for the analysis of atmospheric conditions that contribute to non-homogenous turbulent conditions along the path. Lastly, scintillation index measurements derived from image processing algorithms along single and double pass are assessed to determine the fidelity of such a system for optical tracking.

9614-11, Session 4

Lunar laser ranging: atmospheric limitations and upgrading SLR stations

Douglas G. Currie, Univ. of Maryland, College Park (United States)

The Lunar Laser Ranging Program (LLRP), using data obtained by ranging to the retroreflector arrays deployed during the Apollo missions, has produced most of the best tests of Gravitation and General Relativity. This data is being used to address theories of Dark Matter and Dark Energy. With deployment of the next generation anchored "Lunar Laser Ranging Retroreflector Arrays for the 21st Century" (LLRRA-21), the accuracy of the science results will ultimately be determined by the effects of the earth's atmosphere through which the laser pulse propagates. The ultimate limitations for range measurements will be the jitter, or short term fluctuations, for the single photoelectron (SPE) ranges and the biases of the normal points produced by multiple ranges taken in a short time interval. The former is due to turbulence and the cells with different temperatures. The long term latter effect is caused by atmospheric spatial gradients in temperature and pressure. The recent improvements in the estimates of both the SPE jitter using the GLAD software and additional analysis that improved the estimates of the magnitude of bias estimates and the accuracy of the these estimates. At present, the several Satellite Laser Ranging (SLR) stations have the equipment to accomplish the most accurate laser ranging. We will discuss the relation between the atmospheric propagation effects and the existing equipment configurations of these several SLR stations. Finally, we will address some other applications of the effects of the atmospheric induced jitter, in particular, the role in 3D imaging of satellites.

9614-12, Session 4

Different atmospheric effects causing FSO link attenuation: experimental results and modelling in Czech Republic

Ondrej Fiser, Institute of Atmospheric Physics of the ASCR, v.v.i. (Czech Republic) and Czech Technical Univ.

in Prague (Czech Republic); Vladimir Brazda, Institute of Atmospheric Physics of the ASCR, v.v.i. (Czech Republic)

Different Atmospheric Effects Causing FSO Link Attenuation - Experimental Results and Modelling in Czech Republic

The six year FSO link attenuation measurement concurrently with most important meteorological parameters was performed at our mountain observatory Milesovka. In this contribution we summarize and classify different atmospheric phenomena after the FSO link attenuation quantity. For all particular phenomena the CD curves, typical events and simple dependences on relevant atmospheric parameter(s) are presented. We consider the following phenomena (approximate attenuation in dB in brackets):

1. Fog and cloud (hundreds dB)

This attenuation is modelled in the dependence on meteorological visibility. Examples distinguishing cloud and fog are discussed. Visibility is measured by sensors as well as by videocamera, results are compared.

2. Rain and snow (tens dB)

Rain rate as an attenuation predictor is measured by rain gauge and videodistrometer.

3. Atmospheric turbulence (unit dB)

We evaluate this attenuation through the signal redistribution due to refractivity index in-homogeneity in the dependence on both: structure index and Rytov formula as well as on selected wind parameters derived from 3D sonic anemometer. Correlation of both approaches is acknowledged.

4. Clear air attenuation due to water vapour (unit dB or less)

So called "Clear air attenuation" is caused by invisible atmospheric gasses especially through water vapour. This attenuation depends on the air humidity, temperature and pressure or on "sonic temperature," which is measured by the 3D sonic anemometer.

9614-13, Session 5

Determining beam properties at an inaccessible plane using the reciprocity of atmospheric turbulence

William Nelson, Chensheng Wu, Christopher C. Davis, Univ. of Maryland, College Park (United States)

A turbulent, atmospheric channel can be considered to be exactly reciprocal at any instance in time. Reciprocity is a powerful property that can be used to compensate for the distortions caused by turbulence such as beam scintillation, spreading, and wander. In free-space optical communication systems, reciprocity can be used by phase conjugating a beacon beam propagating from the receiver to the transmitter. However, this strategy would not work in directed energy (DE) systems where the target is uncooperative and the transmitter and receiver are located in the same plane. Theoretical work by Lukin and Charnotskii [Sov. J. Quantum Electron., 12(5), 602 (1982)] has shown that reciprocity principles indicate that certain properties of the beam incident on a target fluctuate synchronously with the intensity distribution reflected from the target. Here we extend this analytically pure treatment using a combination of simulations and experiments. We show that there exists a correlation between the intensity imaged by the receiver and properties of the beam incident on the target. Furthermore, we find that the intensity at a specific location can be used to drive an adaptive optics system that corrects for atmospheric distortions.

9614-14, Session 5

Entropy studies on beam distortion by atmospheric turbulence

Chensheng Wu, Jonathan Ko, Christopher C. Davis, Univ. of Maryland, College Park (United States)



When a beam propagates through atmospheric turbulence over a known distance, the target beam profile deviates from the projected profile of the beam on the receiver end. Intuitively, the unwanted distortion indicates the information carried by the atmospheric turbulence itself. And this information is crucial for guiding adaptive optic systems and improving beam propagation results. In this paper, we propose a 2D entropy function based on the image from a plenoptic sensor to describe the information about atmospheric turbulence. When no correction is applied, the value of the entropy function will increase when the turbulence gets stronger and decrease when the turbulence gets weaker. And at the same level of turbulence, when corrections are applied, the entropy function will decrease with good correction and increase with bad correction. Therefore, the entropy function can be used to analyze the turbulence distortion and evaluate performance of AO systems. In fact, it serves as an image metric that can tell the improvement of beam correction in each iteration step. In addition, it points out the limitation of the AO system at optimized correction as well as the minimum information needed for wavefront sensing to achieve certain levels of correction. In this paper, we will demonstrate the definition of the entropy function and how it is related to evaluating information (randomness) carried by atmospheric turbulence and how this information (randomness) is suppressed by some AO devices in performing correction.

9614-15, Session 5

Analogue holographic wavefront sensor: a performance analysis

Andreas Zepp, Szymon Gladysz, Rui Almeida de Sa Barros, Fraunhofer-Institut für Optronik, Systemtechnik und Bildauswertung (Germany); Wolfgang Osten, Univ. Stuttgart (Germany) and Institut für Technische Optik (Germany); Karin U. Stein, Fraunhofer-Institut für Optronik, Systemtechnik und Bildauswertung (Germany)

The efficiency of laser communications systems is significantly limited by atmospheric effects. Notably challenging scenarios like a long horizontal path or strong scintillation lead to high failure rates of the electro-optical systems. Adaptive optics (AO) methods and components developed for astronomical applications cannot fulfill these higher requirements.

The so-called Holographic Wavefront Sensor (HWFS) is a promising alternative for measuring the wavefront deformation of a laser beam. The basic elements of the HWFS are a diffraction pattern and a fast photodetector like a photodiode array. With these components the aberrations present in the beam are measured directly. The advantages of the HWFS are the high bandwidth (MHz range) and the possibility to use it in strong turbulence where scintillation is a limiting factor for the SHS.

In this paper we show the realization of an analogue HWFS. Core of the sensor is a photosensitive plate. We discuss the benefits and disadvantages in comparison to the digital HWFS. To analyze the performance of the sensor, we studied the effect of residual tip / tilt on the sensor response and the dependency on the detector size. For the challenging applications like laser communications the behavior of a wavefront sensor in the presence of scintillation is a very important criterion. We present experimental results to analyze the influence of scintillation on the analogue HWFS. We are now working on integration of the HWFS in an AO system. In the field of laser communications this can lead to optimized fiber coupling and with this to higher bandwidths and a better light efficiency.

9614-16, Session 5

Atmospheric turbulence induced by hot metal objects

Miranda van Iersel, TNO (Netherlands); Henny E. T. Veerman, Alexander M. van Eijk, TNO (Netherlands)

A CUBI is a simple geometric metal object that is placed in an outdoor environment. The (daily) temperature evolution of the individual facets is

monitored as function of environmental parameters, such as solar irradiance and ambient temperature. This provides insight in the parameters that have the strongest effects on the thermal signature of the CUBI. The CUBI is also imaged by thermal cameras, which provide insight in the amount of air turbulence that is generated by the radiance of the hot facets, as well as the effect of this turbulence on image quality. The amount of turbulence can be compared with the ambient turbulence as calculated by standard bulk theories.

9614-17, Session 5

An adaptive optics approach for laser beam correction in turbulence utilizing a modified plenoptic camera

Jonathan Ko, Chensheng Wu, Christopher C. Davis, Univ. of Maryland, College Park (United States)

Adaptive optics has been widely used in the field of astronomy to correct for atmospheric turbulence while viewing images of celestial bodies. The slightly distorted incoming wavefronts are typically sensed with a traditional Shack-Hartmann sensor and then corrected with a deformable mirror. Although this approach has proven to be effective for astronomical purposes, a new approach must be developed when correcting for the deep turbulence experienced in ground to ground based optical systems. We propose the use of a modified plenoptic camera as a wavefront sensor capable of accurately reconstructing an incoming wavefront that has been significantly distorted by strong turbulence conditions (Cn2>10-13 m-2/3). An intelligent correction algorithm can then use this reconstructed wavefront information to drive a deformable mirror capable of correcting the major distortions in the wavefront. After the large distortions have been corrected, a secondary mode utilizing a stochastic parallel gradient descent algorithm can take over to fine tune the wavefront correction. This two-part algorithm can find use in free space optical communication systems as well as for image correction purposes.

9614-18, Session 6

Estimating refractive index structure parameter (Cn2) profiles in the atmosphere: a framework based on fractal interpolation (Invited Paper)

Sukanta Basu, Ping He, North Carolina State Univ. (United States)

The refractive index structure parameter (Cn2) is commonly used for the quantification of optical turbulence intensity. Over the years, various specialized instruments (e.g., thermosonde, SCIDAR) have been developed for the accurate measurement of Cn2 in the atmosphere. In parallel, a number of empirical models have also been proposed for the reliable estimation of Cn2. For example, the popular Submarine Laser Communications (SLC) model was developed based on averaged Cn2 measurements on Mt. Haleakala, Hawaii. In contrast, the Critical Laser Enhancing Atmospheric Research I (CLEAR I) model was based on observational data from the New Mexico desert. Given that these empirical Cn2 models are site-specific and time-invariant, their applicability to the other regions of the world is questionable.

In this study, we propose a novel Cn2 estimation framework and demonstrate its prowess by validating our predicted results against the measured Cn2 data from the Hawaii 2002 thermosonde campaign by the Air Force Research Laboratory. The salient features of this framework are: (i) ability to capture realistic spatio-temporal variations of Cn2 based on local meteorological settings; (ii) assumption of quasi-universal vertical scaling of temperature fields; (iii) application of the so-called fractal interpolation function technique for statistical downscaling; and (iv) utilization of coarse-resolution temperature and pressure profiles. These profiles can be readily obtained from weather balloons (aka radiosondes), satellite-based soundings (e.g., AIRS), and numerical weather prediction model-generated



output from across the globe.

We would like to emphasize that our proposed Cn2 estimation approach only requires temperature and pressure profiles as input. In contrast, the well-known Cn2 model proposed by Air Force Geophysics Laboratory (AFGL) relates Cn2 to the profiles of wind speed, temperature, and pressure. Since the measurement and/or modeling of wind speed is usually challenging, our approach is expected to be less error-prone and more reliable than the AFGL model.

9614-19, Session 6

Mesoscale modeling of optical turbulence utilizing novel Cn2 parameterizations

Ping He, Sukanta Basu, North Carolina State Univ. (United States)

Small-scale fluctuations of refractive index, commonly known as optical turbulence, can have significant impacts on optical wave propagation in the atmosphere (e.g., beam wandering, scintillation). The intensity of optical turbulence is characterized by the refractive index parameter (Cn2). Accurate numerical modeling of Cn2 is a challenging task since one needs to capture atmospheric scales ranging from the inertial sub-range (on the order of 1 m) to the propagation range (on the order of 100s of km). This modeling difficulty can be further aggravated by the presence of complex atmospheric phenomena (e.g., coherent wake vortices, low-level jets).

In this study, we perform state-of-the-art mesoscale modeling of optical turbulence utilizing two novel Cn2 parameterizations. One of these parameterizations is based on the fractal interpolation function technique and utilizes a quasi-universal vertical scaling of temperature fields. We utilized high-resolution observational data for its development. The other parameterization has its root in the so-called gradient-based similarity theory. We have developed this particular parameterization using an extensive synthetic turbulence database. Numerous direct numerical simulations (DNS) and large-eddy simulations (LES) were performed to create this unique database. It contains both continuous and nitermittent turbulence events and spans a wide-range of Reynolds and Richardson numbers.

In order to document the strengths and weaknesses of our newly proposed Cn2 parameterizations, we have selected several realistic cases from the Hawaii 2002 thermosonde campaign by the Air Force Research Laboratory. The Weather Research and Forecasting (WRF) model (coupled with the Cn2 parameterizations) is employed to simulate these cases. Relatively high spatial resolution (innermost grid with one km grid-spacing) is used for all the runs. For model validation, we primarily make use of the thermosonde-based Cn2 and other meteorological data. For completeness, we also report the performance of a few conventional Cn2 parameterizations (e.g., HV-5/7, AFGL) in this study.

9614-20, Session 6

The Havemann-Taylor Fast Radiative Transfer Code (HT-FRTC) and its Applications

Jean-Claude Thelan, Stephan Havemann, Warren J. Lewis, Met Office (United Kingdom)

The HT-FRTC is a component of the Met Office Neon Tactical Decision Aid (TDA). Within Neon the HT-FRTC has for a number of years been used to predict the IR apparent thermal contrasts between different surface types as observed by an airborne sensor. To do this, the FRTC is supplied with the inherent temperatures and spectral properties of these surfaces (i.e. ground target(s) and surrounding background).

A strength of the HT-FRTC is its ability to take into account the detailed properties of the atmosphere, which in the context of Neon tends to be provided by a Numerical Weather Prediction (NWP) forecast model. Incorporated into the HT-FRTC is an exact treatment of atmospheric

scattering based on spherical harmonics. This allows the treatment of different aerosol and cloud types. Recent developments even account for rain and falling snow.

The HT-FRTC has been extended to cover the spectral range of the Photopic and NVG sensors. One aim here is to give the user guidance on the expected light levels, especially at night, again taking the atmospheric conditions into account. A recent development allows such predictions during twilight.

The user of the code can add new sensors by simply supplying files that contain their sensor's spectral properties.

The HT-FRTC works in Principal Component space which significantly reduces the computational requirements regarding memory and time.

Other applications of the HT-FRTC include simulations of satellite and airborne hyperspectral sounders. The HT-FRTC is also used as the forward model in variational retrieval schemes of atmosphere and surface parameters.

9614-21, Session 6

A parameterization of littoral fog

Joshua J. Rudiger, SPAWARSYSCEN Pacific: San Diego (United States); John S. deGrassie, Space and Naval Warfare Systems Ctr. Pacific (United States)

A microphysical parameterization for fog is developed based upon meteorological measurements such as visibility, droplet number concentration, liquid water content, temperature, relative humidity and atmospheric pressure. The potential use of shipboard laser weapons and increasing use of free-space optical communication systems in many different operating environments require accurate models of aerosols and how they affect these systems. Developing a fog model increases the predictive effectiveness for assessing a given system's performance. It will, for example, aid in predicting the performance of imaging systems, the amount of power scattered off-axis, and, more generally, increase the accuracy of the optical properties such as extinction and absorption. Here we develop a microphysical parameterization for fog modeling applications based upon observations of littoral fog events thereby increasing the predictive accuracy of atmospheric propagation models.

9614-22, Session 7

The study of full link duplexing of UV NLOS scattering channel

Gang Chen, Linchao Liao, Univ. of California, Riverside (United States)

In this paper, the full link duplexing of UV NLOS scattering channel is studied comprehensively. We first conduct a serial of experiment to investigate the self-interference effect of different wavelengths in UV-C band under different configuration geometries. Then we propose a method for self-interference cancelation (SIC) of UV NLOS communication system. Through simulation, it is shown that both the throughput and point-to-point bit-error-rate (BER) of UV NLOS mesh network are obviously improved after adopting the proposed SIC method.

9614-23, Session 7

Massive MIMO visible light communication system via hemispherical lens on hemispherical beehive structure receiver

Gang Chen, Tian lang, Univ. of California, Riverside (United States)

With the development of internet of things, Visible Light Communication (VLC) is the missing piece of this inevitable technology. However, current VLC systems lack the adequate date rate and reliability. By utilizing massive



Multiple Input Multiple Output (MIMO) technology with the proposed hemispherical lens on hemispherical beehive structure (HBS) receiver, we can achieve the significant diversity channel gain in our VLC system which increases the communication speed substantially. Via classical optics, we are able to derive a model to determine the channel gain of the HBS receiver based on the number of indoor transmitter. The simulation result shows images from transmitters to HBS receiver are distinguishable based on different angle of incidence which confirms that there is a significant spatial diversity for the proposed VLC systems.

9614-24, Session 7

Optical design of communication simulator for orbital angular momentum based freespace link with an adaptive optics receiver

Alonzo J. Espinoza, Garret Odom, Wenbo Gao, Milorad Cvijetic, Yuzuru Takashima, The Univ. of Arizona (United States)

Free-space optical links employing Orbital Angular Momentum (OAM) multiplexing is gathering attention because of its ability to spatially multiplex a number of modes by utilizing orthogonality of wavefront structure of Laguerre-Gaussian (LG) modes. Thus enhancement in data rate is expected for both classical and guantum communication channels. Since the multiplexing is based on the phase profile of the wavefront, optical aberration induced by air turbulences increases cross talk among the modes. This phase aberration is considered as one of the obstacles which prevents OAM multiplexed links from being adopted in, for example, ground to ground communication. We determined that the channel capacity is recovered by employing adaptive optics (AO) with sparse selection of OAM modes. In this paper, we report experimental verification of effectiveness of OAM communication with the AO system by using specially made chamberbased simulator which creates air turbulence in a well-controlled manner. The simulator consists of air chamber, air-heater and cooler, transmitter with two OAM modes, and a receiver with an adaptive optics system followed by a single stage Mach-Zehnder based interferometric detector. Computer generated holograms (CGHs) as well as spiral phase plates (SPPs) to create LG modes are designed and fabricated for visible wavelengths for initial testing, and then for 1550nm for final testing. The CGHs and SPPs are fabricated using a mask-less lithography tool. To determine the best option for our application the diffraction efficiency of CGHs and SPPs to produce the desired OAM modes are tested. Cross talk evaluation results and channel capacity estimation are presented.

9614-25, Session 7

The turbulence effects analysis in vehicular optical communication

Gang Chen, Zening Li, Univ. of California, Riverside (United States)

In the vehicular optical communication, hot vehicle exhaust and highspeed air flow can cause severe turbulence to degrade the optical link performance. In this paper, the effects brought in by exhaust and air flow are studied separately. Parameters like exhaust shape, size, temperature as well as the vehicle velocity and sharp have been taken into consideration. Theoretical analysis results based on existing Gamma-Gamma model are compared with the practical measurements. The BER performance has also been discussed under the turbulence case.

9614-26, Session 7

Terrestrial FSO links: channel model classification using neural networks and a case study on the effect of rain

Geetha Prakash, PES Institute of Technology (India); Sripati U. Acharya, Muralidhar Kulkarni, National Institute of Technology, Karnataka (India)

Free Space Optical (FSO) systems are being actively considered as viable options for seamless integration between backhaul optical fiber links and RF or copper links used for last mile connectivity. However, adverse atmospheric conditions can affect the performance and distance over which the link can operate reliably. FSO channel models are chosen based on the atmospheric parameters. In this paper we have developed a novel classification technique using a Radial Basis Function Neural Networks (RBFNN) with a multivariate Gaussian Function to classify FSO channel models. We have also used interpolation techniques, so far not used to model FSO channel models to reconstruct distribution functions for comparison and tested their accuracy by least mean square distance. Simulation results for classification show excellent agreement when compared with the actual distribution function. RBFNN techniques show a Correct Classification Rate (CCR) of above 90 % as compared to 70% with the reconstruction techniques.

FSO systems can suffer outages in the presence of heavy fog, smog and haze. However, since conditions like heavy fog, smog or haze do not manifest at most places in India, these limitations do not limit the widespread deployment of FSO links in our country. However, many places in India (north east and the western coast) see very heavy rainfall for about four to six months in a year. We have studied the effects of rainfall on propagation characteristics of outdoor optical wireless links by taking into account statistics of rainfall in Dakshina Kannada district , Karnataka, India where Surathkal is located which is affected by heavy rainfall for about four to six months in a year. This is broadly representative of many locations on the west coast of India. We observe that the attenuation during heavy rainfall is quite high and may lead to extremely low levels of the received signal or complete erasure of the transmitted data.

Reduced intensity levels could lead to drop in Bit Error Rate (BER) performance. With the validation through simulation in this paper, on the use of Luby Transform (LT) codes in FSO links, we suggest that if LT codes are used in areas prone to rainfall, it would help in the recovery of dropped packets and would also improve the BER performance.

9614-28, Session PWed

Testing resistance modulation formats for FSO communication in turbulent environment, with used simulation box

Ale? Vanderka, Jan Látal, Lukas Hajek, Jan Vitasek, Petr Koudelka, Stanislav Hejduk, Vladimir Va?inek, V?B-Technical Univ. of Ostrava (Czech Republic)

In this article the authors team deals with problems of modulation formats for Free Space Optical (FSO) Communications. FSO communications have high bandwidth, low signal attenuation, quick installation, security, unlicensed band and low cost. In FSO communication occurs due to the influence of atmospheric effect (attenuation, and fluctuation the received power signal, influence turbulence). Here will be dealing modulation schemes OOK (On-off keying) and Subcarrier Intensity Modulation (SIM) based on a BPSK (Binary Phase Shift Keying). In which will studied their characteristic and effect of atmospheric influence on the received signal. This results in decreased Eye-Diagram, Signal-to-Noise Ratio (SNR) and Bit Error Rate (BER). To evaluate the modulation formats in atmospheric turbulence is used simulation box with heat and wind sources.



9614-29, Session PWed

The performance of coherent receiver controlled by the phase lock base in dual rate free-space laser communication

Xiaoping Ma, Jianfeng Sun, Peipei Hou, Wei Lu, Qian Xu, Liren Liu, Shanghai Institute of Optics and Fine Mechanics (China)

The performance of free-space coherent communication is seriously influenced by atmospheric turbulence leading to the distorted wave-front of incident light, the reduced homodyne detection efficiency and bit error rate in the Satellite-to-Ground Laser link. The technique of differential phase shift keying (DPSK) modulation is applied into demodulating phase information in the optical signal receiver. The dual rate free-space receiving structure on the base of Mach-Zehnder delay interferometer without lens is used suitably for differential delay which is equal to the one bit corresponding to a certain data rate. Delay distance at the interference receiver is varied with transmission rate from satellite to ground. Differential information is obtained by the subtraction of the two successive wave-front phases when made to interfere. However, the phase demodulation is extremely sensitive to phase fluctuating. Because of the incident light through atmospheric turbulence, light wave-front because jittered in temporal and spatial domain rapidly. In this paper, the dual rate free-space laser communication receiver with phase lock to stable signal light phase is proposed, increasing the homodyne efficiency and decreasing the bit error rate. The structure are depicted in detail and the experimental results is shown to prove the significance of the phase lock in satellite-to-ground laser link.

9614-30, Session PWed

Evaluation of FSO link throughput in Qatar under harsh environment

Syed Jawad Hussain, Abir Touati II, Mohammed Elamri III, Farid Touati IV, Qatar Univ. (Qatar)

Free-Space Optics (FSO) is a wireless technology that enables the optical transmission of data though the air. FSO is emerging as a promising alternative or complementary technology to fiber optic and wireless radio-frequency (RF) links due to its high-bandwidth, robustness to EMI, and operation in unregulated spectrum. These systems are envisioned to be an essential part of future generation heterogeneous communication networks. Despite the vibrant advantages of FSO technology and the variety of its applications, its widespread adoption has been hampered by rather disappointing link reliability for long-range links due to atmospheric turbulence-induced fading and sensitivity to detrimental climate conditions. A major challenge of such systems is to provide a strong backup system with soft-switching capabilities when the FSO link becomes down. Using the same medium for backup will not help, in the case of the link cut, because most likely the same technology will be cut as well. This is the reason why we decided to create a different medium RF as a backup.

The specific objective of this work is to study for the first time in Qatar and the GCC the link capacity, link availability, and link outage of an FSO system with RF back up (i.e. hybrid FSO/RF) under harsh environment.

In order to analyze the two transport media, we have ported Embedded Linux on FPGA and designed a network sniffer application that can run into FPGA. We installed new FSO/RF terminals and configure and align them successively. In the reporting period, we carry out measurement and relate them to weather conditions. The experimental results, when compared to studies which have been carried out before in Europe and North America, show different behavior

9614-31, Session PWed

Statistical prediction of the atmospheric behavior for free space optical link

Lukas Hajek, Jan Látal, Ale? Vanderka, Andrej Liner, Stanislav Hejduk, Petr Koudelka, Vladimír Va?inek, Jan Vitasek, V?B-Technical Univ. of Ostrava (Czech Republic)

The atmosphere is unstable and unpredictable environment, where are continual changes of the air refractive index. These changes cause fluctuation of optical power at the receiver site. The prediction of behavior of the atmosphere and effect of this behavior on the FSO link is very complicated or even impossible. Aim of this article is focused to statistical analysis of measured level signal RSSI of the FSO link and atmospheric properties measured by hydro-meteorological station. For finding probability distribution function PDF of measured data the statistical analysis tools were used. Next part of article is focused on determination of the linear regression model to calculate level of RSSI depending on the atmospheric properties. Two empirical equations are result for day and night time. These equations describe behavior of signal RSSI in 30 days interval. Finally, comparison of the obtained mathematical model with real measured data of RSSI was introduced for one week before and one week after the analyzed time interval.

9614-32, Session PWed

Modulation of radio signal using laser beam

Mohammad M. Anwar, Asiatic Society of Bangladesh (Bangladesh)

Radio signal can be modulated using laser beam as career wave by converting radio frequency in to laser beam using laser beam radio frequency conversion transducer and then producing interference for getting modulated wave and transmitting through a transmitter for sending long distance transmittance q switched or pulsed laser for efficient radio communication.we will use any receiver for demodulated laser beam for getting radio wave by using another transducer that will convert laser beam to original radio frequency and transmit in the local area by amplifying signal and transmitting from laser demodulation substation that can be in fm radio signal .

9614-33, Session PWed

Performance analysis of OOK receiver with a GSM laser source in space to ground optical communication link

Mengnan Li, Liying Tan, Jing Ma, Siyuan Yu, Jiajie Wu, Qi Wang, Harbin Institute of Technology (China)

In practice, due to the laser device own reason and the inevitable error of the processing technic, the laser source emitted from the communication terminal is represented as partially coherent laser. In space to ground optical communication link, the variation of the source coherent parameter and the zenith angle has effects on the incident optical intensity at the receiver aperture. With full consideration of both the average optical intensity and scintillation, the statistical distribution of the optical intensity is given with different wavelength, beamwidth and zenith angle. The effects of the source coherent parameter on the performance of OOK receiver is systematically analyzed. The average bit error rate (BER) is obtained in the presence of the degradation of the source coherent degree. The results manifest that the performance degrades seriously with the increasing source coherent parameter or the zenith angle, while the degradation is less with a smaller wavelength or a bigger beamwidth. The work is hoped to improve the redundancy design of the optical communication receiver system.



9614-34, Session PWed

Orthogonal phase modulation with self homodyne detect laser communication method for the satellite-to-ground link

Jianfeng Sun, Peipei Hou, Xiaoping Ma, Liren Liu, Shanghai Institute of Optics and Fine Mechanics (China)

Signal laser propagation will pass through the random atmosphere turbulence channel in satellite-to-ground laser communication application. The turbulence will cause the wavefront distortion in the receiver telescope front. For direct detection laser communication system, atmospheric turbulence can affect the coupling efficiency from space laser to the detector. For coherent detection laser communication system, Atmosphere turbulence not only affects the coupling efficiency, but also can seriously reduce the heterodyne detection efficiency. Coherent detection communication receiver must use small aperture telescopes or large aperture telescope with adaptive wavefront compensation system.

To mitigate the influence of the atmosphere turbulence, we proposed a new method base orthogonal phase modulation with self homodyne detect. This method can not only mitigate the influence of the turbulence, but also adjust the communication date rate steplessly. The experiment results show that the method is very suitable to the satellite-to-ground link.

Conference 9615: Quantum Communications and Quantum Imaging XIII



Sunday - Wednesday 9 -12 August 2015

Part of Proceedings of SPIE Vol. 9615 Quantum Communications and Quantum Imaging XIII

9615-1, Session 1

Recent progresses in quantum imaging real applications (Invited Paper)

Marco Genovese, Istituto Nazionale di Ricerca Metrologica (Italy)

Recent progresses in Quantum Imaging Real Applications

I.Ruo Bechera, A.Meda, E.Moreva, P.Traina, I.Degiovanni, G.Brida, Marco Genovese

Quantum imaging is, together with quantum key distribution, the quantum technology more mature for practical applications [1,2,3,4].

In this talk, after a general introduction to the argument, we will present two recent results achieved in INRIM laboratories paving the way for next future commercial use of these techniques.

The first exploits non-classical photon statistics of single nitrogen-vacancy color centers in diamond for realising super-resolution. A little more in detail we demonstrate that the measurement of high order correlation functions allows overcoming Abbe limit.

The second exploit ghost imaging [4] in a specific case of practical interest, i.e. in measuring magnetic structures in garnets. Since it is of large interest to perform these measurements in cryogenic regime a direct imaging is difficult. An acquisition through an optical fiber would be much simpler, but spatial resolution would be lost. The use of ghost imaging through correlated beams would permit recovering spatial information of the light that passed through the sample and the fiber.

[1] G.Brida, M. Genovese, I. Ruo Berchera, NaturePhotonics 4,227 (2010).

[2] E.Lopaeva, I.Ruo Berchera, I.Degiovanni, S.Olivares, G. Brida, M. Genovese PRL110,153603 (2013)

[3] D. Gatto Monticone et al., PRL 113, 143602 (2014)

[4] T. B. Pittman, Y. H. Shih, D. V. Strekalov, and A. V. Sergienko,

Phys. Rev. A 52, R3429 (1995); G.Brida et al., Phys. Rev. A 83, 063807 (2011);

9615-2, Session 1

Two-mode squeezed light source for quantum illumination and quantum imaging

Genta Masada, Tamagawa Univ. (Japan)

Quantum illumination is a recently developed target detection scheme by using quantum entanglement and expected to provide improvement in error probability for discrimination of target present or absent even in a lossy and noisy environment. The original idea was firstly proposed in the case of entangled photon pair and extended to the case of Gaussian states. We are developing high quality two-mode squeezed light as a quantum entanglement resource for exploring the possibility of quantum illumination radar system and expecting to apply to quantum imaging.

Two-mode squeezed light is a non-classical state of the electro-magnetic field and can be generated by combining two independent single-mode squeezed lights by using a beam splitter with relative phase of 90 degrees between each optical field. It shows strong correlation between quadrature phase amplitudes in each mode. In order to reveal the quadrature entanglement in the actual experiment, it is important to generate highly squeezed light.

To generate single-mode highly squeezed light, we employ a sub-threshold optical parametric oscillator (OPO) which includes a nonlinear optical crystal for the second order nonlinear interaction. Especially, we implement an OPO including a periodically polled potassium titanyl phosphatecrystal (PPKTP) with bow-tie configuration of optical cavity and create two-mode squeezed light for quantum radar such as quantum illumination and quantum imaging.

9615-3, Session 1

Quantum imaging at ARL (Invited Paper)

Ronald E. Meyers, U.S. Army Research Lab. (United States)

No Abstract Available

9615-4, Session 2

Quantum repeaters for long distance quantum communication (*Invited Paper*)

Liang Jiang, Sreraman Muralidharan, Linshu Li, Yale Univ. (United States); Norbert Lutkenhaus, Univ. of Waterloo (Canada); Jungsang Kim, Duke Univ. (United States); Mikhail D. Lukin, Harvard Univ. (United States)

Quantum repeaters (QRs), as a promising approach for long distance quantum communication, can overcome both loss and operation errors, and exponentially speedup the communication rate. Loss errors can be suppressed by heralded entanglement generation (HEG) or quantum error correction (QEC). Operation errors can be corrected by heralded entanglement purification (HEP) or QEC. Both HEG and HEP requires twoway classical signaling, while QEC only requires one-way communication.

Depending on the methods used to suppress loss and operation errors, we can classify various QRs into three generations. The first generation of QRs uses HEG and HEP to suppress loss and operation errors. The second generation uses HEG to suppress loss errors and QEC to correct operation errors. The third generation of QRs relies on QEC to correct both loss and operation errors.

To compare different quantum repeater protocols, we need to consider both temporal and physical resources, which are characterized by the key generation rate and the total number of qubits. By introducing the cost function to characterize both temporal and physical resources, we can systematically compare three generations of QRs for various experimental parameters, including coupling efficiency, gate fidelity, and gate times. We have identified different parameter regions with drastically different architectural designs of quantum repeaters with different possible physical implementations. This will provide a guideline for the optimal design of quantum networks over global scales.

9615-5, Session 2

An ion-cavity interface for quantum networks (Invited Paper)

Tracy E. Northup, Bernardo Casabone, Konstantin Friebe, Klemens Schüppert, Florian Ong, Moonjoo Lee, Dario Fioretto, Univ. of Innsbruck (Austria); Rainer Blatt, Leopold-Franzens-Univ. Innsbruck (Austria) and Institut für Quantenoptik und Quanteninformation (Austria)

Trapped ions are a promising platform for local quantum information processing, but as stationary qubits, they are not well suited for quantum communication. Optical cavities offer a coherent interface between matter and light, enabling the transfer of quantum information from stationary qubits onto photons for long-distance distribution.

We demonstrate such an interface by coupling trapped ions to a cavity and have recently shown that a quantum state can be faithfully transferred from an ion onto a photon. In particular, this transfer can be improved by taking advantage of a collective effect between multiple ions, namely, superradiant emission into the cavity. In this proof-of-principle experiment, we tune the phase of a two-ion entangled state between sub- and superradiance. The



superradiant coupling is then used to enhance the transfer of quantum information onto a photon from a logical qubit encoded in the two ions.

Finally, prospects for linking together distant ions in cavities via a quantum network will be discussed. Toward this goal, I will outline a fiber-based ion-cavity experiment which should allow access to the single-ion strong-coupling regime.

9615-6, Session 2

Narrowband correlated single photon source for quantum communications and quantum memory applications from a cavity referenced to cesium atoms (Invited Paper)

Oliver Slattery, Lijun Ma, Paulina Kuo, Xiao Tang, National Institute of Standards and Technology (United States)

Spontaneous parametric down conversion (SPDC) is commonly used to produce degenerate photon pairs (both photons are the same wavelength) and non-degenerate pairs (each photon are different wavelengths), naturally broadened to hundreds of gigahertz or a terahertz. For successful interaction with atomic ensembles, the interacting photon must achieve a very narrow linewidth, in the order of tens of megahertz. For long distance quantum communications, the transmitting photons must be within a telecommunications band. We describe narrowband non-degenerate SPDC sources with one photon at a telecommunications wavelength (near 1310 nm) and the second photon at a wavelength suitable for quantum memory via integration with an atomic (Cesium) ensemble. A cavity narrowed nondegenerate correlated photon pair source can interface quantum memory and quantum communications applications.

The experiment includes a non-linear periodically poled bulk crystal (lithium niobate) pumped at 532 nm and the resulting pairs of correlated photons near 895 nm and 1310 nm, respectively. The single pass (no cavity) linewidths are several nm. By introducing the crystal into a cavity and by relying on the principle of the conservation of energy in the non-linear interaction, the effect is to limit the generation of the pairs to the linewidths matching the resonant modes of the cavity. The resonating cavity is locked to the D1 transition of the Cesium atom. The resulting linewidth at exactly 894.3-nm will be significantly narrower than the single pass linewidth.

Applications include quantum repeaters and the advancement of quantum computer networks.

9615-7, Session 3

Enabling transmitter and receiver technology for free-space quantum key distribution (Invited Paper)

David Woolf, Joel M. Hensley, Physical Sciences Inc. (United States)

The need for unconditionally secure communication links has been growing as traditional encryption techniques become less secure due to advances in computation. Quantum Key Distribution (QKD) is an enabling framework through which secure communication can be achieved. For free-space QKD, a primary challenge exists in detecting single-photons against a sky background, particularly during the daytime. In order to do this, a spectrally narrow, on-demand, and bright single photon source must be paired with a detector capable of significant temporal, spatial and spectral filtering. Here, we report on our development of a transmitter-receiver pair consisting of a spectrally-narrow, cavity coupled diamond color center single photon source and a detector containing a two-stage atomic line filter (ALF) built from isotopically pure Rubidium (Rb) vapor cells. The emitter and receiver are capable of producing a sub-GHz spectral linewidth for emission and detection respectively, which is a 50x improvement over the current state of the art and will enable the construction of high data-rate, unconditionally secure free space data links.

9615-8, Session 3

Secure satellite communication using multi-photon tolerant quantum communication protocol

Bhagyashri A. Darunkar, Nikhil V. Punekar, Pramode K. Verma, The Univ. of Oklahoma - Tulsa (United States)

This paper proposes and analyzes the potential of a multi-photon tolerant quantum communication protocol to secure satellite communication. For securing satellite communication, quantum cryptography is the only known unconditionally secure method. A number of recent experiments have shown feasibility of satellite-aided global quantum key distribution (QKD) using different methods such as: Use of entangled photon pairs, decoy state methods, and entanglement swapping. The use of single photon in these methods restricts the distance and speed over which quantum cryptography can be applied.

Contemporary quantum cryptography protocols like the BB84 and its variants suffer from the limitation of reaching the distances of only Low Earth Orbit (LEO) at the data rates of few kilobits per second. This makes it impossible to develop a general satellite-based secure global communication network using the existing protocols. The method proposed in this paper allows secure communication at the heights of the Medium Earth Orbit (MEO) and Geosynchronous Earth Orbit (GEO) satellites. The benefits of the proposed method are two-fold: First it enables the realization of a secure global communication network based on satellites and second it provides unconditional security for satellite networks at GEO heights. The multi-photon approach discussed in this paper ameliorates the distance and speed issues associated with quantum cryptography through the use of contemporary laser communication (lasercom) devices. This approach can be seen as a step ahead towards global quantum communication.

9615-9, Session 3

Channel models for QKD at higher photon flux levels based on spatial entanglement of twin beams in PDC

Marina Mondin, Politecnico di Torino (Italy); Fred Daneshgaran, California State Univ., Los Angeles (United States); Ivo P. Degiovanni, Marco Genovese, Ivano Ruo Berchera, Istituto Nazionale di Ricerca Metrologica (Italy)

Twin beams generated by Parametric Down Conversion (PDC) exhibit quantum correlations that have been effectively used as a tool for many applications including calibration of single photon detectors and QKD applications [1]. Within QKD applications, the natural setup of quantization of Charge Coupled Device (CCD) detection areas and subsequent measurement of the correlation statistic needed to detect the presence of the eavesdropper Eve, leads to a set of QKD parallel channel models that are either binary or multilevel Discrete Memoryless Channels (DMC). This work explores the derivation of proper channel models for this application starting from measured data, the evaluation of the associated channel capacity, and the application of polar codes for information reconciliation over the resulting parallel DMCs.

[1] Fred Daneshgaran ; Marina Mondin; Inam Bari , "FEC Coding for QKD at Higher Photon Flux Levels Based on Spatial Entanglement of Twin beams in PDC" Proc. SPIE 9225, Quantum Communications and Quantum Imaging XII, 922501

9615-10, Session 3

A modified quantum secret sharing algorithm for distributing two-party secret keys (Invited Paper)

Warren P. Grice, Phil Evans, Benjamin Lawrie, Oak

Conference 9615: Quantum Communications and Quantum Imaging XIII



Ridge National Lab. (United States); Matthieu Legre, id Quantique SA (Switzerland); Pavel Lougovski, William Ray, Brian Williams, Bing Qi, A. Matthew Smith IV, Oak Ridge National Lab. (United States)

We have developed and demonstrated a novel method for distributing random secret information based on N-party single-qubit Quantum Secret Sharing (QSS). Unlike QSS, however, our method does not require a meeting between N-1 of the participants. In addition, our method permits any two participants to establish a secure key known only to them. We have tested our new protocol with N = 3 parties on a single quantum channel using a commercial QKD system developed by ID Quantique. We demonstrate how any two out of the N participants can build a secret key by using partial information from each other and with collaboration from the remaining N ? 2 parties. We note that our protocol allows for the creation of two-party secret keys were standard QSS does not, and it significantly reduces the number of resources (single photon detectors, lasers and dark fiber connections) needed to implement single photon QKD.

9615-11, Session 4

Twin photon source: spatio-temporal properties

Joyee Ghosh, Indian Institute of Technology, Delhi (India) and ICFO-The Institute of Photonic Sciences (Spain); Gabriel Molina-Terriza, ICFO-The Institute of Photonic Sciences (Spain) and Macquarie Univ. (Australia); N. Piro, ICFO-The Institute of Photonic Sciences (Spain) and École Polytechnique Fédérale de Lausanne (Switzerland); L. Dubreuil, Juan P. Torres, ICFO-The Institute of Photonic Sciences (Spain); Juergen Eschner, ICFO-The Institute of Photonic Sciences (Spain) and Univ. des Saarlandes (Germany)

We propose a method to study the spatio-temporal properties of degenerate photon pairs emitted in SPDC, using temperature variation. The photons can be distinguished. We relate these to the measured Hong-Ou-Mandel dip of the photons.

9615-12, Session 4

EIT quantum memory based on Cs Atom (*Invited Paper*)

Lijun Ma, Oliver Slattery, Paulina Kuo, Xiao Tang, National Institute of Standards and Technology (United States)

Quantum memory is an important device to realize long distance quantum communication and linear quantum computing. Quantum memory based on Electromagnetically-induced transparency (EIT) is one of most promising approaches to implement such device.

EIT is a nonlinear optical phenomenon in atoms with a ? energy level structure. In this energy structure, a signal field carries the quantum information while another strong coupling field is used to control the atomic system. The two fields couple excited level to their respective ground levels, and can store and retrieve a pulse of light. The kind of storage/retrieval process is known to be able to preserve certain quantum properties of the light. The memory media can be either warm vapor or cold trapped atoms.

Currently, most work on the EIT based quantum memory use Rb atoms. However, the transition wavelengths of Cs are suitable for quantum communication systems. The 852 nm Cs transition corresponds to the wavelength of the first generation optical communication systems, while the 895 nm Cs transition wavelength, corresponds to a popular photon pair (895+1310 nm) generated by spontaneous parametric down conversion with 532 nm pump wavelength. EIT quantum memory with Cs atoms would have many potential applications in quantum communication systems. We will present our work on EIT quantum memory with both warm vapor and trapped cold Cs atoms, and characterize their performance.

9615-13, Session 4

Hybrid quantum photonic applications of nanodiamond

Brant C. Gibson, RMIT Univ. (Australia)

The approach for combining NV quantum emitters [1,2] with photonic structures has been developed by embedding NDs into tellurite (TZN) glass, which is then drawn into fiber. This approach allows improved efficiency of the NV emitter to be coupled to a bound mode in the fiber [3] and significantly enhances device robustness. Tellurite glass was selected as the host material as it is liquid at relatively low temperatures (600-700 deg C), which minimizes ND oxidation while enabling the NDs to be mixed into the glass melt [4]. Tellurite glasses transmit light in the NV center excitation and emission wavelength range (500-800 nm), and have a high refractive index (n=2.0), which enhances the capture of the NV emission in the fiber core. In this work, the origin of loss in ND-doped tellurite glass was explored [5]. Based on this understanding, the loss of ND-doped tellurite fibers was reduced by more than an order of magnitude down to 10 dB/m across the 600-800 nm wavelength range while preserving functional NDs in the glass [6]. Using optimal fabrication conditions, future fibers with low loss and active, embedded NDs will be used to investigate single photon emission and propagation of quantum information along the fibers, which have the potential to become the photonic backbones for quantum applications. References

[1] J. M. Taylor, et al., Nature Phys. 4, 810-816 (2008).

[2] L P McGuinness, et al., New J. Phys. 15, article 073042 (2013).

[3] M. R. Henderson, et al., Opt. Express 19, 16182-16194 (2011).

[4] M. R. Henderson, et al., Adv. Mater. 23, 2806-2810 (2011).

[5] H. Ebendorff-Heidepriem, et al., Opt. Mater. Express 4, 2608–2620 (2014).

[6] Y. Ruan, et al., Opt. Mater. Express 5, 73-87 (2015).

9615-14, Session 5

New opportunities for quantum storage in diamond (Invited Paper)

Philip R. Hemmer, Texas A&M Univ. (United States)

Nitrogen-vacancy (NV) color centers in diamond have shown great promise for quantum information applications. However the NV has limitations that have slowed the development of quantum repeaters. For this reason, other solid-state emitters have been explored recently such as rare earth doped crystals and color centers in diamond like the silicon-vacancy (SiV). In this talk I will review the recent work on coherent population trapping (CPT) in SiV and discuss the advantages and dis-advantages compared to the NV for quantum storage applications.

9615-15, Session 5

Quantum vacuum emission from a moving refractive index front (*Invited Paper*)

Maxime Jacquet, Friedrich Koenig, Univ. of St. Andrews (United Kingdom)

A thermal flux of light is constantly emitted from the quantum vacuum at the horizon of black holes [1]; sadly it is too feeble to ever be detected. However, it is possible to create optical analogues of the event horizon in which spontaneous emission of photons from the quantum vacuum can be observed [2].

We theoretically investigate the spontaneous emission of light from the

Conference 9615: Quantum Communications and Quantum Imaging XIII



vacuum in a nonlinear dielectric modelled by two joint multi-branch dispersive media that differ in their refractive index. Our aim is to develop further an existing analytical model [3] to describe the scattering of vacuum modes at the Refractive Index Front (RIF) that separates these regions.

We show that under certain conditions, set by the velocity and height of the RIF in the dielectric, there exists a frequency window over which the scattering process resembles black hole emission: the RIF acts as a point of non-return for modes of the fields and quanta are emitted from the vacuum in a unique mode that propagates away from the RIF.

We study the properties of the eigenmodes in all different possible scattering configurations at the RIF and compute the spectra of emission from the vacuum. We investigate the influence of the RIF height and velocity in the medium on the characteristics of this emission and calculate the number of photons created from the vacuum.

[1] Hawking, Nature 1974.

[2] Philbin et al., Science 2008.

[3] Finazzi and Carusotto, PRA 2013.

9615-16, Session 5

A solid state spin-wave optical quantum memory

Margherita Mazzera, Mustafa Gündo?an, Patrick M. Ledingham, Kutlu Kutluer, ICFO - Institut de Ciències Fotòniques (Spain); Hugues de Riedmatten, ICFO - Institut de Ciències Fotòniques (Spain) and Institució Catalana de Recerca i Estudis Avançats (Spain)

Rare earth doped crystals (REC) are promising candidates as quantum memories as they offer coherence properties comparable to atomic systems, but free of the drawbacks deriving from the atomic motion. The research on REC quantum memories has been so far mostly focused on the mapping of quantum bits to optical collective excitations. However, this leads to short lived and mostly pre-determined storage. We report here on the spin-wave storage and on-demand retrieval of weak coherent states of light at the single-photon level in a Pr3+ doped Y2SiO5 crystal. The storage protocol employed is the atomic frequency comb scheme, which relies on the creation of a periodic absorption structure within the inhomogeneously broadened transition of Pr3+ at 606 nm. In order to suppress the noise created by the control pulses, we employ different filtering stages, including spatial, temporal and narrow-band spectral filtering. The latter is implemented by burning a spectral hole in a second Pr3+: Y2SiO5 crystal. Adopting this strategy we achieve a signal-to-noise ratio > 10 for singlephoton-level weak coherent pulses. Furthermore we demonstrate the coherent storage and on-demand read-out of time-bin gubits containing less than one photon per pulse with conditional fidelities (i.e. assuming that a photon is reemitted) larger than the classical threshold, taking into account the Poissonian statistics of the input fields and the finite memory efficiency. These results are promising in view of the spin-wave storage of quantum states of light and of the use of solid state memories in quantum repeater architectures.

9615-17, Session 5

Quantum nonlinear optics with optical nanofibers

Daniel E. Jones, James D. Franson, Todd B. Pittman, Univ. of Maryland, Baltimore County (United States)

Single-photon nonlinearities are useful for quantum computation, quantum communications, and quantum information processing. Optical nonlinearities have been demonstrated at the single-photon level using systems such as Rydberg Blockades, cavity QED, etc; however, more robust, single-pass experiments are also desirable. Examples of such systems include hollow-core fibers filled with atomic vapors and sub-wavelength diameter tapered optical nanofibers surrounded by atomic vapors. The underlying principle of such systems is the confinement of the optical mode to very small cross-sectional areas over very long distances. This allows the realization of very high intensities and nonlinearities at ultra-low powers approaching the single-photon level.

In this talk, we will review our recent work with tapered optical nanofibers in rubidium vapor, including demonstrations of saturated absorption, two-photon absorption, and electromagnetically induced transparency (EIT) at ultralow (-nW) power levels. The ability to achieve these nonlinear processes at such low powers is promising for the use of optical nanofibers for quantum information processing with single photons and/or weak coherent states.

9615-18, Session 5

Single "atom-like" defects in silicon carbide for future quantum photonics (Invited Paper)

Stefania Castelletto, RMIT Univ. (Australia)

Defects are common in many materials and some were regarded as detrimental. Recently with the advent of ultra-sensitive detectors, superresolution microscopy advanced methodologies, optical single spin magnetic resonance and advanced material synthesis and doping, some of conventional semiconductors intra-band gap defects such as NV centre in diamond and their nanostructured counterpart are revealed to be a disruptive discovery for nanoscale sensing in physics, biology and quantum technology. I will present equivalent centres in a similar semiconductor, silicon carbide (SiC). SiC harbour similar defects as NV in diamond, and we have recently identified the first single photon emission in 4H-SiC attributed to a carbon-antisite vacancy pairs. I will show more recent results on single defects SiC nanoparticles, tetrapods and SiC devices providing novel information on their physics and atomistic structure. The fundamental understanding of these defects is essential for their engineering and deployment in next generation multifunctional sensors. References

S. Castelletto, B.C. Johnson., N. Stavrias, A. Gali A. & T. Ohshima, Nature Materials 13, 151-156 (2014)

S. Castelletto, B. Johnsons, A. Boretti, Advanced Optical Materials 1 (9), 609-625 (2013)

S. Castelletto, B. C. Johnson, C. Zachreson, I D. Beke, I. Balogh, T. Ohshima, I. Aharonovich, A. Gali, ACS Nano, 2014, 8 (8), pp 7938–7947

S. Castelletto, Z. Bodrog, A. P. Magyar, A. Gentled A. Gali, I. Aharonovich, Nanoscale, 2014,6, 10027-10032

9615-19, Session 5

Boson sampling with integrated photonics

Fabio Sciarrino, Univ. degli Studi di Roma La Sapienza (Italy)

Boson Sampling is a specialized task which consists in sampling from the output distribution of a system of non-interacting bosons evolving through a linear unitary transformation. It is believed that simulating Boson Sampling experiments (even approximately) with a classical approach is computationally hard, since it requires the calculation of permanents of square matrices. This task represents a promising approach to show the computational capabilities of quantum mechanics in systems of smaller-size than an universal guantum computer, whose large-scale version is currently far with the present technology. This task is naturally solved by photons evolving through a linear optical interferometers and coincidence detection at the output. The recent progresses in photonics technology have lead to the first experimental implementations of Boson Sampling experiments in small-scale system, and to an experimental study of bunching phenomenon in multi-photon interferometers. At variance with other computational tasks, such as factoring of large integer numbers, due to its very complexity there is no-trivial way to certify the correct operation of a Boson Sampling device



where the size of the system increases. Hence it is crucial to identify suitable strategies to correctly discriminate Boson Sampling events from data sampled from other alternative distributions.

. Crespi, R. Osellame, R. Ramponi, D. J. Brod, E. F. Gal-vao, N. Spagnolo, C. Vitelli, E. Maiorino, P. Mataloni, and F. Sciarrino, "Integrated multimode interferometers with arbitrary designs for photonic boson sampling", Nature Photonics 7, 545 (2013).

- N. Spagnolo, C. Vitelli, M. Bentivegna, D. J. Brod, A. Crespi, F. Flamini, S. Giacomini, G. Milani, R. Ramponi, P. Mataloni, R. Osellame, E. F. Galvao, and F. Sciarrino, "Experimental validation of photonic Boson Sampling", Nature Photonics 8, 615 (2014).

9615-20, Session 6

Experimental demonstration of delayedchoice decoherence suppression (Invited Paper)

Jong-Chan Lee, Hyang-Tag Lim, Kang-Hee Hong, Youn-Chang Jeong, Pohang Univ. of Science and Technology (Korea, Republic of); Myungshik Kim, Imperial College London (United Kingdom); Yoon-Ho Kim, Pohang Univ. of Science and Technology (Korea, Republic of)

Wheeler's delayed-choice experiment illustrates vividly that the observer plays a central role in quantum physics by demonstrating that complementarity or wave-particle duality can be enforced even after the photon has already entered the interferometer. The delayed-choice quantum eraser experiment further demonstrates that complementarity can be enforced even after detection of a quantum system, elucidating the foundational nature of complementarity in quantum physics. However, the applicability of the delayed-choice method for practical quantum information protocols continues to be an open question. Here, we introduce and experimentally demonstrate the delayed-choice decoherence suppression protocol, in which the decision to suppress decoherence and even after the detection of a qubit. Our result suggests a new way to tackle Markovian decoherence in a delayed manner, applicable for practical entanglement distribution over a dissipative channel.

9615-21, Session 6

Hong-Ou-Mandel interference for the orbital angular momentum Bell States: a high dimensional analysis

Yingwen Zhang, Filippus S. Roux, CSIR National Laser Ctr. (South Africa); Thomas Konrad, Univ. of KwaZulu-Natal (South Africa); Megan Agnew, Jonathan Leach, Heriot-Watt Univ. (United Kingdom); Andrew Forbes, CSIR National Laser Ctr. (South Africa)

Hong-Ou-Mandel (HOM) interference is a fundamental component in many quantum information protocols and one of the defining features of quantum science. Traditional HOM measurements are implemented in two-dimensional Hilbert spaces and are used to filter anti-symmetric components from an input state. Here, we are able to filter the antisymmetric components from a high-dimensional entangled field. We use Dove prisms to control the precise form of the high-dimensional two-photon state and reveal state-specific constructive and destructive quantum interference. This work paves the way for high-dimensional processing of multi-photon quantum states, for example, in teleportation beyond qubits. Further, this work highlights the role that the symmetry of the state, rather than the distinguishability of the individual photons, plays in HOM interference

9615-23, Session 6

Quasi-Bell entangled coherent states and its quantum discrimination problem in the presence of thermal noise (Invited Paper)

Kentaro Kato, Tamagawa Univ. (Japan)

We are interested in whether or not entangled coherent states are applicable to quantum information-communication technologies as an information processing resource in practical situation. For this question, we discussed the effect of channel loss to the so-called quasi-Bell entangled coherent states in the context of the quantum reading scheme at the past conference (Proc.SPIE 88750P, 2013).

In this study, the effect of thermal noise to the quasi-Bell entangled coherent states is discussed. We first investigate physical properties of the quasi-Bell entangled coherent states such as the photon statistics of it, in the presence of thermal noise. Secondly a quantum discrimination problem of the quasi-Bell entangled coherent states under the influence of thermal noise is discussed in accordance with quantum signal detection theory. Then the error probability of the quantum optimum discrimination for such thermal states will be shown. Finally, we will discuss the combination of the effects from the channel loss and the thermal noise.

9615-24, Session 7

Low-power optical communication: approaching the quantum limit (Invited Paper)

Konrad Banaszek, Univ. of Warsaw (Poland)

We discuss selected strategies to reach the maximum transmission rate, defined by the Holevo bound, of a lossy narrowband optical channel under the constraint of a low mean photon number. When direct detection is used at the output, the ultimate capacity can be approached by optimizing pulse position modulation (PPM) encoding with respect to the symbol length. An approximate analytical formula for the PPM transmission rate is presented, which quantifies the effects of photon statistics in terms of the g(2) normalized second-order intensity correlation function of the light source. The highly imbalanced instantaneous power distribution in PPM encoding can be remedied by the use of binary phase shift keying (BPSK) employing the recently proposed collective receiver based on Hadamard words. It is shown that for collective BPSK encoding, the transmission rate in the presence of phase noise is equivalent to that of PPM with super-Poissonian light statistics, retaining enhanced scaling with the mean photon number compared to individual detection.

9615-25, Session 7

Security loopholes in a free-spece quantum communication receiver (Invited Paper)

Vadim Makarov, Shihan Sajeed, Poompong Chaiwongkhot, Jean-Philippe Bourgoin, Univ. of Waterloo (Canada); Thomas D. Jennewein, Univ. of Waterloo (Canada) and Canadian Institute for Advanced Research (Canada); Norbert Lütkenhaus, Univ. of Waterloo (Canada)

Quantum key distribution (QKD) is perfectly secure in theory, however practical implementations are challenging and harbor physical imperfections that open up security loopholes. Free-space QKD can be used to communicate between earth-based stations, ships, aircrafts, or a satellite. The latter allows to make a global QKD network using the satellite as a trusted relay between a network of ground stations. In free-space QKD, a four-state polarization analyser is commonly used at the receiver station. We study imperfections of this complex optical component that may open

Conference 9615: Quantum Communications and Quantum Imaging XIII



security loopholes. One dangerous imperfection is that the sensitivity of receiver's detectors depends differently on the spatial mode of incoming photons. Consequently, an attacker can control the spatial mode to break security. We identify experimentally the sources of efficiency mismatch in the optical scheme. We then model a practical intercept-and-resend attack and show that it would break security in most situations. We show experimentally that adding a spatial filter at the receiver's entrance is an effective countermeasure. However we subsequently demonstrate a counter-attack to this countermeasure. Other types of imperfections also exist in this type of QKD receiver.

9615-26, Session 7

Hybrid quantum systems and entanglement (Invited Paper)

Christian Kurtsiefer, National Univ. of Singapore (Singapore)

No Abstract Available

9615-27, Session 7

Experimental investigation on local environment effects on the quantum teleportation fidelity (Invited Paper)

Laura T. Knoll, Instituto de Investigaciones Científicas y Técnicas para la Defensa (Argentina); Christian T. Schmiegelow, UNIDEF (CITEDEF-CONICET) (Argentina); Miguel A. Larotonda, Instituto de Investigaciones Científicas y Técnicas para la Defensa (Argentina)

Quantum teleportation relies on entanglement as the quantum resource to be able to communicate with fidelities beyond the classical limit. Nevertheless, the entangled resource may be afflicted by local noise, affecting it's ability to serve as the entangled resource for quantum teleportation. We obtain experimental data on the influence of different local environments on the ability of an initially entangled pair of qubits to act as a teleportation resource after it has been afflicted by noise.

We access to selected conditions on the noise parameter space, both theoretically and experimentally, where an already noisy protocol can be made practically insensitive to a further addition of noise. The experimental results are based on a photonic implementation of the quantum teleportation algorithm, with a polarization-entangled pair acting as the quantum resource. The state to be teleported is an additional qubit encoded in the path internal degree of freedom of Alice's photon. Interactions with different local environments on both sides of the system are either implemented with an extra qubit as the environment, or simulated as a weighed average of pure states.

We compare our experimental results with the theoretical predictions, and by performing quantum process tomography we can calculate the fidelity of the quantum teleportation scheme and evaluate the effect of local environments.

9615-28, Session 8

Deploying quantum light sources on nanosatellites: lessons and perspectives

Alexander Ling, National Univ. of Singapore (Singapore)

The Small Photon Entangling Quantum System (SPEQS) is an integrated entangled photon system where the pump, photon pair source (based on SPDC) and detectors are combined within a single optical tray and electronics package that is no larger than 10 cm x 10 cm x 3 cm. This footprint enables the SPEQS instrument to be placed onboard nanosatellites or the CubeLab structure aboard the International Space Station. The purpose of the SPEQS instrument is to understand the different environmental conditions that may affect the operation of an entangled photon source in low earth orbit. This understanding is crucial for the construction of cost-effective entanglement distribution or QKD type experiments that utilize nanosatellite architecture and compact entangled photon systems. We will discuss the challenges, lessons we have learned over 3 years of development and testing and also the perspectives for future advanced experiments.

9615-29, Session 8

Photonic quantum computing

Jeremy L. O'Brien, Univ. of Bristol (United Kingdom)

Of the various approaches to quantum computing, photons are appealing for their low-noise properties and ease of manipulation at the single qubit level; while the challenge of entangling interactions between photons can be met via measurement induced non-linearities. However, the real excitement with this architecture is the promise of ultimate manufacturability. All of the components---inc. sources, detectors, filters, switches, delay lines---have been implemented on chip, and increasingly sophisticated integration of these components is being achieved. We will discuss the opportunities and challenges of a fully integrated photonic quantum computer.

9615-30, Session 8

Novel fiber based entangled photon sources and protocols

Ronald E. Meyers, U.S. Army Research Lab. (United States)

No Abstract Available

9615-31, Session PWed

Twin photons: spatial and temporal properties by coincidence detection

Joyee Ghosh, Indian Institute of Technology, Delhi (India)

Narrowband entangled photon pair sources based on spontaneous parametric down-conversion are an important tool in many quantum information processing applications. The thorough characterization of the spatio-temporal properties of the emitted photon pairs is crucial to establish their full control. In this paper we show a method to characterize the spatial and temporal properties of these photons using a filtering system combined with temperature scanning of the nonlinear crystal. We then relate the measured spatio-temporal properties to the measured Hong-Ou-Mandel

interference dip of the paired photons, measured in a parallel experiment. By studying the spatio-temporal properties of the generated photons, we show, in particular, that the emitted photons can be distinguished due to their different spectra.

9615-32, Session PWed

Quantum repeater research at NIST

Xiao Tang, Oliver Slattery, Lijun Ma, Paulina Kuo, Alan Mink, National Institute of Standards and Technology (United States)

Quantum repeaters are indispensable modules for connecting distributed quantum systems to form a scalable architecture for an entanglement-based distributed quantum network. Recognizing that distributing, maintaining, and utilizing quantum entanglement is foundational to any quantum network and the necessary building blocks that must be implemented in a quantum repeater. The main critical technical challenges for realization of a quantum repeater include high-efficiency coupling between flying qbits

Conference 9615: Quantum Communications and Quantum Imaging XIII



and stationary qbits, quantum memory with high efficiency, high fidelity and long storage time, and quantum teleportation/Bell state measurement with high visibility.

To overcome these challenges, the NIST quantum communication team has focused on the development of the required building blocks for the realization of quantum repeaters as following:

1. Active quantum interface: for generating non-degenerated entangled photon pairs, in which one photon is at a telecom wavelength and the other is at a desired atomic transition line with narrowed linewidth and stabilized frequency.

2. Passive quantum interface: for converting existing single photons at the telecom wavelengths to a desired atomic transition line, or vice versa.

3. Photon pair sources based on four-wave mixing (FWM) in micro silica toroid: for generating narrowband photon pairs directly placed at a desired atomic transition line.

4. Photon interference studies: to prepare for Bell state measurements, and quantum teleportation.

5. Quantum memory: newly launched research based on Cs warm cells and cold atomic ensembles.

6. Quantum error correction and post processing algorithms.

An overview of the research efforts for quantum repeaters and networks at NIST will be presented.

9615-33, Session PWed

Preparation and characterization of optically transparent and photoluminescent electrospun nanofiber composed of carbon quantum dots and poly(acrylonitrile) blend with poly(acrylic acid)

Hak Yong Kim, Chonbuk National Univ. (Korea, Republic of)

Electrospun PAN/PAA/CQDs(poly(acrylonitrile)/ poly(acrylic acid)/ Carbon Quantum Dots composite NFs were successfully prepared by incorporating CQDs in the pre-electrospinning PAN/PAA polymer solution. It was demonstrated that CQDs were uniformly distributed inside the polymer matrix without sacrificing their optical properties as well as without disturbing the morphology of NFs too. Therefore, CQDs were found to successful conversion of NFs from non-luminescent state to multicolor emission to display blue, green and red color upon excitation by different excitation energy. These results will lead to develop a new family of advanced product of carbon based QDs and polymer such as anticounterfeiting, UV protector, multi-functional textile, optoelectronic devices, biological labeling, and damage detection for composite structures. The composite NFs have also exhibited some UV absorption capability through compromisation of optical transparency. This property has enabled the composite to function as UV shielding material through further research.

9615-34, Session PWed

Characterization of teleportation experiments

Ronald E. Meyers, U.S. Army Research Lab. (United States)

No Abstract Available

Conference 9616: Nanophotonics and Macrophotonics for Space Environments IX



Part of Proceedings of SPIE Vol. 9616 Nanophotonics and Macrophotonics for Space Environments IX

9616-1, Session 1

Stand-off molecular composition analysis (Invited Paper)

Gary B. Hughes, California Polytechnic State Univ., San Luis Obispo (United States); Philip M. Lubin, Peter Meinhold, Univ. of California, Santa Barbara (United States); Hugh O'Neill, Ventura College (United States); Travis Brashears, Qicheng Zhang, Janelle A. Griswold, Jordan C. Riley, Caio Motta, Univ. of California, Santa Barbara (United States)

Molecular composition of distant stars is explored by observing absorption spectra. The star produces blackbody radiation that passes through the molecular cloud of vaporized material surrounding the star. Characteristic absorption lines are discernible with a spectrometer, and molecular composition is investigated by comparing spectral observations with known material profiles. Most objects in the solar system-asteroids, comets, planets, moons-are too cold to be interrogated in this manner. Molecular clouds around cold objects consist primarily of volatiles, so bulk composition cannot be probed. Additionally, low volatile density does not produce discernible absorption lines in the faint signal generated by low blackbody temperatures. This paper describes a system for probing the molecular composition of cold solar system targets from a distant vantage. The concept utilizes a directed energy beam to melt and vaporize a spot on a distant target, such as from a spacecraft orbiting the object. With sufficient flux (~10 MW/m2), the spot temperature rises rapidly (to ~2,500 K), and evaporation of all materials on the target surface occurs. The melted spot creates a high-temperature blackbody source, and ejected material creates a molecular plume in front of the spot. Bulk composition is investigated by using a spectrometer to view the heated spot through the ejected material. Spatial composition maps could be created by scanning the surface. Applying the beam to a single spot continuously produces a borehole, and shallow sub-surface composition profiling is also possible. Initial simulations of absorption profiles with laser heating show great promise for molecular composition analysis.

9616-2, Session 1

Orbital simulations on the deflection of near earth asteroids by directed energy (Invited Paper)

Qicheng Zhang, Univ. of California, Santa Barbara (United States); Kevin J. Walsh, Southwest Research Institute (United States); Carl Melis, Univ. of California, San Diego (United States); Gary B. Hughes, California Polytechnic State Univ., San Luis Obispo (United States); Philip M. Lubin, Univ. of California, Santa Barbara (United States)

Laser ablation of an asteroid on a collision course with Earth produces a cloud of eiecta which exerts a thrust on the asteroid, deflecting it from its original trajectory. The DE-STAR system provides such a thrust by illuminating an Earth-targeting asteroid from afar with a "stand-off" system consisting of a large phased-array laser in Earth orbit. A much smaller version of the same system called DE-STARLITE travel alongside the target, operating in a "stand-on" mode, slowly deflecting it over a long period of time. Such a stand-on system would also permit directing the thrust in any desired direction through careful positioning of the laser relative to the asteroid. We present orbital simulations comparing the effectiveness of both systems across a range of laser and asteroid parameters. Simulated parameters include magnitude, duration and, for the stand-on system, direction of the thrust, as well as the size and orbital characteristics of the target asteroid. These simulations indicate that deflection distance is, in general, proportional to the magnitude of thrust, proportional to the square of the laser on time, and inversely proportional to the mass. Furthermore, deflection distance shows strong dependence on thrust direction with optimal direction varying with the the asteroid's orbital eccentricity. As one example, we consider a 325 m asteroid in an orbit of eccentricity e=0.2; given 15 years of warning, a force of just 2 N from a stand-on DE-STARLITE system is sufficient to deflect the asteroid by 2 Earth radii. We discuss numerous scenarios and discuss a practical implementation of such a system consistent with current launch vehicle capability.

OPTICS+

OPTICAL ENGINEERING+

APPLICATIONS

SPIE. PHOTONICS

9616-3, Session 1

Directed energy deflection laboratory measurements (Invited Paper)

Travis R. Brashears, Phillip M. Lubin, Univ. of California, Santa Barbara (United States); Gary B. Hughes, California Polytechnic State Univ., San Luis Obispo (United States); Jonathan Y. Suen, Peter Meinhold, Caio A. Motta, Janelle A. Griswold, Qicheng Zhang, Miikka Kangas, Payton Batliner, Alexander A. Lang, Jordan C. Riley, Alex McDaniel, Univ. of California, Santa Barbara (United States)

Laboratory studies of the effectiveness of directed energy planetary defense as a part of the DE-STAR (Directed Energy System for Targeting of Asteroids and exploRation) program are presented. Directed energy "stand-off" and "stand-on" systems are proposed that consist of a modular array of kilowattclass lasers powered by photovoltaics, and are capable of heating a spot on the surface of an asteroid to the point of vaporization. Mass ejection, as a plume of evaporated material, creates a reactionary thrust capable of diverting the asteroid's orbit. In a series of papers, a theoretical basis for asteroid diversion has been developed and numerical simulations have been performed to investigate the thrust produced by material evaporating from the surface of an asteroid. In the DE-STAR concept, the asteroid itself is used as the deflection "propellant". This study presents results of experiments designed to measure the thrust created by evaporation from a laser directed energy spot. A vacuum chamber was constructed to simulate space conditions, and a torsion balance that holds an "asteroid" sample was installed. The sample is illuminated with a fiber array laser with flux levels up to 60 MW/m2 which simulated a mission-level flux. The measured thrust is compared to our model results. We discuss scaling issues associated with small-scale laboratory testing vs. full-scale missions.

9616-4, Session 1

Simulations of directed energy thrust on rotating asteroids

Janelle A. Griswold, Isabella Johansson, Philip M. Lubin, Univ. of California, Santa Barbara (United States); Gary B. Hughes, California Polytechnic State Univ., San Luis Obispo (United States); Hugh O'Neill, Ventura College (United States); Peter Meinhold, Jonathan Y. Suen, Jordan C. Riley, Caio A. Motta, Qicheng Zhang, Travis R. Brashears, Univ. of California, Santa Barbara (United States)

Asteroids that threaten Earth could be deflected from their orbits using directed energy to vaporize the surface; the ejected plume creates a reaction thrust that alters the asteroid's orbit. One concern regarding directed energy deflection is the rotation of the asteroid as this will reduce the average thrust magnitude and modify the thrust direction. Flux levels required to evaporate surface material depend on surface material composition and albedo, thermal and bulk mechanical properties of the asteroid, and rotation rate. The observed distribution of asteroid rotation rates is used, along with an estimated range of material and mechanical

Conference 9616: Nanophotonics and Macrophotonics for Space Environments IX



properties, as input to a 3D thermal-physical model to calculate the resultant thrust vector. The model uses a directed energy beam striking the surface of a rotating sphere with specified material properties, beam profile and rotation rate. The model calculates thermal changes in the sphere, including vaporization and mass ejection of the target material. The amount of vaporization is used to determine a thrust magnitude that is normal to the surface at each point on the sphere. As the object rotates beneath the beam, vaporization decreases as the temperature drops and causes both a phase shift and magnitude decrease in the average thrust vector. A surface integral is calculated to determine the thrust vector, at each point in time, producing a 4D analytical model of the expected thrust profile for rotating objects.

9616-5, Session 2

Local phase control for a planar array of fiber laser amplifiers (*Invited Paper*)

Patrick Steffanic, Benjamin T. Johannes, Gary B. Hughes, California Polytechnic State Univ., San Luis Obispo (United States); Philip M. Lubin, Peter Meinhold, Jonathan Y. Suen, Univ. of California, Santa Barbara (United States); Hugh O'Neill, Ventura College (United States); Miikka Kangas, Travis R. Brashears, Qicheng Zhang, Janelle A. Griswold, Jordan C. Riley, Caio A. Motta, Univ. of California, Santa Barbara (United States)

Arrays of phase-locked lasers have been developed for numerous directedenergy applications. Phased-array designs are capable of producing higher beam intensity than similar sized multi-beam emitters, and also allow beam steering and beam profile manipulation. In phased-array designs, individual emitter phases must be controllable, based on suitable feedback. Most current control schemes rely on feedback from the target: phases of individual emitters are adjusted to maximize flux, determined by sensing the target surface temperature. Such power-return schemes have limited scalability for target distance, number of emitters and feedback response time. This paper describes a design and control scheme that relies only on feedback from the array structure itself. A scalable geometry is based on individual hexagonal frames for each emitter; each frame cell consists of a conventional lens mounted in front of the fiber tip. A rigid phase tap structure is placed across two adjacent lenses, and physically connects the two emitter frame cells. The tap senses the exit phase of both emitters, providing information to the phase controller. The phase tap structures also include capacitive proximity sensors that measure the relative position of the tap and lens surfaces. Relative local position data, in combination with theoretical vibration modes of the compound mechanical structure, allows accurate prediction of the relative global position of emitters across the array, providing additional constraints to the phase controller. For target acquisition, infrared sensors occupy some frame cells instead of emitters. The approach is scalable for target distance and number of emitters without loss of control.

9616-6, Session 2

Orbital simulations of laser-propelled spacecraft

Qicheng Zhang, Univ. of California, Santa Barbara (United States); Kevin J. Walsh, Southwest Research Institute (United States); Carl Melis, Univ. of California, San Diego (United States); Gary B. Hughes, California Polytechnic State Univ., San Luis Obispo (United States); Philip M. Lubin, Univ. of California, Santa Barbara (United States)

Spacecraft accelerate by directing propellant in the opposite direction. In the traditional approach, the propellant is carried on board in the form of material fuel. This approach has the drawback of being limited in Delta v by the amount of fuel launched with the craft, a limit that does not scale

well to high Delta v due to the massive nature of the fuel. Directed energy photon propulsion solves this problem by eliminating the need for on-board fuel storage. We discuss our system which uses a phased array of lasers to propel the spacecraft which thus contributes no mass to the spacecraft beyond that of the reflector, enabling a prolonged acceleration and much higher final speeds. This paper compares the effectiveness of such a system for propelling spacecraft into interplanetary and interstellar space across various laser and sail configurations. Simulated parameters include laser power, optics size and orbit as well as payload mass, reflector size and the trajectory of the spacecraft. As one example, a 50 GW laser with 10 km optics could propel a 1 kg craft past Neptune (~30 au) in 5 days at 4% the speed of light. However, even lasers down to 10 kW power and 1 m optics show noticeable effect on gram-class payloads, boosting their altitude in low-Earth orbits by several kilometers per day.

9616-7, Session 2

Directed energy propulsion of wafer scale spacecraft for interstellar missions

Travis R. Brashears, Philip M. Lubin, Univ. of California, Santa Barbara (United States); Gary B. Hughes, California Polytechnic State Univ., San Luis Obispo (United States); Caio A. Motta, Kyle McDonough, Sebastian Roland, Alexander A. Lang, Qicheng Zhang, Univ. of California, Santa Barbara (United States)

In the nearly 60 years of spaceflight, we have accomplished incredible feats of exploration but we have barely left the solar system with Voyager achieving 17 km/s or 0.006% c in 38 years. As remarkable as this is, we will never reach even the nearest stars with our current propulsion technology. We have to radically rethink our strategy or give up our dreams of reaching the stars. We discuss an approach using directed energy to propel small wafer scale spacecraft to relativistic speeds to allow for the first interstellar missions. The technology is both modular and scalable, allowing a roadmap that starts with modest directed energy systems and builds to full interstellar capability. This offers a range of missions both interplanetary and leading to interstellar. The directed energy drive system is provided by a phased array of lasers while the spacecraft uses a radical departure from conventional designs and places a complete mission on a wafer including, power from an embedded radio nuclear thermal generator (RTG), PV, laser communications, imaging, photon thrusters for attitude control and other sensors. As one example, a future 50 GW laser array consisting of 1 - 10 kw meter scale sub elements with a 10km baseline can propel a wafer scale spacecraft with a 1m laser sail to about 26% the speed of light in about 10 minutes, reach Mars in 30 minutes, pass Voyager I in days, and reach Alpha Centauri in about 15 years. No other known technology offer this possibility.

9616-8, Session 2

Solar lens mission concept with directed energy propulsion

Travis R. Brashears, Philip M. Lubin, Univ. of California, Santa Barbara (United States)

We describe a mission concept to get to use our Sun as a gravitational lens, starting at a distance of about at 550AU, to image with extremely high angular resolution. In theory using the gravitational lens of the Sun will allow sub nano radian resolution. The concept uses an orbital phased-array laser powered by solar PV, as a directed energy photon drive to propel low-mass wafer scale spacecraft.. With recent photonic advances a complete mission can be placed on a wafer including, powered from an embedded radio nuclear thermal generator (RTG) or laser driven PV, laser communications, imaging, photon thrusters for attitude control and many other sensors. As one example, a future 200 MW laser array consisting of 1 - 10 kw meter scale sub elements with a 100m baseline can propel a 10 gram wafer scale spacecraft with a 3m laser sail at 60AU/year allowing a mission to the solar lens in about a decade of flight. Directed energy propulsion of low-mass



spacecraft gives us an opportunity to explore far outside our solar system and offers a scalable solution to even larger systems for interstellar flight. This system offers a very large range of missions from wafer scale payload launches of about 10 per day to kg scale payloads at 1 per day at 13 AU/ year.

9616-9, Session 3

Fiber Bragg gratings in microstructured optical fibers: fabrication challenges and applications (Invited Paper)

Francis Berghmans, Thomas Geernaert, Tigran Baghdasaryan, Hugo Thienpont, Vrije Univ. Brussel (Belgium)

The turn of the 21st century has marked the introduction of a new type of optical fiber technology that relies on so called 'microstructured optical fibers' (MOFs). Such fibers are optical waveguides formed with an array of air holes that run along the entire fiber length. MOFs exhibit unprecedented design flexibility when compared to conventional optical fibers and their properties can be tailored to answer specific application requirements. This has led to the development of supercontinuum sources, high power short pulsed fiber lasers and new fiber based optical sensors. A current hot topic in optical fiber technology research is the development of all-MOF based devices, including for example MOF based lasers and MOF based sensors. To do so one is currently investigating the combination of fiber Bragg grating (FBG) technology with MOF technology. Fabricating FBGs inside MOFs has proven not to be straightforward. The holey structure in the cladding of the MOF appears to be a spoilsport for laser based photo-inscription, as it prevents the laser radiation to reach the fiber core in an adequate manner. The intention of this paper is to review sensor applications of microstructured optical fiber Bragg gratings and to take a look at various possibilities for improving the fabrication of FBGs in MOFs with emphasis on IR femtosecond pulse laser photo-inscription methods.

9616-10, Session 4

Effects of degradation on the performance of a triphenylene based liquid crystal organic semiconductor (Invited Paper)

Nathan J. Dawson, Michael S. Patrick, Kyle Peters, Kenneth D. Singer, Case Western Reserve Univ. (United States); Sanjoy Paul, Brett Ellman, Kent State Univ. (United States); Rachael Matthews, Emily Pentzer, Case Western Reserve Univ. (United States); Robert J. Twieg, Kent State Univ. (United States)

We report on the effects of degradation on the charge transport properties of a discotic liquid crystal organic semiconductor, hexapentyloxyltriphenylene (HAT5). Time-of-Flight (TOF) measurements are performed in the hexagonal ordered columnar mesophase, where pristine samples show nearly nondispersive transport due to the quasi-onedimensional transport in this mesophase. We observe how the transient properties change in samples aged over a decade. These aged samples trap charges near the interfaces in TOF cells and show greater signs of dispersive transport. These transient features are used to characterize the interfacial traps and bulk transport properties, where we use a simple model to exactly reproduce the transient behavior for a wide range of sample degradation.

It is shown that only a small amount of impurity is required for interfacial trapping. Experiments show that the interfacial trapping depends greatly on the pump wavelength with respect to the absorption curve, which confirms that the interfacial traps have microscopic length inside the HAT5. Pulse delay experiments show that ion build-up at the interface is not responsible for the creation of traps. The degradation is not found to be oxidation related, where absorbance and mass spectrometry measurements confirm a different route of degradation for the current set of aged material. We

further discuss the properties of HAT5 exposed to either ozone or moisture, and we discuss future plans to study the effects of radiation and further exposure to ozone on the transport properties of organic semiconducting materials.

9616-11, Session 4

Impact of ionizing radiation on organic photovoltaic cells

Camron G. Kouhestani, Team Technologies, Inc. (United States); Roderick A. B. Devine, Team Technologies. Inc. (United States); Kenneth E. Kambour, Leidos (United States); Duc D. Nguyen, COSMIAC (United States); Gang Li, Yang Yang, Univ. of California, Los Angeles (United States); Yue Wu, Solarmer Energy, Inc. (United States)

Organic semiconductor based photovoltaic (OPV) cells potentially offer significant advantages over classical inorganic semiconductor based cells for some space based applications; specifically where criteria such as weight, flexibility and conformity are concerned. Applications in areas such as space technology represent a potential niche market where OPVs may be competitive to inorganic solar cells even though they have lower power conversion efficiencies. An example is cube satellites where power requirements are in the 10's of watts. Our particular interest, then, concerns the applicability of organic photo-cells for use in space based solar panels. It must be recognized that "unusual" conditions will exist (such as ionizing radiation, extremes of thermal cycling, etc.) – such issues are not generally addressed by the organic photo-cell community.

We have examined ionizing radiation effects in two organic photovoltaic materials for total accumulated doses up to 300 krads(SiO2). We find that the primary effect of irradiation on the characteristics of the archetypical material P3HT:PCBM characteristics is to decrease the apparent open circuit voltage, Voc, whereas in the material CS-9:PCBM, we found that the Voc increases with the accumulation of radiation. We have also compared the relaxation time during the accumulation of radiation between the two materials and found that the P3HT material remained constant, but the CS-9 material followed the Voc trend. These effects are explored in the following report. Los Angeles

9616-12, Session 4

Using complementary tools to characterize the effects of radiation in electro-optic polymeric materials (*Invited Paper*)

Javier Perez-Moreno, Skidmore College (United States)

Understanding the fundamental mechanisms behind the radiation resistance of polymers and molecules would allow us to taylor new materials with enhanced performance in space and adverse environments. Previous studies of the radiation effects on polymer-based photonic materials indicate that they are very dependent on the choice of polymer-host and guestchromophores. The best results have been reported from the combination of CLDI as a guest-chromophore doped in APC as host polymer, where improvement of the performance was observed upon gamma-irradiation at moderate doses. In this paper, we report on the different complementary tools that have been tried to characterize the origin of such enhancement: characterization of the nonlinear responses (SHG and electro optic), characterization of chemical properties, and application of an all-optical protocol. We derive some general conclusions by contrasting the results of each characterization, and propose complementary experiments based on microscopy techniques.



9616-13, Session 5

Proton irradiation of MWIR HgCdTe/ CdZnTe

Stephen Fahey, Silviu Velicu, Ramana Bommena, Jun Zhao, EPIR Technologies, Inc. (United States); Vincent M. Cowan, Christian P. Morath, Air Force Research Lab. (United States); Sivalingam Sivananthan, EPIR Technologies, Inc. (United States)

High performance infrared sensors are vulnerable to slight changes in defect densities and locations. For example in a space application where such sensors are exposed to proton irradiation capable of generating point defects the sensors are known to suffer significant performance degradation. The degradation can generally be observed in terms of dark current density and quantum efficiency degradations. Here we report results of MVIR HgCdTe/CdZnTe single element diodes dark current densities and quantum efficiencies before and after exposure to a beam of 63MeV protons at room temperature to a total ionizing dose of 100krad(Si). We find the irradiated diodes show some signs of damage in dark current and quantum efficiency (QE). We see the performance change for individual devices, the development of a bias-dependent quantum efficiency (QE), and dark currents with different qualitative shape after dosing, as well as changes in the dark current density histogram shape for a small number of diodes.

9616-14, Session 5

MWIR unipolar barrier photodetectors based on strained layer superlattices

David A. Ramirez, Stephen A. Myers, Elena Plis, SKINfrared LLC (United States); Christian P. Morath, Vincent M. Cowan, Air Force Research Lab. (United States); Sanjay Krishna, The Univ. of New Mexico (United States)

In this work, we report on the design, growth, and fabrication of MWIR photodetectors based on InAs/GaSb Type-II superlattice. We have designed, grown, and fabricated band-structure engineered MWIR photodetectors based on the pBiBn and pBn architectures. The devices have been characterized using the most relevant radiometric figures of merits. In addition, we have characterized the degradation of the performance of the devices after exposing the devices to 63 MeV proton radiation to a total ionizing dose of 100 kRads (Si).

9616-15, Session 5

Empirical trends of minority carrier recombination lifetime vs proton radiation for rad-hard IR detector materials

Geoffrey Jenkins, Air Force Research Lab. (United States)

The continuous effort to improve space-based infrared (IR) detectors has led to a search for greater fundamental understanding of radiation damage phenomena on key material properties. The material parameter of interest in this paper is the minority carrier recombination lifetime (MCRL), which is directly related to detector performance and can be empirically determined. As radiation damage is incurred upon a detector structure, the MCRL can be significantly affected, and tracking this in a step-wise, in-situ fashion at a radiation source can reveal rates of defect introduction. This has been accomplished by the development of a portable MCRL measurement system employing time resolved photoluminescence (TRPL) while maintaining operational temperatures. Using this methodology is more insightful than the so-called 'bag tests' due to complex parameter changes witnessed with annealing as temperatures change. In addition to the system description, MCRL data on IR detectors from its inaugural deployment at a proton radiation source are analyzed and reveal a linear relationship between inverse MCRL and proton fluence.

9616-16, Session 5

Low-frequency, noise spectrum measurements of mid-wave infrared nBn detectors with superlattice absorbers

Eli Garduno, Christian P. Morath, Vicent M. Cowan, Air Force Research Lab. (United States)

Type-II Strained Layer Superlattice (T2SLS) infrared photodetectors have been in ongoing development over the last decade with the goal of achieving lower dark currents and higher operating temperatures when compared to mercury cadmium telluride (MCT). The theoretically longer Auger recombination lifetime of T2SLS has potential to lower dark current, but the presence of Shockley-Read-Hall defects limits the recombination lifetime far below the Auger-limit. In order to reduce SRH-recombination, unipolar barriers have been incorporated into the energy bands of T2SLS materials in different forms, such as nBn, to improve performance. Here, noise spectra are presented for varyingly sized, near 90% quantum efficiency, nBn mid-wave infrared (MWIR) detectors with superlattice absorbing layers grown by MBE. Noise spectrum measurements are used to evaluate device performance and reveal mechanisms contributing to low frequency noise that often exceeds predictions based on ideal shot noise. Voltage and temperature dependent noise spectra were taken using an external trans-impedance amplifier combined with an internal, cooled impedance converter and feedback resistor.

9616-17, Session 5

InAs/GaSb type II strained-layer superlattice (T2SLS) vertical transport and radiation tolerance

Mitch C. Malone, The Univ. of New Mexico (United States) and Air Force Research Lab. (United States); Christian P. Morath, Air Force Research Lab. (United States); Sanjay Krishna, The Univ. of New Mexico (United States)

Theoretical calculations predict InAs/GaSb Type II strained-layer superlattice (T2SLS) materials can perform comparably to state-of-the-art HgCdTe infrared (IR) detectors, making them a possible candidate for spacebased IR sensing applications. However, several fundamental properties of these materials are still not fully understood, including the multi-carrier, electrical transport characteristics perpendicular to the superlattice plane and its proton radiation tolerance characteristics. Here, a preliminary study of the radiation tolerance characteristics of the vertical minority carrier electron transport in p-type InAs/GaSb T2SLS materials is presented. T2SLS materials were investigated via variable field magneto-resistance measurements before and after room temperature 63 MeV proton irradiation up to 100 kRad(Si). Transport was measured in magnetic fields up to ±9 T over a temperature range of 10-300 K. Quantitative mobility spectrum analysis (QMSA) and multi-carrier fitting routines were then employed to extract mobility, conductivity, and carrier concentrations from pre- and postrad samples. A discussion of building a helium gas recovery system for the magnet dewar used in this study is also given.

9616-18, Session 6

High power VCSEL devices for atomic clock applications (Invited Paper)

Laurence S. Watkins, Jean-Francois Seurin, Chuni Ghosh, Delai Zhou, Guoyang Xu, Bing Xu, Alexander Miglo, Princeton Optronics, Inc. (United States)

We are developing VCSEL technology that can deliver >100mW in single frequency at wavelengths 780nm, 795nm and 850nm etc. Small aperture VCSELs with few mW output have found major applications in atomic clock experiments. Using an external cavity three mirror configuration we have



been able to operate larger aperture VCSELs with >70mW power in single frequency operation.

The VCSEL is mounted in a fiber pigtailed package with the external mirror mounted on a shear piezo. This VCSEL operates in single frequency and can be tuned by a combination of piezo actuator, temperature and current. Mode-hop free tuning over >30GHz frequency span has been obtained. Spectrum measurements show single frequency operation and demonstrate sidemode suppression of 50dB.

A Rb cell locker has been set up and the VCSEL locked to the Rb85 line using the DAVLL method. The short window linewidth was measured using the self-heterodyne method. Linewidths of <100kHz were obtained. A saturable absorption experiment was assembled and the stabilized VCSEL slowly scanned within the Rb85 transition with a 5 second timespan. The transmission probe measurement shows the 6 lines in the hyperfine structure. This measurement was used to determine the linewidth of ~1MHz for a 200mS time window. It also indicates the wavelength stability is <1MHz.

A fully package version of the high power VCSEL is being developed which will include a miniature version of the DAVLL locker inside the package.

9616-19, Session 6

A multi-channel tunable source for atomic sensors (Invited Paper)

Matthew S. Bigelow, Tony D. Roberts, Shirley McNeil, Todd Hawthorne, Philip R. Battle, AdvR, Inc. (United States)

We have designed and completed initial testing on a laser source suitable for atomic interferometry from compact, robust, integrated components. Our design is enabled by capitalizing on robust, well-commercialized, low-noise telecom components with high reliability and declining costs which will help to drive the widespread deployment of this system. The key innovation is the combination of current telecom-based fiber laser and modulator technology with periodically-poled waveguide technology to produce tunable laser light at rubidium D1 and D2 wavelengths (and expandable to other alkalis) using second harmonic generation (SHG). Unlike direct-diode sources, this source is immune to feedback at the Rb line eliminating the need for bulky high-power isolators in the system. In addition, the source has GHz-level frequency agility and in our experiments was found to only be limited by the agility of our RF generator. As a proof-of principle, the source was scanned through the Doppler-broadened Rb D2 absorption line. With this technology, multiple channels can be independently tuned to produce the fields needed for addressing atomic states in atom interferometers and clocks. Thus, this technology could be useful in the development cold-atom inertial sensors and gyroscopes.

9616-20, Session 6

Miniature atomic clock for space applications (Invited Paper)

Lute Maleki, OEwaves, Inc. (United States)

This paper will present a novel architecture for a high performance atomic clock based on the use of miniature optical whispering gallery mode (WGM) resonators. Following the approach of stabilizing a laser local oscillator to an optical transition in an atom or ion, as used in advanced atomic clock, a semiconductor laser is used for stabilization to the D1 line of Rb atoms, held in a small vapor cell. The laser is injection locked to a WGM resonator to reduce its linewidth. To produce the RF output of the clock, a second WGM resonator excited with a second cw semiconductor laser produces an optical frequency comb that is demodulated on a fast photodiode. Locking the Rb transition transfers the stability of the atomic transition to the RF output of the clock. In this way, a miniature all-optical atomic clock is realized. Details of the operation of the clock and application of the architecture to other atomic systems, such as a ytterbium ion, will be described.

9616-21, Session 6

Radiation studies on silicon photonic ring resonators

Sharon M. Weiss, Shweta Bhandaru, Shuren Hu, Daniel M. Fleetwood, Vanderbilt Univ. (United States)

Silicon ring resonators are considered to be among the most important building blocks for emerging optical interconnect technology, and are expected to complement, or in some cases replace, microelectronics components. In this work, we evaluate the performance of silicon ring resonators exposed to 10-keV x-ray and 662-keV gamma radiation. Unpassivated rings having no native oxide exhibit a distinct, dosedependent response, which can lead to a more than 10 dB change in transmission for an x-ray or gamma ray total ionizing dose near 145 krad(SiO2). Silicon ring resonators that have been passivated with native oxide or a polymer coating exhibit no dose-dependent response, but are sensitive to ambient temperature fluctuations. The role of surface passivation in the radiation sensitivity of silicon ring resonators will be discussed in detail. It is believed that surface oxidation is accelerated in the presence of high energy radiation but, at room temperature conditions, the surface oxidation is limited to a terminal native oxide. With appropriate temperature compensation considerations, passivated silicon photonic ring resonators are likely to perform reliably in harsh radiation environments.

9616-22, Session 6

Compact, highly sensitive optical gyros and sensors with fast-light (Invited Paper)

Caleb A. Christensen, Anton Zavriyev, Malcolm Cummings, A. Craig Beal, Mark Lucas, Michael J. Lagasse, MagiQ Technologies, Inc. (United States)

Fast-light phenomena can enhance the sensitivity of an optical gyroscope of a given size by several orders of magnitude, and could be applied to other optical sensors as well. MagiQ Technologies has been developing a compact fiber-based fast light Inertial Measurement Unit (IMU) using Stimulated Brillouin Scattering in optical fibers with commercially mature technologies. We will report on our findings, including repeatable fast-light effects in the lab, numerical analysis of noise and stability given realistic optical specs, and methods for optimizing efficiency, size, and reliability with current technologies. The technology could benefit inertial navigation units, gyrocompasses, and stabilization techniques, and could allow high grade IMUs in spacecraft, unmanned aerial vehicles or sensors, where the current size and weight of precision gyros are prohibitive. By using photonic integrated circuits and telecom-grade components along with specialty fibers, we also believe that our design is appropriate for mass production without further advances in the state of the art.

9616-23, Session 7

Polymer light harvesting composites for optoelectronic applications (Invited Paper)

Sam-Shajing Sun, Dan Wang, Norfolk State Univ. (United States)

Polymer based optoelectronic composites and thin film devices exhibit great potential in space applications due to their lightweight, flexible shape, high photon absorption coefficients, and robust radiation tolerance in space environment. Polymer/dye composites appear promising for optoelectronics applications due to potential enhancements in both light harvesting and charge separation. In this study, the optoelectronic properties of a series of molecular dyes paired with a conjugated polymer P3HT were investigated. Specifically, the solution PL quenching coefficients (Ksv) of dye/polymer follows a descending order from dyes of Hemin, Protoporphyrin, to TCPP. In optoelectronic devices made of the P3HT/dye/PCBM composites, the short circuit current densities Jsc as well as the overall power

Conference 9616: Nanophotonics and Macrophotonics for Space Environments IX



conversion efficiencies (PCE) also follow a descending order from Hemin, Protoporphyrin, to TCPP, despite Hemin exhibits the intermediate polymer/ dye LUMO offset and lowest absorption coefficient as compared to the other two dyes, i.e., the cell optoelectronic efficiency did not follow the LUMO offsets which are key electron transfer driving forces. This study reveals that too large LUMO offset or electron transfer driving force may result in smaller PL quenching and optoelectronic conversion efficiency, this could be another experimental evidence for the Marcus electron transfer model, particularly for the Marcus 'inverted region'. It appears an optimum electron transfer driving force or strong PL quenching appears more critical than absorption coefficient for optoelectronic conversion devices.

9616-24, Session 7

MEMS based solutions for an integrated and miniaturized multi-spectrum energy harvesting and conservation system (Invited Paper)

Heath A. Berry, Eric G. Borquist, Mitchell Belser, Radiance Technologies, Inc. (United States); Sandra Zivanovic, Leland Weiss, Louisiana Tech Univ. (United States)

As the mission of NASA shifts and expands, so too does the need for reliable, energy harvesting technology. Moving further out into the realms of space requires efficient use of the energy present in this unique, and more often than not, harsh environment. This paper describes the development of a unique system consisting of three unique energy harvesting technologies which utilize multiple MEMS and materials development based approaches which are being integrated together using a system-in-package approach. By developing multiple scavenging approaches, NASA will be able to harvest energy from multiple waste energy sources, namely environmental vibrations, thermal energy, and solar flux.

For this system, solar harvesting is accomplished through the use of an amorphous silicon thin-film solar cell with a special metal-dielectric composite electrode (MDCE) that enhances photovoltaic action through excitation of surface plasmons. Additionally, a MEMS-based heat exchanger has been developed for use in conjunction with TEGs as heat sinks for thermal capture. These micro-channel heat exchangers have advantages with respect to transport phenomena, size, and manufacturing. The MHE is one part of the thermal scavenging device. A thermal energy storage system has been fabricated to store excess thermal energy. This energy can be used after the thermal source is removed from the process. Finally, a MEMS based vibration capture element has also been developed for vibration rich environments. All three of these energy capture technologies are being integrated together for a flexible platform which can facilitate the remote collection and transmission of pertinent environmental and mission data.

9616-25, Session 8

Towards ultra-lightweight photonics using atomically thin semiconductors

Vinod M. Menon, The City College of New York (United States)

In this talk I will present an overview of nanophotonic technologies that can be realized using atomically thin two-dimensional semiconductors. Specific applications areas such as light emitters, detectors and ultrafast modulators will be discussed. The different types of two-dimensional materials and their advantages in the different application areas will also be highlighted.

9616-26, Session 8

Radiation damage effects in a CMOS TDI image sensor

Joseph E. Rushton, Konstantin D. Stefanov, Andrew D.

Holland, The Open Univ. (United Kingdom)

Time Delay and Integration (TDI) is used to increase the signal to noise ratio in image sensors when imaging fast moving objects. One important TDI application is in Earth observation from space. In order to operate in the space radiation environment, the effect that radiation damage has on the performance of the image sensors must be understood.

This work looks at prototype TDI sensor pixel designs, produced by e2v technologies. The sensor is a CCD-like charge transfer device, allowing inpixel charge summation, produced on a CMOS process. The use of a CMOS process allows potential advantages such as lower power consumption, smaller pixels, higher line rate and extra on-chip functionality which can simplify system design. CMOS also allows a dedicated output amplifier per column allowing fewer charge transfers and helping to facilitate higher line rates than CCDs.

In this work the effect on the pixels of radiation damage from high energy protons, at doses relevant to a low Earth orbit mission, is presented. This includes the resulting changes in Charge Transfer Efficiency (CTE) and dark signal.

9616-27, Session 9

Microscopic model for studying radiation degradation of electron transport and photodetection devices (Invited Paper)

Danhong Huang, Air Force Research Lab. (United States); Fei Gao, Univ. of Michigan (United States); David A. Cardimona, Christian P. Morath, Vicent M. Cowan, Air Force Research Lab. (United States)

A microscopic-level model is proposed for exploring degraded performance in electron transport and photodetection devices, based on pre-calculated results as initial conditions for meso-scale approaches, including ultrafast displacement cascade, intermediate defect stabilization and cluster formation, and slow defect reaction and migration. The steady-state spatial distribution of point defects in a mesoscopic-scale layered system will be studied by taking into account the planar dislocation loops and spherical neutral voids as well. The electronic structure of point defects will also be computed by employing density-functional theory for both energy levels within energy gap and their localized wave functions. These theoretical efforts are expected to be crucial in fully understanding the physical mechanism for identifying defect species, performance degradations, and the development of mitigation strategies. Additionally, verification of the current model by device characterization is discussed.

9616-28, Session 9

Atomistic- and meso-scale simulations of radiation effects in photodetection devices (Invited Paper)

Fei Gao, Efrain Hernandez-Rivera, Univ. of Michigan (United States); Danhong Huang, Air Force Research Lab. (United States)

Atomistic- and meso-scale models are developed to study behavior of defect evolution in compound semiconductors, which gives rise to performance degradation of electron photo-response. Large-scale molecular dynamics (MD) simulations are used to investigate defect generation, clustering and distribution, as well as their mobilities and stabilities in compound semiconductors. A kinetic Monte Carlo method is employed to follow the evolution of clusters and their interaction with microstructures at time scale much longer than possible with MD simulation. Based on these simulations, defect/property relationships, the effects of defects on transport processes and the aggregation of defects to form complex nanostructures are expect to be established. We also describe how the fundamental mechanisms and knowledge gained from atomic- and mesoscale simulations can be used to inform rate-diffusion theory or cluster



dynamics in the form of initial conditions. This enables us to determine the steady-state distribution of point defects in a mesoscopic layered-structured system, thus allowing the development of a multi-timescale theory to study radiation degradation in electronic and optoelectronic devices.

9616-29, Session 9

Surface conduction in InAs and GaSb

Daniel E. Sidor, Gregory R. Savich, Gary W. Wicks, Univ. of Rochester (United States)

III-V semiconductor materials belonging to the 6.1 Å family (InAs, GaSb, AISb, and their alloys and superlattices) are increasingly used to produce high performance MWIR and LWIR photodetectors. Barrier architecture detectors fabricated from these materials exhibit competitively low dark current densities compared to state-of-the-art pn-based structures. Appropriately placed unipolar barriers within these structures serve to block dark currents arising from growth- and/or processing-related defects. They are also effective at blocking dark currents arising from radiation-induced defects, such as those occurring in space-bound systems.

A challenge inherent to working with these materials is their conducting surfaces: InAs possesses an n-type surface, and GaSb possesses a p-type surface. Care must therefore be taken to avoid fabricating structures in which surface conduction pathways unintentionally shunt bulk conduction. The detrimental effects of conducting surfaces become more significant as device size is reduced, making this a particularly important consideration for applications where detector package size and weight are constrained.

This work presents a fundamental investigation of the surface conduction pathways occurring in devices fabricated from InAs and GaSb. The component of current due to surface conduction is extracted from current-voltage measurements by its dependence on device size and temperature. InAs is found to have a temperature-independent surface conductivity greater than 10^-7 reciprocal ohm-square. The surface conductivity of GaSb is an order of magnitude smaller than that of InAs at room temperature, and when cooled it decreases with a thermal activation energy of approximately 90 meV, which is equal to the known separation between the valence band and surface Fermi level. The temperature dependences of the surface conductivities of the two materials indicate that the surface of InAs is degenerate and the surface of GaSb is non-degenerate.

Extensions of these findings to 6.1 Å alloys and superlattices will be discussed.

9616-30, Session 9

Radiation effects on Yb:YLF crystals used in cryogenic optical refrigerators

Kyle W. Martin, Applied Technology Associates (United States); Tom Fraser, John E. Hubbs, Vicent M. Cowan, Air Force Research Lab. (United States); Seth D. Melgaard, Mansoor Sheik-Bahae, The Univ. of New Mexico (United States)

Optical cooling of solids is a promising and innovative method to provide cryogenic cooling to infrared sensors. Currently insulator crystals, specifically ytterbium-doped yttrium- lithium-fluoride (Yb:YLF), have shown the most promise for cooling to low temperatures. This method has demonstrated cooling below the National Institute of Standards and Technology (NIST) cryogenic temperature definition of less than 123 K. Optical refrigeration utilizes a phenomenon called anti-Stokes fluorescence to generate cooling power. Incident laser light is absorbed by the cooling crystal and photons are spontaneously emitted at a higher, and thus more energetic, frequency. The difference in frequency is proportional to the cooling power of the crystal. Anti-Stokes cooling is highly dependent on doping percentages and YLF crystal purity and structure. Space based infrared sensors and their coolers live in a harsh radiation environment. To ensure that radiative effects on cooling crystal background absorption and resonant absorption parameters is minimal we subjected two samples to a

total ionizing dose of 100 Krad and 1 Mrad, and compared cooling crystal efficiency parameters before and after dosing.

9616-31, Session 9

Potential of CdSiP2 for enabling midinfrared laser sources

F. Kenneth Hopkins, Air Force Research Lab. (United States); Peter G. Schunemann, Kevin T. Zawilski, BAE Systems (United States); Nancy C. Giles, Air Force Institute of Technology (United States); Larry E. Halliburton, West Virginia Univ. (United States)

Laser sources operating near a wavelength of four microns are important for a broad range of space and airborne applications. Efficient solid-state laser sources, demonstrating the highest power, are based upon nonlinear optical (NLO) conversion using the NLO crystal ZnGeP2. However, a related NLO crystal, CdSiP2, is now under investigation by several groups around the world due to its potential to out-perform ZnGeP2. The crystal's characteristics as well as efforts to understand the crystal's defects that presently limit NLO performance will be discussed.

9616-32, Session 9

Deflection of uncooperative targets using laser ablation

Nicolas Thiry, Massimiliano Vasile, Univ. of Strathclyde (United Kingdom)

Owing to their ability to move a target in space without requiring propellant, laser-based deflection methods have gained attention among the research community in the recent years. With laser ablation, the vaporized material is used to push the target itself allowing for a significant reduction in the mass requirement for a space mission. Specifically, this paper addresses two important issues which are thought to limit seriously the potential efficiency of a laser-deflection method: the impact of the tumbling motion of the target as well as the impact of the finite thickness of the material ablated in the case of a space debris. In this paper, we developed a steady-state analytical model based on energetic considerations in order to predict the efficiency range theoretically allowed by a laser deflection system in absence of the two aforementioned issues. A numerical model was then implemented to solve the transient heat equation in presence of vaporization and melting and account for the tumbling rate of the target. This model was also translated to the case where the target is a space debris by considering material properties of an aluminium T6061 alloy and adapting at every time-step the size of the computational domain along with the recession speed of the interface in order to account for the finite thickness of the debris component. The comparison between the numerical results and the analytical predictions allow us to draw interesting conclusions regarding the momentum coupling achievable by a given laser deflection system both for asteroids and space debris in function of the flux, the rotation rate of the target and its material properties.

SPIE. OPTICS+ PHOTONICS **Conference 9617: Unconventional Imaging and Wavefront Sensing XI**

Wednesday - Thursday 12-13 August 2015

Part of Proceedings of SPIE Vol. 9617 Unconventional Imaging and Wavefront Sensing 2015

9617-4, Session PWed

Development of an extreme adaptive optics testbench using a self-referenced Mach-Zehnder wavefront sensor

Christian Delacroix, Magali Loupias, Maud P. Langlois, Michel Tallon, Éric M. Thiébaut, Ctr. de Recherche Astrophysique de Lyon (France)

Extreme adaptive optics (XAO) has severe difficulties meeting the high speed (>1kHz), accuracy and photon efficiency requirements. An innovative high order adaptive optics system using a self-referenced Mach-Zehnder wavefront sensor allows counteracting these limitations. This sensor estimates the wavefront phase by measuring intensity differences between two outputs, with a lambda/4 path length difference, but is limited by its dynamic range. During the past few years, such an XAO system has been studied by our team in the framework of 8-meter class telescopes. In this work, we report on our latest results with the XAO testbed recently installed in our lab, and dedicated to high contrast imaging with 30m-class telescopes (such as the E-ELT or the TMT). A woofer-tweeter architecture is used in order to deliver the required high Strehl ratio (>95%). It consists of a 12x12 deformable mirror and a 512x512 spatial light modulator, characterized using both mono- and polychromatic light. We present our latest simulation and laboratory demonstration results, including components characterization, close loop performance, and sensitivity to calibration errors. This work is carried out in synergy with the validation of fast iterative wavefront reconstruction algorithms, and the optimal treatment of phase ambiguities in order to mitigate the dynamical range limitation of such a wavefront sensor.

9617-16, Session PWed

Single wave-front sensor control deformable mirrors: theory and experiment

Ye Hongwei, Shen Feng, Zhou Rui, Institute of Optics and Electronics (China)

Adaptive optics (AO) systems are used in image systems to compensate the phase disturbance caused mainly by atmospheric turbulence. The compensation performance of AO system largely depends on the fitting capability of the deformable mirror (DM). In the same work condition, large correction stroke and high spatial performance are demanded simultaneously. This demand is difficulty to satisfy with single DM. It's perfectly feasible by disassemble the control voltage of the ideal compensation wave-front to control many deformable mirrors work together. There are some papers analyzing the compensation effect using many deformable mirrors. Such as the scheme using double deformable mirrors to avoid the instability of thermal blooming phase correction was studied in Ref. The double deformable mirrors adaptive optics system which corrects the turbulence and the scintillation was discussed in Ref. In this paper, we will deduce a kind of decoupling algorithms. By disassemble the control voltage of the compensation wave-front to make double or many deformable mirrors work together. Low spatial frequency deformable mirror (LFDM) compensate the low order wave-front aberration using the Zernike decomposition the actuators control voltages of high spatial frequency deformable mirror(HFDM). High spatial frequency deformable mirror (HFDM) compensate all the residual aberration using the directgradient algorithm. the dynamic models of Zernike modal compensation for the direct-gradient algorithm were established in this paper. By using the theoretic model, A single wave-front sensor Control double deformable mirrors were tested on a adaptive optical system including 45-element deformable mirror and 199-element deformable mirror in channel turbulence. The experiment data proved that the single wave-front sensor

control double mirrors adaptive optical system could improve ability of large wave-front compensation.

OPTICAL ENGINEERING+

APPLICATIONS

9617-17, Session PWed

Direct detection of phase coded signal for ranging in synthetic aperture LADAR

Guangyu Cai, Jianfeng Sun, Yu Zhou, Xiaoping Ma, Peipei Hou, FuChuan Liu, Liren Liu, Shanghai Institute of Optics and Fine Mechanics (China)

Ranging ability has always been the fundamental function of Ladar, which has also integrated the detection of other information including Doppler frequency shift in ranging Doppler ladar, imaging in synthetic aperture ladar and three-dimensional imaging ladar etc.. Traditional mechanisms using phase coded optical waveforms for ranging compression in coherent ladar generally adopted local oscillator for heterodyne detection to demodulate the delayed modulation signal, which requires complex receiving structure as well as the master and local oscillators' high frequency stability.

A new detection structure similar to the direct-detection of DPSK signals was proposed in which two orthogonal polarized beams were split with one-bit delay mutually before interference and entering a balanced heterodyne receiver. The one bit difference form of the compressible codes were loaded on the phase modulator in order to demodulate the correct waveform. Various compressible sequences were verified and high precision ranging results were achieved. A relatively higher detection sensitivity was accomplished compared to the intensity modulated direct detection(IM-DD) sequence coding method which was also conducted in the experiment. In addition to the rich waveform diversity which could be tailored to various detecting applications and the high repetition frequency common to the phase coded ranging methods, there are unique advantages of this receiving structure such as the cancellation of the phase errors and frequency shift introduced in the propagation process by the two interfered receiving arms. Moreover, the polarization based detection structure also provided compatibility to the down-looking synthetic aperture ladar with its ranging capability.

9617-18, Session PWed

Imaging signal-to-noise ratio of synthetic aperture LADAR

Liren Liu, Shanghai Institute of Optics and Fine Mechanics (China)

In a synthetic aperture ladar (SAL) the detected optoelectronic signal is temporal, but the output is a 2D image in the time-frequency and distance domain due to the focusing algorithm for imaging. Thus the resulted SNR in an image is different from the SNR in the reception which was well estimated before. So it is interesting to find the 2D SNR in the image space.

In this paper in terms of the photocurrent statistics the noise power spectrum of photocurrent as well as the other sources is first established, and then the relation of the image in power to the noise power background in the orthogonal direction of travel is mathematically figured out, which are connected with the transfer function of detector circuit, the integration time for focusing and the image width in this direction. The SNR is further accumulated along the travel direction. The 2D imaging SNR is derived for the down-looking SAL and side-looking SAL using the p-i-p photodiode or the avalanche photodiode. It is therefore seen that the imaging SNR is inherently enhanced in comparison with the SNR in the reception, the transfer function bandwith should be large enough to stabilize the image intensities and the increase of the integration time will increase both the image intensity and SNR.

On this base, we can correctly design a SAL system with the suitable

parameters such as the received optical power of signal, the dark-current noise, the transfer function of detector circuit, the integration time for focusing and the 2D image width.

9617-19, Session PWed

Improvement of the signal-to-noise ratio in static-mode down-looking synthetic aperture imaging LADAR

Zhiyong Lu, Jianfeng Sun, Ning Zhang, Yu Zhou, Guangyu Cai, Liren Liu, Shanghai Institute of Optics and Fine Mechanics (China)

This paper presents a static mode synthetic aperture imaging ladar. The static mode synthetic aperture imaging ladar in which the target and carrying-platform were kept still during the collection process was proposed and demonstrated. The return signal energy can be collected with more time due to the target is irradiated continuously. The signal-to-noise ratio can be enhanced in this mode synthetic aperture imaging ladar. Compare to the traditional side-looking and trip-mode down-looking synthetic aperture imaging ladar, which can't keep the beam locating on the same target all the time, the static mode synthetic aperture imaging ladar has an advantage to the system sensitivity. We could obtain the remote target image at very low return levels. In the experiment, the target is 10m distance from the transmitting telescope, and power of the laser is about 3mW. The target image is rebuilt in different collected time. As the increasing of the illumination time, the clearer image is reconstructed. This technique has a great potential for applications in extensive synthetic aperture imaging ladar fields.

9617-21, Session PWed

Measurement of polarization parameters of the targets in synthetic aperture imaging LADAR

Qian Xu, Jianfeng Sun, Wei Lu, Peipei Hou, Zhiwei Sun, Zhiyong Lu, Xiaoping Ma, Liren Liu, Shanghai Institute of Optics and Fine Mechanics (China)

Synthetic aperture imaging ladar (SAIL) is the most possible optical method to provide centimeter-class resolution with a real aperture size of a few meters in thousand kilometers. Recently the techniques of SAIL have been found more attention and increasing applications in the field of remote sensing. In the SAIL, the polarization state change of the backscattered light will affect the image quality. Polarization state of the reflected field is always determined by the interaction of the light and the materials on the target plane, which related to the permittivity, roughness, even the surface structure of the material. The Stokes parameters can provide the information both on light intensity and on polarization state, thus can be recognized as the ideal quantities for characterizing the above features. In this paper, a measurement system of the polarization characteristic for the SAIL target materials is designed, which uses a laser operating at the wavelength of 1030nm. The results are expected to be useful in target identification and recognition.

9617-22, Session PWed

A balanced APD photodetection technology for large field of view coherent receiver

Guo Zhang, Zhou Yu, Jianfeng Sun, Baoliang Li, Liren Liu, Guang-Yu Cai, Shanghai Institute of Optics and Fine Mechanics (China) In the Siegman antenna theory, the effective aperture integrated over all possible arrival directions (all solid angle) is essentially the signal wavelength squared. Improving only the solid angular field of view or the effective aperture does not improve the final SNR, so increasing the field of view and the effective receiving aperture while ensuring a higher signal to noise ratio of the received signal has become a key limitation of coherent receiver in large field of view and high sensitivity photodetection application.

SPIE. PHOTONICS

OPTICAL ENGINEERING+ APPLICATIONS

Currently, the near-infrared single photon detection system has high sensitivity. It can detect weak near-infrared optical signal, but the nearinfrared single photon detection system needs avalanche photodiode(APD) operating in Geiger mode, however, the coherent receiver requires APD to operate in linear mode, so designing a system for coherent receiver to increase the photodetection field of view and sensitivity is very important.

In this paper a kind of balanced APD photodetection system which uses APD operating in the linear mode as a photoelectric conversion unit to improve the photodetection sensitivity and balanced photodetection technology to improve the signal to noise ratio for coherent receiver system is designed. Theoretical analysis of the key specifications of the balanced APD photodetection system including stability, noise equivalent power, gain, bandwidth, etc. is given. Corresponding optical detection system to verify its advantages of greatly improving the field of view and sensitivity, which satisfy the coherent receiver's requirements.

9617-23, Session PWed

Resampling technique in the orthogonal direction for down-looking SAIL

Guangyuan Li, Jianfeng Sun, Zhiyong Lu, Ning Zhang, Guang-Yu Cai, Zhiwei Sun, Liren Liu, Shanghai Institute of Optics and Fine Mechanics (China)

The down-looking synthetic aperture imaging ladar(SAIL) with a transmitter of two coaxial and scanned polarization-orthogonal beams of spatial spherical and parabolic phase difference and a receiver of self-heterodyne detection in laboratory and outdoor has been constructed and demonstrated. The implementation of synthetic aperture imaging uses quadratic phase history reconstruction in the travel direction and linear phase modulation reconstruction in the orthogonal direction through Fourier transform.

The linear phase modulation in the orthogonal direction of travel is generated by the shift of two cylindrical lens in the two polarizationorthogonal beams. Therefore, the fast-moving of two cylindrical lens is necessary for airborne down-looking SAIL to match the aircraft flight speed and to realize the compression of the orthogonal direction, but the quick stop and the quick start of the cylindrical lens must greatly damage the motor. To reduce the damage, we make the motor move like a sinusoidal curve to make it more realistic movement, and propose a resampling interpolation imaging algorithm, through which we can transform the nonlinear phase to linear phase.

Three different resampling interpolation methods are analyzed, and we get good reconstruction results of point target and area target in laboratory compared with the results under linear phase modulation. The influences on imaging quality in different sampling positions when the motor make a sinusoidal motion are analysed. At last, we performe a comparison of the results of the two cases in resolution.

9617-24, Session PWed

A demonstrator of all-optronic multifunctional down-looking synthetic aperture LADAR

Wei Lu, Zhiyong Lu, Zhiwei Sun, Ning Zhang, Jianfeng Sun, Lijuan Wang, Liren Liu, Shanghai Institute of Optics and Fine Mechanics (China)

Conference 9617: Unconventional Imaging and Wavefront Sensing XI



A synthetic aperture ladar can provide two-dimensional active imaging of centimeter-class resolution at a long range. Recently an idea of downlooking synthetic aperture ladar (DL SAL) was developed, which represents a completely new structure of SAL and has the important features such as a big coverage with an enhanced receiving aperture and little influence from atmospheric turbulence and other factors. However a DL SAL has much bigger coverage area than a side-looking SAL, a flow of high-resolution images will produce a large amount of data. It is thus predicted that the further improvement to enhance the processing speed from data acquisition to image reconstruction by using an all optical sensing-to-processing chain is useful.

In this paper, the design and laboratory experiment of a demonstrator of alloptronic DL SAL is presented. The demonstrator consists of a DL SAL unit with an optical scanner for transmitting and receiving beams and an optical processor. The designed DL SAL unit is able to function in one of the stripmap mode, spotlight mode or static mode. The optical processor is simple in construction and reconstructs the image in real time and in parallel. From the experiments the ultra-fast processing capability from image acquisition to real-time reconstruction is shown, the all-optical design would provide a compact, lightweight and on-board DL SAL system.

The DL SAL unit uses two coaxial orthogonally polarized beams in transmitter and polarization interference based self-heterodyning detection in receiver. And the linear phase modulation necessary to obtain the target range information in the orthogonal direction of travel is generated by the projection of two cylindrical lenses with a mutual shifting and the quadratic phase modulation necessary to achieve the target phase history in the travel direction is produced by the projection of other two cylindrical lenses, movable if needed. By managing the mutual movement of the SAL and target, the scanner and the cylindrical lenses, therefore, different working modes can be realized. In principle the acquired 2D data is processed to reconstruct the 2D image of target in terms of a focusing algorithm with the Fourier transform in the crossed direction and the matched filtering with a conjugate quadric phase of phase history in the travel direction. Accordingly, the optical processor is designed as an astigmatic optical system, which reduces to a 4-f Fourier transform system in the plane containing the orthogonal direction of travel and functions the free-space propagation with the Fresnel diffraction in the plane containing the travel direction thus to yield the matched filtering with a guadric phase. A spatial light modulator is used as the input interface of the processor, on which the 2D data output from the DL SAL unit are displayed, so that the focused 2D image of the target is visually observed on the processor output plane. A SAL works inherently on the propagation condition of far-field. The experimental verification and test of the all-optronic DL SAL demonstrator in the laboratory space is carried out in a simulated far-field condition by using an optical collimator with a lens of long focal length. Various experimental results are resulted.

9617-25, Session PWed

Dual-mode photosensitive arrays based on integration of liquid crystal microlenses and CMOS sensors for obtaining intensity images and wavefronts

Qing Tong, Yu Lei, Huazhong Univ. of Science and Technology (China)

As we all know, because the index of refraction of the conventional microlens array (MLA) is not variable, the wavefront sensor based on the conventional MLA can only obtain the intensity image with low-resolution when it is used to test the wavefront information simultaneously. So we use the dual-mode photosensitive arrays based on the liquid crystal (LC) MLA and CMOS sensors to obtain both intensity images with high-resolution and wavefronts. The LC MLA is adjoining to the CMOS sensors. When the voltage is applied the LC MLA forms an array of spots on the focal plane, and the LC MLA without voltage looks like a piece of glass. Therefore the dual-mode photosensitive arrays can work between an imaging mode and a wavefront mode by switching the voltage off and on. Moreover we can test the wavefronts in a certain area with a certain resolution and the wavefronts or images in other areas with other resolutions at the same time by using the LC MLA with multi-layered and divisional top patterned electrodes. The field

of the view of the LC MLA is also variable by changing the voltage in theory. Now we are doing the experiments to compare the composite wavefronts of the object exposured in a white light source (ARC LAMP SRC F/1 COLL COND, Newport Corporation) with the wavefronts of the same object in tricolor laser sources (Red: 671nm; Green: 532nm; Blue: 473nm, Changchun New Industries Optoelectronics Tech. Co., Ltd (CNI)), to prove that the composite wavefronts of the white light can be used to test the wavefront information. And we will do the researches mentioned before in the next work. Because of the absorption of the indium tin oxide (ITO) to the infrared (IR) light is very strong, the LC MLA with ITO electrode can only be used in the visible spectrum now, however we are finding other material to replace the ITO, so that the LC MLA can be used in the IR.

9617-26, Session PWed

Some characteristics of the E-ELT's "sodium LGSs"

Nourredine N. Moussaoui, Univ. des Sciences et de la Technologie Houari Boumediene (Algeria)

The characteristics of the sodium Laser Guide Stars "LGSs" could be severely affected by the action of several parameters. We propose in this paper to estimate the effect of some parameters on the "sodium LGSs" of the European-Extremely Large Telescope "E-ELT". The laser guide star photon return flux and consequently the laser power requirement are driven by the spot elongation. It is essential to know the evolution of this parameter, in order to optimize the characteristics of the sodium laser guide star. The angular spot elongation as observed on the ground is evaluated taking into account the temporal evolution of the mesospheric sodium layer. The sodium layer thickness and its centroid height impact strongly the LGSs spot size.

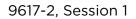
The magnitude of these guide stars could be severely affected by the earth's magnetic field. Even the intensity of this field is not very strong; it can cause a transfer of the atomic population from one sublevel to another one. This is called a redistribution of the atomic population between the magnetic sublevels. So, we have to take into account this effect in the determination of the "sodium LGSs" characteristics. In this paper, we present an analytical approach to calculate the occupation probabilities of the sodium magnetic sublevels in presence of a magnetic field. We focus on the magnetic sublevels of the sodium D2a transitions. This work aims to estimate the effect of the geomagnetic field on the characteristics of the "sodium LGSs" produced by circularly polarized laser beam.

9617-1, Session 1

Multi-conjugate adaptive optics (MCAO): analysis and assessment

Katharine J. Jones, WBAO Consultant Group (United States)

Multi-conjgate Adaptive Optics (MCAO) is an essential approach to wavefront sensing and control. The concept of MCAO corrects each "layer" of the atmosphere independently. Correction devices (deformable mirrors) are placed in "series" and assigned one layer of atmosphere to correct the isoplanatic patch. MACAO can be approached two ways: with multi-guide stars or multi; ayer correction. The objective of this paper is to analyze both approaches and assess their effectiveness to achieve their goals. Wavefront correction is being carried out in the Large Binocular Telescope (LBT) by means of multiple Laser Guide Stars. Multi-Ilayer correction is being achieved by the Solar telescope GREGOR. The Large Binocular Telescope achieves MCAO by using two different Laser Guide Stars. Il uses four Rayleigh beacons at 532 nm for each of two 8.4 m component telescopes. Six Rayleigh guide stars are oriented as equilateral triangles. Sodium LGS AO correction will be added to the LBT at a later stage at 589 nm. The Solar telescope GREGOR achieves MCAO by employing three deformable mirrors at different levels above the ground in series. This paper will analyzed both multi-wavelength and multi-level MCAO for effectiveness in compensating turbulence for distortion correction.



Wavefront-sensor tomography for measuring spatial coherence

Bohumil Stoklasa, Libor Motka, Jaroslav Rehacek, Zdenek Hradil, Palacky Univ. Olomouc (Czech Republic); Luis Lorenzo Sánchez-Soto, Univ. Complutense de Madrid (Spain)

The operation of wavefront sensors is most often understood in an oversimplified geometrical-optics framework, which is much the same as assuming full coherence of the detected signal. However, this is not a complete picture: even in the simplest instance of beam propagation, the knowledge of the coherence features turns out to be essential. We confine ourselves to the example of the Shack-Hartmann (SH) sensor. An incoming light field is dividend into a number of sub-apertures by a microlens array that creates focal spots, registered in a CCD camera. The deviation of the spot pattern from a reference measurement allows the local direction angles to be derived, which in turn enables the reconstruction of the wavefront. Unfortunately, this geometric picture breaks down when the signal is partially coherent, because the very notion of a single wavefront becomes somewhat ambiguous: the signal has to be conceived as a statistical mixture of many wavefronts. To circumvent this difficulty, we observe that these sensors provide a simultaneous detection of position and angular spectrum (i.e., directions) of the incident radiation, which is determined by the position of the detected signal on the CCD. In other words, SH measurements are pertinent examples of simultaneous unsharp position and momentum measurements, a question of fundamental importance in quantum theory. In this contribution we will point out that common wavefront sensors can be utilized for measuring mutual coherence and hence 3D imaging of partially coherent fields provided quantum state reconstruction techniques are adopted for data processing.

9617-5, Session 1

Digital holography wave-front sensing in the presence of strong atmospheric turbulence and thermal blooming

Mark F. Spencer, Air Force Research Lab. (United States); Michael J. Steinbock, Air Force Institute of Technology (United States)

Digital holography wave-front sensing shows distinct potential for directedenergy and remote-sensing applications. For instance, digital holographic detection provides access to the amplitude and wrapped phase associated with an optical field. From the wrapped phase, one can estimate the atmospheric aberrations present and perform adaptive-optics compensation and high-resolution imaging. This paper develops wave-optics simulations which explore the estimation accuracy of digital holography wave-front sensing in the presence of strong atmospheric turbulence and thermal blooming. Specifically, this paper models plane-wave propagation pthrough varying atmospheric conditions along a horizontal propagation path and formulates the field-estimated Strehl as a function of the log-amplitude variance, the distortion number, and the ratio of the detector plane pixel size to the coherence diameter. Such results will allow one to assess the number of pixels needed in a detector array when using digital holography detection in the presence of strong atmospheric turbulence and thermal blooming.

9617-6, Session 1

Artificial turbulence generation by means of different types of piezoceramic deformable mirrors

SPIE. PHOTONICS

OPTICAL ENGINEERING+ APPLICATIONS

Alexis V. Kudryashov, Anna Lylova, Julia Sheldakova, Vadim Samarkin, Active Optics Night N Ltd. (Russian Federation)

No Abstract Available

9617-27, Session 1

Three-dimensional polarimetric imaging in a snapshot

Sudhakar Prasad, Z. Yu, The Univ. of New Mexico (United States)

A recent proposal [1] based on encoding the axial depth of a narrowband point source in the angle of rotation of its off-axis image has greatly enhanced the prospects of full three-dimensional (3D) localization of point sources over a large 3D field with high transverse and axial resolution. This new approach has added to the host of other rotating point spread functions (PSFs), including the double-helix [2,3] and corkscrew PSFs [4], already available for 3D localization, particularly for application to single-molecule biological microscopy. Combining information about the 3D location and polarization state of the source is of vital interest in this application, in which the polarimetric information may uniquely reveal the nature of the local biological environment of the source dipole [5]. In other applications, such as remote sensing, such combined information may localize with high contrast specularly reflecting objects against a diffusely scattering background [6]. In the present work, we carefully treat the non-paraxial nature of light propagation over a large imaging aperture in high numerical-aperture (NA) microscopy using the rotating PSF of Ref. [1]. Such propagation is attended by nontrivial vector dependences of the radiation fields, which can encode information about the full 3D dipolar state of the emitter in the spatial brightness distribution, or its image, acquired by the microscope sensor. By placing a phase mask with a zoned spiral phase structure in a conjugate plane of the imaging aperture [1], one can create a coherent superposition of approximate Bessel beams of varying orbital angular momentum (OAM) guantum numbers and thus also acquire information about the 3D spatial location of the emitter via the center and angle of rotation of the PSF that results from the focusing of such a superposition. We describe the results of our theoretical work and simulations based on this theory for acquisition and recovery of joint 3D polarimetric information of point dipole emitters in a large 3D field in the snapshot mode, which offers the promise of rapid, perhaps video-rate, polarimetric 3D localization microscopy. The use of a g-plate [7], which is a fixed-wave phase plate but with a local axis of birefringence that rotates with the azimuthal angle coordinate of the position on the plate, allows conversion of the spin angular momentum (SAM) of the imaging beam, which is directly controlled by the state of polarization of the dipole emitter, into a corresponding OAM state. Combining a g-plate with the spiral phase mask of the type proposed in Ref. 1 then permits the acquisition of 3D polarimetric information without the need for high-NA microscopy, and opens the way for its use in typically ultralow-NA telescopic imaging as well. We shall also briefly discuss a theoretical analysis of this model and computer simulations exploiting it for joint 3D polarimetric-localization imaging in a snapshot.

9617-7, Session 2

Geometric superresolution by scanning two rect masks - with relative path difference

Ihtsham U. Haq, National Physical and Standard Lab.



(Pakistan) and Pakistan Institute of Engineering and Applied Sciences (Pakistan) and Pakistan Council of Scientific and Industrial Research (Pakistan); Asloob A. Mudassar, Pakistan Institute of Engineering and Applied Sciences (Pakistan); Ihtram U. Haq, Univ. of Karachi (Pakistan)

Today, in everyday imaging in science and research, a digital imager – despite of its lower resolution than conventional film camera, is the first choice due to its obvious advantages. Assuming the imaging system to be diffraction limited, this low resolution is due to two geometrical characteristics of the detector array (CCD/CMOS) used in it at image plane. These two characteristics are pitch and non-zero pixel size – which do sampling and averaging of optical information over pixel spatial area respectively and dictates geometric resolution limit of digital imager.

In this paper, we are proposing a geometric superresolution technique based on scanning of composite rect masks (CRM) over CCD. The two different composite masks are realized from two component Rect masks by introducing zero and single subpixel path difference between them. The CRM are scanned over CCD by half pixel in subpixel steps. The CRM optically codes the image over CCD- which is then decoded computationally from recorded coded digital images to get a super-resolved image – which is spatially enhanced in resolution by subpixel factor. This virtually replaces each CCD pixel by a matrix of subpixels. The decoding process is executed in just one mathematical step. The widths of the component Rect masks are set to achieve maximum SNR – keeping the system deterministic under relative scanning of these masks over CCD.

The 2D simulation results are presented – showing an improvement in resolution by given super-resolution factor - in both x and y directions. Increasing the super-resolution factor more makes the result more close to original. The given superresolution technique can be applied to microscopy, medical imaging, machine vision, industrial inspection, metrology (dimensional metrology, optical metrology), defense, satellite imaging and astronomy.

9617-8, Session 2

Laboratory validation of a sparse aperture image quality model

Philip S. Salvaggio, Rochester Institute of Technology (United States)

The majority of image quality studies in the field of remote sensing have been performed on systems with conventional aperture functions. These systems have well-understood image quality tradeoffs, characterized by the General Image Quality Equation (GIQE). However, in order to continue pushing the boundaries of imaging, more control over the system's pointspread function is needed. Examples include sparse apertures, synthetic apertures, coded apertures and phase elements. As a result of the nonconventional point spread functions of these systems, post-processing becomes a critical step in the imaging process and artifacts arise that are more complicated than simple edge overshoot. Previous research at the Rochester Institute of Technology's Digital Imaging and Remote Sensing Laboratory has resulted in a modeling methodology for sparse and segmented aperture systems, the validation of which will be the focus of this work. This methodology has predicted some unique post-processing artifacts that arise when a sparse aperture system is used over a large (panchromatic) spectral bandpass. Since these artifacts are unique to sparse aperture systems, they have not yet been observed in any real-world data. In this work, a laboratory setup and initial results for a model validation study will be presented. Initial results will focus on the validation of spatial frequency response predictions and verification of post-processing artifacts. The goal of this study is to allow the artifact predictions of this model to be used in image quality studies of non-conventional systems, such as aperture design optimization and the signal-to-noise vs. post-processing artifact tradeoff resulting from choosing a panchromatic vs. multispectral system.

9617-9, Session 2

Multiple-baseline detection of a geostationary satellite with the Navy precision optical interferometer

J. Tom Armstrong, Ellyn K. Baines, Henrique R. Schmitt, Sergio R. Restaino, James H. Clark, U.S. Naval Research Lab. (United States); James A. Benson, Donald J. Hutter, Bob T. Zavala, U.S. Naval Observatory (United States)

Using the Navy Precision Optical Interferometer (NPOI), we have made the first multiple-baseline interferometric detection of a satellite.

The observations, carried out during the March 2015 glint season, succeeded in detecting the DirecTV-7S satellite with interferometer baseline lengths of 8.8 m and 9.8 m and wavelengths from 850 nm to 550 nm, corresponding to a resolution of ~0.02 arcsec, or 4 m at geostationary altitude. This is the first multiple-baseline interferometric detection of a satellite.

9617-10, Session 3

Spectrum engineering for ultrafast imaging

Eric Huang, Qian Ma, Zhaowei Liu, Univ. of California, San Diego (United States)

Conventional imaging techniques use arrays of light detectors to capture an image. However, in order to record the image, each of these detectors must be read electronically. As a result, the ultimate imaging speed of a conventional camera is usually limited to the electronic bandwidth of the readout circuit, which is often too slow to view many processes of interest. A relatively new technique called Compressive Sensing, on the other hand, provides a method for greatly reducing the number of samples needed to take an image, potentially offering an avenue to increase imaging speed. However, current compressive sensing methods work by sampling an image with spatial light modulators, which rely on arrays of electronically controlled optical modulators that are often many orders of magnitude slower than the light detectors used to measure them. Here, we show an experimental demonstration of a method which uses devices with a recently developed ultrafast spatial light modulator that can reach frame rates in the megahertz range. This method can also be applicable to nanoscale structures for the combination of both high-speed and high-resolution imaging.

9617-11, Session 3

Remote sensing solution using 3-D flash LADAR for automated control of aircraft

Brian J. Neff, U.S. Air Force (United States)

Laser Radar imagers known as FLASH LADAR sensors can be designed to provide 2-D and 3-D images of a scene in a single pulse from the laser illuminator. For 3-D sensors, the benefit of having range and intensity for every pixel in the image is obvious, and there are numerous civilian and military applications of interest. This effort will present test results from a 3-D FLASH Laser Radar (LADAR) imaging system flown onboard a small cargo aircraft. The imaging system will be used to image both airborne and ground based targets to demonstrate the utility of 3-D FLASH LADAR for a variety of missions. Previous research employing scanning LADAR for airborne targets yielded disappointing results. However, scanning LADAR is not optimized for imaging environments where both the host platform and target are moving independent of each other. This work will demonstrate that 3-D FLASH LADAR is optimized for this imaging environment, as range and orientation can simultaneously be determined with great precision. Being able to determine range and orientation will be imperative for tasks such as automated aerial refueling. Additionally, images of ground based targets of interest will be collected for analysis and



development of techniques for various missions such as utility line surveys and automated landing of aircraft. Finally, this work seeks to gather and make publicly available a large collection of images for further development and advancement of the technology.

9617-12, Session 3

Experimental method of generating electromagnetic Gaussian Schell-model beams

Matthew J. Gridley, Milo W. Hyde IV, Air Force Institute of Technology (United States); Mark F. Spencer, Air Force Research Lab. (United States); Santasri Basu, Air Force Institute of Technology (United States)

The purpose of this research effort is to experimentally generate an electromagnetic Gaussian Schell-model beam from two coherent linearly polarized plane waves. The approach uses a sequence of mutually correlated random phase screens on phase-only liquid crystal spatial light modulators at the source plane. The phase screens are generated using a published relationship between the screen parameters and the desired electromagnetic Gaussian Schell-model source parameters. The approach is verified by comparing the experimental results with published theory and numerical simulation results. This work enables the design of an electromagnetic Gaussian Schell-model source with prescribed coherence and polarization properties.

9617-13, Session 3

Laser beam propagation and wavefront correction in turbid media

Alexis V. Kudryashov, Ilya Galaktionov, Julia Sheldakova, Active Optics Night N Ltd. (Russian Federation)

No Abstract Available

9617-14, Session 4

Transparent-conductor/oxide/silicon plasmonic photocapacitor for spectral imaging

Farnood Khalilzadeh-Rezaie, Christian W. Smith, Michael S. Lodge, Janardan Nath, Univ. of Central Florida (United States); Justin W. Cleary, Air Force Research Lab. (United States); Masahiro Ishigami, Robert E. Peale, Univ. of Central Florida (United States)

We demonstrate a single pixel of a potential compact spectral imager based on electronic detection of surface plasmon polaritons (SPPs). The technology exploits the angle- and wavelength-dependent excitation of SPPs on one surface of a Kretschmann prism coupler to generate the necessary spectral selection. The SPPs are then detected by a close-coupled transparent-conductor/silicon-oxide/silicon photocapacitor. The transparent conductor, which so far has been graphene or thin gold, is used to detect and control photo-generated charge accumulation at the Si/SiO2 interface. A small negative bias applied on the transparent conductor extinguishes the response. The resulting device potentially enables an ultra compact spectral imager. Though this demonstration is made at visible wavelengths, the method is readily extendable to infrared and even mm-waves.

9617-15, Session 4

Light field modulation of computational ghost imaging with defocus blur

Weiliang Zhang, Wenwen Zhang, Qian Chen, Guohua Gu, Nanjing Univ. of Science and Technology (China)

In recent years, as a new imaging method, ghost imaging has many features that are not included in conventional imaging. The main advantage is the ability to resist the atmospheric turbulence effect partially and separate object from image. Computational ghost imaging eliminates the need for experimental aspects of the reference arm and calculates the virtual reference field by Huygens - Fresnel diffraction theory. It has been emphasized in many papers that the distance between the reference arm and the measuring arm must be consistent. However, we cannot confirm the distance between the object and light source in advance, which often leads to defocus blur effect of the final reconstructed image. In order to solve this problem, we put forward secondary computational ghost imaging based on light field modulation.

The spatial distribution of beam produced by the light source does not need to be measured and recorded by additional detectors (CCD), and the beam is directly modulated by spatial light modulator (SLM). Firstly, we use the low resolution stochastic matrix to modulate the light field and obtain a severely blurred image in accordance with the correlated imaging algorithm. Then we use the high resolution stochastic matrix for further modulation by setting the weighting ratio of the blurred image. The final reconstructed images not only suppress the defocus blur, but also improve the ability of anti-atmospheric turbulence. Further studies have shown that defocus blur of three-dimensional objects still can be eliminated by our method.

SPIE PHOTONICS

CONNECTING MINDS. ADVANCING LIGHT.



OPTICS + PHOTONICS

The latest research in optical engineering and applications, nanotechnology, sustainable energy, and organic photonics

MARK YOUR CALENDAR

WWW.SPIE.ORG/OP2016

San Diego Convention Center San Diego, California, USA

Conferences & Courses 28 August–1 September 2016 Exhibition 30 August–1 September 2016